
2007 Abstracts

Twenty-Ninth Annual Meeting of the American Society for Bone and Mineral Research

**Hawaii Convention Center
Honolulu, Hawaii, USA
September 16-19, 2007**

The *Journal of Bone and Mineral Research* (ISSN: 0884-0431) provides a forum for papers of the highest quality pertaining to all areas of the biology and physiology of bone, the hormones that regulate bone and mineral metabolism and the pathophysiology and treatment of disorders of bone and mineral metabolism. The *Journal of Bone and Mineral Research* is the official journal of the American Society for Bone and Mineral Research and is published monthly plus a special issue in September by the American Society for Bone and Mineral Research, 2025 M Street, N.W., Suite 800, Washington, DC 20036-3309, USA. Address reprint/offprint inquiries to the Sheridan Press at US (717) 632-8448 x 8167. Periodicals postage paid in Washington, DC, and additional offices. POSTMASTER SEND ADDRESS CHANGES TO: Journal of Bone and Mineral Research, P.O. Box 2759, Durham, NC 27715, USA. 2007 Subscription Rates: U.S.: Personal \$495.00; Institutional: \$615.00; Canada/Mexico: Personal \$515.00; Institutional \$645.00; Overseas: Personal \$570.00; Institutional: \$665.00. Single issue \$50.00. Subscription term is January - December.

Claims for missing issues will be serviced at no charge if received within six months of issue date {journal@jbmr.org, or fax (US) 919-620-8465}. Duplicate copies cannot be sent to replace issues not delivered because of failure to notify publisher of change of address. Please notify ASBMR of new address six (6) weeks in advance of moving date. All subscriptions are payable in advance in U.S. funds drawn on a U.S. bank. If not fully satisfied, notify publisher for a refund on all unmailed issues.

Address advertising and commercial reprint inquiries to Mr. Steve Kavalgian, Mill River Media LLC, 141 Boston Post Rd. Old Lyme, CT 06371-1303, USA; (860) 434-6889 (phone); (860) 434-9744 (fax); millrivermedia@aol.com (e-mail). Advertisements are subject to editorial approval.

No responsibility is assumed, and responsibility is hereby disclaimed, by the American Society for Bone and Mineral Research and the *Journal of Bone and Mineral Research* for any injury and/or damage to persons or property as a matter of products liability, negligence or otherwise, or from any use or operation of methods, products, instructions or ideas presented in the *Journal*. Independent verification of diagnosis and drug dosages should be made. Discussions, views and recommendations as to medical procedures, choice of drugs and drug dosages are the responsibility of the authors. Advertisers are responsible for compliance with requirements concerning statements of efficacy, approval, licensure, and availability.

The *Journal of Bone and Mineral Research* is a **Journal Club™** selection. The *Journal* is indexed by *Index Medicus*, *Current Contents/Life Science*, *CABS (Current Awareness in Biological Sciences)*, *Excerpta Medica*, *Cambridge Scientific Abstracts*, *Chemical Abstracts*, *Reference Update*, *ScienceCitation Index*, and *Nuclear Medicine Literature Updating and Indexing Service*. Copyright © 2007 by the American Society for Bone and Mineral Research. For permission to reproduce copyrighted materials from the *Journal*, send requests to Deputy Director of Publications David Allen (david@jbmr.org), or mail the *Journal of Bone and Mineral Research*, P.O. Box 2759, Durham, NC 27715, USA; (919) 620-0681 (phone); (919) 620-8465 (fax). For libraries and other users registered with the Copyright Clearance Center, please contact the Copyright Clearance Center, 222 Rosewood Drive, Suite 910, Danvers, MA 01923, USA; www.copyright.com; (978) 750-8400 (phone); (978) 750-4470 (fax).

GUIDELINES FOR ABSTRACT READERS

The *JBMR* Supplement 1 Abstracts serves as a compiled version of the Abstracts. Authors submit their own abstracts and are charged a fee to do so. Each abstract must be sponsored by a current ASBMR member. Authors are responsible for the accuracy of the content that they post. Authors are responsible for ensuring compliance with applicable human subject and animal subject procedures. When an abstract is submitted, one person is identified as the Presenting Author, the person who is expected to present the abstract at the ASBMR Annual Meeting.

The ASBMR depends upon the honesty of the authors and presenters and relies on their assertions that they have had sufficient full access to the data to be and are convinced of its reliability. In accordance with the rules of Federation of American Societies for Experimental Biology (FASEB), the ASBMR expects that authors and presenters:

- Will disclose any conflicts of interest, real or perceived.
- Should disclose any relationship that may bias one's presentation or which, if known, could give the perception of bias.
- Will affirm, for any study funded by an organization with a proprietary or financial interest, that they had full access to all the data in the study.
- Are responsible for the content of abstracts, presentations, slides, and reference materials.
- Keep the planning, content and execution of abstracts, speaker presentations, slides, abstracts and reference materials free from corporate influence, bias, or control.
- Should give a balanced view of therapeutic options by providing several treatment options, whenever possible, and by always citing the best available evidence.
- Should disclose when any commercial product is not labeled for the use under discussion or that the product is still investigational.

The ASBMR:

- Will note those speakers who have disclosed relationships, including the nature of the relationship and the associated commercial entity.
- Peer-review the abstracts according to categories, but only to determine which will be selected for oral presentation, for poster presentations, or for any awards. Abstracts are not otherwise subject to any quality or content review by ASBMR or *JBMR*.
- Expects the audience for the Abstracts to be researchers, physicians, clinicians and other allied health professionals.
- Protects the Abstracts by copyright, and prohibits the reproduction, distribution, or transmission of the abstracts without the express written permission of ASBMR.
- Embargoes the Abstracts for public release in written, oral and electronic communications until one hour after the abstract has been presented.

Disclaimer. All authored abstracts, findings, conclusions, recommendations, or oral presentations are those of the author(s) and/or speaker(s) and do not reflect the views of the American Society for Bone and Mineral Research or imply any endorsement. No responsibility is assumed, and responsibility is hereby disclaimed, by the American Society for Bone and Mineral Research for any injury and/or damage to persons or property as a matter of products' liability, negligence or otherwise, or from any use or operation of methods, products, instructions or ideas presented in the abstracts or at the ASBMR Annual Meeting. Independent verification of diagnosis and drug dosages should be made. Discussions, views and recommendations regarding medical procedures, choice of drugs, and drug dosages are the responsibility of the authors and presenters.

TABLE OF CONTENTS

General Information	xviii
 FRIDAY, SEPTEMBER 14, 2007	
Day-at-a-Glance	xxxvi
 SATURDAY, SEPTEMBER 15, 2007	
Day-at-a-Glance	xxxvi
 SUNDAY, SEPTEMBER 16, 2007	
Day-at-a-Glance	xxxvii
 MONDAY, SEPTEMBER 17, 2007	
Day-at-a-Glance	xxxix
 TUESDAY, SEPTEMBER 18, 2007	
Day-at-a-Glance	xli
 WEDNESDAY, SEPTEMBER 19, 2007	
Day-at-a-Glance	xlii
 Abstracts Key	 S1
Abstracts	S2
Author Index	S511



JBM^R Journal of Bone and Mineral Research

Official Journal of the American Society for Bone and Mineral Research

Editor-in-Chief

John A Eisman
Sydney, Australia

Associate Editors

Sylvia Christakos
Newark, NJ, USA

Pamela Gehron Robey
Bethesda, MD, USA

Gerard Karsenty
Houston, TX, USA

Shigeaki Kato
Tokyo, Japan

Huibert AP Pols
Rotterdam, The Netherlands

G David Roodman
Pittsburgh, PA, USA

Clifford Rosen
Bangor, ME, USA

Andrew F Stewart
Pittsburgh, PA, USA

Rajesh V Thakker
Headington, Oxford, UK

Editors Emeritus

Marc K Drezner, Madison, WI, USA
Lawrence G Raisz, Farmington, CT, USA

Managing Editor David Allen, 3209 Guess Rd, Suite 201, Durham, NC 27705, USA, phone: (919) 620-0681, fax: (919) 620-8465, email: journal@jbm^r.org

Editorial Board

Yousef Abu-Amer, *USA*
H Clarke Anderson, *USA*
John JB Anderson, *USA*
Troels T Andreassen, *Denmark*
Zvi Bar-Shavit, *Israel*
Paolo Bianco, *Italy*
Joseph P Bidwell, *USA*
Neil Binkley, *USA*
Lynda Bonewald, *USA*
Brendan F Boyce, *USA*
M Leonor Cancela, *Portugal*
Xu Cao, *USA*
Marco Cecchini, *Switzerland*
Timothy Chambers, *United Kingdom*
Chantal Chenu, *United Kingdom*
Roberto Civitelli, *USA*
Bart L Clarke, *USA*
Juliet E Compston, *United Kingdom*
Steven R Cummings, *USA*
Hong-Wen Deng, *USA*
Gabriel DiMattia, *Canada*
Patricia Ducey, *USA*
Thomas A Einhorn, *USA*
Ghada El-Hajj Fuleihan, *Lebanon*
Solomon Epstein, *USA*

Kenneth G Faulkner, *USA*
Nicola Fazzalari, *Australia*
Serge L Ferrari, *Switzerland*
Lorraine Fitzpatrick, *USA*
Tatiana Foroud, *USA*
Mark Forwood, *Australia*
Peter A Friedman, *USA*
Seiji Fukumoto, *Japan*
Edith M Gardiner, *Australia*
Louis C Gerstenfeld, *USA*
Matthew T Gillespie, *Australia*
Ted S Gross, *USA*
Jerome J Guicheux, *France*
Theresa A Guise, *USA*
Geoffrey N Hendy, *Canada*
Michael F Holick, *USA*
Lexie Shannon Holliday, *USA*
Suzanne M Jan de Beur, *USA*
Teppo LN Järvinen, *Finland*
Sundeep Khosla, *USA*
Douglas P Kiel, *USA*
Robert F Klein, *USA*
Tatsuya Kobayashi, *USA*
Christopher S Kovacs, *Canada*
Paul H Krebsbach, *USA*

William Landis, *USA*
Nancy E Lane, *USA*
Craig B Langman, *USA*
Brendan Lee, *USA*
Mary B Leonard, *USA*
Anne C Looker, *USA*
Sharmila Majumdar, *USA*
Koichi Matsuo, *Japan*
Laurie K McCauley, *USA*
Christian Meier, *Switzerland*
Ralph A Meyer Jr, *USA*
Karl Michaelsson, *Sweden*
Leif Mosekilde, *Denmark*
Toshitaka Nakamura, *Japan*
Tally Naveh-Many, *Israel*
Tuan V Nguyen, *Australia*
Riko Nishimura, *Japan*
J Patrick O'Connor, *USA*
Regis O'Keefe, *USA*
Lynne A Opperman, *USA*
Roberto Pacifici, *USA*
A Michael Parfitt, *USA*
Eleftherios P Paschalis, *Austria*
John M Pettifor, *South Africa*
Anthony A Portale, *USA*

Richard L Prince, *Australia*
L Darryl Quarles, *USA*
Stuart H Ralston, *United Kingdom*
D Sudhaker Rao, *USA*
Helmtrud I Roach, *United Kingdom*
F Patrick Ross, *USA*
Janet E Rubin, *USA*
Isidro Salusky, *USA*
Philip N Sambrook, *Australia*
H Wayne Sampson, *USA*
Ernestina Schipani, *USA*
Ego Seeman, *Australia*
Marcus J Seibel, *Australia*
Eileen M Shore, *USA*
Stuart Silverman, *USA*
Frederick R Singer, *USA*
Ethel S Siris, *USA*
Malcolm Snead, *USA*
Larry J Suva, *USA*
Shu Takeda, *Japan*
Sakae Tanaka, *Japan*
Dwight A Towler, *USA*
Connie M Weaver, *USA*
Thomas J Wronski, *USA*
John J Wysolmerski, *USA*

www.jbm^ronline.org

AMERICAN SOCIETY FOR BONE AND MINERAL RESEARCH (ASBMR)

OFFICERS

President: Steven R. Goldring, M.D.
Past-President: Elizabeth Shane, M.D.
President-Elect: Barbara Kream, Ph.D.
Secretary-Treasurer: Keith Hruska, M.D.
Past Secretary-Treasurer: Marc Drezner, M.D.

COUNCILORS

Maria Luisa Brandi, M.D., Ph.D.	<i>Term expires 2009</i>	René Rizzoli, M.D.	<i>Term expires 2007</i>
Roberto Civitelli, M.D.	<i>Term expires 2009</i>	Janet Rubin, M.D.	<i>Term expires 2008</i>
Michael J. Econs, M.D.	<i>Term expires 2008</i>	Thomas Spelsberg, Ph.D.	<i>Term expires 2007</i>
Theresa Guise, M.D.	<i>Term expires 2007</i>	René St. Arnaud, Ph.D.	<i>Term expires 2009</i>
Mark C. Horowitz, Ph.D.	<i>Term expires 2008</i>	John Eisman, M.B.B.S., Ph.D.	<i>Ex Officio</i>

ASBMR STAFF

Greg Akroyd, <i>Marketing and Communications Manager</i>	Alison Gershen, <i>Association Coordinator</i>
David Allen, <i>Deputy Director of Publications</i>	Cara Hill, <i>Registration Assistant</i>
Gretchen Bretsch, <i>Project Manager</i>	Melissa Huston, <i>Senior Convention Manager</i>
Kimberly Buffington, <i>Exhibits Coordinator</i>	Matthew Kilby, <i>Senior Publications Assistant</i>
Angela Cangemi, <i>Senior Program Associate</i>	Kelly Marks, <i>Convention Manager</i>
Marc Charon, <i>Senior Director of Finance</i>	Earline Marshall, <i>Senior Grants Administrator</i>
Danielle Danko, <i>Marketing and Communications Associate</i>	Maureen McBride, <i>Association Associate</i>
Lisa Dittrich, <i>Director of Publications</i>	Rebecca Myers, <i>Program Manager</i>
Ann L. Elderkin, P.A., <i>Executive Director</i>	Elizabeth Nall, <i>Housing Coordinator</i>
Aaron Fennell, <i>Editorial Assistant</i>	Janine O'Donnell, <i>Senior Association Associate</i>
Douglas Fesler, <i>Associate Executive Director</i>	Wayne Horton, <i>Registration Coordinator</i>
Bill Gaskill, <i>Senior Accountant</i>	

ASBMR BUSINESS OFFICE

2025 M Street, NW
Suite 800
Washington, DC 20036-3309
USA
Tel: +1 (202) 367-1161
Fax: +1 (202) 367-2161
E-mail: asbmr@asbmr.org
Internet: <http://www.asbmr.org>

ASBMR PUBLICATIONS OFFICE

P.O. Box 2759
Durham, NC 27715-2759
USA
Tel: +1 (919) 620-0681
Fax: +1 (919) 620-8465
E-mail: journal@jbm.org
Internet: www.jbmronline.org

2007 PROGRAM COMMITTEE

President: Steven R. Goldring, M.D.
Program Co-Chair: Harald Jueppner, M.D.
Program Co-Chair: Juliet Compston, M.D., FRCP

Disclosures:

Dr. Compston - Consultant for Crescent Diagnostics, Procter & Gamble, Novartis, Servier, Shire Alliance for Better Bone Health, Lilly, Amgen, Pfizer, Nycomed, and Medivir, Research grant from Procter & Gamble, and Speaker's Bureau for Procter & Gamble, Servier, Alliance for Better Bone Health, Lilly, and Nycomed
Dr. Goldring - Research grants and consulting fees from Merck, Procter & Gamble Pharmaceuticals, and NPS Allelix; Speaker's bureau, Merck.
Dr. Jueppner - Nothing to disclose.

2007 ABSTRACT REVIEWERS

John Adams, M.D.
 Douglas Adams, Ph.D.
 Judith Adams, MBBS, FRCR
 Robert Adler, M.D.
 Kristina Akesson, M.D., Ph.D.
 Maureen Ashe
 Roland Baron, D.D.S., Ph.D.
 Murat Bastepe, M.D., Ph.D.
 Douglas Bauer, M.D.
 Matthew Beckman, Ph.D.
 Teresita Bellido, Ph.D.
 Clemens Bergwitz, M.D.
 John Bilezikian, M.D.
 Alessandro Bisello, Ph.D.
 Dennis Black, Ph.D.
 Robert Blank, M.D., Ph.D.
 Peter Bodine, Ph.D.
 Jean-Jacques Body, M.D., Ph.D.
 Georges Boivin, Ph.D.
 Lynda Bonewald, Ph.D.
 Roger Bouillon, M.D., Ph.D.
 Mary Boussein, Ph.D.
 Maria Luisa Brandi, M.D., Ph.D.
 Nathalie Bravenboer, Ph.D.
 Felix Bronner, Ph.D.
 Jacques Brown, M.D., FRCP
 Laura Calvi, M.D.
 Xu Cao, Ph.D.
 Geert Carmeliet, M.D., Ph.D.
 Thomas Carpenter, M.D.
 Wenhan Chang, Ph.D.
 Daniel Chappard, M.D., Ph.D.
 Roland Chapurlat, M.D., Ph.D.
 Qian Chen, Ph.D.
 Charles Chesnut, M.D.
 Sylvia Christakos, Ph.D.
 Ung-Il Chung, M.D., Ph.D.
 Luisella Cianferotti, M.D.
 Roberto Civitelli, M.D.
 Bart Clarke, M.D.
 Jackie Clowes, M.D., Ph.D.
 David E. C. Cole, M.D., Ph.D.
 Peter Croucher, Ph.D.
 Tim Cundy, M.D.
 Pierre Delmas, M.D., Ph.D.
 Marie Demay, M.D.
 Adolfo Diez-Perez, M.D., Ph.D.
 Linda Dimeglio, M.D., M.P.H.
 Paola Divieti Pajevic, M.D., Ph.D.
 Marc Drezner, M.D.
 Hicham Drissi, Ph.D.
 Colin Dunstan, Ph.D.
 Richard Eastell, M.D., FRCP
 Michael Econs, M.D.
 Reinhold Erben, M.D., D.V.
 Ken Faulkner, Ph.D.
 Murray Favus, M.D.
 Jian Feng, M.D., Ph.D.
 Virginia Ferguson, Ph.D.
 David Findlay, Ph.D.
 James Fleet, Ph.D.
 Roger Francis, M.D.
 Leopold Fröhlich, Ph.D.
 Masafumi Fukagawa, M.D., Ph.D.
 Dana Gaddy, Ph.D.
 Deborah Galson, Ph.D.
 Thomas Gardella, Ph.D.
 Patrick Garnero, Ph.D.
 Juerg Gasser, Ph.D.
 Matthew Gillespie, Ph.D.
 Carlotta Glackin, Ph.D.
 Francis Glorieux, M.D., Ph.D.
 Francesca Gori, Ph.D.
 Francesco Grassia
 Agamemnon Grigoriadis, Ph.D.
 Theodore Hahn, M.D.
 Stephen Harris, Ph.D.
 Geoffrey Hendy, Ph.D.
 Janet Hock, BDS, Ph.D.
 Lorenz Hofbauer, M.D.
 Michael Holick, M.D., Ph.D.
 Ingrid Holm, M.D., M.P.H.
 Mark Horowitz, Ph.D.
 Keith Hruska, M.D.
 Muneaki Ishijima, M.D., Ph.D.
 Sophie Jamal, M.D., Ph.D.
 Suzanne Jan De Beur, M.D.
 Muhammad Javaid, MBBS, Ph.D.
 Robert Jilka, Ph.D.
 Robert Josse, M.D.
 Ivo Kalajzic, M.D., Ph.D.
 David Karasik, Ph.D.
 Hiroshi Kawaguchi, M.D., Ph.D.
 Gordon Klein, M.D., M.P.H.
 Stavroula Kousteni, Ph.D.
 Christopher Kovacs, M.D., FRCPC, FACP
 Richard Kremer, M.D., Ph.D.
 Henry Kronenberg, M.D.
 Rajiv Kumar, M.D.
 Nancy Lane, M.D.
 Craig Langman, M.D.
 Eleanor Lederer, M.D.
 Mary Leonard, M.D.
 Thomas Linkhart, Ph.D.
 Phyllis Luvall, Ph.D.
 Stavros Manolagas, M.D., Ph.D.
 Joan Marini, M.D., Ph.D.
 Kevin Martin, MBBS
 Thomas John Martin, M.D., D.Sc.
 Laura Masi, M.D., Ph.D.
 Laurie Kay McCauley, D.D.S., Ph.D.
 Eugene McCloskey, M.D., MRCP, M.B.
 Madhusmita Misra, M.D., M.P.H.
 Takeshi Miyamoto, M.D., Ph.D.
 Ralph Mueller, Ph.D.
 Gregory Mundy, M.D.
 Robert Nissenson, Ph.D.
 Brendon Noble, Ph.D.
 Charles O'Brien, Ph.D.
 Susan Ott, M.D.
 Merry Jo Oursler, Ph.D.
 Millan Patel, M.D.
 John Pettifor, MBBS, Ph.D.
 Carol Pilbeam, M.D., Ph.D.
 Anthony Portale, M.D.
 Richard Prince, FRACP, M.D.
 Sylvain Provot, Ph.D.
 L. Darryl Quarles, M.D.
 Lawrence Raisz, M.D.
 Stuart Ralston, MBChB, M.D.
 Jonathan Reeve, D.M., D.Sc.
 David Reid, M.D., FRCP
 Paul Roschger, Ph.D.
 Christian Roux, M.D.
 Alisha Rovner
 Yves Sabbagh, Ph.D.
 Cheryl Sanchez, M.D.
 Arndt Schilling, M.D.
 Ernestina Schipani, M.D., Ph.D.
 Ego Seeman, M.D., FRACP
 Peter Selby, M.D., FRCP
 Deborah Sellmeyer, M.D.
 Eileen Shore, Ph.D.
 Justin Silver, M.D., Ph.D.
 Stuart Silverman, M.D.
 Natalie Sims, Ph.D.
 Timothy Skerry, Ph.D., D.V.M.
 Anna Spagnoli, M.D.
 Paula Stern, Ph.D.
 Matthew Stewart, Ph.D.
 Larry Suva, Ph.D.
 Masamichi Takami, Ph.D.
 Simon Tang
 Sotirios Tetradis, Ph.D., D.D.
 J.H. Tobias, M.D., MRCP
 Anna Tosteson, Sc.D.
 Florence Tremollieres, M.D., Ph.D.
 Charles Turner, Ph.D.
 Andre Van Wijnen, Ph.D.
 Peter Vestergaard, M.D., Ph.D.
 Leanne Ward, M.D.
 Connie Weaver, Ph.D.
 Felix Werner Wehrli, Ph.D.
 Robert Weinstein, M.D.
 Deborah Wenkert, M.D.
 Kenneth White, Ph.D.
 Michael Whyte, M.D.
 Bart Williams, Ph.D.
 Laura Zanello, Ph.D.
 Guang Zhou, Ph.D.

ASBMR COMMITTEES AND REPRESENTATIVES

ADVOCACY COMMITTEE

Lynda F. Bonewald, Ph.D., *Chairperson*
Joseph P. Bidwell, Ph.D.
Stephen E. Harris, Ph.D.
Marc C. Hochberg, M.D., M.P.H.
Mary B. Leonard, M.D.
Laura R. McCabe, Ph.D.
Lilian I. Plotkin, Ph.D.
Paula H Stern, Ph.D., *Ex Officio*
Barbara E. Kream, Ph.D., *Council Liaison*

ANCILLARY PROGRAM COMMITTEE

Thomas L. Clemens, Ph.D., *Chairperson*
Elizabeth Barrett-Connor, Ph.D.
Lora Giangregorio
Richard Kremer, M.D., Ph.D.
Sharmila Majumdar, Ph.D.
Robert Pignolo, M.D., Ph.D.
Hiroshi Takayanagi, M.D., Ph.D., *Ad Hoc*
Michael J. Econs, M.D., *Council Liaison*

ARCHIVES COMMITTEE

Frederick R. Singer, M.D., *Chairperson*
Jane E. Aubin, Ph.D.
Arnold J. Kahn, Ph.D., M.S.
Gregory R. Mundy, M.D.
Sevgi B. Rodan, Ph.D.
Lawrence G. Raisz, M.D., *Ad Hoc*
Paula H. Stern, Ph.D., *Ad Hoc*
Thomas Spelsberg, Ph.D., *Council Liaison*

EDUCATION COMMITTEE

Teresita M. Bellido, Ph.D., *Chairperson*
Julia Billiard, Ph.D.
Jan M. Bruder, M.D.
Laura M. Calvi, M.D.
Christopher S. Kovacs, M.D., FRCPC, FACP
Benjamin Z. Leder, M.D.
Susan M. Ott, M.D.
Merry Jo Oursler, Ph.D.
René Rizzoli, M.D., *Council Liaison*

ETHICS ADVISORY COMMITTEE

Julie Glowacki, Ph.D., *Chairperson*
Thomas L. Clemens, Ph.D.
David Goltzman, M.D.
Lawrence G. Raisz, M.D.
Clifford J. Rosen, M.D.
Elizabeth Shane, M.D., *Ex Officio*
Murray J. Favus, M.D., *Ad Hoc*
Ghada El-Hajj Fuleihan, M.D., M.P.H., *Ad Hoc*
Michael J. Econs, M.D., *Council Liaison*

FINANCE COMMITTEE

Keith A. Hruska, M.D., *Chairperson*
Diane M. Cullen, Ph.D.
Steven R. Goldring, M.D.
Ted S. Gross, Ph.D.
Barbara Kream, Ph.D.
Anna Teti, Ph.D.
Marc K. Drezner, M.D., *Ex Officio*
Mark C. Horowitz, Ph.D., *Council Liaison*

LOCAL ARRANGEMENTS COMMITTEE

Richard Wasnich, M.D.
Frank Singer, M.D.

MEMBERSHIP DEVELOPMENT COMMITTEE

Andre J. van Wijnen, Ph.D., *Chairperson*
Xu Cao, Ph.D.
Wenhan Chang, Ph.D.
Hicham Drissi, Ph.D.
Suzanne M. Jan de Beur, M.D.
Melissa A. Kacena, Ph.D.
Caroline Silve, M.D., Ph.D.
Kenneth E. White, Ph.D.
Akira Yamaguchi, D.D.S., Ph.D.
Matthew Brown, MBBS, M.D., *Ad Hoc*
Thomas Spelsberg, Ph.D., *Council Liaison*

PROFESSIONAL PRACTICE COMMITTEE

Stuart L. Silverman, M.D., *Chairperson*
Robert Adler, M.D.
Catherine M. Gordon, M.D.
Bente L. Langdahl, M.D., Ph.D.
Silvina Levis, M.D.
Kenneth W. Lyles, M.D.
David M. Reid, M.D., FRCP
Laura Tosi, M.D.
Janet Rubin, M.D., *Council Liaison*

2007 PROGRAM COMMITTEE

Steven R. Goldring, M.D., *President*
Juliet E. Compston, M.D., FRCP, *Co-Chair*
Harald Jueppner, M.D., *Co-Chair*

2008 PROGRAM COMMITTEE

Barbara Kream, Ph.D., *President*
Philip Osdoby, Ph.D., *Co-Chair*
Rajesh Thakker, M.D., FRCP, *Co-Chair*

PUBLICATIONS COMMITTEE

Joseph Lorenzo, M.D.
Robert D. Blank, M.D., Ph.D.
Seiji Fukumoto, M.D., Ph.D.
Stavroula Kousteni, Ph.D.
Joan C. Marini, M.D., Ph.D.
Mark S. Nanes, M.D., Ph.D.
Eileen Shore, Ph.D.
John J. Wysolmerski, M.D.
Sakamuri V. Reddy, Ph.D., *Ad Hoc*
John Eisman, MBBS, Ph.D., *Ex Officio*
Clifford J. Rosen, M.D., *Ex Officio*
Rene St.-Arnaud, Ph.D., *Council Liaison*

PRIMER EDITORIAL BOARD

Clifford J. Rosen, M.D., *Chairperson*
Thomas L. Clemens, Ph.D.
Juliet E. Compston, M.D., FRCP
Pierre D. Delmas, M.D., Ph.D.
Marie Demay, M.D.
Theresa A. Guise, M.D.
Suzanne M. Jan De Beur, M.D.
Richard W. Keen, M.D., Ph.D.
Laurie Kay McCauley, D.D.S., Ph.D.
Socrates Papapoulos, M.D.
Vicki Rosen, Ph.D.
Ego Seeman, M.D., FRACP
Rajesh V. Thakker, M.D., FRCP

SCIENCE POLICY COMMITTEE

Larry Suva, Ph.D., *Chairperson*
Lorena M. Havill, Ph.D.
Sophie A. Jamal, M.D., Ph.D.
Robert Marcus, M.D.
F. Patrick Ross, Ph.D.
Kristine M. Wren, Ph.D.
Matthew T. Gillespie, Ph.D., *Ad Hoc*
Philip A. Osdoby, Ph.D., *Ad Hoc*
Lynda F. Bonewald, Ph.D., *Ex Officio*
Stuart L. Silverman, M.D., *Ex Officio*
Theresa A. Guise, M.D., *Council Liaison*
Roberto Civitelli, M.D., *Council Liaison*

WOMEN IN BONE AND MINERAL RESEARCH COMMITTEE

Nicola Partridge, Ph.D., *Chairperson*
John P. Bilezikian, M.D.
Juliet E. Compston, M.D., FRCP
Janine A. Danks, Ph.D.
Deborah L. Galson, Ph.D.
Carol C. Pilbeam, M.D., Ph.D.
Shonni J. Silverberg, M.D.
Jennifer J. Westendorf, Ph.D.
Maria Luisa Brandi, M.D., Ph.D., *Council Liaison*

ASBMR REPRESENTATIVES TO FASEB

Paula H. Stern, Ph.D.
FASEB Board

Larry Suva, Ph.D.
Science Policy Committee

Felicia Cosman, M.D.
Clinical Research Subcommittee, Science Policy Committee

Nicola Partridge, Ph.D.
NIH Issues Subcommittee, Science Policy Committee

Philip A. Osdoby, Ph.D.
Training and Career Resources, Science Policy Committee

Jane B. Lian, Ph.D.
Excellence in Science Award Committee

Robert D. Blank, M.D., Ph.D.
Research Conferences Advisory Committee

Suzanne M. Jan de Beur, M.D. (2008)
FASEB Publications and Communications Committee

Gloria Gronowicz, Ph.D. (2007)
FASEB Federal Funding Consensus Conference Representative

Bernard P. Halloran, Ph.D.
FASEB Federal Funding Consensus Conference Representative

John J. Wysolmerski, M.D.
FASEB Editorial Board

ASBMR REPRESENTATIVES TO OTHER GROUPS

Nancy Lane, M.D.
U.S. Bone and Joint Decade

Shonni J. Silverberg, M.D.
National Osteoporosis Foundation
Interspecialty Medical Council

Murray J. Favus, M.D.
National Osteoporosis Foundation
Subcommittee on Guidance to Physicians to Reduce Fracture Risk

Marjorie M. Luckey, M.D.
National Osteoporosis Foundation
Subcommittee on Implementation of New Guidelines for Practicing Physicians

Steven R. Goldring, M.D.
Sister Societies Forum

Barbara Kream, Ph.D.
Sister Societies Forum

PAST PRESIDENTS

Louis V. Avioli, M.D.	1979-1980	Steven L. Teitelbaum, M.D.	1992-1993
Lawrence G. Raisz, M.D.	1980-1981	Henry M. Kronenberg, M.D.	1993-1994
Claude D. Arnaud, M.D.	1981-1982	Ernesto Canalis, M.D.	1994-1995
Stephen M. Krane, M.D.	1982-1983	John P. Bilezikian, M.D.	1995-1996
William A. Peck, M.D.	1983-1984	Gregory R. Mundy, M.D.	1996-1997
Paula H. Stern, Ph.D.	1984-1985	Michael Rosenblatt, M.D.	1997-1998
B. Lawrence Riggs, M.D.	1985-1986	Jane E. Aubin, Ph.D.	1998-1999
Norman H. Bell, M.D.	1986-1987	David Goltzman, M.D.	1999-2000
Gideon A. Rodan, M.D., Ph.D.	1987-1988	Robert Marcus, M.D.	2000-2001
John G. Haddad, Jr., M.D.	1988-1989	Robert R. Recker, M.D.	2001-2002
Armen H. Tashjian, Jr., M.D.	1989-1990	Clifford J. Rosen, M.D.	2002-2003
Frederick R. Singer, M.D.	1990-1991	Robert A. Nissenson, Ph.D.	2003-2004
Mark R. Haussler, Ph.D.	1991-1992	Sylvia Christakos, Ph.D.	2005-2006
		Elizabeth Shane, M.D.	2006-2007

PAST SECRETARY-TREASURERS

Norman H. Bell, M.D.	1977-1985	Steven R. Goldring, M.D.	1997-2000
Gregory R. Mundy, M.D.	1985-1991	Andrew F. Stewart, M.D.	2000-2004
Arnold J. Kahn, Ph.D.	1991-1997	Marc Drezner, M.D.	2004-2007

PAST COUNCILORS

Constantine Anast, M.D.	1980-1982	Frederick S. Kaplan, M.D.	1997-2000
Claude D. Arnaud, M.D.	1979-1980	Sundeep Khosla, M.D.	2002-2005
Andrew Arnold, M.D.	1999-2002	Stephen M. Krane, M.D.	1979-1981
Jane E. Aubin, Ph.D.	1991-1994	Barbara E. Kream, M.D.	1985-1988
Roland Baron, D.D.S., Ph.D.	1991-1994	Henry M. Kronenberg, M.D.	1986-1989
Daniel Bikle, M.D., Ph.D.	2003-2006	Barbara Lukert, M.D.	2001-2004
John P. Bilezikian, M.D.	1987-1990	Jane B. Lian, Ph.D.	1991-1994
Dennis M. Black, Ph.D.	2001-2004	Robert Marcus, M.D.	1995-1998, 1999-2002
Lynda F. Bonewald, Ph.D.	1995-1998	T.J. Martin, M.D.	1987-1990
Arthur E. Broadus, M.D., Ph.D.	1990-1993	Stephen Marx, M.D.	1983-1986
Ernesto Canalis, M.D.	1989-1992	Toshio Matsumoto, M.D.	1999-2002
Janet M. Canterbury, M.D.	1981-1984	Gregory R. Mundy, M.D.	1983-1985, 1995-1997
Jane Cauley, Ph.D.	2003-2006	Robert Nissenson, Ph.D.	1993-1996
Sylvia Christakos, Ph.D.	1989-1992	Anthony W. Norman, Ph.D.	1980-1982
Thomas L. Clemens, Ph.D.	1998-2001	Philip A. Osdoby, Ph.D.	1997-2000
Jack W. Coburn, M.D.	1981-1984	Susan M. Ott, M.D.	1988-1991
David V. Cohn, Ph.D.	1982-1985	A. Michael Parfitt, M.D.	1990-1993
Cary W. Cooper, Ph.D.	1980-1981	Nicola C. Partridge, Ph.D.	1993-1996
Steven R. Cummings, M.D.	1996-1999	William A. Peck, M.D.	1979-1981
Bess Dawson-Hughes, M.D.	1996-1999	John T. Potts, Jr., M.D.	1979-1981
Hector F. DeLuca, Ph.D.	1979-1980	Paul A. Price, Ph.D.	1986-1989
Marie Demay, M.D.	2000-2003	Robert R. Recker, M.D.	1995-1998
Richard Eastell, M.D., F.R.C.P.	2000-2003	Pamela Gehron Robey, Ph.D.	1992-1995
John Eisman, MBBS, Ph.D.	1994-1997	Gideon A. Rodan, M.D., Ph.D.	1984-1986
Murray J. Favus, M.D.	1992-1995	Sevgi B. Rodan, Ph.D.	1990-1993
David Feldman, M.D.	1982-1986	Vicki Rosen, Ph.D.	2003-2006
Lorraine A. Fitzpatrick, M.D.	1998-2001	Michael Rosenblatt, M.D.	1988-1991
Francis Glorieux, M.D., Ph.D.	1988-1991	Elizabeth Shane, M.D.	1994-1997
Julie Glowacki, Ph.D.	1999-2002	Dolores M. Shoback, M.D.	1998-2001
Steven R. Goldring, M.D.	1993-1996	Ethel Siris, M.D.	1996-1999
Ralph S. Goldsmith, M.D.	1980-1983	Eduardo Slatopolsky, M.D.	1980-1983
David Goltzman, M.D.	1984-1988	Paula H. Stern, Ph.D.	1980-1983
Maxine Gowen, Ph.D.	2000-2003	Andrew F. Stewart, M.D.	1994-1997
Susan Greenspan, M.D.	2002-2005	Gary Stein, Ph.D.	2002-2005
John G. Haddad, Jr., M.D.	1982-1985	Gordon J. Strewler, M.D.	1992-1995
Mark R. Haussler, Ph.D.	1982-1985	Larry Suva, Ph.D.	2001-2004
Hunter H. Heath III, M.D.	1985-1988	Armen H. Tashjian, Jr., M.D.	1979-1982
Helen L. Henry, Ph.D.	1985-1988	John D. Termine, Ph.D.	1984-1987
Keith A. Hruska, M.D.	1989-1992	Marian F. Young, Ph.D.	1997-2000
Arnold J. Kahn, Ph.D.	1986-1989	Robert Wasserman, Ph.D.	1984-1987
		Glenda Wong, Ph.D.	1984-1987

THE FULLER ALBRIGHT AWARD

Supported by an educational grant from sanofi-aventis

Michael F. Holick, M.D., Ph.D.	1980	Roberto Civitelli, M.D.	1994
Mark R. Haussler, Ph.D.	1981	Roberto Pacifici, M.D.	1995
Stephen Marx, M.D.	1982	Clinton T. Rubin, Ph.D.	1996
Gregory R. Mundy, M.D.	1982	René St-Arnaud, Ph.D.	1997
Edward M. Brown, M.D.	1983	Shigeaki Kato, Ph.D.	1998
Helen L. Henry, Ph.D.	1984	Theresa A. Guise, M.D.	1999
Henry M. Kronenberg, M.D.	1985	Dwight Towler, M.D., Ph.D.	2000
Michael Rosenblatt, M.D.	1986	Charles H. Turner, M.D.	2001
Michael P. Whyte, M.D.	1987	Nobuyuki Udagawa, M.D.	2002
Rajiv Kumar, M.D.	1988	Patricia Ducy, Ph.D.	2003
Timothy Chambers, M.D.	1989	Hiroshi Takayanagi, Ph.D.	2004
Michael A. Levine, M.D.	1990	Mary Bouxein, Ph.D.	2005
Dean T. Yamaguchi, M.D., Ph.D.	1991	Hong-Wen Deng, Ph.D.	2006
Andrew Arnold, M.D.	1992	Kenneth White, Ph.D.	2007
Pamela G. Robey, Ph.D.	1993		

THE LOUIS V. AVIOLI FOUNDERS AWARD

Supported by an educational grant from Merck & Co., Inc.

Stavros Manolagas, M.D., Ph.D.	2000	Ernesto Canalis, M.D.	2004
Gerard Karsenty, M.D.	2001	Gino Segre, M.D.	2005
Roland Baron, D.D.S., Ph.D.	2002	Andrew Arnold, M.D.	2006
Edward Brown, M.D.	2003	David Roodman, M.D., Ph.D.	2007

THE FREDERIC C. BARTTER AWARD

Supported by an educational grant from GlaxoSmithKline Consumer Healthcare

Jack Coburn, M.D.	1986	Robert Lindsay, MBChB, Ph.D.	1997
Constantine Anast, M.D.	1987	B.E. Christopher Nordin, M.D., Ph.D.	1998
Charles Y.C. Pak, M.D.	1988	Pierre Meunier, M.D.	1999
Arthur E. Broadus, M.D., Ph.D.	1989	John P. Bilezikian, M.D.	2000
B. Lawrence Riggs, M.D.	1990	Joseph Melton, III, M.D.	2001
Eduardo Slatopolsky, M.D.	1991	Ego Seeman, M.D., FRACP	2002
Norman H. Bell, M.D.	1992	Robert R. Recker, M.D.	2003
Francis H. Glorieux, M.D., Ph.D.	1993	Pierre Delmas, M.D., Ph.D.	2004
Robert P. Heaney, M.D.	1994	John Kanis, M.D.	2005
A. Michael Parfitt, M.D.	1995	Sundeep Khosla, M.D.	2006
C. Conrad Johnston, Jr., M.D.	1996	Michael Whyte, M.D.	2007

THE SHIRLEY HOHL SERVICE AWARD

Supported by an educational grant from sanofi-aventis

Louis V. Avioli, M.D.	1997	Marc K. Drezner, M.D.	2003
Norman H. Bell, M.D.	1998	Jane B. Lian, Ph.D.	2004
Murray J. Favus, M.D.	1999	Julie Glowacki, Ph.D.	2005
Arnold J. Kahn, Ph.D.	2000	Paula Stern, Ph.D.	2006
Lawrence G. Raisz, M.D.	2001	Philip Osdoby, Ph.D.	2007
Nicola C. Partridge, Ph.D.	2002		

THE WILLIAM F. NEUMAN AWARD

Supported by an educational grant from sanofi-aventis

Gerald D. Aurbach, M.D.	1981	Anthony W. Norman, Ph.D.	1995
Paul L. Munson, Ph.D.	1982	Melvin Jacob Glimcher, M.D.	1996
D. Harold Copp, M.D., Ph.D.	1983	Tatsuo Suda, D.D.Sc., Ph.D.	1997
Roy V. Talmage, Ph.D.	1984	Steven L. Teitelbaum, M.D.	1998
Hector F. DeLuca, Ph.D.	1985	Gregory R. Mundy, M.D.	1999
Lawrence G. Raisz, M.D.	1986	R. Graham Russell, M.D.	2000
John T. Potts, Jr., M.D.	1987	Harold M. Frost, M.D.	2001
Louis V. Avioli, M.D.	1988	B. Lawrence Riggs, M.D.	2002
Stephen M. Krane, M.D.	1989	Henry M. Kronenberg, M.D.	2003
Robert H. Wasserman, Ph.D.	1990	Jane E. Aubin, Ph.D.	2004
Claude D. Arnaud, M.D.	1991	Mark R. Haussler, Ph.D.	2005
Herbert A. Fleisch, M.D.	1992	Jane Lian, Ph.D., and Gary Stein, Ph.D.	2006
Gideon A. Rodan, M.D., Ph.D.	1993	Lance Lanyon, Ph.D., BVSc	2007
Thomas John Martin, M.D., D.Sc.	1994		

THE GIDEON A. RODAN EXCELLENCE IN MENTORSHIP AWARD

Supported by an educational grant from Merck & Co., Inc.

Gideon A. Rodan, M.D., Ph.D.	2001	Barbara Kream, Ph.D.	2005
Sylvia Christakos, Ph.D.	2002	B. Lawrence Riggs, M.D.	2006
Webster S. S. Jee, Ph.D.	2003	Thomas John Martin, M.D., D.Sc.	2007
Claude Arnaud, M.D.	2004		

ASBMR EARLY CAREER EXCELLENCE IN TEACHING AWARD

Sharon Nickols-Richardson, Ph.D., R.D.	2006	Catherine Gordon, M.D.	2007
--	------	------------------------	------

ASBMR CAREER ENHANCEMENT AWARDS

Supported by an educational grant from Roche and GSK

Roberta Faccio, Ph.D.	2005	Anja Nohe, Ph.D.	2006
David Karasik, Ph.D.	2005	Deborah Novack, M.D., Ph.D.	2006
Baojie Li, Ph.D.	2005	Matthew Stewart, Ph.D.	2006
Jiake Xu, M.D., Ph.D.	2005	Shoshara Yakar, Ph.D.	2006

RAISZ-DREZNER FIRST AUTHOR JOURNAL AWARDS

James R. Cavey, B.Sc.	2005	Jennifer L. Fiori, Ph.D.	2006
Xuesong Chen, Ph.D.	2005	Guillaume E. Beranger, Ph.D.	2006
Claudia Riedt, Ph.D.	2005		

2006 ASBMR BRIDGE FUNDING RESEARCH GRANT RECIPIENTS

Sulin Cheng, Ph.D.	John Eisman, MBBS, Ph.D.
Roberto Pacifici, M.D.	Vincent Everts, Ph.D.
Alexander Lichtler, Ph.D.	Julie Pasco, Ph.D.
Thomas Lang, Ph.D.	Jonathan Reeve, D.M., DSc.
Roberto Civitelli, M.D.	Anna Teti, Ph.D.

2007 ASBMR MOST OUTSTANDING ABSTRACT AWARD

Supported by an educational grant from GlaxoSmithKline

Shingo Sato, M.D.

2007 ASBMR AWARD FOR OUTSTANDING RESEARCH IN THE PATHOPHYSIOLOGY OF OSTEOPOROSIS

Supported by an educational grant from GlaxoSmithKline

Ulrike Moedder, Ph.D.

2007 ASBMR PRESIDENT'S BOOK AWARD

Yasushi Oshima, M.D.

2007 SHUN-ICHI HARADA YOUNG INVESTIGATOR AWARD

Supported by donations in honor of Shun-ichi Harada, M.D.

Christian Graeff

Li Kong, M.D.

Manisha C. Yadav, Ph.D.

2007 ASBMR YOUNG INVESTIGATOR AWARD RECIPIENTS

Co-Supported by educational grants from the Alliance for Better Bone Health (Procter & Gamble Pharmaceuticals and sanofi-aventis), GlaxoSmithKline, GlaxoSmithKline Consumer Healthcare, Immunodiagnostics Systems, Merck & Co., Inc., Roche and GSK, sanofi-aventis, and Wyeth Pharmaceuticals.

Yutaro Asaba, M.D.
Dustin M. Baldrige
Joyce Y. Belcher
Estelle Bianchi
Dana Bliuc, MMed
Karine Briot, M.D.
Alesha B. Castillo, Ph.D.
Peggy M. Cawthon, Ph.D.
Wai Wilson Cheung, Ph.D.
John T. Chow, M.D.
Lieve Coenegrachts
Jodi N. Dowthwaite, Ph.D.
Melita M. Dvorak, Ph.D.
Feyza Engin
Carlo Galli, D.D.S.
Ignacio Garcia-Tuñón, Ph.D.
Katherine Gunter, Ph.D.
Eric Hesse, M.D.
Makoto Hirata, M.D.
Edward C. Hsiao, M.D., Ph.D.
Yuji Ito, M.D., Ph.D.
Mitsuyasu Iwasawa, M.D.
Catherine E. Jones, Ph.D.
Ivo Kalajzic, M.D., Ph.D.
Firas M. Kara, M.D.
Lisa J. Kidd, BVSc

Lauren A. Kingsley, B.A.
Salman Kirmani, MBBS
Jiarong Li
Katarina M. Lindahl, M.D.
Michael Mannstadt, M.D.
Takehiko Matsushita, M.D., Ph.D.
Yuichi Nagase, M.D.
Kelsey N. Retting
Glenn C. Rowe, Ph.D.
Qi Shen, M.D., Ph.D.
Leslie Spangler, VM.D., Ph.D.
Gary J. Spencer, Ph.D.
Astushi Sugita, M.D.
Yi Tang
Masakazu Terauchi, M.D., Ph.D.
Bich N. H. Tran
Angela R. Venn
Weiguang Wang, M.S.
Yalei Wu, Ph.D.
Weirong Xing, Ph.D.
Zhenqiang Yao, M.D.
Baohong Zhao
Yan Zhong, B.S.
Junling Zhuang, M.D., Ph.D.

2007 SUPPORTERS

The ASBMR gratefully acknowledges the following companies for their support:

DIAMOND LEVEL SUPPORTERS

Amgen, Inc.

Eli Lilly and Company

GOLD LEVEL SUPPORTER

Alliance for Better Bone Health

(Procter & Gamble Pharmaceuticals and sanofi-aventis)

SILVER LEVEL SUPPORTERS

Pfizer, Inc.

Roche and GSK

BRONZE LEVEL SUPPORTERS

Abbott

Merck & Co., Inc.

Novartis Pharmaceuticals Corporation

FRIEND LEVEL SUPPORTERS

GlaxoSmithKline

GlaxoSmithKline Consumer Healthcare

Immunodiagnostic Systems

Merck Research Laboratories

Mission Pharmacal Company

Procter & Gamble Pharmaceuticals

sanofi-aventis

Wyeth Pharmaceuticals

2007 EXHIBITORS

Abbott	Merck & Co., Inc.
Allevia AG	Micro Photonics/Skyscan
Alliance for Better Bone Health	MicroMRI, Inc.
ALPCO Diagnostics	Mindways Software, Inc.
Amgen	Mission Pharmacal Company
AquaStep	National Osteoporosis Foundation (NOF)
Asahi Kasei Pharma Corporation	NIH Osteoporosis & Related Bone Diseases-NRC
Bio-Imaging Technologies, Inc.	Nordic Bioscience a/s
Bioquant Image Analysis Corporation	Novartis Pharmaceuticals Corporation
BioVendor Laboratory Medicine, Inc.	OrthoMetrix, Inc.
Charles River Laboratory, Preclinical Services	Osteometrics, Inc.
Diasorin	Pacific Biometrics, Inc.
Duke Clinical Research Institute (DCRI)	Paget Foundation
Dyets, Inc.	Perceptive Informatics, Inc.
Echo Medical Systems, LLC	Pharmatest Services Ltd.
Eli Lilly and Company	Quidel Corporation
Elsevier/Saunders/Mosby	Ratoc System Engineering Co., Ltd.
FASEB MARC Program	Roche and GSK
Faxitron X-Ray Corporation	Roche Diagnostics
Foundation for Osteoporosis Research & Education (FORE)	Scanco Medical AG
GE Healthcare Lunar	Siemens Medical Solutions USA
Genzyme	Springer
Hologic, Inc.	Upsher-Smith Laboratories, Inc.
Immuno-Biological Laboratories, Inc. (IBL-America)	Wyeth Pharmaceuticals
Immunodiagnostic Systems (IDS)	Xradia, Inc.
Immutopics International, LLC	
International Bone and Mineral Society	
International Osteopetrosis Association (IOA)	
International Society for Clinical Densitometry (ISCD)	
Jarrow Formulas, Inc.	
Juvent	
Kamiya Biomedical Company	
KUREHA Special Laboratory Co., LTD.	
Kyphon Inc.	
Lonza	
Mayo Clinical Trial Services	
MDS Pharma Services	
medi	

*As of 7/19/07

GENERAL INFORMATION

ASBMR MEETING LOCATION

All ASBMR 29th Annual Meeting sessions will take place in the Hawaii Convention Center, unless otherwise stated. The Hawaii Convention Center is located at 1801 Kalakaua Avenue Honolulu, Hawaii, USA.

COPYRIGHT

Abstracts submitted to the ASBMR 29th Annual Meeting and published in the Abstracts supplement to the Journal of Bone and Mineral Research are copyrighted by the American Society for Bone and Mineral Research. Reproduction, distribution, or transmission of the abstracts in whole or in part, by electronic, mechanical or other means, or intended use, is prohibited without the express written permission of the American Society for Bone and Mineral Research. All inquiries regarding copyrighted material or reprint orders should be directed to Lisa Dittrich, Director of Publications, American Society for Bone and Mineral Research, E-mail: lisa@jbmr.org, Tel: (919) 620-0681; Fax: (919) 620-8465, Postal Address: 3209 Guess Road, Suite 201, Durham, NC 27705, USA.

DISCLAIMER

All authored abstracts, findings, conclusions, recommendations, or oral presentations are those of the author(s) and do not reflect the views of the ASBMR or imply any endorsement. No responsibility is assumed, and responsibility is hereby disclaimed, by the American Society for Bone and Mineral Research for any injury and/or damage to persons or property as a matter of products liability, negligence or otherwise, or from any use or operation of methods, products, instructions, or ideas presented in the materials herein (2007 Abstracts). Independent verification of diagnosis and drug dosages should be made. Discussions, views, and recommendations as to medical procedures, choice of drugs, and drug dosages are the responsibility of the authors.

AUDIO- AND VIDEOTAPING

ASBMR expects that attendees respect each presenter's willingness to provide free exchange of scientific information without the abridgement of his or her rights or privacy and without the unauthorized copying and use of the scientific data shared during his or her presentation. In addition, ASBMR expects that attendees will respect Exhibitors' desires not to have their products or booths photographed or videotaped.

The use of cameras, audio-taping devices, and videotaping equipment is strictly prohibited within all Scientific Sessions, the Exhibit Halls, and Poster Sessions without the express written permission of the ASBMR Convention Management. Unauthorized use of the taping equipment may result in the confiscation of the equipment or the individual may be asked to leave the session or Exhibit Hall. These rules are strictly enforced.

USE OF ASBMR NAME AND LOGO

ASBMR reserves the right to approve the use of its name in all material disseminated to the media, public and professionals. ASBMR's name, meeting name, and meeting logo may not be used without permission. Use of the ASBMR logo is prohibited without the express written permission of the ASBMR Executive Director. All ASBMR corporate supporters and exhibitors should share their media outreach plans with the ASBMR Executive Director before release.

No abstract presented at the ASBMR 29th Annual Meeting may be released to the press before its official presentation date and time. Press releases must be embargoed until one hour after the presentation. (See ASBMR Embargo Policy below).

ASBMR MEETING CONTENT AND EMBARGO POLICY

Abstracts submitted to the ASBMR 29th Annual Meeting are embargoed — that is, unavailable for public release in written, oral and electronic communications — until one hour *after* the abstract has been presented.

The ASBMR is sensitive to issues of commercial confidentiality and relevant aspects of the U.S. Securities and Exchange Commission (SEC) regulations. Therefore, the ASBMR reminds all readers that all must adhere to the U.S. Securities and Exchange Commission regulations and treat all scientific information as confidential until the embargo has been lifted – one hour after the abstract has been presented. Any reader of, or listener to, ASBMR Annual Meeting content may be viewed as an “insider” by the SEC due to knowledge of information included in abstracts, particularly clinical trial abstracts. SEC regulations may call for criminal penalties for using such information.

ASBMR'S EXPECTATION OF AUTHORS AND PRESENTERS

Through ASBMR meetings, the Society promotes excellence in bone and mineral research. Toward that end, ASBMR expects that all authors and presenters affiliated with the ASBMR 29th Annual Meeting and the 2007 Ancillary Program will provide informative and fully accurate content that reflects the highest level of scientific rigor and integrity.

The ASBMR depends upon the honesty of the authors and presenters and relies on their assertions that they have had sufficient full access to the data and are convinced of its reliability.

Furthermore, the ASBMR expects that:

- Authors and presenters will disclose any conflicts of interest, real or perceived.
- Authors and presenters describing a study funded by an organization with a proprietary or financial interest must affirm that they had full access to all the data in the study. By so doing, they accept complete responsibility for the integrity of the data and the accuracy of the data analysis.
- The content of abstracts, presentations, slides, and reference materials must remain the ultimate responsibility of the author(s) or faculty.
- The planning, content and execution of abstracts, speaker presentations, slides, abstracts and reference materials should be free from corporate influence, bias, or control.
- All authors and presenters (invited and abstracts-based oral and poster presenters) should give a balanced view of therapeutic options by providing several treatment options, whenever possible, and by always citing the best available evidence.

In addition, ASBMR's meeting evaluations will seek feedback regarding commercial bias at ASBMR Annual Meeting sessions, including the 2007 Ancillary Program.

CONTINUING MEDICAL EDUCATION CREDITS

This activity has been planned and implemented in accordance with the Essential Areas and Policies of the Accreditation Council for CME through the joint sponsorship of The Federation of American Societies for Experimental Biology (FASEB) and the ASBMR. FASEB is accredited by the Accreditation Council for Continuing Medical Education to sponsor continuing medical education for physicians.

The Federation designates this educational activity for a maximum of 38 AMA PRA Category 1 CreditsTM. Each physician should claim only those credits that he or she actually spent in the activity. CME application forms are included in the *On-site Program* book. CME forms should be sent to:

FASEB Office of Scientific Meetings and Conferences
9650 Rockville Pike
Bethesda, Maryland 20814
USA
Tel: (301) 634-7010
Fax: (301) 634-7014

CME Mission Statement and Meeting Objective

The ASBMR 29th Annual Meeting is designed to allow members to present new developments in education, research and clinical practice related to bone and mineral metabolism. The program objectives include updating attendees on the recent advances in osteoporosis and other diseases of bone and mineral metabolism, steroid hormones and receptors, calciotropic and phosphotropic hormones, cancer and bone, bone acquisition and pediatric bone disease, cartilage and connective tissue matrix, bone biomechanics and growth factors.

As a result of their attendance, participants should have enhanced their knowledge of osteoporosis, other diseases of bone, basic bone biology and its correlation to mineral metabolism, as well as their ability to treat and care for their patients. Attendees should have developed a clearer understanding of the interrelationship among basic research, clinical research and patient care through the discussions that are expected to take place. The ASBMR 29th Annual Meeting program should produce an enhanced appreciation of the investigative, diagnostic and therapeutic aspects of metabolic bone disorders.

Target Audience

The program is designed for researchers, physicians, clinicians, and allied health professionals with interests in endocrinology, physiology, cell biology, pathology, molecular biology, genetics, epidemiology, internal medicine, rheumatology, orthopedics, dentistry, nephrology, and pharmacology.

DISCLOSURE/CONFLICT OF INTEREST

The ASBMR is committed to ensuring the balance, independence, objectivity and scientific rigor of all its individually sponsored or industry-supported educational activities. Accordingly, the ASBMR adheres to the requirement set by the Federation of American Societies for Experimental Biology (FASEB) that audiences at FASEB-sponsored educational programs be informed of a presenter's (speaker, faculty, author, or contributor) academic and professional affiliations, and the disclosure of the existence of any significant financial interest or other relationship a presenter has with the manufacturer(s) of any commercial product(s) discussed in an educational presentation. When an unlabeled use of a commercial product, or an investigational use not yet approved for any purpose is discussed during the presentation, it is required that presenters disclose that the product is not labeled for the use under discussion or that the product is still investigational. This policy allows the listener/attendee to be fully knowledgeable in evaluating the information being presented. The Program will note those speakers who have disclosed relationships, including the nature of the relationship and the associated commercial entity.

All authors of submitted abstracts completed the disclosure statement in the online submission program. Invited speakers who are not required to submit an abstract received a form that they completed and returned.

Disclosure includes any relationship that may bias one's presentation or which, if known, could give the perception of bias. This includes relevant financial relationships of a spouse or partner. These situations may include, but are not limited to:

DISCLOSURE KEY

1. stock options or bond holdings in a for-profit corporation or self-directed pension plan
2. research grants
3. employment (full or part-time)
4. ownership or partnership
5. consulting fees or other remuneration
6. non-remunerative positions of influence such as officer, board member, trustee, or public spokesperson
7. receipt of royalties
8. speaker's bureau
9. other

Disclosures for invited speakers and abstract presenters are provided at the end of the session listing for invited speakers (see *On-Site Program* book) and directly after the body of an abstract for abstract submissions. If there is no conflict of interest or disclosure listed, this means that the invited speaker and/or abstract presenter indicated no conflicts to disclose.

The disclosure information will correspond to the key above. If disclosures are given, the company name, along with the respective disclosure relationship number will be listed (for example: Company Name 2, 8.)

2007 ABSTRACTS BOOK

The *2007 Abstracts* book is distributed on-site at the Annual Meeting to all ASBMR members and non-member attendees. Non-member subscribers to *JBMR* will receive the *2007 Abstracts* book by mail. ASBMR members who do not attend the Annual Meeting will receive their copy of the *2007 Abstracts* book by mail following the meeting. The entire ASBMR Scientific Program (invited speaker sessions, lectures, and abstract-based oral and poster presentation information), as well as the 2007 Ancillary Program (Working Groups and Industry-Supported Symposia), are included in full detail in the *On-Site Program* book and on the ASBMR website at www.asbmr.org. **We encourage you to make use of the 2007 Abstracts On-line that is accessible via the ASBMR website at www.asbmr.org. A complimentary hard copy of the 2007 Abstracts book in PDF format will be available for download for all ASBMR members and pre-registered attendees via the ASBMR website as well.**

2007 ABSTRACTS-ON-CD-ROM (ABSTRACTS 2VIEW™)

Supported by an educational grant from Amgen, Inc.

The Abstracts on CD-ROM is also a search tool which allows customized searches of the ASBMR abstracts. The CD-ROM will be included in the ASBMR Annual Meeting delegate bags.

ASBMR ABSTRACTS ONLINE

*Supported by an educational grant from the Alliance for Better Bone Health
(Procter & Gamble Pharmaceuticals and sanofi-aventis)*

The Abstracts Online program, which is accessible through the ASBMR website at www.asbmr.org, is an Internet-based search tool. The program allows the creation of a personalized itinerary for the ASBMR 29th Annual Meeting program and allows customized searches of abstracts.

AWARD PRESENTATIONS

The following ASBMR Awards will be presented immediately following the morning Plenary Symposia and Plenary Lectures in Kamehameha Hall III in the Hawaii Convention Center - the ASBMR Gideon A. Rodan Excellence in Mentorship Award, the Fuller Albright Award, the Louis V. Avioli Founders Award, the Frederic C. Bartter Award, the William F. Neuman Award, and the Shirley Hohl Service Award. Please refer to the schedule found in the inside cover of this book for award presentation times.

ASBMR VIRTUAL EXHIBIT HALL

The ASBMR Virtual Exhibit Hall (www.asbmrexhibits.com) showcases Exhibitors and their products, many of which are present at this year's ASBMR 29th Annual Meeting. Visitors to the ASBMR Virtual Exhibit Hall are able to learn more about Exhibitor's products and services, easily contact them for further information, and enjoy an Exhibit Hall experience at their leisure year-round.

CYBER CAFÉ

Supported by Eli Lilly and Company

The Cyber Café, located in the Exhibit Hall, has full Internet capability and enables attendees to search the Internet and check their email. The Cyber Café will be open during published Poster Hall hours.

NIH LOUNGE

If you are looking for another opportunity to ask U.S. National Institutes of Health and Center for Scientific Review staff about your grant proposal or idea, please plan to visit the Meet-the-NIH Lounge in Kamehameha Hall I & II (Exhibit Hall) of the Hawaii Convention Center and get your questions answered. Program staff from the National Institute and Musculoskeletal and Skin Diseases (NIAMS), the National Institute of Diabetes and Digestive and Kidney Diseases (NIDDK), the National Cancer Institute (NCI), the National Institute of Dental and Craniofacial Research (NIDCR), National Institute on Aging (NIA), Center for Scientific Review (CSR), National Institute of Child Health and Human Development (NICHD), and more will be on-hand, by appointment, to meet with you. Be sure to sign up for open time slots on-site.

YOUNG INVESTIGATOR LOUNGE

All Young Investigator Annual Meeting attendees are cordially invited to drop by the Young Investigator Lounge located in Kamehameha Hall I and II (Exhibit Hall) of the Hawaii Convention Center. Expand your network of colleagues and make new friends.

RECEPTION FOR NEW INVESTIGATOR/NEW MEMBER/FIRST-TIME ATTENDEES

Sponsored by the ASBMR Membership Development Committee

The New Investigator/New Member/First-Time Attendee Reception will be held concurrently with the Welcome Reception and the Plenary Poster session in the Young Investigators Lounge located in the Poster area of Kamehameha Hall I and II (Exhibit Hall) in the Hawaii Convention Center. ASBMR leadership and Senior Investigators will be in attendance for a meet and greet. The purpose of this event is to assist attendees with opportunities to meet other new attendees as well as familiarize themselves with ASBMR leadership. The event has been organized to promote interactions among junior investigators. Wine and cheese will be available.

NEW INVESTIGATOR/NEW MEMBER BREAKFAST

*Sponsored by the ASBMR Membership Development Committee
Supported by an educational grant from Merck & Co., Inc.*

The New Investigator/New Member Breakfast will be held on Monday, September 17, 2007, from 7:00 am to 8:00 am, in Room 316AB of the Hawaii Convention Center. New Investigators (those early in their careers) and new ASBMR members are invited to join the ASBMR Membership Development Committee and colleagues for an informational breakfast. Highlights will include opening remarks by ASBMR President, Dr. Steven Goldring, an overview of the Annual Meeting program by Program Co-Chairs: Drs. Juliet Compston and Harald Jueppner, and a special presentation by Women in Bone and Mineral Research Committee (WBMRC) Chair Dr. Nicola Partridge. Program directors from U.S. NIH Institutes and Centers, along with ASBMR member senior scientists, and representatives from several ASBMR committees will be available for discussion at specially marked tables. Attendees should look for table signs advertising a specialty or NIH Institute or Center of interest, which include: National Institute on Aging (NIA), National Institute of Arthritis and Musculoskeletal and Skin Diseases (NIAMS), National Institute of Child Health and Human Development (NICHD), National Institute of Dental and Craniofacial Research (NIDCR), National Cancer Institute (NCI), National Institute of Diabetes and Digestive and Kidney Diseases (NIDDK), and Center for Scientific Review (CSR). Or attendees can make their own signs to join with colleagues who have similar interests. New Investigators and first time attendees are encouraged to pick up a "New Investigator/ First Time Attendee" ribbon, which will be distributed at the entrance to the room. Breakfast will be provided.

JOINT ECTS/ASBMR SESSION ON OSTEONECROSIS OF THE JAW

This joint session organized by ASBMR and the European Calcified Tissue Society (ECTS) will take place on Tuesday, September 18, 2007, from 12:30 pm to 2:00 pm in Kamehameha Hall III of the Hawaii Convention Center. This unique and timely symposium will feature talks on “ONJ, Fear of ONJ and the Treatment of Osteoporosis,” “The Influence of ONJ on the Use of Bisphosphonates in Cancer Patients” and “Possible Pathophysiological Mechanisms in ONJ: Separating Fact from Fiction.”

SPECIAL SESSION FOR ALLIED HEALTH PROFESSIONALS Featuring an overview of the 29th Annual Meeting by Lawrence G. Raisz, M.D.

Supported by an educational grant from Roche and GSK

This session will be held on Monday, September 17, 2007, from 12:00 noon to 2:00 pm, in Room 313A of the Hawaii Convention Center. This special session is of interest to allied health professionals, first time meeting attendees, individuals new to the field, nurses, clinical research study coordinators, physical therapists and/or those seeking guidance in navigating through the extensive ASBMR program. An overview of the ASBMR 29th Annual Meeting will be given along with lectures on “Bisphosphonates: New Insights into Mechanisms of Action and Therapy Potency” and “Bisphosphonate Therapy: Common Clinical Issue.” There is no additional fee or registration required for this session, nor will food and beverages be served. However, you are welcome to purchase lunch from the concession area in Kamehameha Hall I and II (Exhibit Hall) of the Hawaii Convention Center.

THE “INS AND OUTS” OF RESEARCH FUNDING

Co-Sponsored Career Workshop Session by the ASBMR Education and Membership Development Committees

The Career Workshop Session will be held on Wednesday, September 19, 2007, from 12:30 pm to 2:00 pm, in the Kalakaua Ballroom C of the Hawaii Convention Center. This year's program is titled, “The Ins and Outs of Research Funding.” U.S. and international new investigators (those early in their research careers) and attendees with an interest in learning more about research funding are urged not to miss this workshop on the “ins and outs” of funding—from the National Institutes of Health (NIH) and minority opportunities available to new researchers—to insight on the peer-review process, strategies for writing a successful grant and how career paths can affect prospects for funding. There is no additional fee or registration required for this session, nor will food and beverages be served. However, you are welcome to purchase lunch from the concession area in Kamehameha I & II (Exhibit Hall) of the Hawaii Convention Center.

CLINICAL ROUNDTABLES/CLINICAL SESSION

The Clinical Roundtables/Case Conferences feature a focused discussion on topical issues of clinical relevance for the practicing clinician. Each session features two speakers and includes a panel discussion. Clinical sessions include topical issues of clinical relevance, followed by either a clinical roundtable or point/counterpoint discussion. The Clinical Roundtable/Case Conference sessions include: “Sequential Therapy: Antiresorptives Before and After Anabolics” and “Management of Bone Disease in Patients Undergoing Organ Transplantation.” See the schedule for session times and location. There is no additional fee or registration required for these sessions. Food and beverages will not be served; however, you are welcome to purchase lunch from the concession area in Kamehameha I & II (Exhibit Hall) of the Hawaii Convention Center.

Special Debate

This year's special Clinical Session will be in a debate format on the topic of “Excessive Suppression of Bone Remodeling by Antiresorptive Agents - Fact or Fiction?” argued by Ego Seeman, M.D, FRACP and Socrates Papapoulos, M.D. The session will take place on Sunday, September 16, 2007, from 1:00 pm to 2:00 pm in Kamehameha Hall III of the Hawaii Convention Center.

MEET-THE-PROFESSOR SESSIONS

The Meet-the-Professor Sessions are a series of informal sessions designed to provide an opportunity for meeting attendees to interact with experts in an intimate setting and discuss specific clinical and research topics. The Meet-the-Professor program has been expanded in order to increase the number of attendees who are able to participate in these sessions. The schedule allows for many Meet-the-Professor sessions to be given twice during the program.

New this year, registration will not be required, however space is extremely limited. There are no additional fees for these sessions. Interested individuals are welcome to attend these sessions on a first-come, first-served basis. Room restrictions and professor preferences will dictate number of attendees. Food and beverages will not be served; however, you are welcome to purchase lunch from the concession area in Kamehameha Hall I & II (Exhibit Hall) of the Hawaii Convention Center.

THE WOMEN IN BONE AND MINERAL RESEARCH EVENT

Sponsored by the ASBMR Women in Bone and Mineral Research Committee

Supported by educational grants from Merck & Co., Inc.

The Women in Bone and Mineral Research Event will be held on Tuesday, September 18, from 7:00 pm to 8:00 pm in Room 316 AB of the Hawaii Convention Center. This event is open to all attendees interested in furthering women's participation in the bone and mineral research field, and in the ASBMR. The ASBMR Women in Bone and Mineral Research Committee (WBMRC) was established in 2005. This committee is charged with mentoring women in the Society with respect to career advancement, academic promotions, combining a career with family, etc. This year's event will feature Dr. Diane Wara from the University of California, San Francisco, who will be speaking on issues of women in leadership and implementing institutional change for women. Dinner and wine will be served. Advanced registration and a fee are required for this event, so sign up at your earliest convenience on-site at the Registration Desk in the Main Lobby of the Hawaii Convention Center.

CHALLENGES AND OPPORTUNITIES FACING NIH PEER REVIEW: A VISION FOR INSURING ITS STRATEGIC NATIONAL VALUE

U.S. National Institutes of Health (NIH) Center for Scientific Review (CSR) Director Antonio Scarpa, M.D., Ph.D. will be making a presentation on the changes the CSR is initiating in the NIH peer review system on Sunday, September 16, 2007, from 3:45 pm to 4:45 pm in Kalakaua Ballroom C of the Hawaii Convention Center. The CSR is the portal for NIH grant applications and its review for scientific merit, receiving nearly 80,000 applications a year and recruiting more than 18,000 external experts to review them in study sections and advisory councils. The CSR mission is to see that NIH grant applications receive fair, independent, expert and timely reviews-free from inappropriate influences-so that NIH can fund the most promising research. Dr. Scarpa's presentation will describe the new efforts CSR is instituting to shorten the review process, recruit and retain the best reviewers and foster a culture more favorable to innovative applications.

NIH CENTER FOR SCIENTIFIC REVIEW: WHAT REALLY HAPPENS AT STUDY SECTION?

This workshop will take place on Monday, September 17, 2007, from 1:30 pm to 2:30 pm in Room 311 of the Hawaii Convention Center and will provide an overview of the NIH grant review process and insights into what happens at study section and council, who can review, the skills needed to serve as an effective grant reviewer and what is involved in a grant review. Through this workshop and other activities, the U.S. NIH Center for Scientific Review (CSR) hopes to increase the pool of experienced investigators willing to serve on study sections and review different types of bone-related grants, including basic, translational and clinical grants. The discussion at this informal, interactive session will be led by a panel of bone grant study section chairs and NIH representatives.

WELCOME RECEPTION AND PLENARY POSTER SESSION

Supported by an educational grant from Merck & Co., Inc.

On Sunday, September 16, 2007, from 5:00 pm to 6:45 pm, attendees and registered guests are invited to attend the ASBMR Welcome Reception and Plenary Poster Session in Kamehameha Hall I & II (Exhibit Hall) of the Hawaii Convention Center. Simply display your badge for admission. Guests may purchase a badge for \$30 at registration, which will allow entrance to the Welcome Reception and Exhibit Hall.

ASBMR SOCIAL EVENT

The ASBMR Social Event will take place at 8:00 pm on Tuesday, September 18, 2007, at the Royal Hawaiian Hotel, a legendary Waikiki Beach hotel known as "The Pink Palace of the Pacific." The social event will feature a live band and unique cultural entertainment. Drinks, light hors d'oeuvres and desserts will be served.

Tickets are required and can be purchased for \$30, if available tickets remain. The Royal Hawaiian Hotel is within walking distance to the ASBMR hotels. Shuttle busing will be provided only at the conclusion of the event to the Hilton and Ala Moana Hotels. The event will take place outside on the Ocean Lawn and inside the Monarch Ballroom. Appropriate shoes are recommended.

ASBMR FUN RUN/WALK

Supported by Novartis Pharmaceuticals Corporation

On Wednesday, September 19, 2007, from 6:00 am to 7:00 am delegates and guests of the ASBMR 29th Annual Meeting will have an opportunity to participate in a 5K Fun Run/Walk. Whether participants choose to walk or run, they will find this event a terrific way to begin a busy day. There is no cost to participate. Tickets are required and are available at the ASBMR meeting registration area in the Hawaii Convention Center. Please stop by the Hospitality Desk in the ASBMR meeting registration area on Tuesday, September 18, 2007, from 11:00 am to 6:30 pm to pick up your T-shirt (first 250 ticket holders), sign a waiver form and learn more about transportation.

REGISTRATION HOURS

All on-site registration will take place in the Main Lobby of the Hawaii Convention Center.

Saturday, September 15, 2007	9:00 am - 5:00 pm
Sunday, September 16, 2007	7:00 am - 6:30 pm
Monday, September 17, 2007	7:00 am - 5:30 pm
Tuesday, September 18, 2007	7:00 am - 5:30 pm
Wednesday, September 19, 2007	7:00 am - 5:30 pm

EXHIBIT HALL HOURS

The Exhibit Hall is located in Kamehameha Hall I & II of the Hawaii Convention Center. For meeting attendees, lunch will be available for purchase in the hall during Exhibit hours.

Sunday, September 16, 2007	5:00 pm - 6:45 pm
Monday, September 17, 2007	9:30 am - 4:30 pm
Tuesday, September 18, 2007	9:30 am - 4:30 pm
Wednesday, September 19, 2007	9:30 am - 4:30 pm

ASBMR TELEPHONE NUMBERS

Management Office	Tel: (808) 792-6521
Registration Desk	Tel: (808) 792-6520
Media Office	Tel: (808) 792-6522
Media Office	Fax: (808) 792-6525

SPEAKER READY ROOM

Supported by an educational grant from Mission Pharmacal Company

Speakers must check into the Speaker Ready Room 24 hours in advance of their presentation. At that time, speakers may review their slides. The Speaker Ready Room is located in Manoa 304A of the Hawaii Convention Center. Review of slides must occur at least 24 hours prior to your presentation. The Speaker Ready Room will be open during the following times:

Speaker Ready Room Hours

Saturday, September 15, 2007	9:00 am – 5:00 pm
Sunday, September 16, 2007	7:00 am – 6:00 pm
Monday, September 17, 2007	7:00 am – 6:30 pm
Tuesday, September 18, 2007	7:00 am – 6:00 pm
Wednesday, September 19, 2007	7:00 am – 6:00 pm

SPEAKER LOUNGE

*Supported by an educational grant from the Alliance for Better Bone Health
(Procter & Gamble Pharmaceuticals and sanofi-aventis)*

The Speaker Lounge will be located in Makiki 302AB of the Hawaii Convention Center. The lounge provides a relaxing atmosphere for the oral presenters and invited speakers to rest, mingle with one another, and to catch up on office work. The room will be equipped with computers, fax, copier, phone/modem lines, snacks and beverages, sofas and chairs. The Speaker Lounge will be available from Sunday, September 16, to Monday, September 17, from 7:00 am to 4:00 pm. and Tuesday, September 18, to Wednesday, September 19, from 7:00 am to 5:00 pm.

POSTER SESSIONS

All poster sessions will be held in Kamehameha Hall I & II (Exhibit Hall) of the Hawaii Convention Center. Authors must be at their posters for one hour and a half of the designated poster sessions on Monday through Wednesday and must be available to answer questions during this period. Authors of odd-numbered posters should be present from 11:30 am to 1:00 pm on their designated days. Authors of even-numbered posters should be present from 1:00 pm to 2:30 pm.

Poster numbers are listed in the *2007 Abstracts* book prefixed with a letter that denotes the day of presentation, i.e., M (Monday), T (Tuesday), W (Wednesday). These letters are not posted on the boards. **Presenters should mount their posters on the board bearing their assigned numbers, disregarding the letter prefix. ASBMR accepts no liability for posters or poster materials and will not adjudicate disputes between abstract presenters.**

Plenary Poster presenters and Young Investigator Award recipients presenting posters should mount their posters on Sunday, September 16, 2007, between 3:00 pm and 4:45 pm. Plenary Poster presenters and Young Investigator Award recipients presenting posters are expected to be present during the Welcome Reception and Plenary Poster Session on Sunday, September 16, from 5:00 pm to 6:45 pm. Plenary Poster presenters and Young Investigator Award recipients presenting posters will follow the odd/even hours for presenters during Poster Session I on Monday, September 17, 2007. Plenary Posters will remain posted until Monday, September 17 at 6:30 pm. Young Investigator Award posters will remain posted for the duration of the meeting.

Please note that children 12 years of age and under will not be permitted in the poster area or the Exhibit Hall at any time.

Presenter Check-in:

Since only poster presenters are allowed in the Exhibit/Poster Hall during the below poster set-up and dismantle hours, please go to the Poster Presenter Check-in Table to receive a security pass. The table will be located in front of Kamehameha Hall II of the Hawaii Convention Center. To speed the check-in process, please have your poster board number ready.

- **NOTE: Posters remaining after Poster Dismantling times will be discarded.**
- **Young Investigator Award Posters remain up through Wednesday, September 19.**

Please adhere to these scheduled times to maximize interaction for other attendees:

POSTER PRESENTATION SCHEDULE

	Poster Set-Up	Posters Open	Authors Present	Dismantle Posters
Sunday, Sept. 16 Welcome Reception/ Plenary Poster Session	3:00 - 4:45 pm	5:00 pm – 6:45 pm	5:00 - 6:45 pm Plenary Posters & YIA Award Posters	Do not dismantle.
Monday, Sept. 17 Poster Session I	7:30 – 8:00 am	8:00 am – 6:30 pm	11:30 am - 1:00 pm for Odd # 1:00 pm - 2:30 pm for Even #	6:30 – 7:00 pm Monday Posters Plenary Posters
Tuesday, Sept. 18 Poster Session II	7:30 – 8:00 am	8:00 am – 6:00 pm	11:30 am - 1:00 pm for Odd # 1:00 pm - 2:30 pm for Even #	6:00 – 6:30 pm Tuesday Posters
Wednesday, Sept. 19 Poster Session III	7:30 – 8:00 am	8:00 am – 4:30 pm	11:30 am - 1:00 pm for Odd # 1:00 pm - 2:30 pm for Even #	4:30 – 5:00 pm Wednesday Posters YIA Award Posters

ASBMR MEMBERSHIP

The ASBMR Exhibit Booth is #704 in the Exhibit Hall. Come by and meet the ASBMR staff, pick up information about the Society, check out the online version of the *Journal of Bone and Mineral Research*, and order copies of the 6th Edition of the *Primer on Metabolic Bone Diseases and Disorders of Mineral Metabolism*.

The ASBMR Membership Counter will be located in the ASBMR meeting registration area in the Main Lobby of the Hawaii Convention Center and will be prepared to accept 2008 ASBMR membership renewal payments.

ASBMR JOB PLACEMENT SERVICE

The ASBMR Job Placement Service is easily accessible year-round online. You can access the most up-to-date job and candidate listings using the ASBMR Job Placement Service Website. Simply submit your resume or job announcement using the online forms at **www.asbmr.org**. After your forms are submitted and payment is received, you will be able to use your self-assigned login name and password to access the Online Placement Service database anytime you wish.

Employers enrolled in the service will be entitled to display unlimited job announcements online and onsite at the meeting on the bulletin board located in the ASBMR meeting registration area in the Main Lobby of the Hawaii Convention Center. In addition, employers will have access to candidates' Curricula Vitae.

Employers and candidates may request further information by accessing the ASBMR Online Job Placement Service at www.asbmr.org.

ASBMR MEDIA OFFICE

The ASBMR Media Office will be in operation during the ASBMR 29th Annual Meeting to facilitate media-related activities during the meeting. The Media Office will be located in Palolo 306A in the Hawaii Convention Center.

Media Office - Hours of Operation

Saturday, September 15, 2007	2:00 pm - 5:00 pm
Sunday, September 16, 2007	8:00 am - 5:00 pm
Monday, September 17, 2007	8:00 am - 5:00 pm
Tuesday, September 18, 2007	8:00 am - 5:00 pm
Wednesday, September 19, 2007	8:00 am - 5:00 pm

SPECIAL NOTICES — SAFETY TIPS

- Remove your convention badge outside the meeting sites. Do not wear your badge outside or advertise that you're a visitor and not familiar with your surroundings.
- Walk with another person rather than alone. Avoid alleys, walkways between buildings, and deserted parking lots.
- Remain alert, be aware of your surroundings, and carry your handbag in front of you.
- While in your hotel room, always lock your door. Know where emergency exits are in your hotel.
- Place any valuables in a hotel safety deposit box rather than leaving them in your room or carrying them with you.
- Keep a copy of your passport and travel papers in a safe place.

DOES THE ASBMR HAVE YOUR EMAIL ADDRESS?

All important ASBMR Annual Meeting materials can be found on the ASBMR Website... and we will broadcast email to everyone on our correspondence list early notice of the Call for Abstracts, *Preliminary Program*, Registration and Housing information, Abstracts Online, and more! **So you don't miss out** on early notices and regular updates, please send all your contact information to the ASBMR, including your email address.

American Society for Bone and Mineral Research

2025 M Street, NW, Suite 800
Washington, DC 20036-3309, USA

Tel: (202) 367-1161

Fax: (202) 367-2161

E-mail: ASBMR@asbmr.org

Internet: www.asbmr.org

ANNUAL MEETING EVALUATION

The 2007 Annual Meeting Evaluation will be accessible online following the 29th Annual Meeting. An email will be sent to all meeting attendees who provided their email addresses at the time of registration. The email will provide a hyperlink to the online evaluation site. It will also be accessible via the ASBMR website at www.asbmr.org. We strongly encourage and welcome all attendees to provide us with feedback on the meeting. Your input is very important to us.

FUTURE ASBMR MEETING DATES

ASBMR 30th Annual Meeting

Palais des congrès de Montréal
Montreal, Quebec, Canada
September 12-16, 2008

ASBMR 31st Annual Meeting

Colorado Convention Center
Denver, Colorado, USA
September 11-15, 2009

ASBMR 32nd Annual Meeting

Metro Toronto Convention Center
Toronto, Ontario, Canada
October 15-19, 2010

ABSTRACT-BASED AWARDS

2007 ASBMR Most Outstanding Abstract Award

1061	Central Control of Bone Remodelling by Neuromedin U: A Mediator of the Leptin-dependent Regulation of Bone Formation	<u>S. Sato</u> ^{*1} , <u>S. Takeda</u> ¹ , <u>R. Hanada</u> ^{*2} , <u>M. Iwasaki</u> ^{*1} , <u>H. Inose</u> ¹ , <u>A. Kimura</u> ^{*1} , <u>K. Kangawa</u> ^{*3} , <u>M. Kojima</u> ^{*2} , <u>K. Shinomiya</u> ^{*1} . ¹ Orthopaedic Surgery & 21COE Program, Tokyo Medical and Dental University, Tokyo, Japan, 2Molecular Genetics, Institute of Life Science, Kurume University, Kurume, Japan, 3Biochemistry, National Cardiovascular Center Research Institute, Osaka, Japan.
------	--	---

2007 ASBMR Award for Outstanding Research in the Pathophysiology of Osteoporosis

1235	Deletion of Steroid Receptor Coactivator-2 (TIF-2) Results in Skeletal Resistance to Estrogen but a High Bone Mass Phenotype Due to Concomitant Resistance to PPAR	<u>U. I. Moedder</u> ¹ , <u>D. G. Fraser</u> ^{*1} , <u>A. Sanyal</u> ¹ , <u>M. Gehin</u> ^{*2} , <u>P. Chambon</u> ^{*2} , <u>B. W. O'Malley</u> ^{*3} , <u>C. J. Rosen</u> ⁴ , <u>T. C. Spelsberg</u> ¹ , <u>S. Khosla</u> ¹ . ¹ Mayo Clinic, Rochester, MN, USA, ² Institut de Génétique et de Biologie Moléculaire et Cellulaire, Illkirch, France, ³ Baylor College of Medicine, Houston, TX, USA, ⁴ Jackson Labs, Bar Harbor, ME, USA.
------	--	---

2007 ASBMR President's Book Award

1181	Molecular Interaction Between Bcl-xL and Bnip3 Determines the Cell Fate of Hypertrophic Chondrocytes	<u>Y. Oshima</u> ¹ , <u>T. Akiyama</u> ^{*1} , <u>M. Iwasawa</u> ¹ , <u>Y. Nagase</u> ¹ , <u>L. Hennighausen</u> ^{*2} , <u>K. Nakamura</u> ¹ , <u>S. Tanaka</u> ¹ . ¹ Orthopaedic Surgery, The University of Tokyo, Tokyo, Japan, ² Laboratory of Genetics and Physiology, National Institutes of Health, Bethesda, MD, USA.
------	--	--

2007 ASBMR Shun-ichi Harada Young Investigator Awards

1062	ECM1, a Direct Targeting Molecule of PTHrP, Is a Novel Potent Mediator of Chondrogenesis	<u>L. Kong</u> ^{*1} , <u>Y. Zhang</u> ^{*1} , <u>B. Jiang</u> ^{*2} , <u>Y. Xie</u> ^{*2} , <u>J. Q. Feng</u> ² , <u>T. Kobayashi</u> ^{*3} , <u>H. M. Kronenberg</u> ¹ , <u>C. Liu</u> ¹ . ¹ Department of Orthopaedic Surgery, New York University, New York, NY, USA, ² Department of Biomedical Sciences, Baylor College of Dentistry, Texas A&M University System Health Science Center, Dallas, TX, USA, ³ Endocrine Unit, Massachusetts General Hospital, Boston, MA, USA.
1236	Increased Bone Mineral Density in Transgenic Mice Over-expressing Tissue-nonspecific Alkaline Phosphatase	<u>M. C. Yadav</u> ^{*1} , <u>S. Narisawa</u> ^{*1} , <u>K. Johnson</u> ^{*2} , <u>R. Terkeltaub</u> ^{*2} , <u>N. Pleshko Camacho</u> ³ , <u>J. L. Millan</u> ¹ . ¹ OncoDevelopmental Biology, Burnham Institute for Medical Research, La Jolla, CA, USA, ² VAMC/UCSD, La Jolla, CA, USA, ³ The Hospital for Special Surgery, New York, NY, USA.
1267	Bone Apposition in Patients on Teriparatide Treatment Is Preferably Directed to Skeletal Regions of Local Structural Weakness: Assessment by High Resolution CT Based Finite Element Analysis In Vivo	<u>C. Graeff</u> ¹ , <u>P. Zysset</u> ^{*2} , <u>F. Marin</u> ^{*3} , <u>C. C. Glüer</u> ¹ . ¹ Medical Physics, Diagnostic Radiology, Universitätsklinikum Schleswig Holstein, Campus Kiel, Kiel, Germany, ² Institute for Lightweight Design and Structural Biomechanics, Vienna University of Technology, Vienna, Austria, ³ Medical Research, Eli Lilly & Co, Europe, Madrid, Spain.

2007 ASBMR Young Investigator Awards

1001	Identification of a Novel TGF-beta Dependent-Prometastatic Signature Mediating Bone Colonization	<u>I. Garcia-Tunon</u> ^{*1} , <u>S. Vicent</u> ^{*1} , <u>D. Luis-Ravelo</u> ^{*1} , <u>I. Anton</u> ^{*1} , <u>C. Zanduetta</u> ^{*1} , <u>S. Martinez</u> ^{*1} , <u>J. De Las Rivas</u> ^{*2} , <u>F. Lecanda</u> ¹ . ¹ Division of Oncology, Center for Applied Medical Research, Pamplona, Spain, ² Bioinformatics, CIC, Salamanca, Spain.
1003	Role of Hypoxia in Cancers that Metastasize to Bone: HIF1 Enhances TGF Signaling and Expression of Prometastatic Factors CXCR4 and VEGF	<u>L. A. Kingsley</u> , <u>P. G. J. Fournier</u> , <u>J. M. Chirgwin</u> , <u>T. A. Guise</u> . Internal Medicine, University of Virginia, Charlottesville, VA, USA.
1004	Osteoclasts in Myeloma Are Derived From Gr-1+CD11b+ Mononuclear Cells of the Bone Marrow Niche	<u>J. Zhuang</u> ¹ , <u>L. Yang</u> ^{*2} , <u>J. R. Edwards</u> ¹ , <u>C. M. Edwards</u> ¹ , <u>G. R. Mundy</u> ¹ . ¹ Vanderbilt Center for Bone Biology, Nashville, TN, USA, ² Cancer Biology, Vanderbilt University, Nashville, TN, USA.
1019	A Stone Mouse: Transgenic Expression of an Engineered Gs-coupled Receptor in Osteoblasts Produces Increased Bone Mass	<u>E. C. Hsiao</u> ¹ , <u>B. Boudignon</u> ² , <u>P. W. Chang</u> ^{*1} , <u>M. Benscik</u> ^{*2} , <u>J. Peng</u> ^{*2} , <u>C. Manalac</u> ^{*1} , <u>B. Halloran</u> ² , <u>B. Conklin</u> ^{*1} , <u>R. Nissenson</u> ² . ¹ Gladstone Institutes, University of California, San Francisco, CA, USA, ² Endocrine Unit, VA Medical Center, San Francisco, CA, USA.
1023	Bone Cell Autonomous Effects of Osteoactivin/Gpnb In Vivo	<u>J. Y. Belcher</u> , <u>M. C. Rico</u> , <u>I. Arango-Hisijara</u> , <u>S. Salihoglu</u> [*] , <u>K. B. Buck</u> [*] , <u>S. Abdelmagid</u> , <u>A. Sanjay</u> , <u>S. N. Popoff</u> , <u>F. F. Safadi</u> . Anatomy and Cell Biology, Temple University, Philadelphia, PA, USA.
1027	Novel Mechanism of Vitamin D Receptor (VDR) Activation: Histone H3 Lysine 9 Methyltransferase Is a Transcriptional Coactivator for VDR	<u>Y. Zhong</u> [*] , <u>S. Christakos</u> . Biochemistry and Molecular Biology, UMDNJ-New Jersey Medical School, Newark, NJ, USA.
1031	Dominant-Negative GCMB Mutations Cause Hypoparathyroidism	<u>M. Mannstadt</u> ¹ , <u>G. Bertrand</u> ^{*2} , <u>B. Grandchamp</u> ^{*2} , <u>H. Jueppner</u> ¹ , <u>C. Silve</u> ² . ¹ Endocrine Unit, Massachusetts General Hospital, Boston, MA, USA, ² Faculté de Médecine, Hôpital Xavier Bichat, Paris, France.
1037	Is Bone Strength a Simple Function of Muscle, or Does Other Mechanical Loading Play a Role?	<u>J. N. Douthwaite</u> ¹ , <u>P. P. E. Flowers</u> ^{*2} , <u>J. A. Kanaley</u> ^{*3} , <u>R. M. Hickman</u> ^{*1} , <u>J. A. Spadaro</u> ¹ , <u>T. A. Scerpella</u> ¹ . ¹ Orthopaedic Surgery, SUNY Upstate Medical University, Syracuse, NY, USA, ² Engineering, Syracuse University, Syracuse, NY, USA, ³ Exercise Science, Syracuse University, Syracuse, NY, USA.

1050	Risk of Subsequent Fracture Depends on Bone Mineral Density and Fracture Type: A 15-Year Prospective Study	D. Bliuc, N. Nguyen, T. V. Nguyen, J. A. Eisman, J. R. Center. Bone and Mineral Program, Garvan Institute of Medical Research, Sydney, Australia.
1067	Targeted Deletion of a Distant Transcriptional Enhancer of the RANKL Gene Reduces Bone Remodeling and Increases Bone Mass	C. Galli ¹ , P. E. Cazer ^{*1} , L. A. Zella ² , J. A. Fretz ^{*2} , J. W. Pike ² , R. S. Weinstein ¹ , S. C. Manolagas ¹ , C. A. O'Brien ¹ . ¹ Center for Osteoporosis and Metabolic Bone Diseases, University of Arkansas for Medical Sciences and Central Arkansas Veterans Healthcare System, Little Rock, AR, USA, ² Department of Biochemistry, University of Wisconsin, Madison, WI, USA.
1072	TGF1 Induces Migration of Mesenchymal Stem Cells in Coupling Bone Resorption and Formation	Y. Tang, X. Wu, S. Xie [*] , L. Zhao [*] , C. Wan [*] , Z. Shi [*] , X. Feng, X. Peng [*] , M. Wan, X. Cao. Pathology, University of Alabama at Birmingham, Birmingham, AL, USA.
1077	Clinical Risk Factors for Incident Vertebral Fractures: Data from the Six-Year Prospective OPUS Study	K. Briot ¹ , C. Roux ¹ , S. Kolta ¹ , R. Eastell ² , D. M. Reid ³ , D. Felsenberg ⁴ , C. C. Gluer ³ . ¹ Rheumatology, Cochin Hospital, Paris, France, ² University of Sheffield clinical sciences centre, Sheffield, United Kingdom, ³ Department of Medicine and Therapeutics, University of Aberdeen, Aberdeen, United Kingdom, ⁴ Diagnostic Radiology, Free University Berlin, Berlin, Germany, ⁵ Medical Physics, Department of Diagnostic Radiology, University Hospital Schleswig-Holstein, Campus Kiel, Kiel, Germany.
1084	Role for Estrogen Receptor-Beta in Trabecular Bone Mechanotransduction	A. B. Castillo ¹ , J. M. Doyle ^{*1} , M. R. Allen ² , C. H. Turner ¹ . ¹ Biomedical Engineering, Indiana University Purdue University, Indianapolis, IN, USA, ² Anatomy and Cell Biology, Indiana University School of Medicine, Indianapolis, IN, USA.
1098	Functional Analysis of Bcl-xL in Osteoclasts by Osteoclast-Specific Deletion of bcl-x Gene in Mice	M. Iwasawa ¹ , Y. Nagase ¹ , T. Miyazaki ¹ , T. Akiyama ¹ , Y. Kadono ¹ , M. Nakamura ¹ , Y. Oshima ¹ , T. Yasui ^{*1} , T. Nakamura ^{*2} , S. Kato ^{*2} , K. Nakamura ¹ , S. Tanaka ¹ . ¹ Department of Orthopaedic Surgery, The University of Tokyo, Tokyo, Japan, ² The Institute of Molecular and Cellular Biosciences, The University of Tokyo, Tokyo, Japan.
1107	Targeted Disruption of Ephrin B1 in Osteoblasts Reduces Bone Size in Mice	W. Xing, K. Govoni, A. Kapoor [*] , S. Mohan. J.L. Pettis VA Medical Center and Loma Linda Univ, Loma Linda, CA, USA.
1121	PTH-Regulated Gene Expression in the Mouse Skeleton Suggest a Role for Ephrins in PTH Anabolism versus Catabolism	E. N. Bianchi [*] , R. Rizzoli, S. L. Ferrari. Div. of Bone Diseases, Geneva University Hospital, Geneva, Switzerland.
1124	Adenosine and Osteoporosis: Adenosine A ₁ Receptor Blockade Reverses Bone Loss in Ovariectomized Mice and Deletion of Adenosine A _{2A} Receptors Leads to Diminished Bone Density	F. M. Kara ^{*1} , S. B. Doty ^{*2} , A. Boskey ^{*2} , B. Fredholm ^{*3} , B. N. Cronstein ¹ . ¹ Medicine, NYU School of Medicine, NYC, NY, USA, ² Hospital for Special Surgery, NYC, NY, USA, ³ Karolinska Institute, Stockholm, Sweden.
1139	Evidence for Lineage Dependent Non-canonical Wnt Signal Transduction by Bone Cells	G. J. Spencer [*] , P. G. Genever [*] . Department of Biology, University of York, York, United Kingdom.
1141	ERK1 and ERK2 Are Essential for Osteoblast Differentiation	T. Matsushita ^{*1} , G. Landreth ^{*2} , S. Murakami ¹ . ¹ Orthopaedics, Case Western Reserve University, Cleveland, OH, USA, ² Neurosciences, Case Western Reserve University, Cleveland, OH, USA.
1145	Transcription Factor IRF-8 Is a Negative Regulator of Osteoclast Differentiation In Vitro and In Vivo	B. Zhao ^{*1} , M. Takami ¹ , A. Yamada ^{*1} , X. Wang ^{*1} , K. Nakao ^{*2} , T. Tamura ^{*3} , K. Ozato ^{*4} , H. Takayanagi ⁵ , R. Kamijo ¹ . ¹ Department of Biochemistry, School of Dentistry, Showa University, Tokyo, Japan, ² Laboratory for Animal Resources and Genetic Engineering, Center for Developmental Biology, RIKEN, Kobe, Japan, ³ Department of Physiology, Osaka City University Graduate School of Medicine, Osaka, Japan, ⁴ Laboratory of Molecular Growth Regulation, National Institute of Child Health and Human Development, NIH, Bethesda, MD, USA, ⁵ Department of Cell Signaling, Graduate School, Tokyo Medical and Dental University, Tokyo, Japan.
1146	The Small GTPase cdc42 Enhances Osteoclastogenesis and Bone Resorption	Y. Ito ¹ , Y. Zheng ^{*2} , J. F. Johnson ^{*2} , L. Yang ^{*2} , S. L. Teitelbaum ¹ , F. P. Ross ¹ , H. Zhao ¹ . ¹ Department of Pathology and Immunology, Washington University, St. Louis, MO, USA, ² Division of Experimental Hematology, University of Cincinnati, Cincinnati, OH, USA.
1148	NF-B2 Limits TNF-induced Osteoclastogenesis Through Precursor Cell Cycle Regulation	Z. Yao, L. Xing, B. Boyce. Pathology, University of Rochester, Rochester, NY, USA.
1151	Activation of BMP Signaling by the FOP ACVR1 R206H Mutation	Q. Shen ^{*1} , M. Xu ^{*1} , S. C. Little ^{*2} , F. S. Kaplan ¹ , M. C. Mullins ^{*2} , E. M. Shore ¹ . ¹ Orthopaedics, University of Pennsylvania, Philadelphia, PA, USA, ² Cell and Developmental Biology, University of Pennsylvania, Philadelphia, PA, USA.
1158	Asymmetry in Leg Power Increases Non-spine and Hip Fracture Risk in Older Men: The Osteoporotic Fractures in Men (MrOS) Study	P. M. Cawthon ¹ , T. L. Blackwell ^{*1} , B. Chan ^{*2} , K. Winters-Stone ^{*2} , E. Barrett-Connor ^{*3} , K. Ensrud ^{*4} , E. S. Orwoll ^{*2} . ¹ Research Institute, California Pacific Medical Center, San Francisco, CA, USA, ² Oregon Health and Science University, Portland, OR, USA, ³ University of California, San Diego, CA, USA, ⁴ University of Minnesota, Minneapolis, MN, USA.
1160	Aortic Calcifications Correlate with Volumetric Bone Mineral Density and Bone Microstructure in Men: A Population-Based Study	J. T. Chow ^{*1} , S. Khosla ¹ , L. J. Melton ¹ , E. J. Atkinson ^{*3} , A. E. Kearns ¹ . ¹ Endocrinology, Mayo Clinic College of Medicine, Rochester, MN, USA, ² Epidemiology, Mayo Clinic College of Medicine, Rochester, MN, USA, ³ Biostatistics, Mayo Clinic College of Medicine, Rochester, MN, USA.

1169	Specific Inhibition of the VEGF Homologue Placental Growth Factor Is Protective Against Osteolytic Bone Metastasis in Mice	<u>L. Coenegrachts</u> ^{*1} , <u>C. Maes</u> ¹ , <u>I. Stockmans</u> ^{*1} , <u>T. Guise</u> ² , <u>R. Bouillon</u> ¹ , <u>P. Carmeliet</u> ^{*3} , <u>G. Carmeliet</u> ¹ . ¹ Laboratory of Experimental Medicine and Endocrinology, K.U.Leuven, Leuven, Belgium, ² Dept. of Internal Medicine, University of Virginia, Charlottesville, VA, USA, ³ Center for Transgene Technology and Gene Therapy, VIB, K.U.Leuven, Leuven, Belgium.
1183	Atf4 Regulates Chondrocyte Proliferation and Differentiation by Direct Targeting <i>Indian Hedgehog</i> Transcription	<u>W. Wang</u> [*] , <u>X. Yang</u> . Center for Bone Biology, Departments of Medicine and Pharmacology, Vanderbilt University, Nashville, TN, USA.
1193	Decreases in Cortical Thickness, and not Changes in Trabecular Microstructure, Are Associated with the Pubertal Increase in Forearm Fractures in Girls	<u>S. Kirmani</u> , <u>L. McCready</u> [*] , <u>M. Holets</u> [*] , <u>P. R. Fischer</u> [*] , <u>B. L. Riggs</u> , <u>L. J. Melton</u> , <u>S. Khosla</u> . Mayo Clinic, Rochester, MN, USA.
1196	Sequencing of Collagen I in Three Patients with Multiple Fractures of Unknown Aetiology Reveals Novel Mutations Causing Osteogenesis Imperfecta with Normal to High BMD	<u>K. Lindahl</u> [*] , <u>H. Brändström</u> , <u>A. Kindmark</u> [*] , <u>Ö. Ljunggren</u> [*] . Medical Sciences, Endocrinology, Uppsala, Sweden.
1201	Enhancement of Prognosis of Osteoporotic Fractures by Genetic Marker: Contribution of the Collagen I alpha 1 Gene.	<u>B. H. Tran</u> [*] , <u>N. D. Nguyen</u> , <u>S. A. Frost</u> [*] , <u>J. R. Center</u> , <u>J. A. Eisman</u> , <u>T. V. Nguyen</u> . Bone and Mineral Research Program, Garvan Institute of Medical Research, Sydney, Australia.
1212	Dimorphic Effects of Notch Signaling in Bone Homeostasis	<u>F. Engin</u> ¹ , <u>T. Yang</u> ¹ , <u>G. Zhou</u> ¹ , <u>T. Bertin</u> ^{*1} , <u>M. Jiang</u> ^{*1} , <u>Y. Chen</u> ^{*1} , <u>L. Wang</u> ² , <u>H. Zheng</u> ^{*1} , <u>Z. Yao</u> ³ , <u>B. Boyce</u> ³ , <u>B. Lee</u> ⁴ . ¹ Molecular and Human Genetics, Baylor College of Medicine, Houston, TX, USA, ² Pediatrics, Baylor College of Medicine, Houston, TX, USA, ³ Pathology and Laboratory Medicine, University of Rochester, Rochester, NY, USA, ⁴ Molecular and Human Genetics, Baylor College of Medicine, Howard Hughes Medical Institute, Houston, TX, USA.
1215	Pericytes Derived from Adipose Tissue; Characterization and Evaluation of their Osteogenic Potential	<u>I. Kalajzic</u> ¹ , <u>L. Wang</u> ¹ , <u>X. Jiang</u> ^{*1} , <u>K. Lamothe</u> ^{*2} , <u>L. H. Aguila</u> ^{*2} , <u>D. W. Rowe</u> ¹ . ¹ Dept. of Reconstructive Sciences, Uni. of Conn. Health Center, Farmington, CT, USA, ² Dept. of Immunology, Uni. of Conn. Health Center, Farmington, CT, USA.
1224	Type III Sodium-Dependent Phosphate Transporter Controls Endochondral Ossification Through Regulating Chondrocyte Apoptosis	<u>A. Sugita</u> ¹ , <u>S. Kawai</u> ¹ , <u>T. Hayashibara</u> ^{*1} , <u>H. Yoshikawa</u> ² , <u>T. Yoneda</u> ¹ . ¹ Biochemistry, Osaka University Graduate School of Dentistry, Suita, Japan, ² Orthopedics, Osaka University Graduate School of Medicine, Suita, Japan.
1238	Activation of Renin-Angiotensin System Induces Osteoporosis Independently of Hypertension	<u>Y. Asaba</u> ^{*1} , <u>M. Ito</u> ² , <u>K. Watanabe</u> ¹ , <u>S. Takeshita</u> ¹ , <u>J. Ishida</u> ^{*3} , <u>Y. Nimura</u> ^{*4} , <u>A. Fukamizu</u> ^{*3} , <u>K. Ikeda</u> ¹ . ¹ Department of Bone and Joint Disease, National Center for Geriatrics and Gerontology (NCGG), Obu, Japan, ² Department of Radiology, Nagasaki University School of Medicine, Nagasaki, Japan, ³ Center for Tsukuba Advanced Research Alliance (TARA), University of Tsukuba, Tsukuba, Japan, ⁴ Department of Surgery, Nagoya University Graduate School of Medicine, Nagoya, Japan.
1246	Temporal Pattern of Gene Expression and Histology of Stress Fracture Healing in the Rat Ulna-Loading Model	<u>L. J. Kidd</u> ^{*1} , <u>A. Stephens</u> ^{*1} , <u>J. S. Kuliwaba</u> ^{*2} , <u>N. L. Fazzalari</u> ² , <u>M. R. Forwood</u> ¹ . ¹ School of Biomedical Science, The University of Queensland, Brisbane, Australia, ² Division of Tissue Pathology, Institute of Medical and Veterinary Science and Hanson Institute, Adelaide, Australia.
1247	GSK-3 Inhibits Osteoblastic Bone Formation Through Suppression of Runx2 Transcriptional Activity by the Phosphorylation at a Specific Site	<u>M. Hirata</u> , <u>F. Kugimiya</u> , <u>N. Kawamura</u> , <u>S. Ohba</u> , <u>K. Nakamura</u> [*] , <u>H. Kawaguchi</u> , <u>U. Chung</u> . Sensory & Motor System Medicine & Tissue Engineering, University of Tokyo, Tokyo, Japan.
1248	Overexpression of DeltaFosB Decreases Adipose Mass in a Non-Cell Autonomous Manner by Increasing Energy Expenditure Independently of Bone Cells	<u>G. C. Rowe</u> ^{*1} , <u>L. Neff</u> ^{*1} , <u>T. Green</u> ^{*2} , <u>H. Saito</u> ^{*1} , <u>C. Choi</u> ^{*3} , <u>G. Shulman</u> ^{*3} , <u>E. Nestler</u> ^{*2} , <u>W. Horne</u> ¹ , <u>R. Baron</u> ¹ . ¹ Orthopaedics, Yale University, New Haven, CT, USA, ² Psychiatry, University of Texas Southwestern Medical Center, Dallas, TX, USA, ³ Internal Medicine, Yale University, New Haven, CT, USA.
1250	Zfp521, a D2D FosB-interacting Protein, Is a Novel Inhibitor of Runx2 Activity with Opposite Effects on Osteoblasts and Bone Formation <i>In Vitro</i> and <i>In Vivo</i>	<u>E. Hesse</u> , <u>M. Wu</u> [*] , <u>G. C. Rowe</u> [*] , <u>L. Neff</u> [*] , <u>W. C. Horne</u> , <u>R. Baron</u> . Orthopaedics and Cell Biology, Yale University School of Medicine, New Haven, CT, USA.
1261	Mutations in <i>CRTAP</i> or <i>P3H1</i> Cause Dysregulation of Prolyl-3-hydroxylation and Recessive Osteogenesis Imperfecta	<u>D. Baldridge</u> ^{*1} , <u>U. Schwarze</u> ^{*2} , <u>R. Morello</u> ¹ , <u>J. Lenington</u> ^{*1} , <u>T. K. Bertin</u> ^{*1} , <u>D. R. Eyre</u> ² , <u>M. Weis</u> ^{*2} , <u>A. Green</u> ^{*3} , <u>J. Walsh</u> ^{*3} , <u>D. Lambert</u> ^{*3} , <u>D. Krakow</u> ^{*4} , <u>D. L. Rimoim</u> ^{*4} , <u>D. H. Cohn</u> ^{*4} , <u>P. H. Byers</u> ^{*2} , <u>B. Lee</u> ¹ . ¹ Molecular and Human Genetics, Baylor College of Medicine, Houston, TX, USA, ² University of Washington, Seattle, WA, USA, ³ Our Lady's Hospital, Dublin, Ireland, ⁴ Cedars Sinai Medical Center, Los Angeles, CA, USA.
1263	A Novel Central Mechanism in Uremic Bone Disease	<u>W. Cheung</u> ^{*1} , <u>C. Vanek</u> ² , <u>U. T. Iwaniec</u> ^{*3} , <u>R. T. Turner</u> ^{*3} , <u>R. Klein</u> ^{*2} , <u>R. Mak</u> ^{*1} . ¹ Pediatrics, University of California at San Diego, La Jolla, CA, USA, ² Bone and Mineral Unit, Oregon Health and Science University, Portland, OR, USA, ³ Nutrition and Exercise Sciences, Oregon State University, Corvallis, OR, USA.
1272	Is Antidepressant Use Associated with Bone Loss or Fractures in Postmenopausal Women?	<u>L. Spangler</u> ^{*1} , <u>D. Scholes</u> ¹ , <u>R. Brunner</u> ^{*2} , <u>J. Robbins</u> ^{*3} , <u>S. Reed</u> ⁴ , <u>K. Newton</u> ^{*1} , <u>J. Melville</u> ^{*4} , <u>A. LaCroix</u> ⁵ . ¹ Group Health, Seattle, WA, USA, ² University of Nevada, Reno, NV, USA, ³ University of California, Sacramento, CA, USA, ⁴ University of Washington, Seattle, WA, USA, ⁵ Fred Hutchinson Cancer Research Center, Seattle, WA, USA.
1283	Deletion of Subunit b1 in Osteoblast Reveals Novel Role for Calcineurin in Bone Formation	<u>A. R. Venn</u> [*] , <u>H. Yeo</u> [*] , <u>J. M. McDonald</u> , <u>T. L. Clemens</u> , <u>M. Zayzafoon</u> . Department of Pathology, University of Alabama at Birmingham, Birmingham, AL, USA.
1290	Regulation of Skeletal Homeostasis by Anti-apoptotic Molecule Bcl-2	<u>Y. Nagase</u> ¹ , <u>M. Iwasawa</u> ¹ , <u>T. Akiyama</u> ¹ , <u>Y. Kadono</u> ¹ , <u>T. Miyamoto</u> ² , <u>Y. Oshima</u> ¹ , <u>M. Nakamura</u> ¹ , <u>T. Yasui</u> ¹ , <u>K. Nakamura</u> ¹ , <u>S. Tanaka</u> ¹ . ¹ Orthopaedic Surgery, University of Tokyo, Tokyo, Japan, ² Orthopaedic Surgery, Cell differentiation, Keio University School of medicine, Tokyo, Japan.

1291	Distinct Roles of ITAM Signaling in Bone Remodeling in Various Bony Microenvironments	<u>Y. Wu¹, J. Torchia^{*2}, W. Yao³, N. E. Lane³, L. L. Lanier^{*1}, M. C. Nakamura², M. B. Humphrey¹</u> . ¹ Microbiology and Immunology, University of California, San Francisco, San Francisco, CA, USA, ² Medicine, VA Medical Center, San Francisco, CA, USA, ³ Medicine, University of California, Davis, Sacramento, CA, USA, ⁴ Medicine, University of Oklahoma Health Science Center, Oklahoma City, OK, USA.
1295	Conditional Ablation of Parathyroid Hormone Related Peptide (PTHrP) in Mammary Epithelial Cells Inhibits Breast Cancer Progression	<u>J. Li^{*1}, A. Karaplis², P. Siegel^{*1}, V. Papavasiliou^{*1}, W. Muller^{*1}, R. Kremer¹</u> . ¹ Dept. of Medicine, McGill University Health Centre, McGill University, Montreal., PQ, Canada, ² Dept of Medicine, Jewish General Hospital, McGill University, Montreal., PQ, Canada.
1298	T-lymphocytes Amplify the Anabolic Action of Intermittent PTH Treatment by Regulating Osteoclast Formation	<u>M. Terauchi, Y. Gao, S. Galley, X. Yang*, K. Page*, E. Shah*, M. N. Weitzmann, R. Pacifici</u> . Division of Endocrinology, Metabolism and Lipids, Emory University School of Medicine, Atlanta, GA, USA.
S171/ M171	BMP Canonical Signaling Through Receptor Smads 1 and 5 Is Required for Endochondral Bone Formation	<u>K. N. Retting^{*1}, R. R. Behringer^{*2}, K. M. Lyons¹</u> . ¹ Orthopaedic Surgery, UCLA, Los Angeles, CA, USA, ² Molecular Genetics, University of Texas M.D. Anderson Cancer Center, Houston, TX, USA.
S223/ M223/ O223	Conditional Ablation of the Osteoblast Calcium-Sensing Receptor Causes Abnormalities in Skeletal Development and Mineralization	<u>M. M. Dvorak¹, C. Tu^{*1}, H. Elalieh^{*1}, T. Chen^{*1}, B. Liu^{*1}, B. E. Kream^{*2}, D. D. Bikle¹, W. Chang¹, D. M. Shoback¹</u> . ¹ Department of Medicine, University of California, San Francisco, CA, USA, ² Department of Medicine, University of Connecticut Health Center, Farmington, CT, USA.
S493/ M493	Structural Implications of Low-Magnitude Mechanical Stimulation in a Pilot Study of Patients with Renal Osteodystrophy Evaluated with the MRI-based Virtual Bone Biopsy	<u>C. E. Jones^{*1}, F. W. Wehrli¹, J. F. Magland^{*1}, C. T. Rubin², S. A. Nihtianova^{*3}, M. B. Leonard³</u> . ¹ University of Pennsylvania, Philadelphia, PA, USA, ² State University of New York, Stony Brook, NY, USA, ³ Children's Hospital of Philadelphia, Philadelphia, PA, USA.
S530/ M530	Jump Starting Skeletal Health: Bone Increases from Jumping Exercise Persist Seven Years Post Intervention	<u>K. B. Gunter^{*1}, A. Baxter-Jones^{*2}, R. Mirwald^{*2}, H. C. Almstedt^{*3}, S. Durski^{*1}, A. A. Fuller-Hayes^{*1}, C. M. Snow¹</u> . ¹ Department of Nutrition and Exercise Sciences, Oregon State University, Corvallis, OR, USA, ² College of Kinesiology, University of Saskatchewan, Saskatoon, SK, Canada, ³ Department of Natural Science, Loyola Marymount University, Los Angeles, CA, USA.

HOW THE PROGRAM WAS SELECTED

The President and Program Co-Chairs began the process of developing the program for this meeting in the second quarter of 2006. During this process we have greatly appreciated the advice and suggestions of the previous President, Elizabeth Shane, and the previous Program Co-Chairs Andrew Arnold and Susan Greenspan. We also extend our thanks to the Chairs and Panels of each Abstract Review Category who played a major role in formulating the program for our meeting.

Program overview

As in previous years, the program will contain a combination of oral presentations, poster sessions, symposia, State-of-the-Art Lectures, Meet-the-Professor sessions and workshops. There will be a total of 324 oral presentations selected from the 1,878 abstracts submitted. The 15th Gerald D. Aurbach Memorial lecture will be given by Sir Michael Berridge, FRS, whose discovery of the molecule inositol triphosphate (IP3) and its role in the calcium signaling pathway was a major breakthrough in scientific research. The Louis V. Avioli Memorial Lecture will be given by Tatsuo Suda, D.D.S., Ph.D., who has made numerous key contributions to our current knowledge of bone biology, particularly with regard to osteoclast maturation and function.

New features

This year's program contains two new features. First, there will be a session of "oral posters," in which 24 abstracts (12 clinical and 12 basic science) will be presented in parallel sessions on Sunday. The purpose of these sessions will be to provide the authors of the highest-ranked posters a unique opportunity to present the major findings of their work in a fast-paced oral session. Each speaker will be given three minutes (and will be allowed no more than four slides) to present the key findings of his/her abstract, followed by two minutes of discussion. These oral poster sessions are a well-tried format in some national and international meetings and we hope that they will be well received at the forthcoming Honolulu meeting.

The second new feature of our meeting is that we are staging a debate on Sunday to address the very topical issue of whether long-term suppression of bone turnover has adverse effects on bone strength. The title of this debate is "Excessive Suppression of Bone Remodeling by Anti-resorptive Agents - Fact or Fiction?" and the discussants will be Ego Seeman, M.D., FRACP and Socrates Papapoulos, M.D.

MTP sessions

Based on feedback that was received after last year's meeting, we are continuing with the large number of Meet-the-Professor Sessions (18 clinical, repeated once, and 13 basic science). Feedback indicated that the system of reserving attendance in advance was unsatisfactory because many individuals who had signed up for the session did not attend, which left seats unfilled and those without tickets either waiting in line outside the rooms or deciding not to attend because they assumed they would not be able to participate without a ticket. This year we have therefore decided that attendance should be on a "first-come, first-serve" basis, which hopefully will ensure fairer access. There are also two Clinical Workshops, one on the management of bone disease after organ transplantation and on combined or sequential anabolic and anti-resorptive therapy.

Symposia and State-of-the-Art Lectures

This year there will be seven symposia (three plenary, two clinical and two basic) and two State-of-the-Art Lecture sessions. The topics of the Plenary symposia will be imaging, bone quality and drug development and all three will cover a broad range of clinical and scientific aspects. The State-of-the-Art Lectures will cover the role of stem cells in bone research and the regulation of mineral ion homeostasis and bone metabolism in chronic kidney disease. In choosing the topics for the symposia and State-of-the-Art lectures we have used feedback from the 2006 meeting and advice from its Program Committee. We also have a joint session with the ECTS on Tuesday, which is focused on osteonecrosis of the jaw and will address the pathophysiology and management of this disorder.

How the abstracts and posters were selected

Categories for abstract submission were similar to those of last year, although some modifications were made based on the numbers of abstracts previously submitted within individual categories. 1883 abstracts were submitted, but only 1878 were reviewed due to withdrawals. The abstracts were split evenly between clinical and basic categories. A Poster and Category Chairperson and a panel of approximately 10 reviewers for each category were selected by the President and the Program Co-Chairs. The assigned category of all submitted abstracts was checked by the Category Chair and reassignment made, where appropriate, by the Program Co-Chairs. All reviewers were blinded to the authorship and affiliations of the abstracts and a 5 point score system was used. Reviewers were instructed to refrain from reviewing abstracts for which they were in conflict. Scores were tabulated by Coe-Truman Technologies, ASBMR's abstract processing vendor; these scores were then used to select the oral program by the Program Co-Chairs and the President, along with the President-Elect, Barbara Kream, and next year's Annual Meeting Co-Chairs, Rajesh Thakker and Phil Osdoby.

The over-arching principle in assembling the oral program was to select abstracts based on their scores. The highest-rated abstracts within each category were selected for the concurrent oral sessions unless the authors preferred a poster presentation; and the next tiers of highly ranked abstracts were assigned to the Oral Poster sessions and Plenary Poster Sessions, respectively. Each category had representation on the oral program that was based on the number of abstracts submitted, which resulted in roughly similar numbers with only minor differences in the spread of scoring in the different categories.

Awards

The Society, assisted by corporate support and donations, offers a number of awards, such as the ASBMR Young Investigator Awards, including the new Shun-Ichi Harada Young Investigator Awards, the ASBMR Outstanding Abstract Award, the ASBMR Award for Outstanding Research in the Pathophysiology of Osteoporosis, and the ASBMR President's Book Award. As in previous years, these awardees have been selected based on abstract score and eligibility.

Disclosure of potential conflicts of interest

The 2007 Program Committee and ASBMR staff worked together to comply with the Updated Standards for Commercial Support of the U.S. Accreditation Council for Continuing Medical Education (ACCME). The ASBMR receives its Continuing Medical Education (CME) credits through the Federation of American Societies for Experimental Biology (FASEB), which is accredited by the ACCME. All speakers, session chairs and Program Committee members are required to provide a disclosure of potential conflicts of interest.

Acknowledgements

We are extremely grateful to the ASBMR office staff for their invaluable help and support in planning the program, particularly Rebecca Myers, Angela Cangemi, Melissa Huston and Karen Hasson. We would also like to thank Judie Spalding of Coe-Truman Technologies (ASBMR's abstract processing vendor) for her assistance. We wish to thank the Category Chairs, Poster Chairs, and reviewers for the quality and timeliness of their reviewing and the President and Co-Chairs of the 2006 and 2008 ASBMR meeting for their support and helpful advice. All these individuals have made major contributions to the planning of what we believe is an outstanding scientific program for the 2007 meeting. We hope that you enjoy it as much as we have putting it together!

Sincerely,

Steven R. Goldring, M.D., *President*

Harald Jueppner, M.D., *Program Co-Chair*

Juliet Compston, M.D., FRCP, *Program Co-Chair*

ABSTRACT PRESENTATION KEY

Abstract #	Session Type	Date	Presentation Time	Room
1001-1006	Concurrent Oral 1	Monday, Sept. 17, 2007	10:00 – 11:30 am	Kalakaua Ballroom C
1007-1012	Concurrent Oral 2	Monday, Sept. 17, 2007	10:00 – 11:30 am	Kamehameha Hall III
1013-1018	Concurrent Oral 3	Monday, Sept. 17, 2007	10:00 – 11:30 am	Kalakaua Ballroom AB
1019-1024	Concurrent Oral 4	Monday, Sept. 17, 2007	10:00 – 11:30 am	Room 312
1025-1030	Concurrent Oral 5	Monday, Sept. 17, 2007	10:00 – 11:30 am	Room 313 A
1031-1036	Concurrent Oral 6	Monday, Sept. 17, 2007	10:00 – 11:30 am	Room 311
1037-1042	Concurrent Oral 7	Monday, Sept. 17, 2007	2:30 – 4:00 pm	Room 312
1043-1048	Concurrent Oral 8	Monday, Sept. 17, 2007	2:30 – 4:00 pm	Room 313 A
1049-1054	Concurrent Oral 9	Monday, Sept. 17, 2007	2:30 – 4:00 pm	Kalakaua Ballroom AB
1055-1060	Concurrent Oral 10	Monday, Sept. 17, 2007	2:30 – 4:00 pm	Kamehameha Hall III
1061-1066	Concurrent Oral 11	Monday, Sept. 17, 2007	2:30 – 4:00 pm	Kalakaua Ballroom C
1067-1072	Concurrent Oral 12	Monday, Sept. 17, 2007	2:30 – 4:00 pm	Room 311
1073-1080	Concurrent Oral 13	Monday, Sept. 17, 2007	4:30 – 6:30 pm	Kalakaua Ballroom AB
1081-1088	Concurrent Oral 14	Monday, Sept. 17, 2007	4:30 – 6:30 pm	Kalakaua Ballroom C
1089-1096	Concurrent Oral 15	Monday, Sept. 17, 2007	4:30 – 6:30 pm	Kamehameha Hall III
1097-1104	Concurrent Oral 16	Monday, Sept. 17, 2007	4:30 – 6:30 pm	Room 311
1105-1112	Concurrent Oral 17	Monday, Sept. 17, 2007	4:30 – 6:30 pm	Room 312
1113-1120	Concurrent Oral 18	Monday, Sept. 17, 2007	4:30 – 6:30 pm	Room 313 A
1121-1126	Concurrent Oral 19	Tuesday, Sept. 18, 2007	10:00 – 11:30 am	Kalakaua Ballroom C
1127-1132	Concurrent Oral 20	Tuesday, Sept. 18, 2007	10:00 – 11:30 am	Kalakaua Ballroom AB
1133-1138	Concurrent Oral 21	Tuesday, Sept. 18, 2007	10:00 – 11:30 am	Room 312
1139-1144	Concurrent Oral 22	Tuesday, Sept. 18, 2007	10:00 – 11:30 am	Kamehameha Hall III
1145-1150	Concurrent Oral 23	Tuesday, Sept. 18, 2007	10:00 – 11:30 am	Room 311
1151-1156	Concurrent Oral 24	Tuesday, Sept. 18, 2007	10:00 – 11:30 am	Room 313 A
1157-1162	Concurrent Oral 25	Tuesday, Sept. 18, 2007	2:30 – 4:00 pm	Kamehameha Hall III
1163-1168	Concurrent Oral 26	Tuesday, Sept. 18, 2007	2:30 – 4:00 pm	Kalakaua Ballroom AB
1169-1174	Concurrent Oral 27	Tuesday, Sept. 18, 2007	2:30 – 4:00 pm	Room 311
1175-1180	Concurrent Oral 28	Tuesday, Sept. 18, 2007	2:30 – 4:00 pm	Kalakaua Ballroom C
1181-1186	Concurrent Oral 29	Tuesday, Sept. 18, 2007	2:30 – 4:00 pm	Room 313 A
1187-1192	Concurrent Oral 30	Tuesday, Sept. 18, 2007	2:30 – 4:00 pm	Room 312
1193-1198	Concurrent Oral 31	Wednesday, Sept. 19, 2007	10:00 -11:30 am	Room 311
1199-1204	Concurrent Oral 32	Wednesday, Sept. 19, 2007	10:00 -11:30 am	Kalakaua Ballroom AB
1205-1210	Concurrent Oral 33	Wednesday, Sept. 19, 2007	10:00 -11:30 am	Kamehameha Hall III
1211-1216	Concurrent Oral 34	Wednesday, Sept. 19, 2007	10:00 -11:30 am	Room 313 A
1217-1222	Concurrent Oral 35	Wednesday, Sept. 19, 2007	10:00 -11:30 am	Room 312
1223-1228	Concurrent Oral 36	Wednesday, Sept. 19, 2007	10:00 -11:30 am	Kalakaua Ballroom C
1229-1234	Concurrent Oral 37	Wednesday, Sept. 19, 2007	2:30 – 4:00 pm	Kamehameha Hall III
1235-1240	Concurrent Oral 38	Wednesday, Sept. 19, 2007	2:30 – 4:00 pm	Kalakaua Ballroom C
1241-1246	Concurrent Oral 39	Wednesday, Sept. 19, 2007	2:30 – 4:00 pm	Room 311
1247-1252	Concurrent Oral 40	Wednesday, Sept. 19, 2007	2:30 – 4:00 pm	Kalakaua Ballroom AB
1253-1258	Concurrent Oral 41	Wednesday, Sept. 19, 2007	2:30 – 4:00 pm	Room 313 A
1259-1264	Concurrent Oral 42	Wednesday, Sept. 19, 2007	2:30 – 4:00 pm	Room 312
1265-1270	Concurrent Oral 43	Wednesday, Sept. 19, 2007	4:30 - 6:00 pm	Kamehameha Hall III
1271-1276	Concurrent Oral 44	Wednesday, Sept. 19, 2007	4:30 - 6:00 pm	Kalakaua Ballroom AB
1277-1282	Concurrent Oral 45	Wednesday, Sept. 19, 2007	4:30 - 6:00 pm	Room 311
1283-1288	Concurrent Oral 46	Wednesday, Sept. 19, 2007	4:30 - 6:00 pm	Kalakaua Ballroom C
1289-1294	Concurrent Oral 47	Wednesday, Sept. 19, 2007	4:30 - 6:00 pm	Room 312
1295-1300	Concurrent Oral 48	Wednesday, Sept. 19, 2007	4:30 - 6:00 pm	Room 313 A
O21-O504	Oral Posters (Clinical and Basic)	Sunday, Sept. 16, 2007	3:45 pm - 4:45 pm	Basic: Kalakaua Ballroom AB Clinical: Kamehameha Hall III
S001-S535	Plenary Posters	Sunday, Sept. 16, 2007 Monday, Sept. 17, 2007	5:00 pm - 6:45 pm	Kamehameha Hall I & II

M001-M535	Poster Session I	Monday, Sept. 17, 2007	Odd: 11:30 am – 1:00 pm Even: 1:00 pm – 2:30 pm	Kamehameha Hall I & II
T001-T521	Poster Session II	Tuesday, Sept. 18, 2007	Odd: 11:30 am – 1:00 pm Even: 1:00 pm – 2:30 pm	Kamehameha Hall I & II
W001-W521	Poster Session III	Wednesday, Sept. 19, 2007	Odd: 11:30 am – 1:00 pm Even: 1:00 pm – 2:30 pm	Kamehameha Hall I & II
WG1-WG3	Vitamin D Working Group	Sunday, Sept. 16, 2007	7:00 pm – 10:00 pm	Room 313 C
WG4-WG8	Pediatric Bone and Mineral Working Group	Sunday, Sept. 16, 2007	7:00 pm – 10:00 pm	Room 316 C
WG9-WG12	Physical Activity and Falls Working Group	Sunday, Sept. 16, 2007	7:00 pm – 9:10 pm	Room 313 A
WG13-WG20	Adult Bone and Mineral Working Group	Monday, Sept. 17, 2007	7:00 pm – 10:00 pm	Room 316 AB
WG21-WG23	Working Group on Osteoporosis and Rheumatic Diseases	Monday, Sept. 17, 2007	7:00 pm – 9:00 pm	Room 313 C
WG24-WG33	Musculoskeletal Rehabilitation in Patients with Osteoporosis Working Group	Wednesday, Sept. 19, 2007	6:30 pm – 9:30 pm	Room 316 C
WG34-WG39	Working Group on Patient Education and Adherence to Treatment	Wednesday, Sept. 19, 2007	6:30 pm – 9:30 pm	Room 312
WG40-WG41	Muscle and Bone Working Group	Monday, Sept. 17, 2007	7:00 pm – 10:00 pm	Room 316 C

FRIDAY, SEPTEMBER 14, 2007

DAY-AT-A-GLANCE

Time/Event/Location

**ANCILLARY PROGRAM - THE INTERNATIONAL
SOCIETY FOR CLINICAL DENSITOMETRY (ISCD)**

Separate registration and fee required

7:00 am - 7:30 am

ISCD Registration and Continental Breakfast

HILTON: South Pacific Ballroom Foyer

7:30 am - 11:00 am

**ISCD Bone Densitometry Course: Clinician and Technologist Courses -
General Session**

HILTON: South Pacific Ballroom III & IV

11:00 am - 5:30 pm

ISCD Bone Densitometry Clinician Course

HILTON: South Pacific Ballroom III & IV

11:00 am - 5:45 pm

ISCD Bone Densitometry Technologist Course

HILTON: South Pacific Ballroom II

SATURDAY, SEPTEMBER 15, 2007

DAY-AT-A-GLANCE

Time/Event/Location

**ANCILLARY PROGRAM - THE INTERNATIONAL
SOCIETY FOR CLINICAL DENSITOMETRY (ISCD)**

Separate registration and fee required

7:00 am - 7:30 am

ISCD Registration and Continental Breakfast

HILTON: South Pacific Ballroom Foyer

7:30 am - 11:15 am

ISCD Bone Densitometry Clinician Course

HILTON: South Pacific Ballroom I

7:30 am - 11:00 am

ISCD Bone Densitometry Technologist Course

HILTON: South Pacific Ballroom II

11:45 am - 2:00 pm

ISCD Bone Densitometry Clinician Certification Exam

HILTON: South Pacific Ballroom I

11:45 am - 1:00 pm

ISCD Bone Densitometry Technologist Exam

HILTON: South Pacific Ballroom II

12:30 pm - 6:15 pm

ISCD Vertebral Fracture Assessment Course

HILTON: South Pacific Ballroom III & IV

ASBMR REGISTRATION

9:00 am - 5:00 pm

**Hawaii Convention Center
Registration Area**

SUNDAY SEPTEMBER 16, 2007

DAY-AT-A-GLANCE

Time/Event/Location

(All events will be held at the Hawaii Convention Center, unless otherwise noted.)

7:00 am - 6:30 pm

Registration Open

Main Lobby

8:00 am - 9:30 am

Plenary Symposium I: Emerging Technologies in Functional Bone Imaging

Kamehameha Hall III

9:30 am - 11:00 am

Symposium A (Basic): Novel Insights into Bone Metabolism through Genetics

Kalakaua Ballroom AB

9:30 am - 11:00 am

Symposium B (Clinical): Inhaled Steroids, Aromatase Inhibitors, and TZDs: All Bad for the Bone?

Kamehameha Hall III

11:00 am - 11:15 am

Break

Main Lobby

11:15 am - 11:20 am

Presentation of the Shirley Hohl Service Award

Kamehameha Hall III

11:25 - 11:30 am

Presentation of the Louis V. Avioli Memorial Founders Award

Kamehameha Hall III

11:30 am - 12:30 pm

Louis V. Avioli Memorial Lecture

Kamehameha Hall III

12:30 pm - 1:30 pm

Meet-the-Professor Sessions

Rooms 301-309

No ticket required.

1:00 pm - 2:00 pm

Debate: Excessive Suppression of Bone Remodeling by Antiresorptive Agents - Fact or Fiction?

Kamehameha Hall III

2:00 pm - 3:30 pm

Symposium C (Basic): Osteocytes and the Regulation of Phosphorous Homeostasis

Kalakaua Ballroom AB

2:00 pm - 3:30 pm

Symposium D (Clinical): Anabolics: Pathways for the Future

Kamehameha Hall III

3:30 pm - 3:45 pm

Break

Ballroom Lobby and Main Lobby

3:45 pm - 4:45 pm

Oral Posters (Basic)

Kalakaua Ballroom AB

3:45 pm - 4:45 pm

Oral Posters (Clinical)

Kamehameha Hall III

3:45 pm - 4:45 pm

Challenges and Opportunities Facing NIH Peer Review: A Vision for Insuring Its Strategic National Value

Kalakaua Ballroom C

5:00 pm - 6:45 pm

Welcome Reception & Plenary Poster Session

Kamehameha Hall I & II

5:00 pm - 6:45 pm

Posters Open

Kamehameha Hall I & II

5:00 pm - 6:45 pm

Exhibits Open

Kamehameha Hall I & II

5:00 pm - 6:45 pm

New Investigator/New Member/First-Time Attendee Reception

Kamehameha Hall I & II, Young Investigators Lounge

Ancillary Program - Working Groups

7:00 pm - 9:00 pm

***In Vivo* Working Group**

Room 312

7:00 pm - 10:00 pm

Vitamin D Working Group

Room 313 C

7:00 pm - 9:30 pm

Nutrition and Bone Health Working Group

Room 316 AB

7:00 pm - 10:00 pm

Pediatric Bone and Mineral Working Group

Room 316 C

7:00 pm - 9:10 pm

Physical Activity and Falls Working Group

Room 313 A

SUNDAY SEPTEMBER 16, 2007
DAY-AT-A-GLANCE

Time/Event/Location

(All events will be held at the Hawaii Convention Center, unless otherwise noted.)

Ancillary Program - Industry-Supported Symposia (ISS)

7:00 pm - 9:15 pm

**Osteoporosis Assessment and Treatment: New Evidence
and Future Directions**

Sheraton Waikiki: Maui Ballroom

7:00 pm - 10:00 pm

**Providing Quality Osteoporosis Therapy: Navigating the
Shifting Landscape of Bisphosphonates**

Hilton: Tapa Ballroom and Palace Lounge

7:00 pm - 10:00 pm

**Current Standards and Novel Understandings in the
Management of Bone Loss: The RANK/RANKL/
OPG Pathway and Its Clinical Potential**

Sheraton Waikiki: Kauai Ballroom

MONDAY, SEPTEMBER 17, 2007
DAY-AT-A-GLANCE

Time/Event/Location

(All events will be held at the Hawaii Convention Center, unless otherwise noted.)

7:00 am - 5:30 pm

Registration Open

Main Lobby

7:00 am - 8:00 am

New Investigator/New Member Breakfast

Room 316 AB

8:00 am - 6:30 pm

Posters Open

Kamehameha Hall I & II

8:00 am - 8:10 am

Welcome and Announcements

Kamehameha Hall III

8:10 am - 8:15 am

Presentation of the Gideon A. Rodan Excellence in Mentorship Award

Kamehameha Hall III

8:15 am - 9:45 am

Plenary Symposium II: Bone Quality: Age-Related Changes in Collagen and Mineral

Kamehameha Hall III

9:30 am - 4:30 pm

Exhibits Open

Kamehameha Hall I & II

9:45 am - 10:00 am

Break

Kamehameha Hall I & II

10:00 am - 11:30 am

Concurrent Oral Sessions

1) Cancer and Bone I

Kalakaua Ballroom C

2) Osteoporosis Treatment (Preclinical) I

Kamehameha Hall III

3) Osteoporosis Pathophysiology I

Kalakaua Ballroom AB

4) Mouse Mutants and Bone

Room 312

5) VDR and Other Regulators of Calcium Transport

Room 313 A

6) Genetic Disorders

Room 311

11:30 am - 12:30 pm

Meet-the-Professor Sessions

Rooms 301 - 309

No ticket required.

11:30 am - 2:30 pm

Poster Session I

(Presentations M001 - M536)

11:30 am - 1:00 pm Odd numbers

1:00 pm - 2:30 pm Even numbers

Kamehameha Hall I & II

12:00 pm - 2:00 pm

Special Session for Allied Health Professionals: Featuring an Overview of the 29th Annual Meeting by Lawrence G. Raisz, M.D.

Room 313 A

12:30 pm - 1:30 pm

Clinical Roundtable/Case Conference

Kamehameha Hall III

1:30 pm - 2:30 pm

NIH Center for Scientific Review Workshop: What Really Happens at Study Section?

Room 311

1:30 pm - 2:30 pm

Meet-the-Professor Sessions

Rooms 301 - 309

No ticket required.

2:30 pm - 4:00 pm

Concurrent Oral Sessions

7) Bone Acquisition and Pediatric Bone Disease I

Room 312

8) Osteocyte Biology

Room 313 A

9) Epidemiology I: Hip Fractures

Kalakaua Ballroom AB

10) Osteoporosis Treatment (Clinical) I: Bisphosphonates

Kamehameha Hall III

11) Chondrogenesis and Osteogenesis

Kalakaua Ballroom C

12) Bone and Stem Cells

Room 311

4:00 pm - 4:30 pm

Break

Kamehameha Hall I & II

MONDAY, SEPTEMBER 17, 2007
DAY-AT-A-GLANCE

Time/Event/Location

(All events will be held at the Hawaii Convention Center, unless otherwise noted.)

4:30 pm - 6:30 pm

Concurrent Oral Sessions

13) Osteoporosis Assessment I

Kalakaua Ballroom AB

14) Bone Biomechanics and Quality I

Kalakaua Ballroom C

15) Osteoporosis Treatment (Clinical) II: Combination Therapy

Kamehameha Hall III

16) Osteoclastogenesis

Room 311

17) Bone and Cartilage

Room 312

18) Calcium and Phosphate Regulation

Room 313 A

Ancillary Program - Working Groups

7:00 pm - 10:00 pm

Adult Bone and Mineral Working Group

Room 316 AB

7:00 pm - 10:00 pm

Biochemical Markers of Bone Turnover Working Group

Room 313 A

7:00 pm - 10:00 pm

Bone Remodeling and Stress Fracture Working Group

Room 312

7:00 pm - 9:10 pm

Non-Invasive Assessment of Bone Microarchitecture Working Group

Room 311

7:00 pm - 9:00 pm

Working Group on Osteoporosis and Rheumatic Diseases

Room 313 C

7:00 pm - 10:00 pm

Muscle and Bone Working Group

Room 316 C

Ancillary Program - Industry-Supported Symposia (ISS)

7:00 pm - 10:00 pm

Critical Challenges and Landmark Advances in Osteoporosis

Hilton: Tapa Ballroom

7:00 pm - 9:30 pm

Osteoporosis: Opportunity for Better Outcomes

Hilton: Coral Ballroom, Salons 3-5

7:00 pm - 9:00 pm

When Osteoporosis Is the Wrong Diagnosis: New Insights Linking Vitamin D, PTH, and Bone to Cardiovascular Health

Sheraton Waikiki: Maui & Kauai Ballrooms

TUESDAY, SEPTEMBER 18, 2007

DAY-AT-A-GLANCE

Time/Event/Location

(All events will be held at the Hawaii Convention Center, unless otherwise noted.)

7:00 am - 5:30 am

Registration Open

Main Lobby

8:00 am - 6:00 pm

Posters Open

Kamehameha Hall I & II

8:00 am - 8:05 am

Presentation of the William F. Neuman Award

Kamehameha Hall III

8:10 am - 8:15 am

Presentation of the Fuller Albright Award

Kamehameha Hall III

8:20 am - 8:25 am

Presentation of the Frederic C. Bartter Award

Kamehameha Hall III

8:30 am - 9:30 am

Gerald D. Aurbach Memorial Lecture

Kamehameha Hall III

9:30 am - 10:00 am

Break

Kamehameha Hall I & II

9:30 am - 4:30 pm

Exhibits Open

Kamehameha Hall I & II

10:00 am - 11:30 am

Concurrent Oral Sessions

19) Osteoporosis Treatment (Preclinical) II

Kalakaua Ballroom C

20) Osteoporosis Treatment (Clinical) III: New Approaches

Kalakaua Ballroom AB

21) Osteoporosis Pathophysiology II

Room 312

22) Osteoblast Regulation I

Kamehameha Hall III

23) Osteoclast Signaling I

Room 311

24) Disease Mechanisms

Room 313A

11:30 am - 12:30 pm

Meet-the-Professor Sessions

Rooms 301 - 309

No ticket required.

11:30 am - 2:30 pm

Poster Session II

(Presentations T001 - T521)

11:30 am - 1:00 pm Odd numbers

1:00 pm - 2:30 pm Even numbers

Kamehameha Hall I & II

12:30 pm - 2:00 pm

Joint ECTS/ASBMR Session on Osteonecrosis of the Jaw

Kamehameha Hall III

1:30 pm - 2:30 pm

Meet-the-Professor Sessions

Rooms 301 - 309

No ticket required.

2:30 pm - 4:00 pm

Concurrent Oral Sessions

25) Epidemiology II: :Men

Kamehameha Hall III

26) Osteoporosis Assessment II

Kalakaua Ballroom AB

27) Cancer and Bone II

Room 311

28) Bone and Cartilage Development

Kalakaua Ballroom C

29) Chondrocyte Regulation

Room 313 A

30) PTH/PTHrP

Room 312

4:00 pm - 4:30 pm

Break

Kamehameha Hall I & II

4:30 pm - 6:00 pm

State-of-the-Art Lectures A (Basic): Bone and Stem Cells

Kalakaua Ballroom C

4:30 pm - 6:00 pm

State-of-the-Art Lectures B (Basic/Clinical): Mineral Ion Homeostasis and Early Stages of Chronic Kidney Disease

Kalakaua Ballroom AB

6:00 pm - 7:00 pm

ASBMR Annual Business Meeting

Room 312

7:00 pm - 8:00 pm

The Women in Bone and Mineral Research Committee Event

Room 316 AB

8:00 pm - 11:00 pm

ASBMR Social Event

Royal Hawaiian Hotel, 2259 Kalakaua Avenue

WEDNESDAY, SEPTEMBER 19, 2007

DAY-AT-A-GLANCE

Time/Event/Location

(All events will be held at the Hawaii Convention Center, unless otherwise noted.)

6:00 am - 7:00 am

ASBMR Fun Run/Walk

Ala Moana Beach Park

7:00 am - 5:30 pm

Registration Open

Main Lobby

8:00 am - 4:30 pm

Posters Open

Kamehameha Hall I & II

8:00 am - 9:30 pm

Plenary Symposium III: How Can We Find New Drugs for the 21st Century?

Kamehameha Hall III

9:30 am - 10:00 am

Break

Kamehameha Hall I & II

9:30 am - 4:30 pm

Exhibits Open

Kamehameha Hall I & II

10:00 am - 11:30 am

Concurrent Oral Sessions

31) Bone Acquisition and Pediatric Bone Disease II

Room 311

32) Epidemiology III: Genetic and Hormonal Factors

Kalakaua Ballroom AB

33) Osteoporosis Treatment (Clinical) IV: Anti-resorptives

Kamehameha Hall III

34) Bone Cell Development

Room 313 A

35) Sex Steroids and Bone

Room 312

36) Mouse Genetic Models

Kalakaua Ballroom C

11:30 am - 12:30 pm

Meet-the-Professor Sessions

Rooms 301 - 309

No ticket required.

11:30 am - 2:30 pm

Poster Session III

(Presentations W001 - W521)

11:30 am - 1:00 pm Odd numbers

1:00 pm - 2:30 pm Even numbers

Kamehameha Hall I & II

12:30 pm - 1:30 pm

Clinical Roundtable/Case Conference

Kamehameha Hall III

12:30 pm - 2:00 pm

The "Ins and Outs" of Research Funding

Kalakaua Ballroom C

1:30 pm - 2:30 pm

Meet-the-Professor Sessions

Rooms 301 - 309

No ticket required.

2:30 pm - 4:00 pm

Concurrent Oral Sessions

37) Osteoporosis Treatment (Preclinical) III

Kamehameha Hall III

38) Osteoporosis Pathophysiology III

Kalakaua Ballroom C

39) Bone Biomechanics and Quality II

Room 311

40) Osteoblast Regulation II

Kalakaua Ballroom AB

41) Regulators of Bone Formation

Room 313 A

42) Metabolic Bone Disorders

Room 312

4:00 pm - 4:30 pm

Break

Kamehameha Hall I & II

4:30 pm - 6:00 pm

Concurrent Oral Sessions

43) Osteoporosis Treatment (Clinical) V: Effects on Bone Quality

Kamehameha Hall III

44) Epidemiology IV: Postmenopausal Women

Kalakaua Ballroom AB

45) Osteoporosis Assessment III

Room 311

46) Osteoblast Regulatory Mechanisms

Kalakaua Ballroom C

47) Osteoclast Signaling II

Room 312

48) Hormones and Bone

Room 313 A

WEDNESDAY, SEPTEMBER 19, 2007
DAY-AT-A-GLANCE

Time/Event/Location

(All events will be held at the Hawaii Convention Center, unless otherwise noted.)

Ancillary Program - Working Groups

6:30 pm - 8:30 pm

Molecular Biology and Pathology of Bone Working Group

Room 311

6:30 pm - 9:30 pm

**Working Group on Musculoskeletal Rehabilitation in
Patients with Osteoporosis**

Room 316 C

6:30 pm - 9:30 pm

**Working Group on Patient Education and Adherence to
Treatment**

Room 312

DISCLOSURE/CONFLICT OF INTEREST

The ASBMR is committed to ensuring the balance, independence, objectivity and scientific rigor of all its individually sponsored or industry-supported educational activities. Accordingly, the ASBMR adheres to the requirement set by the Federation of American Societies for Experimental Biology (FASEB) that audiences at FASEB-sponsored educational programs be informed of a presenter's (speaker, faculty, author, or contributor) academic and professional affiliations, and the disclosure of the existence of any significant financial interest or other relationship a presenter has with the manufacturer(s) of any commercial product(s) discussed in an educational presentation. When an unlabeled use of a commercial product, or an investigational use not yet approved for any purpose is discussed during the presentation, it is required that presenters disclose that the product is not labeled for the use under discussion or that the product is still investigational. This policy allows the listener/attendee to be fully knowledgeable in evaluating the information being presented. The Program will note those speakers who have disclosed relationships, including the nature of the relationship and the associated commercial entity.

All authors of submitted abstracts completed the disclosure statement in the online submission program. Invited speakers who are not required to submit an abstract received a form that they completed and returned.

Disclosure includes any relationship that may bias one's presentation or which, if known, could give the perception of bias. This includes relevant financial relationships of a spouse or partner. These situations may include, but are not limited to:

DISCLOSURE KEY

- 1) stock options or bond holdings in a for-profit corporation or self-directed pension plan
- 2) research grants
- 3) employment (full or part-time)
- 4) ownership or partnership
- 5) consulting fees or other remuneration
- 6) non-remunerative positions of influence such as officer, board member, trustee, or public spokesperson
- 7) receipt of royalties
- 8) speaker's bureau
- 9) other

Disclosures for invited speakers and abstract presenters are provided at the end of the session listing for invited speakers (see On-Site Program book) and directly after the body of an abstract for abstract submissions. If there is no conflict of interest or disclosure listed, this means that the invited speaker and/or abstract presenter indicated no conflicts to disclose.

The disclosure information will correspond to the key above. If disclosures are given, the company name, along with the respective disclosure relationship number will be listed (for example: Company Name, 2, 8.).

ABSTRACTS KEY	
1001-1300	Concurrent Oral Presentation
O#	Oral Poster Presentation
S#	Sunday Plenary Poster Presentation
M#	Monday Poster Presentation
T#	Tuesday Poster Presentation
W#	Wednesday Poster Presentation
*(Asterisk)	Denotes Non-ASBMR Membership

1001

Identification of a Novel TGF- β Dependent-Prometastatic Signature Mediating Bone Colonization. I. Garcia-Tunon^{*1}, S. Vicent^{*1}, D. Luis-Ravelo^{*1}, I. Anton^{*1}, C. Zandueti^{*1}, S. Martinez^{*1}, J. De Las Rivas^{*2}, F. Lecanda¹. ¹Division of Oncology, Center for Applied Medical Research, Pamplona, Spain, ²Bioinformatics, CIC, Salamanca, Spain.

Bone represents a frequent target organ of metastasis in a variety of solid tumors including lung. We have recently developed a rapid and selective model in which to identify genes implicated in bone metastasis of lung cancer. After intracardiac inoculation (i.c.) in nude mice, highly metastatic subpopulations (HMS) were selected with increase prometastatic activity. Microarray expression analysis revealed a novel metastatic gene signature of differentially expressed genes in HMS vs parental. Four overexpressed genes in all HMS were further validated by real time qPCR. These genes encode signaling molecules (such as TCF4 and PRKD3) and cell anchorage related proteins (MCAM, and putative adhesion molecule SUSD5). To delineate their functional contribution in metastatic activity we assessed metastatic area by X-ray image analysis and μ CT scan of retrovirally transduced simple, double and triple gene combinations. I.c. of single overexpressors TCF4, PRKD3 or SUSD5 induced a significant increase in metastatic area as compared to mock cells ($p < 0.01$). Furthermore, i.c. of triple overexpressors in nude mice synergistically induced a dramatic increase in prometastatic activity, with prominent osteolytic lesions and metastatic area ($p < 0.001$), whereas cell homing activity to bone was unaltered. This multigenic signature was also ineffective promoting cell proliferation and subcutaneous tumor growth. By contrast, intratibial injection of triple overexpressors induced aggressive bone colonization leading to overt osteolytic lesions as compared to mock cells ($p < 0.001$). These results were correlated with high osteoclastogenic activity induced by conditioned medium of triple overexpressors. Furthermore, TCF4 and SUSD5 were strongly up-regulated in a coculture system mimicking in vivo tumor-stroma interactions, an effect that was further abrogated by an anti-TGF- β peptide. Interestingly, after i.c. of HMS, in vivo treatment with a specific anti-TGF- β peptide severely reduced tumor burden (X-ray analysis and μ CT scans) and osteolytic activity of tumor cells (osteoclast number) compared to an irrelevant peptide and vehicle treated animals. These studies identified a novel signature involving several genes that act cooperatively promoting strong osseous colonization, partially mediated by high osteoclastogenic activity. This multifunctional program is strongly enhanced by TGF- β , which plays a critical role in perpetuating a "vicious cycle" involved in metastatic progression.

Disclosures: I. Garcia-Tunon, None.

This study received funding from: FIS, ISCIII-RETIC RD06/0020, Gov. Navarra.

1002

Osmosensing Receptor TRPV4 Mediates Cancerinduced Bone Pain. H. Wakabayashi^{*1}, L. Wang^{*2}, T. Matsubara^{*2}, A. Mizuno^{*3}, M. Suzuki^{*3}, A. Uchida^{*1}, T. Yoneda¹. ¹Orthopaedic Surgery, Mie University Graduate School of Medicine, Tsu, Japan, ²Biochemistry, Osaka University Graduate School of Dentistry, Suita, Japan, ³Pharmacology, Jichi Medical School, Tochigi, Japan.

Bone pain is becoming a major clinical problem as survival of cancer patients is extended. Bone pain can be caused by noxious chemical and/or mechanical stimuli produced by cancer cells and associated inflammatory cells. H^+ is among such a noxious chemical stimulus. It has been shown that the acidic microenvironment caused by H^+ release by bone-resorbing osteoclasts induces bone pain through an activation of the acid sensing receptors such as transient receptor potential vanilloid 1 (TRPV1). TRPV4 is a transducer of hypo-osmotic stimuli in primary nociceptive afferents. Recent studies using TRPV4^{-/-} mice suggest a critical role of TRPV4 in mechanosensing. Since TRPV4 has 45% homology with TRPV1, we reasoned that TRPV4 is also involved in the pathogenesis of cancer-induced bone pain. In the present study, we investigated the role of TRPV4 in the induction of bone pain associated with cancer colonization in bone. We established an animal model of cancer-induced bone pain in which cancer cells were directly inoculated into the marrow cavity of tibiae. Three behavioral assays including the measurement of paw withdrawal latency, grip force and hind-limb lifting (flinching) were employed to evaluate bone pain. Tumor-inoculated hind-limbs displayed hyperalgesia, decreased grip force and increased flinching as the tumor enlarged, whereas non-tumor-bearing hind-limbs showed no changes. Of note, there was significant reduction in paw withdrawal latency, grip force and flinching in tumor-inoculated hind-limbs in TRPV4^{-/-} mice compared with WT mice, despite that tumor growth and area of osteolytic lesions did not differ between TRPV4^{-/-} and WT mice.

The expression of immunoreactive neurons for pERK, a widely-used molecular marker for neural activation by noxious stimuli, was increased in the ipsi-lateral dorsal root ganglia (DRG) compared with the contra-lateral DRG in WT mice. p-ERK immunoreactive neurons were significantly decreased in the DRG in TRPV4^{-/-} mice compared with WT mice. Hypo stimuli increased p-ERK expression in neuron-like F11 cells that expressed TRPV4 mRNA but not TRPV1 by RT-PCR. Ruthenium red, which is a non-selective TRPV4 inhibitor, decreased p-ERK expression induced by hypo stimuli. In conclusion, our results suggest that TRPV4 as well as TRPV1 plays an important role in inducing bone pain associated with cancer cell colonization in bone. TRPV4 might be a new molecular target for the development of novel analgesics in cancer-induced bone pain.

Disclosures: H. Wakabayashi, None.

1003

Role of Hypoxia in Cancers that Metastasize to Bone: HIF1 α Enhances TGF β Signaling and Expression of Prometastatic Factors CXCR4 and VEGF. L. A. Kingsley, P. G. J. Fournier, J. M. Chirgwin, T. A. Guise. Internal Medicine, University of Virginia, Charlottesville, VA, USA.

Several cancers frequently metastasize to bone, where the microenvironment is hypoxic and rich in growth factors, such as transforming growth factor (TGF) β . TGF β stimulates tumor secretion of proteins that activate osteoclastic bone resorption, angiogenesis and tumor homing to bone. Many of the same proteins are also regulated by hypoxia-inducible factor (HIF)1 α . We hypothesized that hypoxia-induced HIF1 α enhances the effects of TGF β on cancer metastases to bone.

First, we determined that bone metastases were hypoxic. Mice with MDA-MB-231 breast cancer bone metastases were injected prior to euthanasia with pimonidazole, which forms insoluble adducts in hypoxic cells. Immunohistochemical staining of decalcified sections showed that tumor cells adjacent to bone were hypoxic. Next, we determined by Western blot that hypoxia (1% O₂) culture conditions induced the expression of HIF1 α by TGF β -responsive cancer cells which metastasize to bone: MDA-MB-231, PC-3 prostate cancer and 1205Lu melanoma.

Effects of hypoxia and TGF β on promoters of bone metastatic factors VEGF and CXCR4 were studied using luciferase constructs. Both factors are known to be increased by hypoxia. MDA-MB-231 cells and HepG2 hepatocarcinoma cells were treated \pm 5ng/ml TGF β and \pm 1% O₂ and lysates assayed for luciferase after 24hrs. Activity of both promoters was increased by TGF β or 1% O₂. Combined treatment resulted in further promoter activation. Promoter activities correlated with increased mRNAs by quantitative real-time PCR (Q-PCR). These results suggest that TGF β and HIF1 α cooperatively regulate prometastatic gene expression.

We cotransfected cDNAs for HIF1 α and the TGF β signaling proteins Smads 2, 3, 4 and assayed for CXCR4 and VEGF promoter activity. Overexpression of HIF1 α and Smads resulted in greater than 10-fold activation of the promoters by combined treatment with TGF β and 1% O₂, providing further evidence for crosstalk between TGF β and hypoxia signaling pathways. Finally, TGF β target gene expression in MDA-MB-231 cells treated \pm TGF β and \pm 1% O₂ was surveyed by Q-PCR. Hypoxia decreased two negative regulators of TGF β signaling, Smad7 and SnoN, in addition to upregulating VEGF and CXCR4. Thus, hypoxia may potentiate TGF β actions by down-regulating inhibitors of the Smad signaling pathway. Our results provide evidence for HIF1 α and TGF β crosstalk in vitro and suggest that these two pathways may cooperatively promote bone metastasis in vivo.

Disclosures: L.A. Kingsley, None.

1004

Osteoclasts in Myeloma Are Derived From Gr-1+CD11b+ Mononuclear Cells of the Bone Marrow Niche. J. Zhuang¹, L. Yang^{*2}, J. R. Edwards¹, C. M. Edwards¹, G. R. Mundy¹. ¹Vanderbilt Center for Bone Biology, Nashville, TN, USA, ²Cancer Biology, Vanderbilt University, Nashville, TN, USA.

When cancer cells are resident in bone, they initiate a vicious cycle with osteoclasts (OCs) which perpetuates their growth and aggressive behavior. OCs are critical for the maintenance of the vicious cycle, since they control not only bone destruction associated with cancer, but also the aggressive behavior of tumor cells. It has recently been recognized that tumor cells grow in distant sites because they induce non-malignant cells to establish a "pre-metastatic niche" for tumor cells to later engraft. But nothing is yet known for bone. Primitive bone marrow mononuclear cells, called myeloid immune suppressor cells (MISCs), which suppress immune reactivity, are important niche components. MISCs belong to the myelomonocytic lineage with surface markers of CD11b and Gr-1. We hypothesize that MISCs are precursors of OCs recruited by tumors to assist in the establishment of the vicious cycle. To test this hypothesis, we used the well-characterized 5TGM1 murine myeloma model. 5TGM1-GFP transfected myeloma cells were inoculated by tail vein injection. MISCs were assessed by FACS at weeks 1, 2, 3, 4 after tumor cell inoculation. The percentage of Gr-1+CD11b+ cells in marrow, spleen and blood in the tumor group began to increase significantly on week 2 compared with the control group. On week 4, this increase was much greater (60.9 \pm 7.8% vs 37.7 \pm 8.6% $p < 0.05$ in marrow; 21.1 \pm 4.84% vs 2.4 \pm 0.85% $p < 0.05$ in spleen; 23.1 \pm 4.27% vs 5.4 \pm 1.1% $p < 0.05$ in blood) and paralleled the myeloma burden in bone and spleen. We sorted the Gr-1+CD11b+ cells from the spleen of tumor and non-tumor bearing mice. MISCs were induced into multinucleated TRAP positive OCs in medium containing M-CSF (25ng/ml) and RANKL (50ng/ml). The number of OCs derived from tumor MISCs was dramatically greater than those from control mice after 2 weeks of culture (13 \pm 2 per x200 field vs no more than 3). MISCs lost the Gr-1 and CD11b markers and gained CD51 and calcitonin receptor as they differentiated into mature OCs. These cells caused resorption pits on dentine discs, demonstrating they were functional OCs. We co-cultured sorted MISCs with 5TGM1 cells in a transwell plate (8um pore). MISCs markedly stimulated migration of GFP+ myeloma cells at 24h compared with non-MISCs (12.5 \pm 2.08 vs 3.75 \pm 0.83 per x200 field, $p < 0.05$). Our data suggest that MISCs are increased significantly in marrow, spleen and blood of myeloma-bearing mice and parallel the appearance of lytic bone lesions. These MISCs differentiate avidly and rapidly into functional OCs. These results have a number of implications, including the possibility of reducing bone lesions in myeloma and other malignancies by depleting specific subpopulations of osteoclast precursors.

Disclosures: J. Zhuang, None.

1005

Collapse of the Vascular Bone Remodeling Compartment Is a Key Process in the Development of Myeloma-induced Osteolysis. T. L. Andersen^{*1}, T. E. Sondergaard^{*1}, K. Søe^{*1}, T. Plesner^{*2}, J. Delaisse¹. ¹Clinical Cell Biology (KBC), Vejle Hospital, Southern Denmark University, Vejle, Denmark, ²Department of Hematology, Vejle Hospital, Southern Denmark University, Vejle, Denmark.

Bone remodeling is a tightly coupled process where bone formation follows bone resorption to maintain the integrity of the bones throughout life. Bone remodeling occurs in a specialized vascular bone remodeling compartment (VBRC), separated from the marrow compartment by a cellular wall. In the case of myeloma-induced osteolysis, bone formation does not follow and compensate for the increased bone resorption. This uncoupling is a major hallmark of multiple myeloma (MM). Here we report that VBRCs often are disrupted in MM and that this destabilization correlates with: 1) an uncoupling of bone resorption and bone formation, 2) the presence of bone osteolysis as shown by x-rays, 3) direct cell contact between MM cells coming from the marrow compartment and osteoclasts, leading to the formation of myeloma-osteoclast hybrid cells.

We have established through bone histomorphometric analysis of the VBRC, eroded surfaces (ES), and osteoid surfaces (OS), that MM patients showing less than 75% ES in VBRC have a significantly increased ES/BS (20% vs 11%) and a significantly decreased OS/BS (15% vs 26%) compared to patients with more than 75% ES in VBRC. Interestingly, the collapse of VBRCs correlated significantly with the number of osteolytic lesions demonstrated by X-ray, as patients with no osteolytic lesions showed 80% of the ES in VBRC, while patients with more than 5 osteolytic lesions showed only 58% of the ES in VBRC.

We have previously reported that the myeloma-osteoclast hybrid cells account for more than 35% of the osteoclasts present in MM patients by identifying nuclei within osteoclasts having translocations specific for the MM cell clone. Here we show that the disruption of VBRC is a critical event in the generation of hybrid cells. This allows a direct contact between the MM cells of the marrow compartment and the resorbing osteoclast resulting in fusion of these two cell types.

In vitro, we mimicked the VBRC wall by establishing a confluent G₀-arrested mono-layer of MC3T3 cells and tested its response to TGFβ or MM cells. Both addition of TGFβ and co-cultures with MM cells disrupted the confluent layer of MC3T3 cells mimicking the destabilization of the VBRC wall.

In conclusion the VBRC is a micro-anatomical structure that is important for the integrity of the bone remodeling process and its collapse is a key event in the development of MM bone disease. The VBRC is disrupted in MM, potentially both directly and indirectly by MM cells, favoring the development of osteolytic lesions and the formation of myeloma-osteoclast hybrid cells.

Disclosures: T.L. Andersen, None.

1006

Accelerated Bone Resorption, Due to Dietary Calcium Deficiency, Promotes Tumor Growth in a Murine Model of Breast Cancer Bone Metastasis. Y. Zheng, H. Zhou, J. R. K. Modzelewski^{*}, R. Kalak^{*}, J. M. Blair^{*}, M. J. Seibel, C. R. Dunstan. Bone Research Program, ANZAC research Institute, University of Sydney, Sydney, Australia.

The skeleton is a major site of breast cancer metastases. High bone turnover increases risk of disease progression and death. However, there is no direct evidence that high bone turnover is causally associated with the establishment and progression of metastases. In this study, we investigate the effects of high bone turnover on tumor growth in a rodent model of bone metastasis.

Female nude mice were fed a diet containing normal (0.6%) ('Normal-Ca') or low (0.1%) ('Low-Ca') calcium content starting on day -3. Mice were concurrently treated with vehicle or recombinant osteoprotegerin (OPG; 1mg/kg/day sc; n = 16/group). Three days later (day 0), 50,000 TxSA cells (a bone-seeking variant of MDA-MB-231 cells) were implanted by intra-tibial injection and mice were followed until day 17.

On day 0, mice receiving 'Low-Ca' had increased serum PTH and TRAcP5b levels, indicating secondary hyperparathyroidism and high bone turnover, which was maintained until day 17. Treatment with OPG increased serum PTH but profoundly reduced bone resorption. On day 17, in mice receiving 'Low-Ca' alone, lytic lesion area, tumor area and cancer cell proliferation increased by 43%, 24% and 24%, respectively compared to mice receiving 'normal Ca' (p < 0.01). In contrast, OPG treatment completely inhibited lytic lesions, reduced tumor area, decreased cancer cell proliferation and increased cancer cell apoptosis.

We conclude that increased bone turnover, due to dietary calcium deficiency, promotes tumor growth in bone, independent of the action of PTH. These findings have clinical implications as breast cancer patients, much like the older population in general, frequently have a low dietary calcium intake and high bone turnover.

Disclosures: C.R. Dunstan, Amgen 1.

This study received funding from: The National Health and Medical Research Council of Australia (NHMRC project grant #352332).

1007

ATF4 Is Required for the Anabolic Actions of PTH on Bone In Vivo. S. Yu¹, M. Luo^{*1}, R. T. Franceschi², D. Jiang^{*3}, J. Zhang¹, K. Patrene^{*1}, K. D. Hankenson⁴, G. D. Roodman¹, G. Xiao¹. ¹Medicine, University of Pittsburgh, Pittsburgh, PA, USA, ²Periodontics and Oral Medicine, University of Michigan, Ann Arbor, MI, USA, ³Periodontics and Oral Medicine, University of Michigan, Ann Arbor, MI, USA, ⁴University of Pennsylvania, Philadelphia, PA, USA.

Parathyroid hormone (PTH) is a potent stimulator of bone formation and a proven anabolic agent for the treatment of osteoporosis. However, the mechanism whereby PTH increases bone formation remains poorly understood. Activating transcription factor 4 (ATF4) is a critical factor for bone formation during development and throughout postnatal life. This study examined if ATF4 is required for the anabolic actions of PTH on bone using an Atf4^{-/-} mouse model. Five-day-old wt and Atf4^{-/-} mice were given daily subcutaneous injections of vehicle (saline) or hPTH(1-34) (0.04 µg/g body weight) for 28 days. In wt mice, µCT analyses of femurs show that this PTH regimen significantly increased bone volume/tissue volume (BV/TV, 4.3-fold), trabecular thickness (Tb.Th, 50%), trabecular numbers (Tb.N, 1.5-fold), cortical thickness (Cort.Th, 77%), and cross sectional area (CSA, 24%) and decreased trabecular spacing (Tb.Sp, 1.7-fold). These PTH effects were dramatically reduced or completely abolished in the absence of ATF4. Histological analyses show that PTH displayed potent anabolic effects on tibiae, vertebrae, and calvariae, which were significantly reduced in Atf4^{-/-} mice. At the molecular level, PTH markedly increased levels of osteocalcin (Ocn) and bone sialoprotein (Bsp) mRNA of long bones as measured by quantitative real-time RT/PCR. This increase was completely abolished in the absence of ATF4. This study demonstrates that ATF4 is required for the anabolic actions of PTH on bone in vivo and also suggested that modulation of the levels and activity of ATF4 may have therapeutic significance for the treatment of metabolic bone diseases such as osteoporosis.

Disclosures: S. Yu, None.

1008

Rac2 Knockout Mice Have an Augmented Anabolic Response to PTH. T. Kawano^{*}, B. Sun^{*}, J. Wu^{*}, I. Karl. Department of Medicine, Yale University, New Haven, CT, USA.

Rac2 is a small GTPase that is required for CSF1-dependent osteoclast chemotaxis. Rac2^{-/-} mice have increased bone mass, and osteoclast-like cells prepared from these animals have reduced basal resorptive capacity. Histomorphometric analysis has demonstrated a trend towards increased numbers of osteoclasts while osteoblast number is normal. Recent studies have suggested that cells of the osteoclast lineage are necessary for the full anabolic effect of PTH to be manifest. We hypothesized that since osteoclast precursors would be normal or increased in Rac2^{-/-} animals while mature osteoclast function was impaired, the anabolic effect of PTH might be enhanced in these animals. To test this idea, adult Rac2^{-/-} mice and wild-type C57Bl/6 mice were treated with either a single daily sc injection of h(1-34) PTH (80ng/g body weight) or vehicle for 4 weeks, and BMD measured after 0, 2 and 4 weeks of treatment. At the end of 2 weeks the PTH-treated Rac2^{-/-} mice showed a greater increase in spine, femur and total body BMD compared to baseline than did the wild-type mice (3.9±6.8% vs. 1.6±6.5%, 9.0±5.7% vs. 5.8±5.3% and 7.2±3.1% vs. 4.9±2.5%; spine, femur, total body respectively; M±SD). After 4 weeks of treatment this difference was the same or greater (7.4±4.1% vs. 3.7±6.6%, 23.6±9.0% vs. 7.4±6.5% and 13.5±3.4% vs. 5.4±2.6%; spine, femur, total body respectively; M±SD). Further, when compared to vehicle-treated Rac2^{-/-} animals, the PTH-treated Rac2^{-/-} mice showed significantly greater mean increases in bone mass as compared to the increment in BMD observed in PTH-treated wild-type compared to vehicle-treated wild-type mice (6.7% vs. 1.8%; 16.2% vs. 3.8%; and 9.5% vs. 3.5% spine, femur and total body). Consistent with our hypothesis, serum CTX at 4 weeks was significantly lower in the PTH-treated Rac2^{-/-} animals than in the PTH-treated wild-type mice (13.8±2.9 vs. 22.4±9.5 ng/ml; M±SD). While the detailed cellular mechanisms that underlie this effect are not yet clear, these data support the notion that subtly altering osteoclast function may be a feasible way to improve the anabolic response to PTH. Further, since Rac2 is restricted in its expression to hematopoietic tissue it could represent a reasonable target for drug discovery.

Disclosures: T. Kawano, None.

1009

RANK Ligand Inhibition by Denosumab Prevents Cortical Bone Loss in a Murine Model of Glucocorticoid-induced Osteoporosis. L. C. Hofbauer¹, U. Zeitze², M. Schoppert¹, M. Skalic², M. Stolina³, P. J. Kostenuik³, R. G. Erben². ¹Philipps-University, Marburg, Germany, ²University of Veterinary Medicine, Vienna, Austria, ³Amgen Inc., Thousand Oaks, CA, USA.

Osteoporosis is a frequent and severe complication of systemic glucocorticoid therapy, and in vitro studies suggest that RANK ligand (RANKL) represents a potential mediator. We examined the ability of Denosumab (DMab), a fully human monoclonal antibody against RANKL, to prevent glucocorticoid-induced osteoporosis in mice. DMab does not inhibit murine RANKL, so knockin mice were created by replacing exon 5 of the murine RANKL gene with a chimeric 5th exon (murine non-coding and human coding regions). These mice exclusively express a chimeric RANKL protein that is inhibited by Denosumab. Male huRANKL mice (8 months old) received slow-release pellets containing either vehicle or prednisolone (PRED, 5 mg) which was released at a mean dose of 2.1 mg/kg/d over 4 weeks. HuRANKL mice were treated with denosumab (10 mg/kg, twice/week, s.c.) or vehicle (PBS) starting 3-4 days after pellet implantation. In addition, two groups of wild-type mice (Black Swiss/129) were treated with subcutaneous slow release pellets containing vehicle or PRED. Four weeks later all mice were killed after in vivo double fluorochrome labeling. Renal handling of sodium, potassium, and phosphate was unchanged by PRED or denosumab in huRANKL mice. However, PRED increased renal excretion of calcium in wild-type and huRANKL mice. PRED treatment also significantly increased urinary deoxypyridinoline (DPD) excretion as well as serum and bone TRAP5b activity, and denosumab treatment prevented these increases. For example, protein extracts of the whole humerus contained 11.7 ± 2.7 , 17.3 ± 5.1 , and 7.7 ± 7.5 U/g TRAP5b activity (mean \pm SD) in huRANKL mice receiving vehicle, PRED, or PRED + denosumab, respectively (all $P < 0.05$). Quantitative computed tomography (pQCT) revealed that PRED induced significant bone loss in the axial and appendicular skeleton mainly by thinning of cortical bone, consistent with increased endocortical bone resorption. Trabecular BMD and cancellous bone area remained unchanged in PRED-treated mice. Treatment with denosumab completely prevented PRED-induced cortical bone loss in the L4 vertebrae and in the distal femoral metaphysis without impairing biomechanical properties as determined by three-point bending tests in femurs. In summary, PRED treatment caused cortical bone loss that was consistent with increased osteoclastic bone resorption. Treatment of huRANKL knock-in mice with denosumab, a fully human anti-RANKL antibody, prevented glucocorticoid-induced bone loss in association with suppression of bone resorption.

Disclosures: L.C. Hofbauer, None.

1010

A Small Molecule Inhibitor of the Wnt Antagonist Secreted Frizzled-Related Protein (SFRP)-1 Stimulates Bone Formation. P. V. Bodine¹, B. Stauffer¹, H. Ponce-de-Leon¹, R. A. Bhat¹, A. Mangine¹, L. M. Seestaller-Wehr¹, R. A. Moran¹, J. Billiard¹, S. Fukayama², B. S. Komm³, K. Pitts³, G. Krishnamurthy³, A. Gopalsamy³, M. Shi³, J. C. Kern⁴, T. J. Commons⁴, M. A. Wilson⁴, G. S. Welmaker⁴, E. J. Trybulski⁴, W. J. Moore⁴. ¹Women's Health & Musculoskeletal Biology, Wyeth Research, Collegeville, PA, USA, ²Women's Health & Musculoskeletal Biology, Wyeth Research, Cambridge, MA, USA, ³Chemical & Screening Sciences, Wyeth Research, Pearl River, NY, USA, ⁴Chemical & Screening Sciences, Wyeth Research, Collegeville, PA, USA.

Canonical Wnt signaling has been demonstrated to increase bone formation by enhancing osteoblast proliferation, differentiation and activity, while suppressing apoptosis. Consequently, Wnt pathway components have been pursued as potential drug targets for metabolic bone diseases like osteoporosis. Deletion of the Wnt antagonist SFRP-1 in mice activates canonical signaling in bone and increases trabecular bone formation in aged animals. We have developed small molecules that bind to and inhibit SFRP-1 in vitro and demonstrate robust anabolic activity in an ex vivo organ culture assay. A library of over 400,000 compounds was screened for inhibitors of human SFRP-1 using a cell-based functional assay that measured activation of canonical Wnt signaling with an optimized T cell factor (TCF)-luciferase reporter gene assay. One of the hits in this screen, a diarylsulfone sulfonamide, bound to human SFRP-1 with a $K_d = 0.3$ μ M in a tryptophan fluorescence quenching assay. This compound inhibited human SFRP-1 with an $EC_{50} = 2.2$ μ M in the cell-based functional assay, but did not impede other SFRP family members. Moreover, the compound did not antagonize the activity of a SFRP-1 construct that lacked the C-terminal netrin domain, suggesting that this region contains the binding site. The compound also increased total bone area in a murine calvarial ex vivo assay at a concentration of 1.0 μ M. Optimization of this high throughput screening hit for binding and functional potency as well as metabolic stability and other pharmaceutical properties led to improved lead compounds. One of these leads bound to SFRP-1 with a $K_d = 0.08$ μ M and inhibited SFRP-1 with an $EC_{50} = 0.7$ μ M. Moreover, it increased total bone area in the murine calvarial ex vivo assay at concentrations as low as 0.001 μ M. Low oral bioavailability of this compound limited its in vivo evaluation in mice and rats. This work demonstrates the feasibility of developing small molecules that inhibit SFRP-1 and stimulate canonical Wnt signaling to increase bone formation.

Disclosures: P.V. Bodine, Wyeth Research 1, 3.
This study received funding from: Wyeth Research

1011

A Bisphosphonate Analog that Lacks Anti-Remodeling Activity Prevents Osteocyte and Osteoblast Apoptosis In Vivo. L. I. Plotkin, J. Goellner, K. Vyas^{*}, R. S. Shelton^{*}, R. A. Wynne^{*}, R. S. Weinstein, S. C. Manolagas, T. Bellido. Center for Osteoporosis and Metabolic Bone Diseases, Univ Arkansas for Medical Sciences and Central Arkansas Veterans Healthcare System, Little Rock, AR, USA.

A major effect of bisphosphonates (BPs) on bone is inhibition of resorption resulting from their ability to induce osteoclast death or interfere with osteoclast function. Nonetheless, BPs also prevent osteocyte and osteoblast apoptosis in vitro and in vivo, but the contribution of the latter property to the overall beneficial skeletal effects of these agents remains unknown. We compared herein the effect of IG9402, a BP analog that preserves osteoblast and osteocyte viability but does not induce osteoclast apoptosis in vitro, with that of alendronate, a classic BP that affects osteoclasts as well as osteoblasts and osteocytes. Swiss Webster mice (7-8 per group) were implanted with placebo or prednisolone (GC) pellets (2.1 mg/kg/d) for 10 days, and were injected daily with saline or 2.3 μ mol/kg/d alendronate or IG9402, starting 3 days prior to pellet implantation. Alendronate decreased the serum levels of C-telopeptide and osteocalcin, markers of bone resorption and formation, respectively, as well as the levels of osteocalcin and collagen1A1 mRNA in vertebral bone. On the other hand, IG9402 did not affect serum levels of C-telopeptide or osteocalcin nor bone mRNA levels of osteocalcin or collagen1A1. Moreover, whereas alendronate decreased cancellous bone formation rate from 0.43 ± 0.25 to 0.09 ± 0.03 μ m²/ μ m/d ($p < 0.05$), IG9402 did not affect it significantly (0.39 ± 0.04 μ m²/ μ m/d). These findings are consistent with a decrease in bone remodeling resulting from inhibition of resorption by alendronate but not by IG9402. Furthermore, the increase in osteoblast and osteocyte apoptosis induced by GC (from 5.6 ± 2.5 to $15.1 \pm 6.0\%$ and 3.1 ± 1.7 to $7.1 \pm 1.1\%$, respectively, $p < 0.05$) was prevented not only by alendronate, as previously shown, but also by IG9402. In addition, GC induced a significant decrease in the load required to break the 6th lumbar vertebra (68.1 ± 11.6 to 47.1 ± 8.5 N, $p = 0.006$) and a decrease that was non-significant in the compression stress (27.8 ± 5.3 to 21.2 ± 4.9 in MPa $p = 0.095$); and both alendronate and IG9402 prevented the decreased ability of the vertebrae to sustain load induced by GC. We conclude that preservation of osteoblast and osteocyte apoptosis by bisphosphonates is an important, but heretofore unappreciated, mechanism of the beneficial effect of these drugs on bone. Preservation of bone strength without inducing osteoclast apoptosis by IG9402 opens new possibilities for the treatment of bone fragility in conditions in which a decrease in bone remodeling is undesirable.

Disclosures: L.I. Plotkin, None.

This study received funding from: NIH and University of Arkansas for Medical Sciences.

1012

VDRM 1: A Tissue-Selective, Non-Secosteroidal Vitamin D Receptor Modulator with Improved Therapeutic Window of Bone Efficacy over Hypercalcemia. Y. L. Ma, Y. K. Yee^{*}, Q. Zeng^{*}, A. Schmidt^{*}, D. E. Coutant^{*}, R. J. Barr^{*}, L. I. Boone^{*}, S. R. Chintalacharuvu^{*}, J. A. Dodge^{*}, H. U. Bryant, M. Sato. Eli Lilly and Company, Indianapolis, IN, USA.

The active form of vitamin D3 and analogs have been shown to be beneficial for osteoporosis, autoimmune diseases and cancer treatment in animal models; however, the narrow therapeutic window between therapeutic efficacy and hypercalcemia has limited their clinical utility. We have identified an orally active, tissue selective, non-secosteroidal, VDR ligand to be a potent agonist in bone, while having modest calcemic effects in vivo. When compared to 1,25(OH)2D3 in vitro, VDRM 1 was 10 fold less potent in inducing RXR-VDR heterodimerization (3.9 and 38 nM, respectively) and 100 fold less potent in inducing osteocalcin expression in a reporter gene assay (0.2 and 20 nM, respectively), but VDRM 1 was >300 fold less active than 1,25 (OH)2D3 in inducing epithelial cell calcium channel 2 (CAT1) gene expression in Caco-2 cells (3.3 and 1062 nM, respectively). In 7 months old, one month post ovariectomized (Ovx), osteopenic rats, two months of VDRM 1 treatment dose dependently restored Ovx induced loss of vertebral BMD to Sham levels at 0.73 μ g/kg/d. Hypercalcemia was not observed until about 4.6 μ g/kg/d in these animals. Biomechanical analyses showed that VDRM 1 improved bone strength (ultimate load) of lumbar vertebra, femoral midshaft and the femoral neck to significantly above Sham control levels. Static and dynamic histomorphometry showed a dose dependent reduction of both resorption and formation activity in the proximal tibial metaphysis; however a dose-dependent stimulation of the periosteal bone formation rate of > 2 fold was observed on the cortical surface. Histopathology evaluation indicated a 17 fold separation between the bone efficacy and soft tissue calcification in these Ovx rats. Taken together, these animal data suggest that VDRM 1 may have promise to treat postmenopausal women with osteoporosis.

Disclosures: Y.L. Ma, Eli Lilly 3.

1013

Disruption of Hypoxia Inducible Factor-1 α in Osteoblasts Exacerbates Ovariectomy Induced Bone Loss in Mice. L. Deng^{*1}, X. Liu^{*1}, C. Wan², J. Wang^{*1}, J. Qi^{*1}, T. Luo^{*1}, J. Wang^{*1}, Q. Zhou^{*1}, Y. Zhu^{*1}, L. Wei^{*1}, T. L. Clemens². ¹Shanghai Institute of Traumatology and Orthopaedics, Ruijin Hospital, Shanghai Jiaotong University School of Medicine, Shanghai, China, ²Pathology, University of Alabama at Birmingham, Birmingham, AL, USA.

Postmenopausal and senile osteoporosis are associated with decreased skeletal blood flow, reduced capillary networks and impaired endothelial cell function. Vasoactive agents can attenuate oophorectomy-induced bone loss, suggesting that estrogen normally regulates the vascular supply to bone. Angiogenesis during bone development and repair is controlled by the hypoxia inducible factor-1 α (HIF-1 α) which transcriptionally activates VEGF and other proangiogenic proteins. In this study, we examined the contribution of the HIF-1 α pathway on estrogen action in mouse bone in vitro and in vivo. Treatment of wild-type primary mouse osteoblasts with estradiol increased HIF-1 α and VEGF protein expression in a time and concentration dependent manner; these effects were more pronounced under hypoxic conditions. To examine the role of HIF-1 α on osteoblast differentiation, primary osteoblasts carrying floxed HIF-1 α alleles were infected with adenovirus constructs expressing Cre to disrupt HIF-1 α . Osteoblasts lacking HIF-1 α had reduced the levels of VEGF, Runx2, OC and ALP, and decreased RANKL mRNA levels consistent with recent reports that hypoxia regulates osteoclast activity through HIF-1-RANKL interactions. To examine the role of HIF-1 α in vivo, mice carrying an osteoblast specific mutation of HIF-1 α were subjected to ovariectomy. At baseline, HIF-1 α mutants had modestly reduced bone volume, mineral apposition rate, osteoblast numbers, and increased osteoclast numbers relative to control mice. Following ovariectomy, HIF-1 α mutants exacerbated bone loss by histomorphometry and microCT (BV/TV -1.33 fold, trabecular thickness -1.27 fold, and mineral apposition rate -1.13 fold, n=4, P<0.05) and an increase in osteoclast numbers (+1.20 fold) versus controls. These results support the hypothesis that estrogen normally regulates HIF-1 α and that loss of proangiogenic HIF-1 α signaling exacerbates bone loss following ovariectomy.

Disclosures: L. Deng, None.

1014

Deletion of PYK2 Led to High Bone Mass Through a Positive Balance Between Bone Formation and Resorption in Aged Mice. M. Li, D. T. Crawford^{*}, H. Qi^{*}, H. A. Simmons, Y. Li^{*}, D. R. Healy^{*}, E. A. Smith, L. Buchbinder, T. A. Brown. Cardiovascular and Metabolic Diseases, Pfizer Global Research and Development, Groton, CT, USA.

We have recently found that PYK2, a tyrosine kinase, plays an inhibitory role in bone formation. Genetic deletion of PYK2 (PYK2^{-/-}) resulted in increased bone formation and bone mass in adult mice. However, it is not known if the PYK2^{-/-} phenotype persists with age and how the bone performs biomechanically. Therefore, we characterized the skeletal phenotype of female PYK2^{-/-} mice at 12 months of age. There were no differences in body weight and femur length between PYK2^{+/+} and PYK2^{-/-} mice, demonstrating that PYK2 is not essential for bone growth. Three dimensional μ CT analysis of trabecular bone of 2nd lumbar vertebra showed that trabecular bone volume per total volume, trabecular number, thickness, and connectivity density were significantly increased in PYK2^{-/-} mice by +300%, +74%, +149%, and +80%, respectively. In contrast, trabecular separation was significantly decreased by -36% in PYK2^{-/-} mice. These data indicate that PYK2^{-/-} mice had higher cancellous bone mass and improved microarchitecture than PYK2^{+/+} controls. Histomorphometric analysis was performed on the 5th lumbar vertebral bodies. Consistent with μ CT findings, cancellous bone volume, trabecular number and thickness were significantly higher whereas trabecular separation was lower in the PYK2^{-/-} mice than those of PYK2^{+/+} controls. Osteoclast surface and number were significantly lower by -40% and -39%, respectively, suggesting a decrease in bone resorption in the PYK2^{-/-} mice. However, these mice had a +36% and +69% significant increase in tissue referent bone formation rate and ratio of mineralizing surface/osteoclast surface, respectively, which combined with the increased bone mass suggested a positive balance between bone formation and resorption in PYK2^{-/-} mice. Biomechanical properties were examined in the femoral diaphysis, a cortical bone site, and lumbar vertebra body, a cancellous bone site, by four point bending and compression tests, respectively. Maximum load and stiffness were significantly increased by +27% and +24%, respectively in the femurs of PYK2^{-/-} mice. Similarly, maximum load and energy were significantly higher in the lumbar vertebra of PYK2^{-/-} mice. These data indicate that PYK2^{-/-} mice not only had high bone mass but superior structural properties than PYK2^{+/+} controls in both cancellous and cortical bone sites. In summary, deletion of PYK2 caused a positive balance between bone formation and resorption, resulting in augmentation of bone mass and biomechanical properties. Our findings in aged mice indicate that the positive impact of PYK2 inhibition persists with aging.

Disclosures: M. Li, Pfizer Inc. 3.

1015

β -adrenergic Signaling Requires Bone Matrix Protein OPN to Suppress Bone Formation and to Activate Bone Resorption. M. Nagao^{*1}, Y. Saita^{*1}, J. Nagata^{*1}, Y. Izu^{*1}, T. Hayata^{*1}, H. Hemmi^{*2}, Y. Ezura^{*1}, K. Nakashima^{*1}, H. Kurosawa^{*3}, M. Noda^{*1}. ¹Dept Morecular Pharmacology, Medical Research Institute, Tokyo Medical and Dental University, Chiyoda-ku, Tokyo, Japan, ²MTT Program, Tokyo Medical and Dental University, Chiyoda-ku, Tokyo, Japan, ³Orthopedics, Juntendo University School of Medicine, Bunkyo-ku, Tokyo, Japan.

Sympathetic nervous system controls bone mass through the action of β -adrenergic signals that suppress bone formation and stimulate bone resorption. Sympathetic tone would exert its effects through the activation of osteoclast differentiation and in part facilitation of hematopoietic cell progenitor mobilization. Osteopontin (OPN), one of the major components of noncollagenous matrix proteins in bone, has been shown to promote cell adhesion and negatively regulate stem cell niche. However, the role of OPN in bone loss induced by sympathetic signaling via β -adrenergic receptors is unknown. We therefore investigated how signaling of a β -adrenergic agonist, isoproterenol (ISO) signaling, interacts with OPN signaling in bone. MC3T3E-1 cells were treated with 10uM isoproterenol and this treatment decreased OPN expression levels after 2 hours and it reached down to one-third of initial levels after 8 hours, whereas expression levels of RANKL were increased about 20 folds at 2 hours. These observations suggest that OPN may play a role in ISO-induced bone loss. Therefore, to explore the involvement of OPN in ISO-induced bone loss in vivo, ISO was administered into 9 weeks old wild type (WT) and OPN^{-/-} mice. Administration of ISO for 3 weeks reduced trabecular bone mass (BV/TV) in WT mice based on uCT analysis. In contrast, such reduction was not observed in OPN^{-/-} mice. Histomorphometric analysis showed that ISO treatment decreased bone formation rate(BFR) and mineral apposition rate(MAR) in WT mice. In contrast, OPN deficiency suppressed ISO-induced reduction in BFR and MAR. Since OPN is involved in bone resorption, we examined osteoclasts in OPN^{-/-} mice. ISO treatment increased the number and surface of TRAP positive cells in WT mice. In contrast, OPN deficiency suppressed ISO treatment-induced increase in these parameters of osteoclasts. These data indicated that deficiency of OPN blocks β -stimulant-induced bone loss. In conclusion, OPN plays a critical role in β -adrenergic signaling-induced bone loss in vivo via modulation of both bone formation and bone resorption.

Disclosures: M. Nagao, None.

1016

The Basis for Osteoporosis in the Aldehyde Reductase Knockout Mouse. K. H. Gabbay^{*1}, K. M. Bohren^{*1}, R. Morello², J. Song^{*1}. ¹Pediatrics, Baylor College of Medicine, Houston, TX, USA, ²Molecular & Human Genetics, Baylor College of Medicine, Houston, TX, USA.

The aldehyde reductase enzyme (AKR1A4 - GR) knockout (GRKO - GR^{-/-}) mouse develops an age-related (>1 year) osteoporosis phenotype with spontaneous fractures that preferentially affect females. There is a marked acceleration of the phenotype in GR^{-/-} males after castration (CX) and in females after ovariectomy (OVX), and upon induction of streptozotocin diabetes. Both GR and a related enzyme, aldose reductase (AR) are able to reduce D-glucuronate to L-gulonate which is converted to ascorbic acid (ASC) by gulonolactone oxidase (GULO). Our data identify GR as the main source of L-gulonate for ASC synthesis in the mouse. AR has a secondary role indicated by a double knockout model, AR/GRKO, which recapitulates the clinical features of the GULO knockout model (GULO KO) with rapid onset of scurvy in both genders and death at 8-10 weeks of age. While the AR/GRKO and GULO KO models have absolute deficiencies, the GR^{-/-} mice have a moderate ASC deficiency. They show a marked decrease of trabecular (Tb) bone with hypertrophy of dysplastic mesenchymal cell masses, and absence of osteoblasts (Ob) at the growth plate. These cell masses (presumably dysplastic Ob) resolve and form disorganized osteoid after ASC feeding. Serial DEXA measurements in CX GR^{-/-} mice placed on regular diet (ASC content =0) show a statistically significant (p<0.001) decrease in bone mineral density (BMD). The bone phenotype is prevented by dietary ASC. Quantitative bone histomorphometry shows statistically significant decreases in bone volume, trabecular thickness and number with a marked increase in osteoclast (Oc) activity and number in CX GR^{-/-} mice after 3 weeks on regular diet. ASC administration after CX significantly suppresses Oc activity and number below those observed in intact GR^{-/-} levels on regular diet. We propose that the limited ASC synthesis in the GR^{-/-} mouse is adequate for normal skeletal development, but results in an uncoupling of bone homeostasis (formation and resorption) when the mice are subjected to stress. Thus, CX, OVX, or diabetes in the GR^{-/-} mice increase bone resorption in the face of reduced ASC availability, resulting in severe osteoporosis and fractures. ASC suppresses Oc activity and number in addition to promoting the differentiation of Ob. We suggest that oxidative stress in CX, OVX and diabetes is the common effector pathway for osteoclastogenesis. The GRKO model permits differentiation between the pro-osteoblastic activity of ASC and its additional anti-oxidant properties. This mouse model is relevant to understanding the role of ASC in bone homeostasis and the development of osteoporosis in normal and diabetic populations.

Disclosures: K.H. Gabbay, None.

This study received funding from: The Harry & Aileen Gordon Foundation.

1017

Risedronate Prevents Bone Loss in Breast Cancer Survivors: A Two-Year, Randomized, Double-Blind, Placebo-Controlled Clinical Trial. S. L. Greenspan¹, K. T. Vujevidich¹, R. Bhattacharya², S. Perera³, A. Brufsky¹, B. C. Lembersky¹, V. Vogel¹. ¹Medicine, University of Pittsburgh, Pittsburgh, PA, USA, ²Medicine, University of Kansas, Kansas City, KS, USA, ³Medicine/Biostatistics, University of Pittsburgh, Pittsburgh, PA, USA.

Chemotherapy induced menopause and aromatase inhibitors (AI) are associated with bone loss and increased risk for osteoporotic fractures in breast cancer survivors. Little data are available on the efficacy of oral antiresorptive therapy to prevent this. The REBBeca Trial was a single center, 2-year, randomized, double-blind, placebo-controlled trial to evaluate the efficacy of once weekly oral risedronate (RIS) 35mg, for the prevention of bone loss in newly postmenopausal women, following chemotherapy induced menopause for nonmetastatic breast cancer. All received calcium and vitamin D. Outcomes included changes in spine and hip bone mineral density (BMD, Hologic Discovery A) and bone resorption assessed by urinary NTX. 97% of the 87 women (mean age 50 years) randomized had normal or low bone mass by WHO criteria. At baseline, 71% were on tamoxifen and 16% were on an AI. Baseline clinical characteristics and BMD were similar between the 2 groups. During year 2, 49% of women were started on an AI by their oncologist. After 24 months, women in the PLB group had significant losses of BMD at the spine and hip sites ($p<0.05$) that were not observed in the RIS group (Table). At 24 months, BMD was significantly higher at the lateral spine and hip sites in women on RIS compared to PLB (2.3-2.4%, $p<0.05$; Table). In a secondary analysis we compared the response in women ever on an AI (+AI, $n=47$) and never on an AI (No AI, $N=40$) to their respective PLB group. Women on RIS No AI or RIS + AI had BMD 1.5 and 4.0% greater at the hip compared to women in the PLB No AI or PLB + AI groups respectively ($p<0.05$; Table). Women on RIS No AI had BMD 3.7% greater at the lateral spine compared to women in the PLB No AI group ($p<0.05$). Bone resorption was significantly lower in the women on RIS. We conclude that once weekly oral RIS improves BMD and prevents excess bone resorption in breast cancer survivors, even in women on an AI.

Table: Mean percent change \pm standard error in BMD or Marker at 24 months

	Spine	Lateral Spine	Total Hip	Trochanter	NTX
RIS all	0.4 ± 0.8	0.1 ± 1.1	0.9 ± 0.6	1.1 ± 0.8	-6.5 ± 10.4
PLB all	-1.2 ± 0.7	$-2.4 \pm 1.1^*$	$-1.6 \pm 0.4^{**}$	$-1.4 \pm 0.4^{**}$	$39.4 \pm 14.4^{**}$
Adjusted Difference all	1.4 ± 0.8	$2.3 \pm 1.2^+$	$2.4 \pm 0.5^{++}$	$2.4 \pm 0.7^{++}$	$-33.8 \pm 14.4^*$
Adjusted Difference No AI	1.1 ± 1.2	$3.7 \pm 1.8^+$	$4.0 \pm 0.8^{++}$	$3.6 \pm 1.0^{++}$	-26.3 ± 21.5
Adjusted Difference +AI	1.9 ± 1.0	1.8 ± 1.5	$1.5 \pm 0.7^+$	$1.8 \pm 0.9^+$	$-43.4 \pm 18.6^+$

* $p<0.05$, ** $p<0.01$ from baseline, + $p<0.05$, ++ $p<0.01$ RIS vs. PBO

Disclosures: S.L. Greenspan, Procter and Gamble 2, 5.

This study received funding from: Procter and Gamble/Investigator Initiated.

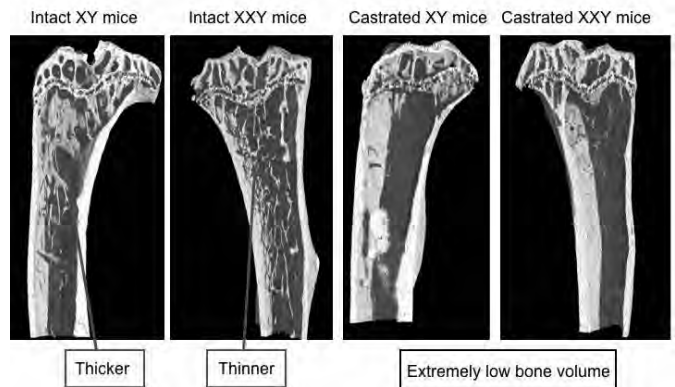
1018

XXY Mice Have an Osteoporotic Phenotype. P. Y. Liu¹, R. Kalak², Y. Lue³, K. Erkkila³, U. Simanainen¹, H. Zhou², A. Hikim³, D. Handelsman¹, M. Seibel², C. Wang³, R. Swerdloff³, C. Dunstan². ¹Andrology, ANZAC Research Institute, Concord, Australia, ²Bone Biology, ANZAC Research Institute, Concord, Australia, ³Endocrinology, Harbor UCLA Medical Center, Los Angeles, CA, USA.

Klinefelter's syndrome is the most common chromosomal aneuploidy in men (XXY karyotype, 1:600 live births) and is characterised by infertility and androgen deficiency, cognitive impairment and osteoporosis. The extent to which skeletal changes are due to sex hormone deficiency or arise directly from gene over-dosage cannot be easily determined in humans. To answer this question, we generated XXY mice through a complex 4-generation breeding scheme.

Eight intact XXY mice and 9 XY littermate controls, and 8 castrated XXY mice and 8 castrated XY littermate controls, were sacrificed at one year of age. Castration occurred 6 months prior to sacrifice. Tibiae were harvested and examined by mCT and histomorphometry. Blood testosterone was assayed by radioimmunoassay.

Compared to intact XY controls, XXY mice had a lower bone volume (6.8 ± 1.2 vs $8.8 \pm 1.7\%$, mean \pm SD, $P=0.01$) and trabeculae were thinner (50 ± 4 vs 57 ± 5 mm, $P=0.007$). Trabecular separation (270 ± 20 vs 270 ± 20 mm), osteoclast number relative to bone surface (2.4 ± 1.0 vs 2.7 ± 1.5 / mm²) and blood testosterone concentrations (5.3 ± 4.7 vs 2.5 ± 3.9 ng/mL) did not differ significantly. These mCT, histomorphometric and blood parameters were similar between castrated XXY and castrated XY mice. As expected, castration drastically decreased relative bone volume ($P<0.001$), trabecular thickness ($P=0.05$), trabecular separation ($P<0.01$) and blood testosterone concentrations ($P<0.001$) with equivalent effects in XY and XXY mice.



In conclusion, XXY mice replicate many features of human Klinefelter's syndrome making them a useful model for studying bone, as well as testis and behaviour (1). Testosterone deficiency may not fully explain the bone phenotype in the non-castrate state as XXY mice show both reduced bone volume and similar blood testosterone levels. These data suggest that novel genes, that escape X inactivation, contribute to bone loss, and when identified, may provide unique molecular targets for the management of osteoporosis.

(1) Lue Y, et al 2005 XXY mice exhibit gonadal and behavioral phenotypes similar to Klinefelter syndrome. *Endocrinology* 146:4148-4154

Disclosures: P.Y. Liu, None.

1019

A Stone Mouse: Transgenic Expression of an Engineered Gs-coupled Receptor in Osteoblasts Produces Increased Bone Mass. E. C. Hsiao¹, B. Boudignon², P. W. Chang¹, M. Benscik², J. Peng², C. Manalac¹, B. Halloran², B. Conklin¹, R. Nissenson². ¹Gladstone Institutes, University of California, San Francisco, CA, USA, ²Endocrine Unit, VA Medical Center, San Francisco, CA, USA.

Activation of the G-protein coupled PTH/PTHrP receptor (PPR) in osteoblasts can elicit a marked increase in bone formation and bone mass. The PPR is capable of activating multiple G protein pathways; however the specific signals responsible for the anabolic effects of the PPR are not fully understood. To address this problem, we engineered a novel GPCR ("Rs1") that activates the Gs/cyclic AMP pathway and displays constitutive Gs-linked signaling in transfection experiments of cultured cells. Rs1 was targeted to osteoblasts in vivo using a ColI 2.3kb promoter fragment combined with the TetO/TetA (TetOff) system. Expression of Rs1 in maturing osteoblasts from conception was sufficient to induce a dramatic anabolic skeletal response. Mutant mice displayed a 2-5 fold increase in femoral bone volume as compared to age and sex-matched littermate controls at 3 weeks. Whole body DEXA demonstrated a 3-fold increase in BMD in 9-week-old mice over controls (0.14 g/sq cm vs. 0.05 g/sq cm, respectively); microCT imaging confirmed a massive and generalized increase in mineralized bone by 9 weeks of age. Histomorphometry showed a marked increase in bone cellularity and osteoid with disorganized trabecular bone and loss of the cortical shell. Serum markers of bone metabolism were elevated in the mutant mice as compared to wildtype controls, including alkaline phosphatase at 3 weeks (970.6 ± 306.8 vs 251.6 ± 27.1 IU/L), and osteocalcin (507.2 ± 86.6 vs 131.6 ± 45.3 ng/ml) and pyridinoline cross links (2.45 ± 0.64 vs 1.28 ± 0.07 nmol/ml) at 9 weeks. No skeletal phenotype was observed in mice where Rs1 expression was suppressed by doxycycline administration from conception through the first 4 weeks of postnatal life. Our results indicate that Gs-GPCR signaling in osteoblasts during the first 4 weeks of life can produce a massive and progressive increase in bone formation and bone mass. The observed phenotype of these mice differs significantly from that of fibrous dysplasia and of transgenic mice expressing a constitutively-active form of the PPR, suggesting that G-protein signaling may interact with other crucial pathways to regulate bone formation. Our model provides a novel approach to activating the Gs pathway in osteoblasts and may indicate an anabolic pathway that could be used to maximize acquisition of peak bone mass for the treatment of osteoporosis.

Disclosures: E.C. Hsiao, None.

1020

Impaired Bone Formation in Mice Lacking the G Protein Subunit Gs α in Early Osteoblasts Leads to Marked Bone Fragility. J. Y. Wu¹, S. Rodda², N. A. Sims³, I. J. Poulton³, M. Chen⁴, L. S. Weinstein⁴, A. P. McMahon², H. M. Kronenberg¹. ¹Endocrine Unit, Massachusetts General Hospital, Boston, MA, USA, ²Department of Molecular and Cellular Biology, Harvard University, Cambridge, MA, USA, ³St. Vincent's Institute of Medical Research, Fitzroy, Australia, ⁴Metabolic Diseases Branch, National Institute of Diabetes and Digestive and Kidney Diseases, Bethesda, MD, USA.

Gs α is a ubiquitous heterotrimeric G protein subunit that mediates signaling downstream of numerous G protein-coupled receptors, including the parathyroid hormone (PTH)/PTH-related peptide (PTHrP) receptor (PPR). We have deleted Gs α in osteoblast progenitors expressing osterix, a transcription factor expressed early in osteoblastogenesis. Osterix-Cre:Gs α (fl/fl) mice have markedly decreased trabecular and cortical bone mass, and experience fractures of the posterior ribs and long bones by the first day of life, leading to early postnatal lethality. Histomorphometric analysis reveals a significant (70%) reduction in trabecular bone volume, with reduced trabecular thickness and number, and osteoblast surface and numbers are dramatically diminished by 87% in mutant mice. We have previously shown that micro-computed tomography of cortical bones revealed increased cortical porosity in Gs α conditional knockout mice. Double calcein labeling demonstrates abnormal woven cortical bone in the absence of Gs α . Sirius red staining followed by analysis under polarized light confirms a striking absence of lamellar bone in cortical bones from mutant mice. Similarly, calvariae of conditional knockout mice are notable for markedly increased porosity and aberrant persistence of woven bone. TRAP staining of trabecular, cortical and calvarial bones do not demonstrate any increase in osteoclasts, and serum TRACP 5b levels are significantly reduced in mutant mice, suggesting that this phenotype cannot be attributed to enhanced bone resorption. Furthermore, osteoclast surface and numbers are not increased in mutant mice. Taken together, these results suggest that mice lacking Gs α early in the osteoblastic lineage have abnormal and/or inadequate bone formation affecting both intramembranous and endochondral bones. The resulting failure to remodel woven bone into lamellar bone may underlie the profound fragility of Gs α -deficient bones.

Disclosures: J.Y. Wu, None.

This study received funding from: NIH.

1021

Designer G Protein Coupled Receptors Suggest Opposing Roles for Gs and Gi Signaling in Osteoblasts. S. M. Millard¹, J. Peng¹, M. Bencsik¹, A. Storer¹, W. Lu¹, T. J. Wronski², B. Conklin³, R. A. Nissenson¹. ¹Endocrine Research Unit, Veteran's Affairs Medical Center, San Francisco, CA, USA, ²Department of Physiological Sciences, University of Florida, Gainesville, FL, USA, ³Department of Medicine, University of California, San Francisco, San Francisco, CA, USA.

Designer GPCRs are powerful tools for dissecting the functional roles of specific G protein signaling pathways. We utilized two such receptors, Ro1 which signals through the Gi pathway and Rs1 which signals through the Gs pathway, to examine the role of these pathways in osteoblasts. Transgenic expression of Ro1 in osteoblasts using the 2.3 kb-Col1 promoter resulted in a dramatic osteopenic phenotype. Histomorphometric analysis of the proximal tibia revealed no change in the numbers of osteoblasts or osteoclasts on the bone surface, but decreased mineral apposition and bone formation rates were evident in Ro1 mice compared to littermate controls (Male BFR: 23.98 \pm 3.83 vs 36.46 \pm 1.44, Female BFR: 31.88 \pm 2.47 vs 44.32 \pm 4.57, p values <0.001). Osteoblast specific Ro1 transgene expression was tet-regulatable (tet-off system), allowing for the controlled expression of Ro1 in primary bone marrow stromal cell (BMSC) cultures. Induction of Ro1 expression in BMSC failed to influence osteoblast specific gene expression or formation of mineralized colonies, even in the presence of spiradoline, a synthetic agonist that activates Gi signaling by Ro1. These findings indicate that Gi signaling in osteoblasts in vivo has a marked negative effect on bone formation, apparently independent of cell autonomous inhibition of osteoblast function. To examine the role of Gs/cAMP signaling in osteoblasts, we have employed Rs1, a modified 5HT4 receptor that signals through Gs/cAMP in response to the synthetic drug RS23597, but not in response to 5HT (serotonin). The ability of Rs1 signaling to mimic cAMP dependent PTH responses was assessed in the osteoblast-like cell line Ros17/2.8. RS23597 induced an increase in intracellular cAMP, increased mRNA expression of the cAMP early response gene, ICER, and repressed Dickkopf1 mRNA expression in cells transiently transfected with Rs1. Neither 5HT treatment nor treatment with RS23597 in the absence of Rs1 expression produced these effects. This demonstrates that Rs1 is a suitable designer GPCR for assessing the role of Gs signaling in osteoblasts. Transgenic expression of Rs1 in osteoblasts in vivo produces a marked increase in bone mass, implying that the Gs/cAMP pathway is a major positive anabolic signaling pathway in osteoblasts. The contrasting phenotypes of the osteoblast-specific Ro1 and Rs1 transgenic mice are suggestive of critical and opposing roles for Gi and Gs signaling in osteoblast biology, the mechanisms of which are yet to be clearly delineated.

Disclosures: S.M. Millard, None.

This study received funding from: NIH grant DK072071, VA Merit Review award (to R.A. Nissenson).

1022

Severe Osteopenia in PERK-Knockout Mice Is Due to Impaired Osteoblast Differentiation Associated with Reduction of Type II RUNX2 Expression. J. Wei^{*}, X. Sheng^{*}, B. McGrath^{*}, D. R. Cavener. Biology, Penn State University, University Park, PA, USA.

PERK deficiency in human (Walcott-Rallison Syndrome) causes multiple skeletal dysplasias and severe osteopenia. As revealed by Micro-CT analysis, PERK deficient mice show a remarkable reduction in trabecular bone mineralization and cortical bone thickness as early as postnatal day 2. The expression of osteoblast markers (Alkaline phosphatase, Osteocalcin and Type I Collagen) was found to be significantly down-regulated in Perk KO mice by ~60-70% compared to wild-type littermates, and osteoclast markers were also reduced. To aid in the in situ identification of mature osteoblasts, the Col2.3GFP transgene was introduced into Perk KO mice. We found that the reduction in the expression of the osteoblast markers in Perk KO mice was the result of fewer mature osteoblasts and lower expression of osteoblast-specific genes per osteoblast. No increase in cell death was observed in KO mice, thus indicating that major defect in Perk-/- osteoblasts was abnormal or incomplete differentiation. A reduction of osteoblast markers was also seen in osteoblast-specific Col2.3 Perk KO mice, suggesting that PERK intrinsically regulates osteoblast differentiation. PERK is well known as a positive translational regulator of certain genes, including the transcription factor ATF4, which contain 5' upstream open reading frame (uORF) in their mRNAs. ATF4 was recently shown to be important in bone development and in regulating amino acid metabolism genes in osteoblasts. However, we found that in bone tissue of Perk KO mice, ATF4 mRNA and protein are normally expressed as well as its downstream amino acid metabolism genes. Another potential candidate for PERK-dependent regulation is RUNX2-type II, which contains five uORFs in its 5' UTR. In Perk-/- primary osteoblast culture, protein level of RUNX2-II is 50-30% of WT, while mRNA level is 80-90% of WT. Furthermore, DTT, a ER stress inducer, can strongly up-regulate RUNX2-II expression in both MC3T3-E1 and WT primary osteoblast, but only mild induction is seen in Perk-/- osteoblast, suggesting translation of RUNX2-II is PERK dependent. In summary our results illustrate that PERK is essential to normal osteoblast differentiation and reduction of type II RUNX2 possibly accounts for the osteoblast defects observed in Perk-/- mice. Supported by NIH AR49816 (D.R.C.).

Disclosures: J. Wei, None.

1023

Bone Cell Autonomous Effects of Osteoactivin/Gpnmb In Vivo. J. Y. Belcher¹, M. C. Rico¹, I. Arango-Hisijara¹, S. Salihoglu¹, K. B. Buck¹, S. Abdelmagid¹, A. Sanjay¹, M. C. Nakamura², S. N. Popoff¹, F. F. Safadi¹. ¹Anatomy and Cell Biology, Temple University, Philadelphia, PA, USA, ²University of California, San Francisco, San Francisco, CA, USA.

Osteoactivin/Glycoprotein nmb (OA/gpnmb) is a transmembrane glycoprotein. The protein is synthesized, processed and heavily glycosylated by osteoblasts. Its expression is associated with increased osteoblast differentiation and matrix mineralization. We have previously shown that OA/gpnmb expression in osteoblasts is regulated by BMP-2 through the Smad-1 signaling pathway. In this study, we used a mouse model with a naturally occurring mutation in the OA/gpnmb gene resulting from a premature stop codon that leads to the production of a truncated OA/gpnmb protein with no biological functions. OA/gpnmb mutant mice develop osteoporosis with age when compared to normal, wild type (WT) littermates. Histological and micro-CT measurements of femurs in mutant mice revealed a decrease in bone volume (BV/TV), trabecular number (Tb.N), and trabecular thickness in OA/gpnmb mutants compared to WT controls. Primary osteoblasts were generated from newborn OA/gpnmb and WT mice and examined for their differentiation ex vivo. All markers for early (alkaline phosphatase activity and collagen type I expression) and late (nodule formation, matrix mineralization and osteocalcin production) osteoblast differentiation were significantly reduced in the OA/gpnmb mutant osteoblasts compared to controls. We also examined bone marrow stromal cells isolated from OA/gpnmb and WT mice and testing their ability to differentiate into osteoblasts. Colony forming unit-fibroblasts (CFU-F) and CFU-osteoblasts (OB) (determined by alkaline phosphatase staining) were significantly reduced in mutant compared to WT mice. These data suggest that OA acts as positive regulator of osteoblast differentiation and function in vivo. We next examined osteoclast differentiation using a co-culture system established using normal osteoblasts as feeder cells and bone marrow (monocyte/macrophage) obtained from either OA/gpnmb mutant or WT mice in the presence of 1,25(OH)₂ vitamin D₃ and PGE2. Osteoclast formation/differentiation was determined by TRAP-staining and actin ring formation. Co-culture of bone marrow cells isolated from OA/gpnmb mutant mice and WT osteoclasts showed marked increase in osteoclast numbers and size when compared to osteoclasts generated from normal bone marrow cells and normal osteoblasts. These data suggest the OA/gpnmb acts as a negative regulator of osteoclast formation in vivo. Collectively, these data suggest that OA/gpnmb acts to regulate bone remodeling by positively affecting osteoblastogenesis and negatively regulating osteoclastogenesis in vivo.

Disclosures: J.Y. Belcher, None.

This study received funding from: NIAMS/NIH.

1024

Characterization of Osteoblast-Specific capn4 Knockout Mice. M. Shimada¹, P. A. Greer^{2*}, A. P. McMahon^{3*}, E. Schipani¹. ¹Endocrine Unit, Massachusetts General Hospital and Harvard Medical School, Boston, MA, USA, ²Pathology, Queen's University, Kingston, ON, Canada, ³Molecular & Cellular Biology, Harvard University, Cambridge, MA, USA.

We have previously demonstrated that the calpain small subunit directly binds the intracellular C-terminal tail (C-tail) of the PTH1R at a site near its N-terminus, and it cleaves PTH1R at its C-tail in a calcium- and ligand- dependent manner in cell lysates and in intact cells. Moreover, the absence or reduction of calpain activity reduces PTH-mediated intracellular cAMP accumulation in both embryonic fibroblasts expressing PTH1R and MC3T3-E1 cells.

The universal knockout mice of capn4, a gene encoding the calpain small subunit, are embryonic lethal. Thus, to investigate calpain's role in cells of osteoblast lineage which express PTH1R, in vivo, we established osteoblast-specific capn4 knockout mice by mating capn4fl/fl mice with mice expressing Cre under the control of osterix promoter (osx-cre). Thereafter, capn4fl/fl and capn4+ indicate floxed and wild-type alleles of capn4, respectively. Efficiency of Cre recombinase, as assessed by real-time PCR of genomic DNA, was approximately 85%. Osx-cre;capn4fl/fl mice were phenotypically normal at birth and fertile. Whole skeletal analysis of newborn mice showed that osx-cre;capn4fl/fl mice had no patterning defect, but they displayed smaller body size and a delay in mineralization of calvaria compared to either control or osx-cre;capn4fl/+ littermates. Body weight of osx-cre;capn4fl/fl mice stayed significantly lower than those of osx-cre;capn4+/+ and capn4fl/fl mice at least up to 12 weeks of age. Detailed histological analyses showed that tibias of osx-cre;capn4fl/fl mice had reduced trabecular bone and lower expression of both osteoblast-specific markers including type I collagen, collagenase 3, osteopontin and osteocalcin, and osteoclast makers such as tartrate-resistant acid phosphatase in comparison to control littermates. Consistent with these data, bone mineral density, as measured by dual-energy X-ray absorptiometry, was also significantly lower in femurs of osx-cre;capn4fl/fl male mice than in controls at 12 weeks old. Preliminary histomorphometric analysis confirmed that osx-cre;capn4fl/fl mice had significantly lower bone volume/total volume ratio and trabecular number with concomitant increase in trabecular spacing when compared to control littermates. Collectively, these results suggest that capn4 plays a critical role in bone development and remodeling in vivo.

Disclosures: M. Shimada, None.

This study received funding from: NIH/NIDDK.

1025

Overexpression of Human VDR in the Intestine Rescues the Hypocalcaemia-Related Phenotype of VDR Knockout Mice. Y. Xue^{*}, J. C. Fleet. Dept. of Foods and Nutrition, Purdue University, West Lafayette, IN, USA.

Vitamin D Receptor (VDR) knockout mice have reduced intestinal calcium absorption (Ca Abs) and develop severe hypocalcaemia and rickets when fed a standard 0.72% Ca chow diet. A highly bioavailable, 2% Ca, 20% lactose rescue diet that bypasses the transcellular Ca Abs pathway partially rescues this phenotype and reveals the importance of vitamin D-regulated intestinal Ca Abs in whole body Ca metabolism. To further study the role of VDR-mediated intestinal Ca absorption in Ca and bone metabolism, we generated transgenic (TG) mice with intestine-specific expression of hemagglutinin-tagged human VDR (HA-hVDR) driven by a 12.4 kb fragment of the villin promoter. Two TG lines, HV1 and HV2, were characterized. HA-hVDR mRNA and protein expression was detected from duodenum (Dd) to colon in TG mice; intestinal VDR protein was increased by 2- and 8- fold in HV1 and HV2, respectively, compared to the wild-type (WT) mice. In contrast a small level of HA-hVDR mRNA was seen in kidney of HV1 and HV2 and no HA-hVDR mRNA was seen in any other tissue. The HV2 line was used to examine whether TG expression could recover the VDR knockout (-/-) mouse phenotype. VDR +/-, TG +/- (control), VDR -/-, TG +/- (recovered KO or TG/KO) and VDR -/-, TG -/- (KO) mice were fed a standard chow diet for 8 or 12 weeks. At the 12 weeks of age, KO mice were growth arrested, developed alopecia, and had severe rickets. TG/KO mice also developed alopecia but growth and bone density were completely recovered. Serum Ca and PTH in TG/KO mice were completely restored to control levels. Serum 1,25(OH)₂D₃ and renal CYP27B1 mRNA levels were dramatically elevated in KO (100X and 400X above control, respectively). In TG/KO, these endpoints were restored to normal (CYP27B1 mRNA) or near normal (serum 1,25(OH)₂D₃, 7X above control levels). Intestinal expression of calbindin D_{9k} and TRPV6 mRNA levels were reduced in KO but recovered in TG/KO mice. In contrast, renal CYP24 mRNA levels were only partially recovered (25% control levels) in TG/KO. At 8 wks, basal Ca Abs in the Dd of TG/KO was 26% higher than controls and both lines increased Ca Abs after treatment with 1,25 (OH)₂D₃ (25 ng/100g body, 9 h; 29.94% vs. 51.46% in controls; 37.81% vs. 52.36% in TG/KO). Surprisingly, while 1,25 (OH)₂D₃ treatment significantly induced CYP24 (Dd, kidney), calbindin D_{9k} (Dd), and TRPV6 (Dd) mRNA in both control and TG/KO, the response in TG/KO was blunted. Our data demonstrate that restoration of active VDR-mediated Ca Abs throughout the intestine is necessary to recover the phenotype of VDR KO mice. This further shows the critical importance of the intestine in controlling whole body Ca metabolism.

Disclosures: Y. Xue, None.

This study received funding from: NIH awards DK54111 and CA101113 to JCF.

1026

Studies Using Nullmutant Mice Reveal Active Intestinal Calcium Transport in the Absence of Calbindin-D_{9k} or TRPV6. B. S. Benn^{1*}, P. Dhawan^{1*}, A. Porta^{1*}, X. Peng^{1*}, M. Hediger^{2*}, J. Peng^{3*}, G. Oh^{4*}, S. Christakos¹. ¹Biochemistry and Molecular Biology, UMDNJ- New Jersey Medical School, Newark, NJ, USA, ²Institute of Biochemistry and Molecular Medicine, University of Berne, Berne, Switzerland, ³Department of Medicine, University of Alabama, Birmingham, AL, USA, ⁴Laboratory of Cardiovascular Genomics, Ewha Woman's University, Seoul, Republic of Korea.

To study the role of the calcium binding protein calbindin-D_{9k} and the epithelial calcium channel TRPV6 in intestinal calcium absorption, calbindin-D_{9k} and TRPV6 nullmutant mice were generated. Nullmutation was verified by RT-PCR and Western blot analyses. When fed a standard rodent chow diet, TRPV6 knockout (KO) mice and calbindin-D_{9k} KO mice have serum calcium levels similar to those of wild type (WT) mice (~ 9 mg Ca⁺⁺/dl). In the TRPV6 KO mice, however, there is a 3 fold increase in serum PTH and 2.4 fold increase in serum 1,25(OH)₂D₃ levels. Levels of calbindin-D_{9k} mRNA and protein in intestine were not significantly different in TRPV6 KO mice compared to WT nor were levels of intestinal TRPV6 mRNA significantly different in calbindin-D_{9k} KO mice compared to WT. However, in calbindin-D_{9k} KO mice there is a significant 2-3 fold increase in renal calbindin-D_{28k} mRNA and protein (vs. WT), suggesting that renal calbindin-D_{28k} is compensating for the lack of renal calbindin-D_{9k}. Active intestinal calcium absorption was measured using the everted gut sac method and the first 5 cm of the duodenum of WT or nullmutant mice. Under low dietary calcium conditions [mice were fed a low calcium (0.02%) diet from weaning for 4 weeks] there was a 4.4, 4.1 and 2.8 fold increase in calcium absorption in the duodenum of WT, calbindin-D_{9k} and TRPV6 KO mice respectively [n=5-18/group; p>0.1 WT vs. calbindin-D_{9k} KO and p<0.05 WT vs. TRPV6 KO on the low calcium diet]. Duodenal calcium absorption was increased 2.2 +/- 0.1 fold in the calbindin-D_{9k}/TRPV6 double knock out mice fed the low calcium diet (p<0.05 WT vs. double KO). Calcium absorption was not stimulated by low dietary calcium in the ileum of the WT or KO mice. In addition to low dietary calcium, 1,25(OH)₂D₃ administration (three injections of 1,25(OH)₂D₃ 100ng/100g body weight; 48, 24 and 12h prior to sacrifice) to vitamin D deficient mice also resulted in a significant increase in duodenal calcium absorption (1.8 - 2.4 fold; p<0.05 compared to vitamin D deficient mice and p>0.1 among all groups) in WT, calbindin-D_{9k}, and TRPV6 KO mice. This study provides evidence for the first time using nullmutant mice that significant active intestinal calcium transport occurs in the absence of calbindin-D_{9k} or TRPV6, thus challenging the dogma for the need for calbindin-D_{9k} and TRPV6 for vitamin D induced active intestinal calcium transport.

Disclosures: B.S. Benn, None.

1027

Novel Mechanism of Vitamin D Receptor (VDR) Activation: Histone H3 Lysine 9 Methyltransferase Is a Transcriptional Coactivator for VDR. Y. Zhong^{*}, S. Christakos. Biochemistry and Molecular Biology, UMDNJ-New Jersey Medical School, Newark, NJ, USA.

Acetylation of core histone tails plays an essential role in transcriptional activation by nuclear hormone receptors. In addition to acetylation, methylation also occurs on core histones. The H3 specific lysine 9 methyltransferase G9a has been reported to function as a co-repressor of transcription by associating with transcriptional repressors. Here we report a novel mechanism of VDR receptor activation where G9a functions as a transcriptional activator in the 1,25(OH)₂D₃ regulation of 25-hydroxyvitamin D₃ 24 hydroxylase (24(OH)ase). Using COS-7 cells transfected with VDR and the rat 24(OH)ase promoter (-298/+74) and treatment with suboptimal 1,25(OH)₂D₃, increasing concentrations of G9a (0.02 - 0.2 ug) alone or in combination with the H3 specific arginine methyltransferase CARM1/PRMT4 (0.2 ug) had little effect on VDR mediated transcription. Expression of GRIP-1 (a p160 coactivator) alone (0.05 ug) or in combination with CARM1 (0.2 ug) or G9a (0.2 ug) stimulated transcription a maximum of 3 fold above the 1,25(OH)₂D₃ induced response. However transfection of G9a (0.2 ug) in combination with GRIP-1 (0.05 ug) and CARM1 (0.2 ug) resulted in a significantly greater enhancement of 1,25(OH)₂D₃ induced 24(OH)ase transcription 7- 8 fold above the 1,25(OH)₂D₃ induced response (p<0.01 compared to each enzyme alone or in combination or compared to activation with GRIP-1; maximal 1,25(OH)₂D₃ induced transcription was 60-70 fold). The synergy was dependent on 1,25(OH)₂D₃ and VDR. When either a mutant of CARM1, E267Q, or a mutant of G9a, that lacked enzymatic activity, was transfected, synergistic coactivator function was reduced. *In vitro* translation and co-immunoprecipitation studies have indicated that GRIP-1 binds directly to CARM1 and indirectly to G9a. When the GRIP-1 mutant AAD2 (which lacks the binding site for CARM1) was used, synergy was not observed, indicating a critical role of GRIP-1 in recruiting the secondary coactivators for VDR mediated transcriptional activation. Results of ChIP assays indicated that G9a is associated with the 24(OH)ase VDRE (-151/-137). Using the mouse 1α hydroxylase promoter and transfection in AOK-B50 kidney cells, we found that G9a can act as a repressor of PKA activation. These findings suggest that the histone modification induced by GRIP-1 can result in G9a acting as a transcriptional activator and that activation or repression depends on the context of transcription factors at a specific promoter. Our findings also suggest, for the first time, that cooperativity between histone methyltransferases and p160 coactivators may play a fundamental role in VDR mediated transcriptional activation.

Disclosures: Y. Zhong, None.

1028

Intracrine Synthesis and Action of 1,25-dihydroxyvitamin D Rescues Toll-like Receptor Suppression of Innate Immunity. S. Ren¹, L. Nguyen^{*1}, P. Liu^{*2}, R. L. Modlin^{*2}, J. S. Adams¹, M. Hewison¹. ¹Endocrinology, Diabetes and Metabolism, Cedars-Sinai Medical Center, Los Angeles, CA, USA, ²Division of Dermatology, UCLA, Los Angeles, CA, USA.

Vitamin D can act as a versatile modulator of the immune system by suppressing adaptive T-cell responses whilst stimulating macrophage innate immunity. We have shown recently that the latter involves toll-like receptor (TLR)-mediated induction of the enzyme 1 α -hydroxylase (CYP27b1) and concomitant autocrine metabolism of 25-hydroxyvitamin D (25D₃) to 1,25-dihydroxyvitamin D₃ (1,25D₃) by macrophages. This enhances innate immunity by stimulating expression of the antibacterial protein cathelicidin (LL37). Here we have used human macrophages cultured in the presence of autologous human serum to assess the effects of circulating 25D₃ levels on LL37 and beta-defensin 4 (DEFB4), another antibacterial peptide associated with innate immunity. Peripheral blood mononuclear cells were isolated from the patients as part of an established IRB protocol. Adherent monocytic cells were then isolated from non-adherent lymphocytes in serum-free medium and re-cultured in medium containing 10% of the patient's own serum. Under these conditions treatment with ligand to either TLR2 (19 kDa lipoprotein [19 kDa], 1ng/ml) or TLR4 (LPS, 100 ng/ml) suppressed expression of LL37 20-fold (p<0.001, n=9) and 32-fold (p<0.001, n=6) respectively. Analysis of patient vitamin D metabolites showed that suppression of LL37 by 19 kDa was inversely correlated with the patient's serum 25D₃ level (R=-0.801, p=0.009), indicating that intracrine conversion of patient 25D₃ to 1,25D₃ protected against inhibition of LL37. Monocytes cultured in autologous serum showed relatively high levels of CYP27b1 expression, and addition of exogenous 25D₃ (100 nM) alone increased expression of mRNA for LL37 (17-fold, p<0.001, n=10). Furthermore, co-treatment with exogenous 25D₃ (100 nM) rescued the suppressive effects of 19 kDa and LPS on LL37 expression (68-fold and 75-fold respectively for 19 kDa and LPS relative to cells treated with TLR ligand alone). Parallel analysis of DEFB4 showed that, in contrast to LL37, expression of this innate immunity gene was induced by either 19 kDa or LPS (349- and 86-fold respectively), and this response was unaffected by co-treatment with 25D₃. In summary, we have shown that high concentrations of TLR ligands act to suppress expression of antibiotic LL37, possibly as a mechanism by which pathogens can evade innate immunity. However, increased serum levels of 25D₃ protect against this pathogenic evasion mechanism. These data emphasize further the importance of intracrine metabolism of 25D₃ as a pivotal mechanism for normal human innate immunity.

Disclosures: S. Ren, None.

1029

Barrier Site Metabolism of Vitamin D: A Mechanism for Protection Against Inflammatory Bowel Disease. S. Wu, L. Nguyen*, S. Ren, R. F. Chun, J. S. Adams, M. Hewison. Endocrinology, Diabetes and Metabolism, Cedars-Sinai Medical Center, Los Angeles, CA, USA.

The active form of vitamin D, 1,25-dihydroxyvitamin D₃ (1,25(OH)₂D₃) is a versatile immunomodulator. In addition to suppression of adaptive T-cell responses, 1,25(OH)₂D₃ is also a potent inducer of innate antibacterial activity in macrophages. Both of these mechanisms are dependent on localized synthesis of 1,25(OH)₂D₃ via the enzyme 1 α -hydroxylase (CYP27b1). We have postulated that this autocrine/paracrine response is crucial to innate and adaptive immune responses at 'barrier sites' where cells have routine contact with pathogen-associated molecular patterns. To test this hypothesis we have used dextran sodium sulfate (DSS) to induce a gastrointestinal barrier challenge in mice, thereby generating symptoms of inflammatory bowel disease (IBD). Wild type (+/+) BL6 mice treated with 2.5% DSS in water for 7 days followed by 2 days recovery showed a decrease in weight of 8.0 \pm 4.4% compared to weight at day 0. Analysis of colonic tissue from these animals showed no change in expression of the Th2 cytokine interleukin-10 (IL-10), but there were increased levels of mRNA for the inflammatory cytokine, IL-1 (14.4-fold, p<0.001). This was associated with a parallel rise in CYP27b1 expression, at the level of mRNA (2.1-fold, p=0.003) and protein (the latter defined by immunohistochemistry). Analysis of sera from the DSS-treated animals showed no change in circulating levels of 25-hydroxyvitamin D₃, but these mice exhibited significantly lower levels of 1,25(OH)₂D₃ (42 pg/ml) when compared to untreated mice (58 pg/ml) (p=0.013). DSS-treatment of mice +/- for the CYP27b1 gene resulted in a similar loss of weight to WT mice (7.1 \pm 5.2% compared to 6.5 \pm 0.6% weight gain in control mice). By contrast, mice with ablation of the CYP27b1 gene (-/-) exhibited a striking weight loss of 23.8 \pm 3.9% when treated with DSS, compared to 2.1 \pm 2.0% weight gain in untreated -/- mice. The enhanced sensitivity of CYP27b1 -/- mice to DSS treatment was associated with increased colonic expression of mRNA for both IL-1 (20-fold compared to DSS-treated +/- mice) and IL-10 (8-fold compared to DSS-treated +/- mice). Increased expression of IL-1 and IL-10 in DSS-treated CYP27b1 -/- mice relative to +/- mice was also observed in spleens from these animals but not kidneys. This study provides further evidence of a role for vitamin D in protecting against the onset of IBD. In particular, our data show that a crucial determinant of this protective effect is the expression of CYP27b1 in affected tissues, including both the colonic epithelium and immune system.

Disclosures: M. Hewison, None.

1030

Molecular Mechanisms of 1 α ,25(OH)₂ Vitamin D₃-induced ATP Release in Osteoblasts. P. Biswas*, L. P. Zanello*. Biochemistry, UC,Riverside, Riverside, CA, USA.

Steroid hormones including 1 α ,25(OH)₂ vitamin D₃ (1,25D) are known to modulate bone cell populations and their activities. Changes in osteoblast to osteoclast ratios have

been identified as a possible cause of some bone diseases. Some therapeutic approaches aim at reduction of osteoclast generation or activity, which to a large extent is governed by factors released by osteoblasts. One such factor is ATP. ATP released by osteoblasts at localized sites, exerts autocrine/paracrine signaling and modulates osteoclast functions. However, molecular mechanisms of ATP release and its regulation are not fully known. Our study describes rapid exocytotic release of ATP induced by the steroid hormone 1,25D in osteoblastic rat ROS 17/2.8 and human Saos-2 cells. Single exocytotic events were monitored in real time with time-lapse videomicroscopy on live osteoblasts stained with quinacrine, which has high affinity for ATP stores. Physiological concentrations of 1,25D (1-10 nM) caused a 3 fold and 5 fold increase of ATP release respect to vehicle in ROS 17/2.8 cells and Saos-2 cells respectively. We found that 1,25D-induced ATP release is vesicular. Pretreatment of cells with 1 mM NEM and 100 μ M monensin, both agents known to interfere with vesicular transport and release, almost completely abolished 1,25D-induced ATP exocytosis. By means of siRNA silencing of the vitamin D receptor (VDR), we demonstrated that a classic VDR is required for 1,25D potentiation of Ca²⁺ and Cl⁻ channels coupled to ATP exocytosis. In addition, we found that an increase in intracellular Ca²⁺ induced by 1,25D is also required for 1,25D-mediated ATP secretion. The L-type Ca²⁺ channel blocker nifedipine (2 μ M) reduced 1,25D induction of ATP exocytosis by about 80%, while the L-type Ca²⁺ channel agonist S(-) BayK8644 (0.5 μ M) and depletion of internal calcium stores with thapsigargin (3 μ M) caused a significant increase in ATP release. Involvement of 1,25D-induced increase in intracellular Cl⁻ in 1,25D-mediated ATP release was determined by pretreatment of cells with the Cl⁻ channel blocker DIDS (200 μ M). We found that DIDS almost completely inhibited the 1,25D-induced ATP secretion. Furthermore, siRNA silencing of the CIC-3 voltage-gated chloride channel in ROS 17/2.8 cells significantly reduced 1,25D-stimulation of ATP release. Our findings provide for the first time, a signaling mechanism for the rapid release and increase of localized ATP concentrations in bone, and its regulation by the steroid hormone 1,25D.

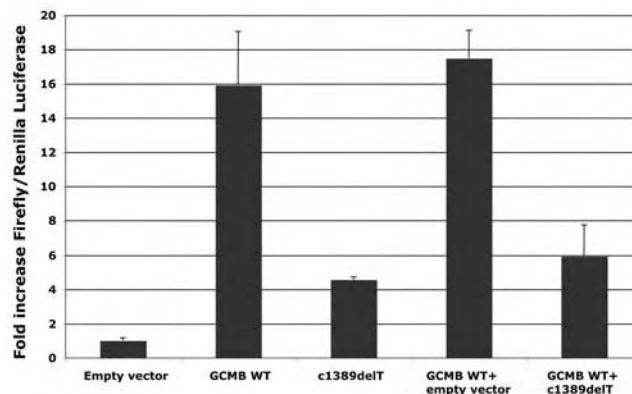
Disclosures: P. Biswas, None.

This study received funding from: USPHS grant DK-071115-01.

1031

Dominant-Negative GCMB Mutations Cause Hypoparathyroidism. M. Mannstadt¹, G. Bertrand^{*2}, B. Grandchamp^{*2}, H. Jueppner¹, C. Silve². ¹Endocrine Unit, Massachusetts General Hospital, Boston, MA, USA, ²Faculté de Médecine, Hôpital Xavier Bichat, Paris, France.

Glial cells missing (GCM), which was first discovered in the fruit fly, belongs to a small family of transcription factors that are key developmental regulators. The rodent GCM ortholog, Gcm2, is exclusively expressed in parathyroid glands and was shown to be a key regulator of parathyroid gland development since mice homozygous for ablation of Gcm2 fail to form parathyroid glands and consequently develop hypocalcemia and hyperphosphatemia; heterozygous animals are phenotypically normal. Consistent with these findings, homozygous mutations in GCM2, the human homolog of Gcm2, provided a plausible explanation for several cases of familial autosomal recessive hypoparathyroidism; importantly, heterozygous carriers of these mutations were healthy. We now report the identification of heterozygous GCM2 mutations as the cause of autosomal dominant hypoparathyroidism in two unrelated families with several affected members; in both families, mutations in the genes encoding parathyroid hormone and the calcium-sensing receptor were excluded. Because of the dominant mode of inheritance, we therefore considered the possibility of dominant negative GCM2 mutations. Indeed, direct nucleotide sequence analysis of GCM2 led to the identification of two novel, heterozygous mutations in genomic DNA of the affected, but not in the unaffected individuals in each family. Both heterozygous GCM2 mutations are single nucleotide deletions within GCM2 exon 5 (c1389delT and c1399delC) that introduce a frame-shift resulting in the truncation of the C-terminal GCM2 region, which contains the putative transactivation domain. To further elucidate the mechanism through which these heterozygous GCM2 mutations cause autosomal dominant hypoparathyroidism, we tested in HEK and DF-1 cells whether the mutant GCM2 inhibits the actions of the wild-type transcription factor using a GCM2-activated luciferase reporter. These experiments demonstrated that both GCM2 mutants impaired dose-dependently the transactivation capacity and thus the biological activity of wild-type GCM2; when expressed alone, the mutants exhibited a reduced capacity to activate the reporter. These findings strongly indicate that the newly discovered GCM2 mutants have dominant-negative properties.



Luciferase reporter assay using chicken fibroblast DF-1 cells. Results from triplicate wells; bars denote standard deviation.

Disclosures: M. Mannstadt, None.

1032

TβRI Inhibitor Rescues Uncoupled Bone Resorption and Formation Caused by TGF-β1 Mutations in Camurati-Engelmann Disease. X. Wu¹, Y. Tang¹, W. Lei^{*1}, W. Van Hul², T. R. Nagy^{*3}, M. Wan¹, X. Cao¹. ¹Pathology, University of Alabama at Birmingham, Birmingham, AL, USA, ²Medical Genetics, University of Antwerp, Antwerp, Belgium, ³Nutrition Sciences, University of Alabama at Birmingham, Birmingham, AL, USA.

TGFβ1, the most abundant cytokine deposited in bone matrix, plays a critical role in bone, but its exact function in the bone milieu is still unclear. Previously, we found that TGF-β1 is activated during bone resorption to induce migration of osteoprogenitors for bone formation as a coupling factor. Camurati-Engelmann Disease (CED) is an inherited bone disease associated with amino acid substitutions in the latency-associated peptide (LAP), but not in the mature TGFβ1 peptide. In examining cellular function of six different CED-derived TGFβ1, we found that mutations in LAP cause premature release of mature TGFβ1 upon secretion. As a result, TGFβ1 mutants exhibit much more potent effects on migration of osteoprogenitors than WT TGFβ1, suggesting its potential disturbance of coupling of bone resorption and formation. Indeed, CED TGFβ1 mutants are hyperactive for inducing phosphorylation of Smad2 and luciferase transcription activity. To examine whether premature release of active TGFβ1 uncouples bone resorption and formation, we generated a CED mutant and WT TGFβ1 transgenic mice driven by 2.3 kb Col I osteoblast-specific promoter. High levels of active TGFβ1 were detected only in bone marrow and matrix of the TGFβ1 mutant mice. A typical progressive diaphyseal dysplasia was observed in the tibia of one month-old TGFβ1 mutant mice. More than 95% mice had tibial fractures by 3 months of age. X-ray and μCT analysis revealed that very high bone density was present at certain areas whereas severe bone resorption was shown at other regions, indicating that bone resorption and formation is uncoupled. No significant differences were observed in bone mineral density (BMD), osteoclast and osteoblast activity between WT and CED transgenic mice, suggesting that premature release of active TGFβ1 interrupts coupling in TGFβ1 mutant mice. Most importantly, treatment of TGFβ1 mutant mice with the inhibitor of TGFβ type I receptor (TβRI) for 6 weeks rescued the uncoupled bone resorption and bone formation and completely prevented tibial fractures in TGFβ1 mutant mice. Taken together, CED-derived TGFβ1 mutations cause premature release of active TGFβ1 as well as uncoupling bone resorption and bone formation. TβRI inhibitor could be used as a potential agent for the treatment of CED patients.

Disclosures: X. Wu, None.

1033

RUNX2 Trinucleotide Repeat Mutations Are Associated with Decreased Bone Density and Altered Protein Function. A. Stephens^{*1}, J. Doecke^{*1}, S. Ralston², R. Prince³, G. Nicholson⁴, P. Sambrook⁵, M. Osato^{*6}, N. Morrison¹. ¹School of Medical Science, Griffith University, Gold Coast, Australia, ²Rheumatic Diseases Unit, University of Edinburgh, Edinburgh, United Kingdom, ³Department of Endocrinology and Diabetes, University of Western Australia, Perth, Australia, ⁴Department of Medicine, Geelong Hospital, University of Melbourne, Geelong, Australia, ⁵Department of Rheumatology, Royal North Shore Hospital, St Leonards, Australia, ⁶Institute of Molecular and Cell Biology, Proteos, Singapore.

The RUNX2 transcription factor is essential for osteoblast differentiation and chondrocyte maturation. Rare mutations within RUNX2 cause the dominantly inherited skeletal disorder cleidocranial dysplasia which is characterized by gross dysgenesis of the skeleton. A unique feature of RUNX2 is the polyglutamine and polyalanine (poly Q/A) domain encoded by a trinucleotide repeat sequence. Such repeat sequences are prone to strand slippage resulting in high mutation rates. We hypothesized that mutations within the RUNX2 poly Q/A domain would exist and these variants would be associated with altered bone density and protein function. 4361 DNA samples were obtained from multiple epidemiological studies of bone density. Bone density was measured by DEXA and ultrasound and expressed as Z-scores around the appropriate age-adjusted mean. A total of 21 subjects were identified as being heterozygous for a wild type 23Q/17A allele and a poly Q/A repeat variant allele. Deletions (15Q and 16Q) and insertions (30Q and 23A) were identified. Collectively Q/A repeat variants presented with significantly lower Femoral Neck BMD (DEXA) displaying a 0.65 SD decrease ($n = 21$, $p = 0.0004$) and lower bone density as measured by quantitative ultrasound of similar magnitude (-0.79 SD, $n = 8$, $p = 0.031$). To understand the mechanism via which the rare mutations were decreasing bone density, functional analyses were carried out on 23Q (WT), 16Q and 30Q RUNX2. The ability of the proteins to bind to the RUNX2 DNA binding site was assessed by EMSA. The analysis did not reveal any obvious changes in the DNA binding capacities of the mutant proteins. However, reporter gene analysis using the mouse osteocalcin promoter revealed significant decreases in the transactivation function of 16Q and 30Q. Finally, the ability of the proteins to localise to the nucleus was assessed. Subcellular analysis revealed the 16Q and 30Q proteins displayed defective nuclear localisation compared to WT. We have identified a new class of functionally relevant RUNX2 variants that occur at collective frequency of ~0.5%. These mutations are associated with significantly lower bone density and altered protein function.

Disclosures: A. Stephens, None.

1034

A Constitutively Activated BMP Receptor, ALK2, Induces Heterotopic Bone Formation in Patients with Fibrodysplasia Ossificans Progressiva (FOP). T. Fukuda¹, M. Kohda^{*2}, K. Kanomata^{*1}, J. Nojima¹, J. Kamizono^{*3}, H. Oda^{*4}, K. Nakayama^{*5}, A. Ohtake^{*6}, K. Miyazono^{*7}, E. Jimi⁸, I. Owan^{*9}, Y. Okazaki^{*2}, T. Katagiri¹. ¹Division of Pathophysiology, Saitama Medical Univ., RCGM, Saitama, Japan, ²Division of Translational Research, Saitama Medical Univ., RCGM, Saitama, Japan, ³Department of Pediatric Emergency, Kitakyusyu city Yahata Hospital, Fukuoka, Japan, ⁴Department of Orthopedic Surgery, Saitama Medical Univ., Saitama, Japan, ⁵Department of Endocrinology and Diabetes, Saitama Medical Univ., Saitama, Japan, ⁶Department of Pediatrics, Saitama Medical Univ., Saitama, Japan, ⁷Department of Molecular Pathology, Univ. of Tokyo, Tokyo, Japan, ⁸Department of Bioscience, Kyushu Dental College, Fukuoka, Japan, ⁹Department of Orthopedic Surgery, Univ. of Ryukyus, Okinawa, Japan.

Fibrodysplasia Ossificans Progressiva (FOP) is a rare autosomal dominant disorder of skeletal malformations and progressive heterotopic bone formation in muscle. Particularly, heterotopic bones were markedly induced in traumatic injury and inflamed area. Recently, the 617G>A and its related mutations were identified in ALK2, one of the BMP type I receptors, in patients with FOP. However, the functional changes of the mutant ALK2 proteins were not elucidated. In the present study, we examined genetic mutations of the ALK2 gene in Japanese patients with FOP and analyzed biochemical alterations of the mutant ALK2. The identical 617G>A heterozygous mutation, which causes a substitution mutation of Arg206 to His, was found in the ALK2 gene in all of the patients examined. Transient overexpression of ALK2(R206H) in C2C12 myoblasts induced phosphorylation and nuclear accumulation of Smad1/5/8 and transactivation of their target gene, Id1. ALK2(R206H) inhibited maturation of myoblasts to myosin heavy chain-positive myocytes. In contrast, ALP activity was synergistically induced by co-expression of ALK2(R206H) and Smad1 or Smad5 in C2C12 myoblasts. Treatment of C2C12 cells overexpressing ALK2(R206H) with BMP-4 or BMP-7 further increased the ALP activity. Co-transfection of Smad7, but not Smad6, suppressed the induction of ALP activity by ALK2(R206H). Moreover, we found that expression of the BMP signaling molecules were up-regulated during muscle regeneration *in vivo*. Taken together, these results clearly indicated that ALK2(R206H) is an active BMP receptor and constitutively transduces intracellular signaling of BMPs. It was also suggested that ALK2(R206H) cooperatively induces the heterotopic bone formation with BMP ligands and/or BMP signaling molecules induced at the sites of muscle regeneration. Smad7 might be a therapeutic target of FOP to inhibit BMP signaling induced by ALK2(R206H).

Disclosures: T. Fukuda, None.

1035

Regulation of the Transcription Factor Pitx1 and its Role in Osteoarthritis Pathogenesis. C. Picard^{*1}, B. Azeddine^{*1}, D. Wang^{*1}, J. Martel-Pelletier^{*2}, J. Fernandes^{*3}, F. Moldovan^{*4}, A. Moreau⁵. ¹Research Center CHU Sainte-Justine, Montreal, PQ, Canada, ²Osteoarthritis Research Unit, CHUM Hôpital Notre-Dame, Montreal, PQ, Canada, ³Research Center, Hôpital du Sacré-Coeur, Montreal, PQ, Canada, ⁴Department of Stomatology, Université de Montréal, Research Center CHU Sainte-Justine, Montreal, PQ, Canada, ⁵Department of Stomatology & Biochemistry, Université de Montréal, Research Center CHU Sainte-Justine, Montreal, PQ, Canada.

The presence of Pitx1, a homeodomain transcription factor, during development of periparticular regions giving rise to the hip and knee joints prompted us to investigate its putative role in Osteoarthritis (OA) pathogenesis. Our previous study demonstrated that partial inactivation of Pitx1 gene led to a progressive formation of OA-like lesions in aging Pitx1^{+/−} mice. Indeed, a loss of Pitx1 expression was observed only in cartilage of OA patients when compared to controls. The purpose of this study is to identify the mechanisms responsible for the down regulation of Pitx1 expression in primary OA. Search for mechanisms turning off Pitx1 expression led us to identify a mutation (−3727 C→T) present only in OA patients and localized into an E2F-response element within the human pitx1 promoter. Electrophoretic mobility shift assays were performed with nuclear extracts prepared from OA and matched control articular chondrocytes and allowed the detection of a protein complex bound to either the wild-type probe or the probe containing the mutated E2F-like site. Off-rate analysis revealed that such mutation increased the stability of the bound complex. To identify proteins part of this complex, we performed DNA pull down assays followed by peptide digestion coupled to mass spectrometry analysis, which allowed the detection of Prohibitin (PHB-1), Prohibitone (PHB-2) and BCL-6 interacting co-repressor (BCoR). PHB-1 plays a role in the maintenance of mitochondrial function and localizes as well as in the nucleus where it facilitates cellular senescence by recruiting specific co-repressors to inhibit E2F target genes. The pathophysiological relevance of PHB-1 was further supported by the detection of an aberrant nuclear accumulation of PHB-1 by immunohistochemistry methods only in OA articular chondrocytes, while the co-localisation *in vivo* of PHB-1 and BCoR on this E2F site was confirmed in OA articular chondrocytes by ChIP assays. The recruitment of this repressor complex was independent of the presence of the mutation suggesting that nuclear accumulation of PHB-1 could be a primary mechanism leading to OA onset. Collectively, these data define an unrecognized and crucial role for Pitx1 in OA pathogenesis and the recruitment of a novel repressor complex switching off its expression in OA.

Disclosures: C. Picard, None.

This study received funding from: Canadian Institutes of Health Research.

1036

Mice with a Truncation Mutation Affecting the UBA Domain of SQSTM1 Develop Several Phenotypic Features Paget's Including Focal Lytic Lesions, and Increased Bone Turnover In Vivo. J. A. Rojas^{*1}, A. Daroszewska^{*1}, R. Layfield^{*2}, M. Helfrich³, R. J. Van't Hof^{*1}, S. H. Ralston¹. ¹Rheumatic Diseases Unit, University of Edinburgh, Edinburgh, United Kingdom, ²Institute of Neuroscience, University of Nottingham, Nottingham, United Kingdom, ³Bone Research Group, University of Aberdeen, Edinburgh, United Kingdom.

Introduction: Paget's disease of bone (PDB) is characterized by focal increases in bone turnover and mutations affecting the Sequestosome 1 gene (SQSTM1) are an important cause of this condition.

Methods: Here we report upon our preliminary analysis of the skeletal phenotype of mice with a truncating mutation at codon 409 (S409X) of the SQSTM1 gene which deletes most of the UBA domain.

Results: We studied 6 wild type and 11 mutant mice carrying a S409X mutation of SQSTM1. Five were heterozygous and 6 were homozygous for the mutation. The age range of animals was 13.5 ± 0.25 months (range 12-15 months). Analysis of the femur and tibia by microCT examination ex-vivo showed large focal lytic lesions in 3/5 heterozygotes and 2/6 homozygotes, although smaller lytic lesions were observed in other mutants such that 9/11 of the animals which carried mutations (81.8%) had lytic lesions of the lower limbs. Three animals had more than one lytic lesion. Lesions of the type seen in the S409X mutant mice were not observed in control littermates. Histological analysis of lesions revealed evidence of increased bone turnover. Moreover bone histomorphometry of the tibial metaphysis showed a dramatic increase in bone turnover in homozygous mutants. There was a 3-fold increase in osteoclast number from 1.2 ± 0.5 /mm² in WT to 4.5 ± 0.8 /mm² in mutant ($p < 0.01$) and a two fold increase in eroded surface from 6.1 ± 2.0 % to 13.2 ± 1.8 % ($p < 0.01$). Osteoblast numbers were also increased from 15.2 ± 4.0 /mm² in WT to 37.5 ± 5.0 /mm² in mutant ($p < 0.01$). Studies in vitro showed a 8.6 ± 14.4 % increase in RANKL-induced osteoclast formation in mutant mice compared with WT ($p = 0.03$), but there was no difference in osteoblast growth between genotypes.

Conclusions: Mice carrying a S409X truncating mutation of the SQSTM1 gene exhibit several features that are reminiscent of PDB including increased bone turnover, focal lytic lesions in the lower limbs, and show increased osteoclast formation in vitro. Further studies are in progress to conduct more detailed characterisation of these mice but our data suggest that the S409X mutant mice may represent an animal model of PDB.

Disclosures: J.A. Rojas, None.

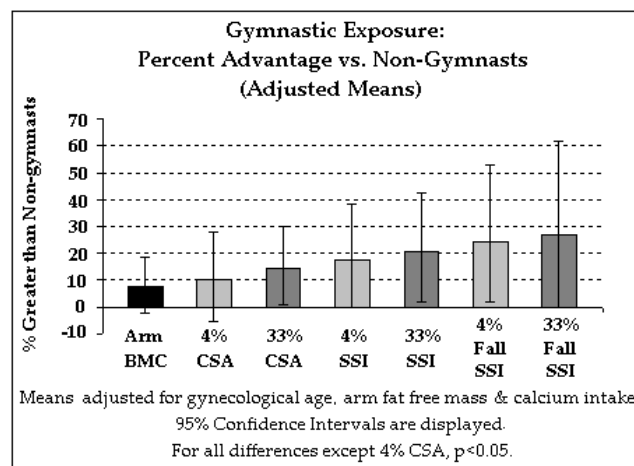
1037

Is Bone Strength a Simple Function of Muscle, or Does Other Mechanical Loading Play a Role? J. N. Dowthwaite¹, P. P. E. Flowers^{*2}, J. A. Kanaley^{*3}, R. M. Hickman^{*1}, J. A. Spadaro¹, T. A. Scerpeila¹. ¹Orthopedic Surgery, SUNY Upstate Medical University, Syracuse, NY, USA, ²Engineering, Syracuse University, Syracuse, NY, USA, ³Exercise Science, Syracuse University, Syracuse, NY, USA.

Many researchers tout muscular forces as the primary impetus for bone formation, but weight-bearing and impact-loading may also yield bone adaptations. We hypothesize that childhood gymnastic loading is linked to high arm BMC, bone diameter and bone strength, independent of arm lean mass (FFM), a surrogate for muscle size.

The Institutional Review Board of SUNY Upstate Medical University approved the project, and subjects/guardians assented/consented to participation. Total body DXA and pQCT radius scans were performed on 33 post-menarcheal girls. Non-dominant arm FFM and BMC were measured by DXA (Hologic QDR 4500W). Non-dominant polar strength-strain indices (SSI) and total bone cross sectional areas (CSA) were measured by pQCT at 4% and 33% distal radius sites. Forearm length was measured with a ruler. Calcium intake was assessed by food frequency questionnaire. Gynecological age was calculated as time from menarche to scan date. Focal outcomes were: non-dominant total arm DXA BMC; pQCT SSIs, total bone CSAs and fall SSIs (SSI/ (weight * forearm length)) at 4% and 33% radius sites. Gymnasts and ex-gymnasts (ex/gymnasts) had spent at least 5 hours per week in gymnastic training for at least 2 years out of the past 10 years. ANOVA compared means for ex/gymnasts (n= 19) vs. non-gymnasts (n= 14); ANCOVA adjusted for gynecological age, calcium intake and arm FFM.

Age, maturity, body size and calcium intake did not differ by gymnastic group. Arm FFM was a strong, consistent correlate of bone outcomes ($R > 0.53-0.79$, $p < 0.003$). All bone outcomes were greater in ex/gymnasts than non-gymnasts with large effect sizes (all $p < 0.02$, Cohen's $d > 0.98$). Gymnastics effects were large regardless of ANCOVA adjustment ($p < 0.05$, Cohen's $d > 0.78$), but arm FFM adjustment tempered 4% CSA significance ($p = 0.08$, large $d = 0.67$). Muscle and bone properties are closely related, and arm FFM is a useful gauge of upper extremity bone characteristics. However, gymnastic exposure acts as an independent factor in bone growth, linked to elevated bone accrual, geometry and strength. Thus, mechanical loading from non-muscular sources is a distinct and important determinant of human skeletal structure.



Disclosures: J.N. Dowthwaite, None.

This study received funding from: NIH NIAMS; OREF.

1038

Negative Effect of Dietary Protein Intake on Bone Mass Accretion in Chinese Pubertal Girls with Low Calcium Intake. Q. Zhang^{*1}, H. Greenfield^{*2}, G. S. Ma^{*1}, K. Zhu², X. Q. Du^{*2}, L. H. Foo^{*2}, X. Q. Hu^{*1}, C. T. Cowell^{*3}, D. R. Fraser^{*2}. ¹Chinese Center for Disease Control and Prevention, Beijing, China, ²University of Sydney, Sydney, Australia, ³Children's Hospital at Westmead, Sydney, Australia.

The aim of this study was to assess the relationship between background nutrient intakes and bone mass accrual in a longitudinal study including two-year milk supplementation trial and three-year follow-up study in Chinese pubertal girls.

Total 757 girls (aged 10.1 yr) were divided into three groups, supplied with either 330 ml calcium fortified milk (n=238) or milk fortified with calcium and vitamin D (n=260) on each school day for 24 mo, or consuming habitual diet without milk supplementation as controls (n=259). Over 24 mo, each subject consumed 144 ml/d supplementary milk on average, containing calcium 245 mg/d with/without vitamin D 3.33µg/d. Of 698 subjects completing the supplementation trial, 504 subjects agreed to be re-examined at 36 mo after supplement cessation.

All indices were measured at 0, 12, 24, 48 and 60 mo from the baseline. Bone mass of the forearm and whole body was measured with dual energy X-ray absorptiometry (DXA, Norland XR-36). Nutrient intakes were assessed by a three-day food record (including two weekdays and one weekend day).

Continuous variables were logarithm-transformed to observe the proportional association after adjustment for corresponding baseline value, pubertal development at baseline, age at each survey, physical activity percentage distribution at each survey, and clustering by schools. A linear mixed model in SAS program was used with $P < 0.1$ as the standard for retention in backward elimination regression. Subjects from all groups and subjects from the control groups (representing typical urban girls in China at puberty) were analyzed separately to identify the influential components.

Most positive effects of milk supplementation on total body and proximal forearm became significant after 24 mo supplementation, and disappeared at two or three yr after supplementation withdrawal. During the five-year study, the background calcium intake (440 mg/d on average, independently of that from the milk supplement) positively influenced bone mineral content (BMC) at total body (TB), proximal forearm (PF) and distal forearm (DF), bone area (BA) at PF and DF, as well as bone mineral density (BMD) at DF. However, negative associations were observed between protein intake (55 mg/d on average) and BMC at TB, PF and DF, BA at PF, as well as BMD at DF.

In summary, besides the effects of milk supplementation, a higher background calcium intake had a positive effect on bone mass accrual, while higher protein intakes appeared to diminish bone mass accrual in Chinese pubertal girls perhaps in association with their low calcium intakes.

Disclosures: Q. Zhang, None.

This study received funding from: Nestlé Foundation and Danone China.

1039

Sexual Dimorphism in Radial and Longitudinal Bone Growth Differ by Tempo and Magnitude: A Study in Male-Female Co-twins Pairs. S. Iuliano-Burns¹, J. Hopper^{*2}, R. Zebaze¹, E. Seeman¹. ¹Endocrinology, Austin Health / University of Melbourne, West Heidelberg, Australia, ²Epidemiology, University of Melbourne, Parkville, Australia.

An individual's bone trait position on the sample distribution influences fracture risk. Fracture risk is lower in males than females, in part due to sex differences in bone achieved during growth. We studied within pair differences in bone structure and mass in 61 dizygotic (DZ) boy-girl twin pairs aged 7 - 18 years to test the hypothesis that sexual dimorphism in bone traits emerge at puberty and are negligible prior to puberty. Total body and posterior anterior lumbar spine (LS) BMC and mid-femoral shaft (FS) dimensions were measured using DEXA. Regional BMC was acquired for the total body scan. Height was measured using a Holtain Stadiometer, and limb lengths using a Harpenden anthropometer. 41 twin pairs were pre- and 20 pairs were or peri/post-pubertal based on Tanner staging (pubic hair, genital development). Within pair comparisons were performed using unpaired t-tests. Contrary to the hypothesis, sexual dimorphism in bone structure and BMC was evident before puberty. BMC was 2-8% greater in the male than female depending on the site measured ($p < 0.05$). LS width (not height) was greater in boys than girls before puberty (3.3 ± 0.03 v 3.0 ± 0.03 mm, $p < 0.001$). Similarly, mid-FS periosteal widths (not femoral length) were higher in boys than girls (15.6 ± 0.3 v 14.5 ± 0.3 mm, $p < 0.01$), resulting in greater slenderness (bone width / length) at the femur in females than males ($p < 0.1$, NS). These existing differences remained during and after puberty. Sexual dimorphism in BMC and structure is detectable prior to puberty challenging the notion that the dimorphism is driven only by differences in sex hormones.

Disclosures: S. Iuliano-Burns, None.

1040

A School-based Physical Activity Intervention Positively Affects Change in Imax in Pre- and Early Pubertal Boys. H. M. Macdonald^{*1}, D. M. L. Cooper¹, S. A. Kontulainen², H. A. McKay¹. ¹Orthopaedics, University of British Columbia, Vancouver, BC, Canada, ²University of Saskatchewan, Saskatoon, SK, Canada.

Bone structural adaptations to physical activity during growth are not well understood. We previously reported a strong trend for greater gain in peripheral QCT (pQCT)-derived bone strength (density-weighted polar section modulus, SSI) at the tibial midshaft in boys who participated in a school-based physical activity intervention compared with control boys.¹ The objective of the present study was to further explore the structural adaptations underpinning the trend for bone strength gains. Participants were 202 boys aged 9-11 years from 10 schools that were randomly assigned to control (CON, 3 schools, n = 63 boys) and intervention (INT, 7 schools, n = 139 boys) groups. Boys in INT schools participated in 60 minutes of additional classroom physical activity each week, which included a simple, progressive, high-impact bone-loading program (Bounce at the Bell), over 11 months. We used ImageJ (1.37v) with a threshold of 480 mg/cm³ to process the grayscale pQCT images (XCT-2000) from the tibial midshaft (50% site) and determine the maximum and minimum second moments of area (Imax, Imin, mm⁴) and the cortical area (CoA, mm²) by quadrant (anterior, medial, lateral and posterior). The quadrants were defined according to the pixel coordinates about the cross-sectional centroid. We used a mixed linear model (group = fixed effect, school = random effect) to compare change in Imax, Imin and CoA (by quadrant) between CON and INT boys after adjusting for baseline bone value, change in tibial length and maturity at followup. Boys were 10.2 ± 0.6 years at baseline and the majority (60%) were prepubertal (Tanner stage 1). Boys in the INT group had a significantly greater gain in Imax than CON boys ($+ 365.7$ mm⁴; 95% CI: 83.5 to 647.9). Boys in the INT group also tended to have a greater gain in Imin, but the difference between groups was not statistically significant ($+ 109.3$ mm⁴; 95% CI: -25.4 to 243.9). Underpinning the greater gain in Imax in INT boys was a slightly greater gain (1-1.5%) in CoA in the anterior, medial and posterior quadrants although the differences between groups were not statistically significant. Change in CoA in the lateral quadrant was similar between CON and INT boys. Our school-based intervention effectively increased bending strength (Imax) at the tibial midshaft in young boys. Together with the tendency for quadrant-specific changes in CoA, these data suggest regional variation in the bone response to AS! BC. Our findings are consistent with expected patterns of bone formation induced by bending loads in the anterior-posterior direction.

1. Macdonald HM et al. JBMR 2007; 22:434-46.

Disclosures: H.M. Macdonald, None.

1041

High Protein Intake Enhances the Positive Influence of Physical Activity on Bone Mineral Content in Pre-Pubertal Boys. T. Chevalley, S. Ferrari, J. P. Bonjour, R. Rizzoli. Service of Bone Diseases, Department of Rehabilitation and Geriatrics, Geneva University Hospitals, Switzerland.

Physical activity is an important lifestyle determinant of bone mineral mass acquisition. Its influence during childhood can be modulated by nutrition, particularly by protein and calcium intakes. We analyzed the relationship between physical activity levels and protein intake, as compared to calcium intake, on bone mineral mass in 232 healthy pre-pubertal boys (age: 7.4 ± 0.4 yrs; standing height: 125.7 ± 5.9 cm; body weight: 25.3 ± 4.6 kg, mean \pm SD). Bone mineral content (BMC) was measured by dual X-Ray absorptiometry (DXA) at 6 skeletal sites: radial metaphysis; radial diaphysis; femoral neck; trochanter; femoral diaphysis and L2-L4 vertebrae. Physical activity, protein and calcium intakes were 242 ± 94 kcal.d⁻¹, 1.79 g.kg BW.d⁻¹ (a value about twice the usual recommended dietary allowance), and 752 ± 263 mg.d⁻¹, respectively. In univariate analysis, correlation coefficients r between physical activity, protein and calcium intakes, and the BMC sum of the 6 skeletal sites were 0.33 ($p=0.0001$), 0.26 ($p=0.0001$), and 0.16 ($p=0.013$), respectively. By multiple regression analysis, physical activity (β adjusted = 0.292, $p < 0.0001$) and protein intake (β adjusted = 0.224, $p=0.007$) remained correlated to BMC, whereas calcium intake was not (β adjusted = -0.027 $p=0.740$). Very similar results were found at the 6 individual skeletal sites. Within the group with protein intake above the median (2.0 g.kg BW.d⁻¹), increased physical activity from 168 to 321 kcal.d⁻¹ was associated with greater total BMC Z-score ($+0.6$, $p=0.0005$). In contrast, in the group with protein intake below the median (1.5 g.kg BW.d⁻¹) increased physical activity from 167 to 312 kcal.d⁻¹ was not associated with a significantly greater total BMC Z-score ($+0.2$, $p=0.371$). The interaction between physical activity and protein intake was close to statistical significance for total BMC Z-score ($p=0.055$) and total radius BMC ($p=0.054$), and significant for femoral neck BMC ($p=0.012$). In keeping with the results derived from multiple regression analysis, the increased physical activity on total BMC Z-score was not influenced by difference in calcium intake (above the median: i.e. 945 mg d⁻¹; below the median: i.e. 555 mg d⁻¹). No significant interaction ($p=0.754$) was detectable for total BMC Z-score as well as for any of the 6 skeletal sites between physical activity and calcium intake. In conclusion, in healthy pre-pubertal boys the influence in increased physical activity on bone mineral content appears to be enhanced by protein intake within a range above the usual recommended allowance.

Disclosures: T. Chevalley, None.

1042

Determinants of Bone Mass and Fracture in Adolescent Children: Early Life, Prepubertal and Current Factors. G. Jones, K. L. Hynes^{*}, S. Foley, J. Flynn^{*}. Menzies Research Institute, Hobart, Australia.

Fractures are common in children while variation in peak bone mass contributes approximately two thirds of fracture risk in later life. Reports in prepubertal children suggested that maternal smoking during pregnancy, breastfeeding and birth weight were all determinants of early bone mass and/or fracture but it is unclear if this persists through puberty. The aim of this study was to examine the role of early life, prepubertal and current factors in the determination of bone mass and fracture in adolescent male and female children.

During 2004/5, 415 16 year old Southern Tasmanian children were studied. Early life factors were available from a 1988 study of risk factors for SIDS (smoking during pregnancy, weight gain, age at birth, birthweight, duration of breastfeeding, period of gestation, anthropometrics and socioeconomic variables). Data were also available from age 8 (bone mass and body composition by DXA, physical activity, sun exposure). Bone mass was assessed at age 16 at the total body, femoral neck and spine using an Hologic Delphi densitometer and at the heel by a Sahara ultrasound densitometer. Fractures were collected by questionnaire (site, age, circumstances) with confirmation from medical records.

Of the 415 children, 160 (39%) had a fracture. In multivariate analysis, bone mass at age 16 was predicted by breastfeeding (3% higher at hip and total body), birth weight (hip and total body), lean mass, sports participation, shuttle run and standing long jump at age 8 (hip and total body) as well as bone mass at age 8. Fracture (particularly those involving the upper limb) was predicted by breastfeeding (HR yes v no 0.69, $p=0.02$) (but not birth weight) and bone mass at age 8 (total body and spine, HR 1.5-2.5/SD). No significant associations with either bone mass or fracture were present for maternal smoking during pregnancy or sun exposure at age 8. Both DXA and heel ultrasound measures at age 16 were also able to discriminate those with and without prevalent fracture (especially those involving the upper limb, OR 1.3-1.8/SD).

These unique data provide strong support to indicate that bone mass in adolescence can be influenced by environmental factors both breastfeeding in early life as well as during childhood where physical activity is most important. In addition, both breastfeeding during early life and bone mass assessed by DXA at age 8 were strong predictors of fracture while heel ultrasound is also reduced in those with fracture. These results suggest that osteoporosis and fracture prevention programs should commence very early in the life cycle.

Disclosures: G. Jones, None.

This study received funding from: NHMRC.

1043

Targeted Deletion of E11/gp38 in Osteocytes Results in Increased Skeletal Size and Bone Mineral Density. D. Guo^{*1}, Y. Mishina^{*2}, J. Feng¹, M. Ray^{*2}, G. Scott^{*2}, M. Harris³, L. Bonewald¹. ¹Oral Biology, UMKC, Kansas City, MO, USA, ²Molecular Developmental Biology, NIEHS, Research Triangle Park, NC, USA, ³Department of Periodontics, UTHSCSA, San Antonio, TX, USA.

As the osteoblast differentiates into an osteocyte, a dramatic change in morphology occurs from polygonal to dendritic. E11/gp38 is a membrane glycoprotein highly expressed in the embedding osteocyte that appears to be responsible for dendrite formation and elongation due to fluid flow shear stress. Therefore, we hypothesized that a reduction of E11 in the osteocyte would be detrimental as the cell would have less capacity for communication and viability. Conventional deletion results in lethality at birth due to a lung defect, therefore to determine function in osteocytes, postnatal targeted deletion of the E11 gene was performed by generation of E11 flx/flx mice (5' loxp site in SacI of exon 1 non-coding region, 3' loxp site in BstEII of intron 1) crossed with mice expressing the osteocalcin promoter driving CRE. The first cKO mouse showed approximately 10% greater body weight than its control littermate at 1 to 3 months of age. Bone mineral density was also 10–20% higher in the E11cKO mouse as determined by PIXIMUS analysis, confirmed by microCT and radiography. Histomorphometric analysis showed a 10% reduction in osteocyte density in ulnar cortical bone compared to control. To validate that E11 was deleted in bone, immunostaining was performed showing dramatic reduction in expression in bone. Furthermore, scanning electron microscopy of acid-etched ulnae embedded in resin revealed an irregular lacuno-canalicular network dramatically different from the uniformly distributed lacunae in control cortical bone. In addition to fewer lacunae, fewer canaliculi per lacunae were observed in the E11 cKO. These observations further support the role of E11 in dendrite formation, however suggest that a reduction in dendrite formation may actually maintain the osteoblast in the matrix producing stage for an extended time before embedment in matrix resulting in greater bone mass.

Disclosures: D. Guo, None.

This study received funding from: NIH.

1044

Dynamic Imaging of Fluorescently Tagged Osteoblast and Osteocyte Populations Integrates Mineralization Dynamics with Osteoblast to Osteocyte Transition. S. L. Dallas¹, P. A. Veno^{*1}, L. F. Bonewald¹, D. W. Rowe², I. Kalajzic^{*2}. ¹Univ. of Missouri Kansas City, Kansas City, MO, USA, ²Univ. of Connecticut Health Ctr, Farmington, CT, USA.

A well accepted model of osteocyte differentiation proposes that the osteoblast becomes trapped within an osteoid matrix, followed by mineralization of the matrix to entomb the osteocyte within its lacuna. Thus, osteocyte differentiation and bone mineralization occur simultaneously and may be interrelated. As a model to understand the dynamic process of osteocyte to osteoblast transition and how this integrates with mineralization, we have performed automated time lapse imaging in mineralizing bone cell cultures from transgenic mice with fluorescently tagged osteoblast and osteocyte populations. Calvarial cells from neonatal mice expressing a Dmp1-GFP transgene as a marker for osteocytes, a 3.6kb Col1a1-DsRed transgene as a marker for osteoblasts or both transgenes together, were cultured with ascorbate and β -glycerol phosphate (β GP) to promote mineralization. Mineral deposition was monitored using differential interference contrast optics or using alizarin red as a vital stain for calcium. Mineral deposition was found to occur exclusively at sites where small clusters of 4–20 cells expressed the Dmp1-GFP transgene and the boundary of the mineralized area followed the boundary of the GFP+ve cell clusters. The kinetics of mineralization were quantified by time lapse imaging in conjunction with thresholding of image stacks. After addition of β GP there was a lag phase of 10–20h followed by a rapid period of mineral deposition that lasted 10–14h before reaching a plateau. A large amount of membrane ruffling and mitosis within the nodule preceded mineral deposition. There was also a high degree of cell motility within the nodule, with a subpopulation of Dmp1-GFP+ve cells, presumably representing embedded cells, remaining stationary throughout the imaging period. A large number of cells switched on Dmp1-GFP expression just prior to or during mineralization, suggesting transition from an osteoblast to an osteocyte-like phenotype. The osteocytic nature of these cells was confirmed by immunostaining for the early osteocyte marker, E11. Interestingly, the Col1a1-DsRed and Dmp1-GFP transgenes identified two distinct cell populations with little overlap. The majority of cells that turned on the Dmp1-GFP osteocyte marker during mineralization were derived from a cell type that did not express high amounts of the Col1a1-DsRed transgene. Together, these data suggest that mineralization is directed by a cell type that is already transitioning into an osteocyte and suggest that mineralization and osteocyte differentiation are simultaneous, interrelated and possibly non-extricable processes.

Disclosures: S.L. Dallas, None.

1045

Dynamic Imaging in Living Calvaria Reveals the Motile Properties of Osteoblasts and Osteocytes and Suggests Heterogeneity of Osteoblasts in Bone. P. A. Veno¹, D. P. Nicoletta², I. Kalajzic³, D. W. Rowe³, L. F. Bonewald¹, S. L. Dallas¹. ¹Univ. of Missouri Kansas City, Kansas City, MO, USA, ²Southwest Res. Inst., San Antonio, TX, USA, ³Univ. of Connecticut Health Ctr, Farmington, CT, USA.

Osteocytes, once thought to be quiescent cells, are now known to be mechanoresponsive, capable of modifying their microenvironment and play a key role in phosphate homeostasis. We have shown that osteocytes within their lacunae may be highly dynamic and show motions of their cell body and dendrites. To determine the dynamic interactions between osteoblasts and osteocytes and understand the role of cell motility in their function we have performed dynamic imaging using mice with fluorescently tagged osteocyte and osteoblast populations.

Calvarial explants from 5–12 day old mice expressing a Dentin matrix protein 1-GFP (Dmp1-GFP) transgene in osteocytes, a 3.6kb Col1a1-DsRed transgene in osteoblasts or both together, were imaged by time lapse fluorescent microscopy. Osteoblasts on the bone surface were highly motile and continually moved randomly with a mean velocity of 5.3 μ m/h. We have previously shown that this motility drives assembly of extracellular matrix proteins. Three distinct motile cell populations were observed on the bone surface. The majority of motile cells were red only (Col1a1DsRed+ve) with smaller populations that were green only (Dmp1GFP+ve) or red and green (GFP/DsRed dual expressing). 65% of the osteocytes showed motions of their cell bodies within their lacunae, with deformations between 4–12% and 98% of the osteocytes extended and retracted their dendrites. Alizarin red staining confirmed that these motions occurred in osteocytes within mineralized lacunae. Transient dendritic connections appeared to be made between adjacent osteocytes and between osteocytes and surface cells. Osteocytes also extended dendrites beyond their canaliculi into vascular channels and resorption pits and appeared to contact cells in these spaces. Osteocytes exposed during bone resorption underwent cell death or migrated out of their lacunae into the resorbed area. Dynamic imaging was next combined with immunostaining to correlate expression of specific markers with the motile history of the cell. In the case of E11, an early osteocyte marker, this revealed distinct cell populations. 75% of Dmp1-GFP+ve surface motile cells and 100% of the partially embedded osteocytes with dendrite motion expressed E11. In contrast, 14% of embedded osteocytes with dendrite motion were E11+ve.

These data suggest that osteocytes and osteoblasts are more motile than previously known and suggest heterogeneity of osteoblasts on the bone surface. A surface motile cell expressing Dmp1-GFP and E11 appears to represent a precursor cell that is destined to become an osteocyte.

Disclosures: P.A. Veno, None.

1046

Control of the SOST Bone Enhancer by PTH Via MEF2 Transcription Factors. O. Leupin^{*1}, I. Kramer^{*1}, N. M. Colette^{*2}, G. G. Loots^{*2}, F. Natt^{*1}, M. Kneissel¹, H. Keller¹. ¹Musculoskeletal Disease Area, Novartis Institutes for BioMedical Research, Basel, Switzerland, ²Chemistry, Materials and Life Sciences Directorate, Lawrence Livermore Laboratory, Livermore, CA, USA.

The SOST gene encodes for sclerostin, an osteocyte-secreted key inhibitor of bone formation. SOST expression is restricted to osteocytes in adult bone and requires the presence of a distant enhancer that is deleted in Van Buchem disease patients, which are characterized by a generalized progressive bone overgrowth. Parathyroid hormone (PTH) has been shown to suppress endogenous SOST expression in UMR-106 bone cells and in adult bone in vivo. Recently, we have reported that PTH completely inhibited the transcriptional activity of the SOST bone enhancer, but only marginally affected the proximal promoter using transient transfection reporter gene assays in UMR-106 cells. Footprint and functional mutation analysis revealed a myocyte enhancer factor 2 (MEF2) response element that is essential for enhancer activity. Furthermore, gel retardation assays and antibody-induced supershifts demonstrated direct binding of MEF2 transcription factors. Here, we show that the MEF2 response element is sufficient for enhancer activity. It conferred comparable enhancer activity as the full length enhancer sequence. Moreover, its activity was fully suppressed by PTH in a manner similar to the full length enhancer sequence. Expression of MEF2 transcription factors in bone was detected by quantitative RT-PCR and in situ hybridization. Expression levels of MEF2A, B, C and D in femur and UMR-106 cells were similar to those in heart and brain, two known MEF2-expressing tissues. Furthermore, immunohistochemistry demonstrated co-expression of MEF2s and sclerostin in UMR-106 cells and in osteocytes of adult bone in vivo. Overexpression of MEF2C in reporter gene assays had no effect on the activity of the proximal SOST promoter, but stimulated the SOST enhancer activity about 3-fold. Conversely, co-expression of a dominant negative MEF2C mutant protein inhibited enhancer activity by 55% in UMR-106 cells. Finally, siRNA-mediated knockdown of MEF2A, C and D suppressed endogenous SOST expression by 65, 59 and 84%, respectively, in UMR-106 bone cells. Combinations of siRNAs against MEF2A&C, A&D, C&D led to increased inhibition of SOST expression reaching levels similar to those observed with SOST-specific siRNAs. These data suggest that MEF2 transcription factors control SOST expression in osteocytes and mediate PTH responsiveness. Hence, MEF2 transcription factors are implicated in the regulation of adult bone mass.

Disclosures: H. Keller, Novartis 1, 3.

This study received funding from: Novartis.

1047

Target Ablation of PTH/PTHrP Receptor in Osteocytes. P. P. Divieti¹, W. F. Powell^{*1}, T. Kobayashi¹, S. E. Harris², F. Bringhurst¹. ¹Endocrine Unit, Mass General Hospital, Harvard Medical School, Boston, MA, USA, ²Department of Periodontic, University of Texas Health Center at San Antonio, San Antonio, TX, USA.

Osteocytes are the most abundant cells in bone, but their relative inaccessibility and the lack of good in vitro cell models have impeded progress in understanding their functional roles. Parathyroid hormone (PTH) is known to act upon osteocytes via both PTH/PTHrP receptors (PPRs), specific for the amino-terminal PTH (and PTHrP) sequence, and CPTHrPs, which recognize amino-truncated forms of the hormone.

To study the role of PTH and PTHrP activation of PPRs in osteocytes we have conditionally ablated PPRs in osteocytes using the Cre-LoxP technique. We first generated three independent lines of transgenic mice in which the tamoxifen inducible Cre-recombinase (Cre-ERT2) is driven by an osteocyte-specific promoter (the 10Kb region of DMP1 promoter). The function, induction and specificity of the DMP1-Cre-ERT2 transgene was evaluated by mating male and female transgenics with homozygous Rosa26R Cre-reporter mice. The dams were injected with tamoxifen (2 mg) at day 17.5 dpc, and X-Gal staining was performed in newborn pups. All osteocytes were positive for the X-Gal staining demonstrating that the promoter was functional and Cre-dependent recombination could be fully induced upon tamoxifen injection. Cre-recombinase mRNA expression was confirmed by RT-PCR analysis of RNA from newborn calvarial bones. Two 10Kb-DMP1-Cre-ERT2 lines were mated with PPR(f/f) animals to create double heterozygotes, which then were mated with PPR(f/f) mice to generate DMP1-Cre/PPR(f/f) animals. To assess for PPR deletion in osteocytes we assessed down regulation of SOST expression in 4 and 8 week old mice (WT and PPRKO) fed a low calcium diet (0.2% Ca) for 1 or 2 weeks to induce secondary hyperparathyroidism. All animals were injected with tamoxifen (0.5 mg every 2 days for up to 2 weeks), and ionized and total calcium were measured at the end of the study period. Long bones and calvaria were fixed, decalcified and analyzed by immunohistochemistry for SOST expression. As expected, SOST expression remained readily detectable in KO mice but was greatly suppressed in WT animals, consistent with successful deletion of the PPR in osteocytes. Further studies to evaluate message levels of SOST and other PTH-regulated genes are currently underway. In summary, we have established a mouse model in which PPR expression can be specifically ablated in osteocytes. These mice will provide an excellent model to dissect the roles of PPRs in osteocytes. Furthermore, the 10Kb-DMP1-Cre-ERT2 mice can be used to delete additional genes of interest from this specific bone cell population

Disclosures: P.P. Divieti, None.

1048

Mutations in LRP5 β -Propeller 1 Block Sclerostin (SOST) Mediated Inhibition of the LRP5-Wnt-TCF Signals in U2OS Osteoblast-like Cells. B. M. Bhat, V. E. Coleburn*, P. J. Yaworsky*, P. V. N. Bodine, S. Harada. Women's Health & Musculoskeletal Biology, Wyeth Research, Collegeville, PA, USA.

Loss of function mutations in the Sclerostin (SOST) gene are linked to Sclerosteosis and van Buchem disease which exhibit progressive growth of dense bone that can lead to clinical complications. However, heterozygous SOST mutations are clinically normal despite having high bone mass (HBM). The specific effect of SOST on bone formation was further demonstrated by increased bone mineral density in SOST knockout mice, osteopenia in SOST transgenics and complete reversal of ovariectomy induced bone loss in rats by SOST antibodies. Osteocyte secreted SOST was considered to be an antagonist of BMP-signaling, but recent studies indicate that this effect is preceded by the inhibition of LRP5-Wnt signaling. It is now well established that an HBM trait in humans is associated with mutations in LRP5 β -propeller 1, among its four β -propellers. Additionally, by in vitro studies we have shown along with others that the HBM-like mutations in LRP5 confer resistance to Dkk1, a secreted inhibitor of LRP5-Wnt- β -catenin signaling. Interestingly, Dkk1 interacts with LRP5 propellers 3 and 4 region while SOST binds to propellers 1 and 2. To investigate the LRP5-SOST interaction further, we studied several LRP5 mutants generated within all four β -propellers. These included the HBM-mutant LRP5G171V, and its structurally equivalent site mutants created within and outside the propeller 1. The analysis involved transient co-transfection assays using a Wnt- β -catenin responsive TCF-reporter and LRP5 or its mutant cDNAs in U2OS bone cells. In addition, we compared the potential role of Kremen2 in modulating Dkk1 and SOST function. Our results indicate that Kremen2 is essential for the inhibition of the LRP5-mediated TCF signal by Dkk1 while SOST mediated inhibition is Kremen independent. It is interesting to observe that Dkk1 and Kremen2 inhibited TCF activity of all three Wnts (1, 3a & 10b) tested while SOST inhibited only Wnt1 and Wnt10b. Out of the eight LRP5 mutants, only those in β -propeller 1 showed resistance to SOST and further supports the specificity of the SOST interaction with β -Propeller 1. In conclusion, the study demonstrates that inhibition of LRP5-Wnt- β -catenin signaling can be dependent on the co-expression of Kremens and the antagonists Dkk1 or SOST. Moreover, the analysis shows the importance of LRP5 β -propeller 1 and specific Wnts in SOST function. Continued investigations would lead to better understanding of LRP5 signaling and the role of different antagonists in maintaining bone homeostasis.

Disclosures: B.M. Bhat, None.

1049

Increased Mortality in Patients with a Hip Fracture - Effect of Pre-morbid Conditions and Post-fracture Complications. P. Vestergaard^{*1}, L. Rejnmark², L. Mosekilde². ¹The Osteoporosis Clinic, Aarhus Amtssygehus, Aarhus, Denmark, ²Department of Endocrinology and Metabolism C, Aarhus Amtssygehus, Aarhus, Denmark.

Background: Patients with a hip fracture have a significant excess mortality. However, it remains unclear if the mortality is linked to the pre-morbid conditions or to complications to the fracture.

Aim: To investigate the causes of mortality after a hip fracture.

Material and methods: All subjects with a hip fracture in Denmark between 1977 and 2001 compared with three age- and gender-matched subjects from the general population. Co-morbidity at the time of fracture and causes of death were evaluated.

Design: Historic cohort study.

Results: A total of 169,145 fracture cases were compared to 524,010 controls. The cases had a much higher prevalence of co-morbidity than the controls. The mortality rate was twice as high in fracture cases compared with controls (HR=2.26, 95% CI: 2.24-2.27). Adjustments for confounders only changed the excess mortality risk little. The mortality after the hip fracture was divided into two categories: an excess mortality of 19% within the first year following the fracture (relative survival=0.81 compared to controls), and an excess mortality of 1.8% per year (relative survival 0.982) for every additional year following the fracture. The major causes of the excess mortality were due to complications to the fracture event (70.8% within the first 30 days). Elderly hip fracture patients were more likely to die from trauma related factors than younger patients.

Conclusions: Patients with a hip fracture have a pronounced excess mortality risk. The major cause was linked to the fracture event and not to pre-existing co-morbidity.

Disclosures: P. Vestergaard, None.

This study received funding from: Helga and Peter Kornings Foundation.

1050

Risk of Subsequent Fracture Depends on Bone Mineral Density and Fracture Type: A 15-Year Prospective Study. D. Bliuc, N. Nguyen, T. V. Nguyen, J. A. Eisman, J. R. Center. Bone and Mineral Program, Garvan Institute of Medical Research, Sydney, Australia.

Half of all fractures occur in people with non-osteoporotic BMD (T-score > -2.5). Any osteoporotic fracture increases re-fracture risk, yet, there is no information on re-fracture risk for different T-scores and how normal or osteopenic BMD affects that risk. This study therefore aimed to examine re-fracture risk according to BMD for all types of osteoporotic fractures in 1374 women and 871 men aged 60+ from the Dubbo Osteoporosis Epidemiology Study (April 1989 - May 2005).

BMD was measured at baseline at spine and hip, and all osteoporotic fractures and deaths were recorded. Fractures were classified into hip, vertebral, major (proximal humerus, distal femur, proximal tibia, pelvis, multiple rib) and minor (all other peripheral fractures excluding digits). Subsequent fracture rates were calculated according to gender, fracture type, and BMD T-score and compared with initial fracture rate of a BMD-matched group. There were 520 incident fractures in women (35% osteopenia and 57% osteoporosis) and 198 in men (44% osteopenia and 25% osteoporosis) during 14,203 and 9,709 person-years, respectively. Following initial fracture 176 women and 48 men had subsequent fractures (2683 and 808 person-years, respectively).

Absolute re-fracture risks were highest for women and men with osteoporosis [86 (72-103) and 135 (87- 209); RR: 1.4 (1.1- 1.7) and 2.9 (1.7- 4.9), respectively] and still increased for osteopenia [40 (30- 55) and 52 (32- 83); RR: 1.5 (1.1- 2.1) and 2.5 (1.5- 4.3) respectively], but for those with normal BMD there was no significant increase in re-fracture risk [RR: 2.1 (0.9- 4.6) and 1.7 (0.8- 3.7) respectively]. As for overall re-fracture risk the increase in relative risk was 2-fold higher for men than women.

In women and men with hip and vertebral fracture¹, re-fracture risk was increased irrespective of BMD, except in the few men with normal BMD where over 50% died within 3 years.

There was an overall increased re-fracture risk following initial fracture in women and men with osteopenia and osteoporosis. Hip and vertebral fractures were associated with the highest re-fracture risk. Neither women nor men with normal BMD had an increased re-fracture risk following minor fractures. These results should help guide physicians in treatment decisions following initial fracture.

¹ Center et al (2007) JAMA 4:387-94.

Disclosures: D. Bliuc, None.

1051

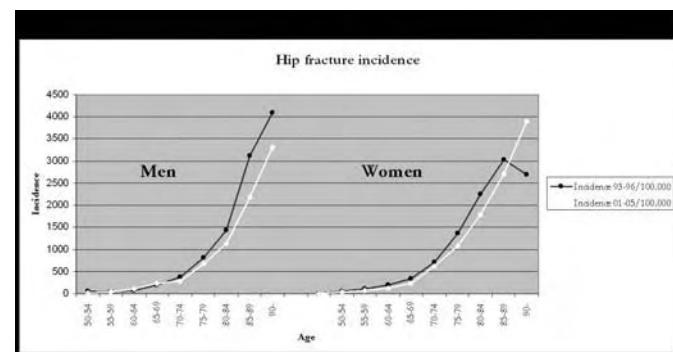
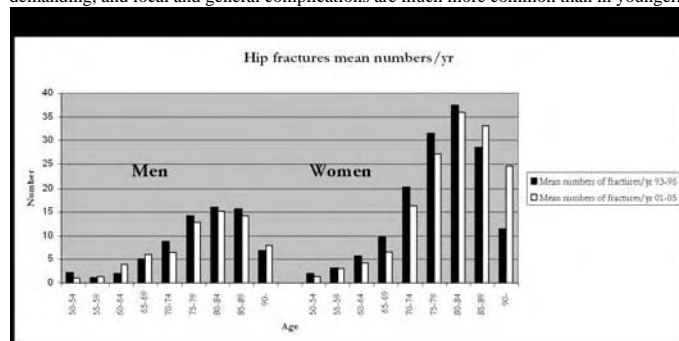
Decline in Age Adjusted Hip Fracture Incidence but a Drastic Increase in Hip Fractures Among the Very Oldest. Hip Fracture Curve Is Right-shifting. U. Bergström¹, Y. Gustafson², H. Jonsson¹, U. Pettersson¹, O. Svensson¹. ¹Dept of Orthopaedics, Umeå, Sweden, ²Dept of Community Med. and Rehab. Geriatric Medicine, Umeå, Sweden.

Introduction: Hip fracture incidence decreases in Europe and N. America. Is there a decreasing trend in all age groups or is just the fracture curve drifting?

Material and methods: This population-based material includes all hip fracture patients 1993-2005, ≥50 years, admitted to Umeå University Hospital: a total of 2,919 (31% men). The absolute numbers of fractures and incidence were mean value over the time periods 93-96 and 01-05.

Results: The overall hip fracture incidence was showing a declining trend, for the periods 93-96, 97-00 and 01-05: for women (men) 706 (390), 709 (314), and 625 (317) hip fractures per 100,000. However, the absolute numbers of hip fractures per year did not change over time. A 50% increase in absolute fracture rate was noted in women age 90 or older (11.5 hip fractures/year (93-96) and 24.6 hip fractures/year (01-05). The latter fracture rate can be compared with the absolute number of hip fractures in women age 75-79 (27.2 fractures/year 01-05) (Table 1). The incidence was also increasing during this period of time, from 2700/100,000 to 3900/100,000 among the women ≥ 90 years (Table 2). In men there were a declining trend in both incidence and absolute numbers, only a small increase of absolute fractures were noted among men ≥ 90 years.

Conclusion: Though the absolute incidence shows a declining secular trend, the absolute fracture rate and incidence are increasing among the very oldest. Women ≥ 90 now account for the same number of hip fractures every year as women 75-79 years. There seems to be a right shift and skewing of the hip fracture distribution towards the very oldest. This is probably due to the increased number of the octo- and nonagenarians, perhaps also to a better general- and bone health among the septuagenarians. This changed pattern will further strain the scarce orthopaedic and geriatric resources- surgery is more technically demanding, and local and general complications are much more common than in younger.



Disclosures: U. Bergström, None.

1052

Ethnic Variations in Hip Geometry Among Women at Baseline from the Women's Health Initiative. D. A. Nelson¹, T. J. Beck², C. E. Lewis³, T. Bassford⁴, J. A. Cauley⁵, M. S. LeBoff⁶, S. B. Going⁴, Z. Chen⁴. ¹Wayne State University, Detroit, MI, USA, ²Johns Hopkins University, Baltimore, MD, USA, ³University of Alabama, Birmingham, AL, USA, ⁴University of Arizona, Tucson, AZ, USA, ⁵University of Pittsburgh, Pittsburgh, PA, USA, ⁶Brigham and Women's, Boston, MA, USA.

The risk of osteoporotic fracture varies among ethnic groups in the U.S., presumably due to differences in bone mechanical strength. African Americans suffer fewer osteoporotic fractures than whites although fracture susceptibility is less well studied in other groups. Our objective was to describe ethnic differences in bone geometry, and possible contributing factors, using hip structure analysis (HSA) of the femoral neck (FN), shaft (FS) and intertrochanteric (IT) regions based on data from the Women's Health Initiative (WHI). Baseline data included DXA of bone and soft tissue, body size, lifestyle, and medical history in 10,516 women representing four ethnic groups (non-Hispanic White-NHW, African-American-AA, Mexican-American-MA, Native-American-NA), ages 50 to 79. Geometry was adjusted for age, height, weight and % lean mass (see FN results in Table).

Hip geometry measurements in FN region (adjusted)	NHW (N=8206)		AA (N=1476)		MA (N=704)		NA (N=130)	
	Mean	SD	Mean	SD	Mean	SD	Mean	SD
Cross sectional area (cm ²)	2.04	0.003	2.15*	0.008	2.03	0.012	2.07	0.028
Outer diameter (cm)	3.02	0.216	2.98*	0.005	3.02	0.008	3.01	0.018
Section modulus (cm ³)	0.916	0.002	0.948*	0.004	0.904	0.006	0.916	0.015
Buckling ratio	12.6	2.937	11.7*	0.070	12.6	0.100	12.4	0.23

*P<0.001 vs. NHW

Compared to NHW, AA women had consistently narrower femora with smaller buckling ratios at all regions. Geometric strength differences were variable: bending resistance (section modulus) was higher in FN but lower in IT and FS, while axial resistance (bone cross-sectional area) was higher in the FN and IT and lower in the FS. Neither MA nor NA women differed from NHW at the FN, but both had higher axial and bending resistance at the IT. MA women had slightly higher bending resistance at the FS. There appear to be ethnic differences in size adjusted femur strength parameters but the clearest advantage for AA women is in their lower buckling ratio. This suggests that they may be less susceptible to loss of strength due to local buckling compared to NHW. Geometric strength differences in MA and NA compared with NHW are less clear and are reduced by adjustment for selected skeletal dimensions in the hip.

Disclosures: D.A. Nelson, None.

This study received funding from: NIAMS.

1053

Risk Factors for Falls in Older Community-dwelling Women. K. A. Faulkner¹, J. A. Cauley¹, J. M. Zmuda¹, D. P. Landsittel², S. R. Cummings³, S. A. Studenski⁴, M. C. Nevitt³. ¹Epidemiology, University of Pittsburgh, Pittsburgh, PA, USA, ²Duquesne University, Pittsburgh, PA, USA, ³University of California San Francisco, San Francisco, CA, USA, ⁴University of Pittsburgh, Pittsburgh, PA, USA.

Identifying risk factors for a single fall is difficult due to accidents. The purpose of the study is to identify risk factors for more frequent incident falls among women with no recent history of falling. Study participants included 9,704 older community-dwelling women who were enrolled in the Study of Osteoporotic Fractures. The analysis sample consisted of 6,750 women (70% of median age (IQR) =72 years (67-75) who had no history of falls in past 12 months. A wide range of potential risk factors were assessed at baseline including 1) age, body mass index (BMI), height and education, 2) medical conditions, 3) medications, 4) lifestyle and 5) neuromuscular function. Data on the number of falls were self-reported every four months using post-card mailings over four years (97% complete) and fall rates were calculated (# falls/woman-years). Poisson regression models with Generalized Estimating Equations were used to calculate the Risk Ratio (RR), or ratio of fall rates. Step-wise building of a multivariate model was performed from 46 potential risk factors that all were minimally adjusted for age, clinic, height, BMI, and education. In the analysis sample including non-fallers at baseline, the average annual fall rates were 344 falls per every 1,000 woman-years. We identified the several risk factors for more frequent falls (p<0.05 for all), including having a high school education (RR= 1.03, vs. no high school education), higher number of Instrumental Activities of Daily Living (IADLs) with difficulty (RR=1.14, per 1 IADL), faster usual-paced walking speed (RR=1.07, per 1 SD), self-reported physician diagnosis of arthritis (RR=1.11), self-reported fear of falling (RR=1.22), and the current use of antidepressants (RR=1.25) and anticonvulsants (RR=1.46). Protective factors for more frequent falls (p<0.05 for all) included taller height (RR= .95, per 2 inches) and a higher number of step-ups completed in 10 seconds (RR=.93, per 1 SD). The RR indicates the increased risk (or decreased risk) in the average rate of falling that is associated with a given factor. Hence, the use of antidepressant and anticonvulsant medications is associated with fall rates 22% and 46% higher, respectively, compared to not using the medications. In conclusion, among older women with no recent history of falls, potentially modifiable risk factors for more frequent falls include the use of antidepressant and anticonvulsant medications, fear of falling, weaker muscle power and poorer functional status.

Disclosures: K.A. Faulkner, None.

1054

Age Effects on Hip Structure: Results in 636 WOMEN AGED 20 to 97. J. K. Brown¹, C. E. Cann^{*1}, R. L. Prince². ¹Mindways Software Inc., Austin, TX, USA, ²Sir Charles Gairdner Hospital, Perth, Australia.

The effects of age on three dimensional bone structure remains uncertain. 636 women, recruited from ten centres across the USA, had a standard, clinical, whole-body CT scan to develop reference data for QCT for regulatory purposes. Slices were taken at 2.5 - 3.0 mm intervals, pixel size 0.75mm and results normalized using a proprietary phantom. Images were analysed using Mindways CTXA Hip Version 3 software with partial volume correction. The CV error for the various measures was under 3%. The data relating bone structure to age is shown in the table.

Total Hip Site	Age Standardised Coefficient	Age ⁻¹ Standardized Coefficient	R ²
Total Mass	0.69 ^{xx}	-1.02 ^{xxx}	0.12
External volume	0.70 ^{xx}	NS	0.12
Total volumetric density	NS	-0.64 ^{xxx}	0.38
Cortical mass	0.66 ^{xx}	-1.02 ^{xxx}	0.19
Cortical volume	0.52 ^{xx}	-0.93 ^{xxx}	0.19
Cortical volumetric density	0.93 ^{xxx}	-0.79 ^{xxx}	0.04
Trabecular mass	0.47 ^{xx}	-0.60 ^{xxx}	0.30
Trabecular volume	0.47 ^{xx}	NS	0.30
Trabecular volumetric density	-0.47 ^{xx}	NS	0.44

^{xx} P < 0.01, ^{xxx} P < 0.001

Bone mass in the various compartments decreased with age as a quadratic by about 40% from age 20. The external bone volume and trabecular (marrow) volume increased with age linearly from age 20 by about 30%, while the cortical volume decreased with age as a quadratic. Volumetric density decreased with age in the total and trabecular compartment, but the cortical volumetric density data increased slightly with age. The changes at the total hip were representative of the changes at the femoral neck, trochanter and intertrochanter sites except for trochanter trabecular mass which was constant with age.

Bone mass at the hip falls from age 20 but the rate increases with age probably reflecting an effect of estrogen deficiency at menopause. However the external size of the hip increases from age 20 likely independent of changes in sex hormone levels. The cortical mass and volume decrease with age in such a way that there is little apparent change in cortical density consistent with thinning of the cortex with age.

Thus age effects on hip bone mass differ in critical respects to age effects on bone volume. Increases in external volume throughout life may increase bone strength and delay the onset of hip fracture.

Disclosures: J.K. Brown, Mindways Software Inc. 3, 4.

1055

Efficacy and Safety of Zoledronic Acid 5 mg in Preventing Fractures in Men and Women With Prevalent Hip Fracture: The HORIZON-Recurrent Fracture Trial. K. Lyles¹, C. Colon-Emeric^{*1}, J. Magaziner², J. Adachi³, C. Pieper^{*1}, L. Hyldstrup^{*4}, C. Mautalen⁵, C. Recknor⁶, K. Moore^{*1}, C. Lavechia^{*7}, J. Zhang^{*7}, P. Mesenbrink^{*7}, E. Eriksen⁸, S. Boonen⁹. ¹Duke Univ Med Ctr, Durham, NC, USA, ²Univ of Maryland, Baltimore, MD, USA, ³McMaster Univ, Hamilton, ON, Canada, ⁴Hvidovre Hospital, Univ of Copenhagen, Copenhagen, Denmark, ⁵Centro de Osteopatias Medicas, Buenos Aires, Argentina, ⁶United Osteoporosis Centers, Gainesville, GA, USA, ⁷Novartis Pharmaceuticals Corp, East Hanover, NJ, USA, ⁸Novartis Pharma AG, Basel, Switzerland, ⁹Univ of Leuven, Leuven, Belgium.

Hip fractures put patients at risk for future fracture and increased mortality. HORIZON-RFT is an international, multicenter, randomized, double-blind, placebo-controlled, parallel group trial assessing whether zoledronic acid (ZOL) 5 mg reduces subsequent clinical fractures in men and women ≥50 yrs of age with a prevalent hip fracture. Inclusion/exclusion criteria as previously described (Colon-Emeric et al. CMRO 2004;20:903). Patients received loading dose vitamin D2 or D3 and daily supplements of 800-1200 IU vitamin D3 and 1000-1500 mg elemental calcium. Patients were followed until 211 had experienced confirmed new clinical fractures (the primary efficacy endpoint). Of 2127 patients randomized, 2111 were treated with once-yearly IV infusions of ZOL 5 mg (N=1054) or placebo (PBO; N=1057). Baseline characteristics were similar between groups. Median age was 76 yrs (range, 50-98); 76% were women. Clinical fractures occurred in 231 patients (92 ZOL, 139 PBO) for a 2-yr cumulative event rate of 8.59% (ZOL) and 13.88% (PBO), based on Kaplan-Meier estimates, and a relative risk reduction of 35% (HR=0.65; 95% CI: 0.50-0.84; P=.0012). ZOL reduced risk for clinical vertebral and non-vertebral fractures relative to PBO by 46% (HR=0.54; 95% CI: 0.32-0.92; P=.0210) and 27% (HR=0.73; 95% CI: 0.55-0.98; P=.0338), respectively. ZOL reduced risk of hip fractures by 30% relative to PBO (HR=0.70; 95% CI: 0.41-1.19; P=.1815 [NS]). Overall incidence of AEs and SAEs was comparable between treatment groups. No significant differences were seen in any cardiovascular parameters or long-term renal function. No cases of ONJ were reported. Death occurred in 101/1054 ZOL patients (9.58%) vs 141/1057 PBO patients (13.34%), yielding a 28% lower mortality risk in ZOL relative to PBO (HR=0.72; 95% CI: 0.56-0.93, P=.0117). In conclusion, this trial showed that subjects with a prevalent hip fracture treated with an annual IV infusion of ZOL experienced significantly fewer clinical fractures compared with placebo. In addition, ZOL had a favorable safety profile and was well tolerated. Finally, this is the first trial to demonstrate a mortality benefit for an antiresorptive agent.

Disclosures: K. Lyles, Novartis, Procter & Gamble Sanofi-Aventis, Amgen 2; Novartis, Procter & Gamble Sanofi-Aventis, Merck, Amgen, Bone Medical LTD 5; Novartis, Dr. Lyles is co-inventor with Novartis Pharmaceuticals on a use patent for zoledronic acid US Provisional Patent Application No. 60-411,067. 9. This study received funding from: Novartis Pharma AG, Basel Switzerland.

1056

Risk Factors for Serious Adverse Events (SAEs) of Atrial Fibrillation in the HORIZON-PFT Trial of Zoledronic Acid. S. R. Cummings¹, P. Mesenbrink^{*2}, E. F. Eriksen³, R. Eastell⁴, D. M. Black⁵. ¹San Francisco Coordinating Center, C.P.M.C. Research Institute and University of California, San Francisco, San Francisco, CA, USA, ²Novartis Pharmaceuticals Corp, East Hanover, NJ, USA, ³Novartis Pharma AG, Basel, Switzerland, ⁴University of Sheffield, Sheffield, United Kingdom, ⁵San Francisco Coordinating Center, University of California San Francisco, San Francisco, CA, USA.

Findings from 2301 HORIZON-PFT Trial of zoledronic acid in postmenopausal women with osteoporosis (but not the 2310 Trial in elderly women with hip fracture) and from the Fracture Intervention Trial (FIT) of alendronate raise a possibility that use of bisphosphonates (BPs) might be associated with an increased risk of atrial fibrillation SAEs (defined as events resulting in hospitalization, disability, or judged to be life-threatening).

The 2301 Trial included 7714 women with osteoporosis treated with annual infusions of 5 mg of zoledronic acid or placebo for 3 years. Women who had taken a bisphosphonate for ≥1 year must have stopped for at least 2 years before enrollment. Previous bisphosphonate use was reported by 1161 or 14.5% of participants (type, dose and duration were not recorded). Arrhythmias were adjudicated by a panel of cardiologists. In an exploratory analysis using this dataset, we selected the best set of risk factors for atrial fibrillation by building stepwise proportional hazards models from age, baseline cardiovascular history, prior BP use and other potential risk factors after fixing treatment and study stratum into the model.

Significant risk factors for atrial fibrillation SAEs included congestive heart failure (CHF), tachyarrhythmia, age and previous use of bisphosphonates. The incidence of atrial fibrillation SAEs was 2.2% with prior BP use vs. 1.6% for no use. In an additional analysis, prior bisphosphonate use was not significantly associated with all (serious and non-serious) atrial fibrillation AEs.

Risk Factors for Atrial Fibrillation Serious Adverse Events		
Factor	Hazard Ratio (95% CI)	P-value
Treatment*	2.35 (1.43, 3.88)	0.001
Age (per year)	1.07 (1.02, 1.11)	0.002
CHF	2.86 (1.12, 7.25)	0.028
Tachyarrhythmia	6.01 (3.23, 11.2)	<0.001
Past BP use	1.81 (1.05, 3.13)	0.034

*Assignment to zoledronic acid vs. placebo

Older women with CHF and tachyarrhythmias have an increased risk of atrial fibrillation. This observational analysis suggests that women who have previously used bisphosphonates might have an increased risk for atrial fibrillation SAEs. This possibility needs additional investigation.

Disclosures: S.R. Cummings, Amgen, Novartis, Lilly, and Pfizer 2; Lilly, Merck, Zelos, Organon, and Amgen 5.

This study received funding from: Novartis.

1057

Efficacy of Continued Alendronate for Fractures in Women without Prevalent Vertebral Fracture: The FLEX Trial. A. V. Schwartz¹, D. C. Bauer¹, J. A. Cauley², K. E. Ensrud³, L. Palermo¹, R. B. Wallace^{*4}, M. C. Hochberg⁵, A. C. Feldstein⁶, A. Lombardi⁷, S. R. Cummings⁸, D. M. Black¹. ¹University of California, San Francisco, San Francisco, CA, USA, ²University of Pittsburgh, Pittsburgh, PA, USA, ³VA Medical Center & University of Minnesota, Minneapolis, MN, USA, ⁴University of Iowa, Iowa City, IA, USA, ⁵University of Maryland, Baltimore, MD, USA, ⁶Kaiser Permanente Northwest Center for Health Research, Portland, OR, USA, ⁷Merck & Co. Inc., Rahway, NJ, USA, ⁸California Pacific Medical Center, San Francisco, CA, USA.

The Fracture Intervention Trial (FIT) found that 4 years of alendronate (ALN) in women without prevalent vertebral fracture reduced the risk of non-vertebral fractures (NVF) in those with femoral neck (FN) T-score ≤ -2.5 but not in those with higher BMD. In the main results of the FIT Long Term Extension trial (FLEX), 10 years of ALN did not significantly reduce the risk of NVFs, compared with 5 years of ALN. Continuing ALN reduced the risk of clinical vertebral fractures but not the risk of x-ray defined vertebral fractures. We tested whether the long term effect of ALN on fracture among women without a prevalent vertebral fracture differs by FLEX baseline FN T-score.

In FLEX, 1099 women randomized to ALN in FIT (mean previous duration 5 years) were re-randomized to placebo (40%) or ALN 5 (30%) or 10 (30%) mg/d for an additional 5 years. The ALN groups were combined in these analyses. At FLEX baseline, 723 women (66%) did not have a prevalent vertebral fracture. We analyzed fracture results in this group, excluding 3 women without baseline hip BMD. Interaction models used continuous FN T-score.

Among women without vertebral fracture at FLEX baseline, we found significant

interactions between FLEX baseline FN T-score and treatment for NVF (table). Continuation of ALN reduced NVF in women with FLEX baseline FN T-score ≤ -2.5 but not in women with T-score > -2 . Results for clinical vertebral or morphometric vertebral fracture did not differ significantly by FN T-score at FLEX baseline.

Risk (95% CI) of Non-Vertebral Fracture among Women without Prevalent Vertebral Fracture			
FLEX Baseline FN T-score	N	Risk Difference	Relative Risk
FN T > -2	333	4.01% (-3.22, 11.24)	1.41 (0.75, 2.66)
-2.5 $<$ FN T ≤ -2	203	-3.46% (-13.30, 6.39)	0.79 (0.37, 1.66)
FN T ≤ -2.5	184	-13.32%* (-25.46, -1.18)	0.50* (0.26, 0.96)
Interaction (p-value)		0.049	0.019

*p<0.05

This post hoc analysis suggests that continuing alendronate for 10 years instead of stopping after 5 years reduces the risk of non-vertebral fracture in women without prevalent vertebral fracture whose FN T-score, achieved after 5 years of ALN, is ≤ -2.5 , but does not reduce risk of NVF in women whose T-score is > -2 . These results are similar to those previously reported for 4 years of ALN use.

Disclosures: A.V. Schwartz, GSK 5.
This study received funding from: Merck.

1058

Giant Osteoclast Formation After Long-Term Oral Aminobisphosphonate Therapy for Postmenopausal Osteoporosis. R. S. Weinstein, T. M. Chambers*, E. A. Hogan*, W. W. Webb*, C. A. Wicker*, S. C. Manolagas. Center for Osteoporosis, Central Arkansas Veterans Healthcare System, Univ of Ark for Med Sci, Little Rock, AR, USA.

Treatment of postmenopausal osteoporosis with aminobisphosphonates leads to progressive increases in bone density and a reduction in the incidence of new fractures. The efficacy of these drugs is believed to result from their ability to promote osteoclast apoptosis. However, bone specimens taken from non-human primates and patients treated with long-term aminobisphosphonates often show little or no effect of the drugs on the number of osteoclasts. We examined bone biopsies from 26 women with postmenopausal osteoporosis after a 3-yr double-blind, randomized, placebo-controlled trial of 10 mg/d of oral alendronate (ALN) for the prevention of postmenopausal bone loss. We report that in the subjects receiving ALN, osteoid perimeter, bone formation rate and biochemical markers of bone remodeling decreased whereas bone density increased as expected. Strikingly, osteoclast number was significantly increased in the subjects receiving ALN compared with those receiving placebo: 0.114 osteoclasts per mm cancellous perimeter \pm 0.078 SD, $n = 9$ vs. 0.059 \pm 0.038, $n = 17$, $p = 0.012$. In the ALN group, most of the osteoclasts were in superficial resorption cavities. Unexpectedly, giant osteoclasts were present in 4 out of the 9 (44%) of the ALN-treated subjects. Specifically, in these 4 subjects, 19% (13/68) of the osteoclasts observed were unusually large and had as many as 15 to 30 nuclei, as compared to 3 to 8 nuclei in the normal-sized osteoclasts of the placebo group. None of the subjects receiving placebo exhibited such cells (0/91). The atypical osteoclasts were partially detached from bone and they were clearly separated from the cancellous bone by unidentified mononuclear cells interspersed between them and the bone surface. In addition, the ruffled borders of the giant cells were distorted or missing. Further, the giant osteoclasts demonstrated positive nuclear in situ end labeling (ISEL) indicative of apoptosis, as well as nuclear condensation, fragmentation and peripheral beading. We conclude that long-term treatment with ALN decreases osteoclast resorptive ability rather than number, possibly by disrupting the ruffled border. Moreover, such treatment gives rise to a previously unrecognized cell phenotype: an apoptotic, excessively nucleated, colossal osteoclast, with apparent resistance to the phagocytosis that normally results from the detachment of cells from the bone matrix. Although these abnormal cells may well be dysfunctional and of no direct danger to the patient, awareness of the condition is crucial because giant osteoclasts could lead to a mistaken diagnosis of Paget's disease or hyperparathyroidism.

Disclosures: R.S. Weinstein, Merck 8.

1059

Effect of Daily Oral Minodronate on Vertebral Fractures in Japanese Postmenopausal Women with Established Osteoporosis: A Randomized Placebo-Controlled Double-Blind Study. T. Matsumoto¹, H. Hagino², M. Shiraki³, M. Fukunaga⁴, T. Nakano⁵, K. Takaoka⁶, H. Morii⁶, Y. Ohashi⁷, T. Nakamura⁸. ¹University of Tokushima Graduate School of Health Biosciences, Tokushima, Japan, ²Tottori University, Yonago, Japan, ³Research Institute and Practice for Involuntional Diseases, Nagano, Japan, ⁴Kawasaki Medical School, Okayama, Japan, ⁵Tamana Central Hospital, Kumamoto, Japan, ⁶Osaka City University, Osaka, Japan, ⁷University of Tokyo, Tokyo, Japan, ⁸University of Occupational and Environmental Health, Kitakyushu, Japan.

Minodronate (ONO-5920/YM529), a potent bisphosphonate, has been shown to increase the lumbar bone mineral density (BMD) of postmenopausal women with established osteoporosis. However, its efficacy in reducing osteoporotic fractures has not been evaluated. The present study was undertaken to examine the efficacy and safety of daily oral minodronate on the risk of vertebral and other fractures in subjects with established osteoporosis.

Seven hundred and four postmenopausal Japanese women at 55 to 80 years of age with one

to five vertebral fractures and BMD below 80% of the young adult mean were enrolled in this study. The subjects were randomly assigned to receive either daily 1 mg minodronate ($n=359$) or placebo ($n=345$) for 26 months. All the participants received daily supplements of 600 mg calcium and 200 IU vitamin D₃. Daily oral 1 mg minodronate for 26 months, compared with placebo, reduced the cumulative incidence of new vertebral fractures (10.4 vs 24.0%; $p<0.0001$) by 58.9% (95% CI, 36.6-73.3%) over 26 months. Because a large number of vertebral fractures occurred during the first 6 months in both groups (20 and 27 in minodronate and placebo groups, respectively), the cumulative incidence of new vertebral fractures from 6 to 26 months was reduced by 74.1% (4.7% vs 16.6%; $p<0.0001$) by minodronate treatment. A non-significant reduction in the incidence of overall clinical fractures was observed by 26 months of minodronate treatment (9.4 vs 13.8%). Minodronate treatment also reduced height loss both after 12 months (1.2 mm vs 3.4 mm in placebo) and 26 months (3.7 mm vs 6.8 mm). Bone turnover markers were suppressed by about 50% after 6 months of minodronate treatment, and remained suppressed thereafter. The overall safety profile including gastrointestinal safety was similar between the two groups. These results demonstrate that daily oral minodronate is safe, well-tolerated, and is effective in reducing vertebral fracture incidence in postmenopausal women with established osteoporosis. Because the dose of minodronate in reducing fracture incidence was low, further studies are warranted to evaluate the efficacy of intermittent administration of higher oral doses of minodronate on osteoporotic fractures.

Disclosures: T. Matsumoto, ONO Pharmaceutical Co., Ltd. 5; Astellas Pharma Inc. 5; Chugai Pharmaceutical Co., Ltd. 5; Eli Lilly Japan K.K. 5.

1060

Efficacy of Clodronate on Fracture Risk in Women Selected by 10-year Fracture Probability. E. McCloskey¹, H. Johansson^{*1}, A. Oden^{*1}, S. Aropuu^{*2}, T. Jalava^{*2}, J. Kanis¹. ¹University of Sheffield, Sheffield, United Kingdom, ²Bayer Schering Pharma, Berlin, Germany.

Treatments for osteoporosis are commonly targeted to patients with low bone mineral density. The WHO tool for fracture prediction estimates an individual's probability of fracture in the next 10 years from clinical risk factors, with or without BMD measurement. To determine if patients identified at high risk by the algorithm are responsive to anti-resorptive treatment, we examined the effects of the bisphosphonate, clodronate, on fracture incidence during 3 years of treatment across the range of fracture probabilities estimated by the WHO tool.

5212 women aged 75 years and older, randomly selected from the local population were randomised, regardless of the presence or absence of osteoporosis, to receive 3 years of therapy with clodronate (BONFOS[®]) 800mg daily p.o. or an identical placebo. The 10-year probability of fracture in each woman was computed using baseline clinical risk factors including BMI, prior fracture, glucocorticoid use, parental hip fracture, smoking, alcohol and secondary osteoporosis. Femoral neck BMD measurements were also obtained at baseline. The interaction between probability of fracture and treatment efficacy to reduce the incidence of all osteoporosis-related fractures was determined using Poisson regression analysis.

Complete clinical risk factor data were available in 3974 women (76.2% of the cohort). The 10-year probability for osteoporotic fracture without BMD was 20.0 \pm 7.3% (mean \pm SD) with the range 7.3-72.8%. The probability for osteoporotic fracture with BMD was 18.1 \pm 8.6% (mean \pm SD) with the range 1.4-73.0%. The interaction between fracture probability and treatment efficacy was not significant when probability was assessed either with or without BMD ($p=0.098$ and $p=0.11$ respectively). A non-significant trend was observed for greater fracture reduction at higher fracture probability, with or without the use of BMD. For example, women lying at the 75th percentile of fracture probability in the absence of BMD had a fracture probability of 24% and treatment reduced the risk of fracture by 23% over 3 years (HR 0.77, 95%CI 0.63-0.95). In those with a fracture probability of 30% (90th percentile), the fracture risk reduction was 31% (HR 0.69, 0.53-0.90). We conclude that the estimation of an individual's 10-year probability of fracture identifies patients at high risk of fracture who will respond to bisphosphonate therapy.

Disclosures: E. McCloskey, Bayer Schering Pharma 2, 8.
This study received funding from: Bayer Schering Pharma.

1061

Central Control of Bone Remodelling by Neuromedin U: A Mediator of the Leptin-dependent Regulation of Bone Formation. S. Sato^{*1}, S. Takeda¹, R. Hanada^{*2}, M. Iwasaki^{*1}, H. Inose¹, A. Kimura^{*1}, K. Kangawa^{*3}, M. Kojima^{*2}, K. Shinomiya^{*1}. ¹Orthopaedic Surgery & 21COE Program, Tokyo Medical and Dental University, Tokyo, Japan, ²Molecular Genetics, Institute of Life Science, Kurume University, Kurume, Japan, ³Biochemistry, National Cardiovascular Center Research Institute, Osaka, Japan.

Leptin inhibits bone formation through a hypothalamic relay and the sympathetic nervous system (SNS). However, hypothalamic target molecule of leptin remains to be elucidated. Neuromedin U (NMU) is an anorexigenic neuropeptide whose expression is induced by leptin. In this study, we investigated the role of NMU on bone remodelling and the possible crosstalk between NMU signalling pathway and leptin-SNS pathway. NMU deficient mice (NMU^{-/-} mice) exhibited a 30% increase in bone mass compared to wild-type (wt) mice. Bone formation in NMU^{-/-} mice was increased as revealed by higher bone formation rate and osteoblast surface. Indeed, in vivo, osteoblast mitotic index analyzed by BrdU incorporation was significantly increased in NMU^{-/-} mice. In contrast, bone resorption parameters of NMU^{-/-} mice were comparable to those of wt mice. In vitro, differentiation or proliferation of primary osteoblasts isolated from NMU^{-/-} mice was similar to those from wt mice. In addition, treatment with varying concentrations of NMU did not affect osteoblast function, suggesting the lack of direct effect of NMU on osteoblast. In contrast, continuous intracerebroventricular infusion (ICV) of NMU to NMU^{-/-} mice decreased bone volume significantly, indicating the central nature of NMU's action on bone formation. Leptin ICV decreased bone volume and bone formation in wt mice, as previously reported. However, and surprisingly, leptin ICV paradoxically increased bone formation and osteoblast number in NMU^{-/-} mice. Likewise, injection of isoproterenol, a beta agonist, reduced bone mass in wt mice. However, NMU^{-/-} mice were resistant to the antiosteogenic activity of isoproterenol. Furthermore, NMU/Adrb2 (gene encoding beta2 adrenergic receptor) double heterozygote mice had higher bone mass than Adrb2 single heterozygote mice or NMU single heterozygote mice. Collectively, our study shows that NMU inhibits osteoblast proliferation and bone formation through the central nervous system. Moreover, it suggests that NMU mediates the antiosteogenic action of the leptin-SNS pathway.

Disclosures: S. Sato, None.

1062

ECM1, a Direct Targeting Molecule of PTHrP, Is a Novel Potent Mediator of Chondrogenesis. L. Kong^{*1}, Y. Zhang^{*1}, B. Jiang^{*2}, Y. Xie^{*2}, J. Q. Feng², T. Kobayashi^{*3}, H. M. Kronenberg³, C. Liu¹. ¹Department of Orthopaedic Surgery, New York University, New York, NY, USA, ²Department of Biomedical Sciences, Baylor College of Dentistry, Texas A&M University System Health Science Center, Dallas, TX, USA, ³Endocrine Unit, Massachusetts General Hospital, Boston, MA, USA.

Chondrogenesis is controlled by cellular interactions with surrounding matrix proteins and growth factors that mediate cellular signaling pathways. In a functional genetic screen for proteins associating with cartilage oligomeric matrix protein, we identified a novel extracellular matrix protein, ECM1 (extracellular matrix protein 1), a molecule that had previously been linked to lipid proteinosis and lichen sclerosis, a common chronic inflammatory condition. We verified this novel interaction using in vitro pulldown and in vivo coimmunoprecipitation assays and demonstrated that these two proteins colocalized on the cellular surface of primary human chondrocytes. Using RT-PCR and western blotting assays, we showed that both mRNA and protein levels of ECM1 were upregulated during differentiation of chondrocytes. ECM1 significantly inhibited mRNA levels of both early and later genes critical for chondrogenesis such as Sox9 (78% reduction), collagen type II (82% reduction), and collagen X (90% reduction) and repression of ECM1 via the siRNA silencing markedly enhanced the expression of Collagen X in the course of chondrogenesis (22 and 5 fold in ADTC5 and 10T1/2 mesenchymal stem cells respectively). To determine the potential mechanisms by which ECM1 negatively regulates chondrogenesis, we studied the effects of ECM1 on PTHrP (an essential negative regulator for later chondrogenesis) and IHH (a positive regulator of chondrogenesis). ECM1 induced PTHrP 5- to 18-fold and inhibited IHH (50% reduction) during chondrogenesis. We further showed that PTHrP induced mRNA levels of ECM1 (28-fold) in chondrocytes. Importantly, knocking down ECM1 mRNA levels via the siRNA silencing or blocking ECM1 protein activity via anti-ECM1 antibodies completely abolished the effects of PTHrP on chondrogenesis in vitro. Using an immunohistochemistry assay, we showed that ECM1 was expressed throughout the chondrocyte zone of growth plates and articular cartilage and that ECM was no longer detectable in PTHrP null growth plates at day E18.5 in vivo. Last, we demonstrated that both mRNA and protein levels of ECM1 were upregulated in arthritis using microarray, real-time PCR and western blotting assays. Our findings demonstrate for the first time that ECM1, a direct downstream molecule of PTHrP in cartilage, is a novel negative regulator of chondrocyte differentiation and suggest that ECM1 may also plays an important role in the pathology of arthritis.

Disclosures: L. Kong, None.
This study received funding from: NIH.

1063

Regulation of Chondrocyte Hypertrophy and Bone Mineral Density by Matrilin-3 Through Modulating Bone Morphogenetic Protein Signaling Pathways. X. Yang^{*1}, L. van der Weyden^{*2}, L. Wei^{*1}, Z. Wang^{*1}, A. Bradley^{*2}, Q. Chen¹. ¹Brown University, Providence, RI, USA, ²Wellcome Trust Sanger Institute, Cambridge, United Kingdom.

Regulation of the entrance to and the exit from the hypertrophic stage of chondrocyte differentiation during endochondral ossification is crucial to the normal development and mineralization of a long bone. Mis-regulation of hypertrophy leads to chondrodysplasia. Important regulators of chondrocyte hypertrophy include growth factors such as bone morphogenetic proteins (BMPs) and extracellular matrix (ECM) proteins. Matrilin-3 (MATN3) is a member of the matrilin family, a group of the adhesive ECM proteins. Mutations in the human gene of MATN3 result in a variety of skeletal diseases including multiple epiphyseal dysplasia, spondylo-epi-metaphyseal dysplasia, and hand osteoarthritis. To determine the function of matrilin-3 in endochondral ossification, we examined the consequences of both knocking out MATN3 and over-expressing MATN3 in hypertrophic chondrocytes. In MATN3 KO mice, the hypertrophic zone of the embryonic tibial growth plate was expanded in comparison to its wildtype littermates. Thus, the lack of matrilin-3 leads to mis-regulation of chondrocyte differentiation in the developing epiphyseal growth plate. By 18 weeks of age MATN3 null mice had a significantly higher total body and knee joint bone mineral density (BMD) than wild-type littermates. Aged MATN3 null mice were much more predisposed to develop severe osteoarthritis than their wild-type littermates. Conversely, Over-expression of MATN3 in embryonic chondrocytes during their transition to hypertrophy led to reduced expression of Col X mRNA, a marker of chondrocyte hypertrophy. Deletion of the cis-acting element in the Col X promoter indicated that the 5' distal region containing BMP responsive elements was necessary and sufficient to mediate the inhibitory effect of MATN3 on Col X. This suggests that MATN3 inhibition of Col X expression is mediated by the BMP pathways. Immunoprecipitation pull-down assay detected BMP-2 in a complex with MATN3 in the conditioned medium of MATN3 transfected cells, suggesting MATN3 may inhibit BMP signaling by interacting and sequestering BMP-2 extracellularly. Interestingly, increased BMP signaling in MATN3 KO mice was indicated by an increase of phosphorylated Smad1 in the growth plate. Our data revealed that MATN3 plays a negative role in regulating chondrocyte hypertrophy by modulating BMP signaling. It suggest a novel pathological mechanism by which matrix defects lead to abnormal BMP signaling that ultimately affects ossification, bone mineral density, and skeletal development and aging.

Disclosures: Q. Chen, None.
This study received funding from: NIH/NIA.

1064

Perlecan Modulates FGF and VEGF Signaling and Is Essential for Vascularization in the Development of the Cartilage Growth Plate. M. Ishijima¹, E. Arikawa-Hirasawa^{*2}, K. Hozumi^{*1}, N. Suzuki^{*1}, K. Kosaki^{*1}, T. Matsunobu^{*1}, Y. Yamada^{*1}. ¹Laboratory of Cell and Developmental Biology, National Institute of Dental and Craniofacial Research, National Institute of Health (NIH), Bethesda, MD, USA, ²Research Institute for Diseases of Old Age, Juntendo University School of Medicine, Tokyo, Japan.

Perlecan (Perl) is a heparan sulfate proteoglycan that is expressed in all basement membranes and in cartilage. Perl-deficiency in mice and humans causes lethal chondrodysplasia, indicating that Perl is essential for cartilage development. However, the precise function of Perl in cartilage development is unknown. The purpose of this study is to investigate the mechanism of Perl functions in growth plate development. Here, we describe the critical role of Perl in FGF/VEGF signaling and angiogenesis in growth plate formation. The Perl^{-/-} growth plate is short with severely impaired endochondral bone formation. Chondrocyte proliferation is reduced, and the hypertrophic matrix is disorganized. Although chondrocytes are differentiated, the expression of FGF downstream genes is dysregulated. We found that both FGFR3 and FGFR1 were activated in the Perl^{-/-} growth plate. Expression of VEGF, a FGF/FGFR target gene, was upregulated by Perl^{-/-} hypertrophic chondrocytes, suggesting that the lack of vascularization into the hypertrophic zone is not due to the reduced VEGF expression. We demonstrated that Perl bound VEGFR but not VEGF. Expression of the Perl transgene specifically in cartilage of Perl^{-/-} mice rescued the perinatal lethality of Perl^{-/-} mice, and vascularization into the growth plate was restored, indicating that perlecan in the growth plate is critical in this process. These results suggest that Perl in the growth plates activates VEGFR signaling of endothelial cells for vascularization into the growth plate. Thus, we conclude that perlecan plays a critical role in endochondral bone formation via modulating FGF/VEGF signaling and promoting angiogenesis.

Disclosures: M. Ishijima, None.

1065

Genetic and Pharmacologic Activation of the Hypoxia Inducible Factor Pathway Promotes Angiogenesis and Accelerates Bone Regeneration. C. Wan¹, S. R. Gilbert², Y. Wang¹, X. Cao^{*1}, X. Shen^{*1}, G. Ramaswamy^{*3}, K. A. Jacobsen^{*4}, Z. S. Alaql^{*4}, L. C. Gerstenfeld⁴, T. A. Einhorn⁴, A. W. Eberhardt^{*3}, L. Deng^{*1}, T. L. Clemens¹. ¹Pathology, University of Alabama at Birmingham, Birmingham, AL, USA, ²Orthopaedic Surgery, University of Alabama at Birmingham, Birmingham, AL, USA, ³Biomedical Engineering, University of Alabama at Birmingham, Birmingham, AL, USA, ⁴Boston University School of Medicine, Boston, MA, USA.

Angiogenesis is critical for bone formation and occurs in close spatial and temporal association with osteogenesis during skeletal development and regeneration. Osteoblasts sense fluctuations in oxygen tension and respond to hypoxia by activating the hypoxia-inducible factor-1 α (HIF-1 α) pathway, which in turn activates vascular endothelial growth factor (VEGF) and other angiogenic gene programs. In this study, we applied genetic and pharmacologic strategies to manipulate HIF-1 α levels in osteoblasts and determine its role in bone regeneration. Overexpression of HIF-1 α was achieved by deleting VHL, a key component of the E3 ubiquitin degradation pathway. Mice overexpressing HIF-1 α (Δ VHL) or lacking HIF-1 α (Δ HIF-1 α) in osteoblasts were subjected to distraction osteogenesis (DO) and bone vascularity and regeneration were measured by angiography and CT. HIF overexpressing Δ VHL mice showed increased vascularity (2.4 fold in vessel volume/total volume, VV/TV), increased VEGF expression and CD31 staining and markedly increased (1.6 fold) BV/TV after consolidation compared with control littermates. Three point bending testing showed increased peak load to failure (3.5 fold) of the Δ VHL bones compared with controls. Concomitant treatment of the Δ VHL mice with VEGF receptor 1 and 2 neutralizing antibodies during distraction markedly attenuated both the angiogenic and osteogenic phases of the repair process. By contrast, Δ HIF-1 α mice exhibited decreased vascularity (2 fold in VV/TV) and decreased bone volume (1.7 fold) in the distraction gap after consolidation compared to control littermates. To pharmacologically induce HIF-1 α , we screened a series of prolyl hydroxylase inhibitors for their ability to activate a HIF-responsive reporter gene. Two compounds, desferrioxamine (DFO) and L-mimosine were then evaluated for their bone regenerative efficacy by local injection in the DO model. Wild type mice receiving DFO, but not L-mimosine, exhibited significantly increased vascularity (2.3 fold in VV/TV) and increased bone (1.5 fold in BV/TV) in the distraction gap compared to vehicle treated mice. We conclude that activation of the HIF pathway accelerates bone healing by stimulating both angiogenesis and osteogenesis. Our results demonstrate the feasibility of developing HIF-1 α activating agents to facilitate bone regeneration.

Disclosures: C. Wan, None.

This study received funding from: NIH grant R01 AR049410(TLC) and P30AR046031(SRG).

1066

Over-expression of Runx2 in Mesenchymal Cells Enhanced Bone Formation but Inhibited Cartilage Formation and Limb Development. C. A. Yoshida^{*}, T. Maeno^{*}, N. Kanatani^{*}, T. Fujita^{*}, S. Izumi^{*}, T. Komori^{*}. Department of Cell Biology, Unit of Basic Medical Sciences, Nagasaki University Graduate School of Biomedical Sciences, Nagasaki, Japan.

Runx2 is an essential transcription factor for skeletal development. Although the roles of Runx2 in osteoblast differentiation and chondrocyte maturation have been extensively studied, the functions of Runx2 at an early developmental stage, when multipotent mesenchymal cells commit to the osteoblastic or the chondrocytic cell lineage, still remain to be investigated. To clarify this issue, we prepared Runx2 transgenic mice using a 2.5kb Prx1 promoter, which drove Runx2 expression to mesenchymal cells in calvarium, limb primordia, maxilla, mandible, and neck. At embryonic day (E) 13.5 skeletal preparations of Runx2 transgenic mice, but not wild-type mice, displayed calcification of calvarial tissues. At E15.5 Runx2 transgenic mice showed brain hernia due to a fusion of the frontal, parietal, and occipital bones. Furthermore, at this stage, the absence of the sternum, resulted in heart and liver hernia. Histological examination of transgenic mice at E12.5, revealed abnormal Col1 α expression and mineralization in the calvarium and neck. Development of the limbs in Runx2 transgenic mice was clearly inhibited, and the level of inhibition ranged from mild to a complete abrogation of cartilage formation. Limb buds of Runx2 transgenic embryos at E10.5 showed reduced or undetectable expression levels of Fgf8, Shh, and Fgf4 but augmented apoptotic cells in the ectoderm compared to those of wild type mice, indicating that apical ectodermal ridge formation was inhibited. These data demonstrate that Runx2 is able to induce differentiation of mesenchymal cells into osteoblasts in presumptive regions of bone formation and even in ectopic areas but to inhibit the differentiation of mesenchymal cells into chondrocytes. Further, our findings indicate that Runx2 can disturb limb development by inhibiting the formation of apical ectodermal ridge.

Disclosures: C.A. Yoshida, None.

This study received funding from: Ministry of Education, Culture, Sports, Science, and Technology, Japan.

1067

Targeted Deletion of a Distant Transcriptional Enhancer of the RANKL Gene Reduces Bone Remodeling and Increases Bone Mass. C. Galli¹, P. E. Cazer^{*1}, L. A. Zella², J. A. Fretz^{*2}, J. W. Pike², R. S. Weinstein¹, S. C. Manolagas¹, C. A. O'Brien¹. ¹Center for Osteoporosis and Metabolic Bone Diseases, University of Arkansas for Medical Sciences and Central Arkansas Veterans Healthcare System, Little Rock, AR, USA, ²Department of Biochemistry, University of Wisconsin, Madison, WI, USA.

Previous in vitro studies, using BAC-based transcriptional reporter constructs and ChIP-on-chip assays, indicated that PTH and 1,25(OH) $_2$ D $_3$ stimulate murine RANKL expression in stromal/osteoblastic cells via an evolutionarily-conserved transcriptional enhancer. This enhancer is located 76 kb upstream from the transcription start site and is designated the RANKL distal control region (DCR). To determine the significance of this enhancer for control of RANKL expression and bone homeostasis, we created knock-out (KO) mice in which the 2 kb DCR was eliminated by gene targeting. DCR null mice were viable, fertile, and, in contrast to RANKL KO mice, were not osteopetrotic. Nonetheless, deletion of the DCR reduced PTH- and 1,25(OH) $_2$ D $_3$ -stimulation of RANKL mRNA and osteoclast formation in primary bone marrow cultures. Consistent with this, stimulation of RANKL mRNA in bone by a single injection of either PTH or 1,25(OH) $_2$ D $_3$ was blunted in DCR KO mice. DCR deletion also reduced basal RANKL mRNA levels in bone, thymus, and spleen. Spinal and femoral bone mineral density (BMD) was elevated in both male and female mice lacking the DCR beginning at 2 months of age and remained elevated up to at least 6 months of age, with the difference in BMD between genotypes remaining relatively constant during this time period. The increase in spinal BMD was approximately 9% in 5-month-old mice and was associated with a 28% increase in vertebral compression strength. Histomorphometric analysis of lumbar vertebra revealed reduced osteoclast and osteoblast formation leading to a low rate of bone remodeling similar to that observed in humans and mice with hypoparathyroidism. Moreover, deletion of the DCR increased trabecular number and thickness and decreased trabecular separation, suggesting that reduced remodeling of the primary spongiosa during growth may be responsible for the increase in bone volume. Consistent with this finding, DPD excretion in urine was reduced in DCR KO mice. However, circulating calcium and PTH levels were similar in wild-type and DCR-deficient mice, demonstrating that PTH control of RANKL is not required for calcium homeostasis under basal conditions. Taken together, these findings demonstrate that PTH control of RANKL expression via the DCR is a critical determinant of the rate of bone remodeling and provide new insights into the relationship, or lack thereof, between the calcium regulating actions of PTH and its effects on the skeleton.

Disclosures: C. Galli, None.

1068

Oncostatin M Is an Essential Stimulus of Bone Formation and Osteoclastogenesis. N. A. Sims, E. C. Walker^{*}, I. J. Poulton^{*}, N. E. McGregor^{*}, M. T. Gillespie, T. J. Martin. St. Vincent's Institute of Medical Research, Melbourne, Australia.

The gp130 receptor is common to many cytokines, including IL-6, IL-11, LIF and cardiotrophin-1 (CT-1) which are all important for regulating bone mass in vivo. Murine oncostatin M (OsM) signals through gp130 bound to a specific receptor, OsMR. Osteoblasts express OsMR, and OsM has been reported to increase osteoclast formation by dramatically increasing their RANKL production. The effects of OsM on bone formation however, are not clearly defined.

To determine whether OsM action is essential for bone formation in vivo, we studied the bone phenotype of 10 week-old OsMR deficient mice. While cortical dimensions and density were not altered, male and female OsMR null mice demonstrated a 75% increase in trabecular bone volume in the distal tibia and 4th lumbar vertebrae. Femoral trabecular BMD was also elevated (by 40%) in both males and females. This was associated with a significant (30%) reduction in osteoclast surface and reduced bone resorption, consistent with the known effect of OsM on osteoclast generation in co-cultures. Bone formation was also significantly reduced, evidenced by low osteoid thickness (reduced to 30%), osteoblast surface (reduced to 60%) and bone formation rate (halved). In contrast, the number of marrow adipocytes was elevated ~4 fold.

To determine the effects of OsM on bone formation, Kusa 4b10 murine stromal cells were treated with OsM (1.25-10ng/ml) for 14 to 21 days. Under mineralising conditions, OsM treatment dose-dependently increased mineralisation; doses as low as 1.25 ng/ml more than doubled alkaline phosphatase activity and alizarin red staining compared to untreated controls. In contrast, under adipogenic conditions adipocyte formation was more than halved. Both the reduced adipogenesis and increased bone formation with OsM treatment are consistent with the opposite observations in OsM-deficient animals.

To identify targets of OsM, we studied its effects on gene expression by undifferentiated Kusa4b10 cells and Kusa4b10 cells differentiated along the osteoblast lineage for 17 days. In both systems, there was a 90% reduction in PPARgamma at 24 hours and a rapid 20-fold increase in C/EBPdelta (but no change in C/EBPbeta) expression within 1 hour of OsM administration. Since C/EBPdelta has been shown to synergise with runx2 to enhance osteocalcin transcription we investigated the effect of OsM on a 6xOSE-luciferase reporter construct in UMR106-06 cells. We detected a dose-dependent increase in reporter activity in response to OsM that was maximal by 6 hours and equivalent to levels observed with 1,25D3 and CT-1.

This reveals a critical role for OsMR in maintaining normal levels of bone resorption and bone formation in vivo, as well as an inhibitory role in adipocyte differentiation.

Disclosures: N.A. Sims, None.

1069

Zfp521, a D2DFosB-interacting Protein, Regulates Chondrocyte Differentiation Downstream of PTHrP. D. Correa, R. Kiviranta, L. Neff*, W. C. Horne, R. Baron. Orthopaedics, Yale University, New Haven, CT, USA.

Chondrocytes are derived from mesenchymal precursor cells through a tightly regulated differentiation process. The paracrine factor PTHrP and the transcription factor Runx2 are key regulators in this program and have opposing actions in prehypertrophic chondrocytes, with PTHrP inhibiting and Runx2 favoring chondrocyte differentiation. We identified the zinc finger protein Zfp521, a 180 kDa protein consisting of 30 kruppel-like zinc fingers, as a $\Delta 2\Delta$ FosB-interacting protein in a yeast-two hybrid screen of an osteoblast cDNA library. In situ hybridization with a Zfp521-specific probe showed that Zfp521 is expressed in mesenchymal condensations as early as day E12.5 and in the developing growth plates of long bones, as well as in osteoblasts. Immunostaining detected Zfp521 mainly in PTHrP receptor (PTH1R)-expressing prehypertrophic chondrocytes. In the well-established ATDC5 cell model of in vitro chondrogenesis, the endogenous expression of Zfp521 was observed primarily at the stage of transition from prehypertrophic to hypertrophic chondrocytes, with a peak around the third week of culture, sharing again a similar pattern of expression with the PTH1R. Transient overexpression of Zfp521 in the ATDC5 cells inhibited chondrogenic differentiation, with decreased Alcian Blue staining and impaired cartilage nodule formation at day 12 of culture. This effect was comparable to the inhibitory effect of PTHrP(1-34). Treatment with PTHrP(1-34) did not increase the Zfp521-induced inhibition of nodule formation in these cells, suggesting that PTHrP and Zfp521 might share the same signaling pathway. Consistent with this hypothesis, stimulation of ATDC5 cells with PTHrP(1-34) and Forskolin promoted Zfp521 expression, regardless of the stage of differentiation, and inhibited chondrocyte progression from prehypertrophic to hypertrophic stages. In contrast, PTHrP(7-34), a known competitive antagonist of PTHrP(1-34), downregulated Zfp521 expression suggesting that it blocked the auto/paracrine effect of PTHrP(1-34), including its positive influence on Zfp521 expression. Additionally, PTHrP(1-34) but not PTHrP(7-34) had a negative effect on Runx2 expression during the differentiation of the ATDC5 cells. Therefore, based on Zfp521's negative effect on chondrogenesis, its pattern of expression in the growth plate and in the ATDC5 model, and its upregulation by PTHrP(1-34), we propose that Zfp521, which antagonizes the transcriptional activity of Runx2, lies downstream of PTHrP at the control point of the progression from prehypertrophic to hypertrophic chondrocytes in the growth plate.

Disclosures: D. Correa, None.

1070

Insulin Promotes Osteoblast Differentiation Independent from IGF-1 Signaling and Its Receptor Is Required for Normal Post Natal Bone Acquisition. K. Fulzele*, Z. Liu*, C. Wan*, W. Zhang*, J. Bruening*, T. L. Clemens*. ¹Department of Pathology, University of Alabama at Birmingham, Birmingham, AL, USA, ²Department of Mouse Genetics and Metabolism, Institute for Genetics, Center of Molecular Medicine, University of Cologne, Cologne, Germany.

Defective bone formation is common in patients with insulin-dependent diabetes mellitus, suggesting that insulin normally exerts anabolic actions in bone. Previous studies suggested that insulin might exert direct effects on osteoblast proliferation and apoptosis. However, because insulin can cross-activate the IGF-1 receptor (IGF-1R), which also functions in bone, it has been difficult to establish direct (IGF-1 independent) actions of insulin in osteoblasts. In this study, we first compared the effects of insulin and IGF-1 on differentiation of primary osteoblasts in vitro. Primary calvarial mouse osteoblasts expressing normal levels of IGF-1R (WT) or deficient in IGF-1R (IGF-1R KO) were differentiated in osteogenic medium with or without insulin or IGF-1. In WT osteoblasts, expression of IGF-1R mRNA declined with differentiation whereas insulin receptor (IR) mRNA remained constant. WT osteoblasts treated with insulin differentiated more rapidly than those treated with IGF-1, as evidenced by increased ALP activity and von Kossa staining. Insulin induced robust activation of Akt and GSK3 β that were not dependent on IGF-1R since they were also observed in IGF-1R KO osteoblasts. Moreover, insulin, but not IGF-1, upregulated expression of Runx2 in WT and KO cells suggesting that insulin promotes differentiation of the primary osteoblasts via the Akt-Runx2 pathway. To investigate the effects of insulin in bone in vivo, we selectively disrupted the IR in osteoblasts using Cre-loxP recombination. Mice carrying floxed IR alleles were mated with a mouse expressing the Cre recombinase driven by the human osteocalcin promoter to generate IR osteoblast-specific knock out mice. Micro-CT analysis of femurs from 3-week-old male OC-Cre IR floxed mice (N=4) showed that bone volume was significantly decreased in IR KO mice compared with IR-floxed littermates. Taken together, our results suggest that insulin exerts direct actions on osteoblasts and signaling through its receptor is required for normal post-natal bone acquisition in vivo. We predict that the loss of insulin action in osteoblasts during states of insulin resistance may contribute to defective bone formation seen in patients with diabetes.

Disclosures: K. Fulzele, None.

This study received funding from: Veterans Administration Merit Review Grant.

1071

Osteogenic Stem Cell Homing to Sites of Endochondral Bone Formation. C. M. Foulletier-Dilling*, A. M. Wada*, Z. Lazard*, M. E. Dickinson*, A. R. Davis¹, F. H. Gannon², M. H. Heggeness^{3,4}, E. A. Olmsted-Davis¹. ¹Cell and Gene Therapy, Baylor College of Medicine, Houston, TX, USA, ²Molecular Physiology, Baylor College of Medicine, Houston, TX, USA, ³Orthopedic Surgery and Pathology, Baylor College of Medicine, Houston, TX, USA, ⁴Orthopedic Surgery, Baylor College of Medicine, Houston, TX, USA.

Using a model of de novo bone, we recently demonstrated the recruitment of bone marrow derived cells of myeloid lineage to undergo chondrogenesis and osteogenesis. Their differentiation program appears to be dictated by the local micro-environment established in the tissues prior to stem cell engraftment. However, these cells must first mobilize from the bone marrow into the circulation and target the site of new bone formation. This process requires the cells to pass through the vessel wall, known as extravasation, into the target tissue. Receptor/integrins on the stem cell surface specifically bind corresponding molecules on specialized endothelial cells. We induce endochondral bone formation in the mouse hind limb by delivery of cells transduced with adenovirus to express BMP2. Immunohistochemical analysis of tissues isolated from the model prior to bone/cartilage formation, revealed the synthesis of new vessels simultaneous with specific temporal expression of several molecules known to be involved in extravasation. Microarray analysis of the tissue surrounding the bone induction site confirmed a specific enhancement in these genes including SDF-1, CXCR4, CD44, Mac1, and E-selectin. To further confirm the formation of new vessels, we utilized mice possessing a cassette consisting of the VEGF receptor (flk-1) promoter driving the expression of nuclear yellow fluorescent protein (YFP). Previous reports suggest that flk1 expression is somewhat restricted to endothelial cells present on smaller newly forming vessels. Our initial characterization of these mice confirmed YFP expression on subpopulations of CD31⁺ endothelial cells. Quantification of the flk-H2B:YFP⁺ in tissues isolated from either the region receiving cells transduced with either AdBMP2 or a control adenovirus, showed a significant increase in YFP expression as compared to the control. We observed this increase as early as two days after induction prior to the appearance of stem cells within the tissues. The results collectively suggest the ability of BMP2 to both recruit the necessary chondro-osseous stem cells but also establish the essential vasculature for extravasation and engraftment into the tissues. This is the first report demonstrating a specific mechanism for stem cell homing for the production of endochondral bone, a process that is essential for tissue engineering, but also provides novel targets for treatment of heterotopic bone formation, and bone metastases.

Disclosures: C.M. Foulletier-Dilling, None.

This study received funding from: NIBIB: RO1EB005173 and DOD:PRO33169.

1072

TGF β 1 Induces Migration of Mesenchymal Stem Cells in Coupling Bone Resorption and Formation. Y. Tang, X. Wu, S. Xie*, L. Zhao*, C. Wan*, Z. Shi*, X. Feng, X. Peng*, M. Wan, X. Cao. Pathology, University of Alabama at Birmingham, Birmingham, AL, USA.

Bone is continuously remodeled by the balanced processes of bone resorption and concomitant bone formation. The recruitment of osteoprogenitors to the site of bone resorption is the initial event necessary for coupling of bone resorption and formation. However, such factor(s) for the coupling process is not clear. Here we demonstrate that TGF β 1 released from bone matrix during osteoclastic bone resorption induces migration of stro-1⁺ primary human bone marrow mesenchymal cells (MSCs). Migration of MSCs was examined in coupling with in vitro osteoclastic bone resorption. Osteoclastic bone resorption-conditioned medium (CM) stimulates migration of MSCs, whereas CM from monocytes/macrophage or osteoclasts without bone slices had no effect. Importantly, addition of an antibody against TGF β 1 inhibited the migration, but antibodies against TGF β 2, TGF β 3, FGF-1, FGF-2, FGF-3, or noggin did not affect the migration. Western blot analysis revealed that only bone resorption-CM contains active TGF β 1. In addition, bone resorption-CM prepared from TGF β 1^{-/-} mice did not induce migration of MSCs. The results indicate that TGF- β 1 released and activated during osteoclastic bone resorption is a key factor in inducing MSCs migration.

In characterization of the mechanism of TGF β 1-induced migration of MSCs, we found that Smad signaling promotes cell migration through TGF β 1 type I receptor (T β RI). T β RI specific inhibitor (SB-431542) blocks the migration. Importantly, injection of the T β RI inhibitor in the rat tibia reduced bone formation dose-dependently as demonstrated by X-ray, μ CT and histomorphometry. TGF β 1 activates RhoA which induces formation of focal adhesion and results in reduction of migration of MSCs. Injection of RhoA inhibitor (Y-27632) in the rat tibia stimulated bone formation. The T β RI-mediated migration mechanisms were also confirmed in MSCs isolated from either T β RII or Smad4 conditional knockout mice. Finally, the TGF β 1^{-/-} mice was crossed with immuno-deficient Rag2^{-/-} mice to prevent the early death of the TGF β 1^{-/-} mice due to organ failure of with inflammatory disease. The adult TGF β 1^{-/-} mice exhibited smaller trabecular bone volume and thickness, and larger trabecular bone space. Histology staining showed lack of preosteoblasts at the surface of trabecular bone. Moreover, TRAP staining of mature osteoclasts confirmed an absence of preosteoblasts around the mature osteoclasts on the surface of trabecular bone. Thus, TGF β 1^{-/-} mice exhibit significant bone loss with features characteristic of uncoupled bone resorption and formation, which indicates that TGF β 1 functions as a primary coupling factor for bone formation and resorption.

Disclosures: Y. Tang, None.

1073

Bone Turnover Markers and Prediction of Fracture: Nine-Year Follow-Up Study of 1040 Elderly Women. K. K. Ivaska, P. Gerdhem, K. Åkesson, K. J. Obrant. Department of Orthopaedics, Lund University, Malmö, Sweden.

High level of bone turnover has been suggested to be a risk factor for future fracture. The aim of this study was to investigate if biochemical markers of bone turnover are associated with long-term incidence of fracture in elderly women followed prospectively for a mean of nine years.

The ability of bone turnover markers to predict future fracture was studied in a population-based sample of 1040 randomly recruited elderly women, all 75-years of age at inclusion (the Malmö OPRA study). Six bone turnover markers (S-TRACP5b, S-CTX-I, S-OC[1-49], S-TotalOC, S-boneALP, urinary osteocalcin (U-OC)) were measured at baseline and after a new sampling one year later, at the age of 76. Prospective fractures were recorded and verified.

During the mean follow-up of 9.0 years (range 7.4 -10.9), a total of 364 women sustained prospectively at least one fracture, including 116 hip fractures and 103 clinical vertebral fractures. Women in the highest tertile for S-TRACP5b, S-CTX-I or U-OC had significantly greater risk for sustaining fracture when compared to women in the lowest tertile. The hazard ratio for any prospective fracture was 1.3-1.4 ($p<0.05$), depending on marker. The results were consistent when we analyzed resorption markers measured at one-year follow-up visit and the incidence of any prospective fracture during the remaining follow-up time of mean 7.9 years (range 6.3 - 9.9). Similar tendency for increased risk was observed when hip fractures or vertebral fractures were analyzed separately, but it did not reach statistical significance. The associations to hip or vertebral fracture became, however, significant with hazard ratios up to 2.0 ($p<0.05$), when we used the average value of two marker measurements (baseline and one-year visit). Bone formation markers S-OC[1-49], S-TotalOC and S-boneALP were not associated with prospective fractures.

We conclude that elevated levels of bone resorption markers S-TRACP5b, S-CTX-I and U-OC are consistently associated with increased fracture risk for up to a decade in elderly women.

Disclosures: K.K. Ivaska, None.

1074

Biochemical Markers of Bone Turnover, Hip Bone Loss and Non-spine Fracture in Men: A Prospective Study. D. C. Bauer¹, P. Garnero², S. L. Harrision³, J. A. Cauley⁴, R. Eastell⁵, K. E. Ensrud⁶, E. Barrett-Connor⁷, E. S. Orwoll⁸. ¹UCSF, San Francisco, CA, USA, ²Synarc, Lyon, France, ³CPMC Research Institute, San Francisco, CA, USA, ⁴University of Pittsburgh, Pittsburgh, PA, USA, ⁵University of Sheffield, Sheffield, United Kingdom, ⁶University of Minnesota, Minneapolis, MN, USA, ⁷UCSD, San Diego, CA, USA, ⁸OHSU, Portland, OR, USA.

Previous studies have found that biochemical markers of bone turnover are independently associated with fracture risk in older women, but few prospective data exist in men.

We performed a nested case-cohort analysis within the Osteoporotic Fractures in Men (MrOS) study to determine if men with higher levels of bone turnover had accelerated bone loss or an elevated risk of fracture. Among the 5,995 MrOS subjects enrolled at baseline (mean age: 72.2 \pm 6.1), 440 men had documented non-spine fractures during a mean follow-up of 5.1 yr. Hip BMD (Hologic QDR4500) was measured at baseline and after a mean follow-up of 4.6 yr. Using fasting baseline serum stored at -190C, bone turnover (PINP, Roche Diagnostics; TRACP 5b, SBA-Sciences; and beta CTX, Roche Diagnostics) was measured on 428 fracture cases (including 82 hip fractures) and 943 randomly selected men. Bone loss (in the randomly selected men) and fracture outcomes were examined in multivariate models adjusted for age and clinic.

Hip bone loss was greater among men in the highest quartile of PINP (>45.6 ng/mL), TRACP 5b (>3.7 U/L) or CTX (> 0.494 ng/mL). For example, total hip bone loss was 0.6% per year among those in the highest quartile of PINP and 0.4% per year among those in the lower 3 quartiles ($p=0.002$). Compared to men without fracture, those with one or more non-spine fracture during follow-up were older (75.5 yr. vs. 73.7) and had lower total hip BMD (0.89 gm/cm² vs. 0.96), but had similar BMI (27.2 kg/m² vs. 27.3). Elevated PINP, but not TRACP 5b or CTX, was associated with an increased risk of fracture, particularly in the highest quartile (Table). Further adjustment for baseline hip BMD attenuated the associations between PINP and fracture, and they were no longer statistically significant.

We conclude that higher levels of bone turnover are associated with greater hip bone loss in older men, but increased turnover is not independently associated with the risk of hip or non-spine fracture. Our findings suggest that a single serum measurement of bone turnover may not be useful to predict hip or non-spine fracture risk in this population.

	RH (95% CI)		RH (95% CI)	
	adjusted for age and clinic (highest vs. 3 lower quartiles)		adjusted for age, clinic and BMD (highest vs. 3 lower quartiles)	
	Non-spine	Hip	Non-spine	Hip
PINP	1.42 (1.10, 1.84)	2.17 (1.29, 3.65)	1.19 (0.91, 1.56)	1.23 (0.65, 2.32)
TRACP 5b	1.07 (0.81, 1.40)	0.91 (0.52, 1.59)	0.93 (0.70, 1.24)	0.65 (0.35, 1.20)
beta CTX	1.15 (0.88, 1.49)	1.45 (0.87, 2.40)	0.93 (0.71, 1.22)	0.89 (0.50, 1.59)

Disclosures: D.C. Bauer, None.

This study received funding from: NIAMS.

1075

Quantitative Ultrasound Predicts Incident Vertebral and Hip Fractures at Least as Strongly as DXA: The OPUS Study. C. C. Glüer¹, R. Barkmann¹, T. Blenk^{2*}, A. Stewart^{3*}, S. Kolta^{4*}, J. Finigan^{5*}, C. Graeff¹, J. v. d. Gabelentz^{2*}, R. Eastell³, D. M. Reid³, C. Roux⁴, D. Felsenberg². ¹Medical Physics, Diagnostic Radiology, University Hospital Schleswig-Holstein, Campus Kiel, Kiel, Germany, ²Charité Universitätsmedizin, Berlin, Germany, ³University of Aberdeen, Aberdeen, United Kingdom, ⁴René Descartes University, Paris, France, ⁵University of Sheffield, Sheffield, United Kingdom.

In the Osteoporosis & Ultrasound (OPUS) study we recruited a population-based sample of 2409 women (ages 55 to 81 years) from 5 European cities. Baseline examinations included dual-x-ray absorptiometry (DXA) of the lumbar spine and the total hip and Quantitative Ultrasound (QUS) of the heel using 4 devices (Lunar Achilles+, Osteometer DTU-one, Quidel/Metra QUS-2, and DMS UBIS 5000) and of the finger using one device (IGEA DBM Sonic BP). At baseline and 6 years later 1566 women underwent repeat spinal radiography for assessment of incident vertebral fractures and reported hip fractures since the baseline visit. Incidence of osteoporotic vertebral fractures was centrally assessed in Berlin according to standard radiological and semiquantitative assessment (vertebral height reduction $>20\%$). We examined the association of the baseline measurements with incident fractures by calculating standardized odds ratios (sOR, per one SD decrease of population variance, adjusted for age) from logistic regression models. There were 67 incident vertebral osteoporotic fractures and 11 incident hip fractures (no major trauma). Prediction based on Speed of Sound (SOS) results was somewhat stronger than for Broadband Ultrasound Attenuation (BUA) or DXA but the differences were not significant (ROC analysis). Finger measurements did not show significant associations with incident fractures. In multivariate age-adjusted vertebral fracture models including both SOS and BMD, only spinal BMD but not total hip BMD contributed independently of SOS (e.g. sOR=1.6, $p<0.03$ for DTU-one SOS and sOR=1.3, $p<0.04$ for DXA spine BMD).

Predictor variable	Age-adj. sOR Vert Fr	Age-adj. sOR Hip Fr
DXA spine BMD	1.5 (1.2-1.8)***	1.3 (0.8-2.1)
DXA total hip BMD	1.5 (1.5-2.0)**	2.6 (1.4-5.0)**
Achilles+ BUA	1.4 (1.04-1.8)*	1.9 (1.1-3.5)*
DTU-one BUA	1.5 (1.2-1.8)***	2.0 (1.3-3.2)**
UBIS 5000 BUA	1.5 (1.2-1.8)**	1.8 (1.0-3.0)*
QUS-2 BUA	1.6 (1.2-2.1)**	2.0 (1.1-3.4)*
Achilles+ SOS	1.7 (1.2-2.3)**	2.9 (1.4-6.4)**
DTU-one SOS	1.8 (1.4-2.4)****	2.9 (1.4-6.4)**
UBIS 5000 SOS	1.6 (1.3-2.2)***	2.7 (1.2-5.7)*
Achilles+ Stiffness Index	1.6 (1.2-2.1)**	2.5 (1.2-5.1)**
DBM BP AD-SoS	1.1 (0.9-1.3)	1.2 (0.8-1.8)

* $p<0.05$, ** $p<0.01$, *** $p<0.001$, **** $p<0.0001$

Conclusion: Calcaneal QUS methods, best evaluated based on SOS, predict incident vertebral and hip fractures at least as well as central DXA approaches.

Disclosures: C.C. Glüer, GE Medical 5; IGEA 2, 5.

This study received funding from: Sanofi-Aventis, Demetech, DMS, Eli Lilly, GE Medical, IGEA, Novartis, OSI/Osteometer Mediatech, Procter & Gamble Pharmaceuticals, Pfizer, Quidel/Metra, Roche.

1076

Abdominal Aortic Calcification (AAC) on Vertebral Fracture Assessment (VFA) Images Predicts Incident Myocardial Infarction and Stroke Independent of Clinical Cardiovascular Disease Risk Factors. J. T. Schousboe¹, B. C. Taylor², D. P. Kiel³, K. E. Ensrud², K. E. Wilson⁴, E. V. McCloskey⁵. ¹Park Nicollet Health Services, Minneapolis, MN, USA, ²Minneapolis VAMC, Minneapolis, MN, USA, ³Hebrew SeniorLife, Harvard Medical School, Boston, MA, USA, ⁴Hologic, Inc, Bedford, MA, USA, ⁵University of Sheffield, Sheffield, United Kingdom.

The risk for cardiovascular disease (CVD) among older women is not adequately captured by traditional clinical CVD risk factors. Lateral spine images obtained on bone densitometers intended for VFA can detect abdominal aortic calcification, an important additional subclinical marker of CVD.

Objective: To estimate the association between AAC scored on VFA images and subsequent MI and stroke in women age 75 years or older participating in a randomized trial of clodronate versus placebo after adjustment for traditional risk factors.

Methods: 408 women sustaining either a fatal or non-fatal MI or stroke during the median 4-year study follow-up period were selected as cases, and an equal number of controls were randomly selected from the remainder of the study population. 732 (89.7%) had a baseline VFA with adequate space visualized anterior to the lumbar spine such that AAC could be scored by a single reader using a previously validated 24-point scale and a simplified 8-point scale, blinded to case status and covariate data. Covariates were systolic BP, LDL and HDL cholesterol, triglycerides, smoking, presence of diabetes, renal function, self-reported diagnoses of hypertension, angina, prior stroke, and health status. Missing covariate data was statistically imputed.

Results: Using logistic regression models, the multivariate-adjusted odds ratios of incident MI/stroke for the top and middle tertiles compared to the bottom tertile of AAC score were;

Outcome Measure	Odds Ratio (95% Confidence Interval) vs. Bottom Tertile (reference)	
	Middle Tertile	Top Tertile
AAC-24	1.14 (0.79 - 1.65)	1.74 (1.19 - 2.56)
AAC-8	1.42 (0.98 - 2.05)	1.76 (1.22 - 2.55)

Results for the subset with complete covariate data (n=420) were very similar.

Conclusion: AAC scored on lateral VFA images is a predictor of incident MI and stroke independent of other clinical risk factors. Since bone densitometry is indicated for all women age 65 and older, VFA imaging offers an opportunity to measure this subclinical indicator of cardiovascular disease in the female population at very little marginal cost.

Disclosures: J.T. Schousboe, Hologic, Inc. 2; Amgen, Inc. 5; Merck, Inc. 5.

This study received funding from: Hologic, Inc.

1077

Clinical Risk Factors for Incident Vertebral Fractures: Data from the Six-Year Prospective OPUS Study. K. Briot¹, C. Roux¹, S. Kolta¹, R. Eastell², D. M. Reid³, D. Felsenberg⁴, C. C. Gluer⁵. ¹Rheumatology, Cochin Hospital, Paris, France, ²University of Sheffield clinical sciences centre, Sheffield, United Kingdom, ³Department of Medicine and Therapeutics, University of Aberdeen, Aberdeen, United Kingdom, ⁴Diagnostic Radiology, Free University Berlin, Berlin, Germany, ⁵Medical Physics, Department of Diagnostic Radiology, University Hospital Schleswig-Holstein, Campus Kiel, Kiel, Germany.

Fractures related to osteoporosis represent a strong public health burden. Low bone mineral density explains only a part of the fracture risk; clinical risk factors play an important role. Many clinical risk factors are identified, but responsibility of some of them needs to be clarified. The objective of the study was to identify clinical risk factors for incident vertebral fractures. Using the 6-years data from the Osteoporosis and Ultrasound study (OPUS), a multi-centre wide study, 2409 European postmenopausal ambulatory women 55-81 years old with baseline clinical risk factors assessment (age, weight, current smoking, personal or familial previous fracture, corticosteroids, medical diseases, physical activity), and bone mineral density (BMD) measurements, were included in the analysis. Spine X-rays were performed using standardized procedures and assessed in a central facility. Incident vertebral fractures (defined as >20% vertebral height reduction and radiological signs of osteoporotic fracture) occurred in 67 women during the six years of follow-up. We performed logistic regression analysis on each of the potential risk factors, with adjustment for age. We chose for multivariate analysis those risk factors that were statistically significant ($p \leq 0.05$). In the age-adjusted multivariate analysis, several clinical factors were significantly associated with incident vertebral fractures, independently of BMD value: age (per 10 years) (sOR=1.7; 95% CI, 1.0-2.7; $p<0.04$), previous fall (sOR=1.4; 95% CI, 1.0-1.9; $p<0.04$), previous paternal hip fracture (sOR=3.0; 95% CI, 1.5-5.9; $p<0.002$), and current intake of proton pump inhibitor therapy (omeprazole) (sOR=1.9; 95% CI, 1.2-2.9; $p<0.006$). There was a trend for an association with previous low traumatic fracture (sOR=1.3; 95% CI, 1.0-1.8; $p<0.08$). Using data from a cohort of ambulatory postmenopausal European women, we showed that few clinical risk factors are associated with an increase risk of incident vertebral fracture over 6 years; two of them (paternal hip fracture and current intake of omeprazole) have not been observed in prospective studies before. This 6-year prospective study results confirm recent data from case-control studies: proton pump inhibitor therapy appeared to be associated with an increase risk of vertebral fractures.

Disclosures: K. Briot, None.

1078

Validation of Ten-Year Fracture Risk Prediction in a Large Clinical Cohort. W. D. Leslie¹, J. F. Tsang², L. M. Lix³. ¹Dept of Medicine, University of Manitoba, Winnipeg, MB, Canada, ²University of Manitoba, Winnipeg, MB, Canada, ³Manitoba Centre for Health Policy, University of Manitoba, Winnipeg, MB, Canada.

Absolute 10-year fracture risk is the preferred method for fracture risk assessment. The validity of applying published fracture rates from one population to another population is uncertain.

Women age 47.5 y or older at the time of baseline femoral neck BMD (N=20579, 1990-2002) were identified in a database containing all clinical DXA test results for the Province of Manitoba, Canada. Individual 10 y fracture risk was predicted from age-only and age+BMD (NHANES-III femoral neck T-score) using published 10 y fracture risk for Swedish women. Health service records were assessed for the presence of non-trauma 'osteoporotic' fracture codes (hip, clinical spine, wrist, humerus) subsequent to BMD testing (86447 person-y follow up, 1173 patients with osteoporotic fractures). Fracture rates were derived for subgroups stratified by age (5 y strata) and estimated risk (5% strata). 10 y fracture rates were computed directly by the Kaplan-Meier method (10 y continuous data) and by the actuarial method (two 5 y periods with adjustments for aging, death and expected BMD loss). Direct and actuarial methods gave nearly identical point estimates, but the latter were more precise.

There was a strong linear correlation between predicted and observed fracture rates based upon age-only (weighted $r=0.95$) and age+BMD (weighted $r=0.99$). For age strata 50 to 75, and for estimated risk strata from 0-5% to 20-25%, the confidence intervals overlapped the line of identity. For women age >77.5 or estimated risk >25%, observed exceeded estimated fracture rates. This is explained by healthy selection bias whereby elderly women referred for BMD testing have lower mortality than expected, hence more years at risk for fracture. Corrected for survival bias, women age >77.5 had observed fracture rates no different than predicted.

In conclusion, Swedish 10-year fracture risk data are generally applicable to the Canadian female population referred for BMD testing, though fracture rates may be underestimated in the oldest and highest risk subgroups due to healthy selection bias.

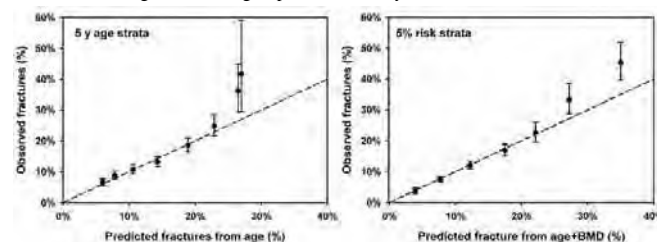


Figure: Predicted 10-year fracture risk versus observed fracture rates (actuarial method) for age-only (left, 5 y age strata from 50 to 85) and age+BMD (right, 5% risk strata for estimated risk, from 0-5% to >30%). Dotted line is the line of identity.

Disclosures: W.D. Leslie, Merck Frosst Canada Ltd; Sanofi-Aventis; Procter & Gamble Pharmaceuticals Canada, Inc. 2, 5, 8.

1079

Bone Mineral Density and Hip Fracture: A Revisit with Time-varying Effects. T. V. Nguyen, N. D. Nguyen, S. A. Frost^{*}, J. R. Center, J. A. Eisman. Bone and Mineral Research Program, Garvan Institute of Medical Research, Sydney, Australia.

All previous studies of association between BMD and fracture were based on a single measurement, and assumed that BMD do not change. The assumption is clearly untenable since BMD is known to decrease with advancing age. The present study sought to estimate the magnitude of association between BMD and hip fracture risk taking into account the time-dependent bone loss.

A cohort of 782 women and 566 men aged 60+ years who have had at least two BMD measurements preceding a hip fracture was studied. The individuals have been followed-up for a median period of 15 years with an average of 5 BMD measurements (GE Lunar DPX) per subject. During the follow-up period, 77 women and 23 men had sustained at least one hip fracture. The Cox's proportional hazards model with time-varying covariates was used to evaluate the absolute risk of fracture for an individual conditioned on the individual's age, history of prior fracture and fall, and BMD measurements.

For a given risk profile, in addition to baseline BMD, bone loss further increased the risk of hip fracture in an individual. For example, a 70-year old woman with baseline BMD T-score of -2.0, and with a prior fracture and a fall is estimated to have the 5-year and 10-year risk of hip fracture of 6.8% and 10.6%, respectively. However, conditional on an annual bone loss is 1%, her 5-year and 10-year risks of hip fracture increase to 7.7% and 14.3%, respectively. Using this time-varying approach, it is possible to construct a full profile of BMD and fracture risk.

These data suggest that to accurately assess the risk of hip fracture in an individual, the dynamic nature of BMD should be considered. The present model takes into account the time-varying effect of BMD, and can therefore be used for individualizing the risk of hip fracture for any given unique risk profile

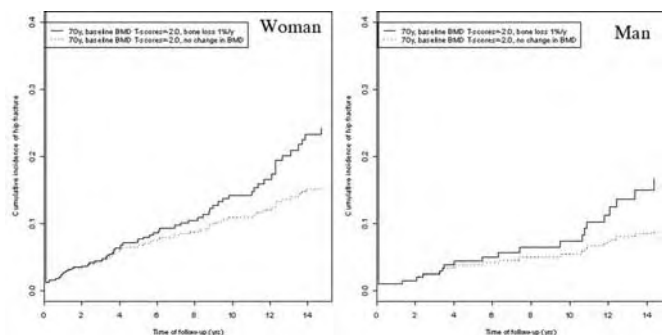


Figure 9: Cumulative incidence of fracture stratified by baseline BMD and time-dependent BMD

Disclosures: T.V. Nguyen, None.

This study received funding from: National Health and Medical Research Council, Australia.

1080

Clinical Validation of a Simplified Absolute Fracture Risk Algorithm in Canadian Women. W. D. Leslie¹, J. F. Tsang², L. M. Lix³. ¹Dept of Medicine, University of Manitoba, Winnipeg, MB, Canada, ²University of Manitoba, Winnipeg, MB, Canada, ³Manitoba Centre for Health Policy, University of Manitoba, Winnipeg, MB, Canada.

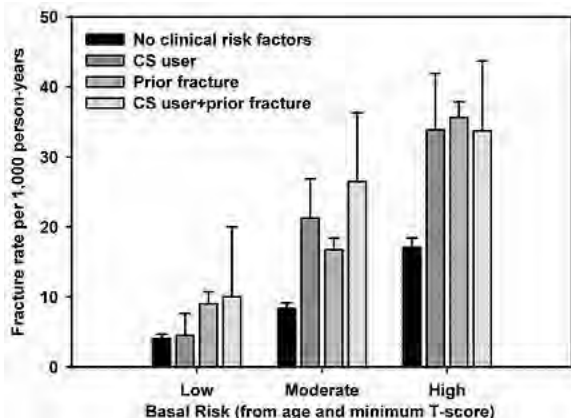
Absolute 10 y fracture risk based upon multiple factors is the preferred method for assessment. A simplified risk assessment system from gender, age, minimum T-score, and two clinical risk factors (CRFs) - prior fracture and systemic corticosteroid (CS) use - has been used in Canada since 2005. The current study was undertaken to validate this system in the Canadian female population.

16,205 women of white ethnicity age 50 y or older at the time of baseline BMD (1998-2002) were identified in a population-based database containing all clinical DXA test results for the Province of Manitoba, Canada. Individual basal 10 y fracture risk (from age and minimum T-score lumbar spine, femur neck, trochanter, total hip) was categorized as low (<10%), moderate (10-20%) or high (>20%). Health service records since 1987 were assessed for non-craniofacial non-trauma fracture codes prior to BMD (N=5,224). CS use was defined as possession for 90d or more during the year prior to BMD testing at a prednisone-equivalent mean daily dose of 7.5mg or greater (N=616). Fracture rates (per 1,000 person-y) after BMD testing were calculated from non-trauma fracture codes for the hip, clinical spine, wrist, or humerus (collectively designated 'osteoporotic', N=757).

In women without CRFs, fracture risk predicted from age and BMD alone showed a significant gradient in observed fracture rates (low 4.1±0.6, moderate 8.4±0.8, high 17.1±1.3 per 1,000 person-y; p-for-trend <.0001). There was an incremental increase in incident fracture rates from a prior fracture (13.9 per 1,000 person-y, p<.0001) or recent CS use (8.4 per 1,000 person-y, p=.0077). Site of prior fracture further stratified fracture risk ('osteoporotic' 25.9 vs all other sites 5.5 per 1,000 person-y, p<.0001). Lower dose CS use (<7.5mg daily) had no observed effect on fracture rates. A Cox proportional hazards model gave: HR basal risk moderate 1.94 (1.61-2.34) and high 4.51 (3.73-5.45) vs low (ref); CS use 1.54 (1.16-2.05); prior 'osteoporotic' fracture 2.68 (2.26-3.17) vs other fracture 1.41 (1.17-1.71).

This simplified fracture risk assessment system provides an assessment of fracture risk that is broadly consistent with observed fracture rates.

Figure: Observed fracture rates (SE bars) in relation to age, BMD and two clinical risk factors.



Disclosures: W.D. Leslie, Merck Frosst Canada Ltd; Sanofi-Aventis; Procter & Gamble Pharmaceuticals Canada, Inc. 2, 5, 8.

1081

Leptin-deficient (ob/ob) Mice Exhibit Increased Bone Mechanosensitivity and Corresponding Osteoblasts Show Increased Anabolic Shear Stress Responses In Vitro. K. H. W. Lau¹, S. Kapur¹, M. Amoui¹, X. Wang¹, C. Kesavan¹, S. Mohan¹, D. J. Baylink². ¹Loma Linda VAMC, Loma Linda, CA, USA, ²Loma Linda Univ., Loma Linda, CA, USA.

We sought to test the hypothesis that the leptin receptor (Lepr) pathway plays an important role in bone mechanosensitivity based on the rationales that Lepr is located within one of the mouse genetic loci that showed mechanosensitivity modulating effects and that Lepr signaling is essential for skeletal maturation and metabolism. To test this hypothesis, the osteogenic response to loading (in the form of 2-week four-point bending) in tibia of adult female ob/ob mice [in C57BL/6J (B6) background] was compared with those in adult female B6 tibia. To adjust for the 14% greater bone size in ob/ob mice, the load was adjusted to produce similar levels of mechanical strain (2129 $\mu\epsilon$ at 9N for ob/ob mice vs. 2500 $\mu\epsilon$ at 6N for B6 mice). This mechanical strain was insufficient to produce a bone anabolic response in B6 mice; whereas in ob/ob mice this strain increased total BMC (16%), cortical area (22%), content (29%), and thickness (28%), and BMD (8%) [p<0.05 for each]. To further test if leptin deficiency would enhance osteogenic response to mechanical stimuli, the effects of a 30-min fluid shear (20 dynes/cm²) on [³H]thymidine incorporation (TdR) and Erk1/2 phosphorylation in ob/ob osteoblasts were compared to those of wild-type (WT) littermates and B6 mice. While the shear stress increased TdR and Erk1/2 in osteoblasts of B6 and WT littermates (each by ~2-fold, p<0.05), the stimulation in ob/ob osteoblasts was greater (> 3-fold, p<0.05 vs. B6 osteoblasts). In addition, 2-hr pretreatment of ob/ob osteoblasts with 100 ng/ml of leptin completely abrogated the enhanced mitogenic response. Because it has been reported that the mechanism whereby mechanical stimuli act to stimulate proliferation involves upregulation of genes of the IGF-I, Wnt, BMP/TGF β , and estrogen receptor pathways, we next determined whether the Lepr pathway acts upstream to these 4 pathways by assessing the effects of the fluid shear on the expression levels of representative genes of these pathways in ob/ob and B6 osteoblasts (by real-time PCR). The upregulation of each test gene of the 4 pathways in ob/ob osteoblasts was much greater (p<0.05) than those in B6 osteoblasts. The 2-hr leptin pretreatment also abrogated the shear stress-induced upregulation of these genes in ob/ob osteoblasts. Conclusions: 1) In vivo, the Lepr pathway inhibits the anabolic responses to mechanical loading which is consistent with increased basal values for bone size in the ob/ob mouse, 2) In vitro, the Lepr pathway also has a negative modulating role in the mechanosensitivity of mouse osteoblasts, and 3) The Lepr pathway acts upstream of 4 selected major anabolic pathways to modulate mechanosensitivity.

Disclosures: K.H.W. Lau, None.

This study received funding from: Department of Defense.

1082

Denosumab (AMG 162), a Fully Human RANKL Antibody, Improves Cortical and Cancellous Bone Mass and Bone Strength in Ovariectomized Cynomolgus Monkeys. M. S. Ominsky¹, J. Schroeder¹, S. Y. Smith², D. J. Farrell¹, J. E. Atkinson¹, P. J. Kostenuik¹. ¹Amgen Inc., Thousand Oaks, CA, USA, ²Charles River Laboratories Preclinical Services Montreal, Inc., Montreal, PQ, Canada.

Denosumab, a fully human monoclonal antibody that inhibits RANKL, decreases bone resorption and increases bone mineral density (BMD) in postmenopausal women participating in clinical studies. Denosumab was shown to cause similar responses in adult ovariectomized (OVX) cynomolgus monkeys (cynos). We now describe the consequences of these changes on bone strength.

One month after OVX or sham surgery, OVX cynos (9 to 16 years old) were treated with vehicle (OVX-Veh) or denosumab (25 or 50 mg/kg, SC, once/month) for 16 months (n=14 to 20/group). Sham controls were treated with vehicle (n=17). After sacrifice, ex vivo DXA and pQCT scans were taken of the intact right femur, L3-L4 vertebral bodies, and L5-L6 vertebral 5mm cancellous cores. Destructive testing was performed by 3-point bending of the femur diaphysis and humeral cortical beams, shearing of the femur neck, and compression of the lumbar vertebral specimens. Statistically significant differences between the denosumab and OVX-Veh groups are reported as P<0.05 by ANOVA.

Compared with OVX-Veh, both doses of denosumab were associated with greater BMC at the femur neck (+19% to 22%), L3-L4 bodies (+23% to 25%), L5-L6 cores (+29% to 30%), and femur diaphysis (+10% to 11%). Both doses of denosumab were associated with significantly greater peak load for femur neck (19% to 34%), L3-L4 bodies (54% to 55%), and L5-L6 cores (69% to 82%), compared with OVX-Veh. Both doses of denosumab were associated with significantly greater stiffness for femur neck (21% to 26%), L3-L4 bodies (39% to 46%), L5-L6 cores (61% to 62%), and femur diaphysis (15% to 16%), compared with OVX controls. Intrinsic (material) properties for cortical sites were derived from geometric data and extrinsic (whole bone) strength parameters. Intrinsic strength parameters of femur diaphysis and humerus cortical beams were similar in OVX-Veh and treatment groups, and the relationship between femur diaphysis vBMC and peak load was strong and similar among all groups ($r^2=0.79$ to 0.91). For the lumbar vertebral bodies and cancellous cores, significant positive correlations were found between vBMC and yield load for all groups ($r^2=0.57$ to 0.84).

In summary, long term (16-month) denosumab therapy increased bone mass and density at both cortical and cancellous sites in ovariectomized cynomolgus monkeys. These increases were highly correlated with improvements in the extrinsic strength of cortical and cancellous sites. The results suggest that in this study, denosumab improves bone strength primarily by increasing bone mass.

Disclosures: M.S. Ominsky, Amgen Inc. 1, 3.

This study received funding from: Amgen, Inc.

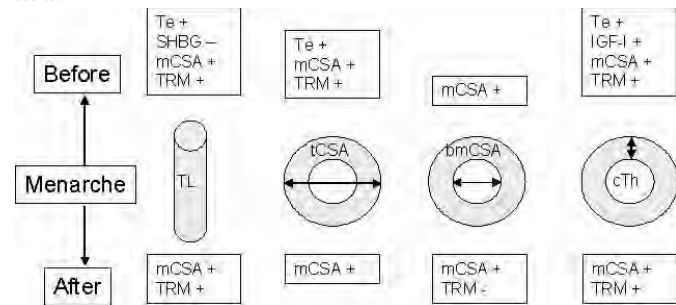
1083

Concerted Growth of Bone Length and Width - Influence of Sex Hormones, IGF-1 and Muscle Size. S. Cheng¹, Q. Wang¹, P. Rakkila^{*1}, M. Alen^{*1}, A. Mahonen^{*2}, H. Kröger², H. Suominen¹, A. Lyytikäinen¹, E. Völgyi^{*1}, U. M. Kujala^{*1}, F. Tylavsky³, E. Seeman⁴. ¹Univ. of Jyväskylä, Jyväskylä, Finland, ²Univ. of Kuopio, Kuopio, Finland, ³Univ. of Tennessee, Memphis, TN, USA, ⁴Univ. of Melbourne, Melbourne, Australia.

Bone growth is determined by genetic and environmental factors. The effect of mechanical loading on growth in bone width and length has not been specifically addressed. We hypothesized that 1) sex hormones and IGF-I correlate with bone growth prior to puberty, since hormone levels are changing rapidly, but correlate less well after puberty when levels vary less; and 2) loading, as reflected by muscle size, correlates with bone width and length throughout growth. 258 girls aged 11.2 yrs at baseline were followed on average for 6.5 years. Left tibial shaft was scanned using pQCT (XCT2000). Tibial length (TL) was determined from whole body DXA scans. Serum 17 β -estradiol (E2), testosterone (Te) and IGF-I concentrations were assessed using immunofluorometry and serum sex hormone binding globulin (SHBG) using time-resolved fluoroimmunoassays.

In hierarchical multiple regression models the growth of tibial length, total cross-sectional area (tCSA), bone marrow cavity area (bmCSA) and cortical thickness (cTh) were explained by E2, Te, IGF-I, SHBG, muscle cross-sectional area (mCSA), and time relative to menarche (TRM). The results of these models are summarized in the Fig. There was no correlation between E2 and bone size measures either before or after menarche. mCSA correlated positively with IGF-I and negatively with SHBG both before and after menarche. Te was positively associated with TL, tCSA and cTh before menarche. Of the hormones studied none were associated with bone variables after menarche. Interestingly, TRM was negatively associated with the bmCSA but was not associated with tCSA after menarche. This implies increased periosteal apposition in the long bone shaft as the girls age. The moderate correlation found between TL and tCSA ($r^2=0.44$) was partly due to growth asynchrony between the two.

The results support our hypothesis that before and after menarche bone growth in length and width are influenced differently by hormones and mechanical loading. Mechanical loading is the dominant factor throughout the pubertal period. Hormones may have an indirect influence on bone growth via their regulatory role on muscle mass based on our results.



Disclosures: S. Cheng, None.

This study received funding from: ASBMR Bridge Funding, Academy of Finland and Finnish Ministry of Education.

1084

Role for Estrogen Receptor-Beta in Trabecular Bone Mechanotransduction. A. B. Castillo¹, J. M. Doyle^{*1}, M. R. Allen², C. H. Turner¹. ¹Biomedical Engineering, Indiana University Purdue University, Indianapolis, IN, USA, ²Anatomy and Cell Biology, Indiana University School of Medicine, Indianapolis, IN, USA.

Recent studies suggest that estrogen receptor beta (ERb) plays a role in bone mechanotransduction at cortical bone sites. To determine whether ERb plays a role in trabecular bone mechanotransduction, 16-wk-old wildtype and ERb^{-/-} female mice were subjected to 28 days of tail suspension (TS). Age-matched, normally-loaded (NL) mice served as controls. Trabecular bone microarchitecture in the distal femur was evaluated using high-resolution computed tomography (vivaCT40, Scanco Medical), and the following parameters were calculated: bone volume/total volume (BV/TV), connectivity density (Conn.D), trabecular number (Tb.N, 1/mm), trabecular thickness (Tb.Th, mm), trabecular spacing (Tb.Sp, mm) and structure model index (SMI). Data were checked for normality and constancy of variance and analyzed using a 2-factor ANOVA with a Fisher's PLSD post-hoc analysis. TS had a significant factor effect on all variables ($p<0.001$) and resulted in significantly different BV/TV, Conn.D, Tb.N and SMI in TS wildtype and ERb^{-/-} when compared to NL controls (Table I). Genotype had a significant factor effect on BV/TV ($p=0.029$), Tb.Sp ($p=0.029$) and SMI ($p<0.001$). TS wildtype and ERb^{-/-} mice exhibited a 38% and 60% decrease in BV/TV, an 8% and 24% increase in Tb.Sp, respectively, when compared with NL controls. Disuse results in a decrease in osteoblast number and activity with no change in osteoclastic activity in most cases. Estrogen inhibits bone turnover by suppressing both osteoblastogenesis and osteoclastogenesis. The fact that TS ERb^{-/-} mice showed a greater loss in BV/TV compared to wildtype mice implies that signaling via ERb may normally inhibit disuse-related osteoclastic activity in the trabecular bone compartment. The role of ERb in disuse-related osteoclastic activity remains unclear. Taken together, these data implicate a role for ERb^{-/-} in disuse bone loss

and suggest that ERb plays a role in trabecular bone mechanotransduction.

	Trabecular Bone Microarchitecture in the Distal Femur			
	Wildtype		ERb ^{-/-}	
	NL (n=13)	TS (n=10)	NL (n=10)	TS (n=11)
BV/TV	0.043±0.004	0.026±0.003 (a)	0.038±0.004	0.016±0.003 (b,c)
Conn.D	37.420±6.373	10.797±2.866 (a)	27.351±7.551	2.058±0.666 (b)
Tb.N (1/mm)	3.549±0.072	3.288±0.095 (a)	3.538±0.108	2.909±0.123 (b)
Tb.Th (mm)	0.034±0.001	0.031±0.001	0.035±0.001	0.031±0.002
Tb.Sp (mm)	0.284±0.006	0.306±0.009	0.285±0.008	0.351±0.015 (b,c)
SMI	3.111±0.057	3.377±0.074 (a)	3.239±0.050	3.744±0.050 (b,c)

Data are presented as mean±standard error

NL= normally loaded; TS = tail suspension

(a) vs. NL wildtype, $p<0.05$

(b) vs. NL ERb^{-/-}, $p<0.05$

(c) vs. TS wildtype, $p<0.05$

Disclosures: A.B. Castillo, None.

This study received funding from: NIH.

1085

Effects of One Year Treatment with PTH (1-34) on Bone Microstructure at the Ultradistal Radius. S. Kirmani, M. Holets*, S. Khosla. Mayo Clinic, Rochester, MN, USA.

Previous studies have shown a beneficial effect of PTH (1-34) on bone density and fracture rate reduction in women with osteoporosis. Compared to placebo, a 13% and 6% increase in areal BMD (aBMD) using DXA was seen at the spine and hip, respectively (NEJM 344: 1434, 2001). At the distal radius, there was no significant effect on aBMD with the 20 μ g/d dose, but at the 40 μ g/d dose, there was a 2% decrease as compared to placebo. Using pQCT, a subset of women from the same trial had a 5-7% increase in cortical bone area, but no significant change in cortical vBMD or cortical thickness (JBMR 18:539, 2003). Despite these data on changes in BMD, there are sparse data on possible effects of PTH therapy on bone microstructure, and the available data are limited to studies using bone biopsies from the iliac crest. Thus, to further define effects of PTH on bone microstructure, we used high resolution 3D-pQCT (XtremeCT, Scanco AG, voxel size ~90 microns) to measure bone microstructural variables at the ultradistal radius in 7 women with osteoporosis (mean age, 74 yrs) at baseline and 1 yr after initiation of 20 μ g/d of PTH (1-34) (Forteo) for osteoporosis. None of the women suffered a fracture during the 1 year of treatment. Compared to baseline, we noted a 6.9% increase in bone volume/tissue volume (BV/TV) (Table, $P = 0.035$). This was similar in magnitude to the 5.7% change noted at the iliac crest in women treated for 3 years with PTH (JBMR 16:1846-1853). Two-thirds of this increase in BV/TV was due to an increase in trabecular thickness (Tb.Th), and only one-third due to an increase in trabecular number (Tb.N). There was a trend towards a decrease in cortical thickness (C.Th) and cortical volumetric BMD (vBMD). In summary, these data represent the first assessment of trabecular microstructure at the wrist following PTH therapy, and they demonstrate that (1) changes in trabecular parameters seen at the radius are very similar to those previously reported at the iliac crest; and (2) the beneficial effects of PTH (1-34) on trabecular bone seem to result primarily from increased trabecular thickness, with the minor apparent increase in trabecular number seen likely due to coalescence of the thickened trabeculae.

Subject	Age	Percent Change From Baseline				
		BV/TV	Tb.Th	Tb.N	C.Th	Cortical vBMD
1	72	0.69	-2.23	2.99	-5.46	-1.68
2	57	2.87	3.86	-0.96	-0.85	0.87
3	80	9.98	-1.13	11.2	2.62	-0.17
4	77	7.37	3.04	4.2	-4.81	-5.4
5	82	20.2	13.9	5.58	-3.05	-0.86
6	78	1.56	4.07	-2.42	-1.04	0
7	74	5.65	9.83	-3.8	0.49	0.04
Mean (\pm SEM)	74 (\pm 3)	6.9 (\pm 2.5)	4.5 (\pm 2.2)	2.4 (\pm 2)	-1.7 (\pm 1.1)	-1.03 (\pm 0.79)
P value		0.035	0.08	0.27	0.17	0.24

Disclosures: S. Kirmani, None.

1086

Glucocorticoids, Aging and Bone Hydration: New Insights into Qualitative Aspects of Bone Strength. R. S. Weinstein, J. Goellner, T. M. Chambers*, E. A. Hogan*, S. B. Berryhill*, R. Shelton*, W. W. Webb*, C. A. Wicker*, S. C. Manolagas. Central Arkansas Veterans Healthcare System, Center for Osteoporosis, University of Arkansas for Medical Sciences, Little Rock, AR, USA.

Both aging and glucocorticoid excess are associated with a decline in bone strength that is greater than the decline in bone mass. In addition, both conditions may decrease the water content of bone, as determined by the intensity of an inert aqueous fluorescent tracer (Procion red), which provides a visible outline of the lacunocanalicular network, following injection into the tail vein. Prompted by these lines of evidence, we obtained femora (including bone marrow) from 15 C57BL/6 mice at 4 months of age and placed them in a vacuum chamber for 50 hours at 4° C. Contralateral femora from the same animals were maintained in normal saline at the same temperature. Compared to zero time, there was a $58.7 \pm 3.0\%$ (SD) reduction of total weight in the femora, as early as 24 hours, and weights remained stable thereafter, indicating that maximum water removal was accomplished by this time point. We next determined the biomechanical properties of the femora during 3-point bending of the wet versus the vacuum dried femora taken from the same animals. Loss of wet weight reduced the average breaking stress by 33.7% and toughness (i.e. the work required to break the bone) by 59%. In agreement with this line of evidence, prednisolone administration to 8 month old C57BL/6 mice ($n = 3$) for 7 days (a time period insufficient to affect bone mass) decreased Procion fluorescence by 71%, as compared to placebo control. This effect was prevented in transgenic mice overexpressing the enzyme 11β -HSD2 in the context of an OG2 promoter, a model for deflecting glucocorticoid action from osteoblasts. In a second experiment with C57BL/6 mice ($n = 16$), crystallinity determined by Fourier transformation infrared microscopy (FTIRM) as well as strength decreased in mice receiving prednisolone for 28 days; and the two measures were directly correlated ($r = 0.53$; $p < 0.03$). Moreover, both the decrease in crystallinity and strength were prevented in the 11β -HSD2 transgenic animals. Lastly, Procion red epifluorescence was decreased by more than 40% in 31 month old as compared to 4 month old female or male C57BL/6 animals ($p < 0.001$). In addition, the mRNA levels in bone of 11β -HSD1 - the enzyme that locally amplifies glucocorticoid action, was increased by 1.8 fold between 8 and 31 month old mice and were inversely related to strength ($r = -0.67$, $p < 0.05$). These results lend strong support to our working hypothesis that skeletal water volume may protect against mechanical failure by means of hydraulic stiffening; and that both aging and glucocorticoid excess compromise bone strength, in part by decreasing skeletal hydration.

Disclosures: R.S. Weinstein, Merck 8.

1087

Effects of Mechanical Loading and Estrogen Are Structurally Distinct. J. Jokihaara¹, I. Pajamäki¹, H. Sievänen^{*2}, P. Kannus^{*2}, T. Vuohelainen^{*1}, T. L. N. Järvinen^{*1}. ¹University of Tampere, Tampere, Finland, ²UKK-Institute, Tampere, Finland.

The objective was to study the effects of effects of estrogen and locomotion on trabecular bone structure. We hypothesized that the independent and potentially interactive effects of these two factors should become distinct after separate or simultaneous inclusion of their influence; i.e. using the classic 2×2 factorial study design.

Accordingly, 30 three-week old littermates of female rats were first randomly assigned into bilateral ovariectomy (E-) or sham surgery (E+), after which the left hindlimb of each rat was cast immobilized (L-) while the contralateral (right) hindlimb served as normally loaded control (L+). After eight-week study period, trabecular structure of the distal femoral metaphysis was analyzed with micro-computed tomography. To eliminate the inherent bias arising from comparisons between animals differing in body weight and size, all data pertaining to bone mechanical competence was equalized in terms of the animal's apparent loading environment by using the body weight and femoral length as covariates. Loading increased bone size ($P=0.002$), while estrogen was not associated with changes in bone size ($P=0.280$). Both factors displayed a significant stimulatory effect on trabecular bone volume ($P=0.001$ and $P=0.003$, respectively). Further, both factors increased trabecular number ($P=0.006$ and $P=0.007$, respectively) while only loading increased trabecular thickness ($P<0.001$ and $P=0.244$, respectively) and only estrogen decreased trabecular separation ($P=0.775$ and $P=0.004$, respectively).

The anabolic effects of loading and estrogen were shown to be independent and the mechanisms of action of these two factors were distinct: loading alone (E-L+) resulted in thickening of individual trabeculae and estrogen effect (E-L-) was discernible as a denser (less spacing) trabecular meshwork. Moreover, when the factors were combined (E+L+), the effects add up. In conclusion, our results show that there is a structural dimorphism in the skeletal actions of estrogen and loading so that the actions of these two factors are independent and additive in nature.



Disclosures: J. Jokihaara, None.

1088

Transgenic Overexpression of OPG Results in Increased Bone Mass and Strength and Decreased Bone Turnover in One-Year-Old Female Rats. M. S. Ominsky, F. J. Asuncion, M. Barrero, Q. Niu*, T. J. Corbin*, D. Dwyer*, K. S. Warmington*, M. Grisanti, H. Tan*, X. Li, M. Stolina, P. J. Kostenuik. Metabolic Disorders and Laboratory Animal Research, Amgen Inc., Thousand Oaks, CA, USA.

RANK ligand (RANKL) is an essential mediator of bone resorption, and its activity is inhibited by osteoprotegerin (OPG). We created transgenic (Tg) rats to study the long-term impact of increased circulating levels of OPG on bone turnover, volume, density, and strength. CD rats were engineered to overexpress full-length soluble rat OPG via a liver promoter. Serum OPG levels in female Tg rats ($n=32$) were up to 260-fold greater than the mean value (257 ± 16 pg/ml) found in wildtype (WT) controls ($n=23$). At 1 year of age, rats were injected with fluorochrome labels for dynamic histomorphometry, bled for biomarker analyses, scanned by DXA, and sacrificed. Lumbar vertebra 2 (L2) was used for histomorphometry, and L5 was scanned by microCT and subjected to destructive mechanical testing.

In normal WT rats, there were no significant correlations between log serum OPG levels and lumbar BMD, serum TRAP-5b, serum osteocalcin, bone formation rate, or bone strength parameters. In contrast, log serum OPG in OPG-Tg rats had significant ($P<0.01$) and positive linear correlations with lumbar BMD ($r^2=0.53$), BV/TV ($r^2=0.77$), trabecular number ($r^2=0.93$), and peak load ($r^2=0.54$). Log serum OPG in OPG-Tg rats had significant ($P<0.01$) and negative linear correlations with serum TRAP-5b ($r^2=0.64$), serum osteocalcin ($r^2=0.35$), and bone formation rate ($r^2=0.51$).

Tg rats with the highest levels of serum OPG (OPG-hi, 50- to 260-fold greater than the mean value for WT controls; $n=15$) had 70% lower osteoclast surface and 91% lower bone formation rates in L2 compared with WT controls ($P<0.001$). Despite the profound suppression of bone turnover, the vertebra of the OPG-hi rats had 56% greater peak load, 62% greater stiffness, and 53% greater energy absorption compared with WT controls ($P<0.01$). To approximate material properties, apparent strength parameters were derived by normalizing to bone volume. Apparent toughness was similar between WT and Tg groups, while apparent strength was significantly higher in the OPG-hi group versus WT ($P<0.01$).

In summary, 1 year of OPG overexpression led to marked changes in bone turnover, volume, density and strength that were consistent with the suppression of bone resorption. The dose-dependent suppression of resorption in OPG-Tg rats was accompanied by a secondary coupling-related suppression of bone formation. Rats with the highest levels of OPG overexpression had the greatest reductions in bone turnover parameters, and the greatest improvements in extrinsic bone strength with no evidence of impairment of material properties.

Disclosures: M.S. Ominsky, Amgen Inc. 1, 3.
This study received funding from: Amgen, Inc.

1089

Comparison of the Effects of Teriparatide and Alendronate on Parameters of Total Hip Strength as Assessed by Finite Element Analysis: Results from the Forteo and Alendronate Comparison Trial. T. M. Keaveny¹, P. F. Hoffmann^{*2}, D. L. Kopperdahl², D. W. Donley^{*3}, K. Krohn³, E. V. Glass^{*3}, B. H. Mitlak³. ¹University of California, Berkeley, CA, USA, ²O.N. Diagnostics, Berkeley, CA, USA, ³Eli Lilly and Company, Indianapolis, IN, USA.

Biomechanical computed tomography (BCT) uses finite element analysis of QCT scans to provide non-invasive measures of femoral strength and density plus a strength: density ratio that can be considered a measure of bone "quality". Teriparatide [rPTH (1-34), TPTD] 20 µg/d and alendronate 10 mg/d (ALN) were previously shown to have positive effects on vertebral strength as assessed by BCT during a randomized, double-blind, 18-month study in postmenopausal women with osteoporosis. The purpose of the present analysis was to extend these studies to analysis of proximal femoral strength for a simulated sideways fall. Using the QCT scans, volumetric density from QCT and strength from BCT were determined for the total hip and for the trabecular and cortical compartments, and a strength: density ratio was calculated. In the TPTD group, whole total hip density was not significantly different from baseline at any time point, however, at 18 months trabecular density significantly increased 5.1% and cortical density significantly decreased 1.0% from baseline. In the ALN group, density was not significantly different from baseline at any time point for any compartment. Total hip strength significantly increased 5.9% from baseline at 18 months in the TPTD group, and strength did not significantly change from baseline at any time point in the ALN group. No significant changes were seen in the strength measures associated with isolated changes in the cortical or trabecular compartments. The strength: density ratio significantly increased 4.1% from baseline at 18 months in the TPTD group, whereas no significant changes were seen for ALN. In conclusion, total hip strength at 18 months significantly increased in the TPTD group and did not significantly change in the ALN group. This significant biomechanical effect for TPTD was associated with a significant decrease in cortical density and a somewhat larger increase in trabecular density.

Table: Median percent change from baseline (Interquartile range) at 6 and 18 months

	Alendronate 10mg/day		Teriparatide 20µg/day	
	6 month (N = 21)	18 month (N = 19)	6 month (N = 27)	18 month (N = 22)
Bone Density (mg/cm ³)				
Whole Total Hip	-0.5 (-1.0, 1.6)	0.4 (-2.5, 2.7)	0.4 (-1.4, 1.8)	1.1 (-0.5, 3.1)
Total Hip Trabecular	-0.7 (-1.5, 1.4)	0.0 (-3.4, 1.5)	1.8 (-1.4, 5.2)	5.1** ‡ (1.5, 9.1)
Total Hip Cortical	0.0 (-1.4, 2.0)	0.0 (-2.3, 2.0)	-0.9 (-3.4, 1.3)	-1.0* (-4.0, -0.3)
Strength (N)				
Whole Total Hip	1.0 (-2.2, 5.2)	1.0 (-5.2, 3.0)	2.9 (-4.7, 6.8)	5.9* (-2.8, 9.9)
Total Hip Trabecular	-1.0 (-2.4, 3.3)	-0.6 (-4.4, 1.4)	0.7 (-2.0, 2.3)	2.5 (-2.8, 4.8)
Total Hip Cortical	0.4 (-1.2, 1.8)	-0.5 (-2.4, 1.3)	0.3 (-4.1, 2.2)	-0.2 (-1.5, 2.5)
Strength: Density Ratio (N cm ³ /mg)	1.0 (-1.8, 3.9)	0.3 (-2.7, 2.5)	2.1 (-1.4, 4.8)	4.1* (0.0, 7.8)

*P<0.05, **P<0.005 within treatment from baseline; ‡P<0.005 between treatments

Disclosures: T.M. Keaveny, Merck, Amgen, GSK, Novartis, Pfizer 5; P&G, Merck, Pfizer, Novartis, Lilly, NPS, Teijin 2; O.N. Diagnostics 4.

This study received funding from: Eli Lilly and Company.

1090

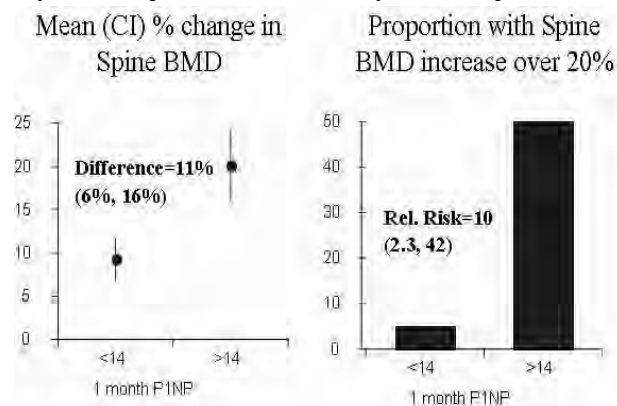
Prediction of 24 Month Change in BMD on PTH Followed by Alendronate: The PaTH Study. D. M. Black¹, D. C. Bauer¹, L. Palermo¹, C. J. Rosen², S. L. Greenspan³, J. P. Bilezikian⁴. ¹UC San Francisco, San Francisco, CA, USA, ²MECORE, St. Joseph Hospital, Bangor, ME, USA, ³University of Pittsburgh, Pittsburgh, PA, USA, ⁴Columbia University, New York, NY, USA.

We previously reported the PaTH study results for postmenopausal women on 2 years of parathyroid hormone (PTH 1-84, 100 µg daily) used either alone or in combination with alendronate (ALN, Black et al., NEJM, 2005). The treatment group that received 1 year of PTH (1-84) followed by 1 year of ALN had the largest mean spine BMD change of 12%, but response varied, with 17% of women having BMD increases over 20%. Previous PaTH analyses have examined predictors of 1 year BMD change while on PTH therapy. This analysis aimed to identify early predictors of response over 2 years in women taking 1 year of PTH followed by 1 year of ALN.

This analysis included 53 women assigned to 1 year of PTH 1-84 followed by 1 year of ALN. The main endpoint was 2 year change in (DXA) spine BMD. Potential predictors included baseline variables (age, BMI, bone marker levels (serum CTX, PINP, Bone ALP), serum chemistries) and early 1- and 3-month on-treatment bone marker values. We used univariable analyses (logistic regression) with change in BMD (>20%) as the outcome adjusted for significant covariates. Bone markers were categorized into highest quartile vs. lower 3 quartiles combined.

The following baseline factors had weak, but significant relationships to the 24-month change in BMD: age, BMI and serum calcium. Baseline bone markers were not significantly associated, but bone marker values at 1 and 3 months after start of treatment were very strongly related to BMD change at 24 months. While all 3 bone markers were associated with 24 month BMD change, PINP was most strongly correlated. The figure

compares 24 month % change in spine BMD in those with 1 month PINP levels in the highest quartile (>142ng/ml) vs. those in the lower 3 quartiles (≤142ng/ml):



The data show that those in the highest quartile of PINP at 1 month were 10 times more likely to show an increase in DXA BMD of ≥20% at 24 months. This relationship was confirmed with multivariable adjustment. In addition to 1-month bone marker values, the 3-month values and change from baseline to 1 and 3 months were similarly predictive of 2 year BMD change. In conclusion, a single measurement of PINP as early as 1 month after initiation of PTH therapy strongly predicts 2 year spine BMD response to 1 year of PTH followed by 1 year of ALN.

Disclosures: D.M. Black, NPS Pharmaceuticals 5; Novartis Pharmaceuticals 2; Merck & Co., Inc. 8; Roche/GSK 2, 5.

This study received funding from: N01 AR92245; NIAMS-045.

1091

Patients Previously Treated with Risedronate Demonstrate Greater Responsiveness to Teriparatide than Those Previously Treated with Alendronate: The OPTAMISE Study. P. Miller¹, R. Lindsay², N. Watts³, S. Meeves^{*4}, T. Lang^{*5}, P. Delmas⁶, J. Bilezikian⁷. ¹Colorado Center for Bone Research, Lakewood, CO, USA, ²Helen Hayes Hospital and Columbia University, West Haverstraw, NY, USA, ³University of Cincinnati College of Medicine, Cincinnati, OH, USA, ⁴sanofi-aventis US Inc., Bridgewater, NJ, USA, ⁵Center for Molecular and Functional Imaging, University of California, San Francisco, CA, USA, ⁶Inserm Research Unit 831 and Université de Lyon, Lyon, France, ⁷Columbia University College of Physicians and Surgeons, New York, NY, USA.

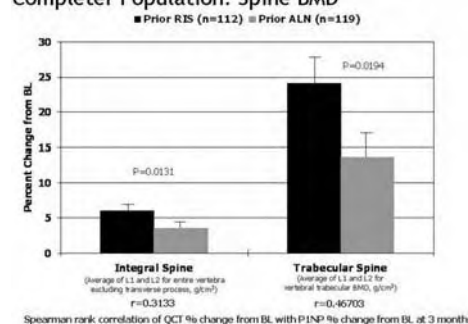
Previous or simultaneous treatment with alendronate (ALN) has been shown to blunt or delay the anabolic response to teriparatide (TPTD). It is not known if the effect is the same with other bisphosphonates. OPTAMISE evaluated the anabolic effect of TPTD in postmenopausal women previously treated for ≥24 months with risedronate (RIS) or ALN.

Post-RIS (n=146) and post-ALN (n=146) subjects were stratified by duration of prior therapy, discontinued their bisphosphonate and were treated with TPTD (20 µg/d SQ) for 12 months. We measured bone turnover markers (BTMs) and bone mineral density (BMD) by DXA and QCT. At baseline, BTMs were higher in the post-RIS group (P<0.05); otherwise, the groups were comparable for key characteristics including BMD by DXA and QCT. Compared with post-ALN subjects, post-RIS changes in BTMs were significantly greater at Months 1-5 (P<0.05, including primary endpoint of PINP change at Month 3), and for BMD by DXA at Month 12 at the spine (P<0.05) and hip (P<0.01). Results were not related to duration of prior bisphosphonate therapy, baseline BTMs, or baseline BMD. Post-RIS subjects showed a 76% greater increase in QCT of trabecular bone at the spine (24.1% vs 13.7%, P=0.0230; Figure). Spine QCT changes correlated with PINP changes at 3 months (r=0.47). TPTD was well-tolerated with a similar incidence of adverse events between groups.

When switched to teriparatide, subjects previously treated with risedronate showed a greater QCT response that correlated with a more pronounced, early increase in PINP as compared with those previously treated with alendronate. Our findings support differences between these bisphosphonates that affect subsequent response to the anabolic effects of teriparatide.

QCT 12-Month Percent Changes from BL

Completer Population: Spine BMD



Disclosures: P. Miller, Alliance for Better Bone Health 2, 5, 8.

This study received funding from: The Alliance for Better Bone Health.

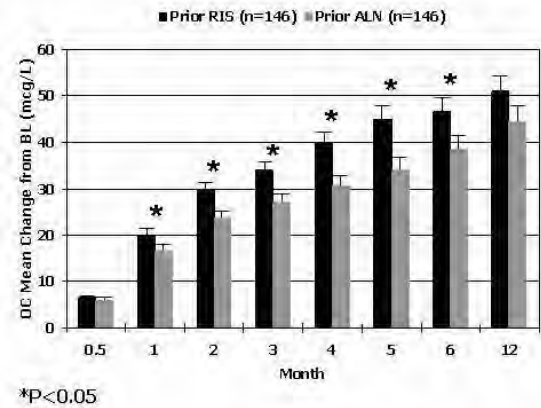
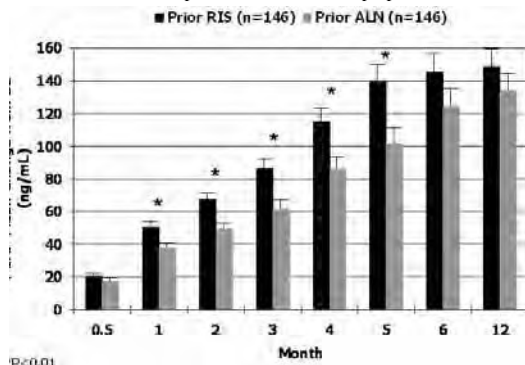
Bone Turnover Markers Demonstrate Greater Earlier Responsiveness to Teriparatide Following Treatment with Risedronate Compared with Alendronate: The OPTAMISE Study. P. Delmas¹, N. Watts², P. Miller³, D. Cahall⁴, J. Bilezikian⁵, R. Lindsay⁶. ¹Inserm Research Unit 831 and Université de Lyon, Lyon, France, ²University of Cincinnati College of Medicine, Cincinnati, OH, USA, ³Colorado Center for Bone Research, Lakewood, CO, USA, ⁴sanofi-aventis, Bridgewater, NJ, USA, ⁵Columbia University College of Physicians & Surgeons, New York, NY, USA, ⁶Helen Hayes Hospital and Columbia University, West Haverstraw, NY, USA.

Previous treatment with alendronate (ALN) has been shown to blunt or delay the anabolic response to teriparatide (TPTD). It is not known if the effect is the same with other bisphosphonates. OPTAMISE evaluated the anabolic effect of TPTD on bone turnover markers (BTM) in postmenopausal women previously treated for ≥ 24 months with risedronate (RIS) or ALN.

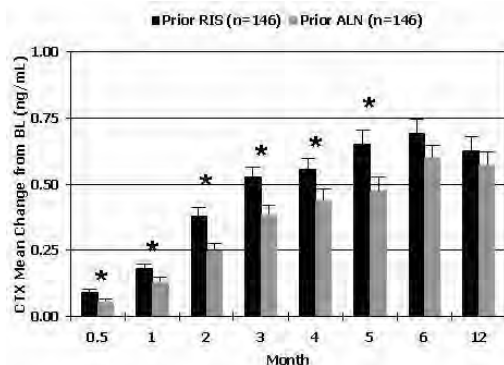
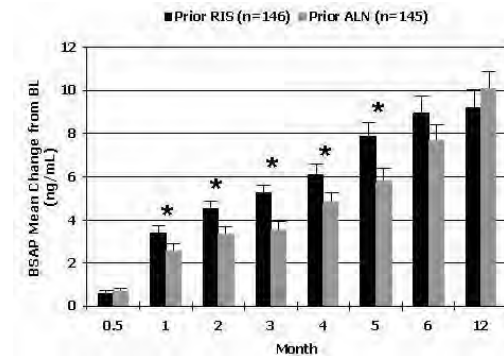
Post-RIS (n=146) or post-ALN (n=146) patients were stratified by duration of prior bisphosphonate therapy, and after discontinuation were treated with TPTD (20 μ g/d SQ) for 12 months. We measured N-terminal propeptide (P1NP, primary endpoint change at Month 3), bone-specific alkaline phosphatase (BAP), osteocalcin (OC), serum CTX and urine NTX in both groups.

Baseline BTMs were significantly higher in the post-RIS group ($P<0.05$); otherwise the groups were comparable for key characteristics, including duration of prior therapy. Absolute changes in P1NP were significantly greater for post-RIS than post-ALN groups during Months 1-5 (Figure 1). Comparable results were observed for BAP, OC, CTX and NTX (Figure 2). Results were consistent regardless of duration of prior therapy or baseline BTMs. TPTD was well-tolerated with a similar incidence of adverse events between groups.

In response to treatment with TPTD, subjects previously treated with RIS showed greater increases in BTMs compared with those previously treated with ALN. The increase in the resorption markers occurred as early as the increase in formation markers, but to a lesser extent. Our findings suggest differences between these bisphosphonates in which RIS allows the skeleton to be more responsive to the anabolic properties of TPTD.



Disclosures: P. Delmas, Alliance for Better Bone Health 2, 5, 8.
This study received funding from: The Alliance for Better Bone Health.



1093

Teriparatide Reduces Bone Microdamage Accumulation in Postmenopausal Women Previously Treated with Alendronate. H. Dobnig¹, J. J. Stepan², D. B. Burr³, A. F. Fahrleitner-Pammer¹, J. Li³, A. Sipos⁴, M. Sato⁴, I. Pavo⁴. ¹Endocrinology and Nuclear Medicine, Medical University of Graz, Graz, Austria, ²Institute of Rheumatology, Charles University Faculty of Medicine, Prague, Czech Republic, ³Department of Anatomy and Cell Biology, Indiana University School of Medicine, Indianapolis, IN, USA, ⁴Lilly Research Laboratories, Indianapolis, IN, USA.

Suppression of bone turnover by bisphosphonates is associated with increased bone microdamage accumulation in animal models. It has been demonstrated at the baseline analysis of the present study, that after adjustment for potential confounders, crack density (Cr.D) was elevated in alendronate (ALN) treated patients compared with treatment naïve (TN) patients. In addition, an association of microdamage accumulation with low bone mineral density was only present in ALN treated patients. To assess effects of bone formation on bone quality, our objective was to investigate the change in microdamage accumulation in iliac crest biopsies by teriparatide (TPTD) in these previously TN patients and in those switched from ALN to TPTD. Sixty-six postmenopausal women with osteoporosis (mean age of 68.0 years and mean BMD T-score of -1.7 at total hip and -2.8 at lumbar spine; 62% with prevalent fractures) entered this prospective, non-randomized study and started with 24-month 20 µg/day subcutaneous TPTD treatment in monotherapy: thirty-eight stopped previous ALN treatment (10 mg/day or 70 mg/week for a mean duration of 63.6 months) and switched to TPTD while twenty-eight were treatment naïve (TN) previously. Paired biopsies with two intact cortices were collected and analyzed for microdamage accumulation at baseline and after 24-month TPTD administration in 13 TN and 18 ALN treated patients. A within-group t-test comparing the mean percent change was carried out on log-transformed data. Following 24 months of teriparatide treatment, Cr.D, crack surface density (Cr.S.D) and crack length (Cr.L) were decreased in previously ALN treated patients while only Cr.L was reduced in former TN patients (Table). The changes in microdamage accumulation parameters were not statistically different between the two groups. Our data indicate that TPTD reduces microdamage accumulation in iliac crest biopsies of patients previously treated with ALN.

All mean+/-SD, %change on log-transformed data				
		Baseline	After TPTD	P-value
Crack Density (/mm ²)	Treatment naïve (N=13)	0.56+/- 0.6	0.71+/-0.6	0.33
Crack Density (/mm ²)	ALN (N=18)	0.91+/-0.7	0.66+/-0.8	0.05
Crack Surface Density (µm/mm ²)	Treatment naïve (N=13)	28.7+/-35	26.7+/-24	0.79
Crack Surface Density (µm/mm ²)	ALN (N=18)	44.5+/-33	28.3+/-43	0.01
Crack Length (µm)	Treatment naïve (N=13)	46+/-10	36+/-5	0.01
Crack Length (µm)	ALN (N=18)	48+/-10	35+/-10	<0.001

Disclosures: H. Dobnig, Eli Lilly 8; Sanofi-Aventis 2, 8.
This study received funding from: Eli Lilly.

1094

Year 3 Effects on Bone Mass in Women using Bisphosphonates after PTH Therapy: Follow-up Results from the PaTH II Study. T. F. Hue¹, J. P. Bilezikian², K. E. Ensrud³, S. L. Greenspan⁴, C. J. Rosen⁵, L. Palermo¹, T. F. Lang¹, D. M. Black¹. ¹University of California, San Francisco, San Francisco, CA, USA, ²Columbia University, New York, NY, USA, ³University of Minnesota, Minneapolis, MN, USA, ⁴University of Pittsburgh, Pittsburgh, PA, USA, ⁵Maine Center for Osteoporosis Research & Education, St. Joseph Hospital, Bangor, ME, USA.

We previously reported the results of the 2-year PaTH trial of 238 postmenopausal women comparing 1 year of therapy with either parathyroid hormone (PTH 1-84, 100 µg daily) alone, the bisphosphonate, alendronate (ALN), alone or the two in combination, followed by 1 year of ALN or placebo (Black et al., NEJM, 2004; NEJM, 2005). At 24 months, 1 year of PTH followed by 1 year of ALN resulted in the largest increases in areal bone mineral density (BMD) at the spine and hip, by dual-energy x-ray absorptiometry (DXA). This group also showed the greatest BMD increase in trabecular spine BMD by quantitative computed tomography (QCT). PaTH II was a 1-year observational study designed for a 3rd year of follow-up in women originally randomized into PaTH (from 4 sites: ME, MN, NY, and PA) to assess if BMD continues to increase or is maintained in those treated with PTH followed by a bisphosphonate. After completion of PaTH, 60% (n=109) of the 182 women in follow-up were prescribed a bisphosphonate (ALN or resoridronate). In addition, 90% of the 182 remained on calcium/vitamin D supplements. Results are presented for the 109 participants who used a bisphosphonate (BIS) during year 3 (months 25-36).

Women who used Bisphosphonates in year 3 (n=109): BMD Mean Percent Changes by DXA and QCT[†]

Treatment Group	PaTH				PaTH II			
	% Changes from baseline to year 2				% Changes from baseline to year 3			
Yr 1 Treatment	PTH	PTH	PTH/BIS	BIS	PTH	PTH	PTH/BIS	BIS
Yr 2 Treatment	Placebo	BIS	BIS	BIS	Placebo	BIS	BIS	BIS
Yr 3 Treatment					BIS	BIS	BIS	BIS
DXA BMD								
Spine	+5.9*	+11.2*	+7.9*	+8.1*	+8.9*	+11.5*	+10.1*	+9.4*
Total hip	+0.05	+4.6*	+3.4*	+3.0*	+1.7	+5.1*	+3.3*	+3.7*
QCT BMD								
Trabecular spine	+19.6*	+29.7*	+9.0*	+3.5	+10.7	+26.6*	+8.1	+3.3
Trabecular hip	+7.8	+13.9*	+14.7*	+5.8	-4.8	+15.1*	+15.1*	+2.4
Cortical hip	-2.6*	-1.4	-1.3	-1.4	-3.6*	-3.5*	-3.2*	-3.4*

* Mean change within group, p-value < 0.05

† QCT scans were not measured in participants at the New York site. PaTH (months 0-24), n= 95;

PaTH II (months 25-36), n=76.

The results suggest that BMD increases were maintained with BIS use in year 3 (for groups B & C), after 1 year of PTH followed by 1 year of BIS or the two in combination, followed by 1 year of BIS. However, women (in group A) who received PTH for 1 year, had no treatment the following year, and then took BIS in year 3, lost approximately 50% of their previous gain (from months 0-24) in trabecular spine BMD. Group A also had a loss of all gains in trabecular hip BMD and reverted to below the mean baseline level. We conclude that treatment of up to 2 years with bisphosphonate, immediately following 1 year of daily PTH, appears to maintain bone mass gains from the initial anabolic therapy in postmenopausal osteoporotic women.

Disclosures: T.F. Hue, None.

This study received funding from: NIAMS-NIH and NPS Pharmaceuticals.

1095

Teriparatide Improves Bone Microarchitecture in Postmenopausal Women Previously Treated with Alendronate. J. Li¹, D. B. Burr¹, J. J. Stepan², H. Dobnig³, A. Fahrleitner-Pammer³, A. Sipos⁴, T. Mullarney⁴, M. Westmore⁴, M. Sato⁴, I. Pavo⁴. ¹Department of Anatomy and Cell Biology, Indiana University School of Medicine, Indianapolis, IN, USA, ²Institute of Rheumatology, Charles University Faculty of Medicine, Prague, Czech Republic, ³Department of Internal Medicine, Medical University of Graz, Graz, Austria, ⁴Lilly Research Laboratories, Indianapolis, IN, USA.

Teriparatide stimulates mineral apposition resulting in increased trabecular bone volume and cortical thickness in postmenopausal women with osteoporosis who were not treated previously with antiresorptive agents. Patients previously on alendronate (ALN) may have a delayed response to teriparatide (TPTD) as measured by an increase in serum levels of biochemical markers of bone formation activity and bone mineral density (BMD). Our aim was to investigate the effect of teriparatide on bone microarchitecture in patients after long-term ALN treatment. Sixty-six postmenopausal women with osteoporosis (mean age of 68.0 years and mean BMD T-score of -1.7 at total hip and -2.8 at lumbar spine; 62% with prevalent fractures) entered a prospective, non-randomized study. Thirty-eight had been switched from previous ALN treatment (10 mg/day or 70 mg/week for a mean duration of 63.6 months) while twenty-eight were treatment naïve (TN). All patients were subsequently treated with TPTD (20 µg/day, subcutaneously) as monotherapy for 24 months. Iliac crest bone biopsies were collected at baseline and endpoint and were analyzed by two-dimensional (2D) histomorphometry (N=35) and three-dimensional (3D) microcomputed tomography (µCT, N=45). Mean activation frequency, an indicator of bone turnover was increased from baseline in both TN and ALN treated patients (mean change, mean % change, within-group p-value: 0.165 cycles/year, 138%, p=0.002 and 0.212 cycles/year, 359%, p<0.001 for TN and ALN respectively). The more accurate µCT 3D indices demonstrated an increase in both trabecular and cortical thickness (Table). There was no difference in 3D changes between the two patient groups. Our results show that after 24 months of treatment, TPTD therapy improves bone microstructure in patients, irrespective of whether they had received prior ALN antiresorptive therapy.

	Treatment naïve (N=16)		Alendronate treated (N=29)	
	% change*	P-value#	% change*	P-value#
Trabecular thickness (mm)	30.4 (30)	0.001	30.8 (53)	0.004
Trabecular number (/mm)	36.7 (179)	0.298	12.7 (54)	0.254
Trabecular separation (mm)	3.1 (36)	0.600	10.4 (75)	0.536
Cortical thickness (mm)	37.8 (59)	0.048	31.7 (63)	0.011
Total cortical area (mm ²)	28.2 (53)	0.545	42.8 (77)	0.026

* mean (standard deviation)

p-value from within-group t-test comparing mean percent change to zero (untransformed or log-transformed data depending on observed data distribution)

Disclosures: J. Li, Eli Lilly & Co. 2.

This study received funding from: Eli Lilly and Company.

1096

Unusual Osteoclast Morphology in Teriparatide-treated Patients Who Have Been Pretreated with Alendronate. D. W. Dempster¹, H. Zhou¹, J. W. Nieves¹, N. Barbuti^{*1}, M. Bostrom^{*2}, F. Cosman¹, R. Lindsay¹. ¹Regional Bone Center, Helen Hayes Hospital, West Haverstraw, NY, USA, ²Hospital for Special Surgery, New York, NY, USA.

It has long been established that osteoblasts signal to osteoclasts. Recent observations suggest that signaling also occurs in the opposite direction, from osteoclasts to osteoblasts (Karsdal et al, JBMR 2007). Such signaling almost certainly plays an important role in mediating the stimulatory effect of anabolic agents, such as teriparatide (TPTD) on bone formation and may also be influenced by prior treatment with antiresorptive agents such as bisphosphonates. The purpose of the present study is to define better the effects of TPTD and prior treatment with the bisphosphonate alendronate on osteoclasts. We recruited 37 women with osteoporosis (16 treatment naïve; 21 pretreated with alendronate for at least one year. The two groups were randomized to control or TPTD (20 mcg/day). Iliac crest biopsies were taken either prior to TPTD treatment (n=11), after 7.5 weeks (n=13), or after 7.5 months (n=13). Biopsies were analyzed without knowledge of treatment assignment. During the morphometric analysis, osteoclasts with unusual morphology were observed in a number of subjects. These cells were approximately twice the size of normal osteoclasts, and contained many more nuclei (up to 27 per cell profiles). They were frequently not attached to the bone surface or were separated from it by lining cells. They were often not associated with Howship's lacunae, or the lacunae were shallow. We refer to them as large, inactive osteoclasts (LI.Oc). LI.Oc were observed in only 1 of 13 subjects at 7.5 weeks but were commonly seen on cancellous, endocortical or both surfaces at 7.5 months.

Group	Number of Subjects	Number of Subjects with LI.Oc
Alendronate Pre-TPTD	6	2
Alendronate Post-TPTD	8	8
Naïve Pre-TPTD	5	1
Naïve Post TPTD	5	1

LI.Oc were observed in 33% of ALN treated patients prior to TPTD treatment, in 100% of patients in whom ALN was followed by TPTD, and in only 20% of naïve patients both before or after TPTD treatment. We conclude that treatment with ALN followed by TPTD results in an increase in LI.Oc. We hypothesize that, by 7.5 months, TPTD enhances osteoclast recruitment, but the resorptive capacity of these osteoclasts is inhibited by ALN. Osteoclast nuclear number and size increase as a compensatory response to inhibition of activity. While resorptive function is inhibited, signaling to osteoblasts remains intact as bone formation is markedly increased by TPTD in ALN-treated subjects (see abstract from our group, this meeting)

Disclosures: D.W. Dempster, None.

1097

The Aging Associated Gene SIRT-1 Regulates Osteoclast Formation and Bone Mass In Vivo. J. R. Edwards¹, K. Zainabadi^{*2}, F. Eleftheriou¹, L. Connelly³, F. Yuli^{*3}, T. S. Blackwell^{*3}, E. Alt^{*2}, L. Guarente^{*2}, G. R. Mundy¹. ¹Center for Bone Biology, Vanderbilt University Medical Center, Nashville, TN, USA, ²MIT, Cambridge, MA, USA, ³VUMC, Nashville, TN, USA.

Progressive bone loss is a universal accompaniment of aging and involves multiple mechanisms. As the aging process has a powerful genetic component we questioned if genes associated with aging had a direct role in controlling bone mass. We examined the role of the longevity gene Sir2 which directly regulates lifespan in *S. cerevisiae*, *C. elegans* and *Drosophila*, in the control of vertebrate bone remodeling. The mammalian homolog of Sir2 is the highly conserved histone deacetylase Silent Information Regulator T-1 (SIRT-1). We examined the phenotype of SIRT-1 null mice using Piximus, μ CT scanning, histomorphometric analysis, bone resorption and cell proliferation assays of primary bone cells from SIRT-1 null and WT mice. In addition, the effect of SIRT-1 agonists and inhibitors on normal osteoclast formation and Nf κ B activity were studied using a GFP-tagged Nf κ B-reporter (NGL) mouse model, and q-PCR used to assess SIRT-1 expression in bone extracts from the SAM P6 osteoporotic mouse model. The phenotype of these mice was striking. Skeletal tissues from 1, 4 and 11 month SIRT-1 null mice showed up to 40% decrease in BV/TV by μ CT analysis (p<0.001) and 46% decrease in BMD (p<0.01) compared to WT. Histomorphometric analysis of undecalcified SIRT-1 null L3-4 vertebrae supported μ CT data showing up to 44% decrease in BV/TV (p<0.001). TRAP staining demonstrated a 27% increase in osteoclast surface/bone surface compared to WT animals (p<0.05). When cells extracted from normal bone marrow were treated with M-CSF (30ng/ml), RANKL (50ng/ml) and the SIRT-1 inhibitor Nicotinamide (10mM) the number and size of VNR+, TRAP+ multinucleated cells formed and resorption of dentine slices was significantly increased. The SIRT-1 agonist Resveratrol (1uM) demonstrated a decrease in osteoclast formation (p<0.05). In agreement with pharmacological data, primary bone marrow cells isolated from SIRT-1 null mice also formed TRAP+ multinucleated cells at significantly increased rates compared with WT cells. Isolated bone marrow cells from NGL mice treated with M-CSF, RANKL and Nicotinamide showed a x10 increase in fluorescence (p<0.05). Resveratrol treatment reduced GFP expression to a level lower than that of RANKL treatment alone (p<0.05) suggesting that Nf κ B is a downstream target of SIRT-1. In addition, bone extracts from SAM P6 mice showed a 7.5 fold decrease in SIRT-1 expression compared to SAM R1 controls (p<0.001). This data suggests that SIRT-1 activity regulates osteoclast formation and bone mass through the release of Nf κ B from SIRT-1 inhibition. These findings identify a new molecular link between aging and osteoporosis.

Disclosures: J.R. Edwards, None.

1098

Functional Analysis of Bcl-xL in Osteoclasts by Osteoclast-Specific Deletion of bcl-x Gene in Mice. M. Iwasawa¹, Y. Nagase¹, T. Miyazaki¹, T. Akiyama¹, Y. Kadono¹, M. Nakamura¹, Y. Oshima¹, T. Yasui^{*1}, T. Nakamura^{*2}, S. Kato^{*2}, K. Nakamura¹, S. Tanaka¹. ¹Department of Orthopaedic Surgery, The University of Tokyo, Tokyo, Japan, ²The Institute of Molecular and Cellular Biosciences, The University of Tokyo, Tokyo, Japan.

Osteoclasts undergo rapid apoptosis without trophic factors, such as macrophage colony-stimulating factor (M-CSF) and receptor activator of NF- κ B ligand (RANKL). However, the molecular events implicated in these processes still remain elusive. Bcl-2 family proteins are central regulators of apoptosis, and include pro- and anti-apoptotic members. Bcl-xL is an anti-apoptotic member of the Bcl-2 family, which is generated by alternative splicing of bcl-x gene, and suppresses apoptosis in many cell types. To investigate the role of Bcl-xL in osteoclasts, we generated osteoclast-specific Bcl-xL knock-out (cKO) mice by mating bcl-x flox/flox mice with Cathepsin K-Cre mice, in which Cre recombinase gene was knocked into a single allele of the cathepsin K gene locus. Expression of Bcl-xL was specifically reduced in osteoclasts derived from cKO mice (-/-OCs) compared to those from wild-type littermates (+/+OCs), but not in osteoblasts or other tissues. Osteoclasts differentiated normally from cKO mouse bone marrow cells in the presence of RANKL and M-CSF. However, -/-OCs exhibited increased cell death and Caspase-3 activity after cytokine withdrawal. In spite of their susceptibility to apoptosis, -/-OCs showed higher bone-resorbing activity than +/+ OCs as determined by pit formation assay. These phenotypes of -/-OCs were restored by adenoviral introduction of Bcl-xL. We further analyzed the effect of Bcl-xL deficiency in osteoclast differentiation using RNA interference technique, and found that osteoclast differentiation was not affected by Bcl-xL knockdown. cKO mice were alive at birth and were obtained at predicted Mendelian frequencies. Although they grew normally with no apparent morphological abnormalities, they exhibited a decrease in trabecular bone volume after 8 weeks, and developed significant osteopenia at 1 year of age as determined by radiological (soft X-ray and bone densitometry) and histological analysis. Histomorphometric analysis of distal femur revealed that the eroded surface/bone surface (ES/BS) was significantly increased in the cKO mice, while bone formation markers were equivalent to those of wild-type mice. From these observations, we conclude that Bcl-xL deficiency in OCs leads to decrease of bone volume through increased bone resorbing activity, despite of increased apoptosis. Bcl-xL plays a pivotal role in both survival and bone-resorbing activity of osteoclasts, thus creating a novel link between anti-apoptotic molecule and skeletal homeostasis.

Disclosures: M. Iwasawa, None.

1099

ADAM8 Binds $\alpha_9\beta_1$ to Increase OCL Formation and Function by Interacting with Pyk2 and Activating Paxillin. G. Lu¹, K. Patrene^{*1}, V. Garcia-Palacios¹, J. Anderson^{*1}, C. Boykin^{*2}, D. Del Prete^{*3}, J. J. Windle^{*2}, G. D. Roodman⁴. ¹Medicine/Hem-Onc, University of Pittsburgh, Pittsburgh, PA, USA, ²Human Genetics, Virginia Commonwealth University, Richmond, VA, USA, ³Human Anatomy & Histology, University of Bari Medical School, Bari, Italy, ⁴Medicine/Hem-Onc, University of Pittsburgh and VA Pittsburgh Healthcare System, Pittsburgh, PA, USA.

We have previously identified ADAM8 (A Disintegrin and Metalloproteinase 8) as a novel osteoclast (OCL) stimulator whose disintegrin domain mediates its stimulatory effects. Further, we identified integrin $\alpha_9\beta_1$, which is expressed both on OCLs and their precursors, as a receptor of ADAM8. Since α_9 integrin only forms heterodimers with β_1 , and β_1 knockout (KO) mice are embryonic lethal, we determined whether there are other receptors for ADAM8 by assessing osteoclastogenesis in α_9 -/- mice, as well as in human bone marrow cells infected with an α_9 integrin shRNA lentivirus. Bone marrow cells from α_9 -/- mice and human OCL precursors infected with α_9 shRNA formed decreased numbers of OCL which were small and had disrupted actin rings. When bone marrow non-adherent cells and spleen cells from 7-day-old α_9 -/- mice were infected with a full length human α_9 construct, normal numbers of OCLs formed. Further, bone marrow cells from α_9 -/- mice failed to respond to treatment with soluble ADAM8, whereas, wild type bone marrow cells formed OCLs in the presence of soluble ADAM8. These data suggest that expression of full length α_9 integrin can rescue the α_9 KO phenotype in OCL formation. To determine the mechanisms responsible for the stimulatory effects of ADAM8 on osteoclastogenesis, we used an ADAM8 disintegrin domain GST fusion protein to identify the proteins that interact with ADAM8. This GST fusion protein can stimulate osteoclast formation to the same level as the full length ADAM8. GST ADAM8 protein pull-down assays with OCL precursor lysates demonstrated that protein tyrosine kinase 2 (Pyk2) formed a complex with the ADAM8 disintegrin domain. The identity of Pyk2 in the complex was confirmed by peptide mass fingerprinting (MS/MS). Further, we found that treatment of wild type OCL cultures with ADAM8 for 5 to 10 minutes induced transient tyrosine phosphorylation (pY118) of paxillin. Paxillin phosphorylation was not detected in α_9 -/- OCL cultures. These results demonstrate that α_9 is the only receptor for ADAM8, and suggest that ADAM8/ $\alpha_9\beta_1$ increases OCL formation and function through interacting with Pyk2 and signaling through paxillin.

Disclosures: G. Lu, None.

This study received funding from: NIH.

1100

RANKL Stimulates Osteoclasts to Release the Lymphatic Growth Factor, VEGF-C, and Enhances Osteoclastic Bone Resorption Through an Autocrine Mechanism. R. Guo, Q. Zhang, Y. Lu*, E. M. Schwarz, B. F. Boyce, L. Xing. University of Rochester, Rochester, NY, USA.

Osteoclasts (OCs) are bone-resorbing cells, which mediate normal bone remodeling and pathologic bone loss, such as in rheumatoid arthritis (RA). Recent studies indicate that OCs also function as immunomodulators and secrete cytokines that contribute to inflammation and autoimmunity. To investigate if OCs produce angiogenic factors in RA, we performed microarray analysis using purified CD11b⁺/Gr-1⁻ osteoclast precursors (OCPs) from blood and bone marrow of TNF transgenic (TNF-Tg) arthritic mice and wt littermates. Among 50 angiogenic factors examined, VEGF-C expression was significantly increased in TNF-Tg mice (6-fold vs wt cells). VEGF-C is a recently identified lymphatic growth factor, but little is known about its role in bone. Here, we examined if osteoclastogenic cytokines regulate VEGF-C production by OCs and if VEGF-C affects OC function. We cultured wt spleen cells with M-CSF for 3 days to generate OCPs, treated them with RANKL or TNF, and examined expression of VEGF members by real-time RT-PCR. Both RANKL (12.1 \pm 0.5 fold) and TNF (3.5 \pm 0.2 fold) stimulated OCP expression of VEGF-C, but not of other VEGFs. RANKL also stimulated mature OCs to produce VEGF-C (40 \pm 1 fold). RANKL failed to induce VEGF-C expression in NF- κ B p50/p52 double knockout OCPs. In an EMSA assay, RANKL promoted nuclear protein binding to a putative NF- κ B binding sequence from the mouse VEGF-C promoter. To determine if VEGF-C affects OC function, we treated OCPs with VEGF-C or over-expressed VEGF-C by retrovirus infection and cultured them on bone slices. VEGF-C increased OC resorption pit area, but not OC numbers. To test if VEGF-C works as an autocrine factor, OCPs were treated with RANKL plus the VEGF-C specific receptor inhibitor, VEGFR3-Fc, or VEGFR2-Fc, which inhibits other VEGFs. VEGFR3-Fc, but not VEGFR2-Fc, reduced RANKL-mediated OC pit formation (pit area (mm²)/slice: IgG 2.1 \pm 0.25; VEGFR3-Fc 0.8 \pm 0.1; VEGFR2-Fc 2.1 \pm 0.22) and had no effect on OC numbers. Furthermore, immunostaining of joint sections from RA patients or TNF-Tg mice showed that OCs expressed high levels of VEGF-C and that lymphatic vessel numbers were increased in joints of the TNF-Tg mice. In summary, RANKL stimulates OCs and OCPs to release large amounts of VEGF-C, which enhances OC bone resorption by binding to the VEGF-C receptor on OCPs and OCs. Thus, VEGF-C is a RANKL-induced autocrine factor for OC function. Importantly, our study indicates that RANKL and OCs may directly affect lymphangiogenesis through VEGF-C signaling, which will require further investigation given the importance of the lymphatic system in inflammation and tumor metastasis.

Disclosures: R. Guo, None.

This study received funding from: NIH.

1101

TRPV4 Affects Bone Remodeling by Regulating Calcium Signaling Required for Osteoclast Activity. R. Masuyama¹, J. Vriens², S. Torrekens¹, K. Moermans¹, A. Vanden Bosch¹, R. Bouillon¹, B. Nilius², G. Carmeliet¹. ¹Laboratory of Experimental Medicine & Endocrinology, Katholieke Universiteit Leuven, Leuven, Belgium, ²Department of Cell Biology, Division of Physiology, Katholieke Universiteit Leuven, Leuven, Belgium.

Intracellular calcium [Ca²⁺]_i signaling is necessary for osteoblast and osteoclast function implying that calcium permeable channels are implicated in local bone remodeling rather than in systemic calcium homeostasis. TRPV4 is a widely expressed Ca²⁺ entry channel of the "Transient Receptor Potential" (TRP) family of cation channels. We detected TRPV4 expression in both osteoblasts and osteoclasts. To elucidate whether TRPV4-mediated [Ca²⁺]_i signaling is important for bone, TRPV4 deficient mice were investigated. Lack of TRPV4 did neither affect systemic calcium homeostasis nor endochondral bone development. However, an increased bone mass (+60%) was observed by histomorphometry in 12-week-old TRPV4^{-/-} tibiae (P<0.01), which was associated by a decreased osteoclast surface (-40%) compared to WT mice (P<0.05). In addition, calcitonin receptor mRNA levels were decreased in TRPV4^{-/-} femora (P<0.05), consistent with decreased serum CTX levels (P<0.05). At the other hand, osteoblast function was not different between genotypes as evidenced by unaltered serum osteocalcin levels and dynamic bone histology. Also, RANKL/OPG mRNA expression in the femur was not altered. These data suggest that TRPV4 promotes osteoclastogenesis cell-autonomously. Accordingly, multinuclearity evaluated by the number of mature osteoclasts containing more than 10 nuclei was decreased in cultures of TRPV4^{-/-} bone marrow-derived hematopoietic cells (P<0.01) treated with RANKL and MCSF. This was associated with decreased resorption activity (-60%) in TRPV4^{-/-} osteoclasts compared to WT osteoclasts (P<0.05) assessed by culturing osteoclasts on apatite-coated disks. In these polarized osteoclasts on apatite disks, TRPV4 localized at the apical membrane as shown by vertical reconstruction of confocal microscope scanning images. Furthermore, the TRPV4-specific agonist, 4 α -PDD, evoked [Ca²⁺]_i influx specifically in large mature WT osteoclasts, but not in small WT osteoclasts containing less than 5 nuclei or TRPV4^{-/-} osteoclasts. Noteworthy, TRPV4 inactivation resulted in lower basal [Ca²⁺]_i in osteoclasts measured at 37°C. In addition, treatment with TRPV4 agonists induced NFATc1 mRNA expression accompanied by increased calcitonin receptor mRNA expression in cultured WT osteoclasts.

In summary, our findings provide evidence that TRPV4 maintains [Ca²⁺]_i homeostasis, osteoclast maturation and function, and therefore contributes to normal bone remodeling.

Disclosures: R. Masuyama, None.

1102

Cell-cell Fusion of Osteoclasts Is Stimulated in DC-STAMP Transgenic Mice. R. Iwasaki^{*1}, T. Miyamoto², H. Kawana^{*3}, T. Nakagawa^{*3}, T. Suda^{*4}. ¹Department of Cell Differentiation, Dentistry and Oral Surgery, Keio University School of Medicine, Tokyo, Japan, ²Department of Cell Differentiation, Musculoskeletal Reconstruction and Regeneration Surgery, Keio University School of Medicine, Tokyo, Japan, ³Department of Dentistry and Oral Surgery, Keio University School of Medicine, Tokyo, Japan, ⁴Department of Cell Differentiation, Keio University School of Medicine, Tokyo, Japan.

Osteoclasts are multinuclear giant cells derived from hematopoietic stem cells in the presence of M-CSF and RANKL. The multinucleation of osteoclasts is induced by a cell-cell fusion of mononuclear osteoclasts. Recently, we have isolated DC-STAMP (Dendritic Cell Specific Transmembrane Protein), a seven transmembrane protein, as an essential molecule for osteoclast cell-cell fusion. Osteoclasts in DC-STAMP deficient mice show complete lack of cell-cell fusion in osteoclasts (J. Exp Med, 2005). Since the osteoclast differentiation molecules such as TRAP and CathepsinK, and the transcriptional factors such as c-fos and NFATc1 were not suppressed in DC-STAMP deficient compared with wild-type osteoclasts, DC-STAMP is specifically required for osteoclast cell-cell fusion. However, it is not yet characterized the mechanisms of cell-cell fusion via DC-STAMP. Here we generated DC-STAMP transgenic mice (Tg) under the control of an actin(CAG) promoter to express DC-STAMP ubiquitously in vivo. 95 lines of offspring were generated by the embryo microinjection, and the presence of the transgene in the offsprings was tested by PCR of tail DNA using transgene specific primers. 10 transgenic founder lines were established, and DC-STAMP expression was detected in various tissues of DC-STAMP Tg mice such as liver, muscle and brain, all of which do not express DC-STAMP physiologically. Interestingly, ectopic cell-cell fusion was not observed in liver and muscle, and the multinucleation of myotube was not stimulated by the forced expression of DC-STAMP in Tg mice.

Indeed defects of osteoclast cell-cell fusion in DC-STAMP deficient mice was rescued by crossing with DC-STAMP Tg mice in vivo and in vitro. In vitro osteoclast formation assay, the number of multinuclear cells as well as the number of nuclei in each multinuclear cell were significantly upregulated in osteoclasts of Tg mice compared with that of wild-type littermates. The cell-cell fusion was not induced even in the cells derived from Tg bone marrow in the presence of M-CSF alone, while the addition of RANKL in turn induced hyper-multinucleation of osteoclasts. Taken together our results suggest that DC-STAMP promotes cell-cell fusion in a tissue specific manner, and DC-STAMP induces a cell-cell fusion downstream of RANKL-RANK cascade in osteoclasts.

Disclosures: R. Iwasaki, None.

1103

Characterization of Osteoclast Inhibitory Peptide-1 (OIP-1/hSca) Binding to Fc Gamma Receptor II B (Fc γ R₂) on Osteoclast Precursor Cells. S. Shanmugarajan¹, C. Beeson^{*2}, S. V. Reddy¹. ¹Charles P. Darby Children's Research Institute, Charleston, SC, USA, ²Pharmaceutical Sciences, Medical University of South Carolina, Charleston, SC, USA.

We have previously identified and characterized the osteoclast inhibitory peptide-1 (OIP-1/hSca) as an autocrine/paracrine inhibitor of osteoclast differentiation. OIP-1 is also known as RIG-E or TSA-1, a member of Ly-6 gene family. We have recently demonstrated that mice targeted with the OIP-1/hSca expression to the osteoclast lineage develop osteopetrosis bone phenotype. We have also shown that OIP-1 c-peptide region is critical for osteoclast (OCL) inhibitory activity; however a cognate receptor/membrane protein which interacts with OIP-1 in osteoclast precursor cells is unknown. Evidence suggests a functional physical association between TSA-1 and Fc gamma receptor II B (Fc γ R₂) on the surface of activated B-cells. Immunoreceptor tyrosine-based activation motif (ITAM) bearing adapter proteins such as Fc γ R₂ and DAP12 play a critical role in OCL development. We therefore, hypothesized that OIP-1 binding to Fc γ R₂ on osteoclast precursor cells inhibit OCL differentiation. We examined binding of the OIP-1 c-peptide to RAW 264.7 osteoclast progenitor cells using FACS analysis. Fluorescein conjugated OIP-1 c-peptide (10 μ M) binds to these cells indicating the presence of a surface receptor or membrane protein partner in these cells. Co-immune precipitation and subsequent mass spectrometric analysis identified OIP-1 associated to Fc γ R₂ expressed in RAW264.7 cells. Confocal microscopy analysis demonstrated co-localization of fluorescein conjugated OIP-1 c-peptide with Fc γ R₂ expressed on the cell membrane in osteoclasts formed in RAW 264.7 and OIP-1 mouse bone marrow cultures. An ELISA binding assay confirmed that the OIP-1 c-peptide forms a 1:1 complex with recombinant Fc γ R₂ protein characterized by an equilibrium dissociation constant of K_d = 5 \pm 1 μ M. We further examined if OIP-1 signals through Fc γ R₂ to inhibit OCL differentiation. siRNA suppression of Fc γ R₂ expression in RAW 264.7 cells rescues OIP-1 c-peptide inhibition of RANKL stimulated OCL differentiation in vitro. We further show that OIP-1 c-peptide (100 ng/ml) treatment of RAW 264.7 and OIP-1 transgenic mouse bone marrow derived preosteoclast cells suppresses (6-fold) RANKL induced ITAM phosphorylation. Taken together, our results suggest OIP-1 binding to Fc γ R₂ in preosteoclasts inhibits osteoclast differentiation through suppression of ITAM phosphorylation. Thus, OIP-1 is an important physiologic regulator of osteoclast development and may have therapeutic utility for bone diseases with high bone turnover such as osteoporosis and Paget's disease of bone.

Disclosures: S. Shanmugarajan, None.

This study received funding from: NIH.

1104

Calcium and Phospholipase C γ 2 Signaling Regulates RANKL-induced Osteoclastogenesis. Y. Chen¹, X. Wang², L. Di³, G. Fu³, Y. Chen³, L. Bai³, J. Liu¹, H. Liu¹, L. Ma¹, X. Feng¹, Y. He³, R. Wen³, J. M. McDonald⁴, D. Wang³, H. Wu². ¹Pathology, MCP, University of Alabama at Birmingham, Birmingham, AL, USA, ²Pediatric Dentistry, University of Alabama at Birmingham, Birmingham, AL, USA, ³Blood Research Institute of Wisconsin, Milwaukee, WI, USA, ⁴Pathology and VA medical center, University of Alabama at Birmingham, Birmingham, AL, USA.

Activation of calcium and phospholipase γ (PLC γ) signaling has been demonstrated in osteoclastogenesis stimulated by the receptor activator of NF κ B ligand (RANKL). Inhibition of PLC γ blocks RANKL-induced Ca²⁺ release from intracellular stores. PLC γ 1 is ubiquitously expressed, whereas its highly homologous PLC γ 2 is primarily expressed in hematopoietic cell lineages, including osteoclasts. With the use of the PLC γ 2 knock out (PLC γ 2^{-/-}) mice, we investigated the role of PLC γ 2 on bone homeostasis in vivo and RANKL-induced osteoclastogenesis in vitro.

Bone morphology of mice was characterized by dual-energy X-ray absorptiometry, MicroCT and histomorphometry analyses. Increased bone mineral density was demonstrated in PLC γ 2^{-/-} relative to wild-type mice. Quantitative measurements of the ratio of trabecular bone volume to tissue volume showed a 2-fold increase in PLC γ 2^{-/-} mice. Bone perimeter and trabecular numbers were increased and trabecular space was decreased in PLC γ 2^{-/-} mice. The increased bone volume was associated with a decreased number of osteoclasts and decreased relative osteoclast surface. Moreover, upon stimulation by RANKL in vitro, the PLC γ 2^{-/-} bone marrow macrophage precursors showed increased expression of early osteoclast markers tartrate-resistant acid phosphatase (TRAP) and Cathepsin K (Cath K), but failed to differentiate into mature multinucleated osteoclasts with expression of the later osteoclast marker calcitonin receptor (CTR). Moreover, lack of PLC γ 2 severely impaired RANKL-induced activation of NF- κ B, AP-1, and NFATc1, the transcription factors involved in osteoclastogenesis. Thapsigargin that is known to increase calcium induced the expression of TRAP, CathK and CTR, and partially restored the RANKL-induced osteoclastogenesis, indicating that PLC γ related calcium signaling is critical for the late stages of RANKL-induced osteoclastogenesis. Further, a retrovirus-mediated gene transduction of PLC γ 2 but not PLC γ 1 restored RANKL-induced osteoclastogenesis of PLC γ 2^{-/-} cells. Therefore, PLC γ 2 plays an important and unique role in RANKL-mediated osteoclastogenesis.

Taken together, PLC γ 2 is essential for RANKL signaling, and its deficiency leads to defective osteoclastogenesis. Characterization of the role of PLC γ 2 in RANKL-induced osteoclastogenesis is important for osteoporosis prevention and therapy.

Disclosures: Y. Chen, None.

1105

Nell-1, a Key Functional Mediator of Runx2, Partially Rescues Craniofacial Defects in Runx2 Haploinsufficient Mice. X. Zhang¹, K. Ting¹, C. M. Cowan², H. Lee³, J. Wong¹, T. Hsu¹, D. Pathmanathan¹, S. Kuroda³, C. Soo⁴. ¹Dental&Craniofacial Research Institute, University of California, Los Angeles, Los Angeles, CA, USA, ²Department of Bioengineering, University of California, Los Angeles, Los Angeles, CA, USA, ³Department of Structural Molecular Biology, Institute of Scientific and Industrial Research, Osaka University, Osaka, Japan, ⁴Department of Plastic and Reconstructive Surgery, University of Southern California, Los Angeles, CA, USA.

Mesenchymal stem cell commitment to an osteochondroprogenitor lineage requires Runx2. Heterozygous Runx2 mice (Runx2^{+/-}) manifest delayed membranous bone development/ossification, causing open anterior and posterior fontanelles, a phenotype similar to cleidocranial dysplasia (CCD) in humans. We have recently demonstrated that craniosynostosis associated protein, Nell-1, is a direct transcriptional target of Runx2. The purpose of this study was to investigate the functional relationship of Nell-1 and Runx2 in craniofacial bone development via in vitro, ex vivo and in vivo experiments. To determine if Nell-1 could functionally compensate for Runx2 absence, Runx2^{-/-} calvarial cells were infected with adenoviral (Ad) Nell-1 (AdNell-1). To determine if Nell-1 was required for Runx2 activity, Nell-1 siRNA were applied on wild-type calvarial cells infected with AdRunx2. Osteoblastic differentiation was assessed by real-time PCR, ALP activity, and von Kossa. To determine if Nell-1 could stimulate mineralization on explanted Runx2^{+/-} mice calvaria, in situ calcein deposition was monitored after recombinant Nell-1 (rNell-1) application. Lastly, to determine if Nell-1 could compensate for Runx2 haploinsufficiency, Nell-1 overexpression mice (Nell-1^{overexp}) were mated to Runx2^{+/-} mice and the progenies were evaluated by skeletal staining, micro-CT, histology, and immunohistochemistry. The results show that Nell-1 induced delayed Alp and Opn upregulation, but no mineralization in Runx2^{-/-} calvarial cells. Meanwhile, Nell-1 siRNA inhibited Alp and Ocn upregulation, ALP activity, and mineralization in AdRunx2 infected wild-type calvarial cells. Furthermore, rNell-1 significantly increased ossification in calvarial explants from Runx2^{+/-} mice. Finally, increased calvarial bone growth as evidenced by smaller anterior fontanelle, narrower sagittal suture width and significantly thicker parietal bone plate were apparent in the Nell-1^{overexp}/Runx2^{+/-} progenies. In conclusion, Nell-1 serves as a key functional mediator of downstream Runx2 effects in supporting full preosteoblastic calvarial cell differentiation and inducing craniofacial bone development.

Disclosures: X. Zhang, co-founder of Bone Biologics, Inc. 4.

This study received funding from: NIH/NIDCR, March of Dimes Birth Defect Foundation, Thomas R. Bales Endowed Chair.

1106

Role of BMP2 in Postnatal Bone Biology: Conditional Knock-Out (cKO) of BMP2 Using the 3.6 Collagen Type IA1 - Cre Model. W. Yang¹, D. Guo², J. Gluhak¹, M. A. Harris¹, A. Lichtler³, B. Kream³, J. Edwards⁴, G. R. Mundy⁴, Y. Mishina⁵, S. E. Harris¹. ¹UTHSCSA, San Antonio, TX, USA, ²UMKC, Kansas City, MO, USA, ³UCONN Health Center, Farmington, CT, USA, ⁴Vanderbilt U, Nashville, TN, USA, ⁵LRDT, NIEHS/NIH, Research Triangle Park, NC, USA.

BMP2 is expressed in early and late osteoblasts and has been shown to accelerate bone regeneration in adults. Genetic data have demonstrated an association of polymorphisms in the BMP2 gene with increased fracture risk and osteoporosis. However, the postnatal function and mechanism of endogenous BMP2 in bone formation has not been established due to the embryonic lethality of BMP2-null mice at 10.5dpp. Thus to define the function of BMP2 in skeleton postnatally, we created a BMP2 floxed mouse model with loxP sites flanking exon 3. Mice embryos with the BMP2 floxed homozygous allele and with the Mox2-Cre allele, which is active at the blastula stage, have the same phenotype as the global BMP2-null model, lethal around 10.5 dpc along with the absence of chorion and defective heart development. This BMP2 floxed model now allows us to remove BMP2 spatiotemporally with various Cre-Loxp recombination models. With 3.6Colla1-Cre recombinase that target early collagen type 1 expressing osteoblasts, BMP2 expression is not detected in osteoblasts and osteocytes in the BMP2 cKO mice. Removal of BMP2 from osteoblasts postnatally results in skeletal defects in vertebrae, ribs, craniofacial bones, and long bones. BMP2 cKO mice show a pronounced osteopenia with reduced radio-opacity and a 12-25% reduced BMD in bones from 2 weeks to 6 months of age. The vertebrae and humeri are revealed to be the most sensitive bones to the removal of BMP2 in osteoblasts. Quantitation μ CT analysis on tibia of 1-month BMP2 cKOs has shown a 33% reduction in the vBV/TV and a 24% reduction in the trabecular number. Furthermore by histology evaluation, we observed the reduction of the trabecular bone and decreased amounts of mineralized bone matrix. Reduced osteoclast activity and number were also detected in BMP2 cKO mice at 1 month. This suggests that deletion of BMP2 in osteoblasts is linked to disruption of bone remodeling. Deletion of BMP2 and a 30% reduction of Osterix expression were also determined in bone extracts from calvaria, humeri, and femurs by Northern analysis. By in situ hybridization, we detected reduced mRNA expression levels of BMP4, Osterix and DLX5 in bone associated osteoblasts. Further investigation on dynamic bone formation rates and detailed histomorphometric analysis is underway. Collectively, our results suggest BMP2 action is upstream of BMP4 in these collagen producing osteoblasts and BMP2 is necessary but not sufficient for the continued differentiation of osteoblasts to stages required for production of mineralized bone postnatally.

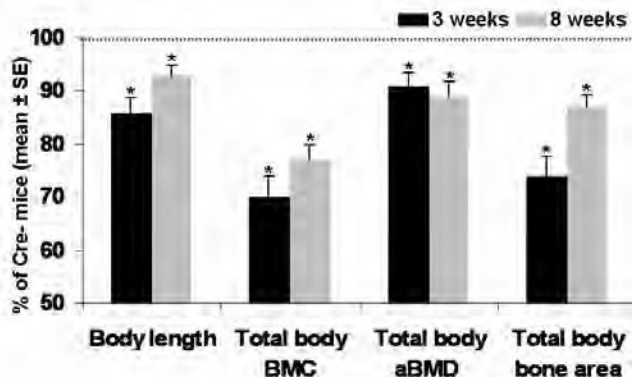
Disclosures: W. Yang, None.

This study received funding from: NIH.

1107

Targeted Disruption of Ephrin B1 in Osteoblasts Reduces Bone Size in Mice. W. Xing, K. Govoni, A. Kapoor*, S. Mohan, J.L. Pettis VA Medical Center and Loma Linda Univ, Loma Linda, CA, USA.

Mutations of Ephrin B1 (Efnb1), a ligand for Ephrin B tyrosine kinase receptors, in humans caused craniofrontonasal syndrome while deletion of Efnb1 gene in mice resulted in perinatal lethality and defects in skeletal patterning. Based on these findings that Efnb1 is required for survival of mice and bone development, we hypothesized that Efnb1 produced by osteoblasts plays a key role in the attainment of peak bone mass. To test this hypothesis, we used a Cre-loxP approach to disrupt Efnb1 specifically in osteoblasts (Obs). Transgenic mice expressing Cre recombinase under the control of the promoter/enhancer unit of Col1a2 gene were crossed with Efnb1 loxP mice to generate Cre+ (Efnb1 disruption) and Cre- (control) loxP homozygous mice. Cre expression was limited to type I collagen producing cells of mesenchymal origin. Western blot confirmed that Efnb1 was expressed in Obs isolated from calvariae of Cre- mice, but not Cre+ mice. The skeletal phenotypes of mice (n = 10 to 19) were characterized by PIXImus measurements at 3 & 8 weeks of age as shown below. An asterisk indicates a significant difference between Cre+ and Cre- mice (P < 0.05).



pQCT analysis of femurs at 8 weeks of age revealed that periosteal and endosteal circumferences were reduced by 22 and 16%, respectively, in the femurs of Cre+ mice vs. corresponding littermate control mice (P < 0.01). In contrast, total volumetric BMD was not affected indicating that the reduction in aBMD by PIXImus was caused by reduced bone size. Because ephrin ligands are known to regulate tissue renewal and tumor cell progression, we tested the prediction that Efnb1 regulates bone size by influencing cell proliferation. Accordingly, overexpression of Efnb1 in MC3T3-E1 cells increased cell number by 32% compared to GFP control (P < 0.05). In summary: 1) Targeted disruption of efnb1 in Obs results in decreased peak bone mass caused predominantly by reduced bone size; 2) Overexpression of Efnb1 in Obs increased cell number. In conclusion, our data provide the first experimental evidence that efnb1 is a critical regulator of bone size in mice and may be an important regulator of osteoblast proliferation.

Disclosures: W. Xing, None.

This study received funding from: US Army DAMD17-03-2-0021.

1108

mTOR Signaling: A Novel Molecular Mechanism Underlying Wnt's Anabolic Effects on Osteogenesis. H. Ouyang¹, K. Inoki^{2*}, X. Zhang¹, T. Zhu^{2*}, C. Bennett^{3*}, C. Lindvall⁴, B. O. Williams⁴, O. A. MacDougald³, K. Guan^{2*}. ¹Cardiology, Restorative Sciences and Endodontics (CRSE), University of Michigan, Ann Arbor, MI, USA, ²Life Sciences Institute, University of Michigan, Ann Arbor, MI, USA, ³Department of Molecular and Integrative Physiology, University of Michigan, Ann Arbor, MI, USA, ⁴Laboratory of Cell Signaling and Carcinogenesis, Van Andel Research Institute, Grand Rapids, MI, USA.

The canonical Wnt signaling plays a critical role in regulating osteogenesis. It inhibits GSK3, resulting in stabilization of β -catenin, a transcription factor important for cell growth-related gene expression. Little knowledge exists as to whether Wnt signaling also regulates protein synthesis, in addition to its role in gene transcription. The mammalian target of rapamycin (mTOR) is a serine/threonine kinase that controls cell growth and protein translation via phosphorylating the molecular components of translation apparatus, such as S6K, S6 and 4EBP. TSC2 is an upstream inhibitor for mTOR; mutation in TSC2 causes tuberous sclerosis complex, an autosomal dominant genetic disorder featured by hamartoma formation in multiple tissues. Here, we reported that Wnt signaling stimulated the mTOR signaling in osteoblasts, both in vivo and in vitro. Wnt3a increased phosphorylation of S6K and S6 in a time- and dose-dependent manner in osteoblasts. Wnt10b stable expression in mouse bone marrow stromal cells also activated mTOR. Consistently, Wnt10b transgenic mice displayed greater mTOR activities than the wild type animals, in vivo. These inductions occurred in a β -catenin-independent manner. Overexpression of a constitutively active form of β -catenin failed to induce mTOR activities, and Wnt3a stimulated mTOR signaling in MEF cells null for β -catenin. Moreover, GSK3 phosphorylated TSC2 in a manner dependent on AMPK, a serine/threonine kinase that acts as a sensor for intracellular energy level. Such phosphorylation enhanced TSC2 inhibition on mTOR. Wnt stimulated the mTOR signaling via inhibiting

GSK3 phosphorylation of TSC2. Importantly, inhibition of mTOR by rapamycin, a specific inhibitor for mTOR, blocked Wnt signaling-induced osteoblastic proliferation and biomineralization, in vitro. Taken together, these results show that Wnt stimulates protein translation machinery and cell growth by activating mTOR signaling. Furthermore, they reveal a role of TSC2/mTOR signaling in Wnt-induced osteogenesis, therefore suggesting a therapeutic value of rapamycin in treating osteosclerotic dysplasia associated with activated Wnt signaling. (This work is supported by grants from NIH (Guan, KL, Ouyang, HJ), and American Association of Endodontists (Ouyang, HJ).)

Disclosures: H. Ouyang, None.

This study received funding from: NIH, American Association of Endodontists.

1109

IGF-I Signaling Is Required for Postnatal Growth Plate Development. Y. Wang¹, H. Z. ElAlieh^{1*}, E. Nakamura^{2*}, M. Nguyen^{2*}, S. Mackem^{2*}, D. D. Biale¹, W. Chang¹. ¹Endocrine Unit, University of California, San Francisco/VA Medical Center, San Francisco, CA, USA, ²Laboratory of Pathology, Center for Cancer Research, NCI, NIH, Bethesda, MD, USA.

Studies of mice with global knockouts genes encoding the insulin-like growth factor-I (IGF-I) and IGF-I receptor (IGF-IR) support a critical role for IGF-I signaling in skeletal development. These mice are born dwarf with severely deformed skeletons and with a high perinatal mortality rate. It is assumed that the lack of local IGF-I/IGF-IR signaling is the main cause for much of the skeletal phenotype in these mice, but systemic derangements are likely to contribute as well. To investigate the role of IGF-I signaling in postnatal GP development, we generated mice ($Tam^{Cre}IGF-IR^{-/-}$) with tamoxifen (Tam)-inducible, cartilage-specific knockout of IGF-IR gene by breeding floxed IGF-IR mice with mice carrying a cDNA encoding Cre recombinase fused to a mutated estrogen responsive element. The transcription of this cDNA is controlled by a type II collagen promoter. $Tam^{Cre}IGF-IR^{-/-}$ mice were viable and fertile without injection of tamoxifen. To knockout the IGF-IR postnatally, we injected the $Tam^{Cre}IGF-IR^{-/-}$ mice with tamoxifen (0.2 mg/mouse) at day 5, day 7, day 9 and day 11 after birth. Bones from the $Tam^{Cre}IGF-IR^{-/-}$ mice and their wild-type littermates (WT) were harvested at day 14 for analysis. Tamoxifen-injected $Tam^{Cre}IGF-IR^{-/-}$ mice were smaller in size (70% of WT) at day 14. Histology showed disorganized proliferating zone, shortened hypertrophic zone (62% of WT), and reduced proliferation (by 60%) in the proliferating zone in tibial GPs of the $Tam^{Cre}IGF-IR^{-/-}$. The protein levels of chondrocyte differentiation markers type II collagen and type X collagen, and the levels of chondrocyte differentiation regulator Indian Hedgehog (Ihh) were also decreased in these mice as assessed by immunohistochemistry. Our data indicate that IGF-I/IGF-IR signaling pathway regulates postnatal GP development by stimulating chondrocytes proliferation and differentiation, support the idea that local IGF-I/IGF-IR signaling is essential for the growth and maturation of chondrocytes in the postnatal periods, and is required for the orderly progression of GP maturation.

Disclosures: Y. Wang, None.

1110

Beta Blockade Mitigates Bone Loss During Energy Restriction Partially via Leptin. K. Baek*, J. Stallone*, S. Bloomfield. Department of Health & Kinesiology and Department of Nutrition, Texas A&M University, College Station, TX, USA.

Leptin is a candidate for responsible for linking energy metabolism to bone mass. In previous work, we demonstrated that energy restriction (ER) is a major contributor to the bone loss during global food restriction. Also, we observed decreased serum leptin during mild food restriction, which may be due to reduced adipocyte number/size and/or sympathetic nervous system (SNS) activation of beta-adrenoreceptors during ER, inhibiting release of leptin from adipocytes. In the present study, we tested whether beta-adrenoreceptor blockade attenuates bone loss during energy restriction and whether such an effect is associated with changes in serum leptin level and leptin localization in bone tissues. Female, 4-mo-old Sprague-Dawley rats were acclimatized to new AIN-93M purified diet for 8 weeks, then assigned into four groups (n=10 each): 2 groups of 40% energy restriction treated with vehicle (ERVEH; saline) or beta-blocker (ERBB; DL-propranolol, Sigma; 250 μ g/kg \cdot hr) via drinking water during 12 weeks, and 2 groups of ad-lib fed controls treated with the same 2 agents (CONVEH, CCBB, respectively). On days 0 and 84, peripheral computed tomography (pQCT) assessed proximal tibial volumetric bone mineral density (vBMD) and geometry, and dual energy X-ray absorptiometry (DXA) assessed total body fat, lean mass, and total body and spine BMD. Sagittal sections of proximal femur were analyzed by standard immunohistochemistry for assessing leptin expression in marrow adipocytes and leptin localization in bone cells. All animal procedures were approved by Texas A&M University Laboratory Animal Care Committee. Over 84 days, CONVEH and CCBB rats gained, but ERVEH and ERBB rats lost body fat mass (+4.8%, +10.08% vs -14.4% and -11.9%, respectively), but lean mass did not change in any group. Reduction in serum leptin (by ELISA) in ERVEH rats was mitigated in ERBB rats (-5.32 vs -1.15ng/ml, respectively). The decline in proximal tibia cancellous vBMD observed in ERVEH rats was attenuated in ERBB rats (-85.24 vs -53.94 mg/cm³, respectively). Spine BMD (by DXA) did not change in any group over 84 days. More leptin expression was observed in bone marrow adipocytes in groups showing higher serum leptin level and higher cancellous vBMD. In the same groups, more bone lining cells, osteocytes and chondrocytes in cartilage also stained positive for leptin. In conclusion, beta blockade mitigated metaphyseal bone loss during energy restriction and also attenuated reductions in serum levels and bone tissue-specific localization of leptin. These data suggest a contributory role for beta-adrenoreceptor signaling via adipocytes in the bone response to energy restriction.

Disclosures: K. Baek, None.

This study received funding from: DOD.

1111

Collagen/Annexin V Interactions Regulate Growth Plate Chondrocyte Mineralization. H. Kim, T. Kirsch, Orthopaedics, University of Maryland School of Medicine, Baltimore, MD, USA.

Mineralization of growth plate cartilage is crucial for normal bone formation. Therefore, an understanding of the mechanisms regulating mineralization is important. We have shown that annexins (II, V and VI) form Ca^{2+} channels in growth plate chondrocytes enabling the initiation of mineralization. In addition, binding of annexin V to types II and X collagen stimulates annexin V Ca^{2+} channel activities. In this study we hypothesized that type II or type X collagen matrix stimulates mineralization of growth plate chondrocytes via binding and activating annexin V channel properties resulting in increased intracellular Ca^{2+} concentration, $[\text{Ca}^{2+}]_i$. Increased $[\text{Ca}^{2+}]_i$ then stimulates mineralization related events. To test this hypothesis, we treated growth plate chondrocytes with vitamin C to stimulate collagen synthesis in the absence or presence of 3,4-dehydro-L-proline (inhibitor of collagen fibril formation and secretion). On the other hand we cultured growth plate chondrocytes on type I or type II collagen coated dishes in the absence or presence of an annexin V specific Ca^{2+} channel blocker (K-201). We measured $[\text{Ca}^{2+}]_i$, expression of mineralization-related genes, alkaline phosphatase (APase) activity and the degree of mineralization. Vitamin C stimulated type II and X collagen synthesis, APase activity and mineralization of growth plate chondrocytes, whereas 3,4-dehydro-L-proline inhibited the stimulation of these events in vitamin C-treated cells. Vitamin C also led to an increase of $[\text{Ca}^{2+}]_i$ in growth plate chondrocytes, whereas 3,4-dehydro-L-proline inhibited this increase. Flow cytometric and co-immunoprecipitation experiments revealed that annexin V is cell surface exposed and interacts with types II and X collagen. Culturing growth plate chondrocytes on type I or type II collagen coated dishes increased $[\text{Ca}^{2+}]_i$, APase activity and the degree of mineralization compared to the levels of cells cultured on non-coated dishes. K-201, a specific annexin V channel blocker, inhibited increase of $[\text{Ca}^{2+}]_i$ of growth plate chondrocytes cultured on type II collagen coated dishes but not on type I collagen coated dishes. Furthermore, overexpression of full length annexin V, which binds to types II and X collagen, was more effective in stimulating APase activity, MMP-13 expression and mineralization of growth plate chondrocytes than overexpression of N-terminus deleted mutant annexin V, which binds to type X collagen but not to type II collagen. In conclusion, our findings reveal that types II and X collagen via binding to annexin V stimulate annexin-mediated Ca^{2+} influx, thereby regulating growth plate chondrocyte Ca^{2+} homeostasis and ultimately mineralization events.

Disclosures: H. Kim, None.

This study received funding from: NIH.

1112

Runx1, Co-activator of Sox5, Sox6 and Sox9 (the Sox trio) Regulates Chondrogenic Differentiation. F. Yano¹, T. Ikeda¹, T. Saito², N. Ogata¹, S. Takeda³, A. Kimura³, S. Ohba¹, F. Kugimiya², K. Nakamura², T. Takato¹, H. Kawaguchi², U. Chung¹. ¹Division of Tissue Engineering, Faculty of Medicine, University of Tokyo, Tokyo, Japan, ²Department of Sensory and Motor System Medicine, Faculty of Medicine, University of Tokyo, Tokyo, Japan, ³Department of Orthopedics, Tokyo Medical and Dental University, Tokyo, Japan.

Aiming at clinical applications to cartilage regeneration, we previously screened natural and synthetic compound libraries and found that a thienindazole derivative small compound T-198946 (TM) strongly induced chondrogenic differentiation without inducing hypertrophy. To clarify its transcriptional targets and signal transduction mechanism, we screened for the target molecules of TM by a microarray analysis using undifferentiated mesenchymal C3H10T1/2 cells treated with TM for 48 hours. Compared to the control, 581 genes were up-regulated by TM, among which Runx1, Sox5, and Sox6 were especially markedly induced. Real-time RT-PCR analysis confirmed that expressions of Runx1, Sox5, and Sox6 were strongly induced by TM treatment. To investigate the functional contribution of Runx1 to chondrocyte differentiation, Runx1 was adenovirally overexpressed, but it did not induce endogenous expression of chondrogenic markers in C3H10T1/2 cells. However, when Runx1 was combined with Sox5, Sox6 and Sox9 (the Sox trio), it enhanced induction of chondrogenic differentiation and cartilage matrix synthesis without inducing hypertrophy, mimicking effects of TM treatment. On the other hand, silencing of Runx1 reduced effects of TM on chondrogenic differentiation. We analysed the effects of Runx1 on the human type II collagen promoter containing putative binding motif for Runx family transcriptional factors. Luciferase-reporter assay using several deletion constructs identified the region containing the binding site of Runx1 at -293 to -288bp, which is highly conserved among species in the proximal promoter and distinct from the Sox9 responsive element. Immunoprecipitation analysis showed that Runx1 physically associated with Sox 5, 6 and 9 proteins. Immunohistochemistry revealed that Runx1, Sox5, 6, and 9 were co-localized in the proliferative and pre-hypertrophic chondrocytes of the mouse growth plate. These data suggest that Runx1 cooperatively works with the Sox trio to induce chondrogenic differentiation. Elucidation of the molecular network of TM targets may help realize to the realization of the regenerative medicine of permanent cartilage.

Disclosures: F. Yano, None.

1113

A Homozygous Missense Mutation in Human KLOTHO Causes Severe Tumoral Calcinosis, but not Premature Aging. S. Ichikawa^{*1}, E. A. Imel¹, M. L. Kreiter^{*2}, X. Yu¹, D. S. Mackenzie^{*1}, A. H. Sorenson^{*1}, R. Goetz^{*3}, M. Mohammadi^{*3}, K. E. White¹, M. J. Econs¹. ¹Indiana University School of Medicine, Indianapolis, IN, USA, ²Children's Memorial Hospital and Feinberg School of Medicine, Northwestern University, Chicago, IL, USA, ³New York University School of Medicine, New York, NY, USA.

Familial tumoral calcinosis is a rare metabolic disorder characterized by ectopic calcifications and hyperphosphatemia. The known genetic causes of tumoral calcinosis are inactivating mutations in the genes encoding fibroblast growth factor 23 (FGF23) and GalNAc transferase 3 (GALNT3). Klotho (KL)-deficient mice were originally reported to model early aging; however, these mice manifest a biochemical phenotype similar to Fgf23-null mice and tumoral calcinosis patients.

We examined a 13-year-old girl with severe tumoral calcinosis with significant dural and carotid artery calcifications. This patient had defects in mineral ion homeostasis with marked hyperphosphatemia, hypercalcemia, and elevated parathyroid hormone (PTH). Serum FGF23 concentrations were markedly elevated [16,140 pg/mL intact (NL<71 pg/mL) and 10,900 RU/mL C-terminal (NL<149 RU/mL)], suggesting resistance to the actions of FGF23 as the cause of the observed hyperphosphatemia. However, there were no features of premature aging.

Mutational analysis was performed for the calcium sensing receptor (CASR), FGF23, GALNT3, and KL. We identified a homozygous missense mutation (His193Arg) in the KL gene of the patient. Analysis of the mutation in the context of published glycosidase structures revealed that the mutated histidine 193 is at the base of the catalytic site. Substitution of the histidine residue to arginine should destabilize the tertiary folding of the KL domain, attenuating the production of membrane-bound and secreted KL. Indeed, compared to wild-type KL, cell surface expression and secretion of mutant KL was drastically reduced in vitro. Immunoprecipitation analysis of the FGF23-KL-FGFR1 ternary complex revealed that only minute amounts of mutant KL bound to FGF23. Furthermore, stimulation of HEK293 cells expressing wild-type KL with FGF23 resulted in a 56-fold increase in mRNA of early growth response-1 (EGR1), a downstream mediator of FGF23 signaling, whereas EGR1 expression was reduced by ~80% in cells expressing mutant KL (p<0.0001).

In summary, our clinical and molecular findings demonstrate that human loss-of-function mutations in KL impair the bioactivity of FGF23 to signal via its cognate FGF receptors and lead to severe tumoral calcinosis, rather than premature aging as previously reported in the KL-deficient mice. Thus, KL plays an essential role in FGF23-mediated phosphate and vitamin D metabolism in humans.

Disclosures: S. Ichikawa, None.

1114

Phosphate-Independent Effects of Fgf-23 on Skeletogenesis. D. Sitara¹, C. Bergwitz², S. Kim^{*1}, R. Erben³, H. Jüppner², B. Lanske¹. ¹Developmental Biology, Harvard School of Dental Medicine, Boston, MA, USA, ²Endocrine Unit, Massachusetts General Hospital and Harvard Medical School, Boston, MA, USA, ³Natural Sciences, University of Veterinary Medicine, Vienna, Austria.

Phosphate homeostasis is regulated by hormones such as parathyroid hormone (PTH), 1,25-dihydroxyvitamin D₃ (1,25(OH)₂D₃) and fibroblast growth factor-23 (Fgf23). Each of these factors can modulate directly or indirectly the activity of sodium-dependent phosphate co-transporter proteins (NaPi) located in kidney and intestine, affecting both renal and intestinal phosphate handling and thereby influencing overall mineral ion homeostasis. Fgf23 ablation leads to a complex phenotype, including hyperphosphatemia, elevated 1,25(OH)₂D₃ and suppressed PTH serum levels, accompanied by enhanced renal tubular phosphate reabsorption through NaPi2a and NaPi2c, leading to abnormal bone mineralization and soft tissue calcifications.

Using genetically modified mice we have now demonstrated an inverse correlation between Fgf23 and NaPi2a; homozygous ablation of NaPi2a from Fgf23^{-/-} mice to generate Fgf-23^{-/-}/NaPi2a^{-/-} double mutants resulted in urinary phosphate-wasting and hypophosphatemia at 6 weeks of age but normal phosphate levels at 3 weeks, despite significantly elevated 1,25(OH)₂D₃ serum levels. This data suggest that altered phosphate homeostasis in Fgf23^{-/-} mice is a NaPi2a-dependent process. Histological analysis of tibial bone sections from Fgf23^{-/-}/NaPi2a^{-/-} double mutants revealed a close resemblance to the findings in Fgf23^{-/-} bones, i.e. hypermineralization of the primary spongiosa together with severe osteoidosis in secondary spongiosa and cortical bone. To further investigate these findings, we examined the expression of genes associated with skeletal development. In Fgf23^{-/-} bones, we observed an up-regulated expression of osteopontin and dental matrix protein-1 (Dmp-1), two sibling proteins known to affect bone mineralization; expression of these genes in Fgf23^{-/-}/NaPi2a^{-/-} double mutants is currently underway.

We are furthermore in the process of evaluating NaPi2c expression, which may be up-regulated to compensate for the loss of NaPi2a in the double mutants, leading to normal serum phosphate levels in Fgf23^{-/-}/NaPi2a^{-/-} double mutants at 3 weeks of age. Moreover, since PTH is known to decrease NaPi2a expression, we are studying the in vivo role of PTH in Fgf23-mediated phosphate homeostasis and skeletogenesis.

In conclusion, our current findings suggest that Fgf23 not only exhibits endocrine functions by regulating phosphate homeostasis through its actions on the kidney, but it also affects skeletogenesis through yet undefined autocrine/paracrine actions.

Disclosures: D. Sitara, None.

1115

The Role of the Type IIc Sodium-dependent Phosphate Transporter (Npt2c), which Is Involved in Hereditary Hypophosphatemic Rickets with Hypercalciuria (HHRH). H. Segawa^{*1}, A. Onitsuka^{*1}, M. Kuwahata^{*1}, E. Aramaki^{*1}, J. Furutani^{*1}, I. Kaneko^{*1}, Y. Tomoe^{*1}, S. Kuwahara^{*1}, N. Amizuka², M. Matsumoto^{*3}, K. Miyamoto¹. ¹Molecular Nutrition, Health Biosciences, The Univ. of Tokushima Graduate School, Tokushima, Japan, ²Center for Transdisciplinary Research, Niigata University, Niigata, Japan, ³Molecular Immunology, Enzyme Research, University of Tokushima, Tokushima, Japan.

Primary loss of inorganic phosphate (Pi) from the kidneys results in hypophosphatemia, the severity of which is directly related to the degree of secondary bone mineralization defects. Two transporters (Npt2a and Npt2c) are expressed exclusively in the proximal convoluted tubule and are regulated by Pi intake, PTH, and FGF23 levels. The type IIa Na/Pi cotransporter (Npt2a) play a major role in reabsorption (70-80%), while type IIc Na/Pi transporter (Npt2c) is more important in weaning animals and less so in adult animals. While the renal Npt2a play a major role in renal Pi reabsorption, Npt2a null (Npt2a^{-/-}) mice do not exhibit rickets/osteomalacia. More recently, linkage analyses have suggested that hereditary hypophosphatemic rickets with hypercalciuria (HHRH) may arise from mutation(s) in the NPT2c/SLC34A3 gene. The goal of the present study was to characterize the role of renal Pi wasting in bone disorders by studying mice deficient in the Npt2c gene, which is the pathogenic protein involved in HHRH. Homozygous mutants (Npt2c^{-/-}) mice are viable, fertile and do not display any gross physical or behavioral abnormalities. Npt2c^{-/-} mice exhibit hypercalcemia, hypercalciuria, and elevation of plasma 1,25-dihydroxyvitamin D3 levels. Interestingly, the levels of plasma fibroblast growth factor 23 (FGF23) levels were significantly reduced in Npt2c^{-/-} mice. However, histologic examination of bone samples from Npt2c^{-/-} mice failed to identify typical features of advanced rickets. Since Npt2c KO mice exhibited abnormally phosphate/calcium homeostasis, our results support that Npt2c may be involved in phosphate/calcium homeostasis.

The further studies required to clarify the mechanism of rickets/osteomalacia which caused by Npt2c-genetic abnormality.

Disclosures: H. Segawa, None.

1116

Molecular Analyses of DMP1 Mutants Causing Autosomal Recessive Hypophosphatemic Rickets (ARHR). E. G. Farrow¹, S. I. Davis^{*1}, X. Yu¹, L. M. Ward², K. E. White¹. ¹Medical and Molecular Genetics, Indiana University School of Medicine, Indianapolis, IN, USA, ²Pediatrics, Children's Hospital of Eastern Ontario, Ottawa, ON, Canada.

Heritable disorders of hypophosphatemia involving FGF23 result from mutations in several genes. We previously demonstrated that the recessive mutations M1V (A1>G) and 1484-1490 deletion (del) in Dentin Matrix Protein-1 (DMP1) cause the novel disorder autosomal recessive hypophosphatemic rickets (ARHR), associated with elevated serum FGF23. The goals of the current studies were to understand the effects of the ARHR mutations on DMP1 and to test the regulation of DMP1 expression. Western analyses of wild type DMP1 following transient transfection into cells demonstrated that DMP1 is normally expressed equally in the cellular lysates and the media. In contrast, the ARHR 1484-1490del mutant was primarily detected in the media whereas the M1V mutant was only detected in the cellular lysates. In order to investigate the ARHR mutations on DMP1 intracellular trafficking, transfected cells were fluorescently co-stained for DMP1 in parallel with staining for the trans-golgi network (TGN), ER, and nucleus. Wild type and 1484-1490del mutant DMP1 localized to the TGN, consistent with their cellular secretion. The M1V mutant did not localize to the TGN but filled the entire cell due to loss of the highly conserved DMP1 signal peptide. We obtained the same results with these constructs produced as fusion proteins with V5 tags or untagged, in HEK293, UMR106, and MC3T3 cells. The last 18 amino acids of DMP1 are highly conserved and are replaced by 33 novel residues due to a frameshift caused by the 1484-1490del mutation. We deleted the last 18 DMP1 residues to determine the role of the C-terminus in processing. This truncated DMP1 acted the same as the wild type species, and had balanced intra- and extracellular expression. Therefore, the unbalanced expression of 1484-1490del DMP1 is a function of the 33 novel residues, and not a consequence of deleting the last 18 native residues. UMR-106 cells were treated with excess phosphate or with 1,25(OH)₂ vitamin D (1x10⁻⁷M) for 4 h to test endogenous DMP1 response. qRT-PCR showed a 2-3 fold increase in DMP1 mRNA compared to control cells with both treatments. In summary, our studies of the ARHR DMP1 mutants illustrate that modifications to the signal peptide and to the C-terminus of DMP1 affect cell processing, and that DMP1 is responsive to metabolites that also control FGF23 production. The alterations in DMP1 secretion due to the ARHR mutations provide unique insight into domains of DMP1 critical for normal biological function.

Disclosures: E.G. Farrow, None.

1117

Vascular Calcification and Aortic Gene Expression Are Consistent with Hyperphosphatemia in OPG-Deficient Mice. S. Morony¹, Z. Zhang^{*2}, Y. Tintut², P. J. Kostenuik¹, L. L. Demer². ¹Amgen Inc., Thousand Oaks, CA, USA, ²Medicine, UCLA, Los Angeles, CA, USA.

Osteoprotegerin (OPG) is a cytokine that suppresses bone resorption by inhibiting the catabolic effects of receptor activator of NF-kappaB ligand (RANKL). OPG-deficient mice [opg^{-/-}] are osteoporotic and exhibit medial calcification of the aorta. This vascular phenotype in opg^{-/-} mice was the first evidence suggesting a protective role for OPG in the vasculature. However, the mechanism of this effect has not been determined and could be an indirect result of high turnover, or the direct result of RANKL or OPG actions within the vasculature. We evaluated these possibilities by assessing vascular calcification, serum calcium/phosphate levels, and aortic gene expression in opg^{-/-} mice and wildtype (WT) controls.

We quantified vascular calcification in opg^{-/-} mice by analyzing aortas ex vivo, using a high-resolution digital radiographic system. Radiographs were scored semi-quantitatively (0 to 5) based on the extent of mineralization, by an investigator blinded to genotype, sex, or age of the mice. No evidence of aortic mineralization was noted in any of the 24 WT aortas; whereas all 27 aortas were calcified in opg^{-/-} mice (mean calcification score = 2.7 ± 1.2). Aortic calcium content was quantified biochemically from a subset of mice, and was elevated 12-fold in opg^{-/-} mice compared to WT controls (p < 0.05).

We found increased serum phosphate (11.5 ± 1.4 mg/dL vs. 9.6 ± 1.1 mg/dL; p < 0.01) and calcium/phosphate product (114 ± 16 mg/dL vs. 94 ± 13 mg/dL; p < 0.01), but normal serum calcium levels (9.9 ± 0.5 mg/dL vs. 9.7 ± 0.4 mg/dL; p = 0.12) in opg^{-/-} mice compared to WT controls. The hyperphosphatemia in opg^{-/-} mice is likely related to increased bone resorption, as RANKL (926 ± 397 vs. 21 ± 22 pg/ml; p < 0.01), TRAP5b (0.10 ± 0.02 vs. 0.05 ± 0.02 AU; p < 0.001), and osteopontin (1736 ± 312 vs. 374 ± 91 pg/ml; p < 0.01) levels were elevated relative to WT controls.

Quantitative PCR was used to evaluate aortic gene expression between opg^{-/-} and WT mice and no difference was noted in expression of bone/cartilage transcription factors, BMP/TGF signaling molecules, or mineral binding/matrix factors. However, consistent with hyperphosphatemia, expression of matrix GLA protein (MGP) in opg^{-/-} mice was increased 90% (p < 0.01) while mRNA for alkaline phosphatase (akp2) was decreased 94% (p < 0.02). Interestingly, mRNA for ectonucleotide pyrophosphatase phosphodiesterase 1 (enpp1), which generates inorganic pyrophosphate (PPi), a mineralization inhibitor, was not increased in opg^{-/-} mice. Thus, the lack of enpp1 induction, together with remodeling-related hyperphosphatemia, may be important etiological factors in the development of vascular calcification in opg^{-/-} mice.

Disclosures: S. Morony, Amgen Inc. 1, 3.

This study received funding from: Amgen, Inc.

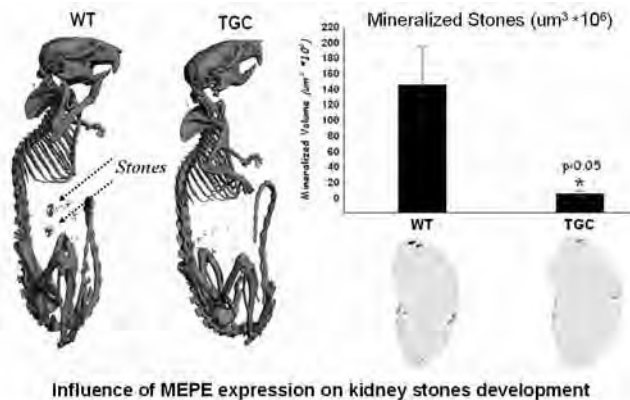
1118

Reduced Kidney-stone Formation and Altered Renal Phosphate-homeostasis in Mice Over-expressing Murine-MEPE. A. Martin¹, V. David¹, L. W. Fisher², A. Hedge^{*1}, P. S. N. Rowe¹. ¹Internal Medicine, Kansas University Medical Center, Kansas City, KS, USA, ²NIDCR-NIH, Bethesda, MD, USA.

Transgenic-mice constitutively over-expressing recombinant murine-MEPE (Col1a1 2.3kb promoter) were used to study the role of MEPE in phosphate mineral-metabolism. Ten 19 week-old transgenic (TGC) male C57Bl6 mice were compared to ten age-matched wild-type (WT) male mice on a high 1% phosphate diet. Biochemical measurements were performed on sera and urine. RT-PCR, western-blots and immunohistochemistry were performed on kidneys to analyse the expression of different markers involved in phosphate-regulation. Computed 3D-microtomography (uCT) was used to assess kidney-stone formation.

Remarkably, despite a low bone-mass phenotype induced by MEPE over-expression, an increase in serum phosphate (WT: 8.1 mg/dL vs. TGC: 11.4 mg/dL, p<0.01) and a mild hypocalcemia (WT: 9.95 mg/dL vs. TGC: 8.96 mg/dL, p<0.05) occurred. Consistent with the increased serum-PO₄, the fractional excretion of phosphate decreased by 66% (p<0.01) and serum PTH decreased by 33% (170 pg/mL to 120 pg/mL, p<0.05). Interestingly, despite a mild hypocalcemia, serum 1,25-(OH)₂-Vit-D₃ was significantly increased (18 pg/mL to 40 pg/mL, p<0.05). Also, increased renal NPT2a Na-dependent co-transporter mRNA levels (+267%, p<0.01) and protein (as measured by western-blots and immunohistochemistry) occurred in transgenic mice, again consistent with the hyperphosphatemia. In contrast transgenic-mice had significantly decreased renal NTP2b and NPT2c mRNA levels (75% and 80% reduction respectively, p<0.05). Phex expression dramatically increased by 4X (p<0.05) in TGC mice. Compared with WT, TGC mice displayed a 700% increase in MEPE expression (protein and mRNA) in the kidney (p<0.05) and a reciprocal decrease in DMP-1 expression (76% decrease, p<0.05). This in combination resulted in a decrease in kidney stones induced by the high-phosphate diet as assessed by 3D-uCT (figure 1; 97% decrease, p<0.05).

In summary, over-expression of MEPE under a Col1a1 2.3kb promoter markedly alters renal-phosphate homeostasis and dramatically influences susceptibility to renal-calcification. Also, these data show an association between MEPE, renal sodium-phosphate co-transporters and susceptibility to kidney-stone formation.



Disclosures: A. Martin, None.

This study received funding from: R01-AR51598-01 & R03-DE015900-01.

1119

Phospholipase C Signaling via the PTH/PTHrP Receptor Is Essential for Normal Full Response to PTH in both Bone and Kidney. J. Guo¹, M. Liu^{1*}, C. C. Thomas¹, D. Yang¹, M. L. Bouxsein², E. Schipani¹, F. R. Bringhurst¹, H. M. Kronenberg¹. ¹Endocrine Unit, Massachusetts General Hospital and Harvard Medical School, Boston, MA, USA, ²Orthopedic Biomechanics Laboratory, Beth Israel Hospital and Harvard Medical School, Boston, MA, USA.

To study role of signaling by distinct second message systems in vivo, we have constructed "knock-in" mice with mutant PTH/PTHrP receptors (PTHR) that can activate adenyl cyclase normally but cannot activate phospholipase C (PLC). We have previously shown that hypertrophic differentiation of chondrocytes is delayed in these so-called DSEL mice. To better understand role of PLC signaling via the PTHR in bone modeling and remodeling we examined the bone phenotype in DSEL mice that were fed either a standard diet or a calcium-deficient diet. Levels of serum PTH, phosphate and total calcium in DSEL mice fed a standard diet were not significantly different from those observed in wild type (WT) mice. Histomorphometric and uCT analysis demonstrate reduced trabecular bone (decreased by 15-20%) in DSEL mice fed a standard diet, and this decrease is associated with a decrease in trabecular number and an increase in trabecular spacing. The mechanisms underlying the low bone mass is not fully understood, since histomorphometric parameters of cell number and bone formation rate are normal in the secondary spongiosa of DSEL tibiae. The decreased bone mass may reflect abnormal modeling, as suggested by indices of increased osteoclast activity in the primary spongiosa, such as increased TRAP activity and mRNAs encoding TRAP and MMP9. Interestingly, DSEL mice fed a low calcium diet was able to develop secondary hyperparathyroidism including elevated serum PTH and substantial bone loss but exhibited a strikingly curtailed peritrabecular stromal cell response (peritrabecular bone marrow fibrosis), whereas WT mice exhibited extensive peritrabecular stromal cell responses to the low calcium diet. Such stromal cells express mRNAs encoding $\alpha 1(I)$ collagen, osteocalcin, and osteopontin, suggesting that they are preosteoblasts. In addition, the mutant mice fed low calcium diet were hyperphosphatemic, in contrast to the fall in blood phosphate in the WT control mice. The DSEL mice also exhibited an attenuated elevation of 1 α -hydroxylase mRNA, despite dramatic elevation of serum PTH in both groups. No significant change in mRNA levels of NaPi2a and NaPi2c was observed in the mutant mice in response to low calcium diet. Levels of FGF23 fell in response to the low calcium diet in both WT and DSEL mice, but on both diets FGF23 levels were not affected by the DSEL mutation. Our findings show that in both kidney and bone, PLC signaling through the PTHR in response to PTH are needed for the normal full responses; molecular analysis of the abnormalities is in progress.

Disclosures: J. Guo, None.

This study received funding from: NIH.

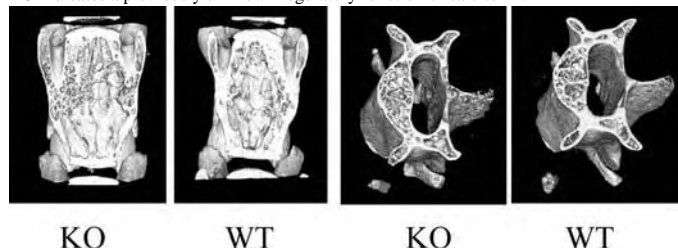
1120

Deletion of the Calcitonin/CGRP Gene Causes a Profound Cortical Resorption Phenotype in Mice. R. F. Gagel, A. O. Hoff, S. E. Huang*, G. J. Cote*. Endocrine Neoplasia & Hormonal Disorders, University of Texas M.D. Anderson Cancer Center, Houston, TX, USA.

There has been confusion regarding the long-term biological effects of calcitonin (CT) deficiency. Prior studies describing CT/CGRP gene or CT Receptor knockout models have provided contradictory phenotypes. To address these inconsistencies we have bred the knockout model (J Clin Invest 2002; F3 generation) into a pure C57/B6 mouse background (F10 generation). In this mouse model exons 2-5 of the mouse CT/CGRP were deleted in the germline by targeted disruption. Analysis of C57/B6 CT/CGRP KO mice (F10 generation) demonstrated a striking phenotype characterized by increased trabecular remodeling, trabecular & cortical thinning, and cortical porosity. The cortical thinning leads to morphological changes of vertebral bodies characterized by a 5% reduction of the height/width ratio ($p < 0.05$) in 12 and 18 month-old animals. The earliest indication of increased remodeling is the presence of a trabecular thinning in 3 & 6 month-old animals.

By 12 months of age a striking phenotype has emerged characterized by trabecular and cortical thinning (25%) with evidence of cortical tunneling (see Figure), collections of osteoclasts, and a 1.5-2-fold increase of serum C-telopeptide. The phenotype is most striking in 12 and 18 month females. Analysis of expressed genes (Affymetrix chip) derived from flushing of marrow with extraction buffer showed > 2-fold increases in CSF2Ra, CSF2Rb2, CCR2, Flotilin 2, Vimentin and > 1.5-fold increases of Prokineticin 2 and NFATc1, all genes involved in monocyte or osteoclast differentiation.

Conclusions: CT/CGRP deficient C57/B6 F10 mice have a profound and progressive phenotype characterized by increased trabecular thinning and cortical remodeling. These mice retain the greater calcemic response to PTH described earlier. Although there is evidence of these effects in 3 & 6 month-old animals, the major histologic effects are observed in older animals, possibly accelerated by gonadal steroid deficiency. The emergence of this phenotype argues persuasively for an important role of the CT/CGRP in the prevention of age-related bone loss and regulation of trabecular remodeling. The modulation of genes important in monocyte and osteoclast differentiation in the CT/CGRP KO indicates a previously unknown regulatory function of calcitonin.



Disclosures: R.F. Gagel, None.

This study received funding from: National Institutes of Health.

1121

PTH-Regulated Gene Expression in the Mouse Skeleton Suggest a Role for Ephrins in PTH Anabolism versus Catabolism. E. N. Bianchi*, R. Rizzoli, S. L. Ferrari. Div. of Bone Diseases, Geneva University Hospital, Geneva, Switzerland.

Intermittent PTH (i.PTH) induces a positive bone mineral balance while continuous PTH (c.PTH) does the opposite, particularly in the cortical bone compartment. The molecular mechanisms for PTH anabolism versus catabolism however remain poorly understood. Bidirectional ephrin signaling mediated by the binding of ephrinB2 ligand (EfnB2) to the ephrinB4 receptor (EphB4) was recently reported to induce osteoblast differentiation and reciprocal inhibition of osteoclast differentiation. This led us to hypothesize that ephrins expression could be up- and down-regulated by, respectively, i.PTH and c.PTH. Using gene expression profiling (Affymetrix Mouse 430A 2.0 Array) of PTH-stimulated primary osteoblasts from neonatal mouse calvariae, we first delineated a set of ephrin ligands (Efn) and receptors (Eph) that was expressed in bone cells. Then, we investigated PTH effects on skeletal gene expression of ephrins in both adult C57/B6J mice and beta-arrestin2 (Arrb2) KO mice, which lack a regulatory protein for PTH-mediated signaling. For this purpose, mice were treated with either daily (s.c.) or continuous (Alzet pump) PTH (80 μ g/kg/day) or vehicle ($n=4$ /gr) for 1 week. RNA was extracted separately from the femur cortical diaphysis (Dia) after flushing of the bone marrow and trabecular metaphysis-epiphysis (Met) region. Targeted gene expression levels of Efn B1 and B2, and Eph A3, A4, B2, B3 and B4, first identified by gene chips analysis in vitro, were analyzed by qRT-PCR (TaqMan MGB probes). Intermittent PTH up-regulated EfnB1, EphB2 and EphB3 1.4 to 1.5 fold in both trabecular and cortical bone compartments, whereas c.PTH did not. In contrast, in Arrb2 KO mice, i.PTH down-regulated the expression of EphA3 and EphA4 in Dia (-1.5x). Moreover, in these mice, c.PTH down-regulated expression of all Efn and Eph (except EphB4) in Dia (-1.4 to -2.5x.) and of EphA3, EphA4 and EphB3 in Met (-1.4 to -1.6x). Interestingly, the profile of EfnB1, EphB2 and EphB3 gene expression induced by PTH paralleled the profile of osteoprotegerin gene (OPG) expression, namely an up-regulation of OPG by i.PTH (2x in Met), but not by c.PTH, in WT mice and a down-regulation (-1.4x in Met and -1.7x in Dia) by c.PTH in KO mice. In summary PTH regulates skeletal gene expression of ephrins and their receptors, which depends on the mode of PTH administration and signaling regulation by beta-arrestins. In turn, up-regulation of ephrins/ephrins receptors, such as EphB3, and OPG by i.PTH should promote osteoblast differentiation and inhibition of osteoclastogenesis. Thereby ephrins could play a role in i.PTH anabolism on both trabecular and cortical bone compartments, while down-regulation of the ephrins system by c.PTH could favor catabolism.

Disclosures: E.N. Bianchi, None.

1122

Treatment with an Anti-Sclerostin Antibody Increased Bone Mass by Stimulating Bone Formation Without Increasing Bone Resorption in Aged Male Rats. X. Li, K. S. Warmington*, Q. Niu*, M. Grisanti, H. Tan, D. Dwyer*, M. Stolina, M. S. Ominsky, W. S. Simonet, P. J. Kostenuik, C. Paszty, H. Z. Ke. Amgen Inc., Thousand Oaks, CA, USA.

Male osteoporosis is becoming more common as the population ages, and decreased bone formation appears to be one of the characteristics of this condition. We previously reported that treatment with an anti-sclerostin antibody (Scl-Ab) stimulated bone formation, restored bone mass and bone strength in aged ovariectomized rats. We now describe the effects of Scl-Ab treatment on bone formation and bone mass in aged gonad-intact male rats. Sixteen-month-old male SD rats were treated s.c. with vehicle or Scl-Ab at 5 or 25 mg/kg, twice a week, for 5 weeks (9-10/group). In vivo bone mineral density (BMD) measurements by DXA showed that rats treated with Scl-Ab at 5 or 25 mg/kg had significantly higher BMD at lumbar vertebrae (+16%; +27%), distal femur (+15%; +20%) and femur-tibia (+9%; +11%) compared with vehicle control. Serum osteocalcin, but not serum CTX-1, was significantly increased in Scl-Ab treated rats as compared with control. Histomorphometric analysis at the proximal tibial metaphysis showed that rats treated with 5 or 25 mg/kg Scl-Ab had significantly greater trabecular bone volume (BV/TV, +133% and +166%, respectively), trabecular thickness, and a significant decrease in trabecular separation compared with vehicle controls. Scl-Ab treated rats had significantly greater osteoblast surface but not osteoclast surface compared with vehicle control. Furthermore, Scl-Ab treated rats had significantly greater mineralizing surface (MS/BS), mineral apposition rate (MAR) and bone formation rate (BFR/BS, +252% and +374% for 5 and 25 mg/kg, respectively) in trabecular bone of proximal tibia. At the tibial shaft increases in endocortical and periosteal bone formation were seen at both the 5 and 25 mg/kg doses, with greater increases seen at the endocortical surface (for 25 mg/kg dose: MS/BS +383% vs +130%, BFR/BS +852% vs +285%). In summary, inhibition of sclerostin by a Scl-Ab increased bone mass and increased bone formation on trabecular, periosteal and endocortical surfaces without evidence of increased bone resorption in aged male rats. These results suggest that anti-sclerostin antibody represents a novel anabolic therapy for age related bone loss in males.

Disclosures: X. Li, Amgen Inc. 1, 3.

This study received funding from: Amgen, Inc.

1123

Gαq Signaling in Osteoblasts Inhibits Bone Formation. N. Ogata¹, Y. Shinoda¹, F. Yano¹, N. Wettschureck^{*2}, S. Offermanns^{*2}, G. V. Segre³, K. Nakamura¹, H. Kawaguchi¹. ¹Sensory and Motor System Medicine, University of Tokyo, Tokyo, Japan, ²Pharmakologisches Institut, University of Heidelberg, Heidelberg, Germany, ³Endocrine Unit, MGH, Boston, MA, USA.

Gas/CAMP/PKA and Gαq/PLC/PKC are known to be the two major signal pathways of PTH. Although accumulated evidence has revealed the anabolic role of the Gas signaling in bone formation, little is known about that of Gαq. To study the role of the Gαq signaling, we initially produced transgenic (Tg) mice that overexpressed the constitutively active Gαq gene exclusively in osteoblasts under the control of 2.3-kb type I collagen α1 chain (COL1A1) promoter. The Tg mice exhibited osteopenia in trabecular and cortical bones with decreased bone formation parameters. Cultured calvarial osteoblasts from the Tg mice showed impairment of differentiation and matrix formation, which was restored by addition of a PKC inhibitor GF109203X. To further explore the role of endogenous Gαq-mediated signaling in bone, we established double knockout (DKO) mice with osteoblast-specific ablation of Gαq and global ablation of Gα11, a Gαq subfamily member that also activates PLC; we did this by crossing Cre transgenic mice under the control of the COL1A1 promoter above (COL1-Cre^{+/+}) and mice with the Gαq gene flanked with loxP / global ablation of Gα11(Gαq^{fl/fl};Gα11^{-/-}). The DKO (COL1-Cre^{+/+};Gαq^{fl/fl};Gα11^{-/-}) mice developed and grew normally without abnormality of major organs. In addition, bone densitometry, 3D-μCT, and histomorphometric analyses showed no significant difference of bone volume or formation in DKO as compared with hetero-knockout of either Gαq (COL1-Cre^{+/+};Gαq^{fl/fl};Gα11^{-/-}) or Gα11 (COL1-Cre^{+/+};Gαq^{fl/fl};Gα11^{-/-}), or the wild-type (COL-Cre^{+/+};Gαq^{fl/fl};Gα11^{+/+}) littermates at 4-20 weeks of age under physiological condition. However, when rhPTH (1-34) (0.08 mg/kg x 5 times x 4 weeks) or the vehicle was subcutaneously injected to 8-week-old mice of all genotypes (n=10/group), the bone densities of the femur, tibia, and L2-5 vertebrae of the PTH group were 12.2, 11.3, and 5.0% higher than the vehicle group (p<0.01 PTH vs. vehicle) in wild-type mice. Although the PTH effect in the Gα11 hetero-knockout mice (12.4, 11.7, and 5.5%) was comparable to WT, it was moderately enhanced by the Gαq hetero-knockout (13.7, 13.1, and 6.7%, P<0.10 vs. wild-type) and significantly by the DKO (15.3, 14.9, and 8.5%, P<0.05 vs. wild-type), indicating dose-dependent stimulation by the Gαq deficiency, but not by Gα11. Taken together, both the gain- and the loss-of-functions of Gαq in osteoblasts clearly demonstrated the inhibitory role of the Gαq signaling in bone formation. Suppression of the Gαq signaling to enhance the PTH anabolic action may lead to a novel treatment of osteoporosis.

Disclosures: N. Ogata, None.

1124

Adenosine and Osteoporosis: Adenosine A₁ Receptor Blockade Reverses Bone Loss in Ovariectomized Mice and Deletion of Adenosine A_{2A} Receptors Leads to Diminished Bone Density. F. M. Kara^{*1}, S. B. Doty^{*2}, A. Boskey^{*2}, B. Fredholm^{*3}, B. N. Cronstein¹. ¹Medicine, NYU School of Medicine, NYC, NY, USA, ²Hospital for Special Surgery, NYC, NY, USA, ³Karolinska Institute, Stockholm, Sweden.

Adenosine regulates a wide variety of physiological processes via interaction with one or more of four G protein-coupled receptors. Because we have previously reported that adenosine A₁ receptors promote fusion of stimulated human monocytes to form giant cells whereas A_{2A} receptor activation inhibits in vitro giant cell formation we determined whether there was a similar requirement for A₁ & A_{2A} receptor occupancy in osteoclast formation.

Spleens were harvested from C57BL/6 female mice (or A₁R knockout mice and their wild type littermates) and splenocytes were cultured in the presence of M-CSF (30 ng/ml) and RANKL (30 ng/ml) with or without various concentrations of the A₁R antagonist DPCPX for 7 days. Cells were stained for tartrate-resistant acid phosphatase (TRAP). The number of TRAP-positive multinucleated cells/well was then enumerated. Histological examination of bones from A₁R, A_{2A} knockout and wild type mice was carried out with both standard (H&E) and immunohistologic (TRAP & Cathepsin K) stains and electron microscopy of bone sections was also carried out. A₁KO and A_{2A} KO mice were analyzed by DEXA (PIXImus) to measure the BMD and by MicroCT. Four week old C57BL/6 mice underwent ovariectomy (OVX) or SHAM surgery; those mice were treated with DPCPX (50 mg/kg/day) or vehicle (VEH) for 5 weeks.

The A₁R antagonist DPCPX inhibits osteoclast formation by as much as 93% in a dose-dependent fashion (P= 0.0012). splenocytes from A₁R KO mice formed almost no osteoclasts in response to M-CSF and RANKL. Histological, pQCT and PIXImus examination from A₁R KO mice shows osteopetrosis, where A_{2A} KO mice shows Osteoporosis. Immunohistological demonstrates that although osteoclasts are present in the A₁R KO mice the osteoclasts are smaller and often not associated with bone. Electron microscopy from A₁KO femur shows an absence of ruffled borders of osteoclasts and resorption of bone. Where A_{2A} mice shows that the osteoclasts are pretty actively in resorbing bone, pQCT and PIXImus scan measurements indicated that by 5 weeks of DPCPX treatment trabecular bone density (TbBD) in the proximal femur increased in both OVX and SHAM compared to VEH. Ex vivo analysis of whole mice by DXA (PIXImus) scan confirmed increased BMD in DPCPX treated mice.

These results indicate that endogenously-released adenosine plays a critical role in regulating bone turnover via interaction with adenosine A₁ & A_{2A} receptors on osteoclasts and their precursor cells. Moreover the A₁ & A_{2A} receptors may be useful targets in treating diseases characterized by excessive bone turnover such as osteoporosis.

Disclosures: F.M. Kara, None.

1125

Effects of Cyclic and Daily PTH in Combination with OPG. A. Iida-Klein¹, S. Johnston^{*1}, Y. Shen², F. Cosman³, R. Lindsay³, D. W. Dempster¹. ¹Regional Bone Center, Helen Hayes Hospital, West Haverstraw, NY, USA, ²MDS Services Inc., Bothell, WA, USA, ³Clinical Research Center, Helen Hayes Hospital, West Haverstraw, NY, USA.

We recently demonstrated that combination of PTH with the anti-resorptive agent alendronate markedly enhances bone strength as well as bone density in mice (Iida-Klein et al, NOF, 2007). Accordingly, we address whether another anti-resorptive agent osteoprotegerin (OPG) has similar effects to alendronate on bone strength as well as density when added to daily or cyclical PTH regimens. We treated 20-week-old, female C57BL/6 mice (n=10/group) for 7 weeks with the following: 1) vehicle [control], 2) OPG-Fc 10 mg/kg/day 2 days/week [OPG], 3) hPTH (1-34) 40 mcg/kg/day [daily PTH], 4) daily PTH in addition to OPG [daily PTH + OPG], 5) PTH and vehicle alternating weekly [cyclic PTH], 6) cyclic PTH in addition to OPG [cyclic PTH + OPG]. We examined the effects of these regimens on femoral and vertebral BMD, bone markers and cortical bone structure of the femur assessed by DXA, biochemical assays and pQCT, respectively. At 7 weeks, all treatment groups markedly increased BMD, and the combination of PTH and OPG additively increased BMD (Table). The positive effect of OPG on vertebral BMD was more marked in the cyclic PTH + OPG group. PTH significantly increased osteocalcin (OC) and mTRAP, while OPG significantly decreased OC and mTRAP. Furthermore, OPG blunted the stimulatory effects of PTH on OC and mTRAP. PTH significantly increased periosteal circumference while OPG tended to decrease endosteal circumference. This effect of OPG at the endocortical site was further enhanced in the presence of PTH as shown by significant decreases in endosteal circumference in the combined groups. At the periosteal site, OPG slightly blunted the PTH-stimulated periosteal expansion. Cortical thickness significantly increased in all groups.

The current study suggests that combination of PTH and OPG may work in a complementary fashion. Combination of these 2 agents in an appropriate protocol in humans may potentially produce more beneficial effects on bone than treatment with either agent alone.

Table 1. Percent increase from control in femoral and vertebral BMD, femoral bone structure and bone markers

	BMD		Osteocalcin	mTRAP	Cortical Thickness	Endosteal Circ.	Periosteal Circ.
	Femur	LV1-6					
OPG	9.1% ^a	16.5% ^b	-42.4% ^b	-65.4% ^b	4.7% ^a	-1.8%	-0.1%
Daily PTH	14.8% ^b	11.8% ^b	472.9% ^b	81% ^b	14.0% ^b	0%	4.9% ^b
Daily PTH + OPG	23.9% ^b	30.1% ^b	-6.8%	-56.3% ^b	22.1% ^b	-5.4% ^b	4.2% ^b
Cyclic PTH	9.4% ^b	2.7% ^a	515.2% ^b	35.6% ^b	6.2% ^b	2.5%	3.8% ^b
Cyclic PTH + OPG	19.4% ^b	31.5% ^b	1.7%	-64.3% ^b	10.9% ^b	-3.2% ^b	2.8% ^a

^a: p<0.05 vs. control, ^b: p<0.01 vs. control.

Disclosures: A. Iida-Klein, Amgen 2.

This study received funding from: Amgen.

1126

A Comparison of Denosumab and Alendronate in Combination with PTH in Ovariectomized Knockin Mice Expressing Humanized RANKL. S. L. Ferrari¹, D. Pierroz¹, N. Bonnet¹, D. Dwyer², M. Stolina², P. Kostenuik². ¹Div. of Bone Diseases, WHO Collaborating Center for Osteoporosis Prevention, Geneva University Hospital, Geneva, Switzerland, ²AMGEN Inc., Metabolic Disorders Research, Thousand Oaks, CA, USA.

Denosumab (DMab, a human Ab versus RANKL), was shown to improve bone volume, density and strength in ovariectomy (OVX) models. The antiresorptive action of DMab typically leads to a secondary increase in serum PTH, which might contribute to Dmab effects on bone. We explored this possibility by examining the endogenous PTH response to DMab or alendronate (ALN), the effects of those therapies on bone density and architecture, and the effects of adding daily PTH to those regimens.

DMab does not inhibit murine RANKL, so studies were performed in knockin mice that express a humanized RANKL gene wherein murine exon 5 was replaced by a human sequence. Adult huRANKL mice (4 months) were sham-operated or OVX, and treated twice weekly (sc) with ALN (100 ug/kg) or Dmab (10 mg/kg) or vehicle (VEH) (n=14-16/group) for 8 weeks. After 4 weeks, half the animals in each group were co-treated with PTH (80 ug/kg/d) or VEH for the remaining 4 weeks. BMD was assessed by DXA at weeks 4 and 8, and trabecular (Tb) and cortical (Ct) microarchitecture of the distal femur was assessed by ex vivo micro-CT at week 8.

Compared to sham, OVX induced a significant loss of whole body (WB) BMD, Tb BV/TV (-74%), number (TbN, -43%), thickness (TbTh, -12%), connectivity (ConnD, -90%) and Ct width (-18%). ALN significantly improved WB BMD, BV/TV and TbN compared to VEH, whereas ALN plus PTH was significantly better than ALN alone on these parameters as well as on TbTh and ConnD. Dmab was statistically superior to ALN alone and equivalent to ALN plus PTH on all Tb bone parameters. Dmab also significantly increased Ct width (+17%), which ALN +/- PTH did not.

The addition of daily PTH to Dmab at week 4 did not significantly change any DXA/microCT parameters compared to 8 weeks of Dmab alone. The lack of additive effects may have been related to the pronounced effects of Dmab monotherapy, which increased WB BMD, BV/TV, TbN and ConnD to levels significantly greater than sham controls. Moreover, Dmab caused a significantly greater increase in serum PTH (1-84) (+250%) and lower serum phosphate at week 4 vs ALN. Circulating PTH levels correlated positively with WB BMD (r=0.62, P<0.001) and Tb BV/TV (r=0.59, p<0.001).

In summary, Dmab was superior to ALN and similar to ALN plus PTH in preventing OVX-related changes of WB BMD, Tb and Ct microarchitecture in huRANKL mice. Intermittent PTH did not further improve Dmab effects, while Dmab induced a significant increase in PTH (1-84) levels and activity. These results support the possibility that endogenous PTH response to Dmab may contribute to its ability to improve bone mass and architecture.

Disclosures: S.L. Ferrari, AMGEN 2, 5; MSD 5, 8.

This study received funding from: Amgen.

1127

GLP-2 Significantly Increases Hip BMD in Postmenopausal Women: A 120-Day study. D. Henriksen¹, P. Alexandersen², B. Hartmann¹, I. Byrjalsen³, J. J. Holst⁴, C. Christiansen¹. ¹Sanos Bioscience A/S, Roedovre, Denmark, ²Center for Clinical & Basic Research, Ballerup, Denmark, ³Nordic Bioscience A/S, Herlev, Denmark, ⁴Department of Medical Physiology, University of Copenhagen, Copenhagen, Denmark.

Glucagon-like peptide-2 (GLP-2) is an intestinal hormone released in response to food intake. We have earlier shown that treatment with GLP-2 for 14 days caused a significant post-administration reduction of bone resorption. This effect was not followed by a change in bone formation and s-osteocalcin levels were unaffected by treatment.

We now present a randomized, placebo-controlled 120-day phase II trial with 160 postmenopausal women. The aim was to test the sustainability of above findings over a longer treatment period and to evaluate the potential for long-term treatment with GLP-2. The study subjects were osteopenic (BMD T-score, -2.5 < T ≤ -1.0) at one or more of the regions: lumbar spine, femoral neck, or total hip. The objectives were relative change from baseline of total hip and spine BMD, as well as pharmaco-dynamic changes in bone resorption (s-CTX) and formation (s-osteocalcin) over the 120 days. Subjects received daily bedtime injections of 0.4, 1.6, or 3.2 mg GLP-2, or placebo. All subjects received supplements of calcium and vitamin D. Treatment with GLP-2 resulted in a dose dependent increase in total hip BMD from baseline, which reached statistical significance (p=0.006) in the 3.2 mg GLP-2 group compared to placebo. This dose dependent relationship in BMD was also seen at the trochanter, (p=0.01, 3.2 mg group). All GLP-2 doses levels elicited an acute and sustained reduction of the nocturnal rise in s-CTX seen in the placebo group. The reduction in the s-CTX level was greater at Day 120 than at Day 1 indicating an overall improved suppression of bone resorption during the 120 days treatment. At Treatment Day 120, all GLP-2 groups had a greater, and highly statistically significant, (p<0.0001) reduction in AUC_{0-4h} for s-CTX compared to placebo.

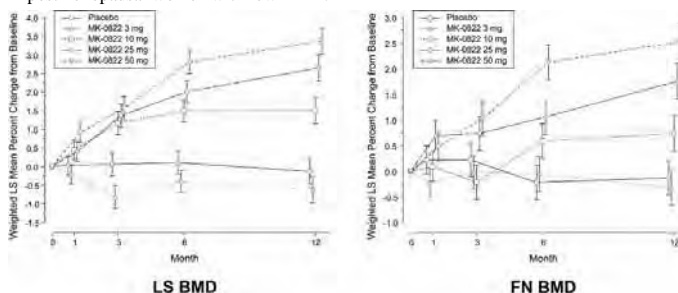
None of the study participants developed any detectable antibodies against GLP-2 and no tachyphylaxis was observed. Overall, it was concluded that the treatment with GLP-2 for 120 consecutive days was effective, well-tolerated and safe. In conclusion, the results suggest that GLP-2 acutely disassociates the two processes of bone remodelling and thereby increases the bone calcium (ossification) balance, particularly at the hip. The favourable effect of GLP-2 on the BMD of the hip suggests that an agent with this mode of action could prove a valuable new treatment for osteoporosis.

Disclosures: D. Henriksen, Sanos Bioscience A/S 3.

1128

A Randomized, Double-Blind, Placebo-Controlled Study of a Cathepsin-K Inhibitor in the Treatment of Postmenopausal Women with Low BMD: One Year Results. H. G. Bone¹, M. McClung², N. Verbruggen³, A. Rybak-Feiglin⁴, C. DaSilva⁴, A. C. Santora⁴, A. Ince⁴. ¹Michigan Bone and Mineral Center, Detroit, MI, USA, ²Oregon Osteoporosis Center, Portland, OR, USA, ³Merck Research Laboratories, Brussels, Belgium, ⁴Merck Research Laboratories, Rahway, NJ, USA.

Cathepsin K, a cysteine protease abundantly expressed in osteoclasts, is necessary for bone collagen degradation. MK-0822, a selective inhibitor of cathepsin K, has been shown to rapidly and reversibly decrease bone resorption in both preclinical and short-term clinical studies. In order to evaluate the safety, tolerability and efficacy of weekly doses of placebo, 3, 10, 25 or 50 mg of MK-0822 on BMD and biochemical indices of bone turnover, a 1+1 year dose-ranging trial is ongoing in postmenopausal women with low BMD. We present 12-month data here. Postmenopausal women (N=399) with BMD T-scores ≤ -2.0 and ≥ -3.5 at lumbar spine (LS), femoral neck (FN), trochanter, or total proximal femur were randomized to receive placebo or 1 of 4 doses of MK-0822. Mean age was 64.2 ± 7.8 years. The mean LS T-score was -2.2 ± 0.8, the FN T-score was -1.9 ± 0.7, and the urinary N-telopeptide/creatinine ratio was 44.1 ± 21.2 nmol/mol. Treatment produced dose-related increases in BMD from baseline. The highest dose of MK-0822 tested (50 mg) resulted in a 3.4% increase in LS BMD (Figure), a 2.5% increase in femoral neck BMD, and a 58% reduction in uNTx/Cr. The safety profile of MK-0822 was generally favorable. There were no dose-related trends in any adverse experiences (AEs). Rash was reported in 8.4% and 3.8% of those in the placebo and 50 mg arms, respectively. Among participants in the placebo arm, 9 discontinued the study due to AEs, and 4 discontinued due to AEs considered drug-related. By contrast, 4 and 0 participants in the 50 mg arm were in each of these AE categories, respectively. In summary, 12 months of MK-0822 treatment was generally safe and well-tolerated and increased LS and FN BMD in postmenopausal women with low BMD.



Disclosures: H.G. Bone, Merck & Co., Inc. 2, 8.

This study received funding from: Merck & Co., Inc.

1129

Anti-Sclerostin Antibody Increases Markers of Bone Formation in Healthy Postmenopausal Women. D. Padhi¹, B. Stouch¹, G. Jang¹, L. Fang¹, M. Darling¹, H. Glise², M. Robinson³, S. Harris⁴, E. Posvar¹. ¹Amgen Inc, Thousand Oaks, CA, USA, ²UCB SA (Pharma), Braine-l'Alleud, Belgium, ³UCB-Celltech, Slough, United Kingdom, ⁴Seaview Research, Miami, FL, USA.

Genetic evidence, along with gene expression, cell biology and pharmacology data, demonstrate that the osteocyte-secreted protein, sclerostin, negatively regulates osteoblasts and plays a key role in controlling bone formation and bone mass throughout life. In this blinded, placebo-controlled, rising single dose study, 48 healthy postmenopausal women were randomized (3:1) to receive a single SC dose (0.1, 0.3, 1, 3, 5, or 10 mg/kg) of a sclerostin neutralizing monoclonal antibody (scl-mAb) or placebo. Blood samples were collected up to 85 days postdose for determination of serum scl-mAb, BSAP, osteocalcin, P1NP and CTx concentrations.

Scl-mAb pharmacokinetics (PK) were non-linear with dose (eg. for the 30-fold increase in dose from 0.1 to 3 mg/kg, mean exposure based on the maximum serum scl-mAb concentrations or area under the serum concentration-time curve increased approximately 60- to 100-fold). Preliminary pharmacodynamic (PD) data for doses of 0.1 to 10 mg/kg scl-mAb are available. Dose-related increases in the bone formation markers P1NP, osteocalcin and BSAP were observed (relative to placebo), with mean percentage change from baseline for these markers of approximately 60 to 100% at 3 mg/kg by 21 days. A trend of dose-related decreases in serum CTx was also observed.

In conclusion, scl-mAb PK following SC administration in healthy postmenopausal women was nonlinear with dose, as observed with other mAbs. Single doses of scl-mAb resulted in significant increases in bone formation markers relative to placebo and a trend of dose related decreases in serum CTx. Scl-mAb was well tolerated following administration of single SC doses. These data support continued clinical investigation of sclerostin inhibition as a potential therapeutic strategy for conditions that will benefit from increased bone formation.

Disclosures: D. Padhi, Amgen 1, 3.

1130

Ostabolin-CTM Increases Lumbar Spine and Hip BMD after 1 Year of Therapy: Results of a Phase II Clinical Trial. A. Hodsman¹, H. Bone², C. Gallagher³, D. Kendler⁴, J. P. Brown⁵, S. Greenspan⁶, C. L. Barclay⁷, P. Morley⁸, R. Anderson⁷, B. R. MacDonald⁸. ¹St. Joseph's Hospital, London, ON, Canada, ²Michigan Bone and Mineral Clinic, Detroit, MI, USA, ³Creighton University, Omaha, NE, USA, ⁴ProHealth Clinical Research Center, Vancouver, BC, Canada, ⁵Laval University, Quebec, PQ, Canada, ⁶University of Pittsburgh, Pittsburgh, PA, USA, ⁷Zelos Therapeutics, Ottawa, ON, Canada, ⁸Zelos Therapeutics Inc., West Conshohocken, PA, USA.

Ostabolin-C (OC) is a cyclic analogue of parathyroid hormone (PTH) (1-31) that has demonstrated marked increases in bone mineral density (BMD) and bone strength in long term preclinical studies, without inducing hypercalcemia. 261 postmenopausal women aged 45-75 years with a BMD T score at lumbar spine (LS) or femoral neck ≤ -2 were randomized into a double blind, placebo controlled dose ranging study investigating the safety and efficacy of 4 months of treatment with OC. Subjects received placebo, 7.5, 15, 30 or 45 $\mu\text{g/day}$ by subcutaneous injection. 198 study subjects elected to continue into a blinded extension study of 8 additional months. The primary endpoint was change in LS-BMD at 1 year. Secondary measures included change in BMD at the hip, biomarkers of bone turnover, and safety measures, including the occurrence of hypercalcemia. OC caused a striking, dose-dependent increase in LS-BMD that was evident by month 4. 79% of subjects in the 45 μg group had an early BMD response (defined as $\geq 3\%$ increase after 4 months). BMD measurements at all proximal femur sites were also increased at 4 months in the 45 μg group. At month 12, LS-BMD was further increased in all active treatment groups with a maximum mean % increase of 11.0 % in the 45 μg group compared to a 0.17 % increase in placebo ($p < 0.001$). At month 12, 97% of subjects in the 45 μg group had an increase in LS-BMD of $\geq 3\%$. At month 12, total hip BMD increased by 2.4% in the 45 μg group compared to a 1.2% decrease in placebo ($p < 0.001$). The BMD effects at all doses were accompanied by commensurate significant increases in biomarkers of bone formation that were detectable at the earliest measured timepoint (4 weeks). Mean % change in P1NP was $> 120\%$, and osteocalcin was $> 100\%$, above baseline throughout the study. Compliance with study drug was $> 93\%$ in all dose groups. The most commonly reported adverse event was mild nausea, as seen with other PTH analogues. This adverse event usually occurred early in the treatment period. Few serious adverse events occurred. Most episodes of hypercalcemia were mild. Hypercalcemia $> 11.0 \text{ mg/dL}$ was infrequent, and only observed with higher incidence than placebo in the 45 μg group. The observed clinical profile, including a marked early BMD response at both hip and spine, indicates that OC has the potential to be a highly effective treatment for osteoporosis.

Disclosures: A. Hodsman, Zelos Therapeutics Inc. 1, 5.
This study received funding from: Zelos Therapeutics Inc.

1131

Dose-dependent Increases in Endogenous Parathyroid Hormone Concentrations After Administration of a Calcium Sensing Receptor Antagonist to Normal Volunteers: Potential for an Oral Bone Forming Agent. D. Ethgen¹, J. Phillips¹, C. Baidoo¹, C. Matheny¹, A. Roshak¹, R. Marquis¹, G. Stroup², S. Kumar¹, P. Bhatnagar¹, W. F. Huffman¹, V. S. Kitchen¹, M. Gowen², L. A. Fitzpatrick¹. ¹GlaxoSmithKline, Collegeville, PA, USA, ²GlaxoSmithKline, King of Prussia, PA, USA.

Brief antagonism of the calcium-sensing receptor (CaR) in the parathyroid gland results in transient stimulation of endogenous parathyroid hormone (PTH) release, a profile known to stimulate bone formation. SB-423557 is an ethyl ester precursor of SB-423562. Upon administration, SB-423557 is converted into its corresponding acid, SB-423562. Both molecules are potent calcium-sensing receptor antagonists that are being investigated for the treatment of osteoporosis as a novel oral bone forming agent. This first clinical study administering SB-423557 orally to healthy male volunteers was designed as a single-blind, placebo-controlled, crossover, randomized (with respect to placebo), dose-rising study. Fifty-four subjects participated in two study sessions separated by ≥ 7 days. In random order, subjects received placebo in one study session, and single oral dose SB-423557 in the other. Dose levels were 5, 10, 20, 50, 100, 200, 400 and 500 mg ($n=5-6$, except $n=12$ for 50 mg group). Blood samples for pharmacokinetic and pharmacodynamic analyses were obtained over a 24-h period after each dose. Elevations in plasma PTH closely followed the time-course of SB-423562 concentrations in blood (SB-423557 generally was undetectable). The duration of PTH elevation (defined as PTH levels \geq twice the pre-dose level) was usually under 8 hours. At SB-423557 doses of 100 mg and above, PTH exposure ($\text{AUC}_{0-24 \text{ h}}$) was on average, 10% to 48% higher compared to placebo. The mean maximum post-dose PTH concentration ranged from 38% to 285% higher relative to placebo; median time to maximum concentration (T_{max}) ranged from 1.01 h to 2.26 h. At doses of 50 mg and higher, relative to placebo, a 1.8- to 4.2-fold increase in PTH levels compared to baseline was noted at the T_{max} . There were no significant effects on serum calcium levels. SB-423557 was generally well tolerated at all doses and no serious adverse events were reported. There were no notable differences among regimens with regard to adverse events frequency, safety laboratory values, vital signs or 12-lead ECG interval values outside the threshold ranges. In conclusion, the observed transient rises in PTH after single oral doses of a CaR antagonist, SB-423557, constitutes an early proof-of-concept in man, and provides the basis for further development of this class of compounds for delivering an oral bone forming treatment to osteoporotic patients.

Disclosures: D. Ethgen, GlaxoSmithKline 3.

1132

A Single Dose of ACE-011 Is Associated with Increases in Bone Formation and Decreases in Bone Resorption Markers in Healthy, Postmenopausal Women. J. Ruckle¹, M. Jacobs¹, W. Kramer², R. Kumar³, K. Underwood³, R. S. Pearsall³, A. Pearsall³, J. Seehra³, C. Condon³, M. L. Sherman³. ¹Covance Clinical Research, Honolulu, HI, USA, ²Kramer Consulting, LLC, North Potomac, MD, USA, ³Accelaron Pharma, Inc., Cambridge, MA, USA.

ACE-011 is a fusion protein consisting of the extracellular domain of the human type II activin receptor IIA (ActRIIA) linked to the Fc portion of human IgG1. ACE-011 binds to activin with a K_d of 50 pM. Nonclinical studies in ovariectomized mice treated with ActRIIA fused to the Fc region of a murine IgG have shown improvements in bone architecture and strength. Histomorphometry studies have demonstrated an anabolic effect. A randomized, double-blind, placebo-controlled study was conducted to evaluate ACE-011 administered to healthy, postmenopausal women. Forty-eight subjects were randomized in cohorts of 6 to receive either a single dose of ACE-011 or placebo (5 active:1 placebo). Dose levels ranged from 0.01 to 3.0 mg/kg intravenously and 0.03 to 0.1 mg/kg subcutaneously. All subjects were followed for 120 days. Subjects were excluded from study participation if they took medications affecting bone metabolism within 6 months of study entry. Safety evaluations were conducted following each cohort to determine dose escalation. In addition to pharmacokinetic (PK) analyses, the biologic activity of ACE-011 was also assessed by measurement of biochemical markers of bone formation and resorption, and FSH levels. No serious adverse events were reported in this study. Adverse events (AEs) were generally mild and transient. Preliminary analysis of AEs included headache, elevated laboratory values, cold symptoms, emesis or vomiting, intravenous infiltration, and hematoma at injection site. PK analysis of ACE-011 displayed a linear profile with dose, and a mean half-life of approximately 25-32 days. The absorption after SC dosing was essentially complete. ACE-011 caused a rapid, sustained dose-dependent increase in serum levels of bone-specific alkaline phosphatase, and a dose-dependent decrease in C-terminal type 1 collagen telopeptide and tartrate-resistant acid phosphatase 5b levels. These bone biomarker changes were sustained for at least 29 days at the highest dose levels tested. There was also a dose-dependent decrease in serum FSH levels consistent with inhibition of activin.

A single dose of ACE-011 given to healthy postmenopausal women was safe and well-tolerated for the range of dose levels tested. The prolonged PK and pharmacodynamic effects suggest that intermittent dosing would be appropriate for future studies. ACE-011 is a first-in-class novel osteoanabolic agent with biological evidence of both an increase in bone formation and a decrease in bone resorption.

Disclosures: J. Ruckle, None.

This study received funding from: Accelaron Pharma, Inc.

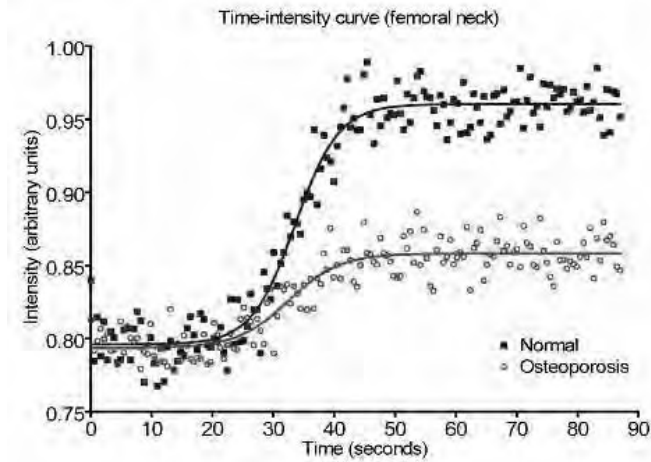
1133

Compromised Bone Marrow Perfusion in Osteoporosis. J. F. Griffith¹, D. K. W. Yeung¹, P. K. Tsang¹, K. C. Choi², T. C. Y. Kwok³, A. T. Ahuja¹, K. S. Leung⁴, P. C. Leung⁵. ¹Diagnostic Radiology and Organ Imaging, The Chinese University of Hong Kong, Prince of Wales Hospital, Shatin, Hong Kong, ²School of Public Health, The Chinese University of Hong Kong, Prince of Wales Hospital, Shatin, Hong Kong, ³Community and Family Medicine, The Chinese University of Hong Kong, Prince of Wales Hospital, Shatin, Hong Kong, ⁴Orthopaedics and Traumatology, The Chinese University of Hong Kong, Prince of Wales Hospital, Shatin, Hong Kong, ⁵Jockey Club Centre for Osteoporosis Care and Control, The Chinese University of Hong Kong, Prince of Wales Hospital, Shatin, Hong Kong.

Background: There may be a link between bone blood flow and osteoporosis. This study of the proximal femur investigates the relationship between bone mineral density (BMD), bone fat content, bone and muscle perfusion.

Methods: 120 healthy female subjects (mean age, 74 years) underwent DXA, proton (¹H) MR spectroscopy, and dynamic contrast-enhanced MRI. Marrow fat content was measured at the femoral head, neck and shaft. Perfusion indices (maximum enhancement, E_{max} and enhancement slope, E_{slope}) in the proximal femur (head, neck, shaft and acetabulum) and adductor muscle were measured. Correlation between T-score, fat content and perfusion indices was examined.

Results: Perfusion indices were significantly reduced in subjects with osteoporosis (Table) compared to subjects with osteopenia or normal BMD (Figure).



Adductor muscle perfusion was not affected by change in BMD (E_{max} , $r = -0.061$; E_{slope} , $r = -0.057$). As marrow perfusion decreased in the proximal femur, marrow fat increased. For normal BMD subjects, perfusion parameters in the femoral head were 1/3 those in the femoral neck or shaft and 1/5 those in the acetabulum.

Conclusion: Perfusion in the proximal femur is reduced in osteoporotic subjects compared to osteopenic and normal subjects. This reduction in perfusion occurs only within the bone and not in the extrasosseous tissues.

Pearson correlation coefficient between T-score, perfusion indices and fat content.			
		Vs. T-score	Vs. Fat content
Enhancement maximum (slope)	Femoral head	0.264* (0.402**)	-0.614** (-0.549**)
	Femoral neck	0.424** (0.405**)	-0.855** (-0.768**)
	Femoral shaft	0.242* (0.174)	-0.653** (-0.647**)
	Acetabulum	0.550** (0.521**)	
Marrow fat content	Femoral head	-0.334**	
	Femoral neck	-0.370**	**p<0.01
	Femoral shaft	-0.412**	*p<0.05

Disclosures: J.F. Griffith, None.

1134

Neuropeptide Y Protects the Skeleton from Stress-induced Bone Loss. P. A. Baldock^{*1}, S. Allison^{*1}, T. Karl^{*2}, D. Pierroz³, D. Lin^{*2}, A. Sainsbury^{*2}, R. Enriquez^{*1}, S. Ferrari³, H. Herzog^{*2}, J. Eisman¹. ¹Bone Program, Garvan Institute of Medical Research, Sydney, NSW, Australia, ²Neuroscience Program, Garvan Institute of Medical Research, Sydney, NSW, Australia, ³Service and Laboratory of Bone Diseases, Geneva University Hospital, Geneva, Switzerland.

Bone responses to stress are not well studied beyond corticosteroid-related effects. Neuropeptide Y has anxiolytic actions, attenuating the psychological effects of stress. Interestingly, the major Y-receptor mediating these anti-stress actions is the Y2 receptor, also known to control bone mass. We therefore investigated how the NPY pathway may modulate skeletal responses to physiological stress.

Behavioral stress responses in NPY^{-/-} mice were examined using established models. Skeletal response to stress was examined at 14 weeks in male NPY^{-/-} and wild type mice after 4 week low and high stress protocols. All mice were kept in a low stress environment until the age of 9 weeks. Following this, the "stress" groups were involved in a protocol that necessitated regular handling and other known stressors in mice, including rectal temperature, glucose tolerance test, 24h fasting and metabolic cage studies. Control mice remained in the lower stress environment.

Anxiety-like behaviours in the open field and light-dark tests, both standard methods for determination of explorative and anxiety-related parameters, were much greater in NPY^{-/-} mice.

As expected, whole body, femoral (53 ± 2 mg/mm² vs 65 ± 2 , $p < 0.05$) and tibial BMD was greater in NPY^{-/-} mice compared to wild type in low stressed group, coincident with greater cortical volume and thickness. Greater cancellous bone volume in distal femoral ($16.7 \pm 1.5\%$ vs 11.6 ± 0.9 , $p < 0.01$), and lumbar vertebral metaphyses was coincident greater mineral apposition rate in NPY^{-/-} mice (1.9 ± 0.1 μ m/d vs 2.8 ± 0.1 , $p < 0.0005$).

In the "stressed" groups, body weight was reduced in NPY^{-/-} mice (30.1 ± 1 g vs 25.5 ± 1 g, $p < 0.0001$), with decrements in lean and fat mass, with no decrease in wild type. A mild cancellous response was evident in wild type mice, with trabecular number reduced but no significant loss of cancellous bone volume. However, in "stressed" NPY^{-/-} mice there was a marked decrease in cancellous bone volume compared to low stressed NPY^{-/-} mice ($16.7 \pm 1.5\%$ vs 13.2 ± 0.7 , $p < 0.01$), again associated with reduced trabecular number. Importantly, mineral apposition rate was also reduced in "stressed" NPY^{-/-} mice, but still remained greater than wild type (1.6 ± 0.1 μ m/d vs 2.4 ± 0.1 , $p < 0.0001$).

In summary, these data suggest that NPY plays a powerful role in regulating the effects of stress. Diminishing levels of NPY may enhance the bone loss induced by stress. This may explain a mechanism for bone loss associated with stress in otherwise healthy individuals.

Disclosures: P.A. Baldock, None.

This study received funding from: NHMRC

1135

Fat-1 Gene Prevents Ovariectomy Induced Bone Loss by Modulating Osteoclastogenesis. M. M. Rahman, A. Bhattacharya*, J. Banu, G. Halade*, G. Fernandes*. Medicine/CI, UTHSCSA, San Antonio, TX, USA.

Consumption of n-3 fatty acids (FA) positively influences on calcium and bone metabolism. Beneficial effects of n-3 FA on bone mineral density (BMD) have been reported in mice, rats and humans, but the precise mechanisms involved have not been described. In this study, we investigated the effect of fat-1 gene on ovariectomy induced bone loss. fat-1 gene encodes for an n-3 desaturase enzyme that can synthesize n-3 FA from n-6 FA. Ovariectomized (OVX) and sham operated wild type (WT) C57BL/6 (B6) mice and fat-1 transgenic B6 mice were fed a diet containing 10% CO. After 24 weeks on diets, BMD was analyzed by dual energy x-ray absorptiometry. fat-1 OVX mice had significantly higher BMD in distal femoral metaphysis, proximal tibial metaphysis, femoral diaphysis, and lumbar vertebra as compared to WT OVX mice. Pro-inflammatory cytokines TNF-alpha, IL-6 and IL-1 beta and anti-inflammatory cytokine IL-10 were analyzed in LPS stimulated bone marrow (BM) culture supernatant by ELISA. Significantly lower level of IL-1 beta, TNF-alpha and IL-6, and higher level of IL-10 expression was found in fat-1 OVX mice compared to WT OVX mice. LPS stimulated NF-kappaB activation was also analyzed in BM cells. NF-kappaB activation was found significantly less in fat-1 OVX mice compared to WT OVX mice. We also examined the LPS stimulated inducible nitric oxide synthase (iNOS) expression and nitric oxide (NO) production in BM cells. Interestingly, LPS treated NO production in BM culture supernatant and iNOS protein expression in BM cells was significantly higher in fat-1 OVX mice as compared to WT OVX mice. Moreover, fat-1 transgenic, nontransgenic and WT BM cells were cultured in the presence of n-6 fatty acid (linoleic acid) with RANKL to differentiate into TRAP +ve cells. Interestingly, fat-1 transgenic BM cells generated significantly less TRAP +ve osteoclast like cells compared to fat-1 nontransgenic and WT B6 BM cells. We offer further the mechanisms involved in preventing the bone loss in OVX mice by n-3 FA using a fat-1 transgenic mouse model.

Disclosures: M.M. Rahman, None.

This study received funding from: NIH.

1136

A CD40L Mediated Cross-talk Between T Cells and Stromal Cells Is Required for Estrogen Deficiency and PTH to Induce Bone Loss. Y. Gao, M. Terauchi, K. Page*, X. Yang*, F. Grassi, S. Galley, E. Shah*, M. R. Ryan, M. N. Weitzmann, R. Pacifici. Division of Endocrinology, Metabolism and Lipids, Emory University School of Medicine, Atlanta, GA, USA.

Activated T cells induce bone loss in inflammation and estrogen (E) deficiency by secreting RANKL, TNF, and IFN γ . T cells also regulate bone marrow (BM) stromal cells (SCs) via surface receptors, but the relevance of T cell membrane signals in bone diseases is unknown. Herein we investigated a) if T cells regulate the capacity of SCs to support osteoclast (OC) formation through CD40L, a T cell costimulatory molecule which binds to SC expressed CD40 receptors, and b) the role of CD40L/CD40 signaling in the bone loss induced by ovariectomy (ovx) and in vivo continuous PTH treatment (cPTH). As compared to T cell replete controls, SCs from nude mice and WT mice immunodepleted of T cells in vivo produce less M-CSF, RANKL, and TNF and supported the formation of fewer OCs when cocultured with BM macrophages (BMMs) from WT mice. Moreover, ovx and cPTH upregulate the osteoclastogenic activity of SCs from control, but not T cell deficient mice, demonstrating that E and PTH regulate SC function through T cells. OvX and cPTH upregulate the T cell expression of CD40L and the SC expression of CD40 by 2-3 fold. CD40 expression is equally increased by IFN γ and TNF, cytokines produced in large amounts by T cells of ovx mice, suggesting that ovx upregulates CD40 expression through these factors. PTH induced OC formation in cocultures of BMMs and SCs is equally enhanced by soluble CD40L and WT T cells, while CD40L -/- T cells are ineffective. Moreover, neutralizing anti CD40L mAb blocks the T cell potentiation of PTH induced OC formation, and the capacity of T cells from ovx mice to increase the formation of OCs in cocultures of SCs and BMMs from intact mice, demonstrating a role for CD40L in PTH and ovx induced OC formation. Analysis by μ CT reveals that CD40L -/- mice are completely protected against the loss of trabecular and cortical bone induced by ovx and cPTH, respectively. Thus, CD40L plays a key role in both ovx and PTH induced bone loss. When T cells from WT and CD40L -/- mice were adoptively transferred into TCR β -/- mice, a strain lacking $\alpha\beta$ T cells, cPTH stimulated bone resorption leading to cortical bone loss in hosts reconstituted with WT T cells, but not in those reconstituted with CD40L -/- T cells, thus demonstrating the specific role of T cell expressed CD40L. In summary, CD40L/CD40 costimulation is a novel pathway by which T cells regulate SC function and OC formation. Upregulation of the osteoclastogenic activity of SCs by T cell expressed CD40L is pivotal for the osteoclastogenic response to PTH and E deficiency. Understanding the cross-talk between T cells and SCs may thus yield novel therapeutic strategies for postmenopausal and PTH induced bone loss.

Disclosures: Y. Gao, None.

1137

Ovariectomy Decreases Bone Mass in Young and Old Female Athymic Mice. W. M. Kozlow, K. Mohammad, C. R. McKenna*, H. Walton*, M. Niewolna*, T. A. Guise. Internal Medicine, University of Virginia, Charlottesville, VA, USA.

Ovariectomy (OVX) has been reported to have no effect on trabecular bone mass in female athymic (nude) mice because these mice lack T cells⁽¹⁾. However, recent data has demonstrated trabecular, but not cortical, bone loss 4 weeks after OVX in 6-week-old female nude mice⁽²⁾. The effect of OVX on bone mass in female nude mice may be related to mouse age at the time of surgery.

To determine the effect of mouse age (at the time of OVX) on bone mass, 4-week-old (young) and 16-week-old (old) female BALB-c nude mice were randomized to OVX or sham surgery (sham). Bone mineral density (BMD), as assessed by Lunar PIXImus, was assessed at baseline and every 2 weeks thereafter. At 20 weeks, the young OVX mice had decreased BMD at the total body ($p=0.0056$), spine ($p<0.0001$) and proximal tibia ($p<0.0001$) compared to the sham mice. Decreased BMD was noted as early as 2 weeks after OVX in the total body and proximal tibia, and by 4 weeks after OVX in the lumbar spine. Although there was no difference in BMD at the distal femur, BMD was surprisingly increased at the mid femur ($p<0.0001$) in the OVX mice compared to the sham mice. However, histomorphometry demonstrated no difference in trabecular bone volume at the distal femur or proximal tibia between the OVX mice and sham mice.

Twenty weeks after surgery, the old OVX mice had decreased BMD at the total body ($p=0.0048$), spine ($p<0.0001$), mid femur ($p=0.0409$) and distal femur ($p<0.0001$) as compared to the sham mice. Decreased BMD was noted as early as 2 weeks after OVX in the total body and distal femur, and by 4 weeks after OVX in the lumbar spine and mid femur. There was no difference in BMD at the proximal tibia.

At 20 weeks, differences between the OVX and sham mice were greater in the young mice versus the old mice: 3.4% versus 1.5% total body; 18.3% versus 9% spine; 9.2% versus 1.1% mid femur; 3.8% versus 6.1% distal femur; 20.1% versus 6.6% proximal tibia.

Bone marrow cultures from OVX mice exhibited a greater number of colony forming unit (CFU)-fibroblasts ($p<0.0001$ for young and old), CFU-osteoblasts ($p<0.0001$ young, $p=0.0001$ old) and TRAP-positive osteoclasts ($p=0.0005$ young) compared to sham mice.

These experiments show that OVX does have an effect on bone mass at multiple sites in female nude mice. OVX-induced decreases in bone mass were seen in both young and old female nude mice, but the differences between the OVX and sham mice were more profound in the younger mice as compared to the older mice. Bone marrow cultures revealed that the lower bone mass was associated with increased bone turnover.

⁽¹⁾ Cenci S et al. J Clin Invest. 2000;106: 1229-37.

⁽²⁾ Lee S-K et al. J Bone Miner Res. 2006; 21:1704-12.

Disclosures: W.M. Kozlow, None.

This study received funding from: Department of Defense.

1138

IGF-I Carrier Components Determine Skeletal Integrity Via Direct and Indirect Mechanisms. S. Yakar¹, W. Mejia^{*1}, Y. Kawashima^{*1}, H. Sun^{*1}, M. L. Bouxsein², C. J. Rosen³. ¹Mount Sinai School of Medicine, New York, NY, USA, ²Beth Israel Deaconess Medical Center, Boston, MA, USA, ³The Jackson Laboratory, Bar Harbor, ME, USA.

Serum IGF-I is secreted mainly by the liver and circulates bound to IGF-binding proteins (IGFBPs, predominantly IGFBP-3) in binary complexes and bound to IGFBP-3 and the acid labile subunit (ALS) in a ternary complex. To delineate the role of IGF-I circulatory complexes in skeletal integrity, we employed three mouse lines that have reduced circulating IGF-I: liver-specific IGF-I deficient (LID) mice; ALS knockout (ALSKO) mice, and IGFBP-3 knockout (BP3KO) mice. Bone micro-architecture is profoundly affected in the different IGF-I mutants; LID mice exhibit minor reductions in trabecular BV/TV% (~10%), but significantly lower areal BMD and mid-diaphyseal cortical thickness. In contrast, gene inactivation of the ALS, leads to a marked decrease in trabecular BV/TV% (~20%), with no changes in cortical thickness and reduced cross-sectional area. In contrast to both LID and ALSKO mice, BP3KO mice have ~30% decreases in trabecular bone volume fraction with no changes in cortical bone thickness or diaphyseal cross-sectional geometry. To determine what mechanisms may be operative in the skeleton of the IGF-I deficient mice we studied marrow cells and their ability to form osteoblasts(OB) and osteoclasts (OC). ALSKO and BP3KO exhibited an increase in OB differentiation as assessed by alkaline phosphatase staining, whereas marrow stromal cells from LID mice did not differ from controls. OC differentiation was enhanced in BP3KO mice as reflected by increased TRAP positivity compared to control mice. In contrast, ALSKO mice exhibited reductions in OC number and activity as assessed by pit formation assay. In support of the latter, real time PCR for OC markers revealed a decrease in TRAP and cathepsin K expression in ALSKO cultures consistent with impaired differentiation of macrophage precursors. Taken together, these results suggest direct yet diverse effects of ALS and IGFBP-3 on OB and OC differentiation and activity. Alternatively it is conceivable that ALS and IGFBP-3 may have indirect effects on bone via alterations in the hematopoietic-monocytic lineage that are modulated by marrow stromal cells.

Disclosures: S. Yakar, None.

1139

Evidence for Lineage Dependent Non-canonical Wnt Signal Transduction by Bone Cells. G. J. Spencer*, P. G. Genever*. Department of Biology, University of York, York, United Kingdom.

Wnt signaling has emerged as an important determinant of bone mass, regulating osteoblast and osteoclast formation and activity. Most studies have focused on the transcriptional effects of canonical Wnt signaling although Wnts are also known to signal through non-canonical pathways, evoking changes in intracellular calcium and activation of protein kinase signaling cascades. Using a combination of Affymetrix microarray analysis and RT-PCR we have identified expression of Wnt ligands (Wnt5a), Fzd receptors (Fz 1, 3 and 7) and PKC isoforms required for non-canonical Wnt signal transduction in human mesenchymal stem cells (MSCs). Exposure of MSCs to the prototypical non-canonical Wnt ligand Wnt5a (conditioned medium, 10-50%) during osteogenic differentiation induced by dexamethasone, ascorbate and β -glycerol phosphate, significantly reduced cell numbers ($p<0.001$) and increased alkaline phosphatase activity ($p<0.01$), supporting a role for non-canonical signaling in stimulating osteogenesis. In contrast, exposure to the canonical ligand Wnt3a stimulated proliferation and inhibited osteogenesis. By confocal imaging, western blotting and immunolocalization we demonstrated that exposure of MSCs to Wnt5a (10-500ng/ml) caused a rapid, thapsigargin-sensitive increase in intracellular calcium and potentially stimulated the phosphorylation of PKC isoforms PKC δ , PKC α/β and PKD/PKC μ . Wnt5a also stimulated the phosphorylation and nuclear translocation of the transcription factor CREB without affecting p42/44 MAPK activity. Significantly, using cultures of rat primary calvarial osteoprogenitors we were unable to demonstrate any stimulatory effect of Wnt5a on intracellular calcium, proliferation or osteogenic differentiation, although Wnt3a remained inhibitory. These data strongly suggest that uncommitted MSCs respond to non-canonical signals to promote osteogenesis with loss of responsiveness soon after the onset of differentiation, while anti-osteogenic effects of Wnt3a are independent of lineage commitment state. As potential anabolic therapies depend on their specificity for osteogenesis we determined whether cells of the osteoclast lineage also respond to non-canonical Wnts. Using RAW264.7 cells we showed that exposure to Wnt5a (10-500ng/ml) potentially increased p42/44 MAPK activity and phosphorylation of JNK, PKC α , PKC α/β and PKD/PKC μ , without affecting CREB. These data have wide implications for our understanding of Wnt signaling in bone; non-canonical Wnts promote osteogenesis but also have potential to affect osteoclastogenesis and bone resorption through common activation of PKC isoforms but differential effects on the activity of CREB, MAPK and JNK.

Disclosures: G.J. Spencer, None.

This study received funding from: The Wellcome Trust.

1140

Reciprocal Regulation of Dkk1 Gene Transcription by Msx2 and c/EBP α . S. Cheng, O. L. Sierra, D. A. Towler. Division of Bone and Mineral Diseases, Washington University School of Medicine, St. Louis, MO, USA.

Msx2 plays an important role in craniofacial bone formation, osteoblast gene transcription, and osteogenic-adipogenic differentiation. We previously demonstrated that Msx2 inhibits gene transcription via 3 mechanisms: (a) antagonistic protein-protein interactions with a multiprotein complex containing Runx2, Ku antigen, and MINT, (b) inhibitory interactions with TFII-F, a PolII-dependent transcription initiation and elongation factor, and (c) inhibitory protein-protein actions with c/EBP α that preclude PPAR γ 2 expression and adipogenic differentiation. We also demonstrated that Msx2 promotes calvarial osteogenesis in part via suppression of Dkk1, with concomitant activation of canonical Wnt signaling. Msx2 pro-osteogenic actions are abrogated by treatment with Dkk1 protein or transduction with a Dkk1-expressing retrovirus. We wished to examine the mechanisms that mediate Msx2 inhibition of Dkk1. Using 10T1/2 cells transduced with Msx2 retrovirus or primary calvarial osteoblasts from CMV-Msx2 transgenic mice, we find that Msx2 suppresses Dkk1 gene expression. Western blot analyses confirm reduction of Dkk1 levels in Msx2-expressing cells (30% of control). Conversely, "knock-down" of endogenous Msx2 levels in 10T1/2 cells with Msx2 siRNA enhances Dkk1 transcription. Msx2 variants with either increased (P148H) or absent (T147A) intrinsic DNA binding activity demonstrate that Msx2 inhibits Dkk1 transcription via antagonistic protein-protein interactions. Systematic 5'- and 3'-deletion analyses of the Dkk1 promoter (LUC reporter) mapped Msx2-dependent suppression to nucleotides +165 to +234 relative to the transcription initiation site. Increased expression of the adipogenic transcription factor c/EBP α sequesters Msx2, and upregulates Dkk1 gene transcription. Chromatin immunoprecipitation (ChIP) assays demonstrate that Msx2 reduces the stable interaction of PolII with Dkk1 gene. Inhibition is distinctly enhanced with distance downstream of the transcription initiation site, indicating that both initiation and elongation must be affected by Msx2. Thus, Msx2 promotes osteogenesis and prevents adipogenic gene expression in part via paracrine Dkk1 signals. Msx2 suppression of Dkk1 promotes canonical Wnt signaling and osteogenic differentiation. Conversely, inhibition of Msx2 by c/EBP α upregulates Dkk1, inhibits canonical Wnt signaling, and promotes adipogenic differentiation. Stable association of PolII with the Dkk1 gene is negatively regulated by Msx2, and represents an important transcriptional regulatory step during osteogenic differentiation of calvarial mesenchymal progenitors.

Disclosures: S. Cheng, None.

1141

ERK1 and ERK2 Are Essential for Osteoblast Differentiation. T. Matsushita^{*1}, G. Landreth^{*2}, S. Murakami¹. ¹Orthopaedics, Case Western Reserve University, Cleveland, OH, USA, ²Neurosciences, Case Western Reserve University, Cleveland, OH, USA.

To examine the roles of ERK MAPK in bone formation, we inactivated ERK2 using the Cre-loxP system. Inactivation of ERK2 in mesenchymal cells using the Prx1-Cre transgene in the ERK1-null background caused severe bone defects in the limbs and calvaria. In severely affected long bones, no distinct cortical bone was formed. The lambdoid suture in calvaria failed to close postnatally. While normal levels of Runx2, Osterix, Atf4, and Col1a1 expression were observed in situ hybridization, Osteocalcin expression was abolished. These observations indicate that osteoblast differentiation was blocked after Osterix expression and before differentiation into fully mature osteoblasts. Furthermore, loss of ERK1 and ERK2 caused ectopic cartilage formation in the perichondrium, strongly suggesting that osteo-chondroprogenitor cells in the perichondrium were arrested in their differentiation into osteoblasts and instead differentiated into chondrocytes. Immunohistochemical analysis showed decreased beta-catenin protein levels in the perichondrium, suggesting reduced Wnt signaling. Loss of ERK1 and ERK2 in chondrocytes also resulted in severe disorganization of the epiphyseal cartilage. While the cartilage anlage was normally formed, chondrocytes failed to form columnar structures in the growth plate. There was a striking widening of the zone of hypertrophic chondrocytes. Furthermore, TRAP-positive osteoclasts were decreased, suggesting MAPK-mediated regulation of osteoclastogenesis by mesenchymal cells. Similar cartilage phenotype was observed when ERK2 was inactivated using the Col2a1-Cre transgene in the ERK1-null background. As a complementary experiment, we generated transgenic mice that express a constitutively active mutant of MEK1 under the control of a prx1 promoter. The transgene was expressed in the developing limb bud, the perichondrium and periosteum of the long bones, and the lambdoid suture in the cranium. These mice showed a delay in the formation of cartilage anlage, synostosis of long bones, fusion of carpal and tarsal bones, and accelerated closure of the lambdoid suture. These mice showed a thickening of Runx2-expressing periosteum and a dramatic increase in the cortical bone formation. Our observations indicate that ERK1 and ERK2 are essential for osteoblast differentiation, and increased MAPK signaling promotes bone formation. ERK1 and ERK2 inhibit ectopic cartilage formation in the perichondrium, and increased MAPK signaling inhibits the formation of cartilage anlage. Based on these observations, we propose that ERK1 and ERK2 play essential roles in the lineage specification of mesenchymal cells.

Disclosures: T. Matsushita, None.

1142

Polycystin-1 Selective Activation of Runx2-II Isoform Transcription Is Mediated Through the Calcium-PI3K-Akt Pathway. Z. S. Xiao, S. Q. Zhang^{*}, B. S. Magenheimer^{*}, J. P. Calvet^{*}, L. D. Quarles. The Kidney Institute, University of Kansas Medical Center, Kansas City, KS, USA.

The presence of primary cilia and polycystins 1 (PC1) and 2 (PC2) in osteoblasts and osteocytes, suggest that these molecules may form a mechanosensing complex in bone. At present, data supporting this hypothesis is limited to the observation that PC1-deficient (Pkd1 mutant) mice have osteopenia that is associated with a selective decrease in the expression of the Runx2-II isoform in bone. To further establish the role of primary cilia and polycystins in regulating bone cell function, we investigated PC1 and PC2 expression in primary cilia and examined the signal transduction pathways linking PC1 to Runx2-II expression in osteoblasts. Using immunofluorescent staining with antibodies to PC1, PC2, and the primary cilium marker alpha tubulin, we found that PC1 and PC2 co-localize to primary cilia in MC3T3-E1 osteoblasts. To further establish the role of Runx2-II in mediating PC1 effects on bone, we crossed heterozygous Pkd1 and Runx2-II mutant mice to create double heterozygous mice that are deficient in both PC1 and Runx2-II. Double heterozygous Pkd1 and Runx2-II mice exhibited a significantly greater reduction in bone mineral density than their heterozygous littermates, supporting the functional role of Runx2-II as a downstream signal for PC1 regulation of osteoblast function in vivo. To investigate the intracellular pathways linking PC1 to Runx2-II, we examined the effects of over-expressed PC1 C-tail constructs on P1 and P2 promoter-luciferase activity, intracellular calcium levels and PI3K/Akt pathways in MC3T3E1 osteoblasts. We found that PC1 C-tail constructs resulted in a significant increase in intracellular calcium and Runx2 P1 but not P2 promoter activity. Site-directed mutagenesis of critical amino acids in the coil-coil domain of the PC1 C-tail construct necessary for coupling to PC2 completely abolished PC1 C-tail-stimulated Runx2-II P1 promoter activity. Moreover, both PI3K (LY294002) and Akt inhibitors blocked the ability of PC1 C-tail constructs to increase Runx2-II P1 promoter activity. Additional promoter analysis identified a PC1 responsive region in an area between positions -420 to -350 that contains both putative NF1 and AP-1 binding sites. These findings indicate that a primary cilia-polycystin complex is present and is selectively coupled to Runx2-II gene expression in osteoblasts through intracellular calcium and PI3K-AKT signaling pathways.

Disclosures: Z.S. Xiao, NIAMS (R01-AR049712) and NIDDK (P50-DK057301) 2. This study received funding from: NIAMS (R01-AR049712) and NIDDK (P50-DK057301).

1143

Identification of the Homeobox Protein, Prx1 (MHox), as a Regulator of Osterix Expression and Mediator of TNF Action. X. Lu^{*1}, G. R. Beck², L. C. Gilbert^{*1}, T. P. Conrads^{*3}, M. J. Kern^{*4}, M. S. Nanes¹. ¹Div Endocrinology, Dept Medicine, Emory Univ / VAMC, Atlanta, GA, USA, ²Div Endocrinology, Dept Medicine, Emory Univ, Atlanta, GA, USA, ³Div Clin Pharm, Hillman Cancer Inst, Univ Pittsburgh, Pittsburgh, PA, USA, ⁴Dept Cell Biology and Anatomy, MUSC, Charleston, SC, USA.

A network of transcription factors (TF) regulates the commitment of pluripotent mesenchymal cells to the osteoblast lineage. Identifying these factors is key to understanding skeletal development and lifelong renewal of bone forming cells. Osterix (Ox, SP7) is an important TF required for late chondrocyte and osteoblast differentiation as deletion results in a cartilaginous skeleton. We recently described the transcriptional regulation of Ox by defining 2 upstream promoters that direct synthesis of 2 mRNA species. A potent TNF/MAPK sensitive suppressor region was identified within the Ox promoter that was highly protein bound, inactivated by mutation, and functionally transferable to another promoter. We considered that identification of the proteins bound to the suppressor would reveal early TF regulators of osteoblast differentiation. Nuclear extracts from TNF-treated and untreated mesenchymal cells (C3H) were incubated with a DNA-Sepharose probe containing the 18 bp suppressor sequence. Tryptic fragments of the bound proteins were analyzed using tandem mass spectroscopy. Candidate TF were identified by subtraction analysis of identified protein fragments from the 2 treatment groups. 7 transcription factors were found among 62 unique nuclear proteins in the murine genome database. ChIP assay confirmed specific binding of some but not all of these to the Ox promoter suppressor region. One TF, the paired related homeobox protein (Prx1, MHox), had previously been shown to have a critical role in skeletal development and a compound loss of Prx1/Prx2 (S8) function was reported to have limb deformation, impaired ossification, and facial defects (Martin Genes Dev 1995; Lu Dev Biol 1999; Peterson Dev Dyn 2005). PCR revealed expression of Prx1 in primitive mesenchymal cell lines including C3H, C2C12, and MC3T3. TNF induced a 2 fold increase in Prx1 expression without affecting expression of Prx2. To determine the role of Prx1 in the TNF suppression of Ox, C3H cells were treated with a silencing RNA to Prx1 (siPrx1). siPrx1 specifically silenced basal Prx1 mRNA and blocked TNF stimulation of Prx1. Treatment of C3H cells with siPRX1 completely abrogated TNF suppression of Ox mRNA expression. In MC3T3, siPRX1 increased basal Ox expression 6 fold and partially prevented inhibition by TNF. These results identify Prx1 as an important inhibitor of Ox transcription and a mediator of TNF/MAPK inhibition of Ox expression in early osteoblast progenitors.

Disclosures: M.S. Nanes, None.

1144

TIEG: A Novel Mediator of Runx2 Expression and Activity in Osteoblasts. J. R. Hawse¹, M. Subramaniam¹, D. G. Monroe¹, J. B. Lian², G. S. Stein², A. J. van Wijnen², M. J. Oursler¹, T. C. Spelsberg¹. ¹Biochemistry and Molecular Biology, Mayo Clinic, Rochester, MN, USA, ²Department of Cell Biology, University of Massachusetts Medical School, Worcester, MA, USA.

TGFβ Inducible Early Gene-1 (TIEG) is a member of the Kruppel-like family of transcription factors that is highly expressed and regulates a multitude of genes in osteoblasts. Through the development of TIEG-null mice (TIEG^{-/-}), we have identified a critical role for TIEG in bone as these animals display a severe osteopenic phenotype. TIEG^{-/-} calvarial osteoblasts have reduced expression levels of Runx2 and other important osteoblast marker genes as well as significant defects in their mineralization capacity. Through the use of transient transfection and ChIP assays, we have demonstrated that TIEG directly binds to, and activates, the Runx2 promoter, and we have shown that the DNA binding domain of TIEG is necessary for this regulation. Since TIEG is known to be targeted for proteasomal degradation by SIAH, an E3 ubiquitin ligase, we created 2 point mutations in the TIEG protein that abolishes the interaction of TIEG with SIAH and ultimately increases its stability. Interestingly, this mutation results in further activation of the Runx2 promoter indicating that the stability of TIEG plays a critical role in the regulation of Runx2 expression. Additionally, transfection of wild-type calvarial osteoblasts with a TIEG specific siRNA significantly decreases the expression of Runx2 and conversely, overexpression of TIEG induces Runx2 transcription. Runx2 adenoviral infection of TIEG^{-/-} osteoblasts restores Runx2 expression and significantly increases their mineralization capacity. Through the use of co-immunoprecipitation studies, we have demonstrated that TIEG is also capable of interacting with Runx2. This interaction is further confirmed through the use of transient transfection assays in which TIEG co-activates Runx2 binding elements (OSE₂) in the presence of Runx2 protein. Since Runx2 regulates the expression of important osteoblast marker genes such as osterix and osteocalcin, and since these genes exhibit decreased expression in TIEG^{-/-} osteoblasts, these studies imply that TIEG may play an important role in co-activating their expression in concert with Runx2. Collectively, these data demonstrate that TIEG directly regulates the expression and activity of Runx2 in osteoblasts and suggest that the decreased expression of Runx2 in TIEG-null mice is, at least in part, responsible for the observed osteopenic phenotype. Finally, a novel mechanism for the regulation and modulation of Runx2 expression and activity in osteoblasts is revealed.

Disclosures: J.R. Hawse, None.

1145

Transcription Factor IRF-8 Is a Negative Regulator of Osteoclast Differentiation In Vitro and In Vivo. B. Zhao^{*1}, M. Takami¹, A. Yamada^{*1}, X. Wang^{*1}, K. Nakao^{*2}, T. Tamura^{*3}, K. Ozato^{*4}, H. Takayanagi⁵, R. Kamijo¹.

¹Department of Biochemistry, School of Dentistry, Showa University, Tokyo, Japan, ²Laboratory for Animal Resources and Genetic Engineering, Center for Developmental Biology, RIKEN, Kobe, Japan, ³Department of Physiology, Osaka City University Graduate School of Medicine, Osaka, Japan, ⁴Laboratory of Molecular Growth Regulation, National Institute of Child Health and Human Development, NIH, Bethesda, MD, USA, ⁵Department of Cell Signaling, Graduate School, Tokyo Medical and Dental University, Tokyo, Japan.

RANK signaling regulates the expressions of various transcription factors involved in osteoclast differentiation including NFATc1. However, little is known about transcription factors that negatively regulate osteoclast differentiation. In this study we identified a transcription factor, IRF-8 (also referred to as ICSBP), which is controlled by RANK signaling. IRF-8 was expressed in bone marrow or spleen-derived macrophages that are capable of differentiating into osteoclasts in response to RANKL stimulation. When the macrophages were stimulated with RANKL, the expression level of IRF-8 decreased within 8 hours, which is earlier than the increase of NFATc1 expression. Overexpression of IRF-8 in macrophages by retrovirus vectors completely inhibited RANKL-induced osteoclast differentiation, indicating that IRF-8 is a negative regulator of osteoclast differentiation. In IRF-8 deficient mice, a significant increase in osteoclast number and severe osteoporosis due to high turnover of bone metabolism were observed. Macrophages prepared from IRF-8 deficient mice differentiated into osteoclasts by stimulation with 1/20-1/4 of the concentrations of RANKL used for wild type. Cocultures of osteoblasts with IRF-8-deficient bone marrow cells produced a significantly larger number of osteoclasts than that with wild-type bone marrow cells. Analysis using immunoprecipitation, EMSA and promoter assay revealed that IRF-8 interacted with NFATc1 and attenuated transcriptional activity of NFATc1 by interfering with the binding of NFATc1 to its target DNA sequence. Furthermore, toll-like receptor ligands such as LPS, CpG ODN, peptidoglycan and poly(I:C)RNA inhibited osteoclast differentiation by macrophages prepared from wild-type mice although the ligands failed to inhibit that prepared from IRF-8 deficient mice. These results suggest that IRF-8 is a critical negative regulator reduced by RANK signaling in the early phase of osteoclast differentiation. Since IRF-8 deficient mice showed severe osteoporosis, IRF-8 also contributes to physical bone homeostasis in vivo. Furthermore, our data imply that IRF-8 plays an important role in inflammatory bone destruction induced by virus and bacterial infection.

Disclosures: B. Zhao, None.

1146

The Small GTPase cdc42 Enhances Osteoclastogenesis and Bone Resorption. Y. Ito¹, Y. Zheng^{*2}, J. F. Johnson^{*2}, L. Yang^{*2}, S. L. Teitelbaum¹, F. P. Ross¹, H. Zhao¹. ¹Department of Pathology and Immunology, Washington University, St. Louis, MO, USA, ²Division of Experimental Hematology, University of Cincinnati, Cincinnati, OH, USA.

Osteoclasts (OCs) degrade bone by polarized secretion of protons and cathepsin K, a process requiring cytoskeletal reorganization. Cdc42, a small GTPase, is hypothesized to control formation of the OC actin cytoskeleton. Since global deletion of cdc42 leads to early embryonic lethality its impact on bone biology cannot be evaluated directly. Our observation, however, that the osteoclastogenic cytokines M-CSF and RANKL activate cdc42 led us to investigate further. Cycling of cdc42 between inactive GDP-bound and active GTP-bound forms is regulated by specific guanine nucleotide exchange factors that enhance GDP/GTP exchange and GTPase-activating proteins (GAPs) that stimulate its intrinsic GTPase activity, respectively. To define the role of cdc42 in OCs we examined first cdc42 gain-of-function mice, which were produced by deleting cdc42GAP globally. The animals die soon after birth, precluding direct analysis of their OC phenotype. To overcome this problem we transplanted WT or cdc42GAP-deficient OC precursors present in fetal liver cells into irradiated WT mice and sacrificed them after four months. Compared to WT controls cdc42GAP^{-/-} bone marrow macrophages (BMMs) undergo accelerated proliferation in response to M-CSF and differentiate into increased numbers of OCs in the presence of M-CSF and RANKL. Furthermore, cdc42GAP null mature OCs exhibit less apoptosis and OCs cultured on bone exhibit greater resorptive capacity than WT cells (medium CTx levels). Confirming a role for cdc42 in organizing the OC cytoskeleton, the number of RANKL-induced actin rings at the sealing zone of cdc42GAP^{-/-} OCs cultured on bone is greater than in WT cells. Last, RANKL induces formation of a Par3/Par6/APK complex downstream of cdc42 activation. Reflecting these in vitro observations, mice containing cdc42GAP^{-/-} OC precursors have lower bone mass, more osteoclasts and higher levels of bone resorption. Having established a cdc42 gain of function phenotype, we turned to OCs lacking cdc42. To this end, we isolated BMMs from cdc42^{flx/flx} mice and deleted the small GTPase by transduction in vitro with retroviral Cre. In contrast to gain of function cells, proliferation of cdc42 null BMMs is decreased in response to M-CSF, apoptosis is increased in pre-OCs and M-CSF/RANKL-induced differentiation largely absent. Given these obverse phenotypes we conclude that cdc42 a) increases OC precursor proliferation and differentiation; b) suppresses apoptosis in pre- and mature OCs; c) promotes organization of the OC actin cytoskeleton on bone and hence d) enhances bone resorption.

Disclosures: Y. Ito, None.

1147

IkB α -Deficient Mice Display Increased Osteoclast Formation and Activity and Bone Loss In Vivo. J. R. Edwards¹, L. Connelly², W. Han^{*3}, L. C. Dumitrescu¹, T. S. Blackwell^{*3}, E. Yull^{*2}, G. R. Mundy¹. ¹Center for Bone Biology, Vanderbilt University Medical Center, Nashville, TN, USA, ²Cancer Biology, VUMC, Nashville, TN, USA, ³Immunology, VUMC, Nashville, TN, USA.

The Rel-NF κ B transcription factor family regulates numerous growth factors including those that control osteoclast (Oc) formation. Rel dimers are sequestered in the cytoplasm by inhibitor κ B (IkB) proteins, predominantly IkB α . As this vital regulatory molecule mediates the transcriptional activity of NF κ B, we hypothesized that IkB α may directly regulate bone mass by controlling Oc formation. The bone phenotype of IkB α -genetically modified mice was examined by whole body imaging, histomorphometric analysis, bone resorption and cell proliferation assays, molecular and protein analysis of primary bone cells and purified immortalized macrophages. IkB α ^{-/-} mice die shortly after birth. Alizarin red/alcian blue whole body preparations of 4 day pups showed a severe skeletal growth defect and μ CT scanning revealed a 23% decrease in BV/TV compared to +/+ pups. Mature 4mth IkB α ^{+/-} mice were compared to +/+ animals using histomorphometry, Pixmap and μ CT scanning. IkB α ^{+/-} mice showed a profound decrease in BMD and BV/TV ($p < 0.01$). Histomorphometric analysis of undecalcified IkB α ^{+/-} L3-4 vertebrae supported μ CT data showing a BV/TV of 9.2 ± 0.3 compared to 15.4 ± 1.6 in +/+ mice ($p < 0.05$). The Oc surface/bone surface ratio in +/+ mice was 6.3 ± 2.4 while +/+ mice displayed 4.3 ± 0.4 ($p < 0.05$). In vitro culture of +/+ marrow cells showed increased dentine resorption and Oc formation rates than +/+ cells. TRAP staining of +/+ cells stimulated with M-CSF (30ng/ml) and RANKL (50ng/ml) formed 48.6 TRAP+ cells/well, while +/+ cells formed 33.5 TRAP+ cells/well over 5 days ($p < 0.05$). To accurately study Oc formation in IkB α KO cells, we immortalized macrophages isolated from IkB α ^{-/-} and +/+ pups. While IkB α +/+ macrophages appeared typically small and spherical the morphological appearance of IkB α ^{-/-} cells were larger and often multinucleated. Calcitonin receptor, NFATc1 and c-src mRNA expression were increased in IkB α ^{-/-} cells which proliferated at twice the rate of +/+ cells ($p < 0.001$). Gel zymography showed a 2-fold increase in MMP-9 in media conditioned by IkB α ^{-/-} macrophages compared to +/+ cells. M-CSF decreased proliferation of -/- cultures by 71% ($p < 0.001$) and increased TRAP+ multinucleated cells by 30% while +/+ cell proliferation increased 33% ($p < 0.005$). RANKL and M-CSF treatment increased TRAP+ multinucleated cells in both cell lines, indicating that RANKL augments Oc formation in precursor cells with constitutive NF κ B activation through alternative pathways. We conclude that IkB α deletion increases Oc formation and activity and decreases bone mass in vivo by its effects on bone resorption.

Disclosures: J.R. Edwards, None.

1148

NF- κ B2 Limits TNF-induced Osteoclastogenesis Through Precursor Cell Cycle Regulation. Z. Yao, L. Xing, B. Boyce. Pathology, University of Rochester, Rochester, NY, USA.

RANKL and TNF are the only cytokines known to directly induce osteoclastogenesis without stromal cells in vitro. However, TNF consistently generates fewer and smaller osteoclasts (OCs) than RANKL and stimulates fewer OCs than RANKL in vivo, suggesting that it may work through different mechanisms from RANKL or induce inhibitors in osteoclast precursors (OCPs) during culture. Both cytokines activate the canonical (p65 and p50) and non-canonical (p52 and RelB) NF- κ B pathways, which typically control different biologic processes by regulating transcription of different target genes. In the non-canonical pathway p52 is generated from its precursor protein, p100 (NF- κ B2), but the role of this pathway in OC formation has not been fully investigated. To address this issue, we examined the expression of NF- κ B p65, p50, p52 and RelB during TNF- and RANKL-induced OC differentiation from 4 to 96 hrs, in which mature OCs started to form at ~48 hrs. Both cytokines increased mRNA expression of p65 and p50 temporarily from 1 to 4 hours and of p52 and RelB from 4 hrs to 72 hrs, and these gradually decreased thereafter. TNF and RANKL induced a similar pattern of p65, p50 and RelB protein expression. RANKL increased protein levels of p52, but not p100. In contrast and importantly, TNF increased both p52 and p100 protein levels in whole cell lysates from 8 to 72 hours. Previous studies have shown that exit from the cell cycle is a necessary step for OC terminal differentiation and involves NF- κ B. TNF also activates cyclin D1 through NF- κ B p52/RelB to stimulate cell proliferation. To determine if TNF induction of fewer OCs than RANKL requires NF- κ B2 and involves cyclin D1, we first treated OCPs from wt and NF- κ B2^{-/-} mice that lack both p52 and p100 expression with TNF or RANKL. TNF induced significantly fewer OCs from wt cells than RANKL (120 ± 13 vs 585 ± 29) and significantly more TRACP-negative cells. Importantly, TNF generated similar OC numbers (365 ± 20 vs 410 ± 18) and resorption pit area/bone slice (2.5 ± 0.6 vs 2.8 ± 0.8) and fewer TRACP-negative cells than RANKL from NF- κ B2^{-/-} spleen cells. Furthermore, TNF induced more OCs from cyclin D1^{-/-} than wt OCPs (369 ± 40 vs 173 ± 18 per well). We conclude that TNF limits differentiation of OCPs through mechanisms involving NF- κ B2 and cyclin D1. Thus, NF- κ B2 may function as a negative regulator of osteoclastogenesis by controlling proliferation of OCPs to limit excessive bone resorption mediated by TNF in various bone diseases.

Disclosures: Z. Yao, None.

1149

Wnt5a Enhances RANKL-induced Osteoclastogenesis. K. Maeda^{*1}, Y. Kobayashi^{*2}, T. Mizoguchi^{*2}, Y. Nakamichi², T. Yamashita², S. Kinugawa^{*2}, N. Udagawa³, K. Marumo^{*1}, N. Takahashi². ¹Department of Orthop. Surg., The Jikei Univ., Tokyo, Japan, ²Institute for Oral Science, Matsumoto Dental Univ., Shiojiri, Japan, ³Department of Biochemistry, Matsumoto Dental Univ., Shiojiri, Japan.

Wnts exert two types of signals, β -catenin (β -cat)-dependent (canonical) and β -cat-independent (non-canonical) pathways. Combinations of their putative receptors, frizzleds and their co-receptors, LRP5/6 or Ror2, determine which pathway to use. The β -cat pathway has been reported to suppress bone resorption due to up-regulation of OPG expression and suppression of RANKL expression in osteoblasts. However, the roles of the non-canonical pathway in bone resorption are not elucidated. Here, we analyzed the effect of Wnt5a, a non-canonical Wnt ligand, on osteoclast formation. (1) Wnt5a enhanced RANKL-induced osteoclast formation from mouse bone marrow macrophages (BMM ϕ), RAW264.7 cells and human CD14-positive monocytes in a dose-dependent manner. (2) Wnt5a activated c-Jun N-terminal kinase and protein kinase C, but failed to increase the cytoplasmic accumulation of β -cat in BMM ϕ . (3) The role of Ror2, a co-receptor of Wnt5a, in osteoclast formation was examined using short hairpin RNA interference. The knockdown of Ror2 abolished the stimulatory effect of Wnt5a on RANKL-induced osteoclast formation in the BMM ϕ culture. (4) GST-soluble Ror2 (sRor2) specifically bound to Wnt5a in a pull down assay. Addition of sRor2 to the BMM ϕ culture also abolished the stimulatory effect of Wnt5a on RANKL-induced osteoclast formation. (5) Semi-quantitative RT-PCR analysis revealed that the expression level of Wnt5a mRNA was much higher in osteoblasts than in BMM ϕ . (6) sRor2 inhibited $1\alpha,25$ -dihydroxyvitamin D₃-induced osteoclast formation in co-cultures of osteoblasts and BMM ϕ in a dose-dependent manner. These results suggest (1) that Wnt5a activates the non-canonical pathway but not the canonical one in BMM ϕ , and (2) that Wnt5a secreted by osteoblasts promotes osteoclast formation through Ror2. Rheumatoid arthritis (RA) synovium has been shown to strongly express Wnt5a. Taken together, our results indicate that Wnt5a is involved not only in physiological bone remodeling but also in pathological bone loss in RA. Wnt5a represents a potential novel therapeutic target for RA to suppress excessive bone loss.

Disclosures: K. Maeda, None.

1150

Osteoclast Formation and Osteolysis Are Promoted by the AMP-activated Protein Kinase (AMPK) Activator Aminoimidazole-4-carboxamide Ribonucleoside (AICAR) In Vivo. J. M. W. Quinn¹, S. Tam^{*2}, N. A. Sims¹, H. Saleh^{*1}, N. E. McGregor^{*1}, I. J. Poulton^{*1}, B. E. Kemp^{*3}, M. T. Gillespie¹, B. J. W. van Denderen^{*1}. ¹St. Vincent's Institute, Fitzroy, Australia, ²Dept of Medicine, The University of Melbourne, Fitzroy, Australia, ³CSIRO Molecular and Health Technologies, Parkville, Australia.

AMPK serves to maintain whole body and cellular energy balance in response to hormonal and metabolic stress signals. We have investigated the effect of pharmacological activation of AMPK by AICAR on osteoclast (OC) formation and function in vitro and in vivo.

AICAR (200uM) increased OC formation by approximately 40% in murine bone marrow cell cultures maximally stimulated by RANKL (100ng/ml) and MCSF (30ng/ml); with lower RANKL levels (20ng/ml) AICAR increased OC formation up to 50-fold. Osteoclast formation was not increased by adenosine, adenosine antagonists or re-uptake inhibitors, consistent with AICAR acting independently of the adenosine signaling pathway. Increased OC formation with AICAR was also observed in RANKL stimulated cultures of spleen cells, bone marrow macrophages, RAW264.7 cells and in osteoblast/bone marrow co-cultures stimulated by dihydroxy vitamin D₃. AICAR stimulated phosphorylation of the AMPK substrate acetyl-CoA carboxylase in bone marrow macrophages. However, AICAR did not alter OC survival or the amount of dentine resorbed per OC.

We investigated AICAR actions in vivo, using a protocol previously employed to investigate AMPK activation in skeletal muscle. Male C57Bl/6 mice (12 weeks old) received daily intraperitoneal injections of AICAR (500mg/kg) or saline (controls) and their tibia examined by histomorphometry at 28 days. We found significantly reduced (49.5%) trabecular bone mass (BV/TV) in AICAR treated mice, with 2.2-fold greater OC numbers (OcS/BS). Trabecular number (Tb.N) was much decreased but trabecular thickness (Tb.Th) was not altered. Osteoblast numbers (ObS/BS) were also 2.8-fold higher with AICAR treatment and osteoid surface increased.

In summary, AICAR promotes OC progenitor differentiation, and causes high turnover osteopenia in vivo that is consistent with increased OC formation and a coupled increase in osteogenesis. These results are consistent with AMPK playing a role in bone physiology by modulating bone cell differentiation.

Disclosures: J.M.W. Quinn, None.

1151

Activation of BMP Signaling by the FOP ACVR1 R206H Mutation. Q. Shen^{*1}, M. Xu^{*1}, S. C. Little^{*2}, F. S. Kaplan¹, M. C. Mullins^{*2}, E. M. Shore¹. ¹Orthopaedics, University of Pennsylvania, Philadelphia, PA, USA, ²Cell and Developmental Biology, University of Pennsylvania, Philadelphia, PA, USA.

Fibrodysplasia ossificans progressiva (FOP), a rare genetic disorder of heterotopic ossification, results in profound decreased mobility of affected individuals. ACVR1, a bone morphogenetic protein (BMP) type I receptor, is mutated in FOP, with a single recurrent missense mutation in the GS activation domain (c.617G>A; R206H) in all patients with classic disease features (malformation of the great toe and progressive heterotopic ossification). In order to examine the functional effects of the FOP ACVR1 mutation, His-tagged control (c.617G) and mutant (c.617A) ACVR1 constructs were generated. Expression in COS-7 cells was confirmed by immunoblot analysis. As expected, cells transfected with control ACVR1 showed ligand-dependent activation of BMP signaling with increased phosphorylation of Smad1/5/8. Signaling occurred specifically through the BMP/Smad pathway. By contrast, cells transfected with mutant ACVR1 showed ligand-independent activation of BMP pathway signaling in Smad phosphorylation and luciferase reporter assays. To investigate the interaction of mutant ACVR1 with FKBP12, a GS domain binding protein that prevents leaky type I BMP receptor activation in the absence of ligand, we co-transfected COS-7 cells with FKBP12 and control or mutant ACVR1 constructs, followed by co-immunoprecipitation with FKBP12 antibodies and immunoblot analysis for ACVR1. We found reduced binding of FKBP12 to mutant ACVR1, suggesting that increased BMP pathway activity in cells with mutant ACVR1 is due at least in part to decreased binding of the inhibitory factor FKBP12. To complement these in vitro studies, in vivo functional analyses tested the ability of ACVR1 to rescue the zebrafish Alk8 (homolog of human ACVR1) knockout (lost-a-fin). Transient expression of control ACVR1 RNA in zebrafish embryos partially rescued (~75%) the lost-a-fin phenotype. However, mutant ACVR1 induced a ventralized phenotype in the embryos, demonstrating an over-compensation of the knockout phenotype and indicating hyper-activation of BMP signaling. In conclusion, these data show that the FOP ACVR1 c.617G>A mutation causes elevated ligand-independent activity of the BMP pathway and support that decreased binding of the FKBP12 inhibitory protein to the mutant receptor is a mechanism leading to increased BMP signaling and heterotopic ossification in FOP.

Disclosures: Q. Shen, None.

1152

Measles Virus Nucleocapsid Gene Expression Is Required for Abnormal Osteoclast Activity in Paget's Disease of Bone. N. Kurihara¹, Y. Hiruma¹, K. Yamana², C. Rousseau^{*3}, J. Morissette^{*3}, J. P. Brown³, G. D. Roodman⁴. ¹Medicine/Hem-Onc, University of Pittsburgh, Pittsburgh, PA, USA, ²Biomedical Research, Teijin, Tokyo, Japan, ³CHUL Res Center, Laval University, Quebec City, PQ, Canada, ⁴Medicine/Hem-Onc, VA Pittsburgh Healthcare System and University of Pittsburgh, Pittsburgh, PA, USA.

Paget's disease (PD) is one of the most exaggerated examples of abnormal bone remodeling, but its etiology is unclear. Both a genetic and a viral etiology for PD have been suggested. The viral etiology is based on: 1) the detection of Measles Virus Nucleocapsid (MVNP) mRNA and protein in osteoclasts (OCL) from PD lesions, 2) studies showing that transfection of normal human OCL precursors with the MVNP gene results in formation of PD-like OCL, and 3) transgenic mice expressing MVNP targeted to the OCL lineage (TRAP-MVNP mice) develop PD-like bone lesions. However, the role of MVNP in the abnormal OCL formation present in PD patients is unclear. To determine the requirement of MVNP for the abnormal OCL activity in PD, we tested MVNP mRNA expression by RT-PCR in OCL precursors from bone marrow of normals and PD patients and the effect of a previously validated antisense construct targeted to 5' end of the MVNP mRNA (AS-MVNP, J Inf Dis 176:258,1997) on OCL formation, bone resorption, and the enhanced $1,25$ -(OH)₂D₃ responsiveness in OCL precursors from patients carrying the most common genetic mutation linked to PD (p62^{P392L}). OCL precursors from 5 of 8 PD patients expressed MVNP, and MVNP was not detected in 6 normals. AS-MVNP transduced OCL precursor cells from 2 patients with PD that expressed MVNP or normals were cultured in methylcellulose with recombinant GM-CSF and G418. G418-resistant CFU-GM-derived cells were then cultured with varying concentrations of $1,25$ -(OH)₂D₃ or RANKL. OCL precursors from PD were hyper-responsive to $1,25$ -(OH)₂D₃, RANKL and TNF- α compared to normals. AS-MVNP transduced OCL precursors from PD patients treated with $1,25$ -(OH)₂D₃ or RANKL formed 60-70% fewer OCL and had lower nuclear numbers compared to OCL formed from scrambled antisense transduced OCL precursors. AS-MVNP had no effect on normal OCL formation compared to scrambled antisense controls, and scrambled antisense transduced PD cells formed PD-like OCL. Further, expression of TAF_{II}17 mRNA, a VDR coactivator present in PD but not normal OCL, was decreased by 70% with transfection of AS-MVNP compared to scrambled vector transduced PD OCL precursors. These data demonstrate that AS-MVNP blocked the abnormal OCL formation in cultures from patients with PD and decreased the hyper-sensitivity of PD OCL precursors to $1,25$ -(OH)₂D₃ and RANKL. These results support a pathologic role for MVNP in PD.

Disclosures: N. Kurihara, None.

This study received funding from: NIH.

1153

TSH Is Both Anti-Resorptive and Anabolic In Vivo. L. Sun¹, J. Iqbal^{1*}, L. L. Zhu^{1*}, K. Yamoah^{1*}, A. Arabi^{1*}, B. S. Moonga^{1*}, T. F. Davies^{1*}, H. C. Blair², E. Abe¹, M. Zaidi¹. ¹Mount Sinai Bone Program, Department of Medicine, Mount Sinai School of Medicine, New York, NY, USA, ²Department of Pathology, University of Pittsburgh, VA Medical Center., Pittsburgh, PA, USA.

We have shown that the deletion of the TSH receptor (TSHR), even in a haploinsufficient state, causes high-turnover bone loss (Abe et al. Cell, 2003). We have further demonstrated that this osteoporosis and enhanced osteoclastogenesis is reversed by genetically ablating TNF α in double TSHR^{-/-}/TNF α ^{-/-} mutants. In vitro, we showed that TSH inhibits osteoclast formation and function, as well as TNF α expression (Hase et al., Proc. Natl. Acad. Sci. 2006). Here, we show that the in vivo administration of recombinant human TSH (Genzyme), 0.7 μ g/mouse, three times a week prevents bone loss following ovariectomy, as well as increases bone mass in sham-operated controls. A lower dose of TSH (0.07 μ g/mouse) increased bone mass in sham-operated controls, but not in ovariectomized mice. The effect of high dose TSH, 0.7 μ g/mouse, was however, less marked, reflecting persistent elevations in serum thyroid hormones. Identical results were obtained by administering estrogen pellets (0.56 μ g/mouse) or daily recombinant human PTH (0.56 μ g/mouse). Ex vivo cultures of bone marrow cells 8 weeks post-cessation showed highly significant reductions in osteoclast formation and expression of the osteoclast differentiation markers TRAP, integrin β_3 , cathepsin K, calcitonin receptor and NFATc1. We also found evidence for an anabolic action ex vivo in bone marrow stromal cell cultures; CFU-F and CFU-OB formation were dramatically increased with 0.07 and 0.7 μ g/mouse doses, again 8 weeks post-cessation. To further substantiate the anti-resorptive component of TSH action, we investigated mice with functionless TSH receptors, TSHR^{hwt} mice. Ex vivo osteoclast formation was significantly enhanced in both TSHR^{hwt} mutants and heterozygotes. This enhanced osteoclast differentiation was suppressed by TSH in heterozygous and wild type mice, but not in homozygous mutants, thus confirming TSH-specificity. In conclusion, TSH exhibits both anti-resorptive and anabolic actions in vivo.

Disclosures: L. Sun, None.

1154

Atorvastatin Inhibits Lipid Induced Aortic Valve Calcification and Osteoporosis via the Lrp5/Wnt Mediated Pathways in Vivo and In vitro. N. M. Rajamannan¹, F. C. Caira^{1*}, A. L. Flores^{1*}, C. P. Dolehide^{1*}, L. B. Arterburn^{1*}, M. Subramaniam², T. C. Spelsberg². ¹Cardiology, Northwestern University, Chicago, IL, USA, ²Biochemistry, Mayo Clinic, Rochester, MN, USA.

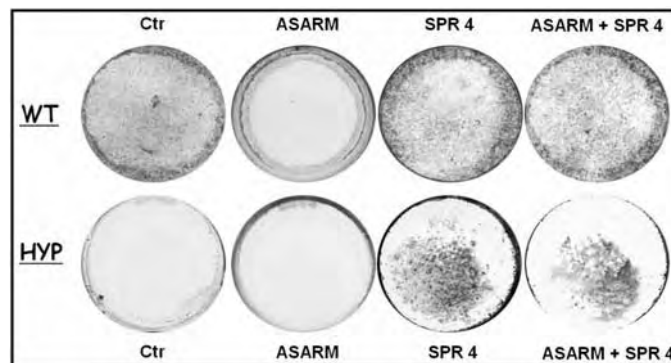
Atherosclerosis and osteoporosis are the leading causes of morbidity and mortality in the aging population in the United States. Evidence indicates that hyperlipidemia plays a paradoxical role in these disease processes. However, the hyperlipidemic mechanisms of atherosclerotic calcification and decrease bone mass are not well understood. We hypothesize that hyperlipidemia plays a role in cardiovascular calcification and osteoporosis. We propose to test this hypothesis in an experimental hypercholesterolemia model and further test if statins play a protective role in this process. LDLR^{-/-} mice (n=100) were treated with Group I (n=20) normal diet, Group II (n=20) 1.25% chol diet (w/w), and Group III (n=20) 1.25% (w/w) chol diet+atorv, to determine the development of calcification in the hearts and osteoporosis in the bones. The aortic valve and aorta (AVA) was examined for myofibroblast cell proliferation, calcification, and bone matrix markers by immunohistochemistry and RTPCR. Bone formation was assessed by micro Computed Tomography (microCT), calcein injection, osteocalcin, cbfa-1 and osteopontin expression. We also have an in vitro model of aortic valve (AV) myofibroblasts cells and bone MC3T3 cells treated with osteogenic media to determine the expression of bone development and measure the signaling markers in these ossifying cells. The cholesterol diet induced complex bone formations by microCT in the calcified AVA with an increase in cellular proliferation, osteopontin, osteocalcin and cbfa-1 expression. Atorvastatin reduced bone formation, cellular proliferation and cbfa-1 levels and calcification in the AVA. Ex vivo analysis of calcein label demonstrated an increase in calcein label (4+) in the hypercholesterolemia AVA and the periosteal femoral bone surface with attenuation of the calcein label (1+) with atorvastatin therapy in the AVA and the femoral bones. (Calcein Scale =1-4, 4+=severe label, 1+=minimal label). The in vitro aortic valve myofibroblast cells and MC3T3 cells developed bone in the presence osteogenic media at 40 days. Cbfa1, Lrp5 and Osteopontin are increased in the osteogenic treated AV and MC3T3 cells as compared to the controls. Alizarin Red confirmed the presence mineralizing nodules in culture. Experimental hypercholesterolemia induces cardiovascular calcification and increased bone turnover which is attenuated by atorvastatin and mediated in part by an osteoblast pathway in the cardiovascular tissues. This model may have future implications in the treatment of cardiovascular calcification and osteoporosis with statin therapy.

Disclosures: N.M. Rajamannan, None.
This study received funding from: NIH.

1155

Degradation of MEPE, DMP1 & Release of SIBLING ASARM-peptides (minhibins): ASARM-peptide(s) Are Directly Responsible for Defective Mineralization in HYP. V. David¹, A. Martin¹, J. Laurence^{1*}, M. D. McKee², L. W. Fisher³, A. Hedge^{1*}, P. S. N. Rowe¹. ¹Kansas Uni Med Center, Kansas City, KS, USA, ²McGill University, Montreal, PQ, Canada, ³NIDCR, Bethesda, MD, USA.

Binding of MEPE to PHEX results in proteolytic protection and prevents release of a small protease resistant MEPE-peptide (ASARM peptide). This peptide is a potent inhibitor of mineralization (minhibin) in vivo and in vitro and also occurs in DMP1, a related SIBLING protein. Thus, in Hyp, increased osteoblastic-proteases and the absence of PHEX may contribute to increased ASARM-peptide release from DMP1 and MEPE. We therefore evaluated the effects of ASARM-peptide and a small synthetic PHEX-Peptide (SPR4; 4.2 kDa) on mineralization of co-cultures of HYP and wild-type (WT) bone marrow stromal cells (BMSCs). The ASARM peptide binds to the PHEX Zn-binding motif as confirmed by surface plasmon resonance (SPR) and 2D H1/N15 NMR. Also, SPR4 peptide mimics the minimal PHEX Zn-motif site and binds specifically to the ASARM peptide. Interactions between SPR4 and ASARM peptide largely determine the bound conformation, whereas the ASARM-phosphate moieties stabilize the interaction, increasing the binding strength. When cultured individually for 21 days, Hyp BMSCs displayed reduced mineralization compared to WT (-87%; p<0.05). When co-cultured, both Hyp and WT cells failed to mineralize. ASARM-peptide induced a similar pattern in WT cells (-78%), and treatment with SPR4 peptide or an anti-ASARM neutralizing-antibodies completely corrected the mineralization defect. SPR4-peptide had no effect on WT mineralization without ASARM-PO4 peptide. In HYP BMSCs, SPR4-peptide increased mineralization nodules by >66%. Anti-ASARM neutralizing antibodies had similar effects to the SPR4 peptide. Moreover, ASARM treatment also decreased PHEX mRNA expression in WT-cells (-72%; p<0.05) and protein as detected by immunohistochemistry (-80%; p<0.05). SPR4 co-treatment reversed this by preventing ASARM binding to PHEX. Also, western-blots of Hyp calvariae revealed massive degradation of both MEPE and DMP1 protein as compared to the WT. Similar results were obtained by immunohistochemistry in Hyp and ASARM BMSCs treated cultures and a significant correction occurred after SPR4 peptide co-treatment or treatment. We conclude that degradation of MEPE and DMP-1 and release of acidic ASARM-peptides are chiefly responsible for the mineralization defect in HYP.



Effect of ASARM and SPR4 on mineralization

Disclosures: V. David, None.

This study received funding from: R01-AR51598-01 & R03-DE015900-01.

1156

Circulating Osteogenic Precursor Cells of Hematopoietic Origin. R. J. Pignolo¹, R. K. Suda^{1*}, D. Porter^{1*}, E. M. Shore², F. S. Kaplan³. ¹Medicine, University of Pennsylvania, Philadelphia, PA, USA, ²Genetics and Orthopaedic Surgery, University of Pennsylvania, Philadelphia, PA, USA, ³Medicine and Orthopaedic Surgery, University of Pennsylvania, Philadelphia, PA, USA.

Mesenchymal precursors with osteogenic potential reside in a variety of tissues. We previously demonstrated that circulating osteogenic precursor (COP) cells can be identified from peripheral blood as a population of CD 14/type I collagen⁺/CD 45⁺ mononuclear adherent cells that can produce bone in vivo upon subcutaneous injection into immunodeficient mice. We further showed that higher numbers of COP cells occur in patients with fibrodysplasia ossificans progressiva (FOP) who had recent episodes of ectopic bone formation, compared to either patients with stable disease or unaffected individuals. We now show that human COP cells are of hematopoietic origin. COP cells isolated from patients who underwent sex-mismatched bone marrow transplantation (BMT), including one FOP patient, were examined for both X and Y chromosomes by fluorescence in situ hybridization (FISH) and for COP cell-specific markers by immunofluorescence using antibodies against type I collagen/CD34, type I collagen/CD45, or type I collagen/CD13. Virtually 100% of circulating cells that became adherent in culture were of donor origin. Of these cells, 79-89% expressed markers consistent with their identity as COP cells. We also demonstrated by immunofluorescence the presence of type I collagen⁺/CD45⁺ COP cells in lesions of heterotopic ossification found in FOP. Our

data suggest that bone-formation is not exclusively derived from cells of the mesenchymal lineage, but that circulating cells of hematopoietic origin can also serve as osteogenic precursors.

Disclosures: R.J. Pignolo, None.

1157

Arterial Oxygen Saturation During Sleep and the Risk of Fractures, Falls and Mortality in Older Men. J. A. Cauley¹, T. Blackwell², S. Redline³, D. Bauer⁴, K. Ensrud⁵, S. Ancoli-Israel⁶, E. Haney⁷, H. Fink⁸, E. Orwoll⁷, K. Stone². ¹University of Pittsburgh, Pittsburgh, PA, USA, ²California Pacific Medical Center, San Francisco, CA, USA, ³Case Western Reserve University, Cleveland, OH, USA, ⁴University of California San Francisco, San Francisco, CA, USA, ⁵University of Minnesota, Minnesota, MN, USA, ⁶University of California, San Diego, San Diego, CA, USA, ⁷Oregon Health Sciences University, Portland, OR, USA, ⁸Veterans Affairs Medical Center, Minneapolis, MN, USA.

Low arterial oxygen saturation has been linked to poor neuromuscular function and could be a risk factor for falls and fractures.

To test this hypothesis, we studied 2,911 men (mean age 76.4 y) enrolled in the Osteoporotic Fractures in Men (MrOS) Sleep study. Oxygen saturation (SaO₂) during sleep was measured by finger pulse oximetry (Nonin, MN) during a home polysomnography test over one night. Sleep time was assessed by neurophysiological monitoring and staged using standard criteria. Men were divided into groups based on the percent of sleep time that SaO₂ was below 90%: <1% (referent); 1 to <3.5%; 3.5 to <10% and ≥10%. Incident falls were reported every four months for 1 year; recurrent falls defined as ≥ 2 falls. Incident non-spine fractures and deaths were ascertained during 2.2 years of ≥95% complete follow-up. Logistic regression (falls) and Cox Proportional Hazards models (fractures/deaths) were used to estimate the Relative Risk (RR) and 95% Confidence Interval. We initially adjusted for age, weight, race and clinic.

819(28.1 %) men reported at least one fall; 396(13.6%) men reported two or more falls; 94(3.2%) men experienced an incident fracture and 75(2.6%) men died over the follow-up period. More time at SaO₂ <90% (i.e., more time spent at lower levels of oxygen saturation) was associated with an increased risk of falls, recurrent falls, non-spine fractures and death, Table. Additional adjustment for BMD, history of COPD, smoking, neuromuscular function and self-reported health status had little effect on our results (data not shown). Further adjustment of the fracture models for falls in the past 12 months did not appreciably change the results.

We conclude that greater time spent at nocturnal desaturation levels below 90% is an independent risk factor for falls, fractures, and death in older men. Further trials should determine if identification of these men for treatment could reduce these clinical events.

	Any Fall		≥ 2 Falls		Fracture		Death	
	(n)	RR ⁺ (95% CI)	(n)	RR (95% CI)	(n)	RR (95% CI)	(n)	RR (95% CI)
<1% (n=1410)	(359)	referent	(166)	referent	(31)	referent	(25)	referent
1 to <3.5% (n=767)	(210)	1.04 (0.85-1.27)	(101)	1.10 (0.84-1.45)	(29)	1.66 (0.98, 2.78)	(22)	1.63 (0.91, 2.9)
3.5 to <10% (n=374)	(115)	1.21 (0.93,1.57)	(58)	1.33 (0.95,1.86)	(19)	2.23 (1.23,4.03)	(13)	2.01 (1.05,4.18)
≥10% (n=360)	(135)	1.58 (1.21,2.06)	(71)	1.77 (1.26,2.46)	(15)	1.67 (0.87,3.23)	(15)	2.59 (1.30,5.16)
p (trend)		0.001		0.0009		0.03		0.004

⁺RR is used to represent Odds Ratio for logistic models; Relative Hazard for Cox models.

Disclosures: J.A. Cauley, Merck & Company 2, 8; Novartis Pharmaceuticals 2, 5; Eli Lilly & Company 2, 5, 8; Pfizer Pharmaceuticals 2.

This study received funding from: NIH.

1158

Asymmetry in Leg Power Increases Non-spine and Hip Fracture Risk in Older Men: The Osteoporotic Fractures in Men (MrOS) Study. P. M. Cawthon¹, T. L. Blackwell¹, B. Chan², K. Winters-Stone², E. Barrett-Connor³, K. Ensrud⁴, E. S. Orwoll². ¹Research Institute, California Pacific Medical Center, San Francisco, CA, USA, ²Oregon Health and Science University, Portland, OR, USA, ³University of California, San Diego, CA, USA, ⁴University of Minnesota, Minneapolis, MN, USA.

In older men, decreased leg power is associated with an increased risk of falls and fractures. Asymmetry, or the difference in power between the left and right legs, may also influence fall and fracture risk in older men.

To test the hypothesis that greater asymmetry in leg power increases the risk of fracture, we measured leg power (Nottingham Power Rig) in the right and/or left leg in 5,443 men age ≥65. Men were followed for an average of 1 year for falls and 4.7 years for non-spine fractures. Asymmetry was calculated as the absolute percent difference in maximal leg power between the right and left legs, and categorized into quartiles. Men in the highest quartile of asymmetry (quartile 4, most difference between legs) were compared to men with less difference in leg power (quartiles 1-3, referent group). Men who were unable to complete the leg power measures on one leg due to injury or weakness were included in the highest asymmetry group. During follow-up, 387 non-spine fractures (including 63 hip)

were validated. Frequent fallers (N=596) were men who fell two or more times in the year after baseline. Proportional hazards models estimated fracture risk; logistic regression was used for falls outcomes. Confounding variables were selected using backward selection. Total hip bone mineral density (BMD) was measured by dual x-ray absorptiometry (DXA). Average maximal leg power was 208.3 watts. Average asymmetry was 9.8% (range: 0% - 86%). 95 men (1.7%) completed leg power measures on only one leg. A difference in leg power of 13.5% or higher represented the highest quartile of asymmetry. In multivariate models, men with greatest asymmetry had a 73% increased risk of hip fracture and a 28% increased risk of non-spine fracture. Men with the greatest asymmetry had a modest increase in risk for frequent falls in age-adjusted models, but in multivariate models this association was smaller in magnitude and no longer reached significance. (Table) In summary, asymmetrical leg power was found to be a novel risk factor for fractures in older men. Assessment of asymmetry in leg power may be worth pursuing when evaluating fracture risk in older men.

Table. Likelihood of falls and relative hazard of fracture for men with asymmetrical leg power

	Frequent faller	Non-spine fracture	Hip Fracture
Age, clinical center adjusted	1.29 (1.07, 1.55)	1.36 (1.10, 1.68)	1.96 (1.19, 3.22)
Multivariate adjusted*	1.16 (0.96, 1.41)	1.28 (1.04, 1.59)	1.73 (1.04, 2.88)

Falls models adjusted for age, clinical center, walking for exercise, diabetes, osteoarthritis, stroke, overall leg power, self-rated health and physical activity score.

Non-spine fracture models adjusted for age, clinical center, walking for exercise, BMI, race, overall leg power, total hip BMD.

Hip fracture models adjusted for age, clinical center, BMI, heart attack, stroke, overall leg power, total hip BMD.

*Referent group is men with more symmetrical leg power

Disclosures: P.M. Cawthon, None.

This study received funding from: NIAMS, NIA, NCI.

1159

SSRI Use Is Associated with Increased Risk of Fracture Among Older Men. E. M. Haney¹, N. Parimi², S. J. Diem³, K. E. Ensrud³, J. A. Cauley⁴, E. S. Orwoll¹, M. M. Bliziotes¹. ¹Department of Medicine, Oregon Health & Science University, Portland, OR, USA, ²California Pacific Medical Center, San Francisco, CA, USA, ³University of Minnesota, Minneapolis, MN, USA, ⁴University of Pittsburgh, Pittsburgh, PA, USA.

Selective serotonin reuptake inhibitors (SSRIs) have the potential for direct effect on bone because they block the serotonin transporter that is present in osteoclasts, osteoblasts, and osteocytes. SSRI use has been associated with lower bone mineral density (BMD) in men. The purpose of this analysis was to examine the association between SSRI use and fracture.

MrOS is a prospective cohort study of 5,995 U.S. men ages 65 and older from six clinical sites. This analysis used data from 4,156 men who participated in the baseline visit and Visit 2, approximately 4 years later. SSRI users were defined as those participants reporting SSRI use at either baseline or Visit 2. Combination antidepressant users and those using another antidepressants were excluded. We performed Cox-proportional hazards regression. Initially, we included variables that were significantly associated with SSRI use in univariate analyses. Then we restricted the covariates to those that influenced the parameter estimate for SSRIs and fracture in order to achieve the most parsimonious model.

236 (6.3%) men reported use of SSRIs at either baseline or Visit 2. 323 (7.6%) men had at least one fracture. Adjusting for age, race, weight, clinic site, hip BMD, and depressive symptoms using the baseline SF-12 mental summary score, SSRI use was associated with an increased hazard rate of any non-spine fracture (HR=2.2, 1.6-3.0, p<0.0001). Multivariate models including the above variables plus all significant covariates also indicated an increased HR for SSRIs (HR 2.2, 1.6-3.1, p<0.0001). Excluding users of benzodiazepines, non-benzodiazepine anticonvulsants, and osteoporosis medications and substituting the Geriatric Depression Scale measured at Visit 2 for the SF-12 mental summary score did not change the results. The final model included SSRI use, age, weight, total hip BMD, history of fracture, and history of falls (HR 1.8, 1.2-2.6, p=0.003).

Our results suggest that SSRI use in a population of community-dwelling elderly men is associated with fracture. Given the widespread use of these drugs, further investigation into the mechanism for this association is important.

Disclosures: E.M. Haney, None.

This study received funding from: National Institutes of Health: U01 AR45580, U01 AR45614, U01 AR45632, U01 AR45647, U01AR 45654, U01 AR 45583, U01 AG 18197, M01 RR000334, R01 AR052018, K23 AR051926.

1160

Aortic Calcifications Correlate with Volumetric Bone Mineral Density and Bone Microstructure in Men: A Population-Based Study. J. T. Chow^{*1}, S. Khosla¹, L. J. Melton², E. J. Atkinson^{*3}, A. E. Kearns¹. ¹Endocrinology, Mayo Clinic College of Medicine, Rochester, MN, USA, ²Epidemiology, Mayo Clinic College of Medicine, Rochester, MN, USA, ³Biostatistics, Mayo Clinic College of Medicine, Rochester, MN, USA.

Calcification of the vasculature has been epidemiologically linked with bone loss and osteoporosis. Data in men has been sparse, with studies primarily utilizing conventional radiography and absorptiometry for calcification and bone density determination, respectively. We herein present the first population-based assessment relating volumetric bone mineral density (vBMD) and bone microstructure to aortic calcification (AC) in men, utilizing advanced imaging techniques.

Using QCT, vBMD and calcification in the abdominal aorta were quantified in 321 men from an age-stratified sample of Rochester, Minnesota residents. High-resolution 3-D pQCT imaging at the radius was used to define trabecular bone volume/tissue volume (BV/TV), trabecular thickness (Tb.Th), trabecular number (Tb.N), and trabecular separation (Tb.Sp). Subjects were analyzed in 2 groups based on age: <50 or ≥50 years.

AC was present in 285 subjects (89%), with the prevalence rapidly increasing after age 50. In men ≥50 years of age, but not <50 years of age, AC correlated with lower vertebral and femur neck vBMD. The negative correlation was not significant after adjustments for age, body mass index (BMI), and smoking status (ever). In subjects ≥50, AC correlated with lower BV/TV and Tb.Th, but not after multivariate adjustment, while a negative correlation with Tb.N persisted after adjustment. Conversely, AC correlated with higher Tb.Sp, and this relationship also continued to be significant after multivariate adjustment. Our findings support an age-dependent association between AC and vBMD in men. This population-based study of men may provide a more accurate representation of vascular and bone biology, as potential confounding factors in women such as menopause are not present. We also present the novel finding of a relationship between vascular calcification and bone microstructure beyond the 5th decade of life. The association of AC to lower Tb.N and higher Tb.Sp is especially interesting, given our previous observation that Tb.N and Tb.Sp appear to be constant throughout life in a general population of men. Further studies are required to establish the pathophysiologic process leading to this association.

Table 1 - Unadjusted and Age/BMI/Smoking Status-Adjusted Correlation Coefficients Relating AC with vBMD and Microstructural Parameters

Parameter	< 50 years	≥ 50 years
QCT vBMD		
Vertebral Trabecular	-0.03/0.15	-0.35***/0.02
Femur Neck		
• Total	0.02/0.16	-0.24***/0.01
• Trabecular	-0.05/0.08	-0.27***/0.05
• Cortical	0.06/0.20*	-0.16*/-0.05
3-D pQCT microstructure		
BV/TV	-0.17/-0.06	-0.25***/-0.14
Tb.N (1/mm)	0.32***/0.10	-0.24**/-0.15*
Tb.Th (mm)	-0.33***/-0.12	-0.18*/-0.09
Tb.Sp (mm)	-0.22*/-0.06	0.25***/0.16*

*P < 0.05, **P < 0.01, ***P < 0.001

Disclosures: J.T. Chow, None.

1161

Diabetes and Fracture Risk in Older Men: The Osteoporotic Fractures in Men (MrOS) Study. A. V. Schwartz¹, E. S. Strotmeyer², T. Dam^{*3}, D. E. Sellmeyer¹, D. C. Bauer¹, K. E. Ensrud⁴, A. R. Hoffman^{*5}, L. M. Marshall⁶, E. Barrett-Connor⁷, L. Palermo¹, E. S. Orwoll⁶, S. R. Cummings⁷. ¹University of California, San Francisco, San Francisco, CA, USA, ²University of Pittsburgh, Pittsburgh, PA, USA, ³University of California, San Diego, La Jolla, CA, USA, ⁴VA Medical Center & University of Minnesota, Minneapolis, MN, USA, ⁵VA Palo Alto Health Care System, Palo Alto, CA, USA, ⁶Oregon Health & Science University, Portland, OR, USA, ⁷California Pacific Medical Center, San Francisco, CA, USA.

In older women type 2 diabetes (DM) is associated with increased fracture risk in spite of average or higher BMD compared with non-diabetic women. Since limited data are available for men, we investigated DM and fracture risk in participants from the Osteoporotic Fractures in Men (MrOS) Study, a cohort of community dwelling, ambulatory men aged ≥65 years recruited at 6 U.S. sites during 2000-2002. DM was defined as self-report of a previous physician diagnosis or use of hypoglycemic medication. Men who first reported DM at a follow-up visit were excluded (N=288). Of the remaining 5,707 participants, 663 (11.6%) had DM at baseline, including 80 who reported insulin use (Ins DM). Those with DM were less likely to be white (78% Ins DM, 82% No Ins DM, 90% non-DM), had higher total hip BMD (0.99 g/cm² Ins DM, 1.00 No Ins DM, 0.95 non-DM) and BMI (29.5 kg/m² Ins DM, 28.9 No Ins DM, 27.1 non-DM) and were more likely to have fallen in the previous year (44% Ins DM, 25% No Ins DM, 20% non-DM). Average age (73.7 ± 5.9 yrs) was similar. During an average follow up of 5.3 years, 420 men reported at least one non-vertebral fracture. Incidence rates (per 100 person-years) were 3.00 (Ins DM), 1.40 (No Ins DM), and 1.37 (non-DM). The most common fractures were rib, hip and wrist. Risk of first non-vertebral fracture was assessed with proportional hazards models, adjusted for age, race, clinic, total hip BMD, BMI, use of bone-active medications, and then falls. Risk estimates were not reduced by excluding 153 men who reported thiazolidinedione use, associated with fracture risk in diabetic women, at any visit.

Model adjusted for:	Insulin use	Oral hypoglycemic use, no insulin	No hypoglycemic use
Age, race, clinic	2.64 (1.48, 4.71)	1.08 (0.75, 1.58)	1.04 (0.57, 1.90)
+ potential confounders	2.49 (1.38, 4.49)	1.01 (0.66, 1.53)	1.05 (0.52, 2.12)
+ falls	2.18 (1.21, 3.95)	0.97 (0.64, 1.47)	1.04 (0.51, 2.10)

Compared with non-diabetic men, fracture risk was increased in older diabetic men on insulin therapy but not among others with diabetes, even after adjusting for more frequent falls. Insulin use may be a marker of increased diabetes-related complications in older men.

Disclosures: A.V. Schwartz, None.

This study received funding from: NIAMS, NIA, NCI.

1162

Mapping the Prescripiome to Fractures in Men: A National Analysis of Prescription History and Attributable Risk. B. Abrahamsen¹, K. Brixen².

¹Department of Medicine F, Copenhagen University Hospital Gentofte, Hellerup, Denmark, ²Department of Endocrinology, Odense University Hospital, Odense, Denmark.

Despite the large number of pharmaceutical products on the market, studies linking exposure to medicines to fracture risk are generally undertaken in a manner similar to candidate gene studies and not to the more conservative genetic mapping, despite the risk of mass significance. To stress the similarity between pharmacoepidemiology and genetics, we coined the term prescripiome to describe the entire complement of prescription drugs redeemed by an individual.

We identified all men aged 50+ years who presented with a fracture at any hospital in the country in the year 2000 and retrieved information about prescriptions redeemed in the preceding 5y in fracture patients (n= 15,716) and matched controls (n=47,149). All level-4 ATC groups were included as independent variables in the same logistic regression analysis with fracture as the dependent variable.

The greatest increase in hip fracture risk was observed in patients exposed to antiepileptics (odds ratio OR 1.80, 95% CI [1.53-2.12], population attributable risk PAR 1.4%), opioids (1.40 [1.23-1.59], PAR 1.4%), dopaminergics (1.87 [1.46-2.39], 0.6%), hormone antagonists (2.20 [1.14-4.28], 0.1%), anti-depressants (1.53 [1.37-1.71], 3.5%), insulin (1.87 [1.50-2.33], 1.2%), loop diuretics (1.37 [1.20-1.57], 3.6%) and anti-psychotics (1.51 [1.26-1.80], 1.0%). The risk of spine fractures were particularly increased in users of most classes of analgesics, cardiac glycosides, systemic and topical glucocorticoids and hormone antagonists.

Medications predisposing to hip fracture differed from those associated with increased risk of spine fractures. Most classes of analgesics were more widely used in patients who subsequently sustained fractures, but drugs affecting the nervous system were key contributors to hip fracture risk while anti-hormonal agents were more important as predictors of vertebral fracture. The advantage of this type of analysis is that it provides a conservative approach, while facilitating discovery of new associations between prescription history and subsequent fracture. The disadvantage of the method is that weak associations may be missed, especially where drugs belonging to the same level-4 ATC class have opposite effects on risk.

Disclosures: B. Abrahamsen, Roche 2; Nycomed 5; Servier 8; Merck 8.

1163

Skeletal Size and Fracture Risk in a Large Clinical Cohort. W. D. Leslie¹, J. F. Tsang^{*2}, L. M. Lix^{*3}. ¹Dept of Medicine, University of Manitoba, Winnipeg, MB, Canada, ²University of Manitoba, Winnipeg, MB, Canada, ³Manitoba Centre for Health Policy, University of Manitoba, Winnipeg, MB, Canada.

DXA is affected by skeletal size with smaller bones giving lower areal BMD (aBMD) despite equal volumetric BMD. Whether this size effect confounds the use of aBMD as a diagnostic and fracture risk assessment tool is unclear.

We identified 16205 women of white ethnicity age 50 y or older undergoing baseline hip assessment with DXA (1998-2002) from a population-based database which contains all clinical DXA test results for the Province of Manitoba, Canada. Total hip aBMD and T-scores (NHANES-III) were categorized according to quartile in total hip area (Q1=smallest, Q4=largest). Longitudinal health service records were assessed for the presence of non-trauma 'osteoporotic' fracture codes (hip, clinical spine, wrist, humerus) during mean 3.1 y after BMD testing (757 osteoporotic fractures, 186 hip fractures).

Total hip area strongly affected diagnosis with much higher rates in Q1 (15.5%) than Q4 (8.9%). However, incident fracture rates in women with T≤-2.5 were constant across area quartiles. Age was a potential confounder that correlated positively with area (r=0.12, p<.0001). When age was not included in a Cox regression model, Q1 appeared to have a lower rate of osteoporotic fractures (HR 0.80, 95% CI 0.66-0.98, reference Q4) and hip fractures (HR 0.63, 95% CI 0.43-0.94) for a given aBMD. In age-adjusted regression models, aBMD was strongly predictive of osteoporotic fractures (HR per SD 1.83, 95% CI 1.68-1.99) and hip fractures (HR per SD 2.80, 95% CI 2.33-3.35) but there no independent effect of bone area (categorical or continuous). Including height and/or weight as covariates did not change the results. Models that assessed bone area and BMC covariates together, or simple volume-adjustments, were no better than aBMD alone for fracture prediction.

We conclude that aBMD categorizes a substantially higher fraction of women with smaller bone area as being osteoporotic despite younger age. Observed fracture rates correlate equally well with aBMD across all bone area quartiles when adjusted for age.

Table: Osteoporosis diagnosis (T≤-2.5) and fracture rates (for osteoporotic women)

according to total hip area quartile (Q1=smallest, Q4=largest).

	Q1 (N=4052)	Q2 (N=4051)	Q3 (N=4050)	Q4 (N=4052)	p-for-trend
Osteoporosis diagnosis	15.5%	11.0%	9.8%	8.9%	<.0001
Any osteoporotic fracture	13.5%	11.9%	14.1%	13.4%	NS
Hip fracture	4.8%	5.4%	5.6%	5.6%	NS

Disclosures: W.D. Leslie, Merck Frosst Canada Ltd; Sanofi-Aventis; Procter & Gamble Pharmaceuticals Canada, Inc. 2, 5, 8.

1164

High Resolution Peripheral Quantitative CT (HRpQCT) of the Radius Reflects Iliac Crest Biopsy Measures of Microstructure and Mechanical Competence. A. Cohen¹, D. W. Dempster², R. Mueller³, X. E. Guo¹, X. H. Zhang^{*1}, A. J. Wirth^{*3}, G. H. van Lenthe^{*3}, D. J. McMahon¹, H. Zhou^{*2}, M. R. Rubin¹, J. P. Bilezikian¹, R. R. Recker⁴, E. Shane¹. ¹Columbia University, New York, NY, USA, ²Helen Hayes Hospital, West Haverstraw, NY, USA, ³University of Zurich, Zurich, Switzerland, ⁴Creighton University, Omaha, NE, USA.

The newly available HRpQCT instrument (Scanco Medical AG) has sufficiently high resolution (<100µm) to permit in vivo assessment of trabecular (Tb) architecture at the radius (RAD) and tibia (TIB). Finite element analysis (FEA) can be applied to HRpQCT data to quantify bone mechanical competence (Young's moduli; E), where E is a surrogate for bone strength.

Study goal: To evaluate relationships between structural parameters and Young's moduli assessed by HRpQCT of the RAD and TIB and those measured by 2D histomorphometry (2DH) and 3D microCT (Scanco µCT40) of iliac crest biopsies, and to determine whether HRpQCT images accurately reflect histomorphometric analyses.

Biopsies and HRpQCT scans were performed in 37 individuals (10 men, age 22-76) with normal BMD, or with osteoporosis or hypoparathyroidism. Cortical thickness (CtWi) was measured by 2DH and HRpQCT, while Tb indices, including Tb bone volume (BV/TV), number (TbN), thickness (TbTh), separation (TbSp) were assessed by 2DH, microCT and HRpQCT. In a subset (n=24), FE models created by voxel-to-element conversion were used to calculate apparent E (longitudinal) for microCT and E in 3 directions for HRpQCT. Structural Measures: BV/TV, TbN, TbTh, and TbSp by 2DH correlated well with comparable microCT measures on biopsies (r=0.85, 0.82, 0.71, 0.80, respectively; all p<0.0001). RAD HRpQCT measures of BV/TV, TbN and TbSp correlated significantly with 2DH of biopsies (r=0.47, 0.41, 0.42; p<0.02). In contrast, at the TIB only BV/TV correlated significantly with 2DH of biopsies (r=0.37, p<0.05). CtWi by 2DH correlated with RAD (r=0.42; p=0.01) and TIB (r=0.54; p<0.001) HRpQCT. MicroCT measurements of BV/TV, TbN and TbSp correlated with similar RAD (r=0.41, 0.50, 0.63; all p<0.02), but not TIB, HRpQCT.

Mechanical competence: Apparent E (longitudinal) calculated from microCT correlated with E in three directions calculated from RAD (r=0.65; p<0.001) but not TIB (r=0.17; NS) HRpQCT.

In summary, there are strong relationships between comparable measures performed on iliac crest biopsies by 2DH and 3D microCT, and also between most 2DH and microCT parameters at the iliac crest and HRpQCT of the RAD. Parameters from TIB HRpQCT did not correlate well with biopsies. E calculated on biopsies correlated well with E calculated on RAD, but not TIB HRpQCT.

We conclude that RAD HRpQCT correlates well with bone biopsy structural parameters and can be considered as a non-invasive surrogate measure of bone strength.

Disclosures: E. Shane, None.

This study received funding from: NIH/NIAMS.

1165

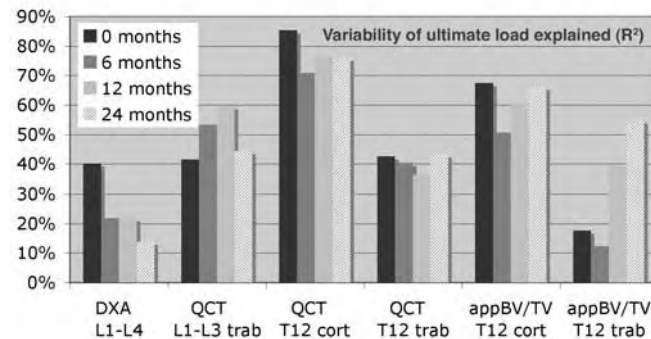
QCT and High Resolution CT Are Better Surrogate Measures of Bone Strength than DXA for Patients on Teriparatide Treatment: Results from the EUROFOR Study. C. C. Glüer¹, C. Graeff¹, T. Nickelsen^{*2}, P. Zysset^{*3}.

¹Med. Phys., Diagn. Radiology, UKSH, Kiel, Germany, ²Eli Lilly, Europe, Bad Homburg, Germany, ³Inst. for Lightweight Design and Struct. Biomechanics, Vienna University of Technology, Wien, Austria.

The deficiencies of DXA for monitoring osteoporosis treatment are well established. Treatment induced increases in BMD only partially reflect reductions in fracture risk. As an alternative approach, structural strength of the vertebrae can be estimated by digital finite element analysis (FEA). We investigated (1) whether this performance problem of DXA would manifest itself as a reduction in the correlation between DXA and structural strength in teriparatide (TPTD) treated compared to untreated patients and (2) whether QCT or High Resolution CT (HRCT) might show more consistent correlations in treated and untreated patients, indicating that they would be better techniques for monitoring treatment effects.

In the Eurofors multi-center study, a subset of 23 patients on 24 months of treatment with TPTD (20 µg per day) was measured with DXA (L1-4), QCT (L1-3), and HRCT (T12). FEA of the T12 vertebrae was used to calculate ultimate load under axial compression. Using StructuralInsight software developed in-house, regions of the vertebral cortical rim (outer 3mm) and inner trabecular volume were segmented. Volumetric BMD (QCT) and structural measures (apparent BV/TV, from HRCT) were calculated for T12. QCT analyses on L1-3 were performed by Mindways QCTPro.

At baseline DXA explained 40% of bone strength but this was reduced to only 14% after 2 years of TPTD treatment. QCT based BMD and HRCT based BV/TV associations with bone strength were maintained or even shown improvements: at 24 months these measures explained 43-76% of bone strength.



We conclude that in patients on teriparatide treatment DXA loses its ability to estimate bone strength but that QCT and HRCT maintain a high correlation with bone strength. Our results indicate that CT based assessments may offer substantial advantages over DXA in assessing treatment effects on bone strength, specifically for TPTD.

Disclosures: C.C. Glüer, None.

This study received funding from: Eli Lilly.

1166

Development of a Clinical Nomogram for Individualizing 5-year and 10-year Risks of Fracture. N. D. Nguyen, S. A. Frost*, J. R. Center, J. A. Eisman, T. V. Nguyen. Bone and Mineral Research Program, Garvan Institute of Medical Research, Sydney, Australia.

Although many risk factors of fracture have been identified, the translation of these risk factors into a prognostic model that can be used in primary care setting has not been well realized. The present study sought to develop a nomogram that incorporates non-invasive risk factors to predict 5-year and 10-year absolute risks of fracture for an individual man and woman.

The Dubbo Osteoporosis Epidemiology Study was designed as a community-based prospective study, with 1358 women and 858 men aged 60+ years as at 1989. Baseline measurements included femoral neck bone mineral density (FNBM), prior fracture, a history of falls and body weight. Between 1989 and 2004, 426 women and 149 men had sustained a low-trauma fracture. Two prognostic models based on the Cox's proportional hazards analysis were considered: model 1 included age, BMD, prior fracture and falls; and model 2 included age, weight, prior fracture and falls.

Analysis of the area under the receiver operating characteristic curve (AUC) suggested that model 1 (AUC=0.75 for both sexes) performed better than model 2 (AUC = 0.72 for women and 0.74 for men). Using the models' estimates, various nomograms were constructed for individualizing the risk of fracture for men and women. If the 5-year risk of 10% or greater is considered "high risk", then virtually all 80 years old men with BMD T-scores < -1.0 or 80 years old women with T-scores < -2.0 were predicted to be in the high risk group. A 60 years old woman's risk was considered high risk only if her BMD T-scores ≤ -2.5 and with a prior fracture; however, no 60 years-old men are in the high risk regardless of their BMD and risk profile.

These data suggest that the assessment of fracture risk for an individual can not be based on BMD alone, since there are various combinations of factors that could substantially elevate an individual's risk of fracture. The nomograms presented here can be useful for individualizing the short- and intermediate-term risk of fracture and identifying high-risk individuals for intervention to reduce the burden risk of fracture in the general population.

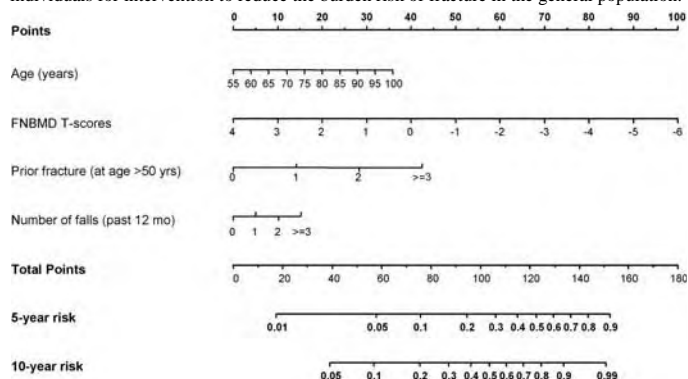


Figure: Nomogram for predicting 5-year and 10-year probability of any osteoporotic fracture for individual women

Disclosures: N.D. Nguyen, None.

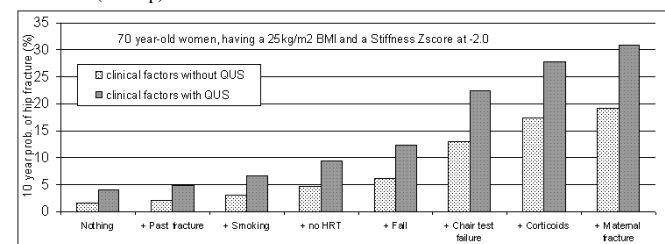
This study received funding from: National Health and Medical Research Council, Australia.

1167

Ten-year Probability of Osteoporotic Hip Fracture in Elderly Women Combining Clinical Factors and Heel Bone Ultrasound: A New Model From the EPISEM Prospective Cohort. C. Durosier^{*1}, M. Krieg², A. Schott^{*3}, J. Kanis^{*4}, D. Hans¹. ¹Nuclear Medicine, University Hospital, Geneva, Switzerland, ²Outpatient Clinic, University Hospital, Lausanne, Switzerland, ³Medical Information, Hospices Civils of Lyon, Lyon, France, ⁴WHO Collaborating Centre for Metabolic Bone Diseases, Sheffield University, United Kingdom.

Many independent clinical risk factors (CRF) have been identified that contribute to the osteoporotic hip fracture risk above that reflected by BMD. However, DXA is not always available. Prospective studies shown that heel bone ultrasound (HBU) predicts hip fracture equally well as hip BMD. In addition we demonstrated that combining CRF with HBU improves the 10-year probability of hip fracture (ASBMR 2006). The aim of our study is to recalculate the probability considering additional CRF present in the current WHO model for central DXA.

We built a database "EPISEM" (12958 women aged 70 to 97 years) by grouping the EPIDOS (French) and SEMOF (Swiss) cohorts. At baseline, all women had been measured by the HBU Achilles+ (GE-Lunar), and questioned for their osteoporosis CRF. During a mean follow-up of 3.2 ± 0.9 years (\pm SD), 307 women reported a hip fracture. Covariates included age and time since start of follow-up. The association of risk factors with the risk of hip fracture and possible interactions were examined using a Poisson regression model, which included only the significant ones. Stiffness HBU was expressed as Z-scores. Gradient of risk per standard deviation of the model was calculated as well as the 10-year probability of hip fracture of all possible combination of selected CRF and Stiffness HBU. The following independent predictors were kept: Stiffness HBU, BMI, past fracture, fall within a year, chair test, past HRT, current smoking, current corticoids intake and hip fracture in mother. Gradient of risk of the model per one standard deviation decrease varies from 1.5 to 2.7 when considering a baseline age of 70 up to 95 years. An example of probability of a 70-year-old woman is given in the figure below according to the number of risk factors (sum-up).



The association of CRF and HBU clearly improves the detection of elderly women at high risk. Thresholds corresponding to an equivalent of -2.5 T-score of the femoral neck are been defined enabling the identification of women likely to benefit of a treatment initiation. Clinical evaluation is underway to further validate such model.

Disclosures: C. Durosier, None.

1168

Establishing a Reference Range for Bone Turnover Markers in 635 healthy, Young, Pre-menopausal Women from UK, France, Belgium and the USA. S. J. Glover¹, M. Gall², O. Schoenborn-Kellenberger³, P. Garnero⁴, S. Boonen⁵, J. A. Cauley⁶, D. M. Black⁷, P. D. Delmas⁸, R. Eastell¹. ¹Academic Unit of Bone Metabolism, University of Sheffield, Sheffield, UK, United Kingdom, ²Novartis Pharmaceuticals Incorporated, East Hanover, NJ, USA, ³Novartis Pharma AG, Basel, Switzerland, ⁴SYNARC, Lyon, France, ⁵Leuven University Center for Metabolic Bone Diseases & Division of Geriatric Medicine, Katholieke Universiteit Leuven, Leuven, Belgium, ⁶University of Pittsburgh, Pittsburgh, PA, USA, ⁷Department of Epidemiology and Biostatistics, University of California, San Francisco, CA, USA, ⁸INSERM Research Unit 831, University of Lyon, Lyon, France.

Bone turnover markers (BTMs) are important in determining fracture risk in women with postmenopausal osteoporosis. Robust reference ranges are required for the interpretation of BTMs in large phase III fracture trials, such as the Horizon-PFT study of zoledronic acid. The aims of the study were to: a) establish reference intervals for crosslinked C-telopeptides of type I collagen (beta CTX), crosslinked N-telopeptides of type I collagen (NTX), bone alkaline phosphatase (bone ALP) and procollagen type I N propeptide (PINP) in healthy young pre-menopausal women; and b) study the effect of geographical location on BTMs. We recruited 635 women from 4 countries that participated in the Horizon-PFT study (UK, France, Belgium, US). The women were 30 to 40 years of age (mean 34.6), with regular cyclic menses. Subjects completed a medical and lifestyle questionnaire. The reference ranges are shown in the table and were obtained using the IFCC methodology.

Measurement	Reference interval, 95% CI	Lower limit, 90%CI	Upper limit, 90%CI
Serum CTX, ng/mL	0.114 - 0.628	0.100 ; 0.131	0.548 ; 0.721
Urinary NTX/Cr, nmol/mmol Cr	9.22 - 51.81	8.03 ; 10.57	45.16 ; 59.44
Serum bone ALP, ug/L	5.15- 15.32	4.48 ; 5.92	13.33 ; 17.61
Serum PINP, ug/L	16.3 - 78.2	15.5 ; 17.3	74.0 ; 82.7

Beta CTX was significantly higher in France than UK ($p=0.01$) and PINP was higher in France and Belgium than UK ($p<0.001$) and higher in France than US ($p<0.01$) by ANOVA. We found several differences between countries in BMI, previous numbers of pregnancies, and in the proportion of women who were current smokers, regular exercisers and consuming alcohol regularly (ANOVA, all $p<0.05$), which might explain the differences in BTMs. The proportion of current smokers was higher in France than in UK ($p<0.01$) and smoking was associated with significantly higher levels of beta CTX and PINP ($p<0.05$). In conclusion we have established reference ranges for 4 BTMs based on an international study of pre-menopausal women and have identified differences in BTMs, BMI, smoking habit, pregnancies, exercise and alcohol consumption between countries.

Disclosures: S.J. Glover, None.

This study received funding from: Novartis.

1169

Specific Inhibition of the VEGF Homologue Placental Growth Factor Is Protective Against Osteolytic Bone Metastasis in Mice. L. Coenegrachts^{*1}, C. Maes¹, I. Stockmans^{*1}, T. Guise², R. Bouillon¹, P. Carmeliet^{*3}, G. Carmeliet¹. ¹Laboratory of Experimental Medicine and Endocrinology, K.U.Leuven, Leuven, Belgium, ²Dept. of Internal Medicine, University of Virginia, Charlottesville, VA, USA, ³Center for Transgene Technology and Gene Therapy, VIB, K.U.Leuven, Leuven, Belgium.

Osteolytic bone metastasis comprises of several stages including tumor cell migration, tumor growth, angiogenesis and bone resorption. Bone marrow (BM) stromal cells and osteoclasts contribute to metastasis progression and both cell types express VEGFR-1, the receptor for the VEGF homologue Placental Growth Factor (PlGF). We recently reported that PlGF is important for fracture repair by stimulating angiogenesis and bone remodeling. Given this multi-functionality of PlGF in bone pathology, we investigated its role in osteolytic metastasis.

MDA-MB231 human breast cancer cells, which express VEGFR-1, were intracardiac injected in nude mice treated for 3 weeks with an anti-murine PlGF antibody (mPlGF-Ab) or an isotopic control antibody (a kind gift of Thrombogenics NV, Leuven, Belgium).

Administration of mPlGF-Ab significantly reduced the number of mice with osteolytic lesions as analyzed by radiography (mPlGF-Ab: 7/13 vs. control: 11/11; $p<0.05$). In particular, the number of affected bones was significantly reduced by mPlGF-Ab treatment (mPlGF-Ab: 0.92 vs. control: 3.54, of 4 bones (tibia-femur) analyzed per mouse; $p<0.001$). Histomorphometry confirmed these results and additionally showed that tumor size in mPlGF-Ab treated mice with osteolytic lesions was reduced compared to the control group. These data suggest that preferentially early phases of bone metastasis and tumor growth are inhibited by mPlGF-Ab treatment.

Mechanistic investigation revealed that murine BM stromal cells expressed increased PlGF mRNA and protein levels (species-specific qRT-PCR, ELISA) when cultured in vitro adjacent to human MDA-MB231 cells for 3 and 6 days ($p<0.001$) but not when cultured separated by a membrane. This observation can explain the significantly increased mPlGF mRNA expression in bone, 2 weeks after tumor cell injection, the time when metastases become histological detectable. In addition, already one week after tumor cell injection, osteoclast surface (TRAP) was decreased in mPlGF-Ab treated mice compared to control treatment. In agreement, C-telopeptide serum levels, a bone resorption marker, were significantly reduced in mPlGF-Ab treated mice 3 weeks after tumor cell injection. Moreover, osteoclast differentiation in vitro was significantly impaired by inhibition of PlGF activity.

In conclusion, these data suggest that mPlGF promotes osteolytic bone metastasis by affecting tumor growth and by stimulating bone resorption.

Disclosures: L. Coenegrachts, None.

1170

Imatinib Mesylate Suppresses Bone Metastases by Inhibiting Osteoclasts through Blockade of M-CSF Signals. T. Hiraga, H. Nakamura. Histology and Cell Biology, Matsumoto Dental University, Nagano, Japan.

Imatinib mesylate (imatinib), also known as Glivec or STI-571, is a potent and selective inhibitor of the tyrosine kinases, Bcr-Abl, c-Kit and platelet-derived growth factor receptors (PDGFRs), and is widely and successfully used for the treatment of chronic myeloid leukemia and gastrointestinal stromal tumor. Recently, it has been reported that imatinib also targets the macrophage colony-stimulating factor (M-CSF) receptor c-Fms. M-CSF signals are critical for the differentiation of osteoclasts. Furthermore, it is widely accepted that osteoclasts play central roles in the development and progression of bone metastases. These findings led us to hypothesize that imatinib may have beneficial effects on bone metastases. Co-immunoprecipitation assays showed that imatinib inhibited the M-CSF-induced phosphorylation of c-Fms in the osteoclast precursor cells, RAW264.7 and mouse bone marrow macrophages (BMM ϕ), as well as the PDGF-induced PDGFR phosphorylation in MDA-MB-231 human breast cancer cells. Imatinib also suppressed osteoclast-like cell formation in BMM ϕ cultures treated with RANKL/M-CSF and mouse bone marrow cultures treated with parathyroid hormone-related protein (PTHrP) in a dose-dependent manner. However, imatinib did not affect the RANKL-induced cell signals, phosphorylation of I κ B α and ERK, in RAW264.7 and BMM ϕ , and the PTHrP-induced RANKL expression in mouse primary bone marrow stromal cells, suggesting that the imatinib-decreased osteoclast-like cell formation was caused by the blockade of M-CSF signals but not RANKL signals. Of note, imatinib also inhibited osteoblast differentiation determined by alkaline phosphatase activity and alizarin red staining; however, the minimum effective dose was approximately 10 times higher than the dose required to inhibit osteoclast differentiation. Finally, we examined effects of imatinib on bone metastases using a well-characterized animal model. Radiographic and histomorphometric analyses demonstrated that imatinib significantly decreased the bone metastases of MDA-MB-231 in a dose-dependent manner. Consistent with the *in vitro* results, osteoclast number was significantly reduced in the bone metastases in imatinib-treated animals. The development of MDA-MB-231 tumors in the mammary fat pad was also suppressed by the imatinib treatment. In conclusion, these results suggest that imatinib reduced bone metastases by inhibiting osteoclasts through the blockade of M-CSF signals, in addition to the direct anti-tumor effects through the inhibition of known tyrosine kinases. The results also suggest that imatinib may have a protective effect against cancer treatment-induced bone loss.

Disclosures: T. Hiraga, None.

1171

Treatment with Heparanase III Inhibits the Growth of Myeloma Tumors in Bone. Y. Yang^{*1}, L. Suva², Z. Shriver^{*3}, G. Venkataraman^{*3}, R. Sasisekharan^{*4}, J. Epstein^{*5}, S. Yaccoby⁵, J. Shaughnessy^{*5}, R. Sanderson^{*1}. ¹Pathology, UAB, Birmingham, AL, USA, ²Orthopedic Surgery, UAMS, Little Rock, AR, USA, ³Momenta Pharmaceuticals, Inc., Cambridge, MA, USA, ⁴Division of Bioengineering and Environmental Health, MIT, Cambridge, MA, USA, ⁵Myeloma Institute for Research and Therapy, Little Rock, AR, USA.

Bacterial heparinase III (HepIII) is an enzyme that degrades heparan sulfate and has anti-tumor activity in animal models of melanoma and lung carcinoma. We tested HepIII for its effect against myeloma tumors because the syndecan-1 heparan sulfate proteoglycan is expressed by all myeloma tumors and is shed into the myeloma microenvironment where it binds to and regulates the activity of numerous growth factors. Through these activities, syndecan-1 plays a major role in promoting myeloma growth, metastasis and angiogenesis. Recombinant HepIII was purified to homogeneity, cleared of endotoxins and tested for anti-myeloma activity utilizing two *in vivo* models of the disease; a subcutaneous model in which cells of the CAG human myeloma cell line were injected into SCID mice and a SCID-hu model in which primary tumor cells isolated from myeloma patients were injected into fragments of human bone implanted in SCID mice. In addition to treatment with the recombinant HepIII enzyme, we also tested the anti-tumor activity of fragments of heparan sulfate generated by treating purified syndecan-1 with HepIII. Treatment of tumor-bearing animals with HepIII (15 mg/kg/day) or HepIII-generated fragments of heparan sulfate (0.8 mg/kg/day) was accomplished by twice daily injections for 4 weeks. The levels of human immunoglobulin light chain in murine sera were assessed as an indicator of tumor burden. The results demonstrated that treatment with either Hep III or Hep III-generated heparan sulfate fragments significantly inhibited tumor growth of both the cell line (subcutaneous model) and primary tumors (SCID-hu model). All 8 myeloma patient samples tested were inhibited by the treatment, with Hep III and Hep III-generated heparan sulfate fragments reducing tumor burden by 83% (P=0.003) and 78% (P=0.02), respectively. MicroCT scanning of the human bones revealed that inhibition of tumor growth by Hep III was associated with prevention of the bone destruction associated with myeloma. Importantly, the treated animals showed no sign of adverse side effects. We conclude that Hep III and Hep III-generated fragments of heparan sulfate significantly inhibit tumor growth and cancer-related bone resorption *in vivo*. These results indicate that targeting heparan sulfate may be an effective therapeutic approach for myeloma.

Disclosures: Y. Yang, NIH 2.

This study received funding from: National Cancer Institute.

1172

Intermittent PTH Treatment Inhibits Development and Progression of Primary Myeloma by Promoting Bone Formation in the SCID-rab Model. A. Pennisi^{*}, X. Li^{*}, M. Zangari^{*}, S. Yaccoby. Myeloma Institute for Research and Therapy, University of Arkansas for Medical Sciences, Little Rock, AR, USA.

Myeloma (MM) is associated with severe bone disease that likely contributes to tumor progression. We have previously demonstrated that whereas osteoclasts support MM growth osteoblasts have negative impact on survival of MM cells (Yaccoby et al., Haematologica 2006). The aims of the study were to investigate the effect of intermittent parathyroid hormone (PTH 1-34) treatment on bone formation and MM growth, and the consequences of PTH pretreatment on MM progression in our SCID-rab model for primary MM (Yata & Yaccoby, Leukemia 2004). SCID-rab mice were engrafted with MM cells from 5 patients. Upon establishment of MM growth, as monitored by measurement of human monoclonal immunoglobulins (hIg) in mice sera and by x-rays, mice were subcutaneously injected with PTH (0.3 mg/kg/day) or saline for 4-6 weeks. Overall, whereas BMD of the myelomatous bones in saline-treated hosts was markedly reduced by 22 \pm 7% (p<0.03), it was increased by 6 \pm 6 % from pretreatment level in PTH-treated hosts (p<0.02 saline vs. PTH-treated hosts). The bone anabolic effect of PTH was evident in 4 of 5 experiments and was associated with reduced MM growth only in hosts whose implanted bone had increased BMD from pretreatment level (242 \pm 87 vs. 875 \pm 186 μ g/ml hIg in controls, p<0.01). PTH, however, significantly increased BMD of the nonmyelomatous, uninvolved, murine femur by >12% (p<0.017) from pretreatment level in all experiments, regardless of tumor burden level in the remote myelomatous implanted bone. In additional experiments hosts received PTH or saline (10 mice/group), 4 weeks prior to and 8-12 weeks after the injection of 3 patient's derived MM cells. PTH pretreatment prior to injection of MM cells increased BMD of the nonmyelomatous implanted bones by 48 \pm 11% (p<0.001). Following inoculation of MM cells, BMD of the implanted bone in PTH-treated hosts remained significantly higher than in saline-treated hosts (p<0.002). In all 3 set of experiments, pretreatment with PTH resulted in delayed engraftment and growth of MM cells. We further confirmed by qRT-PCR that type-1 PTH receptor was not expressed by MM cells. *In vitro* PTH had no direct effect on MM cell growth and in contrast to Saos-2 osteosarcoma cells PTH did not protect MM cells from serum starvation-induced growth inhibition, indicating that PTH inhibitory effect on MM is indirectly mediated through creation of an inhospitable environment for MM cells. We conclude that increased bone formation by PTH contributes to controlling MM growth and that pretreatment with PTH, in addition to improving skeletal complications, may be a promising approach to prevent MM progression.

Disclosures: A. Pennisi, None.

This study received funding from: NCI, MMRF.

1173

Anti-myeloma Response of the Proteasome Inhibitor, Bortezomib, Is Associated with Reduced Osteoclastogenesis and Increased Osteoblastogenesis and Bone Mass in Myelomatous Bones. A. Pennisi^{*}, X. Li^{*}, B. Barlogie, M. Zangari^{*}, S. Yaccoby. Myeloma Institute for Research and Therapy, University of Arkansas for Medical Sciences, Little Rock, AR, USA.

The ubiquitin-proteasome pathway regulates differentiation of bone cells and myeloma (MM) growth. Bortezomib is a novel proteasome inhibitor with promising efficacy, even in patients with refractory MM. We recently reported that anti-MM response of bortezomib is associated with increased circulating alkaline phosphatase in MM patients (Zangari et al., BJH 2005). The aim of this study was to investigate the effect of bortezomib on bone remodeling and tumor growth in our SCID-rab model for primary MM (Yata & Yaccoby, Leukemia 2004). SCID-rab mice were engrafted with MM cells from 14 patients. MM growth was monitored by measurement of human monoclonal immunoglobulins (hIg) in mice sera, by x-rays and by live animal imaging using luciferase-expressing MM cells. MM-bearing mice were injected subcutaneously with bortezomib (0.5 mg/kg twice a week) or saline for 4-8 weeks. Whereas all control mice had increased hIg levels, bortezomib reduced hIg in 7/14 experiments by 70 \pm 7% from pretreatment levels and delayed growth in additional 3 experiments. Overall, tumor burden in control- and bortezomib-treated mice was increased by 519 \pm 85% and 202 \pm 68% from pretreatment, respectively (p<0.003). Whereas in control mice BMD of the implanted bone was reduced by 15.2 \pm 5.7%, in bortezomib-treated hosts it increased by 5.4 \pm 11% from pretreatment (p<0.03). Increased bone formation by bortezomib was more profound in responding hosts (r=-0.58 between BMD and hIg changes in responding hosts) and was not observed in hosts responding to melphalan. Furthermore, clinical response and bone histomorphometric changes (assessed by micro-CT) in patients who received bortezomib as a single agent were consistent with bortezomib's effects in mice engrafted with MM cells from those patients. Histological examination revealed increased numbers of osteocalcin-expressing osteoblasts (34 \pm 7 vs. 13 \pm 3 in controls, p<0.03) and reduced numbers of multinucleated TRAP-expressing osteoclasts (10 \pm 3 vs. 28 \pm 7 in controls, p<0.02) in myelomatous bones from bortezomib-treated hosts. We further demonstrated that bortezomib (2.5-5 nM) directly induced differentiation of human MSCs into osteoblasts and prevented formation of TRAP-expressing multinucleated osteoclasts (p<0.03) via downregulation of NF-kappaB activity in osteoclast precursors. We conclude that bortezomib promotes bone formation in MM by simultaneously inhibiting osteoclastogenesis and stimulating osteoblastogenesis, and thus, is a potent agent for treating MM and its associated bone disease.

Disclosures: A. Pennisi, None.

This study received funding from: NCI, MMRF, Millennium Pharmaceuticals.

1174

WISP-1/CCN-4 a Novel Target for Inhibiting Prostate Cancer Growth in Bone. C. I. Inkson*, T. M. Kilts*, L. W. Fisher, M. F. Young. Craniofacial and Skeletal Diseases Branch, National Institute of Dental and Craniofacial Research, Bethesda, MD, USA.

WISP-1/CCN-4 is a member of CCN family of cysteine-rich secreted proteins implicated in the progression of breast, colonic and gastric cancers. Recent studies indicate that WISP-1 can regulate osteogenic progenitor cell function in vitro and in vivo. The goal of our study was to examine WISP-1 expression in prostate tumors, and then to test the possibility that by inhibiting WISP-1 we could reduce prostate tumor growth. We have developed an antibody to WISP-1 which was used to localize WISP-1 expression in various grades of prostate cancer and normal prostate tissue. WISP-1 expression was found predominantly in early to mid stage cancers, mostly localized to large areas of stromal tissue within these tumors that co-localized with areas of alpha-SMA expression. Expression was also apparent in some transformed ductal epithelial cells and small blood vessels. However, only weak expression of WISP-1 could be observed in normal prostate tissue. Next we tested whether our antibody could block WISP-1 activity thereby preventing tumor growth of the PC3 prostate cancer cells in vivo. To do this, PC-3 cells containing a luciferase gene (PC3-luc) were incubated with 100ug/10,000 cells WISP-1 affinity purified antibody (ab), an iso-type control ab, or PBS for 1 hour and then injected subcutaneously to form tumors in nude mice. The extent of tumor development was analysed by measurement of growth dimensions using callipers, as well as by measurement of luciferase expression using the Xenogen Live Bioluminescent Imaging System. Twice weekly intra-peritoneal (IP) injections of 100ug WISP-1 ab suppressed the size and growth rate of these subcutaneous growths in comparison to mice treated with 100ug of a control ab or PBS. In a second approach, we used an intra-cardiac (IC) injection model to test the possibility that by inhibiting WISP-1 we could obstruct growth of circulating prostate cells in the bone microenvironment. PC3-luc cells were pre-treated with 100ug/10,000 cells WISP-1 ab, control ab or PBS and then administered via IC injection into nude mice (N=6 per treatment). Bioluminescence was analyzed over a 4 week period to determine tumor formation and growth. Cells pre-incubated with the WISP-1 ab had significantly less tumor establishment than PBS or control ab pre-treated cells, and unlike the untreated cells, tumors were limited to the craniofacial region. Furthermore, twice weekly IP injection of 100ug WISP-1 antibody suppressed the growth rate of these tumors compared to control ab or PBS-injected mice. Our data implies WISP-1 may play a role in prostate cancer growth in bone and may prove a novel target for future therapeutics.

Disclosures: C.I. Inkson, None.

This study received funding from: IRP-NIDCR, NIH.

1175

Hypoxia-Inducible Factor 2 α Induces Type X Collagen and Promotes Hypertrophic Differentiation of Chondrocytes. T. Saito¹, T. Ikeda^{*2}, A. Higashikawa¹, Y. Kawasaki¹, A. Kan¹, M. Ushita¹, S. Ohba², F. Yano², K. Nakamura¹, U. Chung², H. Kawaguchi¹. ¹Sensory & Motor System Medicine, University of Tokyo, Tokyo, Japan, ²Division of Tissue Engineering, University of Tokyo, Tokyo, Japan.

Although hypertrophic differentiation of chondrocytes is a crucial process in endochondral ossification, the underlying molecular mechanism remains unclear. The present study initially performed the screening of transcription factors using HeLa cells transfected with a luciferase-reporter construct containing a 1.2 kb human promoter of type X collagen (COL10A1), the representative marker for hypertrophic chondrocytes. Among over 200 transcription factors known to be expressed in chondrocytes, we identified hypoxia-inducible factor 2 α (HIF2A) as the strongest transactivator of the COL10A1 promoter. The activity was more than twice that of Runx2, a representative transcription factor of COL10A1. In vivo expression of HIF2A was shown by immunohistochemistry to be localized in the pre-hypertrophic and hypertrophic chondrocytes of the mouse growth plate. In addition, during differentiation of cultured mouse chondrogenic cell line ATDC5 in the presence of insulin, the HIF2A mRNA level determined by real-time RT-PCR was increased simultaneously with that of COL10A1. To investigate the functional relevance of HIF2A to chondrocyte hypertrophy, we established stable lines of ATDC5 cells overexpressing HIF2A or the dominant negative (DN) HIF2A mutant through retroviral introduction. The COL10A1 mRNA level, as well as ALP and Alizarin red stainings, were increased by the HIF2A overexpression, whereas all were decreased by the DN mutant overexpression, as compared with respective GFP-introduced control cells. We further examined the mechanism of induction of COL10A1 by HIF2A. Among several hypoxia-responsive elements in the COL10A1 promoter, site-directed mutagenesis analysis determined the responsive region of HIF2A in intron 1. Electrophoretic mobility shift assay revealed specific binding of in vitro-translated HIF2A protein with the oligonucleotide probe of the region, but not with the mutated probe. The competition assay using unlabeled probes and the super-shift assay using the antibody to HIF2A confirmed the specific binding of HIF2A and the region. Furthermore, the chromatin immunoprecipitation assay confirmed their in vivo binding. In conclusion, the present study identified HIF2A as a potent transcription factor for COL10A1 and hypertrophic differentiation of chondrocytes. Elucidation of the signaling related to the HIF2A / COL10A1 axis will lead to further understanding of the molecular network of chondrocyte differentiation during endochondral ossification.

Disclosures: T. Saito, None.

1176

Expression of Ca²⁺ Receptors in Cartilage Is Essential for Embryonic Skeletal Development In Vivo. C. Tu*, H. Elalieh*, T. Chen*, B. Liu*, M. Hamilton*, D. Shoback, D. Bikle, W. Chang. Endocrine Research Unit, VAMC, University of California San Francisco, San Francisco, CA, USA.

The Ca²⁺ receptor (CaR), a G-protein coupled receptor, is expressed in the growth plate with highest levels in the mineralizing hypertrophic zone. In cultured growth plate chondrocytes (GPCs), CaRs are critical for promoting terminal differentiation. Their impact on growth plate development in vivo is unclear. GPCs from a general CaR-knockout mouse (^{CaR}^{-/-}) (Ho et al, Nature Med, 1993) express alternatively spliced CaRs lacking exon 5 and respond to changes in the extracellular [Ca²⁺] ([Ca²⁺]_e) comparable to wild-type (wt) GPCs -- suggesting an incomplete knockout. Severe hypercalcemia and hyperparathyroidism and early death have precluded definitive assessment of CaR function in postnatal growth unless the hyperparathyroidism was corrected. To address this, we generated cartilage-specific CaR^{-/-} (^{CaR}^{CaR}^{-/-}) mice using Cre/lox recombination by inserting loxP sites flanking CaR exon 7, which encodes the transmembrane and intracellular loops of the CaR, and injecting the construct into mouse ES cells. CaRs transcribed from CaR exon 1-6 cDNA did not reach the membrane, respond to high [Ca²⁺]_e, or block signaling by wt CaRs. Germline transmission of the floxed-CaR (CaR^{lox/lox}) was achieved. Cre recombinase (Cre) could excise CaR exon 7 when CaR^{lox/lox} GPCs were infected with adenoviruses expressing Cre. ^{CaR}^{CaR}^{-/-} mice were made by breeding CaR^{lox/lox} mice with transgenic (Tg) mice expressing Cre driven by a Col(II) promoter [Col(II)-Cre] and backcrossing to CaR^{lox/lox} mice to generate homozygous knockouts. Homozygous knockout is embryonic lethal: no ^{CaR}^{CaR}^{-/-} mice were born alive in 25 litters (~200 pups) or found at embryonic (E) stages 14-16 (6 litters). In 56 embryos (6 litters for E12 and E13), only 2 homozygous ^{CaR}^{CaR}^{-/-} mice were found. Both showed delayed formation of primary ossification centers and unmineralized calvariae and long bones. To study the role of CaRs in postnatal growth, we bred CaR^{lox/lox} mice with Tg ^{CaR}^{ER^{Cre}} mice which express cDNA encoding a fusion protein (Cre-ER^{Tam}) containing Cre and a mutated ligand-binding domain of the estrogen receptor conferring tamoxifen (Tam) sensitivity. The Cre-ER^{Tam} is controlled by a mouse Col(II) promoter for cartilage-specific expression. Homozygous ^{CaR}^{Cre-ER^{Tam}}/CaR^{lox/lox} mice are viable and fertile. Two consecutive maternal injections of 4OH-Tam 2-4 days before birth induced excision of CaR exon 7 in neonates. Analyses of Tam-induced ^{CaR}^{CaR}^{-/-} mice are in progress. This work shows for the first time a non-redundant role for CaRs in growth plate development in vivo and indicate that exon 5-less CaRs can compensate for the loss of full-length CaR in the ^{CaR}^{CaR}^{-/-} mice.

Disclosures: W. Chang, None.

1177

Conditional Deletion of Fibronectin in Osteoblasts Reveals Distinct Roles in Orchestrating Assembly of Bone ECM Proteins and in Osteoblast Differentiation. Q. Chen¹, J. Zhao^{*1}, M. R. Dallas^{*1}, D. M. Pacicca^{*2}, R. Fassler^{*3}, S. L. Dallas¹. ¹Univ. of Missouri, Kansas City, Kansas City, MO, USA, ²Children's Mercy Hospitals & Clinics, Kansas City, MO, USA, ³Max Planck Institute of Biochemistry, Martinsried, Germany.

Fibronectin (FN) is an extracellular matrix (ECM) glycoprotein that is expressed at sites of bone formation and is important for osteoblast function. Conventional knockout of the FN gene is early embryonic lethal and therefore its role in the skeleton is unclear. Previous studies using FN-null embryonic fibroblasts differentiated with BMP2 have shown that FN was required for osteoblast mineralization, through its role in controlling assembly of multiple bone ECM proteins. To further determine the role of FN in the skeleton we have used an in vivo and in vitro conditional knockout approach. Mice with a deletion of FN in osteoblasts (FNcKO) were generated by crossing FN floxed mice with mice expressing Cre recombinase driven by the 3.6kb Col1a1 promoter. The numbers of FNcKO live births were 60% less than expected, suggesting lethality. Surviving FNcKO mice were fertile but were smaller than control littermates, with a 10-35% reduction in body weight. At 6wks, the FNcKO mice showed a 3-10% reduction in the length and width of the tibia and femur and reduced cortical thickness. Bone mineral density and bone mineral content of the whole body, spine, femur and tail vertebrae were significantly decreased. 100% of the FNcKO mice showed a kinky tail phenotype, ranging from involvement of a single vertebra to involvement of all tail vertebrae. Occasionally, a curved spine phenotype was also observed, resembling congenital scoliosis. Decreased FN in the skeleton was associated with decreased staining for type I collagen and decorin. A key role for FN in bone ECM assembly was confirmed in FN floxed primary osteoblast cultures infected with adenovirus expressing Cre (Ad-CMV-Cre) to achieve an in vitro deletion of FN. The Ad-CMV-Cre-infected cultures showed a 90% reduction of FN compared to untreated or Ad-CMV-GFP treated controls. Lack of FN was associated with reduced alkaline phosphatase (AlkP) and impaired assembly of bone ECM proteins, including type I collagen, decorin, biglycan, LTBP1 and fibrillin-1, a known regulator of BMPs. Both AlkP expression and assembly of ECM proteins were rescued by addition of intact FN to the cultures, but not by a panel of shorter FN fragments, covering the complete FN molecule. BMP2 alone rescued AlkP expression but not the assembly of bone ECM proteins. These data suggest that FN is critical for normal development of the skeleton and for normal osteoblast function and is a key regulator of assembly of bone ECM proteins. The effects of FN on differentiation may be mediated by BMP2, while those on ECM assembly may be BMP2-independent.

Disclosures: Q. Chen, None.

1178

Connective Tissue Growth Factor (CTGF) Causes Osteopenia In Vivo. A. Smerdel-Ramoya, S. Zanotti, L. Stadmeier*, E. Canalis. Research, Saint Francis Hospital and Medical Center, Hartford, CT, USA.

CCN are highly conserved proteins, which include Cyr 61, connective tissue growth factor (CTGF). Nephroblastoma overexpressed (Nov) and Wnt induced secreted proteins. CCN proteins are expressed in skeletal cells and ctgf null mutations have demonstrated that CTGF plays a role in developmental chondrogenesis in vivo. However, the function of CTGF in the post natal skeleton is not known. To define the function of CTGF in the skeleton in vivo, we created transgenic mice expressing CTGF under the control of a 3.8 kilobase fragment of the human osteocalcin promoter in an FVB genetic background. Two transgenic lines were established. Four week old CTGF transgenic mice were compared to wild type littermate controls of identical age, sex and genetic composition. CTGF overexpression was confirmed in calvarial extracts by real time RT-PCR, which revealed 150 times higher levels of CTGF mRNA in transgenics than control mice. CTGF transgenics exhibited osteopenia, with a 50% decrease in trabecular bone volume, due to a decrease in trabecular number. This phenotype was analogous in male and female CTGF transgenics. There was a 20% increase in osteoclast surface/bone surface and osteoclast number/perimeter, and a tendency toward an increase in eroded surface/bone surface, without a compensatory increase in mineral apposition rate or bone formation rate. Osteoblast number/perimeter and surface were not changed. To examine the mechanism for the lack of a bone forming response, marrow stromal cells from CTGF transgenics were studied. Confirming the BMP antagonistic activity of CTGF, cells from CTGF transgenics displayed a reduced response to BMP on mothers against decapentaplegic (Smad) 1/5 phosphorylation, and a modest reduction in alkaline phosphatase activity. In conclusion, CTGF overexpression in vivo causes osteopenia, by enhancing bone resorption and preventing a bone forming response, possibly by antagonizing BMP signaling.

Disclosures: A. Smerdel-Ramoya, None.

This study received funding from: Dept. Veterans Affairs.

1179

Selective Deletion of Fibronectin in Osteoblasts Affects Bone Density and Osteoblast Function. A. Bentmann*, N. Kawelke*, I. Nakchbandi².

¹University of Heidelberg, Heidelberg, Germany, ²University of Heidelberg and Max-Planck Institute for Biochemistry, Heidelberg, Germany.

Bone extracellular matrix consists mainly of collagen (90%), with fibronectin consisting only a small portion. In vitro data however have established an absolute requirement for fibronectin for the assembly of collagen to take place. We therefore postulated a defect in matrix assembly that may affect bone density in mice in which fibronectin is deleted in the osteoblasts.

Mice that are homozygous for fibronectin die in utero. We therefore used the Cre-loxP strategy to produce mice that are deficient in fibronectin produced by the osteoblasts. Mice with the genotype collagen alpha1(I)-Cre (1.6 kb)/+ were mated with mice carrying the fibronectin floxed gene (fibronectin floxed/floxed) over two generations to obtain mice with the following genotype: alpha1(I)-Cre (1.6 kb)/+ _fibronectin floxed/floxed. These mice will delete fibronectin in cells that express collagen alpha1(I); i.e., osteoblasts. At 4 months of age female mice were euthanized and bones harvested for further analysis.

There was a significant decrease in bone mineral density of the femur in conditional knockout mice (cKO) as measured using peripheral quantitative computer tomography in total bone (6% decrease in bone mineral density compared to controls; n=14 for controls and 8 for cKO, p<0.01), and in trabecular bone (12% decrease, p<0.05). Histomorphometry showed a 50% increase in osteoblast number adjusted to bone surface (27 ± 2 in cKO vs. 17 ± 1 in controls, n=5 for both, p<0.05), a 34% increase in osteoid surface adjusted to bone surface (p<0.01), a 15% decrease in the osteoid surface per osteoblast (p<0.005), and a 64% increase in mineralization lag time (p<0.05).

In summary, production of fibronectin by osteoblasts is required for a normal bone mineral density in female mice. In the absence of fibronectin production each osteoblast lays down less osteoid than a normal osteoblast, but due to the presence of a larger number of osteoblasts more osteoid gets laid down. This osteoid lags behind in its mineralization confirming in vitro data that fibronectin is required for normal mineralization by osteoblasts (Moursi A. et al. 1996 and Chen Q et al. 2006).

These data suggest that fibronectin production by osteoblasts via a feedback loop regulates osteoblast number, production of matrix and mineralization. Thus we were able to prove in vivo a role for locally produced fibronectin in modulating osteoblasts, and to show that fibronectin production by collagen alpha1(I) expressing osteoblasts mediates 6% of bone mineral density of the total bone and 12% of trabecular bone density in adult female mice.

Disclosures: A. Bentmann, None.

This study received funding from: AR0514769, AR46545, MTF.

1180

Mis-expressions of SOX9 During Skeletogenesis Lead to Accelerated Adipogenesis in Transgenic Mice. B. Liang¹, D. Chen^{*1}, B. Lee², G. Zhou¹.

¹Department of Orthopaedics, Case Western Reserve University, Cleveland, OH, USA, ²Department of Molecular and Human Genetics, Baylor College of Medicine, Houston, TX, USA.

During development mesenchymal cells can differentiate into adipocytes, chondrocytes, myoblasts, and osteoblasts as determined by different cell-type specific transcription factors. Among them SOX9 is a positive regulator for chondrogenesis while RUNX2 acts as a transcriptional activator essential for osteoblasts differentiation and chondrocytes maturation. RUNX2 also represses adipocytes differentiation and RUNX2 deficiency in chondrocytes showed enhanced adipogenesis. We have previously reported that SOX9 could severely inhibit RUNX2 function in the osteoblasts of a Col1a1-SOX9 transgenic mouse model in which SOX9 was specifically expressed in osteoblasts by a 2.3kb Col1a1 promoter. In this study to investigate the effects of SOX9 on mesenchymal stem cells (MSCs) differentiation, we isolated MSCs from the bone marrows of Col1a1-SOX9 transgenic mice and induced adipocytes and osteoblasts differentiation in vitro. While there were no significant differences in the number of osteoblast precursor cells by alkaline phosphatase assay between wild-type and transgenic mice, Col1a1-SOX9 MSCs exhibited decreased osteogenic differentiation by Alizarin Red staining. Interestingly Col1a1-SOX9 MSCs also displayed enhanced adipocytes differentiation by Oil Red-O staining. To directly investigate inhibitory effects of SOX9 on RUNX2 during chondrocytes hypertrophy, we have also generated a novel Col10a1-SOX9 transgenic mouse model in which SOX9 is specifically expressed in hypertrophic chondrocytes driven by a 10kb Col10a1 promoter. In monolayer culture of rib hypertrophic chondrocytes (HC) isolated from 6-day-old mice, expression of Col10a1, a downstream target of RUNX2, was decreased by 55% in Col10a1-SOX9 transgenic mice by quantitative RT-PCR. Additionally mineralized hypertrophic cartilage areas were significantly reduced by 10% (p<0.05) in 10-week-old proximal tibia of Col10a1-SOX9 transgenic mice by von Kossa staining. Furthermore in comparison with wild-type mice, Col10a1-SOX9 HC culture also displayed increased adipogenesis with more lipid droplets accumulation by Oil Red-O staining and higher expression levels of adipogenic genes including C/EBPα, PPARγ2, SCD1 and Glut4. In conclusion, our work suggests that during mesenchymal cells differentiation repression of RUNX2 function by SOX9 not only results in impaired osteogenesis and hypertrophic cartilage mineralization, it also leads to enhanced adipogenesis via relieving RUNX2 inhibition of adipocytes differentiation.

Disclosures: B. Liang, None.

1181

Molecular Interaction Between Bcl-xL and Bnip3 Determines the Cell Fate of Hypertrophic Chondrocytes. Y. Oshima¹, T. Akiyama^{*1}, M. Iwasawa¹, Y. Nagase¹, L. Hennighausen^{*2}, K. Nakamura¹, S. Tanaka¹.

¹Orthopaedic Surgery, The University of Tokyo, Tokyo, Japan, ²Laboratory of Genetics and Physiology, National Institutes of Health, Bethesda, MD, USA.

During endochondral ossification, chondrocytes undergo hypertrophic differentiation and die by apoptosis. The level of inorganic phosphate (Pi) elevates at the site of cartilage mineralization, and previous studies have proposed that Pi entry into hypertrophic chondrocytes may act as an apoptogen. The Bcl-2 family proteins, which consist of pro- and anti-apoptotic members, are major regulators of mitochondria-initiated apoptosis. To investigate their role in determining the cell fate of chondrocytes, we used chondrogenic ATDC5 cells that differentiate into hypertrophic state in the presence of insulin. When differentiated ATDC5 cells were treated with Pi, they mineralized the surrounding matrix and underwent rapid apoptosis as evidenced by nuclear condensation, Caspase-3 & 7 activation, and Lamin proteolysis. With this system, we analyzed the role of pro- and anti-apoptotic Bcl-2 members in chondrocyte apoptosis. Among 15 pro-apoptotic Bcl-2 members, 7 molecules increased their expression levels during the course of hypertrophic differentiation, and two in response to Pi stimulation. Of these, gene silencing of a proapoptotic BH3-only molecule bnip3 by RNA interference significantly suppressed Pi-induced apoptosis. Conversely, among anti-apoptotic members examined, overexpression of bcl-xL suppressed, and its knockdown promoted apoptosis. The susceptibility to apoptosis by bcl-xL knockdown was partially restored by simultaneous silencing of bnip3. Pi treatment markedly upregulated the protein level of Bnip3 without affecting Bcl-xL levels. Bnip3 was associated with Bcl-xL and attenuated its anti-apoptotic effect in chondrocytes. Immunohistological examination of murine growth plates revealed that Bcl-xL expressed uniformly in the growth plate chondrocytes, whereas Bnip3 expression was exclusively localized in the hypertrophic chondrocytes. Finally, we generated chondrocyte-specific bcl-xL knockdown mice using the Cre-loxP recombination system, and provided evidence that the hypertrophic chondrocyte layer was markedly shortened in those mice owing to massive chondrocyte apoptosis and that the mice exhibited dwarfism as a result. Furthermore, Bnip3 expression was decreased in hypertrophic chondrocytes in mice fed with a low phosphate diet, and the abnormalities in the growth plate were almost completely rescued. In summary, increase in Pi levels in hypertrophic zone causes upregulation of Bnip3 in chondrocytes, which binds to Bcl-xL and consequently impairs its anti-apoptotic effect, and finally causes apoptosis of the cells.

Disclosures: Y. Oshima, None.

1182

p63 Plays a Central Role in Cartilage Development by Directly Regulating Key Genes for Chondrogenesis. T. Ikeda¹, H. Kawaguchi², T. Saito², A. Kan², F. Yano¹, M. Ushita², Y. Kawasaki², K. Nakamura^{*2}, U. Chung¹. ¹Div of Tissue Engineering, Graduate School of Medicine, The Univ of Tokyo, Tokyo, Japan, ²Orthop Surg, Graduate School of Medicine, The Univ of Tokyo, Tokyo, Japan.

To understand the molecular network underlying chondrogenic differentiation, we identified the embryonic SOX6 promoter and its core enhancer CES6. Using the 4 x CES6 as bait for bio-panning of cartilage-derived phage display libraries, we identified a p53 family gene p63 as a CES6-binding transcription factor. Luciferase-reporter assay revealed that p63 transactivated not only SOX6 promoter, but also promoters of type II collagen (COL2A1) and SOX9. Among the three alternative splicing variants α , β and γ , p63 β exhibited the strongest activity. When multi-tissue expression was evaluated by real-time RT-PCR, p63 was mainly expressed in the tracheal cartilage, testis and prostate. Overexpression of p63 in non-chondrogenic cell line HeLa caused rapid induction of SOX6 and COL2A1 expressions, which were 2-3 fold greater than that by overexpression of SOX9, the representative transcription factor for chondrogenesis. Furthermore, retroviral overexpression of p63 into de-differentiated mouse costal cells after a long period of culture induced their re-differentiation to chondrocytes with enhanced Alcian blue staining and increased COL2A1, SOX6 and SOX9 mRNA levels. By combining luciferase-reporter assay, electrophoretic mobility shift assay, and chromatin immunoprecipitation, we identified the direct binding sites of p63 β in CES6 of SOX6 and in the proximal promoters of the SOX9 and COL2A1. The identified sequences were 1-2 bp different from the known p53 binding motif "RRRCWWGYYY". To further learn the endogenous function of p63, we investigated the skeleton of p63 knockout (p63^{-/-}) mouse embryos that exhibited severe short limb deformities. The expressions of SOX6, SOX9 and COL2A1 were rarely detectable in limb buds of p63^{-/-} embryos around E12-13 by whole mount in situ hybridization. Although a small cartilage was barely formed after E17, the SOX6, SOX9 and COL2A1 expressions were decreased compared to those in the wild-type littermates. Since BrdU uptake was comparable between p63^{-/-} and wild-type limb buds, the impaired cartilage development by the p63 deficiency may be due to a defect in chondrogenic differentiation, but not in proliferation, of mesenchymal cells. In conclusion, we identified a novel chondrogenic transcription factor p63 which may play a central role in cartilage development by directly regulating key genes for chondrogenesis like SOX6, SOX9 and COL2A1. Further understanding of molecular network related to p63 will herald a new era of cartilage regenerative medicine.

Disclosures: T. Ikeda, None.

1183

Atf4 Regulates Chondrocyte Proliferation and Differentiation by Direct Targeting Indian Hedgehog Transcription. W. Wang^{*}, X. Yang. Center for Bone Biology, Departments of Medicine and Pharmacology, Vanderbilt University, Nashville, TN, USA.

Indian Hedgehog plays a critical role in growth plate biology, and understanding the regulation of its expression is important for our understanding of endochondral bone formation. In studies on Atf4, a CREB-related transcription factor required for osteoblast differentiation and function (Yang & Karsenty, 2004), we noted evidence that Atf4 also affects cartilage biology. For example, Atf4-deficient (Atf4^{-/-}) mice are small in size with shorter limbs suggesting a defect in endochondral bone formation. We found that Atf4 whose cell-specificity is regulated at protein level (Yang et al., 2004) is expressed in chondrocytes by Western blot analysis using an antibody against Atf4. To determine whether Atf4 mutant mice display abnormalities of growth plate chondrocytes, we examined Atf4^{-/-} newborns in details by histological analysis, BrdU-labeling of dividing cells, and in situ hybridization. Compared to their wildtype counterparts, Atf4^{-/-} newborns exhibit 1) a delay in hypertrophic mineralization, 2) an expansion of the hypertrophic zone, 3) a decrease in BrdU positive proliferating chondrocytes, and 4) a dramatic decrease in the expression of the Indian Hedgehog (Ihh), a key regulator coordinating the chondrocyte proliferation and differentiation in endochondral bone formation in the prehypertrophic chondrocytes. Consistent with these in situ hybridization results, we also detected a decrease in Ihh mRNA expression in the Atf4^{-/-} chondrocytes. Based on these observations we hypothesize that Atf4 may play a central role in controlling chondrocyte proliferation and differentiation by direct targeting Ihh transcription. To test this hypothesis, we cloned a 5 kb promoter fragment of the Ihh gene from a BAC genomic DNA clone and made 5 Ihh promoter driven-luciferase reporter constructs that contain different lengths of the Ihh promoter sequences. Co-transfection assays using these reporter constructs and Atf4 expression vector showed that ATF4 indeed was able to transactivate the Ihh promoter with maximal observed activation in a reporter construct containing 742 base-pairs of the Ihh proximal promoter sequence, pIhh742-Luc. By visual scanning we found 9 putative Atf4 binding sites (A1 to A9) within this fragment. Gel retardation assays showed that Atf4 bound strongly to A9 and weakly to A1 to A8. Deletion of A9 led to a decrease in ATF4 transactivation activity on the pIhh742-Luc by 60%, suggesting that Atf4 activates the Ihh gene through A9. Taken together, our findings identify Atf4 as a physiological activator of Ihh gene and a regulator of chondrocyte proliferation and differentiation by directly targeting Ihh gene transcription.

Disclosures: W. Wang, None.

1184

Trps1 Transcription Factor Regulates Chondrocyte Hypertrophy and Perichondrial Mineralization through Repression of Runx2. D. Napierala¹, K. Sam^{*1}, R. Morello¹, T. Bertin^{*1}, Q. Zheng¹, T. Sibai^{*1}, R. Shivdasani^{*2}, B. Lee¹. ¹Molecular and Human Genetics, Baylor College of Medicine, Houston, TX, USA, ²Dana-Farber Cancer Institute and Harvard Medical School, Boston, MA, USA.

Mutations involving the TRPS1 gene cause tricho-rhino-phalangeal syndrome (TRPS) characterized by short stature, cone-shaped epiphyses, premature closure of growth plates and distinctive craniofacial appearance. During mouse skeletal development Trps1 is highly expressed in chondrogenic mesenchymal condensations, prehypertrophic chondrocytes, joint mesenchyme and perichondrium. Trps1 is a transcription repressor that contains nine zinc-fingers including GATA-type and Ikaros-type domains. To elucidate the role of Trps1 in endochondral bone formation, we analyzed Trps1 mutant mice deleted for the GATA DNA-binding domain (Trps1 Δ GT mice). Histological analysis of long bones of E18.5 embryos showed reduced size of bone marrow cavity due to expansion of cartilaginous part in homozygous Trps1 Δ GT mice. Morphometric analyses and RNA in situ hybridization demonstrated that zones of proliferating, prehypertrophic and hypertrophic chondrocytes are elongated in Trps1 Δ GT mice in comparison with WT littermates. Moreover, the Trps1 mutant mice demonstrated advanced mineralization of perichondrium. Both mineralization and chondrocytes maturation are regulated by the Runx2 transcription factor, therefore we tested the potential interaction of Trps1 and Runx2 in vitro. Cotransfection experiments demonstrated that Trps1 can repress the Runx2-mediated transactivation of the target reporter. Moreover, the C-terminal part of the Trps1 protein physically interacts with the runt domain of Runx2 in the GST pull-down assay. In conclusion, our data indicate that Trps1 regulates the growth plate mineralization and chondrocyte hypertrophy, and that could be partially through the repression of the Runx2 protein function.

Disclosures: D. Napierala, None.

This study received funding from: NIDCR.

1185

Identification of a Novel Chondrogenic Factor Sorting Nexin 19 Using a Real-Time Fluorescence Monitoring Cell Line ATDC5-S2RD5. A. Kan, T. Ikeda, T. Saito, U. Chung, H. Kawaguchi. Sensory & Motor System Medicine, Tissue Engineering, University of Tokyo, Tokyo, Japan.

To identify chondrogenic factors, the present study initially attempted to establish a monitoring system that could detect chondrogenic differentiation in a precise, noninvasive and real-time manner. For this purpose, we identified a 49 bp region including a SOX9 binding enhancer in intron 1 of type II collagen (COL2A1) gene, which was highly conserved among human, mouse and rat. We then established several lines of mouse chondrogenic ATDC5 cells stably transfected with four tandem copies of the 49 bp region cloned upstream of the COL2A1 promoter and DsRed2 fluorescence reporter gene. Among them, we selected a clone ATDC5-S2RD5 that fluoresced not only upon chondrogenic stimulation by insulin, but also by BMP-2, TGF β , and SOX9 / SOX6 co-transfection. This cell line was confirmed to show increases in COL2 mRNA level and Alcian blue staining by the stimulations above. We then created retroviral expression libraries from human tracheal cartilage and mouse embryos, and applied the ATDC5-S2RD5 cell line to the expression cloning for their screening. Among several genes that caused fluorescence in the system, sorting nexin (SNX) 19, a member of the SNX family, intracellular transportation proteins whose insufficiency causes skeletal dysplasia in human, exhibited strong fluorescence. Multi-tissue expression analysis by real-time RT-PCR confirmed the SNX19 expression in cartilage, and the subcellular localization was shown to be limited in the cytoplasm by immunostaining with an anti-myc-FITC antibody in HeLa cells overexpressing myc-SNX19. To learn the functional relevance of SNX19 to chondrogenic differentiation, we established ATDC5 cells and mouse primary costal cells overexpressing SNX19 or the siRNA through retroviral transfection. COL2 mRNA level by real-time RT-PCR and the promoter activity by luciferase-reporter assay were increased by the SNX19 overexpression, whereas they were decreased by the knockdown. Among signaling molecules ERK, p38 MAPK, JNK, Akt, I κ B, Smads and GSK3 β , the SNX19 overexpression enhanced phosphorylation of p38. SB203580, a specific inhibitor of p38, suppressed COL2 expression induced by the SNX19 overexpression. In conclusion, we established a real-time fluorescence monitoring cell line for chondrogenesis ATDC5-S2RD5. Using it, we identified a novel chondrogenic factor SNX19 which was a cytoplasmic protein related to the p38 signaling. Further screening of molecules using this monitoring cell line will elucidate the molecular network underlying chondrogenic differentiation.

Disclosures: A. Kan, None.

1186

Osteal Macrophages: Novel Regulators of Bone Formation. L. J. Raggatt¹, M. K. Chang^{*1}, K. A. Alexander^{*1}, J. S. Kuliwaba², N. L. Fazzalari², D. A. Hume^{*1}, A. R. Pettit¹. ¹Institute for Molecular Bioscience, Cooperative Research Centre for Chronic Inflammatory Diseases, University of Queensland, Brisbane, QLD, Australia, ²Institute of Medical and Veterinary Sciences and Hanson Institute, University of Adelaide, Adelaide, SA, Australia.

Resident tissue macrophages are an integral component of many tissues and are important in immunity, homeostasis and repair. Macrophages have been implicated in both bone destruction and osteophyte formation in bone diseases, suggesting these cells may also be associated with osteal tissues. We report here that resident tissue macrophages (referred to as OsteoMacs) are present on the endosteal surface of human trabecular bone. We have extended these observations using the murine tissue macrophage marker F4/80 to investigate fully the anatomical distribution of OsteoMacs in mouse bones. Immunohistochemistry demonstrated F4/80⁺ OsteoMacs are intercalated in bone lining tissues. OsteoMacs were also closely associated with bone remodelling units in the secondary spongiosa but are not TRAP⁺ mononuclear osteoclast precursors. Importantly, OsteoMacs formed a cell layer over bone forming osteoblasts (OB, collagen type 1⁺ and osteocalcin⁺) on growing cortical surfaces. Histomorphometric analysis showed that on cortical endosteal surfaces 75.9±5.3% of the OB bone surface was covered by a F4/80⁺ cell 'canopy', indicating that OsteoMacs and OB are intimately associated in vivo and that OsteoMacs may regulate OB function. We examined the effect of OsteoMacs on OB functional responses to elevated extracellular calcium (eCa²⁺), as eCa²⁺ is unique to the bone microenvironment and induces macrophage expression of the osteo-inductive molecule BMP-2. Using a co-culture system of macrophages with OB, in either direct contact or separated using transwells, we demonstrated that OB mineralization occurred in response to eCa²⁺ only in the presence of macrophages. At no stage were OB exposed to the classical differentiation agents ascorbate and beta-glycerolphosphate, yet macrophage enhanced OB mineralization occurred rapidly (7 days). Conditioned medium from eCa²⁺ stimulated macrophages also induced mineralization of OB cultures, indicating that macrophages produce a soluble factor that enhances OB mineralization. However addition of recombinant noggin or soluble BMPRI to co-cultures did not inhibit macrophage-induced OB mineralization, indicating that BMP-2 is not the osteo-inductive molecule. These observations suggest macrophages detect changes in eCa²⁺ and consequently produce soluble factor(s) that drive OB mineralization. We propose that OsteoMacs are an integral component of osteal tissues and play a novel role in bone homeostasis through regulating OB function and orchestrating bone formation.

Disclosures: L.J. Raggatt, None.

1187

Upregulation of Calcium-sensing Receptor Gene Expression by the Proinflammatory Cytokine, Interleukin-6: In Vivo and In Vitro Studies. L. Canaff^{*}, K. Schorr^{*}, G. N. Hendy. Medicine, McGill University, Montreal, PQ, Canada.

Increased calcium-sensing receptor (CASR) expression in parathyroid gland, thyroid C-cells, and kidney tubule leads to a decrease in the extracellular calcium set-point, thereby reducing parathyroid hormone (PTH) secretion and renal calcium reabsorption and increasing calcitonin secretion resulting in reduced circulating calcium levels. Hypocalcemia is common in critically ill patients with burn injury and/or sepsis. In such patients, circulating levels of cytokines are increased, with those of interleukin-6 (IL-6) being most marked. In the present study, we have examined the ability of IL-6 to affect the expression of the CASR. In vivo, in the rat, parathyroid, thyroid and kidney CASR mRNA levels increased after intraperitoneal injection of IL-6. Peak values occurred at 16h and remained elevated at 24h. This was associated with decreased circulating calcium and PTH levels. Further in vitro studies were conducted. The human CASR gene has two promoters (P1 and P2) yielding transcripts having alternative 5' untranslated regions (1A and 1B), but encoding the same receptor protein. Activities of human CASR P1 and P2 promoter/luciferase reporter constructs transfected into proximal tubule HKC cells and TT thyroid C-cells were stimulated ~2-3 fold by IL-6. The P1 construct contains 1439 bp upstream of the transcription start (+1), the 638 bp exon 1A and 242 bp of exon 2 before the ATG translation start site. Transfection of P1 deleted and mutated constructs into TT cells revealed that a Stat element within exon 1A accounted for ~70% of the induction by IL-6. Cotransfection of Stat1 (Y701F) or Stat3 (Y705F) dominant negative constructs markedly reduced (~70%) IL-6-stimulated upregulation of the P1 promoter. Pretreatment of TT cells with the MAPK pathway inhibitor U0126 (10 microM) led to significant loss (~30%) of IL-6 upregulation of all the P1 promoter constructs including an exon 1A Stat mutant. The P2 construct has 460 bp upstream of the transcription start (+1), the 259 bp exon 1B and 242 bp of exon 2 before the ATG translation start site. Transfection of P2 deletion constructs into TT cells showed that sequence within -341 to +220 is required for IL-6 responsiveness. There are no Stat elements in the P2 promoter or exon 1B but Sp1 elements are present at the transcription start site (+1). Cotransfection of Sp1 and/or Stat1 or Stat3 dominant negative constructs abolished IL-6 responsiveness of the P2 promoter. In conclusion, a variety of elements in the CASR gene promoters mediate transcriptional upregulation by IL-6, with Stat and MAPK independently and additively controlling promoter P1, and Stat regulating promoter P2 via Sp1.

Disclosures: L. Canaff, None.

1188

The Role of Caspase-3 in the Anabolic Actions of PTH in Bone. J. Yamashita¹, D. Yang¹, K. Yamashita^{*1}, E. T. Keller², L. K. McCauley¹. ¹University of Michigan School of Dentistry, Ann Arbor, MI, USA, ²University of Michigan Medical School, Ann Arbor, MI, USA.

Caspase-3 is a crucial component in the signaling of programmed cell death, cell survival, and cell cycle in a variety of cells. It has been reported that caspase-3 functions in osteogenic differentiation of bone marrow stromal cells and that the activation of caspase-3 is essential for osteoclast differentiation. Intermittent PTH is a powerful bone anabolic agent, but the exact mechanisms of PTH action are unclear. It has been hypothesized that PTH may extend the life span of osteoblasts by suppressing apoptosis and the long-living osteoblasts would contribute to enhanced mineral matrix deposition. Because caspase-3 is a pro-apoptotic factor, suppression of caspase-3 could enhance the anabolic effect of PTH in bone. However, the role of caspase-3 in PTH actions is not known. In this study we tested the hypothesis that inhibition of caspase-3 enhances anabolic actions of PTH in bone. Caspase-3 deficient mice were genotyped and the expression of caspase-3 protein verified by Western blotting of spleen lysate. Histomorphometric analysis of the tibiae of day-21 mice showed no significant difference in bone area (%) between caspase-3 wild type (+/+) and knockout (-/-) mice. Calvarial osteoblasts were isolated from caspase-3 +/+ and -/- mice. Cell enumeration showed no difference between caspase-3 +/+ and -/- osteoblasts over the 9 day culture period. To characterize apoptosis of osteoblasts, cells were treated with staurosporine and relative cell numbers versus control were assessed. Caspase-3 -/- osteoblasts ex vivo showed more resistance to staurosporine-induced cell death than +/+, suggesting an important role of caspase-3 in osteoblast survival. To determine the role of caspase-3 in bone formation in response to PTH, daily administration of PTH (50µg/kg/day) was performed on +/+ and -/- mice from day-4 to day-21 of age. Peripheral quantitative computed tomography and histomorphometric analyses showed that both caspase-3 +/+ and -/- mice responded to PTH with substantially increased bone area when compared to vehicle-control groups. Such increased bone mass was more significantly pronounced in caspase-3 -/- mice than +/+ (p<0.05). To further determine whether the inhibition of caspase-3 augments anabolic effect of PTH in osteoporotic bone, caspase-3 +/+ and -/- mice (9 weeks old) were ovariectomized and PTH (80µg/kg/day) administered for 21 days. Daily PTH administration significantly increased bone mass in both genotypes with greater anabolic effect in -/- than +/+ bone. These results suggest that the inhibition of caspase-3 may enhance the anabolic actions of PTH in bone. Caspase-3 could be a target for the prevention and treatment of osteoporosis in conjunction with PTH therapy.

Disclosures: J. Yamashita, None.

1189

Dissection of the Mechanisms of PTH-mediated Inhibition of Sodium-dependent Phosphate Transport Using a Long-acting PTH(1-28) Analog. S. Nagai, M. Okazaki^{*}, J. T. Potts, H. Jüppner, T. J. Gardella. Endocrine Unit, Massachusetts General Hospital and Harvard Medical School, Boston, MA, USA.

PTH reduces the reabsorption of inorganic phosphate (Pi) largely through its effects on sodium-dependent phosphate transporters (NaPi-IIa and NaPi-IIc) in renal proximal tubule (PT) cells. The mechanisms by which PTH regulates transporter function in these cells are not clear, particularly in terms of the signaling and protein-trafficking pathways utilized. We now investigated these processes by utilizing a new PTH analog, [Ala^{1,2}, Aib³, Gin¹⁰, Har¹¹, Trp¹⁴, Arg¹⁹]hPTH(1-28)NH₂ {M-PTH(1-28)} that binds to the PTH receptor more stably than does PTH(1-34). The capacity of the analog to inhibit phosphate uptake in opossum kidney (OK) cells, a model PT cell line, was first assessed by a routinely used 4-hour incubation protocol. M-PTH(1-28) inhibited Pi uptake to the same extent (~60%) as did PTH(1-34) (ligand concentrations = 1x10⁻⁷ M). Phosphate transport was then assessed at various time points after incubating the cells with ligand for only 10 minutes followed by extensive rinsing before measuring Pi uptake. Using this protocol, Pi uptake was maximally inhibited by PTH(1-34) two hours after wash-out and returned to basal by 24 hours. In cells treated with M-PTH(1-28), Pi uptake was again maximally inhibited at 2 hours, but remained suppressed for at least 24 hours. Analysis of cAMP production showed that the response to PTH(1-34) diminished to basal by 1 hour after wash-out, whereas that of M-PTH(1-28) continued for at least 6 hours. PTH(1-34) is known to induce the removal of NaPi-IIa from the surface of OK cells; confocal microscopy showed that whereas NaPi-IIa surface expression was restored by 24 hours in cells treated with PTH(1-34), it was completely absent in cells treated with M-PTH(1-28). To explore these differences in ligand activity in vivo, PTH(1-34) and M-PTH(1-28) were injected subcutaneously into mice, and serum Pi was measured. Both ligands suppressed Pi levels maximally at 2 hours, but where Pi levels returned to normal by 4 hours in PTH(1-34)-treated mice, they remained suppressed for 6 hours in M-PTH(1-28)-treated mice. The data show that persistent binding of a PTH agonist to the PTH receptor in renal PT cells can lead to sustained cAMP signaling and sustained down-regulation of NaPi-IIa. The mechanisms by which PTH regulates NaPi-IIa expression and function in PT cells are incompletely understood, but the formation of cAMP appears to be a key signaling event. Moreover, the recovery process occurs more slowly than expected, particularly when assessed with the new analog, M-PTH(1-28). This new PTH analog should be useful in exploring the underlying mechanisms further.

Disclosures: S. Nagai, None.

1190

Analysis of PTH-PTH Receptor Interaction Mechanisms Using a New, Long-Acting PTH(1-28) Analog Reveals Selective Binding to Distinct PTH Receptor Conformations and Biological Consequences In Vivo. M. Okazaki*, S. Nagai, T. Dean*, J. T. Potts, T. J. Gardella. Endocrine Unit, Massachusetts General Hospital, Boston, MA, USA.

The PTH/PTHrP receptor (PTHR) is likely to exist in multiple protein conformations. This raises the possibility that different PTH or PTHrP ligands could bind selectively to distinct PTHR conformations and thereby produce different biological effects. Based on recent radioligand binding data, we hypothesize that the PTHR can adopt a novel PTHR conformation, termed R0, that is uncoupled from heterotrimeric G protein but yet can form highly stable complexes with certain PTH ligands, including PTH(1-34). In contrast, PTHrP(1-36) and M-PTH(1-15) (M = Aib1,3,Gln10,Har11,Ala12,Trp14), bind only poorly to R0, and instead bind predominantly to PTHRs in a G protein-coupled conformation (RG). We further hypothesize that R0 can isomerize to RG, and thus contribute to ligand activity. For example, stable binding of a ligand to R0 could result in signaling responses in cells long after the initial ligand-binding event. To test these hypotheses, we investigated the structural features in the ligand and receptor that underlie stable binding to R0 in vitro, and we explored the biological relevance of such binding in vivo. One analog to emerge from the studies was [Ala1,12,Aib3,Gln10,Har11,Trp14,Arg19]hPTH(1-28)NH2 (M-PTH(1-28)). In R0 binding assays, performed using membranes expressing the rat PTHR, 125I-PTH(1-34) tracer radioligand, and in the presence of GTPγS, M-PTH(1-28) bound with 80-fold higher affinity than did PTH(1-34), and more than 200-fold higher than did M-PTH(1-15) or unmodified PTH(1-28). In ROS17/2.8 cells, M-PTH(1-28) produced a more prolonged cAMP response than did the latter three peptides. When injected subcutaneously into mice (50 nmole/Kg), M-PTH(1-28) produced a more prolonged hypercalcaemic response than did PTH(1-34): blood Ca++ induced by PTH(1-34) peaked at 2 hours and returned to vehicle control at 4 hours; whereas, that induced by M-PTH(1-28) peaked at 3 hr, and did not return to control until at least 6 hours. Overall, the studies support the hypothesis that the PTHR can form a stable R0 conformation, and that the extent to which a ligand (e.g. PTH or PTHrP) binds this conformation can determine the biological actions of that ligand in vivo. The capacity of a ligand to bind to R0 requires interaction to the both the juxtamembrane and N-terminal regions of the PTHR, because both the "M" modifications and the 16-28 segment of M-PTH(1-28) are required. Further exploration of the conformational states possible for the PTHR should improve our understanding of how this receptor functions in normal and pathological physiology.

Disclosures: M. Okazaki, Chugai Pharmaceutical Co., Ltd. 2.

This study received funding from: NIH DDK 11794.

1191

Parathyroid Hormone Expression Is Negatively Regulated by FGF23 in Primary Bovine Parathyroid Cells. T. Krajisnik¹, P. Björklund², R. Marsell², O. Ljunggren¹, G. Akerstrom², K. B. Jonsson², G. Westin², T. E. Larsson¹. ¹Uppsala University Hospital, Dept. of Medical Sciences, Uppsala, Sweden, ²Uppsala University Hospital, Dept. of Surgical Sciences, Uppsala, Sweden.

Fibroblast Growth Factor-23 (FGF23) is a circulating protein that regulates serum levels of inorganic phosphate as well as 1,25(OH)2D3. FGF23 is elevated in chronic kidney disease (CKD), as a response to the prevailing hyperphosphatemia. In addition, high serum FGF23 in CKD is a predictor of future secondary hyperparathyroidism, although the reason for this association is unknown. The objective of the current study was to investigate the effect of FGF23 on parathyroid glands in vitro. For this purpose, we used primary isolates of bovine parathyroid cells. Recombinant FGF23 was produced by transient transfection of the hFGF23(R176Q)-pcDNA3.1-V5-His-TOPO plasmid into COS-7 cells. Conditioned serum-free medium was collected and analyzed for intact FGF23 concentration using an intact FGF23 ELISA. Control medium was obtained by transfection of the pcDNA3.1(+) expression vector. Importantly, we found that Klotho, a FGF23 receptor co-factor, was abundantly expressed in bovine parathyroid cells, as detected by RT-PCR. FGF23-stimulation of parathyroid cells at concentrations of 400-2000 pg/mL was followed by a 2-7-fold increase in Egr-1 mRNA level, a marker of FGF23 signaling (p<0.05). FGF23 potently and dose-dependently decreased the PTH mRNA level within 12 hours in the concentration range 400-2000 pg/mL (p<0.01). In agreement, FGF23 dose-dependently decreased PTH protein secretion into conditioned media at concentrations 700-2000 pg/mL (p<0.05). Finally, FGF23 did not alter cell viability or apoptosis, as determined by flow cytometry analysis. A small but significant increase in cell proliferation was observed (p<0.001), as measured by tritium-labelled thymidine incorporation. We conclude that FGF23 is a potent negative regulator of PTH mRNA expression and protein secretion. Our data indicate that increased FGF23 levels in CKD may, in part, inhibit secondary hyperparathyroidism. This potentially defines a novel function of FGF23 in CKD, besides the previously established role in ameliorating hyperphosphatemia by promoting renal Pi excretion.

Disclosures: T. Krajisnik, None.

1192

Geranylgeranylation Promotes Osteoblast Survival and Is Involved in Anti-apoptotic Effects of PTH. T. Yoshida*, P. H. Stern. Department of Molecular Pharmacology and Biological Chemistry, Northwestern University Feinberg School of Medicine, Chicago, IL, USA.

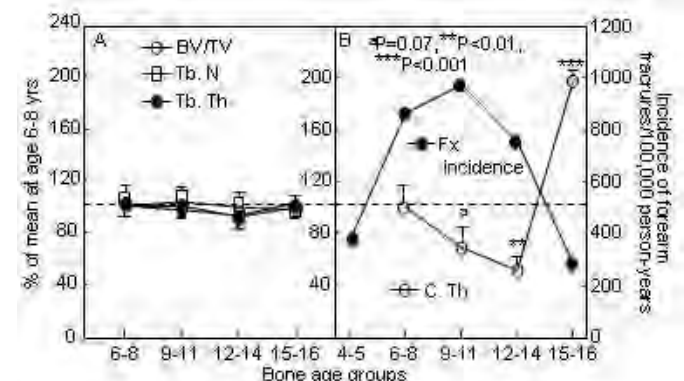
We have previously described a Gα12/Gα13-RhoA-phospholipase D pathway in osteoblastic cells, and found that the pathway is stimulated by parathyroid hormone (PTH). It was therefore of interest to determine the role of the pathway in osteoblast cell function and in parathyroid hormone action on osteoblasts. Studies in other tissues indicate that the pathway is involved in cell survival and influences the apoptotic cascade. Covalent attachment of geranylgeranyl moieties from the donor geranylgeranylpyrophosphate (GGPP) leads to the activation of RhoA, and several studies show that reducing the cellular pool of GGPP by inhibition of HMG-CoA reductase leads to apoptosis. These reports led us to investigate whether the pathway, and specifically geranylgeranylation, could be involved in osteoblast survival and in the anti-apoptotic effects of PTH. We used the geranylgeranyl group donor geranylgeraniol (GGOH) and the geranylgeranyltransferase inhibitor GGTI-2166 as tools to study this. Preosteoblastic MC3T3-E1 cells were seeded at a density of 250,000 cells/well in 6-well plates, and serum starved for 24 hr, a stimulus leading to apoptosis and elevated caspase-3 activity, a central step in the apoptosis cascade. Subsequent treatment with PTH for 6 hr markedly decreased caspase-3 activity. Effects were seen at PTH concentrations as low as 10 pM. In contrast to the effects of short-term exposure, overnight treatment with PTH was not effective. The response to PTH was density-dependent and was attenuated in higher density cultures. GGOH (10 μM) mimicked the effect of PTH, decreasing caspase-3 activity in serum-starved cells. The effects of PTH or fetal bovine serum to decrease caspase-3 activity were antagonized by GGTI-2166, 10 and 30 μM. In cultures of primary mouse osteoblasts, PTH promoted cell survival after serum starvation, as measured by trypan blue exclusion, and the geranylgeranyltransferase inhibitor GGTI-2166 antagonized the protective effect of PTH. These results suggest that GGPP is critical for osteoblast survival. In addition to direct effects through Gα12/Gα13-coupled receptors, we speculate that the PTH effect on survival and on PLD could be mediated through increases in a cellular pool of GGPP.

Disclosures: T. Yoshida, None.

1193

Decreases in Cortical Thickness, and not Changes in Trabecular Microstructure, Are Associated with the Pubertal Increase in Forearm Fractures in Girls. S. Kirmani, L. McCready*, M. Holets*, P. R. Fischer*, B. L. Riggs, L. J. Melton, S. Khosla. Mayo Clinic, Rochester, MN, USA.

We previously demonstrated that forearm fractures in girls peak between age 8 and 11 years, during the time of maximal pubertal growth (JAMA 2003;290:1479). The structural basis for this increase is unclear but may be related to the transient cortical thinning and increased porosity related to increased calcium demands during maximal growth. It is also possible that there may be alterations in trabecular microstructure during puberty that reduce bone strength. To address these possibilities, we used high-resolution 3D pQCT (XtremeCT, Scanco, voxel size ~90 microns) to assess trabecular and cortical bone parameters in healthy girls aged 7-16 yrs (n=46) without a prior history of fracture. Subjects were classified into 4 groups based on bone age (BA) assessed using hand and wrist x-rays: Group I (BA, 6-8 yrs, n = 8), Group II (BA, 9-11 yrs, n = 15), Group III (BA, 12-14 yrs, n = 13), and Group IV (BA, 15-16 yrs, n = 10). There were no significant differences (P > 0.2) in trabecular parameters (bone volume/total volume, BV/TV; trabecular number, Tb.N; or trabecular thickness, Tb.Th) through the course of puberty, expressed as a percentage of the mean value in Group I (Panel A of figure). By contrast, there were marked but transient decreases in cortical thickness (C.Th) which decreased by 50% during puberty (P < 0.005 for group I vs. group III, P = 0.07 for group I vs. group II) before rising sharply by 89% at the end of puberty (P < 0.005 for group I vs. group IV). This pattern was a mirror image of the previously described rise in distal forearm fractures in this population (Panel B), and there were similar changes in cortical vBMD (data not shown).



Our findings, which represent the first direct assessment of trabecular and cortical structure during growth in children, thus demonstrate that: (1) perhaps surprisingly, puberty is associated with minimal changes in trabecular microstructure, suggesting that these parameters may be established very early in life; and (2) the transient increase in distal

forearm fractures during growth in girls is largely explained by temporary cortical thinning (and perhaps increased cortical porosity). Further studies are needed to define the mechanisms underlying these alterations in cortical parameters as well as preventive measures that may attenuate these changes and, hence, distal forearm fractures during growth.

Disclosures: S. Kirmani, None.

This study received funding from: Thrasher Research Fund.

1194

Vitamin D Receptor Gene Polymorphisms Modulate the Musculo-Skeletal Response to Vitamin D Supplementation in Healthy Girls. A. Arabi¹, Z. Mahfoud^{1,2}, L. Zahed³, J. Maalouf¹, M. Nabulsi⁴, M. Choucair¹, G. El-Hajj Fuleihan¹. ¹Calcium Metabolism and Osteoporosis Program, American University of Beirut, Beirut, Lebanon, ²Epidemiology and Population Health, American University of Beirut, Beirut, Lebanon, ³Pathology and Laboratory Medicine, American University of Beirut, Beirut, Lebanon, ⁴Pediatrics, American University of Beirut, Beirut, Lebanon.

Associations between Vitamin D receptor (VDR) genotypes and bone mass have been reported. Our group showed a beneficial effect of vitamin D (Vit D) supplementation on bone mass in girls¹. This effect was mediated by changes in height, bone area and lean mass¹. Whether the musculo-skeletal response to Vit D is modulated by polymorphisms in VDR gene has not been previously assessed.

The relationship between VDR gene polymorphisms and the musculo-skeletal response to Vit D supplementation was evaluated in 168 girls (10-17 years), randomly assigned to placebo (n=55), Vit D3 1400 IU/week (n=58) or Vit D3 14000 IU/week (n=55), for one year¹. Calcium intake was similar between groups¹.

VDR genotypes were determined using BsmI, TaqI and ApaI restriction enzymes. Bone mass at the spine (LS), hip, forearm (FA) and total body (TB), and lean mass were measured by DXA at baseline and at one year.

Because the response to Vit D3 was not dose dependent¹, Vit D3 groups (low and high dose) were combined in the analyses. VDR gene polymorphisms using BsmI restriction enzyme were associated with percent changes in height, LS BMC, femoral neck BMC (FN BMC) and TB BMC, FN area, TB area, TB BMD and FA BMD in the Vit D3 group but not in the placebo group. The least increments were observed in the BB genotype (Table). There was no difference in changes in lean mass between genotypes. The relationship between VDR genotypes and changes in BMD and BMC remained significant after adjustment for menarcheal status, changes in lean mass, in height or in bone area.

Similar relationships between skeletal response and VDR were obtained with TaqI restriction enzyme. The least increments were observed in the tt genotype. No such relationship was observed when VDR genotypes were determined using ApaI restriction enzyme.

In conclusion, polymorphisms in the VDR gene may modulate the skeletal response to vitamin D supplementation in healthy adolescent girls.

¹ El-Hajj Fuleihan et al, J Clin Endocrinol Metab, 2006.

Table showing the percent changes BMC in placebo or Vitamin D3 group, according to VDR genotype

	Placebo			Vitamin D3 group		
	BB	Bb	bb	BB	Bb	bb
FN BMC	-0.06±8.6	3.9±6.3	5.8±7.3	1.4±5.7*	4.7±7.7	6.9±8.5*
LS BMC	10.0±9.6	11.0±8.2	10.0±8.7	8.0±7.4*#	14.1±11.9*	16.4±10.7#
TB BMC	7.8±9.0	6.1±7.0	7.6±7.0	3.7±7.1#*	9.8±8.6*	12.4±8.7#

*, # Significant differences between the two genotypes by ANOVA and post-hoc analyses.

Disclosures: A. Arabi, None.

This study received funding from: Nestle Foundation; Merck KGaA.

1195

Growth and Response to Active Vitamin D and Phosphorus Treatment Is Highly Associated with Haplotype of the Vitamin D Receptor Promoter in X-linked Hypophosphatemic Rickets. F. Jehan, M. Nguyen*, O. Walrant-Debray*, C. Sinding*, M. Garabedian*. Hopital Saint Vincent de Paul, Inserm U561, Paris, France.

X-linked hypophosphatemic rickets is a monogenic disease characterized by bone deformities, growth retardation, dental anomalies, urinary phosphate wasting, low serum 1,25-dihydroxyvitamin D3 and hypocalciuria. Treatment with phosphorus and 1-hydroxylated forms of vitamin D cures, or prevents, bone deformities, and improves calcium/phosphorus status. However, its beneficial effect on growth retardation remains controversial, mainly due to wide variations of individual expressivity of the disease. We have hypothesized that natural genetic variations (polymorphisms and/or haplotypes) could explain some of the variability in growth impairment and treatment responses. We considered variants in the promoter region of the vitamin D receptor (VDR) gene as a good target, since we found association between VDR promoter variants and growth in healthy adolescents girls (d'Alesio et al., Hum Mol Genet, 2005 14: 3539-48), and since variants influencing VDR expression are likely to influence responses to vitamin D treatment in hypophosphatemic patients.

Methods. We analyzed the VDR promoter haplotype structure in a large cohort of hypophosphatemic rickets patients treated since early childhood with phosphate and 1-hydroxylated vitamin D derivatives (n=52 including 16 patients now adults), that we have clinically and biologically followed from diagnosis on.

Results: 1) A clear association was observed between adult height (expressed as SD scores) and VDR Hap1 haplotype (Hap1+: -0.82±0.40, Hap1-: -2.59±0.26; mean ± SE; p<0.004). The Hap1 effect on growth was highly significant as early as 4 years of age (p<0.004). It was independent of the gender, vitamin D and phosphate daily dosages, and age at onset of treatment. No such effect was observed by breaking the cohort with the two other major haplotypes of the VDR promoter.

2) Urinary calcium excretion increased with the 1-(OH)D dosage in all patients during childhood. But the sensitivity to treatment was clearly Hap1 dependent. With 1 microgram per day of 1-OH vitamin D, the mean urinary calcium/creatinine ratio for each patient was normal in Hap1+ children (0.36±0.20 mmol/mmol, n=26) and already elevated in Hap1- children (0.76±0.35, n=10, mean ± SD, p<0.0001 vs. Hap1+). Other biological values were similar in the two Hap1 groups (serum calcium, phosphorus, 25-(OH)D, and 1,25-(OH)2D).

Conclusion: variations in the clinical and biological expressivity of the hypophosphatemic rickets may be explained, at least in part, by natural genetic variants on the VDR promoter that may regulate the VDR protein expression, and hence the patient sensitivity to vitamin D treatment.

Disclosures: F. Jehan, None.

1196

Sequencing of Collagen I in Three Patients with Multiple Fractures of Unknown Aetiology Reveals Novel Mutations Causing Osteogenesis Imperfecta with Normal to High BMD. K. Lindahl*, H. Brändström, A. Kindmark*, Ö. Ljunggren*. Medical Sciences, Endocrinology, Uppsala, Sweden.

Osteogenesis imperfecta (OI) is a heterogeneous genetic disorder with an incidence of approximately 1/15 000 individuals. In general, patients with OI have low Bone Mineral Density (BMD) and an increased susceptibility to fracture. Clinical features of OI also include blue sclerae, dentinogenesis imperfecta, deafness and hyper mobile joints. Phenotypes range from mild to lethal. In more than 90% of cases the disorder is due to a dominant mutation in one of the two genes that encode collagen type I, COL1A1 and COL1A2. Mild OI is usually the result of a mutation that leads to a premature stop codon, which subsequently leads to too little, but structurally normal collagen. In contrast, the more severe OI phenotypes are often de-novo mutations leading to an exchange of a glycine residue for an amino acid with a bulkier side chain. Patients with multiple fractures, but no other clinical signs of OI, pose a diagnostic problem, especially when BMD is normal. It is debated whether collagen sequencing should be performed as a routine in these cases.

In this study, we have sequenced COL1A1 and COL1A2 in three patients who had suffered more than 15 fractures, but had a BMD in the normal to high range. None of the patients had any clinical signs of OI and despite extensive investigation neither of the patients had a clinical diagnosis explaining their fragile bones.

DNA was extracted from whole blood using a commercially available kit. Exons and flanking intron sequences of COL1A1 and COL1A2 were sequenced using standardised sequencing with ABI3130XL using 110 primer pairs.

Three novel mutations were found: Asp1219Asn, was detected at the splice site of the carboxy-terminal propeptide of the COL1A1 gene, Gln1206Termination in COL1A1 and Gly757Ser in COL1A2. Control sequence ruled out the possibility of a naturally occurring polymorphism and the mutations were not previously reported in the collagen database.

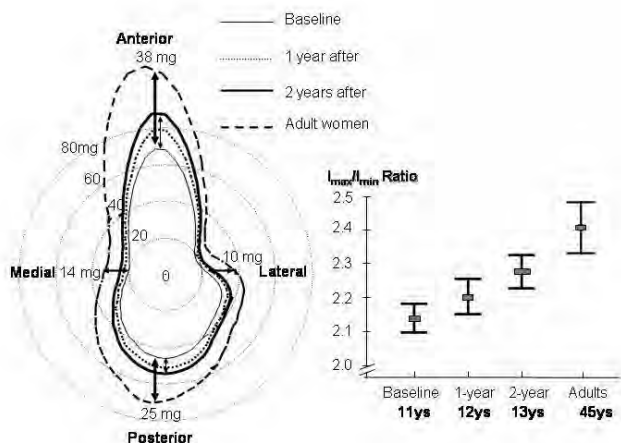
These findings indicate that sequencing of collagen type I is valuable in patients with multiple fractures of unknown aetiology. Furthermore, BMD is not necessarily low or strictly correlated to bone strength in OI.

Disclosures: K. Lindahl, None.

1197

Bone Traits Are Determined Early in Life but Adapt During Growth to Accommodate Local Loading Circumstances. Q. Wang¹, S. Cheng², E. Seeman¹. ¹Medicine/Austin Health, University of Melbourne, Melbourne, VIC, Australia, ²Department of Health Sciences, University of Jyväskylä, Jyväskylä, Finland.

Bone structure determines the loads tolerated but the loads imposed also determine its structure. We hypothesized that: 1) the position of an individual's bone trait is established prior to puberty and remained in the position, 2) bone shape changes to accommodate prevailing loads, 3) bone strength and the loads imposed increase in proportion with age so their ratio is independent of age. In 258 10-13yrs healthy girls, peripheral quantitative computed tomography (Stratec XCT-2000) was used to determine the cross sectional structure of the left tibial shaft and muscle size during 2 years. Mothers of 108 of these girls were also studied. Height, lower leg length, bone traits such as total tibial cross sectional area (CSA) and cortical thickness increased with age but trait variances - the magnitude of the dispersion around the age-specific mean did not. The relative position of bone trait, whether at the 5th, 50th or 95th percentile, was established prior to puberty. In 60-70% individuals their bone traits remained in their percentile after 2 years; the other 30-40% individuals their bone trait's percentile increased or decreased. The change in the percentile of muscle CSA or in lean tissue mass (from DXA) correlated with the change in the percentile of bone traits ($r=0.5-0.6$). Periosteal apposition added more than twice the amount of bone anteriorly (18 mg) and posteriorly (10 mg) than medially (5 mg) and laterally (4 mg) increasing tibial ellipticity. Bending strength of tibial shaft thus increased more in the antero-posterior (Imax) than medio-lateral direction (Imin); the ratio Imax/Imin increased by 7% over the 2 years ($p<0.001$) and was 13% higher in the mothers than in girls at baseline ($p<0.001$) (Fig). Imax increased with age and correlated with the estimated load imposed (tibial length X weight) ($r=0.73$). The ratio Imax/estimated load was independent of age reflecting proportional age-related increases in the structural determinants of bone strength and the load imposed. In conclusion, we infer that skeletal structure in one individual as a result of genetic variability is already expressed before puberty. In this setting, skeletal development is adaptive throughout growth so that load applied modifies bone shape accommodating that load efficiently.



Disclosures: Q. Wang, None.
This study received funding from: Academy of Finland.

1198

Extraction Socket Healing in Pediatric Patients Treated with Pamidronate: A Retrospective Chart Review. C. J. Chahine^{*1}, M. Cheung^{*2}, T. W. Head^{*1}, S. Schwartz^{*3}, F. Rauch², F. H. Glorieux². ¹Oral and Maxillofacial Surgery, McGill University, Montreal, PQ, Canada, ²Genetics Unit, Shriners Hospital for Children, Montreal, PQ, Canada, ³Pediatric Dentistry, Montreal Children's Hospital, Montreal, PQ, Canada.

Osteonecrosis of the jaw (ONJ) has been described in adults who have received bisphosphonates, but its occurrence in children has not been reported. In the present study we evaluated whether ONJ has occurred in any of the pediatric patients who received pamidronate therapy at the Shriners Hospital for Children in Montreal. 338 patients had received pamidronate treatment. Dental follow up data were obtained on 49 patients (16 females) who had undergone tooth extraction (age at last follow up: 2 to 24 years, mean 12.8 years). The indication for pamidronate use included osteogenesis imperfecta (N = 46), fibrous dysplasia (N = 1), hypercalcemia (N = 1), and muscular dystrophy (N = 1). A total of 181 teeth had been extracted (145 primary teeth, 36 permanent teeth). 19 of the teeth required surgical extraction with flap elevation, bone removal, and tooth sectioning. Prophylactic antibiotic use was implemented in 10 patients. The indication for dental extraction was impacted teeth (N = 16), fractured teeth (N = 11), decay or odontogenic abscess (N = 38), retained primary teeth (N = 67), and ectopic eruption or pre-orthodontic therapy (N = 49). The mean cumulative dose of pamidronate prior to dental extraction was 40.6 mg/kg. The mean duration of pamidronate treatment prior to dental extraction was 4.5 years. 100 teeth were extracted during active treatment. The mean interval of time between the last pamidronate dose prior to dental extraction and first pamidronate dose following dental extraction was 55 and 61 days, respectively. 81 teeth were extracted an average of

1.6 years after the last dose of pamidronate. All of the patients were followed post-operatively with a mean of 2.6 years (range: 1 month to 10 years). Adequate healing as judged by the treating dentist's clinical evaluation was noted on post-operative visits in all patients. There was no evidence of delayed healing, exposed bone, or ONJ in any patient. In conclusion, we did not detect any cases of ONJ in this large pediatric patient population with long-term pamidronate exposure.

Disclosures: C.J. Chahine, None.

1199

Large-scale Analysis of Association Between Polymorphisms in the LRP-5 and -6 Genes and Bone Mineral Density and Fracture. J. B. J. van Meurs^{*1}, T. A. Trikalinos^{*2}, S. H. Ralston^{*3}, F. Rivadeneira^{*1}, J. P. A. Ioannidis^{*2}, A. G. Uitterlinden^{*1}, The Genomos Study Group^{*4}. ¹Internal Medicine, Erasmus Medical Center, Rotterdam, The Netherlands, ²Hygiene and Epidemiology, University of Ioannina, Ioannina, Greece, ³Rheumatic Diseases, University of Edinburgh, Rotterdam, United Kingdom, ⁴For more information: Http://www.genomos.eu/, The Netherlands.

Objective: Mutations in the low-density lipoprotein receptor-related protein 5 (LRP5) gene cause rare syndromes characterized by altered bone mass. Common LRP5 variants may affect bone mass and fracture risk, but the magnitude of the association has been debated. The objective of this study was to generate large-scale evidence on whether common variants of LRP5 and its close homologue LRP6 are associated with bone mineral density (BMD) and fracture-risk.

Methods: We performed a prospective meta-analysis of participant-level data from 18 centers on 37,760 men and women. We assessed the association of common LRP5 (Val667Met, Ala1330Val) and LRP6 (Ile1062Val) variants with lumbar spine (LS) BMD, femoral neck (FN) BMD, all prevalent fractures, and prevalent vertebral fractures. Genotyping was standardized across centers. Unadjusted analyses with generalized linear mixed models allowed for random effects across center-gender strata. Adjustments for sex, age, weight, height, menopausal status and hormone replacement therapy were also performed. Fracture risks were also adjusted for BMD.

Results: LS-BMD decreased by 0.02 g/cm² per 667Met allele copy ($p=3.3 \times 10^{-8}$), and by 0.014 g/cm² per 1330Val copy ($p=2.6 \times 10^{-9}$). The corresponding decrease for FN-BMD was 0.011 and 0.008 g/cm² ($p=5.0 \times 10^{-6}$ and $p=3.8 \times 10^{-5}$). For both LS and FN this corresponds to approximately 0.1 SD difference in BMD. For fractures, the strongest association was seen for vertebral fracture risk (OR=1.26 [95%CI: 1.05-1.24] and 1.12 [95%CI: 1.01-1.24] per allele for Val667Met and Ala1330Val, respectively), but an effect was present also for all fractures (OR 1.14 [95%CI: 1.05-1.24] and 1.06 [95%CI: 1.01-1.12] per allele, respectively). The fracture risks were partly attenuated by adjustment for differences in BMD. Haplotype analysis of the two LRP5 variants indicated independent effects of both variants on BMD. The LRP6 Ile1062Val polymorphism was not associated with any of the phenotypes.

Conclusions: In this very large genetic association study of more than 37,000 subjects we show that common variants of the LRP5-gene are consistently associated with both BMD and fracture risk across different Caucasian populations. The magnitude of the effect is modest, but highly significant. LRP5 is the first gene to reach a genome-wide significance level for a phenotype related to osteoporosis.

Disclosures: J.B.J. van Meurs, None.
This study received funding from: European Commission, grant QLK6-CT-2002-02629.

1200

Serum DHEA Is Independently of Estradiol and Testosterone Related to Incident Fractures in Elderly Men - The MrOS Sweden Study. C. Ohlsson¹, L. Vandenput¹, A. Holmberg², H. Mallmin³, E. Orwoll⁴, A. Oden^{*5}, A. Eriksson¹, M. Lorentzon¹, M. Stenstrom^{*1}, M. K. Karlsson², Ö. Ljunggren⁶, F. Labrie^{*7}, D. Mellström¹. ¹Center for Bone Research at the Sahlgrenska Academy, Dpts of Internal Medicine and Geriatrics, Gothenburg University, Gothenburg, Sweden, ²Dpt of Orthopaedics, Malmö University Hospital, Lund University, Malmö, Sweden, ³Dpt of Surgical Sciences, Uppsala University, Uppsala, Sweden, ⁴Bone and Mineral Unit, Oregon Health and Sciences University, Portland, OR, USA, ⁵Consulting Statistician, Gothenburg, Sweden, ⁶Dpt of Medical Sciences, Uppsala University, Uppsala, Sweden, ⁷Laboratory of Molecular Endocrinology and Oncology, Laval University, Quebec, PQ, Canada.

The enzymes required to transform adrenal-derived dehydroepiandrosterone (DHEA) into androgens and/or estrogens are expressed in several peripheral target tissues such as bone and muscle. The impact of serum DHEA for bone health in elderly men is unclear. The aim of the present study was to determine the relationship between serum DHEA and incident fractures in elderly men of MrOS Sweden (n=3014, 75.4 ± 3.2 years). Incident X-ray verified fractures at major non-vertebral osteoporosis-related sites (hip 39, distal radius 29, proximal humerus 16 and pelvis 8 fractures) were identified in 82 subjects with an average follow-up of 3.3 years. Serum levels of DHEA, estradiol and testosterone were analyzed by validated gas chromatography/mass spectrometry assays (n=2640). Serum SHBG was measured using an immunoradiometric assay.

Multivariate proportional hazards regression analysis was used to assess the independent relationship of DHEA to fracture risk. In age-adjusted analyses, baseline DHEA was inversely related to incident fracture risk (hazard ratio (HR) per SD decrease in DHEA = 1.43; CI 1.17-1.75). As serum estradiol and serum testosterone were inversely and SHBG was directly related to incident fracture risk, these parameters were included in the

analyses of the independent relationship between DHEA and incident fracture risk. Interestingly, the relationship between DHEA and incident fracture risk was not affected by adjustment for estradiol, testosterone and SHBG (HR per SD decrease in DHEA = 1.40; CI 1.13-1.74). Neither inclusion of total hip BMD (HR per SD decrease in DHEA = 1.36; CI 1.11-1.67) nor inclusion of BMI (HR per SD decrease in DHEA = 1.45; CI 1.18-1.77) in the model affected the association between DHEA and incident fractures.

In conclusion DHEA is an independent predictor of incident non-vertebral fractures at major osteoporosis-related sites in elderly men. Because this association was independent from changes in BMD, one may speculate that adrenal-derived DHEA could influence neuromuscular function and thereby fracture risk in elderly men.

Disclosures: C. Ohlsson, None.

1201

Enhancement of Prognosis of Osteoporotic Fractures by Genetic Marker: Contribution of the Collagen I alpha 1 Gene. B. H. Tran*, N. D. Nguyen, S. A. Frost*, J. R. Center, J. A. Eisman, T. V. Nguyen. Bone and Mineral Research Program, Garvan Institute of Medical Research, Sydney, Australia.

Given the time-invariant nature of the genetic information and BMD and age-related nature of fracture risk, a short-term absolute risk approach is more meaningful and appropriate than a relative risk-based approach. The present study was aimed at developing a prognostic model for predicting 5-y and 10-y of fracture risks in elderly women by incorporating genetic marker information.

COL1A1 genotypes (GG, GT and TT) were determined in 915 women of Caucasian background aged 60+ years as at 1989, who have been followed for up to 17 years (1989-2006). Low trauma, non-pathological fractures were recorded. Femoral neck bone mineral density (FNBMD) was measured by dual energy X-ray absorptiometry (GE-LUNAR DXA) at baseline and expressed as T-scores. A series of nomograms for predicting 5-year and 10-year risk of fractures including any fracture, hip and vertebral fractures for an individual woman were developed by using Cox's proportional hazards model.

The proportion of individuals with GG, GT and TT genotypes in the population of 63%, 32% and 5%, respectively, which was consistent with Hardy-Weinberg equilibrium law. In the multivariable Cox's proportional hazards model, the risk ratio for COL1A1 TT (vs. G allele) and any, hip and vertebral fractures were 3.07 (1.47-6.43), 7.07 (2.37-21.14) and 4.45 (1.89-10.47), respectively, after adjusting for age and FNBMD. The area under the curves for prediction models for any fracture, hip and vertebral fractures were 0.68, 0.85 and 0.69, respectively. Using the models' parameters, various nomograms were constructed for individualizing the risk of any, hip and vertebral fractures. A woman with the TT genotype had an absolute fracture risk equivalent to a 20-year older counterpart without the TT genotype independence of BMD. Similarly, a woman homozygous for the T allele had an absolute risk approximately equivalent to a woman with the same age without the genotype but with 1SD lower in FNBMD.

These data suggest that in women the effect of COL1A1 TT genotype (5% in the population) is equivalent to an effect of 20-year increase in age or one SD lower in BMD. The incorporation of COL1A1 genotypes could enhance the short-term prognosis of osteoporotic fracture in women.

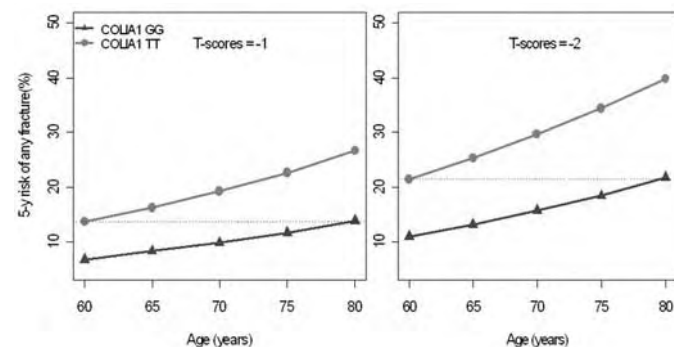


Figure: 5-y risk of any fracture in women, stratified by age, BMD and COL1A1 genotype

Disclosures: B.H. Tran, None.

This study received funding from: National Health and Medical Research Council, Australia.

1202

Serum 25 Hydroxy Vitamin D 25(OH) and the Risk of Hip Fractures: The Women's Health Initiative (WHI). J. A. Cauley¹, A. LaCroix², L. Wu³, J. Lee⁴, M. Horowitz⁵, D. Bauer⁶, R. Jackson⁷, M. Danielson⁸, M. LeBoff⁹, F. Stranczyk¹⁰, S. Cummings¹¹. ¹University of Pittsburgh, Pittsburgh, PA, USA, ²University of Washington, Seattle, WA, USA, ³University of California, Davis, Davis, CA, USA, ⁴University of California San Francisco, San Francisco, CA, USA, ⁵Ohio State University, Ohio, OH, USA, ⁶Harvard University, Cambridge, MA, USA, ⁷University of Southern California, Los Angeles, CA, USA, ⁸University of San Francisco, San Francisco, CA, USA.

Vitamin D deficiency is common in older persons, especially in home based populations, in general medical inpatients and in women with acute hip fracture. To test the hypothesis that serum measures of 25(OH)D predict the likelihood of hip fracture in

community dwelling women, we performed a nested case control study in the WHI Observational Study Cohort. We excluded women who had a history (hx) of hip fracture or used hormones or other osteoporosis medications at baseline. A total of 39,793 women met these criteria. We randomly chose 400 women who had an incident hip fracture, confirmed by medical record over a median of 7.1 y. A control was selected for each case, matched on baseline age (+/- one year), race/ethnicity and date of blood draw (within 75 days). 25(OH)D was measured in fasting baseline serum using DiaSorin kits. The sensitivity of the assay was 1.5ng/ml; interassay coefficients of variation ranged 8.6% to 12.5%. Conditional logistic regression models were conducted to evaluate the association between hip fractures and Vitamin D. Odds ratio (OR) with 95% confidence intervals (CI) were estimated per SD and across quartiles of 25(OH)D (defined by the distribution in controls) with p values for tests of linear trend. We adjusted for potential confounders. The mean age of cases and controls was 70.8 years; 95% were White. 25(OH)D levels ranged from 3.7 to 48.6 ng/ml. The mean (SD) Vitamin D level (ng/ml) in the cases was 22.4 (8.1) and 23.8 (7.2) in the controls, p=0.007. The risk of hip fractures was 77% higher among women whose 25(OH)D was <19ng/ml (Table). Additional adjustment for other risk factors for fracture had no effect. In conclusion, low serum 25(OH)D levels are an independent prognostic risk factor for hip fracture in community dwelling postmenopausal women.

Odds ratio (95% CI) for hip fracture

Vit D	Unadjusted	MV-adj*
Per SD (7.7ng/ml) increase	0.81 (0.70, 0.94)	0.79 (0.66, 0.94)
p for linear trend	p=0.006	p=0.009
Number of missing pairs (total=400)	1	18
Quartiles (according to control group)		
1 st quartile (<19.04 ng/ml)	1.73 (1.14, 2.62)	1.77 (1.09, 2.87)
2 nd quartile (19.04 - <24.09 ng/ml)	1.06 (0.71, 1.58)	1.15 (0.73, 1.80)
3 rd quartile (24.09-<28.29 ng/ml)	0.77 (0.50, 1.20)	0.79 (0.49, 1.26)
4 th quartile (28.29+ ng/ml (ref))	1	1

*Multivariate adjustment includes age, BMI, parental hx of hip fracture, personal hx of fractures, smoking, alcohol, calcium and Vitamin D intake.

Disclosures: J.A. Cauley, Merck & Company 2, 8; Novartis Pharmaceuticals 2, 5; Eli Lilly & Company 2, 5, 8; Pfizer Pharmaceuticals 2.

This study received funding from: NHLBI.

1203

Variation in the FLNB Gene Regulates Bone Density in Two Populations of Caucasian Women. S. G. Wilson¹, B. H. Mullin², M. R. Jones³, I. M. Dick⁴, F. Dudbridge⁵, T. D. Spector⁶, R. L. Prince⁷. ¹Endocrinology, Sir Charles Gairdner Hospital, Nedlands, Australia, ²MRC Biostatistics Unit, Cambridge, United Kingdom, ³Twin Research and Genetic Epidemiology, King's College London, London, United Kingdom, ⁴Medicine and Pharmacology, The University of Western Australia, Nedlands, Australia.

Based on our previous linkage data showing that genes in the chromosome 3p14-21 region are associated with osteoporosis¹ and data that mutations of the Filamin B (FLNB) gene are the cause of osteochondrodysplasias including Larsen's Syndrome, Boomerang Dysplasia and atelosteogenesis type I & III, recently confirmed by KO studies in mice, we have undertaken a detailed study of the effects of variation in the FLNB gene sequence on bone structure. Filamin B is a cytoskeleton protein involved in actin polymerisation and participates in its interaction with signal transduction pathways. Thus the aim of this study was to evaluate the role of variation in the FLNB gene in regulating bone mass and the propensity to osteoporotic fracture. This hypothesis was tested in two large cohorts, firstly 771 women from the GENOS sib-pair study, identified on the basis of an osteoporotic proband and previously used in linkage analysis, and secondly a population-based cohort of 1192 unrelated Caucasian women from the CAIFOS/CARES study. Hip bone density was measured by DXA (Hologic QDR 4500). Genotyping for the family study was by GoldenGate Assay (Illumina Inc.) and in the population study used MALDI-ToF (Sequenom Inc.). Association between BMD and genotype in the family study was assessed using the FBAT program and in the population-based cohort used ANOVA. Genotype effect on fracture rate was examined using a Chi-square test. Haplotype analysis was undertaken using UNPHASED software. Nine SNPs covering the LD in the FLNB gene were studied in the family-based cohort, of which four (rs7637505, rs9822918, rs2177153 and rs2001972) showed an association with age corrected BMD at both femoral neck (P = 0.02-0.0002) and total hip (P = 0.02-0.0006). Six SNPs were taken forward to the population-based replication study of which, rs9822918 (P = 0.02-0.003) and rs2177153 (P = 0.02) showed association with BMD. The difference in mean BMD for alleles of rs2177153 was 3.9-44.9%. Fewer prevalent fractures were observed in individuals homozygous for the G allele of rs2177153 (P = 0.015). Our data shows that genetic variation in the FLNB gene is associated with differences in bone mass and this has been replicated in two independent cohorts of Caucasian women. These results suggest that understanding the mechanism may lead to greater insight into bone cell biology and new therapies.

1. Wilson SG et al., 2003 Am. J. Hum. Genet. 72:144-155.

Disclosures: S.G. Wilson, None.

This study received funding from: NHMRC Project No. 294402.

1204

Genetic and Environmental Effects on Muscle Cross-Sectional Area and Structural Strength of Tibia in Older Female Twins. T. Mikkola^{*1}, S. Sipilä^{*2}, T. Rantanen^{*1}, H. Sievänen³, H. Suominen¹, J. Kaprio^{*4}, M. Koskenvuo^{*4}, M. Kauppinen^{*2}, A. Heinonen¹. ¹Department of Health Sciences, University of Jyväskylä, Jyväskylä, Finland, ²Finnish Centre for Interdisciplinary Gerontology, University of Jyväskylä, Jyväskylä, Finland, ³Bone Research Group, UKK Institute for Health Promotion Research, Tampere, Finland, ⁴Department of Public Health, University of Helsinki, Helsinki, Finland.

The aims of this study were to estimate to what extent individual differences in cross-sectional area of the lower leg muscles (mCSA), bending strength of tibial shaft (BSIb) and compressive strength of distal tibia (BSIc) are influenced by genetic and environmental factors in older women, and to investigate whether the associations between these traits are due to common genetic or environmental factors.

The mCSA, BSIb and BSIc values were measured with peripheral quantitative computed tomography from 102 monozygotic (MZ) and 113 dizygotic (DZ) 63-76-year-old female twin pairs. Quantitative genetic models were used to decompose the phenotypic variances into common and trait-specific additive genetic (A), shared environmental (shared by the sisters, C) and individual environmental (unique to each sister, E) factors.

The pairwise correlations of the MZ and DZ twins were 0.73 and 0.42 for mCSA, 0.73 and 0.50 for BSIb and 0.73 and 0.56 for BSIc, respectively. The age-adjusted multivariate independent pathway model showed that the total relative contributions of A, C and E were 75%, 0% and 25% for mCSA, 55%, 20% and 25% for BSIb and 40%, 37% and 23% for BSIc, respectively. In addition, the model showed that a genetic factor, common to all three traits accounted for 75% (95% CI: 66-82%) of the variance in mCSA, 17% (8-27%) of that in BSIb and 8% (2-17%) of that in BSIc. BSIb and BSIc had a shared environmental factor in common which accounted for 20% (9-35%) and 37% (20-53%) of the variances in BSIb and BSIc, respectively. A common individual environmental factor accounted for 5% (2-11%) of the variance in mCSA, 22% (13-33%) of that in BSIb and 13% (7-22%) of that in BSIc. The remaining variances were attributable to trait-specific genetic factors and trait-specific individual environmental factors.

In older women, cross-sectional area of the lower leg muscles, tibial bending strength and tibial compressive strength share common genetic and environmental effects. The total influence of genes is strong on muscle area and weaker on tibial strength indices. These results suggest that in older women the same genetic and environmental factors may predispose to or protect from both sarcopenia and bone fragility.

Disclosures: T. Mikkola, None.

This study received funding from: Finnish Ministry of Education.

1205

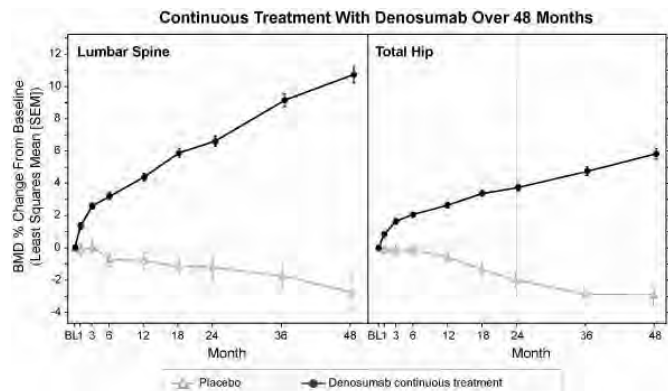
Effect of Denosumab on Bone Mineral Density and Bone Turnover Markers: 48-Month Results. P. Miller¹, M. Bolognese^{*2}, E. M. Lewiecki^{*3}, M. McClung⁴, B. Ding^{*5}, Y. Liu⁵, J. San Martin⁵. ¹Colorado Center for Bone Research, Lakewood, CO, USA, ²Bethesda Health Research Center, Bethesda, MD, USA, ³New Mexico Clinical Research & Osteoporosis Center, Albuquerque, NM, USA, ⁴Oregon Osteoporosis Center, Portland, OR, USA, ⁵Amgen Inc., Thousand Oaks, CA, USA.

Denosumab is an investigational fully human monoclonal antibody that reduces bone turnover by inhibiting RANKL, an essential mediator of osteoclast formation, function, and survival. An ongoing phase 2 study in postmenopausal women with low bone mineral density (BMD) showed that denosumab increased BMD and reduced bone turnover markers (BTM) during the first 24 months of therapy. We report 48-month results of denosumab continuous treatment, discontinuation, and rechallenge.

After 24 months, subjects were reassigned. Those who continued on denosumab were switched from other denosumab dosing regimens to 60 mg Q6M (continuous treatment). Those who received denosumab 210 mg Q6M were switched to placebo (PBO) for the rest of the study (discontinuation), and those on 30 mg Q3M were switched to 12 months of PBO followed by 12 months of 60 mg Q6M (rechallenge). Subjects in the PBO arm remained on PBO, and those in the alendronate (ALN) arm discontinued ALN and were followed. Changes in BMD, BTM, and safety were assessed at 48 months.

BMD data from 229 subjects were available for this interim analysis. After 48 months, continuous denosumab treatment resulted in sustained BMD gains from baseline. Lumbar spine BMD % change from baseline at month 48 was 10.6% for denosumab vs -2.7% for PBO (between-group difference: 13.4%, $P < .001$). BMD also increased at the total hip with denosumab (5.8% vs -2.9%; between-group difference: 8.7%, $P < .001$; Figure). Denosumab discontinuation was associated with a BMD decrease to values near baseline. Rechallenge with denosumab increased BMD to an extent similar to initial therapy. In subjects who discontinued ALN, a slight decline of BMD was observed. Continuous denosumab therapy led to sustained reduction of BTM from baseline. BTM increased upon denosumab discontinuation and decreased with rechallenge. Adverse event rates were similar among treatment groups over 48 months.

These data indicate that RANKL inhibition with denosumab led to continued gains in BMD and suppression of BTM relative to PBO over 48 months, which appeared to be reversible with discontinuation and responsive with rechallenge.



Disclosures: P. Miller, Amgen Inc. 2, 5, 8; P&G 2, 5, 8; sanofi-aventis 2, 5, 8; Roche 2, 5, 8.

This study received funding from: Amgen Inc.

1206

Efficacy of Bazedoxifene in Reducing New Vertebral Fracture Risk in Postmenopausal Women with Osteoporosis: Results From a 3-Year, Randomized, Placebo- and Active-Controlled Clinical Trial. S. L. Silverman¹, C. Christiansen², H. K. Genant³, J. R. Zanchetta⁴, I. Valter^{*5}, T. J. de Villiers^{*6}, G. Constantine^{*7}, A. A. Chines⁷. ¹Osteoporosis Medical Center, Clinical Research Center, Beverly Hills, CA, USA, ²Center for Clinical and Basic Research (CCBR), Ballerup, Denmark, ³University of California, San Francisco, and Synarc, San Francisco, CA, USA, ⁴University of El Salvador, Metabolic Research Institute, Buenos Aires, Argentina, ⁵CCBR, Tallinn, Estonia, ⁶Panorama MediClinic, Capetown, South Africa, ⁷Wyeth Pharmaceuticals, Collegeville, PA, USA.

Bazedoxifene (BZA), a novel selective estrogen receptor modulator (SERM), is currently in clinical development for the prevention and treatment of postmenopausal osteoporosis. We report the results of a 3-year, Phase III study that evaluated the effect of BZA therapy on the incidence of new vertebral fracture compared with placebo (PBO) and raloxifene (RLX) in postmenopausal women with osteoporosis.

This study enrolled generally healthy postmenopausal women aged 55-85 years with lumbar spine (LS) or femoral neck (FN) T-scores ≤ -2.5 and no prevalent vertebral fractures or LS or FN T-scores

≥ -4.0 with prevalent vertebral fractures. Participants were randomized to receive 20 mg/d or 40 mg/d BZA, 60 mg/d RLX, or PBO and received supplemental calcium (1200 mg) and vitamin D (400 IU). The primary efficacy outcome was the incidence of new vertebral fractures after 36 months; secondary outcomes included non-vertebral fractures (NVFs).

A total of 7492 women (mean age \pm SD, 66.4 \pm 6.7 years) were randomized and received ≥ 1 dose of study medication. At baseline, mean LS T-score was -2.4, mean total hip T-score was

-1.4, and 56% of women had ≥ 1 prevalent vertebral fracture (mostly mild). The 3-year incidences of new vertebral fracture, based on Kaplan-Meier estimates, were 2.3%, 2.5%, 2.3%, and 4.1% in the BZA 20 mg, BZA 40 mg, RLX 60 mg, and PBO groups, respectively, with a relative risk reduction for new vertebral fracture of 42% ($P=0.015$), 37% ($P=0.031$), and 42% ($P=0.012$), respectively, versus PBO. There was overall no treatment effect on NVFs. In a post-hoc analysis of women with FN T-score ≤ -3.0 or ≥ 1 moderate or multiple vertebral fracture ($n=1782$), NVF incidence was 3.0%, 3.8%, 5.9% and 6.3% in BZA 20 mg, 40 mg, RLX 60 mg and PBO groups, respectively. Relative to PBO, BZA 20 mg reduced NVF incidence by 52% ($P=0.045$). Similar reduction was observed when both BZA doses were combined (46% reduction, $P=0.037$).

We conclude that BZA treatment significantly reduces the risk of new vertebral fractures, and in subjects at higher risk for fractures, BZA is associated with a significant reduction in NVFs.

Disclosures: S.L. Silverman, Novartis, Eli Lilly, Wyeth, Roche, Procter & Gamble, Merck 2; Roche, Novartis, Merck, Procter & Gamble, Wyeth 5; Eli Lilly, Merck, Procter & Gamble, Roche 8; Compumed (member, Board of Directors) 9.

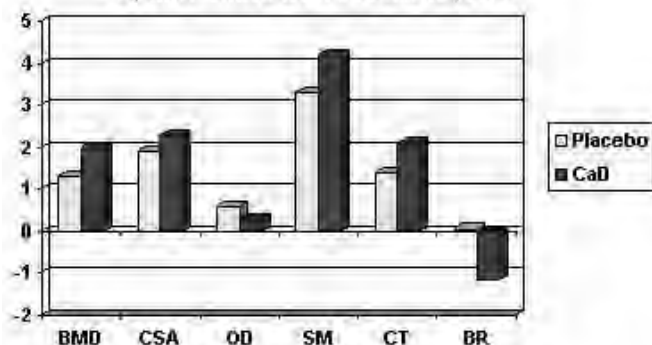
This study received funding from: Wyeth Pharmaceuticals.

1207

The Effect of Calcium plus Vitamin D Supplement on Hip Geometric Structures: Results from the Women's Health Initiative CaD Trial. Z. Chen¹, T. J. Beck², N. C. Wright¹, A. Z. LaCroix³, J. A. Cauley⁴, C. E. Lewis⁵, T. Bassford^{*1}, M. S. LeBoff⁶, R. D. Jackson^{*7}. ¹U of Arizona, Tucson, AZ, USA, ²Johns Hopkins Univ., Baltimore, MD, USA, ³Fred Hutchinson Cancer Research Center, Seattle, WA, USA, ⁴U of Pittsburgh, Pittsburgh, PA, USA, ⁵U of Alabama, Birmingham, AL, USA, ⁶Brigham and Women's Hospital, Boston, MA, USA, ⁷Ohio State Univ., Columbus, OH, USA.

A previous report has shown that calcium and vitamin D (CaD) supplementation caused a small but significantly improvement in bone mineral density (BMD) among healthy postmenopausal women who participated in the CaD trial of the U.S. nationwide Women's Health Initiative Study (WHI). The purpose of this study was to investigate the effect of CaD intervention on femoral bone strength as measured by hip structure analysis (HSA) in the same sample. The WHI CaD trial was designed for women to take either the CaD supplement (containing calcium carbonate (500 mg as elemental calcium) with vitamin D₃ (200 IU)) or matching placebo twice daily (GlaxoSmithKline Consumer Healthcare, Parsippany, NJ) depending on their randomization assignment. The analysis included participants (n = 1,731) at three WHI bone density centers. HSA in the femoral narrow neck (FNN), intertrochanter (IT), and femoral shaft (FS) regions were done using the validated Beck's method on hip scans from dual-energy x-ray absorptiometry. Women in the CaD arm were similar to women in the placebo arm in baseline characteristics, such as age (62.2 vs. 62.3 year), height (161.81 vs. 161.75 cm) and body weight (76.2 vs. 75.2 kg). Percent changes in HSA measurements at FNN from baseline to year3 are presented in the Figure. Results from multiple linear regression analysis after adjusting for baseline HSA measure suggest significant CaD intervention effects on HSA measurements in the FNN region during the first three years of the intervention (p<0.05). Overall CaD reduced the expansion of outer diameter (OD) and increased buckling ratio (BR). Meanwhile, section modulus (SM) and cortical thickness (CT) were significantly improved by CaD intervention. Higher cross-sectional area (CSA) were also observed in the CaD arm, but the intervention effect was not statistical significant. Adjusting for hormone interventions did not change the findings. Interestingly, the CaD effect on bone strength was limited to the FNN region. In conclusion, CaD intervention has significant and skeletal-site specific benefits on bone strength.

Figure 1. Percent change in HSA measurements by intervention from baseline to year 3



Disclosures: Z. Chen, None.

This study received funding from: NIAMS R01-AR049411.

1208

Denosumab Increases Bone Mineral Density in Patients with Rheumatoid Arthritis: 12-month Results. R. K. Dore^{*1}, E. Hurd^{*2}, W. Palmer^{*3}, W. Shergy^{*4}, N. Lane^{*5}, S. Cohen^{*6}, L. Zhou^{*7}, R. Newmark⁷, W. Tshuji^{*7}. ¹Robin K. Dore, Inc., Anaheim, CA, USA, ²Arthritis Centers of Texas, Dallas, TX, USA, ³Westroads Medical Group, Omaha, NE, USA, ⁴Rheumatology Associates of North Alabama, Huntsville, AL, USA, ⁵UC Davis Medical Center, Sacramento, CA, USA, ⁶Metroplex Center for Clinical Research, Dallas, TX, USA, ⁷Amgen, Inc., Thousand Oaks, CA, USA.

Rheumatoid arthritis (RA) is characterized by articular and periarticular bone erosions and systemic bone loss. RANKL is a key factor implicated in the bone destruction associated with many diseases, including RA. In clinical studies, denosumab, a fully human monoclonal antibody, inhibits RANKL and increases bone mineral density (BMD) in postmenopausal women with low bone mass. As part of a study to determine the effects of denosumab on joint destruction in patients with RA, the effect of denosumab on systemic bone loss was examined. Patients with mild to moderately active RA for at least 6 months with manifest erosions and maintained on methotrexate (MTX) were randomly assigned to treatment with subcutaneous injections of placebo or denosumab (60 or 180 mg) every 6 months. BMD was measured by dual-energy x-ray absorptiometry (DXA) at baseline, 1 month, 6 months, and 12 months. Adverse events were monitored throughout the study. A total of 227 patients were enrolled in the study (78 placebo, 73 denosumab 60 mg, 76

denosumab 180 mg). Average lumbar spine BMD T-score at baseline was (mean \pm SD) -0.50 \pm 1.58. Approximately one-third of patients used steroids at screening and one-fifth of all patients used bisphosphonates during the study; uses of both were balanced among groups. An additional 5% of patients in each treatment group had previously used bisphosphonates. At 12 months, denosumab significantly increased BMD at the lumbar spine, total hip, femoral neck, and trochanter compared with placebo (Table). Adverse events occurred with similar frequency among the treatment groups. Flare of RA was the most common adverse event.

All statistical comparisons were based on a repeated-measures model adjusting for treatment, visit, baseline use of steroid, previous use of biologic, baseline value, and visit by treatment interaction.

In summary, denosumab treatment increased BMD in patients with RA at 12 months and showed similar frequency and severity of adverse events across treatment groups. These results are consistent with those observed at 6 months.

Least-Squares Mean (\pm SE) Percent Change from Baseline in BMD at 12 Months			
Skeletal site	Placebo (n = 74)	Denosumab 60 mg (n = 70)	Denosumab 180 mg (n = 71)
Lumbar spine	0.76 \pm 0.39	3.01 \pm 0.38 ^a	4.05 \pm 0.39 ^a
Total hip	-0.35 \pm 0.29	1.60 \pm 0.28 ^a	1.75 \pm 0.28 ^a
Femoral neck	-0.61 \pm 0.44	1.28 \pm 0.44 ^b	1.48 \pm 0.44 ^b
Trochanter	-0.30 \pm 0.44	2.05 \pm 0.44 ^a	2.20 \pm 0.44 ^a

^a P \leq 0.001 versus placebo
^b P = 0.010 and 0.004 versus placebo for the 60-mg and 180-mg groups, respectively

Disclosures: R.K. Dore, Merck 2, 5, 8; Eli Lilly 2, 5, 8; Roche 2, 5, 8; Amgen 2.

This study received funding from: Amgen, Inc.

1209

Efficacy of Bazedoxifene for Prevention of Postmenopausal Osteoporosis: Results of a 2-Year, Phase III, Placebo- and Active-Controlled Study. P. D. Miller¹, C. Christiansen², H. C. Hoek^{*2}, D. L. Kendler³, E. M. Lewiecki⁴, G. Woodson⁵, M. Ciesielska^{*6}, A. A. Chines⁶, G. Constantine^{*6}, P. D. Delmas⁷.

¹University of Colorado Medical Center, Denver, CO, USA, ²Center for Clinical and Basic Research, Ballerup, Denmark, ³Osteoporosis Research Centre, Vancouver, BC, Canada, ⁴New Mexico Clinical Research & Osteoporosis Center, Inc, Albuquerque, NM, USA, ⁵Atlanta Research Center, Decatur, GA, USA, ⁶Wyeth Pharmaceuticals, Collegeville, PA, USA, ⁷University of Lyon and INSERM Research Unit 831, Lyon, France.

Bazedoxifene (BZA) is a novel selective estrogen receptor modulator (SERM) currently in clinical development as monotherapy for prevention and treatment of postmenopausal osteoporosis and in combination with conjugated estrogens for the treatment of menopausal symptoms and prevention of postmenopausal osteoporosis. In preclinical studies, BZA maintained skeletal mass without stimulation of the mammary gland or endometrial tissue. This 2-year, Phase III study was designed to assess the efficacy and safety of 3 BZA doses compared with placebo (PBO) and raloxifene (RLX) in the prevention of postmenopausal osteoporosis.

Healthy postmenopausal women (N=1583; mean age: 57 y) with lumbar spine or femoral neck BMD T-scores no less than -2.5 (mean: -1.2) were randomized to 1 of 5 groups: BZA 10, 20, or 40 mg, PBO, or RLX 60 mg. All women received 600 mg elemental calcium. The primary outcome was percent change in lumbar spine BMD at 24 months; secondary outcomes included BMD at other skeletal sites and serum bone turnover markers.

All BZA doses and RLX prevented bone loss, whereas PBO was associated with significant reductions in BMD. The difference in percent change of lumbar spine BMD from baseline to 24 months relative to PBO was 1.08%, 1.41%, 1.49%, and 1.50% for 10 mg, 20 mg, 40 mg BZA and 60 mg RLX, respectively (P<0.001 for all comparisons). Comparable BMD responses were observed with BZA at other skeletal sites. Significant decreases in serum osteocalcin and C-telopeptide levels from baseline and relative to PBO were observed as early as 3 months and remained sustained through study end (P<0.001). By month 24, median serum osteocalcin levels decreased from baseline by 21%, 22%, 22%, and 27% with BZA 10, 20, and 40 mg, and RLX, respectively, and 6% with PBO (P<0.001 vs baseline for each); median serum C-telopeptide levels decreased by 25%, 24%, 22%, and 32% with respective BZA doses and RLX and 13% with PBO (P<0.001 vs baseline for each). Overall, BZA was well tolerated and exhibited a favorable safety profile.

In conclusion, this study demonstrated that treatment with BZA, a new SERM, prevented bone loss, reduced bone turnover, and was generally well tolerated in postmenopausal women with normal or low BMD.

Disclosures: P.D. Miller, Procter & Gamble Pharmaceuticals, Sanofi-Aventis Pharmaceuticals, Roche Pharmaceuticals, Eli Lilly, Merck & Co., Novartis Pharmaceuticals, Amgen 2; Procter & Gamble Pharmaceuticals, Sanofi-Aventis Pharmaceuticals, Roche Pharmaceuticals, Eli Lilly, Merck & Co., Novartis Pharmaceuticals, Amgen, NPS, GlaxoSmithKline 5, 8.

This study received funding from: Wyeth Pharmaceuticals.

1210

The Effect of a Single Large Oral Dose of Cholecalciferol on Serum 25-hydroxyvitamin D Levels in Humans. M. Ilahi, L. A. G. Armas, R. P. Heaney. Endocrinology, Diabetes & Metabolism, Creighton University Medical Center, Omaha, NE, USA.

We report results of work to quantify the response of 25-hydroxyvitamin D to a large oral dose of cholecalciferol. Large intermittent doses of vitamin D have been shown to reduce fracture risk and to elicit good patient compliance. However, the time course of the serum 25(OH)D response has never been measured and hence both the safety and the optimum frequency of dosing are uncertain.

This study included two groups, an older group of 20 subjects (age 61-84 yrs, 15 females, 5 males) and a younger group of 10 subjects (age 27-47yrs, 6 females, 4 males). The subjects were healthy with limited sun exposure. Data were collected from October to March. Subjects were dosed at baseline with 100,000 IU of cholecalciferol as a single oral dose. Blood for 25-hydroxyvitamin D was drawn throughout the ensuing 16 weeks. Blood for calcium was drawn through the first 5 days.

Baseline levels of 25(OH)D were 59.4 nmol/L (median; interquartile range 55.6-75.1) in the older group and 63.7 nmol/L (median; interquartile range 57.1-78.4) in the younger group. 25(OH)D increased to 92.1 nmol/L (median; interquartile range 81.1-104.6) in the older age group, and to 102.8 nmol/L (median; interquartile range 91.6-126.2) in the younger age group. Both groups reached peak 25(OH)D levels at day 7. In most of the subjects the mean 25(OH)D remained above 80 nmol/L for 70 days. Only two subjects in the older age group did not reach 80 nmol/L throughout the study. The incremental rise of 25(OH)D in the older age group was 28.7 nmol/L (median; interquartile range 24.0-37.9). In the younger age group the incremental rise of 25(OH)D was 36.5 nmol/L (median; interquartile range 28.0-52.1). Calcium at baseline for both the older and younger group was 9.5 mg/dl (median; interquartile range 9.4-9.8). Calcium levels during the first week of supplementation remained below baseline.

In summary, one large oral dose of 100,000 IU of cholecalciferol raises and maintains 25(OH)D above 80 nmol/L in most subjects for 70 days without raising serum calcium levels. No subject achieved a 25(OH)D level above what would commonly be found in outdoor workers at the end of summer. Even a dose this large will not raise 25(OH)D above 80 nmol/L in more severely vitamin D deficient subjects. We conclude that doses of 100,000 IU cholecalciferol are safe and that the optimum frequency of dosing is at least every 60-70 days.

Disclosures: M. Ilahi, None.

This study received funding from: Research Fund of Creighton University.

1211

Akt1 Contributes to Maintenance of Bone Mass and Turnover by Inhibiting Apoptosis of Osteoblasts Through FoxO3a/Bim Axis. N. Kawamura, F. Kugimiya*, T. Kadowaki*, K. Nakamura, U. Chung, H. Kawaguchi. Sensory & Motor System Medicine, Tissue Engineering, and Metabolic Diseases, University of Tokyo, Tokyo, Japan.

We found that mice lacking a phosphoinositide-dependent serine-threonine protein kinase Akt1 (Akt1^{-/-}) exhibited low-turnover osteopenia through dysfunctions of osteoblasts and osteoclasts: the former through increased susceptibility to apoptosis and decreased differentiation with impaired transactivity of Runx2, and the latter through suppressed RANKL expression in osteoblasts and cell-autonomous defects in osteoclasts. This study sought to learn the molecular mechanism underlying the enhanced apoptosis in Akt1^{-/-} osteoblasts. Among apoptosis-related molecules that are known to be possible substrates of Akt, transcription factors FoxO3a and FoxO1 were expressed in primary osteoblasts and MC3T3-E1 cells. Although these factors showed nuclear entry after serum deprivation, only that of FoxO3a was enhanced in Akt1^{-/-} osteoblasts as compared to wild-type (WT) osteoblasts. Meanwhile, overexpression of the constitutively active form of Akt1 (Akt1CA) in osteoblasts stimulated the cytoplasmic FoxO3a phosphorylation and inhibited the nuclear entry. The increased apoptosis and caspase-3 activity of Akt1^{-/-} osteoblasts after serum deprivation were restored by introduction of a dominant-negative form of FoxO3a (FoxO3aDN). Among the candidate molecules of the transcriptional target of FoxO3a: Fas ligand, Bim, and Bcl-xL, only Bim mRNA and protein levels were increased after serum deprivation, followed by the induction of cleaved caspase-3, in osteoblasts. The cleaved caspase-3 induction was suppressed by silencing of Bim through RNA interference. Actinomycin D canceled the Bim increase after serum deprivation, indicating the transcriptional regulation. The Bim promoter activity determined by luciferase-reporter assay was enhanced by FoxO3a, and endogenous Bim expression was stimulated by overexpression of FoxO3a while inhibited by FoxO3aDN, indicating that Bim is a transcriptional target of FoxO3a in osteoblasts. Akt1CA overexpression suppressed the Bim transactivation by FoxO3a and endogenous Bim induction after serum deprivation. The Bim induction which was higher in Akt1^{-/-} osteoblasts than WT was restored by the FoxO3aDN transfection. We therefore conclude that Akt1 inhibits osteoblast apoptosis through phosphorylation of FoxO3a and prevention of the nuclear entry, leading to impaired transactivation of pro-apoptotic Bim. Taken all together, Akt1 was established as a crucial regulator of osteoblasts and osteoclasts to maintain bone mass and turnover via several pathways.

Disclosures: N. Kawamura, None.

1212

Dimorphic Effects of Notch Signaling in Bone Homeostasis. F. Engin¹, T. Yang¹, G. Zhou¹, T. Bertin^{*1}, M. Jiang^{*1}, Y. Chen^{*1}, L. Wang², H. Zheng^{*1}, Z. Yao³, B. Boyce³, B. Lee⁴. ¹Molecular and Human Genetics, Baylor College of Medicine, Houston, TX, USA, ²Pediatrics, Baylor College of Medicine, Houston, TX, USA, ³Pathology and Laboratory Medicine, University of Rochester, Rochester, NY, USA, ⁴Molecular and Human Genetics, Baylor College of Medicine, Howard Hughes Medical Institute, Houston, TX, USA.

Evolutionarily conserved Notch signaling plays a critical role in diverse developmental and physiological processes including cell fate determination, differentiation, proliferation, and apoptosis. Dysregulation of Notch pathway has been associated with many different diseases including spondylocostal dysostosis and cancer. However, its in vivo function during mesenchymal cell differentiation, and specifically in bone homeostasis remains largely unknown. Here, we show that osteoblast-specific gain of Notch1 function results in severe osteosclerosis. Transgenic mice over-expressing Notch1 intra cellular domain (N1ICD) from the Col1a1 promoter have increased proliferation of immature osteoblasts that produce immature woven bone. Under these pathological conditions, Notch stimulates early osteoblastic proliferation by up-regulating Cyclin D, Cyclin E and Osterix. Notch also regulates osteoblastic terminal differentiation by directly binding Runx2, an essential transcription factor for osteoblastogenesis, and repressing its transactivation function. Consistent with this proliferative effect, human osteosarcomas show evidence of increased Notch signaling and its inhibition by a gamma-secretase inhibitor in vitro decreases the proliferation of human osteosarcoma cells. In contrast, loss of all physiologic Notch signaling in osteoblasts, generated by deletion of Presenilin 1 and 2 in osteoblasts, is associated with late onset, age-related osteoporosis. Double knock-out mice show decreased expression of Osteoprotegerin (Opg) expression indicating an increased osteoblast-dependent osteoclastic activity. Moreover, co-culture and flow cytometric analyses reveal increased differentiation of osteoclast precursors explaining the low bone mass phenotype in these mice. Together, these findings highlight the potential dimorphic effects of Notch signaling in bone homeostasis, and importantly, they may provide direction for novel therapeutic applications.

Disclosures: F. Engin, None.

This study received funding from: HIN grants ES11253 (B. Lee), HD22657 (B. Lee), DE0

1213

Osteoblasts in Adult Bone use Slug for Regeneration and Repair but not Remodelling. J. G. Mount*, S. Allen*, M. Muzylak*, L. E. Lanyon, A. Goodship*, I. M. McGonnell*, J. S. Price. Veterinary Basic Sciences, Royal Veterinary College, London, United Kingdom.

The zinc finger transcription factor Slug was first described as a marker of pre-migratory and migratory neural crest in the embryo. It is a member of the highly conserved Snail family of transcription factors, originally thought to be involved exclusively in developmental functions. Snail family members have not been identified in adult bone and have not been ascribed any function in osteoblasts. We recently identified a range of neural crest markers, including Slug, in the periosteum from which deer antlers regenerate (these are the only bones that repeatedly regenerate in adult mammals). This led us to further explore the role of Slug in bone. We also studied the relationship between Slug and Wnt signaling since there is a LEF/TCF binding site in Slug's promoter and during development it is regulated by Wnts.

Immunocytochemistry was used to co-localize Slug and activated β -catenin (β cat) in mesenchymal progenitors in the foetal primordia of antlers and in osteoblasts on the frontal bone on which antlers develop. Slug and β cat also co-localized in osteoblasts in foetal long bones. Slug could not be detected in any adult deer or rodent bones, however, in healing adult rat fractures it was identified in periosteal progenitors. Similarly, in regenerating adult antlers Slug and β cat localized in mesenchymal progenitors and in osteoblasts. This suggests that Slug may have distinct roles at early and late stages of skeletal cell differentiation. Interestingly, Slug was not detected in cartilage in regenerating antlers, nor in cartilage in fracture callus. This indicates that its down-regulation is required for chondrogenesis.

In order to investigate the relationship between Slug expression, osteogenesis and chondrogenesis, periosteum-derived progenitor cells (PDPs) were cultured under osteogenic or chondrogenic conditions. Slug expression increased as osteoblast differentiation increased (determined by changes in Osterix and Runx-2 expression), whereas its expression decreased with chondrocyte differentiation (determined by changes in Sox9 and type II collagen). Wnt/ β catenin signaling is known to control cell fate determination in mesenchymal cells and in PDP cells activation of Wnt signaling by LiCl decreased Slug expression.

In conclusion, we have shown, to our knowledge for the first time, that in adults Slug has a role in osteoblasts during bone regeneration and repair, but not remodeling. We also present evidence that Slug is involved in the regulation of mesenchymal cell fate by Wnt/ β catenin signaling. The study also affirms that in adults developmental mechanisms are recapitulated during bone regeneration and fracture repair.

Disclosures: J.G. Mount, None.

This study received funding from: BBSRC.

1214

MicroRNA Expression Profiling and Function During In Vitro Osteogenesis. G. J. Spencer*, P. G. Genever*. Department of Biology, University of York, York, United Kingdom.

Understanding molecular mechanisms that control osteogenic differentiation is central to the development of novel therapies aimed at bone remodelling such as osteoporosis. Many studies have successfully identified critical factors involved in initiating and maintaining lineage-specific transcriptional changes although the role of post-transcriptional gene silencing during osteoblast differentiation remains unclear. MicroRNAs (miRNAs) are a superfamily of evolutionary conserved, small non-coding RNAs that bind to the 3' UTR of mRNAs inhibiting protein translation and influencing a broad range of biological roles, instrumental in conferring tissue identity and function. In this study we aimed to determine expression and investigate the function of miRNAs during osteogenesis in vitro. Expression was determined by microarray analysis of 984 known and predicted miRNAs using RNA isolated from undifferentiated rat primary calvarial osteoblast progenitors or cells induced to differentiate in the presence of osteogenic supplements (dexamethasone, ascorbic acid and β -glycerolphosphate) over 21 days. Differentiation was confirmed by induction of alkaline phosphatase, von-Kossa positive mineralization and qRT-PCR, revealing temporally relevant changes in expression of osteogenic markers (cbfa-1, alkaline phosphatase, type-I collagen, osteopontin and osteocalcin). Analyses revealed constitutive expression of 20 miRNAs, 5 miRNAs specifically expressed in osteoblast progenitors but down regulated during osteogenesis and 35 miRNAs absent from progenitors and expressed in mature osteoblasts. The functional role of miRNAs was determined using anti-mir microRNA inhibitors transfected into rat calvarial osteoblast progenitors before osteogenic stimulation. Inhibition of miRNA, let7i, constitutively expressed throughout osteogenesis, significantly reduced alkaline phosphatase activity and impaired osteoblast differentiation as determined by changes in gene expression by qRT-PCR. In contrast, inhibition of progenitor specific mir298 promoted osteoblast differentiation and reduced osteoblast numbers as determined by viability assays. Bioinformatic analyses of let7i and mir298 targets using predictive algorithms revealed components of the Wnt, Notch and BMP signaling pathways, suggesting the endogenous function of let7i in promoting osteoblast differentiation, and mir298 in inhibiting differentiation and promoting proliferation may be mediated by specific regulation of these signaling pathways. Together these data provide evidence for an important functional role of miRNAs during osteogenesis which may have pervasive implications for our understanding of bone biology.

Disclosures: G.J. Spencer, None.

This study received funding from: The Wellcome Trust.

1215

Pericytes Derived from Adipose Tissue; Characterization and Evaluation of their Osteogenic Potential. I. Kalajzic¹, L. Wang¹, X. Jiang^{*1}, K. Lamothe^{*2}, L. H. Aguila^{*2}, D. W. Rowe¹. ¹Dept. of Reconstructive Sciences, Uni. of Conn. Health Center, Farmington, CT, USA, ²Dept. of Immunology, Uni. of Conn. Health Center, Farmington, CT, USA.

We have shown that pericytes/myofibroblast expand following osteoblast ablation. This was assessed by a dramatic increase in a population of cells within the bone marrow that was positive for smooth muscle actin (SMAA), SM22 and exhibited a myofibroblastic phenotype. To further substantiate these observations and test the hypothesis that pericytes from non-calcified tissues have osteoprogenitor potential we have obtained SMAA-GFP transgenic mice that direct GFP towards smooth muscle cells and pericytes. We have characterized the GFP expression in bone and other tissues. A few SMAA-GFP positive cells detected in bone were localized to microvasculature in the periosteum and in a few locations within the trabecular area within bone marrow space. We have confirmed the close relationship of SMAA+ cells in periosteum with the underlying endothelial cells by CD31 immunohistochemistry. Utilizing SMAA-GFP, we observed rich vascular network in muscle and adipose tissue. In adipose tissue, two levels of SMAA+ cells were closely associated with CD31+ staining; a smooth muscle layer of blood vessels, and extensive capillary network.

Phenotypic analysis against cell surface markers expressed in mesenchymal progenitor cells showed that 50% of freshly isolated SMAA-GFP+ cells from adipose tissue were CD45-/Sca1+. Culturing for 6 days enriched this CD45-/SMAA+/Sca1+ mesenchymal progenitor population to 80%. In addition, SMAA+ cells were negative for c-kit and CD11b.

Bone marrow and adipose derived stromal cells isolated from SMAA-GFP mice were purified by FACS to generate SMAA-GFP+ and GFP- populations. Following induction to osteogenesis and adipogenesis, expression of bone and fat markers was restricted to SMAA-GFP+ population. This in vitro data confirmed that SMAA-GFP+ cells differentiated into osteoblasts and adipocytes. To confirm the ability of SMAA-GFP positive cells derived from adipose tissue to generate mature osteoblasts in an in vivo model, we have utilized dual transgenic mice obtained by breeding a SMAA(green) with osteoblast specific Col2.3(blue). Following FACS isolation, pure SMAA-GFP+/2.3GFP- cells were transplanted by direct intra marrow injection into GFP negative recipient mice. One month after the injection histological analysis of transplanted bones reveals the presence of numerous osteoblasts (Col2.3GFP+) localized to bone surface and closely associated with new bone formation as detected by underlying deposition of xylenol orange. Our result confirms that a pericyte population from adipose tissue has osteoprogenitor potential with the ability to generate mature bone lineage cells.

Disclosures: I. Kalajzic, None.

1216

Oxidative Stress-induced Vascular Calcification Is Associated with Increased Expression of Receptor Activator of Nuclear Factor κ B Ligand (RANKL). C. Byon^{*1}, X. Feng¹, T. L. Clemens¹, J. M. McDonald², Y. Chen¹.

¹Pathology, MCP, University of Alabama at Birmingham, Birmingham, AL, USA, ²Pathology and VA medical Center, University of Alabama at Birmingham, Birmingham, AL, USA.

Oxidative stress plays a critical role in the pathogenesis of atherosclerosis, including the development of atherovascular calcification, a prominent feature of atherosclerosis. Enhanced osteogenic differentiation of vascular smooth muscle cells (VSMC) is associated with oxidative stress in vitro. Further, increased expression of RANKL is present in calcified vessels. Thus, we determined the effects of oxidative stress on the expression of RANKL and its role in VSMC calcification.

VSMC were explanted from the aorta of C57BL6 mice and the smooth muscle (SM) cell identity was confirmed by immunofluorescent staining with SM α -actin antibody. VSMC were exposed to osteogenic media for 3 weeks and mineralization was determined by von Kossa staining. H_2O_2 , at concentrations of 0.05 mM to 0.4 mM, were used to induce oxidative stress. The expression of RANKL, alkaline phosphatase (ALP), type I collagen (Col I), and osteocalcin (OC) was determined by real-time PCR and RT-PCR. The effect of oxidative stress on RANKL promoter activity was determined with a series of deletion mutants of RANKL promoter-luciferase reporters. All experiments were performed with VSMC at passage 5 to 8. H_2O_2 increased intracellular peroxide production in VSMC as determined by dichlorofluorescein fluorescence. VSMC mineralization was induced by H_2O_2 in a dose-dependent manner (fold increase at 0.05 mM=1.5 \pm 0.7, 0.3 mM=6.0 \pm 1.4, and 0.4 mM=16.0 \pm 1.4 compared with control, n = 4, p<0.05). Increased expression of bone-associated proteins including ALP, Col I and OC and decreased expression of SM- α actin were demonstrated when VSMC were exposed to 0.4 mM H_2O_2 (fold increase in ALP=8.7 \pm 1.2, Col I=6.6 \pm 0.9, and OC=5.3 \pm 1.4 compared with control, n = 4, p<0.05). In addition, a 33-fold increase in the expression of RANKL and no change in osteoprotegerin (OPG) was demonstrated in VSMC exposed to 0.4 mM H_2O_2 (n = 4). Luciferase-reporter assay revealed an oxidative stress-responsive region between -400 and -200 in RANKL promoter. Addition of RANKL (100 ng/ml) or OPG (50 ng/ml) protein into the osteogenic media did not affect VSMC calcification; and oxidative stress-enhanced calcification was not blocked in VSMC from RANKL knock out mice.

In summary, oxidative stress decreased the expression of SM α -actin and increased the expression of bone-associated proteins and calcification in VSMC. Oxidative stress induced the expression of RANKL via its promoter region located between -400 and -200. Elevation of RANKL during VSMC calcification did not mediate the effect of oxidative stress on VSMC calcification.

Disclosures: Y. Chen, None.

1217

Androgens Act Directly via the Androgen Receptor in Mineralizing Osteoblasts to Regulate Bone Turnover and Maintain Trabecular Bone in Male Mice. R. A. Davey¹, M. Chiu^{*1}, C. Chiang^{*1}, A. J. Moore^{*2}, E. Doust^{*1}, C. Ma^{*1}, T. L. Clemens³, H. A. Morris³, J. D. Zajac³.

¹Medicine, AH, University of Melbourne, Heidelberg, Victoria, Australia, ²Hanson Institute, Adelaide, Australia, ³Pathology, University of Alabama at Birmingham, Birmingham, AL, USA.

Androgens play a key role in skeletal growth and bone maintenance, however the relative contribution of their actions via the androgen receptor (AR) versus the estrogen receptor (ER) remains unclear. Our recent data using Collagen 1a1 2.3kb-AR knockout mice (KO) provides strong evidence for a role of androgens acting directly via the AR in mature osteoblasts to maintain trabecular bone (1). The aim of this study was to define the target cells of androgen action via the AR in bone using mice in which the DNA-binding actions of the AR are deleted specifically in terminally differentiated, mineralizing osteoblasts (mOBL-ARKOs).

mOBL-ARKO mice were generated by breeding mice with a floxed exon 3 of the AR gene (2) with osteocalcin-Cre mice. The phenotype of male mOBL-ARKOs and littermate controls (wild-type, AR floxed, osteocalcin-Cre) was assessed by histomorphometry in the distal femoral metaphysis at 6, 12 and 24 wks of age (n=10/group).

mOBL-ARKOs had normal femur length, body weight, testis and seminal vesicle mass compared to controls. Deletion of the AR specifically in mineralizing osteoblasts resulted in 22-38% decreases in trabecular number (TbN) at 6, 12 and 24 wks of age (P<0.05) in the secondary spongiosa. At 6 wks of age, this loss of TbN resulted in a 36% decrease in trabecular bone volume (BV/TV) (P<0.01). In contrast, BV/TV in mOBL-ARKOs did not differ from controls at 12 and 24 wks of age, as they were able to maintain or increase trabecular thickness (P<0.05), suggesting a compensatory mechanism to prevent further bone loss in the absence of AR action in mineralizing osteoblasts. The loss of TbN observed at all ages is likely to be due to increased bone resorption, evident from 12 wks of age as measured by serum X-laps (P<0.05). Although the mean X-laps was higher in mOBL-ARKOs at 6 wks of age (mean \pm SE; wild-type: 92 \pm 6; mOBL-ARKO: 122 \pm 15, n=10), this did not reach significance (P=0.07). Trabecular bone parameters in the primary spongiosa were unaffected in mOBL-ARKOs indicating that the accrual of new bone is not dependent on the DNA-binding actions of the AR in mineralizing osteoblasts.

Our findings conclusively demonstrate that in addition to the well-established actions of androgens via aromatization to estrogen, androgens also act directly via the AR in osteoblasts. We have now shown that androgens also act directly via the AR in mineralising osteoblasts to maintain trabecular bone mass by regulating bone turnover.

References:

- 1) Notini AJ, et al. JBM 2007; 22:347-56;
- 2) Notini AJ et al. J Mol Endo 2005; 35:547-55.

Disclosures: R.A. Davey, None.

1218

Local Over Expression of Aromatase in Osteoblasts Leads to Clearly Increased Bone Mass. K. Sjogren*, N. Andersson, S. Movérare-Skrtic*, C. Swanson, C. Ohlsson. Division of Internal Medicine, Medicine, Goteborg, Sweden.

Testosterone (T) is of importance for the regulation of peak bone mass and age-dependent bone loss in males. The effects of T on bone can either be direct or mediated via local aromatization of T to estrogen (E2), followed by activation of estrogen receptors (ERs) in osteoblasts.

To investigate the importance of high local formation of E2 in osteoblasts, we developed a transgenic mouse model that over-expresses the human aromatase gene under the control of the rat type I alpha I procollagen promoter (Coll-Aro mice). This promoter will direct the aromatase expression to late osteoblasts in bone.

Measurements of aromatase expression in bone by quantitative real-time PCR showed that the system works and that Coll-Aro mice have a high and specific expression of human aromatase in bone. The bone specific expression of aromatase was supported by that serum E2 levels were unaffected in both male and female Coll-Aro mice and that the uterine weight was unaffected in female mice. At 11 weeks of age, male Coll-Aro mice exhibited a dramatic increase in cortical bone mineral content as analysed in the diaphyseal region in femur (+28%, $p < 0.001$) while there was no effect in female mice as measured by peripheral quantitative computed tomography (pQCT). The increased cortical bone mineral content in the male Coll-Aro mice was mainly due to increased cortical thickness (+21%, $p < 0.001$) but also to a slightly increased cortical volumetric BMD (+6%, $p < 0.001$). Detailed analysis of the tibia by μ CT revealed an increase in trabecular thickness (+9%, $p < 0.05$) in male Coll-Aro mice.

In conclusion, we show that bone-specific anabolic estrogenic effects can be achieved without systemic adverse effects by increasing the expression of aromatase specifically in bone. Based on the fact that aromatase expression in osteoblasts and breast/uterus is dependent on different promoters one may speculate that development of tissue specific inducers of aromatase expression in bone might result in bone-anabolic effects without systemic adverse effects.

Disclosures: K. Sjogren, None.

1219

Modulation of Mouse RANKL Gene Expression by Runx2 and Vitamin D3. R. Kitazawa, K. Mori, T. Kondo, S. Kitazawa. Division of Pathology, Kobe University, Graduate School of Medicine, Kobe, Japan.

The expression of receptor activator of nuclear factor- κ B ligand (RANKL) in osteoblastic cells is regulated by bone-seeking hormones such as PTH and vitamin D3. Runx2 is a master gene for osteoblastic differentiation and, at the same time, modulates osteoclastogenesis by regulating RANKL gene through the proximal (-378/-354, -214/-194 and -200/-180) and the distal (conserved noncoding sequence located 76 kb upstream of exon 1) runx2 sites. To elucidate the precise mechanism whereby runx2 and vitamin D3 regulate RANKL expression, we studied the function of runx2 on chromatin structure and on the proximal binding sites using mouse osteoblastic cell lines derived from normal (ST2) and runx2-deficient mice (C6).

Quantitative RT-PCR revealed that although the expression of RANKL mRNA in the steady-state was higher in runx2-deficient C6 cells than in ST2, it increased 20-fold in ST2, but only 1.8-fold in C6 by an 8-hour D3 treatment. Additionally, runx2 knock down in ST2 by siRNA resulted in an increase in the steady-state expression of RANKL mRNA and a decrease in the inducible effect of D3. Conversely, restoration of Runx2 by the Tet-On system in C6 decreased steady-state RANKL expression and increased the inducible effect of vitamin D3.

The exogenous transfected 2 kb promoter-reporter construct (2k-luc) showed 60% of the steady-state activity in C6 compared with that in ST2. Vitamin D3 increased the promoter activity of 2k-luc in ST2, but not in C6. Forced expression of runx2 by Tet-On system in C6 increased the steady-state activity of 2k-luc and its response to D3. Transfection of the mutated constructs with any one, two or all of the three proximal runx2 sites, depending on the number of mutated sites, decreased both the steady-state activity and the inducible effect of vitamin D3 in ST2, but not in C6. These data suggest that runx2 may exert a positive effect on the activity of the proximal 2kb promoter and its response to vitamin D3. We then assessed the acetylation status of the area spanning 40 kb upstream of the basic promoter in ST2 and C6 by ChIP assay with anti-acetylated H3 and H4 histone antibodies. Whereas H3 and H4 histone acetylation was detected even in the steady-state in C6, it was detected only in the presence of vitamin D3 in ST2, suggesting that constitutive histone acetylation of the 5' flanking region of the RANKL gene due to runx2-deficiency in C6 may cause its higher expression at the steady-state than in ST2.

Although runx2 may suppress RANKL gene by condensing chromatin structure, it exerts a positive effect in D3-induced RANKL transcription when the proximal runx2 sites are accessible to runx2 by D3 treatment. Thus, RANKL expression in stromal/osteoblastic cells is keenly regulated in response to vitamin D3 by transactivating the gene at two different levels.

Disclosures: R. Kitazawa, None.

This study received funding from: Japanese Ministry of Education, Sports and Culture.

1220

Sex Steroids Hormone Receptors in Osteoclasts Mediate Osteoprotective Effects by Regulating Its Life Cycle. Y. Imai¹, T. Nakamura², T. Matsumoto^{3*}, S. Takeda⁴, K. Igarashi^{5*}, T. Fukuda^{6*}, Y. Yamamoto^{2*}, J. Kanno^{5*}, K. Takaoka⁶, T. J. Martin⁷, P. Chambon^{8*}, S. Kato³. ¹Laboratory of Nuclear Signaling, Institute of Molecular and Cellular Biosciences, The University of Tokyo, Department of Orthopaedic Surgery, Osaka City University Graduate School of Medicine, Tokyo, Japan, ²Laboratory of Nuclear Signaling, Institute of Molecular and Cellular Biosciences, The University of Tokyo, Tokyo, Japan, ³Laboratory of Nuclear Signaling, Institute of Molecular and Cellular Biosciences, The University of Tokyo, ERATO, JST, Tokyo, Japan, ⁴Tokyo Medical and Dental University, Tokyo, Japan, ⁵Division of Cellular and Molecular Toxicology, National Institute of Health Sciences, Tokyo, Japan, ⁶Department of Orthopaedic Surgery, Osaka City University Graduate School of Medicine, Osaka, Japan, ⁷St. Vincent's Institute of Medical Research, Fitzroy, Australia, ⁸Institut de Genetique et de Biologie Moleculaire et Cellulaire and Institut Clinique de la Souris, Illkirch, France.

Sex steroids, estrogen and androgen, have the osteoprotective effect and prevents bone loss such as post-menopausal osteoporosis. However the molecular mechanism of how these are accomplished remains to be elucidated. Here we report critical roles of osteoclastic androgen receptor (AR) in males and osteoclastic estrogen receptor alpha (ER α) in females in mediating the actions of sex steroids on bone.

We selectively ablated AR and ER α in differentiated osteoclasts (AR^{ΔOC/Y} and ER^{ΔOC/ΔOC}) using Cathepsin K-Cre knock-in mice. AR^{ΔOC/Y} males exhibited clear bone loss in plain X-ray and 3D-CT, similar to the osteoporotic bone phenotype. Also in DEXA, femurs of AR^{ΔOC/Y} males showed low bone mineral density. Bone histomorphometric analysis revealed significant increase of osteoclast surface, osteoclast number and eroded surface in AR^{ΔOC/Y} males when compared to the control. In addition, MAR and BFR were increased in AR^{ΔOC/Y} males, these results suggested that AR^{ΔOC/Y} males had a high turnover osteoporotic phenotype. In *in vitro* study, quantitative RT-PCR showed that mRNA expression of Fas ligand (FasL) was facilitated in AR-overexpressed primary cultured osteoclasts treated with DHT, although the expression of Fas was not altered. Likewise, osteoclastic ER α appeared to mediate the osteoprotective estrogen action in females, but not males.

From these findings, we presume that the osteoprotective actions of sex steroids are mediated at least in part through osteoclastic AR in male and ER α in female, and that sex steroids regulate the life span of mature osteoclasts by controlling Fas/FasL related cell death signaling.

Disclosures: Y. Imai, None.

This study received funding from: JST, ERATO.

1221

Control of Estradiol-Directed Gene Transactivation by an Intracellular Estrogen Binding Protein and an Estrogen Response Element Binding Protein. H. Chen, M. Hewison, J. S. Adams. Endocrinology, Diabetes and Metabolism, Cedars-Sinai Medical Center, Los Angeles, CA, USA.

Experiments of nature have helped to illuminate the key pathways associated with metabolism and signal transduction of steroid hormones. In recent studies we have used the steroid hormone resistance exhibited by New World primates (NWP) to identify entirely novel mechanisms associated with intracellular trafficking and DNA targeting of steroid hormones. NWP exhibit resistance to estrogens that is associated with overexpression of an estrogen response element binding protein (ERE-BP) and an intracellular estradiol binding protein (IEBP). The NWP ERE-BP shows homology with human heterogeneous nuclear ribonucleoprotein C like protein, whilst IEBP shows homology with human hsp27. Although ERE-BP acts as a competitor for ERE occupancy by liganded estrogen receptor-alpha (ER), the function of IEBP/hsp27 is less clear. In new studies using human breast cells we show that IEBP/hsp27 can regulate estrogen signaling: 1) as a protein chaperone for ER; 2) as a cytosolic decoy for estradiol (E₂) binding; 3) by binding to ERE-BP and modulating the temporal organization of ERE occupancy by the ER and ERE-BP. IEBP/hsp27 was able to bind E₂ with relatively high affinity (K_d=0.25 nM). This was similar to that observed with estron (0.1 nM), whereas the selective estrogen receptor modulator tamoxifen showed no binding to IEBP/hsp27. Studies using ER^{ΔVE} MCF-7 cells showed that, in the absence of E₂, IEBP/hsp27 and ER were localized predominantly in the cytoplasm, with both translocating to the nucleus in the presence of E₂. GST-pulldown analyses confirmed binding of ER to IEBP/hsp27 but also revealed indirect association between ER and ERE-BP. Protein-protein interaction of IEBP/hsp27 and ERE-BP was confirmed by immunolocalization, as well as yeast 2-hybrid and GST-pulldown analyses. These studies also showed that normal E₂ responses in MCF-7 cells involve cycling of the IEBP/hsp27-ERE-BP complex between the cytosol and nucleus. Over-expression of either IEBP/hsp27 or ERE-BP suppressed E₂-mediated transcription in ER^{ΔVE} cells. This was associated with abnormal subcellular distribution of the IEBP/hsp27-ERE-BP complex, which resulted in concomitant dysregulation of ERE occupancy by ER and ERE-BP as determined by chromatin immunoprecipitation. We hypothesize that IEBP/hsp27 and ERE-BP not only cause hormone resistance in NWP but are also crucial to normal estrogen signaling in human cells. In particular, protein-protein interaction between IEBP/hsp27 and ERE-BP in both cytosolic and nuclear compartments appears to be essential to the regulation of their individual actions on ER signaling.

Disclosures: H. Chen, None.

1222

Estradiol Mediates Rescue of the Dominant-negative Effects of Estrogen Response Element-binding Protein In Vivo. H. Chen, M. Hewison, L. Nguyen*, J. S. Adams. Endocrinology, Diabetes and Metabolism, Cedars-Sinai Medical Center, Los Angeles, CA, USA.

Biological responses to estrogens are dependent on the integrated actions of various proteins, including the estrogen receptor (ER), that regulate the transcription of estrogen response element (ERE)-containing target genes. We have identified a naturally occurring antagonist of this mechanism that functions by competing with ER for ERE occupancy. The hnRNP-like protein, termed an ERE-binding protein (ERE-BP), is constitutively over-expressed in cells from estrogen-resistant New World primates. In order to verify that ERE-BP legislates estrogen resistance *in vivo*, we generated transgenic mice that specifically over-express varying levels of ERE-BP in breast tissue under the control of whey acidic protein gene promoter. Female transgenic mice with high levels of ERE-BP were unable to nurse their pups, none of which survived to weaning unless were fostered. Mice expressing intermediate and low levels of ERE-BP in breast had progressively more estrogen-driven breast development and lactational capacity. We hypothesized that escape from the dominant-negative action of ERE-BP on the breast was dictated by relative balance in ERE-BP expression levels and the concentration of estrogen available to the dominant-positive-acting ER. To test this hypothesis, four-week-old ERE-BP-high female mice were implanted subcutaneously with a capsule containing 7.2mg/21day-release estradiol (E2) or placebo. Analysis of 8-week-old mice breast whole-mounts and histology showed that E2-treated ERE-BP mice exhibited a 4.5-fold increase in mammary gland branch number ($p<0.001$) and 3.7-fold increase in duct number ($p<0.05$) compared with the placebo-infused controls. Analysis of postpartum breast whole-mounts and histology showed that E2-treated ERE-BP mice demonstrated more than a doubling in milk-containing lumina and a 3.0-fold increase in lobule-alveolae and duct formation ($p<0.02$) compared to placebo-infused ERE-BP mice, consistent with improved mammary gland differentiation. These data emphasize that 1) ERE-BP is a potent attenuator of estrogen-directed bioactivity and 2) increased circulating levels of E2 can rescue the host from the suppressive effects of ERE-BP *in vivo*, confirming *in vitro* data from our group. In summary, we have shown for the first time that there exists a reciprocal, dominant-positive:dominant-negative relationship between E2-liganded ER and ERE-BP *in vivo*. Although our experiments have focused on breast tissue, we hypothesize that ERE-BP is a crucial determinant of ERE-directed estrogen responses throughout the body.

Disclosures: H. Chen, None.

1223

Bax-deficient Mice Exhibit Marked Increase in Callus Size and Cartilage During Endochondral Repair of Femur Fractures. C. H. Rundle, X. Wang*, J. E. Wergedal, M. H. C. Sheng, R. M. Porte*, K. H. W. Lau, S. Mohan. Research (151), J.L. Pettis VAMC, Loma Linda, CA, USA.

While it is clear that endochondral bone formation during fracture repair involves the spatial and temporal regulation of the proliferation and differentiation of multiple cell types, there is suggestive evidence that the spatial and temporal regulation of apoptosis is also critical. Accordingly, this study evaluated the effects of Bax (a pro-apoptotic gene) deficiency on fracture repair. Healing of femoral fractures (created by three-pointed bending) in adult Bax KO [in a C57BL/6 (B6) genetic background] and B6 control mice was monitored by pQCT and histomorphometry. Bax KO mice developed larger calluses with increased cartilage area [3-fold at 7 days ($p<0.003$); 2-fold at 14 days ($p<0.05$)]. The bone mineral content (BMC) of Bax KO calluses was also greater than B6 calluses [\sim 2-fold each at 14 days ($p<0.004$), 21 days ($p<0.04$), and 28 days ($p<0.0008$)]. Cell counts within the cartilage area of the healing calluses showed that the enlarged cartilage in the Bax KO callus was due to an increase in chondroblast number and not cell size. To evaluate whether the BAX deficiency-related impairment of apoptosis accounted for the difference, the number of apoptotic cells in the cartilage within the healing callus was determined by the TUNEL assay. There was no significant difference in the percentage of apoptotic cells, indicating that the large increase in chondroblast number could not be due to differences in chondroblast apoptosis alone and suggesting that Bax deficiency also increased chondroblast proliferation during early fracture healing. There were also more osteoclasts on the woven bone surfaces of Bax KO mice during callus remodeling at 21 days (25%, $p<0.004$) and 28 days (33%, $p<0.05$). The callus size and BMC of Bax KO mice returned to B6 levels at 35 days. To identify a mechanism for the increase in chondroblasts, whole genome gene expression analysis was performed at 14 days post-fracture. There were no significant expression changes in genes associated with mitochondrial apoptosis, with the exception of the Bik-like gene (2.3-fold increase, $p<0.05$), suggesting a compensatory function for this gene. Consistent with the greater prehypertrophic chondrocyte content of early fracture cartilage, the expression of collagen-2 and collagen-9 (3-fold, $p<0.05$ for each), but not collagen-10, was elevated. Conclusions: 1) Bax deficiency enhanced cartilage formation, bone formation and remodeling during fracture repair, suggesting that Bax is a negative regulator of these processes, and 2) Bax deficiency increased chondroblast proliferation, suggesting that Bax may regulate fracture repair through a mechanism independent of its pro-apoptotic action.

Disclosures: C.H. Rundle, None.

1224

Type III Sodium-Dependent Phosphate Transporter Controls Endochondral Ossification Through Regulating Chondrocyte Apoptosis. A. Sugita¹, S. Kawai¹, T. Hayashibara^{*1}, H. Yoshikawa², T. Yoneda¹.

¹Biochemistry, Osaka University Graduate School of Dentistry, Suita, Japan,

²Orthopedics, Osaka University Graduate School of Medicine, Suita, Japan.

Previous studies reported that phosphate levels in growth plate increased as chondrocyte differentiation advances. Cartilage differentiation is markedly disturbed in X-linked hypophosphatemia (XLH), a dominant disorder of phosphate homeostasis. These results suggest a critical role of phosphate in chondrocyte differentiation. Extracellular phosphate is incorporated into cells through the sodium-dependent phosphate transporter (NPT). Growth plate chondrocytes express type IIa NPT (Npt2a) and type III NPT (Pit-1). It is therefore likely that these NPTs are involved in the regulation of chondrocyte differentiation. However, which NPT is a major player is currently unknown. Phosphonoformic acid (PFA), a non-selective competitive inhibitor of NPT, reduced ³²P uptake and suppressed apoptosis in mouse primary rib chondrocytes. PFA also inhibited chondrocyte apoptosis *in vivo*. Of interest, PFA decreased intracellular levels of ATP, which is essential for the activation of caspase-9 and caspase-3, leading to the progression of apoptosis. To investigate the specific role of phosphate in chondrocyte apoptosis, we knocked-down Npt2a or Pit-1 using small interfering double-stranded RNA (siRNA). siPit-1 significantly decreased ³²P uptake, intracellular ATP levels, caspase-9 and caspase-3 activity, followed by reduced apoptosis. As a consequence, calcification of chondrocytes was diminished. In contrast, siNPT2a showed no effects. Both siPit-1 and siNPT2a did not affect early stages of chondrocyte differentiation. Finally, we examined the effects of Pit-1 overexpression on apoptosis in chondrocytes of Hyp mice that are a mouse homologue of human XLH and exhibit reduced Pit-1 expression and apoptosis in cartilage compared with wild-type mice. Overexpression of Pit-1 significantly increased ³²P uptake in Hyp chondrocytes. In conjunction, it also increased intracellular ATP levels, caspase-9 and caspase-3 activation and apoptosis in Hyp chondrocytes. In conclusion, our results suggest phosphate uptake through Pit-1 specifically modulates the activation of ATP-dependent caspase signaling pathway, which in turn controls apoptosis and calcification of chondrocytes, thereby regulates endochondral ossification.

Disclosures: A. Sugita, None.

1225

The 7B2 Protein Regulates FGF-23 Degradation and Production in X-linked Hypophosphatemia (XLH). B. Yuan*, M. Takaiwa*, Y. Xing*, J. J. Meudt*, M. K. Drezner*. Department of Medicine, Endocrinology Section, University of Wisconsin, Madison, WI, USA.

The mechanism by which inactivating PHEX mutations increase serum FGF-23 remains unknown. However, FGF-23 may be processed at a subtilisin-like proprotein convertase (SPC) cleavage site (RXXR). Indeed, we reported mice treated 5 days with an SPC inhibitor, Decanoyl-Arg-Val-Lys-Arg-chloromethyl ketone (Dec), develop inhibition of FGF-23 degradation and elevation of serum FGF-23, as well as abnormal Pi homeostasis and vitamin D metabolism, characteristic of XLH. Yet, these studies did not reveal increased FGF-23 mRNA, failing to recapitulate the mechanism underlying abnormal serum FGF-23 in XLH. Thus, we further investigated if abnormal SPC activity can create both aberrant FGF-23 cleavage and production. Initially, we explored if SPC2 and helper protein 7B2 truly alter FGF-23 degradation, using HEK293 cells transfected with recombinant FGF-23 cDNA and co-transfected with SPC2 and 7B2 alone or together. After 48 hours Western blotting indicated neither SPC2 nor 7B2 alone altered FGF-23 degradation. However, transfection with SPC2 and 7B2 increased C-terminal fragments of FGF-23 in cell culture medium (2.14 ± 0.18 vs 1.0 ± 0.08 ; $p<0.01$) and decreased intact FGF-23 in cell lysates (0.48 ± 0.4 vs 1.02 ± 0.2 ; $p<0.05$), confirming that diminished SPC2/7B2 activity may increase serum FGF-23 levels. Subsequently, we explored if SPC2/7B2 inhibition altered FGF-23 mRNA production. Incubation of immortalized osteoblasts with 25 μ M Dec for 12h inhibited FGF-23 degradation, but more importantly increased FGF-23 mRNA (3.9 ± 0.9 vs 1.2 ± 0.2 ; $p<0.001$). Surprisingly, altered FGF-23 degradation and production corresponded with decreased 7B2 active protein (0.53 ± 0.01 vs 1.77 ± 0.1 ; $p<0.001$) and mRNA (0.61 ± 0.09 vs 1.04 ± 0.14 ; $p<0.001$). These observations suggest that decreased 7B2 not only reduces FGF-23 degradation but up-regulates production. To confirm this possibility we assessed 7B2 in hyp-mice, the murine homolog of XLH. The hyp-mice have decreased osseous production of 7B2 mRNA (0.45 ± 0.02 vs 1.06 ± 0.05 ; $p<0.01$) and reduced 7B2 active protein (0.68 ± 0.04 vs 1.0 ± 0.08 ; $p<0.01$). Further, we found that administration of 25 μ M Dec to normal mice for 12-days not only resulted in the HYP biochemical phenotype, but in a significant decrease in osseous 7B2 mRNA (0.84 ± 0.05 vs 1.0 ± 0.12 ; $p<0.05$), an expected decrease of FGF-23 degradation and an increase in FGF-23 mRNA (2.23 ± 0.12 vs 1.16 ± 0.02 ; $p<0.01$). Our observations indicate that decreased 7B2 production and accordingly 7B2 active protein in osteoblasts result in the sustained elevation of circulating FGF-23 in XLH due both to the direct effects of SPC2/7B2 on FGF-23 cleavage and to likely downstream effects of SPC2/7B2, which increase FGF-23 mRNA production.

Disclosures: B. Yuan, None.

This study received funding from: NIH.

1226

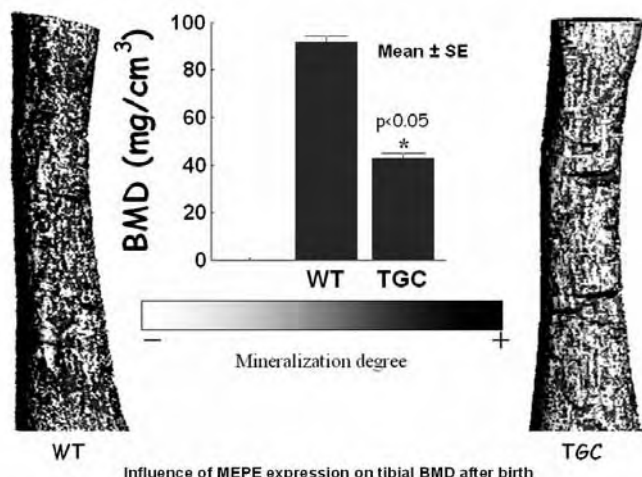
Abnormal Bone Mineralization, Osteoclastogenesis & Bone Turnover in Transgenic Mice Overexpressing MEPE. V. David¹, A. Martin¹, L. W. Fisher², A. Hedge¹, P. S. N. Rowe¹. ¹Internal Medicine, Kansas University Medical Center, Kansas City, KS, USA, ²NIDCR-NIH, Bethesda, MD, USA.

Matrix extracellular phosphoglycoprotein (MEPE) is a SIBLING-protein involved in bone-mineralization. Although increased MEPE expression occurs in several bone-mineral and renal-phosphate handling diseases, its precise physiological role is unknown.

In this study, we constructed transgenic-mice overexpressing murine-MEPE (Col1a1 2.3kb promoter) and used them as a model-system to test whether MEPE influences bone-mineralization in vivo. We analyzed bone-phenotypes of male-transgenic (TGC) and wild type (WT) C57BL6 newborn, 5 week-old and 19 week-old adult mice (n=10).

Protein (western-blot) and mRNA (RT-PCR) measurements confirmed a 50X over-expression of MEPE in bone. Newborn mice overexpressing MEPE displayed a low bone-mass phenotype (see figure, 53% decrease in BMD, $p<0.001$). Abnormal bone-growth also occurred at 5 weeks as assessed by femur length (5% decrease, $p<0.01$) and growth plate width (+26%; $p<0.05$). In older animals, X-ray densitometry and 3D-microtomography analyzes (uCT) showed MEPE over-expression results in a lower tibial bone-mineral density (6% decrease, $p<0.01$) and cortical thickness (10% decrease, $p<0.01$). In contrast, TGC mice had a significantly reduced vertebral trabecular bone-volume (8%, $p<0.05$). Despite an increase in PHEX (+300%, $p<0.05$) and other osteocyte and osteoblast specific markers, MEPE over-expression resulted in reduced bone-remodeling. Specifically, TGC mice displayed lowered bone-formation rate (34% decrease in BFR/BS, $p<0.05$), reduced osteoclast number (33% decrease N.Oc/B.Pm, $p<0.01$), as well as serum and urinary bone-resorption markers (CTX and PYD, -50%, $p<0.05$). Also, BMSCs from MEPE transgenic-mice failed to mineralize in vitro as measured by alizarin-red staining. Interestingly, a 5X increased mRNA expression of DMP1 (a related SIBLING-protein) occurred in transgenic bone.

In summary, our findings show bone over-expression of MEPE negatively impacts bone-mineralization, hinders bone-growth and reduces bone-resorption and modeling age-dependently. Also, an indirect or direct negative effect on osteoclastogenesis plays a key role in the transgenic phenotype.



Disclosures: V. David, None.

This study received funding from: RO1-AR51598-01 & R03-DE015900-01.

1227

FGF Receptors 3 and 4 Are Not Physiologically Relevant FGF23 Targets in the Kidney. S. Liu, L. Vierthaler*, W. Tang*, J. Zhou*, L. D. Quarles. Internal Medicine/The Kidney Institute, University of Kansas Medical Center, Kansas City, KS, USA.

Fibroblast growth factor 23 (FGF23) is a phosphaturic factor that exerts its biological effects on the kidney proximal tubule, leading to suppression of the sodium-dependent phosphate transport and production of 1,25(OH)₂D and to rickets/osteomalacia. FGF23 activation of target tissues appears to require the co-expression of FGF receptors and klotho, a transmembrane beta-glucuronidase. Klotho binds to the c splice isoforms of FGF receptors 1, 3 and 4, and the resulting FGF receptor:klotho complex creates the functional FGF23 receptor. The proximal tubule restricted location of the FGF receptor 3c implicates this receptor as the physiologically relevant target for FGF23 in the kidney. To confirm the role of FGF receptor 3 in mediating FGF23-dependent kidney effects, we crossed Hyp mice, which have elevated circulating FGF23 levels due to an inactivating Phe mutation, onto FGFR3-null mice. Consistent with their high circulating FGF23 levels, Hyp mice compared to wild-type (WT) littermates exhibited low serum phosphate (5.5 ± 0.2 mg/dL in Hyp vs. 8.9 ± 0.2 mg/dL in WT, $P < 0.01$) and serum 1,25 (OH)₂D levels (132 ± 25 pM in Hyp vs. 197 ± 23 pM in WT, $P = 0.08$), reduced Npt2a expression in the proximal tubules, and low bone mineral density (BMD) due to the presence of osteomalacia. In contrast, neither the serum phosphate nor 1,25(OH)₂D levels were altered in FGF receptor 3 null mice. More importantly, ablation of the FGF receptor 3 in Hyp mice failed to correct

the hypophosphatemia, aberrant 1,25(OH)₂D levels, reduced Npt2a expression or decreased BMD. In similar studies, ablation of FGF receptor 4 in Hyp mice also failed to correct the effects of excess FGF23. To explore the role of FGFR1 and klotho in mediating the proximal tubule response to FGF23, we performed immunohistology of mouse kidneys using FGFR1 and klotho specific antibodies. Consistent with previous reports, we found that both FGFR1 and klotho are predominately expressed in the distal rather than the proximal tubule. Our findings suggest that neither FGFR3 nor FGFR4 are responsible for the renal actions of FGF23. Moreover, the co-localization FGFR1 with klotho in the distal tubule would require the presence of a distal to proximal tubular autocrine pathway to explain FGF23 inhibition of renal phosphate absorption and 1,25(OH)₂D production by the proximal tubule. Further studies are needed to determine whether FGFR1c in the distal tubule or a novel receptor in the proximal tubule mediate the renal effect of FGF23.

Disclosures: S. Liu, None.

This study received funding from: RO1-AR45955 and P20 RR-17708.

1228

Alox5 Null Mice Have Reduced Cortical Bone Density, Altered Bone Turnover and Low Serum IGF-I. V. E. DeMambro¹, L. G. Horton¹, C. L. Ackert-Bicknell¹, W. G. Beamer¹, M. C. Horowitz², C. J. Rosen¹. ¹The Jackson Laboratory, Bar Harbor, ME, USA, ²Yale University School of Medicine, New Haven, CT, USA.

We previously reported that a congenic mouse strain, B6.C3-6T, which carries a 30 cM QTL region from C3H on Chr 6. B6.C3-6T, has reduced serum IGF-1, decreased areal BMD and low trabecular BV/TV, with enhanced marrow adiposity. A candidate gene in this QTL is Alox5 (Lipoxygenase 5), which by sequencing in 6T, has a truncated 3'UTR. Alox5 was also reported to be a prime candidate gene for BMD and fat mass in a B6 x DBA analysis, although phenotyping was limited in the Alox5 nulls (-/-) by small numbers of mice(1). To test the hypothesis that Alox5 polymorphisms could contribute to the 6T phenotype, we raised Alox5-/- (n=20) mice on a pure B6 background and compared them with littermate +/- (n=20) controls. At 16 weeks, male and female Alox5-/- had decreased aBMD ($p<0.05$) by DXA; % body fat was lower in the male -/- vs +/- ($p<0.05$) but did not differ in the females. Femoral pQCT revealed that both male and female Alox5-/- mice had decreased total vBMD, reduced periosteal and endosteal circumferences, and thinner cortices ($p<0.05$ vs gender matched +/-). Femur length was not affected. MicroCT40 of the femur revealed a decrease in both Bone Area and Bone Surface at the midshaft of female and male -/- mice, while analysis of the distal femur showed that male Alox5-/- mice had slightly reduced BV/TV ($p=0.08$ vs +/-) due to a decrease in trabecular thickness ($p<0.05$ vs +/-), without changes in trabecular number. Female Alox5-/- mice had an increase in distal femoral BV/TV ($p<0.05$ vs +/-) and connectivity density ($p<0.05$ vs +/-) with a trend towards increased trabecular number and decreased trabecular spacing. Histomorphometry of female -/- tibias at 8wks of age showed decreased osteoblasts/osteoid perimeter ($p=0.02$ vs +/-) and a slightly reduced Bone Surface/Bone Volume ($p=0.10$ vs +/- controls). Both male and female Alox5-/- had a 15-20% reduction in serum IGF-1 ($p<0.05$ vs +/-) while osteocalcin levels tended to be lower in the females -/- ($p=0.10$ vs +/-) but not in the males -/-. In vitro studies of marrow stromal and bone marrow cells from 10wk Alox5-/- females demonstrated reduced CFU-AP+ colonies ($p<0.05$ vs +/-), as well as less TRAP+ multinucleated osteoclasts compared to controls. In summary, Alox5-/- mice have in vivo and in vitro evidence of altered bone turn over, as well as compartment specific changes in the skeleton. Polymorphisms in the Alox5 gene may contribute to the unique skeletal phenotype of 6T, and may be important in peak bone acquisition.

Disclosures: V.E. DeMambro, None.

This study received funding from: NIAMS 45433.

1229

Weekly Administration of a Novel Parathyroid Hormone - Collagen Binding Domain Fusion Protein Increases Bone Mineral Density by More Than 15 Percent in Normal Mice. T. Ponnappakkam¹, O. Matsushita^{2*}, J. Sakon³, R. C. Gensure¹. ¹Pediatrics, Ochsner Clinic Foundation, New Orleans, LA, USA, ²Microbiology and Parasitology, Kitasato University School of Medicine, Tokyo, Japan, ³Chemistry and Biochemistry, University of Arkansas, Fayetteville, AR, USA.

Parathyroid hormone (PTH) is an anabolic bone agent which has been shown to be superior to bisphosphonate compounds in the treatment of osteoporosis; however, bisphosphonates are currently the first line treatment for this disorder primarily because of dosing convenience and more favorable side-effect profile. Bisphosphonates accumulate in the bone, allowing them to be efficacious with weekly/monthly oral dosing or yearly intravenous dosing. PTH, on the other hand, is quickly metabolized in the bloodstream and must therefore be given by daily subcutaneous injection. To prolong the retention of PTH in the bone, and thus prolong its duration of action and minimizing systemic side-effects, we have synthesized a fusion protein (PTH-CBD) of human PTH(1-33) and the collagen binding domain of ColH collagenase, derived from Clostridium histolyticum. In-vitro collagen binding assays indicate that the PTH-CBD fusion protein retains its ability to bind collagen. PTH-CBD also stimulates cAMP accumulation with similar potency and efficacy to human PTH(1-34) in LL-CPK cells stably transfected with the parathyroid hormone receptor (PTH-CBD: Kd = 2×10^{-8} M, Emax = 390 ± 54 pmol/well; PTH(1-34): Kd = 1.5×10^{-8} M, Emax = 357 ± 60 pmol/well). Weekly injections of PTH-CBD in normal young female C57BL/6J mice (Jackson Laboratories) for 8 weeks resulted in a 16.7 ± 4.5 percent ($p<0.01$, N=6) increase in spinal bone mineral density (BMD), vs. 7.3 ± 7.1 percent for PTH(1-34) (NS, N=6) and 4.9 ± 6.7 percent for vehicle control (NS, N=8). BMD was also measured in excised spines after sacrifice, and there was again a significant increase seen after PTH-CBD treatment vs. vehicle control (15.4% increase, 74.8 ± 3.0 vs. 64.9 ± 1.5 mg/cm², $p<0.05$). The PTH(1-34) group showed no significant change in BMD vs.

vehicle control (67.7 \pm 2.5 vs. 64.9 \pm 1.5 mg/cm², NS). There were no side effects observed in either treatment group; the animals did not develop hypercalcemia and there was no evidence of bone tumors in whole-body DEXA scans or in excised bone tissues at the end of the study. In-vivo efficacy of longer (i.e. monthly) dosing intervals of PTH-CBD is currently being assessed. This novel fusion protein represents an application of a new concept in drug design, combining individual protein domains to create an agent with unique properties. PTH-CBD allows the superior anabolic effect of parathyroid hormone in the treatment of osteoporosis to be obtained with a more convenient dosing interval, at least in mice.

Disclosures: R.C. Gensure, None.

1230

ACE-011, A Soluble Activin Receptor Type IIA Fusion Protein, Increases BMD and Improves Microarchitecture in Cynomolgus Monkeys. R. J. Fajardo¹, M. L. Bouxsein¹, A. E. Pearsall², A. Grinberg², M. Davies², T. Monnell², J. Ucran², M. Barazza², C. Kelly², D. Khanzode², K. Underwood², R. Kumar², R. S. Pearsall². ¹Beth Israel Deaconess Medical Center and Harvard Medical School, Boston, MA, USA, ²Accelaron Pharma, Cambridge, MA, USA.

Until recently, the role of activin, a member of the TGF- β superfamily, in bone metabolism was unclear. We have reported that treatment with an activin antagonist, a soluble form of the extra cellular domain of activin type IIA receptor (ActRIIA) fused to a murine IgG-Fc fragment, increases bone formation in normal mice and reverses bone loss in OVX mice. However, the pharmacokinetics of human ActRIIA-IgG-Fc (ACE-011) and its effects on bone mass in a larger animal model with a physiology more similar to humans has been lacking. To address this, female young adult Cynomolgus monkeys were used 1) to assess the pharmacokinetic (PK) properties and tolerability of ACE-011, and 2) to assess skeletal effects of ACE-011 treatment. In the PK study, a single dose of ACE-011 (1, 10 and 30 mg/kg) was administered by subcutaneous (SC) injection. Tolerability and PK parameters were assessed over a 28-day period. ACE-011 showed linear pharmacokinetic parameters across the 3 dose levels tested in the 28-day study. The half-life of ACE-011 was found to be 7 to 10 days. A single subcutaneous dose of ACE-011 up to 30 mg/kg was well tolerated, as were multiple doses (7) at 10 mg/kg over a 3-month period. In the efficacy study, monkeys were treated with ACE-011 (10 mg/kg, SC, bi-weekly) or VEH for 3 months (n=5/gr). At the conclusion of the study bones were harvested for ex vivo assessment of bone density and structure using DXA, pQCT, and μ CT. Compared to VEH, 3-months treatment with ACE-011 administration significantly increased BMD, trabecular bone density and structure in the axial and appendicular skeleton. BMD of the 5th lumbar vertebral body by DXA was 13.2% higher in ACE-011 vs. VEH (p<0.01). MicroCT analysis of the same bone revealed that ACE-011 treatment led to an increase in trabecular BV/TV (+16.2%, p<0.01), trabecular number (+13%, p=0.07), and a decrease in structure model index (7 fold decrease, p<0.01) relative to VEH. At the distal femur, compared to VEH, BMD by DXA was increased 15.3% (p=0.052), whereas trabecular bone density by pQCT was increased 79.5% (p<0.01). In summary, these results indicate that soluble ActRIIA (ACE-011) has a PK profile consistent with intermittent dosing, and that biweekly treatment with ACE-011 significantly improves bone density and structure at multiple skeletal sites in monkeys. These data provide strong rationale for further investigations into the use of ACE-011 as a new anabolic agent for the treatment of skeletal fragility.

Disclosures: R.S. Pearsall, Accelaron Pharma 3.
This study received funding from: Accelaron Pharma.

1231

Treatment with an Anti-Sclerostin Antibody Directly Stimulates Bone Formation in a Dose-Dependent Manner in Ovariectomized Rats with Established Osteopenia. X. Li, K. S. Warmington*, Q. Niu*, M. Grisanti, H. Tan, W. S. Simonet, P. J. Kostenuik, C. Paszty, H. Z. Ke. Amgen Inc., Thousand Oaks, CA, USA.

We previously reported that sclerostin inhibition via an anti-sclerostin antibody (Scl-Ab) increased bone formation, restored bone mass and bone strength in aged ovariectomized (OVX) rats with established osteopenia. In the present study, using osteopenic OVX rats, we examined the effects of various Scl-Ab doses on bone mass and bone formation. Six-month-old female SD rats were sham-operated or OVX and left untreated for 5 months. OVX rats were then treated with vehicle or Scl-Ab at 1, 2.5, 5, 10, 25 mg/kg (twice a week, s.c.) for 5 weeks (10/group). Xylenol orange (XO, 90 mg/kg) was injected s.c. the day before and the day of treatment initiation in order to detect mineralization and bone formation for the initial effects of treatment. Calcein and tetracycline were injected s.c. 12 and 2 days before necropsy, respectively. Histomorphometric analysis at the 2nd lumbar vertebral body showed that Scl-Ab treated groups had greater trabecular bone volume (BV/TV, +14 to +69%) in a dose-dependent manner compared with OVX control. There was a significantly higher osteoblast surface in OVX rats treated with 5 or 25 mg/kg of Scl-Ab compared with OVX control. However, osteoclast surface did not differ significantly between all doses of Scl-Ab treated OVX rats and OVX control. Qualitatively, OVX rats treated with Scl-Ab had more bone surface labeled with XO than Sham or OVX rats treated with vehicle. Almost all of the XO labeled bone surface in Scl-Ab treated animals was followed by new bone formation and calcein-tetracycline labels, indicating that Scl-Ab directly stimulates the trabecular bone formation without prior activation of bone resorption. Scl-Ab treated OVX rats had greater mineralizing surface (MS/BS, +76 to +288%), mineral apposition rate (MAR, +8 to +60%) and bone formation rate (BFR/BS, +101 to +546%) according to the measurement of calcein-tetracycline labels in a dose-dependent manner compared with OVX control. Qualitatively, an "over-filling" in trabecular bone remodeling was observed, illustrating that Scl-Ab increases bone formation on trabecular remodeling surfaces. These results

reveal that treatment with a Scl-Ab in OVX rats increases the formation mode of trabecular bone modeling and also increases bone formation on trabecular remodeling surfaces without increasing bone resorption.

Disclosures: X. Li, Amgen Inc. 1, 3.
This study received funding from: Amgen Inc.

1232

Sclerostin Inhibition Leads to Increased Periosteal and Endocortical Bone Formation as well as Decreased Cortical Porosity in Aged Ovariectomized Rats. Q. Niu^{*1}, K. S. Warmington^{*1}, M. Grisanti¹, H. Tan¹, M. S. Ominsky¹, W. S. Simonet¹, M. Robinson^{*2}, P. J. Kostenuik¹, H. Z. Ke¹, C. Paszty¹, X. Li¹. ¹Amgen Inc., Thousand Oaks, CA, USA, ²UCB-CellTech, Slough, United Kingdom.

We previously reported that treatment with a sclerostin antibody (Scl-Ab) stimulated trabecular bone formation, restored bone mass and bone strength in aged ovariectomized (OVX) rats. Cortical bone is known to be a major contributor to bone strength, so we used dynamic histomorphometry to examine the effects of sclerostin inhibition on cortical bone formation. Six-month-old female SD rats were sham-operated or OVX and left untreated for 13 months. OVX rats were then treated s.c. with vehicle or a Scl-Ab at 25 mg/kg, twice a week, for 5 weeks (9-12/group). Calcein and tetracycline were given by s.c. injection 10 and 3 days before necropsy, respectively. Left femurs were collected and femoral midshaft cross-sections were prepared for dynamic histomorphometry. Scl-Ab treated OVX rats had decreased marrow cavity area (-17%) and increased cortical bone area (+14%) compared with OVX controls. Mineralizing surface (MS/BS), mineral apposition rate (MAR) and bone formation rate (BFR/BS) were determined. Scl-Ab-treated OVX rats had significantly greater bone formation on periosteal (MS/BS +155%, MAR +84%, BFR/BS +339%) and endocortical surfaces (MS/BS +372%, MAR +145%, BFR/BS +913%) compared with OVX controls. In addition to examining periosteal and endosteal surfaces, we looked at the effect of Scl-Ab treatment on intracortical surfaces. Cortical porosity was quantitated by determining the total porosity area for all pores with a diameter greater than 40 μ m. Expressed as percent of cortical area (Ct.Ar), the OVX control group had increased porosity area (Po.Ar/Ct.Ar, +1124%) as compared to sham controls. As compared to OVX control rats, Scl-Ab treatment decreased porosity area (to sham levels) and significantly increased MS/BS (+205%), MAR (+49%) and BFR/BS (+504%) on the intracortical surfaces. These results suggest that the decreased porosity in Scl-Ab treated OVX rats is due to increased bone formation on the intracortical surfaces. In summary, sclerostin inhibition stimulated periosteal and endocortical bone formation, and also reduced cortical porosity by increasing bone formation on intracortical surfaces of aged OVX rats with established osteopenia. These results suggest that treatment with anti-sclerostin antibody has the potential to improve cortical geometry and bone strength by promoting bone formation on periosteal, endocortical and intracortical surfaces in patients with low bone mass.

Disclosures: X. Li, Amgen Inc. 1, 3.
This study received funding from: Amgen, Inc.

1233

Comparison of a Soluble Activin Receptor Type IIA (ACTRIIA), PTH and Zoledronate, for Treatment of Established Bone Loss in OVX Mice. E. Rosen^{*1}, E. Canalis², L. Stadmeier^{*2}, E. Cory^{*1}, V. Glatt¹, R. S. Pearsall³, M. L. Bouxsein^{*1}. ¹Beth Israel Deaconess Medical Center and Harvard Medical School, Boston, MA, USA, ²St. Francis Hospital and Medical Center, Hartford, CT, USA, ³Accelaron Pharma, Cambridge, MA, USA.

We previously reported that treatment with an activin antagonist, a soluble form of the extra cellular domain of activin receptor type IIA fused to a murine IgG-Fc fragment (RAP-011), induced new bone formation and reversed bone loss in OVX mice. Here, we compare the skeletal effects of RAP-011 to known anabolic (PTH(1-34)) and antiresorptive (zoledronate, ZOL) therapies. 8-wk old female C57BL/6 mice were OVX or SHAM-OVX, and allowed to lose bone for 8 wks. OVX mice were then randomized to receive RAP-011 (10 mg/kg, I.P. 2x/wk), PTH (80 μ g/kg, s.c. 5x/wk), ZOL (single I.P. injection, 20 μ g/kg) or vehicle (VEH, I.P., 2x/wk) for 6 weeks (n=8-10/gr). In two other groups (VEH and RAP-011), treatment was stopped after 6 wks, and mice were sacrificed 6 wks later. Skeletal response was assessed by PIXImus, microCT and histomorphometry. Total body BMD increased significantly in PTH, RAP-011, and ZOL versus baseline but was unchanged in VEH and SHAM. By microCT, trabecular (Tb) BV/TV at the distal femur was higher than VEH in RAP-011 and ZOL, but not PTH. Histomorphometry of the distal femur revealed that bone formation rate was increased only in RAP-011 (1.4-fold, p=0.03 vs VEH). Osteoblast number increased in PTH (1.4-fold, p=0.014) but not in RAP-011 or ZOL, while osteoclast number decreased in RAP-011 (p=0.03) and ZOL (p<0.01), but not PTH. Eroded surface was increased in PTH, but not other treatments. At the 5th lumbar vertebral body, Tb BV/TV was significantly greater in RAP-011 (+30%), PTH (+35%) and ZOL (+21%) than VEH (p<0.001 for all). Tb number was increased in PTH and RAP-011, but not ZOL. Vertebral compressive strength was higher in all treatment groups compared to VEH (p<0.001 for all), whereas work-to-failure was significantly increased by PTH and RAP-011, but not ZOL. Six weeks after cessation of treatment, vertebral and femoral Tb BV/TV remained increased in RAP-011 vs VEH. Altogether these data indicate that in adult OVX mice with established bone loss, treatment with an activin antagonist (RAP-011) increases bone volume, trabecular number and bone formation rate without enhancing bone resorption. The pattern of skeletal response to RAP-011 differed from PTH and from ZOL, suggesting that activin inhibition represents a novel mechanism for restoration of bone mass following estrogen deficiency.

Disclosures: M.L. Bouxsein, Accelaron Pharma 2, 5.
This study received funding from: Accelaron Pharma.

1234

Intermittent PTH Has Increased Anabolic Effects in Cyclooxygenase-2 Knockout Mice. M. Xu, Q. Gao*, O. Voznesensky*, S. Choudhary, V. Diaz-Doran*, L. Raisz, C. Pilbeam. Endocrine Division and Musculoskeletal Institute, University of Connecticut Health Center, Farmington, CT, USA.

Because PTH induces cyclooxygenase (COX)-2 and prostaglandin (PG) E_2 production and because PGE $_2$ and PTH can both increase bone formation, we hypothesized that COX-2 knockout (KO) mice would have decreased anabolic response to PTH compared to wild type (WT) mice. Five-month old male WT (27) and KO (24) mice in a CD-1 background were injected with vehicle (control) or PTH (80 µg/kg, 1-34 hPTH) daily for 22 d and euthanized 3 h after the last injection. Bone mineral density (BMD) was measured by DXA in vivo at beginning and end. KO mice weighed 10% less than WT mice ($p < 0.01$) and had 20% less body fat than WT mice ($p < 0.01$). There was no difference in femur BMD between WT and KO before PTH. Comparing each mouse to itself, PTH increased femur BMD 6.0% ($p < 0.01$) in WT mice and 11.4% ($p < 0.01$) in KO mice, and the increase was significantly greater ($p < 0.05$) in KO mice. PTH increased the BMD of ex vivo vertebrae (L1-L5) 11% ($p < 0.05$) in KO mice but only 6% (NS) in WT mice. On µCT of ex vivo bones no change in BV/TV was seen in PTH-treated WT or KO mice. However, PTH increased trabecular thickness in vertebrae and distal femurs 15-20% ($p < 0.01$) in WT mice and 21-25% ($p < 0.01$) in KO mice. Femur cortical thickness ($p < 0.01$) and area ($p < 0.05$) were less in KO (0.25 mm, 1.15 mm 2) compared to WT mice (0.29 mm, 1.28 mm 2). PTH increased cortical thickness and area 25-30% ($p < 0.01$) in KO mice but the increase (3-7%) in WT was not significant. Dynamic histomorphometry of the distal femur showed that, compared to controls, PTH significantly ($p < 0.01$) increased (1) MAR from 0.85 to 1.85 µ/d in WT mice and from 0.78 to 2.46 µ/d in KO mice and (2) BFR/BS from 0.23 to 0.77 µ 3 /µ 2 /d in WT mice and from 0.24 to 1.32 µ 3 /µ 2 /d in KO mice. PTH increased resorption similarly in WT and KO mice. Compared to controls, PTH increased (1) osteoclast surface in WT (7.4% vs 17.9%, $p < 0.01$) and KO mice (6.7% vs 13.0%, $p < 0.01$); (2) serum calcium 10% ($p < 0.05$) in both WT and KO mice; and (3) serum TRAP levels 1.8- to 2-fold ($p < 0.01$) in both WT and KO mice. Analysis of mRNA in tibiae by real time PCR at end of experiment showed no differences in COX-1 in any group. Alkaline phosphatase, Runx2, and RANKL mRNA were increased and OPG mRNA decreased by PTH in both WT and KO mice. Compared to controls, PTH decreased SOST mRNA in KO mice (RQ values, 8.0 vs 2.6, $p < 0.01$) but not significantly in WT mice (RQ values, 6.7 vs 4.1). In summary, PTH increased BMD of femur and spine to a greater degree in COX-2 KO mice than in COX-2 WT mice. Effects of PTH on trabecular bone volume were similar in WT and KO mice. We speculate that absence of COX-2 expression may increase the anabolic response to PTH primarily in cortical bone.

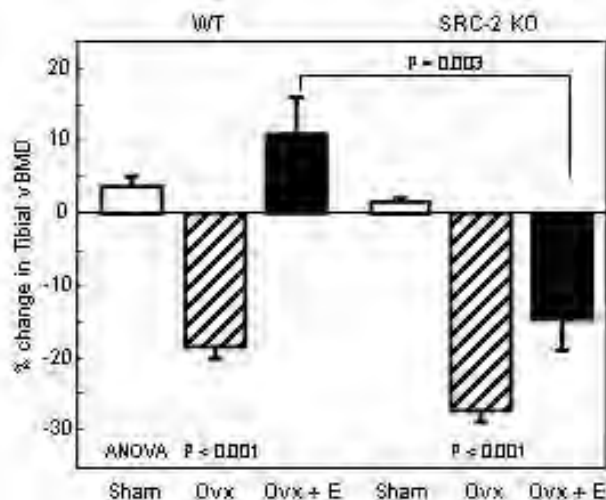
Disclosures: M. Xu, None.

This study received funding from: NIH DK-48361 and AR-47673.

1235

Deletion of Steroid Receptor Coactivator-2 (TIF-2) Results in Skeletal Resistance to Estrogen but a High Bone Mass Phenotype Due to Concomitant Resistance to PPAR γ . U. I. Moedder¹, D. G. Fraser¹, A. Sanyal¹, M. Gehin², P. Chambon², B. W. O'Malley³, C. J. Rosen⁴, T. C. Spelsberg¹, S. Khosla¹. ¹Mayo Clinic, Rochester, MN, USA, ²Institut de Génétique et de Biologie Moléculaire et Cellulaire, Illkirch, France, ³Baylor College of Medicine, Houston, TX, USA, ⁴Jackson Labs, Bar Harbor, ME, USA.

Both the estrogen receptor (ER) and PPAR γ regulate bone metabolism and there is increasing evidence for cross-talk between these receptors. Clinically, PPAR γ agonists are associated with increased bone loss and fractures in postmenopausal women, but not in men. Since steroid receptor coactivator (SRC)-2 enhances both ER and PPAR γ activity, we examined the consequences of deletion of SRC-2 on bone using SRC-2 knock out (KO) mice. To assess the skeletal response to estrogen (E), wild type (WT) or SRC-2 KO mice ($n = 7-10$ per group) were studied following sham surgery, ovariectomy (ovx) or ovx following treatment with a physiological concentration of E $_2$ (2.5 µg/kg/d) for 2 months. While both WT and SRC-2 KO mice lost similar amounts of bone following ovx, the same dose of E $_2$ was much less effective in preventing ovx-induced bone loss in the SRC-2 KO compared to the WT mice (Figure).



Despite this defect in E action, SRC-2 KO mice clearly had a high bone mass phenotype under basal conditions (BV/TV [mean \pm SEM] at the femur metaphysis of 22.2 ± 3.4 %, vs. 12.4 ± 1.3 % for the WT, $P = 0.02$) with a marked decrease in bone marrow adipocytes (AV/TV of 0.6 ± 0.1 % vs. 1.3 ± 0.3 % for the WT, $P = 0.03$). These data suggest that, in the SRC-2 KO mice, endogenous PPAR γ ligands may be less effective at inhibiting bone formation. Consistent with this, in the presence of the PPAR γ agonist, rosiglitazone (1µM), bone marrow cultures from SRC-2 KO mice formed significantly more mineralized nodules (by 93 ± 34 %, $P = 0.02$) compared to cultures from WT mice. Collectively, these findings demonstrate that SRC-2 may be a key coregulator linking ER and PPAR γ signaling pathways in bone. While loss of SRC-2 leads to skeletal E resistance, the concomitant resistance to PPAR γ appears to be dominant, resulting in a net increase in bone mass and reduction in bone marrow adipocytes. To the extent that the ER and PPAR γ may compete for limiting cellular concentrations of SRC-2, loss of E following the menopause may lead to the observed susceptibility to thiazolidinediones (TZD)-induced bone loss in postmenopausal women by increasing the availability of SRC-2 to enhance PPAR γ signaling in bone.

Disclosures: U.I. Moedder, None.

1236

Increased Bone Mineral Density in Transgenic Mice Over-expressing Tissue-nonspecific Alkaline Phosphatase. M. C. Yadav¹, S. Narisawa¹, K. Johnson², R. Terkeltaub², N. Pleshko Camacho³, J. L. Millan¹. ¹Oncodevelopmental Biology, Burnham Institute for Medical Research, La Jolla, CA, USA, ²VAMC/UCSD, La Jolla, CA, USA, ³The Hospital for Special Surgery, New York, NY, USA.

We have recently reported that the rickets and osteomalacia characteristic in tissue-nonspecific alkaline phosphatase (TNAP)-deficient mice (Akp2 $^{-/-}$ mice) results from highly increased levels of the calcification inhibitor PPI, a natural substrate of TNAP, and from the concomitant increase in the expression of skeletal osteopontin (OPN), another calcification inhibitor. These studies suggested the possibility of manipulating the PPI/OPN axis as a means of affecting calcification. In this paper, we have tested this axis by surmising that transgenic mice over-expressing TNAP might be able to achieve tissular expression of TNAP sufficiently high to be able to lower circulating PPI and OPN concentrations to enhance bone mineral density (BMD) in these animals. Transgenic mice were generated by expressing human TNAP cDNA under control of the Apolipoprotein E promoter, which drives expression of TNAP primarily in the post-natal liver. We examined the expression levels of TNAP in tissues from mice carrying one copy or two copies of the ApoE-Tnap transgene and also from [Akp2 $^{-/-}$; ApoE-Tnap] mice, and examined the ability of their primary osteoblasts to calcify in culture. MicroCT analysis was used to measure BMD in long bones, vertebrae and calvaria. TNAP expression in ApoE-Tnap mice was major in the liver and kidney as expected, with lower but yet detectable levels in bone, brain and lung. Serum AP concentrations were 10 to 50-fold higher than age-matched sibling control wild-type (WT) mice. As predicted, serum levels of PPI and OPN were reduced in the transgenic animals. Furthermore, microCT analysis of femur, vertebrae and calvaria revealed higher BMD in cancellous bone of ApoE-Tnap+ and ApoE-Tnap+/+ mice compared to WT mice. Thus, we show that increases in tissular and circulating levels of TNAP lead to higher BMD by reducing the effective levels of the calcification inhibitors PPI and OPN. These data provide a mechanistic interpretation for the correlation between AP and BMD that has been observed in humans and mice. Furthermore, these studies suggest that administering recombinant TNAP may serve as a novel therapeutic approach for osteoporosis.

1Harvey et al., Elevated osteopontin levels contribute to the hypophosphatasia phenotype in Akp2 $^{-/-}$ mice. J. Bone Min. Res. 21: 1377-1386 (2006).

2Murshed et al., Broadly expressed genes accounts for the special restriction of ECM mineralization to bone. Genes Dev. 19: 1093-1104 (2005).

Disclosures: M.C. Yadav, None.

1237

The Retinoblastoma-Related Pocket Protein Rbl2 Is a Candidate Gene for a Quantitative Trait Locus Affecting Peak Bone Mass and Strength in Mice. R. F. Klein, E. A. Larson*, W. J. Wagoner*, D. A. Olson*, A. S. Carlos*. Bone and Mineral Unit, Oregon Health & Science University, Portland, OR, USA.

We previously identified a QTL on chromosome 8 (Chr 8) associated with variation in peak bone mineral density (BMD) in C57BL/6 (B6) and DBA/2 (D2) mice. A chromosomal fragment containing the Chr 8 QTL interval (61.6 Mb - 111.7 Mb) was transferred from D2 onto a B6 genetic background by selective breeding. Comparison of the resulting congenic strain (B6.D2^{DM231.113}) with the background B6 strain, established that the D2 interval on Chr 8 conferred increased bone mass and strength. Peak whole body, femoral and vertebral BMD (determined by DXA in 20-wk-old male mice) were, respectively, 11%, 23% and 16% greater in the congenic (D2 allele-bearing; $n=10$) mice compared to the background B6 ($n=9$) mice (all t-tests $p < 0.0001$). MicroCT analysis of mid-shaft femoral geometry revealed 18% greater cross-sectional area, 10% greater cortical thickness and 47% increased moment of inertia in congenic mice compared to background mice (all $p < 0.0001$). Consistent with the increased bone density and geometry, femoral failure load (determined by 3-point bending) of the congenic mice was increased 40% compared to the background mice ($p < 0.0001$). The Chr 8 introgressed region is homologous with a human genomic region (16q11.1-q23) linked with variation in both bone density and circulating osteocalcin levels suggesting that the effects on bone mass at this chromosomal region may be mediated through genes affecting bone remodeling. Serum osteocalcin levels (determined by RIA) were increased 53% (92 ± 5 ng/ml vs. 60 ± 4 ng/ml, $p < 0.0001$) in the B6.D2^{DM231.113} congenic strain compared to the

background strain. Based on synteny between human genome sequence and the murine Chr 8 introgressed region, we identified Rbl2 (residing at 16q12.1 in the human genome and at 94 Mb on Chr 8 in the mouse genome), which encodes the retinoblastoma p130 pocket protein, as a positional candidate gene for the observed variation in bone traits. Sequencing of the Rbl2 gene identified 5 nonsynonymous amino acid variants, one of which (exon 20; position 1023) involved a substitution of alanine (B6) for serine (D2). The transcriptional activity of p130 is influenced by post-translational phosphorylation at serine and threonine residues raising the possibility that this polymorphism may alter p130 function. Given the important role the family of retinoblastoma proteins plays in coordinating skeletal development through their effects on osteogenic differentiation, we hypothesize that Rbl2 is an important determinant of bone mass in mice and that inherited variation in the activity of retinoblastoma proteins may explain some proportion of the natural variation in peak bone density and strength in humans.

Disclosures: R.F. Klein, Merck & Co. 8; Procter & Gamble, Inc. 8; sanofi-aventis 8; Eli Lilly & Co., Inc. 8.

1238

Activation of Renin-Angiotensin System Induces Osteoporosis Independently of Hypertension. Y. Asaba^{*1}, M. Ito², K. Watanabe¹, S. Takeshita¹, J. Ishida^{*3}, Y. Nimura^{*4}, A. Fukamizu^{*3}, K. Ikeda¹. ¹Department of Bone and Joint Disease, National Center for Geriatrics and Gerontology (NCGG), Obu, Japan, ²Department of Radiology, Nagasaki University School of Medicine, Nagasaki, Japan, ³Center for Tsukuba Advanced Research Alliance (TARA), University of Tsukuba, Tsukuba, Japan, ⁴Department of Surgery, Nagoya University Graduate School of Medicine, Nagoya, Japan.

Osteoporosis and cardiovascular disease are major health problems worldwide. Although low BMD has been associated with deaths from stroke, the relationship between blood pressure and BMD is controversial and the underlying mechanism remains elusive. We have studied the role of the renin-angiotensin system (RAS) in bone metabolism using Tsukuba Hypertensive Mice (THM) overexpressing the human renin and angiotensinogen genes. THM exhibited elevated circulating angiotensin II (Ang II), high blood pressure (140 +/- 10 mmHg vs. 118 +/- 10 mmHg in WT) and low trabecular bone volume, as determined by microCT-40, at 3 and 6 months old. The trabeculae of THM were characterized by microarchitectural alterations such as decreases in trabecular thickness and connectivity and increases in trabecular separation and structure model index. Bone histomorphometry at the proximal tibia revealed the number of osteoclasts and eroded surface were significantly elevated compared with wild-type mice, and the bone formation rate was also increased, pointing to a state of high bone turnover. Interestingly, single transgenic mice overexpressing the human renin gene were normotensive but exhibited lower bone mass. Together with the expression of angiotensin converting enzyme (ACE) in bone by RT-PCR, it was suggested that local RAS is sufficient to induce osteoporosis independently of hypertension. Ang II had no direct effect on osteoclastogenesis from isolated bone marrow macrophages (with RANKL/M-CSF), but stimulated the formation of TRAP-positive osteoclasts in co-cultures of bone marrow cells and osteoblasts, pointing to an indirect mechanism through osteoblasts. Both the AT1 and AT2 receptors were expressed in osteoblasts, in which Ang II had increased RANKL and VEGF expression. Knockdown of AT2 by siRNA inhibited osteoclastogenesis in co-culture, while that of AT1 caused a paradoxical increase, suggesting a functional interaction between the 2 receptors. Accordingly, treatment of THM mice in vivo with an ACE inhibitor (enalapril) improved but an AT1 blocker (losartan) exacerbated osteoporosis. In conclusion, activated RAS is a contributing factor to the pathogenesis of osteoporosis, and certain anti-RAS drugs may be an effective therapy for the co-morbidity of hypertension and osteoporosis with aging.

Disclosures: Y. Asaba, None.

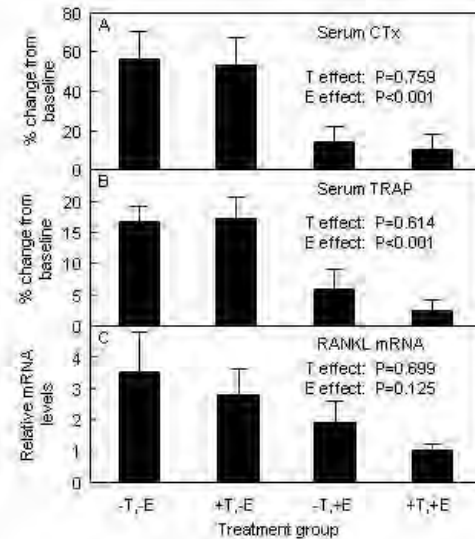
1239

Effects of Testosterone and Estrogen on Bone Resorption Markers and RANKL mRNA Levels in Bone Marrow Osteoblastic Cells in Men. A. Sanyal, K. Hoey*, J. Peterson*, E. Atkinson*, L. McCready*, M. Oursler, S. Khosla. Mayo Clinic, Rochester, MN, USA.

Previous studies have shown that in men, estrogen (E) may be a more potent inhibitor of bone resorption than testosterone (T), although this remains controversial. In addition, while it is clear that RANKL is a key regulator of bone resorption, possible effects of T and E on RANKL production in men have not been defined. Thus, to characterize further possible differential effects of T and E on bone resorption and on RANKL production in vivo, we studied 59 elderly men (mean age, 67 yrs) using a previously validated experimental paradigm in which the men were made hypogonadal with GnRH, endogenous E production was suppressed with the aromatase inhibitor letrozole, and sex steroid levels maintained with exogenous T or E supplementation. Following serum collections for the bone resorption markers, CTx and TRAP 5b, the men had withdrawal of both T and E (-T, -E), were replaced with T alone (+T, -E) but with continuation of letrozole to block aromatization of T to E, E alone (-T, +E) or both (+T, +E) for 3 weeks and the serum collections were repeated. In addition, bone marrow aspirates were performed and osteoblast lineage cells isolated by magnetic activated cell sorting (MACS) using an antibody against alkaline phosphatase (AP). RNA was extracted from the cells and RANKL mRNA levels quantified using quantitative PCR. Panel A shows the percent changes in serum CTx, panel B shows the percent changes in serum TRAP 5b, and panel C shows the relative RANKL mRNA levels in the AP positive cells isolated from the subjects in the 4 groups.

As is evident, while there were clear effects of E on both resorption markers, T did not regulate either marker. The pattern of changes in RANKL mRNA levels in the AP positive cells was similar to the changes in the bone resorption markers, although due to the variability of these measurements, there was only a trend for an E effect. Collectively, these findings are consistent

with the hypothesis that, at physiological concentrations, E has greater suppressive effects on bone resorption than T and that these differences are likely mediated, at least in part, by regulation of RANKL production. The use of more highly purified cell populations (e.g., additional purification using fluorescent activated cell sorting following MACS) should reduce the variability of the mRNA assessments and allow for clearer definition of the mediators of sex steroid action in vivo.



Disclosures: A. Sanyal, None.

This study received funding from: NIH AG04875.

1240

Increased Plasma Osteoprotegerin (OPG) Concentrations Are Associated with Indices of Bone Strength of the Hip: The Framingham Study. E. J. Samelson^{*1}, K. E. Broe¹, S. Demissie^{*2}, E. J. Benjamin^{*3}, R. S. Vasan^{*3}, J. Massaro^{*3}, S. Kathiresan^{*3}, C. J. O'Donnell^{*3}, T. J. Beck^{*4}, D. Karasik^{*1}, D. P. Kiel^{*1}. ¹Inst for Aging Research, Hebrew SeniorLife, Boston, MA, USA, ²Biostatistics, BUSPH, Boston, MA, USA, ³Framingham Heart Study, Framingham, MA, USA, ⁴Johns Hopkins, Baltimore, MA, USA.

OPG is an important regulator of bone turnover though its effects on osteoclastogenesis, yet little is known about the significance of circulating OPG concentrations with respect to bone strength in humans. Therefore, we evaluated the cross-sectional association between plasma OPG and femoral neck bone density (FN BMD) and geometry in a large cohort of women and men.

Participants included 1379 post-menopausal women and 1165 men, age 50+ years, in the Framingham Offspring Study. Information was obtained from exams performed 1996-2001. DXA (Lunar DPX-L) scans were used to evaluate FN BMD and geometry. Hip structure analysis was used to determine subperiosteal width, section modulus (bending strength), cross-sectional area (compression strength), and BMD at the narrow neck (NN) region. Plasma OPG concentrations were measured by ELISA (Biomedica, Austria). Sex-specific analysis of covariance was used to calculate means and assess linear trend in BMD and geometry values across OPG quartiles, adjusted for age, height, body mass index, current smoking, diabetes, coronary heart disease, osteoporosis medications, estrogen use (women), and NN BMD (for geometry outcomes).

Mean age of participants was 64 years (range, 50-89 years). OPG concentrations were greater in women (median 5.75 pmol/L; interquartile range (IQR) 4.85-6.84) than men (median 5.32; IQR 4.38-6.47) and increased with age. Multivariable-adjusted mean FN BMD in women increased from the lowest to the highest OPG quartile (Table; trend, p<0.01). However, no linear trend between FN BMD and OPG was observed in men (trend, p=0.34). Section modulus, width, and cross-sectional area increased with OPG in men (trend, p<0.01), whereas no association between hip geometry indices and OPG was observed in women.

Increased OPG concentrations were associated greater bone density in women and with favorable geometry features in men. These results suggest that higher OPG concentration may indicate greater skeletal strength in women and men, possibly through reducing bone loss in women and through increasing periosteal apposition in men.

ADJUSTED MEAN FEMORAL NECK BONE DENSITY* AND GEOMETRY INDICES** BY OPG QUARTILE

OPG Quartile	Women (N=1379)				Men (N=1165)			
	FN BMD (g/cm ²)	Cross-Sectional Area (cm ²)	Width (cm)	Section Modulus (cm ³)	FN BMD (g/cm ²)	Cross-Sectional Area (cm ²)	Width (cm)	Section Modulus (cm ³)
1 (low)	0.85	2.27	3.35	1.33	0.98	2.77	3.74	1.79
2	0.85	2.22	3.29	1.28	0.97	2.83	3.82	1.87
3	0.86	2.23	3.29	1.28	0.98	2.83	3.81	1.85
4 (high)	0.88	2.25	3.29	1.31	0.96	2.85	3.86	1.91
Trend, p	<0.01	0.45	0.11	0.41	0.34	<0.01	<0.01	<0.01

*Adjusted for age, height, body mass index, current smoking, diabetes, coronary heart disease, osteoporosis medications, estrogen use (women).

**Additionally adjusted for NN BMD.

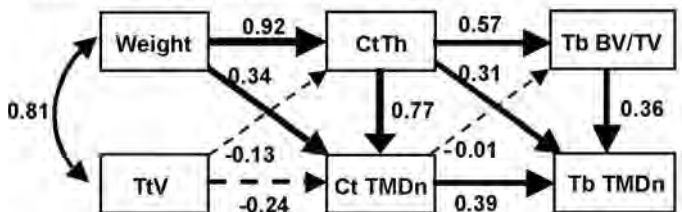
Disclosures: E.J. Samelson, None.

1241

Coadaptation Among Trabecular and Cortical Traits Contribute to Genetic Variation Affecting Bone Size in Recombinant Inbred Mouse Vertebral. S. M. Tommasini¹, B. Hu^{2*}, J. H. Nadeau³, K. J. Jepsen². ¹CUNY Graduate Center, New York, NY, USA, ²Mount Sinai School of Medicine, New York, NY, USA, ³Case Western Reserve University School of Medicine, Cleveland, OH, USA.

A previous study showed that randomization of A/J (A) and C57BL/6J (B) genomic regions resulted in adult Recombinant Inbred (RI) mice having mechanically functional femora with different sets of morphological and tissue-quality traits. This suggested that multiple traits were coordinated to ensure mechanical functionality. Analysis of RI strains has the potential for determining if similar biological controls exist for the construction of vertebrae. To test the hypothesis that trabecular, cortical, and compositional traits of the vertebral body are functionally related, we examined vertebrae from 20 genetically randomized female AXB/BXA RI mouse strains (n=5/genotype; age=16wks). Trabecular traits (bone volume fraction, Tb BV/TV; number; thickness; spacing), cortical traits (cortical thickness, CtTh), tissue mineral density (TMDn), and total vertebral volume (TtV = bone vol + marrow vol) of the L4 vertebral body were measured using micro-CT (GEMS). A correlation analysis using the mean values for each RI strain revealed that 30% of the correlations examined were significant. Thus, many bone traits covaried after genetic randomization. A Path Analysis was conducted using the mean Z-scores of each RI strain. Directed paths (Fig 1) identified important interactions among total vertebral size, cortical thickness, and mineral density similar to that observed in femora, such that larger vertebrae (greater TtV) tended to have thinner cortices with lower mineral content, whereas smaller vertebrae had thicker cortices with higher mineral content. Further, the Path Analysis highlighted important functional relationships between cortical and trabecular components such that vertebrae with thicker cortices had higher Tb BV/TV and Tb TMDn, and vertebrae with thinner cortices had lower Tb BV/TV and Tb TMDn. These results suggest that there are critical biological controls that co-adapt the set of cortical, trabecular, and compositional bone traits so that vertebrae are sufficiently stiff for daily loading. Therefore, this approach provides important new insight showing how genetic variation in trabecular architecture is functionally related to genetic variation in cortical traits.

Fig 1. Path analysis showing causal (straight arrows) and non-causal (curved arrows) relationships among body weight, total vertebral volume (TtV), cortical thickness (CtTh), cortical tissue mineral density (Ct TMDn), trabecular bone volume fraction (Tb BV/TV), and trabecular tissue mineral density (Tb TMDn). Path coefficients based on Z-transformed data.



$$CtTh = 0.92 \text{ Weight} - 0.13 \text{ TtV}, R^2 = 0.67$$

$$Ct \text{ TMDn} = 0.77 \text{ CtTh} + 0.34 \text{ Weight} - 0.24 \text{ TtV}, R^2 = 0.84$$

$$Tb \text{ BV/TV} = 0.57 \text{ CtTh} - 0.01 \text{ Ct TMDn}, R^2 = 0.32$$

$$Tb \text{ TMD} = 0.36 \text{ Tb BV/TV} + 0.31 \text{ CtTh} + 0.39 \text{ Ct TMD}, R^2 = 0.87$$

$$\text{Chi-square} = 1.30, \text{ df} = 4, \text{ p-value} = 0.86, \text{ RMSEA} = 0.00$$

Disclosures: S.M. Tommasini, None.

1242

Correlation Between Growth Patterns and Material Composition Leads to Preferred Sets of Adult Bone Traits. C. Price, H. W. Courtland, K. J. Jepsen. Mount Sinai School of Medicine, New York, NY, USA.

The specific combination of bone size, shape, and material composition observed in adulthood is predictive of whole bone mechanical properties and fracture risk. However, it is unknown how certain combinations of adult bone traits arise. Knowledge of how specific trait combinations arise is important because while most sets of bone traits satisfy the mechanical demands of daily loading certain sets are preferred under extreme loading conditions. Therefore, the goal of this investigation was to determine how different combinations of adult bone traits develop in inbred mouse femora. Variability in periosteal and endosteal surface growth results in different combinations of adult bone traits. To determine how surface movement influences bone shape and size we plotted femoral polar moment of inertia (J_0) against cortical area (CtAr) for A, B6, and C3H inbred mice from 1 to 112-days of age. Power law regression analysis ($J_0 = A \cdot CtAr^B$) demonstrated that B6 mice constructed femora in a more "structurally efficient" manner resulting in a greater femoral J_0 for a given CtAr. A and C3H femora exhibited similar structural efficiencies of growth that were reduced in comparison to B6. Analysis of bone surface movement demonstrated that strain-specific differences in the structural efficiency

of growth resulted from variability in the relative rates of periosteal and endosteal expansion.

To test if the structural efficiency of growth could be extrapolated from adult data sets we validated a generalized power law regression with a fixed exponent ($J_0 = A \cdot CtAr^{1.44}$) that utilized only adult bone CtAr and J_0 values. We observed significant variability in structural efficiency of growth (A) among a cohort of 8 inbred mouse strains and 18 A, B6, and C3H reciprocal cross offspring/founders. Using this panel we also identified a significant correlation between the structural efficiency (SE) of growth and measures of ash content ($\text{ash} = -0.09 \cdot SE + 0.70, r^2 = 0.30, p < 0.01$). Thus, femora with more efficient growth patterns exhibited lower ash content values than those with less efficient growth patterns. This correlation between measures of material composition and structural efficiency was further confirmed by an analysis of previously published data including 29 different inbred mouse strains [1]. Together, these results suggest that surface growth patterns and material composition are co-adapted during bone growth. This investigation also provides new insight into bone adaptation and bone fragility and suggests mechanisms by which growth patterns can be used to establish preferred sets of (or robust) adult bone traits (high CtAr, high J_0 , and low ash).

[1] Wergedal, et al., 2005 Bone

Disclosures: C. Price, None.

1243

Heritability of Bone Microstructure in Women. S. L. Ferrari, T. Chevalley, J. P. Bonjour, R. Rizzoli. Div. of Bone Diseases, WHO Collaborating Center for Osteoporosis Prevention, Geneva University Hospital, Geneva, Switzerland.

Areal bone mineral density (BMD) has a 60-80% heritability (h^2) in humans. Bone microarchitecture, another major constituent of bone strength, is also highly heritable in inbred strains of mice. Because bone microstructure is difficult to assess in humans, the proportion of the population-based variance for trabecular and cortical bone traits explained by additive genetic factors is currently unknown. We measured cortical (Ct) and trabecular (Tb) bone structure at distal radius and tibia in 103 mother-daughter pairs using high-resolution (82 microns) peripheral computed tomography (HR-pQCT, Scanco, Switzerland). BMD was evaluated by DXA at radius, hip and spine. H^2 (%) was calculated as twice the beta coefficient of the linear regression between maternal and offspring values. The sample consisted of 103 young European-Caucasian females (mean age \pm SD, 20.4 \pm 0.6 yrs) and their mothers, of whom 53 were pre- (48.1 \pm 3.2 yrs) and 50 post-menopausal (53.3 \pm 3.2 yrs; 5.0 \pm 3.4 yrs since menopause, YSM). H^2 estimates for body weight, height and BMD were in the expected range, from a lowest 42% and 50% for total and ultradistal (UD) radius BMD, to a highest 70% and 84% for total hip and trochanter BMD, respectively. Heritability of cross-sectional area (CSA), as evaluated by HR-pQCT, was 62% at radius and as high as 96% at tibia, a weight-bearing site. Concerning tibia bone microstructure, h^2 values equal or greater than 50% were found for Tb bone density (BV/TV), Tb number (TbN), as well as Tb and Ct thickness (TbTh, CtTh), whereas h^2 was much lower for cortical volumetric density (D.Ct). However, TbTh and D.Ct had h^2 values of 79% and 48%, respectively, in daughters with pre-menopausal mothers, but of less than 20% in those with post-menopausal mothers, indicating that increased bone turnover may promptly overcome genetic effects on these traits. At radius, h^2 of 50% or greater was found for Tb BV/TV and TbN in all pairs, and for CtTh and D.Ct in pre-menopausal mother-daughter pairs only. Since DXA and HR-pQCT evaluate the same ROI at distal radius, bone microstructural traits were then adjusted by multiple linear regressions for UD radius BMD in addition to height, weight, age and YSM, leading to the following adjusted h^2 values at radius: BV/TV, 52%, TbN, 49%, CtTh, 58%, CSA, 44%, D.Ct 32% and TbTh < 10%.

In summary, we report for the first time the heritability of bone microstructure in humans, including the evidence that additive genetic effects may contribute specifically to these traits, i.e. independently of body size and BMD. Heritability for BMD, CSA and TbTh being more robust at weight-bearing sites, it suggests a genetic influence on the skeletal response to loading.

Disclosures: S.L. Ferrari, None.

This study received funding from: Swiss National Science Foundation.

1244

Spatio-Temporal Dynamics of a Single Bone Remodeling Unit. M. D. Ryser^{*1}, N. Nigam^{*1}, S. V. Komarova². ¹Mathematics and Statistics, McGill University, Montreal, PQ, Canada, ²Dentistry, McGill University, Montreal, PQ, Canada.

Bone remodeling occurs asynchronously at multiple sites in the mature skeleton and involves bone resorption by osteoclasts, followed by formation of new bone by osteoblasts. At each location, osteoclasts and osteoblasts are organized in Bone Remodeling Units (BRUs), which contain 10-20 osteoclasts in the leading front followed by 1000 - 2000 osteoblasts. BRUs exist much longer than individual osteoclasts and osteoblasts, traveling for 2-6 mm at a rate of 20-40 μ m/day. To analyze BRU progression, we developed a mathematical model that describes changes in osteoclast and osteoblast numbers in time and space while taking into account autocrine and paracrine interactions among these cells. We assumed that basal level of a pro-resorptive cytokine RANKL may change locally due to microfracture or external stimulus. The changes in osteoclast numbers were modeled to result from osteoclast formation, death and movement via diffusion and convection in response to RANKL field. The cutting cone was modeled as a free-boundary value problem with appropriate Stefan conditions. The changes in osteoblast numbers were modeled to result from osteoblast formation and death, whereas the necessity for osteoblast active movement was investigated. RANKL antagonist OPG was modeled to be produced by mature osteoblasts and to diffuse with different rates both through bone tissue and

through the liquid interface between osteoblasts and osteoclasts. The evolution of the cutting cone arising from this model was studied using numerical simulations. We have found that our model successfully recapitulates spatial and temporal dynamics observed in vivo in a cross-section of the bone. The formation and movement of osteoclasts were most strongly affected by RANKL produced by cells resident to quiescent bone, such as lining cells, osteocytes and stromal cells. Coupling of osteoclasts to osteoblasts allowed for sufficient recruitment of osteoblasts to remodeled surfaces, in such way that a diffusion term describing the directional movement of osteoblasts was not necessary. OPG diffusion through bone was critical in determining the direction of BRU movement. RANKL produced by osteoblasts was found to have little effect on activation of BRU, but was most important in preventing OPG from diffusing through the liquid interface between osteoblasts and osteoclasts, and inhibiting osteoclast activation. Thus, our model demonstrates that taking into account spatial organization of BRUs provides new insights into the roles of RANKL and OPG in regulating bone turnover. In the future, this model will allow in silico analysis of the impact of cytokines, growth factors and potential therapies on the process of bone remodeling.

Disclosures: M.D. Ryser, None.

This study received funding from: CIHR/IMHA/TAS and NSERC.

1245

Rapamycin Differentially Alters the Skeletal Response to PTH and Mechanical Loading. P. J. Niziolek^{*1}, S. M. Murthy^{*2}, S. N. Ellis^{*2}, K. B. Sukhija^{*3}, T. A. Hornberger^{*3}, C. H. Turner¹, A. G. Robling². ¹Department of Biomedical Engineering, Purdue University, Indianapolis, IN, USA, ²Department of Anatomy, Indiana University, Indianapolis, IN, USA, ³Department of Bioengineering, University of California - San Diego, San Diego, CA, USA.

Exercise-induced skeletal muscle hypertrophy requires signaling through the mTOR pathway. Likewise, bone cells may respond to exercise through the mTOR pathway, but this hypothesis has not yet been tested. PTH-induced bone hypertrophy requires IGF signaling (an upstream effector of mTOR), but the downstream components of this PTH-stimulated cascade are less certain. We investigated whether the bone-building effects of intermittent PTH require functional mTOR signaling, by treating mice with rapamycin, a selective inhibitor of mTOR activity, during a 6-wk course of daily PTH. We also investigated whether the anabolic effects of mechanical stimulation in bone require functional mTOR signaling, as they do for skeletal muscle, by subjecting mice to ulnar loading in the presence of rapamycin.

Female C57BL/6J mice were implanted with sustained-release rapamycin (or placebo) pellets, then treated with [A] either 0 (vehicle), 30, 60, or 90 µg/kg PTH 1-34 7dy/wk for 6 wk, or [B] mechanical loading of the right ulna for 3 consecutive days, (2 Hz; 2400 µε). PTH treated mice were measured for skeletal effects using DEXA, pQCT, and µCT; serum Trap 5b was measured via ELISA. Loaded mice were measured for MS/BS, MAR, and BFR/BS in the right and left ulnar midshaft via fluorochrome histomorphometry.

Rapamycin reduced BMC modestly but significantly. PTH induced significant dose-responsive gains in bone mass in the presence of rapamycin, albeit to a lesser degree than in placebo pellet animals. Trabecular bone mass and morphology in the distal femur (BV/TV, Tb.N, vBMD) followed similar trends as was observed for whole-body DEXA. Serum Trap 5b measurements indicated that resorption was enhanced significantly in the rapamycin-treated mice, particularly in those given PTH. Mechanical loading increased mineralizing surface similarly in rapamycin and non-rapamycin treated mice, but rapamycin treatment significantly suppressed load-induced mineral apposition rates and bone formation rates by 34% and 38% (p<0.05), respectively.

The anabolic effects of PTH appear to occur in the presence of rapamycin. Most of the disparity in PTH-induced bone gain between rapamycin and non-rapamycin treated mice can be attributed to the enhanced resorptive response induced by rapamycin. The reduced osteogenic response to mechanical loading in the rapamycin-treated mice suggests that mTOR participates in bone cell mechanical signal transduction cascades. Our data indicate that bone and muscle share a common exercise-induced pathway.

Disclosures: P.J. Niziolek, None.

1246

Temporal Pattern of Gene Expression and Histology of Stress Fracture Healing in the Rat Ulna-Loading Model. L. J. Kidd^{*1}, A. Stephens^{*1}, J. S. Kuliwaba^{*2}, N. L. Fazzalari², M. R. Forwood¹. ¹School of Biomedical Science, The University of Queensland, Brisbane, Australia, ²Division of Tissue Pathology, Institute of Medical and Veterinary Science and Hanson Institute, Adelaide, Australia.

Rat ulnar loading has become a central tool in the investigation of bone fatigue injury and remodelling, however this model has not yet been fully characterised. The aim of this study was to undertake a detailed examination of the histology, histomorphometry and gene expression of the healing and remodelling process initiated by rat ulnar fatigue-loading. In a group of 30 female Wistar rats cyclic ulnar loading was stopped at a fatigue level of 10% increase in displacement. Ulnae were harvested 2, 4 or 6 weeks following loading. All animals developed a fatigue fracture of the distal diaphysis of the loaded ulna. These were of a consistent configuration and position with a "U" shaped, incomplete, "stress" fracture on the medial cortex of the bone. Fracture healing involved direct remodelling that progressed along the fracture line as well as woven bone proliferation at the site of the fracture. Remodelling was greatest at 2 weeks and it originated at the region of the fracture line closest to the periosteal exit.

Real-time PCR was performed on the ulnae from 40 rats in which a stress fracture was created. Rats were euthanized following 4 hours, 24 hours, 4 days, 7 days and 14 days (n=8/group). A control group did not undergo loading. At 4 hours post fracture there was peak increased mRNA expression (p<0.05), compared to non-loaded controls, for IL-6 (400 fold increase), OPG (11 fold), COX-2 (6 fold) and VEGF (2 fold). At 24 hours there was peak mRNA expression of IL-11 (48 fold). At 4 days there was a significant increase in mRNA expression of SDF-1 (4 fold), SOST (3 fold), and BMP-2 (6 fold). At 7 days there was peak mRNA expression of RANK-L (12 fold). Other genes that showed a marginal increase in mRNA expression were BAX, Bcl-2, Collagen 10, COX-1, IGF-1, Runx-2, TNFα and IL-1, all with 2-3 fold increases, peaking at 4 days post fracture. mRNA expression of RANK-L, OPG and COX-2 was also increased in the opposite, unloaded, left limb suggesting a systemic response in bones distant to the site of injury.

These results show that rat ulna-loading is an excellent model for creating stress fractures and initiating remodelling. The gene expression results demonstrated a clear temporal cascade of important signalling events that occurred during fracture healing and remodelling. Dramatic, early up-regulation of IL-6 and IL-11 suggests their central role in initiating later signalling events. Prominent, up-regulation of COX-2, VEGF, OPG, SDF-1, BMP-2 and SOST prior to peak expression of RANK-L indicates the likely importance of these factors in mediating and possibly co-ordinating directed remodelling.

Disclosures: L.J. Kidd, None.

This study received funding from: NHMRC.

1247

GSK-3β Inhibits Osteoblastic Bone Formation Through Suppression of Runx2 Transcriptional Activity by the Phosphorylation at a Specific Site. M. Hirata, F. Kugimiya, N. Kawamura, S. Ohba, K. Nakamura*, H. Kawaguchi, U. Chung. Sensory & Motor System Medicine & Tissue Engineering, University of Tokyo, Tokyo, Japan.

GSK-3β is known to be a kinase involved in bone formation signalings like Wnt and Akt. To investigate the role of GSK-3β in bone, we initially investigated the skeletal phenotype of GSK-3β-deficient mice. Although the homozygous deficient mice were embryonically lethal, the heterozygous deficient (Gsk-3β^{+/-}) mice developed and grew normally; however, bone densitometry, 3D-μCT, and histomorphometric analyses revealed that Gsk-3β^{+/-} mice showed increased bone mass with enhanced bone formation as compared to the wild-type littermates. In Gsk-3β^{+/-} calvarial osteoblast cultures, the differentiation and function determined by ALP, Alizarin red and von Kossa stainings, and mRNA levels of osteoblastic markers were enhanced, while the proliferation was unaffected. Similarly, addition of lithium chloride or SB216763, selective inhibitors of GSK-3β, stimulated the bone formation parameters above. Meanwhile, overexpression of wild-type GSK-3β or a constitutively active form of GSK-3β (CA-GSK-3β) suppressed the parameters, although the kinase-inactive form of GSK-3β (KI-GSK-3β) overexpression did not affect it. Neither CA-GSK-3β overexpression, genetic GSK-3β insufficiency, nor GSK-3β inhibitors altered the expression or subcellular localization of Runx2, a master gene for osteoblast differentiation. However, the luciferase reporter assay revealed that the Runx2-dependent transcription was attenuated by wild-type GSK-3β or CA-GSK-3β overexpression, but not by KI-GSK-3β, whereas it was enhanced by GSK-3β inhibitors. Binding with the oligonucleotide probe of OSE2 / osteocalcin promoter by electrophoretic mobility shift assay was enhanced in nuclear extracts from Runx2-overexpressing osteoblasts from Gsk-3β^{+/-}, as compared to those from wild-type. To learn the contribution of phosphorylation of Runx2 by GSK-3β, we generated phosphorylation-deficient mutants of Runx2 at the five consensus sites, and found that a specific mutant at S369-S373-S377 cancelled the inhibition of Runx2 transactivity by CA-GSK-3β. Finally, when Runx2^{+/+} mice were crossed with Gsk-3β^{+/-} mice to generate the compound deficient mice (Gsk-3β^{+/-};Runx2^{+/+}) or were administered lithium chloride from E7.5, the cleidocranial dysplasia was significantly rescued, confirming the interaction between Runx2 and GSK-3β in vivo as well. In conclusion, GSK-3β was shown to inhibit the Runx2 transcriptional activity through the phosphorylation at S369-S373-S377, causing the suppression of osteoblast differentiation and bone formation.

Disclosures: M. Hirata, None.

1248

Overexpression of DeltaFosB Decreases Adipose Mass in a Non-Cell Autonomous Manner by Increasing Energy Expenditure Independently of Bone Cells. G. C. Rowe^{*1}, L. Neff^{*1}, T. Green^{*2}, H. Saito^{*1}, C. Choi^{*3}, G. Shulman^{*3}, E. Nestler^{*2}, W. Horne¹, R. Baron¹. ¹Orthopaedics, Yale University, New Haven, CT, USA, ²Psychiatry, University of Texas Southwestern Medical Center, Dallas, TX, USA, ³Internal Medicine, Yale University, New Haven, CT, USA.

Overexpression of Δ FosB in mice under the control of the enolase 2 promoter (ENO2), which drives expression in bone, fat and the brain, results in increased bone formation and decreased adipose mass, due to a reduction of the size of the individual adipocytes and not their number. To determine whether this effect on fat was linked to the bone phenotype, we generated mice which overexpress Δ FosB under the control of the osteocalcin promoter (OG2). These mice failed to recapitulate the adipose phenotype, demonstrating that the effect on adipocytes is independent of the increased bone formation. Since differentiation of the adipocytes was unimpaired we then explored whether the function of the adipocyte or the metabolic status of the ENO2- Δ FosB mice may be altered. To determine if the decrease in adipose mass was due to a cell autonomous effect within the adipocyte we generated a mouse overexpressing Δ FosB under the control of the adipocyte protein 2 promoter (aP2). Again, these mice did not recapitulate the decrease in adipose mass observed in the ENO2- Δ FosB mice, eliminating the possibility that the decrease in size of the adipocytes was due to a cell-autonomous defect. These results lead us to explore the metabolic status of the ENO2- Δ FosB mice: in contrast to the OG2- Δ FosB and aP2- Δ FosB mice, the ENO2- Δ FosB mice exhibited an improved glucose tolerance and an increased sensitivity to insulin. Furthermore metabolic analysis of the ENO2- Δ FosB mice revealed an increase in energy expenditure that was not present in the aP2- Δ FosB mice. Since the effect of Δ FosB on the regulation of adipose mass and energy expenditure was not due to its expression in either the osteoblast or adipocyte lineages, these results opened the possibility of a central effect of Δ FosB. We found that Δ FosB is overexpressed in the arcuate nucleus (ARC) of the hypothalamus in the ENO2- Δ FosB mice. Since the hypothalamus has been identified as a key regulator of both adipose and bone mass, we then examined the possibility of Δ FosB regulating adipose mass centrally. Stereotaxic injections were performed using adeno-associated viruses to target Δ FosB to the ARC of the hypothalamus. Six weeks post injection the mice injected with Δ FosB exhibited a significant reduction in body weight compared to control injected mice. This suggests that Δ FosB is able to alter adipose mass in a non-cell autonomous manner by altering the hypothalamic regulation of energy expenditure independent of the osteoblast.

Disclosures: G.C. Rowe, None.

1249

Inhibition of Wnt Signaling by Osterix. C. Zhang¹, J. Lyons^{*2}, K. Sinha^{*1}, P. McCrea^{*2}, X. Zhou^{*1}, B. de Crombrughe¹. ¹Molecular Genetics, University of Texas MD Anderson Cancer Center, Houston, TX, USA, ²Biochemistry and Molecular Biology, University of Texas MD Anderson Cancer Center, Houston, TX, USA.

During mouse embryonic development both the osteoblast-specific transcription factor Osterix (Osx) and Wnt/ β -catenin signaling are required for osteoblast differentiation. To explore whether Osx also plays a role in control of osteoblast proliferation, we compared BrdU incorporation in wild type and Osx-null E18.5 calvaria and examined the proliferation rates of primary calvarial cells isolated from wild type and Osx-null E18.5 embryos. BrdU incorporation in calvaria and proliferation of calvarial cells were markedly increased in Osx-null mice. In addition, overexpression of Osx in C2C12 mesenchymal cells resulted in slower growth. These experiments suggested the hypothesis that Osx could control osteoblast proliferation.

A microarray comparison of RNA expression profiles of wild type and Osx-null calvarial cells from E18.5 embryos revealed that expression of the Wnt inhibitor, Dkk1, which is high in wild type osteoblasts, was abolished in calvarial cells of Osx-null embryos. Moreover, expression of several Wnt target genes such as c-Myc and cyclin D1 increased in Osx-null calvarial cells. These findings suggested the hypothesis that Osx might inhibit Wnt pathway activity. Several lines of evidence, indeed, support this hypothesis. In vitro transfection studies in HEK293 cells demonstrated that Osx activated the Dkk1 promoter. In other transfection experiments Osx inhibited expression of the β -catenin-induced TOPFLASH reporter. In addition, Osx also inhibited β -catenin-induced secondary axis formation in Xenopus embryos. Moreover, in calvaria of Osx^{-/-} mice, which harbor the TOPGAL reporter transgene, β -galactosidase activity of the reporter was increased, suggesting that Osx inhibits the Wnt pathway in osteoblasts in vivo. Coimmunoprecipitation experiments showed that Osx interacted with Tcf, a DNA-binding partner of β -catenin. Gel shift assay indicated that Osx was able to disrupt Tcf binding to DNA. Thus our observations suggest that Osx has the ability to inhibit Wnt/ β -catenin signaling through several mechanisms. We speculate that the proposed inhibition by Osx of osteoblast proliferation might be a consequence of the Osx-mediated control of Wnt/ β -catenin activity.

Disclosures: C. Zhang, None.

1250

Zfp521, a D2D FosB-interacting Protein, Is a Novel Inhibitor of Runx2 Activity with Opposite Effects on Osteoblasts and Bone Formation In Vitro and In Vivo. E. Hesse, M. Wu^{*}, G. C. Rowe^{*}, L. Neff^{*}, W. C. Horne, R. Baron. Orthopaedics and Cell Biology, Yale University School of Medicine, New Haven, CT, USA.

The identification of novel molecules or pathways that contribute to the regulation of bone formation in vivo is essential for the development of future anabolic drugs. Overexpression of Δ FosB leads to a striking osteosclerotic phenotype in vivo and to the increased expression of osteoblast (OB) markers and bone nodule formation in vitro (Sabatatos, Nat Med, 6:985, 2000). We recently reported that the further N-terminally truncated and AP1 transcription-inactive isoform Δ 2 Δ FosB induces the same phenotype as Δ FosB in vivo. We therefore proceeded to a yeast two-hybrid screen and identified the zinc finger protein Zfp521, a 180 kDa protein consisting of 30 kruppel-like zinc fingers, as a Δ 2 Δ FosB-interacting protein. In situ hybridization and immunocytochemistry showed that Zfp521 is expressed at the periphery of mesenchymal condensations as early as day E12.5. At later stages of bone development, Zfp521 is strongly expressed in chondroblast and OB precursors in the perichondrium and periosteum, as well as in prehypertrophic chondrocytes, OB and osteocytes. In vitro, Zfp521 expression repressed, whereas RNAi-mediated depletion of Zfp521 enhanced, in vitro OB differentiation, nodule formation and mineralization. Co-immunoprecipitation studies revealed that Runx2 interacts with Zfp521, and we identified zinc fingers 6-10 and 26-30 as interacting sites. Moreover, in vitro overexpression of Runx2 dose-dependently rescued the Zfp521 induced repression of the OB phenotype, suggesting that Zfp521 acts as a Runx2 antagonist. Consistent with this hypothesis, Zfp521 strongly repressed the transcriptional activity of Runx2 in a reporter assay as well as the expression of Runx2 target genes (Runx2 itself, alkaline phosphatase, and other OB markers). Surprisingly, and despite the fact that Zfp521 inhibits OB differentiation in vitro, over-expressing Zfp521 in transgenic mice under the control of the OB-specific osteocalcin promoter resulted in a marked increase in bone volume and bone formation as measured by histomorphometry. Therefore, based on the well known functional duality of Runx2, which is required for OB differentiation at early stages of bone development while inhibiting OB maturation at later stages (Liu, J Cell Biol, 155:157, 2001; Geoffroy, Mol Cell Biol, 22:6222, 2002), we propose that Zfp521 both inhibits early OB differentiation and promotes late stages of OB maturation and bone formation by antagonizing Runx2 activity. Thus, the balance between Zfp521 and Runx2 could determine the rate of osteoblast differentiation and bone formation during development and in the adult skeleton.

Disclosures: E. Hesse, None.

1251

Cox-2 Deficiency Impairs Periosteal Progenitor Cell Activation and Differentiation Rescued by Ep4 Agonist. X. Zhang, C. Xie^{*}, M. Xue^{*}, A. Naik^{*}, E. Schwarz, R. J. O'Keefe. Orthopaedics, University of Rochester, Rochester, NY, USA.

We previously showed that genetic ablation of cyclooxygenase-2 (COX-2) resulted in delayed and defective fracture healing in mice. In this study, we evaluated COX-2 expression in the bone repair microenvironment and its critical role for activation and expansion of local progenitor cells following skeletal injury. In a stabilized femoral fracture healing model, COX-2 mRNA was increased at day 3 prior to chondrogenesis and peaked at day 7 in early chondroprogenitors and proliferating chondrocytes. Coincident with COX-2 expression, initiation and completion of periosteum mediated endochondral bone repair was markedly delayed in COX-2^{-/-} mice, as evidenced by delayed appearance of PCNA positive periosteal progenitor cells at day 3, marked reduction of Col2a1 gene expression at day 5, and deficient angiogenesis and osteogenesis at day 14. The deficient activation of periosteum bone repair in COX-2^{-/-} mice resulted in the development of fibrotic non-unions in live 4mm segmental cortical bone graft transplantations. Minimal periosteal response was found on the wild-type (WT) or COX-2^{-/-} (KO) graft when transplanted into a KO host. In contrast, the transplantation of a wild type live graft into a wild type host defect resulted in abundant bone formation and neovascularization on grafted surface. An intermediate amount of periosteal bone formation with increased amount of cartilage formation was found on the graft when transplanting a KO graft into a WT host, suggesting the requirement of COX-2 in the local microenvironment for the normal initiation and progression of periosteal bone repair. To rescue the deficient periosteal response in COX-2^{-/-} mice, an EP4 agonist CP-734432 was administered via periosteal injection. The delivery of EP4 agonists during the early phase of fracture healing reversed the impaired fracture healing in COX-2^{-/-} mice. PGE2 and agonists of EP2 or EP4 receptor potentially increased phosphorylation of ERK1/2 in mouse bone marrow stromal cells and primary sternal chondrocyte cultures. The activation of the MAPK/ERK pathway led to rapid induction of early growth response gene (EGR-1). Treatment with PGE2 and EP agonists also induced the phosphorylation of GSK3 β at serine 9 in the same cultures with further induction of the active form of β -catenin. Taken together, our data strongly suggest that transient induction of COX-2 functions as an essential early signal for initiation and completion of endochondral bone healing through targeting of the periosteal progenitor cell population. These signals are necessary for early events in repair and are a potential target for the treatment of impaired skeletal healing.

Disclosures: X. Zhang, None.

This study received funding from: AR051469, AR46545, MTF.

1252

TRIP-1: An Important Co-Regulator of Bone Formation in Skeletal Remodeling. D. Metz-Estrella*, T. Sheu*, R. Mroczek*, J. Puzas. Orthopaedics, University of Rochester, Rochester, NY, USA.

TGFbeta receptor interacting protein (TRIP-1) is an intracellular signaling cofactor with high affinity for fragments of tartrate resistant acid phosphatase (TRAP). TRAP, when bound to TRIP-1 activates the TGFbeta signaling pathway and leads to an increase in markers of bone formation in osteoblasts. This may be one way that osteoblasts recognize resorption lacunae during remodeling. Pull down assays also show that TRIP-1 interacts with intermediates of the BMP pathway (i.e. Smad1) and that this interaction is inversely related to the level of activation in the pathway. Based on these findings we hypothesize that TRIP-1 is a pleiotropic regulator of Smad-dependent pathways during bone remodeling.

To further investigate the mechanism by which TRIP-1 influenced signaling we identified regions in the Smads that bind to TRIP-1. Our results show that the MH1 domain of Smad3 is mainly involved in the physical interaction with TRIP-1 and that this interaction leads to a large increase in its phosphorylation.

In regard to its pleiotropic nature TRIP-1 also activates a BMP-specific reporter in osteoblasts. When this same reporter is transfected into Smad4-deficient cells, TRIP-1 expression leads to a greater than 50 fold induction. Moreover, co-localization experiments have shown that TRIP-1 associates with phosphorylated Smad1, 5, 8 in the nuclei of osteoblasts.

To understand the *in vivo* role of TRIP-1 we used a mouse model in which TRIP-1 can be over expressed in osteoblasts using the TetOn system. In these mice, induction of TRIP-1 expression in the calvarium led to an approximate three fold increase in bone volume ($p<0.001$) and a three fold increase in mineral apposition rate ($p<0.001$).

These results provide evidence to conclude that TRIP-1 is an important co-regulator of the Smad pathways and may control, in part, bone formation at sites of remodeling.

Disclosures: J. Puzas, None.

1253

Serum IGFBP-2 (IGF binding protein-2) Is a Marker of Bone Turnover; In Vivo Evidence from the IGFBP-2 Null Male Mouse. V. E. DeMambro¹, D. Clemmons², W. G. Beamer¹, M. L. Bouxsein³, E. Canalis⁴, C. J. Rosen¹. The Jackson Laboratory, Bar Harbor, ME, USA, ²University of North Carolina, Chapel Hill, NC, USA, ³Beth Israel Deaconess Medical Center, Boston, MA, USA, ⁴St. Francis Hospital & Medical Center, Hartford, CT, USA.

IGFBP-2 is a 36kD IGF binding protein with strong affinity for hydroxyapatite and extracellular Matrix proteins. It circulates in relatively high concentrations, and increases with age, and malnutrition. IGFBP-2 is expressed in most tissues including bone and combined with IGF-I can stimulate bone formation in experimental animals. A recent study highlighted a direct correlation between serum IGFBP-2 and bone turnover markers in both men and women. However, the mechanism of this effect is unknown. To understand the role of IGFBP-2 in the mammalian skeleton we generated IGFBP-2 null (-/-) mice that were backcrossed 10 generations onto C57BL/6J. We then performed skeletal and metabolic phenotyping at 8 and 16 weeks and compared the nulls to +/+ littermates. Male BP2-/- mice had shorter femurs at 16 wks and had greater % body fat than +/+ ($p<0.05$). However, they were not insulin resistant and had normal glucose tolerance. Serum IGF-I in the BP2-/- mice was 10% higher than +/+ ($p<0.05$) at 8 but not 16 wks. Hepatic expression of IGFBP-1,3,4,5,6 was higher in the -/- at 6wks than +/+ mice ($p<0.05$). BP2-/- mice at 8 weeks had reduced total bone area and cortical thickness by microCT with a 17% reduction in trabecular BV/TV vs +/+ ($p<0.01$). This was almost entirely due to reduced trabecular thickness ($p<0.01$) rather than change in trabecular #. Serum osteocalcin was suppressed by 40% in BP2-/- vs +/+ ($p<0.01$) and both CFU-AP+ pre-OBs and TRAP+ osteoclasts were significantly less abundant *in vitro* than +/+ cells from littermates. Moreover, null mice have 20% smaller spleens and less B220+ mononuclear cells in marrow and spleen than +/+. Histomorphometry at 16 wks revealed there were significantly less osteoblasts/BPm ($p<0.01$) and less osteoclasts/BPm ($p<0.05$) in BP2-/- than +/+ mice. Mineralizing surface/bone surface in BP2-/- was markedly reduced ($p<0.001$), as was the overall bone formation rate/BSd (-45%, $p<0.001$) but MAR was not different. In summary, IGFBP-2 null mice have a skeletal phenotype that is directly related to bone turnover and mostly likely begins with impaired OB recruitment. Recent work suggests that IGFBP-2 can bind to the $\alpha_v\beta_3$ integrin receptor, independent of IGF-I, and may suppress PTEN expression. Conversely, IGFBP-2 may mediate its action by transporting IGF-I to its receptor on stromal cells leading to enhanced OB differentiation. Studies are ongoing to assess whether recombinant IGF-I or IGFBP-2 can rescue the *in vitro* or *in vivo* phenotypes. Nonetheless, circulating IGFBP-2 may become a useful marker of bone turnover.

Disclosures: V.E. DeMambro, None.

This study received funding from: NIAMS 45433.

1254

Chemokine Receptor CCR-1 Deficient Mice Have a High Turnover Osteoporosis that Is Greater in Females than in Males. J. Lorenzo, J. Kalinowski*, S. Jastrzebski*, S. K. Lee*. Medicine, University of Connecticut Health Center, Farmington, CT, USA.

Chemokine receptor CCR1 is expressed on osteoclasts and binds the ligands CCL3 (macrophage inflammatory protein 1 α , MIP-1 α) and CCL9 (MIP-1 γ). Previous *in vitro* results demonstrated that MIP-1 α and MIP-1 γ stimulate osteoclast formation and mobility. To better understand the *in vivo* effects of CCR1 and its ligands on bone, we examined mice that were globally deficient in CCR1 (CCR1 KO). Animals were examined for changes in bone mass, bone turnover and the ability of bone marrow cells to form osteoclast-like cells (OCL) *in vitro*. CCR1 KO and wild type (WT) mice were in a C57BL/6 background. Bone mass was measured by micro-CT. Changes in bone cells were determined by histomorphometry. Global bone turnover was assessed by measuring serum c-terminal telopeptide (CTX), a measure of bone resorption, and osteocalcin (OCN), a measure of bone formation. *In vitro* osteoclastogenesis was assayed in bone marrow cultures, treated with M-CSF and RANKL (30 ng/ml for each) for 4 days. Mice were examined at 9-10 weeks of age and females (F) and males (M) were analyzed separately. Based on the previous *in vitro* data, we anticipated that CCR1 KO mice would have increased bone mass and low turnover. Instead we found that both F and M CCR1 KO mice had decreased vertebral trabecular bone mass, with the greatest effect in females (BV/TV was decreased 15.8% in F and 8.4% in M, trabecular thickness was decreased 12.2% in F and 3% in M, $p<0.05$ for all). Femoral cortical bone thickness was also significantly decreased in F and M CCR1 KO mice by 10% for both ($p<0.05$). There was no significant difference in femoral trabecular bone mass between either F or M CCR1 KO and WT. In the femurs of F mice there were increases in the osteoclast surfaces (29.2%), the number of osteoclasts per unit bone surface (22.8%) and osteoblast surfaces (43.3%) ($p<0.05$ for all). In the femurs of M mice there were no significant differences in histomorphometric indices between CCR1 KO and WT. CCR1 KO mice also had increased serum turnover markers. In F CCR1 KO mice serum CTX was 36% greater while OCN was increased by 49% over WT ($p<0.05$ for both). Increases in serum CTX and OCN in M CCR1 KO mice were also seen but were less (20% and 39%, respectively, $p<0.05$ for both). OCL formation *in vitro* in bone marrow cell cultures was similar in F CCR1 KO and WT cultures. In contrast, in M cells, there was an 18% decrease in OCL formation relative to WT cells ($p<0.05$). These results demonstrate that CCR1 KO mice have a high turnover osteoporotic phenotype, which is markedly greater in female than in male mice. These findings imply that complex mechanisms, which are not dependent on the ability of CCR1 ligands to stimulate osteoclasts, are responsible for the observed bone phenotype of CCR1 KO mice.

Disclosures: J. Lorenzo, None.

1255

Selective Deletion of the Membrane-bound Colony Stimulating Factor 1 Isoform In Vivo Does Not Affect Estrogen-deficiency Bone Loss in Mice. G. Yao, J. Wu*, K. Insogna. Yale University, New Haven, CT, USA.

It has been reported that a neutralizing antibody to CSF1 completely prevents ovariectomy (OVX)-induced bone loss in mice. There are two isoforms of CSF1, soluble (sCSF1) and membrane-bound (mCSF1), but their individual biological functions are unclear. It has been reported that estrogen-withdrawal increases levels of IL-1 and TNF in bone marrow, which induce the formation of a stromal cell population producing high levels of secreted CSF1. However, others have found that estrogen-withdrawal selectively up-regulates expression of mCSF1 and down-regulates sCSF1 expression in rat bone marrow cultures. To explore the role of CSF1 isoforms in estrogen-deficiency bone loss, we have generated mCSF1 knock-out mice. Isoform-specific RT-PCR confirmed the absence of transcripts for mCSF1 in bone tissue isolated from these animals and western blot analysis demonstrated similar amounts of sCSF1 secreted by osteoblasts isolated from mCSF1 k/o and wild-type mice. The mCSF1 k/o mice had higher femur BMD than wild-type controls. Five month-old mCSF1 k/o and wild-type female mice underwent ovariectomy (OVX) or sham-OVX. One month after surgery, femoral and spinal BMD (determined by DEXA) were reduced by 7% and 5% respectively in OVX-wild-type animals as compared to sham-OVX wild-type mice. OVX mCSF1 k/o mice showed similar 5% and 8% reductions in femoral and spinal BMD respectively compared to sham-OVX mCSF1 k/o animals. We next used real time PCR to quantitate expression of transcripts for mCSF1 and sCSF1 in RNA isolated from bones of OVX or sham-OVX wild-type mice. When data from three separate experiments were analyzed, OVX induced a significant 4-fold increase in the expression of sCSF1 while mCSF1 expression was either unchanged or changed minimally. In summary, our findings indicate important non-redundant functions for the two isoforms of CSF1. In particular, it appears that the mCSF1 isoform is not involved in estrogen-deficiency bone loss although this isoform is essential for normal bone remodeling since, in its absence, bone density is increased. In contrast our data suggest that sCSF1 could play a key role in estrogen-deficiency bone loss.

Disclosures: G. Yao, None.

This study received funding from: NIH.

1256

Point Mutation of Endofin at PP1c-Binding Domain (F872A) Stimulates Bone Formation in Transgenic Mice: A Negative Feedback Regulation of BMP Signaling. F. Zhang^{*1}, W. Shi^{*1}, T. Qiu¹, X. Wu¹, J. Chen^{*2}, J. Si^{*3}, M. Wan¹, X. Cao¹. ¹Pathology, University of Alabama at Birmingham, Birmingham, AL, USA, ²Pharmacology, Tongji Medical School, Wuhan, China, ³Pathology, Shihezi University School of Medicine, Shihezi, China.

Smad anchor for receptor activation (SARA) facilitates TGF β signaling by recruiting and presenting Smad2/3 to the receptor complex. SARA does not bind Smad1 and hence does not enhance bone morphogenetic protein (BMP) signaling. We identified Endosome-associated FYVE-domain protein (endofin) acts as a Smad anchor for receptor activation in BMP signaling. We have shown that endofin binds Smad1 preferentially and enhances Smad1 phosphorylation and nuclear localization upon BMP stimulation. Silencing of endofin by RNAi resulted in a reduction in BMP-dependent Smad1 phosphorylation. We also demonstrate that endofin contains a protein-phosphatase-binding motif, which recruits protein phosphatase 1 (PP1c) to negatively modulate BMP signals through receptor dephosphorylation of BMP type I receptor. Point mutation of endofin at PP1c-binding domain (F872A) almost abolished the interaction between PP1c and endofin. As a result, BMP signaling was sensitized and osteoblast differentiation was enhanced.

To further determine whether this endofin mutant affects osteoblast activity and bone formation in vivo, transgenic mice were generated in which this mutant (F872A) was overexpressed in osteoblasts driven by 2.3 kb Col I promoter. Significant bone formation in transgenic mice was observed. The expression of the mutant endofin (F872A) was detected in 4 different transgenic lines with Western blot. X-ray analysis revealed that bone density of the entire skeleton is elevated at 4-month-old age of all 4 transgenic lines. Analysis of femur by μ CT shows that trabecular volume (BV/TV) is increased by 11 percent more in comparison to their wild type littermates. Consistently, the trabecular bone thickness and number are also significantly increased, whereas the trabecular bone separation is decreased. To examine whether the effect of this endofin mutant on bone formation is due to BMP signaling change, Smad1 phosphorylation was detected in osteoblasts. Immunostaining of tibia sections demonstrate that the level of phosphorylated Smad1 was enhanced in osteoblasts from the transgenic mice. Taken together, the recruitment of PP1c to endofin functions as a negative feedback regulation of the BMP signaling pathway. Disruption of PP1c binding motif of endofin by point mutation leads to an elevated level of phosphorylated Smad1 and augment of bone formation in transgenic mice.

Disclosures: F. Zhang, None.

1257

Molecular Mechanisms for BMP-2 Transcription by the Hedgehog Pathway. M. Zhao¹, R. L. Chandler^{*2}, J. Liu^{*1}, G. R. Mundy¹, D. P. Mortlock^{*2}. ¹Medicine/Clinical Pharmacology, Vanderbilt University, Nashville, TN, USA, ²Molecular Physiology & Biophysics, Vanderbilt University, Nashville, TN, USA.

The Hedgehog pathway is essential for normal developmental patterning from drosophila to man. This pathway mediates effects via the Gli family of transcriptional activators, and one of its major downstream target genes is BMP-2. We have previously examined the molecular mechanisms by which Gli2 transactivates BMP-2 through the 5' flanking promoter region from -2712 to +165 (Zhao et al., 2006, MCB), but did not find good evidence for discrete functional binding sites. We have thus now examined much larger genomic regions flanking the murine BMP-2 gene. Two BAC clones, namely 5'BAC-LacZ and 3'BAC-LacZ, spanning from -185 to +53kb and -2.7 to +207kb of upstream and downstream respectively of the gene, were modified by inserting a LacZ reporter cassette in the place of exon 3 of BMP-2 coding region. Using transgenic mice which contain the BAC-LacZ genes, we have found that each BAC clone directs distinct BMP-2 expression patterns. Strikingly, we found that the regulatory sequence located more than 53kb 3' to the promoter is required for BMP-2 expression in osteoblast progenitors during skeletal development. To refine the location of the osteoblastic element, we have generated transgenics that carry 3'BAC-LacZ with different deletions. We found that deletion of +132 to +168kb region completely abolished LacZ-positive osteoblasts in long bones. Finally, a conserved 656bp region, namely ECR1, located within +155 to +160kb from the BMP-2 promoter, was identified as an osteoblast-specific enhancer of BMP-2 expression, shown by LacZ staining in both endochondral and intramembranous bones of ECR1 transgenic mice. Sequence analysis of the ECR1 fragment shows a putative Gli-response element. Thus, we examined the effect of Gli2 on ECR1 regulation of BMP-2 transcription. We made two chimeric reporter constructs by linking ECR1 to the BMP-2 promoter (2.7kb) or SV40 promoter (0.2kb). Luciferase assays showed that ECR1 addition increased Gli2 stimulation of BMP-2 promoter activity. We also found that Gli2 significantly enhanced the activities of 3'BAC-LacZ and ECR1-LacZ genes that were stably transfected into the osteoblastic MC3T3-E1 cells. These results strongly suggest that the 3' genomic sequence from +155 to +160kb of BMP-2 gene, covering a cis-enhancer ECR1, is required for osteoblast progenitor-specific BMP-2 expression, and the Hedgehog signaling mediator Gli2 enhances BMP-2 transcription in osteoblasts through this region. The identification of this enhancer should clarify regulatory mechanisms that control BMP-2 transcription in osteoblasts during skeletal development and postnatal bone formation.

Disclosures: M. Zhao, None.

1258

Absence of sFRP1, an Antagonist of Wnt Signaling Accelerates Fracture Healing. T. Gaur¹, J. J. Wixted^{*2}, S. Hussain^{*1}, D. Ayers^{*2}, P. V. N. Bodine³, G. S. Stein¹, J. B. Lian¹. ¹Department of Cell Biology and Cancer Center, University of Massachusetts Medical School, Worcester, MA, USA, ²Department of Orthopedics, University of Massachusetts Medical School, Worcester, MA, USA, ³Women's Health and Musculoskeletal Biology, Wyeth Research, Collegeville, PA, USA.

Bone fractures are the frequent consequence of trauma and pathological bone conditions (osteoporosis, diabetes and cancer). Fracture healing is a complex regenerative process and delayed process in aging and diseased bone results in clinical complications. Several clinical studies as well as transgenic mouse models have shown that the Wnt pathway supports bone formation. We examined the role of Wnt signaling in improving fracture repair using a knockout mouse model for the Wnt antagonist secreted frizzled related protein 1 (sFRP1-KO). We also used the chemical inducer LiCl to activate canonical Wnt signaling in wild type mice. A transverse fracture in the right tibia was generated in WT and sFRP1-KO mice. Healing was monitored at regular intervals by radiographic analyses. Bone samples were collected at 7, 11, 14, 21 and 28 days post fracture for histological and gene expression analyses for assessing the progression of bone formation and remodeling. Fracture healing was achieved completely in WT mice by 28 days post fracture but significantly accelerated in the sFRP1-KO mouse with appearance of new bone formation beginning at day 11. Both radiographic and histological analyses showed that on day 7, the initial callus appeared similar, but by day 11, reduced callus formation with increased cartilage tissue and trabecular bone bridging the fracture occurred in sFRP1-KO mice. After day 11, bone remodeling (by TRAP staining) was much more robust in the sFRP1-KO. Radiography identified union of the fracture by day 21 in the sFRP1-KO mice, in contrast to the WT fracture which still exhibited presence of cartilaginous callus along with formation of new bone. Enhanced fracture healing was observed in WT mice treated with LiCl. Gene expression analyses using RNA from callus tissues showed reduced TNF α levels suggesting less inflammation in KO mice fractures. Lower levels of chondrocyte proliferation markers (Col2a1 and Sox9) and mild induction of bone markers (Runx2, osteocalcin, osteopontin and Colla1) were observed in sFRP1-KO mice, consistent with less chondroid tissue and more bone formation in sFRP1-KO mice by histology. Bone remodeling markers, MMP9, TRAP and VEGF were slightly elevated in sFRP1-KO mice, suggesting mechanisms for accelerated healing. Our studies establish a direct improvement of fracture repair by increasing Wnt signaling and also provide a possibility for modulation of the Wnt pathway to achieve better fracture healing in compromised clinical cases.

Disclosures: T. Gaur, Wyeth Research, Inc. 2.

This study received funding from: Wyeth Research.

1259

Enzyme Replacement Therapy for Murine Hypophosphatasia. J. L. Millan¹, S. Narisawa^{*1}, I. Lemire^{*2}, T. P. Loisel^{*2}, G. Boileau^{*3}, P. Leonard^{*2}, M. D. McKee⁴, P. Crine², K. Johnson^{*5}, R. Terkeltaub^{*5}, N. Pleshko Camacho⁶, M. P. Whyte⁷. ¹Oncodevelopmental Biology, Burnham Institute for Medical Research, La Jolla, CA, USA, ²Enobia Pharma, Inc., Montreal, PQ, Canada, ³University of Montreal, Montreal, PQ, Canada, ⁴McGill University, Montreal, PQ, Canada, ⁵VAMC/UCSD, La Jolla, CA, USA, ⁶The Hospital for Special Surgery, New York, NY, USA, ⁷Shriners Hospitals for Children and Washington University, St. Louis, MO, USA.

Hypophosphatasia (HPP) is the inborn-error-of-metabolism that features rickets or osteomalacia due to loss-of-function mutation within the tissue-nonspecific alkaline phosphatase (TNALP) gene. Consequently, there is extracellular accumulation of the mineralization inhibitor inorganic pyrophosphate (PPI), one of TNALP's natural substrates. HPP features a remarkable range of severity spanning (most severe to mildest) perinatal, infantile, childhood, adult, and odontohypophosphatasia forms, classified (historically) according to age at diagnosis. TNALP null mice (Akp2^{-/-}) phenocopy infantile HPP remarkably well, as they are born with a normally mineralized skeleton, but develop radiographically apparent rickets at about 6 days of age, and die between day 12-16 suffering severe skeletal hypomineralization and episodes of apnea and epileptic seizures attributable to disturbances in pyridoxal 5'-phosphate (vitamin B6) metabolism. There is no established medical therapy for HPP. Case reports of enzyme replacement therapy (ERT) using intravenous (i.v.) infusions of ALP-rich plasma from Paget's bone disease patients and purified placental ALP have described failure to rescue affected infants. It seems that ALP activity must be increased not in the circulation, but in the skeleton itself. This hypothesis is supported by beneficial outcomes for two girls with infantile HPP following marrow cell transplantation where perhaps some TNALP-containing cells were introduced throughout the skeleton. Here, we report survival without significant skeletal or dental disease or seizures in TNALP knockout mice undergoing enzyme replacement therapy (ERT) from birth with a bone-targeted form of recombinant TNALP (sALP-FcD10). Short-term and long-term efficacy studies with daily s.c. injections of 1, 2, or 8.2 mg/kg sALP-FcD10 for 15, 19 and 52 days showed homing of sALP-FcD10 to bone tissue and normal circulating PPI concentrations with preservation of skeletal and dental architecture (assessed by radiographs, microCT, and histology) as well as increased life span and well-being. This bone-homing, recombinant form of human TNALP prevents lethal HPP in TNALP knockout mice. Our findings represent the first successful use of ERT for a heritable primary disease of the skeleton, and are a foundation for therapeutic trials for human HPP.

Disclosures: J.L. Millan, Enobia Pharma, Inc. 5.

This study received funding from: Enobia Pharma, Inc.

1260

Treatment of Osteogenesis Imperfecta in Adults with Teriparatide: Results of an 18-month Prospective Observational Trial. J. D. Ringe¹, H. Faber^{*1}, P. Farahmand^{*1}, T. N. Nickelsen². ¹Medizinische Klinik IV, Klinikum Leverkusen, Leverkusen, Germany, ²Medical Department, Lilly Deutschland GmbH, Bad Homburg, Germany.

Osteogenesis imperfecta (OI) is a genetic disorder of connective tissue characterized by brittle bones and a susceptibility to fracture from normal impacts of daily living or inadequate trauma. It has been shown that an antiresorptive therapy with bisphosphonates has beneficial effects on the clinical outcome of OI, especially in children. So far there is a lack of data on the use of osteoanabolic drugs in this disorder.

The aim of the ongoing "Teriparatide in Osteogenesis Imperfecta" trial (TOI-trial) is to study the efficacy of an anabolic treatment with teriparatide (rPTH-1-34) in adults with clinically symptomatic disease. In this 18-month prospective, observational, single center trial we included 10 patients (6 men, 4 women) above the age of 30 years (mean age 44.9) with a T-score <-3.0 at the lumbar spine and <-2.0 at the total hip, and at least one prevalent vertebral and one non-vertebral fracture. Fluoride, bisphosphonates or alfacalcidol had been used previously over different intervals, but during the last 6 months only calcium and vitamin D were given. During the study, all patients received daily subcutaneous injections of 20µg teriparatide plus oral supplements of 1200 mg calcium and 800 IU vitamin D per day.

Baseline characteristics of patients included a mean height of 154.1 cm, mean weight 66.3 kg, average T-scores of -4.03 at the lumbar spine and -3.24 at the hip, and a mean number of 1.5 new vertebral and 0.8 non-vertebral fractures per patient during the last year before intervention.

BMD measured at 6-month intervals showed highly significant increases at both sites and amounted to an average gain of 10.8% at the lumbar spine and 8.4% at the total hip after 18 months. During the 18 months we observed only one new vertebral and two non-vertebral fractures. This is remarkable in relation to the respective average fracture rates during the last year before starting teriparatide injections. There was a significant decrease in back pain. Moderate, transient adverse events occurred in 5 of 10 patients.

All patients will be followed during a subsequent antiresorptive therapy up to month 36. These very positive preliminary results should encourage further, controlled trials with an anabolic therapy in osteogenesis imperfecta.

Disclosures: J.D. Ringe, Eli Lilly and Company 8.

1261

Mutations in CRTAP or P3H1 Cause Dysregulation of Prolyl-3-hydroxylation and Recessive Osteogenesis Imperfecta. D. Baldrige^{*1}, U. Schwarze^{*2}, R. Morello¹, J. Lenington^{*1}, T. K. Bertin^{*1}, D. R. Eyre², M. Weis^{*2}, A. Green^{*3}, J. Walsh^{*3}, D. Lambert^{*3}, D. Krakow^{*4}, D. L. Rimoin^{*4}, D. H. Cohn^{*4}, P. H. Byers^{*2}, B. Lee¹. ¹Molecular and Human Genetics, Baylor College of Medicine, Houston, TX, USA, ²University of Washington, Seattle, WA, USA, ³Our Lady's Hospital, Dublin, Ireland, ⁴Cedars Sinai Medical Center, Los Angeles, CA, USA.

Osteogenesis imperfecta (OI) or brittle bone disease is a genetic condition caused by mutations in the type I collagen genes (COL1A1 or COL1A2). Quantitative or structural type I collagen alterations lead to recurrent fractures. Prolyl 3-hydroxylases, such as P3H1, are recently identified enzymes that hydroxylate a unique proline residue in the α -helical domain of fibrillar collagens like type I collagen. CRTAP, or cartilage-associated protein, interacts with P3H1, and Crtp null mice display an OI-like phenotype and lack fibrillar collagen prolyl 3-hydroxylation. The purpose of this study is to identify additional genetic causes of osteogenesis imperfecta.

In our study of 70 OI subjects we report a spectrum of recessively-inherited phenotypes, including OI types II and III, caused by mutations in either CRTAP (two patients) or mutations in P3H1 (six patients). The latter group includes a mutation in the Irish Traveller population, a community with a high degree of consanguinity and which has a prevalence of OI of approximately 2%. The mutations lead to loss-of-function, including premature termination, frameshift, and splice site alterations that result in a severe decrease of mRNA, as well as decreased collagen prolyl-3-hydroxylation by mass spectrometry, as demonstrated in patient fibroblasts. MS analysis of collagen from bone shows a 50% decrease in prolyl-3-hydroxylation in a patient with a P3H1 mutation, while a patient with a CRTAP mutation shows a 95% reduction. This suggests that there may be partial functional redundancy among the family of prolyl-3-hydroxylase enzymes and therefore as yet undiscovered less severe phenotypes from loss of function of each of these genes. However, expression of the cofactor CRTAP may be essential for complete enzymatic activity of the complex in vivo. Clinically, one patient with a P3H1 mutation was treated with IV bisphosphonates and showed prolonged survival. Hence, osteoclastic inhibition may be a viable strategy for treatment of OI due to abnormal 3-prolyl-hydroxylation. These results demonstrate a genetic basis for recessive OI and help to explain the apparent recurrence of OI to unaffected parents previously attributed primarily to germline mosaicism. In summary, loss of function of CRTAP or P3H1 leads to the severe OI phenotype including types II and III.

Disclosures: D. Baldrige, None.

1262

Expression of Osteocalcin by Circulating Endothelial Progenitor Cells Predicts Endothelial Dysfunction or Structural Coronary Artery Disease. U. I. Moedder, M. Gössl^{*}, A. Lerman^{*}, S. Khosla. Mayo Clinic, Rochester, MN, USA.

Increasing evidence indicates a link between bone and the vasculature, and bone marrow as well as circulating cells with osteogenic potential have been identified by staining for the osteoblastic marker, osteocalcin (OCN). Endothelial progenitor cells (EPCs) contribute to vascular repair, but repair of vascular injury may result in calcification, which is also a marker for future coronary events. A previous preliminary study (Bull Exp Biol Med. 139:266, 2005) found that circulating cells staining for another bone-related protein, osteonectin, were present in the circulation of 7 subjects with coronary artery disease (CAD) but absent from the circulation of 4 control subjects. Thus, in the present study, we tested whether patients with coronary atherosclerosis had increases in circulating EPCs expressing an osteogenic phenotype, as assessed by OCN staining. We studied 59 patients undergoing invasive coronary assessment. Subjects were defined as controls (no significant structural coronary lesions, normal endothelial function, n = 11) versus two groups with coronary atherosclerosis: early coronary atherosclerosis (defined as no significant structural coronary lesions but abnormal endothelial function, n = 19) and late coronary atherosclerosis (defined as severe, multi-vessel coronary artery disease [CAD], n = 29). Peripheral blood mononuclear cells were analyzed using flow cytometry following staining for EPC markers (CD133, CD34, vascular endothelial growth factor receptor 2/kinase insert domain receptor [KDR]) and OCN. Compared to controls, patients with early or late coronary atherosclerosis had significantly higher percentages of EPCs which co-stained for OCN, particularly in the population containing relatively late EPCs (CD133-/CD34+/KDR+, by 8- and 5-fold, P = 0.0006 and 0.012, respectively). In unadjusted logistic regression models, a doubling of these OCN positive EPCs was associated with an odds ratio of 1.8 (95% confidence interval, 1.2-2.7) for having CAD; following adjustment for age, sex, and statin use, the corresponding odds ratio was 4.2 (95% confidence interval, 1.5-12.1); by comparison, the analogous odds ratios for the currently used marker for coronary atherosclerosis, high sensitivity C-reactive protein, were 0.9 (0.7-1.3) and 1.2 (0.7-1.9), unadjusted and age, sex, and statin use adjusted, respectively. Thus, a higher percentage of EPCs co-stains for OCN in patients with coronary atherosclerosis as compared to subjects with normal endothelial function and no structural CAD. These findings have potential implications for the mechanisms of vascular calcification and for the development of novel markers for coronary disease.

Disclosures: U.I. Moedder, None.

1263

A Novel Central Mechanism in Uremic Bone Disease. W. Cheung^{*1}, C. Vanek², U. T. Iwaniec^{*3}, R. T. Turner^{*3}, R. Klein^{*2}, R. Mak^{*1}. ¹Pediatrics, University of California at San Diego, La Jolla, CA, USA, ²Bone and Mineral Unit, Oregon Health and Science University, Portland, OR, USA, ³Nutrition and Exercise Sciences, Oregon State University, Corvallis, OR, USA.

Bone disease is common in patients with uremia. In this study, we tested whether leptin signaling, via the hypothalamic melanocortin system, is an important cause of uremic bone disease. We performed sub-total nephrectomy (N) or sham operation (S) in 8-week-old wild-type (WT, C57BL/6J), leptin deficient (ob/ob), leptin receptor deficient (db/db) and melanocortin receptor 4 knockout (MC4-RKO) mice. Additional WT-N mice were treated with agouti-related protein (AgRP, a MC4-R antagonist) or vehicle (V). Secondary hyperparathyroidism in uremic mice was minimized by administering a low phosphorus and high calcium diet. WT-N mice were fed ad libitum and all other mice were pair-fed to WT-N mice. Changes in whole body composition were assessed by DXA at the beginning and at the end of the 6-week study. Excised left femoral composition was determined by DXA and x-ray microtomographic scanning. Femoral strength was assessed by 3-point bending. Architecture of right femora was analyzed by mCT. WT-N, ob/ob-N, db/db-N, MC4-RKO-N, WT-N/V and WT-N/AgRP mice were uremic based on increased blood urea nitrogen and creatinine levels. WT-N mice displayed a uremic bone phenotype characterized by decreased femoral length, bone mineral content/density and failure load. mCT evaluation demonstrated reduced total femoral volume, cortical area and thickness in WT-N mice. The uremic bone phenotype was attenuated in ob/ob and db/db mice; nephrectomy in these animals did not result in significant differences in femoral bone composition and architecture compared to controls. Uremic bone disease was also attenuated by central MC4-R deficiency. MC4-RKO-N mice had no change in bone parameters compared with MC4-RKO-S mice. We also tested the effect of central MC4-R antagonism in the WT-N mice. Uremic bone disease in WT-N was ameliorated by central administration of AgRP. In summary, leptin signaling through the central melanocortin system may play an important role in the pathogenesis of uremic bone disease. These findings may have significant clinical and pharmacotherapeutic implications.

mCT analysis of right femur. Data are expressed as means \pm SEM. #p<0.0015; *p<0.003

	Total femur (cortical + cancellous) bone volume (mm ³)	Cortical bone area (mm ²)	Cortical bone marrow area (mm ²)	Cortical bone thickness (mm)
WT-N (n=7)	13.20 \pm 0.24#	0.51 \pm 0.01*	1.03 \pm 0.02	0.134 \pm 0.004*
WT-S (n=7)	16.74 \pm 0.64	0.68 \pm 0.03	0.96 \pm 0.05	0.178 \pm 0.010
MC4-RKO-N (n=7)	23.09 \pm 0.67	0.91 \pm 0.02	1.01 \pm 0.05	0.226 \pm 0.004
MC4-RKO-S (n=6)	21.61 \pm 0.70	0.86 \pm 0.01	0.91 \pm 0.06	0.225 \pm 0.004
WT-N/V (n=7)	12.90 \pm 0.27#	0.56 \pm 0.01#	1.06 \pm 0.04#	0.144 \pm 0.004#
WT-N/AgRP (n=8)	17.46 \pm 0.28	0.68 \pm 0.01	0.89 \pm 0.03	0.185 \pm 0.003

Disclosures: W. Cheung, None.

1264

Threonine 137 Is an Important Determinant of Sodium-Phosphate Co-transport in Human NaPi-IIc. G. Jaureguiberry^{*1}, T. O. Carpenter², S. Forman^{*3}, H. Jüppner¹, C. Bergwitz¹. ¹Endocrine Unit, Massachusetts General Hospital, Boston, MA, USA, ²Dept. of Pediatrics and Endocrine Unit, Yale School of Medicine, New Haven, CT, USA, ³Dept. Anesthesiology, Massachusetts General Hospital, Boston, MA, USA.

We recently reported homozygous and compound heterozygous loss-of-function mutations in SLC34A3/NaPi-IIc, as the cause for hereditary hypophosphatemic rickets with hypercalciuria (HHRH). A previously reported male affected by HHRH (Pediatrics 1989; 84:276-280) was found to carry a novel SLC34A3 mutation, T137M c.410C>T(p.T137M), on the maternal allele and the deletion g.4225_50del on his paternal allele. In addition to rickets and typical biochemical abnormalities, he also suffered from recurrent kidney stones prior to therapy with phosphate or vitamin D analogs. His mother, who is a heterozygous carrier of T137M, also had one renal stone during pregnancy, but both parents were otherwise healthy. To permit functional analysis of T137M and g.4225_50del in vitro, we generated expression plasmids encoding enhanced green-fluorescence protein (EGFP) followed, in-frame, by cDNAs encoding wild-type or mutant human NaPi-IIc, i.e. EGFP-hNaPi-IIc, EGFP-[M137]hNaPi-IIc, or EGFP-[V446Stop]hNaPi-IIc. The V446Stop mutant showed a complete loss-of-function when assayed for surface expression and sodium-dependent [33P]-uptake in *Xenopus* oocytes. Conversely, EGFP-[M137]hNaPi-IIc was well expressed in apical patches, the renal brush border membrane equivalent of opossum kidney cells, and it was properly inserted into the cell membrane when the mutant cRNA was injected into oocytes. However, when quantified by confocal microscopy, oocyte membrane fluorescence was reduced to 50% compared to EGFP-hNaPi-IIc. After correction for surface expression, the rate of [33P]-uptake by oocytes mediated by EGFP-[M137]hNaPi-IIc was decreased by an additional 60%. In comparison to wild-type, function of this NaPi-IIc mutant was thus reduced to 30%, which, taken together with complete loss-of-function by g.4225_50del on his second allele appears to be sufficient to explain the phenotype in our patient. Two-electrode studies indicated that EGFP-[M137]hNaPi-IIc is non-electrogenic and the stoichiometry of simultaneous [33P]- and [22Na]-uptake was unaltered when compared to EGFP-hNaPi-IIc. However, EGFP-[M137]hNaPi-IIc displayed a significant phosphate-independent inward-directed sodium-leak, which appears to be insensitive to phosphonoformic acid (PFA) and changes in extracellular pH, factors known to inhibit sodium-dependent phosphate co-transport. M137 may thus reduce the rate of phosphate uptake by uncoupling sodium-phosphate co-transport, suggesting that this amino acid residue has an important functional role in human NaPi-IIc.

Disclosures: G. Jaureguiberry, None.

This study received funding from: National Kidney Foundation.

1265

Alendronate Impairs Angiogenesis and Bone Formation During the Early Stages of Bone Healing in an Animal Model for Osteonecrosis of the Jaw. J. I. Aguirre, S. M. Vanegas*, M. K. Altman*, S. E. Franz*, M. E. Leal, T. J. Wronski. Physiological Sciences, University of Florida, Gainesville, FL, USA.

Osteonecrosis of the jaw (ONJ) is a bone disorder characterized by persistent areas of exposed, necrotic bone in the oral cavity after jaw trauma, dental surgery, or tooth extraction. ONJ is most frequently observed in cancer patients that receive high doses of nitrogen-containing bisphosphonates (BPs) IV to inhibit bone metastases. It has also been reported to occur, although with lower incidence, in postmenopausal women undergoing treatment for osteoporosis with lower doses of orally-administered BPs. Despite the association of BPs with ONJ, the pathophysiology of this condition is not well understood. Since tooth extraction has been identified as a risk factor for ONJ, we propose to use BP-treated rats as a novel animal model to test the hypothesis that BPs inhibit angiogenesis and delay filling of the root socket with new bone after tooth extraction. Intact female rats at 2.5 months of age were injected SC twice weekly with either vehicle, a low dose of alendronate (15 µg/kg bw), or a high dose of alendronate (150 µg/kg bw). The 10-fold difference in these doses is roughly equivalent to the difference between osteoporosis and oncology doses for other BPs. Treatments were administered for 3 weeks before the first mandibular molar was extracted in each rat, and continued during a post-extraction period of 10 days. The left mandibles were then collected to assess the effects of alendronate on bone healing by determining osteo- and angiogenesis within the distal root socket by quantitative histomorphometry. We found that both the low and high doses of alendronate decreased woven bone volume within the root socket by approximately 50% compared to vehicle-treated rats. In addition, alendronate induced significant decreases in osteoid and osteoblast surfaces by approximately 45% and 30% at the low and high doses, respectively. In contrast, no significant difference was observed in osteoclast surface with either dose. Remarkably, both the low and high doses of alendronate decreased blood vessel area by 30% and 45%, and blood vessel number by 40% and 35%, respectively. Along the mesial and distal alveolar bone surfaces at the margins of the distal root socket, both doses of alendronate significantly decreased mineralizing surface, but no difference was observed in osteoclast surface. These findings indicate that alendronate impairs angiogenesis and bone formation during the early stages of bone healing after tooth extraction in female rats. Furthermore, these findings provide evidence for use of tooth extraction in rats as an animal model for BP-associated ONJ.

Disclosures: J.I. Aguirre, None.

1266

Nitrates and BMD Among Canadian Men and Women. S. A. Jamal¹, D. Goltzman², D. A. Hanley³, A. Papaioannou⁴, J. C. Prior⁵, R. G. Josse¹. ¹Medicine, University of Toronto, Toronto, ON, Canada, ²Medicine, McGill University, Montreal, PQ, Canada, ³Medicine, University of Calgary, Calgary, AB, Canada, ⁴Medicine, McMaster University, Hamilton, ON, Canada, ⁵Medicine, University of British Columbia, Vancouver, BC, Canada.

Cross sectional studies suggest that compared to nonusers, postmenopausal women using nitrates have higher BMD and a decreased fracture risk. We used data from a population-based cohort study, The Canadian Multicentre Osteoporosis Study (CaMos), to determine the relationship between nitrate use and bone loss among men and women in a prospective manner. Subjects were 50 years and older, not using bone active agents at the baseline visit. Medication use was assessed by questionnaire at baseline and subjects classified as nitrate users if they used any of: isosorbide dinitrate, mononitrate or nitroglycerin at least once a day every day. We excluded subjects who reported use of nitroglycerin (tablet or spray) exclusively on an "as needed" (prn) basis. BMD at the lumbar spine, total hip and femoral neck was measured at baseline and five years later.

We used linear regression models, stratified by gender and adjusted for age and weight to determine the change in BMD at the total hip, femoral neck and lumbar spine (L1 to L4) from baseline. Results are expressed as the annualized percent change in nitrate users compared with nonusers.

BMD measurements were obtained in 1449 men; 14 men reported nitrate use. BMD measurements were obtained in 2682; 35 women reported nitrate use. The majority of the cohort was Caucasian (95%). The mean age of the men in our cohort was 66.3 ± 9.5 years; the mean age of the women was 68.2 ± 9.3 years. The men weighed 81.2 ± 13.8 kg and the women weighed: 68.9 ± 13.9 kg. Among both men and women, nitrate users were significantly older and weighed significantly less than nonusers.

At all BMD sites and among both men and women, nitrate users lost less bone mass than nonusers. For example, among men, nitrate users had a 1.3% (95% Confidence Interval [CI]: 0.6 to 3.7) annual increase in total hip BMD while nonusers lost 0.9% (95% CI: 0.5 to 1.1) at the total hip. At the lumbar spine nitrate users had a 1.2 % (95% CI: 0.5 to 4.1) increase in BMD while nonusers gained 0.6% (95% CI: 0.3 to 1.1) at the lumbar spine. Women who used nitrates had a 2.8% (95% CI: 0.4 to 5.2) increase in total hip BMD compared to nonusers who lost 1.9% (95% CI: 1.7 to 2.1). Nitrate users also had a 1.4 % (95% CI: 1.1 to 4.0) increase in lumbar spine BMD compared to nonusers who gained 0.5% (95% CI: 0.4 to 0.7).

Our analysis demonstrates that nitrate use is associated with increases in BMD among both men and women 50 years and older. These findings are consistent with earlier studies and strengthen the need for a randomized trial to determine the effects of nitrates on fracture.

Disclosures: S.A. Jamal, None.

1267

Bone Apposition in Patients on Teriparatide Treatment Is Preferably Directed to Skeletal Regions of Local Structural Weakness: Assessment by High Resolution CT Based Finite Element Analysis In Vivo. C. Graeff¹, P. Zysset^{*2}, F. Marin^{*3}, C. C. Glüer¹. ¹Medical Physics, Diagnostic Radiology, Universitätsklinikum Schleswig Holstein, Campus Kiel, Kiel, Germany, ²Institute for Lightweight Design and Structural Biomechanics, Vienna University of Technology, Vienna, Austria, ³Medical Research, Eli Lilly & Co, Europe, Madrid, Spain.

The concepts of skeletal adaptation to loads, such as Wolff's law and Frost's mechanostat, are well established. High resolution computed tomography (HRCT) combined with finite element (FE) analysis technique provide new tools to study these concepts non-invasively in vivo. We investigated at which locations within vertebral bodies new bone is preferentially added under teriparatide treatment, hypothesizing that bone apposition induced by teriparatide is not solely governed by existing bone material acting as a scaffold but is controlled by mechanical needs, e.g. happens preferentially in areas of high strain.

In 27 patients participating in the EUROFORs study we studied the relationship of local baseline strain and subsequent increases in bone mass during 6 months of teriparatide (TPTD, 20 µg per day) treatment. HRCT scans of T12 were performed at 0 and 6 months. Voxel by voxel, we correlated baseline FE-calculated strains (and, for comparison, local apparent bone volume as assessed by HRCT, appBV/TV) with subsequent locally site-matched increases in bone mineral density (BMD) by employing image registration methods. For the FE analysis the entire segmented vertebrae were converted into finite elements of 1.3 mm isotropic resolution and relative von Mises strains were calculated by dividing local strain by global strain applied to the whole vertebra.

Results shown in figure 1 confirm our hypothesis: a sharp increase in BMD with increasing local strain, then converging (left) and a less pronounced upturned U-shaped relation to baseline app.BV/TV

1269

Effects of 2 Year Teriparatide Treatment on 3-D Femoral Neck Bone Distribution, Geometry and Bone Strength: Results from the Eurofors Study. J. Borggrefe^{*1}, C. Graeff¹, T. N. Nickelsen², F. Marin^{*2}, J. del Pino^{*3}, J. Kekow^{*4}, R. Mörcke^{*5}, C. C. Glüer¹. ¹Med. Phys., Diagn. Radiology, UKSH, Kiel, Germany, ²Eli Lilly & Co, Bad Homburg, Germany, ³Internal Medicine, Hospital ClAnico, Salamanca, Spain, ⁴Fachkrankenhaus Rheumatologie, Vogelsang, Germany, ⁵Endokrinolog. Praxis, Magdeburg, Germany.

A DXA-based analysis of treatment-induced changes in bone strength of the proximal femur has limitations due to the complex 3-D bone structure, the projectional imaging and limited spatial resolution. We studied teriparatide (TPTD) induced changes in bone distribution, geometry (periosteal apposition occurring?), and bone strength based on 3-D QCT of the femoral neck.

We examined 53 patients treated for 24 months with TPTD (20 µg/d) in the EUROFORs study with 3 subgroups of women, based on prior antiresorptive treatment: treatment-naïve; pre-treated; and pre-treated with inadequate response. In addition to DXA femoral neck BMD (aBMD [g/cm³]), CT scans of the proximal femur were obtained at 0, 6, 12, and 24 months and were analyzed with Mindways' QCTPRO BIT software. The QCT neck region was defined semiautomatically by six reformatted 1mm slices positioned perpendicular to the neck axis and with a consistent position along that axis based on neck excentricity criteria. Cortical (vBMDcor [mg/cm³]) and trabecular (vBMDtra [mg/cm³]) bone density were evaluated in regions segmented by a fixed threshold. Minimum section modulus (Z1 [cm³]) was calculated as measure of bending strength, buckling ratio (BR) as measure of risk of buckling (high risk if BR>10), and cross sectional area (CSA [cm²]) to evaluate geometric changes.

Strength in bending and buckling did not change in the first 12 months and improved significantly at 24 months, independent of type of pre-treatment. No significant change in periosteal bone geometry was observed. Treatment effects were more favourable in individuals at higher baseline risk: the improvement in Z1 was larger at lower baseline Z1; absolute BR reduction over 2 years was -0.8 in high risk subjects (baseline BR>10) compared to -0.2 in other subjects (p<.05), resulting in a 29% reduction of subjects (16 vs 21) in the high risk category.

We conclude that 24 months of TPTD treatment improves bone strength of the proximal femur both with regard to bending and buckling, with larger protective effects in subjects at higher risk.

Table 1: Baseline data and TPTD-induced changes. ^{ns}:p<0.2, ^{*}:p<.05, ^{**}:p<.01, ^{***}:p<.001

	aBMDfin	vBMDcor	vBMDtra	CSA	Z1	BR
baseline	.57±.009	554±36	81±13	9.6±1.0	0.47±0.01	9.47±0.29
diff. 6mo	-9% ^{ns}	-6.8%***	-2.1%**	-0.3% ^{ns}	+0.0% ^{ns}	+0.7% ^{ns}
diff. 12mo	+2.4%*	-6.3%***	+3.4%***	-1.3% ^{ns}	-3.3% ^{ns}	-1.4% ^{ns}
diff. 24mo	+4.2%***	-1.9%***	+5.4%***	-0.5% ^{ns}	+3.0%*	-4.6%***

Disclosures: J. Borggrefe, None.

This study received funding from: Eli Lilly.

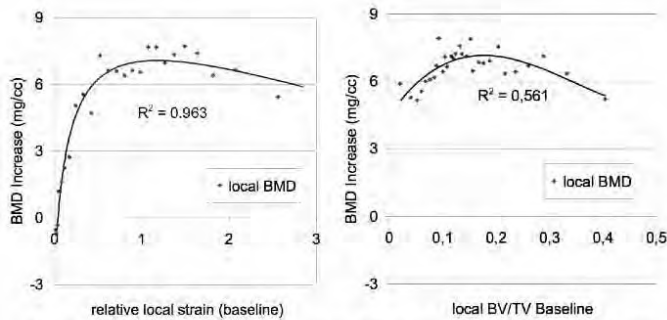


Figure 1: BMD changes as function of baseline strain (left) and appBV/TV (right). Each point represents 2.5% of the total number of voxels.

We conclude that bone apposition under TPTD treatment is not uniform but directed to skeletal regions of local structural weakness. This represents a microstructural, non-invasive, visual and quantitative demonstration of the validity of the biomechanical concepts of bone tissue response to local strains, in accordance with Wolff's law and Frost's mechanostat.

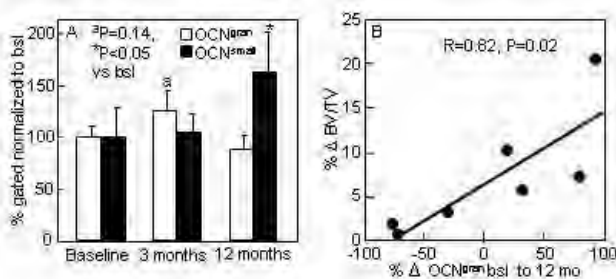
Disclosures: C. Graeff, None.

This study received funding from: Eli Lilly & Company.

1268

Changes in Circulating Osteoblast Lineage Cells Following PTH (1-34) Therapy and Correlation with Changes in Trabecular Bone Mass. S. Kirmani, M. Drake, U. Moedder, J. Peterson*, S. Khosla. Mayo Clinic, Rochester, MN, USA.

Using flow-cytometry, we previously demonstrated a five-fold increase in circulating osteoblast progenitor cells in pubertal boys compared to adult males (NEJM 352:1959-1966). We recently further classified these osteocalcin (OCN) positive cells into two distinct populations: small, relatively agranular cells that co-stained for the stem cell marker, CD34 (OCN^{small}, which may represent a less differentiated cell population), and larger, more granular cells that were CD34 negative (OCN^{gran}, which may represent a more differentiated cell population) (Bone 40:1370-1377). To evaluate the effects of PTH therapy on these cells, we studied 8 women at baseline, 3 months and 12 months after starting 20 mcg/day rh 1-34 PTH (Forteo). All 8 subjects completed the baseline and 3 month visit, and 7 of the 8 completed the 12 month visit. Panel A in the figure shows the changes in the OCN^{small} and OCN^{gran} cells. At 3 months, there was no significant change in the OCN^{small} cells, but a trend for an increase (of 26%, P = 0.14) in the OCN^{gran} cells. However, at 12 months, this pattern was reversed, with the OCN^{small} cells showing a marked increase (of 64%, P = 0.016), and the OCN^{gran} showing a decrease back to baseline levels. Interestingly, the percent change in OCN^{gran} cells between 0 and 12 months was highly positively correlated (R = 0.82, P = 0.02) with changes in bone volume/tissue volume (BV/TV) as assessed by high resolution 3D-pQCT (Xtreme CT, Scanco) in these patients (Panel B). The mean (± SEM) increase in BV/TV in the subjects who had an increase in the OCN^{gran} cells between baseline and 12 months was 10.8 ± 3.25% as compared to 1.7 ± 0.6% in the subjects who had a decrease in these cells (P = 0.066). To the extent that the OCN^{small} cells and OCN^{gran} cells represent less as compared to more differentiated osteoprogenitor populations, respectively, our findings suggest that PTH initially expands the population of more mature osteoprogenitor cells, whereas over a longer period of time this effect wanes, and more immature cells are recruited along the osteoblast pathway. Sustained increases in the more differentiated cells appear to be predictive of larger gains in trabecular bone volume, although further studies characterizing the relative osteoblastic differentiation of the OCN^{small} vs. OCN^{gran} are needed to test this hypothesis.



Disclosures: S. Kirmani, None.

1270

Effect of Vitamin-D3 and Calcium on Fracture Risk in 65-71 Year Old Women in a 3-Year Randomized Clinical Trial - Preliminary Results of the OSTPRE-Fracture Prevention Study. K. T. J. Salovaara¹, M. Tuppurainen¹, T. Rikonen¹, M. Kärkkäinen^{*1}, J. Sirola^{*1}, R. Honkanen^{*1}, E. Alhava^{*2}, H. P. Kröger³. ¹Bone and Cartilage Research Unit, University of Kuopio, Kuopio, Finland, ²Department of Surgery, University Hospital of Kuopio, Kuopio, Finland, ³Department of Orthopedic, Trauma and Handsurgery, University Hospital of Kuopio, Kuopio, Finland.

Although Ca+Vitamin D supplementation has been shown to prevent fractures in the elderly, the effect of such a supplementation on fracture prevention in younger ambulatory postmenopausal women is still debatable. The aim of this population level intervention was to determine whether daily Vitamin-D3 800 IU and Ca 1000 mg administered in two daily doses (Calcichew-D3 forte 500 mg/400IU, Leiras Nycomed Ltd. Finland) could decrease the incidence of fractures in postmenopausal women.

The women within the OSTPRE-cohort who were 65 years or older on 30.11.2002 (n = 5553) were asked regarding their willingness to participate in a randomized controlled trial with questions about medications, health disorders and health behaviour. Of the questionnaires that were adequately completed with written consent, 3432 subjects were randomized to have either Ca+Vit D supplementation (n=1718) or no supplementation (n=1714) for 3 years. Primary end points were number of falls and fractures. Fracture data was collected from the entire cohort by telephone interviews once a year and also from a subsample every 4 months. All self reported fractures were included in the analysis. Risk of fracture (HR) was calculated using Cox proportional hazards model. The study was approved by the local ethics committee.

Mean age of women was 67.4 (SD 1.8, range 65-71). At baseline (n = 3432) there were no statistically significant differences in age, weight, bone mineral density, HRT-use, hormonal status, age at menopause, smoking habits, alcohol use or functional capacity. A total of 290 fractures were reported including 144 osteoporotic fractures (vertebral n=26, hip n=10, distal forearm n=82 and humerus n=26). The incidence of distal forearm fractures was lower (1.86 %) in the intervention group compared to the control group (2.68%) (p = 0.107, chi square test). In the Cox regression model (n = 2946) the hazard ratios (HR with 95% CI) in the intervention group compared to the control group were 0.84 (0.65-1.08) for all fractures, 0.74 (0.51-1.06) for osteoporotic fractures and 0.60 (0.37-0.98) for distal forearm fractures, respectively.

In conclusion, this population level intervention study suggests that daily Vitamin-D3 and Calcium supplementation has a trend towards fracture reduction in all fractures and particularly osteoporotic fractures in postmenopausal women.

Disclosures: K.T.J. Salovaara, None.

This study received funding from: Leiras Nycomed, Finnish Academy, Kuopio University Hospital EVO-grant.

1271

Long Term Risk Factors for Incident Vertebral Fractures In Healthy Older Women After 15 Years of Follow-up: The Study of Osteoporotic Fractures. T. A. Hillier¹, J. A. Cauley², M. C. Nevitt³, J. H. Rizzo^{*1}, K. L. Pedula^{*1}, K. K. Vesco^{*1}, M. C. Hochberg⁴, S. R. Cummings³. ¹Center for Health Research, Kaiser Permanente, Portland, OR, USA, ²U Pittsburgh, Pittsburgh, PA, USA, ³CPMC Research Institute and UCSF, San Francisco, CA, USA, ⁴U Maryland, Baltimore, MD, USA.

Vertebral fractures (Vfx) are associated with morbidity and mortality in older white women, yet little is known about their long-term risk factors.

We therefore performed a comprehensive assessment of potential risk factors in 2,286 women age 65 or older without baseline Vfx enrolled in the Study of Osteoporotic Fractures. Women who returned after 15 years of follow-up represented 76% (3572/4702) of survivors, 64% (2286/3572) of whom had repeat lateral thoracic and lumbar spine films. Incident Vfx were defined as $\geq 20\%$ and $\geq 4\text{mm}$ decrease in vertebral height at any level. More than 50 risk factors were evaluated, including known short-term predictors of vertebral fractures and long-term predictors of non-spine fracture. Risk factors associated univariately with incident Vfx (p<0.10) were further tested using backward stepwise regression to determine the final multivariable logistic regression model.

During a mean of 15 (SD 0.70) years of follow-up, 324 (14%) of women developed an incident vertebral fracture. Age, BMD, history of fracture since age 50, and falls remained significant risk factors (p<0.05) for incident Vfx (Table). DXA BMD at total hip and spine were both significantly associated with incident Vfx; spine BMD had a higher point estimate and was used in the final model. Other risk factors for non-spine fracture, such as alcohol, smoking, physical activity, and estrogen or glucocorticoid use, were not independent predictors.

Long-Term Incident Vfx Risk Multivariable model:	Odds Ratio (95% CI)
Age (per 5 years)	1.6 (1.4, 1.9)
Spine BMD*	1.8 (1.6, 2.1)
Fall during first year of follow-up	1.4 (1.1, 1.9)
Fracture since age 50	1.5 (1.2, 1.9)

*per standard deviation decrease

Among women who survived to age 80 and above, only four factors were independent predictors of new Vfx during 15 years of follow-up. Our results suggest a single BMD is highly predictive of long-term vertebral fracture risk, and that efforts to prevent vertebral fracture in healthy older women should focus on BMD and on falls.

Disclosures: T.A. Hillier, None.

This study received funding from: the National Institute of Aging (NIA) and National Institute of Arthritis, Musculoskeletal, and Skin Diseases (NIAMS): 2R01AG027574-22A1, R01 AG005407, R01AG027576-22, 2R01AG005394-22A1, AG05407, AG05394, AR35583, AR35582, AR35584.

1272

Is Antidepressant Use Associated with Bone Loss or Fractures in Postmenopausal Women? L. Spangler^{*1}, D. Scholes¹, R. Brunner^{*2}, J. Robbins^{*3}, S. Reed⁴, K. Newton^{*1}, J. Melville^{*4}, A. LaCroix⁵. ¹Group Health, Seattle, WA, USA, ²University of Nevada, Reno, NV, USA, ³University of California, Sacramento, CA, USA, ⁴University of Washington, Seattle, WA, USA, ⁵Fred Hutchinson Cancer Research Center, Seattle, WA, USA.

A link between depression and bone outcomes has been postulated. The association may be the result of common physiologic systems, similar risk factors, or medication use. Literature on the association between antidepressant medication (ADM) use and BMD is limited and most research on the association with fracture relies on automated data.

We assessed these associations in 93,676 postmenopausal women (50 to 79 years old) enrolled in the WHI Observational Study, followed an average of 7.4 years. Participants brought current medications to the interviews and ADM was recorded. We further categorized ADM as selective serotonin reuptake inhibitors (SSRIs) and all other types for some analyses. To assess self-reported fractures of the hip (adjudicated), spine, wrist, and "other" skeletal sites we used Cox survival models controlling for exercise, cardiovascular disease, analgesic use, and fracture history. To assess 3-year changes in hip, spine, and whole body BMD in 6441 women enrolled at the 3 densitometry clinics we used linear regression models that included baseline BMD and hormone therapy. In addition, all models adjusted for depressive symptoms (Burnam's screen), age, menopause duration, race, physical function, smoking, height and weight.

At baseline, 8% of women were using ADM (4% SSRI). Overall, no significant associations were seen between ADM and 3-year changes in BMD at any skeletal site after adjustment. There was a positive association between ADM and increase risk of self-reported spine fractures (HR for SSRI =1.25 CI .96 - 2.05; HR for other ADM = 1.45 CI 1.17-1.81) and fractures at other skeletal sites (HR for SSRI = 1.32 CI 1.21 - 1.45; HR for other ADM =1.16 CI 1.06 -1.27) (Table 1). Controlling for falls had little effect on these associations. No associations were observed between ADM and hip or wrist fracture. The results from this sizeable study of generally healthy postmenopausal women provide additional evidence for an association between ADM and increased risk of fracture at some skeletal sites.

Table 1. Antidepressants use (ADM) and adjusted hazard ratios for fracture

Anatomic site of fracture	Adjusted hazard ratio for fracture (referent group =women not using antidepressants)	p-value	95% Confidence interval
Hip (1,132 hip fractures)	1.14	0.28	0.90 to 1.45
Spine (1,607 spine fractures)	1.36	0.001	1.14 to 1.63
Wrist (2,867 wrist fractures)	1.15	0.06	0.99 to 1.33
Other sites (11,128 fractures at other skeletal sites)	1.24	<0.001	1.15 to 1.32

Disclosures: L. Spangler, None.

1273

Functional Decline after Incident Wrist Fracture: The Study of Osteoporotic Fractures. B. J. Edwards¹, D. Dunlop^{*1}, J. Song^{*1}, H. A. Fink², J. Cauley³. ¹Medicine, Feinberg School of Medicine, Northwestern University, Chicago, IL, USA, ²Medicine, Geriatric Research Education and Clinical Center, Veterans Affairs Medical Center, Minneapolis, MN, USA, ³Medicine, University of Pittsburgh, Pittsburgh, PA, USA.

Wrist fractures are common fractures that occur in post-menopausal women. Little is known about the effect of wrist fractures on functional decline. Analyses included 7,694 participants of the Study of Osteoporotic Fractures (SOF), a multicenter observational study of women aged > 65 years. Functional activity was by self-report and measured ability to perform five activities: walking, climbing stairs, preparing meals, shopping, and doing heavy housework. The items are rated on a four point scale from no difficulty (0), mild (1) and moderate difficulty (2), to unable to perform (3). We calculated global function (0-15), and targeted upper extremity function (0-9 from cooking, heavy housekeeping and shopping).

Participants who did not sustain a vertebral or hip fracture or wrist fracture prior to baseline and participated in as at least one (range 1-5) follow-up visits through 1998. (N=7,694) We track wrist fracture status at each visit to utilize longitudinal information and to include records from women who contribute function data both prior to and following an incident wrist fracture. Longitudinal multiple regression analyses with generalized estimating equations (GEE) are used to estimate annual decline in function

over time.

Age-adjusted average annual rates of global functional decline were almost 3 times greater following a wrist fracture and remained significantly higher controlling for BMI, and health status (Table 1). Similarly, wrist fractures resulted in significantly greater decline in upper extremity function (Table 2)

Table 1 Average Annual Decline in Global Function by Incident Wrist Fracture Status

Adjustment Factors	Sustained Incident Wrist Fracture		Comparison of average decline in function for women with and without wrist fracture
	Yes	No	
Age	0.37	0.13	p=0.003
Age+BMI+Health	0.27	0.02	p=0.001

Table 2: Average Annual Decline in Upper Extremity Function by Incident Wrist Fracture Status

Adjustment Factors	Sustained Incident Wrist Fracture		Comparison of average decline in function for women with and without wrist fracture
	Yes	No	
Age	0.58	0.34	p=0.002
Age+BMI+Health	0.46	0.20	p=0.007

Women with incident wrist fractures had statistically significant functional decline independent of age, BMI and baseline health.

Disclosures: B.J. Edwards, Merck 2; Procter and Gamble 2, 8; Roche 8; GSK 8.
This study received funding from: NIH.

1274

Fracture Risk Increases after Cancer Diagnosis in Postmenopausal Women: Results from the Women's Health Initiative. Z. Chen¹, M. Maricic¹, A. K. Aragaki², C. P. Mouton³, A. M. Lopez⁴, L. A. Arendell¹, T. Bassford⁵, R. T. Chlebowski⁵. ¹Univ. of Arizona, Tucson, AZ, USA, ²Fred Hutchinson Cancer Research Center, Seattle, WA, USA, ³Howard University, Washington, DC, USA, ⁴Arizona Cancer Center, Tucson, AZ, USA, ⁵UCLA, Los Angeles, CA, USA.

The primary aim of this study was to investigate changes in fracture and fall risk after breast cancer (BC) or other cancer (OC) diagnosis. This was a prospective study in the Women's Health Initiative (WHI) cohort. Participants included 145,886 postmenopausal women who had no cancer history at baseline and were enrolled in either the Observational Study (OS) or the Clinical Trials (CT). They were followed up to 9 years and classified into no-cancer, incident BC and incident OC group. Hip fractures were adjudicated for both OS and CT, while the remaining fractures were only adjudicated in the CT group. Falls were self-reported. Hazards ratio (HR) and confidence interval (CI) were computed from Cox Proportional Hazards Models. The results suggest that fracture and fall risk increases after cancer diagnosis (Table 1). In comparison to women without a cancer history, hip fracture risk was significantly higher after BC diagnosis (HR =1.51 CI(1.13-2.54)) or OC diagnosis (HR = 2.03 (1.62-2.54)), but the annual incidence rates of hip fractures before a cancer diagnosis were comparable between groups after adjusted for age, hormone use, health and other lifestyle factors. Risk of fall also increased with either a BC (HR = 1.16 (1.08-1.25)) or OC diagnosis (HR = 1.27 (1.19-1.36)). Although fall was a risk factor for fracture, the increased number of falls did not explain the elevated hip fracture risk. The relative risk for vertebral, forearm or total fractures were all elevated after either BC or OC diagnosis; however, the increased risk reached statistical significant (p<0.05) only for vertebral and total fractures in the other cancer group. In conclusion, postmenopausal women have a significantly elevated risk for fracture and fall after a cancer diagnosis. However, the increased risk of fall is not the major contributor to this higher fracture risk observed in the incident cancer cases. Future study should investigate the impact of cancer prognosis and cancer treatment on the observed increased risk of fracture and fall associated with cancer.

Table1. Age-adjusted Annualized Percentages of Fractures and Falls Before and After Cancer Diagnosis (n=146,959)

		Annualized Percent				
	Phase	Hip Fracture	Forearm Fracture	Vertebral Fracture	Total Fracture	>= 2 Falls
No Cancer (N = 132840)		0.15%	0.47%	0.19%	1.24%	4.72%
Other Cancer (N = 8242)	Before	0.15%	0.42%	0.34%	1.45%	5.06%
	After	0.40%	0.53%	0.48%	1.89%	5.76%
Breast Cancer (N = 4804)	Before	0.13%	0.43%	0.16%	1.12%	4.89%
	After	0.25%	0.50%	0.30%	1.36%	5.30%

Disclosures: M. Maricic, None.
This study received funding from: NIH.

1275

Impact of Adherence to Osteoporosis Medications on Fracture Rates: A Population-based Study. S. Jaglal¹, D. Thiruchelvam², G. Hawker³. ¹Rehabilitation Science, University of Toronto, Toronto, ON, Canada, ²Institute for Clinical Evaluative Sciences, Toronto, ON, Canada, ³Medicine, University of Toronto, Toronto, ON, Canada.

The purpose of this study was to examine if current efforts at managing osteoporosis led to a reduction in fracture in elderly men and women in Ontario, Canada. Specifically we determined the impact of differing levels of adherence to osteoporosis medications on subsequent fracture in a population-based study. Ontario residents over the age of 65 have universal access to Medicare and to certain osteoporosis medications. We identified all persons aged 67 and older who initiated an osteoporosis medication between April 1, 2002 - March 31, 2004 and who did not have a drug claim for an osteoporosis medication (bisphosphonate or SERM) during the 2 years prior to initiation date (N=90,723). We excluded patients with erroneous records (prescribed 1 pill for 1 day, n=866 or adherence > 120%, n = 4,605), prescription for salmon calcitonin (n=687), history of Paget's, epilepsy, cancer, pathological fracture (n=163), discharged to nursing home (n=2,458) or died before the end of the 2 year followup period from medication initiation (n=7,859) for a final cohort of 74,085 patients. The main predictor was fracture in the period after the initiation of medication. The Medication Possession Ratio (MPR) defined as the no. days supplied from first to last prescription / length of followup (730 days). This was defined at 4 cut-offs, 30%, 50%, 67% and 80%. The outcome was fracture in the period after the initiation of medication. There were 1751 (2.4%) fractures. Logistic regression analyses were conducted for each refill compliance cut-off adjusted for age, sex, BMD, no. of non-osteoporosis medications, and no. of physician visits in 2 year period prior to initiation of treatment, BMD after initiation of treatment, and Charlson co-morbidity index. Only 80% and 67% refill compliance were statistically significantly associated with fracture reduction: Odds ratio (80%) = 0.85, p = 0.046; Odds ratio (67%) = 0.85, p = 0.013. Age <75 (OR = 0.63), being female (OR = 0.54), having had a BMD prior to treatment (OR = 0.85) and one after (OR = 0.89) were also statistically significantly associated with fracture reduction. In conclusion, patients who are at least 67% adherent with their osteoporosis medications over a two-year period are less likely to fracture. Other factors associated with fracture reduction are younger age, female sex, and BMD testing. These are important findings, which confirm at a population level previous reports based on selected clinical trials patients. We now have evidence to show decision-makers that if we continue our efforts to monitor treatment and increase adherence even bigger gains in fracture reduction might be possible.

Disclosures: S. Jaglal, None.
This study received funding from: Institute for Clinical Evaluation Sciences.

1276

Clinical Low-Trauma Fractures Cluster in Time in Postmenopausal Women. P. Geusens¹, T. van Geel², G. Dinant². ¹Internal Medicine/Rheumatology, University Hospital Maastricht and UHasselt, Maastricht, The Netherlands, ²Department of General Practice, University Maastricht, Maastricht, The Netherlands.

Objective. Postmenopausal women with a fracture history have an increased risk for new fractures. Some studies indicate that this risk is highest immediately after a fracture. We assessed during a 10-year follow-up the time relation between a first and second clinical fracture.

Study design. Population-based study in 10 general practice centers, including 4203 postmenopausal women, aged between 50 and 80 years at baseline, who completed a questionnaire about the incidence of radiographically confirmed clinical low-trauma fractures, analysed by multiple Cox regression.

Main outcome measures. The time frame between start of menopause, a first and second low-trauma clinical fracture.

Results. 924 women sustained at least one fracture after menopause, of whom 243 had a second fracture. The fracture probability for a first fracture within 1, 5, 10 and 20 years from the menopause on was 1.0 (0.7-1.3), 3.5 (3.0-4.1), 7.9 (7.1-8.7) and 19.0% (17.6-20.3). The fracture probability for a second fracture within 1, 5, 10 and 20 years following a first fracture was 6.1 (4.5-7.6), 15.9 (13.4-18.4), 27.1 (23.8-30.5) and 40.2% (35.4-45.0), respectively.

Of all first fractures, 4.3% (3.0-5.6) occurred within one year after menopause, 15.5% (13.2-17.8) within 5 years and 33.9% (30.9-36.9) within 10 years. Of all second fractures, 22.6% (17.7-27.5) occurred within one year after a first fracture, 53.9% (48.1-59.8) within 5 years and 79.8% (75.2-84.5) within 10 years.

Conclusion. In postmenopausal women, low-trauma clinical fractures cluster in time. Twenty percent of second fractures occur within 1 year after a first fracture, half within 5 years and 80% within 10 years. Prevention of a second fracture is therefore indicated soon after a first fracture has occurred.

Disclosures: P. Geusens, None.

1277

Tri-partite Relationships Between Bone, Cartilage and Adipogenic Changes Contribute to Bone Loss. N. H. Kulkarni^{*1}, T. Wei^{*1}, B. Han^{*1}, M. A. Schreivweis^{*1}, K. A. Brune^{*1}, T. A. Christopher^{*1}, J. A. Wolos^{*1}, A. Harvey^{*1}, D. L. Sterchi^{*1}, B. Gitter^{*1}, S. Chandrasekhar^{*1}, T. J. Martin², H. U. Bryant¹, Y. L. Ma¹, P. G. Mitchell^{*1}, J. E. Hale^{*1}, J. E. Onyia¹. ¹Eli Lilly and Company, Indianapolis, IN, USA, ²SVIMR, Fitzroy, Victoria, Australia.

Ovariectomy (Ovx) or estrogen withdrawal leads to an increase in bone turnover resulting in osteopenia. A hallmark of this process includes changes in bone, cartilage and adipogenic markers. While the bone markers are well studied in osteopenia, the regulation of cartilage and adipogenic markers remain poorly understood. Here, we present a comprehensive longitudinal evaluation of the anatomical (BMD), biochemical and molecular changes in bone, cartilage and adipogenic markers in rat Ovx model. Female, 6-month old rats were Ovx or sham-operated and sacrificed at 2, 4, 6, 8 and 12 weeks post-Ovx. The left femur was analyzed for BMD and the right metaphyseal femora were used for mRNA analysis of bone, cartilage and adipogenic/lipid metabolism markers. Biochemical markers of bone and cartilage turnover (PINP, CTX-I, CTX-II) and leptin, an adipogenic marker, were measured in the serum. Ovx-induced decrease in distal metaphyseal BMD was evident at 2 weeks with a steady decline over 12 weeks and was consistent with observed histological decrease in bone volume and increase in marrow adiposity. Serum PINP, CTX-I and CTX-II robustly increased 3.5-, 1.8-, and 4.7- fold respectively in 2 weeks and returned to near sham levels by 12 weeks. The levels of serum leptin increased, most evident in 6 weeks and was sustained over time consistent with increased adiposity. The mRNA levels of 15 osteogenic markers (alkaline phosphatase, collagens α_1 (I), α_1 (V), osteocalcin, etc) initially increased with maxima at 6 weeks and thereafter decreased below sham levels; whereas the expression levels of osteoblast-derived resorption indicator (OPG/RANKL ratio) steadily declined reminiscent of BMD. Interestingly, a steady decrease in the expression levels of chondrocytic markers (collagen α_1 (II), (X), aggrecan, COMP, cdnap) were observed. In contrast, markers of 7 adipogenic/lipid metabolism (LPL, FABP4, SCD1, PEPCK, leptin, etc) increased significantly and persisted with time. Overall, gene expression changes in these markers were consistent with biochemical markers and pathological changes in Ovx-induced osteopenia. Gene expression markers (bone, cartilage and adipogenic) independently showed a correlation of $r^2=0.55$; 0.58; 0.52 respectively to BMD, whereas a combination of these markers increased the correlation to $r^2=0.91$. These results suggest that the relationship between bone, cartilage, and adipogenic changes underscore osteopenia and should together be leveraged as markers to better model the disease process.

Disclosures: N.H. Kulkarni, Eli Lilly and Company 3.

1278

Bone Mineral Density in Hip and Spine by Quantitative CT and Previous History as Predictors of Incident Low Trauma Fractures in Elderly Men and Women. K. Siggeirsdottir^{*1}, T. Aspelund^{*1}, G. Sigurdsson¹, B. Jonsson^{*2}, B. Mogensen^{*3}, G. Eiriksdottir^{*1}, S. Sigurdsson^{*1}, L. Launer^{*4}, T. Harris^{*4}, T. F. Lang⁵, V. Gudnason^{*1}. ¹Icelandic Heart Association, IS-201 Kopavogur, Iceland, ²University Hospital, Malmö, Sweden, ³University of Iceland, IS-101 Reykjavik, Iceland, ⁴National Institute on Aging, Bethesda, MD, USA, ⁵University of California, San Francisco, CA, USA.

The experience with QCT in prospective population studies is limited. We have studied the predictive power of QCT of hip and lumbar spine in the AGES-REYKJAVIK Study, a cohort of 67-85 year old men (n=829) and women (n=1088) drawn from an established population based cohort. 4 detector Siemens CT system with 1 mm slices was used and for this analysis integral BMD in femoral neck and vertebral centrum in L₁+L₂ was used. All low trauma fractures during 3.7 years follow-up were validated by medical and radiological records, altogether 44 fractures in 36 men and 121 fractures in 104 women. Baseline information on previous fractures, falls during the last twelve months, medications, body mass index and measured grip strength were among several variables included in a Cox-proportional hazards model (see table).

Significant variables	Hazard ratio (95% CI)	
	Females	Males
Δ 5-years in age	NS	1.6** (1.0-2.3)
Femoral neck BMD/SD	1.8** (1.4-2.3)	2.0** (1.4-2.8)
Previous fracture	1.7** (1.1-2.6)	2.9** (1.4-6.0)
Falling/12 months	2.2** (1.4-3.4)	2.9* (1.4-6.2)
Grip strength/SD	1.7* (1.1-2.5)	NS

*p<0.05, **p<0.01

The results show that the risk of all osteoporotic fractures almost doubled in both sexes per one standard deviation below the mean in femoral neck BMD whereas lumbar spine BMD did not add further to the prediction. Increase in age after 67 seems to be mainly a risk factor amongst men. Previous osteoporotic fractures and falling during the last twelve months were strong risk factors in both sexes whereas grip strength reached only significance in women. The area under the ROC curve (aROC) was 0.83 (0.78-0.88) for men, using the above variables, and 0.72 (0.76-0.77) for women. Using hip BMD increased the aROC curve significantly both for men (p=0.03) and women (p=0.0230). Grip strength did not improve diagnostic capacity. We conclude that volumetric BMD at the femoral neck measured by QCT is an important risk factor for all osteoporotic fractures.

Disclosures: G. Sigurdsson, None.

This study received funding from: NIH NO1-AG-1-2100.

1279

Fracture Risk Index After Falling: A Selection Strategy for Fracture Reduction Through Falls Prevention in the Frail Elderly. P. N. Sambrook¹, J. S. Chen^{*1}, L. M. March¹, J. M. Simpson^{*2}, M. J. Seibel³. ¹Institute of Bone & Joint Research, University of Sydney, Sydney, Australia, ²School of Public Health, University of Sydney, Sydney, Australia, ³ANZAC Research Institute, University of Sydney, Sydney, Australia.

This study aims to develop and evaluate a fracture risk index after falling for use in the frail elderly. We assessed risk factors at baseline and prospectively recorded falls and falls-related fractures in 2005 institutionalized older people. Each fall was treated as a study unit and a fracture as an outcome. To account for within-subject correlation between falls, the generalized estimating equations approach (specified a binomial distribution and a log link) was used to identify fracture predictors after falling. Relative risk (RR) for a risk factor was assigned as a weight. A baseline weighting of one was given if a resident did not have the risk factor. Fracture score was calculated by multiplying the weights of all independent risk factors in a person. The score is a RR compared to residents without the risk factors. The subjects (1532 females & 473 males) were older and frail, with a mean age of 87 (SD = 7.1) years and 45% living in nursing homes. Over a mean of 1.55 years, 6646 falls were reported by 1342 subjects and 308 fractures by 270 subjects, giving an incidence rate of 214 and 9.9 per 100 person years for falls and fractures respectively. The independent risk factors were lower broadband ultrasound attenuation, lower weight, longer lower leg length, better balance, intermediate-care residence, a history of fracture and lack of report of a fall in the past year. The risk score corresponded well with fracture risk. Fracture rate was 1.1 per 100 falls for 13.8% of falls with a mean score of 3.1 compared to a rate of 9.9 for 14.4% of falls with a mean score of 20.0, a multiplicative increase of 8.8. In order to identify residents who would be at high risk of both falls and fractures from baseline, the risk score was multiplied by a falls risk score calculated using the falls risk index proposed by the Fracture Risk Epidemiology in the frail Elderly (FREE) study (Chen et. al. A multivariate regression model predicted falls in residents living in intermediate hostel care. J Clin.Epidemiol. 58:503-508, 2005). The results showed that 34% of highest risk residents (i.e. highest combined score) had incidence rates of 249 and 16.2 per 100 person years for falls and fractures respectively and accounted 56% of the total fractures. The rates were 30% and 125% higher in falls and fractures respectively compared to the rest of the sample. Prevention strategies on fracture reduction through fall prevention should be directed to those at highest risk in both falls and fractures. The index could help to rationalize the provision of falls prevention programs in the frail elderly.

Disclosures: P.N. Sambrook, None.

This study received funding from: NHMRC of Australia.

1280

Finite Element Analyses Based on In Vivo HR-pQCT Images of the Radius Tend to Improve Wrist Fracture Prediction. S. Boutroy^{*1}, B. Van Rietbergen^{*2}, E. Sornay-Rendu^{*1}, F. Munoz^{*1}, M. L. Bouxsein³, P. D. Delmas¹. ¹INSERM Unit 831 and Université de Lyon, Lyon, France, ²Department of Biomedical Engineering, Eindhoven University of Technology, Eindhoven, The Netherlands, ³Orthopedic Biomechanics Laboratory, Beth Israel Deaconess Medical Center, Boston, MA, USA.

We recently reported that attributes of cortical (Ct) and trabecular (Tb) architecture contribute to skeletal fragility, partially independently of areal BMD (Sornay-Rendu, JBMR 2007; Boutroy, JCEM 2005). Integrated assessment of bone strength by finite element analysis (FEA) may further contribute to the prediction of fracture risk. To test this, we performed FEA on in vivo HR-pQCT images of the distal radius (XtremeCT, Scanco Medical AG) in 33 women (73 ± 6 yrs) who previously sustained a fragility fracture of the wrist (fx) and 33 age-matched controls, from the OFELY cohort. We found that areal BMD; total, Tb and Ct volumetric BMD; Tb number, separation, thickness and distribution; as well as Ct thickness were significantly worse in fx cases than controls, ranging from -6% to 73%. FEA-derived stiffness, apparent modulus and estimated failure load were 15-16% lower in fx than in controls (p < 0.05). In both groups, the load was mostly carried by the cortex, from 60% (distal region) to 91% (proximal region). Tb bone carried 9 to 22% more load in controls than in fx, implying that the load distribution was more uniform in controls. To reduce the number of variables, we conducted a principal components (PC) analysis with varimax rotation in the 66 women. The first PC included stiffness, apparent modulus, estimated failure load, areal and volumetric BMD and Ct thickness, explaining 51% of the variance. PC2 combined Tb architecture: number, separation and distribution, and explained 13% of the variance. An additional 10% of the variance was explained by the distribution of the load between Ct and Tb bone (PC3). We used univariate logistic regression to compute odds ratio (OR) for the PC: PC1=2.27 [1.16-4.44], PC2=2.22 [0.97-5.09] and PC3=2.21[0.99-4.98]. The OR for combination of PC1 and PC2 was 4.72 [1.54-14.28], but the addition of PC3 did not reach significance (p=0.27). Altogether these results indicate that FEA may provide information about skeletal fragility and fracture risk not assessed by BMD or architecture measurements alone. In particular, the load distribution between Ct and Tb bone, assessed by FEA, seems very promising for improving wrist fracture prediction independently of BMD and microarchitecture. These data provide strong rationale for additional studies testing the ability of FEA based on HR-pQCT to predict fracture risk.

Disclosures: S. Boutroy, None.

1281

Height Loss Predicts Fractures in Middle Aged and Older Men and Women: European Prospective Investigation Into Cancer-Norfolk Population Cohort Study. A. Moayyeri^{*1}, A. Welch^{*1}, R. N. Luben^{*1}, N. J. Wareham^{*2}, S. Bingham^{*3}, K. T. Khaw^{*1}. ¹Department of Public Health and Primary Care, Institute of Public Health, School of Clinical Medicine, The University of Cambridge, Cambridge, United Kingdom. ²MRC Epidemiology Unit, The University of Cambridge, Cambridge, United Kingdom. ³MRC Dunn Human Nutrition Unit, The University of Cambridge, Cambridge, United Kingdom.

With effective interventions available for fracture prevention, a major clinical issue is identification of individuals at greatest fracture risk for preventive interventions. Height loss among middle aged men and women can be easily measured in outpatient clinics and may contribute to fracture risk prediction. We aimed to assess measured height loss and fracture incidence in a prospective observational population study. Height was measured in men and women in the Norfolk cohort of the European Prospective Investigation into Cancer (EPIC-Norfolk) between 1993 and 1997 and was repeated between 1997 and 2000. Incident fractures up to 2006 were ascertained by hospital record linkage. Height loss and known risk factors of fracture were entered into Cox proportional hazards models to determine their independent contribution to the risk of fracture. In 14,921 men and women aged 42-82 years, during follow-up period of 7.1 (SD 0.7) years, there were 390 fractures, including 122 hip fractures. Annual height loss in the group of fracture sufferers (1.8 mm, SD 0.3) was significantly greater than other participants (0.9 mm, SD 0.2; $p < 0.001$). Participants with annual height loss > 0.5 cm had an age and sex-adjusted hazard ratio of any fracture of 1.76 (95%CI 1.16-2.67) and of hip fracture of 2.08 (95%CI 1.07-4.05) compared to those with no height loss. In multivariate models, 1 cm of height loss per year was associated with a hazard ratio of 1.86 (95% CI 1.28-2.72) for all fractures and 2.24 (95%CI 1.23-4.09) for hip fracture independent of age, sex, past history of fracture, smoking, body mass index, alcohol intake, and heel ultrasound measures. Annual height loss of 1 cm was comparable to having a past history of fracture and equivalent to being about 14 years older in chronological age in terms of magnitude of relationship with fracture risk. Middle aged and older men and women with annual height loss > 0.5 cm are at increased risk of hip and total fracture. Serial height measurements can easily be incorporated in routine clinical practice and may contribute to the development of practical fracture risk assessment tools.

Disclosures: A. Moayyeri, None.

This study received funding from: Medical Research Council and Cancer Research UK.

1282

Hip Muscle Cross-Sectional Area and Attenuation: Association with Hip Fracture. T. F. Lang¹, X. Cheng^{*2}, C. Li^{*1}, A. Koyama^{*1}, T. Harris^{*3}, Y. Lu^{*1}. ¹Radiology, University of California, San Francisco, San Francisco, CA, USA, ²Radiology, Beijing Ji Shui Tan Hospital, Beijing, China. ³Epidemiology and Biometry, National Institute on Aging, Bethesda, MD, USA.

Purpose: Falling is an important risk factor for hip fracture, and the strength of the hip musculature is crucial for recovery of stability after loss of balance. We hypothesized that the size (cross-sectional area (CSA)) of hip muscle from hip QCT and adipose infiltration of muscle (defined by CT x-ray attenuation of the hip muscles), acting as surrogate measures for hip muscle function, would correlate with hip fracture independently of age and body size.

Methods: To test the hypothesis, we compared CT scans of the contralateral hip in 45 women (mean age 74.71 ± 5.94) imaged within 48 hours of their hip fractures to 66 age-matched control subjects (mean age 70.70 ± 4.66). A volumetric CT scan encompassing the proximal part of the femur was analyzed for total percentage of fat tissue in the in the CT field of view and for the CSA and lean tissue Hounsfield Unit (HU) values of the hip extensor, abductor, adductor and flexor muscles. The CT scan was also analyzed to compute areal bone mineral density (aBMD) of the hip bone. Logistic regression analyses were employed to determine differences between fracture subjects and controls in body composition measures after adjustment for age, height, and BMI. Receiver-operator curve (ROC) analyses were employed to determine if combinations of aBMD and body composition were better discriminators of hip fracture than aBMD alone.

Results: Subjects with hip fractures were on average 5 years older ($p < 0.001$) had 8% lower BMI ($p < 0.05$), 8% lower percentage fat ($p < 0.0001$) and roughly 20% lower extensor and adductor CSA values than controls ($p < 0.0001$). Despite having lower total adiposity, they had higher muscle adiposity as indicated by lower lean tissue attenuation in all four muscle groups, with statistically significant differences in the adductor, abductor and flexor groups ($0.00001 < p < 0.02$). After adjustment for age and BMI, the fracture subjects had lower total % fat, smaller extensor and adductor CSA values, and greater adipose infiltration (lower attenuation) in the adductor ($0.001 < p < 0.05$). ROC analyses showed that models combining percent fat, muscle CSA and muscle attenuation values with aBMD had higher AUC values than models containing only aBMD (0.97 vs 0.88 , $p < 0.001$).

Conclusions: Reduced total adiposity and increased hip muscle adiposity appear to be independent correlates of hip fracture, and combination of skeletal and body composition variables appears to enhance diagnostic efficacy compared to skeletal variables alone.

Disclosures: T.F. Lang, None.

This study received funding from: Eli Lilly.

1283

Deletion of Subunit b1 in Osteoblast Reveals Novel Role for Calcineurin in Bone Formation. A. R. Venn^{*}, H. Yeo^{*}, J. M. McDonald, T. L. Clemens, M. Zayzafoon. Department of Pathology, University of Alabama at Birmingham, Birmingham, AL, USA.

We recently reported that the pharmacological inhibition of calcineurin (Cn) by low concentrations of Cyclosporin A increases osteoblast differentiation in vitro and bone mass in vivo. To determine whether Cn exerts direct actions in osteoblasts, we generated mice lacking Cnb1 (Cn regulatory subunit) in osteoblast ($\Delta Cnb1^{OB}$) using Cre-mediated recombination methods. Transgenic mice expressing Cre-recombinase, driven by human osteocalcin promoter, were crossed with homozygous mice that express loxP-flanked-Cnb1 ($Cnb1^{flf}$). Micro-CT analysis of tibiae at three months showed that $\Delta Cnb1^{OB}$ mice had dramatic increases in bone mass compared to controls. Histomorphometric analysis showed significant increases in mineral apposition rate (67%), bone volume (32%), trabecular thickness (29%) and osteoblast numbers (68%), as well as 40% decrease in osteoclast numbers as compared to the values from control mice. To delete Cnb1 in vitro, primary calvarial osteoblasts, harvested from $Cnb1^{flf}$ mice, were infected with adenovirus expressing the Cre-recombinase. Cre-expressing osteoblast had a complete inhibition of Cnb1 protein levels, but differentiated and mineralized more rapidly than control, GFP-expressing cells. Deletion of Cnb1 increased expression of osteoprotegerin and decreased expression of RANKL. Co-culturing Cnb1-deficient osteoblast with wild type osteoclast demonstrated that osteoblast lacking Cnb1 failed to support osteoclast differentiation in vitro. Taken together, our findings demonstrate that the inhibition of Cnb1 in osteoblasts increases bone mass by directly increasing osteoblast differentiation and indirectly decreasing osteoclastogenesis.

Disclosures: A.R. Venn, None.

This study received funding from: NIH Grant P30-AR46031 and NIH grant P01-CA098912.

1284

Conditional Knockouts in Early and Mature Osteoblasts Reveal a Critical Role for Ca^{2+} Receptors in Bone Development. W. Chang¹, C. Tu^{*1}, T. Chen^{*1}, B. Liu^{*1}, H. Elalieh^{*1}, M. Dvorak¹, T. Clemens², B. Kream³, B. Halloran¹, D. Bikle¹, D. Shoback¹. ¹Endocrine Research Unit, VAMC, University of California San Francisco, San Francisco, CA, USA, ²University of Alabama, Birmingham, AL, USA, ³University of Connecticut Health Center, Farmington, CT, USA.

Ca^{2+} receptors (CaRs), which detect changes in extracellular $[Ca^{2+}]$ ($[Ca^{2+}]_e$) in parathyroid and kidney cells, are also expressed in osteoblasts (OBs) during differentiation. In vitro studies support a role for CaRs in mediating high $[Ca^{2+}]_e$ -induced changes in proliferation, chemotaxis, and gene expression in OBs, but their impact on skeletal development in vivo is unclear. We generated mice with conditional knockout of CaRs in early committed or mature OBs by breeding a novel mouse line carrying floxed-CaR ($CaR^{flox/flox}$) gene alleles with transgenic mice expressing Cre recombinase (Cre) under the control of 2.3 kb type 1 collagen ($2.3Col1-Cre$) or 3.5 kb human osteocalcin (OC) promoters ($OC-Cre$), respectively. Resulting $2.3Col1-Cre/CaR^{flox/flox}$ and $OC-Cre/CaR^{flox/flox}$ mice were born in normal Mendelian ratios with the $2.3Col1-Cre/CaR^{flox/flox}$ mice demonstrating severe growth retardation, clearly visible by 3 days of age. At 21 days of age, weights of $2.3Col1-Cre/CaR^{flox/flox}$ mice were $\approx 30\%$ of their wild-type (wt) littermates. They had smaller, undermineralized skeletons by whole-mount alcian blue and alizarin red staining with significant reductions in bone volume (BV) and bone mineral density (BMD) in femur and vertebrae by micro-computed tomography (μ CT). Goldner and von Kossa staining revealed excessive amounts of unmineralized osteoid in both metaphyses and diaphyses of the long bones from $2.3Col1-Cre/CaR^{flox/flox}$ vs wt mice. Defective mineralization was evident in newborns and persisted postnatally in $2.3Col1-Cre/CaR^{flox/flox}$ mice suggesting that CaRs are essential for both prenatal and postnatal bone development. Quantitative real-time PCR demonstrated significant reductions in OC RNA level (by $\approx 50-65\%$) and increases in RUNX2 and RANKL expression (by $\approx 50\%$) in calvariae and humeri from $2.3Col1-Cre/CaR^{flox/flox}$ vs wt mice without changes in RNA expression of Col1 and osteopontin, supporting a role for CaRs in OB maturation. Width of the hypertrophic zone in growth plate was reduced in $2.3Col1-Cre/CaR^{flox/flox}$ mice, indicating delayed growth plate development which could contribute to their growth retardation. In contrast, growth curves of $OC-Cre/CaR^{flox/flox}$ mice were comparable to wt littermates. Analyses of bone micro-architecture by μ CT revealed no significant changes in BV, BMD, and structure parameters in the $OC-Cre/CaR^{flox/flox}$ mice. These studies confirm a critical role for CaRs at early stages of bone development potentially by promoting OB maturation.

Disclosures: W. Chang, None.

1285

Inadequate Bone Adaptation in Bone Cell Specific Connexin43 Deficient Mice. Y. Zhang*, A. F. Taylor*, E. M. Paul*, A. Davison*, S. K. Bronson*, H. J. Donahue. Penn State University, College of Medicine, Hershey, PA, USA.

Previous in vitro studies suggest that gap junction (GJ) deficiency affects bone metabolism possibly resulting in osteopenia. We examined the hypothesis that connexin 43 (Cx43), the predominate Cx in bone, deficiency in murine osteoblasts and osteocytes results in osteopenia. Osteoblast/osteocyte specific Cx43 knockout (KO) mice were generated by breeding Cx43 null mice (Cx43^{-/-}) with mice expressing Cre recombinase under the control of the human osteocalcin promoter (OC-Cre) and with mice in which the Cx43 gene is flanked by two loxP sites (Cx43^{fl/fl}). Our breeding strategy resulted in littermates with Cx43 deleted from osteoblasts (conditional knockout, KO, Cx43^{fl/fl};OC-Cre), a single functional allele of Cx43 in osteoblasts (heterozygous equivalent, HET, Cx43^{fl/+};OC-Cre), or with two functional alleles in all cell types (wild type equivalent, WT, Cx43^{fl/fl}). All mice examined were 3 weeks old. GJ intercellular communication (GJIC) was dramatically reduced in osteoblastic cells isolated from KO relative to HET or WT, suggesting that we had indeed deleted Cx43 expression in osteoblastic cells. MicroCT of humeri and femora revealed that bones from KO mice were osteopenic, relative to WT or HET mice. KO displayed periosteal expansion, cortical thinning, increased porosity and an approximately 8% and 26% reduction in bone mineral density and bone volume over total volume, respectively. More importantly, three point bending revealed that the failure stress of femora from KO mice was reduced approximately 41% and 27% relative to WT and HT, respectively. Our results demonstrate successful conditional deletion of the Cx43 gene in osteoblasts and osteocytes and confirm previous in vitro data suggesting that Cx43 is largely responsible for GJIC between osteoblastic cells. More importantly, microCT and mechanical testing revealed osteopenia in osteoblast/osteocyte specific Cx43 deficient mice. The exact mechanism by which Cx43 deficiency results in osteopenia was not investigated in this study. However, the remarkable similarity between bones from KO mice and those from mice experiencing disuse osteopenia, together with our previous in vitro data demonstrating that GJIC contributes to bone cell response to load induced biophysical signals, suggests that bones from KO mice were unable to properly adapt to loads engendered during normal ambulation, which, as confirmed by behavioral studies, all genotypes examined were experiencing. In any case, these in vivo data confirm in vitro data suggesting Cx43 mediated GJIC is critical for normal bone adaptation and emphasize the physiological relevance of GJs in bone.

Disclosures: Y. Zhang, None.

This study received funding from: NIH.

1286

Low Bone Mass in Mice with Null Mutation in TG-interacting Factor (TGIF): Impaired Osteoblast Function. M. K. Crook¹, K. S. Mohammad¹, G. A. Clines¹, L. Bartholin², T. Melhuish², C. R. McKenna¹, M. Niewolna¹, L. J. Suva³, A. Carver³, D. Wotton², T. A. Guise¹. ¹Department of Internal Medicine, University of Virginia, Charlottesville, VA, USA, ²Department of Biochemistry and Molecular Genetics, University of Virginia, Charlottesville, VA, USA, ³University of Arkansas for Medical Sciences, Little Rock, AR, USA.

TGIF (TG interacting factor) is a transcriptional corepressor of both TGF β and retinoic acid signaling. Mutations in the TGIF gene can lead to holoprosencephaly, a severe defect in craniofacial development. TGIF-null mice had developmental and skeletal abnormalities including growth retardation, domed skulls, twisted noses, and defects in vertebrae, ribs and sternum. Loss of TGIF may enhance responses to TGF β and retinoic acid, both of which can adversely affect bone. Therefore, we studied bone remodeling in TGIF^{-/-} and wild-type (WT) littermates in the C57BL/6J mice. Skeletal assessment revealed that the TGIF^{-/-} mice had significantly less trabecular bone by DXA (PIXImus), microCT and histomorphometry. Low bone mass was associated with increased osteoclast activity, reduced osteoblast number and bone formation rates. Primary osteoblasts from TGIF^{-/-} compared to WT mice had reduced expression of two late markers, osteocalcin and bone sialoprotein, and increased expression of the early marker Col1A, assessed by quantitative real-time PCR, suggesting that complete osteoblast differentiation was impaired in TGIF^{-/-} mice. To evaluate if the low bone mass seen in TGIF^{-/-} mice was due to enhanced TGF β signaling, we treated TGIF^{-/-} and WT mice for 10 weeks with a small molecule inhibitor of the TGF β receptor I kinase, which significantly reduces TGF β 1-dependent phosphorylation of Smad proteins and increase bone mass in normal mice. As expected, inhibitor treatment versus vehicle significantly increased bone mineral density (BMD) in WT mice at total body (p=0.0005), tibia (p<0.0001), femur (p=0.0046) and spine (p=0.0005). In contrast, BMD was not increased at any site in the TGIF^{-/-} mice treated with inhibitor versus vehicle. There was no difference in phosphoSmad2 staining in the bones of TGIF^{-/-} compared to WT mice.

The data suggest that reduced bone mass in TGIF^{-/-} mice is due to impaired osteoblast differentiation and increased osteoclast activity. We hypothesized that the effects were due to enhanced activity of TGF β and/or retinoic acid due to loss of TGIF repression. However, we found no evidence of increased TGF β signaling, nor were the bone abnormalities reversed by a TGF β receptor kinase inhibitor. The mechanism responsible for the abnormal bone remodeling requires further elucidation and may involve increased retinoic acid signaling.

Disclosures: M.K. Crook, None.

1287

Skeletal Phenotype in Transgenic Mice Over-Expressing CTGF in Cells of the Osteoblast Lineage. J. A. Arnott, E. Nuglozeh*, K. B. Buck*, F. F. Safadi, S. N. Popoff. Anatomy and Cell Biology, Temple University School of Medicine, Philadelphia, PA, USA.

CTGF has recently emerged as an important growth factor in osteogenesis, demonstrated by its ability to promote proliferation, matrix production and differentiation in cultures of osteoblasts. Since most of the data concerning the role of CTGF in osteogenesis has come from in vitro studies, in this study we generated transgenic mice in which CTGF is over-expressed under control of the truncated 3.6kb collagen type I (pOBCol3.6) promoter (CTGF^{pOBCol3.6} mice). This promoter was chosen because it is expressed early during osteoblast differentiation. The targeting vector used to generate transgenic mice also contained LacZ (to identify cells expressing the transgene) and an enhancer element to boost CTGF expression. The presence of the transgene was determined by PCR of tail DNA using transgene specific primers. Six lines were established by mating founder mice with C57/Blk6 wild type (WT) mice. Multiple tissues were used to examine specificity of transgene expression using PCR with transgene specific primers, followed by confirmation of CTGF mRNA expression levels by Northern blot analysis. Transgene expression was highest in long bone and calvaria, with lower levels of expression in other type I collagen producing tissues (lung and skin). Two of the transgenic lines with different CTGF expression levels were used for analysis of the skeletal phenotype. Mice from one line survive, however, mice from the other line die within a few days after birth. Line one showed a 3-4 fold (moderate expression) increase and line two showed a >7-8 fold (high expression) increase in CTGF protein levels in bone when compared to age matched WT mice. Histological and morphometric examination of the distal femoral metaphysis from TG mice with moderate over-expression of CTGF exhibited significant increases in trabecular bone volume associated with increased osteoid thickness and osteoblast activity/numbers compared to WT mice. Increased thickness of the periosteum with increased numbers of osteoprogenitor cells was also observed in TG compared to WT bone. Primary cultures of osteoblasts derived from these TG mice also exhibited enhanced differentiation (ALP staining and mineralization) compared to WT cultures. Surprisingly, examination of bones from transgenic mice over-expressing CTGF at very high levels demonstrated an increase in osteoclast number and size. These data suggest that the precise effects of CTGF on bone cell differentiation and function depend on the magnitude of CTGF over-expression. Moderate levels of CTGF have a direct effect on osteoblasts to promote bone formation, while high levels favor the formation of osteoclasts, perhaps indirectly through a RANK-L dependent mechanism.

Disclosures: S.N. Popoff, None.

1288

The Human Type 1a2 Procollagen Nuclear Targeting Sequence Together with Human Runx2 Enhancer Elements Drives Robust Expression in Transgenic Mouse Osteoblasts. D. D. Strong*, C. Strivers*, K. Howard*, S. Kleinman*, T. A. Linkhart. MDC, J.L. Pettis Memorial VA Med Ctr., Loma Linda, CA, USA.

Translocation of plasmid DNA into the nucleus is an important rate-limiting step affecting transgene expression levels in non-dividing cells. Inclusion of a SV40 viral DNA nuclear targeting sequence (DTS) in plasmid vectors enhances nuclear import efficiency and increases transgene delivery and expression in vitro and in vivo. Plasmid nuclear import involves cellular transcription factors that bind in the cytoplasm to viral DTSs and translocate the DNA by a nuclear localization signal/importin dependent process. We identified a sequence in the human type 1 alpha 2 procollagen promoter (hCol1a2) (-312 to +45) that stimulated osteoblast (Ob) specific nuclear entry of plasmid DNA but not into the nuclei of fibroblasts or chondrocytes. We used this hCol1a2-based nuclear import sequence together with an enhancer sequence derived from the human Runx2 promoter to increase Ob-specific promoter activity and retain nuclear entry activity. We found that the hRunx2-hCol1a2 promoter linked to the luciferase reporter (pGL3Basic vector) demonstrated three-fold more activity than the hCol1a2 promoter alone in transient transfection assays of Obs. To test the specificity and strength of expression of the hCol1a2 and hRunx2-hCol1a2 promoters in vivo we took advantage of Cre-loxP technology and created transgenic (Tg) mouse lines to characterize expression patterns of the promoters in the postnatal skeleton. Specifically the Cre recombinase (Cre) transgene was linked to either the hCol1a2 or the hRunx2-hCol1a2 promoter in the pTurbo-Cre vector (T. Ley) that expresses Cre fused to a nuclear localization signal sequence to facilitate recombination. Multiple lines of Tg mice were prepared and Cre expression was assessed by crossing Cre Tg mice with Rosa26LacZ (R26R) reporter mice to allow expression of beta-galactosidase following Cre activation. Using these mice, we found Cre activity in distinct cell populations in skeletal tissues, including Obs lining the bone surface and in osteocytes. The Runx2-hCol1a2 promoter expressed higher levels of Cre than the hCol1a2 promoter and Cre expression levels and patterns were comparable to mCol1a1-Cre Tg animals (from Dr. Karsenty) crossed to R26R animals and analyzed in parallel. The Tg lines showed that the Ob-specific nuclear entry sequence (\pm hRunx2 enhancer) was also a strong promoter in Ob lineage cells. The hCol1a2 promoter not only contains a novel Ob-specific DTS, useful for development of nonviral expression vectors to increase transgene expression in Obs but also acts as a strong promoter in vivo to drive Ob-specific transgene expression in skeletal tissues.

Disclosures: D.D. Strong, None.

1289

Tec Tyrosine Kinases Are Essential For Osteoclast Differentiation. M. Shinohara*, T. Koga*, K. Okamoto*, H. Takayanagi. Cell Signaling, Tokyo Medical and Dental University, Tokyo, Japan.

Osteoclasts are multinucleated cells that originate from bone marrow-derived monocyte/macrophage precursor cells (BMMs). The differentiation of BMMs to osteoclasts is mainly regulated by three signaling pathways activated by receptor activator of nuclear factor κ B ligand (RANKL), macrophage colony-stimulating factor (M-CSF) and immunoreceptor tyrosine-based activation motif (ITAM). RANKL and its costimulatory receptors of the immunoglobulin superfamily cooperatively stimulate the tyrosine phosphorylation of ITAM in DNAX-activating protein 12 (DAP12) and Fc receptor common γ subunit (FcR γ). However it has been unclear how RANKL contributes to the activation of the tyrosine kinase cascade downstream of ITAM. In this study, a genome-wide screening for non-receptor tyrosine kinases revealed selective expression of Tec and Btk, which are essential for B cell development. Notably, Tec^{-/-}Btk^{-/-} mice exhibited an osteopetrotic phenotype due to severe impairment of osteoclast differentiation. In vitro analysis demonstrated that Tec and Btk are essentially required for the osteoclast differentiation in a cell autonomous manner. Tec kinases are activated by RANKL stimulation and recruited to a lipid raft to form an osteoclastogenic complex with RANK, adaptor proteins such as BLNK and ITAM-harboring adaptors, which mediates the activation of PLC γ -calcium signaling-NFATc1 pathway. Furthermore, Tec^{-/-}Btk^{-/-} mice are resistant to ovariectomy-induced bone loss. Thus, this study identifies the importance of Tec kinases in the osteoclast differentiation and may provide a molecular basis for a novel therapeutic strategy for bone diseases.

Disclosures: M. Shinohara, None.

1290

Regulation of Skeletal Homeostasis by Anti-apoptotic Molecule Bcl-2. Y. Nagase¹, M. Iwasawa¹, T. Akiyama¹, Y. Kadono¹, T. Miyamoto², Y. Oshima¹, M. Nakamura¹, T. Yasui¹, K. Nakamura¹, S. Tanaka¹. ¹Orthopaedic Surgery, University of Tokyo, Tokyo, Japan, ²Orthopaedic Surgery, Cell differentiation, Keio University School of Medicine, Tokyo, Japan.

Anti-apoptotic molecule Bcl-2 resides on mitochondrial outer membrane, and inhibits apoptosis by suppressing cytochrome c release from mitochondria. Although several studies have uncovered the importance of Bcl-2 in maintaining skeletal integrity, detailed cellular and molecular mechanisms still remain elusive. We investigated the role of Bcl-2 on bone metabolism by analyzing bcl-2-deficient mice. Bcl-2^{-/-} (KO) mice were dwarf at 3 weeks of age compared to wild type (WT) littermates, and radiographic analysis of long bones showed a sclerotic lesion at the metaphysis and an atrophic change at the diaphysis. The histomorphometric study revealed that KO mice showed an increase in primary spongiosa due to a decrease in the number of osteoclasts and eroded surface. Many KO osteoclasts were found unattached to primary spongiosa, whereas WT osteoclasts were largely juxtaposed to bone in vivo. The proportion of osteoclast precursors in bone marrow cells which were positive for c-Fms, Mac1 and c-Kit was not different between KO mice and WT littermates as determined by flow cytometry. However, NFATc1 induction in response to RANKL stimulation was impaired in M-CSF-dependent osteoclast precursors obtained from KO mice, which led to a delayed differentiation into mature osteoclasts. KO osteoclasts exhibited an increased cell death and higher Caspase-3 activity after cytokine withdrawal, and their bone-resorbing activity was impaired as determined by pit formation assay as compared to WT osteoclasts in spite of their normal actin ring formation. These abnormalities were restored by retroviral introduction of Bcl-2. In addition to such cell-autonomous defect in bone resorption, bone formation of KO mice was also impaired, which caused an atrophic bone lesion at the diaphysis and reduced calcein double labeling. KO mice exhibited a decrease in osteoblast surface/bone surface, mineral apposition rate and bone formation rate by histomorphometric analysis. KO osteoblasts exhibited an increased cell death, and expression of osteoblastic markers such as type I collagen, alkaline phosphatase and osteocalcin was reduced in primary osteoblasts obtained from KO mouse calvaria, and their mineralization was attenuated. Serum deprivation induced Caspase-3 activation in KO osteoblasts at higher levels, which indicated an increased susceptibility to apoptosis. Collectively, Bcl-2 promoted the differentiation, activity and survival of both osteoclasts and osteoblasts, and plays an essential role in maintaining skeletal homeostasis.

Disclosures: Y. Nagase, None.

1291

Distinct Roles of ITAM Signaling in Bone Remodeling in Various Bony Microenvironments. Y. Wu¹, J. Torchia², W. Yao³, N. E. Lane³, L. L. Lanier¹, M. C. Nakamura², M. B. Humphrey⁴. ¹Microbiology and Immunology, University of California, San Francisco, San Francisco, CA, USA, ²Medicine, VA Medical Center, San Francisco, CA, USA, ³Medicine, University of California, Davis, Sacramento, CA, USA, ⁴Medicine, University of Oklahoma Health Science Center, Oklahoma City, OK, USA.

Immunoreceptor tyrosine-based activation motif (ITAM) signaling mediated by DAP12 or Fc ϵ receptor γ chain (FcR γ) has been shown to be critical for osteoclast differentiation and maturation under normal physiological conditions. Their function in pathological conditions is unknown. We studied the role of ITAM signaling during rapid bone remodeling induced by

ovariectomy (OVX) in wild-type (WT), DAP12^{-/-}, FcR γ ^{-/-} and DAP12^{-/-}FcR γ ^{-/-} mice. Six weeks after OVX, DAP12^{-/-}FcR γ ^{-/-} mice showed resistance to lumbar vertebral body (LVB) trabecular bone loss, while WT, DAP12^{-/-} and FcR γ ^{-/-} had significant LVB bone loss. In contrast, all ITAM-deficient mice responded to OVX with bone loss in both femur and tibia of approximately 40%, relative to basal bone volumes (Table 1). DAP12^{-/-}FcR γ ^{-/-} mice showed the greatest absolute loss of trabecular bone after OVX, losing more than twice as much bone volume as WT, DAP12^{-/-} and FcR γ ^{-/-} (Table 1). Only WT mice developed significant cortical bone loss after OVX. In vitro studies showed microenvironmental changes induced by OVX are indispensable for enhanced osteoclast formation and function. Cytokine changes, including TGF β and TNF α , were able to induce osteoclastogenesis independent of RANKL in bone marrow-derived macrophages (BMMs) from WT but not DAP12^{-/-} and DAP12^{-/-}FcR γ ^{-/-} mice. Follicle-stimulating hormone (FSH) stimulated RANKL induced osteoclast differentiation from BMMs in WT, but not DAP12^{-/-} and DAP12^{-/-}FcR γ ^{-/-} mice.

Our study demonstrates that whereas ITAM signaling is critical for normal bone remodeling, estrogen deficiency induces an ITAM-independent bypass mechanism allowing for enhanced osteoclastogenesis and activation in specific bony microenvironments.

Table 1. Bone loss in distal femur, six weeks after OVX, n=5 in each group.

	Wild-type	DAP12 ^{-/-}	FcR γ ^{-/-}	DAP12 ^{-/-} FcR γ ^{-/-}
BV/TV _{SHAM}	5.7%	20.6%	11.7%	56.3%
BV/TV _{OVX}	2.9%	12.1%	6.7%	35.0%
Δ	-2.8%	-8.4%	-5.0%	-21.3%
Δ / BV/TV _{SHAM} (x100%)	-49	-41	-43	-38

Disclosures: Y. Wu, None.

This study received funding from: NIH, VAMC.

1292

Osteoclast Specific Ablation of Dicer Suppresses Bone Resorption and Increases Bone Mass. F. Mizoguchi¹, T. Nakamura², T. Hayata¹, H. Hemmi³, Y. Ezura¹, K. Nakashima⁴, N. Miyasaka⁴, B. Harfe⁵, S. Kato², M. Noda¹. ¹Molecular Pharmacology, Medical Research Institute, Tokyo Medical and Dental University, 21st Century COE Program, Tokyo, Japan, ²Institute of Molecular and Cellular Biosciences, University of Tokyo, Tokyo, Japan, ³MTT Program, Tokyo Medical and Dental University, Tokyo, Japan, ⁴Department of Medicine and Rheumatology, Tokyo Medical and Dental University, Tokyo, Japan, ⁵Department of Molecular Genetics and Microbiology, University of Florida College of Medicine, Gainesville, FL, USA.

Micro RNAs (miRNA) are endogenous non-coding RNAs of ~22 nucleotides in length. miRNAs regulate the expression of genes by binding 3'-UTR regions of the targets, and have been reported to be involved in fine tuning of biological events, such as cell proliferation, differentiation and cell death in both physiological and pathological conditions. Osteoclastogenesis is a complex process where multiple transcription factors and cytokines are involved. However, the role of miRNAs in osteoclastogenesis is totally unknown. It was reported that simple loss-of-function approaches will be less fruitful for studying miRNA function due to their high level of possible redundancy (B. Harfe. PNAS 2005). RNaseIII enzyme Dicer is one of the key molecules that process pre-miRNAs to mature miRNAs while dicer knock out mice are embryonic lethal. To examine the role of miRNAs in osteoclastogenesis, we specifically knocked out dicer in these cells by crossing conditional allele (Dicer flox) with Cathepsin K-Cre knock-in allele. Mutant mice survived normally during perinatal period. However, during the growth period, body weight gain was less and body size was smaller by about 20 % than control Cre-negative littermates at the age of 7 weeks. Bone mineral density (BMD) levels at the distal 1/3 of the femora in mutant mice were increased by about 20 % than control littermates. In contrast, BMD levels of whole femora were similar between mutant mice and control mice. Thus, the effects of dicer KO appears to be more in cancellous bone. In fact, 3-dimensional micro CT analyses revealed that dicer deficiency in osteoclasts increased BV/TV levels by about 20% compared to control littermates. Further analyses revealed that 3D-thickness of the trabecular bone was specifically increased in mutant mice, while the levels in the number of trabeculi in mutant mice were similar to those in control mice. Histological analysis revealed that TRAP positive cells in trabecular bone (Oc/BS, N.Oc/BS) were decreased in mutant mice by about 30% compared to control littermates. These results indicated that dicer is required for the maintenance of osteoclastic activities in bone. Thus, miRNAs play a regulatory role in these cells to determine the levels of bone resorption.

Disclosures: F. Mizoguchi, None.

1293

Rab3D Recruits the Dynein Complex to Secretory Vesicles in Osteoclasts Through Direct Interaction with Tctex-1. N. J. Pavlos¹, J. Xu¹, A. Carrello^{*1}, R. Jahn^{*2}, M. H. Zheng¹. ¹Department of Orthopaedic Surgery, The University of Western Australia, Perth, Australia, ²Department of Neurobiology, The Max Planck Institute for Biophysical Chemistry, Goettingen, Germany.

Targeted intracellular trafficking of osteolytic enzymes and degraded bone matrix substrates to and from the ruffled border of bone-resorbing osteoclasts requires coordinated interplay between carrier vesicles, motor proteins and the cytoskeletal network. We have previously shown that Rab3D, an exocytic-related small GTPase, regulates a post-TGN vesicle transport step that is required for the maintenance of the ruffled border membrane and bone resorption (1). Here, to investigate the complement of effectors through which Rab3D elicits its biological function, we have employed a yeast two-hybrid system to screen for candidate Rab3D-interacting proteins. Using the N-terminal of Rab3D as "bait" we identified Tctex-1, a 14 kDa light chain of the cytoplasmic dynein motor complex, as a putative effector molecule. Specific interaction between Rab3D and Tctex-1 was confirmed by GST-pull-down, immunoprecipitation and colocalization studies. Furthermore, yeast two-hybrid analysis demonstrated that Tctex-1 specifically associates with Rab3 family members via an interaction with the Switch II/GTP-binding motif. Consistently, bioluminescence resonance energy transfer (BRET) analyses demonstrated that Tctex-1 preferentially binds to the active (GTP-bound) forms of Rab3 GTPases *in vivo*. Moreover, overexpression of wild-type and constitutively active Rab3D led to the recruitment of Tctex-1 and other subunits of the dynein/dynactin complex to secretory vesicle membranes. Disruption of cytoplasmic dynein by dynamin overexpression redistributed Golgi-associated Rab3D to peripheral vesicles. Similarly, depolymerization of microtubules with nocodazole altered the spatial distribution Rab3D-bearing vesicles and impaired Rab3D-Tctex-1 interaction *in vivo*. These data demonstrate that Tctex-1 is a bona fide Rab3 binding protein and that Tctex-1 may cooperate with Rab3D to recruit the dynein motor complex to membrane micro-domains, thereby regulating the sorting and microtubule-dependent targeting/recycling of post-Golgi secretory vesicles to/from the ruffled border during osteoclast-mediated bone resorption.

1. Pavlos, N.J., Xu, J., Riedel, D., Yeoh, J.S.G., Teitelbaum, S.L., Papadimitriou, J.M., Jahn, R., Ross, F.P., Zheng, M.H. (2005) *Mol. Cell. Biol.* 25, 5253-5269

Disclosures: N.J. Pavlos, None.

1294

Mice with a Myeloid Lineage-Specific Deletion of IKK β Demonstrate Both In Vivo and In Vitro Defects in Osteoclastogenesis. J. E. Otero^{*1}, M. Al-hawagri^{*1}, S. Dai^{*1}, J. Vacher^{*2}, M. Pasparakis^{*3}, Y. Abu-Amer¹. ¹Orthopedic Surgery and Cell Biology & Physiology, Washington University School of Medicine, Saint Louis, MO, USA, ²Institut de Recherches Cliniques de Montreal, Montreal, PQ, Canada, ³Molecular Biology, EMBL, Monterotondo, Italy.

Nuclear Factor kappa B (NF- κ B) is a family of transcription factors that regulates various cellular and physiological processes such as inflammatory signaling, immune system development, and cell survival. NF- κ B activity is controlled by two upstream kinases, IKK α and IKK β . NF- κ B is also essential for osteoclast development and survival, evidenced by the osteopetrotic phenotype displayed by mice doubly deficient in subunits NF- κ B1 and NF- κ B2. The significance of upstream regulation of NF- κ B in the context of osteoclastogenesis *in vivo* has been unclear given the embryonic and early postnatal lethal phenotypes of mice deficient in IKK β and IKK α , respectively. Furthermore, the only published report of a conditional deletion of IKK β relevant to osteoclastogenesis utilizes an inducible system, in which specificity of deletion is uncertain. We report for the first time that a myeloid lineage-specific deletion of IKK β using the Cre-loxP system renders mice defective in both *in vivo* and *in vitro* osteoclastogenesis. Cre recombinase driven by the promoter for myeloid-specific marker, CD11b, deletes loxP-flanked IKK β in bone marrow macrophages to a degree sufficient to drastically reduce the IKK β mRNA level compared to that observed in CD11b Cre-negative, loxP-flanked IKK β controls. Furthermore, IKK β protein levels are undetectable in both bone marrow and spleen osteoclast precursors from CD11b Cre-positive, loxP-flanked IKK β mice. The defect in osteoclastogenesis appears to be due to developmental and survival defects, since knockout bone marrow macrophages form less osteoclasts in response to RANKL and are also more sensitive to RANKL and pro-inflammatory cytokine, TNF- α , induced apoptosis. Furthermore, retroviral transduction of a dominant-negative form of IKK β into wild-type bone marrow macrophages blocks basal and TNF- α stimulated osteoclastogenesis. Interestingly, although IKK β protein is undetectable in spleen macrophages, no defect in *in vitro* osteoclastogenesis has been observed, which suggests that the microenvironment of macrophages in the spleen pre-programs osteoclast precursors to differentiate into osteoclasts independently from IKK β activity. These findings support the conclusion that IKK β is required for osteoclast development and survival in a cell-autonomous manner. Furthermore, our results substantiate IKK β as a target in the treatment of inflammatory bone loss and validate the CD11b promoter as a tool for transgenic expression of genes in cells of the myeloid lineage.

Disclosures: J.E. Otero, None.

1295

Conditional Ablation of Parathyroid Hormone Related Peptide (PTHrP) in Mammary Epithelial Cells Inhibits Breast Cancer Progression. J. Li^{*1}, A. Karaplis², P. Siegel^{*1}, V. Papavasiliou^{*1}, W. Muller^{*1}, R. Kremer¹. ¹Dept. of Medicine, McGill University Health Centre, McGill University, Montreal, PQ, Canada, ²Dept of Medicine, Jewish General Hospital, McGill University, Montreal, PQ, Canada.

Breast cancer, the second leading cause of cancer death in women, is frequently associated with increased circulating PTHrP levels in late stage of the disease. However, a causal relationship between breast tumor progression and PTHrP has not yet been established. Here, we used the Cre/LoxP recombination system to disrupt PTHrP function in the mammary epithelium of a transgenic mouse model of human breast cancer (PyVMT). In this model hyperplasia occurs at 4-5 weeks, adenocarcinoma at 7-8 weeks and pulmonary metastasis at 12-13 weeks in 100% of animals. Mice carrying a conditional PTHrP allele in which the fourth coding exon was flanked by LoxP recombination sites were backcrossed on an FVB background. These mice were first crossed with the PyVMT mammary tumor model and then with a separate transgenic strain expressing Cre in the mammary epithelium (MMTV/Cre) both on an FVB background. Targeted excision of the PTHrP allele was confirmed using molecular and histological approaches. Ablation of PTHrP in normal FVB animals did not interfere with the initial stages of mammary ductal outgrowth. Ablation of PTHrP in PyVMT animals significantly delayed tumor onset as demonstrated by Kaplan Meier analysis. At age 50 days, 50% of control animals (PyVMT-PTHrP^{fllox/fllox}-Cre⁻ and PyVMT-PTHrP^{fllox/+}-Cre⁻) had a palpable tumor as compared to age 67 days ($p < 0.005$) in heterozygous (PyVMT-PTHrP^{fllox/+}-Cre⁺) and 78 days ($p < 0.001$) in homozygous (PyVMT-PTHrP^{fllox/fllox}-Cre⁺) animals. In addition tumor growth slowed significantly over time with a significant reduction observed in both PyVMT^{fllox/+}-Cre⁺ and PyVMT-PTHrP^{fllox/fllox}-Cre⁺ animals at all time points. Tumor weight at sacrifice (13 weeks) was significantly reduced in homozygous ($67 \pm 5\%$ reduction, $p < 0.001$) and heterozygous animals ($48 \pm 8\%$ reduction, $p < 0.005$) as compared to controls. Finally, metastatic spread to lungs at sacrifice was seen in 14/14 control animals, 0/13 homozygous animals and 6/14 heterozygous animals. Molecular and immunohistochemical analysis of tumor tissues revealed an 80% inhibition of markers of tumor progression including cyclin D1, Neu/Erb2 and Ki67 in homozygous PyVMT-PTHrP^{fllox/fllox}-Cre⁺ animals and a 40% reduction in heterozygous PyVMT-PTHrP^{fllox/+}-Cre⁺ animals as compared to controls.

In summary these studies provide a direct demonstration that PTHrP is critical for the initiation and progression of mammary tumorigenesis *in vivo*.

Disclosures: J. Li, None.

1296

The 57 kDa C-terminal Fragment of Dentin Matrix Protein 1 (DMP1) Retains All Biological Activity: Osteocytic Regulation of Pi Homeostasis Through FGF23. Y. Lu¹, S. Liu², S. Yu³, Y. Xie^{*3}, J. Zhou^{*2}, L. D. Quarles², L. F. Bonewald¹, J. Q. Feng³. ¹Oral Biology, School of Dentistry, UMKC, Kansas City, MO, USA, ²The Kidney Institute, KU Medical Center, Kansas City, KS, USA, ³Baylor College of Dentistry, Dallas, TX, USA.

Patients with Autosomal Recessive Hypophosphatemic Rickets (ARHR) were found to have mutations in DMP1. Like Dmp1-null mice, these patients exhibit osteomalacia, renal Pi wasting and elevated FGF23 expression in osteocytes. The intact DMP1 protein has never been purified from bone, only 37 kDa N-terminal and 57 kDa C-terminal fragments. To determine if one of these fragments is biologically active, we re-expressed the 57 kDa C-terminal fragment of DMP1 in Dmp1-null animals using the 3.6 kb Col 1 promoter. Re-expression of the full-length DMP1 was performed as a control. To validate successful re-expression in osteoblasts/osteocytes, *in situ* hybridization and immunohistochemistry were performed showing highly elevated expression in osteoblasts/osteocytes as compared to endogenous DMP1 which is more highly expressed in osteocytes. The Dmp1-null phenotype was fully corrected with introduction of either the full-length molecule (two independent lines) or the 57 kDa fragment (two independent lines). Defects in the Dmp1-null mice such as shortened long bones, disorganized growth plate, diffuse fluorochrome labeling of matrix, disorganized osteocyte lacuno-canalicular network, etc. where found to be corrected in either the full-length or the 57 kDa fragment rescued mice using approaches such as X-ray, uCT, procion red injection, TEM, backscatter SEM, von Kossa, and resin-casted SEM approaches. Biochemical analysis further confirmed that high FGF23 (13-fold elevation in Dmp1-null mice as compared to controls), low serum Pi (40% decrease), and low serum calcium (8.9% decrease) levels were restored to control levels in both full-length and 57 kDa animals by 7 weeks of age. Preliminary studies suggest DMP1 regulation of FGF23. In summary, our findings show that the 57 kDa fragment is the biologically active form of DMP1. We are in the process of determining if the biological activity of DMP1 resides in the carboxy terminus as mutations were identified in the last 20 amino acids of DMP1 in the ARHR patients.

Disclosures: Y. Lu, None.

This study received funding from: NIH.

1297

Parathyroid Hormone Activates β -catenin Signaling Through LRP5/6. M. Wan, C. Yang*, H. Yuan*, X. Wu*, C. Lu*, C. Chang*, X. Cao. Pathology, University of Alabama at Birmingham, Birmingham, AL, USA.

Parathyroid hormone (PTH) plays a primary role in regulating calcium homeostasis and is the only anabolic treatment for osteoporosis in clinical. PTH (1-84) or its analog PTH (1-34) binds to the PTH/PTHrP receptor (PTH1R) and activates Gas and G α q, leading to the activation of PKA and PKC respectively. However, the mechanism accounting for the anabolic actions of PTH on bone is still not clear. Here we show that PTH induces the recruitment of LRP5/6, coreceptors of Wnt canonical signaling, to PTH1R to stabilize β -catenin, which is known to positively regulate osteoblast activity and bone formation. PTH stimulated β -catenin-responsive luciferase reporter and elevated the levels of β -catenin protein in both cytoplasm and nucleus in osteoblastic UMR106 cells and embryonic kidney epithelial HEK 293 cells, indicating that treatment of PTH stabilizes β -catenin protein and promotes its nucleus translocation. To further clarify the mechanism, immunoprecipitation assays demonstrated that PTH induced the interaction of PTH1R with LRP5/6 as well as the formation of ternary complex of PTH ligand, PTH1R and LRP5/6. The extracellular domains of LRP5 or LRP6 act as dominant negative mutants to inhibit the formation of the triple complex. PTH-induced recruitment of LRP5/6 resulted in phosphorylation LRP5/6 at their intercellular PPPSP motifs, which is required for the subsequent binding of Axin to LRP5/6. Interestingly, addition of the inhibitors of either PKA or PKC blocked PTH-induced LRP5/6 phosphorylation, indicating that both PKA and PKC signals are required for optimal activation of LRP5/6 signaling. Moreover, PTH-induced activation of LRP5/6 was confirmed in xenopus system. Coinjection of PTH and PTH1R mRNAs significantly enhanced the efficiency of secondary axis induction by LRP5 and LRP6 to 18% and 25%, respectively.

Activation of LRP5/6- β -catenin signaling by PTH was also examined in vivo. Injection of PTH in rats stimulated phosphorylation of LRP5/6 in 30 minutes and peaked at 8 hours. Levels of both β -catenin and phosphorylated LRP5/6 were significantly increased in the osteoblasts of trabecular bone sections when PTH was intermittently administered for 28 days in mice, correlating with increased bone formation. Neither β -catenin nor phosphorylated LRP5/6 level was stimulated with continuous PTH treatment for the same period of time. These findings reveal that coreceptors LRP5/6 mediate PTH-activated β -catenin signaling in a similar way as in canonical Wnt pathway in osteoblasts, and imply that this pathway is one of the key elements in mediating the anabolic bone effect of PTH.

Disclosures: M. Wan, None.

1298

T-lymphocytes Amplify the Anabolic Action of Intermittent PTH Treatment by Regulating Osteoclast Formation. M. Terauchi, Y. Gao, S. Galley, X. Yang*, K. Page*, E. Shah*, M. N. Weitzmann, R. Pacifici. Division of Endocrinology, Metabolism and Lipids, Emory University School of Medicine, Atlanta, GA, USA.

Intermittent PTH treatment (iPTH) stimulates bone formation by targeting stromal cells (SCs) and osteoblasts (OBs), but osteoclasts (OCs) are now known to be the source of a key permissive signal, as iPTH fails to exert its anabolic activity in the absence of OCs. T cells have been shown to be required for continuous PTH treatment to induce OC formation and bone resorption, suggesting the possibility that T cells may regulate the anabolic activity of iPTH by modulating OC formation. To investigate this hypothesis 5 week-old C57BL/6 T cell receptor β knock-out mice (TCR β -/-), a strain which lacks $\alpha\beta$ T cells, were treated with iPTH by injecting sq human PTH 1-34, 80 μ g/kg/day for 4 weeks. Prospective in vivo BMD measurements by DXA revealed that iPTH caused a larger increase in femur BMD in congenic WT controls than in TCR β -/- mice (45.5% vs. 33.8%, $p < 0.05$). μ CT analysis of the femoral metaphysis showed that iPTH induces a greater increase in trabecular BV/TV in WT than in TCR β -/- mice (25.0% vs. 16.8%; $p < 0.05$). Trabecular number, separation and thickness were also differentially affected by iPTH in WT and TCR β -/- mice. The blunted response of TCR β -/- mice to iPTH was confirmed by 4-point bending tests which showed that iPTH increases femoral stiffness in WT, but not in TCR β -/- mice. Measurements of serum levels of osteocalcin, a marker of bone formation, and of CTX, a marker of resorption revealed that iPTH stimulates both bone formation and resorption in WT mice while it had no effect in TCR β -/- mice. Furthermore, in vivo iPTH treatment failed to stimulate the formation of CFU-ALP, an index of the number of SCs with osteogenic potentials, in whole bone marrow (BM) from TCR β -/- mice. PTH also caused a 3-fold lower increase in ex vivo formation of OCs in TCR β -/- mice as compared to WT mice. These findings demonstrate that T cells potentiate the capacity of iPTH to stimulate OB and OC formation. Additional FACS studies revealed that in vivo iPTH treatment increases by 2-fold intracellular RANKL levels in BM CD4+ and CD8+ T cells, while in vitro PTH treatment upregulates T cell RANKL expression in cocultures of T cells and SCs, but not in purified T cells alone. Thus, PTH stimulates T cell RANKL expression by targeting SCs. In summary, the data demonstrate that PTH stimulated SCs induce the production of RANKL by T cells, suggesting that T cell produced RANKL contributes to PTH induced osteoclastogenesis, and indicating that T cells potentiate the bone anabolic activity of iPTH by promoting the formation of OCs, a lineage required for iPTH to stimulate bone formation.

Disclosures: M. Terauchi, None.

1299

Movements Within the Parathyroid Hormone Receptor (PTH1R) Upon PTH Binding. B. E. Thomas¹, A. Wittelsberger¹, P. Monaghan^{*1}, D. F. Mierke^{*2}, M. Rosenblatt¹. ¹Tufts University School of Medicine, Boston, MA, USA, ²Department of Molecular Pharmacology, Brown University, Providence, RI, USA.

Defining the nature of the parathyroid hormone (PTH)-PTH receptor (PTH1R) interaction is key to understanding the role of PTH in physiology, disease, and facilitating the discovery of therapeutic agents which work through the PTH1R. The PTH-PTH1R interaction leads to receptor (Rc) activation, signal transduction, and expression of PTH bioactivity. Since the hormone docks distant from intracellular G proteins, changes resulting from PTH binding to the extracellular face of PTH1R must converge into a conformational shift at the cytoplasmic PTH1R-G protein interface. We set out to determine the motions of transmembrane (TM) domains of PTH1R induced by PTH and the sequence of events that trigger Rc activation. We engineered Cys-substitutions into TMs postulated to play a critical role in Rc activation. Promotion of disulfide crosslinking by PTH indicates that two TMs are brought sufficiently close to form a linkage not possible in the "inactive" state. We chose to study the dynamics of TM2 and TM7 motion by creating a series of PTH1R mutants, each of which contains a Cys pair with potential to span TM2 to TM7 superimposed on a PTH1R template which contains a c-myc "tag" for purposes of detection and a Factor Xa (FXa) cleavage site. The PTH1R template displays binding and PTH-stimulated adenylyl cyclase activity comparable to native PTH1R. PTH1R mutants were exposed to PTH-(1-34), followed by Factor Xa cleavage. The appearance/disappearance of a low MW band (~23 kDa) was monitored using anti-c-myc antibody. A decreased quantity of the band indicates new disulfide formation. For one TM2/TM7 pair, F238C/F447C, mild oxidation promoted disulfide formation. But addition of PTH decreased disulfide linkage, indicating that the Cys pair in TM2 and TM7 are near each other in the inactive state of Rc, but move apart upon binding PTH. These data are supported by molecular modeling insights: bound PTH causes disruption of interaction between residues at position 238 in TM2 and 447 in TM7, suggesting that F238 and F447 move apart to accommodate the bound hormone. For the K240C/F447 pair, disulfide linkage is promoted by PTH binding, indicating that the Cys pair moves even closer. One experiment provides demonstration of the sensitivity of this approach: placement of Cys in TM2 at position 241 instead of 240 precludes disulfide formation with Cys 447. Since the TMs have a helical structure, insertion of Cys one position removed places the sulfhydryl function one-third way around the helix, away from the favorable spatial arrangement of the 240/447 pair. These studies begin to elucidate the molecular mechanisms by which PTH triggers activation of PTH1R.

Disclosures: B.E. Thomas, None.

1300

Bone Mineralization and Vitamin D Inadequacy. Histomorphometric Analysis of Iliac Crest Bone Biopsies and Circulating 25-hydroxyvitamin D in 648 Patients. M. Priemel¹, T. Kladde^{*1}, S. Kessler^{*1}, S. Seitz^{*1}, K. Püschel^{*2}, T. Schinke¹, M. Amling¹. ¹Trauma Surgery and Center of Biomechanics, University Medical Center Hamburg, Hamburg, Germany, ²Forensic Medicine, University Medical Center Hamburg, Hamburg, Germany.

The estimated required circulating 25-hydroxyvitamin D (25[OH]D) to maintain skeletal health range between 12 and 40 ng/ml. This wide range is based on many studies that have used the relationship between low 25[OH]D and increased secretion of parathyroid hormone (PTH) to determine a plausible threshold. PTH is however only one measurable index of skeletal health and we reasoned, that histomorphometric analysis of iliac crest bone biopsies would be another and even more direct approach to assess bone health. Thus to get an answer as to the circulating levels of 25[OH]D that should be ensured, and to assess the prevalence of vitamin D insufficiency we measured 25[OH]D serum levels and performed transiliac crest bone biopsies (8mm diameter) in 648 patients (388 males, mean age: 58.8 years, and 260 females, mean age: 68.6 years) who had no signs of secondary osteopathies at autopsy. All biopsies were undecalcified embedded and histologically processed. Static structural analysis was performed using the Osteomeasure system according to ASBMR standard. Analysis included bone volume (BV/TV), osteoid volume (OV/BV), osteoid surface (OS/BS), trabecular thickness (Tb.Th), trabecular number (Tb.N), and trabecular separation (Tb.Sp). Statistical analysis consisted of testing for the lack of correlation and the similarity of the correlation coefficient in males and females. The histologic results demonstrate an unexpected high prevalence of mineralization defects. Indeed 37.35% of the analyzed patients presented with an OS/BS of more than 20%. Based on the definition described by Delling in 1975 that an OV/BV of >1.2% is pathologic 46.76% of the biopsies presented with manifest skeletal mineralization defects. Even a more conservative threshold with a pathologic increase in OV/BV of > 2% was detected in 27.62% of the patients. Most interestingly these mineralization defects were found independent of BV/TV, throughout all ages and affected both sexes. While we could not establish a minimum 25[OH]D level that was inevitably associated with manifest mineralization defects, we did not find pathologic accumulation of osteoid in any patient with circulating 25[OH]D levels above 30ng/ml. Therefore our data demonstrate that the prevalence of vitamin D deficiency and manifest mineralization defects is extremely high in the European population. In case of vitamin D supplementation, the dose given should ensure that circulating levels of 25[OH]D reach a threshold of 30 ng/ml.

Disclosures: M. Priemel, None.

O021

Marrow Adipogenesis and Osteoblastogenesis Reflect Global Energy Utilization Through Activation of PPARG and Modulation by 'Clock' Genes in a Genotype Specific Manner. C. L. Ackert-Bicknell¹, V. E. DeMambro¹, M. L. Bouxsein², M. C. Horowitz³, E. Canalis⁴, C. J. Rosen¹. ¹The Jackson Laboratory, Bar Harbor, ME, USA, ²Beth Israel Deaconess Medical Center, Boston, ME, USA, ³Yale University School of Medicine, New Haven, CT, USA, ⁴St. Francis Hospital and Medical Center, Hartford, CT, USA.

The relationship between marrow adipogenesis and bone formation is critical for understanding osteoporosis. We generated a congenic mouse (6T) with C3H alleles from a QTL on mouse Chr 6 introgressed on a 99.5% C57BL/6J(B6) background. 6T have reduced BMD, impaired osteoblast(OB) differentiation, more marrow adiposity, but low body temp, and unresponsiveness (i.e. thermal output) to stimulation by a $\beta 3$ agonist. An inversion in C3H, and polymorphisms in genes at the break point [115.38-116.38 Mb between Pparg and Alox5], prompted us to hypothesize that genes in this region influence OB and adipocyte(Ad) function. To test this, we fed 3 wk B6 and 6T mice an 11%(LF) or 60% fat(HF) diet for 13 wks and studied metabolic and skeletal parameters. On a HF diet, B6 gained wt and became insulin resistant with no change in BV/TV by μ CT, while 6T showed no change in wt or insulin secretion, but lost trabecular bone ($p<0.001$ vs B6). Histomorphometry comparing HF to LF diets revealed that B6 had suppressed bone formation, reduced osteoclast #, increased marrow Ads (2.1 fold higher), but no change in BV/TV. In contrast 6T on HF had a 1.5 fold increase in OB#, but no change in Ad #, despite a 30% reduction in BV/TV. Expression profiling (using a 2x2 statistical design:genotype x diet)revealed that 21 genes were differentially regulated in liver; and 64 in bone (marrow+bone). Most were histones, but in 6T liver on HF, Ccrn4l (a 'clock' gene) was 2 fold up-regulated; $p=1.0 \times 10^{-6}$, while in 6T bone, uncoupling protein-1(Ucp-1) was increased nearly 3 fold; $p=1.0 \times 10^{-6}$. 2 candidate genes within the 1Mb region on Chr 6 were suppressed in 6T bone on the HF diet: March 8, a membrane protein ($p<0.0005$, vs B6) and Raf1 ($p<0.007$ vs B6). In the liver, two downstream targets of Pparg, Fasn, and Srebp, as well as ephrinA1 and SOCS-2, were increased by a HF diet in 6T($p<0.05$ vs B6). In summary, we found genotype-specific skeletal and marrow responses to HF. In 6T, HF caused bone loss despite recruitment of more OBs, but in B6, even with marrow adipogenesis, and a reduced bone formation rate, BV/TV was preserved. Expression profiles demonstrated that a HF diet activated Pparg in a strain-specific manner, likely through recruitment of co-activators that differentially influenced Ad and OB function. In 6T, greater UCP-1 expression (a marker of brown fat), and enhanced insulin sensitivity imply distinct physiologic roles for marrow fat (i.e. energy use:6T vs storage: B6) influenced by Chr 6 genes and modulated by 'clock' proteins.

Disclosures: C.L. Ackert-Bicknell, None.

This study received funding from: niams 45433

O064

Estrogen Receptor α Is Required for Strain-Related β -Catenin Signaling in Osteoblasts. V. J. Armstrong*, M. Muzylak*, A. Sunter*, G. Zaman*, L. K. Saxon, J. S. Price, L. E. Lanyon. Veterinary Basic Sciences, The Royal Veterinary College, London, United Kingdom.

Wnt/ β -catenin signaling has been implicated in the regulation of bone mass through its involvement in bone cells' response to their mechanical environment [1]. Since Estrogen Receptor α (ER α) is also involved in bones' response to loading [2], we investigated whether strain induced signaling through ER α uses the same pathway as β -catenin. Western blot and immuno-cytochemical analysis showed that in ROS 17/2.8 cells a short period of dynamic strain in vitro increased the levels of activated β -catenin (β cat) in the cytoplasm and within 1 hour stimulated its translocation to the nucleus. These changes in β cat were paralleled by inhibitory phosphorylation of GSK-3 β . Strain, and the GSK-3 β inhibitor LiCl, also induced a significant increase in TCF/LEF transcriptional activity. In contrast, estrogen had no influence on the level or distribution of β cat, nor any effect on TCF/LEF activation. Nuclear translocation of β cat and TCF/LEF activation stimulated by both strain and LiCl were inhibited by the ER modulator ICI 182,780, which also reduced strain-induced nuclear accumulation of ER α . The ER modulator Tamoxifen also inhibited LiCl stimulated nuclear translocation of β cat.

In primary cultures of osteoblast-like cells derived from the long bones of Wild Type mice and those lacking ER β , β -catenin was similarly activated and translocated to the nucleus in response to strain and LiCl. In these cells this response was blocked by ICI 182,780. In contrast, in cultures of osteoblast-like cells from mice lacking ER α neither strain nor LiCl stimulated nuclear accumulation of β cat. ICI 182,780 had no effect in these cells.

These data show that in osteoblastic cells exposure to strain causes similar activation of β -catenin, its translocation to the nucleus, and regulation of transcription as GSK-3 β inhibition by LiCl. These changes require ER α but not ER β . To our knowledge these are the first data to demonstrate that in osteoblasts ER α is required for these cells' responses to strain involving Wnt/ β -catenin. Reduced effectiveness of bone cells' responses to bone loading, associated with decline in bio-available estrogen and ER α , may contribute to the failure to maintain structurally appropriate bone mass in osteoporosis in both men and women. This failure may in part be due to reduced effectiveness of Wnt/ β -catenin signaling.

1. Sawakami K, et al (2006) J Biol Chem 281(33):23698

2. Lee K, et al (2003) Nature 424:389

Disclosures: V.J. Armstrong, None.

This study received funding from: BBSRC.

O099

Expression of OCZF Directed by the Cathepsin K Promoter Affects Bone Mass and Osteoclast Formation in Transgenic Mice. T. Shobuiké*, T. Kukita², K. Nagata^{*2}, J. Teramachi^{*2}, M. Asagiri³, H. Takayanagi³, A. Kukita¹. ¹Saga University, Saga, Japan, ²Oral Biological Science, Kyushu University, Fukuoka, Japan, ³Cell Signaling and COE Program, Tokyo Medical and Dental University, Tokyo, Japan.

We previously isolated the OCZF cDNA encoding Kat-6 antigen specifically expressed in rat osteoclast. The OCZF gene product is a member of POK protein family that contains two domains of POZ/BTB and zinc finger in their N- and C-terminal region respectively, and that is shown to be involved in various cellular processes. Suppression of OCZF by antisense RNA inhibits osteoclast differentiation in vitro, indicating that OCZF is involved in osteoclastogenesis, but in vivo role in the process is not clear. To this end we generated transgenic mice, which expressed OCZF under the control of mouse cathepsin K promoter. Nine transgenic mice were identified among the offspring by PCR and Southern blot analysis of mouse tail genomic DNA. Transgene expression was verified by RT-PCR using osteoclasts differentiated in vitro from bone marrow at 10 weeks of age. Two lines of the transgenic animals exhibited relatively high transgene expression, and were further investigated. The c-fos and NFATc1 protein exhibit higher levels during differentiation into osteoclasts in vitro from bone marrow of the transgenic mice than that of normal littermates. Micro-CT and peripheral quantitative CT (pQCT) analyses and histomorphometry of femur were performed in mice at 6 weeks of age. Micro-CT imaging demonstrates a reduction in trabecular bone volume in the transgenic mice relative to normal littermates. pQCT analyses also demonstrate a reduction in bone mineral density and bone mineral content especially in trabecular bone with a decrease in strength strain index, whereas those in cortical bone were slightly affected. Consistently, von Kossa staining shows a smaller mineralized area in the transgenic mice than in normal littermates. Histological analyses with tartrate-resistant acid phosphatase staining and calcein labeling indicate an increase in the number of osteoclast, whereas bone formation rate did not significantly change. These results suggest that OCZF has an important role in osteoclastogenesis in vivo.

Disclosures: T. Shobuiké, None.

O112

Transgenic Overexpression of Osteoclastic Protein-tyrosine Phosphatase, PTP-oc, in Cells of Osteoclastic Lineage Led to Increased Bone Resorption and Marked Reduction in Trabecular Bone Mass and Density in Adult Mice. M. H. C. Sheng, M. Amoui*, A. K. Srivastava, J. E. Wergedal, K. H. W. Lau, Loma Linda VAMC, Loma Linda, CA, USA.

Past in vitro studies have suggested that the structurally unique osteoclastic transmembrane PTP-oc acts as a positive regulator of osteoclast activity. This study sought to determine whether transgenic (TG) overexpression of PTP-oc in cells of osteoclastic lineage would increase (\uparrow) bone resorption and decrease (\downarrow) bone mass or density (BMD) in adult mice. To generate TG mice, a TG construct containing the rabbit PTP-oc cDNA driven by a tartrate-resistant acid phosphatase (TRACP)-1C promoter was injected into the pronucleus of fertilized ova, which were implanted into pseudo-pregnant B6D2F1 mice. TG founders, identified by a PCR-based genotyping assay using primers that span unique regions of TRACP-1C promoter and rabbit PTP-oc sequence, were bred with C57BL/6J mice to produce F2 mice. Ten-week-old male F2 progenies were extensively followed for pQCT, histological, and serum resorption marker analyses. The body weight of TG mice was 10% less ($p<0.05$, $n=8$ each) than that of wild-type (WT) littermates. pQCT analyses of the femur revealed that TG mice had 30% \downarrow in trabecular BMD ($p<0.002$). Histologic analyses at the secondary spongiosa in the femur of 9 TG and 7 WT littermates confirmed that TG mice showed 35% \downarrow in trabecular surface (Tb.Pm, $p<0.01$), 27% \downarrow in % trabecular area (Tb.Ar, $p<0.05$), 11% \downarrow in trabecular number (Tb.N, $p<0.05$), and 36% \uparrow in trabecular separation (Tb.Sp, $p<0.005$). The lumbar vertebra of 12 TG mice, when compared to 8 WT littermates, also showed 20% \downarrow in Tb.Pm ($p<0.005$), 17% \downarrow in Tb.N ($p<0.003$) and 35% \uparrow in Tb.Sp ($p<0.004$). Consistent with an \uparrow in bone resorption, the serum c-telopeptide level of TG mice ($n=14$) was 25% ($p<0.05$) higher than that of littermates ($n=11$). That the number of osteoclasts and the length of TRACP-labeled bone surface per total bone surface were not different suggested that TG overexpression of PTP-oc increased osteoclast activity rather than osteoclast differentiation. The same phenotype was confirmed in a second TG line. In congruent with an \uparrow in osteoclastic activity, the average pit area created by osteoclasts derived from bone marrow cells of 10-week-old male TG mice in response to RANKL and MCSF in the pit formation assay was $\sim 50\%$ greater ($p=0.008$) than those by osteoclasts of WT littermates ($n=8$ each). However, the TRACP activity per cellular protein in osteoclasts derived from the two groups of mice was not different. In summary, TG overexpression of PTP-oc in cells of osteoclastic lineage led to a marked reduction in trabecular bone mass in adult mice due to an \uparrow in osteoclastic activity. These findings provide compelling in vivo evidence that PTP-oc is a positive regulator of osteoclastic activity.

Disclosures: M.H.C. Sheng, None.

This study received funding from: Veterans Administration.

O142

CITED1 Ablation Impairs Endochondral Bone Formation During Embryonic Development. D. Yang, J. Guo*, R. Bringham*. Endocrine Unit, Massachusetts General Hospital, Boston, MA, USA.

CITED1 (CBP/P300 interacting Transactivator with Glutamic Acid [E]/ Aspartic Acid [D]-Rich C-terminal domain) is a transcriptional cofactor located on the X chromosome. We previously observed that CITED1 expression is rapidly and transiently induced by PTH1R activation in osteoblasts and that cultured osteoblasts from mice lacking CITED1 display abnormal differentiation in vitro. To determine the possible role of CITED1 in early bone development, we have analyzed endochondral bone formation in tibiae from CITED1-knockout (KO) embryonic mice in which the CITED1 gene is replaced with a functional LacZ/Neo cassette and bred into the 129Sv background for five generations. The tibiae of CITED1 KO mice were shorter than those of wild type (WT) littermates, and bone volume and the extent of trabeculae in CITED1 KO tibiae at E18.5 and post-natal day 1 (P1) were significantly reduced, as shown by von Kossa staining and histology. At E15.5, the regions of overall chondrogenesis and of chondrocyte hypertrophy, demonstrated by Col II and Col X expression respectively, were not different in WT and KOs; but bone formation, shown by Col I in situ analysis, appeared slightly earlier inside the tibia and expanded wider in perichondral region in the WT. Osteopontin (OPN) is expressed by late hypertrophic chondrocytes and osteoblasts within the primary and secondary spongiosa. Relative to WT, the length of the central region of OPN expression was reduced in all KO bones from E15.5 through P1, accounting for the foreshortening of the overall bone length. In situ hybridization and LacZ staining analysis showed strong expression of CITED1 in this same central region of the developing bones but not in adjacent chondrocytes. We conclude that CITED1 expression, probably by cells of the osteoblast lineage, is important for normal endochondral bone formation and that loss of functional CITED1 expression leads to a reduction in the rate of bone formation. Whether this defect reflects impaired activity of osteoblasts that normally express CITED1 and/or loss of an indirect effect on chondrocyte proliferation and/or differentiation, which could involve PTHrP, remains to be investigated.

Disclosures: D. Yang, None.

O157

Biglycan and Fibromodulin Control Bone Mass by Regulating Osteoclast Differentiation Through Bone Marrow Stromal Cells. Y. Bi*, T. M. Kilts*, A. C. Griffin*, M. F. Young. National Institute of Dental and Craniofacial Research, National Institutes of Health, Bethesda, MD, USA.

Members of the Small Leucine-Rich Proteoglycan (SLRP) family populate numerous sites in the musculoskeletal system including tendon, cartilage and bone, but, their precise role in these tissues is still unclear. Previous work showed that mice with combined deficiencies in two SLRPs, biglycan (bgn) and fibromodulin (fmod), acquire osteoarthritis and ectopic tendon ossification. Here we show that the bgn-0/fmod-/- mice have delayed bone formation during development judged by alizerin red/alcian blue staining and severe age-dependent osteopenia determined by X-ray and microCT analyses. In order to understand the molecular basis for this osteopenia, osteogenic bone marrow stromal cells (BMSCs) were isolated and examined. Colony-forming unit fibroblastic (CFU-F) analysis, which estimates the number of osteogenic stem cells, showed no significant differences between WT and bgn-0/fmod-/- mice. Further, in vitro osteogenesis assays showed that Ca2+ accumulation was increased in the bgn-0/fmod-/- BMSC cultures compared to WT BMSCs. Western analysis of the BMSC protein extracts showed that the bgn-0/fmod-/- cells had increased levels of Runx2 compared to WT controls. The bgn-0/fmod-/- BMSCs also had increased BMP-2 and TGF-beta1 signaling indicated by increased levels of p-smad1 and p-smad2/3 in the presence of BMP-2 and TGF-beta1 compared to WT BMSCs, respectively. Furthermore, in vivo bone formation was not significantly different between WT and bgn-0/fmod-/- BMSCs transplanted subcutaneously into immuno-compromised mice. From these data, we concluded that the decreased bone mass in bgn-0/fmod-/- mice was not primarily due to a defect in osteogenesis. We next determined whether the osteopenia in bgn-0/fmod-/- mice could be due to increased differentiation and/or activity of osteoclasts. To test this, sections of long bone and BMSC transplants were stained for Tartrate-Resistant Acid Phosphatase (TRAP), an osteoclast marker. The number of TRAP positive cells was higher in bone and in vivo BMSC transplants from bgn-0/fmod-/- mice. Osteoclastogenesis was assessed by adding bone marrow suspensions to plates in which BMSC had formed individual colonies and showed that greater numbers of colonies in the bgn-0/fmod-/- cultures supported formation of TRAP-positive multinucleated cells compared to WT. In summary, we have shown that bgn and fmod when depleted in combination have a negative influence on bone mass by increasing osteoclast formation and function and thereby pointing to the possibility that these SLRPs could be novel targets to modulate bone turnover.

Disclosures: Y. Bi, None.

This study received funding from: IRP-NIDCR, NIH.

O165

Rescue of MT1-MMP Expression in Cartilage Increases Survival, Chondrocyte Proliferation and Bone Formation in MT1-MMP Deficient Mice. L. Szabova*, S. Yamada*, K. Holmbeck*. CSDB/MMPU, NIDCR, Bethesda, MD, USA.

Membrane type-1 matrix metalloproteinase (MT1-MMP) is a potent collagenase essential for proper remodeling of collagen rich tissues. Mice deficient for MT1-MMP (KO) are dwarfs with severe fibrosis of connective tissues, bone loss and retention of embryonic cartilages in the skull due to impaired degradation of unmineralized type I and II collagens. Here we define the contribution of disrupted cartilage remodeling in the development of the MT1-MMP-deficient phenotype. Specifically, we created transgenic mice where MT1-MMP expression was selectively re-introduced in cartilage tissues using a transgene driven by the type II collagen promoter/enhancer. We have bred these mice into the MT1-MMP-deficient background and evaluated the developmental effects of MT1-MMP expression in the cartilage tissue of otherwise MT1-MMP deficient mice. Cartilage specific MT1-MMP expression in KO mice resulted in complete rescue of the pre-weaning death observed in KO mice, increased body weight and prolonged survival. Transgenic KO mice further displayed increased bone formation in the skull compared to KO mice. Strong expression of the MT1-MMP transgene increased chondrocyte proliferation in the epiphyseal growth plate, which resulted in increased growth of the long bones. Increased bone formation quite unexpectedly coincided with expression of the transgene in a subset of bone cells. Expression of type II collagen was documented in bone cells of normal mice using in situ hybridization and immunostaining thus documenting that transgene expression was not ectopic, but mirrored the normal expression pattern of type II collagen. This finding explains the increased bone formation observed in transgenic KO mice since MT1-MMP is necessary for maintaining the bone formation. In conclusion, reintroduction of MT1-MMP in the cartilage of MT1-MMP KO mice results not only in cartilage specific expression, but also directs transgene expression in a subset of bone cells thereby facilitating increased bone formation. These bone cells are most likely the descendants of a common progenitor of bone cells and chondrocytes expressing type II collagen and support our previous observation that some chondrocytes can differentiate into bone cells. Our data suggest that MT1-MMP provides type II expressing chondrocytes and bone cells with the necessary collagenolytic activity required for chondrocyte proliferation and bone formation in vivo.

Disclosures: L. Szabova, None.

O179

Sclerostin Overexpression Impairs Limb Patterning. N. M. Collette*, R. M. Harland*, G. G. Loots*. Biosciences and Biotechnology Division, Lawrence Livermore National Laboratory, Livermore, CA, USA, ²Department of Molecular and Cellular Biology, University of California, Berkeley, CA, USA.

Sclerostin (SOST) is a negative regulator of bone formation that has been described as both a BMP- and WNT- antagonist. Loss of SOST function causes sclerosteosis (MIM 269500), a condition of severe progressive bone overgrowth. Using transgenic mice expressing human SOST from a bacterial artificial chromosome (BAC) we have demonstrated that SOST over-expression causes decreased bone formation and results in osteopenia, similar to the over-expression of other BMP antagonists such as Noggin and Gremlin. These mice also exhibit severe limb patterning defects that are dose-dependent and range from the loss of a single posterior digit to the loss and/or fusion of many distal limb skeletal elements. The apical ectodermal ridge (AER) relays cell-cell signals to the underlying differentiating limb mesenchyme, a place of SOST expression initiated as early as E9.5. To determine how elevated levels of SOST impair proper limb patterning, we have examined AER and cartilage markers by measuring mRNA levels by in situ hybridization. We find FGF8, a major AER signaling molecule and underlying mesenchymal markers BMP2, Gli1, Pax1, HoxD12 and gremlin expression to be perturbed in SOST transgenic mice. In addition, skeletal analysis of double mutant animals show that over-expression of SOST fails to complement loss of BMP antagonists (Gremlin and Noggin) essential for limb patterning and chondrogenesis, resulting in more dramatic skeletal defects than single mutants alone, suggesting that SOST action in the limb parallels the BMP-pathway. This work is supported by NIH RO1 HD047853 and the work has been performed under the auspices of the U.S. Department of Energy by the University of California, Lawrence Livermore National Laboratory Contract No. W-7405-Eng-48. UCRL-ABS-229990

Disclosures: N.M. Collette, None.

This study received funding from: NIH RO1 HD047853.

O185

TNF- α Upregulates Aortic BMP2-Msx2-Wnt Signaling in Diabetic LDLR-/- Mice. J. S. Shao, C. F. Lai, Z. Al-Aly*, J. Cai*, E. Huang*, S. L. Cheng, D. A. Towler. Dept. of Internal Medicine, Washington University School of Medicine, St. Louis, MO, USA.

Aortofemoral calcification is prevalent in type II diabetes (T2DM), tracking metabolic syndrome parameters and increasing the risk for lower extremity amputation. LDLR-/- mice fed high fat diets (HFD) develop obesity, T2DM, and accumulate aortic calcium - the latter mediated via osteogenic mechanisms that resemble craniofacial mineralization. HFD upregulate aortic BMP2 and Msx2-Wnt signaling cascades that promote mineralization in neural crest-derived skeletal tissues. Administration of recombinant purified BMP2 augments aortic Msx2-Wnt signaling in TOPGAL reporter mice, and promotes aortic calcium deposition in LDLR-/- mice. Low-grade inflammation, including elevated circulating TNF- α , is characteristic of obesity with T2DM, therefore, we examined the relationships between TNF- α and aortic BMP2-Msx2-Wnt signaling in the LDLR-/- model. HFD feeding promotes obesity, hyperglycemia, and hyperlipidemia -- and upregulated serum TNF- α and haptoglobin in male LDLR-/- mice. Oxidative stress, reflected in serum 8-F- α -isoprostane (8-IsoP) levels, was increased, with concomitant upregulation of aortic BMP2 (2.5-fold), Msx2 (2.5-fold), Wnt3a (10-fold), and Wnt7a (14-fold) gene expression (all $p < 0.01$, 2-tailed t-test). Treatment of diabetic LDLR-/- mice with the TNF- α antagonist infliximab (10 μ g / gm twice weekly, 5 animals per group) did not reduce obesity, hyperleptinemia, or hyperglycemia; however, serum 8-IsoP and haptoglobin levels were significantly decreased. Moreover, aortic BMP2, Msx2, Wnt3a, and Wnt7a expression and aortic calcium accumulation were concomitantly and significantly reduced by infliximab treatment (all $p < 0.05$). Administration of sodium salicylate, an alternative anti-inflammatory strategy, also reduced serum haptoglobin and aortic Msx2 gene expression. Finally, C57BL/6 mice with arterial smooth muscle TNF- α expression augmented by a SM22- TNF- α transgene accumulate significantly higher levels of aortic BMP2, Msx2, Wnt3a, and Wnt7a mRNAs vs. their non-transgenic sibling cohorts. Furthermore, 80% of SM22-TNF α ; TOPGAL mice exhibit aortic betagalactosidase reporter staining vs. 0% of their non-transgenic TOPGAL siblings ($p=0.05$ with Yates' chi-square correction), indicating net enhanced mural Wnt signaling by the SM22-TNF α transgene. Thus, inflammatory TNF- α signals promote pro-calcific BMP2-Msx2-Wnt programs in the aortic tissues of diabetic LDLR-/- mice. Strategies that inhibit inflammation-induced arterial BMP2-Msx2-Wnt signals may improve aortofemoral physiology and reduce lower extremity amputation risk in T2DM.

Disclosures: D.A. Towler, National Institutes of Health 2; Barnes-Jewish Hospital Foundation 2; Wyeth 5; GlaxoSmithKline 5.
This study received funding from: National Institutes of Health.

O223

Conditional Ablation of the Osteoblast Calcium-Sensing Receptor Causes Abnormalities in Skeletal Development and Mineralization. M. M. Dvorak¹, C. Tu^{*1}, H. Elalich^{*1}, T. Chen^{*1}, B. Liu^{*1}, B. E. Kream^{*2}, D. D. Bikle¹, W. Chang¹, D. M. Shoback¹. ¹Department of Medicine, University of California, San Francisco, CA, USA, ²Department of Medicine, University of Connecticut Health Center, Farmington, CT, USA.

The calcium-sensing receptor (CaR) is a G protein-coupled receptor essential for maintenance of calcium homeostasis. Defining the role for the osteoblast CaR in vivo, using global full-length CaR knockout models, is complicated by metabolic disturbances and the potential for compensation by a CaR splice variant identified in these mice. To circumvent these issues, we generated Flox-CaR^{+/+} mice, in which loxP sites flank exon 7 that encodes the transmembrane and signaling domains of the receptor. Osteoblast-specific inactivation of the CaR was achieved by mating Flox-CaR^{+/+} mice to transgenic mice expressing Cre-recombinase, under control of the 3.6 kb fragment of the rat $\alpha 1(I)$ collagen promoter (Col1-Cre). Col1-Cre^{+/+}/Flox-CaR^{+/+} mice exhibited growth delay from birth and died within four weeks. At 21 days, the skeletal phenotype was hallmarked by hypomineralization, evident by von Kossa staining and micro-computed tomography (μ CT) analysis, which revealed significant reductions in bone volume/tissue volume (BV/TV; $\downarrow \sim 75\%$), bone mineral density (BMD; $\downarrow > 90\%$), segmented BMD ($\downarrow \sim 20\%$), trabecular number ($\downarrow \sim 40\%$), trabecular thickness ($\downarrow \sim 30\%$) and connectivity density ($\downarrow \sim 80\%$) in the secondary spongiosa of the distal femur ($n=6$, $p<0.05$, ANOVA), compared to controls. The changes were comparable, although less extensive in the L4 vertebra. The cortical compartment of the femur was also affected, with significant decreases in BV ($\downarrow \sim 60\%$), cortical thickness ($\downarrow \sim 70\%$), BMD ($\downarrow \sim 45\%$), and segmented BMD ($\downarrow \sim 15\%$) and markedly increased cortical porosity ($\sim 70\%$), compared to controls ($n=6$, $p<0.05$, ANOVA). Histology of femora from Col1-Cre^{+/+}/Flox-CaR^{+/+} mice revealed severe hyperostoidosis (Goldner staining) as well as trabeculation of the cortex (Von Kossa staining). Reduced mineral content could be secondary to increased turnover, with inadequate mineralization of newly made osteoid. This is consistent with quantitative real-time PCR (qPCR) analysis of humeri and calvaria that indicate significant increases in markers of proliferation (cncd1), osteoblast differentiation (collagen I, alkaline phosphatase, osteopontin), mineralization (anklylosis protein, ectonucleotide pyrophosphatase/phosphodiesterase 1) and regulators of osteoclastogenesis (RANK-L, osteoprotegerin); ($n=3-5$, $p<0.05$, ANOVA). Our findings indicate a critical role for the skeletal CaR in the control of bone mineralization in early postnatal skeletal development.

Disclosures: M.M. Dvorak, None.

O262

Novel Vitamin D3 Analogs (DLAMs) Antagonize Bone Resorption Via Suppressing RANKL Expression in Osteoblasts. M. Inada, K. Tsukamoto*, M. Takita, M. Hirata, A. Hoshino*, T. Tominari*, K. Nagasawa*, C. Miyaura. Department of Biotechnology and Life Science, Tokyo University of Agriculture and Technology, Koganei, Tokyo, Japan.

Active vitamin D3, 1 α , 25(OH)2D3 (D3), has been proposed to regulate bone remodeling through bone formation and resorption that is maintaining calcium levels in blood serum. Recently new aspects of D3 activities have been reported in bone resorption, inhibition of osteoclast differentiation via interference of c-fos and NFATc1 expression. The other aspect was found in D3 analogs, synthetic modification at C2 position of D3 that is enhancing bone formation and bone mass. Here we show newly synthesized analogs, 1 α ,25(OH)2D3-26,23-lactam, (23S,25S)-DLAM-1P and DLAM-2P, that has a lactam moiety in the side chain, perfectly antagonized D3-induced osteoclast (Oc) differentiation. In computer docking simulation estimated DLAM-1P bind to VDR, lactam moiety in DLAM-1P may interfere VDR helix-12 folding at the site of Phe-422 (ligand binding domain). Oc formation was assessed by mouse co-culture system. We first examined antagonistic effects of DLAMs on Oc formation induced by D3. When simultaneous treatment of DLAM-1P (10-7M to 10-5M) and D3 (10-8M), DLAM-1P clearly suppressed the number of TRAP+ Ocs in a dose-dependent manner. To understand the mechanism of action of DLAM-1P, we analyzed mRNA expression of RANKL, a sole molecule for Oc differentiation. DLAM-1P clearly suppressed the D3-induced expression of RANKL mRNA in osteoblasts. In organ culture using mouse calvaria, bone resorbing activity (calcium release) induced by D3 was clearly suppressed by adding DLAM-1P that is associated with less induction of RANKL mRNA. The other analog DLAM-2P has shown similar activities to DLAM-1P. Therefore, DLAM analogs act on osteoblasts as an antagonist of D3 to suppress RANKL dependent Oc differentiation in the cell and the organ, suggesting the DLAMs are novel candidate for the treatment of pathological bone loss such like osteoporosis. Further modification will require for the therapeutic compound, enhancing bone formation and inhibition of RANKL expression beside minimum modification in DLAMs structure, e.g. installing substituents on its C2 position.

Disclosures: M. Inada, None.

O272

Characterization of the Bone Phenotype in CIC-7 Deficient Mice. A. V. Neutzsky-Wulff^{*1}, K. Henriksen¹, A. Snel^{*1}, T. J. Jentsch^{*2}, J. Fuhrmann^{*2}, P. Lange^{*2}, C. Christiansen³, M. A. Karsdal¹. ¹Nordic Bioscience, Herlev, Denmark, ²MDC/FMP, Berlin, Germany, ³CCBR, Ballerup, Denmark.

Loss of the chloride channel CIC-7 leads to severe osteopetrosis. CIC-7 is believed to play a role in the ability of the osteoclasts to acidify the resorption lacuna, and thereby their ability to resorb bone. We therefore examined the bone phenotype of CIC-7 knockout (KO) mice in vitro and in vivo in detail, and compared it to the phenotype of oc/oc mice.

CIC-7 KO, oc/oc mice, and their corresponding wildtype littermates (WT) were sacrificed at 4-5 weeks of age. Bones and spleens were dissected and used for isolation of osteoclasts. The isolated cells were differentiated into mature osteoclasts on bone using M-CSF and RANKL. Cell culture supernatants were collected for measurements of CTX-I, TRACP and gelatinase activity by zymography. Cells were fixed and TRACP stained and the resorption pits were counted. Biochemical markers of resorption (CTX-I), osteoclast number (TRACP 5b), and osteoblast activity (ALP) were measured in serum of CIC-7 KO, oc/oc mice and the corresponding WT. Osteoblastogenesis in vitro was investigated using calvarial osteoblasts. In addition, bones were used for histological examination of TRACP positive osteoclasts with respect to number and morphology. Furthermore, osteoblast numbers and morphology were examined.

The osteoclasts from the CIC-7 KO mice were unable to resorb bone, as measured by CTX-I and by counting of resorption pits. Measurements of TRACP activity, as well as TRACP staining, showed the presence of equal numbers of osteoclasts in WT and KO cultures. Gelatinase activity was similar in both genotypes. Furthermore, the morphology of the KO cells was normal. Histological investigation of TRACP stained bone sections of both CIC-7 KO and oc/oc mice, indicated an elevated number of large osteoclasts present compared to WT. The serum TRACP levels were increased by 250% in CIC-7 KO and oc/oc mice, whereas the resorption per osteoclast was reduced to 50% of the WT level. Finally, the serum ALP level in KO and oc/oc mice was increased by 30%, whereas no differences in osteoblast function were observed in vitro.

In summary, the osteoclasts from CIC-7 KO mice differentiate normally and form actin rings, but fail to resorb bone in vitro. In vivo, the osteoclasts are larger and more numerous, however, show no signs of resorption. Interestingly, an elevation of TRACP, a marked reduction in resorption per osteoclast, and elevated ALP level were observed in serum from both CIC-7 KO and oc/oc mice, showing increased signs of bone formation despite the low resorption. These findings indicate that the osteoclasts, and not their activity, control osteoblastic activity.

Disclosures: A.V. Neutzsky-Wulff, None.

O293

Parathyroid Hormone-Related Protein Induces Bone Pain Through Stimulation of Proton-Secretion in Osteoclasts. L. Wang*, H. Wakabayashi*, T. Hiraga*, T. Yoneda. Department of Biochemistry, Osaka University Graduate School of Dentistry, Osaka, Japan.

Bone pain is the most common complication associated with bone metastases. Of note, clinical studies reported that inhibitors of osteoclasts such as bisphosphonates (BPs) efficiently reduced bone pain, suggesting a causative role of osteoclasts. Parathyroid hormone-related protein (PTH-rP), a potent stimulator of osteoclasts, has been implicated in bone metastasis. Activated osteoclasts are known to release protons via the $\alpha 3$ type vacuolar- H^+ -ATPase ($\alpha 3$ V- H^+ -ATPase) to dissolve bone minerals, thereby inducing acidosis in the neighboring environment. Acidosis is a well-known cause of pain. These results collectively suggest that PTH-rP is associated with bone pain through stimulating osteoclastic bone resorption. Repeated subcutaneous injections of PTH-rP caused increased osteoclastic bone resorption in the metatarsal bones and hyperalgesia in the hind-paw. Immunohistochemical examination revealed that the hyperalgesia was associated with increased protein expression of the transient receptor potential channel-vanilloid subfamily member 1 (TRPV1) and phosphorylated-ERK (p-ERK) in the ipsi-lateral dorsal root ganglions (DRGs) and c-Fos in the spinal dorsal horn. The hyperalgesia and elevated protein expression were significantly reduced by a most potent BP zoledronic acid, recombinant human OPG, a specific inhibitor of the V- H^+ -ATPase FR167356 and an antagonist of TRPV1 activation I-RTX, respectively. Finally, TRPV1 knockout mice exhibited reduced PTH-rP-induced hyperalgesia. Relevant to bone pain in bone metastases of breast cancer, we developed an animal model in which the MDA-MB-231 human breast cancer cells that produces large amounts of PTH-rP were directly inoculated into the tibial marrow cavity in nude mice. These mice showed hyperalgesia in the ipsi-lateral hind-paw and a monoclonal antibody to PTH-rP reduced the hyperalgesia. These results suggest that PTH-rP produced by metastatic cancer cells plays a part in causing bone pain through stimulation of proton-secretion in osteoclasts, thereby activating the acid-sensing receptors such as TRPV1 that are expressed in the nociceptive neurons innervating bone.

Disclosures: L. Wang, None.

O309

Myeloma Cells Decrease EphB4 Expression in Osteoblasts; A Novel Mechanism for Regulation of Bone Formation in Multiple Myeloma. A. L. Bates*, G. R. Mundy, C. M. Edwards. Vanderbilt Center for Bone Biology, Vanderbilt University, Nashville, TN, USA.

Multiple myeloma is associated with a destructive osteolytic bone disease, characterized by an increase in osteoclastic bone resorption and a reduction in osteoblastic bone formation. The increase in bone resorption in myeloma is well characterized; however the precise cellular and molecular mechanisms which mediate the reduction in bone formation and the uncoupling of bone resorption from bone formation are poorly understood. Recently, a novel mechanism has been suggested for coupling between osteoblasts and osteoclasts during normal bone homeostasis due to bidirectional signaling between the ligand ephrin B2, expressed by osteoclasts, and its receptor EphB4, expressed by osteoblasts. The interaction between EphB4 and ephrin B2 resulted in inhibition of osteoclast activity by reverse signaling through ephrin B2 on osteoclasts and stimulation of osteoblast differentiation and bone formation by forward signaling through EphB4 on osteoblasts (Zhao et al. 2006). Since the normal coupling of bone resorption to bone formation is dysregulated in multiple myeloma, we hypothesized that this may be mediated by modifications in the EphB4/ephrin B2 receptor/ligand interaction. To study bone formation in multiple myeloma in vivo, we used the 5TGM1 murine model of myeloma. 5TGM1 myeloma cells were inoculated by i.v. injection into C57BL/6J mice, resulting in homing of myeloma cells to the bone marrow, and development of an osteolytic bone disease. In addition to the well characterized increase in osteoclastic bone resorption, the bone disease was associated with a significant reduction in osteoblast number and rates of bone formation ($p < 0.01$). Real time PCR demonstrated expression of EphB4 mRNA in 5TGM1 myeloma cells, C2C12 and 2T3 osteoblasts, with a 2-fold increase in expression in 5TGM1 myeloma cells when compared with C2C12 or 2T3 cells. Western blotting demonstrated expression of EphB4 protein in C2C12 and 2T3 cells. Treatment of C2C12 or 2T3 cells with conditioned media from 5TGM1 myeloma cells resulted in a significant reduction in expression of EphB4 in both C2C12 and 2T3 cells, suggesting that myeloma cells release a soluble factor which down-regulates EphB4 in osteoblasts. In conclusion, we have shown that the development of myeloma bone disease in the 5TGM1 murine model of myeloma is associated with a reduction in bone formation, and that 5TGM1 myeloma cells can down-regulate EphB4 expression in osteoblasts. This raises the possibility that the reduction in bone formation associated with myeloma bone disease is mediated by a reduction in EphB4 expression and thus disruption of the normal coupling of bone resorption and bone formation.

Disclosures: C.M. Edwards, None.

O358

Endogenous Sex Hormones and Incident Fracture Risk in Older Men: The Dubbo Osteoporosis Epidemiology Study. C. Meier¹, T. V. Nguyen², D. J. Handelsman^{3,4}, C. Schindler^{4,5}, M. M. Kushnir^{6,7}, A. L. Rockwood^{8,9}, W. A. Meikle^{6,7}, J. R. Center², J. A. Eisman², M. J. Seibel⁷. ¹Division of Endocrinology, University Hospital Basel, Switzerland, ²Bone and Mineral Research Program, Garvan Institute of Medical Research, Sydney, Australia, ³Department of Andrology, ANZAC Research Institute, Sydney, Australia, ⁴Institute of Social and Preventive Medicine, University of Basel, Switzerland, ⁵ARUP Institute for Clinical and Experimental Pathology, Salt Lake City, UT, USA, ⁶Department of Medicine and Pathology, University of Utah, Salt Lake City, UT, USA, ⁷Bone Research Program, ANZAC Research Institute, Sydney, Australia.

One third of osteoporotic fractures occur in men. Data on the influence of gonadal hormones on incident fracture risk in elderly men are limited. The present study examined the prospective relationship between serum levels of testosterone (T) and estradiol (E2) and future fracture risk in elderly men as part of the long-term observational Dubbo Osteoporosis Epidemiology Study of community-dwelling men over 60 years followed prospectively since 1989. This analysis included men who had serum samples for baseline measurements ($n=609$, 70.6%) with follow-up of 5.8 years (up to 13 yrs) closing in 2005. Clinical risk factors, including bone mineral density (BMD) and lifestyle factors were assessed at baseline. Serum T and E2 were measured by tandem mass spectrometry (LC-MS/MS). The incidence of low-trauma symptomatic fracture was ascertained by X-ray record.

During follow-up, 113 men suffered at least one low-trauma fracture. Fracture risk was increased in men with reduced T levels (hazard ratio [HR] 1.33; 95%CI: 1.09, 1.62). After adjustment for SHBG, both low serum T (HR 1.48; 95%CI: 1.22, 1.78) and serum E2 (HR 1.21; 95%CI: 1.00, 1.47) were associated with increased overall fracture risk. After further adjustment for major fracture risk factors (age, weight or BMD, fracture history, smoking status, calcium intake and SHBG), lower T was still associated with increased risk of hip (HR 1.88; 95%CI: 1.24, 2.82) and non-vertebral (HR 1.32; 95%CI: 1.03, 1.68) fracture. By contrast, lower E2 was only associated with increased fracture risk in the presence of body weight (HR 1.25; 95%CI: 1.02, 1.54), but not at any site after adjustment for BMD (HR 1.19; 95%CI: 0.69, 1.03).

In community-dwelling men over 60 years of age, serum T, but not E2, is an independent predictor of osteoporotic fracture and its measurement may provide additional clinical information for the assessment of fracture risk in elderly men.

Disclosures: C. Meier, None.

O360

Respiratory Function Is Associated with Bone Ultrasound Measures and Hip Fracture: European Prospective Investigation Into Cancer-Norfolk Population Cohort Study. A. Moayyeri¹, R. N. Luben², S. Bingham^{2,3}, A. Welch¹, N. J. Wareham³, S. Kaptoge¹, J. Reeve¹, K. T. Khaw¹. ¹Department of Public Health and Primary Care, Institute of Public Health, School of Clinical Medicine, The University of Cambridge, Cambridge, United Kingdom, ²MRC Dunn Human Nutrition Unit, The University of Cambridge, Cambridge, United Kingdom, ³MRC Epidemiology Unit, The University of Cambridge, Cambridge, United Kingdom.

Forced expiratory volume in 1 second (FEV1), an easily obtainable measure of respiratory function in clinics, has been shown to be associated with physical activity. We hypothesized that FEV1 is linked with bone health. In the context of the European Prospective Investigation into Cancer-Norfolk study, 14,800 participants aged 42-81 in 1997-2000 were evaluated by spirometry and heel ultrasound and were followed for fracture outcomes up to July 2007. After excluding participants with history of pulmonary diseases, among 5,555 men and 6,935 women (mean age 62.1 \pm 9.0), FEV1 significantly correlated with heel broadband ultrasound attenuation (BUA; Pearson $r=0.403$; $p<0.001$) and velocity of sound (VOS; $r=0.269$; $p<0.001$). The association remained significant in sex-stratified linear regression models after adjustment for age, history of fracture, height, body mass index, smoking status and alcohol consumption (standardized Beta coefficient -0.057 and $p<0.001$ in men; Beta -0.075 and $p<0.001$ in women). Mean adjusted FEV1 among 109 hip fracture patients (2.00 \pm 0.60 liter) was significantly lower than that of other participants (2.49 \pm 0.71 liter; t -test $p<0.001$). In a Cox proportional hazards regression model, FEV1 was a significant predictor of hip fracture after adjustment for age, sex, history of fracture, height, body mass index, smoking and alcohol consumption (hazard ratio for 1 standard deviation [700 ml in 1 second] decrease in FEV1 -1.39 , 95%CI 1.03-1.88, $p=0.029$). Among 6197 current and former smoker participants, hazard ratio for 1 standard deviation decrease in FEV1 was 1.67 (95%CI 1.11-2.57, $p=0.014$). Middle aged and older men and women with lower respiratory function appear to be at increased risk of osteoporosis and hip fracture. The observed association might be related to the level of physical activity or deformities in thoracic spine related to osteoporosis. Given the feasibility and affordability of spirometry in general practices, it can be used to improve the identification of high risk groups at the first point of care.

Disclosures: A. Moayyeri, None.

This study received funding from: Medical Research Council and Cancer Research UK.

O373

Changes in Hip Geometric Structures with Aging--Longitudinal Data Analysis from the Women's Health Initiative Observational Study. T. Bassford^{*1}, T. J. Beck², G. Wu^{*1}, J. A. Cauley³, A. Z. LaCroix^{*4}, C. E. Lewis⁵, Z. Chen¹. ¹University of Arizona, Tucson, AZ, USA, ²Johns Hopkins University, Baltimore, MD, USA, ³University of Pittsburgh, Pittsburgh, PA, USA, ⁴Fred Hutchinson Cancer Research Center, Seattle, WA, USA, ⁵University of Alabama-Birmingham, Birmingham, AL, USA.

Fracture risk increases with age. In addition to bone loss, change in the distribution of bone mass is another significant factor associated with bone fragility. The objective of this study was to investigate the relationship between aging and changes in hip geometry derived from hip structure analysis (HSA). A prospective study in an ethnically diverse subcohort of 5,856 postmenopausal women enrolled in the Observational Study of the Women's Health Initiative was conducted. Eligible subjects were between 50 and 79 years of age and had completed bone scans using Dual-energy X-ray Absorptiometry (DXA). The Beck HSA software was used to estimate bone mineral density (BMD), cross-sectional area (CSA), outer diameter (OD), section modulus index (SM), average cortical thickness (CT) and buckling ratio (BR) for the femoral narrow neck (FNN), intertrochanter (IT) and proximal femoral shaft regions (FS). Analyses showed that BMD, CSA, SM and CT were all significantly lower and the OD and BR measures were significantly higher in the older age group in comparison to the younger age group at baseline ($p < 0.01$). Results from paired t-test indicated significant changes in all HSA measures from baseline to year 6 (Table). Interestingly, both the bone bending strength (SM) and the likelihood of cortical failure under compression (BR) increased significantly over this same time frame, suggesting a complex process with changes in the hip geometry associated with aging. The rates of changes in HSA measures varied by age group and by femoral site. For example, OD expansion in all regions was significantly larger in the 60-69 or 70-79 years age group in comparison to the 50-59 years age group. While significant age differences in the change of other HSA measures were only observed in the FNN region. In conclusion, hip geometric structures change significantly with aging and the rate of changes varies by age and femoral site. The impacts of these changes on hip bone strength are complicated and remained to be investigated.

FNN	Baseline	Year 6	Change	*P-value
BMD (g/cm ²)	0.719 ± 0.130	0.713 ± 0.136	-0.006 ± 0.070	<0.001
CSA (cm ²)	0.204 ± 0.365	0.205 ± 0.391	0.007 ± 0.208	0.037
Outer diameter (cm)	2.997 ± 0.209	3.033 ± 0.228	0.035 ± 0.139	<0.001
SM (cm ³)	0.910 ± 0.190	0.935 ± 0.220	0.025 ± 0.133	<0.001
CT (cm)	0.137 ± 0.026	0.136 ± 0.028	-0.001 ± 0.014	<0.001
BR	12.3 ± 2.84	12.6 ± 3.04	0.344 ± 1.647	<0.001

*p-value from paired t-test

Disclosures: T. Bassford, None.

This study received funding from: NIAMS R01-AR049411.

O386

Oral Treatment with the Calcium Receptor Antagonist SB-423557 Causes PTH Release in Multiple Species and Positive Bone Forming Effects in the Rat. S. Kumar¹, X. Liang¹, J. A. Vasko^{*1}, G. B. Stroup², S. J. Hoffman¹, V. R. Vaden^{*2}, H. Haley^{*2}, J. Fox³, E. F. Nemeth³, A. M. Lago^{*2}, J. F. Callahan^{*2}, P. Bhatnagar^{*1}, W. F. Huffman^{*1}, M. Gowen². ¹GlaxoSmithKline, Collegeville, PA, USA, ²GlaxoSmithKline, King of Prussia, PA, USA, ³NPS, Salt Lake City, UT, USA.

Antagonists of the parathyroid calcium receptor (calcilytics) stimulate the secretion of PTH. Previously, we demonstrated the ability of an orally active calcilytic compound to cause sustained increases in circulating levels of endogenous PTH and to stimulate bone formation and resorption (without a net increase in bone formation) in the ovariectomized (OVX) rat. In the present study, a prodrug approach has been used to preserve oral bioavailability and yield a calcilytic with a shorter half-life in vivo. SB-423557 is the ethyl ester prodrug of SB-423562 that, when administered orally to rats, dogs or monkeys, caused a dose-dependent, transient increase in circulating levels of endogenous PTH. In order to examine the bone forming effect of SB-423557, six-month-old female rats received OVX or sham surgery and were untreated for 6 weeks to allow osteopenia to develop and then treated orally daily with either vehicle, SB-423557 (50 mg/kg), or with rat PTH(1-34) (5 µg/kg SC) for 12 weeks. Plasma levels of PTH peaked at 10-60 min following oral administration of 50 mg/kg SB-423557 (3-fold, C_{max} of 40-60 pM) and returned to baseline by 2-3 hours. SC administration of rat PTH(1-34) resulted in a systemic C_{max} of 127-240 pM at 10 minutes post-injection. SB-423557 significantly and completely prevented additional OVX-induced loss of BMD in the lumbar spine and partially prevented trabecular BMD loss in the proximal tibia by 39% (ns) compared to OVX controls. Histomorphometric analysis indicated greater trabecular bone area (36%, ns) in the spine and increased cortical area (72%) and endocortical bone formation rate (220%) with no effect on the eroded perimeter of the distal tibia in the SB-423557 treated rats compared to vehicle-treated OVX animals. Serum osteocalcin increased (ns) with SB-423557 treatment with no effect on urinary deoxypyridinoline levels. In addition, treatment with SB-423557 resulted in greater ultimate strength (ns), toughness, and elastic modulus of a lumbar vertebral body and at the femoral diaphysis compared to OVX controls. Treatment with PTH(1-34) also completely prevented the OVX-induced loss in bone mass, BMD, and strength. These data provide a proof of principle for stimulation of bone formation following daily brief antagonism of the calcium receptor in the OVX rat and support the potential use of these agents to treat disorders of bone metabolism such as osteoporosis.

Disclosures: S. Kumar, GlaxoSmithKline 3.

O390

β2 Adrenergic Receptor Deficiency Enhances Bone Mass in by Antagonizing Against Aging-induced Bone Loss and Blunts Anabolic Effects of PTH on Osteoblasts. R. Hanyu^{*1}, Y. Saita^{*1}, J. Nagata^{*1}, Y. Izu^{*1}, T. Hayata^{*1}, H. Hemmi^{*2}, S. Takeda^{*3}, Y. Ezura^{*1}, K. Nakashima^{*1}, H. Kurosawa^{*4}, M. Noda^{*1}. ¹Department of Molecular Pharmacology, 21st Century COE Program, MRI, Tokyo Medical and Dental University, Chiyoda-ku, Tokyo, Japan, ²MTT Program, MRI, Tokyo Medical and Dental University, Chiyoda-ku, Tokyo, Japan, ³Department of Orthopedics, 21st Century COE Program, Tokyo Medical and Dental University, Chiyoda-ku, Tokyo, Japan, ⁴Department of Orthopedics, Juntendo University school of Medicine, Bunkyo-ku Tokyo, Japan.

Soaring of the aged population in modern world increases the fraction of aged population with diseases and thus in bone field, leads to increase in osteoporosis incidence. Loss of bone mass is accelerated with age regardless of gender. Osteoporotic patients with their bone mass levels at their nadir require treatment to increase bone mass through the activation of bone formation. PTH has been proven to be efficacious in increasing bone mass. However, its efficacy in the highly aged population such as those over 80 years of age in human have not yet been fully elucidated. In mice, aged models of over one year old, indicate lower bone mass than younger adult animals regardless of the gender. Recently, sympathetic nervous system was reported to regulate bone mass in mice. However, these reports always indicate the effects of adrenergic system on young adult mice. Therefore, the purpose of this paper is examine the effects of β2 adrenergic system and PTH on the bone mass in aged mice. Aged (54 weeks old) female mice null for β2 adrenergic receptor (Adrb2^{-/-}) and wild type (WT) were used. Mice were treated with vehicle or PTH (80µg/kg/day sc) for 4 weeks (5 days/week). The base line bone mass levels in these aged mice were significantly reduced compared to young adult mice. Aged Adrb2^{-/-} mice exhibited higher total body BMD, trabecular bone volume fraction(BV/TV), cortical bone volume compared with aged WT mice. In WT, PTH treatment significantly increased the levels of total body BMD, 3D-BV/TV, mineral apposition rate (MAR) and bone formation rate (BFR). In contrast, in aged Adrb2^{-/-} mice, PTH failed to increase the levels of BMD and BV/TV. Analyses on aged Adrb2^{-/-} mice also revealed that PTH failed to enhance BFR and MAR. Importantly, Adrb2 deficiency increased cortical bone volume compared to WT while this parameter was no longer enhanced by PTH in the mutant mice. Regarding bone resorption side, Oc.S/BS, N.Oc/BS were similar regardless of the genotype or PTH treatment. In conclusion, we found that in one year old aged female mice, β2 adrenergic receptor signal operates to reduce bone mass, while β2 adrenergic signaling is required for the anabolic actions of PTH on bone formation.

Disclosures: R. Hanyu, None.

O409

Decreased Bone Turnover and Porosity Are Associated with Improved Bone Strength in Ovariectomized (OVX) Cynomolgus Monkeys Treated with Denosumab, a Fully Human RANKL Antibody. M. S. Ominsky¹, J. Schroeder^{*1}, J. Jolette^{*2}, S. Y. Smith², D. J. Farrell^{*2}, J. E. Atkinson¹, P. J. Kostenuik¹. ¹Amgen Inc., Thousand Oaks, CA, USA, ²Charles River Laboratories Preclinical Services Montreal, Inc., Montreal, PQ, Canada.

Denosumab (DMab), a fully human monoclonal antibody against RANKL, was previously shown to decrease biochemical markers of bone turnover and increase bone mineral density in adult OVX cynomolgus monkeys. We now report from that study the effects of DMab on bone turnover at the histologic level, and their relationships with bone strength. One month after surgery, OVX cynos (9-16 years old) were treated with either vehicle (OVX-Veh) or DMab (25 or 50 mg/kg, SC, once/month) for 16 months (n=14-20/group). Sham controls were treated with vehicle (n=17). Double fluorochrome labels were injected prior to iliac and rib biopsies (at month 6 and 12), and prior to sacrifice. Histomorphometry was performed on these biopsies, the tibial diaphysis, and cancellous bone in L2 vertebra and the proximal femur. Cancellous bone turnover was increased in OVX-Veh animals, based on significantly greater mineralizing surface (MS/BS), bone formation rate (BFR), and activation frequency at the lumbar spine, iliac crest, and femur neck ($P < 0.05$ vs Sham). Both doses of DMab fully prevented these OVX-related changes while reducing values significantly below those of sham controls ($P < 0.05$). Osteoclast and osteoblast surfaces were 78-100% lower in the lumbar spine, iliac crest, and femur neck of DMab groups, while eroded surface was decreased by 45-93% ($P < 0.05$ vs OVX-Veh). Cortical bone turnover was also increased in OVX-Veh cynos, as shown by significantly greater cortical porosity, labeled perimeter, and BFR at the endocortical and haversian surfaces of the tibial diaphysis and rib ($P < 0.05$ vs Sham). Both doses of DMab fully prevented these OVX-related changes, while reducing labeled perimeter and BFR significantly below sham control levels ($P < 0.05$). Prolonged DMab-related turnover suppression was associated with significant increases in strength parameters at the lumbar vertebrae, femur neck, and femur diaphysis ($P < 0.05$ vs OVX-Veh). Regression analysis of all groups combined demonstrated significant inverse relationships between the strength of L5-L6 cores (yield load) and mineralizing surface ($r^2 = 0.44$) or eroded surface in L2 ($r^2 = 0.37$; $P < 0.001$). Cortical porosity in the tibia was negatively correlated with peak load at the femur diaphysis ($r^2 = 0.21$; $P < 0.001$). In summary, denosumab treatment of OVX cynos was associated with significant decreases in histomorphometric indices of bone turnover. These changes were accompanied by significant improvements in bone strength at cortical and cancellous sites.

Disclosures: P.J. Kostenuik, Amgen, Inc. 1, 3.
This study received funding from: Amgen Inc.

O423

Efficacy of Adding Teriparatide versus Switching to Teriparatide in Postmenopausal Women with Osteoporosis Previously Treated with Raloxifene or Alendronate. F. Cosman¹, R. A. Werners², C. Recknor³, K. F. Mauck^{*2}, L. Xie^{*4}, E. V. Glass^{*4}, J. H. Krege⁴. ¹Helen Hayes Hospital, West Haverstraw, NY, USA, ²Mayo Clinic, Rochester, MN, USA, ³United Osteoporosis Centers, Gainesville, GA, USA, ⁴Eli Lilly and Company, Indianapolis, IN, USA.

In patients previously treated long term with antiresorptive drugs, information regarding the relative efficacy of adding teriparatide (TPTD, 20 mcg/d) versus switching to TPTD is not available. Postmenopausal women with osteoporosis previously treated for at least 18 months with alendronate (ALN, 70 total mg/week, median treatment duration 37.3 months) or raloxifene (RLX, 60 mg/d, median treatment duration 36.9 months) were randomized to either add TPTD or switch to TPTD for 6 months. A preplanned 12-month extension of this study is currently ongoing. Efficacy results included markers of bone turnover and DXA BMD. Baseline BMD and other characteristics were well matched with the exception that previous ALN patients had lower baseline bone turnover than previous RLX patients (Table). Adding TPTD conferred smaller increases in bone turnover versus switching to TPTD; these differences were more marked between the groups previously treated with ALN. However, adding TPTD conferred greater increases in BMD versus switching to TPTD; these differences were again more marked between the groups previously treated with ALN. All regimens were well tolerated. In conclusion, an anabolic response to TPTD was observed in patients previously treated with ALN or RLX regardless of whether the previous antiresorptive drug was continued or discontinued. In general, greater bone turnover was achieved by switching from antiresorptive to TPTD, while greater BMD increase was achieved by continuing antiresorptive during TPTD treatment.

Table: Baseline and change from baseline after 6 Months of TPTD Treatment.

Variable	Alendronate Pretreated			Raloxifene Pretreated		
	TPTD (N=50)	TPTD+ALN (N=52)		TPTD (N=49)	TPTD+RLX (N=47)	
BL	6-Mo Δ	BL	6-Mo Δ	BL	6-Mo Δ	BL
PINP (μg/L)	27.101.5 (400.9%*)	30.21.5 (69.1%*)	43.103.0 (245.7%*)	42.62.5 (125.4%*)		
BSAP (U/L)	5.11.9 (73.3%*)	0.3.1 (16.1%*)	25.9.7 (38.6%*)	27.8.1 (30.6%*)		
CTx (ng/ml)	0.10.40 (231.0%*)	0.10.05 (28.6%*)	0.30.37 (136.1%*)	0.20.14 (64.6%*)		
LS DXA BMD (g/cm ²)	0.80.012 (1.9%*)	0.80.033 (4.5%*)	0.80.034 (4.2%*)	0.80.037 (4.6%*)		
FN DXA BMD (g/cm ²)	0.60.0001 (0.1%)	0.60.004 (0.7%)	0.60.002 (0.3%)	0.60.012 (1.9%*)		
TH DXA BMD (g/cm ²)	0.7-0.007 (-0.8%)	0.70.009 (1.4%*)	0.70.003 (0.5%)	0.70.013 (1.8%*)		

For bone markers, values are median baseline, median absolute change from baseline (% change). For BMD, values are mean baseline, mean absolute change from baseline (% change). BL, baseline; PINP, amino-terminal propeptide of type I collagen; BSAP, bone specific alkaline phosphatase; CTx, C-terminal telopeptide of type I collagen; LS, lumbar spine; FN, femoral neck; TH, total hip. P-values are based on percent changes. *P<0.001 and **P<0.05 within group from baseline; †P<0.001 and ‡P<0.05 between groups within a stratum.

Disclosures: F. Cosman, Eli Lilly and Company 2, 5, 8; Merck 5, 8.
This study received funding from: Eli Lilly and Company.

O435

Mechanistic Bases of Bone Mineral Density Increase During Alendronate Therapy. D. Vashishth¹, P. Chavassieux², G. Boivin², P. D. Delmas². ¹INSERM Unite 831 Universite de Lyon France & Rensselaer Polytechnic Institute, Troy, NY, USA, ²INSERM Unite 831 Universite de Lyon, Lyon, France.

An increase in the mean degree of tissue mineralization (DMB) occurring through secondary mineralization has been proposed to increase bone mineral density (BMD) during bisphosphonate (BP) therapy [1]. In this study we conducted additional analyses on human iliac crest biopsies obtained as part of alendronate (ALN) clinical trials [2] to identify the mechanistic bases of BMD increase.

Out of a group of 16 patients on a three-year ALN-therapy [1], we identified two groups of 5 patients each showing lower (8.5 %) and higher (13.3%) bounds of BMD increase but no difference in baseline BMD. For all 10 patients, previously prepared microradiographs were reanalyzed to measure the mean degree of tissue mineralization (DMB) at the osteonal and interstitial compartments in both cortical and cancellous bone tissues. Based on a moving average analysis, six fields each of cortical and cancellous bone tissues were randomly selected for measurement from each biopsy. The average values for patients in each group within osteonal and interstitial compartments were compared between and across cortical and cancellous bone tissues. All DMB measurements were also tested for correlation with standard histomorphometric measures of bone structure (BV/TV, Tb.Th, Tb. Separation, Tb.N), osteoclast activity (EV/BV, E-Depth, Oc#/BS), osteoid (OS/BS, OV/BV, OTh), and bone formation (MAR, BFR/BS, FP) reported previously [2].

The low-BMD-gain group demonstrated no difference between the osteonal and interstitial bone compartments within cortical or cancellous bone tissues but demonstrated a higher DMB in cancellous than in cortical tissue (p<0.05). In contrast, the high-BMD-gain group showed higher DMB in interstitial than in osteonal compartment for both cortical and cancellous tissues as well as a higher DMB in cancellous than in cortical tissue (p<0.05). Out of all the DMB measures in cortical and cancellous tissues, only cortical bone interstitial level DMB correlated to bone formation rate (BFR/BS) (r = -0.86; p = 0.006) and formation period (FP) (r = -0.75; p = 0.04). In conclusion, this study demonstrates that the effects of ALN-therapy are more evident in

cancellous than in cortical bone. Moreover since the interstitial level DMB is at least partially dependent on the duration of secondary mineralization, and negatively correlated to formation parameters, slow bone formation rate and longer bone formation period produce conditions conducive to complete secondary mineralization and consequently larger BMD gain.

References: [1] Boivin et al. Bone. 2000 5: 687-94. [2] Chavassieux et al. JCI 1997 100:1475-80.

Disclosures: D. Vashishth, Merck 5.

This study received funding from: INSERM, France & NIH Grants AR49635, AG 20618.

O498

Thioredoxin-1 Overexpression Attenuates Streptozotocin-induced Diabetic Osteopenia in Mice: A Novel Role of Oxidative Stress and Therapeutic Implications. Y. Hamada^{*1}, H. Fujii^{*1}, R. Kitazawa², S. Kitazawa², M. Fukagawa¹.

¹Division of Nephrology and Kidney Center, Kobe University School of Medicine, Kobe, Japan, ²Division of Molecular Pathology, Department of Biomedical Informatics, Kobe University School of Medicine, Kobe, Japan.

Diabetes mellitus is associated with increased risk of osteopenia and bone fracture. However, the mechanisms accounting for diabetic bone disorder still remain to be clarified. Moreover, there are few effective treatments for this disease. We have previously reported that streptozotocin-induced diabetic mice develop low turnover osteopenia associated with increased oxidative stress in diabetic condition (BONE 2007). Therefore, in order to determine the role of oxidative stress in the development of diabetic osteopenia, we investigated the effect of thioredoxin-1 (TRX) overexpression, a major intracellular antioxidant, on the development of diabetic osteopenia using TRX transgenic mice (TRX-Tg). TRX-Tg was C57BL/6 mice that carry the human TRX transgene under the control of β-actin promoter.

Eight-week-old male TRX-Tg and wild type littermates (WT) were intraperitoneally injected with either streptozotocin or vehicle alone. Mice were classified into four groups: 1) non-diabetic WT, 2) Non-diabetic TRX-Tg, 3) diabetic WT, and 4) diabetic TRX-Tg. After 12 weeks of streptozotocin treatment, the physical properties of femora, and the parameters of bone histomorphometry of tibiae were assessed. Oxidative stress in the whole body as well as in the bone was evaluated.

TRX overexpression did not affect either body weights or hemoglobin A1c levels both in the diabetic mice and in the non-diabetic mice. There were no significant differences in renal function, and serum levels of calcium, phosphate, and intact parathyroid hormone among four groups. Urinary excretion of 8-hydroxydeoxyguanosine (8-OHdG), a marker of oxidative DNA damage, was significantly elevated in diabetic WT, which was attenuated in diabetic TRX-Tg. Immunohistochemical staining for 8-OHdG was clearly intensified in the bone tissue of diabetic WT compared with non-diabetic WT. In contrast, staining was attenuated in diabetic TRX-Tg. TRX overexpression partially restored reduced bone mineral density and prevented the suppression of bone formation (OV/BV, OS/BS, Ob.S/BS, O.Th, MAR, and BFR/BS) observed in diabetic WT. These results suggest that increased oxidative stress in diabetic condition contributes to the development of diabetic osteopenia. Furthermore, our findings indicate that suppression of increased oxidative stress by TRX induction can be a therapeutic approach for treatment of diabetic osteopenia.

Disclosures: Y. Hamada, None.

O504

Time Sequence of Secondary Mineralization and Microhardness of Bone in an Ewe Model. Y. Bala^{*}, D. Farlay^{*}, C. Simi^{*}, P. J. Meunier, P. D. Delmas, G. Boivin. INSERM Unité 831, Université de Lyon, Lyon, France.

The degree of mineralization is a major determinant of the mechanical resistance of bone (Follet et al. 2004, Bone 34:783-9). Mineralization begins by a rapid primary mineralization followed, after the full completion of the Basic Structural Units (BSUs), by a secondary mineralization phase, i.e., a slow and gradual maturation of the mineral component leading to complete mineralization of newly formed BSUs (Meunier & Boivin 1997, Bone 21:373-7). The duration of primary mineralization has been evaluated by several authors but the time sequence of secondary mineralization is still poorly investigated [Fuchs et al. 2005, J Bone Miner Res 20 (Suppl.1):325]. Our aim was to determine the time course of secondary bone mineralization in ewe, an animal model having an Haversian bone tissue with a remodeling activity close to the Human one (Chavassieux et al. 1997, Bone 20:451-5). 18 ewes (4.5±0.4 years, INRA, Theix, France) received every six months for 30 months fluorescent labelings following the schedule: T0 double tetracycline, T6 single fluorescein, T12 triple tetracycline, T18 double fluorescein, T24 single tetracycline, T30 double alizarin labeling in order to date the age of the BSUs. Transiliac bone samples have been taken on each ewe after T18 and T30 labelings, then embedded in methyl methacrylate. Microradiography (Boivin & Meunier 2002, Calcif Tissue Int 70:503-11) performed on 100±1 μm-thick sections allowed the measurement of the focal Degree of Mineralization of Bone (DMB g/cm³) on 505 different BSUs in which the duration of the mineralization was precisely determined by labeling. Microhardness using a Vickers indenter under a load of 25g for 10s (Hv kg/mm²) was measured on 367 among the 505 BSUs [Bala et al. 2006, J Bone Miner Res 21(suppl.1):S332]. DMB measured at primary mineralization (0.76±0.10 g/cm³) significantly increased during the first 6 months (+26%, p<0.0001). Then, DMB increased more slowly until 30 months to reach a mean of 1.20±0.12 g/cm³. DMB measured at the end of the primary mineralization corresponded to 64% of the final mineralization. DMB after 6 and 12 months were 85% and 91% of the final DMB, respectively. Secondary mineralization is thus the fastest during the first year. Hv followed a similar trend, with a rapid increase during the first six months (+32%, p<0.0008), then a slow increase until 30 months. Hv and DMB are strongly and positively correlated (r²=0.52, p<0.0001). The time course of secondary mineralization can be divided into two parts having separated trends, a rapid increase during the first year then a slowdown of mineralization until 30 months. Mineralization explains a great part of the hardness of bone at BSU level.

Disclosures: G. Boivin, None.

S002

Oxidized Metabolites of Polyunsaturated Fatty Acids Stimulate Osteoblast Apoptosis via both PPAR γ -dependent and -independent Mechanisms. R. L. Jilka, M. Almeida, R. Wynne*, L. Han, S. C. Manolagas. Center for Osteoporosis and Metabolic Bone Diseases, Central Arkansas Veterans Healthcare System, University of Arkansas for Medical Sciences, Little Rock, AR, USA.

Age-related loss of bone mass and strength in mice is accompanied by increased reactive oxygen species (ROS) in the bone marrow, increased osteoblast apoptosis, and decreased osteoblast number; but the underlying mechanisms are unknown. The level of expression of the lipoxygenase Alox15, and the nuclear hormone receptor PPAR γ , is inversely related to bone mass in mice; and the expression of these genes increases with aging. Alox15, as well as ROS, oxidize polyunsaturated fatty acids (PUFAs) to generate PPAR γ ligands such as 9-hydroxyoctadecadienoic acid (9-HODE) and 12-hydroxyicosatetrenoic acid (12-HETE). Oxidized PUFAs are further metabolized to form 4-hydroxynonenal (4-HNE), which can form pro-apoptotic protein and DNA adducts, and can further increase oxidative stress. Here, we examined the impact of these PUFA metabolites on the apoptosis of C2C12 uncommitted osteoblast progenitor cells and OB-6 osteoblastic cells. We found that 9-HODE or 12-HETE stimulated apoptosis of C2C12 cells after 6 hours and of OB-6 cells after 16 hours, as measured by caspase-3 activity. This effect required 0.5 to 5 μ M of 9-HODE or 12-HETE, which is near their binding constant for PPAR γ 2. Using osteoblastic OB-6g2 cells that express PPAR γ 2 under the control of the tet-OFF promoter, we found that the pro-apoptotic effect of both metabolites required the presence of this transcription factor. Six hours of treatment with 4-HNE also stimulated apoptosis of C2C12 and OB-6 cells at physiologic concentrations (10–40 μ M). Unlike 9-HODE and 12-HETE, however, the pro-apoptotic effect of 4-HNE did not require PPAR γ 2. Using pharmacologic inhibitors, we further determined that 4HNE-stimulated apoptosis required p38 MAP kinase, and that neither MEK nor JNK MAP kinases were involved. 4-HNE-induced apoptosis was prevented by the antioxidant N-acetyl cysteine. Moreover, treatment of C2C12 cells with 40 μ M 4-HNE for 1 hour increased phosphorylation of p66^{Sbc}, a ROS-sensitive adaptor protein known to directly activate apoptosis. Based on these findings, we hypothesize that an age-related increase in the production of oxidized lipids such as 9-HODE and 13-HETE stimulate apoptosis of osteoblasts and osteoblast progenitors via activation of PPAR γ 2; and downstream PUFA metabolites like 4-HNE further increase oxidative stress and stimulate apoptosis of these cells. In view of the role of lipid oxidation in atherosclerosis and increasing epidemiologic evidence linking atherosclerosis and osteoporosis, it is tempting to speculate that these diseases share a common pathologic basis.

Disclosures: R.L. Jilka, Radius Health, Inc. I.

S004

The Role of Fas/Fas Ligand System in Estrogen Deficiency-induced Osteoporosis. N. Kovacic¹, V. Grubisic^{*1}, K. Mihovilovic^{*1}, I. K. Lukic¹, D. Grcevic^{*2}, V. Katavic^{*1}, P. Croucher³, A. Marusic^{*1}. ¹Department of Anatomy, Zagreb University School of Medicine, Zagreb, Croatia, ²Department of Physiology and Immunology, Zagreb University School of Medicine, Zagreb, Croatia, ³Academic unit of Bone Biology, University of Sheffield Medical School, Sheffield, United Kingdom.

The aim of this study was to estimate the role of Fas/Fas ligand system in vivo in the pathogenesis of estrogen deficiency induced bone loss.

We first analyzed the expression of Fas gene by quantitative PCR in bones and bone cell cultures from wild-type mice, four weeks after the ovariectomy (ovx). Then we performed ovx in mice deficient for Fas gene (Fas^{-/-}) and their wild-type controls. After four weeks we analyzed: 1) standard histomorphometric parameters of their femora, 2) differentiation of osteoblast (Obl) and osteoclasts (Ocl) in vitro from their bone marrow progenitors. Obl and Ocl differentiation was estimated histochemically (number of alkaline phosphatase positive Obl colonies, and number of TRAP-positive Ocl-like cells), and according to the expression of Obl (Runx2, alkaline phosphatase, osteocalcin and osteoprotegerin) and Ocl (RANK, calcitonine receptor) differentiation genes.

Our results showed that after four weeks, gene expression of Fas was increased in bone and mature Obl cultures from ovx (0.36 \pm 0.06 and 2.6 \pm 0.05 respectively) compared to sham operated animals (0.31 \pm 0.01 and 1.8 \pm 0.76, p<0.05). A mild decrease in Fas expression was also observed in the Ocl cultures from ovx animals. Trabecular bone volume was generally significantly higher in Fas^{-/-} mice (p=0.01, t-test) than in wild-type controls. Furthermore, trabecular volume significantly decreased in wild-type mice four weeks after ovx (p=0.01, t-test), and remained unaltered in Fas^{-/-} mice (p=0.67, t-test). Mean number of TRAP-positive Ocl on bone surface of wild-type mice increased four weeks after ovx (p=0.03), whereas this number was unchanged in Fas^{-/-} mice (p=0.27). OvX also significantly increased osteoclastogenesis in vitro in wild-type animals but this effect was absent in Fas^{-/-} mice. Osteoblastogenesis in vitro was stimulated by ovx in both animal strains, but this effect was more pronounced in Fas^{-/-} mice. Obl differentiation genes were had similar expression patterns in sham operated and ovx mice, although Fas^{-/-} mice Obls generally had higher expression levels of Obl differentiation genes compared to wild-type controls. Our findings point to the conclusion that Fas/Fas ligand system may have an important role in the pathogenesis of postmenopausal osteoporosis and modulation of its effects on bone cells may contribute to the development of new strategies for osteoporosis treatment.

Disclosures: N. Kovacic, None.

S010

Osterix as a Regulator of Bone Formation and Maintenance. J. Kim¹, W. Baek^{*1}, M. Lee^{*1}, H. Akiyama^{*2}, Z. Zhang^{*3}, B. de Crombrughe³. ¹Department of Molecular Medicine, Kyungpook National University School of Medicine, Daegu, Republic of Korea, ²Department of Orthopaedics, Kyoto University, Kyoto, Japan, ³Department of Molecular Genetics, University of Texas M. D. Anderson Cancer Center, Houston, TX, USA.

Osterix (Osx) is a zinc-finger containing transcription factor which is essential for osteoblast differentiation and bone formation. Osx null mutant by gene targeting shows a complete absence of intramembranous and endochondral bone formation. Disruption of Osx has led to perinatal lethality, hence preventing the study for the importance of Osx in bones that are developing or formed. Here, we examined the role of Osx in developing bones after bone collar formation using the time-specific and site-specific Cre/loxP system. Osx was inactivated in osteoblasts by Col1a1-Cre with the activity of Cre recombinase under the control of 2.3-kb collagen promoter. Low bone mass was observed in mouse bones at the age of 2 months. Bone forming rate by Calcein double labeling was shown a remarkable reduction, while single labeling surface was increased in endosteum and trabecular of mouse lumbar. The analysis of Deoxyypyridinoline (DPD) crosslinks in the urine, which reflects osteoclast activity in vivo, was not significantly changed in Osx-inactivated mice. These results demonstrated that Osx inactivation decreased the function of osteoblasts to synthesize and regulate the deposition and mineralization of bone extracellular matrix, whereas it was not affected to osteoclast differentiation and activity in vivo. We also studied the role of Osx in intact bones after birth by generating Osx inactivation in osteoblasts using inducible Cre system. Bone volume was decreased and bone forming rate was reduced in mice which Osx was inactivated in osteoblasts of already formed bones after birth by 4-OHT administration. Thus, this study suggests that Osx plays a significant role in regulating bone formation and maintenance. To better understand the role of Osx in cellular mechanisms, we are investigating the interrelation between osteoblasts and osteoclasts derived from Osx-inactivated mice.

Disclosures: J. Kim, None.

This study received funding from: Korea Research Foundation Grant funded by Korea Government (MOEHRD, Basic Research Promotion Fund) (KRF-2005-204-E00006) and Grain Korea 21 Project in 2007.

S016

Overexpression of Osteoblast Specific Angiopoietin1 Increases Bone Mass. T. Suzuki^{*1}, T. Miyamoto², N. Fujita^{*3}, M. Yagi^{*3}, K. Ninomiya^{*1}, R. Iwasaki^{*4}, Y. Toyama^{*3}, T. Suda^{*3}. ¹Cell Differentiation and Orthopaedics Surgery, Keio University, Tokyo, Japan, ²Orthopaedics Surgery and Musculoskeletal Reconstruction and Regeneration Surgery, Keio University, Tokyo, Japan, ³Orthopaedics Surgery, Keio University, Tokyo, Japan, ⁴Department of Dentistry and Oral Surgery, Keio University, Tokyo, Japan, ⁵Cell Differentiation, Keio University, Tokyo, Japan.

Angiogenesis has been considered to play an important role in the bone formation. However, relationship between angiogenesis and bone formation is poorly understood. Angiopoietin1 (Angpt1) is an essential molecule of angiogenesis, is expressed in osteoblasts. To understand the effect of Angpt1 on bone formation in vivo, we generated a transgenic mouse overexpressing Angpt1 in osteoblasts under the control of mouse 2.3kb alpha 1 collagen promoter. 51 lines of offspring were generated by the embryo microinjection. The presence of the transgene in the offsprings was tested by PCR of tail DNA using transgene specific primers. 16 transgenic founder lines were established by mating founders with C57/BL6 wild type mice. Angpt1 expression was confirmed by RT-PCR with mRNA extracted from long bones, and Western blotting with protein extracted from calvaria. CD31-positive endothelial cells were increased in tibial trabecular area of 6-weeks-old Angpt1 transgenic mice compared with wild-type controls. Microcomputed tomography analysis showed that bone mineral density and bone volume/total volume were significantly increased, while trabecular spacing was significantly decreased in 8-weeks-old Angpt1 transgenic mice compared with wild-type controls. Immunohistochemistry using alkaline phosphatase (ALP) antibody showed increase of ALP activity in femoral trabecular area of 8-weeks-old Angpt1 transgenic mice compared with wild-type controls. Furthermore, tartrate resistant acid phosphatase (TRAP) staining showed TRAP activity of 8-weeks-old transgenic mice femoral trabecular area is higher than wild-type controls. Overall, these data showed that Angpt1 overexpression in osteoblasts induced angiogenesis of the trabecular area, which results in increased bone mass in vivo.

Disclosures: T. Suzuki, None.

S021

Marrow Adipogenesis and Osteoblastogenesis Reflect Global Energy Utilization Through Activation of PPARG and Modulation by 'Clock' Genes in a Genotype Specific Manner. C. L. Ackert-Bicknell¹, V. E. DeMambro¹, M. L. Bouxsein², M. C. Horowitz³, E. Canalis⁴, C. J. Rosen¹. The Jackson Laboratory, Bar Harbor, ME, USA, ²Beth Israel Deaconess Medical Center, Boston, ME, USA, ³Yale University School of Medicine, New Haven, CT, USA, ⁴St. Francis Hospital and Medical Center, Hartford, CT, USA.

The relationship between marrow adipogenesis and bone formation is critical for understanding osteoporosis. We generated a congenic mouse (6T) with C3H alleles from a QTL on mouse Chr 6 introgressed on a 99.5% C57BL/6J(B6) background. 6T have reduced BMD, impaired osteoblast(OB) differentiation, more marrow adiposity, but low body temp, and unresponsiveness (i.e. thermal output) to stimulation by a $\beta 3$ agonist. An inversion in C3H, and polymorphisms in genes at the break point [115.38-116.38 Mb between Pparg and Alox5], prompted us to hypothesize that genes in this region influence OB and adipocyte(Ad) function. To test this, we fed 3 wk B6 and 6T mice an 11%(LF) or 60% fat(HF) diet for 13 wks and studied metabolic and skeletal parameters. On a HF diet, B6 gained wt and became insulin resistant with no change in BV/TV by μ CT, while 6T showed no change in wt or insulin secretion, but lost trabecular bone ($p<0.001$ vs B6). Histomorphometry comparing HF to LF diets revealed that B6 had suppressed bone formation, reduced osteoclast #, increased marrow Ads (2.1 fold higher), but no change in BV/TV. In contrast 6T on HF had a 1.5 fold increase in OB#, but no change in Ad #, despite a 30% reduction in BV/TV. Expression profiling (using a 2x2 statistical design:genotype x diet)revealed that 21 genes were differentially regulated in liver; and 64 in bone (marrow+bone). Most were histones, but in 6T liver on HF, Ccrn4l (a 'clock' gene) was 2 fold up-regulated; $p=1.0 \times 10^{-6}$, while in 6T bone, uncoupling protein-1(Ucp-1) was increased nearly 3 fold $p=1.0 \times 10^{-6}$. 2 candidate genes within the 1Mb region on Chr 6 were suppressed in 6T bone on the HF diet: March 8, a membrane protein ($p<0.0005$, vs B6) and Raf1 ($p<0.007$ vs B6). In the liver, two downstream targets of Pparg, Fasn, and Srebp, as well as ephrinA1 and SOCS-2, were increased by a HF diet in 6T ($p<0.05$ vs B6). In summary, we found genotype-specific skeletal and marrow responses to HF. In 6T, HF caused bone loss despite recruitment of more OBs, but in B6, even with marrow adipogenesis, and a reduced bone formation rate, BV/TV was preserved. Expression profiles demonstrated that a HF diet activated Pparg in a strain-specific manner, likely through recruitment of co-activators that differentially influenced Ad and OB function. In 6T, greater UCP-1 expression (a marker of brown fat), and enhanced insulin sensitivity imply distinct physiologic roles for marrow fat (i.e. energy use:6T vs storage: B6) influenced by Chr 6 genes and modulated by 'clock' proteins.

Disclosures: C.L. Ackert-Bicknell, None.

This study received funding from: NIAMS 45433

S023

Osterix Mediates Mesenchymal Progenitor Cell Differentiation into Osteoblasts Downstream of PTH During Bone Repair. L. A. Kaback*, Y. Jiang*, A. Naik*, C. Hock*, E. M. Schwarz, S. Bukata, R. J. O'Keefe, H. Drissi. Orthopaedics, University of Rochester, Rochester, NY, USA.

We investigated the mechanisms underlying the effects of PTH on bone repair. We hypothesize that PTH accelerates fracture healing through induction of the zinc finger transcription factor Osterix (Osx), thereby inducing mesenchymal stem cell (MSC) commitment towards osteogenesis. Our real time RT-PCR data show that Osx transcripts are up-regulated upon intermittent PTH treatment of osteoblast progenitors 24, 36 and 72 hours in culture compared to untreated controls, concomitant with that of osteoblast phenotypic genes. Continuous PTH treatment strongly inhibits Osx mRNA levels and osteoblast markers at all time points. Daily injections of mice with the anabolic PTH drug, Forteo, or saline for up to 14 days was performed. Bone marrow derived MSCs cultured from Forteo treated and control mice revealed accelerated osteoblast maturation with increased alkaline phosphatase and Von Kossa staining. Analyses of RNA extracted from these MSCs shows that Osx expression in marrow cultures from Forteo treated mice was dramatically up-regulated compared to control samples. Furthermore, Runx2 levels were also up-regulated in the Forteo treated samples along with markers of osteoblast differentiation. Together, these results indicate that in vivo treatment with Forteo mimics the anabolic effects of PTH observed in vitro. The cellular distribution of Osx during fracture repair was determined immunohistochemically in response to Forteo. Our results show that after 7 days of Forteo exposure, Osx protein is maintained in the periosteal cells and confined in the immature chondrocytes while absent from the hypertrophic chondrocytes in the fracture callus. By 10 to 14 days post-fracture, Osx persists in mesenchymal progenitor cells as well as in the immature chondrocytes, and in osteoblasts embedded in the newly formed bone in the control calluses. However, this representation of Osx is intensified in the Forteo treated animals. We harvested RNA from fracture callus of mice treated or not with Forteo. Our real time RT-PCR data show a progressive induction of Osx transcripts which becomes maximal after 10 days of treatment, but is down-regulated 14 and 21 days post-fracture. Additionally, while Runx2 regulation parallels that of Osx in these calluses, type I collagen and osteocalcin continue to be up-regulated 14 days post-fracture. Together, our results suggest that PTH may accelerate fracture repair through MSC differentiation into mature osteoblasts in response to Osx enhanced expression. Signaling and transcriptional mechanisms behind this PTH mediated regulation of Osx is currently under investigation.

Disclosures: H. Drissi, None.

S025

Analysis of Krox20 Gene Regulation Reveals Srf Function in Bone and Cooperation with NFAT1. M. Frain^{*1}, A. Nordheim^{*2}, P. Charnay^{*1}. ¹Ecole Normale Supérieure, Inserm U 784, Paris, France, ²Department of Molecular Biology, Tuebingen University, Institute of Cell Biology, Tuebingen, Germany.

The Krox20 gene encodes a zinc finger transcription factor that plays a key role in regulating bone formation. We have shown that Krox20 is expressed in a subpopulation of growth plate hypertrophic chondrocytes and in differentiating osteoblasts and that Krox20 conditional knockout mice develop severe osteopenia.

To investigate the mechanisms of Krox20 transcriptional regulation in bone, we have used a transgenic mice approach and identified a bone-specific enhancer in the 5' flanking region of the mouse Krox20 gene which spans 860 bp and recapitulates Krox20 expression during bone development. Combining phylogenetic footprinting analyses and in vitro and in vivo experiments, we have defined three types of regulatory elements within the enhancer: Krox20 binding sites involved in a direct positive autoregulatory loop, Runx2 binding sites modulating Krox20 expression and a 13 bp A/T rich essential for Krox20 activation in both osteogenic and chondrogenic cells. This key regulatory element is conserved among vertebrates and contains partially overlapping canonical binding sites for two transcription factors: Srf (Serum Response Factor) and NFAT (Nuclear Factor of Activated T-cells) known to control several developmental processes. Gel-shift, transfection experiments and mutational analyses have shown that Srf and NFAT1/c2 are both required for initiation of Krox20 expression in the two bone-forming cells. Our data are consistent with recent studies showing that NFAT1 controls endochondral bone formation (Koga et al, Nat Med 8, 880-5, 2005). We have pursued our studies by establishing Srf spatio-temporal expression pattern in the developing bone. We have found that Srf is expressed in hypertrophic chondrocytes and in differentiating osteoblasts and precedes Krox20 activation in these cell types. To genetically establish that Srf lies upstream of Krox20 in the regulatory cascade, we have created a Srf conditional mutant inactivating Srf in hypertrophic chondrocytes and differentiating osteoblasts. We have found that the Srf conditional mutant shows a reduced level of Krox20 expression in the developing bone.

Altogether, our studies demonstrate that Srf and NFAT1 constitute upstream regulators of Krox20 in bone and highlight a novel role for Srf in regulating skeletogenesis.

Disclosures: M. Frain, None.

S027

Role of Dlx3 in Bone: Study of Inducible Cre Mediated Dlx3 Inactivation in Mice. M. Islam^{*1}, X. Jiang^{*1}, H. Li^{*1}, M. S. Kronenberg^{*1}, D. J. Adams^{*1}, M. M. Morasso^{*2}, A. C. Lichtler¹. ¹University of Connecticut Health Center, Farmington, CT, USA, ²NIAMS, National Institute of Health, Bethesda, MD, USA.

Dlx3 is a member of Dlx family of transcription factors. Trichodonto osseous dysplasia, a human genetic anomaly, is caused by mutation of Dlx3 gene. This condition has distinct bone findings, which suggests that Dlx3 has a role in bone formation and metabolism. Studies in our lab also show that Dlx3 is highly expressed in mature osteoblast and osteocytes. Universal knock out of the gene causes embryonic lethality, so we have created a bone specific Dlx3 null mice using cre-LoxP recombination. We have used a transgenic mouse model in which a 3.6 kb type I collagen promoter drives constitutive or tamoxifen inducible (CreERT2) cre. In the constitutive model, cre is active in multiple tissues including bone, skin and tendon, and sometime in early embryonic development. Because of this lack of specificity, we focused on inducible cre mediated floxed Dlx3 knockout mouse model. Here the cre transgene is fused to a mutated estrogen receptor gene. Although cre activity in this model should require tamoxifen; we found that inducible cre transgenic mice show strong bone specific cre activity without tamoxifen in vivo and in calvarial osteoblast (mCOB) and bone marrow stromal cell (BMSC) cultures. Dlx3 mutant mice show distinct trabecular and cortical bone changes. In a microCT study of femur, there was a trend of increase bone volume fraction (BV/TV) and trabecular number while trabecular spacing and thickness was decreased in the mutant mice compared to age matched controls. Femoral cortical bone in microCT showed a trend of age related increase in cortical porosity in the mutant mice starting at 3 weeks of age. In histological bone sections it appeared that there were more osteocytes in the femoral cortical bone. Dynamic histomorphometry did not show a difference in mineral apposition rate (MAR), but did show a significant decrease of mineralized surface in the trabecular compartment of mutant mice. Expression of bone marker genes is currently being studied. We believe that Dlx3 plays a role towards the end stages osteoblast differentiation pathway, hence downstream to Runx2 and osterix transcription factors.

Disclosures: M. Islam, None.

This study received funding from: National Institute of Health.

S029

OASIS, an Endoplasmic Reticulum Stress Transducer, Is Involved in Normal Bone Formation. T. Murakami¹, S. Kanemoto^{*1}, S. Kondo^{*1}, A. Wanaka^{*2}, K. Imaizumi^{*1}. ¹Division of Molecular and Cellular Biology, Department of Anatomy, Faculty of Medicine, University of Miyazaki, Miyazaki, Japan, ²Department of Anatomy and Neuroscience, Nara Medical University, Nara, Japan.

OASIS (Old Astrocyte Specifically Induced Substance) is a basic leucine zipper (bZIP) transcription factor of the CREB/ATF family with a transmembrane domain that allows it to associate with the ER. In our previous report, we identified OASIS as a novel endoplasmic reticulum (ER) stress transducer in astrocytes. The molecule is cleaved at the membrane in response to ER stress, and its cleaved amino-terminal cytoplasmic domain, which contains the bZIP domain, translocates into the nucleus where it activates the transcription of target genes such as GRP78/BiP. To assess the role of OASIS in vivo, we generated OASIS knockout mice. OASIS^{-/-} mice were viable, but exhibited growth retardation. In macroscopic observation on OASIS^{-/-} mice, they exhibited deformity of limb bones and swellings in joint. Analysis of in situ hybridization showed that OASIS mRNA was detected not only in astrocytes but also in bones. From the results of histopathological examination of osseous tissues, OASIS deficiency resulted in abnormal bone formation with significant loss of bone mass. Electron microscopic analysis indicated the expansion of rough ER and accumulation of a large amount of secreted materials in the ER lumen in OASIS^{-/-} osteoblast. In contrast, none of the structural changes were observed in osteocytes, osteoclasts and chondrocytes. These results suggested that abnormality of bone formation in OASIS^{-/-} mice was caused by disturbance of production or secretion of bone matrix in osteoblasts. Next, we examined expression, production and secretion of bone matrix in primary osteoblast. OASIS proteins were highly expressed in primary osteoblasts. Secretion rate of osteopontin was decreased in ^{-/-} osteoblasts compared with WT, while that of osteocalcin was increased. These results showed that OASIS^{-/-} osteoblasts were disturbed production and secretion of bone matrix. Taken together, these findings indicate that OASIS is required for normal bone formation and its deficiency causes osteogenesis imperfecta.

Disclosures: T. Murakami, None.

S031

Identification of a Novel Wnt/ β -Catenin Response Element in the Osteoprotegerin Gene Promoter and its Regulation with Bone Morphogenetic Protein-2 Signaling. M. Sato^{*1}, A. Nakashima^{*1}, M. Nashimoto^{*2}, A. Ishisaki^{*1}, Y. Yawaka^{*3}, M. Tamura¹. ¹Biochemistry and Molecular Biology, Grad. Sch. Dent. Med., Hokkaido University, Sapporo, Japan, ²Department of Applied Life Sciences, NUPALS, Niigata, Japan, ³Dentistry for Children and Disabled Person, Grad. Sch. Dent. Med., Hokkaido University, Sapporo, Japan.

Wnt/ β -catenin signaling plays a role in the developing skeletal system. However, the exact mechanisms by which Wnt/ β -catenin signaling regulates bone remodeling remain to be elucidated. Our previous studies demonstrated that an interaction between β -catenin and Smad was crucial for Wnt-mediated regulation of the BMP-2 responsive gene expression, and that BMP-2 up-regulated Wnt-induced lymphoid enhancing factor 1/T cell factor (Lef1/Tcf)-dependent TopFlash transcriptional activity in the C2C12 cell line. Also, Wnt/ β -catenin signaling regulates expression of osteoprotegerin (OPG) and receptor activator of NF κ B ligand (RANKL) in osteoblasts. In this study, we investigated the mechanism of how OPG expression is induced by Wnt/ β -catenin signaling in osteoblasts. OPG expression was induced by over-expression of Wnt3a or activated β -catenin in mesenchymal pluripotent C2C12 cells or osteoblastic MC3T3-E1 cells. In these cultures, BMP-2 synergistically enhanced OPG expression. Silencing of glycogen synthase kinase-3 β by siRNA or sgRNA (tRNAseZL-utilizing gene silencing method) also increased OPG levels in the culture supernatant from C2C12 cells estimated by ELISA assay. To investigate the mechanisms of the Wnt/ β -catenin signaling activated OPG gene transcription, we have cloned an approximately 1.5-kilobase pair genomic DNA fragment corresponding to the 5'-flanking promoter region of the murine OPG gene. Activated β -catenin results in a 10-15 fold increase in reporter gene transcription activity of the 1.5-kilobase fragment by transient transfection assay performed in C2C12 cells. Deletion analyses revealed that a proximal 253-base pair region in the promoter was required for Wnt/ β -catenin responsiveness. In this region, we identified four putative Lef1/Tcf binding sites, which meet with a consensus sequence reported to be recognized by Lef1/Tcf proteins. Using site-directed mutation analyses, functional Lef1/Tcf binding site was identified in these regions. Smad protein was involved and interacted with the Wnt/ β -catenin responsive element on the OPG promoter in response to BMP-2 stimulation. A chromatin IP assay indicated that β -catenin regulates transcription of OPG via a promoter region at their site. These results show that OPG is a target gene for Wnt/ β -catenin signaling and that its induction is mediated by a novel Wnt/ β -catenin response element of the OPG gene promoter.

Disclosures: M. Sato, None.

S033

Expression of a Hypomorphic Allele of FIAT (Factor Inhibiting ATF4-mediated Transcription) Improves Long Bone Mechanical Properties. V. W. C. Yu^{*}, R. St-Arnaud. Genetics Unit, Shriners Hospital for Children, Montreal, PQ, Canada.

We have recently cloned and characterized FIAT, a 66 kDa leucine zipper protein that dimerizes with the basic domain-leucine zipper transcription factor ATF4 to form inactive dimers that cannot bind DNA. Overexpression of FIAT in osteoblasts of transgenic mice inhibited osteocalcin gene transcription and reduced osteoblastic activity, leading to osteopenia (J Cell Biol 169: 591; 2005). Reciprocally, inhibition of FIAT expression in osteoblasts, using siRNA technology, results in a higher transcriptional activity from the osteocalcin promoter, augmented collagen type I secretion, and enhanced mineralization. Together, these results support the role of FIAT in regulating ATF4 activity in osteoblasts and confirm the importance of FIAT in the modulation of osteoblast activity. To further assess the physiological role of FIAT, we have used the technique of homologous recombination in ES cells to engineer an allele of FIAT in which the first exon, containing the translational start site, was flanked by lox P sites. Mice carrying the floxed FIAT allele were crossed to transgenic mice expressing the Cre recombinase under the control of the collagen type I promoter (Col I-Cre) for osteoblast-specific inactivation. Since the FIAT gene maps to the X chromosome, initial characterization of the mutant phenotype was performed in Col I-Cre;FIAT^{Y/f} male mice. Mutant mice showed only 20% reduction of FIAT expression as measured by RT-qPCR, suggesting that we have engineered a hypomorphic allele and not a true null. The reduction in FIAT expression was statistically significant, however. Despite this moderate reduction in FIAT mRNA levels, the mutant mice showed significantly increased osteocalcin gene transcription and a trend towards increased bone volume. When the biomechanical properties of the mutant bones were tested using three-point bending, we measured significant increases in ultimate force and work to failure. These results show that even a small reduction in FIAT expression significantly improves long bone mechanical properties and suggest that FIAT represents an interesting target for therapeutic intervention to increase bone strength in osteoporotic patients.

Disclosures: R. St-Arnaud, None.

This study received funding from: NIH-NIAMS.

S036

Mechanical Loading Induced Wnt/ β -catenin Signaling Is Compromised in ER α -/- Mouse Tibia- In Vivo Microarray Analysis. G. Zaman^{*}, L. K. Saxon, M. Muzylak^{*}, J. S. Price, L. E. Lanyon. Basic Sciences, The Royal Veterinary College, London, United Kingdom.

Postmenopausal osteoporosis represents a failure of bone cells to adapt bone mass and architecture to withstand loading without fracture. A number of studies have shown that the adaptive response of bone to mechanical loading is deficient in the absence of estrogen receptor associated with estrogen deficiency. Wnt/ β -catenin signalling is one of the pathways shown to regulate bone formation during growth and in response to mechanical load.

In order to identify the genes and signal pathways responsible for the loading-related osteogenic response, we used the RNG-MRC 25k mouse microarray analysis to compare differential gene expression in the right and left (loaded, 12N at 2Hz for 60 cycles and not loaded) tibiae of WT and ER α -/- mice after a single period of dynamic axial loading. This transient exposure to dynamic strain change has been shown to produce an osteogenic response in mice.

RNA was extracted at 3, 8, 12 and 24 hours after loading from control and loaded tibiae. In WT mice there were 663, 539, 173 and 33 differentially regulated genes at 3, 8, 12 and 24 hours respectively after loading. Lists of differentially regulated genes were loaded into Ingenuity Pathways Analysis software. Canonical pathway analysis of the sets of genes differentially regulated showed that a number of catabolic and anabolic pathways were affected. Six genes previously reported to be involved in the Wnt/ β -catenin pathway (WNT2B, FZD2, GNAQ, PPP2R3A, CREBBP, RAR γ) were differentially expressed in loaded versus control bones 3 hours after treatment (expression of 10 genes changing over a period of 24 hours). This differential expression was less evident at 8 and 12 hours after loading and returned to the levels observed in the contra-lateral control limb 24 hours after treatment.

In ER α -/- mice the number of differentially regulated genes was much lower at each time point after loading (17, 122 and 8 genes at 3, 8 and 24 hours respectively). Only one Wnt/ β -catenin related gene (RAR γ) in ER α -/- mice showed a change in its expression between loaded and control bones at 3 hours and none at 24 hours. The gene expression profile in response to mechanical loading in WT mice confirms the regulation of a number of genes involved in Wnt/ β -catenin signalling. The reduction in the number of Wnt/ β -catenin-related genes differentially regulated by loading in the absence of ER α suggests a role for ER α in early loading-related activation of the Wnt/ β -catenin signalling in bone cells. Diminished effectiveness of loading-related Wnt/ β -catenin activity due to reduced ER α activity, as would occur with estrogen deficiency, may contribute to less effective control of structurally appropriate bone mass in osteoporosis in both men and women.

Disclosures: G. Zaman, None.

This study received funding from: The Wellcome Trust.

S039

Prostaglandin E₂ (PGE₂) Increases a Specific Subset of Primitive Hematopoietic Cells In Vivo. B. J. Frisch*, B. J. Gigliotti*, J. M. Weber*, R. J. O'Keefe, C. T. Jordan*, L. M. Calvi. University of Rochester School of Medicine, Rochester, NY, USA.

Parathyroid Hormone (PTH) stimulates osteoblastic cells (OBs) in the bone marrow (BM) microenvironment, expanding hematopoietic stem cells (HSCs) through activation of the Notch receptor. Similarly, we previously demonstrated that PGE₂ increases the Notch ligand Jagged1 in OBs, and does so through Protein Kinase A (PKA) activation. Therefore, we hypothesized that PGE₂ could also expand HSC in vivo. To test whether PGE₂ regulates HSC, we treated mice with intermittent intraperitoneal PGE₂ or vehicle. Several schedules were tested to maximize the PGE₂ effect on the HSC-enriched lineage-Sca-1+ c-kit+ (LSK) cells in BM. At the end of each treatment, peripheral blood (PB) was analyzed and mice were euthanized (n=8 mice per treatment group). BM was harvested from one of the hindlimbs, while the contralateral limb was fixed for microCT and histologic analysis. Flow cytometric analysis demonstrated a time and dose dependent increase in BM LSK, which was maximal at day 16 with bid PGE₂ vs vehicle (0.11 vs 0.04% BM mononuclear cells, P=0.0061). At this dose, there was no significant PGE₂-dependent bone anabolic effect either histologically or by micro-CT. Maximal LSK expansion was superior to PTH-dependent HSC stimulation (approximately 350 vs 100% increase in LSK). When the more mature hematopoietic progenitor population was quantified using the CFU-C assay in vitro, there was no difference between PGE₂- and vehicle-treated animals. Similarly, there were no significant PGE₂ effects on Hct, Plts or WBC counts compared to vehicle. Therefore PGE₂-dependent cell expansion was not global across differentiated subsets, but was restricted to primitive hematopoietic cells, similar to the effects of PTH in vivo. Competitive transplantation of irradiated recipients was then performed to assess the engraftment, proliferation, and self-renewal properties which define HSC. Cells derived from PGE₂-treated mice demonstrated superior contribution to all hematopoietic lineages at 3 weeks after transplantation (33.3 vs 23.5% PB mononuclear cells, P=0.0045), but this increase was not persistent at 12 weeks. This surprising result suggests that PGE₂ selectively expands a subpopulation of HSC, the short-term HSCs (or ST-HSCs), which have highly proliferative properties, but limited self-renewal. Further studies will determine if this effect is mediated by osteoblastic Jagged1 or by other niche components. This finding implicates for the first time the existence of specialized niches regulating subsets of HSC. These novel data therefore increase our understanding of the HSC niche, which could be exploited clinically for specifically targeted ST-HSC expansion.

Disclosures: B.J. Frisch, None.

This study received funding from: NIDDK, Pew Foundation, Wilmot Cancer Research Fellowship.

S041

Cell Cooperation Between Human OsteoProgenitor Cells and Endothelial Cells in Tissue Engineering. M. Grellier*, C. Bourget*, R. Bareille*, P. L. Granja*, M. A. Barbosa*, J. Amédée*. INSERM U577 - University V. Segalen Bordeaux 2, Bordeaux, France, ²INEB - Instituto de Engenharia Biomédica - University of Porto, Porto, Portugal.

Bone is a dynamic tissue that constantly undergoes remodelling which requires interactions between bone cells. However, the intimate association of the vascular endothelium with osteogenic cells appears necessary to modulate bone formation and degradation balance. The purpose of this work is to study the cell communication between osteoblast and endothelial cells before to apply this strategy for bone tissue engineering. To investigate that, Human OsteoProgenitor (HOP) and Human Umbilical Vein Endothelial Cells (HUVEC) were co-cultured in direct contact and compared to isolated cultures. We analysed the regulation of cell communication, studying the expression of Connexin 43 and VE-cadherin, by Quantitative-PCR and the localization of beta-catenin, by immunostaining. We investigated genes involved in extracellular matrix organisation (ECM) such as MMP-1, TIMP-1, VEGF and TGFbeta-1. We followed cell migration by time lapse. We used an extrusion system to encapsulate cells inside beads of alginate. After 24 hours of co-culture, HOP and HUVEC form specific multicellular networks which suggest an ECM reorganisation and cell migration. The expression of Connexin 43 is up-regulated while VE-cadherin expression is down regulated in co-culture compared to HUVEC culture. We observed a modification of the beta-catenin distribution when cells are in direct contact: beta-catenin is cytoplasmic in HOP culture and localised to the membrane after 6 hours of co-culture while its expression, analysed by western blot, was unchanged. MMP1 and TIMP1 results suggest that the co-culture could enhance a production of an ECM and both VEGF and TGFbeta-1 are upregulated in co-culture. We observed by time lapse that HUVEC are able to migrate through HOP filopodes. These results suggest that ECM remodelling occurred when endothelial and osteoblastic cells are in direct contact. This mechanism could be due either to a regulation of cell communication between HOP and HUVEC or/and to a production of growth factors involved in cell migration and ECM remodelling. A better knowledge of this cell to cell cross-talk will be helpful for the development of a vascularised bone tissue for tissue engineering. Preliminary data obtained using alginate microspheres revealed that these cells entrapped inside such beads are still able to proliferate after one week of culture and their implantation into a critical size bone defect allows us to evaluate this newly bone regeneration strategy.

Disclosures: M. Grellier, None.

S043

Progressive Ankylosis Gene (ank) Regulates Osteoblast Differentiation. T. Kirsch¹, H. Kim¹, J. A. Winkles². ¹Orthopaedics, University of Maryland School of Medicine, Baltimore, MD, USA, ²Surgery, University of Maryland School of Medicine, Baltimore, MD, USA.

The progressive ankylosis gene (ank) is a transmembrane protein that transports intracellular pyrophosphate (PP_i) to the extracellular milieu. Human mutations of ank lead to craniometaphyseal dysplasia (CMD), a disease, which is characterized by the overgrowth of craniofacial and long bones, suggesting that Ank plays a role in the regulation of osteoblast differentiation. To determine the role of Ank in osteoblast differentiation, we suppressed Ank expression in osteoblastic MC3T3 cells using siRNA or studied the osteoblastic differentiation of bone marrow stromal cells isolated from the bone marrow of ank/ank mice, which express a truncated, non-functional Ank protein, or wild type littermates. MC3T3 cells mineralized within 20 days after the addition of vitamin C and β-glycerolphosphate. Ank gene and protein expression in these cells was the highest at 3 days and declined afterwards, whereas alkaline phosphatase (APase) expression and activity increased on day 8 and was the highest between day 17 and day 20. Suppression of Ank expression in MC3T3 cells using siRNA led to a decrease of APase expression and activity. Suppression of Ank expression in these cells also resulted in a decrease of the expression of bone-related genes, including type I collagen, bone sialoprotein, and osteocalcin. In addition, the expression of the transcription factor osterix was downregulated in Ank expression suppressed MC3T3 cells, whereas runx 2 expression in these cells was upregulated. Bone marrow stromal cells isolated from bone marrow of ank/ank mice and wild type littermates were cultured in the presence of 100 μg/ml ascorbate phosphate for various days and analyzed by staining for APase enzyme activity and van Kossa to determine mineralized colonies. The number of APase activity positive and van Kossa stained colonies was markedly reduced in bone marrow stromal cell cultures from ank/ank mice compared to the number of APase activity and van Kossa positive colonies in bone marrow stromal cell cultures from wild type littermates. These findings suggest that Ank is a positive regulator of differentiation events towards a mature osteoblastic phenotype and Ank appears to act upstream of osterix. Loss of Ank function in osteoblastic precursor cells results in an arrest of cells in a premature osteoblastic stage, in which they express high levels of runx2 and low levels of osterix.

Disclosures: T. Kirsch, None.

This study received funding from: National Institutes of Health.

S045

Wnt5A Signals Through Ror2 to Promote Osteoblastogenesis. Y. Liu, B. Rubin*, P. V. N. Bodine, J. Billiard. Women's Health and Musculoskeletal Biology, Wyeth Research, Collegeville, PA, USA.

Wnts are a large family of growth factors that regulate important cellular events by signaling through both canonical/beta-catenin pathway and non-canonical pathways. While activation of canonical Wnt signaling has been implicated in osteoblast physiology, very little is known about the role of non-canonical pathways in osteoblasts. Ror2 is an orphan receptor tyrosine kinase that induces osteogenic commitment and differentiation of pluripotent mesenchymal stem cells (MSCs). We and others have shown that both canonical and non-canonical Wnts bind Ror2, but their ability to activate Ror2 signaling has not been examined. Here we tested if canonical or non-canonical Wnts induce downstream signaling of the Ror2 receptor and lead to increased osteogenesis. We used purified recombinant non-canonical Wnt5A and canonical Wnt3A that bound Ror2 equally well in pull-down assays. We found that Wnt5A, but not Wnt3A, induced homo-dimerization of Ror2 and stimulated tyrosine phosphorylation of the Ror2 substrate 14-3-3β scaffold protein. Treatment of pluripotent human MSCs with Wnt5A dose-dependently induced formation of the mineralized extracellular matrix, which is the ultimate phenotype of an osteogenic tissue. Down-regulation of Ror2 expression by short hairpin RNA greatly inhibited Wnt5A-induced mineralization, indicating that Wnt5A effect is mediated at least in part through activation of the Ror2 receptor. Finally, using mouse calvarial ex vivo organ culture model, we demonstrated that treatment with Wnt5A results in significantly increased bone formation in this complex system.

In summary, we identify Wnt5A as the ligand that activates the Ror2 receptor tyrosine kinase signaling pathway and promotes osteogenic commitment and differentiation of pluripotent stem cells.

Disclosures: Y. Liu, Wyeth 3.

This study received funding from: Wyeth.

S047

Growth Inhibition of Osteoblast Progenitors by Runx2 Depends on Its C-Terminal Regulatory Domain and Is Accompanied by Changes in G-Protein Coupled Signaling Pathways. N. Teplyuk, M. Galindo*, V. Teplyuk*, D. W. Young*, D. Lapointe*, M. van der Deen*, J. Pratap, S. K. Zaidi*, A. Javed, J. L. Stein*, J. B. Lian, G. S. Stein, A. J. van Wijnen. Department of Cell Biology and Cancer Center, University of Massachusetts Medical School, Worcester, MA, USA.

The runt-related transcription factor Runx2 mediates osteogenic cell fate determination, as well as stimulates anabolic activities and inhibits the proliferative potential of osteoblasts. The levels of Runx2 change during the cell division cycle, and preferential expression of Runx2 in G1 may control the responsiveness of osteoblasts to extracellular signals that influence commitment to enter a new proliferative cycle. Runx2 elicits biological responses in osteoblasts by acting as the end-point effector of multiple signaling axes, including the Src/Yes-Yap, TGF β /BMP-Smad and CDK-cyclin pathways, which each converge at nuclear matrix-associated transcriptional sites. Here we addressed what functions of Runx2 protein are required for cell growth suppression, and what genes are regulated by Runx2 to control osteoblast growth. We first examined the biological phenotypes of osteoblastic progenitors upon introduction of Runx2 proteins with mutations that affect interactions with co-factors that transduce cell signals and/or control transcriptional activation or repression. These Runx2 point mutants were introduced into Runx2 null mouse calvarial cells using adenoviral vectors that permit efficient transient expression of Runx2 proteins. Wild type Runx2 or point mutants that can not interact with Yap or Smad or the nuclear matrix each inhibit growth of Runx2 null cells. Thus, several key signaling pathways are dispensable for growth suppression by Runx2. A point mutation in the runt-homology DNA binding domain establishes that cell growth control requires direct regulation of putative Runx2 target genes. Deletion of the C-terminal VWRPY repressor domain reduces but does not abolish growth suppressive potential indicating that both gene activation and repression contribute to the anti-proliferative effect of Runx2. Affymetrix gene expression profiling shows that the C-terminus of Runx2 is required for the induction of its classical targets (e.g., osteocalcin, osteopontin, MMP13), but also a number of genes involved in cell cycle related pathways, including multiple components of G-protein coupled receptor signaling. Because defects in Gs-signaling have been linked to fibrous dysplasia (FD), our data suggest that Runx2 may contribute to the hyper-proliferation of mesenchymal cells characteristic of FD.

Disclosures: A.J. van Wijnen, None.

S049

Regulation of Osteoblast Differentiation by MicroRNA. H. Inose¹, S. Takeda², A. Kimura^{*2}, S. Sato^{*1}, K. Shinomiya^{*1}. ¹Department of Orthopaedics, Tokyo Medical and Dental University, Tokyo, Japan, ²TICOE, Tokyo Medical and Dental University, Tokyo, Japan.

MicroRNAs (miRNA) regulate the expression of genes by binding and modulating the translation of specific mRNAs. They have been shown to be critical in the development of organisms and cell proliferation. However, their role in osteoblast differentiation remains to be elucidated. In this study, we aimed to identify miRNAs expressed in osteoblasts and investigate their role in osteoblast differentiation. C2C12 cells were induced to differentiate into osteoblasts by BMP2 treatment. Using miRNA microarray, we performed comprehensive analysis of miRNAs. Most of the known miRNAs were expressed in C2C12 cells. Among these, we focused on several miRNAs whose expression was reduced during the course of osteoblast differentiation as potential negative regulators for osteoblast differentiation. We confirmed that they were also expressed in primary osteoblasts and their expression was downregulated along differentiation. To address their physiological role, we manipulated their expression in osteoblasts and examined the effect. Indeed, forced expression of those miRNAs in primary osteoblasts significantly repressed osteoblast differentiation as demonstrated by reduced alkaline phosphatase activity and expression of osteoblastic genes. Conversely, inhibition of the activity of those miRNAs by antisense miRNA oligonucleotide promoted osteoblast differentiation. We further examined their potential target using in silico approach and verified that those candidates are, bona fide, target genes of the miRNAs by in vitro experiments. Taken together, our results suggest that miRNA is a physiological regulator of osteoblast differentiation and manipulating their activity would lead to a development of a novel therapy for increasing bone formation.

Disclosures: H. Inose, None.

S052

Mesenchymal Stem Cells from Aging C57BL/6 Exhibit Increased Oxidative Stress and Defective Replication: Correction of Both by Provision of an Extracellular Matrix from Young Mice. X. Chen, C. M. Skinner*, E. Ambrogini*, L. Han, M. Almeida, S. C. Manolagas, R. L. Jilka. Center for Osteoporosis and Metabolic Bone Diseases, Central Arkansas Veterans Healthcare System, Univ. of Arkansas for Medical Sciences, Little Rock, AR, USA.

The supply of osteoblasts depends on the replication of mesenchymal stem cells (MSCs) and their commitment to the osteoblast lineage. It has been shown previously that a cell-free extracellular matrix (ECM) made by marrow stromal cells greatly increases the frequency of MSCs by promoting their replication and restraining their differentiation. And, it has been reported that age-related bone loss in C57BL/6 mice is associated with decreased osteoblast number and bone formation, as well as increased oxidative stress in the bone marrow. Here, we have examined whether aging and oxidative stress negatively impact the number and ex vivo replication of MSCs using femoral marrow cells from 3-month old (young) and 18-month old (old) female C57BL/6 mice. We report that the number of MSCs in marrow from old mice, measured by their ability to form a colony of osteoblastic cells (CFU-OB), was 5-10% lower as compared to young mice. Moreover, MSCs from old mice exhibited a replication defect during 6 days of culture on plastic, as measured subsequently upon re-plating and determination of CFU-OBs. Thus, whereas CFU-OB from young mice increased during this period by 1.8 fold, MSCs from old mice did not. As a result, the frequency of CFU-OB in the expanded population of cells from old mice was only 30% of that of young mice. In parallel cultures of marrow cells maintained for 6 days on an ECM made by marrow stromal cells from 2 month old mice, the number of CFU-OB from both young and old mice increased indistinguishably (14 \pm 2, and 16 \pm 2 fold, respectively). Further, the intracellular level of reactive oxygen species (ROS), quantified using dichlorodihydrofluorescein diacetate, was 20% higher in cultures from old mice, as compared to young, when the cultures were performed on plastic. Fascinatingly, ROS levels in cultures from young and old mice were reduced by 30% and 50%, respectively, when cells were maintained on the ECM. Consistent with these ex vivo results, oxidative stress induced by administration of buthionine sulfoxide to 6-month old C57BL/6 mice for 4 weeks reduced femoral CFU-OB number by 30-50%. Based on these findings, we hypothesize that the increased oxidative stress associated with old age exhausts a limited pool of MSC osteoblast progenitors, and that the old ECM itself, and/or the factors embedded in it, may contribute to the increased oxidative stress. Moreover, we suggest that culture of aging MSCs on an ECM may improve their number and quality, thereby optimizing the effectiveness of autologous MSC administration for therapeutic applications.

Disclosures: X. Chen, None.

S056

AMP-kinase Activator (AICAR) and Rho-kinase Inhibitor (hydroxyfasudil) Induce the Differentiation and Mineralization of Osteoblastic MC3T3-E1 Cells via Inhibiting the Mevalonate Pathway and Enhancing BMP-2 Expression. I. Kanazawa*, T. Yamaguchi, S. Yano, M. Yamauchi, M. Yamamoto, T. Sugimoto. Internal Medicine 1, Shimane University Faculty of Medicine, Izumo, Japan.

AMP-activated protein kinase (AMPK) and Rho kinase (ROK) have recently attracted widespread attention due to their beneficial anti-diabetic and anti-atherosclerotic effects. AMPK is known to modulate the mevalonate pathway via suppressing HMG-CoA reductase, and ROK comprises this pathway and acts in its downstream. Although the inhibition of the mevalonate pathway by statins is well known to stimulate bone formation via enhancing BMP-2 expression, the effects of AMPK activator and ROK inhibitor on bone metabolism by modulating the pathway are still unclear. We investigated the effects of pharmacological AMPK activator (5-amino-imidazole-4-carboxamide-riboside; AICAR) and ROK inhibitor (hydroxyfasudil; HF) on the differentiation and mineralization of osteoblastic MC3T3-E1 cells. AMPK activation by AICAR (0.1-0.5mM) was confirmed by Western blot. AICAR significantly stimulated ALP activity, and promoted mRNA expressions of both collagen-I and osteocalcin (OC) by real-time PCR as well as mineralization by von Kossa and Alizarin Red stainings. Moreover, AICAR significantly stimulated BMP-2 mRNA expression in dose- and time-dependent manners. Simultaneous addition of either mevalonate or geranyl-geranyl pyrophosphate (GGPP), which also comprise the mevalonate pathway and act in the downstream of HMG-CoA reductase, significantly antagonized BMP-2 and OC mRNA expressions and mineralization enhanced by AICAR. On the other hand, inhibition of ROK by HF (10-5-10-4M) also stimulated OC mRNA expression and mineralization through enhancing BMP-2 mRNA expression in dose- and time-dependent manners. In conclusion, the suppression of mevalonate pathway by AICAR and HF promoted the differentiation and mineralization of osteoblastic MC3T3-E1 cells via enhancing BMP-2 expression. Our present findings suggest that modulation of the mevalonate pathway might be useful for not only creating anti-diabetic or anti-atherosclerotic drugs but also developing new drugs promoting bone formation for the treatment of osteoporosis.

Disclosures: I. Kanazawa, None.

S058

Molecular Mechanisms of Lysophosphatidic Acid-Stimulated Osteoblastic Cell Chemotaxis. S. A. Karagiosis*, L. K. Opreko*, W. B. Chrisler*, N. J. Karin. Biological Sciences Division, Pacific Northwest National Laboratory, Richland, WA, USA.

Our focus is the understanding of molecular mechanisms of lysophosphatidic acid (LPA)-induced osteoblastic cell chemotaxis. We hypothesize that LPA exerts anabolic effects on bone mass through the stimulation of pre-osteoblast migration, and that LPA is therefore a factor that supports bone repair. Osteoblast progenitor cells must migrate to injury sites where they elaborate mineralized matrix in the compromised region. LPA is released by activated platelets at the site of injury, and we have shown that this lipid factor is a potent chemotactic agent for MC3T3-E1 pre-osteoblasts [Masiello et al. (2006) Bone 39:72-82]. LPA-stimulated MC3T3-E1 cells exhibit dramatic changes in morphology and F-actin architecture, including robust stress fiber formation. We investigated the role of phosphatidylinositol-3 kinase (PI3K), which is essential in many other cells for driving the initial cytoskeletal rearrangements and cell polarization required for cell locomotion. We found a dose-dependent reduction in LPA-induced migration upon treatment with the PI3K inhibitor, LY294002. The distribution of two actin regulatory proteins, zyxin and arp2/3, was also consistent with our hypothesis. Zyxin was enriched at the newly-formed stress fibers in LPA-treated pre-osteoblasts and to focal adhesions and filopodia tips. The arp2/3 complex immunolocalized to sites of dynamic F-actin assembly in lamellipodia and filopodia. The propagation of ERK1/2 activation is required for the coordinated-migration of cells during epithelial wound healing [Matsubayashi et al. (2004) Curr. Biol. 12:731-735]. MC3T3-E1 cell ERK1/2 exhibited two waves of phosphorylation upon LPA stimulation: a rapid transient wave and a more sustained wave. Using live cell imaging of osteoblasts expressing low levels of ERK1-GFP, we observed ERK1 nuclear translocation upon LPA addition. LPA-induced cell motility was not blocked by an inhibitor of ERK1/2 activation. Additionally, we demonstrate that LPA-induced ERK1/2 activation and migration are independent of EGF receptor transactivation in osteoblasts. We conclude that PI3K-associated cytoskeletal changes, but not ERK1/2 phosphorylation or EGF receptor transactivation, are essential for LPA-stimulated MC3T3-E1 cell migration.

Disclosures: S.A. Karagiosis, None.

This study received funding from: U.S. Department of Energy.

S060

Proliferation and Differentiation of Periosteal Osteoblast Progenitors Are Differentially Regulated by Sex Steroids and Intermittent PTH Administration. M. Ogita, E. Dworakowski*, J. P. Bilezikian, S. Kousteni. Division of Endocrinology College of Physicians & Surgeons, Department of Medicine, Columbia University Medical Center, New York, NY, USA.

The periosteum is recognized as a homeostatic and therapeutic target for actions of sex steroids and intermittent parathyroid hormone (PTH) administration. However, the mechanisms by which estrogens suppress but androgens and PTH promote periosteal expansion are not known. In this report, we show that intermittent PTH(1-34), within 16 days of treatment, upregulates the expression and activity of alkaline phosphatase (AP) in periosteal cells isolated from the surface of murine or rat long bones. Similar to PTH, dihydrotestosterone (DHT) dose-dependently stimulates AP activity. The stimulatory action of PTH or DHT on AP activity is suppressed by inhibitors of ERKs, BMP-2 and Wnt signaling. In contrast, 17 β -estradiol (E_2) has no effect by itself; but dose-dependently attenuates PTH- or BMP-2-induced stimulation of AP expression or activity. E_2 also attenuates the stimulatory effect of PTH or BMP-2 on AP, osteocalcin, as well as Smad6 and axin2 expression in primary periosteal cells. In agreement with these in vitro observations, administration of intermittent PTH (40 ng/g) or a bone protective dose of DHT (300 ng/g) to ovariectomized adult C57BL/6 mice, induces, within 1 hour, phosphorylation of Smad1/5/8 in the periosteum as assessed by western blot analysis of femoral periosteal lysates. A replacement dose of E_2 (30 ng/g) has no effect by itself but suppresses PTH-induced phosphorylation of Smads. None of the 3 hormones affect Smad phosphorylation in trabecular bone from the femurs of the same experimental animals. In contrast to its pro-differentiating effects, PTH suppresses proliferation of primary periosteal osteoblast progenitors. E_2 , not only promotes proliferation, but attenuates the anti-proliferative effect of PTH. Finally, all 3 hormones protect periosteal osteoblasts from apoptosis induced by etoposide, TNF α or dexamethasone. These observations suggest that the different effects of sex steroids and PTH on the periosteum result from opposing actions on the recruitment of early periosteal osteoblast progenitors. Intermittent PTH and androgens promote osteoblast differentiation from periosteum-derived mesenchymal progenitors by actions that require ERK, BMP and Wnt signaling. Estrogens promote the expansion of early osteoblast progenitors but inhibit their differentiation by osteogenic agents such as PTH or BMP-2. The property of estrogens to increase periosteal osteoblast precursor number, yet retain them in an undifferentiated state may reflect actions of the hormone on a cell population distinct from that affected by PTH.

Disclosures: S. Kousteni, Radius 1.

S062

P2X7 Receptors on Osteoblasts Couple to Production of Lysophosphatidic Acid: A Novel Signaling Axis Promoting Osteogenesis. N. Panupinthu¹, J. T. Rogers¹, L. Zhao², F. Possmayer², S. M. Sims¹, S. J. Dixon¹. ¹CIHR Group in Skeletal Development and Remodeling, The University of Western Ontario, London, ON, Canada, ²Obstetrics & Gynaecology, The University of Western Ontario, London, ON, Canada.

Nucleotides are released in response to mechanical stimuli and signal through P2 receptors. P2X7 receptors are ATP-gated cation channels that, under certain conditions, induce formation of large membrane pores. Targeted disruption of the gene encoding the P2X7 receptor diminishes periosteal bone formation and impairs response of the skeleton to mechanical loading. Our goal was to investigate the pathways underlying the actions of P2X7 receptors on osteogenesis. Benzoylbenzoyl-ATP (BzATP, an agonist more potent than ATP at P2X7 receptors) induced pore formation in live cells on the surface of calvariae from wild-type (WT), but not P2X7 receptor knockout (KO) mice. When rat calvarial cells were differentiated to form bone-like nodules in vitro, BzATP induced pore formation in cells associated with these nodules. These data indicate that functional P2X7 receptors are present in cells of the osteoblast lineage. BzATP, but not equivalent concentrations of UTP (P2Y agonist) or inorganic phosphate, accelerated the appearance of alkaline phosphatase activity and promoted mineralization in rat calvarial cell cultures. Moreover, expression of genes encoding osteocalcin and osteonectin was significantly enhanced in BzATP-treated cultures. Next, calvarial cells from WT and KO mice were differentiated in the absence of exogenous nucleotides. Alkaline phosphatase activity and mineralization were markedly reduced in KO compared to WT cultures, without significant difference in cell numbers. Transcript levels of osteocalcin, osteonectin and osteocalcin were also suppressed in KO compared to WT cultures. These changes were accompanied by increased levels of the adipocyte markers PPAR γ and lipoprotein lipase. Using thin layer chromatography, we found that BzATP activates production of the potent lipid mediator lysophosphatidic acid (LPA) through activation of phospholipases D and A₂. The specific LPA receptor antagonist VPC-32183 suppressed LPA-induced elevation of cytosolic free calcium in rat calvarial cells. Importantly, the same concentration of VPC-32183 abolished the stimulatory effects of BzATP on mineralization and expression of osteocalcin and osteonectin. We conclude that P2X7 receptors on osteoblasts enhance bone formation through a cell autonomous mechanism. Furthermore, a novel signaling axis links P2X7 receptors to production of LPA, which in turn stimulates osteogenesis. These findings explain the role of P2X7 receptors in skeletal development and mechanotransduction.

Disclosures: N. Panupinthu, None.

This study received funding from: The Canadian Institutes of Health Research (CIHR).

S064

Estrogen Receptor α Is Required for Strain-Related β -Catenin Signaling in Osteoblasts. V. J. Armstrong*, M. Muzylak*, A. Sunter*, G. Zaman*, L. K. Saxon, J. S. Price, L. E. Lanyon. Veterinary Basic Sciences, The Royal Veterinary College, London, United Kingdom.

Wnt/ β -catenin signaling has been implicated in the regulation of bone mass through its involvement in bone cells' response to their mechanical environment [1]. Since Estrogen Receptor α (ER α) is also involved in bones' response to loading [2], we investigated whether strain induced signaling through ER α uses the same pathway as β -catenin. Western blot and immuno-cytochemical analysis showed that in ROS 17/2.8 cells a short period of dynamic strain in vitro increased the levels of activated β -catenin (β cat) in the cytoplasm and within 1 hour stimulated its translocation to the nucleus. These changes in β cat were paralleled by inhibitory phosphorylation of GSK-3 β . Strain, and the GSK-3 β inhibitor LiCl, also induced a significant increase in TCF/LEF transcriptional activity. In contrast, estrogen had no influence on the level or distribution of β cat, nor any effect on TCF/LEF activation. Nuclear translocation of β cat and TCF/LEF activation stimulated by both strain and LiCl were inhibited by the ER modulator ICI 162,780, which also reduced strain-induced nuclear accumulation of ER α . The ER modulator Tamoxifen also inhibited LiCl stimulated nuclear translocation of β cat. In primary cultures of osteoblast-like cells derived from the long bones of Wild Type mice and those lacking ER β , β -catenin was similarly activated and translocated to the nucleus in response to strain and LiCl. In these cells this response was blocked by ICI 162,780. In contrast, in cultures of osteoblast-like cells from mice lacking ER α neither strain nor LiCl stimulated nuclear accumulation of β cat. ICI 162,780 had no effect in these cells. These data show that in osteoblastic cells exposure to strain causes similar activation of β -catenin, its translocation to the nucleus, and regulation of transcription as GSK-3 β inhibition by LiCl. These changes require ER α but not ER β . To our knowledge these are the first data to demonstrate that in osteoblasts ER α is required for these cells' responses to strain involving Wnt/ β -catenin. Reduced effectiveness of bone cells' responses to bone loading, associated with decline in bio-available estrogen and ER α , may contribute to the failure to maintain structurally appropriate bone mass in osteoporosis in both men and women. This failure may in part be due to reduced effectiveness of Wnt/ β -catenin signaling.

1. Sawakami K, et al (2006) J Biol Chem 281(33):23698

2. Lee K, et al (2003) Nature 424:389

Disclosures: V.J. Armstrong, None.

This study received funding from: BBSRC.

S068

Effects of PTH(1-34) on Primary Osteocytes. S. Banerjee^{*1}, S. Shaheen^{*1}, S. E. Harris², F. R. Bringhurst¹, P. Divieti¹. ¹Endocrine Unit, Massachusetts General Hospital, Boston, MA, USA, ²Department of Periodontic, University of Texas Health Center, San Antonio, TX, USA.

Parathyroid hormone (PTH) induces a plethora of effects on bone cells, depending on the mode and timing of administration. While continuous PTH in vivo induces catabolic effects, including rapid bone turnover, intermittent treatment increases bone mass (anabolic effect). At the cellular level, continuous treatment with PTH inhibits osteoblast differentiation while intermittent treatment promotes it. Osteocytes play a major "mechanosensory" role and PTH is known to influence the output of this mechanosensory response and to delay osteocyte apoptosis. PTH exerts its classical effects via activation of a G-protein coupled receptor, the PTH/PTHrP receptor (PPR) that recognizes and is fully activated by the first 34 amino acids of the hormone. Osteocytes also express CPTHRS, which recognize amino-truncated forms of the hormone.

In this study we compared the effects of continuous vs intermittent activation of PPRs in osteocytes in vitro. Cells were isolated enzymatically from calvariae of 4-day-old transgenic mice in which the green fluorescent protein (GFP) is driven by the 8Kb promoter of dentin matrix protein 1 (DMP1). Primary bone cells cultured for 10 days before sorting them for GFP+ (osteocytes) and GFP- (predominantly osteoblasts) populations.

We have previously shown that both PPRs and CPTHRS were expressed in GFP+ cells and that their expression was 2-3 fold higher than in GFP- cells, suggesting that both PPRs and CPTHRS might play an important role in osteocyte functions. Cyclic AMP accumulation in response to PTH(1-34) was also present in these cells. The expression of selected osteocytic marker proteins - Sclerostin (SOST), DMP1 and the membrane mucoprotein Podoplanin (E11) was analyzed following intermittent vs continuous PTH treatment in vitro. Unsorted calvarial cells were treated with 10nM PTH(1-34) for 2 hr every second day (intermittent) or continuously (refed with fresh PTH every 2 days) for 10 days before FACS analysis. Continuous PTH reduced the percentage of GFP+ cells, increased expression of SOST and reduced that of DMP1 and E11 in the GFP+ population. Intermittent PTH decreased SOST and E11 but increased DMP1. We conclude that terminal differentiation of osteoblasts is inhibited by continuous PTH exposure in vitro and that the osteocyte phenotype is sensitive to different temporal patterns of PTH exposure.

Disclosures: P. Divieti, None.

This study received funding from: NIH.

S073

Rho GTPase Signaling Pathways in Osteoclasts: Wrch1/rho Role In Cell Adhesion and Osteolysis. A. Blangy, H. Brazier^{*}, S. Ory^{*}, S. Stephens^{*}, G. Pawlak^{*}. CNRS UMR 5237 CRBM, CNRS Montpellier France

Rho GTPase signaling pathways regulate essential aspects of osteoclast biology through the regulation of actin cytoskeleton dynamics. In particular they control osteoclast adhesion by regulating podosome organization and sealing zone architecture, thereby modulating osteolysis. We established the expression pattern of all Rho GTPases and Rho GTPase activator during osteoclast differentiation, identified novel genes induced during osteoclastogenesis and confirmed their importance in osteoclast by retrovirus-mediated RNA interference (Brazier et al., 2006, JBM, 21(9) 1387-1398).

In particular we reported that the expression of Wrch1/RhoU is highly induced during osteoclastogenesis but absent in macrophages, suggesting an specific role for the GTPase in osteoclasts. Using retrovirus-mediated infection of osteoclast precursors, we now report that Wrch1/RhoU localizes to osteoclast adhesion structures: it colocalized with vinculin around isolated podosomes and the podosome belt. Furthermore, when osteoclasts were seeded on mineralized matrices, we observed Wrch1/RhoU association with the sealing zone. The distribution of Wrch1/RhoU was identical in RAW264.7 cell or mouse bone marrow derived osteoclasts. We expressed constitutively active (Q107L) and inactive (T63N) mutants of Wrch1/RhoU in osteoclasts and showed that the GTPase associates with the podosomes and the sealing zone requires in its active GTP bound form. We next examined the influence of Wrch1/RhoU on adhesion structure and sealing zone formation. Using dynamic imaging on live cells, we have shown that Wrch1/RhoU influences the distribution and amount of adhesion structures, that it modifies integrin linked signaling and affects cell migration. We will also present how the modification of Wrch1/RhoU activity by mutant expression or lentivirus-mediated gene silencing in osteoclasts affects their migration and osteolytic activity on mineralized matrix.

Our results show that Wrch1/RhoU associates with osteoclast adhesion structures and the sealing zone and affect their ability to migrate and to resorb mineralized matrix. To establish its importance in the maintenance of bone homeostasis, we are currently generating mouse strains bearing a conditional knock out of Wrch1/RhoU gene in the osteoclast lineage.

Disclosures: A. Blangy, None.

This study received funding from: ARC, CNRS, ARP.

S082

An Osteoclast Niche Is Composed of 5-FU-insensitive Osteoclast Precursors In Vivo. T. Mizoguchi^{*1}, A. Muto^{*2}, A. Hosoya^{*3}, T. Yamashita¹, Y. Kobayashi^{*1}, T. Ninomiya^{*1}, Y. Nakamichi¹, N. Udagawa⁴, M. Ito^{*1}, N. Takahashi¹. ¹Institute for Oral Science, Matsumoto Dental Univ., Shiojiri, Japan, ²Department of Periodontology, School of Dentistry, Aichi Gakuin Univ., Nagoya, Japan, ³Department of Oral Histology, Matsumoto Dental Univ., Shiojiri, Japan, ⁴Department of Biochemistry, Matsumoto Dental Univ., Shiojiri, Japan.

We have shown that cell cycle progression and subsequent cell cycle arrest in osteoclast precursors are required for their differentiation into osteoclasts. The quiescent osteoclast precursors were named "postmitotic osteoclast precursors (pOCPs)" (JBM 21 Suppl 1: F259, 2006). We also showed that osteoblasts prepare the osteoclast niche, which supports a long-term survival of pOCPs. pOCPs in the osteoclast niche differentiated into osteoclasts without cell cycle progression in response to several stimuli including RANKL administration. These findings suggest that, like hematopoietic stem cells, pOCPs should be resistance to 5-fluorouracil (5-FU), which induces apoptosis of cells having high proliferative potential. Here, we examined effects of 5-FU administration in mice on the osteoclast differentiation from pOCPs in bone. 5-FU was administered intravenously to mice for 6 days. Mice received intraperitoneal injections of 2MD (a highly potent analog of $1\alpha, 25(\text{OH})_2\text{D}_3$) for additional 2 days. To discriminate between proliferating and quiescent cells, mice were given 5'-bromo-2'-deoxyuridine (BrdU) in drinking water during the period of 2MD administration. Tibiae and serum samples were collected from mice. Bone marrow cells were recovered from tibiae and subjected to cellular analysis. Sections of tibiae were subjected to histological analysis using TRAP and BrdU staining. TRAP5b activity, a marker of osteoclastic activity, and calcium concentrations in serum were measured using the respective assay kits. (1) The number of monocytes and lymphocytes in the bone marrow was markedly decreased by 5FU administration. (2) 2MD administration scarcely affected the bone marrow cellularity, but significantly increased the number of TRAP-positive osteoclasts in tibiae even after treatment with 5FU. None of the nuclei in osteoclasts incorporated BrdU. In contrast, BrdU-positive nuclei in chondrocytes were detected in growth plates. (3) Serum TRAP5b activity was significantly increased in mice injected with 2MD even after administration of 5-FU. Serum calcium levels were also increased in response to 2MD in the 5-FU-treated mice. These results suggest that osteoclasts, induced by administration of 2MD, differentiated from 5-FU-insensitive pOCPs. Our observations support the hypothesis that quiescent pOCPs exist in the osteoclast niche.

Disclosures: T. Mizoguchi, None.

S084

The RANK Cytoplasmic Motif, IVVY⁵³⁵⁻⁵³⁸, Plays an Essential Role in TNF α - and IL-1-induced Osteoclastogenesis. J. Jules, Z. Shi^{*}, W. Liu^{*}, S. Wang^{*}, X. Feng. Pathology, University of Alabama at Birmingham, Birmingham, AL, USA.

RANKL and its cognate receptor RANK play a pivotal role in osteoclastogenesis. RANK, a member of the TNFR family, possesses three cytoplasmic motifs that recruit various TNFR-associated factors (TRAF) to transmit downstream signaling pathways to regulate osteoclastogenesis. Recently, a TRAF-independent RANK cytoplasmic motif (IVVY⁵³⁵⁻⁵³⁸) was shown to play an essential role in osteoclastogenesis by committing bone marrow macrophages (BMMs) to the osteoclast lineage. Notably, both TNF α and IL-1 utilize TRAFs to activate signaling, but they are unable to mediate osteoclastogenesis in the presence of M-CSF. However, TNF α and IL-1 can induce osteoclastogenesis from BMMs exposed to permissive levels of RANKL in the presence of M-CSF, indicating that TNF α -/IL-1-mediated osteoclastogenesis requires prior priming of BMMs by RANKL. Therefore, we hypothesize that it is the RANK motif IVVY⁵³⁵⁻⁵³⁸ that plays a role in priming BMMs in TNF α -/IL-1-mediated osteoclastogenesis. To address the issue, we used a previously established chimeric receptor approach. The receptor comprises human Fas external domain linked to the transmembrane and cytoplasmic domains of mouse RANK. When the chimera was expressed in BMMs from C3H mice, the clustering of the chimera induced by a human Fas activating antibody (hFas-AB) activates the RANK intracellular domain of the chimera without affecting its endogenous RANK on the BMMs. Since hFas-AB recognizes only human Fas, it does not activate endogenous mouse Fas on BMMs. We developed two chimeric receptors: Ch-1 and Ch-2. While Ch-1 comprises the human Fas external domain linked to the transmembrane and intracellular domains of normal RANK, Ch-2 contains an inactivating mutation in the RANK motif. BMMs expressing Ch-1 or Ch-2 were pre-treated with hFas-AB for 18 hours in the presence of M-CSF, followed by treatments with TNF α or IL-1 in the presence of M-CSF for 96 hours. The assays showed that only the chimeric receptor containing the normal RANK motif (Ch-1) was able to incite osteoclastogenesis, indicating that the RANK motif IVVY⁵³⁵⁻⁵³⁸ plays an important role in priming BMMs in TNF α -/IL-1-mediated osteoclastogenesis. To further address the issue, we are currently inserting a RANK fragment containing IVVY⁵³⁵⁻⁵³⁸ to TNFR1. If the addition of the RANK fragment renders TNFR1 to be able to mediate osteoclastogenesis, the data will provide firm proof that IVVY⁵³⁵⁻⁵³⁸ is involved in TNF α -/IL-1-mediated osteoclastogenesis. Significantly, these studies may establish IVVY⁵³⁵⁻⁵³⁸ as a potent therapeutic target for bone loss in rheumatoid arthritis.

Disclosures: J. Jules, None.

S086

Dok-1 and Dok-2 Deficiency Enhances Bone Resorption and Modulates the Geometry of Bone In Vivo. A. Kawamata¹, A. Inoue², Y. Ezura³, K. Nakashima¹, T. Amagasa³, Y. Yamanashi², M. Noda¹. ¹Department of Molecular Pharmacology, 21st Century COE Program, MRI, Tokyo Medical and Dental University, Tokyo, Japan, ²Department of Cell Regulation, MRI, Tokyo Medical and Dental University, Tokyo, Japan, ³Maxillofacial Surgery, Tokyo Medical and Dental University, Tokyo, Japan.

Dok-1 and Dok-2 are adaptor proteins acting downstream of protein tyrosine kinases (Yamanashi et al. Cell 1997). Both Dok-1 and Dok-2 are mainly expressed in the cells of hematopoietic lineage (DiCristofano et al. JBC 1998) and suppress Ras-Erk signaling (Yasuda et al. JEM 2004). Dok-1 and Dok-2 also suppress TLR4 signaling in innate immunity (Shinohara et al. JEM 2005). Recently, defects in Dok-7, another family member were shown to be involved in congenital myasthenic syndromes (Beeson et al. Science 2006). However, the functions of Dok-1 and Dok-2 in bone are not understood. The aim of this paper is to elucidate the role of Dok-1 and Dok-2 in bone metabolism. Dok-1 or Dok-2 single deficient mice did not show overt phenotypes possibly because of overlapping functions of Dok-1 and its closest family member, Dok-2. Thus, we analyzed bone in Dok-1 and Dok-2 double-deficient (dKO) mice. Dok-1/2 double deficient mice revealed reduction in the levels of cortical bone thickness and cortical bone volume in the femora of 9-week-old mice compared to wild type (WT). In addition, Dok-1/2 deficiency increased periosteal perimeters and endosteal perimeters in the mid shaft of femora. Possibly as a result of these changes, bone mineral density levels in femur of dKO mice were similar to those in WT. For cancellous bone envelope, bone volume and mineralized nodule formation in ex vivo bone marrow cultures were similar between dKO and WT. Histomorphometrical analysis of the dynamic bone parameters indicated that the levels of mineral apposition rate (MAR) and bone formation rate (BFR) in cortical bone of Dok-1/2 dKO mice were similar between dKO and WT. To understand the role of Dok-1/2 in bone resorption, we measured urine deoxypyridinoline (Dpyr), a marker of bone resorption. Double Dok-1/2 deficiency significantly increased Dpyr levels in urine. Intriguingly, the levels of the number of TRAP positive cells per bone surface were similar between dKO and WT, suggesting that Dok-1 and Dok-2 would be involved in the suppression of osteoclastic function specifically without altering osteoclast number. In conclusion, we identified that the novel signaling molecules Dok-1 and Dok-2 suppress bone resorption and are involved in the maintenance of bone geometry.

Disclosures: A. Kawamata, None.

S090

RNA Interference Machinery Is Essential for Osteoclastogenesis. T. Sugatani, K. A. Hruska. Department of Pediatrics, Washington University Medical School, St. Louis, MO, USA.

RNA interference (RNAi) is an evolutionarily conserved pathway, central to a broad spectrum of biological phenomena, including development, stem cell differentiation, transcriptional gene silencing, heterochromatin formation, and transposon silencing. RNAi is triggered by small RNAs such as microRNAs and small interfering RNAs (siRNAs) that regulate gene expression by translational inhibition and mRNA degradation. However, the biological function of the RNAi-related pathway in osteoclastogenesis is not completely understood. Here we show that RNAi machinery is essential for osteoclastogenesis. Moreover, microRNA-223 expression in bone marrow macrophages (BMMs) is critical for osteoclastogenesis. To investigate whether RNAi machinery is a key function in osteoclastogenesis, we focused on the function of Dicer and Argonaute 2 in the RNAi-related pathway. Endogenous small non-coding microRNAs are processed by Dicer from precursor microRNAs. Then, these small double-stranded RNAs assemble into the RNA-induced silencing complex (RISC), which contains Ago 2, Dicer and other cellular factors. Activated RISC finds its target mRNA and affects mRNA translation or stability. We employed a retroviral system for delivery of Dicer or Ago 2 siRNA into primary BMMs, and osteoclasts were induced by RANKL. The knockdown of Dicer or Ago 2 expression attenuated cell proliferation in BMMs. Moreover, the knockdown of Dicer or Ago 2 expression in BMMs suppressed the number of TRAP-positive multinucleated osteoclasts formed compared with scrambled siRNA as a control. However, TRAP expression was not blocked by the knockdown of Dicer or Ago 2 expression. These results indicate that RNAi machinery regulates TRAP-positive multinucleated osteoclast formation. We have reported that microRNA-223 is expressed in RAW264.7 cells, and the overexpression of precursor microRNA-223 in cells blocks TRAP-positive multinucleated osteoclast formation and bone resorption. Here, we examined the effect of the overexpression of microRNA-223 in primary BMMs using a retroviral system. The overexpression of precursor microRNA-223 in BMMs suppressed the number of TRAP-positive multinucleated osteoclasts formed, demonstrating that the continuous expression of microRNA-223 in BMMs results in the inhibition of TRAP-positive multinucleated osteoclast formation. Thus, we provide the first evidence that the Dicer and Ago 2-related RNAi machinery is important for the formation of TRAP-positive multinucleated osteoclasts. In particular, the regulation of microRNA-223 expression in osteoclast precursors during osteoclastogenesis may be critical for osteoclast differentiation and function.

Disclosures: T. Sugatani, None.

S093

The Mechanism of RANKL-evoked $[Ca^{2+}]_i$ Oscillations Mediated by RGS10 in Osteoclast Differentiation. S. Yang, Y. Li. Cytokine Biology, The Forsyth Institute, Harvard School of Dental Medicine, Boston, MA, USA.

Increased osteoclastic resorption leads to many bone diseases, including osteoporosis and rheumatoid arthritis. To better understand the mechanisms underlying osteoclast-based diseases and design relevant therapies, it is necessary to unveil the molecular basis of osteoclast differentiation and function as well as the regulatory mechanisms of osteoclast signaling. In our previous work, we have characterized RANKL-induced signaling protein, Regulator of G-protein Signaling 10 (RGS10) and found it is predominantly expressed in osteoclasts. Impaired osteoclast differentiation in RGS10-deficient ($RGS10^{-/-}$) mice with severe osteopetrosis indicates the essential role of RGS10 for RANKL-evoked $[Ca^{2+}]_i$ oscillations in osteoclast differentiation. However, the mechanism underlying how RGS10 regulates the RANKL-evoked $[Ca^{2+}]_i$ oscillations and NFATc1 expression in osteoclast differentiation still remains unclear. In this study, we focused on the mechanism of RANKL-evoked $[Ca^{2+}]_i$ oscillations mediated by RGS10 in osteoclast differentiation. Our data demonstrated that RGS10 interacts with calmodulin in a Ca^{2+} -dependent manner. Ca^{2+} /calmodulin complexes are formed at high $[Ca^{2+}]_i$ and compete for the PIP₃ binding site on the RGS10 protein to regulate $[Ca^{2+}]_i$ oscillations and activity of PLC γ . Calcineurin inhibitor, FK506, inhibited the rescue effect of RGS10 reintroduction in RANKL-induced $RGS10^{-/-}$ BMMs and the formation of TRAP⁺ cells from $RGS10^{-/-}$ BMMs driven by RGS10 ectopic expression without RANKL induction. Ectopic expression of NFATc1 rescues impaired osteoclast differentiation in $RGS10^{-/-}$ mice, indicating that RGS10 acts upstream of Calcineurin and NFATc1. Our results revealed a working model: PIP₃ specifically binds RGS10 at low $[Ca^{2+}]_i$ to inhibit RGS10 activity. When RANKL activates ITAM and PLC γ , which hydrolyzes PIP₂ to generate inositol 3-phosphate (IP₃), Ca^{2+} /calmodulin complexes are formed at high $[Ca^{2+}]_i$ and the complexes compete for the PIP₃ binding site on the RGS10 protein to restore RGS10 activity, which in turn regulates PLC γ activity. The dual regulation of RGS10 activity can cause $[Ca^{2+}]_i$ oscillations, implying the mechanism for RGS10-mediated modification of intracellular $[Ca^{2+}]_i$ oscillations that activate calcineurin (CN) and NFATc1 for osteoclast terminal differentiation. To our knowledge, this is the first in vivo model revealing the mechanism of $[Ca^{2+}]_i$ oscillation regulation by RGS10. The essential role of RGS10 selectively involved in RANKL-induced $[Ca^{2+}]_i$ oscillations in osteoclast differentiation may offer a very specific and powerful therapeutic target for treatment of bone diseases caused by excessive bone resorption.

Disclosures: S. Yang, None.

S096

A Dramatic Increase in Hematopoiesis and Angiogenesis in Bone Marrow of Rescued RANKL-Deficient Mice by Expression of Soluble RANKL Transgene. H. Yasuda¹, A. Minamida², J. M. Penninger³, Y. Iwakura².

¹Nagahama Institute for Biochemical Science, Oriental Yeast Co., Ltd., Shiga, Japan, ²Institute of Medical Science, University of Tokyo, Tokyo, Japan, ³Institute of Molecular Biotechnology of the Austrian Academy of Sciences, Vienna, Austria.

Receptor activator of NF- κ B ligand (RANKL) is a key regulator of osteoclastogenesis, lymphocyte development and lymph node (LN) organogenesis. RANKL is a membrane-bound ligand but its soluble form is released from different type of cells by shedding. In humans increases of serum sRANKL level were reported in patients with rheumatoid arthritis and juvenile Paget's disease. RANKL knockout (KO) mice showed severe osteopetrosis, with no osteoclasts, marrow spaces, or tooth eruption, and exhibited profound growth retardation. These mice also showed defects in early differentiation of T and B cells, and lacked all LNs. We previously reported that most of all abnormalities in RANKL KO mice were rescued by expression of soluble RANKL (sRANKL) transgene by mating the KO mice with sRANKL transgenic (TG) mice. The purpose of this study is to analyze the bone marrow cells appeared in the rescued mice (hereafter called TG/KO mice). The histological analysis of the TG/KO mice revealed that a dramatic increase in hematopoiesis and angiogenesis in their bone marrow cavities. The ratio of Ter119+ cells (erythroid cells), Mac1+ cells (macrophages), Gr-1+ cells (granulocytes), and Thy1.2+ cells (T cells) increased in the flow cytometry, respectively. In contrast, the ratio of B220+ cells (B cells) decreased. These results suggested the possibility of a lineage shift from B cells to others. The increase in hematopoiesis and angiogenesis was observed only in TG/KO mice, but not in TG mice, suggesting that the phenotypic changes were not directly caused by overexpression of sRANKL. RT-PCR analysis revealed that the sRANKL transgene was expressed in T-cells, B-cells, and macrophages, but not in osteoblasts in the TG/KO and TG mice. Numerous TRAP+ multinucleated cells were formed in bone marrow macrophage culture of TG/KO and TG mice in the presence of M-CSF without addition of sRANKL. Addition of OPG inhibited the osteoclast formation. Together, these results suggest that sRANKL acts on bone marrow macrophages in an autocrine fashion. TRAP+ cells were observed only in the bone surface in TG/KO mice, suggesting that the hypothetical factors besides RANKL regulated the localization of osteoclasts. In conclusion, the TG/KO mice showed a marked increase in hematopoiesis and angiogenesis accompanied with a lineage shift from B cells to other cell populations in the rescued bone marrow cavities and these mice would represent a good animal model studying the formation of bone marrow.

Disclosures: H. Yasuda, Oriental Yeast Co., Ltd. 3.

S099

Expression of OCZF Directed by the Cathepsin K Promoter Affects Bone Mass and Osteoclast Formation in Transgenic Mice. T. Shobuiké^{*1}, T. Kukita², K. Nagata^{*2}, J. Teramachi^{*2}, M. Asagiri³, H. Takayanagi³, A. Kukita¹. ¹Saga University, Saga, Japan, ²Oral Biological Science, Kyushu University, Fukuoka, Japan, ³Cell Signaling and COE program, Tokyo Medical and Dental University, Tokyo, Japan.

We previously isolated the OCZF cDNA encoding Kat-6 antigen specifically expressed in rat osteoclast. The OCZF gene product is a member of POK protein family that contains two domains of POZ/BTB and zinc finger in their N- and C-terminal region respectively, and that is shown to be involved in various cellular processes. Suppression of OCZF by antisense RNA inhibits osteoclast differentiation in vitro, indicating that OCZF is involved in osteoclastogenesis, but in vivo role in the process is not clear. To this end we generated transgenic mice, which expressed OCZF under the control of mouse cathepsin K promoter. Nine transgenic mice were identified among the offspring by PCR and Southern blot analysis of mouse tail genomic DNA. Transgene expression was verified by RT-PCR using osteoclasts differentiated in vitro from bone marrow at 10 weeks of age. Two lines of the transgenic animals exhibited relatively high transgene expression, and were further investigated. The c-fos and NFATc1 protein exhibit higher levels during differentiation into osteoclasts in vitro from bone marrow of the transgenic mice than that of normal littermates. Micro-CT and peripheral quantitative CT (pQCT) analyses and histomorphometry of femur were performed in mice at 6 weeks of age. Micro-CT imaging demonstrates a reduction in trabecular bone volume in the transgenic mice relative to normal littermates. pQCT analyses also demonstrate a reduction in bone mineral density and bone mineral content especially in trabecular bone with a decrease in strength strain index, whereas those in cortical bone were slightly affected. Consistently, von Kossa staining shows a smaller mineralized area in the transgenic mice than in normal littermates. Histological analyses with tartrate-resistant acid phosphatase staining and calcein labeling indicate an increase in the number of osteoclast, whereas bone formation rate did not significantly change. These results suggest that OCZF has an important role in osteoclastogenesis in vivo.

Disclosures: T. Shobuiké, None.

S103

Potential Role of Rab3D-Calmodulin Interaction in Osteoclastic Bone Resorption. J. Xu, T. Cheng*, N. Pavlos*, E. Ang*, M. H. Zheng. Orthopaedic Surgery, The University of Western Australia, Nedlands, WA, Australia.

Osteoclastic bone resorption is a highly dynamic process that requires the tight ordering of intracellular trafficking events in order to maintain the structural and functional polarization of the ruffled border and basolateral domains. Rab3 proteins are a subfamily of GTPases, known to mediate membrane transport in eukaryotic cells and play a role in exocytosis. Our recent data indicates that Rab3D modulates a post-TGN trafficking step that is required for osteoclastic bone resorption (1). Here, to identify down-stream regulatory molecules of Rab3D, we have performed a yeast two-hybrid screen. Amongst several candidate Rab3D-interacting proteins identified, Rab3D was found to associate with calmodulin, an established regulator of osteoclastic bone resorption. As an initial effort to better define the interaction between Rab3D and calmodulin, we generated several mutants of Rab3D which interfere with the GDP/GTP nucleotide exchange (Rab3DQ81L, Rab3DNI35I) and/or membrane attachment of Rab3D (Rab3D-CXC). By in vivo bioluminescence resonance energy transfer (BRET) assay, Calmodulin was found to associate equivalently with wild-type Rab3D as well as Rab3DNI35I and Rab3DCXC variants. Overexpression of constitutively-active Rab3D (Rab3DQ81L) enhanced this interaction suggesting that the active form of Rab3D (i.e. GTP-bound) might recruit additional effector molecules which further potentiate its binding to calmodulin. In an attempt to address the impact of calmodulin activity on Rab3D-calmodulin interaction and osteoclastic bone resorption, we performed complementary BRET and in vitro bone resorption assays in the presence of the calmodulin inhibitor, calmidazolium chloride. Interestingly, we show that suppression of calmodulin activity via calmidazolium chloride impairs the association of Rab3D with calmodulin, an affect that correlates with a disruption in osteoclastic bone resorption. We propose that the recruitment of calmodulin by Rab3D might be an important requirement for osteoclast-mediated bone resorption. 1. Pavlos, N.J., Xu, J., Riedel, D., Yeoh, J.S.G., Teitelbaum, S.L., Papadimitriou, J.M., Jahn, R., Ross, F.P., Zheng, M.H. (2005) Mol. Cell. Biol 25, 5253-5269

Disclosures: J. Xu, None.

This study received funding from: NHMRC.

S110

TNFR1 and 2 Differentially Regulates Inflammatory Bone Resorption Induced by LPS In Vivo. M. H. Mian^{*1}, K. Aoki², N. Alles^{*1}, H. Saito^{*2}, K. Ohya². ¹Center of Excellence program for Frontier Research on Molecular Destruct. and Reconst. of Bone, Tokyo Medical and Dental University, Tokyo, Japan, ²Department of Hard tissue Engineering, Section of Pharmacology, Tokyo Medical and Dental University, Tokyo, Japan.

Chronic bone infection is often complicated by severe osteolysis. It has been reported that TNF receptors differentially regulate osteoclastogenesis, where TNFR1 accelerate and TNFR2 inhibit osteoclastogenesis (Abu-Amer et al, J Biol Chem, 2000). But whether these receptors influence bone resorbing activity of osteoclast differentially is yet to be

elucidated. The purpose of this study was to investigate bone resorbing activity through TNFR1 and TNFR2 in vitro as well as to clarify the role of these receptors on inflammatory bone resorption in vivo. We examined the roles of TNF receptors using bone marrow cells in vitro as well as in LPS induced local bone resorption model in vivo. For in vitro study, pit formation assay in dentin slices using a confocal microscope was performed to check the functional osteoclast activity of TNFR1 and TNFR2 upon stimulation of TNF- α . Average pit depth in Wild type (WT) and TNFR1 deficient (KO) culture influenced by TNF- α were not significantly changed, but significant increase in average pit depth were observed in TNFR2 KO culture. For in vivo study, 10 mg/kg LPS was injected subcutaneously on calvaria of TNFR1KO, TNFR2 KO, and their WT mice, sacrificed on day 5 after the LPS injections. Calvariae, tibiae and femurs were dissected. The calvarial BMD measured by DXA in LPS-injected group was significantly decreased in WT and TNFR2 KO mice compared to the control. In contrast, there was no significant decrease of calvarial BMD in TNFR1 KO mice. On the other hand, the significant decrease on the BMD of tibiae and femurs measured by peripheral quantitative computed tomography (pQCT) was observed in TNFR2 KO mice, but no significant decrease was observed in WT and TNFR1 KO mice. The results of urinarydeoxyypyridinoline reflected these resorption and histomorphometric analyses of tibia shows the significant increase of osteoclast number in TNFR2 KO mice by LPS injection. These BMD data were confirmed by μ -CT analyses. The present data indicate that TNFR1 plays the pivotal role for inducing local bone resorption induced by LPS and TNFR2 might have a protecting role in inflammatory bone resorption process.

Disclosures: M.H. Mian, None.

S112

Transgenic Overexpression of Osteoclastic Protein-tyrosine Phosphatase, PTP-oc, in Cells of Osteoclastic Lineage Led to Increased Bone Resorption and Marked Reduction in Trabecular Bone Mass and Density in Adult Mice. M. H. C. Sheng, M. Amoui*, A. K. Srivastava, J. E. Wergedal, K. H. W. Lau. Loma Linda VAMC, Loma Linda, CA, USA.

Past in vitro studies have suggested that the structurally unique osteoclastic transmembrane PTP-oc acts as a positive regulator of osteoclast activity. This study sought to determine whether transgenic (TG) overexpression of PTP-oc in cells of osteoclastic lineage would increase (\uparrow) bone resorption and decrease (\downarrow) bone mass or density (BMD) in adult mice. To generate TG mice, a TG construct containing the rabbit PTP-oc cDNA driven by a tartrate-resistant acid phosphatase (TRACP)-IC promoter was injected into the pronucleus of fertilized ova, which were implanted into pseudo-pregnant B6D2F1 mice. TG founders, identified by a PCR-based genotyping assay using primers that span unique regions of TRACP-IC promoter and rabbit PTP-oc sequence, were bred with C57BL/6J mice to produce F2 mice. Ten-week-old male F2 progenies were extensively followed for pQCT, histological, and serum resorption marker analyses. The body weight of TG mice was 10% less ($p < 0.05$, $n = 8$ each) than that of wild-type (WT) littermates. pQCT analyses of the femur revealed that TG mice had 30% \downarrow in trabecular BMD ($p < 0.002$). Histologic analyses at the secondary spongiosa in the femur of 9 TG and 7 WT littermates confirmed that TG mice showed 35% \downarrow in trabecular surface (Tb.Pm, $p < 0.01$), 27% \downarrow in % trabecular area (Tb.Ar, $p < 0.05$), 11% \downarrow in trabecular number (Tb.N, $p < 0.05$), and 36% \uparrow in trabecular separation (Tb.Sp, $p < 0.005$). The lumbar vertebra of 12 TG mice, when compared to 8 WT littermates, also showed 20% \downarrow in Tb.Pm ($p < 0.005$), 17% \downarrow in Tb.N ($p < 0.003$) and 35% \uparrow in Tb.Sp ($p < 0.004$). Consistent with an \uparrow in bone resorption, the serum c-telopeptide level of TG mice ($n = 14$) was 25% ($p < 0.05$) higher than that of littermates ($n = 11$). That the number of osteoclasts and the length of TRACP-labeled bone surface per total bone surface were not different suggested that TG overexpression of PTP-oc increased osteoclast activity rather than osteoclast differentiation. The same phenotype was confirmed in a second TG line. In congruent with an \uparrow in osteoclastic activity, the average pit area created by osteoclasts derived from bone marrow cells of 10-week-old male TG mice in response to RANKL and mCSF in the pit formation assay was ~50% greater ($p = 0.008$) than those by osteoclasts of WT littermates ($n = 8$ each). However, the TRACP activity per cellular protein in osteoclasts derived from the two groups of mice was not different. In summary, TG overexpression of PTP-oc in cells of osteoclastic lineage led to a marked reduction in trabecular bone mass in adult mice due to an \uparrow in osteoclastic activity. These findings provide compelling in vivo evidence that PTP-oc is a positive regulator of osteoclastic activity.

Disclosures: M.H.C. Sheng, None.

This study received funding from: Veterans Administration.

S114

The CaMK-CREB Pathway Regulates Osteoclast Differentiation and Function. A. Suematsu¹, K. Sato^{*2}, T. Nakashima^{*1}, S. Takemoto-Kimura^{*3}, K. Aoki⁴, K. Ohya⁴, A. Yamaguchi⁵, T. A. Chatila^{*6}, H. Bito^{*3}, H. Takayanagi¹. ¹Department of Cell Signaling, Tokyo Medical and Dental University, Tokyo, Japan, ²Division of Rheumatology and Applied Immunology, Saitama Medical University, Saitama, Japan, ³Department of Neurochemistry, University of Tokyo, Tokyo, Japan, ⁴Department of Hard Tissue Engineering, Tokyo Medical and Dental University, Tokyo, Japan, ⁵Department of Oral Pathology, Tokyo Medical and Dental University, Tokyo, Japan, ⁶The David Geffen School of Medicine at the University of California at Los Angeles, Los Angeles, CA, USA.

Calcium (Ca^{2+}) signaling is critical for the regulation of various cellular events. Intracellular Ca^{2+} binds to calmodulin, and the Ca^{2+} /calmodulin complex activates Ca^{2+} /calmodulin-dependent kinases (CaMKs) as well as phosphatases such as calcineurin. We

revealed the importance of calcineurin-nuclear factor of activated T cells (NFAT) pathway in osteoclastogenesis. However, it remains unclear whether CaMKs play a crucial role in bone homeostasis. Here we examined the role of CaMKs in osteoclast differentiation and function. Because knockdown of CaMKIV had a suppressive effect on RANKL-induced osteoclastogenesis, we analyzed the bone phenotype of CaMKIV-deficient mice. We observed an increase in bone volume in CaMKIV-deficient mice, which resulted from the reduction in osteoclast number. In vitro osteoclastogenesis in CaMKIV-deficient cells stimulated with RANKL was also reduced. We focused on cAMP response element (CRE)-binding protein (CREB) as a physiological substrate of CaMK in the osteoclast differentiation. CREB was phosphorylated and activated through CaMKIV after RANKL stimulation. The pharmacological inhibition of CaMKs suppressed osteoclast differentiation and downregulated the expression levels of c-fos, which is required for the induction of NFATc1. Furthermore, CREB together with NFATc1 induced the expression of osteoclast-specific genes. Finally, we explored the possibility whether modulation of CaMK activity can be used as therapeutic target in an ovariectomy (OVX) mice. The reduction in bone volume associated with an increase in osteoclast number in OVX mice was ameliorated by systemic administration of CaMK inhibitor. These results indicate that both kinases and phosphatases downstream of Ca^{2+} signaling cooperatively regulate the transcriptional program of osteoclast differentiation and function. Thus, inhibition of the CREB-CaMK pathway may be a new therapeutic target for various bone diseases.

Disclosures: A. Suematsu, None.

S118

Thyroid Hormone-induced Terminal Differentiation of Growth Plate Chondrocytes Involves IGF-1 Modulation of Canonical Wnt Signaling. L. Wang^{*1}, Y. Y. Shao^{*1}, R. T. Ballock². ¹Department of Biomedical Engineering, Cleveland Clinic, Cleveland, OH, USA, ²Departments of Orthopaedics and Biomedical Engineering, Cleveland Clinic, Cleveland, OH, USA.

Thyroid hormone is a potent regulator of skeletal maturation in the growth plate. Wnt signaling has also been recognized as an important signal transduction pathway in regulating terminal differentiation of growth plate chondrocytes into hypertrophic cells. Wnt ligands and β -catenin have been shown to promote chondrocyte maturation in the chick growth plate. Since thyroid hormone is a known stimulator of IGF-1 receptor expression, and IGF-1 has been described as a stabilizer of β -catenin in other cell types, we hypothesize that thyroid hormone may regulate terminal differentiation of growth plate chondrocytes in part by stimulating Wnt/ β -catenin signaling pathway through the modulation of IGF-1/IGF-1R signaling.

Three-dimensional pellet cultures of 2-day old rat growth plate chondrocytes were maintained in serum-free medium. Thyroid hormone treatment upregulated Wnt-4 mRNA expression, increased the accumulation of β -catenin and upregulated β -catenin target gene Runx2/cbfa1. Both Wnt4 conditioned medium and adenovirus expressing stabilized β -catenin increased the markers of hypertrophy alkaline phosphatase (ALP) activity and Col10a1 mRNA expression in growth plate chondrocytes. Blocking Wnt ligand/receptor interactions with Wnt inhibitors Frzb/sFRP3 or DKK1 decreased the T3-induced increases of β -catenin accumulation and inhibited the maturation-promoting effects of T3 in growth plate cells. IGF-1R mRNA expression was upregulated by thyroid hormone treatment in growth plate cells. Incubation of the cells with recombinant IGF-1 protein or IGF-1R adenovirus not only resulted in increases of β -catenin accumulation and upregulation of Wnt4 and Runx2 mRNA expression, but also increased ALP activity and Col10a1 mRNA expression in growth plate chondrocytes. The IGF-1 receptor inhibitor picropodophyllin (PPP) inhibited T3-induced increases of Wnt4 mRNA as well as T3-mediated hypertrophy of growth plate chondrocytes.

These data demonstrate that thyroid hormone promotes terminal differentiation of growth plate chondrocytes in part through IGF-1 modulation of the canonical Wnt signaling pathway.

Disclosures: R.T. Ballock, None.

S121

Proteasome Inhibition Induces Permanent Growth Retardation and Apoptosis in Growth Plate Chondrocytes. E. E. Eriksson, F. Zaman^{*}, A. S. Chagins^{*}, D. Chrysis^{*}, L. Sälvendahl^{*}. Women and Child Health, Pediatric Endocrinology, Stockholm, Sweden.

Proteasome inhibitors, a new class of anti-cancer drugs has recently been approved for multiple myeloma treatment in adults and is under clinical trial in pediatric cancers. However, any specific side effects on normal bystander tissues in children are unknown. The objective of this research was to study the effects of the proteasome inhibitors, MG262 and the clinically used proteasome inhibitor, Velcade on linear bone growth in young mice (male, 5 weeks old) and in fetal rat metatarsal bones. To address this question, C57B and NMRI mice were treated with the proteasome inhibitors, Velcade and MG262, in a clinical relevant dose. We followed the linear bone growth of the mice longitudinally and observed permanent growth retardation. To elucidate the underlying mechanisms, we used a transgenic mouse model expressing a green fluorescent protein reporter allowing monitoring the ubiquitin/proteasome system. MG262 treatment results in accumulation of the green fluorescent protein in the growth plate and increased apoptosis in stem-cell like chondrocytes. To further prove local effect of proteasome inhibition on linear growth, fetal rat metatarsal bones were cultured in presence of either Velcade or MG262. These experiments also showed bone growth retardation and increased chondrocyte apoptosis. To understand the apoptotic pathways induced by proteasome inhibitors in chondrocytes, we used rat- and human chondrocytic cell lines that both were found to undergo apoptosis upon proteasome inhibitor treatment. A pan-caspase inhibitor (Z-VAD-fmk) suppressed MG262-mediated apoptosis by 32% in rat and 35% in human chondrocytes. Together with

early up-regulation of p53 and apoptosis inducing factor (AIF) these observations suggest involvement of both caspase-dependent and independent apoptosis. Indeed, apoptosis was suppressed by 30% employing p53-sequence specific siRNA. In short, we conclude that impairment of the ubiquitin/proteasome system causes permanent growth retardation by inducing massive apoptosis in chondrocytes in vivo and in vitro, an effect which is both dependent and independent of caspases. Our findings suggests that proteasome inhibitors have to be cautiously used in growing children and that involvement of p53 in chondrocyte apoptosis opens targets for new potential ways to rescue growth.

Disclosures: E.E. Eriksson, None.

S123

The Regulation of Chondrocyte Proliferation, Function, and Differentiation by Akt Signaling Pathways. T. Fujita^{*}, S. Rokutanda^{*}, N. Kanatani^{*}, C. Yoshida^{*}, T. Komori^{*}. Cell Biology, Nagasaki university, Nagasaki, Japan.

Akt is a broadly expressed multifunctional protein, but its roles in chondrocytes still remain to be clarified. We investigated chondrocyte proliferation, function, and differentiation in transgenic mice expressing myristoylated Akt (myrAkt) by Col2a1 promoter. Chondrocyte proliferation was enhanced in the reservoir zone, but it was reduced in the proliferative zone, in which an increase in matrix production was observed. Chondrocyte maturation was enhanced in the spine and sphenoid but inhibited in the long bones. Accelerated chondrocyte proliferation by IGF-I was inhibited by FoxO3a, and an inhibitory effect of Akt on chondrocyte proliferation was abolished by rapamycin, a mTOR specific inhibitor, suggesting that Akt-FoxO and Akt-mTOR axes functioned as a proliferative pathway in the reservoir zone and as an anti-proliferative pathway in the proliferative zone, respectively, in myrAkt transgenic mice. The enhanced matrix synthesis by myrAkt was blocked by rapamycin, indicating that Akt-mTOR pathway plays an important role in matrix synthesis. FoxO3a overexpression mildly enhanced chondrocyte maturation, and lithium, a GSK3 inhibitor, inhibited it in long bone of wild-type mice. Further, the stimulatory effect of Akt on chondrocyte maturation in spine was abolished by rapamycin. These results indicate that Akt-FoxO and -GSK3 β pathways are involved in the negative regulation of chondrocyte maturation in long bone but Akt-mTOR pathway is involved in the positive regulation of chondrocyte maturation in spine. These results demonstrate that Akt regulates chondrocyte proliferation, matrix synthesis, and chondrocyte maturation depending on the skeletal elements and the maturational stages of chondrocytes.

Disclosures: T. Fujita, None.

S127

Transcriptional Regulation of Type X Collagen by Runx2: Molecular Network Underlying Chondrocyte Hypertrophy Causing Osteoarthritis. A. Higashikawa, T. Saito, S. Kamekura^{*}, S. Ohba, T. Ikeda, K. Nakamura, U. Chung, H. Kawaguchi. Sensory & Motor System Medicine, University of Tokyo, Tokyo, Japan.

Chondrocyte hypertrophy is essential not only for physiological skeletal development and growth, but also for pathological disorders like osteoarthritis (OA). When we created an experimental mouse OA model by producing instability in the knee joint through surgical transection of the medial collateral ligament and resection of the medial meniscus, Runx2 expression determined by immunostaining and real-time RT-PCR was induced in chondrocytes at the superficial and middle layers of joint cartilage as early as 2 weeks, which was not observed in the sham-operated joint. Most of the Runx2-positive chondrocytes then expressed type X collagen (COL10), the representative marker of hypertrophic differentiation, at 2-4 weeks, and thereafter produced collagenases causing degradation of the cartilage matrix. In heterozygous Runx2-deficient mice, however, COL10 expression, as well as the subsequent collagenase expression and matrix degradation, was suppressed under the OA induction, indicating that Runx2 contributes to the pathogenesis of OA through chondrocyte hypertrophy. COL10 mRNA level, as well as Alizarin-red and von Kossa stainings, were markedly increased by the Runx2 overexpression, whereas they were decreased by the dominant negative Runx2 overexpression, in the cultures of respective stable lines of mouse chondrogenic ATDC5 cells. In HeLa cells transfected with a luciferase-reporter gene construct containing a 4.5 kb fragment of the human COL10 promoter region, the transcriptional activity was enhanced by co-transfection with Runx2. Deletion analysis using a series of 5'-deletion constructs of the COL10 promoter identified the core responsive element to Runx2 to be within 10 bp around the -80 bp region (HY-box). The transcriptional activity of Runx2 was suppressed by a site-directed mutagenesis in the HY-box. The tandem-repeat constructs responded to Runx2 depending on its repeat number. Electrophoretic mobility shift assay showed specific binding of nuclear extracts from Runx2-overexpressed COS7 cells with the wild-type HY-box oligonucleotide probe, but not with the mutated probe. Cold competition with an excess of unlabelled wild-type probe, but not with the unlabelled mutated probe, suppressed formation of the complex. In addition, the complex underwent a supershift by the antibody to Runx2, confirming the specific binding of the HY-box and Runx2. In conclusion, we identified the Runx2-responsive region HY-box in the COL10 promoter. Studies on molecules related to Runx2 / HY-box will lead to elucidation of the molecular network underlying chondrocyte hypertrophy and OA pathogenesis.

Disclosures: A. Higashikawa, None.

S130

Inhibitory Smad6 and Smad7 Differently Regulate Cartilage Formation. T. Iwai¹, J. Murai^{*1}, H. Yoshikawa¹, N. Tsumaki². ¹Orthopaedic Surgery, Osaka University Graduate School of Medicine, Osaka, Japan, ²Cartilage and Bone Biology, Osaka University Graduate School of Medicine, Osaka, Japan.

TGF- β / BMP signals are mediated by Smad proteins. Biochemical studies have revealed that Smad6 inhibits BMP signaling, whereas Smad7 inhibits both TGF- β and BMP signaling. Transgenic / knockout mouse studies showed that BMP signals are definitely necessary for cartilage formation, whereas importance of TGF- β signals in cartilage formation is controversial. In this annual meeting last year, we reported generation of conditional transgenic mice overexpressing Smad7 in cartilage. Smad7 overexpression inhibited cartilage formation and delayed chondrocyte hypertrophy. In the present study, we further clarified roles of Smads 6 and 7. In situ hybridization analysis revealed that the expression levels of both Smad6 and Smad7 were low in cartilage compared with those in surrounding soft tissues and bone. To investigate the importance of this Smad7 down-regulation in cartilage during endochondral bone formation, we analyzed transgenic mice (Tg) overexpressing Smad 6 or Smad7. In situ hybridization analysis showed elevated expression of Smad 6 in cartilage of Smad6 Tg and elevated expression of Smad7 in cartilage of Smad7 Tg. Cartilage size was normal in Smad6 Tg, but significantly reduced in Smad7 Tg. We next cultured mesenchymal cells derived from 12.5 d.p.c. limb buds and induced cartilaginous nodule formation in the presence of rhBMP2 in micromass system. Cartilaginous nodule formation induced by exogenous BMP2 was prohibited in mesenchymal cells prepared from Smad7 Tg, but not in those from Smad6 Tg. Real-time RT-PCR analysis of the cells in micromass culture showed that the Smad6 expression level in Smad6 transgenic mesenchymal cells was 1.7 times higher than wild-type mesenchymal cells and that the Smad7 expression level in Smad7 Tg was 1.8 times higher. The expression level of Sox9 was normal in Smad6 transgenic cells, but dramatically reduced in Smad7 transgenic cells. Cartilaginous nodule formation induced by rhBMP2 in wild-type mesenchymal cells was inhibited by addition of the SB203580 (inhibitor of p38 MAPK pathway), but not by addition of the SB431542 (inhibitor of TGF- β pathway). Immunoblot analysis of ATDC5 cells showed that BMP-induced phosphorylation of ATF2 was repressed by overexpression of Smad7 but not by overexpression of Smad6. In general, BMP stimulate cartilage formation and chondrocyte hypertrophy. Smad6 Tg showed that BMP signals for chondrocyte hypertrophy is mediated by Smad 1/5/8 that Smad6 blocks. The present results suggest that BMP signals for cartilage formation are mediated by Smad-independent pathways. This pathways could be inhibited by Smad7 but not Smad6. The p38 MAPK pathways may be one of candidates for this pathway.

Disclosures: T. Iwai, None.

S133

Analysis of the Role of Runx1 in Chondrocyte Differentiation using Chondrocyte-specific Runx1 Deficient Mice. A. Kimura^{*1}, S. Takeda^{*1}, S. Sato^{*2}, M. Iwasaki^{*2}, H. Inose^{*1}, K. Sinomiya^{*1}. ¹21COE, Dept. of Orthopedics, Tokyo Medical and Dental University, Tokyo, Japan, ²Dept. of Orthopedics, Tokyo Medical and Dental University, Tokyo, Japan.

Chondrocyte differentiation is a multistep process essential for endochondral bone formation.

The transcription factor Runx family is involved in chondrocyte differentiation. Namely, Runx2 accelerates chondrocyte differentiation and Runx3 also regulates chondrocyte maturation in collaboration with Runx2. However, the physiological role of the other member Runx1 in chondrocyte differentiation remains to be elucidated. We previously reported that all Runx genes are expressed in cells of chondrocyte lineage in mouse embryo. In this study, we tried to address the role of Runx1 in chondrocyte differentiation, in vivo, by generating mice deficient for Runx1 specifically in chondrocyte, since mice lacking Runx1 die in the midgestation stage.

We generated Runx1-floxed mice (Runx1^{fl/fl}) harboring loxP sites surrounding exon4 which encodes DNA binding domain of Runx1 by gene targeting. By crossing them with Col1a1-Cre transgenic mice that drive cre expression by chondrocyte-specific Col1a1 promoter, we obtained chondrocyte-specific Runx1 deficient (Col1a1-Cre/Runx1^{fl/fl}) mice.

Successful deletion of Runx1 in Col1a1-Cre/Runx1^{fl/fl} mice was confirmed by southern blot analysis of genomic DNA. Unexpectedly, Col1a1-Cre/Runx1^{fl/fl} mice were grossly normal. By skeletal preparation at birth, Col1a1-Cre/Runx1^{fl/fl} mice were indistinguishable from wild-type mice, namely the size of the body and calcification of the skeleton were similar. Histologically, Col1a1-Cre/Runx1^{fl/fl} embryos showed no overt abnormality. We also analyzed them by In situ hybridization analysis using molecular markers expressed in chondrocytes such as Col1a1, ColXa1 and Indian hedgehog, but we did not detect any abnormality.

Taken together, this study show that Runx1 is not necessary for chondrocyte differentiation and the absence of Runx1 may be compensated by Runx2 and Runx3.

Disclosures: A. Kimura, None.

S136

Osteoprotegerin Negatively Regulates Chondroclast Formation and Recruitment in Endochondral Ossification. N. Ota¹, H. Takaishi^{*1}, J. Takito^{*1}, T. Kimura^{*2}, Y. Okada^{*2}, K. Matsuzaki¹, H. Yasuda^{*3}, H. Kawaguchi⁴, Y. Toyama^{*1}. ¹Orthopaedic Surgery, Keio University School of Medicine, Tokyo, Japan, ²Pathology, Keio University School of Medicine, Tokyo, Japan, ³Nagahama Institute for Biochemical Science, Oriental Yeast, Shiga, Japan, ⁴Orthopaedic Surgery, University of Tokyo, Tokyo, Japan.

Osteoprotegerin (OPG) is a decoy receptor for receptor activator of NF- κ B ligand (RANKL). It has been suggested that RANKL expression in hypertrophic chondrocytes is involved in the formation and activation of chondroclasts, which function in resorption of cartilaginous matrix at the growth plates. The fracture repair process closely resembles normal development of the skeleton during embryonic bone formation. We previously reported the accelerated fracture healing in OPG deficient mice (OPG KO) via the rapid resorption of cartilaginous callus due to the enhanced chondroclast recruitment. The purpose of the present study was to further investigate the role of OPG in endochondral ossification using the chondrocytes obtained from OPG KO and wild type (WT). Newborn rib chondrocytes were disseminated as feeder cells in the presence of 1,25-dihydroxy vitamin D3 and PGE2, and cocultured with spleen cells, in order to examine inducing effects of chondrocytes on the chondroclast formation. Strikingly, OPG KO-derived chondrocytes induced numerous TRAP positive multinucleated cells in a coculture system with spleen cells isolated from WT. In contrast, WT-derived chondrocytes could not induce any TRAP positive cells. Addition of recombinant OPG to the coculture system decreased the chondroclastogenesis in a concentration dependent manner. RT-PCR analysis showed that WT chondrocytes increased RANKL mRNA in response to PTHrP, FGF-18, PGE2, IL-1 and TNF- α . On the other hand, TGF- β increased the expression of OPG. Next, we examined whether the chondrocytes fully differentiated in atelocollagen pellets could induce chondroclastogenesis. Cartilage pellets from OPG KO cocultured with RAW 264.7 cells induced TRAP positive multinucleated cells in the presence of 10 ng/ml RANKL, while WT cartilage pellets did not. ELISA measurements indicated that the OPG KO-derived cartilage pellets produced the significant level of soluble RANKL. Finally, the transplantation assay of the cartilage pellets under the kidney capsules of adult OPG KO revealed the remarkable recruitment of TRAP positive cells around the OPG KO-derived cartilage pellets, which were subsequently replaced by osseous tissues. These observations suggest that RANKL and OPG expression in chondrocytes is regulated by various cytokines and inflammatory mediators, and OPG might controls the process of endochondral ossification as a negative regulator of chondrocyte dependent chondroclastogenesis.

Disclosures: N. Ota, None.

S142

CITED1 Ablation Impairs Endochondral Bone Formation During Embryonic Development. D. Yang, J. Guo^{*}, R. Bringhurst^{*}. Endocrine Unit, Massachusetts General Hospital, Boston, MA, USA.

CITED1 (CBP/P300 interacting Transactivator with Glutamic Acid [E]/ Aspartic Acid [D]-Rich C-terminal domain) is a transcriptional cofactor located on the X chromosome. We previously observed that CITED1 expression is rapidly and transiently induced by PTH1R activation in osteoblasts and that cultured osteoblasts from mice lacking CITED1 display abnormal differentiation in vitro. To determine the possible role of CITED1 in early bone development, we have analyzed endochondral bone formation in tibiae from CITED1-knockout (KO) embryonic mice in which the CITED1 gene is replaced with a functional LacZ/Neo cassette and bred into the 129Sv background for five generations. The tibiae of CITED1 KO mice were shorter than those of wild type (WT) littermates, and bone volume and the extent of trabeculae in CITED1 KO tibiae at E18.5 and post-natal day 1 (P1) were significantly reduced, as shown by von Kossa staining and histology. At E15.5, the regions of overall chondrogenesis and of chondrocyte hypertrophy, demonstrated by Col II and Col X expression respectively, were not different in WT and KO; but bone formation, shown by Col I in situ analysis, appeared slightly earlier inside the tibia and expanded wider in perichondral region in the WT. Osteopontin (OPN) is expressed by late hypertrophic chondrocytes and osteoblasts within the primary and secondary spongiosa. Relative to WT, the length of the central region of OPN expression was reduced in all KO bones from E15.5 through P1, accounting for the foreshortening of the overall bone length. In situ hybridization and LacZ staining analysis showed strong expression of CITED1 in this same central region of the developing bones but not in adjacent chondrocytes. We conclude that CITED1 expression, probably by cells of the osteoblast lineage, is important for normal endochondral bone formation and that loss of functional CITED1 expression leads to a reduction in the rate of bone formation. Whether this defect reflects impaired activity of osteoblasts that normally express CITED1 and/or loss of an indirect effect on chondrocyte proliferation and/or differentiation, which could involve PTHrP, remains to be investigated.

Disclosures: D. Yang, None.

S146

A Spontaneous Mutation (Dhe) in the Mouse Lmna Gene Results in Hypoplastic Cranial Sutures and Under-mineralization of the Skeleton. L. R. Donahue¹, D. Liu^{*1}, M. Curtain^{*1}, J. Hurd^{*1}, C. Marden^{*1}, C. A. MacKay^{*2}, P. R. Odgren^{*2}. ¹The Jackson Laboratory, Bar Harbor, ME, USA, ²University of Massachusetts Medical School, Worcester, MA, USA.

The Lmna gene encodes the nuclear lamins A and C, which, along with lamin B, constitute the proteinaceous nuclear envelope. Lmna mutations are associated with connective tissue disorders, including cardiomyopathies, muscular dystrophies, lipodystrophies, progeria and bone abnormalities. We discovered a new mutation in mouse Lmna that demonstrates a critical role for Lmna in cranial suture development and skeletal mineralization. Dhe, (Dominant hair and ears) is a semi-dominant mutation in exon 1 of Lmna (L52R). Dhe/+ mice exhibit a sparse coat, small ear pinnae, hypoplastic cranial sutures, and under-mineralization of the skeleton.

To assess suture formation we used X-ray, histological, and in situ analyses. Skeletal mineralization was measured by DEXA and X-ray.

DEXA showed that areal BMD is lower in Dhe/+ than in controls (Dhe/+ 0.037; +/- 0.045 g/cm²). Under-mineralization can be seen in radiographs of axial and appendicular skeleton. In X-rays of Dhe/+ skulls, the premaxillary/maxillary and cranial vault sutures, and the entire parietal bone, are clearly visible and radiolucent, indicating severe hypomineralization.

Microscopic examination revealed severely hypomorphic sutures in Dhe/+ skulls. The bony plates fail to overlap, the cells and connective tissue connecting the bones are loosely organized and hypoplastic, and suture material is poorly attached.

Extracellular matrix gene expression by in situ hybridization assessed with probes for expression of type I collagen mRNA in bone matrix and type III collagen mRNA in the fibrous suture matrix revealed gross deficiency of collagen gene expression. In controls, rows of osteoblasts on bone surfaces were intensely stained for col I. Bone synthesis was highly polarized, with active bone synthesis confined to specific surfaces, indicating a high degree of site specificity to the production of bone in the cranium. In contrast, Dhe/+ mice had extremely low levels of col I mRNA at the cranial sutures, consistent with a pronounced deficiency of bone synthesis. In +/- mice, the fibroblastic cells inhabiting the suture expressed high levels of col III, consistent with the production of dense connective tissue in the suture proper. In Dhe/+, the level was extremely low, consistent with the loose strands of connective tissue connecting the cranial bones. These observations provide evidence that there is a severe loss of extracellular matrix synthesis at the cellular level in osteoblasts and sutural fibroblasts. Thus, Lmna is critical to normal cranial bone and suture formation and to skeletal mineralization.

Disclosures: L.R. Donahue, None.

This study received funding from: NIH R01 grant: EYO15073 to Dr. Donahue.

S148

Body Mass Influences Bone Mass Independent of Leptin Signaling. U. T. Iwaniec¹, S. Boghossian^{*2}, R. T. Turner¹, S. P. Kalra^{*2}. ¹Nutrition and Exercise Sciences, Oregon State University, Corvallis, OR, USA, ²Neuroscience, University of Florida, Gainesville, FL, USA.

Skeletal growth and turnover are coupled to energy balance via incompletely understood mechanisms. Anorexia is associated with low bone mass, whereas obesity correlates with increased bone mass. Leptin, a hormone produced by fat cells, functions as a sentinel of energy balance and may be a potential mediator of the effects of fat mass on bone mass. The objective of this study was to determine whether increased weight due to increased fat intake increases bone mass, and, if so, whether this requires central leptin signaling. Leptin-deficient ob/ob mice were used in the experiment. In order to replete hypothalamic leptin, 8-10 week-old ob/ob mice were injected in the hypothalamus with a recombinant adeno-associated virus containing the leptin gene (rAAV-lep) or a control vector, rAAV-GFP (green fluorescent protein). The mice were maintained on a regular control diet (RCD) for 7 weeks and then subdivided into groups (n=8-9/group) and either continued on the RCD or fed a high fat diet (HFD, 45 kcal% fat; D12451, Research Diets) for 8 weeks. Bone mass and architecture were evaluated by μ CT. Administration of rAAV-lep resulted in decreased body weight, increased femur length and total femur volume, and reduced cancellous bone volumes in the distal femur and lumbar vertebra, indicating that leptin affects multiple aspects of bone growth and architecture. Body weight increased (P<0.003) with high fat intake (+18%), irrespective of rAAV treatment; mice administered rAAV-GFP weighed 56 \pm 2g on RCD and 66 \pm 2g on HFD, while mice administered rAAV-lep weighed 28 \pm 3g on RCD and 33 \pm 2g on HFD. Total femur bone volume increased with HFD in leptin-deficient rAAV-GFP mice (P<0.001, 14.3 \pm 0.6 mm³ vs. 18.2 \pm 0.4 mm³) and there was a tendency for an increase in total femur bone volume in HFD-fed rAAV-lep-treated mice (P<0.06, 16.2 \pm 0.2 mm³ vs. 17.1 \pm 0.4 mm³). Distal femur and vertebral cancellous bone volume were not altered by diet. There was a significant correlation between body weight and total femur bone volume in wildtype mice fed normal diets (data not shown). Taken together, these findings suggest that increased body weight has a positive effect on total femur bone mass that is independent of dietary fat and leptin signaling.

Disclosures: U.T. Iwaniec, None.

This study received funding from: NIH.

S150

Phenotypic Analysis of the Crtp^{-/-} Mice: The First Animal Model for Recessive Osteogenesis Imperfecta. R. Morello¹, J. N. Lenington^{*2}, S. Kakuru^{*1}, M. Jiang^{*3}, Y. Chen^{*3}, D. R. Keene^{*4}, B. Lee³. ¹Molecular and Human Genetics, Baylor College of Medicine, Houston, TX, USA, ²Pediatrics, Baylor College of Medicine, Houston, TX, USA, ³Howard Hughes Medical Institute, Houston, TX, USA, ⁴Shriners Hospital for Children, Portland, OR, USA.

We recently described the phenotype of the Crtp^{-/-} mice. These mice exhibit a severe osteochondrodysplasia, with low bone mass, kyphosis and shortening of the long bones. Crtp interacts with prolyl 3-hydroxylase 1 (P3h1) and is essential for proper type I and II collagens post-translational modification. Importantly, the phenotype of Crtp^{-/-} mice closely resembles that of OI patients and mutations in the CRTAP gene cause recessive osteogenesis imperfecta (OI). In this study we extended the phenotypic analysis of our mutant mice in order to obtain a better understanding of the Crtp role during development and adulthood. Adult skeletal preparations showed marked craniofacial abnormalities in the Crtp null mice, consisting of shortening and compression of the anterior portion of the cranium with occasional asymmetry causing malocclusion and overgrowth of the incisor teeth. The skin showed increased laxity compared to WT littermates: a histological analysis revealed a decreased thickness of the dermis while at the ultrastructural level, areas of decreased matrix density as well as collagen fibrils with increased diameter were visible. Histological analysis of visceral organs showed evidence of abnormal lung morphology, with alveolar dilatation associated with thinning of the alveolar walls. Moreover, the kidney glomerular basement membrane appeared to have an expanded lamina lucida at the expenses of the lamina densa, suggesting perhaps an additional Crtp role in the regulation of type IV collagen modification. Finally, loss of Crtp causes a chondrodysplasia with rhizomelic shortening of long bones. Interestingly, BrdU incorporation studies of the growth plate point to a slight increase in chondrocyte proliferation in the zeugopod growth plates of E15.5 Crtp null mice compared to controls. Our studies point to a broad spectrum of connective tissue disease that can arise from loss of CRTAP and altered collagen 3-prolyl-hydroxylation.

Disclosures: R. Morello, None.

S152

Female, But Not Male, TIEG-Null Mice Display Severe Osteopenia and Abnormal Cancellous Bone Microarchitecture. M. Subramaniam¹, J. R. Hawse¹, U. T. Iwaniec², S. F. Bensamoun^{*3}, K. D. Peters^{*1}, N. M. Rajamannan⁴, M. J. Oursler¹, R. T. Turner², T. C. Spelsberg¹. ¹Biochemistry and Molecular Biology, Mayo Clinic, Rochester, MN, USA, ²Department of Nutrition and Exercise Sciences, Oregon State University, Corvallis, OR, USA, ³Genie Biologique, Universite de Technologie de Compiègne, Compiègne, France, ⁴Department of Cardiology, Northwestern University Medical School, Chicago, IL, USA.

TGF β Inducible Early Gene-1 (TIEG), also classified as Krüppel-like transcription factor-10 (KLF-10), was originally cloned from human osteoblasts and has been shown to play an important role in osteoblast growth and differentiation. To better understand the biological role of TIEG in the skeleton, we generated TIEG-null (TIEG^{-/-}) mice. Calvarial osteoblasts isolated from TIEG^{-/-} mice express reduced levels of Runx2 and other important osteoblast marker genes and have significant defects in their mineralization capacity relative to wild-type (WT) controls. Through the use of PIXImus and pQCT analysis, we have demonstrated that the femurs and tibias of two-month-old C57Black6 female TIEG^{-/-} mice display significant decreases in numerous bone parameters including total bone mineral content, density and area, relative to WT littermates. However, no differences were observed for any of these bone parameters in male mice. In order to further characterize the bone phenotype of female TIEG^{-/-} mice, we performed mechanical 3-point bending tests. These studies revealed that the femurs of TIEG^{-/-} mice are much weaker when compared to WT littermates. Micro-CT analysis of femurs of two-month-old TIEG^{-/-} and WT mice revealed a highly significant 9% decrease in total femur bone mass (cortical + cancellous bone) in the TIEG^{-/-} mice compared to WT littermates. Histomorphometric evaluation of the distal femur revealed that TIEG^{-/-} mice also display a 31% decrease in cancellous bone area, which is primarily due to a 22% decrease in trabeculae number. At the cellular level, TIEG^{-/-} mice exhibit a 42% reduction in bone formation rate which is almost entirely due to a reduction in double labeled perimeter. Differences in the mineral apposition rate were not detected between WT and TIEG^{-/-} mice. Interestingly, we have demonstrated that TIEG is regulated by estrogen in an ER β isoform-specific manner in osteoblasts. Since ER β is primarily expressed in cancellous bone, and since TIEG^{-/-} mice display significant defects in cancellous bone in a gender specific manner, we speculate that the estrogen regulation of TIEG may play a vital role in this phenomenon. Taken together, these findings suggest that TIEG^{-/-} mice are osteopenic mainly due to a decrease in total osteoblast number and support a critical role for TIEG in skeletal development and/or homeostasis.

Disclosures: M. Subramaniam, None.

S157

Biglycan and Fibromodulin Control Bone Mass by Regulating Osteoclast Differentiation Through Bone Marrow Stromal Cells. Y. Bi*, T. M. Kilts*, A. C. Griffin*, M. F. Young. National Institute of Dental and Craniofacial Research, National Institutes of Health, Bethesda, MD, USA.

Members of the Small Leucine-Rich Proteoglycan (SLRP) family populate numerous sites in the musculoskeletal system including tendon, cartilage and bone, but, their precise role in these tissues is still unclear. Previous work showed that mice with combined deficiencies in two SLRPs, biglycan (bgn) and fibromodulin (fmod), acquire osteoarthritis and ectopic tendon ossification. Here we show that the bgn-0/fmod-0 mice have delayed bone formation during development judged by alizerin red/alcian blue staining and severe age-dependent osteopenia determined by X-ray and microCT analyses. In order to understand the molecular basis for this osteopenia, osteogenic bone marrow stromal cells (BMSCs) were isolated and examined. Colony-forming unit fibroblastic (CFU-F) analysis, which estimates the number of osteogenic stem cells, showed no significant differences between WT and bgn-0/fmod-0 mice. Further, in vitro osteogenesis assays showed that Ca²⁺ accumulation was increased in the bgn-0/fmod-0 BMSC cultures compared to WT BMSCs. Western analysis of the BMSC protein extracts showed that the bgn-0/fmod-0 cells had increased levels of Runx2 compared to WT controls. The bgn-0/fmod-0 BMSCs also had increased BMP-2 and TGF- β 1 signaling indicated by increased levels of p-smad1 and p-smad2/3 in the presence of BMP-2 and TGF- β 1 compared to WT BMSCs, respectively. Furthermore, in vivo bone formation was not significantly different between WT and bgn-0/fmod-0 BMSCs transplanted subcutaneously into immuno-compromised mice. From these data, we concluded that the decreased bone mass in bgn-0/fmod-0 mice was not primarily due to a defect in osteogenesis. We next determined whether the osteopenia in bgn-0/fmod-0 mice could be due to increased differentiation and/or activity of osteoclasts. To test this, sections of long bone and BMSC transplants were stained for Tartrate-Resistant Acid Phosphatase (TRAP), an osteoclast marker. The number of TRAP positive cells was higher in bone and in vivo BMSC transplants from bgn-0/fmod-0 mice. Osteoclastogenesis was assessed by adding bone marrow suspensions to plates in which BMSC had formed individual colonies and showed that greater numbers of colonies in the bgn-0/fmod-0 cultures supported formation of TRAP-positive multinucleated cells compared to WT. In summary, we have shown that bgn and fmod when depleted in combination have a negative influence on bone mass by increasing osteoclast formation and function and thereby pointing to the possibility that these SLRPs could be novel targets to modulate bone turnover.

Disclosures: Y. Bi, None.

This study received funding from: IRP-NIDCR, NIH.

S160

Implication of Two Matrix Proteins in Bone Healing: Osteopontin (OPN) and Bone Sialoprotein (BSP). L. Monfoulet*, J. Fricain*, L. Malaval*, J. Aubin*, O. Chassande*. ¹INSERM U577 - Univ Victor Segalen Bordeaux2, bordeaux, France, ²INSERM U890 - Univ Jean Monnet, St Etienne, France, ³Medical Genetics and Microbiology, Faculty of Medicine, University of Toronto, Toronto, ON, Canada.

Bone fracture healing involves a well characterized cascade of events that includes: hematoma, inflammation, "soft" callus, neovascularization, callus mineralization and remodelling of the "hard" callus to generate mature lamellar bone. This complex sequence of biological processes is controlled by chemotactic factors, growth factors and bone matrix proteins. Our study is focused on two major non-collagenous bone matrix proteins belonging to the Small Integrin-Binding Ligand N-linked Glycoprotein (SIBLING) family: osteopontin and Bone Sialoprotein. OPN promotes angiogenesis, inhibits bone mineralization, and regulates osteoclast function. BSP is involved in osteoclast adhesion and differentiation, in matrix mineralization, and mediates endothelial cell migration and angiogenesis. Together, these data suggest that BSP and OPN can play an important role in bone fracture healing. To investigate the role of these proteins of bone healing, we used mice knockout for the OPN or BSP genes. We developed a new model of bone healing in mice which consists in a 0.9 mm diameter cortical defect in the femoral diaphysis. Micro-computed tomography was used to quantify mineralization at 14 and 21 days. Histology (at 14 and 21 days) and quantitative RT-PCR (at 10 days) were used to evaluate cellular functions related to ECM formation, bone formation and remodelling. We also established primary cultures of osteoblasts from mutant and wild type bone marrow, characterized by quantitative RT-PCR and alkaline phosphatase activity. Using micro-CT, we have demonstrated in BSP-0 mice a significant delay of bone healing as showed by a slower decrease of the Bone Volume / Tissue Volume (BV/TV) volume within the defect. At 10 days, RT-PCR analysis reveals a lower expression of osteocalcin mRNA in BSP-0 mice compared to wild-type mice. These preliminary results suggest that the delay in bone healing observed in BSP-0 mice could be due to a decreased osteoblast activity. In contrast, the OPN-0 mice show an advanced bone healing in comparison with wild-type. We have also developed primary cultures of mouse Bone Marrow Stromal Cells to investigate the role of this bone matrix protein on osteoblast differentiation. The first results tend to show that OPN deficiency accelerates differentiation into mature osteoblasts. This early differentiation could explain the advanced bone healing observed by microCT in OPN-0 mice. In summary, our results reveal antagonist roles for these two major bone matrix proteins during the process of bone healing.

Disclosures: L. Monfoulet, None.

S163

Delayed Cartilage and Bone Remodeling During Fracture Healing in Matrix Metalloproteinase 13 Null Mutant Mice. C. Colnot¹, D. J. Behonick², S. Lieu¹, Z. Xing¹, R. Marcucio¹, Z. Werb², T. Miclau¹. ¹Orthopaedic Surgery, University of California San Francisco, San Francisco, CA, USA, ²Anatomy, University of California San Francisco, San Francisco, CA, USA.

Adult bone does not heal through the production of scar tissue rather through a regenerative process, that recapitulates early skeletal development. Matrix metalloproteinase 13 (MMP13, collagenase-3) is an extracellular matrix (ECM) protease whose preferred substrates include the major components of cartilage and bone ECM. MMP13 has been shown to be important for skeletal development via endochondral ossification (1). This observation led us to question the role of MMP13 in skeletal repair. We compared bone healing in Mmp13^{-/-} and wild type mice during non-stable, stable fracture repair and cortical defect healing. In order to understand which cell types were affected by the Mmp13^{-/-} mutation, we examined the expression profile of Mmp13 during bone healing using in situ hybridization. In addition, we transplanted bone marrow from wild type mice into Mmp13^{-/-} mice and compared healing to Mmp13^{-/-} mice, which received bone marrow from a Mmp13^{-/-} donor. Tissues were analyzed by cellular, molecular and histomorphometric analyses on paraffin tissue sections.

We show that MMP13 is required for proper resorption of hypertrophic cartilage and normal bone remodeling during non-stabilized fracture healing, which occurs via endochondral ossification (Fig. 1). Transplant of bone marrow from wild type mice is not sufficient to rescue the Mmp13^{-/-} healing phenotype. These results indicate that impaired healing is intrinsic to cartilage and/or bone and is not due to defects in osteoclasts. These results are consistent with the expression of Mmp13 which is restricted to hypertrophic chondrocytes and osteoblasts but absent from osteoclasts. Furthermore, Mmp13^{-/-} mice also exhibit a delay in bone remodeling during healing of stabilized fractures and cortical defects via intramembranous ossification, demonstrating that the bone phenotype is independent from the cartilage phenotype. Overall, our findings demonstrate that MMP13 is crucial for normal production and remodeling of cartilage and bone during adult fracture repair.

1. Stickens D et al. Development 131:5883-95, 2004

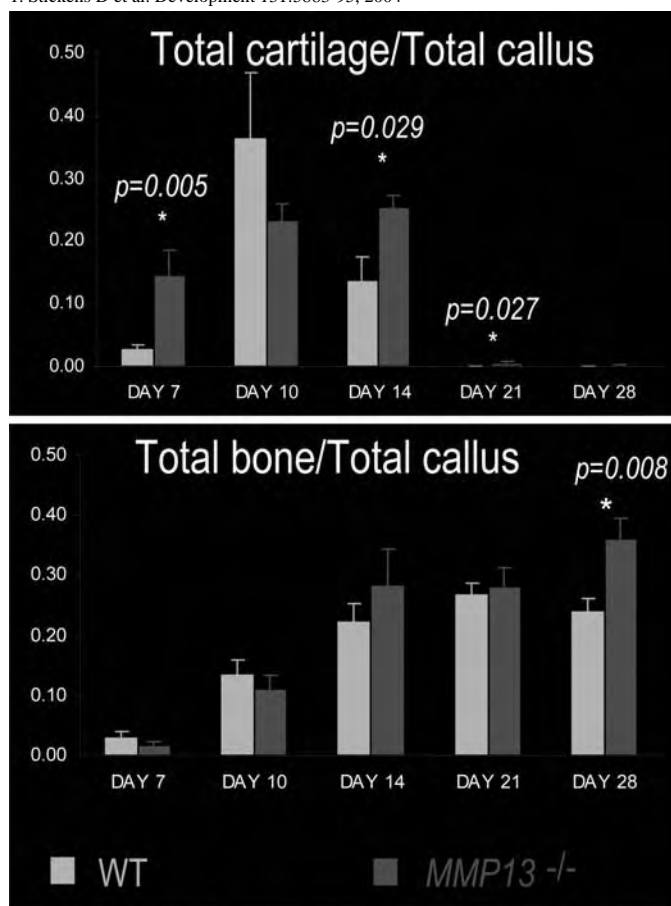


Fig.1: Histomorphometric measurements indicating increased amount of cartilage at days 7, 14 and 21 post fracture and increased amount of bone at day 28 in the Mmp13^{-/-} compared to wild type control

Disclosures: C. Colnot, None.

This study received funding from: NIH.

S165

Rescue of MT1-MMP Expression in Cartilage Increases Survival, Chondrocyte Proliferation and Bone Formation in MT1-MMP Deficient Mice. L. Szabova*, S. Yamada*, K. Holmbeck*. CSDB/MMPU, NIDCR, Bethesda, MD, USA.

Membrane type-1 matrix metalloproteinase (MT1-MMP) is a potent collagenase essential for proper remodeling of collagen rich tissues. Mice deficient for MT1-MMP (KO) are dwarfs with severe fibrosis of connective tissues, bone loss and retention of embryonic cartilages in the skull due to impaired degradation of unmineralized type I and II collagens. Here we define the contribution of disrupted cartilage remodeling in the development of the MT1-MMP-deficient phenotype. Specifically, we created transgenic mice where MT1-MMP expression was selectively re-introduced in cartilage tissues using a transgene driven by the type II collagen promoter/enhancer. We have bred these mice into the MT1-MMP-deficient background and evaluated the developmental effects of MT1-MMP expression in the cartilage tissue of otherwise MT1-MMP deficient mice. Cartilage specific MT1-MMP expression in KO mice resulted in complete rescue of the pre-weaning death observed in KO mice, increased body weight and prolonged survival. Transgenic KO mice further displayed increased bone formation in the skull compared to KO mice. Strong expression of the MT1-MMP transgene increased chondrocyte proliferation in the epiphyseal growth plate, which resulted in increased growth of the long bones. Increased bone formation quite unexpectedly coincided with expression of the transgene in a subset of bone cells. Expression of type II collagen was documented in bone cells of normal mice using *in situ* hybridization and immunostaining thus documenting that transgene expression was not ectopic, but mirrored the normal expression pattern of type II collagen. This finding explains the increased bone formation observed in transgenic KO mice since MT1-MMP is necessary for maintaining the bone formation. In conclusion, reintroduction of MT1-MMP in the cartilage of MT1-MMP KO mice results not only in cartilage specific expression, but also directs transgene expression in a subset of bone cells thereby facilitating increased bone formation. These bone cells are most likely the descendants of a common progenitor of bone cells and chondrocytes expressing type II collagen and support our previous observation that some chondrocytes can differentiate into bone cells. Our data suggest that MT1-MMP provides type II expressing chondrocytes and bone cells with the necessary collagenolytic activity required for chondrocyte proliferation and bone formation *in vivo*.

Disclosures: L. Szabova, None.

S169

Identification of a Novel Stem Cell for Bone and Cartilage of the Myeloid Lineage. Z. W. Lazard*, C. M. Fouletier-Dilling*, F. H. Gannon², M. H. Heggeness*, E. A. Olmsted-Davis¹, A. R. Davis¹. ¹Cell and Gene Therapy, Baylor College of Medicine, Houston, TX, USA, ²Orthopedic Surgery and Pathology, Baylor College of Medicine, Houston, TX, USA, ³Orthopedic Surgery, Baylor College of Medicine, Houston, TX, USA.

We have previously shown that osteoblasts can be derived from hematopoietic stem cells (HSC), through mesenchymal progenitors. In this study, we focused on identifying the pathway that leads from a bone marrow HSC to a mesenchymal progenitor for bone and cartilage. To better characterize this process, we used a BMP2 inductive model which recruits chondro-osseous progenitors in the mouse to a heterotopic location. In this bone formation model, cells transduced with an adenovirus expressing BMP2 were implanted into the muscle in the mouse hind limb. Bone formation occurs rapidly, with cartilage appearing within 6 days and mineralized osteoid detected by 7 days after implantation of the transduced cells. Initial characterization of the tissues isolated three days after induction showed a substantial increase in tentative progenitors. These cells possessed the marker of the donor HSCs used to repopulate the bone marrow in ablated recipients, suggesting they were bone marrow derived. Cells isolated from the day 4 tissues were capable of undergoing osteogenic or chondrogenic differentiation *in vitro*. Immunohistochemical and microarray analysis of these tissues showed specific elevation in genes associated both with mesenchymal stem cells (CD44, CXCR4) as well as myeloid cells (CD11b, CD68, CD166) in tissues receiving the AdBMP2 transduced cells as compared to those receiving cells transduced with an empty vector. To further delineate the tentative myeloid origin of these progenitors we performed heterotopic bone assays in mice which express myeloid restricted β -galactosidase. In these mice cre recombinase is expressed by the myeloid specific LysM gene promoter which can remove the intervening DNA sequence between the LacZ gene promoter and its transcriptional start site leading to permanent activation. Analysis of the tissues shows specific β -galactosidase activity in the tentative progenitors, as well as the mature chondrocytes, and osteoblasts in the heterotopic bone as well as adjacent skeletal bone. Since these bone marrow derived cells must circulate to reach the heterotopic location, we next attempted to purify these from peripheral blood. Results showed significant elevation in both myeloid and mesenchymal stem cell markers on peripheral blood mononuclear cells by 3 days after induction of bone formation. The data collectively demonstrates a novel myeloid progenitor, easily isolated from peripheral blood, that is recruited for endochondral bone formation.

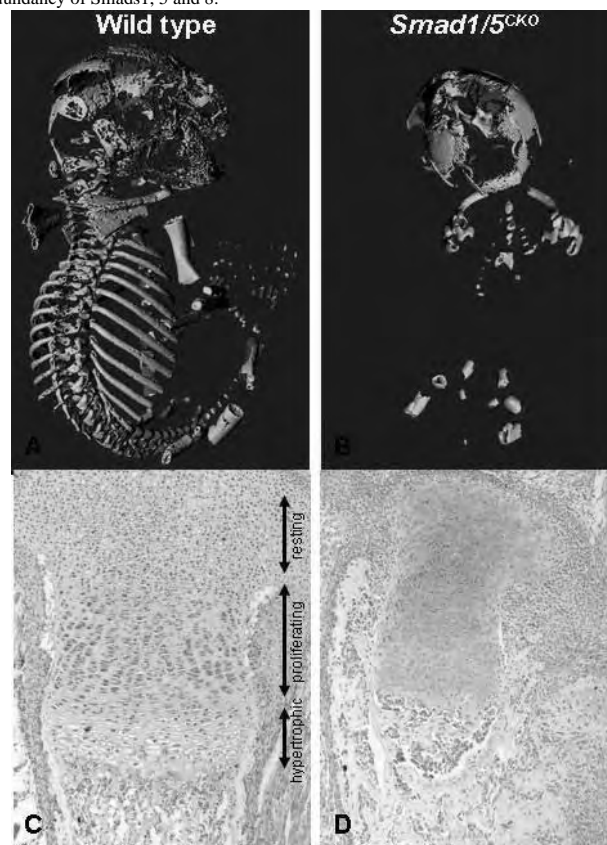
Disclosures: Z.W. Lazard, None.

This study received funding from: NIBIB: R01EB005173 and DOD: PRO33169.

S171

BMP Canonical Signaling Through Receptor Smads 1 and 5 Is Required for Endochondral Bone Formation. K. N. Retting*, R. R. Behringer*, K. M. Lyons¹. ¹Orthopaedic Surgery, UCLA, Los Angeles, CA, USA, ²Molecular Genetics, University of Texas M.D. Anderson Cancer Center, Houston, TX, USA.

Transforming growth factor- β (TGF β) superfamily members including bone morphogenetic proteins (BMP) play multiple roles during endochondral bone formation. It is believed that TGF β superfamily members signal predominantly through canonical Smad pathways during chondrogenesis. The BMP family activates Smads 1, 5 and 8. We have found nuclear localization of BMP R-Smads in proliferating and differentiating chondrocytes in the growth plate and in primary cultures. These and other studies establish that BMP signaling is required for chondrogenesis. R-Smads share structural homology, yet the extent to which Smad proteins are functionally redundant, regulate distinct targets, and control endochondral bone formation *in vivo* is unknown. To study the role of BMP R-Smads during chondrogenesis, we generated knockout models of Smads 1, 5 and 8 individually and in combination. It has been reported that Smad8 null mice have no obvious defects. Because mice null for either Smad1 or 5 die too early in embryogenesis for chondrogenesis analysis, we conditionally deleted Smads 1, 5 and 8 in endochondral elements utilizing the cartilage-specific collagen II-Cre. Cartilage-specific loss of Smad1 as well as the combined loss of Smads1 and 8 results in apparently normal mice. However, Smad1 (fx/fx);Smad5 (fx/fx);Col2Cre mutant mice exhibit severe chondrodysplasia, resulting in lethality at birth. Smad1/5^{CKO} mutants display little to no mineralization of the axial skeleton. The dramatically shortened limbs lack an organized growth plate and display excessive growth in the bone collar. These data demonstrate that canonical Smad signaling is required for endochondral bone formation, and suggest that Smads 1 and 5 exhibit functional redundancy. The phenotype is more severe than that seen in Smad4 (fx/fx);Col2Cre mice, challenging the dogma, at least in chondrocytes, that co-Smad4 is required to mediate Smad signaling through TGF β and BMP pathways. Furthermore, skeletal defects in the Smad1/5^{CKO} are not as severe as the cartilage-specific knockout of BMP receptors, indicating that BMP signaling is not completely abolished. We are currently testing these hypotheses. Overall, these data demonstrate the importance of the BMP canonical Smad pathway in chondrogenesis and answer the questions of functional redundancy of Smads1, 5 and 8.



Absence of endochondral bone formation in Smad1 (fx/fx);Smad5 (fx/fx);Col2Cre mice. Wild type (A,C) and mutant (B,D) littermates at P0; MicroCT scan (A,B); proximal tibia stained with Alcian blue and nuclear fast red (C,D).

Disclosures: K.N. Retting, None.

S176

Role of TROY in Tooth Development. N. Yamaguchi¹, H. Ichioka^{*1}, S. Toyosawa^{*2}, H. Harada^{*3}, R. Nishimura¹, T. Yoneda¹. ¹Biochemistry, Osaka University Graduate School of Dentistry, Suita, Japan, ²Oral Pathology, Osaka University Graduate School of Dentistry, Suita, Japan, ³Oral Anatomy 2, Iwate Medical University School of Dentistry, Morioka, Japan.

Mutations of ectodysplasin (Eda), a member of TNF family, cause hypohydrotic ectodermal dysplasia (HED), characterized by ectodermal abnormalities, including sweat glands defects, impaired hair formation, anodontia/oligodontia, and amelogenesis imperfecta. It is also demonstrated that the receptor for Eda/Edar and an adaptor protein of Edar EDARADD are responsible for HED. Spontaneous mutations of the Eda, Edar or EDARADD gene in mice also develop HED like phenotype. These results indicate a critical role of Eda/Edar/EDARADD signal in the tooth development. Eda/Edar/EDARADD transduces signals into cytoplasm through TRAF6. Mice deficient in TRAF6 gene showed more severe ectodermal abnormalities than tabby mice which have a mutation in the Eda gene. We therefore hypothesized that an additional pathway plays a role in the tooth development through TRAF6. Because a TNF receptor family member, TROY, which has 33% homology to Edar and directly binds to TRAF6, is expressed in tooth germ, we examined whether TROY plays a critical role in tooth development associated with TRAF6.

We first determined the expression of TROY in tooth germs. RT-PCR analyses demonstrated the expression of TROY in tooth germs of E13 or 14 days mouse embryos. In addition, we also found that Nogo Receptor 66-1 and LINGO-1, both of which function as co-receptors of TROY, were expressed in tooth germs, suggesting an involvement of TROY in the tooth development. To understand the role of TROY in the tooth development, we generated soluble TROY (sTROY), which consists of only an extracellular domain of TROY, and thus is expected to function as a decoy receptor for TROY, and determined its effect on the development of tooth germs of mice in organ culture system. Treatment with sTROY clearly impaired growth of tooth germs. Furthermore, sTROY markedly inhibited expression of phenotypic markers of ameloblast such as ameloblastin, amelogenin, and Sp6. These results suggest that TROY is involved in ameloblast differentiation. To determine downstream pathways of TROY involved in the tooth development, we next examined whether p38 and JNK pathways, which are well-known downstream pathways of TRAF6, are involved in the tooth development. We observed that p38 inhibitor (SB203580) and JNK inhibitor (SP600125) dramatically inhibited the development of tooth germs and reduced expression of ameloblastin at transcriptional level. In conclusion, our data suggest that TROY plays an important role in the tooth development, especially in ameloblast differentiation, presumably through p38 and JNK pathways.

Disclosures: N. Yamaguchi, None.

S179

Sclerostin Overexpression Impairs Limb Patterning. N. M. Collette^{*1}, R. M. Harland^{*2}, G. G. Loots¹. ¹Biosciences and Biotechnology Division, Lawrence Livermore National Laboratory, Livermore, CA, USA, ²Department of Molecular and Cellular Biology, University of California, Berkeley, CA, USA.

Sclerostin (SOST) is a negative regulator of bone formation that has been described as both a BMP- and WNT- antagonist. Loss of SOST function causes sclerosteosis (MIM 269500), a condition of severe progressive bone overgrowth. Using transgenic mice expressing human SOST from a bacterial artificial chromosome (BAC) we have demonstrated that SOST over-expression causes decreased bone formation and results in osteopenia, similar to the over-expression of other BMP antagonists such as Noggin and Gremlin. These mice also exhibit severe limb patterning defects that are dose-dependent and range from the loss of a single posterior digit to the loss and/or fusion of many distal limb skeletal elements. The apical ectodermal ridge (AER) relays cell-cell signals to the underlying differentiating limb mesenchyme, a place of SOST expression initiated as early as E9.5. To determine how elevated levels of SOST impair proper limb patterning, we have examined AER and cartilage markers by measuring mRNA levels by in situ hybridization. We find FGF8, a major AER signaling molecule and underlying mesenchymal markers BMP2, Gli1, Pax1, HoxD12 and gremlin expression to be perturbed in SOST transgenic mice. In addition, skeletal analysis of double mutant animals show that over-expression of SOST fails to complement loss of BMP antagonists (Gremlin and Noggin) essential for limb patterning and chondrogenesis, resulting in more dramatic skeletal defects than single mutants alone, suggesting that SOST action in the limb parallels the BMP-pathway. This work is supported by NIH RO1 HD047853 and the work has been performed under the auspices of the U.S. Department of Energy by the University of California, Lawrence Livermore National Laboratory Contract No. W-7405-Eng-48. UCRL-ABS-229990

Disclosures: N.M. Collette, None.

This study received funding from: NIH R01 HD047853.

S182

Lysophosphatidic Acid Induces Osteocyte Dendrite Outgrowth. S. A. Karagiosis^{*}, N. J. Karin. Biological Sciences Division, Pacific Northwest National Laboratory, Richland, WA, USA.

Osteocytes form an extensive mechanosensory network in bone matrix and communicate intercellularly via gap junctions established at dendrite termini. These membrane extensions are thought to be essential for osteocyte function, but the mechanisms that govern dendrite formation are not known. We previously demonstrated that osteoblasts, the progenitors of osteocytes, are highly responsive to the lipid growth factor lysophosphatidic acid (LPA). LPA-treated MC3T3-E1 osteoblastic cells developed membrane structures that resemble osteocyte dendrites [Masiello et al. (2006) Bone 39:72-82], and we predicted that LPA would promote osteocyte membrane outgrowth. We developed a method to measure osteocyte dendritogenesis in vitro using a modified transwell assay and determined that LPA is a potent stimulator of dendrite outgrowth in MLO-Y4 osteocytes. The stimulatory effects were dose-dependent with maximal outgrowth observed within a physiological range of LPA. The LPA-induced increase in dendrite formation was blocked by the specific LPA-receptor antagonist K16425 and by pertussis toxin. LPA-treated osteocytes exhibited distinct rearrangements of the actin cytoskeleton and a more stellate morphology than control cells. These data are the first evidence for the regulation of dendrite formation by a soluble factor. Osteocytes in vivo are encased in bone matrix, rendering them non-motile. However, LPA promoted MLO-Y4 cell chemotaxis, suggesting that commonalities exist between the intracellular signaling pathways that regulate dendrite outgrowth and cell motility. Bone cells in vivo encounter platelet-derived LPA in regions of bone damage, and we postulate that this lipid factor is important for re-establishing osteocyte connectivity during fracture repair. We also found that MC3T3-E1 cells, primary mouse calvarial osteoblasts and MLO-Y4 osteocytes express autotaxin, a lysophospholipase that catalyzes the generation of LPA. This indicates that bone cells may be exposed to LPA under conditions other than the response to bone damage, and that this lipid growth factor may have broader roles in the control of skeletal homeostasis.

Disclosures: S.A. Karagiosis, None.

This study received funding from: U.S. Department of Energy.

S185

TNF-alpha Upregulates Aortic BMP2-Msx2-Wnt Signaling in Diabetic LDLR-/- Mice. J. S. Shao, C. F. Lai, Z. Al-Aly^{*}, J. Cai^{*}, E. Huang^{*}, S. L. Cheng, D. A. Towler. Dept. of Internal Medicine, Washington University School of Medicine, St. Louis, MO, USA.

Aortofemoral calcification is prevalent in type II diabetes (T2DM), tracking metabolic syndrome parameters and increasing the risk for lower extremity amputation. LDLR-/- mice fed high fat diets (HFD) develop obesity, T2DM, and accumulate aortic calcium - the latter mediated via osteogenic mechanisms that resemble craniofacial mineralization. HFD upregulate aortic BMP2 and Msx2-Wnt signaling cascades that promote mineralization in neural crest-derived skeletal tissues. Administration of recombinant purified BMP2 augments aortic Msx2-Wnt signaling in TOPGAL reporter mice, and promotes aortic calcium deposition in LDLR-/- mice. Low-grade inflammation, including elevated circulating TNF-alpha, is characteristic of obesity with T2DM, therefore, we examined the relationships between TNF-alpha and aortic BMP2-Msx2-Wnt signaling in the LDLR-/- model. HFD feeding promotes obesity, hyperglycemia, and hyperlipidemia -- and upregulated serum TNF-alpha and haptoglobin in male LDLR-/- mice. Oxidative stress, reflected in serum 8-F-alpha-isoprostane (8-IsoP) levels, was increased, with concomitant upregulation of aortic BMP2 (2.5-fold), Msx2 (2.5-fold), Wnt3a (10-fold), and Wnt7a (14-fold) gene expression (all p < 0.01, 2-tailed t-test). Treatment of diabetic LDLR-/- mice with the TNF-alpha antagonist infliximab (10 ug / gm twice weekly, 5 animals per group) did not reduce obesity, hyperleptinemia, or hyperglycemia; however, serum 8-IsoP and haptoglobin levels were significantly decreased. Moreover, aortic BMP2, Msx2, Wnt3a, and Wnt7a expression and aortic calcium accumulation were concomitantly and significantly reduced by infliximab treatment (all p < 0.05). Administration of sodium salicylate, an alternative anti-inflammatory strategy, also reduced serum haptoglobin and aortic Msx2 gene expression. Finally, C57BL/6 mice with arterial smooth muscle TNF-alpha expression augmented by a SM22- TNF-alpha transgene accumulate significantly higher levels of aortic BMP2, Msx2, Wnt3a, and Wnt7a mRNAs vs. their non-transgenic sibling cohorts. Furthermore, 80% of SM22-TNFalpha; TOPGAL mice exhibit aortic beta-galactosidase reporter staining vs. 0% of their non-transgenic TOPGAL siblings (p=0.05 with Yates' chi-square correction), indicating net enhanced mural Wnt signaling by the SM22-TNFalpha transgene. Thus, inflammatory TNF-alpha signals promote pro-calcific BMP2-Msx2-Wnt programs in the aortic tissues of diabetic LDLR-/- mice. Strategies that inhibit inflammation-induced arterial BMP2-Msx2-Wnt signals may improve aortofemoral physiology and reduce lower extremity amputation risk in T2DM.

Disclosures: D.A. Towler, National Institutes of Health 2; Barnes-Jewish Hospital Foundation 2; Wyeth 5; GlaxoSmithKline 5.

This study received funding from: National Institutes of Health.

S191

IGF-I Engineered Bone Marrow Mesenchymal Stem Cells Improve the Fracture Healing Process. F. Granero-Molto¹, J. A. Weis¹, L. D. O'Rear¹, M. I. Miga², A. Spagnoli¹. ¹Pediatrics, Vanderbilt University, Nashville, TN, USA, ²Biomedical Engineering, Vanderbilt University, Nashville, TN, USA.

Healing failure occurs in 20% of the fractures. The reasons why fractures do not heal are mostly unknown. Limitations in adult stem cells (MSC) and growth factor imbalance play critical roles. The purpose of this study is to determine the regenerative ability of bone marrow (BM) MSC engineered to express IGF-I in a rodent fracture healing model. MSC, isolated from BM of syngenic FVB male mice, were retrovirally infected and selected either to stably express human des-IGF-I (MSC-IGF-I) or empty vector (MSC). Syngenic female mice (8-10 weeks old) were subjected to a three point bending stabilized tibia fracture and then transplanted either with 10⁶ MSC-IGF-I or MSC by IV tail injection. Fractured females were also used as controls (no cells). Fractured tibias were analyzed longitudinally by μ CT scan (Scanco 40 μ m). Fracture mechanoproperties were determined by distraction biomechanical testing (BMT) (ELF 3100, Bose). Callus cross-sections were subjected to histological and in-situ hybridization studies for cartilage and bone markers. As shown in Table I, fractured mice transplanted with MSC-IGF-I showed a significant improvement of the biomechanical properties of the callus with an increase in peak force, modulus of elasticity and energy to peak compared to controls.

	MSC-IGF-I (n=3)	MSC (n=4)	No cells (n=4)
Peak Force (N)	5.00 \pm 1.32 ^{*#}	2.63 \pm 0.96	1.86 \pm 0.55
Modulus of Elasticity (N/mm)	41.12 \pm 1.02 ^{*#}	11.95 \pm 9.76	19.39 \pm 9.35
Energy to Peak (N*mm)	0.36 \pm 0.18 ^{*#}	0.49 \pm 0.11	0.14 \pm 0.05

Table I. MSC-IGF-I transplant improves fracture healing. BMT performed 14 days after fracture/transplant. *p<0.05 vs MSC; #p<0.05 vs no cells.

As determined by μ CT analyses, fractured mice transplanted with MSC-IGF-I showed a significant increase in total, new high and low mineralized bone volumes (Table II).

	MSC-IGF-I (n=3)	MSC (n=3)	No cells (n=2)
New High Mineralized Bone (NH) (mm ³)	2.71 \pm 0.45 ^{*#}	2.02 \pm 0.47	1.93 \pm 0.07
New Low Mineralized Bone (NL) (mm ³)	6.91 \pm 2.24 [#]	3.43 \pm 0.61	3.69 \pm 1.26
Total Bone Volume (B+NH+NL) (mm ³)	13.72 \pm 2.22 [*]	9.32 \pm 1.15	9.26 \pm 1.32

Table II. MSC-IGF-I transplant increases callus bone mineralized volumes. μ CT analyses performed 14 days after fracture/transplant. *p<0.05 vs MSC; #p<0.05 vs no cells.

In-situ hybridization showed that in mice transplanted with MSC-IGF-I, the increase in biomechanical properties and bone callus volumes was associated with an increase of collagen-1 and 10 expression. We conclude that MSC-IGF-I transplant improves fracture repair increasing the fracture mechanoproperties, bone volumes and bone/cartilage gene expression. Our studies provide critical data to implement a novel therapeutic approach in patients with fracture healing failure transplanting MSC engineered to express IGF-I.

Disclosures: F. Granero-Molto, None.
This study received funding from: NIH-NIDDK.

S202

E-Selectin Ligand 1 Negatively Regulates TGF β in the Golgi During Skeletogenesis. T. Yang¹, R. Mendoza-Londono¹, H. Lu¹, K. Li¹, B. Keller¹, M. Jiang¹, Y. Chen¹, T. Bertin¹, B. Dabovic², D. B. Rifkin³, J. Hick⁴, A. L. Beaudet¹, B. Lee¹. ¹Molecular and Human Genetics, Baylor College of Medicine, Houston, TX, USA, ²Department of Cell, New York University Medical Center, New York, NY, USA, ³New York University Medical Center, New York, NY, USA, ⁴Dept. Pathology, Baylor College of Medicine, Houston, TX, USA.

Transforming growth factor β (TGF β) signaling is critical for the regulation of growth and differentiation during development and disease. Its context dependent action is specified by numerous control mechanisms at the extracellular level and downstream of ligand-receptor interactions, but little is known about the regulation of its post-translational trafficking. E-Selectin Ligand-1 (ESL-1), the cysteine rich protein originally isolated as a ligand for E-Selectin, was found to interact with FGFs and to be co-purified with TGF β 1 in a large protein complex. To elucidate the in vivo function of ESL-1, we mutated Esl-1 gene in mice by conventional knock-out strategy. The newborn and adult Esl-1^{-/-} mice are notably smaller with narrow chests and generalized shortening and thinning of the long bones, ribs and spine. By histological analysis, P1 Esl-1^{-/-} mice showed shortening of the growth plates in both the proliferating zone and hypertrophic zone. Further molecular biology assays show that ESL-1 acts as a negative regulator of TGF β production by binding TGF β precursors in the Golgi in a cell autonomous fashion. In vivo, loss of ESL-1 function causes increased TGF β signaling resulting in decreased cell proliferation and delayed terminal differentiation in the cartilaginous growth plate, independent of effects on BMP and FGF signaling. Moreover, in vivo genetic models of gain vs. loss of TGF β signaling in the growth plate confirm this effect. These data identify a novel cellular mechanism for regulating TGF β during skeletogenesis and cartilage homeostasis.

Disclosures: T. Yang, None.
This study received funding from: Arthritis Foundation.

S208

Klotho Ablation Completely Reverses the Biochemical and Skeletal Alterations in FGF23(R176Q) Transgenic Mice. X. Bai, H. Fu*, D. Qiu*, D. Goltzman, A. C. Karaplis. Department of Medicine, McGill University, Montreal, PQ, Canada.

Recently, we described the generation of a murine model of FGF23(R176Q) overexpression (FGF23^{tg}) and the associated biochemical and bone histological changes consistent with abnormal vitamin D metabolism and rickets. In this study, we have sought to use the mouse genetic approach to clarify the role of Klotho in the metabolic derangements associated with FGF23(R176Q) overexpression. To this end, we have crossed mice heterozygous for the hypomorphic Klotho allele (Kl^{-/-}) and Fgf23^{tg} mice to obtain Fgf23^{tg} transgenic mice homozygous for the Kl-hypomorphic allele (Fgf23^{tg}/Kl^{-/-}). Mice were sacrificed on day 50 post partum and serum, urine, and tissues were procured for analysis and comparison to Fgf23^{tg} WT, and Kl^{-/-} controls. From 4 weeks onward, Fgf23^{tg}/Kl^{-/-} mice were clearly distinguishable from Fgf23^{tg} mice and exhibited a striking phenotypic resemblance to the Kl^{-/-} controls. Their average body weight was 12.5 g \pm 0.7 (N=12), similar to that of Kl^{-/-} mice (12.7 g \pm 0.6; N=12) and significantly different from Fgf23^{tg} (18.6 g \pm 0.3; N=12) and WT controls (23.5 g \pm 0.5; N=12). Similarly, their average life span was dramatically diminished compared to Fgf23^{tg} mice (59.6 days vs. ~2 years) but comparable to that of Kl^{-/-} mice (62.4 days). Serum analysis for calcium (12.04 \pm 0.30 vs. 11.19 \pm 0.12 vs. 10.27 \pm 0.11 mg/dl), phosphorus (13.74 \pm 0.66 vs. 15.87 \pm 0.44 vs. 6.43 \pm 0.27 mg/dl), PTH (46.67 \pm 0.58 vs. 48.24 \pm 1.19 vs. 84.23 \pm 11.37 pg/ml), 1,25(OH)₂ vitamin D₃ (164.30 \pm 13.71 vs. 159.3 \pm 14.11 vs. 73.33 \pm 8.49 pg/ml), and alkaline phosphatase activity (163.30 \pm 15.59 vs. 125.40 \pm 26.20 vs. 611.3 \pm 66.04 IU/L) further confirmed the serum biochemical resemblance between the Fgf23^{tg}/Kl^{-/-} and Kl^{-/-} mice and their distinct difference from that of Fgf23^{tg} controls, respectively. Serum intact FGF23 levels also paralleled this pattern (371,500 \pm 16,500 vs. 336,000 \pm 32,300 vs. 2,544 \pm 463 pg/ml) among animals of the three genotypes. The characteristic bony changes associated with FGF23(R176Q) overexpression were also dramatically reversed by the absence of Klotho. Hence, frontal view of 3D reconstructed proximal end of Fgf23^{tg}/Kl^{-/-} tibia obtained using microCT showed complete reversal of the wide, unmineralized growth plate observed in the Fgf23^{tg} mice. Improved skeletal mineralization was also confirmed on histological sections of the Fgf23^{tg}/Kl^{-/-} epiphyseal region of femurs with complete absence of the profound osteomalacic changes apparent in trabecular and cortical bone in animals expressing FGF23(R176Q). In summary, our findings confirm the pivotal role of Klotho in the mechanism of action of FGF23 as its concomitant ablation fully reverses the complete spectrum of biochemical and skeletal disturbances attributed to FGF23.

Disclosures: X. Bai, None.

S210

1,25(OH)₂D₃ Inhibits Bone Nodule Mineralization Through the FGF23-Mediated ERK Pathway in Rat Calvaria Osteoblast Cultures. T. Minamizaki¹, Y. Yoshiko¹, H. Wang¹, S. Suzuki¹, K. Kozai², J. E. Aubin³, N. Maeda¹. ¹Oral Growth & Developmental Biology, Hiroshima University Graduate School of Biomedical Sciences, Hiroshima, Japan, ²Pediatric Dentistry, Hiroshima University Graduate School of Biomedical Sciences, Hiroshima, Japan, ³Molecular and Medical Genetics, University of Toronto, Toronto, ON, Canada.

Vitamin D, or its active metabolite 1,25-dihydroxyvitamin D₃ (1,25(OH)₂D₃), plays a major role in the regulation of mineral homeostasis and affects bone metabolism, but separating direct effects on osteoblasts and bone from indirect effects via other cell types and organs has been difficult in humans and animal models. However, osteoblasts possess a specific receptor for 1,25(OH)₂D₃ and 1,25(OH)₂D₃ affects many osteoblast functions including proliferation, extracellular matrix synthesis, etc. In the well-established rat calvaria (RC) osteoblast model, we found that 1,25(OH)₂D₃ inhibits bone nodule mineralization, concomitant with upregulation of production of fibroblast growth factor (FGF)23, a phosphate-regulating factor responsible for several phosphaturic disorders; we also found that overexpression of FGF23 in RC cells inhibits bone nodule mineralization. We therefore hypothesized that FGF23 may be involved in 1,25(OH)₂D₃-dependent mineralization defects in the RC osteoblast model. To test this hypothesis, we first confirmed that RC osteoblasts expressed Klotho, a senescence-related protein and FGF receptor (FGFR)s, which together are necessary for FGF23-specific signaling. 1,25(OH)₂D₃ (0.1~10 nM) upregulated FGF23 production in nodule-forming osteoblastic cells but not proliferating progenitor cells, and this activity was enhanced by 10 mM β -glycerophosphate, a stimulator of mineralization. We next prepared conditioned media from 10 nM 1,25(OH)₂D₃-treated (CM-D; FGF23, \geq 10,000 pg/ml) and -untreated (CM-C; FGF23, approx. 20 pg/ml) RC osteoblast cultures. As predicted, CM-D but neither CM-C nor 1,25(OH)₂D₃ at reduced concentrations in CM-D (\leq 0.4 nM) inhibited bone nodule mineralization in a dilution dependent manner (1:50-1:200). Neutralizing anti-FGFR antibody, SU5402 (an inhibitor of tyrosine kinase activity of FGFR1) and U0126 (an inhibitor of extracellular signaling-related kinase (ERK)) all rescued the mineralization defects seen in both CM-D and 1,25(OH)₂D₃ (10 nM)-treated RC osteoblast cultures. These effects were, at least in part, mimicked by either small interfering (si)RNA knockdown of FGF23 or siRNA knockdown of Klotho. Thus, our observations suggest that 1,25(OH)₂D₃ inhibits bone nodule mineralization through an FGF23-induced ERK pathway in RC osteoblast cultures.

Disclosures: T. Minamizaki, None.

S212

FGF-7 Is a Potent In Vivo Phosphaturic Agent in Rats. A. Shaikh*, T. Berndt*, R. Kumar. Nephrology Research, Mayo Clinic Rochester, Rochester, MN, USA.

FGF-7 has been identified as a tumor-derived phosphatonin on the basis of its ability to inhibit Na⁺ dependent phosphate uptake in cultured renal epithelia. Its bioactivity in vivo is unknown. The purpose of this study was to compare the phosphaturic effect of fibroblast growth factor-7 (FGF-7) to that of FGF-23 in rats with intact parathyroid glands. Rats were anesthetized and prepared for clearance studies to determine the glomerular filtration rate and fractional excretion of phosphate following infusion of protein or vehicle. After a 90-minute stabilization period, a control 30-minute clearance sample was collected and then either vehicle (saline, n=8), recombinant FGF-7 (0.1nmol/kg/hr, n=4) or recombinant FGF-23 (1 nmol/kg/hr, n=8) were infused intravenously. Glomerular filtration rate remained stable in all groups. The fractional excretion of phosphate (FEP) was unchanged in rats receiving vehicle alone (control vs. experimental period, 21±4 to 26±4%). Infusion of full length FGF-23 at a dose of 1 nmol/kg/hr increased FEP from 14±3% to 32±5%. Infusion of 0.1 nmol/kg/hr of FGF-7 increased FEP from 25±7% to 42±5%.

We conclude that FGF-7 increases phosphate excretion in vivo at a 10-fold lower dose than FGF-23. FGF-7 is likely to be responsible for the abnormal phosphate metabolism seen in some patients with tumor-induced osteomalacia in which tumors elaborate FGF-7 but not FGF-23.

Disclosures: A. Shaikh, None.

S214

The Role of Npt2c in Renal Pi Reabsorptive Process of Npt2a KO Mice. Y. Tomoe*, H. Segawa*, S. Sugino*, M. Ito*, S. Tatsumi, M. Kuwahata*, K. Miyamoto. Molecular Nutrition, Health Biosciences, The University of Tokushima Graduate School, Tokushima, Japan.

The proximal tubule is the major site of renal Pi reabsorption. The rate-limiting step in Pi reabsorption is a sodium-dependent step that occurs in the luminal brush border membrane (BBM). Two transporters (Npt2a and Npt2c) are expressed exclusively in the proximal convoluted tubule and are regulated by Pi intake, PTH, and FGF23 levels. The type IIa Na/Pi cotransporter (Npt2a) play a major role in reabsorption (70-80%), while type IIc Na/Pi transporter (Npt2c) is more important in weaning animals and less so in adult animals. Recently, mutation of the human Npt2c gene has shown to cause hereditary hypophosphatemic rickets with hypercalciuria (HHRH), implicating that the NPT2c plays an important role in renal Pi reabsorption in human and may be a key determinant of plasma Pi concentration. In this study, we examined administration of FGF23, which is a strong Pi diuresis factor, to Npt2a KO mice to determine the role of Npt2c in renal Pi reabsorptive process using naked DNA methods. As described previously, the levels of plasma FGF23 concentration were kept extremely low in the Npt2a KO mice when compared with wild-type (WT) mice. The levels of plasma FGF23 protein was markedly increased in Npt2a KO mice injected FGF23R179Q. FGF23R179Q induced severe hypophosphatemia, and markedly decreased renal Na/Pi transport activity, and Npt2c protein levels in Npt2a KO mice when compared with WT mice (FGF23R179Q group) 4 days after administration. FGF23R179Q suppressed the levels of intestinal Na/Pi transport activity in WT mice. However, intestinal Na/Pi transport activity were similar when compared Npt2a KO (FGF23R179Q group), and Npt2a KO (Mock group). These results suggested that Npt2a KO mice retain the capacity to reabsorb Pi at a rate that can be explained by the presence of Npt2c. Renal Npt2c is a major Na/Pi transporter in Npt2a KO mice.

Disclosures: Y. Tomoe, None.

S217

Protein-PTH mRNA Interactions that Determine PTH mRNA Stability in Secondary Hyper- and Hypoparathyroidism. M. Nechama*, I. Z. Ben-Dov*, J. Silver, T. Naveh-Manly. Minerva Center for Calcium and Bone Metabolism, Hadassah Hebrew University Medical Center, Jerusalem, Israel.

Hypocalcemia, uremia and hypophosphatemia regulate PTH gene expression, PTH secretion and parathyroid cell proliferation. Gene expression can be regulated at the transcriptional or post-transcriptional level. Serum Ca²⁺ and P regulate PTH gene expression post-transcriptionally by changes in mRNA stability. A low serum Ca²⁺ and uremia result in increased protein-PTH mRNA binding of a stabilizing complex and increased PTH mRNA levels in vivo. A low P has the opposite effects. We have previously identified two trans acting proteins, AU rich binding factor 1 (AUF1) and Upstream of N-ras (Unr) that bind a specific conserved cis element in the PTH mRNA 3'- untranslated region (UTR) and stabilize PTH mRNA. Here we use both in vitro degradation assays with rat parathyroid extracts and transfected heterologous cells to characterize the mechanisms of PTH mRNA decay and to identify the ribonucleases that determine PTH mRNA stability. mRNA decay can be exonucleolytic from either the 5' or 3' end of the mRNA or endonucleolytic by cleavage in the mRNA body. We show that PTH mRNA is endonucleolytically cleaved by parathyroid extracts and is a substrate for the endonuclease PMR1. PMR1 co-immunoprecipitates with the 3' to 5' exonucleolytic complex, the exosome. Knock-down of an exosome component by siRNA prevents PMR1-mediated degradation of PTH mRNA. Similarly, exosome immunodepletion in parathyroid extracts prevents PTH mRNA endonucleolytic degradation. PMR1 also interacts with the mRNA decay-promoting protein KSRP that binds PTH mRNA and decreases PTH mRNA levels in transfected cells. Significantly, the association of KSRP with PTH mRNA is increased in parathyroid glands from rats fed a phosphorus restricted diet where PTH mRNA is unstable, compared to parathyroid glands from rats fed a calcium-restricted diet or uremic rats, where PTH mRNA is stable. We suggest that KSRP recruits a degradation complex to

degrade PTH mRNA and determine PTH mRNA stability and levels in response to changes in Ca²⁺ and P. Phosphorous restriction increases PTH mRNA association with KSRP generating a degradation complex that accelerates PTH mRNA decay and decreases PTH mRNA levels. Calcium depletion and uremia lead to formation of a stabilizing complex on PTH mRNA, consisting of AUF1 and Unr. This complex competes for the association of PTH mRNA with the degrading complex and leads to increased PTH mRNA stability and levels. This is the first identification of the molecular mechanisms whereby protein-RNA interactions determine PTH mRNA stability and levels in response to changes in serum Ca²⁺ and P and experimental uremia.

Disclosures: T. Naveh-Manly, None.

S219

The Calcium-Sensing Receptor Regulates PMCA2 Activity in Mammary Epithelial Cells: A Mechanism for Calcium-Stimulated Calcium Transport into Milk. J. N. VanHouten, J. J. Wysolmerski. Yale University, New Haven, CT, USA.

Milk contains a great deal of calcium. Mammary epithelial cells secrete calcium into milk via a high capacity transepithelial transport system that is only partly understood. Prior experiments have demonstrated that calcium can stimulate its own transport from the maternal circulation into milk. Activation of the calcium-sensing receptor (CaR) at the basolateral surface of mammary epithelial cells promotes transepithelial calcium transport and also stimulates bulk milk production in mice. In this study, we investigated the mechanism by which CaR signaling affects calcium transport across mammary epithelial cells. The plasma membrane calcium ATPase, isoform 2 (PMCA2), has been reported to be the major calcium pump responsible for the transport of calcium into milk. We confirmed that expression of the PMCA2bw splice variant is upregulated in the mammary gland during lactation. Immunofluorescence and immuno-electron microscopy demonstrated that PMCA2 is found only at the apical surface of mammary epithelial cells. Milk calcium was reduced by 70% in homozygous Dfw-2J mice, which carry a loss-of-function mutation in the PMCA2 gene (Atp2b2). These data confirm that PMCA2 is critical for calcium transport into milk. Therefore, we sought to determine whether PMCA2 is a downstream target of CaR signaling in mammary epithelial cells. In cultured primary and EpH4 mouse mammary epithelial cells, CaR stimulation by extracellular calcium or the calcimimetic, gadolinium, had no discernable effect on PMCA2 expression, mRNA splicing, or localization. However, activation of the CaR increased calcium-dependent ATPase activity in mammary epithelial cell plasma membrane preparations. Knockdown of PMCA2 expression with siRNA showed that PMCA2 accounts for the preponderance of calcium-ATPase activity in mammary epithelial cells. Furthermore, siRNA-mediated ablation of CaR expression in mammary epithelial cells eliminated the ability of extracellular calcium or gadolinium to elicit an increase in plasma membrane calcium-dependent ATPase activity. These results demonstrate that activation of the CaR on the basolateral aspect of mammary cells increases PMCA2 activity in the apical membrane and provide a mechanism for the regulation of transepithelial calcium transport by calcium in the lactating mouse mammary gland.

Disclosures: J.N. VanHouten, None.

S223

Conditional Ablation of the Osteoblast Calcium-Sensing Receptor Causes Abnormalities in Skeletal Development and Mineralization. M. M. Dvorak*, C. Tu*, H. Elalieh*, T. Chen*, B. Liu*, B. E. Kream*, D. D. Bikle*, W. Chang*, D. M. Shoback*. ¹Department of Medicine, University of California, San Francisco, CA, USA, ²Department of Medicine, University of Connecticut Health Center, Farmington, CT, USA.

The calcium-sensing receptor (CaR) is a G protein-coupled receptor essential for maintenance of calcium homeostasis. Defining the role for the osteoblast CaR in vivo, using global full-length CaR knockout models, is complicated by metabolic disturbances and the potential for compensation by a CaR splice variant identified in these mice. To circumvent these issues, we generated Flox-CaR^{+/+} mice, in which loxP sites flank exon 7 that encodes the transmembrane and signaling domains of the receptor. Osteoblast-specific inactivation of the CaR was achieved by mating Flox-CaR^{+/+} mice to transgenic mice expressing Cre-recombinase, under control of the 3.6 kb fragment of the rat $\alpha 1(I)$ collagen promoter (Col1-Cre). Col1-Cre^{+/+}/Flox-CaR^{+/+} mice exhibited growth delay from birth and died within four weeks. At 21 days, the skeletal phenotype was hallmarked by hypomineralization, evident by von Kossa staining and micro-computed tomography (μ CT) analysis, which revealed significant reductions in bone volume/tissue volume (BV/TV; \downarrow 75%), bone mineral density (BMD; \downarrow 90%), segmented BMD (\downarrow 20%), trabecular number (\downarrow 40%), trabecular thickness (\downarrow 30%) and connectivity density (\downarrow 80%) in the secondary spongiosa of the distal femur (n=6, p<0.05, ANOVA), compared to controls. The changes were comparable, although less extensive in the L4 vertebra. The cortical compartment of the femur was also affected, with significant decreases in BV (\downarrow 60%), cortical thickness (\downarrow 70%), BMD (\downarrow 45%), and segmented BMD (\downarrow 15%) and markedly increased cortical porosity (~70%), compared to controls (n=6, p<0.05, ANOVA). Histology of femora from Col1-Cre^{+/+}/Flox-CaR^{+/+} mice revealed severe hyperostoidosis (Goldner staining) as well as trabeculation of the cortex (Von Kossa staining). Reduced mineral content could be secondary to increased turnover, with inadequate mineralization of newly made osteoid. This is consistent with quantitative real-time PCR (qPCR) analysis of humeri and calvaria that indicate significant increases in markers of proliferation (ccnd1), osteoblast differentiation (collagen I, alkaline phosphatase, osteopontin), mineralization (anklylosin protein, ectonucleotide pyrophosphatase/phosphodiesterase 1) and regulators of osteoclastogenesis (RANK-L,

osteoprotegerin); (n=3-5, p<0.05, ANOVA). Our findings indicate a critical role for the skeletal CaR in the control of bone mineralization in early postnatal skeletal development.

Disclosures: M.M. Dvorak, None.

S227

Calcium Sensing Receptor Plays Significant Role in Protection Against Hypercalcemia. L. Kantham¹, S. Quinn^{*1}, O. Egbuna¹, J. Pang^{*1}, R. Butters^{*1}, M. Pollak^{*2}, E. M. Brown¹. ¹Medicine / Endocrine, Brigham & Women's Hospital, Boston, MA, USA, ²Medicine / Renal division, Brigham & Women's Hospital, Boston, MA, USA.

The calcium sensing receptor (CaR) plays a pivotal role in controlling the secretion of parathyroid hormone (PTH), which, in turn, via its direct and indirect actions on kidney, bone and intestine restores and maintains normal extracellular ionized calcium levels. To date, there is only limited understanding of the functions of CaR expressed in tissues other than the parathyroid. Mice homozygous for knockout of the CaR were unsuitable for such studies as they die from lethal hyperparathyroidism. As an alternative, we employed single and double knock out (KO) mouse models, specifically mice lacking PTH alone (CaR^{+/+}PTH^{-/-}), both CaR and PTH (CaR^{-/-}PTH^{-/-}), and wild type (CaR^{+/+}PTH^{+/+}) of the same genetic background for studies to gain insight into CaR-specific functions in the absence of confounding actions of CaR-mediated changes in PTH.

In the first set of experiments, 3-4 month old adult male mice were fed ad lib with regular chow containing 0.8% calcium and 0, 1 or 2% CaCl₂ containing water for one week. Measurement of serum calcium (SCa) levels revealed marked differences between the three genotypes. As expected, CaR^{+/+}PTH^{+/+} mice maintained their SCa levels close to 9.5 mg/dL under all conditions. The CaR^{+/+}PTH^{-/-} and CaR^{-/-}PTH^{-/-} mice were hypocalcemic, showing SCa of 6.8 and 6.2 mg/dL, respectively, in the absence of added calcium in the water. However, the SCa level rose to 8.3 in the CaR^{+/+}PTH^{-/-} mice and to over 10 mg/dL in the CaR^{-/-}PTH^{-/-} mice when they received water containing 1% CaCl₂. On 2% CaCl₂ water, the CaR^{+/+}PTH^{-/-} mice showed a SCa (9.5 mg/dL) in the normal range. In contrast the SCa increased markedly to 14 mg/dL in the CaR^{-/-}PTH^{-/-} mice. The results indicate that despite the lack of PTH, CaR is able to defend the mice against hypercalcemia in the face of an increased oral load of calcium. It is known that severe phosphate deficiency induces hypercalcemia and we tested the response of these mice to a phosphate deficient diet (containing 1% calcium) and plain water for one week. Once again we noted significant differences between mice expressing the CaR and those that did not. The wild type and CaR^{+/+}PTH^{+/+} mice maintained near normal SCa levels of 9-10 mg/dL, whereas those in the CaR^{-/-}PTH^{-/-} mice reached 15 mg/dL. Further investigation revealed that the calcitonin response to hypercalcemia induced by increased oral calcium load was normal in the control mice but was severely blunted in the CaR^{-/-}PTH^{-/-} mice. Thus the CaR defends effectively against hypercalcemia induced by a calcium load even in the absence of CaR-mediated changes in PTH secretion. Ongoing studies are directed at further characterization of the mechanism(s) by which it does so.

Disclosures: L. Kantham, None.

S233

The Small GTPase RhoA and its Effector Kinase ROCK Mediate Actin Cytoskeleton Reorganization Leading to Osteocyte Anoikis by Glucocorticoids. L. I. Plotkin, K. Vyas*, S. C. Manolagas, T. Bellido. Center for Osteoporosis and Metabolic Bone Diseases, Univ Arkansas for Medical Sciences and Central Arkansas Veterans Healthcare System, Little Rock, AR, USA.

Glucocorticoids (GC) induce osteocyte apoptosis by activating the focal adhesion-related kinase Pyk2 and its downstream target, the kinase JNK, which in turn counteract pro-survival signaling mediated by the focal adhesion kinase FAK. This results in osteocyte detachment-induced apoptosis or anoikis. We report herein that the retraction of osteocyte cytoplasmic processes and cell rounding that precede GC-induced apoptosis of osteocytic MLO-Y4 cells are associated with rapid disruption of stress fibers and formation of peripheral actin rings, as visualized by confocal microscopy of cells stained with Alexa Fluor-conjugated phalloidin. The small GTPase family of proteins has been shown to transduce extracellular signals into actin cytoskeleton reorganization, ultimately controlling cell morphology and diverse cellular functions, including apoptosis. Consistent with a role of small GTPases in GC actions on osteocytes, the GC-induced apoptosis, changes in cell shape as well as actin reorganization were abolished by pharmacological inhibition of the small GTPase RhoA or its effector kinase ROCK with p75^{NTR} or Y-27632, respectively. On the other hand, inhibition of another small GTPase Rac1 with NSC23766 did not prevent GC effects. Furthermore, whereas GC did not induce apoptosis in cells expressing a kinase deficient dominant negative Pyk2 (K-Pyk2), expression of a constitutively active (ca) RhoA mutant, as well as two different ca JNK mutants, rescued GC-induced apoptosis in cells expressing K-Pyk2. These results indicate that Pyk2 activation by GC results in activation of both RhoA and JNK. Moreover, the ca RhoA rescued GC-induced apoptosis in cells expressing a dn JNK mutant, whereas the ca JNK mutants were unable to rescue GC-induced apoptosis in cells treated with the ROCK inhibitor. These results indicate that activation of JNK precedes RhoA/ROCK activation. We conclude that the small GTPase RhoA and its downstream kinase ROCK act downstream of Pyk2 and JNK activation by GC in a pathway that leads to rapid reorganization of the actin cytoskeleton. The resulting changes in cell morphology lead to osteocyte detachment-induced apoptosis or anoikis.

Disclosures: L.I. Plotkin, None.

This study received funding from: NIH.

S235

Col3.6-HSD2 Transgenic Mice: A Glucocorticoid Loss-of-Function Model Spanning Early and Late Osteoblast Differentiation. M. Yang^{*1}, J. R. Harrison², D. J. Adams³, B. E. Kream¹. ¹Medicine, University of Connecticut Health Center, Farmington, CT, USA, ²Craniofacial Sciences, University of Connecticut Health Center, Farmington, CT, USA, ³Orthopaedic Surgery, University of Connecticut Health Center, Farmington, CT, USA.

Glucocorticoids (GC) exhibit complex regulatory effects on bone remodeling. To elucidate the role of endogenous GC signaling in mature osteoblasts, we previously developed Col2.3-HSD2 transgenic (TG) mice in which a 2.3-kb Col1a1 promoter fragment drives expression of 11 β -hydroxysteroid dehydrogenase type 2 (11 β -HSD2), which metabolizes biologically active GC. Col2.3-HSD2 TG mice showed decreased vertebral trabecular and femoral cortical bone mass, due in part to impairment of osteoblast differentiation. The goal of the present study was to characterize the bone phenotype of Col3.6-HSD2 TG mice in which a longer 3.6-kb Col1a1 promoter fragment drives 11 β -HSD2 expression more widely in the osteoblast lineage. Serum corticosterone was unchanged in 7-week-old TG females. Skeletal parameters were assessed by dual energy X-ray absorptiometry and microcomputed tomography. Compared to WT littermates, TG mice showed reductions of 20% in vertebral trabecular bone volume, 10-17% in femoral and tibial sub-periosteal area, and 20-40% in sub-endosteal area. TG calvarial osteoblast (mCOB) and bone marrow stromal cell (BMC) cultures had decreased alkaline phosphatase and mineral staining, and reduced pOBCol3.6-GFP transgene expression, a marker of early osteoblast differentiation. Northern blot and real time PCR showed that Col1a1, bone sialoprotein and osteocalcin expression were decreased by 56%, 73% and 72%, respectively, in TG cultures. To study osteoclast formation, BMCs were treated with RANKL and mCSF for 3-7 days. Col3.6-HSD2 TG cells showed lower osteoclast number at day 4, but higher osteoclast number at day 6 and 7, suggesting delayed osteoclast formation and/or suppression of osteoclast apoptosis. To determine gene pathways affected by 11 β -HSD2 transgene, RNA of 7-week-old WT and TG female vertebrae was assessed by microarray analysis. Modest (1.5- to 2-fold) but significant effects were seen on genes of the TGF β , IGF and FGF pathways. TG bone had increased cathepsin K and c-fms expression, markers of the osteoclast lineage. In summary, Col2.3-HSD2 and Col3.6-HSD2 mice showed a similar low bone mass phenotype and impaired ex vivo osteoblast differentiation; in addition, Col3.6-HSD2 mice showed an altered tempo of ex vivo osteoclast formation. Based on the phenotypic similarities between the Col2.3-HSD2 and Col3.6-HSD2 models, we conclude that endogenous GC signaling is required for optimal bone mass acquisition by acting primarily on the later stages of osteoblast differentiation.

Disclosures: M. Yang, None.

This study received funding from: National Institutes of Health.

S239

Intermittent PTH Stimulates Osteoblastic Cells Even in the Absence of Osteoclasts. P. H. Luiz de Freitas¹, M. Li², T. Ninomiya^{*3}, M. Nakamura^{*3}, K. Oda^{*4}, R. Takagi^{*1}, N. Udagawa^{*3}, T. Maeda^{*5}, N. Amizuka². ¹Oral and Maxillofacial Surgery, Niigata University, Niigata, Japan, ²Center for Transdisciplinary Research, Niigata University, Niigata, Japan, ³Institute for Oral Science, Matsumoto Dental University, Shiojiri, Japan, ⁴Biochemistry, Niigata University, Niigata, Japan, ⁵Oral and Maxillofacial Anatomy II, Niigata University, Niigata, Japan.

PTH anabolic actions affect both components of the bone remodeling cycle. We aimed to determine if the increase on osteoblastic activity seen after intermittent PTH treatment in vivo is solely result of the hormone's actions on osteoblasts, or if it also depends on coupling to, and/or enhancement of, osteoclastic activities. Eight-week-old ICR male mice were divided in control and PTH injection groups. Age-matched c-fos knockout female mice, an osteopetrotic strain without osteoclasts, were similarly grouped. Injection groups received PTH (120 μ g/kg, sc) daily for 14 days, while controls received only saline. Under anesthesia, animals were fixed with an aldehyde solution and had their bones extracted for histological processing, i.e., tartrate-resistant acid phosphatase (TRAP) reaction, alkaline phosphatase (ALP) and PTH/PTHrP receptor (PTH-R) immunohistochemistry, as well as for transmission electron microscopy (TEM). The picture of PTH treatment in ICR mice was one of increased bone content with longer, thicker and interconnected trabeculae. Compared to their controls, injection samples had a thicker ALP-positive preosteoblastic layer lining their bone surfaces. Number of TRAP-positive cells did not differ considerably between control and injection groups, while PTH-R positivity was increased in the latter. TEM imaging revealed at least two categories of cells of the preosteoblastic layer according to their morphology: endoplasmic reticulum (ER)-rich cells and ER-poor ones. Collated to their controls, PTH-injected c-fos knockouts exhibited more ALP-positive cells on their bone surfaces. It has been suggested that osteoclastic cells may play an active role on the anabolic actions of PTH, but our data pointed to another direction: PTH-driven osteoblastic anabolism seems to be independent of osteoclast presence and/or activity, yet the outcomes of hormonal administration might be less dramatic when bone resorption is hindered. We have shown that intermittent PTH stimulates cells of the osteoblastic line even if osteoclasts are ablated, substantiating the idea that anabolic effects of PTH are independent of osteoclastic presence.

Disclosures: P.H. Luiz de Freitas, None.

S241

Ablation of IGF-I Signaling Disrupts the Communication Between Osteoblasts and Osteoclasts. Y. Wang¹, H. Z. ElAlich^{*1}, W. Chang¹, T. L. Clemens², D. D. Bikle¹. ¹Endocrine Unit, University of California, San Francisco/ VA Medical Center, San Francisco, CA, USA, ²Department of Pathology, University of Alabama at Birmingham, Birmingham, AL, USA.

We and others have shown that insulin-like growth factor-I (IGF-I) has been regulates the functions of both osteoblasts (OB) and osteoclasts (OCL). Our previous studies demonstrated that IGF-I was required for normal OBs proliferation, differentiation and stimulated osteoclastogenesis both directly and/or through the interaction between OBs and OCL precursors to support OCL formation. Furthermore, IGF-I signaling is required for PTH stimulation of bone formation, an action that appears to require the OCL as well as IGF-I. However, the mechanisms by which IGF-I signaling is responsible for the cellular communication between OBs and OCLs has not been evaluated. Recent studies identified bidirectional signaling between OBs and OCLs mediated by ephrin B2 in OCLs and EphB4 in OBs. To address whether such signaling was involved in IGF-I action, we used Cre-mediated conditional gene targeting techniques to delete IGF-I receptor (IGF-IR) in vitro and in vivo. Bone marrow stromal cells (BMSC) were isolated from the mice bearing the loxP-flanked IGF-I receptor (IGF-IR) alleles in exon 3 (IGF-IR floxed mice). To inactivate IGF-IR, BMSCs were infected with 10 PFU/cell recombinant adenoviruses expressing a functional Cre (Cre-ADV) at day 12 for 2 days. Quantitative real-time PCR (Q-PCR) analysis demonstrated that the mRNA levels of IGF-IR in the BMSCs were reduced by 95% with Cre-ADV infection. mRNA levels of ephrin B2 and Eph B4 were decreased by 78% and 71%, respectively in the cultures infected by Cre-ADV (IGF-IR^{-/-}). PTH treatment (100 ng/ml, 2 hrs) significantly increased the mRNA levels of both ephrin B2 (2.6 fold) and EphB4 (4 fold) in the cultures infected by vehicle (IGF-IR^{+/+}), but these effects were abolished in the IGF-IR^{-/-} cultures. For the in vivo studies, 3 month old mice with a bone specific IGF-IR null mutation (OB IGF-IR^{-/-}) (floxed IGF-IR x osteocalcin promoter driven Cre recombination) and their normal littermates (controls) were treated with vehicle or PTH (80 µg/kg bw/day for 2 weeks). As analyzed by Q-PCR, mRNA levels of ephrin B2 and EphB4 were decreased by 44% and 48% respectively in bone tissue of the OB IGF-IR^{-/-} mice. PTH significantly increased the mRNA levels of ephrinB2 and EphB4 in the control mice (1.6 fold and 3.5 fold, respectively), but induced no changes in the mRNA levels of these 2 molecules in the OB IGF-IR^{-/-} mice. Our data indicate that the IGF-IR is critical for the communication between OBs and OCLs mediated by bidirectional ephrin signaling to stimulate OBs differentiation and osteoclastogenesis, suggest that this action is required for PTH stimulated bone turnover.

Disclosures: Y. Wang, None.

S244

Androgenic Effects on Bone and Body Composition Depend on Concerted and Additive Activation of both AR and ERα: Evidence from a New Male Mouse Model with Combined Disruption of both AR and ERα. F. Callewaert^{*}, K. Venken^{*}, J. Ophoff^{*}, K. De Gendt^{*}, S. Boonen, R. Bouillon, G. Verhoeven^{*}, D. Vanderschueren. Katholieke Universiteit Leuven, Leuven, Belgium.

During puberty, androgens increase bone and muscle mass but lower fat mass. Both androgen receptor (AR) and estrogen receptor-α (ERα) activation are likely to be involved in these characteristic male phenotypic changes, but the relative contribution of these sex steroid receptors is unclear. In the present study, we characterized bone and body phenotype of male AR-ERα double KO (AR-ERαKO) mice in comparison with ARKO, ERαKO and wildtype (WT) littermates. Tibial bone mineral density and geometry and whole-body composition were assessed weekly by in vivo pQCT and DEXA, respectively, until 16 weeks of age. Results were analyzed by repeated measures ANOVA and expressed as % difference vs. WT. Disruption of the AR decreased body weight gain (-14%, $p < 0.01$) without additional effect of ERα disruption. Interestingly, body composition was independently affected in ARKO or ERαKO mice; ERα disruption (but not AR disruption) increased fat mass in ERαKO or AR-ERαKO mice from 8 weeks of age (+36% and +30%, resp., $p < 0.01$), whereas combined AR and ERα disruption caused additive reductions of lean body mass (-24%, $p < 0.01$). However, ARKO and ERαKO mice showed divergent effects on trabecular BMD; disruption of the AR or ERα decreased (-64%, $p < 0.01$) and increased (+14%, $p < 0.01$) cancellous bone density, respectively. The cancellous bone gain in ERαKO mice appeared entirely AR dependent since no increase was observed in AR-ERαKO mice. In contrast, cortical bone mass acquisition was impaired in ARKO or ERαKO mice as reflected by a significantly decreased cross-sectional area (-8% and -6%, resp., $p < 0.01$) and periosteal perimeter (-4% and -3%, resp., $p < 0.01$). Moreover, combined disruption of the AR and ERα further reduced cortical bone expansion; an additional decrease in cross-sectional area (-14%, $p < 0.01$), periosteal perimeter (-5%, $p < 0.01$) and strength strain index (-29%, $p < 0.01$) was observed in AR-ERαKO mice. Disruption of the ERα, not AR, also lowered serum IGF-I in ERαKO (-23%, $p < 0.01$) and AR-ERαKO mice (-10%, $p < 0.01$), which may explain its additive negative impact on periosteal bone expansion. Our data indicate that combined disruption of the AR and ERα has an additive effect on cortical bone growth as well as lean body mass compared to ARKO or ERαKO mice. Therefore, we conclude that activation of both AR and ERα are needed for optimal acquisition of cortical bone mass and lean mass. However, AR activation alone is able to maintain cancellous bone mass, whereas ERα activation lowers fat mass and increases serum IGF-I.

Disclosures: F. Callewaert, None.

S246

Factors Produced in Ovary Inhibit Musculoskeletal Growth and Promote Adipogenesis During Puberty: Potential Mediation by Non Estrogenic Actions. K. E. Govoni, R. B. Chadwick^{*}, J. E. Wergedal, S. Mohan, J. L. Pettit VAMC and Loma Linda University, Loma Linda, CA, USA.

To test if the pubertal surge in estrogen is essential for the increased growth hormone (GH)/insulin-like growth factor (IGF) action and bone accretion during puberty, we evaluated the consequence of ovariectomy in prepubertal mice on skeletal changes and GH/IGF axis during puberty. C57BL/6J mice were ovariectomized (OVX) or SHAM operated at 3 weeks of age ($n = 6$ to 7) and skeletal changes measured prior to and 3 weeks after surgery. A 57% reduction ($P = 0.01$) in uterine size confirmed the effectiveness of OVX. Prepubertal OVX caused a 12% increase in the body weight ($P = 0.01$), 15% increase in lean total body mass ($P < 0.01$), and 18% reduction in percent total body fat ($P < 0.01$). Abdominal body fat was reduced by 43% in OVX group ($P = 0.01$). PIXImus analysis revealed a 12% increase in total body BMC and bone area ($P < 0.02$). pQCT analysis of femur mid diaphyseal region revealed an 8% increase in cross sectional area ($P = 0.07$), but no effect on vBMD. Femur length was increased by 3% ($P < 0.01$). We next determined if the absence of ovarian hormones during puberty influences puberty-induced increase in serum IGF-I level. We found that neither serum level of IGF-I (298 ± 21 vs. 277 ± 19 ng/ml in SHAM vs. OVX, respectively) or local IGF-I expression (1.12 ± 0.14 and -1.23 ± 0.13 fold change vs. SHAM in bone and muscle, respectively) were altered in OVX mice at 3 weeks post surgery ($P \geq 0.30$). To identify the potential pathways by which ovarian factors negatively regulate their effects on the musculoskeletal system, we performed a whole genome microarray analysis of mRNA from the femurs of OVX and SHAM mice at 3 weeks post surgery. A total of 223 genes were significantly ($P \leq 0.05$) regulated in the bones of OVX mice. We observed significant upregulation ($P \leq 0.05$) of expression of regulators (osterix, ephrinA1, formin2) and markers (Colla2, thrombospondin2, lumican) of osteoblast differentiation in the bones of OVX mice. In contrast, OVX resulted in significant downregulation ($P < 0.05$) of genes (lipoprotein lipase, stearyl-Coenzyme A desaturase 1, caveolin1) which are known to be upregulated in adipocytes. In conclusion: 1) Female mice exhibit male-like features (bone, muscle and adipose) in the absence of ovarian hormones during puberty; 2) The increase in GH/IGF production during puberty is not dependent on estrogen production; 3) Expression of genes involved in osteoblast and adipocyte differentiation was altered in OVX mice during puberty; and 4) Based on these data and the published data that bone size is not increased in estrogen receptor-α knockout female mice, we speculate that factors besides estrogen may be responsible for the inhibitory effects of ovarian factors on the musculoskeletal system during puberty.

Disclosures: S. Mohan, None.

This study received funding from: National Institute of Health Grant AR048139.

S248

The Purinergic P2X₇ Receptor Is Responsible for Ovariectomy-induced Bone Loss in Mice. S. Petersen^{*1}, S. Syberg^{*1}, Z. Henriksen^{*1}, P. Schwarz², J. B. Jensen^{*1}, O. H. Sorensen^{*1}, N. R. Jorgensen¹. ¹Endocrinology and Clinical Biochemistry, Copenhagen University Hospital Hvidovre, Hvidovre, Denmark, ²Research Center for Ageing and Osteoporosis, Copenhagen University Hospital Glostrup, Glostrup, Denmark.

The purinergic P2X₇ receptor is an ATP-gated cation channel that is primarily expressed in cells of hematopoietic origin such as osteoclasts and macrophages, but also in mature osteoblasts. It has been shown to have important functions both in the regulation of osteoblastic bone formation and in the formation and activity of osteoclasts. The aim of this study was to elucidate possible gender-differences in bone mass between P2X₇ genotypes as well as the role of the receptor in the bone loss accompanying estrogen-withdrawal.

Two groups of C57BL mice with the following P2X₇ genotype: P2X₇^{+/+} (Wt), P2X₇^{-/-} (He) P2X₇^{-/-} (Ho) were examined. The first group (A) was sacrificed at 120 days of age ($n=159$, 76 males, 83 females). The second group (B) contained all females and were ovariectomized (OVX) ($n=36$) at 120 days of age with one month additional follow up for effect of OVX. At sacrifice, both groups had determination of bone mineral density (BMD) and bone mineral content (BMC) using a PIXImus densitometer as whole body BMD/BMC and right femur BMD/BMC.

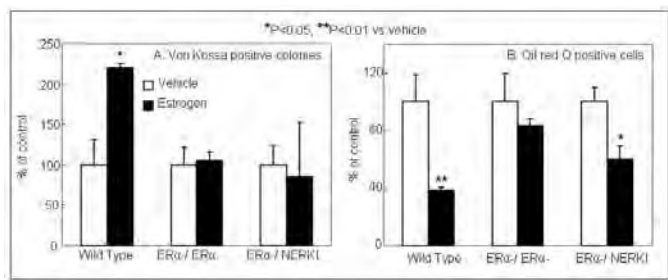
In order to determine the role of the P2X₇ receptor in gender-differences in bone mass we compared bone mass values for the genotypes in group A. For the Wt animals, males had highly significant BMC/BMD than females (p -values < 0.01), while in the P2X₇ null mice only slight differences between genders could be found, and only for BMC of the femur (Mean \pm SEM: 0.037 ± 0.001 vs. 0.035 ± 0.0005 , p -value: 0.04), despite significantly higher weight in males compared to females in all genotype groups. For group B, a significant bone loss (5%) was found one month after OVX in the Wt group compared to baseline, but no change in BMD/BMC values could be detected in the He or Ho groups in response to OVX. In conclusion, as expected differences were found in bone mass between male and female mice. Interestingly, these differences were not present in mice with a deletion of the P2X₇ receptor. Furthermore, P2X₇ null mice were protected against OVX-induced bone loss compared to their Wt littermates. Thus, the P2X₇ receptor appears to be involved in the effects of sex hormones on the regulation of bone metabolism.

Disclosures: S. Petersen, None.

S250

Classical ER α Signaling Is Essential for Estrogen Mediated Enhancement of Osteogenesis but not for Inhibition of Adipogenesis. F. A. Syed, D. G. Fraser*, M. J. Oursler, S. Khosla. Endocrinology, Mayo Clinic College of Medicine, Rochester, MN, USA.

Previous studies have demonstrated that estrogen (E) enhances osteoblastic and inhibits adipocytic differentiation of bone marrow stromal cells (BMSCs). ER α can signal either via the "classical" pathway requiring direct binding to E response elements (EREs) or through indirect, "non-classical" pathways involving protein-protein interactions. We have previously demonstrated (JBMR 20:1992, 2005; Endocrinology 148:1902, 2007) that mice with a deleted ER α allele and a knock-in of a mutant ER α that cannot bind EREs on the other allele (ER α -/NERKI) have osteopenia and decreased bone formation rates, suggesting that ERE signaling may be essential for E effects on bone formation. Interestingly, in contrast to the generally observed inverse relationship between bone mass and marrow fat, ER α -/NERKI mice have osteopenia but no increase and, in fact, a decrease in bone marrow fat: adipocyte volume/total volume (AV/TV) at the proximal tibial metaphysis of $2.3 \pm 0.2\%$ vs. $14.6 \pm 1.6\%$ for wild type (WT) mice, $P < 0.05$, suggesting dissociation of ER α signaling on bone vs. fat. To test this, we exposed primary BMSC cultures from female WT, ER α -/ER α -, and ER α -/NERKI mice to osteogenic (dex, β -glycerolphosphate, and ascorbate) and adipogenic (rosiglitazone) media in the absence or presence of estradiol (10^{-8} M). Mineralization was assessed using von kossa staining and adipogenesis using oil red O staining. As is evident (Figure, panel A), while E clearly increased the number of osteoblastic colonies in WT cultures, it was totally ineffective in doing so in the ER α -/ER α - or ER α -/NERKI cultures. By contrast, while E inhibited adipogenesis in WT and was ineffective in the ER α -/ER α - cultures, it was able to inhibit adipogenesis in the ER α -/NERKI cultures (panel B). Collectively, our in vivo and in vitro findings demonstrate that ERE signaling is essential for E effects on enhancing bone formation but not for inhibition of adipogenesis, consistent with dissociation of the signaling pathways involved in these effects. Further studies to characterize the different pathways by which E mediates effects on osteogenesis vs. adipogenesis are currently underway.



Disclosures: F.A. Syed, None.

S253

Internalization of Vitamin D Binding Protein (DBP) by Human Monocytes. R. F. Chun, S. Ren, J. S. Adams, M. Hewison. Endocrinology, Diabetes and Metabolism, Cedars-Sinai Medical Center, Los Angeles, CA, USA.

Convention holds that 25-hydroxyvitamin D₃ (25D₃) and 1,25-dihydroxyvitamin D₃ (1,25D₃) enter target cells by passive diffusion in their 'free' form. However, recent studies have shown that DBP-bound 25D₃ can also enter cells by facilitated endocytosis. In proximal tubule and breast epithelial cells this mechanism provides a conduit for delivery of substrate 25D₃ to the vitamin D-activating CYP27b1 α -hydroxylase. Here we used fluorescent Alexa-tagged DBP, which retains the capacity to bind 25D₃ specifically, to show that DBP is also internalized by monocytes, a cell type that exhibits classical extrarenal metabolism of 25D₃ to 1,25D₃ via the 1 α -hydroxylase. Human peripheral blood mononuclear cells were cultured in the presence of granulocyte-macrophage colony stimulating factor (10 U/ml) for 1, 3 or 7 days. During this time monocytes showed increased expression and activity of the CYP27b1 α -hydroxylase with sustained Alexa-DBP uptake at levels 2-4-fold higher than control cell autofluorescence. Uptake of Alexa-DBP was observed when fluorescence-activated cell sorting (FACS) was gated for monocyte sub-populations, but no uptake was observed when cell populations were gated for lymphocyte sub-populations, indicating that uptake was specific for human monocytes. In day-1 and day-3 populations of cells DBP uptake was more pronounced in cells positive for the macrophage marker CD14. However, in day-7 populations, DBP uptake was also observed in CD14-negative dendritic cells. To determine whether uptake of DBP by monocytes was megalin-mediated, as observed in kidney and breast cells, monocytes were preincubated with receptor-associated protein (RAP), an antagonist of megalin-mediated endocytosis. RAP reduced Alexa-DBP internalization in megalin-rich BN16 rat yolk epithelial cells but had no effect on DBP uptake in monocytes, highlighting a megalin-independent means for DBP uptake in these cells. In summary, these data indicate that: 1] human monocyte/macrophages and DCs are capable of internalizing DBP by megalin-independent means; and 2] internalization of DBP occurs in monocytes, macrophages and dendritic cells. We propose that DBP-mediated uptake of 25D₃ is a crucial mechanism in defining the immunomodulatory actions of 25D₃. Furthermore, the presence of this mechanism in different types of human mononuclear cells suggests that DBP-mediated uptake of 25D₃ is important for vitamin D effects on both innate and adaptive immunity.

Disclosures: R.F. Chun, None.

S255

Curcumin: A Novel Nutritionally-Derived Ligand of the Vitamin D Receptor with Implications for Colon Cancer Chemoprevention and Bone Health. L. Bartik*, G. K. Whitfield², M. J. Kaczmarek*, C. A. Haussler², M. R. Haussler², P. W. Jurutka³. ¹Biochemistry & Molecular Biophysics, University of Arizona, Tucson, AZ, USA, ²Basic Medical Sciences, University of Arizona College of Medicine, Phoenix, AZ, USA, ³Integrated Natural Sciences, Arizona State University, Phoenix, AZ, USA.

The nuclear vitamin D receptor (VDR) mediates the actions of 1,25-dihydroxyvitamin D₃ (1,25D₃) to alter gene transcription in several target tissues, including intestine and bone. Recently, the secondary bile acid, lithocholate, was recognized as a VDR ligand. Using reporter gene and mammalian two-hybrid systems, we identified curcumin (CM), a turmeric-derived bioactive polyphenol, as a likely additional novel ligand for VDR. CM (10^{-5} M) activated transcription of a luciferase plasmid containing the distal vitamin D responsive element from the human CYP3A4 gene comparably to 1,25D₃ (10^{-8} M) in transfected human colon cancer cells (Caco-2). While CM also stimulated transcription via a retinoid X receptor (RXR) responsive element, activation of the glucocorticoid receptor by CM was negligible. Competition binding assays with radiolabeled 1,25D₃ confirmed that CM binds directly to VDR, obviating the possibility that it acts only via RXR. In mammalian two-hybrid assays employing transfected Caco-2 cells, CM (10^{-5} M) increased the ability of VDR to recruit RXR and the steroid receptor coactivator (SRC-1) by 10- and 9.6-fold, respectively, an action consistent with the promotion of transcriptional initiation of VDR-regulated genes. Small intestine and colon are important VDR-containing tissues, and frequent consumption of curry-containing foods can result in chronic, long-term exposure to significant levels of CM at these sites. Therefore, it is hypothesized that such diets can result in modest and sustained VDR/CM-mediated transcriptional activation of key target genes in the intestine. If this effect extends to genes involved in calcium transport, such as TRPV6, this may explain the beneficial effects of CM on bone, and our preliminary quantitative real time PCR (RT-PCR) data reveal CM-mediated upregulation of TRPV6 in Caco-2. Moreover, numerous studies have shown intestinal chemoprotection by CM via a variety of mechanisms; 1,25D₃ has known anticancer properties in the intestine potentially due, in part, to VDR activation of CYP-mediated xenobiotic detoxification and/or up-regulation of p21. Using RT-PCR, we demonstrate a significant increase in the levels of p21 mRNA in Caco-2 cells treated with either 1,25D₃ or CM. Thus, our results raise the novel possibility that nutritionally-derived CM facilitates intestinal chemoprotection and enhanced bone health via direct binding to VDR and activation of strategic target genes.

Disclosures: P.W. Jurutka, None.

S259

Molecular Analysis of Two Novel Mutations in the Vitamin D Receptor Corepressor, Hairless, and Expression of Rat Hairless in E. coli. J. C. Hsieh¹, C. A. Sheedy*, D. R. Mathern*, S. A. Slater*, G. K. Whitfield², C. A. Haussler², M. R. Haussler². ¹Biochemistry & Molecular Biophysics, University of Arizona, Tucson, AZ, USA, ²Basic Medical Sciences, University of Arizona, Phoenix, AZ, USA.

Mammalian hairless (hr) is expressed primarily in skin and brain tissues. Its gene product (Hr) is postulated to be involved in hair follicle progression and regeneration, as well as in brain development. Hr interacts with the thyroid hormone receptor (TR) and the orphan nuclear receptor, ROR α , inhibiting the ability of these receptors to activate transcription. Our recent work demonstrated that Hr also inhibits vitamin D receptor (VDR)-mediated transactivation in human keratinocytes. Two novel autosomal recessive Hr mutations, G985W and Δ AK (a C-terminal deletion), have been reported to cause hair loss in mice. The mutated residues are highly conserved in human, macaque, mouse, and rat species. To test whether the G985W and Δ AK rat Hr (rHr) mutants inhibit VDR and TR action, plasmids expressing the relevant proteins were cotransfected into COS-7 cells. Data revealed that the G985W mutation abolished the ability of Hr to repress TR- and VDR-mediated transactivation. On the contrary, the Δ AK mutant lost the ability to repress TR-mediated transactivation, but retained strong repression of 1,25-VDR-mediated transcription. Pull-down assay demonstrated that both rHr mutants interact well with human VDR. These results provide new insight into the Hr repression mechanism, including the functional, but not VDR-association, involvement of Gly985 in the repression of VDR- and TR-mediated transactivation. Second, the requirement of the C-terminal Ala-Lys residues in rHr for repression of TR- but not VDR-mediated transactivation, implies a clear difference in how Hr modulates the activity of these two nuclear receptors. Third, the hair loss phenotype exhibited by the Δ AK mutant is presumably caused by a defect in Hr function that is downstream of VDR-Hr binding. To further probe Hr-VDR interactions, we next overexpressed rHr. Previous characterization of Hr has been hampered by the limited availability of sufficient quantities of this large, labile protein. Consequently, full-length rHr was overexpressed in E. coli. A 4 kb fragment of the rHr cDNA was subcloned into the pT7-7 expression vector and transformed into E. coli BL21(DE3)pLys S cells. The 130 kDa rHr was well expressed in this bacterial system and its authenticity was confirmed by mass spectrometry. The expression yield of rHr in this system was approximately 2-3% of total protein. This E. coli-expressed rHr will provide a resource for future functional studies of the molecular mechanism whereby Hr influences VDR- and TR-mediated target gene transcription.

Disclosures: J.C. Hsieh, None.

This study received funding from: National Institutes of Health NIDDK.

S262

Novel Vitamin D3 Analogs (DLAMs) Antagonize Bone Resorption Via Suppressing RANKL Expression in Osteoblasts. M. Inada, K. Tsukamoto*, M. Takita, M. Hirata, A. Hoshino*, T. Tominari*, K. Nagasawa*, C. Miyaura. Department of Biotechnology and Life Science, Tokyo University of Agriculture and Technology, Koganei, Tokyo, Japan.

Active vitamin D3, 1 α , 25(OH)2D3 (D3), has been proposed to regulate bone remodeling through bone formation and resorption that is maintaining calcium levels in blood serum. Recently new aspects of D3 activities have been reported in bone resorption, inhibition of osteoclast differentiation via interference of c-fos and NFATc1 expression. The other aspect was found in D3 analogs, synthetic modification at C2 position of D3 that is enhancing bone formation and bone mass. Here we show newly synthesized analogs, 1 α ,25(OH)2D3-26,23-lactam, (23S,25S)-DLAM-1P and DLAM-2P, that has a lactam moiety in the side chain, perfectly antagonized D3-induced osteoclast (Oc) differentiation. In computer docking simulation estimated DLAM-1P bind to VDR, lactam moiety in DLAM-1P may interfere VDR helix-12 folding at the site of Phe-422 (ligand binding domain). Oc formation was assessed by mouse co-culture system. We first examined antagonistic effects of DLAMs on Oc formation induced by D3. When simultaneous treatment of DLAM-1P (10-7M to 10-5M) and D3 (10-8M), DLAM-1P clearly suppressed the number of TRAP+ Ocs in a dose-dependent manner. To understand the mechanism of action of DLAM-1P, we analyzed mRNA expression of RANKL, a sole molecule for Oc differentiation. DLAM-1P clearly suppressed the D3-induced expression of RANKL mRNA in osteoblasts. In organ culture using mouse calvaria, bone resorbing activity (calcium release) induced by D3 was clearly suppressed by adding DLAM-1P that is associated with less induction of RANKL mRNA. The other analog DLAM-2P has shown similar activities to DLAM-1P. Therefore, DLAM analogs act on osteoblasts as an antagonist of D3 to suppress RANKL dependent Oc differentiation in the cell and the organ, suggesting the DLAMs are novel candidate for the treatment of pathological bone loss such like osteoporosis. Further modification will require for the therapeutic compound, enhancing bone formation and inhibition of RANKL expression beside minimum modification in DLAMs structure, e.g. installing substituents on its C2 position.

Disclosures: M. Inada, None.

S265

Targeted Inactivation of the Vitamin D Receptor by Caspase-3. P. J. Malloy*, D. Feldman. Department of Medicine, Stanford University, Stanford, CA, USA.

Calcitriol inhibits the growth of many cells including breast, colon, ovarian, pancreatic, and prostate cancer cells by causing cell cycle arrest and in some cells by inducing apoptosis. In breast cancer cells, calcitriol induces apoptosis by a caspase independent mechanism. On the other hand, in prostate cancer cells, calcitriol induction of apoptosis involves activation of caspase activity. Calcitriol actions are mediated by the vitamin D receptor (VDR) a member of the steroid-thyroid-retinoid receptor superfamily of nuclear transcription factors. In LNCaP prostate cancer cells induction of apoptosis by staurosporine abolished [³H]1,25(OH)₂D₃-binding and VDR protein suggesting to us that the VDR might be targeted for inactivation by caspases, a family of cysteine proteases that are activated during apoptosis. We identified a potential caspase-3 cleavage site (DxxDS) in helix H2n (D₁₉₅MMDS₁₉₉) in the VDR ligand-binding domain. Mutations (D195A, D198A and S199A) were generated in the putative caspase-3 cleavage site and their effects on caspase cleavage of VDR examined. In reporter gene assays, all of the VDR mutants exhibited transactivation activity similar to the WT VDR. COS-7 cells transfected with WT and mutant VDR cDNA expression vectors were then treated with staurosporine and VDR examined by western blot. A 22 kDa cleavage fragment was detected on western blot from cleavage of the WT VDR and the S199A mutant VDR but not the D195A or D198A mutant VDRs. Addition of the caspase-3 specific inhibitor z-DEVD-FMK prevented cleavage of the WT VDR in vivo. Treatment of transfected COS-7 cells with calcitriol also resulted in cleavage of the WT VDR but not the D198A mutant VDR. Calcitriol-induced cleavage of the WT VDR was blocked with z-DEVD-FMK demonstrating that calcitriol activates caspase-3 in these cells. In vitro treatment with caspase-3 resulted in the cleavage of WT VDR and S199A but not D195A or D198A mutant VDRs. WT VDR was also cleaved by caspase-6, and -7 but not caspase-8 in vitro. In conclusion, our results demonstrate that the VDR is cleaved by caspase-3 in vivo. We further demonstrate that calcitriol induces caspase-3 activity that results in the cleavage of the VDR. Our results suggest that activation of caspase-3 by calcitriol, while contributing to apoptosis may also may limit the apoptotic effects of calcitriol in cells that express caspase-3. Since caspases also regulate the activity of many proteins under non-apoptotic conditions, the inactivation of VDR by caspases may be of general importance as a mechanism to limit calcitriol activity.

Disclosures: P.J. Malloy, None.

S268

Phe377del Mutation in the Ank Gene Causes Craniometaphyseal Dysplasia (CMD)-like Phenotype in Knock-in Mice. I. Chen*, J. C. Wang*, E. J. Reichenberger. Reconstructive Sciences, UCHC, Farmington, CT, USA.

Craniometaphyseal dysplasia (CMD) is a rare craniofacial disorder characterized by progressive thickening of craniofacial bones concurrent with widened and radiolucent metaphyses in long bones. Mutations for autosomal dominant CMD have been identified in the human ANK gene (ANKH). ANK serves as a pyrophosphate (PPi) transporter regulating intra and extracellular PPi levels. To date, little is known about the pathogenesis of CMD and medical therapies of CMD show limited effect. We have generated a knock-in (KI) mouse model expressing a deletion mutation (Phe377del) in the Ank gene, the most common mutation found in our CMD patients. The purpose of this study is to characterize the progression of bone phenotype in these mice.

Ank^{-KI} and Ank^{KI/KI} mice appear normal at birth. Ank^{KI/KI} mice begin to weigh less than their respective wild type and Ank^{-KI} littermates after weaning. Within four to five weeks they develop a stiff, flat-footed gait, similar to phenotypes in Ank^{ank/ank} and Ank null mice. Decreased mobility of joints becomes more severe with age and they die around 6 months of age. Radiographically, bones from 1, 3 and 6 month-old Ank^{KI/KI} mice show increased radiopacity of cranial vault, base, facial bones, and mandibles; widening of metaphyses with increased radiolucency in femurs; fusion of joints in paws; narrowing of inter-disc space of vertebrae. Most Ank^{-KI} mice are indistinguishable from wild type mice but bones from 3 or 6 month-old heterozygous mice develop an intermediate phenotype. Skulls and jaws from 3 month-old Ank^{KI/KI} mice show significantly increased bone mineral density and bone mineral content. MicroCT results from skulls, femurs and mandibles of 3 month-old Ank^{KI/KI} mice show hyperostosis of calvariae and cranial base, narrowing of cranial neural foramina; significant decrease in trabecular number and bone volume fraction (BVf) of club-shaped femurs; increased BVf but decreased cortical density of mandibles compared to wild type and Ank^{-KI} mice. Dynamic histomorphometry analysis of femurs from 10 week-old Ank^{KI/KI} mice shows a marked decrease in mineral apposition rate. These observations suggest that the Ank mutation causing the CMD-like phenotype may be in a dose and time-dependent manner. These Ank knock-in mice can be used as a model for CMD.

Based on the similar joint phenotype to Ank null mice, we hypothesize that the CMD-causing mutant Ank is a loss of function mutation. The unique CMD-like phenotype in these mice suggests that a second molecular mechanism, rather than solely an abnormality in the extracellular pyrophosphate level, is involved in CMD pathogenesis.

Disclosures: I. Chen, None.

This study received funding from: AR49539.

S270

BMP Signaling in Osteoblasts Negatively Regulates Canonical Wnt Signaling to Reduce Bone Mass During Embryonic Bone Development. N. Kamiya¹, L. Ye², T. Kobayashi³, Y. Mochida⁴, M. Yamauchi⁴, H. Kronenberg³, J. Feng², Y. Mishina^{*1}. ¹LRDT, NIEHS/NIH, Research Triangle Park, NC, USA, ²Oral Biology, University of Missouri-Kansas City, Kansas City, MO, USA, ³Endocrine Unit, Massachusetts General Hospital and Harvard Medical School, Boston, MA, USA, ⁴Dental Research Center, University of North Carolina, Chapel Hill, NC, USA.

Bone morphogenetic proteins (BMPs) have been believed to be osteogenic inducers over 40 years, because of their ability to induce ectopic endochondral bone formation after subcutaneous implantation. However, physiological function of BMP signaling in osteoblasts remains largely unknown, because mice with germline mutations in genes encoding BMPs or BMP receptors that are predominantly expressed in bone (i.e., BMP2, BMP4, BMPRIA, and ACVRI) die in early embryonic stages before bone development. In the present study, we focused on function of BMP signaling during embryonic bone development using loss-of-function and gain-of-function strategies for BMP receptor IA (BMPRIA) in mice. We unexpectedly found that BMP signaling in osteoblasts restrained bone mass through regulation of canonical Wnt signaling.

BMP receptor type IA (BMPRIA or ALK3) is one of three type I receptors for BMPs and is predominantly expressed in bone. Since homozygous mice for a null mutation in Bmpr1a die at embryonic day 7.5, we rescued the embryonic lethality by generating a bone-specific knockout of Bmpr1a using tamoxifen inducible Cre-loxP system. Interestingly, under the physiological loss of BMPRIA signaling in osteoblasts, bone mass was increased and osteoclastogenesis was reduced concomitantly. Moreover, canonical Wnt signaling was upregulated due to a dramatic reduction in some of the Wnt inhibitors. Treatment with one of the Wnt inhibitors ex vivo rescued the phenotype of Bmpr1a-deficient bones with concomitant reduction of canonical Wnt signaling. In addition, upregulation of BMPRIA signaling in osteoblasts increased the expression of the Wnt inhibitor and increased osteoclastogenesis through OPG/RANKL pathway. Lastly, the bone phenotype of Bmpr1a-deficient mice was rescued by upregulation of BMPRIA signaling in mice with concomitant reduction of canonical Wnt signaling and an increase in osteoclastogenesis. These data indicate that BMP signaling in osteoblasts negatively regulates canonical Wnt signaling and positively regulates osteoclastogenesis through OPG/RANKL pathway to reduce bone mass during embryonic bone development. This study provides the first evidence of the molecular mechanism how these two major signaling pathways, BMP and Wnt, interact specifically in bones. We believe this study will provide innovative understanding of the physiological function of BMP signaling in bone biology.

Disclosures: N. Kamiya, None.

S272

Characterization of the Bone Phenotype in CIC-7 Deficient Mice. A. V. Neutzsky-Wulff^{*1}, K. Henriksen¹, A. Snel^{*1}, T. J. Jentsch^{*2}, J. Fuhrmann^{*2}, P. Lange^{*2}, C. Christiansen³, M. A. Karsdal¹. ¹Nordic Bioscience, Herlev, Denmark, ²MDC/FMP, Berlin, Germany, ³CCBR, Ballerup, Denmark.

Loss of the chloride channel CIC-7 leads to severe osteopetrosis. CIC-7 is believed to play a role in the ability of the osteoclasts to acidify the resorption lacuna, and thereby their ability to resorb bone. We therefore examined the bone phenotype of CIC-7 knockout (KO) mice in vitro and in vivo in detail, and compared it to the phenotype of oc/oc mice.

CIC-7 KO, oc/oc mice, and their corresponding wildtype littermates (WT) were sacrificed at 4-5 weeks of age. Bones and spleens were dissected and used for isolation of osteoclasts. The isolated cells were differentiated into mature osteoclasts on bone using M-CSF and RANKL. Cell culture supernatants were collected for measurements of CTX-I, TRACP and gelatinase activity by zymography. Cells were fixed and TRACP stained and the resorption pits were counted. Biochemical markers of resorption (CTX-I), osteoclast number (TRACP 5b), and osteoblast activity (ALP) were measured in serum of CIC-7 KO, oc/oc mice and the corresponding WT. Osteoblastogenesis in vitro was investigated using calvarial osteoblasts. In addition, bones were used for histological examination of TRACP positive osteoclasts with respect to number and morphology. Furthermore, osteoblast numbers and morphology were examined.

The osteoclasts from the CIC-7 KO mice were unable to resorb bone, as measured by CTX-I and by counting of resorption pits. Measurements of TRACP activity, as well as TRACP staining, showed the presence of equal numbers of osteoclasts in WT and KO cultures. Gelatinase activity was similar in both genotypes. Furthermore, the morphology of the KO cells was normal. Histological investigation of TRACP stained bone sections of both CIC-7 KO and oc/oc mice, indicated an elevated number of large osteoclasts present compared to WTs. The serum TRACP levels were increased by 250% in CIC-7 KO and oc/oc mice, whereas the resorption per osteoclast was reduced to 50% of the WT level. Finally, the serum ALP level in KO and oc/oc mice was increased by 30%, whereas no differences in osteoblast function were observed in vitro.

In summary, the osteoclasts from CIC-7 KO mice differentiate normally and form actin rings, but fail to resorb bone in vitro. In vivo, the osteoclasts are larger and more numerous, however, show no signs of resorption. Interestingly, an elevation of TRACP, a marked reduction in resorption per osteoclast, and elevated ALP level were observed in serum from both CIC-7 KO and oc/oc mice, showing increased signs of bone formation despite the low resorption. These findings indicate that the osteoclasts, and not their activity, control osteoblastic activity.

Disclosures: A.V. Neutzsky-Wulff, None.

S275

Identification of Single Nucleotide Polymorphisms (SNPs) Contributing to Bone Mineral Density and Fractures: A DNA Microarray Based Study. L. Gennari¹, D. Tejedor^{*2}, D. Merlotti¹, V. De Paola¹, A. Cadaval^{*2}, G. Martini¹, F. Valleggi¹, B. Franci^{*1}, S. Campagna^{*1}, B. Lucani^{*1}, L. Simon^{*2}, A. Martinez^{*2}, R. Nuti¹. ¹Internal Medicine, Endocrine-Metabolic Sciences and Biochemistry, University of Siena, Siena, Italy, ²Progenika Biopharma SA, Derio, Spain.

Osteoporosis is a complex polygenic disorder determined by the interaction between multiple genes and environmental risk factors, each with a small to modest effect. Traditional single candidate gene approach was only able to figure out a very small fraction of the whole genetic background of bone mass and fractures. We performed a DNA microarray-based analysis allowing the simultaneous study of 113 single nucleotide polymorphisms (SNPs) of 54 genes, which have been selected by their potential impact on bone metabolism. BMD and other phenotypes relevant to the pathogenesis of osteoporosis, such as ultrasound properties of bone, bone volume, bone turnover markers and sex hormone levels were evaluated in a population-based cohort of 904 postmenopausal women and elderly men. Moreover, 125 consecutive patients with non traumatic fractures were also investigated. Relationship between the selected clinical outcomes and the patient's pattern of SNPs was analysed by logistic regression. For each clinical outcome the optimal predictive model, based on a weighted combination of SNPs and disease characteristics and aimed resulting in a very high (95%) specificity, was selected. We identified 19 major SNP associated with BMD of whom 7 were non -sex-specific and 12 sex-specific. In particular SNPs at LRP-5, CYP19, ESR2, PPARalpha, and CYP11B1 genes were preferentially involved in determining BMD in males and SNPs at ESR1, SRD5A2, AR, IGF1, and IL-6 appeared to be female specific. Moreover, in females 2 SNPs (ESR1 and IL-6) were specific for spine BMD and 2 for hip BMD (AR and SRD5A2). In males, LRP-5 and CYP19 SNPs affected both femoral and lumbar BMD, while PPARalpha SNP mainly regulated BMD at the spine. Interestingly, 7 SNPs were associated with non-traumatic fractures independently of BMD. The most consistent associations with non-vertebral fractures were observed in IntegrinBeta3 and COL1A2 SNPs. In contrast, ESR1, TNFalpha, ADRB2, COMT, IL-6, and CYP19 were associated with both vertebral and non vertebral fractures. Importantly, different associations of SNPs were able to discriminate between the presence or the absence of non-traumatic fractures in the analysed population with a specificity of 95%, sensitivity 57% or 55%, and a likelihood ratio of 11.4 or 11.0 in males and females, respectively. The validation of these associations in larger samples could result useful for the identification of patients at higher fracture risk.

Disclosures: L. Gennari, None.

S277

Genome-Wide Measure of Pleiotropy Among Osteoporosis-Related Traits in the Framingham Study. D. Karasik¹, Y. K. Cho², L. A. Cupples^{*2}, D. P. Kiel¹, S. Demissie^{*2}. ¹IFAR, Hebrew SeniorLife, Boston, MA, USA, ²Biostatistics, BU Sch Public Health, Boston, MA, USA.

There have been no genome-wide association studies (GWAS) for osteoporosis-related traits using high-density genotyping platforms published to date. Such a GWAS may be used to examine pleiotropic associations of single nucleotide polymorphisms (SNPs) with BMD and bone geometric (BG) indices.

We used the Affymetrix 100K SNP GeneChip marker set in the Framingham Heart Study (FHS) to examine genetic associations with BMD and BG indices of the hip. We evaluated 70,987 autosomal SNPs with genotypic call rates $\geq 80\%$, HWE $p \geq 0.001$, and MAF $\geq 10\%$. In 1141 phenotyped members of FHS families (495 men and 646 women, mean age 62.5 yrs), using multivariable-adjusted residual trait values, we used linear regression analysis with generalized estimating equations (GEE), as well as family-based association tests (FBAT), to test associations between SNPs and BMD and BG traits. Variance components analysis (SOLAR) was performed to estimate genetic correlations (ρ_{Gc}) among these traits.

We searched for SNPs associated with pairs of bone traits and presented the proportion of SNPs associated with the first trait that are also associated with the second trait.

We found that at a pre-specified significance threshold α , BMD traits (measured at femoral neck, FN, and trochanter, TR) share 23% at $\alpha = 0.001$ (36% at 0.01 level) associated SNPs in GEE analysis, as is expected from the high $\rho_{Gc} = 0.84$ between them (Table). There are almost no such SNPs that share associations with both hip BMD and BG traits (femoral neck and shaft width, N and S WID, and neck length, FNL), despite substantial ρ_{Gc} among these traits (ranging -0.25 to -0.44). Also, the BG traits shared a surprisingly small percentage of associated SNPs.

In conclusion, GWAS offers an unbiased strategy to identify new candidate genes for osteoporosis, but also may be used to better understand how related phenotypes potentially share the same genetic determinants. These results need to be replicated in other GWAS samples.

	FN BMD	TR BMD	FNL	N WID	S WID
FN BMD		0.84***	0.149	-0.44***	-0.25*
TR BMD	23.3 (35.6)		0.141	-0.38***	-0.32**
FNL	1.0 (2.3)	0.5 (2.2)		-0.04	0.28*
N WID	0 (3.1)	0.5 (3.2)	0 (1.7)		0.44***
S WID	0 (2.8)	1.0 (3.0)	0 (1.7)	0 (3.0)	

Above diagonal - Genetic correlations (ρ_{Gc}) * $p < 0.05$; ** $p < 0.005$; *** $p < 0.0001$

Below diagonal - % associations shared by the phenotypes at $\alpha = 0.001$ (0.01 level)

Disclosures: D. Karasik, None.

This study received funding from: NHLBI/NIAMS/NIA.

S279

LRP5 G171V Mutation and Age-Related Bone Fragility. M. P. Akhter, D. M. Cullen, R. R. Recker. Medicine, Creighton University, Omaha, NE, USA.

It is well documented that aging has significant impact on the mechanical properties of bone in the human skeleton. In an animal model, we characterized bone structural and strength properties to determine if the LRP5 G171V mutation will protect against bone loss associated with Aging. Seventy two female mice representing two genotypes [(all bred to C57BL/6 mice), WT (Lrp5+/+, wild type), HBM (High bone mass with LRP5 G171V mutation)] and three age groups (4, 18, 22 months) were used (Table). At the time of necropsy fourth lumbar (L4) vertebral bodies were collected and then scanned using micro-CT (μ CT-40, Scanco) to quantify trabecular bone structural properties. The vertebral bodies were then mechanically tested in compression (along cranial-caudal direction) at 3mm/min displacement rate using an Instron-5543 testing device. We analyzed the trabecular bone structure and strength data using the General Linear Model (SPSS, IL) for univariate analysis to test for differences ($P < 0.05$) due to age and genotype. There was age-related loss in vertebral body structure and strength (Table). By 18 months of age, vertebral body trabecular bone structure (BV/TV) declined 28% in HBM mice and 54% in WT mice. In addition, HBM (33-60% decrease) and WT (47-57% decrease) mice lost significant structural strength (ULT, YLD, STIFF) by 18 months (Table). However, the decline between the 18 and 22 month age groups was not significant for either bone structure or strength within each genotype. HBM's trabecular bone structure (BV/TV) and strength remained significantly elevated at each age group (Table). These data suggest that the HBM mice (Lrp5 G171V mutation) experienced similar rates of bone loss with age but maintained both structural and strength advantage over the WT mice.

Age (month)	4		18		22	
Variable/ Genotype	HBM	WT	HBM	WT	HBM	WT
BV/TV	0.61 \pm 0.05	0.5 \pm 0.03 ^b	0.44 \pm 0.07 ^a	0.23 \pm 0.04 ^{ab}	0.49 \pm 0.05 ^a	0.24 \pm 0.06 ^{ab}
ULT (N)	46.5 \pm 9.20	18.9 \pm 5.9 ^b	19.0 \pm 3.2 ^a	10.0 \pm 5.6 ^{ab}	24 \pm 6.1 ^a	11.0 \pm 3.6 ^{ab}
YLD (N/mm)	35.0 \pm 8.30	13.9 \pm 5.5 ^b	15.3 \pm 4.3 ^a	6.0 \pm 3.9 ^{ab}	14.7 \pm 6.4 ^a	6.9 \pm 3.4 ^{ab}
STIFF (N/mm)	251 \pm 57	154 \pm 73 ^b	168 \pm 59 ^a	74 \pm 51 ^{ab}	161 \pm 61 ^a	97 \pm 40 ^{ab}

(Mean \pm SD); BV/TV=bone volume to total volume ratio; ULT/YLD=ultimate/yield load; STIFF=stiffness; ^aDifferences due to age (compare to 4mo) within each genotype ($P < 0.05$); ^bDifferences due to genotype within each age group ($P < 0.05$)

Disclosures: M.P. Akhter, None.

This study received funding from: The State of Nebraska LB595 Funds.

S281

LRP5 Mutations Are Associated with Osteoporosis, Impaired Glucose Tolerance and Hypercholesterolemia. A. Saarinen^{*1}, T. Saukkonen^{*2}, M. Somer^{*3}, C. M. Laine^{*2}, S. Toivainen-Salo^{*4}, A. Lehesjoki^{*1}, O. Mäkitie^{*2}.

¹Folkhälsan Institute of Genetics, University of Helsinki, Helsinki, Finland, ²Hospital for Children and Adolescents, University of Helsinki, Helsinki, Finland, ³The Family Federation of Finland, Helsinki, Finland, ⁴Helsinki Medical Imaging Center, Helsinki University Hospital, Helsinki, Finland.

LRP5 and LRP6 are coreceptors in the Wnt signaling pathway. Homozygous mutations in LRP5 cause osteoporosis-pseudoglioma syndrome (OPPG), characterized by severe osteoporosis and blindness. Heterozygous LRP5 mutations may also result in reduced bone mass. Recently mutations in LRP6 have been associated with coronary artery disease and metabolic syndrome. We have assessed bone health and glucose and lipid metabolism in a large Finnish OPPG pedigree with several heterozygous carriers of LRP5 mutations. DNA samples were collected from 30 family members, two of whom had OPPG. The exons and exon-intron boundaries of LRP5 were sequenced. Skeletal phenotype was assessed in 29 subjects by fracture history, bone mineral density (BMD) and spinal radiographs. Fasting blood samples were collected and oral and intravenous glucose tolerance tests were performed to assess glucose and lipid metabolism in individuals with LRP5 mutations.

Two different missense mutations were identified. The subjects with OPPG (aged 52 yrs and 58 yrs) were homozygous for R570W. One subject (age 85 yrs) was a compound heterozygote for R570W and R1036Q; she had normal vision but severe osteoporosis. Six subjects were heterozygous for R570W and three, for R1036Q; their median age was 59 yrs (15 - 72 yrs) and median BMI 26 kg/m². No mutations were found in 18 family members; their median age was 48 yrs (20 - 67 yrs) and median BMI 26 kg/m². Patients with two LRP5 mutations had multiple spinal and peripheral fractures and low BMD. The nine heterozygous LRP5 mutation carriers had significantly lower median BMD Z-scores at the lumbar spine (-1.0 vs +0.4, P=0.002) and femoral neck (-0.8 vs +0.75, P=0.009), more often vertebral fractures (44% vs 17%) and more peripheral fractures than those 18 without mutations. Of the 11 subjects with LRP5 mutation(s) six subjects (55%) had abnormal glucose tolerance: five had diabetes and one, impaired glucose tolerance. Intravenous glucose tolerance tests suggested impaired beta cell function; no insulin resistance was observed. Six subjects (55%) had hypercholesterolemia; three of them were on medication.

In addition to osteoporosis we found an unexpectedly high prevalence of diabetes and hypercholesterolemia in subjects with LRP5 mutations. These results link mutations in LRP5 to risk factors of coronary artery disease and implicate LRP5 as a novel gene that plays a role in glucose dependent insulin secretion from pancreatic beta cells.

Disclosures: A. Saarinen, None.

S288

Association Study Between Polymorphism Across the Osteoprotegerin Gene and Osteoporotic Phenotypes. S. Jurado^{*1}, N. Garcia-giral^{*1}, L. Agueda^{*2}, M. Bustamante^{*2}, A. Supervia^{*1}, M. A. Checa^{*1}, L. Perez-edo^{*1}, G. Salo^{*1}, M. J. Peña^{*1}, I. Aymar^{*1}, J. M. Garces^{*1}, S. Balcells^{*2}, D. Grinberg^{*2}, L. Mellibovsky^{*1}, A. Diez-perez^{*1}, X. Nogues^{*1}. ¹URFOA IMIM Universitat Autònoma de Barcelona, Hospital del Mar, Barcelona, Spain, ²Genetics Department, Universitat de Barcelona, Barcelona, Spain.

Osteoprotegerin (OPG) is a key regulator of bone resorption in the OPG/RANK/RANKL system. Therefore, the study of polymorphisms in the OPG gene is relevant in relation to osteoporosis. The aim of the present study is to evaluate common variation across the OPG genomic region using a haplotype-based approach.

A total of 964 postmenopausal women from Hospital del Mar of Barcelona (BARCOS cohort) were recruited and anthropometric features, together with bone mineral density (BMD) and osteoporotic fracture data, were recorded. Cases were consecutive unselected women attending to the Menopause Unit outpatient clinics in our institution. Secondary causes of metabolic bone disease were ruled out. BMD was measured with HOLOGIC QDR 4500 SL at lumbar spine (LS) and femoral neck (FN) sites. Twenty four single nucleotide polymorphisms (SNPs) were selected from haplotypic blocks obtained from the second phase of HapMap (CEU). Genotyping was performed by SNPlex at CeGen facilities, Biomedical Research Park of Barcelona. Haplotype frequencies were obtained using the PHASE software. Statistical analyses included ANCOVA for BMD and logistic regression for fractures (SPSS for windows statistical package v.12.0). Additive, recessive and dominant models were considered in all cases.

Twelve out of the 24 SNPs yielded significant statistical results (p value < 0.05) for LS BMD, FN BMD and/or osteoporotic fracture. These SNPs are located between the promoter region and intron 1, and belong to five different haplotypic blocks. Haplotypes within these blocks were also found to be associated with the different bone phenotypes. While none of the SNPs was associated with the three phenotypes, three of them were associated with both FN BMD and fracture, and two with FN and LS BMD.

In conclusion, genetic variants at the promoter and intron 1 of the OPG gene were found related to BMD and fracture risk in Spanish postmenopausal women, suggesting a role for regulatory SNPs in this gene for bone mass and / or fragility determination.

Disclosures: X. Nogues, None.

S291

Inhibition of Osteolytic Bone Metastases in Breast Cancer with a Cathepsin K Inhibitor. G. Wesolowski¹, M. Pickarski¹, G. Neusch^{*1}, P. Leung^{*1}, R. Oballa^{*2}, M. Percival^{*2}, W. Black^{*2}, L. T. Duong¹. ¹Bone Biology & Osteoporosis, Merck Res. Labs., West Point, PA, USA, ²Merck Res. Labs., Pointe-Claire-Dorval, PQ, Canada.

Breast and prostate cancer commonly metastasize to bone, resulting in bone loss, bone pain and fracture. Orally active cathepsin K inhibitors are currently being developed as potent bone resorption inhibitors for the treatment of osteoporosis. The standard of care, I.V. bisphosphonates, provides proof-of-concept for the use of potent antiresorptives for the treatment of metastatic bone disease. High expression of Cat K has also been detected in metastatic breast carcinoma, which suggests a role of Cat K in tumor invasion. L-006235 is a potent inhibitor of Cat K, with IC₅₀ of 0.2, 0.5, 12 and 22 nM against human, rabbit, rat and mouse Cat K, respectively, and of rabbit osteoclastic bone resorption, with IC₅₀ of 5 nM. Previously, L-235 was shown to be lysosomotropic, resulting to potential inhibition of other cathepsins, including Cat B, at high concentration in vivo. In this study, oral L-006235 was evaluated up to 100 mg/kg/day and compared to zoledronic acid (ZOL, 7.5 µg/kg, sc, wky) for the prevention of osteolytic lesions and tumor growth in the intra-tibial engraftment model of MDA-MB-231 breast carcinoma cells in nude rats. Progression of osteolysis and tumor burden were monitored by radiography and evaluated by µCT and histological analyses over 6 weeks. Compared to vehicle, L-006235 at 10, 30 and 100 mg/kg dose-dependently inhibited tumor-induced bone volume loss by 18%, 22%, and 43% (p<0.001), respectively, with full protection at the highest dose which was comparable to the efficacy of ZOL (45%). Compared to vehicle, L-006235 also reduced tumor growth by 29%, 40% and 63% (p<0.001), versus a 56% reduction with ZOL. In this study, L-006235 at 30 and 100 mg/kg also reduced cortical disruption, tumor necrosis, and tumor cell migration from the original injection site. Taken together, these data suggest that cathepsin K inhibitors provide potent anti-resorptive efficacy and, compared to the current standard of care, may potentially have added benefits in reducing tumor invasion, and preventing bone metastases associated with breast cancer.

Disclosures: L.T. Duong, Merck & Co. 3.

S293

Parathyroid Hormone-Related Protein Induces Bone Pain Through Stimulation of Proton-Secretion in Osteoclasts. L. Wang^{*}, H. Wakabayashi^{*}, T. Hiraga^{*}, T. Yoneda. Department of Biochemistry, Osaka University Graduate School of Dentistry, Osaka, Japan.

Bone pain is the most common complication associated with bone metastases. Of note, clinical studies reported that inhibitors of osteoclasts such as bisphosphonates (BPs) efficiently reduced bone pain, suggesting a causative role of osteoclasts. Parathyroid hormone-related protein (PTH-rP), a potent stimulator of osteoclasts, has been implicated in bone metastasis. Activated osteoclasts are known to release protons via the a3 type vacuolar-H⁺-ATPase (a3 V-H⁺-ATPase) to dissolve bone minerals, thereby inducing acidosis in the neighboring environment. Acidosis is a well-known cause of pain. These results collectively suggest that PTH-rP is associated with bone pain through stimulating osteoclastic bone resorption. Repeated subcutaneous injections of PTH-rP caused increased osteoclastic bone resorption in the metatarsal bones and hyperalgesia in the hind-paw. Immunohistochemical examination revealed that the hyperalgesia was associated with increased protein expression of the transient receptor potential channel-vanilloid subfamily member 1 (TRPV1) and phosphorylated-ERK (p-ERK) in the ipsi-lateral dorsal root ganglions (DRGs) and c-Fos in the spinal dorsal horn. The hyperalgesia and elevated protein expression were significantly reduced by a most potent BP zoledronic acid, recombinant human OPG, a specific inhibitor of the V-H⁺-ATPase FR167356 and an antagonist of TRPV1 activation I-RTX, respectively. Finally, TRPV1 knockout mice exhibited reduced PTH-rP-induced hyperalgesia. Relevant to bone pain in bone metastases of breast cancer, we developed an animal model in which the MDA-MB-231 human breast cancer cells that produces large amounts of PTH-rP were directly inoculated into the tibial marrow cavity in nude mice. These mice showed hyperalgesia in the ipsi-lateral hind-paw and a monoclonal antibody to PTH-rP reduced the hyperalgesia. These results suggest that PTH-rP produced by metastatic cancer cells plays a part in causing bone pain through stimulation of proton-secretion in osteoclasts, thereby activating the acid-sensing receptors such as TRPV1 that are expressed in the nociceptive neurons innervating bone.

Disclosures: L. Wang, None.

S295

Runx2 Regulates the Indian Hedgehog-PTHrP Pathway in Breast Cancer Cells. J. Pratap, J. Dobson*, A. J. van Wijnen, J. L. Stein*, G. S. Stein, J. B. Lian. Department of Cell Biology and Cancer Center, University of Massachusetts Medical School, Worcester, MA, USA.

Runx2 is expressed in hypertrophic chondrocytes and osteoblasts and is essential for bone formation. However, Runx2 is also highly expressed in bone metastatic cancer cells compared to non-metastatic cells. Importantly, Runx2 upregulates several metastatic markers (MMPs and VEGF) in cancer cells and a loss of function mutation of Runx2 prevents the osteolytic lesions formed by breast cancer cells in vivo. To further understand how Runx2 participates in the osteolytic process mediated by cancer cells, we investigated the effect of Runx2 on key components of the "vicious cycle". The vicious cycle of metastatic bone disease involves overproduction of PTHrP (Parathyroid hormone related protein) by tumor cells in the bone microenvironment, resulting in osteoclastic bone resorption. The resorbed bone releases TGF- β thereby stimulating tumor-cell proliferation and consequently continuing the vicious cycle. In the growth plate chondrocytes, Indian hedgehog (IHH) regulates PTHrP expression. Here, we show, following transduction of Runx2 expressing adenovirus that Runx2 activates endogenous levels of IHH more than 10 fold compared to 3-4 fold activation of other Runx2 target genes (VEGF, MMP9, MMP13 and osteocalcin) in MDA-MB-231 cells detected by real time PCR analysis. Runx2 also increased PTHrP levels 2-3 fold. The C-terminal deletion mutant of Runx2 (lacking the activation domain) failed to induce IHH and PTHrP levels in MDA-MB-231 breast cancer cells, as well as Runx2 target genes. In a time course analysis, we find Runx2 was able to activate IHH levels within 6hr of Runx2 expression in MDA-MB-231 cells. Consistent with these findings, depletion of Runx2 by siRNA decreases endogenous IHH and PTHrP levels produced by breast cancer cells. Blocking the Hedgehog signaling pathway using cyclopamine also inhibits Runx2 mediated activation of PTHrP which suggests that PTHrP upregulation by Runx2 is via IHH signaling events. We confirmed Runx2 recruitment on the IHH promoter in breast cancer cells by chromatin immunoprecipitation assays. Runx2 binds to a proximal (-0.5Kb) and distal site (-1.4Kb) of human IHH promoter. We propose that metastatic cancer cells by having higher levels of Runx2 are able to activate components of the vicious cycle as well as target genes that promote tumor progression in bone and increases bone loss. Thus this master regulator of bone formation is also a significant mediator of the metastatic activities of cancer cells and deserves consideration for targeted inhibition in tumor cells as a therapeutic approach to prevent the osteolytic bone disease.

Disclosures: J. Pratap, None.

S298

Osteonecrosis of Jaw Under Bisphosphonate Therapy: Patient Profile and Risk Assessment. T. I. Jung*, J. von der Gablentz*, B. Hoffmeister*, S. Mundlos*, P. Fratzl*, M. Amling*, M. J. Seibel*, D. Felsenberg*. ¹Zentrum für Muskel- und Knochenforschung (ZMK), Charité - Universitätsmedizin, Berlin, Germany, ²Clinic for Oral, Maxillofacial and Plastic Surgery, Charité - Universitätsmedizin, Berlin, Germany, ³Institute for Medical genetics, Charité - Universitätsmedizin, Berlin, Germany, ⁴Department of Biomaterials, Max Planck Institute of Colloids and Interfaces, Potsdam-Golm, Germany, ⁵Centre for Biomechanics and Skeletal Biology, University Hospital, Hamburg-Eppendorf, Germany, ⁶ANZAC Research Institute, University of Sydney, Sydney, Australia.

The objective of the ongoing German Register for Osteonecrosis of the Jaw (ONJ) was to explore the development of ONJ as a serious adverse event of bisphosphonate (BP) treatment. A standardized questionnaire was used to analyze all cases that were officially reported within Germany up until 31 Dec 2006. Focus was placed on 1) demographics, 2) primary disease incl. its therapy 3) BP intake 4) dental status 5) diagnosis of ONJ and outcome of ONJ therapy. We included cases with osteomyelitis or ONJ while cases due to radiotherapy were excluded.

In 383 reported cases, patients were 63.4 \pm 8.3 years old and women were affected twice as often. They suffered from malignant disease (78.4%), osteoporosis (8.2%), or a combination of both (13.4%). Common malignant diseases were breast cancer (46.7%), multiple myeloma (30.1%) and prostate cancer (13.5%). Patients had previously received chemotherapy (68.9%), radiotherapy (62.3%) and glucocorticosteroids (47.5%). The majority (67.2%) was treated with a single BP: Zoledronate (79.7%) or Pamidronate (12.4%). Two BPs were administered consecutively to 30.7% of the patients: Pamidronate/Zoledronate (53.5%). ONJ occurred after 23.8 \pm 17.6 (Zoledronate) or 36.4 \pm 20.0 (Pamidronate) months of BP treatment. Patients presented clinically with infection (33.3%), mucosal changes (21.4%), wound healing disturbance (21.4%), exposed bone (11.9%) and pathological dental status (46.2%). Histological signs were infection (51.9%) and osteonecrosis (34.2%) while radiologists diagnosed osteolysis (19.5%) and osteomyelitis (14.3%). Dental management included surgical (45.3%) or conventional (13.2%) methods, or a combination of both (41.6%). Success rate was highest (17.0%) for the combination therapy.

The etiopathogenesis of ONJ remains unclear but is likely to be complex. A discrete increase in osteoporotic patients was noted but high-risk patients received BPs due to their malignant disease. The occurrence of ONJ might be reduced by adjusting the guidelines of bisphosphonate treatment and by defining algorithms for the dental management of high-risk patients.

Disclosures: T.I. Jung, Elsbeth Bonhoff Foundation 2.
This study received funding from: Elsbeth Bonhoff Foundation.

S300

The SABRE (Study of Anastrozole with the Bisphosphonate Risedronate) Study: 12-Month Analysis. R. Eastell¹, C. Van Poznak*, R. A. Hannon¹, G. Clack³, M. Campone*, J. R. Mackey*, J. Apffelstaedt on behalf of the SABRE Investigators*, ¹Academic Unit of Bone Metabolism, University of Sheffield, Sheffield, United Kingdom, ²Dept of Internal Medicine, University of Michigan, Michigan, MI, USA, ³AstraZeneca, Macclesfield, United Kingdom, ⁴Site Hospitalier Nord de Nantes, Centre René Gauducheau, Nantes, France, ⁵Dept of Oncology, University of Alberta, Edmonton, AB, Canada, ⁶Dept of Surgery, University of Stellenbosch, Tygerberg, South Africa.

The SABRE study (NCT00082277) evaluated the effects of the bisphosphonate risedronate on bone mineral density (BMD) and bone turnover in postmenopausal women with hormone receptor-positive early breast cancer treated with anastrozole. Patients were stratified according to baseline risk of fracture by lumbar spine and hip T-scores. High-risk (H) patients (T-score < -2.0 for spine or hip, or those deemed high-risk by the investigator) received anastrozole (A) 1 mg/day plus risedronate (R) 35 mg/week orally. Moderate-risk (M) patients (T-score < -1.0 for spine or hip but \geq -2.0 for both) were randomized in a double-blind manner to receive A plus either R or placebo (P). Low-risk (L) patients (T-scores \geq -1.0 at both sites) received A alone. All patients received calcium and vitamin D. Bone turnover was assessed using serum procollagen type I amino terminal peptide (PINP), bone alkaline phosphatase (bALP), and serum C-terminal crosslinking telopeptide of type I collagen (sCTX). Percentage change in BMD is shown in the table. BMD increased significantly in H and decreased significantly in L. In M, a significant difference was seen between treatment groups for lumbar spine (p < 0.0001) and total hip (p = 0.002, analysis of covariance).

In M, there was a significant difference in the percentage changes in bone markers between treatment groups (A + R sCTX -43.73, PINP -47.56, bALP -23.91 vs A + P 5.18, -7.65, 1.61 respectively; p < 0.0001 for all). Incidences of adverse events (AEs) were comparable between M treatment groups (A + R 88%, A + P 86%; serious AEs A + R 5%, A + P 5%). In postmenopausal women with breast cancer who are already at moderate to high risk of fragility fracture, and are scheduled for treatment with anastrozole, bone health can be managed according to established guidelines. In this study, for patients already at risk, risedronate at the licensed dose was sufficient to prevent a decrease in BMD and an increase in bone turnover.

	Stratum / treatment	N	Estimated % change in BMD from baseline to 12 months (95% CI)
Lumbar spine	L/A only	35	-0.62 (-1.93, 0.71)
	M/A+P	65	-0.41 (-1.11, 0.29)
	M/A+R	73	+1.71 (0.85, 2.58)
	H/A+R	36	+3.36 (2.05, 4.69)
Total hip	L/A only	35	-0.35 (-1.37, 0.68)
	M/A+P	65	-0.09 (-0.66, 0.47)
	M/A+R	73	+1.29 (0.69, 1.90)
	H/A+R	37	+1.53 (0.37, 2.71)

A, anastrozole; CI, confidence intervals; P, placebo; R, risedronate

Disclosures: R. Eastell, Astra Zeneca 2, 5, 8; Alliance for Better Bone Health 2, 5, 8.
This study received funding from: SABRE was funded by AstraZeneca and Aventis.

S303

In Vivo Inhibition of Osteosarcoma Growth by Notch Pathway Inhibition. T. Setoguchi*, M. Tanaka*, S. Komiya*. Department of Orthopaedic Surgery, Kagoshima University, Kagoshima, Japan.

The Notch signaling pathway functions as an organizer in embryonic development. Genetic analysis has demonstrated a critical role for the Notch pathway in morphogenesis. Recent studies have shown constitutive activation of the Notch pathway in various types of malignancies. However, it remains unclear whether this pathway is activated in human bone tumor. Here, we examined the expression of the Notch pathway components by RT-PCR and immunohistochemical staining. RT-PCR and immunohistochemistry for Notch1-4, Jagged, Dll, Hes, and Hey was performed using human osteosarcoma cell lines and human osteosarcoma samples. And also, we investigated the effects of Notch pathway inhibition on osteosarcoma growth using pharmacologic inhibitors of γ -secretase (GSI) in vitro and in vivo. Cell viability was examined by MTT method. In order to determine the effects of Notch blockade in vivo, we examined the formation of tumor xenografts using osteosarcoma cell line and nude mice. RT-PCR revealed high expression of Notch-1, 2, Jagged1 Hes, and Hey in all of osteosarcoma cell lines. And also, 7 osteosarcoma human samples also showed high expression of notch signaling molecules mRNAs. In addition, immunohistochemistry showed high expression of Notch-1C in nucleus of osteosarcoma cell lines and human osteosarcoma samples. And also, expression of Jagged and Hes was observed in osteosarcoma cell lines and human osteosarcoma samples. MTT assay showed that GSI suppresses the growth of the osteosarcoma cell lines in vitro (Fig.1). In addition, intraperitoneally GSI administration dramatically inhibited the osteosarcoma xenografts growth in vivo (Fig.2). Our data indicate that the Notch pathway is a new candidate for therapeutic target of osteosarcoma.

Fig.1

γ -secretase inhibitor suppresses the growth of osteosarcoma cell lines

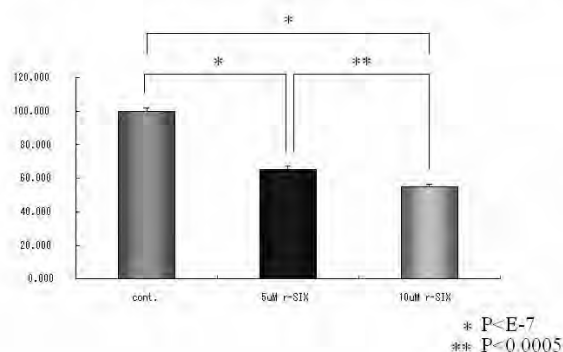
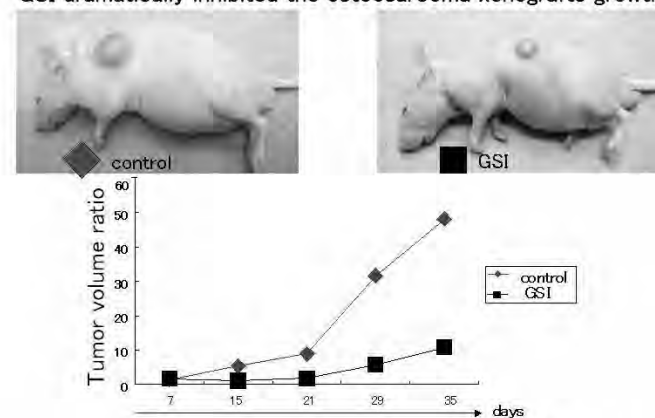


Fig.2

GSI dramatically inhibited the osteosarcoma xenografts growth



Disclosures: T. Setoguchi, None.

This study received funding from: Japan Society for the Promotion of Science.

S305

Transforming Growth Factor β Receptor I Kinase Inhibitor Reduces the Development and Progression of Melanoma Bone Metastases. K. S. Mohammad¹, D. Javelaud², E. G. Stebbins³, M. Niewolna¹, C. R. McKenna¹, X. Peng¹, L. A. Kingsley¹, P. G. J. Fournier¹, L. S. Higgins³, D. H. Wong³, A. Mauviel², T. A. Guise¹. ¹Internal Medicine, University of Virginia, Charlottesville, VA, USA, ²INSERM U697, Paris, France, ³Scios Inc., San Francisco, CA, USA.

Melanoma often metastasizes to bone, where it is exposed to high concentrations of TGF- β . Constitutive Smad signaling occurs in human melanoma. Because TGF- β

promotes metastases to bone by several solid tumors, we hypothesized that TGF- β could promote melanoma metastases to bone. Consistent with this, overexpression of the inhibitory Smad7 blocked the capacity of 1205Lu melanoma cells to form bone metastases by preventing the TGF- β induction in vitro of genes known to mediate osteolytic breast cancer bone metastases such as PTHrP, IL-11, CXCR4 and osteopontin and by blocking the induction of TGF- β target genes PTHrP, IL-11 and CTGF in bone metastases in vivo. We next tested the effect of a small molecule inhibitor of TGF- β receptor I kinase (TGF- β RI), SD-208 on development and progression of bone metastases due to 1205Lu melanoma. This inhibitor effectively reduced bone metastases due to MDA-MB-231 breast cancer. In vitro, SD-208 blocked TGF- β induction of Smad3 phosphorylation relative activity of the TGF- β (Smad)-responsive promoter CAGA in several melanoma lines: 1205Lu, WM852, 501mel and 888mel as well as invasion through matrigel by 1205Lu. We therefore hypothesized that pharmacologic blockade of TGF- β signaling using SD-208, would be effective treatment for melanoma metastasis to bone. Nude mice were inoculated with 1205Lu melanoma cells into the left cardiac ventricle and treated with SD-208 (20 and 60 mg/kg po qd administered via oral gavage) in either prevention or treatment protocol. In the former, SD-208 (60mg/kg/d), started 2 days before tumor inoculation, prevented the development of osteolytic bone metastases compared with vehicle. In the latter, mice given SD-208 (60mg/kg/d) after confirming the presence of osteolytic lesions by radiography, had significantly smaller osteolytic lesions vs. vehicle treated mice ($p=0.0009$). These data indicate that therapeutic targeting of TGF- β may decrease the osteolytic bone metastases caused by malignant melanoma by mechanisms similar to those implicated in breast cancer osteolysis.

Disclosures: K.S. Mohammad, None.

S307

RANKL Inhibition Blocks Lung Cancer-induced Osteolytic Lesions and Reduces Skeletal Tumor Burden in Both RANK-Expressing and RANK-Negative Lung Cancers. R. Miller¹, J. Jones¹, M. Tometsko¹, M. Chaisson-Blake¹, M. Roudier², W. Dougall¹. ¹Department of Hematology/Oncology Research, Amgen Inc., Seattle, WA, USA, ²Department of Pathology, Amgen Inc., Seattle, WA, USA.

Bone metastasis is a serious complication of lung cancer and occurs in 30% of patients. Tumor cells interact with the bone microenvironment to induce osteoclastogenesis, leading to bone destruction and release of growth factors that have the potential to feed back to the tumor growth. RANK ligand (RANKL) is essential for osteoclast formation, function, and survival. Tumor cell-mediated osteolysis occurs ultimately via induction of RANKL within the bone stroma, and inhibition of RANKL in animal models of breast or prostate cancer bone metastasis blocks tumor-induced osteolysis and prevents the increase in bony tumor burden. Another role for RANK and RANKL in promoting metastasis to bone has recently been proposed, in which RANK-expressing tumor cells migrate into the bone environment via RANKL acting as a chemotactic factor (Holstead-Jones et al. 2006). We examined a panel of lung cancer cell lines to develop a model of lung cancer in bone. Lung cancer cell lines that expressed RANK included H146, H2107, H2108, H1975, H2126, while H526 and H1299 were negative for RANK, as determined by flow cytometry. Using bioluminescent imaging (BLI) and intracardiac challenge, we observed that several lung cancer lines became established and progressed in the bone, resulting in osteolytic lesions. The growth in bone and development of osteolytic lesions occurred with both RANK-expressing (H2126, H1975) and RANK-negative (H1299) cell lines. We treated mice bearing either H1299 (RANK-negative) or H1975 (RANK-positive) with the RANKL inhibitor OPG-Fc at early or late timepoints. OPG-Fc completely blocked the radiographically-evident osteolytic lesions induced by either cell line at all time points tested. In addition, RANKL inhibition blocked the skeletal tumor progression of the H1299 lung cancer line as determined by longitudinal BLI analysis and histomorphometry. In conclusion, these results clearly show that both RANK-expressing and RANK-negative lung tumor cells lead to bone metastasis. The ability of RANK expression on tumor cells to further promote bone metastasis will require additional studies. These results demonstrate that, irrespective of RANK expression on tumor cells, RANKL is a required factor for the tumor-induced osteolytic lesions caused by each lung cancer tested in vivo. RANKL inhibition reduced skeletal tumor burden of the H1299 lung cancer line, presumably via the indirect mechanism of blocking tumor-induced osteoclastogenesis and resultant production of growth factors from the bone microenvironment.

Disclosures: R. Miller, Amgen Inc. 1, 3.

This study received funding from: Amgen, Inc.

S309

Myeloma Cells Decrease EphB4 Expression in Osteoblasts: A Novel Mechanism for Regulation of Bone Formation in Multiple Myeloma. A. L. Bates*, G. R. Mundy, C. M. Edwards. Vanderbilt Center for Bone Biology, Vanderbilt University, Nashville, TN, USA.

Multiple myeloma is associated with a destructive osteolytic bone disease, characterized by an increase in osteoclastic bone resorption and a reduction in osteoblastic bone formation. The increase in bone resorption in myeloma is well characterized; however the precise cellular and molecular mechanisms which mediate the reduction in bone formation and the uncoupling of bone resorption from bone formation are poorly understood. Recently, a novel mechanism has been suggested for coupling between osteoblasts and osteoclasts during normal bone homeostasis due to bidirectional signaling between the ligand ephrin B2, expressed by osteoclasts, and its receptor EphB4, expressed by osteoblasts. The interaction between EphB4 and ephrin B2 resulted in inhibition of osteoclast activity by reverse signaling through ephrin B2 on osteoclasts and stimulation of

osteoblast differentiation and bone formation by forward signaling through EphB4 on osteoblasts (Zhao et al. 2006). Since the normal coupling of bone resorption to bone formation is dysregulated in multiple myeloma, we hypothesized that this may be mediated by modifications in the EphB4/ephrin B2 receptor/ligand interaction. To study bone formation in multiple myeloma in vivo, we used the 5TGM1 murine model of myeloma. 5TGM1 myeloma cells were inoculated by i.v. injection into C57BlK^a.wRij mice, resulting in homing of myeloma cells to the bone marrow, and development of an osteolytic bone disease. In addition to the well characterized increase in osteoclastic bone resorption, the bone disease was associated with a significant reduction in osteoblast number and rates of bone formation ($p < 0.01$). Real time PCR demonstrated expression of EphB4 mRNA in 5TGM1 myeloma cells, C2C12 and 2T3 osteoblasts, with a 2-fold increase in expression in 5TGM1 myeloma cells when compared with C2C12 or 2T3 cells. Western blotting demonstrated expression of EphB4 protein in C2C12 and 2T3 cells. Treatment of C2C12 or 2T3 cells with conditioned media from 5TGM1 myeloma cells resulted in a significant reduction in expression of EphB4 in both C2C12 and 2T3 cells, suggesting that myeloma cells release a soluble factor which down-regulates EphB4 in osteoblasts. In conclusion, we have shown that the development of myeloma bone disease in the 5TGM1 murine model of myeloma is associated with a reduction in bone formation, and that 5TGM1 myeloma cells can down-regulate EphB4 expression in osteoblasts. This raises the possibility that the reduction in bone formation associated with myeloma bone disease is mediated by a reduction in EphB4 expression and thus disruption of the normal coupling of bone resorption and bone formation.

Disclosures: C.M. Edwards, None.

S311

Prevention and Treatment of Hypogonadism-associated Bone Loss and Bone Metastases by OPG-Fc in a Model of Mixed Osteolytic/Osteoblastic Metastases. S. S. Padalecki¹, B. Grubbs¹, B. Goins¹, A. Soundarajan¹, G. R. Mundy², W. Dougall³. ¹UTHSCSA, San Antonio, TX, USA, ²VUMC, Nashville, TN, USA, ³Amgen, Inc., Cambridge, MA, USA.

Bone resorption plays an important role in the development of osteoblastic metastases. Osteoclastic bone resorption results in the release of potent growth factors from bone. Androgen ablation, the standard treatment for men with advanced prostate cancer, increases systemic bone resorption and releases these growth factors from bone. As a result it also likely makes the skeleton a more fertile environment for prostate cancer metastasis. We have previously shown that increased osteoclastic bone resorption due to hypogonadism causes a more fertile environment for mixed osteolytic/osteoblastic bone metastases utilizing a mouse model which mimics the clinical situation of men rendered hypogonadal as a result of treatment for prostate cancer. To investigate the potential of OPG-Fc in preventing and treating bone loss due to hypogonadism and mixed bone metastases, male nude mice underwent orchiectomy or sham surgery 4 weeks prior to intracardiac inoculation with TSU-PR1 bladder cancer cells that cause mixed bone metastases. The potential of OPG-Fc in prevention of bone loss and mixed bone metastases was assessed by treating mice 3X weekly with OPG-Fc or vehicle from the time of surgery. To determine the efficacy of treating existing bone metastases with OPG-Fc, treatments were not started until 75% of the mice had evidence of bone metastases by radiograph. Radiographs, bone mineral density, 99mTc-MDP MicroSPECT imaging and bone histomorphometry were used to assess bone turnover and tumor osteolysis. As expected, hypogonadism resulted in lower bone mineral density and increased bone turnover compared with sham-controls. This was prevented by OPG-Fc. TSU-PR1 bone metastases were increased and developed faster in hypogonadal mice treated with vehicle compared to sham-controls. OPG-Fc decreased bone metastases in hypogonadal TSU-PR1-inoculated mice when used in a preventative fashion but had no effect on soft tissue metastases or survival. When OPG-Fc was used to treat existing bone metastases, it resulted in a decrease in radiographic lesion number and area. This work provides in vivo evidence that OPG-Fc not only prevents bone loss due to androgen deprivation and reduced bone metastases in a prevention scenario, but suggests it also may lessen the severity of existing bone metastases. These data support the hypothesis that increased bone resorption due to androgen deprivation may result in a more fertile environment for the development of bone metastases. Bone resorption inhibitors, such as OPG-Fc, may benefit hypogonadal men with advanced prostate cancer to prevent and treat bone loss as well as skeletal metastases.

Disclosures: S.S. Padalecki, Amgen, Inc. 2.
This study received funding from: Amgen, Inc.

S316

Serum Pentosidine Level Is Positively Associated with the Presence of Vertebral Fractures in Postmenopausal Women with Type 2 Diabetes. M. Yamamoto, T. Yamaguchi, M. Yamauchi, S. Yano, T. Sugimoto. Department of Internal Medicine 1, Shimane University Faculty of Medicine, Izumo, Japan.

Despite higher BMD than healthy subjects, patients with type 2 diabetes mellitus (2DM) have an increased risk of fractures, suggesting that BMD was not sensitive enough to assess the risk of fractures. However, there are no useful methods for assessing the bone fragility in 2DM. Recently, bone content of pentosidine, which is one of well-known advanced glycation end-products, is known to be negatively associated with bone strength. In this study, an association between serum pentosidine levels and the presence of vertebral fractures were examined in diabetic patients whose bone fractures lack their predictive markers. Ninety-four male and 76 postmenopausal female patients with 2DM within normal creatinine levels were examined by bone mineral density (BMD) at the lumbar spine, femoral neck and one-third of radius as well as spine radiographs, and by measurement of

biochemical parameters including serum pentosidine, serum bone-specific alkaline phosphatase (BAP) and urinary levels of N-telopeptide (uNTX). Thirty-three male and 20 female had vertebral fractures. Serum pentosidine level significantly increased with age in the diabetic men and women ($r = 0.232$, $p = 0.026$ and $r = 0.319$, $p = 0.006$, respectively). Comparison between diabetic subjects with and without vertebral fractures revealed no significant differences in BMD values at any sites or biochemical parameters such as BAP or uNTX in both genders. In contrast, serum pentosidine levels in women with vertebral fractures were significantly higher than in those without fractures ($0.0440 \pm 0.0136 \mu\text{g/ml}$ vs $0.0321 \pm 0.0118 \mu\text{g/ml}$, $p < 0.001$). Multivariate logistic regression analysis adjusted for age, body weight, body height, HbA1c, serum creatinine and diabetic duration showed that serum pentosidine level was identified as an independent factor associated with the presence of vertebral fractures in postmenopausal women with diabetes as shown in Table.

Associations between the presence of vertebral fractures and serum pentosidine levels in 2DM			
Pentosidine level	OR	(95% CI)	P
Male	0.76	(0.44-1.30)	0.3087
Female	3.33	(1.42-7.84)	0.0059 **

Serum pentosidine level, but not BMD, seems to be useful for assessing the risk of vertebral fractures in postmenopausal diabetic women, and may reflect bone quality in this group.

Disclosures: M. Yamamoto, None.

S321

Factors Predicting Osteoporosis Treatment Initiation in a Regionally-Based Clinical Cohort. W. D. Leslie¹, J. F. Tsang², L. M. Lix³. ¹Dept of Medicine, University of Manitoba, Winnipeg, MB, Canada, ²University of Manitoba, Winnipeg, MB, Canada, ³Manitoba Centre for Health Policy, University of Manitoba, Winnipeg, MB, Canada.

BMD testing is used by many clinical practice guidelines to identify those at high fracture risk and to guide osteoporosis therapy (OTx) initiation. We hypothesized that OTx initiation would show large step increases at discrete cutoffs corresponding to proposed T-score intervention thresholds (e.g., -1.5, -2.0 or -2.5). Women age 50 y or older who had not been dispensed any OTx medication in the year prior to baseline DXA (1998-2002) were identified in a regionally-based database which contains all clinical DXA test results for the Province of Manitoba, Canada. Women with independent indications for OTx (previous glucocorticosteroid use or non-traumatic fractures of the hip, spine, wrist or humerus) were excluded. The rate of OTx initiation in the year after BMD (1 or more pharmacy dispensations) was studied using descriptive and logistic regression methods. 3826 of the 8654 women (44.2%) were dispensed OTx in the year after BMD. OTx initiation increased progressively as BMD decreased (8.2% normal, 41.0% osteopenic, 78.5% osteoporotic, p -for-trend < .00001). Contrary to expectation, there was a gradient response to OTx initiation rather than step increases at conventional T-score intervention thresholds. A small step increase occurred at a T-score of -1.0 but this is not generally considered as an OTx initiation threshold in the absence of other indications. In a logistic regression model BMD was strongly associated with OTx ($p < .00001$) while age ($p > .2$), weight or BMI ($p > .2$), and fracture (excluding hip, spine, wrist or humerus) in the last year ($p > .2$) were not. Similar results were seen when spine and hip T-scores were considered separately, or when OTx initiation was defined as 2 or more pharmacy dispensations. We conclude that physicians rely heavily on the BMD T-score to decide on OTx initiation. Although many clinical practice guidelines suggest that age in addition to other risk factors should be considered in OTx decision-making, we did not see evidence of this. More explicit methods of reporting fracture risk may be required to assist physicians in selecting patients likely to derive the largest benefit from OTx.

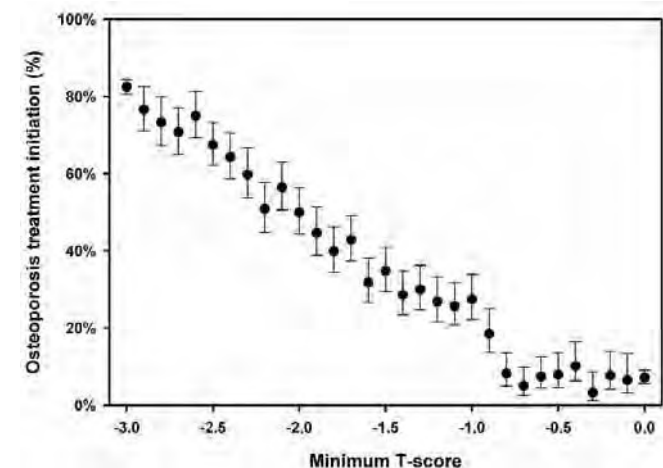


Figure: Osteoporosis treatment (OTx) initiation according to T-score (minimum spine and hip).

Disclosures: W.D. Leslie, Merck Frosst Canada Ltd; Sanofi-Aventis; Proctor & Gamble Pharmaceuticals Canada, Inc. 2, 5, 8.

S323

Utility of Lumbar Spine DXA Scanning in Women Undergoing Asymptomatic Osteoporosis Screening. V. Pao*, D. E. Sellmeyer, Medicine/Endocrinology, University of California San Francisco, San Francisco, CA, USA.

The International Osteoporosis Foundation recommends osteoporosis screening with bone mineral density (BMD) be conducted at the hip. The planned WHO fracture risk assessment model includes femoral neck BMD. Previous studies of research populations have suggested that lumbar BMD may be affected by degenerative changes and contribute little additional information to fracture risk assessment. To determine the utility of spine BMD in asymptomatic postmenopausal women undergoing routine clinical osteoporosis screening, we conducted a retrospective chart review of women over age 50 years who were referred for screening via dual x-ray absorptiometry (DXA) scanning at the UCSF Osteoporosis Center during 12 consecutive months. Women were excluded if they had a known secondary cause of bone loss or were on medications known to affect bone. We categorized each DXA as normal, osteopenia, or osteoporosis at the lumbar spine, femoral neck, and total hip according to the WHO T-score definitions. We also recorded patient demographics and specialty of referring physician. Patient characteristics were analyzed across categories of bone density using ANOVA.

The average age of the 744 participants was 65.7 ± 9.4 (mean \pm SD) years; 65% were Caucasian and 21% were Asian. DXA results showed 18.5% of the women had normal bone mineral density (BMD) at all three sites while 57.2% had osteopenia (T-score between -1 and -2.5) at one or more sites and 24.2% had osteoporosis (T-score < -2.5) at one or more sites. Compared to women with normal BMD, women with osteoporosis were more likely to be of Asian or Caucasian ethnicity ($p < 0.001$), have a smaller BMI ($p < 0.001$), and have a past history of back pain ($p = 0.009$). Osteoporotic patients were less likely to be taking calcium and vitamin D ($p = 0.02$) and more likely to have a history of fracture ($p = 0.003$). The majority of the patient population was referred by their primary care provider (64.1%), followed by gynecologists, endocrinologists, and rheumatologists. Orthopedic surgeons referred only 0.1% of patients. Of women who had normal BMD readings at both the total hip and femoral neck, 9.3% had osteopenia or osteoporosis at the lumbar spine. The average lumbar spine T-score among these women was -1.6 ± 0.5 . Many health care providers limit screening for osteoporosis to hip and femoral neck measurements. However, in our study a significant proportion of women had osteopenia or osteoporosis at the lumbar spine despite having normal BMD at the hip and femoral neck. These women would be expected to have an increased risk for vertebral fracture and would be missed if screening were limited to the hip site. Consideration should be given to regularly including the lumbar site when conducting routine osteoporosis screening in asymptomatic women.

Disclosures: D.E. Sellmeyer, None.

S330

In Vivo Assessment of 3-Dimensional Bone Micro Architecture with HR-pQCT in Patients with and without Fractures. H. Radspieler¹, I. Frieling², M. Neff³, R. Fischer⁴, M. Zulliger³, M. A. Dambacher⁵. ¹Center of Osteoporosis Munich, Muenchen, Germany, ²Center of Osteoporosis Hamburg, Hamburg, Germany, ³Center of Osteoporosis Zurich, Zurich, Switzerland, ⁴Klinik Eppendorf, Hamburg, Germany, ⁵ZORG, Zurich, Switzerland.

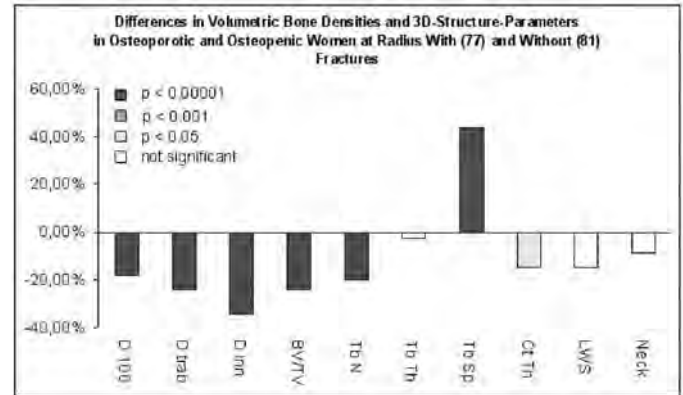
Measurement of areal bone mineral density (BMD/DXA) with derived T-scores may not be sufficient to evaluate the individual fracture risk. HR-pQCT reveals volumetric cortical and trabecular bone density and structural parameters as BV/TV, trabecular thickness and separation and cortical thickness.

We examined more than 200 women in the centres of osteoporosis in Hamburg and Munich with normal (T-Score > -1 SD), osteopenic (-2.5 SD $>$ T-score < -1.0 SD) or osteoporotic (T-score < -2.5 SD) BMD measured with DXA. In all patients volumetric BMD and trabecular architecture of the radius and tibia were measured by HR-pQCT (XtremeCT[®], SCANCO Medical AG).

Women with and without fractures showed no significant differences in height and weight but in age (68 vs. 63 y). The median T-scores from DXA measurements in women with and without fractures showed no significant differences (lumbar spine: -2.2 and -2.1, total hip: -2.2 and -2.2, neck: -2.0 and -1.8, respectively).

However, selective and region specific trabecular densities as well as structure parameters measured by HRpQCT differed significantly in osteopenic and osteoporotic women with and without fractures. The mean total density was lower in women with fracture than in women without fractures (D100, 247 vs. 291 mg/ml, $p < 0.001$), as well as the mean trabecular density (Dtrab, 94 vs. 123 mg/ml, $p < 0.001$) and the mean inner trabecular density (Dinn, 49 vs. 75 mg/ml, $p < 0.001$). Furthermore structure parameters in patients with fractures showed significantly increased trabecular separation (TbSp, 678 vs. 548 μ m, $p < 0.001$) and significantly decreased trabecular number (TbN, 1.3 vs. 1.6/mm, $p < 0.001$) as well as BV/TV (7.8 vs. 10.3%, $p < 0.001$) and significantly decreased cortical thickness (CtTh, 623 vs. 735 μ m, $p < 0.05$) with visible inhomogeneity of trabecular structure.

In conclusion, high-resolution peripheral computed tomography might help to predict fracture risk in osteopenic and osteoporotic patients. Especially in patients with osteopenia (according WHO-definition), the T-score seems to underestimate the fracture risk.



Disclosures: H. Radspieler, None.

S332

Use of DXA-Based Structural Engineering Models of the Proximal Femur to Predict Hip Fracture. L. Yang¹, N. Peel², J. Clowes¹, E. V. McCloskey¹, R. Eastell¹. ¹Academic Unit of Bone Metabolism, University of Sheffield, Sheffield, United Kingdom, ²Metabolic Bone Centre, Northern General Hospital, Sheffield, United Kingdom.

Several DXA-based structural engineering models of the proximal femur have been developed to estimate stress due to sideways falls. Their usefulness in predicting hip fracture has not yet been established and we therefore evaluated these models as diagnostic tools for hip fracture.

We recruited 51 consecutive female patients presenting to the orthopaedic ward with low-trauma hip fracture (ages 58-81); 30 of the fractures had occurred at the femoral neck (FN), 17 were classified as trochanteric (TR) and 4 fracture sites were not specified. For each case we selected 3 age-height and weight-matched controls from a population-based cohort. The hip DXA scans were analysed using a special version of Hologic's software that produces a pixel-by-pixel BMC map. Curved-beam, curved composite beam and finite element (FE) models were generated and the stress calculated at each pixel. The elastic modulus and yield stress of the models were determined according to Keyak (Keyak et al. Clin Orthop Relat Res 437: 219-28). Index of fracture risk (IFR) was defined at each pixel as the stress divided by the yield stress. The maximum and mean IFR in the FN, narrowest FN, middle trochanter (MT), trochanter and total hip were calculated. The usual hip structure analysis (HSA) parameters were also calculated. Logistic regression was performed followed by ROC analysis, expressed as area under the curve (AUC), to identify the best discriminators between cases and controls. Analysis was performed regarding hip fracture as a homogeneous condition and repeated separately for FN and TR fractures.

TH BMD, FN axial length (AL), MT cortical thickness (CTH) and mean IFR (avgIFR) from the FE models were identified as best predictors. Specificity for hip fracture was consistently high (93-99%). The sensitivity and AUC are shown in the Table where * indicates AUCs that are significantly ($p < 0.05$) different from that with TH BMD alone as predictor.

In conclusion, this study suggests that HSA and FE models can enhance hip fracture discrimination over TH BMD alone. Preliminary analyses suggest their contribution may differ between FN and TR fractures but further evaluation is required.

	Model 1	Model 2	Model 3	Model 4
All hip fractures				
Sensitivity (%)	33	45	59	61
AUC	0.778	0.848*	0.877*	0.885*
Femoral Neck fractures				
Sensitivity (%)	23	40	53	57
AUC	0.806	0.850	0.908*	0.913*
Trochanteric fractures				
Sensitivity (%)	6	24	N/A	N/A
AUC	0.774	0.816		

Model 1: TH BMD; Model 2: TH BMD + MT CTH

Model 3: Model 2 + FNAL; Model 4: Model 3 + MT avgIFR

Disclosures: L. Yang, None.

S336

Longitudinal Rate of Change in Bone Mineral Density by Age for Men and Women. L. Langsetmo¹, C. Berger¹, D. A. Hanley², J. Prior³, W. P. Olszynski⁴, J. Brown⁵, L. Joseph⁶, A. Tenenhouse⁶, D. Goltzman⁶. ¹CaMos, Montreal, PQ, Canada, ²University of Calgary, Calgary, AB, Canada, ³University of British Columbia, Vancouver, BC, Canada, ⁴University of Saskatchewan, Saskatoon, SK, Canada, ⁵Laval University, Ste-Foy, PQ, Canada, ⁶McGill University, Montreal, PQ, Canada.

The objective of this study was to estimate the average rate of change in bone mineral density (BMD) of the lumbar spine and hip as a function of age for men and women 25-85

years old. The source population was a longitudinal cohort of 9423 community-dwelling Canadian adults recruited from randomly selected households within a 50 km radius of nine cities across Canada. BMD of the lumbar spine and hip (total hip, femoral neck, trochanter, and Ward's triangle) was measured at baseline and 5-year follow-up for all age groups and at 3-year follow-up for those 40-60 years old. The study excluded anyone without repeat BMD measurement (n=2665), over 85 years (n=179), or with more than 3 months corticosteroid use (n=211). A direct calculation or linear regression was used to estimate individual rate of change. A separate analysis was done for men and women and further stratified by use of anti-resorptives. The average rate of BMD change was calculated based on 5-year age intervals and used to construct age trajectories for the rate of bone loss.

The main age-dependent changes for women are a period of accelerated bone loss in those 40-54 years old, increased loss at hip sites in those over 70 years old, and a sustained increase in BMD of the lumbar spine in those over 65 years old. The main age-dependent changes for men are increased loss at all sites in those 25-39 years old, increased loss at hip sites in those over 65 years old, and a sustained increase in lumbar spine BMD in those over 40 years old. Different hip sites had similar but not parallel trajectories. The maximal femoral neck BMD loss for women not using anti-resorptives was an average 0.0077 (95% CI: 0.0062-0.0091) g/cm² per year in the 50-54 year age group and for men not using anti-resorptives was an average 0.0060 (95% CI: 0.0032-0.0088) g/cm² per year in the 25-29 year age group. In contrast, the femoral neck BMD loss for women using anti-resorptives was an average 0.0026 (95% CI: 0.0017-0.0035) g/cm² per year in the 50-54 year age group. Mean rates of bone loss for anti-resorptive users were lower than non-users for both men and women 50-79 years old. The differences between users and non-users were statistically significant for women but not men. The overall pattern of bone loss with age is substantially different in men and women with different periods of increased bone loss. Understanding the timing of maximal bone loss may enable better strategies in prevention and management of osteoporosis.

Disclosures: L. Langsetmo, None.

S339

Impact of Herbal Remedies for Menopause on Bone Mineral Density: The Herbal Alternatives for Menopause (HALT) Trial. K. M. Newton¹, A. Z. LaCroix², S. D. Reed³, L. C. Grothaus⁴, J. W. Lampe⁵, K. Ehrlich⁶. ¹Group Health Center for Health Studies, Seattle, WA, USA, ²Fred Hutchinson Cancer Research Center, Seattle, WA, USA, ³Obstetrics and Gynecology, University of Washington, Seattle, WA, USA.

While estrogen therapy is associated with decreased fracture risk, evidence regarding the effects of soy isoflavones on bone mineral density (BMD) is mixed, and the influence on BMD of herbal approaches used for menopause symptoms is unknown. The purpose of this study was to evaluate the effects of herbal approaches for menopause symptoms on hip and spine BMD.

We enrolled 351 peri and postmenopausal women, aged 45-55, in Washington state, into the HALT study, a 5-arm randomized controlled trial comparing 3 herbal therapies and hormone therapy to placebo. Entry criteria included ≥ 2 hot flashes and/or night sweats per day. Over 95% completed the month 6 BMD, 93% the month 12. Women were randomly assigned to: 1) black cohosh (160 mg daily); 2) multibotanical with black cohosh (200 mg daily) and 9 other ingredients; 3) multibotanical plus dietary soy counseling; 4) conjugated equine estrogen 0.625 mg \pm medroxyprogesterone acetate 2.5 mg daily (HT); or 5) placebo. Outcome measures were BMD of the lumbar spine and total hip measured by DXA at baseline, 6, and 12 months. We used maximum likelihood (mixed models) to compare mean percent change from baseline for herbs and hormone therapy vs. placebo, adjusted for age, body mass index (kg/m²), dietary calcium and baseline BMD. Compared to placebo, the multibotanical plus dietary soy was associated with a significant decrease in hip and spine BMD at 6, but not 12 months. Compared to placebo, HT had no significant effect on hip BMD but was associated with a significant increase in spine BMD at 6 and 12 months.

Black cohosh and the multibotanical with black cohosh had no impact on hip or spine BMD, Table 1.

Table 1. Percent BMD Change From Baseline

	Hip 6 Months	Hip 12 Months	Spine 6 Months	Spine 12 Months
Black Cohosh n=79	-0.59%	-0.22%	-1.11%	-1.72%
Multibotanical n=74	-0.72%	-1.23%	-1.57%	-2.23%
Multi + Soy n=78	-0.94%	-1.21%	-1.72%*	-2.42%
HT n=32	-0.28%	0.77%	2.10%†	1.17%‡
Placebo n=83	-0.23%	-0.54%	-0.65%	-1.48%

Change in intervention vs. change in placebo *P=0.03, †P=0.0001, ‡P=0.002

We conclude that black cohosh alone or as part of a multibotanical preparation has no impact on BMD of the total hip or lumbar spine, and that black cohosh taken in combination with other herbs and soy diet may negatively impact spine BMD.

Disclosures: K.M. Newton, None.

S342

Effects of Functional Single Nucleotide Polymorphism in the Tissue-Nonspecific Alkaline Phosphatase Gene (787T>C) Associated with BMD. M. Goseki-Sone¹, N. Sogabe², K. Oda³, H. Nakamura⁴, H. Orimo⁵, T. Hosoi⁶. ¹Department of Food and Nutrition, Japan Women's University, Tokyo, Japan, ²Division of Biochemistry, Niigata University, Graduate School of Medical and Dental Sciences, Niigata, Japan, ³Department of Chemistry, Gakushuin University, Tokyo, Japan, ⁴Division of Molecular Genetics and Nutrition, Department of Biochemistry and Molecular Biology, Nippon Medical School, Tokyo, Japan, ⁵Department of Advanced Medicine, National Center for Geriatrics and Gerontology, Aichi, Japan.

Human alkaline phosphatases (ALPs) are classified into four types: tissue-nonspecific, intestinal, placental, and germ cell types. Previously, we identified polymorphisms of the TNSALP gene 787T>C (Y246H) associated with BMD among 501 postmenopausal women. There was a significant difference in the BMD and the score of BMD adjusted for age and body weight (Z-score) among haplotypes, which was lowest among 787T homozygotes, highest among 787T>C homozygotes, and intermediate among heterozygotes. In subgroups divided by age, haplotypes were significantly associated with the BMD in older postmenopausal women. These results indicated that the effect of haplotypes on the BMD depended on age. In the present study, we have investigated the effects of amino acid substitution on the biosynthesis and the catalytic properties of the protein translated from the 787T>C gene, and three-dimensional structure-related effects on calcium. Furthermore, we explored the possibility that the TNSALP gene may contribute to phosphate metabolism in humans by measuring serum concentrations of bone-specific ALP (BAP), osteocalcin, calcium, phosphorus, and FGF-23 (phosphatonin). As the results, TNSALP (787T) and TNSALP (787T>C) were synthesized similarly as a high-mannose-type 66-kDa form, and became an 80-kDa form in an in vitro translation system. Expression of the 787T>C TNSALP gene using mouse marrow stromal cells (ST2) demonstrated that the protein translated from 787T>C exhibited an ALP-specific activity similarly to that of 787T. Interestingly, the Km value for TNSALP in cells transfected with the 787T>C TNSALP gene was decreased significantly compared to that of cells bearing the 787T gene (p<0.01). Moreover, we demonstrated the associations among the levels of serum BAP and phosphorus in 60 healthy young males. The level of serum BAP was significantly correlated with serum phosphorus in 787T (p<0.01), but not in 787T>C homozygotes. These results suggest that TNSALP variation may be an important determinant of age-related bone loss in humans, and that the phosphate metabolism pathway may provide a novel target for the prevention and treatment of osteoporosis.

Disclosures: M. Goseki-Sone, None.

S344

The Effect of Nutritional Calcium on the Risk of Postmenopausal Fractures Varies with Age. A 15-year Follow-up of the OSTPRE Cohort.

R. J. Honkanen¹, K. Salovaara², M. Kärkkäinen¹, M. T. Tuppurainen³, H. P. Kröger⁴, E. M. Alhava⁴. ¹BCRU, Clinical Research Center, University of Kuopio, Kuopio, Finland, ²Surgery, Kuopio University Hospital, Kuopio, Finland, ³Gynaecology, University Central Hospital of Kuopio, Kuopio, Finland, ⁴Surgery, University Central Hospital of Kuopio, Kuopio, Finland.

We have previously shown that nutritional calcium (Ca) prevents early postmenopausal distal forearm fracture (DFF). The purpose was to examine the stability of this Ca effect with age.

The study population consisted of those 9403 OSTPRE cohort women (born in 1932-41) who responded to all four enquiries: in 1989 (N=13100), in 1994 (N=11798), in 1999 (N=10977) and in 2004 (N=9403). Self-reported follow-up fractures were validated by perusal of patient records: 777 women recorded fractures in 1989-94, including 279 women with DFF and 6 women with hip fracture; the number of women with fractures in 1999-2004 was 835, including 322 women with DFF and 28 women with hip fracture. Self-reported dairy Ca intake (forming about 75 % of overall nutritional Ca intake) was used as a measure of nutritional Ca intake. Logistic regression was used as the statistical method.

Mean Ca intake was 827(SD 391) mg/day in 1989 and 848 (SD370) mg/day in 1999. Ca intake did not predict fractures in general in 1989-94 or in 1999-2004. It protected from DFF in 1989-94 (p=0.001 for continuous Ca variable) (with OR of 0.68 (95% CI 0.51-0.92) at Ca intake of 500-999 mg and OR of 0.57 (0.40-0.81)) at Ca intake >999 mg compared to women with Ca intake <500 mg) but not in 1999-2004 (p=0.353 for continuous Ca variable). However, a joint effect of high Ca intake and HRT on the incidence (%) of DFF was seen even in late postmenopausal women in 1999-2004:

	Ca intake in 1999			P value*
HRT in 1999	<500 mg	500-999 mg	>999 mg	
No	4.0 %	4.1 %	3.8 %	0.679
Yes	3.4 %	2.2 %	1.3 %	0.019

*trend test

In addition, Ca intake strongly protected from hip fracture in 1999-2004 (p=0.001 for continuous Ca variable) with OR of 0.27 (0.13-0.59) at Ca intake of <500 mg and OR of 0.08 (0.02-0.34) at Ca intake >999 mg compared to Ca intake of <500 mg. Adjusting for weight, height, fracture history, HRT, time of menopause and number of health disorders did not affect these fracture risks. Ca intake did not protect from fractures at other sites. The protective effect of nutritional Ca on distal forearm fracture risk is more easily seen in early than late postmenopausal women, whereas the effect on the risk of hip fracture becomes apparent later with increasing incidence of hip fractures.

Disclosures: R.J. Honkanen, None.

This study received funding from: Academy of Finland.

S347

Leg Lean Mass and Risk of Hip Fracture: The Framingham Study. M. T. Hannan, K. E. Broe*, R. R. McLean*, D. P. Kiel. HSL Institute for Aging Research, Boston, MA, USA.

While bone density is a potent risk factor for fracture, few data exist on lean muscle mass and risk of hip fracture. Low lean mass, or 'sarcopenia', has been associated with reduced muscle strength and lower functioning in elders. We examined whether leg lean mass predicted risk of hip fractures in women of the Framingham Original Cohort with the hypothesis that lower lean mass of the legs would be associated with increased hip fracture risk even after adjustment for major confounders. Men were not included as too few hip fractures occurred in men and their lean mass measures were different from women.

432 women of the Original Cohort had leg lean mass (kg) measured in 1992-93 using whole body DXA (Lunar DPX-L) and were followed for incident hip fracture. Fracture information through 12/31/2003 was provided by the Framingham Fracture Registry (incident hip fractures ascertained by interview, record reviews and confirmed by x-ray). Number of person-years was determined from DXA scan date to hip fracture, last contact, death, or end of follow-up. Cox proportional hazards regression was used to calculate hazard ratios (HR) and 95% confidence intervals (CI) estimating the risk of hip fracture for each kg increase in leg lean mass. Covariates (baseline) included age, weight, height, physical activity (PASE score), calcium and vitamin D intake and femoral neck bone mineral density (BMD).

Mean age was 78 yrs (range: 72-92 y); 49 hip fractures occurred over follow-up. Mean leg lean mass for these women was 11.38 kg (range 7.2-17.0). Leg lean mass was significantly inversely correlated with age, and significantly positively correlated with weight, height, physical activity and BMD. In Cox regression model adjusting for age, weight and height, leg lean mass predicted subsequent hip fracture, HR=1.46 (95% CI: 1.15, 1.85). Further adjustment for physical activity, calcium and vitamin D intake did not change these results. Adding femoral neck BMD to the model attenuated the risk somewhat: for each kg increase in leg lean mass in women, the risk of hip fracture increased by 30% (HR=1.30, 95% CI: 1.01, 1.67).

In sum, leg lean mass predicted hip fracture in elderly women even after adjusting for BMD. While not supporting our hypothesis, these unexpected results may reflect that those elderly women with greater lean mass were more physically active and were more apt to fall and fracture (ie, adjusting for physical activity may not have fully adjusted for increased opportunity to fall & fracture). Also, perhaps a lower fracture risk exists for middle-age adults but not the geriatric women we studied (ie, hip fracture risks change with age). Further studies should examine lean mass and fractures in men as well as change in physical activity and falls for risk of hip fractures in elders.

Disclosures: M.T. Hannan, None.

This study received funding from: NIH.

S349

Burden of Hip and Wrist Fractures: Incidence Estimates of Non-traumatic Fractures in Older Women and Men in North America, Western Europe, Australia, and Japan. C. Strader*, C. W. Shinoff*, M. S. Anthony*, L. A. Fitzpatrick*. The Mattson Jack Group, St. Louis, MO, USA, ²Amgen Inc., Thousand Oaks, CA, USA.

Fractures in older men and women lead to increased risk of subsequent fractures and mortality. Current international estimates of non-traumatic fracture incidence are not readily available, but are needed to estimate the burden of osteoporotic disease. We estimated the annual incidence of non-traumatic hip and wrist fractures in women >50 and men >60 years of age. A literature review and web-search was conducted to find studies that quantified fracture incidence in the United States, Canada, United Kingdom, Germany, France, Italy, Spain, Australia, and Japan. Data from the National Health and Nutrition Examination Survey (NHANES) 1999-2002 were used to estimate the ratio of site-specific non-traumatic fractures to total hip and wrist fractures. Non-traumatic fractures were defined as a fall from standing height or less. If the country-specific fracture studies did not exclude traumatic fractures, the site-specific NHANES ratio of non-traumatic to total fractures was used to estimate site and country-specific non-traumatic fracture incidence rates. Census data were used to standardize the age-, gender-, and country-specific incidence data to the 2005 country-specific population. Non-traumatic hip fracture incidence was 1-6 fold higher and wrist fracture incidence 3-8 fold higher in women compared to men (Table 1). Hip fracture incidence was highest for women in Germany and wrist fracture rates were highest in US women. Hip and wrist fracture rates increased with age for both men and women.

Table 1. Annual Non-Traumatic Hip and Wrist Fracture Incidence Estimates in Women >50 and Men >60 Years of Age (per 10,000 population)

Country	Hip fractures		Wrist fractures	
	Women	Men	Women	Men
United States	36.8	12.7	52.9	8.1
Canada	26.0	7.6	27.5	8.2
United Kingdom	38.5	7.8	32.5	4.7
Germany	42.4	6.7	42.5	5.3
France	27.9	5.7	19.3	3.3
Italy	22.1	4.4	21.3	2.9
Spain	28.2	6.1	20.0	3.6
Australia	34.0	28.1	24.2	3.5
Japan	17.5	3.5	20.2	2.8

Fractures in older women and men represent a significant problem globally. Projected to the 2005 census, there are about 500,000 non-traumatic hip fractures and 537,000 non-traumatic wrist fractures annually in women older than 50 and men older than 60 years of age in these 9 countries. Differences in rates between countries could be due to inherent biologic differences, differences in fracture ascertainment, or differences in environmental factors, such as strategies for preventing fractures. As the population ages, these rates will continue to increase.

Disclosures: C. Strader, Amgen Inc. 5.

This study received funding from: Amgen Inc.

S351

Chronic Proton Pump Inhibitor Use Is Not Associated with an Increased Risk of Osteoporotic Fracture. L. E. Targownik*, W. D. Leslie¹, L. M. Lix*, C. J. Metge*, H. J. Prior*, S. Leung*. ¹Internal Medicine, University of Manitoba, Winnipeg, MB, Canada, ²Community Health Sciences, University of Manitoba, Winnipeg, MB, Canada, ³Pharmacy, University of Manitoba, Winnipeg, MB, Canada.

Proton pump inhibitors (PPIs) are commonly prescribed medications used for the treatment and prevention of a variety of gastrointestinal diseases. They are believed to decrease gastrointestinal absorption of dietary calcium, and are also postulated to stimulate osteoclast activity. Therefore, PPIs are a putative risk factor for the development of osteoporosis and osteoporotic fracture. Results of studies linking PPI use to osteoporotic fracture are conflicting.

We used the Manitoba Health Research Data Repository to perform a nested case-control study. Cases, defined as patients admitted for a hip/proximal femoral fracture between 1996-2004, were matched to controls with no history of osteoporotic fracture (hip, spine, wrist) on age, sex, medical comorbidity and ethnicity (Aboriginal vs. non-Aboriginal). PPI exposure was obtained from the provincial pharmacy database, and tracked for either 1, 2, or 4 years prior to the index date. Subjects were considered to be continuously exposed to PPIs if there was documented PPI use over >70% of days in the exposure period of interest (1, 2, and 4 years prior to event), and unexposed if PPIs were used <10% of the time during the exposure period of interest. Conditional logistic regression was performed to obtain odds ratios and confidence intervals, adjusted for pertinent covariates.

Numbers of cases and controls for each exposure period and both the unadjusted and adjusted odds ratios are displayed in the table below. We did not detect an association between PPI use and hip fracture over 1, 2 or 4 years of prior exposure.

PPIs do not appear to be an important risk factor for the development of hip fracture. Further studies are required in other populations to confirm our findings.

PPI Exposure and Odds of Developing Hip Fracture				
Duration of Exposure	# Cases	# Controls	Crude Odds Ratio (95% CI)	Adjusted Odds Ratio (95% CI)
Lead-In Time			PPI exposed vs. PPI unexposed	(PPI exposed vs. PPI unexposed)
1 year	13378	40048	1.10 (1.00 - 1.23)	1.04 (0.93 - 1.16)
2 years	11067	33182	1.08 (0.95 - 1.22)	1.00 (0.88 - 1.13)
4 years	7172	21465	1.17 (0.97 - 1.40)	1.11 (0.92 - 1.35)

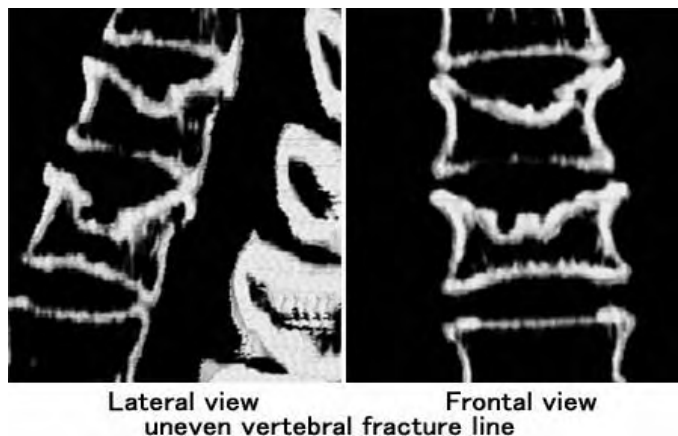
Disclosures: L.E. Targownik, None.

This study received funding from: Canadian Institutes of Health Research.

S353

Vertebral Fracture Lines Are Not Smooth, but Mixtures of Multiple Schmorl's Nodes and Endplate Perforations. T. Okamoto*, S. Okamoto¹, H. Noguchi*, H. Suzuki*, N. Otsu*, A. Itabashi*. ¹SORF Okamoto Clinic, Oita, Japan, ²Noguchi Thyroid Clinic and Hospital Foundation, Beppu, Japan, ³Suzuki Orthodontic Office, Nagasaki, Japan, ⁴Saitama Center of Bone Research, Saitama, Japan.

Although vertebral fracture cannot occur without mechanical compression, discussion on what exactly is the primary causative factor of vertebral depression has been conspicuously absent. The 3-D models revealed that the vertebral endplates of fractured vertebrae are rarely smooth and are compromised with multiple Schmorl's nodes and endplate perforations. The TV X-ray fluoroscopy was performed on 2,600 female patients with osteoporosis in one outpatient clinic in Oita, Japan. Care was taken to adjust the posture of each patient to align the vertebrae in right angle to the film. Also we created computerized 3-D renderings of 1280 cases comprised of post-menopausal women aged 45-85, primarily of patients of osteoporosis and osteoarthritis, and healthy female controls aged 20-40. The digital 3-D models were constructed from helical CT data and examined for morphologic characteristics. The 3-D models revealed that the vertebral endplates of post-menopausal women are frequently compromised with perforated indentations. We calculated the ratio of the perforations to the area of the endplates and found that the there was a significant correlation between the perforation/endplate area ratio and the number of years after menopause. The space enclosing the vertebral disc actually expands while the rims of the vertebrae converge. What has conventionally been known as fish-shaped vertebral fractures may in fact be secondary to the herniation of the disk nucleus into the weakened vertebral body of the osteoporotic spine. The so-called wedge type fractures appear to be the result of rim destruction due to direct contact between the vertebral rims after narrowing of intervertebral space. The multiple perforations which appears just after menopause, and gradually enlarge, are eroding vascular pathways which nourish the vertebral disc through the vertebral medulla. To avoid inaccurate diagnosis of vertebral fractures, a better grasp of the vertebral structure as a complex three-dimensional entity is definitely necessary.



Disclosures: T. Okamoto, None.

S356

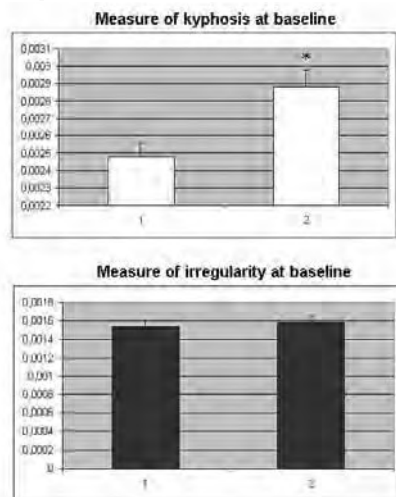
Computer Based Measure of Kyphosis Predicts Fractures in the Thoracic Spine of Postmenopausal Women. P. C. Pettersen¹, M. de Bruijne², J. Chen¹, Q. He¹, L. B. Tankó³, C. Christiansen⁴. ¹Radiology, Center for Clinical and Basic Research, Ballerup, Denmark, ²Department of Computer Science, University of Copenhagen, Copenhagen, Denmark, ³Clinical Research, Center for Clinical and Basic Research, Ballerup, Denmark, ⁴Nordic Bioscience, Herlev, Denmark.

The aim of this study is to investigate whether recently introduced computer-based measures of the degree of kyphosis and irregularities in vertebral alignment of the thoracic spine are independent contributors to fragility fractures.

This was a case control analysis including 126 healthy elderly women, 63 of whom maintained skeletal integrity, whereas 63 sustained a thoracic fracture over the mean observation period of 4.8 years. None of the women received ongoing osteoporosis treatment and the cases and controls were matched for age, follow-up, spine BMD L1-L4 (DEXA), and body weight. Lateral X-rays acquired at baseline and follow-up were digitised and the corner points on each vertebra from Th4 to L1 were marked. Spine curvature at each vertebra level was characterized by the curvature (1/radius) of the circle connecting its center with the centers of neighbors. The degree of kyphosis is defined as the mean curvature of the thoracic spine (Th5 to Th12). The sum of differences between the individual curvatures and the mean curvature defined irregularity of vertebral alignment.

Kyphosis presented a statistically significant difference between the two groups at baseline (fig1 p=0.002), and the measure of kyphosis was increased from baseline in the fracture group (p=0.02). The analyses of irregularities along the thoracic spine did not show differences between the two groups at baseline (fig1). However, the measure of irregularity of vertebral alignment increased in those sustaining a vertebral fracture (p=0.0001). The mean values and SD are shown in figure 1.

The measure of kyphosis, but not the measure of irregularity, can predict fragility fractures in the thoracic spine of postmenopausal women, independent of age, body weight and spine BMD. The observation of increasing irregularity of vertebrae alignment is considered as a consequence of irregular anterior wedge accentuation due to either remodeling or fragility fractures. Secondly, this observation indicates that the herein presented computer based diagnostic tool could be a useful supplement to existing approaches to fracture prediction.



Disclosures: P.C. Pettersen, None.

S358

Endogenous Sex Hormones and Incident Fracture Risk in Older Men: The Dubbo Osteoporosis Epidemiology Study. C. Meier¹, T. V. Nguyen², D. J. Handelsman³, C. Schindler⁴, M. M. Kushnir⁵, A. L. Rockwood⁶, W. A. Meikle⁶, J. R. Center², J. A. Eisman², M. J. Seibel⁷. ¹Division of Endocrinology, University Hospital Basel, Switzerland, ²Bone and Mineral Research Program, Garvan Institute of Medical Research, Sydney, Australia, ³Department of Andrology, ANZAC Research Institute, Sydney, Australia, ⁴Institute of Social and Preventive Medicine, University of Basel, Switzerland, ⁵ARUP Institute for Clinical and Experimental Pathology, Salt Lake City, UT, USA, ⁶Department of Medicine and Pathology, University of Utah, Salt Lake City, UT, USA, ⁷Bone Research Program, ANZAC Research Institute, Sydney, Australia.

One third of osteoporotic fractures occur in men. Data on the influence of gonadal hormones on incident fracture risk in elderly men are limited. The present study examined the prospective relationship between serum levels of testosterone (T) and estradiol (E2) and future fracture risk in elderly men as part of the long-term observational Dubbo Osteoporosis Epidemiology Study of community-dwelling men over 60 years followed prospectively since 1989. This analysis included men who had serum samples for baseline measurements (n=609, 70.6%) with follow-up of 5.8 years (up to 13 yrs) closing in 2005. Clinical risk factors, including bone mineral density (BMD) and lifestyle factors were assessed at baseline. Serum T and E2 were measured by tandem mass spectrometry (LC-MS/MS). The incidence of low-trauma symptomatic fracture was ascertained by X-ray record.

During follow-up, 113 men suffered at least one low-trauma fracture. Fracture risk was increased in men with reduced T levels (hazard ratio [HR] 1.33; 95%CI: 1.09, 1.62). After adjustment for SHBG, both low serum T (HR 1.48; 95%CI: 1.22, 1.78) and serum E2 (HR 1.21; 95%CI: 1.00, 1.47) were associated with increased overall fracture risk. After further adjustment for major fracture risk factors (age, weight or BMD, fracture history, smoking status, calcium intake and SHBG), lower T was still associated with increased risk of hip (HR 1.88; 95%CI: 1.24, 2.82) and non-vertebral (HR 1.32; 95%CI: 1.03, 1.68) fracture. By contrast, lower E2 was only associated with increased fracture risk in the presence of body weight (HR 1.25; 95%CI: 1.02, 1.54), but not at any site after adjustment for BMD (HR 1.19; 95%CI: 0.69, 1.03).

In community-dwelling men over 60 years of age, serum T, but not E2, is an independent predictor of osteoporotic fracture and its measurement may provide additional clinical information for the assessment of fracture risk in elderly men.

Disclosures: C. Meier, None.

S360

Respiratory Function Is Associated with Bone Ultrasound Measures and Hip Fracture: European Prospective Investigation Into Cancer-Norfolk Population Cohort Study. A. Moayyeri¹, R. N. Luben¹, S. Bingham², A. Welch¹, N. J. Wareham³, S. Kaptoge¹, J. Reeve¹, K. T. Khaw¹. ¹Department of Public Health and Primary Care, Institute of Public Health, School of Clinical Medicine, The University of Cambridge, Cambridge, United Kingdom, ²MRC Dunn Human Nutrition Unit, The University of Cambridge, Cambridge, United Kingdom, ³MRC Epidemiology Unit, The University of Cambridge, Cambridge, United Kingdom.

Forced expiratory volume in 1 second (FEV1), an easily obtainable measure of respiratory function in clinics, has been shown to be associated with physical activity. We hypothesized that FEV1 is linked with bone health. In the context of the European Prospective Investigation into Cancer-Norfolk study, 14,800 participants aged 42-81 in 1997-2000 were evaluated by spirometry and heel ultrasound and were followed for fracture outcomes up to July 2007. After excluding participants with history of pulmonary diseases, among 5,555 men and 6,935 women (mean age 62.1±9.0), FEV1 significantly correlated with heel broadband ultrasound attenuation (BUA; Pearson r=0.403; p<0.001) and velocity of sound (VOS; r=0.269; p<0.001). The association remained significant in sex-stratified linear regression models after adjustment for age, history of fracture, height, body mass index, smoking status and alcohol consumption (standardized Beta coefficient=-0.057 and p<0.001 in men; Beta=0.075 and p<0.001 in women). Mean adjusted FEV1 among 109 hip fracture patients (2.00±0.60 liter) was significantly lower than that of other participants (2.49±0.71 liter; t-test p<0.001). In a Cox proportional hazards regression model, FEV1 was a significant predictor of hip fracture after adjustment for age, sex, history of fracture, height, body mass index, smoking and alcohol consumption (hazard ratio for 1 standard deviation [700 ml in 1 second] decrease in FEV1=1.39, 95%CI 1.03-1.88, p=0.029). Among 6197 current and former smoker participants, hazard ratio for 1 standard deviation decrease in FEV1 was 1.67 (95%CI 1.11-2.57, p=0.014). Middle aged and older men and women with lower respiratory function appear to be at increased risk of osteoporosis and hip fracture. The observed association might be related to the level of physical activity or deformities in thoracic spine related to osteoporosis. Given the feasibility and affordability of spirometry in general practices, it can be used to improve the identification of high risk groups at the first point of care.

Disclosures: A. Moayyeri, None.

This study received funding from: Medical Research Council and Cancer Research UK.

S362

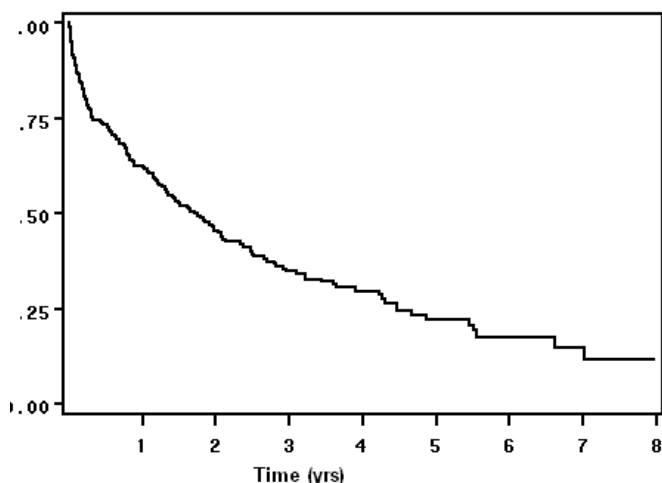
Competing Risk of Subsequent Fracture and Death After Hip Fracture in Nursing Home (NH) Residents. S. Berry, K. Broe, D. Kiel. IFAR, Hebrew SeniorLife, Boston, MA, USA.

Prior studies have demonstrated an increased risk of subsequent fracture among community dwellers with hip fracture. It is unclear whether this is also true in NH residents given the high burden of co-morbidities and associated competing risk of mortality. Therefore, we described the incidence of second fractures and the competing risk of death following a hip fracture in a large NH.

Participants were 218 consecutive residents (49 men, 169 women) of Hebrew Rehabilitation Center, a 725 bed long term care facility in Boston, MA, with a hip fracture between 1/1/1999 and 12/31/2006. Fractures were identified from a review of mandated injury files (excluding fractures associated with malignancy, Paget's disease, or prosthesis; n=3). Second fractures included any fracture occurring after the initial fracture, excluding toe and hand fractures. Baseline characteristics were obtained from administrative databases in the three months preceding the initial hip fracture. Subjects were followed from initial hip fracture until second fracture, death, discharge, or 12/31/2006. A Wilcoxon rank sum compared baseline age among subjects with second fracture and subjects who died without second fracture. Cumulative incidence estimates, taking into account the competing risk of death, described the incidence of second fractures.

At baseline, 82% of subjects had 0-1 major co-morbidities, and 35% were functionally intact or had mild impairment. Over a median follow-up of 11 months (range, 2 d- 8 yrs), 17% of subjects (7 men, 31 women) experienced a second fracture (17 hip, 5 leg, 2 ankle, 5 arm, 5 pelvic, 2 clinical vertebral, 1 skull, 1 clavicle), and 55% of subjects (30 men, 90 women) died. Subjects with second fracture were younger than subjects who died without second fracture (median 88 yrs vs. 91 yrs, p=0.02). Five percent of subjects experienced a second fracture within six months, and 10% experienced a second fracture within 1 yr of the initial hip fracture. In contrast, 27% of subjects died within 6 months, and 37% died within 1 yr of the initial hip fracture (Kaplan-Meier estimates). In conclusion, the striking mortality among NH residents with minimal co-morbidities and hip fracture highlights the importance of hip fractures as a sentinel event in the NH. Among NH residents who survive a hip fracture, second fractures are common. Future studies should focus on identifying likely survivors with sufficient quality of life to target secondary fracture prevention.

Survival after a hip fracture among NH residents



Disclosures: S. Berry, None.

S364

Factors Influencing the Diagnosis and the Treatment of Osteoporosis Following a Fragility Fracture. L. Bessette¹, J. P. Brown¹, S. Jean^{*2}, K. S. Davison¹, M. Beaulieu^{*3}, M. Baranci^{*4}, J. Bessant^{*5}, L. Ste-Marie^{*6}. ¹Laval University, Quebec, PQ, Canada, ²INSPQ, Quebec, PQ, Canada, ³Merck Frosst, Montreal, PQ, Canada, ⁴sanofi aventis, Montreal, PQ, Canada, ⁵P&G Pharma, Montreal, PQ, Canada, ⁶U. of Montreal, Montreal, PQ, Canada.

ROCQ (Recognizing Osteoporosis and Its Consequences in Québec) revealed that 73% of women 50y and over are not provided anti-fracture therapy following fragility fracture. This study's objectives were to determine predictors of osteoporosis (OP) diagnosis (DX) and treatment (TX) 6 to 8 months after fragility fracture.

At phase 1, women were recruited at cast or outpatient clinics in 17 hospitals 0 to 16 weeks following fracture. Consenting patients were contacted by phone to answer a short questionnaire to classify them as having either experienced a fragility or traumatic fracture. During the first phone contact, there was no reference to the possible association between the fracture and OP and no investigation or intervention was proposed. At phase 2, 6-8 months following fracture, women were contacted again by phone to complete a questionnaire on demographic features, clinical characteristics and risk factors for OP. The DX (informed of OP and/or BMD measurement with diagnosis of OP) and TX (bisphosphonates, raloxifene, nasal calcitonin or teriparatide) rates of OP were determined

via this questionnaire. This analysis included only women with a fragility fracture who were not receiving OP TX at phase 1.

Of the 1273 women who completed phase 1, 1001 (79%) sustained a fragility fracture; 818 were not on treatment at phase 1 and completed the phase 2 questionnaire. Overall, 79% of these participants had not received a DX of osteoporosis or were without OP TX at phase 2. The highest rate of DX and TX of OP was observed between 0-5 months following fracture and decreased considerably thereafter. In multivariate analyses, the results of BMD tests before or after the fracture event (p<0.0001) and mobility problems (p=0.03) were the only variables that influenced the DX of OP. The BMD test result was the strongest predictor (p<0.0001) of TX followed by the fracture site (hip, femur and pelvis; p=0.015) and vitamin D supplements at the time of fracture (p=0.035). All other risk factors for OP such as age, fracture history after age 40, family history of OP, and comorbidities did not influence the DX or TX rate. No demographic and clinical features or OP risk factors were significantly associated with the decision to send women for a BMD testing following fracture.

Despite the evidence clearly showing that the occurrence of a fragility fracture represents a greater risk of future fragility fracture than a low BMD measurement, physicians based their decision to treat on BMD results and not on the clinical event (fragility fracture).

Disclosures: L. Bessette, Merck Frosst Canada 2, 5, 8; The Alliance for Better Bone Health (P&G and sanofi-aventis) 2, 5, 8; Eli Lilly 2, 5, 8; Novartis Pharma 2, 5, 8. This study received funding from: Merck Frosst, P&G Pharmaceuticals, sanofi-aventis, Eli Lilly, Novartis.

S366

A Comparison of the Effects of Thiazide Diuretics and Angiotensin Converting Enzyme Inhibitors on Fracture Risk - A Randomised Controlled Trial. T. Winzenberg¹, K. Willson^{*2}, P. Ryan^{*2}, M. Nelson^{*1}, G. Jones¹. ¹Menzies Research Institute, Hobart, Australia, ²Adelaide University, Adelaide, Australia.

Observational evidence suggests that antihypertensives, particularly thiazide diuretics may affect bone and fracture risk. However head-to-head comparisons of the effects of different antihypertensives on fracture risk to inform choice of antihypertensive are lacking. We aimed to prospectively compare the effects of thiazide diuretics and angiotensin converting enzyme (ACE) inhibitors on fracture risk.

The second Australian National Blood Pressure trial is a prospective, randomized, open-label study which was conducted in 6083 hypertensive Australian family practice patients aged 65-84 years. Subjects were followed for a median of 4.1 years. Family practitioners (FPs) were responsible for the stepwise management of antihypertensive treatment, guided by study protocols for drug choices and the study's blood pressure treatment goals. Management was to conform to the randomized treatment assignment. Patients were randomised to initially receive either diuretic (hydrochlorothiazide recommended first-line) or ACE inhibitor (enalapril recommended first-line), but the choice of the specific agent and dose was made by the FP. Fractures were a secondary outcome, and were ascertained from FPs' records. Relative risks (RR) were calculated using log-binomial Generalized Estimating Equations, using both intention-to-treat and per-protocol analyses. In the diuretic group, 251 subjects had a fracture (8.3%), compared to 236 (7.8%) in the ACE group. There was no evidence of a difference in fracture rates between those patients randomised to diuretic and those to ACE with the age- and sex-adjusted RR for fracture in the diuretic compared to ACE groups being 1.06 (95% CI 0.90-1.25) for all fractures and 1.16 (95% CI 0.72-1.86), 1.02 (95% CI 0.66-1.57) and 1.15 (95% CI 0.82-1.62) for hip, vertebral and upper limb fractures respectively, in intention-to-treat analyses. Per protocol analysis examining treatments received and comparing use of thiazides, indapamide or either of these diuretics with use of neither of these agents demonstrated similar results, again with no differences in fracture rates.

There is no evidence to suggest that either thiazide diuretics or ACE inhibitors are superior to each other for reducing fracture risk in elderly hypertensive patients, or that choice of hypertensive therapy should be influenced by concerns about effects on fracture risk. Treatment of hypertension should still be guided by current best practice recommendations taking into account other significant co-morbidities.

Disclosures: T. Winzenberg, None.

S368

Vasomotor Symptoms Are Related to Lower Bone Mineral Density (BMD): A Longitudinal Analysis. C. J. Crandall¹, S. Crawford^{*2}, R. Thurston^{*3}, E. Gold^{*4}, J. Johnston^{*3}, G. Greendale¹. ¹University of California, Los Angeles, CA, USA, ²University of Massachusetts, Worcester, MA, USA, ³University of Pittsburgh, Pittsburgh, PA, USA, ⁴University of California, Davis, CA, USA.

Vasomotor symptoms (hot flashes or night sweats, VMS) are common in perimenopausal and postmenopausal women. We determined within each menopause transition stage whether women with vasomotor symptoms had lower BMD than women without VMS.

We analyzed longitudinal data from 2136 participants of the Study of Women's Health Across the Nation, a cohort study of Caucasian, African American, Japanese, and Chinese women. At baseline, women were aged 42 to 52 years, had intact uterus and ≥1 ovary, and were pre- or early peri-menopausal. Menopausal stage and VMS were assessed by annual questionnaire. We defined frequent VMS as reporting VMS for >5 days in the past 2 weeks. Menopause stages were premenopausal (no change in menstrual regularity), early perimenopausal (decreased regularity in past 3 months), late perimenopausal (no menses in past 3-11 months), or postmenopausal (no menses for ≥12 months). Using data from

baseline to annual follow-up visit 5 in repeated measures mixed models, we determined the association between VMS (any vs. none, frequent vs. infrequent) and BMD (by DXA) within each menopause status category.

After controlling for age, menopausal stage, cumulative time in each menopausal stage, ethnicity, study site, and baseline menopause stage, postmenopausal women with any VMS had lower lumbar (0.007g/cm² lower, P=0.002) and lower total hip (0.004 g/cm² lower, P=0.04) BMD than postmenopausal women without VMS. Compared to early perimenopausal women without VMS, early perimenopausal women with any VMS had lower femoral neck BMD (0.003g/cm² lower, P<0.0001). Premenopausal women with any VMS had lower femoral neck BMD (0.003g/cm² lower, P=0.02), compared to premenopausal women without VMS. Results from analyses of women with frequent vs. infrequent VMS were similar. Lumbar and total hip BMD were not different among premenopausal women with any VMS compared to premenopausal without VMS, or among early perimenopausal women with any VMS compared to early perimenopausal women without VMS. Results from analyses additionally controlled for baseline weight, height, and weight change were similar for any vs. no VMS, and frequent vs. infrequent VMS.

Within each menopause transition stage, women with VMS had lower BMD than women without VMS. Effects varied by anatomical site, being most evident in postmenopausal women at the lumbar spine and total hip, and among premenopausal and early perimenopausal women at the femoral neck. Even at the earliest menopause transition stages, women with VMS are at risk for greater bone loss than women without VMS.

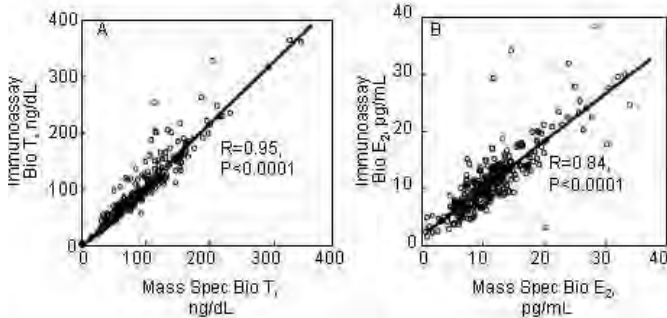
Disclosures: C.J. Crandall, None.

This study received funding from: SWAN has grant support from the NIH, DHHS, through the NIA, the NINR and the NIH ORWH. (Grants NR004061; AG012505, AG012535, AG012531, AG012539, AG012546, AG012553, AG012554, AG012495). Crandall was supported by NIH grant #s 5K12AG01004 from the NIA.

S369

Comparison of Sex Steroid Measurements in Men by Mass Spectrometry vs. Immunoassay: Relationships with Cortical and Trabecular Volumetric BMD. S. Khosla, R. J. Singh*, L. J. Melton, S. Achenbach*, J. Peterson*, B. L. Riggs. Mayo Clinic, Rochester, MN, USA.

While immunoassays (IA) have been used extensively for measurement of serum testosterone (T) and estradiol (E₂) levels, there is concern about their specificity, particularly at low E₂ levels as present in men. Thus, we developed and validated mass spectroscopic (MS) measurements of T and E₂ and used this method to measure T and E₂ levels in a population-based sample of men (n = 313), age 22 to 91 yrs. We compared the MS levels with values previously obtained using IAs and, to test the biological relevance of E₂ measured by the two techniques, related bioavailable (bio, or non-SHBG bound) E₂ to cortical and trabecular volumetric BMD (vBMD) at various skeletal sites using QCT. Panels A and B show the relationships between the bio T and bio E₂ levels determined using either the MS or IA for the T and E₂ measurements. Bio T measurements using the two methods were highly correlated, but the correlation was weaker for bio E₂.



Since, based on IAs, we previously postulated the existence of a "threshold" bio E₂ level for E effects on cortical, but not trabecular, bone we reanalyzed these relationships for values below vs. above the median levels for bio E₂ in men > 60 yrs (8.6 pg/ml and 8.1 pg/ml for the MS and IA, respectively); the Table shows the respective correlation coefficients. As is evident, for both assays, vertebral trabecular vBMD showed similar correlations with bio E₂ in subjects with low or high bio E₂ levels, whereas femur neck cortical vBMD was correlated with bio E₂ at low, but not high bio E₂ levels. In summary, although E₂ measurements with IAs correlate less well with the MS measurements than do the T measurements in men, these data indicate that the fundamental relationships with BMD for E₂ observed with the IAs are also present with the MS measurements. Thus, while MS is considered the "gold standard", the lower cost and greater accessibility of IAs justifies their ongoing use to assess sex steroid levels, at least in men.

		Vertebral vBMD	trabecular vBMD	Femur vBMD	neck vBMD	cortical vBMD
Bio E ₂ below the median	MS-derived bio E ₂	R = 0.25, P = 0.021		R = 0.22, P = 0.044		
	IA-derived bio E ₂	R = 0.27, P = 0.012		R = 0.29, P = 0.009		
Bio E ₂ above the median	MS-derived bio E ₂	R = 0.26, P < 0.001		R = 0.06, P = 0.398		
	IA-derived bio E ₂	R = 0.23, P < 0.001		R = 0.01, P = 0.888		

Disclosures: S. Khosla, None.

S371

Morphometric Vertebral Fracture Status and WHO Predictors of Fracture Risk. P. Chen^{*1}, J. H. Krege^{*1}, D. Goltzman^{*2}, J. C. Prior^{*3}, A. Tenenhouse^{*2}, J. P. Brown^{*4}, M. Papadimitropoulos^{*1}, N. Kreiger^{*5}, W. P. Olszynski^{*6}, R. G. Josse^{*5}, J. D. Adachi^{*7}. ¹Eli Lilly and Company, Indianapolis, IN, USA, ²McGill Univ, Montreal, PQ, Canada, ³Univ of British Columbia, Vancouver, BC, Canada, ⁴Laval University, Ste-Foy, PQ, Canada, ⁵Univ of Toronto, Toronto, ON, Canada, ⁶Univ of Saskatchewan, Saskatoon, SK, Canada, ⁷McMaster Univ, Hamilton, ON, Canada.

The WHO tool considers BMD, age, prior clinical fragility fracture, current smoking, alcohol use, family history of osteoporosis, and glucocorticoid use to assign a 10-year absolute fracture risk [Kanis et al. Osteopor Int 2002; 13:527-36]. We assessed the information gained from consideration of baseline morphometric vertebral fracture (MVF) status and some of the likely WHO risk factors. Data were from 4744 subjects aged >50yr (3452 women, 1292 men) with baseline and 5-yr radiographs from the Canadian Multicentre Osteoporosis Study (CaMos), a prospective, randomly-selected, population-based cohort. Using the CaMos method [Jackson et al. Osteopor Int 2000; 11:680-87], MVF status was defined as: a) present or absent; b) number; c) maximum severity (normal=0, mild=1, moderate or severe=2); and d) spinal deformity index (SDI, sum of severity scores of T4 to L4). Incident vertebral fractures were identified via baseline and 5-year lateral spine radiographs and non-vertebral fractures by an annual questionnaire with medical confirmation. Logistic regression analyses were performed to assess the prediction of 5-yr risk of any fragility fractures (vertebral or non-vertebral) using individual WHO risk factors and MVF status. In univariate analyses, age, BMD, family history, glucocorticoid use, prior clinical fragility fracture and MVF status were statistically significant predictors. As the results were similar, multivariate analyses were performed in men and women together. This analysis of the statistically significant factors showed MVF status, especially greater number or severity of vertebral deformities or higher SDI, provided the greatest discrimination of risk (Table). MVF was the most important predictor of 5-yr fracture risk in this population-based cohort.

Odds ratios (95% CI) for baseline significant risk factors. Analyses were repeated with MVF status defined as yes/no, maximum severity, number, and SDI.

	Yes/No	Severity	Number	SDI
Age (per year)	1.03 (1.02, 1.04)	1.03 (1.02, 1.04)	1.03 (1.02, 1.04)	1.03 (1.02, 1.04)
Femoral neck T-score (per unit decrease)	1.20 (1.10, 1.30)	1.18 (1.08, 1.28)	1.19 (1.09, 1.29)	1.18 (1.09, 1.29)
Family history	1.25 (1.03, 1.52)	1.25 (1.03, 1.52)	1.23 (1.01, 1.49)	1.24 (1.02, 1.51)
Glucocorticoid use	1.05 (0.56, 1.95)	1.03 (0.55, 1.93)	1.01 (0.54, 1.88)	1.04 (0.56, 1.94)
Prior clinical fracture	1.50 (1.24, 1.81)	1.47 (1.21, 1.78)	1.48 (1.22, 1.79)	1.47 (1.21, 1.78)
MVF status	Yes=2.04 (1.72, 2.40)	1=1.60 (1.30, 1.97) 2=2.61 (2.08, 3.27)	1=1.88 (1.55, 2.28) 2=2.50 (1.93, 3.24)	1=1.63 (1.30, 2.04) 2=2.33 (1.77, 3.06) ≥3=2.71 (2.01, 3.65)

Disclosures: P. Chen, Eli Lilly and Company 1, 3.

This study received funding from: Eli Lilly and Company.

S373

Changes in Hip Geometric Structures with Aging--Longitudinal Data Analysis from the Women's Health Initiative Observational Study. T. Bassford^{*1}, T. J. Beck², G. Wu^{*1}, J. A. Cauley³, A. Z. LaCroix^{*4}, C. E. Lewis⁵, Z. Chen¹. ¹University of Arizona, Tucson, AZ, USA, ²Johns Hopkins University, Baltimore, MD, USA, ³University of Pittsburgh, Pittsburgh, PA, USA, ⁴Fred Hutchinson Cancer Research Center, Seattle, WA, USA, ⁵University of Alabama-Birmingham, Birmingham, AL, USA.

Fracture risk increases with age. In addition to bone loss, change in the distribution of bone mass is another significant factor associated with bone fragility. The objective of this study was to investigate the relationship between aging and changes in hip geometry derived from hip structure analysis (HSA). A prospective study in an ethnically diverse subcohort of 5,856 postmenopausal women enrolled in the Observational Study of the Women's Health Initiative was conducted. Eligible subjects were between 50 and 79 years of age and had completed bone scans using Dual-energy X-ray Absorptiometry (DXA). The Beck HSA software was used to estimate bone mineral density (BMD), cross-sectional area (CSA), outer diameter (OD), section modulus index (SM), average cortical thickness (CT) and buckling ratio (BR) for the femoral narrow neck (FNN), intertrochanter (IT) and proximal femoral shaft regions (FS). Analyses showed that BMD, CSA, SM and CT were all significantly lower and the OD and BR measures were significantly higher in the older age group in comparison to the younger age group at baseline ($p < 0.01$). Results from paired t-test indicated significant changes in all HSA measures from baseline to year 6 (Table). Interestingly, both the bone bending strength (SM) and the likelihood of cortical failure under compression (BR) increased significantly over this same time frame, suggesting a complex process with changes in the hip geometry associated with aging. The rates of changes in HSA measures varied by age group and by femoral site. For example, OD expansion in all regions was significantly larger in the 60-69 or 70-79 years age group in comparison to the 50-59 years age group. While significant age differences in the change of other HSA measures were only observed in the FNN region. In conclusion, hip geometric structures change significantly with aging and the rate of changes varies by age and femoral site. The impacts of these changes on hip bone strength are complicated and remained to be investigated.

FNN	Baseline	Year 6	Change	*P-value
BMD (g/cm ³)	0.719 ± 0.130	0.713 ± 0.136	-0.006 ± 0.070	<0.001
CSA (cm ²)	0.204 ± 0.365	0.205 ± 0.391	0.007 ± 0.208	0.037
Outer diameter (cm)	2.997 ± 0.209	3.033 ± 0.228	0.035 ± 0.139	<0.001
SM (cm ³)	0.910 ± 0.190	0.935 ± 0.220	0.025 ± 0.133	<0.001
CT (cm)	0.137 ± 0.026	0.136 ± 0.028	-0.001 ± 0.014	<0.001
BR	12.3 ± 2.84	12.6 ± 3.04	0.344 ± 1.647	<0.001

*p-value from paired t-test

Disclosures: T. Bassford, None.

This study received funding from: NIAMS R01-AR049411.

S375

Relationships Between Lower-Limb Physical Function and Bone Mineral Density in Community-Dwelling Older People. T. Komatsu^{*1}, H. Park¹, D. Nozaki^{*1}, S. Kashiwaguchi^{*2}, T. Kamitani^{*2}, C. Okada^{*3}, Y. Mutoh^{*1}.

¹Department of Physical and Health Education Graduate School of Education, The University of Tokyo, Tokyo, Japan, ²Department of Orthopedic Surgery, Tokyo Koseinenkin Hospital, Tokyo, Japan, ³Department of Rehabilitation, Tokyo Koseinenkin Hospital, Tokyo, Japan.

The Fall Prevention Program was established in 1997 to decrease falls and fall-related fractures in community-dwelling older people. We investigated the relationship between lower-limb physical function, such as gait function and single-leg stance, and osteoporosis (Komatsu, 2006). Four hundred and eighty-four older adults (average age 71.0±3, 52.5±8.9kg, BMI 22.3±3.3) participated in the Fall Prevention Program between December, 1997 and January, 2007. The bone mineral density (BMD) of the femoral neck was measured by dual-energy X-ray absorptiometry using the Hologic co. QDR2000. The subjects were classified into four groups according to BMD by the WHO criteria: normal, osteopenia, osteoporosis and severe osteoporosis. For the linear relationship, that calculated the partial correlation coefficients. Analyses of covariance (ANCOVA) assessed independent associations between the BMD and the lower-limb physical function after controlling the effect of the age. Moreover the logistic regression analysis was used to determine odds ratios and their 95% confidence intervals adjusted by age for the BMI in order to assess association between the osteoporosis and the lower-limb physical function. The probability less than 5% significance was assumed to be significant by using the Statistical Package for Social Science (Ver.15.0). A significant correlation was observed between the BMD and the lower-limb physical function ($r = -0.567$, $p = 0.013$). Subjects who are in the lowest quartile of the maximum gait speed were 1.96 folds more at risk of osteoporosis than the highest quartile (Table1). Therefore, we concluded that gait speed is an important factor in determining fall and fracture risk (Kanis, 2005). In this study of community-dwelling older people who participated in the Fall Prevention Program, the relationship between gait speed and osteoporosis was explained.

Table 1 Age and sex adjusted odds ratio (95% confidence interval) for the estimated risk of osteoporosis in quartiles (Q1-Q4) of rapid gait speed

	Gait speed	Odds ratio (95% CI)
Q1	≤ 1.59	1.96 (1.20-2.96)
Q2	1.5-1.82	1.18 (0.64-2.14)

Disclosures: T. Komatsu, None.

S377

Associations Between Body Composition and Hip Geometry in Postmenopausal Women in the Women's Health Initiative. S. Going^{*1}, T. Beck^{*2}, L. Arendell^{*1}, J. Cauley^{*3}, B. Lewis^{*4}, T. Bassford^{*1}, Z. Wang^{*5}, A. LaCroix^{*6}, T. Lohman¹, Z. Chen^{*1}. ¹Univ of AZ, Tucson, AZ, USA, ²Johns Hopkins Univ, Baltimore, MD, USA, ³Univ of Pittsburgh, Pittsburgh, PA, USA, ⁴Univ of Alabama, Birmingham, AL, USA, ⁵Columbia Univ, New York, NY, USA, ⁶Fred Hutchinson Cancer Research Center, Seattle, WA, USA.

Body weight (wt) and composition are associated with bone mass and bone mineral density (BMD) and likely also affect bone strength through associations with other structural features. While ethnic differences in mass and BMD have been described, differences in structural parameters and their association with soft tissue composition are not well studied. The aim of this study was to assess the associations among measures of body composition and hip geometry (HG) in non-Hispanic White, African American, Hispanic and Native American postmenopausal women (n=5,761) aged 50 to 79 y, in the observational arm of the WHI. Participants' mean age, wt and height (ht) at baseline was 63.7 ± 7.5 y, 72.7 ± 17.1 kg, and 161.4 ± 6.5 cm respectively. Whole-body fat (FM) and lean soft tissue (LSTM) masses and BMD were measured by dual energy x-ray absorptiometry. HG measures, estimated with Hip Structural Analysis (HSA), included femur narrow neck, inter-trochanter, and shaft cross-sectional area (CSA), outer diameter (OD), section modulus (SM), cortical thickness (CT) and buckling ratio (BR). The means and standard deviations of HG measures in the femoral narrow neck region by the quartile of baseline LSTM (table) suggest increased bone strength with higher LSTM.

	Baseline Lean Soft Tissue Mass			
	Quartile 1 mean (st. dev)	Quartile 2 mean (st. dev)	Quartile 3 mean (st. dev)	Quartile 4 mean (st. dev)
Narrow Neck Cross-sectional area (cm ²)	1.81 (0.28)	1.92 (0.30)	2.10 (0.33)	2.30 (0.39)
Narrow Neck Out diameter (cm)	2.93 (0.19)	3.00 (0.20)	3.03 (0.21)	3.08 (0.23)
Narrow Neck Section modulus (cm ³)	0.78 (0.14)	0.86 (0.15)	0.94 (0.18)	1.06 (0.23)
Narrow Neck Cortical thickness (cm)	0.12 (0.02)	0.13 (0.02)	0.14 (0.03)	0.15 (0.03)
Narrow Neck Buckling ratio	13.3 (2.9)	13.1 (3.1)	12.3 (2.7)	11.5 (2.7)

*Quartiles, Q2-Q4 (except for Q2& 3 of OD) were sig. different from Q1 after adjusted for age, ethnicity, HT, WT ($p < 0.05$).

Linear regression was used to assess the association of baseline LSTM and FM with baseline, year 3 and year 6 HG, with baseline wt, ht, physical activity (PA), age and ethnicity as covariates. Body wt and composition, age and ethnicity were significantly correlated with HG LSTM and FM were related positively to BMD, CSA, OD, SM and CT, and negatively to BR at all sites at all years. LSTM explained more variance in HG (adj R²=0.4 to .41) than FM (adj R²=0.01-.03). The associations were not confounded by age, ethnicity, PA or baseline ht and wt. In conclusion, HSA measurements are significantly related to soft tissue composition, especially LSTM in postmenopausal women.

Disclosures: S. Going, None.

This study received funding from: NIH/NIAMS.

S379

Recognition of Postmenopausal Women at Risk of Fracture Using BMD and Clinical Risk Factors: Results from a Northern Italian Multicenter Study. A. Giusti¹, A. Barone^{*1}, G. Pioli², G. Girasole³, G. Bianchi³, E. Palummeri^{*1}, M. Pedrazzoni⁴. ¹Gerontology, Galliera Hospital, Genova, Italy, ²Gerontology, ASMN, Reggio Emilia, Italy, ³Rheumatology, La Colletta Hospital, Arenzano, Italy, ⁴Internal Medicine, University of Parma, Parma, Italy.

Objectives: To estimate the prevalence of 4 internationally validated independent clinical risk factors (CRFs) (low body mass index (BMI), prior history of fragility fracture, family history of fracture, current smoking) for fragility fractures in a cohort of Italian postmenopausal women and evaluate the impact of the combined assessment of CRFs with bone mineral density (BMD) measurement on risk stratification.

Subjects: Postmenopausal women examined in 3 osteoporosis centers from Northern Italy (Arenzano, Genoa, Parma) over a period of 2 years.

Methods: All women answered a standardized questionnaire to assess smoking habits,

history of prior fragility fractures at any site and fractures of the spine, ribs, distal forearm, humerus and hip in first-degree relatives. Each subject underwent anthropometric assessment to calculate BMI. BMD measurements of lumbar spine (L1-L4) and total hip were obtained by dual-energy x-ray absorptiometry. The relative risk (RR) of fracture versus the general population was modeled as a function of BMD only and BMD plus CRFs, using published data from Kanis et al. (Bone, 2004; Osteoporos Int, 2005).

Results: 10068 post-menopausal women were included in the study (mean age \pm standard deviation, 63.3 \pm 8.7 years; range 45-97). The overall population was divided in subgroups according to the number of prevalent CRFs: the proportion of women with 0, 1, 2 and ≥ 3 prevalent CRFs was 53.1%, 36.1%, 9.8% and 1%, respectively. Overall 4702 women (46.9%) presented at least one risk factor. The most frequent risk factor was a prior history of fragility fracture (21.8%), followed by a parental history of fracture (16.7%), current smoking (14.7%) and BMI < 20 kg/m² (5.6%). As expected, the relative prevalence of some risk factor varied with age. In particular, the proportion of women with a prior fragility fracture increased progressively with age; whereas the percentage of current smokers decreased.

The addition of CRFs to BMD improved risk stratification as compared to BMD alone. The effect was modest in women with only one CRF (RR based on BMD: 1.2; RR based on BMD plus CRFs: 1.7), but more marked in women with 2 CRFs (a 2-fold increase in RR from 1.4 to 2.9) and in women with ≥ 3 prevalent CRFs (a 3-fold increase from 1.7 to 5.4).

Conclusion: The prevalence of risk factors in this cohort of postmenopausal Italian women is similar to that observed in international population-based studies. The addition of CRFs to BMD resulted in a clinically significant increase in the gradient of risk in about 10% of subjects.

Disclosures: A. Giusti, None.

S381

Hip Geometric Structure Is Weaker in Anemic Women--Results from the Women's Health Initiative Observational Study. G. Wu^{*1}, T. J. Beck², T. Bassford^{*1}, J. A. Cauley³, A. Z. LaCroix^{*4}, C. E. Lewis⁵, Z. Chen¹. ¹University of Arizona, Tucson, AZ, USA, ²Johns Hopkins University, Baltimore, MD, USA, ³University of Pittsburgh, Pittsburgh, PA, USA, ⁴Fred Hutchinson Cancer Research Center, Seattle, WA, USA, ⁵University of Alabama-Birmingham, Birmingham, AL, USA.

Anemia is a common health problem in the U.S. older population and it is associated with increased hip fracture risk. The influence of anemia to bone geometric structures is unknown. This study used baseline data from participants of the Women's Health Initiative Observational Study to examine the association between hip geometric structure and anemia. Participants were age 50-79 years and postmenopausal women who came from different ethnic backgrounds. Only participants who had hemoglobin measurements (Hb) and hip bone density scans on dual-energy x-ray absorptiometry at one of the three WHI bone mineral density (BMD) centers were included in this study (n = 5,617). The Beck's hip structure analysis (HSA) method was used to measure BMD, cross-sectional area (CSA), outer diameter (OD), section modulus (SM), cortical thickness (CT) and buckling ratio (BR) in the femoral narrow neck (FNN), intertrochanter (IT) and femoral shaft (FS) region. Anemia was defined as Hb concentrations less than 12 gm/dl based on the definition by the World Health Organization (WHO). Overall, 6.8% of the participants were anemic and the rate of anemia varied by age and ethnicity. The results from multiple regression analyses showed that, after adjustment for age, height, weight, ethnicity, hormone use, physical activity and total body percent lean mass, women with anemia tend to have lower BMD, CSA, SM, CT, and higher BR in all the three femoral regions compared to women with a normal Hb level. However, statistically significant differences by anemic status were only observed for the SM and BR measure in the IT region (Table 1). Compared to the FNN and FS region, the differences in HSA measures were more obvious at the FN. In conclusion, hip geometric structure differs by anemic status and the differences seem bigger in the IT region than in the FNN and FS region.

Table 1. Baseline hip geometric measurement by anemia status

	Normal (N=5237)	Anemia (N=380)	p
	Mean \pm SE	Mean \pm SE	
Intertrochanter			
BMD (g/cm ³)	0.714 \pm 0.002	0.703 \pm 0.006	0.104
Cross-sectional area (cm ²)	3.451 \pm 0.008	3.395 \pm 0.030	0.072
Outer diameter (cm)	5.088 \pm 0.004	5.079 \pm 0.016	0.582
Section modulus (cm ³)	2.856 \pm 0.007	2.790 \pm 0.027	0.020
Cortical thickness (cm)	0.289 \pm 0.001	0.283 \pm 0.003	0.072
Buckling ratio	10.394 \pm 0.032	10.646 \pm 0.122	0.047

*Means are adjusted for age, weight, height, ethnicity, whole body percent lean mass, hormone use and physical activity

Disclosures: G. Wu, None.

This study received funding from: NIAMS R01-AR049411.

S383

How Should Hypercalciuria Be Defined? N. M. Maalouf, M. A. Cameron*, K. Sakhaee, Charles and Jane Pak Center for Mineral Metabolism, University of Texas Southwestern Medical Center, Dallas, TX, USA.

Background: Although hypercalciuria is a well-established risk factor for nephrolithiasis and is frequently considered in the differential of secondary osteoporosis, its definition has been debated and the "normal range" for urinary calcium excretion is not clearly defined. The most commonly used definitions for hypercalciuria are based on

absolute calcium excretion and weight-based calcium excretion. We examined whether the prevalence of hypercalciuria differs according to the definition used in a cohort of healthy individuals.

Methods: 24-hour urinary calcium excretion was measured in 149 healthy individuals with no history of kidney stones, while on an unrestricted diet. Absolute hypercalciuria (AHC) was defined as urinary calcium excretion exceeding 250 mg or 300 mg of calcium per day for women and men respectively. Weight-based hypercalciuria (WBHC) was defined as calcium excretion greater than 4 mg/kg of body weight per day. The prevalence of hypercalciuria was evaluated using both definitions, and was examined within the following body mass index (BMI) categories: normal, BMI < 24.9 Kg/m², overweight, BMI 25-29.9 Kg/m², and obese, BMI > 30 Kg/m².

Results: The cohort was composed of 46 individuals with normal BMI, while 52 were overweight and 51 were obese. For the entire cohort, mean BMI was 28.3 \pm 6.6 Kg/m², mean 24-hr urine calcium was 163.0 \pm 94 mg/day, or 2.09 \pm 1.10 mg/Kg/day. The prevalence of AHC was 15.4% while the prevalence of WBHC was 6.7% (p=0.016). Weight based urine calcium excretion did not vary significantly between the 3 groups of BMI (2.10 \pm 1.12 mg/Kg/day for normal BMI, 2.06 \pm 1.10 mg/Kg/day for overweight, and 2.10 \pm 1.11 mg/Kg/day for obese). On the other hand, absolute urine calcium excretion increased significantly with increasing BMI (125.5 \pm 66.0 mg/day for normal BMI, 157.7 \pm 73.3 mg/day for overweight, and 202.0 \pm 117.9 mg/day for obese). Accordingly, the prevalence of hypercalciuria varied significantly between BMI categories using the AHC but not the WBHC definition.

Urinary Calcium Excretion and Prevalence of Hypercalciuria According to BMI

	Urine Calcium mg/d	mg/kg	Prevalence of Hypercalciuria	
			AHC (%)	BWCH (%)
BMI<25	125.5 \pm 66.0†	2.10 \pm 1.12	2.2	4.3
BMI 25-29.9	157.7 \pm 73.3*	2.06 \pm 1.10	11.5*	5.7
BMI>30	202.0 \pm 117.9*,†	2.10 \pm 1.11	31.4*,†,‡	9.8

* p< 0.05 vs. BMI<25

† p< 0.05 vs. 25<BMI<29.9

‡ p<0.05 for prevalence of AHC vs BWCH within same BMI category

Conclusions: The prevalence of hypercalciuria depends on the definition used, particularly in obese patients. These results should be considered in the evaluation of calcium excretion in patients with nephrolithiasis and osteoporosis. Further studies are needed to establish the optimal definition of hypercalciuria.

Disclosures: N.M. Maalouf, None.

S386

Oral Treatment with the Calcium Receptor Antagonist SB-423557 Causes PTH Release in Multiple Species and Positive Bone Forming Effects in the Rat. S. Kumar¹, X. Liang¹, J. A. Vasko^{*1}, G. B. Stroup², S. J. Hoffman¹, V. R. Vaden^{*2}, H. Haley^{*2}, J. Fox³, E. F. Nemeth³, A. M. Lago^{*2}, J. F. Callahan^{*2}, P. Bhatnagar^{*1}, W. F. Huffman^{*1}, M. Gowen². ¹GlaxoSmithKline, Collegeville, PA, USA, ²GlaxoSmithKline, King of Prussia, PA, USA, ³NPS, Salt Lake City, UT, USA.

Antagonists of the parathyroid calcium receptor (calcilytics) stimulate the secretion of PTH. Previously, we demonstrated the ability of an orally active calcilytic compound to cause sustained increases in circulating levels of endogenous PTH and to stimulate bone formation and resorption (without a net increase in bone formation) in the ovariectomized (OVX) rat. In the present study, a prodrug approach has been used to preserve oral bioavailability and yield a calcilytic with a shorter half-life in vivo. SB-423557 is the ethyl ester prodrug of SB-423562 that, when administered orally to rats, dogs or monkeys, caused a dose-dependent, transient increase in circulating levels of endogenous PTH. In order to examine the bone forming effect of SB-423557, six-month-old female rats received OVX or sham surgery and were untreated for 6 weeks to allow osteopenia to develop and then treated orally daily with either vehicle, SB-423557 (50 mg/kg), or with rat PTH(1-34) (5 µg/kg SC) for 12 weeks. Plasma levels of PTH peaked at 10-60 min following oral administration of 50 mg/kg SB-423557 (3-fold, C_{max} of 40-60 pM) and returned to baseline by 2-3 hours. SC administration of rat PTH(1-34) resulted in a systemic C_{max} of 127-240 pM at 10 minutes post-injection.

SB-423557 significantly and completely prevented additional OVX-induced loss of BMD in the lumbar spine and partially prevented trabecular BMD loss in the proximal tibia by 39% (ns) compared to OVX controls. Histomorphometric analysis indicated greater trabecular bone area (36%, ns) in the spine and increased cortical area (72%) and endocortical bone formation rate (220%) with no effect on the eroded perimeter of the distal tibia in the SB-423557 treated rats compared to vehicle-treated OVX animals. Serum osteocalcin increased (ns) with SB-423557 treatment with no effect on urinary deoxypyridinoline levels. In addition, treatment with SB-423557 resulted in greater ultimate strength (ns), toughness, and elastic modulus of a lumbar vertebral body and at the femoral diaphysis compared to OVX controls. Treatment with PTH(1-34) also completely prevented the OVX-induced loss in bone mass, BMD, and strength.

These data provide a proof of principle for stimulation of bone formation following daily brief antagonism of the calcium receptor in the OVX rat and support the potential use of these agents to treat disorders of bone metabolism such as osteoporosis.

Disclosures: S. Kumar, GlaxoSmithKline 3.

S388

Prior Alendronate Treatment Does Not Inhibit the Early Stimulation of Osteoblast Activity in Response to Teriparatide. R. Lindsay¹, F. Cosman¹, H. Zhou², J. W. Nieves¹, M. Boström³, N. Barbuto^{*1}, D. W. Dempster². ¹Clinical Research Center, Helen Hayes Hospital, West Haverstraw, NY, USA, ²Regional Bone Center, Helen Hayes Hospital, West Haverstraw, NY, USA, ³Department of Orthopaedics, Hospital for Special Surgery, New York, NY, USA.

Several studies suggest that the bone density response to PTH treatment is blunted in subjects previously treated with alendronate. The present study evaluates the effects of teriparatide (TPTD) on bone formation variables from iliac crest biopsies in subjects who were either treatment naïve or pretreated with alendronate (ALN). We recruited 25 postmenopausal women with osteoporosis (12 treatment naïve; 13 pretreated with alendronate for at least 1 yr (mean age 63)). The two groups were randomized to control or TPTD (20mcg/day). All underwent iliac crest bone biopsy 7.5 weeks after randomization. We used quadruple tetracycline labeling as previously described (JBMR 2006) to provide longitudinal data on bone formation in each subject. Biopsies were read with the observer blinded to treatment group. Groups were well matched for demographics and indices of cancellous and cortical bone structure. In ALN- treated patients, mineral apposition rate (MAR), mineralized perimeter (Md.Pm) and bone formation rate (BFR) were lower at baseline than in naïve patients.

	MAR		BFR		MdPm	
	Pre	Post	Pre	Post	Pre	Post
Cancellous						
Naïve	0.73 0.06	± 0.88 0.06	± 0.016 0.004	± 0.054 0.015	± 2.16 0.41	± 5.78 ± 1.32
ALN	0.38 0.14	± 0.84 0.05	± 0.005 0.003	± 0.035 0.013	± 0.78 0.39	± 4.25 ± 1.63
Endocortical						
Naïve	0.69 0.05	± 0.86 0.07	± 0.049 0.014	± 0.141 0.034	± 6.69 1.69	± 15.73 ± 3.50
ALN	0.32 0.11	± 0.58 0.13	± 0.006 0.003	± 0.049 0.015	± 1.21 0.39	± 6.36 ± 1.70

After TPTD, the absolute increment in MAR was dramatic in the ALN group, increasing approximately 80-120% above baseline in cancellous bone and on the endocortical surface (Table). MAR also increased significantly with TPTD in the naïve group (21-25%), but the increments were not as marked as in ALN subjects. The absolute increases in BFR and Md.Pm were similar in ALN and naïve groups in cancellous bone but were larger in the naïve group on the endocortical surface due to the higher baseline Md.Pm. However, the percentage increments in all bone formation variables were greater on both envelopes in the ALN compared to the naïve group. We conclude that the increments in the work rate of osteoblast teams (MAR) in response to early treatment with TPTD are greater following ALN pretreatment than in naïve subjects. However, the extent of bone forming surface is overall larger in naïve subjects, perhaps providing an explanation for the possible blunting of the BMD effect in ALN treated women given TPTD.

Disclosures: R. Lindsay, Eli Lilly & Company 2, 8.

This study received funding from: Primary funding, NIH; Product, Eli Lilly.

S390

β2 Adrenergic Receptor Deficiency Enhances Bone Mass in by Antagonizing Against Aging-induced Bone Loss and Blunts Anabolic Effects of PTH on Osteoblasts. R. Hanyu^{*1}, Y. Saita^{*1}, J. Nagata^{*1}, Y. Izu^{*1}, T. Hayata^{*1}, H. Hemmi^{*2}, S. Takeda^{*3}, Y. Ezura^{*1}, K. Nakashima^{*1}, H. Kurosawa^{*4}, M. Noda^{*1}. ¹Department of Molecular Pharmacology, 21st Century COE Program, MRI, Tokyo Medical and Dental University, Chiyoda-ku, Tokyo, Japan, ²MTT Program, MRI, Tokyo Medical and Dental University, Chiyoda-ku, Tokyo, Japan, ³Department of Orthopedics, 21st Century COE Program, Tokyo Medical and Dental University, Chiyoda-ku, Tokyo, Japan, ⁴Department of Orthopedics, Juntendo University School of Medicine, Bunkyo-ku Tokyo, Japan.

Soaring of the aged population in modern world increases the fraction of aged population with diseases and thus in bone field, leads to increase in osteoporosis incidence. Loss of bone mass is accelerated with age regardless of gender. Osteoporotic patients with their bone mass levels at their nadir require treatment to increase bone mass through the activation of bone formation. PTH has been proven to be efficacious in increasing bone mass. However, its efficacy in the highly aged population such as those over 80 years of age in human have not yet been fully elucidated. In mice, aged models of over one year old, indicate lower bone mass than younger adult animals regardless of the gender. Recently, sympathetic nervous system was reported to regulate bone mass in mice. However, these reports always indicate the effects of adrenergic system on young adult mice. Therefore, the purpose of this paper is examine the effects of β2 adrenergic system and PTH on the bone mass in aged mice. Aged (54 weeks old) female mice null for β2 adrenergic receptor (Adrb2^{-/-}) and wild type (WT) were used. Mice were treated with vehicle or PTH (80µg/kg/day sc) for 4 weeks (5 days/week). The base line bone mass levels in these aged mice were significantly reduced compared to young adult mice. Aged Adrb2^{-/-} mice exhibited higher total body BMD, trabecular bone volume fraction(BV/TV), cortical bone volume compared with aged WT mice. In WT, PTH treatment significantly increased the levels of total body BMD, 3D- BV/TV, mineral apposition rate (MAR) and bone formation rate (BFR). In contrast, in aged Adrb2^{-/-} mice, PTH failed to

increase the levels of BMD and BV/TV. Analyses on aged Adrb2^{-/-} mice also revealed that PTH failed to enhance BFR and MAR. Importantly, Adrb2 deficiency increased cortical bone volume compared to WT while this parameter was no longer enhanced by PTH in the mutant mice. Regarding bone resorption side, Oc.S/BS, N.Oc/BS were similar regardless of the genotype or PTH treatment. In conclusion, we found that in one year old aged female mice, β2 adrenergic receptor signal operates to reduce bone mass, while β2 adrenergic signaling is required for the anabolic actions of PTH on bone formation.

Disclosures: R. Hanyu, None.

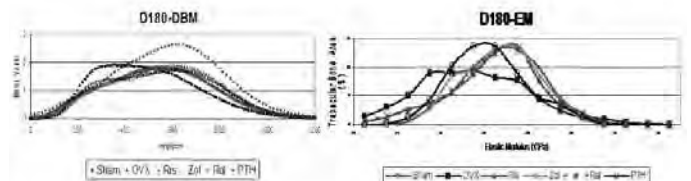
S392

PTH Improves Bone Strength in an Osteoporosis Model Through Increasing Mineralized Matrix Yet the Elastic Modulus of the Trabecular Surface Is More Heterogeneous than Observed with Anti-Resorptive Agents. Z. Cheng¹, W. Yao¹, K. J. Koester^{*2}, M. Balooch^{*2}, R. O. Ritchie^{*2}, N. E. Lane¹. ¹Center for Healthy Aging, UC Davis Medical Center, Sacramento, CA, USA, ²Materials Science and Engineering, Materials Sciences Division, Lawrence Berkeley National Laboratory, Berkeley, CA, USA.

Current approved medical treatments for osteoporosis reduce fracture risk to a greater degree than predicted from changes in bone mineral density (BMD). Based on these observations, we hypothesize that these bone active agents improve bone strength by altering material properties of the bone.

Methods. 18-month-old female Fischer rats were ovariectomized (OVX) or sham-operated and were untreated for 60 days to induce osteopenia before they were treated with single doses of risenedronate (iv., 500µg/kg), zoledronic acid (iv., 100µg/kg), continuous raloxifene (2mg/kg, po., 3x/wk), hPTH (1-34) (25µg/kg, sc., 3x/wk) or vehicle. Groups of animals were sacrificed after d60 and d180 of treatment. Measurements of bone quality from the proximal tibial metaphyses (PTM) included µCT, the degree of bone mineralization (DBM), mineral heterogeneity index (MHI); localized elastic modulus (EM) mapping of select trabecular surface by scanning probe microscopy, and bone compression testing from a lumbar vertebral body (LVB).

Results. The bone volume (BV/TV), DBM, EM and compressive bone strength were significantly lowered at d60 post-OVX (pretreatment, day 0 study) than at baseline. At d60 all treatments restored bone material measurements (BV/TV, DBM, EM and compressive bone strength) and no differences between OVX + anti-resorptives and OVX + PTH were observed. However, at d180 OVX + PTH further increased BV/TV (+30% from d 60), DBM, MHI and bone strength to baseline levels. EM mapping of PTM from the OVX + vehicle and OVX + PTH at d180 had significant heterogeneity with higher percentage of high and low EM areas than sham. Moreover, at d180 there was a higher percentage of high EM in OVX + PTH compared to other OVX + anti-resorptives and whole bone strength was higher. Therefore, these data suggest that localized changes in the material properties of bone after PTH, differs from anti-resorptive agents, and while the EM of the matrix is more heterogeneous, the overall result in greater bone strength. Additional studies are needed to correlate these preclinical findings with the clinical efficacy of these agents in osteoporosis.



Disclosures: Z. Cheng, None.

This study received funding from: R01 AR043052-078, 1K12HD05195801, DE AC-02 05CH11231.

S394

The Use of RAP-011, a Novel Bone Anabolic Agent, in Combination with Parathyroid Hormone or Zoledronic Acid Using a Mouse Model of Established Bone Loss. M. Cornwall-Brady^{*}, M. Mangini^{*}, D. Barbosa^{*}, L. Mazzola^{*}, T. Marvell^{*}, J. Milling^{*}, B. Haigis^{*}, R. Kumar^{*}, K. Underwood^{*}, R. S. Pearsall. Acceleron Pharma, Cambridge, MA, USA.

RAP-011, a novel soluble receptor fusion protein based on the activin receptor type IIA was previously reported to increase bone density in vivo (Pearsall et al, J Bone Min. Res. 21(S1) 2006). Here, we investigate the efficacy of RAP-011 compared with parathyroid hormone (PTH) or zoledronic acid (ZOL).

Eight week old C57BL/6 mice were ovariectomized (OVX) or sham operated (SHAM). 8 weeks after surgery all mice were analyzed by dual-energy x-ray absorptiometry (DEXA) prior to treatment. Mice were administered either RAP-011 (IP, 10 mg/kg, biw), PTH (SC, 80 µg/kg/day) or a single dose of ZOL (IP, 20 µg/kg).

Study 1 included 48 OVX (16 each treated with PBS, RAP-011, PTH) and 8 SHAM mice. After six weeks of treatment, half of each group received a single IP dose of the ZOL. The bone mineral density (BMD) of each animal was measured 0, 6, 10, 14 and 18 weeks after treatment initiation. This study demonstrated an increase in total body BMD of 3.6%, 4.2%, 7.6%, and 10.0% in SHAM VEH, OVX VEH, OVX-RAP-011 and OVX PTH respectively after 6 weeks of treatment. Four weeks after ZOL dosing DEXA results showed an additional increase (relative to week 6 results) of 4.7%, 4.6%, and 1.3% in OVX groups treated with PBS, RAP, and PTH respectively. In groups that did not receive ZOL

treatment the BMD changes were 2.4%, 1.9%, 2.0% and -3.6% for SHAM VEH, OVX VEH, OVX RAP-011 and OVX PTH mice respectively.

Study 2 included 32 OVX (8 each treated with PBS, RAP, PTH, and a combination of both RAP-011 and PTH), 24 Sham (8 each PBS, RAP-011 and PTH). DEXA was performed at weeks 0 and 6. In this study we show an increase in total body BMD of 2.8%, 4.6%, 9.8% and 13.3% for OVX groups treated with PBS, RAP-011, PTH and the combination of both RAP-011 and PTH, respectively. SHAM groups had total body BMD changes of -0.1%, 8.0% and 6.9% for PBS, RAP-011 and PTH respectively.

Consistent with our previously reported results, these data show that total body BMD increased significantly after 6 weeks of treatment with either RAP-011 or PTH. Subsequent treatment with ZOL resulted in equivalent increases in BMD in groups that were previously treated with RAP-011 or PBS. These results indicate that RAP-011 does not alter the bone microenvironment in such a way as to preclude the use of antiresorptive therapy. DEXA results also indicate that the total body BMD increase as a result of a combination treatment with both RAP-011 and PTH was larger than either the RAP-011 or PTH treatment alone in both SHAM and OVX mice. The results of these two studies provide evidence that RAP-011 can be used in combination with other currently approved therapies.

Disclosures: M. Cornwall-Brady, Acceleron Pharma 1, 3.

S397

Endogenously Produced n-3 Fatty Acids (Fat-1 transgene) Protects Bone after Ovariectomy in Mice. J. Banu¹, A. Bhattacharya², G. Halade¹, M. Rahman¹, G. Fernandes¹. ¹Med/Clinical Immunology & Rheumatology, University of Texas Health Science Center at San Antonio, San Antonio, TX, USA, ²Department of Cellular and Structural Biology, University of Texas Health Science Center at San Antonio, San Antonio, TX, USA.

Aging is associated with bone loss leading to escalating the risk of fractures. Recently, there is growing interest in identifying nutritional supplements that can be more effective in preventing age-related as well as postmenopausal bone loss with minimum side-effects. There is increasing evidence on the beneficial effects of n-3 fatty acids in the prevention of postmenopausal bone loss. In 2004, a novel transgenic mouse model (fat-1) that could convert n-6 fatty acids to n-3 fatty acids was produced. We studied bone loss after ovariectomy in this mouse model and their wild type counterparts (C57BL/6).

Fat-1 transgenic and wild type C57BL/6 mice were used in this study. Female mice were 8 weeks old when they were either ovariectomized or sham operated. They were maintained in the laboratory for 6 months and then sacrificed. Serum alkaline phosphatase and osteocalcin were measured. The femur, tibia and lumbar were analyzed using peripheral quantitative computed tomography (PQCT) densitometry.

Serum alkaline phosphatase (ALP) was decreased significantly in the wild type mice after ovariectomy. The fat-1 mice had lower ALP when compared to the wild type mice, but after ovariectomy there was no further decrease in the enzyme levels. Osteocalcin levels were not significantly altered after ovariectomy in the wild type mice and fat-1 mice.

In wild type mice, there was significant loss of bone after ovariectomy in the neck of the femur and proximal tibial metaphysis. However, in the fat-1 transgenic mice there was significantly less bone loss after ovariectomy in the neck of the femur and proximal tibial metaphysis. In the femoral diaphysis, fat-1 transgenic mice had significantly higher bone mass when compared to that of the wild type mice. The tibia fibular junction did not show any differences between the wild type and transgenic mice. Similarly, ovariectomy did not affect the pure cortical bone in both wild type and transgenic mice.

We conclude that endogenously produced n-3 fatty acids can attenuate postmenopausal bone loss significantly in the femur followed by the tibia and this bone loss is mainly due to decreased endocortical resorption.

Disclosures: J. Banu, None.

This study received funding from: NIH.

S399

Vitamin K Supplementation in Postmenopausal Women with Osteopenia: The ECKO Trial. A. M. Cheung¹, L. E. Tile¹, Y. Lee², G. Tomlinson³, G. Hawker⁴, J. Scher¹, H. Hu¹, R. Vieth⁵, L. Thompson⁶, S. A. Jamal², R. Josse². ¹Osteoporosis, University Health Network, Toronto, ON, Canada, ²Osteoporosis, St. Michael's Hospital, Toronto, ON, Canada, ³Medicine, University Health Network, Toronto, ON, Canada, ⁴Osteoporosis, Women's College Hospital, Toronto, ON, Canada, ⁵Pathobiology and Laboratory Medicine, Mt. Sinai Hospital, Toronto, ON, Canada, ⁶Nutrition, University of Toronto, Toronto, ON, Canada.

BACKGROUND: Vitamin K has been widely promoted as a supplement for decreasing bone loss in postmenopausal women, but the long-term benefits and potential harm are unknown.

METHODS: We performed a 2-year single-centre placebo-controlled double-blind randomized trial involving 440 postmenopausal women with osteopenia: 217 received 5mg of vitamin K1 daily and 223 received placebo daily. Outcome measures included bone mineral density (BMD), bone turnover markers, fragility and non-fragility fractures, long-term adverse effects and health-related quality of life. The study was extended for earlier participants for a maximum duration of up to 4 years because of interest in long-term safety and fractures.

RESULTS: Bone mineral densities decreased by -1.28% and -1.22% (p=0.84) at the lumbar spine and -0.69% and -0.88% (p=0.51) at the total hip in the vitamin K and placebo groups over two years, respectively. There were no significant differences in changes in

BMDs at any site between the vitamin K and the placebo groups over the 2 to 4-year duration of the trial. Vitamin K supplementation did increase serum vitamin K levels (22.6% versus 2.0%, p<0.0001) and carboxylation of osteocalcin (-21.4% versus -2.0%, p<0.0001) and lowered total osteocalcin levels (bone formation marker) (-13.2% versus -0.1%, p<0.0001); however, it did not change C-telopeptide (6.2% versus -1.2%, p=0.10). There were fewer cancers (3 versus 12, p=0.02) and fewer clinical fractures in the vitamin K group (9 versus 20, p=0.04). Health-related quality of life was not significantly different between the two groups.

CONCLUSIONS: Daily vitamin K supplementation for 2 to 4 years did not protect against age-related decline in BMD in postmenopausal women with osteopenia. There were lower incidences of fractures and cancer

with vitamin K supplementation. Further studies are required to confirm these findings. (ClinicalTrials.gov number, NCT00150969)

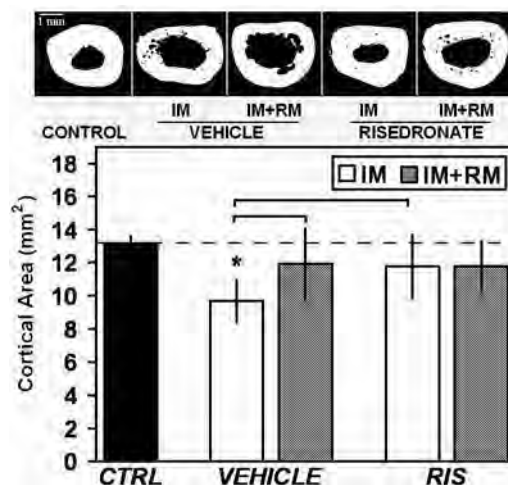
Disclosures: A.M. Cheung, None.

This study received funding from: Canadian Institute for Health Research.

S403

Bisphosphonate Treatment During Long-Term Disuse Blunts the Recovery Response of Bone to Restored Weight-Bearing. J. C. Fritton¹, C. Y. Li¹, X. Zhang¹, D. Laudier¹, R. Mann², M. B. Schaffler¹. ¹Leni & Peter W. May Department of Orthopaedics, Mount Sinai School of Medicine, New York, NY, USA, ²Bronx VA Medical Center, New York, NY, USA.

Bone retention with bisphosphonates (BIS) may set the stage for improved recovery from disuse osteoporosis. We previously found that risedronate (RIS) treatment attenuates approximately half of cortical bone loss associated with long-term immobilization. The purpose of this study was to test whether bone that remains after RIS-treatment during long-term immobilization better recovers its architecture after restoration of mechanical usage. Right forelimbs of 5-7 year-old retired breeder female Beagles (N=27) were immobilized (IM) with splints as in our previous studies. Dogs were treated daily with either RIS (0.5 mg/kg, p.o., provided by P&G Pharmaceuticals) or sterile-water vehicle for 6 months, after which tissues were obtained. In remaining animals, RIS treatment was stopped and splints removed. Remobilized (RM) dogs were allowed 12 months of unrestricted weight-bearing. Age-matched dogs served as controls. Cortical bone structure was assessed by μ CT scanning of third metacarpals at 20- μ m resolution. Calibrations determined bone mineral density (BMD) values; structural analyses used a global BMD threshold of 600 mg/cc. Cross-sectional properties obtained at the mid-shaft included cortical bone, marrow cavity and total areas, and polar moments of inertia. Effects were tested by ANOVA with post-hoc PLSD comparisons (p<0.05, data shown as Means \pm SD). RIS treatment prevented approximately 60% of the bone loss due to IM. RM of vehicle-treated dogs restored significant amounts of cortical bone lost during disuse. Surprisingly, despite discontinuation of RIS, a similar remobilization response was absent in the animals drug-treated during IM.



BIS have long half-lives (on the order of years) and thus have effects after active dosing has stopped. This may underlie the impaired response of RIS-treated bone to restored loading. The decision to use BIS in prevention of bone loss during long-term immobilization (e.g., bed rest or space flight) must include consideration of side effects. Our results indicate that these side effects include an impairment of the ability of cortical bone to respond appropriately to the reintroduction of mechanical loading.

Disclosures: J.C. Fritton, None.

This study received funding from: NSBRI & NIH.

S405

Combination Treatment with a Selective Androgen Receptor Modulator (SARM) and a Bisphosphonate has Additive Effects in Osteopenic Female Rats. E. G. Vajda, A. Hogue*, K. N. Griffiths*, W. Y. Chang*, K. Burnett*, K. Marschke*, D. E. Mais*, B. Pedram*, Y. Shen*, A. van Oeveren*, F. J. López*. Ligand Pharmaceuticals, San Diego, CA, USA.

Recent clinical trials with bisphosphonates and PTH have not supported the hypothesis that combination treatments with antiresorptive and anabolic agents would lead to synergistic activity. We hypothesized that combination treatment with a SARM, LGD3303, and a bisphosphonate would be beneficial. In vitro, LGD3303 is a potent androgen that shows little or no cross-reactivity with related nuclear receptors. In male rats, LGD3303 has tissue selective properties, increasing the levator ani muscle weights above eugonadal levels at high doses, but having greatly reduced activity on the prostate, never increasing the ventral prostate weight above eugonadal levels. To assess bone effects, three month-old female SD rats were ovariectomized (OVX) and allowed to develop osteopenia for 8 weeks. Rats were orally dosed with vehicle, LGD3303, alendronate sodium, or the combination from week 8 to 20 post-OVX (all dosed at 3 mg/kg/day). LGD3303 and combination treatment significantly increased gastrocnemius muscle weight, unlike alendronate. All three treatments increased whole femur BMD and BMC measured by DEXA. BMC was significantly higher with LGD3303 and combination treatment (19.0% and 19.9% increase, respectively) compared to alendronate (8.3% increase). At the lumbar spine, LGD3303 and alendronate increased BMD (10.8% and 7.6% increase, respectively), but combination treatment restored it to near sham levels (18.0% increase). Similarly, elevations in bone strength at the femur and lumbar spine were also observed with all treatments; however the combination had the largest increase, particularly at the lumbar spine. Histomorphometry confirmed that LGD3303 and combination treatment significantly increased mid-femur periosteal bone formation (75.9% and 74.2%, respectively), whereas alendronate (6.3%) was nearly inactive. In contrast, all three treatments suppressed cancellous bone remodeling at the lumbar spine and increased trabecular bone volume. Collectively, these results indicate that LGD3303 and alendronate have positive effects on cancellous bone, but the combination treatment is the most effective at suppressing bone turnover and improving spinal strength and bone density. Muscle and cortical bone were unaffected by alendronate, whereas LGD3303 has anabolic activity which is unaltered by combination treatment with alendronate. At every measured site, combination treatment was as effective as either single agent and in some cases showed significant added benefit.

Disclosures: E.G. Vajda, Ligand Pharmaceuticals 3.

S409

Decreased Bone Turnover and Porosity Are Associated with Improved Bone Strength in Ovariectomized (OVX) Cynomolgus Monkeys Treated with Denosumab, a Fully Human RANKL Antibody. M. S. Ominsky¹, J. Schroeder^{*1}, J. Jolette^{*2}, S. Y. Smith², D. J. Farrell^{*2}, J. E. Atkinson¹, P. J. Kostenuik¹. ¹Amgen Inc., Thousand Oaks, CA, USA, ²Charles River Laboratories Preclinical Services Montreal, Inc., Montreal, PQ, Canada.

Denosumab (DMab), a fully human monoclonal antibody against RANKL, was previously shown to decrease biochemical markers of bone turnover and increase bone mineral density in adult OVX cynomolgus monkeys. We now report from that study the effects of DMab on bone turnover at the histologic level, and their relationships with bone strength.

One month after surgery, OVX cynos (9-16 years old) were treated with either vehicle (OVX-Veh) or DMab (25 or 50 mg/kg, SC, once/month) for 16 months (n=14-20/group). Sham controls were treated with vehicle (n=17). Double fluorochrome labels were injected prior to iliac and rib biopsies (at month 6 and 12), and prior to sacrifice. Histomorphometry was performed on these biopsies, the tibial diaphysis, and cancellous bone in L2 vertebra and the proximal femur.

Cancellous bone turnover was increased in OVX-Veh animals, based on significantly greater mineralizing surface (MS/BS), bone formation rate (BFR), and activation frequency at the lumbar spine, iliac crest, and femur neck (P<0.05 vs Sham). Both doses of DMab fully prevented these OVX-related changes while reducing values significantly below those of sham controls (P<0.05). Osteoclast and osteoblast surfaces were 78-100% lower in the lumbar spine, iliac crest, and femur neck of DMab groups, while eroded surface was decreased by 45-93% (P<0.05 vs OVX-Veh).

Cortical bone turnover was also increased in OVX-Veh cynos, as shown by significantly greater cortical porosity, labeled perimeter, and BFR at the endocortical and haversian surfaces of the tibial diaphysis and rib (P<0.05 vs Sham). Both doses of DMab fully prevented these OVX-related changes, while reducing labeled perimeter and BFR significantly below sham control levels (P<0.05).

Prolonged DMab-related turnover suppression was associated with significant increases in strength parameters at the lumbar vertebrae, femur neck, and femur diaphysis (P<0.05 vs OVX-Veh). Regression analysis of all groups combined demonstrated significant inverse relationships between the strength of L5-L6 cores (yield load) and mineralizing surface (r²=0.44) or eroded surface in L2 (r²=0.37; P<0.001). Cortical porosity in the tibia was negatively correlated with peak load at the femur diaphysis (r²=0.21; P<0.001).

In summary, denosumab treatment of OVX cynos was associated with significant decreases in histomorphometric indices of bone turnover. These changes were accompanied by significant improvements in bone strength at cortical and cancellous sites.

Disclosures: P.J. Kostenuik, Amgen, Inc. 1, 3.
This study received funding from: Amgen Inc.

S411

Bone Effects of Cathepsin K Inhibitor in Ovariectomized Rhesus Monkeys. P. Masarachia, S. Pun*, D. Kimmel. Molecular Endocrinology and Bone Biology, Merck Research Laboratories, West Point, PA, USA.

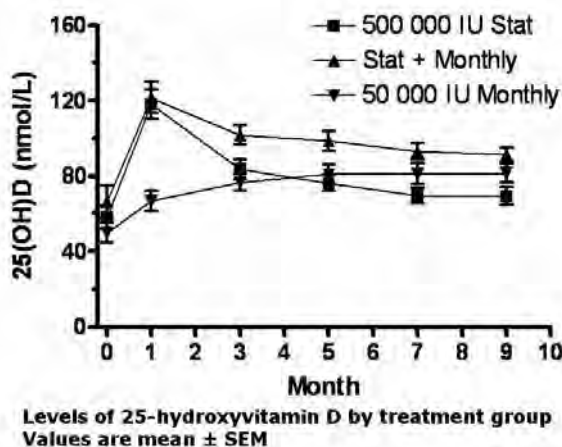
Cathepsin K (CatK), a cysteine protease highly expressed in osteoclasts, degrades type I collagen. CatK inhibitors, by slowing bone matrix degradation that follows the demineralization phase of bone resorption, may be useful as anti-resorptive agents for treating osteoporosis. The objective of this study was to evaluate bone mineral density (BMD) and bone turnover in newly-ovariectomized (OVX) non-human primates treated with CatK inhibitor MK-0822. Rhesus monkeys (age 12-19 yrs) were assigned to four groups (N=10-11): (1) vehicle-treated intact; and OVX treated with (2) vehicle, (3) 6mg/kg/d or (4) 30 mg/kg/d MK-0822. Daily oral dosing started on ~day 11 following OVX. BMD of spine and hip were measured (DXA, Hologic DiscoveryA) at baseline and 11 months. Calcein (12 mg/kg, SC) was given on the 18th and third days before obtaining right transilial (TIBx) and ninth rib (RBx) biopsies. Specimens were embedded undecalcified and sectioned at 6µm or 100µm. Both trabecular (TB) and endocortical surfaces (EC) were used for standard histomorphometric endpoints. BMD declined significantly at the spine and femoral neck after OVX. This BMD decline was prevented by 30mg/kg/d MK-0822. In both TIBx and RBx, double-labeled surface (DLS/BS) was elevated by OVX and reduced vs. OVX by ~80-90% (P<0.01) by both 6 and 30 mg/kg/d MK-0822. In RBx, Haversian turnover tended to be elevated by OVX and reduced by 30 mg/kg/d MK-0822. In TIBx, mineralizing surface (MS/BS, %) and mineral apposition rate (MAR) decreased vs. OVX for both doses in both TB and EC compartments (P<0.01). All treatment effects were significant except MAR in the TB compartment. Bone formation rate (BFR) tended to increase with OVX, and was decreased relative to OVX by MK-0822; differences were significant for both doses in the TB compartment but only for 6 mg/kg in EC compartment. Osteoid thickness (Os.Th, µm) and surface (OS/BS, %) were increased ≥50% (P<0.05) by OVX and decreased vs. OVX for both MK-0822 doses (P<0.05) in both compartments. The distribution of osteoid thicknesses was shifted to thicker seams by OVX, but was similar to intact animals with MK-0822. In RBx, both osteoclast covered (OcS/BS) and non-osteoclast covered eroded surface (ES/BS) were significantly lower with MK-0822 treatment. In animals with higher amounts of osteoid surface, osteoclasts were seen adjacent to osteoid surfaces with the same low frequency in all groups. MK-0822 reverses the OVX-induced rise in bone turnover in the TB and EC bone of the rib and ilium at 6 and 30mg/kg/d, but reduces rib cortical bone turnover only at 30mg/kg/d, the only dose that preserved spine and hip BMD. We conclude that both doses of MK-0822 reduced TB turnover in biopsy sites and the higher dose tested prevented OVX-induced loss of BMD at osteoporosis fracture sites.

Disclosures: P. Masarachia, None.

S415

A Comparison of Three High Dose Oral Vitamin D₃ Supplementation Regimens. C. J. Bacon*, G. D. Gamble*, A. M. Horne*, I. R. Reid. Faculty of Medical and Health Sciences, University of Auckland, Auckland, New Zealand.

Vitamin D insufficiency is recognized as a major clinical problem in the elderly. Most previous supplementation studies have provided daily calciferol doses of 400-800 IU/day. It may take considerable time on these doses for many elderly people to attain recommended levels of 25-hydroxyvitamin D [25(OH)D]. The purpose of this study was to compare the magnitude and time-course of 25(OH)D response to three high dose vitamin D₃ regimens. Sixty-three elderly people, aged 81.6±6.7 years (mean±sd), were recruited on discharge from general medical wards. They were randomly assigned to supplementation with either a single dose of 500 000 IU (Stat), 500 000 IU stat plus 50 000 IU monthly (Stat+Monthly), or 50 000 IU monthly alone (Monthly), in a double-blind trial. The figure shows 25(OH)D levels throughout the study. Baseline 25(OH)D was 58±32 nmol/L and was not different between groups. Mixed-model analysis of variance showed significant Month, Group, and Month x Group interaction effects (p<0.001). At one month, 25(OH)D in the Stat and Stat+Monthly groups rose to 120±33 nmol/L compared to 67±24 nmol/L in the Monthly group. The maximum 25(OH)D level reached at one month was 220 nmol/L, from a baseline level of 136 nmol/L. Three other individuals attained levels >150 nmol/L. The Monthly group reached a plateau of approximately 80±20 nmol/L after five months. At the end of the study only the Stat+Monthly and Monthly groups maintained mean levels >80 nmol/L. In order to rapidly increase 25(OH)D to recommended levels and sustain these levels in frail elderly, a loading dose followed by regular supplementation is preferable to regular supplementation alone.



Disclosures: C.J. Bacon, None.

This study received funding from: New Zealand Health Research Council.

S419

Teriparatide Administration Following Antiresorptive Therapy (BBB-Study): Changes in 3D Microarchitecture, Mineralization and Remodeling at the Iliac Crest After 6 Months. B. Jobke¹, B. Muche², A. J. Burghardt¹, J. Semler², G. Delling³, T. M. Link¹, S. Majumdar¹. ¹MQIR - Dept. of Radiology, University of California, San Francisco, CA, USA, ²Dept. of Osteology, Immanuel-Hospital, Berlin, Germany, ³Inst. for Pathology, Hannover, Germany.

The purpose of this investigation is to obtain more information regarding the onset and duration of new bone formation that result in architectural changes under recombinant human parathyroid hormone 1-34 (rhPTH = teriparatide) following inadequate response to long-term bisphosphonate (BP) therapy for osteoporosis.

Materials and Methods: 25 female osteoporotic patients (age 69 ± 9 years) self-administered teriparatide (20 µg/d), for an ongoing treatment period of 18 months, after long-term BP use (mean duration 40 ± 22 months). In this single center clinical trial, to date, 13 paired iliac crest biopsies (Jamshidi technique) were obtained at baseline (M0) and 6 months (M6) at alternating sides. Tetracycline double-labeled and PMMA embedded biopsies were analyzed semi-quantitatively using light microscopy. Bone volume fraction (BV/TV), structural parameters (Conn.D, SMI, Tb.N, Tb.Th, Tb.S, TBPf) and tissue mineralization (mgHA/ccm) were assessed using µCT (MicroCT 40).

Results: Teriparatide application led to a significant increase in bone remodeling units at M6 compared to M0: in 10/13 (77%) patients an increase was found, in 2/13 there was no change and in 1/13 a decrease in bone turnover was documented. 4 patients showed minor forms of local endosteal fibrosis and 3 had a moderate surface osteoidosis at M6. Pairwise changes in the degree of tissue mineralization did not differ from M0 (p=0.945; mean change: -1.5% to 1087 mgHA/ccm ± 30), independent of bone turnover status. Pairwise changes in BV/TV and 'structure model index' (SMI) improved significantly (p=0.014 and p=0.046, respectively). The average increase in bone volume fraction was +1.8%. Increases in bone volume fraction >2% compared to M0 were observed in 62% (8/13). **Discussion:** Despite previous long-term suppression of bone turnover with BP, rhPTH considerably stimulated or balanced bone turnover after 6 months of treatment. In contrast to previous reports there was no detectable decrease in tissue mineralization under osteoanabolic rhPTH treatment. This observation may be due to a relatively small gain in new mineralized bone at M6. It appears that an early gain in bone volume at M6 was best represented by BV/TV whereas most changes in structural parameters were not significant yet. Our results from the iliac crest are consistent with findings from previous clinical trials which found high levels of bone formation markers at M6 with a subsequent improvement in bone stability.

Disclosures: B. Jobke, Travel grant from: Eli Lilly 9.

This study received funding from: Eli Lilly.

S421

Pulmonary Delivery of the Parathyroid Hormone Analogue Ostabolin-C™ Stimulates Markers of Bone Formation in Postmenopausal Women. P. Morley¹, J. Bishop¹, R. Anderson¹, C. L. Barclay¹, D. Krause¹, G. Morelli², M. Newhouse³, N. Sadrzadeh⁴, M. Eldon⁴. ¹Zelos Therapeutics Inc., Ottawa, ON, Canada, ²MDS Pharma Services, Montreal, PQ, Canada, ³McMaster University, Hamilton, ON, Canada, ⁴Nektar Therapeutics, San Carlos, CA, USA.

Ostabolin-C is a cyclic analogue of human parathyroid hormone (PTH) (1-31) that has demonstrated marked increases in bone mineral density of the lumbar spine and hip in a 1-year subcutaneous (SC) injection Phase II clinical trial. Pulmonary delivery will improve compliance with PTH therapy, especially in patients averse to self-injection. In the present

study, the pharmacokinetic (PK), safety and efficacy profile of Ostabolin-C inhalation powder (OCIP) was evaluated in healthy postmenopausal female volunteers using a randomized, double-blind, placebo-controlled single and 28-day repeat escalating dose study design. Seventy two subjects (49-105 kg; 47-74 years of age) in 9 cohorts of 6 OCIP and 2 placebo treated subjects received a single inhalation of OCIP (dose range 0.1-1.6 mg/day) or placebo powder followed by 28-days of daily inhalation of OCIP or placebo for 7 of the 9 cohorts. Pre- and post-dose urinary cAMP, PINP, osteocalcin, CTx, NTx, ECG vital signs, spirometry, adverse events (AEs) and plasma Ostabolin-C levels were recorded. Following administration of OCIP using the Nektar T326 inhaler, C_{max} and AUC increased proportionally with dose while T_{max} and t_{1/2} were dose independent. There was no accumulation with repeat dosing and PK profiles of OCIP and SC Ostabolin-C were similar. Biological activity, measured by urinary cAMP, showed significant dose-dependent increases from pre- to post-dose on Day 1 that were maintained with repeat dosing. Significant dose-dependent increases in PINP and osteocalcin were observed on Day 28. There was no change in the markers of bone resorption CTx or NTx. The safety profile was consistent with PTH class effects, i.e., headache and nausea were the most commonly reported AEs and a dose-dependent increase in heart rate was recorded. There were no treatment-emergent pulmonary or cardiovascular AEs, no effect on pulmonary function and no clinically relevant laboratory abnormalities. Tolerability was poor in subjects receiving 1.2 mg or greater due to PTH class AEs. Serial total serum calcium (0.25-24 hours post-dose) in subjects dosed with 0.8 or 1.2 mg demonstrated a pharmacological effect on serum calcium only at the 1.2 mg dose. This first-in-human trial of inhaled Ostabolin-C demonstrates that it is well tolerated and stimulates cAMP and markers of bone formation to the same extent as SC Ostabolin-C. Inhaled Ostabolin-C represents a convenient alternative to daily injections for patients who require PTH therapy.

Disclosures: P. Morley, Zelos Therapeutics Inc. 1, 3, 4.

This study received funding from: Zelos Therapeutics Inc.

S423

Efficacy of Adding Teriparatide Versus Switching to Teriparatide in Postmenopausal Women with Osteoporosis Previously Treated with Raloxifene or Alendronate. F. Cosman¹, R. A. Wermers², C. Recknor³, K. F. Mauck⁴, L. Xie⁴, E. V. Glass⁴, J. H. Krege⁴. ¹Helen Hayes Hospital, West Haverstraw, NY, USA, ²Mayo Clinic, Rochester, MN, USA, ³United Osteoporosis Centers, Gainesville, GA, USA, ⁴Eli Lilly and Company, Indianapolis, IN, USA.

In patients previously treated long term with antiresorptive drugs, information regarding the relative efficacy of adding teriparatide (TPTD, 20 mcg/d) versus switching to TPTD is not available. Postmenopausal women with osteoporosis previously treated for at least 18 months with alendronate (ALN, 70 total mg/week, median treatment duration 37.3 months) or raloxifene (RLX, 60 mg/d, median treatment duration 36.9 months) were randomized to either add TPTD or switch to TPTD for 6 months. A preplanned 12-month extension of this study is currently ongoing. Efficacy results included markers of bone turnover and DXA BMD. Baseline BMD and other characteristics were well matched with the exception that previous ALN patients had lower baseline bone turnover than previous RLX patients (Table). Adding TPTD conferred smaller increases in bone turnover versus switching to TPTD; these differences were more marked between the groups previously treated with ALN. However, adding TPTD conferred greater increases in BMD versus switching to TPTD; these differences were again more marked between the groups previously treated with ALN. All regimens were well tolerated. In conclusion, an anabolic response to TPTD was observed in patients previously treated with ALN or RLX regardless of whether the previous antiresorptive drug was continued or discontinued. In general, greater bone turnover was achieved by switching from antiresorptive to TPTD, while greater BMD increase was achieved by continuing antiresorptive during TPTD treatment.

Table: Baseline and change from baseline after 6 Months of TPTD Treatment.

Variable	Alendronate Pretreated				Raloxifene Pretreated			
	TPTD (N=50)	6-Mo Δ	TPTD+ALN (N=52)	6-Mo Δ	TPTD (N=49)	6-Mo Δ	TPTD+RLX (N=47)	6-Mo Δ
PINP (µg/L)	27.5	101.5 (400.9%*)	30.0	21.5 (69.1%*†)	43.0	103.0 (245.7%*)	42.0	62.5 (125.4%*†)
BSAP (U/L)	20.1	11.9 (73.3%*)	20.3	3.1 (16.1%*†)	25.1	9.7 (38.6%*)	27.1	8.1 (30.6%*)
CTx (ng/ml)	0.16	0.40 (231.0%*)	0.18	0.05 (28.6%*†)	0.31	0.37 (136.1%*)	0.28	0.14 (64.6%*†)
LS DXA BMD (g/cm ²)	0.86	0.012 (1.9%**)	0.82	0.033 (4.5%*†)	0.84	0.034 (4.2%*)	0.84	0.037 (4.6%*)
FN DXA BMD (g/cm ²)	0.66	0.0001 (0.1%)	0.66	0.004 (0.7%)	0.66	0.002 (0.3%)	0.67	0.012 (1.9%**)
TH DXA BMD (g/cm ²)	0.72	-0.007 (-0.8%)	0.73	0.009 (1.4%*†)	0.72	0.003 (0.5%)	0.73	0.013 (1.8%*†)

For bone markers, values are median baseline, median absolute change from baseline (% change). For BMD, values are mean baseline, mean absolute change from baseline (% change). BL, baseline; PINP, amino-terminal propeptide of type I collagen; BSAP, bone specific alkaline phosphatase; CTx, C-terminal telopeptide of type I collagen; LS, lumbar spine; FN, femoral neck; TH, total hip. P-values are based on percent changes. *P<0.001 and **P<0.05 within group from baseline; †P<0.001 and ‡P<0.05 between groups within a stratum.

Disclosures: F. Cosman, Eli Lilly and Company 2, 5, 8; Merck 5, 8.

This study received funding from: Eli Lilly and Company.

S425

Correlations between Bone Turnover Markers and BMD in Patients treated with Teriparatide or Alendronate for Glucocorticoid-induced Osteoporosis. A. L. Burshell¹, R. Möricke², R. Correa-Rotter³, P. Chen^{*4}, M. R. Warner^{*4}, J. H. Kregge⁴. ¹Endocrinology, Ochsner Clinic Foundation, New Orleans, LA, USA, ²Clinical Research Laboratory, Magdeburg, Germany, ³Nephrology and Mineral Metabolism, National Medical Science and Nutrition Institute, Mexico City, Mexico, ⁴Lilly Research Laboratories, Eli Lilly and Company, Indianapolis, IN, USA.

Correlations between bone turnover markers and BMD were assessed in a double-blind, active-comparator study of anabolic versus antiresorptive treatment for glucocorticoid-induced osteoporosis (GIOP). Men and women taking ≥ 5 mg/d prednisone equivalent for ≥ 3 months prior to screening were randomized to teriparatide (TPTD) 20 mcg/d (N=214) or alendronate (ALN) 10 mg/day (N=214) for 18 months. Markers of bone formation included N-terminal and C-terminal propeptide of type I procollagen (PINP and PICP) and bone-specific alkaline phosphatase (BSAP), and a resorption marker, carboxy-terminal telopeptide of type I collagen (CTX). Morning fasting blood specimens were measured at baseline and at 1 and 6 months. Lumbar spine (LS) and femoral neck (FN) BMD were measured by DXA at baseline and 18 months. Spearman correlation coefficients were calculated for baseline and changes from baseline in biomarkers at 1 and 6 months with changes from baseline in BMD at 18 months (Table). Baseline median glucocorticoid dose was 7.8 and 7.5 mg/d in the ALN and TPTD group, respectively; mean (\pm SD) LS BMD T-score was -2.5 ± 1.0 and -2.4 ± 1.0 in the ALN and TPTD group, respectively. In the ALN group, baseline markers were correlated with change in FN BMD, 1 and 6 month change in PINP and CTX were negatively correlated with increases in FN BMD, and 1 month change in CTX was negatively correlated with increased LS BMD. In the TPTD group, increases in PINP were correlated with gains in LS and FN BMD. In conclusion, bone turnover at baseline was correlated with FN BMD response to ALN but not to TPTD. In the ALN group, decreases in markers were correlated with gains in FN BMD. In the TPTD group, increased PINP was correlated with increased LS and FN BMD. These results demonstrate the opposite mechanism of action of TPTD and ALN in patients treated for GIOP.

Table: Correlation coefficients: baseline markers and the change in markers versus the change in lumbar spine (LS) or femoral neck (FN) BMD

Marker	Time (month)	Alendronate		Teriparatide	
		Lumbar spine	Femoral neck	Lumbar spine	Femoral neck
BSAP	0	-0.01 (66)	0.29 (66)*	-0.03 (61)	0.21 (60)
	$\Delta 1$	0.06 (58)	0.08 (58)	0.04 (52)	0.19 (52)
	$\Delta 6$	-0.19 (63)	-0.05 (63)	0.19 (59)	0.18 (58)
PINP	0	0.02 (72)	0.44 (69)*	0.14 (78)	0.03 (78)
	$\Delta 1$	0.02 (71)	-0.30 (69)*	0.33 (77)*	0.34 (77)*
	$\Delta 6$	-0.13 (70)	-0.34 (67)*	0.23 (77)	0.30 (77)*
PICP	0	0.14 (66)	0.36 (66)*	0.19 (62)	-0.06 (61)
	$\Delta 1$	0.02 (58)	-0.06 (58)	0.18 (53)	0.13 (53)
	$\Delta 6$	-0.15 (63)	-0.15 (63)	0.04 (60)	-0.03 (59)
CTX	0	-0.05 (69)	0.30 (68)*	-0.13 (68)	0.05 (67)
	$\Delta 1$	-0.32 (60)*	-0.29 (59)*	0.16 (57)	0.05 (57)
	$\Delta 6$	-0.21 (62)	-0.28 (62)*	0.18 (59)	0.21 (58)

*P<0.05; (n)

Disclosures: A.L. Burshell, Eli Lilly and Company 2.
This study received funding from: Eli Lilly and Company.

S427

Antagonism of Calcium Sensing Receptor Stimulates Dose-related Release of Endogenous Parathyroid Hormone in Normal Volunteers: A Proof of Concept Study. D. Ethgen¹, T. Danoff^{*1}, M. Schultz^{*1}, D. Tenero^{*1}, A. Anderson^{*1}, G. B. Stroup², S. Kumar¹, A. M. Lago^{*2}, J. F. Callahan^{*2}, P. Bhatnagar^{*1}, W. F. Huffman^{*1}, M. Gowen², L. A. Fitzpatrick¹. ¹GlaxoSmithKline, Collegeville, PA, USA, ²GlaxoSmithKline, King of Prussia, PA, USA.

Calcium sensing receptor antagonists (calcilytics) are a new class of drugs that stimulate bone formation through a PTH-mediated mechanism. Preclinical investigation has shown that briefly antagonizing the calcium receptor (CaR) on the parathyroid gland results in a transient secretion of endogenous PTH, a profile that stimulates bone formation.

SB-423562 is a small molecule with potent short-lived CaR antagonist activity. This was the first clinical study administering this compound to healthy male volunteers. Safety and tolerability, as well as preliminary pharmacokinetics and pharmacodynamics of a single IV administered rising doses were investigated.

A single 10-minutes IV infusion of SB-423562 (dose range 0.02 to 5.0 mg) in 28 healthy adult male humans resulted in a strong dose-related transient PTH release at varying dose levels.

Pharmacokinetic measurements showed that SB-423562 was quantifiable for 0.25 h post-dose (155 μ g dose) up to 3 h post-dose (5.0 mg dose). SB-423562 area under the concentration-time curve (AUC) and maximal observed plasma concentration (C_{max}) increased in an approximately dose-proportional manner. The elimination half-life, where estimated, was <1 h. Total clearance was moderate (approximately 500 mL/min). Volume of distribution was approximately 20 L.

SB-423562 produced a strong endogenous PTH release profile, particularly at 1.25 mg, 2.5

mg and 5.0 mg. Mean T_{max} was 15 minutes or less. Duration of effect was typically less than 1 h. A 3- to 5.5-fold increase in PTH levels relative to baseline was observed with the 1.25, 2.5 and 5.0 mg doses at 10-15 minutes post infusion. At the higher doses (0.625 to 5 mg), a PTH profile was produced that is consistent with bone forming effects observed with previous experience with SC administered PTH (1-34). A dose related effect was observed on total and ionized serum calcium levels.

SB-423562 was generally safe and well tolerated in healthy male volunteers, no deaths, serious adverse events or withdrawals due to adverse events were reported during the study. There were no apparent differences observed across regimen for safety laboratories values, blood pressure and heart rate.

These data provide a proof of principle that a small molecule with CaR antagonizing properties delivered to healthy male subjects can generate endogenous PTH release in a profile compatible with a long term bone forming effect. Further work is ongoing to develop a formulation allowing the oral delivery of this class of drugs to osteoporotic patients.

Disclosures: D. Ethgen, GlaxoSmithKline 3.

S430

Low Energy Femoral Diaphyseal Fractures Associated with Alendronate Use. B. Lenart^{*}, A. Neviasser^{*}, M. G. Peterson^{*}, F. Edobor-Osula^{*}, B. Schreck^{*}, C. Chang^{*}, D. G. Lorich^{*}, J. M. Lane. Orthopedic Surgery, Hospital for Special Surgery, New York, NY, USA.

The purpose of this study was to elucidate a correlation between prolonged alendronate use and low energy subtrochanteric and shaft fractures in postmenopausal women.

We performed a retrospective case-control study to investigate our hypothesis. Cases were defined as postmenopausal women with low energy subtrochanteric/shaft fractures verified by xray who presented from 2000-2007 at a university hospital. Controls were postmenopausal women matched by age, race and body mass index with low energy intertrochanteric or femoral neck fractures. Forty one cases were identified and matched to 82 controls, one intertrochanteric and femoral neck fracture each. Patients with diseases or drugs known to affect bone metabolism were excluded.

Alendronate use occurred at a rate of 36.6% in the cases, significantly higher than the 11% observed in controls (p<.001) with an odds ratio of 4.68 for subtrochanteric/shaft fractures with alendronate use (95% CI, 1.83-11.98). Furthermore, alendronate was the bisphosphonate prescribed in each of the cases, which was significantly different than that expected based on 2003 estimates of proportion of bisphosphonates prescribed (p=.042). Logistic regression analysis showed that calcium and alendronate were most significantly associated with cases (p=.09 and p=.003 respectively). Baseline characteristics of cases and controls were similar except serum calcium, which was significantly lower in the cases (p=.02). Patients with subtrochanteric/shaft fractures taking alendronate also shared a common xray fracture pattern, defined as a simple or oblique fracture with cortical thickening and beaking of the cortex on one side. This xray pattern was highly associated with alendronate use (p<.001) with an odds ratio of 15.33 (95% CI, 3.06-76.90). Patients with the xray pattern had an average duration of alendronate use of 7.3 years, while that for those on alendronate without the xray pattern was 2.8 years (p<.001). Wilcoxon survival analysis yielded significantly different cumulative survival without fracture between these two groups (p=.003). By Spearman's rank correlation, duration of alendronate use was significantly correlated to the ratio of the cortical thickness to diameter (p<.001).

Alendronate treatment historically reduces the rate of hip fracture by 50%. Our study demonstrates that alendronate may actually increase the risk of low energy subtrochanteric and shaft fractures with prolonged use. While this data does not prove a causal relationship, it provides strong evidence that a correlation exists between prolonged alendronate use and femoral diaphyseal fractures.

Disclosures: B. Lenart, None.

S432

The Effect of Risedronate on Risk of Clinical Fracture Among Patients with Prior Hip Fracture. M. R. McClung^{*1}, A. Grauer², X. Zhou^{*2}, P. D. Miller^{*3}, S. Boonen^{*4}. ¹Oregon Osteoporosis Center, Portland, OR, USA, ²Procter & Gamble Pharmaceuticals, Mason, OH, USA, ³Denver Osteoporosis Center, Denver, CO, USA, ⁴University Hospital Leuven, Leuven, Belgium.

Previous hip fracture is a risk factor for subsequent fractures. In this analysis, the anti-fracture efficacy of risedronate was examined among patients with previous hip fracture at baseline.

A total of 339 postmenopausal women between ages 70-79 years with low BMD in HIP trials (McClung, MR et al. 2001 NEJM) had a history of at least one hip fracture prior to study entry. These subjects were treated with either placebo (PLC) or risedronate (RIS) 2.5mg or 5 mg daily. The incidence of osteoporosis-related clinical fracture, defined by the occurrence of the radiographically confirmed clinical vertebral fracture or radiographically confirmed non-traumatic non-vertebral fracture was calculated using Kaplan-Meier survival estimates over a 3 year period and was compared between placebo- and risedronate-treated subjects. Treatments were compared using log rank test, and the risk ratio and its 95% confidence interval were obtained using a Cox regression model stratified for study.

Subjects' mean age was 75 years, and their mean femoral neck (FN) and lumbar spine (LS) T-scores were -3.1 and -3.2 SD, respectively. Baseline characteristics were well balanced between the 3 treatment groups. Over the 0-3 year period, the clinical fracture incidences were 28.4%, 14.9% and 13% for the PLC, RIS 2.5mg and RIS 5mg groups, respectively. Relative to the placebo group, RIS 5mg and 2.5 mg statistically significantly reduced the risk for clinical fracture over 0-3 year period (p<0.05). The risk ratio of clinical fracture was 0.5 for both the risedronate 5mg and 2.5 daily groups relative to the placebo group.

Risedronate treatment was well tolerated in HIP trial.

Risedronate significantly reduced the risk of clinical fracture among women with postmenopausal osteoporosis with prior hip fracture.

Table: Incidence of Clinical Fracture (According to Kaplan-Meier Survival Estimates) among Patients with Prevalent Hip Fracture

Placebo	Ris 2.5mg	Ris 5 mg	Ris 2.5 or 5 mg
27/111 (28.4%)	15/122 (14.9%)	12/106 (13.0%)	27/228 (14.1%)
	0.50 (0.26, 0.95)	0.50 (0.25, 1.00)	0.50 (0.29, 0.86)
	p=0.031	p=0.048	p=0.011

Disclosures: M.R. McClung, Procter & Gamble Pharmaceuticals 5.

S434

The Effects of Zoledronic Acid 5 mg Once-Yearly on Bone Remodeling and Structure in Osteoporotic Women Are Consistent Across Age. R. R. Recker¹, P. Delmas², I. Reid³, S. Boonen⁴, J. Halse⁵, P. Garcia⁶, J. Supronik⁷, M. Lewiecki⁸, L. Ochoa⁹, P. Miller¹⁰, F. Hartl¹¹, J. A. Gasser¹¹, P. Mesenbrink¹², H. Hu¹², E. Eriksen¹¹. ¹Creighton Univ. Osteoporosis Res. Center, Omaha, NE, USA, ²Univ. of Lyon, INSERM Res. Unit 831, Lyon, France, ³Univ. of Auckland, Auckland, New Zealand, ⁴Univ. Ziekenhuizen K.U., Leuven, Belgium, ⁵Osteoporoseklínikken, Oslo, Norway, ⁶Hosp. Univ., Monterrey, Mexico, ⁷Sniadecki Hosp., Bialystok, Poland, ⁸New Mexico Clin. Res. & Osteoporosis Center, Albuquerque, MN, USA, ⁹OSTEOSOL COMOP, Col. Hipodromo, Mexico, ¹⁰Colorado Center for Bone Res., Lakewood, CO, USA, ¹¹Novartis Pharma AG, Basel, Switzerland, ¹²Novartis Pharmaceuticals Corp, East Hanover, NJ, USA.

In the pivotal fracture trial establishing the antifracture efficacy of once-yearly infusions of zoledronic acid (ZOL) 5 mg in women with postmenopausal osteoporosis aged 64-89, we tested whether tissue level responses to ZOL differed with age by analyzing changes in bone remodeling and bone structure between treatment and placebo (PLB) in 3 age groups: < 70, 71-74 and ≥ 75 yrs. Bone remodeling indices were assessed in tetracycline labeled biopsies obtained from 43 patients on ZOL and 49 on PLB (Table 1). Prior to histomorphometric analysis, trabecular bone structure and cortical thickness were assessed on intact biopsy cores by µCT in 50 patients on ZOL and 49 on PLB.

Table 1. Differences (Δ%) in key remodeling and structural indices between ZOL and PLB groups across 3 age groups after 3 yrs.

	<70			70-74			≥75		
	ZOL	PLB	Δ%	ZOL	PLB	Δ%	ZOL	PLB	Δ%
Remodeling indices	n=20	n=19		n=13	n=12		n=10	n=18	
Ac.f yr ⁻¹	0.16	0.66	-75.8	0.1	0.32	-68.8	0.08	0.28	-71.4
MAR µm/day	0.62	0.53	17.0	0.661	0.494	33.8	0.48	0.51	-5.9
MS/BS %	1.67	9.42	-82.3	0.98	4.91	-80.0	0.49	4.57	-89.3
BFR/BV mm ³ /mm ³ /yr	0.064	0.318	-79.9	0.051	0.139	-63.3	0.035	0.144	-75.7
OS/BS %	6.54	21.9	-70.1	9.18	15.46	-40.6	3.86	17.88	-78.4
Structural indices	n=25	n=19		n=15	n=12		n=10	n=18	
BV/TV %	17	13.6	25.0	16.2	13.3	21.8	14.3	13.1	9.2
Tb.N mm ⁻¹	1.28	1.23	4.1	1.38	1.22	13.1	1.27	1.21	5.0
Tb.Sp. mm	0.78	0.81	-3.7	0.71	0.83	-14.5	0.79	0.82	-3.7
Tb.Th mm	0.17	0.15	13.3	0.16	0.16	0.0	0.15	0.15	0.0
Ct.Th mm	0.82	0.73	12.3	0.8	0.72	11.1	0.82	0.78	5.1

In the PLB group bone turnover, reflected in activation frequency (Ac.f) and mineralizing surface (MS/BS) decreased with increasing age. Despite this, ZOL induced consistent reductions by 71%, 69%, and 76% across the 3 age groups. Differences between other histomorphometric indices: osteoid surface (OS/BS), mineral appositional rate (MAR), and volume referent bone formation rate (BFR/BV), were stable across age groups. Structural parameters (bone volume (BV/TV), trabecular number (Tb.N), trabecular spacing (Tb.Sp), trabecular thickness (Tb.Th) and cortical thickness (Ct.Th)) indicated preservation of bone structure in patients on ZOL in all age groups, albeit the numerical differences were lower in the oldest age group.

In conclusion, changes in bone remodeling and preservation of bone structure after 3 yrs of treatment with once-yearly doses of ZOL 5 mg iv are similar across all age groups in postmenopausal women aged 64-89 yrs.

Disclosures: R.R. Recker, Novartis Pharma AG 5.

This study received funding from: Novartis Pharma AG.

S435

Mechanistic Bases of Bone Mineral Density Increase During Alendronate Therapy. D. Vashishth¹, P. Chavassieux², G. Boivin², P. D. Delmas². ¹INSERM Unite 831 Université de Lyon France & Rensselaer Polytechnic Institute, Troy, NY, USA, ²INSERM Unite 831 Université de Lyon, Lyon, France.

An increase in the mean degree of tissue mineralization (DMB) occurring through secondary mineralization has been proposed to increase bone mineral density (BMD) during bisphosphonate (BP) therapy [1]. In this study we conducted additional analyses on human iliac crest biopsies obtained as part of alendronate (ALN) clinical trials [2] to identify the mechanistic bases of BMD increase.

Out of a group of 16 patients on a three-year ALN-therapy [1], we identified two groups of 5 patients each showing lower (8.5 %) and higher (13.3%) bounds of BMD increase but no difference in baseline BMD. For all 10 patients, previously prepared microradiographs were reanalyzed to measure the mean degree of tissue mineralization (DMB) at the osteonal and interstitial compartments in both cortical and cancellous bone tissues. Based on a moving average analysis, six fields each of cortical and cancellous bone tissues were randomly selected for measurement from each biopsy. The average values for patients in each group within osteonal and interstitial compartments were compared between and across cortical and cancellous bone tissues. All DMB measurements were also tested for correlation with standard histomorphometric measures of bone structure (BV/TV, Tb.Th, Tb. Separation, Tb.N), osteoclast activity (EV/BV, E-Depth, Oc#/BS), osteoid (OS/BS, OV/BV, OTh), and bone formation (MAR, BFR/BS, FP) reported previously [2]. The low-BMD-gain group demonstrated no difference between the osteonal and interstitial bone compartments within cortical or cancellous bone tissues but demonstrated a higher DMB in cancellous than in cortical tissue (p<0.05). In contrast, the high-BMD-gain group showed higher DMB in interstitial than in osteonal compartment for both cortical and cancellous tissues as well as a higher DMB in cancellous than in cortical tissue (p<0.05). Out of all the DMB measures in cortical and cancellous tissues, only cortical bone interstitial level DMB correlated to bone formation rate (BFR/BS) (r = -0.86; p = 0.006) and formation period (FP) (r = -0.75; p = 0.04).

In conclusion, this study demonstrates that the effects of ALN-therapy are more evident in cancellous than in cortical bone. Moreover since the interstitial level DMB is at least partially dependent on the duration of secondary mineralization, and negatively correlated to formation parameters, slow bone formation rate and longer bone formation period produce conditions conducive to complete secondary mineralization and consequently larger BMD gain.

References: [1] Boivin et al. Bone. 2000 5: 687-94. [2] Chavassieux et al. JCI 1997 100:1475-80.

Disclosures: D. Vashishth, Merck 5.

This study received funding from: INSERM, France & NIH Grants AR49635, AG20618.

S437

Mineralization Status of Bone Matrix in Postmenopausal Women During a 10-year Alendronate Treatment Period. P. Roschger¹, G. Mair², N. Fratzl-Zelman¹, P. Fratzl², D. Kimmel³, K. Klaushofer¹, A. LaMotta³, A. Lombardi³.

¹Ludwig Boltzmann Institute of Osteology at the Hanusch Hospital of WGKK and AUVA Trauma Centre Meidling, 4th Med. Dept., Hanusch Hospital, Vienna, Austria, ²Max Planck Institute of Colloids and Interfaces, Dept Biomaterials, Potsdam, Germany, ³Merck Research Laboratories, Rahway, NJ, USA.

Knowledge of the effects of long-term antiresorptive treatment on bone material quality is an important issue for the safety and optimal duration of treatment. Mineralization density distribution (BMDD) as well as mineral particle thickness, both important composite parameters of bone material, were studied by quantitative backscattered electron imaging (qBEI) and small angle x-ray scattering (SAXS). Previously published data of biopsies from Phase III alendronate studies of 2 or 3 years treatment duration (placebo, n=12, alendronate (ALN), n=12) were compared to data obtained from the FLEX study (fracture intervention trial long-term extension) (5 yrs ALN + 5yrs placebo, n=14 and 10 yrs ALN, n=16). The mean (CaMean) and the most frequent calcium (CaPeak) concentration, the heterogeneity in mineralization (CaWidth) and the amount of low mineralized bone area (primary mineralization) (CaLow) were determined. ALN treatment for 5 yrs, followed by 5 yrs of placebo treatment resulted in an increase of CaMean (+3.5%) and CaPeak (+2.4%) compared to the group treated with placebo for 2 or 3 yrs. Continuous treatment with ALN for 10 years did not further increase CaMean and CaPeak. Remarkably, the decrease in CaWidth (-14.5 %) observed with 2 or 3 yrs ALN treatment was reversed after 5 yrs and 10yrs ALN treatment, respectively. This transient narrowing of the BMDD around 3 yrs is consistent with computer modeling of BMDD and indicates the effect on BMDD by the sudden decrease in bone turnover during ALN treatment. In none of the investigated cases CaMean and CaPeak values did exceed those of normal adult trabecular bone, nor did the mean mineral particle thickness parameter get out of the normal range (3.5 to 4.2 nm). Our data support the hypothesis that antiresorptive treatment with ALN should be maintained for 3 to 5 years and that there are no negative effects on bone matrix mineralization even with longer treatment.

Disclosures: P. Roschger, None.

This study received funding from: Merck.

S440

Bisphosphonates Adherence and Fracture Risk: Time-Dependent Relationships from 103,038 Bisphosphonate Users in the U.S. J. R. Curtis¹, A. Westfall^{*1}, H. Cheng¹, E. Delzell^{*1}, K. Lyles², K. G. Saag¹. ¹University of Alabama at Birmingham, Birmingham, AL, USA, ²Duke University, Durham, NC, USA.

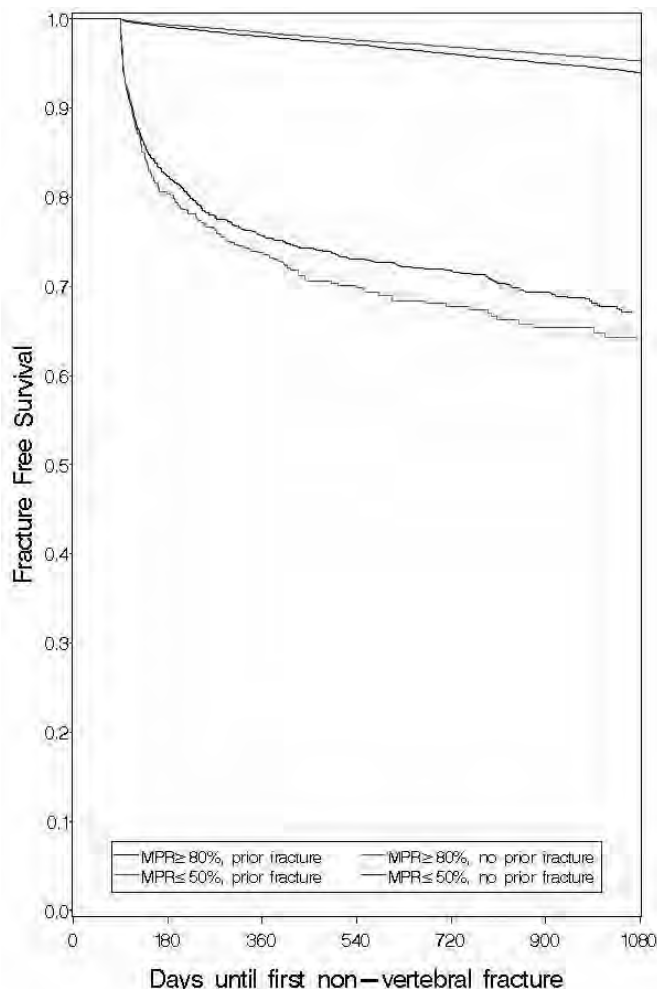
Background: There is high interest in determining if there is a 'threshold' level of real-world adherence to bisphosphonate (BP) therapy, after which additional fracture (fx) risk reduction is minimal.

Methods: Using the claims and pharmacy databases of a large consolidated health plans database, we identified persons initiating alendronate or risedronate (no use in prior 6 months) and calculated adherence as a Medication Possession Ratio (MPR: number of days of BPs dispensed divided by the calendar time since BP initiation (the index date)). Claims data identified non-vertebral fx's occurring after the index date. Survival analyses compared fx rates of persons with MPR $\geq 80\%$ (adherent) vs. those with MPR $\leq 50\%$ (non-adherent) at 90 days, stratifying by history of fx in the 6 months prior to the index date. We then examined fx rate by 10% increments of MPR and characterized MPR in a time-dependent fashion in sequential 3 month intervals. This analysis was repeated excluding those who did not have BPs dispensed for at least 90 days with the expectation that these 'very non-adherent' individuals might confound the adherence-fx relationship.

Results: We identified 103,038 new BP users, mean age 62.2 ± 8.2 (SD) years. Overall, there was a significant relationship between adherence and fx risk ($p < 0.0001$ between adherence groups); survival curves stratified by prior fx (yes/no) are shown (Figure). At 3 years, the absolute fx rate of the adherent vs. the non-adherent was 4.6% vs. 5.6% (number needed to treat = 103). Among those with prior fx, the rate was 35.8 vs. 38.9% (number needed to treat = 32).

The relation between adherence (in 10% increments) and fx was linear with no inflection point observed. After excluding patients who did not have BPs dispensed for at least 90 days, the relation between adherence and fx was curvilinear with an inflection point at MPR = 40-50%.

Conclusions: Adherence with BPs is an important determinant of fx rates, although the number of adherent patients needed to treat to prevent one fx is strongly determined by additional risk factors such as prior fx. The overall relation between adherence and fx is monotonic; although, likely subject to unmeasured confounding. However, even after partially accounting for this confounding, the incremental benefit in fx risk reduction with increasing adherence remained.



Disclosures: J.R. Curtis, Novartis 2; Amgen 2; Merck 2, 5, 8; Procter & Gamble 5, 8. This study received funding from: Novartis.

S443

Modeling the Contribution of Long-term Persistence with Weekly or Yearly Bisphosphonate Treatment to Fracture Outcomes. S. Rietbroek^{*1}, M. Olson², T. van Staa^{*1}. ¹General Practice Research Database, London, United Kingdom, ²Novartis Pharmaceuticals, Basel, Switzerland.

Purpose: The objective of this study was to evaluate the impact of improving long-term persistence on fracture outcomes.

Methods: The study population included patients prescribed alendronate or risedronate in the UK General Practice Research Database (GPRD). Individualised probabilities of fracture and death during bisphosphonate therapy and of treatment persistence were estimated by age, gender, dosage regimen, calendar year and clinical risk factors using Cox-regression. Persistence was calculated by measuring repeat prescribing. A unique patient-based pharmacoeconomic model was then developed using these probabilities. By varying the persistence probabilities in a simulation, the fracture outcomes with different scenarios of persistence were then evaluated. The model included seven different fracture types, with weighting of different types by post-fracture mortality. The outcomes were simulated over a 4-year period (maximum of 3 years of bisphosphonate use followed by 1 year of offset). It was assumed that the bisphosphonate users had experienced similar fracture reductions as observed in clinical trials and that weekly and yearly bisphosphonates had similar relative rates of fracture risk reduction.

Results: The study population included 43,525 patients. The 1-year persistence for weekly bisphosphonate in the model was 56.7% and 3-year persistence 35.3%. Modeling showed that improvement of the 3-year persistence by 20% (over current persistence in GPRD) would prevent an additional 41.3 hip fractures per 10,000 patients with weekly treatment. If weekly treatment (with refill at 4 week periods) was substituted with yearly treatment (refill once a year), an additional 28.7 hip fractures (per 10,000 patients) would be prevented. If 3-year persistence improved by 20% with yearly treatment, an additional 75.7 hip fractures would be prevented compared to monthly bisphosphonates. The effects of this substitution were largest in elderly patients and in women. Yearly bisphosphonates would prevent an additional 64.8 hip fractures in women aged 80+ compared to weekly bisphosphonates (with equal 3-year persistence), while this number was 3.5 in men aged 40 to 49. **Conclusion:** This study found that the switch of weekly to yearly bisphosphonates may prevent additional fractures due to the longer treatment.

Disclosures: T. van Staa, Novartis Pharmaceuticals 2.

This study received funding from: Novartis Pharmaceuticals.

S447

Bone Material Characteristics in Osteoporotic Postmenopausal Women after 3-year Treatment with Strontium Ranelate. C. Li^{*1}, P. Roschger², R. Zoehrer^{*2}, I. Manjubala^{*1}, E. P. Paschalis², N. Fratzl-Zelman², P. Fratzl^{*1}, K. Klaushofer². ¹Max Planck Institute of Colloids and Interfaces, Department of Biomaterials, 14424 Potsdam, Germany, ²Ludwig Boltzmann Institute of Osteology at the Hanusch Hospital of WGKK and AUVA Trauma Centre Meidling, 4th Medical Department, Hanusch Hospital, Vienna, Austria.

Three-year treatment of postmenopausal osteoporotic women with strontium ranelate is reported to reduce the risk of vertebral and hip fractures by 41% and 36%, respectively. The underlying mechanism of strontium may involve an effect on bone material properties. Biopsies (kindly provided by Servier) from osteoporotic women treated for 3 years with strontium ranelate (n=6) or placebo (n=6) were investigated using complementary nondestructive scanning methods like quantitative backscattered electron imaging (qBEI), x-ray microanalysis (EDX), scanning small- and wide-angle x-ray scattering (sSAXS/sWAXS), and Fourier transform microspectroscopy (FTIRM). qBEI gray level histograms of strontium ranelate-treated subjects showed a distinct shift to bone material with higher average atomic number compared with placebo-treated subjects, which is consistent with the incorporation of Sr (Z=38), which has a higher atomic number than calcium (Z=20). EDX analysis of small selected areas (10x10 μm) within individual bone packet areas revealed that Sr was present in a molar fraction up to 6 %, exclusively in bone packets newly formed during strontium ranelate treatment, while the old bone packets (most likely generated before strontium ranelate treatment was started) had only marginal amounts of Sr (close to the detection limit of the method). As previously shown by others, global mean bone Sr content obtained by destructive chemical analysis was $1.56\% \pm 0.30\%$ (Sr/Sr+Ca %mol/mol). WAXS line scans across the bone packets detected an increase in the hydroxyapatite crystal lattice spacing (c-axis) consistent with the number of Ca atoms replaced by Sr atoms (up to 0.5 of the 10 calcium ions composing each unit cell replaced by 0.5 Sr ions), indicating that Sr is incorporated into the bone mineral. Area scans by sSAXS failed to reveal any Sr-dependent changes in mean mineral particle thickness (3.1 to 3.6 nm). FTIRM analysis of trabecular bone did not detect any differences in collagen cross-link ratio (pyr/deH-DHLNL) between placebo and strontium ranelate treatment. In conclusion, after 3 years of treatment with strontium ranelate, strontium was only found in newly formed bone, with preservation of examined bone material characteristics.

Disclosures: K. Klaushofer, None.

This study received funding from: Servier.

S452

Vitamin-D 800 IU/Day + Calcium 1000 mg Supplementation Decreases the Risk of Falling Among Postmenopausal Ambulatory Women - A Population-based, Randomized, 3-Year Study (OSTPRE-FPS). M. Kärkkäinen^{*1}, M. Tuppurainen¹, T. Rikkonen^{*1}, K. Salovaara², J. Sirola^{*2}, R. Honkanen¹, E. Alhava^{*3}, H. Kröger². ¹Bone and Cartilage Research Unit, University of Kuopio, Kuopio, Finland, ²Department of Orthopaedics and Traumatology, Kuopio University Hospital, Kuopio, Finland, ³Department of Surgery, Kuopio University Hospital, Kuopio, Finland.

Vitamin D insufficiency and subsequent secondary hyperparathyroidism are common especially in Northern latitude. Vitamin D insufficiency has been related to low bone mass, falls and fractures. In this 3-year population-based randomized trial (OSTPRE-FPS) we hypothesized that Vitamin-D and Calcium supplementation improves muscle strength, functional capacity and decreases falls in ambulatory postmenopausal women.

The present study population consisted of 606 ambulatory women age varied from 66 to 71 years (mean (SD) 68.5 (1.7)) who belong to the OSTPRE-FPS cohort (n=3432). The intervention group (n=292) obtained Cholecalciferol 800 IU/d + Calcium 1000 mg/d supplementation (Calcichew-D3 Forte, Leiras-Nycomed Ltd) for 3 years and the control group (n=314) received no supplementation.

Falls (ICD10 W00-W19) were recorded based on phone inquiry done at 4 months intervals. The functional capacity tests included: standing-on-one-foot, squat down, chair rising, standing eyes closed 10s, fast regular walk 10m, tandem walk 6m, grip and leg extension strength measurements.

A total of 873 falls in 364 subjects were recorded during the 3-year follow up. There were 381 falls in 165 women in Vitamin D-supplementation group and 492 falls in 199 women in the control-group. Thus, the vitamin-D and calcium supplementation decreased the incidence of falls by 23 % (p=0.039). Results in chair rising test and leg extension strength improved in the supplementation group (p=0.002 and p<0.001, respectively) but the difference between the groups did not reach statistical significance.

In conclusion, Cholecalciferol 800 IU + Calcium 1000 mg supplementation is effective in fall prevention among ambulatory postmenopausal women. The positive effect may be mediated through improvements in lower extremity muscle strength and balance.

Disclosures: M. Kärkkäinen, None.

This study received funding from: Leiras-Nycomed Ltd, Academy of Finland, EVO grant of the Kuopio University Hospital.

S459

Antiinflammatory Role of Osteoprotegerin (OPG) in the Pathophysiology of Osteoporosis and Arteriosclerosis. C. Kasperk¹, U. Liegibel^{*1}, U. Sommer^{*1}, U. Wolf^{*1}, I. Grafe^{*1}, L. Basler^{*2}, P. Nawroth^{*1}, P. J. Meeder^{*2}. ¹Internal Medicine I, Endocrinology, University of Heidelberg, Heidelberg, Germany, ²Orthopedic Surgery, University of Heidelberg, Heidelberg, Germany.

Osteoporosis and arteriosclerosis are associated diseases which have numerous genetic, cellular and epidemiological characteristics in common, e.g. OPG^{-/-} mice develop osteoporosis and arteriosclerosis (Bucay et al. Genes Develop 12:1260, 1998). Previously, we demonstrated that mechanical stress by cellular elongation exerts a stimulatory effect on OPG production of osteoblastic cells Liegibel et al. J Exp Med 196:1387, 2002). We hypothesized that there is a biphasic response of the OPG gene to mechanical stress in osteoblastic (OC) and endothelial cells (EC) and that OPG exerts an antiinflammatory action on bone and endothelial cell metabolism implicating a direct effect of OPG on OC and EC. We exposed primary human OC and EC (HUVEC) to elongation stress (ES) using a Flexer cell device. ES up to 2.5 % of initial cell length stimulated OPG production in OC (200 % of control) and had no effect on OPG in EC. ES > 10 % inhibited OPG production in OC down to 50 % and in EC to 15 % of control. OPG increased ERK-1 and -2 phosphorylation and α v β 3 integrin production in OC and EC, effects which could be inhibited by antiRANKL antibodies and the MAP kinase inhibitor PD98059, respectively. The proinflammatory cytokine TNF α stimulated IL-6 production in OC and EC which could be inhibited by an OPG co-treatment in both cell types. Interestingly, TNF α and IL-1 β decreased alkaline phosphatase activity (AP) in OC but increased AP in EC. However, a combined treatment of OC and EC with the proinflammatory cytokines TNF α or IL-1 β together with OPG converted the cytokines' effects on AP and thus exerted a stimulation of AP in OC whereas in EC the AP activity was significantly decreased by the cytokine-OPG co-treatment. In order to clarify antiinflammatory OPG effects we examined a possible action of OPG on I κ B and observed a stimulatory action of OPG on I κ B production in OC and EC. In summary, in both OC and EC (1) ES exerts a biphasic effect on OPG production, (2) OPG directly activates MAP kinases and stimulates α v β 3 integrin and I κ B production, (3) TNF α and IL-1 β stimulate IL-6 production which can be inhibited by OPG co-treatment, and (4) TNF α and IL-1 β decreased AP in OC but increased AP activity in EC; OPG-co-treatment converted the inhibitory action of TNF α and IL-1 β and thus resulted in a stimulation of AP in OC and decreased AP activity in EC. In conclusion, OPG is an antiinflammatory cytokine which exerts direct effects on OC and EC metabolism. Locally decreased OPG production may contribute to localized osteoporosis in bone and to mineralization processes closed to branching blood vessels.

Disclosures: C. Kasperk, None.

S466

Alpha/Beta-T Cells Do Not Modulate Androgen Withdrawal-induced Bone Loss in Aged Rats. R. G. Erben, K. Mildner^{*}, C. Schüller^{*}, M. Skalicky^{*}. Dept. of Natural Sciences, University of Veterinary Medicine, Vienna, Austria.

T lymphocytes are thought to play an important role in the regulation of bone turnover. To explore further the role of T lymphocytes in sex steroid deficiency-induced bone loss, we developed a T cell depletion model in aged Fischer rats. Twelve-month-old male Fischer 344 rats were either thymectomized (TX) or sham-operated (SHAM-TX). Beginning 2 weeks postsurgery, TX rats received 3 intraperitoneal injections (every 3 days) of 20 mg/kg of a monoclonal mouse anti-rat antibody directed against the rat α / β -T cell receptor. SHAM-TX animals received 20 mg/kg of a non-immune monoclonal mouse isotype control antibody. T cell depletion was monitored by FACS analysis of peripheral blood. Three weeks after T cell depletion, TX and SHAM-TX rats were orchietomized (ORX) or sham-operated (SHAM). All animals were killed 2 months post-ORX after fluorochrome double labeling. The data were analyzed by two-way analysis of variance (ANOVA), determining the influence of the factors TX and ORX and their mutual interaction.

FACS analysis revealed that intraperitoneal injection of TX rats with high dose anti-rat α / β -T cell receptor antibody resulted in a lasting depletion of circulating α / β -T cells. As expected, 2-way ANOVA showed that ORX induced pronounced loss of total and trabecular bone mineral density (BMD) of the proximal tibial metaphysis and of the fourth lumbar vertebral body measured by peripheral quantitative computed tomography (pQCT), 2 months post-ORX. TX by itself had no influence on tibial or vertebral BMD, and significant two-way interactions between the factors TX and ORX were lacking. The ORX-induced bone loss and the increase in bone resorption as measured by urinary collagen crosslink excretion were identical in T cell-depleted TX and in T cell replete SHAM-TX rats. Thus, our study provides evidence that circulating α / β -T cells are not involved in the up-regulation of bone turnover and the subsequent bone loss induced by androgen withdrawal in aged male rats.

Disclosures: R.G. Erben, Schering 2, 5; Procter & Gamble 2; Amgen 2; AiCuris 5.

This study received funding from: German Research Foundation.

S468

High Cardiovascular Risk in Men with Increased Bone Resorption or Low Bone Mass. P. Szulc, P. D. Delmas. INSERM 831, Hôpital E. Herriot, Lyon, France.

Recent studies suggest the existence of an association between bone mineral density (BMD) and cardiovascular disease. We studied the predictive value of BMD and biochemical bone turnover markers (BTM) for major cardiovascular events (myocardial infarction, stroke) in 628 men aged 50 years and over in whom 61 such events occurred during an 8-year follow-up. At baseline, BMD was measured at the lumbar spine, hip, whole body and distal forearm. After adjustment for age and co-morbidities, lower BMD at all sites of measurement was associated with an increased risk of cardiovascular event (O.R. = 1.25 to 1.55 per 1 standard deviation decrease, p<0.04-0.002). Low BMD, defined by T-score<-1, was associated with a twofold increase in the cardiovascular risk, e.g. whole body BMD - O.R. = 2.63, 95% C.I.: 1.49-4.65, p<0.001). Elevated levels of the urinary markers of bone resorption were defined by 1 standard deviation above the mean in men aged 50 to 60 years. After adjustment for age, co-morbidities, serum creatinine concentration and season, elevated levels of urinary markers of bone resorption were associated with a higher risk of the cardiovascular event (total deoxypyridinoline - O.R. = 2.90, 95% C.I.: 1.41-5.98, p<0.005; free deoxypyridinoline - O.R. = 2.24, 95% C.I.: 1.13-4.44, p<0.03; β -CTX-I - O.R. = 2.37, 95% C.I.: 1.09-5.16, p<0.03). Bone formation markers did not predict the cardiovascular event.

To the best of our knowledge, this is the first study showing that the increased bone resorption is associated with an increased risk of myocardial infarction and stroke in elderly men. We also confirm that low BMD is associated with an increased cardiovascular risk in elderly men.

Disclosures: P. Szulc, None.

S471

Homocysteine Levels and Risk of Hip Fracture in Postmenopausal Women with Poor Renal Function: The Women's Health Initiative Observational Study. M. S. LeBoff¹, R. Narweker^{*1}, A. LaCroix^{*2}, L. Wu^{*2}, R. Jackson^{*3}, J. Lee^{*4}, D. C. Bauer^{*5}, C. Kooperberg^{*2}, J. Cauley^{*6}, S. Cummings^{*7}.

¹Endocrine-Hypertension, Brigham and Women's Hospital, Boston, MA, USA, ²Fred Hutchinson Cancer Research Center, Seattle, WA, USA, ³Ohio State University, College of Medicine and Public Health, Columbus, OH, USA, ⁴University of California, Davis, CA, USA, ⁵San Francisco Coordinating Center, CPMC Research Institute, San Francisco, CA, USA, ⁶University of Pittsburgh, Pittsburgh, PA, USA, ⁷University of California, San Francisco, CA, USA.

Hip fractures are the most serious osteoporotic fractures leading to disability and increased mortality. Recent studies suggest that high homocysteine levels are associated with an increased risk of fractures, although the mechanisms are not fully understood. Women with decreased renal function, as measured by cystatin-C, have elevated homocysteine levels and an increased risk of hip fractures. To assess the relationship between homocysteine levels and renal function on hip fracture risk, we conducted a nested case-control study in the Women's Health Initiative Observational Study (WHI-OS). The WHI-OS, is a multiethnic study among American women (n=93,676) aged 50-79 years at study entry. We selected 400 incident cases of hip fracture and 400 controls matched on age, ethnicity, and blood draw date among women not on treatment for osteoporosis including hormone use at baseline. These analyses were adjusted for body mass index, parental hip fracture history, treated diabetes, alcohol use, smoking, history of stroke, and calcium intake. Serum homocysteine levels were measured using a high-performance liquid chromatography assay. Serum cystatin-C was measured using the Dade Behring BN-II nephelometer with a particle-enhanced immunonephelometric assay (interassay co-efficient of variation=5.7%, sensitivity=0.02 mg/L). The risk of hip fracture increased 1.36-fold (1.13, 1.63) for each SD increase in serum homocysteine level. In multivariate models adjusted for potential confounders, women in the highest quartiles of both homocysteine and cystatin-C (n=111) had a 2.77-fold higher risk of hip fracture (1.60, 4.81) as compared to women in the lowest three quartiles of both homocysteine and cystatin-C (p=0.025 for the interaction). However, women in the highest quartile of homocysteine but lower three quartiles of cystatin-C had an OR= 0.85 (0.53, 1.37) of hip fracture. In summary, high homocysteine levels confer a substantial increased risk of subsequent hip fracture mainly among women with poor renal function.

Disclosures: M.S. LeBoff, None.

This study received funding from: NIH.

S477

Mutations in p62 Linked to Paget's Disease Make the Bone Microenvironment Highly Osteoclastogenic. Y. Hiruma¹, N. Kurihara¹, M. A. Subler^{*2}, H. Zhou³, D. W. Dempster³, S. Ishizuka⁴, G. D. Roodman⁵, J. J. Winkler^{*2}. ¹Medicine/Hem-Onc, University of Pittsburgh, Pittsburgh, PA, USA, ²Human Genetics, Virginia Commonwealth University, Richmond, VA, USA, ³Regional Bone Center, Helen Hayes Hospital, New York, NY, USA, ⁴Teijin Biomedical Research, Tokyo, Japan, ⁵Medicine/Hem-Onc, VA Pittsburgh Healthcare System and University of Pittsburgh, Pittsburgh, PA, USA.

Bone lesions in Paget's Disease (PD) are characterized by abnormal osteoclasts (OCL), markedly increased bone resorption and formation and increased RANKL expression in the bone microenvironment. Genetic factors contribute to the pathogenesis of PD, with mutations in the p62 gene being the most frequently linked to PD. p62 plays a critical role in NF- κ B and p38 MAPK activation induced by TNF- α and RANKL, but the contributions that mutations in p62 make to the abnormalities in OCL and the marrow microenvironment in PD are unclear. To address this question, we generated p62^{P394L/P394L} knock-in (KI) mice that express the most frequent p62 mutation in PD and compared these animals to wild-type (WT) mice. KI mice did not develop PD-like lesions in vivo. However, OCL formation in unfractionated marrow cultures from KI mice was increased and OCL formed at much lower concentrations of RANKL, TNF- α and 1,25-(OH)₂D₃, similar to marrow cultures from PD patients. Since the p62^{P394L} mutation in KI mice was expressed in both OCL precursors and marrow stromal cells, we then cultured highly purified OCL precursors (CFU-GM) and marrow stromal cells from KI mice separately to determine their respective contribution to the enhanced OCL formation. Purified KI OCL precursors were hyper-responsive to RANKL and TNF- α and formed increased numbers of OCL compared to WT. However, unlike PD patients, KI OCL precursors were not hyper-responsive to 1 α ,25-(OH)₂D₃. We then treated stromal cells from WT and KI mice with 1 α ,25-(OH)₂D₃ and determined the levels of RANKL expression. KI marrow stromal cells expressed high levels of RANKL and RANKL mRNA compared to WT. To determine the mechanism responsible for increased RANKL expression, we then examined the effects of the p62^{P394L} on activation of downstream signaling pathways induced by 1 α ,25-(OH)₂D₃ in stromal cells. 1 α ,25-(OH)₂D₃ increased p38 MAPK activity in KI stromal cells, and p38 inhibitors as well as a VDR genomic antagonist decreased RANKL expression. 1 β ,25-(OH)₂D₃, which blocks nongenomic actions of 1 α ,25-(OH)₂D₃, also decreased RANKL expression. These results show that expression of p62^{P394L} in marrow stromal cells markedly increases RANKL production via p38 MAPK and genomic and nongenomic actions of VDR. They also suggest that p62^{P394L} enhances RANKL production by the marrow microenvironment in PD and predisposes but is not sufficient to induce PD.

Disclosures: Y. Hiruma, None.

This study received funding from: NIH.

S482

Mast Cell Migration to Bone Surfaces Precedes and Appears Essential for PTH-induced Peritrabecular Fibrosis. K. Marley¹, M. B. Lowry^{*2}, S. Lotinun^{*1}, U. T. Iwaniec¹, R. T. Turner¹. ¹Oregon State University, Corvallis, OR, USA, ²Microbiology, Oregon State University, Corvallis, OR, USA.

Increased mast cell number is associated with osteoporosis, osteopetrosis and marrow fibrosis. However, no cause and effect relationship has been established between the mast cell and any of these metabolic bone diseases. The presence of mast cells at sites of bone turnover and degranulating mast cells in the immediate vicinity of osteoclasts in rats led to investigation of the mast cell's role in the skeletal response to parathyroid hormone (PTH). Intermittent increases in PTH (iPTH) are anabolic to bone whereas chronic increases in PTH (cPTH) result in multiple skeletal abnormalities (parathyroid bone disease), including focal bone resorption, impaired mineralization and peritrabecular marrow fibrosis. We now report compelling evidence that the mast cell mediates many of the actions of PTH on bone: 1) cPTH induced severe bone disease in rats but not in 3 mouse strains (C57BL6, DBA2, WBB6F1) lacking mature bone marrow mast cells. In addition, the effects of iPTH and cPTH on osteoblasts (OB) and osteoclasts (OC) were greatly attenuated in mice compared to rats. 2) Both iPTH and cPTH resulted in rapid migration of mast cells to bone surfaces in rats with the mast cells adhering to OB in response to iPTH, and to fibroblasts in response to cPTH. In a time-course study, cPTH induced rapid mast cell migration to bone surfaces. By day 3, mast cells at the bone surface were increased 3-fold but peritrabecular fibrosis was not detected until day 5. This suggests that mast cell signaling stimulates fibroblast proliferation and facilitates migration of fibroblasts to bone surfaces. In support of this hypothesis, mast cells produce PDGF, a profibrotic cytokine. Administration of Trapidil, a PDGF receptor antagonist, did not impede mast cell migration to bone surfaces but suppressed cPTH-induced fibrosis, suggesting a critical chemotactic role for this mast cell-derived factor on fibroblasts. 3) Kit signaling mediates mast cell migration. OB lineage cells produce kit ligand (stem cell factor) which is chemotactic to mast cells. The Kit antagonist Gleevec prevented mast cell migration to bone surfaces and inhibited fibrosis. 4) Kit signals through phosphatidylinositol 3-kinase (PI3K) to initiate mast cell degranulation. The PI3K inhibitor wortmannin dramatically reduced fibrosis in rats treated with cPTH, suggesting a critical role for this pathway in cPTH-induced fibrosis. Taken together, these findings indicate that mast cell migration to bone surfaces precedes and is obligatory for cPTH-induced peritrabecular fibrosis and suggest that mast cells potentiate the bone anabolic effects of iPTH as well as the catabolic effects of cPTH.

Disclosures: K. Marley, None.

S484

Marked Improvement of Cortical Bone Geometry After Parathyroidectomy in Postmenopausal Women with Primary Hyperparathyroidism. M. Yamauchi¹, R. Nomura^{*2}, H. Kaji², S. Yano¹, T. Yamaguchi¹, T. Sugimoto¹. ¹Internal Medicine 1, Shimane University Faculty of Medicine, Izumo, Japan, ²Division of Endocrinology/Metabolism, Neurology and Hematology/Oncology, Kobe University Graduate School of Medicine, Kobe, Japan.

Cortical bone geometry is one of the most important factors of bone quality. It has been reported that recombinant human PTH(1-34) treatment induced beneficial changes in cortical geometry and our cross-sectional study from women with primary hyperparathyroidism (pHPT) revealed that endogenous PTH excess markedly affected cortical bone geometry (JCEM 2003). On the other hand, our six-year longitudinal study in postmenopausal women with pHPT revealed that parathyroidectomy (PTX) led to marked and sustained increase in bone mineral density (BMD) (Clin Endocrinol 2004). However, no data have been available about geometric changes of cortical bone after PTX in pHPT. In the present study, we assessed the longitudinal effects of removal of endogenous PTH excess on cortical bone geometry in pHPT postmenopausal patients with PTX and compared them with age-, body height and weight-, postmenopausal period-matched normal women. Twenty pHPT postmenopausal women (mean: age 63.6yr, Ca 12.0mg/dl, iPTH 267pg/ml) and thirty control women (age 64.6yr) participated in this study. We assessed volumetric BMD, architectural parameters of cortical bone and SSIP (polar strength strain index) by pQCT at the site of radius. Measurements of pQCT were performed at the time of enrollments and were repeated 1 year after PTX in pHPT group, and 1 year thereafter in control group. During 1-year period, total BMD and cortical BMD significantly decreased in control group (-2.1%, -1.3%), but increased in pHPT group (+2.9%, +1.6%), respectively. Significant decreases in cortical thickness and area were also observed in control group (-3.0%, -2.5%). In contrast, pHPT group showed significant increases in cortical thickness and area (+8.5%, +7.6%) as well as SSIP (+6.2%) during the follow-up period. In conclusion, the present longitudinal study showed that there were significant beneficial changes in vBMD, cortical bone geometry and bone strength in pHPT postmenopausal women, whereas age-related thinning of cortical bone as well as decrease of vBMD were observed in control group. The present findings suggest that the removal of sustained PTH excess markedly affects cortical bone geometry and that PTX in pHPT improve the bone strength by amelioration of cortical bone geometry as well as increase in BMD.

Disclosures: M. Yamauchi, None.

S487

Long-Term Propranolol Improves Bone Mineral Content and Lean Body Mass in Pediatric Burn Patients. L. K. Branski^{*1}, D. N. Herndon^{*1}, W. B. Norbury^{*1}, M. G. Jeschke^{*1}, R. P. Mlcak^{*1}, G. L. Klein². ¹Surgery, University of Texas Medical Branch and Shriners Burns Hospital, Galveston, TX, USA, ²Pediatrics, University of Texas Medical Branch and Shriners Burns Hospital, Galveston, TX, USA.

Burn injury over 40% total body surface area (TBSA) causes marked hypermetabolism and episodic increases in catecholamine production as part of the stress response. The aim of our study was to evaluate the effects of propranolol (Prop) given over the first 12 months post-burn on total body bone mineral content (TBMC) and lean body mass (LBM). Forty-nine (49) children, ages 2-18 yr with burns $\geq 40\%$ TBSA were enrolled and randomized to receive Prop (n=24) or placebo (Cont, n=25). Prop was titrated to achieve a reduction in heart rate by 15%. TBMC and LBM were measured by dual energy x-ray absorptiometry (DXA) using a 4500A absorptiometer (Hologic, Waltham MA) at hospital discharge, 6, 9, and 12 months post-burn. Results were calculated as % discharge (baseline) values. Statistical analysis used two-way ANOVA with post-hoc Tukey's test for inter-group comparisons and one-way repeated measures ANOVA with post-hoc Bonferroni's t-test for intra-group comparisons to baseline values. Prop increased LBM and TBMC and body weight ($p < 0.02$) vs Cont at 12 months post-burn. Within the Prop group, LBM and body weight increased vs baseline at 9 months, while TBMC increased at 12 months compared to baseline ($p < 0.02$). Within the Cont group, patients showed an increase in LBM and body weight at 12 months ($p < 0.05$) compared to baseline. We conclude that long-term use of propranolol has a beneficial effect on bone acquisition due to its effects on increased lean body mass and secondary skeletal loading and/or an inhibition of the episodic increase in endogenous catecholamine production that may promote bone resorption and inhibit bone formation.

Disclosures: G.L. Klein, None.

This study received funding from: NIH.

S489

Bone Morbidity at Diagnosis among Children with Acute Lymphoblastic Leukemia. L. M. Ward¹, N. Shenouda^{*1}, N. Alos², S. Atkinson³, C. Clarkson^{*4}, R. Couch^{*5}, E. Cummings^{*6}, R. Grant^{*7}, C. Rodd⁸, D. Stephure^{*9}, S. Taback^{*10}, M. Matzinger^{*1}, F. Rauch⁸, and the STOPP Consortium^{*11}. ¹University of Ottawa, Ottawa, ON, Canada, ²Université de Montréal, Montréal, PQ, Canada, ³McMaster University, Hamilton, ON, Canada, ⁴University of Western Ontario, London, ON, Canada, ⁵University of Alberta, Edmonton, AB, Canada, ⁶Dalhousie University, Halifax, NS, Canada, ⁷University of Toronto, Toronto, ON, Canada, ⁸McGill University, Montréal, PQ, Canada, ⁹University of Calgary, Calgary, AB, Canada, ¹⁰University of Manitoba, Winnipeg, MB, Canada, ¹¹Canadian Pediatric Bone Health Working Group, Ottawa, ON, Canada.

Children with acute lymphoblastic leukemia (ALL) can manifest vertebral compression at diagnosis; however, the frequency and pattern of vertebral fractures, as well as their relationship to bone mineral density (BMD), has not been systematically studied. We therefore evaluated bone morbidity in 116 newly diagnosed children (age (mean \pm SD) 6.6 \pm 4.1 years; 62 boys) with ALL (pre-B cell ALL: N=102; T-cell ALL: N=14), who were enrolled in the STeroid-induced Osteoporosis in the Pediatric Population (STOPP) study, a prospective research program comprising 11 Canadian pediatric tertiary care centers. All patients underwent lateral thoracolumbar spine x-rays and BMD studies within 30 days of diagnosis. Forty-one patients (35%) had a total of 113 vertebral compression fractures (90 thoracic, 23 lumbar), as independently assessed by two radiologists at the coordinating site. Twenty-eight patients (68%) had one or two vertebral fractures, 10 patients (25%) had three to seven fractures and 3 patients (7%) had between nine and twelve fractures. Vertebrae T6 and T7 were most commonly affected and accounted for 41 of the 113 fracture events (36%). Ninety-two of the fractures (81%) were graded as mild, 17 (15%) as moderate and 4 (4%) as severe. Eighty-six of the compressed vertebrae (76%) had an anterior wedge configuration. Children with vertebral compression fractures had lower mean lumbar spine areal BMD z scores than those without fractures (-1.5 \pm 1.4 versus -0.67 \pm 1.3; $P < 0.05$). Mean height z scores did not differ between the two groups (0.3 \pm 1.19 for those with fractures; 0.31 \pm 1.25 for those without; $P = 0.9$). Only 14 of the 41 patients with vertebral compressions (34%) reported back pain. Thus, significant overt skeletal morbidity is common in newly diagnosed children with ALL, but is asymptomatic in the majority of cases.

Disclosures: L.M. Ward, None.

This study received funding from: Canadian Institutes for Health Research.

S493

Structural Implications of Low-Magnitude Mechanical Stimulation in a Pilot Study of Patients with Renal Osteodystrophy Evaluated with the MRI-based Virtual Bone Biopsy. C. E. Jones^{*1}, F. W. Wehrli¹, J. E. Magland^{*1}, C. T. Rubin², S. A. Nihtianova^{*3}, M. B. Leonard³. ¹University of Pennsylvania, Philadelphia, PA, USA, ²State University of New York, Stony Brook, NY, USA, ³Children's Hospital of Philadelphia, Philadelphia, PA, USA.

Renal osteodystrophy (ROD) is a pervasive disorder of bone metabolism that results in impaired trabecular architecture, loss of cortical bone, and increased fracture rates. In this

double blind, placebo-controlled pilot study we examined the hypothesis that low magnitude mechanical stimulation (LMMS) increases bone volume fraction and improves the structural integrity of the trabecular bone in ROD. A total of 30 dialysis patients were randomized to daily (20 min/day) LMMS treatment with an active device (0.3g, 30 Hz), or a placebo device. Micro-MRI scans were performed in the distal tibial metaphysis at a voxel size of 137x137x410 μm^3 using a custom designed 3-D spin echo pulse sequence at baseline and after 6 months of treatment. The images subsequently underwent a cascade of processing steps, comprising the virtual bone biopsy, resulting in a final voxel size of 45x45x135 μm^3 and BV/TV was computed. After skeletonization of the images was performed (so that trabecular plates were converted to surfaces and rods to curves), the data were subjected to digital topological analysis. This algorithm establishes the topological identity of each voxel as belonging to a curve, surface or junction between the two fundamental types. To date, repeat MRI scans have been obtained on 10 LMMS and 11 placebo-treated subjects. Fig. 1 illustrates the wide range of structural abnormalities in some of the study subjects at baseline. In patients treated with the active LMMS device, TB/TV was increased 2.8% ($p = 0.02$) while the surface-to-curve ratio (S/C, ratio of all surface-type divided by all curve-type voxels) was increased 8.0 percent ($p = 0.03$), indicating a relative increase in plates over rods. Similarly, the erosion index (a measure of loss of connectivity) was decreased 6.9% ($p = 0.03$) suggesting improved trabecular connectivity. No significant changes were noted in the placebo group. The observed changes are commensurate with the treatment's anabolic effect resulting in improved bone quality and hence potentially reduced risk of fracture. These data are the first showing structural implications of LMMS treatment in patients with renal disease assessed with in vivo structural imaging.

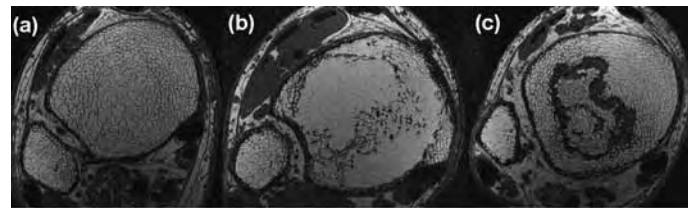


Fig. 1. Transverse μMR images through the distal tibia in three patients: relatively normal bone (a), severely disconnected network (b); presence of marrow fibrosis (c).

Disclosures: C.E. Jones, None.

S498

Thioredoxin-1 Overexpression Attenuates Streptozotocin-induced Diabetic Osteopenia in Mice: A Novel Role of Oxidative Stress and Therapeutic Implications. Y. Hamada^{*1}, H. Fujii^{*1}, R. Kitazawa², S. Kitazawa², M. Fukagawa¹. ¹Division of Nephrology and Kidney Center, Kobe University School of Medicine, Kobe, Japan, ²Division of Molecular Pathology, Department of Biomedical Informatics, Kobe University School of Medicine, Kobe, Japan.

Diabetes mellitus is associated with increased risk of osteopenia and bone fracture. However, the mechanisms accounting for diabetic bone disorder still remain to be clarified. Moreover, there are few effective treatments for this disease. We have previously reported that streptozotocin-induced diabetic mice develop low turnover osteopenia associated with increased oxidative stress in diabetic condition (BONE 2007). Therefore, in order to determine the role of oxidative stress in the development of diabetic osteopenia, we investigated the effect of thioredoxin-1 (TRX) overexpression, a major intracellular antioxidant, on the development of diabetic osteopenia using TRX transgenic mice (TRX-Tg). TRX-Tg was C57BL/6 mice that carry the human TRX transgene under the control of β -actin promoter.

Eight-week-old male TRX-Tg and wild type littermates (WT) were intraperitoneally injected with either streptozotocin or vehicle alone. Mice were classified into four groups: 1) non-diabetic WT, 2) Non-diabetic TRX-Tg, 3) diabetic WT, and 4) diabetic TRX-Tg. After 12 weeks of streptozotocin treatment, the physical properties of femora, and the parameters of bone histomorphometry of tibiae were assessed. Oxidative stress in the whole body as well as in the bone was evaluated.

TRX overexpression did not affect either body weights or hemoglobin A1c levels both in the diabetic mice and in the non-diabetic mice. There were no significant differences in renal function, and serum levels of calcium, phosphate, and intact parathyroid hormone among four groups. Urinary excretion of 8-hydroxydeoxyguanosine (8-OHdG), a marker of oxidative DNA damage, was significantly elevated in diabetic WT, which was attenuated in diabetic TRX-Tg. Immunohistochemical staining for 8-OHdG was clearly intensified in the bone tissue of diabetic WT compared with non-diabetic WT. In contrast, staining was attenuated in diabetic TRX-Tg. TRX overexpression partially restored reduced bone mineral density and prevented the suppression of bone formation (OV/BV, OS/BS, Ob.S/BS, O.Th, MAR, and BFR/BS) observed in diabetic WT. These results suggest that increased oxidative stress in diabetic condition contributes to the development of diabetic osteopenia. Furthermore, our findings indicate that suppression of increased oxidative stress by TRX induction can be a therapeutic approach for treatment of diabetic osteopenia.

Disclosures: Y. Hamada, None.

S504

Time Sequence of Secondary Mineralization and Microhardness of Bone in an Ewe Model. Y. Bala*, D. Farlay*, C. Simi*, P. J. Meunier, P. D. Delmas, G. Boivin. INSERM Unité 831, Université de Lyon, Lyon, France.

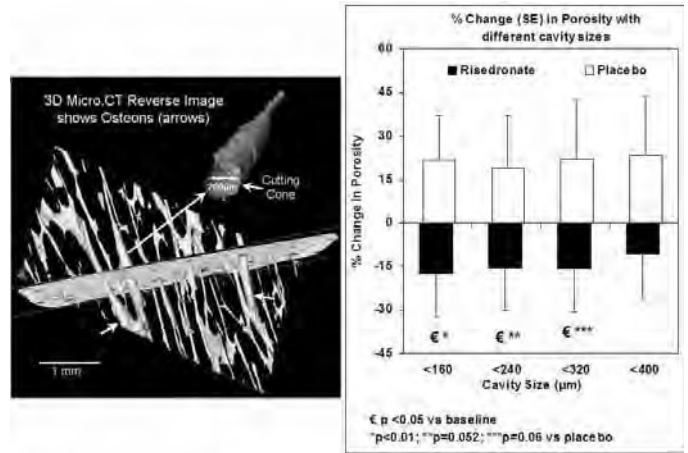
The degree of mineralization is a major determinant of the mechanical resistance of bone (Follet et al. 2004, Bone 34:783-9). Mineralization begins by a rapid primary mineralization followed, after the full completion of the Basic Structural Units (BSUs), by a secondary mineralization phase, i.e., a slow and gradual maturation of the mineral component leading to complete mineralization of newly formed BSUs (Meunier & Boivin 1997, Bone 21:373-7). The duration of primary mineralization has been evaluated by several authors but the time sequence of secondary mineralization is still poorly investigated [Fuchs et al. 2005, J Bone Miner Res 20(Suppl.1):325]. Our aim was to determine the time course of secondary bone mineralization in ewe, an animal model having an Haversian bone tissue with a remodeling activity close to the Human one (Chavassieux et al. 1997, Bone 20:451-5). 18 ewes (4.5±0.4 years, INRA, Theix, France) received every six months for 30 months fluorescent labelings following the schedule: T0 double tetracycline, T6 single fluorescein, T12 triple tetracycline, T18 double fluorescein, T24 single tetracycline, T30 double alizarin labeling in order to date the age of the BSUs. Transiliac bone samples have been taken on each ewe after T18 and T30 labelings, then embedded in methyl methacrylate. Microradiography (Boivin & Meunier 2002, Calcif Tissue Int 70:503-11) performed on 100±1 µm-thick sections allowed the measurement of the focal Degree of Mineralization of Bone (DMB g/cm³) on 505 different BSUs in which the duration of the mineralization was precisely determined by labeling. Microhardness using a Vickers indenter under a load of 25g for 10s (Hv kg/mm²) was measured on 367 among the 505 BSUs [Bala et al. 2006, J Bone Miner Res 21(suppl.1):S332]. DMB measured at primary mineralization (0.76±0.10 g/cm³) significantly increased during the first 6 months (+26%, p<0.0001). Then, DMB increased more slowly until 30 months to reach a mean of 1.20±0.12 g/cm³. DMB measured at the end of the primary mineralization corresponded to 64% of the final mineralization. DMB after 6 and 12 months were 85% and 91% of the final DMB, respectively. Secondary mineralization is thus the fastest during the first year. Hv followed a similar trend, with a rapid increase during the first six months (+32%, p<0.0008), then a slow increase until 30 months. Hv and DMB are strongly and positively correlated (r²=0.52, p<0.0001). The time course of secondary mineralization can be divided into two parts having separated trends, a rapid increase during the first year then a slowdown of mineralization until 30 months. Mineralization explains a great part of the hardness of bone at BSU level.

Disclosures: G. Boivin, None.

S508

Risedronate Reduces Osteonal Cortical Porosity in Osteoporotic Women. B. Borah*, T. Dufresne*, J. Nurte*, P. Chmielewski*, R. Phipps*, M. Lundy*, X. Zhou*, M. Bouxsein*, E. Seeman*. ¹Procter & Gamble Pharmaceuticals, Mason, OH, USA, ²Ortho Biomechanics Lab, Harvard Medical School, Boston, MA, USA, ³Austin Health, University of Melbourne, Melbourne, Australia.

Measurements of cortical porosity include 1) Haversian canals (diam. <50 µm), 2) the remodeling spaces of the osteons (diam. ~100 to 300 µm) in the intra-cortical envelope, and 3) larger cavities (diam. >380 µm) primarily in the endocortical envelope. In this study, we evaluated the effect of risedronate on cortical porosity in transiliac biopsies from osteoporotic women. Paired biopsies taken at baseline and after 5 years risedronate treatment (5 mg/day, n=28) or placebo (n=21) were imaged by micro-CT at 8 µm isotropic resolution. The cavities were then stratified by size, as determined by the minor axis length of the holes in the 2D slices. Porosity was averaged over 10 to 14 slices ~300 µm apart and was calculated as the area of cavities expressed as a percentage of the total cortical bone area. The porosity at baseline was not statistically different between placebo and risedronate for any pore size. Compared to baseline, 5 years treatment with risedronate caused a significant 15% reduction in porosity for cavities of ≤320 µm diameter (p<0.05, Figure), an effect likely to be the result of reduced osteonal remodeling. In the placebo group, porosity from cavities in this same size range increased by ~20% compared to baseline (not significant). The between group difference was significant or approached significance for cavities ≤320 µm diameter (p=0.01 - 0.06). The reduction of porosity by risedronate was not significant when cavities >400 µm were included. These larger cavities produce trabecularization of the inner cortex and cortical thinning. It appears that due to the variability of the age-related changes in the endocortical trabecularization, treatment-related reduction of porosity cannot be reliably assessed from measurements made throughout the cortex. These findings indicate that risedronate reduces cortical porosity by reducing the birth rate of new osteons or by filling in the remodeling spaces in osteons that existed prior to treatment.



Disclosures: B. Borah, Procter & Gamble Pharmaceuticals 3.

S512

LRP5 G171V Mutation Protects Against Disuse-Related Trabecular Bone Fragility. M. P. Akhter, D. M. Cullen, R. R. Recker. Medicine, Creighton University, Omaha, NE, USA.

Fragility fracture risk is greater in people with low bone mass or osteoporosis. In addition, a sedentary (disuse or lack of exercise) lifestyle choice may further deteriorate low bone mass associated with osteoporosis. We have shown (#F171 ASBMR-06) that disuse causes far greater loss in bone volume fraction (BV/TV) in the KO mice (67%) than in the HBM mice (14%). In this study, we characterized trabecular bone strength properties to determine if the LRP5 G171V mutation will protect against bone loss associated with disuse. Forty eight adult (4 mo.) male mice representing three genotypes (all bred to C57BL/6 mice): WT (Lrp5^{+/+}, wild type), KO (Lrp5^{-/-} knockout), HBM (High bone mass with LRP5 G171V mutation) were randomly divided between control and Disuse groups. The mice in the disuse group were hind limb suspended in individual cages for 4 weeks. All mice were inspected daily to assure compliance, adequate food intake, and general health. Femurs were collected and frozen in saline for biomechanical strength testing. A 1.26 mm diameter indenter was used to measure trabecular bone strength at the distal femur site (testing rate of 3mm/min, Instron 5543). We analyzed the data using the General Linear Model for univariate analysis to test for differences (P<0.05) due to disuse within each genotype. Trabecular bone strength declined in all the three genotypes (Table). Bone strength variables (ultimate load [ULT], yield load [YLD], stiffness [STIF]) were lower in the disuse group as compared to their controls within each genotype (HBM, WT, and KO). Disuse-related loss in strength (ULT) was 48%, 51% and 74% in HBM, WT and KO mice respectively. In addition, trabecular bone strength (ULT, YLD, STIF) in HBM mice remained elevated as compared to both WT and KO within each treatment group (Control & Disuse). Similar to trabecular bone structure data (reported previously), the already fragile KO has a large decrease in trabecular bone strength (74%), and the HBM losses were moderate with final bone strength remaining well above normal for the wild type mice. The mice with the LRP5 G171V mutation (HBM) did show a significant response to disuse demonstrating mechanosensitivity. However, the relative advantage in trabecular bone strength (ULT, YLD) between HBM and KO went from 10 fold in the control mice to 20 fold after disuse (Table). These data suggest that the HBM genotype (LRP5 G171V mutation) is relatively protected against disuse-related bone fragility.

(Mean ± SD)	Control			Disuse		
Indent test (distal femur)	HBM	WT	KO	HBM	WT	KO
ULT (N)	34.3 ± 7.5	5.1 ± 1.3 ^b	3.5 ± 0.7 ^b	17.7 ± 1.6 ^a	2.5 ± 0.7 ^{ab}	0.9 ± 0.3 ^{ab}
YLD (N)	24.3 ± 2.4	2.9 ± 0.9 ^b	2.3 ± 0.4 ^b	12.4 ± 1.8 ^a	1.8 ± 0.6 ^{ab}	0.6 ± 0.4 ^{ab}
STIF (N/mm)	190 ± 51	48 ± 14 ^b	53 ± 8 ^b	149 ± 39	32 ± 13 ^{ab}	8 ± 3 ^{ab}

^aDifferences due to Disuse (P < 0.05); ^bDifferent from HBM within each group (P < 0.05)

Disclosures: M.P. Akhter, None.

This study received funding from: The State of Nebraska LB595 Funds.

S514

Beta-Adrenergic Receptor Agonist Administration During Hindlimb Unloading Attenuates Losses in Bone Geometry, Structure, and Mechanical Properties. J. M. Swift*, J. T. Ali*, J. L. Stallone*, H. A. Hogan*, S. A. Bloomfield*. ¹Health and Kinesiology, Texas A&M University, College Station, TX, USA, ²Mechanical Engineering, Texas A&M University, College Station, TX, USA.

A major challenge to long-duration spaceflight is the significant bone loss that occurs in weightbearing limbs. The rodent hindlimb unloading (HU) model effectively simulates the deleterious effects of microgravity on the skeleton. In addition, HU results in significant declines in blood flow and increases in vascular resistance in unweighted hindlimb bone. Previously, we demonstrated that dobutamine (DOB), a beta-adrenergic receptor agonist (ADRB), given during simulated microgravity significantly blunts decreases in femoral

midshaft cortical bone area and polar moment of inertia (CSMI). The purpose of this study was to assess the effectiveness of DOB in attenuating HU-associated losses in tibiae and femora bone content, density, area, and strength during 28 days of unloading. Male Sprague-Dawley rats, aged 6-mo, were assigned to either a normal cage activity (CC) or HU group (n=24/group). Animals were given one daily bolus dose (4 mg/kg BW/d) of DOB (n=12) or an equal volume of saline (VEH; n=12). In vivo peripheral quantitative computed tomography (pQCT) scans were taken at the proximal tibia metaphysis (PTM) and tibial mid-diaphysis on anaesthetized animals on days 0 and 28 to reveal geometric and structural changes. Post-sacrifice, hindlimb bones were excised for determination of mechanical properties using an Instron 1125 device; ex vivo pQCT scans were performed at the femoral neck (FN) and mid-diaphysis. At the PTM, HU resulted in similar reductions in total bone mineral content (BMC) in animals treated with VEH (-17%) and DOB (-15%); however, reductions in total volumetric bone mineral density (vBMD) were only evident in HU+VEH (-9%). Total BMC, total area, and CSMI were significantly higher at FN in HU+DOB vs. HU+VEH (+18%, +23%, and +52%, respectively). Mechanical testing of FN revealed that HU+DOB exhibited a significantly higher ultimate load (+25%) as compared to HU+VEH. No significant changes in mid-diaphyseal tibia bone structure or area during HU were evidenced by in vivo pQCT scans, but 3-point bending to failure revealed a significantly higher ultimate load (+46%) in HU+DOB vs. HU+VEH. Ex vivo pQCT scans of mid-diaphyseal femora revealed significantly higher total BMC (+7%), total area (+5%), and CSMI (+10%) in DOB-treated rats subjected to 28-day HU vs. HU alone. These results suggest that DOB administration during HU prevents significant declines in total vBMD at PTM and produces a higher midshaft tibia ultimate load. We speculate that these positive effects may be attributed to ADRB-mediated vasodilation, improving blood flow to bone during unloading.

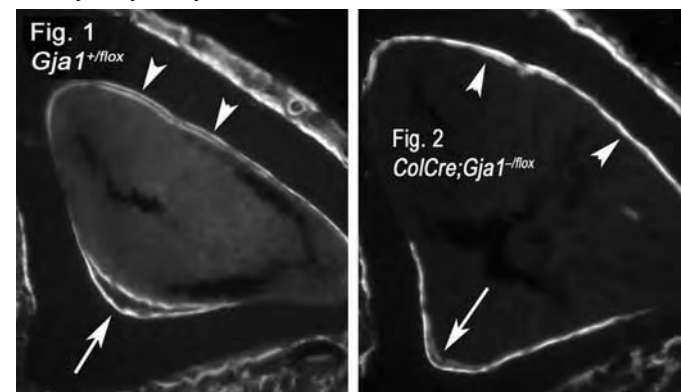
Disclosures: J.M. Swift, None.

This study received funding from: The National Space Biomedical Research Institute through NASA NCC 9-58.

S518

Attenuated Response to Skeletal Load in Connexin43 Deficient Mice. S. K. Grimston, M. D. Brodt*, M. J. Silva, R. Civitelli. Bone and Mineral Diseases, Washington University in St. Louis, St. Louis, MO, USA.

In vitro data suggest that connexin43 (Cx43) plays an important role in mechanotransduction. We reported that the anabolic response to parathyroid hormone is attenuated in mice with conditional ablation of the Cx43 gene (Gja1) in osteoblasts, obtained using a Cx43^{fllox}/LacZ gene replacement model and a 2.1 kb fragment of the $\alpha_1(I)$ collagen promoter to drive Cre (ColCre;Cx43^{fllox}). We tested the hypothesis that the anabolic response of the skeleton to mechanical loading is also dependent on Cx43. Four-month-old female mice were anesthetized and subjected to an in vivo 3-point bending protocol on the tibia, 5 days a week for 2 weeks. ColCre;Gja1^{fllox} mice had significantly greater marrow area, total tissue area, and thinner cortices than wild type equivalent Gja1^{fllox} mice. However, area moment of inertia was similar (0.130±0.059 versus 0.128±0.054 mm⁴, respectively), suggestive of adaptive responses similar to aging bone in Gja1 deficient mice. In Gja1^{fllox} mice, the loading regimen produced abundant new bone formation at the endocortical surface, as evidenced by double calcein labeling (injected ip on days 5 and 12), proportional to the estimated strain applied (1600 $\mu\epsilon$), with maximal effects at the apex (tension) and on the lateral aspect (compression) (arrows and arrowhead in Fig. 1, respectively). Conversely, there were predominantly single labels in ColCre;Gja1^{fllox} mice (Fig. 2). Accordingly, mineral apposition rate (MAR) and bone formation rate were significantly lower (p<0.05) in ColCre;Gja1^{fllox} (1.02±0.97 $\mu\text{m}/\text{day}$; 83.5±84.12 $\mu\text{m}^3/\mu\text{m}^2/\text{yr}$) relative to Gja1^{fllox} mice (1.86±0.65 $\mu\text{m}/\text{day}$; 192.23±89.5 $\mu\text{m}^3/\mu\text{m}^2/\text{yr}$), with heterozygous Gja1^{fllox} mice showing intermediate values (1.86±0.94 $\mu\text{m}/\text{day}$; 150.54±120.89 $\mu\text{m}^3/\mu\text{m}^2/\text{yr}$). Relative to the unloaded contralateral leg, MAR increased in the loaded leg by 67±16% (p<0.01) in Gja1^{fllox} mice, and 19±22% (n.s.) in ColCre;Gja1^{fllox} mice. Loading also stimulated the formation of periosteal woven bone on the surface subject to pressure, and this was also less evident in the conditionally ablated ColCre;Gja1^{fllox} (22.7±4.4%) relative to Gja1^{fllox} mice (31.3±13.1%; p<0.05). Thus, deletion of Gja1 prevents full anabolic response to in vivo skeletal physical loading. Cx43 is critical for bone's rapid adaptive response to mechanical stimuli.



Disclosures: S.K. Grimston, None.

This study received funding from: NIH AR41255.

S523

The Lrp5 Gain of Function Mutation Is Associated with an Increased Osteogenic Response to Loading in Trabecular as well as Cortical Bone in Female but not Male Mice. L. K. Saxon, T. Sugiyama, J. Price, L. E. Lanyon. Veterinary Basic Sciences, Royal Veterinary College, London, United Kingdom.

The Lrp5 gain of function G171V mutation (Lrp5⁺) is associated with increased sensitivity to mechanical loading in cortical bone [1], however it is not known if the same occurs in trabecular bone. We therefore used our mouse tibial loading model [2] to investigate the effect of loading on trabecular and cortical bone in male and female Lrp5⁺ mice.

The right tibiae of 17-week-old male (n=6) and female (n=7) Lrp5⁺ and WT mice were subjected to a short period of dynamic axial loading for 40 cycles/day, 10 Hz, 3 days a week for 2 weeks. Strain gauges bonded to the medial mid-shaft were used to determine the magnitude of the load required to apply similar strains within each group. Differences in trabecular bone volume (BV/TV), number (Tb.N), thickness (Tb.Th), total bone area (TA), cortical area (CA), periosteal perimeter (Pp), endocortical perimeter (Ep), moment of inertia (MMI), and cortical thickness (C.Th) in the loaded (right) versus non-loaded (left) tibia were measured using microCT.

In male Lrp5⁺ mice all measured parameters in control bones were higher than in WT except C.Th (p<0.001). To engender 850 $\mu\epsilon$ a 19.8N load was applied to Lrp5⁺ and 10.5N to WT. In WT males loading increased Pp, CA, MMI, Tb.Th (p<0.05) whilst in Lrp5⁺ mice loading only increased C.Th (p<0.05); all other measures showed no loading-related difference. The magnitude of loading-related change between Lrp5⁺ and WT mice was only different for periosteal perimeter (3.9 vs -1.3%, p<0.001).

In female Lrp5⁺ mice all measured parameters were also higher than in WT (p<0.001). A load of 19.8N applied to the tibia of Lrp5⁺ mice and 9N to WT mice induced 1100 $\mu\epsilon$. All loaded WT tibiae showed gains in Pp, CA, MMI (p<0.05), and all parameters increased except Tb.N in Lrp5⁺ mice (p<0.05). In cortical bone the magnitude of the loading response was higher in the Lrp5⁺ mice compared with WT (TA 10.1 vs 1.2%, CA 17.7 vs 1.2%; Pp 5.5 vs -3.1%; Ep 10.4 vs -2.4%; MMI 21.7 vs -3.0%; C.Th 9.1 vs 4.1%, p<0.05). The gains in BV/TV were also greater in Lrp5⁺ mice. This was due to increased trabecular thickness not number (BV/TV 16.8 vs 5.6%; Tb.Th 17.5 vs 2.7%, p<0.05; Tb.N -0.5 vs 3.1%).

In conclusion, the G171V mutation results in a more robust bone phenotype in male mice. However, at the strain levels we used there was no difference from WT in their osteogenic response to loading in trabecular bone, and only a small difference in cortical bone. By contrast, in females the G171V mutation results in both a more robust bone phenotype and increased sensitivity to loading in trabecular and cortical bone.

1. Akhter et al Bone 2004

2. DeSouza et al Bone 2005

Disclosures: L.K. Saxon, None.

S525

Bone Adaptation to Impact Loading - Significance of Loading Intensity. A. Vainionpää*, R. Korpelainen*, J. Leppälou*, T. Jämsä*. ¹Department of Medical Technology, University of Oulu, Oulu, Finland, ²Department of Sports Medicine, Oulu Deaconess Institute, Oulu, Finland, ³Department of Physiology, University of Oulu, Oulu, Finland.

It is important to find efficient strategies for prevention of osteoporosis and fragility fractures as the prevention with medication is impossible at the population level. Exercise is one of the major prevention strategies even though the optimal loading patterns of bone have not yet been clearly defined in terms of bone loading forces in clinical settings. Our aim was to study the effects of impact loading on bone and assess the intensity and amount of efficient impact loading.

We conducted a 12 month population-based exercise intervention in 120 premenopausal women aged 35 to 40 years. The women were randomized equally to exercise (EG) and control groups (CG). The exercise regimen consisted of supervised, progressive high-impact exercises three times per week and an additional home program. Bone mineral density (BMD) in the proximal femur was measured by dual x-ray absorptiometry and bone geometry in the mid-femur was quantified by computed tomography (QCT). Also bone turnover was examined by using biochemical markers (TRACP-5b, PINP and Uncoupling Index). Daily impact loading was continuously recorded with a novel accelerometer-based measurement device and analyzed as the daily number of impacts within five acceleration ranges between 0.3 g to 9.2 g (g=acceleration of gravity, 9.81 m/s²).

Regular impact exercise increased the femoral neck BMD by 1.5 % (p=0.003) and led to geometric adaptations by increasing the mid-femur periosteal circumference by 0.2 % (p=0.03) when compared to controls. It also altered bone turnover balance in favour of bone formation. The women with the highest number of impacts at the intensity level above 4 g had the greatest increment in proximal femur BMD. The number of impacts needed exceeding this level was 60 impacts per day. Impacts exceeding 2.5 g were associated with increased periosteal circumference and enhanced bone turnover favouring bone formation.

According to our results, impact loading has significant dose- and intensity dependent effect on weight-bearing bones. The threshold for improving BMD in the hip is 60 impacts per day exceeding 4 g, while geometric adaptation and bone turnover activation can be achieved with lower intensity levels. Impacts required for osteogenic effects can be obtained during habitual exercise training. These thresholds for osteogenic exercise give tools to promote efficient exercise patterns to be included in everyday routines and personal activities, thus increasing the potential to affect in community level.

Disclosures: A. Vainionpää, None.

This study received funding from: Tekes, Finland; Newtest Ltd, Finland.

S528

Gene Polymorphisms, Bone Mineral Density and Bone Mineral Content in Children: The Iowa Bone Development Study. M. C. Willing¹, T. L. Burns², J. C. Torner², E. Letuchy², S. Santiago-Parton¹, K. F. Janz³, T. Marshall⁴, J. M. E. Gilmore⁴, J. J. Warren⁴, S. M. Levy⁴. ¹Pediatrics, University of Iowa Carver College of Medicine, Iowa City, IA, USA, ²Epidemiology, College of Public Health, Iowa City, IA, USA, ³Health and Sports Studies, College of Liberal Arts, Iowa City, IA, USA, ⁴Preventive and Community Dentistry, College of Dentistry, Iowa City, IA, USA.

We examined associations of candidate gene polymorphisms with bone mineral density (BMD) and content (BMC) in a cohort of 412 healthy non-Hispanic white children participating in the Iowa Bone Development Study. Whole body (WB), hip and spine BMD and BMC were determined using a Hologic QDR 4500a densitometer for 213 girls and 199 boys age ~11 years. Candidate genes included the type I collagen genes (COL1A1 and COL1A2), osteocalcin, osteonectin (SPARC), osteopontin, vitamin D receptor (VDR), estrogen receptor (ER), androgen receptor (AR), IGF-1, IGF-2, PTR, PTHR and LRP5. Gender-combined and gender-specific prediction models for bone measures that included age, weight, height, dichotomous Tanner stage (and gender) were developed using multiple linear regression analysis and residuals were calculated. COL1A2 genotype (identified by one or more of the following: RsaI, Intron 12 VNTR, 5'(CA)_n-CGCACA(CG)_m(CA)_nGT_x3') was found to have the strongest and most consistent association with adjusted BMD/BMC measures. When stratified by gender, COL1A2 genotype was associated with WB BMC, spine BMC, and hip BMD in both boys and girls, as well as with hip BMC in girls. IGF-2 (6815 A/T), osteocalcin (C/T promoter), PTHRT3 (AAAG) and VDR (Bsm-I) genotypes were also associated with some bone measures in the combined analyses, but the associations differed by gender. In girls, osteocalcin and IGF-2 genotypes were associated with hip BMC and BMD and with WB BMC and hip BMD, respectively. PTHR genotype was associated with all bone measures except spine BMC in the combined analyses, but results only reached significance in girls. In contrast, VDR (Bsm-I) genotype was associated with hip BMD only in boys, and COL1A1 (RsaI) genotype was associated with spine BMD, hip BMC and BMD only in boys. Gender-specific quartiles of the BMD/BMC residuals were determined and an association analysis using the recursive partitioning technique represented by the nonparametric classification tree approach was used to identify candidate genotypes associated with high vs. low quartile status. Significant gene x gene interaction effects involving PTHR and each of the following: IGF-1, IGF-2, COL1A2, and osteonectin were identified for spine BMD, particularly in girls. Our data suggest that genetic variation at multiple genetic loci is important in bone accrual in children. Combinations of individual genotypes may also impact BMD and BMC.

Disclosures: J.M.E. Gilmore, None.

S530

Jump Starting Skeletal Health: Bone Increases from Jumping Exercise Persist Seven Years Post Intervention. K. B. Gunter¹, A. Baxter-Jones², R. Mirwald², H. C. Almstedt³, S. Durski¹, A. A. Fuller-Hayes¹, C. M. Snow¹. ¹Department of Nutrition and Exercise Sciences, Oregon State University, Corvallis, OR, USA, ²College of Kinesiology, University of Saskatchewan, Saskatoon, SK, Canada, ³Department of Natural Science, Loyola Marymount University, Los Angeles, CA, USA.

Evidence suggests that bone mineral increases attributable to exercise training prior to puberty may confer a significant advantage into adulthood. However, there is a dearth of supportive prospective longitudinal data. We assessed the change in bone mineral content (BMC) at the left proximal femur over eight years in children who participated in a seven-month jumping intervention and who were pre-pubertal at study onset. We hypothesized that jumpers would accrue and retain more BMC compared to controls and therefore be at a considerable advantage in optimizing peak bone mass accrual. Subjects were drawn from the BUGSY study (Building Growing Skeletons in Youth), an ongoing mixed longitudinal study of bone mineral accretion in growing children initiated in the fall of 1997. Participants were recruited from local elementary schools in Corvallis, Oregon and were randomly assigned within classrooms to either an intervention (jumping) or control (stretching) group. Subjects were assessed at baseline, at the end of the intervention (7 months) and at approximately 19 months. Participants were reassessed at 31, 43, 55, 67, 79 and 91 months from study entry for a total of nine measurement occasions over approximately 8 years. Bone mineral content was assessed by dual-energy X-ray absorptiometry. Multi-level random effects models were constructed and used to predict change from study entry in BMC at each measurement occasion. We were able to utilize data from a total of 421 DXA scans on 57 individuals who were measured on 3 or more occasions. At 7 months, the intervention group had 3.6% more total hip bone accrual than the non-intervention group ($p < 0.05$), once the effects of change in age, height and weight were accounted for. The effects of the intervention, in terms of percentage contribution to A total hip BMC, decreased at each measurement occasion thereafter. After an average of 7.6 years, the intervention group had 1.4% more total hip bone accrual than the non-intervention group, once the effects of change in age, height and weight were accounted for ($p < 0.05$). This provides the first evidence that changes in BMC attributable to short-term exercise undertaken prior to puberty persist more than 7 years following exercise cessation in growing children. If the benefits are sustained into adulthood, effectively increasing peak bone mass, this could have substantial effects on fracture risk.

Disclosures: K.B. Gunter, None.

This study received funding from: National Institutes of Health RO1 AR45655-08.

S533

Regular Physical Activity Has Only Temporary Effect on Bone Gain in Pubertal Girls: A 6.5 Year Follow-up Study. E. Völgyi¹, F. A. Tylavsky², H. Suominen¹, S. M. Cheng¹, A. Lyytikäinen¹, M. Alén¹, U. M. Kujala¹, H. Kröger³, S. Cheng¹. ¹Department of Health Sciences, University of Jyväskylä, Jyväskylä, Finland, ²Health Science Center; Preventive Medicine, University of Tennessee, Memphis, TN, USA, ³Department of Surgery, Kuopio University Hospital, Kuopio, Finland.

The effects of exercise on bone gain in early puberty have been proven in many different short intervention studies. Whether effects found in early puberty can be sustained until early adulthood in children who are not in athletic training is still debatable. The purpose of this study is to evaluate the relationship between physical activity and bone gain in girls and the relationship with their mothers' physical activity level and bone characteristics. The study subjects consisted of 258 10-13-year old girls with maturation status of I-III at the baseline. They were followed on average of 6.5 years and their results reflect the entire follow-up period. In addition, a group of these girls' mothers ($n=108$, mean age 44yrs) had measurement twice within a 3.5 year interval. Bone area (BA), mineral content (BMC) and density (BMD) of the total femur (TF), femoral neck (FN), and lumbar spine (L2-L4) were assessed by DXA (Prodigy, GE Lunar). The level of leisure time physical activity (PA) was assessed by questionnaire. We only compared those with consistently low (LPA, < 2 times & hours/wk, $n=92$ 0mo, $n=65$ 12mo, $n=92$ 24mo, $n=25$ 36mo, $n=26$ 84mo), to those consistently high (HPA, > 4 times & hours/wk, $n=101$ 0mo, $n=71$ 12mo, $n=71$ 24mo, $n=22$ 36mo, $n=26$ 84mo) PA groups at each measurement point. No differences were found in age, relative weight and height, and in Tanner stage between the HPA and LPA groups in girls through-out the follow-up. Those girls in the HPA group had higher BMC ($p=0.017$, t-test) of the FN at 24mo, and BMD of the FN at 0mo ($p=0.033$), 12mo ($p=0.01$) and 24mo ($p=0.029$) than that of the LPA group. There were no differences in BA from any of the bone sites between PA groups at any follow-up time point. By age 17.9 years the differences in BMC and BMD of FN, TF or L2-4 between the HPA and LPA had vanished. When we compared the girl's PA with the mother's PA (paired), we found PA levels were associated only at baseline but not in other time points. The agreement between mothers and daughters for LPA was 71% and for HPA was 56% ($p=0.043$, χ^2 analysis). They reached the mean value of the mothers ($n=108$ at 36mo) only in FN BMD ($p>0.05$). There were no differences in FN BMC, TF BMD, L2-4 BMD, FN BA and L2-4 BA ($p>0.05$). Daughters had lower TF BMC ($p=0.001$), TF BA ($p<0.001$) and L2-4 BMC ($p<0.001$) compared to mothers. Our results indicate that the higher BMC and BMD value due to HPA during puberty may be temporary or participating physical activity more than 4 times and 4 hours a week was not sufficient to impact on bone gain.

Disclosures: E. Völgyi, None.

This study received funding from: ASBMR Bridge Funding, Academy of Finland and Finnish Ministry of Education, Juho Vainio Säätiö, Finnish and Hungarian Government Scholarship Pool (CIMO).

S535

Bone Density at Age of Peak Bone Mass in Women Is Not Associated with History of Childhood Fractures. S. M. Ott¹, A. Z. LaCroix², L. E. Ichikawa³, L. Spangler¹, D. Scholes⁴. ¹U of WA, Seattle, WA, USA, ²U of WA and Fred Hutchinson, Seattle, WA, USA, ³Group Health, Seattle, WA, USA, ⁴U of WA and Group Health, Seattle, WA, USA.

A recent large study of ten-year-old children found that low bone mineral density (BMD) predicted fracture incidence. Peak bone mass is attained during late teenage years at the hip and in the mid-twenties at the spine. Whether childhood fractures are related to the bone density during adolescence or young adulthood has not been as well studied. We therefore examined this in a cross-sectional study of 606 adolescents and young women aged 14-30 years. Members of Group Health, a Washington State HMO, were selected from the health plan computerized databases based on prescriptions for oral contraceptive use and age. We mailed letters of invitation to participate in a study of bone health. BMD (DEXA) was measured at the hip, spine, and whole body. Data on previous fractures and other factors related to bone health were collected via interview and a written questionnaire. Potential subjects with severe health problems, known metabolic bone disease, recent pregnancy, or use of prednisone or progesterone-only birth control methods were excluded. Overall, 51% of the cohort was 14-18 years of age. 206 of 606 subjects (34%) reported at least one fracture; there were a total of 336 fractures. Most common sites were ankle, wrist and toe. Fractures were most common at age 11 when 4.2% of the subjects experiences their first fracture. Ninety percent of the fractures occurred before age 17. The fracture history differed by racial background: 9% of Black subjects, 11% of Asian and 39% of Whites and other races reported history of fracture. Previous fractures occurred in 32% of subjects who were currently underweight and 40% of those who were currently obese; 41% who had weight loss greater than ten pounds in the past; in 46% of subjects with asthma, in 33% of those with menarche older than age 13, and in 43% of those who had a relative with a history of fractures.

The BMD was not lower at the hip, spine, or whole body in the adolescents or young women who had a history of fracture: total hip BMD was .993 g/cm² in those with a fracture history vs .986 in those without; at the spine the results were 1.023 vs 1.019 and at the whole body 1.103 vs 1.096, respectively. Similar findings were seen in teens as in young adults, with slightly higher bone density in the fracture cases at all three measurement sites. Adjusting for age, race, BMI, calcium intake, physical activity, and current smoking status did not alter the findings. Our data show that history of fracture is common, reported in about a third of otherwise healthy young women. At the age of peak bone mass women in this study with childhood fractures did not have lower bone density than those without fractures.

Disclosures: S.M. Ott, None.

This study received funding from: NIH.

M001

PTHrP Induces Mitogen-Activated Protein Kinase Phosphatase-1 in Differentiated Bone Marrow Stromal Cells, Mouse Osteoblast and Cementoblast Cell Lines. N. S. Datta, R. Kolailat*, G. Pettway*, J. Berry*, L. K. McCauley. Periodontics and Oral Medicine, University of Michigan, Ann Arbor, MI, USA.

This study investigated the signaling mechanisms of Parathyroid hormone (PTH) and PTH related protein (PTHrP) during osteogenic cell proliferation and differentiation. Mitogen-activated protein kinases (MAPKs) play a critical role in this process. In order to understand the up-stream signaling pathways, the role of MAP kinase phosphatase-1 (MKP-1) in regulating MAPKs, cyclin D1 and osteoblast cell growth arrest were studied. Analysis of MAPK activity revealed down-regulation of cyclin D1 (5-10 fold), p38 and ERK1/2 phosphorylation after PTHrP stimulation in differentiated mouse MC3T3-E1 osteoblasts. Interestingly, MKP-1 was induced concurrently with the attenuation of p38 and ERK1/2 phosphorylation. Real-time PCR and western blot analysis revealed 4-8 fold increase in MKP-1 expression following PTHrP stimulation (15 min to 4h) compared to vehicle controls in differentiated osteoblasts. Using different pharmacological inhibitors and activators of cAMP/PKA and PKC pathways both cAMP and PKC were implicated in the PTHrP regulation of MKP-1. MKP-1 expression was also induced in differentiated primary bone marrow stromal cells (BMSCs) and OCCM cementoblast cells (tooth root lining cells phenotypically similar to osteoblasts). Microarray analysis of ectopic ossicles (implanted BMSCs) generated in mice, demonstrated down-regulation of MKP-1 in less differentiated ossicles following acute injection of PTH. In contrast, there was an increase in MKP-1 expression by real-time PCR following three weeks of anabolic PTH treatment in more differentiated ossicles. These findings highlight MKP-1 as a potential regulator of the PTH and PTHrP response in osteoblasts and may be an important target gene in the anabolic action of PTH in bone.

Disclosures: N.S. Datta, None.

This study received funding from: NIH grants DE016865 and DK53904.

M002

See Sunday Plenary Number S002

M003

Odd-Skipped Related 2 Functions in Cell Proliferation. S. Kawai, M. Yamauchi*, A. Amano*. Department of Oral Frontier Biology, Osaka University Graduate School of Dentistry, Suita-Osaka, Japan.

The drosophila pair-rule gene Odd-skipped encodes a zinc finger transcription factor required for accurate segment formation in the drosophila embryonic development. Mammalian homologues, Odd-skipped related 1 (Osr1) and Osr2, were expressed in limb, branchial arches, kidney, eye, and dermis. Osr2 is known to play a critical role in the secondary palate development. We previously reported the function of Osr2 in the bone using transgenic mice. In this study, we analyzed more detailed functional role of Osr2. Osr2 was found to be highly expressed in multipotent mesenchymal C3H10T1/2 cells. The expression level of Osr2 by C3H10T1/2 cells was examined under various culture condition. Osr2 expression remarkably increased by the serum starvation along the growth arrest, whereas, the expression decreased promptly by the serum re-addition. Next, the DNA methylation of Osr2 promoter was analyzed with the sodium bisulfite sequencing method, and histone acetylation on Osr2 promoter was also analyzed with the chromatin immunoprecipitation. The expression of Osr2 in the serum starvation, the confluent growth arrest, and the serum re-addition was found to be regulated by DNA methylation in the Osr2 promoter as well as by the histone acetylation. Moreover, Osr2 was observed to be localized in the cellular nuclear euchromatin with the confocal laser scanning microscope. Osr2 was participated in the maintenance at the G0 state that corresponded in the quiescent state at the cell cycle by the flow cytometry. These findings indicate that Osr2 play an important role in cell proliferation, especially in G0 regulation which is thought the entrance of the osteoblastic cell differentiation.

Disclosures: S. Kawai, None.

M004

See Sunday Plenary Number S004

M005

Grx5 Regulates Osteoblast Cell Functions by Protecting Against Oxidative Stress. G. R. Linares, W. Xing, K. E. Govoni, T. T. Nguyen*, S. Chen*, S. Mohan. JLP VAMC and LLU, Loma Linda, CA, USA.

There is now increasing evidence which suggest an important role for reactive oxygen species (ROS) in a variety of pathological situations including osteoporosis. However, little is known on the molecular components of the oxidative stress pathway or their functions in bone. Based on our recent findings that the newly identified member of glutaredoxin (Grx) family, Grx5, is highly expressed in bone and induced by growth hormone and the published findings that Grx5 protects yeast against oxidative stress, we proposed the hypothesis that Grx5 protects osteoblasts (Obs) from oxidative stress. We

found that treatment of MC3T3-E1 Obs with CdCl₂, an inhibitor of Grx activity, increased apoptosis in a dose dependent manner with a 2.5 fold increase ($P < 0.001$) at 1 μ M dose. To verify that the CdCl₂ effects on Ob apoptosis is caused by inhibition of Grx5 activity, we treated MC3T3-E1 Obs with Grx5 siRNA or control siRNA and evaluated effects on apoptosis. Grx5 expression decreased ($P < 0.01$) 80 and 40% at 24 & 72 hrs, respectively, after treatment with Grx5 siRNA. In contrast, neither Grx1 nor Grx2 expression was altered by Grx5 siRNA treatment. Grx5 siRNA treatment decreased osteocalcin expression by 50% ($P < 0.01$) and increased apoptosis by 40% ($P < 0.01$) as determined by DNA fragmentation assay. To identify the molecular pathway by which Grx5 regulates Ob functions, we tested based on findings in yeast that Grx5 deficiency results in impaired biogenesis of Fe-S cluster, a critical co-factor for a large number of regulatory proteins. Accordingly, mitochondrial aconitase activity, which is dependent on Fe-S cluster, was decreased by 37% ($P < 0.01$) in Grx5 siRNA treated cells. Since reduced formation of Fe-S cluster would lead to increased level of free iron, a competitive inhibitor of Mn-SOD (a key mitochondrial enzyme that scavenges ROS) we measured MnSOD activity in Grx5 deficient Obs. Mn-SOD activity was significantly reduced in Grx5 siRNA treated cells (0.89 ± 0.11 vs. 2.04 ± 0.05 U/mg protein; $P < 0.001$). Because estradiol treatment has been shown to protect Obs against oxidative stress and increase Grx5 expression (1.5 fold, $P < 0.05$), we evaluated the consequence of Grx5 overexpression on Obs. We found that Grx5 overexpression using retroviral vectors protected MC3T3-E1 cells against H₂O₂-induced apoptosis and formation of ROS (50 & 40% reduction; $P < 0.01$). Furthermore, Grx5 overexpression increased mineralized nodule formation in MC3T3-E1 cells (23% increase; $P < 0.01$). Our findings are consistent with the hypothesis that Grx5 is an important determinant of Ob cell functions and acts via a molecular pathway that involves regulation of Fe-S cluster formation, Mn-SOD activity, and ROS generation.

Disclosures: G.R. Linares, None.

M006

ROS Expression in Osteoblasts of NOS1, 2 and 3 Knock Out Mice. H. Watanabe, Y. Sugawara, T. Yanagisawa*. Ultrastructural Science, Tokyo Dental College, Chibacity, CHIBA, Japan.

Oxygen is converted to reactive oxygen species (ROS) and nitric oxide (NO) with high reactivity, and reacted with proteins and genes, affecting cell metabolism and intracellular transport. Bone tissues are readily affected by the gas environment, but reports on the effects of the gas environment on osteoblasts have been rare. In this study, we examined the protein levels of various NO and ROS synthetases (NOX) in normal mice and NOS1 (n-NOS), NOS2 (i-NOS), and NOS3 (e-NOS) knock-out (KO) mice, and evaluated the interrelationships among various NO and ROS synthetases. After 5-week-old normal mice and NOS1, 2, and 3 KO mice were anesthetized, immunohistochemical evaluations were performed using NOXO, NOXA, NOX4, and NQO antibodies. In osteoblasts of the control mice, the NOXO, NOXA, and NQO expression was negative, but NOX4 expression was weakly positive. Both NOXO and NOXA were expressed in NOS2 and NOS3 KO mice, also suggesting the expression of NOX1. Furthermore, since the expression of NOX4 and NQO were strongly positive in NOS2 and NOS3 KO mice, the presence or absence of i-NOS and e-NOS is considered to be involved in the generation of ROS in osteoblasts.

Disclosures: H. Watanabe, None.

M007

Rapamycin Inhibits Osteoblast Proliferation and Differentiation in MC3T3-E1 Cells and Primary Mouse Bone Marrow Stromal Cells. U. K. Singha*¹, Y. Jiang*², S. Yu*¹, M. Luo*¹, Y. Lu*¹, J. Zhang*¹, G. D. Roodman*¹, G. Xiao*¹. ¹Medicine, University of Pittsburgh, Pittsburgh, PA, USA, ²Pharmacology, University of Pittsburgh, Pittsburgh, PA, USA.

While the roles of the mammalian target of rapamycin (mTOR) signaling in regulation of cell growth, proliferation, and survival have been well documented in various cell types, its actions in osteoblasts are poorly understood. In this study, we determined the effects of rapamycin, a specific inhibitor of mTOR, on osteoblast proliferation and differentiation using MC3T3-E1 preosteoblastic cells (MC-4) and primary mouse bone marrow stromal cells (BMSCs). Rapamycin significantly inhibited proliferation in both MC-4 cells and BMSCs at a concentration as low as 0.1 nM. Western blot analysis shows that rapamycin treatment markedly reduced levels of cyclin A and D1 protein in both cell types. In differentiating osteoblasts, rapamycin dramatically reduced osteoblast-specific osteocalcin (Ocn), bone sialoprotein (Bsp), and osterix (Osx) mRNA expression, ALP activity, and mineralization capacity. However, the drug treatment had no effect on these parameters when the cells were completely differentiated. Importantly, rapamycin markedly reduced levels of Runx2 protein in both proliferating and differentiating but not differentiated osteoblasts. Finally, overexpression of S6K in COS-7 cells significantly increased levels of Runx2 protein and Runx2 activity. Taken together, our studies demonstrate that mTOR signaling affects osteoblast functions by targeting osteoblast proliferation and the early stage of osteoblast differentiation.

Disclosures: G. Xiao, None.

M008

Effects of Traumatic Brain Injury on Bone Formation/Remodeling During Fracture Healing in a Rat Model. I. Arango-Hisijara¹, E. R. Kulick^{*2}, S. Rehman^{*3}, M. B. Elliott^{*4}, M. F. Barbe⁴, R. F. Tuma^{*2}, F. F. Safadi¹, S. N. Popoff¹, W. G. DeLong³. ¹Anatomy and Cell Biology, Temple University School of Medicine, Philadelphia, PA, USA, ²Physiology, Temple University School of Medicine, Philadelphia, PA, USA, ³Orthopaedic Surgery and Sports Medicine, Temple University Hospital, Philadelphia, PA, USA, ⁴Physical Therapy, Temple University, Philadelphia, PA, USA.

Previous studies have established that traumatic brain injury can enhance the process of fracture healing. In this study, we examined the effects of traumatic brain injury on bone formation in the fracture callus and on circulating factors that can influence bone remodeling and/or angiogenesis. Ten week old Male Sprague-Dawley rats were separated into four groups: 1) Control; 2) Standard closed femoral fracture (Fx); 3) Low impact traumatic brain injury combined with Fx (LiHtx/Fx); 4) High impact traumatic brain injury combined with Fx (HiHtx/Fx). Rats were injected with calcein at 5 and 2 days prior to being euthanized at 2 weeks post-treatment. Histological analysis of the brains stained with cresyl violet confirmed diffuse axonal injury in both Htx groups; The HiHtx group displayed more axonal injury and neuronal apoptosis compared to the LiHtx group. Radiographic examination of the fracture callus demonstrated greater bony consolidation in the brain injured LiHtx/Fx and HiHtx/Fx compared to Fx rats. Histological analysis of the fracture callus demonstrated greater amounts of periosteal (intramembranous) and endochondral bone formation occurring in the brain injured LiHtx/Fx and HiHtx/Fx compared to Fx rats. Calcein labeling demonstrated a significant increase in bone formation rates in the brain injured rats, providing direct evidence that brain injury can increase bone formation at the fracture site. Serum osteocalcin was also measured with a significant increase in the LiHtx/Fx and HiHtx/Fx groups compared to the Fx group. Analysis of other circulating factors revealed significant increases in TGFβ1, MCP-1, TNFα, IL-1β, IL-6, and leptin levels in the LiHtx/Fx and HiHtx/Fx groups compared to the Fx group. TNFα, IL-1β and IL-6 are osteoclastogenic factors suggesting that remodeling of the fracture callus occurs earlier in the brain injured LiHtx/Fx and HiHtx/Fx compared to Fx rats. High levels of TGFβ1 and MCP-1 could stimulate proliferation of osteoprogenitor cells, and high levels of leptin have been shown to increase VEGF expression resulting in enhanced angiogenesis that is a requirement for accelerated fracture healing. In conclusion, traumatic brain injury accelerates bone formation and remodeling during fracture healing and changes in circulating levels of factors known to influence bone cell development/function may mediate, in part, the acceleration of fracture repair.

Disclosures: I. Arango-Hisijara, None.

M009

TWEAK Is a Regulator of Human Osteoblast Function. G. J. Atkins¹, C. Vincent^{*1}, K. J. Weldon^{*1}, D. R. Haynes^{*2}, C. Holding^{*2}, T. S. Zheng^{*3}, A. Evdokiou^{*1}, D. M. Findlay¹. ¹Discipline of Orthopaedics and Trauma, University of Adelaide, Adelaide, Australia, ²Discipline of Pathology, University of Adelaide, Adelaide, Australia, ³Biogen Idec Inc., Boston, MA, USA.

TNF-like weak inducer of apoptosis (TWEAK), a member of the TNF superfamily is pro-angiogenic, pro-inflammatory and proliferative for endothelial and other cell types. We recently showed that TWEAK is a novel mediator of mouse collagen-induced arthritis and have identified TWEAK expressing cells in human rheumatoid arthritis (RA) tissues. The aim of this work was to investigate a potential role for TWEAK in human bone remodeling.

Human primary osteoblasts (OB) were found, by flow cytometry, to express high levels of the TWEAK receptor, Fn14. OB also expressed abundant TWEAK mRNA. Treatment of OB with exogenous TWEAK was highly proliferative. TWEAK dose-dependently suppressed OCN mRNA expression and increased both the RANKL:GAPDH and the RANKL:OPG mRNA ratios. Time-course studies under mineralising conditions showed that TWEAK suppressed the osteogenesis-related genes OCN and BSP-1 early in cultures, corresponding with the period in which RANKL expression was increased. Whereas RANKL induction was transient (up to day 9), OCN, BSP-1 and type I collagen mRNA expression were inhibited throughout the mineralisation period (up to day 21). Consistent with this, continuous TWEAK exposure inhibited *in vitro* mineralisation by OB and induced the expression of sclerostin, which has been shown to inhibit bone formation via BMP/Wnt signalling. TWEAK stimulated mitogen-activated protein kinase (MAPK) activity in primary osteoblasts, inducing phosphorylation of ERK-1/2 and JNK, but not p38 MAPK. TWEAK had only a slight effect on NFκB signalling and did not invoke the Akt survival pathway. We also found that TWEAK significantly modifies the osteoblast response to TNFα, suggesting that in an inflammatory situation the outcome may vary, dependent on the relative amounts of these cytokines present. Our results suggest that TWEAK is a novel regulator of bone turnover and are consistent with a role for TWEAK in inflammatory bone loss pathologies, such as RA, where its persistent presence may be anti-anabolic.

Disclosures: G.J. Atkins, None.

M010

See Sunday Plenary Number S010

M011

Lysyl Oxidase Regulates Collagen Quality and Quantity in MC3T3-E1 Cell Culture System. P. Atsawasuwan^{*}, Y. Mochida, M. Yamauchi. Dental Research Center, University Of North Carolina at Chapel Hill, Chapel Hill, NC, USA.

Lysyl oxidase (LOX) is an amine oxidase critical in stabilizing collagen fibrils in tissues including bone. To obtain further insights into the function of this enzyme in osteoblastic cells, we established and characterized the MC3T3-E1 (MC) derived clones stably overexpressing LOX. MC cells were transfected with pcDNA3.1-V5/His containing coding sequence of mouse LOX and several stable clones expressing higher levels of LOX (S clones) were generated. The overexpression of LOX was verified by Western blot analysis with anti-V5 antibody and anti-LOX antibody. Five S clones and two control groups (MC cells and those transfected with an empty vector) were selected and analyzed. Based on MTS assay at day 1, 3 and 5 of culture, all S clones showed the proliferation rate comparable to that of controls. In another set of experiment, the clones and control cells were cultured in α-MEM in the presence of 10% fetal bovine serum, 2mM β-glycerophosphate and 50 μg/ml ascorbic acid for up to 4 weeks. At appropriate time points of culture, cell-matrices were analyzed for collagen content (week 0, 1) and cross-links (wk 2 and 4) by high performance liquid chromatography, fibrillogenesis (wk 3) by transmission electron microscopy and *in vitro* mineralization (wk 0, 1, 2, 3 and 4) by Alizarin-red S staining. The quantitative cross-link analysis revealed that two major cross-links (dihydroxylysinonorleucine and pyridinoline), the major aldehyde (hydroxyllysine aldehyde) and a total number of aldehydes (free + cross-linked) were significantly increased in S clones in comparison to controls demonstrating higher LOX activities in these clones. However, the collagen content in all S clones was significantly decreased. Consistent with this, the number and diameter of collagen fibrils in S clones were significantly fewer and smaller than those of controls. Furthermore, the onset of mineralization was markedly delayed in S clones. These findings indicate that LOX plays crucial roles not only in collagen stability but also in collagen synthesis. The latter function could be due in part to the ability of LOX to bind and modulate transforming growth factor β1 (TGF-β1) function as we have recently reported. These dual functions of LOX may have significant impact on matrix organization and mineralization in bone.

Disclosures: P. Atsawasuwan, None.

This study received funding from: NIH grants DE10489 and AR052824.

M012

Calcitonin and Teriparatide for Vertebral Fracture Pain. A. Bazarra-Fernandez^{*}. ObGyn, Juan Canalejo University Hospital, La Corunna, Spain.

Background: Fractures, especially vertebral fractures, are a common complication of osteoporosis, leading to significant pain.

Aim: To compare the pain release induced by osteoporotic vertebral fracture, through teriparatide and teriparatide plus calcitonine.

Methods: We performed a study to compare the analgesic effect of 20 mcg teriparatide versus 20 mcg teriparatide plus metered dose intranasal spray 200IU/activation calcitonin in two groups between postmenopausal women undergoing osteoporosis with vertebral fracture. A 10-point visual analog pain scale (1 = least to 10 = most painful) and a four-point pain grade (grade 1 = least to grade 4 = most painful) were used to measure the pain perception.

Results: The mean pain scores for the teriparatide and teriparatide plus calcitonin were 2.3 ± 1.1 and 8.5 ± 1.1 , respectively ($P < 0.05$), while the pain grades for teriparatide and teriparatide plus calcitonin were 1.5 ± 0.3 and 3.5 ± 0.4 , respectively ($P < 0.05$). In teriparatide group, analgesics were requested, but in teriparatide plus calcitonin group no analgesics were requested ($P < 0.001$).

Conclusion: Using teriparatide is more expensive than other osteoporosis treatment. Studies show that taking a bisphosphonate with hormone replacement therapy (HRT), results in increased bone mass when compared to taking either a bisphosphonate or estrogen alone. Besides, calcitonin is better for osteoporotic vertebral fracture pain release than HRT. However, a larger investigation will be needed to achieve more significant case number.

Disclosures: A. Bazarra-Fernandez, None.

M013

Osteoblasts from Serotonin Transporter Knockout Mice Display Reduced Growth and Mineralization Capacity. M. M. Bliziotis, K. M. Wiren. Medicine, Oregon Health and Science University/pvanc, Portland, OR, USA.

Recent studies in bone have demonstrated the presence of functional pathways for both responding to and regulating the uptake of serotonin (5-HT). This is of high clinical importance given the role of the serotonergic system in affective disorders, and the wide use of pharmacologic agents that target the 5-HT system to manage these disorders. In addition to the presence of 5-HT receptors, osteoblasts, osteoclasts and osteocytes all possess the serotonin transporter (5-HTT). Binding and uptake studies have demonstrated the 5-HTT in osteoblastic and osteocytic cells to be functional and highly specific for 5-HT uptake. Immunohistochemistry of sections of whole bone from rat tibia demonstrated the

in situ expression of 5-HT receptors and the 5-HTT in osteoblasts and osteocytes. Additional evidence for a role of 5-HT signaling in the growing skeleton was more recently provided by animal studies. Using two differing animal models, Warden et al. (Endocrinology 2005) found that mice with a life-long null mutation of the gene encoding for the 5-HTT displayed a consistent skeletal phenotype of reduced mass, altered architecture, and inferior mechanical properties. This finding was confirmed in a second model wherein inhibition of the 5-HTT using a SSRI resulted in reduced bone mineral accrual during growth. In both models, the skeletal phenotype resulted from a reduction in bone formation indicating an osteoblastic defect.

We have investigated the phenotype of osteoblastic cells from 5-HTT knockout mice in vitro. Calvaria from wild type and 5-HTT^{-/-} neonatal mice were isolated and osteoblast populations derived with serial collagenase digestion. Cell growth curves, alkaline phosphatase expression and mineralization capacity (as assessed by alizarin red staining of osteoblast cultures) were assessed.

Cells from 5-HTT^{-/-} mice demonstrated reduced growth capacity in the first week of culture, with approximately 30-60% reduction in growth as assessed by cell counts. Alkaline phosphatase activity was also reduced by 20% in the 5-HTT^{-/-} cells at day 14 of culture. Finally, mineralization capacity was reduced by 20% at day 23 in culture in the 5-HTT^{-/-} cells.

We conclude that the reduced bone formation rates and osteopenia observed in young 5-HTT^{-/-} mice is due, at least in part, to a cell autonomous defect in osteoblasts which results in reduced cell growth, alkaline phosphatase activity and mineralization capacity. The mechanism whereby this defect is expressed is unknown. Given the widespread use of drugs that target the 5-HTT, elucidation of the effects of disruption of this transporter on bone is of major clinical significance.

Disclosures: M.M. Blizotes, None.

M014

Strontium Ranelate Effects in Human Osteoblasts Support its Uncoupling Effect on Bone Formation and Bone Resorption. T. C. Brennan^{*1}, M. S. Rybchyn^{*1}, P. Halbout^{*2}, A. D. Conigrave^{*3}, R. Mason^{*1}. ¹School of Medical Sciences (Physiology) and Bosch Institute, University of Sydney, Sydney, Australia, ²Rheumatology, Institut de Recherches Internationales Servier, Courbevoie, France, ³School of Molecular and Microbial Biosciences, University of Sydney, Sydney, Australia.

Strontium ranelate reduces the risk of vertebral and hip fractures in post-menopausal women. Previous studies have shown that strontium ranelate increases bone formation and decreases bone resorption. In the current study, we investigated the uncoupling effect of strontium ranelate in primary human osteoblasts (HOB). For this, we assessed the strontium ranelate effects on indirect markers of bone formation (HOB proliferation, alkaline phosphatase (ALP) activity), on the regulation of osteoclastogenic signals by osteoblasts (OPG mRNA level and RANKL mRNA and protein level) and on HOB lifespan. HOB were cultured in Dulbecco's modified Eagles medium with 10% fetal bovine serum, adapted to serum-free and calcium-free medium for 24h, and then treated with strontium ranelate in physiological Ca²⁺ (1mM). After a 48h-treatment, strontium ranelate increased HOB proliferation, assessed by thymidine incorporation, in a dose-dependent manner, up to 3.8-fold with 2 mM Sr²⁺ (p<0.01). ALP activity was increased after 72 h with strontium ranelate by almost 2 fold (1 and 2 mM, p<0.01). After only 24 h, strontium ranelate dose-dependently increased OPG mRNA expression, by qRT-PCR, up to 1.9-fold with 2 mM Sr²⁺ (p<0.001). Under the same conditions, RANKL mRNA expression was dramatically decreased compared with RANKL expression observed in vehicle: remaining expression was below 25% with strontium ranelate concentrations ≥ 0.1mM (p<0.001). These results were confirmed at the protein level by RANKL-specific western blotting. Finally, strontium ranelate increased HOB survival under oxidative stress conditions induced by peroxide (0.1 mM, p<0.05, 1 and 2 mM, p<0.01), and decreased serum deprivation-induced apoptosis as measured by caspase 3 and caspase 7 activities (0.1 and 1.0 mM, p<0.05). In conclusion, strontium ranelate, at strontium concentrations close to those observed in patients treated with the therapeutic dose of 2g/day, increases human osteoblast replication, differentiation and the ability to withstand stress, parameters associated with promotion of bone formation. In parallel, human osteoblasts stimulated by strontium ranelate express more OPG and less RANKL, thereby decreasing their capability to stimulate osteoclastogenesis. Overall, these results strongly support the dissociation effect of strontium ranelate on bone formation and bone resorption in human osteoblasts.

Disclosures: T.C. Brennan, None.

M015

Primary Murine Osteoblast Cultures Contain Macrophages that Enhance Osteoblast Mineralisation. M. Chang^{*}, A. R. Pettit^{*}, K. Schroder^{*}, V. M. Ripoll^{*}, D. A. Hume^{*}, L. Raggatt^{*}. Institute for Molecular Bioscience, University of Queensland, St. Lucia, QLD, Australia.

Delineation of the phenotype and functional capacity of osteoblasts (OBs) has been widely studied using primary OBs harvested via enzymatic digestion of neonatal rodent calvaria (calvarial OBs). Previous studies have suggested heterogeneity within this cell preparation and reported immune functions that are not traditionally performed by mesenchymal cells. These immune functions have been attributed to the OB, however, the heterogeneous nature of the culture has not been considered. We have demonstrated that macrophages are a significant population in standard calvarial OBs using cells isolated from MacGreen mice (macrophages express an eGFP transgene driven by a myeloid restricted promoter). Microarray analysis of differentiating calvarial OB cultures (day 5, 14 and 21) confirmed a large number of macrophage-associated genes at all time points.

Clustering analysis using microarray datasets representing nearly all tissues and cell lineages (symatlas.gnf.org) linked the gene expression profiles of calvarial OBs to macrophages and osteoclasts. Immunocytochemistry and flow cytometry confirmed that calvarial OB preparations co-isolated a population of F4/80⁺ macrophages that persist and expand during OB differentiation in vitro. Multiple passaging did not eliminate macrophages from these cultures. Bone explant cultures were also examined as an alternative approach to generating primary OBs and were similarly shown to contain F4/80⁺ macrophages. Given these observations, and our recent data demonstrating that macrophages are intercalated within bone lining tissues, we hypothesised that macrophages and OBs cooperate in the control of bone metabolism. To delineate the cooperative and distinct functional roles of macrophages and OBs, we used magnetic-assisted cell sorting to generate a population of highly enriched calvarial OBs by removing haematopoietic cells. The majority of cells removed via this method expressed the F4/80 macrophage marker. Strikingly, macrophage removal significantly decreased both osteocalcin mRNA expression levels and in vitro mineralisation (von Kossa staining) in enriched OB differentiation cultures. The presence of a persistent population of macrophages within primary OB cultures raises the possibility that our existing understanding of in vitro OB biology has been influenced by the contribution of this cell population. Our data provide evidence that macrophages regulate OB function and specifically enhance mineralisation in vitro.

Disclosures: M. Chang, None.

M016

See Sunday Plenary Number S016

M017

Atm Regulates Osteoblast Differentiation Through the BMP-Smad1/5/8 Pathway. J. F. Chau^{*}, N. Rasheed^{*}, S. Wang^{*}, B. Li^{*}. Institute of Molecular and Cell Biology, Singapore, Singapore.

Ataxia telangiectasia mutated (Atm) is a tumor suppressor that plays a critical role in DNA damage response and is required for genome integrity. In addition, Atm deficient mice have been shown to suffer from osteoporosis (Hishiya et al. Bone 37:497, 2005; Rasheed et al. Hum. Mol. Genet 15:1938, 2006). It was found that Atm deficient osteoblast showed decreased expression of osterix, an essential transcription factor for osteoblast differentiation, leading to the defective osteoblast differentiation in the Atm deficient mice. It is known that osterix is induced by BMPs through the canonical Smad1/5/8 and non-canonical MAPK signaling pathways. As Atm deficiency diminished the BMP induced up-regulation of osterix, we propose that Atm participates in the BMP activated signaling pathways. We found that BMP2 treatment can activate Atm and the activation of Smad1/5/8 was compromised in Atm deficient osteoblast and MEF as detected by Western blotting. This phenomenon was also observed in normal cells treated with wortmannin or caffeine, inhibitors to phosphatidylinositol 3-kinase related kinases (PIKKs), a family of proteins that Atm belongs to. Treatment of wortmannin or caffeine also decreased the protein level of Id1, a known target of BMP-Smad1/5/8 signaling pathway. The results strongly suggest that Atm controls osteoblast differentiation through the BMP signaling pathway.

Disclosures: J.F. Chau, None.

This study received funding from: A-star.

M018

The Effect of Calcium Channel Antagonists on Bone Metabolism in Aged Male and Female Brown Norway Rats. D. L. DeMoss^{*}, B. D. Kidd^{*}, M. J. Harmon^{*}, L. A. Ashley^{*}, G. C. Howard^{*}, A. J. Auxier^{*}, E. D. Nickel^{*}. Biological Sciences, Morehead State University, Morehead, KY, USA.

Bone metabolism is invariably correlated with calcium transport indicating that calcium channels are a potential point of regulation for skeletal remodeling. Calcium channel antagonists are utilized therapeutically and experimentally to decrease the influx of calcium into cells by blocking voltage-regulated L-type calcium channels. Previous experimental evidence has suggested that calcium channel antagonists decrease osteoblastic activity, thus decreasing the activity of the bone forming cells at a time when bone formation is already exceeded by bone resorption, exacerbating the situation. Therefore, the established principle that bone formation decreases following the attainment of peak bone mass, illustrates the need for a more comprehensive understanding of the action calcium channel antagonists have on bone turnover. Experimentation utilized male and female Brown Norway Rats six months of age to compare the effects of estrogen and the antagonists on blood pressure and bone turnover from skeletal compartments. In order to evaluate the positive or negative impact of various calcium channel antagonists on bone loss, bone resorption parameters were compared between normal males and females, and those receiving calcium channel antagonists (diltiazem, nifedipine, verapamil). The models utilized to study bone turnover were the pharmacokinetic loss of the tracer ³H-tetracycline, a compound deposited in the active mineralization front and freely released in urine, the measurement of various bone degradation markers in urine collected throughout the experimental period and organ isotope extraction. The data suggest significant differences between sexes and antagonist impact on the turnover of calcium from multiple calcium pools.

Disclosures: D.L. DeMoss, None.

This study received funding from: NIH-INBRE 5P20RR17481-06.

M019

Protein Kinase D Is an Essential Mediator During Osteoblast Differentiation. D. N. Y. Fan, W. M. W. Cheung, A. W. C. Kung. Department of Medicine, The University of Hong Kong, Hong Kong, China.

Protein kinase D, also known as PKC μ , is a serine/threonine protein kinase that responds to phorbol esters and diacylglycerol. Using MC3T3-E1 cells, we demonstrated that PKD is activated during DMSO-induced osteoblast differentiation. We further demonstrated that prolonged activation of protein kinase C pathways alone, i.e. in the absence of osteogenic inducers such as BMP-2 and/or DMSO, is sufficient to induce bone formation in preosteoblast cells in vitro. In this study, we examined the functional roles of PKD in osteoblastogenesis. Phorbol 12-myristate 13-acetate (PMA) activates most PKCs including PKD. Treatment of MC cells with PMA enhances osteoblast differentiation as indicated by increased ALP activity and bone nodules formation. Treatment with Gö6976, a specific inhibitor for PKD, at 0.02 and 0.2 μ M resulted in a significant dose-dependent decrease in alkaline phosphatase (ALP) activity during osteoblast differentiation of MC cells mediated by DMSO, BMP2 or PMA. Bone nodule formation was attenuated simultaneously. Semi-quantitative RT-PCR analyses demonstrated that Gö6976 treatment resulted in reduced Runx2, Osterix and ALP transcript expression in MC cells. However, a general PKC inhibitor Gö6983 that does not inhibit PKD showed little effect on osteoblast differentiation, suggesting that PKD is crucial in the process. To confirm the functional roles of PKD, we overexpressed wild-type (PKD-WT), constitutively active (PKD-CA) and dominant negative (PKD-DN) PKD in MC cells and examine the effect of PKD modulation on osteoblast differentiation. In the absence of osteogenic inducers, MC cells transfected with PKD-CA resulted in enhanced bone nodules formation as compared to the PKD-DN transfectants. These findings are in good concordance to our previous observations that PKD activation alone is sufficient for inducing osteoblast differentiation. Using both pharmacological and PKD overexpression studies, our findings suggested that PKD plays essential roles in osteoblast differentiation and that osteoblast differentiation can be modulated via the activation of PKD.

Disclosures: D.N.Y. Fan, None.

This study received funding from: AO Research Fund of the AO Foundation, Matching Grant and HKU foundation of the University of Hong Kong.

M020

Tumor Necrosis Factor- α Stimulated Msx2 Expression in C2C12 Cells. H. Lee*, H. Ryoo, K. Woo, G. Kim*, J. Baek. Department of Cell and Developmental Biology, Seoul National University School of Dentistry, Seoul, Republic of Korea.

Tumor necrosis factor- α (TNF- α) is a pro-inflammatory cytokine that is involved in local and systemic bone loss through both stimulation of osteoclastic bone resorption and inhibition of osteoblastic bone formation. Although previous reports have shown that TNF- α inhibit osteoblast differentiation via enhanced Runx2 degradation, we could observe TNF- α -mediated inhibition of alkaline phosphatase (ALP) activity in Runx2-nulled calvarial cells. Msx2 has been shown to suppress ALP activity via counteracting the ability of Dlx5 to activate ALP promoter. Therefore we examined the effect of TNF- α on Msx2 expression in C2C12 cells. As previously reported, either Msx2 overexpression or TNF- α treatment suppressed BMP2-induced ALP activity in C2C12 cells. TNF- α enhanced the mRNA and protein level of Msx2. TNF- α -mediated Msx2 induction was not suppressed by cycloheximide treatment. BAY-11-7082, an NF- κ B inhibitor, suppressed TNF- α -mediated Msx2 induction but SP600125, a JNK inhibitor, did not. BAY-11-7082 partially reversed TNF- α -mediated inhibition of ALP activity. These results suggest that stimulation of Msx2 expression may be involved in TNF- α -mediated inhibition of osteoblast differentiation, at least in part.

Disclosures: J. Baek, None.

M021

See Sunday Plenary Number S021

M022

A Novel R131G RUNX2 Mutation Causing Cleidocranial Dysplasia Disrupts Heterodimerization with Core Binding Factor- β . H. Kim*, M. Han*, K. Lim*, A. J. van Wijnen², J. L. Stein², J. B. Lian², G. S. Stein², J. Choi¹. ¹Biochemistry & Cell Biology, Kyungpook Natl. Univ. School of Medicine, Skeletal Diseases Genome Research Center, Daegu, Republic of Korea, ²Cell Biology, UMASS Medical School, Worcester, MA, USA.

Cleidocranial dysplasia (CCD) is caused by haploinsufficiency of the RUNX2 gene. In previous study (Kim HJ et al, J Cell Physiol 207:114-122, 06), we found a novel R131G RUNX2 mutation from CCD patient. Here, we showed functional analysis of this RUNX2 R131G mutation with respect to molecular mechanism. RUNX2 R131G mutation is located in RUNT DNA binding domain and it also located within putative nuclear localization signal. Therefore, we determined mutant RUNX2 with regard to nuclear localization, DNA binding, heterodimerization with partner protein core binding factor- β (CBF- β) and transactivation function against downstream target gene osteocalcin promoters. In nuclear localization function, RUNX2 R131G mutation had normal nuclear localization function, which was confirmed by transient transfection of HA-tagged mutant

RUNX2 into CHO and HeLa cells by in situ immunofluorescent staining. With regard to DNA binding activity, RUNX2 R131G mutant had normal DNA binding activity, which was shown by electrophoresis mobility shift assay. Third, heterodimerization function of mutant RUNX2 with CBF- β was disrupted in cotransfection assays. Finally, RUNX2 R131G mutant showed loss of transactivation function on osteocalcin promoter reporter assay while RUNX2 wild type showed high transactivation function. Collectively, R131G mutation of RUNX2 causes CCD phenotype through the loss of heterodimerization with the partner protein CBF- β without abnormalities of nuclear localization, and DNA binding.

Disclosures: J. Choi, None.

M023

See Sunday Plenary Number S023

M024

Estrogen Suppression of Adipogenesis Is Mediated by TGF- β . K. B. Clifton, S. Khosla, M. J. Oursler. Endocrine Research Unit, Mayo Clinic, Rochester, MN, USA.

Osteoblasts and bone marrow adipocytes originate from a common mesenchymal precursor. Investigators have hypothesized that a shunting of the common precursor cell away from the osteoblast and towards the adipocyte may be partly responsible for bone loss with aging, and we have hypothesized that estrogen deficiency with age may be responsible for this shift. While estrogen and transforming growth factor- β (TGF- β) have been shown to enhance osteoblast and inhibit adipocyte differentiation, the exact mechanism(s) by which estrogen may regulate these processes is not yet clear. Peroxisome proliferator-activated receptor- γ (PPAR γ) is a member of the nuclear receptor super-family; it is known to be the master regulator of adipocyte differentiation. We tested the hypothesis that estrogen may play a role in regulating adipogenesis by suppressing expression of PPAR γ , and that its effects are mediated, at least in part, by TGF- β . The bipotential mouse bone marrow stromal cell line, ST2, was used to address this hypothesis. In time course experiments, ST2 cells were treated with estrogen, TGF- β , or the corresponding vehicle from 1 hour up to 12 days. Expression of PPAR γ was significantly reduced ($p < 0.05$) by TGF- β treated ST2 cells compared to the vehicle treatment at the 24 hour time point and each time point thereafter. Similarly, estrogen suppressed PPAR γ expression compared to both the vehicle treated and untreated cells after 48 hours of treatment. ST2 cells were cultured in adipogenic medium for 6 days. Treatment with estrogen or TGF- β reduced PPAR γ expression. Moreover, co-treatment with estrogen and a chemical TGF- β signaling inhibitor partially restored expression of PPAR γ . To examine possible molecular mechanisms by which estrogen and TGF- β regulate PPAR γ expression, cells were infected with dominant negative (dn) Smads 2 and 3, dn MEK, and dn PAK2 to block Smad-dependent and Smad-independent pathways. Both estrogen- and TGF- β -regulated repression of PPAR γ were partially disrupted by blocking the Smad 3 and the Smad-independent PAK2 pathways. These results are consistent with the hypothesis that estrogen may play a role in regulating adipogenesis, and that its effects are mediated, at least in part, by TGF- β through both Smad dependent and Smad-independent signaling pathways.

Disclosures: K.B. Clifton, None.

This study received funding from: NIH.

M025

See Sunday Plenary Number S025

M026

Regulation of RUNX2 Translation by 5'- and 3'-UTR Binding Proteins. N. Elango*, S. Sudhakar*, M. S. Katz. GRECC, VA Medical Center, San Antonio, TX, USA.

RUNX2, the major regulator of osteoblast differentiation, is expressed as two isoforms (RUNX2-I and RUNX2-II) encoded by two mRNAs differing only in their 5'-UTRs and initial coding regions. Recent studies show that RUNX2 gene expression is regulated at the translational level, and RUNX2-I is translated earlier during osteoblast differentiation than RUNX2-II. Since a 3961 nucleotide-long 3'-UTR is common to both mRNAs and the two 5'-UTRs are distinct, we hypothesize that the 3'-UTR contains a common translational regulatory motif and the two 5'-UTRs contain isoform-specific motifs. We have found by deletion analysis that the region between 2000 and 3000 nucleotides of the 3'-UTR contains a negative regulatory motif. Gel retardation assays reveal a 75 kDa protein, expressed in osteoblastic cells (UMR-106, ROS 17/2.8) but not precursors (ST2), binding to a pyrimidine-rich sequence within the 2000-3000 nucleotide region. Using RNA affinity chromatography we have purified six proteins from UMR-106 cells, including a 75 kDa protein, that bind to the pyrimidine-rich sequence. A high level of luciferase expression by RUNX2-I reporter plasmid but not RUNX2-II reporter mRNA in transfected osteoblasts (Elango et al, J Cell Biochem 99:1108, 2006) suggests that nuclear factor(s) bound to the 5'-UTR of RUNX2-I mRNA during transcription (but absent from in vitro transcribed reporter mRNA) are essential for translation. We have purified from UMR-106 cells by RNA affinity chromatography three proteins that bind to the RUNX2-I 5'-UTR. Translation of RUNX2-I but not RUNX2-II in early osteoblastic cells (UMR-106) expressing both RUNX2 mRNAs suggests that RUNX2-II translation is suppressed until later stages of differentiation. Gel retardation assays show that stem-loop structures of RUNX2-II mRNA 5'-UTR bind proteins expressed in early osteoblasts (UMR-106) but not precursors (ST2) or mature osteoblastic cells (ROS 17/2.8); these proteins may

function as suppressors of RUNX2-II translation in early osteoblasts. Based on these findings, we postulate: 1) translation of both RUNX2 mRNAs is suppressed in precursors by 3'-UTR binding protein(s); 2) RUNX2-I is translated early in osteoblastogenesis upon expression of a 75 kDa pyrimidine-rich region binding protein and removal of suppression. RUNX2-I translation is also enhanced by RUNX2-I 5'-UTR binding proteins; 3) translation of RUNX2-II is suppressed during early osteoblast differentiation by the transient expression of proteins binding to the RUNX2-II 5'-UTR. Our studies provide a model by which 3'- and 5'-UTR binding proteins control sequential translation of the two RUNX2 isoforms and thereby regulate the course of osteoblast differentiation.

Disclosures: N. Elango, None.

This study received funding from: VA Merit Award.

M027

See Sunday Plenary Number S027

M028

Dlx5 Overexpression Promotes Early Odontoblast Maturation. V. L. S. Ferrer^{*1}, Y. Kawano², H. T. Li¹, H. Chin^{*1}, L. Wang^{*3}, A. C. Lichtler¹.

¹Genetics and Developmental Biology, University of Connecticut Health Center, Farmington, CT, USA, ²Division of Oral Anatomy, Niigata University, Niigata, Japan, ³Institute of Molecular Biology, Academia Sinica, Taipei, Taiwan.

Dlx5 is a member of the Dlx gene family of transcription factors, which have been shown to be important for the differentiation of osteoblasts and chondrocytes and the development of craniofacial structures including teeth. To further understand the role of Dlx5 in vivo, our laboratory generated transgenic mice overexpressing Dlx5 driven by the osteoblast- and odontoblast-directed 3.6 kb fragment of the type I Collagen promoter (3.6Col1a1). We have previously reported that 3.6Col1a1-driven Dlx5 overexpression results in accelerated mandibular enamel and dentin mineralization in 7-week-old mouse incisor. Enamel highlighting of micro-CT 3D reconstruction of the mandible showed initiation of enamel mineralization at the level of the 3rd molar in transgenics in contrast to the wildtype enamel, which begins at the level of the 1st molar. Light micrographs showed that transgenic odontoblasts exhibited advanced maturation, displaying the distinct lack of polarity seen in wild-type early, functional odontoblasts.

To further analyze the phenotype, we examined transgenic mice at earlier time points (1, 3, and 5 weeks) to determine the onset of the phenotype. MicroCT revealed no significant differences in enamel and dentin mineralization at these time points. However, light micrographs showed that the odontoblast phenotype is apparent as early as 1 week.

Further histological analysis of 7-week-old transgenic incisors revealed that as odontoblast differentiation progresses towards the incisal end, the odontoblasts become highly disorganized and eventually are indistinguishable from the pulp. The corresponding dentin lacks the parallel arrangement of the dentinal tubules. Predentin in the incisal area is diminished or absent, leading to jagged and thinner dentin and, ultimately, exposed pulp. Trichrome staining revealed ectopic collagen formation in the pulp adjacent to the dentin. Undecalcified sections of calcein and xylenol orange labeled incisors showed that the formations are ectopic mineralizations. The wavy pattern of labeling, which appears at the incisal tip in the wild-type incisor, begins at the middle third of the transgenic incisor.

These observations suggest that 3.6Col1a1-driven Dlx5 overexpression promotes early odontoblast maturation. However, this early maturation results in the eventual loss of recognizable odontoblast morphology and irregularity and depletion of dentin matrix formation, leading to exposed pulp chamber.

Disclosures: V.L.S. Ferrer, None.

This study received funding from: NIH.

M029

See Sunday Plenary Number S029

M030

Positive and Negative Regulation of Osteoblast Differentiation by the SWI/SNF Chromatin Remodeling Complex. S. Flowers^{*1}, N. G. Nagl^{*1}, H. Guo^{*1}, G. R. Beck², E. Moran¹.

¹Fels Institute for Cancer Research and Molecular Biology, Temple University School of Medicine, Philadelphia, PA, USA, ²Division of Endocrinology, Metabolism and Lipids, Emory University School of Medicine, Atlanta, GA, USA.

Osteoblast differentiation requires reprogramming of gene expression to activate tissue specific gene expression and to effect coordinated withdrawal from the cell cycle. Chromatin remodeling is an important part of this process, in which the SWI/SNF complex uses the energy of ATP hydrolysis to disrupt nucleosome architecture, thereby altering the accessibility of gene promoters to transcription factors. The SWI/SNF complex is essential for both positive and negative gene regulation events, which has complicated analysis of its molecular mechanisms of action. A manner by which the complex might distinguish functions is suggested by the occurrence of two subunits as pairs of related alternatives. To test this concept, we used siRNA technology to deplete MC3T3-E1 pre-osteoblast cells of each subunit. The alternative pairs include the largest subunits of the complex, p270/ARID1A and its close relative ARID1B, which are members of the ARID family of DNA

binding proteins. The other subunit that occurs as a mutually exclusive pair is the ATPase itself, which can be either BRM, or the BRM-related protein BRG1.

This approach successfully distinguished complexes with distinct roles in osteoblast differentiation. The p270/ARID1A subunit was revealed as diagnostic of a complex with a repressor role during cell cycle withdrawal. In contrast, complexes containing the ARID1B subunit play an important positive role in cell cycle activity. The high level of c-myc expression seen in MC3T3-E1 pre-osteoblasts is dependent on the integrity of ARID1B-containing complexes, while differentiation-associated repression of c-myc depends on complexes containing the p270/ARID1A subunit. Chromatin immunoprecipitation (ChIP) assays indicate the c-myc promoter is a direct target of the SWI/SNF complexes, and that depletion of either ARID subunit impairs the association of other important regulators with the c-myc promoter. Likewise, depletion of the ATPase subunits reveals separation of key functions. Both ATPases contribute to cell cycle withdrawal, but they have very distinct functions in tissue specific gene expression and the onset of mineralization. The osteocalcin promoter is a direct target of SWI/SNF complexes, and the ATPases distinguish complexes with different roles in its regulation. These analyses give insight into the molecular mechanisms that underlie lineage determination, and the timing and coordination of the differentiation process.

Disclosures: S. Flowers, None.

M031

See Sunday Plenary Number S031

M032

Regulation of RUNX2 at the Nuclear Lamina. P. M. Fonseca¹, G. Zhou^{*1}, Q. Zheng^{*1}, H. Kingston^{*2}, M. Tassabehji^{*2}, B. Lee¹. ¹Molecular Human Genetics, Baylor College of Medicine, Houston, TX, USA, ²St. Mary's Hospital, Manchester, United Kingdom.

RUNX2 is a member of the RUNT family of transcription factors. It is essential for osteoblast formation and chondrocyte maturation. Loss of function mutations in RUNX2 result in the human skeletal disorder cleidocranial dysplasia (CCD). RIP (CBFA1/RUNX2-Interacting Protein) was isolated in a screening of a human osteosarcoma cDNA library using a yeast two-hybrid approach. Two families with rearrangements involving chromosome 8q - where RIP maps - have been reported to have a CCD-like phenotype. In transient transfection experiments, RIP down-regulated the transactivation by RUNX2 in a dose-dependent manner in both 10T1/2 cells and ROS17/2 cells. RIP is mainly localized in the nucleus and it was identified as a component of the nuclear envelope in proteomic screens. The major components of the nuclear envelope are lamins, which are intermediate filaments with an important role in nuclear organization, cell division, apoptosis and transcriptional regulation. Interestingly, mutations in A-type lamins and lamin-associated proteins result in several laminopathies such as mandibuloacral dysplasia (MAD). MAD presents clinical features such as acroosteolysis, dental crowding, hypoplastic clavicles and delayed closure of the fontanels, partially phenocopying CCD. We hypothesize that the skeletal defects observed in these patients are due to the disruption of lamin interactions with transcriptional regulators relevant in bone formation such as RIP and RUNX2. GST pull-down experiments showed an interaction between LaminA/C and RIP, as well as the RUNT domain of RUNX2. The tail domain, which is mutated in MAD patients, is responsible for the interaction. Moreover, LaminA/C could repress RUNX2 transactivation of reporter genes in COS7 cells in a dosage-sensitive way. Mutant versions of lamin carrying MAD mutations seem to lose their repressive action. These mutants had altered binding properties. These data suggest a novel mechanism for transcription regulation of skeletogenesis involving sequestration of a RUNX2 complex at the nuclear lamina. In order to study the effects of A-type lamins on osteoblast differentiation, we are currently generating a C2C12 stable cell line overexpressing laminA/C and we will also knock-down the gene in pre-osteoblastic cells.

Disclosures: P.M. Fonseca, None.

This study received funding from: Fundacao Ciencia e Tecnologia, Portugal.

M033

See Sunday Plenary Number S033

M034

Metnrl: A New Secreted Protein Inhibit Differentiation of MG-63. W. Y. Gong^{*1}, Y. Liu^{*2}, R. M. Zheng^{*1}, G. X. Qiu^{*2}, S. Q. Lin¹. ¹Obstetric and Gynecology, Peking Union Medical College Hospital, Peking Union Medical College, Chinese Academy of Medical Science, Beijing, China, ²Orthopaedic Surgery, Peking Union Medical College Hospital, Peking Union Medical College, Chinese Academy of Medical Science, Beijing, China.

It has been reported that AP-1 transcription factor complex modulates the function of osteoblasts and osteoclasts which participate in bone formation and bone resorption respectively. So in our previous study, we constructed a high-throughput assay method based on the AP-1 signaling pathway dual-luciferase reporter system to screen new function gene expressing in fetal osteoblasts. We found one gene (GMSS555) without reporting function in PUBMED inhibited the activation of AP-1 (<50% compare to empty vector). After analysis with basic local alignment tool (BLAST), this gene is noted "Meteorin, glial cell differentiation regulator-like (METRNL)". Now in this experiment, we cloned this gene and studied whether it could influence the differentiation of MG63. The full-length cDNA of METRNL contains an open reading frame encoding 312 amino acids with a putative signal peptide of 45 aa. Northern blotting revealed that a 1.5kb mRNA was constitutively but lowly expressed in most normal adult tissues. The recombinant METRNL was isolated from BL21 codon plus and used to immunize rabbits to raise polyclonal antibodies. Western blot detected an about 34 kDa protein in culture supernatant of CHO cells stably transfected with ORF of METRNL. Immunohistochemistry analysis demonstrated that METRNL was mainly expressed by the undifferentiated osteoblasts and chondrocytes. To study the function of METRNL in osteoblasts, we established stable MG63 cells that express the METRNL tagged with EGFP at its COOH-terminus. After cultured in osteogenic supplement (containing b-Glycerolphosphate/dexamethasone/ascorbic acid-2-phosphate) for 14 days, the METRNL transfected MG63 produces lower matrix than mock-transfected and parent MG63. Real time PCR assays showed METRNL inhibited the ALP and osteocalcin mRNA expression ($p < 0.05$). Our study indicated that METRNL expressed mainly in undifferentiated cells and can inhibited transcription activity of AP-1, and reduced the differentiation of human osteoblastic MG63.

Disclosures: W.Y. Gong, None.

M035

TIEG Suppresses Osteoblast Cell Proliferation Through Modulation of the TGF β /Smad Signaling Pathway and Repression of E2F1 Gene Expression. J. R. Hawse¹, M. Subramaniam¹, J. Pirngruber^{*2}, N. M. Rajamannan³, M. J. Oursler¹, S. A. Johnsen^{*2}, T. C. Spelsberg¹. ¹Biochemistry and Molecular Biology, Mayo Clinic, Rochester, MN, USA, ²Department of Molecular Oncology, Gottingen Center for Molecular Biosciences, Gottingen, Germany, ³Department of Cardiology, Northwestern University Medical School, Chicago, IL, USA.

TGF β Inducible Early Gene-1 (TIEG) is a member of the Kruppel-like family of transcription factors that was originally identified in osteoblasts. This transcription factor regulates the expression of many genes and plays a critical role in bone formation and maintenance. We have demonstrated that TIEG suppresses the expression of Smad7 following TGF β treatment of osteoblasts and that this suppression does not occur in the absence of TIEG. Further, transient transfection of osteoblasts with a TIEG expression construct results in suppression of Smad7 promoter activity. Through the use of yeast-2-hybrid and co-immunoprecipitation assays, we have shown that TIEG directly interacts with mSin3a, a well characterized co-repressor. In order to determine if TIEG recruits mSin3a to the Smad7 promoter, we performed time course ChIP assays. These studies revealed that TIEG and mSin3a are recruited to the Smad7 promoter within 60 minutes of TGF β treatment, and that phosphorylated polymerase II is displaced from the Smad7 promoter within 30 minutes of treatment. Interestingly, the HDAC proteins do not appear to be involved in this process since they are not recruited to this promoter region and since TSA, an inhibitor of HDAC activity, does not relieve the repression of Smad7 by TIEG. Since we have demonstrated a central role for TIEG in the TGF β /Smad signaling pathway, and since this pathway is known to be an important regulator of cell proliferation, we sought to determine TIEG's role in the proliferation of osteoblast cells. Overexpression of TIEG in osteoblasts results in a significant decrease in cell proliferation by approximately 50%. Additionally, calvarial osteoblasts isolated from TIEG^{-/-} mice proliferate more rapidly relative to osteoblasts isolated from wild-type littermates. To further characterize this proliferative response, we examined the role of TIEG in regulating the activity of the E2F1 promoter, a well known pro-proliferative gene. Transient transfection assays demonstrate that TIEG drastically decreases the activity of this promoter in osteoblasts. Taken together, these data demonstrate a central role for TIEG in suppressing the expression of Smad7 leading to enhancement of the Smad signaling pathway. TIEG is also shown to play a critical role in regulating osteoblast cell proliferation, and potentially osteoblast differentiation, possibly as a result of TGF β /Smad signaling and E2F1 expression.

Disclosures: J.R. Hawse, None.

M036

See Sunday Plenary Number S036

M037

TFIIA, ATF4, and Runx2 Synergistically Activate Osteoblast-specific Osteocalcin Gene Expression. S. Yu¹, Y. Jiang^{*2}, M. Luo^{*1}, Y. Lu¹, J. Zhang¹, G. D. Roodman¹, G. Xiao¹. ¹Department of Medicine, University of Pittsburgh Medical Center (UPMC), Pittsburgh, PA, USA, ²Department of Pharmacology, University of Pittsburgh Medical Center (UPMC), Pittsburgh, PA, USA.

Runx2, a member of the runt homology domain family of transcription factors, is a master regulator of osteoblast function and bone formation. Mice lacking Runx2 have no mineralized skeleton due to a complete lack of mature osteoblasts. The expression level of Runx2 protein is regulated by a number of factors including BMPs, FGF-2, IGF-1, TNF- α , TGF- β , and PTH, all of which play important roles in osteoblasts and bone both in vitro and in vivo. In addition, the activity of Runx2 protein is positively or negatively modulated through protein-protein interactions. Activating transcription factor 4 (ATF4) is an osteoblast-enriched factor which regulates the terminal differentiation and function of osteoblasts. ATF4 knock-out mice have reduced bone mass and bone mineral density (severe osteoporosis) throughout their life. To identify proteins interacting with Runx2, we used a yeast two-hybrid system and identified TFIIA, a general transcriptional factor, as a Runx2-interacting factor. While pull-down assays confirmed that TFIIA physically interacted with Runx2 when both factors were coexpressed in COS-7 cells, surprisingly, it did not activate or inhibit Runx2-dependent transcriptional activity. In contrast, TFIIA unexpectedly activated ATF4, which we recently identified as a Runx2-interacting protein, in a dose-dependent manner. Deletion analysis found that this activation required the presence of the C-terminal 15 amino acid residues of ATF4 molecule. Finally, TFIIA, ATF4, and Runx2 synergistically stimulated the 0.657-kb mOG2 (mouse osteocalcin gene 2) promoter activity and endogenous osteocalcin mRNA expression. In summary, this study demonstrates a novel mechanism through which bone-specific transcription factors and general transcription factors cooperate in regulating osteoblast-specific gene expression.

Disclosures: S. Yu, None.

M038

siRNA Specific Knockdown of Lamin A/C Inhibits Osteogenic Differentiation of Human Mesenchymal Stem Cells. R. Akter¹, D. Rivas¹, Y. Dong², H. Drissi², G. Duque³. ¹Lady Davis Institute for Medical Research, Montreal, PQ, Canada, ²Orthopaedics, University of Rochester, Rochester, NY, USA, ³Medicine/Geriatrics, McGill University, Montreal, PQ, Canada.

Recent studies have indicated the role of lamin A/C, a component of nuclear lamina, in premature ageing with severe bone loss. Mutations in the gene encoding lamin A/C have shown a deficit in the number of both osteoblasts and osteocytes. We have previously shown that lamin A/C expression levels are reduced in the aging osteoblasts in vivo. However, no study has evaluated the direct role of lamin A/C in osteogenic differentiation of mesenchymal stem cells (MSC). In this study, we hypothesize that reduced expression of lamin A/C has a negative impact on osteogenic differentiation of human MSC. We inhibited lamin A/C using different doses of lamin A/C siRNA (200-800 nM) in MSC committed to differentiate into osteoblasts. Cells treated with vehicle but without the siRNA/oligo were used as a control. The level of siRNA was determined by western blot and RT-PCR. We found that up to 400nM did not have any inhibitory effect, but 600 and 800nM successfully inhibited lamin A/C without affecting cell survival. After 10 days of lamin A/C knockdown, cells were stained with alizarin red (mineralization) and alkaline phosphatase. Additionally, expression of osteocalcin, cbfa1 and lamin A/C were determined by RT-PCR and western blot. Finally, nuclear blebbing, a typical finding of lamin A/C inhibition, was quantified by propidium iodine staining. We found that lamin A/C knockdown induces higher level of nuclear blebbing and significantly reduces alizarin red staining ($p < 0.01$) and alkaline phosphatase activity ($p < 0.01$) in osteogenic differentiating MSC. Additionally, expression of cbfa1 and osteocalcin was reduced in lamin A/C knockdown cells. Overall, to identify the potential mechanism, gel-shift assay analyses were pursued. We found that lamin A/C knockdown affects the DNA/protein interaction of the binding sites in the cbfa1 promoter. In conclusion, our results suggest that lamin A/C is a new factor required for the osteogenic differentiation of MSC and that lamin A/C directly interacts with the cbfa1 transcription pathway.

Disclosures: R. Akter, None.

This study received funding from: Canadian Institutes for Health Research.

M039

See Sunday Plenary Number S039

M040

Osteofornin Enhances Gap Junction Communication of Human Preosteoblastic Cells in Culture. L. X. Bi, E. Mainous, Y. Zeng^{*}, W. J. Buford^{*}. Dpts. of Surgery & Orthopaedics, UTMB, Galveston, TX, USA.

Gap junctions provide a cell-to-cell low resistance conduction pathway for coordination of tissue function. Composed of nonselective channels they allow passage of ions, nucleotides, and other small molecules. Our previous study has shown that marrow sac cells (preosteoblasts) which separate the bone from marrow display intercellular gap junctions (Bi LX JBMR 17: SA219 Suppl. 1, 2002). To investigate activities of gap

junction affected by osteoformin (polyaspartate), we examined the levels of fluorescence recovery after photobleaching (FRAP) using a laser scanning confocal microscope. Human preosteoblast cells were cultured in a minimum essential medium [a-MEM] and 10% fetal bovine serum with or without osteoformin (5ug/ml) for 3 days. The cells were loaded with 5,6-carboxyfluorescein diacetate,acetoxymethyl ester (5,6-CFDA/AM, 5 µg/ml) for FRAP at 37°C for 30 minutes and then de-esterified by washing with phosphate buffered saline before photobleaching. The FRAP was examined using a laser scanning confocal microscope with a 488-nm wavelength light from an argon laser (LSM microscope) and recorded every 5 seconds in 60 seconds after photobleaching. Osteoformin enhanced levels of intercellular gap junction communication by 68-72% ($P<0.01$) compared to that of the control group. To confirm that the fluorescein crosses the gap junction channel, a gap junctional blocker (carbenoxolone, 150 µg/ml) was used. Carbenoxolone blocked the effect of osteoformin on human preosteoblasts. We conclude that osteoformin significantly enhances intercellular gap junction communication which is associated with exchange of regulatory ions and osteoblast differentiation in vitro. It might be an important regulator of bone formation by accelerating fracture and bone defect healing, and controlling bone diseases.

Disclosures: L.X. Bi, None.

M041

See Sunday Plenary Number S041

M042

Osteogenic Differentiation of Circulating Endothelial Progenitor Cells. T. Bick^{*1}, N. Rozen^{*2}, E. Dreyfuss^{*1}, M. Soudry^{*1}, D. Lewinson¹. ¹Research Institute for Bone Repair, Orthopaedic Surgery A, Rambam-Health Care Campus, Haifa, Israel, ²Research Institute for Bone Repair, Rambam-Health Care Campus, Haifa, Israel.

The dramatic potential of circulating endothelial progenitor cells (EPC) to heal a large bone defect (critical-sized gap in sheep tibiae, see abstract: Healing of Critical-sized Bone Defects by Endothelial Progenitor Cells. By D. Lewinson et al) led us to investigate whether EPC might be induced to transform into osteogenic cells. Peripheral mononuclear fraction of circulating sheep and human mononuclear cells were isolated using LymphoprepTM (Axis-Shield, Oslo, Norway), seeded on fibronectin-coated plates (Sigma-Aldrich, MS, USA), and cultured in EBM-2 media supplemented with EGM-2MV SingleQuote (Clonetics, Cambrex Bio Science, MD, USA). The endothelial nature of adherent colonies was identified by incorporation of Dil-acetylated LDL (Molecular Probes, Oregon, USA), tube formation on Matrigel (BD Labware, MA, USA) and immunostaining for von Willebrand factor (Dako, Glostrup, Denmark). EPC were expanded and cultured in plastic dishes or seeded into polyethylene glycol/fibrinogen hydrogel scaffolds. Cultures were incubated either in DMEM/F12 (1:1) containing 10% FCS or in an osteogenic differentiation media - DMEM/F12 (1:1) containing 10% FCS, Dexamethasone 10^{-7} M/L, ascorbic acid 5×10^{-3} M/L and β -glycerophosphate 10^{-2} M/L. Changes in cell morphology, nodule formation, von Kossa (vK) and alizarin red (AR) staining as well as osteocalcin (OC) immunohistochemistry served to identify osteoblastic differentiation. Nodular aggregates formation was evident in osteogenic media-incubated sheep EPC already by 1 week. These nodular aggregates stained positively by vK, AR and OC. However, human EPC, when cultured in the same conditions showed very intensive staining of equal intensity over all the confluent culture by AR with many more intensively-stained small noduli. vK staining showed many granular deposits dispersed all over the culture plate. In contrast to sheep EPC, not only the nodular aggregates but most of human EPC stained by both vK and AR. Control cultures of both human and sheep EPC showed minimal background staining. Phase contrast microscopy of sheep EPC-seeded scaffolds demonstrated that the cells were distributed homogeneously throughout the scaffold and formed tube-like structures by 1 week in both media. However the cell-seeded scaffolds cultured in osteogenic media showed prominent nodular aggregates. vK and AR staining were not informative because the scaffold itself retained the stain. Our results support a possible mechanism that explains the potential of blood derived EPC in tissue engineering for bone regeneration.

Disclosures: T. Bick, None.

M043

See Sunday Plenary Number S043

M044

Differential Effects of Secreted Frizzled-related Proteins (sFRPs) and Wnt Inhibitory Factor (WIF)-1 on Osteoblastic Differentiation of Mouse Pluripotent Mesenchymal Cell Line. S. W. Cho, S. J. Heo, H. J. Sun, O. K. Choi, J. Y. Yang, H. Y. Cho, S. W. Kim, C. S. Shin. Department of Internal Medicine, Seoul National University College of Medicine, Seoul, Republic of Korea.

Secreted Frizzled-related proteins (sFRPs) are modulators of Wnt signaling which plays a role in development, apoptosis and tumorigenesis. sFRPs bind directly to the wnts proteins and appear to antagonize the effects of wnts by sequestering them from their receptor. Although overexpression of sFRP-1 in human osteoblasts has been shown to antagonize Wnt-signaling and accelerates apoptosis, a recent report demonstrated that sFRP-3 is a potent stimulator of osteoblast differentiation. This study was undertaken for

definitive assessment of contribution of different sFRPs and WIF-1 in osteoblast differentiation and function. Treatment of C3H10T1/2 cells with sFRP1, -2, -3, and -4 in the presence of Wnt-3A conditioned medium did not show significant difference in alkaline phosphatase (ALP) activity compared to vehicle treated cells. However, WIF-1 strongly inhibited the ALP activity in a dose-dependent manner [5nM, 10nM, 50nM, 100nM; 0.141 ± 0.002 , 0.105 ± 0.026 , 0.041 ± 0.003 , 0.022 ± 0.003 mU/mg protein, $p < 0.05$]. To further investigate the role of cell-associated sFRPs, we have transduced C3H10T1/2 cells with retroviral vector for sFRPs and WIF-1. Consistent with the previous data, sFRP-1, -2, -3, and -4 did not result in significant difference in ALP activity compared to empty virus transduced cells during osteoblastic differentiation using β -glycerophosphate and ascorbic acid. In contrast, overexpression of WIF-1 significantly inhibited the ALP activity compared to control cells at day 14 of culture [10.078 ± 1.835 vs 18.368 ± 3.848 mU/mg protein, $p < 0.05$]. BrdU uptake assay and caspase-3 assay showed that treatment of sFRPs and WIF-1 did not affect cell proliferation or apoptosis. In conclusion, we were not able to demonstrate that sFRP1-4 inhibit osteoblastic differentiation of mesenchymal cells. On the other hand, WIF-1 has consistently exhibited negative effects on osteoblastic differentiations of mouse pluripotent mesenchymal cells.

Disclosures: S.W. Cho, None.

M045

See Sunday Plenary Number S045

M046

Mesenchymal Stem Cell Concentration and Bone Repair: Pitfalls from Bench to Bedside. A. V. Cuomo^{*1}, M. Virk², F. Petrigliano^{*1}, E. Morgan^{*3}, C. Kang^{*4}, J. R. Lieberman². ¹UCLA, Los Angeles, CA, USA, ²University of Connecticut, Hartford, CT, USA, ³Orthopaedic Surgery, Boston University, Boston, MA, USA, ⁴Orthopaedic Surgery, UCLA, Los Angeles, CA, USA.

PURPOSE: This is a preclinical trial comparing the osteogenic potential of mesenchymal stem cell enriched bone marrow aspirate (enrBMA) versus unprocessed BMA mixed with demineralized bone matrix (DBM) in a critical-sized athymic rat femoral defect model.

METHODS: The buffy coat was extracted from 8 human BMA donors to obtain the enrBMA. The MSCs concentration was estimated by counting fibroblast colony forming units (f-CFU). Lyophilized DBM allograft (Osteofil-RTTM) was mixed with saline, BMA, enrBMA, or recombinant human bone morphogenetic protein-2 (rhBMP-2) (10ug) and was used to treat a 6mm critical-sized femoral defect in athymic rats. A total of 59 rats were divided into 6 groups (Table 1). Radiographs at 4, 6, 8, and 12 weeks were graded for bone healing by 3 independent observers. All animals were sacrificed at 12 weeks for microCT and histomorphometry.

RESULTS: The BMA and enrBMA from all 8 donors averaged 1072 ± 991 f-CFUs/mL and 6503 ± 6953 f-CFU/mL, respectively. All 10 defects healed in the positive control groups (II, VI) with rhBMP-2 (Table 1). One defect healed in each experimental group (III-V). The radiographic scores did not differ between time-points (data not shown) and the bone volume (BV) and mineral density (MD) did not differ between groups IV and V. The wide radiographic variability of defect healing in Groups IV and V did not correlate with the concentration of f-CFU's, the lot number of the DBM, or the age or sex of the BMA donor. Histomorphometry showed more dense trabecular and cortical bone in groups III-V than in group II.

CONCLUSION: Although enrBMA may demonstrate superior bone healing in certain clinical situations, this pre-clinical study cannot support the use of enrBMA when mixed with DBM to reliably heal critical-sized bone defects. The results of this study introduces one or more possibilities: (1) a higher number of MSC may be required for healing critical-sized defects; (2) an enhanced osteoinductive signal is required in the setting of critical-sized defects that cannot be overcome by enrBMA and DBM alone, and (3) the carrier used did not provide the optimal environment to promote cell growth and signaling. Importantly, this study identifies potential pitfalls when adapting the use of MSC to treat humans in a clinical setting.

Table 1. Radiographic (XR), MicroCT Bone Volume (BV), and Mineral Density (MD) Scores

Group	Healed defect/ group*	12 week XR**	BV (mm ³)	MD (mg HA/ccm)
I Defect only	0/5	2.2(±0.9)	-	-
II ACS+rhBMP-2	5/5	5.0(±0.0)	-	-
III DBM+Saline	1/10	3.4(±0.6)	-	-
IV DBM+BMA	1/17	3.2(±0.7)	77.0(±35.3)	1148(±139)
V DBM+enrBMA	1/17	3.1(±0.9)	87.9(±29.6)	1145(±137)
VI DBM+rhBMP-2	5/5	4.8(±0.4)	117.0(±18.3)	1149(±127)

*number of 100% healed defects per total animals per group.

**XR bone healing score: 0 = none, 1 = 0%-25%, 2 = 26%-50%, 3 = 51%-75%, 4 = 76%-99%, and 5 = 100%

Disclosures: A.V. Cuomo, Medtronic Sofamor Danek 2.

This study received funding from: Medtronic Sofamor Danek.

M047

See Sunday Plenary Number S047

M048

The Effect of Caloric Restriction on Bone of Aging Rats Is Exerted Through the Stimulation of Sirtuins. G. Duque¹, D. Rivas², F. Picard^{*3}, S. Miard^{*3}, M. Lafontaine-Lacasse^{*3}, G. Ferland^{*4}, P. Gaudreau^{*4}. ¹Medicine/Geriatics, McGill University, Montreal, PQ, Canada, ²Lady Davis Institute for Medical Research, Montreal, PQ, Canada, ³University of Laval, Quebec, PQ, Canada, ⁴University of Montreal, Montreal, PQ, Canada.

Caloric restriction (CR) in combination with soy protein is reported to inhibit adipose genes in peripheral fat and to increase bone mass in mice and rats. The mechanisms that explain these effects remain unknown. After the recent finding that Sirt1, a member of the Sirtuins family, acts as a repressor of PPAR γ 2 in peripheral fat, we hypothesize that CR combined with soy protein diet reduce adipogenesis in bone through the upregulation of Sirt1 and its co-factors. In this study, male Sprague Dawley rats (8 month-old) were fed for 12 months with either casein or soy protein and exposed to a CR of 40% in comparison to the rats fed to satiety. A control group was fed ad libitum. Changes in body mass index (BMI), weight, length and serum leptin were quantified. At 20 months of age, animals (n=20 per group) were sacrificed and tibiae were obtained for immunohistochemistry, immunofluorescence and in-situ hybridization for Sirt1 and its co-factor AEBP1. Additionally, bone marrow expression of PPAR γ 2 and CEBP α was also quantified. Our results showed that CR induced a significant reduction in weight, body mass index and serum leptin levels in both casein and soy protein fed groups as compared with the ad libitum groups (p<0.001). We found that in the CR rats fed with soy protein there is a significantly higher expression of both Sirt1 and AEBP1 detected by both in-situ hybridization and immunohistochemistry as compared with casein and ad libitum fed rats (p<0.01). Additionally, levels of both PPAR γ 2 and CEBP α expression were significantly reduced in the soy protein group (p<0.01). Our results indicate that the combination of CR and soy protein has an inhibitory effect on bone marrow adipogenesis through the stimulation of Sirtuins (Sirt1 and co-factor AEBP1) thus suppressing the expression of PPAR γ 2. These findings provide the basis for further investigation on the role of Sirtuins in age-related bone marrow adipogenesis.

Disclosures: G. Duque, None.

This study received funding from: Canadian Institutes for Health Research.

M049

See Sunday Plenary Number S049

M050

Bespoke Bioceramic Scaffolds Support Mesenchymal Stem Cell Growth and Osteogenic Differentiation. J. Dyson^{*1}, P. Genever^{*2}, K. Dalgarno^{*3}, D. Wood^{*1}. ¹Leeds Dental Institute, University of Leeds, Leeds, United Kingdom, ²Department of Biology, University of York, York, United Kingdom, ³School of Mechanical and Systems Engineering, University of Newcastle, Newcastle, United Kingdom.

There is a clinical need for new bone replacement materials which combine long implant life with complete integration and appropriate mechanical properties. Apatite-wollastonite (A-W) is a bioactive glass-ceramic that shows excellent biocompatibility in vivo and similar mechanical properties to bone. Selective laser sintering (SLS) is a rapid prototyping technology used to produce intricate porous three-dimensional scaffolds to match the exact geometry of a patient's graft site, and can be applied to A-W powder. Mesenchymal stem cells (MSCs) can be induced to undergo osteogenic differentiation to mature bone-forming osteoblasts making MSCs attractive candidates for orthopaedic tissue engineering applications. We have used human MSCs to populate porous A-W scaffolds produced by SLS to create bespoke bone replacements.

MSCs were cultured on A-W scaffolds for up to 21 days. Confocal and scanning electron microscopy (SEM) were used to determine optimal seeding densities, to demonstrate that MSCs adhered and retained viability on the surface and penetrated into the pores of A-W scaffolds over 21 days culture. We identified a significant increase (p<0.01) in the number of MSCs growing on the scaffolds over 7 days. Using BrdU incorporation we demonstrated that $28.4\% \pm 2.6$ of MSCs proliferated over a period of 24 hours. Using real-time PCR we analyzed the expression of osteogenic markers by MSCs cultured in the absence of osteogenic supplements on A-W scaffolds compared to tissue culture plastic. We identified up to a 3-fold increase in cbfa1, 4-fold increase in alkaline phosphatase, 8-fold increase in type-I collagen, 170-fold increase in osteopontin, 1-fold increase in osteocalcin and a 14-fold increase in osteonectin expression on A-W compared to plastic at different time points over 21 days (p<0.05). At all time points the expression of osteogenic markers was equivalent to or significantly greater on A-W than plastic. We also identified significantly higher (p<0.01) alkaline phosphatase activity at days 7 and 14 compared to a calcium phosphate scaffold. Bespoke A-W scaffolds were engineered with a central channel to increase cell penetration in dynamic culture. Confocal microscopy and SEM were used to demonstrate that MSCs adhered to the scaffolds and retained viability for 21 days culture and cell in-growth was facilitated. These results indicate for the first time the biocompatibility and osteo-supportive capacity of SLS-generated A-W scaffolds and their potential as a bone replacement material.

Disclosures: J. Dyson, None.

This study received funding from: White Rose.

M051

Enhanced Mesenchymal Stem Cell Properties in Dynamic Three-Dimensional Cultures. J. E. Frith^{*1}, B. Thompson^{*2}, P. G. Genever^{*1}.

¹Department of Biology, University of York, York, United Kingdom, ²Smith and Nephew Research Centre, York, United Kingdom.

Mesenchymal stem cells (MSCs) are multipotent progenitor cells with the ability to self renew and differentiate along the osteogenic, adipogenic and chondrogenic lineages. This makes them good candidates for a range of therapeutic applications. MSCs are routinely cultured as monolayers attached to tissue culture plastic but there are indications that they lose their capacity for proliferation and differentiation after prolonged culture periods. We have grown MSCs as three-dimensional (3D) spheroids under dynamic conditions in both spinner flasks and a NASA rotating wall vessel (RWV). We hypothesised that increased cell-cell interactions, potential for communication and conditions of shear-stress and mass transfer may more closely mimic the in vivo environment to improve retention of stem cell properties.

We have shown that human MSCs spontaneously aggregate when prevented from adhering to culture plastic. These aggregates compact over a period of seven days into dense spheroids with decreased cell size and altered cell surface antigen expression compared to parallel monolayer MSCs, as shown by SEM and flow cytometric analysis. Live/dead staining confirmed that the cells remained viable in both spinner flasks and RWV culture after 7 days of dynamic culture. MSCs were cultured as monolayers and as spheroids in spinner flasks and the RWV in osteogenic medium for a period of 21 days. Staining showed the presence of alkaline phosphatase in all cultures from 7 days onwards with von Kossa-positive discrete staining for mineralised deposits in both dynamic 3D cultures, but not monolayers, at 14 and 21 days. RNA was extracted at 7, 14 and 21 days for analysis of osteogenic marker expression by qRT-PCR. As compared to monolayers, expression of Cbfa1 and osteocalcin was increased in 3D culture across all time points and expression of osteonectin and osteopontin was increased after 21 days. Increases in alkaline phosphatase and type-I collagen were also present in RWV cultures after 14 and 21 days. A comparison of adipogenic differentiation showed lipid droplet accumulation, by Oil red O staining, in dynamic 3D cultures after just seven days with accumulation in monolayers not occurring until 21 days. qRT-PCR analysis of adipogenic marker expression showed increased expression of C/EBP α and FABP4 in spinner flasks and of PPAR γ , LPL, C/EBP α and FABP4 in RWV cultures. Together these results show that dynamic 3D methods are viable for MSC culture and that both osteogenic and adipogenic differentiation potential are enhanced as compared to standard monolayer cultures.

Disclosures: J.E. Frith, None.

This study received funding from: BBSRC and Smith and Nephew.

M052

See Sunday Plenary Number S052

M053

Increasing Osteoblast Number Is Not Sufficient to Enhance the Function of the Hematopoietic Stem Cell Niche. S. Lymperti, A. Cope^{*}, F. Dazzi^{*}, N. Horwood. Kennedy Institute of Rheumatology, London, United Kingdom.

The regulation of haemopoietic stem cell (HSC) fate requires a specialized microenvironment in the bone marrow (BM) cavity called the HSC niche. Accumulating evidence indicates that osteoblasts (OB) are a key component of this niche, regulating HSC number and differentiation state. In this study the role of OB in the niche was further investigated by manipulating their activity with strontium (Sr). Since Sr increases osteoblast activity whilst inhibiting osteoclast differentiation and function, we hypothesized that Sr would improve the HSC supporting capacity of the niche.

Sr, like PTH, promoted bone nodule formation (alizarin red S and Von Kossa staining) and increased production of runx2 mRNA by RT-PCR in primary OB cultures. Administration of Sr to mice resulted in elevated levels of serum osteocalcin as measured by ELISA. Sr-treated mice showed increased bone volume and trabecular thickness defined by micro-CT analysis. In terms of haemopoiesis, Sr-treated mice exhibited increased numbers of haemopoietic progenitor cells compared to untreated control mice as assessed by colony forming unit-cells assay. However, no difference in primitive HSC numbers was detected between the two groups as evaluated by long term culture-initiating cells assay and FACS analysis for lin⁻, sca1⁺, c-kit⁺ cells. When Sr-treated mice were used as donors in HSC transplantation experiments, no difference in HSC engraftment ability was observed. However, when treated mice were used as recipients a delayed recovery was observed. Therefore despite an augmenting effect on OB function, the administration of Sr had no influence on primitive HSC, although the number of haemopoietic progenitors was higher than untreated controls.

It was recently shown that osteoclasts are important in stress-induced mobilization of haemopoietic stem and progenitors cells. The impaired engraftment of HSC observed in Sr-treated recipients, together with the fact that strontium inhibits osteoclastic resorption, implies that BM space could be intimately linked to the effect of bone remodeling whereby factors released from the bone matrix or produced by the osteoclasts themselves are required to provide signals that maintain the stem cell niche. In conclusion, we have shown that, although osteoblasts are indeed key functional component of the niche, an increase in their activity is not enough to expand the stem cell pool size. Therefore, we propose that active osteoclasts and balanced bone remodeling are required for the generation of the optimal HSC niche.

Disclosures: S. Lymperti, None.

This study received funding from: Leukemia Research Fund.

M054

Alteration of Endothelin-1 Effects on Calvarial Osteoblastic Cells from Connexin-43-deficient Mice. G. Geneau^{*1}, C. Niger^{*2}, N. Defamie^{*1}, S. Rodriguez^{*1}, M. Mesnil^{*1}, L. Cronier^{*1}. ¹UMR 6187, Institute of Physiology and Cellular Biology, CNRS, University of Poitiers, Poitiers, France, ²Department of Orthopaedics, University of Maryland School of Medicine, Baltimore, MD, USA.

Gap junctional intercellular communication (GJIC) is known to permit coordinated cellular activities during development and differentiation processes. Accordingly GJIC dysfunction or mutations of gap junction protein (connexin, Cx) genes have been implicated in human pathologies. In bone, in vitro and in vivo studies have demonstrated the implication of Cx43 expression and GJIC in osteoblastic differentiation and in the mineralization process (i.e. Schiller et al., 2001; Chung et al., 2006). Cumulated data support the fact that Cx43 expression is very important for normal bone formation and regulation of cellular responses to hormones/growth factors stimulation and to mechanical load. In this context, since Endothelin-1 (ET1) has been also implicated in the control of osteoblast proliferation/differentiation and in some bone pathologies like prostatic metastasis, the possible cross talk between Cx43 and ET1 was investigated in cultured calvarial osteoblastic cells (OB) isolated from Cx43^{-/-} and Cx43^{+/+} mice.

Interestingly, microcomputed tomographic analysis of 3days-old Cx43^{-/-} mice confirmed the hypomineralization observed in Cx43^{-/-} embryos by Civitelli's group. However, this delayed ossification was restricted to calvaria and in vitro characterization demonstrated that Cx43 protein expression, GJIC, alkaline phosphatase (ALP) activity, osteocalcin mRNA level and mineral deposits were significantly reduced in Cx43^{-/-} OB compared to Cx43^{+/+} OB. Pharmacological approaches using specific antagonists and agonist and quantitative RT-PCR using specific primers for ET1 receptor subtypes (ETA and ETB) revealed that the partial deletion of Cx43 gene was not related to a decrease or a modification in the expression of both receptor subtypes in OB. ET1 (10⁻⁸M) induced an inhibitory effect on OB differentiation in both genotypes whereas this peptide has a mitogenic effect only in Cx43^{+/+} OB. Moreover, the ET1 inhibitory effect on cell differentiation was correlated to a reduced Cx43 expression (-22%) and GJIC (-46%) in Cx43^{+/+} OB. Surprisingly, this correlation was not demonstrated in Cx43^{-/-} OB, suggesting an alternative regulatory pathway. The link between ET1 effect and GJIC was confirmed in the presence of a well-known uncoupler (18-AGA; 30 µM) in the culture medium of Cx43^{+/+} OB cells. In conclusion, these data strongly suggest that the level of Cx43 expression influences the osteoblastic response to ET1.

Disclosures: G. Geneau, None.

This study received funding from: Ligue Régionale contre le cancer.

M055

Modulation of P2X₇ Receptors in Human Osteoblasts by Oestrogen and Corticosteroids. M. Al-qallaf^{*1}, E. J. Kidd^{*1}, B. A. J. Evans². ¹Welsh School of Pharmacy, Cardiff University, Cardiff, United Kingdom, ²Child Health, Cardiff University, Cardiff, United Kingdom.

The P2X₇ receptor (P2X₇R) is usually identified by the greater affinity of dibenzoyl ATP (DBzATP) compared to ATP. Prolonged activation of the P2X₇R results in the formation of a non-selective pore in the cell membrane permeable to molecules as large as 900 Da. Oestrogen has been shown to inhibit osteoblast apoptosis, and hence increase their activity and lifespan. Additionally, oestrogen has been shown to inhibit osteoblast proliferation, an action believed to be through the oestrogen receptor-α. Interestingly, oestradiol has been found to exert non-genomic inhibition of the human P2X₇R in transfected CV-1 monkey kidney cells. The aims of this project were to investigate the modulation of P2X₇R expression and function by oestrogen and dexamethasone in human osteoblasts.

We have studied the effects of pre-incubating (30 minutes or 2 days) human osteoblasts with oestradiol or dexamethasone on P2X₇R expression and function using a cell line representing a late stage of osteoblast differentiation (SaOS2). To investigate the effect of oestradiol and dexamethasone on P2X₇R expression, Western blotting was performed. P2X₇R function was studied by measuring pore formation upon activation with ATP using the YO-PRO 1 (a dye that fluoresces on binding to nucleic acids) uptake method.

Dexamethasone (5 µM) and oestradiol (10 µM) were found to have no effect on P2X₇R protein expression. Concentration-effect curves (CEC) for ATP using the YO-PRO 1 assay gave EC₅₀ values of 0.36 mM ± 0.12. Oestradiol and dexamethasone were found to have no effect on the ATP EC₅₀ values, but they decreased the maximum YO-PRO 1 uptake induced by the agonist. Oestradiol significantly decreased maximum YO-PRO 1 uptake after pre-incubation for 30 minutes and 2 days by 22 and 38%, respectively. Dexamethasone significantly decreased maximum YO-PRO 1 uptake after 30 minutes incubation by 19%, but had no effect following a 2 day pre-incubation.

The results show that the P2X₇R expression at the protein level is not modulated by oestradiol or dexamethasone. However, oestradiol was found to have an inhibitory action on P2X₇R function after 30 minutes and 2 days pre-incubation. A non-classical, non-genomic mechanism must be responsible for the action of dexamethasone and oestradiol after 30 minutes incubation. The effect of the 2 day incubation with oestradiol could be genomic or non-genomic. These effects of oestradiol and dexamethasone on the P2X₇R might be important mechanisms for their modulation of osteoblast function. Further experiments are required to elucidate the function of the P2X₇R in these cells.

Disclosures: M. Al-qallaf, None.

M056

See Sunday Plenary Number S056

M057

Silencing Dkk1 Expression Rescues Dexamethasone-induced Bone Loss In Vitro. J. S. Butler¹, C. J. Hurson^{*1}, R. T. Moon^{*2}, J. M. O'Byrne^{*3}, P. P. Doran^{*1}. ¹UCD School of Medicine & Medical Science, Mater Misericordiae University Hospital, Dublin, Ireland, ²Howard Hughes Medical Institute, University of Washington School of Medicine, Seattle, WA, USA, ³Dept of Trauma & Orthopaedic Surgery, Royal College of Surgeons in Ireland, Dublin, Ireland.

Osteoporosis is a common skeletal disorder characterised by a reduced bone mass and a progressive micro-architectural deterioration in bone tissue leading to bone fragility and susceptibility to fracture. The Wnt/β-catenin pathway is a major signaling cascade in bone biology, playing a key role in regulating bone development and remodeling, with aberrations in signalling resulting in disturbances in bone mass.

Our objectives were to assess the gene expression profile of primary human osteoblasts (HOBs) exposed to dexamethasone with a view to identifying key genes driving bone mass regulation and to assess the effects of the Wnt antagonist Dickkopf-1 (Dkk1) on the bone profile of primary human osteoblasts exposed in vitro to dexamethasone.

HOBs were cultured in vitro and exposed to 10⁻⁸M dexamethasone over a time course of 4hr, 12hr and 24hr. RNA isolation, cDNA synthesis, in vitro transcription and microarray analysis were performed. Microarray data was validated by quantitative real time RT-PCR. Dkk1 expression was silenced using small interfering RNA (siRNA). Quantitative RT-PCR was performed to confirm gene knockdown. Control and Dex-treated HOBs were compared with respect to bone turnover. Markers of bone turnover analyzed included alkaline phosphatase activity, calcium deposition, osteocalcin expression, along with cell proliferation and cellular apoptosis.

Global changes in HOB gene expression were elicited by dexamethasone. Development associated gene pathways were co-ordinately dysregulated with the expression profile of key genes of the Wnt Pathway significantly altered. Dkk1 expression in HOBs was increased in response to dexamethasone exposure with an associated reduction in alkaline phosphatase activity, calcium deposition and osteocalcin expression. Silencing of Dkk1 expression, as confirmed by quantitative RT-PCR, was associated with an increase in alkaline phosphatase activity and calcium deposition, along with increased cell proliferation and reduced cellular apoptosis.

Dkk1 is an antagonist of Wnt/β-catenin signalling and plays a key role in regulating bone development and remodeling. Silencing the expression of Dkk1 in primary human osteoblasts has been shown to rescue the effects of dexamethasone-induced bone loss in vitro. The pharmacological targeting of the Wnt/β-catenin signaling pathway offers an exciting opportunity for the development of novel anabolic bone agents to treat osteoporosis and disorders of bone mass.

Disclosures: J.S. Butler, None.

M058

See Sunday Plenary Number S058

M059

Glucocorticoid Suppresses the Differentiation of Osteoblasts by Enhancing the Expressions of BMP Antagonists, Follistatin and Dan, and Pretreatments with Alendronate and PTH Abolish this Process. K. Hayashi^{*}, T. Yamaguchi, S. Yano, M. Yamauchi, M. Yamamoto, T. Sugimoto. Internal Medicine 1, Shimane University Faculty of Medicine, Izumo, Japan.

Glucocorticoid-induced osteoporosis (GIO) is known to be caused by the suppression of osteoblast-mediated osteogenesis, and to be effectively treated by bisphosphonate and parathyroid hormone (PTH). However, the exact mechanisms by which glucocorticoid(GC) suppresses osteoblast functions, or alendronate and PTH cure GIO are still unclear. The impaired BMP-Runx2 signal is known to be one of candidates for the suppression of osteogenesis by GC. The present study was performed by using osteoblastic MC3T3-E1 cells in order to clarify the mechanisms by which GC modulated this signal pathway and whether or not bisphosphonate as well as PTH antagonized GC-induced effect on this process. Dex (10⁻⁷M) significantly inhibited the proliferation of the cells through Day 7 by cell counting and BrdU incorporation. Dex (10⁻⁹ - 10⁻⁷ M) also strongly and dose-dependently suppressed the mineralization of the cells at Days 21 and 28 by Alizarin red stain and von Kossa stain. Real-time PCR revealed that Dex (10⁻⁷ M) reduced the mRNA expressions of type I collagen, osteocalcin, and Runx2. In contrast, mRNA expressions of BMP antagonists, Follistatin and Dan, were increased by Dex (10⁻⁷ M). Western blotting also revealed that protein expressions of Dan and follistatin were increased by Dex (10⁻⁷ M). The addition of a neutralizing antibody for Dan partially reversed the Dex-induced suppression of mineralization of the cells. Moreover, pretreatments of the cells with alendronate (10⁻⁸ M) or human PTH-(1-34) (10⁻⁸ M) also reversed the Dex-induced enhancement in mRNA expression of follistatin and Dan. The present findings suggest that Dex may inhibit the differentiation of osteoblasts by suppressing the BMP signal pathway through enhanced expressions of its antagonists, follistatin and Dan, and that the effectiveness of bisphosphonate and PTH in treating GIO may be partly explained by the abolishment of this process.

Disclosures: K. Hayashi, Merk & Co., Inc. 2.

This study received funding from: Merck & Co., Inc.

M060

See Sunday Plenary Number S060

M061

ChIP-on-chip Analysis Reveals Novel Glucocorticoid Response Genes Adjacent to Genomic Binding Sites for Steroid Hormone Receptor in Osteoblastic Cells. K. Horie-Inoue^{*1}, K. Takayama^{*2}, S. Inoue². ¹Division of Gene Regulation and Signal Transduction, Research Center for Genomic Medicine, Saitama Medical University, Saitama, Japan, ²Department of Geriatric Medicine, Graduate School of Medicine, University of Tokyo, Tokyo, Japan.

Glucocorticoid causes secondary osteoporosis by increasing bone resorption and impairing bone formation. Investigation of the glucocorticoid-dependent gene regulatory network in osteoblasts will provide useful information to elucidate the pathophysiology of glucocorticoid-induced osteoporosis. Glucocorticoid receptor (GR) belongs to the nuclear receptor superfamily, and functions as a ligand-induced transcriptional factor that regulates the expression of its target genes by recognizing and binding to the steroid hormone response elements (SHREs) in the gene regulatory regions. The prototypic consensus SHRE is a palindromic sequence that consists of two hexameric half-sites arranged as inverted repeats with a 3-bp spacer. Besides GR, other steroid hormone receptors for androgen, mineralocorticoid, and progesterone can also recognize and bind to the identical consensus SHREs. In the present study, we investigate whether novel glucocorticoid response genes can be identified in the vicinity of SHREs that have been previously validated as androgen response elements. Using chromatin immunoprecipitation (ChIP) assay combined with DNA microarray technique (ChIP-on-chip), we identified 10 bona-fide androgen-dependent SHREs in human prostate cancer LNCaP cells in the genomic regions that are being investigated by the ENCYCLOPEDIA OF DNA ELEMENTS (ENCODE) project. We examined whether these SHREs in the ENCODE regions could also recruit GR ligand-dependently and the expression of their adjacent genes could be modulated by glucocorticoid in osteoblastic Saos2 cells. Among the genes in the vicinity of the SHREs, pepsinogen C (PGC) and UDP glucuronosyltransferase 1A1 (UGT1A1) mRNAs were up-regulated by >2-fold in Saos2 cells (4.6-fold and 2.9-fold, respectively) in response to dexamethasone (10 nM) treatment for 6 h. The SHREs in the proximal upstream region of PGC and the 17-kb upstream region of UGT1A1 were shown to recruit GR ligand-dependently by ~2-fold in response to dexamethasone treatment for 1 h. The present data suggest that the systemic investigation of functional SHREs by ChIP-on-chip analysis is useful to identify novel glucocorticoid response genes in osteoblastic cells, which may play roles in the pathogenesis of glucocorticoid-induced osteoporosis as well as in the physiological hormone regulation.

Disclosures: K. Horie-Inoue, None.

M062

See Sunday Plenary Number S062

M063

Acid-induced Stimulation of COX-2 and RANKL in Osteoblasts Is Mediated by IP₃. N. S. Krieger, A. C. Michalenka*, K. LaPlante Strutz*, D. A. Bushinsky. Medicine, University of Rochester, Rochester, NY, USA.

Chronic metabolic acidosis stimulates net calcium (Ca) efflux from bone by regulation of osteoblastic activity leading to stimulation of osteoclastic resorption. This acid-induced bone resorption is mediated primarily by stimulation of osteoblastic cyclooxygenase 2 (COX2) mRNA and subsequent prostaglandin E₂-mediated increase in RANKL. We hypothesize that extracellular [H⁺] transduces its intracellular signal through a G protein-coupled proton sensing receptor, OGR1, recently identified in osteoblasts and coupled to inositol trisphosphate (IP₃)-mediated Ca release. We have shown previously that acid-induced bone Ca efflux from neonatal mouse calvariae is inhibited by TMB-8 and 2-APB, both of which inhibit IP₃ mediated Ca signaling. To further define the signaling pathway that responds to H⁺, we now demonstrate that these inhibitors also block osteoblastic COX2 and RANKL production. Neonatal mouse calvariae were incubated for 48h in Met (pH ~7.11) or neutral (Ntl, pH ~7.40) medium in the absence or presence of 100 μM TMB-8 or 50 μM 2-APB. Medium was changed at 24 h. As before, incubation in Met induced a marked increase in net Ca efflux and this bone resorption was significantly blocked by each inhibitor. In parallel, immunoblot analysis shows a significant increase in COX2 protein at 48h in calvariae in response to Met compared with Ntl (Ntl=0.37±0.04, Met=1.18±0.16, normalized to actin, p<0.05). This increase in COX2 protein was also significantly inhibited by treatment with TMB-8 (Met + TMB-8 = 0.13±0.05) or 2-APB (Met + 2-APB=0.20±0.10). Our previous studies have shown that the increase in COX2 in response to Met occurs within 6h in primary osteoblastic cells isolated from the calvariae. We now demonstrate that incubation of cells for 6h in the presence of TMB-8 also significantly inhibits the acid-induced increase in COX2 mRNA, as measured by realtime PCR (Ntl=2.49±0.47, Met=5.70±1.19, Met + TMB-8=1.54±0.27 normalized to actin). Acid stimulation of osteoblastic COX2 protein, measured by immunoblot analysis, was also inhibited by TMB-8 and 2-APB (Ntl=0.84±0.11, Met=1.18±0.11, Met + TMB-8=0.43±0.05, Met + APB= 0.61±0.08, normalized to actin). Increases in RANKL in response to Met occur downstream of stimulation of COX2. In primary cells Met increased RANKL mRNA compared to Ntl after 48h and this stimulation of RANKL mRNA was significantly inhibited in the presence of TMB-8 (Ntl=3.27±0.59, Met=7.81±2.02, Met + TMB-8=1.87±0.56, normalized to actin). Thus, our results are consistent with a requirement for a H⁺-induced increase in osteoblastic IP₃-stimulated Ca release from intracellular stores which would stimulate production of COX2 and then RANKL, leading to the subsequent increase in osteoclastic bone resorption.

Disclosures: N.S. Krieger, None.

This study received funding from: NIH, RRI.

M064

See Sunday Plenary Number S064

M065

ATP Is Released From Human Osteoblasts By Multiple Mechanisms. J. A. Gallagher¹, J. P. Dillon^{*1}, P. M. Wilson^{*1}, H. E. Burrell^{*1}, M. J. Hayton^{*1}, W. D. Fraser², A. Gartland³. ¹Human Anatomy and Cell Biology, University of Liverpool, Liverpool, United Kingdom, ²Clinical Chemistry, University of Liverpool, Liverpool, United Kingdom, ³Bone Biology, University of Sheffield, Sheffield, United Kingdom.

There is a growing recognition that extracellular ATP is one of the most important regulators of bone cell function. Multiple P2 receptor subtypes are expressed by bone cells and these regulate many functions including osteoblast proliferation and gene expression, osteoclast formation and resorptive capacity, and apoptosis of both osteoblasts and osteoclasts. Recent evidence indicates that extracellular ATP plays a pivotal role in mechanotransduction in bone, signalling in part through the P2X7 receptor. Less is known about how ATP is released into the bone microenvironment. We used a combination of end-point and real-time assays, utilising luciferin/luciferase bioluminescence, to monitor release of ATP into the extracellular environment from osteoblast cell lines, SaOS-2, MG63 and Te85, as well as primary human osteoblasts. Real-time assays revealed that ATP is released into the medium constitutively and that this release is exquisitely sensitive to changes in fluid flow. In response to increased flow, there was a rapid rise in ATP concentration in medium bathing the cells, followed by a slower decline back to resting levels. At steady state, the concentration of ATP in the medium of cultures of osteosarcoma cells lines was usually less than 5 nM ATP. In contrast, the ATP concentration in the medium of cultures of primary osteoblasts was up to six fold higher, depending on the donor. The concentration of ATP in medium is a function of ATP release from cells and degradation by ectonucleotidases. End-point assays revealed that fluid flow in the form of medium displacement resulted in a rise in the concentration of ATP which correlated with the number of displacements. After six displacements there was an approximate 10-fold increase in control cultures and 16-fold in cultures treated with ionomycin. Treatment with N-ethylmaleimide inhibited constitutive and fluid displacement-stimulated release, probably by blocking N-ethylmaleimide sensitive factor, a protein that regulates membrane fusion events in exocytosis. Addition of a monoclonal antibody that blocks the action of the P2X7 receptor had variable effects on extracellular concentration of ATP, both in control and fluid displacement cultures, but it was never completely effective in blocking ATP release. These data demonstrate that ATP release varies between osteoblastic cell lines, can be stimulated by fluid flow and is mediated by more than one mechanism. The effect of fluid flow on ATP release could be a key factor in mechanotransduction in bone.

Disclosures: J.A. Gallagher, None.

M066

Microstructural Variation in the Bone Matrix and Cell Attachments Modify Strain Amplification on the Osteocyte. A. R. Bonivitch¹, L. E. Bonewald², D. P. Nicoletta¹. ¹Mechanical and Materials Engineering, Southwest Research Institute, San Antonio, TX, USA, ²School of Dentistry, University of Missouri-Kansas City, Kansas City, MO, USA.

Osteocytes make up over 90% of all bone cells and are hypothesized to be the mechanosensors in bone that mediate the effects of loading. Measurements of bone strain in humans using strain gages have been used for strain applications in *in vitro* bone cell experiments. The limitation of applying this strain magnitude to cells *in vitro* is that the *in vivo* strain gage measurements represent continuum measures of bone deformation. Clearly, bone is not a continuum, but heterogeneous, especially at the spatial level of bone cells. Microstructural inhomogeneities result in inhomogeneous strain fields in which local tissue strains are magnified. The objective of this study was to investigate how microstructural bone tissue strains may be transmitted to an embedded osteocyte and its cell processes and to determine how changes in the perilacunar bone tissue structure and properties affect osteocyte strain and deformation. Previously we had created a parametric finite element model composed of an osteocyte lacuna, canaliculi, perilacunar tissue, and surrounding bone tissue. This model showed that a decrease in perilacunar tissue elastic modulus amplifies the perilacunar tissue strain and canalicular deformation. As the perilacunar elastic modulus decreases with glucocorticoid treatment, this may change the level of strain perceived by the osteocyte. In the present model, an osteocyte, cell processes, and glycoalyx attachments to the cell and cell processes were added. A displacement was applied to the model resulting in a global strain of 2000 microstrain and 27 simulations were performed with varying osteocyte and cell process moduli, perilacunar tissue moduli, and glycoalyx and cell process attachment stiffness. Maximum strain levels in the osteocyte reached over 10,000 microstrain, 5 times the applied macroscopic strain of 2000 microstrain. Similar strain levels had been observed in lacunae in bone slices previously. Maximum strain within the osteocyte was found to occur on the cell membrane, parallel to the plane of applied strain. Maximum osteocyte strain was found to increase with a decrease in perilacunar tissue modulus and decrease with an increase in perilacunar tissue modulus consistent with perilacunar tissue strains in the earlier model. A decrease in the osteocyte, glycoalyx, and cell process stiffness led to a decrease in the maximum strain transmitted to the osteocyte. In summary, this model can predict the influence of each component of the osteocyte structure and microenvironment on location and magnitude of cellular and dendrite deformation.

Disclosures: A.R. Bonivitch, None.

This study received funding from: NIH/NIAMS.

M067

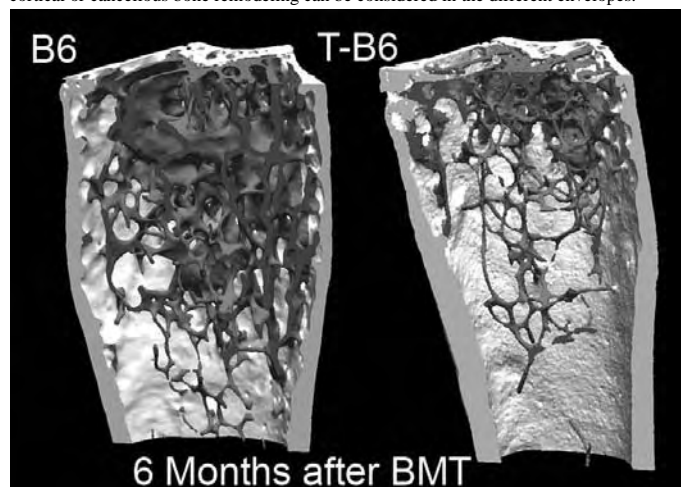
Bone Microarchitecture of Irradiated and Bone Marrow Transplanted Mice. A. Dumas^{*1}, M. Brigitte^{*2}, M. F. Moreau^{*1}, M. F. Baslé^{*1}, R. K. Ghérandi^{*2}, D. Chappard¹. ¹Faculté de Médecine, INSERM, EMI 0335, Angers, France, ²Faculté de Médecine, Université Paris XII, INSERM, EMI 0011, Créteil, France.

Osteopenia and osteoporosis are complications of renal, hepatic, cardiac and bone marrow transplants. Bone loss is attributed to transplant-related treatments (ciclosporine, glucocorticoids...) whether they act directly on bone cells or they deregulate the hormonal system. Total body irradiation provokes hypogonadism and increases osteoclast number and activity without increase in bone formation.

We investigated the effects of total body irradiation and bone marrow transplantation (BMT), without additional treatment, on bone mass and microarchitecture in a murine model. C57Bl/6 (B6) mice were lethally irradiated and within 1 day received syngeneic bone marrow cells expressing the green fluorescent protein. Transplanted mice (T-B6) and age-control B6 mice were euthanized 1, 3 and 6 months after BMT. Bone mass (BV/TV), mean cortical thickness (Ct.Th), trabecular characteristics (Tb.Th, Tb.N, Tb.Sp, Tb.Pf and SMI) were analyzed by microCT at the distal femur.

One month after irradiation and BMT, T-B6 presented a 56.9% bone loss compared to B6 at the same age. T-B6 did not restore their bone mass with time whereas BV/TV of B6 increased. The difference in bone mass between both groups reached 80.8% six months after BMT. Bone microarchitecture was altered in T-B6 mice: Tb.N dramatically decreased 1 month after BMT, Tb.Sp increased whereas Tb.Th was reduced after 6 months. The trabecular bone was less connected with fewer plates. Ct.Th increased significantly with time and, 6 months after BMT, T-B6 had cortical bone of the femoral diaphysis significantly thicker than age-matched B6 (+16%).

Our findings suggest that transplanted bone cells do not restore of the irradiation-induced trabecular bone loss despite an increase in cortical thickness. Effects of irradiation on cortical or cancellous bone remodeling can be considered in the different envelopes.



Disclosures: A. Dumas, None.

M068

See Sunday Plenary Number S068

M069

Lacunocanalicular Fluid Flow and Regulation of Basic Multicellular Unit Activity. G. C. Goulet^{*1}, D. M. L. Cooper^{*2}, D. Coombe^{*3}, D. L. Thomas^{*4}, J. G. Clement^{*4}, R. F. Zernicke^{*5}. ¹Schulich School of Engineering, University of Calgary, Calgary, AB, Canada, ²Department of Orthopaedics, University of British Columbia, Vancouver, BC, Canada, ³Computer Modelling Group, Ltd., Calgary, AB, Canada, ⁴School of Dental Science, University of Melbourne, Melbourne, Australia, ⁵Schulich School of Engineering; Departments of Kinesiology and Medicine, University of Calgary, Calgary, AB, Canada.

Human bone is continuously regenerated through remodeling. This process is carried out by a complex mediator mechanism called the Basic Multicellular Unit (BMUs). Cortical BMUs proceed by osteoclastic excavation of a resorption space (cutting cone) followed by new bone formation by osteoblasts (closing cone). Current theories suggest that the BMU is strain and/or fluid-flow regulated [1,2,3]. While these regulatory models have focused on idealized forms, BMU morphology is variable, including unidirectional, bidirectional, and branched forms. The purpose of this study was to examine strain and fluid flow in relation to realistic BMU forms directly observed in human cortical bone by 3D micro-CT imaging. Computational models were developed in STARS, a coupled finite difference fluid flow and finite element mechanics simulator (Computer Modelling Group, Ltd., Calgary, AB, Canada). Models of a unidirectional and branched BMU were generated. These were subjected to compressive loads, which induced fluid flow through

the simulated lacunocanalicular porosity. Upon loading, fluid flowed from the high-pressure bone matrix into the low-pressure porosity of the BMU. Consistent with previous models, the unidirectional canal model displayed decreased strain in front of the cutting cone, and increased strain behind it. Similarly, the branched model demonstrated strain reduction in front of both cutting cones and increased strain behind them. However, the branched morphology also displayed a similar reduction in strain at the fork where it divided. Fluid stasis has been implicated as a regulating mechanism in BMU activity, whereby decreased osteocytic stimulation results in reduced production of nitric oxide, inducing apoptosis, which subsequently signals the recruitment of osteoclasts. The inter-branch strain shielding and related reduction in fluid flow observed in the branched BMU poses a challenge to this regulatory model since the region between resorption spaces would also be prone to osteocyte apoptosis and osteoclastic activity, effectively eliminating the branched structure. Therefore, strain and related fluid flow alone may not be sufficient to explain BMU regulation.

[1] Smit and Burger (2000). *J Bone Miner Res*, 15, 301-307. [2] Burger et al. (2003). *J Biomech*, 36, 1453-1459. [3] Smit et al. (2002). *J Bone Miner Res*, 17, 2021-2029.

Disclosures: G.C. Goulet, None.

This study received funding from: Natural Sciences and Engineering Research Council; Alberta Heritage Foundation for Medical Research; Wood Professorship in Joint Injury Research.

M070

Increased Expression of Anti-adhesive PODXL in TIEG Knock-Out Osteoclast Precursors Delays Osteoclast Formation and Reduces Osteoclast Size. M. Cicek¹, A. Vrabel^{*1}, M. Subramaniam², T. C. Spelsberg², M. J. Oursler¹. ¹Endocrine Research Unit, Mayo Clinic, Rochester, MN, USA, ²Department of Molecular Biology and Biochemistry, Mayo Clinic, Rochester, MN, USA.

TIEG is a Krüppel-like transcription factor gene which was originally cloned from human osteoblasts as an early response gene to TGF- β treatment. As reported previously, TIEG^{-/-} mice have decreased cortical bone thickness and lower vertebral volume, increased spacing between the trabeculae in the femoral head, and a lower breaking strength compared to wild-type mice. Therefore we investigated the role of TIEG in the osteoclasts that may be responsible for bone phenotype in TIEG^{-/-} mice. In vitro cultures of mouse marrow treated with RANKL and M-CSF, we found that osteoclasts differentiated more slowly and formed reduced numbers of osteoclasts compared to wild type precursors. Moreover, TIEG^{-/-} osteoclasts were significantly smaller than wildtype osteoclasts. Flow cytometry analyses showed that there was no difference in CD11b+ and/or RANK+ and/or c-fms+ in osteoclast precursors in freshly harvested marrow cells between the genotypes. These data led us to hypothesize that loss of TIEG reduced the capacity of TIEG^{-/-} precursors to differentiate into mature osteoclasts. We therefore investigated the role of the anti-adhesive glycosylated cell-membrane protein podocalyxin (PODXL) in osteoclastogenesis in vitro in TIEG^{-/-} and wildtype precursor differentiation. We found that TIEG^{-/-} precursors have increased expression of PODXL relative to the wildtype. Adding RANKL and M-CSF to the in vitro model significantly reduced the expression of PODXL in TIEG^{-/-} precursors, suppressing expression relative to that of wildtype cells. Parallel treatment of wildtype precursors did not reveal any effect on PODXL expression in these cells. These data suggest that the reduced ability of TIEG^{-/-} osteoclast differentiation may be due to an increased expression of anti-adhesive PODXL in these cells. We conclude that TIEG expression may be critical in controlling the rate of osteoclast differentiation and that increased PODXL expression in TIEG^{-/-} may be a key factor in the reduced differentiation and/or the size of TIEG^{-/-} osteoclasts.

Disclosures: M. Cicek, None.

M071

Regulation of Integrin Expression by NFATc1 and PU.1 in Osteoclasts. T. N. Crotti¹, M. R. Flannery^{*1}, J. D. Fleming^{*1}, S. R. Goldring², K. P. McHugh¹. ¹Rheumatology and Orthopaedics, Beth Israel Deaconess Medical Center, Boston, MA, USA, ²Hospital for Special Surgery, New York, NY, USA.

Beta-3 and beta-5 integrins play important and contrasting roles in osteoclast (Oc) differentiation and are accordingly reciprocally regulated. The integrin beta-5 is expressed by pre-Ocs and has an inhibitory role in Oc differentiation, as beta-5 knockout mice display enhanced Oc formation. The beta-3 integrin is expressed by mature Ocs and is required for normal Oc function.

NFATc1 is a RANKL-induced and Ca⁺⁺-regulated transcription factor critical for Oc differentiation. NFATc1 with PU.1, an ETS family transcription factor, regulate expression of distinct target genes in Oc differentiation. We provide here direct evidence that NFATc1 and PU.1 are involved in the reciprocal regulation of integrin expression during Oc differentiation.

To test the involvement of NFATc1 in beta-3 integrin expression, we generated mouse beta-3 promoter/reporter constructs (-1350 to +34bp; mB3-1350) which include a composite NFAT and PU.1 binding site conserved from mouse and man. The mB3-1350 construct was trans-activated >60X by co-transfected NFATc1 in RAW264.7 cells, consistent with our previous report on regulation of the human beta-3 promoter. Trans-activation was abolished by deletion to -1084, and further deletions were similarly unresponsive. Direct binding of NFATc1 and PU.1 to the mouse beta-3 promoter was demonstrated by EMSA. Consensus NFAT and PU.1 oligos competed, while oligos with mutant NFAT or ETS sites failed to compete. The identity of the protein moieties was verified by supershift with anti-NFATc1 and PU.1 antibodies. Mutation of either the NFAT or PU.1 binding site, in the context of mB3-1350, abrogated NFATc1 trans-activation. The specificity of PU.1, among ETS family members, to induce mB3-1350 was demonstrated by co-transfection in HEK293 cells. NFATc1 trans-activation of the mB3-1350 promoter was specifically facilitated by PU.1. NFATc1 had no effect when co-transfected with Ets-1, ESE1, or Elf, however Ets-1 and Elf mediated the highest basal expression.

We previously reported that TAT-mediated transduction with a dominant-negative (dn)NFATc1 construct dose-dependently blocked spreading of mouse osteoclasts and inhibited expression of the endogenous beta-3 integrin gene. In addition to this, we find reciprocal dose-dependent induction of the endogenous beta-5 integrin by TAT-dnNFATc1. The mouse beta-3 integrin gene is therefore a specific target of NFATc1 during RANKL-induced Oc differentiation through direct binding of NFATc1 and PU.1 to specific sites in the beta-3 promoter. Furthermore, NFATc1 function is coupled with, and required for, down-regulation of the beta-5 integrin gene Oc cells.

Disclosures: T.N. Crotti, None.

This study received funding from: The author of this paper holds a National Health and Medical Research Council (Aust) CJ Martin Fellowship (I.D. 200078). This work was supported in part by National Institute of Health Grants NIAMS R01 AR45472 (to SRG), NIAMS R01 AR47229 (to KPM).

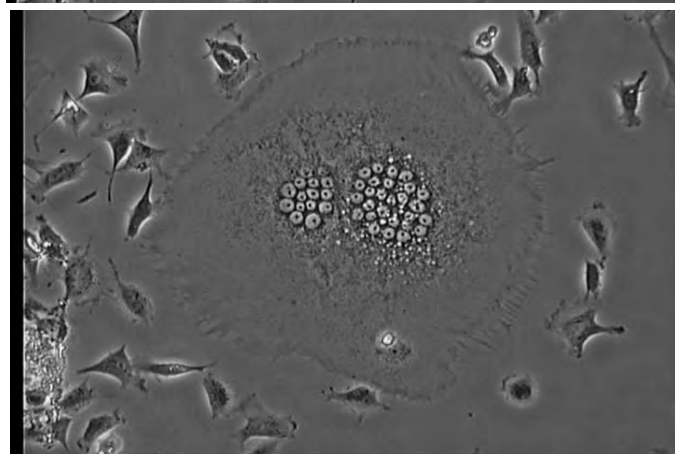
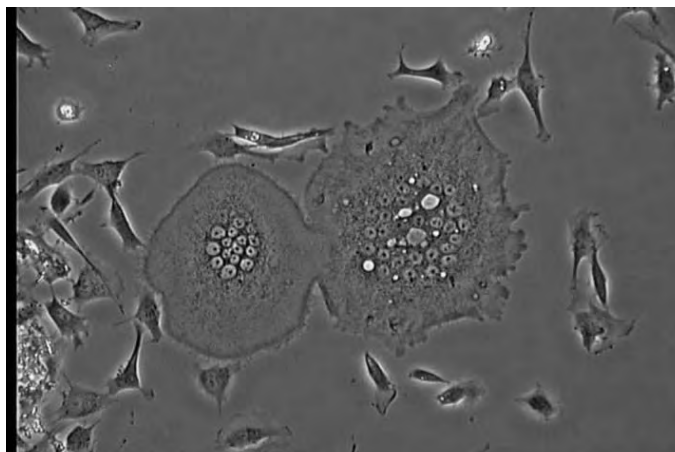
M072

The Decisive Moment of Osteoclast Fusion and Apoptosis Captured Under a Microscope Connected with Time-Lapse Motion Video Picture. A. Itabashi¹, T. Ohnuma^{*2}, Y. Takada^{*1}. ¹Saitama Center for Bone Research, Kumagaya, Japan, ²Yone Production, Tokyo, Japan.

Osteoclasts are multinucleated bone cells that are formed by multiple cell fusions. Mature osteoclasts undergo several cycles of activation and inactivation, where bone is resorbed in the active state and osteoclasts migrate in the resting state, eventually, the cells die apoptotically. However, there are few pictures or videos that captured the moment of osteoclast fusion or apoptosis. In this study, we tried to capture those pictures in collaboration with a science movie company.

We first observed mouse calvarial bone cells under a microscope connected with time-lapse motion video picture in organ culture conditions continuously for more than 96 hours. We could observe osteoblast division and bone matrix formation. We could also capture the decisive moment of osteoclast fusion using isolated rabbit osteoclasts with stromal cells. Osteoclasts had many cell processes folding in and sticking out from their cell surfaces, and moved around in a culture dish actively. When the cell process made contact with that of the other osteoclast, rapid movements between those processes were observed. Often they separated again after some conversation between them. But some cells started to make continuous contact with each other, with busy communication through cell membranes. And then one part of cell membrane overlapped with other cell membrane, and cell contents started to mingle and multiple nuclei from each osteoclast assembled to form a giant multinucleated osteoclast. The huge osteoclast moved around actively as one cell and it could be maintained in the plastic dish under culture conditions for several hours, then rapidly decreased movement. After that, spontaneous apoptosis occurred in that cell with cell shrinkage and fragmentation of nuclei.

Using time-lapse video picture system under regular culture conditions for certain amount of time, we can observe the way the osteoclasts fuse and die. This can contribute to understand the mechanism of osteoclast fusion and apoptosis.



Disclosures: A. Itabashi, None.

M073

See Sunday Plenary Number S073

M074

Tropomyosin-2/3 Regulate the Intracellular Scaffold of Osteoclasts. P. Kotadiya^{*}, B. K. McMichael, T. Singh^{*}, B. S. Lee. Physiology and Cell Biology, The Ohio State University, Columbus, OH, USA.

Tropomyosins (Tms) are actin-binding proteins that stabilize microfilaments and inhibit or recruit binding of other actin-associated proteins. In nonmuscle cells, over twenty alternately spliced isoforms are expressed from four distinct genes, namely the alpha gene (Tm-2, -3, -5a/b, -6), the beta gene (Tm-1), the gamma/5NM gene (Tms NM-1 to NM-11), and the delta/Tm-4 gene (Tm-4). Recent studies have indicated that individual Tm isoforms are distributed to different intracellular locations where they regulate specific actin pools. Therefore, the goal of this work is to determine the roles of tropomyosin isoforms in mature osteoclast activity.

Our previous studies showed that at least eight Tm isoforms are expressed in osteoclasts and that some of these, including Tm-2 and 3, are not present in monocyte-macrophage precursors but are upregulated during osteoclastogenesis. These isoforms differ by only a few amino acids; therefore, reagents that distinguish between them are limited. However, Tm-2 is present in osteoclasts at levels about four-fold higher than Tm-3. Immunocytochemical analysis showed that they are dispersed throughout the interior of osteoclasts and are only loosely intercalated in the podosomes and actin rings. To analyze the role of Tm-2/3 in osteoclasts, the effects of both Tm-2/3 suppression and overexpression have been studied in these cells. It was found that cells treated with Tm-2/3-specific siRNAs covered a greater surface area, but contained the same number of nuclei, as control cells. These results suggest that loss of Tm-2/3 results in increased cell spreading. This hypothesis is supported by data showing that the siRNA-treated cells are flattened relative to controls. These cells also are greatly diminished in their motility in Transwell assays. Additionally, resorption assays illustrated that the total resorption area was similar in Tm-2/3-suppressed cells and controls, but the siRNA-treated cells generated fewer, but larger, resorbed areas. On the other hand, increasing Tm-2 levels by overexpression also distorted cell shape. On glass, these cells were distinctly more spherical than controls and lacked podosomes. Instead, these overexpressing cells contained patches of actin and sometimes stress fibers at their base. This in turn led to decreased motility by these cells. In summary, these findings indicate that Tm-2/3 are involved in regulating cell shape and motility, likely due to stabilization of actin microfilaments that create a cellular scaffold.

Disclosures: P. Kotadiya, None.

M075

Effect of Pore Size and Surface Modification of the Circular Poly-Ethylene Glycol(PEG) Polymer Scaffold on Adhesion of Cultured Human Ligamentum Flavum Cells. C. Lee^{*1}, H. Kim^{*1}, J. Lee^{*1}, M. Nan^{*1}, J. Park^{*2}, E. Moon^{*2}, S. Park^{*3}, H. Kim^{*2}, J. Jahng^{*2}, S. Moon^{*2}, H. Lee^{*2}, H. Chun^{*4}, H. Kim^{*2}. ¹Orthopaedic Surgery, Brain Korea 21 Medical Science Graduate School of Yonsei University, Seoul, Republic of Korea, ²Orthopaedic Surgery, Yonsei University College of Medicine, Seoul, Republic of Korea, ³Orthopaedic Surgery, Korea University College of Medicine, Seoul, Republic of Korea, ⁴Mechanical Engineering, School of Mechanical Engineering of Yonsei University, Seoul, Republic of Korea.

Tissue engineering requires viable cells and cellular-compatible scaffold. Poly-Ethylene Glycol(PEG) polymer is a probable option of scaffold with its unique advantages. Nevertheless, it is still needed to be characterized that the effect of surface modification with making pore with various size and coating with collagen. Hence, we report the effect of surface modification by circular pore and type I collagen coated to cellular attachment and viability of ligamentum flavum (LF) cells. Human LF tissue was harvested, digested, and cultured. Poly-Ethylene Glycol(PEG) hydrogel micropatterns were fabricated from PEG by using a photomask illuminated with UV light. Collagen-coated PEGs were made by immersion in type I collagen solution. Then LF cells (1×10^5) were seeded on PEG with various pore size (50, 100, 200 μ m) with or without collagen coating. After 2 days' incubation, adherent cells were imaged in SEM. Cellular viability was assessed by live/dead cell viability kit. Most LF cells were found at the base of pore, however, some patches of cells were found on the surface of PEG and inner surface of the PEG pore. No visible cellular adhesion was noted in PEG with the pore size of 50 μ m. However, in PEG with the pore size of 100 and 200 μ m there is marked cellular adhesion to the surface of PEG and even inner surface of the PEG pore. Surface modification of PEG with type I collagen renders more efficient adhesion of LF cells on the modified surface of PEG. Even with collagen coating, PEG with pore size of 50 μ m failed to show any significant cellular adhesion. Adhered cells on the surface of PEG were all viable in all experiment group. In summary, PEG scaffold with the pore size of 100 and 200 μ m was non-toxic to the LF cell and provided suitable surface for LF cell adhesion. Surface modification with type I collagen facilitated process of cellular adhesion to PEG surface. New modification such as one sided sealing of the pore is need for more efficient cellular containment within PEG pore.

Disclosures: C. Lee, None.

M076

Myosin X Regulates Osteoclast Adhesion Through Linkage of Podosomes and Microtubules. B. K. McMichael¹, R. E. Cheney^{*2}, B. S. Lee¹. ¹Physiology and Cell Biology, The Ohio State University, Columbus, OH, USA, ²Cell and Molecular Physiology, University of North Carolina at Chapel Hill, Chapel Hill, NC, USA.

Osteoclasts generate two distinct actin-based adhesion structures--podosomes for migration, and the actin ring of the sealing zone for resorption. Although podosomes are actin-based structures, their patterning is microtubule dependent. In this study, the role of myosin X (myo10) in osteoclast adhesion was assessed. Myo10 is an unconventional myosin that consists of a motor domain, three light chain binding domains, and a unique tail consisting of pleckstrin homology domains (PH), a myosin tail homology 4 domain (MyTH4), and a FERM domain. The multifaceted myo10 has been shown to bind many osteoclast regulatory proteins including microtubules, β 1/ β 3/ β 5 integrins, products of PI3 kinase, and VASP, along with binding actin via the motor domain. Initial immunocytochemical analysis of osteoclasts showed myo10 to be localized immediately adjacent to, but not overlapping, podosome belts and the actin ring, suggesting a potential role in positioning of these structures. To analyze its role, myo10 expression was inhibited in both RAW264.7 and mouse marrow derived osteoclasts via RNA interference. Myo10 suppression resulted in diminished spreading of osteoclasts cultured on glass. Suppression also led to a decrease in the size of the actin ring with an even greater decrease in bone resorption and motility. Further, inhibition of myo10 levels resulted in a microtubule-based podosome patterning defect. When microtubules of osteoclasts were depolymerized by cold treatment, both siRNA-treated and control cells showed redistribution of podosomes away from the cell periphery. However, when allowed to recover, the siRNA-treated cells, unlike the control cells, could not distribute their podosomes back to the periphery even though they reformed the microtubule network. These results suggest that myo10 may act as a link between podosomes and microtubules through its tail domains. Indeed, detailed immunocytochemical analysis of osteoclasts during podosome positioning shows myo10 localized between podosomes and the surrounding microtubule system. Over-expression of sections of the tail, either PH, MyTH4, or FERM alone or in combination, caused formation of aberrant podosomes while over-expression of all three domains had a dominant negative effect similar to the phenotype manifested in the siRNA-treated cells. These results taken together clearly suggest a role for myo10 in linking the microtubule network to podosomes through its tail domain.

Disclosures: B.K. McMichael, None.

M077

Expression and Possible Role of PVR/CD155/ Necl-5 in Osteoclastogenesis. I. Morita, S. Kakehi^{*}, K. Nakahama. Cellular Physiological Chemistry, Tokyo Medical and Dental University, Tokyo, Japan.

Osteoclast, the bone-resorbing cell, is differentiated from hematopoietic precursors via two-step cell-cell interactions; interaction between osteoclast precursor and stromal cell, and interaction among osteoclast precursors. We have previously reported that some adhesion molecules have a crucial role in these interactions. Recently, poliovirus receptor (PVR, CD155, Necl-5) was reported to play important roles in cell adhesion and migration. However, there is no report of PVR in osteoclastogenesis. Here, we examined the expression of PVR and its ligand, DNAX accessory molecule-1 (DNAM-1, CD226) in osteoclast precursor, mature osteoclast and stromal cell. We found that the PVR was constitutively expressed in both osteoclast cells and stromal cells. The expression of PVR was not changed at various stages of osteoclast formation. In contrast, the expression of DNAM-1 was observed in mononuclear cells and was down-regulated during osteoclastogenesis. Moreover, multinucleated osteoclast formation was inhibited by treatment with extracellular domain of DNAM-1 (ED-DNAM-1) as a soluble ligand for PVR, but mononuclear preosteoclast formation was not affected. Especially, during the 7-days cultivation, osteoclast formation was suppressed by the treatment with ED-DNAM-1 on days 6 and 7, when mononuclear preosteoclast fused into multinucleated osteoclasts. This suppression was abrogated partially by small interfering RNA specific for PVR. These results indicated that the binding of PVR with DNAM-1 negatively regulates osteoclast formation via inhibition of cellular fusion caused by PVR mediated signaling. Our report may suggest the possibility of a new therapy for bone loss diseases by activation of PVR signaling.

Disclosures: I. Morita, None.

This study received funding from: JSPS COE Program.

M078

Spacio-Temporal Analysis of Osteoclastogenesis Using Co-culture System. K. Nakahama¹, S. Ichinose^{*2}, I. Morita¹. ¹Cellular Physiological Chemistry, Tokyo Medical and Dental University, Tokyo, Japan, ²Instrumental Analysis Research Center, Tokyo Medical and Dental University, Tokyo, Japan.

The mechanism of osteoclast differentiation has been well studied in vivo and in vitro. But, in our knowledge, little is known about the spacio-temporal aspects of preosteoclast differentiation into multinuclear osteoclast. To examine the spacio-temporal aspects of osteoclastogenesis, the stromal cells and spleen-derived mononuclear cells were labeled with calcein-AM and CellTracker Orange CMRA respectively. The spleen-derived mononuclear cells were co-cultured on the confluent stromal cells. In this co-culture system, tartrate-resistant acid phosphatase (TRAP)-positive multinuclear osteoclasts were observed under the stromal cells after 5-days culture without stimulation. Confocal microscopic observation revealed that mononuclear cells migrated under stromal cells after 6-hrs co-culture. Surprisingly, in addition to the paracellular migration (migration via cell junction), transcellular migration (migration via stromal cell body) of spleen-derived mononuclear cell was detected. These two types of migrations were confirmed using scanning electron microscopy. Immunocytochemical study showed strong expression of intercellular adhesion molecule-1 (ICAM-1) and its counter receptor macrophage antigen-1 (Mac-1) on spleen-derived mononuclear cell, but not on stromal cells at 24-hrs after co-culture. The polarized localization of ICAM-1 indicated that ICAM-1 plays some roles in the migration of spleen-derived mononuclear cells. Two-days after co-culture, some aggregated mononuclear cells expressed ICAM-1 at cell-cell adhesion sites. After 5-days co-culture of the cells, multinucleated TRAP-positive osteoclasts were formed. Interestingly, we also detected the localization of ICAM-1 at cell-cell association site among osteoclasts. ICAM-1 localization in some osteoclasts was observed at apical surface of the membrane. Collectively, these results suggest that preosteoclasts will migrate under the stromal cells paracellularly and transcellularly, thereafter they will fuse each other. There may be suitable conditions at basolateral side of stromal cells. Polarized localization of ICAM-1 on osteoclast would indicate some important roles in migration and fusion of preosteoclasts.

Disclosures: K. Nakahama, None.

This study received funding from: JSPS COE Program.

M079

HMGB1 Regulates Actin Cytoskeleton Organization and RANKL-induced Osteoclastogenesis in a Manner Dependent on RAGE. Z. Zhou¹, D. Ferguson², J. Xie¹, C. Xi¹, D. Stern², L. Mei¹, W. Xiong¹. ¹Institute of Molecular Medicine and Genetics, Medical College of Georgia, Augusta, GA, USA, ²University of Cincinnati, Cincinnati, OH, USA.

High-mobility group box 1 (HMGB1), a non-histone nuclear protein, is released by macrophages into the extracellular milieu consequent to cellular activation. Extracellular HMGB1 has properties of a pro-inflammatory cytokine via its interaction with receptor for advanced glycation endproducts (RAGE) and/or toll-like receptors (TLR2 and TLR4). Although HMGB1 is highly expressed in macrophages and differentiating osteoclasts, its role in osteoclastogenesis remains largely unknown. Here we present evidence for a function of HMGB1 in this event. HMGB1 is released from macrophages in response to RANKL stimulation, and is required for RANKL-induced osteoclastogenesis *in vitro* and *in vivo*. In addition, HMGB1, like other osteoclastogenic cytokines (e.g., TNF α), enhances RANKL-induced osteoclastogenesis *in vivo* and *in vitro* at sub-threshold concentrations of RANKL, which alone would be insufficient. The role of HMGB1 in osteoclastogenesis is mediated largely by its interaction with RAGE, and regulation of α v β 3 integrin signaling and osteoclastic actin ring formation. Together, HMGB1-RAGE signaling appears to be important in regulating osteoclastic actin cytoskeleton reorganization, thereby participating in RANKL-induced osteoclastogenesis. These observations provide a new link between inflammatory mechanisms and bone resorption.

Disclosures: Z. Zhou, None.

M080

Precursor Analyses of CD11c⁺Dendritic Cells-derived Osteoclasts. M. Alnaeeli^{*}, D. Mahamed^{*}, J. Park^{*}, Y. Teng^{*}. Department of Microbiology & Immunology and Eastman Department of Dentistry, University of Rochester, Rochester, NY, USA.

Inflammation-induced osteoclastogenesis is a well established osteoimmunological phenomenon, whereby osteoclasts (OC) frequency and activity become elevated under inflammatory conditions. Dendritic cells (DC) are professional antigen presenting cells that not only infiltrate bone tissues during inflammation, but are also suggested to share common precursors with OC. Previously we reported and characterized the *in vitro* development of TRAP⁺ CT-R⁺ cathepsin-K⁺ CD11c⁺ MHC-II⁺ multinucleated functional OC from murine CD11c⁺DC (called; DDOC), in response to RANKL and bacterial or protein antigens during immune interactions [J. Immunol. 177(5): 3314-26 & JBM, in press, 06/2007]. Here, we aimed to study the clonal characteristics of DDOC by determining their OC precursor frequency and proliferative capability. We employed colony forming unit assay and limiting dilution analysis, using purified murine bone marrow-derived CD11c⁺DC (purity $\geq 98\%$) in the presence of 100ng/ml RANKL & 10 μ g/ml sonicated antigens of *Aggregatibacter* (*Actinobacillus*) *actinomycetemcomitans*; an anaerobic human pathogen. After 5 days culture and when compared to the controls, the purified CD11c⁺DC: i) did not manifest any proliferative capability ($p=0.003$), and ii) had an estimated precursor frequency of $8.4 \pm 0.06\%$, based on the number of TRAP⁺ multinucleated (≥ 3 nuclei) OC yielded. To investigate the physiological relevance of the DDOC phenomenon, we studied the osteoclastogenic potential of murine CD11c⁺DC *in vivo*. Interestingly, after the injection of carboxyfluorescein succinimidyl ester-labelled freshly purified DC onto mouse calvarias, we found CFSE⁺ TRAP⁺ multinucleated OC-like cells associated with higher local bone loss, compared to the control groups, suggesting that CD11c⁺DC can become TRAP⁺ multinucleated OC under inflammatory conditions *in vivo*. Furthermore, our immunohistochemical analysis detected the presence of CD11c⁺ multinucleated OC-like cells on the subchondral bone surfaces of the arthritic joints in DBA mice but not healthy controls. Collectively, these findings support the possible development of DDOC at the osteo-immune interface, which may be an integral part of the mechanisms underlying inflammation-induced osteoclastogenesis in inflammatory bone disorders such as rheumatoid arthritis and periodontal disease.

Disclosures: M. Alnaeeli, None.

This study received funding from: CIHR Grant MOP-37960 and NIH Grant DE 15786 to Y-T A Teng.

M081

In Vivo Activation of Toll-Like Receptor 9 Modulates Osteoclastogenesis. A. Amcheslavsky^{*}, Z. Bar-Shavit. Experimental Medicine and Cancer Research, Hebrew University, Jerusalem, Israel.

Toll-like receptor (TLR) ligands are pathogen-derived molecules that activate the innate immune response. Many studies have shown that activation of these receptors in osteoclast lineage cells accelerates osteoclast formation and activity. In recent years, several groups have shown that pathogen-derived molecules such as peptidoglycan, viral RNA (mimicked by poly-IC), lipopolysaccharides and bacterial DNA (mimicked by CpG-oligodeoxynucleotides [CpG-ODNs]), the ligands of TLR2, 3, 4 and 9, respectively, inhibit RANKL-induced osteoclastogenesis under certain conditions. *In vitro* studies led to the hypothesis that activation of TLRs in early osteoclast precursor cells inhibits their differentiation, while in cells that have been primed with RANKL and have already begun their osteoclastic differentiation, TLR ligands are potent stimulators of osteoclastogenesis. In the present study, we examine how *in vivo* administration of the TLR9 ligand CpG-ODN impacts osteoclastogenesis. Mice were injected, either *i.p.* or *i.v.*, with the TLR9 ligand CpG-ODN. Bone marrow cells were harvested 1-7 days later and an osteoclastogenesis assay was performed. No effect was observed 1 day

after injection, but in all other treatments the injection of CpG-ODN increased the number of osteoclasts formed in response to RANKL. Consistent with previous *in vitro* findings, osteoclast differentiation was greater in cells harvested from BALB/c mice injected with CpG-ODN than in cells from C57BL/6-injected mice. CpG-ODN did not exert any effect when injected to TLR9 knockout mice. The failure to identify conditions under which CpG-ODN inhibits osteoclast differentiation can be explained in two ways. Either, this effect occurs only *in vitro*, or both inhibition and stimulation of osteoclastogenesis take place *in vivo*, but the stimulatory effect is more pronounced and, therefore, a net inhibitory effect is not observed. Since the inhibitory effect of CpG-ODN is exerted on early precursors, we injected mice with 5-fluorouracil (5FU), which is known to enrich the bone marrow with early stem cells. Indeed, a reduction in osteoclast differentiation was observed when CpG-ODN was injected into 5FU-treated mice. Thus, TLR9 activation *in vivo* confirms the effect observed *in vitro*. The inhibition of osteoclast differentiation in early precursor cells may play a role in reducing the excessive bone loss caused by pathogenic infection and shifting the balance between the bone and immune systems during infection to recruit the immune system.

Disclosures: A. Amcheslavsky, None.

M082

See Sunday Plenary Number S082

M083

CreatinE Kinase Brain Type (CK-B) Involves in the Bone Resorptive Activity of Osteoclast Activity through by Regulating the V-ATPase and Rho Activity. E. Chang¹, J. Ha¹, F. Oerlemans², H. Kim¹, B. Wieringa², Z. Lee¹, H. Kim¹. ¹Department of Cell and Developmental Biology, College of Dentistry, BK21 and DRI, Seoul National University, Seoul, Republic of Korea, ²Department of Cell Biology, Nijmegen Centre for Molecular Life Sciences, Radboud University Medical Centre, Nijmegen, Netherlands Antilles.

Osteoclasts, responsible for bone resorption, differentiate from the hematopoietic precursor cells of the monocyte/macrophage lineage. Receptor activator of nuclear factor- κ B ligand (RANKL), in the presence of M-CSF, mediates osteoclast formation and activation through binding to its receptor RANK on osteoclast precursor cells. Some proteins highly expressed in osteoclasts have been suggested as molecular targets for development of anti-bone resorptive drugs. Previously, we identified through a proteomics approach that the brain type cytoplasmic creatine kinase (CK-B) is greatly increased in osteoclasts. In this study, we found that inhibition of CK-B blocked V-ATPase and Rho activity, resulting in the decrease of *in vitro* bone-resorbing activity of osteoclasts. *In vivo* experiments with a CK inhibitor also showed a reduced bone resorption in ovariectomized rat model. Using CK-B (-/-) KO and wild-type (WT) mice, we investigated the V-ATPase and Rho activity and *in vitro* bone-resorbing activity on dentine slice. Compared with that in WT mice, both the V-ATPase and Rho activity was decreased in KO osteoclasts. In aged mice, BMD in femur was significantly more increased in KO than in WT mice. These data reveal that CK-B, up-regulated in osteoclasts, plays an important role for bone resorbing activity of osteoclasts. Therefore, CK-B might be a good target for anti-resorptive drug development.

Disclosures: E. Chang, None.

M084

See Sunday Plenary Number S084

M085

Jagged1-Notch2 Signaling Promotes Osteoclast Differentiation In Vitro. H. Fukushima¹, A. Nakao¹, F. Okamoto¹, H. Kajiya¹, E. Jimi², K. Okabe¹. ¹Physiological Science & Molecular Biology, Fukuoka Dental College, Fukuoka, Japan, ²Molecular Signalling & Biochemistry, Kyusyu Dental College, Fukuoka, Japan.

Notch related genes play a key role in various cell differentiation processes. Expression of Notch receptors in hematopoietic cells and expression of their ligands in bone marrow stromal cells suggests a possible role for Notch signaling in the regulation of osteoclastogenesis. However, the role of this Notch signaling pathway is unclear. Expression of Notch2 is upregulated during osteoclast differentiation, on the other hand, expression of Jagged1 of the Notch ligand family increases in osteoclasts and primary osteoblasts stimulated with osteoclast differentiation factors. To assess the involvement of Notch signaling in osteoclastogenesis, we generated RAW264.7 cells to permit the conditional induction of Notch2 specific shRNA using tetracycline-induced expression. Induction of Notch2 shRNA resulted in suppression of RANKL-induced osteoclast differentiation. Transient transfection of constitutively active intracellular domain of Notch2 in bone marrow macrophages increased NFATc1 activity and osteoclast differentiation. Treatment with Jagged1 activated Notch2 signaling and osteoclastogenesis. The selective γ -secretase inhibitor, L685,458 suppressed Notch signaling activity and RANKL-induced osteoclast differentiation from bone marrow macrophages. Furthermore, the intracellular domain of Notch2 was found to interact with p65 and p50 in NF κ B signaling but not c-Fos. RBPJ κ , a transcription factor in the downstream Notch signaling pathway, possesses a consensus sequence near the NF κ B binding site of NFATc1/P1 promoter. Activation of Notch2

increased the promoter activity of RANKL-induced NFATc1/P1 in RAW264.7 cells. Co-activation of Notch2 and p65 also activated NFATc1/P1 promoter. These data suggest that Notch2 interacts with Jagged1 and promotes osteoclastogenesis via activation of NFATc1 and NFkB signaling in osteoclast precursor cells.

Disclosures: H. Fukushima, None.

M086

See Sunday Plenary Number S086

M087

Extracellular Matrix Proteins Affect both Osteoclast Formation and Resorptive Activity. A. Gramoun^{*1}, D. P. Trebec², N. Azizi^{*1}, J. Sodek^{*1}, M. F. Manolagas¹. ¹Faculty of Dentistry, University of Toronto, Toronto, ON, Canada, ²Department of Biochemistry, University of Toronto, Toronto, ON, Canada.

Tissue destruction in arthritis is associated with bone loss and elevated levels of the extracellular matrix (ECM) proteins in affected joints. Osteoclasts (OCs), the bone resorbing multinucleated cells, are formed by fusion of mononuclear precursors. The ECM proteins, vitronectin (VN), fibronectin (FN) and osteopontin (OPN), all implicated in arthritis, interact with OCs through the integrin $\alpha\beta3$. To determine the effects of VN, FN and OPN on OC formation and resorptive activity RAW 264.7 (RAW) cells were plated and differentiated (using 100 ng/ml RANKL) on dishes or OsteologicTM slides precoated with 0.01-20 μ g/ml FN, VN, and OPN; concentrations shown not to affect cell proliferation. After 96 hours of differentiation, dose response experiments showed that OC number on VN and FN remained significantly lower than those on OPN and the uncoated controls. Measuring tartrate-resistant acid phosphatase (TRAP) activity levels revealed that only VN and OPN attenuated differentiation up to 72 hours. Furthermore, counting the number of mononuclear TRAP+ cells (preOCs) at 48 hours and large OCs (> 10 nuclei) at 96 hours showed that while FN did not affect preOC number, it significantly decreased OC formation and multinucleation compared to the uncoated control. OPN on the other hand, had the opposite effect. Resorption studies revealed that both FN and OPN increased the total area of resorption and resorptive activity/OC by 40% compared to VN and the uncoated control groups. Further, FN increased the released TRAP/OC in cultures. Nitric oxide levels (as measured by Griess reagent) were significantly elevated by FN but not in any of the other groups. When cells were differentiated for 3 days then incubated with 1 μ g/ml of the anti-rat $\alpha\beta3$ antibody, VNR149, (or its IgG control) for 24 hours, VNR149 significantly increased the total OC number on FN compared to its control by 37% while VN, OPN and the control groups showed a significant decrease in OC numbers. We also observed that OCs on FN had a 1.5 fold increase in $\alpha\beta3$ cell surface expression compared to uncoated group, as determined by flow cytometry. In conclusion, despite its inhibitory effect on preOC fusion and OC formation, FN significantly enhanced resorption/OC. FN's induction of nitric oxide and the increased $\alpha\beta3$ expression, could both explain the increased OC activity. VN attenuates both differentiation and preOC fusion thus decreasing OC formation. This results in an overall reduction in total resorption and resorption per OC. Early effects of OPN on osteoclastogenesis are similar to VN. Beyond 48 hours, OPN promotes both the formation and fusion of preOCs resulting in an elevation of resorption.

Disclosures: A. Gramoun, None.

M088

Suppression of Osteoclastogenesis by N,N-dimethyl-D-erythro-sphingosine: A Sphingosine Kinase Inhibition-Independent Action. H. Kim^{*}, Y. Lee^{*}, E. Chang^{*}, H. Kim^{*}, S. Hong^{*}, Z. Lee^{*}, J. Ryu^{*}, J. Ko, H. Kim. Cell and Developmental Biology, College of Dentistry, BK21 and DRI, Seoul National University, Seoul, Republic of Korea.

N,N-dimethyl-D-erythro-sphingosine (DMS) competitively inhibits sphingosine kinase (SPHK) and has been widely used to assess the role of SPHK during cellular events including motility, proliferation, and differentiation. In the present study, the effect of DMS on the differentiation of bone marrow macrophages (BMMs) to osteoclasts was investigated. When the osteoclast precursor cells were treated with DMS, the receptor activator of nuclear factor kappa B ligand (RANKL)-induced osteoclastogenesis was completely blocked. Surprisingly, however, knock-down of SPHK by siRNA in BMMs did not reduce osteoclastogenesis. Furthermore, both overexpression of SPHK and exogenous addition of sphingosine-1-phosphate, the product of SPHK activity, failed to overcome the anti-osteoclastogenic effect of DMS. These results suggest that DMS inhibited osteoclastogenesis independently of SPHK. Subsequent characterization of the DMS-mediated suppression of osteoclastogenesis revealed that DMS did not affect RANKL-induced activation of JNK, p38, NF- κ B, and Ca^{2+} oscillation. On the other hand, DMS strongly inhibited two separate signaling pathways, the RANKL-induced activation of ERK and Akt, which eventually converged on the transcription factors c-Fos and NFATc1. There was significant increase in the osteoclast formation in the presence of DMS when BMMs were overexpressed with c-Fos, suggesting that c-Fos was a critical downstream target of DMS for the inhibition of osteoclastogenesis. Taken together, our data demonstrate that DMS has an anti-osteoclastogenic function independently of its SPHK inhibitory activity. Considering previously reported anti-cancer properties of DMS, our study may also propose that DMS is an ideal drug candidate for bone metastases, for which osteoclastic bone-resorption is crucial.

Disclosures: H. Kim, None.

M089

PIAS3 Negatively Regulates RANKL-induced Osteoclastogenesis. T. Hikata¹, H. Takaishi^{*1}, M. Matsumoto^{*2}, H. Takayanagi^{*3}, A. Yoshimura^{*4}, H. Asahara^{*5}, Y. Toyama^{*1}. ¹Department of Orthopaedic Surgery, School of Medicine, Keio, University, Tokyo, Japan, ²Department of Molecular Biology, Saitama Medical School, Saitama, Japan, ³Department of Cellular Physiological Chemistry, Tokyo Medical Dental University, Tokyo, Japan, ⁴Division of Molecular and Cellular Immunology, Medical Institute of Bioregulation, Kyusyu University, Kyusyu, Japan, ⁵Department of Innovative Surgery, National Center for Child Health and Development, Tokyo, Japan.

It is known that protein inhibitor of activated STAT3 (PIAS3) not only inhibits the DNA binding activity of STAT3 in the JAK/STAT signaling pathway, but also interacts with MITF that is an important transcription factor for the osteoclast differentiation, and to regulate the gene expression in the downstream. We found that PIAS3 was widely expressed in RAW 264.7, bone marrow-derived monocyte/macrophage lineage cells (BMMs) and mouse primary osteoblasts (POB). To clarify the physiological role of PIAS3 in the bone resorption, we examined the biological effect of PIAS3 on RANKL-induced osteoclastogenesis in the culture systems using hematopoietic osteoclast precursors. Retroviral gene transduction of PIAS3 in RAW264.7 and BMMs drastically inhibited the formation of the multinucleated TRAP-positive osteoclasts. PIAS3 also suppressed the expression of osteoclast differentiation markers such as TRAP and Cathepsin K, and attenuated the protein expression of c-Fos and NFATc1 during RANKL-induced osteoclastogenesis. In PIAS3-transduced RAW264.7, the suppression of c-fos and NFATc1 DNA-binding activity was observed using ELISA-based screening system for the several transcription factors regulating osteoclast differentiation. To confirm further the functional roles of PIAS3 in osteoclast-specific gene regulation, we performed reporter gene assays using 293T and Cos7 cells. PIAS3 suppressed NFATc1, PU.1, and MITF-induced promoter activity of the TRAP and CathepsinK in a dose dependent manner. PIAS3 also produced dose-dependent inhibition of MITF-induced c-Fos promoter activity. ChIP assays showed that overexpression of PIAS3 in RAW264.7 inhibited MITF binding to the c-Fos promoter region mediated by RANKL treatment as compared to the mock-transduced control. Furthermore, siRNA knockdown of PIAS3 led to accelerated expression of RANKL in the POB stimulated with IL-6 and sIL-6R. Taken together, our results demonstrate that a possible role of PIAS3 as a negative transcriptional regulator in osteoclastogenesis directly and indirectly. These results may offer molecular approaches for the treatment of inflammatory bone destruction.

Disclosures: T. Hikata, None.

M090

See Sunday Plenary Number S090

M091

Osteoclast Differentiation During Medullary Bone Formation Period in Japanese Quail Bone Marrow Cell Culture. S. Hiyama, E. Yamanishi^{*}, M. Watanabe^{*}, T. Uchida^{*}. Department of Oral Biology, Hiroshima University Graduate School of Biomedical Sciences, Hiroshima, Japan.

Medullary bone is a unique tissue of female birds, that is formed in the long bone marrow cavity to reserve and provide for calcium of egg-shell. This bone is remodeling during the reproductive period. On the other hand, when male birds are once injected estrogen (E2) into male birds, medullary bone is formed by osteoblasts that are derived by bone lining cells and immediately resorbed by osteoclasts. However, it is not clear why osteoclasts can differentiate rapidly, and can resorb to medullary bone. To address this question, we isolated to bone marrow cells (BMC) from femurs of male Japanese quails that injected E2 at 3 (Day3), 2 (Day2), 1 (Day1), and 0 days (Day0) before slaughter, and cultured with or without RANKL & M-CSF for 4 and 8 days. At culture 4 days, in either of the presence or the absence of RANKL & M-CSF, TRAP-positive mononuclear cells were existed. TRAP-positive multinucleated cells were slightly found in RANKL & M-CSF treated BMCs. TRAP-positive multinucleated cells were increased from culture 4 days to 8 days at BMCs of each Day. However, these cells in the absence of RANKL & M-CSF were small compared with these cells in the presence of RANKL & M-CSF. In Day3 RANKL & M-CSF treated BMCs, there was much number of TRAP-positive multinucleated cells in comparison with other Days BMCs, and these cells were very large. To confirm that these BMCs were expressed the transcription factors, NFATc1 and c-Fos, RT-PCR analysis was carried out. Although c-Fos mRNA was expressed all Days BMCs, non-RANKL & M-CSF treated BMCs were very low expressed and RANKL & M-CSF treated BMCs were high expressed. The expression of NFATc1 mRNA was increased in RANKL & M-CSF treated BMCs during culture, but not expressed in non-treated BMCs. Furthermore, to evaluate the ability to resorb of bone in these cells, we cultured with these cells on the calcium-phosphate coated culture dishes. In the absence of RANKL & M-CSF, resorption area was almost observed to neither BMCs of each Day. However, the area of resorption was recognized in RANKL & M-CSF treated BMCs, especially Day3 BMCs. In addition, bone resorption activity was inhibited by osteoprotegerin, as a decoy receptor of RANKL. Our results suggest that osteoclast precursor cells increase in the bone marrow cavity during medullary bone formation. Moreover osteoclast differentiation may be regulated by osteoblasts that formed medullary bone.

Disclosures: S. Hiyama, None.

M092

Actin Binding Activity in the B Subunit Is Required for Sorting Vacuolar H⁺-ATPase (V-ATPase) in Osteoclasts. L. S. Holliday¹, J. Zuo^{*1}, R. Ricofort^{*1}, E. Serrano^{*1}, A. Cooper^{*1}, S. S. Grieshaber^{*2}, ¹Orthodontics, University of Florida College of Dentistry, Gainesville, FL, USA, ²Oral Biology, University of Florida College of Dentistry, Gainesville, FL, USA.

Actin binding activity is required for transport of virally-expressed B1 subunit of the vacuolar H⁺-ATPase (V-ATPase) to the ruffled membranes of osteoclasts(1). We are seeking the mechanistic basis for this requirement. Gel filtration chromatography, immunoprecipitations, differential detergent extractions, differential centrifugations and Native Blue gel electrophoresis were used to determine the assembly state of V-ATPases that bound actin in osteoclasts. Cholera toxin beta chain, which binds ganglioside GM1 (GM1), lysotracker probes and anti-V-ATPase subunit antibodies were used to probe the pathways responsible for ruffled membrane formation in murine osteoclasts. V-ATPase subunit B1 and B1mut (which does not bind actin) were expressed using adeno-associated virus. LY294002 was used to block phosphatidylinositol-3 kinase activity. Our results were consistent with B subunit interacting with actin only as part of intact, membrane-associated V-ATPases. This suggests that the actin binding activity is required for sorting V-ATPases into a specific vesicular trafficking pathway. GM1 was identified as a "surprising" marker for V-ATPase-rich vesicles in inactive osteoclasts and for ruffled membranes of resorbing osteoclasts. GM1 is normally endocytosed from the plasma membrane and sorted into a retrograde pathway through the golgi to the endoplasmic reticulum. Virally-expressed B1 subunit co-localized extensively with GM1, but B1mut did not. Sorting along this retrograde pathway has been reported to require the activity of vps34p (class III PI 3-kinase) and phosphatidylinositol 3-phosphate 5-kinase (PIKfyve). When PI 3-kinases were blocked using LY294002, large vacuoles that were rich in GM1 and V-ATPases quickly became apparent, a result consistent with disruption of the retrograde pathway. We also found that PIKfyve was upregulated 5-fold during osteoclastogenesis suggesting it plays an important role in osteoclasts. Our data indicate that the actin binding activity of subunit B of V-ATPase enables sorting of V-ATPases away from their default locations in the endocytic pathway into GM1-rich vesicles that then fuse with the plasma membrane as osteoclasts activate to form ruffled membranes. We are testing the hypothesis that this actin-dependent sorting targets V-ATPases into the vps34p/PIKfyve-dependent retrograde pathway, which may have been adapted in osteoclasts for the formation of ruffled membranes.

1. Zuo J, Jiang J, Chen SH, Vergara S, Gong Y, Xue J, Huang H, Kaku M, Holliday LS / 2006, J Bone Miner Res 21:714-721.

Disclosures: L.S. Holliday, None.

This study received funding from: NIH NIAMS R01 AR-47959.

M093

See Sunday Plenary Number S093

M094

Alterations in MicroRNAs and GW Bodies Are Associated with Osteoclastogenesis. J. Zuo^{*1}, A. Jakymiw^{*2}, K. M. Pauley^{*2}, E. K. Chan^{*2}, L. S. Holliday¹, ¹Orthodontics, University of Florida College of Dentistry, Gainesville, FL, USA, ²Oral Biology, University of Florida College of Dentistry, Gainesville, FL, USA.

Understanding and manipulating osteoclastogenesis requires knowing the mechanisms that regulate gene expression during this process. MicroRNAs, small endogenous RNAs, about 22 nucleotides in length, are thought to use the elements of the RNA-interference pathway to post-transcriptionally down-regulate the expression of protein-coding genes. Recent reports have identified GW bodies (mammalian P bodies) as sites that are important for microRNA-dependent regulation. We screened for differential expression of microRNAs in RAW 264.7 cells grown with or without treatment with recombinant Receptor Activator of Nuclear Factor Kappa B-ligand (RANKL) using a microRNA microarray. Some results were then confirmed by real time PCR. GW bodies, sites of microRNA-based regulation were identified using specific antibodies. We identified 9 microRNAs that were strongly downregulated (expressed to not expressed) and 6 microRNAs that were strongly upregulated (not expressed to expressed) in response to RANKL during osteoclastogenesis. In addition, the members of the let-7 family were expressed at high levels in both stimulated and unstimulated RAW cells, and all increased from 2-3 fold in response to RANKL. Six of the twelve subunits of vacuolar H⁺-ATPase as well as a number of other proteins known to be upregulated during osteoclast formation are predicted targets (MIRANDA and TargetScan 3.1, Sanger Institute) of one or more of the downregulated microRNAs. MicroRNAs 146 and 155, which have been reported to be upregulated during inflammatory responses in macrophages, were strongly upregulated in response to RANKL. GW bodies increased in number in RAW 264.7 cells as they differentiated into osteoclast-like cells. In summary, our data support the hypothesis that regulation of gene expression by microRNAs plays a role in osteoclastogenesis. Understanding this regulation may identify novel categories of pharmaceuticals for the treatment of osteoclast-mediated diseases.

Disclosures: L.S. Holliday, None.

This study received funding from: University of Florida College of Dentistry Seed Grant.

M095

Molecular Cloning and Characterization of Mouse RANK Gene Promoter Region. J. Ishii^{*1}, R. Kitazawa¹, T. Kondo¹, K. Mori¹, K. P. McHugh², S. Kitazawa¹, ¹Division of Pathology, Kobe University Graduate School of Medicine, Kobe, Japan, ²Beth Israel Deaconess Medical Center, Orthopaedic Research, Boston, MA, USA.

Receptor Activator of NF- κ B (RANK), expressed on osteoclasts and their precursors, is a receptor for RANK ligand (RANKL), a membrane-bound cytokine expressed in stromal/osteoblastic cells; signals transduced by RANK-RANKL interaction are prerequisite for differentiation, activation and maintenance of osteoclasts. To elucidate the mechanism regulating RANK gene expression during osteoclastogenesis, we cloned and characterized the 5'-flanking region of the mouse RANK gene. A 6-kb fragment containing this region was subcloned from a BAC clone and sequenced. The transcription start sites were determined by the 5'-RACE method. A 1-kb fragment upstream of the transcription start sites was ligated to the promoterless and enhancerless pGL3-basis vector (pGL3-RANK) and transfected into the mouse monocyte/macrophage cell line, RAW264.7, by the liposome mediated technique. The transfected cells were subjected to luciferase assay. Transient transfection studies showed significant pGL3-RANK promoter activity in RAW 264.7 cells. The basic promoter region of the mouse RANK gene lacked canonical TATA boxes but contained four Sp-1 binding sites located at -98, -79, -65, and -58, and four transcription start sites located at -54, -41, -27, and -23 upstream of the translation start site. Putative binding sites for PU.1 (-480), CRE/AP-1 (-240), E-box (-510, -260, -100), and NFAT (nuclear factor of activated T cells) (-720, -550, -370) were located within the 1-kb fragment of the transcription start sites. Co-transfection studies with the use of the expression vectors of MTF and PU.1 revealed that MTF and PU.1 increased RANK promoter activity three-fold and two-fold, respectively, and six-fold synergistically. Since lipopolysaccharide (LPS) is one of the factors that influences RANK gene expression in osteoclasts and their precursors, we examined the molecular mechanism whereby LPS affects RANK expression. Quantitative real-time RT-PCR showed that the expression of RANK as well as MTF and PU.1 mRNA was suppressed by treatment with LPS. Mirroring the decrease of MTF and PU.1 mRNA to 70% by LPS treatment, transient transfection studies with pGL3-RANK revealed that short-term treatment with LPS also decreased the promoter activity to 70%. We therefore speculated that RANK gene expression is influenced by two transcription factors, MTF and PU.1, both of which are prerequisite for macrophage and osteoclast differentiation, and that LPS suppresses the RANK gene, at least in part, by downregulating the expression of MTF and PU.1 genes.

Disclosures: J. Ishii, None.

This study received funding from: Japanese Ministry of Education, Culture, Sports, Science and Technology.

M096

See Sunday Plenary Number S096

M097

Iron Uptake Through the Transferrin Receptor 1 Promotes Osteoclast Differentiation and Function. K. Ishii^{*1}, S. Takeshita¹, N. Shimohata^{*2}, M. Ito³, H. Aburatani^{*4}, S. Taketani^{*5}, K. Iwai^{*2}, K. Ikeda¹, ¹Department of Bone and Joint Disease, National Center for Geriatrics and Gerontology (NCGG), Obu, Japan, ²Department of Molecular Cell Biology, Osaka City University Graduate School of Medicine, Osaka, Japan, ³Department of Radiology, Nagasaki University School of Medicine, Nagasaki, Japan, ⁴Genomescience Division, University of Tokyo School of Medicine, Tokyo, Japan, ⁵Department of Biotechnology, Kyoto Institute of Technology, Kyoto, Japan.

Osteoclasts are acid-secreting polykaryons that are rich in mitochondria. However, how mitochondrial biogenesis is stimulated during osteoclast development remains unknown. Gene expression analysis with mouse genome arrays containing 39,000 transcripts revealed transferrin receptor (TfR) 1 mRNA, which was barely detectable in bone marrow macrophages (BMMs), was markedly induced along with osteoclast differentiation. Electrophoretic mobility shift assays revealed binding of iron regulatory protein (IRP)2 to iron-responsive element (IRE) in the TfR1 mRNA 3'UTR to be markedly increased during osteoclastogenesis. Thus, IRP2 senses a heme/iron deficient state in osteoclasts and, by binding to IRE of TfR1, leads to the upregulation of TfR1 through stabilization of its mRNA. Through the increased TfR1 on the cell surface, the addition of holo-Tf as well as apo-Tf markedly stimulated the formation of TRAP-positive osteoclasts from BMMs dose dependently, which effect was inhibited by iron chelation with desferrioxamine (DFO). The pit area resorbed by mature osteoclasts was also significantly increased by Tf and decreased by DFO, suggesting that TfR1 on osteoclasts is functional, and that iron uptake through TfR1 not only promotes osteoclast formation but also the bone-resorbing function of mature osteoclasts. Gene chip analysis disclosed that almost all of the mRNAs coding for respiratory complexes I-V of mitochondria were concomitantly upregulated during osteoclastogenesis. As many of these heme-containing proteins are involved in electron transport, the mitochondrial membrane potential was increased by RANKL, which was markedly enhanced by Tf. Finally, pre-treatment of OVX mice with DFO significantly inhibited bone loss and the level of a bone resorption marker, CTX, suggesting that iron is an important regulator of osteoclastic bone resorption in vivo. In conclusion, uptake of iron through TfR1 and subsequent incorporation of heme/iron into mitochondrial respiratory proteins are critical for osteoclast development and bone-resorbing function.

Disclosures: K. Ishii, None.

M098

Role of P-Rex1 in Osteoclast Differentiation. H. Kang*¹, D. Wu*². ¹Genetics and Developmental Biology, University of Connecticut Health Center, Farmington, CT, USA, ²Pharmacology, Yale University, New Haven, CT, USA.

Guanine nucleotide exchange factors (GEFs) directly activate Rho family GTPases in response to various extracellular stimuli and play a crucial role in actin cytoskeleton rearrangement, an essential part for the differentiation and function of osteoclasts. Despite of presumed implication of GEFs in osteoclast biology, in vivo role of GEFs in osteoclasts has been poorly demonstrated. Here, we test possible involvement of P-Rex1 in osteoclast formation and ultimately in bone remodeling. P-Rex1 was identified as a phosphatidylinositol (3,4,5) trisphosphate- and Gbetagamma-regulated GEF for Rac that is implicated in chemotactic response in neutrophils. In order to examine the role of P-Rex1, P-Rex1 knockout mice were generated by inactivating Dbl homology domain, which is an essential region for GEF function to activate target Rho GTPases. Osteoclast differentiation of bone marrow-derived macrophages (BMMs) was induced by recombinant RANKL (receptor activator of NF- κ B ligand). The osteoclast formation was estimated using tartrate-resistant acid phosphatase (TRAP) staining. BMMs from P-Rex1 knockout mice showed a defect in forming TRAP-positive multinuclear cells (controls were syngenic wild-type mice). This result suggests that P-Rex1 is among the regulators for development of functional multinuclear TRAP-positive osteoclasts. Given the fact that nitrogen-containing bisphosphonates, which target small G proteins in osteoclasts, are used as antiresorptive agents in the treatment of metabolic bone diseases, identification of key GEFs in osteoclasts may contribute to more specific pharmaceutical targeting of small G proteins.

Disclosures: H. Kang, None.

This study received funding from: NIH.

M099

See Sunday Plenary Number S099

M100

BMP-2-Inducible Osterix Increases Osteoblastic CSF-1 and RANKL/OPG Ratio to Induce Osteoclast Maturation. C. C. Mandal¹, G. Ghosh-Choudhury*², H. Drissi³, N. Ghosh-Choudhury⁴. ¹Pathology, UTHSCSA, San Antonio, TX, USA, ²Medicine, UTHSCSA, GRECC, STVHCS, San Antonio, TX, USA, ³Orthopaedics, University of Rochester Medical Center, Rochester, NY, USA, ⁴Pathology, UTHSCSA, STVHCS, San Antonio, TX, USA.

Bone remodeling results from balanced action of osteoblasts and osteoclasts. BMP-2-inducible master transcription factor osterix (Ox) is essential for osteoblast differentiation and mature bone formation. Through a paracrine cytokine signaling loop, osteoblasts contribute to differentiation and maturation of osteoclasts by producing two critical factors, CSF-1 and RANKL. Expression of Ox in two different mesenchymal progenitor cells, 2T3 and C2C12, resulted in increased expression of CSF-1 and RANKL mRNA. In contrast, Ox reduced mRNA expression of osteoprotegerin (OPG), a RANKL antagonist and negative regulator of osteoclast differentiation. To investigate the mechanism, we tested the effect of Ox on CSF-1, RANKL and OPG transcription using luciferase reporter constructs driven by these promoters. BMP-2 as well as Ox independently increased transcription of CSF-1 and RANKL, while OPG transcription was significantly reduced. However, expression of Ox additively increased CSF-1 and RANKL transcription and prevented transcription of OPG. Thus osteoblast-specific Ox maintains significantly high RANKL-OPG ratio. In an effort to elucidate the mechanism, Genomatix analysis of the CSF-1 promoter revealed the presence of consensus Ox binding site between -287 bp and -246 bp (from transcription start site). Nuclear extracts prepared from BMP-2-stimulated C2C12 cells were tested in electrophoretic mobility shift assay (EMSA) using ³²P-labeled double stranded oligonucleotide representing this Ox site in the CSF-1 promoter. BMP-2 significantly increased protein-DNA complex formation, the specificity of which was determined by cold competition analysis. Use of Ox antibody in EMSA showed the presence of Ox in the DNA-protein complex. To further characterize the role of Ox in osteoclastogenesis, we stably transfected HA-tagged Ox into C2C12 and 2T3 cells respectively. Anti-HA immunoblotting of the cell lysates confirmed expression of Ox in both these cells. These cells were used in coculture assay to examine their osteoclastogenic property. Both C2C12 and 2T3 cells overexpressing Ox significantly increased TRAP positive multinucleated osteoclast formation. Together these data for the first time show a mechanism for the master transcription factor Ox action, which regulates expression of osteoblastic cytokines CSF-1, RANKL and OPG. Furthermore, we provide the first direct evidence confirming the contribution of Ox in osteoclast maturation.

Disclosures: C.C. Mandal, None.

This study received funding from: NIAMS, VA.

M101

Use of Nanogels as a Drug Delivery System for Tumor Necrosis Factor- α Antagonist in Murine Bone Resorption Model. C. N. R. Alles*¹, M. H. Mian*¹, N. S. Soysa*¹, H. Saito*², K. Aoki², K. Akiyoshi*¹, K. Ohya².

¹Center of Excellence for Frontier Research on Molecular Destruction and Reconstruction of Bone, Tokyo Medical and Dental University, Tokyo, Japan, ²Section of Pharmacology, Tokyo Medical and Dental University, Tokyo, Japan.

Our previous study has shown that a TNF antagonist peptide (WP9QY/W9) inhibits RANKL-induced bone resorption (J Clin Invest 116:1525-1534, 2006). Easy degradation in serum is a major drawback in clinical application of this peptide. On the other hand nanogels have emerged as a promising carrier in delivering proteins and peptides. Hence we hypothesized cholesterol group-bearing pullulan (CHP) nanogel as a candidate in delivering TNF- α antagonist in vivo. We reported previously (C.N.R. Alles et al. ASBMR 2006) using C57BL/6J mice on low Ca diet injected with veh, CHP nanogel, W9 or CHP-W9 complex, that twice a day subcutaneous injections of the CHP-W9 complex prevented the reduction in BMD in mice on low Ca diet. From these BMD data it was not clear whether the formation was increased or the resorption is decreased. To this end histomorphometry was performed at the sites of metaphysis of tibiae. CHP-W9 complex prevented the decrease of bone volume parameters significantly: trabecular volume ($p < 0.001$), trabecular thickness ($p < 0.05$) and trabecular number ($p < 0.001$) and prevented the increase of trabecular separation ($p < 0.001$) compared to low Ca-veh group. CHP-W9 complex prevented the increase of osteoclast surface ($p < 0.05$) and number ($p < 0.05$) to bone surface brought by low Ca as well. Conversely the complex substantially mitigated the increase of osteoblast surface to bone surface ($p < 0.005$) and mineral apposition rate (MAR) ($p < 0.005$). Similarly the bone resorption parameter, urine deoxypyridinoline in low Ca-veh group ($p < 0.05$) was significantly increased compared to the normal Ca-veh and CHP-W9 complex groups. To further confirm the in vivo complexation of W9 with CHP nanogel, in vitro stability test was performed. W9 was easily dissolved in alkali whereas it tends to aggregate in low pH. By using Dynamic Light Scattering (DLS) analysis, we observed the association of peptide with nanogels. When peptide is added with CHP nanogel, even at pH 6.5, W9 could completely dissolve in nanogels. Taken together these results suggested that the twice a day subcutaneous injection of CHP-W9 complex was effective in preventing the bone resorption brought by low Ca feeding as agreeing with previous study which use 8x/day injections. This implied that the complex was stable in serum and achieved a constant release corroborating our in vitro data. Hence our study confirmed that nanogels could be used as an effective carrier to deliver W9 peptide.

Disclosures: C.N.R. Alles, None.

M102

Development of Cell-Based Assays for Identifying Antiresorptive Compounds Targeting RANK Signaling through High Throughput Screening. J. Ashley*¹, Z. Shi*¹, E. Mills*¹, D. Clements*¹, T. Chen*², X. Feng¹. ¹Dept. of Pathology, University of Alabama at Birmingham, Birmingham, AL, USA, ²Dept. of Chemical Biology & Therapeutics, St. Jude Children's Research Hospital, Memphis, TN, USA.

Current antiresorptive drugs either lack satisfactory efficacy or cause serious side effects. The unraveling of the RANKL/RANK/OPG system has provided an opportunity to develop more effective antiresorptive drugs, but agents currently under development targeting RANK/RANKL interactions are likely to have side effects due to the role of the system in other biological processes. We recently identified three functional TRAF-binding motifs (Motif 1: PFQEP³⁶⁹⁻³⁷³, Motif 2: PVQEET⁵⁵⁹⁻⁵⁶⁴ and Motif 3: PVQEQG⁶⁰⁴⁻⁶⁰⁹) in the RANK cytoplasmic domain. While Motif 2 and Motif 3 are very potent in mediating osteoclast formation and function, Motif 1 plays a minimal role in these processes, instead being the primary actor in RANKL-mediated immune function. Thus, Motifs 2 and 3 can serve as potent and specific antiresorptive targets.

We have developed cell-based high throughput screening (HTS) assays for identifying compounds inhibiting Motifs 2 and 3 signaling. The assays contain three key components: RAW264.7 (RAW) cells, an NF- κ B-responsive luciferase reporter, and a chimeric receptor consisting of human Fas external domain linked to the transmembrane and cytoplasmic domains of normal or mutant RANK. First, we established a RAW cell line stably expressing the luciferase reporter, which showed a 6-fold induction of luciferase activity in response to RANKL treatment. We then prepared and expressed the following chimeric receptors in the stable RAW cell line: M2 (Motifs 1 and 3 in RANK domain are mutated), M3 (Motifs 1 and 2 in RANK domain are mutated). Cells expressing M2 or M3 can be used in HTS for identifying compounds inhibiting Motifs 2 and 3, respectively. For example, treatment of the cells expressing M2 with anti-human Fas antibody (hFas-AB) causes recruitment of TRAF3 to Motif 2, leading to the formation of a signaling complex and activation of NF- κ B, which, in turn, activates the luciferase reporter. If a compound blocks the TRAF3-Motif 2 interaction or the formation of signaling complex, no NF- κ B will be activated by the M2 receptor and subsequent reporter activation will be reduced. Preliminary data indicate that cells expressing M2 and M3 can induce ~1.5-fold reporter activity following hFas-AB treatment. We have also developed additional assays for hit follow up and are now improving assay efficiency by optimizing hFas-AB concentration and treatment time as well as selecting subclones with higher levels of induction. In addition, we are seeking partnerships with groups interested in utilizing our assays.

Disclosures: J. Ashley, None.

M103

See Sunday Plenary Number S103

M104

Cytoplasmic Terminus of a V-ATPase Accessory Subunit Ac45 Is Required for Proper Interaction with V0 Domain Subunits and Efficient Osteoclastic Bone Resorption. T. Cheng^{*1}, H. Feng^{*1}, K. H. M. Yip^{*1}, N. J. Pavlos^{*1}, A. Carrello^{*1}, R. Seeber^{*2}, K. Eidne^{*2}, M. H. Zheng¹, J. Xu¹. ¹Centre for Orthopaedic Research, University of Western Australia, Perth, Australia, ²Western Australia Institute for Medical Research, University of Western Australia, Perth, Australia.

Solubilization of mineralized bone by osteoclasts is largely dependent on the acidification of the extracellular resorption lacuna driven by vacuolar type proton pump (V-ATPases) polarized within the ruffled border membranes. V-ATPases consist of two functionally and structurally distinct domains, V1 and V0. The peripheral cytoplasmically oriented V1 domain drives ATP hydrolysis which necessitates the translocation of protons across the integral membrane bound V0 domain. Here, we demonstrate that an accessory subunit, Ac45, interacts with the V0 domain and contributes to V-ATPase-mediated function in osteoclasts. Consistent with its role in intracellular acidification, Ac45 was found to be localized to the ruffled border region of polarized resorbing osteoclasts and enriched in pH-dependent endosomal compartments which polarized to the ruffled border region of actively resorbing osteoclasts. Interestingly, truncation of the 26aa-residue cytoplasmic tail (aa437-463) of Ac45 (Ac45C-mutant) which encodes an autonomous internalization signal was found to impair bone resorption in vitro. Furthermore, immunoprecipitation and bioluminescence resonance energy transfer (BRET) analysis revealed that although both wild type Ac45 and Ac45C-mutant were capable of associating with V-ATPase subunits a3, c, c', and d, deletion of the cytoplasmic tail altered its binding affinity with a3, c' and d. In all, our data suggest that the cytoplasmic terminus of Ac45 contains essential elements necessary for its proper interaction with V-ATPase and efficient osteoclastic bone resorption.

Disclosures: T. Cheng, None.

M105

Modeling Role of ER in Transcellular Calcium Flux in Bone Resorbing Osteoclasts. H. K. Datta. Institute of Cellular Medicine, Newcastle University, Newcastle upon Tyne, United Kingdom.

It has been shown that Ca^{2+} produced in the osteoclast (OC) hemivacuole by the action of secreted acid is continually transported to the basolateral surface; thus, preventing accumulation of the cation in the resorptive lacuna. Ca^{2+} may be taken up through store-operated Ca^{2+} channels in the basal membrane, the site of the resorptive hemivacuole, and is pumped into the basal endoplasmic reticulum (ER) by Ca^{2+} -ATPases. Ca^{2+} then diffuses through the lumen of the ER from the base to the apical region, where it is released into the cytosol via specific Ca^{2+} channels i.e. inositol 1,4,5-triphosphate (IP_3) and ryanodine receptors. Ca^{2+} is then pumped out of the cell by plasma membrane Ca^{2+} -ATPases which are located in the apical membrane. The route through the lumen of the ER is attractive because of the abundance of calreticulin, a high capacity Ca^{2+} -binding protein which is involved in Ca^{2+} homeostasis. In view of these observations, we attempted to define the role of ER and have modeled the calcium disposal through bone resorbing osteoclast. The modeling was performed using Virtual Cell Software, available from National Resource for Cell Analysis and Modeling (NRCAM), at the website: <http://www.nrcam.uchc.edu>. The model is comprised of four physiological structures, namely hemivacuole, cytosol, ER and extracellular fluid space, giving four respective resolved geometric subdomains. For these resolved structure mixed boundary conditions Neuman and Dirichlet were chosen. The kinetics of calcium pumps and channels are given by linear equation; SERCA pump uptake is modelled by a Hill type equation and channels influx is catalyzed by reaction described by the Michaelis-Menton equation. 2-D geometry involves extensive network, two exact mirror image of the osteoclast-hemivacuole; the line of symmetry of two opposing actively resorbing osteoclast therefore passes through the resorptive hemivacuole. Other relevant parameters, such as constants, functions, and volumes were selected based on published literature. The results of simulations experiments were compared with the experimental observations, and were found to successfully mimic in vivo observations, such as elevated $[\text{Ca}^{2+}]_{\text{ER}}$ and maintenance of $[\text{Ca}^{2+}]_i$ within known physiological range but with high localized $[\text{Ca}^{2+}]_i$ (so-called calcium puffs) near the hemivacuole site. Perturbation experiments performed established a critical role of the ER and its key components in the transcellular Ca^{2+} -transport and buffering. The model has ER which is functionally continuous unit, where Ca^{2+} released from the apical ER is quickly replenished from the base. In conclusion, OC provides an excellent model to test recent suggestion that ER is an important conduit for the transcellular transport of Ca^{2+} in polarized cells.

Disclosures: H.K. Datta, None.

M106

Tetracyclines [Doxycycline(Dox) and Minocycline(Mino)] Effectively Inhibit Osteoclast Differentiation and Function. S. Kinugawa^{*1}, M. Koide², T. Ninomiya^{*2}, H. Nakamura³, Y. Kobayashi², N. Takahashi², N. Udagawa⁴. ¹Graduate School of Oral Medicine, Matsumoto Dental University, Siojiri, Japan, ²Institute for Oral Science, Matsumoto Dental University, Siojiri, Japan, ³Department of Oral Histology, Matsumoto Dental University, Siojiri, Japan, ⁴Department of Biochemistry, Matsumoto Dental University, Siojiri, Japan.

Tetracyclines (Dox and Mino) are widely used in the treatment of periodontal disease to suppress the growth of bacteria. Tetracyclines also have been shown to prevent bone loss, but the mechanism of action of tetracyclines to inhibit bone resorption is not elucidated. Here, we examined how tetracyclines inhibit bone resorption. We found that both Dox and Mino directly acted on osteoclast (OC) precursors to inhibit their differentiation into OCs, and on mature OCs to inhibit their function.

(1) Increasing concentrations of Dox and Mino were added to co-cultures of mouse bone marrow cells (BMCs) and osteoblasts (OBs) in the presence of PGE_2 and $1\alpha,25(\text{OH})_2\text{D}_3$. Both Dox and Mino dose-dependently inhibited OC formation induced by PGE_2 and $1\alpha,25(\text{OH})_2\text{D}_3$. (2) Effects of Dox and Mino on RANKL and COX-2 mRNA expression in OB cultures were examined by RT-PCR. Treatment of OBs with $1\alpha,25(\text{OH})_2\text{D}_3$ up-regulated RANKL mRNA expression. Dox and Mino added to OB cultures failed to affect $1\alpha,25(\text{OH})_2\text{D}_3$ -induced RANKL mRNA expression. Neither Dox nor Mino induced OB COX-2 mRNA expression. (3) Mouse bone marrow macrophages (BMMs) and human CD14-positive monocytes were cultured as OC precursors in the presence of RANKL and M-CSF with increasing concentrations of Dox and Mino. RANKL and M-CSF stimulated mouse and human OC formation. Dox and Mino dose-dependently inhibited mouse and human OC formation with the complete inhibition at 20 $\mu\text{g}/\text{ml}$ of either compound. (4) When mouse OCs were cultured on dentine slices, they formed many resorption pits on the slices in the presence of OBs. Addition of Dox and Mino at 20 $\mu\text{g}/\text{ml}$ also inhibited the pit-formation activity of OCs. (5) Western blot analysis demonstrated that the treatment of BMMs with lipopolysaccharide stimulated phosphorylation of ERK, a MAP kinase, which was completely inhibited by pretreatment with Dox and Mino. Thus, both Dox and Mino directly inhibited differentiation and function of not only mouse but also human OCs. These inhibitory effects on bone resorption are proposed to be associated with the suppression of MAP kinases. These results suggest that Dox and Mino have great therapeutic potential for the periodontal therapy to suppress alveolar bone loss.

Disclosures: S. Kinugawa, None.

M107

M-CSF Receptor C-fms Antibody Inhibits Mechanical Stress-Induced Root Resorption. H. Kitaura, Y. Fujimura^{*}, M. Yoshimatsu^{*}, T. Eguchi^{*}, H. Kohara^{*}, N. Yoshida^{*}. Division of Orthodontics and Dentofacial Orthopedics, Nagasaki University Graduate School of Biomedical Sciences, Nagasaki, Japan.

Root resorption is occurred during orthodontic treatment, and lead to serious problem. However, because a suitable experimental animal model has been lacking, the biological mechanism is not clearly understood. We established mechanical stress-induced osteoclastogenesis model in mice using orthodontic tooth movement in which an Ni-Ti coil spring was inserted between the upper incisors and the upper first molar. And we found root resorption was occurred in this model during mechanical loading. The formation of osteoclasts depends on macrophage-colony-stimulating factor (M-CSF) and a ligand for the receptor activator of necrosis factor κB (RANKL). It has recently been reported that administration of an antibody of the M-CSF receptor c-fms completely blocked pathological osteoclastogenesis and bone erosion induced by TNF administration or inflammatory arthritis. This study aimed to examine the effect of monoclonal anti-c-fms antibody to a root resorption in mechanical stress-induced osteoclastogenesis model. We injected 10 micro gram anti-c-fms antibody in PBS daily into a local site for 12 days during mechanical loading. We assessed the root resorption of upper first molar after mechanical loading and carried out histological observations. The amount of the root resorption was evaluated by measuring the resorption area at disto-buccal root of the first molar by an electron microscope. Anti-c-fms antibody significantly inhibited root resorption after mechanical loading ($p<.01$). Further, the number of osteoclasts stained for TRAP on the root surface in the anti-c-fms antibody injected group was markedly reduced compared with controls. The results suggested that M-CSF and/or its receptor are potential therapeutic targets in mechanical stress-induced osteoclastogenesis, and that injection of an anti-c-fms antibody might be useful for inhibition of mechanical stress-induced root resorption.

Disclosures: H. Kitaura, None.

M108

A Possible Suppressive Role of Galectin-3 in Osteoclastic Bone Destruction Accompanying Adjuvant-induced Arthritis in Rats. Y. Li^{*1}, J. Teramachi^{*1}, K. Nagata^{*1}, Z. Wu^{*1}, A. Kukita², A. Akamine¹, T. Kukita¹. ¹Faculty of Dental Science, Kyushu University, Fukuoka, Japan, ²Faculty of Medicine, Saga University, Saga, Japan.

Galectin-3 is a β -galactoside-binding animal lectin having pleiotropic effects on cell growth, differentiation and apoptosis. This lectin has shown to be involved in phagocytosis by macrophages and inflammation. Here we investigated an involvement of galectin-3 in the regulatory process of inflammatory bone resorption in rats with adjuvant-induced arthritis accompanying severe bone destruction in the ankle joints. The protein level of galectin-3 in the ankle-joint-extracts was markedly augmented at week 3 after adjuvant injection, at the time when severe bone destruction was observed. Immunohistochemical

analysis revealed an extremely high expression of galectin-3 in macrophages and granulocytes infiltrated in the area of severe bone destruction in the distal tibia. To estimate a role of galectin-3 in osteoclastogenesis and osteoclastic bone resorption, recombinant galectin-3 was added to *in vitro* systems. Exogenously added recombinant galectin-3 markedly inhibited the formation of osteoclasts in cultures of murine osteoclast precursor cell line (RAW-D cells) as well as in rat bone marrow culture systems for evaluating osteoclastogenesis in a carbohydrate-independent manner. This inhibition was not observed by heat-inactivated galectin-3 and by galectin-7. Although recombinant galectin-3 did not affect signaling through MAP-kinases and NF- κ B, it specifically suppressed the induction of NFATc1, a key transcription factor required for osteoclastogenesis. Furthermore, galectin-3 significantly inhibited dentin resorption by mature osteoclasts. Thus, abundant galectin-3 observed in the area of severe bone destruction could act as a negative regulator for the up-regulated osteoclastogenesis accompanying inflammation, that would contribute to prevention of excess bone destruction.

Disclosures: T. Kukita, None.

M109

P2X7 Nucleotide Receptors Couple to Isoform-Specific Activation of PKC in Osteoclasts: Spatio-Temporal Patterning of PKC Translocation Revealed by Live-Cell Imaging. S. Armstrong, A. Pereverzev*, S. M. Sims*, S. J. Dixon. Physiology and Pharmacology, University of Western Ontario, London, ON, Canada.

Nucleotides, released from cells in response to mechanical or inflammatory stimuli, signal through P2 nucleotide receptors in many cell types including osteoclasts. Osteoclasts express functional P2X7 receptors -- calcium-permeable channels that are activated by high concentrations of extracellular ATP. Targeted disruption of the gene encoding the P2X7 receptor leads to increased resorption and reduced skeletal response to mechanical stimuli. However, little is known about the signaling pathways stimulated by P2X7 receptors in osteoclasts. Our purpose was to investigate whether P2X7 receptors couple to activation of protein kinase C (PKC). An early step in activation of PKC involves translocation, with many PKC isoforms moving from the cytosol to the plasma membrane. RAW264.7 mouse monocytic cells were differentiated with RANKL and transiently transfected with plasmids encoding PKC-EGFP fusion proteins or the fluorescent protein EGFP alone. Live-cell confocal imaging was used to monitor changes in the distribution of PKC isoforms in the resulting multinucleated osteoclast-like cells. Within 20-40 s, benzoylbenzoyl-ATP (BzATP, 150 μ M, a relatively potent P2X7 receptor agonist) induced translocation of PKC α to the basolateral membrane. Translocation was transient with duration of 5-10 min. In contrast to BzATP, the PKC activator phorbol myristate acetate (PMA) induced sustained translocation of PKC α . UTP (150 μ M) or ATP (10 μ M), which activate several P2 receptors other than P2X7, failed to induce translocation of PKC α ; whereas, ATP (3 mM, a concentration sufficient to activate P2X7) caused translocation. Translocation was inhibited by the selective P2X7 antagonist Brilliant Blue G. These data are consistent with involvement of P2X7 receptors. To investigate the role of cytosolic calcium, we simultaneously monitored PKC α location and calcium concentration. BzATP induced transient rise in cytosolic calcium that was temporally correlated with translocation of PKC α . Moreover, removal of extracellular calcium prevented translocation induced by BzATP, but not by PMA. BzATP induced translocation of PKC α and PKC β I, which are both calcium-dependent PKC isoforms. In contrast, BzATP did not induce translocation of the calcium-independent isoform PKC δ . These findings establish that activation of P2X7 receptors induces calcium-dependent translocation of PKC to the basolateral membrane domain of osteoclasts, an aspect of spatio-temporal signaling not previously recognized. Thus, ATP -- released in response to inflammatory or mechanical stimuli -- may signal through specific PKC isoforms to regulate osteoclast functions *in vivo*.

Disclosures: S. Armstrong, None.

This study received funding from: The Canadian Arthritis Network & Canadian Institutes of Health Research.

M110

See Sunday Plenary Number S110

M111

Novel Pro-Survival Functions of the Kruppel-Like Transcription Factor Egr2 in Promotion of M-CSF-Mediated Osteoclast Survival Downstream of the MEK/ERK Pathway. E. W. Bradley*¹, M. M. Ruan*², M. J. Oursler². ¹Biochemistry and Molecular Biology, Mayo Clinic, Rochester, MN, USA, ²Endocrine Research Unit, Mayo Clinic, Rochester, MN, USA.

M-CSF promotes differentiation and survival of cells within the monocyte/macrophage cell lineage, including bone resorbing multinucleated osteoclasts. As osteoclast survival is in part mediated by M-CSF, determining the molecular mechanisms of M-CSF-promoted osteoclast survival is crucial in treating pathological bone loss. However, the signaling mechanism M-CSF utilizes to support osteoclast survival is poorly characterized. This study addressed activation of MEK/ERK, a signaling pathway implicated in controlling osteoclast survival, in response to M-CSF and identified a novel pro-survival downstream effector of this pathway. M-CSF transiently activated the MEK/ERK pathway, an effect blocked by chemical inhibition of MEK1/2 or adenoviral expression of dnMEK1. M-CSF also induced expression of two Kruppel-like transcription factors, Egr1 and Egr2. Induction of both Egr1 and Egr2 expression was blocked through chemical inhibition of MEK1/2. To determine if one of these Egr transcription factors was a potential downstream mediator of the M-CSF-activated MEK/ERK pathway, the nuclear Egr1 and Egr2 corepressor Nab2 was employed to inhibit the function of

both Egr1 and Egr2. In addition, the difference between Nab2 expression alone or Nab2 expression in combination with MEK inhibition by U0126 was examined. While both Nab2 and MEK inhibition increased osteoclast apoptosis, a concomitant increase in osteoclast apoptosis with Nab2 expression in combination with MEK1/2 inhibition treatment was not evident. These data suggest a role for Egr1 and/or Egr2 in M-CSF-promoted osteoclast survival and demonstrate the necessity of Egr family members in the promotion of MEK-dependant osteoclast survival. Both Egr1 and Egr2 were therefore pursued as downstream effectors of MEK/ERK mediated osteoclast survival downstream of M-CSF. Two forms, a wild-type (wt) and a mutant form (ca) lacking the Nab corepressors binding site, were utilized. Expression of wtEgr2 and caEgr2, not wtEgr1 or caEgr1, reduced the basal rate of osteoclast apoptosis. In addition, expression caEgr2 bypassed the block of M-CSF-promoted osteoclast survival mediated through MEK1/2 inhibition. M-CSF therefore promotes osteoclast survival through activation of the MEK/ERK pathway and induction of Egr2, providing a novel function of Egr2 in the promotion of cell survival.

Disclosures: E.W. Bradley, None.

M112

See Sunday Plenary Number S112

M113

Disruption of WASP-Associated Signaling Complex Formation Leads to Defects in Sealing Ring Formation and Bone Resorption in Osteoclasts. T. Ma*, M. A. Chelliah. Department of BMS Rm 7207 South Dental School, University of Maryland, Baltimore, MD, USA.

Wiscott-Aldrich Syndrome protein (WASP) has a unique regulatory role in sealing ring formation and bone resorption in osteoclasts. The activities of different kinases have been correlated to the phosphorylation of WASP and osteoclast bone resorption. The purpose of this study was to identify the WASP domain that regulates osteoclast function *in vitro*. TAT-mediated delivery of different WASP domains and full-length WASP into osteoclasts was performed. Transduction of TAT-fused full-length WASP peptide induced Arp2/3 complex formation, F-actin content, sealing ring formation and bone resorption largely as compared with other peptides containing different WASP domains. Transduction of WASP peptides containing basic, verpulin-central, pTyr294, and proline-rich regions exhibited inhibitory effects at various levels on the processes listed above. The ability to resorb bone by WASP peptides containing basic, verpulin-central, and proline-rich regions was reduced and the resorbed area matched the size of the sealing ring. However, osteoclasts transduced with WASP peptide containing pTyr294aa demonstrated total loss of sealing ring-like structures but displayed actin-rich clusters at the peripheral edge that contains filopodia-like projections. Abnormal cytoskeletal changes have been coupled with the reduced capacity for bone resorption *in vitro*. The resorption pits were small, simple, and superficial. Taken together, these findings suggest that modulation of phosphorylation state of Tyr294aa assists in integrating multiple signaling molecule and pathways that partake in the assembly of sealing ring

Disclosures: M.A. Chelliah, None.

This study received funding from: NIH-NIAMS RO1AR46292 to MAC.

M114

See Sunday Plenary Number S114

M115

Regulation of RANKL-induced MAP Kinase Activation by Reactive Oxygen Species. H. Choi¹, H. Yu¹, J. Shin¹, S. Lee². ¹Life and Pharmaceutical Sciences, Ewha Womans University, Seoul, Republic of Korea, ²Division of Life and Pharmaceutical Sciences, Center for Cell Signaling & Drug Discovery Research, Ewha Womans University, Seoul, Republic of Korea.

Osteoclasts (OCs) are multinucleated hematopoietic cells that resorb bone and are essential for bone homeostasis. Signaling between receptor activator of NF- κ B ligand (RANKL) and TNF (tumor necrosis factor) receptor-associated factor (TRAF) 6 is essential for differentiation of bone marrow monocyte/macrophage (BMM) lineage cells into osteoclasts. Here, we show that enhanced intracellular reactive oxygen species (ROS) levels by RANKL in BMM are dependent on the binding strength between RANK and TRAF6. ROS generation was decreased in overexpression of modified RANK (E342/449A and E342/375/449A) in TRAF6-binding sites, but not in reconstitution of wild-type RANK which has normal interaction between RANK and TRAF6. Consistently, MAPKs activation including ERK, JNK and p38 were attenuated by the modified RANK expression. To examine whether MAPK phosphatases (MKPs) play a role in the negative regulation of MAPKs through inactivation by ROS, we first investigated expression of MKPs in BMM through quantitative real-time PCR. The mRNA expression levels of MKP1 and MKP3 were much higher than other MKPs. We found MKP1 regulates JNK activation and MKP3 controls JNK and p38 activation in response to RANKL in 293-TR cells that express Flag epitope-tagged RANK inducibly in 293 cells. Moreover overexpression of catalytic mutant of MKP1 and MKP3 prompted osteoclast differentiation. These results suggest that MKPs including MKP1 and MKP3 might be an intracellular signal modulator for osteoclast differentiation between ROS and MAPKs.

Disclosures: H. Choi, None.

This study received funding from: BK 21 fellowship.

M116

Mice Overexpressing Nucleolar PTHrP Driven by Type II Collagen Promoter Show Disordered Distribution of Chondrocytes in the Epiphyseal Cartilage. N. Amizuka¹, T. Komori², K. Oda³, D. Goltzman⁴, A. Karaplis⁴, M. Li¹. ¹Center for Transdisciplinary Research, Niigata University, Niigata, Japan, ²Division of Cell Biology, Nagasaki University, Nagasaki, Japan, ³Division of Biochemistry, Niigata University, Niigata, Japan, ⁴Faculty of Medicine, McGill University, Montreal, PQ, Canada.

The main pathway for parathyroid hormone-related peptide (PTHrP) action is that of extracellular secretion and subsequent activation of the cell membrane-bound PTH/PTHrP receptor. PTHrP has also been reported to translocate into nucleoli, and modulate cellular functions through its nuclear/nucleolar actions. PTHrP molecule, lacking the signal sequence but encompassing the nucleolar targeting signal, was shown to successfully translocate into nuclei and nucleoli, without following the secretory pathway in transfected chondrocytic cell line, CFK2. When this nuclear form of PTHrP cDNA tagged with the myc epitope was inserted into a type II collagen promoter/enhancer cassette and transfected in primary cultured chondrocytes from mouse epiphyseal cartilage, PTHrP and myc immunoreactivity was observed in their nuclei and nucleoli, but not in the cytoplasmic region. Based on these experiments, we generated mice overexpressing nucleolar PTHrP, which is driven by the type II collagen promoter. Transgenic mice at 18-19 day-old fetal stages were sacrificed, and the transgene was examined by PCR using specific primers recognizing the DNA sequence from the C-terminal region of myc-tagged PTHrP. Immunohistochemistry for PTHrP and myc demonstrated their localization to be restricted to nuclei and nucleoli of resting and proliferative chondrocytes, but not in hypertrophic cells. The width of the resting, proliferative and hypertrophic zones of the tibial and femoral epiphyses, as well as cell proliferation estimated by statistical analysis for PCNA (proliferating cell nuclear antigen)-immunopositive cells were not different between transgenic and wild-type fetuses. In addition, the width of the type X collagen-positive hypertrophic zone in transgenic mice was similar to that of wild type mice. Therefore, unlike PTHrP's receptor-mediated pathway, nucleolar PTHrP appeared not to dynamically affect proliferation or differentiation of chondrocytes. However, chondrocytes of various sizes were present in the lower region of proliferative zone were irregularly distributed. In summary, overexpression of the nuclear form of PTHrP appears to influence the distribution of chondrocytes rather than their proliferation or differentiation in mouse epiphyseal cartilage.

Disclosures: N. Amizuka, None.

M117

Induction of kinin B₁ Receptor in Osteoarthritis Is Performed by Vasoactive Peptide Endothelin-1. H. L. Attalah¹, D. Debois², C. A. Manacu³, N. Newman⁴, A. Moreau⁵, F. Moldovan⁵. ¹Faculty of Dentistry of Montreal University, Research Center CHU Ste Justine Hospital, Canada, PQ, Canada, ²Pharmacology, University of Montreal, Canada, PQ, Canada, ³Research Center CHU Ste Justine Hospital, Canada, PQ, Canada, ⁴University of Montreal, Canada, PQ, Canada, ⁵Dentistry Faculty of Montreal University, Research Center CHU Ste Justine Hospital, Canada, PQ, Canada.

Endothelin-1 (ET-1) and kinin B₁ receptors are involved in pain. ET-1 and B₁ receptor activate similar signalling pathways, and their expression is under the control of the pro-inflammatory mediators that are key molecules for Osteoarthritis (OA) pathophysiology. Kinins are potent agonists that participate in inflammatory and pain responses to insults by acting through the inducible B₁ receptor. We hypothesize that ET-1 has a specific role in OA pathophysiology in the early phase by promoting cartilage degradation and late phase by inducing B₁R expression leading to thereby exacerbating inflammation and pain induction in late stage OA.

Analysis of B₁R expression in synovial tissues of OA patients by immunohistochemistry and in situ hybridization revealed that its presence locally dependent on the level of tissue inflammation since its expression appears to be directly regulated by inflammatory mediators such as ET-1 and IL1 β . We also observed that B₁R co-localizes with ET-1 in both endothelial cells and type A synoviocytes (macrophage like cells). In OA chondrocytes, western blotting revealed p70S6 and p85S6 kinases and the p70S6 kinase is phosphorylated by ET-1, and that this phosphorylation is inhibited by rapamycin. Both of which act on mitogen-activated signalling pathways downstream of phosphoinositide 3-kinase (PI3K), and are targets of rapamycin FRAPm/TOR. Activation of PI3K-Akt and Ras-Raf MEK-ERK signalling cascades by ET-1 is thought to play an important role in cartilage matrix degradation via the activation of MMP-1 and MMP-13 which specifically cleave OA cartilage collagen.

These results prompted us to propose that ET-1 over expression in OA synovial tissues contributes to B₁R up-regulation, although it remains unclear whether such an effect is solely due to elevated ET-1 levels. These data point toward a possible role of ET-1 in inflammatory pain. Thus, ET-1 is potentially attractive therapeutic target for OA pathology characterised by a chronic pain.

Disclosures: H.L. Attalah, None.

This study received funding from: The Arthritis Society.

M118

See Sunday Plenary Number S118

M119

Hydrostatic Loading of Growth Plate Chondrocytes in Vitro. Y. Y. Shao^{*1}, J. Welter², L. Wang^{*3}, R. T. Ballock⁴. ¹Department of Biomedical Engineering, Cleveland Clinic, Cleveland, OH, USA, ²Department of Biology, Case Western Reserve University, Cleveland, OH, USA, ³Department of Biomedical Engineering, Cleveland Clinic, Cleveland, OH, USA, ⁴Departments of Orthopaedics and Biomedical Engineering, Cleveland Clinic, Cleveland, OH, USA.

Objective: It is well-established that mechanical forces can influence the behavior of cartilage chondrocytes, however little is known about the response of growth plate chondrocytes to these mechanical forces. The objective of this study was to examine the effects of hydrostatic compression on the behavior of growth plate chondrocytes by testing the hypothesis that hydrostatic loading would inhibit proliferation and differentiation of these cells through modulation of the Ihh-PTHrP feedback loop.

Methods and Results: Epiphyseal chondrocytes were isolated from the distal femoral growth regions of two day old Sprague-Dawley rats and cultured as three-dimensional cell pellets (3x10⁵ cells/pellet) for five days. The pellets were then either subjected to hydrostatic compression or cultured as unloaded controls. A custom-designed mechanical loading system was used apply an intermittent 1MPa hydrostatic compression force (1 hour on, 1 hour off) for 1 or 2 days at 37°C and 5% CO₂. After the compression period, AQ 96 proliferation assays were carried out immediately for analysis of cell viability, while others were frozen for later testing. The growth plate chondrocytes subjected to hydrostatic compression increased proliferation more than the control cells after one day of loading, but were identical to control samples after two days. Real-time quantitative RT-PCR analysis demonstrated that type X collagen (ColX) expression was increased by 12 fold in the loaded samples after one day of compression, while Ihh mRNA was up-regulated more than 6-fold and expression of patched (Ptc) and runt-related transcription factor (RunX2) were both increased two-fold. In addition, Ihh expression was also examined after shorter periods of compression (0.5, 1, 2, and 4 hours), Ihh expression increased 1.5 fold in response to the compression as early 30 minutes following application of the hydrostatic load. Measurement of caspase 3/7 activity and immunoblotting of Bcl₂ protein failed to reveal any increase in apoptotic activity in the hydrostatically loaded pellets compared to the unloaded controls.

Conclusions: Our results show that in vitro hydrostatic compression can stimulate Ihh expression, chondrocyte proliferation and terminal differentiation in growth plate chondrocytes cultured as three-dimensional cell pellets.

Disclosures: R.T. Ballock, None.

M120

Establishment of a Rat Culture System for Studying the Morphological Diversity of Hypertrophic Chondrocytes. K. Chen^{*}, L. Tatarczuch^{*}, Y. Ahmed^{*}, M. Mirams^{*}, C. N. Pagel^{*}, E. J. Mackie. School of Veterinary Science, The University of Melbourne, Parkville, Australia.

During endochondral ossification, hypertrophic chondrocytes exist in two forms, "dark" and "light" cells. We have recently observed that these cells undergo two different forms of non-apoptotic physiological cell death (PCD) in horse growth cartilage, and have established a culture system for studying hypertrophy and death of equine chondrocytes. The aim of the current study was to develop a culture system using rodent chondrocytes in order to study differences between dark and light cells and their modes of death. Chondrocytes were isolated from femoral epiphyseal cartilage from neonatal rats and cultured as pellets in the presence of triiodothyronine (T3) in 0.1% FCS. After 14 days, the pellets were examined by light and electron microscopy. The proportion of hypertrophic light chondrocytes was double that of hypertrophic dark chondrocytes. Hypertrophic light chondrocytes from the T3-treated pellets could be purified through centrifugation in a gradient concentration of Ficoll-PaqueTM Plus. The microarray technique was performed to compare the difference in gene expression between the purified hypertrophic light chondrocytes and the mixed hypertrophic dark and light cells in the T3-treated pellets. A number of genes of interest have been selected for validation by real-time PCR. These include genes encoding Egr2 and tissue plasminogen activator, which appear to be more highly expressed in light cells than dark cells, and periostin and osteoglycin, which appear to be more highly expressed in dark cells than light cells. Staurosporine induces apoptosis in many cell types, but when staurosporine was added to pellets cultured in 10% FCS, apoptotic chondrocytes were rarely observed. Instead, there was an increase in the proportion of dark cells dying by the process observed for these cells in vivo. Staurosporine significantly down-regulated mRNA expression of type X collagen, type II collagen, runx2 and aggrecan. Fewer dark cells were seen in chondrocyte cultures from rats than in those from horses, which is probably due to the fact that very few dark cells are observed in neonatal growth cartilage from rats. This will be a useful system for studying molecular mechanisms of chondrocyte hypertrophy and death.

Disclosures: K. Chen, None.

M121

See Sunday Plenary Number S121

M122

Role of the Transcription Factor Lbh in Endochondral Bone Formation. K. L. Conen¹, S. Nishimori^{*1}, S. Provot², H. M. Kronenberg¹. ¹Endocrine Unit, Massachusetts General Hospital, Harvard Medical School, Boston, MA, USA, ²Department of Anatomy, University of California, San Francisco, CA, USA.

In endochondral bone formation, mesenchymal condensations develop into chondrocytes that proliferate and form the fetal growth plate. As round, flat and hypertrophic chondrocytes they undergo progressive, well-ordered stages of differentiation. All differentiation steps are characterized by the synthesis of stage-specific matrix proteins and the expression of different transcription factors (TF). In order to study the transcriptional control of endochondral bone formation we previously analyzed genes expressed in discrete layers of the mouse newborn (NB) growth plate using microarray analyzes. There the TF limb-bud-and-heart (Lbh) appeared to be expressed predominantly in hypertrophic chondrocytes. Lbh is thought to act as a transcriptional co-activator and is highly conserved among species. It has a to date uncharacterized role in endochondral bone formation. In situ hybridization (ISH) of sections of NB mouse tibia confirmed that Lbh is expressed in hypertrophic chondrocytes. We therefore investigated whether Lbh has a key regulating role in the induction of the differentiation steps from flat to hypertrophic chondrocytes in an experimental model, providing advantages for a relatively easy and fast testing: The fetal growth plate of chicken embryos at E10, a time when growth cartilage and bone become visible. Our hypothesis is that Lbh plays a key role in hypertrophic chondrocyte differentiation. We have begun to use the avian Replication-Competent ASLV long terminal repeat with Splice acceptor (RCAS) retroviral vector strategy. Lbh cDNA samples have been cloned into this RCAS virus. We infect chicken limb buds at E3-E3.5 in ovo and then analyze the effect of Lbh by comparing the gross aspect of E10 infected limbs compared to the uninfected contralateral limb using skeletal preparations and ISH. Whole-mount ISH of Lbh in the chicken system revealed an early signal in the entire outgrowing limb buds of E4.5 chickens. This signal subsequently remains visible only in the fetal growth plate area between E6 and E10. These data suggest a possible role of Lbh in chondrogenesis of chicken and mouse endochondral bone formation.

Disclosures: K.L. Conen, None.

M123

See Sunday Plenary Number S123

M124

Effect of Removal of Nucleus Pulposus Cells on the Annulus Fibrosis of the Intervertebral Disc. C. Dahia^{*1}, A. Durrani¹, E. Mahoney^{*1}, C. Wylie^{*2}. ¹Orthopaedic Surgery, Cincinnati Children's Hospital and Medical Center, Cincinnati, OH, USA, ²Developmental Biology, Cincinnati Children's Hospital and Medical Center, Cincinnati, OH, USA.

The relationship between the nucleus pulposus and the Annulus fibrosis in normal differentiation and maintenance of the IVD is not clearly understood. We studied the effect of removal of NP cells on the AF.

The NP's were surgically aspirated from L2-L3 and L3-4 discs of 2-week old male mice (during the period of rapid postnatal vertebral growth), using a 27-gauge syringe. L4-5 discs in the same mice were sham-operated (needle insertion without aspiration) as controls. The effects on the IVD were assayed 2-8 weeks after the surgery. 8 µm cryosections were collected in the coronal plane and histological analysis was carried out using H&E staining. Cell proliferation and cell death was determined by phospho Histone H3 (PH3) and active caspase-3 staining respectively.

5-weeks following removal of the NP cells there was significant collapse of the IVDs (Fig-B) from which the NP had been removed, compared with those of sham-operated controls (Fig-A). By 7-weeks, fibrocartilage cells derived from the AF were invading the disc space, which became completely filled by 8 weeks. Growth of the disc was reduced in both cranio-caudal and transverse diameters by 30%, compared to control discs. Mitotic cells were absent in the AF indicating that AF cells stopped proliferating in the absence of NP cells. A large number of activated caspase-3 positive cells were found in AF cells 8 weeks after removal of NP cells (Fig-D), compared to sham controls (Fig-C).

Removal of NP cells leads to invasion of the disc space, and its fibrosis by AF cells, decreased proliferation and increased cell death of the AF cells, and decrease in disc growth. These data suggest a requirement for the NP cells in normal differentiation and growth of the AF cells.

Disclosures: C. Dahia, None.

This study received funding from: Children's Hospital Research Foundation.

M125

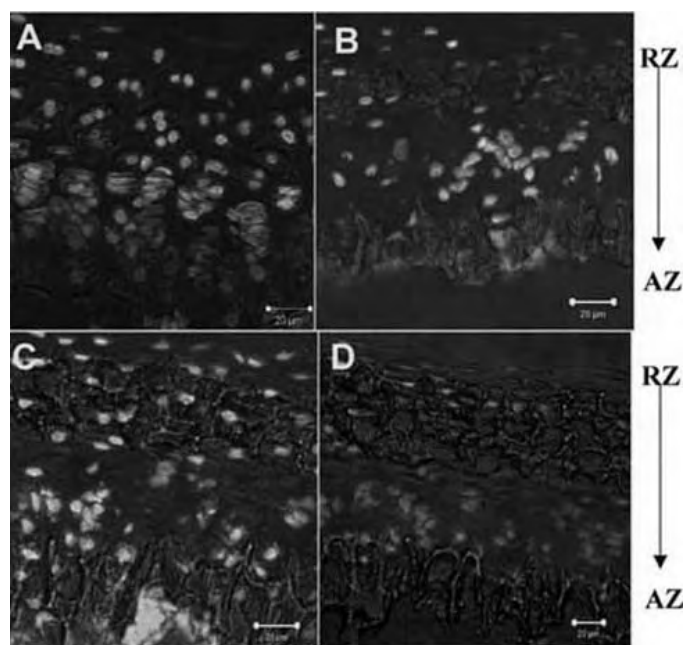
Spatial and Temporal Localization of Components of the TGF-beta, BMP, IHH and FGF Signaling Pathways in the Postnatal Mouse Lumbar Vertebral Growth Plate (LVGP). C. Dahia^{*1}, E. Mahoney^{*1}, A. Durrani¹, C. Wylie^{*2}. ¹Orthopaedic Surgery, Cincinnati Children's Hospital and Medical Center, Cincinnati, OH, USA, ²Developmental Biology, Cincinnati Children's Hospital and Medical Center, Cincinnati, OH, USA.

Little is known about postnatal spine growth. A number of signaling pathways have been shown by gene targeting in the mouse to be important in the growth of fetal long bones. The objective of this study was to find out if these signaling pathways are present in postnatal LVGP, and their expression pattern during growth and aging.

8 µm cryosections in the coronal plane from decalcified LVGP of 1-12 weeks old male FVB mice were analyzed by H&E and alkaline phosphatase (AP) staining. Cell proliferation & cell death was determined by phospho-histone H3 (PH3) & TUNEL assay, respectively. Immunolocalization of components of the TGFβ1&2, BMP2&4, IHH & FGF2 pathways was carried out using confocal microscopy.

PH3 positive staining disappeared from the proliferative zone chondrocytes (PZc) of LVGP at 3-weeks indicating cessation of cell proliferation. Membrane localization of IHH (Fig-A) & its receptor PTC-1 was observed on the PZc of LVGP only until 2-weeks of age. Between 2-12 weeks of age, active TGFβ1&2 signaling was present at the junction of PZc and early hypertrophic zone chondrocytes (HZc) of the LVGP, as shown by staining for its activated downstream intermediate (p)Smad2/3 (Fig-B). BMP2&4 pathways were active only in the HZc (Fig-C) of the LVGP at all ages. Staining for its active downstream molecule, pSmad1/5/8 (Fig-D), decreased from 3-weeks onwards, but did not disappear. FGF2 signaling was observed to be active only in the HZ of the LVGP of 2-week old mice and decreased with age. Intensity of AP staining increased in the HZc from 2-week onwards.

Our data suggests that IHH regulates the proliferation of PZc in the LVGP. TGFβ signaling regulates the transition of PZc to HZc. FGF signaling is seen only in the HZ indicating it may play a role in regulating HZc. Active BMP & AP signaling seen only in the HZc in all ages suggests its role in the maintenance of the extracellular matrix.



Disclosures: C. Dahia, None.

This study received funding from: Children's Hospital Research Foundation

M126

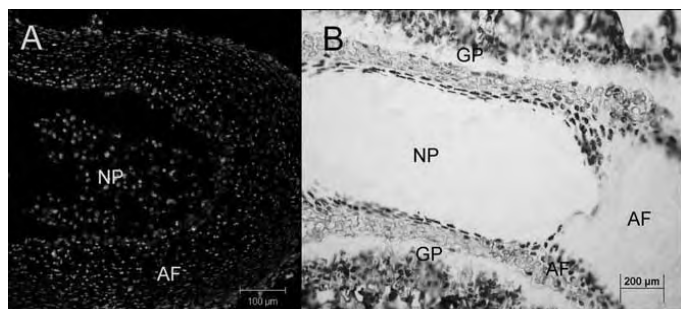
Histological and Molecular Analysis of the Growth and Differentiation of the Mouse Lumbar Intervertebral Disc. C. Dahia^{*1}, E. Mahoney^{*1}, A. Durrani¹, C. Wylie^{*2}. ¹Orthopaedic Surgery, Cincinnati Children's Hospital and Medical Center, Cincinnati, OH, USA, ²Developmental Biology, Cincinnati Children's Hospital and Medical Center, Cincinnati, OH, USA.

Intervertebral disc (IVD) degeneration is the most common cause of back pain. We wish to understand the cellular and molecular mechanisms of disc growth and development in mouse.

8µm thick coronal and transverse cryosections, from lumbar vertebrae (LV) of 1-48 weeks old male mice, were analyzed by H&E and alkaline phosphatase (AP) staining. Physical growth of the discs was measured using a 1mm graticule. The number and thickness of the layers of the annulus fibrosus (AF), was measured using DIC optics. Cell proliferation and death was determined by phospho Histone H3 (PH3) and TUNEL staining, respectively. Immunolocalization of components of the TGFβ, BMP and Shh pathways was carried out using confocal microscopy.

Growth of the IVD paralleled that of the vertebral column, being most rapid between birth and 3 weeks, and plateauing off by 9 weeks of age. Proliferating cells were found until 3 weeks of age in both the AF and NP (Fig-A). During the first week, the AF became divided into a mineralized component over the vertebral bodies, which stained positively for AP, and non-mineralized component between the vertebrae (Fig-B). Cells in the mineralized component also became hypertrophied. Apoptosis was only found in the NP. DIC imaging revealed that the number of layers of AF increased from 1-2 weeks of age, after which each layer becomes very thick due to the extracellular matrix secreted by them. The number of AF layers decreased in the IVDs of older mice. TGFβ as well as BMP signaling pathway was active in the NP as well as the AF cells, while Shh was secreted by the NP and fibrous AF cells but acted on the mineralized AF cells.

The IVDs grow coordinately with the vertebrae. Both components of the disc grow, and then involute with age. The AF becomes divided into a mineralized and non-mineralized component during growth. Active cell signaling pathways like BMP, TGFβ and Shh suggests that these cells are actively involved in disc maintenance.



Disclosures: C. Dahia, None.

This study received funding from: Children's Hospital Research Foundation.

M127

See Sunday Plenary Number S127

M128

Non-covalent Interaction of MMP13 and LTBP1 in a Unique TGFβ Large Latent Complex Produced by Hypertrophic Chondrocytes. B. N. Dragann^{*1}, V. L. Scheinfeld^{*1}, S. M. Routson^{*1}, B. M. Mentzer^{*1}, P. M. Mattioli^{*1}, A. H. Selim², D. M. Appelt^{*1}, M. D'Angelo¹. ¹Center for Chronic Disorders of Aging, PCOM, Philadelphia, PA, USA, ²Department of Biology and Physics, KFUPM, Dhahran, Saudi Arabia.

Our lab has shown that hypertrophic chondrocytes produce a unique TGFβ2 large latent complex that contains collagenase 3 (MMP13) in non-covalent association with latent TGFβ binding protein (LTBP1). In this study, we investigate hypertrophic chondrocyte production of the elements of this unique TGFβ2 large latent complex. Hypertrophic chondrocytes from the avian sterna were cultured 5 days in serum-free alginate. RNA, conditioned media, cell-associated matrix (isolated after release of the chondrocytes from alginate), and cell extracts were analyzed for TGFβ2, MMP13 and LTBP1. Immunoblot analysis revealed the presence of immunoreactive bands for TGFβ2, MMP13 and LTBP1 in the cellular extracts. Assembly into the extracellular matrix and secretion of the components was indicated by the presence of immunoreactive bands for all three proteins in the cell-associated matrix and conditioned media fraction. Immunocytochemistry demonstrated the presence of TGFβ2, MMP13 and LTBP1 in association with the cells and in a pericellular staining pattern. In order to determine whether MMP13 binds non-covalently to LTBP1 of the TGFβ large latent complex, primary monolayer cultures of hypertrophic chondrocytes were double-labeled with antibodies against MMP13 and LTBP1. Optical serial sections were collected from these cells and the images deconvoluted into three-dimensional micrographs. LTBP1 and MMP13 were present both intracellularly and in association with the extracellular matrix between cells. In addition, the fluorescent signal indicated substantial co-localization of the two proteins within the extracellular matrix of the cultures. For additional confirmation, we produced a biotin-

labeled peptide corresponding to the C-terminal hemopexin domain of MMP13 that bioinformatics indicated could interact non-covalently with the C-terminal EGF-calcium domains of LTBP1. Protein from hypertrophic chondrocyte tissue was extracted from day 17 avian upper sternum and immunoprecipitated with antibody to LTBP1. Dot blot analysis of the immunoprecipitate showed binding of the biotin-labeled MMP13 peptide with proteins in the tissue extracts. These data demonstrate that the components of the unique TGFβ2 large latent complex are produced and secreted by hypertrophic chondrocytes and are present in compartments that are characteristic of extracellular matrix assembly. In addition, these data confirm that MMP13 can interact with LTBP1 and underscores the candidacy of MMP13 in the unique mechanism of activation of TGFβ by hypertrophic chondrocytes.

Disclosures: M. D'Angelo, None.

M129

Twist1 Stage-specifically Regulates Chondrocyte Differentiation Downstream of TGF-β and Wnt Signaling. Y. Dong, Y. Chang^{*}, D. Y. Soung, R. O'Keefe, E. Schwarz, H. Drissi. Orthopaedics, University of Rochester, Rochester, NY, USA.

We investigated the molecular mechanisms underlying the transition between immature and mature chondrocytes downstream of TGF-β and canonical Wnt signals. We used two developmentally distinct chondrocyte models isolated from the caudal portion of embryonic chick sternum or chick growth plates. Lower sternal chondrocytes exhibited immature phenotypic features, while growth plate extracted cells display a hypertrophic phenotype. TGF-β significantly induced β-catenin in immature chondrocytes, while it repressed it in mature chondrocytes. TGF-β further enhanced canonical Wnt-mediated transactivation of the Topflash reporter expression in lower sternal chondrocytes. However, it time-dependently inhibited Topflash activity in growth plate chondrocytes. Our immunoprecipitation experiments showed that TGF-β induced Smad3 interaction with TCF-4 in immature chondrocytes, while it inhibited this interaction in mature chondrocytes. Similar results were observed by chromatin IP showing that TGF-β differentially shifts TCF-4 occupancy on the Runx2 promoter in lower sternal chondrocytes versus growth plate chondrocytes. To further determine the molecular switch between immature and hypertrophic chondrocytes, we assessed the expression and regulation of Twist1 and Runx2 in both cell models upon treatment with TGF-β and Wnt3a. We show that Runx2 and Twist1 are differentially regulated during chondrocyte maturation. Furthermore, while TGF-β induced Twist1 in mature chondrocytes, it inhibits Runx2 expression in these cells. Opposite effects were observed upon Wnt3a treatment which predominates over TGF-β effects on these cells. Finally, over-expression of chick Twist1 in mature chondrocytes dramatically inhibited their hypertrophy. Together, our findings show that Twist1 may be an important regulator of chondrocyte progression towards terminal maturation in response to TGF-β and canonical Wnt signaling.

Disclosures: H. Drissi, None.

M130

See Sunday Plenary Number S130

M131

Role of Fe³⁺ Ion and Ferritin on Differentiation of Chondrocytes at the Stage of Calcification. H. Hagiwara¹, N. Hashimoto^{*2}, T. Ohno^{*2}, K. Yamazaki^{*1}, H. Okumura^{*3}, T. Ito^{*3}. ¹Dept. of Biomedical Engineering, Toin University of Yokohama, Yokohama, Japan, ²Dept. of Bioscience and Biotechnology, Tokyo Institute of Technology, Yokohama, Japan, ³Health Effects Research, Energy and Environment Research, Japan Automobile Research Institute, Tsukuba, Japan.

Fe ions are major contents of metal in our body. However, there is a little information about the effect of Fe ions on bone metabolism. In the present study, we examined the effects of Fe³⁺ ion and ferritin, a storage protein of Fe³⁺ ion in cells, on the differentiation and mineralization of cultured chondrocytes, ATDC5 cells. At first, we monitored the expression pattern of ferritin mRNA with RT-PCR during the culture period of ATDC5 cells. Ferritin mRNA was expressed in ATDC5 cells, from day 21, at the late stage of culture. We used ferric ammonium citrate (FAC) as a donor of Fe³⁺ ion and desferrioxamine (DFO) as a chelator of Fe³⁺ ion. Both chemicals did not affect the production of proteoglycan by ATDC5 cells. By contrast, FAC inhibited the deposition of calcium by ATDC5 cells and DFO accelerated it. Furthermore, FAC inhibited the expression of MMP13 mRNA, a differentiation marker at a late stage of differentiation of chondrocytes. In addition, DNA microarray methods revealed that Fe³⁺ ion regulated the expression of collagen mRNAs in ATDC5 cells. These results suggested that Fe³⁺ ion might play an important role on chondrocyte differentiation and mineralization.

Disclosures: H. Hagiwara, None.

This study received funding from: Grants-in-Aid for Scientific Research from the Ministry of Education, Science, Sports, and Culture of Japan.

M132

A Novel Tumor Necrosis Factor- α Responsive CCAAT/Enhancer-binding Protein Site Regulates Cartilage Cd-Rap Expression. T. Imamura^{*1}, A. McAlinden^{*2}, K. Terada^{*1}, H. Miyahara^{*1}, Y. Iwamoto^{*3}, L. J. Sandell^{*2}. ¹Orthopaedic Surgery, Kyushu Medical Center, Fukuoka, Japan, ²Orthopaedic Surgery, Washington Univ., St. Louis, MO, USA, ³Orthopaedic Surgery, Kyushu Univ., Fukuoka, Japan.

Objective. Rheumatoid arthritis is characterized by an inflammatory process in the synovium resulting in progressive destruction of the affected joints. Cytokines such as Tumor Necrosis Factor (TNF)- α and Interleukin 1 (IL-1)- β regulate inflammation, causing functional impairment. Previous studies in our laboratory have shown that expression of cartilage characteristic genes, such as cartilage-derived retinoic acid sensitive protein (Cd-rap) and Type II collagen (Col2a1), are repressed by IL-1 β by a process involving a CCAAT/Enhancer binding protein (C/EBP) site. The aim of this study is to investigate the mechanism of TNF- α induced inhibition of cartilage gene expression by studying regulation of the Cd-rap gene.

Methods. Rat chondrosarcoma (RCS) cells were transiently transfected with cDNA constructs encoding Cd-rap in the presence of TNF- α . Expression of C/EBP β , Sox9 and p300 after treatment with TNF- α were examined by RT-PCR and Western blot in RCS cells and primary human articular chondrocytes. The effect of TNF- α on endogenous binding of C/EBP β or Sox9 to the Cd-rap promoter was examined by chromatin immunoprecipitation (ChIP) assays.

Results. We identified a new C/EBP binding site in the Cd-rap promoter (position -1059 to -1046). Binding of C/EBP to this site was regulated by TNF- α , but not IL-1 β , resulting in down-regulation of Cd-rap expression. This effect was reversed by mutational inactivation of the C/EBP motif. In addition, the activation potential of Sox9 and CBP/p300 on the Cd-rap promoter was enhanced after mutation of the new C/EBP binding site, indicating that blockage of this site would increase transcription.

Conclusion. TNF- α regulates the expression and/or DNA binding potential of key positive and negative-acting transcription factors that control the expression of the cartilage matrix gene, Cd-rap.

Disclosures: T. Imamura, None.

This study received funding from: NIH.

M133

See Sunday Plenary Number S133

M134

OPG Inhibits Cartilage Degradation in a Knee Instability Mice Model. A. Kadri^{*}, H. Ea^{*}, B. Uzan^{*}, C. Bazille^{*}, M. Ah Kioon^{*}, F. Liote^{*}, M. E. Cohen-Solal. Hopital Lariboisiere, INSERM U606, Paris, France.

Osteoarthritis (OA) is a focal rheumatic disease characterised by cartilage destruction. Mechanical stress and several other local factors are responsible for cellular and molecular changes that contribute to matrix proteolysis. Proteases as aggrecanases (ADAMTS-4 and ADAMTS-5) participate to chondrolysis in OA. Subchondral bone (SCB) may be involved in the pathogenesis of OA. We used a meniscectomy-induced OA model in mice in order to assess to the changes of SCB and the effects of inhibition of cytokines involved in bone and cartilage remodeling (IL1ra and OPG). Ten week-old C57/BL6 male mice underwent medial meniscectomy of the right knees (Mnx) and the left knees were sham-operated (sham). Mice were separated in 3 groups and received intraperitoneal injections of PBS, OPG (10mg/kg) or IL1ra (100mg/kg) twice a week for 6 weeks. At sacrifice, serial sagittal sections of decalcified knees were performed to assess OA score, ADAMTS expressions and micro-architecture of SCB. At the tibia, OA score was increased in Mnx compared to sham-operated mice in PBS group (0.5 ± 0.27 vs 1.9 ± 0.41 , $p < 0.05$). Compared to PBS-treated mice with Mnx, OA score was not altered with IL1ra (1.9 ± 0.41 vs 2.29 ± 0.84), but was decreased by OPG (1.9 ± 0.41 vs 0.17 ± 0.17 , $p < 0.05$). In PBS-treated mice, the number of ADAMTS-4+ cells was significantly enhanced in Mnx compared to sham (64.6 ± 2.1 vs $35.9 \pm 1.6\%$ of total cells, $p < 0.0001$) as well as ADAMTS-5+ cells (47.3 ± 1.9 vs 78.9 ± 2.7 $p < 0.0001$). The number of positive cells in Mnx was then expressed using sham as referent (Δ ADAMTS). Compared to PBS, Δ ADAMTS-4+ cells were lower with IL1ra and OPG (0.81 ± 0.78 vs 0.51 ± 0.12 , vs 0.46 ± 0.29 respectively). Δ ADAMTS-5+ cells were also lower with IL1ra (0.67 ± 0.08 vs 0.42 ± 0.1) and further decreased with OPG (0.67 ± 0.08 vs 0.26 ± 0.09 , $p < 0.05$). In PBS treated-mice, BV/TV was decreased in Mnx vs sham knees ($39 \pm 0.36\%$ vs $49 \pm 0.48\%$) along with an increased Marrow Star Volume (Ma.Sv: $8.9 \cdot 10^3 \pm 3.4 \cdot 10^3$ vs $3.7 \cdot 10^3 \pm 1.5 \cdot 10^3$) suggesting increased bone resorption. In Mnx knees, IL1ra did not change BV/TV ($39 \pm 0.36\%$ vs $42 \pm 0.46\%$), whereas it was increased with OPG ($39 \pm 0.36\%$ vs $53 \pm 0.59\%$). Only OPG decreased Ma.Sv compared to PBS treated-mice ($1.3 \pm 0.37 \cdot 10^3$ vs $8.9 \pm 3.4 \cdot 10^3$, $p < 0.05$).

In conclusion, meniscectomy induces cartilage degradation and increases aggrecanase expressions. This was associated with an increased bone resorption. Inhibition of bone resorption by OPG prevents matrix cartilage degradation and the increase of protease expressions. These data suggested that increased bone resorption at SCB could be implicated in the pathogenesis of OA at early stage. Targeting specifically the inhibition of bone resorption might lead to the prevention of OA.

Disclosures: A. Kadri, None.

M135

Therapeutic Effect of KHB9 on Cartilage Degradation and Inflammation in Collagenase-induced Rabbit Osteoarthritis. D. Kim¹, J. Huh^{*2}, Y. Baek^{*2}, J. Lee^{*2}, D. Choi^{*2}, D. Park^{*2}. ¹Internal Medicine, Kyung Hee University Hospital, Seoul, Republic of Korea, ²Acupuncture & Moxibustion, College of Oriental Medicine, Kyung Hee University, Seoul, Republic of Korea.

The aim of this study was to determine the therapeutic effects of an herb medicine, KHB9 on osteoarthritis. We investigated whether KHB9 could suppress the disease progression of collagenase-induced osteoarthritis (CIA) in rabbits.

The right knees of rabbits were injected intra-articularly with collagenase, and rabbits were orally administrated with distilled water, KHB9 (50, 100, 400 mg/kg) or celecoxib (100 mg/kg) once a day for 28 days after the initiation of the CIA induction. The knee joints were evaluated by gross morphology and histology. Target gene expression was analyzed by RT-PCR such as proteoglycan, MMPs, and cyclooxygenases (COX) in knee joints. Also, we measured glycosaminoglycan (GAG) release, MMPs activity, PGE₂ production by colorimetric analysis. COX-1 and COX-2 protein expression were confirmed by immunohistochemistry.

Histological evaluation showed that KHB9 dose-dependently suppressed damage in cartilage and synovium as compared with the control. The mRNA expression of proteoglycan, MMP-1, MMP-3, and COX-2 was dose-dependently decreased, whereas COX-1 expression not affected. As well, GAG release and matrix degradation enzymes including MMP-1 and MMP-3 activities, and PGE-2 production significantly reduced at a dose-dependent manner.

This study indicates that KHB9 play a protective role against cartilage degradation and anti-inflammatory effect in rabbits with OA. The role may be achieved through the down regulation of the MMP-1, MMP-3, PGE2 and COX-2 activity, and expression in CIA rabbit model.

Disclosures: D. Kim, None.

This study received funding from: A grant of the Oriental Medicine R&D Project, Ministry of Health & Welfare, Republic of Korea.

M136

See Sunday Plenary Number S136

M137

Gene-Trap Mutagenesis Revealed the Involvement of Vinculin in Chondrogenic Differentiation in ATDC5 Cells. T. Koshimizu^{*1}, M. Kimata^{*1}, K. Tachikawa^{*1}, K. Ozono², T. Michigami¹. ¹Department of Bone and Mineral Research, Osaka Medical Center and Research Institute for Maternal and Child Health, Osaka, Japan, ²Department of Pediatrics, Osaka University Graduate School of Medicine, Osaka, Japan.

Gene-trap mutagenesis is based on the idea that the random insertion of a trapping vector may disturb the function of inserted genes. In the current study, to identify the genes involved in chondrocytic differentiation, we have applied this method to a chondrogenic mesenchymal cell line, ATDC5. As the trap vector, we used pPT1-geo, which lacks its own promoter and enhancer, but contains a lacZ-neo fusion gene geo as a reporter and selection marker. The reporter activity reflects the expression level of the trapped gene. We screened the isolated clones for high β -galactosidase activity, and the selected clones were subjected to the chondrogenic induction to evaluate the phenotypical changes. 5'-RACE was performed to identify the gene trapped in each clone. In clone #4-17, the trap vector pPT1-geo was integrated in intron 13 in the gene encoding vinculin. Vinculin is a cytoskeletal protein and occurs in multimolecular complexes that are thought to function in adhesion and/or signaling between the extracellular milieu and the cell, via integrins and cadherins. Since vinculin-knockout mice are embryonic lethal, the roles of vinculin in skeletogenesis remain unclear. As the result of integration of pPT1-geo, a truncated vinculin lacking carboxyl-terminal paxillin-binding domain fused to geo product was produced from the trapped allele, and Western blotting confirmed that both wild-type and the truncated vinculin were expressed in #4-17. There was no apparent morphological change in the clone. When cultured in the differentiation medium, #4-17 exhibited impaired nodule formation and less accumulation of cartilaginous matrices. RT-PCR analyses revealed that the expression of chondrocytic marker genes including Col2a1 and PTHrP was reduced in the clone, although that of SOX9 was retained. The expression of wild-type vinculin in the parental ATDC5 and that of lacZ in #4-17 were elevated during the culture in differentiation medium, suggesting the involvement of vinculin in chondrocytic differentiation. Integrin-stimulated FAK autophosphorylation was markedly enhanced in the clone #4-17, demonstrating the aberrant signaling transduction induced by adhesion to extracellular matrix, while the phosphorylation state of paxillin was not obviously changed. Taken together, the phenotypical changes caused by trapping of vinculin gene indicated its critical roles in chondrocytic differentiation, and enhanced the indispensability of the signals from extracellular matrix in the process.

Disclosures: T. Koshimizu, None.

M138

Effect of Vertebroplasty Filler Materials on Viability and Gene Expression of Mouse and Human Nucleus Pulposus Cells. Á. Lazáry¹, P. Varga^{*1}, G. Speer^{*2}, K. Bácsi^{*2}, B. Balla^{*2}, J. Kósa^{*2}, Z. Nagy², I. Takács², P. Lakatos².
¹Center of Spinal Disorders, Buda Health Center, Budapest, Hungary, ²1st Department of Internal Medicine, Semmelweis University, Budapest, Hungary.

Consequences of intradiscal cement leakage - often occur after vertebral cement augmentation for the treatment of vertebral compression fractures - are still unknown. In this study, we have investigated the influences of vertebroplasty filler materials (polymethylmethacrylate-, calcium phosphate- and calcium sulfate based bone cement) on isolated nucleus pulposus cells. Cell viability of cultured human nucleus pulposus cells were measured after treatment with vertebroplasty filler materials. Gene expression profile of selected genes was determined with quantitative real-time PCR. The widely used polymethylmethacrylate and calcium phosphate cement significantly decreased cell number in a dose- and time-dependent manner (e.g. cell number was reduced by 79% in human cultures in case of 2 day treatment of 0.1% v/v polymethylmethacrylate) while calcium sulfate cement affected cell viability less. Expression of genes involved in matrix metabolism of nucleus pulposus - aggrecan, collagens, small proteoglycans -, as well as important transcription factors have also significantly changed due to treatment (e.g. 2.5-fold decrease in aggrecan expression was determined in human cultures due to polymethylmethacrylate treatment). Our results suggest that intradiscally leaked bone cement - depending on the type of applied material - can accelerate the degeneration of nucleus pulposus resulting in a less flexible disc. This process may increase the risk of a subsequent new vertebral fracture, the main complication of vertebral augmentation. In conclusion, avoiding of cement leakage and development of vertebroplasty filler material that does not interfere with vital gene expression and cell viability would be desirable.

Disclosures: Á. Lazáry, None.

This study received funding from: NKFP-1A/002/2004, NKFP-1A/007/2004, ETT-55059.

M139

Regulation of Matrix Metalloproteinase (MMP)-9 Expression by MMP-12 in Interleukin-1 β -treated Articular Chondrocytes. H. Oh, M. Lee^{*}, J. Chun^{*}. Department of Life Science, Gwangju Institute of Science and Technology, Gwangju, Republic of Korea.

Interleukin (IL)-1 β is a major pro-inflammatory cytokine that causes destruction of articular cartilage via induction of several matrix-metalloproteinases (MMPs). MMPs play an essential role in pathological extracellular matrix (ECM) breakdown in arthritic cartilage. In primary culture articular chondrocytes and cartilage explants, IL-1 β caused induction of several MMPs such as MMP-1, -3, -9, -12, and -13, whereas expression of other MMPs including MMP-2, -14, and -15 was not affected. Because the role of MMP-12 in chondrocytes remains largely unknown, we examined the signaling mechanisms and the role of IL-1 β -induced expression of MMP-12 in primary culture articular chondrocytes. Among the mitogen-activated protein (MAP) kinases, extracellular signal-regulated kinase and p38 kinase mediated expression and activation of MMP-12, whereas c-Jun N-terminal kinase regulated MMP-12 activation without effects on its expression. MMP-12 expression by IL-1 β was also mediated by nuclear factor kappa enhancer binding protein (NFkB). Because ECM fragments produced by MMP action were known to regulate expression of several MMPs, we next examined the role of MMP-12 in expression of other MMPs in chondrocytes. Exogenous MMP-12 in IL-1 β -treated chondrocytes caused both expression and secretion of MMP-9, which is known to degrade proteoglycan and denatured type II collagen. However, MMP-12 did not affect of MMP-9 expression in absence of IL-1 β . Taken together, our results suggest that IL-1 β causes expression and activation of MMP-12 through signaling pathway involving MAP kinases and NFkB, and activated MMP-12 may contribute to cartilage destruction by increasing MMP-9 expression.

Disclosures: H. Oh, None.

M140

BMP4 in Postnatal Alveolar Bone Formation and Tooth Cytodifferentiation: Conditional Deletion of BMP4 with the 3.6 Collagen type 1a-Cre Model. J. Gluhak-Heinrich¹, L. Martineze^{*1}, W. Yang¹, J. Zhang², J. Feng³, D. Guo³, A. Lichtler⁴, B. Cream⁴, M. Harris¹, S. Harris¹. ¹UTHSCSA, San Antonio, TX, USA, ²Univ. of Vanderbilt, Nashville, TN, USA, ³UKMC, Kansas City, MO, USA, ⁴UCONN, Farmington, CT, USA.

Bone morphogenetic protein 4 (BMP4) is essential for early tooth and bone development in the postnatal animal. Smad1/5/8 plays a central role in BMP4 signaling, with other transcription factors like: Runx2, Dlx5 and Osx. BMP4 conditional knockout (Bmp4 cKO) leads to mice with reduced bone and osteopenia, as well as reduction in dentin formation during tooth cytodifferentiation. The mechanisms by which BMP4 deficiency leads to defects during bone and tooth cytodifferentiation have not been explored. The objective of this study was to determine the biologic effect of postnatal BMP4 deficiency on tooth and alveolar bone formation and mineralization. To obtain 3.6collagen1a-Cre/BMP4cKO mice, we crossed 3.6 collagen1a-Cre mice with BMP4 floxed mice. Deletion of BMP4 (by excision of exons 3 and 4) occurs in collagen producing osteoblasts and odontoblasts of progeny cells. BMP4cKO mice and their sibling controls were selected for phenotype characterization using analytical methods including X-ray, histological techniques, in situ hybridization, and immunocytochemistry. Our results show that by day 12, BMP4cKO mice display reduced size of calvarias and osteopenia in alveolar bone of the mandible, a 99% decrease in immunoreactivity of

phospho-Smad1/5/8 and reduced DMP1 mRNA in the odontoblasts. By day 18, BMP4cKO mice show 82% reduction of BMP4 mRNA with changed odontoblast morphology and dental tubule formation and 45% decrease in Dlx5 mRNA. Osterix expression was reduced 84% and DSPP 67% in odontoblasts. Amelogenin was reduced 60-80% in ameloblasts in one month old BMP4cKO mice. Dentin thickness was reduced 40% and enamel formation was delayed, although the 3.6 Colla1-Cre shows no activity in ameloblasts at any stage. In conclusion, our results indicate that the absence of BMP4 in osteoblasts and odontoblasts impairs mineralization of the calvaria and mandible, greatly delays the processes of dentinogenesis and amelogenesis. Delayed enamel formation was associated with BMP4 deficiency in odontoblasts and reduced dentin formation, suggesting that disruption in odontoblast differentiation by lack of BMP4 leads to disruption in amelogenesis or enamel formation. These results support the concept that odontogenesis is tightly linked to amelogenesis and is controlled by BMP4. Elucidation of downstream targets for BMP4 signaling using our BMP4cKO mice may provide novel strategies for enhancing bone and tooth integrity.

Disclosures: J. Gluhak-Heinrich, None.

This study received funding from: AR46798 and DE16949.

M141

Angiotensin II Suppresses Bone Mass via AT1 receptor in Long Bones of Adult Mice. Y. Izu, T. Hayata, H. Hemmi^{*}, J. Nagata, Y. Ezura, K. Nakashima^{*}, M. Noda. Department of Molecular Pharmacology, Medical Research Institute, Tokyo Medical and Dental University, Tokyo, Japan.

Angiotensin II (Ang II), a major effector peptide of the renin angiotensin system, controls blood pressure and body fluid homeostasis. Ang II, derived from Angiotensin I by angiotensin converting enzyme (ACE), binds to its receptors comprised of two major subtypes, angiotensin II type 1 (AT1) and type 2 (AT2). Ang II induces vasoconstriction and sodium retention through AT1 activation, whereas it induces vasodilation and tissue regeneration through AT2 activation. In rodents, two type 1 receptors (AT1a and AT1b) are encoded by distinct genes, although both receptors are pharmacologically identical. In human, clinical and epidemiologic studies suggested that Ang II might have functions to regulate bone metabolism. Indeed, Ang II inhibits differentiation of osteoblasts and matrix calcification in vitro through AT1 activation. In addition, Ang II stimulates osteoclastic bone resorption in a bone marrow cell culture system. However, physiological roles and actions of Ang II in bone metabolism in vivo remain unclear. In order to examine whether Ang II signaling is involved in bone metabolism in vivo, we first examined if its specific receptors, AT1 and AT2, are expressed in the bone of adult mice (9 weeks old). By immunohistochemical approach, we identified AT1 and AT2 expressions in both osteoblasts and osteoclasts in adult long bones. These observations suggest that Ang II may directly regulate osteoblast and osteoclast function in vivo. Additionally, to distinguish physiological roles of AT1 and AT2 in bone in vivo, specific receptor antagonist for AT1, losartan (peroral administration of 10 mg/kg/day) or for AT2, PD123319 (intraperitoneal injection of 10 mg/kg/day) was administered into adult mice (9 weeks old). 3D-micro-CT analysis further revealed that losartan inhibited of AT1 enhanced the levels of bone mineral density (BMD) and cancellous bone volume (BV/TV) in hind limbs. In contrast, blockade of AT2 by PD123319 tended to reduce the levels of both BMD and cancellous BV/TV. These data suggest that Ang II signalings through AT1 and AT2 exhibit opposite roles in bone metabolism in the adult mice.

Disclosures: Y. Izu, None.

M142

See Sunday Plenary Number S142

M143

Identification of Translationally Controlled Tumor Protein (TCTP) as a Nuclear Matrix Protein in Osteoblasts. Y. Jung^{*1}, J. Jeong^{*1}, N. Park^{*1}, K. Lee^{*1}, A. J. van Wijnen², J. B. Lian², J. L. Stein², G. S. Stein², J. Choi¹. ¹Biochemistry & Cell Biology, Kyungpook Natl. Univ. School of Medicine, Skeletal Diseases Genome Research Center, Daegu, Republic of Korea, ²Cell Biology, UMASS Medical School, Worcester, MA, USA.

The composition of nuclear matrix proteins changes as the osteoblast differentiates. To isolate nuclear matrix proteins unique to the bone phenotype, we analyzed nuclear matrix proteins from the primary cultures of rat calvarial osteoblasts by two-dimensional gel electrophoresis at two different stages: proliferation (day3) and differentiation (day 18). We characterized a protein (20 kDa; pI 4.76) that was detected only in the nuclear matrix of differentiated osteoblasts. By MALDI-TOF mass spectrometry and microsequencing, this protein was identified as the TCTP. Expression of TCTP was detected both in vitro bone cell cultures and in vivo bone tissues. In Northern blot analysis, TCTP mRNA expression was detected from early stage to late differentiation stage with no change of its level during the differentiation of human or rat primary cultured osteoblasts. In Western blot analysis, TCTP expression was not changed during osteoblast or chondrocyte differentiation. However, TCTP was detected only in the nuclear matrix fractions of differentiated osteoblasts. In immunohistochemical staining, TCTP was detected in both osteoblasts and chondrocytes in long bone of 17.5 days mouse embryo. These results suggest that TCTP may play an important role in the nucleus during osteoblast differentiation.

Disclosures: Y. Jung, None.

M144

Expression of Splice Variants of Collagen XII in Human Osteoblast-like Cells. A. Kamada¹, T. Ikeo¹, Y. Yoshikawa¹, I. Tamura^{*1}, S. Goda^{*1}, E. Domae^{*1}, Y. Takaishi¹, T. Miki². ¹Biochemistry, Osaka Dental University, Hirakata, Japan, ²Geriatric Medicine, Osaka City University, Osaka, Japan.

Type XII collagen, which is a fibril-associated collagen (FACIT), is characterized by a short triple-helical domain with three extended noncollagenous NC3 domains, and may contribute to the stability of collagen I fibrils. Little is known about the role of this FACIT collagen in bone metabolism. In this study, we demonstrated collagen XII gene expression in human osteoblast-like cells, and the influence of beta-glycerolphosphate (BGP) as a biomineralization-inducing agent on the expression of splice variants, which have a long or short NC3 domain.

Two sets of primers and probe for a large variant specific site and a common site in collagen XII NC3 domain were designed based on cDNA sequences in the Gene Bank database. RNA was extracted from cells cultured with or without BGP for 0, 2, 7 days. The expression levels of mRNA were assessed using real-time quantitative RT-PCR technique. The mRNA expression of alpha1(XII) in intact normal human osteoblasts (NHOB) and human osteoblast-like osteosarcoma cells (SaOS2) was confirmed by RT-PCR and agarose gel electrophoresis. Western blot analysis also showed the protein expression of both the long and short form of alpha1(XII) in osteoblast-like cells. When cells were cultured with BGP, mRNA expression levels of alpha1(I), osteocalcin and ALP increased compared with controls ($p < 0.05$). In contrast, the level for the long variant of alpha1(XII) was significantly lower than that in controls two days after BGP stimulation ($p < 0.05$). It is known that the long form NC3 domain of collagen XII can carry glycosaminoglycans and bind to tenascin, while collagenous domains attach to collagen I. Our results clarify that collagen XII gene is transcribed in human osteoblast-like cells, and indicate that the transcription control of splice variants may be concerned with bone formation.

Disclosures: A. Kamada, None.

M145

Murine Bone Loss Following Local Irradiation. E. R. Bandstra¹, S. Judex², M. E. Vazquez^{*3}, T. A. Bateman¹. ¹Bioengineering, Clemson University, Clemson, SC, USA, ²Biomedical Engineering, SUNY Stony Brook, Stony Brook, NY, USA, ³Medical Department, Brookhaven National Laboratory, Upton, NY, USA.

Spaceflight presents a complex set of challenges to the skeletal system. Unloading is a well documented stressor that results in bone loss. The impacts of radiation on bone have not been well studied. On long-duration exploratory missions, astronauts will be exposed to higher doses of ionizing radiation from both solar and cosmic sources, ranging from protons to iron ions. We have recently identified that multiple spaceflight-relevant types of radiation, approaching doses astronauts will be exposed to on exploratory missions, cause profound trabecular bone loss. This study aims to investigate the effects of local (head only) irradiation on regional and systemic bone. Male C57BL/6 mice were irradiated with 1GeV/n HZE ⁵⁶Fe at 16 weeks of age at the NASA Space Radiation National Laboratory. The radiation was collimated such that the head received 2.4 Gy and the rest of the body, including humerus and tibia, received 14% (33.6 cGy) of the total dose delivered. The mice were sacrificed 8 weeks after irradiation. MicroCT analysis was performed on the trabecular and cortical bone of the proximal humerus and tibia. Within the humerus, a significant 15.1% decline in trabecular volume fraction was observed compared to the control group. However, no differences were observed within the tibia compared to control (insignificant decline in trabecular volume fraction of 4%). Analysis of the cortical bone revealed a 4.2% decrease in bone volume with a 6.5% increase in cortical porosity in the proximal humerus, with no significant cortical changes in the proximal tibia. The bone loss in the humerus, without corresponding loss in the tibia, indicates either a differential response of these bones or a greater loss in bones anatomically closer to higher doses of radiation. Previous work has not found changes in cortical bone following similar doses of low-LET radiation, possibly indicating cortical bone changes are LET-dependent. In contrast, previous studies of radiation at these doses have not shown an LET-dependent response in trabecular bone. Another important contribution of this study is the demonstration of bone loss in mice that are near peak bone mass. Our previous studies examined mice irradiated at 9 weeks of age when the skeletal system is rapidly growing. Radiation-induced bone loss in the mature skeleton further demonstrates that this challenge represents a potential concern for astronauts on long-duration exploratory missions, and should be studied to further characterize the bone loss following irradiation, identify causal mechanisms, and develop countermeasures.

Disclosures: E.R. Bandstra, None.

This study received funding from: National Space Biomedical Research Institute.

M146

See Sunday Plenary Number S146

M147

Fracture Threshold in Breast Cancer Patients Treated with Adjuvant Aromatase Inhibitors. F. Bertoldo^{*}, L. Dalle Carbonare^{*}, S. Zenari^{*}, S. Pancheri^{*}, M. Zanatta^{*}, B. Giovanazzi^{*}, M. T. Valenti^{*}, V. Lo Cascio. Biomedical and Surgical Sciences, Medicina D, University of Verona, Verona, Italy.

Aromatase inhibitors (AI) in the adjuvant treatment of breast cancer patients is notoriously associated with an increased risk of fractures as opposed to tamoxifene therapy (ATAC trial). Prospective studies evaluating the long-term effects of AI treatment on bone mineral density (BMD) showed a relatively modest decrease in BMD after 2 years of treatment and no patients with normal BMD at baseline became osteoporotic at the end of observation. Actually it is not clear which patients should receive preventive measures. The latest ASCO guidelines identified BMD as a valid tool in treatment decision making. As the value of BMD T-score ≤ -2.5 for fracture threshold is applicable only for postmenopausal osteoporosis (PMO), and pathophysiology underlying AI induced bone loss may be different from PMO, we planned a pilot cross-sectional study to assess the BMD fracture threshold in AIs treated women. We compared lumbar and femoral neck BMD (Hologic Discovery A), vertebral fracture (vFX) prevalent number, Spine deformity Index (SDI), bone turnover markers among 21 breast cancer patients treated for one year with AIs (AI group), 96 PMO patients (PMO group) and 42 breast cancer patient not treated with AIs (BC group). The groups were comparable for age (52 ± 5 y.o, 52 ± 6 and 51.8 ± 4 respectively) height and BMI. The three group did not differ for the number of prevalent vFX and SDI. Lumbar spine BMD T-score was -2.21 ± 0.5 in AI group, -2.53 ± 0.3 in PMO group and -2.49 ± 0.5 in BC group ($p = 0.042$ ANOVA). Among marker of bone turnover, CTX was significantly higher in AI group than in PMO and BC groups (0.684 ± 0.123 , 0.427 ± 0.185 and 0.408 ± 0.210 respectively; $p = 0.036$ ANOVA). A weak inverse correlation between CTX and spine BMD T-score was found only in PMO and BC group ($r = 0.48$ and $r = 0.32$ respectively). These preliminary data suggest that independent predictive factors of fracture risk, i.e. high bone turnover, could increase BMD fracture threshold in AIs treated patients compared to PMO patients or BC patients not treated with AI.

Disclosures: F. Bertoldo, None.

M148

See Sunday Plenary Number S148

M149

Identification of Proteins that Interact with the Collagen Type XI (α 1) Amino Terminal Domain. R. J. Brown^{*}, J. R. T. Oxford. Biomolecular Research Center and Department of Biology, Boise State University, Boise, ID, USA.

The extracellular matrix of articular cartilage is composed of collagens, proteoglycans and a variety of noncollagenous, nonproteoglycan molecules which interact to ultimately contribute to the structural integrity, compressibility and tensile strength of the tissue. The ultimate goal of our investigation was to examine the potential interactions of the amino terminal domain (NTD) of collagen. Utilizing the recombinant aminoproteptide common to each of the collagen α 1(XI) isoforms, proteins extracted from bovine articular cartilage were separated by affinity chromatography. Molecules extracted from the articular cartilage and enriched by their association with the surface of the collagen fibril were identified by tandem mass spectrometry. Proteins enriched by the association with the surface of the α 1(XI) collagen fibril were predominantly: the collagen types IX, XII and XIV; the extracellular matrix proteins, COMP (thrombospondin-5), thrombospondin-1, matrilin-1 (CMP), chondroadherin, PARP, matrilin-3, chondrocalcin and proteoglycans; biglycan and fibromodulin. The results presented here provide evidence that the NTD of collagen α 1(XI) may associate, either directly or indirectly, with a variety of cartilage matrix constituents in the connective tissue and suggest the possibility that this region of collagen α 1(XI) may add structural support bridging the environment between chondrocytes and the surrounding extracellular matrix or play a role in fibrillogenesis.

Disclosures: R.J. Brown, None.

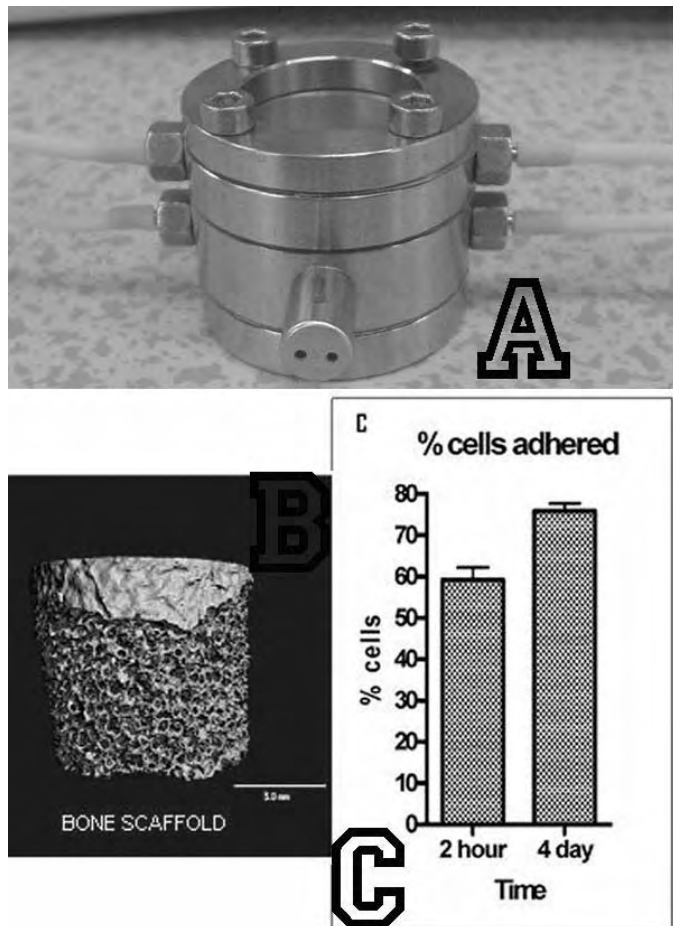
M150

See Sunday Plenary Number S150

M151

Bioreactor Design for Osteochondral Tissue. S. Cartmell¹, J. Gittings², I. Turner², J. Chaudhuri³, M. Ellis³, S. Waters⁴, L. Cummings⁴, N. Kuiper¹, V. Michael¹. ¹Institute of Science and Technology in Medicine, University of Keele, Stoke on Trent, United Kingdom, ²Department of Mechanical Engineering, University of Bath, Bath, United Kingdom, ³Department of Chemical Engineering, University of Bath, Bath, United Kingdom, ⁴Division of Applied Mathematics, University of Nottingham, Nottingham, United Kingdom.

Bioreactor design for the culture of tissue-engineered constructs is essential for the production of functional tissue. Co-cultures of cartilage and bone tissue together have been shown to be beneficial compared to monocell cultures. We have developed a bioreactor for culturing osteoblasts/chondrocytes together (A). Two separate bone and cartilage culture chambers are assembled together with the bone/cartilage separated by a silicone membrane. This system allows nutrient administration via two separate methods to allow scale up of larger tissues. Media is perfused to the chambers whilst a PLGA porous fibre runs through the bone scaffold delivering extra nutrients via diffusion. Through this fibre, a temperature/oxygen sensor will be introduced to the samples, allowing monitoring of cellular activity. Non-invasive lactate and glucose culture media analysis also allows further quantification. Porous calcium-phosphate scaffolds (15mm x 10mm) and Chitosan hydrogel substrates (15mm x 6mm) are used to support the bone/cartilage cells. The bone scaffold (B) mimics the arrangement in an articulating joint where the porous trabecular bone is covered with a shell of dense cortical bone which, in turn, interfaces with the cartilage component. It is hypothesised that the cap to the porous scaffold will restrict mixing between the bone and cartilage media. Static experiments have been performed by seeding bone scaffolds with MG-63 cells. Mathematical modelling of the bone chamber and porous scaffold has been performed. Preliminary seeding data reveal 59% and 76% of cells were adherent on the scaffold after 2 hours and 4 days in culture respectively (C). Numerical simulations were able to visualise the fluid distribution through the bone chamber, and determine the optimum chamber size and inlet/outlet configuration to achieve minimal regions of stagnation, while maintaining shear stress below the threshold (5-15 dyne/cm²). This sophisticated co-culture bioreactor has the potential to significantly improve the functionality of tissue-engineered osteochondral plugs.



Disclosures: S. Cartmell, None.

M152

See Sunday Plenary Number S152

M153

A Novel Model of Impaired Fracture Healing. T. S. Gross¹, S. L. Poliachik^{*1}, S. E. Nork^{*1}, S. D. Bain². ¹Orthopaedics and Sports Medicine, University of Washington, Seattle, WA, USA, ²MDS Pharma Services, Bothell, WA, USA.

The biological pathways responsible for normal fracture repair are well understood. However, the causal factors leading to unsuccessful fracture healing are ill defined and poorly understood. Based on recent data indicating that transient muscle paralysis rapidly induces bone loss in mice, we hypothesized that a transient loss of muscle function superimposed upon a closed femur fracture in rats would lead to delayed fracture healing. To test this hypothesis, Sprague-Dawley female rats (age: 4 months, n=14) underwent a standard closed femur fracture with a Kirschner wire inserted through the right femur diaphysis prior to blunt guillotine impact. Following radiographic confirmation of the location and disposition of all fractures, 7 rats were given a single injection of Botox in their right quadriceps (2 Units/100g, 1/2 of dose 5 mm proximal, 1/2 dose 5 mm distal to the fracture site). The remaining 7 rats received identical volume Saline injections. All rats were allowed to ambulate freely, with 10 rats killed at 4 wk (n=5/grp) and 4 rats killed at 6 wk (n=2/grp). Following sacrifice, right femurs were radiographed and micro-CT scans were obtained of all right and left femurs (1.6 cm region centered at the mid-diaphysis, 21 µm voxel). For each animal, callus volume and the polar moment of inertia (pMOI) of the callus were determined by contrast with the contralateral intact left femur. Botox induced quadriceps paralysis significantly diminished fracture callus volume compared to Saline treated rats at 4 wk (-42.1%, p=0.003) and 6 wk (-39.9%, p=0.05). Similarly, callus pMOI was profoundly reduced in Botox treated rats compared to Saline treated rats (4 wk: -60.0%, p<0.001; 6 wk: -49.8%, p=0.03). Radiographic examination indicated an absence of bone union in 6 of 7 Botox treated rats, while all Saline treated rats demonstrated clear evidence of bone union across the fracture gap. These data clearly demonstrate that transient muscle paralysis of a single muscle group adjacent to the femur leads to impaired fracture healing. Further, the lack of callus formation in the Botox rats was not spatially confined to the anterior cortex adjacent to the quadriceps. As diminished muscle function following trauma or due to aging have both been associated with poor fracture healing, this novel model holds potential to directly impact clinical care by exploring why normal muscle function is required for successful fracture healing.

Disclosures: T.S. Gross, None.

M154

Formation of Haversian-Type Bone and Blood Vessels Guided by the Artificial ECM of Vasculature-Inducing Geometry. T. Kaku¹, H. Kobayashi^{*1}, S. Iku^{*2}, K. Nemoto^{*2}, T. Miyata^{*2}, Y. Kuboki^{*3}. ¹Oral Pathology, Health Sciences University of Hokkaido, Hokkaido, Japan, ²Koken Bioscience Institute, Hokkaido, Japan, ³Koken Bioscience Institute & Hokkaido University, Hokkaido, Japan.

We have proposed that geometrical property of the artificial extracellular matrices (ECM) must be taken into consideration for successful development of tissue engineering (JBJS 83A:S1-105-115, 2001). Geometry is defined in this case as the three dimensional (3D) structure of artificial ECM at the order of micrometer, which can direct growth of tissues and organs in vivo and in vitro. Previously we have reported that honeycomb-shaped hydroxyapatite (HC-HAP) with the pores less than 100-µm induced endochondral ossification, while one with 350-µm pores induced direct bone formation. By the fact that a single large blood vessels was always noticed in the center of the 350-µm pores of HC-HAP, we attempted to direct the haversian-type bone formation by an artificial ECM with similar geometry to HC-HAP but with biodegradable property. We chose a honeycomb-shaped collagen product (HC-COL) (Honeycomb sponge, Koken, Japan). HC-COL was cut into block-form, combined with the purified BMP cocktail (500 µg) or rhBMP-2 (5 µg) and implanted into rat skin. HC-COL was calcified with a series of the solutions, which contained calcium and phosphate to obtain the hydroxyapatite-coated honeycomb collagen (HAP-HC-COL), which was also implanted into the skin. Two weeks after implantation, it was found that the concentric layered osteogenesis occurred within the each tunnels of HC-COL/BMP, the centers of which, there was a single large blood vessel. The structure was reminded us the haversian system. More interestingly, HAP-HC-COL itself (without BMP) induced the concentric fibrous tissue formation with a blood vessel in the center of the tunnel. Although bone formation was not observed. It was concluded that the characteristic 3D-structure (vasculature-inducing structure) of HC-COL or HAP-HC-COL induced vasculature first, irrespective of the presence of BMP. Then bone formation will occur if the mesenchymal cells were differentiated into osteoblasts by BMP.

Disclosures: T. Kaku, None.

M155

Mineral and Matrix Characteristics in Mice with LRP5 G171V Mutation. N. P. Camacho¹, M. P. Akhter². ¹Imaging & Spectroscopy Lab, The Hospital for Special Surgery, New York, NY, USA, ²Medicine, Creighton University, Omaha, NE, USA.

Greater bone density and strength has been reported in mice with the LRP5 G171V mutation. We characterized femoral cortical bone properties to determine if the LRP5 G171V mutation differences in mineral and matrix properties as compared to wild type (WT). Sixteen female mice (4 mo.) representing two genotypes (WT=wild type, HBM=High bone mass with LRP5 G171V mutation) were used. Femoral mineral and matrix properties were analyzed by Fourier transform infrared imaging spectroscopy (FT-IRIS). This allows information on mineral, collagen, and carbonate content and

distribution to be obtained at ~ 7 μm spatial resolution from PMMA-embedded bone sections. Infrared vibrations of both the mineral (a poorly crystalline carbonated apatite (HA)) and matrix phases (primarily Type I collagen) were monitored simultaneously. The ratio of the area of the HA phosphate ν_1 , ν_2 absorbance from 900 to 1200 cm^{-1} , to the area of the protein amide I absorbance from 1590 to 1720 cm^{-1} was calculated to obtain the relative amounts of mineral and protein present (min:matrix), a parameter previously shown to be correlated to ash weight. The carbonate-to-mineral ratio (carb:min), an indicator of carbonate content of the mineral phase, was calculated as the ratio of the area of the carbonate ν_2 absorbance from 850 to 890 cm^{-1} to the area of the phosphate ν_1 , ν_2 absorbance. Crystallinity of the mineral phase was calculated by ratioing the intensity of the absorbance at 1030 cm^{-1} to that at 1020 cm^{-1} , a parameter previously shown to be related to the apatite crystal length in the c-axis direction. The crosslink (Xlink) parameter, related to the ratio of mature to immature collagen crosslinks, was obtained by ratioing the intensity of the absorbance at 1660 cm^{-1} to that at 1686 cm^{-1} . We analyzed the data using the Student's t test for differences due to genotype. There were no differences in FT-IRIS determined bone parameters, except for the Xlink parameter, which tended to be greater in the HBM mice compared to the WT mice ($p = 0.08$). An increase in this collagen parameter likely reflects increased mature crosslinks, a finding which could be consistent with the greater bone strength previously reported in the HBM mice. Further investigations will focus on how the relatively increased crosslinks in HBM mice influence their bone intrinsic material properties as measured by nano-indentation at ultrastructural level.

FT-IRIS (mid-shaft femur)	HBM	WT
Min:Mat	6.95 \pm 0.63	6.53 \pm 0.82
Car/Pho	0.010 \pm 0.002	0.0093 \pm 0.002
XLink	4.23 \pm 0.41	3.89 \pm 0.29 ^a
Crystallinity	1.1 \pm 0.03	1.12 \pm 0.065

(Mean \pm SD), ^a Compared to HBM ($P = 0.08$)

Disclosures: M.P. Akhter, None.

M156

Secreted Phosphoprotein-24 Is Converted from an Inhibitor to a Functional Enhancer During BMP-Directed Osteoblastogenesis. M. J. Beckman¹, S. C. Ramage¹, A. Maiti², O. Korchynski². ¹Biochemistry and Molecular Biology, Virginia Commonwealth University, Richmond, VA, USA, ²Orthopaedic Surgery, Virginia Commonwealth University, Richmond, VA, USA.

Bone morphogenetic proteins (BMPs) are members of the TGF β family and key regulators of osteogenesis. BMPs signal through their cognate receptors to SMAD proteins that transduce the signals to activate genes crucially important to osteogenesis. Secreted phosphoprotein-24 (Spp24) is a 24 kDa bone matrix protein isolated from demineralized bovine bone matrix. Spp24 has known homology domains to both cystatin and TGF β receptor type II (T β RII), and like many bone matrix proteins has numerous sites for glycosylation as well as serine and threonine phosphorylation. The T β RII domain of Spp24 has shown a low affinity binding to BMP-2. A truncated form of Spp24 has been shown to possess osteoinductive character and enhance BMP activity. Overexpression of mouse Spp24 (mSpp24) inhibited various BMPs' signaling at early time points. We hypothesize that Spp24 is converted to a more active factor that can enhance later stages of BMP-mediated osteoblastogenesis. This concept was tested using an adult human bone marrow mesenchymal stem cell model (MSC). A mouse Spp24 adenovirus (Adv5CMV-mSpp24) construct was used to transduce MSCs with 100% efficiency for long duration. MSC differentiation to osteoblasts (OB) was induced and maintained by controlled treatment with BMP-2/7 heterodimer dosed over a 14 day period, resulting in fully differentiated OB cells. The experimental design was a 2 x 2 factorial of Adv5CMV-LacZ control, LacZ plus BMP-2/7, mSpp24, and mSpp24plus BMP-2/7. All groups were also co-transduced with a BMP-specific response element reporter to assay BMP-Smad-induced signaling and β -galactosidase for normalization. Results demonstrated marked repression of BMP signaling by mSpp24 after 3 days in culture. By day 7, the mSpp24 repression of BMP signaling was not evident. However, at the subsequent time points, particularly on day 10, the effect of mSpp24 was to significantly enhance BMP signaling. Western blots were performed with the HA-tagged mSpp24 protein product at 3, 7, 10 and 14 days. The results of this analysis revealed a truncated 18 kDa fragment of mSpp24, representing the putative active form, appearing by day 7 and increased at day 10. In conclusion, these data indicate that Spp24 plays an antagonistic role to osteogenic signaling until it is modified in a yet unspecified manner to create this smaller 18 kDa form that is capable of enhancing BMP activity. Our study confirms earlier work by Wozney that described a slow release factor capable of regulating BMP-mediated osteogenesis and later by Murray that Spp18 is the active fragment.

Disclosures: M.J. Beckman, None.

M157

See Sunday Plenary Number S157

M158

Cross-Talk Between CTGF and TGF- β 1 in Mesenchymal Stem Cell Condensation. F. Del Carpio-Cano^{*1}, J. Y. Belcher¹, K. B. Buck^{*1}, J. A. Arnot¹, R. A. DeLa Cadena^{*2}, S. N. Popoff¹, F. F. Safadi¹. ¹Anatomy and Cell Biology, Temple University, Philadelphia, PA, USA, ²Physiology, Temple University, Philadelphia, PA, USA.

Condensation or the aggregation of mesenchymal stem cells (MSCs) precedes chondrocyte differentiation and is required for cartilage formation. CTGF is a matricellular protein that has been found to be expressed during MSC condensations in vivo. It has been shown that TGF- β 1 regulates CTGF expression and that CTGF acts as a downstream mediator of TGF- β 1 effects on extracellular matrix production. It has also been reported that CTGF has the ability to bind TGF- β 1 and modulates its effects. Using C3H10T1/2 MSCs as a model for mesenchymal condensation, we have shown previously that TGF- β 1 induces MSC condensation in vitro associated with increased matrix production, proliferation and migration and this induction is mediated by CTGF. In this study, we were interested to examine whether CTGF overexpression can mediate MSC condensation in the absence or presence of TGF- β 1. C3H10T1/2 MSCs were infected with adenovirus over-expressing CTGF tagged with GFP achieving a 6-7 fold increase in CTGF mRNA and protein expression. Adenovirus expressing only GFP was used as control. Cells overexpressing CTGF did not show any MSC condensation. Surprisingly, TGF- β 1 induced MSC condensation was inhibited in cells overexpressing CTGF. These results suggest that a fine equilibrium of CTGF expression is required for TGF- β 1-induced MSC condensation. We next examined the effect of CTGF overexpression on MSC adhesion and spreading associated with vinculin localization at focal adhesion and actin cytoskeletal reorganization. Cells overexpressing CTGF spread more robustly with an increased punctuated signal of vinculin at sites of focal adhesion with the formation of lamellipodia when compared to cells infected with GFP virus. We next examined the signaling pathway associated with MAP Kinase family to evaluate differences between TGF- β 1-induced MSC condensation and the inhibitory effect of CTGF overexpression on MSC condensation. Phosphorylated P38, Jnk and Erk were increased in the GFP-infected MSCs treated with TGF- β 1. However, MSCs infected with GFP-CTGF and treated with TGF- β 1 showed only an increase in phosphorylated Jnk and Erk but not P38. These findings indicate that p38 MAPK may mediate MSC condensation by TGF- β 1. Further studies are warranted to modulate P38 expression to elucidate the interaction between CTGF and TGF- β 1 in regulating MSC condensation.

Disclosures: F. Del Carpio-Cano, None.

This study received funding from: Pennsylvania Dept. of Health and NIAMS/NIH.

M159

The Three Dimensional ¹H NMR Structure of Bovine Lead Ion-Bound Osteocalcin and Implications for Lead Toxicity. L. Li^{*1}, C. M. Gundberg², T. L. Dowd^{*3}. ¹National Institute of Environmental Health Science, Research Triangle Park, NC, USA, ²Orthopedics, Yale University School of Medicine, New Haven, CT, USA, ³Chemistry, Brooklyn College of the City University of New York, Brooklyn, NY, USA.

Structural information on the effect of Pb²⁺ on proteins under physiologically relevant conditions is largely unknown. We have solved the three dimensional structure of bovine lead coordinated osteocalcin, a bone protein from a target tissue, using ¹H 2D NMR techniques and suggested a molecular mechanism for lead toxicity. The protons in the 49 amino acid sequence were assigned using 2D homonuclear NMR experiments. Lead, at a stoichiometry of only 1:1, was shown to induce a tertiary structure in the protein similar to that induced by Ca²⁺ at a stoichiometry of 3:1. The structure of Pb²⁺-osteocalcin consists of an unstructured N terminus and a C-terminal hydrophobic core (residues 16-49) formed by long range hydrophobic interactions. Elements of secondary structure within residues 16-49 include a type III turn (residues 27-30) and a α_1 helix (residues 31-34). Residues 21-26 formed loose turns with helical characteristics. The 3 Glu residues project from the same face of the helical turns and are surface exposed. The genetic algorithm -molecular dynamics simulation approach was used to place 1 lead ion on the NMR derived structure. The lead ion was coordinated by side chain oxygen ions of OE3 and OE4 of Glu 24 and the side chain oxygen ions of OE1 and OE2 of Glu 21. The best correlation of the distances between the uncoordinated Glu oxygen ions is with the intercalcium distance of 9.43 Å in hydroxyapatite. This mineral binding is similar to what was proposed from the structure of Ca²⁺-osteocalcin. A comparison of Pb²⁺- and Ca²⁺-osteocalcin indicates Pb²⁺ may induce conformational changes and subsequent molecular processes in proteins prematurely. Lead exposure may alter the amount of mineral bound osteocalcin contributing to abnormal bone remodeling. This may play a role in the increased bone resorption and decreased bone density observed in bones from lead exposed animals.

Disclosures: T.L. Dowd, None.

This study received funding from: NIH.

M160

See Sunday Plenary Number S160

M161

The Biological Trials of Hyaluronic Acid on Osteoclast Differentiation Induced by IL-1. M. Hirata¹, M. Kobayashi^{1*}, K. Miyazaki^{2*}, C. Miyaaura¹, M. Inada¹. ¹Department of Biotechnology and Life Science, Tokyo University of Agriculture and Technology, Tokyo, Japan, ²Seikagaku Corporation, Tokyo, Japan.

Hyaluronic acid (HA) is a component of extra cellular matrix (ECM) in cartilage, polymer of a glycosaminoglycan organized the network with majority of agrican. In human bone marrow, HA produced in both stromal and hematopoietic lineage of cells, the capacities could be counted on regulating cellular response for bone cells. In bone ECM, HA present as a high molecular size, however, the functional effect of HA on osteoclast differentiation is still unclear. Here we demonstrate that the roles of HA in osteoclast differentiation induced by IL-1. When the co-culture of primary osteoblasts from newborn calvaria and bone marrow cells from tibiae in the presence of IL-1, TRAP (Tartrate Resistant Acid Phosphatase) positive multinucleated cells were formed 7 days of culture. HA single treatment did not alter the proliferation of osteoblast/stromal cells. In the presence of IL-1 (2 ng/ml) and HA (900 KDa, 1 mg/ml), however, the number of TRAP positive cells was decreased. RT-PCR was performed using primer sets of RANKL (as an inducible ligand on osteoblast) and NFATc1 (inducible transcriptional factor on osteoclast differentiation). The result showed RANKL expression induced by IL-1 was suppressed in the presence of HA. NFATc1 expression slightly decreased in the culture. To identify further mechanisms of the HA, ex vivo calvarial organ culture was performed. Calvarial bone from day 4 old mice were dissected into 2 portions (control vs. challenge group) of culture, bone resorbing activity was measured by cultured medium calcium. When the presence of IL-1 (2ng/ml) in culture, bone resorbing activity was increased and the activity was suppressed by the simultaneous treatment with HA (900 KDa, 1 mg/ml). These results suggested HA attenuated IL-1 induced RANKL production in osteoblast, following NFATc1 expression was suppressed in osteoclast precursors sequentially decrease the number of mature osteoclast. The potentials shown in the presented study suggested that HA could apply various inflammatory diseases as an inhibitor of bone loss.

Disclosures: M. Hirata, None.

M162

The Inhibitor of Metalloproteinases TIMP-1 Rescues the Strong Bone Loss Induced by Runx2 Overexpression in Mice. C. Schiltz*, C. Prouillet*, C. Marty*, M. De Vernejoul, V. Geoffroy. Hôpital Lariboisière, INSERM U606, Paris Cedex 10, France.

The Runx2 gene is essential for osteoblast differentiation and function. Runx2 deficiency results in complete lack bone formation and overexpression of Runx2 in cells of the osteoblastic lineage to severe osteoporosis. Osteoblastic matrix metalloproteinases (MMPs) have been reported to be required for normal bone resorption. Several lines of evidence suggest that osteoblastic MMPs could take part of the increased bone resorption observed in mice after overexpression of Runx2. The goal of our study was to define using transgenic approach whether inhibition of osteoblastic MMPs can reduce the bone loss induced by Runx2.

We examined the rescue of the severe osteopenic phenotype in Runx2 mice by overexpressing the MMPs inhibitor TIMP-1 (tissue inhibitor of metalloproteinase 1) specifically in osteoblasts. 1-, 4- and 8-month-old females with the different genotypes (WT, Runx2, TIMP-1 and TIMP-1/Runx2) were generated. Bone density was measured by DXA and by pQCT for all mice. Microarchitecture and formation and resorption parameters were evaluated in 1- and 4-month-old females by histomorphometry. Primary osteoclasts were differentiated ex vivo from bone marrow or co-cultured with primary osteoblasts isolated from calvaria. Primary osteoblasts were also used to evaluate gene expression by qPCR.

Bone density analysis indicated that TIMP-1 overexpression is efficient at reducing bone loss observed in Runx2 mice but only in 4- and 8-month-old females. The rescue and prevention of bone loss in TIMP-1/Runx2 mice were visible at the long bones and the caudal vertebrae. Histomorphometry analysis on trabecular bone indicated that this rescue in 4-month-old TIMP-1/Runx2 females was due to a decrease of the resorption activity (decreased trabecular separation and osteoclastic surfaces) and a sustained osteoformation (increased trabecular thickness and maintained BFR) compared to Runx2 mice. In addition, we also reported a partial rescue of the cortical bone loss (increased cortical thickness and outer bone diameter) in TIMP-1/Runx2 mice compared to Runx2 mice. Our ex vivo study showed that the ability of osteoclastic cell to differentiated is reduced in TIMP-1/Runx2 mice compared to Runx2 mice due to a reduction in the expression of RANK-L by TIMP-1/Runx2 osteoblastic cells.

In conclusion, we showed that TIMP-1 overexpression in the runx2 background mainly reduces bone resorption (decrease osteoclasts differentiation and activity) and maintains bone formation in trabecular and cortical bone. Our results indicate that osteoblastic MMPs are partly responsible for the bone loss in mice overexpressing Runx2.

Disclosures: V. Geoffroy, None.

This study received funding from: ANABONOS consortium (Sixth Framework Programme of the European community).

M163

See Sunday Plenary Number S163

M164

Identification of Novel Transcription Factors Necessary for Chondrocyte Hypertrophy. A. M. Ionescu, A. B. Lassar*. BCMP, Harvard Medical School, Boston, MA, USA.

To date, only two families of transcription factors are known to regulate chondrogenesis, Sox and Runx family members. The early steps of chondrogenesis, including mesenchymal condensation and expression of chondrocyte-specific extracellular matrix proteins are critically regulated by Sox9, Sox5, and Sox6. In contrast, the latter steps of chondrogenesis appear to be regulated by Runx2 and/or Runx3. Runx2 is expressed in chondrocytes as they initiate chondrocyte hypertrophy, and loss of this factor in genetically engineered mice severely delays chondrocyte maturation in a number of developing bones.

Interestingly, recent work in the Lassar lab has demonstrated that expression of exogenous Runx2 fails to activate expression of endogenous collagen X in naïve somites, but can activate expression of this gene in somites that have been induced to initiate the chondrocyte differentiation program. Consistent with this result, I have found out that Runx2 and Smad1 (which transduces BMP signals) are only able to induce the expression of a Col X-luciferase reporter in upper sternal chondrocytes (USCs) but not in fibroblasts (CEFs) isolated from chicken embryos, in the presence of exogenous BMP signals. This suggests that hypertrophic chondrocytes express another factor that is required for the expression of Col X.

To identify a chondrocyte-specific DNA binding factor(s), a series of overlapping 40 bp oligomers that cover the Col X enhancer were used in an EMSA to detect DNA binding activities that are specifically present in primary chondrocytes but are absent from fibroblasts. This analysis led to the identification of a Fast Mobility Complex (FMC) that binds to 4 sites in the collagen X regulatory sequences, a Slow Mobility Complex (SMC) that binds to 2 sites and Sox 5 which binds in multiple places along the collagen X regulatory sequences. Mutational analysis of these binding sites indicated that the FMC sites are necessary for efficient induction of a Col X-luciferase reporter by co-transfected Runx2 and Smad1 in chondrocytes. Moreover, 4-fold reiteration of one of the Fast Mobility Complex binding sites (FMC3) placed upstream of Col X-promoter proximal sequences (4x FMC3-Col X-luciferase), led to chondrocyte-specific induction of the downstream luciferase reporter by co-transfected Runx2 and Smad1. Thus, our immediate focus consists in identification and characterization of the proteins that comprise FMC3. The successful identification of FMC3 will lead to the identification of new hypertrophy-specific factors which, if inhibited, could reverse chondrocyte hypertrophy which is pathologically induced during osteoarthritis.

Disclosures: A.M. Ionescu, Arthritis Foundation postdoctoral fellowship 2.

This study received funding from: Arthritis Foundation.

M165

See Sunday Plenary Number S165

M166

Alpha-2-Macroglobulin Is a Novel Substrate for ADAMTS-7 and ADAMTS-12 and Inhibits Their Degradation of Cartilage Oligomeric Matrix Protein. Y. Luan^{1*}, D. R. Howell^{2*}, L. Kong^{2*}, C. Liu². ¹Orthopaedic Surgery, New York University, New York, NY, USA, ²New York University, New York, NY, USA.

Degradative fragments of cartilage oligomeric matrix protein (COMP) have been observed in both osteoarthritis and rheumatoid arthritis. We previously reported that ADAMTS-7 and ADAMTS-12, two members of ADAMTS (a disintegrin and metalloprotease with thrombospondin motifs) family, sharing the similar domain organization in the family, degraded COMP in vitro and were significantly induced in the cartilage and synovium of arthritic patients (Liu, et al, FASEB J. 2006; 20(7):988 and Liu, et al, J. Biol. Chem. 2006; 281(23):15800). In this study we further demonstrated the importance of COMP degradation by ADAMTS-7 and ADAMTS-12 in vivo, since i) the size of the COMP fragments produced by either ADAMTS-7 or ADAMTS-12 is similar to that of COMP-degradative fragments seen in the patients with osteoarthritis; ii) antibody blocking assay indicated that specific antibodies against ADAMTS-7 or ADAMTS-12 dramatically inhibits TNF- α -induced COMP degradation in the cultured cartilage explants and iii) suppression of ADAMTS-7 or ADAMTS-12 expression using siRNA silencing approach in the human chondrocytes also markedly prevents COMP degradation. Furthermore, we revealed that α_2 -Macroglobulin (α_2 M) is a novel substrate for ADAMTS-7 and ADAMTS-12 based on the observations that both metalloproteinases were able to cleave α_2 M in a dose-dependent manner, which gave rise to the cleavage products with the molecular weights of 180 and 105 kDa respectively. More significantly, α_2 M inhibits both ADAMTS-7- and ADAMTS-12-mediated COMP degradation in a dose-dependent manner; thus α_2 M represents the first endogenous inhibitor of ADAMTS-7 and ADAMTS-12.

Disclosures: Y. Luan, None.

This study received funding from: NIH.

M167

MT3-MMP Is a Major Mesenchymal Collagenase Essential for Skeletal Development. J. Shi*, M. Son*, S. Yamada*, L. Szabova*, S. Kahan*, K. Chrysovergis*, L. Wolf*, A. Surmak*, K. Holmbeck*. CSDB/MMPU, NIDCR, Bethesda, MD, USA.

Peri-cellular remodeling of mesenchymal extracellular matrices is considered a prerequisite for mesenchymal cell proliferation, motility and development. Here we explore the molecular mechanisms responsible for collagen remodeling in the skeleton and peri-skeletal tissues of the mouse. We demonstrate that membrane-type 3 MMP, MT3-MMP, is expressed in mesenchymal tissues of the skeleton and in peri-skeletal soft connective tissue. Consistent with these observations MT3-MMP-deficient mice display growth inhibition tied to a decreased viability of mesenchymal cells in skeletal tissues. We document that MT3-MMP works as a major collagenolytic enzyme, enabling cartilage and bone cells to cleave high-density fibrillar collagen and modulate their resident matrix to make it permissive. Collectively, these data uncover a novel extracellular matrix remodeling mechanism required for proper function of mesenchymal cells. The physiological significance of MT3-MMP is highlighted in mice double deficient for MT1-MMP and MT3-MMP. Double deficiency transcends the combined effects of the individual single deficiencies and leads to severe embryonic defects in palatogenesis and bone formation incompatible with life. These defects are directly tied to loss of indispensable collagenase activities required in mesenchymal tissues for extracellular matrix remodeling and cell proliferation during embryogenesis. Based on these observations we conclude that peri-cellular collagen remodeling mediated by the MT1-MMP/MT3-MMP synergizing duo of collagenases is essential for skeletogenesis and palatogenesis in the mouse and demonstrates the requirement for embryonic remodeling of collagen.

Disclosures: J. Shi, None.

M168

BMP-2 Induces Sustained Expression of COX-2 in MC3T3-E1 Osteoblasts. K. A. Blackwell*, P. Hortschansky*, L. G. Raisz*, C. C. Pilbeam*. ¹Endocrine Division and Musculoskeletal Institute, University of Connecticut Health Center, Farmington, CT, USA, ²Leibniz Institute for Natural Product Research and Infection Biology, Hans-Knöll-Institute (HKI), Jena, Germany, ³Endocrine Division and Musculoskeletal Institute, University of Connecticut Health Center, Farmington, CT, USA.

BMP-2 potently stimulates osteoblastic differentiation. We have shown that BMP-2 induces cyclooxygenase-2 (COX-2) expression in murine primary calvarial osteoblasts via a Runx2 binding site at -267/-261 bp in the COX-2 promoter and that the full anabolic response to BMP-2 requires the induction of COX-2 and production of prostaglandin (PG) E₂ in osteoblasts. To study further the mechanisms by which BMP-2 regulates COX-2 mRNA and by which PGE₂ may contribute to effects of BMP-2, we treated MC3T3-E1 osteoblastic cells with vehicle, BMP-2 (300 ng/ml), PGE₂ (1 µM), or BMP-2 + PGE₂ and measured COX-2 mRNA by real time PCR. To prevent effects of endogenous PGE₂ induced by BMP-2, all experiments were performed in the presence of the COX-2 selective inhibitor, NS-398 (0.1 µM). Although the induction of COX-2 is generally transient, BMP-2 induced elevation of COX-2 mRNA was more sustained: 2.9-fold at 4 h, 3.0-fold at 8 h and 2.6-fold at 24 h. PGE₂ alone had no significant effect on COX-2 mRNA levels. However, the addition of PGE₂ to BMP-2 increased the elevation of COX-2 mRNA, relative to BMP-2 treatment alone, by 1.3-fold at 4 h, 1.5-fold at 8 h, and 2.5-fold at 24 h. To assess the role of promoter regulation by BMP-2 in these effects, we used MC3T3-E1 cells stably transfected with 371 bp of the COX-2 promoter fused to the luciferase gene. BMP-2 transiently stimulated luciferase activity by 2.7-fold at 4 h, with levels returning to baseline at 24 h. At 4 h, PGE₂ alone had a small effect on luciferase activity (1.6-fold) and addition of PGE₂ to BMP-2 further amplified luciferase levels by 1.6-fold over BMP-2 alone. Similar to BMP-2 treatment alone, levels returned to baseline by 24 h. Similar results were obtained with MC3T3-E1 cells stably transfected with 3 kb of the COX-2 promoter fused to the luciferase gene. Measurement of mRNA degradation after treatment with inhibitors of transcription indicated that neither BMP-2 or BMP-2 + PGE₂ stabilized COX-2 mRNA compared with controls or PGE₂ alone. These results suggest that BMP-2 may transcriptionally elevate COX-2 expression not only via the proximal promoter region (-300 bp), which stimulates the transient expression of COX-2, but also via distal elements (> -3 kb), which stimulate more sustained expression of COX-2. Additionally, PGE₂ enhances both the transient and sustained induction of COX-2 mRNA by BMP-2.

Disclosures: K.A. Blackwell, None.
This study received funding from: NIH DK-48361L.

M169

See Sunday Plenary Number S169

M170

Craniofacial Reconstruction with Bone Morphogenetic Protein-2. A. Docherty Skogh, C. Arnander*, T. Engstrand*. Plastic and Reconstructive Surgery, Karolinska University Hospital, Stockholm, Sweden.

The purpose of this study is to report the effectiveness and safety of using titanium mesh combined with chitosan-heparin sponge and rhBMP-2(InductOs) for the reconstruction of large through-and-through cranial defects in humans. Previous to this, a study of boneformation in Sprague Dawley rats was performed that showed very good results with the above mentioned carrier system.

Methods: Three patients were operated on and subsequently followed up with CT scans, clinical examination and histological samples. The patients had frontotemporal or parietal defects ranging from 54 to 117 cm(2) resulting from postoperative infection and necrosis of the bone following removal of neoplasms, cerebral aneurysms or haemorrhage. The first patient had received radiation to the operating field. The patients were reconstructed with (1) titanium mesh, chitosan-heparin sponge on the dura mater with 4 mg rhBMP-2, chitosan-heparin sponge with 8 mg rhBMP-2 on the titanium mesh, (2) titanium mesh, chitosan-heparin sponge with 12 mg rhBMP-2 on the dura mater, (3) titanium mesh, chitosan-heparin sponge with 10 mg rhBMP-2 on the titanium mesh. All the patients were followed up by clinical examination and repeated CT scans for a minimum of 8 months. Histological samples were taken from two of the patients.

Results: All the patients had signs of postoperative infection and were given antibiotics. One patient experienced hair loss in the operating field two months postoperatively. The hair grew back uneventfully a month later. Two of the patients had exposure of the titanium mesh and were reoperated once and five times respectively. The latter patient required free flap surgery to get the wound to finally heal. CT scans showed calcification of the dura mater in the operating field, but no signs of boneformation in two of the patients. The third patient showed ongoing boneformation after eight months and CT scans are to be repeated thirteen months postoperatively.

The histological samples taken six and nine months postoperatively showed no sign of boneformation or angiogenesis.

Conclusions: Titanium mesh combined with chitosan-heparin sponge and rhBMP-2 (InductOs) appears to be a potential way to reconstruct significant craniofacial defects. The patients did have quite a lot of complications postoperatively, in particular the patient with the chitosan-heparin sponge and rhBMP-2 directly on the dura mater. The chitosan seems to cause an inflammatory response that impairs the healing of the wound. In one patient local hair loss was seen, most likely due to the effect of BMP-2. This study illustrates the difficulties of translating the results from studies on rodents to humans, and also the need for a more inert carrier system.

Disclosures: A. Docherty Skogh, None.

M171

See Sunday Plenary Number S171

M172

Acid Swelling Overcomes Osteogenesis Inhibition of Xenogeneic Collagenous Matrix Delivery System used for Naturally-Derived Bone Morphogenetic Protein Complex. B. Rothman*, E. Olivier*, N. Duneas*. ¹Altis Biologics (Pty) Ltd, Pretoria, South Africa, ²School of Pharmacy, Tshwane University of Technology, Pretoria, South Africa, ³Biomedical Sciences, Tshwane University of Technology, Pretoria, South Africa.

The bone morphogenetic proteins (BMPs) are pleiotropic morphogens belonging to the greater transforming growth factor-β (TGF-β) superfamily of growth factors responsible for embryonic patterning as well as post-natal tissue regeneration.

BMPs require a safe and effective delivery system to bring about osteogenesis in clinical settings. Native porcine bone matrix-derived insoluble collagenous bone matrix (ICBM) was treated with various protocols involving organic acid and proteases (pepsin) to determine whether the chemical swelling of the matrix and telopeptide reduction would reduce the inflammatory response in the xenogeneic host, which has been associated with inhibition of the biologic activity of BMPs.

Native and treated porcine ICBM samples were combined with various doses of naturally derived porcine BMP complex and implanted intra-muscularly and subcutaneously in rodents in order to study bone formation. Histological examination of tissue specimens retrieved 12 days post implantation showed that the degree of inflammation induced by native porcine ICBM is high, and bone induction was inhibited at high doses of up to 50mg porcine BMP complex per gram delivery system. In contrast, acetic acid treated porcine ICBM was found to be an effective delivery system for BMPs, dose dependently stimulating bone formation and alkaline phosphatase activity, a specific enzyme marker for bone formation, at dose ranges of between 0 to 12mg porcine BMP complex per gram delivery system.

Porcine ICBM that was treated successively with acetic acid followed by enzyme digestion using porcine gastric mucosa-derived pepsin showed only a slight improvement in bringing about osteoinduction (not significant p>0.05). A striking observation was that the inflammatory response to chemically and/or enzymatically treated ICBM was dose dependently reduced by increasing concentrations of porcine BMP complex. The data demonstrate that chemical swelling plays a major part in improving xenogeneic ICBM for use as a BMP delivery system. This work will assist in the development of xenogeneic derived collagenous matrices with improved host immuno-compatibility which may function as safe and effective delivery systems for BMPs to be used in the clinical repair and regeneration of bone defects in humans.

Disclosures: N. Duneas, Altis Biologics 1, 2, 4.
This study received funding from: National Research Foundation RSA.

M173

Xenogeneic Bone Morphogenetic Protein Complex Enhances Allogeneic Demineralised Bone Matrix Osteoinductivity in Rats. N. Duneas¹, B. Rothman², E. Olivier³, G. U. Mohangi⁴. ¹Biomedical Sciences, Tshwane University of Technology, Pretoria, South Africa, ²Altis Biologics, Pretoria, South Africa, ³School of Pharmacy, Tshwane University of Technology, Pretoria, South Africa, ⁴School of Dentistry, University of Pretoria, Pretoria, South Africa.

Demineralised Bone Matrix (DBM) is a widely used allograft material in a variety of clinical settings, including bone voids, as bulking agent for autogenous bone graft material, and orthopaedic and periodontal defects. DBM promotes osteogenesis due to its content of bone morphogenetic proteins (BMPs), a family of morphogens classified under the larger transforming growth factor- β superfamily of growth and differentiation factors. The BMPs induce and regulate bone formation during embryogenesis and in postnatal life during regeneration and healing of traumatic bone defects. We present data that show in animal models that allogeneic DBM can be fortified with xenogeneically sourced BMP complex to improve DBM performance. Rat DBM was fortified with BMP complex purified from porcine diaphyseal bone. BMP complex contains a number of BMPs, and is standardized with respect to hBMP-2 content determined by commercial ELISA kit. Implantation of 25 mg rat allogeneic DBM fortified with 0, 3, 6 and 12 mg BMP complex per gram of DBM resulted in dose dependant upregulation of bone formation on day 12 as scored histologically and against alkaline phosphatase activity, an enzyme marker specific for bone formation. The data may assist in developing tissue banked DBM that is fortified by the adsorption of xenogeneically sourced BMP complex, thereby improving the performance of human sourced DBM.

Disclosures: N. Duneas, Altis Biologics 2, 4.

This study received funding from: National Research Foundation, RSA.

M174

Oxidative Stress Suppresses Osteoblastogenesis by Antagonizing Wnt/ β -catenin and BMP Signaling. M. Almeida, E. Ambrogini, L. Han, M. Martin-Millan, V. Lowe*, A. Warren*, R. L. Jilka, S. C. Manolagas. Center for Osteoporosis and Metabolic Bone Diseases, University of Arkansas for Medical Sciences and Central Arkansas Veterans Healthcare System, Little Rock, AR, USA.

Increased levels of reactive oxygen species (ROS) in aging female or male C57BL/6 mice are temporally associated with progressive loss of bone strength and mass, decreased osteoblast (Ob) number and bone formation rate and increased Ob and osteocyte apoptosis. Moreover Axin2 and OPG mRNA expression is decreased and GADD45 is increased in the bone of old as compared to young C57BL/6 female mice, consistent with compelling in vitro evidence that ROS attenuate Wnt/ β -catenin signaling by diverting β -catenin from TCF- to FOXO-mediated transcription. To test directly the hypothesis that increased oxidative stress decreases osteoblastogenesis, 5 month-old C57BL/6 mice were injected intraperitoneally twice daily (5 days a week) for a total of 6 weeks with 2 mM / Kg of L-buthionine-(S,R)-sulphoximine (BSO), a specific inhibitor of glutathione synthesis. Additionally, 20 mM of BSO was provided in their drinking water. At the end of the experiment, several markers of oxidative stress were determined along with osteoblastogenesis. ROS levels increased and glutathione reductase activity decreased in the bone marrow, while p66^{bc} phosphorylation increased in vertebral lysates, in mice treated with BSO as compared to saline treated controls. Moreover, BSO treatment promoted a decrease in osteoblastogenesis as measured by the number of colony forming units-osteoblasts in ex vivo bone marrow cultures. In addition, treatment of C2C12 cell with H₂O₂ for 24 h inhibited osteoblastogenesis induced by Wnt3a, as measured by alkaline phosphatase (AP) activity. Furthermore, overexpression of a plasmid encoding FOXO3a abrogated AP activity induced by Wnt3a. Conversely, silencing FOXOs using siRNA for FOXO 1, 3a, and 4, up-regulated the basal levels of AP activity. Activation of osteoblastogenesis induced by BMP-2 was also blocked by exposure of C2C12 cells to H₂O₂ for 24 h. This effect was associated with abrogation of BMP-2 induced Smad1/5/8 phosphorylation by H₂O₂ as determined by Western blotting. Taken together with evidence that the replication of mesenchymal stem cell progenitors of osteoblasts is decreased in old as compared to young mice, presented elsewhere in this meeting, these results strongly support the hypothesis that aging, and specifically oxidative stress, decreases osteoblastogenesis and thereby bone formation by antagonizing Wnt/ β -catenin and BMP-signaling.

Disclosures: M. Almeida, None.

M175

Evaluation of Bone Phenotype in Mice Carrying Adenomatous Polyposis Coli (APC^{min}) Gene Mutation. Q. Su¹, S. Pun¹, B. Pennypacker¹, C. Winkelmann², O. A. Flores¹, H. Glantschnig¹, D. B. Kimmel¹, F. Chen¹.

¹Molecular Endocrinology, Merck Research Laboratories, West Point, PA, USA, ²Imaging, Merck Research Laboratories, West Point, PA, USA.

The identification of LRP5 mutations that are associated with high or low bone mass in humans has triggered great interest in studying Wnt signaling in bone formation. Current information clearly demonstrates that the canonical Wnt/ β -catenin pathway plays a crucial role in regulating bone mass. Reducing the inhibitory effects of Wnt-signaling antagonists

like Dkk1, SFRP1 or SOST which indirectly increase β -catenin in the nucleus has been shown to increase bone mineral density (BMD). LiCl inhibition of glycogen synthase kinase-3 β which stabilizes β -catenin was also reported to increase BMD in mice and humans by a mechanism that is likely independent of membrane Wnt signaling. Heterozygous mice with APC loss of function gene mutation (APC^{min/+}) also have high levels of nuclear β -catenin. In this study, we investigated the bone phenotype in APC^{min/+} mice by evaluating bone mass and genes related to bone function in comparison to wild type (wt) controls.

BMD of wt and APC^{min/+} mice femurs at 9 weeks and 16 weeks were measured using PIXIMUS. Tibia RNA samples from the above mice were analyzed for gene expression via Taqman.

At 9 weeks of age, no difference in BMD between wt and APC^{min/+} mice was detectable in the distal or central femur. However, at 16 weeks of age, BMD in the distal femur was significantly increased by 5% in APC^{min/+} mice vs. the wt controls (P-value of 0.0107). Gene expression studies of bone (tibia) samples from 9-week old mice showed that both Dkk1 and SOST expression levels were ~7 folds higher in APC^{min/+} mice compared to wt-control. This could indicate negative regulatory feedback mechanism to counter a constitutively active APC mutation. In addition, markers for osteoblast function COL1A1, ALP, OC and osteoclast function OPG, TRACP5, CatK were all ~2 - 4 folds increased in tibia of APC^{min/+} mice. This effect was transient as at 16 weeks of age differences in the above genes between wt and APC^{min/+} were insignificant, with the exception of SOST transcript levels which remained slightly elevated (~2 folds).

In conclusion, increased β -catenin activity derived from APC^{min} locus results in subtle but measurable change in BMD at discrete skeletal sites. Constitutive cytoplasmic Wnt pathway activation resulted in a transient increase in bone cell activities.

Disclosures: F. Chen, Merck Research Laboratories 1, 3.

M176

See Sunday Plenary Number S176

M177

Is Erythropoietin a Regulator of Bone Density and Serum Calcium in Elderly Men? - Mr Os Sweden. M. Ethnérsson¹, U. Lerner², H. Nilsson-Ehle³, H. Wadenvik³, M. Lorentzon¹, M. Karlsson⁴, Ö. Ljunggren⁵, E. Orwall⁶, U. Smith³, C. Ohlsson¹, D. Mellström¹. ¹Center for Bone research at the Sahlgrenska Academy, Göteborg University, Göteborg, Sweden, ²Oral Cell Biology, Umeå University, Umeå, Sweden, ³Medicine, Göteborg University, Göteborg, Sweden, ⁴Orthopedics, Lund-Malmö University, Malmö, Sweden, ⁵Medical Sciences, Uppsala University, Uppsala, Sweden, ⁶Bone and mineral Unit, Oregon Health and Sciences University, Portland, OR, USA.

Erythropoietin (EPO) is the main regulator of the erythropoiesis. Erythrocytes and osteoclasts are derived from the same hematopoietic stem cell. With increasing age there is a decline in haemoglobin resulting in an increasing EPO. The aim of the present study is to investigate if erythropoietin, EPO, is related to bone density and serum calcium in elderly men in the Göteborg part of the Mr Os Sweden cohort (n=1010, age 69-80).

Haemoglobin (Hb), EVF and white blood cell count were analyzed in 1010 men between 69-80 years of age. Blood samples were drawn after 10 hours of fasting and non-smoking in the morning. Serum and plasma were placed in a 80°C freezer. Plasma erythropoietin was analyzed with an ELISA method Quantikine IVD, R & D system, Inc, Minneapolis in 980 men. Bone density was measured with a Hologic 4500A.

Mean plasma EPO was 11,51 (9,1) IU/L. We found that EPO inversely correlated to Hb r = -0,324 (p < 0,0001) and EPO increased with age, r = 0,11 p < 0,001. EPO directly correlated to all bone mineral density (BMD)-sites (p < 0,001) and to PTH r = 0,18 (p = 0,0001) and indirectly to serum calcium r = -0,13 (p < 0,001). EPO correlated indirectly to lung function (FEV1,0) and renal function (cystatin C) but also directly to inflammatory parameters IL-6 and CRP (p < 0,001) but not to vitamin D, phosphate or sex hormones.

Height, weight, age, Hb, kidney function, PTH, vitamin D, phosphate were included in regression models for bone mineral density (BMD). EPO was an independent predictor of Hip total BMD β = 0,123, p < 0,001, trochanter BMD β = 0,108, p < 0,001, femoral neck β = 0,143 p < 0,0001 and lumbar spine BMD β = 0,0701 p < 0,05.

A multiple regression model with EPO, PTH, age, phosphate, albumin and cystatin C showed that EPO was an independent predictor of serum calcium β = -0,08 p < 0,01. A multiple regression model with EPO, serum calcium, albumin, phosphate, age, cystatin C showed that EPO was an independent predictor of PTH β = 0,119 (p < 0,0001).

In conclusion we found an inverse correlation between EPO and Hb and EPO increases with age. EPO correlated directly to bone mineral density at all sites and to PTH and indirectly to serum calcium even after multiple regression models taking in consideration several possible covariates. These novel findings indicate that EPO might be involved in the regulation of BMD and calcium metabolism in elderly men.

Disclosures: M. Ethnérsson, None.

M178

FGF2 and TGFβ1 Have Opposite Effects on the Mural Cell Phenotype of CD146⁺ BMSCs. A. Funari^{*1}, S. Michienzi^{*2}, B. Sacchetti^{*3}, S. Cersosimo^{*3}, M. Riminucci^{*1}, P. Bianco². ¹Experimental Medicine, University of L'Aquila, L'Aquila, Italy, ²Experimental Medicine and Pathology, University of La Sapienza, Rome, Italy, ³Fondazione Parco Biomedico S.Raffaele, Rome, Italy.

CD146⁺ Bone Marrow Stromal Cells (BMSC) include skeletal stem cells and are closely associated with sinusoids either in human bone marrow (hBM) and in heterotopic ossicles. Factors regulating proliferation and differentiation of CD146⁺ BMSC are unknown. In this work, we analyzed the effects of FGF2 and TGFβ1 on CD146⁺ BMSC morphology, proliferation and gene expression. Furthermore, we investigated the pattern of expression of FGF2 and TGFβ1 in the ossicle as compared to human bone. FGF2 stimulated BMSC proliferation and downregulated most mRNAs characteristic of mural cell phenotype, including: α-SMA; caldesmon 1; calponins; desmin; PDGF-R beta; basement membrane proteins such as SMOC1 and COL4A1. Of note, FGF2 treatment upregulated VEGF, that promotes cell migration and inhibits apoptosis and a group of sphingosine-1-phosphate receptors including EDG1 that is involved in endothelial cell differentiation and in the proliferative and migratory response of mural cells. All these genes were oppositely regulated by TGFβ1, which stabilizes mural cells and nascent vessels. In the hBM, FGF2 and TGFβ1 are produced by connective tissue cells, embedded in the matrix and either released upon matrix degradation, or activated by proteases (TGFβ1). To assess the expression of the two factors during ectopic osteogenesis, heterotopic ossicles were generated by BMSC transplantation in SCID mice and harvested at different time points. Immunohistochemistry was performed by using antibodies against FGF2, TGFβ1, activated TGFβ1 and human mitochondria antigen. As in the hBM in vivo, in the ossicle either FGF2 and TGFβ1 were expressed in mesenchymal and osteoblastic cells in the developing marrow space. High levels of immunoreactivity for TGFβ1 were also observed in marrow adipocytes which derive from adventitial reticular cells. Active TGFβ1 was not observed in the cell types immunoreactive for the latent form and was specifically detected in a peri-sinusoidal location and in the nascent bone. This result is consistent with its extracellular activation. In conclusion, we have shown that CD146⁺ BMSCs have a mural phenotype in vivo and in vitro and that is strengthened by TGFβ1 and downregulated by FGF2. Both factors are expressed in the ossicle with the same spatial layout observed in post-natal human trabecular bone. The activation of TGFβ1 is detected at the sites of pericyte-endothelial contact where active TGFβ1 induces the expression of SMC/pericyte markers by mesenchymal cells and inhibits proliferation of ECs.

Disclosures: A. Funari, None.

M179

See Sunday Plenary Number S179

M180

Demonstration of an Anabolic Effect of Prostaglandin E₂ on Bone in CD-1 Mice. Q. Gao^{*}, M. Xu, P. Zhan^{*}, C. B. Alander^{*}, C. C. Pilbeam, L. G. Raisz. Endocrine Division and Musculoskeletal Institute, University of Connecticut Health Center, Farmington, CT, USA.

Previous studies have shown that treatment with prostaglandin E₂ (PGE₂) can lead to increased bone resorption and bone loss in C57BL/6 mice. However, dynamic histomorphometric analyses in these mice showed that osteoblast function was also stimulated, as indicated by increased mineral apposition rate (MAR) and bone formation rate (BFR/BS). To determine if there can be a true anabolic effect of PGE₂ on bone in mice with an appropriate dose and duration of treatment, 9 week old CD-1 male and female mice were injected intraperitoneally with vehicle or PGE₂ (3 mg/kg, 2 times a week for 4 weeks) and euthanized 5 days after the last injection. Body weight, serum calcium and total protein were not significantly changed between vehicle and treatment groups. By dynamic histomorphometric analysis of distal femurs, PGE₂ treatment in both gender groups showed an increase in MAR compared to vehicle treated animals (1.44 ± 0.01 vs. 1.03 ± 0.07 μ/d in males and 2.04 ± 0.04 vs. 1.31 ± 0.27 μ/d in females, n=5-6, p<0.05). BFR/BS was also increased in both males and females (0.52 ± 0.06 vs. 0.27 ± 0.05 μ³/μ²/d in males and 0.74 ± 0.05 vs. 0.38 ± 0.10 μ³/μ²/d in females, p<0.01). Double labeled surface was similar in vehicle treated males and females, and increased significantly from 13.7 % to 26.6 % with PGE₂ treatment. In contrast to previous experiments, there was no loss of trabecular bone volume (BV/TV) in males treated with PGE₂ and there was a trend for an increase in females (3.4 vs. 6.2 % p=0.06). Tibial mRNA was collected at the end of the experiment. Samples were reverse transcribed and RQ values for mRNA calculated by real time PCR. There was an increase in BMP-2 expression in the PGE₂ treated group compared to vehicle (1.45 ± 0.16 vs. 0.99 ± 0.12, p<0.05, n=11-12, pooled male and female data). RUNX-2 expression was also increased in the PGE₂ treated group (1.19 ± 0.11 vs. 0.91 ± 0.06, p<0.05). These results indicate that an anabolic response to PGE₂ treatment can be obtained in mice. This model can be used to study the effects of PGE₂ or selective agonists, as well as the effects of deletion of COX-2 or prostaglandin receptors, on the murine skeleton.

Disclosures: Q. Gao, None.

This study received funding from: 5R01AR018063-31.

M181

TNF-alpha/CCL3-5/CCR5 Cascade Mediates RANKL+ Cells Migration in Inflammatory Bone Resorption. G. P. Garlet^{*1}, C. R. B. Cardoso^{*2}, S. B. Ferreira^{*1}, C. E. P. Repeke^{*1}, M. J. Avila-Campos^{*3}, A. P. Campanelli^{*1}, J. S. Silva^{*4}. ¹Department of Biological Sciences, School of Dentistry of Bauru, São Paulo University -FOB/USP, Bauru - SP, Brazil, ²Department of Biochemistry and Immunology, School of Medicine of Ribeirão Preto, São Paulo University - FMRP/USP, Ribeirão Preto - SP, Brazil, ³Department of Biological Sciences, Institute of Biomedical Sciences - São Paulo University - ICB/USP, Bauru - SP, Brazil, ⁴Department of Biochemistry and Immunology, School of Medicine of Ribeirão Preto - FMRP/USP, Ribeirão Preto - SP, Brazil.

Inflammatory immune reactions in response to periodontopathogens are thought to protect the host against infection, but may trigger inflammatory bone resorption in periodontium, in a milieu characterized by high levels of the pro-inflammatory cytokine TNF-α and inflammatory cells expressing the osteoclastogenic factor RANKL. Thus, we examined the mechanisms by which TNF-α drives RANKL+ cells migration to bone resorption focus, and therefore modulates the outcome of A. actinomycetemcomitans-induced periodontal disease in WT and genetically modified C57BL/6 mice. Our results showed that TNF-αp55 deficiency results in significantly decreased levels of chemokines CCL3, 4 and 5, and RANKL (evaluated by ELISA), associated with a lower inflammatory infiltrate and less alveolar bone loss. Flow cytometry analysis demonstrate that majority (72%) of RANKL+ leukocytes in inflammatory infiltrate are T cells (CD3+), and that RANKL+ cells are also highly positive (61%) to CCR5, a receptor whose ligands include CCL3-5. Interestingly, CCL3-knockout mice presented a minor decrease in RANKL+CCR5+ cells and in bone loss. However, CCL3 knockout mice presented similar levels of CCL4-5 in the periodontal tissues than WT mice, suggesting a redundancy of these chemokines in determining CCR5+ cell migration. Conversely, the absence of CCR5 resulted in pronounced reduction in the number of leukocytes and RANKL+ cells, and decreased RANKL levels and bone loss, suggesting an important role for this chemokine receptor in the migration of RANKL+ leukocytes to inflammatory focus surrounding alveolar bone. Our results demonstrate a cytokine-chemokine(s)-chemokine receptor cascade involved in inflammatory bone resorption: TNF-α induces the expression of the chemokines CCR3-5, which mediates the chemoattraction of CCR5+RANKL+ cells to periodontal tissues, and consequently leads to bone resorption. Therefore, chemokines and their receptors are potential targets to therapeutic intervention in inflammatory bone diseases.

Disclosures: G.P. Garlet, None.

This study received funding from: FAPESP #06/00534-1.

M182

See Sunday Plenary Number S182

M183

Relationship of Serum Cytokines and Monocyte Gene Expression to Bone Mineral Density and Content in Postmenopausal Women. E. R. Gertz^{*1}, N. Silverman^{*1}, C. P. Kirschke^{*2}, J. W. Stewart^{*3}, L. N. Hanson^{*3}, L. Huang^{*2}, D. L. Alekel³, M. D. Van Loan². ¹Dept Nutrition, UC Davis, Davis, CA, USA, ²USDA, ARS, WHNRC, Davis, CA, USA, ³Dept Food Science and Human Nutrition, ISU, Ames, IA, USA.

The dynamic balance of bone formation and resorption can be influenced by cytokine and gene interactions. The purposes of our study were to 1) examine the relationships among inflammatory markers, monocyte gene expression, and bone mineral density (BMD) and content (BMC) and 2) determine the contributions of inflammatory markers and gene expression to BMD and BMC in healthy postmenopausal women not taking hormones. Serum samples were obtained from a subsample of 81 women who were enrolled in a 3-yr clinical trial. BMD and BMC from the lumbar spine, total hip, and femoral neck were assessed by dual energy x-ray absorptiometry. Inflammatory markers were: cortisol, IL-1, IL-4, IL-6, IL-7, IL-8, INF-γ, G-CSF, GM-CSF, and TNF-α. Serum cytokines were measured by a cytokine multiplex immunoassay (LINCplex; Millipore). Quantitative PCR was performed on a PRISM ABI 7900HT Sequence Detection System using TaqMan Assay-on-Demand kits for IFN-β, c-Fos, and β-Actin (Applied Biosystems). Genes were quantitated by an absolute standard curve method and normalized to the expression of β-Actin. Cytokine and gene expression data were transformed for normality. We observed a negative association between femoral neck BMC with TNF-α (p<0.05) and a positive association with cortisol (p<0.05). Total hip and femoral neck BMDs were associated with c-Fos gene expression (p<0.05 and p<0.01, respectively). Gene expression of IFN-β was found to be significantly and negatively associated with femoral neck BMC (p<0.05). The contribution of inflammatory markers and gene expression to BMD and BMC was examined using stepwise multiple regression: Total hip BMC=16.294 + 0.446(weight) - 0.879(BMI) + 1.137(c-Fos) Total hip BMD=0.61 + 0.002(weight) + 0.021(c-Fos) Femoral neck BMC=4.075 + 0.013(weight) - 0.181(IFN-β) - 0.384(TNF-α) Femoral neck BMD=0.312 + 0.002(weight) + 0.027(c-Fos) + 0.006(Cortisol) + 0.007(IL-6) In conclusion, c-Fos, IFN-β, TNF-α, cortisol, and IL-6 were significant contributors to hip and femoral neck BMC and BMD and may be important factors in bone health for postmenopausal women. Supported by funds from NIAMS/NIH (AR046922) and USDA,ARS,WHNRC.

Disclosures: E.R. Gertz, None.

M184

Epigenetic Mechanisms Are Involved in the Cytokine-induced de novo Expression of IL-1 beta in Human Articular Chondrocytes In Vitro. K. Hashimoto^{*1}, S. Kokubun^{*1}, E. Itoi¹, H. I. Roach². ¹Department of Orthopaedics, Tohoku University, Sendai, Japan, ²Bone & Joint Research Group, University of Southampton, Southampton, United Kingdom.

Inflammatory cytokines, such as IL-1 β , TNF- α and oncostatin M (OSM), induce abnormal expression of proteases in articular chondrocytes in vitro, analogous to the cytokine-induced abnormal expression in OA chondrocytes in vivo. Previous studies had shown that the latter was associated with loss of DNA methylation (Arthritis & Rheumatism 52:3110-3124) at specific CpG sites in the relevant promoters. DNA methylation at crucial CpG sites usually silences the gene and is replicated during cell division by the maintenance methyl transferase DNMT1. Since loss of methylation is a pre-requisite for gene induction, we hypothesized that the cytokines-induced IL-1 β expression also included DNA de-methylation. Human chondrocytes, isolated from the femoral articular cartilage of six non-OA patients, did not express proteases, IL-1 β or TNF- α , but did express collagen II, aggrecan and DNMT1. The cells from each patient were divided into 5 groups: non-culture; no additions (cultured control); + IL-1 β (10ng/ml); + 5-aza-deoxycytidine (5-aza-dC, 2 μ M); + TNF- α (10ng/ml) combined with OSM (10ng/ml). 5-aza-dC is a non-specific de-methylation agent, which was used for comparison with the effects of cytokines. After 4-5 weeks of culture, mRNA expression and the % of DNA methylation at -289bp were quantified, after initial studies had identified this CpG site to be of crucial importance.

Before culture, 60-66% of cells were methylated, i.e. only 40% of the cells could theoretically respond to inductive factors. However, complete absence of IL-1 β expression suggested that the right inductive factors were not present in these non-OA chondrocytes. Culture per se induced slight expression (set to 1) and some loss of methylation (30-40% still methylated). As expected, 5-aza-dC caused a further 20% loss of methylation, but this corresponded only to a 4-8 fold induction of expression. Remarkably, IL-1 β induced its own expression with a 15-190 fold increase and only 4-25% of cells remaining methylated. However, the greatest effect was seen with the combined TNF- α /OSM treatment, which increased IL-1 β expression 300-1700 fold and abolished methylation. Expression of DNMT1 was reduced considerably by culture alone, but further by cytokine treatment. This study is the first to correlate quantitatively mRNA expression and loss of DNA methylation. The results suggest that inflammatory cytokines are able to cause de-methylation, which leads to increased transcription. The challenge for the future will be to determine the mechanisms of the cytokine-induced loss of DNA methylation.

Disclosures: K. Hashimoto, None.

M185

See Sunday Plenary Number S185

M186

Identification of TNF- α Shedding Enzyme in Macrophages. A. Hikita¹, R. Suzuki^{*1}, S. Tohma^{*1}, S. Tanaka^{*1}, N. Fukui^{*1}. ¹Clinical Research Center, National Hospital Organization Sagami Hospital, Kanagawa, Japan, ²Orthopaedic surgery, The University of Tokyo, Tokyo, Japan.

Tumor necrosis factor- α (TNF- α) is a cytokine that plays pivotal roles in the pathologies of various inflammatory diseases such as rheumatoid arthritis and Crohn's disease. TNF- α is first synthesized as a membrane-bound protein, and converted into a soluble form by proteolytic cleavage. These two forms are shown to bind to two TNF receptors with different affinities to exert different biological activities. A disintegrin and metalloproteinase 17 (ADAM17), which is also known as TNF- α converting enzyme (TACE), is considered to be a primary sheddase for TNF- α . However, the significance of this enzyme in macrophages is not fully investigated while macrophages are the primary cells for TNF- α production in rheumatoid arthritis. Considering that the activity of TNF- α differs between the membrane-bound form and the soluble form, it is important to identify the sheddase(s) for TNF- α in macrophages.

In order to identify the sheddase(s), we developed an assay system using a plasmid containing cDNA for secreted placental alkaline phosphatase (SEAP) fused with the cDNA coding the stalk region of mouse TNF- α . The TNF- α -SEAP plasmid was transfected into HEK293 cells together with the expression vectors for various matrix metalloproteinases (MMPs) (MMP-1, 2, 3, 7, 9, 11, 13, 19, 23, 28, MT1, 2, 3, 4, 5, 6-MMP) and ADAMs (ADAM9, 10, 17, 19), and the TNF- α shedding activity of these proteinases was detected as alkaline phosphatase activity in the culture media. In this assay, ADAM9, 10, 17, MMP7, MT1, 2, and 3-MMP showed shedding activities for TNF- α . Among these proteinases, the expression of ADAM9, 10, 17 and MT1-MMP was detected at substantial levels in mouse macrophages by real-time PCR. Then the plasmids for these proteinases were transfected to 293 cells together with a full-length TNF- α expression vector, and the occurrence of shedding was evaluated by the appearance of soluble TNF- α in the culture media, which was detected by Western blotting. As predicted by the TNF- α -SEAP system, the occurrence of shedding was observed with all four proteinases with the full length TNF- α . Among these proteinases, suppression of ADAM10 by siRNA resulted in a significant reduction in the TNF- α shedding.

These results suggest that, besides ADAM17, ADAM10 also works as a dominant sheddase for TNF- α in macrophages. The results also suggest that other proteinases such as ADAM9 and MT1-MMP can be the sheddases for TNF- α , depending on the biological situations. It may be notable that several other proteinases can take the place of ADAM17 as a sheddase for TNF- α .

Disclosures: A. Hikita, None.

M187

Lysophosphatidic Acid Promotes Maturation and Survival in Rat Growth Plate Chondrocytes. J. L. Hurst-Kennedy^{*1}, J. Greene^{*2}, Z. Schwartz², B. D. Boyan². ¹School of Biology, Georgia Institute of Technology, Atlanta, GA, USA, ²Department of Biomedical Engineering, Georgia Institute of Technology, Atlanta, GA, USA.

The bioactive phospholipid metabolite lysophosphatidic acid (LPA) has been implicated in a number of cellular processes including wound healing, smooth muscle contraction, cell proliferation, survival, and migration. Recent studies have shown that LPA is a potent stimulator of osteoblast maturation as well. LPA is derived from phosphatidic acid (PA), which is produced by the action of phospholipase D (PLD). One physiological regulator of PLD in growth plate cartilage cells is the vitamin D metabolite 24,25-dihydroxyvitamin D3 [24R,25(OH)₂D₃]. When resting zone chondrocyte cultures are treated with 24R,25(OH)₂D₃, PLD activity is increased, resulting production of diacylglycerol (DAG), as well as increased PKC activity, increased cellular maturation and increased cell survival. DAG is a metabolite of LPA, suggesting that LPA acts as a second messenger during the promotion of chondrocyte differentiation and survival in growth plate cartilage cells. The purpose of this study was to determine if chondrocytes produce LPA and if so, whether LPA signaling mediates chondrocyte maturation and survival and the mechanisms involved. To investigate this, we used resting zone chondrocytes isolated from the rat costochondral cartilage growth plate as a model system. 24R,25(OH)₂D₃ treatment regulated LPA production in a dose-dependent manner. These cells were shown to express the LPA receptors LPA1, LPA3, LPA5, and peroxisome proliferator-activated receptor gamma (PPAR- γ). LPA treatment also promoted an increase in two markers of chondrocyte differentiation: alkaline phosphatase activity and proteoglycan sulfation. Furthermore, apoptosis induced by phosphate and the protein kinase C (PKC) inhibitor chelerythrine was attenuated by LPA. Western Blot analysis indicated that LPA decreased the abundance of the tumor-suppressor protein p53. LPA treatment regulated the expression of the p53-target genes Bcl-2 and Bax to enhance cell survival. Collectively, these data suggest that LPA signaling promotes cellular maturation and survival in resting zone chondrocytes demonstrating a novel function of LPA signaling in 24R,25(OH)₂D₃-mediated chondrogenesis.

Disclosures: J.L. Hurst-Kennedy, None.

This study received funding from: Children's Healthcare of Atlanta Pediatric Hospital.

M188

Continuous Infusion of Insulin-like Growth Factor-I into the Epiphysis of the Tibia. A. Abbaspour, S. Takata, Y. Matsui, M. Takahashi^{*}, S. Katoh^{*}, N. Yasui^{*}. The Department Of Orthopedics, The University of Tokushima, Tokushima, Japan.

We have developed a method to promote longitudinal bone growth at the level of a specific growth-plate in young rabbits. Twenty-four male young rabbits weighing about 500 grams were divided into three groups, one-week treatment of IGF-I (n=5), two-week treatment of IGF-I (n=5), and four-week treatment of IGF-I (n=14). Insulin-like growth factor-I was continuously infused by means of an osmotic pump into the bone marrow cavity of the proximal epiphysis of the left tibia. In the epiphysis of right tibia, normal saline was infused continuously as a control. Longitudinal growth of the tibia was monitored by weekly-taken soft X-ray. After 4 weeks of treatment, the animals were sacrificed for histological examination and peripheral QCT (pQCT) analysis. Radiological measurement showed a 2-mm overgrowth of the tibia after 4 weeks of treatment, while histological analysis demonstrated a 15% increase in the thickness of the selected growth-plate. The local infusion of IGF-I increased the numbers of both proliferative and hypertrophic chondrocytes and promoted hyperplasia of bony trabeculae within the epiphysis. Bone mineral density (BMD) at the proximal metaphysis of the tibia was also significantly higher in both 2 weeks and 4 weeks treatment of IGF than in control sides. The distribution of material infused locally into the epiphysis was simulated by the infusion of Indian ink using the same methodology (osmotic pump) as that for IGF-I. Most of the dye remained within the bone marrow cavity of the epiphysis, but a portion infiltrated into the growth-plate, reaching the deep layer of the physal chondrocytes and primary spongiosa of the metaphysis. These results suggest that the method reported here is a valid one for delivering cytokines or growth factors to the selected growth-plate and for controlling the growth and differentiation of physal chondrocytes.

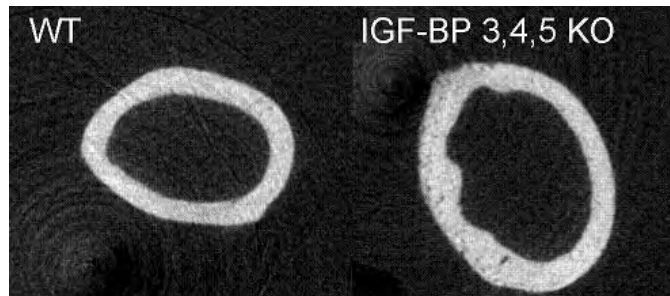
Disclosures: A. Abbaspour, None.

M189

IGF-Binding Protein 3, 4 and 5 Triple Knock-out Mice Have Larger Bones. B. M. Boudignon^{*1}, M. Qin^{*2}, J. Pintar^{*2}, B. P. Halloran¹. ¹Endocrine unit, Veteran Affairs Medical Center San Francisco, San Francisco, CA, USA, ²Department of Neuroscience and Cell Biology, University of Medicine and Dentistry of New Jersey, Piscataway, NJ, USA.

IGF-I, the most abundant growth factor in the bone microenvironment, plays an important role in maintaining normal bone structure and mass. The activity of IGF-I is regulated by a family of IGF-binding proteins (IGF-BP 1-6). All 6 BPs have crucial roles in association with IGF-I and in some cases can modulate cell metabolism independent of IGF-I. Animals (C57BL6/129ReJ mixed background) harboring targeted defects in IGF-BP-3,4,5 have been developed and provide a unique opportunity to study the role of these BPs in metabolism and whole animal physiology (Ning et.al, Mol. Endo., 20:2173, 2005).

Triple KO animals are slightly smaller and have reductions in serum total and bioactive IGF-I of 55% and 63%, respectively. To study the role of BP-3,4,5 in bone we examined bone structure and density in wild type and triple KO mice using microCT analysis. Femurs from triple KO animals were longer, and tissue volume of the secondary spongiosa in the distal femoral metaphysis was increased by more than 30%. Fractional bone volume and segmented bone mineral density remained unchanged. Tissue, bone and marrow volumes of the femoral midshaft were all significantly increased by nearly 20% whereas bone fraction remained unchanged. Whereas the endocortical surface of the femoral diaphysis in wild type animals displayed a smooth curvature, the surface in the triple KO mice was irregular and wavy (see fig.) These results suggest that the combined global loss of BP-3,4,5 results in an increase in bone size (length, volume and diaphyseal diameter) but proportionately with normal bone volume despite low serum IGF-I and reduced body weight.



Disclosures: B.M. Boudignon, None.

M190

In Vivo Models To Study IGF-1 Receptor Dynamics Of Bone Stem Cells. B. C. Bragdon^{*1}, K. Young^{*1}, L. G. Horton^{*2}, R. Gundersen^{*1}, C. J. Rosen^{*2}, A. Nohe¹. ¹University of Maine, Orono, ME, USA, ²Jackson Laboratory, Bar Harbor, ME, USA.

Insulin-like Growth Factor- I (IGF-I) is a critical peptide in skeletal growth and consolidation. In detail IGF-I is key in the differentiation of bone marrow stromal cells (BMSCs) into osteoblasts. Current research indicates that localization of the IGF-I receptor in specific regions of the membrane does effect the specificity of signaling. However research is lacking the correlation between membrane domain dynamics, osteoblast differentiation and osteoporosis. Using the Family of Image Correlation Spectroscopy (FICS) we showed that membrane domain dynamics are altered in bone marrow stromal cells derived from mice exhibiting an age related osteoporotic phenotype, B6.C3H-6T (6T). 6T contains the wild type C57BL/6J (B6) background with an inversion of a segment of chromosome 6. This inversion includes Ppar gamma. Ppar gamma is a key mediator of adipogenesis. The mouse also has low serum IGF-I and reduced bone density which is characteristic of age related osteoporosis. Using FICS we observed an increase in cluster density (number of clusters per unit area) of both the membrane domains and IGF-I receptors, while the percent of co-localization was unchanged in the BMSCs. Our data indicated that the receptors as well as the membrane domains reshuffle on the membrane. This shuttling is crucial for their function. Especially caveolae flask-shaped invaginations of the plasma membrane are effected. Utilizing reporter gene assays with reporters for major down stream signaling pathways we showed significant differences in IGF-I signaling in 6T mice versus control. Further our data showed that cholesterol content and lipid composition are altered in 6T mice measured by HPLC and cholesterol assays. These results point to the importance of lipid balance and cholesterol in IGF-I signaling. Our data indicated that membrane, receptor dynamics are affected in mice exhibiting an osteoporotic phenotype.

Disclosures: B.C. Bragdon, None.

M191

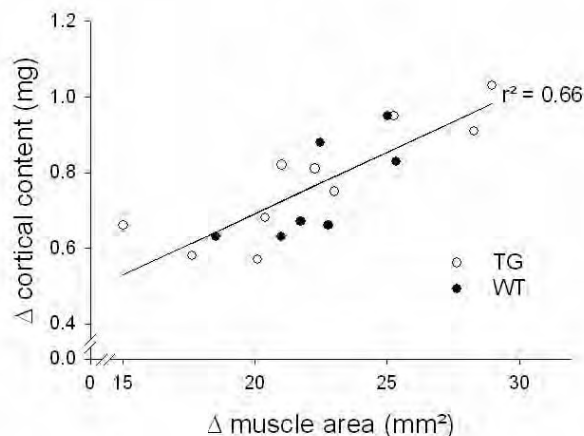
See Sunday Plenary Number S191

M192

Systemic IGF-I Shows Concerted Anabolic Actions on Bone and Muscle: Evidence from Male Mice with Liver-Specific Overexpression of IGF-I. F. Callewaert^{*1}, K. Venken^{*1}, J. Ophoff^{*1}, L. Liao^{*2}, S. Boonen¹, R. Bouillon¹, J. Xu^{*2}, D. Vanderschueren¹. ¹Katholieke Universiteit Leuven, Leuven, Belgium, ²Department of Molecular and Cellular Biology, Baylor College of Medicine, Houston, TX, USA.

Serum IGF-I is principally derived from the liver and stimulates not only bone but also muscle during growth. We questioned to what extent overexpression of IGF-I by the liver affects bone and muscle mass and how the changes in bone and muscle are interrelated. To answer this question, transthyretin (TTR)-IGF-I transgenic mice and controls were evaluated longitudinally. Tibial bone mineral density and whole-body composition were assessed weekly by in vivo pQCT and DEXA, respectively, until 16 weeks of age. Transgenic mice showed 21% higher serum IGF-I during the entire experiment ($p < 0.01$). The increased serum IGF-I level was accompanied by enhanced lean body mass (+7% vs.

controls, $p < 0.01$) and muscle cross-sectional area (+10% vs. controls, $p < 0.01$). In addition, cortical bone mass (but not trabecular bone mass) and strength strain index were 7% and 12% greater in transgenic mice, respectively ($p < 0.01$). Regression analysis was performed to assess the impact of hepatic IGF-I overexpression on cortical bone mass and bone strength in relation to changes in muscle mass. Cortical bone mass and bone strength were very strongly related to changes in muscle cross-sectional area in both transgenic and control mice ($p=0.0001$), as represented by the figure, which shows the relationship between changes (Δ in figure, week16 - week4) in cortical content and muscle cross-sectional area. Moreover, regression analysis showed that the difference in cortical bone mass and bone strength between transgenic and control mice did not persist after correction for changes in muscle mass so that changes in bone and muscle mass during growth were proportionate in transgenic mice versus control mice. In conclusion, our data indicate that systemic IGF-I shows significant and concerted anabolic actions on both bone and muscle.



Disclosures: F. Callewaert, None.

M193

Local Application of GH and IGF-I Have a Similar Effect on Intramembranous Bone Healing in a Rat Femur Osteotomy Model - A Comparative Study. M. Huening¹, T. Lindner^{*1}, A. Flyvbjerg^{*2}, W. Weichert^{*3}, M. Raschke^{*1}, H. Bail^{*1}. ¹Dept. of Trauma and Orthopaedic Surgery, Charité, Berlin, Germany, ²Medical Department (Diabetes and Endocrinology), Kommunehospital, University Aarhus, Aarhus, Denmark, ³Dept. of Pathology, Charité, Berlin, Germany.

Previous studies showed that systemic application of growth hormone GH stimulates bone and fracture healing. According to the "somatomedin-hypothesis" liver-derived IGF-I exerts this effect as the main endocrine transmitter of GH on physiological bone formation whilst the "dual-effector-theory" hypothesizes an additional direct effect of GH on longitudinal bone growth. To test these theories we performed an in-vivo study to elucidate the local effects of GH and IGF-I on callus formation.

A monolateral external fixator was mounted to the left femurs of 72 adult SD-rats followed by a standardized osteotomy creating a 0.3 mm gap. Three groups were created that received either GH, IGF-I or vehicle via mini-osmotic pumps with a tube routed to the osteotomy.

group I: phosphate buffer

group II: 100 µg/kg bodyweight/day IGF-I

group III: 100 µg/kg bodyweight/day rh-GH

Femurs of each group (n=8) were harvested after 7, 14 and 21 days and processed for histological and histomorphometrical analysis. Sections were stained and evaluated with a semi-quantitative histological score regarding bone formation and gap bridging at all time-points. In addition histomorphometrical measurement were performed after 21 days with an image analysis system.

While no difference for bone formation and gap bridging between groups was detectable after 7 days, scores appeared to be higher for groups II and III after 14 and 21 days with a significant higher score for group II compared to group I after 21 days.

Histomorphometry displayed a significant increase of callus area and mineralized callus area in groups II and III compared to group I. The cartilage area and the cartilaginous share were nearly doubled in the vehicle group compared to groups II and III. The structure of the callus, represented by the callus bone density and the callus diameter were not different between the three groups after 21 days.

In conclusion our study demonstrates that both, local application of GH and IGF-I increase hard callus formation in the process of bone healing. Moreover both agents change the callus composition towards a lower share of cartilage. The results also strongly suggest that GH exerts a direct, non-liver mediated effect on bone healing which is comparable to the effect induced by IGF-I. Our findings clearly support the hypothesis that the "dual-effector-theory" is not only applicable for longitudinal bone growth but also for intramembranous bone healing.

Disclosures: M. Huening, None.

This study received funding from: Deutsche Forschungsgemeinschaft (DFG Hu 876/1-1)

M194

Cortical Bone Is Positively Associated with Serum IGF-I and Testosterone and Negatively with Fibrinogen in Men and Women. K. L. L. Landin-Wilhelmsen¹, P. Trimpou^{*2}, S. Lindstrand^{*1}, A. G. Nilsson¹, A. Odén^{*2}, L. W. Wilhelmsen^{*2}. ¹Section for Endocrinology, Sahlgrenska University Hospital, Göteborg, Sweden, ²Sahlgrenska University Hospital, Institution of Medicine, Göteborg, Sweden.

Lower calcaneal ultrasound values predict fractures during follow-up. The purpose was to analyse factors of importance for the ultrasound variables in a random population sample of men and women aged 25-64 years, 54% women, from the 1995 World Health Organisation (WHO) MONItoring of trends and determinants in Cardiovascular disease (MONICA) study in Gothenburg, Sweden. The baseline examination in 1995 included history of fractures, physical activity at work and during leisure time, psychological stress, smoking habits, coffee consumption, BMI, blood pressure, total cholesterol, HDL-cholesterol, ApoA, ApoB, triglycerides, fibrinogen, CRP, IGF-I, IGFBP-1, IGFBP-3, osteocalcin, procollagen, estradiol, free estradiol, testosterone, free testosterone, PTH, procollagen, SHBG, and insulin. The calcaneal ultrasound (LUNAR Achilles) variables were: Stiffness, Speed Of Sound (SOS) and Broadband Ultrasound Attenuation (BUA). We have previously shown that leisure time physical activity was positively associated with calcaneal cortical bone. In the present analysis we analysed the additional influence of selected blood variables and hormones. The table shows number of individuals with results available (n), partial correlation coefficients [r] and p-values.

	Stiffness			SOS			BUA		
	n	r	p	n	r	p	n	r	p
Fibrinogen	546	-0.080	0.0618	543	-0.090	0.0360	542	-0.052	0.2269
IGF-I	348	0.170	0.0014	345	0.158	0.0032	344	0.131	0.0150
Testosterone	330	0.139	0.0114	327	0.162	0.0033	326	0.084	0.1302
Free testosterone	328	0.105	0.0575	325	0.128	0.0209	324	0.017	0.7607

All calcaneal ultrasound variables were associated with IGF-I, SOS and stiffness with testosterone, whereas SOS was negatively associated with fibrinogen. A more detailed analysis of relations to gender showed that testosterone was important for the ultrasound variables in both men and women.

In summary, out of a large series of hormones IGF-I and testosterone were positively associated with calcaneal cortical bone. Fibrinogen, indicating chronic inflammation, was negatively associated with cortical bone.

Disclosures: K.L.L. Landin-Wilhelmsen, None.

M195

The Role of IGF-I and IGFBP-1 Status and Secondary Hyperparathyroidism in Relation to Osteoporosis in Elderly Swedish Women. H. S. Salminen¹, M. Sää^{*2}, H. Ringertz^{*3}, L. Strenger^{*1}. ¹Centre for Family and Community Medicine, Karolinska Institutet, Huddinge, Sweden, ²Department of Endocrinology, Metabolism and Diabetes, Karolinska Institutet, Stockholm Sweden, Sweden, ³Department of Surgical Sciences, Institution of Diagnostic Radiology, Karolinska Institutet, Stockholm, Sweden.

Our aim was to investigate among elderly women the relationship to osteoporosis of calcium-regulating hormones and anabolic growth factors. A population-based cross-sectional study of 350 elderly women (mean age 73 years). Measurements of bone mineral density (BMD) of the left hip, lumbar spine and heel and risk markers for osteoporosis were studied. The BMD values showed significant inverse relationship with the values of insulin-like growth factor binding protein (IGFBP-1) at all sites of measurement and significant positive relationship with the values of insulin-like growth factor-I (IGF-I) at all sites with the exception of the lumbar spine. There was no significant association between the values of BMD and the values of 25-hydroxy vitamin D (25(OH)D). The use of loop diuretics was strongly and significantly associated with elevated levels of PTH (OR 4.4, P<0.001). The anabolic growth factors IGF-I and IGFBP-1 showed a stronger association with the BMD values than the calcium regulating hormones 25(OH)D and PTH. In this study the use of loop diuretics was a more important cause of secondary hyperparathyroidism than vitamin D status.

Analysis of regression between BMD, vitamin D, PTH and IGF-I and IGFBP-1

Variable	IGF-I slope	p-value	IGFBP-1 slope	p-value
BMI (kg/cm2)	-0.0010	0.79	-0.0505	<0.0001
BMD(g/cm2)				
neck	0.0572	0.001	-0.0557	<0.0001
total hip	0.0706	0.001	-0.0804	<0.0001
lumbar spine	0.0538	0.057	-0.0687	<0.0001
heel	0.0269	0.010	-0.0350	<0.0001
25-OH vitamin D (nmol/L)	0.0534	0.28	0.0392	0.66
PTH (pg/ml)	-0.0532	0.23	0.0015	0.99

Disclosures: H.S. Salminen, None.

M196

Opposing Effects of Growth Hormone and Alcohol on Bone Marrow Adiposity and Cancellous Bone Mass and Turnover Reveal a Critical Role for the Local Action of Growth Hormone in the Reciprocal Relationship between Adipocyte and Osteoblast Differentiation. R. T. Turner, P. J. Menaghy^{*}, G. Maddalozzo^{*}, U. T. Iwaniec. Nutrition and Exercise Sciences, Oregon State University, Corvallis, OR, USA.

Cancellous bone loss is accompanied by an increase in bone marrow adiposity. Adipocytes and osteoblasts are derived from a common progenitor cell, and adipocytes produce cytokines (e.g., IGF-I) and adipokines (e.g., leptin) which affect bone turnover. Thus, it is possible that the formation of fat and reduction in bone are regulated by a common factor. Excessive alcohol consumption is known to result in bone loss and marrow adiposity. We evaluated the effects of alcohol in a rat model in which the caloric intake of the animals fed the alcohol and control diets was the same. Alcohol consumption decreased % body fat and bone mass but increased bone marrow adiposity. Alcohol consumption reduced IGF-I mRNA levels in liver and bone, suggesting that growth hormone (GH) signaling may play a causal role in the observed reciprocal relationship between bone marrow adiposity and bone mass. We further investigated this relationship in hypophysectomized (HYPOX) rats. HYPOX of rapidly growing male rats reduced bone formation and led to cancellous osteopenia in tibiae. Despite a large reduction in body weight, there was a dramatic increase in bone marrow adiposity (from <1% to >50% marrow volume). Similar changes were observed in sexually mature male and female HYPOX rats. GH (0.8 mg/kg/d) normalized bone formation and bone mass, skeletal expression of IGF-I, and bone marrow adiposity in HYPOX rats. In contrast, administration of IGF-I (200 ug/kg/d) to HYPOX rats had no effect on either bone formation or adiposity, and administration of PTH (80 ug/kg/d) to HYPOX rats increased bone formation and increased the skeletal expression of IGF-I but had no effect on adiposity. To rule out estrogen deficiency as a contributing factor, we administered GH to: 1) HYPOX, 2) ovariectomized (OVX) + HYPOX and 3) estrogen-replaced OVX + HYPOX rats. In each case, GH was effective in reversing the effects of HYPOX on bone and adiposity. Taken together, these findings demonstrate that GH, a key hormone in the integration of energy production and expenditure, regulates the balance between bone and adiposity by enhancing bone formation and inhibiting adipocyte differentiation. Furthermore, the absence of a positive response to IGF-I treatment suggest that GH acts directly on osteoblasts and adipocytes.

Disclosures: R.T. Turner, None.

This study received funding from: NIH.

M197

Transforming Growth Factor β Stimulates New Bone Formation in Neonatal Mouse Calvariae via Suppression of Dickkopf-1. L. M. Bevelock^{*}, K. L. Clines^{*}, J. M. Chirgwin, T. A. Guise, G. A. Clines. Internal Medicine, University of Virginia, Charlottesville, VA, USA.

Wnt signaling is important in normal bone remodeling and the pathogenesis of bone metastases. The secreted Wnt inhibitor dickkopf-1 (DKK1) contributes to the dysregulation of bone formation in cancer metastases. Increased DKK1 in multiple myeloma is associated with osteolytic bone disease and suppressed bone formation, while tumor-produced endothelin-1 (ET-1) suppresses secretion of DKK1 from osteoblasts, contributing to the abnormal new bone formation associated with osteoblastic metastases. However, little is known about the local control of DKK1 expression. We hypothesized that the Dkk1 promoter in osteoblasts is regulated by TGF β , a factor abundant in the bone microenvironment.

We first examined regulation of Dkk1 transcription by TGF β . C3H10T1/2 pre-osteoblastic cells were transfected with a Dkk1 promoter/luciferase construct and treated with 5ng/ml TGF β , which decreased promoter activity threefold (p=0.04). TGF β significantly inhibited DKK1 protein secretion from neonatal mouse calvariae at 2d and 4d, as determined by ELISA. This was associated with an increase in new bone formation, osteoblast number and osteoblast nuclear phosphoSmad2 staining compared to control (p<0.001). Recombinant DKK1 protein (50 ng/ml) blocked TGF β -stimulated new bone formation (p<0.001). TGF β treatment of neonatal calvarial mouse osteoblasts increased β -catenin nuclear staining, indicating activation of canonical Wnt signaling.

TGF β can signal via Smad-dependent and -independent pathways. We mutated two putative Smad-binding elements (SBEs) within the Dkk1 promoter and transfected mutant and wild-type promoters into C3H10T1/2 cells. Mutation of the individual SBEs did not reverse TGF β repression of Dkk1 transcription, suggesting a possible Smad-independent mechanism.

Our data from cells and calvarial organ cultures contrast with previous studies in whole animals, where inhibition of TGF β signaling increases osteoblast activity and bone mass. In solid tumor metastases to bone, TGF β is released from the bone matrix by osteoclastic bone resorption, and promotes metastases by stimulating tumor cell production of pro-metastatic factors. The paradoxical stimulation of calvarial organ cultures suggests that effects of TGF β on bone are context-dependent. In calvariae ex vivo TGF β can stimulate bone formation by suppressing DKK1 and activating Wnt signaling through Smad-dependent and -independent mechanisms. Further studies are needed to elucidate the context-dependent effects of TGF β on osteoblast function and the role of DKK1.

Disclosures: L.M. Bevelock, None.

M198

NF- κ B-Regulated Gene Expression and Kinase Phosphorylation Oscillate Rapidly Over Time. J. Iqbal*, L. Sun, M. Zaidi. Mount Sinai Bone Program, Department of Medicine, Mount Sinai School of Medicine, New York, NY, USA.

For the first time, we show that the expression of any eukaryotic gene, in our case NF- κ B regulated genes, and kinase phosphorylation oscillate with time. The closest to this paradigm is gene expression phasicity noted over days, not over hours, as we describe. Our fundamental observation is that TNF α -induced mRNA expression is dynamic, undergoing rapid oscillations over hours. Expression of the "early genes" c-fos and IL-6 was enhanced transiently within 30 minutes of TNF- α application. Expression of "late genes", namely Mn-SOD and RANTES genes was oscillatory beginning 3 hours post-TNF α . A third group, "continual genes", namely IkB α , A-20 and MIP-2 α showed robust induction, but unlike c-fos and IL-6, continued to display oscillations over 8 hours. We also show that, whereas the early oscillatory profiles induced by TNF α and RANK-L can almost be superimposed, "continual genes" failed to oscillate after 4 hours of RANK-L. These results indicate that TNF superfamily members not only trigger a distinct pattern of oscillations for different gene groups, but that oscillatory behavior is ligand-specific. Second, we found that the phosphorylation of signalling molecules was dynamic, with parallel, but distinct, waves of activation. Intracellular phospho-flow cytometry showed that p65, JNK and p38 phosphorylation oscillated for up to 8 hours, while ERK1/2 displayed a single wave. The only period where all four molecules displayed an overlapping phosphorylation was during the first signaling wave. Furthermore, p38 and p65 phosphorylation were in unison. However, their oscillations were slower than JNK1/2 phosphorylation within the first 3 hours, but at 4 hours, the three became aligned. Finally, we showed that a super-repressor of IkB α altered the amplitude and frequency of kinase phosphorylation. The amplitude of JNK phosphorylation was increased and oscillation frequency altered. ERK1/2 phosphorylation was converted from a monophasic to oscillatory frequency in unison with JNK for the first 3 hours. ERK1/2 did not show any appreciable phosphorylation after 4 hours, while JNK1/2 phosphorylation continued to oscillate. These latter results suggest that NF- κ B negatively modulates both the amplitude and frequency of JNK and ERK1/2 phosphorylation. In conclusion, we show that TNF superfamily members induce robust ligand-specific oscillations in NF- κ B regulated genes and phosphorylation of downstream kinases. This constitutes a novel paradigm through which cells can use multiple signaling molecules to coordinate gene expression and so regulate time-resolved physiological processes, such as chemokine and cytokine secretion.

Disclosures: J. Iqbal, None.

M199

New Insights into the Determination of Smads Signaling by TGF β Superfamily. B. Kim*, J. Lee*, H. Park*, S. Lee*, M. Lee*, H. Koo*, W. Yoon*, J. Kim*, H. Ryoo*, J. Cho*. ¹Biochemistry, School of Dentistry, Kyungpook National University, Daegu, Republic of Korea, ²Department of Cell and Developmental Biology, School of Dentistry, Seoul National University, Seoul, Republic of Korea.

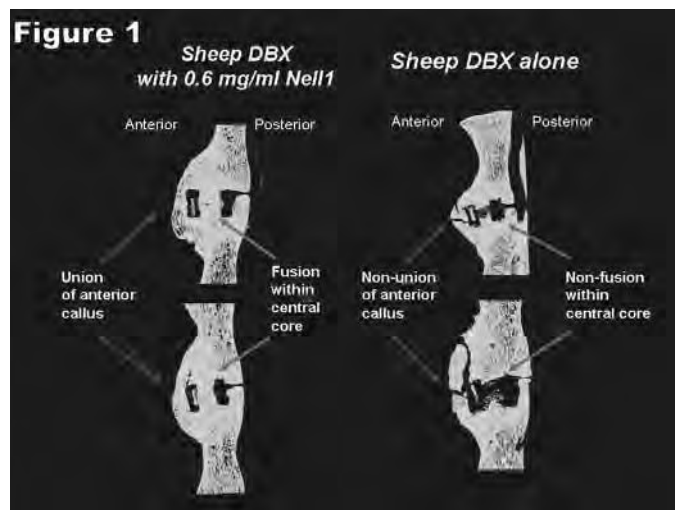
A considerable number of studies have been done on TGF β superfamily / Smad pathway. But, the mechanisms how to specify Smads in response to TGF β and BMP stimuli is still unknown. In this study, we have used a combined method of the enrichment of phosphoproteins with proteomics strategy to discover those mechanisms. In early stage (at 30 min) after stimuli, we purified phosphoproteins from premyoblasts C2C12 cells using antibody-based phosphoaffinity column for the identification of the phosphoproteins regulated by BMP-2 or TGF β 1. We have identified about 1600 potential phosphoproteins using by GeLC-MS/MS. Interestingly, we detected that both Smad1 and Smad2 are temporally phosphorylated by opposite signals (that is, Smad2 by BMP-2, Smad1 by TGF β 1). This phosphorylation level, however, rapidly decreased (from 30 min to 1hr), and dramatically restored by proteasome inhibitor MG132 pretreatment. These data suggest that ubiquitination-proteasomal degradation system would play a key role in the early events of TGF β signal transduction. In the proteome data analysis, several ubiquitination / deubiquitination enzymes were identified. HECT-domain E3 ligases Nedd4 and Nedd4L, deubiquitin enzymes UCHL3/4 and USP4 respectively. Nedd4L was identified as a unique phospho-protein by BMP-2, but Nedd4 was detected commonly in both BMP-2 and TGF β 1 stimulation. The Smads ubiquitination by Nedd4 has not been elucidated yet. So, we hypothesized that temporally phosphorylated-Smads would be polyubiquitinated by Nedd4 family (that is, p-Smad1 by Nedd4, p-Smad2 by Nedd4L) in TGF β signaling pathway and degraded by proteasome. When coexpressed together with Nedd4, wild type Smad1 was polyubiquitinated and constitutive phospho-Smad1 mutant (DVD) is more polyubiquitinated than non-phospho Smad1 mutant (AVA). In addition, ALP (Alkaline phosphatase) staining confirmed that overexpressed Nedd4 suppress transdifferentiation of BMP-2 induced C2C12. Overall, our results suggested that TGF β 1 induced phospho-Smad1 was selectively ubiquitinated by Nedd4 and followed by proteasomal degradation. We argue that Nedd4 ubiquitin E3-ligase family would serve as 'modulators' of the TGF β activated Smad signaling pathway determination by ubiquitination-proteasomal degradation system.

Disclosures: B. Kim, None.

M200

NELL-1 Promotes Bone Formation in a Sheep Spinal Fusion Model. S. S. Lu*, J. Whang*, X. Zhang*, B. Wu*, S. Turner*, H. B. Seim*, K. Ting*, J. C. Wang*, C. Soo*. ¹School of Dentistry and Medicine, University of California-Los Angeles, Los Angeles, CA, USA, ²Veterinary Science, Colorado State University, Fort Collins, CO, USA.

NELL-1 is a Runx2 regulated secretory protein with marked osteochondrogenic cell specificity. NELL-1 exhibited comparable osteoinductivity to bone morphogenetic protein 2 (BMP-2) in a rodent calvarial defect model when placed on poly(lactic-co-glycolic acid) scaffolds. The purpose of this study was to test NELL-1 the osteoinductivity in a sheep interbody fusion model and to establish preliminary dose ranges. Eight sheep divided into four groups underwent interbody fusion at L4-L5 and at L5-L6 with a radiolucent vertebral spacer (2 animals/group; 4 sites/group). The control group was filled with sheep demineralized bone matrix (DBX) and saline within and around each vertebral spacer. The other three groups received sheep DBX mixed with NELL-1 at final concentrations of 0.3, 0.6, and 1.5 mg/ml within and around the vertebral spacers. To assess spine fusion, X-rays (0, 2, and 3 months), CT images (2 and 3 months), and microCTs (explanted 3 month specimens) were obtained. Spinal fusion criteria were either > 50% contiguous bone volume within the spacer or contiguous bone formation within the callus totaling > 1/3 anterior vertebral body circumference. All animals were sacrificed at 3 months after surgery. The results showed significantly increased bone formation in NELL-1 treated animals relative to controls. CT images at three months demonstrated successful spinal fusion in 100% of the 0.6mg/ml NELL-1 dose sites and none of the controls. Representative post-sacrifice microCT images of L5-6 from two controls (right) and two NELL-1 animals (left) also confirmed this finding (Figure 1). MicroCT analysis of central bone within the spacers revealed increased bone density and bone volume in NELL-1 specimens relative to controls. We conclude that all three NELL-1 doses induced significantly more bone formation than controls. 0.6mg/ml NELL-1 appears to induce the most robust bone, and this initial finding will be investigated in a larger follow-on study. Overall, NELL-1/DBX at the 3 month time point may induce comparable sheep interbody fusion to published BMP-2 studies carried out to the 6 month time point.



Disclosures: S.S. Lu, None.

This study received funding from: UC-Discovery Grant & Bone Biologics.

M201

TGF-beta Suppresses POEM Expression in Osteoblasts. A. Miyazono^{*1}, A. Yamada^{*1}, N. Morimura^{*2}, D. Suzuki^{*1}, M. Kobayashi^{*3}, M. Takami¹, K. Tezuka⁴, M. Yamamoto³, R. Kamijo¹. ¹Department of Biochemistry, Showa University, Tokyo, Japan, ²Laboratory for Comparative Neurogenesis, RIKEN Brain Science Institute, Saitama, Japan, ³Department of Periodontology, Showa University, Tokyo, Japan, ⁴Graduate School of Medicine, Gifu University, Gifu, Japan.

POEM (preosteoblast epidermal growth factor-like repeat protein with MAM domain), also known as nephronectin, is an extracellular matrix protein that is thought to play a critical role in the development and functions of various tissues, such as those of the kidney, bone, muscle, and endocrine organs, through interaction with other extracellular molecules. In the present study, we found that transforming growth factor-beta (TGF-beta) dose-dependently and strongly inhibited POEM expression in mouse osteoblastic cell lines, MC3T3-E1 and UAMS-32. Inhibition of POEM expression by TGF-beta could be seen at concentrations exceeding 10 pg/ml. The time-dependent effects of TGF-beta on the reduction of POEM expression were further examined using 1 ng/ml of TGF-beta. A decrease in POEM mRNA was detected at 3 hours after the addition of TGF-beta and the decrease continued up to 24 hours, demonstrating that the TGF-beta induced decrease of POEM gene expression occurs in both time- and dose-dependent manners. When the cells were pretreated with a selective inhibitor of ALK5 (TGF-beta R1, a TGF-beta type 1 receptor) prior to the addition of 1 ng/ml of TGF-beta, down-regulation of POEM expression was completely blocked. These results suggest that regulation of POEM expression by TGF-beta occurs via TGF-beta R1. Further, bone morphogenetic protein-2 (BMP-2) slightly blocked the effect of TGF-beta toward the reduction of POEM expression. TGF-beta is a key regulator of bone matrix properties and composition, and it inhibits the expression of RUNX2 which is a critical transcriptional regulator of osteoblast differentiation in MC3T3-E1. Therefore to elucidate the relationship between the inhibition of osteoblast differentiation and reduction of POEM expression by TGF-beta, effect of TGF-beta on the expressions of alkaline phosphatase (ALP), osteocalcin, and bone sialoprotein (BSP) were examined. Each of those genes was down-regulated by TGF-beta in a manner consistent with that of POEM mRNA. These results indicate that POEM is a novel marker gene for osteoblast differentiation similar to others, such as ALP, osteocalcin, and BSP. In addition, reduced POEM expression may contribute to the inhibition of osteoblast differentiation by TGF-beta.

Disclosures: A. Miyazono, None.

M202

See Sunday Plenary Number S202

M203

A Novel Activin/Nodal-binding Protein, G11, Inhibits Matrix Mineralization in Osteoblasts. Y. Mochida, D. Parisuthiman^{*}, M. Katafuchi^{*}, P. Atsawasuwan^{*}, M. Kaku^{*}, M. Yamauchi. Dental Research Center, University of North Carolina at Chapel Hill, Chapel Hill, NC, USA.

Transforming growth factor-beta (TGF-β) superfamily consists of three major sub-families including TGF-β, bone morphogenetic protein (BMP) and activin/nodal, and they are known to be potent effectors in almost all crucial biological/developmental/regenerative events. Currently, however, the presence of activin/nodal and, if present, their roles in osteoblasts are largely unknown. In an effort to identify TGF-β superfamily binding proteins, we have taken a bioinformatics approach and just identified a novel gene, G11. The gene structure of G11 is related to chordin family. To investigate the potential function of G11 in osteoblasts, first, its expression pattern during cell differentiation and matrix mineralization was analyzed by quantitative real time PCR. Second, MC derived clones overexpressing G11 (S clones) were established and characterized by analyzing cell proliferation and in vitro mineralization. The phenotypes of S clones were evaluated by comparing to those of two control groups, i.e. MC and a clone transfected with an empty vector (EV clone). The data demonstrated that G11 was highly expressed in the early differentiation stage, i.e. at day 7 in mineralization medium, and decreased thereafter. The cell proliferation rate in S clones was not affected. However, in vitro mineralization in S clones was significantly delayed in comparison to those of controls. In order to gain mechanistic insights into an inhibitory function of G11, the interaction between G11 and TGF-β superfamily members (TGF-β1, -β2, -β3, BMP-2, -4, -6, -7, inhibin-ba, -bb and nodal; all were expressed in MC) was examined by immunoprecipitation-Western blotting. The data demonstrated that G11 was strongly bound to activin/nodal, and furthermore, G11 enhanced activin/nodal-induced Smad2 phosphorylation in MC cells. These results indicate that G11 is a novel chordin-like extracellular protein expressed in osteoblasts, and that it inhibits in vitro matrix mineralization possibly through its early interaction with activin/nodal.

Disclosures: Y. Mochida, None.

This study received funding from: NIH grants, DE10489 and AR052824.

M204

Collagen Binding Characteristics of Collagen Binding Domain from Clostridium Histolyticum Class I Collagenase. J. Sakon^{*1}, P. S. T. Leena^{*1}, O. Matsushita^{*2}. ¹Biochemistry, University of Arkansas, Fayetteville, AR, USA, ²Molecular Biology, Kitasato University School of Medicine, Kanagawa, Japan.

Weekly intraperitoneal injection of a fusion protein of PTH(1-33) with CBD for 8 weeks in mice showed 15% BMD increase. Clostridium histolyticum ColG collagenase activated by Ca²⁺ is responsible for extensive tissue destruction, and the CBD is a segment of the multi-domain enzyme. Binding of two Ca²⁺ on CBD is co-operative and is both enthalpically and entropically driven ($K_{d1} = 2.13 \mu\text{M}$; $K_{d2} = 4.63 \mu\text{M}$). Structures in the presence and absence of Ca²⁺ have been solved at ultrahigh resolution (<1.2 Å). N-terminus 14 residues of CBD adopt an alpha-helical conformation; however, an addition of Ca²⁺ unwinds the linker into a new beta-strand. To rule out the crystal-packing artifact, NMR titration studies were done and they confirm the conformational changes upon addition of Ca²⁺. The changes in Stokes and hydrodynamic radii as measured by size exclusion chromatography and dynamic light scattering experiments showed drastic transition upon Ca²⁺ addition. With Ca²⁺ CBD becomes thermally stable ($T_m > 90^\circ\text{C}$), less susceptible to proteolysis and stable against chemical denaturants. Collagen binding affinity of CBD was detected only in the presence of Ca²⁺. Mutagenesis experiments identified a cluster of Tyr residues involved in collagen binding. The Tyr-rich surface becomes accessible upon Ca²⁺ binding. Co-crystallization of collagen:CBD have yielded no crystals thus far. Docking experiment of CBD with collagen-like peptide G(POG)₆ resulted in 3 different binding orientations. NMR titration of CBD against G(POG)₁₀ eliminated one of the probable in silico orientations. N¹⁵ enriched CBD and unlabeled (POG)₁₀ were used for the titration experiment. Studies thus far demonstrate the drastic structural changes accompanied upon secretion of the enzyme from a bacteria to infected tissues. They also provide atomic insights into how CBD interacts with extracellular collagen.



Disclosures: J. Sakon, None.

This study received funding from: NIH-COBRE.

M205

Smad4 Has a Direct Apoptogenic Role at the Mitochondria. H. Yuan^{*1}, T. Qiu¹, J. Huang^{*2}, X. Cao¹, M. Wan¹. ¹Pathology, University of Alabama at Birmingham, Birmingham, AL, USA, ²Shihezi University School of Medicine, Shihezi, China.

Smad4, originally isolated from the human chromosome 18q21, is a key factor in transducing the signals of the TGF-β superfamily of growth hormones, which is an important player in regulating bone homeostasis and cancer cell growth and apoptosis. Smad4 plays a pivotal role in mediating antimitogenic and proapoptotic effects of TGF-β, but the mechanisms by which Smad4 induces apoptosis are elusive. Here we report that Smad4 directly translocates to the mitochondria of apoptotic tumor cells.

Smad4 overexpression significantly promotes, whereas Smad4 gene silencing by siRNA inhibits, TGF-β- and UV-induced apoptosis in two pancreatic cancer cell lines. To further clarify the mechanism by which Smad4 induces apoptosis, we found that a fraction of Smad4 translocates to mitochondria upon TGF-β treatment or UV exposure by Western blot analysis of cytosol and mitochondrial Smad4 protein. Smad4 mitochondria translocation was also confirmed by Smad4 colocalization with Mitotracker Red observed by confocal fluorescence microscope.

To examine the functional significance of mitochondrial Smad4 localization in apoptosis, we searched for mitochondria proteins that have physical interactions with Smad4 using yeast two-hybrid screening approach. DNA sequence analysis identified 34 positive clones, five of which encoded subunits in mitochondria complex IV, i.e. one clone encoded cytochrome c oxidase (COX)II, three clones encoded COXIII and one clone encoded COXVb. The data indicate that Smad4 might associate with mitochondria proteins and may have mitochondria-related function. Strong interaction between Smad4 with COXII was verified in yeast by β-gal activity assays and in mammalian cells by immunoprecipitation assays. Importantly, we isolated the mitochondrial portion and confirm the interaction between COXII and Smad4 in mitochondria upon TGF-β treatment or UV exposure. COXII is encoded by mitochondrial DNA, synthesized in the mitochondria, and inserted into the inner membrane by mitochondrion-dependent

pathways. COXII also has been shown to bind directly to cytochrome c and is speculated to regulate apoptosis through this affinity for cytochrome c. The association of Smad4 with COXII in mitochondria demonstrated in the present study implies that Smad4 may regulate cell apoptosis by directly targeting mitochondria.

Disclosures: H. Yuan, None.

M206

Arkadia, an E3 ubiquitin Ligase, Represses Skeletal Muscle Differentiation Through Enhancement of Myostatin and TGF-beta Signaling. H. Yuzawa^{*1}, D. Koinuma^{*1}, S. Maeda¹, M. Takahata^{*1}, M. Hayashi^{*1}, K. Miyazawa^{*2}, K. Yamamoto^{*3}, T. Imamura¹. ¹Department of Biochemistry, The Cancer Institute of the Japanese Foundation For Cancer Research, Tokyo, Japan, ²Department of Molecular Pathology, Graduate School of Medicine, University of Tokyo, Tokyo, Japan, ³Department of Orthopaedic Surgery, Tokyo Medical University, Tokyo, Japan.

Myostatin belongs to transforming growth factor (TGF)-beta family, and act as a negative regulator of skeletal muscle differentiation. Myostatin knockout mice cause dramatic and wide spread increase in skeletal muscle, and naturally occurring myostatin mutations in cattle breeds lead to a heavy muscle condition due to hyperplasia and hypertrophy. Regulation of Myostatin signaling is thus a matter of physiological and pathological importance. However, how positive and negative regulators affect myostatin signaling is still not fully understood. Here we investigated the function of Arkadia in Myostatin signaling during myoblast differentiation. Arkadia was originally identified as an intracellular protein that is essential for formation of a mammalian node during mouse development through enhancement of Nodal signaling. In addition, we have previously reported that Arkadia is an E3 ubiquitin ligase that degrades an inhibitory Smad, Smad7, to enhance TGF-beta family signaling. In the present study, we first showed that mouse myoblast C2C12 cells express increased level of Myostatin and TGF-beta3 during myoblast differentiation. Adenoviral-mediated expression of Arkadia effectively enhanced suppression of myoblast differentiation by Myostatin and TGF-beta3, as determined by myotube formation and target gene expression, including myosin heavy chain. We further examined the role of endogenous Arkadia by lentiviral shRNA knockdown system, and showed that loss of endogenous Arkadia enhances myotube formation. Moreover, protein level of endogenous Smad7 was elevated by knockdown of Arkadia suggesting that Arkadia represses skeletal muscle differentiation through modulation of negative feedback mechanisms. In conclusion, we propose a physiological role of Arkadia as an important negative regulator of myoblast differentiation through enhancement of TGF-beta family signaling. Investigation of expression and activity of Arkadia is thus required in the future.

Disclosures: H. Yuzawa, None.

M207

The Duodenum Rapidly Senses and Modulates Renal Phosphate Reabsorption Via Novel PTH- and Phosphatonin-Independent Pathways. T. Berndt^{*}, L. Thomas^{*}, T. Craig^{*}, S. Sommer^{*}, X. Li^{*}, E. Bergstralh^{*}, R. Kumar. Nephrology Research, Mayo Clinic Rochester, Rochester, MN, USA.

The mechanism by which phosphorus homeostasis is preserved during alterations in dietary phosphate intake is not completely understood. Net phosphorus balance in mammals is maintained by the absorption of phosphate in the duodenum and jejunum and by the tubular reabsorption of phosphate by the kidney. We have previously demonstrated that renal phosphate reabsorption is altered by the infusion of phosphate into the duodenum by PTH- and phosphatonin-independent pathways. In order to localize the segments of the gastrointestinal tract responsible for this response, we infused phosphate either into the duodenum or the stomach of anesthetized rats previously fed a normal phosphate diet and measured renal phosphate reabsorption following the infusion. After a control clearance, sodium phosphate was administered into the duodenum (n=7) or the stomach (n=6). Five, ten, twenty, and thirty minutes following the infusion of sodium phosphate, renal phosphate reabsorption was measured. The administration of phosphate into the duodenum resulted in rapid and significant increases in the fractional excretion of phosphate (FEP) at 10, 20, and 30 minutes. Basal FEP (mean±SD) was 28.4±8.6%, 5 min = 28.7±7.9%, 10 min = 31.9±7.6%, 20 min = 41.8±9.9%, 30 min = 44.0±11.4%, resulting in a slope/min of 0.6±0.3, P=0.0037. The administration of sodium chloride did not alter the fraction excretion of phosphate in similarly prepared rats (FEP 23.7±7.2%, 20.2±4.0%, 21.6±6.9%, 24.5±8.5% and 24.6±5.4%, resulting in a slope/min of 0.096±0.09, P=0.066). This effect is independent of PTH and the phosphatonins, FGF-23 and sFRP-4. When sodium phosphate was infused into the stomach, no change in the fraction excretion of phosphate was observed (FEP was 26.3±6.6%, 25.9±8.0%, 27.4±7.8%, 27.8±6.6%, 29.0±5.8%, resulting in a slope/min of 0.083±0.28, P=0.46). Our results show that a phosphate sensing mechanism exists in the duodenum but not in the stomach that rapidly decreases renal phosphate reabsorption following the ingestion of a high phosphate meal.

Disclosures: T. Berndt, None.

M208

See Sunday Plenary Number S208

M209

Transgenic Mice Overexpressing sFRP-4 Have Low Bone Mass but Do Not Exhibit Disturbed Phosphate Homeostasis. H. Y. Cho^{*}, H. J. Sun^{*}, J. Y. Yang^{*}, H. J. Choi^{*}, J. H. Ahn^{*}, S. W. Cho, S. W. Kim, S. Y. Kim^{*}, C. S. Shin. Internal Medicine, Seoul National University College of Medicine, Seoul, Republic of Korea.

Secreted frizzled-related protein-4 (sFRP-4) is a member of secreted modulators of wnt signaling pathways that regulate biological processes ranging from developmental cell fate, cell polarity and tumorigenesis. Moreover, sFRP-4 has recently been recognized to play important roles in the pathogenesis of oncogenic osteomalacia as a potential phosphatonin. To investigate the role of sFRP-4 in bone metabolism in postnatal life, we have generated transgenic mice that overexpress sFRP-4 under the control of the serum amyloid P (SAP) promoter, which drives transgene expression postnatally. Transgene expression was identified in various tissues including serum, bone, liver and kidney in transgenic mice. At 10 week of age, the serum phosphorus concentration and urinary phosphorus excretion in transgenic mice were not significantly different from those of wild-type mice in both female and male. However, transgenic female mice exhibited decreased bone mineral density (0.045 ± 0.001 , $P < 0.05$) and bone mineral content (0.407 ± 0.026 , $p < 0.05$) compared to wild type female mice. Body fat contents were not different between wild-type and transgenic mice. On histological examination, transgenic mice showed decreased osteoid mass, thickness, decreased growth plate width and prolonged reversal phase. Histomorphometric analysis revealed that transgenic mice had decreased osteoid volume ($P < 0.05$), osteoid thickness ($P < 0.05$), and mineralization lag time ($P < 0.05$) compared to wild type mice. There was no difference in bone resorption parameters. Whereas difference in the mRNA expression of Na/P cotransporters, Npt2a and Npt2c, were not apparent, the 1- α -hydroxylase expression was increased in transgenic mice. Our data do not support the role of sFRP-4 as a phosphatonin but suggest a direct effects of sFRP-4 on new bone formation without disrupting phosphate homeostasis.

Disclosures: H.Y. Cho, None.

M210

See Sunday Plenary Number S210

M211

Evaluation of FGF 23 (c-terminal and intact) ELISA Kits in End-stage Renal Disease Patients. W. J. Fassbender¹, M. Hanfland-Schmidt^{*1}, J. Windolf^{*2}, U. C. Stumpf². ¹Department of Internal Medicine, Hospital z. HI. Geist, Kempen, Germany, ²Department of Traumatology and Handsurgery, University Hospital, Duesseldorf, Germany.

Hyperphosphataemia, calcitriol deficiency and secondary hyperparathyroidism (sHPT) are common complications in end-stage chronic kidney disease (CKD). Fibroblast Growth Factor 23 (FGF-23) is a phosphaturic peptide that also inhibits renal 1 α -hydroxylase activity and tubular phosphate reabsorption by inhibition of sodium-dependant renal phosphate transport. Consequences are the decrease of serum 1,25 dihydroxyvitamin D3 and phosphaturia. Therefore FGF 23 plays a role in hyperphosphataemia associated with CKD and may be involved in the pathogenesis of sHPT. Increased FGF 23 may contribute to maintaining normal serum phosphate levels in the face of advancing CKD, but up to a reduction of a creatinine clearance lower than 30 ml/min the capacity of this regulative mechanism ends and hyperphosphataemia results. Within end-stage renal disease we find markedly increased serum FGF 23 associated with hyperphosphataemia, phosphaturia and decreased serum calcitriol and sHPT.

Material and methods: We evaluated the actual in Europe available ELISA kits for FGF 23 (c-terminal and intact, "Human Intact FGF 23 ELISA Kit" and "Human FGF 23 (C-Term) ELISA Kit", Immutopics) for assessment of serum and EDTA-plasma in patients requiring dialysis, as expected with high serum FGF 23 levels compared with values derived from a normal collective of healthy persons with normal renal function. Furthermore preanalytical testing for stability of FGF 23 was performed by comparing samples which were stored at -20° C with samples stored for 6 days at -4° C.

Dialysis patients: 23 patients, 17 male, 6 female, age: 36 - 79 years (mean age: 62,13). Collective of healthy subjects: 17 subjects, 8 male, 9 female, age: 24 - 56 years, (mean age: 33,41).

Results: Dialysis patients: mean values serum FGF 23 15,32 pg/ml (intact) and 2774 U/ml (c-terminal, arithmetic mean). Mean values in EDTA-plasma FGF 23 (intact) 271 pg/ml; FGF 23 (c-terminal) 2606 U/ml; collective of healthy subjects: mean serum values FGF 23 0,64 pg/ml (intact) and 13,67 U/ml (c-terminal, arithmetic mean). Mean values of EDTA-plasma FGF 23 (intact) 13,09 pg/ml; FGF 23 (c-terminal) 19,18 U/ml.

Discussion: The parallel investigation of serum and EDTA-plasma FGF 23 certifies the advantage of EDTA-plasma in subjects with intact renal function. The significantly increased levels of FGF 23 in patients requiring dialysis demand dilution of the samples. Further investigations concerning age-related changes of serum FGF 23 should be performed. The feed-back mechanism of FGF 23 and serum 1,25 dihydroxyvitamin D3 implements possible future therapeutical options within the treatment of sHPT.

Disclosures: W.J. Fassbender, None.

M212

See Sunday Plenary Number S212

M213

Venous Sampling for FGF23 as a Tool for Pre-Operative Localization of Tumors Giving Rise to Hypophosphatemic Osteomalacia. E. Hagström^{*1}, P. A. Westerberg^{*2}, G. Toss^{*3}, T. Lindhe^{*2}, Ö. Ljunggren², T. E. Larsson². ¹Dept. of Surgical Sciences, Uppsala University Hospital, Sweden, ²Dept. of Medical Sciences, Uppsala University Hospital, Sweden, ³Dept. of Medicine, Linköping, Sweden.

Tumor-induced hypophosphatemic osteomalacia (TIO) is a rare paraneoplastic syndrome, characterized by hypophosphatemia, low or inappropriately normal 1,25(OH)2D3 and rickets/osteomalacia. Increased serum level of Fibroblast Growth Factor-23 (FGF23) has been identified as the causative factor for TIO. In this study, we report on the diagnostic difficulties and tumor localization in a 55-year old male with presumable TIO.

Primary imaging studies, including CT/MRI scans and octreotide scintigraphy, failed to localize the tumor, however consistently elevated FGF23 levels were found (180-220 pg/mL). Venous sampling, followed by intact FGF23 analysis, revealed locally increased FGF23 level in the left femoral vein (343 pg/mL). Octreotide scintigraphy of the upper left leg revealed a 20 mm large tumor located at the left lateral condyle of the femur. Surgical resection of the tumor normalized serum phosphate and vitamin D within 5-10 days, however serum FGF23 declined from 292 to 12 pg/mL 24 hours after surgery. Pre-operative bone mineral density (BMD), as determined by DXA analysis, revealed a T-score of -1.6 in lumbar spine and -1.16 in total hip. Lumbar spine BMD was increased by 25% two months after tumor resection. Notably, our patient post-operatively developed a secondary hyperparathyroidism, which may reflect a transient hypocalcemia related to increased bone mineralization. In conclusion, our study demonstrates the diagnostic complexity and difficulties in localizing small TIO tumors. Venous sampling for FGF23 followed by octreotide scintigraphy may constitute a powerful tool for tumor localization in subjects with hypophosphatemic osteomalacia.

Disclosures: E. Hagström, None.

M214

See Sunday Plenary Number S214

M215

Rise in FGF-23 Precedes 1-84PTH and Linear Decline in Calcitriol Precedes Rise in FGF-23 in Non-diabetic Predialysis Patients. T. Hamano^{*}, K. Tomida^{*}, S. Mikami^{*}, N. Fujii^{*}, T. Ito^{*}, E. Imai^{*}. Nephrology, Osaka University Hospital, Suita, Japan.

Today fibroblast growth factor-23 (FGF-23) was found to be another phosphaturic hormone derived from osteocyte and osteoblast. The reduction in calcitriol synthesis by phosphate load can be explained by the increase in FGF-23. Although many study measured FGF-23 using a two-site ELISA that detects carboxyl-terminal portion of FGF-23, full-length FGF-23 (intact FGF-23) at different glomerular filtration rate (GFR) is not well documented in large cohort. Our aim is to know at what level of GFR intact FGF-23 and 1-84PTH increase and serum calcitriol decrease significantly. In this cross-sectional observational study (OVIDS-CKD; Osaka Vitamin D Study in patients with CKD), we enrolled non-diabetic patients in outpatients nephrology clinic at two major hospitals in Osaka. Patients who were or had been receiving glucocorticoid, bisphosphonate, vitamin D, calcium, or hormone replacement therapy were excluded. We measured serum phosphorus, calcium, albumin, intact FGF-23, whole PTH, calcitriol, and 25-hydroxyvitamin D (25OHD). We check the relationship of fold increase of two phosphaturic hormones and change in other parameters with estimated GFR (eGFR). Patients were divided into 9 groups by eGFR.

In this study 574 patients were enrolled. In comparison with patients with eGFR more than 80 mL/min/1.73m², intact FGF-23, 1-84PTH, and serum phosphorus increased significantly in those with eGFR<60, eGFR<50, and eGFR<30 mL/min/1.73m², respectively. In patients with eGFR<50 mL/min/1.73m², steeper rise in 1-84PTH was observed than intact FGF-23. Whereas serum 25OHD had no correlation with eGFR at all, significant decline in serum calcitriol was observed even in patients with eGFR<80 compared to those with eGFR>80 mL/min/1.73m². Multiple linear regression analysis revealed that significant positive contributors to serum calcitriol were eGFR, 1-84PTH, and 25OHD. Negative contributor was intact FGF-23. The significant decline in calcitriol was found even when significant rise in intact FGF-23 was not observed. Therefore the reduction of calcitriol synthesis in earlier stage of CKD seemed not to be explained by the fact that FGF-23 decrease 1 α -hydroxylase in proximal tubules. There might be another mechanism for calcitriol decline in this early CKD stage. The earliest sign for phosphate overload relative to viable nephron numbers was compensative rise in intact FGF-23, not in serum 1-84PTH. Given the origin of this two phosphaturic hormones, this fact might suggest that the bone is more sensitive to minimal phosphate overload than the parathyroid glands. Significant linear decline in calcitriol with CKD progression precedes significant rise in FGF-23.

Disclosures: T. Hamano, None.

M216

Comparison of Rapid Intraoperative Parathyroid Hormone to IRMA in Patients with Hyperparathyroidism. M. Al Mukaddam^{*}, C. Albany^{*}, C. Hajj-Shahine^{*}, G. El-Hajj Fuleihan. Calcium Metabolism and Osteoporosis Program, American University of Beirut-Medical Center, Internal Medicine, Beirut, Lebanon.

The use of rapid intact parathyroid hormone (iPTH) assay is central to the success of minimally invasive parathyroidectomy. Comparing information obtained with this assay and the classical immunoradiometric PTH assay (IRMA) is limited.

142 blood samples collected from 71 patients referred to a tertiary care center for parathyroidectomy were analyzed. PTH levels on the intraoperative blood samples (pre- and post- gland excision) were concomitantly measured with the rapid and the classical IRMA kits. The classical IRMA kit utilizes monoclonal antibodies specific for the mid and C terminal part 39-84 and polyclonal antibodies specific to the N terminal moiety of PTH (CIS Bio International, Gif sur Yvette, France). The rapid iPTH was performed with the electrochemoluminescence immunoassay "ECLIA" (Roche Elecsys 2010 analyzer, Roche Diagnostics, Indianapolis, USA). It employs two monoclonal antibodies that react with epitopes in the amino acid regions 26-32 and 37-42 of PTH.

ECLIA assay (y) values strongly correlated with IRMA assay (x) values; y=1.63x -63.86 (r = 0.956, p<0.0001, pre- gland excision) and y=1.31x +4.22 (r=0.938, p<0.0001, 10-15 minutes post gland excision). This correlation was also evident with the percentage drop in PTH level using the above assays y=0.96x+0.51 (r =0.944, p<0.0001). Both assays yielded similar prediction of cure using the 50% drop as cut-off. However, mean pre- and post-gland excision PTH were significantly higher by ECLIA than IRMA, suggesting a systematic difference between the two assays, that is independent of mean PTH levels.

	PTH by ECLIA Median (min-max)	PTH by IRMA Median (min-max)	P value	%CV mean \pm SD
Pre-excision	177 pg/ml (39-3130)	129pg/ml (28-1648)	<0.0001*	22 \pm 16
Post-excision	39 pg/ml (9-452)	27pg/ml (2-265)	<0.0001*	31 \pm 22
% PTH Drop	77% (5-95)	80% (18-98)	NS	5 \pm 1

* paired t-test on log transformed values of PTH, NS: Not Significant

The manufacturers report a normal range for PTH of 15-65 pg/ml with ECLIA, which is very similar to the normal range for IRMA assay of 8-76 pg/ml. However, this study reveals that there is significant difference in the values obtained with the two assays, and underscores the importance of using the same assay when monitoring patients. Further studies should be implemented to elucidate sources of discrepancies between the two assays.

Disclosures: M. Al Mukaddam, None.

M217

See Sunday Plenary Number S217

M218

Ability of XL α s to Mimic Gs α in Mediating Parathyroid Hormone Signaling In Vivo. C. Aydin¹, L. F. Fröhlich^{*2}, D. Ozturk^{*1}, M. Bastepe¹.

¹Endocrine Unit, Department of Medicine, Massachusetts General Hospital, Harvard Medical School, Boston, MA, USA, ²Institute of Pathophysiology, University of Veterinary Medicine, Vienna, Austria.

XL α s, an imprinted, paternally expressed variant of the α -subunit of the stimulatory G protein (Gs α), can mediate parathyroid hormone (PTH)-induced adenylyl cyclase activation and, thus, is able to replace Gs α in transfected cells. However, XL α s knockout mice show phenotypes that are significantly different from those observed in Gs α knockout mice, suggesting that XL α s is unable to mimic Gs α in vivo. To address this question, we generated a transgenic mouse strain in which the rat type-I γ -glutamyltranspeptidase promoter was employed to target XL α s expression to the proximal tubule, a major site of PTH action. Southern blots identified five different founders (rptXL α s mice), and Northern blots showed that the F1 generation from two of the founders (G14 and G28) expressed transgenic rat XL α s mRNA at the age of two months. In G14 rptXL α s mice, but not in wild-type littermates, RT-PCR using whole kidney total RNA and primers common to both mouse and rat XL α s mRNA yielded a specific amplicon, whose sequence matched the cDNA sequence of rat XL α s. Western blots using a polyclonal antibody against the C-terminus of XL α s detected the XL α s protein in membrane extracts from the proximal tubules of the G14 rptXL α s mice but not of wild-type littermates. Endogenous Gs α mRNA levels appeared similar in transgenic and wild-type animals, which was determined by real-time RT-PCR using total RNA isolated from the proximal tubule. In contrast, the level of 1 α -hydroxylase mRNA, a downstream target of Gs α -mediated PTH signaling, was elevated in the G14 rptXL α s mice compared to wild-type littermates. These findings suggest that proximal tubular PTH actions that typically rely on Gs α signaling are enhanced in the G14 rptXL α s mice without changes in Gs α levels, providing strong evidence for the ability of XL α s to function in a manner similar to Gs α in vivo. Since XL α s mRNA is disrupted by most paternal mutations that disrupt Gs α mRNA and is preserved when those mutations are maternal, the Gs α -like activity of XL α s may be important in the pathogenesis of disorders associated with altered Gs α activity, such as pseudohypoparathyroidism, Albright's Hereditary Osteodystrophy, and fibrous dysplasia of bone.

Disclosures: C. Aydin, None.

This study received funding from: NIH/NIDDK (KO1 DK062973 to MB).

M219

See Sunday Plenary Number S219

M220

Estrogen Deficiency and PTHrP Infusion Do Not Fully Reproduce the Bone Loss of Lactation. S. Brian*, P. Dann*, J. Wysolmerski. Endocrinology and Metabolism, Yale University, New Haven, CT, USA.

Lactation is associated with increased bone turnover and rapid bone loss. Suckling inhibits GnRH secretion, causing hypogonadotropic hypogonadism and low circulating levels of estradiol. In addition, the lactating mammary gland secretes PTHrP into the circulation. Estrogen replacement in lactating mice reduces bone loss by 60%, while disrupting the PTHrP gene in the lactating mammary gland reduces bone loss by 50%. Therefore, we hypothesized that the combination of estrogen deficiency and PTHrP excess is sufficient to explain bone loss in lactating mothers. To test this hypothesis, we attempted to reproduce lactational bone loss in nulliparous mice by suppressing estrogen and raising PTHrP levels. We administered 100 micrograms of leuprolide acetate twice daily to induce hypogonadotropic hypogonadism and lower estrogen levels. PTHrP(1-36) was infused at a rate of 10 pmol/hr using Alzet miniosmotic pumps. We studied 5 groups of mice: 1) lactating controls, 2) nulliparous controls, 3) PTHrP-treated, 4) leuprolide-treated, and 5) combined PTHrP and leuprolide. All mice were CD-1's between 11 and 14 weeks of age at the beginning of the experiment. BMD was measured by DXA prior to the start of the treatments and again after 11 days, and in lactating mice on day 1 and day 11 postpartum. After 11 days, mice were sacrificed and blood and urine were collected. As expected, lactating mice had lower estradiol levels (4.2pg/ml) than did randomly cycling virgins (13.7 pg/ml). Importantly, leuprolide-treated mice also had suppressed levels of estradiol (3.5 pg/ml) that were equivalent to those of lactating mice. Infusion of PTHrP led to mild hypercalcemia. Urinary C-telopeptide excretion (corrected for creatinine) (CTX) was elevated for all groups as compared to non-lactating controls. However, treatment with leuprolide, PTHrP or the combination did not raise CTX levels as high as those measured in lactating mice. BMD declined by 22% at the spine, 19% at the femur and 16% for the total body in lactating mice. PTHrP treatment caused losses of 8.0% at the spine, 8.7% at the femur and 8.0% at the total body. Interestingly, leuprolide treatment alone caused no bone loss and bone loss in the combined leuprolide and PTHrP group was no worse than with PTHrP treatment alone (5.0% at the spine, 5.1% at the femur and 7.0% for the total body). In conclusion, infusion of PTHrP combined with hypogonadotropic estrogen deficiency does not reproduce the extremely rapid rate of bone loss observed during lactation. These data suggest that either antecedent pregnancy or some other aspect of lactation magnifies bone loss caused by estrogen deficiency and PTHrP.

Disclosures: S. Brian, None.

M221

Activation of the Calcium Sensing Receptor With Cinacalcet Increases Serum Gastrin Levels in Healthy Older Subjects. L. Ceglia, S. S. Harris, H. Rasmussen*, B. Dawson-Hughes. Bone Metabolism Laboratory, Jean Mayer USDA Human Nutrition Research Center on Aging at Tufts University, Boston, MA, USA.

Gastric acidity is postulated to enhance calcium absorption since calcium is better dissolved at low pH. Extracellular calcium stimulates gastrin and gastric acid secretion in humans. Ex vivo studies indicate that the calcium sensing receptor (CaR), which is expressed on the surface of human G cells and parietal cells, may be involved in this regulation. We evaluated whether cinacalcet (C), a CaR agonist, compared to placebo (P) would increase serum gastrin level (G) and basal gastric acid output (BAO) in healthy subjects.

17 subjects age 47-70 were placed on a metabolic diet with fixed protein, calcium, phosphorus, sodium, magnesium, potassium and vitamin D for 18 days. We measured G, BAO, intact parathyroid hormone (PTH), and 24-hr urine calcium-to-creatinine excretion ratio (Ca/Cr) at baseline (day 8, following a run-in period) and post-intervention (day 18). C was titrated to 30 mg daily. G was measured by the Diasorin method. Gastric volume, pH and acid mEq were measured to calculate BAO.

Mean G was similar in the 2 groups at baseline (C = 33.1 ± 13.9 (SD) pg/ml (n=9), P = 38.5 ± 13.9 pg/ml (n=8)). However, mean change in G differed (C = 7.0 ± 7.3 pg/ml, P = -4.6 ± 6.8 pg/ml, p = 0.004). Mean BAO at baseline was similar in the 2 groups (C = 2.14 ± 1.77 mEq/hr, P = 2.43 ± 1.56 mEq/hr), and mean change in BAO did not differ significantly (C = 1.32 ± 2.37 mEq/hr, P = -0.24 ± 1.08 mEq/hr, p = 0.109). In the group as a whole, change in G correlated with change in BAO (r = 0.530, p = 0.029 (n=17)). Baseline mean PTH was similar in the 2 groups (C = 43.9 ± 16 pg/ml, P = 47.8 ± 18.0 pg/ml), and as expected mean change in PTH differed (C = -26.9 ± 11.7 pg/ml, P = 14.3 ± 17.0 pg/ml, p = <0.0001). Ca/Cr did not differ significantly at baseline in the 2 groups (C = 84.9 ± 59.9 mg/g, P = 114.3 ± 80.1 mg/g, p = 0.401), but mean change in Ca/Cr was significantly different (C = 17.9 ± 24.6 mg/g, -12.2 \pm 24.3 mg/g, p = 0.023).

These results show that activation of the CaR with cinacalcet stimulates gastrin secretion, and that an increase in gastrin is associated with a rise in basal gastric acid output in healthy older subjects. The impact of these changes on calcium absorption requires further investigation.

Disclosures: L. Ceglia, None.

This study received funding from: Jean Mayer Human Nutrition Research Center on Aging at Tufts University.

M222

The Discriminative Power of the 24h-Calcium/Creatinine Clearance Ratio (CCCR), the 24h-Calcium/Creatinine Ratio (CR) and the 24h-Calcium Excretion (CE) for the Separation Between Familial Hypocalciuric Hypercalcemia (FHH) and Primary Hyperparathyroidism (PHPT). S. E. Christensen¹, P. H. Nissen^{*2}, P. Vestergaard¹, L. Heickendorff^{ff2}, L. Mosekilde¹. ¹Dept. of Endocrinology, C., Aarhus University Hospital, THG, DK-8000 Aarhus C., Denmark, ²Dept. of Clinical Biochemistry, Aarhus University Hospital, THG, DK-8000 Aarhus C., Denmark.

Introduction: The 24h-urine calcium/creatinine clearance ratio (CCCR) is used clinically to separate familial hypocalciuric hypercalcemia (FHH) from primary hyperparathyroidism (PHPT).

A CCCR < 0.01 is often considered to indicate FHH, whereas a CCCR > 0.02 may be diagnostic for PHPT. Values between 0.01 and 0.02 are probably inconclusive. The simpler 24h-urine calcium/creatinine ratio (CR) and the 24h-urine calcium excretion (CE) have also been used. However, the discriminative powers of the different indices have not been sufficiently evaluated in well-defined subsets of patients.

Objective: To evaluate the diagnostic powers of CCCR, CR and CE in separating FHH from PHPT, using ROC curve analyses and overlap performance analyses.

Materials: We included 59 hypercalcemic FHH-patients characterized by clinically significant mutations in the CaSR gene and 97 hypercalcemic patients with surgically verified PHPT. All patients had a plasma creatinine (P-Cr) level < 150 pmol/l.

Methods: We calculated the CCCR as (P-Ca / 24h-U-Ca) x (24h-U-Cr / P-Cr), the CR as 24h-U-Ca/ 24h-U-Cr (mmol/mmol) and the CE as 24h-U-Ca (mmol/24h).

In FHH, all protein coding exons in the calcium sensing receptor gene (CaSR) were sequenced and aligned to GenBank reference sequence NM_000388.

Results: Highly significant differences between the two groups were found for all three indices (p<0.001). The table reports the ROC curve analyses. CCCR had the largest area under the ROC curve and a slightly higher sensitivity and specificity at the optimal separation point compared to the CR and CE.

ROC analyses	curve	Optimal separation point	Sensitivity	Specificity	Area under ROC curve
CCCR		<0.015	0.78	0.83	0.856
CR (mmol/mmol)		<0.45	0.71	0.86	0.831
CE (mmol/24h)		<5.5	0.76	0.72	0.800

CCCR < 0.01 had a positive predictive value of 0.89 for FHH, whereas CCCR > 0.02 had positive predictive value for PHPT of 0.93. Overlap performance analyses supported a two step diagnostic approach based on CCCR determination in all patients with CaSR gene analyses in those with CCCR < 0.02

Conclusions:

The diagnostic differentiation between PHPT and FHH should be based on CCCR determination with CaSR analyses in all patients with CCCR < 0.02.

Disclosures: S.E. Christensen, None.

M223

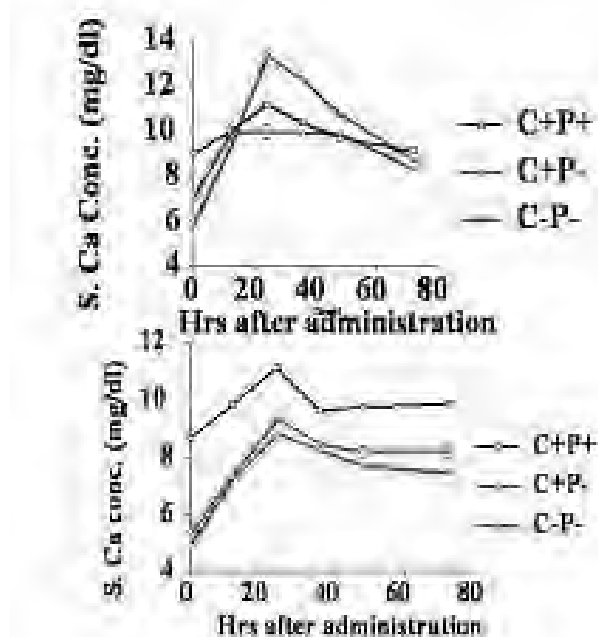
See Sunday Plenary Number S223

M224

The Calcim-Sensing Receptor (CaSR) Dampens the Calcemic Response to Exogenous 1,25 (OH)₂vitamin D In Vivo Independent of Parathyroid Hormone (PTH). O. Egbuna¹, L. Kantham², S. Quinn², J. Pang^{*2}, R. Butters^{*2}, M. Pollak^{*3}, E. Brown². ¹Divisions of Endocrinology and Nephrology, Brigham and Womens's Hospital and Beth Israel Deaconess Med Ctr, Boston, MA, USA, ²Division of Endocrinology, Brigham and Womens's Hospital, Boston, MA, USA, ³Division of Nephrology, Brigham and Womens's Hospital, Boston, MA, USA.

The CaSR has known actions on the parathyroid gland, parafollicular C-cell, and kidney. Our studies of the adaptations of mice with targeted disruption of the PTH gene (CaR^{-/-}PTH^{-/-} aka PTH KO), both the PTH and CaR genes (CaR^{-/-}PTH^{-/-} aka DKO) or wild type mice (CaR^{+/+}PTH^{+/+} aka WT) to exogenous 1,25 (OH)₂ vitamin D₃ have revealed striking phenotypes that provide new insights on the roles of the CaR and PTH in calcium homeostasis. The 3 groups mice were given 0.5 ng/g BW of 1,25 (OH)₂vitamin D₃ by intraperitoneal injection, and the calcemic response over 72 hrs analyzed. Injections were given while the mice were given free access to a calcium replete diet [0.6% calcium (Ca) w/w chow and plain water] and repeated after conditioning the mice for 18-72 hrs on a Ca-deficient diet (0.01% Ca in the chow and plain water) prior to injection. Peak calcemic responses were observed in all genotypes on either diet at 24 hrs post injection. On the Ca replete diet (top figure), there was a 125% increase in serum calcium (SCa) in the DKO mice at 24 hrs. The increase in SCa was substantially less marked in the (PTH KO) (+41%), and less in the WT mice (+25%). On the Ca deplete diet (lower figure), the calcemic response at 24 hrs in the DKO mice was much less robust- +37%, and was similar to that in the PTH KO mice (+39%) but again was greater than that in the WT mice (+13%).

Lack of the CaSR renders mice lacking PTH markedly more sensitive to the calcemic action of vitamin D₃ than mice lacking PTH alone or WT mice. This exaggerated response appears selective for vitamin D-mediated intestinal Ca absorption rather than bone resorption, since it was observed on a Ca replete but not a Ca deplete diet. Additional factors that may contribute to the increased vitamin D sensitivity of the DKO mice are impaired secretion of calcitonin and decreased renal Ca excretion, although the latter could not explain the differences in the responses on the Ca replete and deplete diets.



Disclosures: O. Egbuna, None.

This study received funding from: NIH-NIDDK.

M225

Testin, a Novel Binding Partner of the Calcium-Sensing Receptor. A. L. Magno^{*1}, B. K. Ward^{*2}, E. Ingley^{*1}, A. D. Conigrave³, T. Ratajczak^{*2}.

¹Western Australian Institute for Medical Research, University of Western Australia, Perth, Australia, ²Endocrinology and Diabetes, Sir Charles Gairdner Hospital, Perth, Australia, ³School of Molecular and Microbial Biosciences, University of Sydney, Sydney, Australia.

The calcium-sensing receptor (CaR) is a G protein-coupled receptor that can respond to a diverse range of stimuli. Besides its integral role in calcium homeostasis, the CaR is involved in a wide variety of cellular processes through its mediation of different intracellular signalling pathways. To elucidate the mechanisms that convert the various extracellular stimuli for the CaR to specific intracellular responses we used the CaR intracellular tail as bait in a yeast two-hybrid screen of a mouse haemopoietic cell line

library. Identified in this library screen was testin, a protein that has been proposed to act as a tumour suppressor and is involved in cell adherence. Testin is a triple LIM domain protein that localises to focal adhesions and actin stress fibres. LIM domains are composed of two zinc fingers that mediate protein interactions important in coordinating specific signalling pathways. Three distinct clones of testin containing a 61 amino acid overlapping region were identified. This overlapping region incorporates the second zinc finger of the first LIM domain. Yeast two-hybrid based deletion mapping studies revealed that testin binds to the membrane-proximal region of the CaR tail, a domain critical for activation of several intracellular signalling pathways. The interaction between the CaR and testin in a mammalian system was confirmed in coimmunoprecipitation studies using lysates from HEK293 cells transiently expressing FLAG-tagged CaR and EGFP-tagged testin. The focus of our current studies is to investigate the possible colocalization of the CaR and testin at focal adhesions and/or actin stress fibres in conjunction with experiments examining testin's potential modulating role in CaR-mediated activation of the mitogen-activated protein kinase, phosphatidylinositol 3-kinase and Rho pathways. In this regard, we have preliminary evidence that overexpression of testin reduces CaR-mediated extracellular signal-regulated kinase phosphorylation in HEK293 cells stably expressing the CaR. In conclusion, we have identified the LIM domain protein, testin, as a novel interaction partner for the CaR that may regulate CaR-mediated signalling linked to the cytoskeleton.

Disclosures: A.L. Magno, None.

M226

Regulation of Calcium-Sensing Receptor by Glial Cells Missing 2 in Hyperplastic Parathyroid Cells. M. Mizobuchi^{*1}, C. S. Ritter^{*1}, G. Sicard^{*2}, E. Slatopolsky¹, A. J. Brown¹. ¹Renal, Washington University School of Medicine, St Louis, MO, USA, ²Surgery, Washington University School of Medicine, St Louis, MO, USA.

Glial cells missing 2 (Gcm2) is the key regulating transcription factor for parathyroid gland development. The continued expression of high levels of Gcm2 in mature parathyroid glands suggests that it is required for maintenance of parathyroid cell differentiation. The role of Gcm2 in parathyroid cell physiology, however, has not been fully investigated. In preliminary studies, we confirmed that Gcm2 mRNA continued to be expressed in hyperplastic parathyroid cells placed in culture. Western blot analysis of the human parathyroid tissue using a polyclonal antibody for Gcm2 revealed a band of approximately 57 kDa, the predicted size of the Gcm2 protein. We then examined the effects of Gcm2 silencing on cultured human parathyroid cells. Collagenase-dispersed human parathyroid cells from patients with chronic kidney disease were placed in monolayer cultures, and treated with lentivirus expressing shRNA for human Gcm2 for 24 hours. Fresh medium was added and the cells were harvested after 48 hours. RNA was analyzed for Gcm2, PTH, vitamin D receptor (VDR), calcium-sensing receptor (CaR) and proliferating cell nuclear antigen (PCNA) mRNAs by qPCR. Gcm2 mRNA was decreased by 75 ± 4 % (p < 0.01; mean of 3 cultures). Immunoblot analysis confirmed the decrease in Gcm2 as well. VDR, PTH and PCNA were not significantly affected by Gcm2 silencing, but CaR mRNA was consistently reduced by 48 ± 9% (p < 0.01). Further analysis of CaR mRNA indicated that transcripts containing Exon 1B, derived by transcription from CaR promoter 2, were down-regulated by the Gcm2 silencing. These results indicate that one function of Gcm2 is to maintain high levels of CaR expression in parathyroid cells. Further studies are underway to identify other targets of Gcm2 action.

Disclosures: M. Mizobuchi, None.

M227

See Sunday Plenary Number S227

M228

Calcilytics Block the Suppressive Effect of Calcimimetics on PTH mRNA Levels in Bovine Parathyroid Cells. B. T. Brinton^{*1}, M. Chan^{*1}, J. Li^{*1}, T. Le-Capling^{*1}, R. Fantáske^{*1}, E. F. Nemeth². ¹NPS Pharmaceuticals, Toronto, ON, Canada, ²Dept. Pharmaceutical Sciences, University of Toronto, Toronto, ON, Canada.

Extracellular calcium is the primary regulator of parathyroid cell function and most, if not all its actions are mediated by the calcium receptor (CaR). Thus, activation of CaR by the calcimimetic compound NPS R-568 decreases PTH secretion, PTH mRNA levels, and parathyroid cell proliferation elicited by hypocalcemic conditions. CaR antagonists (calcilytics) increase PTH secretion but, under normocalcemic conditions, do not appear to increase parathyroid cell proliferation. The effects of the calcilytic compound NPS 89636 on PTH synthesis (mRNA levels) in parathyroid cells is reported here. Dissociated bovine parathyroid (bPT) cells were cultured in media containing 0.9 mM phosphate and various concentrations of extracellular calcium (0.5 to 3 mM) in the presence or absence of NPS R-568 and/or NPS 89636. PTH mRNA levels were determined by real time quantitative PCR. Levels of PTH mRNA were similar following incubation of bPT cells for 24 hrs in media containing 0.5 or 1.8 mM calcium but were reduced by 70% at an extracellular calcium concentration of 3 mM (n=4; p=0.0001). The addition of NPS R-568 to cells cultured for 24 hrs in 1.8 mM calcium reduced PTH mRNA levels by 80%. These inhibitory effects of NPS R-568 were concentration-dependent (IC₅₀ = 42 nM) and stereoselective (no effect with 1 uM NPS S-568) and were essentially the same as our previous results using Northern blots to quantify PTH mRNA. The stability of PTH mRNA, as assessed by comparison to mRNA half-life at 1.8 mM extracellular calcium,

was reduced 2.8-fold by 3 mM extracellular calcium and 4.3-fold by 300 nM NPS R-568. The inhibitory effect of 3 mM extracellular calcium was completely blocked by NPS 89636 in a concentration-dependent manner ($EC_{50} = 21$ nM). The calcilytic similarly blocked the inhibitory effect of 300 nM NPS R-568 on PTH mRNA levels and shifted the NPS R-568 concentration-response curve to the right. By itself, NPS 89636 did not significantly affect PTH mRNA levels at extracellular calcium concentrations of 0.5 or 1.8 mM. Secretion of PTH, however, was stimulated by NPS 89636 (30-300 nM) at extracellular calcium concentrations of 1.25 to 2 mM. The ability of a calcilytic compound to completely block the effects of extracellular calcium on PTH secretion and mRNA levels demonstrates that both these effects are mediated solely through the CaR. In contrast to PTH secretion, levels of PTH mRNA appear to be maximally elevated at extracellular calcium levels of 1.8 mM and can be lowered but not further increased by compounds that act on the CaR.

Disclosures: E.F. Nemeth, NPS Pharmaceuticals 1, 5.
This study received funding from: NPS Pharmaceuticals.

M229

Role of G-alpha-q in Parathyroid Gland Function Elucidated by Mouse Genetic Approaches. M. Pi, Q. Luo*, L. D. Quarles. The Kidney Institute, KUMC, Kansas City, KS, USA.

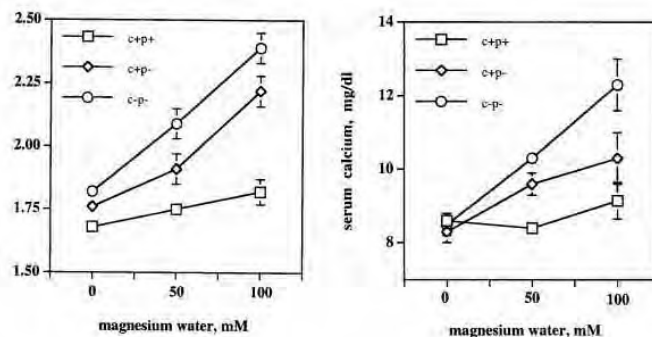
The calcium-sensing receptor (CASR) is a heptahelical receptor coupled to G-alpha-i and G-alpha-q. CASR regulates parathyroid gland (PTG) function, including PTH secretion and production as well as chief cell hypertrophy and hyperplasia. The specific and/or separate functions of G-alpha-q and G-alpha-i in regulating these different aspects of PTG function have not been elucidated. To investigate the role of G-alpha-q in the PTG, we initially assessed serum PTH levels in heterozygous G-alpha-q-deficient mice. We found that G-alpha-q-deficient mice had small but significant elevation of serum PTH levels compared to wild-type littermates. Next, we created transgenic ($Tg^{PTHp-Gqloop}$) mice using the human PTH promoter to drive the overexpression of a dominant negative Gqloop mini-gene to selectively disrupt G-alpha-q function in the PTG. We found that the gross appearance, body weight and survival of the $Tg^{PTHp-Gqloop}$ mice were indistinguishable from that of wild-type littermates. We also found that the Gqloop messenger RNA was expressed in parathyroid gland but not in other tissues of the $Tg^{PTHp-Gqloop}$ mice. Adult $Tg^{PTHp-Gqloop}$ mice exhibited a ~ 2-fold increase in basal serum PTH levels compared to wild-type mice (43 ± 5 pg/ml vs 25 ± 2 pg/ml; $p=0.001$), as well as increased PTH mRNA levels in PTG containing tissue. However, stimulation of PTH secretion by lowering the serum calcium with EGTA (300 microM/kg body weight) resulted in identical maximum levels of serum PTH in $Tg^{PTHp-Gqloop}$ and wild-type mice, but the percentage increment in PTH levels was less in $Tg^{PTHp-Gqloop}$ due to the higher baseline PTH values. Of interest, CASR mRNA expression was increased in the PTG, but decreased in the kidney of $Tg^{PTHp-Gqloop}$ compared to wild-type mice. In conclusion, we have demonstrated that the selective targeting of the PTG to investigate signaling mechanisms downstream of CASR is feasible. Our observations suggest a role for G-alpha-q in the regulation of PTH and CASR expression in the PTG, but fail to identify G-alpha-q-dependent regulation of PTH secretion in response to hypocalcemic stimuli. Studies are ongoing to determine if further reductions of G-alpha-q, achieved by crossing $Tg^{PTHp-Gqloop}$ onto heterozygous G-alpha-q-deficient mice, will uncover additional effects of G-alpha-q in CASR-dependent signaling. In addition, future studies will use the PTH promoter to separately target G-alpha-i to investigate its function in mediating CASR effects on PTG function.

Disclosures: M. Pi, None.
This study received funding from: P20-RR017686 and R01-AR37308.

M230

Intact Calcium-Sensing Receptor and PTH Genes Are Required to Regulate the Extracellular Magnesium and Calcium Concentrations Independently. S. Quinn*, O. Egbuna, L. Kantham, R. Butters*, J. Pang*, M. Pollak*, E. M. Brown. Medicine, Brigham and Women's Hospital, Boston, MA, USA.

Although the systems governing Ca^{2+} and Mg^{2+} homeostasis share elements in common, e.g., a common mechanism for paracellular reabsorption in the renal cortical thick ascending limb, the circulating levels of these two divalent cations are generally regulated independently of one another. We have studied the adaptations of mice with targeted disruption of the PTH gene ($CaR^{+/+}PTH^{-/-}$), both the PTH and CaR genes ($CaR^{-/-}PTH^{-/-}$) or wild type mice ($CaR^{+/+}PTH^{+/+}$) to variations in calcium or magnesium intake. The results have revealed striking phenotypes that shed light on the roles of the CaR and PTH in permitting independent regulation of Ca^{2+} and Mg^{2+} . When maintained on sufficient calcium intake to sustain normocalcemia, $CaR^{-/-}PTH^{-/-}$ mice show a dose-dependent, 55% and 33% increases in both blood Ca^{2+} and Mg^{2+} , respectively, when Mg^{2+} in the water is increased to 50 and then 100 mM (Figure 1). $CaR^{+/+}PTH^{-/-}$ mice show similar, but less marked increases of 24 and 26%, respectively, while wild type mice show 6% and 9% changes. Increasing Ca^{2+} in the water from 0% to 1% and then 2%, produces analogous changes in both blood Ca^{2+} and Mg^{2+} , elevating the two divalent cations by 106% and 50%, respectively, in the $CaR^{-/-}PTH^{-/-}$ mice, by 53% and 17% in the $CaR^{+/+}PTH^{-/-}$ mice and by 6% and 3% in the wild type mice (not shown). Thus loss of both PTH and the CaR results in an apparent "default" mode, in which increased intake of either Ca^{2+} or Mg^{2+} elevates the blood levels of both divalent cations. This defect is less severe when only PTH is missing, but the full capacity to maintain constancy of both Ca^{2+} and Mg^{2+} in the face of markedly increased oral loads of one or the other requires both PTH and the CaR.



Disclosures: S. Quinn, None.
This study received funding from: NIH.

M231

Deletion of the 25 Hydroxy Vitamin D 1 α Hydroxylase from Mice Expressing the Null Mutation for the Calcium Sensing Receptor Converts a Hypercalcemic to a Hypocalcemic Hyperparathyroid Phenotype. C. Richard*, D. Miao*, R. Samadifam*, Y. Wang*, G. N. Hendy*, D. Goltzman*. ¹Dept of Medicine, Calcium Laboratory, McGill University, Royal Victoria Hospital, Montreal, PQ, Canada, ²Department of Human Anatomy, Nanjing Medical University, Nanjing, China, China.

The calcium sensing receptor (CaSR) is functional mainly in the parathyroid gland and kidney, but likely as well in other tissues such as the gastrointestinal tract and the skeleton. These tissues are also target sites for the action of 1,25-dihydroxyvitamin D [$1,25(OH)_2D$]. Mice which are heterozygous or homozygous for the calcium sensing receptor null mutation ($CaSR^{+/+}$ and $CaSR^{-/-}$ respectively) develop hypercalcemia and hyperparathyroidism to a moderate or severe degree, respectively. Mice which are homozygous for targeted deletion of the 25 hydroxyvitamin-D 1 α -hydroxylase [$1\alpha(OH)ase^{-/-}$] which synthesizes $1,25(OH)_2D$ develop hypocalcemia, hyperparathyroidism and rickets but survive long term. To assess the interactions between the important calcium regulating molecules, CaSR and $1,25(OH)_2D$, we created compound mutants of the CaSR and 1 $\alpha(OH)ase$ mutants and assessed their growth, biochemistry and skeletal morphology. $CaSR^{+/+};1\alpha(OH)ase^{+/+}$ mice grew normally and exhibited normal longevity. $CaSR^{+/+};1\alpha(OH)ase^{-/-}$ mice developed severe rickets and osteomalacia as assessed by faxitron x-ray analysis and von Kossa staining of the skeleton but survived at least 2 months. $CaSR^{+/+};1\alpha(OH)ase^{-/-}$ mice developed even more severe rickets, osteomalacia and growth retardation but also survived long term. BMD, assessed by PIXIMUS, was reduced by 68% in the lumbar spine and by 49% in the femur compared to wild type mice, but only by 58% and 38% in the lumbar spine and femur respectively of the $CaSR^{+/+};1\alpha(OH)ase^{-/-}$ mice. Although $CaSR^{-/-};1\alpha(OH)ase^{+/+}$ mice develop severe hypercalcemia and most die before or shortly after weaning, deletion of the 1 $\alpha(OH)ase$ in $CaSR^{-/-};1\alpha(OH)ase^{-/-}$ mice facilitated survival for at least 2 months although these animals exhibited the most severe growth retardation, rickets and osteomalacia of all mutants. All mutant animals showed evidence of hyperparathyroidism with $CaSR^{+/+};1\alpha(OH)ase^{+/+}$ and $CaSR^{-/-};1\alpha(OH)ase^{+/+}$ mice displaying hypercalcemia. In contrast, $CaSR^{+/+};1\alpha(OH)ase^{-/-}$ mice and $CaSR^{-/-};1\alpha(OH)ase^{-/-}$ mice were severely hypocalcemic (serum calcium 1.28 and 1.27mM respectively). The results indicate that the phenotypic manifestations of hyperparathyroidism may be markedly influenced by the vitamin D status of animals with CaSR mutations, confirm that elimination of hypercalcemia sustains longevity in mice homozygous for the CaSR null mutation, and suggest that mutations in the CaSR contribute to worsening of skeletal mineralization.

Disclosures: C. Richard, None.

M232

Periarticular Bone Loss in Arthritis: Role of Synovial Glucocorticoid Generation. M. S. Cooper¹, R. Hardy^{*1}, E. H. Rabbitt^{*1}, N. J. Gittoes¹, M. Hewison², C. D. Buckley^{*1}, K. Raza^{*1}, P. M. Stewart^{*1}. ¹University of Birmingham, Birmingham, United Kingdom, ²Cedars-Sinai Medical Centre, Los Angeles, CA, USA.

Periarticular osteoporosis is a common feature of inflammatory arthritis. This feature is related to disease activity and is associated with uncoupling of bone resorption from formation. We previously hypothesised that local glucocorticoid generation within osteoblasts in response to inflammation may underlie this bone loss. An alternative possibility is that excess glucocorticoids are generated from other joint tissues. Primary synovial fibroblasts express the 11 β -hydroxysteroid dehydrogenase type 1 (11 β -HSD1) enzyme that generates the active glucocorticoids cortisol and prednisolone from their inactive counterparts cortisone and prednisone suggesting that synovium might generate glucocorticoids. We have now explored this hypothesis by characterizing glucocorticoid metabolism in synovial tissue explants from patients with rheumatoid arthritis (RA) and osteoarthritis (OA).

Glucocorticoid metabolism was examined in synovial tissue taken from subjects with OA (n=8) or RA (n=12) during orthopedic surgery using radiolabelled steroids and TLC. Immunohistochemistry was used to identify the cellular distribution of enzymes. The functional consequences of enzyme activity on IL-6 production were examined by ELISA.

All synovial biopsies had substantial capacity to activate glucocorticoids (cortisone to cortisol and prednisone to prednisolone) which was blocked by a specific 11 β -HSD1 inhibitor confirming 11 β -HSD1 expression. No difference in steroid metabolism was seen between samples from RA and OA subjects. In patients with RA, synovial cortisol generation increased with the ESR of the tissue donor ($R^2=0.4$, $p<0.05$). 11 β -HSD1 activity had functional consequences with cortisone able to decrease synovial IL-6 production in tissue from patients with RA or OA ($31\pm15\%$ for RA, $36\pm9\%$ for OA, both $p<0.05$). Steroid inactivation was also apparent in synovium and was not blocked by inhibition of 11 β -HSD1. Using immunohistochemistry 11 β -HSD2 expressing cells were identified in RA synovium and expression colocalized with the monocyte marker CD68. This pattern was distinct from 11 β -HSD1 which was expressed in fibroblasts.

Synovial tissue metabolises glucocorticoids with the predominant effect being glucocorticoid activation and this increases with inflammation. Endogenous glucocorticoid production in the joint is likely to regulate tissue inflammation but in excess might detrimentally impact on periarticular bone integrity. Additionally, a subset of immune cells expressing 11 β -HSD2 within synovium will be resistant to cortisol/prednisolone through steroid inactivation and this could perpetuate synovial inflammation.

Disclosures: M.S. Cooper, None.

M233

See Sunday Plenary Number S233

M234

The Effects of Glucocorticoid on BMP-2 and BMP-7 Expressions in Bone and Kidney. L. Cui¹, L. Zhou^{*1}, T. Wu^{*2}. ¹Department of Pharmacology, Guangdong Medical College, Zhanjiang, Guangdong, China, ²Guangdong Key Laboratory for R & D of Natural Drugs, Guangdong Medical College, Zhanjiang, Guangdong, China.

Aims: To determine the effects of long-term over dose of glucocorticoid (GC) on the genes and proteins expressions of bone morphogenetic proteins (BMP)-2 and BMP-7 in the bone tissue and kidneys of rats, to explore the relationships between BMPs changes in kidney-blood-bone and osteoporotic, hence to evaluate the roles of BMP-2 and BMP-7 in GC-induced osteoporotic. **Methods:** Three months-old Sprague-Dawley male rats were divided to control, GC-treated, GC-treated plus Danshen and GC-treated plus epimedium groups. Rats were oral gavages prednisone (3.2mg/kg/d) in the morning and the other treatments in the afternoon for three months. At endpoint, all rats were sacrificed for the collections of blood, bone and kidneys. The bone histomorphometry parameters in proximal tibial metaphyseal (PTM) were measured. The contents of BMP-7 and BMP-2 in blood serum were determined. RT-PCR was applied to test gene expressions of BMP-2 and BMP-7 mRNA and Immunohistochemistry was applied to analyze the expression locations and quantities of BMP-2 and BMP-7 in kidney and femoral bone. **Results:** Glucocorticoid induced bone loss by decreasing 28.96% ($P<0.01$) in trabecular area and 14.53% in trabecular thickness and 17.93% in trabecular number in PTM respectively, the trabecular separation increased 27.97% ($P<0.05$) when compared with control. Simultaneously, glucocorticoid decreased the gene and protein expressions of BMP-2 and BMP-7 in femoral bone ($P<0.05$), however, it decreased BMP-7 expression but increased BMP-2 expression in kidney ($P<0.05$). Glomerulus and collecting duct atrophy and protein cast were seen in kidneys of glucocorticoid treated rats. The contents of BMP-7 and BMP-2 in blood serum were decreased in the glucocorticoid treated rats. There was a positively correlation ($P<0.05$) in expressions of BMP-7 among kidney, blood and bone mass and a negatively correlation ($P<0.05$) in expressions of BMP-2 between kidneys and bone mass. Traditional Chinese medicine Danshen and epimedium can prevented glucocorticoid induced bone loss by regulating BMP-2 and BMP-7 expressions in bone and kidneys. **Conclusions:** Glucocorticoid induce bone loss in rats and down-regulated the expressions of BMP-2 and BMP-7 in bone tissue, down-regulated BMP-7 but up-regulated BMP-2 expression in kidney. BMP-2 and BMP-7 may play an important role in the mechanism of glucocorticoid induced osteoporosis. Some kidneys action Traditional Chinese medicine can prevented glucocorticoid induced osteoporosis by regulating the BMPs expressions in bone and kidneys.

Disclosures: L. Cui, None.

This study received funding from: Guangdong Science & Technology Project.

M235

See Sunday Plenary Number S235

M236

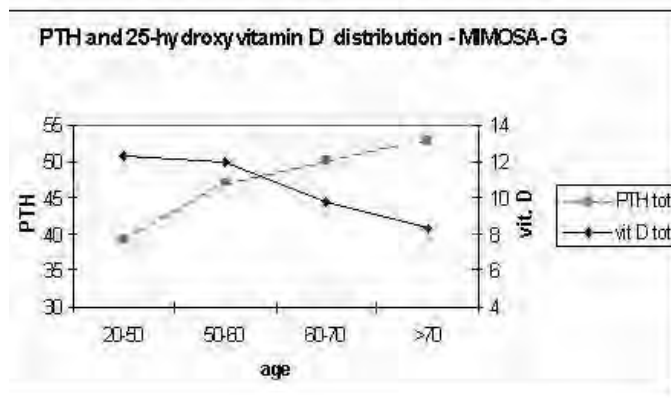
A Vitamin D Deficiency in an Italian Central Town Normal Population (MIMOSA-G project). P. De Remigis^{*1}, P. Ranieri^{*1}, A. De Remigis^{*1}, B. De Laurentiis^{*2}, M. Lattanzio^{*2}, L. Vianale^{*1}. ¹Endocrine Unit, General Hospital, Chieti, Italy, ²Endocrine Laboratory Unit, General Hospital, Chieti, Italy.

In the context of MIMOSA (Mineral Metabolism Osteoporosis in Abruzzo) project, a study was carried out about the correlation between 25-hydroxyvitamin D and PTH levels, in order to unveil vitamin-D deficiency and to schedule a prophylaxis program.

200 healthy subjects were considered; this population, belonged to a town (Guardagrele) of 9970 inhabitants, located in Abruzzo, a Central Italian Region, was selected from a randomized group of 820 subjects, who had ultrasound BMD screening, on the basis of normal t-score at QUS and ruling out other risk factors for osteoporosis, by questionnaire (this project is called MIMOSA-G, because it is restricted to total people of Guardagrele). The population was homogeneous for environmental factors and nutritional intake, of both genders, ranged from 20 to 85 yrs. They were subdivided in four groups of 25 members, for each gender: a) ranged from 20-50 yrs b) 50-60 c) 60-70 d) over 70. The blood samples were taken in winter; 25-hydroxyvitamin D and PTH were assayed by chemiluminescent method.

In our population of healthy individuals, calcidol levels are decreasing very significantly from 12.3 ng/ml (young people group) to 8.31 (the oldest one). There is not differences between male and females at any different age classes we considered. On the other hand, in parallel way, PTH levels are increasing significantly from 39.2 pg/ml in young people to 52.9 pg/ml in older ones, showing that a condition of secondary compensatory hyperparathyroidism is realizing by aging.

25-hydroxyvitamin D and PTH levels are negative correlated (correlation coefficient of 0.18). The threshold of 25-hydroxyvitamin D, above which the correlation becomes not significant, is 30 ng/ml (to be considered our biological reference). 50.2% of subjects show a level of 25-hydroxyvitamin D below 8 ng/ml. The profile of 25-hydroxyvitamin D graphic indicates the level of a vitamin D is sharply declining in general population over 60 yrs (more evident in females, while in man the curve is smoother), putting at risk of femoral fractures people for secondary hyperparathyroidism. Vitamin D deficiency is shown in Abruzzo severe over all in aged population probably due to inadequate exposure in winter and also insufficient dietary compensation.



Disclosures: P. De Remigis, None.

M237

The Protective Effects of Mechanical Strain on Osteocyte Viability Is Mediated by the Effects of Prostaglandin on the cAMP/PKA and the β -Catenin Pathways. Y. Kitase^{*}, M. L. Johnson, L. F. Bonewald. Oral Biology, School of Dentistry, UMKC, Kansas City, MO, USA.

Mechanical loading has been shown to prevent or reduce osteocyte cell death or apoptosis in vitro and in vivo. Fluid flow shear stress (FFSS) has been shown to reduce osteocyte apoptosis in response to glucocorticoid (GC). As GC induced osteoporosis is the second most common form of osteoporosis, we sought to identify the molecular mechanisms responsible for the protective effect of mechanical loading. Application of FFSS (16 dynes/cm²) significantly inhibited apoptosis of osteocyte-like MLO-Y4 cells induced by dexamethasone (Dex, 10⁻⁶ M). We hypothesized that PGE₂ is a protective factor for osteocytes as osteocytes release PGE₂ within minutes in response to FFSS. The protective effect of FFSS on Dex-induced apoptosis was significantly inhibited by indomethacin (10⁻⁶ M) while exogenous PGE₂ (10⁻⁶ M) significantly prevented apoptosis induced by Dex. The use of PGE₂ receptor agonists (butaprost, PGE, alcohol, sulprostone) and antagonist (AH6809) showed that the EP2 receptor was responsible. Dex was found to inhibit EP2 receptor and COX-2 expression and PGE₂ production as determined by gene array, real-time PCR and ELISA. As the EP2 receptor is known to signal through the classical cAMP/PKA pathway, the cAMP analog, 8Br-cAMP (100 μ M) was tested and found to protect against Dex-induced cell death. However, the PKA inhibitor H89 (5 μ M) only partially abrogated the protective effects of PGE₂. As recent studies suggest that PGE₂

can activate the β -catenin signaling pathway in addition to the classical cAMP/PKA pathway, LiCl (10 mM) was tested and found to protect against Dex induced cell death equivalent to FFSS and PGE₂. FFSS, PGE₂, and LiCl increased phosphorylation of both GSK-3 α and β . Wortmannin (1 μ M), a PI3K inhibitor, but not H89, reduced the phosphorylation of GSK-3. FFSS, PGE₂, and LiCl induced nuclear translocation of β -catenin. These studies provide evidence that osteocyte production of PGE₂ in response to mechanical shear stress is protective against GC induced osteocyte cell death, not only through the classical cAMP/PKA pathway, but also the PI3K/GSK-3/ β -catenin pathway. It will be important to determine if increased mechanical loading alone or in combination with therapeutics will reduce or prevent the detrimental effects of GC on osteocyte viability and bone integrity.

Disclosures: Y. Kitase, None.

M238

PTHrP Regulates Antimicrobial Peptide Production by Skin Keratinocytes. L. J. Defetos¹, D. W. Burton¹, J. Schaubert^{*2}, S. Tu^{*1}, R. A. Dorschner^{*2}, R. L. Gallo^{*2}. ¹Medicine, Veterans Administration San Diego Healthcare System and University of California, San Diego, CA, USA, ²Dermatology, Veterans Administration San Diego Healthcare System and University of California, San Diego, CA, USA.

PTHrP is expressed in normal skin keratinocytes at relatively high levels, but its function in this tissue is not well studied. Reports have demonstrated that PTHrP expression is increased in skin inflammation and that PTHrP contributes to the progression of other inflammatory diseases, such as rheumatoid and osteoarthritis. In this study, we investigated the interaction of PTHrP with antimicrobial peptides made by keratinocytes. We altered the amount of PTHrP that was expressed by an immortalized keratinocyte cell line (HaCaT) using transfection to increase expression and siRNA techniques to inhibit it. Real-time PCR was used to measure the levels of cellular antimicrobial peptides, including cathelicidin and α - and β -defensins. PTHrP 1-139, 1-141, and 1-173 transfection into HaCaT cells stimulated cathelicidin mRNA expression. While all three isoforms had a stimulatory effect, it was greatest for PTHrP 1-173 (150%), least for PTHrP 1-139 (50%), and intermediate for PTHrP 1-141 (80%), compared to vector control cells. Deletion of the 1-32 domain in the PTHrP expression plasmids prevented the increase in cathelicidin. No PTHrP effects were observed on α - or β -defensin mRNA expression. Inhibition studies using siRNA duplexes targeted to PTHrP 16-22, included in all three isoforms, demonstrated an 89% and 65% decrease in PTHrP and cathelicidin expression, respectively, compared to control (non-silencing) siRNA duplex targeted to a non-mammalian protein from *Thermotoga maritima*. Our results demonstrate that PTHrP regulates the expression of cathelicidin in keratinocytes and that both the 1-32 and 140-173 amino acids of PTHrP are required for the maximal stimulatory effect on cathelicidin expression. These data illustrate the contribution of keratinocyte-derived PTHrP to the immune defense of skin. The known interactions of vitamin D with PTHrP posit a novel regulatory network also involving toll receptors for the innate immune pathway in skin and perhaps other tissues.

Disclosures: L.J. Defetos, None.

This study received funding from: Department of Veterans Affairs and NIH.

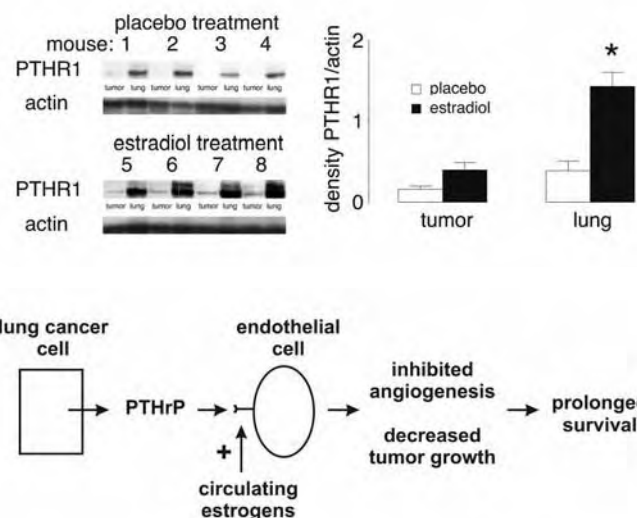
M239

See Sunday Plenary Number S239

M240

Sex Effects on PTHR1 in Non-Small Cell Lung Carcinoma. R. H. Hastings^{*}, A. Ko^{*}, R. Quintana^{*}, Y. Rascon^{*}. VA San Diego Healthcare System, San Diego, CA, USA.

Parathyroid hormone-related protein (PTHrP) is associated with increased survival in women with non-small cell lung carcinoma but not in men (Hastings et al. Clin Cancer Res 2006; 12:499-506). The sex dependence could arise from hormonal mechanisms, since lung carcinomas express receptors for gonadal steroids and estrogen is known to upregulate the type 1 PTH receptor (PTHrP1). This project tested the effects of estrogen on PTHR1 expression in orthotopic A549 lung adenocarcinomas model in female athymic mice. A549 cells express PTHrP, PTHR1 and estrogen receptor beta. Experimental animals received a subcutaneous estradiol pellet (0.72 mg/60 d to increase serum estradiol levels from control levels of <40 pmol/L, a known anomaly in athymic mice, to over 300 pmol. Immunoblots demonstrated significantly increased PTHR1 protein levels in estradiol-treated lung (Figure 1, $P < 0.01$) at 4 wks after tumor implantation. Estrogen also increased levels in lung carcinomas compared to controls, but the differences were not significant. At this point, our working hypothesis points to pulmonary endothelial cells as the site of estradiol action in lung. PTHrP 1-34 is known to stimulate endothelial cell apoptosis and to decrease tumor angiogenesis (Bakre, Nature Med 2002; 8:995-1003). Thus, the model in Figure 2 could explain the sex-selective association between lung carcinoma PTHrP expression and prolonged survival in female patients. Tumor-derived PTHrP would act on endothelial cells to inhibit angiogenesis, as a result slowing tumor growth and leading to longer survival. The effect would manifest predominantly in females because of estrogen-dependent increases in endothelial PTHR1. Studies are underway to test these hypotheses.



Disclosures: R.H. Hastings, None.

This study received funding from: Flight Attendants Medical Research Foundation, Dept. of Veterans Affairs.

M241

See Sunday Plenary Number S241

M242

Teriparatide [rhPTH(1-34)] Speeds Fracture Healing and Initiates Healing of Non-unions in Humans. E. N. Schwartz, D. M. Steinberg^{*}. Northern California Institute for Bone Health, Inc., Oakland, CA, USA.

Teriparatide (TPTD) stimulates osteoblast function. Osteoblast function is a key to fracture healing. Numerous studies have shown increased fracture healing with TPTD in a variety of experimental models. In these studies, intermittent low dose TPTD increased callus formation, increased production of bone matrix proteins and increased other potential mechanisms of fracture healing.

There is anecdotal information that TPTD may enhance fracture healing in humans. Accordingly, a variety of acute traumatic fractures (n = 20) of multiple body sites including a stress fracture of the femoral shaft, a fracture of a metacarpal, a fracture of the ankle and a fracture of the thumb all healed within a window of 3-5 weeks when healing of each fracture was estimated to take 6-8 weeks. Fracture healing was assessed by x-ray and CT scanning.

Additionally, these same mechanisms of enhanced fracture healing might also be useful in cases of fracture non-union. Accordingly, a variety of patients with different sites and lengths of time of non-union (n = 10) were treated by intermittent low dose TPTD. These included sites such as navicular bone in the ankle (2 fractures), the ischium, the distal tibial shaft, and other sites. About 50% of the non-unions had been previously operated on (ORIF). About 50% of the treated TPTD non-unions went on to partial or complete fracture healing based on x-ray, CT scanning or operative findings.

The risk factors for healing and non-healing of non-unions are not completely understood at this time.

The cases discussed indicate a possible role for TPTD in acute and stress fracture healing and a possible role in healing of certain fracture non-unions in humans.

Disclosures: E.N. Schwartz, Merck Pharmaceuticals 2, 5, 8; Proctor & Gamble 2, 5; Novartis 2, 5; Amgen 2, 5.

M243

The Effect of Estrogens on Bone Marrow Adipogenesis: A New Role for Sirtuins in Age-Related Bone Loss. A. Elbaz¹, D. Rivas¹, G. Duque². ¹Lady Davis Institute for Medical Research, Montreal, PQ, Canada, ²Medicine/Geriatrics, McGill University, Montreal, PQ, Canada.

Estrogens (E₂) are known to increase bone mass through the regulation of osteoclastic activity. In the case of age-related bone loss, the role of E₂ remains unclear since the predominant feature of this type of bone loss is not a higher level of osteoclastic activity but the infiltration of bone marrow by fat. In this study, we investigated whether E₂ have an effect on bone marrow adipogenesis and if this potential effect is exerted through the regulation of Sirt1 a recently reported suppressor of PPAR γ 2 in visceral and subcutaneous fat. We hypothesize that E₂ have an inhibitory effect on bone marrow adipogenesis through the induction of Sirt1 expression. To examine this hypothesis, young (5 month) and aged (24 month) female C57Bl/6J mice (n=10 per group) were either gonadally-intact, ovariectomized (OVX) or OVX and E₂ (estradiol-3,17- β -diol Steroids Inc., Witten, NH, USA) treated (OVX/E₂) to produce mean circulating levels of E₂ of 12 to 18 ng/ml. After three weeks of treatment, mice were sacrificed and both side tibia and femur dissected and fixed. Hematoxylin/Eosin (H/E), Toluidine Blue and oil red-O stainings were performed. Additionally, expression of Sirt1 was determined by immunofluorescence. Post-mortem uterus weight was taken as an index of the effect of estrogen deprivation (OVX) or supplementation (E₂ treatment) and was significantly reduced ($P < 0.05$) in OVX group (44 ± 1 mg, mean \pm s.e.m) compared to intact (76 ± 2 mg) or OVX/E₂ mice (64 ± 3 mg). We found significant differences in fat volume between old OVX and old OVX/E₂ with a significant reduction seen in the treated mice ($p < 0.001$). In contrast, no differences were found between the young groups. Additionally, we found that the reduction in bone marrow fat volume in OVX/E₂ mice correlated with high levels of Sirt1 expression and with reduced levels of PPAR γ 2 ($p < 0.01$) within the bone marrow. In summary, we have assessed the effect of estrogen on bone marrow adipogenesis in a model of young and old OVX mice. We have found that estrogens only inhibited bone marrow fat infiltration in old mice and that this effect is associated with higher levels of Sirt1 expression. This is an initial step in the understanding of the effect of estrogens on bone marrow adipogenesis through the activation of Sirtuins.

Disclosures: A. Elbaz, None.

This study received funding from: Quebec Network on Aging Research-Nutrition Axis.

M244

See Sunday Plenary Number S244

M245

Genetic Determinants of Serum Levels of Free Estradiol and Free Testosterone in Young Adult Swedish Men - The GOOD Study. A. Eriksson¹, M. Lorentzon¹, S. Nilsson², L. Vandenput¹, F. Labrie³, C. Ohlsson¹. ¹Center for Bone Research at the Sahlgrenska Academy, Göteborg University, Göteborg, Sweden, ²Division of Mathematical Statistics, Chalmers University of Technology, Göteborg, Sweden, ³Laboratory of Molecular Endocrinology and Oncology, Laval University, Quebec, PQ, Canada.

Sex hormones are important for skeletal growth and maintenance. Genetic factors are important regulators of serum sex hormone levels. However, the magnitude of contribution to this regulation from individual genes is not well known. The aim of this study was to investigate which sex hormone-related genes are the most important ones for regulation of calculated free serum estradiol (E2) and testosterone (T) levels, as a result of genetic variations, in young adult men. We used the Gothenburg Osteoporosis and Obesity Determinants (GOOD) study, a population-based study consisting of 1068 young men, age 18.9 ± 0.6 yrs (mean \pm SD). E2 and T in serum were analyzed using gas chromatography/mass spectrometry (GC-MS). Serum SHBG levels were measured using IRMA. Free E2 (FE2) and free T (FT) were calculated using a method described by Vermeulen et al (1), taking the concentrations of T, E2 and SHBG into account, and assuming an albumin concentration of 43 g/l. Genomic DNA was extracted from whole blood. We selected 51 candidate genes coding for hypothalamic and pituitary hormones regulating sex steroid secretion, enzymes involved in synthesis, metabolism or conversion of sex steroids, sex steroid receptors and carrier proteins. Single nucleotide polymorphisms (SNPs) with a minor allele frequency $\geq 5\%$ were selected from HapMapData Rel 21a/phaseII using a pairwise correlation method ($r^2 \geq 0.80$) including 10 kb upstream and 5 kb downstream of each gene. Genotyping was performed on the Illumina Bead Station Platform and was successful in $\geq 95\%$ of the study subjects in 626 of 765 selected SNPs ($\sim 81.8\%$). For FE2 the most strongly correlated SNP was found in CYP19. For FT the corresponding SNP was found in the FSHR (follicle stimulating hormone receptor) gene. An SNP in LHCG (luteinizing hormone/choriogonadotropin receptor) was the second most strongly correlated SNP for both FE2 and FT2. For each of these genes linear regression with all genotyped SNPs included were performed. Backward elimination was used to build the best models. For FE2 the best models of SNPs in CYP19 and LHCG explained 2.7 % and 2.9 % respectively of variation in serum levels ($p < 0.001$). For FT SNPs in FSHR and LHCG explained 4.0 % and 2.7 % respectively ($p < 0.001$). In conclusion, genetic variations in CYP19 and FSHR are important determinants of FE2 and FT respectively, in young Swedish men. Genetic variations in LHCG are important determinants of both FE2 and FT.

(1) Vermeulen A, et al. 1999. J Clin Endocrinol Metab 84:3666-3672

Disclosures: A. Eriksson, None.

M246

See Sunday Plenary Number S246

M247

Equol Producers After Soy Challenge Is Related to High Bone Turnover in Premenopausal Women. H. Kwak^{*1}, M. Kim^{*2}, C. Hwang^{*1}, S. Lee^{*1}, M. Jung^{*1}, Y. Kang^{*1}, C. Yim^{*1}, S. Park^{*1}, H. Yoon¹, K. Han^{*1}. ¹Laboratory of Endocrinology, Cheil Hospital and Women's Healthcare Center, Kwandong University College of Medicine, Seoul, Republic of Korea, ²Department of Internal Medicine, Marynoll General Hospital, Inje University School of Medicine, Busan, Republic of Korea.

Soybean isoflavones, the main phyto-estrogen, have been known to be able to modulate the action of endogenous estrogens and metabolism of phyto-estrogens might be affected by the menstrual cycles in premenopausal women. There have been few studies about metabolism of soy isoflavones and metabolites activity on bone in premenopausal women, therefore, we investigated the effect of isoflavones on bone turnover markers after challenge of soy isoflavones in premenopausal women. Premenopausal women were randomly assigned to receive either a 120mg soy extract-containing capsule (isoflavone group) or a lactose-containing capsule as placebo once a day for 3 menstrual cycles. Food records, blood samples, and 24hr urine collections were obtained from each subject at the beginning and end of the study. The isoflavone group showed increased concentrations of urinary isoflavone metabolites (equol, diadzein, genistein and dihydrodaidzein) after administration of soy extract-containing capsules compared to the placebo group. A bone formation marker, serum osteocalcin (OC) was increased after treatment in the isoflavone group compared to the placebo group, but the change of a bone resorption marker, urine deoxypyridinoline (DPD) after treatment was not different between two groups. As urinary isoflavone metabolites showed large inter-individual variation, we performed subgroup analyses according to previous studies. Equol is one of the isoflavone metabolites known to have high activity as diadzein or genistein, so that we divided the isoflavone group into the non-equol producer group (< 1000 nmol/l of urinary equol) and the equol producer group (> 1000 nmol/l of urinary equol). Serum OC was significantly increased after treatment in the equol producer group compared to the placebo and non-equol producer groups. And levels of urine DPD didn't change after soy challenge in the equol producer group, however, decreased in the placebo and non-equol producer groups. In conclusion, these data suggested that some premenopausal women who have ability to produce high amount of equol from soy isoflavones would result in relatively enhanced bone turnover rate after soy isoflavone intake and high-dose equol might have anti-estrogenic effects on bone metabolism in premenopausal women.

Disclosures: C. Hwang, None.

M248

See Sunday Plenary Number S248

M249

Activation of Farnesoid X Receptor in Breast Cancer Cell Lines by Bone-Derived Lipid. F. Journe¹, C. Chaboteaux^{*1}, V. Durbecq^{*1}, D. Larsimon^{*1}, G. Laurent^{*2}, J. J. Body¹. ¹Institut Bordet, Brussels, Belgium, ²Université de Mons-Hainaut, Mons, Belgium.

The skeleton is the most common site for metastasis of breast cancer. Cancer cells enhance the destruction of the bone matrix and increase the release of many growth factors and cytokines that stimulate metastatic cells proliferation. This vicious cycle is the key mechanism underlying the development of bone metastases. Recent data indicate that bone tissue also contains bile acids (BAs), which are accumulated from serum and which could stimulate the migration of breast tumor cells towards bone (Silva, J Lipid Res 2006). BAs are physiological ligands for farnesoid X receptor (FXR). FXR is a nuclear receptor involved in the regulation of BA metabolism in liver and intestine. In this context, it has been shown to heterodimerize with the retinoid X receptor (RXR). We have recently demonstrated the presence of FXR in human breast cancer specimens. In postmenopausal breast cancer patients, we found a correlation between FXR expression and that of estrogen receptor (ER) and proliferation markers. In the present study, we determined the effects of FXR activation by chenodeoxycholic acid (CDCA) in breast cancer cells, and examined its expression in bone metastasis specimens. We found that 50 μ M CDCA stimulated the proliferation of ER(+) MCF-7 cells cultured in steroid-free medium (EC50=15 μ M), while it had no effect on ER(-) MDA-MB-231 cells. Antiestrogens completely suppressed the mitogenic effect of CDCA in MCF-7 cells. Moreover, CDCA downregulated ER by 40% and stimulated the transactivation of progesterone receptor (PgR) by 316% in MCF-7 cells. Antiestrogens completely abolished PgR induction, and FXR gene silencing (siRNA) inhibited CDCA-stimulated cell proliferation as well as PgR induction. CDCA did not compete with [3H]-17 β -estradiol for binding to human recombinant ER immobilized on hydroxylapatite gel. In addition, FXR immunoprecipitation and subsequent ER demonstration by Western blotting revealed physical interaction between both receptors within 30 min. Finally, bone metastases from 32 breast cancer patients were examined for FXR expression by immunohistochemistry. FXR was expressed in 58% of bone metastasis specimens. In conclusion, our data reveal a positive crosstalk between FXR and ER, which accounts for FXR-mediated ER activation and subsequent mitogenic effects of FXR agonists in MCF-7 cells. Therefore, because of significant FXR and ER expressions in bone metastases of breast cancer, bone-derived lipids might contribute to the vicious cycle of tumor-induced osteolysis, especially in postmenopausal or estrogen-depleted cancer patients.

Disclosures: F. Journe, None.

M250

See Sunday Plenary Number S250

M251

Degeneration of Intervertebral Disc in Ovariectomized Rats. M. Kato¹, N. Fujita^{*1}, N. Hosogane^{*1}, H. Takaishi^{*1}, J. Takito^{*1}, T. Kikuchi^{*2}, M. Matsumoto^{*3}, K. Chiba^{*1}, Y. Toyama^{*1}. ¹Orthopaedic Surgery, Keio University School of Medicine, Tokyo, Japan, ²National Hospital Organization Murayama Medical Center, Tokyo, Japan, ³Department of Musculoskeletal Reconstruction and Regeneration Surgery, Keio University School of Medicine, Tokyo, Japan.

The intervertebral discs, which consists of water-rich nucleus pulposus and lamellar annulus fibrosus, degenerate with age and become source of low back pain. Estrogen deficiency in postmenopausal state closely associates with osteoporosis and may induce vertebral fractures. The purpose of this study is to investigate whether and how estrogen is involved in the degenerative process of the intervertebral discs. Eight-week-old female Wistar rats were sham operated (Sham) or ovariectomized (OVX). We collected the nucleus pulposus (NP) and the annulus fibrosus (AF) from the intervertebral discs at 1 week, 2 weeks, 3 months, 7 months, and 1 year after the operation. Histological observations at 7 months after the surgery indicated that the cell number of the NP and AF decreased significantly in OVX rats than that in Sham rats. Lamellar structure of the AF was disorganized in OVX rats. T2 weighted MRI images at 1 year after the surgery exhibited lower signal intensity of the NP of OVX rats than that of Sham rats. RT-PCR detected the expression of estrogen receptors (ER) α and ER β , in both the NP and AF. Immunofluorescence using confocal microscope revealed the nuclear localization of ER α and ER β in AF cells. In AF cells, nuclear localization of exogenously transfected DsRed-tagged ER α tended to aggregate under estradiol treatment and disperse under estrogen antagonist, ICI182780, administration. Real-time RT-PCR indicated that the expression level of type II collagen of the AF and NP in OVX rats was approximately 0.4 points lower ($P<0.05$) than that in Sham rats at 2 weeks and 7 months after the surgery. Decreased type II collagen mRNA expression and histological evidence of degeneration in the intervertebral discs of OVX rats suggests that menopause is one of the factors inducing disc degeneration and that estrogen may be involved in intervertebral disc homeostasis.

Disclosures: M. Kato, None.

M252

Co-Chaperone Potentiation of Vitamin D Receptor-Mediated Transactivation: A Role for Bag-1 as an Intracellular Binding Protein for 1,25-Dihydroxyvitamin D₃. R. F. Chun, M. Gacad^{*}, L. Nguyen^{*}, M. Hewison, J. S. Adams. Endocrinology, Diabetes and Metabolism, Cedars-Sinai Medical Center, Los Angeles, CA, USA.

In recent studies we have proposed that mitochondrial metabolism and nuclear signaling of vitamin D metabolites are not simply dependent on intercompartmental concentration gradients of free hormone in the target cell, but instead involve protein chaperones that interact with and traffic vitamin D metabolites to specific intracellular destinations. For example, the constitutively-expressed member of the heat shock protein-70 family (hsc70) is able to bind both 25-hydroxyvitamin D₃ (25D₃) and 1,25-dihydroxyvitamin D₃ (1,25D₃), potentiating 25D₃ metabolism and 1,25D₃-mediated gene transactivation. Hsc70 also recruits and interacts with the co-chaperone protein BAG-1. Competitive ligand binding assays showed that, like hsc70, recombinant BAG-1 is able to bind 25D₃ (K_d=0.57 nM) and 1,25D₃ (K_d=0.19 nM) with high affinity. To investigate the functional significance of this, we transiently overexpressed the naturally-occurring short (S), medium (M) and long (L) variants of BAG-1 in human, 1 α -hydroxylase (CYP27b1)-expressing kidney HKC-8 cells stably transfected with a 1,25D₃-responsive 24-hydroxylase (CYP24) promoter-reporter construct. Physiologically relevant concentrations of 25D₃ (200 nM) and 1,25D₃ (5 nM) were able to induce CYP24 promoter activity in these cells. CYP24 reporter activity was amplified 1.5-2.0-fold following over-expression of BAG-1S, L or M. By contrast, BAG-1 isoforms had no effect on metabolism of 25D₃ to either 1,25D₃ or 24,25D₃ by HKC-8 cells, indicating that the induction of CYP24 promoter activity by 25D₃ and potentiation of this effect by BAG-1 involves intracrine conversion to 1,25D₃. Further studies showed that transfection of HKC-8 cells with cDNA for BAG-1S in which the hsc70-binding domain was mutated resulted in decreased binding of 1,25D₃ leading to a concomitant loss of potentiation of CYP24 promoter transactivation. Similar loss or promoter-reporter activity in the presence of mutant BAG-1S was not observed for 25D₃ which retained binding to this form of BAG-1S. These data 1] highlight a novel role for BAG-1 as an intracellular binding protein for 1,25D₃ and 2] suggest that BAG-1 is able to potentiate vitamin D receptor (VDR)-mediated transactivation by acting as a nuclear chaperone for exogenous or endogenously synthesized 1,25D₃. We postulate that hsc70 and BAG-1 interact to provide a chaperone complex for 1,25D₃, but not 25D₃, thereby providing a novel mechanism for fine tuning the intracellular actions of the hormone.

Disclosures: R.F. Chun, None.

M253

See Sunday Plenary Number S253

M254

Expression of the 1,25-Dihydroxyvitamin D₃ Receptor in Multiple Tissues in Adult and Developing Danio rerio (Zebrafish). T. Craig^{*}, R. Kumar. Nephrology Research, Mayo Clinic Rochester, Rochester, MN, USA.

The receptor for 1,25-dihydroxyvitamin D₃ (VDR) mediates many of the functions of 1,25-dihydroxyvitamin D₃ in cellular growth and development and mineral homeostasis. In order to better understand the functions of VDR, we utilized zebrafish (*Danio rerio*) as a model organism in which investigations of both adults and developing embryos are facile compared to larger vertebrates. Immunohistochemistry was carried out in decalcified male and female zebrafish adults (5 months age) and in developing fertilized embryos at 72 hours using antibodies against VDR. Mounted sections from formalin-fixed paraffin-embedded tissue blocks were treated with a polyclonal antibody raised in rabbits against the VDR or pre-immune rabbit control serum. Anti-rabbit HRP secondary antibody/diaminobenzidine (DAB) staining, with hematoxylin, as a counter-stain was used to visualize the primary antibody bound to the receptor. We observed intense staining for the VDR in epithelial cells of the intestine, oropharynx, cells covering gill lamellae, osteoblasts, osteocytes, pharyngeal teeth, kidney tubules (but not glomeruli), rods and cones of the retina, spinal cord, and epithelia of the olfactory organ. Less intense staining was observed in the ovaries and testes, with large areas of testes without immunostaining for the receptor.

We conclude that the VDR is expressed in calcium and phosphate transporting epithelia of the intestine, gills, and kidney and in osteoblasts, teeth, and neural cells. The use of zebrafish as a model may allow performance of experiments specific to the VDR that are difficult to carry out in other vertebrates.

Disclosures: T. Craig, None.

M255

See Sunday Plenary Number S255

M256

A Significant Higher Risk for Fall-Associated Fractures with a Creatinine Clearance Below 65. L. C. Dukas^{*1}, E. Schacht², M. Runge^{*3}. ¹Acute Geriatric University Clinic, Kantonsspital Basel, Basel, Switzerland, ²Zurich Osteoporosis Research Group ZORG, Zurich, Switzerland, ³Center for Muscle and Bone Research, Aerpah Klinikum, Esslingen, Germany.

A Creatinine clearance of <65ml/min. is associated with decreasing balance and muscle power and an increased risk for falls. In this study we investigated if a Creatinine clearance of <65ml/min. is also associated with a higher fracture incidence. In a cross-sectional study in 1781 German men and women treated for osteoporosis, we assessed the association between the Creatinine clearance and the risk for fractures within the last 12 months. The Creatinine clearance was calculated using the established Cockcroft-Gault formula. Results are from spearman correlation analyses and logistic regression analyses. The p-values are two-sided. 1410 women and 371 men aged 60 years and older with a mean BMI of 26kg/m² and a mean Creatinine clearance of 60.2ml/min. participated in this study. A Creatinine clearance of <65ml/min. was significantly associated with a 44% higher fall associated fracture incidence compared to a Creatinine clearance of >65ml/min. Participants with a Creatinine clearance of <65ml/min. had significantly more vertebral fractures ($P=0.008$), hip fractures ($p=.002$) and fractures of the radius ($p=.002$) but not significantly more fractures in other localization ($p=0.08$), compared to participants with a Creatinine clearance of >65ml/min. We found no association between the Creatinine clearance and non-fall associated fractures ($p=.49$). We are the first to describe, that patients with a low Creatinine clearance of <65ml/min have a significant higher increased risk for falls and a higher increased risk for fall associated fractures, compared to patients with a Creatinine clearance of >65ml/min. Since the higher risk for falls, associated with a Creatinine clearance of <65ml/min., is due to decreasing calcitriol serum levels, we hypothesize that also the higher fall-associated fracture incidence observed with a Creatinine Clearance of <65ml/min., is due to decreasing calcitriol serum levels.

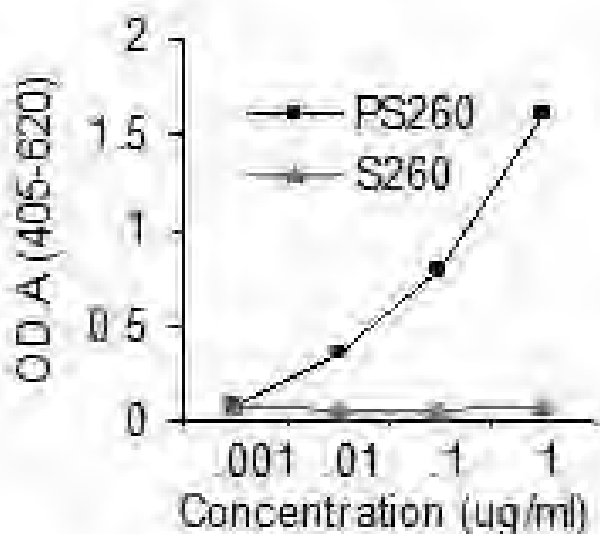
Disclosures: L.C. Dukas, Teva Pharmaceutical Industries 2.

This study received funding from: TEVA Pharmaceutical Industries..

M257

Examination of Human Retinoid X Receptor alpha Phosphorylation at Serine 260 Using Specific Antibodies in Cancer Cell Lines and Tumor Tissues. D. C. Huang, X. F. Yang*, L. Nguyen-Yamamoto, R. Kremer. Department of Medicine, Royal Victoria Hospital and McGill University, Montreal, PQ, Canada.

The retinoid X receptor alpha (RXR α) is a member of the nuclear receptor superfamily which regulates transcription of target genes through its heterodimerization with several partners including the vitamin D receptor. In previous studies, we have shown that phosphorylation of serine 260 of the human RXR α disrupts signaling and induces resistance to ligand activation of several partners of RXR α . Here we report the development of novel polyclonal antibodies which specifically react with phosphoserine residue 260 of human RXR α (PS260). Antiserum raised against PS260 or non-phosphorylated human RXR α S260 were purified with PS260 or S260 affinity columns. Specificity of antibodies against PS260 was examined by ELISA and demonstrated selective reactivity with PS260 peptide (Figure). We next examined hRXR α phosphorylation at serine 260 in several cell lines in which MAPKinase/Erk is activated prior to and following treatment with the MAPKinase inhibitor U0126 and showed a strong decrease in hRXR α serine 260 phosphorylation. We next examined human tissues from breast, colon and lung cancers by Western blot analysis using PS260, S260 and ERK antibodies. A strong correlation was observed between ERK expression and hRXR α phosphorylation at serine 260. Furthermore, a positive correlation was observed between tumor staging and hRXR α phosphorylation. Overall, our data indicate that antibodies specifically raised against phosphorylated hRXR α at serine 260 may be useful indicators of tumor progression of several types of cancers.



Disclosures: D.C. Huang, None.

M258

Role of TRPV 6 and β -Glucuronidase in 1,25(OH) $_2$ D $_3$ - and PTH-Stimulated Calcium Uptake in Intestinal Epithelial Cells. R. C. Khanal*, N. M. Smith*, T. M. Sterling*, S. Tunsophon*, I. Nemere. Nutrition and Food Sciences, Utah State University, Logan, UT, USA.

We have found that 1,25(OH) $_2$ D $_3$ -stimulated 45 Ca uptake can be demonstrated in isolated intestinal cells of adult chickens, and that the response is mediated by the 1,25D $_3$ -MARRS receptor, but not the VDR, as judged by preincubation with the appropriate antibodies. Such cells retain hormone-stimulated PKA, believed to mediate 45 Ca uptake, but lack steroid-stimulated PKC, believed to mediate efflux. PKC mediated efflux is supported by the observation that in freshly isolated cells from young chicks, 1,25(OH) $_2$ D $_3$ -stimulated 45 Ca uptake can only be demonstrated in cells pretreated with calphostin C, since without the PKC inhibitor, steroid-stimulated uptake is matched by efflux. Moreover, treatment of such cells with phorbol ester rapidly stimulated 45 Ca efflux. We have also discovered that cultured intestinal cells exhibited hormone stimulated PKC activity after 50 h, but it was diminished by 64 h, and lost by 72 h. Using the 72 h cultured cell model system, we have verified that 300 pM 1,25(OH) $_2$ D $_3$ stimulated 45 Ca uptake, and that this response is inhibited by pretreatment with Ab099 against the receptor. To further study the mechanism of calcium uptake, we found that 1,25(OH) $_2$ D $_3$ also stimulated the release of β -glucuronidase, a lysosomal marker enzyme and activator of TRPV calcium transporters. Moreover, treatment of isolated enterocytes with β -glucuronidase stimulated 45 Ca uptake in the absence of hormone. To determine whether the PKA signal transduction pathway is responsible for exocytosis of β -glucuronidase, we treated cells with PTH-known to activate PKA but not PKC in the chick model system-forskolin, or phorbol ester. PTH and forskolin-both of which stimulate 45 Ca uptake-were each found to stimulate β -

glucuronidase release, while phorbol ester had no effect. Finally, using siRNA to either TRPV 6 or β -glucuronidase abolished 1,25(OH) $_2$ D $_3$ -stimulated 45 Ca uptake, relative to controls transfected with scrambled siRNA.

Disclosures: R.C. Khanal, None.

M259

See Sunday Plenary Number S259

M260

Derepression of CYP27B1 Gene Expression Mediates DNA-Demethylation. M. Kim*, I. Takada*, K. Takeyama*, S. Kato. Institute of Molecular and Cellular Biosciences, Tokyo, Japan.

25(OH)D $_3$ 1 α -hydroxylase (CYP27B1) gene is a key enzyme in vitaminD synthesis, hydroxylating 25(OH) $_2$ D $_3$ to the active form of vitaminD, 1 α ,25(OH) $_2$ D $_3$. 1 α ,25(OH) $_2$ D $_3$ negatively regulates gene expression through Vitamin D receptor(VDR) binding to promoter, while PKA signaling activated by parathyroid hormone induced gene expression. The transactivation function by VDRE, a bHLH transcriptional factor recognizing negative VDRE in CYP27B1 promoter(1 α nVDRE), was found to be suppressed by liganded VDR/HDAC co-repressor complex(EMBO J. 23, 1598, 2004). We further reported that Dnmts interacts with VDRE /VDR/HDAC co-repressor complex, 1 α ,25(OH) $_2$ D $_3$ -dependent transrepression of CYP27B1 gene links repressive histone modification with epigenetic DNA methylation.

Now we reports that DNA methylation and demethylation have a critical role of CYP27B1 gene regulation. ChIP assay showed that Dnmt and HDAC sequentially interacts with 1 α nVDRE, and then sequential changes in DNA methylation pattern were occurred. However, DNA methylation status couldn't induced of heterochromatin formation of CYP27B1 gene, instead that, DNA demethylation occurred on CYP27B1 promoter by depleting of 1 α ,25(OH) $_2$ D $_3$. Furthermore, demethylation was increased when activates PKA signaling under cAMP pathway. Demethylation was observed later for one hour since 1 α ,25(OH) $_2$ D $_3$ is depleted. These changes occurred in the absence of cell growth or cell division. Furthermore, demethylation was inhibited by a treatment with actinomycin, a transcription inhibitor. These results suggest that this demethylation links to transcriptional mechanism. Thus, we propose the presence of demethylase enzyme that removes 1 α ,25(OH) $_2$ D $_3$ -induced DNA methylation.

Disclosures: M. Kim, None.

This study received funding from: ERATO, Japan Science and Technology Agency.

M261

Personal Ultraviolet Exposure and Vitamin D Synthesis. M. G. Kimlin, A. Brodie, C. A. Lang. Institute of Health and Biomedical Innovation, Queensland University of Technology, Brisbane, Australia.

The association between exposure to ultraviolet radiation and the synthesis of Vitamin D [25(OH)D] is an area that is under increasing scrutiny. It is currently assumed that incidental UV exposure, particularly in a sunny climate should provide adequate vitamin D status for the population.

This research was undertaken to test this assumption among healthy free-living adults aged 19 to 82 years, in southeast Queensland, Australia (27°S), during late February/early March 2007 (Australian summer). 42 adults (17 males, median age 43 years) participated in this project, by having a blood sample taken to assess baseline serum 25(OH)D status and answering a self-reported questionnaire which sought demographic data and information about sun exposure. Participants were distributed with UV dosimeters to assess personal sun exposure. A second blood sample at 48-hour post-baseline blood, was collected along with the used UV dosimeters. This research was approved by Queensland University of Technology Human Research Ethics Committee and conducted under the guidelines of the Declaration of Helsinki.

The mean blood serum 25(OH)D at baseline was 75nm/L (min., 16, max., 160 nm/L) and 48 hours post baseline was 79nm/L (min., 21, max., 183 nm/L). The median personal UV exposure in the first 24 hours (as measured with the UV dosimeters) was 1.05 MED (minimal erythemal dose) with a range of 0 MED to 15.8 MED and in the final 24 hours the median personal UV exposure was 1.92 MED with a range of 0.2 MED to 7.4 MED. No significant correlation was found between personal UV exposure over the 48 hour period and change in 25(OH)D status between baseline and final collection. Additionally, self reported time in the sun (during this 48 hour period) was not related to change in 25(OH)D status. No relationships were also found between sunscreen use, age or gender. These results suggest that short term sun exposure does not impact on the 25(OH)D status, even though high exposures were of such intensity to promote the production of 25(OH)D.

Disclosures: M.G. Kimlin, None.

This study received funding from: Institute of Health and Biomedical Innovation.

M262

See Sunday Plenary Number S265

M263

Seasonal Skin Colour Variations and the Impact on Vitamin D Status. C. A. Lang¹, A. Brodie¹, S. Harrison^{*2}, M. G. Kimlin¹. ¹Institute of Health and Biomedical Innovation, Queensland University of Technology, Brisbane, Australia, ²Skin Cancer Research Group, James Cook University, Townsville, Australia.

The influence of sunlight exposure on Vitamin D [25(OH)D] status is an intriguing and complex question. The current theory is that incidental UV exposure, particularly in a sunny climate should provide adequate 25(OH)D, however, an individual's characteristics, such as skin colour also contributes to an individual's potential to synthesize 25(OH)D. The aim of this research was to investigate the relationship between skin colour and 25(OH)D status of healthy adults in the 2007 summer and the 2006 winter in Queensland, Australia (27°S). A sample of blood was collected to assess 25(OH)D status at each time point. Skin colour was determined using a Minolta 2500D spectrophotometer recording spectral skin reflectance on the dorsum of the hand, forehead and upper inner arm. Melanin Density (MD) was calculated using the formula described by Dwyer et al. This research was approved by Queensland University of Technology Human Research Ethics Committee and conducted under the guidelines of the Declaration of Helsinki. Sixty participants (18m / 42f) with a median age 53 years (18 to 87 years) completed both summer and winter cross-sectional surveys. 53% described themselves as having a fair complexion, 25% medium and 18% an olive/dark complexion. There were 60% of the sample with an adequate (>50nm/l) 25(OH)D level in winter compared with 86.7% in summer (p=0.005). Vitamin D levels in winter (median 53.5 nm/l, interquartile range (IQR) 40.3nm/l) were significantly lower (z = -4.28, p<0.001) than summer (median 72.0 nm/l, IQR 38.8 nm/l). There was a median seasonal difference in 25(OH)D of 16.0 nm/l, with a wide range (-43.0 to 69 nm/l) that was not associated with age, gender, occupation or self reported skin colour. Median MD levels of a high UV exposure site (forehead) were significantly lower (z = -3.59, p<0.001) in winter (median 2.55 (IQR 1.74) than summer (median 3.02, IQR 1.61). There was a significant inverse correlation between the winter levels of forehead MD and 25(OH)D status (r=-0.353, p=0.006) and no correlation between the summer forehead MD and 25(OH)D (r = 0.012, p=0.927). These results indicate that seasonal variations in skin colour, due to seasonal exposure, cannot be used as a crude indicator for 25(OH)D status. Why the forehead MD was correlated in winter but not summer remains unanswered. Further research is required into the interactions between the solar UV environment and Vitamin D synthesis, particular with respect to seasonal variability of skin colour.

Disclosures: C.A. Lang, None.

This study received funding from: Institute of Health and Biomedical Innovation.

M264

Vitamin D₂ Supplementation Suppresses Endogenous Levels of 25-Hydroxyvitamin D₃; Clinical Application of A New, Direct Immunoassay for the Specific Detection of 25-Hydroxyvitamin D₃. B. Li^{*1}, I. Byrjalsen¹, C. Christiansen¹, P. Glendenning^{*2}, D. Henriksen^{*3}, S. Vasikaran^{*2}, P. Qvist¹. ¹Nordic Bioscience A/S, Herlev, Denmark, ²Department of Core Clinical Pathology & Biochemistry, Royal Perth Hospital, Perth, Australia, ³Sanos Bioscience A/S, Roedovre, Denmark.

The nutritional vitamin D status is assessed on the basis of 25-hydroxyvitamin D (25(OH)D) levels in circulation, however there is no consensus on the relative potency of the two main vitamin D forms, D₃ and D₂. Therefore it is important to have available specific data for the endogenous form 25(OH)D₃ as well as for the corresponding D₂ forms. The present study was performed to determine the circulating levels of 25(OH)D₃ during vitamin D₂ and D₃ supplementation, respectively, using a new, direct immunoassay specific for 25-hydroxyvitamin D₃.

Serum samples were obtained at baseline and three months after supplementation with vitamin D₃ (39 participants, 400-800 IU/day) and vitamin D₂ (45 participants, 1000 IU/day), respectively. 25(OH)D₃ levels were determined by a new direct, vitamin D₃ specific ELISA based on polyclonal antibodies with <1% cross-reactivity to 25(OH)D₂ (Nordic Bioscience Diagnostics A/S, Herlev, Denmark). The direct 25(OH)D₃ ELISA demonstrated excellent correlation (r=0.95) to 25(OH)D₃ levels determined by HPLC through the Vitamin D External Quality Assessment Scheme (DEQAS, UK).

In the vitamin D₂ treated group, the relative levels of 25(OH)D₃ increase 21% (post vs pre treatment in individuals) after 3 months treatment (P<0.01). In contrast, vitamin D₂ supplementation induced 15% reduction (post vs pre treatment in individuals) compared to pre-treatment (P<0.01). The data suggest, that the decrease of 25(OH)D₃ level in vitamin D₂ group could be caused by the vitamin D₂ supplementation, which could give rise to competition between vitamin D₂ and vitamin D₃ for the substrate of vitamin D 25-hydroxylase.

Further studies are needed to confirm the suppression of endogenous vitamin D₃ levels during vitamin D₂ supplementation and its clinical relevance.

Disclosures: B. Li, Nordic Bioscience A/S 3.

M265

See Sunday Plenary Number S265

M266

Fetal Hypervitaminosis D Results in Neonatal Lethality. L. Lieben^{*}, R. Van Looveren^{*}, R. Bouillon, G. Carmeliet. Laboratory of Experimental Medicine & Endocrinology, K.U.Leuven, Leuven, Belgium.

1,25(OH)₂vitaminD₃ [1,25(OH)₂D₃] is the major regulator of calcium homeostasis but is dispensable for fetal bone development. Hypervitaminosis D is deleterious during adult life but its effect on embryonic development is still enigmatic. To this end, vitamin D receptor deficient (VDR^{-/-}) females, showing highly elevated serum 1,25(OH)₂D₃ levels (p<0.001 vs. VDR^{+/+} mothers) were mated with VDR^{+/+} males generating offspring that either can (VDR^{+/+}) or cannot respond (VDR^{-/-}) to possible high 1,25(OH)₂D₃ levels.

VDR^{-/-} mice conceived less frequently, but both genotypes were born in the anticipated Mendelian ratio (47% VDR^{+/+} and 53% VDR^{-/-} pups). Although genotypes were indistinguishable in appearance and weight at birth, 97% of VDR^{+/+} pups died immediately thereafter. Further analyses were therefore performed at embryonic day 18.

No manifest difference in serum calcium levels was observed between genotypes. Surprisingly, bone mass was decreased in VDR^{+/+} embryos, whereas it was normal in VDR^{-/-} embryos. More specifically, femoral calcium content was decreased by 30% in VDR^{+/+} fetuses as compared to VDR^{-/-} littermates and to VDR^{+/+} embryos of VDR^{+/+} mother (p<0.001). This is primarily due to reduced cortical bone volume as shown by histomorphometry (-50% vs. VDR^{+/+} fetuses of VDR^{+/+} mother; p<0.001). Transplacental calcium transport was significantly decreased in VDR^{+/+} fetuses (-20%; p<0.05), although no difference was found in the placental TRPV6 and calbindin-D_{9k} mRNA level between genotypes. In addition, amniotic fluid calcium levels were increased in VDR^{+/+} embryos (1.2x; p<0.001) despite increased TRPV5 mRNA expression (5x; p<0.001) compared to VDR^{-/-} littermates. These data indicate that bone mineralization is impaired in VDR^{+/+} fetuses of VDR^{-/-} mothers, associated with normocalcemia and increased calcium excretion.

A likely explanation are the increased 1,25(OH)₂D₃ levels detected both in VDR^{-/-} (14x) and VDR^{+/+} fetuses (9x) of VDR^{-/-} mothers compared to VDR^{+/+} embryos of VDR^{+/+} mothers (p<0.001), suggesting diffusion of 1,25(OH)₂D₃ through the maternal-fetal barrier. VDR^{+/+} fetuses responded to this elevated 1,25(OH)₂D₃ level with increased mRNA level of fibroblast growth factor 23 in the femur (5x; p<0.001) and 24-hydroxylase in the kidney (1.7x; p<0.05) and decreased renal expression of 1α-hydroxylase (-80%) as compared to VDR^{+/+} embryos of VDR^{+/+} mothers.

In conclusion, our data indicate that 1,25(OH)₂D₃ diffuses through the maternal-fetal barrier and that fetuses control their serum 1,25(OH)₂D₃ levels by activating feedback loops. Moreover, excessive 1,25(OH)₂D₃ is toxic for the fetus resulting in decreased bone mineralization and neonatal lethality.

Disclosures: L. Lieben, None.

M267

Effect of Hypercalciuria on Bone Density and Strength in Genetic Hypercalciuria Stone-Forming Rats. M. D. Grynaps¹, A. Ng^{*1}, S. D. Waldman^{*2}, D. A. Bushinsky³. ¹Pathology, Mount Sinai Hospital Research Institute, Toronto, ON, Canada, ²Chemical Engineering, Queens University, Kingston, ON, Canada, ³Nephrology/Medicine, University of Rochester, Rochester, NY, USA.

Hypercalciuria is the most common metabolic abnormality in patients with calcium (Ca) containing kidney stones. Patients with hypercalciuria often excrete more Ca than they absorb, indicating a net loss of total body Ca, almost certainly derived from bone. A number of studies have shown a decrease in bone mineral density (BMD) and an increase in fracture rate in hypercalciuric stone formers compared to controls. However, in human stone formers it is difficult to determine if the reduction in BMD is due to a primary bone disorder or to any number of dietary factors that may be altered in stone formers over their lifetime. To study the independent effect of hypercalciuria on bone, we utilized the genetic hypercalciuric stone-forming (GHS) rats which were established by successively inbreeding the most hypercalciuric progeny of hypercalciuric Sprague-Dawley rats. Sixteen 46th generation female GHS and control (Ctl) rats were placed in metabolic cages and fed a 1.2 % Ca diet for 6 weeks, and then their femurs, tibiae, humeri and lumbar spines were studied for BMD, histomorphometry, image analysis and mechanical tests. All comparisons are to Ctl rats. Urine Ca excretion was significantly greater in the GHS rats. BMD in both the femur and vertebrae (L1-L5) was significantly lower in the GHS rats. In the femur, trabecular bone volume and thickness were significantly lower in the GHS rats; however, trabecular number was not altered. Neither osteoid volume nor osteoid surface was altered in GHS rats. In the femur, the number of end points, multiple points, the length of node-to-free struts and the length of the node-to-node struts were each significantly higher in the GHS rats. In the humeri, failure stress was not different; however, failure strain and toughness were lower and modulus of elasticity higher in the GHS rats. Cortical and trabecular hardness was lower in the GHS compared to Ctl. Backscattered imaging (BSE) revealed that the GHS rat cortical bone is more mineralized than that of Ctl. Thus, the GHS rats, fed an ample Ca diet, have reduced bone mineral density with reduced trabecular volume, mineralized volume and thickness and their bones are more brittle and fracture prone, indicating that hypercalciuric stone-forming rats have an intrinsic bone disorder that is not secondary to diet.

Disclosures: D.A. Bushinsky, None.

This study received funding from: NIH.

M268

See Sunday Plenary Number S268

M269

Seasonal Changes in Bone and Body Mass in C57BL/6J Inbred Mice Are Gender and Compartment Specific. K. M. Delahunty^{*1}, L. G. Horton¹, H. F. Coombs^{*1}, W. G. Beamer¹, M. L. Bouxsein², C. J. Rosen¹. ¹The Jackson Laboratory, Bar Harbor, ME, USA, ²Beth Israel Deconess Medical Center, Boston, MA, USA.

Seasonal bone loss in humans has been thought due to changes in vitamin D. We previously reported that C57BL/6J (B6) mice at The Jackson Laboratory had lower areal (a)BMD, measured by DXA, in Winter versus Summer despite no changes in 25OH vitamin D. However, these data were obtained retrospectively. To test the hypothesis that seasonal bone loss occurs in B6 and to characterize physiological changes, we performed a cross sectional study in July 2006 (Summer), and February 2007 (Winter) using 16 week B6 virgin female (n=20-24) and male (n=18-21) mice from the same colony and animal room. We measured morphometric phenotypes by DXA, total femoral volumetric (v)BMD by pQCT, trabecular bone by Micro CT40, and serum IGF-I by RIA. The mice were fed the defined NIH31 diet, 16% fat by kcal, and unrefined for nutrient sources.

Female body weight, percent body fat and femur length did not show seasonal changes, but serum IGF-I was 25% lower in Winter than in Summer (p<0.006). In Winter, males had higher body weight (p<0.013), but no increase in percent body fat or femoral length, while serum IGF-I was reduced (~25%, p<0.001). Total femoral vBMD was also lower in Winter than Summer for both females (p=0.017) and males (p<0.01). But in the mid shaft of the femur, during Winter males had markedly reduced percent bone area (p<0.003) accompanied by expansion of periosteal (p=0.005) and endosteal (p<0.002) circumferences. Females in Winter had no changes at the mid shaft, but a decrease in total femoral mineral (p=0.042). By contrast for the distal femur, females had significantly lower BV/TV in Winter than in Summer (p=0.02), with fewer trabeculae (p=0.02), more spacing (p=0.03), and lower connectivity density (p<0.05); males had no seasonal changes in trabecular bone. Summary: Seasonal changes in bone, body mass and IGF-I occur in B6 mice despite controlled conditions that include: a) constant diet, b) 14:10hr light:dark cycle, c) minimal changes in humidity, and d) constant room temperatures. Seasonal changes in males resulted in compensation for Winter bone loss by expansion of periosteum and preservation of trabecular bone. In females, both BMC and trabecular bone were decreased in the Winter. Mechanistically, the cues - environmental or endogenous - driving these skeletal changes are unknown. Further studies that control for factors such as nutrient composition, are necessary to gauge the true magnitude of seasonal change, the mechanisms involved, and the relevance for future mouse and human studies.

Disclosures: L.G. Horton, None.

This study received funding from: NIAMS 45433.

M270

See Sunday Plenary Number S270

M271

Genetic Interaction Between p53 and Atm in Bone Development. Y. Hu^{*}, W. Leong^{*}, B. Au^{*}, B. Li. Institute of Molecular and Cell Biology, Singapore, Singapore.

p53 and Atm play critical roles in DNA damage response with p53 being a target of the Atm kinase. Recent studies show that p53 is a negative regulator of osteoblast differentiation, osteoblast-dependent osteoclastogenesis and bone remodeling (Wang et al. J Cell Biol 172:115, 2006; Zambetti et al. J Cell Biol 172:795, 2006; Lengner et al. J Cell Biol 172:909, 2006). p53(-/-) mice display a high bone mass phenotype; p53(-/-) osteoblasts show accelerated differentiation and increased expression of osteoblast-specific transcription factor, osterix. On the other hand, Atm plays a positive role in regulating expression of osterix. Atm(-/-) mice show reduced bone mass, decreased bone formation rate and defective differentiation of osteoblasts (Rasheed et al. Hum. Mol. Genet. 15:1938, 2006; Hishiyama et al. Bone 37:497, 2005). To study the relationship of these two genes in bone development, we generate p53 and Atm double knockout mice. By using calcein double labeling method we found P53(-/-)Atm(-/-) mice have a high bone mass, increased bone formation rate. The p53(-/-) Atm(-/-) osteoblasts show accelerated differentiation justified by ALP and Von Kossa staining. The cells also show increased expression of osterix but not Runx2. Overall, these results indicate that p53 may function downstream of Atm in regulating bone development.

Disclosures: Y. Hu, None.

This study received funding from: A-Star.

M272

See Sunday Plenary Number S272

M273

A Functional RNAi Screening for Runx2-regulated Genes Corresponding to Ectopic Bone Formation in Human Spinal Ligaments. M. Kishiya^{*1}, K. Furukawa^{*1}, K. Kanemaru^{*1}, H. Kudo^{*2}, T. Numasawa^{*2}, T. Yokoyama^{*2}, S. Toh^{*2}, S. Motomura^{*1}. ¹Pharmacology, Hirosaki University School of Medicine, Hirosaki, Japan, ²Orthopaedic Surgery, Hirosaki University School of Medicine, Hirosaki, Japan.

Ossification of the posterior longitudinal ligament of the spine (OPLL) is characterized by ectopic bone formation in the spinal ligaments which enlarges with time and compresses spinal cord, resulting a serious neurological symptoms. We have previously reported that osteoblast differentiation keyfactor (Runx2) were enhanced in OPLL cells. To clarify a role of Runx2 in the ectopic ossification, effects of osteogenic medium (OS:48h) and RNA interference (using siRNAs targeted to Runx2) on gene expressions were analyzed by genome-wide linkage analysis (microarray) and the results were confirmed by real-time PCR in the ligament cells derived from tissues of OPLL and non-OPLL (CSM; Cervical spondylotic myelopathy) patients obtained during surgery to decompress the spinal cord for myelopathy.

Microarray demonstrated 22 candidate genes regulated by Runx2 in OPLL cells. In addition to osteogenic markers, any chondrogenic markers and angiogenic markers were influenced by OS induction and RNAi for Runx2. Particularly, Aggrecan-1 and angiopoietin-1 were significantly increased by OS induction in OPLL cells but not in non-OPLL cells and decreased by siRNAs for Runx2, but Runx2 were not decreased by siRNAs for angiopoietin-1. Furthermore, VEGF-A down-regulated by OS induction was up-regulated by siRNA for Runx2 or angiopoietin-1.

In our study, we suggested that OPLL development result in forming the metaplasia of spinal ligament cells and was derived through a mechanism of endochondral ossification. Furthermore, angiopoietin-1 and VEGF-A is downstream of Runx2 both in OPLL cells and osteoblasts. In our present study, we investigated any circulation factors in OPLL patients. OPLL patients was bleeding tendency in the perioperative period. Particularly, blood loss after surgery was significantly increased than non-OPLL patients. Other factors (function of platelets, coagulation abnormality, Hypertension, operation time...et al) was not significant between OPLL patients and non-OPLL patients. These data supported that OPLL patients find abnormality of microangiogenic function.

At least we can say that there is some remarkable relation in OPLL development. Signaling pathway between skeletogenesis and vasculogenesis or angiogenesis could have been on contact with Runx2, events that may regulate angiogenesis, and OPLL growth. These data may become a key to elucidate the disease state of OPLL between ectopic bone formation and angiogenesis. Angiopoietin-1 may play an important role in the disease state of OPLL.

Disclosures: M. Kishiya, None.

M274

Dwarfism: A Comparative Analysis of Bone Mineral Density. D. C. Andrade^{*1}, M. G. Pippa^{*2}, S. R. Eis³, C. A. Brandao⁴, C. A. Zerbin². ¹Clinical Research, Centro Paulista de Investigação Clínica, Sao Paulo, Brazil, ²Rheumatology, Hospital Heliopolis, Sao Paulo, Brazil, ³Clinical Research, Centro de Diagnóstico e Pesquisa da Osteoporose do Espírito Santo, Vitoria, Brazil, ⁴Bone Densitometry, Fleury Medicina e Saúde, Sao Paulo, Brazil.

Dwarfism is a medical condition which result in short stature. It refers to an adult height of 4 feet 10 inches or under and can be caused by a wide variety of conditions, most of which are genetic. The most common type, accounting for 70% of all cases of short stature, is called achondroplasia. This one results from a spontaneous mutation in one gene or a child can inherit the gene from a parent who has achondroplasia. Characteristically, the arms are shorter than the forearms and the thighs are shorter than the legs, although trunk growth is nearly normal. Little is known about bone mass adjusted for body size and body composition compartments in children with dwarfism. Our objective was to evaluate the influence of short high in bone mineral density (BMD). We compared BMD results of dwarfs with a normal population. Twenty females and males dwarfs and were studied. All of them were submitted to dual-energy X-ray absorptiometry (DXA) in order to analyze BMD of lumbar spine. Control group was formed by normal females and males, that were matched by sex and age. Areal BMD was measured and reported in g/cm². Adjusted BMD was calculated by the relation between bone mineral content (BMC)/ height and results were given in g/m². Apparent BMD (App BMD) was calculated according to Bachrach. Variables were evaluated as descriptive patterns. The adherence to normal curve was evaluated by Kolmogorov Smirnov test. To compare the difference of quantitative variables between dwarfs and control group the Student t test was used. The effective P value to be considered significant was < 0.05. Data were analysed using the statistical computer program Minitab version 15.0%. Dwarf population showed lower means for all anthropometric values, but BMI [(weight = 52.8 Kg); (height = 1.23 m); (BMI = 34.4 Kg / m²)] when compared to control group [(weight = 65.3 Kg); (height = 1.62 m); (BMI = 34.4 Kg / m²)]. Analysing bone mass we observed that there were no significant differences between Dwarfs and control group concerning to areal L1-L4 BMD (1.035 g/cm²; 1.122 g/cm²) p = 0.158, L1-L4 Z-score (-0.71 SD; -0.44 SD) p = 0.532, and L1-L4 App BMD (0.308 g/cm²; 0.313 g/cm²) p = 0.735. Dwarfs presented lower values of L1-L4 BMC (48.40g) and L1-L4, area BMD (45.65) when compared to control group L1-L4 BMC (58.50g) p = 0.040; L1-L4 area BMD (51.67g) p = 0.026. Interestingly Adjusted L1-L4 was higher in Dwarfs when compared to controls (0.837 g/cm² / 0.697 g/cm² respectively), p = 0.001. Our results suggest BMD in Dwarfs should be based on analysis of adjusted L1-L4 BMD instead of App BMD.

Disclosures: D.C. Andrade, None.

M275

See Sunday Plenary Number S275

M276

Analysis of Cranial Defect Healing in CXCR2 Receptor2 Knock-out (CXCR2^{-/-}) Mice. D. S. Bischoff^{*1}, T. Sakamoto^{*1}, N. S. Makhijani^{*1}, H. E. Gruber², D. T. Yamaguchi¹. ¹Research Service, VA Greater Los Angeles Healthcare System, Los Angeles, CA, USA, ²Orthopaedic Surgery, Carolinas Medical Center, Charlotte, NC, USA.

The potential role of CXC chemokines bearing the glu-leu-arg (ELR⁺) motif in bone repair was studied using a mouse cranial defect (CD) model in CXCR2^{-/-} mice. Inflammation is the initial step in bone repair. ELR⁺ CXC chemokines are released by inflammatory cells and serve as angiogenic factors. Previously we have shown that osteogenic differentiation of hMSCs increases expression of the ELR⁺ CXC chemokine, IL-8 (CXCL8). CXCL8 signals through the CXCR2 receptor in mice. We created 1.8 mm CDs in 6 week old male CXCR2^{-/-} and wild-type (WT) mice and allowed the CDs to repair over a 12-week period. CXCR2^{-/-} mice were significantly reduced in size and weight compared to their WT littermates. Weight, length, and DEXA measurements were taken (total, femur, tibia, radius, humerus, and vertebrae) before surgery and 6 and 12 weeks after surgery. CXCR2^{-/-} mice were significantly smaller in weight (54% of WT at 6 weeks, 75% at 12 and 18 weeks, p<0.0001) and length from base of tail to nose tip (82% at 6 weeks, 90% at 12 and 18 weeks, p<0.0004). DEXA analysis indicated that bone mineral density (BMD) and bone mineral content (BMC) were significantly decreased in CXCR2^{-/-} mice in all bones, and total area (TA), bone area (BA), total tissue mass (TTM), and lean body mass (LBM) significantly decreased in all with the exception of the vertebrae. There was no difference in % fat between CXCR2^{-/-} and WT mice. Normalizing for the size differences with weight or LBM, BMD is significantly decreased in CXCR2^{-/-} mice only at 6 weeks whereas BMC is slightly increased in the CXCR2^{-/-} mice at 18 weeks of age. CDs were analyzed using the BIOQUANT system. Although the CDs were not completely healed even after 12 weeks, preliminary analysis indicates that there was significant bone in-growth in both the CXCR2^{-/-} and WT CDs. Old and new bone were identified using polarized light and quantitated for numbers of osteocytes (OCy) and blood vessels (BV) around the original CD. New bone in CXCR2^{-/-} mice had more OCy than WT (2618 vs 2049 OCy/ μm^2). CXCR2^{-/-} old bone had about half as many OCy as new bone but still more than WT old bone (1282 vs 1043 OCy/ μm^2). In new bone, the number of BV in WT was ~2X more than seen in CXCR2^{-/-} (43 vs 20 BV/ μm^2). The number of BV in the old bone was more closely matched (9 vs 11 BV/ μm^2 for WT and CXCR2^{-/-} respectively). Conclusion: CXCR2^{-/-} mice have 1) reduced weight and size; 2) reduced BMD at 6 weeks of age but not at later time points; 3) increased BMC at 18 weeks of age; 4) increased number of OCy in new bone; and 5) decreased number of BV in new bone.

Disclosures: D.S. Bischoff, None.

This study received funding from: VA Merit Review.

M277

See Sunday Plenary Number S277

M278

Significant Lower Balance and Muscle Power Performance and Higher Risk for Falls in Elderly People with a Decreasing Creatinine Clearance. L. C. Dukas^{*1}, E. Schacht², M. Runge^{*3}. ¹Acute Geriatric University Clinic, Kantonsspital Basel, Basel, Switzerland, ²Zurich Osteoporosis Research Group ZORG, Zurich, Switzerland, ³Center for Muscle and Bone Research, Aerpah Klinikum, Esslingen, Germany.

A Creatinine clearance (CrCl) of <65ml/min. is associated with a significant increased risk for falls. In a German study a decreasing creatinine clearance was associated with significantly decreasing muscle power and balance. We assessed this association in a multinational study. For this cross-sectional study data were collected from 7 European countries including Russia. 1190 women and 127 men aged 60 years and older with a mean BMI of 27.2kg/m² and a mean CrCl of 58.6ml/min., freshly diagnosed and therefore untreated for osteoporosis, participated in this study. The CrCl was calculated using the established Cockcroft-Gault formula. Results are from spearman correlation analyses and from logistic regression analyses. The p-values are two-sided.

A decreasing CrCl was multivariate controlled significantly associated with lower performance in the Timed-up-and-go test (TUG) (corr-0.1341, p<.0001) and in the Chair Rising test (corr-0.1266, p<.0001). Performance in the Tandem Stand was not associated with the CrCl. A CrCl of <65ml/min. was multivariate controlled a significant risk factor for falls.

We found a significant correlation between decreasing CrCl and lower performance in balance and muscle power tests. However, contrary to the findings in another study the performance in the Tandem Stand test was not significantly associated with a decreasing CrCl. Furthermore we found that a CrCl<65ml/min is, independent from the performance in muscle and balance tests, a significant risk factor for falls. Our results together with the results from already published studies allows us to suggest a low CrCl of <65ml/min. to be a diagnostic tool to identify elderly frail patients.

Disclosures: L.C. Dukas, Teva Pharmaceutical Industries 2.

This study received funding from: TEVA Pharmaceutical Industries.

M279

See Sunday Plenary Number S279

M280

Candidate Genes of Every Known QTL of BMD in Whole Mouse Genome. Q. Xiong^{*}, Y. Jiao, W. Gu. Departments of Orthopaedic Surgery - Campbell Clinic, University of Tennessee Health Science Center, Memphis, TN, USA.

One difficulty in the identification of candidate genes for QTL is that the genomic region of a QTL is generally considered as too large to search the candidate genes. In this study, we systematically examined all the genes in each of QTL of BMD identified from mouse study.

Methods: To identify every QTL, literature search was conducted with key words "Bone" and "QTL" in PubMed for every publication up to January 2007. Genes within a QTL region are obtained from Ensembl database (<http://www.ensembl.org/index.html>). For every known gene in QTL, their potential connection with BMD was evaluated by searching information from Online Mendelian Inheritance in Man (OMIM) at <http://www.ncbi.nlm.nih.gov/entrez/query.fcgi?db=OMIM> and PubMed at <http://www.ncbi.nlm.nih.gov/entrez/query.fcgi?db=PubMed>. Searching terms are the combination of the symbol of the gene with any of those eight key words: bone mineral density, BMD, bone strength, bone size, osteoporosis, osteoblast, osteoclast, and fracture.

Results: We obtained candidate genes for every known BMD QTL. A total of 74 BMD QTL cover 1,210,895,314 bp genomic sequence which is roughly 46% of the total mouse genome sequences. Every autosomal chromosome except chromosome 8, contains at least one BMD QTL. Within the 1,210,895,314 genomic sequences of total of 74 BMD QTL, a total of 15,075 genes have been located. Among all those genes, 290 have been nominated as candidate genes according our bioinformatics search. For any potential candidate, at least the abstract of one reference was read to confirm the link between the gene and BMD. For a gene with more than one reference that indicates its candidacy, at least two references were read and cited in this study. Many BMD QTL have been located on the gene rich regions of the genome. The average gene density through whole mouse genome is about one gene per 95,977 bp. Within the total of 1,210,895,314 BMD QTL genome sequences, there is about one gene per 80,324 bp, while in the genome region outside of BMD QTL regions, there is about one gene per 114,894 bp.

Discussion and Conclusion: Our search reveals that a very large number of candidate genes exists within QTL regions. For most of them, we do not aware any report on the investigation or even being listed as candidates. The other important finding is that the association between polymorphism of many candidate genes and BMD has been reported in human studies. As the rapid development of technologies and genome projects such as knockout of genes in whole mouse genome, information of gene function accumulates in an unexpected speed. Those information should be useful for our gene identification of QTL. A comprehensive search of candidate genes for known QTL may provide unexpected benefit for QTL studies.

Disclosures: W. Gu, None.

M281

See Sunday Plenary Number S281

M282

Identification of the CACNA2D2 Gene on Chromosome 3p21 as a Novel Susceptibility Gene for Osteoporosis. Q. Huang^{*1}, C. Cheung^{*1}, P. Fong^{*2}, M. Ng^{*1}, W. Mak^{*2}, V. Chan^{*1}, P. Sham^{*2}, A. Kung¹. ¹Medicine, The University of Hong Kong, Hong Kong, China, ²Genome Research Center, The University of Hong Kong, Hong Kong, China.

Evidence of linkage of chromosome 3p to bone mineral density (BMD) has been previously reported in individual as well as meta-analysis of genome wide linkage scans. To identify the quantitative trait loci gene underlying BMD variation at chromosome 3p, we performed a region-wide association study with 200 single-nucleotide polymorphisms (SNPs) across 6Mb of chromosome 3p21 in 1,243 case-control Chinese subjects. The cases were subjects with low BMD (Z-scores ≤ -1.28 , equivalent to the lowest 10 percent of the population) at either the L1-4 lumbar spine or femoral neck. Control subjects had high BMD (Z-score $\geq +1.0$) at the corresponding sites. Two hundred tag SNPs were selected and genotyped using the high-throughput Sequenom genotyping platform. One hundred thirty-five SNPs met quality control criteria (genotyping call rate >0.9, minor allele frequency > 0.01, duplicate error rate <0.02 and Hardy-Weinberg equilibrium p values >0.01) and were analyzed for the high-throughput Sequenom genotyping platform. Binary logistic regression analyses were performed to test for associations between each SNP genotype and BMD. Haplotype association analyses were performed by WHAP. Five SNPs (rs11918619, rs1471217, rs2336664, rs7626551, and rs2257216) were associated with spine BMD and two SNPs (rs2236953, rs2624839) with femoral neck BMD (p<0.01) in single marker associations. The region that contained 6 SNPs, located within the CACNA2D2 gene, showed the strongest association with femoral neck BMD in the haplotype analyses (permutation p<0.002). In addition, we consistently detected significant associations for the haplotype CCGATGCCAC of the CACNA2D2 gene with BMD at the spine, trochanter and total hip region. Our results suggest that CACNA2D2, which encodes a voltage-dependent calcium channel subunit, is a novel susceptibility gene for BMD variation in Chinese and is likely to be involved in the pathogenesis of osteoporosis. Replication study is currently being conducted in Japanese population.

Disclosures: Q. Huang, None.

M283

Lack of Major Survival Benefit of Vitamin D Receptor Gene Polymorphisms. A. Arabi¹, L. Zahed^{2*}, Z. Mahfoud^{3*}, J. Maalouf¹, M. Choucair^{4*}, M. Nabulsi^{4*}, G. El-Hajj Fuleihan¹. ¹Calcium Metabolism and Osteoporosis Program, American University of Beirut, Beirut, Lebanon, ²Pathology and Laboratory Medicine, American University of Beirut, Beirut, Lebanon, ³Epidemiology and Population Health, American University of Beirut, Beirut, Lebanon, ⁴Pediatrics, American University of Beirut, Beirut, Lebanon.

Vitamin D has recently emerged as an important risk factor for several health problems associated with increased mortality. Vitamin D receptor (VDR) is widely expressed in most immune cell types and other tissues, and prostate, breast and colon cancer cells exhibit increased levels of VDR protein when compared to their normal counterparts. This raises the possibility that some VDR genotypes may be associated with higher mortality rate and therefore their frequency distribution may decrease in the surviving elderly. The aim of this study was to look for a survival benefit of VDR gene polymorphisms by comparing the genotype frequencies in children to those in the elderly in a population of the same ethnic background.

Data from 203 elderly subjects aged 65-85 years who participated in a population-based study assessing the prevalence of osteoporosis, and data from 336 children aged 10-17 years who participated in a vitamin D trial were used. In both groups, polymorphisms in the VDR gene were assessed with the restriction enzymes BsmI, TaqI and ApaI.

The frequency distributions of VDR genotypes were similar to those reported in white populations. The heterozygote genotype for all enzymes was the most frequent in both age groups (Table 1). The frequencies of genotypes in both age groups were in Hardy-Weinberg equilibrium. There was no difference in the frequency distribution of VDR genotypes between the young and the elderly, both by gender and in the overall group.

The lack of difference in the frequency distribution of VDR genotypes between the children and the elderly within the same population renders the role of VDR as a major modulator of the relationship between vitamin D and conditions associated with high mortality unlikely.

Table 1. Frequency distribution of VDR genotypes according to the restriction enzyme in children and in the elderly*

		Children	Elderly
Bsm	bb	110 (33%)	62 (31%)
	Bb	169 (50%)	96 (48%)
	BB	56 (17%)	43 (21%)
Apa	aa	53 (16%)	23 (12%)
	Aa	161 (48%)	102 (50%)
	AA	122 (36%)	78 (38%)
Taq	tt	47 (14%)	39 (20%)
	Tt	170 (51%)	99 (48%)
	TT	119 (35%)	66 (32%)

* No significant difference between the children and the elderly within gender or in the overall group.

Disclosures: A. Arabi, None.

M284

The Decreased Activity of Lactase Phlorizin Hydrolase and Bone Mineral Density in Postmenopausal Women. K. Bácsi*, J. P. Kósa*, B. Balla*, Á. Lazáry, Z. Nagy, I. Takács, G. Speer*, P. Lakatos. First Department of Internal Medicine, Semmelweis University, Budapest, Hungary.

The CC genotype of the -13910 T/C dimorphism (LCT) related to lactose intolerance and decreased calcium absorption from gut is accompanied with reduced activity of lactase phlorizin hydrolase. We hypothesized that the altered calcium absorption throughout life has an impact on bone mineral density (BMD) of postmenopausal women. We studied 200 osteoporotic, 235 osteopenic and 160 healthy women. Genotyping, osteodensitometry at the lumbar spine, total hip, femur head, Ward's triangle and radius as well as serum calcium measurements were carried out in all subjects. The -13910 T/C polymorphism was significantly associated with the BMD at the Ward's triangle (Z-score (TT) = 0.082±0.787, Z-score (TC) = -0.179±0.829, Z-score (CC) = -0.334±0.871; p=0.028) and in a recessive model at the radius (Z-score (TT+TC) = 0.406±1.322, Z-score (CC) = 0.105±1.415; p=0.038) in the whole study population. Similar relationship was seen at the femoral head (Z-score (TT+TC) = 0.595±1.02, Z-score (CC) = 0.148±1.063; p=0.013) but only in the unified groups of osteoporotic and healthy women. Also, we found significant association between genotypes and both the total hip density (Z-score (TT) = -0.717±0.841, Z-score (TC) = -1.106±0.877, Z-score (CC) = -1.003±0.826; p=0.043) and the Ward's triangle density (Z-score (TT) = -0.375±0.606, Z-score (TC) = -0.819±0.485, Z-score (CC) = -0.88±0.541; p=0.015) in osteoporotic and osteopenic patients together. All results remained significant after adjustment for menopausal age and body mass index. We could not detect any associations between genotypes and BMD at the lumbar spine in the study groups. Our data suggest that the -13910 T/C dimorphism might have an influence on bone mass at cortical but not trabecular bone.

Disclosures: K. Bácsi, None.

This study received funding from: ETT 022/2006, NKFP-1A/007/2004, NKFP-1A/002/2004.

M285

An Interaction Between Dietary Fat and Polymorphisms in a Previously Undetected, Alternate 3' UTR of the PPARG Gene Influences Bone Mass in Both Mice and Humans. C. L. Ackert-Bicknell¹, J. Graber^{1*}, K. Cho², S. Demissie^{2*}, J. Ordoñez^{3*}, W. G. Beamer¹, D. P. Kiel⁴, C. J. Rosen¹. ¹The Jackson Laboratory, Bar Harbor, ME, USA, ²Boston University School of Public Health, Boston, MA, USA, ³Tufts University, Boston, MA, USA, ⁴Hebrew SeniorLife, Boston, MA, USA.

We previously identified a Quantitative Trait Locus (QTL) for volumetric BMD on mouse Chromosome (Chr) 6 and now name Peroxisome Proliferator-Activated Receptor-gamma (Pparg) as a likely candidate gene. The B6.C3H-6T (6T) congenic mouse was created for the purpose of understanding the biology underlying this QTL and was generated by introgressing a 30 cM region of Chr 6 from C3H/HeJ (C3H) onto C57BL/6J (B6). Female 6T mice have low BMD and increased adipocyte infiltration in bone marrow. PPARG is a nuclear receptor known to be key for maturation of adipocytes. Existing annotation of PPARG indicated a 3' Untranslated Region (3' UTR) with an approximate length of 210 nucleotides (nt). Examination of the pattern of evolutionary conservation downstream of this site led us to predict a previously undetected alternative 3' processing site that would result in a longer (~3450 nt) 3' UTR. We have sequenced the genomic region between the two 3' processing sites and found 25 polymorphisms in C3H, when compared to B6. Dietary fat is able to activate PPARG and female 6T mice fed a high fat diet (60% fat) have lower aBMD than low fat (11% fat) fed 6T mice. There is no difference in aBMD in B6 mice fed the two diets. Using Real Time RT-PCR, we examined expression of Pparg transcripts containing this alternate 3' UTR in bone. There was no difference between B6 mice fed the low and high fat diets, (fold = 1.52±0.4, p = 0.318) and between B6 and 6T mice fed a low fat diet (fold = 1.8±0.6, p = 0.18). 6T mice fed high fat had a 4.3±1.4 fold increase compared to B6 mice fed low fat (p = 0.036) and a 2.25±0.6 fold increase compared to 6T mice fed low fat (p=0.016). We examined 13 SNPs in the PPARG gene in the Framingham Offspring Cohort. For three of these SNPs, rs1152004, rs1175381 and rs1186464, we found a significant interaction with dietary fat intake for the phenotype of DXA BMD of the trochanter region in women. SNPs rs1152004 and rs1175381 are located in a region of high evolutionary conservation very near to the alternative 3'-processing site in PPARG. The usage of alternative 3' UTR can affect transcript stability and translation efficiency. These findings suggest that dietary fat has a significant influence on BMD but is dependent on alleles in the rare, extended 3' UTR of PPARG.

Disclosures: C.L. Ackert-Bicknell, None.

This study received funding from: NIAMS 45433.

M286

Association of Luteinizing Hormone Receptor Polymorphism with Bone Mineral Density in Young Men - Results from Odense Androgen Study. C. L. Brasen^{1*}, T. L. Nielsen^{2*}, B. Abrahamson³, L. Christiansen^{4*}, C. Hagen^{2*}, M. Andersen^{2*}, K. Brixen², L. Bathum^{1*}. ¹Dept. of Biochemistry, Pharmacology and Genetics, Odense Universitetshospital, Odense C, Denmark, ²Department of Endocrinology, Odense Universitetshospital, Odense C, Denmark, ³Department of Medicine & Endocrinology, Copenhagen University Hospital Gentofte, Hellerup, Denmark, ⁴Department of Epidemiology, Institute of Public Health, University of Southern Denmark, Odense C, Denmark.

The N312S polymorphism in the luteinizing hormone receptor (LHR) has previously been shown to be associated with genital undermasculinization. We investigated the hypothesis, that the N312S polymorphism in LHR is associated with bone mineral density (BMD).

We genotyped 783 healthy men aged 20-29 years from the population-based Odense Androgen Study for the N312S polymorphism in LHR and investigated association with BMD in the spine, hip, truncus and extremities as well as whole body BMD. 406 of the participants underwent MRI scans to determine visceral and subcutaneous adipose tissue (VAT and SAT), muscle tissue and femoral compacta area. We furthermore tested for association with testicular volume, height, lean body mass, carboxy-terminal telopeptide of type I collagen (ICTP), bone-specific alkaline phosphatase (bone ALP), luteinizing hormone, testosterone, oestrogen, dihydrotestosterone (dht) and androstenedione.

Genotype distribution (AA, 0.20; AG, 0.48; GG, 0.32) was consistent with the Hardy-Weinberg equilibrium. Using the entire study group, we found significant association between LHR alleles and testicular-volume (p=0.03) as well as with BMD in spine (p=0.04) and trend association between LHR alleles and BMD in truncus and whole body BMD.

Stratifying participants into "sedentary" and "non-sedentary", we found that in the sedentary participants (n=615), LHR N312S was significantly associated with testicular volume, BMD in spine, truncus, and whole body. The results also indicated a trend association with BMD in hip and extremities, as well as the level of ICTP.

Additional stratification by smoking showed that in the group of sedentary ever-smokers (n=199) LHR alleles were significantly associated with BMD in spine, truncus, extremities and whole body, (p<0.01 for all), ICTP (p=0.04) and bone ALP (p=0.002). The difference in mean BMD in the spine equals 5.9%. Furthermore there was a trend association with BMD in hip and lean body mass. Finally we found a trend association with VAT, SAT and femoral compacta area.

These findings strengthen the hypothesis that the LHR N312S polymorphism is associated to genital undermasculinization and hereby low BMD. More studies are needed to verify these results. Interaction with other polymorphisms will be discussed.

Disclosures: C.L. Brasen, None.

M287

Study of 7 Polymorphisms Genes (LCT, MTHFR, COLIA-1 and Promoters of RANKL, OPG, IL-6 and TCIRG1) Previously Described as Linked to Osteoporotic Fractures: Lack of Association in French Women.

V. Breuil¹, D. Quincey², J. Testa³, C. Albert¹, C. H. Roux¹, Z. Mroueh², H. Cham¹, O. Brocq¹, C. Grisot¹, L. Euler-Ziegler¹, G. Carle². ¹Rheumatology, CHU de Nice - Medical School, Nice, France, ²CNRS - Faculté de Médecine, GEPITOS-Université de Nice Sophia Antipolis, Nice, France, ³Informatique Médicale, CHU de Nice - Medical School, Nice, France.

Osteoporosis (OP) is have a strong genetic determination and numerous polymorphisms are reported to be associated with it. However, these associations depend on the population studied. Thus, we tested in a French population 7 genes polymorphisms [Lactase Transferase (LCT), RANKL promoter, Collagen 1 α (COLIA-1), OPG promoter, IL-6 promoter, methylenetetrahydrofolate reductase (MTHFR), and TCIRG1 promoter] previously reported to be associated with OP fractures.

Two groups of postmenopausal women were selected, 50 to 80 years old: one control group free of OP fracture and with normal BMD (T-score >-1 SD at hip and spine) in without any anti-OP treatment, and one group of OP women with at least one fracture and a low BMD (T-score <-2.5 SD at hip and/or spine); secondary OP were excluded. For each patient, genomic DNA was isolated from peripheral blood and polymorphisms genotyped by PCR and restriction analysis. The univariate statistical analysis used Chi² or Fisher test (qualitative variables) and Kruskal-Wallis (quantitative variables); the multivariate analysis used logistic regression.

159 women (89 OP and 70 controls) were enrolled. The 2 groups were similar regarding age of menopause, statine, betablockers, neuroleptics or antidepressants use. In the OP group, there was significant higher rate of family history of OP, higher age, age of puberty and loss of height, as well as significant lower weight, height, body mass index, high blood pressure. In the OP group, 47 vertebral fractures and 62 non vertebral fractures were recorded. The analysis of each polymorphism didn't show any significant differences between the 2 groups. To take in account the polygenic pattern of the disease, we tested whether the OP group presented significantly more polymorphisms on the 7 genes than the control group and failed to detect any difference. However, we found a significant association between the polymorphism of IL-6 or TCIRG1 promoter and family history of OP ($p=0.01$), as well as other polymorphisms associated with hyperlipidaemia, height, loss of height, BMI, and diabetes.

In our French population, we did not found the polymorphisms associations with OP fractures previously described. This could be related to the sample size, even if some of the previous studies enrolled a similar number of subjects, or, as previously described for numerous polymorphisms, to a geographical factor.

Disclosures: V. Breuil, None.

This study received funding from: PHRC régional du CHU de Nice, Lilly.

M288

See Sunday Plenary Number S288

M289

A Haplotype-Based Analysis of the LRP5 Gene in Relation to Osteoporosis Phenotypes. L. Agueda¹, X. Nogues², M. Bustamante¹, S. Jurado², N. Garcia-Giral², J. Garces², L. Mellibovsky², S. Balcells¹, A. Diez-Perez², D. Grinberg¹. ¹Genetics, University of Barcelona, CIBERER, IBUB, Barcelona, Spain, ²URFOA, IMIM, Hospital del Mar, Autonomous University of Barcelona, Barcelona, Spain.

LRP5 encodes the low-density lipoprotein receptor-related protein 5, a transmembrane protein involved in Wnt signaling. In bone, LRP5 is an important regulator of osteoblast growth and differentiation, affecting peak bone mass in vertebrates. Rare mutations in LRP5 result in severe phenotypes associated with bone. Whether common variants in LRP5 are associated with normal BMD variation or osteoporosis phenotypes remains controversial. In this study, we employed a haplotype-based approach to comprehensively examine the contribution of common variation at the LRP5 genomic region to osteoporosis susceptibility.

A total of 24 SNPs were selected to cover a 150 kb genomic region including the LRP5 gene and flanking regions, about 7 kb at each side. Most of these SNPs were tag-SNPs selected based on HapMap-CEU data. The remaining were either missense changes or SNPs previously studied by others. Genotyping was performed using SNPlex or TaqMan methodologies. Association, both at single SNP or block-haplotype level, was tested against LS-BMD, FN-BMD and osteoporotic fracture in a cohort of 964 Spanish postmenopausal women (BARCOS cohort). Statistical methods included ANCOVA and logistic regression.

At the single SNP level, a significant association with LS BMD was found for SNP#1, located in the promoter region ($p=0.011$, recessive model). The SNP#6 (intron 1) was associated with both LS BMD ($p=0.025$, additive model) and FN BMD ($p=0.031$, recessive model). Three SNPs, SNP#11 (intron 1; $p=0.007$, additive model), SNP#13 (intron 5; $p=0.041$, recessive model) and SNP#15 (intron 5; $p=0.019$, recessive model) were significantly associated with the risk of osteoporotic fracture, with ORs of 1.70, 1.66 and 1.79, respectively. In general, haplotype analyses did not provide additional information to that obtained from SNP analyses. The only exception was one block-haplotype (tagged by SNPs 10, 11 and 12), which showed a significant association with LS BMD ($p=0.043$), while none of the tag-SNPs gave a significant result on their own.

In conclusion, we found that genetic variation in the first half of the LRP5 genomic region was associated with osteoporotic phenotypes in the BARCOS cohort.

Disclosures: X. Nogues, None.

M290

An $\alpha_v\beta_3$ Integrin Antagonist (MK-0429) Inhibits Osteolytic Lesions in Breast Cancer and Melanoma Lung Metastases. M. Pickarski, G. Wesolowski, G. Neusch*, T. Prueksaritanont*, L. T. Duong. Merck Res. Labs., West Point, PA, USA.

There is significant evidence to support multiple roles of $\alpha_v\beta_3$ integrin in mediating osteoclastic bone resorption, tumor progression and metastasis. Increased expression of $\alpha_v\beta_3$ in several tumors, including breast cancer and melanoma, is correlated with a greater metastatic potential and the development of bone metastases. Previously, we demonstrated the efficacy of MK-0429 as a safe, well tolerated, orally active antiresorptive in reversing estrogen-deficiency induced bone loss in preclinical animal models and in postmenopausal women. Here, we evaluated the efficacy of MK-0429 in inhibiting the proliferation of breast cancer (BrCa), prostate cancer (PCa) and melanoma cells.

Cell Lines	BrCa		PCa		Melanoma	
	MDA-MB-231	22RV1	PC3-M	DU145	B16-F10	
IC ₅₀ nM	639 \pm 370	488 \pm 360	863 \pm 475	736 \pm 196	96 \pm 61	

MK-0429 also inhibited MDA-MB-231 breast cancer (IC₅₀ = 2.1 nM) and PC3-M prostate cancer (IC₅₀ = 4.1 nM) cell migration to vitronectin; and blocked MDA-231 matrigel invasion (IC₅₀ = 7.0 nM), comparable to its potency to inhibition of osteoclastic bone resorption in vitro (IC₅₀ = 12 nM). In this study, MK-0429 was evaluated in the prevention of bone metastasis growth using the intra-tibial engraftment model of MDA-MB-231 breast carcinoma in nude rats. Bone loss and skeletal tumor growth were determined by μ CT and histology over a 6-week period. Compared to vehicle, treatment with oral MK-0429 at 100, and 300 mg/kg, bid, significantly prevented osteolytic lesions by 22 and 42%, respectively, compared to 45% with zoledronic acid (ZOL, 7.5 μ g/kg, sc, wky). Compared to vehicle, MK-0429 also reduced tumor volume by 40 and 66%, vs. a 56% reduction with ZOL. MK-0429 significantly inhibited cortical disruption, tumor necrosis, tumor infiltration between the trabecular bone plates, and invasion of the bone marrow. While having no effect on melanoma growth in an s.c. xenograft model, MK-0429 reduced the incidence of B16-F10 pulmonary metastases by 60% vs. vehicle. Taken together, these data show that MK-0429 had both anti-resorptive and anti-metastatic activities in preclinical models of breast cancer bone metastasis, as well as extraskelatal activity in blocking melanoma lung metastasis. Compared to the i.v. bisphosphonates, MK-0429 may represent a novel oral therapy for the treatment of patients with bone metastasis.

Disclosures: L.T. Duong, Merck & Co. 3.

M291

See Sunday Plenary Number S291

M292

Prevalence of Vitamin D Insufficiency in Patients with Breast Cancer. N. Napoli, C. Ma, S. Vattikuti*, M. R. Azadfar*, A. Rastelli, M. Ellis*, R. C. Armamento-Villareal. Medicine, Washington University School of Medicine, St. Louis, MO, USA.

Previous studies have shown that aromatase inhibitor therapy in patients with ER+/PR+ breast cancer is associated with bone loss and increased incidence of fractures. As these studies were not designed to investigate skeletal outcomes as the primary endpoint, the vitamin D status of these patients remains undetermined. The objective of our study is to determine the incidence of vitamin D deficiency in patients with newly-diagnosed breast cancer who are about to initiate aromatase inhibitor therapy. We have recruited 80 postmenopausal patients (69 Caucasians, 11 African-Americans) between 40 to 80 years old from March 2006 to March 2007, with newly-diagnosed Stage 1 to 11a, ER+/PR+ breast cancer who will be initiated on aromatase inhibitors by their oncologists. Table 1 shows the clinical data of the whole study population. Baseline vitamin D levels were available in 70 patients. Analysis of serum vitamin D levels showed that 60 out of 70 patients (85.7%) of which 51 were Caucasians and 9 were African-Americans, have insufficient levels, i.e. <30 ng/ml (31 patients between 20-30 ng/ml, 25 between 10-19 ng/ml and 4 have <10 ng/ml). The vitamin D levels were significantly lower in African-Americans compared to Caucasians (16.3 ± 10.8 ng/ml vs 22.3 ± 8.3 ng/ml, $p=0.04$). Analysis according to the time of presentation showed no seasonal variation in vitamin D levels (April to September = 23.2 ± 9.1 vs October to March = 20.5 ± 8.8 ng/ml, $p=0.24$). In summary, insufficient vitamin D levels is common among patients with breast cancer perhaps from a combination of poor sunlight exposure (from lack of physical activity) and poor intake (from lack of appetite). The prevalence of vitamin D insufficiency appears to be higher in our cohort than what has been reported in the literature for otherwise healthy postmenopausal women without breast cancer (Holick MF, et al. J Clin Endocrinol Metab. 2005 Jun;90(6):3215-24. Epub 2005 Mar 29). Low vitamin D levels may aggravate bone loss from aromatase inhibitors, thus, routine vitamin D determination followed by appropriate supplementation may be necessary in breast cancer patients, most especially in those who will be starting aromatase inhibitor therapy.

Clinical data of the whole study population (N=80)	
Age (years)	62.6 \pm 9.6
Years since menopause	16.8 \pm 15.5
Menopausal age (years)	47.6 \pm 7.4
Body mass index (kg/m ²)	30.7 \pm 6.1
Waist To Hip ratio	0.86 \pm 0.06
Calcium (mg/dl)	9.7 \pm 0.5
Alkaline Phosphatase(IU/l)	91 \pm 33.5
Vitamin D(ng/ml)	21.4 \pm 8.9

Disclosures: N. Napoli, None.

M293

See Sunday Plenary Number S293

M294

6-Thioguanine Acts on Gli2 to Decrease PTHrP Expression and Osteolysis. M. P. Nguyen¹, J. A. Sterling², A. J. Roberts^{3*}, G. R. Mundy². ¹Department of Medicine, Vanderbilt University, Nashville, TN, USA, ²Center for Bone Biology, Department of Clinical Pharmacology, Vanderbilt University, Nashville, TN, USA.

Breast and lung tumor cells frequently metastasize to bone, where they cause osteolytic bone destruction. Parathyroid hormone-related peptide (PTHrP) has been identified as one of the major mediators of osteolysis and hypercalcemia in tumors that metastasize to bone. Thus, compounds that inhibit tumor cell production of PTHrP can potentially be clinical treatments for osteolytic metastases. Our laboratory has previously demonstrated that guanosine nucleotides, represented by 6-thioguanine (6-TG), reduces PTHrP production, tumor-induced osteolysis, and tumor burden in bone. 6-TG was identified from screening a diverse library of small molecular weight chemicals that inhibit PTHrP promoter activity, using a cell-based screen with PTHrP promoter as the molecular target (Gallwitz et al, JCI 2002). This observation raises the possibility that 6-TG or a related compound may be effective in reducing PTHrP production by cancer cells and thus provides a useful therapeutic approach to hypercalcemia and osteolysis caused by PTHrP excess. In this study, we have attempted to determine the molecular mechanism by which 6-TG inhibits the PTHrP promoter. Recently, we have found that PTHrP production in cancer cells is regulated by activation of the developmental Hedgehog (Hh) pathway, specifically by the Hh pathway transcriptional activator, Gli2. We hypothesized that 6-TG inhibits PTHrP through regulating Gli2 expression. To test this hypothesis we utilized the osteolytic and PTHrP producing tumor cells, RWG2, a human squamous cell carcinoma, and MDA-231, breast carcinoma cells. We treated these cells with either 6-TG or purine as a negative control. We found that 6-TG treatment of RWG2 and MDA-231 human cancer cells decreases Gli2 expression by Western blot and real-time PCR by approximately 10-fold. These effects correlated with decreases in PTHrP expression by real-time PCR and PTHrP promoter-luciferase activity. Since 6-TG can decrease Gli2 mRNA expression, it is also possible that 6-TG directly affects Gli2 promoter activity. We have therefore cloned the Gli2 promoter to determine if 6-TG can repress Gli2 promoter activity in osteolytic tumor cells. Currently, our data demonstrates that 6-TG inhibits PTHrP through regulating Gli2, suggesting that specific inhibitors of Gli2 expression may be a potential approach for treating osteolytic metastases.

Disclosures: M.P. Nguyen, None.

M295

See Sunday Plenary Number S295

M296

Non-Canonical Hedgehog Signaling Regulates Gli2 and PTHrP Expression in Osteolytic Cancer Cells. J. A. Sterling¹, S. S. Padalecki², B. G. Grubbs², M. P. Nguyen¹, A. J. Roberts^{3*}, B. O. Oyajobi², G. R. Mundy¹. ¹Center for Bone Biology, Vanderbilt University, Nashville, TN, USA, ²University of Texas Health Science Center, San Antonio, TX, USA.

Cancer cells cause osteolysis and hypercalcemia by over-production of PTHrP. We have shown previously that PTHrP expression and osteolysis by cancer cells are regulated by Gli2, a Hedgehog (Hh) signaling molecule. Gli2 is a developmental protein mis-expressed in some tumors. Understanding whether Gli2 expression in cancer cells is regulated through Hh receptor signaling or other mechanisms is important for target-based drug approaches for inhibiting Hh signaling and PTHrP in osteolytic breast cancer. To clarify this, we have used several approaches. We examined cancer cells associated with increased PTHrP expression for expression of Hh signaling receptors and determined the effects of specific receptor antagonists. The absence of these receptors would indicate the Hh pathway is stimulated independently of Hh ligand. We also determined the effects of antagonists specific for Gli2. Hh molecules utilize two receptors Smoothened (Smo), the signaling receptor, and Patched (Ptc). We found that osteolytic MDA-231 human breast cancer cells express Ptc but do not express Smo. Without the presence of the signaling receptor, the observed increase in Gli2 is unlikely due to canonical signaling. To verify that Gli2 is not regulated by canonical Hh signaling, we utilized the Hh antagonist cyclopamine. Cyclopamine had no effect on growth of MDA-231 cells in vitro and did not decrease Gli2 or PTHrP expression by real-time PCR. When athymic nude mice were inoculated with MDA-MB-231 cells via the intracardiac route, and treated with 10mg/kg/day of cyclopamine, there was no inhibitory effect on tumor-induced osteolysis. However, overexpression of intracellular molecules that modulate Hh signaling by down-regulating Gli2 protein in MDA-231 cells decreased PTHrP expression. Specifically, Suppressor of Fused (SuFu), a protein that binds to Gli2 and prevents it from translocating to the nucleus, blocked Gli2 stimulation of PTHrP, while a dominant-negative SuFu increased PTHrP promoter activity. Furthermore, overexpression of a dominant-negative β -TrCP, the E3 ligase which targets Gli2 for ubiquitination and proteasomal degradation, increased PTHrP promoter activity by inhibiting the degradation of Gli2. Together, our data confirm that Gli2 mediates PTHrP expression, and that Gli2 expression is not driven by signals initiated by Hh in breast cancer. Although these data suggest Hh antagonists such as cyclopamine will not be effective treatments for osteolytic bone metastases, they do indicate the potential utility of targeting Gli2 degradation.

Disclosures: J.A. Sterling, None.

M297

TGF β Drives Expression of Osteogenic Molecules in Bone Metastatic Breast Cancer Cells: A Potential Mechanism for Breast Cancer Osteomimicry. M. Ni^{1*}, J. A. Sterling², A. Roberts^{3*}, L. Lin^{3*}, G. R. Mundy², R. L. Caldwell⁴. ¹Department of Pharmacology, Vanderbilt University School of Medicine, Nashville, TN, USA, ²Department of Medicine/Clinical Pharmacology, Vanderbilt University School of Medicine, Nashville, TN, USA, ³Department of Pharmacology, Vanderbilt University School of Medicine, Nashville, TN, USA, ⁴Orthopaedics and Rehabilitation, Vanderbilt University School of Medicine, Nashville, TN, USA.

As tumor cells leave the primary environment, expression of molecules important for homing to the targeted organ ensues. For bone metastatic cancer cells, these molecules are similar to those expressed by bone cells, a process called osteomimicry. They include Runx2 and other molecules in the Wnt/B-catenin pathway which are important in osteoblast differentiation. Several groups have reported similar findings, yet the significance of these molecules is unclear. We have previously demonstrated that osteolytic breast cancer cells express the Hedgehog (Hh) signaling molecule Gli2, which drives BMP2 expression and the Wnt/B-catenin pathway in osteoblasts. We hypothesized that expression of BMP2 and Wnt/B-catenin pathway components are dependent on activation of the Hh pathway in breast cancer cells. We found that wild type (WT) MDA-MB-231 human breast cancer cells express Gli2 and BMP2. Since breast cancer cells in bone are exposed to high concentrations of TGF- β , we examined these cells for Gli2 and BMP2 regulation by TGF- β . We also examined MDA-MB-231 cells deficient in TGF- β signaling (DN-TGF- β RII). In WT MDA-MB-231 cells, we found high levels of BMP2 expression that were increased after TGF- β treatment. BMP2 expression was absent in DN-TGF- β RII cells. We found TGF- β treatment increases BMP receptor type II (BMPRII) expression in WT cells, suggesting that bone metastatic breast cancer cells are able to respond to the observed increase in BMP2. To determine if TGF- β could increase BMP2 signaling, we tested the effect of TGF- β on a SMAD6 promoter-reporter construct, revealing that TGF- β increases activity from the SMAD6 promoter. Contrary to other tumor cell types that exhibit decreased proliferation after BMP2 treatment, cell proliferation assays did not indicate a BMP2-mediated growth inhibition in WT breast cancer cells. We then examined an MDA-MB-231 clone over-expressing a dominant-negative, kinase-deficient BMPRII and found decreased tumor cell proliferation compared to WT cancer cells. Our data suggest that the Hh pathway, and specifically Gli2, may drive expression of downstream molecules implicated in osteomimicry, and that the process is enhanced by TGF- β expression in the bone metastatic microenvironment.

Disclosures: J.A. Sterling, None.

This study received funding from: Vanderbilt University Tumor Microenvironment Network and Developmental Funds from the Department of Orthopaedics and Rehabilitation.

M298

See Sunday Plenary Number S298

M299

Fracture Risk Factors in Breast Cancer Survivors with Chemotherapy-induced Amenorrhea. K. M. Winters-Stone^{*1}, L. Nail^{*1}, A. Schwartz^{*2}, K. Witzke^{*3}. ¹School of Nursing, Oregon Health & Science University, Portland, OR, USA, ²School of Nursing, Arizona State University, Tempe, AZ, USA, ³Kinesiology, California State Univ., San Marcos, CA, USA.

Premenopausal breast cancer survivors (BCS) who experience chemotherapy-induced amenorrhea may have elevated fracture risk due to both chemotherapy and hypoestrogenism. Low estrogen is associated with bone loss and possible neuromuscular declines, whereas chemotherapy for breast cancer is also associated with bone loss, and with weight gain and neurological symptoms. Our pilot study aimed to describe the baseline and one-year change in fractures, falls and bone health in breast cancer survivors with premature menopause within one year following treatment completion. We collected baseline and one year follow-up data to describe changes in fractures and risk factors over time in premenopausal women with early stage breast cancer who experienced chemotherapy-related loss of menstrual cycles (N=47; mean age: 46 yrs; 12.2±4.5 mos. post-chemotherapy). Data on premenopausal, cancer-free controls (N=30; mean age: 41 yrs) were used as a reference group. Bone health was assessed by measuring bone mineral density (BMD) of the proximal femur (hip) and lumbar spine via DXA (Hologic Discovery Wi) and by measuring bone turnover via levels of serum osteocalcin (OC) and urinary deoxypyridinoline cross-links (Dpd). DXA data were also described as T-scores derived from spine and hip BMD values categorized as either normal (≥1) or low (<1). Baseline fall and fracture history were assessed retrospectively by questionnaire and prospectively over 12-months by monthly postcards. Comparisons between groups were determined by ANCOVA on baseline and 12 month values, adjusting for group differences in age and by chi-square for frequency data. There were no significant differences between groups for spine or hip BMD at either time point. However, more BCS were classified as having low spine BMD compared to controls both at baseline 39% vs. 17% for BCS and controls, respectively, p=.06 and at follow-up (44% vs. 20% for BCS and controls, respectively, p<.05). Levels of both OC and Dpd were significantly greater in BCS versus controls both at baseline and at 12-mos. follow-up (p<.01). In BCS, 11% had a history of fracture at baseline compared with 3% of controls (n.s.) and fracture rates over 1 yr were similar between groups. At baseline 42% of BCS had fallen in the last year compared to 50% of controls (n.s.), but over 1 year 70% of BCS experienced 1+ falls compared to 43% of controls (p=.05). Prematurely menopausal breast cancer survivors should be screened for bone health and fall history and if positive should be considered for therapeutic intervention to decrease fracture risk, such as exercise and/or medication.

Disclosures: K.M. Winters-Stone, None.

This study received funding from: PHS Grant 5 M01 RR00334 and the OHSU Medical Research Foundation.

M300

See Sunday Plenary Number S300

M301

Bone Metastases Select for Integrin $\alpha 2 \beta 1$ Negative Cells in Prostate Cancer Cell Line DU145. J. Yin, K. Tracy*, Y. Ward*, K. Kelly*. National Cancer Institute, Bethesda, MD, USA.

The metastatic process involves making and breaking contacts with different extracellular matrix (ECM) components in the primary tumor and metastatic sites. ECM binding is mediated by cell surface integrins. The integrin expression patterns in prostate cancer bone metastasis have not been well studied. To determine whether changes in integrin expression affect prostate cancer metastasis to bone, we studied the integrin expression profile of bone tropic cells in a xenograft model of prostate cancer metastasis. DU145 cells expressing the Ras effector mutant, Ras^{V12G37}, gain the ability to colonize bone, in part as a result of activating the Ral Pathway. Ras signaling through growth factor receptors is commonly activated in prostate cancer progression, and Ral is an important downstream pathway of Ras. All clones isolated from bone metastasis had increased bone metastatic activity compared with the parental DU145/Ras^{V12G37} cells as evidenced by development of more and larger bone metastases at earlier times. The DU145 cell line expresses low levels of integrin $\alpha 1$, and high level of integrin $\alpha 2$, αv , $\beta 1$, and $\beta 3$. Although over-expression of Ras^{V12G37} in a polyclonal population of DU145 cells did not significantly alter the expression of integrins $\alpha 1$, αv , $\beta 1$ and $\beta 3$, about 10% of cells demonstrated loss of integrin $\alpha 2$ expression. Interestingly, integrin $\alpha 2$ expression was lost in 4 out of 5 cell lines isolated from bone metastases, indicating selection within the population for rare $\alpha 2 \beta 1$ negative cells. In addition, loss of integrin $\alpha 2$ expression was correlated with high Ras expression and high RalA activity. We then performed cell adhesion assays on several ECM components including collagens I and IV, laminin and fibronectin. All isolated bone metastatic cell lines with low integrin $\alpha 2$ expression lost adhesiveness to collagen I and IV, while adhesion to laminin or fibronectin remained unchanged. These results suggest that cells with higher RalA activity and loss of integrin $\alpha 2$ are selected in the development of bone metastasis. Downregulation of integrin $\alpha 2$ has been observed in prostate cancer patients, and v-Ras has been shown to down-regulate integrin $\alpha 2$ expression. Our results indicate that high Ras activity and/or loss of integrin $\alpha 2$ may be a marker of prostate cancer bone metastasis.

Disclosures: J. Yin, None.

This study received funding from: NCI.

M302

Up-regulation of TACE in Monocytes Ameliorates their Deflected Differentiation into Osteoclasts and Dendritic Cells in Myeloma. M. Abe¹, M. Hiasa^{*2}, S. Kido¹, K. Takeuchi^{*1}, K. Kitazoe^{*1}, A. Oda^{*1}, H. Amou^{*1}, K. Kagawa^{*1}, T. Hashimoto^{*1}, S. Ozaki^{*1}, T. Matsumoto¹. ¹Department of Medicine and Bioregulatory Sciences, University of Tokushima Graduate School of Medicine, Tokushima, Japan, ²Orthodontics and Dentofacial Orthopedics, University of Tokushima Graduate School of Medicine, Tokushima, Japan.

Monocytes are a common precursor for both osteoclasts (OC) and dendritic cells (DC). M-CSF and RANK ligand induce osteoclastogenesis from monocytes, while GM-CSF and IL-4 in combination trigger the differentiation of DC. We demonstrated that GM-CSF and IL-4 up-regulate TNF-alpha converting enzyme (TACE) expression and activity in monocytes, which cleaves membrane-bound M-CSFR to disrupt M-CSF signaling and inhibit induction of osteoclastogenesis. Multiple myeloma (MM) cells affect the reciprocal regulation of monocytic differentiation into OC and DC lineages towards OC lineage to cause devastating bone destruction and immune suppression in MM. In the present study, we therefore explored a role of up-regulation of TACE in monocytes in the skewed induction of OC and DC differentiation by MM cells. GM-CSF and IL-4 up-regulated the levels of soluble M-CSFR in the co-cultures of monocytes with U266 MM cells. Addition of TAPI-0, a TACE inhibitor, substantially reduced the soluble M-CSFR levels enhanced by GM-CSF and IL-4, suggesting that up-regulation of TACE by GM-CSF and IL-4 mediates cleavage of cell-surface M-CSFR on monocytes in the presence of MM cells. Importantly, the GM-CSF and IL-4 treatment also disrupted osteoclastogenesis in rabbit bone cell cultures enhanced by U266 MM cells as well as by M-CSF and RANK ligand. Addition of TAPI-0 restored the MM cell-mediated osteoclastogenesis suppressed by GM-CSF and IL-4. In contrast, TAPI-0 potently suppressed CD1a+ DC differentiation induced by GM-CSF and IL-4 in the presence of MM cells. These results suggest that up-regulation of TACE by GM-CSF and IL-4 is able to disrupt osteoclastogenesis enhanced by MM cells, while inducing DC formation. Therefore, GM-CSF and IL-4 in combination or other alternatives to up-regulate endogenous TACE activity in monocytes may have a potential as a novel therapeutic maneuver to drive into DC lineage the monocytic differentiation deflected to OC lineage in MM.

Disclosures: M. Abe, None.

M303

See Sunday Plenary Number S303

M304

In Vitro Effects of Zoledronic Acid Alone or in Combination with Radiation Therapy on Cells of the Metastatic Bone Environment. S. A. Arrington, B. S. Margulies*, E. R. Fisher*, M. J. Allen. Orthopedic Surgery, SUNY Upstate Medical University, Syracuse, NY, USA.

The specific aim of this current study was to determine the effect of zoledronic acid (ZA) on individual cell types involved in the metastatic bone environment. In addition we wanted to analyze whether ZA increased breast cancer cell sensitivity to radiation therapy. Mouse marrow stromal cells (ST2), mouse osteoblast-like cells (MC3T3), and human breast cancer cells (F10) were cultured with up to 100µM of ZA for two and seven days. Additionally, F10 cells were treated 24 hours after seeding with radiation (0 Gy to 20 Gy) alone or in combination with 5 µM ZA. Cells were assayed 7 days post-treatment. Cell viability was measured using an MTT assay. Treatment affects on cell cycle were analyzed using flow cytometry. ZA caused a dose-dependent decrease in cell viability with IC₅₀ ranging from 55 µM (F10 cells) to 7 µM (ST2 cells) and 5 µM (MC3T3 cells) 7 days post-treatment. This indicates that F10 breast cancer cells are less sensitive to ZA. F10 cells treated with 5 Gy radiation in combination with ZA showed significant decreases in cell viability compared to cells treated with 5 Gy alone (p=0.0406). Cell cycle analysis revealed G2/M arrest in ST2 cells treated with 5 µM ZA, whereas F10 cells displayed an increase in G0/G1. F10 cells treated with radiation showed a dose dependent increase in G2/M arrest, which was further increased by the addition of 5 µM ZA (Figure 1). These results indicate that when F10 cells are exposed to ZA, they may be blocked from entering S-phase. There was a dramatic increase of cells in G2/M after treatment with 10 Gy and 5 µM ZA, compared to treatment with 10 Gy alone. Taken together these results indicate that even though breast cancer cells are less sensitive to the effects of ZA, compared to marrow stromal cells and osteoblasts, ZA is still effective in causing disruptions to the cell cycle and decreasing cell viability. These effects are further enhanced when ZA is combined with radiation therapy. These findings correlate well with previous work in our mouse model, which also demonstrated decreased tumor damage in tumor-burdened bones treated with radiation and ZA compared to radiation alone.

Disclosures: S.A. Arrington, None.

This study received funding from: CDMRP Department of Defense.

M305

See Sunday Plenary Number S305

M306

Anti-tumor Actions of 2-Methoxyestradiol Is Accompanied by an Increase in Osteoprotegerin Expression in Osteosarcoma Cells. M. Benedikt*, J. P. Szatkowski*, K. L. Shogren*, G. Sarkar*, M. J. Yaszemski, A. Maran. Orthopedic Research, Mayo Clinic, Rochester, MN, USA.

Osteosarcoma is the most common bone malignancy that primarily affects children and young adults. About 30% of patients diagnosed with osteosarcoma will develop metastatic disease. Although a combination of surgery and adjunctive chemotherapy has resulted in improved survival rates, the mortality rate remains very high. 2-Methoxyestradiol (2-ME), a naturally occurring metabolite of 17 β -estradiol has been implicated in the inhibition of tumor cell proliferation. Previous results show that 2-ME did not affect the growth of normal osteoblasts in vivo and in vitro, but inhibited the proliferation and induced apoptosis in osteosarcoma cells. Several recent studies have demonstrated that the expression of bone remodeling proteins osteoprotegerin (OPG) and receptor activator of nuclear factor kappa B ligand (RANKL) are altered in different human cancers. To investigate whether the OPG/RANKL system is involved in the anti-tumor actions of 2-ME, we studied the expression of OPG protein in 2-ME-treated human osteosarcoma cells. Western blot analysis showed that OPG protein levels increased by 2-fold in 2-ME (10 μ M)-treated MG63 osteosarcoma cells. Furthermore a tumorigenic estrogen metabolite, 16 α -hydroxyestradiol which does not induce cell death, had no effect on OPG protein levels. Our results also show that 2-ME treatment increased OPG protein levels in TE85, KHOS, 143B, ROS, SAOS, LM8 human osteosarcoma cells. Thus, these findings suggest that there may be a close association between OPG regulation and 2-ME-mediated cell death in osteosarcoma cells.

Disclosures: M. Benedikt, None.

This study received funding from: National Institute of Health and Mayo Clinic.

M307

See Sunday Plenary Number S307

M308

C-terminal PTHrP(109-119) in Human Serum and Urine Is a Useful Biomarker for Malignancies. D. Burton*¹, C. Chalberg*¹, K. C. Smith*¹, R. L. Fitzgerald², D. A. Herold², L. J. Deftos¹. ¹Medicine, Veterans Administration San Diego Healthcare System and University of California, San Diego, CA, USA, ²Pathology, Veterans Administration San Diego Healthcare System and University of California, San Diego, CA, USA.

Since PTHrP is the most common oncoprotein secreted by human cancers it is a logical biomarker for many malignancies. However, most serum immunoassays for PTHrP can only detect this oncoprotein when it is markedly elevated, usually late in the course of the cancer. This lack of sensitivity limits the clinical value of contemporary PTHrP assays, both research and commercial. In order to address this limitation, we applied newly-developed PTHrP immunoassays to the measurement of PTHrP in the serum and urine of human subjects. We utilized PTHrP immunoassays with differing immunochemical formats to evaluate the PTHrP signature in the serum and urine of patients with calcium and skeletal disorders. In the present study, we collected serum or urine samples from over 200 patients that were either normo- or hypercalcemic (Ca²⁺ > 10.6 mg/dL). We employed three human PTHrP epitope-specific immunoassays directed against human PTHrP amino acids 1-34, 38-64 and 109-119 with assay limits of detection of 2.0, 0.6 and 0.8 fmol/tube, respectively. The PTHrP(1-34) (N-PTHrP) species was undetectable in all urine specimens tested, while the PTHrP(38-64) form averaged 0.025 pmol/L. The PTHrP(109-119) (C-PTHrP) fragment was the most readily detectable form of PTHrP present in urine, averaging 0.52 pmol/L in our patient survey. Similar PTHrP fragment ratios were observed in the sera. Serum C-PTHrP levels ranged from undetectable to 3.1 nmol/L. Cancer patients had higher serum C-PTHrP levels than normal, non-tumor bearing subjects (p < 0.05). There was not a significant correlation between serum Ca²⁺ and serum C-PTHrP, which likely indicates inactivation by proteolysis of the hypercalcemia inducing N-PTHrP fragment. We next analyzed the serum and urine PTHrP from cancer patients using size-exclusion chromatography (Sephacryl S100 beads). Immunoreactive C-PTHrP peaks were observed in both fluids, but the N-PTHrP assay did not detect any PTHrP in the fractions. These results demonstrate the stability of the C-PTHrP species in biological fluids and the processing of the N-PTHrP species. Extension of our studies should lead to the development of testing procedures that may be useful in the early diagnosis and clinical management of patients with PTHrP-expressing cancers.

Disclosures: D. Burton, None.

This study received funding from: Department of Veterans Affairs.

M309

See Sunday Plenary Number S309

M310

The Ubiquitin-Proteasome Pathway Is Dysregulated in Myeloma Cells in the Bone Microenvironment In Vivo. C. M. Edwards, J. A. Fowler, R. L. Caldwell, A. L. Bates*, J. R. Edwards, J. Zhang*, D. E. Foehr*, R. Parker*, A. Roberts*, G. R. Mundy. Vanderbilt Center for Bone Biology, Vanderbilt University, Nashville, TN, USA.

There is abundant evidence that myeloma cells are dependent on host cells for their aggressive behavior in vivo. Recent basic and clinical data shows that myeloma cells are exquisitely sensitive to proteasome inhibition, suggesting that the ubiquitin-proteasome pathway, which is present in all cells, is critical for myeloma cell growth and survival. We hypothesized that activity of the ubiquitin-proteasome pathway in myeloma cells may be increased by and dependent on host cells. We have examined this new concept using the well-characterized 5TGM1 murine model of myeloma. 5TGM1-GFP cells were inoculated into C57Bl/KaLwRij mice, resulting in tumor growth within the bone marrow and development of the characteristic osteolytic bone disease of myeloma. 5TGM1-GFP cells were then isolated from the bone marrow of myeloma-bearing mice by FACS and compared with pre-inoculation cells. A significant increase in chymotrypsin-like proteasome activity was found in 5TGM1 myeloma cells following in vivo growth in bone, as compared to the pre-inoculation cells. Protein profiling by MALDI mass spectrometry revealed a number of regulated proteins, including a reduction in free ubiquitin in myeloma cells following in vivo growth in bone. This decrease in free ubiquitin expression was confirmed by western blotting. Real time PCR demonstrated no significant difference in expression of ubiquitin mRNA in myeloma cells following in vivo growth in bone, suggesting post-translational regulation of ubiquitin in the bone microenvironment. Consistent with an increase in proteasome activity, a decrease in expression of β -catenin, which is degraded by the proteasome, was also demonstrated in myeloma cells isolated from bone when compared to the pre-inoculation cells. Treatment of pre-inoculation 5TGM1 myeloma cells with conditioned media from 14M1 stromal cells, which were isolated from myeloma-bearing mice, demonstrated a significant increase in proteasome activity suggesting the involvement of a soluble factor released from the host microenvironment in mediating the increase in proteasome activity. Our data demonstrate that the ubiquitin-proteasome pathway is dysregulated in myeloma cells within the bone microenvironment in vivo, associated with a reduction in free ubiquitin and an increase in proteasome activity. This suggests that the ubiquitin-proteasome pathway in myeloma cells may be controlled by host factors, and that these host-tumor interactions may contribute to the survival of myeloma cells within the bone microenvironment in vivo.

Disclosures: C.M. Edwards, None.

M311

See Sunday Plenary Number S311

M312

Prevalence of Secondary Causes of Osteoporosis Among Breast Cancer Patients with Osteoporosis and Osteopenia. P. M. Camacho¹, A. Dayal^{*1}, J. Diaz^{*1}, E. Nabhan^{*1}, M. Agarwal^{*2}, J. Norton^{*3}, P. Robinson^{*4}, K. S. Albain^{*4}. ¹Endocrinology and Metabolism, Loyola University Chicago, Maywood, IL, USA, ²Medicine, Christ Hospital, Oak Lawn, IL, USA, ³Cancer Center, Loyola University Chicago, Maywood, IL, USA, ⁴Hematology/Oncology, Loyola University Chicago, Maywood, IL, USA.

Purpose: The main objective of this study was to determine the prevalence of secondary causes of osteoporosis among breast cancer patients being evaluated for osteopenia (low bone mass) and osteoporosis.

Methods: We conducted a retrospective chart review of 238 postmenopausal women consecutively referred to Loyola University Medical Center Endocrinology clinics from 2000-2005, for the management of osteoporosis or osteopenia. Patients were divided into two groups: those without a history of breast cancer or NBC group (N=174), and those with breast cancer or BC group (N=64). The BC group was comprised of patients with early stage breast cancer in the midst of or considering adjuvant hormonal therapy with aromatase inhibitors. Histories and biochemical data from their initial consultation were analyzed. Statistical analysis of each patient population was performed to elucidate the prevalence of secondary causes of osteoporosis in patients with breast cancer relative to the group of patients without breast cancer.

Results: The demographics of the two groups differed in age (64.2 \pm 14.2 in NBC versus 59.5 \pm 10.6 in BC group, p=0.015), mean weight (63.5 \pm 13.7 in NBC versus 73.62 \pm 20.95 kg in BC, p < 0.001), 25 OH Vitamin D levels (28.7 \pm 13.1 in NBC versus 34.03 \pm 15.1 ng/ml in BC, p = 0.019) and degree of bone loss (spine T score of -1.966 \pm 1.34 in NBC versus -0.918 \pm 1.41 in BC, p < 0.001). The presence of at least one secondary cause of osteoporosis was seen in 78.1% of the breast cancer patient group (excluding cancer-related therapies), and in 77% of the non-breast cancer group. Newly diagnosed metabolic bone disorders were seen in 57.8% of the breast cancer population. The most common secondary cause in both groups was vitamin D deficiency, which was seen in 37.5% of the breast cancer group and 51% of the non-breast cancer group. In the BC group, this was followed by idiopathic hypercalciuria (15.6% versus 8% in NBC, trend towards higher prevalence in BC than the NBC group p=0.085), normocalcemic hyperparathyroidism (3.1%) and primary hyperparathyroidism (1.6%).

Conclusion: We found a high prevalence of secondary causes of osteoporosis among breast cancer patients undergoing or considering adjuvant hormonal therapy with aromatase inhibitors. Previously published reports of bone loss and fractures seen in patients on such

agents may have been partly due to the presence of these disorders. It is prudent to obtain a baseline DXA and to screen patients with breast cancer for secondary causes of bone loss.

Disclosures: P.M. Camacho, None.

This study received funding from: Proctor and Gamble.

M313

Environmental Influences on Variability in Levels of Bone Turnover Markers. O. S. Donescu¹, M. C. Battie^{*2}, T. Videman^{*3}. ¹Research, Toronto Rehabilitation Institute at University of Toronto, Toronto, ON, Canada, ²Physical Therapy, University of Alberta, Edmonton, AB, Canada, ³Rehabilitation Science, University of Alberta, Edmonton, AB, Canada.

Biochemical markers may capture the imbalance between bone formation and resorption and may also allow quantitative evaluation of rates of bone loss. Therefore, determinants of marker levels may also provide insights into factors influencing bone turnover and osteoporosis. The aim of the study was to estimate the influence of environmental factors (e.g. lifetime physical activities at work and leisure time, calcium intake, smoking, alcohol and coffee consumption) in determining procollagen type I amino-terminal propeptide (PINP), type I collagen carboxy-terminal telopeptide (ICTP) and urinary amino-terminal type I collagen telopeptide (NTx) marker levels in 147 monozygotic (MZ) and 153 dizygotic (DZ) male twin pairs.

Biochemical markers of bone turnover originating from type I procollagen synthesis or type I collagen breakdown were examined in men using a classic twin study design based on MZ and DZ twins. An extensive, structured interview was conducted to obtain data on exposure to suspected environmental and behavioral risk factors, such as recent and lifetime experiences of smoking, alcohol, coffee consumption, dietary calcium intake, lifetime leisure time activities and sport participation, sitting at work, job heaviness, as well as medical history and medication use. Clinical examinations of each subject were also conducted, including dual magnetic resonance imaging (MRI) of the lumbar spine, serum and urine samples (obtained over a one and a half-day period) and lifting tests. After excluding subjects with medical conditions or taking medications thought to influence biological variation of markers, 98 MZ and 108 DZ male twin pairs were left. Subjects age ranged from 40-56 years (48 +/- 7.9) for MZ and 42-56 (49 +/- 6.7) for DZ twins.

The effect of dietary calcium, smoking, coffee and alcohol, as well as lifetime physical activity (e.g. leisure time activities, sport participation, occupational loading) were not significant determinants of biochemical marker levels in this group of adult men. The genetic and environmental variance in bone markers PINP, NTx and ICTP was largely independent from the environmental or behavioral factors studied, suggesting that these factors have a minor influence in bone formation and degradation in men. In conclusion, possible interventions focusing on these behavioral factors in adulthood might be of limited value in targeting bone resorption or formation.

Disclosures: O.S. Donescu, None.

M314

Monitoring Therapy: Are Bone Resorption Markers (BRM) During Osteoporosis Treatment with Bisphosphonates Within the Lower Half of the Premenopausal Range? D. A. Eekman^{*1}, H. J. G. M. Derikx^{*2}, I. E. M. Bultink^{*1}, A. P. van Zanten^{*3}, W. F. Lems¹. ¹Rheumatology, VU University Medical Center, Amsterdam, The Netherlands, ²Rheumatology, Slotervaart Hospital, Amsterdam, The Netherlands, ³Clinical Chemistry, Slotervaart Hospital, Amsterdam, The Netherlands.

Background and objectives: Although oral bisphosphonates (OB) are efficacious, adherence to anti-osteoporotic treatment is generally poor. It has been suggested that adequate monitoring of the effects of therapy with BRM has a positive effect on adherence (1). We observed in which proportion of patients, diagnosed with osteoporosis and treated with an OB, the urinary excretion of the total fraction of deoxypyridinoline (DPD) is in the lower half of the premenopausal range. (2)

Patients and methods: all consecutive patients visiting the osteoporosis outpatient clinic of the Slotervaart hospital using an OB for at least three months were enrolled. Urine samples were collected by asking the patients to collect their fasting second morning-void. Total DPD was determined by high performance liquid chromatography using commercial reagents (Chromsystems, München, Germany). Day to day variation of this technique is lower than 8 %. The mean (SD) urinary excretion of DPD is 9.3 (2.2) µmol/mmol creatinine, based on fasting second morning-void samples of 35 healthy premenopausal women at 3 consecutive moments. Results: 38 patients were enrolled, 31 women and 7 men, mean age (SD) 69 (11) years. The mean BMD (SD) of the spine and hip was 0.800 (0.147) g/cm² and 0.704 (0.086) g/cm², respectively. All patients were treated with bisphosphonates: alendronate (22), risedronate (11), ibandronate (5).

The mean (SD) urinary excretion of DPD was 8.86 (6.44) µmol/mmol creatinine. In 71% of the patients the DPD excretion was below the premenopausal mean (<9.3 µmol/mmol creatinine).

Conclusion: In our ongoing study in patients with osteoporosis chronically treated with bisphosphonates, bone resorption was within the premenopausal range in more than 70% of the patients: the (biological) target of therapy.

Our data illustrate that measuring BRM is feasible in a non-academic outpatient clinic, and suggest that measurement of urinary excretion of DPD might be a valuable tool to improve adherence to therapy.

References:

- 1) Delmas E.P. et al J Clin Endocrinol Metab. 2007 Apr;92(4):1296-304
- 2) Eastell R. Delmas E.P. J Bone Miner Res. 2005 Jul;20(7):1261-2;

Disclosures: D.A. Eekman, None.

M315

Changes in Bone Resorption Markers During Osteoporosis Treatment with Oral Bisphosphonates. D. A. Eekman^{*1}, H. J. G. M. Derikx^{*2}, I. E. M. Bultink^{*1}, A. P. van Zanten^{*3}, W. F. Lems¹. ¹Rheumatology, VU University Medical Center, Amsterdam, The Netherlands, ²Rheumatology, Slotervaart Hospital, Amsterdam, The Netherlands, ³Clinical Chemistry, Slotervaart Hospital, Amsterdam, The Netherlands.

Background: Adherence to anti-osteoporotic treatment is generally poor; it has been suggested that monitoring therapy with measurement of bone resorption markers (BRM) might improve it. (1) In large observational studies it has been shown that already after 3 months of therapy, BRM can be decreased by more than 30%. (1) Several BRM are available; we investigated the changes in the total fraction of deoxypyridinoline (DPD) during treatment with bisphosphonates.

Objectives: to observe in daily practice in which proportion of patients, diagnosed with osteoporosis and subsequently treated with bisphosphonates, the urinary excretion of DPD has decreased by 30% or more, at least 3 months after starting with therapy.

Patients and methods: in this ongoing project, all consecutive patients who come to the osteoporosis outpatient clinic of the Slotervaart Hospital and start with bisphosphonates are enrolled. Urine samples are collected by asking the patients to collect their second fasting urine. DPD is determined by high performance liquid chromatography using commercial reagents (Chromsystems, München, Germany). Day to day variation of this technique is lower than 8 %. Reference values were determined in a group of 35 healthy premenopausal women as 6.6 - 15.4 µmol DPD / mmol creatinine.

Results: so far 19 patients are enrolled, 18 women and 1 man, mean (SD) age 67 (15) years. The mean BMD of the spine was 0.806 g/cm² and of the hip 0.699 g/cm². All patients started with bisphosphonates: alendronate (7), risedronate (5), ibandronate (6) and pamidronate (1). Seventy-nine percent of the patients were treated with calcium/vitamin D.

During anti-osteoporotic treatment the mean (SD) decrease in urinary excretion of DPD was 36% (18). In 12 of the 19 patients (63%), the urinary excretion decreased by more than 30%.

In 6 of the 7 patients we found an explanation for the non-occurrence of a decrease in bone resorption: secondary osteoporosis in 3 and in 3 patients it appeared that they had not taken their medication adequately.

Conclusion: In 63 % of the patients we found a favourable bone marker response. In the others we found either a cause for secondary osteoporosis, or a failure in adherence to therapy.

We think that this ongoing project (so far in a limited number of patients) emphasizes that it might be useful to use the markers of bone resorption during osteoporosis treatment with bisphosphonates in daily practice.

Reference:

- 1) Delmas E.P. et al J Clin Endocrinol Metab. 2007 Apr;92(4):1296-304

Disclosures: D.A. Eekman, None.

M316

See Sunday Plenary Number S316

M317

Markers of Bone Turnover in Peripubertal Girls. K. M. Fagerlund^{*1}, M. Lehtonen-Veromaa^{*2}, T. Möttönen^{*3}, A. Leino^{*4}, J. Viikari^{*3}, H. K. Väänänen^{*1}, J. M. Halleen⁵. ¹Institute of Biomedicine, Department of Anatomy, University of Turku, Turku, Finland, ²Paavo Nurmi Center, Sport and Exercise Medicine Unit, Department of Physiology, University of Turku, Turku, Finland, ³Department of Medicine, Turku University Central Hospital, Turku, Finland, ⁴Central Laboratory, Turku University Central Hospital, Turku, Finland, ⁵Pharmatest Services Ltd, Turku, Finland.

Puberty is a time of large increase in bone mass and it is associated with high values of bone turnover markers. During puberty, bone turnover is affected by bone remodeling, bone modeling and growth. Little research has been conducted on serum levels of bone turnover markers of children at different ages. We studied changes in bone turnover markers and their association with changes in bone mineral density (BMD) in peripubertal girls. A total of 170 healthy peripubertal Caucasian girls aged 10-19 years were included in the study. The following serum markers of bone turnover were measured: TRACP 5b, a marker of osteoclast number; C-terminal cross-linked telopeptides of type I collagen (CTX), a marker of osteoclast activity; bone-specific alkaline phosphatase (BAP), a marker of osteoblast number; and procollagen I N-terminal propeptide (PINP), a marker of osteoblast activity. The mean activity of a single osteoclast was determined at each age group using the resorption index CTX/TRACP 5b, and the mean activity of a single osteoblast using the formation index PINP/BAP. Turnover index was calculated as the ratio of CTX/PINP. BMD was measured from lumbar spine (LBMD) and femoral neck (FBMD) at baseline, 2 and 6 years. All bone turnover markers correlated significantly with each other and with LBMD and FBMD. Highest levels of all bone turnover markers were observed at the age of menarche (10-12 years). The values decreased during aging until they reached the normal adult levels at the age of 17. BAP and TRACP 5b decreased at a similar rate, while PINP decreased at a higher rate and CTX at a lower rate. As a result, the resorption index and turnover index increased and the formation index decreased up to the age of 17. These results demonstrate that bone turnover markers decrease and correlate significantly with BMD in growing children. The number of osteoclasts and the number of osteoblasts is decreased at a similar rate. However, osteoblast activity is decreased at a higher rate than osteoclast activity, and the mean activity of a single osteoblast is decreased, while the mean activity of a single osteoclast is increased up to the age of 17.

Disclosures: K.M. Fagerlund, None.

M318

Association of Serum FGF-23 and Urinary γ -glutamyltransferase (GGT) with Bone Mineral Density: Hiroshima Cohort Study. S. Fujiwara¹, W. Ohishi^{*1}, N. Masunari^{*1}, K. Ikeda². ¹Clinical Studies, Radiation Effects Research Foundation, Hiroshima, Japan, ²Bone and Joint Disease, National Center for Geriatrics and Gerontology (NCGG), Obu, Japan.

Recently, γ -glutamyltransferase (GGT) was identified as a novel bone-resorbing factor (J Biol Chem 2004, Endocrinology 2007), and its urinary excretion correlated with bone resorption activity in the body (Bone 2006). Fibroblast growth factor (FGF)-23 has emerged as an endocrine regulator of phosphate and vitamin D metabolism, and is a product of osteocytes. The objective of this study was to determine if serum FGF-23 and urinary GGT are related to bone mineral density (BMD) in a population-based cohort. The study population consisted of 1,380 subjects (478 men and 902 women) aged 59 to 101 years old (average age 72.3), followed up by biennial health examinations. Serum FGF-23, and urinary CTX and NTX were measured by ELISA kits. GGT activity in the urine was determined by autoanalyzer and corrected for creatinine concentration. BMD was measured in the spine and the hip by dual X-ray absorptiometry (QDR-4500, Hologic). Multiple linear regression was used for analysis. The study protocol was approved by the ethics committee of the Radiation Effects Research Foundation, and written informed consent was obtained from all participants. Serum FGF-23 concentration was found to increase with age, but no sex difference was observed. Serum FGF-23 concentration correlated positively with body weight and serum creatinine concentration, and negatively with height. After adjusting for age, sex, and body weight, serum FGF-23 concentration was associated positively with spinal BMD ($p=0.01$). Urinary GGT excretion was higher in men than in women, and increased with age with marginal significance ($p=0.08$). Positive correlation was observed between urinary GGT and urinary CTX ($p<.0001$) and NTX ($p<.0001$). After adjusting for age, sex, and body weight, urinary GGT was associated negatively with spinal ($p=0.05$) and hip BMD ($p=0.02$). It is thus concluded that serum FGF-23 and urinary GGT are potential makers for bone metabolism.

Disclosures: S. Fujiwara, None.

This study received funding from: National Institute of Biomedical Innovation.

M319

A New Specific Immunoassay for Intact Serum TRACP5b Demonstrates Increased Sensitivity in Osteoporosis. Y. Lhoste^{*}, P. Vergnaud^{*}, P. Garnero. Synarc, Lyon, France.

Tartrate resistant acid phosphatase 5b (TRACP5b) is secreted by osteoclastic cells and is closely related to TRACP isoenzyme 5a which is mainly derived from macrophages. Current immunoassays for circulating TRACP 5b use antibodies that recognize both intact and fragmented TRACP5a and 5b, selectivity for TRACP5b being partly achieved by performing the measurements at optimal pH for TRACP5b. Recently a new immunoassay (Metra® TRACP5b, Quidel Corporation) has been developed. It uses two monoclonal antibodies raised against purified bone TRACP5b that shows limited crossreactivity for purified TRACP5a. One antibody captures active intact TRACP5b and the other eliminates interference of inactive fragments. The activity of TRACP5b is assessed using the substrate 2-chloro-4-nitrophenyl phosphate (CNPP) which is more specific for TRACP 5b than pNPP used in existing assay. The aim of this study was to evaluate the analytical and clinical performance of this new specific TRACP5b ELISA (M-TRACP5b) in postmenopausal osteoporosis.

The M-TRACP5b assay exhibited a cross-reactivity of only 8.5% for circulating heparin-chromatography purified TRACP 5a. The intra and inter assay coefficients of variation were below 6%. Analytical dilution of serum samples and recovery of spiked human bone purified TRACP5b ranged from 84 to 101% and 95 to 106%, respectively. The sensitivity of the test has been determined at 0.08 U/L. Intra-patient coefficient of variation assessed on 14 untreated postmenopausal women sampled 3 times over 2 months was 12%. In 103 healthy untreated pre and postmenopausal women, serum M-TRACP5b correlated significantly ($r=0.84$, $p<0.0001$) with the existing SBA-TRACP5b (SBA-Sciences). Serum M-TRACP5b increased by an average of 174% (3.32 ± 1.07 vs 1.21 ± 0.47 U/L, $p<0.001$) in 48 untreated postmenopausal women compared to 55 healthy premenopausal women aged from 35 to 45 years. When expressed as SDs from the mean of premenopausal levels (T-score), postmenopausal levels were significantly higher for M-TRACP5b than SBA-TRACP5b (mean T-score: +4.5 vs +2.9, $p<0.001$). After 3 months of treatment of 42 osteoporotic women with alendronate (oral 10 mg/day), the decrease of serum M-TRACP5b was significantly larger than that of SBA-TRACP5b [median (25, 75 pct): -44% (-62, -29%) vs -28% (-37%, -9%), $p<0.001$]. In conclusion, the new ELISA for intact TRACP5b has a low cross-reactivity with circulating TRACP5a, demonstrates good analytical performances and is highly sensitive to detect changes of osteoclastic number/activity following menopause or bisphosphonate therapy.

Disclosures: P. Garnero, None.

M320

Effect of Diet and Exercise-induced Weight Loss on Regional and Total Body BMD of Obese Subjects. H. S. Barden¹, M. K. Oates^{*2}, R. Huizenga^{*3}. ¹GE Healthcare, Madison, WI, USA, ²Mary K Oates MD, Santa Maria, CA, USA, ³Cedars Sinai Medical Center, Los Angeles, CA, USA.

The effect of weight loss on bone densitometry measurements is a topic of interest for subjects and clinicians participating in weight loss programs. Some researchers have suggested that dual-energy x-ray absorptiometry (DXA) measurement of bone mineral

content (BMC) or bone area in obese subjects might be compromised by potentially negative effects of increased soft tissue thickness and increased x-ray attenuation on bone edge detection. The Lunar iDXA (GE Healthcare) uses a high-definition detector to provide improved image quality, precision and accuracy, especially in obese subjects. Recently, obese subjects participating in a weight-loss reality television show were measured with iDXA at the beginning and end of the 8-month program.

We measured 25 female and 22 male subjects at total body, lumbar spine (L1-L4) and proximal femur before and after the weight loss and aggressive exercise program. Average (SD) weights at baseline were 110 kg (9.7 kg) and 152 kg (20.0 kg) for females and males, respectively. Average (SD) weight losses were 27.5 kg (12.1 kg) and 49.3 kg (20.0 kg) for females and males, respectively. Percent weight losses for females and males were ~25% and 32%, respectively.

BMD change with weight loss was minimal (-1% or less) for total body and total femur. Lumbar spine BMD increased 1.5% and 6% for females and males, respectively. Average changes in bone areas were negligible (<0.4%) for all regions, indicating consistent edge detection with changing body weight and no magnification errors due to changes in distance of the bone above tabletop. Regressions of BMD and Area change with weight loss were non-significant for total body and total femur. There was a significant increase in BMD with weight loss in men at the spine. It is unclear if the larger increase in spine BMD seen in men vs women, despite losing a greater percent of their total weight, is related to observed greater weight-bearing aerobic and weight-lifting exercise, greater initial percentage lean mass or hormonal differences.

We conclude that bone results with the iDXA appeared relatively unaffected by rapid, large changes in weight in these very obese subjects. BMD changes were minimal for all regions with the exception of L1-L4 in men, and bone area changes for all regions were negligible. Table 1. Bone Densitometry Changes with Weight Changes in Obese Subjects

		Females	Males
		% Change (SD)	% Change (SD)
Total Body	BMD	-0.4% (1.5%)	-0.8% (2.6%)
	BMC	-0.7% (1.8%)	-1.0% (2.3%)
	Area	-0.3% (1.9%)	-0.1% (1.9%)
Spine L1-L4	BMD	1.5% (3.0%)	6.4% (4.2%)
	BMC	1.2% (4.1%)	6.3% (5.2%)
	Area	-0.3% (1.6%)	-0.2% (2.6%)
Total Femur	BMD	-1.1% (2.4%)	-0.4% (3.3%)
	BMC	-1.2% (2.7%)	-0.2% (3.7%)
	Area	-0.1% (1.5%)	0.2% (1.7%)

Disclosures: H.S. Barden, GE Healthcare 3.

M321

See Sunday Plenary Number S321

M322

Association Of Vitamin D Status With Bone Mineral Density Considering Seasonal Changes of Vitamin D. S. Choi^{*}, B. Kim^{*}. Family Practices and Community Health, Ajou University Hospital, Suwon, Republic of Korea.

Vitamin D deficiency that causes secondary hyperparathyroidism has been considered as major contributor for osteoporosis. Serum 25-hydroxyvitamin D level has seasonal changes. We assessed whether low random serum 25-hydroxyvitamin D level can indicate vitamin D deficiency that leads low bone mineral density considering seasonal variation. Subjects for this study were 2,878 women who had periodic health examination in Ajou university hospital. We measured serum 25-hydroxyvitamin D level by radioimmunoassay and bone mineral density by DEXA.

Serum 25-hydroxyvitamin D levels were high in summer and autumn, low in winter and spring. However, serum 25-hydroxyvitamin D levels did not reflect bone mineral density at any season.

Serum 25-hydroxyvitamin D levels on a spot represent the transient vitamin D status, not vitamin D status affecting long term bone mineral density. When 25-hydroxyvitamin D levels are used to detect the vitamin D deficiency, the cautious interpretation should be necessary.

Serum 25-OHVD levels in groups by BMD			
BMD in L2-L4 spines	n (%)	mean \pm SD	P-value
Normal	1740 (60.5)	15.630 \pm 7.8720	0.618
Osteopenia	861 (29.9)	15.949 \pm 8.7178	
osteoporosis	277 (9.6)	15.898 \pm 8.9077	

Serum 25-OHVD levels in groups by BMD-Summer			
BMD in L2-L4 spines	n (%)	mean \pm SD	P-value
normal	380 (58.3)	18.262 \pm 8.6388 ^a	0.029
osteopenia	202 (31.0)	19.998 \pm 10.2690 ^{a,b}	
osteoporosis	70 (10.7)	20.714 \pm 9.4021 ^b	

Serum 25-OHVD levels in groups by BMD-Fall			
BMD in L2-L4 spines	n (%)	mean \pm SD	P-value
normal	395 (65.7)	18.880 \pm 7.7681 ^a	0.018
osteopenia	161 (26.8)	20.272 \pm 9.2000 ^a	
osteoporosis	45 (7.5)	16.476 \pm 8.5364 ^b	

Serum 25-OHVD levels in each season			
	n(%)	Mean \pm SD	P-value
Spring (March-May)	748 (26.0)	12.897 \pm 6.9835 ^a	0.01
Summer (June-Aug)	652 (22.7)	19.063 \pm 9.2906 ^b	
Fall (Sep-Nov)	601 (20.9)	19.074 \pm 8.2740 ^b	
Winter (Dec-Feb)	877 (30.5)	13.445 \pm 6.4856 ^a	

Disclosures: S. Choi, None.

M323

See Sunday Plenary Number S323

M324

Longitudinal Patterns in Bone Mass Measurement Among U.S. Medicare Beneficiaries.

J. R. Curtis¹, L. Carbone², H. Cheng¹, B. Hayes³, A. Laster⁴, R. Matthews⁵, K. G. Saag¹, R. Sepanski⁵, B. Tanner⁶, C. Womack³, E. Delzell¹. ¹University of Alabama at Birmingham, Birmingham, AL, USA, ²Veterans Affairs Medical Center, Memphis, TN, USA, ³University of Tennessee, Memphis, TN, USA, ⁴Arthritis & Osteoporosis Consultants of the Carolinas, Charlotte, NC, USA, ⁵University of Tennessee, Nashville, TN, USA, ⁶Vanderbilt University, Nashville, TN, USA.

Background: The rising burden of osteoporosis has increased the importance of bone mass measurement (BMM). We examined longitudinal changes in BMM among older U.S. Medicare beneficiaries.

Methods: Using Medicare data (1999-2004), we studied beneficiaries age \geq 65 with part A+B, not HMO (A+B-HMO) and in the 5% sample. We identified central DXA claims performed in a physician office (non-facility) or hospital (facility); peripheral DXA; or other BMM. The number of persons with \geq 1 test/yr was divided by the number of beneficiaries to derive the % of eligible persons tested. The number of tests was multiplied by 20 to derive annual national estimates. For persons eligible in 2004, we added data from earlier years to obtain a cumulative prevalence of DXA utilization.

Results: The number of BMM tests are shown (Table); use of central DXA approximately doubled over 5 years, and ~2/3 were performed in physician offices. The proportion of beneficiaries receiving any BMM each year increased from 5.4% (1999) to 8.5% (2004); utilization among women from 8.5% to 13.2%; among men from 0.9% to 2.0%; among blacks from 2.3% to 5.2%; and among whites from 5.7% to 8.8%.

In 2004, there were an estimated 2.24 million central DXA scans; utilization among persons age 65-69, 70-79, and \geq 80 was 9.1%, 9.6%, and 6.8%. Across regions, DXA utilization in 2004 was highest in the South (8.9%) and lowest in the Midwest (7.9%). Among persons eligible in 2004, adding 1-5 prior years increased the cumulative prevalence of DXA utilization from 7.7% to 15.5% (1 extra year), 19.8%, 23.9%, 28.8%, and 29.6% (5 extra years).

Conclusions: The proportion of eligible U.S. Medicare beneficiaries age \geq 65 with A+B-HMO receiving BMM each year increased more than 50% from 1999-2004. A majority of scans were performed in physician offices. Data from only one year substantially underestimated BMM utilization; after aggregating up to 6 years of data, approximately 30% of beneficiaries received any BMM. Ongoing work will examine how these longitudinal patterns are affected by changes in DXA reimbursement.

	1999	2000	2001	2002	2003	2004
Central DXAs, non-facility	815,520	947,840	1,090,060	1,267,960	1,376,160	1,464,360
facility	400,000	504,840	600,940	693,840	759,400	775,020
Peripheral DXAs non-facility	118,640	97,060	79,320	77,620	69,320	68,400
facility	14,800	17,600	17,900	16,600	17,000	19,320
Any other BMM	49,120	48,700	55,000	53,780	89,920	89,740
A+B-HMO persons age \geq 65 receiving any BMM, %	1,375,740	1,596,040	1,824,300	2,085,480	2,282,060	2,374,240
	5.4	6.2	6.9	7.7	8.3	8.5

Disclosures: J.R. Curtis, Merck 5, 8; Proctor & Gamble 5, 8; Roche 5, 8; Amgen 2. This study received funding from: Amgen.

M325

Quantitative Computed Tomography (QCT) of the Forearm Using Clinical CT Scanners.

K. Engelke¹, W. Timm¹, B. Stampa¹, E. Paris¹, T. Fuerst², C. Libanati³, H. K. Genant². ¹Synarc, Hamburg, Germany, ²Synarc, San Francisco, CA, USA, ³Amgen, Thousand Oaks, CA, USA.

This study aimed to demonstrate that clinical CT scanners can be used to determine BMD and geometrical parameters at the distal forearm. Dedicated pQCT scanners are typically used to assess BMD at the distal forearm from

single or limited peripheral skeleton slices. pQCT scanners use low power x-ray tubes, thus an evaluation of a larger volume requires long (several minutes) scanning time, increasing the likelihood of motion artifacts. In contrast, clinical whole body spiral CT scanners allow scanning of a 10 - 20 cm forearm section in seconds improving patient comfort and data acquisition quality.

We used a 120 kV, 1 mm slice thickness, pitch 1 scan protocol to image 10 cm of the forearm starting 0.5 cm distally of the radial styloid. BMD, cortical thickness and some geometrical parameters from single CT slices were measured using the Geanie software (Commit Inc. Finland). Custom software allowed extracting an arbitrary number of slices perpendicular to the radial axis at preconfigurable distances from the styloid process. A dedicated phantom developed in cooperation with QRM GmbH, Germany, was used for simultaneous calibration of the CT values to BMD. BMD accuracy as assessed from 110 scans of a European Forearm Phantom (EFP) was $3.0 \pm 3.6\%$.

We report cross sectional data from 252 postmenopausal women with QCT and DXA forearm scans. QCT analysis included 3 ultra distal slices (udQCT) located 10 mm proximal to the ulna styloid (distal end of the udDXA region), 1 distal slice (dQCT) located 20 mm proximal to the ulna styloid (proximal end of the udDXA region) and 1 mid slice (midQCT) located 40 mm proximal to the ulna styloid within the distal third of the midDXA region.

Along the radial axis, total radial BMD significantly changed for QCT from udQCT to dQCT by +105% and from dQCT to midQCT by +63%. The corresponding BMD change for DXA from udDXA to midDXA was +48%. Correlations (r^2) between QCT and DXA were: udQCT - udDXA: 0.46, average (udQCT and dQCT) - udDXA: 0.5, midQCT - midDXA: 0.48. A separate analysis of the cortex was performed for the distal and mid QCT slices. At the ultra distal location the cortex is too thin to be reliably analyzed. Cortical thickness significantly increased from distal to mid by +55%, trabecular BMD changed (n.s.) by -10%.

In conclusion forearm QCT, using clinical CT scanners, allows for an accurate and differential analysis of BMD along the axis of the radius. In addition QCT allows separate cortical and trabecular measurements, as well as the provision of radial geometrical parameters. Forearm QCT presents valuable information beyond that provided from simple projectional forearm DXA measurements.

Disclosures: K. Engelke, None.

M326

Trabecular Bone Structural Analysis Using 64 Multi-Detector CT Scanner.

P. K. Saha¹, O. I. Saba², M. Hudson¹, A. Pick¹, G. El-Khoury¹, E. A. Hoffman¹. ¹University of Iowa, Iowa City, IA, USA, ²Siemens Medical Center Solutions USA, Inc., Iowa City, IA, USA.

Several studies have demonstrated association of skeletal diseases including osteoporosis and osteoarthritis with trabecular bone (TB) architectural changes. Multi-detector CT scanner (MDCT) is clinically widely available, less expensive, easy to use and fast to perform and has a low effective dose of about 0.05 mSv. The present study evaluates the role of MDCT for computing TB structural parameters. We imaged distal tibia in a cadaveric left leg of a 102 Y female using a Siemens Sensation 64 MDCT scanner at 120 kVp & 140 mAs to adequately visualize the bony structures. After scanning in a helical mode with a slice thickness of 0.6 mm and collimation of 12 x 0.6 mm, data was reconstructed at 0.3 mm slice thicknesses with a normal cone beam method utilizing a very sharp algorithm of U75u to achieve high image resolution. Three scans with pixel size of 0.15, 0.21 and 0.21 mm were acquired after repositioning the specimen each time. Imtek Micro-cat II was used for mCT imaging (28.8 μ m isotropic voxel) after removing soft tissue and dislocating tibia from the ankle joint. Three MDCT scans were used for reproducibility while the first scan was used for comparison with mCT data. Images were subjected to 3 sequential steps: 1) Bone volume fraction (BVf) computation using local thresholding, 2) resampling at 0.15 mm isotropic voxel using shape-based interpolation and 3) 3D rigid body registration. MDCT TB images have shown high visual agreement with TB architecture in mCT images (Figures 1a and b) and 3D continuity of TB structures is visible in longitudinal slices (Figure 1c). Ten cylindrical regions (ROI) each of 3.75 mm radius and length were chosen over TB region at 8 mm above distal cortical endplate. Four parameters, namely, bone volume/tissue volume (BV/TV), skeletal density (SkD), surface-curve ratio (SCR) and erosion index (EI) were computed for each ROI. Intra class correlations of three MDCT scans are 0.95, 0.97, 0.93 and 0.93 for BV/TV, SkD, SCR and EI while the r^2 values of linear correlation between MDCT and mCT data are 0.84, 0.87, 0.87, 0.98. Preliminary results of this study show high potential of MDCT as a modality for analyzing TB architecture.

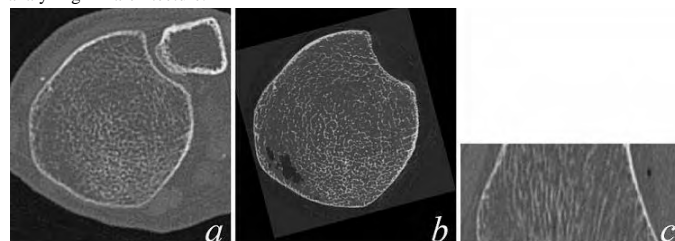


Figure 1 A transverse slice in 64 MDCT (a) and mCT (b) images of TB after 3D registration. (c) A longitudinal image slice from the MDCT data.

Disclosures: P.K. Saha, None.

This study received funding from: Start-up fund, Radiology, University of Iowa.

M327

Abnormal Trabecular Microarchitecture and Mechanical Competence in Premenopausal Women with Idiopathic Osteoporosis (IOP) Can Be Detected by High Resolution Peripheral Quantitative Computed Tomography (HRpQCT). A. Cohen¹, R. R. Recker², X. E. Guo³, X. H. Zhang^{*3}, J. Lappe^{*2}, H. F. Eisenberg^{*1}, D. J. McMahon¹, E. Shane¹. ¹Medicine, Columbia University, New York, NY, USA, ²Medicine, Creighton University, Omaha, NE, USA, ³Biomedical Engineering, Columbia University, New York, NY, USA.

IOP is an uncommon disorder in which young otherwise healthy individuals sustain low trauma fractures. In a retrospective biopsy study of premenopausal (PrM) women with IOP, we found reduced bone formation, increased resorption and, disrupted trabecular (Tb) architecture. We are now conducting a prospective study of the pathogenesis of decreased bone quality and mechanical competence in PrM IOP.

HRpQCT (XtremeCT, Scanco Medical AG) is a new imaging technology (resolution<100µm) that distinguishes cortical from Tb bone and yields in vivo measurements of Tb microstructure previously obtained only by bone biopsy. HRpQCT images can be subjected to finite element analyses (FEA) to determine elastic moduli (stiffness; E) in 3 directions. These E correlate well with mechanical strength.

To date, we have performed HRpQCT scans of radius and tibia in 8 IOP subjects (IOPs) and 9 healthy controls (C) (Table). IOPs and C had normal serum and urine calcium, PTH and 25-OHD; 2 causes of IOP were excluded by clinical/laboratory evaluation.

HRpQCT: At the radius, cortical density and thickness (Th) were similar in IOPs and C. In contrast, Tb number was 19% lower and separation 33% higher in IOPs, while Tb Th did not differ. The Tb network was also more heterogeneous (SD 1/TbN). Tibial cortical Th and Tb number were 20% and 26% lower respectively; Tb separation was 47% higher while Tb Th did not differ. At both sites, Tb density tended to be lower.

FEA: E's were lower in IOPs, but only significantly at the tibia. Variability of these measures was high.

In summary, our preliminary HRpQCT data show that PrM women with IOP have fewer, more widely separated trabeculae of similar thickness. This suggests that loss of entire Tb elements may underlie the more heterogeneous Tb network, decreased stiffness and increased fracture risk. It is not clear why decreased stiffness was found only at the tibia, as weightbearing would be expected to mitigate some of these differences. Future studies will focus on the pathogenesis of differences in Tb structure and mechanical competence. HRpQCT is a sensitive tool for investigation of bone microstructure and strength.

	Radius			Tibia		
	IOP	Control	p	IOP	Control	P
Cortical Density (mgHA/cm ³)	923.9±41.3	901.6±40.2	NS	878.3±54.8	913.0±41.9	NS
Cortical Thickness (mm)	0.77±0.10	0.82±0.14	NS	0.98±0.22	1.23±0.16	0.02
Tb Density (mgHA/cm ³)	129.0±45.6	162.3±22.5	0.07	127.0±43.1	158.11±24.84	0.08
Tb Number (1/mm)	1.66±0.38	2.06±0.24	0.02	1.49±0.48	2.01±0.36	0.02
Tb Thickness (mm)	0.06±0.01	0.07±0.01	NS	0.07±0.02	0.07±0.01	NS
Tb Separation (mm)	0.57±0.14	0.43±0.06	0.02	0.66±0.21	0.45±0.10	0.03
SD of 1/Tb Number (network inhomogeneity)	0.25±0.09	0.16±0.02	0.02	0.41±0.33	0.20±0.06	NS
Elastic Moduli						
E11 (anterior/posterior)	268 ± 183	419 ± 179	NS	136 ± 67	267 ± 133	0.05
E22 (medial-lateral)	508 ± 391	637 ± 320	NS	204 ± 96	398 ± 151	0.02
E33 (longitudinal)	944 ± 684	1149 ± 604	NS	629 ± 214	982 ± 295	0.03

Disclosures: E. Shane, None.

This study received funding from: NIH/NIAMS.

M328

Peripheral Quantitative Computed Tomography (pQCT) Reproducibility of Volumetric Bone Density Measurements at the Radius and Tibia in Healthy Women. K. A. Szabo-Davenport¹, J. D. Adachi², D. Inglis^{*3}, L. Giangregorio^{*4}, C. Webber^{*5}, R. Tozer^{*6}, C. Gordon^{*7}, A. Papaioannou¹. ¹Department of Medical Sciences, McMaster University, Hamilton, ON, Canada, ²Department of Medicine, St. Joseph's Healthcare, McMaster University, Hamilton, ON, Canada, ³Department of Civil Engineering, McMaster University, Hamilton, ON, Canada, ⁴Department of Kinesiology, University of Waterloo, Waterloo, ON, Canada, ⁵Department of Nuclear Medicine, McMaster University, Hamilton, ON, Canada, ⁶Department of Pathology and Molecular Medicine, McMaster University, Hamilton, ON, Canada, ⁷Department of Radiology, McMaster University, Hamilton, ON, Canada.

Peripheral quantitative computed tomography (pQCT) allows the assessment of volumetric bone mineral density (vBMD) and the ability to separately evaluate cortical and trabecular bone compartments at peripheral sites. The objective of this cross-sectional study was to determine the in vivo reproducibility of vBMD measurements of the upper and lower extremity bones in healthy pre- and post-menopausal women via pQCT. Thirty women were recruited to participate in this study; 15 had scans taken of their non-dominant tibia and 15 had scans taken of their non-dominant radius. To better understand differences in bone density, distal (4% site) and diaphyseal sites of the radius (20% site) and tibia (38% site) were examined for trabecular and cortical bone. Trabecular vBMD (TRAB_DEN in mg/cm³), total vBMD (TOT_DEN in mg/cm³) and cortical vBMD (CRT_DEN in mg/cm³) were evaluated at all four sites. For each outcome, the root mean squared coefficient of variation (RMSCV) was calculated. In this population, the distal tibia gave the most favorable RMSCV for TOT_DEN and TRAB_DEN, while the

diaphyseal tibia gave the most favorable RMSCV for CRT_DEN. The data presented here suggest that pQCT scans at the tibia provide more reproducible measurements of total, cortical and trabecular bone.

	Root Mean Squared Coefficient of Variation (%)		
	TRAB_DEN	CRT_DEN	TOT_DEN
Radius 4%	2.0	2.2	5.1
Radius 20%	3.8	0.5	3.3
Tibia 4%	1.6	0.9	1.5
Tibia 38%	5.1	0.3	3.7

Disclosures: K.A. Szabo-Davenport, None.

This study received funding from: Canadian Institutes of Health Research (CIHR) Skeletal Health Training Award and an Ontario Graduate Scholarship (OGS) to K.S.-D.

M329

Novel MRI-Based Technique for Quantifying Cortical Bone Water and Porosity In-Vivo. A. Techawiboonwong^{*1}, H. K. Song^{*1}, B. S. Zemel^{*2}, F. W. Wehrli¹. ¹University of Pennsylvania, Philadelphia, PA, USA, ²The Children's Hospital of Philadelphia, Philadelphia, PA, USA.

Cortical bone porosity is known to increase with age and to correlate inversely with mechanical strength. Measurement of porosity requires invasive techniques -- typically histology from sections or synchrotron µCT -- since typical pore sizes range from tens of micrometers (Haversian canals and osteocyte lacunae) to sub-micrometer (canaliculi). However, all pore spaces are occupied by water, which can be measured with suitable magnetic resonance imaging (MRI) techniques. However, surface interactions and diamagnetism of the mineral relative to water cause extremely short signal lifetime of the signal ($T_2 < 500\mu s$). Here we demonstrate the potential of a new MRI technique to quantify bone water (BW) as a new parameter of bone quality. In contrast to the signal void shown with conventional MRI for the tibial mid-shaft (Fig. 1a), ultrashort-TE radial images in conjunction with an external reference (containing 10% volume of H₂O in D₂O) allow BW quantification (Fig. 1b). MR images were obtained from women ages 20-40 years and 60-80 years (N=5 each) on a 3T scanner at a voxel size of 0.3x0.3x8mm³ in 9 minutes scan time. BW concentration was computed as $(I_{bone}/I_{ref})C_{ref}$ where C_{ref} is the H₂O concentration of the reference and I_{bone} and I_{ref} are the signal intensities corrected for losses during the excitation and spin relaxation. BW (vol %) was 27% larger in the older group (24.04±1.1 vs 17.44±2.2, p=0.0003). In contrast, BMD measured by pQCT at the same location was 1.122±0.033 versus 1.191±0.018 g/cm³, a difference of only 6% (p=0.003). The method was validated in situ in cortical bone of adult sheep where the H₂O fraction was controlled by graded exchange through immersion of the bone in H₂O/D₂O mixtures of varying volume fraction. Total BW was found to be ~19%. The linearity and goodness of fit ($r^2 > 0.99$) suggest the method to be highly accurate and precise (Fig. 2). It is concluded that our technique can quantify BW in vivo as a new index of bone quality.

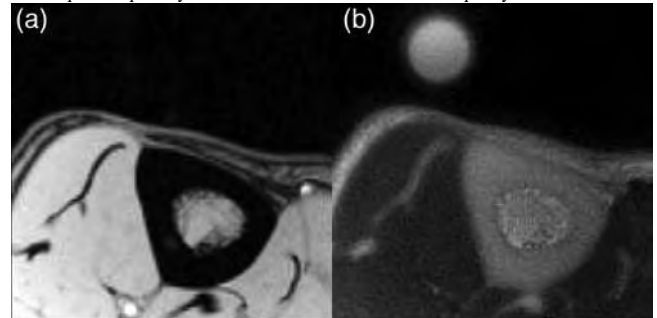


Figure 1. Axial MR images of tibial mid-shaft acquired with (a) conventional gradient-echo; (b) ultrashort-TE radial MRI technique showing for cortical bone; circular structure on top of Fig. b is the reference sample.

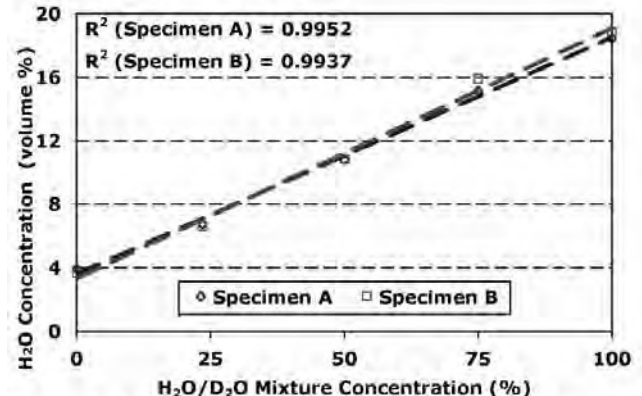


Figure 2. Bone-water concentration quantified from MR images of sheep tibia specimens after graded isotopic exchange with D₂O.

Disclosures: A. Techawiboonwong, None.

M330

See Sunday Plenary Number S330

M331

Clinical Utility of Radiographic Texture Analysis (RTA) Performed on Densitometric Calcaneal Images. T. J. Vokes¹, M. Giger^{*2}. ¹Medicine/Endocrinology, University of Chicago, Chicago, IL, USA, ²Radiology, University of Chicago, Chicago, IL, USA.

RTA is an image-based non-invasive method of evaluating bone structure through computerized analysis of trabecular pattern of bone radiographs. We have applied RTA to calcaneal images obtained using a portable densitometer. RTA yields the following features: Fourier based measurements including RMS (root mean square variation, a measure of the variability in the radiographic texture pattern, the relative difference in the contrast between light and dark areas), and its directional measure, sdRMS (standard deviation of RMS) which is a measure of anisotropy of the trabecular pattern, and FMP (first moment of the power spectrum, a measure of the trabecular pattern's spatial frequency); and Minkowski fractal (MINK), a measure of roughness-smoothness of the trabecular pattern. 1) In 812 patients (739 female) referred for BMD at the University of Chicago we examined which biologic factors influence RTA. 2) In a subset of 331 postmenopausal women who had no secondary causes of and were not receiving treatment for osteoporosis, we determined how well RTA differentiated 48 women with from 283 women without vertebral fracture detected on VFA (Vertebral Fracture Assessment - densitometric spine image).

1) Relationship between RTA and biologic factors: In a multivariate regression analysis all RTA features were associated with age and weight ($p < 0.0001$ for all except $p = 0.02$ for MINK and age) while only MINK and RMS were associated ($p < 0.0001$) with heel BMD. 2) Utility of RTA in assessing fragility. In a univariate logistic regression analysis with presence of prevalent vertebral fractures as a binary outcome the separation between women with and without vertebral fractures using RTA and using BMD measurement were similar ($p = 0.002$ and $p < 0.001$ for sdRMS and MINK, respectively; $p = 0.01$, $p = 0.003$ and $p < 0.001$ for spine, heel and hip BMD, respectively). In a multivariate logistic regression, there was a significant association of vertebral fractures with RTA, BMD, and age with odds ratio (OR) of having a vertebral fracture of 2.0 for each decade increase in age ($p < 0.001$), OR=1.8 for 1 unit decrease in hip BMD T-score ($p = 0.003$), and OR=1.7 for 1 standard deviation decrease in sdRMS ($p = 0.003$) or MINK ($p = 0.008$).

These results suggest that RTA of heel images obtained using a portable densitometer characterizes bone properties not measured by BMD and that RTA provides assessment of fragility that is not captured by the currently used measurements such as BMD and clinical risk factors (age). Addition of RTA to BMD and clinical risk factors may improve the stratification of fracture risk.

Disclosures: T.J. Vokes, None.

This study received funding from: NIH.

M332

See Sunday Plenary Number S332

M333

Bone Varies the Spatial Distribution of its Mass, Rather Than its Mass, to Optimise Strength and Minimize Bulk. R. Zebaze¹, A. Jones^{*2}, A. Bohte^{*1}, Q. Wang^{*1}, M. Knackstedt^{*2}, E. Seeman¹. ¹Austin Health, Melbourne, Australia, ²ANU, Canberra, Australia.

Modelling and remodelling allow bones to adapt to the loading environment by modifying the spatial distribution of their mass rather than the mass itself. We hypothesized (i.) spatial distribution of cortical bone along the femoral neck (FN) as quantified by the variability in cortical thickness (CTh) around the cross sectional (CS) perimeter and along FN length is a better predictor of the cortical bone area (an indicator of axial compressive strength) than the average CTh, the commonly used estimator of cortical area, apparent density and strength indices. (ii.) The amount of material needed to optimise strength is minimized by varying the distribution of bone as compared to having a constant CTh around the CS perimeter.

The spatial distribution of cortical bone was quantified every 300 μ m along the FN (~200 slices/per specimen) using high-resolution micro-QCT in specimens from 13 Caucasian females (mean age 69 years). For each slice, CTh was measured at every degree around the CS perimeter and along the FN. The average FN CTh, the SD of CTh distribution (CTh SD), cortical area and total cross sectional area (TCSA) were computed for each specimen. Also, the CS perimeter was directly measured at 3 points: the neck-shaft junction, mid-FN and neck-head junction and FN CS perimeter was computed as the average of the 3 measurements. The estimated FN cortical area in the hypothetical situation where the cortical bone was uniformly distributed was calculated as FN average cortical thickness * FN CS perimeter.

In a model multivariate including CTh SD, average CTh and TCSA, CTh SD was the best predictor of cortical area $r = 0.76$ ($p < 0.01$); average CTh was not an independent predictor of cortical area. The estimated cortical area derived using the average CTh uniformly distributed around the perimeter (as done in all studies) was $46 \pm 6\%$ ($p < 0.05$) larger than the true (measured) cortical area. The greater the CTh SD, the greater the minimization achieved (i.e., the difference estimated - true cortical area correlated with CTh SD $r = 0.6$, $p < 0.05$).

Point specific modelling and remodelling on the endosteal and periosteal surfaces produce the variability in CTh needed to adapt bone to its loading conditions and so determines cortical area. Varying the spatial distribution of bone mass in this way minimizes the amount of material

needed to optimise strength while avoiding the energy cost and loss of mobility incurred by bulk. Rather than using means, the use of CTh SD may provide more information concerning the heterogeneity in structure so fundamental to its strength. Recognition of the importance of the spatial distribution of bone is essential for understanding the pathogenesis of bone fragility.

Disclosures: R. Zebaze, None.

M334

The Femoral Neck Is No Drinking Straw: Heterogeneity in Structure Is Not Captured Using the Hip Structural Analysis. R. Zebaze¹, A. Jones^{*2}, A. Bohte^{*1}, A. Ghasem-Zadeh^{*1}, M. Knackstedt^{*2}, E. Seeman¹. ¹Austin Health, Melbourne, Australia, ²ANU, Canberra, Australia.

Indirect estimates of femoral neck (FN) structure using hip structure analysis (HSA) are used to predict fracture, estimate age related changes in indices of bone strength, and responses to therapy. These estimates must accurately reflect FN structure and its diversity as this diversity accounts for differences in FN fragility in individuals differing by age, height, weight, race and sex. To determine whether single indices of FN structure and strength derived using HSA reflect the diversity of FN structure and strength, we measured cortical thickness (C.Th) at every degree around the perimeter of each of the ~200 cross sections (CS) along the FN, their total cross sectional area (CSA), shape, cortical area, and section modulus (Z) directly from tomographic images from a high-resolution micro-QCT obtained in postmortem specimens from 13 Caucasian females (mean age 69 years). The structure of the narrow neck (NN) and mid-FN was examined.

A single C.Th failed to capture the structural diversity within a CS. The coefficient of variation of C.Th around the CS averaged 80% (range 54 - 130%) depending on the cross section and varied within and between specimens. Along the FN, from slice to slice, there were varying large and small differences in external and internal architecture within or between specimens not captured by a single depth, width, total CSA or shape, cortical area (or cortical fraction), C.Th or Z. The structure of one CS resembled an adjacent one modestly. For example, two CS around the mid-FN separated by 1mm differed in Z by 12 to 30%. In a region of ± 1 mm to the mid-FN, in ~90% of cases, there was a difference in the average C.Th between at least two CS.

The NN used in HSA varied between specimens, was more distal in individuals with larger NSA ($r = 0.53$, $p < 0.05$) and corresponded to the mid-FN in 2 of 13 specimens; in most cases, NN and mid-FN were not comparable. The average C.Th at the NN and mid-FN differed by 5-23% depending on the specimen. Even greater differences in indices of strength were noted between these two cross sections. In ~65% of the specimens, the NN or mid-FN average C.Th differed from the average whole FN C.Th.

Interpretation of FN structure using HSA inadequately reflects the structural diversity and strength of the FN. The NN is not a constant referent predictive of the diverse structure of the FN and use of the HSA should be viewed with scepticism. Methods to quantify FN structural diversity may help to define the structural basis of bone strength and better predict fracture and treatments effects.

Disclosures: R. Zebaze, None.

M335

Resting Energy Expenditure: A Stronger Marker than Body Weight for BMD in Caucasian Women but Not in Men--The Rancho Bernardo Study. A. Afghani^{*1}, E. Barrett-Connor². ¹College of Health Sciences, Touro University International, Cypress, CA, USA, ²Department of Family and Preventive Medicine, School of Medicine, University of California, San Diego, La Jolla, CA, USA.

The association between resting energy expenditure (REE) and bone mineral density (BMD) has been reported in African-American women, who tend to have lower REEs compared with Caucasian women. The relation between REE and BMD has not been reported in Caucasian adults. 996 postmenopausal Caucasian women and 686 men aged 36-97 years participated in this community-based study. BMD of the lumbar spine (L1-L4), total hip, and total body was measured using dual energy x-ray absorptiometry. REE was calculated using the Harris-Benedict equation; waist and hip girth were measured by standard protocol; grip strength was measured by isometric dynamometry. REE was significantly lower in women than in men (1220 versus 1566 kcal/day, $p < 0.0001$). After adjusting for lean mass, however, REE was significantly higher in women than in men (1407 versus 1296 kcal/day, $p < 0.0001$). In stepwise multiple linear regressions adjusted for estrogen therapy, waist girth, hip girth, and grip strength, REE's contribution to the BMD variances were as follows:

	Spine BMD	Hip BMD	Total Body BMD
Women	13%	31%	30%
Men	0.05%	22%	21%

In women, when body weight replaced REE in the models, weight became the strongest covariate of BMD, but weight explained 9% less of the variance in hip BMD and 6% less of the variance in total body BMD than did REE. The contribution of weight to the variance of spine BMD was the same as the contribution of REE. In men, when body weight replaced REE in the models, there was no change in the variance of hip BMD, but weight explained 9.5% more of the variance in spine BMD and 3% more of the variance in total body BMD than did REE. In this Caucasian cohort, more of the variance in BMD is explained by REE than by weight in women, but in men, weight explains more of the variances in spine and in total body BMD than does REE.

Disclosures: A. Afghani, None.

This study received funding from: National Institute on Aging Grant AG07181.

M336

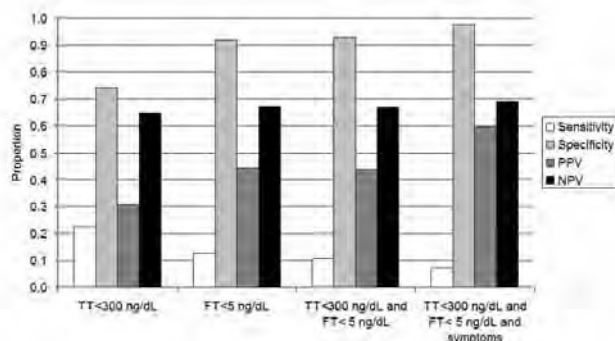
See Sunday Plenary Number S336

M337

Presence of Symptoms in Men with Low Testosterone Levels Improves Prediction of Low BMD. A. B. Araujo¹, T. G. Travison¹, B. Z. Leder², G. R. Esche^{*1}, J. B. McKinlay^{*1}. ¹New England Research Institutes, Watertown, MA, USA, ²Endocrine Unit, Massachusetts General Hospital, Boston, MA, USA.

While recent data show that measurement of bone mineral density (BMD) may be indicated in men with low testosterone (T), T is seldom measured in the absence of symptoms suggestive of androgen deficiency (AD). We examined associations between T, free T, symptoms suggestive of AD, and proximal femur BMD in a racially diverse sample of 1,219 randomly-selected men aged 30-79 y. BMD was measured by dual X-ray absorptiometry. Low BMD was defined as femoral neck or total hip BMD T-score < -1. T and sex hormone-binding globulin (SHBG) were measured by immunoassay, and free T was calculated from T and SHBG concentrations using the mass action equations. Subjects were considered symptomatic if they reported low libido, erectile dysfunction, or two or more of the following non-specific symptoms: sleep disturbance, depressed mood, lethargy, or diminished physical performance. We defined symptomatic AD as the combination of symptoms and serum total T < 300 ng/dL and serum free T < 5 ng/dL. We examined the proportions of men with low BMD in these risk groups, and calculated measures of sensitivity, specificity, positive predictive value (PPV), and negative predictive value (NPV). Mean age among the 991 men with complete sex steroid data was 47 ± 12 y (790 men had complete symptom data). Twenty-five percent of men had low total T, 10% had low free T, 8% had low total and free T, 20% were symptomatic, and 4% had symptomatic AD. Prevalence of low BMD was 34%, which varied considerably by risk group: low total T (30.6%), low free T (44.3%), low total and free T (43.7%), and symptomatic AD (59.7%). The screening characteristics of these measures are shown in the Figure. All measures had low sensitivity (<25%). Specificity was generally high at ≥ 74%. NPV ranged between 54%-69%. Finally, PPV was highest among men with symptomatic AD. In summary, the low prevalence, poor sensitivity, and relatively low PPV of biochemical hypogonadism in our diverse population appears to limit its utility as a screening test for low BMD. Conversely, men who are both biochemically hypogonadal and who report symptoms suggestive of AD have a higher prevalence of low BMD, yielding a higher PPV than for men with low total or free T (alone or in combination). Bone mineral density measurements may thus be indicated in these patients

Disclosures: A.B. Araujo, None.



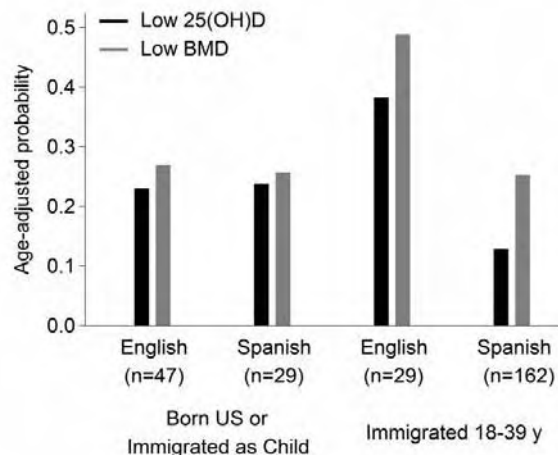
This study received funding from: NIA: AG20727; NIDDK: DK 56842.

M338

Vitamin D Deficiency, Low Bone Mineral Density, and Acculturation in Hispanic Men. A. B. Araujo¹, T. G. Travison¹, G. R. Esche^{*1}, M. F. Holick², T. C. Chen², J. B. McKinlay^{*1}. ¹New England Research Institutes, Watertown, MA, USA, ²Boston Univ Medical School, Boston, MA, USA.

Health disparities occurring within ethnic groups are generally ignored, but in evolving populations such differences may have major public health implications. We examined serum 25-hydroxyvitamin D (25(OH)D) and bone mineral density (BMD) in 360 Puerto Rican, Dominican, Central American, and South American men ages 30-79 y. We examined variation in the proportion of men with 25(OH)D deficiency (<20 ng/mL) and low proximal femur BMD (femoral neck or total hip BMD T-score < -1) by ethnicity, acculturation (language preference and immigration status), and other risk factors. 25(OH)D deficiency was most common among men of Puerto Rican (26%) descent, compared with Dominican (21%), Central American (11%), and South American (9%) men. Percentages with low BMD were: South American (44%), Puerto Rican (34%), Dominican (29%), and Central American (23%). In spite of differences in prevalence of low BMD among the groups, mean differences in BMD were smaller -- with only South American men having significantly lower BMD -- driven mainly by subtle differences in the shape of their BMD distributions. Acculturation displayed a complex but consistent association with 25(OH)D and BMD. While men born in the US or who immigrated as a child did not differ with respect to low 25(OH)D or BMD according to language preference, there were large differences in low 25(OH)D ($p < 0.01$) and BMD ($p = 0.01$) according to language preference among men who immigrated later (see Figure). Multiple

regression models showed that low 25(OH)D and BMD were strongly related to acculturation, and clear differences among the groups with respect to acculturation. However, the explanatory power of acculturation in these differences was largely accounted for by differences in obesity, smoking, physical activity, and other risk factors. There is considerable variation in the skeletal status of male Hispanic ethnic subgroups, which is partly explained by acculturation but more so by differences in lifestyle and health behaviors. When considered in light of US demographic trends, evidence of a rising hip fracture incidence in Hispanics, and the wide range of diseases associated with suboptimal vitamin D status, these data have important implications for fractures, osteoporosis, and the sequelae of vitamin D deficiency.



Disclosures: A.B. Araujo, None.

This study received funding from: NIA: AG 20727; NIDDK: DK 56842; MO RR00533.

M339

See Sunday Plenary Number S339

M340

Prevalence of Vertebral Fractures on Chest Radiographs (CXR) in Elderly African-American and Caucasian Women. B. Bennet^{*1}, O. Ahmed^{*2}, S. Thiel^{*3}, L. Dixon^{*3}, T. Vokes¹. ¹Department of Medicine, University of Chicago, Chicago, IL, USA, ²University of Illinois College of Medicine at Chicago, Chicago, IL, USA, ³Department of Radiology, University of Chicago, Chicago, IL, USA.

Introduction: Hospital discharge claims and population studies report that African-American (AA) women have lower rates of clinical vertebral fractures (Vfx) than Caucasian (CA) women. However, because only 1/3 of radiographically detected Vfx are clinically recognized, and radiographic Vfx have not been examined in AA, the true prevalence of Vfx in AA is not known. Therefore, we compared the prevalence of Vfx detected on routine CXRs in an unselected group of AA and CA female hospital patients.

Methods: Five hundred consecutive lateral CXRs obtained in women ages 60 and over at the University of Chicago were independently evaluated by 3 trained interpreters. Each vertebra was graded using Genant's semiquantitative scale (0=no fracture, 1=mild, 2=moderate and 3=severe compression fracture). Individual vertebra's grades were then added to generate a Spinal Deformity Index (SDI) for each subject. The presence of Vfx was defined by a SDI ≥ 2 from at least 2 of the 3 interpreters. The subjects were labeled with a clinical diagnosis of osteoporosis if the word "osteoporosis" was mentioned in their electronic medical record and with a BMD diagnosis of osteoporosis if they had BMD testing and had T-score ≤ -2.5 at hip or spine. Analysis was restricted to the 418 AA and CA subjects.

Results: Of the 418, 57 (13.6%) had Vfx: 11.9% of 38 AA and 19.4% of 98 CA ($p=0.06$). Only 9 of 57 Vfx (15.8%) detected by our study were mentioned in the official report, with the higher ($p<0.001$) percentage of Vfx reported in CA (4/19 or 21.1%) than in AA (5/38 or 13.2%). Clinical diagnosis of osteoporosis was recorded in 8.9% of study subjects, including 13.3% of CA and 7.5% of AA ($p=0.079$), and in 8/57 (14.0%) of subjects with Vfx. Of 418 subjects, 155 (37.1%) had BMD testing; 31.6% of CA and 38.8% of AA were tested ($p=0.202$). Prevalence of BMD diagnosis of osteoporosis did not differ between the two races: 36/124 (29.0%) in AA and 11/31 (35.5%) in CA ($p=0.49$). Among 57 subjects with Vfx, 19 had BMD testing. BMD diagnosis of osteoporosis was present in 5/6 (83.3%) of CA who had Vfx, but in only 5/13 (38.5%) of AA with Vfx ($p=0.069$).

Conclusion: Although the prevalence of vertebral fractures was lower (but not statistically significant) in AA, they were more likely to have vertebral fractures that were not recognized. Furthermore, they were less likely to have the diagnosis of osteoporosis even if they did have vertebral fractures.

Disclosures: B. Bennet, None.

M341

Examination of the Effect of Dietary Habits on Bone Mineral Density in Healthy Men Aged 15-49 Years Living in the City of Debrecen, Hungary. H. P. Bhattoa^{*1}, A. Balogh². ¹Regional Osteoporosis Center and Department of Clinical Biochemistry and Molecular Pathology, University of Debrecen, Debrecen, Hungary, ²Regional Osteoporosis Center, Department of Obstetrics and Gynecology, University of Debrecen, Debrecen, Hungary.

Diet is known to be one of the most important predictors of bone mineral density, the aim of the present study is to characterize the dietary habits and examine its effects on BMD in a healthy male population aged 15-49 years.

The study protocol expressed a target of enrolling 200 subjects, who were stratified by age into seven 5-year age-bands (15-19, 20-24, 25-29, 30-34, 35-39, 40-44, 45-49 years). The local population based register was used to select a population based random sample. Subjects with a longer than 3 month history of chronic disease affecting bone metabolism were excluded. Other exclusion criteria included previous non-traumatic fracture and prolonged immobilization (>1 month). The subjects were interviewed for approximately one hour according to a modified version of the WHO osteoporosis questionnaire. Information sought included age, socio-demographic status, fracture history (both in the subject and their family), tobacco consumption, physical activity, and dietary calcium, carbohydrate, fat and protein intake. Bone mineral density (BMD) was measured using the DPX-L dual energy X-ray absorptiometry densitometer (Madison, Wisconsin, USA). Bone mineral density was measured at the L2-L4 lumbar spine (LS) and the femur neck (FN). Statistical analysis was performed using SPSS (version 9) for windows.

A total of 177 subjects were enrolled into the study (mean age 39.9 ± 8.7 years). Across the study population, highly significant differences in BMD were observed between the age-band at both skeletal sites ($p < 0.05$). It was not possible to estimate peak bone mass due to the marked fluctuations in mean BMD across the age-bands. The mean LS BMD was lowest in the oldest age-band. The mean FN BMD was highest between 25-29 years and gradually decreased with age, the lowest values being seen in the 35-39 year age-band.

There was a significant correlation between LS BMD and weight, age, daily dietary calcium intake and daily protein intake; FN BMD and weight, age, BMI, dietary calcium, protein, fat and energy intake.

Our findings suggest that among the dietary components examined, daily dietary calcium, protein, fat and energy intake correlated significantly with FN BMD and only the daily dietary calcium and protein intake correlated with LS BMD. The knowledge of the dietary components best responsible for a healthy bone mass may help formulate adequate diet oriented preventive strategies in those between 15-49 years of age as such reduce the burden of osteoporosis later in life.

Disclosures: H.P. Bhattoa, None.

M342

See Sunday Plenary Number S342

M343

Dietary Calcium, Phosphorous, Protein and Bone Metabolism in Korean Postmenopausal Women. H. Chung¹, E. Kim², I. Jeong^{*1}, K. Ahn^{*1}, D. Kim¹, M. Kwon^{*1}, S. Rhee^{*1}, S. Chon^{*1}, S. Oh^{*1}, J. Woo^{*1}, S. Kim^{*1}, J. Kim^{*1}, Y. Kim^{*1}. ¹Kyung Hee University, Seoul, Republic of Korea, ²Fatima Hospital, Daegu, Republic of Korea.

There is a consensus that adequate calcium intake helps to prevent bone resorption and osteoporosis especially in person with low calcium diets. Even though people are concerned about bone health and are encouraged to take calcium supplementation, we believe that most people do not have enough calcium in their diets. The purpose of this study was to determine the nutritional status, urine calcium, bone markers and their relationship in Korean postmenopausal women. The subjects were 80 healthy female with postmenopausal osteopenia and osteoporosis (mean age, 57.8 y). Dietary calcium, phosphorus and protein were measured by 24 hrs recall method and urine calcium, bone markers were measured in fasting. The mean (SD) daily dietary intakes of Ca, P, protein were 603 (204.2) mg, 993 (246.3) mg, 63.9 (16.1) g respectively. Only 5% of the participants had a calcium intake of more than 1000 mg. 51% of the subjects showed 25-OH D of less than 30 ng/mL. The subjects showing hypercalciuria (>300mg/d) was 14.7%. Multiple regression analysis showed that urinary calcium excretion was associated with serum P, CTX, 25-OH D but not dietary Ca. Serum Mg was negatively correlated with osteocalcin ($r = -0.286$, $p = 0.013$), CTX ($r = -0.289$, $p = 0.01$). Nutritional support including calcium supplementation should be required for the most postmenopausal women and should be encouraged in persons who are interested in improving bone health.

Disclosures: H. chung, None.

M344

See Sunday Plenary Number S344

M345

Calcium Intake and the Risk of Osteoporosis and Fractures in French Women. P. Fardellone¹, C. Roux², E. Lespessailles³, F. Cotte^{*4}, A. Gaudin^{*5}. ¹Rheumatology, CHU Hopital Nord, Amiens, 80054, France, ²Rheumatology, Université René Descartes, Hôpital Cochin, Paris, France, ³Rheumatology, CHR Orléans, Orléans, France, ⁴Health Outcomes Studies, GlaxoSmithKline, Marly le Roi, France, ⁵Health Outcomes Studies, GlaxoSmithKline, France, Marly le Roi, France.

Background: The influence of calcium intake from dietary sources on the risk of osteoporosis and fracture prevention is hotly discussed and somewhat confusing.

Objectives: The aim of the study was to assess in French women aged 45 or more years the calcium intake and its relation to osteoporosis and fracture prevalence.

Methods: This study is a cross-sectional observational epidemiological survey carried out in a representative sample of the population of women aged 45 or more years constituted according to the quota method, a stratified random sampling method. Calcium intake from dietary sources was assessed by a validated auto-questionnaire. The investigation on the prevalence of osteoporosis and fractures were conducted by face-to-face home interviews which took place between September and December 2006.

Results: Among the 2,613 interviewed women aged 45 or more years (mean age, 65.8 ± 11.2 years) the prevalence of osteoporosis diagnosed by densitometry was 9.7%. Fractures were reported by 101 subjects (3.9% of the total population and 39.9% of the BMD-diagnosed osteoporotic women). 68.4% of osteoporotic women took supplements of calcium and vitamin D, with no differences between osteoporotic women with fracture or no-fracture history (68.1% vs. 68.6%).

2,135 women returned their questionnaire on calcium intake. The mean calcium intake was $754.1 (+/- 364.2)$ mg/d in the total population, with only 20.1% ingesting more than 1 000 mg/d and 37.2% ingesting less than 600 mg/d. The major single nutrient was milk representing an average daily calcium intake of 137 mg/d ($+/- 230.9$). The mean calcium intake was 795.1 mg/d ($+/- 417.8$) in osteoporotic women ($n=218$), milk representing the most important single nutrient (154.9 mg of calcium/d). These values are not significantly different in comparison with those of the general population.

Conclusion: Calcium intake by French women aged 45 or more years is somewhat low, but is not different between women with or without osteoporosis. The frequency of calcium and vitamin D supplementation is similar in women with fractures and the ones without. These results suggest that in women older than 45 years the diagnosis of osteoporosis or the presence of fractures does not influence the intake of calcium or vitamin D.

Disclosures: P. Fardellone, GlaxoSmithKline 5.

This study received funding from: GlaxoSmithKline.

M346

Height Loss and Decreased Physical Function in Japanese Women: The Hizen-Oshima Study. K. Aoyagi, Y. Abe. Public Health, Nagasaki University, Nagasaki, Japan.

Vertebral fractures lead to subsequent height loss, and previous studies reported that vertebral fractures are associated with decreased physical functioning. However, longitudinal changes of height to physical functioning remain uncertain. We examined the associations of height loss with changes of physical functioning among 373 Japanese women aged 42-91 years. Heights and data on physical functioning were obtained at baseline and at a follow-up examination an average of 3.4 years later. A self-administered questionnaire was used to survey participants about 14 items' difficulty in performing selected basic and instrumental activities of daily living (ADL). Height loss was defined the decrease of 2cm and over between examinations. Decreased physical function was defined as increased difficulty performing 3 or more ADLs. Frequency of height loss increased significantly with age. Height loss was associated with an existence of vertebral deformity at baseline (odds ratio [OR]; 2.28, 95% confidence interval [CI]; 0.96-5.41, $p=0.06$). In age and height at baseline adjusted logistic regression model, height loss was associated with increased difficulty in bending over or picking up a lightweight object (OR; 2.76, 95% CI; 0.91-8.36, $p=0.07$), lifting a 5 kg object from the floor (OR; 2.50, 95% CI; 0.99-6.23, $p=0.05$), reaching an object above her head (OR; 3.85, 95% CI; 1.61-9.20, $p=0.002$), and feeding or dressing herself (OR; 9.28, 95% CI; 1.55-55.34, $p=0.01$). Height loss increased the odds of decreased physical function by 2.4 times (95% CI; 0.9-6.6, $p=0.09$). In conclusion, height loss, possibly due to vertebral fractures, contributes to decreased physical function, as measured by ADLs, independent of age and height at baseline.

Disclosures: K. Aoyagi, None.

M347

See Sunday Plenary Number S347

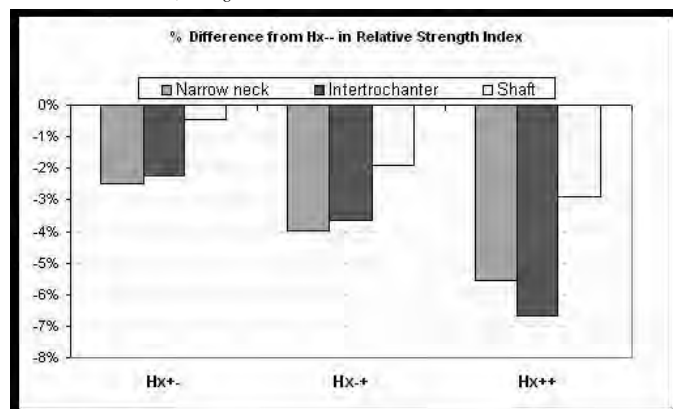
M348

Towards a Weak Bone Phenotype: Comparisons of Load Normalized Section Modulus Among Women With and Without Fracture History in the Women's Health Initiative. T. J. Beck¹, Z. Chen², S. B. Going².

¹Radiology, Johns Hopkins University, Baltimore, MD, USA, ²Epidemiology and Statistics, University of Arizona College of Public Health, Tucson, AZ, USA.

Genetic differences in bone mechanical strength may contribute to fracture susceptibility in life but a clear phenotype of reduced strength is elusive. Low BMD is heritable and associated with increased fracture rates but BMD is a problematic phenotype due to age, gender, site, and body size dependence and an ambiguous relationship to mechanical properties. If a weak bone phenotype does exist, it is probably geometric since most individual differences and effects of age are geometric in nature, that is due to variance in the amount and distribution of bone tissue within bones. Size-corrected section moduli (SM), indices of bending resistance, are continually adapted to prevalent loads throughout life and changes across the lifespan are mainly in response to changing skeletal load. SM appear to maintain an equilibrium with prevalent loads thus a measurable deficiency in that equilibrium may serve as a weak bone phenotype. In this preliminary analysis we used height-adjusted femur section moduli normalized to total body lean mass as a relative strength-load index (cm³/kg). We hypothesized that this index might be diminished among women who suffer bone fractures. Using the Hip Structure Analysis software on DXA scans of the hip, SM were measured at the narrow-neck, intertrochanteric and proximal shaft regions on 6032 multi-ethnic postmenopausal women in the observational cohort of the Women's Health Initiative. Total body lean mass was measured from total body DXA scans. Based on self-reported fracture of any bone prior to enrollment and adjudicated fracture of any bone after enrollment, subjects were divided into four groups: fracture free (Hx-- N=3231), prior fracture only (Hx+- N=1992), new fracture only (Hx+ N=383) and both fractures (Hx++ N=426). Height adjusted indexes in fracture groups were compared to Hx-- (Figure) only the shaft index in Hx++ was non-significant. The results suggest that women who suffer fractures may have a deficit in load response and that this deficit may be greater among women with a history of fracture prior to enrollment and who also suffered new fractures during the observation period. It remains to be seen whether index differences are of genetic origin but the index may prove useful in future genetic studies of fracture susceptibility.

Disclosures: T.J. Beck, Hologic Inc. 7.



This study received funding from: National Institutes of Health.

M349

See Sunday Plenary Number S349

M350

Validation of a Clinical Definition for Fragility Fracture. J. P. Brown¹, L. Bessette¹, S. Jean², K. S. Davison¹, M. Beaulieu³, M. Baranci⁴, J. Bessant⁵, L. Ste-Marie⁶. ¹Laval University, Quebec, PQ, Canada, ²INSPQ, Quebec, PQ, Canada, ³Merck Frosst Canada, Montreal, PQ, Canada, ⁴sanofi-aventis, Montreal, PQ, Canada, ⁵P&G Pharmaceuticals, Montreal, PQ, Canada, ⁶U. of Montreal, Montreal, PQ, Canada.

Despite numerous studies examining the epidemiology of osteoporotic or fragility fracture, there is still no clinical definition available in the literature. Fractures are classically considered to be osteoporotic where the fracture type is associated with decreased bone mineral density (BMD) and its incidence rises with age. This leads to the assumption that all fractures at a particular included site are due to osteoporosis, while fractures at a particular excluded site are unlikely to be osteoporosis-related. An alternative approach is to consider fragility fractures as being osteoporotic based on the mechanism of falling regardless of the site and respective BMD, particularly considering that the majority of fractures occurring in postmenopausal women occur in those with osteopenia or normal BMD.

The aim of this study was to validate a clinical definition for fragility fractures: a fracture occurring spontaneously or following a minor trauma, such as a fall from standing height, a

fall from the sitting position or a fall from laying down on a bed or a reclining deck chair from less than a meter high, a fall after having missed 1 to 3 steps in a staircase, after a movement outside of the typical plane of motion, or coughing. ROCQ (Recognizing Osteoporosis and Its Consequences in Québec) is an ongoing patient health management program aiming to improve the rate of diagnosis and treatment of osteoporosis for women 50+y that have suffered a fragility fracture. To date, 3288 women, mean age (SD) of 65.2 (10.3)y have been recruited 0 to 16 weeks following a fracture either at cast/outpatient clinic in 17 participating hospitals or by mail using the Health Administrative Database of the Province of Quebec (RAMQ) and together have experienced 3485 fracture events. Patients were contacted by phone to answer a short questionnaire to classify them as having either experienced a fragility or traumatic fracture. The proportion of fragility fractures increased progressively with age [73.8% (50-59y), 80.6% (60-69y), 85.5% (70-79y) and 92.8% (80+y)] and was similar between the various types of fracture[wrist (83.0%), humeral (76.1%), ankle (82.6%)], except for a higher proportion at the hip (93.0%), presumably because of its occurrence in older individuals. In conclusion, the proposed clinical definition of fragility fracture based on the mechanism of falling fulfills the criteria for the classical definition without the requirement of a low BMD and should be preferred in epidemiologic and clinical studies of osteoporotic fractures.

Disclosures: J.P. Brown, Merck Frosst Canada 2, 5, 8; The Alliance for Better Bone Health (P & G Pharmaceuticals and sanofi-aventis) 2, 5, 8; Eli Lilly 2, 5, 8; Novartis 2, 5, 8.

This study received funding from: Merck Frosst, P&G Pharmaceuticals, sanofi-aventis, Eli Lilly, Novartis.

M351

See Sunday Plenary Number S351

M352

Spirolactone Use and Risk of Fracture in Men With Congestive Heart Failure. L. D. Carbone¹, J. Cross¹, S. Raza¹, R. Sepanski², S. Dhawan¹, B. Khan¹, M. Gupta¹, K. Ahmad¹, R. Khouzam¹, D. Dishmon¹, J. Nesheiwat¹, W. Christy¹, A. Hajjar¹, W. Nasser¹, M. Khan¹, C. Womack¹, T. Cho¹, A. Haskin¹, K. T. Weber². ¹Veterans Affairs Medical Center (VAMC), Memphis, TN, USA, ²University of Tennessee Health Science Center, Memphis, TN, USA.

Congestive heart failure (CHF), which is mediated in part by activation of the renin-angiotensin-aldosterone system, is a systemic, pro-inflammatory condition that has deleterious effects on multiple tissues, including the skeleton. Observational studies suggest that there is an interrelationship between CHF and osteoporosis. In experimental studies in rats receiving aldosterone/salt treatment, which stimulates the aldosteronism of CHF, we have identified reduced BMD and bone strength. Administration of spironolactone (Spiro) an aldosterone antagonist, attenuated bone loss, and decreased skeletal fragility in these rats. Persons living with CHF are a population at growing risk for osteoporosis, and use of Spiro for treatment of CHF is becoming increasingly common. The purpose of this translational study was to determine the association of Spiro use with incident atraumatic fractures in CHF.

The medical records of all male patients with an ICD-9 diagnosis consistent with CHF from 1999-2005 (n=4735) treated at VAMC, Memphis, TN, were reviewed. Cases were defined as men with CHF who had an incident atraumatic fracture between 1999-2005; controls were men with CHF without incident atraumatic fractures between these years. CHF controls were randomly selected and age and race matched to CHF cases. Information on clinical characteristics and medication use was recorded. Hazard ratios (HRs) with 95% confidence intervals for incident fractures were estimated from Cox proportional hazard models.

We identified 189 CHF cases with an incident fracture and matched these by age and race to 844 CHF controls with no incident fractures. After adjustment for BMI, smoking status, prevalent fractures and use of medications for osteoporosis and CHF, use of Spiro was associated with a significantly lower risk of all fractures (HR 0.481; 95% CI=0.307-.754). Use of Spiro was associated with a significantly decreased risk for nonvertebral (HR 0.393; 95% CI 0.233-0.661), but not vertebral fractures (HR 0.657; 95% CI 0.310-1.395). Both short term (less than or equal to six months) and long term (greater than six months) use of Spiro was associated with a reduced risk for all fractures (p<0.019 for both). Spiro use was associated with a reduced risk of fractures in both systolic and diastolic heart failure.

Short and long-term use of Spiro was associated with a reduced risk of osteoporotic-related fractures in men with CHF. Further longitudinal studies of the effects of Spiro use on osteoporosis in patients with CHF are warranted.

Disclosures: L.D. Carbone, Merck 5, 8; P & G 2, 5, 8; Aventis 8.

M353

See Sunday Plenary Number S353

M354

Identifying Clinical Vertebral Fractures Using Administrative Claims Data: A Validation Study. J. R. Curtis¹, A. Mudano¹, D. H. Solomon², Y. Kim¹, K. G. Saag¹. ¹University of Alabama at Birmingham, Birmingham, AL, USA, ²Brigham and Women's, Boston, MA, USA.

Background: Administrative claims data is often used to identify fracture endpoints in research that examines the effectiveness of osteoporosis therapies. However, the absence of validated claims-based algorithms to identify clinical vertebral compression fractures (VCF) lead to the potential for fracture misclassification.

Methods: Using the claims databases of a multi-state managed care organization from 1/03 - 6/04, we identified patients with ≥ 1 claim for a vertebral compression fracture (ICD9: 805.2, 805.4, 805.8, or 733.13) and excluded patients with claims for malignancies (ICD9: 140.xx to 208.xx, 170.2, 198.5, 203.00, 203.01, 228.09, 238.0, 238.6, 239.2). A random sample of these individuals was selected, and diagnostic radiology reports commonly used to identify VCFs (e.g. x-rays, MRI) prior to or following the initial VCF were requested. Records were reviewed by two independent abstractors to confirm a prevalent VCF. Uncertainties were resolved by consensus among a 3 person review panel. The sensitivity, specificity, and positive predictive value of claims-based criteria were validated against a gold-standard of a radiographically confirmed VCF.

Results: We identified and requested records for 267 patients with ≥ 1 claim for a VCF and received records for 187 persons. Among these individuals, 84% had a confirmed VCF (95% CI 79 - 89%). The diagnostic properties of 3 additional criteria sets compared to the initial screening approach are shown (Table).

Conclusions: The majority of single VCF claims represent confirmed VCF events based on radiographic confirmation. Requiring >1 VCF code or that the VCF code appears after and proximate to radiology claims for specific diagnostic imaging procedures improves the positive predictive value of confirmed VCF events.

	Sensitivity	Specificity	Positive Predictive Value
≥ 1 VCF codes appearing same day or after radiology claim, %	82	50	90
≥ 1 VCF codes appearing same day or within 90 days after radiology claim, %	71	70	93
≥ 2 VCF codes on different days, %	64	80	95

Disclosures: J.R. Curtis, Amgen 2; Novartis 2; Roche 5, 8; Merck 2, 5, 8.

M355

Impact of Incident Hip Fracture on Quality of Life in Older Men: the Osteoporotic Fractures in Men (MrOS) Study. H. A. Fink¹, N. Parimi², B. C. Taylor³, J. T. Schousboe⁴, A. N. A. Tosteson⁵, M. L. Stefanick⁶, K. E. Ensrud³. ¹GRECC, VA Medical Center, Minneapolis, MN, USA, ²California Pacific Medical Center, San Francisco, CA, USA, ³CCDOR, VA Medical Center, Minneapolis, MN, USA, ⁴Park Nicollet Clinic, Minneapolis, MN, USA, ⁵Dartmouth Medical School, Lebanon, NH, USA, ⁶Stanford University Medical Center, Stanford, CA, USA.

Older men with incident hip fractures (fx) often have poor pre-existing health and would be likely to experience health decline unrelated to hip fx. We aimed to estimate the excess decline in self-reported quality of life (QOL) in older men attributable to incident hip fx.

We utilized data from MrOS, a prospective osteoporosis study in men aged ≥ 65 years. Total hip and lumbar spine BMD were measured with DXA. QOL was measured with SF-12 (physical component scale [PCS-12] and mental component scale [MCS-12]) at baseline and visit two (mean interval 4.6 years). Self-reported incident hip fx were centrally confirmed by radiology reports. Linear regression was used to compare change in SF-12 measures between men with incident hip fx and men with no fx. Men with 2+ fx or a nonhip fx were excluded from analyses. Of 5992 men with baseline SF-12 data, 5513 had no incident fx and 48 had an incident hip fx and no other fx. Of men with hip fx, 17 (35%) died before visit two, with 25 of 31 (81%) hip fx survivors completing SF-12 follow-up. At baseline, those with hip fx were older, lighter, less physically active, had more comorbid conditions, lower PCS-12 scores, lower hip BMD, and more often had past fx. Among men with hip fx, those not completing follow-up SF-12 measures appeared less healthy than those with follow-up by all these measures. Among men with baseline and follow-up SF-12 measures, those with incident hip fx experienced a significantly greater mean decline in PCS-12 (-9.1 vs. -2.6, $p=0.02$) but no difference in mean change in MCS-12 (+0.8 vs. -0.5, $p=0.38$). PCS-12 decline appeared greater in men whose hip fx occurred <1 year vs. ≥ 1 year prior to visit two (-15.0 vs. -5.2, $p=0.06$). After adjustment for age, weight, and fall history, PCS-12 decline in men with hip fx overall remained significantly greater than for men without fx.

Among survivors, QOL decline in men with incident hip fx exceeded that in men without fx after accounting for other factors associated with QOL decline. The smaller decline in those with longer fx-to-follow-up intervals suggested that results derived solely from survivors to visit two likely underestimated QOL decline in men after hip fx. Future studies should characterize and distinguish QOL change preceding hip fx and short and long-term post-hip fx QOL change independently attributable to the hip fx.

Disclosures: H.A. Fink, None.

This study received funding from: NIAMS, NIA.

M356

See Sunday Plenary Number S356

M357

Magnification Correction of Vertebral Body Heights During Quantitative Morphometry. A. Mukkananchery*, T. Fuerst, N. Bouzegaou*, G. von Ingersleben, Y. Chen*, C. Wu*, S. Pourfathi*, H. K. Genant. Synarc, Inc., San Francisco, CA, USA.

Vertebral quantitative morphometry (QM) is a common method used to detect incident vertebral fractures in adult women and men. One advantage of QM is the ability to define objective criteria for fracture based on vertebral height changes. However successful QM requires a standardized protocol for point placement and careful training of QM readers. Even with these efforts QM measurements are susceptible to technical errors affecting magnification of the radiographic image. In this study we documented the prevalence of such errors and investigated a technique for magnification correction in QM.

Standardized lateral radiographs of the thoracolumbar spine were acquired at baseline, one year and two years in 4,838 osteoporotic women participating in multi-center clinical trials. Radiographic acquisition was standardized. The films were digitized with a pixel size of 200 microns and QM was performed by trained readers on a proprietary reading workstation. Magnification factors (MF) between images from serial visits were determined by the mean of the ratio of posterior heights at follow-up compared to baseline. When MF was greater than 1 an increase in image size was observed. The MF was then used to adjust vertebral body heights of follow-up images to remove magnification differences and incident fracture was determined using standard criteria (20% change in height from baseline). The identification of an incident fracture by QM methods with and without MF correction was compared to vertebral fractures identified by semiquantitative (SQ) reading by a trained radiologist.

Magnification differences between visits resulted from geometric magnification changes as well as optical magnification changes due to digital x-rays printed at a scale not equal to 100%. Differences between visits exceeded 5% in 30% of subjects in Year 1 while magnification differences greater than 10% occurred in 7% of subjects. Variation increased at Year 2 with 43% and 13% of subjects exceeding these thresholds. Magnification adjustment improved the agreement of QM with SQ by decreasing the number of QM false negative cases by 14 and the number of false positive cases by 75.

Variation in magnification between visits during long term follow-up can be relatively common in spine radiography even with efforts to standardize image acquisition. However, the magnitude of magnification differences and low fracture incidence limits the impact on fracture assessment. SQ reading has greater immunity to magnification differences and is a necessary complement to QM fracture assessment.

Disclosures: T. Fuerst, None.

M358

See Sunday Plenary Number S358

M359

Impact of Incident Vertebral Fractures on Health-Related Quality of Life in Postmenopausal Women: The OPUS Study. M. G. Glüer¹, T. Blenk², C. Graeff¹, D. Felsenberg², C. Roux³, D. M. Reid⁴, R. Eastell⁵, C. C. Glüer¹.
¹Medical Physics, Diagnostic Radiology, University Hospital Schleswig-Holstein, Campus Kiel, Kiel, Germany, ²Charité Universitätsmedizin, Berlin, Germany, ³René Descartes University, Paris, France, ⁴University of Aberdeen, Aberdeen, United Kingdom, ⁵University of Sheffield, Sheffield, United Kingdom.

Health Related Quality of Life (HRQoL) is impaired in patients with vertebral fractures. However, there are no population-based studies with repeated assessment of vertebral fracture and HRQoL at the same time points. We studied the impact of prevalent and/or incident vertebral fractures on HRQoL and compared it with HRQoL changes associated with aging.

In the OPUS study 2409 women were recruited from population-based registers at the 5 participating centers in Aberdeen, Berlin, Kiel, Paris, and Sheffield. At baseline and approximately 6 years later spinal x-rays were obtained and fracture status was assessed by central reading in Berlin (criteria: >20% height reductions and radiological signs of osteoporotic fracture). HRQoL was assessed with the following validated instruments: SF-12 incl. the physical score (PCS-12), EuroHealth, EuroQoL, QUALEFFO-41 (QE) including domain scores, and the symptoms domain of the OQLQ. For all instruments except for QE a lower score implies worse HRQoL.

In a subset of 1285 women (mean age 65.3 at baseline, range 55-80) complete data on vertebral fractures and HRQoL were evaluated. Groups were defined as having no fractures or any fracture, the latter with subgroups of: 'only baseline prevalent fractures', 'only incident fractures', and 'prevalent and incident fractures'.

The table lists those instruments for which at least a trend ($p < 0.2$) for associations was observed. Column 3 represents age-related changes in HRQoL ($^{\circ}$: $p < .05$, ** : $p < .01$, *** : $p < .001$). Columns 4-7 represent HRQoL changes associated with aging and fractures ($^{\circ}$: $p < .2$, * : $p < .05$, ** : $p < .01$ compared to age-related changes of column 3; significance indicates association with fracture and not just aging).

All instruments except for the OQLQ symptoms score revealed some significant reductions in HRQoL. These were similar for incident and prevalent fracture and generally larger if both fractures occurred. HRQoL losses in women with vertebral fractures were independent of the highly significant losses associated with aging.

Score	Mean HRQoL at 0yr, no fx group	HRQoL change 6yr - 0yr				
		No fracture n=1096	Any fracture n=189	Only prev fx n=156	Only inc fx n=33	Prev & inc fx n=22
PCS-12	46.4	-0.9 ^{ns}	-2.3 [*]	-2.2 [°]	-2.8	-2.9
EuroHealth	74.3	-2.4 ^{***}	-4.7 [°]	-4.5	-5.2	-7.7
EuroQoL	72.8	-1.2	-3.6 [°]	-4.1 [°]	-1.3	-14.4 [*]
QE pain	26.4	-1.5 [*]	+1	-6	+3.0	+7.7 [°]
QE physical	12.6	+1.4 ^{***}	+3.3 ^{**}	+3.4 [*]	+2.9	+3.9
QE social	29.1	+2.0 ^{***}	+6.2 ^{**}	+6.7 ^{**}	+4.0	+4
QE mental	32.1	-.9 ^{ns}	+2	+2	+1	+5.0 [*]
QE total	23.5	+6.2 ^{***}	+8.1 ^{**}	+8.2 [*]	+7.9	+9.5 [°]

Disclosures: M.G. Glüer, None.

This study received funding from: Sanofi-Aventis, Demetech, DMS, Eli Lilly, IGEA, GE Medical, Novartis, OSI/Osteometer Mediatech, Procter & Gamble Pharmaceuticals, Pfizer, Guidel/Metra, Roche.

M360

See Sunday Plenary Number S360

M361

Epidemiology of Children's Fractures: A Population-based Study. E. M. Hedström*, P. Michno*, U. Bergström*, O. Svensson. Department of Orthopaedics, Umeå University Hospital, Umeå, Sweden.

Fractures are most common in youth and senescence, when the skeleton is porous with weak points at the physes and metaphyses, respectively. However, there is little published on the general epidemiology of children's fractures. We present the fracture pattern within a population ≤19 years of age, seen at Umeå University Hospital (UUH).

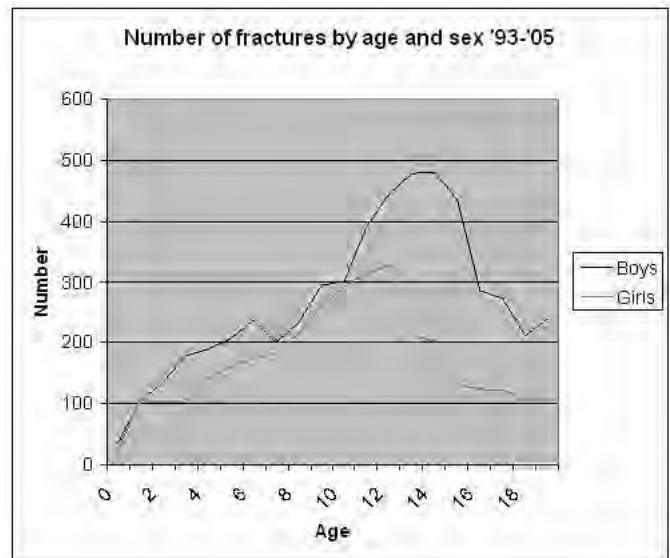
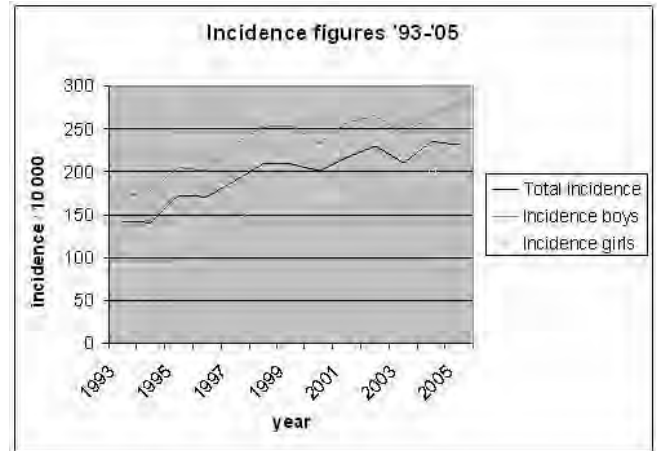
All children sustaining fractures in the Umeå area are seen at UUH which serves as the regional hospital. During the period 1993-2005, when data was collected, the average annual population aged 0-19 in the region was 34,337.

All accidents resulting in injury seen at the hospital were recorded in a database including variables such as age, sex, date of injury, type of injury, mechanism of injury and treatment. From the database we extrapolated 8,768 cases among individuals aged 0-19 where injury resulted in at least one fracture. We then analysed these cases noting incidence rates, fracture type and mechanism of injury, including sex and age related differences.

The yearly incidence rate varied between 141-236 / 10,000 individuals. The minimum incidence rate occurred '94, and the maximum '04. The incidence rate for the whole period was 196 / 10,000 individuals and year. The most common fracture site was the distal

forearm (33%). The most common type of mechanism was falls (58%). The peak incidence occurred at 11-12 years of age in girls and at 13-14 years of age in boys. There was a predominance of boys in the material. The male to female incidence ratio for all fractures and ages was 1.49, a difference which became pronounced in teenage years, being most obvious in the 15 year olds where the male to female incidence ratio was 3.17.

Like in old age, children's fractures are due to both intrinsic and extrinsic factors, but we also have factors due to growth and changes in motor skills and activities. A better description of the epidemiology and possible age, sex and gender specific differences is necessary for optimal targeting of injury preventive measures in the future.



Disclosures: E.M. Hedström, None.

M362

See Sunday Plenary Number S362

M363

Hyperkyphosis and Physical Function in Older Community Dwelling Women: The Study of Osteoporotic Fractures (SOF). M. Huang¹, L. Palermo², K. Stone³, S. R. Cummings³, D. M. Kado¹. ¹Division of Geriatrics, Department of Medicine, UCLA, Los Angeles, CA, USA, ²Univ. of San Francisco, San Francisco, CA, USA, ³Research Institute, California Pacific Medical Center, San Francisco, CA, USA.

Maintaining physical functional ability is an important prerequisite for preserving independence in later life. Hyperkyphosis, or an increased thoracic curvature, is commonly observed in older persons and may be an important determinant of poor physical function. While the Cobb angle method is currently the standard kyphosis measure, data from studies demonstrating an association between hyperkyphosis and physical function have relied on gross clinical observations of stooped posture, and have not taken into consideration possible confounders such as underlying vertebral fractures. Therefore, we sought to determine the cross-sectional association between hyperkyphosis and self-reported and objectively measured physical function in a cohort of 1196 older women aged 65 or older who had radiographs available to measure Cobb angle kyphosis. The digitized Cobb angle (T4-T12) derived from supine lateral thoracic spine plain films was used to

calculate the degree of kyphosis. Participants were an average of 68.8 years old (SD= 3.3) and had a mean kyphosis angle of 44.6 degrees (SD = 12.1). Regression models were used to evaluate association between kyphosis and 1) self-reported being on feet \leq 4 hours/day (yes/no); 2) self-reported functional status (any difficulty in performing six tasks: walking 2-3 blocks, climbing or descending 10 steps, preparing meals, heavy housework, and shopping); 3) measured walking speed; and 4) grip strength. No significant findings between hyperkyphosis and being on feet \leq 4 hours/day or walking speed were detected. However, with each 10 degree increase of kyphosis, women were 1.13-fold more likely to report functional difficulty (95% CI: 1.00 - 1.28, $p = 0.05$) after adjustment for age, clinic, weight, height, physical activity, alcohol, health status, diabetes, and arthritis. Furthermore, with each 10 degree increase in kyphosis, there was 0.2 kg decline in grip strength ($p=0.01$) after adjustment for age, clinic, body mass index, weight, physical activity, health status, diabetes, and arthritis. Similarly, in multivariable adjusted models, women in the worst Cobb angle quartile were 1.6-fold more likely to be in the worst quartile of grip strength (95% CI: 1.2-2.2, $p = 0.001$). Longitudinal studies will be better able to determine whether hyperkyphosis predicts subsequent decline in physical function.

Disclosures: M. Huang, None.

This study received funding from: NIH-NIAMS NIA RO1 AG24246.

M364

See Sunday Plenary Number S364

M365

Height Loss Is Associated with Impaired Quality of Life in the Elderly. K. Tanaka¹, M. Himeno^{*1}, M. Kishimoto^{*1}, A. Kuwabara^{*1}, Y. Ogawa^{*1}, S. Manabe^{*1}, A. Miseki^{*1}, K. Muto^{*1}, M. Fujii^{*2}, N. Kawai^{*2}, J. Ohta^{*3}, S. Kido^{*1}, K. Yoh^{*4}. ¹Kyoto Women's University, Kyoto, Japan, ²Kayu Shirakawa, Kyoto, Japan, ³Shohakuen, Neyagawa, Japan, ⁴Hyogo Medical University, Hyogo, Japan.

Standing height is one of the essential parameters in the anthropometric assessment of the elderly. For example, it is a prerequisite for the estimation of energy expenditure and body composition. Its measurement is, however, too often difficult in the elderly. Although several equations have been published to estimate the height from other surrogate parameters, currently there is no consensus on the way, or more fundamentally, the validity of estimation. In this paper, we have studied these problems, and additionally the impact of height loss on the quality of life (QOL) of the elderly. Initial study including university students revealed that practically all the parameters well correlated with the standing height. In the following study including 187 subjects (52 males, 135 females, 83.2 \pm 9.5 years old), knee height, forearm length could be measured with accuracy in more than 90% of the subjects. In contrast, standing height, arm span, or demispan could be measured in the limited number of patients. In 52 female subjects, standing height could be measured. From the data from these subjects various equations were prepared, of which, the following one best predicted the standing height; standing height=1.82*knee height+1.39*forearm length-0.32*age+60.14 ($R^2=0.63$, $p<0.01$). Previously published equations exhibited marked discrepancies, especially on the way to incorporate the age-related height loss. Theoretically, there are two classes of height; maximum height and current height. The above-mentioned discrepancy probably reflects that these two heights were not clearly distinguished in the previous studies. Knee height is likely to be a good predictor of maximum height, thus could be a good parameter to be used in calculating the energy expenditure or body composition. Finally, the association of QOL with height was studied. The physical component summary (PCS) of SF-8 was significantly correlated with the current height ($r=0.48$, $p<0.05$), but not with knee height, which suggests that height loss is associated with decreased QOL. In summary, nutritional evaluation of the subjects with height loss are to be done using knee height or forearm length, which well reflects the maximum length.

Disclosures: K. Tanaka, None.

M366

See Sunday Plenary Number S366

M367

Bone Density, Muscle Cross Section and Muscular Power in the Lower Limbs in Healthy Postmenopausal Women, Patients on Corticosteroids and Fracture Patients. P. Schneider, H. Haenschel*, E. Maiweg*, C. Reiners*. Clinic for Nuclear Medicine, University of Wuerzburg, Wuerzburg, Germany.

Purpose: We measured bone density parameters at various sites and muscular performance of the lower limbs to investigate the degree of association of bone and muscle status.

Methods: In 3 groups of females (45-89y.), 126 normal postmenopausal women (PW), 36 corticosteroid patients (CS), and, 24 osteoporotic fx patients (OFX), areal bone density (aBMD) was measured at hip and spine using DXA. Distal radius and femur volumetric bone density (vBMD), bone strength index at the tibia midshaft (BSI), largest calf muscle cross section(CMC) area were measured with pQCT. Maximum muscle force and power of the legs were measured with a ground force reaction device (Soehnle Professional GmbH,

Murrhardt Germany) during maximum force knee-bends over 10 seconds. The ratio of force and power to body weight was also considered. Correlations between parameters were calculated over the entire sample. Between-group differences were tested (Tukey's HSD Test). Significance level was set at $p<0.01$.

Results: In the whole sample aBMD and vBMD parameters correlated significantly ($r=0.50$ to 0.67), highest between lumbar spine and femur neck. Distal radius trabecular vBMD and femur neck aBMD were at $r=0.60$. Muscle force, power and cross section correlated with vBMD's and aBMD's in a range of $r=0.32$ to 0.56 ($p<0.001$). CMC and force or power in the tests ranged from $r=0.43$ to 0.56 . The muscle parameters per body weight did not significantly correlate with bone parameters. Between groups comparison showed aBMD's at femur neck and lumbar spine, tibial trabecular vBMD and tibial BSI to be significantly lower in the OFX as compared to the PW and CS group. No differences were found between PW and CS patients. All muscle parameters except power to weight ratio did not show any significant difference between groups. Power to weight ratio was lower in OFX patients. However, in CS, variance of muscle performance parameters was much larger than in PW. Age was negatively correlated with vBMD's and aBMD's ($r=-0.2$ to -0.36) and with muscle power or force ($r=-0.25$ to -0.5). CMC and BSI did not significantly correlate with age.

Conclusion: Prediction of BMD's was slightly better within DXA assessed sites (hip and lumbar spine) as compared to pQCT, or, between the 2 densitometric methods. The sign. difference of power per body weight ratio in OFX as compared to the PW and CS patients could indicate its importance in prevention of falls leading to fracture. In turn, it could also reflect degradation of muscular fitness following the fracture event, which could increase prospective fracture probability. Prospective fracture probability assessment should therefore also focus on accurate muscular performance assessment.

Disclosures: P. Schneider, Soehnle Professional GmbH 5.

M368

See Sunday Plenary Number S368

M369

See Sunday Plenary Number S369

M370

Vitamin D Insufficiency Is Associated with Lower Bone Density in African American Men. N. Akhter^{*1}, B. Sinnott^{*1}, D. Rao², K. Mahmood^{*1}, S. Kukreja³, E. Barengolts¹. ¹University of Illinois at Chicago, Chicago, IL, USA, ²Henry Ford Hospital, Detroit, MI, USA, ³Jesse Brown VA Medical Center, Chicago, IL, USA.

Prevalence and effects of Vitamin D insufficiency are well studied in women but not in African American (AA) males. In previous studies, a negative correlation between serum 25-hydroxy vitamin D (25-OHD) and bone mineral density (BMD) has been shown in Caucasians and Asians. In AA population despite lower serum 25-OHD and secondary hyperparathyroidism, BMD levels are higher. Thus it is not known whether low serum vitamin D has any deleterious effects on the skeleton in the AA population. In AA women, supplementation with vitamin D over 3 years did not increase BMD (Aloia et al. Arch Intern Med. 2005; 165:1618). There are no previous studies that have examined the effects of low serum 25-OHD on BMD in AA men. In the present study, we report data for 112 male veterans enrolled in an osteoporosis study. We examined prevalence of Vitamin D insufficiency and its correlation with age, serum calcium, body mass index (BMI) and BMD. Serum 25-OHD was measured by chemiluminescence assay (DiaSorin Inc., Stillwater, MN, normal range 15-80 ng/ml). BMD was measured by Lunar Prodigy Densitometer. Serum 25 OHD was sufficient in 48% (Group 1, 25OHD >15 ng/ml) and insufficient in 52% (Group 2, 25OHD ≤ 15 ng/ml) of the subjects. The data are presented in the table:

There was no difference between the two groups for age, BMI, calcium, and BMD. However, within Group 2, 25-OHD level correlated positively with BMD of Spine ($r=0.25$, $P=0.05$), Total Hip ($r=0.23$, $P<0.05$), Ward's triangle ($r=0.25$, $P=0.05$) and Trochanter ($r=0.3$, $P=0.02$). Our study suggests that in African American men, the deleterious effects of vitamin insufficiency on bone may be observed only at very low levels of 25-OHD. Further studies with vitamin D supplementation are needed to elucidate risks and consequences of various degrees of vitamin D deficiency in African American men.

Table 1

Characteristics	Group 1, n = 54 Mean \pm SD	Group 2, n = 58 Mean \pm SD	P value
Age, years	66.5 \pm 15.9	61.5 \pm 11.9	0.06
BMI, kg/m ²	28.5 \pm 5.5	28.9 \pm 4.9	0.69
Calcium, mg/dl	8.9 \pm 0.7	9.09 \pm 0.54	0.33
25-OHD, ng/ml	25.07 \pm 8.07	10.46 \pm 3.09	<0.0001
Hip, g/cm ²	1.09 \pm 0.18	1.08 \pm 0.15	0.55
F neck, g/cm ²	1.02 \pm 0.17	1.03 \pm 0.16	0.78
Spine, g/cm ²	1.29 \pm 0.22	1.21 \pm 0.15	0.22

Disclosures: N. Akhter, None.

M371

See Sunday Plenary Number S371

M372

Factors Influencing Women Persistence with Osteoporosis Treatment After 6 Months of Treatment. V. Breuil¹, P. Fardellone², M. Rossignol³, B. Cortet⁴, F. Liard⁵, F. A. Allaert⁶, F. E. Cotté⁶, A. F. Gaudin⁷. ¹CHRU l'Archet, Nice, France, ²CHU, Amiens, France, ³RRSSS, Montréal, PQ, Canada, ⁴CHRU Roger Salengro, Lille, France, ⁵General Practitioner, Saint-Epain, France, ⁶DIM CHRU, Dijon, France, ⁷GSK, Marly le Roy, France.

A retrospective study carried out by 2029 GPs whose representativeness has been controlled.

The purpose was to describe the persistence of women treated for postmenopausal osteoporosis (PMO) for at least 6 months and factors influencing it. Each of them was requested to describe the first 2 successive postmenopausal osteoporotic women who have been persisting with osteoporosis treatment for at least 6 months during the last year, and to ask them to complete a self administered questionnaire.

3598 women 69.5±8.8 years old were included. Regarding risk factors of osteoporosis, 37.5% had maternal history of osteoporotic fracture, 21.5% an early menopause (<45y old), 19.6% were smoking more than 20 cig/day, 13.8% had a long duration of steroid use (≥ 6 months), 11.7% had a BMI < 19 kg/m² and 10.0% were immobilized more than 3 months. 71.3% of them had at least one osteoporotic fracture and the average number of fractures was 1.1 ± 1.0. They were located in vertebra (50.0%), wrist (48.9%) and hip (10.1%). 83.5% of women received the same treatment since the diagnostic of osteoporosis and were defined as persistent. Persistence was higher with weekly bisphosphonates (WBP) (89.8%) and SERM (84.6%) compare to daily bisphosphonates (DBP) (41.4%). The main reasons for non-persistence were "Treatment intolerance" for women treated with WBP and SERM (respectively 36.0% and 34.6%) and "Treatment strictness" with DBP (55.5%). Univariate analysis showed that "Consideration of PMO as a serious disease" and "Knowledge of PMO risk factors" were significantly higher in persistent patient comparing to non-persistent one (<0.01). Persistent patients had significantly more medical consultations (p<0.001). Women under 70 years were more persistent than the older (<0.05). With both daily or weekly regimens, logistic regression shows that persistence with bisphosphonates increases with the number of previous fracture (3 vs 0): OR=1.9, IC_{95%}=[1.1;3.3] and OR=1.7, IC_{95%}=[1.0;2.8], respectively.

Strictness of dosing regimen and intolerance on therapy appeared to be the main reasons for discontinuing PMO treatments. Otherwise, improving information of women and acknowledgement of PMO severity and consequences could be the major way for enhancing their persistence on therapy.

Disclosures: V. Breuil, None.

This study received funding from: Laboratory GlaxoSmithKline.

M373

See Sunday Plenary Number S373

M374

Elderly Patients with Non-Hodgkin's Lymphoma Who Receive Chemotherapy at Higher Risk for Osteopenia and Osteoporosis. M. E. Cabanillas¹, H. Lu¹, S. Fang², X. L. Du². ¹General Internal Medicine, MD Anderson Cancer Center, Houston, TX, USA, ²Division of Epidemiology, The School of Public Health, The University of Texas Health Science Center at Houston, Houston, TX, USA.

In order to determine the risk of osteopenia and osteoporosis associated with chemotherapy among elderly patients with Non-Hodgkin's Lymphoma (NHL), we studied a cohort of 13,570 patients aged ≥65 years with incident NHL in 1992-1999, identified from the SEER-Medicare linked data. We searched for any diagnosis of osteoporosis or osteopenia 1 year prior to and thereafter the diagnosis of NHL, during the 11 years of follow-up. Of 13,570 patients, 60% received chemotherapy. One year prior to the diagnosis of NHL, there were 335 (4.1%) patients who had claims for osteoporosis in the chemotherapy group versus 272 (5%) subjects in the no chemotherapy group (p=0.012). After diagnosis, patients who received chemotherapy had a statistically significant increase in rates of osteoporosis (10.1%) and osteopenia (8.1%) in the chemotherapy group compared to the no chemotherapy group (8.3% and 4.0%, respectively) (p<0.001). After controlling for ethnicity, age, gender, follow-up time, tumor stage, and geographic location, patients who received chemotherapy had a significantly increased odds ratio of 1.27 (95% CI: 1.12-1.45) for osteoporosis and 1.95 (95% CI: 1.66-2.30) for osteopenia compared to those who did not. In conclusion, this population-based retrospective cohort study demonstrated that chemotherapy was associated with an increased risk of developing osteopenia and osteoporosis in community dwelling elderly patients with NHL.

Osteoporosis and Osteopenia between NHL patients who received chemotherapy versus those who did not

	Received chemotherapy n=8152, n, (%)	Did not receive chemotherapy n=5418, n, (%)	p-value
Osteoporosis (1 year before diagnosis)	335 (4.1)	272 (5.0)	0.012
Osteoporosis (on/after diagnosis, or chemotherapy for those receiving chemotherapy)	822 (10.1)	449 (8.3)	<0.001
Osteopenia (1 year before diagnosis)	196 (2.4)	122 (2.3)	0.565
Osteopenia (on/after diagnosis, or chemotherapy for those receiving chemotherapy)	661 (8.1)	216 (4.0)	<0.001

Disclosures: M.E. Cabanillas, None.

M375

See Sunday Plenary Number S375

M376

Prevalence and Risk Factors of Osteoporosis and Vertebral Fractures in COPD Males. E. Casado¹, M. Gallego², M. Larrosa¹, C. Orellana¹, R. Valls³, E. Berlanga⁴, C. Domingo², J. Gratacós¹. ¹Rheumatology, Hospital Sabadell, Sabadell, Spain, ²Pneumology, Hospital Sabadell, Sabadell, Spain, ³Radiology, UDIAT, Sabadell, Spain, ⁴Laboratory, UDIAT, Sabadell, Spain.

The objective of our study was to determine the prevalence of densitometric osteoporosis (OP) and osteoporotic vertebral fractures in COPD patients. To identify the risk factors for the presence of OP and vertebral fractures in COPD patients.

Inclusion criteria: Male sex, older than 50, COPD defined according to ATS/ERS classification. Patients gave their informed consent to participate in the study. Exclusion criteria: Patients with COPD presenting any other concomitant pulmonary disease. Patients with COPD presenting rheumatologic and/or vertebral disease that may hinder the interpretation of the densitometry. Bone mass measurement was determined by dual-energy x-ray absorptiometry (DXA) at lumbar and femoral sites. OP was defined using the WHO score. X-ray of lumbar and dorsal spine was performed in order to evaluate the presence of vertebral fractures. Analytical parameters that influence the phospho-calcium metabolism were determined: calcemia, phosphoremia, 25-OH-vitamin D, PTH, alkaline phosphatase and testosterone. For each patient, age, weight, height, body mass index (BMI), comorbidities, toxins (cigarettes, alcohol), medications, degree of exposure to sun and daily calcium intake were recorded. Corticosteroids treatments in the previous five years and number of hospitalizations were also recorded.

211 patients were evaluated. Mean age was 66.78 years (50-84). 73 patients had a FEV1 between 50-80% and 138 had a FEV1 <50%. Prevalence of OP and fractures were respectively 41.6% and 33%. Dose of prednisone greater than 675 mg, BMI below 21, low blood levels of 25-OH-vitamin D, and FEV1<30% were associated significantly with OP (p <0.05). When logistic regression was performed only BMI (OR=0.9; 95% CI, 0.84-0.96) and FEV1<30% (OR=3.32; 95% CI, 1.36-8.06) remained in the model. Age, use of corticosteroid and FEV1<30% were associated significantly with vertebral fractures. When logistic regression analysis was performed, age (OR=1.06; 95% CI, 1.01-1.1) and FEV1<30% (OR=4.39; 95% CI, 1.66-11.59) remained in the model. In conclusion, the prevalence of OP and vertebral fractures are higher than expected in general population. COPD severity is an important riskfactor for OP and vertebral fracture.

Disclosures: E. Casado, None.

M377

See Sunday Plenary Number S377

M378

Prevalence and Patterns of Presumed Osteoporosis (OP) Among Older Americans Based on Medicare Data. H. Cheng, L. C. Gary*, J. R. Curtis, M. L. Kilgore*, K. G. Saag*, H. Yun*, R. Matthews*, S. Swaminathan*, M. A. Morrisey*, E. Delzell*. Univ. of AL at Birmingham, B'ham, AL, USA.

Background OP prevalence is rising nationally, with recent prevalence estimates for older white women, based on femoral neck bone mineral density testing, of 13.6% for ages 60-69, 26.0% for ages 70-79 and 47.9% for ages 80+. Medicare data afford opportunities and challenges for studying the epidemiology of OP at a population level.

Methods We used Medicare claims data to estimate the prevalence of presumed OP in 2004 and to determine the contributions to estimated OP prevalence of claims for OP and related fractures. The Medicare Chronic Condition Data Warehouse provided data for an enhanced 5% national sample of beneficiaries. We studied 1,600,877 beneficiaries who were ≥ 65 years of age in 2004, had 12 months of Medicare Parts A and B coverage and were not enrolled in an HMO. We assessed claims for 1999-2004 to identify cases with three definitions (D) of presumed OP: D1, ≥ 1 physician service claim with a diagnosis code for OP or for fracture sites strongly associated with OP (i.e., hip, spine or wrist) in any year; D2, ≥ 1 claim for OP or for fractures strongly or usually associated with OP (e.g. pelvis, humerus, radius/ulna, femur, tibia/fibula or clavicle); D3, ≥ 1 claim for OP or for fractures

strongly, usually or sometimes associated with OP (e.g. ribs, scapula, patella or ankle). Results OP prevalence was 19.1% (D1) to 22.9% (D3) overall and varied by gender, race, age and number of years of data (table). For white women, D1-OP prevalence estimates (by age) were 15.7% (65-69), 26.9% (70-79) and 33.4% (80+). Of all D1 cases, 68% had ≥ 2 physician service claims, 71.4% had claims with diagnosis codes for OP only, 14.4% had claims for both OP and fracture, and 14.2% had claims for fracture but not OP. Among people with fracture claims, only 50% had a diagnosis code for OP. Conclusions Estimates of OP prevalence based on Medicare claims were similar to recent prevalence estimates obtained using bone mineral density testing for white women ages 65-79 years and were 20% (D3)-30% (D1) lower for white women ages 80+. Variation in claims-based prevalence by age, gender and race was similar to that found using other methodological approaches. OP-related fractures accounted for a substantial proportion of presumed OP cases. The low proportion of fracture patients with an OP diagnosis code may reflect low rates of OP testing among post-fracture patients.

Prevalence of presumed osteoporosis in 2004 (definition 1)			
Characteristic	Prevalence (%)	Characteristic	Prevalence (%)
Total	19.1	White women	27.5
Race/ethnicity		White women age	
Black	9.7	65-69	15.7
White	19.8	70-79	26.9
Other	21.9	80+	33.4
Gender, Women	26.5	Years of data	
Men	6.3	6	22.8
Age, 65-69	9.5	4-5	15.0
70-79	18.0	2-3	10.8
80+	26.4	1	5.7

Disclosures: H. Cheng, Amgen 2.
This study received funding from: Amgen.

M379

See Sunday Plenary Number S379

M380

No Ethnic Differences in Vertebral Fractures Were Found Between Caucasians, Mestizos and Other Ethnic Background in the Latin-American Vertebral Osteoporosis Study (LAVOS). P. Clark¹, J. Talavera^{*1}, S. R. Cummings², D. Margarita³, F. Cons-Molina⁴, J. Zanchetta⁵, D. Messina⁶, L. Haddock⁷, S. Ragi⁸, J. Jaller⁹, a. The LAVOS Group¹. ¹Clinical Epidemiology Unit, IMSS, Mexico City, Mexico, ²Coordinating Center, UCSF, San Francisco, CA, USA, ³Clinica de Osteoporosis, Puebla, Mexico, Mexico, ⁴Unidad de Diagnostico de Osteoporosis, Mexicali, Mexico, Mexico, ⁵Instituto de Investigaciones Metabólicas, Buenos Aires, Argentina, ⁶Clinica de Osteoporosis, Buenos Aires, Argentina, ⁷Universidad de Puerto Rico, San José, Puerto Rico, ⁸CEDOES, Brazil, Brazil, ⁹Clinical Epidemiology Unit, Colombia, Barranquilla, Colombia.

Different rates of OP and fractures have been reported between groups with different ethnicity. Our aim was to determine if different ethnic backgrounds were associated with the risk of vertebral fractures in Latin American women.

A population based sampling frames were obtained from 5 countries within the Latin-American Region in women 50 years and older: Argentina, Brazil, Colombia, Mexico and Puerto Rico. A questionnaire to get demographic information, conventional risk factors, ethnic background and some life style characteristics was applied. BMD in two regions and lateral dorsal/lumbar x-rays were obtained in all cases accordingly with international protocols. Digital morphometry was used to determine vertebral deformities by modified Eastell criteria; all readings were concentrated in one center. A total of 1922 women from the five countries were included from which, 969 (50.4%) self-reported to be Mestizo, 748 (38.9%) Caucasians, and (10.7%) others (Black, Amerindians, Asians or native Indians). Prevalence of Vertebral fractures was 15.3% (148) in Mestizos, 15 % (112) in Caucasians and 10.7% (22) in other ethnic backgrounds. Ethnicity did not impact the fracture risk. The observed odds ratio between Mestizo and Caucasian was 0.98 (95% CI 0.74-1.29) and 0.67 (95% CI 0.40-1.10) between Mestizo and others. Conclusions: Ethnicity does not appear to have any impact in the risk of vertebral fractures in community dwelling Latin-American women.

Disclosures: P. Clark, None.
This study received funding from: IOF.

M381

See Sunday Plenary Number S381

M382

Stage-of-Change Model Applied to Osteoporosis Medication Use at the Time of Fragility Fracture. B. G. Escott*, V. Elliot-Gibson*, E. R. Bogoch, D. E. Beaton. Mobility Program Clinical Research Unit, Department of Surgery, Keenan Research Center, Li Ka Shing Knowledge Institute, St. Michael's Hospital, University of Toronto, Toronto, ON, Canada.

The purpose of this study was to explore the readiness of patients who have sustained a fragility fracture to take osteoporosis (OP) medication and to identify differences in patient-related factors associated with the various stages of change.

This was a cross-sectional study of baseline data from a prospective cohort of women ≥ 40 years and men ≥ 50 years presenting to a fracture clinic with a low-trauma fragility fracture. Data collected at baseline via a self-reported survey included demographics, OP risk factors, prior OP investigation, diagnosis, treatment and adherence, OP awareness and health beliefs, and a single-item stage of change question adopted from Mauck (2002). We performed multivariable logistic regression to determine associations between baseline patient-related factors and different stages of change.

629 patients completed survey information and met our criteria. Preliminary analysis of willingness to take OP medication revealed a bimodal distribution at the extremes of Prochaska's stages of change with the majority of patients falling in the pre-contemplation or maintenance stages, the two groups analyzed in this study. 539 of 629 (85.7%) patients were either in the pre-contemplation (n=372 or 69%) or maintenance (n=165 or 31%) stages. Mean age (+/- SD) was 73 years (12) and 81% of subjects were female.

Multivariable analysis (adjusted OR; 95% CI) revealed that age >60 (2.5; 1.1-5.8), female gender (3.5; 1.5-7.5), self-reported history of previous fracture (3.3; 2.0-5.3) and self-described poor bone quality (19.9; 8.4-47.3) were significantly ($p<0.05$) associated with being in the maintenance stage compared to pre-contemplation stage. Previous BMD and OP diagnosis were very strongly associated with maintenance stage of change so were not included in the model. Fracture site and highest level of education were not significantly associated.

Higher stage of change was strongly associated with OP awareness. Patients already aware and caring for their OP were more likely to be >60 , female, have sustained a previous fracture and have greater self-awareness of bone quality. Mauck (2002) found few subjects in the intermediate or later stages of change in women suffering a hip fracture. In our study, the intermediate stages of change were not populated suggesting a need to target two main groups for intervention: maintainers for reinforcement and pre-contemplators to raise awareness. This health behavior could be explained using a simpler dichotomous model of motivation for health behavior change. Ref: Mauck et al. (2002) Osteoporos Int 13: 560-564.

Disclosures: B.G. Escott, None.

M383

See Sunday Plenary Number S383

M384

Southern California Hispanic Women Osteoporosis Education and Screening Project. A. E. Focil*. President, California Hispanic Osteoporosis Foundation (CHOF), Oxnard, CA, USA.

This study identified Hispanic women at risk for osteoporosis to determine 1) if providing a fracture risk assessment in addition to osteoporosis education would motivate them to seek medical help and 2) if acculturation of Hispanic women had an impact on health seeking behavior. 318 postmenopausal Hispanic women of low economic/education status were recruited at osteoporosis screening events in Ventura County, CA. Osteoporosis education and written materials were provided in Spanish. After obtaining written informed consent, all participants received 1) a risk factor questionnaire; 2) an acculturation questionnaire; and 3) a heel peripheral bone density report. The latter half of women screened also received an absolute fracture risk report (AFR). A survey 6 months later (via telephone and in-home interviews) assessed osteoporosis awareness, if medical intervention was sought and if osteoporosis therapy was initiated.

At screening, 14% of Hispanic women in this study were taking estrogen (n = 45), 43% calcium (n = 137), and 21% vitamin D (n = 67). Overall, 38% of the Hispanic women in the study had low bone mass (LBM)/osteopenia (n = 121), 13% were osteoporotic (n = 43), and 31% of women ≥ 65 years old were osteoporotic. Follow-up surveys were completed in 201 out of 318 screened women (63%), 143 in the T-score only group (70%) and 58 from the T-score plus an AFR group (50%). There was no difference detected in the response with "seeking medical help" between women classified with LBM/osteopenia (40%) or osteoporosis (41%). The number of risk factors and/or a T-score with AFR did not have an impact on this parameter. Age, risk factors and a T-score plus AFR did not appear to influence physician ordering an axial DXA and/or prescribing an osteoporosis treatment or the likelihood of patients filling their prescriptions. There was a non-significant trend in the osteoporosis patients to seek medical help, receive an axial DXA, receive a prescription for osteoporosis therapy (30%), and fill the prescription (19%). The acculturation questionnaire showed that 310 out of 318 (97%) participants did not consider themselves as Americanized (75% viewed themselves as being "very Mexican"), reflecting a fairly homogeneous group of Hispanic women. It was therefore not possible to determine if acculturation of Hispanic women had an impact on health seeking behavior.

Providing an AFR did not appear to influence patient or physician behavior. Future studies need to identify factors that will change Hispanic women's and their physicians' behavior related to osteoporosis.

Disclosures: A.E. Focil, Procter & Gamble Pharmaceutical Unrestricted Research Grant to CHOF 2.

This study received funding from: Procter & Gamble Pharmaceutical Unrestricted Research Grant to CHOF.

M385

Effects of Long-Term Treatment with a Prostaglandin E₂ Receptor Subtype 4 Agonist and PTH at Skeletal Sites with Moderate Osteopenia in Aged Ovariectomized Rats. J. I. Aguirre, M. K. Altman*, S. M. Vanegas*, M. F. Rivera*, T. J. Wronski. Physiological Sciences, University of Florida, Gainesville, FL, USA.

Prostaglandin E₂ (PGE₂) is a strong stimulator of bone formation with the ability to restore lost cancellous bone mass in osteopenic ovariectomized (OVX) rats. We and others have shown that a PGE₂ receptor subtype 4 agonist (EP4A) stimulates cancellous bone formation at skeletal sites with severe and moderate osteopenia in aged OVX rats. We also observed that, despite the potent anabolic effect, this agonist was unable to restore cancellous bone mass in aged OVX rats at skeletal sites with severe osteopenia even after long-term treatment (11 weeks). The purposes of this study were to determine the effects of long-term treatment with EP4A at skeletal sites with moderate cancellous osteopenia, and to compare its bone-restorative efficacy with that of PTH treatment. Groups of OVX and sham-operated rats were maintained untreated for 1 year postovariectomy (15 months of age) to develop cancellous osteopenia. OVX rats were then treated SC with vehicle, the EP4A CP-734432 (3 mg/kg) daily, or PTH (80 µg/kg) 5 days/week for a period of 11 weeks. Cancellous bone histomorphometry was performed in the lumbar vertebra (LV) and proximal femur (PF). We found that after 11 weeks of vehicle treatment, OVX rats were moderately osteopenic at both the LV and PF with cancellous bone volumes of 23% and 30%, which corresponded to 60% and 65% decreases compared with the sham-operated controls, respectively. As expected, PTH treatment restored cancellous bone mass to near the level of sham-operated control rats at both skeletal sites. In contrast, EP4A treatment failed to increase cancellous bone mass in aged OVX rats at the LV and PF. Interestingly, osteoblast, osteoid, mineralizing, and osteoclast surfaces were significantly increased in rats treated with EP4A at both skeletal sites, but were unchanged or increased to a much lesser extent in OVX rats treated with PTH. Moreover, whereas EP4A induced significant increases in bone formation rate at both the LV and PF (14- and 4.3-fold, respectively), PTH did not induce significant changes in this variable after 11 weeks of treatment. These findings indicate that although EP4A stimulated cancellous bone formation and bone turnover to a greater extent than PTH, the agonist failed to translate this anabolic response into a restorative effect on cancellous bone at moderately osteopenic sites in aged OVX rats. These findings also suggest that the increase in bone resorption induced by EP4A is in balance with the increase in bone formation so that a net increase in cancellous bone mass failed to occur.

Disclosures: J.I. Aguirre, None.

M386

See Sunday Plenary Number S386

M387

KR62980, a Novel Compound, Enhances Bone Formation Through Promoting Osteoblastogenesis and Inhibiting Osteoclastogenesis. M. Bae, H. Cheon*, J. Lee*, J. Heo*, H. Kim*. Medicinal Science Division, KRICT, Daejeon, Republic of Korea.

The renewal of bone is responsible for bone strength throughout our life as a result of the coordinated actions of two cells, the osteoclast and the osteoblasts. Metabolic bone diseases are considered to be conditions in which this bone resorption-formation balance is lost in favor of increased bone resorption by osteoclasts. Herein, we investigated whether KR62980 exhibits any effects on osteoblast and osteoclast differentiation. KR62980 induced alkaline phosphatase (ALP) activity and increased extracellular matrix calcification in primary osteoblast. Real time RT-PCR analysis revealed that KR62980 also increased the mRNA transcripts of specific genes involved in osteoblastic differentiation, including BSP, OC, ALP and Runx-2. Furthermore, the presence of KR62980 inhibited dose-dependently the osteoclast differentiation by reducing RANKL-induced expression of TRAP and actin ring formation with NFκB inactivation. To reveal sensitivity of KR62980 to changes in anti-osteoporotic activity, 4 week female ddy mice were subjected to ovariectomy (OVX), OVX with daily KR62980 or sham. Mice were imaged on week 8 via Micro-CT. OVX induced a decrease of bone mineral density (BMD) in distal femur over sham (p<0.05), a decrease of BMD which was blocked by daily KR62980 (p<0.01). Taken together, these results suggest that KR62980 deserve attention as potential drugs for treating bone disease.

Disclosures: M. Bae, None.

M388

See Sunday Plenary Number S388

M389

Dual-Action Cathepsin K Inhibitors: Modulation of Human Osteoclast Function. A. J. Westover*, D. Chagnovich, M. W. Long. Velcura Therapeutics, Inc., Ann Arbor, MI, USA.

Cathepsin K (CTSK), a cysteine protease secreted by osteoclasts (OC), is an attractive target for therapies aimed at osteoporosis and other bone diseases. Moreover, the recent demonstration of CTSK's expression in osteoblast (OB) suggests that other functions exist for this enzyme.

VEL-0230 is a dual-action, orally-available CTSK inhibitor that has an anabolic effect on osteoblasts (stimulation of ex vivo and in vivo bone formation) while also acting to disrupt bone resorptive processes. The effects of VEL-0230 on the differentiation and function of human OC were studied by seeding them onto bovine bone slices in the presence or absence of VEL-0230. Evaluation of VEL-0230's actions on OC differentiation indicated that its continuous presence (10 days exposure) failed to affect M-CSF/Rank Ligand-induced OC differentiation and viability over a range of 10nM to 10µM. The actions of VEL-0230 on OC bone resorption were evaluated via collagen telopeptide CTX1 release into the bone-slice supernatant, coupled with the qualitative assessment of OC motility and pit-formation using Toluidine Blue. Levels of the CTX1 and bone pit depth were strongly inhibited by VEL-0230 in a concentration-dependent manner. Likewise, human OCs treated with VEL-0230 failed to migrate across bone surface, etching a shallow singular pit rather than forming the distinctive trail pattern indicative of OC resorption and migration. VEL-0230's mechanism of action (MOA) was investigated by examining its actions on the intracellular processing of CTSK. Cathepsin K is an autocatalytic enzyme that first cleaves its 38 kDa proenzyme to a 27 kDa active enzyme; a subsequent cleavage of this generates a 25 kDa molecule. Western analysis of VEL-0230 (a cell-permeable compound) treated OC shows a concentration-dependent increase in the relative abundance of the 27kDa and a concomitant reduction in the 25 kDa molecule, with little or no apparent change in the relative abundance of the 38 kDa proenzyme. While the relative abundance of the 27kDa form is high, CTSK enzymatic activity is essentially ablated (70% reduction at 1 µM; 100% at 10 µM). We conclude that VEL-0230 inhibits OC function, reducing pit formation, OC migration and collagen degradation without affecting OC differentiation. Mechanistically, this CTSK inhibitor seems to act after its first autocatalytic cleavage exposes the enzyme's active site, preventing further processing and inactivating the mature enzyme. Coupled with its anabolic actions, VEL-0230 represents a novel, dual-action (anabolic & anti-catabolic) therapeutic candidate for diseases such as osteoporosis. Further, this compound may also have therapeutic indications where cell mobility is a factor.

Disclosures: D. Chagnovich, Velcura Therapeutics 1, 3.

M390

See Sunday Plenary Number S390

M391

Effects of Low Dose Parathyroid Hormone on Body Composition, Bone Mass and Turnover and Ectopic Osteoinduction in a Rat Model for Chronic Alcohol Abuse. U. T. Iwaniec¹, C. H. Trevisiol^{1,2}, G. Maddalozzo¹, R. T. Turner¹. ¹Nutrition and Exercise Sciences, Oregon State University, Corvallis, OR, USA, ²Chemical Engineering, Oregon State University, Corvallis, OR, USA.

Parathyroid hormone (PTH) is used clinically to increase bone mass by enhancing bone formation. PTH is also under investigation as a therapy to accelerate fracture repair. We have recently shown that disuse greatly diminishes the bone anabolic response to low-dose (similar to a human therapeutic dose) PTH, suggesting that "life-style" factors may modulate the skeletal response to bone anabolic therapy. The prevalent use of alcohol may represent one of these factors. Chronic alcohol abuse is associated with osteoporosis and impaired fracture healing. Alcohol consumption also inhibits osteoinduction by demineralized allogeneic bone matrix (DABM); DABM is used clinically to facilitate bone fracture repair. Therefore, the present study investigated the effects of alcohol on the bone anabolic response to low-dose PTH: 1) during normal bone turnover, and 2) in a model of DABM-induced bone formation. Three-month-old male Sprague Dawley rats (4 groups; n=10-11 rats/group) were fed control or Lieber-DeCarli liquid diet with 35% of the calories derived from ethanol. The control rats were pair-fed an alcohol-free isocaloric diet. Following a 1 week adaptation to the diets, the rats were implanted subcutaneously with DABM cylinders prepared from femurs and tibiae of rats fed normal rat chow. The rats were then treated with PTH (1 µg/kg/d, 5 d/wk; +/- alcohol) or vehicle (+/- alcohol) for 6 weeks. Body composition was determined on day of necropsy using DXA. Tibiae were processed for histomorphometry. Bone architecture in DABM implants was evaluated by µCT. PTH treatment increased whole body bone mineral content (BMC) and bone mineral density (BMD). The hormone also increased bone formation and bone area/tissue area in the proximal tibial metaphysis. In contrast, PTH had minimal effects on osteoinduction by DABM. Alcohol consumption decreased whole body BMC, fat mass and % body fat. Alcohol also decreased bone formation and bone area/total area in tibia and impaired DABM-mediated osteoinduction. There was no interaction between PTH treatment and alcohol consumption for any of the endpoints measured. Our results suggest that PTH, at a dose rate that increases bone mass in a normal weight bearing bone, is ineffective in enhancing osteoinduction under non weight bearing conditions. In contrast, alcohol inhibited osteoinduction, and reduced bone formation in the presence or absence of therapeutic PTH. These results provide additional evidence that alcohol impairs bone healing and may reduce the efficacy of drugs intended to reverse bone loss.

Disclosures: U.T. Iwaniec, None.

This study received funding from: NIH, DOD.

M392

See Sunday Plenary Number S392

M393

In Silico Identification of Selective Fibroblast Growth Factor-Receptor Modulators. M. E. Leal¹, L. S. Holliday², D. A. Ostrov³, J. I. Aguirre¹, T. J. Wronski¹. ¹Physiological Sciences, University of Florida, Gainesville, FL, USA, ²Orthodontics, University of Florida, Gainesville, FL, USA, ³Pathology, Immunology and Laboratory Medicine, University of Florida, Gainesville, FL, USA.

Basic fibroblast growth factor (bFGF) has promise as a therapeutic agent for the treatment of osteoporosis, but induces side effects including anemia in a rat model. We are seeking small molecules that selectively modulate the fibroblast growth factor receptors (FGFRs) that are present in bone cells. The long-term goal is to identify a selective ligand for an FGFR that induces a stimulatory effect on bone formation with minimal adverse side effects in non-skeletal tissues. Our initial approach involves use of an in silico method to identify FGFR-selective small molecule ligands. We then screened these ligands for effects on growth of BaF3 cells that were stably-transfected with FGFR1c, FGFR2b, and FGFR3c, using a metabolic colorimetric assay. Small molecules identified as interacting with specific receptors were then screened for effects on osteoclast formation in mouse marrow cultures. We initially identified 36 small molecules predicted to interact selectively with FGFR1c and FGFR3c. None were agonists, but several inhibited the growth of BaF3 cells by 50-80% in the presence of bFGF and acidic FGF. From these, we identified one small molecule against FGFR1c (LWOH031c) and one against FGFR3c (LWOH193c) that were selective. LWOH031c reduced osteoclast formation by 80% in mouse marrow cultures in the presence of bFGF and other stimulators, but also reduced bFGF-stimulated proliferation of adherent cells. LWOH193c inhibited osteoclast formation by 80-90%, but did not reduce adherent cell proliferation. We are currently testing the effects of these molecules on bFGF-induced proliferation of calvarial osteoblasts and primary chondrocytes. In conclusion, we have identified small molecules that selectively interact with FGFR1c and FGFR3c to block stimulation by bFGF. Interestingly, both reduced osteoclast formation in mouse marrow cultures in response to bFGF and other stimulators of osteoclastogenesis. The inhibitor of FGFR3c had no detectable effect on proliferation of adherent cells. These molecules may be useful pharmacologically as FGFR-selective inhibitors, or may be derivatized to enable them to serve as selective agonists.

Disclosures: M.E. Leal, None.

This study received funding from: University of Florida.

M394

See Sunday Plenary Number S394

M395

Effects of Intermittent Administration of Parathyroid Hormone (1-34 hPTH) on Distraction Osteogenesis in Rabbits. H. Maruno¹, S. Ichimura², T. Oohata², C. Uchikura², K. Satomi². ¹Orthopaedic, Kyorin Univ, Tokyo, Japan, ²Orthopaedic, Kyorin Univ., Tokyo, Japan.

<Objective> Our study examined the effects of intermittent administration of parathyroid hormone (1-34 hPTH) on distraction osteogenesis. <Materials and Methods> An external fixator was applied to 15 immature white Japanese rabbits and an osteotomy was performed on the right tibia. After a delay of 1-week, the distraction was started at a rate of 0.375 mm twice a day for 2 weeks. Beginning on distraction, hPTH was subcutaneously administered once a day, four days a week for a total of 4 weeks at a dose of 10 µg/kg (group P10) or 30 µg/kg (group P30) to five rabbits per group. Five rabbits received only the vehicle (group C) in the same manner. Seven weeks after osteotomy, the external fixator was removed, and rabbits were sacrificed 1-week later. We analysed the distracted callus by X-ray, DXA, pQCT, and µCT, to evaluate the bone union, BMD, cross section area and the morphology of callus. Three-point bending test was performed to assess biomechanical parameters. <Results> Bone union was found in all rabbits. The average BMD of the distracted callus (mg/mm³) was 321.0, 330.8 and 354.4 for group C, group P10 and group P30, respectively. The total cross section area (mm²) was 63.5, 53.6 and 81.7 and the value of group P30 was significantly larger than those of the other two groups. The cortical cross section area (mm²) of group P30 was largest and was significantly larger than that of group P10. µCT of group C showed the immature trabecular bone in the medullary cavity of the callus and the undefined lamellar formation of cortical bone. On the other hand, in PTH-administered groups, there was less immature trabecular bone in the medullary cavity, and the formation of lamellar structure in cortical bone was accelerated. Three-point bending analysis showed that fracture energy (N•mm) was 168.9, 240.1 and 583.0, respectively, and group P30 demonstrated a significantly larger value than the other two groups. <Discussion> PTH have a remodeling acceleration effect in bone fracture experiments. In relation to distraction osteogenesis, Seebach found an increase in bone mineral content and a stronger callus using rat femur models. The results in this study did not find any significant difference in bone density, but the cross section area and mechanical strength of the distracted callus of group P30 was significantly larger and higher. The morphology of the distracted callus in groups P10 and P30 also suggested a remodeling acceleration effect. We concluded that intermittent administration of PTH could be beneficial to shorten the consolidation period of callus formation in distraction osteogenesis.

Disclosures: H. Maruno, Asahi Kasei Pharma Co. 2.

M396

Calcium Absorption from Commonly Consumed Vegetables in Healthy Thai Women. S. Charoenkiatkul¹, W. Kriengsinos¹, U. Suthutvoravut², C. M. Weaver³. ¹Institute of Nutrition, Mahidol University, Nakhonpathom, Thailand, ²Faculty of Medicine, Ramathibodi Hospital, Mahidol University, Bangkok, Thailand, ³Foods and Nutrition, Purdue University, West Lafayette, IN, USA.

The absorbability of calcium from ivy gourd, green leafy vegetable (*Coccinia grandis* Voigt.) and winged bean young pods (*Psophocarpus tetragonolobus*, (L) DC) were measured in 19 healthy adult women aged 20-45 y, in a three-way, randomized-order, crossover design with an average calcium load of 100 mg and milk as the referent. The test meals were extrinsically labeled with ⁴⁴Ca and given with rice as breakfast after an overnight fast. Absorption of calcium was determined on a blood sample drawn 5 h after ingestion of the test meal. Fractional calcium absorption (X ± SD) was 0.391 ± 0.128, from winged beans, 0.476 ± 0.109 from ivy gourd, and 0.552 ± 0.119, from milk. The difference in fractional calcium absorption for these two vegetables was significant (P<0.05) and the fractional calcium absorption from these two vegetables were both significantly lower than from milk. The difference was partly accounted for by the phytate, oxalate and dietary fiber content of the vegetables. However, the bioavailability of these two vegetables, commonly consumed among Thais, was relatively good compared to milk (71-86% of milk) and could be generally recommended to the public as calcium sources other than milk and Brassica vegetables.

Disclosures: S. Charoenkiatkul, None.

This study received funding from: Thailand Research Fund.

M397

See Sunday Plenary Number S397

M398

Natural Plant Extracts, Gs-Ac and -H, Induce Osteoblast Differentiation and Reduce Osteoclast Differentiation. Y. Chung¹, H. Yoon¹, S. Yun¹, S. Yi¹, Y. Won², Y. Shin³, S. Lee⁴, S. Lee⁵, N. Song⁶, J. Ryu⁶.

¹Endocrinology and Metabolism, Ajou University School of Medicine, Suwon, Republic of Korea, ²Orthopedic Surgery, Ajou University School of Medicine, Suwon, Republic of Korea, ³Endocrinology and Metabolism, Wonju College of Medicine, Wonju, Republic of Korea, ⁴Biochemistry, Eulji University College of Medicine, Daejeon, Republic of Korea, ⁵ISAM Internal Medicine Clinic, Busan, Republic of Korea, ⁶HL Genomics, Yongin, Republic of Korea.

Background: Bone is a dynamic organ that is continuously remodeled by combinational roles of osteoblasts and osteoclasts. Osteoporosis is a disease of imbalance in bone formation (osteoblast) and resorption (osteoclast), which leads to bone loss. We investigated that effects of natural plant extracts GS-Ac and -H on osteoblast and osteoclast differentiation.

Methods: Osteoblastic differentiation was evaluated with alkaline phosphatase (ALP) and mineralization assays. Osteoclastic differentiation was determined with osteoprotegerin (OPG) and tartrate resistant acid phosphatase (TRAP) staining.

Results: GS-Ac and -H (0.1, 0.05 mg/ml) increased ALP activity as 5-7-fold of control in osteoblast. Dexamethasone decreased ALP activity as 1.5-fold of control and GS-Ac, and -H increased as 2.3-10-fold of Dexamethasone. GS-Ac (0.1, 0.05 mg/ml) and GS-H (0.05 mg/ml) increased mineral nodule formation in osteoblast. OPG concentration was increased as 2.5-fold of control. TRAP-positive cells were decreased in GS-Ac treated osteoclast.

Conclusion: GS-Ac and -H promoted osteoblast differentiation and suppressed osteoclast differentiation.

Disclosures: Y. Chung, HL Genomics 2.

This study received funding from: GRRC Project of Gyeonggi Provincial Government, Republic of Korea.

M399

See Sunday Plenary Number S399

M400

Efficiency of Dietary Calcium Use for Skeletal Growth and Mineralization in Young Pigs Fed Diets with Various Phosphorus Concentrations. H. Singh*, D. K. Schneider*, T. D. Crenshaw. Animal Sciences, University of Wisconsin -Madison, Madison, WI, USA.

Efficiency of nutrient use (nutrient retained/consumed) is typically higher in animals fed diets with marginal deficiencies compared with animals allowed adequate intake of the nutrient. However, Ca efficiency was lower in pigs fed diets with a marginal Ca deficiency compared with Ca efficiency of pigs fed diets with excess Ca. The previous study (J Bone Miner Res 20:S193) was designed to assess recovery of skeletal growth in young pigs following a period of deficit growth induced by a Ca deficiency. Dietary P concentrations may have limited the efficiency of Ca use. The current study was designed to assess the impact of dietary P concentrations (either 70, 90, or 120% of requirements) on efficiency of Ca use in young pigs. Diets provided Ca at either 75 or 150% of requirements for each P level. Ca efficiency was estimated from Ca retention predicted with DXA scans (GE Prodigy, using scan modes previously shown accurate for pigs, J Bone Miner Res 20:S332) and dietary Ca consumption over a 27 day trial. In pigs fed diets with 90% of P requirements, Ca efficiency was greater if Ca was limited (75%) than if excess (150%). However, if pigs were fed diets with excess P (120%) no differences in Ca efficiency were detected between Ca levels. Pigs fed diets with only 70% of P requirements failed to gain bone mass over the 27 d trial regardless of the Ca level. Improvements in efficiency of P use were not detected in animals fed diets limited in P regardless of Ca levels. In conclusion, efficiency of Ca use in young pigs is altered by dietary P levels.

Diet Ca, % of required	75			150			
Diet P, % of required	70	90	120	70	90	120	SEM
BMC gain, g/d ^{bc}	-1.36	6.47	9.27	-1.75	4.37	13.11	0.40
Ca intake, g/d ^{abc}	5.9	6.1	7.0	10.0	13.3	10.7	0.48
P intake, g/d ^{bc}	3.7	6.0	8.5	3.8	6.3	7.5	0.28
Ca retention, g/d ^{bc}	-0.52	2.47	3.53	-0.67	1.67	5.00	0.15
P retention, g/d ^{bc}	-0.31	1.46	2.09	-0.40	0.99	2.96	0.09
Ca efficiency ^{abc}	-0.09	0.41	0.50	-0.07	0.13	0.47	0.018
P efficiency ^{abc}	-0.09	0.24	0.25	-0.11	0.16	0.40	0.017

Superscripts within a row denote difference: a. Ca; b. P; or c. Ca X P interactions, P<0.05.

Disclosures: T.D. Crenshaw, None.

M401

Postmenopausal Osteoporosis HRT and Weight Gain. A. Bazarra-Fernandez*. ObGyn, Juan Canalejo University Hospital Trust, Amparo Lopez Jean 13 4^a A, La Coruña, Spain.

Background: Recent studies have found weight gained during menopause increase the risk of high blood pressure, the diabetes, heart disease, and has been strongly linked to increased incidence of breast and other hormone-related postmenopausal malignancies. These healthcare concerns have led to the conception of specific products that target menopausal weight gain.

Aim: Looking over weight gain and osteoporosis treatment in climacteric. Material and methods: 20 women who were 44 to 58 years old have been recruited. BMI was increased to age. Those with an intact uterus have moderate to severe vasomotor symptoms associated with the menopause, moderate to severe symptoms of vulvar and vaginal atrophy and risk of postmenopausal osteoporosis. They were ascribed to equal two 10 women groups. One group was assigned to 2 mg drospirenone /1 mg 17 beta- estradiol hemihydrate. The other group treated with. 40 mg soy bean.

Results: in the women on 2 mg drospirenone /1 mg 17 beta- estradiol hemihydrate medication decreased, moderate to severe symptoms of vulvar and vaginal atrophy vasomotor symptoms associated with the menopause in regard to the other group treated with 40 mg soy bean. They had weight main loss of 3 kg in one year, (P < 0.05).

Conclusions: Human HRT is in relation to decrease osteoporosis. Nobody noted 17 beta-estradiol is in relation to breast cancer. Estradiol is the same oestrogen produced by the ovaries before menopause. Drospirenone has the unique property of reducing water retention often associated with the use of oestrogen and other synthetic progestin hormones. The impact of obesity on hormone replacement therapy is due to many women associate hormones with weight gain. This late medication formula can be beneficial in minimizing uncomfortable symptoms, such as weight gain, hot flashes, night sweats, and mood swings, associated with the natural progression of a woman's life cycle. So, it is due to conduct one great try to make clear and more comprehensible these points.

Disclosures: A. Bazarra-Fernandez, None.

M402

Bone Specific SARMs (Selective Androgen Receptor Modulators) Increased Bone Mineral Density in a Different Manner from Anti-resorptive Agent, Raloxifene with Minimum Effects on the Uterus. K. Furuya¹, N. Yamamoto^{*1}, Y. Ohyabu^{*1}, T. Morikyu^{*1}, A. Iwata^{*1}, H. Ishige^{*2}, K. Kuzutani^{*3}, Y. Taquahashi^{*3}. ¹Drug Discovery Research Lab., Kaken Pharmaceutical, Co., Ltd., Kyoto, Japan, ²Chemistry Lab., Kaken Pharmaceutical, Co., Ltd., Kyoto, Japan, ³Safty Research Lab., Kaken Pharmaceutical, Co., Ltd., Fueda, Japan.

Estrogens and androgens are opposite sex steroid hormones and both affect bone metabolism and uterine homeostasis. Raloxifene is a selective estrogen receptor modulator (SERM) which has estrogenic effects on the bone with reduced side effects on the sexual organs. We have been demonstrated a concept of Selective Androgen Receptor Modulators (SARMs) as useful drugs for a treatment of osteoporosis through proving that anabolic effects on the bone can be separated from virilizing effects. This study compared our new SARM Compound R2 with Raloxifene in the effects on the bone and uterus. Female 12-week old Sprague-Dawley rats were ovariectomized (OVX) and were feed with a low calcium diet for 4 weeks to expedite reduction of the bone mineral density (BMD). Oral administration of Compound R2 (1, 10 mg/kg) or Raloxifene (1 mg/kg) were followed once a day for 8 weeks. Compound R2 significantly increased the BMD at the part between the diaphysis and proximal metaphysis of the femurs at 1 mg/kg, whereas Raloxifene slightly increased the BMD at the distal and proximal metaphysis which are cancellous bone rich parts. Concerning to the effects on the uterus, dihydrotestosterone had a major impact on the uterine muscle and also increased the endometrium. Compound R2 did not show any effects on the uterus at 1mg/kg and displayed minimum effects on the uterine muscle at 10mg/kg. On the other hand, Raloxifene displayed slightly thickening of the endometrium. These results demonstrate that Compound R2 is superior to Raloxifene in bone formation and specificity to the bone, suggesting that SARM is promising for the treatment of severe osteoporosis patients without anabolic effects on the uterus.

Disclosures: K. Furuya, None.

M403

See Sunday Plenary Number S403

M404

Effects of Bazedoxifene Acetate on Bone Loss: A 12-Month Study in Ovariectomized Rats. B. S. Komm¹, P. V. N. Bodine¹, D. R. Minck^{*2}. ¹WHMSB, Wyeth Research, Collegeville, PA, USA, ²Drug Safety, Wyeth Research, Chazy, NY, USA.

Bazedoxifene acetate (BZA) is a novel, stringently screened selective estrogen receptor modulator (SERM) currently in development for the prevention and treatment of postmenopausal osteoporosis and in combination with conjugated estrogens for the treatment of menopausal symptoms and prevention of postmenopausal osteoporosis. We examined the effects of BZA on bone mass/composition, biomechanics, and histomorphology in ovariectomized (OVX), 6-month-old female rats.

In the active treatment groups, 3 doses of BZA (0.15, 0.3, and 1.5 mg/kg/day) were administered to OVX animals by oral gavage for 12 months. Control groups included an untreated baseline group, untreated sham-operated animals, untreated OVX animals, and an estrogen-treated (17 α -ethinylestradiol [EST], 0.03 mg/kg/day) OVX group. Animals assigned to the baseline group received no treatments or procedures and were euthanized within 2 weeks of study initiation for testing. Untreated sham-operated and untreated OVX animals were administered only test vehicle, once daily. Dual energy x-ray absorptiometry (DXA) scans, peripheral quantitative computerized tomography (pQCT), and biomechanical and histomorphometric studies were conducted to assess bone mineral density (BMD), bone mineral content (BMC), and bone architecture and strength. Based on BMD and BMC analyses, BZA protected the skeleton from estrogen-dependent bone loss at several sites, with optimal protection observed with the 0.3 mg/kg/day dose. In vivo DXA data revealed a dose-related response to treatment with BZA for 11 of 12 parameters examined. Treatment with BZA 0.3- and 1.5-mg/kg/day reduced the loss of trabecular BMD at metaphysis (MTrabMDp) observed in OVX controls by 39%-41% and 34%-37%, respectively (P \leq 0.01), as confirmed by pQCT analysis at the tibia and femur; these doses of BZA resulted in more marked reductions in MTrabMDp loss than EST. A significant difference was observed between the BZA 0.3- and 1.5-mg/kg/day treatment groups and the OVX control group in maximal stress on the lumbar vertebra 4 on biomechanical testing (P \leq 0.01); BZA also increased maximum load reached in the neck of the femur, but this effect did not reach statistical significance. Histomorphometric analyses showed differential beneficial effects of treatment with BZA in protecting against the deleterious effects of ovariectomy on the skeleton.

We conclude that BZA, a novel SERM, exhibits a promising therapeutic profile based on demonstration of generally dose-related protective effects on several skeletal parameters in this animal model of accelerated bone loss.

Disclosures: B.S. Komm, Wyeth Pharmaceuticals 1, 3.

This study received funding from: Wyeth Pharmaceuticals.

M405

See Sunday Plenary Number S405

S207

M411

See Sunday Plenary Number S411

M412

Small Organic Molecule Compound Protects Against Inflammatory Bone Loss in a Rat Model of Periodontitis. R. Jin^{*1}, Y. Zhang^{*1}, Y. Liang^{*1}, X. Li^{*1}, R. Bhatt^{*1}, D. Wu^{*2}, J. Zheng^{*3}, L. Xu^{*4}, L. Golub^{*4}, D. Liu¹. ¹Enzo Therapeutics, Inc, Farmingdale, NY, USA, ²Yale University, New Haven, CT, USA, ³St Jude Hospital, Memphis, TN, USA, ⁴School of Dental Medicine, Stony Brook, NY, USA.

The canonical Wnt signaling pathway is initiated by the binding of Wnt proteins to receptor complexes consisting of LDL receptor-related protein (LRP) 5/6 and frizzled protein. An antagonist of the Wnt pathway, Dkk1 protein (Dkk), binds to the third YWTD repeat domain of LRP5 and Kremen, resulting in the removal of this co-receptor with inactivation of the Wnt pathway. Both human and mouse genetic studies provide supporting evidence that LRP5 has an important role in the regulation of bone remodeling. Hypomorphic or null alleles lead to early onset of osteoporosis; whereas, other LRP5 mutation alleles are associated with high bone mass. Our innovative approach combines structural biology, computational screening, and biological assays to identify small molecule compounds that are capable of disrupting LRP5-Dkk interactions and reversing the inhibitory effect of Dkk on Wnt signaling. We have employed a periodontitis model of bone loss to evaluate the effect that our small molecule compound has on protecting against bone resorption. In this model, lipopolysaccharide (LPS) was used to initiate inflammatory-induced alveolar bone loss. Prior to administering LPS between the first and second molar of the maxillae of Sprague Dawley rats, animals were pretreated with a small molecule test compound (SMTC) or vehicle by oral gavage. Animals were then exposed to LPS every other day and treatment with the SMTC was continued daily. Jaws were removed after 10 days, defleshed and stained with Loeffler's methylene blue in order to identify the cemento-enamel junction (CEJ) as a reference point to measure bone height. Histological analysis clearly showed significant bone resorption and root furcation in the LPS-treated animals, and little bone resorption in the LPS plus SMTC-treated animals. Linear measurements from the CEJs to the alveolar bone crest showed a mean bone loss of 0.94 ± 0.08 mm in LPS-treated animals; 0.59 ± 0.04 mm in LPS plus SMTC-treated animals; and 0.54 ± 0.04 in control animals. There were statistically significant differences between the LPS group and the LPS plus SMTC group ($p = 0.00006$) and between the control group and LPS group ($p = 0.00003$). As an indicator of protection, there was no significant difference between the control group and the LPS plus SMTC group ($p = 0.18$). These data clearly show that SMTC protects against bone resorption in an animal model of endotoxin-induced bone loss. This SMTC may represent an attractive potential new class of therapeutic agents for clinical use, and continued investigation is warranted.

**Equal Contribution

***Corresponding Author

Disclosures: D. Liu, Enzo Therapeutics, Inc 3.

This study received funding from: Enzo Therapeutics, Inc.

M413

Vitamin D Supplementation and 25OHD Levels in Long Term Care Residents. R. Crilly^{*1}, M. Mason^{*2}, M. Kloseck^{*3}. ¹Department of Medicine, University of Western Ontario, London, ON, Canada, ²Department of Health and Rehabilitation Sciences, Faculty of Health Science, University of Western Ontario, London, ON, Canada, ³Faculty of Health Sciences, University of Western Ontario, London, ON, Canada.

Osteoporosis is common in long term care patients who contribute about 30% of all hip fractures. Vitamin D supplementation has been shown to reduce hip fractures in these patients. Recent information in the community dwelling elderly has suggested that the doses of vitamin D used need to be higher to achieve the blood levels required to reduce the PTH levels. In LTC patients, where sunshine is a rarity, we hypothesized that the supplementation dose would need to be even higher. To date, 41 patients of 4 nursing homes have consented to participate. Patients were either on no supplementation, 400 IU per day or 1000 IU per day. Patients were on various doses of calcium supplementation (range 0-1500). No change in dose of D or calcium had been made for at least 3 months. Blood was drawn for 25 OHD and PTH levels. Patients with renal impairment shown by a creatinine over 130 nmol/L were excluded. 14 patients were on no vitamin D supplementation, 13 were on 400 IU and 14 on 1000IU. Patients were aged 84.4 ± 6.7 yrs SD (range 71-98 yrs.), with no age difference between the groups, had been in the institution for 35.2 months ± 30 SD (range 9-151) and, where applicable, on the current vitamin D dose for 11.3 ± 1.77 months SD. Mean levels of 25OHD in the three groups were 48.29 ± 19.07 ; 83.46 ± 21.75 ; and 87.4 ± 15.7 nmol/l for the three groups, no supplement; 400IU; and 1000IU respectively. The level for each treatment dose differed from the no-treatment group ($p < .001$) but not from each other. Parathyroid hormone levels on the other hand were similar in all groups (4.41 ± 2.0 ; 6.02 ± 4.16 ; 4.81 ± 2.87 for the zero, 400 and 1000 dose groups respectively), and there was no correlation between 25OHD levels and PTH levels overall. Mean levels of calcium supplementation was lower for those on zero and 400IU of vitamin D (405 ± 356 vs. 320 ± 473 mg/day) compared to those on 1000IU (769 ± 525 mg/day, $p = .044$ and $.031$ respectively). The lower PTH levels in those on no, or lower, vitamin D doses could not be explained by calcium supplementation levels, which was lower in those groups. We conclude on the basis of these unexpected preliminary results that the level of 25OHD levels achieved in LTC

residents is adequate on 400IU of vitamin D, that the PTH levels are lower than expected in those on no vitamin D, and calcium supplementation does not account for this finding.

Disclosures: R. Crilly, Alliance for Better Bone Health 2.

This study received funding from: Alliance for Better Bone Health.

M414

Age Modifies the Impact of Vitamin D3 Supplementation on the 25-OH Vitamin D/ Parathyroid Hormone Ratio. H. J. Florez^{*}, E. P. Cherniack^{*}, O. Gómez-Marín^{*}, B. A. Roos^{*}, S. Levis, B. R. Troen. Miami VAMC, University of Miami Miller School of Medicine, Miami, FL, USA.

Both 25-hydroxyvitamin D (25OH-D) and parathyroid hormone (PTH) are associated with functional outcomes in the elderly. Recent evidence suggests that the 25OH-D/PTH ratio predicts functional recovery after hip fracture in older patients [1]. In a pilot study we evaluated supplementation with 2,000 IU/day of cholecalciferol (D3) for 6 months in elderly men at the Miami VA Medical Center. Participants were randomized to either placebo [$n = 17$, age (mean \pm SD: 79 ± 4 years)] or D3-treatment [$n = 17$, age: 80 ± 4 years]. No significant baseline differences were observed between participants aged 80 years and older compared to those age 70 to 79 years in 25OH-D (28.7 ± 9.1 vs. 29.7 ± 7.3 ng/ml, $p = 0.7$), PTH (48.6 ± 22.1 vs. 42.1 ± 19.6 pg/ml, $p = 0.4$), or the 25OH-D/PTH ratio (730 ± 409 vs. 893 ± 571 , $p = 0.3$). After 6 months of treatment, 25OH-D was higher in both D3-treated age subgroups compared to the placebo subgroups (Table), while no significant differences in PTH values were observed between age and treatment groups. D3 treatment increased the 25OH-D/PTH ratio compared to placebo participants, and the changes in this ratio were significantly higher only among those aged 80 years and older (619 ± 126 in D3-treated vs. -64.5 ± 133.6 in placebo participants, $p < 0.001$). These results suggest that D3 treatment improves 25OH-D levels in all elderly participants. However, the differences in the 25OH-D/ PTH ratio suggest that D3 treatment may provide additional functional benefits in those aged 80 and older. Further studies to characterize the response to D3 therapy in this elderly group are warranted.

25-hydroxyvitamin D (25OH-D) and parathyroid hormone (PTH) at the 6-month follow-up

	Placebo Age<80	Treated age<80	Placebo age≥80	Treated age≥80
25OH-D (ng/ml) †	30 ± 3.2	39.9 ± 3.4	27.4 ± 3.4	45.1 ± 3.2
PTH (pg/ml)	42.9 ± 5.8	43.6 ± 6.1	46.9 ± 6.1	37.1 ± 5.8
25OH-D/PTH †	846 ± 155	1038 ± 164	599 ± 164	1046 ± 155
Δ 25OH-D (ng/ml) †	-0.2 ± 3.5	10.7 ± 3.7	-1.7 ± 3.7	16.9 ± 3.5
Δ PTH (pg/ml)	-3.9 ± 6.2	6.9 ± 6.6	-2.1 ± 6.6	-11.3 ± 6.2
Δ 25OH-D/PTH † *	3.7 ± 125.6	88.3 ± 133.6	-64.5 ± 133.6	619 ± 126

†Group treatment: $p < 0.01$; * age-treatment interaction: $p = 0.03$

[1] Di Monaco M et al., 25-Hydroxyvitamin D, parathyroid hormone, and functional recovery after hip fracture in elderly patients. J Bone Miner Metab 2006; 24:42-47

Disclosures: H.J. Florez, None.

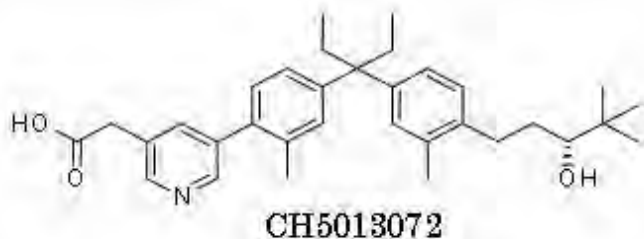
M415

See Sunday Plenary Number S415

M416

Orally-active Nonsecosteroidal Vitamin D Agonists Increased Bone Mass in Ovariectomized Rats without Causing Hypercalcemia. S. Harada^{*1}, S. Takeda^{*1}, A. Sugita^{*1}, M. Ishigai^{*2}, H. Kashiwagi^{*3}, T. Takahashi^{*3}, T. Tamura^{*1}, K. Morikawa^{*3}, E. Ogata^{*4}, E. Ichikawa^{*1}. ¹Pharmaceutical Research Dept. 1, Fuji Gotemba Research Labs. Chugai Pharmaceutical Co., Ltd., Gotemba, Japan, ²Pre-clinical Research Dept, Fuji Gotemba Research Labs. Chugai Pharmaceutical Co., Ltd., Gotemba, Japan, ³Chemistry Research Dept. 1, Fuji Gotemba Research Labs. Chugai Pharmaceutical Co., Ltd., Gotemba, Japan, ⁴Cancer Institute Hospital, Tokyo, Japan.

Secosteroidal vitamin D receptor (VDR) agonists have been used for treatment of psoriasis, secondary hyperparathyroidism and osteoporosis. However, their efficacy is limited due to the development of hypercalcemia. Recently, several nonsecosteroidal compounds were demonstrated to be active as VDR agonists. To identify VDR agonists with less calcemic effects than those of secosteroidal structures, we designed and synthesized about seven hundred nonsecosteroidal VDR agonists using co-crystal structure of VDR and its agonists. In VDR agonists, there were good correlations between epithelial calcium channel 2 (ECaC2) induction in colon cancer cell line (Caco-2) in vitro and urinary calcium excretion in vivo, and also between osteocalcin (OC) secretion in MG63 osteoblast cell line in vitro and response of bone mineral density (BMD) in vivo. Therefore, nonsecosteroidal VDR analogs were first tested for their abilities to induce ECaC2 mRNA in Caco-2 and to induce the secretion of osteocalcin from MG63. Forty compounds which showed strong OC induction with less ECaC2 induction were selected for in vivo evaluations. Six compounds (e.g. CH5013072) significantly increased BMD of spine and femur without inducing hypercalcemia in ovariectomized rats after daily oral administration. Moreover, they decreased bone resorption parameters but had little effect on bone formation parameters. Thus, these nonsecosteroidal VDR agonists will be promising candidates as orally-active and less calcemic drugs for osteoporosis.



	Serum Ca (mg/dl)	Spinal BMD (mg/cm ²)	Femoral BMD (mg/ cm ²)	DPD (nM/CREmM)
SHAM	10.5 ± 0.1	174.2 ± 3.3	179.6 ± 3.1	22.5 ± 3.81
OVX	10.2 ± 0.1	157.6 ± 2 #	166.1 ± 1.4 #	71.94 ± 4.87 #
CH5013072 0.025 µg/kg	10.3 ± 0.1	165.7 ± 3.8	168.3 ± 1.8	68.26 ± 8.64
0.05 µg/kg	10.3 ± 0.1	166.9 ± 2.8	176.9 ± 3 *	47.75 ± 3.57 *
0.1 µg/kg	10.7 ± 0.1 *	172.8 ± 6.3 *	180.4 ± 4.4 *	54.67 ± 7.12
		# p < 0.05 vs Sham, t-test	* p < 0.05 vs OVX, Dunnet's t-test	Mean ± SE (n=8)

Disclosures: S. Harada, None.

M417

Differential Effects of Alfacalcidol in the Distal Tibial Metaphyses of Orchidectomized and Aged Male Rats. X. Y. Tian¹, X. Q. Liu¹, H. Y. Chen¹, R. B. Setterberg^{*1}, M. Li², W. S. S. Jee¹. ¹Division of Radiobiology, University of Utah School of Medicine, Salt Lake City, UT, USA, ²Department of Cardiovascular and Metabolic Disease, Pfizer Global Research and Development, Groton, CT, USA.

The purpose of the study was to compare the effects of alfacalcidol (ALF), a vitamin D analog, on the cancellous bone of distal tibial metaphysis in aged male and orchidectomized (ORX) rats. The distal tibia fuses its epiphyses at 3 months and is primarily a fatty marrow site with a cancellous bone histomorphometric profile similar to that in human iliac crest sites. Seventy male Sprague-Dawley rats were sham or ORX at 18 months of age and then orally treated with vehicle or ALF at 0.1 or 0.2 µg/kg/d, 5 days per week for 12 weeks. Double fluorescent-labeled undecalcified distal tibiae were processed for bone histomorphometry. An age-related increase in bone turnover without bone loss was seen in aged rats. Despite further increased bone turnover, ORX did not cause bone loss in aged rats. Treatment of aged rats with ALF at 0.1 and 0.2 µg/kg/d decreased %eroded perimeter (Er.Pm), mineralizing surface (MS/BS), surface referent bone formation rate (BFR/BS), and bone volume referent bone formation rate (BFR/BV), resulting in non-significant increases in ratio of mineralizing surface/eroded surface (MS/Er.Pm) and trabecular area (Tb.Ar). These data indicate that 12 weeks of treatment with ALF had a positive but moderate effect on the balance between bone formation and resorption in the aged male rats. Treatment of ORX rats with ALF at 0.1 µg/kg/d caused similar changes in the Er.Pm, MS/BS, BFR/BS, and BFR/BV but significantly increased MS/Er.Pm and Tb.Ar. Although treatment of ORX rats with ALF at 0.2 µg/kg/d decreased Er.Pm (-67%), it did not alter MS/BS, BFR/BS, and BFR/BV, resulting in significant increases in MS/Er.Pm (+220%) and Tb.Ar (+47%) compared with aged rats treated with vehicle. When compared with vehicle-treated ORX rats, ALF significantly decreased Er.Pm (-73%), MS/BS (-46%), and BFR/BV (-58%) whereas increased MS/Er.Pm (+173%) and Tb.Ar (+51%). These data revealed that ALF treatment suppressed bone resorption below normal level while maintaining bone formation at normal level, leading to a positive balance between bone formation and resorption and consequently increased bone mass in ORX rats. Thus, the positive effect of ALF is more pronounced in the distal tibia of ORX rats with a higher bone turnover than sham controls. The differential effects of ALF on bone in sham and ORX rats suggest that vitamin D analog such as alfacalcidol is more efficacious at a predominantly fatty marrow skeletal site with high bone turnover.

Disclosures: X.Y. Tian, None.

M418

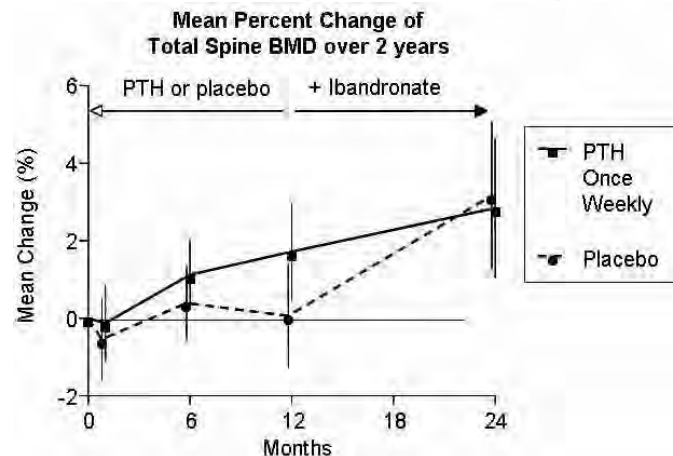
The Effect of Oral Ibandronate Following Weekly PTH: PTH Once Weekly Research Follow-up (POWR II). D. M. Black¹, L. Palermo¹, T. F. Hue¹, S. Majumdar¹, M. L. Bouxsein², C. J. Rosen³. ¹University of California, San Francisco, San Francisco, CA, USA, ²Beth Israel Deaconess Medical Center, Boston, MA, USA, ³MECOR, St. Joseph Hospital, Bangor, ME, USA.

Use of alendronate for one year following one year of daily PTH in the PaTH study led to large increases in BMD during the second year, in postmenopausal women. We recently reported the results from the PTH Once Weekly Research (POWR) study, which demonstrated that PTH 1-84 used once weekly (100 µg) led to an increase of about 2% in DXA spine BMD versus placebo. POWR II is a follow-up study, in which all POWR participants were offered open-label monthly ibandronate (150mg) for 12 months. In the POWR study, 50 women were randomized (1:1) to either one year of PTH 1-84 injections (100 µg weekly, after a 1 month daily loading period) or to placebo. At the end of the year, 48 adherent women were offered 1 year of ibandronate (150 mg/monthly). 43 women chose to take the ibandronate and are included in this analysis. The main endpoint

was changed in DXA spine BMD; secondary endpoints (not reported here) included hip BMD, QCT (hip and spine) and MRI (wrist) assessed trabecular BMD. We hypothesized that those who had been on weekly PTH would experience larger rises in BMD than those on placebo.

During the one year on ibandronate, the group formerly taking weekly PTH had a 1.1% increase in spine BMD compared to 3.1% increase in those who were on placebo injections (p=0.07). Cumulatively over two years (months 0-24), the group given weekly PTH followed by ibandronate increased 2.8% compared to 3.2% for those who had been given placebo then ibandronate (see Figure). Results for other endpoints were similar; showing no significant difference in the change in BMD during the second year regardless of earlier treatment with weekly PTH.

Over 24 months, mean BMD change in women on weekly PTH followed by ibandronate was the same as those on placebo followed by ibandronate. The weak anabolic effect of once weekly PTH achieved after 12 months, was insufficient to yield the subsequent BMD gain at 24 months, as seen with bisphosphonate use after daily PTH therapy in PaTH.



Disclosures: D.M. Black, Roche/GSK 2, 5; NPS Pharmaceuticals 5; Novartis Pharmaceuticals 2; Merck & Co., Inc. 8.

This study received funding from: NIAMS-NIH (POWR), Roche (POWR II).

M419

See Sunday Plenary Number S419

M420

Characteristics of Postmenopausal Women Treated with PTH(1-84) in the TOP Study: Relationship of Baseline Serum and Urine Ca Values to Hypercalcemia and Hypercalciuria. H. A. Bone¹, S. Greenspan², S. Morris³, J. Bilezikian⁴. ¹Michigan Bone and Mineral Clinic, Detroit, MI, USA, ²Osteoporosis Prevention and Treatment Center, Pittsburgh, PA, USA, ³NPS Pharmaceuticals, Parsippany, NJ, USA, ⁴Columbia University College of Physicians and Surgeons, New York, NY, USA.

The TOP study, an 18-month, multinational, randomized, double blind, placebo-controlled trial, assessed the ability of recombinant human PTH(1-84) to reduce vertebral fracture incidence in postmenopausal osteoporotic women. 2679 subjects received daily Ca (700 mg) and vitamin D (400 IU) supplements in addition to either PTH(1-84) 100 µg SC daily or placebo. Inclusion criteria included a serum Ca ≤10.7 mg/dL and a urinary Ca to creatinine ratio of ≤1.0 mmol/mmol at screening, values that generally exceed the upper limits of normal for adults. These limits contrast with criteria for other studies of PTH-like peptides, e.g., teriparatide fracture study [PTH(1-34)] and the PaTH study [PTH(1-84)] in which subjects were excluded if baseline serum and urine Ca values were above normal to any degree (e.g. subjects must have serum calcium <10.2 mg/dL and urinary calcium <300 mg/24 hr). Of the 1286 subjects treated with PTH, 16% had serum Ca >10.2mg/dL and 10% had urine Ca >300 mg/24 hr at baseline, values that would have excluded them from participation in the other trials alluded to. Moreover, 3.1% of subjects had both hypercalcemia and hypercalciuria. Subjects treated with PTH(1-84) with a baseline urine Ca >300 mg/24 hr had an incidence of hypercalciuria at least 2-fold higher than in those with baseline urinary calcium ≤300 mg (>70%). Similarly, individuals treated with PTH(1-84) with baseline serum Ca >10.2 mg/dL had ~2-fold higher likelihood of hypercalcemia (47%). These results help to explain the substantially higher risk for either hypercalcemia and/or hypercalciuria in TOP as compared to the other trials. Although subjects who experienced hypercalcemia or hypercalciuria benefited from PTH by increases in BMD at multiple skeletal sites and a reduced incidence of vertebral fractures, these data emphasize the critical role that inclusion and exclusion criteria play in the interpretation of PTH safety profiles.

Disclosures: H.A. Bone, NPS Pharmaceuticals 5.

This study received funding from: NPS Pharmaceuticals.

M421

See Sunday Plenary Number S421

M422

Early Adjuvant Therapy with Teriparatide after Major Orthopaedic Surgery of Complicated Fractures of Long Bones in Postmenopausal Women: Preliminary Clinical Results. C. F. Corradini^{*1}, F. M. Olivieri^{*2}, C. A. Verdoia^{*1}. ¹Orthopaedic and Traumatologic Clinic, Studies University of Milan, Milan, Italy, ²Nuclear Medicine, Policlinico Mangiagalli IRCSS Foundation, Milan, Italy.

INTRODUCTION: In the last years the postmenopausal population is increasingly afflicted by complicated fractures of long bones. These are represented by two main clinical situations: the sixties woman without any apparent bone metabolic problem that after a comminuted fracture of long bones suffers a series of complication as late consolidation or non union; the second is an eighties with a new on precedent fracture or periprosthetic fracture. In both the untreated metabolic impairment of bones creates always a trouble to the orthopaedic surgeon because of altered mechanical resistance. So the exigency to improve the bone quality has suggested the use of an anabolic agent with a direct action on osteoblasts.

The aim of the study was to evaluate if the adjuvant therapy with teriparatide may improve the clinical outcome of complex fractures in postmenopausal osteoporotic women.

CASES REPORT: we studied a consecutive series of 7 female patients between 63 and 94 years-old presenting a complex fracture of long bones. Biochemical determinations of bone turnover and calcium homeostasis were obtained on admission and 4, 12 and 24 weeks later. Rx of affected segment was repeated at least 2, 4, 6 months. BMD was measured by DXA during hospitalization and at 6 month.

They received daily subcutaneous teriparatide (25 microg) per day, 1000 mg calcium and 400-1200 IU of vitamin D daily as oral supplementation for 6 months from 15 days by operation.

FINDINGS: Four periprosthetic of the femur, one late consolidation of neck treated with intramedullary nail, one non union of the radio-ulna treated with plaques and screws, one re-fracture of the tibia. At 6 month all patients were cured in a range of 12-20 weeks in average 14. The vitamin D was at lower levels but the supplementation was sufficient to normalize. The other biochemical variables of bone formation and resorption peaked within the consolidation process and at 6 months were indistinguishable from baseline. Subjects increased bone mass by 11.4+/-2.4% in the spine, 3.4+/-2.0% in the total hip.

CONCLUSIONS: These data show that an early adjuvant therapy with teriparatide of complicated fractures in postmenopausal women permits an bone consolidation and functional recovery. Nevertheless further studies in humans will be required to define optimal efficacy, it is intriguing the possibility to obtain the fracture healing with a bone anabolic agent.

Disclosures: C.F. Corradini, None.

M423

See Sunday Plenary Number S423

M424

Changes in 25-hydroxy- and 1,25-dihydroxyvitamin D During Treatment with Teriparatide. F. Cosman¹, B. Dawson-Hughes², P. Chen³, J. H. Kregg³.

¹Clinical Research Center, Helen Hayes Hospital, West Haverstraw, NY, USA, ²Jean Mayer US Department of Agriculture, Human Nutrition Research Center on Aging, Tufts University, Boston, MA, USA, ³Lilly Research Laboratories, Eli Lilly and Company, Indianapolis, IN, USA.

Teriparatide (TPTD) treatment improves bone density, architecture, and strength. The objective of this study was to evaluate changes in 25-hydroxyvitamin D (25(OH)D) and 1,25-dihydroxyvitamin D (1,25(OH)₂D) in placebo-controlled TPTD trials in postmenopausal women (1)(n=1637) and men (2)(n=437) with osteoporosis. Subjects were supplemented with 400-1200 IU of vitamin D daily at least 1 month before baseline samples were obtained and then randomized to daily teriparatide 20 (TPTD20) or 40 (TPTD40) mcg or placebo. 25OHD was measured at baseline and 12 months and 1,25(OH)₂D was measured at baseline, 1, 3, 6, and 12 months in a subset of subjects. Lumbar spine BMD was measured at baseline and 18 months. At 12 months, 25OHD concentrations significantly declined (p<0.05 vs placebo) with TPTD20 treatment in women and men (Table). Concentrations of 1,25(OH)₂D increased significantly in both women and men (Table). Peak 1,25(OH)₂D increments occurred after 1 month with smaller increments persisting throughout 12 months of TPTD20 treatment. Results for subjects treated with TPTD40 were similar to those with TPTD20 (data not shown). Serum phosphorous did not change significantly in any group. The decline in 25OHD at 12 months and the increment in 1,25(OH)₂D at 1 month explained only 4% and 7%, respectively, of the variance in BMD response to TPTD. The mechanism for the changes in vitamin D levels may relate to TPTD-induced stimulation of 1-hydroxylase resulting in conversion of 25OHD to 1,25(OH)₂D. We conclude that treatment with TPTD decreases 25OHD and increases 1,25(OH)₂D.

Table. Changes from baseline in levels of 25OHD (ng/mL) and 1,25(OH)₂D (pmol/L) in women and men treated with teriparatide

Study	Treatment	Baseline	1 mo	3 mo	6 mo	12 mo
25(OH)D (Women)	TPTD20 (N=471)	30.8 (24.8,37.0)	NA	NA	NA	-5.6 (-10.4,0.0)*
	Placebo (N=479)	31.2 (25.2,36.8)	NA	NA	NA	0.0 (-6.0,6.0)
25(OH)D (Men)	TPTD20 (N=126)	31.8 (24.8,38.0)	NA	NA	NA	-3.2 (-9.6,3.2)*
	Placebo (N=133)	31.6 (24.0,39.6)	NA	NA	NA	0.4 (-6.8,8.0)
1,25(OH) ₂ D (Women)	TPTD20 (N=167)	98.4 (86.4,120.0)	27.6 (7.2,49.2)*	4.8 (-14.4,26.4)*	13.2 (-16.8,28.8)*	19.2 (-7.2,40.8)*
	Placebo (N=169)	100.8 (84.0,120.0)	-2.4 (-16.8,14.4)	-2.4 (-21.6,19.2)	-1.2 (-22.8,19.2)	-2.4 (-19.2,21.6)
1,25(OH) ₂ D (Men)	TPTD20 (N=144)	93.4 (80.4,120.0)	24.0 (0.44,4)*	9.6 (-9.6,28.8)*	7.2 (-16.8,33.6)*	12.0 (-9.6,37.2)
	Placebo (N=143)	103.2 (88.8,115.2)	0 (-24.0,16.8)	-2.4 (-21.6,14.4)	-2.4 (-24.0,24.0)	4.8 (-12.0,24.0)

* p<0.05 compared to placebo. Results are median (IQR).

1. Neer et al. 2001 N Engl J Med 344:1434-1441.

2. Orwoll et al. 2003 J Bone Miner Res 18:9-17.

Disclosures: F. Cosman, Eli Lilly and Company 2, 5, 8.

This study received funding from: Eli Lilly and Company.

M425

See Sunday Plenary Number S425

M426

Serum Calcium Values After 4 and 24 Weeks of Treatment with Full-Length Parathyroid Hormone PTH(1-84) of Postmenopausal Women with Primary Osteoporosis: The First 125 Patients. M. Diaz-Curiel^{*}. Servicio de Medicina Interna. Fundacion Jimenez Diaz Madrid. Cátedra de Enfermedades Metabólicas, Unidad de Enfermedades Metabólicas Óseas, Madrid, Spain.

Background: The human recombinant parathyroid hormones (PTHs) represent a class of potent anabolic agents for the treatment of primary osteoporosis in postmenopausal women. All forms of PTH administration in this treatment increase serum calcium. However, prior clinical trials with PTH(1-84) resulted in markedly different incidences of hypercalcemia, with the incidence much higher in TOP than in PaTH. The PEAK (Preotact after a bREAK) trial employed inclusion/exclusion criteria aligned with those of the PaTH trial, therefore permitting an assessment of their impact on the incidence of hypercalcemia. **Method:** The PEAK study is an open label, international, multi centre, parallel group, phase III b, randomised trial, investigating lumbar spine BMD changes in postmenopausal women with primary osteoporosis the first year of which all patients are treated with PTH(1-84). The trial will enrol 390 postmenopausal women aged more than 50 years with primary osteoporosis with a lumbar spine T score ≤ -3.0 SD. Consistent with PaTH (but not TOP), woman with documented baseline hypercalcaemia or hypercalciuria, hyperparathyroidism or severe vitamin D deficiency will be excluded from participation in the study.

Results: 125 patients had reached 4 weeks of treatment with PTH(1-84). The majority (81%) of patients had a serum calcium below the upper limit of normal. 14% had mild elevations in serum calcium. 5% was above 2.67 mmol/l and only one of these had marked elevations of serum calcium (>=3.00 mmol/l).

Fourteen patients had reached 24 weeks of treatment with PTH(1-84). The majority of those patients had a serum calcium below the upper limit of normal.

Serum Calcium Values After 4 of Treatment With PTH(1-84)			
Total serum-calcium (mmol/l)	<2.55	2.55-2.67	>2.67
Number	101	18	6
Percentage	81	14	5

Conclusion: The majority of postmenopausal women with primary osteoporosis treated with PTH(1-84) for 4 weeks had a normal total serum calcium.

Disclosures: M. Diaz-Curiel, Servier, Roche, MSD and Lilly 8; Nycomed 5.

This study received funding from: Nycomed.

M427

See Sunday Plenary Number S427

M428

A Meta-Analysis of Individual Patient Data: Significant Reduction in Non-Vertebral Fractures With High- Versus Low-Dose Ibandronate. J. D. Adachi¹, G. Wells^{*2}, S. E. Papapoulos³, A. Cranney, for the SCIENCE Meta-analysis Group^{*2}. ¹McMaster University, Hamilton, ON, Canada, ²Ottawa Health Research Institute, Ottawa, ON, Canada, ³Leiden University Medical Center, Leiden, The Netherlands.

Ibandronate (IBN) 2.5mg daily, providing an annual cumulative exposure (ACE) of 5.5mg (0.6% oral bioavailability), significantly reduces vertebral fracture risk by 62% (p=0.0001) in postmenopausal osteoporosis and non-vertebral fracture risk by 69%

($p=0.013$) in high-risk patients (baseline femoral neck BMD T-score <-3).¹ Non-vertebral fracture efficacy was not shown in the overall study population who were relatively low risk.¹ Analyses of biochemical marker and BMD data obtained with high IBN ACE ($\geq 10.8\text{mg}$) predict that the licensed doses (monthly oral 150mg, quarterly i.v. 3mg [100% bioavailability]) would have significant antifracture efficacy.² To test this, individual patient data meta-analyses were used to assess the effect of different doses of IBN on non-vertebral fractures.

The analyses included all randomized, controlled trials of IBN; variable doses of IBN based on ACE were explored: 12mg, $\geq 10.8\text{mg}$, $\leq 7.2\text{mg}$ (ACE for daily oral 2.5mg). Here we present a time-to-event analysis conducted using Kaplan-Meier methodology comparing high ACEs ($\geq 10.8\text{mg}$) with lower ACEs with data taken from MOBILE and DIVA; hazard ratios (HRs) were derived from a Cox model with adjustments for clinical fracture, age, bone mineral density and study, first with the full model and then stepwise.

A significantly reduced rate of non-vertebral fractures was seen when combined high doses (ACE 12mg and $\geq 10.8\text{mg}$) were compared with ACE 5.5mg (table). In addition, there was a dose-response effect with increasing ACE (7.2-12mg) compared with ACE 5.5mg. Similar results were seen when ACE $\geq 10.8\text{mg}$ was compared with ACE $\leq 7.2\text{mg}$ (HR: 0.634; 95% CI: 0.427, 0.943; $p=0.0243$). Adjustment for covariates had minimal effect.

Overall, treatment effects on non-vertebral fractures were dose dependent. A significant effect on non-vertebral fracture risk reduction was seen when IBN doses providing ACE $\geq 10.8\text{mg}$ were compared with ACEs 5.5mg and $\leq 7.2\text{mg}$. These data indicate improved fracture efficacy for the licensed oral and i.v. doses versus oral daily dosing.

1. Chesnut CH, et al. J Bone Miner Res 2004;19:1241-9.

2. Papapoulos S, Schimmer R. Ann Rheum Dis 2007; ePub ahead of print.

ACE	12mg vs 5.5mg	$\geq 10.8\text{mg}$ vs 5.5mg	$\geq 7.2\text{mg}$ vs 5.5mg
High doses	2mg q2m, 3mg q3m i.v.	150mg/m p.o.; 2mg q2m, 3mg q3m i.v.	50+50mg, 100mg, 150mg/m p.o.; 2mg q2m, 3mg q3m i.v.
Low doses (p.o.)	2.5mg/d	2.5mg/d	2.5mg/d
Patients (n)	1,355	2,137	2,921
Adjusted HR	0.569 (0.324, 0.997)	0.620 (0.395, 0.973)	0.745 (0.504, 1.102)
p value	0.0489	0.0375	0.1402

Disclosures: J.D. Adachi, F. Hoffmann-La Roche Ltd/GlaxoSmithKline 5.

This study received funding from: F. Hoffmann-La Roche Ltd/GlaxoSmithKline.

M429

Fragility Fracture Increases Antidepressant Use among Women 65 Years of Age and Older. J. D. Adachi¹, N. N. Borisov², C. R. Purple², D. T. Gold³.

¹McMaster University, Hamilton, ON, Canada, ²Procter & Gamble Pharmaceuticals, Mason, OH, USA, ³Duke University Medical Ctr., Durham, NC, USA.

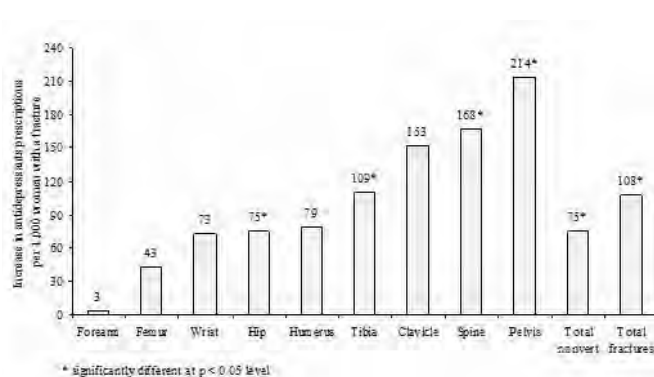
A fragility fracture is often the initiating event in a spiral of life-style altering comorbidities; these may include depression. The objective of this study was to assess antidepressant use among women ages 65 and over before and after fragility fracture in 2 integrated administrative medical claims databases (Ingenix Lab/RxTM and Medstat MarketScan[®]).

A retrospective cohort study was conducted among women with a new non-traumatic closed fracture verified with a diagnostic code between July 1, 2000 and December 31, 2003. The study included fractures at 9 anatomical sites: hip, femur, tibia/fibula, humerus, clavicle, pelvis, forearm, wrist, and spine. The cohort was observed 6 months prior and 6 months after the fracture to identify women who had antidepressant prescriptions.

A total of 19,554 women with a new fragility fracture were identified in the databases during the study period. The mean age was 79 years (SD=8). Nonvertebral fractures represented 77% of all index fragility fractures in this population. Overall, 3.7% more women were using antidepressant drugs 6 months after fragility fracture compared to 6 months before the fracture ($p<0.0001$). Women with a fragility fracture used 108 (SD=60) more prescriptions for antidepressants per 1,000 women after their fracture than before ($p<0.0001$). Specifically, women with fractures of the hip, tibia, pelvis, or spine had the highest significant increases in antidepressant use than women with other fractures (figure).

In this study, fragility fractures had a significant effect on antidepressant use. Women with a fragility fracture were more likely to use antidepressants after their fracture than before with significantly more prescriptions. The increased use of antidepressants might indicate a decreased quality of life associated with a fracture. A treatment for osteoporosis that reduces fracture incidence should reduce the cost associated with prescriptions for antidepressants as well. Therefore, this cost reduction should be considered in the cost-effectiveness analysis of treatments for osteoporosis.

Figure. Antidepressant prescriptions difference (per 1,000 fractured women): 6 months after fragility fracture compared to 6 months before the fracture



Disclosures: J.D. Adachi, Procter & Gamble Pharmaceutical 5.

M430

See Sunday Plenary Number S430

M431

Comparison of Estrogen, Raloxifene and Bisphosphonate Administration for Prevention of Bone Loss in Climacteric Women Complicated with Osteopenia. K. Aisaka, K. Nagasaka*, S. Arita*, K. Itabashi*, Y. Takane*, Y. Ikezuki*, R. Matsuoka*, K. Kohda*. Obstetrics & Gynecology, Odaira Memorial Tokyo Hitachi Hospital, Tokyo, Japan.

Objective: Bisphosphonate (BIS) and SERM (Selective Estrogen Receptor Modulator, raloxifene) have been widely used for the prevention of bone loss in Japan. On the other hand, the hormone replacement therapy (HRT, using estrogens and progestogens) also performed to improve the QOL of the climacteric women even after the WHI report. The present study was performed to compare these medications for the treatment of bone loss and climacteric symptoms.

Subjects & Methods: The ethics committee of our hospital consulted on the protocol and was approved before beginning of the study. 198 patients of the climacteric women complicated with osteopenia were subjected (53.6 \pm 3.9 years old). Then, the subjected patients were divided three groups at random with the enough informed consents. Group A: Administrated BIS (risedronate 2.5mg/day), 76 cases, group B: Administrated SERM (raloxifene 60mg/day), 64 cases, and group C: HRT (conjugated equine estrogen 0.625mg + medroxyprogesterone acetate 2.5mg/day), 58 cases. The changes of BMD values (DXA method), urinary NTx and plasma BAP levels were compared among them.

Results: The percent changes of BMI in the group A, B, C were 1.19 \pm 0.64, 1.06 \pm 0.36, 1.02 \pm 0.54 % (6 months after), and 1.33 \pm 0.53, 1.17 \pm 0.46, 1.15 \pm 0.60 % (12 months after), respectively, and there was a significant increase in the group A ($p<0.025$). The urinary levels of NTx in the group A decreased significantly by the treatment compared to another groups (0, 1, 6 months after treatment): A: 48.6 \pm 15.8 \rightarrow 33.1 \pm 18.7 \rightarrow 24.3 \pm 13.7, B: 50.9 \pm 21.4 \rightarrow 42.9 \pm 29.6 \rightarrow 34.5 \pm 18.5, C: 47.3 \pm 20.2 \rightarrow 44.5 \pm 23.8 \rightarrow 35.7 \pm 20.1 nmolBCE/nmol.cre., $p<0.025$ -0.001). No significant changes were observed in plasma BAP levels among these three groups. The symptom of hot flush was suppressed in the group C, while increased in the group B. Conclusion: It was concluded that the inhibition effect toward bone resorption was the strongest in BIS administrated group. The improvement of the QOL in climacteric women was much better in the HRT group. From these results, BIS should be used for the patients of severe osteopenia, and the HRT should be considerable to precede the QOL of the climacteric women if they had no risks of the breast cancer.

Disclosures: K. Aisaka, None.

M432

See Sunday Plenary Number S432

M433

Risedronate Treatment in Type 2 Diabetic Men with Primary Osteoporosis: A Three-Year Longitudinal Study. L. J. L. Ascanio*. Endocrinology, Endocrinological Foundations, Caracas, Venezuela.

Bisphosphonates have been widely used in the treatment of osteoporosis in women, whereas until now there have been few data on their use in men. The aim of this study was to evaluate the effect of a 3-year risedronate treatment on bone mineral density (BMD) and quantitative ultrasound (QUS) in type 2 diabetic men with primary osteoporosis. We studied 77 osteoporotic men (aged 57.1 ± 10.8 yrs) who completed a 3-year treatment with risedronate (35 mg/once a week) plus calcium (1000 mg/day) ($n = 39$), or calcium alone ($n = 38$). At baseline and at a 12-month interval, we measured BMD at the lumbar spine and femur (femoral neck and total hip) by DXA (Hologic) and speed of sound (SOS), broadband ultrasound attenuation (BUA) and Stiffness (S) at the os calcis by Achilles plus (Lunar). Risedronate treatment had significantly increased lumbar spine BMD by 4.2% at year 1, by 6.3% at year 2, and 8.8% at year 3. BMD at the femoral neck and total hip had increased by 2.1% and 1.6% at year 1, by 3.2% and 2.9% at year 2, and by 4.2% and 3.9% at year 3, respectively. BUA and Stiffness showed a significant increase in the risedronate-treated group at year 2 (3.2% and 4.9%, respectively) and at year 3 (3.8% and 6%, respectively). BMD at the lumbar spine showed the best longitudinal sensitivity whereas longitudinal sensitivity of both QUS at the heel and femur BMD were similar. In conclusion, this study confirms that Risedronate represents an important therapeutic advance in the management of male osteoporosis. BMD at the lumbar spine appears to be the best method for monitoring the effect of risedronate on bone mass in osteoporotic men with type 2 diabetic. Key words: Male osteoporosis _ Risedronate _ Bone mineral density _ Quantitative ultrasound

Disclosures: L.J.L. Ascanio, None.

M434

See Sunday Plenary Number S434

M435

Mechanistic Bases of Bone Mineral Density Increase During Alendronate Therapy. D. Vashishth¹, P. Chavassieux², G. Boivin², P. D. Delmas². ¹INSERM Unite 831 Université de Lyon France & Rensselaer Polytechnic Institute, Troy, NY, USA, ²INSERM Unite 831 Université de Lyon, Lyon, France.

An increase in the mean degree of tissue mineralization (DMB) occurring through secondary mineralization has been proposed to increase bone mineral density (BMD) during bisphosphonate (BP) therapy [1]. In this study we conducted additional analyses on human iliac crest biopsies obtained as part of alendronate (ALN) clinical trials [2] to identify the mechanistic bases of BMD increase.

Out of a group of 16 patients on a three-year ALN-therapy [1], we identified two groups of 5 patients each showing lower (8.5 %) and higher (13.3%) bounds of BMD increase but no difference in baseline BMD. For all 10 patients, previously prepared microradiographs were reanalyzed to measure the mean degree of tissue mineralization (DMB) at the osteonal and interstitial compartments in both cortical and cancellous bone tissues. Based on a moving average analysis, six fields each of cortical and cancellous bone tissues were randomly selected for measurement from each biopsy. The average values for patients in each group within osteonal and interstitial compartments were compared between and across cortical and cancellous bone tissues. All DMB measurements were also tested for correlation with standard histomorphometric measures of bone structure (BV/TV, Tb.Th, Tb. Separation, Tb.N), osteoclast activity (EV/BV, E-Depth, Oc#/BS), osteoid (OS/BS, OV/BV, OTh), and bone formation (MAR, BFR/BS, FP) reported previously [2].

The low-BMD-gain group demonstrated no difference between the osteonal and interstitial bone compartments within cortical or cancellous bone tissues but demonstrated a higher DMB in cancellous than in cortical tissue ($p < 0.05$). In contrast, the high-BMD-gain group showed higher DMB in interstitial than in osteonal compartment for both cortical and cancellous tissues as well as a higher DMB in cancellous than in cortical tissue ($p < 0.05$). Out of all the DMB measures in cortical and cancellous tissues, only cortical bone interstitial level DMB correlated to bone formation rate (BFR/BS) ($r = -0.86$; $p = 0.006$) and formation period (FP) ($r = -0.75$; $p = 0.04$).

In conclusion, this study demonstrates that the effects of ALN-therapy are more evident in cancellous than in cortical bone. Moreover since the interstitial level DMB is at least partially dependent on the duration of secondary mineralization, and negatively correlated to formation parameters, slow bone formation rate and longer bone formation period produce conditions conducive to complete secondary mineralization and consequently larger BMD gain.

References: [1] Boivin et al. Bone. 2000 5: 687-94. [2] Chavassieux et al. JCI 1997 100:1475-80.

Disclosures: D. Vashishth, Merck 5.

This study received funding from: INSERM, France & NIH Grants AR49635, AG20718.

M436

Bisphosphonate Use Increases in Patients with Osteoporosis Following an Integrated Osteoporosis Educational Intervention: Canadian Quality Circle (CQC) National Project. B. Kvern¹, G. Ioannidis², A. Papaioannou³, L. Thabane^{*2}, A. Gafni², A. Hodsman³, D. Johnstone⁴, L. Salach^{*5}, F. Jiwa^{*6}, J. D. Adachi². ¹University of Manitoba, Winnipeg, MB, Canada, ²McMaster University, Hamilton, ON, Canada, ³University of Western Ontario, London, ON, Canada, ⁴P&G Pharmaceuticals, Toronto, ON, Canada, ⁵Ontario College of Family Physicians, Toronto, ON, Canada, ⁶Osteoporosis Canada, Toronto, ON, Canada.

Quality Circles (QCs) methodology was used to improve primary care physicians' (PCPs) management of osteoporosis in accordance with the Osteoporosis Canada 2002 Guidelines. The QCs project involves a small group of people from comparable work environments who identify and analyze work related problems and recommend solutions. The study consists of five phases: wave I data collection, 1st educational intervention, wave II data collection, 2nd educational intervention, and wave III data collection. During the educational intervention, QC's met to discuss how they managed osteoporosis and to participate in an osteoporosis workshop. This interim analysis (wave I & II) evaluated the change in treatment in patients with osteoporosis (defined as a BMD t-score < -2.5). According to the guidelines, therapy should be initiated if a patient has a BMD t-score in the osteoporotic range. A total of 340 (wave I) and 301 (wave II) PCPs formed 34 QCs. For each wave, PCPs gathered data from different patients via chart reviews and a standardized collection form. A total of 8376 (wave I) and 7354 (wave II) patient records were selected at random and analyzed. All patients were women 55 years and older. The generalized estimating equations (GEE) approach was used to evaluate differences in bisphosphonate use in patients with osteoporosis pre and post educational intervention. The cluster variable for the GEE model was physician and the analysis was adjusted for patient's age, fracture status, family history of fracture, early menopausal status and other major and minor risk factors for fracture. An exchangeable correlation matrix was used for the analysis. Odds ratios (OR) and 95% confidence intervals (CI) were calculated. A total of 1774 and 1272 patients had osteoporosis during wave I and wave II, respectively. Of these, 1545 (87.1%) during wave I and 1148 (90.3%) during wave II were treated with a bisphosphonate. The adjusted likelihood of bisphosphonate use increased following the educational intervention for patients with osteoporosis (OR 1.30; 95% CI: 1.06, 1.61). In conclusion, a majority of patients with osteoporosis are being treated with bisphosphonate therapy. However, bisphosphonate use increased in patients with osteoporosis following the educational workshop. The use of bisphosphonates may reduce the future fracture risk of these high risk patients.

Disclosures: B. Kvern, Alliance for Better Bone Health 5, 8.

This study received funding from: Alliance for Better Bone Health.

M437

See Sunday Plenary Number S437

M438

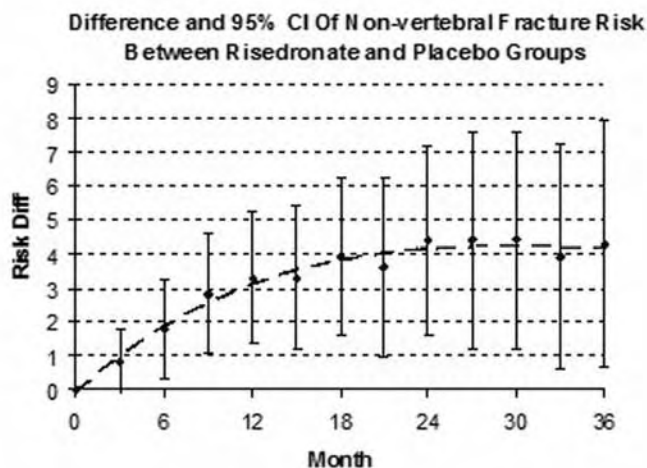
Early and Sustained Non-Vertebral Fracture Efficacy with Risedronate. R. Lindsay¹, C. Roux^{*2}, J. D. Adachi^{*3}, X. Zhou^{*4}, A. Grauer⁴, N. B. Watts⁵. ¹Helen Hayes Hospital, West Haverstraw, NY, USA, ²Cochin Hospital, Rene Descartes University, Paris, France, ³McMaster University, Hamilton, ON, Canada, ⁴Procter & Gamble Pharmaceuticals, Mason, OH, USA, ⁵University of Cincinnati, Cincinnati, OH, USA.

Previous analyses have shown non-vertebral fractures account for 77% of the osteoporosis-related fractures and over 90% of costs. Predicting an osteoporosis-related fracture is not possible. Therefore, treating with an agent that provides both early and sustained fracture protection will provide maximum benefit to patients. The objective of this analysis is to examine whether the non-vertebral fracture efficacy of risedronate meets these criteria.

Analysis population included 1169 postmenopausal women from VERT and ROE & RON trials with low BMD (LS T-score < -2.5 SD), who were treated with at least one dose of either placebo or risedronate 5mg daily. The mean age of the population was 67 years and 58% of the patients had at least one prevalent vertebral fracture at baseline. The fracture endpoint was radiographically confirmed osteoporosis related non-vertebral fracture. Risk difference of osteoporosis-related non-vertebral fracture between the placebo and risedronate 5mg groups was estimated using the difference of the Kaplan Meier (KM) estimators from month 3 through 36. The standard error of the risk difference was approximated by the square root of the sum of the variance of the KM estimators of the placebo and risedronate 5mg groups. The upper and lower bound of the 95% confidence intervals were calculated as the mean plus and minus 1.96 times the standard error of the estimated risk difference.

The findings are consistent with the rapid onset of fracture risk reduction with risedronate treatment. Relative to placebo, risedronate significantly reduced the risk for non-vertebral fracture starting from Month 6 with an absolute risk reduction of 1.8% (95% CI: 0.4%, 3.3%). The magnitude of the difference in the risk for non-vertebral fracture between the placebo and risedronate 5mg groups increased during the first 2 years and remained constant during the 3rd year of the trial with an absolute risk reduction of approximately 4%.

In summary, the results confirmed the risedronate rapid protection benefit against non-vertebral fracture as early as Month 6. Further, the risedronate anti-fracture efficacy was sustained through out the remaining study period.



Disclosures: R. Lindsay, Procter & Gamble Pharmaceuticals 5.

M439

So How Was It? Patient Opinions on Osteoporosis Interventions in the Fracture Clinic Setting. D. E. Beaton, E. R. Bogoch, R. Sujic*, V. Elliot-Gibson*. Mobility Program, St. Michael's Hospital, Toronto, ON, Canada.

Our study aims to understand factors that influence fragility fracture patient's adherence with St. Michael's Hospital Osteoporosis Exemplary Care Program's recommendations for further osteoporosis testing and treatment. Our previous research indicates that coordinator-based interventions are an effective way of preventing future fractures. The results of this study will help identify key variables to consider when evaluating the Ontario Osteoporosis Strategy's Fracture Clinic Screening Program which is based on the coordinator model.

This is a qualitative study using focus-group methodology. Out of 45 patients who were eligible based on the study criteria, 24 patients participated in five focus groups. Transcripts of the five focus groups were transferred to N-Vivo for storing and sorting the data. Transcripts were coded for content and links between descriptive labels were made. By using qualitative method, we are hoping to explore the impact of the Osteoporosis Exemplary Care Program in a much more contextualized fashion.

Emerging results support Anderson's behavioural model of health care utilization. Perceived need and susceptibility were associated with osteoporosis prevention efforts and treatment adherence as reported by the patients involved in the focus groups. The most frequent barriers that patients identified in diagnosis and treatment of osteoporosis included the perceived lack of clear and reliable information regarding the nature of BMD testing and proper treatment as well as the lack of general practitioner's recommendations about osteoporosis care and prevention. Most often cited facilitators of osteoporosis testing and treatment included thorough follow up by an osteoporosis coordinator, accessibility and ease of BMD testing and general practitioners' recommendations for treatment and testing.

General practitioners were named as key influence over the initiation of prevention and treatment of osteoporosis.

Disclosures: D.E. Beaton, None.

M440

See Sunday Plenary Number S440

M441

Improvement of the Persistence with Teriparatide in Postmenopausal Osteoporosis: The French Experience of an Education Program. K. Briot¹, P. Ravaud², S. Liu-Léage³, C. Roux¹. ¹Rheumatology, Cochin Hospital, Paris, France, ²Biostatistics and Epidemiology, Bichat Hospital, Paris, France, ³Lilly France, Suresnes, France.

Several anti-osteoporotic treatments have been proved effective in decreasing the risk of fractures but available data suggest low adherence and persistence rates in patients taking medications for osteoporosis. This can result in failure in treatment efficacy. Several strategies have been developed to improve adherence and persistence. Teriparatide, prescribed 20 µg/day injected subcutaneously, is an anabolic treatment licensed for established postmenopausal osteoporosis. Education program has been developed after its launch, to help elderly women to deal with the pen take and consequently better follow the prescribed treatment. The objective is to assess the efficacy of an education program to improve the persistence with teriparatide in postmenopausal osteoporotic women. This education program has been created by the promotor of teriparatide since its launch of teriparatide in France in September 2004 and it is proposed to each woman who begins the

teriparatide. The program includes injection technique learning, osteoporosis education, observance and persistence assessment. Women are interviewed by regular calling of a nurse, each month the first year and every 3 months the 6 following months. Data about persistence and side-effects are available for the period September 2004 to December 2006. Persistence is defined as the percentage of patients still on treatment at the end of the 18-month course. Since the launch of teriparatide in France in September 2004, 4518 postmenopausal women (mean age 73.6 ± 11.4 years) with osteoporosis (lumbar spine and/or femoral T score ≤ -2.5) and vertebral fractures (4 fractures on average) have participated to the program. At the end of the year 2006, 1951 women have been followed at least 18 months. Of these 1951 women, persistence at 18 months was 82.6%. Main reasons for discontinuation, as declared by the patients, were side-effects (43.8%), wish of the patient (23.8%), physicians' decisions (17%) and deaths (5.3%). Persistence has been compared to the data of the French universal health insurance system; and it has been estimated that persistence at 18 months was closed to 0% for women who have been prescribed teriparatide without any education program. This study shows that an education program can highly improve the persistence with teriparatide at 18 months. Persistence is greater than that of existing oral therapies for osteoporosis, and this high persistence should improve the effectiveness of this therapy.

Disclosures: K. Briot, None.

M442

The Impact of GI Medication Usage with Regard to Discontinuation and Restart Behavior with Oral Bisphosphonates in Three Large US Physician Groups. M. B. Nichol¹, W. W. Chan², T. Dow³, K. H. Kahler², S. Bamford³, L. D. Marks⁴, C. Parise⁴, G. Darah⁵. ¹JMRG Consulting, Encino, CA, USA, ²Novartis Pharmaceuticals Corp., East Hanover, NJ, USA, ³Physician Associates, Pasadena, CA, USA, ⁴Sutter Medical Group, Sacramento, CA, USA, ⁵ProMedica, Toledo, OH, USA.

Purpose: Clinical studies have demonstrated that women at risk of osteoporotic fracture reduce the risk of new osteoporotic fracture with bisphosphonate treatment. However, observational studies have also shown high discontinuation rates with these oral medications. This study investigated the impact of GI medication usage with regard to discontinuation and treatment re-initiation.

Methods: The study was based on a retrospective claims review of data from three large US physician groups. The groups represent a diverse patient base in terms of geographic and organizational considerations. Specifically, the groups are based in Northern and Southern California and Ohio; one is a network of independent physicians in private practice, and two are not-for-profit integrated health care networks. We evaluated the integrated administrative dataset for health plan eligibility as well as drug utilization information.

Results: 5,737 patients were selected for analysis. 4,074 patients (71.0%) initiated therapy on alendronate, and 1,663 patients (29.0%) initiated therapy on risendronate. One-third of women were aged 45 to less than 60, 40% were aged 60 to less than 75, with the remainder 75 and older, with no statistically significant differences by index medication. Approximately 20% of women used GI medications during the one year study period. Duration of GI therapy averaged 176 days (SD 126), with statistically significant differences seen by drug when the medical groups were combined (p = 0.017). Specifically, risendronate initiators averaged 194 days of GI therapy (SD 125) and alendronate initiators averaged 174 days (SD 127). Women typically added GI treatment after approximately three months (mean 93, SD 100) for both medications. Logistic regression analysis showed concurrent GI use was associated with a 74% greater likelihood of discontinuation with bisphosphonate treatment (95% CI: 1.36, 2.22) and a decreased likelihood of re-initiation of bisphosphonate treatment (Odds Ratio 0.76, 95% CI: 0.51, 1.14).

Conclusion: These data revealed that approximately 20% of bisphosphonate users were on GI therapy during the study period. However, rather than acting as a mitigating agent that was associated with better compliance, it appears that GI usage reflected side effect problems that jeopardize persistence. This area deserves further study to determine the direction of cause and effect.

Disclosures: W.W. Chan, Novartis Pharmaceuticals Corp. 1, 3.

This study received funding from: Novartis Pharmaceuticals Corp.

M443

See Sunday Plenary Number S443

M444

Longitudinal Patterns of Adherence with Bisphosphonates. J. R. Curtis¹, A. Westfall^{*1}, H. Cheng¹, E. Delzell^{*1}, K. Lyles², K. G. Saag¹. ¹University of Alabama at Birmingham, Birmingham, AL, USA, ²Duke University, Durham, NC, USA.

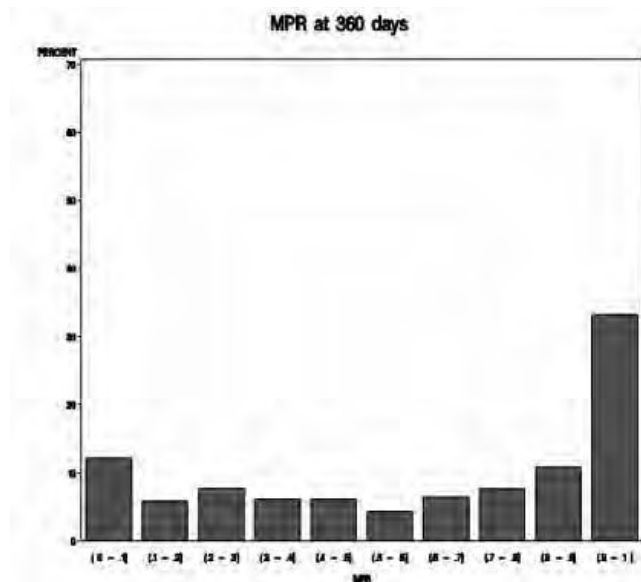
Background: Poor adherence to bisphosphonates (BPs) appears associated with a greater rate of fracture (Fx). Misclassification of adherence and the impact of acute Fx on adherence may compromise interpretation of findings. We examined longitudinal patterns of BP adherence using less restrictive definitions than in some past studies that included an arbitrary definition of discontinuation. We also determined the impact of adherence associated with hip Fx.

Methods: Using claims data of a large consolidated health plan database, we identified persons initiating BPs and calculated adherence as a Medication Possession Ratio (MPR), allowing for BP switching. We compared adherence among individuals initiating weekly vs. daily BPs. MPR was examined at 1, 2, and 3 yrs and was compared among those with no fracture or with hip Fx. We also examined MPR in the 3 and 6 months immediately prior to a hip Fx compared to the 3 and 6 months following this Fx to determine how measured adherence changed following a Fx.

Results: We identified 87,099 new BP users with ≥ 1 year of follow-up. Mean \pm SD age was 60.1 ± 7.8 years. The proportion with MPR $\geq 80\%$ was 44% (Figure), 39%, and 36% at 1, 2, and 3 yrs, respectively. Among persons with MPR $\geq 80\%$ at yr 1, 80% of these had MPR $\geq 80\%$ at yr 2. Those who were initially prescribed weekly BPs had higher 1 yr MPR than those initially prescribed daily BPs (mean = 45% vs. 38%, $p < 0.001$).

Among those with a hip Fx, MPR at years 1, 2, and 3 was 9%, 12%, and 10% lower compared to those without Fx ($p < 0.001$ for each), and MPR in the 3 and 6 months following the hip Fx was -9% and -6% compared to before the hip Fx ($p < 0.0001$ and < 0.0001).

Conclusions: Using a definition of adherence that allowed for switching to different dosages or formulations of BPs, adherence was somewhat better than in past studies but remained suboptimal. Adherence at year 1 was a strong predictor of adherence in subsequent years. Adherence in the 3 and 6 months following a hip Fx was significant lower than immediately prior to the fracture, which may be real or an artifact of a lack of pharmacy data capture during periods that patients are hospitalized or in rehabilitation settings. Analyses that fail to consider adherence in a time-dependent fashion, before Fx occur, may magnify the apparent differences in Fx risk between adherent and non-adherent persons.



Disclosures: J.R. Curtis, Merck 2, 5, 8; Proctor & Gamble 5, 8; Novartis 2; Amgen 2. This study received funding from: Novartis.

M445

A Year-long Study to Demonstrate the Bone Reversal Efficacy of Dried Plums in Postmenopausal Women. B. H. Arjmandi¹, S. Hooshmand¹, S. C. Chai¹, R. L. Saadat^{*1}, L. Devareddy^{*1}, K. Brummel-Smith^{*2}. ¹Nutrition, Food and Exercise Sciences, Florida State University, Tallahassee, FL, USA, ²Department of Geriatric, Florida State University, Tallahassee, FL, USA.

Our findings in rat models of osteoporosis as well as a short-term human study suggest that dried plums are highly effective in preventing and reversing ovarian hormone-deficiency-associated bone loss. Dried plums are rich in polyphenolic compounds and other nutrients that contain high antioxidant properties. Antioxidative properties of dried plum, in part, may be responsible for prevention of bone loss that is in part due to the rise in oxygen-derived free radical formation. It is necessary to confirm the findings of animal studies as well as positive effects of dried plum on biomarkers of bone formation in a relatively long-term clinical study. For this purpose, we are conducting a completely randomized comparative-controlled study to test the hypothesis that daily consumption of

dried plum increases bone mineral density (BMD) of osteopenic women 1 to 10 years postmenopausal. So far, we have recruited 85 (n=144) subjects who are not on hormone replacement therapy and have been randomly assigned to one of two treatment groups: dried plum (100 g/d) or dried apple (comparative control). All study participants are receiving 500 mg elemental calcium plus 250 IU vitamin D daily. BMD and bone mineral content (BMC) of lumbar spine, forearm, hip and whole body are being assessed at baseline and at the end of the study using dual-energy x-ray absorptiometry. Blood and 24-hr urine samples (baseline, 3-, 6-, and 12-month) are also assessed. Physical activity and dietary confounders will be examined as potential covariates. This study will provide critical data about an acceptable and efficacious food alternative to reverse bone loss in menopausal women. Based on our preliminary data, we anticipate subjects that are consuming dried plum will have an average gain of 3% BMD at all sites after one year. The urinary and blood interim analyses will be presented at the time of poster presentation.

Disclosures: B.H. Arjmandi, None.

M446

Analgesic Efficacy of Calcitonin for Vertebral Fracture Pain. A. Bazarra-Fernandez^{*}, ObGyn, Juan Canalejo University Hospital Trust, Amparo Lopez Jean 13 4º A La Coruña, Spain.

Background: Fractures, especially vertebral fractures, are a common complication of osteoporosis, leading to significant pain.

Aim: To compare the pain release induced by osteoporotic vertebral fracture, through teriparatide and teriparatide plus calcitonine.

Methods: We performed a study to compare the analgesic effect of 20 mcg teriparatide versus 20 mcg teriparatide plus metered dose intranasal spray 200IU/activation calcitonin in two groups between postmenopausal women undergoing osteoporosis with vertebral fracture. A 10-point visual analog pain scale (1 = least to 10 = most painful) and a four-point pain grade (grade 1 = least to grade 4 = most painful) were used to measure the pain perception.

Results: The mean pain scores for the teriparatide and teriparatide plus calcitonin were 2.3 ± 1.1 and 8.5 ± 1.1 , respectively ($P < 0.05$), while the pain grades for teriparatide and teriparatide plus calcitonin were 1.5 ± 0.3 and 3.5 ± 0.4 , respectively ($P < 0.05$). In teriparatide group, analgesics were requested, but in teriparatide plus calcitonin group no analgesics were requested ($P < 0.001$).

Conclusion: Using teriparatide is more expensive than other osteoporosis treatment. Studies show that taking a bisphosphonate with hormone replacement therapy (HRT), results in increased bone mass when compared to taking either a bisphosphonate or estrogen alone. Besides, calcitonin is better for osteoporotic vertebral fracture pain release than HRT. However, a larger investigation will be needed to achieve more significant case number.

Disclosures: A. Bazarra-Fernandez, None.

M447

See Sunday Plenary Number S447

M448

The Correction of BMD Measurements for Bone Strontium Content. G. M. Blake. Nuclear Medicine Department, King's College London School of Medicine, London, United Kingdom.

Strontium ranelate is a new oral treatment for osteoporosis associated with large increases in bone mineral density (BMD) compared with alternative therapies such as bisphosphonates. Much of the BMD increase during strontium ranelate treatment is a physical effect caused by the increased attenuation of X-rays due to the accumulation of strontium in bone tissue. The aim of this study was to assess the contribution made by bone strontium content (BSC) to the overall BMD increase by evaluating the percentage F of the BMD change explained by the physical presence of strontium in bone. A value of F less than 100% would provide evidence of the anabolic effect of strontium ranelate as an additional factor contributing to the overall BMD increase. Studies of mixtures of strontium hydroxyapatite (SrHA) and calcium hydroxyapatite (CaHA) scanned on a variety of dual-energy X-ray absorptiometry (DXA) systems show that a 1% molar ratio of SrHA/(CaHA+SrHA) causes a 10% overestimation of BMD. The correction of spine BMD measurements for the physical effects of strontium depends on knowledge of two further factors: (1) bone biopsy measurements of iliac crest BSC; (2) the ratio R of BSC at the DXA site to BSC at the iliac crest measured in animal studies. We used clinical trial data and values of R_{spine} measured in studies of monkeys and beagle dogs to determine values of F_{spine} for 1, 2 and 3 years treatment with strontium ranelate. Based on the average value of $R_{spine} = 0.7$ for male and female monkeys we found values for $F_{spine} = 75\% - 80\%$ for 1, 2 and 3 years of treatment. Using the value of $R_{spine} = 1.0$ from the beagle study gave values of $F_{spine} = 100\%$. Although values of F_{spine} as low as 40% are possible, we conclude that the most likely figure is 75% or greater. However, it is apparent that there are large uncertainties in the correction of BMD results for the effect of bone strontium and that the most important of these is the inference of BSC values at DXA sites from measurements of bone biopsy specimens.

Disclosures: G.M. Blake, None.

M449

Calcium Supplementation Improves Lipid Profile But Does Not Decrease the Incidence of Cardiovascular Events in Postmenopausal Women. M. J. Bolland*, B. Mason*, A. Horne*, R. Ames*, A. Grey, G. Gamble*, R. Doughty*, A. Barber*, I. R. Reid. Department of Medicine, University of Auckland, Auckland, New Zealand.

Previously we have shown that calcium supplementation produces beneficial changes in lipids that might impact upon the incidence of cardiovascular disease. We set out to determine the effect of calcium supplementation on myocardial infarction (MI), stroke, sudden death, and lipids in post-menopausal women.

We carried out a 5 year randomized, placebo-controlled trial of 1g daily calcium citrate supplementation in 1471 post-menopausal women (mean age 74y). MI, stroke, and sudden death events were recorded during the study. Hospital admissions for cardiovascular events were also obtained from a national database. All events were adjudicated by a physician and a cardiologist or neurologist. Serum lipids were measured annually in a substudy of 223 women.

There were increases in the number of women in the calcium group who during the study reported MI (32 vs 14, $P=0.007$), stroke (42 vs 38, $P=0.19$), and the composite endpoint of MI, stroke or sudden death (70 vs 45, $P=0.015$). After adjudication of events and identification of additional unreported events from the national database, the increases in number of women in the calcium group with MI (31 vs 21, $P=0.16$), stroke (34 vs 25, $P=0.23$), and the composite of MI, stroke or sudden death (60 vs 50, $P=0.32$) persisted but were not statistically significant. The relative risk of MI was 1.2 (1.0-1.5), stroke 1.2 (0.9-1.6), and the composite of MI, stroke or sudden death 1.1 (0.9-1.3). There were trends toward an increased rate of MI in the calcium group (11.1 vs 6.6 /1000 patient-years, $P=0.06$), stroke (11.4 vs 7.8 /1000, $P=0.18$), and the composite of MI, stroke, or sudden death (23.2 vs 16.3 /1000, $P=0.05$).

There were trends toward a greater decrease in LDL from baseline in the calcium group over 5 years (9.5% vs 6.2%, $P=0.05$) and a greater increase in HDL (10.4% vs 9.8%, $P=0.11$). There was a greater increase in the HDL:LDL ratio over 5 years in the calcium group ($P=0.015$).

In summary, 5 years of calcium supplementation, 1g daily, in postmenopausal women improved lipid profile but did not reduce the number of cardiovascular events. In fact, there were trends towards an increase in the rate of cardiovascular events in women receiving calcium.

Disclosures: M.J. Bolland, None.

This study received funding from: Health Research Council of New Zealand.

M450

The Effects of UV-B Light on Serum Vitamin D Levels in Humans. L. A. G. Armas¹, R. P. Heaney¹, M. J. Barger-Lux^{*1}, C. Huerter^{*2}, R. Lund^{*3}.

¹Osteoporosis Research Center, Creighton University, Omaha, NE, USA,

²Dermatology Department, Creighton University, Omaha, NE, USA,

³Nephrology Department, Creighton University, Omaha, NE, USA.

We report results of vitamin D levels after 4 weeks of exposure to graded doses of UV-B light delivered by a light booth. The subjects ($n=69$, age 19-49 yr, females = 41, males = 28) were healthy indoor workers with limited non-solar sources of Vitamin D.

Data were gathered from September through June for 2 consecutive years (71% completed the study from January through May). We determined BMI, 25(OH)D, vitamin D, Ca^{2+} and PTH at baseline. The subjects had 90% of their body exposed to broad-band UV-B light from a UV light booth 3 times a week for 4 weeks (12 treatments) in doses ranging from 20mJ to 80mJ per treatment. Serum Vitamin D was drawn at baseline, after 4 weeks of UV-B treatment, and again 4 weeks after completion of UV-B treatment.

At baseline, 80% percent of the subjects had undetectable vitamin D levels. The subjects' median serum vitamin D level was 0 nmol/L (0, 0 interquartile range). At 4 weeks, after 12 treatments with UV-B light, the median vitamin D level was 31.0 nmol/L (19.0, 42.5 interquartile range). Four subjects' vitamin D levels remained at 0 after UV-B treatment despite a median rise in their 25(OH)D levels of 26.6 nmol/L.

At week 8, the median vitamin D level decreased to 0 nmol/L (0, 5.9 interquartile range) with 57% of subjects' levels reaching 0 nmol/L.

The vitamin D response to UV-B light correlated positively with dose of UV-B light and the 25(OH)D level at week 4 and inversely correlated with age, body surface area, and body mass index.

In conclusion, serum vitamin D levels increase in response to UV-B light, but the body needs constant vitamin D input to maintain vitamin D levels. The serum vitamin D levels are quickly depleted by either storage by the body or conversion by the liver to 25(OH)D.

Disclosures: L.A.G. Armas, None.

This study received funding from: Dialysis Clinics, Inc., Endocrine Fellows Foundation.

M451

Daily Versus Monthly Oral Vitamin D2 and D3: Effect on Serum 25OHD Concentration. N. Binkley, D. Gemar, R. Ramamurthy, D. Krueger, M. K. Drezner. University of Wisconsin Osteoporosis Research Program, University of Wisconsin-Madison, Madison, WI, USA.

It is widely assumed that ergocalciferol (D2) is less effective than cholecalciferol (D3) in maintaining normal serum 25 hydroxyvitamin D [25(OH)D] levels. However, data supporting this belief remains limited. The common suboptimal adherence to daily

supplements confounds this problem further since clinicians may elect to utilize high-dose vitamin D supplementation monthly. As only ergocalciferol is available as a high-dose prescription preparation in the US, evaluation of intermittent high-dose D2 supplementation on 25(OH)D status is required. Moreover, the logical hypothesis that appropriate timing of 25(OH)D measurement is required, such that a trough 25(OH)D value is obtained when dosing monthly, has not been tested. With these related considerations in mind, the purpose of this year long randomized, double-blind, placebo-controlled prospective clinical trial is to evaluate the effect of daily dosing of 1,600 IU D2 or D3 versus monthly dosing of 50,000 IU D2 and D3 on serum 25(OH)D concentration and concurrently to investigate the potential importance of obtaining trough 25(OH)D levels in adults over age 65 years. Study inclusion criteria include community dwelling men and women age ≥ 65 years with a serum 25(OH)D concentration between 10-60 ng/ml who were willing to use sunscreen when exposed to the sun. Those with hypercalcemia, hypercalciuria, renal failure, use of drugs interfering with vitamin D metabolism or a history of nephrolithiasis were excluded. Serum 25(OH)D was measured by reverse phase HPLC. At this time, 20 participants, age 74.3 ± 1.8 years (mean/SEM) have been randomized. At baseline, their serum 25(OH)D concentration was 31.1 ± 2.2 ng/ml. After one week of study, serum 25(OH)D concentration increased ($p < 0.001$) by 8.6 ± 0.6 ng/ml and 6.7 ± 1.4 ng/ml at three and seven days following receipt of 50,000 D3, but was not different from baseline in those receiving daily therapy with D2 or D3 or monthly D2. Our preliminary observations support the possibility that therapy with D3 may be more effective. However, as this study is ongoing, additional data, including the effect of intermittent monthly dosing, and the impact of specimen acquisition time relative to monthly dosing of D2 and D3, on serum 25(OH)D concentration will be reported.

Disclosures: N. Binkley, None.

M452

See Sunday Plenary Number S452

M453

Effect of Alfacalcidol on Volumetric Bone Mineral Density Measured by pQCT in Alendronate-Treated Postmenopausal Women with Osteopenia or Osteoporosis: 1 Year Interim Analysis of the ALFA Study. O. Bock¹, H. Boerst^{*1}, M. Runge^{*2}, G. Beller^{*1}, F. Touby^{*1}, J. Tuerk^{*2}, P. Martus^{*3}, E. Schacht^{*4}, J. Hashimoto^{*5}, D. Felsenberg¹. ¹Centre for Muscle and Bone Research, Charité - Campus Benjamin Franklin, Berlin, Germany, ²Centre for Muscle and Bone Research, Aerpah Kliniken Esslingen-Kennenburg, Esslingen, Germany, ³Institute of Biostatistics and Clinical Epidemiology, Charité - Campus Benjamin Franklin, Berlin, Germany, ⁴ZORG - Zurich Osteoporosis Research Group, Zurich, Switzerland, ⁵Bone Disease Area Department, Chugai Pharmaceutical Co.Ltd., Tokyo, Japan.

The purpose of the ALFA (Alfacalcidol & Falls) study (three-year prospective, randomized, double-blind, placebo-controlled trial) is to evaluate the effect of alfacalcidol 1 µg daily on the number of falls in postmenopausal, alendronate-treated, osteopenic or osteoporotic women. A pre-planned one year interim analysis was performed to examine the effect of alfacalcidol on bone mineral density (BMD) by DXA and pQCT.

A total of 278 postmenopausal women (mean age 73.7 years, SD 4.8) received either alfacalcidol 1 µg or placebo daily, in addition to alendronate 70 mg weekly and calcium 500 mg daily. Volumetric BMD (vBMD) at standardized sites of radius and tibia were measured by pQCT (Stratec XCT-2000) at baseline and after 3, 6, 9 and 12 months of treatment.

Baseline characteristics of patients, including age, BMI, bone markers, BMD at lumbar spine (mean T-Score -2.33 vs. -2.40 SD) and hip (mean T-Score -1.40 vs. -1.45 SD) were not significantly different between the two groups.

BMD	Volumetric BMD change from baseline after 1 year (per protocol analysis)		
	alfacalcidol + alendronate	placebo + alendronate	p value (T-test)
radius, trabecular	- 0.83 %	- 0.66 %	0.874
radius, cortical (mid shaft)	+ 0.26 %	- 0.19 %	0.032
tibia, trabecular	+ 0.04 %	- 0.50 %	0.042
tibia, cortical 14%	+ 0.20 %	- 0.25 %	< 0.001
tibia, cortical 38%	+ 0.16 %	- 0.13 %	0.002
tibia, cortical 66%	+ 0.17 %	+ 0.07 %	0.216

A slight, but significant increase of cortical vBMD at the mid shaft radius and the 14% and 38% measurement sites of the tibia was detectable after one year of additional alfacalcidol medication versus placebo in alendronate treated patients. Similar results were found for the trabecular vBMD at the tibia. Results were not significantly different for trabecular vBMD at the radius and cortical vBMD at the 66% measurement site of the tibia.

For the first time, our data showed an additional, potentially beneficial, effect of alfacalcidol 1 µg daily in alendronate-treated postmenopausal women not only on lumbar spine BMD measured by DXA (as reported earlier), but also on several volumetric BMD parameters at the appendicular skeleton. Their long-term change and possible impact on bone strength of the peripheral skeleton will be monitored in the actually ongoing study for three years.

Disclosures: O. Bock, None.

This study received funding from: Chugai Pharmaceutical Co., Ltd (Japan), GRY-Pharma GmbH (Germany) and Teva Pharmaceutical Industries (Israel).

M454

Bone Mineral Density (BMD) and Serum Vitamin D Levels in Patients with Chronic Obstructive Pulmonary Disease (COPD) Without Glucocorticoid Use. C. Franco^{*1}, C. A. M. Kulak¹, P. Gomes^{*1}, S. C. Radominski², V. Z. C. Borba¹, C. L. Boguzewski^{*1}. ¹Endocrinology, UFPR, Curitiba, Brazil, ²Reumatology, UFPR, Curitiba, Brazil.

The evaluation of BMD in patients with COPD is restricted to those in glucocorticoid use or with risk factors. It is not known if COPD per se affects bone mass and increases the risk of fracture. The purpose of this study was to evaluate the BMD, vitamin D levels and spirometric parameters in a group of COPD patients without systemic glucocorticoid (GC) use. We examined 28 women and 21 men (65.4 ± 9.2 years old) with COPD without chronic systemic GC use. Age below 25 years old and patients with any other cause for osteoporosis were excluded. Patients answered to a questionnaire and were submitted to DXA (Hologic QDRW1000) of lumbar spine and femur. The diagnosis of COPD was done by spirometry and blood was collected for laboratory exams. Past history of fractures were present in 22, 4%. The lumbar spine BMD (g/cm²) was 0.794 ± 0.169, femoral neck 0.704 ± 0.143, total femur 0.78 ± 0.15. Low bone mass was presented in 79.6% and 51% presented osteoporosis. There was a correlation between spirometry and BMD: lumbar (R=0, 38 p <0, 01), femoral neck (R=0, 40 p=0, 01), total femur (R=0, 36 p <0, 01). The mean levels of 25 OH vitaminD (25-OHD) was 20.8 ± 1.0 ng/dl, (28, 6% were 25-OHD insufficient; 6% were 25-OHD deficient and 67% had secondary hyperparathyroidism). Patients with oxygen saturation <88% presented lower 25-OHD levels, and who stopped smoking > 49 months had better BMD. In regression analysis, weight, current smoking, sex and time without smoking were related to the worsening of BMD (R² = 0,7) These data suggest that COPD patients present low bone mass, vitamin D insufficiency and increased fracture risk, independent of the GC use.

Disclosures: V.Z.C. Borba, None.

M455

Remodelling of Bone Microarchitecture in Aging Mice Is Associated with Changes in Ephrins Gene Expression. E. N. Bianchi^{*}, R. Rizzoli, S. L. Ferrari. Div. of Bone Diseases, Geneva University Hospital, Geneva, Switzerland.

Continuous bone remodelling leads to prominent losses of trabecular microarchitecture in aging C57BL/6J mice, which mimics the deterioration of bone structure observed in post-menopausal women. The molecular mechanisms involved in this process however remain poorly understood. Binding of ephrin (Efn) B2 to the ephrin receptor (Eph) B4 was recently reported to induce stimulation of osteoblast differentiation and inhibition of osteoclastogenesis. We hypothesized that a decline in ephrins expression could be implicated in the changes of bone microarchitecture observed in aging mice. For this purpose, female C57BL/6J mice were sacrificed at 4 and 12 months of age, and trabecular (Tb) and cortical (Ct) bone microarchitecture analyzed by microCT (Scanco40) at distal and midshaft femur, respectively. RNA was extracted from the same regions of interest, i.e. the diaphysis (Dia) after flushing of the bone marrow and the metaphysis-epiphysis (Met) of femur. Expression levels of Efn B1 and B2 and Eph A3, A4, B2, B3 and B4 genes were determined by quantitative RT-PCR (TaqMan MGB probes).

Tb BV/TV decreased by 60% between 4 and 12 months of age (p=0.0001) associated with a decline in Tb number and connectivity, and an increase in Tb separation (all p<0.001). Meanwhile, Ct volume increased by 20-30%. Overall, Efn and Eph expression levels were higher in Met than Dia and in young compared to older mice. More precisely, expression of EfnB2 decreased by 65% (p<0.0001) in Met and 40% (p<0.02) in Dia with aging, whereas its receptors Eph B2, B3 and A4 decreased by 40% to 70% (p<0.05) in both compartments. In contrast, significant down-regulation (-35% to -50%, p<0.02) of EfnB1 and EphB4 occurred specifically in Met, but not in Dia. We then investigated expression of additional genes associated with osteoclast (OPG, RANKL and TRAP) and osteoblast/osteocyte activity (IGF-1 and SOST). OPG, RANKL and TRAP were more prominently expressed in Met than Dia (p<0.005), and both the RANKL/OPG ratio and TRAP gene expression were significantly down-regulated with age. In contrast, IGF-1 and SOST mRNA levels were twice as high in Dia than Met, and decreased only marginally with age in Dia.

In summary, reciprocal changes in bone geometry and trabecular content and distribution occur in the femur of aging mice. Neither the changes of OPG, RANKL and TRAP, nor those of IGF-1 and SOST can explain the age-related decline of trabecular microarchitecture. However, the decline of ephrins and ephrin receptors gene expression, particularly of EfnB1 and EphB4 in the Tb compartment, might favor uncoupling of bone formation from resorption and remodelling of skeletal microarchitecture.

Disclosures: E.N. Bianchi, None.

M456

Low Vitamin D Level and High Bone Turnover in Aged Type 2 Diabetic Patient. D. Chung, J. Chung^{*}, D. Myung^{*}, D. Cho^{*}, M. Chung^{*}. Internal Medicine, Chonnam National University Medical School, Gwangju City, Republic of Korea.

Bone mineral density in type 2 diabetic patient is known to be variable; such as increased, decreased, or not different from normal subject. Levels of bone turnover markers are also conflicting while several histomorphometric data shows low bone turnover status in diabetic bone. However, recent epidemiologic data showed that osteoporotic fracture rate is increased in type 2 diabetes even in patients with normal or high BMD possibly due to poor bone quality. Bone metabolism in diabetes is thought to be

affected by many factors including glycemic control status, presence of late chronic complications, disorder of calcium and vitamin D metabolism. In this study, we investigated the vitamin D status and bone turnover rate in 53 type 2 diabetic postmenopausal women (69.9±8.1 years, HbA1c was 8.2±2.3%) and 34 non-diabetic postmenopausal women (66.8±8.4 years). 25OHD, serum CTX and other laboratory data were acquired after overnight fasting. BMD was measured at the lumbar spine and femur using dual energy X-ray absorptiometry (Lunar Prodigy Advance). Body mass index and years since menopause were not different between two groups. The 25OHD level was significantly lower (p=0.001) in diabetic women (23.1±11.4 ng/ml) compared to normal subject (32.6±12.3 ng/ml). The serum CTX was significantly higher (p=0.013) in diabetic women (0.61±0.42 ng/ml) compared to non-diabetic women (0.39±0.29 ng/ml). However, the BMD at the spine and femur were not significantly different between two groups. These results suggest low serum vitamin D level and high bone turnover in aged type 2 diabetic patient may contribute to increased probability of osteoporotic fracture.

Disclosures: D. Chung, None.

M457

Multifactorial Etiology of Weak Bones in Type 1 Diabetes (T1DM). K. K. Danielson^{*1}, M. E. Elliott², M. Palta^{*3}. ¹Section of Pediatric Endocrinology, University of Chicago, Chicago, IL, USA, ²Pharmacy Practice Division, University of Wisconsin, Madison, WI, USA, ³Population Health Sciences and Biostatistics & Medical Informatics, University of Wisconsin, Madison, WI, USA.

Our research has demonstrated bone mineral density (BMD) and bone formation to be lower in women with T1DM than in matched controls. We also found that the earliest etiologic effects of T1DM on bone appear at the level of bone turnover. We therefore attempted to delineate the potential pathophysiologic mechanisms altering bone turnover in T1DM. The study included premenopausal women with T1DM enrolled in the Wisconsin Diabetes Registry (n=89). Each participant completed questionnaires, a physical exam, and blood draw to measure HbA1c, parathyroid hormone (PTH), insulin-like growth factor 1 (IGF-1), vitamin D, estradiol, osteocalcin and NTx. An Uncoupling Index (UI) was calculated as the difference between osteocalcin and NTx z-scores. Urinary albumin excretion (UAE; n=61) was collected as a measure of kidney function during the three years prior to the study (mean=1.7 years). The study was approved by the University of Wisconsin institutional review board. Mean age was 28 years (18-45 years) and 98% were Caucasian. Mean disease duration was 16 years and current mean HbA1c was 8.1%. Only 9.8% demonstrated early kidney impairment with elevated UAE (≥20 µg/min). A negative UI was exhibited by 66.3% of the sample, indicating bone resorption was outpacing formation. The final multivariable regression model for bone formation demonstrated several potential etiologic factors to be independently associated with osteocalcin (ng/ml): HbA1c (%; β=-0.3), PTH (10 pg/ml; β=0.4), IGF-1 (10 ng/ml; β=0.1), and logUAE (µg/min; β=0.3). The HbA1c coefficient did not attenuate when PTH, IGF-1, or UAE was added to the final model indicating they did not mediate the association between glycemic control and bone formation. The final model for bone resorption (NTx [nmol BCE/L]) also demonstrated a positive association with logUAE (β=1.6). Lastly, the UI (z-score) was independently associated with PTH (β=0.2) and IGF-1 (β=-0.1). In conclusion, uncoupled bone turnover in T1DM, encompassing low formation and net resorption, appears to be related to the poor glycemic control and low IGF-1 and PTH levels associated with T1DM. The progression of kidney disease, even the early stages as detected in our sample by slightly elevated UAE, may then accelerate this uncoupled bone turnover. These factors may eventually culminate in the low BMD and increased fracture risk seen in T1DM. Fortunately, this multifactorial process provides several potential targets for intervention.

Disclosures: K.K. Danielson, None.

This study received funding from: American Diabetes Association.

M458

Relationship of Bone Turnover Markers, Ovarian Hormones and Cytokines During Menopause. M. P. Desai^{*1}, V. R. Taskar^{*2}, M. Khatkhatay^{*1}. ¹Molecular Immunodiagnostics, National Institute for Research in Reproductive Health, Mumbai, India, ²Clinical, Streehit Karini, Mumbai, India.

Estrogen influences bone remodeling, by modulating the secretion of cytokines. Its deficiency at menopause causes accelerated bone loss and subsequently osteoporosis. The aim of the study was therefore to characterize the changes in cytokines and ovarian hormonal profiles and correlate with bone turnover markers and bone density. This would aid in identification of women at risk for osteoporosis and preventive therapy could be initiated. We studied a cross-sectional age stratified population sample of 124 premenopausal women (age: 21-40yrs), 68 perimenopausal women (age: 36-44 yrs) and 188 postmenopausal women (age: 41-75 yrs) not using any oral contraceptives or on hormone replacement therapy. Serum calcium, phosphorus and PTH were estimated to assess the bone homeostasis while bone mineral density (BMD) of lumbar spine and femoral neck was measured by DEXA. The women in the groups were classified into normal, osteopenic and osteoporotic based on BMD measurements and their ovarian hormonal status. Urinary estrone glucuronide (E₁G) and follicle stimulating hormone (FSH) were estimated by in-house assays, whereas serum interleukins (IL1, IL6 and TNFα) by optimized EIA assays. The bone markers such as Osteocalcin (OC), bone specific alkaline phosphatase (BSAP), urinary type I collagen telopeptide (CTX) and pyridinium crosslink de-oxypridinoline (Dpd) by ELISA kits. The perimenopausal women showed 30% higher CTx excretion (528 ± 126 µg/mol Cr, p<0.01), 28% higher

Dpd levels (5.02 ± 1.20 nMol / mol Cr, $p < .01$), increased levels of urinary FSH (38.6 ± 3.84 m IU / mg Cr, $p < 0.0001$) and IL6 (11.68 ± 2.61 ng/ml, $p < 0.05$) with osteopenic changes on BMD whereas E_1G bone formation markers and BMD though low did not show any significant change. In the osteopenic menopausal women all the bone markers were significantly elevated indicating increased rate of bone remodeling. Of the three cytokines, IL6 increased significantly (15.85 ± 3.5 ng/ml, $p < 0.0001$) correlating well with increased bone turnover (CTx 1126 ± 362 μ g / mol Cr and Dpd 8.49 ± 2.65 nM / mol Cr) while there was marginal increase in TNF α levels (6.5 pg/ml; $p < 0.0056$) only in the osteoporotic women. A significant drop in E_1G (8.99 ng/mgCr; $p < 0.0001$) and BMD measurements with rise in IL 6 was also observed in these women. The data suggests that elevated cytokines (IL 6 and TNF α) and bone resorption markers (CTx and Dpd) are associated with rapid of fall of estrogens in the first decade of menopause leading to postmenopausal osteoporosis. Combination of hormonal profiles, bone resorption markers and cytokines will thus aid in identifying women at risk for osteoporosis.

Disclosures: M.P. Desai, None.

This study received funding from: Department of Family Welfare, Government of India.

M459

See Sunday Plenary Number S459

M460

Relationships Between Leptin, PTH, Vitamin D and Bone Metabolism Markers in Patients with Hip Fracture. A. A. Fisher^{*1}, E. K. Southcott^{*1}, S. L. Goh^{*2}, W. Sriksalanukul^{*1}, M. W. Davis^{*1}, P. N. Smith^{*2}. ¹Department of Geriatric Medicine, The Canberra Hospital, Australian National University, The Canberra Hospital, Woden, ACT, Australia, ²Department of Orthopaedic Surgery, The Canberra Hospital, Australian National University, The Canberra Hospital, Woden, ACT, Australia.

The relationship between leptin and bone metabolism is controversial. The study aim was to investigate leptin-skeletal interactions in older patients with hip fracture (HF), a population not previously studied.

In 207 consecutive patients (mean age 82.1 ± 7.9 years; 75.8% women) with low-energy trauma HF (119/88 cervical/trochanteric) serum concentrations of leptin, 25 hydroxy-vitamin D [25(OH)D], parathyroid hormone (PTH), calcium, phosphorus, magnesium, osteocalcin (OC), bone-specific alkaline phosphatase (BAP) and urine excretion (normalised for urinary creatinine) of free deoxypyridinoline (DPD) and N-terminal cross-linked telepeptide of type 1 collagen (NTx) were measured and clinical data collected prospectively.

Elevated PTH (> 6.5 pmol/L) was present in 53%, 25(OH)D insufficiency (< 50 nmol/L) in 81.6%, excessive bone resorption (increased DPD and/or NTx excretion) in 93.7% and low bone formation (low OC and/or BAP) in 59.2%. Leptin (log-transformed) was significantly and positively correlated with OC ($r = 0.18$; $p = 0.006$) and negatively with NTx ($r = -0.17$; $p = 0.015$) and DPD ($r = -0.14$; $p = 0.037$). In both cervical and trochanteric HF groups, leptin was positively associated with OC, but the association with DPD was significant only in trochanteric HF ($r = -0.30$; $p = 0.009$). Trochanteric compared to cervical HF patients have higher levels of PTH (7.9 ± 6.0 vs 5.9 ± 3.8 pmol/L; $p = 0.005$), but the concentrations of leptin, 25(OH)D and bone turnover markers were similar. Only in cervical HF patients were leptin and PTH positively correlated ($r = 0.26$; $p = 0.005$) and 25(OH)D levels were negatively and significantly correlated with NTx ($r = -0.25$; $p = 0.016$), DPD ($r = -0.31$; $p = 0.002$) and BAP ($r = -0.24$; $p = 0.012$). Other bone metabolism parameters were not associated with leptin in neither group.

These findings suggest that in HF patients there exists a complex relationship between leptin and calciotropic factors, that serum leptin may independently contribute to bone remodelling and is likely to exert different effect on cortical and trabecular bone compartments.

Disclosures: A.A. Fisher, None.

M461

Do Periosteal and Intracortical Responses to Ulmar Fatigue Loading Differ Between Old and Young Rats? J. B. Jones^{*}, R. T. Kitterman^{*}, S. D. Mendenhall^{*}, J. G. Skedros. Dept. of Orthop. Surgery, Univ. of Utah, SLC, UT, USA.

Age-related skeletal deterioration results not only in decreased bone mass but also bone quality. Inadequate modeling responses and/or incomplete infilling of resorption cavities following bone fatigue contribute to this decline in bone mechanical properties. Using the rat ulna fatigue model, we hypothesized that older adult rats would show less periosteal woven bone apposition and resorption space infilling when compared with younger adult rats following mechanical loading. With IACUC approval, 28 male F344 rats (14, 5 month-old, 14, 15 month-old) were obtained from the National Institute on Aging (Bethesda, MD). Eight rats of each age formed the experimental groups and the remaining were used for load/strain calibration. Right forearms were cyclically loaded [Uthgenannt & Silva, J Biomech, 2006] and the contralateral ulnae served as controls. Tetracycline was injected 13 and 3 days prior to sacrifice at 18 days post-loading. Ten transverse sections were then cut from mid-third ulnar diaphyses and mounted on slides. Resorption space areas (Rs.Ar/Ct.Ar), infilling areas (Rs.Inf.Ar/Ct.Ar), and periosteal woven bone area (PWb.Ar/Ct.Ar) were quantified. Kruskal-Wallis ANOVA was employed with significance set at $p < 0.05$. Contrary to our hypothesis that older rats would exhibit less periosteal bone apposition, a larger amount was observed when compared to younger rats (see Table).

Additionally, total resorption area was twice as large in older rats. However, when resorption space infilling area was considered, the older rats showed significantly less infilling than younger rats (33% vs. 55%, see Table). These data suggest that older rats show an imbalance between intracortical resorption and bone formation which leads to net bone loss—a similar phenomenon experienced by aging humans. The finding that older rats exhibit more periosteal woven bone than younger rats implies the possibility of a compensatory mechanism that counteracts the increased cortical porosity. Although a similar interaction between remodeling and modeling has been suggested in humans, the modeling response is relatively subtle [Ural & Vashishth: J Orthop Res 2006]. This demonstrates a limitation when attempting to extrapolate the capacity of bone modeling in 15-month old rats to that in aging humans.

Table: Periosteal modeling, intracortical resorption, and intracortical infilling by age in the rat

	5 month old rats (mean \pm SD)	15 month old rats (mean \pm SD)	
PWb.Ar/Ct.Ar	0.0630 ± 0.0875	0.1578 ± 0.1380	$p < 0.001$
Rs.Ar/Ct.Ar	0.0063 ± 0.0235	0.0129 ± 0.0225	$p = 0.008$
Rs.Inf.Ar/Ct.Ar	0.0035 ± 0.0118	0.0043 ± 0.0065	$p = 0.030$

PWb.Ar/Ct.Ar - periosteal woven bone area / cortical area (mm²/mm²)

Rs.Ar/Ct.Ar - total resorption space area / cortical area (mm²/mm²)

Rs.Inf.Ar/Ct.Ar - resorption space infilling area / cortical area (mm²/mm²)

Disclosures: J.B. Jones, None.

This study received funding from: OREF Grant 01-024.

M462

Increased Active Osteoclasts Are Associated with Acute Cancellous Bone Loss in Adult Mice Exposed to Ionizing Radiation and Musculoskeletal Disuse. H. Kondo¹, R. Mojarrah^{*1}, A. Wang^{*1}, J. Phillips^{*1}, E. A. C. Almeida^{*1}, D. J. Loftus^{*1}, E. Morey-Holton^{*1}, R. K. Globus^{*1}, W. Vercoe^{*1}, C. Limoli^{*2}, N. D. Searby^{*1}. ¹Bone and Signaling Lab, NASA Ames Research Center, Moffett Field, CA, USA, ²Radiation oncology, University of California Irvine, Irvine, CA, USA.

Spaceflight challenges the skeletal health of astronauts by exposure to radiation in microgravity. Hamilton et al. (JAP (2006) 101:789) showed that irradiation alone decreases bone mass in growing mice 4 mo after exposure to 2 Gy vs. controls, as does musculoskeletal disuse. We hypothesize that radiation and disuse share cellular and molecular mechanisms to cause rapid bone loss in the adult. To define dose (1-2 Gy) and time dependence (3 or 10 d) of skeletal responses to radiation, 4 mo old C57/B16 mice were Cs¹³⁷ gamma-irradiated (IR), then marrow cells analyzed for viability by FACS and bones for structure by microCT. In a second study, mice were hindlimb unloaded (HU) or normally loaded (NL) for 7 d; half the mice from each group were IR with 2 Gy 4 d into the unloading period. Bones were analyzed for structure (microCT), osteoclast surface (histomorphometry) and oxidative damage to lipids (peroxidation by malondialdehyde assay). As expected, HU for 7 d decreased cancellous bone compared to NL. Surprisingly, only 3 d after exposure, IR (2 Gy) caused a loss in cancellous BV/TV (~20%), trabecular number, and connectivity similar to 7 d HU. By 10 d after IR, BV/TV was 25% lower than controls at 1 Gy and 35% lower at 2 Gy, showing both dose and time-dependent effects of IR. Cancellous bone loss was similar in mice exposed to IR during HU, compared to mice treated with either IR or HU alone. IR transiently reduced (by 65% at 3 d) numbers of viable marrow cells due to increased apoptosis. IR elevated (by 36%) lipid peroxidation in bone. Osteoclast surface per bone surface increased 113% due to IR, 100% due to HU, and 153% due to both IR and HU compared to NL, indicating stimulated resorption. Hydrogen peroxide treatment of cultured bone marrow cells caused a dose-dependent increase in TRAP+ cells, inhibited by the anti-oxidant, alpha-lipoic acid. Together, these results showed that IR and HU caused similar detrimental effects on cancellous bone structure of adult mice, and shared the cellular mechanism of increasing active osteoclasts. In the short-term, continuous HU did not alter the structural changes caused by radiation, possibly due to depletion of osteoclast precursors by unloading or irradiation alone. Finally, radiation caused oxidative stress in bone tissue that may contribute to increased resorption leading to rapid bone loss. These results have potential clinical relevance to astronauts as well as to cancer patients treated therapeutically with radiation.

Disclosures: H. Kondo, None.

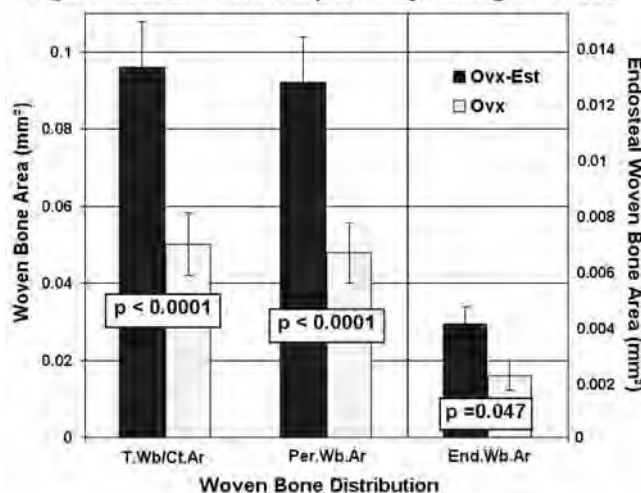
This study received funding from: NASA.

M463

The Periosteal and Endosteal Modeling Process Is Affected by Estrogen Differently in Response to Fatigue Loading Than During Development. S. D. Mendenhall*, J. B. Jones*, R. T. Kitterman*, J. G. Skedros. Dept. of Orthop. Surgery, Univ. of Utah, SLC, UT, USA.

Females are "set up" during skeletal development to have fragile bones later in life. This results primarily from the inhibitory effect of estrogen on periosteal modeling during bone mass acquisition, causing women's bones to be less robust than men's. Delayed pubertal development in female rats increases periosteal bone growth, but results in a minor decline in endosteal modeling [Yingling: Tran Orthop Res Soc 2007]. However, little is known about the effects of estrogen on periosteal/endosteal modeling responses to fatigue loading in rats. Using the rat ovariectomy (Ovx) model, we tested the hypothesis that estrogen-deficient rats would exhibit less endosteal modeling and more periosteal modeling following fatigue loading than Ovx rats that were estrogen-repleted (Ovx-Est). With IACUC approval, 36 five-month-old female F344 rats were obtained--6 for load/strain calibration and 15 for each of the experimental groups. Following Ovx, right forearms were cyclically loaded [Uthgenannt & Silva, J Biomech, 2006] and the contralateral ulnae served as controls. The Ovx Est group received daily β -Estradiol (0.05 mg/kg) injections. All animals received tetracycline injections 13 and 3 days prior to sacrifice at 18 days post-loading. Ten transverse sections were cut from mid-third ulnar diaphyses and mounted on slides. Endosteal woven bone area (End.Wb.Ar), periosteal woven bone area (Per.Wb.Ar), and total woven bone area (T.Wb.Ar) were then quantified. Kruskal-Wallis ANOVA was used with significance at $p < 0.05$. As expected, the Ovx rats had less endosteal bone growth when compared to Ovx-Est rats. Surprisingly, the Ovx-Est rats produced nearly twice as much periosteal woven bone than did Ovx rats (see Figure). These results show an interesting interaction between hormone status and fatigue-induced modeling responses in the rat. Although estrogen inhibits periosteal bone growth during development, heavy mechanical stimuli seem to reverse this role, thereby maximizing the amount of new bone growth on periosteal and endosteal surfaces. Similar anabolic effects of estrogen have been reported in women on estrogen replacement therapy [Vedi et al.: Osteoporos Int 1999]. Further work is needed to validate the rat Ovx model for evaluating novel therapeutic agents that target estrogen's actions on bone.

Figure: Woven Bone Response by Estrogen Status



Disclosures: S.D. Mendenhall, None.

This study received funding from: OREF Grant 01-024.

M464

An Acute 7 Gray Dose of Gamma-Radiation Induces a Profound and Rapid Loss of Trabecular Bone in Mice. J. S. Willey*, D. S. Gridley*, M. J. Pecaut*, R. W. Norrdin*, T. A. Bateman*. ¹Bioengineering Department, Clemson University, Clemson, SC, USA, ²Department of Radiation Medicine, Loma Linda University, Loma Linda, CA, USA, ³College of Veterinary Medicine and Biomedical Sciences, Colorado State University, Fort Collins, CO, USA.

Fracture rates of irradiated bones are elevated in patients receiving radiation therapy for a primary tumor as well as palliative care treatment. The mechanism for the elevated risk of fracture is unclear. Osteoblast death and damaged vascularity have been documented in patients as well as animal models, and contribute to atrophy after irradiation. But the effects of radiation on osteoclast number and function are not well defined. We investigated the effects of acute, high-dose radiation exposure on trabecular and cortical bone to document bone quantity and structural properties at an early time-point post-irradiation. Nine-week old C57BL/6 mice (n=6) received 7 Gray (Gy) gamma-radiation, with nonirradiated controls (n=6). Fourteen days after exposure the animals were euthanized, hind limbs removed, and tibiae analyzed via microCT and histomorphometry. Statistical analyses were performed using t-tests to compare the groups. Profound loss of trabecular bone within the metaphysis was observed. Significant reduction in BV/TV (-

54%), Conn.Dens (-69%), and Tb.N (-26%) were observed in irradiated animals compared with control. No differences were observed in cortical parameters. Decreased growth plate cellularity, disorganized chondrocyte arrangement, and a terminal bar of bone along the distal physal border indicated slow growth among all animals. Oc.S/BS and ES/BS were similar between both groups, with TRAP staining confirming presence of multinucleated osteoclasts. The large difference in the amount of bone between groups and evidence together with evidence of slow growth suggests bone loss as opposed to reduced bone growth. Evidence of stabilized resorption at sacrifice indicates that large declines in bone quantity occurred via increased resorption very early after exposure. Radiation-induced reduction in bone quantity and microarchitecture via elevated resorption could reduce bone quality and may provide insight into the nature of increased fracture rates among radiation therapy recipients.

Disclosures: J.S. Willey, None.

This study received funding from: NSBRI.

M465

Reduced Levels of Serum Insulin Like Growth Factor 1 in Male with Idiopathic Osteoporosis. J. Dewailly*, I. Legroux-Gerot*, M. D'Herbomez*, X. Marchandise*, D. Dewailly*, B. Duquesnoy*, B. Cortet*. ¹Rheumatology, CHRU Hopital Salengro, Lille, France, ²Service de Médecine nucléaire, CHRU Hopital Salengro, Lille, France, ³Endocrinology, CHRU, Lille, France.

Objective: The pathophysiology of idiopathic male osteoporosis remains unknown. The histomorphometric studies suggest reduction of bone formation. A disturbed secretion of IGF-1 could be involved in male idiopathic osteoporosis since IGF-1 has a stimulative effect on the osteoblastic proliferation and on the bone tissue synthesis. Few studies have evaluated the relationship between the circulating concentrations of IGF-1 and bone mineral density, particularly in osteoporotic men, and the results are controversial. The aim of our study was to evaluate the involvement of IGF-1 in idiopathic male osteoporosis and the relationships between bone density and the serum levels of IGF-1 and sex hormones. **Materials and methods:** Serum levels of IGF-1, estradiol, testosterone, SHBG and bone mineral density at lumbar spine, femoral neck and total hip were compared between 79 men with idiopathic osteoporosis and 26 healthy subjects. Inclusion criteria were a densitometric osteoporosis defined by a T-score ≤ -2.5 SD and/or an osteoporotic fracture. The osteoporotic patients were included after exhaustive work-up excluding the principal causes of secondary osteoporosis.

Results: A significant reduction in the mean serum IGF-1 levels was found in osteoporosis patients ($p = 0.02$) that persisted after adjustment for BMI. However, no correlation was found between bone density and the serum IGF-1 levels. The mean SHBG level was higher in osteoporotic patients ($p = 0.001$) thus yielding a reduction in the mean Free Testosterone Index (FTI, total testosterone / SHBG) ($p = 0.002$). These differences remained significant after adjustment for BMI. After adjustment for the FTI, the mean IGF-1 levels between patients and controls were not significantly different. However, after adjustment for the FTI and the BMI in patients, the IGF-1 level was significantly related to the presence of an osteoporotic fracture, thus indicating an independent effect of the IGF-1 level on fracture risk.

Conclusion: Our study confirms the presence of reduced serum IGF-1 levels in male idiopathic osteoporosis. This could be the cause or the consequence of a disturbance in sex hormones with increased SHBG serum level. This confirms the important role of SHBG in the pathophysiology of male osteoporosis.

Disclosures: J. Dewailly, None.

M466

See Sunday Plenary Number S466

M467

Birth Weight Predicts Lean Body Mass and Thus Bmc in Healthy Men at Peak Bone Mass - Results from the Odense Androgen Study. L. Frederiksen*, T. L. Nielsen*, K. Wraae*, H. Claus*, M. Andersen*, K. Brixen*. Endocrinology, Odense University Hospital, Odense, Denmark.

Birth weight has been associated with low bone mass in later life. Previous studies, however, have relied on self-reported data on birth weight, included select populations, or been of a limited size. Moreover, it is unclear if the association between birth weight and bone mass is mediated by body weight, lean body mass, or fat mass.

We hypothesize that birth weight is associated with peak bone mass in men independent of current lean body mass and body weight.

The Odense Androgen Study is a population-based, prospective, observational study on the inter-relationship between endocrine status, body composition, muscle function, and bone metabolism in young men. In brief, 3000 males aged 20-30 years were randomly selected from the civil registration database in Funen County, Denmark, and invited by mail to participate in the study. A total of 2042 men returned the questionnaire, 783 gave written informed consent to participate in the study and the data are presented here. Bone mass measurements (spine, hip, and whole body) were performed using a hologic-4500a densitometer. Data on birth weight, length at birth, and gestational age was retrieved in a national database covering all birth clinics in Denmark in the current period. The relationship between Birth weight, BMC, Lean body mass and fat mass as tested using multiple regression analysis is shown in the table as partial correlation coefficients

Data on birth weight and birth length were available on 754 participants while gestational

age was available on 263 participants (those 20-24 years old). In bivariate analyses, BMC at whole body, spine, and hip were significantly associated with current body weight ($R=0.50$ to 0.30 , $p<0.001$) and birth weight ($R=0.17$ to 0.09 , $p<0.01$). Birth weight was also significantly associated with current body weight ($R=0.09$, $p<0.01$), current lean body mass ($R=0.15$, $p<0.001$) but not current fat mass ($R=-0.04$, NS). No significant difference was found in BMC at any skeletal site in participants born prematurely ($n=26$) and those born at term ($n=237$).

R-values	BMC		
	WB	Spine	Hip
Birth weight	0.08*	-	-
Current fat mass	-0.35***	-0.38***	0.67***
Current lean body mass	0.73***	0.58***	-0.31***
Overall model	0.75***	0.60***	0.67***

* $p<0.05$, ** $p<0.01$, *** $p<0.001$

Birth weight predicts peak bone mass, but this seems to be due to correlation between birth weight and body weight (and lean body mass) in young adult life.

Disclosures: L. Frederiksen, None.

M468

See Sunday Plenary Number S468

M469

Aberrations in Wnt/ β -Catenin Signaling Driving HAART-induced Bone Loss In Vitro. J. S. Butler¹, P. P. Doran^{*1}, R. T. Moon^{*2}, J. M. O'Byrne^{*3}, W. G. Powderly^{*1}. ¹Mater Misericordiae University Hospital, UCD School of Medicine & Medical Science, Dublin, Ireland, ²Howard Hughes Medical Institute, University of Washington School of Medicine, Seattle, WA, USA, ³Dept of Trauma & Orthopaedic Surgery, Royal College of Surgeons in Ireland, Dublin, Ireland.

The advent of highly active anti-retroviral therapy (HAART) had dramatically decreased the rate of HIV-related mortality and significantly extended the life span of patients with AIDS. A variety of metabolic side effects are associated with these therapies, one of which is metabolic bone disease. A higher prevalence of osteopenia and osteoporosis is reported in HIV-infected patients receiving anti-retroviral therapy relative to patients not on therapy. Thus, we decided to investigate the role played by Wnt/ β -catenin signaling in Protease Inhibitor (PI) induced bone loss in vitro.

Our objectives were to assess the gene expression profile of primary human osteoblasts (HOBs) exposed to PIs with a view to identifying key genes driving HAART-induced bone loss and to assess the effects of silencing the Wnt antagonist Dickkopf-1 (Dkk1) on the bone profile of primary human osteoblasts (HOBs) exposed to $5\mu\text{M}$ of IDV and RTV in vitro.

Primary human osteoblasts (HOBs) were cultured in vitro and exposed to $5\mu\text{M}$ of IDV and RTV over a time course of 4hr, 12hr, 24hr and 48hr. Dkk1 expression was silenced using small interfering RNA (siRNA). Quantitative RT-PCR was performed to confirm gene knockdown. Control and PI-treated HOBs were compared with respect to bone turnover. Markers of bone turnover analyzed included alkaline phosphatase activity, calcium deposition and osteocalcin expression, along with cell proliferation and cellular apoptosis. Global changes in HOB gene expression were elicited by IDV and RTV. Development associated gene pathways were co-ordinately dysregulated with the expression profile of key genes of the Wnt Pathway significantly altered. Dkk1 expression in HOBs was increased in response to IDV and RTV exposure with an associated reduction in alkaline phosphatase activity and calcium deposition. Silencing of Dkk1 expression, as confirmed by quantitative RT-PCR, was associated with an increase in alkaline phosphatase activity and calcium deposition, along with increased cell proliferation and reduced cellular apoptosis.

Dkk1 is an antagonist of Wnt/ β -catenin signaling and plays a key role in regulating bone development and remodeling. Silencing the expression of Dkk1 in primary human osteoblasts has been shown to rescue the effects of PI-induced bone loss in vitro. The pharmacological targeting of the Wnt/ β -catenin signaling pathway offers an exciting opportunity for the development of novel anabolic bone agents to treat HAART associated osteopenia/osteoporosis.

Disclosures: J.S. Butler, None.

M470

Bone Mineral Density and Prevalence of Osteoporosis and Fractures in Psoriatic Arthritis. M. Romera, N. Busquets*, J. Rodríguez-Moreno*, C. Gómez-Vaquero*, X. Juanola*, J. M. Nolla*. Rheumatology, Hospital Universitari de Bellvitge, L'Hospitalet, Spain.

Systemic diseases, mainly those involving joints, are known to produce secondary osteoporosis. However, there is little information available about bone mineral density (BMD) and the prevalence of osteoporosis and fractures in patients with psoriatic arthritis (PsA).

The purpose of the study is to evaluate BMD and to quantify the prevalence of osteoporosis and clinical fractures in PsA.

BMD was determined by DXA (Hologic QDR 4.500) in all the patients with PsA regularly evaluated in a tertiary university hospital who were willing to participate in the study;

patients with axial involvement were excluded. All patients underwent a physical examination and a general analytics. We gathered demographic and clinical variables related with BMD and risk of fractures. We also recorded the antecedent of clinical low impact fracture. The activity of PsA was assessed by means of the Modified Health Assessment Questionnaire (HAQm) and the Disease Activity Score 28 (DAS28). The population of reference to calculate T-score and Z-score proceeds from a Spanish database. The diagnosis of osteoporosis was made according to the recommendations of the International Society for Clinical Densitometry.

One hundred and fifty-five patients were included (64 postmenopausal women, 26 premenopausal women and 65 men) with a mean age of 62 ± 8 , 39 ± 7 and 55 ± 14 years, respectively. The clinical forms of PsA were: 1% monoarticular, 44% oligoarticular and 55% polyarticular.

BMD in males under 50 years old was lower than BMD of healthy males of the same age ($p < 0.05$); there were no differences in the other groups of patients. BMD related in a statistically significant way to age, body mass index (BMI), time since the beginning of PsA, number of tender joints, HAQm and DAS28.

The prevalence of osteoporosis in postmenopausal women was 28%; in males above 50 years old, 10%. Fifteen percent of the postmenopausal women and 20% of the males under 50 years old had a BMD below the expected range for their age.

Thirteen percent of the patients had had a clinical fracture. The most frequent localization of the fracture was forearm (7%), followed by vertebra (1%) and hip (1%). Clinical and demographic data were similar in patients with and without fracture. Postmenopausal women had a significantly higher prevalence of fractures.

As a conclusion, patients with PsA, mainly postmenopausal women, have a high prevalence of osteoporosis. BMD correlates with age, BMI and activity of the disease. The frequency of clinical osteoporotic fractures is not negligible. The factors associated to fractures in PsA are similar to those in general population.

Disclosures: C. Gómez-Vaquero, None.

M471

See Sunday Plenary Number S471

M472

Associations of Osteoporotic Spinal Deformity with Back Strength Among Elderly Women in Japan and the United States. M. Hongo¹, M. Sinaki², N. Miyakoshi¹, Y. Shimada^{*1}, E. Itoi^{*3}. ¹Department of Orthopedic Surgery, Akita University, Akita, Japan, ²Department of Physical Medicine and Rehabilitation, Mayo Clinic, Rochester, MN, USA, ³Department of Orthopedic Surgery, Tohoku University, Sendai, Japan.

Kyphosis is associated with diminished daily physical function, increased risk of falls, and increased mortality risk. Back extensor strength (BES) is an important factor in maintaining the sagittal alignment of spine and preventing vertebral fractures. When back exercises are prescribed, it is important to know the associations of the sagittal alignment with BES. However, there is a controversy in the literature regarding the influence of the thoracic and lumbar spinal curvatures on BES or quality of life. We hypothesized that the regional or ethnic factor may influence the relationship between thoracic and lumbar sagittal curve, BES and other factors. The purpose of this cross-sectional study was to assess the associations of osteoporotic spinal deformity with back strength in elderly women in Japan and the United States. Using the same inclusion criteria, 104 Asian women residing in Akita, Japan and 102 Caucasian women residing in Minnesota with postmenopausal osteoporosis were selected for this study. Kyphosis angle of the thoracic and lumbar spine were measured with lateral radiographs. Isometric BES was evaluated using a custom-made dynamometer. Correlations between the kyphosis angle, isometric BES, bone mineral density, physical activity score or quality of life score, the number of vertebral fractures, and grip strengths were analyzed. No significant difference was found in thoracic kyphosis between Akita and Minnesota (43.1° and 44.1° , respectively), whereas lumbar kyphosis angle in Akita was significantly larger than in the Minnesota (-15.4° and -54.0° , $p<0.0001$). In Akita, BES showed significant negative correlation with lumbar kyphosis angle ($r=-0.492$, $p<0.0001$), but no correlation with thoracic kyphosis angle ($r=-0.004$, $p=0.97$). In Minnesota, BES showed significant negative correlation with thoracic kyphosis angle ($r=-0.372$, $p<0.0001$), but no correlation was found with lumbar kyphosis angle ($r=-0.087$, $p=0.362$). In addition, quality of life score in Akita demonstrated significant correlation with lumbar kyphosis, but not with thoracic kyphosis. Physical activity score in Minnesota showed significant negative correlation with thoracic kyphosis, but not with lumbar kyphosis. In conclusion, there was a significant difference in lumbar kyphosis angle between the two countries. Lumbar kyphosis angle has more significant influences in maintaining BES and quality of life among women in Akita, Japan compared with those in Minnesota.

Disclosures: M. Hongo, None.

M473

Secretion of Adipokines and Hypertrophic Changes in Bone Marrow Adipocytes. A. Hozumi^{*1}, M. Osaki^{*2}, H. Shindo^{*2}. ¹Orthopaedic surgery, Nagasaki Memorial hospital, Nagasaki, Japan, ²Orthopaedic surgery, Nagasaki University, Nagasaki, Japan.

Recent analysis of gene expression in subcutaneous and visceral adipose tissue has shown that 20 to 30% of proteins expressed in adipose tissue are associated with genes coding for secretory proteins, and that adipocytes secrete a series of physiologically active substances such as adiponectin, leptin, tumor necrosis factor alpha (TNF α), and plasminogen activator inhibitor type 1 (PAI-1), regulating vital functions [1-7]. Thus, subcutaneous and visceral adipose tissue is regarded as an endocrine organ, and its importance is emphasized. No study has investigated the physiological function of adipocytes present in the bone marrow.

In this study, we established a simple method for the primary culture of bone marrow adipocytes with a suspension culture line, and quantified adipokine gene expression and secretory proteins released in suspension.

(Subjects) The subjects were 8 patients (8 joints) with coxarthrosis or femur neck fracture, with a mean age of 72 years. Subjects comprised 1 male and 7 females. Bone marrow adipocytes were isolated from bone marrow fluid collected on prosthesis insertion.

(Methods) After bone marrow fluid was treated with an enzyme, adipocytes were isolated by centrifugation, and used as an experimental system employing the floating culture method. These adipose cells were histopathologically examined by oil red O staining and Mayer's hematoxylin staining. In addition, we investigated morphological changes in the adipocytes 7 days after dexamethazone (DEX) administration. We examined PPAR γ , adiponectin, leptin, PAI-1, and TNF α mRNA expressions by RT-PCR 24 hours after culture. Concerning adiponectin, PAI-1, and TNF α release in culture medium, we quantified protein levels by ELISA.

(Results) We confirmed that the isolated adipocytes were histologically mature, and that they comprised a uniform cell population. At the gene expression level, various adipokines were detected in all patients, as demonstrated for subcutaneous and omental adipocytes. We confirmed the secretion of adiponectin, PAI-1, and TNF α in culture medium.

Seven days after DEX administration, hypertrophic change of adipocytes was observed in comparison with the control group.

(Discussion) In this study, we initially established a method for the primary floating culture of bone marrow adipocytes. In addition, various cytokines were detected in bone marrow adipocytes, as demonstrated for subcutaneous and omental adipocytes.

This procedure may be useful for investigating mature bone marrow adipocytes.

Disclosures: A. Hozumi, None.

M474

RANKL Signaling in Human Osteoclasts: Effect of P62 Mutations. E. Chamoux¹, J. N. Couture^{*1}, B. G. Lemenchick^{*1}, J. P. Brown^{*2}, S. Roux¹. ¹Rheumatology, Faculty of Medicine, Sherbrooke, PQ, Canada, ²GRMO, CHUL Research Center, Quebec, PQ, Canada.

The discovery of mutations in Paget's disease of bone (PDB), characterized by an increased number of overactive osteoclasts (OC), has now targeted p62 as an important player in RANKL signaling. To date, all the mutations identified in p62 prevent its Ubiquitin Binding Associated (UBA) domain from being functional, thus potentially affecting its degradation and/or signaling capacities. Studies on rodent models concluded that p62 forms complexes with the atypical ζ PKC and other partners after RANKL stimulation. However, the precise role of p62 in osteoclast physiology is not clearly understood yet. For our study, we build p-EGFP-C2 plasmids containing p62 wild-type (p62^{wt}), p62 modified with the most common mutation observed in PDB patients (p62^{P392L}) and p62 with a deleted UBA domain (p62^{ΔUBA}). Human OCs differentiated from cord blood monocytes with RANKL were typically able to resorb around 15% of a bone slice surface. This area was more than 3 times larger for osteoclasts transfected with p62^{wt} or p62^{P392L}. Interestingly, OCs transfected with p62^{ΔUBA} did not resorb bone more than non-transfected OCs or OCs transfected with an empty vector. DAPI staining showed that apoptosis occurred in 44.8 \pm 6.1 % of non-transfected OCs 24h after RANKL withdrawal. Similar results were seen in OCs transfected with p62^{wt} or an empty vector. In contrast, apoptosis was decreased in cells transfected with p62^{P392L} or p62^{ΔUBA} (14.1 \pm 5.7% and 8.3 \pm 4.5% respectively), which suggests that p62 mutations increase cell survival. To better understand early events occurring after RANKL stimulation, we used an antibody recognizing ζ PKC when phosphorylated on the Ser410 (hallmark of its activation) in immunofluorescence studies. RANKL stimulation led to the relocalization of P- ζ PKC from the membrane to the perinuclear area (15 min), then within nuclei (1h). If no difference was observed in cells transfected with p62^{wt}, OCs expressing p62^{P392L} in contrast exhibited P- ζ PKC in their nuclei prior to any stimulation by RANKL, and no change was noticed after RANKL addition. We finally determined that RANKL stimulation induced an important intracellular Ca²⁺ mobilization with an amplitude of 356.5 \pm 34.4 pM Ca²⁺, which was not observed in OCs transfected with p62^{P392L}. Our results underline strong relationships between p62 mutations and modified osteoclast behavior resembling to PDB. We also provide new insights in early events occurring after RANKL stimulation of human osteoclasts, noticeably a possible constitutive activation of ζ PKC, which may help to explain the increased survival and resorption observed in mutated OCs.

Disclosures: E. Chamoux, None.

This study received funding from: CHIR.

M475

Functional Consequences of P62 Mutations in PDB Osteoclasts. J. N. Couture^{*1}, E. Chamoux¹, J. Morissette^{*2}, J. P. Brown^{*2}, S. Roux¹. ¹Rheumatology, Faculty of Medicine, Sherbrooke, PQ, Canada, ²GRMO, CHUL Research Center, Quebec, PQ, Canada.

Mutations in the gene encoding SQSTM1/p62 have been linked to Paget's disease of the bone (PDB), a chronic focal skeletal disorder characterized by an increased number of overactive osteoclasts (Ocs), but the functional consequences of these mutations still need to be understood. All the PDB-associated p62 mutations were mapped to the ubiquitin-associated (UBA) domain of the protein. Studies in rodents have shown that p62 forms complexes with signalling partners upon RANKL stimulation but its exact role in the Ocs physiology remains to be elucidated. For this study, we conducted experiments on osteoclast-like cells differentiated from peripheral blood mononuclear cells isolated from PDB patients previously identified with the p62^{P392L} mutation. We compared our results to normal human osteoclasts differentiated from cord blood monocytes (CBMs), a well established model. PDB Ocs were able to resorb cortical bone when differentiated with 25, 50 or 100 ng/mL RANKL during 21 days. The resorbed surface was at least 3 times greater than that for CBMs with the same doses of RANKL added throughout the differentiation. We hypothesized that increased cell survival may in part explain this hyper-resorption so, using DAPI staining, we evaluated PDB Ocs response to some of the major apoptotic signals for human Ocs. PDB Ocs and CBMs were deprived of growth factors for 72h, then a Fas-activating antibody (400 ng/ml), TGF β 1 (2 ng/ml), and M-CSF (25 ng/ml) were added where appropriate for 24h. 58 \pm 2.3% of CBMs vs 12.5 \pm 4.5% in PDB Ocs were apoptotic in controls. This percentage was 75.2 \pm 3.6% for CBMs in the presence of anti-Fas (400 ng/mL) vs 16.3 \pm 4.5% for PDB Ocs. In the presence of TGF β 1 (2ng/mL), apoptotic CBMs were 78.4 \pm 3.6% vs 28.9 \pm 5.6% for PDB Ocs. Finally, 25.1 \pm 5.6% of CBMs were apoptotic with M-CSF (25 ng/ml) vs 17.2 \pm 3.7% for PDB Ocs. To determine if cellular signalisation upon RANKL activation was affected, we conducted immunofluorescence studies on p62, PKC ζ and the activated form of PDK1. In non-treated cells, p62 has a cytoplasmic localisation but reaches the nuclei within 60 minutes after RANKL addition. We also observed that PKC ζ , pPDK1 were present in the nucleus of PDB Ocs prior to any stimulation. In normal human Ocs, these proteins reach the perinuclear region upon stimulation but are cytoplasmic otherwise. Together, these results strongly suggest that PDB Ocs carrying p62^{P392L} are more resistant to apoptosis and display an altered RANKL signaling compared to normal human osteoclasts. This could explain, at least in part, their functional over-activity.

Disclosures: J.N. Couture, None.

This study received funding from: CHIR.

M476

A Randomised, Active-controlled, 6-month Study of Once Weekly 280 mg Oral Buffered Alendronate Solution for Treatment of Paget's Disease of Bone. M. J. Hooper¹, A. Faustino^{*2}, I. R. Reed³, D. Hosking^{*4}, N. Gilcrest^{*5}, P. Selby^{*6}, M. Wu^{*7}, G. Salzmann^{*7}, J. West^{*7}, A. Leung^{*7}. ¹University of Sydney, Sydney, Australia, ²Servimed, Lda, Lisbon, Portugal, ³Auckland Hospital, Auckland, New Zealand, ⁴Nottingham City Hospital, David Evans Medical Research Centre, Nottingham, United Kingdom, ⁵Princess Margaret Hospital, Canterbury Geriatric Medical Research Trust, Christchurch, New Zealand, ⁶Manchester Royal Infirmary, Vitamin D Research Group, Manchester, United Kingdom, ⁷Merck & Co, Merck Research Laboratories, Rahway, NJ, USA.

Although daily doses of oral bisphosphonates are a safe and effective treatment for Paget's disease of bone (PDB), some patients may experience upper gastrointestinal adverse effects (UGI AEs) or find the dosing requirements onerous and become noncompliant. A once weekly (OW) oral dose of bisphosphonate in buffered solution (OBS) may be as effective, better tolerated and more convenient than daily dosing.

During a 6-month, randomized, double-blind, active-controlled trial, we compared an alendronate (ALN) 280-mg OW OBS with an ALN 40-mg/day tablet for treating PDB. Patients were randomized (2:1) to ALN 280-mg OW OBS or ALN 40-mg/day. The primary endpoint was the mean percent decrease in total serum alkaline phosphatase (SAP) from baseline at 6-months.

At Month 6, the mean change from baseline in SAP was -71.76% with a 95% CI of (-76.77, -65.67) in the ALN 280-mg OW OBS group and -73.18% with a 95% CI of (-79.52, -64.89) in the ALN 40-mg/day tablet group. There was no significant difference between groups during the 6-month period. There was a higher incidence of clinical AEs in the ALN 280-mg OW OBS (78.6%) vs. the ALN 40-mg/day tablet group (66.7%), including drug related AEs (47.6% and 9.5%, respectively), that led to study discontinuation (19.0% and 9.5%, respectively). There was a higher incidence of laboratory AEs in the ALN 280-mg OW OBS group (16.7%) vs. the ALN 40-mg/day tablet group (4.8%), including drug related AEs.

Although ALN 280-mg OW OBS was as safe and effective as ALN 40-mg/day in reducing SAP in patients with PDB, ALN 40-mg/day tablet appears to be better tolerated than ALN 280-mg OW OBS.

Disclosures: M.J. Hooper, Merck & Co. 2.

This study received funding from: Merck & Co.

M477

See Sunday Plenary Number S477

M478

Long-term Effects of Single Zoledronate or Neridronate Infusion in Paget's Disease of Bone. D. Merlotti, L. Gennari, F. Valleggi, V. De Paola, G. Martini, A. Avanzati*, R. Nuti. Internal Medicine, Endocrine-Metabolic Sciences and Biochemistry, University of Siena, Siena, Italy.

Aminobisphosphonates actually represent the most common treatment for Paget's disease of bone (PDB), with the potential for sustained remission. Intravenous regimens with different compounds demonstrated improved efficacy and compliance with respect to oral regimens. However, there have been few head to head randomized trials comparing intravenous bisphosphonates, and it is not demonstrated if these drugs differ in therapeutic efficacy. We recently performed a randomized study comparing intravenous pamidronate to zoledronate or neridronate in 90 subjects with active PDB. We report the results from the trial and the post-trial follow up of patients. At baseline patients were randomly assigned to receive either a 4 mg infusion of zoledronic acid (n=30) or a 30 mg infusion of pamidronate for 2 consecutive days every 3 months (n=60). After 6 months non-responders to pamidronate were crossed over to zoledronate (n=18) or neridronate (n=15, infusion of 100 mg for 2 consecutive days) treatment. Blood samples were collected at baseline and after 1, 3, 6, 12, 15, 18, and 24 months. No bisphosphonate was given after the cross-over, during the extension study. At 6 months, normal ALP levels were achieved in 93% of patients in zoledronate group and in 35% of patients in pamidronate group. Normalization of ALP levels was maintained in 79% and 65% of patients in the zoledronic acid group, after 12 and 24 months follow-up, respectively, while loss of therapeutic response was observed in 2/30 (6%) at 24 months. Among non-responders patients to pamidronate, 14/15 (93%) in the neridronate group and 17/18 (94%) in the zoledronate group achieved a therapeutic response after 6 months from the cross-over. Similar normalization rates were also observed between neridronate (80%) and zoledronate (83%) treated subjects at 6 months. Moreover, at 18 months from cross-over treatment (corresponding to 24 months from the baseline visit) ALP normalization was maintained in 60% and 77% of patients in neridronate or zoledronate group, respectively. In conclusion, single neridronate and zoledronate infusion produced a rapid and sustained control of bone turnover in up to 90% of PDB patients non-responders to pamidronate. This effect was largely independent of pre-treatment disease activity and prior bisphosphonate therapy.

Disclosures: D. Merlotti, None.

M479

Measles Virus Nucleoprotein (MVNP) Enhances NFATc1 Activation During Osteoclastogenesis in Paget's Disease. A. Sarmasik*, Y. Hiruma¹, S. Okumura*, J. P. Brown², J. J. Windle³, G. D. Roodman⁴, N. Kurihara¹, D. L. Galson¹. ¹Ctr for Bone Biol, Dept of Med, Univ of Pittsburgh, Pittsburgh, PA, USA, ²Laval Univ, CHUL Res Center, Quebec City, PQ, Canada, ³Human Genetics, Virginia Commonwealth Univ, Richmond, VA, USA, ⁴Univ of Pittsburgh & VA Pittsburgh Healthcare System, Pittsburgh, PA, USA.

The mechanisms responsible for the dramatically increased numbers of hypermultinucleated osteoclasts (OCL) in Paget's Disease (PD) are just beginning to be understood. To explore the role of the critical osteoclast transcription factor NFATc1 in PD, we determined if NFATc1 expression and activity were affected by measles virus nucleocapsid protein (MVNP), which is implicated in PD. Both OCL precursors from PD patients and normal human OCL precursors transduced with MVNP (MVNP-CFU-GM) are hyper-responsive to RANKL and form pagetic-like OCL in vitro. Furthermore, we have found that in the absence of added RANKL, both OCL precursors from PD patients and MVNP-CFU-GM have an increased amount (2-3 fold) of NFATc1 protein. Transient co-transfections of an NFAT-responsive CTR P3 promoter reporter and MVNP- and NFATc1-expression vectors into RAW264.7 cells reveal that MVNP (2 fold alone) and NFATc1 (50 fold alone) cooperate to activate the P3 reporter 250 fold. Additionally, RANKL treatment of RAW264.7 cells co-transfected with the P3 reporter and MVNP demonstrated that MVNP also cooperates with RANKL (2.5 fold alone) to activate this reporter 15 fold. However, MVNP expression could not help NFATc1 overcome lack of the key NFAT-binding site in the P3 reporter, suggesting that NFAT binding is required for MVNP to cooperate with NFAT to activate the P3-reporter. Comparative EMSA analysis of NFAT activation in osteoclastogenesis cultures using bone marrow monocytes (BMM) from wild-type and TRAP promoter-driven MVNP transgenic mice (MVNP-Tg) reveal that both TNF- α and RANKL induction of NFATc1 activation was increased in MVNP-expressing cells. However, CsA blocked MVNP + RANKL from generating multinucleated TRAP+ OCL, implying that MVNP effects require an intact NFAT activation pathway. A constitutively-active NFATc1 (caNFATc1) retrovirus can induce wild-type mouse BMM to differentiate into OCL in the absence of RANKL at a low level with increased differentiation in the presence of suboptimal levels of RANKL. caNFATc1 transduction into BMM from MVNP-Tg mice revealed cooperative enhancement of OCL differentiation by caNFATc1 and MVNP at no and suboptimal RANKL with more and larger OCLs formed than in the presence of either alone. These data demonstrate that NFATc1 is increased in PD and that MVNP can synergize with NFATc1 to upregulate OCL differentiation in PD. Hence, inhibition of NFATc1 activation may be a possible therapeutic target for PD patients.

Disclosures: A. Sarmasik, None.

This study received funding from: NIH grant P01-AR049363.

M480

Enhanced Levels of FGF-2 and SOCS Signaling Modulates RANK Ligand Expression in Patients with Paget's Disease. K. Sundaram¹, J. Senn¹, D. S. Rao², S. V. Reddy¹. ¹Children's Research Institute, Medical University of South Carolina, Charleston, SC, USA, ²Henry Ford Hospital, Detroit, MI, USA.

Paget's disease of bone (PD) is a chronic focal skeletal disorder characterized by excessive bone resorption followed by disorganized new bone formation. We previously reported measles virus nucleocapsid (MVNP) gene expression in patients with PD. MVNP expression in osteoclast lineage results in Pagetic phenotype in osteoclasts and suggested a pathophysiologic role for MVNP in PD. Enhanced levels of IL-6, M-CSF and endothelin-1 have been associated with PD, and are implicated in pathogenesis. Also, RANK ligand (RANKL), a critical osteoclastogenic factor expressed on marrow stromal/osteoblast cells is upregulated in PD. We have recently demonstrated that heat shock factor-2 (HSF-2) is a downstream target of fibroblast growth factor-2 (FGF-2) to induce RANKL expression in stromal/preosteoblast cells. In this study, we hypothesized that FGF-2 modulates suppressors of cytokine signaling (SOCS) levels to induce RANKL gene expression in PD. We found a significant increase (2.5-fold) in serum FGF-2 levels in patients (n=8) with PD compared with normal subjects (n=10). These results are consistent with previous reports that FGF-2 mRNA expression is elevated in pagetic osteoclasts and bone marrow cells. Interestingly, conditioned media obtained from MVNP transduced normal human bone marrow cells showed a significant increase (3.2 -fold) in the level of FGF-2 compared to empty vector transduced cells. Confocal microscopic analysis further demonstrated that MVNP conditioned media (20%) stimulates HSF-2 nuclear translocation in normal human bone marrow stromal/preosteoblast cells, which was blocked by a neutralizing antibody against FGF-2. We further show that FGF-2 stimulation increased SOCS-1 mRNA (5.2-fold) expression in these cells. We next examined if SOCS play a role in FGF-2 signaling to modulate RANKL gene expression in PD. Real-time PCR analysis demonstrated a significant increase in the levels of SOCS-1 (3.4-fold) and SOCS-3 (3.5-fold) mRNA expression in pagetic bone marrow mononuclear cells compared to normal subjects. In addition, co-expression of SOCS-1 with hRANKL gene promoter-luciferase reporter plasmid in marrow stromal cells demonstrated a significant increase (3.0-fold) of RANKL gene promoter activity without FGF-2 stimulation. These data suggest that enhanced levels of SOCS expression, FGF-2 signaling and cross-talk mechanisms may play an important role in modulating RANKL gene expression in PD. The identification of SOCS and FGF-2 involvement in RANKL gene expression may lead to novel therapeutic targets to control excessive bone turnover in PD.

Disclosures: K. Sundaram, None.

This study received funding from: NIH.

M481

Cardiovascular Manifestations of Primary Hyperparathyroidism. J. Fleischer, M. D. Walker, S. Homma*, T. Rundek*, W. Inabnet*, D. J. McMahon, A. Tineo*, R. Liu*, R. Sacco*, S. J. Silverberg. Columbia University, New York, NY, USA.

Severe primary hyperparathyroidism (PHPT) is associated with cardiovascular (CV) calcification and increased CV mortality. We initiated this prospective observational study of patients who meet NIH surgical criteria and undergo surgery (PTX) to determine whether the mild, frequently asymptomatic PHPT seen today still poses a risk to the CV system, and whether identified abnormalities are reversible. Patients are evaluated pre-PTX and for 2-yr post-PTX. Baseline data on the first 29 patients (72% female; age \pm SD 61 \pm 7 yrs, range: 48-75) and 1 yr post-PTX data (n=5) are available. Baseline serum calcium was 10.5 \pm 0.6 mg/dl and PTH 121 \pm 50 pg/ml. Blood pressure was 121 \pm 15/ 75 \pm 11 mm Hg. Structural changes typical of classical PHPT were uncommon: 5 had valvular calcifications and 4 had increased left ventricular (LV) mass. LV function and wall motion were normal in all. Carotid ultrasound showed plaque in 11 (38%). Carotid intima-medial thickness (IMT), a subclinical marker of atherosclerosis was 0.98 \pm .10 mm in the 75th (\pm 12) percentile of an age/sex/race matched control population. While structural abnormalities were uncommon, functional tests of the heart (diastolic function by mitral pulse wave velocity, deceleration time, tissue doppler E velocity), peripheral vasculature (endothelial function by brachial artery flow-mediated dilation, FMD) and carotid (distensibility [Table]) were revealing. Carotid stiffness and FMD were abnormal. In this small group, FMD improved (4.8 \pm 4.9 to 8.5 \pm 11.7, p=0.08) after PTX. Although mean values for other measures of CV function were normal, 27/29 (93%) had at least one test and 16/29 (55%) had 2 or more tests outside the normal range.

Functional CV Tests			
Functional CV Test	Mean \pm SD	Normal Range	# Abnormal
Mitral Pulse Wave E/A	1.1 \pm .44	.75-1.5	10 (34%)
Deceleration Time (msec)	157.3 \pm 26	>140	8 (28%)
Tissue Doppler E Velocity (cm/sec)	12.3 \pm 3	<15	7 (24%)
FMD (%)	4.8 \pm 3.7	6-10%	19 (66%)
Carotid STRAIN (%)	9.2 \pm 2.9	6-12%	4 (14%)
Carotid STIFFNESS	6.7 \pm 3.4	< 6	14 (48%)

Higher PTH levels were associated with decreased vascular compliance (carotid stiffness: R = 0.37, p=.07; and strain R = -0.61, p=.0009), while serum calcium levels did not predict any CV measures.

In summary, these patients with mild PHPT had abnormal endothelial function and increased carotid stiffness, both of which are risk factors for CV events. Vascular compliance was lowest in those with highest PTH levels. Although the structural CV hallmarks of severe PHPT were not commonly seen, 93% of patients with mild disease had one or more functional CV abnormalities, some of which may improve with PTX. Confirmation and extension of these findings could alter the guidelines for management of PHPT.

Disclosures: J. Fleischer, None.

M482

See Sunday Plenary Number S482

M483

Vitamin D Status Is Inversely Associated with Blood Pressure: Results from the Third National Health and Nutrition Examination Survey. S. E. Judd¹, H. M. Blanck^{*2}, M. S. Nanes³, T. R. Ziegler^{*3}, P. W. F. Wilson^{*3}, V. Tangpricha³. ¹Graduate Division of Biological and Biomedical Sciences, Emory University, Atlanta, GA, USA, ²Division of Nutrition and Physical Activity, Centers for Disease Control and Prevention, Atlanta, GA, USA, ³School of Medicine, Emory University, Atlanta, GA, USA.

The prevalence of both hypertension and vitamin D insufficiency are high in the United States. Recent clinical trials and animal studies have suggested that vitamin D insufficiency may be associated with elevated blood pressure. Using cross-sectional data, we sought to determine whether 25(OH)D levels were related to systolic blood pressure in the National Health and Examination Survey (NHANES) III (1988-1994). We excluded individuals currently taking anti-hypertensive medications to minimize the confounding of blood pressure treatment. This study was conducted in adult blacks and whites with available serum 25(OH)D determinations (N=7699). Blood pressure was classified using the 5 categories from the Joint National Committee 7 with a sixth category added to distinguish normotensives (<110 mmHg) from those with high-normal blood pressure (110-119 mmHg). We used predicted marginals to estimate the conditional means of serum 25 hydroxy vitamin D [25(OH)D] and to test for trend across blood pressure categories. Lower 25(OH)D concentrations were significantly associated with a higher blood pressure category in whites (p<0.001). This trend held upon stratification by age, gender, and BMI except in persons <50 years old. Such an association was not seen in black individuals; however, 92% were vitamin D insufficient, thus limiting the range of values with which to detect an association. Vitamin D insufficiency is associated with higher blood pressure in U.S. whites. Such an association was not seen in U.S. blacks given a higher prevalence of vitamin D insufficiency in this population. These data suggest the need for greater testing, detection and treatment of vitamin D insufficiency in U.S. adults for potential cardiovascular benefits. Further, these data suggest a strong interaction between vitamin D and hypertension suggesting that vitamin D repletion may be beneficial in lowering blood pressure.

Disclosures: S.E. Judd, VA Foundation Grant 2.
This study received funding from: VA Foundation Grant.

M484

See Sunday Plenary Number S484

M485

Molecular Analysis of Histologically Atypical Parathyroid Adenomas: Incipient Malignancies or Fundamentally Benign? K. B. Lauter¹, L. J. Krebs^{*1}, M. R. Rubin², G. G. Fernandez-Ranvier^{*3}, O. H. Clark^{*3}, S. J. Silverberg², A. Arnold¹. ¹University of Connecticut School of Medicine, Farmington, CT, USA, ²Columbia University College of P&S, New York, NY, USA, ³UCSF/Mt.Zion Medical Center, San Francisco, CA, USA.

Whether atypical parathyroid adenomas represent an early stage of parathyroid carcinoma or are fundamentally benign neoplasms is unknown. Atypical parathyroid adenomas possess histological features commonly found in parathyroid cancer (e.g. fibrous bands, mitoses), but lack the definitive diagnostic criteria of distant metastases or invasion of surrounding structures. Mutations of the HRPT2 tumor suppressor gene, encoding parafibromin, are common in clear-cut parathyroid carcinomas and are rare in typical benign parathyroid adenomas. Thus, analysis of non-familial atypical adenomas for HRPT2 mutations could provide insight into their nature and malignant potential.

We examined 13 sporadic atypical adenomas for HRPT2 mutations by direct sequencing of the full 17-exon coding region and splice sites, and for parafibromin expression by immunohistochemistry using antibody 2H1 (Santa Cruz). We found no HRPT2 mutations in any of the 10 fully sequenced atypical adenomas, in striking contrast to the >75% prevalence of inactivating HRPT2 mutations previously detected in definite parathyroid malignancies using identical methodology. Moreover, parafibromin staining was performed in 12/13 atypical adenomas and was strongly or largely positive as quantified with ImageJ software in all 12. This pattern was similar to the positive staining in 21 typical parathyroid adenoma controls and markedly contrasted with the reduced parafibromin staining we observed in three metastatic/invasive parathyroid carcinoma controls.

The absence of detectable HRPT2 inactivating mutations, supported by parafibromin expression patterns, strongly suggests that most non-familial atypical adenomas are fundamentally different from parathyroid carcinomas and, despite their suspicious histologic features, may not share the latter's malignant potential. Our results imply a biological validity for using stringent criteria in defining parathyroid cancer, and suggest caution when considering post-surgical adjuvant therapies for patients with atypical tumors. Our findings also raise the possibility that HRPT2 inactivation might be crucial for conferring the capacity to invade surrounding tissues or to metastasize, whereas histologic features like fibrous bands and mitoses may occur in the absence of HRPT2 inactivation. In summary, disparate patterns of HRPT2/parafibromin status suggest a fundamental difference between atypical sporadic parathyroid adenomas and carcinomas.

Disclosures: K.B. Lauter, None.

M486

Intravenous Administration of Pamidronate Decreases Serum Levels of FGF23 Rapidly in Patients with Osteogenesis Imperfecta. T. Kitaoka¹, N. Namba¹, K. Miura^{*1}, T. Kubota¹, H. Hirai^{*1}, S. Nakajima¹, T. Yamamoto², K. Ozono¹. ¹Department of Pediatrics, Osaka University Graduate School of Medicine, Suita, Osaka, Japan, ²Department of Pediatrics, Minoh City Hospital, Minoh, Osaka, Japan.

Background: Fibroblast growth factor 23 (FGF23) is a recently discovered phosphate (P)-regulating factor responsible for several disorders associated with hypophosphatemia. FGF23 decreases renal P reabsorption by down-regulating sodium P cotransporter type IIa and 25-hydroxyvitamin D-1-alpha-hydroxylase. However, the details of FGF23 regulation and action remain unclear. In this study, we examined the change of FGF23, P, calcium (Ca) and Ca-regulating hormones during the treatment of pamidronate for patients with osteogenesis imperfecta (OI). Subjects & Methods: Six patients with OI (1.4 to 12.1 year old) were included in the study. All patients were treated cyclically with pamidronate for 3 consecutive days, according to the protocol reported by Rauch et al (J Clin Invest 2002). No other medications were taken during intravenous administration. Blood samples were collected at pre- and post-drip infusion of pamidronate at the first and second cycle of treatment. We evaluated the time-course of serum Ca, P, intact PTH (iPTH), 1,25-dihydroxyvitamin D (1,25(OH)₂D) and intact FGF23 (iFGF23) (ELISA, Kainos Laboratories, inc.) values on each cycle. Written informed consent was obtained from the parents. Results: During the first cycle of treatment, serum Ca levels decreased significantly from day 2 post-infusion (-0.84 mg/dl, p<0.05), and serum P levels also decreased from day 1 post-infusion (-0.77 mg/dl, p<0.05). Both iPTH and 1,25(OH)₂D levels increased significantly from day 3 pre-infusion (+140.2 pg/ml and +31.0pg/ml, respectively). In contrast, serum iFGF23 levels decreased from day 2 pre-infusion (-6.75 pg/ml, p<0.05). During the second cycle, iFGF23 declined from the day 1 post-infusion, while serum Ca and P decreased significantly from day 3 pre- and day 1 post-infusion, respectively. Discussion: The reduction in serum Ca and P levels following pamidronate infusion was associated with the inhibition of bone resorption. Interestingly, FGF23 decreased rapidly after pamidronate infusion. It is feasible that the hypophosphatemia attenuated the levels of FGF23. However, it is also possible that pamidronate may directly suppress FGF23 secretion as well as bone resorption, since the decrease in FGF23 at times preceded hypophosphatemia.

Disclosures: T. Kitaoka, None.

M487

See Sunday Plenary Number S487

M488

A Severe Hypertension: A Possible Complication of McCune-Albright Syndrome. Y. Ohata^{*1}, T. Yamamoto¹, T. Michigami², K. Satomura^{*3}, S. Ida^{*3}, K. Ozono⁴. ¹Pediatrics, Minoh City Hospital, Minoh, Japan, ²Bone and Mineral Research, Osaka Medical Center and Research Institute for Maternal and Child Health, Izumi, Japan, ³Pediatrics, Osaka Medical Center and Research Institute for Maternal and Child Health, Izumi, Japan, ⁴Pediatrics, Osaka University Graduate School of Medicine, Suita, Japan.

We describe a female case of McCune-Albright syndrome (MAS) complicated by severe hypertension. She had a previous history of Cushing syndrome and was undertaken surgical removal of bilateral adrenal glands when she was 10 months old. An activating mutation of the Gsα protein (Arg 201 to His) was proved in the stored frozen adrenal tissues. We first observed severe hypertension with the systolic blood pressure of 240 mmHg when she was 9 years old. Laboratory investigation revealed that the levels of serum calcium and phosphate were low (8.5 mg/dl, and 2.9 mg/dl, respectively), and serum alkaline phosphatase was extremely high (8720 U/l). Then, urinary excretion levels of norepinephrine and dopamine were extremely increased by 10 and 4 folds compared to the average levels of the age matched controls respectively. Meta-iodobenzylguanidine (MIBG) scintigraphy proved neither pheochromocytoma nor the residual adrenal glands. Iatrogenic hypertension by the supplemental mineral corticoid was implausible because of the normal plasma rennin activity. Hypertension was ameliorated gradually by the combination therapy of several antihypertensive medications including an angiotensin receptor blocker, a calcium blocker, an alpha blocker and diuretics. Since the Gsα protein regulates the norepinephrine synthesis in the sympathetic nodes, it is plausible that an activating mutation of the Gsα protein in MAS complicated by a Cushing syndrome is associated with the cause of hypertension due to the overproduction of norepinephrine, because both of the sympathetic nodes and the adrenal glands in medulla have the similar origins in the process of embryological development. Also this rare case suggested the possible role of Gsα genes in the primary hypertension.

Disclosures: Y. Ohata, None.

M489

See Sunday Plenary Number S489

M490

Acro-osteolysis and Calcinosis - Possible Role of the Sympathetic Nervous System (SNS) in Pathogenesis and Treatment with Beta-blockers. M. Patel¹, C. Senger², P. Malleson², S. Ichikawa³, M. J. Econs³, K. Mulpuri². ¹Medical Genetics, University of British Columbia, Vancouver, BC, Canada, ²University of British Columbia, Vancouver, BC, Canada, ³Indiana University, Indianapolis, IN, USA.

A 9 year old healthy girl presented with a 1.5 year history of idiopathic, progressive distal acro-osteolysis of all toes. Dystrophic calcification of adjacent soft tissues caused swelling and pain with periodic rupture of a whitish chalky substance through the dorsal skin of the toes. These findings were associated with slightly tight distal phalangeal skin and distal erythema of the fingers and toes. No systemic abnormalities of bone or mineral ion homeostasis were present, no serologic or histologic findings consistent with rheumatologic disease were present and sequencing of the GALNT3 and FGF23 genes did not reveal mutations in the coding regions or at the intron-exon boundaries. Surgical decompression of one toe demonstrated homogeneous calcification surrounded by reactive macrophages. Analysis of a remnant distal phalanx demonstrated abundant periosteal osteoclasts and absence of osteoblasts. As the cellular findings in bone were consistent with hyperactivation of the SNS, the patient was started on 1.5 mg/kg/day propranolol. This was increased every 2 weeks until beta-blockade occurred, confirmed by an absence of exercise-induced tachycardia, at a final dose of 9 mg/kg/day. Treatment for one year was associated with regression of nascent calcification, arrest of osteolysis and partial regrowth of actively resorbing distal phalanges. The biopsied phalanx re-grew and showed no recurrence of acro-osteolysis on treatment.

Disclosures: M. Patel, None.

M491

Low Total and Bioavailable Testosterone Does Not Play a Role in Renal Bone Disease in Men on Hemodialysis. U. Gruntmanis¹, C. V. Odvina², K. Sakhaee², J. E. Zerwekh². ¹Department of Medicine, Division of Endocrinology, UT Southwestern Medical Center and Dallas Veterans Affairs Medical Center, Dallas, TX, USA, ²Center for Mineral Metabolism and Clinical Research, UT Southwestern Medical Center, Dallas, TX, USA.

In previous studies as many as 60% of men on hemodialysis (HD) are found to be hypogonadal. Yet role of low testosterone in complex pathogenesis of renal bone disease has not been defined. In this cross-sectional study our primary goal was to determine if men on HD with low total testosterone (testosterone below 300 ng/dl) have lower BMD than eugonadal men. Second goal was to find out if there is a difference between serum bone formation and resorption markers (bone specific alkaline phosphatase (BSAP), osteocalcin (OC), type 5b tartrate-resistant acid phosphatase (TRAP5b)) between hypogonadal and eugonadal men on HD. Only BSAP and TRAP5b are not dialyzable and therefore are good markers of bone turnover for this population. We analyzed data on 83 men, 52 African Americans, 20 Hispanic, 9 Caucasians and one Indian American. 50 and 33 men were eugonadal and hypogonadal, respectively. Mean age 52.8±8.2, weight 187.6±40.8 lbs, HD length 30.8±26.1 month and was not different between hypogonadal and eugonadal groups.

Results: BMD at lumbar spine (LS), femoral neck (FN), total hip (TH), distal forearm (DF) and BSAP, TRAP5b, OC levels were not different between hypogonadal and eugonadal groups. 43.8% and 82.1% of men were found to be vitamin D deficient (25-D <20ng/ml) or insufficient (25-D<30ng/ml), yet low 25 hydroxy vitamin D (25-D) level did not correlate with intact PTH, BMD at LS, FN, TH, DF and BSAP, TRAP5b, OC levels in our study.

Length of HD did not correlate with weight, total testosterone, bioavailable testosterone, estradiol, 25-D, BMD or bone turnover markers. Weight had very strong positive correlation for BMD at LS (p=0.01), FN (p<0.0001), TH (p<0.0001) and DF (p=0.068) but negative correlation for BSAP (p<0.009), TRAP5b (p<0.03), OC (p=0.4). Intact PTH (i-PTH), had positive correlation with BSAP (p=0.001), OC (p<0.0001), TRAP5b (p=0.08). BSAP as expected, had negative correlation with BMD at TN (p=0.02), DF (p=0.05), but no correlation at FN (p=0.08), LS (p=0.3). TRAP5b also had negative correlation with BMD at FN and TN (p=0.04) but no correlation at DF (p=0.49) and LS (p=0.07).

Conclusions: Total testosterone level does not appear to play significant role in renal bone disease in our study population. We postulate that men on HD who are heavier have lower bone formation and resorption and as a result have higher BMD. This observation did not change after results were adjusted for total testosterone, bioavailable testosterone, estradiol, i-PTH, 1,25-D and 25-D levels.

Disclosures: U. Gruntmanis, None.

This study received funding from: National Osteoporosis Foundation and GCRC USPHS grant M01-RR00633.

M492

Administration of Pravastatin Inhibits Suppressed Osteoblast Dysfunction and Bone Turnover in Uremic Rats. Y. Iwasaki^{*1}, H. Yamato², M. Fukagawa³. ¹Health Sciences, Oita University of Nursing and Health Sciences, Oita, Japan, ²Development, Kureha Special Laboratory Co, Ltd., Fukushima, Japan, ³Nephrology & Dialysis center, Kobe University School of Medicine, Kobe, Japan.

HMG-CoA reductase inhibitors (statins) are widely used for treatment of hypercholesterolemia. Recent studies reveal that statins stimulate bone formation and suppress bone resorption. To evaluate the effect of pravastatin, which is a major statin, on bone formation in low-turnover bone disease with renal failure, we demonstrated bone histomorphometry on our model rats which have low turnover bone. Male SD rats underwent thyroparathyroidectomy (TPTx). The TPTx rats underwent 5/6 nephrectomy (Nx) or sham operations. These rats were continuously infused with rat PTH and injected with L-thyroxine subcutaneously to maintain physiological levels. TPTx-Nx rats simulate adynamic bone disease which is a major type of renal osteodystrophy in chronic dialysis patients. Six weeks after the second Nx, TPTx-Nx rats were assigned to receive pravastatin (Daiichi-Sankyo, Co, Ltd., Japan) at a dosage of 3 or 30 mg/kg body weight per day or vehicle in the diet. By bone histomorphometry, bone formation rate in the TPTx-Nx with vehicle group was reduced to 8% of the TPTx-Sham group. The reduction of bone turnover was ameliorated by pravastatin administration in a dose dependent manner. In the high dose group, the level of osteoblast surface recovered was up to 40% of the TPTx-Sham group. The Serum biochemical parameters, including lipid metabolic parameters, did not change among all the groups. Gene expression of organic anion transporter (OAT)-3, which mediates cellular uptake of pravastatin, was expressed in rat tibiae. In vitro study, we also determined the effect of co-culturing with pravastatin and indoxyl sulfate (IS), which is one of the uremic toxins, on cultured primary osteoblasts. It is known that IS is taken up via OAT-3 and increases free radical production and suppresses cell viability. Free radical production induced by the addition of IS was decreased in the presence of pravastatin in primary cultured osteoblasts. Suppressed osteoblasts cell viability ameliorated in a dose dependent manner. OAT-3 mRNA was expressed in cultured osteoblast. These results suggest that pravastatin ameliorates bone turnover, induced at least in part by suppressed intracellular free radical production and improve osteoblast function.

Disclosures: Y. Iwasaki, None.

M493

See Sunday Plenary Number S493

M494

Tartrate-Resistant Acid Phosphatase Isoforms in End-Stage Renal Disease. A. Jancikla¹, B. Price^{*2}, E. Lederer², L. Yam^{*1}. ¹Medicine, VA Medical Center, Louisville, KY, USA, ²Medicine, University of Louisville, Louisville, KY, USA.

End-stage renal disease (ESRD) is often complicated by chronic inflammation and osteodystrophy. Tartrate-resistant acid phosphatase (TRACP) isoforms 5a and 5b may be suitable serum markers to gauge inflammation and bone resorption respectively.

Methods: Serum was collected from 73 patients (38 male, 35 female) with ESRD just prior to hemodialysis. The mean age was 56±16 years and the mean time on dialysis was 6±5 years. A control group consisted of 36 healthy adults (8 male, 28 female) aged 43±11 years. TRACP 5a and 5b isoforms were estimated by in-house immunoassays. C-reactive protein was estimated by an in-house, high-sensitivity assay using commercially available antibodies and standards. Commercial kits were used to estimate other inflammation and bone markers including fetuin-A, bone-specific alkaline phosphatase (bALP) and cross-linked N-telopeptides of type-I collagen (NTx). Intact parathyroid hormone (iPTH) levels were determined by radioimmunoassay. Bone mineral density (DEXA of calcaneus) was determined at the time of study.

Results: Mean levels of all serum markers were significantly elevated in ESRD except fetuin-A, which was significantly lower than control. Absolute BMD (g/cm²) was no different than control, but the mean T-score was significantly lower in ESRD. TRACP 5a protein correlated with CRP but not fetuin-A or any other bone marker. CRP and fetuin-A were inversely correlated. TRACP 5b correlated positively with all bone markers and inversely with BMD, but not with any inflammation marker. Neither iPTH nor NTx were significantly associated with BMD.

Conclusion: These preliminary data suggest that TRACP isoforms 5a and 5b may be useful markers to estimate the degree of inflammation and bone resorption respectively in ESRD patients on chronic hemodialysis.

Disclosures: A. Jancikla, None.

M495

Albuminuria Predicts Bone Loss in Older Adults: The Rancho Bernardo Study. S. K. Jassal^{*1}, D. von Muhlen², E. Barrett-Connor². ¹Medicine, UCSD & VASDHS, San Diego, CA, USA, ²Family and Preventive Medicine, UCSD, San Diego, CA, USA.

Purpose: There is interest in the association between kidney function and bone health, but prior studies have focused on estimates of creatinine clearance or glomerular filtration rate as predictors. We investigate the cross-sectional and longitudinal association between albuminuria and bone mineral density (BMD), bone loss, and osteoporotic fracture in older community-dwelling adults.

Methods: A cross-sectional and prospective study from the Rancho Bernardo Study. Between 1992 and 1995, 1713 participants (average age 71.3 +/- 11.1 years) completed standardized questionnaires, physical examinations, laboratory testing and bone densitometry; 1023 participants returned for a follow-up visit in 1997-1999, an average of 4.1 (+/-0.9) years later.

Results: Using previously established sex-specific cut-offs, albuminuria (urine albumin/creatinine ratio (ACR) $\geq 17\text{mg/g}$ in men and $\geq 25\text{mg/g}$ in women) was present in 148 men (22%) and 143 women (13.8%) at baseline. In cross-sectional analyses, there was a significant linear association between log transformed ACR (log ACR) and hip BMD in men (Beta (SE) = -0.021 (0.010), $p = 0.034$) and women (Beta (SE) = -0.053 (0.008), $p < 0.001$). These associations were no longer significant after adjusting for age and body mass index (BMI). In prospective analyses, there was an average annual bone loss at the hip of 0.6%. There was a significant association between baseline log ACR and four-year bone loss in men (Beta (SE) = -0.237 (0.089), $p = 0.008$) and women (Beta (SE) = -0.332 (0.0110), $p = 0.003$). These associations persisted after adjusting for age and BMI in both men (Beta (SE) = -0.212 (0.010), $p = 0.018$) and women (Beta (SE) = -0.254 (0.014) $p = 0.026$). At baseline, 180 of 1713 participants (11%) reported at least one clinical fracture of the hip, femur, forearm or wrist; 79 (8%) reported at least one new clinical fractures during follow-up. Log ACR was associated with prevalent clinical fractures in women OR (95% CI) = 1.67 (1.19-2.35), but this did not persist after adjusting for age and BMI. Log ACR was not significantly associated with incident clinical fractures.

Conclusions: ACR was not independently associated with hip BMD in cross-sectional analyses. Baseline ACR, however, predicted four-year bone loss at the hip in both sexes independent of age and BMI. Baseline ACR was associated with prevalent but not with incident clinical fracture, perhaps reflecting the multifactorial etiology of fractures beyond BMD.

Disclosures: S.K. Jassal, None.

This study received funding from: Grant AG07181 from the National Institute on Aging and Grant DK31801 from the National Institute of Diabetes and Digestive and Kidney Diseases. Procter & Gamble Pharmaceuticals Unrestricted Educational Grant.

M496

Osteopenia and Lipodystrophy in HIV-infected Patients. S. Azriel^{*1}, R. Rubio^{*2}, H. Requejo^{*1}, S. Guadaliu^{*1}, E. Jódar¹, G. Martínez¹, F. Hawkins¹. ¹Endocrinology Service, University Hospital 12 de Octubre, Madrid, Spain, ²HIV Unit, University Hospital 12 de Octubre, Madrid, Spain.

Reduced bone mineral density (BMD) and abnormalities in fat redistribution, glucose homeostasis and lipid metabolism are prevalent among HIV-infected patients on highly active antiretroviral therapy (HAART). The relationship between BMD and changes in regional and whole body composition is unclear.

Patients and methods: This was a prospective cohort study. One hundred HIV-infected caucasian outpatients were recruited during a period of 24 months and were studied over 2 years of follow-up. Exclusion criteria were any condition that could cause loss of BMD and use of medications that interfere with mineral metabolism in the past 6 months. 68% of the patients were males, mean age of the cohort was 40 years (SD: 9), mean BMI was 24 kg/m² (SD: 3.6), 95% had undetectable virus load. 77% were taking a HAART regimen (65% included a protease inhibitor), 18% bitherapy (2 nucleoside reverse-transcriptase inhibitors) and 5% were ART-naïve. BMD (lumbar spine, femoral neck, total hip and radius) and body composition (total body fat mass, percent total fat, trunk fat mass, percent trunk fat, lean mass) were assessed by DXA Hologic QDR 4500. Osteopenia/osteoporosis (op/OP) was defined according to WHO criteria. Lipodystrophy was classified according to clinical criteria (patient's self report and physician's evaluation).

Results: The prevalence of op (at any site) in the cohort was 63.6% and 13.1% of OP. Alterations in body fat distribution were described in 38% of the patients: 35% lipoatrophy, 16% lipohypertrophy and 13% mixed anomalies. In the univariate statistical analysis, patients with low lumbar spine BMD (< -1 SD T-score) showed lower total (kg) and % body fat mass ($p = 0.06$ and $p = 0.049$, respectively), and trunk fat mass (kg, %; $p = 0.039$ and $p = 0.047$). Patients with low femoral BMD (at the femoral neck and total hip) also had lower total body fat mass ($p = 0.013$ and $p = 0.003$, respectively). There was no independent association between op/OP and type or duration antiretroviral therapy and lipodystrophy at any site. In the multivariate logistic regression analysis, the total body fat mass was a protective factor for bone loss at lumbar spine [OR: 0.89, 95% CI: 0.82-0.96, $p = 0.003$, for each additional kg]. No significant changes in BMD and in body composition were found after 2 years of follow-up.

Summary: Prevalence of op in HIV-infected patients is high, irrespective of the antiretroviral therapy. Lumbar op is associated with low total body fat mass. Op does not progress after 24 months.

Disclosures: S. Azriel, None.

This study received funding from: Fundación Mutua Madrileña (project n° 2005-072).

M497

Anti-TNF Treatment in Rheumatoid Arthritis Patients Does Not Alter the 1-Year Change in Spine and Hip Bone Mineral Density Compared to Control Patients. P. Boyesen^{*1}, E. Haavardsholm^{*1}, G. Haugeberg^{*2}, T. Kvien¹. ¹Dept of Rheumatology, Diakonhjemmet sykehus, Oslo, Norway, ²Dept of Rheumatology, Sørlandet hospital, Kristiansand, Norway.

An increased bone loss is observed in rheumatoid arthritis (RA) patients. Observational uncontrolled studies have suggested that anti-TNF treatment counteract this loss. The aim of this study was to compare one-year change in hip and spine bone mineral density (BMD) between RA patients receiving anti-TNF treatment and historical RA controls.

Twenty-nine RA patients with clinically active disease starting with anti-TNF treatment were included in the intervention group and 253 RA patients were identified as controls from the Oslo RA register. The controls were matched on a group level for disease duration and age. The BMD of hip and spine was measured by dual energy x-ray absorptiometry (DXA) on the same Lunar Expert machine. The anti-TNF group was examined at baseline and 12 months, the controls were assessed in 1996 and 1998 as part of an epidemiologic study.

Mean (SD) age was 52 (6.2) and 55 (6.2) years in the anti-TNF group and control group respectively, disease duration 10 (6.2) and 10 (6.2) years, 82% and 83% were females, 90% and 49% were rheumatoid factor (RF) positive, mean (SD) disease activity score (DAS-28) was 5.3 (1.3) and 4.7 (1.1), Modified Health Assessment Questionnaire (MHAQ) score 1.7 (0.5) and 1.6 (0.4), ESR 31.8 (19.6) and 21.4 (15.8) mm/hr and 28-swollen joint count 9.8 (5.6) and 8.4 (6.0). The only group differences were RF ($p < 0.001$), ESR ($p = 0.02$) and DAS-28 ($p = 0.01$) (Chi square, t-test). 45% and 42% used disease modifying anti-rheumatic drugs, 14% and 22% estrogens and/or bisphosphonates, 52% and 45% were currently using corticosteroids in the anti-TNF group and control group respectively (Chi square test).

At inclusion 55% and 39% were osteopenic, 3% and 13% osteoporotic in the anti-TNF group and the control group respectively. Annual BMD change was computed. BMD of spine and hip were similar between the groups at baseline (t-test). The one-year change was not statistically significant different between the groups. The mean (SD) change in total hip BMD was -0.9% (3.3) and -0.2% (2.6) ($p = 0.17$) and the spine BMD (L1-L4) -1.0% (5.1) and -0.2% (2.8) ($p = 0.17$) for the anti-TNF group and control group respectively. The hip BMD results remained unchanged when correcting for sex, RF, corticosteroids, bisphosphonates, DAS-28 and MHAQ (regression analysis). The adjusted change in BMD at the spine showed an association between increased loss in BMD and anti-TNF treatment ($p = 0.047$).

In conclusion the one-year bone loss of the hip and spine was similar in RA patients treated with anti-TNF and historical RA controls. This finding may suggest that the mechanisms of bone loss in established RA are not halted by TNF blockade.

Disclosures: P. Boyesen, None.

M498

See Sunday Plenary Number S498

M499

Small Molecule Inducer of Activated CD4+ T Cell Death Inhibits Disease Progression in Collagen-induced Arthritis Models. J. Han^{*1}, H. Sung^{*1}, J. Park^{*1}, S. Lim^{*2}, S. Lee^{*2}, S. Cho^{*3}, H. Kim^{*3}, S. Shim^{*2}, S. Kim¹, S. Ko⁴, S. Chang^{*1}, J. Kim^{*1}. ¹Pharmacology, OSCOTEC Inc., Cheonan, Republic of Korea, ²Medicinal Chemistry, OSCOTEC Inc., Cheonan, Republic of Korea, ³Pharmacokinetics, OSCOTEC Inc., Cheonan, Republic of Korea, ⁴Oral Biochemistry, Dankook University, Cheonan, Republic of Korea.

Rheumatoid arthritis (RA) is a chronic, systemic, inflammatory autoimmune disorder that affects 1% of the adult population worldwide. RA is characterized by the inflammation of synovial joints infiltrated by CD4+ T cells, macrophages, and plasma cells that play major roles in the pathogenesis of the disease. CD4+ T cells responding to an unknown antigen activate macrophages to produce pro-inflammatory cytokines. Therefore, selective elimination of activated CD4+ T cells, but not naive cells, may slow down disease progression with minimum toxicity. To identify small molecules that selectively induce activated CD4+ T cell death, high-throughput screening (HTS) was conducted on 5,680 compounds. From the Hit compound identified from HTS, we generated lead compound (TCK-O-1). TCK-O-1 was found to induce activated T cell death in a dose-dependent manner. The cytotoxic effects of TCK-O-1 to naïve splenocytes were observed only at high concentrations ($> 10\mu\text{M}$), while selective killing effects on activated CD4+ T cells (up to 60 percent) were observed at low concentrations ($< 3\mu\text{M}$). In addition, TCK-O-1 did not show cytotoxic effect on other immune effector cell lines. To examine the effect of TCK-O-1 on disease progression in RA, time course studies were conducted in collagen induced arthritic (CIA) mice. TCK-O-1 was orally (40mg/kg) or subcutaneously (10mg/kg) administered to CIA mice, once a day for 21 days. Administration of TCK-O-1 significantly suppressed the arthritic index and inhibited the activated CD4+ T cell ratio in peripheral blood mononuclear cells (PBMC), but not other immune cells. Therefore, administration of TCK lead compound effectively inhibited disease progression with minimum toxicity. These results suggest that small molecule inducer of activated CD4+ T cell death may be used for the treatment of rheumatoid arthritis. TCK-O-1 is under development as candidate molecules in search for new anti-rheumatoid arthritis drugs.

Disclosures: S. Chang, None.

M500

Can We Predict Structural Damage Progression at 2 Years in Very Early Arthritis? Value of Bone and Cartilage Markers in the Conservatively Treated Community-based Inceptive VERA Cohort. A. Daragon¹, M. Brazier^{*2}, C. Fèvre^{*1}, R. Daveau^{*3}, O. Mejjad^{*1}, P. Boumier^{*4}, A. Gayet^{*5}, F. Tron^{*3}, C. Zarnitsky^{*6}, O. Vittecoq^{*7}, X. Le Loët^{*7}. ¹Rheumatology, CHU - Hôpitaux de Rouen, Rouen, France, ²Rheumatology, CHU, Amiens, France, ³Immunology Laboratory, Inserm U 519, Rouen, France, ⁴College of Rheumatology Picardie, Amiens, France, ⁵College of Rheumatology Haute Normandie, Rouen, France, ⁶Rheumatology, Groupe Hospitalier, le Havre, France, ⁷Rheumatology, CHU - Hôpitaux de Rouen, Inserm U 519, Rouen, France.

Objective: identification of bone and cartilage markers to predict structural damage progression at 2 years in patients with very early arthritis.

Methods: community -based-recruitment (media campaigns) of 310 adults (mean age: 51.8 years ; 68% females) with swelling of 2 or more joints persisting more than 4 weeks, evolving for less than six months (mean: 4.2 months), DMARD and steroids naïve. Then, they were conservatively treated for 2 years. Assessment was made at entry and comprised clinical data (global pain, Ritchie index and swollen joints / 44), CRP, ESR, auto antibodies rheumatoid factors (RF) by agglutination tests and IgM, IgA, IgG, isotypes by Elisa, anti-CCP II, serum pyridinoline (PYD) deoxypyridinoline (DPD), CTX I, Cartilage Oligomeric Matrix Protéin (COMP), osteoprotegerin (OPG) and RANKL. All patients with ACR RA criteria or undifferentiated arthritis were followed except those classified as having defined rheumatism (DR). Criterion of judgment was structural damage progression of erosion with an increase of at least 1 unit at 2 years (measurement was done according to vdH modified erosion Sharp score by two readers).

Results: At 2 years, 213 patients were assessed (29 refused, 1 lost to follow-up; 1 death, 61 classified as DR, 5 with X ray failure): 42 (19.7%) had erosion progression. With univariate analysis, there was a relationship between erosion progression and COMP (p = 0.017), VS (p = 0.003), IgG and IgA (p = 0.007 and 0.005), and anti-CCP II (p < 10⁻⁴). But OPG, CTX I, PYD, DPD, and CRP were not associated with erosion progression. With principal components analysis 75 % patients are correctly classified as progressive or not progressive with these five markers. COMP give a better sensibility (61.5 %) than other markers (52 %). Results of RANKL will be presented.

CONCLUSION: In patients with very early arthritis, conservatively treated, COMP, anti-CCP II, IgA RF, IgG RF, and ESR, are useful to identify patients who will have structural damage progression at 2 years. This population could be a good target for early aggressive treatment.

Disclosures: A. Daragon, None.

This study received funding from: Fondation pour la Recherche Médicale.

M501

Material Properties of Osteoporotic Ewes. E. F. Calton^{*1}, J. MacLeay^{*2}, A. Boskey¹. ¹Hospital for Special Surgery, New York, NY, USA, ²Colorado State University, Fort Collins, CO, USA.

The purpose of this study was to establish baseline material properties for osteoporotic cancellous bone from ovine iliac crest biopsies. Skeletally mature (4-7 yo; 169±29 lb) Rambouillet-Columbia cross-ewes (n=18) were administered a diet to induce metabolic acidosis (MA) and create bone loss similar to that seen in human osteoporosis [MacLeay et al. 2004 J Bone Miner Metab 22:561-8]. Bone densitometry (DXA) measurement of the 4 most caudal vertebrae lumbar spine was performed using a Hologic Delphi QDR dual-energy x-ray absorptiometer (Hologic). Transiliac crest biopsies (8mm dia.) were removed and placed in ethanol. Micro-CT data were collected on the cortical and cancellous regions separately for volumetric bone mineral density measurements. Biopsies were bisected axially with a low-speed saw; half was saved for embedding and histological sectioning and half was prepared for infrared (IR), x-ray diffraction (XRD), and chemical analysis of Ca and PO₄. On the latter half, the cortical ends were removed with the low speed saw. Cancellous bone was defatted using a 1:1 mixture of Chloroform and Methanol and lyophilized 16 hours. The dried and defatted cancellous bone was pulverized using a Spex Mill CertiPrep Freezer/Mill. The XRD line width of the c-axis 002 peak was measured using Cu K α radiation (Bruker AX-8 powder diffractometer, Bruker). FTIR absorbance spectra were collected at 4 cm⁻¹ on pulverized bone formed in KBr pellets (1 wt%). Spectra were baseline corrected and integrated areas were taken for three spectral regions: matrix amide I (1595-1720 cm⁻¹), mineral phosphate v1, v3 (900-1200 cm⁻¹), and carbonate v2 (855-890 cm⁻¹), and area ratios (mineral:matrix and carbonate:phosphate) were calculated. Peak height ratios 1030:1020 cm⁻¹ and 1660:1690 cm⁻¹ were calculated as a measure of crystallinity and collagen cross-linking (maturity), respectively [Paschalis et al. 2001 JBMR 16:1821-8]. Acid hydrolyzed samples were used for phosphate concentration determined by colorimetric assay and for Ca concentration measured by atomic absorption (Perkin Elmer Analyst 100). The values obtained from these measurement methods provide baseline values for cancellous bone from sheep iliac crest biopsies. These values are being used to assess the efficacy of therapeutic interventions on sheep with reduced bone mass and may be useful in determining similar effects in humans with osteoporosis.

Mean Values (n=18)	
Chemical Analysis:	Ca/PO ₄
X-ray Diffraction:	Crystal size (nm)
DXA:	aBMD (g/cm ²)
Micro-CT:	vBMD (mg/cm ³)
IR Parameters:	Mineral-to-matrix ratio
	CO ₃ /PO ₄
	Crystallinity (ratio)
	Cross link ratio

Disclosures: E.F. Calton, None.

This study received funding from: NIH Grant AR043215.

M502

Finite Element Models More Accurately Predict Structural Behavior of Human Cancellous Bone When Using Specimen-Specific Tissue Properties. J. H. Cole¹, E. R. Myers^{*2}, M. C. H. van der Meulen¹. ¹Sibley School of Mechanical and Aerospace Engineering, Cornell University, Ithaca, NY, USA, ²Biomedical Mechanics and Materials, Hospital for Special Surgery, New York, NY, USA.

Osteoporosis affects cancellous bone tissue properties through altered mineralization and changes in chemical composition, which may compromise its structural behavior. Experimental assessments of tissue properties are limited primarily to localized in vitro measurements that likely do not fully capture the in vivo spatial variations. Finite element (FE) models that simulate tissue heterogeneity over a larger region of bone can be used to investigate changes in tissue properties non-invasively. This study examined the effect of changes in tissue material properties on the structural behavior of cancellous bone using architecture- and material-based FE models. Cylindrical cores were drilled from the center of the T12 and L2 vertebrae of 13 female and 11 male human cadavers, ages 56-92, and scanned using micro-computed tomography (microCT) at an 11.6- μ m resolution. Cores were fixed in brass endcaps and tested to failure at 0.5% strain/s, and apparent stiffness was computed. MicroCT bone voxels were coarsened to 68 μ m and directly converted to 8-noded linear brick elements for the gage length region of each cancellous core. A variable tissue modulus (E) was assigned for three sets of models: universal homogeneous (Homo) with E = 20 GPa, specimen-specific homogeneous (SS Homo) with E = f(mean microCT mineral content), and specimen-specific heterogeneous (SS Hetero) with E = f(microCT mineral content at each voxel). A uniform compressive strain of 0.25% was applied to the models, and the resulting apparent stiffness and element tissue strains were computed. FE-predicted stiffness was compared to experimentally-measured stiffness using simple linear regression for each set of models. A significance level of 0.05 was used. Repeated measures ANOVA was used to assess the effect of the assigned modulus on the predicted stiffness and tissue strains. Overall, the heterogeneous tissue modulus ranged 5.2-36.6 GPa and averaged 9.9-13.0 GPa over all models. Model-predicted apparent stiffness was 0.13-1.50 GPa for Homo, 0.10-0.79 GPa for SS Homo, and 0.09-0.79 GPa for SS Hetero models. Compared to Homo models, SS Homo and Hetero models predicted cancellous bone stiffness more accurately (slopes = 0.36, 0.78, 0.78) and explained more variability (r² = 0.29, 0.42, 0.42). A virtual biopsy modeling method allows tissue property variations to be examined non-invasively and may help predict bone fragility in the aging population.

Disclosures: J.H. Cole, None.

M503

Regional Variations in Three-Dimensional Microstructural Properties of Proximal Femoral Trabeculae with Aging. Y. Won¹, B. Min^{*2}, Y. Chung³, W. Cui^{*1}, M. Baek^{*1}, H. Kim^{*4}. ¹Orthopaedics, Ajou University School of Medicine, Suwon, Republic of Korea, ²Orthopaedics, Keimyung University School of Medicine, Daegu, Republic of Korea, ³Endocrinology and Metabolism, Ajou University School of Medicine, Suwon, Republic of Korea, ⁴Orthopaedics, Yonsei University School of Medicine, Seoul, Republic of Korea.

Purpose: The purpose of this study was therefore to explore region-dependent changes in the 3D microstructure of trabecular bone in human proximal femur, with respect to aging.

Materials and Methods: A total of 162 trabecular bone cores were obtained from six regions (femoral head, superior and inferior regions of the neck, and superior/middle and inferior regions of the trochanter) of twenty-seven normal femora of Korean male cadaver donors, aged 40-90 years. These specimens were scanned using high-resolution micro-computed tomography (micro-CT). The following 3D microstructural parameters were calculated: bone volume fraction (BV/TV), trabecular number (Tb.N), thickness (Tb.Th) and separation (Tb.Sp), structure model index (SMI), and degree of anisotropy (DOA).

Results: The results showed that the trabecular morphology changed significantly with age, as well as varied from different regions of the proximal femur. There was a significant decrease in bone volume fraction and an almost identical decrease in trabecular thickness associated with aging at any region. Regional analysis demonstrated a significant difference in BV/TV, Tb.Th, DOA, Tb.Sp, Tb.N between superior and inferior neck, as well as a significant difference in BV/TV, Tb.Sp, DOA, SMI, Tb.N between superior and inferior trochanter.

Conclusions: Age-related changes in bone loss and trabecular microstructure within the male proximal femur are not uniform in this Korean cadaveric population. As a result of mechanical and age-related adaptation, significant regional variations in microstructural properties of trabecular bone are likely to important factors affecting the mechanical properties of the proximal femur.

Disclosures: W. Cui, None.

M504

See Sunday Plenary Number S504

M505

Calcium Density of Bone Correlates with Trabecular Bone Architecture. N. L. Fazzalari¹, B. Ma^{*1}, P. Sutton-Smith^{*1}, J. S. Kuliwaba¹, R. Phipps², I. H. Parkinson^{*1}, A. Badiei^{*1}. ¹Bone and Joint Research Laboratory, Institute of Medical and Veterinary Science and Hanson Institute, Adelaide, Australia, ²Procter & Gamble Pharmaceuticals, Mason, OH, USA.

Many of the skeletal risk factors for fragility fracture have been defined (bone mass, bone geometry, bone architecture, bone mineralisation and bone remodelling). The amount of bone and the degree of mineralisation have been shown to influence the ultimate failure strength of bone independently. In this study we tested if there was any relationship between calcium density of bone ($D_{Ca} = BV/TV \times \% \text{calcium}$) and trabecular bone architecture.

Intertrochanteric cancellous bone cores were obtained from patients undergoing hemiarthroplasty surgery for a subcapital fragility femoral fracture (N=40; 26f, 14m, mean age \pm SD of 81 ± 9 years), and from controls at autopsy (N=10; 2f, 8m, 76 ± 14 years). All samples were imaged by microCT (Skyscan, Belgium) to determine 3D measures of trabecular bone volume (BV/TV), thickness (Tb.Th), separation (Tb.Sp) and number (Tb.N). An age matched subset of 18 fracture cases (13f, 5m, 82 ± 8 years) and 4 control cases (1f, 3m, 79 ± 9 years) were resin-embedded for quantitative backscattered electron imaging (qBSEI) of the degree of mineralisation.

The trabecular bone architecture of the fracture and nonfracture control group was not significantly different. For the pooled group data, Tb.Sp increased exponentially as BV/TV decreased ($y = 3.2 \times 10^{-5} x^2$, $P < 0.001$). Between each group the rate at which Tb.Sp increased was more than three times greater for the fracture group in contrast to the control group. In the pooled group data of the qBSEI analysis, BV/TV did not correlate with %Ca indicating that the measures of bone volume and tissue level mineralisation were independent variables in the bone structural hierarchy. D_{Ca} did positively correlate with Tb.Th and according to the magnitude of r^2 accounted for greater than 25% of the variability in Tb.Th. In contrast, BV/TV accounted for about 10% and %Ca did not account for any variability in Tb.Th. Collectively, these data suggest that Tb.Th may be reactive to changes in D_{Ca} through an interaction between BV/TV and %Ca. It is understood that increased fragility fracture risk is associated with decreased BV/TV and reduced mineralisation of the bone tissue but possible secondary consequent changes in bone architecture have not been investigated to date. D_{Ca} , a composite bone material property provides a novel perspective of bone quality that might help provide a better understanding of fracture risk and treatment efficacy.

Disclosures: N.L. Fazzalari, Procter & Gamble 2, 5.

This study received funding from: Alliance for Better Bone Health.

M506

Role of Microarchitecture on Whole-Vertebral Body Biomechanical Behavior. A. J. Fields*, S. K. Eswaran*, T. M. Keaveny. Mechanical Engineering, University of California, Berkeley, Berkeley, CA, USA.

Trabecular microarchitecture can explain variations in biomechanical properties of isolated trabecular bone specimens, yet the role of microarchitecture on whole-bone biomechanical behavior remains unclear. For the spine, the influence of microarchitecture might be obscured by such factors as cortical shell thickness and overall bone size. The purpose of this study was to assess the role of trabecular microarchitecture with and without such factors on whole-vertebral mechanical behavior.

Human T9 whole vertebral bodies (posterior elements removed) from male (n=5) and female (n=13) cadavers (87.4 ± 5.0 years) were micro-CT scanned at 30-micron resolution. Internal regions (approximately $15 \times 20 \times 10 \text{ mm}^3$) of trabecular bone were analyzed for the standard model-independent microarchitectural parameters (Table). An average cortical shell thickness (Ct.Th) was also measured. Linear, isotropic finite element models (60-micron element size), containing 30-80 million elements each and with assumed uniform bone tissue material properties, were created for each whole vertebra from the micro-CT scans and subjected to uniform compression loading to compute whole-vertebral stiffness (K_{FE}).

Results indicated that total bone volume (BV) was the best independent predictor of whole-vertebral stiffness, followed by cortical thickness (Ct.Th) and then trabecular spacing (Tb.Sp) and SMI (Table). BV/TV was not an independent predictor. Using stepwise multiple regression with all parameters, the model included BV, Tb.Sp, and Conn.D ($R^2 = 0.77 \rightarrow 0.86 \rightarrow 0.92$); when BV was excluded, the model included Ct.Th and SMI ($R^2 = 0.45 \rightarrow 0.62$); and when Ct.Th was also excluded, the model included SMI and Tb.Sp ($R^2 = 0.35 \rightarrow 0.55$).

While these finite element models did not contain any tissue mineralization effects and this elderly cohort was limited in size, this study is unique since it included measures of microarchitecture and whole-vertebral mechanical behavior for the same specimens. We conclude that trabecular microarchitectural parameters have the potential to improve predictions of whole-vertebral biomechanical behavior, although their influence interacts with other vertebral features. Ongoing efforts are extending these studies to a larger and younger cohort.

Table: Pearson correlation coefficients (n=18)

	BV	Tb.N	Tb.Sp	Tb.Th	Conn.D	DA	SMI	Ct.Th	BV/TV
K_{FE}	0.88*	-0.54†	0.59†	0.05	-0.28	0.18	-0.59†	0.67†	0.33
BV	1.00	-0.31	0.35	-0.08	-0.17	0.07	-0.58‡	0.59†	0.40
BV/TV	0.40	0.17	-0.17	-0.01	0.21	-0.08	-0.62†	0.16	1.00

* $p < 0.001$; † $p < 0.01$; ‡ $p < 0.05$

Disclosures: A.J. Fields, None.

This study received funding from: NIH AR49828.

M507

Withdrawn.

M508

See Sunday Plenary Number S508

M509

Assumptions and Limitations in Image-Based Strength Assessment of Bone. T. N. Hangartner. BioMedical Imaging Laboratory, Wright State University, Dayton, OH, USA.

The goal of many bone measurements is the assessment of the likelihood of future fracture. The most commonly used surrogate for strength is density, which can be measured through the attenuation of x-rays. Mechanical testing of machined bone specimens as well as whole bones usually shows an initial linear behavior between load and deformation, leading to a region of reduced resistance to load and eventually reaching the breaking point. Although the initial slope of these curves is tightly related to the material properties of the bone as well as to the architecture and can be estimated with finite-element models, the breaking point is influenced by non-linear features and differs by age and disease state, usually not taken into account.

Computed tomography, through its three-dimensional representation of the bone, has the highest potential to provide the architectural information needed for accurate mechanical simulation. Although average density of the various compartments like trabecular and cortical bone has proven clinically relevant, strength calculations based on the distribution of the bone material are expected to better represent the strength of an individual bone. It is critical, here, to appropriately convert the CT-measured density values to local elastic moduli, a relationship that almost follows a square law. One specific parameter used by some investigators, the strength-strain index, assumes a linear relationship and may, thus, not adequately represent the strength of the bone.

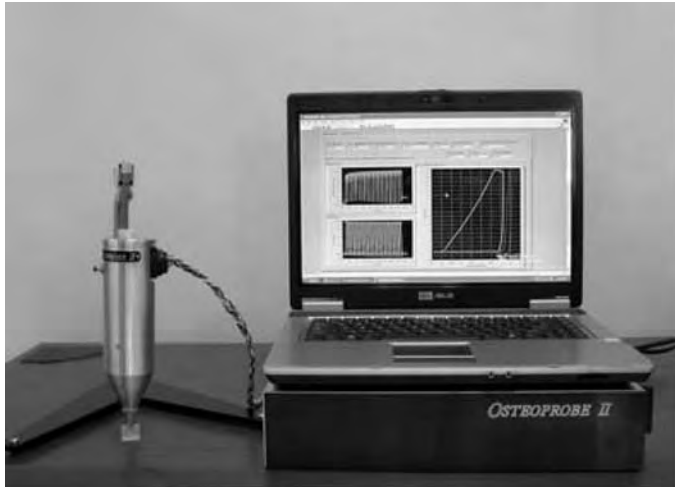
Dual-energy absorptiometry is a two-dimensional imaging method that reflects the third, collapsed dimension in the density value measured at each point in the image. For purely axial loading, as could be assumed in a simplified model of a vertebra, the resistance to loading would be related to the bone mineral content. In the femur, however, the loads are eccentrically applied to the femoral shaft axis, and, thus, major bending stresses occur in the femoral neck. The resistance to a load applied vertically to the center of the femoral head is dictated by the distribution of the bone material in a vertical plane going through the point of force application and the femoral shaft. The projection image of a properly rotated femur provides just that information, and strength calculations based on dual-energy absorptiometry scans have shown tighter relationships with fractures in vitro than simple density measurements. However, current methods assume a linear relationship of density and elastic modulus. Results might be improved if an appropriate power-based relationship is assumed.

Disclosures: T.N. Hangartner, None.

M510

A New Bone Diagnostic Instrument: the Osteoprobe II. P. K. Hansma, P. J. Turner*, B. Drake*, J. Adams*, J. LeLujan*, A. Proctor*, F. Garza de Leon*. Physics, University of California, Santa Barbara, CA, USA.

The Osteoprobe II can measure the material properties of bone even if the bone is covered in tissue because of its novel probe assembly. The probe assembly consists of a reference probe, a 22 gauge hypodermic syringe, and a test probe, a small diameter sharpened rod, which slides through the inside of the syringe. The probe assembly is inserted through the skin to rest on the bone. The distance that the test probe is indented into the bone can be measured relative to the position of the reference probe, which rests on the surface of the bone. Complete force vs. distance curves for bone indentation cycles are automatically generated and analyzed to obtain the material properties of the bone. Cyclic force vs. distance curves reveal differences for bones that differ in their resistance to fracture. The resistance of bone to continuing indentation with cycling is less for bone that has less resistance to fracture, for example, bone that has been baked or irradiated. The resistance of human bone to continuing indentation with cycling is less for bone from an elderly donor than for bone from a young donor. This is consistent with data showing that the fracture toughness is lower for bone from elderly donors compared to bone from young donors². The long range goal is to develop a diagnostic tool to help physicians assess fracture risk in their patients: specifically the contribution to fracture risk due to deterioration of materials properties such as fracture toughness. The availability of this tool could also help in the development of new therapies to mitigate or reverse deterioration.



1. Hansma, P.K., Turner, P., & Fantner, G.E. Bone Diagnostic Instrument. Review of Scientific Instruments 77, 075105 (2006)
2. Nalla, R.K., Kruzic, J.J., Kinney, J.H. & Ritchie, R.O. Effect of aging on the toughness of human cortical bone: evaluation by R-curves. Bone 35, 1240 (2004).
This research was supported, in part, by a grant from the NIH: RO1 GM 065354-05

Disclosures: P.K. Hansma, None.

M511

Lrp5 Gene Expression and Bone Turnover with Disuse. G. K. Alvarez, B. T. Hackfort*, B. McGuckin*, M. P. Akhter, D. M. Cullen. Osteoporosis Research Center, Creighton University, Omaha, NE, USA.

The Lrp5 receptor (low density lipoprotein like receptor protein) is associated with canonical Wnt signaling and bone formation. The G171V mutation in LRP5 is associated with high bone mass and greater sensitivity to increase mechanical loading. Conversely, disuse results in bone loss due to increased osteoclast activity and decreased osteoblast activity. The hypothesis for this study was that variation in Lrp5 expression and specifically the G171V mutation are associated with differences in bone response to disuse. We examined the response in adult virgin female (4.5 ± 0.4mo) mice to four weeks of hindlimb suspension in three mice genotypes: WT (wild type C57BL6, Lrp5+/+), KO (single knock out Lrp5-/-), and HBM (high bone mass due to G171V mutation). Mice within each genotype were randomly assigned to suspension (N=46) or control (N= 43). All mice were allowed free access to food and water. The protocol was approved by the University IACUC. Calcein was injected 10 and 3 days before tissue collection and histomorphometry performed on undecalcified femur cortical bone. Measurements included Area (total, cortical), mineralizing surface (MS/BS), mineral apposition rate (MAR), and bone formation rate (BFR/BS). Differences among genotypes and due to disuse were analyzed by GLM in SPSS with P<0.05. There were no differences among groups in initial body weight (25.6 ± 2.6 g). The controls maintained their weight while the hindlimb mice lost an average of 3.6 g over four weeks. Results are presented in the table below. HBM mice had greater total and cortical bone area in the control femur and this difference was maintained after disuse. Only the KO group showed a significant decrease in cortical bone area. Cortical femur after hindlimb suspension had formation two to four fold lower in all genotypes. Mice with the HBM mutation and Lrp5+/+ maintained cortical bone despite a decrease in bone formation with disuse while the Lrp5+/- mice lost bone with the same relative decrease in formation. These results show that Lrp5 gene may protect against bone loss with removal of force. Lrp5 in regulation of osteoclast activity may be a secondary role in addition to the primary role of bone cell proliferation and differentiation. The disuse-related effects of the G171V mutation were not discernable in this study since bone areal changes in control mice were small.

Variable	Trt	HBM (G171V)	WT (Lrp5+/+)	KO (Lrp5+/-)
Total Area	C	2.13 (0.27)	1.58 (0.10)a	1.57 (0.20)a
	H	2.24 (0.11)	1.55 (0.04)a	1.48 (0.10)a
Cortical Area	C	1.26 (0.23)	0.78 (0.05)a	0.79 (0.13)a
	H	1.28 (0.15)	0.70 (0.04)a	0.67 (0.06)ab
Peri MS	C	23.81 (8.65)	19.29 (11.78)	21.71 (9.09)
	H	9.12 (7.34)b	6.90 (4.80)b	6.58 (6.32)b
Peri BFR	C	65.27 (26.13)	47.16 (29.94)	63.82 (39.90)
	H	18.80 (19.63)b	12.64 (9.96)b	14.61 (16.77)b
Endo MS	C	50.67 (12.42)	49.35 (11.67)	58.12 (13.40)
	H	29.91 (11.22)b	34.57 (15.69)b	33.51 (10.90)b
Endo BFR	C	147.01 (47.51)	143.44 (46.69)	185.84 (51.84)a
	H	86.67 (41.84)b	105.88 (67.65)b	100.01 (36.73)b

Mean (S.D.), a different from HBM P<0.03, b different within genotype due to hindlimb, p<0.05

Disclosures: G.K. Alvarez, None.

This study received funding from: Nebraska Cigarette Taxes.

M512

See Sunday Plenary Number S512

M513

Effect of Hindlimb Unloading on Bone in Two Strains of Mature Mice. B. M. Boudignon*, P. Kurimoto*, B. Orwoll*, B. Halloran. Endocrine Unit, Veteran Affairs Medical Center San Francisco, San Francisco, CA, USA.

Hindlimb unloading is a good model of to study the effects of loss of weight bearing on bone. Numerous studies have shown that hindlimb unloading induces osteopenia, decreases bone formation and increases bone resorption. These studies, however, focused mostly on rapidly growing animals and only a few mouse strains have been compared in adult animal. To examine the effects of hindlimb unloading and mouse strain on bone in mature mice, male C57BL6 and DBA/2 animals, 6 months of age, were permitted normal ambulation or were unloaded for 1, 2 or 4 weeks using the tail suspension method. The femoral distal metaphysis was analyzed using microCT analysis and histomorphometry. Bone marrow cells were collected to examine calcium nodule and osteoclast formation. Basal BV/TV was 50% lower in DBA/2 than C57BL/6J mice and didn't decrease even after 4 weeks of suspension. C57BL/6J mice lost a significant amount of bone after 2 weeks of suspension and this was maintained through week 4. Calcified nodule number decreased dramatically one week after unloading and remained low through week 4. Osteoclast number increased markedly in both strains of mice and normalized after 4 weeks of suspension in the DBA/2 mice but not in the C57BL/6J. Osteoclasts with more than 50 nuclei, believed to be the most active bone resorbing cells, were most increased (nearly 4 times) the first week after hindlimb unloading. Our results show that hindlimb unloading decreases bone mass in mature C57BL/6J mice but not in DBA/2 mice. That basal bone mass was low in the DBA/2 mice might explain why BV/TV was unaffected by unloading. The cell cultures however demonstrated a dramatic effect of unloading on osteoblasts formation and function and osteoclasts formation in both strains. Our results demonstrate that the loss of bone induced by skeletal unloading is strain dependant and in mature mice is associated with changes in both osteoblast and osteoclast function.

Disclosures: B.M. Boudignon, None.

M514

See Sunday Plenary Number S514

M515

Seasonal Changes in the Bone Mineral Density of a Non-hibernating Arctic Rodent Species: The Northern Red-backed Vole, Clethrionomys rutilus. K. T. Stevenson¹, J. D. Mayfield^{*1}, B. M. Barnes^{*1}, I. G. van Tets^{*2}. ¹Biology & Wildlife, University of Alaska Fairbanks, Institute of Arctic Biology, Fairbanks, AK, USA, ²Biological Sciences, University of Alaska Anchorage, Anchorage, AK, USA.

Arctic rodents use a variety of over-wintering strategies to survive the seasonal arctic environment. Some rodents hibernate. These animals decrease their heart rate, metabolic rate, and body temperature, and in some species may not move, eat, drink, urinate, or defecate for five to seven months. Other rodents, "non-hibernators", maintain a constant body-temperature during winter, but reduce their activity and change their diet, social behavior, and physiology in the months leading up to and throughout winter. Both types of rodents could potentially provide models for studying disuse osteoporosis in humans. However, the coupling of reduced activity with maintained metabolic rate and body temperature in non-hibernators resembles the situation of the human patients more closely. Our aim was to determine whether and how bone mineral density (BMD) changed with season in a non-hibernating arctic rodent, the northern redbacked vole, Clethrionomys rutilus. We used dual-energy X-ray absorptiometry (DXA) to measure seasonal changes in the BMD of adult C. rutilus carcasses collected in Alaska at different times of the year. There was no significant effect of season on the BMD of female voles. The BMD of males, however, was highest in spring and fall and lowest in summer and winter, suggesting a decrease in bone strength in male voles as the result of reduced winter activity and an increase in bone strength associated with the onset of the breeding season. Recruitment of younger adults having lower BMDs and the loss of older adults with higher BMDs in summer is likely to have been responsible for the lower BMD values in summer. This evidence of reduced BMD during times of naturally low activity for male C. rutilus suggests that these non-hibernating arctic rodents could serve as models for studies of disuse osteoporosis in humans. To further test this, we will dissect the bones out of the vole carcasses and repeat our analyses on these isolated bones. We will also use DXA to measure the effect of hibernation on long bone remodeling in captive arctic ground squirrels, Spermophilus parryi, to test the suitability of hibernating rodents for similar research. Continuing research on the effects of season and activity on mineral metabolism and deposition in arctic rodents is likely to improve our understanding of disuse osteoporosis.

Disclosures: K.T. Stevenson, None.

This study received funding from: NOAA CIFAR International Polar Year, National Science Foundation, HSF Alaska EPSCoR, The American Society of Mammalogists.

M516

A Novel Partial Weight Suspension System Simulating Mars Gravity Leads to Reduced Bone Mass and Strength in Mice. E. B. Wagner^{*1}, W. Tan^{*2}, K. C. Gosselin^{*2}, M. L. Bouxsein³. ¹Division of Health Sciences and Technology, Harvard-MIT, Cambridge, MA, USA, ²Massachusetts Institute of Technology, Cambridge, MA, USA, ³Beth Israel Deaconess Medical Center and Harvard Medical School, Boston, MA, USA.

The musculoskeletal effects of partial weightbearing, such as expected on the Moon (16%) and Mars (38%), are yet to be quantified. Our novel model of Partial Weight Suspension (PWS) provides the first mechanism for investigating chronic, titrated quadrupedal loading in mice. Suspension is provided by combination of a custom forelimb vest and tail wrap, and can be adjusted to support studies within +/- 5% of a given static loading level. In this study, we examined musculoskeletal adaptation to Mars-analog (38% weightbearing) levels. Adult female BALB/cByJ mice (n=32, 10 weeks old) were randomly assigned to the BASELINE sacrifice group (n=8), MARS suspension group (n=9), JACKET full-weightbearing control group (n=5), or group-housed AGE matched control group (n=10). JACKET mice were singly housed in identical cages and wore the same forelimb vest to mimic any stress induced by the PWS system. JACKET mice were pair-fed based on consumption of MARS, and AGE animals were group housed and fed ad libitum. After 21 days, animals were sacrificed, the gastrocnemius muscle was weighed, and the bone architecture in the distal femur, femoral midshaft, and proximal tibia were assessed by microCT. Femora were tested in 3-point bending to determine biomechanical properties. We found that: 1) Body weight gain did not differ between MARS and AGE-matched controls after an initial adaptation period, suggesting low levels of systemic stress; 2) Gastrocnemius weight and bone architecture did not differ between AGE and JACKET controls; 3) Gastrocnemius weight was significantly decreased in MARS vs AGE-controls (-21.8%, p<0.05); 4) Femoral trabecular BV/TV and mid-shaft cortical thickness were significantly reduced in MARS animals vs controls (BV/TV -20.6%, p<0.01; Cort.Th -8.9%, p<0.001); 5) Bending rigidity and ultimate moment were significantly reduced in MARS animals relative to controls (BR: -13.8%, p<0.005; UltMom: -19.9%, p<0.01). In summary, MARS loading leads to significant muscle and bone loss. Interestingly, trabecular bone loss under MARS weightbearing appears to be attenuated relative to previous reports of bone loss associated with hindlimb suspension.

Disclosures: E.B. Wagner, None.

This study received funding from: NASA.

M517

Fluid Shear Stress and Mechanical Strain Induce a Similar Osteogenic Gene Response via Divergent Signaling Pathways. N. Case¹, Z. Xie^{*1}, B. Sen^{*1}, M. Ma^{*1}, H. Jo^{*2}, J. Rubin¹. ¹Medicine, UNC, Chapel Hill, NC, USA, ²BME, GATech/Emory, Atlanta, GA, USA.

Mechanical loading influences on bone remodeling are well-established with physiologic loading causing net bone gain. The specific forces generated during loading have been postulated to cause equally specific responses: indeed, the few direct comparisons between strain and shear stress have suggested that these forces are not interchangeable. Our previous work has shown that mechanical strain promotes bone formation through repression of RANKL, a necessary factor for osteoclastogenesis, as well as stimulation of Runx2 and osterix, genes that induce osteoblast differentiation and activity. We here ask whether this coordinated regulation of multiple genes associated with bone remodeling is specific to strain: does shear activate the same pattern of osteogenic gene response? Using a modified cone-and-plate shear device, we evaluated the effects of steady fluid flow on regulation of bone remodeling effector genes in the pre-osteoblast CIMC-4 cell line. RANKL mRNA expression was decreased to 0.11 ± 0.03 fold, Runx2 mRNA expression was increased 1.56 ± 0.13 fold and osterix mRNA expression was increased 3.37 ± 0.41 fold in cultures subjected to flow overnight (3 experiments, n=11) as compared to no-flow cultures (p<0.01 all genes). The magnitude of shear-induced changes was \geq strain effects: RANKL repression was 2-3 times lower, Runx2 expression was unchanged and osterix induction was 2 times higher in flow compared to changes observed in strained cultures. We next investigated potential signaling pathways involved in flow-mediated gene regulation. Signaling pathway inhibitors evaluated included MEK inhibitors, PD98059 and U0126, the PI3-kinase inhibitor LY294002, the nitric oxide synthase inhibitor L-NAME and thapsigargin, which empties intracellular calcium stores. While we have previously shown that PD98059 inhibits strain effects on RANKL, Runx2 and osterix, this MEK inhibitor did not affect shear-induced gene changes. As well, shear regulation of RANKL and Runx2 was not altered by treatment with any other inhibitor. Interestingly, shear upregulation of osterix was inhibited by U0126, LY294002 and thapsigargin, but not by L-NAME, indicating that osterix regulation by flow involves at least PI3-kinase and calcium signals. In sum, these data suggest that fluid shear stress and mechanical strain can elicit similar, if not equivalent, cellular responses and that the same biological endpoint can be reached through different means. In conclusion, this work suggests that there is no one dominant biophysical force guiding the response to skeletal loading; rather, a variety of inputs/signaling pathways converge to elicit a summed response that is anti-catabolic and pro-anabolic in bone cells.

Disclosures: N. Case, None.

This study received funding from: NIAMS, NIH.

M518

See Sunday Plenary Number S518

M519

A Novel Role for Nuclear Factor of Activated T Cell (NFATc1) in Bone Mechanotransduction. A. B. Celil Aydemir^{*1}, S. Lee^{*1}, T. R. Gardner^{*1}, J. M. Ahn^{*2}, F. Y. Lee¹. ¹Orthopaedic Surgery, Columbia University, New York, NY, USA, ²Hallym University, Chuncheon of Gangwon, Republic of Korea.

Bone adapts to the changes in its microenvironment. It has been shown that osteoblasts alter cytokine expression in response to mechanical stimuli. However, signal transduction pathways that mediate bone cell response to mechanotransduction have not been elucidated at the transcriptional level. One of the early events of mechanotransduction is the elevation of intracellular calcium, which is upstream of calcium/calmodulin and NFAT signaling. Calcium/calmodulin signaling activates NFATc1, which is a transcription factor. Our bioinformatics analysis shows the presence of putative NFATc1 binding motifs in the promoter region of Cox2, a well-known mechanotransduction mediator. We hypothesize that calcineurin/NFATc1 signaling mediates mechanotransduction in osteoblasts. In this study, we show that fluid shear stress (FSS) induces Cox2 and TNF α expression in bone marrow derived human mesenchymal stem cells (hMSC) and mouse preosteoblasts. Osteoblasts and osteocytes are known to be subject to fluid shear stress in vivo. Cells were subjected to a sinusoidal fluid shear stress of ± 10 dynes/cm² at 1Hz for 15minutes. Concurrently, a clinically relevant hydrostatic pressure of 0.138MPa (1380 dynes/cm²), comparable to pressures found in the hip joint space during gait, was applied to the cells. Proinflammatory gene expression and TNF α release in hMSC were both found to increase in this loading environment. Further, NFATc1 translocates to the nucleus in response to fluid shear stress in hMSC. A peptide inhibitor of NFATc1, Vivit, inhibits the FSS-induced proinflammatory gene expression and NFATc1 nuclear translocation. Our results implicate the involvement of the calcineurin/NFATc1 axis as a novel mediator of bone cell response due to mechanical stimulation.

Disclosures: A.B. Celil Aydemir, None.

This study received funding from: NIH, OREF.

M520

Fluid Flow Shear Stress Promotes Intracellular Assembly and Formation of Connexin 43-forming Channels in Osteocytes. S. Burra¹, A. J. Siller-Jackson¹, L. F. Bonewald², E. Sprague^{*3}, J. X. Jiang¹. ¹Biochemistry, University of Texas Health Science Center, San Antonio, TX, USA, ²Oral Biology, School of Dentistry, University of Missouri, Kansas City, MO, USA, ³Radiology, University of Texas Health Science Center, San Antonio, TX, USA.

Connexin 43 (Cx43) is the major gap junction and hemichannel forming protein in primary osteocytes and osteocyte-like cell line MLO-Y4. Osteocytes are the mechanosensory cells; mechanical signals travel from one osteocyte to other through gap junctions formed at the tips of the dendritic processes of osteocytes. Recent studies by our laboratory and others show that in addition to form gap junction channels, Cx43 forms functional hemichannels, an apposed of halves of gap junctions. Fluid flow shear stress induces the opening of hemichannels associated with the release of prostaglandins. Cx43 protein is abundantly expressed intracellularly as well as along the cell surface. We have previously shown that FFSS appears to enhance the migration of intracellular Cx43 protein towards plasma membrane, resulting in an increase in Cx43 protein on the cell surface. To determine the molecular mechanism of assembly and formation of gap junctions and hemichannels in response to FFSS, sucrose gradient sedimentation analysis was conducted. FFSS induced the assembly of Cx43 into hexamers, the oligomeric forms of Cx43 in forming gap junctions and hemichannels. The localization of Cx43 and its response to FFSS was determined by colocalization analysis with intracellular organelle marker proteins including calnexin (endoplasmic reticulum (ER) marker) and 58K Golgi protein (Golgi marker). Cx43 co-localized with both ER and Golgi markers at static conditions. Cx43 protein plaques, indicative of assembled channels, predominantly localized in the Golgi. Interestingly, upon mechanical stimulation by FFSS, the colocalization of Cx43 plaques in Golgi diminished; instead Cx43 appeared to migrate towards the cell surface. The levels of Cx43 protein on cell surface was quantified by biotinylation approach. When MLO-Y4 cells were subjected to FFSS and the then incubated for various periods of time, surface expression of Cx43 gradually increased over the time and reached maximum after 2 h of incubation. Together, these results combined with functional studies show that FFSS stimulates the assembly and formation of Cx43-forming gap junctions and hemichannels, which will accommodate the response to mechanical stimulation in osteocytes.

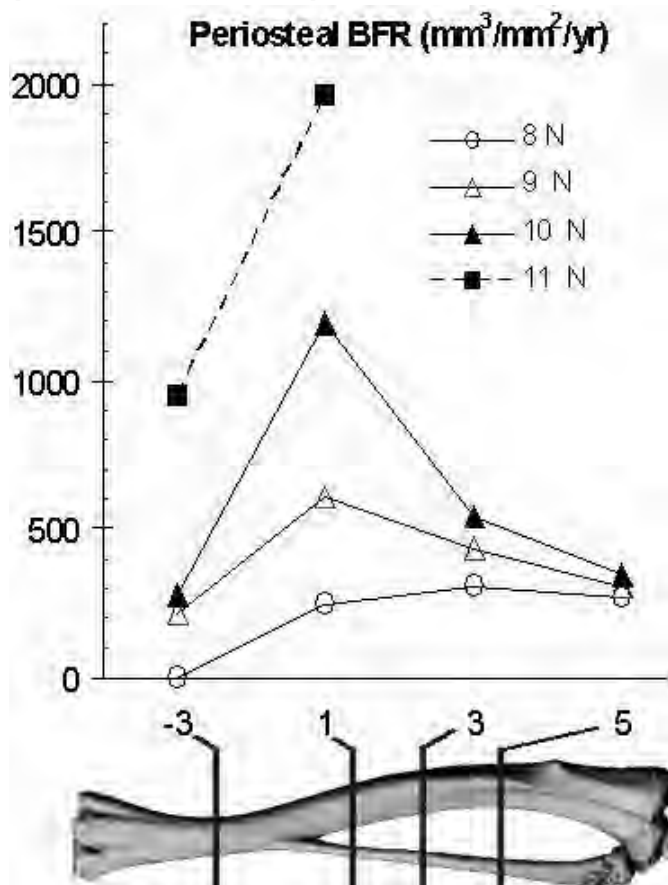
Disclosures: S. Burra, None.

This study received funding from: National Institutes of Health.

M521

In Vivo Tibial Compression Stimulates Bone Formation. D. M. Cullen, G. K. Alvarez, B. T. Hackfort*, B. McGuckin*, M. P. Akhter. Osteoporosis Research Center, Creighton University, Omaha, NE, USA.

Increased exercise stimulates bone formation, but is difficult to model in vivo. Popular noninvasive models include tibial four-point or cantilever bending and ulna compression, but they are limited by the unique load distributions, sample regions, and potential injury. Two papers in Bone 2005, by Fritton and Desousa introduced tibial compression. They presented strain gage data, area, and BMC changes, but did not provide sufficient information to determine appropriate load ranges and sample sites for bone histology. The purpose of this study was to document the bone formation response along the tibia and to demonstrate the load response curve to increasing forces. The load apparatus was modeled after DeSousa with the knee and ankle positioned for force application in the vertical plane with an Enduratec (ELF3200) device. Twenty female C57Bl6 adult mice (5.5±0.4 mo, 30.0±3.2g) were randomized to loads 8, 9, 10, or 11N and then 100 cycles at 2 Hz was applied Mon-Wed-Fri for 3 weeks. Midtibial strains ranged from 1800 to 2500µε. Mice received calcein injections 10 and 3 days before euthanasia to label bone formation for dynamic histomorphometry. Animals loaded from 8-11 N showed no signs of injury. In a test of 12 N loads, 20% of the animals had a stress fracture by day 3 and the group was stopped. Bone sections were selected relative to the tibia fibular junction (TFJ, Fig) with one distal (3 mm) and three proximal (1, 3, 5 mm) sections measured. Differences were seen within animals for loaded and non loaded legs and section location, and among load groups at the periosteal and endocortical surfaces for mineralizing surface (MS), mineral apposition rate (MAR), bone formation rate, and woven bone formation. For all endpoints the responses tended to increase with increased load and the differences in load response were greatest at 3 mm proximal to the TFJ. Difference (Loaded - nonloaded) in periosteal bone formation rate (MS x MAR) is shown in the Figure. Formation increased as applied force increased with the greatest differences seen 3 mm proximal to the TFJ where multiple intergroup comparisons were significant (P<0.01). This study demonstrates that the most load sensitive region for cortical bone histomorphometry is ~ 1 mm proximal to the TFJ, the same region sampled for tibial four-point bending. This area is easily located, reproducible and has a fairly constant shape.



Disclosures: D.M. Cullen, None.

This study received funding from: Grant #AR051365 from NIAMS.

M522

Is Golf a Good Sport for Bone Health in the Elderly? A DPX and High Resolution pQCT Evaluation at both Radius and Tibia Bone Sites. T. Thomas¹, G. Ntougou Assoumou Hourfil², M. Zouch², L. Vico².

¹Rheumatology Department - University Hospital, LBTO INSERM U890, Saint-Etienne, France, ²LBTO INSERM U890, Saint-Etienne, France.

A regular practice of golf may be beneficial for preserving a good bone health in the elderly population, both in the lower limbs because of ground impacts during long walks and in the upper limbs because of impacts transmitted by the club during the swing. Therefore, we conducted a prospective cross-sectional study in men (age range: 60-75) comparing a group of 15 golfers, playing their sport 8 to 12 hours a week for the last 2 years, to a group of 15 walkers, with a similar weekly practice and a group of sedentary men, all appeared for age. Evaluation of bone status was performed using DPX (Hologic Delphi 4500 QDR) and HR-pQCT (Scanco Xtreme CT) for microarchitecture analysis as well as biochemical parameters on fasting blood samples collected early morning. Daily calcium intake and physical activities were assessed by validated questionnaires. The 3 groups were not different in terms of height, weight, BMI and daily calcium intake. Using DPX, we observed that bone mineral content of mid diaphysis radius was significantly higher in the golfer group than in the other groups. There was no statistically significant difference in bone mineral content both at the distal radius and dominant lower limb. The HR-pQCT analysis showed significant differences between groups in central trabecular density (Dtrab), total trabecular density (Dtrab) and trabecular bone volume (BV/TV) both at the dominant radius and tibia. Surprisingly, these parameters were higher in the walker group than in the other groups. On the other hand, cortical density at both bone sites was higher in golfers with a large inter-individual variability. Several factors may partly explain the higher values in trabecular parameters in the walker group. Indeed, total and sport-related annual physical activities were significantly higher in this group compared to the others. Those of golfers were not significantly higher than sedentary group levels. Past physical activity of walker group also was very significantly higher than golfers one while this parameter was significantly lower in sedentary group compared to the others. In addition, testosterone level also was significantly higher in walkers than in other groups and testosterone was significantly and positively related to Dinn ($r = 0.41$, $p < 0.05$).

In summary, our results suggest that golf practice has beneficial effect on the cortical envelope both at the radius and tibia bone sites. The role of past and actual global physical activity seems preponderant on trabecular envelope. Further studies are necessary to confirm a definitive benefit of golf practice on bone health in the elderly.

Disclosures: T. Thomas, None.

This study received funding from: University Hospital of St-Etienne.

M523

See Sunday Plenary Number S523

M524

Eight Months of Twice Weekly Ten Minute Jumping Activity for PE Warm Up Improves Bone in Adolescent Boys and Girls: The POWER PE Study.

B. K. Weeks, C. M. Young*, B. R. Beck. School of Physiotherapy and Exercise Science, Griffith University, Gold Coast, Australia.

High intensity skeletal loading during growth may be an effective strategy to maximise bone accrual and reduce fracture risk in old age. Preventing Osteoporosis With Exercise Routines in Physical Education (POWER PE) was an 8-month randomised controlled school-based exercise intervention designed to apply known principles of effective bone loading to practical opportunities to improve life long musculoskeletal outcomes. We replaced regular warm up activities with jumping in the twice-weekly PE classes of early high school students to observe the effect on bone accrual in adolescent boys and girls. A total of 99 adolescents (46M:53F, 13.8 ± 0.4 years) volunteered to participate in the yearlong study. Most were classified as Tanner IV (53%). Intervention group subjects performed ten minutes of supervised jumping activity in place of regular PE warm up activities. Control subjects performed regular PE warm-up activities directed by their teacher. Anthropometrics, Tanner staging, peak height velocity, muscle strength and power, flexibility, and bone mass (DXA and QUS) were measured at baseline and follow-up. Geometric properties (such as FN cross-sectional moment of inertia and LS index of bone strength) were estimated from DXA measures. Physical activity and dietary calcium were determined by questionnaire. There were no differences in any measured variable between control and intervention groups at baseline. No group differences were detected for 8-month change in anthropometric, maturity, strength, or flexibility variables for boys or girls. At eight months, boys in the intervention group had experienced significant improvements in calcaneal BUA (+5.0%, $p = 0.012$), and fat mass (-10.5%, $p = 0.023$), while controls did not (+1.4% and -0.8% respectively). Girls in the intervention group, however, experienced significant improvements in FN BMC (+13.9%, $p = 0.05$) and LS BMAD (+5.2%, $p = 0.04$), which were not observed in controls (+4.9% and +1.5% respectively). Other bone strength parameters improved significantly for both groups, such that between group comparisons of percent change revealed significant intervention effects only for WB BMC (+10.6% vs +6.3%, $p = 0.029$) for boys. Short duration, regular jumping activity during adolescence appears to improve bone accrual in a sex-specific manner. Boys improved whole body bone mass and BUA, and reduced fat mass, while girls improved bone mass at the hip and spine.

Disclosures: B.K. Weeks, None.

M525

See Sunday Plenary Number S525

M526

Knee Loading Stimulates Wound Healing in Mouse Femora. P. Zhang, Q. Sun*, C. H. Turner, H. Yokota. Biomedical Engineering, Indiana University Purdue University Indianapolis, Indianapolis, IN, USA.

Knee loading is a recently developed loading modality capable of inducing anabolic responses in murine femora and tibiae. The object of this study was to examine whether this loading modality would be useful in stimulating bone healing in mouse femora. Thirty-seven C57/BL/6 female mice (~14 weeks of age; and a body weight of ~20 g) were used for the study. The procedures performed in this study were in accordance with the Institutional Animal Care and Use Committee guidelines. A surgical hole of 0.5 mm in diameter was generated in the left and right femora. The hole penetrated through the anterior and posterior surfaces at 50% (~8 mm) distant from the distal femoral end. From the fourth postoperative day, knee loading was conducted with a custom-made piezoelectric loader, and 0.5-N loads were laterally applied to the left knee at 15 Hz for 3 min/day for 3 consecutive days. The contralateral femur was used as sham-loaded control. Animals were sacrificed 1, 2, or 3 weeks after the surgery. The healing process was evaluated using μ CT (n = 20), pQCT (n = 7), and histomorphometry with calcein labeling (n = 10).

Compared to sham control, the loaded samples clearly showed load-driven enhancement of wound healing. First, knee loading significantly reduced the size of surgical wounds by 14% (p < 0.05), 24% (p < 0.01), and 32% (p < 0.001) in 1, 2, and 3 weeks after the surgery, respectively. Second, pQCT data showed that the total bone density (BMD) was increased from 571 ± 19 mg/cm² (control) to 686 ± 19 mg/cm² (loading) (p < 0.01), and the total bone content (BMC) was elevated from 3.05 ± 0.12 mg/mm (control) to 3.42 ± 0.11 mg/mm (loading) (p < 0.05). Similarly, the cortical bone density was increased from 1057 ± 19 mg/cm² (control) to 1136 ± 10 mg/cm² (loading) (p < 0.01), and the cortical bone content was elevated from 2.25 ± 0.11 mg/mm (control) to 2.73 ± 0.11 mg/mm (loading) (p < 0.01). Lastly, bone formation near the wound was stimulated by loading. In summary, the current study demonstrates that knee loading is capable of enhancing a healing process in the mouse femur. The described knee loading modality might provide a novel strategy to develop mechanical therapies to accelerate bone healing.

Disclosures: P. Zhang, None.

This study received funding from: NIH.

M527

Sex-Specific Bone Surface Changes During Adolescent Growth: pQCT Analysis of the Mid-Tibia. Y. Ahamed*, D. M. L. Cooper, H. A. McKay. Orthopaedics, University of British Columbia, Vancouver, BC, Canada.

The classic studies of Garn and colleagues reported that although growing boys and girls can both exhibit endosteal and periosteal apposition within the diaphysis of the second metacarpal; girls undergo greater endosteal apposition while boys undergo greater periosteal apposition. This suggests a strength advantage for boys as adding bone to the endosteal surface is less mechanically advantageous. Further, this biological "preference" has been viewed as contributing to women's increased bone fragility. Garn's classic studies were conducted using planar measurement techniques and thus were unable to directly assess bone cross-sectional geometry. In a previous study by our group, changes in bone surfaces at the mid-tibia over 20 months (2001-2003) in boys and girls were directly assessed by peripheral quantitative computed tomography (pQCT). This study did not detect any evidence of endosteal formation in either sex in this young sample (mean age = 13.5 (± 0.55) years in 2003) regardless of maturity level. The aim of our current study was to extend this previous work by examining sex-specific changes in bone surfaces across 56 months. We tested the hypothesis that girls add more bone on the endosteal surface compared with boys during adolescence. Subjects were a part of The University of British Columbia Healthy Bones Study. There was no difference between control and intervention groups for pQCT outcomes at the tibia four months after cessation of the exercise intervention. Therefore, both groups were collapsed for the current study which included 69 participants (38 girls, 31 boys) for whom 6 consecutive mid-diaphyseal pQCT (Stratec XCT 2000) scans were available (2001-2006). Mean ages were 12.0 years (± 0.55) at baseline and 16.5 (± 0.56) years as of June 2006. Total bone area (ToA) and medullary canal (MedA) were measured using Stratec XCT software version 5.50. Repeated measures univariate analysis of variance with sex as a factor showed significant increases in ToA and MedA (p < 0.001) in both sexes. Over 56-months ToA increased 42% in boys and 16% in girls. In boys, MedA increased a total of (32%) while the change in MedA for girls was less pronounced (7% increase). Our current findings differ from Garn and colleagues' earlier studies of the second metacarpal but are consistent with our early findings of this cohort when they were less mature that found no evidence of endosteal apposition at the midshaft of either sexes' tibiae. This indicates that endosteal formation of bone does not occur uniformly throughout the skeleton during adolescence and, therefore, may not underlie differences in fragility between the sexes.

Disclosures: Y. Ahamed, None.

This study received funding from: Michael Smith Foundation for Health Research.

M528

See Sunday Plenary Number S528

M529

Distribution of Bone Measures in Children at 11 Years of Age. J. C. Torner*, M. C. Willing², T. L. Burns*, E. Letuchy*, K. F. Janz*, T. Marshall*, J. M. E. Gilmore*, J. J. Warren*, S. M. Levy*. ¹Epidemiology, University of Iowa College of Public Health, Iowa City, IA, USA, ²Pediatrics, University of Iowa Carver College of Medicine, Iowa City, IA, USA, ³Epidemiology, University of Iowa Carver College of Medicine, Iowa City, IA, USA, ⁴Health and Sports Studies, University of Iowa College of Liberal Arts, Iowa City, IA, USA, ⁵Preventive and Community Dentistry, University of Iowa College of Dentistry, Iowa City, IA, USA.

The purpose of this study is to describe and characterize factors of bone development. A cohort of 481 children (251 girls and 230 boys) was evaluated for bone measures of area, bone mineral content (BMC) and density (BMD) using an Hologic 4500a. The children ranged in age from 10.5 to 12.4 years with a mean of 11.2 years. Even within this restricted age range BMD had a wide distribution.

BMD (gm/cm²) by Site

Location	Mean	Low	High
Hip	0.780	0.535	1.18
Spine	0.700	0.457	1.18

The coefficient of variation was 12.7 for hip BMD and 14.3 for spine BMD. Values for BMC were 21.5 (spine), 22.9 (hip), 17.7 (whole body) and 20.9 (whole body without head). Correlations of BMC between hip and other sites were higher (r=0.801) than correlations for BMD (r=0.659). Hip was more strongly correlated with total body BMC than spine was. Regression models for bone measures with gender, height, weight, and dichotomized Tanner stage as predictors showed that weight and height are the most important predictors of BMC levels. For hip and spine BMC and BMD, gender is also highly significant; Tanner stage is statistically significant (p<0.05) for spine BMC and BMD, whole body without head BMC and hip BMD, and marginally statistically significant (0.05<p-value<0.10) for hip BMC and whole body BMC. Overall, gender, body size and Tanner stage explain 56% of variation in spine BMC, 61% of variation in hip BMC, and 71 and 77% of variation in whole body BMC with and without head; they explain between 36 and 41% of variation in BMD measures. Cross-classification of quartiles adjusted by age, height, weight, gender and Tanner Stage showed that hip BMC and whole body BMC without head had the highest agreement for boys and for girls it was spine and whole body BMC. Quartile agreement for boys for BMD was 41.7% and for girls it was 43.4%. For the lowest quartile the lowest agreement was between hip and spine. These results show disparity in bone measures by site and suggest differential factors may be related to development.

Disclosures: J.M.E. Gilmore, None.

M530

See Sunday Plenary Number S530

M531

The Independent Contribution of Physical Activity to Bone Mass During Growth. M. Burrows¹, A. Baxter-Jones², H. M. Macdonald*, R. Mirwald², H. McKay¹. ¹Orthopaedics, University of British Columbia, Vancouver, BC, Canada, ²College of Kinesiology, University of Saskatchewan, Saskatoon, SK, Canada.

A few long-term prospective trials have demonstrated the relationship between physical activity and absolute values for bone mass in children. However, the unique contribution of physical activity to the bone gain trajectory (change in bone mass) is not well understood. We assessed bone mineral content velocity (Δ BMC (g/yr), Hologic QDR4500W) at the lumbar spine (LS), proximal femur (PF), femoral neck (FN) and total body (TB) in 361 boys and girls over 7 years (Healthy Bones Study). We obtained parental consent to assess these children aged 9-12 years at baseline. Lean mass (g) and fat mass (g) were obtained from TB scans. Physical activity score (PA score) was determined from a previously validated self-report questionnaire (PAQ-C). To control for the well-documented maturational differences between adolescent boys or girls of the same chronological age, we determined biological age (chronological age at peak height velocity (APHV determined from cubic spline fits) - chronological age at the time of measurement). If APHV had not occurred it was predicted using an anthropometric based regression equation (Mirwald, 2002). We used multi-level modeling to assess the independent contribution of physical activity to change (Δ) in BMC. Table 1 provides significant predictors (with coefficients) for PF and FN BMC Δ . Most notably, in girls each increment increase in PA score was associated with a 21.6g increase in BMC Δ at the FN (p<0.05). In boys, each increment increase in PA score predicted a 0.55g increase in BMC Δ at the PF (p<0.05). PA was a significant predictor of BMC Δ at the TB for girls only (p<0.05) [Δ TB BMC = $324(51) + 2370 + 104(6.5)\text{yrstart}_i + -13.8(2.1)\text{yrstart}_{2i} + -5.9(1.0)\text{yrstart}_{3i} + 7.9(2.3)\Delta\text{height}_{ij} + 0.02(0.003)\Delta\text{lean mass}_{ij} + 21.6(8.9)\text{physical activity score}_{ij} + e_{0ij}$]. Physical activity was an important predictor of bone mineral accrual across 7 years especially at weight bearing sites in boys and girls.

Table 1. Multi-level modeling significant predictors of BMC change in boys and girls

Δ BMC (g)	Boys (n = 183)	Girls (n = 178)
Total proximal femur (PF)	Δ height - 0.15 ± 0.05	Δ height - 0.17 ± 0.04
	Δ lean mass - 0.0006 ± 0.00005	Δ lean mass - 0.0006 ± 0.00005
	Δ fat mass - 0.0001 ± 0.00003	Δ fat mass - 0.0001 ± 0.00003
	Biological age - 0.55 ± 0.31	Biological age - 0.39 ± 0.30
	Physical activity - 0.42 ± 0.21	Physical activity - 0.30 ± 0.17
Femoral Neck (FN)	Δ height - 0.003 ± 0.006	Δ height - 0.002 ± 0.005
	Δ lean mass - 0.00007 ± 0.000005	Δ lean mass - 0.00007 ± 0.000007
	Δ fat mass - 0.000006 ± 0.000003	Δ fat mass - 0.000001 ± 0.000004
	Biological age - 0.04 ± 0.04	Biological age - 0.003 ± 0.006
	Physical activity - 0.09 ± 0.02	Physical activity - 0.02 ± 0.02

Values are estimated mean coefficients ± SEE (Standard Error Estimate); p<0.05 (mean > 2*SEE). Variables that did not enter were weight, ethnicity, calcium intake and years in study.

Disclosures: M. Burrows, None.

This study received funding from: Canadian Institute of Health Research.

M532

Determination of Bone Mass and Size in Term, Near-Term, and Preterm Boys. H. Abou Samra^{*1}, D. Stevens^{*2}, T. Binkley¹, B. L. Specker¹. ¹EA Martin Program in Human Nutrition, South Dakota State University, Brookings, SD, USA, ²Pediatrics, Sanford Hospital Medical Center, Sioux Falls, SD, USA.

The purpose of the study was to determine whether there are differences in bone mass and size among prepubertal boys who were born term (> 37 weeks), near-term (NT: 34 to 37 weeks), or at preterm (PT, ≤ 34 weeks gestation) and whether differences in strength or activity explained bone differences. Total body (TB), spine (LS) and hip DXA and pQCT measures of the distal tibia were obtained on 24 prepubertal boys aged 5.7 to 8.3 years. In multiple regression analysis, after adjusting for current weight, height, age, percentage body fat (%BF), and jump power, term boys had greater cortical thickness (p=0.03) and area (p=0.01), higher trabecular volumetric bone mineral density (aBMD) (p=0.05), TB BMC (p=0.01), and total hip BMD (p=0.01) than PT boys and higher TB BMC (p=0.01), TB bone area (p=0.04), total hip BMC (p=0.02) and BMD (p=0.01), and femoral neck BMC and BMD (both, p=0.02) than NT boys. There were no differences in activity measures among gestation groups and no group-by-activity interactions. In conclusion, term boys have greater bone size and mass than PT boys and higher bone mass than NT boys at several bone sites. Activity measures did not differ among gestation groups and did not explain bone differences. Our findings, if confirmed in larger populations, may have significant implications for bone health in near- and preterm children, a group that is thought to represent approximately 11.3% of all births.

Disclosures: H. Abou Samra, None.

This study received funding from: EA Martin Endowed Program.

M533

See Sunday Plenary Number S533

M534

Timing of Peak Bone Mass and Bone Mineral Density Are Influenced by High-Level Physical Activity in Young Adults of Both Sexes. S. Breban^{*}, C. Chappard, C. Jaffre^{*}, C. Benhamou. CHR Orleans, INSERM Unit U658, Orleans, France.

Optimization of Peak Bone Mass may help to prevent osteoporosis and sport is known to be beneficial for bone tissue by increasing Bone Mineral Density (BMD). No study has reported effects of physical activity on Peak bone Mass. Thus, the aim of this cross-sectional study was to analyse the influence of physical activity on timing and level of Peak Bone Mass.

70 girls and 90 boys aged 17-28 years participated in this study. The sample included 40 athlete-girls and 60 athlete-boys participating in weightlifting, ball collective sports or judo for more than 6 hours per week (9.6±3.5 hours per week for women and 10.4±3.7 for men). They were age and sex matched with control girls (n=30) and boys (n=30). Bone Mineral Content (BMC, g) and BMD (g/cm²) were measured by DXA (Delphi, Hologic®, Waltham, MA), at lumbar spine (LS) and non dominant femur (total and femoral neck (FN)). We also evaluated whole body (WB) BMC and BMD, with derived analysis of trunk, lower and upper limbs. Height, weight and body composition were derived from these DXA measurements. The timing of Peak Bone Mass was analysed by the inflexions of the age/BMD curves at all bone sites. Our variables were best fitted by second order polynomial regression equations. Thus, the model was expressed as y=ax²+bx+c. The age of maximal bone mass was determined as the maximum of the curve, i.e. when x = -b / 2a. Athletes had higher BMD measurements than controls in both sexes at all bone sites (p<0.05). Consequently all the Peak Bone Mass levels were significantly higher in athletes than controls. BMD peaks were achieved around 21.5 (FN), 22 years (LS), and 24-25 years (WB, upper and lower limbs) in athlete girls; BMD peaks were reached before 17 years for all bone sites except for LS (21.8 years) in control girls. In athlete boys, BMD peaks were reached before 17 years for upper and lower limbs, and ranged from 21.0 years (FN) to 25.5 and 26.0 years respectively for WB and LS. Finally, in control boys, BMD peaks were

reached before 17 years at all bone sites. Timing of Peak Bone Mass was different according to bone sites, sex and athletic or non athletic status. Thus, those results confirm that weight-bearing physical activity lead to a better bone status compared to non athletes, in both sexes and even after puberty. Moreover, our data suggest that the Peak Bone Mass was not reached at all bone sites before 17 years; thus, it is yet possible to optimize BMD and Peak Bone Mass in young adults between 17 and 28 years. High level weight-bearing physical activity seemed to induce a delayed and higher Peak Bone Mass compared to controls.

Disclosures: S. Breban, None.

M535

See Sunday Plenary Number S535

M536

Fat Mass Is Inversely Related to Subsequent Change in Bone Size and Mass in Young Prepubertal Children. K. S. Wosje¹, P. R. Khoury^{*1}, S. R. Daniels^{*2}. ¹Cincinnati Children's Hospital Medical Center, Cincinnati, OH, USA, ²The Children's Hospital, Denver, CO, USA.

Recent literature suggests that whole body fat mass (FM) may be positively related to periosteal bone formation in children. FM was reported to be positively associated with subsequent 2-year changes in whole body bone area (BA) and bone mass (BMC) in 9 year-olds, but this has not been examined in younger children. We hypothesized that there would be a positive relationship between FM at age 3.5 y and changes in BA and BMC from age 3.5 to 7 y, adjusting for race, sex, socioeconomic status [household income (HHI); N = 104 <\$50,000, N = 117 ≥\$50,000], exact age at baseline, change in whole body lean mass (LM), and change in height. 221 children [176 white (45% girls), 45 black (60% girls)] with data available from whole body DXA (Hologic 4500A) scans done within 3 months of both 3.5 and 7 years of age (interval 3.5 ± 0.2 y) as part of a longitudinal study of adiposity development were included. All 442 scans were confirmed by visual inspection of printed output to have no major limb or trunk movement. For the DXA measures of BA and BMC, the skull was excluded because the skull-inclusive whole body data may be affected by differences in relative head size over time within children. LM, height, BA and BMC were expressed as percentage change (Δ) from age 3.5 to 7 y. Data are mean ± SD. In bivariate analysis, FM at age 3.5 y was inversely associated with ΔBA (p<0.001) and ΔBMC (p<0.01). Blacks had greater ΔBA (32 ± 8 vs. 28 ± 6%, p<0.001) and ΔBMC (91 ± 15 vs. 80 ± 13%, p<0.001) than whites; neither ΔBA nor ΔBMC differed by sex or HHI (all p>0.2). In all children, ΔLM was not associated with ΔBA (p=0.1) but was positively associated with ΔBMC (p<0.001). As expected, exact age at baseline was inversely related to ΔBA and ΔBMC (both p<0.001); and Δheight was positively associated with ΔBA and ΔBMC (both p<0.001). In the final multiple regression model, FM at age 3.5 y remained inversely related to ΔBA (p<0.001) and ΔBMC (p<0.001) after adjusting for race, exact age at baseline, ΔLM and Δheight. There was no FM-by-race or FM-by-sex interaction in relation to ΔBA (both p>0.07) or ΔBMC (both p>0.4). Similar findings were obtained when LM, height, BA and BMC were expressed as absolute rather than percentage change from age 3.5 to 7 y, and baseline BA or BMC was included in the model. Our findings were opposite of our hypothesis and conflict with a prior report of a positive relation between FM and subsequent change in BA and BMC among older prepubertal children. Although our study provides indirect evidence that FM does not appear to be positively related to periosteal bone formation during the younger prepubertal years, studies with measures of cortical bone dimensions using pQCT would provide clarification.

Disclosures: K.S. Wosje, None.

This study received funding from: NIH.

T001

Prostaglandin D₂ in Human Bone Formation and Remodelling In Vivo. M. A. Gallant*, C. Wollén*, E. Chamoux, J. Parent*, S. Roux, A. J. de Brum-Fernandes. Division of Rheumatology, Département de Médecine, Faculté de Médecine et des Sciences de la Santé, Université de Sherbrooke, Sherbrooke, PQ, Canada.

Prostaglandin D₂ (PGD₂) is a lipid mediator implicated in several physiological and pathological events. We have previously showed that human osteoblasts produce PGD₂ and that this mediator decreases osteoprotegerin production through the activation of the DP receptor while it decreases RANKL secretion and increases osteoblast migration through the activation of the CRTH2 receptor, both present on osteoblasts (Gallant et al, JBMR 2005, 20:672-81). These results led to the hypothesis that PGD₂ could be an autacoid implicated in bone remodelling and exerting a positive feedback on osteoblasts. Our objective was to determine, in humans, if the PGD₂ stable metabolite 11 β -PGF_{2 α} was increased in conditions of high bone remodelling and formation in vivo.

We determined the levels of urinary 11 β -PGF_{2 α} and serum bone-specific alkaline phosphatase (BAP) and C-terminal collagen I telopeptide (CTX) in 17 patients with traumatic fracture 6 weeks post-fracture as well as in age- and sex-matched controls. Three patients with active untreated Paget's disease of bone and matched controls were also studied.

The age in patients with fracture varied from 18 to 46 (average 29.4 \pm 11.8 years old). Levels of 11 β -PGF_{2 α} were significantly increased in patients with of bone fractures compared to age- and sex-matched controls (59.86 \pm 6.37 vs 41.26 \pm 5.54 ng/mmol creatinine). No significant increases in BAP or CTX were observed in the whole fracture cohort. Men and women fracture subgroups both showed significantly elevated 11 β -PGF_{2 α} levels compared to their respective controls (62.66 \pm 13.51 vs 35.75 \pm 9.03 and 57.90 \pm 6.02 vs 33.16 \pm 3.74 ng/mmol creatinine for men and women, respectively). The women fracture subgroup presented a significant increase in CTX excretion compared to control (0.499 \pm 0.095 vs 0.239 \pm 0.021 ng/ml) but that was not observed in the men subgroup. Correlation analyses showed no significant correlation between 11 β -PGF_{2 α} levels and BAP or CTX in the whole cohort. In patients suffering from Paget's disease of bone, urinary levels of 11 β -PGF_{2 α} were also significantly higher than the controls, however the sample size prevented us from performing statistical analysis. As expected in PDB patients, the level of BAP was also higher than the controls, indicating a high level of bone formation in these patients. These results support our working hypothesis that PGD₂ could be implicated in the control of bone anabolism and remodelling in vivo in humans. They also suggest that the urinary levels of 11 β -PGF_{2 α} could be a sensitive marker of osteoblast activity.

Disclosures: M.A. Gallant, None.

This study received funding from: CUGR.URSC.

T002

Bone Turnover in Late Gestation and Six Months Postpartum. J. P. Greeves¹, J. Achten², A. Jeukendrup³, W. D. Fraser⁴. ¹QinetiQ Ltd, Farnborough, United Kingdom, ²Clinical Sciences Research Institute, Coventry, United Kingdom, ³University of Birmingham, Birmingham, United Kingdom, ⁴University of Liverpool, Liverpool, United Kingdom.

Pregnancy and the postpartum period are associated with a loss of bone mass. The aim of the present study was to monitor changes in bone turnover from late gestation to six months postpartum. The study was approved by the North Birmingham Local Ethics Committee.

Early morning blood samples were obtained after an overnight fast in 15 Caucasian pregnant subjects (Preg) at 31 wk gestation (Gest) and at 8, 17 and 26 wk postpartum (PP). Samples were obtained at the same time points in seven non-pregnant controls (Con) during the follicular phase of the menstrual cycle. At 8 wk PP, ten Preg subjects were breast feeding, four were bottle feeding and one was mixed feeding. At 26 wk PP, four Preg subjects were breast feeding and three were mixed feeding. All subjects were non-smokers and followed a standardised diet for 24-h prior to blood sampling. Pregnant and control subjects were matched for age (mean (SD): 30.5 (3.3) vs 29.8 (3.2) y), pre-pregnancy body mass index (22.2 (0.5) vs 24.1 (2.1) kg-m²) and leisure time physical activity (437 (198) vs 409 (196) kcal-d⁻¹, respectively). Blood samples were analysed for markers of bone resorption (β -CTX), bone formation (P1NP and Bone ALP), and OPG.

Mean (1SD) data for Preg and Con are shown in the Table. There was a significant increase in β -CTX and P1NP from Gest to the PP period in Preg (p<0.05) but no change in Con. In Preg, β -CTX increased from Gest to 8 wk PP (p<0.001) and 17 wk PP (p<0.05), and P1NP remained elevated at all PP time points (p<0.05). Bone ALP increased significantly in Preg from Gest to 8 wk PP (p<0.05). OPG decreased during PP compared with Gest (p<0.01), and was unchanged in Con.

In conclusion, bone turnover was significantly elevated during the postpartum period, compared to 31 wk gestation. Elevated bone turnover helps to provide sufficient calcium for breastfeeding. OPG is the decoy receptor for RANKL and the decrease to control levels postpartum be required to allow RANKL to stimulate osteoclast-mediated bone resorption

Table: Markers of bone turnover (β -CTX, P1NP and bone ALP), and OPG at 31 wk gestation (Gest) and during postpartum (PP) (mean (1SD))

		Gest	8 weeks PP	17 weeks PP	26 weeks PP
β -CTX (μ g-L ⁻¹)	Preg	0.49 (0.24)	0.83 (0.20) [*]	0.88 (0.47) [*]	0.72 (0.37)
	Con	0.40 (0.11)	0.33 (0.11)	0.34 (0.13)	0.32 (0.13)
P1NP (μ g-L ⁻¹)	Preg	49 (28)	104 (48) [*]	119 (65) [*]	108 (65) [*]
	Con	48 (17)	49 (18)	50 (20)	51 (19) [*]
bone ALP (U-L ⁻¹)	Preg	20 (6)	25 (8) [*]	27 (9)	26 (10)
	Con	18 (3)	18 (2) [*]	18 (2) [*]	17 (2) [*]
OPG (pg-mL ⁻¹)	Preg	7.8 (2.5)	5.1 (1.5) [*]	4.6 (1.2) [*]	4.7 (1.2) [*]
	Con	5.0 (1.3) [*]	4.9 (1.1)	4.8 (0.6)	4.8 (0.4)

significant difference from Gest (p<0.05), * (p<0.01), * (p<0.001).
significant difference from Preg (p<0.05), * (p<0.01), * (p<0.001).

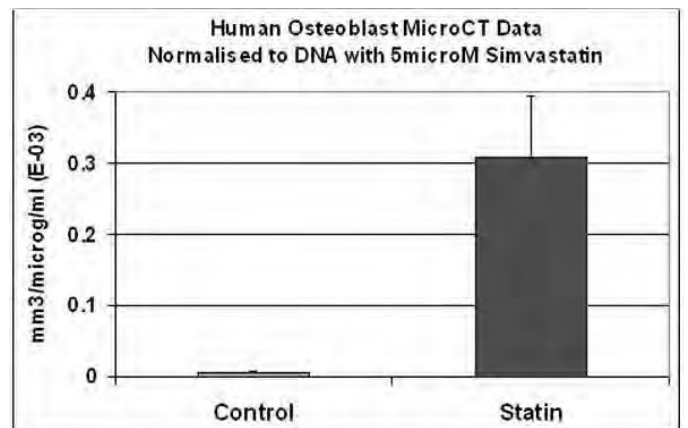
Disclosures: J.P. Greeves, None.

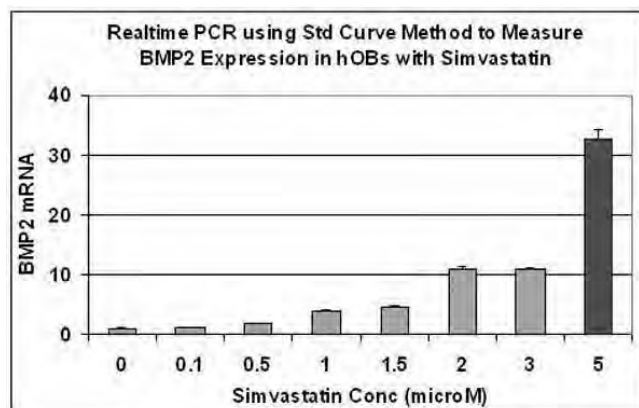
This study received funding from: The Human Capability Domain of the UK Ministry of Defence Scientific Research Programme.

T003

The use of Statins to Enhance Bone Mineralisation and Formation in 2D and 3D Tissue Engineered Constructs. S. Griffiths, S. Cartmell. Institute of Science and Technology in Medicine, University of Keele, Stoke on Trent, United Kingdom.

The culture of human bone cells for tissue engineering has great potential as a therapy for patients suffering from bone loss due to disease or trauma. This study has looked at using simvastatin, for the novel use of enhancing human bone cell tissue engineered constructs in vitro. Statins usually prescribed to lower cholesterol, can also enhance bone differentiation, maturation and matrix formation, with increased expression of BMP2 mRNA locally. Our study used simvastatin as a media supplement for in-vitro 2D and 3D primary human osteoblast seeded constructs, utilising gene expression analysis via Real-time RT-PCR, picogreen DNA assays, MicroCT and calcium analysis. Results of 2D cultures show low statin concentrations (0.001 microM) have a significantly increased proliferative effect in 3 (p=4.5E-05) and 7 day cultures (p=2.5751E-05), with a dosage dependent increase in BMP2 mRNA expression. This effect becomes significant after 1microM, though smaller doses also appear to have an enhancing effect (although this may be a result of increased proliferation). Higher optimised simvastatin concentrations (5microM) significantly reduce osteoblast proliferation (p=0.007), whilst gene expression showed significant increases in BMP2 and osteopontin mRNA suggest an increase in osteoblast differentiation and maturation at 7 days. This may be a result of the statin mechanism interacting with cell cycle regulators, pushing the osteoblasts into the maturation stage. 3D scaffold cultures showed increasing volumes of mineralised matrix production per cell in primary human cell cultures, using 5microM simvastatin as a media supplement. Optimised concentration/timing was then used in 2D cell culture, to maximise proliferation and mineralisation of bone constructs. Mineralisation and calcification were analysed using calcium assay/Von-Kossa staining, whilst picogreen DNA analysis was used for quantitative proliferative data. A further extension of this optimised experiment on a 3D hydroxyapatite scaffold is ongoing, with further analysis via MicroCT and microarray. Results suggest that various statin concentrations could be used with non-diseased bone tissue to enhance proliferation, differentiation and maturation of bone cells, when introduced at various culture periods to enhance mineralisation of extracellular matrix in bone tissue engineered constructs





Disclosures: S. Griffiths, None.

T004

Tartrate-Resistant Acid Phosphatase Is a Negative Regulator of Osteoblast Differentiation. H. C. Roberts^{*1}, R. Crossland^{*1}, T. M. Cox^{*2}, M. J. Evans^{*3}, A. R. Hayman¹. ¹School of Clinical Veterinary Science, University of Bristol, Langford, Bristol BS40 5DU, United Kingdom, ²Addenbrooke's Hospital, University of Cambridge, Cambridge CB2 2QQ, United Kingdom, ³School of Biosciences, University of Cardiff, Cardiff CF10 3US, United Kingdom.

Tartrate-resistant acid phosphatase (TRAP) is a molecule important in both the skeleton and the immune system. It is an iron containing protein expressed by osteoclasts, macrophages, dendritic cells and other cell types including osteoblasts. TRAP is secreted by osteoclasts during bone resorption and its serum activity correlates with the level of resorptive activity in certain bone diseases. We have shown using mice lacking TRAP (-/-) that TRAP is important for the normal development of the skeleton since the gross morphology of the bones in TRAP^{-/-} mice is abnormal. Femoral bones lacking TRAP were stronger and more mineralized and the rate of collagen turnover was increased. Femurs from knockout mice have increased tensile strength, increased MMP-2 activity and contain more total collagen cross-links. Osteoclasts from TRAP^{-/-} animals demonstrate reduced bone resorption in vitro. In this study we aim to determine the role of TRAP in the osteoblast.

We have isolated bone marrow from both TRAP^{-/-} and WT mice and used them in comparative studies. Alkaline phosphatase (ALP) activity was measured enzymatically using p-nitrophenyl phosphate as the substrate, and ALP protein by flow cytometry. Bone marrow cultures were grown to confluency (D-MEM/FCS/antibiotics). The cells were reseeded and the medium supplemented with 50µg/ml ascorbic acid and 50mM β-glycerolphosphate. At selected times cells were analysed for (i) cell viability using the 3-(4,5-dimethylthiazol-2-yl)-2,5-diphenyltetrazolium bromide (MTT)-dye reduction assay. (ii) ALP activity, (iii) mineral deposition (iv) cbfa-1 expression.

Single-colour flow cytometry using a monoclonal antibody to ALP showed that the TRAP^{-/-} cultures had increased numbers of ALP positive cells compared to wild-type (2.4 fold, p<0.05). TRAP^{-/-} bone marrow cells showed an increase in ALP activity compared with WT (1.8 fold, p<0.05). The rate of cell growth in the TRAP^{-/-} cultures was significantly reduced (p<0.05) and cellular morphology was altered. In cultures of TRAP^{-/-} osteoblasts ALP levels were higher and mineralisation occurred earlier after 3-4 days compared with 7-10 days for WT osteoblasts. Conventional PCR demonstrated an increase in the expression of cbfa1 and osteocalcin in TRAP^{-/-} osteoblasts.

In conclusion, TRAP^{-/-} mice have abnormal osteoblast function leading to an increased rate of differentiation and enhanced mineralisation. This work suggests that TRAP is a negative regulator of osteoblast activity.

Disclosures: A.R. Hayman, None.

This study received funding from: The Wellcome Trust.

T005

Independent of Their Resorptive Activity, Osteoclasts Secrete an Activity Promoting Bone Formation and Canonical Wnt Signalling in Osteoblastic Cells. K. Henriksen¹, A. V. Neutsky-Wulff^{*1}, K. D. Hausler^{*2}, M. Ciccomancini^{*2}, C. Christiansen³, M. Gillespie², T. J. Martin², M. A. Karsdal¹. ¹Nordic Bioscience A/S, Herlev, Denmark, ²St. Vincent's Institute of Medical Research, Melbourne, Australia, ³Center for Clinical and Basic Research, CCB, Ballerup, Denmark.

Some osteopetrotic mutations lead to low bone resorption, increased numbers of osteoclasts and increased bone formation, whereas other osteopetrotic mutations lead to low resorption, low numbers of osteoclasts and decreased bone formation. These findings indicate that the osteoclasts independent of their resorptive activity could be sources of anabolic signals for the osteoblasts.

The aim of the current study was to investigate whether osteoclasts secrete bone anabolic signals, and to elucidate the signal transduction involved.

Conditioned media from mature human osteoclasts cultured on either bone slices or plastic

were collected. Measuring TRACP and CTX-I validated osteoclast maturity and resorption. Conditioned media were applied to cultures of MC3T3-E1 preosteoblasts, followed by bone formation assessment by Alizarin red and Von Kossa staining after 20 days' culture. We assessed key osteoblast regulatory pathways by using UMR106.01 cells transiently transfected with several reporter constructs. These were the TOPFlash vector, which contains 8 TCF/LEF response elements, the osteocalcin promoter with x6 tandem OSE repeats (6 x OSE), NFAT, AP-1 and NFκB. In each case appropriate positive control stimuli were used.

Conditioned media from osteoclasts cultured on either bone or plastic stimulated nodule formation by the MC3T3-E1 cells to levels comparable to stimulation with 10ng/mL BMP-2. Conditioned media from osteoclasts cultured on both bone and plastic specifically induced activation of the TCF/LEF response system at a level comparable to induction by 20ng/mL of Wnt3A. The Wnt 3a and conditioned medium signals were equally inhibited by addition of either 100ng/mL of DKK1 or sclerostin, consistent with activation of the canonical Wnt signaling pathway. No activation of the OSE, NFAT, NFκB, or AP-1 reporters was detected, suggesting specific wnt activity.

We present evidence that osteoclasts, independent of their resorptive activity, secrete an activity that stimulates osteoblastic bone formation. The same media contains an activity that signals through the wnt activation cascade, indicating a wnt as a possible anabolic product, i.e. a potential coupling factor, produced by the osteoclasts.

Disclosures: K. Henriksen, None.

T006

Alpha1 and Beta2 Adrenergic Agents Modify RANKL/OPG Expression and Cell Proliferation in Human Osteoblasts and Osteoblastic Cells. H. H. Huang, T. C. Brennan^{*}, M. M. Muir^{*}, R. S. Mason. Department of Physiology and Bosch Institute, University of Sydney, Sydney, Australia.

Previous studies have shown that central control of bone mass is mediated via beta2 receptors of the sympathetic nervous system ⁽¹⁾. Whether alpha adrenergic receptors are expressed in human bone cells is controversial ^(1,2). Takeuchi et al ⁽³⁾ showed that epinephrine increased both RANKL and OPG mRNA expression in murine osteoblast-like cells via beta and alpha adrenergic receptors. The aim of this study is to further investigate alpha and beta adrenergic receptors in human bone cells. Human osteoblastic MG63 cells and primary human fetal bone cells (FBC) were cultured in DMEM with 10% FBS then adapted to serum-free medium for 24 h before treatments were added. Alpha1b and beta2 adrenergic receptors were expressed in MG63 cells and FBC as determined by RT-PCR (alpha1b, beta2) and sequence analysis (alpha1b). In FBC, 10⁻⁵M cirazoline (specific alpha1 agonist) increased OPG and RANKL mRNA expression by 1.43 (p<0.01) and 1.36 (p<0.001) times respectively, while only high-dose cirazoline (10⁻³M) up-regulated OPG (3-4-fold) and RANKL (over 10-fold) in MG63. Fenoterol, (beta2 agonist) at 10⁻⁷M-10⁻⁵M dose-dependently up-regulated OPG mRNA expression (p<0.05) but only 10⁻⁷M fenoterol increased RANKL mRNA expression (p<0.05) in FBC. Phenylephrine (alpha1 agonist) dose-dependently increased cell replication in both FBC (10⁻⁶-10⁻⁴M) and MG63 (10⁻⁶-10⁻⁵M), as did cirazoline in FBC. The beta2 agonist fenoterol suppressed FBC proliferation (10⁻⁶-10⁻⁵, p<0.001). The maximal effects of cirazoline in FBC and phenylephrine in MG63 at 10⁻⁶M on proliferation were partially suppressed by 10⁻⁴M urapidil (alpha1 antagonist). These data indicate that alpha1 adrenergic receptors are present in human bone cells and could play a role in modulation of bone turnover by the sympathetic nervous system in human bone cells.

1. Takeda, S. et al. (2002), Cell 111: 305-317.

2. Togari, A. (2002), Microsc Res Tech 58: 77-84.

3. Takeuchi, T. et al. (2000), Biochem Pharmacol 61: 579-586.

Disclosures: H.H. Huang, None.

T007

An Isoform of Fibronectin Is Responsible for Decreased Bone Formation in Patients with Primary Biliary Cirrhosis and this Effect Is Not Exclusively Mediated by beta1 Integrins. N. Kawelke^{*1}, A. Bentmann^{*1}, N. Hackl^{*1}, P. Feick^{*2}, M. V. Singer^{*2}, I. Nakchbandi³. ¹University of Heidelberg, Heidelberg, Germany, ²University of Heidelberg at Mannheim, Mannheim, Germany, ³University of Heidelberg and Max-Planck Institute for Biochemistry, Heidelberg, Germany.

Patients with chronic cholestatic liver disease experience a decrease in bone formation and density associated with an increase in fracture rates. The cause for this bone loss remains elusive. We have reported that oncofetal fibronectin (oFN) is elevated in patients with primary biliary cirrhosis (PBC) and correlates negatively with circulating osteocalcin levels. To determine a causal relationship between the elevation of oFN and bone loss in subjects with PBC we performed in vitro and in vivo experiments in mice.

Fibronectin (FN) was isolated from amniotic fluid (aFN) and characterized as containing both the EIIIA domain and the glycosylated variable region domain (oFN). In vitro experiments showed that mineralization by osteoblasts is diminished to the same degree whether aFN contained the EIIIA domain or not (71% vs. 78% decrease in mineralization using 100 ug/ml FN). This suggests that the presence of the glycosylated variable region was responsible for the decrease in mineralization.

Injection of aFN in CD1 mice for 10 days (1 mg/day/mouse) resulted in a 17% drop in trabecular BMD compared to controls ($p < 0.05$) as measured by pQCT. There was a 30% decrease in mineralizing surface (MS/BS = 44.7 ± 3.1 in controls vs. 31.2 ± 1.6 % in injected mice, $p < 0.005$), and a decrease of 45% in the number of osteoblasts (Ob.N/mm BS = 18.2 ± 1.4 in controls and 10.0 ± 0.8 in injected mice, $p < 0.05$).

In order to determine whether this effect is mediated by beta1 integrins we repeated the experiment in mice in which beta1 integrin was deleted using the collagen alpha1(I)-cre promoter (Beta1 integrin floxed/floxed-Collagen alpha1(I)-cre/+). Similarly to CD1 mice there was a significant decrease of 50% in the number of osteoblasts when aFN was injected over a period of 10 days (Ob.N/mm BS: 25 ± 3 vs. 13 ± 1 , $p < 0.01$; $n = 8$ controls and 4 injected mice).

In summary, we have shown that 1) in patients with PBC the glycosylated variable region of FN as recognized by the FDC-6 antibody correlates negatively with osteocalcin, 2) decreased mineralization by osteoblasts in vitro is caused by the presence of the same domain, and 3) injection of FN containing this domain in mice results in a significant decrease in osteoblasts number that is not exclusively mediated by the presence of beta1 integrins on the surface of osteoblasts expressing the collagen alpha1(I) promoter.

We therefore propose, that oncofetal fibronectin is responsible for decreased bone formation in patients with primary biliary cirrhosis.

Disclosures: N. Kawelke, None.

T008

Osteogenesis of the Human Ligamentum Flavum by Demineralized Bone Matrix. J. Lee^{*1}, H. Kim^{*2}, C. Lee^{*1}, M. Nan^{*1}, K. Lee^{*2}, S. Moon^{*3}, J. Park^{*3}, H. Kim^{*3}, J. Jahng³, H. Lee^{*3}, H. Kim^{*3}. ¹Orthopaedic Surgery, BK21 Medical Science Graduate School of Yonsei University, Seoul, Republic of Korea, ²Korea Bone Bank, Seoul, Republic of Korea, ³Orthopaedic Surgery, Yonsei University College of Medicine, Seoul, Republic of Korea.

Many attempts have been made to apply demineralized bone matrix for bone regeneration. It has been reported that DBM derived from human tissues induces bone formation and spinal fusion, and that DBM is widely used as a bone graft substitutes in orthopaedic and dental surgery. In addition, Ligamentum flavum (LF) was reported to have osteogenic potential with stimulation of bone morphogenetic protein-2 which is also included in DBM. Although many potential studies for osteogenesis by DBM have been evaluated, osteogenesis of human LF by DBM have not yet been found. In this study, we elucidated the effect of DBM on osteogenesis of human LF. Experimental group (human LF cell culture) was incubated in media solution containing 5mg/ml or 10mg/ml DBM for 2hr, 2day and 7days, and control group was incubated in media which have no DBM. To assess proliferation rate, we performed Alamar blue assay. To assess osteoinductivity, we performed RT-PCR of osteogenic marker gene and von-kossa, alkaline phosphatase (ALP) staining after incubating LF with DBM. DBM, LF and mixture of DBM and LF was implanted to nude mouse. After 28days, H&E staining was performed. Human LF cell cultured with DBM showed increased proliferation without cytotoxicity compared to control in dose-dependent manner. The expression of collagen type I, osteocalcin, osterix, dIIX5, Human MSX2 mRNA demonstrated upregulation of osteogenic phenotype. Also, result of ALP, von-kossa and H&E staining were shown that experimental group, LF by adding the DBM, showed positive osteogenesis compared to control group. We proved that human LF cells cultured with DBM showed increase in proliferation and upregulation of osteogenic phenotypes. Given osteogenic potential of human LF with DBM, autogenous LF can be used for carrier for DBM and bone graft substitute in spinal surgery. The application of mixture DBM and LF will likely be useful in the clinical reconstruction of bone.

Disclosures: J. Lee, None.

T009

Healing of Critical-sized Bone Defects by Endothelial Progenitor Cells. D. Lewinson¹, N. Rozen^{*2}, T. Bick^{*1}, B. Shemian^{*1}, A. Yayon^{*3}, M. Soudry^{*1}. ¹Research Institute for Bone Repair, Orthopaedic Surgery A, Rambam Health Care Campus, Haifa, Israel, ²Research Institute for Bone Repair, Rambam Health Care Campus, Haifa, Israel, ³ProChon BioTech LTD, Ness-Ziona, Israel.

In this study we developed a novel cell therapy method for promoting repair of large bone defects. Our model tested the healing potential of circulating autologous endothelial progenitor cells (EPC) in a critical-sized bone defect created in sheep tibia. Peripheral mononuclear fraction was isolated using LymphoprepTM (Axis-Shield, Oslo, Norway), seeded on fibronectin-coated plates and cultured in EBM-2 media supplemented with EGM-2MV SingleQuote (Clonetics, Cambrex Bio Science, MD, USA). The endothelial nature of adherent colonies was identified by incorporation of Dil-acetylated LDL (Molecular Probes, Oregon, USA), tube formation on Matrigel (BD Labware, MA, USA) and immunostaining for von Willebrand factor (Dako, Glostrup, Denmark). A defect of 3.2 cm was created in the mid-shaft of sheep tibia, partially preserving the periosteum. Two weeks later, a longitudinal wedge was cut along the regenerating tissue filling the gap, 2×10^7 EPC were transplanted into the formed tunnel and covered with the removed scar tissue. Sham-operated sheep served as controls. Bone regeneration was followed during the next three months by x-rays radiography every two weeks. At the end of the experiment, the operated fragment bone was removed and subjected to a detailed qualitative and quantitative 3-D evaluation at a resolution of 36 micrometers using a micro computed tomography (μ CT) imaging system (μ CT 40, Scanco Medical, Bassersdorf, Switzerland). No significant new bone formation was observed radiographically in 4 sham-operated sheep. In contrast, 5 out of six EPC-transplanted sheep showed full bridging at 3 months, starting 2 to 4 weeks post EPC transplantation. Data collected showed an increase of 500% of total tissue volume (TV), 700% of bone volume (BV) in EPC-transplanted gaps vs. sham-operated ones. Material density increased 2-folds both in the entire volume and in the mineralized tissue compartment. We conclude that EPC have a promising potential for healing of large bone defects.

Disclosures: D. Lewinson, ProChon BioTech LTD 2, 3.

This study received funding from: Ministry of Industry & Commerce, Government of Israel and ProChon Bio Tech LTD.

T010

How Does Hypoxia Contribute to the Formation of the External Apical Root Resorption In Vitro? D. Liu, Z. Ou^{*}. Developmental Sciences/Orthodontics, Marquette University, Milwaukee, WI, USA.

Objectives: External apical root resorption (EARR) is commonly seen in orthodontic patients. However, how the EARR is formed under orthodontic force is not known. When a mechanical force is applied to move a tooth, an immediate response is the compression of periodontal ligament, which often leads to occlusion of the capillary blood vessels in it, in turn, forms an ischemia zone within which all the surrounding cells are subjected to hypoxia. Cementoblasts are cementum (first barrier to be attacked during EARR) - forming cells and have been shown to be involved in the repair of EARR. Therefore, we hypothesize that hypoxia plays an active role in the formation of EARR via the regulation of cementoblasts. The purpose of this study is to investigate the effect of hypoxia on the biological responses of cementoblasts in vitro. Methods: OCCM.30 cells - an immortalized murine cementoblastic cell line (from Somerman MJ, U. Washington), were seeded onto glass slides coated with type I collagen ($10 \mu\text{g}/\text{cm}^2$) and grown in α -MEM with 10% FBS. Upon confluent, OCCM.30 cells were starved for 24 hours then subjected to 1% hypoxia challenge while controls were kept under normal culture condition of 95% air and 5% CO_2 . For the early signaling study, after the onset of hypoxia, media were collected at 5 and 15 minutes to determine the release of ATP and PGE_2 . For the long-term functional study, the cells were subjected to 1% hypoxia for 0.5, 1, 3, 6, 12 hours to determine the induction of hypoxia-inducible factor 1- α (HIF-1 α) and production of cyclooxygenase-2 (COX-2) and sclerostin (SOST - a negative regulatory protein for bone formation) by western blot analysis. Paired t test was used to compare hypoxia treated and untreated groups for each parameter with p value being set at 0.05. Results: For the short-term changes, 1% hypoxia induced a drastic release of ATP at 5min followed by increased PGE_2 release at 15min. For the long-term changes, 1% hypoxia significantly induced HIF-1 α production after 3 hours, with a peak reached at 12 hours. COX-2 production was significantly increased after 6 and 12 hours of 1% hypoxia. Interestingly, SOST was for the first time found not only expressed in OCCM.30 cementoblasts but also increased after 6-12 hours of 1% hypoxia. Conclusions: Our data indicate that hypoxia modulates both early molecular signaling and late functional responses of cementoblasts, suggesting its potential role in the modulation of cementum remodeling towards resorption. Clinically, mechanical load exceeding the capillary blood pressure leading to an ischemia-associated hypoxia in periodontal ligament should be avoided to reduce the risk of root resorption during orthodontics. This work was supported by AAOF and EOS research grants.

Disclosures: D. Liu, None.

T011

Indian Hedgehog Is Essential for Postnatal Bone. Y. Maeda^{*1}, R. G. Erben^{*2}, E. Schipani^{*3}, B. Lanske¹. ¹Developmental Biology, Harvard School of Dental Medicine, Boston, MA, USA, ²Department of Natural Science, University of Veterinary Medicine, Vienna, Austria, ³Endocrine Unit, Massachusetts General Hospital and Harvard Medical School, Boston, MA, USA.

Indian hedgehog (Ihh) is essential for chondrocyte proliferation/differentiation and osteoblast differentiation during prenatal endochondral bone formation. Recently we

reported the generation and characterization of tamoxifen-inducible conditional *Ihh* knockout mice (*Col2a1-Cre ER**; *Ihh* d/d), in which the *Ihh* gene was successfully ablated from chondrocytes after birth. Our results demonstrated for the first time that *Ihh* expression in postnatal chondrocytes is essential for maintaining a growth plate, and for sustaining trabecular bone, a normal articular surface, and eventual bone growth after birth. We also showed that Wnt signaling was significantly decreased in these mice suggesting that *Ihh* activates osteoblast differentiation via the Wnt signaling pathway in postnatal life. Loss of trabecular bone in the *Col2a1-Cre ER**; *Ihh* d/d mutants could be secondary to their growth plate abnormalities. To examine the direct role of *Ihh* on postnatal bone formation, maintenance of a growth plate in the mutants would be required. We, therefore, induced deletion of *Ihh* in chondrocytes at P14, after a secondary ossification center was formed. At P21, however, the growth plate was completely lost and time course experiments are being performed now to investigate the kinetics of this event. In order to dissect whether the loss of the growth plate or the lack of *Ihh* signaling itself in chondrocytes is responsible for the decrease in trabecular bone, we are now attempting to rescue the growth plate of the *Col2a1-Cre ER**; *Ihh* d/d animals by mating them to *col2a1*-constitutively active *PTH/PTHrP* receptor transgenic mice (*col2a1-Jansen*). Using such compound mutant mice, we anticipate rescue of the growth plate despite absence of *Ihh* signaling. This will allow us to study specific actions of chondrocyte-derived *Ihh* on postnatal bone.

Disclosures: Y. Maeda, None.

T012

Potential Involvement of Ephrin B2 in the Anabolic Action of PTH in Osteoblasts. E. H. Allan^{*1}, K. D. Hausler^{*1}, J. M. W. Quinn¹, J. Gooi^{*1}, T. Wei^{*2}, J. E. Onyia², N. A. Sims¹, M. T. Gillespie¹, T. J. Martin¹. ¹Bone, Joint & Cancer, St Vincent's Institute, Melbourne, Australia, ²Lilly Research Laboratories, Indianapolis, IN, USA.

The aim was to identify paracrine factors whose production is controlled by PTH and/or PTHrP, using a mouse marrow stromal cell line, Kusa 4b10 that acquires osteoblast features under differentiating conditions. After the appearance of functional PTH1R in Kusa 4b10 cells they were treated with either PTH(1-34) or PTHrP(1-141) for 1, 6 and 24 hours and RNA subjected to Affymetrix whole mouse genome array. The data was analysed statistically by SAM (significance analysis of micro-arrays). Of the 45101 probes used on the micro-array, 4621 probes or 3231 genes with functional annotations were differentially expressed by at least 1.5 fold with false discovery rate < 0.1. These genes were then functionally categorized into 228 groups according to their Gene Ontology. Among genes belonging to the family of Ephrins and their receptors, Ephrin B2 and Eph B2 were up-regulated in response to PTH and PTHrP. The effects were validated using independently prepared RNA samples from differentiated Kusa 4b10 cells, UMR106 rat osteogenic sarcoma cells, and primary mouse calvarial osteoblasts, as well as in vivo using RNA prepared from metaphyseal bone of 3 week-old rats 1.5 and 4 hrs after a single PTH injection. Stimulation of mRNA for Ephrin B2 by PTH and PTHrP was maximal at 4-6 hrs, with a 3-6-fold response. The effect was dose-dependent and the curve shifted to the left with phosphodiesterase inhibition. Western blotting showed a sustained increase in Ephrin B2 protein following treatment of Kusa 4b10 cells with PTH for 6, 12 and 24 hours. Neither IL-11 nor active vitamin D affected Ephrin B2 production. Whereas Ephrin B2 production was clearly regulated in osteoblasts by PTH/PTHrP through a cAMP/PKA mechanism, its baseline production remained unchanged throughout differentiation. No evidence was obtained for regulation by PTH/PTHrP of Eph B4 production, which also remained unchanged throughout differentiation. Eph B2 mRNA was increased 2-fold and Ephrin A5 decreased 2-fold after 6 hrs PTH or PTHrP treatment. Recent evidence implicates osteoclast-derived Ephrin B2 acting through its receptor, EphB4 in osteoblasts, to promote osteoblast differentiation, and through reverse signalling via EphB4 and possibly other members of the receptor family to suppress the formation of osteoclast precursors. The present data raise the possibility that ephrinB2 might act in a paracrine or autocrine manner on the osteoblast under the influence of PTH, and provide a local event related to the anabolic action of PTH.

Disclosures: T.J. Martin, None.

T013

Acceleration of Fracture Healing via Enhanced Vasculogenesis and Osteogenesis Through SCF/cKit Pathway in Lnk-Deficient Mice. T. Matsumoto¹, H. Nishimura^{*1}, Y. Mifune¹, T. Shoji^{*1}, R. Kuroda^{*2}, A. Kawamoto^{*1}, A. Oyamada^{*1}, M. Horii^{*1}, M. Miwa^{*2}, M. Kurosaka^{*2}, T. Asahara^{*1}. ¹Stem Cell Translational Research, Kobe Institute of Biomedical Research and Innovation / RIKEN Center for Developmental Biology, Kobe, Japan, ²Department of Orthopedic Surgery, Kobe University Graduate School of Medicine, Kobe, Japan.

Lnk, with APS and SH2-B, belongs to an intracellular adaptor protein family and was recently proved an essential inhibitory signal molecule of the stem cell factor (SCF)-cKit signaling pathway for self-renewal of stem cells in the findings demonstrating enhanced hematopoietic reconstitution in Lnk-deficient mice. We previously reported that systemic administration of human hematopoietic/endothelial progenitor cell (HPC/EPC)-enriched population induces osteogenesis as well as vasculogenesis and provides a favorable environment for functional bone healing in non-healing fracture model of immunodeficient rat. Therefore, we investigated the hypothesis that a lack of Lnk signaling enhances the regenerative response via vasculogenesis and osteogenesis in fracture healing in Lnk-deficient mice. In radiological and histological evaluations, reproducible model of closed femoral fracture in 10-week-old mice demonstrated more prompt fracture healing in Lnk-

knock out (KO) than wild-type (WT) mice (week2: KO, 70%; WT, 35%, p<0.01, week3: KO, 100%; WT, 90%, n=20). Serial FACS analysis of peripheral blood (PB) demonstrated significantly larger number of Sca1+ Lin- cells, HPC/EPC-enriched fraction (HPC/EPCs), in KO than WT (p<0.05), and significantly increased HPC/EPCs by fracture-stress with the peak at 1 day post-fracture (p<0.05). Among up-regulated gene expressions at the peri-fracture site by cDNA microarray in KO, angiogenesis/vasculogenesis (CD31, VE-cadherin, KDR) and osteogenesis (Osteocalcin, Collagen1A1, Cbfa1/Runx2) related gene expression assessed by real time RT-PCR were significantly enhanced 7 days post-fracture in KO compared to WT (p<0.01). Immunohistochemical staining at the peri-fracture site demonstrated significantly enhanced density of Sca1+ cell-derived endothelial cells (ECs)(Sca1+/CD31+) and osteoblasts (OBs)(Sca1+/Osteocalcin+) 7 days post-fracture in KO compared to WT (p<0.05). Moreover, in addition to a significant higher expression of plasma SCF in KO compared to WT by ELISA (p<0.01), SCF stimulation enhanced these mobilization and incorporation of HPC/EPCs even in WT and more in KO, confirmed by analysis of PB FACS (p<0.05), EC (p<0.05), and OB density (p<0.05). Our data suggest the therapeutic potential of negatively controlling the Lnk system via SCF-cKit pathway for promoting an environment conducive to vasculogenesis and osteogenesis so that fractures can heal promptly.

Disclosures: T. Matsumoto, None.

T014

Withdrawn

T015

Bone Plays an Important Role in the Metabolism of Postprandial Lipoproteins in Mice: Impact on Osteoblast Function. A. Niemeier¹, D. Niedzielska^{*2}, R. Secer^{*2}, A. Schilling^{*3}, M. Merkel^{*4}, C. Enrich^{*5}, P. C. Rensen^{*6}, J. Heeren^{*2}. ¹Orthopaedics, University Medical Center Hamburg-Eppendorf, Hamburg, Germany, ²Biochemistry and Molecular Biology II: Molecular Cell Biology, University Medical Center Hamburg-Eppendorf, Hamburg, Germany, ³Trauma- Hand- and Reconstructive Surgery, University Medical Center Hamburg-Eppendorf, Hamburg, Germany, ⁴Internal Medicine, University Medical Center Hamburg-Eppendorf, Hamburg, Germany, ⁵Biologia Cellular, Facultat de Medicina, Universitat de Barcelona, Barcelona, Spain, ⁶General Internal Medicine, Endocrinology and Metabolic Diseases, Leiden University Medical Center, Leiden, The Netherlands.

Dietary lipids and lipophilic vitamins are transported by postprandial lipoproteins and are required for bone metabolism. Despite that, it remains unknown whether bone cells are involved in the uptake of circulating postprandial lipoproteins in vivo. The current study was designed to investigate a putative participation of bone in the systemic postprandial lipoprotein metabolism in mice, to identify potentially involved cell type populations and to analyze whether lipoprotein uptake affects bone function in vivo.

As a model for the postprandial state, chylomicron remnants (CR) were injected intravenously into mice. Bone was compared to organs with an established role in CR catabolism. CR organ distribution and cellular uptake was analyzed by immunohistochemistry, confocal laser microscopy and electron microscopy. Radiolabeled CR were used for quantification of organ-specific plasma clearance and uptake into primary osteoblasts and hepatocytes. The effect of vitamin K1-enriched CR on plasma osteocalcin was determined by radioimmunoassay.

Next to the liver, bone appeared to contain the most active cells for the uptake of radioactive and fluorescent CR particles from the circulation in vivo. Immunostaining for apoE proved that intact CR particles were taken up in both liver and bone, but not in other organs. Uptake of CR by primary murine osteoblasts and hepatocytes was in a similar range in vitro. Localization studies in bone showed strongest primary binding to sinusoidal endothelial cells, while particle uptake was also observed into macrophages and osteoblasts. Enrichment of injected CR with vitamin K1 resulted in an increase of the degree of osteocalcin carboxylation in vivo.

In conclusion, bone is an organ of major importance in the postprandial lipoprotein metabolism. Bone function in vivo appears to be directly influenced by CR uptake, which has an impact on the secretory function of osteoblasts. This study uncovers a close functional relation between the systemic lipoprotein metabolism and bone metabolism.

Disclosures: A. Niemeier, None.

This study received funding from: Deutsche Forschungsgemeinschaft.

T016

Isolation and Immunohistochemical Analysis of Osteomodulin Expressed in Osteoblast. K. Ninomiya^{*1}, T. Miyamoto², N. Fujita^{*3}, T. Suzuki^{*1}, R. Iwasaki^{*4}, M. Yagi^{*3}, Y. Toyama^{*3}, T. Suda^{*5}. ¹Orthopaedic Surgery and Cell Differentiation, Keio University School of Medicine, Tokyo, Japan, ²Cell Differentiation, Orthopaedic Surgery and Musculoskeletal Reconstruction and Regeneration Surgery, Keio University School of Medicine, Tokyo, Japan, ³Orthopaedic Surgery, Keio University School of Medicine, Tokyo, Japan, ⁴Dentistry and Oral Surgery and Cell Differentiation, Keio University School of Medicine, Tokyo, Japan, ⁵Cell Differentiation, Keio University School of Medicine, Tokyo, Japan.

The bone volume is regulated with the well-controlled balance between bone-resorbing osteoclast and bone-forming osteoblast, which is called coupling. Although coupling is a well-known phenomenon, coupling factor has not been identified. To isolate the coupling factor, we performed microarray and cluster analysis among rat 13 tissues, and isolated osteomodulin (OMD) as a candidate of coupling factor. OMD is an extracellular matrix keratin sulfate proteoglycan that belongs to small leucine-rich repeat proteoglycans (SLRPs). Though OMD is not expressed in osteoclast, the expression of OMD couples with osteoclast markers such as matrix metalloproteinase-9 (MMP-9) and tartrate-resistant acid phosphatase (TRAP) in bone. SLRPs are known to have diverse functions such as regulation of matrix assembly, cell growth, and cell differentiation. In *in vitro*, OMD is expressed in primary osteoblasts and is upregulated during osteoblastic differentiation. To investigate the localization of OMD in *in vivo*, we established an anti-OMD polyclonal antibody. OMD is mainly produced by alkaline phosphatase (ALP) positive osteoblast. The specificity of the anti-OMD antibody was confirmed by the blocked immunoreactivity of the antibody by synthetic peptide. Op/op mice are osteopetrotic because of defective osteoclast formation due to the lack of macrophage colony-stimulating factor (M-CSF) production. Intriguingly, the immunoreactivity of anti-OMD antibody in trabecular bone in op/op mice is weaker than that of wildtype mice. Since osteoblasts do not express c-fms, a M-CSF receptor, the reduced OMD expression in op/op mouse is confirmed based on the lack of coupling due to a defect of osteoclast formation. We also confirmed that expression of OMD in C2C12 cells increased accompanied by an upregulation of ALP activity during osteoblastic differentiation. Because some members of SLRPs inhibit signal of transforming growth factor (TGF), OMD could modulate differentiation of osteoblast and osteoclast by inhibition of TGF signal. Our results suggest that OMD is expressed in osteoblasts especially activated by osteoclast.

Disclosures: K. Ninomiya, None.

T017

Induction of Mineralized Tissues by In Vivo Transplantation of Cultured Rat Dental Pulp Cells in Rat Calvarial Bone Defects. H. Ohba, H. Seto, K. Tokunaga, H. Hama, Y. Inagaki, M. Horibe, E. Takeda, T. Nagata. Health Biosciences, Tokushima, Japan.

Dental pulp tissues have a potency to form mineralized tissues. We investigated the ability of dental pulp cells for mineralized tissue induction *in vitro* and *in vivo*. Dental pulp tissues were extracted from maxillary incisors of male Wistar rats. The tissues were minced and digested with 0.5% trypsin and 0.02% EGTA. Dissociated cells were cultured in Eagle's MEM. After subconfluency, cells were collected and seeded in multi-well plate with or without 2 mM β -GP and 50 μ g/ml ascorbic acid. Alkaline phosphatase (ALP) activity was determined on days 1 and 5 and the von Kossa staining was performed to detect bone nodule (BN) formation on day 20. Also, the association of bone morphogenetic protein (BMP) on such a mineralized tissue formation was determined by ELISA. The subconfluent dental pulp cells were collected and used in the following *in vivo* study. Bone defects were made in male Wistar rat calvaria (hole shape, 3.8 mm diameter). The collected dental pulp cells were transplanted in the defects with collagen sponges including 1% collagen gel (2.5×10^6 cells/ml). After 8 weeks, rat calvariae were taken out and analysed by soft X-ray and histological examinations. Results showed that ALP activity increased and BNs were clearly formed in the dental pulp cell cultures. ELISA assay showed that dental pulp cells produced BMP and the amount of BMP in the condition medium time-dependently increased, showing 3-fold amount of BMP compared to the control on day 15. The soft X-ray and histological examinations revealed that the transplantation of dental pulp cells induced a greater amount of bone-like tissues in the inside of calvarial bone defects than in the controls, showing 4-fold increase of radiopaque area. Hematoxylin and eosin staining demonstrated that there were many osteoblast-like cells around the new-formed tissues. Present findings indicate that bone defects were recovered by the transplantation of dental pulp cells, suggesting that dental pulp cells have a potency to form mineralized tissues in association with BMP production.

Disclosures: H. Ohba, None.

T018

Imatinib Mesylate Inhibits Bone Formation and Decreases Bone Mass In Vivo by Inhibiting PDGFR-Mediated Osteoblast Mitogenesis. S. O'Sullivan^{*1}, D. Naot^{*1}, K. Callon^{*1}, M. Watson^{*1}, G. Gamble^{*1}, M. Karsdal^{*2}, M. Ladefoged^{*2}, J. Cornish¹, P. Browett^{*3}, A. Grey¹. ¹Medicine, University of Auckland, Auckland, New Zealand, ²Nordic Bioscience, Herlev, Denmark, ³Pathology and Molecular Medicine, University of Auckland, Auckland, New Zealand.

Imatinib mesylate, an orally active inhibitor of the c-abl (including bcr/abl), c-kit and platelet-derived growth factor receptor (PDGFR) tyrosine kinases, is in clinical use for the treatment of chronic myeloid leukaemia (CML) and gastrointestinal stromal cell tumours (GIST). Genetic interruption of both c-kit and c-abl signaling in mice induces osteopenia, and treatment with PDGF increases bone mass in rodents, suggesting that imatinib might have adverse effects on the skeleton. *In vitro*, imatinib exerts complex effects in bone cells. It inhibits the proliferation of osteoblast-like cells induced by both low-dose serum and PDGF. Neither addition of SCF, the c-kit ligand, nor siRNA-mediated knockdown of c-abl, alters osteoblast mitogenesis. Imatinib dose-dependently increases osteoblast differentiation, also by inhibiting PDGFR signaling, an observation that might explain the early increase in bone formation markers observed in humans with CML starting therapy with imatinib. In murine bone marrow cultures, imatinib inhibits osteoclastogenesis stimulated by 1,25 dihydroxyvitamin D₃ and partially inhibits osteoclastogenesis induced by treatment with RANKL and M-CSF. Consistent with these findings, imatinib partially inhibits osteoclastogenesis in RANKL-stimulated RAW-264.7 cells. Treatment with imatinib increases the expression of OPG in bone marrow from CML patients, and osteoblastic cells *in vitro*. In order to elucidate the skeletal effects of imatinib *in vivo*, we treated 6 month old Wistar rats with vehicle, imatinib 40mg/kg/day or imatinib 70mg/kg/day, for 5 weeks. Trabecular bone volume, assessed at the proximal tibia by micro-CT, declined by 20% in the imatinib-treated rats ($p < 0.05$ vs vehicle). Serum osteocalcin (Rat-Mid) fell by 40% in response to imatinib therapy ($p < 0.01$ vs baseline). There was no evidence for an anti-resorptive effect of imatinib *in vivo* (CTX-I). Collectively, these results suggest that the dominant skeletal action of imatinib *in vivo* is inhibition of osteoblast mitogenesis by interruption of PDGFR signaling, leading to decreased bone formation and a decline in bone mass. Clinical studies should be undertaken to assess the effect of long-term imatinib therapy on bone mass in humans. These results also suggest that PDGFR signaling in osteoblasts may regulate bone mass *in vivo*.

Disclosures: S. O'Sullivan, None.

T019

Expression of Metalloproteinase-14 Is Pleiotropic on Alkaline Phosphatase Expression in Osteogenic Differentiation. D. Palmieri^{*}, S. Soldano^{*}, S. Zanotti^{*}, D. Lombardini^{*}, P. Manduca. DiBio, University of Genoa, Genova, Italy.

It is known that modulation of the expression of AP and MMP-14 are developmentally regulated during osteogenesis.

We here report that in ROB (rat tibia-derived osteoblasts), during early and pre-mineralization stages of osteogenesis, the modulation of the expression of MMP-14 affects that of AP which later jointly condition the formation of nodules and the mineralization of the osteogenic population. We show that the level of expression of MMP-14 affects pleiotropically the expression of AP by up or down modulating, at transcriptional or post-transcriptional levels the expression of either gene in ROB and in cloned derivative lines. Changes in MMP-14 were obtained by activating antibodies or inhibitors or observed in selected clones:

- 1 - Constitutive expression of MMP-14, obtained by exposure to activating antibodies, determines constitutive expression of AP: no nodules form, no mineralization occurs in the population.
- 2 - Inhibitors of MMP-14 inhibit also the expression of AP: no nodules form, no mineralization occurs in the population.
- 3 - Clones constitutive for MMP-14 are constitutive also for AP: no nodules form, no mineralization occurs in the population.

Vice versa, modulation of the expression of AP by GF or fluorides or by inhibitors has no effect on the expression of MMP-14:

- 1 - Over-induction of AP by F compounds, by IGFII and by ET does not affect the expression of MMP-14: enhanced nodule formation and mineralization occur in the population.
 - 2 - Inhibition of AP by Levamisole or by inhibition of endogenous ET, does not affect the expression of MMP-14: nodules form, but their mineralization is reduced.
 - 3 - Inhibition of AP by Levamisole in clones constitutive for MMP-14 and AP, does not affect the expression of MMP-14: no nodules form, no mineralization occurs.
- In conclusion, at the onset of osteogenesis, MMP-14 expression is pleiotropic on AP, not vice versa. Transient up-modulation of both is required for nodule formation and mineral deposition. Down-modulation of MMP-14 is required for nodule formation. Down modulation of both enzymes is associated with mineralization.

Disclosures: D. Palmieri, None.

This study received funding from: MIUR.

T020

Role of PLF in Remodeling of Bone Following Injury. S. Rani^{*1}, M. F. Barbe¹, A. E. Barr^{*2}, J. Litvin^{*1}. ¹Anatomy and Cell Biology, Temple University, Philadelphia, PA, USA, ²College of Health Professions, Temple University, Philadelphia, PA, USA.

Periostin-Like-Factor (PLF) is expressed in developing bone and is up regulated in adult bones that undergo remodeling due to fractures or repeated high force activity which leads to inflammation followed by injury of the bone. PLF over expression by adenovirus in the bone marrow cavity of rats resulted in increased bone formation. Together, these findings suggest that PLF plays an important role in bone formation. To test the hypothesis that PLF promotes bone formation under conditions of remodeling, tissues obtained from the novel model of Upper Extremity-Work-Related Musculoskeletal Disorder (WMSD) in the rat were obtained and subjected to ELISA, immunostaining and Western blot analysis. Twenty two young adult female Sprague Dawley rats were trained to perform a High Repetition High Force (HRHF) voluntary reaching and pulling task, with a food pellet reward. This task entails pulling a lever isometrically at a target rate of 4 reaches/min with 60% max grip force for 2 hrs/day in four 30 min sessions separated by 1.5 hr each, 3days/week and leads to mechanical loading of bone. Loaded bone responds by remodeling and under extreme situations stress fractures and resorptive spaces develop. Tissues from the reach limbs of performing rats and from randomly selected forelimbs of control rats were obtained at various times and subjected to immunostaining and Western blot analysis. To investigate the expression of pro-inflammatory cytokines ELISA assay was done on the bone of performing and control animals.

PLF protein was markedly up regulated in the bone of the performing limb of animals exposed to high force and repetitive motion, and the spatial pattern of PLF expression varied over the course of remodeling. Its expression peaked at 6 weeks, during the 12 week-work regimen. It was detected in the periosteum which contains mesenchymal pre-osteoblasts of the ulna and radius, in osteocytes and osteoclasts. It was secreted from proliferating and hypertrophied chondrocytes. The pro-inflammatory cytokines TNF- α and IL-1, also peaked in the bone at 6 weeks of task performance, suggesting a link between the PLF up regulation and the inflammation process.

The expression of PLF in bones undergoing remodeling, recovery and repair suggests that PLF plays a significant role in formation and maintenance of bone tissue. Its up regulation concomitant with the presences of high levels of pro-inflammatory mediators also suggests that it has a role in the inflammatory processes. In future experiments the role of PLF in remodeling and inflammation mediated processes will be examined in depth in the WMSD and other fracture repair models.

Disclosures: S. Rani, None.

This study received funding from: NIAMS.

T021

Pitx2 Inhibits Osteoblastic Conversion of Myoblasts Through Interfering the Promoter Activity of Osterix Gene. M. Hayashi^{*1}, S. Maeda¹, H. Aburatani^{*2}, K. Miyazono^{*3}, T. Imamura¹. ¹Department of Biochemistry, The Cancer Institute of the Japanese Foundation for Cancer Research, Tokyo, Japan, ²Genome Science Division, Research Center for Advanced Science and Technology, University of Tokyo, Tokyo, Japan, ³Department of Molecular Pathology, Graduate School of Medicine, University of Tokyo, Tokyo, Japan.

Bone morphogenetic protein (BMP) gives osteoblastic phenotype to myoblast C2C12. The osteoblastic conversion is accompanied by induction of Runx2 and Osterix. However, during the differentiation, C2C12 cannot form calcified bone nodules, which suggests osteoblastic maturation process is inhibited. We have found that induction of Osterix by BMP in C2C12 was transient, which decreased after 24 hours after stimulation. We hypothesized that there may be an inhibitory factor to suppress the expression of Osterix in this period. We screened nuclear proteins of repressors, which were induced late after 24 hours of BMP-stimulation in C2C12, by microarray technique. The expression of paired-like homeodomain transcription factor 2 (Pitx2) up-regulated gradually after 24 hours, and peaked at day four, and remained high level over one week. Since this induction was not seen in osteoblasts and other osteoblastic progenitors, the expression of Pitx2 by BMP may be exclusive to myoblasts. The overexpression of Pitx2 in C2C12 inhibited the induction of Osterix, not Runx2, which was followed by suppressed osteoblastic differentiation. C2C12 cells induced by shRNA for Pitx2, or MEF isolated from Pitx2 null mice showed enhanced induction of Osterix by BMP with elevated expression of ALP, bone sialoprotein and osteocalcin, while no difference on Runx2 was observed. Finally, we found some putative Pitx2 binding elements (PBE) in the promoter of osterix gene, one of which was shown to be functional target for Pitx2 by gel shift and ChIP assays. These results suggest that Pitx2 play a unique role in myoblast to suppress osteoblastic conversion through inhibiting the expression of Osterix. Thus, Pitx2 may be the first therapeutic target for muscle ossifying diseases, such as fibrodysplasia ossificans progressiva, in which cells BMP signaling is tend to be accelerated.

Disclosures: M. Hayashi, None.

T022

TRP Channels Are Both Present and Functional in Human Osteoblast-like Cells. N. C. Henney^{*1}, B. A. J. Evans², A. K. Campbell^{*3}, K. T. Wann^{*1}.

¹Welsh School of Pharmacy, Cardiff University, Cardiff, United Kingdom,

²Department of Child Health, Cardiff University, Cardiff, United Kingdom,

³Department of Medical Biochemistry & Immunology, Cardiff University, Cardiff, United Kingdom.

Transient receptor potential (TRP) cation channels are currently drawing a lot of interest in many tissues, but relatively little interest in bone. TRP channels are mostly non-selective and are generally widely expressed with increased expression in some malignancies¹, and TRPV1 and TRPM8 ligands, for example, may have potential uses as anti-cancer agents² in prostate malignancy. As prostate cancer cells metastasize to and cohabit with bone cells, this area of research is potentially important and deserves attention. The putative roles of TRP channels include growth, repair, metastasis, apoptosis and cell calcium entry - all of which are relevant to osteoblasts. We aim to show that TRP channels are present and active in osteoblast-like cells.

RT-PCR was carried out using intron-spanning primer pairs for TRPV1, TRPV5, TRPV6, TRPM7 and TRPM8 subunits in MG63 and SaOS-2 osteoblast-like cells. Cell proliferation assays were performed over 72 hours to test the effects of known TRP ligands on cell number, using trypan blue exclusion testing and MTS-conversion assay. Patch-clamp analysis was performed on MG63 and SaOS-2 cells using calcium-free and/or sodium gluconate solutions to minimise the confounding influence of other channel subtypes.

RT-PCR has revealed appropriate sized bands for TRPV1, TRPV5, TRPV6, TRPM7 and TRPM8 in MG63 and SaOS-2 cell lines. In cell proliferation assays, $\geq 10 \mu\text{M}$ capsaicin or capsaizipine significantly reduced MG63 cell number ($P < 0.05$), but $1 \mu\text{M}$ capsaizipine antagonises the effects of $\geq 10 \mu\text{M}$ capsaicin. In addition, resiniferatoxin (TRPV1 agonist), SB366791 (TRPV1 blocker) and anandamide (cannabinoid and TRPV1 modulator) all decreased MG63 cell numbers. Patch-clamp analysis has revealed small conductance channels of 18 - 30 pS in excised inside-out patches, and slightly larger conductance channels in cell-attached and inside-out patches at depolarised and hyperpolarised potentials in MG63 and LNCaP (prostate cancer) cells.

Given our preliminary data, we propose that five members of the TRP channel family are expressed in osteoblast-like cell lines, and we show electrophysiological and pharmacological data which lead us to suggest that at least one TRP channel type is active and functional in bone. TRP channels could therefore be new targets in the battle against bone disorders, and some known TRP channel ligands could be included in that armoury.

1: Tsavaler L et al. (2001). Cancer Res 61(9):3760-9

2: Athanasiou A et al. (2007). BBRC 354:50-55

Disclosures: N.C. Henney, None.

T023

A Lymphoid Enhancer Binding Factor (Lef) 1 Isoform Regulates Osteoblast Maturation. L. H. Hoepfner¹, E. D. Jensen^{*2}, J. J. Westendorf³.

¹Graduate Program in Microbiology, Immunology and Cancer Biology,

University of Minnesota, Minneapolis, MN, USA, ²University of Minnesota,

Minneapolis, MN, USA, ³Department of Orthopedic Surgery, Mayo Clinic,

Rochester, MN, USA.

Lymphoid Enhancer Binding Factor (Lef) 1 is a transcription factor linked with the Wnt/LRP5/ β -catenin signaling cascade, which regulates osteoblast proliferation and survival, bone density and skeletal strength. We previously demonstrated that suppression of Lef1 promotes osteoblast mineralization while Lef1 overexpression blocks osteoblast maturation. We also showed that Lef1 blocks Runx2-dependent activation of the osteocalcin promoter. In this study we demonstrate that Lef1 blocks activation from the neighboring Runx2 binding site, even when the sequence is changed from a Runx binding element to a GAL4 DNA binding element. A truncated form of Lef1 (Lef1 ΔN) that lacks the β -catenin binding domain does not repress osteocalcin expression as well as full-length Lef1, even though it retains a functional DNA binding domain. Lef1 ΔN is transcribed from a promoter in the intron between exons 2 and 3 in humans (exons 3 and 4 in mice). Runx2 binds a consensus Runx binding element in this promoter and activates transcription of the Lef1 ΔN transcript. Northern blot analysis indicates that the 2.3 kD Lef1 ΔN transcript is not present in undifferentiated MC3T3-E1 preosteoblasts but becomes detectable after six days of osteogenic stimulation. These data suggest that premature expression of Lef1 ΔN in osteoblast progenitors might block osteoblast differentiation. To test this hypothesis, we stably overexpressed Lef1 ΔN in the murine myo-osteoblast progenitor C2C12 cell line and induced differentiation in osteogenic medium containing ascorbic acid, β -glycerol phosphate, and BMP2. Lef1 ΔN overexpression decreased the rate of alkaline phosphatase production compared to control cells. Together these data suggest that Lef1 ΔN is a Runx2 target gene and an important regulator of osteoblast differentiation. Our model predicts that Lef1 ΔN is normally expressed during the maturation process where it competes with endogenous Lef1 for binding elements and thereby mitigates the Wnt signaling pathway. If expressed earlier, Lef1 ΔN blocks preosteoblast maturation.

Disclosures: L.H. Hoepfner, None.

T024

Orphan Nuclear Receptor Small Heterodimer Partner (SHP) Promotes Osteoblast Differentiation by Regulation of Runx2 Activity. B. Jeong*, I. Bae*, I. Kim*, J. Koh. Dental Science Research Institution and Brain Korea 21 project, School of Dentistry, Chonnam National University, Gwangju, Republic of Korea.

Orphan nuclear receptor small heterodimer partner (SHP) is an atypical member of the nuclear receptor superfamily, regulating transcription of target genes without a conventional DNA binding domain. This study was undertaken to elucidate roles of SHP in osteoblast differentiation. Primary osteoblasts, mesenchymal progenitor cell lines, and C2C12 were cultured with or without BMP2 (300 ng/ml), and SHP expression was determined by RT-PCR analyses. For evaluation of osteoblast differentiation, alkaline phosphatase (ALP) activity, osteocalcin (OC) production, and Alizarin Red staining assays were done with adenoviral infection of BMP2 and/or siRNA-SHP. To examine transcriptional regulatory actions of SHP, 6XOSE- or OG2 promoter was transfected with Runx2 plasmid. During the BMP2-induced osteoblast differentiation of C2C12 cells, SHP mRNA increased. Transient transfection of SHP significantly promoted the Runx2-dependent stimulation of OG2 or OSE promoter. Knocking down SHP expression by adenovirus siRNA-SHP inhibited BMP-2 induction of ALP activity, OC production, and mineralization with down-regulations of ALP, OC and bone sialoprotein mRNA. These results indicate that orphan nuclear receptor SHP may act as a positive regulator of osteoblast differentiation and mineralization.

Disclosures: B. Jeong, None.

This study received funding from: Brain Korea 21 Project for Dental School.

T025

Withdrawn.

T026

Opposing Effects of Glucocorticoids and Wnt Signaling on Krox20 and Mineral Deposition in Osteoblast Cultures. N. Leclerc*¹, T. Noh*¹, J. Cogan*¹, D. B. Samarawickrama*¹, E. Smith*², B. Frenkel¹. ¹Biochemistry and Molecular Biology, University of Southern California, Los Angeles, CA, USA, ²Orthopaedic Surgery, University of Southern California, Los Angeles, CA, USA.

The beneficial anti-inflammatory properties of glucocorticoids (GCs) are associated with inhibition of osteoblast-mediated bone formation, leading to osteoporosis. We previously discovered Krox20 as the transcription factor most strongly repressed by GCs in osteoblast cultures, and showed that GC-inhibition of Osteocalcin (OC) transcription was mediated via suppression of an OC Krox20-binding Enhancer (OKE) located immediately upstream of the Runx2-binding OSE2 site. Because GCs also inhibit Wnt signaling, a major regulator of bone mass, we pursued a possible linkage between GCs, Wnt signaling and Krox20 in osteoblasts.

We first characterized the expression pattern of Krox20 in MC3T3-E1 and primary calvarial osteoblast cultures treated or not with 1 μ M dexamethasone (DEX). RT-qPCR analysis showed that Krox20 expression was the highest during late stages of osteoblast differentiation. DEX decreased Krox20 mRNA to 50 % of control levels within 15 minutes, suggesting a direct effect. Long-term repression of Krox20 by DEX, however, required new protein synthesis, as it was alleviated after a 4 hours cycloheximide treatment. We previously showed that activity of the OKE was absent in undifferentiated osteoblasts and that fibroblasts acquired OKE activity upon forced expression of Runx2. Here, we ruled out the requirement for Runx2 binding in cis -the OKE remained active after the OSE2 site was mutated. We then examined the possibility that Krox20 is regulated by the Wnt signaling pathway. Indeed, Wnt3A stimulated both Krox20 expression and activity of the OKE, whereas two other bone anabolic agents, BMP2 and PTH(1-34), failed to do so. We next addressed the involvement of Wnt signaling in the DEX-repression of Krox20. DEX-inhibition of Wnt signaling was only partially responsible for the 6-fold repression of Krox20 by DEX, as DKK-1 did not completely abolish it but rather reduced it down to 3.7-fold. Finally we asked whether treatment with Wnt3A could antagonize the inhibitory effects of GCs on both Krox20 and the osteoblast phenotype. Wnt3A partially rescued Krox20 expression in DEX-arrested osteoblast cultures and this was associated with rescue of mineralization. However, mineralized nodules only formed when Wnt3A was administered briefly, not chronically, and they were morphologically different from those formed in control cultures.

Our findings are consistent with a role for Krox20 in osteoblast function and suggest that it may contribute to the opposing effects of GCs and Wnt signaling on bone formation.

Disclosures: N. Leclerc, None.

This study received funding from: Arthritis Foundation, National Institutes of Health (AR047052), and J. Harold and Edna L. LaBriola Chair in Genetic Orthopaedic Research at the University of Southern California.

T027

Vimentin Negatively Regulates Osteoblast Differentiation by Inhibiting the Transactivation Activity of Atf4. N. Lian*, X. Yang. Center for Bone Biology, Department of Pharmacology, Vanderbilt University, Nashville, TN, USA.

Our previous work has identified Atf4 as an osteoblast-enriched transcription factor that is required for osteoblast terminal differentiation and function (Yang et al. 2004; Yang and Karsenty, 2004). Atf4 transactivates gene transcription of osteocalcin, an osteoblast-specific and mature osteoblast marker gene, by binding directly to its osteoblast-specific cis-acting element, OSE1. The transactivation activity of Atf4 is positively regulated by phosphorylation by RSK2, a protein kinase whose mutation causes Coffin-Lowry syndrome (CLS). CLS is characterized by mental retardation and skeletal manifestations. In this study we found, by chromatography and mass spectrometry using purified Atf4 protein and osteoblast nuclear extracts, that Atf4 interacts with vimentin, a member of type III intermediate filament proteins. Interaction between Atf4 and vimentin was confirmed by a reciprocal co-immunoprecipitation in COS1 cells that overexpress both Atf4 and vimentin. Vimentin may play a specific role in osteoblast biology since our RT-PCR and Northern hybridization assay results showed that its mRNA expression is enriched specifically in bone and lung. Consistent with published studies vimentin is localized in both cytosol and nucleus as demonstrated by expressing a fusion protein of green fluorescent protein and vimentin in COS1 cells. To determine whether vimentin affects Atf4's transactivation activity, we performed co-transfection assays using osteocalcin promoter-luciferase reporter constructs and expression vectors encoding Atf4 and/or vimentin. Our results showed that vimentin decreased 80% of the activation of the osteocalcin reporter gene by Atf4. This inhibition is specific because vimentin did not affect the transactivation of a reporter gene by FosB, a transcription factor of the AP1 family. Gel retardation assays showed that this inhibition was caused by the fact that vimentin directly interferes with the binding of Atf4 to OSE1. To further determine the function of vimentin in the osteoblast differentiation process, we have established cell lines that stably overexpress Atf4, vimentin or both. Our results revealed that vimentin affects in osteoblast differentiation and function as shown by measurements of alkaline phosphatase activity, mineralization rate, and expression patterns of osteoblastic marker genes. Together our data suggest that vimentin is not only a structural protein that provides mechanical support for the plasma membrane but also acts as a negative regulator of osteoblast differentiation via its interaction with Atf4.

Disclosures: N. Lian, None.

T028

The microRNA miR-26a Targets the SMAD1 Protein During of Human Adipose Tissue-Derived Stem Cells. E. Luzi*, F. Marini*, S. Carbonell Sala*, I. Tognarini*, G. Galli*, A. Falchetti, M. Brandi. Internal Medicine, University of Florence, Florence, Italy.

Human Adipose Tissue-Derived Stem cells (hADSCs) are a cell population capable to differentiate in adipogenic, osteogenic, chondrogenic, myogenic, and neurogenic lineages. Although different studies suggest a high osteogenic potential for hADSCs, the molecular mechanisms that regulate hADSCs differentiation towards osteogenic precursors and subsequent bone-forming osteoblasts is unknown. MicroRNAs (miRNAs) are a family of naturally occurring, evolutionary conserved, small (approximately 19-23 nucleotides), non-protein-coding RNA molecules that negatively regulate post-transcriptional gene expression. miRNAs are estimated to account for >3% of all human genes and to control expression of thousands of target mRNAs, with multiple miRNAs targeting each mRNA. A role for miRNAs has been identified in both physiological and pathological conditions, encompassing metabolism, proliferation, cell death, differentiation, development, and insulin secretion from pancreatic beta cells, viral infection, and cancer. With few exceptions, physiological targets for miRNAs remain to be identified. Understanding miRNAs function is critically dependent on the identification of its targets. Nucleotides 2-8 (referred to as "seed") of the miRNAs are crucial in determining target specificity. Using osteoblast precursors obtained by subcutaneous human adipose tissue we were able to demonstrate that miR-26a levels increased in differentiating osteoblasts and that the inhibition of miR-26a, by 2'-O-methyl-antisense RNA, increased protein levels of the mothers against decapentaplegic homolog 1 (SMAD1) transcription factor in treated osteoblasts, up-regulating bone marker genes and, thus, enhancing osteoblast differentiation. Our data showed that combined expression and functional data suggest a role for miR-26a in the differentiation of hADSCs towards the osteogenic lineage by targeting its predicted target, the SMAD1 protein.

Disclosures: E. Luzi, None.

T029

Osteoblastic Master Regulator Osterix Mediates the Feedback Regulation of BMP-2 Auto-Expression via PI 3 Kinase/Akt Signaling. C. C. Mandal¹, G. Ghosh-Choudhury^{*2}, H. Drissi³, N. Ghosh-Choudhury⁴. ¹Pathology, University of Texas Health Science Center at San Antonio, San Antonio, TX, USA, ²Medicine, UTHSCSA, GRECC, STVHCS, San Antonio, TX, USA, ³Orthopedics, University of Rochester, Rochester, NY, USA, ⁴Pathology, UTHSCSA, STVHCS, San Antonio, TX, USA.

We have recently reported the requirement of phosphatidylinositol 3 kinase (PI3K)/Akt signal transduction in BMP-2-induced osteoblast differentiation and mature bone nodule

formation. BMP-2-inducible Zn-finger transcription factor, osterix (Osx), is required for bone formation during mouse skeletogenesis. The mechanism by which BMP-2 increases Osx expression is not known. BMP-2 increased expression of Osx protein in a time-dependent manner in the cytosol and nucleus of C2C12 cells, concomitant with Osx mRNA expression. PI3K inhibitor, Ly294002, significantly inhibited BMP-2-induced Osx mRNA and protein abundance. Infection of C2C12 cells with adenovirus vectors expressing dominant negative PI3K or PTEN, a negative regulator of PI3K signaling, blocked expression of Osx mRNA and protein in response to BMP-2. Adenoviral-mediated expression of dominant negative Akt kinase (AdDNakt), a target of PI3K, inhibited BMP-2-induced Osx expression. These data for the first time indicate a critical role of PI3K/Akt signaling in osteogenic transcription factor Osx expression during osteoblast differentiation. To investigate the mechanism of Osx expression, we investigated its transcription using reporter construct in which 5'-flanking sequence of Osx gene drives firefly luciferase cDNA (Osx-Luc). Transient transfection of Osx-Luc into C2C12 cells showed increased Osx transcription in response to BMP-2. Analysis of the progressive 5' deletions of the Osx promoter revealed the presence of BMP-2 responsive sequence between -800 bp and -500 bp with respect to the transcription start site. Inhibition of PI3K and Akt kinase activity by Ly294002 or by expression of dominant negative lipid kinase, PTEN and AdDNakt respectively, abolished BMP-2-induced transcription of Osx. BMP-2-induced BMP-2 expression is necessary for sustained osteoblast differentiation. The mechanism is not known. We show that expression of Osx increased the transcription of BMP-2 gene, resulting in BMP-2 protein and alkaline phosphatase protein expression in osteoblasts. Together these results for the first time demonstrate that PI3K/Akt signaling regulates the expression of osteogenic master transcription factor Osx in response to BMP-2. Furthermore, we provide the first evidence that Osx represents the master regulator for BMP-2-induced BMP-2 expression to regulate osteoblast differentiation.

Disclosures: C.C. Mandal, None.

This study received funding from: NIAMS, VA.

T030

Responses of Bone in ANA Knock-out Mice to Ovariectomy. K. Miyai^{*1}, M. Yoneda^{*2}, F. Mizoguchi¹, T. Hayata¹, Y. Ezura¹, K. Nakashima¹, T. Yamamoto^{*2}, M. Noda¹. ¹Department of Molecular Pharmacology, Medical Research Institute, Tokyo Medical and Dental University, Tokyo, Japan, ²Division of Oncology, The Institute of Medical Science, The University of Tokyo, Tokyo, Japan.

Tob, a member of BTG/APRO/TOB family protein, has been reported as a negative regulator of BMP signaling on bone. We have identified that ANA, another member of this family, is expressed in skeletal system, including Meckel's cartilage and cartilages of ribs at E12.5 mice suggesting that ANA plays a role in the proliferation and/or chondrocytic differentiation of the cartilage cells (Yoshida et al. 1998 Oncogene). ANA has been reported to interact with Ca²⁺, whose absence did augment the response of bone to BMP similarly to the observation reported in Tob knock out mice. In fact, Tob knock-out mice revealed alteration in the levels of bone mass after ovariectomy. Based on these observations, we examined whether ANA would be involved in the regulation of bone metabolism. To analyze this point, we examined mice deficient in ANA gene. By crossing heterozygous female and male mutants, progeny pups in each genotype were obtained at normal Mendelian frequency. The growth and appearance of knock-out mice were similar to those in wild type littermates. We assumed that this observation was brought about by compensatory mechanisms covering the expected influence, and hypothesized that certain stress on mouse might reveal its role on bone.

It has been reported that Tob knock-out mice are resistant to reduction of bone volume / tissue volume (BV/TV) in femur after ovariectomy, we therefore examined the effect of ovariectomy on bone mass changes in ANA knock-out mice. BMD levels of femur were similar between ANA knock-out mice and wild type littermates. BV/TV levels in femur were tended to decrease in ANA knock-out mice after ovariectomy, and such trends were similar to those in wild type. In conclusion, unlike Tob knock-out mice, ANA deficient mice responded to ovariectomy similarly to wild type mice.

Disclosures: K. Miyai, None.

T031

Investigation of KCl Cotransport Expression In Canine Osteosarcoma Cell Lines. H. Ochiai. Research Institute of Biosciences, Azabu University, Sagami-hara Kanagawa, Japan.

K-Cl cotransport, defined originally in erythrocytes as Cl-dependent, ouabain-insensitive bidirectional K transport, encoded by four KCC genes, is recognized as a functional and structural reality in various types of cells. As a functional system, KCC is necessary for ionic and volume homeostasis. Since its discovery by swelling erythrocytes in hyposmotic solutions, KCC has been recognized as one of the key K transport membrane proteins affecting regulatory volume decrease (RVD). Although much information on erythrocytes has been reported, little is known about KCC in osteosarcoma cells. In this study, we investigated KCC of two canine osteosarcoma cell lines, parent canine osteosarcoma cell lines (OS) and highly lung metastasizing canine osteosarcoma which was established from five subcutaneous implantation cycles of lung tumor deposits using parent OS (HM-OS). There was no difference in K-Cl cotransport activity in the physiological condition, while NEM revealed significantly higher Rb (K) uptake in HM-OS than OS. Western blot analysis indicated KCC1, KCC3 and KCC4 were expressed in both cells, and KCC3 was especially abundant in HM-OS compared with OS. Insulin-like growth factor 1 (IGF-1) increased KCC activity and mRNA expression in a dose- and time-dependent manner of the three KCCs. This activation was diminished by addition of DIOA, the specific inhibitor of KCC, along with the inhibitory effect of cell growth in both

cells. Retinoid, the vitamin A derivative, induced morphologic differentiation in both canine osteosarcoma cells and enhanced cell flattening and spreading, as well as reduction in cell overlapping. Alkaline phosphatase (ALP) activity and ALP staining were decreased and induced an increase in production of type I collagen. Retinoid-treated HM-OS indicated KCC3 expression was reduced to level of OS.

Disclosures: H. Ochiai, None.

T032

Characterization of Regions Upstream of Exon II of the Human CYP19 (aromatase) Gene that Mediate Regulation by cAMP in Murine Osteoblasts. O. K. Oz¹, T. Hasegawa^{*2}, Y. Zhao^{*1}. ¹Radiology, UT Southwestern Medical Center at Dallas, Dallas, TX, USA, ²Pediatrics, Keio University School of Medicine, Tokyo, Japan.

Estrogen is important for the regulation of bone growth and metabolism in humans. Aromatase P450 (aromatase), the product of the CYP19 gene, catalyzes conversion of androgens to estrogens. Aromatase is expressed in human osteoblasts and cultured fetal osteoblast-like cells. In humans, tissue-specific expression of aromatase is regulated in part, by tissue-specific promoters and by alternative splicing mechanisms. In mice, only two promoters, one specific for brain and one for gonads have been described. Little is known regarding the expression and regulation of aromatase expression in murine bone. Thus, we first wanted to determine if aromatase is expressed in murine long bone. Aromatase transcripts were present in whole bone as determined by RT-PCR. Aromatase protein was detected both in osteoblasts and chondrocytes by immunohistochemistry. To ascertain how aromatase expression is regulated in mouse bone, various amounts (-945/-16 bp to -100/-16 bp) of 5'-flanking DNA and promoter of the human CYP19 gene, upstream of exon II (CYP19_h) were linked upstream of the luciferase cDNA (LUC) for transient transfection studies utilizing MC3T3-E1 osteoblast cells. Forskolin-induced reporter activity was greatest with the -517/-16 LUC construct and the response to cAMP was lost upon deletion to -140 bp. Mutation of cAMP-responsive element-like sequence (CLS) and steroidogenic factor-1 (SF-1) element sequence sites markedly decreased the response to forskolin. A probe containing the CLS was used in electromobility shift assays; two complexes were formed with MC3T3-E1 nuclear extracts (NE), and a cAMP-responsive element binding protein (CREB) antibody was able to compete formation of these complexes. A probe specific for the SF-1 element formed a complex with MC3T3-E1 NE and this could be competed through the use of an SF-1 antibody. The results indicate that aromatase is expressed in mouse bone and the 5'-flanking DNA and Promoter II of the human CYP19 gene is capable of driving expression of aromatase in the MC3T3-E1 osteoblast cells. These results suggest a role for SF-1 in bone homeostasis and that the osteoblast is an extraglandular source of local estrogen that may play an important role in bone metabolism.

Disclosures: O.K. Oz, None.

T033

Snail, a Transcription Factor, Inhibits the Differentiation of Mesenchymal Stem Cells to Osteoblasts. S. Park^{*1}, J. Yook^{*2}, J. Byun^{*1}, Y. Rhee¹, H. Ryoo³, E. Lee^{*1}, S. Lim¹. ¹Internal Medicine, Yonsei University, Seoul, Republic of Korea, ²Oral Pathology, Yonsei University, Seoul, Republic of Korea, ³Cell and Developmental Biology, Seoul National University, Seoul, Republic of Korea.

Mesenchymal stem cells are able to differentiate into several highly specialized cell types, including osteoblasts, adipocytes, myocytes and chondrocytes. Several key transcription factors play a crucial role in commitment process thereby directing the cells along a particular lineage and suppressing the alternative pathways. However, how the key transcription factors in order to specify several distinct lineages are regulated remains a pivotal question. In this study, we examined whether snail, a zinc-finger transcription factor, regulates the differentiation of mesenchymal stem cells. Snail-overexpression decreased the expression of osteoblast marker genes including type I collagen and ALP in C3H10T1/2 mesenchymal cells. And the expression of Runx2, the osteoblast-specific transcription factor, was significantly reduced by Snail-overexpression. The activity of Runx2 was also suppressed by 2 folds after Snail-overexpression in C3H10T1/2 cells. In addition, siRNA against Snail enhanced the activity of Runx2 in C3H10T1/2 cells. Interestingly, osteoblastogenesis was dramatically stimulated after suppression of endogenous Snail expression by siRNA in osteoblastic MC3T3-E1 cells. These results suggested that Snail plays a crucial role in developmental process from the mesenchymal stem cells to osteoblasts.

Disclosures: S. Park, None.

T034

Role of Nuclear Factor I-X Transcription Factor in Regulation of IGFBP-5 and Osteocalcin Expression in Mouse Osteoblasts. L. A. Pérez-Casellas¹, K. E. Govoni², K. D. Howard^{*2}, G. R. Linares³, C. A. Strohbach^{*1}, T. A. Linkhart^{*2}, D. D. Strong². ¹Microbiology, Loma Linda University, Loma Linda, CA, USA, ²Research, Loma Linda VAMC, Loma Linda, CA, USA, ³Physiology, Loma Linda University, Loma Linda, CA, USA.

The Nuclear Factor I (NFI) gene family plays wide reaching roles in viral DNA replication, regulation of gene transcription and development. Gene knockout studies of NFI have shown that nfi-a ^{-/-} mice display mainly neuroanatomical defects, nfi-b ^{-/-} mice show lung and brain defects, nfi-c ^{-/-} caused primarily a disruption of tooth root and underlying mandibular bone development, and nfi-x ^{-/-} mice have brain malformation and also develop a deformation of the spine, due to impaired endochondral ossification and decreased mineralization. We previously reported that the Nuclear Factor I gene family was an important regulator of IGFBP-5 expression in human osteoblast-like cells. Specifically, the isoforms NFI-B and NFI-X significantly activated the IGFBP-5 promoter and siRNA knockdown of NFI-B expression decreased IGFBP-5 mRNA and protein expression. To determine the role of the four NFI isoforms in mouse osteoblast differentiation we evaluated mRNA expression levels in mouse bone marrow stromal cells and mouse osteoblast MC3T3-E1 cells at different stages of differentiation in vitro (αMEM, FBS, Ascorbic Acid and β-glycerolphosphate). We found that all four genes were expressed and their expression levels increased at least 10 fold between day 14 and 21 during differentiation. NFI-x expression was the most abundant in bone marrow stromal cells and differentiated MC3T3-E1 cells and increased the most during differentiation. The increased nfi expression between 14 and 21 days corresponds to previous observations that igfbp-5 expression decreased in MC3T3-E1 cells as the cells fully differentiated and osteocalcin expression increased¹. To determine the role of nfi-x in regulating igfbp-5 expression and osteoblast differentiation, mouse nfi-x expression was inhibited with specific siRNA oligonucleotides in MC3T3-E1 cells. NFI-x mRNA levels were decreased at 48 hrs by 80% and mouse osteocalcin mRNA levels were decreased by 65% compared to non targeting control siRNA. However, nfi-x knockdown caused a 2 fold increase in igfbp-5 mRNA levels. In contrast to stimulating IGFBP-5 promoter activity in human osteoblasts (from an IGFBP-5 luciferase reporter plasmid), nfi-x overexpression in transient transfection experiments did not stimulate promoter activity in MC3T3-E1 osteoblasts. These results suggest an important role for NFI-X in regulating osteoblast differentiation, and that NFI regulation of IGFBP-5 expression may occur by different mechanisms in mouse and human.

(1) Thraill et al. Bone 17:307-313 (1995).

Disclosures: L.A. Pérez-Casellas, None.

T035

Zinc Finger Protein 64 Is a Downstream Target of Runx2 and Regulates Myogenic and Osteogenic Differentiation as a Coactivator of Notch1. K. Sakamoto^{*}, A. Yamaguchi. Section of Oral Pathology, Tokyo Medical and Dental University, Tokyo, Japan.

Runx2 is a crucial transcription factor for osteoblast differentiation. Notch signaling is required for multiple aspects of mesenchymal cell differentiation and it recently has been recognized as an essential regulator of osteogenesis. However, the mechanism to coordinate these signaling pathways is still poorly understood. In this paper, we identified zinc finger protein 64 isoform D (Zfp64) as a novel coactivator of Notch1. Zfp64 was associated with the carboxyl terminal PEST-containing region of Notch1 and was recruited to the promoters of the Notch target genes Hes1 and Hey1, which transactivates these Notch downstream genes. Zfp64 expression, which is under the control of Runx2, was upregulated by direct transactivation of its promoter. During embryo- and organogenesis, Zfp64 is expressed mainly in the mesenchymal cells, including osteoblasts and chondroblasts, but not in myocytes. Zfp64 suppressed the myogenic differentiation of C2C12 cells and promoted their osteoblastic differentiation. Our data demonstrates that Zfp64 is a downstream target of Runx2 and regulates differentiation of osteoblasts and myoblasts as a coactivator of Notch1 by intermediating two signaling pathways between Runx2 and Notch.

Disclosures: K. Sakamoto, None.

T036

Runx2 Transcriptional Activation Domain 3 Supports Synergistic Runx2-MINT Activation of the Osteocalcin FGF Response Element via A DMAT-Sensitive Kinase. O. L. Sierra, S. L. Cheng, D. A. Towler. Bone & Mineral Diseases, Washington Univ Sch Med, St Louis, MO, USA.

MINT, the Mx2-interacting nuclear matrix target protein, is an abundant component of the osteoblastic nuclear matrix. MINT functionally interacts with Runx2 to enhance osteocalcin promoter activity in C3H10T1/2 mesenchymal cells. To study Runx2-MINT interaction in greater detail, we concatamerized the 42-bp element (rat osteocalcin promoter FGF response element; OCFRE) that comprises Runx2 binding sites upstream of the unresponsive RSV minimal promoter (LUC reporter). In co-transfection assays, MINT enhanced Runx2-dependent activation of the OCFRE by 3-4 fold, both in the presence and absence of exogenous FGF2. However, the related family member Runx1 exhibited only 10% the activity of Runx2 in this assay. Deletion of Runx2 N-terminal Activation Domains (AD) AD1 and AD2 did not affect Runx2-MINT interaction. By contrast, Runx2 (1-312) – lacking C-terminal residues 313 to 528 – had significantly reduced activity, indicating that interaction interface with MINT must reside in the C-terminus. A systematic series of Runx1-Runx2 chimeras were generated to

functionally map Runx2-MINT interactions. Runx2 AD1 and AD2 did not convey MINT-dependent activation to Runx1. However, when Runx2 residues 315-402 or 365-402 replaced equivalent domains in the Runx1 C-terminus, both of these Runx1-Runx2 chimeras were capable of augmenting OCFRE activity in the presence of MINT. This region of Runx2, residues 315-402, encodes activation domain 3 (AD3). Inspection of the protein sequence identified multiple potential phosphorylation sites, including cognates for proline-directed protein kinases (PKDs; S319, T326, T407), casein kinase-2 (CK2; S347, S388), and protein kinase C (S330, S364). Alanine scanning mutagenesis was performed in the context of the Runx1-Runx2 chimera. Disruption of S319 and T326 phosphorylation cognates significantly reduced functional Runx2-MINT interactions, indicating that a PDK contributes to transactivation. Other Ala substitutions had no effect. We next examined effects of Ser/Thr protein kinase inhibitors on Runx2-MINT transactivation. Most, including PD98059, had little if any activity. However, the CK2 / Dyrk1 kinase inhibitor 2-dimethylamino-4,5,6,7-tetrabromo-1H-benzimidazole (DMAT) profoundly and dose-dependently abrogated MINT-Runx2 activation and Runx2-transactivation, with an ID50 of 5 uM. By contrast, DMAT did not affect TCF/LEF-dependent transcription. Other CK2 antagonists, such as emodin and apigenin, lacked inhibition. Thus, Runx2 Transcriptional AD3 confers Synergistic Runx2-MINT Activation on the minimally responsive Runx1 protein. MINT-stimulated transcription of AD3 requires the activity of a DMAT sensitive kinase.

Disclosures: O.L. Sierra, None.

This study received funding from: National Institutes of Health/NIAMS.

T037

LMP-1 Accelerates MC3T3-E1 Osteoblast Differentiation in Part Through Modulation of the IGF System. C. A. Strohbach¹, S. T. Chen^{*2}, S. J. Kleinman^{*2}, T. A. Linkhart², D. D. Strong². ¹Loma Linda University, Loma Linda, CA, USA, ²J.L. Pettis VAMC, Loma Linda, CA, USA.

LIM Mineralization Protein (LMP)-1 is a novel intracellular protein that is believed to be a critical regulator of the osteoblast differentiation program. LMP-1 has been shown to promote bone formation in spinal fusion models and enhance fracture repair. LMP-1 has been proposed to act through the induction of osteogenic factors such as BMPs and Runx2. However, the exact mechanism of action of LMP-1 is still unknown. Previously we found that IGFBP6 (BP6) binds intracellular LMP-1, suggesting that LMP-1 interacting with BP6 may affect osteoblast differentiation. The purpose of this study was to determine the effect of LMP-1 overexpression on MC3T3-E1 osteoblast differentiation, and to further elucidate mechanisms of LMP-1 action focusing on the IGF system. MC3T3-E1 osteoblasts were transduced with an MLV-based retroviral LMP-1 or GFP control vector. Expression of LMP-1 was confirmed by Western blot. After transduction, cells were seeded into 6-well plates and stimulated to differentiate by addition of osteogenic media containing ascorbic acid and beta-glycerolphosphate. The effect of LMP-1 on MC3T3-E1 osteoblast differentiation was determined by Alizarin Red staining and real-time PCR analysis of osteoblast marker gene and IGF system component mRNA levels. At 14 days, Alizarin Red staining demonstrated increased nodule formation in cells transduced with LMP-1 compared to GFP. Real-time PCR analysis revealed that LMP-1 significantly increased the mRNA levels of osteocalcin (7-fold), osteonin (4-fold), bone sialoprotein (19-fold), alkaline phosphatase (7-fold), and Runx2 (4-fold) compared to control. Furthermore at 14 days, LMP-1 significantly decreased mRNA levels of components of the IGF system including IGF-1 (36-fold), IGFBP4 (4-fold), IGFBP5 (14-fold), and BP6 (5-fold). Since LMP-1 is an intracellular molecule, we investigated whether LMP-1 effected transcription using pGL3-promoter reporter constructs. Transient co-transfection revealed that LMP-1 dose-dependently inhibited BP6 promoter activity. Furthermore, we found that retroviral overexpression of BP6 in MC3T3-E1 cells inhibited differentiation and nodule formation normally observed after 21 days of culture in osteogenic media. These results suggest that 1) LMP-1 stimulates the production of osteoblast specific proteins and transcription factors, 2) LMP-1 is involved in regulation of the IGF system, and 3) LMP-1 may have a direct effect on BP6 transcription.

Disclosures: C.A. Strohbach, None.

This study received funding from: Department of Veterans' Affairs.

T038

An In Vitro Assay to Assess Secreted Osteogenic Factors from Genetically Engineered Cells. M. Viggswarapu, M. Bargouti^{*}, C. Rogers^{*}, L. Titus, S. D. Boden. Orthopedics, Emory University, Decatur, GA, USA.

LIM Mineralization Protein-1 (LMP-1) is known to induce secretion of osteogenic factors. Optimization of gene transfer protocols, promoter selection, isoform choice and other details have required resource-intensive in-vivo assays to date. The goal of this investigation was to validate an in-vitro assay to measure the osteogenic potential of secreted proteins from genetically engineered cells. To isolate the paracrine effect of secreted osteogenic proteins we chose the non-osteogenic mouse fibroblast (Nor10) cell line as the genetically engineered donor cells. We tested conditioned media (CM) from those cells for their osteogenic potential on freshly isolated rat calvarial osteoblasts (ROBs) and C2C12 pluripotent cells. Nor10 cells were seeded at 2.6x10⁴/cm² in DMEM containing 20% FBS. LMP-1 cDNA was delivered using either a plasmid (pCMV-LMP-1) or Adenovirus (Ad5LMP-1) and grown for 72hrs. CM was collected on day 3 and frozen at -70° until used. The CM was thawed, concentrated 10 fold using 10,000 M_w cut off Centrprep/Centricon concentrators, and sterile filtered. Concentrates were resuspended in fresh complete medium to the original concentration and applied to recipient cells (C2C12 or ROB). C2C12 cells were seeded at 2.1x10⁴/cm² in DMEM containing 10% FBS. Cells were grown for 72 hrs and RNA was harvested. Gene expression was determined by reverse transcription followed by real-time TaqMan PCR analysis. Treatment of C2C12 cells with the CM from Nor10 cells treated with Ad5LMP-1 or pCMV-LMP1 increased BMP2, BMP7 and osteocalcin mRNA

levels. The C2C12 cells, while convenient, do not readily make mineralized bone. Thus, we also tested the osteogenic potential of Nor10 CM on confluent secondary ROB cultures by measuring mineralized nodule formation. Confluent secondary ROB cultures were treated with the CM from LMP-1 overexpressing Nor10 cells and grown for another 14 days. Treatment of ROB with the CM from Nor-10 cells treated with AdLMP-1 or pCMV-LMP1 induced a 5 to 8 fold increase in mineralized bone nodule formation compared with CM from control Nor-10 cultures transduced/transfected with vector alone. In conclusion, these data demonstrate that we can measure the paracrine effects of cells genetically engineered to produce osteogenic factors using a two cell transfer assay. Intermediate markers of osteoblast differentiation (BMPs) and/or mineralized nodule endpoints can be demonstrated.

Disclosures: L. Titus, None.

This study received funding from: VA, NIH and Medtronic.

T039

Osteoblasts Express CSF-1R and Are a Target for CSF-1. Y. Wittrant^{*1}, Y. Gorin^{*2}, K. Woodruff^{*1}, D. Horn^{*1}, S. Mohan^{*1}, H. Abboud^{*2}, S. Werner¹. ¹Pathology, University of Texas Health Science Center and Audie Murphy VA Hospital, San Antonio, TX, USA, ²Nephrology, University of Texas Health Science Center and Audie Murphy VA Hospital, San Antonio, TX, USA.

CSF-1, released by osteoblasts, stimulates the proliferation of osteoclast progenitors via the c-fms receptor (CSF-1R) and, in combination with RANKL, leads to the formation of mature osteoclasts. Whether the CSF-1R is expressed by osteoblasts and mediates specific biologic effects in osteoblasts has not been explored. To examine the CSF-1R in osteoblasts, primary calvarial osteoblasts (OB), isolated from wild-type (wt) and CSF-1 deficient op/op mice, were incubated in the presence and absence of recombinant CSF-1 and analyzed for CSF-1R mRNA and protein by RT-PCR and Western blot, respectively. Wt OB cultures were serum starved for 24 hr and the effect of CSF-1 (0-100 ng/ml) on proliferation and gene expression of RANKL, OPG, CSF-1 and osteocalcin (OC) was determined at 48 hr. In wt bone marrow cultures incubated with 1,25(OH)₂D₃ (10⁻⁸M) and dexamethasone (10⁻⁸M) for 13 days, CSF-1 was tested for its effect on alkaline phosphatase activity (AP), RANKL mRNA and osteoclast formation. Since reactive oxygen species (ROS) influence osteoblast gene expression, studies analyzed the effect of CSF-1 on NADPH oxidase activity, Nox1 and Nox 4 proteins. Results indicate that wt and op/op OB express CSF-1R mRNA and protein and that CSF-1 dramatically reduces CSF-1R protein, but not CSF-1R mRNA, levels. In wt OB, CSF-1 decreased RANKL mRNA in a dose and time dependent manner whereas CSF-1 showed no effect on cell proliferation, OPG, OC or CSF-1 mRNA expression. Incubation of marrow cultures with CSF-1 resulted in a significant decrease in AP activity and RANKL expression and this effect was associated with a decline in TRAP activity and CTR expression. In wt OB, NADPH oxidase activity decreased in response to CSF-1 and correlated with a decline in Nox1 and Nox4 protein levels. Compared to untreated cultures, 1uM DPI (diphenylene iodonium, NADPH oxidase inhibitor) decreased RANKL similar to that observed with CSF-1, and RANKL expression in cultures treated with both CSF-1 and DPI was comparable to each agent alone. These findings provide the first evidence that osteoblasts express CSF-1R and are a target for CSF-1 ligand. CSF-1 may act in an autocrine or paracrine manner to regulate its cognate receptor and osteoblast differentiation. Inhibition of NADPH oxidase activity by CSF-1 likely contributes to the effect of CSF-1 on RANKL. CSF-1-mediated inhibition of RANKL expression on osteoblasts may provide an important mechanism for coupling bone formation/resorption and preventing excessive osteoclastogenesis during normal skeletal growth.

Disclosures: Y. Wittrant, None.

This study received funding from: NIH (AR-42306) and VA's Merit Award.

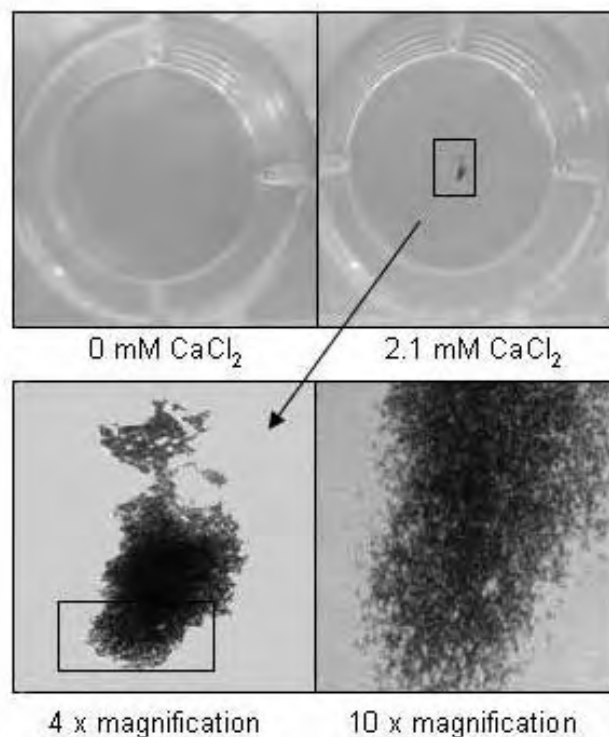
T040

Non-adherent Circulating Progenitor Cells with Osteoblastic Potential Become Adherent in the Presence of Calcium²⁺ and Are able to Mineralize. U. I. Moedder, S. Khosla. Mayo Clinic, Rochester, MN, USA.

Circulating progenitor cells with osteoblastic potential may play an important role both in normal bone remodeling and in mediating vascular calcification. In addition, migration and differentiation of these cells into osteoblasts may be regulated by the release of chemokines, such as stromal cell-derived factor-1 (SDF-1), as well as by increased local calcium²⁺ (Ca²⁺) concentrations, which may be as high as 40 mM at sites of active bone resorption and in areas of vascular injury associated with apoptotic cells. Thus, in the present study, we tested whether non-adherent osteoblast progenitors expressed the SDF-1 receptor, CXCR4, and/or became adherent and formed mineral deposits (as assessed by Von Kossa and Alizarin Red staining) in the presence of Ca²⁺.

Osteocalcin positive cells (OCN^{pos}) were isolated by magnetic activated cell sorting (MACS) and OCN^{pos} cells and mononuclear cells (MNCs) were used as negative controls. Continuous proliferation of the MNCs and OCN^{pos} was observed for up to 7 days in vitro following isolation; however, OCN^{pos} cells failed to proliferate after 24 hours. By flow cytometry, 82% of OCN^{pos} cells coexpressed CXCR4, the exclusive receptor for SDF-1, which is released at sites of vascular injury or fractures. OCN^{pos} cells did not adhere to uncoated culture flasks in the presence of regular growth medium for up to 4 weeks. By contrast, if the culture medium contained an additional 2.1 mM Ca²⁺ for up to 5 days at the beginning of the culture, the cells started to adhere. Subsequently (and following removal of the additional Ca²⁺), these cells mineralized within 21 days in the presence of osteoblast differentiation medium, as determined by Von Kossa and Alizarin Red staining (Figure). By contrast, MNCs and OCN^{neg} cells did not mineralize under these culture conditions. Collectively, these findings support the concept that OCN^{pos} cells may be recruited to sites of bone remodeling and/or vascular injury via the CXCR4-SDF-1 axis and, in the setting of

an increased local concentration of Ca²⁺, be induced to adhere and differentiate into osteoblastic cells.



Disclosures: U.I. Moedder, None.

T041

Human Fetal Bone Cells for Tissue Engineering. M. Montjovent^{*1}, C. Scaletta^{*2}, L. Mathieu^{*3}, D. Pioletti¹, L. Applegate^{*2}. ¹Laboratory of Biomechanical Orthopedics EPFL-HOSR, EPFL, Lausanne, Switzerland, ²Orthopedic Cell Therapy Unit, PAV-03, Centre Hospitalier Universitaire Vaudois and University of Lausanne, Lausanne, Switzerland, ³Laboratory of Composite and Polymer Technology, EPFL, Lausanne, Switzerland.

For clinical bone transplantations, tissue engineering techniques based on the delivery of cells to the defect using scaffold materials are currently investigated. Our aim is to evaluate the possible use of human fetal bone cells for tissue repair. Firstly, fetal bone cells were characterized for their osteoblastic phenotype. Then, fetal bone cells were seeded on scaffolds made of poly-L lactic acid (PLA) and reinforced with b-TCP. Proliferation, ALP enzymatic activity were observed, and in vitro mineralization was assessed. Lastly, scaffolds seeded with fetal cells were tested in vivo in critical size defects in the rat cranial model. The cellular doubling time of fetal bone cells was estimated to be 27 hours, whereas this value was significantly higher for adult bone cells and clearly age dependent. Fetal bone cells receiving a differentiation mix showed a strong induction of ALP activity after 4-6 days of treatment and this observation was also verified at high passage numbers. Adult cells showed a lower induction of ALP enzymatic activity. Extracellular matrix analysis demonstrated that fetal bone cells were able to mineralize PLA/b-TCP scaffolds in vitro. Moreover, repair of craniotomy critical size defect was assessed in vivo and we showed that human fetal bone cells possess a high proliferation potential, are able to differentiate into osteoblasts, and they promote bone repair in vivo when seeded on PLA/b-TCP constructs. The use of fetal bone cells, which have the advantage of a high proliferation capacity, for bone tissue engineering could be an alternative to mesenchymal stem cells.

Disclosures: M. Montjovent, None.

This study received funding from: PNR 46 N404640-101114/1.

T042

Modulation of WNT3A Induced Signaling Through Dual-Specificity Phosphatases. P. V. Nantermet^{*1}, P. Hodor^{*2}, O. Flores^{*1}, H. Glantschnig^{*1}.

¹Bone Biology & Osteoporosis, Merck Research Labs, West Point, PA, USA,

²Molecular Profiling, Merck Research Labs, West Point, PA, USA.

There is substantial evidence for a central role of Wnt-signaling in regulating bone mass accrual. Wnt activates a canonical signaling pathway through β -catenin, likely mediated via LRP5 and LRP6. However, other Wnt-mediated non-canonical signaling components like Ca⁺⁺, protein kinase C and mitogen-activated protein kinases (MAPKs) have also been implicated. Using a mesenchymal pluripotent cell (C3H10T1/2), we observed Wnt3A induced early osteoblastic cell differentiation, which can be blocked by DKK-1. To elucidate the signaling pathways engaged in this cell system, we performed a micro-array analysis in C3H10T1/2 cells treated with WNT3A in the presence or absence of exogenous DKK-1.

Among genes regulated by WNT3A, we identified individual temporal responses of eleven members of the dual-specificity phosphatase (DUSP) family. Despite the amount of information on DUSPs in MAPK signaling, limited information exists on the role of DUSPs in Wnt signaling pathway or on further downstream effects. Within this study we have therefore focused on Dusp 1, 4 and 9 representing early (6 hours), delayed (24 hours) and late (72 hours) responders to WNT3A, respectively.

The WNT3A increased Dusp 1/4/9 expression was blocked only partially by simultaneous addition of DKK1. Experiments using bone marrow derived cells from Lrp5^{-/-} mice revealed that the WNT3A induced increase in Dusp 4/9 transcript levels is independent of LRP5. However, over-expression of a HBM-mutant in HEK293-cells (Lrp5-G171R) seemed to augment WNT3A -induced Dusp 4 transcription. To address DUSP involvement in Wnt/LEF/TCF signaling, we transiently over-expressed Dusp 4/9 in HEK293 cells. No effect of either phosphatase on Lef/TCF signaling was observed in absence of WNT3A, however, WNT3A induced signaling was further augmented by about 50% and 20% by Dusp 4 and Dusp 9 over-expression, respectively. Furthermore, in-vitro knockdown of Dusp 4 and 9 by siRNA indicated crucial roles of DUSP-4/9 in WNT3A mediated Lef/TCF signaling.

In conclusion, we have identified DUSP family members responding to WNT3A treatment and importantly, in the case of DUSP 4/9, cross-talking with canonical Wnt/LEF/TCF signaling pathway. By inference, DUSP mediated control of MAPK's through dephosphorylation, thus might play a role in WNT3A induced C3H10T1/2 osteoblastic cell differentiation.

Disclosures: P.V. Nantermet, None.

T043

Nondestructive Evaluation of Cell Numbers in Bone Marrow Stromal Cells

/ Biodegradable Scaffold Composites Using Ultrasound. K. Oe¹, M. Miwa^{*1}, K. Nagamune^{*1}, Y. Sakai^{*1}, R. Kuroda^{*1}, T. Hasegawa^{*1}, T. Iwakura^{*1}, N. Shibamura^{*1}, Y. Hata^{*2}, M. Kurosaka^{*1}. ¹Department of Orthopedic Surgery, Kobe University Graduate School of Medicine, Kobe, Japan, ²Graduate School of Engineering, University of Hyogo, Himeji, Japan.

Composites of bone marrow stromal cells (BMSCs) and biodegradable scaffold (BS) have been used as a bone graft model. Up to now, the actual number of cells contained in these composites has been difficult to evaluate using nondestructive techniques. In general, ultrasound amplitude through homogeneous material is larger than through heterogeneous material such as BMSCs/BS composites. We developed an ultrasound device to evaluate BMSCs/BS composites.

The ultrasound device has a transmitting probe and a receiving probe attached to the slide gauge frame. Both probes are set to be collinear at opposite sides to propagate ultrasound wave from the transmitting probe to the receiving probe. One of the probes can be moved along the frame to adjust the size of the material to be inserted between them. The ultrasound wave data was recorded by an oscilloscope via an ultrasound pulser/receiver. In this study, we investigated the relationship between the ultrasound amplitude and the actual number of cells, using ultrasound as a nondestructive and quantitative technique. We used BMSCs of S-D rat and examined five experimental groups with different concentrations of BMSCs: 0 (control), 1.0×10^6 , 1.5×10^6 , 2.0×10^6 and 1.0×10^7 cells/ml (n=25). Porous ceramic blocks composed of β -tricalcium phosphate were used as scaffolds. All samples were incubated for 24 hours at 37°C and we evaluated them with the ultrasound device. After measurement by ultrasound device, BMSCs/BS composites were detached with 0.25% trypsin during the destruction of the BMSCs/BS composites for 30 minutes. We counted the BMSCs of all BMSCs/BS composites using a Hemacytometer. We repeated this treatment twice, and considered the total cell count numbers to be the actual number of cells.

Ultrasound amplitude was well correlated to the actual number of cells contained in the BS (r=0.779). The estimation equation ($y=9879x-33290$) was derived from the results. Here, x and y represent the amplitude value and estimated cell number in this study, respectively. The linearity of this estimation equation was validated in the range of seeding cell concentration from 5.8×10^4 to 19.2×10^4 of the cell number. The estimated error for the system was 2.591×10^4 . These results indicate that the ultrasound device we developed is a valuable, convenient, and nondestructive tool for applications in tissue engineering, especially in the generation of artificial bone tissue.

Disclosures: K. Oe, None.

T044

Liganded versus Unliganded Estrogen Receptor: A Potential Explanation for Paradoxical Regulation of Periosteal Expansion by Estrogens. M. Ogita, E. Dworakowski*, J. P. Bilezikian, S. Kousteni. Division of Endocrinology, College of Physicians & Surgeons, Department of Medicine, Columbia University Medical Center, New York, NY, USA.

Many studies in rodents, primates and humans indicate that estrogens suppress periosteal expansion. However, in certain situations, such as in men with aromatase deficiency or in the growing skeleton, low estrogen concentrations may promote directly periosteal expansion or, alternatively, be permissive to the stimulatory effects of androgens or mechanical stimulation. Based on evidence that unliganded and liganded ER α regulate the expression of cytokines like TNF α in an opposite manner, we examined the possibility that ER α may also show different, and opposite, functions to regulate periosteal osteoblast differentiation. We have found that 17 β -estradiol (E₂) has no effect by itself, but attenuates the stimulatory effect of BMP-2 on the expression or activity of alkaline phosphatase and endogenous targets of BMP-2 - and Wnt/ β -catenin-mediated transcription in primary periosteal cells. Dihydrotestosterone (DHT) exerts the opposite effects. However, reduction of ER α expression in primary periosteal osteoblast progenitors using siRNA, dose-dependently attenuates BMP-2 - induced osteoblast differentiation, as measured by AP activity. Pre-treatment with 10^{-8} M of the specific ER inhibitor ICI 182,780, which causes ER degradation, attenuates the stimulatory effect of BMP-2 on AP activity in primary periosteal cells. BMP-2-induced upregulation of Smad1/5/8 phosphorylation is not affected by ICI 182,780; but Smad6 (a transcriptional target of BMP-2), osteocalcin and axin2 (a transcriptional target of Wnt/ β -catenin) expression, measured at 16 days following treatment with ICI 182,780, is attenuated. These results suggest that ER α is a major cellular switch which can either suppress (in the presence of E₂) or stimulate (in the absence of E₂) periosteal bone formation; perhaps by potentiating the beneficial effects of mechanical loading or androgens. We have also found that low doses of E₂ have no effect on periosteal cell differentiation, but in combination with DHT (1-100 pM), induces AP activity in periosteal osteoblast progenitors. Thus, low dose estrogen exposure may mimic the stimulatory actions of unliganded ER α on periosteal expansion. We propose that the dual action of ER α in periosteal osteoblast differentiation may help to explain the apparent paradox of the dose-dependent biphasic response of the periosteum to estrogens.

Disclosures: M. Ogita, None.

T045

Characterization of Bone Tumors in a Mouse Model for Carney Complex.

E. Pavel^{*1}, K. Nadella^{*1}, W. Towns^{*1}, L. Kirschner^{*2}. ¹Human Cancer Genetics, The Ohio State University, Columbus, OH, USA, ²Internal Medicine, Subdivision of Endocrinology, The Ohio State University, Columbus, OH, USA.

Carney Complex (CNC) is an autosomal dominant neoplasia syndrome caused by inactivating mutations in PRKARIA, the gene encoding the type 1A regulatory subunit of protein kinase A (PKA). This genetic defect induces skin pigmentation, endocrine tumors, myxomas, schwannomas and bone tumors termed osteochondromyxomas.

In order to study the link between the PRKARIA mutations and tumor formation, we generated a mouse model of this condition. Prkar1a^{-/-} mice develop bone tumors with high frequency, although the associated molecular changes have not been characterized.

Bone tumors observed in Prkar1a^{-/-} mice were heterogeneous, including elements of myxomatous, cartilaginous and bony differentiation which effaced the normal bone architecture. Immunohistochemical analysis had suggested an osteoblastic origin for the tumor cells which we have confirmed using additional markers. These abnormal cells were typically associated with increased bone remodeling as evidenced by increases in osteoclasts number.

Analysis of primary culture of the tumors confirmed that the tumor cells were derived from the osteoblast lineage; however, fully differentiated functions such as mineralization were impaired and tumor cells exhibited an increase in migratory capability. At the biochemical level, we observed the expected reduction in Prkar1a protein and an increase in PKA activity in tumor cells. Moreover, primary tumor cells demonstrated an increased sensitivity to the growth-promoting effects of PKA activation in the cells.

Examination of gene expression in the tumor cells revealed down-regulation of markers of bone differentiation and increased expression of locally acting growth factors, including members of the Wnt signaling pathway. The role of the Wnt signaling pathway has also been confirmed by observing alterations the subcellular distribution of the relevant signaling molecules. In summary, loss of Prkar1a from the mouse leads to the formation of bone tumors analogous to osteochondromyxomas observed in human patients. Dysregulation of PKA leads to the formation of osteoblast-derived bone tumors through dysregulation of differentiation and upregulation of locally-acting factors involved in cell growth and differentiation.

Disclosures: E. Pavel, None.

T046

Effects of PDE7 and PDE8A Inhibition on the Differentiation of Human Mesenchymal Stem Cell-Derived Osteoblasts. M. H. Pekkinen¹, M. E. B. Ahlström^{*1}, U. Riehle^{*2}, M. M. Huttunen¹, C. J. E. Lamberg-Allardt¹.

¹Department of Applied Chemistry and Microbiology, University of Helsinki, Helsinki, Finland, ²Institute for Biological Chemistry and Nutrition, University of Hohenheim, Stuttgart, Germany.

Cyclic adenosine monophosphate (cAMP) is an important second messenger involved in a variety of cellular responses to extracellular agents such as hormones and neurotransmitter, i.e. in PTH signaling via cAMP. cAMP is known to be inactivated by the cyclic nucleotide phosphodiesterases (PDEs), a superfamily of enzymes divided into 11 known families; designated PDE 1-11. PDEs determine the amplitudes of cyclic nucleotide mediated hormonal responses and modulate the duration of the signal. Osteoporosis, bone loss, typically reflects an imbalance in skeletal turnover so that bone resorption exceeds bone formation. It is important to understand the role of the PDEs in bone cells, because the bone metabolism, and especially bone formation, could be affected via PDEs. The aim of this study was to investigate the influence of PDE7 and PDE8A inhibition in the differentiation and function of human osteoblasts.

Osteoblasts differentiated from human mesenchymal stem cells (hMSC) were cultured and treated for 48 h with small interfering RNAs (si-RNAs) generated from PDE7 and PDE8 PCR products. Total RNA was isolated from the cells and gene expression was assayed with cDNA microarray. Quantitative Real-Time PCR was used to confirm the specific PDE inhibition and the cDNA microarray results. bALP measurements were assayed during differentiation and mineralization was determined by quantitative Alizarin red S staining. On the level of mRNA, PDE7 and PDE8 inhibition by RNA interference (RNAi) decreased the gene expression of PDE7A by 60%, PDE7B by 40% and PDE8A by 30%. The silencing of PDE7 increased the expression of several osteogenic genes, such as β -catenin, osteocalcin, caspase 8, and CREB-5 genes and decreased the expression of the 1,25-dihydroxyvitamin D3 receptor gene. The silencing of PDE8A significantly decreased caspase-8, osteoglycin, BMP-1. Mineralization was increased up to threefold in PDE7 siRNA treated cells compared to control and treatment with the PDE7-selective PDE-inhibitor BRL-50481 also increased the mineralization. Silencing with PDE8A siRNAs had no effect on mineralization.

Our results show that specific gene silencing with the RNAi method is a useful tool for inhibiting the gene expression of specific PDEs and that PDE7 upregulates several osteogenic genes and increases mineralization. PDE7 may play an important role in the regulation of osteoblastic differentiation.

Disclosures: M.H. Pekkinen, None.

T047

Conjugated Linoleic Acid Regulates Osteoblast and Adipocyte Differentiation from Mesenchymal Stem Cells. I. D. Platt^{*1}, L. G. Rao^{*2}, A. El-Soehy^{*1}. ¹Nutritional Sciences, University of Toronto, Toronto, ON, Canada, ²Medicine, University of Toronto, St. Michael's Hospital, Calcium Research Laboratory, Toronto, ON, Canada.

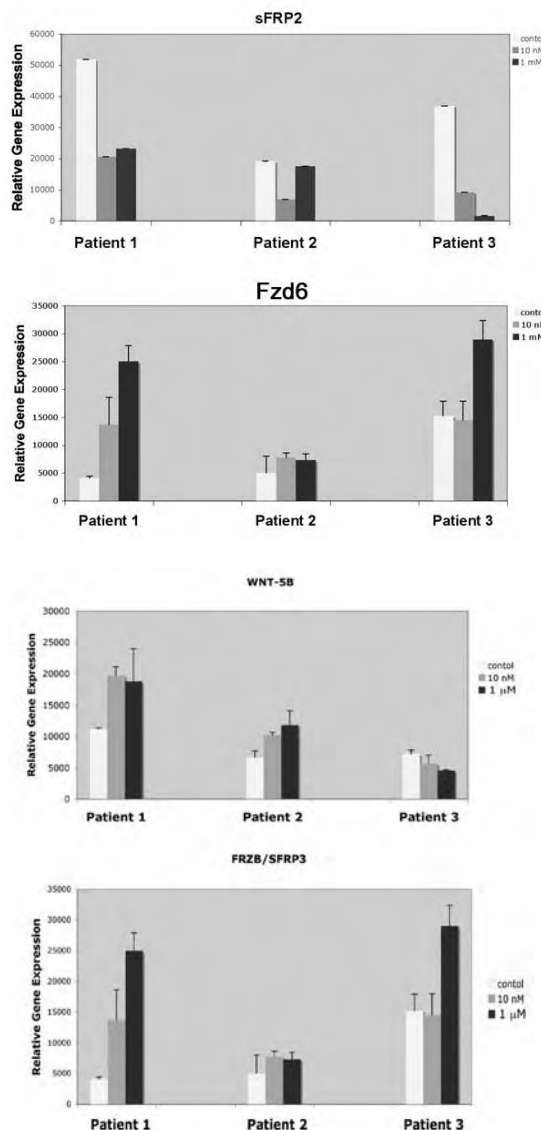
Conjugated linoleic acid (CLA) refers to a group of geometric and positional isomers of linoleic acid. The major isomers are 9cis,11trans (9,11) and 10trans,12cis (10,12) CLA, which are both bioactive and often have different physiological effects. CLA has variable effects on bone formation and on adiposity in vivo and in vitro. Osteoblasts and adipocytes are both derived from mesenchymal stem cells (MSCs), and factors that promote the differentiation of one cell type may inhibit the differentiation of the other type. CLA may be one such factor and the effects of CLA on MSCs are not known. The purpose of this study was to determine whether 9,11 and 10,12 CLA affect markers of osteoblast (alkaline phosphatase (ALP), osteocalcin) and adipocyte (lipid droplet) differentiation from human bone marrow-derived MSCs and alter the expression of genes regulating osteoblast (Wnt10b) and adipocyte (C/EBP α) differentiation from these cells. To determine the effects of CLA on osteoblast differentiation, MSCs were seeded at 3×10^3 cells/cm², and treated 4 days later with 0-50 μ M 9,11 or 10,12 CLA in osteogenic media. Cells were harvested after 11 days in culture for mRNA analysis (Wnt10b, osteocalcin), and for the measurement of ALP activity. Calcium deposition was measured after 18 days in culture. To determine the effects of CLA on adipocyte differentiation, MSCs were seeded at 2×10^4 cells/cm², and treated 4 days later with 0-50 μ M 9,11 or 10,12 CLA in adipogenic media. After 11 days in culture, cells were stained for lipid droplet formation using oil red O, and cells were harvested for mRNA analysis (C/EBP α). Gene expression was determined by real-time RT-PCR and normalized to the expression of β -2-microglobulin. At 12.5 μ M, 10,12 CLA increased Wnt10b expression (~70%), whereas 9,11 CLA decreased its expression (~33%). At 50 μ M, 10,12 CLA increased osteocalcin expression (~85%), calcium deposition (~32%), and ALP activity (~85%), but 9,11 CLA had no effect. At 50 μ M, 10,12 CLA decreased the expression of C/EBP α (~35%), but 9,11 CLA had no effect. However, 9,11 CLA increased oil red O staining at all concentrations and maximally at 50 μ M (~70%). Our results demonstrate that 10,12 CLA increases osteoblast differentiation and decreases adipocyte differentiation from MSCs suggesting that this isomer may prevent bone loss and decrease bone marrow adiposity.

Disclosures: I.D. Platt, None.

T048

Activation of the Non-canonical Wnt Pathway During Human Mesenchymal Stem Cell Osteogenesis: Microarray Expression Analyses to Examine the Effects of Dexamethasone on Cell Differentiation. K. T. Rousche^{*}, A. Derfoul^{*}, J. Helm^{*}, R. S. Tuan^{*}. Cartilage Biology and Orthopaedics Branch, NIH/NIAMS, Bethesda, MD, USA.

Non-canonical Wnts enhance osteogenic differentiation in adult human mesenchymal stem cells (hMSCs). The molecular mechanisms involved in activation of this Wnt pathway during osteoblastic differentiation of hMSCs have yet to be defined. In vitro, glucocorticoids (GCs) are known to maintain differentiation of osteoblasts and to promote osteogenic differentiation of hMSCs. However, administration of high doses of GCs has been shown to suppress growth in children and lead to low bone mineral density and increased fracture risk in adults. To gain insight in the mechanisms of GC action on the differentiation of hMSCs into osteoblasts, we examined the effects of various doses of the GC analog, dexamethasone (DEX), on osteogenic differentiation of hMSCs. The purpose of this study was to identify genes involved in osteogenic differentiation of hMSCs at physiological doses of GCs, as well as genes associated with the inhibition of osteoblast function by therapeutic doses of GCs. We performed DNA microarray analyses of hMSCs cultured in osteogenic conditions in the presence or absence of 10 nM or 1 μ M DEX. Human bone marrow was obtained from the femoral head of patients undergoing hip arthroplasty. hMSCs were cultured in monolayer for 12 days in osteogenic medium in the presence or absence of 10 nM to 1 μ M DEX. Microarray analyses of hMSCs grown in the presence of 10 nM or 1 μ M DEX were performed using Affymetrix human Genome U133 Plus 2.0 chips. Results were analyzed using bioinformatics RAM and MAS softwares. Data suggest that GCs alter expression of non-canonical Wnts, Wnt receptors and Wnt modulators during hMSC osteogenic differentiation. Wnt5b, FRZB (sFRP3), Twist2, and FRZ6, and sFRP2 were differentially expressed during GC-mediated hMSC osteogenesis. Taken together, these data support a distinct role for non-canonical Wnts in MSC osteogenic differentiation. siRNA and functional studies are underway to further support this data.



Disclosures: K.T. Rousche, None.

This study received funding from: Intramural Research Program of NIAMS, NIH.

T049

Cytoplasmic Interaction of p21 with Runx2 During Osteogenic Differentiation of Mesenchymal Stem Cells. P. Muller^{*1}, C. Bergemann^{*1}, U. Bulnheim^{*1}, A. Liebold^{*2}, G. Steinhoff^{*2}, J. Rychly¹. ¹Laboratory of Cell Biology, University of Rostock, Rostock, Germany, ²Department of Heart Surgery, University of Rostock, Rostock, Germany.

Regulating the switch between proliferation and osteogenic differentiation of mesenchymal stem cells is critical for the development of normal bone tissue and more over is of considerable interest in bone tissue engineering using mesenchymal stem cells as vehicles for cell based skeletal therapies. Recent investigations revealed that the protein p21 exhibits multiple functions in addition to its role in cell cycle inhibition. These functions appear to rely on the different cellular localizations and molecular targets. To assess a possible role of p21 in the differentiation of mesenchymal stem cells, we tested the cellular localization of p21 during the osteogenic differentiation of mesenchymal stem cells. Bone marrow derived human mesenchymal stem cells were stimulated to differentiate into osteoblasts by addition of osteogenic differentiation medium (ODM) containing ascorbic acid, glycerolphosphate and dexamethasone. In p21-GFP transfected cells we observed a translocation of p21 from the nucleus to the cytoplasm within 2 hours after addition of ODM. This nuclear export was mediated by CRM1, the major nuclear protein export receptor, because leptomycin B completely blocked the translocation of p21. These experiments further indicated the significance of the CRM1 mediated nuclear export of proteins for the osteogenic differentiation, because inhibition of the export reduced the expression of osteogenic marker proteins and alkaline phosphatase activity. To further assess whether the translocation of p21 is related to known molecules of the cellular machinery that control the osteogenic differentiation we addressed the interaction of p21 with Runx2, the principal osteogenic transcription factor. Coimmunoprecipitation experiments with both nuclear and cytoplasmic fractions revealed that p21 interacts with Runx2 in the cytoplasm during osteogenic differentiation. Blocking the nuclear export of proteins revealed an association of both proteins in the nucleus. We further found that inhibition of the export by leptomycin B with the consequence of blocking osteogenic differentiation did not reduce but rather increased the RNA expression of Runx2. In conclusion, the interaction of p21 with Runx2 in the cytoplasm during osteogenic differentiation suggests that p21 plays a role in the osteogenic differentiation. However, the function of the cytoplasmic interaction of these proteins is not known. We speculate that p21 may act as assembly factor for Runx2 in the cytoplasm to promote or control a nuclear import of Runx2.

Disclosures: J. Rychly, None.

T050

Osteogenesis and Adipogenesis Are Differentially Modulated by PTH and the N- and C-Terminal Fragments of PTH-Related Protein. R. Santiago^{*1}, A. Casado^{*2}, I. Herrera^{*3}, A. Torres^{*3}, P. Esbrit^{*4}, G. Dorado^{*5}, J. M. Quesada^{*1}. ¹UMM, Hospital U. Reina Sofía, Córdoba, Spain, ²Sanyres (Grupo PRASA), Hospital U. Reina Sofía, Córdoba, Spain, ³Servicio Hematología, Hospital U. Reina Sofía, Córdoba, Spain, ⁴Laboratorio de Metabolismo Mineral y Oseo, Fundación Jimenez Diaz, Madrid, Spain, ⁵Dpto. Bioq y Biol Mol, Universidad de Córdoba, Córdoba, Spain.

Chronic or intermittent parathormone (PTH) administration plays different roles on bone. We evaluated the effects of different patterns of exposure to either PTH (1-34), parathyroid hormone-related protein (PTHrP) (1-36), or PTHrP (107-139) on adipogenesis and osteoblastogenesis in vitro. Bone marrow stromal cells were differentiated to osteoblasts (dexamethasone, ascorbic acid and glycerolphosphate) or adipocytes (dexamethasone, indomethacin and isobutylmethylxanthine), in the presence of PTH or the PTHrP peptides (100 nM), added at the beginning or at day 6 up to the end of the study period. Differentiating cell cultures were sampled at 6, 18, and 24 days. The differentiating process was evaluated by measuring alkaline phosphatase (AP) activity and gene expression (by real time PCR) of osteogenic (AP, runx2, type I collagen, osteocalcin, osteoprotegerin, and RANKL) and adipogenic (PPAR γ 2 and LPL) markers. Osteoblast mineralization was assessed by alizarin red staining; and adipocyte by oil red staining. Expression of all osteoblastic factors tested decreased with both PTHrP (1-36) and PTH at day 6. However, addition of these peptides, but not PTHrP (107-139), from this day through the end of the culture period increased the expression of these factors at 18 and 24 days, respectively. This was associated with a decrease in PPAR γ 2 and LPL gene expression induced by either PTHrP (1-36) or PTH within the same time period. On the other hand, continuous treatment with PTHrP (107-139) from the start of cell culture induced adipogenesis, as shown by increased PPAR γ 2 and LPL gene expression at day 18, and decreased the expression of various osteoblastic products at day 24. Moreover, at the latter time period, the number of adipocytes was 20 % higher in cultures supplemented with PTHrP (107-139), but 20 % lower in those treated with either PTHrP (1-36) or PTH from day 6, compared with that in untreated cells. In conclusion, our findings suggest that the effects of PTH and these PTHrP peptides on bone marrow stromal cells depend on their differentiation stage. Thus, PTH and, to a lesser extent, the N-terminal PTHrP fragment induce osteogenesis in cells that are already differentiating. On the other hand, PTHrP (107-139) was not found to be osteogenic, but it enhanced adipogenesis, in our experimental setting.

Supported by: Sanyres (Grupo PRASA), CM0010/05, PAI CTS-413, and SAF2005-05254.

Disclosures: R. Santiago, None.

T051

Effect of 1,25-Dihydroxyvitamin D₃, Retinoic Acid, and Dexamethasone on the Osteoblastic Differentiation of Human Adipose-Derived Stem Cells. M. J. Saran^{*1}, P. A. Zuk^{*2}, W. Huang^{*3}, C. K. Huang^{*4}, M. Hakimi^{*1}, D. S. Bischoff^{*3}, G. H. Rudkin^{*5}, D. T. Yamaguchi¹, T. A. Miller^{*3}. ¹David Geffen School of Medicine, UCLA, Los Angeles, CA, USA, ²Regenerative Bioengineering and Repair Lab, UCLA, Los Angeles, CA, USA, ³Research Service, VA Greater Los Angeles Healthcare System, Los Angeles, CA, USA, ⁴Head & Neck Surgery, UCLA, Los Angeles, CA, USA, ⁵Plastic Surgery, UCLA, Los Angeles, CA, USA.

Human adipose-derived stem cells (ASC) are a promising source of cells for bone tissue engineering; however, the factors that stimulate osteogenic differentiation in human ASC have not been well characterized. Most studies have either been done in animal models or in 2-dimensional (2-D) cultures systems. However, human ASC have been shown to respond differently to the osteogenic supplements than animal ASC. Also, 3-D cultures, as compared to 2-D cultures, are a closer approximation to the 3-D matrix that cells encounter in vivo. The purpose of this study was to investigate the supplements that are commonly used to induce osteogenic differentiation in human ASC, and to compare their actions in 2-D versus 3-D cultures. One million human ASC cells were seeded onto 3-D poly(L-lactide-co-glycolide) (PLGA) scaffolds or 2-D PLGA films. Cells were cultured in osteogenic media in the presence or absence of each of the following supplements: 1,25-Dihydroxyvitamin D₃ (VD) [10nM or 100nM], Retinoic Acid (RA) [1 μ M], or Dexamethasone (Dex) [100nM]. Cells were harvested at 7, 10, and 14 days for RNA extraction. Quantitative real-time RT-PCR was performed to measure mRNA expression of the following osteogenic marker genes: Alkaline Phosphatase (ALP), Osteocalcin (OCN), Bone Sialoprotein (BSP), and Collagen I (Col I). VD increased the expression of all 4 osteogenic marker genes in 3-D cultures compared to control. ALP increased 5-fold on day 14. OCN and BSP increased 2-fold on day 14. Col I increased 3-fold on day 14. 2-D cultures treated with VD followed a similar expression pattern. However, treatment with Dex or RA adversely effected expression of these osteogenic markers in both 2-D and 3-D cultures. On day 7, RA treatment resulted in a 4-fold decrease in ALP expression, an 11-fold decrease in BSP expression, and no change in the levels of OCN mRNA. Similarly, Dex caused a 7-fold decrease in BSP expression and no change in ALP or OCN expression compared to control on day 7. In conclusion, we found that for both 2-D and 3-D cultures, 1,25-Dihydroxyvitamin D₃ promotes the expression of osteogenic marker genes; whereas, Retinoic Acid and Dexamethasone treatment, have no effect or can be detrimental to ASC cell osteogenic differentiation. This is an important step to understanding the best supplements to use to promote human ASC osteogenic differentiation in bone tissue engineering.

Disclosures: M.J. Saran, None.

T052

Microgravity and Bone: Effects of Modeled Microgravity on Osteoblast and Osteoclast Differentiation. R. Saxena^{*1}, G. Pan^{*2}, J. M. McDonald². ¹Department of Cell Biology, University of Alabama at Birmingham, Birmingham, AL, USA, ²Department of Pathology, University of Alabama at Birmingham, Birmingham, AL, USA.

Prolonged microgravity experienced by astronauts on long term space missions is associated with a decrease in bone mass and an increase in risk of fracture. Studies on astronauts during spaceflight indicate that increased bone resorption by osteoclasts and decreased osteoblast activity, are jointly responsible for bone loss. To investigate the effect of microgravity on differentiation of osteoclasts and osteoblasts from precursor cells in space, we used the Rotary Cell Culture System (RCCS) which is a ground based system that is able to simulate microgravity conditions. Using the RCCS, we have demonstrated that modeled microgravity inhibited the expression of osteoblast differentiation genes and increased adipocyte genes in human mesenchymal stem cells incubated under osteogenic conditions. This transformation involves reduced RhoA activity and cofilin phosphorylation, disruption of F-actin stress fibers, and decreased integrin signaling through focal adhesion kinase. We have recently established a unique system to investigate the effects of modeled microgravity on osteoclastogenesis. The mouse macrophage cell line, RAW264.7 was cultured with microcarrier beads in DMEM supplemented with 10% FBS. Cells attached to beads were placed in the RCCS (microgravity treatment) and rotated at 9 rpm for 8 hours and 24 hours. Bead-attached cells placed simultaneously in culture plates were the gravity controls. After incubations, the cells were detached from beads and stimulated with RANKL (Receptor Activator of NF κ B Ligand, 20ng/ml) and allowed to differentiate for 4 days. Differentiated multinucleated osteoclasts were observed under the microscope followed by TRAcP (Tartrate Resistant Acid Phosphatase) staining. Our results show that multinucleated TRAcP-positive osteoclasts derived from microgravity treated cells were increased nearly two-fold compared to that from gravity-treated cells after treatment with RANKL. RT-PCR further demonstrated that TRAcP expression in MMG-treated cells was increased compared to gravity-treated cells. In conclusion, these data indicate that modeled microgravity directly stimulates osteoclastogenesis and inhibits osteoblastogenesis, consistent with the studies of bone loss in humans in microgravity.

Disclosures: R. Saxena, None.

T053

Mesenchymal Stem Cells from Human Adipose Tissue and Bone Marrow: Osteogenic Differentiation and Interaction with Ti6Al4V. I. Tognarini^{*1}, S. Sorace^{*1}, R. Zonfrati^{*1}, G. Galli^{*1}, A. Gozzini^{*1}, S. Carbonell Sala^{*1}, G. Zappoli Thyron^{*1}, A. Carossino^{*1}, S. Ciuffi^{*1}, A. Tanini^{*1}, F. Sbaiz^{*2}, A. Facchini^{*2}, M. Brandi¹. ¹Internal Medicine, University of Florence, Florence, Italy, ²LIMA SpA Medical System, San Daniele del Friuli, Udine, Italy.

In bone tissue engineering and surgery there is a growing need to test the ability of hard biomaterials to control the differentiation of mesenchymal stem cells (MSCs) in order to gain direct bone apposition to implant materials. MSCs, classically used to test implanted biomaterial as Ti6Al4V alloy, are isolated and ex vivo expanded from bone marrow aspirates. Human adipose tissue derived stromal cells may be a better source of MSCs according to their abundance and accessibility. The aim of this study was to evaluate the osteogenic differentiation of adipose tissue and bone marrow-derived MSCs (PA1 and BMC1, respectively) and to compare their response to Ti6Al4V.

The expression of the osteoblastic phenotype was evaluated by monitoring alkaline phosphatase (ALP) activity, expression of osteoblastic markers by quantitative RT-PCR and immunocytochemistry, and calcium mineralization by Calcein staining and Alizarin Red S assay. Cell growth, cytoskeleton morphology and adhesion of differentiated cells on Ti6Al4V were evaluated by cell counting and Laser Scanning Confocal Microscopy analysis (actin, tubulin and vinculin). Human osteoblast-like cells (SaOS-2) were used as control.

Thirty days after the osteogenic induction, near 50% of PA1 cells showed an osteoblastic-like phenotype, whereas almost 100% of BMC1 cells resulted entirely differentiated. BMC1 cells cultured on Ti6Al4V exhibited an increase of ALP activity that was similar to that seen on culture polystyrene (PS), whereas PA1 cells showed a statistically significant increment of this activity on Ti6Al4V compared to that observed on PS. A comparable enhancement of transcript levels of genes involved in osteogenic differentiation was observed in both cell lines on PS and on Ti6Al4V during differentiation. Osteoblastic activity was confirmed at the protein level by osteopontin and osteocalcin immunostaining and at the mineral level by the production of calcium deposits. A good adhesion, cytoskeleton organization, and cell growth on Ti6Al4V were observed in every cell line, but interestingly only PA1 cells showed a higher level of adhesion to Ti6Al4V compared to the control.

In conclusion, the results of this study confirmed that PA1 cells are capable of adhering, proliferating, and differentiating on Ti6Al4V as well as BMC1 cells and support the concept that adipose tissue may represent a valuable alternate source of MSCs to bone marrow for hard tissue regeneration.

Disclosures: I. Tognarini, None.

T054

Identification of Human Circulating Side Population (SP) Cells Co-expressing the Mesenchymal Stromal Cell Marker, Stro-1. A. H. Undale, U. I. L. Moedder, S. Khosla. Mayo Clinic, Rochester, MN, USA.

Stem cells that stain differentially with vital dyes such as Hoechst 33342 are described as side population (SP) cells, which can be distinguished by their capacity to efflux the Hoechst 33342 dye efficiently and by their unique profiles in Hoechst red versus Hoechst blue bivariate fluorescent-activated cell sorting dot plots. SP cells have been identified in a wide variety of mammalian tissues, including murine and human bone marrow and human peripheral blood. These cells can not only regenerate the cells of the hematopoietic lineage but have also been shown to regenerate several mesenchymal lineages, suggesting their pluripotent potential. Studies conducted by Aubin et al (Bone 2006, 38:662) showed that SP cells isolated from fetal rat calvaria were enriched for osteoprogenitor cells.

We undertook the current study to investigate whether SP cells in human peripheral blood expressed the mesenchymal stromal cell marker, Stro-1, which identifies cells with osteogenic potential in human bone marrow. We examined the SP cell population in human peripheral blood mononuclear cells (MNCs) obtained by Ficoll-gradient centrifugation. The SP cell population (mean \pm SEM, n=4) was identified by flow cytometry based on the ability of these cells to efflux Hoechst 33342 and their typical Hoechst 33342 profile. Flow cytometric analyses identified 0.14 ± 0.01 % of MNCs as SP cells. Further phenotypic characterization of the SP cell population was done using a monoclonal Ab to Stro-1. We found that 1.6 ± 0.4 % of the SP cell population expressed Stro-1, so that the total percentage of Stro-1^{pos}/SP^{pos} cells in MNCs was 0.002%. These results thus demonstrate for the first time the presence of the stromal cell marker Stro-1 on a subset of human peripheral blood SP cells. The circulating Stro-1^{pos}/SP^{pos} cells may represent an early mesenchymal stem cell population that could potentially be expanded and have utility in the treatment of metabolic bone diseases.

Disclosures: A.H. Undale, None.

T055

β Trcp1 Ubiquitin Complex Regulates Ihh-promoted Osteoblast Differentiation Through Gli2 Ubiquitination. M. Wada^{*1}, T. Matsubara¹, K. Hata^{*1}, T. Imamura^{*2}, R. Nishimura¹, T. Yoneda¹. ¹Osaka University, Osaka, Japan, ²JFCR Cancer Institute, Tokyo, Japan.

Accumulating data indicate that Indian hedgehog (Ihh) promotes the differentiation of mesenchymal stem cells into osteoblasts. It is also suggested that the transcription factor, Gli2, which is activated by Ihh, plays a role in this differentiation process. Recent studies have reported that an ubiquitin ligase complex consisting of β Trcp1 regulates Gli2 expression, suggesting an involvement of β Trcp1 in the osteoblast differentiation. However, the precise role of β Trcp1 in Ihh/Gli2-promoted osteoblastogenesis is currently unknown. Furthermore, it is also unclear whether and how Ihh signaling regulates ubiquitination of Gli2 in conjunction with β Trcp1. In the present study, we investigated the role of β Trcp1 in the osteoblast differentiation stimulated by Ihh signaling and the relationship between Ihh and β Trcp1 ubiquitination system. Overexpression of β Trcp1 together with protein kinase A (PKA) and glycogen synthase kinase 3 (GSK3 β), both of which are shown to be involved in controlling β Trcp1 activity during Gli2 ubiquitination, truncated Gli2 into the repressor form of 78KD. Overexpression of β Trcp1/PKA/GSK3 β also suppressed transcriptional activity of Gli2, suggesting a negative regulatory role of the β Trcp1 ubiquitin ligase complex in Ihh/Gli2 signaling. We next examined the effects of a mutant β Trcp1 (β Trcp1- Δ F-box), which lacks the F-box domain necessary for ubiquitin ligase complex formation on osteoblast differentiation using the mesenchymal cell line C3H10T1/2. Treatment with Ihh or overexpression of Gli2 promoted osteoblast differentiation in C3H10T1/2 cells. Of note, overexpression of β Trcp1- Δ F-box markedly stimulated the Gli2-induced osteoblast differentiation. However, of interest, β Trcp1- Δ F-box had little effects on the Ihh-induced osteoblast differentiation, raising a possibility that Ihh functions through influencing ubiquitination system upstream of β Trcp1. To investigate this, we focused on GSK3 β that functions upstream of β Trcp1. Since GSK3 β activity is known to be negatively-regulated by phosphorylation, we examined the effects of Ihh on GSK3 β phosphorylation and found that Ihh phosphorylated GSK3 β . Moreover, Fused, the serine/threonine kinase which is one of the essential components of hedgehog signaling, also phosphorylated GSK3 β . Collectively, our results suggest that the β Trcp1 ubiquitin complex modulates the Ihh-promoted osteoblast differentiation by regulating Gli2 ubiquitination and that Ihh down-regulates the β Trcp1 ubiquitination system through inactivation of GSK3 β as a consequence of its phosphorylation by Fused.

Disclosures: M. Wada, None.

T056

Ectoderm Neural Cortex 1, a Wnt Target Gene, Is Expressed in Chondrocytic and Osteoblastic Cells. L. E. Worton¹, Y. Shi^{*2}, E. J. Smith^{*2}, D. G. Little^{*3}, J. P. Whitehead^{*1}, E. M. Gardiner¹. ¹Diamantina Institute for Cancer, Immunology and Metabolic Medicine, Brisbane, Australia, ²Garvan Institute of Medical Research, Sydney, Australia, ³Children's Hospital, Westmead, Sydney, Australia.

The canonical Wnt pathway has been implicated in bone mass regulation; however, few Wnt target genes affecting this process have been elucidated. Ectoderm Neural Cortex 1 (ENC1) is a reported Wnt target gene found to be involved in adipocyte differentiation. ENC1 has also been reported to interact directly with retinoblastoma protein (p110 Rb) and with filamentous actin in various cell lines. Therefore, this study was undertaken to establish a role for ENC1 in bone biology. Transcript profiles of fracture callus tissues collected at early stages in a rabbit model of tibial distraction osteogenesis were generated using human ResGen cDNA arrays. ENC1 expression was up-regulated 40-fold between 2 and 4 or 6 weeks post distraction, correlating with a marked change in callus cellular composition. In 2-week callus, fibroblastic and cartilaginous cells predominated. At 4- and 6-weeks, mature osteoblasts and osteocytes were more abundant, coinciding with a notable increase in bone forming activity. ENC1 transcripts were localized to osteoblastic cells and remnant chondrocytes by in situ hybridization of rabbit 4-week fracture callus sections. Furthermore, in normal mouse bone, ENC1 was expressed in growth plate and articular chondrocytes and in mature periosteal osteoblasts. Quantitative RT-PCR analysis confirmed the expression of ENC1 during the differentiation of primary osteoblastic cultures, and of cultured MC3T3-E1 and Kusa-O 4b10 osteoblastic cells. Expression of ENC1 was also confirmed in osteosarcoma and chondrocytic cell lines. Transient expression of epitope tagged ENC1 in MG63 and SaOS2 osteosarcoma cells and stable over-expression in HEK293 and CHO cell lines showed ENC1 to have a cytoplasmic distribution with staining of a subset of nuclei in MG63 cells. There was no evidence of co-localization with filamentous actin. These results indicate that ENC1 is expressed in chondrocytic and osteoblastic cells and may play a role in Wnt stimulated osteoblastic differentiation.

Disclosures: L.E. Worton, None.

T057

Glucocorticoid-induced Leucine-Zipper (GILZ) Enhances Osteoblast Differentiation of Bone Marrow Mesenchymal Stem Cell by Inhibiting Adipocyte Differentiation. W. Zhang^{*1}, X. Shi². ¹Department of Neurology, The First Affiliated Hospital, Sun Yat-sen University, Guangzhou, China, ²Institute of Molecular Medicine & Genetics, Medical College of Georgia, Augusta, GA, USA.

Mesenchymal stem cells (MSCs) can differentiate into multiple cell lineages including osteoblasts and adipocytes. A recently identified transcription factor, glucocorticoid-induced leucine zipper (GILZ), was shown to inhibit the expression of peroxisome proliferator-activated receptor gamma-2 (PPAR γ 2) and blocks adipocyte differentiation. To investigate the role of GILZ in osteoblast differentiation of MSCs, we isolated bone marrow MSCs from C57BL/6 mice using negative-immuno-depletion and positive-immuno-selection approaches, and overexpressed GILZ in MSCs using retrovirus-mediated gene delivery approach. Our results show that overexpression of GILZ in MSCs increased alkaline phosphatase (ALP) activity and enhanced mineralized bone nodule formation. Consistent to this phenotypic conversion, real-time RT-PCR analysis showed that both basal and differentiation-induced transcripts of the lineage commitment gene Runx2/Cbfa1, as well as osteoblast differentiation marker genes including ALP, type I collagen, and osteocalcin, were all increased in GILZ-expressing cells. In contrast, the mRNA levels of adipogenic PPAR γ 2 and C/EBP α were significantly reduced in GILZ-expressing cells under both osteogenic and adipogenic conditions. In conclusion, results of this study show that GILZ functions as a modulator of MSC differentiation and that GILZ can shift the balance between MSC osteoblast and adipocyte differentiation. These data suggest that GILZ may have therapeutic value for fracture repair and osteoporosis therapy.

Disclosures: W. Zhang, None.

This study received funding from: AHA, Arthritis Foundation.

T058

Partial Rescue of the Vitamin D Deficient Phenotype of 1 α -hydroxylase Gene Knockout Mice by Transplantation of Wild-Type Non-Adherent Bone Marrow-Derived Mesenchymal Stem Cells. Z. Zhang¹, J. Tong^{*1}, D. Goltzman², D. Miao³. ¹Department of Public Health, Suzhou University, Suzhou, China, ²Medicine, McGill University, Montreal, PQ, Canada, ³Institute of Dental Research, Nanjing Medical University, Nanjing, China.

We previously demonstrated that there are non-adherent mesenchymal stem cells (MSCs) in adult bone marrow and that transplantation of non-adherent bone marrow-derived MSCs (NA-BM-MSCs) can rescue lethal-dose irradiated VDR^{-/-} mice by re-constructing a hematopoietic system and repairing damaged tissues. To determine whether the transplantation of NA-BM-MSCs can rescue the phenotype of 1 α (OH)ase^{-/-} mice, 2x10⁶ NA-BM-MSCs from wild-type mice or vehicle (as a control) were transplanted into lethal-dose irradiated female 1 α (OH)ase^{-/-} mice by tail vein injection. Our results show that all control mice irradiated at a 10 Gy dose died within 2 weeks, however, following transplantation of NA-BM-MSCs, 75% and 70% of lethal-dose irradiated mice were viable at 1 and 2 months, respectively. The phenotype of viable 1 α (OH)ase^{-/-} recipients was compared with that of age-matched, non-irradiated wild-type and 1 α (OH)ase^{-/-} mice. 1 α (OH)ase mRNA in kidney was undetectable by RT-PCR in non-irradiated 1 α (OH)ase^{-/-} mice but was detected in viable irradiated 1 α (OH)ase^{-/-} recipients, although levels were lower when compared to levels in non-irradiated wild-type kidney. Serum 1,25(OH)₂D₃ levels were undetectable in non-irradiated 1 α (OH)ase^{-/-} mice and rose to 24% of non-irradiated wild-type mice (96 \pm 11.3ng/L) in viable irradiated 1 α (OH)ase^{-/-} transplant recipients (23 \pm 8.5ng/L). Serum calcium levels rose to 2.08 \pm 0.25mmol/L in viable 1 α (OH)ase^{-/-} recipients from 1.6 \pm 0.18mmol/L in non-irradiated 1 α (OH)ase^{-/-} mice. Skeletal mineralization improved, but did not reach normal levels in viable 1 α (OH)ase^{-/-} recipients as demonstrated by BMD measurement, micro-CT analysis and von Kossa staining of undecalcified sections. In lethal dose irradiated and non-transplanted control 1 α (OH)ase^{-/-} mice, osteoblasts in the endosteum, periosteum and metaphysis were severely damaged, whereas chondrocytes and osteocytes sustained less injury. Osteoblasts were regenerated in viable 1 α (OH)ase^{-/-} recipients. The number of WBC in the peripheral blood and CD4 and CD8 positive cells in spleen were decreased in non-irradiated control 1 α (OH)ase^{-/-} mice but were normalized in viable 1 α (OH)ase^{-/-} recipients. This study indicates that donor NA-BM-MSCs cells can relocate to multiple tissues where they synthesize 1 α (OH)ase and produce 1,25(OH)₂D₃ that contributes to the improvement of serum calcium and skeletal mineralization and where they produce immune cells that contribute to the viability of irradiated 1 α (OH)ase^{-/-} recipients.

Disclosures: Z. Zhang, None.

T059

Tension Stress/Stain Induced Osteogenesis in Canine Leg Lengthening Procedures. J. J. Zhao, J. A. Jacobson^{*}, Y. Jiang. Osteoporosis and Arthritis Lab, Department of Radiology, University of Michigan, Ann Arbor, MI, USA.

We evaluated distraction osteogenesis under stimulation of mechanical tension stress/strain, and ability of various imaging modalities for detection and monitor its progress, since the rate of distraction depends on the successful production of new bone in the distraction gap. Early evaluation of new bone production is important. Overly fast distraction will inhibit new bone formation and mineralization while overly slow distraction will lead to premature consolidation.

Tibial and fibular midshaft osteotomy was performed in 25 adult canines, distracted at the 7th day post-surgery using Ilizarov's equipment at 1 mm daily till reaching 3 cm lengthening, and examined weekly by ultrasound and radiography. Osteotomy of the left tibia without distraction was severed as control. They were euthanized at 3, 5, 7, 9, and 11 weeks post-surgery. The tibias were examined using DXA, CT, MRI, and processed for histomorphometry.

Ultrasound and DXA detected new bone formation within the distraction site as echogenic foci at 2-3 weeks post-surgery. Serial follow-up sonograms showed that echogenicity increased progressively in number and size till coalesced as echodense bone. Radiographs showed linear streaks of new bone formation in the distracted gap at 3-4 weeks, and a bone bridge formed at about 7 weeks post-surgery. CT showed only bony structure while MRI clearly delineated fibrous, cartilaginous, and bony tissues. Histomorphometry showed location-dependent bone formation and remodeling activity. Both intramembranous and endochondral but mainly intramembranous bone formed linearly oriented columns of interconnecting trabecular plates of woven and lamellar types. Bone formation rate, bone volume, and percentage of bone surface covered cuboidal osteoblast were significantly increased within the distraction and osteotomy callus regions compared with controls. At the original cortical bone, periosteal bone formation and increased bone resorption were found. Imaging modalities were highly correlated with histomorphometric measures of cartilage and newly formed bone, and measures of cortical porosity and increased osteoclasts in the original cortical bone ($r^2 = 0.81-0.88$).

In conclusion, tension stress/stain induced distraction osteogenesis represents an oriented continuum of primary gap healing, associated with enhanced bone formation likely resulting from rapid recruitment and activation of bone forming cells and increased surface area available for matrix deposition and mineralization. Ultrasound and DXA can detect bone formation and monitor mineralization process earlier than radiograph in leg lengthening procedures. The imaging findings are strongly correlated with histomorphometric measurement.

Disclosures: J.J. Zhao, None.

T060

PTH Enhances ATP Induced ERK1/2 Activation via a Competitive Mechanism Involving G-protein Coupled Receptor Kinase 2 in Osteoblastic Cells. Y. Gu^{*}, Y. Xing^{*}, H. J. Donahue, J. You. Division of Musculoskeletal Sciences, Department of Orthopaedics and Rehabilitation, The Pennsylvania State University College of Medicine, Hershey, PA, USA.

In vivo studies show that parathyroid hormone (PTH) enhances mechanically induced bone formation. Previously we and other investigators found that osteoblastic cells responded to mechanical loading induced fluid flow by releasing ATP and activating the P2Y purinergic signaling pathway. In addition, in vitro studies demonstrated that co-activation of P2Y and PTH receptors leads to a profound synergism. However, the molecular mechanism of the synergistic effect of ATP and PTH in osteoblastic cells is unclear. P2Y and PTH receptors are both G-protein coupled receptors (GPCR), which are presumably desensitized by G-protein coupled receptor kinase (GRK). Thus, we hypothesized that PTH enhances ATP induced osteoblastic responses by inhibiting the desensitization of P2Y receptors via a competitive mechanism involving GRK. To test our hypothesis, we first employed osteoblastic MC3T3-E1 cells to examine ERK1/2 activation in response to ATP stimulation in the presence of PTH. Our results indicated that, after pretreatment with 50nM PTH, ATP not only increased the peak activation of ERK1/2 at 5 min, but also extended the activation to 10 min and 15 min compared to those without PTH, demonstrating the synergistic effect of ATP and PTH. Secondly, we over-expressed GRK2 in MC3T3-E1 cells and found that ERK1/2 activation at 5 min was significantly decreased compared with that of MC3T3-E1 cells over-expressing an empty vector (control) in the presence of PTH. In contrast, when we over-expressed a GRK2 dominant negative mutant, GRK2/K220R, in osteoblastic cells, the enhancement of ERK1/2 activation at 5 min was increased further compared with that of control MC3T3-E1 cells in the presence of PTH, suggesting that GRK2 is involved in the synergistic effect of ATP and PTH. Finally, PTH has been shown to induce ERK1/2 activation via PKA signaling pathways. Here we tested whether PKA signal pathways are involved in the synergistic effect by using a PKA activator, forskoline, instead of PTH. Our results showed that activating PKA signaling pathway by forskoline did not enhance ATP induced ERK1/2 activation. Furthermore, we demonstrated that PKA inhibitor did not suppress the synergistic effect of ATP and PTH in osteoblastic cells, suggesting that PKA activation is not required for the synergism. Taken together, our results demonstrate that it is not the PTH downstream signaling pathway (PKA), rather the regulation of PTH and P2Y receptors by GRK2 that is responsible for the synergism, suggesting a competitive mechanism involving GRK2 in MC3T3-E1 cells.

Disclosures: Y. Gu, None.

T061

Phosphorylation of Caveolin-1 in Response to Fluid Shear in Osteoblasts Is Mediated by P2X7 Activation. S. Majumdar, K. Czymmek*, E. J. McLaughlin*, R. L. Duncan. Biological Sciences, University of Delaware, Newark, DE, USA.

The anabolic responses of bone to mechanical stimuli are triggered by cellular signaling events that occur within seconds and minutes of initiation of load. One of these early signaling events is the rapid release of ATP, and perhaps other nucleotides, that can bind to purinergic receptors that are essential for mechanotransduction. We have recently shown that the P2X7 receptor is central to the response of bone to exogenous loading, in vivo. We have further shown that binding of the P2X7 receptor activates an entry mechanism capable of cellular uptake of large solutes (>600 Da). Since P2X7 receptors have been associated with lipid rafts in the membrane, we postulated that nucleotide binding to the P2X7 receptor could induce endocytosis via caveolin activation. When 12 dynes/cm² laminar shear was applied to MC3T3-E1 osteoblasts, we found that YO-PRO1, a 629 Da dye, was taken up by the cell within 5 min of the onset of shear, with peak uptake observed at 30 min. Extended application of shear demonstrated that YO-PRO1 uptake subsequently decreased at 45 min. When P2X7 receptors were activated in MC3T3-E1 osteoblasts by the addition of BzATP, the pharmacologic agonist of P2X7, a similar time course of YO-PRO1 uptake was observed. Western blot analysis of MC3T3 cells showed that static controls demonstrated little phosphorylation of caveolin-1 while application of fluid shear stress greatly increased the phosphorylation of caveolin-1. Time course studies demonstrated that phosphorylation of caveolin-1 peaked at 30 min and subsequently decreased at 60 min, which is correlates with our dye uptake experiments. Addition of BzATP also increased caveolin-1 phosphorylation implicating the activation of the P2X7 receptor in the phosphorylation of caveolin. Amino acid sequence analysis of the P2X7 receptor indicates a region which is specific for caveolin binding or interaction, further suggesting an interaction between caveolin and P2X7. These data suggest that caveolin phosphorylation may be a direct function of P2X7 activation and that caveolin phosphorylation triggers an entry mechanism that is large enough to take in large molecules as seen by the dye uptake experiments. Caveolin has been suggested as a scaffold for protein-protein interactions for downstream signaling events. Thus, caveolin phosphorylation may be central to the cellular transduction of a mechanical signal.

Disclosures: S. Majumdar, None.

This study received funding from: NIAMS: AR051901.

T062

Glucocorticoids Stimulate Wnt Expression in Mature Osteoblasts. W. Mak, H. Zhou, C. R. Dunstan, M. J. Seibel. Bone Research Program, ANZAC Research Institute, University of Sydney, Australia.

Differentiation of mesenchymal cells towards the osteoblastic lineage is governed by an array of different factors. Glucocorticoids (GC) have been shown to promote osteoblastic differentiation while Wnt signalling can promote osteoblastogenesis and inhibit adipogenesis. However, whether there is a direct relationship between these signalling pathways has not been fully established. Transgenic (tg) overexpression of 11beta-hydroxysteroid dehydrogenase type 2 (HSD2), a GC inactivating enzyme, under the control of a 2.3kb collagen type I promoter (Col2.3-HSD2) abrogates intracellular GC signalling in mature osteoblasts. We have previously demonstrated that calvarial cell cultures derived from Col2.3-HSD2 tg mice exhibit reduced osteoblastogenesis and retarded Wnt/β-catenin signalling. Here, we have bred Col2.3-GFP mice with Col2.3-11βHSD2 tg mice to generate Col2.3-HSD2-GFP tg and Col2.3-GFP WT mice. We investigated the GC-dependent regulation of Wnts in mature osteoblasts by isolating GFP positive cells using FACS to yield a population of mature osteoblasts. GFP-positive cells were subsequently grown in serum free media. Cultures were treated with a single-dose of 10-8M corticosterone for 0.5, 2, 4, 6 hours. In GFP positive cell cultures derived from WT mice, Wnt7b mRNA expression was up-regulated 4-fold and 3.5-fold following 2 and 4 hrs of treatment, respectively, using real time PCR analysis. Wnt10b mRNA expression was up-regulated 2.5-fold at 2 hrs, and 3-fold at 4 hrs, compared to controls. Up-regulation of Wnt7b and Wnt10b expression was blocked by the addition of cycloheximide, suggesting the requirement for de novo protein synthesis. 10-8M corticosterone had no effect on GFP-positive cells derived from Col2.3-GFP-HSD2 tg mice, with no change in the expression of either Wnt protein. In contrast to mature osteoblasts, enriched precursor cells population (first enzymatic release of the calvaria) derived from either Col2.3-GFP WT or Col2.3-GFP-HSD2 tg calvaria Wnt7b was not detected, while there was only low expression of Wnt10b. We conclude that intact GC signalling in mature osteoblasts, in association with transcriptional regulatory complexes, is essential to stimulate Wnt protein expression and hence osteoblastic differentiation.

Disclosures: W. Mak, None.

This study received funding from: NHMRC.

T063

Prostaglandin E₂ Acts Through EP2/EP4 Receptors to Upregulate RGS2 Expression in Osteoblasts. C. Nunn*, S. J. Dixon, P. Chidiac*. Physiology and Pharmacology, University of Western Ontario, London, ON, Canada.

Prostaglandin E₂ (PGE₂) can stimulate bone formation in vivo and in vitro. Osteoblasts express multiple subtypes of prostaglandin E₂ (PGE₂) receptors, which are coupled to Gq (EP1), Gs (EP2 and EP4) and Gi/o (EP3). RGS (regulators of G protein signaling) proteins suppress signaling via G protein-coupled receptors (GPCRs). Upregulation of RGS2 expression in osteoblasts mediates cross desensitization between receptors coupled to Gs and those coupled to Gq (J Biol. Chem. 281: 32684, 2006). Thus, RGS2 may play an important role in regulating PGE₂ signaling through its different receptor subtypes. The aims of this study were to determine the effects of PGE₂ on RGS2 expression in osteoblasts, and the receptor subtypes which mediate these effects. Primary mouse calvarial osteoblasts were treated with PGE₂ at different concentrations for multiple time points before extraction and quantification of mRNA using real-time RT-PCR. PGE₂ increased RGS2 expression in a time-dependent manner, which was maximal at 1 h (6 fold increase over control) and decreased to control levels within 6 h. This effect of PGE₂ was concentration-dependent, with an EC₅₀ of 2 μM and maximal effect at 10 μM. To determine the receptor subtypes involved, cells were treated with EP receptor subtype-selective agonists (10 μM) for 1 h. Agonists for EP2/EP4 receptor subtypes (butaprost, 11-deoxy-PGE₂) stimulated RGS2 expression to a similar level as PGE₂, whereas agonists selective for EP1 (17-Ph-ω-trinor-PGE₂) and EP3 (sulprostone) receptor subtypes had little effect on RGS2 expression. Furthermore, isoproterenol (which acts through Gs) dramatically increased RGS2 expression, whereas PGF_{2α} (which acts through Gq) had no effect. Taken together, these data establish that RGS2 is upregulated in osteoblasts by PGE₂, acting through its Gs-coupled receptors. PGE₂ has been shown previously to stimulate bone formation via both Gs-coupled and Gq-coupled receptor subtypes. Our findings suggest a mechanism for cross desensitization between Gs- and Gq-coupled receptors stimulated by the same agonist (PGE₂), in which activation of Gs leads to increased expression of RGS2, which in turn suppresses signaling through Gq.

Disclosures: C. Nunn, None.

This study received funding from: Canadian Institutes of Health Research.

T064

ATP Modulation of Mitogen-Activated Protein Kinases (MAPKs) and c-fos Expression in Osteoblastic and Breast Cancer Cells. P. Scodelaro, Bilbao*, S. Katz*, R. Boland, A. Russo de Boland*, G. Santillán*. Biología, Bioquímica & Farmacia, Universidad Nacional del Sur, Bahía Blanca, Argentina.

We previously showed that ATP and UTP increase intracellular calcium concentration ([Ca²⁺]_i) in MCF-7 breast cancer and osteoblastic ROS 17/2.8 osteosarcoma cells. The elevation of [Ca²⁺]_i was due to Ca²⁺ release from inner stores through activation of the PI-PLC/IP₃ pathway. In addition, mechanical stimulation after ATP or UTP but not ADP induced a transient Ca²⁺ influx in both cell lines, suggesting that P2Y_{2/4} receptor activation is required for this mechanical stress-activated Ca²⁺ (SAC) influx. Moreover, ATP-dependent SAC influx mediated the phosphorylation of mitogen-activated protein kinases (MAPKs) ERK1/2, p38 and JNK1 only in ROS 17/2.8 cells. In this work, we investigated the expression of P2Y_{(1,2,4)}} subtype purinoceptors and the participation of PKC and Src family kinases in the activation of MAPKs by ATP in both cell lines. The involvement of ATP dependent SAC influx in the regulation of c-fos expression was examined. RT-PCR studies supported the expression of P2Y₂ subtype receptor in the osteoblastic and breast cells in the osteoblastic and breast cells, while P2Y₁ was not detected neither in MCF-7 nor ROS17/2.8 cells, and P2Y₄ was weakly expressed only in MCF-7 cells. The use of Ro 318220, a PKC inhibitor, showed that PKC participates in the phosphorylation of MAPKs by ATP in both cell lines. Otherwise, the use of PP1 or PP2, Src family kinases inhibitors, involved the participation of such kinases in the phosphorylation of MAPKs by ATP only in ROS 17/2.8 cells, although phosphorylation of Src (Tyr 416) was also observed in MCF-7 cells. Maximum levels of c-fos induction were observed after 30 min treatment with ATP in both cell lines, and the use of Gd³⁺, a SAC influx inhibitor, reduced its expression in ROS17/2.8 but not in MCF-7 cells. These results show that P2Y₂ is the main receptor subtype involved in ATP-dependent SAC influx in osteoblasts and breast cells. Unlike MCF-7 cells, Src family kinases and SAC influx, respectively, participate in MAPKs activation and c-fos expression induced by ATP only in ROS17/2.8 cells.

Disclosures: A. Russo de Boland, None.

T065

Ubc9 Promotes Stability of Smad4 and Regulates BMP Signaling Pathway in Osteoblastic Saos-2 Cells. K. Shimada¹, N. Suzuki², M. Maeno³, M. Eda^{*1}, K. Yamada^{*1}, K. Ito^{*1}. ¹Department of Periodontology, Nihon University School of Dentistry, Tokyo, Japan, ²Department of Biochemistry, Nihon University School of Dentistry, Tokyo, Japan, ³Department of Oral Health Science, Nihon University School of Dentistry, Tokyo, Japan.

Bone morphogenetic proteins (BMPs) play a specific role in osteoblastic differentiation and maturation. BMPs induce receptor-regulated Smads (R-Smads). The R-Smads form complexes with the common-partner Smad, which is Smad4 in mammals. These complexes translocate and accumulate in the nucleus and regulate the transcription of various target genes. However, the function of Smad4 remains unclear. Here, we performed a yeast two-hybrid screen using Smad4 as bait and a cDNA library from human bone marrow to identify the proteins interacting with Smad4. For this screen, full-length human Smad4 was cloned in pGBKT7 vector to express it as a fusion with the GAL4-binding domain, and the cDNA library was screened. Two cDNA clones of full-length Ubc9 were identified. To analyze the function of Ubc9 in the BMP signaling pathway, endogenous Ubc9 was disrupted in human osteoblastic cell line Saos-2 using a 19-nucleotide siRNA and examined its effectiveness in silencing Ubc9 expression. The gene expression of BMP-induced transcription factor genes, including Runx2, Dlx5, Msx2, and Osterix, was examined using real-time reverse-transcribed PCR and the protein levels of Smad4, Smad1 and phospho-Smad1 were determined with SDS-PAGE and Western blotting. Moreover, to observe whether Smad4 was sumoylated or not, Smad4 was overexpressed using pcDNA3.1 vector in Saos-2 cells and the sumoylated-Smad4 was observed with SDS-PAGE and Western blotting using anti-SUMO1 antibody, because Ubc9 was SUMO-conjugating enzymes E2. The efficiency of silencing Ubc9 mRNA level was approximately 70%. The expression of Runx2, Dlx5, Msx2, and Osterix mRNA was markedly inhibited when Ubc9 was silenced. The protein levels of Smad4 and phospho-Smad1 decreased dose-dependently and the level of Smad1 did not change by siRNA for Ubc9. The sumoylated-Smad4 was detected when Smad4 was overexpressed, and the sumoylated-Smad4 was inhibited by the addition of Senp2, SUMO-protease, was added. In conclusion, it is suggested that Ubc9 promotes stability of Smad4 and Smad4 is sumoylated. Ubc9 should be required the upregulation of BMP signaling pathway because the gene expression of the transcriptional factors and the protein levels of phospho-Smad1 inhibit by siRNA for Ubc9.

Disclosures: K. Shimada, None.

T066

Effect of Prostaglandin D₂ on Na-Dependent Phosphate Transport Activity in Osteoblast-like Cells. A. Shogo^{*}, S. Sekiguchi, A. Yokoyama^{*}, K. Inagaki^{*}, H. Kakizawa^{*}, N. Hayakawa^{*}, N. Oda^{*}, A. Suzuki, M. Itoh^{*}. Department of Internal Medicine, Fujita Health University, Aichi, Japan.

Prostaglandins (PGs) are well known to act as autocrine and paracrine factors in microenvironment including bone metabolism. Among them, PGD₂ has been reported to be produced by osteoblasts, and stimulates their proliferation, decreases both osteoprotegerin and RANKL and to induce osteoblast chemotaxis, suggesting the anabolic role of PGD₂ in bone metabolism. We have recently shown that Phosphate (Pi) transporter Pit-1 plays a critical role in the mechanism of the development of the extracellular mineralization of osteoblasts, and Pit-1 has been shown to be expressed in a subpopulation of hypertrophic chondrocyte. The aim of the present study is to investigate the effect of PGD₂ on Pi transport and its intracellular signaling mechanism in mouse calvaria-derived osteoblast-like MC3T3-E1 cells. PGD₂ time- and dose-dependently stimulated Pi transport in MC3T3-E1 cells. A protein kinase C (PKC) inhibitor calphostin C partially suppressed the stimulatory effect of PGD₂ on Pi transport. The selective inhibitors of mitogen-activated protein (MAP) kinases, such as ERK and p38, did not affect PGD₂-induced Pi transport. On the other hand, JNK inhibitor, SP600125, markedly suppressed the enhancement of Pi transport by PGD₂. Both LY294002, a phosphatidylinositol (PI) 3-kinase inhibitors, attenuated PGD₂-induced Pi transport. A selective inhibitor of S₆ kinase, rapamycin, reduced this effect of PGD₂, while Akt kinase inhibitor did not. In summary, these results suggest that PGD₂ stimulates Na-dependent Pi transport activity in osteoblast-like cells. The mechanism responsible for this effect is not mediated by p38 MAP kinase or Akt kinase, but involves activation of PKC, Jun kinase, PI 3-kinase and S₆ kinase.

Disclosures: A. Shogo, None.

T067

AKT's Effects on β -catenin Regulate Osteoblasts' Responses to Mechanical Strain and PTH. A. Sinters^{*}, M. Muzylak^{*}, G. Zaman^{*}, V. J. Armstrong^{*}, L. E. Lanyon, J. S. Price. Veterinary Basic Science, Royal Veterinary College, London, United Kingdom.

Two major influences controlling bone mass and architecture are mechanical loading and PTH. One of the pathways implicated in bones' adaptive responses to load is the canonical Wnt pathway. In vitro we have shown that exposing osteoblastic cells to dynamic strain inhibits GSK3 β phosphorylation of β -catenin (β Cat), thereby allowing its translocation to the nucleus where it regulates transcription. Since regulation of β Cat via GSK3 β inhibition can be controlled by AKT we hypothesised that this effect of strain may be mediated through AKT.

To explore this hypothesis the plastic strips onto which monolayer cultures of UMR106 rat

osteoblast like cells had been seeded were subjected to a short period of dynamic 4-point bending engendering levels of strain sufficient to stimulate proliferation. Western blotting demonstrated that this exposure to strain stimulated a transient increase in the expression of phosphorylated AKT (^pAKT) and phosphorylated GSK3 β (inactive) as well as active (de-phosphorylated) β Cat (^p β Cat). Western blots of nuclear/cytoplasmic fractions showed that the strain-mediated nuclear translocation and activation of β Cat were inhibited by pre-treatment with the phosphatidylinositol 3 (PI3)-kinase inhibitor LY294002. Both LY294002 and the AKT specific inhibitor Triciribene also inhibited strain-related proliferation.

Treatment of UMR cells with high continuous concentrations of PTH (100nM) inhibited strain induced proliferation and reduced both basal and strain-induced levels of ^pAKT. PTH also induced the expression of the phosphatase MAP kinase phosphatase-1 (MKP-1) Since PTH signaling acts in part through protein kinase A (PKA), we treated UMR cells with the PKA inhibitor H89 alone, or in combination with PTH and/or strain. H89 treatment increased basal levels of ^pAKT and inhibited MKP-1 induction by PTH. H89 also resulted in a decrease in levels of total β Cat. In strained cells treated with H89 did not influence the increase in ^pAKT but reduced total β Cat levels, and thus failed to increase levels of activated β Cat. However, a combination of H89, PTH and strain resulted in AKT phosphorylation as well β Cat activation with no decline in total β Cat levels. Taken together, these data suggest that PI3K/AKT signaling is a key mediator of the responses to at least two key influences on osteoblasts. Acting through regulation of β Cat, AKT is integral to osteoblasts' responses to mechanical strain associated with bone formation. The responses of osteoblasts to high levels of PTH associated in vivo with resorption may be the result of PTH inhibiting AKT activation.

Disclosures: A. Sinters, None.

This study received funding from: Wellcome Trust.

T068

Regulation of RANKL Expression by Glucocorticoid in Human Osteoblast-like Cells. F. Hirano, N. Maruyama^{*}, K. Komura^{*}, K. Okamoto^{*}, Y. Makino^{*}, M. Haneda^{*}. Medicine, Asahikawa Medical College, Asahikawa, Japan.

Glucocorticoid-induced osteoporosis remains the most common secondary form of metabolic bone diseases. The soluble and transmembrane cytokines, RANKL, are produced by the osteoblast under hormonal and cytokine control and are essential for osteoclastogenesis and bone resorption. In contrast, osteoprotegerin is known to bind to RANKL and to block the interaction between RANKL and its receptor RANK. Glucocorticoid has been reported to induce RANKL mRNA expression in osteoblasts, although circulating soluble RANKL is reduced by glucocorticoid. The reasons of this discrepancy are still unknown. The purpose of this study was to clarify the regulation of RANKL expression by glucocorticoid in human osteoblast-like cells. We used human osteoblast-like cell line MG-63 and examined effect of glucocorticoid on RANKL expression. Quantitative real-time RT-PCR and ELISA methods revealed that 100 nM dexamethasone (DEX) significantly increased RANKL mRNA expression (15-fold, p<0.05) in MG-63 cells for a time-dependent manner and decreased soluble RANKL protein in supernatant, as expected. In addition, we found that DEX did not influence RANKL transcriptional activity by reporter gene assay using human RANKL promoter. Moreover, Treatment with actinomycin D and DEX markedly prolonged the half-life of RANKL mRNA in MG-63 cells, as compared to treatment with actinomycin D alone (T1/2 = over 24h v.s. 10h), presumably indicating that DEX-induced RANKL mRNA expression is due to the stabilization of RANKL mRNA. Next, we investigated effect of glucocorticoid on the expression of TNF converting enzyme (TACE), a known RANKL shedase. The activity of TACE was dose-dependently reduced by DEX. Moreover, 100 nM DEX significantly decreased both mRNA- and protein-expression of TACE by quantitative real-time RT-PCR and ELISA, respectively. Furthermore, 100 nM DEX clearly induced transmembrane RANKL protein in MG-63 cells by flow cytometry and Western blot analysis, suggesting that DEX-reduced soluble RANKL protein expression in supernatant is associated with the decreases of TACE activity and protein expression in MG-63 cells. In conclusion, we presented glucocorticoid up-regulated RANKL mRNA expression via the stabilization of RANKL mRNA and reduced soluble RANKL expression via the decrease of TACE expression, possibly indicating that glucocorticoid-induced transmembrane RANKL expression in osteoblasts mainly played a pivotal role in osteoclastogenesis.

Disclosures: F. Hirano, None.

T069

Calcitriol Inhibits Marrow Stromal Cell Differentiation into Osteoblasts in a Manner Cooperative with but Independent of TGF-beta. D. Inoue, H. Ochiai^{*}, R. Okazaki. Third Department of Medicine, University of Teikyo School of Medicine, Ichihara-shi, Chiba, Japan.

Vitamin D is essential to skeletal homeostasis, as impaired action of vitamin D, caused by either vitamin D deficiency or loss-of-function mutations of the vitamin D receptor (VDR), leads to rickets/osteomalacia. However, its direct effect on bone cells has not been fully understood. Recent in vivo studies in mice have shown that the absence of VDR has an anabolic effect on bone, suggesting that vitamin D, at least under physiological conditions, is a negative regulator of bone formation. In the present study, we examined effect of vitamin D on early mesenchymal cell differentiation in our previously established culture system in which a bipotential mouse marrow stromal cell line, ST-2, was induced by BMP-2 to differentiate into osteoblasts and adipocytes.

We found that calcitriol or 1,25-dihydroxyvitaminD3 (1,25D) inhibited the BMP-2-induced ALP activity in a dose-dependent manner with the maximal effect being an almost complete inhibition at 10 nM. A physiological level (0.1 nM) of 1,25D readily caused a significant ALP reduction. Interestingly, in the same culture system, 1,25D also inhibited

the BMP-2-induced adipocytic differentiation as assessed by Oil-Red O-positive cell counts. These results indicate that 1,25D has a negative effect on the early phase of osteoblastic differentiation and that this effect is not a result of reciprocally enhanced adipogenesis.

Given the fact that TGF-beta counteracts the BMP stimulation of osteoblastogenesis and is able to modulate the VDR-dependent 1,25D action, we then tested a hypothesis that TGF-beta lies downstream of the anti-osteoblastogenic effect of 1,25D. As expected, TGF-beta inhibited the BMP-2-induced ALP activity in a dose-dependent manner. Suboptimal concentrations of 1,25D and TGF-beta showed additive effects. SB431542, a TGF-beta receptor kinase inhibitor, completely reversed the suppressive effect of TGF-beta, but showed virtually no effect on the effect of 1,25D. Luciferase assays using Id-1 promoter constructs revealed that TGF-beta, but not 1,25D, inhibited BMP-induced Smad-dependent transcription. We therefore conclude that 1,25D inhibits BMP-2-induced early osteoblastic differentiation in a manner cooperative with TGF-beta through a distinct mechanism. Elucidation of the molecular pathway by which 1,25D inhibits the BMP-induced mesenchymal cell differentiation into osteoblasts and adipocytes will not only help understand its physiological role in skeletal homeostasis but may also provide a theoretical basis for the development of novel selective VDR modulators with bone anabolic effects.

Disclosures: D. Inoue, None.

T070

CCN3/NOV Inhibits BMP-2-induced Osteoblast Differentiation by Interacting with BMP and Notch Signaling Pathways. T. Minamizato^{*1}, K. Sakamoto^{*1}, S. Nakamura^{*2}, A. Yamaguchi¹. ¹Section of Oral Pathology, Graduate School of Tokyo Medical and Dental University, Tokyo, Japan, ²Section of Oral and Maxillofacial Oncology, Division of Maxillofacial Diagnostic and Surgical Science, Graduate School of Dental Science, Kyushu University, Fukuoka, Japan.

Several lines of evidence suggest that the CCN family of proteins is involved in regulation of mesenchymal cell differentiation. We demonstrated that CCN3/NOV associated with the Notch1 extracellular domain and inhibited myoblast differentiation through Notch signaling pathway. Further, we reported that Notch signaling is involved in BMP-2-induced osteoblast differentiation. These results prompted us to investigate the role of CCN3 in osteoblast differentiation and its involvement in the BMP and Notch signaling pathways. To explore whether CCN3 participates in regulation of osteoblast differentiation, we first overexpressed CCN3 and/or BMP-2 in MC3T3-E1 cells by adenoviruses. Transduction with CCN3 alone induced no apparent changes in the expression of osteoblast-related markers, whereas cotransduction with BMP-2 and CCN3 significantly inhibited the BMP-2-induced mRNA expression of Runx2, osterix, ALP, and osteocalcin. Immunoprecipitation-western analysis revealed that CCN3 associated with BMP-2. Compared to transduction with BMP-2 alone, cotransduction with BMP-2 and CCN3 attenuated the expression of phosphorylated Smad1/5/8 and the mRNA for Id1, Id2, and Id3, which are target molecules involved in the downstream of BMP signaling. Meanwhile, transduction with CCN3 activated Notch signaling pathway by increasing the expression of cleaved Notch1, an activated form of Notch1, and the mRNA expression of Hes1 and Hey1, the target genes of Notch in MC3T3-E1 cells. Overexpression of CCN3 also increased the promoter activities of Hes1 and Hey1 in C2C12 cells. Since Hey1/Hes1 is reported to inhibit Runx2 promoter activity, we investigated the effects of CCN3 on osteoblast differentiation using Hey1-deficient cells isolated from calvariae of Hey1 knockout mice. The inhibitory effects of CCN3 on the expression of BMP-2-induced osteoblast-related markers were nullified in these cells. Finally, we explored the expression levels of mRNA for CCN3 and proteins for phosphorylated Smad1/5/8 and cleaved Notch1 during bone regeneration in mice. All of these were highly upregulated during bone regeneration. Collectively, the present study indicate that CCN3 exerts inhibitory effects on BMP-2-induced osteoblast differentiation by interacting with the BMP and Notch signaling pathways, and these interaction might be involved in the process of bone regeneration.

Disclosures: T. Minamizato, None.

T071

High Mobility Group Proteins (HMGs) Coupled with TNF α Production Are Essential for Osteoclastogenesis. A. Brebene^{*1}, K. Yamoah^{*1}, A. Arabi^{*1}, H. Amano², G. Dolios^{*3}, R. Wang^{*3}, R. Yanagisawa^{*1}, E. Abe¹. ¹Endocrinology, Mt. Sinai School of Medicine, New York, NY, USA, ²Pharmacology, School of Dentistry, Showa University, Tokyo, Japan, ³Genetics & Genomics Sciences, Mt. Sinai School of Medicine, New York, NY, USA.

We previously have shown that TSHR (Thyroid stimulating hormone receptor) null mice exhibit osteoporosis due to increased osteoclast formation stemming from TNF α overproduction in osteoclast progenitors. Since the enhanced osteoclast formation in the TSHR null mice was normalized in TSHR and TNF α double null mice, TNF α is concluded to be a crucial factor for osteoporosis in TSHR deficiency. We next examined in detail the regulatory mechanisms of TNF α transcription by identifying the responsive sequence of the murine TNF α promoter and the associated transcription factor. HMG2 (high mobility group 2) was identified by mass spectrometry to bind to a specific sequence of the TNF α promoter and its expression level was increased by IL-1/TNF α , or by RANKL treatment in which TNF α expression was also stimulated. HMG2 in addition to HMG1 not only localized in the nucleus but was also secreted, and stimulated cytokine expression (IL-1, IL-6 and TNF α) and RANKL-induced osteoclast formation in a positive feedback manner. As HMG1 or HMG2 expression was suppressed by siRNA, TNF α and TRAP expression were significantly reduced. We also confirmed the parallel expression of

HMGs and TNF α in osteoclast progenitors from TSHR^{-/-} and TSHR^{+/-} mice, which overexpress TNF α , and TNF α ^{-/-} mice, which underexpress it. These results suggest that the newly identified HMGs are crucial factors in the regulation of TNF α expression and osteoclast formation under pathogenic conditions.

Disclosures: A. Brebene, None.

This study received funding from: NIH.

T072

The Suppressive Effect of IL-27 in Osteoclastogenesis. M. Furukawa¹, H. Takaishi^{*1}, S. Sakai^{*1}, M. Yoda^{*1}, H. Takayanagi^{*2}, H. Yoshida^{*3}, Y. Toyama^{*1}. ¹Orthopaedic, Keio university, Tokyo, Japan, ²Department of Cellular Physiological Chemistry, Tokyo Medical Dental University, Tokyo, Japan, ³Department of Biomolecular Sciences, Faculty of Medicine, Saga University, Saga, Japan.

In recent years identification of cytokine of interleukin-12 family advanced, and it became clear to have different point of action depending on a differentiation stage of Th1. Among them, IL-27 is produced from antigen presenting cells and is viewed as inducing initial-phase Th1 differentiation by mediating receptor WSX-1/GP130 as EBI-3 and p28 heterodimers. Bone metabolism and the immune system have a correlative relationship, and both are controlled by various common cytokines in excessive osteoclastogenesis caused by inflammatory diseases, such as autoimmune arthritis. We examined the osteoclastogenesis and participation to Th17 for the purpose of clarifying a role of IL-27 in the inflammatory bone destruction. CD4+T cells were isolated by magnetic cell sorting from mouse spleen cells and were induced to Th17 using the anti-IL-4, anti-IL-12, anti-IFN- γ antibody, and IL-23 after stimulation with immobilized anti-CD3, anti-CD28 antibody. IL-17 expression of Th17 markedly increased by PMA+Ionomycin stimulation, and the stimulation of IL-27 restrained production of IL-17 in induction process from Naive CD4+T cells to Th17. With human and mouse bone marrow macrophages, the expression of p28 was strongly induced by LPS (100ng/ml) stimulation, but no changes were observed in WSX-1. In the mouse primary osteoblasts, IL-27 did not affect for the expression of RANKL, which was induced by D3+ PGE2 or IL-17 stimulation. Human CFU-GM was collected by incubating bone marrow obtained through prosthetic joint replacement surgery in a methylcellulose culture containing GM-CSF and IL-3. In the differentiation process induced by M-CSF+RANKL, IL-27 strongly inhibited the osteoclastogenesis of human CFU-GM in a dose dependent manner. (100ng/ml, 85%). Our study revealed that IL-27 directly inhibited osteoclastogenesis of human CFU-GM. The suppressive effect of IL-27, however, is not selective for IL-17 production in the induction process of Th17, but appears to cover a broad group of proinflammatory cytokines. Therefore, we assume that IL-27 can be used to respond temporally or spatially to the clinical state of an autoimmune disorder, and thus to react with versatility to inflammatory bone destruction.

Disclosures: M. Furukawa, None.

T073

Cascade of Gene Expression Indicates Chemokine MCP-1 Is Essential for Human Osteoclast Formation. R. M. S. Granfar^{*}, A. S. Stephens^{*}, S. R. J. Stephens^{*}, C. J. Day^{*}, N. A. Morrison. Health Science, Griffith University, Gold Coast, Australia.

The chemokine MCP-1 (CCL2) is essential, in human and mouse, for the formation of foreign body giant cells (FBGC), a multinucleated macrophage cell type similar to osteoclasts. We tested the hypothesis that MCP-1 is necessary for human osteoclast differentiation. On comparing chemokine induction by RANKL with that elicited by LPS or TNF- α , where numerous chemokines are strongly induced, it appeared that RANKL induced a restricted repertoire of chemokines in osteoclasts. MCP-1 and MIP- β (CCL4) were strongly induced by RANKL in human osteoclast progenitors within 24 hours (1200 fold and 40 fold respectively). Other chemokines (MIP- α , RANTES and CCL1) peaked later or were not as potently induced. MCP-1 receptor, CCR2b, was also strongly induced by RANKL (500 fold). As CCR2b expression increased through time, MCP-1 mRNA expression decreased, suggesting a feedback autocrine loop in osteoclast precursors.

A truncated form of MCP-1 with 7 amino acids removed (7ND) acts as dominant negative and blocks FBGC formation in mouse and human. Inhibition of MCP-1 autocrine loop signalling using both neutralising antibody and dominant negative MCP-1 (7ND) dramatically suppressed RANKL mediated osteoclast formation. Neutralising antibody to MCP-1 (4 μ g/mL) reduced osteoclast formation from 240 \pm 16 per cm² (control) to 188 \pm 17 (p=0.01) while 7ND (50ng/mL) suppressed osteoclast number to 21 \pm 1 per cm² (p=4.8 \times 10⁻⁸). Not only did 7ND reagent inhibit osteoclast differentiation, it also suppressed bone resorption activity of purified mature human osteoclasts, reducing dentine resorption from 81 \pm 3 to 18 \pm 3 pits per dentine slice (p=0.0002). The presence of 7ND prevented early RANKL mediated induction of JUN, suggesting that the MCP-1 autocrine loop is necessary for osteoclast transcription factor induction. Following the early 24 hour peak of induction of MCP-1 induction, calmodulin-1 was maximally induced at three days exposure to RANKL. Transcription factors NFAT1 and NFAT2 (thought to be essential for osteoclast formation) reached peak induction six days after MCP-1 induction. The fact that 7ND blocked mature osteoclast bone resorption indicates the surprising fact that chemokine signalling may be required for on-going bone resorption. Indeed, treating mature osteoclasts with MCP-1 enhanced bone resorption activity. Taken together, the data suggest that a highly specific assemblage of inflammatory chemokines is necessary for osteoclast differentiation and that continuous chemokine signalling is required for bone resorption.

Disclosures: R.M.S. Granfar, None.

T074

G-CSF Enhances Osteoclast Differentiation and Function. R. M. S. Granfar*, C. J. Day*, N. A. Morrison. School of Medical Science, Griffith University, Southport, Australia.

Osteoclasts (OCs) are critical protagonists for the mobilization of the endosteal niche of hematopoietic stem cells. Granulocyte Colony Stimulating Factor (G-CSF) is a widely applied stem-cell mobilization treatment with clinically documented risk of mild to severe bone loss. If OC activity is required for stem cell mobilization, then G-CSF and potentially other stem cell mobilizers should enhance OC differentiation and bone resorption. The standard human mononuclear cell model of OC formation was used. Cells were cultured in MEM supplemented with 25ng/ml M-CSF. In these conditions, RANKL (20ng/ml) treatment results in OC formation in 14 days. OCs differentiated on collagen coated plates were purified over serum gradients to select for giant cells and then this fraction plated onto sperm whale dentine for bone resorption assays. Recombinant G-CSF (Peprotech) was used at doses up to 25 ng/ml. Markers of OC maturity such as dentine-resorption, multi-nucleation, as well as gene expression and protein presence of tartrate resistant acid phosphatase (TRAP), were analysed.

G-CSF treatment had strong effects on OC biology. As well as stimulating bone resorption activity in mature OCs, G-CSF had an early strong effect on OC size and number. Treatment with RANKL and G-CSF resulted in significantly larger OCs by 7 days when compared to RANKL treated cells ($p=0.0004$). Once RANKL treated OCs had matured (at 14 days) they were almost the same size as OCs treated with RANKL and G-CSF, suggesting that exogenous G-CSF accelerates early OC formation. RANKL and G-CSF increased the TRAP+ multi-nuclear cell count when compared to RANKL treated cells (7d $p=0.00005$ and 14d $p=0.013$). Using real time PCR analysis, TRAP mRNA content was significantly greater in G-CSF treated OCs, consistent with the increased number of TRAP positive cells compared to control treatment with RANKL ($p=0.007$). Continual treatment with RANKL and G-CSF over 21 days significantly increased bone resorption activity measured by pits on dentine slices relative to OCs treated with RANKL alone ($p=0.012$). Similarly, addition of G-CSF significantly stimulated bone resorption in mature purified OCs that had no prior treatment with G-CSF, suggesting that G-CSF receptor is present on mature OCs. Gene array showed RANKL induced G-CSF receptor in OCs (12 fold), consistent with the hypothesis that OCs respond to G-CSF as a result of RANKL mediated induction of G-CSF receptor.

In summary, G-CSF increases osteoclast bone resorption, TRAP expression, cell-size and multinucleation. The osteopenic effect of G-CSF therapy and endosteal hematopoietic stem cell mobilization may be regulated by the same phenomenon; G-CSF stimulation of osteoclast differentiation and bone resorption.

Disclosures: R.M.S. Granfar, None.

This study received funding from: Griffith University.

T075

M-CSF Stimulates Bone Resorbing Activity of Mature Human Osteoclasts Via Increased Activation of AP-1 and NF κ B. J. M. Hodge*, M. A. Kirkland*, G. C. Nicholson. Clinical and Biomedical Sciences: Barwon Health, University of Melbourne, Geelong, Australia.

The critical role of M-CSF in the differentiation of osteoclasts (OC) is well established. In mature OC, M-CSF has been reported to regulate survival and motility, but no clear role in resorptive function has been established. In this study we investigated the role of M-CSF on resorbing activity of mature human OC.

Human OC were generated by treatment of CFU-GM-derived precursors with soluble hRANKL (125ng/mL) and hM-CSF (25ng/mL) for 14-21d. To quantify resorbing activity, mature OC were dissociated from the plastic substrate using a non-enzymatic buffer, settled onto dentine slices and cultured for 72h. Activation of NF κ B and AP-1 was assessed using a sandwich ELISA technique. I κ B α and ERK were assessed by Western analysis.

Neither M-CSF nor RANKL were required for mature OC survival over 72h. However, resorption function was absolutely dependent on the addition of RANKL. Co-treatment with M-CSF had a concentration-dependent biphasic action, greatly augmenting RANKL-induced resorbing activity (+181%) and actin ring formation (+131%) at 25ng/mL. RANKL alone activated NF κ B (+554%). M-CSF had no effect on NF κ B but potentiated RANKL-induced activation (+42%). In contrast, RANKL alone had no effect on AP-1 activation whereas M-CSF stimulated weakly (+63%) and the combination produced a synergistic effect (+171%). M-CSF activated phosphorylation of ERK 1/2, peaking at 5 min, whereas RANKL had no effect alone or in combination with M-CSF. M-CSF had no effect on I κ B α phosphorylation whereas RANKL alone stimulated, with no additional effect in combination with M-CSF. Time-lapse video-microscopy showed no apparent effect of M-CSF on the motility of OC co-treated with RANKL.

We have demonstrated that M-CSF is not required for survival of mature human OC, but it does potently modulate RANKL-induced resorbing activity via NF κ B and AP-1 activation. The molecular mechanism of this effect remains to be determined although we propose a convergence of RANK and fms signaling ("cross-talk") upstream of the critical OC transcription factors NF κ B and AP-1. These findings have important implications for the clinical management of diseases associated with excess bone resorption.

Disclosures: J.M. Hodge, None.

T076

The Effects of IL-12 Related Cytokines, IL-23 and IL-27, on Osteoclast Formation and T Cell Properties. S. Kamiya*¹, T. Fukawa*¹, C. Nakamura*², T. Yoshimoto*³, S. Wada*¹. ¹Clinical Sciences, Josai International University, Chiba, Japan, ²Bio-analytical Chemistry, Josai International University, Chiba, Japan, ³Intractable Immune System Disease Research Center, Tokyo Medical University, Tokyo, Japan.

A number of evidence has shown that bone remodeling process was affected by host immune reactions. Above all, cytokines which could modulate T cell functions were much focused in this area. Interleukin (IL) -23 and IL-27, IL-12-related cytokines, have been shown to be involved in chronic inflammatory diseases by modulating T cell function and to differentiate naive CD4+ T cells to type 1 helper T. Here, we examined the effects of these cytokines on osteoclast (OC) formation induced by M-CSF/RANKL in the presence of T cells. Mouse Bbone marrow macrophage like cells (BMMs) were prepared through incubating bone marrow cells with M-CSF, and were cocultured with activated T cells, which were partially purified from isolated splenocytes by adhesion properties and were stimulated by anti-CD3 antibody (Ab).

When T cells were activated by 0.2 μ g/ml anti-CD3 Ab, and were cocultured with BMMs in the presence of M-CSF/sRANKL, the number of OC was reduced compared with that of co-cultures with innate T cells. The addition of IL-23 and IL-27 in this culture much strongly and significantly inhibited OC formation. Treatment with these cytokines alone also reduced OC formation minimally even in the absence of activated T cells. To understand this phenomenon more precisely, we explored possible factors which could be produced by the activated T cells and modulate OC formation. Although the production of TNF α , IL-4, and IFN γ , detected by ELISA, was not changed in T cells treated with IL-23 or IL-27, the production of IL-10 was increased by ~200% in T cells treated with IL-27 these interleukins. This was not the case for IL-23. In this process, we found that T treatment with IL-27 also significantly reduced sRANKL production in activated T cells. Furthermore, through FACS analysis revealed we found that treatment with IL-27 suppressed the expression of membrane-bound RANKL on the T cells. These effects of IL-27 could not be found in osteoblasts when stimulated by IL-6. The effects of IL-23 are now under investigation.

In this study, we found that IL-23 and IL-27 inhibited OC formation when cocultured with activated T cells. The effects of these interleukins IL-27 would be associated with modified cytokine-expression profile of the T cells. The findings observed in this study would suggest that IL-12 related cytokines may play crucial roles for OC formation in autoimmune-related skeletal diseases.

Disclosures: S. Kamiya, None.

T077

Endogenous TNF α in Osteoclast Precursor Cells Promotes Osteoclastogenesis Via c-Fos and NFATc1 Activation. A. Nakao*¹, H. Fukushima*¹, H. Kajiya*¹, F. Okamoto*¹, S. Ozeki*², K. Okabe*¹. ¹Physiological Science & Molecular Biology, Fukuoka Dental College, Fukuoka, Japan, ²Oral & Maxillofacial Surgery, Fukuoka Dental College, Fukuoka, Japan.

Although TNF α is well known to be an important factor for bone resorption, particularly in inflammatory bone diseases, the relevance of RANKL and TNF α in osteoclastogenesis remains unclear. In this study we examined the mechanism of TNF α induced osteoclastogenesis and its downstream signaling using RT-PCR, ELISA, Western blotting and luciferase activity assay. We show that osteoclastogenesis is suppressed by anti-TNF α - and anti-TNF receptor type I (TNFRI)-antibodies and in TNF α - and TNFRI-deficient mice using in vitro culture systems: (1) co-culture of mouse spleen derived osteoclast precursor cells (pOCs) with osteoblasts, (2) pure pOC culture and (3) RAW264.7 cells in presence of RANKL. In co-culture with TNF α - or TNFRI-deficient osteoblasts and wild type (WT) mouse pOCs, the number of osteoclasts was always reduced compared to that in combination with WT osteoblasts and WT pOCs. When pure pOCs without osteoblasts or RAW 264.7 cells were cultured in the presence of RANKL both TNF α and TNFRI neutralizing antibodies significantly inhibited RANKL-induced osteoclastogenesis. In contrast, addition of TNF α increased RANKL-induced osteoclastogenesis in both culture system. Furthermore, fewer osteoclasts were formed in co-culture with WT osteoblasts and pOCs derived from TNF α - and TNFRI-deficient mice. The number of osteoclasts was recovered by addition of TNF α into cultures of TNF α -deficient pOCs, but not TNFRI-deficient pOCs. We also found that RANKL directly induced TNF α expression and secretion in pOCs and RAW264.7 cells in a time-dependent manner. Endogenous TNF α in pOCs induced c-Fos and NFATc1. Expression rates of NFATc1 and c-Fos were significantly delayed and decreased in TNF α - and TNFRI-deficient pOCs compared to WT pOCs during osteoclastogenesis. These results indicate that TNF α is induced by RANKL in pOCs and serves as an autocrine factor promoting osteoclastogenesis through c-Fos and NFATc1 activation.

Disclosures: A. Nakao, None.

T078

IL-23-Enhanced Osteoclastogenesis Are Mediated by STAT3 and NF- κ B Via Upregulation of RANKL from CD4+T cells. S. Park*, J. Ju*, K. Kang*, I. Kim*, H. Kim*. Internal Medicine, Division of Rheumatology, College of Medicine, The Catholic University of Korea, Seoul, Republic of Korea.

Object. IL-23 is a new proinflammatory cytokine which stimulates T cells to subsequently produce inflammatory molecules, resulting in inflammatory arthritis. This study was undertaken to explore the role of IL-23 in CD4+T cells on RANKL expression and

osteoclastogenic activity.

Method. Joint cells, CD4⁺T cells and Fibroblast like synoviocytes (FLSs) were isolated from IL-1Ra^{-/-}mice. The level of RANKL mRNA were measured with realtime PCR after these cells were treated with various cytokines including IL-23, in combination with inhibitors of the intracellular signal pathway. Osteoclasts precursor cells were cocultured with CD4⁺T cells in the presence of IL-23 and subsequently stained for tartrate-resistant acid phosphatase (TRAP) activity. IL-1Ra^{-/-} mice were injected intra-articularly with a recombinant adenovirus expressing mouse IL-23.

Results. Expressions of IL-23, IL-17 and IL-1 β were increased in arthritic joints of IL-1Ra^{-/-} mice. Coexpression of IL-23, CD4⁺T cells and RANKL in pannus of arthritic joints was revealed by immunohistochemical staining. IL-23 increased expression of both RANKL in the mixed joint cells of IL-1Ra^{-/-}mice. IL-23 enhances the expression of RANKL in CD4⁺T cells. TRAP-positive osteoclastogenesis was enhanced by IL-23-stimulated CD4⁺T cells. Interestingly, IL-23 had the potential to induce osteoclastogenesis in itself without the help of CD4⁺T cells. In vivo, intraarticular injection of adenoviral vector carrying IL-23 accelerated the severity of arthritis in IL-1Ra^{-/-}mice and effected high expression of RANKL at inflammatory joints.

Conclusion. IL-23 induces not only joint inflammation but also bone destruction via RANKL expression in arthritic CD4⁺T cells. The various effects of IL-23 in CD4⁺T cells have an important clinical impact in the view point of joint destruction. The interactions among IL-23, CD4⁺T cells, osteoclasts and RANKL expression may be a potential therapeutic approaches in treating bone destruction in inflammatory diseases.

Disclosures: S. Park, None.

T079

Regulation of Human Osteoclast Precursor Generation by Type II Cytokines and STATs. K. Park-Min^{*1}, M. Humphrey^{*2}, L. B. Ivashki^{*1}.

¹Arthritis and Tissue Degeneration program, Hospital for Special Surgery, New York, NY, USA, ²VAMC, Oklahoma City, OK, USA.

The first step in osteoclastogenesis is M-CSF-mediated generation of osteoclast precursors (pOC) that are responsive to RANKL stimulation from bone marrow progenitors or monocytes. The purpose of this study was to determine if type II cytokines that suppress osteoclastogenesis (IFN- γ , IFN- α/β , IL-10) inhibit human pOC generation and to explore underlying mechanisms. pOC were generated from human monocytes (and in some experiments from murine bone marrow cells) using M-CSF in the presence or absence of IFN- α , IFN- γ , or IL-10, and stimulated with RANKL. OC formation was analyzed by staining for TRAP positive multinucleated cells, OC gene expression was analyzed using real time PCR, and RANK-induced signal transduction was analyzed using immunoblotting. RNA interference and retroviral transduction were used to study the function of OC genes, and the role of Stat1 and Stat3 were investigated using cells from knockout mice. The generation of human pOC was associated with striking increases in expression of RANK and the key costimulatory receptor TREM2. Subsequent RANKL-induced osteoclastogenesis was strongly suppressed by IL-10, IFN- γ , and IFN- α , with concomitant suppression of OC-specific genes such as TRAP and cathepsin K. TREM2 expression in pOC and OC was essentially completely abrogated by IL-10 and IFN- γ ; IFN- γ and IFN- α also suppressed RANK expression. The effects of IL-10 were partially reversed by forced expression of TREM2. IL-10 also suppressed the proximal RANK signaling pathway. Type II cytokines suppress pOC generation by inhibiting expression of TREM2 and RANK. In addition, IL-10 suppresses pOC function by inhibiting signaling responses to RANKL by a mechanism that differs from the previously reported degradation of TRAF6 by IFN- γ . These results yield insights into the molecular regulation of initial steps of osteoclastogenesis by type II cytokines.

Disclosures: K. Park-Min, None.

T080

Skeletal Muscle-specific Overexpression Pregnancy-associated Plasma Protein-A (PAPP-A) Increases Bone Accretion in Mice. J. Wergedal¹, M. Rehage^{*2}, D. Phang^{*2}, W. Xing², B. Bonafede^{*2}, D. Hou^{*2}, S. Mohan¹, X. Qin^{*1}. ¹Department of Medicine, Loma Linda University, Loma Linda, CA, USA, ²Musculoskeletal Disease Center, J. L. Pettis Veterans Affairs Medical Center, Loma Linda, CA, USA.

We have recently reported that osteoblast-specific overexpression of PAPP-A, a protease for IGF binding protein-2, -4 and -5, increased bone size and bone formation rate in mice. On the other hand, somatic growth was not significantly enhanced, which is consistent with the lack of PAPP-A transgene expression in other non-skeletal tissues and the lack of detectable PAPP-A in circulation. In this study we tested the hypothesis that an increase in PAPP-A concentration in blood, as occurring during human pregnancy, would exert an anabolic effect on bone. Overexpression of PAPP-A in skeletal muscle using the human skeletal muscle alpha actin promoter significantly increased skeletal muscle mass at an age of 10 weeks. The PAPP-A transgene was highly expressed in muscle, leading to a significant increase in PAPP-A concentration and IGFBP-4 proteolysis in the blood. Conversely, PAPP-A transgene mRNA was not detected in bone. Compared with the wild-type littermates, transgenic mice exhibited a significant increase ($P<0.01$) in femur total bone content (26% \pm 4), cortical bone content (28.1 \pm 4.6), and cortical bone area (24% \pm 5) determined by pQCT, calvarial BMD (29% \pm 6) measured by DEXA, and calvaria thickness (39% \pm 6). In conclusion, 1) an increase in PAPP-A concentration in circulation can enhance bone accretion, 2) systemic administration of PAPP-A may be of clinical interest for the treatment of osteoporosis.

Disclosures: X. Qin, None.

This study received funding from: VA.

T081

IL-33 Inhibits Osteoclast Formation Indirectly Through Osteoblastic Cells. H. Saleh^{*}, J. M. W. Quinn, T. J. Martin, M. T. Gillespie. Bone, Joint and Cancer Group, St. Vincent's Institute, Fitzroy, Australia.

IL-33 is a proinflammatory factor that induces Th2 cytokine production and is produced by endothelial cells in rheumatoid arthritis. Its receptor is ST2, and a natural soluble form of ST2 has anti-inflammatory actions. Since IL-33 is related to IL-18, an inhibitor of osteoclast (OC) formation, we investigated the actions of IL-33 on osteoclastogenesis in vitro.

We studied IL-33 effects on murine OC formation from the following cell populations that contain haemopoietic progenitors: bone marrow cells, M-CSF dependent non-adherent bone marrow macrophages (BMM), spleen cells and RAW264.7 cells. OC formation from these cells was stimulated either by treatment with RANKL (100ng/ml) plus M-CSF (30ng/ml), or by co-culture with 1,25 dihydroxyvitamin D3-stimulated osteoblastic cells.

In RANKL/M-CSF stimulated cultures, IL-33 dose dependently inhibited OC formation from bone marrow cells and spleen cells, with a maximal effect at 20ng/ml. However, these populations contain large numbers of non-hematopoietic cell types such as stromal cells and lymphocytes. OC formation in cultures of RAW264.7 cells or BMM was not inhibited by IL-33, suggesting that IL-33 does not act directly on these two types of immature myelomonocytic cells to block differentiation. In co-cultures of bone marrow, spleen and BMM populations with osteoblastic cells (primary calvarial osteoblasts or Kusa O osteoblastic cell line), dose dependent inhibition of OC formation by IL-33 was observed with a maximal effect also at 20ng/ml. Since OC formation from RANKL-stimulated BMM was not inhibited by IL-33, this suggests an indirect inhibitory action through the mediation of osteoblastic cells. To investigate whether this involved the induction of a soluble osteoblast-derived inhibitor we co-cultured Kusa O cells and BMM separated by a porous membrane in the presence of 1,25 dihydroxyvitamin D3. IL-33 inhibited OC formation in these cultures even when exogenous RANKL and M-CSF were also added suggesting the inhibition is not mediated by osteoprotegerin (OPG).

Our results indicate that IL-33 is a novel OC inhibitor that acts on osteoblastic stromal cells to induce a soluble inhibitor of OC formation that is not OPG. This points to a significant role for IL-33 and, by extension, its decoy receptor ST2 in bone metabolism.

Disclosures: H. Saleh, None.

T082

Sonic Hedgehog in Fracture Repair and Osteoclast Formation. T. Shimo^{*1}, T. Yuasa², S. Isowa^{*1}, S. Ibaraki^{*1}, M. Enomoto-Iwamoto^{*2}, A. Sasaki^{*1}, A. Yamaguchi^{*1}, M. Pacifici², M. Iwamoto². ¹Oral and Maxillofacial Surgery, Okayama University Graduate School of Medicine and Dentistry, Okayama, Japan, ²Orthopaedic Surgery, Thomas Jefferson University, Philadelphia, PA, USA.

Sonic hedgehog (Shh) was originally identified as a critical factor in antero-posterior skeletal patterning in developing limb and has since been found to influence other essential developmental processes. In previous studies we found that Shh and other hedgehog proteins are transiently expressed in experimental bone fractures, indicating that the factors may be important in skeletal healing and remodeling. To test this hypothesis, we first monitored hedgehog gene expression in a mouse costal bone fracture model and then tested hedgehog protein functions. RT-PCR analysis showed that gene expression of Shh, hedgehog receptor Patched (Ptc) and its signal transducer Gli1 was strongly and coordinately up-regulated within 12h after fracture and lasted up to 48h. Up-regulation of family member Indian hedgehog (Ihh) was detected after 72h. In situ hybridization revealed that Shh transcripts were broadly distributed within the fracture site field by 6h, indicating that Shh expression is part of an acute response mechanism mounted by several local cell types. To gain insight into the nature of the cells responding to Shh, we created rib fractures in hedgehog reporter mice that harbor β -galactosidase linked to the promoter regions of the Ptc gene, a direct target of hedgehogs. Reporter activity was prominent and well distributed throughout the bone marrow of the fractured bone by 24h. Interestingly, reporter activity was particularly intense in many TRAP-positive and multinucleated cells, suggesting that hedgehog signaling is activated during formation and/or function of osteoclasts. To test this possibility directly, bone marrow-derived osteoclast progenitor cell populations were isolated from 5 week old mice and cultured in the presence or absence of exogenous recombinant Shh and/or RANKL. While Shh itself did not induce osteoclast formation in the absence of RANKL, it markedly enhanced osteoclast formation in RANKL-treated cultures as determined by TRAP staining and dentin pit formation assay. The stimulatory effects of Shh on RANKL-induced osteoclast formation were also observed in CD11b(+) and RAW264.7 cell cultures, were inhibited by treatment with hedgehog pharmacological inhibitor cyclopamine, and failed to occur in primary cultures of bone marrow cells lacking the hedgehog signaling receptor Smoothened. The results of the study provide clear evidence that hedgehog signaling is rapidly activated during bone fracture repair and could be part of mechanisms enhancing bone marrow progenitor cell function and, in particular, osteoclast differentiation and action.

Disclosures: T. Shimo, None.

T083

Phenotypical Heterogeneity Between Osteoclasts Involved in the Endochondral Ossification and Bone Remodeling. S. Soeta, Y. Izu, S. Kamiya*, H. Amasaki*, Veterinary Anatomy, Nippon Veterinary Life Science University, Musashino-City, Tokyo, Japan.

Osteoclasts at the chondro-osseous junction of the epiphyseal growth plate play an essential role for replacement of cartilage with bone tissues in the endochondral ossification, and contribute to the longitudinal growth of long bones. Therefore, they are thought to be controlled by a different regulatory mechanism from osteoclasts resorbing bone tissues in the modeling and remodeling process. The purpose of this study is to clarify functional heterogeneity between osteoclasts involved in the endochondral ossification and in the modeling and remodeling process in the long bones. We investigated the expression of RANK, RANKL, Flk-1 (VEGF receptor 1), MMP-9, and MMP-13 immunohistochemically in osteoclasts in the tibiae of new-borne and young male rats. Osteoclasts, detected as TRAP-positive multinucleated giant cells, distributed throughout from epiphysis to diaphysis in the tibiae in rats aged 1 to 42 days. In rats aged 1 to 28 days, osteoclasts at the chondro-osseous junction showed RANK, RANKL and MMP-9-immunoreactivities, but not Flk-1 and MMP-13-immunoreactivities. In rats aged 35 and 42 days, however, osteoclasts at the chondro-osseous junction showed Flk-1 and MMP13-immunoreactivities in addition to RANK, RANKL and MMP-9-immunoreactivities. Osteoclasts on the surface of trabecular bones in the diaphysis showed RANK, RANKL, Flk-1, MMP-9 and MMP-13 immunoreactivities in rats aged 1 to 42 days. From the immunohistochemical observations, osteoclasts may be recruited to the chondro-osseous junction without VEGF-Flk-1 pathway, and absorb the cartilage tissue of the epiphyseal growth plate independent on MMP-13 in the growing period. Therefore, osteoclasts involved in the endochondral ossification in the epiphyseal growth plate may be regulated in a different manner from osteoclasts resorbing bone tissues in the modeling and remodeling process.

Disclosures: S. Soeta, None.

T084

Nicotine and Lipopolysaccharide Stimulate the Formation of Osteoclast-like Cells by Increasing Macrophage Colony-Stimulating Factor and Prostaglandin E₂ Production by Osteoblasts. H. Tanaka*, N. Tanabe*, T. Kawato*, T. Katono*, A. Namba*, N. Suzuki*, M. Motohashi*, M. Maeno*, ¹Department of Oral Health Sciences, Nihon University School of Dentistry, Tokyo, Japan, ²Department of Oral and Maxillo facial surgery, Nihon University School of Dentistry, Tokyo, Japan, ³Department of Biochemistry, Nihon University School of Dentistry, Tokyo, Japan.

Several studies have indicated that one of the causes of alveolar bone destruction with periodontitis is lipopolysaccharide (LPS) from the cell wall of Gram-negative bacteria in plaque and that tobacco smoking may be an important risk factor for the development and severity of periodontitis. The present study was undertaken to determine the effect of nicotine and LPS on the expression of macrophage colony-stimulating factor (M-CSF), osteoprotegerin (OPG), and prostaglandin E₂ (PGE₂) in osteoblasts, and the indirect effect of nicotine and LPS on the formation of osteoclast-like cells. Saos-2 cells were cultured with 10⁻³ M nicotine, or 1 or 10 µg/ml LPS and 10⁻³ M nicotine, for up to 14 days. The gene and protein expression of M-CSF and OPG were determined using real-time PCR and ELISA, respectively. PGE₂ expression was determined using ELISA. The formation of osteoclast-like cells was estimated using tartrate-resistant acid phosphatase (TRAP) staining of osteoclast precursors in culture with conditioned medium from nicotine and LPS-treated Saos-2 cells and the soluble receptor activator of NF-κB ligand (RANKL). M-CSF and PGE₂ expression increased markedly in cells cultured with nicotine and LPS compared with those cultured with nicotine alone. OPG expression increased in the initial stages of culture with nicotine and LPS but decreased in the later stages of culture. The conditioned medium containing M-CSF and PGE₂ produced by nicotine and LPS-treated Saos-2 cells with soluble RANKL increased the TRAP staining of osteoclast precursors compared with that produced by nicotine treatment alone. These results suggest that nicotine and LPS stimulate the formation of osteoclast-like cells via an increase in M-CSF and PGE₂ production and that the stimulation is greater than with nicotine treatment alone.

Disclosures: H. Tanaka, None.

T085

VGLUT1 KO Mice Develop Osteopenia due to an Increase in Osteoclastic Bone Resorption. S. Uehara*, S. Senoh*, M. Nakamura*, T. Ninomiya*, T. Mizoguchi*, Y. Kobayashi*, Z. Hua*, R. H. Edwards*, Y. Moriyama*, N. Takahashi*, N. Udagawa*, ¹Department of Biochemistry, Matsumoto Dental University, Shiojiri, Japan, ²Department of Membrane Biochemistry, Okayama University, Okayama, Japan, ³Institute for Oral Science, Matsumoto Dental University, Shiojiri, Japan, ⁴Departments of Neurology and Physiology, University of California San Francisco School of Medicine, San Francisco, CA, USA.

The vesicular glutamate transporter (VGLUT) is responsible for vesicular storage of L-glutamate, and plays an essential role in L-glutamate-mediated chemical transduction in the central nervous system and some peripheral tissues. We previously reported the role of VGLUT in bone metabolism as follows (EMBO J, 25:4175, 2006): (1) VGLUT1 was expressed in the transcytotic vesicle in osteoclasts, and osteoclasts secreted both L-glutamate and bone degradation products upon depolarization or ATP stimuli in Ca²⁺-and

cAMP-dependent manners. (2) Osteoclasts expressed the metabotropic glutamate receptor (mGluR)8. L-glutamate secreted by osteoclasts inhibited the transcytosis and bone resorbing activity of osteoclasts through the mGluR8 in an autocrine manner. (3) VGLUT1 knock out (KO) mice developed osteopenia. In this study, we investigated the mechanism of L-glutamate secretion from osteoclasts and the cause of osteopenia induced by VGLUT1 deficiency in mice in more detail. The results obtained from this work are as follows: (1) we first examined whether the signaling pathway of cAMP-dependent protein kinase (PKA) is involved in the secretion of L-glutamate from osteoclasts. Osteoclasts obtained from the co-culture of mouse osteoblasts and bone marrow cells were treated with KT-5720, a PKA inhibitor, and stimulated with KCl or ATP to induce L-glutamate secretion. KT-5720 scarcely inhibited the KCl and ATP-induced L-glutamate secretion from osteoclasts. (2) To determine the cause of bone loss in VGLUT1 deficiency in mice, we measured serum levels of TRACP5b (a marker of bone resorption) and alkaline phosphatase (a marker of bone formation) in 8-week-old VGLUT1 KO and wild-type mice. Serum levels of TRACP5b in VGLUT1 KO mice were significantly higher than those in wild-type mice. Serum alkaline phosphatase activities were also increased in VGLUT1 KO mice. These results suggest that osteoclasts secrete L-glutamate through PKA independent pathway, and that bone loss in VGLUT1 KO mice is caused by an increase in bone resorption. The results also suggest that the lack of L-glutamate-mediated signals in bone induces a high turnover bone state. Bone histomorphometry of VGLUT1 KO mice is currently analyzed in our laboratories.

Disclosures: S. Uehara, None.

T086

Tumor Cells Metastatic to Bone Express CSF-1 and Support Osteoclast Survival. K. Yagiz, S. R. Rittling, Cytokine, Forsyth, Boston, MA, USA.

Tumors metastatic to the bone produce factors that cause massive bone resorption mediated by osteoclasts in the bone microenvironment. The mechanisms that explain the increase in bone resorption in metastasis are unclear. We have hypothesized that osteoclasts in the vicinity of tumor cells are "superactivated": superactivated osteoclasts are larger than normal osteoclasts with higher resorptive ability. Colony stimulating factor (CSF-1) is strictly required for the formation and survival of active osteoclasts. Aberrant expression of CSF-1, which can be synthesized as a soluble or a membrane-associated protein, has been found in many cancers correlating with disease progression and malignancy. Here we show that r3T cells, a tumor cell line that forms bone metastasis in mice, express abundant CSF-1 in vitro. FACS analysis with an antibody to CSF-1 as well as RT-PCR confirmed that r3T cells express CSF-1 both a secreted and a membrane-associated protein. Murine osteoclast-like cells co-cultured with either mitomycin-c (MMC) treated or glutaraldehyde fixed r3T cells with cytokine RANKL survived in the absence of added CSF-1. In addition, murine osteoclast-like cells were cultured with r3T conditioned medium (CM). Our results showed that r3T cells supported osteoclast formation by providing adequate amounts of CSF-1 protein. Importantly, direct cell-to-cell contact was required for osteoclast survival. Therefore, drugs that could counteract the effect of CSF-1 might be useful for reducing the osteoclast mediated osteolysis. We suggest that tumor cell production of CSF-1 is one of the mechanism by which tumors cause osteoclast superactivation.

Disclosures: K. Yagiz, None.

T087

Hormonal and Pharmacological Modulation of MT2 Melatonin Receptor Inhibits Osteoclast Maturation and Activity. G. Maillot*, C. Desrochers*, R. Doucet*, E. Levy*, A. Moreau*, ¹Department of Nutrition, Université de Montréal, Research Center CHU Sainte-Justine, Montreal, PQ, Canada, ²Research Center CHU Sainte-Justine, Montreal, PQ, Canada, ³Department of Stomatology & Biochemistry, Université de Montréal, Research Center CHU Sainte-Justine, Montreal, PQ, Canada.

Melatonin (Mel) is known to induce bone formation through osteoblast activation and indirectly through OPG up regulation leading to osteoclast inactivation. However, a direct effect of Mel on osteoclast has never been shown previously. The aim of this study is to investigate the influence of the Mel signaling pathway on osteoclastogenesis and osteoclast activity using in vitro and in vivo models as experimental paradigm. Gene and protein expression of Mel receptor, MT2, were detected in RAW 264.7 cells cultured in presence or absence of RANKL (50ng/ml) whereas MT1 receptor was not detected. Addition of physiological doses of Mel (10⁻⁹ M) decreased by 60% the number of resorption pits and by 69% the total resorbed area although no significant change was observed in the number of TRAP+ cells. Addition of 4-P-PDOT, a MT2 receptor antagonist, blocks the inhibitory action of Mel suggesting that such effect was mediated through Mel signaling activity. Surprisingly, RAW 264.7 cells treated with increasing doses of 4-P-PDOT (10⁻¹⁰ M to 10⁻⁶ M) alone demonstrated a significant decrease in both number of TRAP+ multinucleated cells and resorption pits in a dose dependent-manner. These effects were neither caused by an increased apoptosis nor due to reduced proliferation since no changes were observed between untreated and 4-P-PDOT treated cells. To further investigate the effect of 4-P-PDOT on bone metabolism, we injected 4-P-PDOT (10mg/kg of body weight) after weaning to male C57Bl/6j mice 3 times per week during 4 weeks and performed densitometric (PixiMus II bone densitometer) and histomorphometric analyzes. Preliminary results revealed an increase in bone mineral accretion at the spine and whole body level in treated mice compared to vehicle-injected animals. Overall, these data highlight the importance of the Mel signaling pathway in modulating osteoclast function and show an unrecognized effect of Mel receptor antagonist 4-P-PDOT as a potential anti-osteoporotic drug.

Disclosures: G. Maillot, None.

This study received funding from: Cotrel Foundation Institut de France.

T088

The Osteopetrotic Incisor Absent Rat Exhibits Reduced Osteoclast Activity, Resulting in Normal Endochondral Fracture Union but Delayed Hard Callus Remodeling. M. M. McDonald^{*1}, A. Morse^{*1}, K. Mikulec^{*1}, C. Godfrey^{*1}, S. Tamara^{*2}, D. Little^{*1}. ¹Orthopaedic Research, The Children's Hospital Westmead, Sydney, Australia, ²Science, The University of Technology, Sydney, Australia.

A spontaneous mutation in the incisor absent (ia/ia) rat results in abnormal osteoclasts which display deficient resorption. We investigated the resulting osteopetrotic phenotype to determine the exact age of recovery. Furthermore, we utilized this model to examine fracture repair in the absence of functional osteoclasts.

Samples were harvested from male rats from 3 weeks of age for phenotype analysis. Once the age of recovery was determined, closed fractures were performed in 5 week old male ia/ia and wt/het controls. Harvests were performed at 1, 2 and 3 weeks post fracture, to assess repair within the period of osteoclast dysfunction.

Serum CTX showed decreases up to 9 weeks of age in ia/ia rats ($p < 0.05$), with normalization to control levels at 12 weeks of age. Further, ia/ia primary osteoclast cultures revealed decreased resorption pit formation at 5 and 9 weeks of age compared to control ($p < 0.01$), again normalizing to control levels at 12 weeks.

DEXA scans of tibial metaphyses revealed increases of 40-114% in BMD up to 20 weeks of age in ia/ia rats compared to controls ($p < 0.01$). Histology at this site revealed a constant incline in BV/TV at the proximal region in ia/ia rats such that a 3-fold increase was achieved by 20 weeks compared to controls ($p < 0.01$). In the distal tibial metaphysis however, the BV/TV in the ia/ia rats began to decrease after 9 weeks of age such that it had reduced by half at 20 weeks, suggesting recovery of resorption.

Femur length showed an 11%-14% decrease in ia/ia compared to control rats at all time points examined from 3 weeks of age ($p < 0.01$). However, growth plate height showed a slight increase in ia/ia rats at only 5 weeks of age compared to controls ($p < 0.05$), all other time points showing no differences.

Importantly, initial endochondral fracture union was achieved by 3 weeks post fracture in both ia/ia and controls. QCT revealed significant increases in BMC and volume in ia/ia calluses at 1, 2 and 3 weeks ($p < 0.01$). Controls showed a reduction in callus volume between 2 and 3 weeks, whereas the ia/ia callus volume increased 41%.

In conclusion, the ia/ia rat exhibits a severe osteopetrotic phenotype resulting from reduced osteoclast activity. Recovery from the dysfunctional resorption occurs between 9 and 12 weeks of age. Initial endochondral fracture union was achieved normally in the absence of functional osteoclasts in ia/ia rats, however hard callus remodeling was hindered resulting in a larger, more mineralised callus. This study reveals that osteoclast function is not essential for initial fracture union but is required for hard tissue remodeling.

Disclosures: M.M. McDonald, None.

T089

Normal Endochondral Bone Healing Follows Continuous Bisphosphonate Pre-treatment in a Rat Closed Fracture Model. A. Morse^{*}, M. McDonald^{*}, K. Mikulec^{*}, H. Mai^{*}, C. Munns, D. G. Little^{*}. Orthopaedic Research, The Children's Hospital Westmead, Sydney, Australia.

Long-term Pamidronate (PAM) therapy is the mainstay of treatment for moderate to severe osteogenesis imperfecta (OI). However, these patients can develop a reduced bone turnover state that may affect fracture healing. We aimed to investigate the effects of continuous PAM pre-treatment on bone healing in a rat model of endochondral fracture repair.

9 week old Wistar rats received closed femoral fractures. 4 weeks prior to fracture PAM dosing commenced subcutaneously (SC) at 0.15mg/kg, 0.5mg/kg and 5 mg/kg twice weekly. Harvests were at 2 and 6 weeks post-fracture.

Radiographic union was observed in all 6 week samples and QCT showed increases of 55-92% in callus BMC and 44-77% in callus volume with PAM treatment over saline controls ($p < 0.01$). These increases were attributed to retention of hard callus, with increases in primary callus BV/TV of 68%-84% at 6 weeks compared to saline ($p < 0.01$). In addition, remodeling of the callus was delayed with decreases of 32% and 45% in callus remodeled neo-cortical bone in the 0.5mg/kg and 5mg/kg PAM groups respectively compared to saline ($p < 0.01$).

Histology revealed that endochondral fracture healing followed a normal timeline regardless of PAM treatment. No differences were observed between groups in callus cartilage content at both 2 and 6 weeks post fracture. One 5mg/kg PAM sample showed retained cartilage at 6 weeks, but had no effect on the overall result.

Systemically, PAM dosing lead to increases of up to 4-fold in metaphyseal BV/TV over saline controls at 6 weeks ($p < 0.01$). Endosteal mineral apposition rate (MAR) was reduced by 6 weeks with PAM treatment, the 0.5mg/kg and 5mg/kg groups showing reductions of 30% and 84% respectively compared to saline ($p < 0.01$). Periosteal MAR however showed no changes with PAM treatment at 6 weeks. Small growth deficiencies of 2-5% in femur length were noted with 0.5 mg/kg or 5 mg/kg PAM compared to saline ($p < 0.01$). The growth rate between the 2 and 6 week time points however remained constant, regardless of treatment. Growth plate height was also unaffected by PAM dosing.

In conclusion, continuous PAM pre-treatment was associated with a small decrease in bone formation and a large reduction in bone resorption, leading to a net increase in callus size. However, this lowered bone turnover did not hinder fracture repair, with endochondral union being achieved normally regardless of treatment. These data suggest that long-term BPs, whilst reducing bone turnover, may not interfere with normal endochondral fracture union in healthy individuals, but may hinder long bone growth. Further work is planned with a longer interval of pre-dosing with Pamidronate as well as experiments in animal models of Osteogenesis Imperfecta.

Disclosures: A. Morse, None.

T090

Anti-GGT Antibody Attenuates Osteoclastic Bone Erosion in CIA Mice. Y. Ishizuka^{*1}, S. Moriwaki^{*2}, S. Niida². ¹AC Bio Technologies, Yokohama, Japan, ²Bone & Joint Disease, National Center for Geriatrics & Gerontology, Obu, Japan.

gamma-Glutamyl transpeptidase (GGT/CD224), known as a key enzyme for the catabolism of glutathione and cysteine metabolism, is a newly identified bone-resorbing factor which stimulates osteoclast formation. We found that GGT expression was up-regulated in the inflamed joints of the patients with rheumatoid arthritis (RA). Therefore, we hypothesized that GGT may be involved in the arthritis-related osteolysis. In this study, we demonstrate that the inhibitory effects of anti-GGT monoclonal Ab (GGT-mAb) on the joint destruction in the collagen-induced arthritis (CIA) mice.

Materials and Methods: GGT localization in the synovium of RA patients and CIA mice was determined by immunohistochemistry. In vivo osteoclastogenic activity of GGT was assessed by histological analysis of the rat alveolar bone after infusing the recombinant human GGT (rhGGT) into the jaws. For preparation of CIA mice, DBA/1J mice were immunized with an emulsion containing bovine type II collagen and Mycobacterium tuberculosis in incomplete Freund's adjuvant. GGT-mAbs were generated against rhGGT using BALB/c mice. The GGT-mAbs were administered via i.p. to CIA mice. The therapeutic effects of GGT-mAbs were evaluated by incidence score, arthritic score and histopathological analysis. Role of GGT in osteoclast formation was investigated using cell cultures, microarray analysis and quantitative RT-PCR.

Results: Immunohistochemistry of the inflamed synovium revealed that GGT was detectable in lymphocytes, plasma cells, and macrophages, as well as capillary vessels. The rhGGT-treated rats exhibited marked alveolar bone destruction with an increase in TRAP-positive osteoclasts. Treatment with GGT-mAbs significantly reduced the number of osteoclasts and the severity of osteolysis in CIA mice. In vitro examinations using bone marrow cultures containing 1,25(OH)₂D₃ indicated that the osteoclast development was enhanced through the further up-regulation of RANKL expression mediated by GGT stimulation. Moreover, addition of rhGGT accelerated the osteoclastogenesis in the cultures of bone marrow macrophages maintained with M-CSF and RANKL as compared with those of condition without rhGGT.

Conclusion: This study revealed the involvement of GGT in the bone erosion of CIA mice and contributed to further understanding of the arthritis-related bone loss. Thus, GGT antagonists may be new effective agents for attenuating the joint destruction in RA.

Disclosures: S. Niida, None.

T091

Electroneutral Sodium/Bicarbonate Cotransporter NBCn1 Is Expressed in Rat Osteoclast Ruffled Border Membrane. R. Riihonen¹, I. Song^{*2}, S. Nielsen^{*3}, T. Laitala-Leinonen^{*1}, T. Kwon^{*2}. ¹Bone Biology Research Consortium, Department of Biomedicine, University of Turku, Turku, Finland, ²Department of Biochemistry and Cell Biology, School of Medicine, Kyungpook National University, Daegu, Republic of Korea, ³The Water and Salt Research Center, Institute of Anatomy, University of Aarhus, Aarhus, Denmark.

The aim of this study is to define the expression of the electroneutral sodium/bicarbonate cotransporter NBCn1 in rat osteoclasts and its role for bone resorption. NBCn1 has previously been shown to significantly enhance the cellular uptake of bicarbonate on the basolateral side of the thick ascending limb of the loop of Henle in the kidneys in response to chronic metabolic acidosis, but its function in osteoclasts is unknown.

First, the expression pattern of NBCn1 in bone tissue was determined by analyzing 3-day old rat pup femur and tibia with immunohistochemistry. Additionally, confocal microscopy was utilized to explore the specific localization of NBCn1 in rat osteoclasts. RT-PCR was performed to study NBCn1 mRNA expression in primary rat osteoclasts cultured on bovine bone slices. Moreover, changes of NBCn1 mRNA levels were monitored after exposing osteoclasts to various stimuli such as anoxic conditions, acidic or alkaline culture media and growth factors known to increase the bone resorption rate.

NBCn1 immunostaining was specifically associated with the osteoclast cell membrane facing the bone trabeculae in tissue specimens, and immunocytochemistry revealed a similar expression profile where NBCn1 was exclusively localized in the ruffled border membrane in rat osteoclasts. Using RT-PCR, NBCn1 mRNA expression was detected from rat osteoclast cultures, and the expression levels varied markedly due to changes in the extracellular culture environment.

In conclusion, NBCn1 is localized in the ruffled border membrane of rat osteoclasts and the mRNA expression levels are dependent on the extracellular conditions and the activation status of the osteoclasts. These results suggest a role for NBCn1 in bone resorption, possibly by maintaining an acidic pH in the resorption lacuna by means of bicarbonate uptake during the active bone resorption phase. Thus, we may have found a novel, important player in the osteoclastic bone resorption process and will continue this study by exploring the effects of NBCn1 inhibition on the bone resorption rate.

Disclosures: R. Riihonen, None.

T092

TSG-6, a New Regulator of Bone Remodelling. D. Mahoney^{*1}, K. Mikecz^{*2}, G. Mabiliau^{*1}, N. A. Athanasou¹, T. Ali^{*3}, C. M. Milner^{*3}, A. J. Day^{*3}, A. Sabokbar¹. ¹Botnar Research Centre, University of Oxford, Oxford, United Kingdom, ²Rush University Medical School, Chicago, IL, USA, ³Faculty of Life Sciences, University of Manchester, Manchester, United Kingdom.

TSG-6 (TNF-stimulated gene-6) is a non-constitutively expressed protein which is up-regulated by inflammatory mediators and growth factors. The protein is composed almost entirely of LINK and CUB domains; to date a wide variety of protein and glycosaminoglycan ligands have been identified as associating with the LINK module. Animal models of arthritic disease have indicated TSG-6 has anti-inflammatory properties and may protect against cartilage degradation and bone erosion. To determine the mechanism by which TSG-6 affects bone we have characterised; (i) the in vitro effect of TSG-6 on osteoclast activity and osteoblast differentiation, (ii) its mode of action and (iii) its levels in the synovial fluids of inflammatory bone disorders.

Using ELISA and BIAcore analysis, we have shown that TSG-6 binds to a mediator of osteoclastogenesis, sRANKL, as well as BMPs-2, 4, 5, 6, 7, 13 and 14 which promote osteoblastogenesis. In vitro assays indicate that TSG-6 inhibits RANKL-induced human osteoclast formation and activity in a dose-dependent fashion, similar in manner to that of OPG. Furthermore, bone marrow cells isolated from the long bones of TSG-6 deficient mice, give rise to markedly increased resorption as compared to cells isolated from control animals. We have also shown that TSG-6 inhibits the BMP-2 induced alkaline-phosphatase activity of an osteoblastic cell line. Full-length TSG-6 inhibits osteoclastogenesis and BMP-mediated osteoblast differentiation to a greater extent than the isolated LINK and CUB domains: affinity analysis suggests sRANKL and BMP2 interact at composite binding surfaces between the LINK and CUB modules. Quantification of TSG-6 in the synovial fluid of patients with rheumatoid arthritis, osteoarthritis, pyrophosphate arthropathy and gout showed varying levels (0.1-200 ng/ml).

These findings indicate that TSG-6 is a regulator of bone metabolism which can synchronise osteoblast and osteoclast biology. We hypothesise dual functions for this protein; a homeostatic role in non-inflammatory bone environments through inhibition of osteoblast differentiation, and a role in inflammatory bone disease through prevention of osteoclastogenesis. As such TSG-6 has a potential role for the development of therapeutic strategies in bone diseases.

Disclosures: A. Sabokbar, None.

T093

Diphyllin, a Novel Potent V-ATPase Inhibitor, abrogates Acidification of the Osteoclastic Resorption Lacunae and Bone Resorption. M. G. Sorensen, K. Henriksen, A. V. Neutzsky-Wulff*, C. Christiansen, M. Karsdal. Nordic Bioscience A/S, Herlev, Denmark.

Dissolution of the inorganic phase of bone by the osteoclasts is mediated through the V-ATPase and ClC-7. Inhibition of the osteoclastic V-ATPase or ClC-7 is a novel approach for inhibition of osteoclastic bone resorption. By testing natural compounds in acidification assays using acridine orange, diphyllin was identified as a potent inhibitor of lysosomal acidification in osteoclasts. We characterized diphyllin with respect to potency in a human osteoclastic bone resorption assay, an acid influx assay, and in a V-ATPase assay. For comparison, diphyllin was tested in an osteoblastic bone formation assay.

Human osteoclasts were generated from CD14⁺ monocytes cultured with 25ng/ml M-CSF and RANKL. The effect of diphyllin on lysosomal acidification in human osteoclasts was investigated using the dye acridine orange. The effect of diphyllin on osteoclastic bone resorption was measured as the release of CTX-I and calcium into the supernatant, and by scoring pit area. The number of osteoclasts, the TRACP activity, and the cell viability were measured. Diphyllin was tested in the acid influx assay and the V-ATPase assay using bovine chromaffin granules isolated from the medullae of bovine adrenal glands. The effect of diphyllin on bone formation was investigated using MC3T3 cells cultured in medium supplemented with ascorbic acid and beta-glycerol phosphate.

We found that diphyllin inhibited human osteoclastic bone resorption measured by CTX-I (IC₅₀=14nM, Figure 1A), calcium release and pit area, in face of increased osteoclast numbers (Figure 1B) and increased levels of TRACP activity. Moreover, diphyllin dose dependently inhibited lysosomal acidification in human osteoclasts. In the acid influx assay, diphyllin potently inhibited influx (IC₅₀=0.6nM), which is similar to the effect of bafilomycin. Furthermore, diphyllin inhibited the V-ATPase with an IC₅₀ value of 17nM, compared to 4nM for bafilomycin. Finally, diphyllin showed no effect on bone formation in vitro, whereas bafilomycin was highly toxic.

We have identified a natural compound that potently inhibits the lysosomal acidification and the V-ATPase in osteoclasts and thereby abrogates bone resorption. These findings are in alignment with osteopetrotic patients where acidification and resorption are attenuated that result in increased numbers of osteoclasts.

Figure 1A

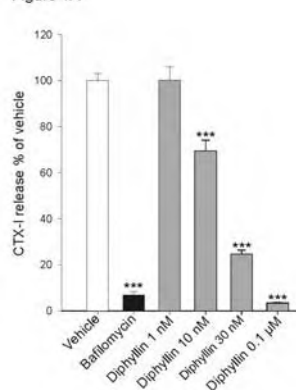
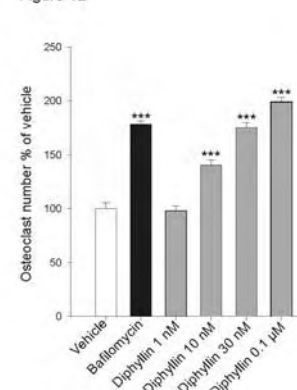


Figure 1B



Disclosures: M.G. Sorensen, None.

T094

Canonical NF-κB Pathway Mediates Osteoclast Bone Resorption Activity.

N. S. Soysa^{*1}, C. N. R. Alles^{*1}, K. Aoki², E. Jimi³, K. Ohya². ¹Center of Excellence for Frontier Research on Molecular Destruction and Reconstruction of Bone, Tokyo Medical and Dental University, Tokyo, Japan, ²Section of Pharmacology, Tokyo Medical and Dental University, Tokyo, Japan, ³Biochemistry, Kyushu Dental College, Kitakyushu, Japan.

NF-κB transcription factor is a key determinant in the orchestration of osteoclast formation, differentiation and survival. Nevertheless the mechanistic basis for NF-κB effect on bone resorbing activity of osteoclast has not fully elucidated yet. Hence the main objective of this study was to find the role of canonical NF-κB pathway in osteoclast resorbing activity using the NBD peptide, an established selective inhibitor of IκB-kinase (IKK). BMM cultured on dentine slices and on cover slips in the presence of RANKL and M-CSF were changed after 3 days with 10µM and 20µM of NBD peptides (Wt). Most of the osteoclasts were fully differentiated when the medium was changed and further cultured for 24 hrs in the presence of the peptides. Osteoclasts were stained for TRAP. Apoptosis was detected by DAPI staining and by TUNEL method and pits were measured by using a confocal microscope system. There was no detectable change in osteoclast numbers after changing the medium. Significant reduction in area of resorption was observed in Wt at 10µM and 20µM concentrations (P<0.01 and P<0.001 respectively). Volume of resorption pit was significantly reduced at 20µM (P<0.001). Volume to area ratio which was independent on osteoclast number was also reduced significantly (P<0.05). No difference in number of apoptotic cells was observed between Wt and control. TRAP was measured in the cell lysate and supernatant to measure the percentage TRAP release. Similarly, Wt significantly reduced TRAP release. Cell migration towards RANKL was reduced in treated samples compared to control assessed by transwell migration assay. Then osteoclasts on cover slips were stained for actin rings. Percentage of osteoclasts with actin rings were markedly reduced in peptide treated group (P<0.001). The levels of TRAP, cathepsin K, MMP-9, NFATc1 and αvβ3 mRNAs analyzed by real-time RT-PCR were significantly reduced in treated samples (p<0.0001). Taken together these results suggest that NBD peptide reduces osteoclast bone resorbing activity, migration and actin ring formation by down regulating above mRNAs and the inhibitory effect on bone resorption was not due to apoptosis, suggesting the vital role of canonical NF-κB pathway in osteoclast activity. Cathepsin K and MMP-9 are NF-κB dependent genes. Also NF-κB binding sites are present within the promoter region of the NFATc1 gene and NFAT binding sites in the TRAP, Cathepsin K, and αvβ3 promoters as well. Therefore the interplay among NF-κB and NFATc1 seems to be crucial in establishment of osteoclast activity.

Disclosures: N.S. Soysa, None.

T095

Dentine Organic Matrix Down-Regulate Osteoclastic Activity in Root Resorption.

W. Sriarj^{*1}, B. J. Varghese^{*1}, K. Aoki², K. Ohya², Y. Takagi^{*1}, H. Shimokawa². ¹Pediatric Dentistry, Tokyo Medical and Dental University, Tokyo, Japan, ²Hard Tissue Engineering, Tokyo Medical and Dental University, Tokyo, Japan.

It has been reported that deciduous tooth roots were more susceptible in resorption than permanent tooth roots, in which resorption did not occur in physiological condition. However, the mechanisms of root resorption are still unclear. Our previous study has shown that osteoclasts cultured on deciduous dentine exhibited a higher level of cathepsin K and MMP-9 mRNA and a higher degree of resorption than cultured on permanent dentine. These could be due to the difference of organic matrices between deciduous and permanent dentine. The purpose of this study is to investigate the effect of organic matrix extracted from bovine deciduous or permanent dentine on the resorptive activity. We extracted dentine organic matrices from bovine deciduous or permanent root dentine using 4M guanidine hydrochloride, pH7.4 (G-ext) then 4M guanidine hydrochloride plus 0.5M EDTA, pH 7.4 (E-ext) sequentially. Osteoclasts, obtained from mouse bone marrow cells co-cultured with osteoblast-rich fraction in α-MEM containing 10% FBS, 1,25-(OH)₂-D₃ and PGE₂, were cultured on the ivory slices

with 500µg/ml of G-ext or E-ext for 48 hours. TRAP positive multinucleated cell number, TRAP activity, resorption pit area and the mRNA level of cathepsin K, TRAP, and MMP-9 were determined. We have found that osteoclasts cultured with both E-ext from deciduous and permanent dentine exhibited lower TRAP positive multinucleated cell number and TRAP activity than G-ext as well as resorption pit area. The mRNA level of cathepsin K, TRAP, and MMP-9 were also down-regulated in osteoclasts cultured with E-ext. Furthermore, permanent dentine E-ext seemed to suppress osteoclastic activity more than deciduous one. These findings suggest that some factors in dentine organic matrices E-ext affect osteoclastic activity in root resorption.

Disclosures: W. Sriarj, None.

T096

Homogenous Fluorescence-based Calcium Assay for the Rapid Determination of In Vitro Bone Resorption. K. E. Renn*, M. J. Brown*. Lonza Walkersville, Inc., Walkersville, MD, USA.

High-throughput assays for measuring in vitro osteoclast-mediated bone resorption are essential tools in the study of bone related diseases. We have developed a homogenous, fluorescence-based assay for the rapid analysis of in vitro osteoclastic activity. The CalciFluor™ Assay quantitatively measures free calcium released during in vitro bone degradation. Normal human osteoclast precursors (OCP) cultured on a human bone substrate in the presence of macrophage-colony stimulating factor (M-CSF) and soluble RANK ligand (sRANKL) exhibit a linear increase in bone degradation over time when assayed using the CalciFluor Assay. Comparable results are obtained when the bone resorption activity of other primary cell types, such as murine bone marrow mononuclear cells, is measured with the assay. Treatment of human OCP with the bisphosphonate alendronate results in a dose-dependent decrease in the amount of calcium released from human bone coated plates. Likewise, OCP cultured in the presence of osteoprotegerin show decreased calcium release from bone, further illustrating that the free calcium elevations result from osteoclast-mediated bone degradation. Results generated with this fluorescent calcium assay are comparable to those obtained with commercially available enzyme immunoassay (EIA) kits detecting collagen degradation products. When the release of either calcium or collagen fragments is measured, actively resorbing osteoclasts show similar time-dependent trends in the amount of bone degraded as well as comparable inhibition profiles in the presence of pharmacologic agents. The CalciFluor Assay is a more rapid, convenient, and economical assay than the current EIA-based assays for bone resorption, and therefore represents an excellent tool for in vitro analysis of osteoclast activity.

Disclosures: M.J. Brown, Lonza Walkersville, Inc. 3.

T097

Lack of Bruton's Tyrosine Kinase Results in Osteoporosis, Despite Defects in Osteoclast Function. L. Danks*, S. Workman*, A. D. Webster*, B. M. Foxwell*, M. Feldman*, N. J. Horwood*. ¹The Kennedy Institute of Rheumatology, Imperial College, London, United Kingdom, ²Department of Immunology, Royal Free and University College Medical School, London, United Kingdom.

Bruton's tyrosine kinase (Btk) is a member of the Tec family of kinases and mutations in Btk result in a rare disease known as X-linked agammaglobulinemia (XLA). These patients have an absence of mature B cells resulting in profound hypogammaglobulinemia and recurrent infections. We have previously shown that Btk is not only involved in B cell responses but also plays a role in inflammatory cytokine production in macrophages, however the role of Btk in osteoclast formation and activation is unknown. As the Tec kinases are regulated by the Src family kinases, which are known to have important actions on osteoclast function, we hypothesised that Btk would be a downstream signaling target of Src kinase. Therefore, we investigated the role of Btk in osteoclast differentiation and activation in vitro and examined the effect of Btk deficiency on the bone phenotype of XLA patients.

Human peripheral blood monocytes were differentiated into osteoclasts in the presence of RANKL and M-CSF. Adenoviral overexpression of Btk/GFP during osteoclast culture on hydroxyapatite slides resulted in an unusual actin ring arrangement, the actin rings were smaller and thicker than those of controls. Lacunar pit formation on dentine slices was dose dependently inhibited, whilst there was no effect on TRAP+ osteoclast formation. Osteoclasts derived from PBMC's or CD14+ precursors of XLA patients, compared to control subjects, exhibited a dose dependent and highly significant decrease in bone resorption activity in response to RANKL despite having a dose dependent increase in TRAP+ osteoclast formation. These results suggest that Btk is important specifically for osteoclast resorption activity. The bone phenotype of the XLA patients was examined using serum markers of bone metabolism and bone density analysis. Surprisingly, XLA patients exhibited an osteoporotic bone phenotype with an average 20% reduction in bone density compared to age matched controls.

Our results provide novel evidence that Btk is an important signaling molecule for normal osteoclast activity in vitro however these patients are osteoporotic in vivo. As B cells play a role in the regulation of basal bone turnover, by providing a reservoir of early osteoclast precursors and by direct expression of osteoclast regulatory cytokines, it is likely that the lack of mature B cells in the XLA patients, and the resulting reduction in OPG levels, are able to override the osteoclast defect in vivo. Thus, our novel finding that XLA patients are osteoporotic suggests that absence of B lymphocytes gives rise to an overall decrease in bone density.

Disclosures: L. Danks, None.

This study received funding from: Arthritis Research Council.

T098

NEMO (IKKγ) Modulates Osteoclastogenesis and Bone Erosion. I. Darwech*, S. Dai*, Y. Abu-Amer. Orthopedic Surgery and Cell Biology & Physiology, Washington University School of Medicine, Saint Louis, MO, USA.

The transcription factor NF-κB is essential for osteoclastogenesis and is considered an immune-modulator of rheumatoid arthritis and inflammatory osteolysis. Activation of NF-κB subunits is regulated by the upstream IκB kinase (IKK) complex which contains, among other proteins, IKK1, IKK2, and IKKγ; the latter also known as NF-κB essential modulator (NEMO). The role of IKK1 and IKK2 in the skeletal development and inflammatory osteolysis has been described, whereas little is known about the role of NEMO in this setting. In this regard, several case reports identified point mutations that led to osteopetrosis and hypodontia or anodontia with conical incisors. NEMO facilitates and integrates upstream stimuli and appears to assign, by yet unknown mechanisms, signal specificity. Typically, signals such as RANKL or TNF prompt oligomerization of NEMO monomers through well-defined domains termed the coiled-coil-2 (CC2) and Lucine zipper (LZ) motifs. This step is a prerequisite for binding to IKKs and further relaying signal transduction. In fact, blocking NEMO binding to IKKs perturbs NF-κB activation, abrogates osteoclastogenesis, and diminishes inflammatory bone erosion. In this study, we asked whether NEMO is essential for osteoclastogenesis of murine marrow macrophages and whether interruption of NEMO oligomerization impedes the process of osteoclast differentiation in vitro and in vivo. To this end, we generated short peptides overlapping the CC2 and LZ motifs and fused them with a carrier peptide to enable cell membrane translocation. Our results show that the CC2 and LZ short peptides specifically bind to NEMO monomers, prevent trimer formation, and render NEMO monomers susceptible for ubiquitin-mediated degradation. Further, CC2 and LZ peptides attenuate RANKL and TNF-induced NF-κB signaling in bone marrow-derived osteoclast precursors. More importantly, these peptides potently inhibit osteoclastogenesis, in vitro, and arrest RANKL-induced calvarial osteolysis, in mice. To further ascertain its role in osteoclastogenesis, we were able to block osteoclastogenesis using NEMO siRNA knockdown approach. Collectively, our data establish that NEMO is essential for osteoclastogenesis and provide the novel finding that inhibition of NEMO assembly leads to its degradation. More importantly, inhibition of NEMO expression impedes osteoclast formation and arrests osteolysis. Thus, NEMO present itself as a promising candidate for therapeutic intervention.

Disclosures: I. Darwech, None.

T099

NFATc1 Mediates the Stimulatory Effects of Post-translationally Modified Bone Sialoprotein on the Resorptive Activity of Rabbit Osteoclasts. H. H. Chen*, J. A. R. Gordon*, A. Pereverzev*, S. M. Sims*, G. K. Hunter*, S. J. Dixon, H. A. Goldberg. CIHR Group in Skeletal Development and Remodeling, The University of Western Ontario, London, ON, Canada.

Cell-adhesion proteins of bone extracellular matrix such as bone sialoprotein (BSP) promote osteoclastogenesis and resorption; however, their mechanism of action has remained elusive. NFATc1 is a transcription factor that plays a critical role in osteoclast differentiation. Our purpose was to determine whether the effects of BSP on osteoclastic resorption involve NFATc1. Osteoclasts were isolated from the long bones of neonatal rabbits. Native BSP (nBSP) from rat long bones (post-translationally modified) and rat recombinant BSP (rBSP, prokaryotically expressed without post-translational modifications) were purified to homogeneity using FPLC. To quantify resorptive activity, osteoclasts were incubated for 24 hours on dentin slices coated with nBSP or rBSP, or uncoated (control). Samples were stained for TRAP activity to determine osteoclast number and then with toluidine blue to determine total area resorbed. In parallel studies, osteoclast attachment and NFATc1 activation were assessed 3 hours after plating on coverslips coated with nBSP or rBSP, or uncoated (control). Immunofluorescence was used to quantify the percentage of osteoclasts demonstrating nuclear localization of NFATc1, which upon activation translocates from the cytosol to the nuclei. Coating of substrates with nBSP or rBSP did not significantly affect the number of osteoclasts attached at 3 or 24 hours. However, nBSP significantly promoted the resorption of dentin slices (2.26 ± 0.26 fold greater than control, mean \pm SEM, $n = 7$), whereas rBSP had no effect (1.06 ± 0.07 fold). Similarly, nuclear localization of NFATc1 was enhanced in osteoclasts plated on coverslips coated with nBSP (1.68 ± 0.05 fold greater than control, $n = 3$), but not with rBSP (1.05 ± 0.03 fold), suggesting a role for NFATc1 in the activation of resorption. To assess the involvement of NFAT in mediating BSP-induced resorption, we used 11R-VIVIT (a cell-permeable peptide inhibitor of NFAT activation). As expected, 11R-VIVIT decreased NFATc1 translocation in osteoclasts bound to nBSP-coated coverslips. Notably, 11R-VIVIT, but not the inactive control peptide 11R-VEET, blocked the stimulatory effect of nBSP on resorptive activity. These findings establish that interaction of osteoclasts with post-translationally modified BSP enhances NFATc1 activation, which in turn stimulates resorption. This is the first direct demonstration that NFAT regulates the resorptive activity of authentic osteoclasts.

Disclosures: S.J. Dixon, None.

This study received funding from: Canadian Institutes of Health Research (CIHR).

T100

AG490, Jak2 Specific Inhibitor, Regulates Osteoclast Survival via Distinct Signaling Pathways. H. B. Kwak*, H. M. Sun*, D. Yang*, H. Kim*, H. Ha*, J. Lee*, Z. H. Lee. Department of Cell and Developmental Biology, School of Dentistry, Seoul National University, Seoul, Korea, Seoul, Republic of Korea.

Osteoclasts are multinucleated cells with the unique ability to resorb bone. Elevated activity of these cells under pathological conditions leads to the progression of bone erosion, such as osteoporosis, periodontal disease, and rheumatoid arthritis. The regulation of osteoclast apoptosis is important for bone homeostasis. In this study, we examined the effect of AG490 (JAK2 specific inhibitor) on osteoclast apoptosis. We show that AG490 inhibits cytochrome c release into cytosol and in turn suppresses caspase-9 and -3 activation, thereby inhibiting osteoclast apoptosis. Also, AG490 stimulated the phosphorylation of ERK and Akt. Adenovirus-mediated overexpression of dominant negative (DN)-Ras and DN-Akt in osteoclasts inhibited the survival of osteoclast despite the presence of AG490. Thus, osteoclast survival in response to AG490 leads to ERK and Akt pathways. Furthermore, constitutive active (CA)-MEK and Myr-Akt suppress the release of cytochrome c into cytosol and inhibit caspase activity. These results suggest that AG490 inhibits caspase activity by activating Akt and ERK and in turn suppresses the apoptosis of osteoclasts.

Disclosures: H.B. Kwak, None.

T101

Expression and Transcriptional Activity of Microphthalmia-Associated Transcription Factor Isoforms During Osteoclastogenesis. M. Murakami¹, Y. Iwata^{*1}, M. Funaba^{*2}. ¹Laboratory of Molecular Biology, Azabu University School of Veterinary Medicine, Sagamihara, Japan, ²Laboratory of Nutrition, Azabu University School of Veterinary Medicine, Sagamihara, Japan.

Microphthalmia-associated transcription factor (Mitf), a member of the basic helix-loop-helix leucine zipper (bHLH-ZIP) transcription factors, is required for proper development of several cell lineages including osteoclasts, melanocytes, retinal pigment cells and mast cells. Mitf has been implicated to be a key regulator of the later steps of osteoclastogenesis, but the role of Mitf is not fully elucidated; although nine distinct Mitf isoforms, which contain an isoform-specific first exon and are identical exons 2 to 9, have been identified at the RNA level, it is unclear whether any isoforms are unique to the osteoclast lineage cells. The present study examined expression of Mitf isoforms in sRANKL-induced osteoclast-like cells. Previous studies have revealed that tartrate-resistant acid phosphatase (Trap) is a transcriptional target of Mitf in osteoclasts. Thus, we also examined factors affecting Trap gene transcription in HepG2 cells that are responsive to Mitf overexpression. Treatment of RAW264 macrophage-like cells with sRANKL (50 ng/ml) for 72 h resulted in the increase in the number of Trap-positive multinucleated cells. Mitf-A and -J but not the other Mitf isoforms (-B, -C, -D, -E, -H, -M and -mc) were expressed in RAW264 cells, irrespective of the treatment with sRANKL. These results indicate that expression of Mitf isoforms is cell-type specific, and that differentiation of osteoclast lineage cells hardly affects expression pattern of Mitf. In addition, Tfe3, another member of the bHLH-ZIP family, was also significantly expressed throughout the differentiation of RAW264 cells. Transcriptional activation assays using luciferase-based reporter gene containing Trap promoter (-2049 +1) revealed that overexpression of Mitf-J/-D/-E but not Mitf-A slightly increased luciferase expression. The overexpression of c-Jun but not c-Fos and JunB increased expression of Trap reporter gene, and synergistic effects of c-Jun and Mitfs (-A and -J/-D/-E) on Trap gene transcription were detected. In contrast, no synergism was observed between Mitf and the other AP-1 component (c-Fos and JunB). Distinct expression of Mitf isoforms and functional interaction between Mitf and the other transcription factor such as c-Jun during the terminal differentiation of osteoclasts suggests discrete regulation of osteoclastogenesis.

Disclosures: M. Murakami, None.

T102

FADD-Caspase-8 aXis Regulates Osteoclast Apoptosis. M. Nakamura, T. Akiyama, K. Nakamura, S. Tanaka. Department of Orthopaedic Surgery, Faculty of Medicine, The University of Tokyo, Tokyo, Japan.

Osteoclasts are terminally differentiated cells and rapidly die through apoptosis in the absence of tropic factors. Apoptosis is genetically programmed cell death to remove unwanted cells from physical status, and is controlled by two distinct signaling pathways; the death receptor-mediated pathway and the mitochondria-mediated pathway. We previously reported that a proapoptotic BH3-only Bcl-2 family member Bim is a key regulator of osteoclast apoptosis, showing the involvement of mitochondrial pathways in the cell death of osteoclasts. On the other hand, the role of the death receptor pathway in osteoclast apoptosis is not fully clarified yet. The death receptor-mediated pathway is activated upon ligand binding to cell surface receptors such as tumor necrosis factor (TNF) receptor that contain cytoplasmic death domains. Ligand binding induces oligomerization of these death domains through ligand-induced receptor trimerization, generates homophilic interaction surfaces for death domain-containing adaptor molecules. FADD (FAS-associated death domain-containing protein) is a universal adapter protein that mediates signaling of death-domain containing members of the TNF receptor superfamily, and plays a critical role in recruiting death-inducing signaling complex and the subsequent activation of initiator caspase-8 and downstream effector caspases. In an attempt to elucidate the role of FADD in osteoclast apoptosis, we constructed an adenovirus vector carrying a dominant negative mutant of FADD (AxFADD-DN), which lacks the death effector domain and therefore cannot activate Caspase-8. Osteoclasts generated in vitro were infected with control adenovirus or AxFADD-DN, which effectively induced FADD-DN expression in the cells, and were subjected to the survival assay. Osteoclasts

overexpressing FADD-DN survived longer than control cells after cytokine depletion, which was associated with the downregulation of Caspase-8 activity. Apoptosis of osteoclasts was also suppressed by a specific inhibitor of Caspase-8, Z-IETD-FMK. These results suggest that death receptor & FADD-mediated pathways are crucial for osteoclast apoptosis. To identify death receptors involving in osteoclast apoptosis, we treated the cells with FasL, TNF- α and TRAIL. However, all of them failed to promote the apoptosis of osteoclasts. Our results suggest that the FADD-Caspase-8 axis critically regulates the apoptosis of osteoclasts, which is activated through previously unknown death receptor ligands.

Disclosures: M. Nakamura, None.

T103

RANKL-induced Expression of TRPV2, Calcium Permeable Channel, Is Involved in Osteoclastogenesis via Calcium Signaling Activation. F. Okamoto*, H. Kajiya, A. Nakao*, K. Okabe. Physiological Science and Molecular Biology, Fukuoka Dental College, Fukuoka, Japan.

Osteoclast differentiation from hematopoietic precursor cells is stimulated by receptor activator of NF- κ B ligand (RANKL) via activation of transcription factors. Nuclear factor of activated T cells (NFAT) c1 is known to be a crucial transcriptional factor for osteoclastogenesis and is activated by calcineurin, a Ca²⁺/calmodulin-dependent phosphatase. Calcium signaling is considered to be an important regulator during osteoclastogenesis. Although it has been shown that RANKL stimulates PLC γ and then releases Ca²⁺ from intracellular Ca²⁺ stores, little is known which intra- and/or extra-cellular pathways induce osteoclastogenesis. Using a DNA microarray, we found that transient receptor potential V2 (TRPV2), a calcium permeable cation channel, was highly expressed in RANKL treated RAW264.7 cells compared to untreated cells. Thus, the aim of present study was to investigate the expression and role of TRPV2 on osteoclastogenesis via calcium signaling. TRPV2 channels were expressed in RAW 264.7 cells and bone marrow macrophages. RANKL significantly increased TRPV2 expression in both cell types 24 h after treatment. To elucidate the electrophysiological function of TRPV2, non-selective cation currents were recorded from RAW264.7 cells using the whole-cell voltage clamp technique. The current density was significantly increased in RANKL treated cells 24 h after treatment compared to untreated cells. Ruthenium red (10 μ M), an inhibitor of TRPV channels, reduced the current density as well as RANKL-induced osteoclastogenesis. Tetracycline-inducible siRNA targeted TRPV2 completely abolished the RANKL-dependent augmentation of non-selective cation currents. Silencing with TRPV2 siRNA in RAW264.7 cells also suppressed RANKL-stimulated osteoclastogenesis. These results suggest that RANKL up-regulates TRPV2 expression which serves as a calcium influx pathway. TRPV2 is involved in the RANKL-evoked calcium signaling and subsequent activation of calcium-dependent transcriptional factors such as NFATc1 and AP-1 promoting osteoclastogenesis.

Disclosures: F. Okamoto, None.

T104

Characterization of the Signaling Complex that Mediates Osteoclastic Activation. J. L. Ross*, T. J. Chambers, K. M. Lawrence*. Department of Cellular Pathology, St George's, University of London, London, United Kingdom.

Although the signals responsible for osteoclast differentiation are well characterized, almost nothing is known of those responsible for the activation and modulation of resorption. Confocal microscopy clearly demonstrates that osteoclasts form actin ring structures on mineralized substrates that differ distinctively from those formed on non-mineralized surfaces. Moreover, osteoclasts secrete enzymes when incubated on bone but not on plastic. These findings show that osteoclasts have the ability to distinguish bone from other surfaces, and that mineralized surfaces are essential for the induction of resorptive behaviour.

There is much evidence that the vitronectin receptor (VNR) and c-src are implicated in bone resorption. Recently, it has become clear that in many cases, best exemplified by the immunological synapse of T cells, cell signaling occurs through the formation of large multi-protein complexes that form dynamic physical associations between surface receptors and intracellular signaling molecules. Identifying the components of the multi-protein complex that controls osteoclast resorption may provide new targets for clinical intervention in the treatment of osteoporosis and related diseases.

We therefore performed co-immunoprecipitation experiments, using antibodies to VNR and c-src, to isolate complexes associated with these molecules in resorbing and non resorbing osteoclasts. Osteoclasts were formed on plastic substrates, lifted into suspension, and sedimented onto plastic or bone surfaces. Protein complexes from osteoclasts incubated on bone versus plastic, and with versus without resorption-inducing cytokines, were then compared.

One and 2D gel electrophoresis showed that several proteins were associated with both VNR and c-src under each of the experimental conditions used.

Interestingly co-immunoprecipitates from resorbing cells yielded proteins which were not seen under conditions of no activation. This suggests that in resorbing osteoclasts, additional proteins are recruited to the signaling complex. Furthermore, other proteins appeared to be complexed with VNR and c-src in non-resorbing osteoclasts but absent in activated cells. This implies that some proteins must be removed from the complex in order for resorption to take place, suggesting a novel resorption block mechanism. In order to identify these proteins we used Western immunoblots to probe for known signaling molecules. Using both co-immunoprecipitation antibodies, IL1 receptor, TRAF6, VNR and c-src were found to be present but equal under all conditions, thus eliminating these as differentially-bound candidates. The unidentified novel proteins are currently being identified by mass spectrometry.

Disclosures: J.L. Ross, None.

T105

Elucidating Mechanisms Leading to Increased Resorptive Activity of Large Osteoclasts in Inflammation. D. P. Trebec¹, A. Gramoun^{*2}, J. N. M. Heersche^{*2}, M. F. Manolson². ¹Department of Biochemistry, University of Toronto, Toronto, ON, Canada, ²Faculty of Dentistry, University of Toronto, Toronto, ON, Canada.

Large osteoclasts (OCs) (≥ 10 nuclei) are prevalent in inflammatory diseases characterized by increased bone resorption (e.g. rheumatoid arthritis and periodontal disease). Previously, we have shown that large OCs express higher levels of the activating receptor interleukin-1 receptor-1 (IL-1R1) while the decoy receptor IL-1R2 was increased in small OCs (2-5 nuclei). In addition, large OCs were found to be more active compared to small OCs in response to interleukin-1 (IL-1 β) (Trebec et al. JCB 101: 205-220, 2007). As a result, our aim was to determine how differential expression of IL-1R1 and IL-1R2 leads to increased resorption in large OCs and if IL-1 α and IL-1 β result in differential effects on OC formation and activity. For all experiments, we used the RAW 264.7 cells differentiated into populations of small and large OCs. In the presence of 50 ng/mL RANKL, RAW cell proliferation rates were unaffected by the addition of IL-1 α/β . IL-1 α (1 ng/mL) and IL-1 β (10 ng/mL) resulted in an increase in TRAP+ cells when added to cultures at day 0 or day 3 but not at day 5. In contrast, TRAP activity revealed no significant differences between the groups. A 2-fold increase in the number of large OCs adopting a "rounded" morphology (indicative of active OCs) was also seen when exposed to 10 ng/mL IL-1 β for 24 hours (less so for IL-1 α) and was reversed with the addition of 50 ng/mL IL-1 receptor antagonist (IL-1ra). Furthermore, similar to previous results shown with 10 ng/mL IL-1 β , large OCs resorbed 3-fold more in the presence of 1 ng/mL IL-1 α . Neither the increase in rounded morphology, inhibition by IL-1ra, nor differences in resorptive activity were evident in small OCs in response to either cytokine. Colocalization of IL-1R1 and the integrin $\alpha v \beta 3$ was observed in OCs, most notably in OCs plated on fibronectin where they adopted a round morphology. Gramoun et al have shown that OCs on fibronectin are hyperactive. In conclusion, there is a differential response between large and small OCs to IL-1, possibly resulting from variations in their IL-1 receptor levels in turn leading to activation of different signalling pathways. IL-1 α was found to be a ~10X more potent than IL-1 β . Colocalization of IL-1R1 and $\alpha v \beta 3$ could also contribute to the differential signalling responses. Elucidating mechanistic differences between large and small OCs may result in novel targets for therapeutics designed to inhibit excessive resorption by large OCs while maintaining normal bone remodelling.

Disclosures: D.P. Trebec, None.

T106

NF- κ B But Not NFATc1 Is Involved in AhR - RANKL Crosstalk in Benzo[a]pyrene-Mediated Inhibition of Osteoclastogenesis. I. Voronov^{*1}, K. Li^{*2}, H. C. Tenenbaum², J. N. M. Heersche^{*2}, M. F. Manolson². ¹Laboratory Medicine and Pathobiology, University of Toronto, Toronto, ON, Canada, ²Faculty of Dentistry, University of Toronto, Toronto, ON, Canada.

Cigarette smoking is a risk factor for impaired bone healing, however, the molecular mechanisms leading to its detrimental effects are not known. Benzo[a]pyrene (BaP) is an environmental pollutant present in high concentrations in cigarette smoke. BaP binds to the aryl hydrocarbon receptor (AhR), a cytosolic transcription factor (TF), and induces expression of several drug-metabolizing enzymes including cytochrome P450 1B1 (CYP1B1). We have demonstrated previously that osteoclastogenesis is suppressed by BaP, and that RANKL, when delivered in high concentration (100 ng/ml) reverses this inhibition and suppresses BaP-mediated gene expression, suggesting possible crosstalk between AhR and RANKL signaling pathways (Voronov et al., Biochem. Pharmacol., 70:300-7, 2005). NF- κ B and NFATc1 are key TFs activated in RANKL-induced osteoclastogenesis. To evaluate the effect of BaP on these TFs, RAW264.7 cells were exposed to 25 or 200 ng/ml RANKL and 10^{-5} M BaP and analyzed by TF activation ELISA kits. TF activity assays demonstrated that BaP inhibited RANKL-mediated NF- κ B activation at 30 min, however, at 60 min, NF- κ B activation levels remained above control levels in BaP-containing groups. In contrast, NFATc1 activity was significantly upregulated by BaP. To determine the effect of BaP on RANKL-mediated nuclear translocation, the cells were analyzed by immunofluorescence (IF) using an anti-p65 or anti-NFATc1 antibodies. IF showed that BaP inhibited RANKL-induced NF- κ B nuclear translocation, but had no effect on NFATc1. To investigate the involvement of NF- κ B and NFATc1 in BaP-mediated gene expression, the cells were cultured in the presence of NF- κ B and NFATc1 inhibitors. RT-PCR revealed that NF- κ B but not NFATc1 inhibitors decreased CYP1B1 expression suggesting that NF- κ B is involved in BaP-mediated CYP1B1 expression. To assess if there is a direct interaction between AhR and NF- κ B, co-immunoprecipitation experiments were performed and revealed an AhR-NF- κ B interaction in the presence of BaP. Based on the above, we speculate that NF- κ B but not NFATc1 is involved in AhR - RANKL signaling crosstalk. We conclude that inhibition of RANKL-induced NF- κ B activation is one of the possible mechanisms of BaP-mediated inhibition of osteoclastogenesis.

Disclosures: I. Voronov, None.

T107

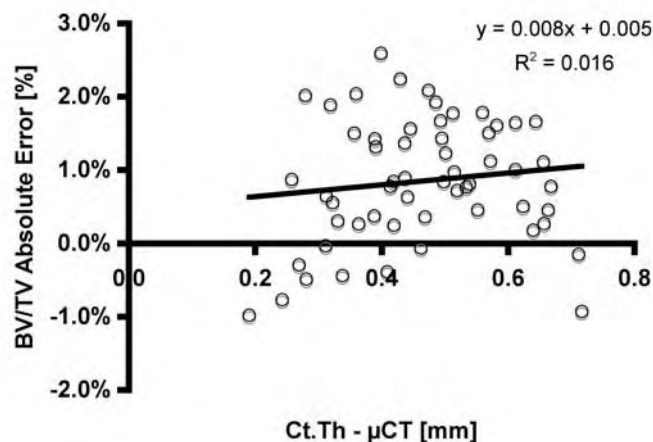
Densitometric Derived Structural Indices in HR-pQCT Are Independent of Cortical Geometry. A. J. Burghardt, K. Davis*, S. Majumdar. Radiology, University of California, San Francisco, San Francisco, CA, USA.

High-resolution peripheral quantitative computed tomography (HR-pQCT) has the potential to be a useful method for the longitudinal evaluation of bone quality in human subjects. Current structure analysis methods for this modality calculate BV/TV based on

the apparent mineral density of the trabecular compartment and an assumed compact bone mineral density of 1200 mg HA/cm³. This requires accurate calibration of bone mineral densities and adequate correction for beam hardening effects. Using an equivalent calibration and beam hardening correction in a micro-tomography device, it has been shown that cortical geometry can introduce a non-negligible bias in apparent density measures [1]. In this study we evaluate the error in calculating BV/TV densitometrically as it relates to cortical geometry and corrections for beam hardening for HR-pQCT. Cadaveric distal radii were acquired from 6 donors and a 1cm length was imaged using HR-pQCT (Scanco XtremeCT, 82 μ m isotropic nominal resolution) and μ CT (Scanco μ CT40, 18 μ m isotropic nominal resolution). For both devices custom beam hardening correction factors were determined using a 200mg HA/cm³ wedge phantom. The datasets were registered based on matching cross sectional areas prior to analysis. BV/TV and Ct.Th measures were determined for each dataset in 1mm increments along the long axis of the bone. BV/TV was calculated densitometrically as $vBMD_{trab}/1200$ mg HA/cm³ for the HR-pQCT images, while a simple voxel counting method was used for the μ CT data. Ct.Th was calculated for the μ CT data using direct 3D methods. As reported elsewhere [2], BV/TV determined densitometrically from calibrated HR-pQCT images was somewhat underestimated compared to the reference μ CT values. The absolute error in BV/TV exhibited minimal dependence on cortical geometry. These results suggest that beam hardening effects related to cortical shell geometry are not a significant source of bias in HR-pQCT based measures of trabecular bone structure.

[1] E. Cory et al, ORS 2007

[2] J.A. MacNeil and S.K. Boyd. Med Eng. Phys. 2007 Epub



Disclosures: A.J. Burghardt, None.

T108

Measurement Protocols for the Non-invasive Assessment of Bone Constituent Properties by Raman Spectroscopy. J. H. Cole¹, M. V. Schulmerich^{*1}, K. A. Dooley^{*1}, J. M. Kriegl^{*2}, E. Daley^{*2}, S. A. Goldstein^{*2}, M. D. Morris¹. ¹Department of Chemistry, University of Michigan, Ann Arbor, MI, USA, ²Department of Orthopaedic Surgery, University of Michigan, Ann Arbor, MI, USA.

Techniques that clinically evaluate bone status may assess the mass and organization of the tissue, but no current method can examine features of bone quality such as mineral and matrix properties in vivo, which contribute vitally to skeletal strength and toughness. Previous studies revealed that bone fragility is associated with changes in composition metrics, such as mineral crystallinity or substitution and collagen cross-linking. We recently developed a non-invasive Raman fiber optic probe that allows us to observe bone spectra through the skin and overlying tissue in animal and human cadaveric limbs. The objective of our study was to improve tissue preparation, optimize probe configuration, and examine our ability to measure bone constituent properties non-invasively in different specimens over a range of overlying tissue depths. Excised limbs from human, mouse, rat, and canine specimens were obtained. For the animal limbs, fur was removed in the region of interest (ROI) using a depilatory agent. Glycerol was applied to the ROI to increase light penetration into overlying tissue, thereby improving the Raman bone spectra. Multiple spectra were acquired on each limb. Following transcutaneous measurements, tissues overlying the bone were removed, and Raman spectra were collected from the exposed bone for validation. The contribution of bone (e.g., mineral and matrix) was separated from that of the overlying tissue (e.g., skin and tendon) using multivariate methods. Standard composition metrics including carbonate/phosphate ratio, mineral/matrix ratio, and collagen cross-link ratio were computed using both band heights and band areas. Band height ratios generally gave better accuracy, because they were less sensitive to errors from baseline correction. Bone composition measurements obtained transcutaneously differed by less than 5% from those obtained on the exposed bone, and the two were not significantly different ($p > 0.05$). The results demonstrate effective measures of bone beneath more than 5 mm of overlying tissue with the expectation of reaching greater depths with further improvements to our system. Non-invasive Raman spectroscopy can accurately assess the contribution of bone composition to bone quality and may prove useful in the clinical assessment of bone fragility.

Disclosures: J.H. Cole, None.

T109

Within Osteons Infrared Parameters Linked to Specific Bone Properties Vary as a Function of Tissue and Animal Age. S. Gourion-Arsiquaud¹, L. M. Havill², A. L. Boskey¹. ¹Research, Hospital for Special Surgery, New York, NY, USA, ²Southwest Foundation for Biomedical Research, San Antonio, TX, USA.

Fractures are the major problem associated with osteoporosis and represent a major concern of public health. Although BMD is used as a clinical predictor of fracture risk, some patients with fracture incident present normal BMD showing that this is not the only factor affected in osteoporosis. Moreover BMD does not allow understanding the underlying mechanisms involved in these bone diseases. Therefore it was important to find other parameters linked to bone quality. Previous studies on healthy and diseased bones using FTIR spectroscopy have validated parameters that reflect the mineral and matrix organization at a molecular level.

Due to constant bone remodeling, there are tissue age variances within the same bone specimen. In this work we analyze the molecular variations of bone as a function of both tissue and animal age. To address this issue we describe changes of parameters inside osteons from baboons of different ages by FTIR-Imaging and for representative samples also using Raman spectroscopy. The osteon was chosen for this study as it is an active remodeling unit, presenting different tissue ages going from its center to the periphery.

The following parameters were examined across individual osteons in femoral samples from 27 baboons aged 0-30 years: Mineral/matrix ratio, a quantitative assessment of the mineral content; Crystallinity ratio linked to the hydroxyapatite (HA) crystal size; Carbonate to phosphate ratio, and Collagen cross-link ratio which represent, respectively, the incorporation of carbonate into the HA lattice and the maturity of collagen. We found that mineral/matrix ratio and crystallinity ratio increase with tissue age whereas carbonate to phosphate ratio decreases. These data improve our knowledge on the mechanisms involved in bone tissue aging. The Raman data validate and complete these IR results. The parameters show a similar trend within osteons regardless the age of the animal. Only the absolute values of these ratios differed. This work demonstrates not only that FTIR imaging allows the co-localization of important mineral and matrix properties of bone at the microscopic level but also that osteon analysis can provide reproducible characterization of these properties. Indeed, this work set up a basis which will permit using normal osteonal data as a baseline against which those of samples from bone disease subjects can be compared. This should allow characterization of which bone properties are associated with the metabolic bone diseases. On the same way osteonal studies should provide information on the efficacy of therapies used in the treatment of bone diseases.

Disclosures: S. Gourion-Arsiquaud, None.

T110

Assessment of Bone Tissue Mineralization: Evaluation of Polychromatic μ CT Mineralization Measurement by Comparison to Synchrotron Radiation μ CT. G. J. Kazakia, A. Burghardt, S. Majumdar. Radiology, UC San Francisco, San Francisco, CA, USA.

The goal of this study was the quantitative evaluation of micro-computed tomography (μ CT)-based measurement of degree of mineralization of bone (DMB). While μ CT systems are used widely to assess bone structure, beam-hardening effects due to the polychromatic source complicate assessment of DMB. Beam-hardening correction algorithms have recently been introduced to overcome this limitation. Synchrotron radiation μ CT (SR μ CT) is an appropriate standard for spatially-resolved DMB evaluation due to the monoenergetic, high flux, parallel beam that provides high spatial resolution and accurate attenuation measurement. Therefore we proposed to compare μ CT data to those obtained by SR μ CT to evaluate the accuracy of μ CT mineralization measurement.

Cylinders of trabecular bone (8 x 4 mm, n = 14) were harvested from proximal femurs, proximal tibiae, and vertebrae of human cadavers in an effort to include a range of structure and mineralization. Specimens were imaged using a desktop μ CT system (μ CT-40, Scanco Medical AG) at a resolution of 8 microns and energy settings optimized for mineralized human trabecular bone (70 kV, 114 mA). Density-calibrated μ CT reconstructions were created using a hydroxyapatite (HA) phantom.

The specimens were then scanned at a synchrotron beamline equipped with a μ CT stage (National Synchrotron Light Source, BNL) at low energy (26keV) with a voxel size of 7.5 microns. Density-calibrated reconstructions were created using the μ CT HA phantom. SR μ CT data were segmented using a global threshold criterion. Segmentation of the μ CT data was performed by matching the volume fraction (BV/TV) determined by SR μ CT analysis. Mean DMB (g/cc) and BMC (g) were calculated for each specimen from the μ CT and SR μ CT reconstructions. Following imaging, ash weight (g) and density (g/cc) were measured using established gravimetric protocols.

Desktop μ CT DMB measurements were well-correlated to SR μ CT DMB values when anatomic sites were considered individually ($R^2 = 0.80$ tibia & vertebra; 0.99 femur) but not when pooled ($R^2 = 0.21$). At all sites evaluated, μ CT underestimated DMB as compared to SR μ CT (12 to 18 %, $p < 0.001$). At all sites, BMC derived from both μ CT and SR μ CT were well-correlated with ash weight ($R^2 = 0.98$). DMB was correlated to ash density only for proximal femur cores ($R^2 = 0.55$ for both μ CT & SR μ CT).

These results suggest that trabecular bone structure is critical in tomography-based determination of mineral density. We found that bone samples from sites with high BV/TV (proximal femur) produce more accurate DMB measures than low BV/TV samples. Partial volume and segmentation artifacts, which are more prevalent in low BV/TV imaging, likely contribute to errors in DMB.

Disclosures: G.J. Kazakia, None.

This study received funding from: NIH.

T111

Analysis of Differing Approaches for the Assessment of Large Scale Transcriptional Profiling of Fracture Healing. J. E. McLean¹, L. J. Silkman¹, T. A. Einhorn¹, T. F. Smith², L. C. Gerstenfeld¹. ¹Orthopaedic Research, Boston University, Boston, MA, USA, ²Biomedical Engineering, Boston University, Boston, MA, USA.

Fracture healing is a synchronous temporal process of one round of endochondral bone formation followed by an extended period of remodeling. The aim of this study was to compare three approaches to the normalization of large scale transcriptional profiling. The methods used were: the profile of unfractured bone as the reference; an exogenously added artificial gene sequence with no known correlate in the mouse genome as reference "alien gene"; and a set of standard genes "housekeeping genes". Standard femur fractures were generated in C57/B6 mice and assessed at days 3, 7, 10, 14, and 21. ~21,000 genes were examined. The hybridization of each spot was assessed using three separate detection channels and spots were measured as a ratio intensities. Separate ratios were determined using the biological reference and the exogenously added Alien gene, which were both co-printed with each gene spot on the chip included with the hybridization cDNAs. Sixty standard genes were empirically compiled based on both their invariant expression from the biological reference and low standard deviation. Sixty genes with the largest ratio differences from their reference for four basic expression patterns increasing, decreasing, and two types of complex behavior over time were used to assess statistical reproducibility of the data. The Alien and biological reference had statistically significant correlation for all sets at ($p < 0.002$). The correlation between the standard genes and the biological reference showed statistical significance (all $p < 0.05$) and was only significant at $p < 0.05$ for two out of four sets of genes that were examined when compared to Alien. The use of the biological reference excludes ratio intensity measurements from being made for all genes that are not actively transcribed in the unfractured bone sample. This analysis method excluded ~2000 mRNAs that are newly transcribed following fracture, as determined via ratio to Alien reference. Using fixed in-spike concentration of Alien also enables absolute ratio intensity measurements of the expressed levels for individual mRNAs to be made. Validation of expressed levels between gene transcripts can be assessed, by examining the ratios of Col1a1 and Col1a2, splice variants of Col2a1 and a selected group of ribosomal subunit proteins. The inherent advantages of using an exogenous reference enables absolute determination of individually expressed mRNAs species to be made and provides the greatest degree of accuracy of both inter-chip and inter-experimental comparisons.

Disclosures: J.E. McLean, None.

This study received funding from: NIH.

T112

Microscopic Imaging of Bone Composition En Block with Synchrotron Infrared Microspectroscopy. L. M. Miller¹, T. C. Feldman², A. Schirmer³, R. J. Smith¹, S. Judex³. ¹National Synchrotron Light Source, Brookhaven National Laboratory, Upton, NY, USA, ²Materials Science and Engineering, Stony Brook University, Stony Brook, NY, USA, ³Biomedical Engineering, Stony Brook University, Stony Brook, NY, USA.

Understanding changes in the chemical makeup of bone is important for diagnosing and treating bone disease. Fourier transform infrared microspectroscopy (FTIRM) is a well-established imaging technique that provides information on both the mineral and matrix composition of bone. One drawback of the technique is that FTIRM data are typically collected in a transmission geometry, thus requiring plastic-embedding and microtoming of very thin (3 - 5 micrometer) sections of bone. In this work, we have established a new method for collecting FTIRM data in a reflection geometry from the surface of a bone block using synchrotron light. This study will demonstrate the accuracy and quality of reflection FTIRM, while investigating spatially-resolved chemical changes in developing mouse bone. Tibiae of female BALB mice were harvested at 8 time points distributed between 1d and 40d of age and embedded in poly methyl methacrylate (PMMA). Thin sagittal sections (3 micrometers) were cut from the surface of each embedded bone. FTIRM was performed on both the thin section and the surface of the sample block in transmission and reflection geometry, respectively. The results from the two imaging methods were compared using visible landmarks present in both the thin section and the embedded bone. Specifically, the mineralization (phosphate/protein ratio), carbonate accumulation (carbonate/phosphate ratio), crystallinity, and collagen cross-linking were assessed. The results of this work will be presented as a validation of this new methodology, which will increase the applicability of FTIRM by expanding its use to those samples that cannot be processed into thin sections for analysis.

Disclosures: L.M. Miller, None.

This study received funding from: U.S. Department of Energy.

T113

Back-Scattered Electron Imaging of Bone Mineralization in Osteoarthritis. P. Sutton-Smith^{*}, N. Fazzalari, J. Kuliwaba, H. Beard^{*}, B. Ma^{*}. Tissue Pathology, Institute of Medical and Veterinary Science, Adelaide, Australia.

Osteoarthritis affects a large proportion of Western society. There is controversy over the degree and nature of bone changes in this disease with presentation of heterogeneous tissue-level morphology. Studies of sub-chondral bone have shown increased bone volume and decreased bone mineralization, but more distal sites have not been systematically

investigated. We have used a quantitative back-scattered electron imaging technique to analyze inter-trochanteric trabecular bone samples from 22 patients (11 males aged 70±12 years, 11 females aged 68±13 years) undergoing total hip replacement for osteoarthritis. These are compared with a group of 20 skeletally normal post mortem controls (12 males aged 60±14 years, 9 females aged 63±14 years) with both groups including only individuals aged greater than 40 years. Bone samples were fixed and embedded in methylmethacrylate resin for histomorphometry. These blocks were then polished, carbon coated and examined in a Philips XL20 scanning electron microscope which was calibrated with carbon/aluminium standards. Data were pooled to create a mineralization distribution for each of the groups, as well as analyzing the weight percent calcium (wt%Ca) and trabecular bone volume fraction (BV/TV[%]) data for individuals. The mineralization of the osteoarthritis group was less than that of the control group (24.2 wt%Ca versus 25.3 wt%Ca, respectively). The osteoarthritis mineralization distribution was a lower, broader curve consistent with the heterogeneous tissue-level morphology characteristic of osteoarthritis. Statistical analysis of individual's values revealed a significant lowering of the weight percent calcium in osteoarthritis compared to controls (24.4 wt%Ca versus 25.1 wt%Ca, respectively, $p<0.001$) concomitant with a significant increase in BV/TV(%) (10.4% versus 7.6%, respectively, $p<0.02$). These results are similar to those reported for sub-chondral bone in osteoarthritis and imply an increased rate of bone turnover associated with a net positive gain in bone volume. These findings at a site distal to the primary disease process have implications for systemic changes of bone metabolism in osteoarthritis.

Disclosures: P. Sutton-Smith, None.

T114

Osthoe Stimulates Pre-osteoblast Proliferation and Differentiation Via BMP-2/RUNX2/SMAD1 Pathway. D. Tang^{*1}, S. Cheng^{*1}, Q. Shi^{*1}, D. Chen², Y. Wang^{*1}. ¹Orthopaedics, Institute of Spine, Shanghai University of Traditional Chinese Medicine, China, ²Orthopaedics, Center for Musculoskeletal Research, University of Rochester, NY, USA.

Osthoe, also named 7-methoxy-8-isopentenoxycoumarin, is a coumarin extracted from *Cnidium fructus*. In the present researches, it has various of pharmacological effects, such as anti-arrhythmia, anti-immunity, anti-apoptosis, anti-tumor, anti-inflammation, etc. It was also found that osthoe has effects on osteoporosis using ovariectomized (OVX) rats and human osteoblast-like cell lines. The purpose of this study was to examine effects of osthoe on the pre-osteoblast related with the dose and find its possible mechanisms for anti-osteoporosis. OCT-1 cells (a pre-osteoblast cell line) were used, cultured with 3 dose of osthoe for 48h, or with purified BMP-2 protein. We first determined the effect of osthoe on cell proliferation by MTT assay. alkaline phosphatase (ALP) activity in the cells was also assayed after appropriate treatment periods. The real time RT-PCR was employed to quantify the changes in mRNA levels for bone morphogenetic protein-2 (BMP-2) and RUNX2 of cells. At last we used the Western Blotting analysis to evaluate the expression of Smad1 protein.

As a result, osthoe (10ug/ml) can promote the OCT-1 cells proliferation, but osthoe (30ug/ml) and osthoe (60ug/ml) had no effect on the proliferation of these cells. Various dose of osthoe can increase the ALP activity of OCT-1 cells, the effect of 30ug/ml was the best, and 10ug/ml followed. From the real time RT-PCR analysis, Various dose of osthoe can enhance the BMP-2 mRNA levels, the effect of 10ug/ml was the best, and 30ug/ml followed. In addition, we found that osthoe (10ug/ml) can enhance the BMP-2 mRNA levels significantly, but osthoe (60ug/ml) decreased the BMP-2 mRNA levels significantly. From the Western Blotting analysis, osthoe (10ug/ml) and osthoe (30ug/ml) can stimulate the expression of Smad1 protein, but osthoe (60ug/ml) had the opposite effect. In this study, we demonstrate that osthoe is a promising agent for anti-osteoporosis, but the effect of osthoe is related with the dose. Only suitable dose of osthoe can stimulate bone formation, while exorbitant dose of osthoe may inhibit bone formation.

Disclosures: D. Tang, None.

T115

A New Approach to Assess Bone Formation Rates and Immunohistochemistry / in situ Hybridization in the Same Bone Specimen. J. Zhang, G. E. Gutierrez, M. Zhao, S. A. Munoz*, J. R. Edwards, G. R. Mundy. Center for Bone Biology, Vanderbilt University, Nashville, TN, USA.

Bone formation rate is the key parameter in the in vivo characterization of osteoblast activity and bone growth/remodeling. The standard procedure to assess new bone formation is to use calcium-seeking fluorochromes which are visualized in undecalcified, plastic embedded sections of bone using fluorescence microscopy. Not only is this method time consuming and laborious, more importantly, it limits the application of immunohistochemistry (IHC)/in situ hybridization (ISH) on the same sections/specimens. Consequently, two separate bones (left and right) of an animal must be used for assessing bone formation or IHC/ISH experiments. This is problematic because we have observed that BMD and structural property differ between left-sided and right-sided bones. This suggests that experiments performed on different bones from the same animal may generate different biological information and lead to inaccurate conclusions. Our goal is to develop methods that enable the evaluation of all bone parameters including bone formation rate, bone/osteoid volume, osteoblast and osteoclast numbers, protein and gene expression profiles (IHC, ISH) using one bone specimen. To achieve this goal, the most challenging problem is to assess bone formation rate in decalcified specimens. We have tested three fluorochromes, two fixation buffers and two decalcification solutions. We found that the visualization of calcein green is superior to calcein blue and alizarin red in formalin fixed, EDTA-decalcified paraffin embedded bone sections; the fixation and decalcification times are also critical for preserving calcein green labeling. All three

fluorochromes were not preserved in ethanol or formalin fixation following acid decalcification. Optimizing the time for different specimens, we have effectively assessed mineral apposition rates and other parameters of bone remodeling, as well as IHC and ISH in the same slides/specimens in different developmental stages of tooth and bone. In conclusion, we have successfully developed a simple method to assess new bone formation rates and protein/gene expression profiles in the same bone specimen. This procedure greatly increases the efficiency and reliability of the results.

Disclosures: J. Zhang, None.

T116

IGF-1 Regulation of Collagen II and Matrix Metalloproteinase-13 Gene Expression in Rat Endplate Chondrocytes via Distinct Signaling Pathways. M. Zhang^{*1}, Q. Zhou^{*1}, Y. Dong², T. Li², Q. Shi^{*1}, Y. Wang^{*1}. ¹Orthopaedics, Institute of Spine, Shanghai University of Traditional Chinese Medicine, China, ²Orthopaedics, Center for Musculoskeletal Research, University of Rochester, NY, USA.

It is well known that IGF-I exerts positive anabolic effects on chondrocytes in vivo and in vitro. However, little is known on IGF-mediated regulation of collagen II, matrix metalloproteinase-13(MMP13) gene expression and the involved intracellular signaling pathway in endplate chondrocytes. In the present study, chondrocytes isolated from normal rat endplate cartilage were stimulated with IGF-1 in monolayer culture. The technique of real-time PCR was employed to quantify the changes in mRNA levels for collagen IIa and mmp13 in rat endplate chondrocytes in response to IGF. The data were normalized to mRNA levels of β -actin, a constitutively expressed gene. Expression of signaling proteins was evaluated by western blot analysis. Cells were also treated with pharmacologic agents that block PI3K and MAPK signaling pathways. IGF-1 increased the collagen IIa mRNA expression in a time- and dose-dependent manner. With the treatment of IGF-1 (100 ng/ml), the expression of collagen IIa mRNA in rat endplate chondrocytes reached the highest value at 24 h and then decreased gradually along with time. IGF-1 (100 ng/ml) increased collagen IIa mRNA levels in rat endplate chondrocytes by 3.89 fold after treatment 24 h. Additionally, IGF-1 decreased MMP13 mRNA expression in rat endplate chondrocytes. IGF-1 (100 ng/ml) decreased MMP13 mRNA level by 0.55 fold after treatment 24 h. Furthermore, IGF-1 activated (phosphorylation) members of both the PI3K pathway and the ERK/MAPK pathway, Akt and ERK1/2. Coincubation of IGF-1 with PI3K inhibitor wortmannin significantly blocked the stimulatory effect of IGF-1 on collagen IIa mRNA expression, but did not significantly inhibit IGF-induced repression of MMP13 mRNA expression. In contrast, the ERK/MAPK inhibitors PD98059 was able to block partially IGF-stimulated collagen IIa mRNA expression, but significantly blocked IGF-induced MMP13 mRNA repression. These data suggested that IGF-1 stimulation of PI3K signaling pathway is responsible for the ability of IGF-1 to increase collagen IIa mRNA expression, and IGF-1 stimulation of ERK/MAPK signaling pathway is responsible for the ability of IGF-1 to inhibit MMP13 mRNA expression.

Disclosures: M. Zhang, None.

T117

Activation ERK1/2 Prevents the FasL-induced Apoptosis Anulus Fibrosus Cells in Insulin-like Growth Factor-1-Treated. Q. Zhou^{*1}, M. Zhang^{*1}, Y. Dong², T. Li², Q. Shi^{*1}, Y. Wang^{*1}. ¹Orthopaedics, Institute of Spine, Shanghai University of Traditional Chinese Medicine, China, ²Orthopaedics, Center for Musculoskeletal Research, University of Rochester, NY, USA.

FasL binds to Fas to induce cell apoptosis. Insulin-like growth factor-1(IGF-1) decreases apoptosis in several cell types. There have been no descriptions showing that through activation Erk1/2, increasing focal adhesion kinase (FAK) expression on anulus fibrosus cells with IGF-1. In this present study, rat anulus fibrosus cell were cultured and treated with antibody FasL, with or without human recombinant IGF-1. Cellular morphology was examined by light microscopy and reverse transcription polymerase chain reaction (RT-PCR). Apoptotic changes were evaluated by transmission electron microscopy, TUNEL staining, and immunostaining of Bax and bcl-2. Real time RT-PCR analysis showed mRNA levels of FAK, collagen II and aggrecan. Values are normalized to β -actin from three independent experiments. Western blot was performed to assay signaling proteins FAK and Erk1/2 phosphorylation and assess its relation to IGF-1. Anulus fibrosus cells expressed collagen II and aggrecan in vitro that maintained cell characteristic in vivo. FasL can induce anulus fibrosus cells apoptosis. TUNEL staining confirmed increased apoptosis ratio in antibody treated cells. Expression of bcl-2 was decreased by FasL, while expression of Bax was increased. FasL treatment caused FAK, collagen II and aggrecan mRNA expression approximately 2.84, 3.43, 3.91-fold down-regulated when compared to untreated controls. Simultaneous treatment with IGF-1 inhibited the effect of FasL on FAK, collagen II and aggrecan mRNA expression, increased 3.63, 11.32, 2.16-fold after treatment 24 hours. FasL treatment inhibited members of ERK/MAPK pathway, Erk1/2 phosphorylation. But not significant affected FAK phosphorylation. Co-treatment of IGF-1 can activate Erk1/2 (phosphorylation) but not significant activate FAK in short time. These data suggested that IGF-1 through activation Erk1/2 and up-regulated the FAK expression protects anulus fibrosus cells from FasL-induced apoptosis.

Disclosures: Q. Zhou, None.

T118

Dominant X-linked Hypophosphatemic Rickets: A New Mutation of PHEX Gene. L. Masi¹, S. Carbonell Sala¹, A. Gozzini¹, I. Pela², A. Amedei¹, A. Falchetti¹, E. Luzi¹, S. Ottanelli¹, M. L. Brandi¹. ¹Internal Medicine, University of Florence, Florence, Italy, ²Pediatric, University of Florence, Florence, Italy.

Hypophosphatemic rickets is a group of disorders with hypophosphatemia, hyperphosphaturia, normal levels of vitamin D and parathyroid hormone (PTH), bone deformities, osteomalacia/rickets. X-linked hypophosphatemic rickets (XLH) is one of the most common form of the familial hypophosphatemic rickets and in 60-80% of cases bear of mutation in PHEX gene (Xp22.2-p22.1). PHEX encodes for an endopeptidase member M13Zn-metalloproteinase family, involved in the regulation of phosphate homeostasis. PHEX inactivating mutations causes XLH. These mutation enable the accumulation of phosphaturic factors and/or mineralization inhibitors. In the present study we describe a 3 years old female referred to our Center, exhibiting clinical features of a clear hyperphosphaturia, hypophosphatemia, normocalcemia, PTH circulating levels at the upper values of the normal range and normal values for vitamin D. She showed deep asthenia, muscle pain and spasms, bowed legs and cranial deformities. The parents feel well and were not consanguineous. The patient and her parents underwent PHEX mutational analysis upon administration of an informed consent from (in case of minor patient signed by legal tutor). Genomic DNA has been extracted by peripheral blood leukocytes. The 22 exons and the intron-exon boundaries of PHEX have been investigated by PCR and direct-sequencing (ABI-Prism 3100) protocol. It has been identified a hemizygous mutation of PHEX IVS1078+1 position, causing nucleotide change in a splice donor site that may cause an abnormal splicing phenomenon. This nucleotide substitution has been never described on PHEX database (<http://www.phexdb.mcgill.ca/>). Up today, no functional analysis for this mutation has been performed. In the present study a mini-gene analysis is undergoing to evaluate the alternative splicing pattern. Finally, we are planning to use cellular models, either obtained from patients and engineered by transfection methods to evaluate the functionality of the mutated gene. These approaches will be helpful to better understand the molecular mechanism of PHEX action and could provide highlight for future targeted therapies.

Disclosures: L. Masi, None.

T119

Analysis of the Function of the CTCF-binding Site Between the Rxrb and the Col11a2 Genes. J. Murai¹, M. Okamoto¹, H. Yoshikawa¹, N. Tsumaki². ¹Orthopaedic Surgery, Osaka University Graduate School of Medicine, Suita, Japan, ²Bone and Cartilage Biology, Osaka University Graduate School of Medicine, Suita, Japan.

The $\alpha 2(XI)$ collagen chain gene (Col11a2) is specifically expressed in cartilage. The 1st intron sequence of the Col11a2 gene acts as the enhancer that activates expression in cartilage and silencer that inactivates expression in non-cartilaginous tissues. The 5'-end of the Col11a2 gene resides very closely to the 3'-end of the retinoid-X-receptor β gene (Rxrb) which is ubiquitously expressed. We hypothesized the enhancer/silencer blocking elements between these genes. So far, almost all of the characterized enhancer blocking elements identified in vertebrates are bound by the CTCF protein. At the last this annual meeting, we reported the CTCF binding site between the Col11a2 and the Rxrb genes. The purpose of this study is to investigate the function of the CTCF binding site. We prepared three transgene constructs by using the human bacterial artificial chromosome (BAC) DNA clone which is 160 kb in length covering entire COL11A2 and RXRB genes. The wild type (WT) construct was generated by placing the LacZ sequence at the downstream of the RXRB gene promoter in the BAC clone. The mutation construct (Mut) was made by introducing 14 bp-substitution mutation in the CTCF binding site in the WT. The deletion construct (Del) was produced by deleting the 507bp sequence around the CTCF binding site in the WT. We generated transgenic mice bearing these constructs and analyzed LacZ expression patterns by staining the 13.5 d.p.c. founder embryos with X-gal. All of the 4 transgenic mice bearing the WT transgene expressed the LacZ gene in all tissues. This ubiquitous expression pattern of the LacZ was consistent with the expression pattern of the endogenous Rxrb gene. On the other hand, 2 out of 3 transgenic mice bearing the Mut and 2 of 4 mice bearing the Del expressed the LacZ genes specifically in cartilage. Abolition of the CTCF-binding site specifically inhibited expression of the LacZ in non-cartilaginous tissues, suggesting that the CTCF-binding site blocks silencer activities of the Col11a2 regulatory sequences. Next, we established stable transformant clones of rat chondrosarcoma cells bearing the WT, Mut and Del BAC DNA respectively. By the real time RT-PCR, we specifically amplified the human RXRB and COL11A2 mRNA sequences that derived from the transgene. The expression levels of the puromycin resistance gene were used as the internal control. The mean expression levels of the RXRB genes of the Mut and Del clones were significantly higher than that of the WT clones. The abolition of the CTCF-binding site increased expression of the RXRB in chondrosarcoma cells, suggesting that the CTCF-binding site blocks enhancer activities of the Col11a2 in cartilage.

Disclosures: J. Murai, None.

T120

Identification of Hs.43125 as an Articular Chondrocyte-Specific Gene. S. Shin^{*}, J. Chun^{*}. Department of Life Science, Gwangju Institute of Science and Technology, Gwangju, Republic of Korea.

Developmental process of endochondral bones is initiated by chondrogenesis of mesenchymal cells and subsequent hypertrophic maturation. During this developmental process, chondrocytes produce a variety of signaling molecules to coordinately regulate cartilage and bone development. We searched expressed sequence tags (ESTs) cluster library of human normal cartilage in Unigene transcriptome database to identify unrevealed signaling molecules which are produced during limb development. Hs.43125 was identified as a novel cartilage-specific gene and selected for functional characterization. Hs.43125 is composed of four different exons and signal peptide sequence for secretion. When myc-tagged Hs.43125 cDNA was ectopically expressed in primary articular chondrocytes, Hs.43125 encodes a 17 kDa secretory. The molecular weight of secreted Hs.43125 was smaller than cellular protein indicating post-translational modification during secretion. In attempt to examine the role of Hs.43125, expression pattern of Hs.43125 was examined during chondrogenesis of mesenchymal cells and hypertrophic maturing of chondrocytes. Hs.43125 expression was low in mesenchymal cells, increased during chondrogenesis and decreased during hypertrophic maturation of chondrocytes in vitro. In situ hybridization analysis also indicated that Hs.43125 is expressed in proliferating chondrocytes of developing cartilage of mouse embryo at 14.5 day. Our results suggest that Hs.43125 may have a role in chondrogenesis, maintenance of differentiated chondrocyte phenotypes, and/or transition of prehypertrophic chondrocytes to hypertrophic chondrocytes.

Disclosures: S. Shin, None.

T121

Carbonic Anhydrase II Regulates Differentiation and Proliferation of Ameloblast via Intracellular pH-dependent Mechanism. X. Wang¹, T. Suzawa¹, M. Nakamura², B. Zhao¹, R. Yasuhara¹, T. Inoue³, Y. M. Masuda⁴, K. Matsumoto⁴, R. Kamijo¹. ¹Department of Biochemistry, Showa University School of Dentistry, Tokyo, Japan, ²Department of Oral Anatomy, Showa University School of Dentistry, Tokyo, Japan, ³Department of Oral Physiology, Showa University School of Dentistry, Tokyo, Japan, ⁴Department of Clinical Cariology & Endodontology, Showa University School of Dentistry, Tokyo, Japan.

This study aimed to clarify the involvement of carbonic anhydrase II (CAII), a zinc metalloenzyme, on ameloblast differentiation and enamel biomineralization. We identified the expression level of CAII mRNA is strongly up-regulated in differentiated enamel epithelial tissues by means of microarray. Immunohistochemical analysis revealed that CAII was expressed intensively in secretory stage ameloblast in enamel epithelium. In an ameloblast primary culture, the CA enzyme activity measurement showed that activity of CA was increased along with differentiation of ameloblast. RT-PCR indicated that the expression level of amelogenin, a marker for secretory ameloblasts, was enhanced by ethoxzolamide (EZA), a CA inhibitor, as well as by CAII antisense oligonucleotide (CAIIASO). In contrast, expression of EMSP-1, a marker for mature ameloblast, was inhibited by them, suggesting that inhibition of CAII activity could inhibit differentiation of ameloblast. MTS assay also showed they promoted proliferation of ameloblast. Inhibition of ameloblast differentiation by EZA and CAIIASO was confirmed by tooth germ organ culture, since they induced disorderly arrayed ameloblasts with poor polarity. Intracellular pH of ameloblast was labeled with BCECF-AM, and was controlled by the K⁺-nigericin method. EZA and CAIIASO elevated intracellular pH in ameloblast, and an artificial decrease of intracellular pH abolished the effects of CAIIASO on ameloblast. These results suggest the novel role of CAII during amelogenesis, that is, controlling differentiation and proliferation of ameloblast. The results also suggest controlling intracellular pH might be primary mechanism of CAII in ameloblast.

Disclosures: X. Wang, None.

T122

Regulation of Matrix Metalloproteinases Expression by EPAS1 in Articular Chondrocytes. S. Yang^{*}, J. Cho^{*}, J. Chun^{*}. Department of Life Science, Gwangju Institute of Science and Technology, Gwangju, Republic of Korea.

We identified and selected for functional characterization of endothelial PAS domain protein 1 (EPAS1), also referred as a hypoxia-inducible factor 2 α , by screening transcriptome database for expressed sequence tags (ESTs) using osteoarthritic cartilage library in unigene. Because EPAS1 plays essential roles in hypoxia and many pathogenic conditions, this study examined a role of EPAS1 in articular chondrocytes. EPAS1 expression was significantly increased in human osteoarthritic cartilage compared with normal cartilage. In primary culture articular chondrocytes, EPAS1 expression was significantly increased during dedifferentiation of chondrocytes caused by interleukin-1 β , epidermal growth factor (EGF), retinoic acid (RA), or serial subculture as monolayer. Dedifferentiation of chondrocyte accompanies induction of several matrix metalloproteinases (MMPs) such as MMP-1, -3, -9, -12, and -13, without effects on MMP-2, -14, and -15 expressions. Upregulation of EPAS1 during dedifferentiation of chondrocyte occurs prior to MMP expression. We, therefore, examined whether EPAS1 mediates upregulation of MMPs. Overexpression of EPAS1 by adenovirus-EPAS1 (Ad-

EPAS1) induced MMP-1, -3, -9, and -13 expressions, whereas expression patterns of MMP2-, -14, and -15 were not changed. Knockdown of EPAS1 by siRNA blocked IL-1 β -induced expression of MMP-3, -9, and -13. Our results suggest that EPAS1 may play a role in cartilage destruction by modulating MMP expression.

Disclosures: S. Yang, None.

T123

Identification and Characterization of MicroRNAs Expressed During Chondrogenesis of Mesenchymal Cells. S. Yu, J. Chun*. Life Science, GIST, Gwangju, Republic of Korea.

microRNAs (miRNAs) play important roles in regulating the expression of specific mRNAs at both transcriptional and posttranscriptional levels. In attempt to understand more information in on-off of mRNA expression during chondrogenesis, we investigated miRNAs expressed in chondrifying mesenchymal cells derived from mouse embryo limb buds. We identified three new miRNAs from chondrifying mesenchymal cell. Among the identified miRNAs, expression of miRNA 542-3t was decreased during chondrogenesis of mesenchymal cells, and its expression was specifically detected in developing cartilage tissue. By computational analyses, 6130401L20Rik was identified as a potential target gene of miRNA 542-3t. Consistent with the expression pattern of miRNA 542-3t, a target gene expression was increased during chondrogenesis, and its expression was detected in developing cartilage. Our results suggest specific that miRNA 542-3t may regulate transcription of mRNAs such as 6130401L20Rik during mammalian limb development.

Disclosures: S. Yu, None.

T124

Effect of Estrogen Deficiency on Gene Expression Pattern in the Bone Tissue of Postmenopausal Versus Premenopausal Healthy Women. B. Balla*¹, J. Kósa*¹, J. Kiss*², A. Borsy*³, J. Podani*⁴, I. Takács¹, Á. Lazáry¹, Z. Nagy¹, K. Bácsi*¹, G. Speer*¹, L. Orosz*³, P. Lakatos¹. ¹1st Department of Internal Medicine, Semmelweis University, Budapest, Hungary, ²Department of Orthopedics, Semmelweis University, Budapest, Hungary, ³Institute of Genetics, Agricultural Biotechnology Center, Gödöllő, Hungary, ⁴Department of Plant Taxonomy and Ecology, Eötvös Loránd University, Budapest, Hungary.

Estrogen deficiency at the time of menopause results in marked increase in bone resorption and formation leading to rapid bone loss. The aim of our investigation was to determine genes characterized by significantly changed mRNA expression rates in postmenopausal vs. premenopausal healthy bone tissue and describe the interrelationship among these genes using multidimensional data analysis. Ten bone tissue samples from postmenopausal non-osteoporotic female patients (mean age: 53.50 \pm 4.12 years, T-score > -1 SD) and seven bone tissue samples from premenopausal healthy women (mean age: 52.14 \pm 2.34 years, T-score > -1 SD) were examined in our study. Messenger RNA was prepared from each sample and reverse transcribed to cDNA. The expression differences of selected 118 genes were analyzed by TaqMan Gene Expression Assay in Real-Time PCR system. Statistical methods were performed using Mann-Whitney U test, canonical variates analysis and principal components analysis (PCA). Mann-Whitney U test indicated significant differences in the expression of 29 genes between post- and premenopausal healthy individuals ($p \leq 0.05$). Twenty eight genes, including extracellular matrix molecules and digesting enzymes (COL2A1, COL3A1, COL5A1, COL5A2, COL9A1, COL12A1, COL15A1, MGP, BGLAP, FN1, MMP13, BMP1), TGF-beta/BMP pathway (BMP1A, TGF2, TGF3, TGFBR2, SMAD4), transcription factors (RUNX2, SP7, TCF7L2, SOX9), growth factors (PDGFA, FGFR1) and other candidate genes (TNFSF11, IL6, ALPL, IGSF4, TRIB2) were significantly upregulated in postmenopausal women compared to premenopausal ones. Only one gene (ENO1) showed downregulation in the bone tissue after menopause. Applying canonical variates analysis the groups of post- and premenopausal patients are separable by 12 genes coding extracellular matrix molecules which have the best discriminatory power. Based on the multiple mRNA expression profiles of 118 genes, post- and premenopausal states could be differentiated by enhanced postmenopausal gene expression rate using PCA. Significant differences observed in gene expression profiles of estrogen deficient human bone tissue provide further insight into the process of postmenopausal changes of bone metabolism. The menopausal states of bone tissue have been unambiguously defined by their complex gene transcription patterns.

Disclosures: B. Balla, None.

This study received funding from: NKFP-1A/007/2004, NKFP-1A/002/2004, ETT 022/2006.

T125

Novel Transcription Factor-like Function of MMP-3/stromelysin-1 that Regulates Connective Tissue Growth Factor (CTGF/CN2) Gene Transcription. T. Eguchi¹, S. Kubota*¹, K. Kawata*¹, Y. Mukudai*¹, T. Yanagita*¹, T. Ohgawara*¹, J. Uehara*², S. Ibaragi*³, M. Takigawa¹. ¹Dept. of Biochemistry and Molecular Dentistry, Graduate School of Medicine, Dentistry and Pharmaceutical Sciences, Okayama University, Okayama, Japan, ²Dept. of Oral & Maxillofacial Rehabilitation, Graduate School of Medicine, Dentistry and Pharmaceutical Sciences, Okayama University, Okayama, Japan, ³Dept. of Oral & Maxillofacial Surgery, Graduate School of Medicine, Dentistry and Pharmaceutical Sciences, Okayama University, Okayama, Japan.

Connective tissue growth factor (CTGF/CN2) is the second member of CCN protein family and a multifunctional growth factor involved in the development and remodeling of matrix-rich tissues such as cartilage and bone. For example, we have shown that CCN2 promotes endochondral ossification by acting on chondrocytes, osteoblasts and endothelial cells. Its expression is extremely high in chondrocytes especially in hypertrophic chondrocytes. Enhanced production of CCN2 in HCS-2/8 human-derived chondrocytic cells is found to be mediated by the TRENDIC (transcription enhancer dominant in chondrocytes). Matrix metalloproteinases (MMPs) are zinc-dependent endopeptidase also involved in the development and remodeling of cartilage and bone. Here, we report that human MMP3/stromelysin-1 in the nucleus binds to the TRENDIC, and displays a transcription factor-like function. The MMP3 was detected in the nuclear extract of the HCS-2/8 cells in vitro, and also in the nucleus of the normal and osteoarthritic chondrocytes in vivo. Externally added recombinant human MMP3 was internalized into the HCS-2/8 cells and translocated to the nucleus. Also, six putative nuclear localization signals were found in MMP3 and were capable of trans-locating the fused green fluorescent protein to the nucleus. MMP3 interacted with enhancer sequences including TRENDIC in the CCN2 promoter. MMP3 overexpression resulted in activating the CCN2 promoter; whereas, a TRENDIC-mutant of the promoter lost the response. Knocking-down of MMP3 also suppressed CCN2 expression. Notably, an MMP3 inhibitor specifically suppressed the CCN2 promoter activity in the cells. Furthermore, we identified several nuclear MMP3 associated proteins (NuMAPs) in the cells. These finding indicates that MMP3 has dual functions. One is as an extracellular matrix-degrading activity. The other is novel transcription factor-like function for CCN2/CTGF, which results in production of ECM. This extra- and intra-cellular, dual function of MMP3 may play an important role in development and matrix remodeling of cartilage and bone.

Disclosures: T. Eguchi, None.

This study received funding from: MEXT, JSPS.

T126

Epigenetic Status Monitored by DNA Methylation in the 5'-flanking Regions of CpG-rich Promoters Are Stable During Chondrogenesis in Pellet Cultures of Pluripotent Human Mesenchymal Progenitor Cells. Y. Ezura¹, I. Sekiya*², T. Muneta*³, M. Noda¹. ¹Department of Molecular Pharmacology, Medical Research Institute, Tokyo Medical and Dental University, Tokyo, Japan, ²Section of Cartilage Regeneration, Graduate School, Tokyo Medical and Dental University, Tokyo, Japan, ³Section of Orthopedic Surgery, Graduate School, Tokyo Medical and Dental University, Tokyo, Japan.

Developmental skeletogenesis requires multistep cellular events, including progenitor cell recruitment, proliferation, differentiation and multiple interactions of different types of cells. The entire actions of the processes are believed to be programmed in the genomic sequence of the cells; however investigations indicating the additional involvement of "epigenetic" regulation also exist. Here, to investigate the possible involvement of "epigenetic" controls of gene expression during skeletogenesis, we analyzed DNA methylation of CpG-rich promoters for several genes, using genomic DNA samples obtained from the experimental chondrogenesis assay of mesenchymal progenitor cells derived from human synovial tissues. Chondrogenic pellet-cultures were performed according to a standard protocol using rhBMP2 and TGF beta in the medium, and genomic DNA was isolated before and after 3 weeks of pellet-culture. This resulted in highly differentiated chondrocytes producing large amount of cartilage matrix. Candidate genes for the epigenetic control were selected by analysis of expression profiling data accomplished by Affymetrix DNA microarray. By searching dramatically upregulated or downregulated genes during the chondrogenesis, 40 genes were chosen. Among them, genes having extreme CpG-rich promoter were examined at first, for the extent of DNA methylation using bisulfite DNA sequencing method. Consistent with previous studies, most of the CpG-rich promoters were hypomethylated in the progenitor cells before pellet-culture, even for the genes completely silenced before differentiation. We observed stable, similar level of methylation after 3 weeks of pellet-culture in most case. In contrast, we detected highly methylated CpG sites in the promoter region of moderate CpG content, like matrilin-4 gene promoter that is transcriptionally repressed before differentiation; however, the methylation levels were similar even after the induction of chondrogenesis despite apparently detectable levels of the expression. We concluded regarding the genes examined in this study that epigenetic status such as DNA methylation would stably exist during chondrogenic differentiation at least in the context of pellet cultures of the human mesenchymal progenitor cells.

Disclosures: Y. Ezura, None.

T127

Bone Remodeling after Achievement of Osseointegration by Titanium Implantation in Rat Maxillae. M. Haga^{*1}, N. Fujii^{*2}, K. Nozawa-Inoue^{*3}, K. Uoshima^{*2}, S. Nomura^{*1}, T. Maeda^{*3}. ¹Div. of Oral Health in Aging and Fixed Prosthodont., Niigata Univ. Grad. Sch. of Med. & Dent. Sci., Niigata, Japan, ²General Dentistry and Clinical Education Unit, Niigata Univ., Niigata, Japan, ³Div. of Oral Anat., Niigata Univ. Grad. Sch. of Med. & Dent. Sci., Niigata, Japan.

Osseointegration is regarded as the most appropriate bone-implant interface as it affords a favorable prognosis over an extended period. Previous reports have indicated the existence of pre-existing bone with empty osteocytic lacunae even after achievement of osseointegration. However, little information is available regarding the fate of this injured bone. It is also unclear whether bone remodeling takes place around the implant. The present study was therefore undertaken to examine the response of the surrounding bone around a titanium implant on an animal model using rat maxillae.

Following extraction of the upper first molars of male Wistar rats (4-week-old; n=80), pure titanium implants were installed in the prepared bone cavities by drilling at 1 month after tooth extraction. Under deep anesthesia, the animals were sacrificed at 1 to 12 months after implantation. Decalcified paraffin sections were processed for double staining with alkaline phosphatase (ALP) and tartrate-resistant acid phosphatase (TRAP). For histologic observations, some sections were stained with hematoxylin and eosin (H-E), or Azan. An additional 14 rats were injected with calcein for dynamic labeling of bone formation at 5 and 20 days before sacrifice. Undecalcified sections were prepared in a cryostat with a tungsten knife.

The present animal model achieved osseointegration between the implants and alveolar bone by 1 month post-implantation, but the injured bone with empty osteocytic lacunae remained in the pre-existing bone. Surface analyses showed that the pre-existing bone with empty osteocytic lacunae decreased gradually to disappear completely at 3 months after implantation. Many ALP-positive osteoblasts and TRAP-reactive osteoclasts localized on the surface of the bone along the implant at 1 month post-implantation and remained until 6 months after implantation. The newly-formed bone around the implants thickened and exhibited the same histological features as compact bone at 3 months. Two calcein-labeled lines were recognizable in the newly-formed bone around implants throughout this observation period.

These morphological data suggest the involvement of bone remodeling in replacing newly-formed immature woven bone and injured pre-existing bone with compact bone around titanium implants.

Disclosures: M. Haga, None.

T128

The Increase of the Mechanical Strength of Novel Unidirectional Porous Hydroxyapatite Ceramics In Vivo. M. Iwasashi¹, M. Sakane¹, Y. Shirai^{*2}, Y. Suetsugu^{*2}, T. Tateishi^{*2}, N. Ochiai^{*1}. ¹Graduate School of Comprehensive Human Sciences, University of Tsukuba, Tsukuba, Japan, ²Biomaterials Center, National Institute for Materials Science, Tsukuba, Japan.

Background While the porous Hydroxyapatite (HAp) ceramic has interconnection between the pores, a few osteogenesis occur at the deep area of the HAp material. We have recently developed a unidirectional pores HAp ceramic, which have continuous interconnection through the material.

Purposes The purposes of this study were to observe osteoconductivity of the novel HAp ceramic, and to evaluate the increase of mechanical strength after implantation in the femur of rabbit.

Materials and Methods: Materials for this study were provided by KURARAY CO., LTD. (Kurashiki, Japan).

Animal experiments were carried out in our university and governmental guidelines for proper conduct of animal experiment. Japanese white rabbits were used in this study. Under intravenous injection of thiopental, the knee joint was exposed. Intramedullary, a tunnel was made with drilling of the femur, the cylindrical unidirectional porous HAp (6mm in diameter, 7mm in height) were implanted in the femur. The direction of the interconnected pore is parallel to the axis of the femur. Two, six and twelve weeks after implantation, the femurs were harvested and the 4×4×5mm HAp samples were cut down. The compression strength was measured using a uniaxial mechanical testing apparatus with speed of 0.5mm/s. The same size samples before implantation were measured as a control. For statistical analysis, Tukey-Kramer test were used and P<0.05 was considered statistically significant. Some of the femurs were used for histological evaluation.

Results: The compression strength of samples before implantation was 13.8±1.4MPa, and that of samples at two, six, and twelve weeks was 10.9±3.9, 21.6±9.2, 47.0±12.7MPa. The compression strength at six and twelve weeks increased significantly. Histologically, new bone and osteogenic cells were observed inside of the HAp after two weeks.

Discussion: The microstructure of unidirectional porous HAp is oval pores 100 ~ 300µm in diameter penetrate through the material. The structure is advantageous not only about compression strength but also migration for osteogenic and angiogenic cells inside of the HAp, and contributed to excellent new bone formation at two weeks. The shape of new bone is columns because osteogenesis occurred along the inner wall of the HAp. Beside, early angiogenesis promote bone remodeling. Hence, the mechanical strength at twelve weeks gained 3.4 times as much as before implantation.

Conclusion: Unidirectional porous HAp has excellent osteoconductivity and increase of mechanical strength with time in vivo.

Disclosures: M. Iwasashi, Materials were provided by Kuraray Co., Ltd. (Kurashiki, Japan) 9.

T129

Identification of Calcyclin Expression in Rat Amelogenesis Using Acp Ddrt-pcr Method. Y. Kawano^{*}, S. Kinoshita-kawano^{*}, K. Nozawa-inoue^{*}, A. Suzuki^{*}, T. Maeda^{*}. Niigata University Graduate School of Medical and Dental Sciences, Niigata, Japan.

Ameloblasts are involved in enamel secretion and mineralization. Unmineralized enamel is secreted by secretory ameloblasts and subsequently mineralized by maturation stage ameloblasts. The transformation from secretory into maturation stage ameloblasts during amelogenesis is presumed to be accompanied by changes in gene expression in each cell type. The goal of this study was to identify the genes expressed specifically in ameloblasts that might be involved in ameloblast differentiation, enamel formation or maturation.

Annealing controlled primers (ACP) differential display PCR screening was performed to compare RNA isolated from secretory ameloblasts with those from maturation stage ameloblasts. Using 120 different combinations of primers, we identified and cloned 36 distinct differential display fragments with sizes ranging from 250 to 1000 bp. Seventeen of 39 differentially expressed genes (DEGs) were sequenced and identified. Seven DEGs have significant sequence similarities to already published genes whose functions in the rat incisor are known. The rest is homologous to genes expressed in other tissues, but is not known to be expressed in the incisor. One of the DEGs showed 100% homology to calcyclin (S100A6).

Calcyclin belongs to a family of S100A calcium binding proteins that bind calcium molecules through conserved EF-hand domains. Recently a wide variety of cellular functions has been attributed to the products of this gene family. In particular, calcyclin has been implicated in intracellular calcium homeostasis and signaling, ion transport, and cell proliferation. Quantitative RT-PCR confirmed that calcyclin has specific expression patterns in differentiating ameloblasts during odontogenesis. Calcyclin mRNA was less expressed in secretory stage, but highly in both early and late maturation stages in rat incisor. Immunohistochemistry also showed that calcyclin proteins are expressed in maturation stage of ameloblasts, but not in papillary layer cells. Furthermore, odontoblasts and cementoblasts showed immunopositive reaction for calcyclin, while osteoblasts on alveolar bone were devoid of immunoreaction.

Using ACP, we found 39 DEGs in secretory and maturation stage ameloblasts. Calcyclin was identified to be 100% homologous to one of the DEGs. We confirmed the existence of calcyclin in the differentiating ameloblasts using qRT-PCR and demonstrated its expression in ameloblasts, odontoblasts and cementoblasts by immunohistochemistry. Our findings suggest a role for calcyclin in amelogenesis, especially in enamel maturation, dentinogenesis, and cementogenesis.

Disclosures: Y. Kawano, None.

T130

The Effects of Heme Oxygenase-1 on Collagen Induced Arthritis Model. H. Kim^{*1}, M. Lee^{*2}, J. Oh^{*3}, J. Kim^{*4}, K. Yun^{*1}. ¹Pathology, Wonkwang University Hospital, Iksan Cholla-bukdo, Republic of Korea, ²Rheumatology, Wonkwang University Hospital, Iksan Cholla-bukdo, Republic of Korea, ³Anatomy, Wonkwang University School of Medicine, Iksan Cholla-bukdo, Republic of Korea, ⁴Orthopaedic Surgery, Wonkwang University Hospital, Iksan Cholla-bukdo, Republic of Korea.

Introduction: Heme oxygenase-1 (HO-1), an inducible heme-degrading enzyme, is expressed by macrophages and endothelial cells in response to various stress. It is also an important mediator of inflammation.

Purpose: To determine the effects of HO-1 modulation on the collagen-induced arthritis (CIA) model and observe the VEGF expression in human synovial fibroblast

Method: DBA/1J mice were treated with an inhibitor of HO-1, tin protoporphyrin IX (SnPP), or with an inducer of HO-1, cobalt protoporphyrin IX (CoPP), from day 1 to day 35 after CIA induction. The clinical evolution of disease was visually monitored. At the end of the experiment, joints were examined for histopathologic changes. VEGF expression in paws were measured by immunohistochemical stain. mRNA expression of VEGF stimulated with TNF- α , CoPP and SnPP, accessed in human synovial fibroblast by RT-PCR

Results: Administration of cobalt protoporphyrin IX significantly induced the inflammatory response, with increased arthritis index and expression of VEGF in paw of arthritis models. Treatment with SnPP significantly reduced the severity of CIA, with inhibition of joint inflammation and cartilage destruction. The expression of VEGF were also significantly reduced by SnPP treatment in paw. CoPPIX as inducer of HO-1, increased VEGF expression dose dependently in synovial fibroblast. In contrast, inhibition of HO-1 activity by SnPPIX reversed CoPPIX-induced VEGF production.

Conclusion: The effects of HO-1 induction in rheumatoid arthritis result in aggravation of arthritis via up-regulation of VEGF. We concluded that inhibition of HO-1 could be a therapeutic target of rheumatoid arthritis

Disclosures: H. Kim, None.

This study received funding from: Wonkwang University grant 2004.

T131

Loss of Annexin VI Affects Endochondral Bone Formation. H. Kim¹, S. E. Moss², T. Kirsch¹. ¹Orthopaedics, University of Maryland School of Medicine, Baltimore, MD, USA, ²Division of Cell Biology, University College London, London, United Kingdom.

Annexin VI is a Ca^{2+} and membrane-binding protein, which is involved in a various cell functions. We have shown that annexin VI is expressed by hypertrophic growth plate chondrocytes and osteoblasts together with other annexins, including annexin II and V. These annexins control Ca^{2+} homeostasis in growth plate chondrocytes and matrix vesicles thereby regulating terminal differentiation and mineralization events (Kirsch 2005 Front Biosci 10:576-581). To determine the exact function of annexin VI in skeletal tissues, we analyzed long bones of annexin VI^{-/-} mice histomorphometrically and analyzed the function of matrix vesicles isolated from long bones of 5 months old mice. Matrix vesicles are released by mineralization-competent growth plate chondrocytes and osteoblasts and these particles initiate the mineralization process. We have shown that annexins II, V and VI have the critical role of mediating influx of Ca^{2+} into the vesicles enabling the formation of the first mineral phase inside the vesicles. Newborn annexin VI^{-/-} mice were ~20% shorter and lighter than wild type littermates. Histomorphometric analysis of the femoral and tibial growth plates of these animals revealed that the lengths of the growth plates (proliferative and hypertrophic zones) were reduced by ~40% in the annexin VI^{-/-} mice compared to the lengths of the growth plates of wild type littermates. The length of the proliferative zone of the annexin VI^{-/-} mice is similar to the length of the proliferative zone of the wild type littermates. However, the length of the hypertrophic zone is markedly reduced in the growth plates of the annexin VI^{-/-} mice. At 4 weeks of age the length of the growth plate in the annexin VI^{-/-} mice was enlarged compared to the length of the growth plates of the wild type littermates, suggesting that endochondral bone formation is delayed in annexin VI^{-/-} mice. At 10 weeks of age the annexin VI^{-/-} mice showed reduced bone volume compared to the bone volume of the wild type littermates. Matrix vesicles isolated from long bones of annexin VI^{-/-} mice contained more annexin II and annexin V than the amount of these annexins in matrix vesicles isolated from wild type littermates. However, vesicles isolated from annexin VI^{-/-} mice contained less Ca^{2+} and P_i than the amount of these mineral ions in vesicles isolated from wild type littermates. In addition, matrix vesicles isolated from annexin VI^{-/-} mice were not able to mineralize in vitro. These findings reveal that annexin VI plays an important regulatory role in terminal differentiation and mineralization events of growth plate chondrocytes and osteoblasts and a loss of annexin VI results in delayed endochondral bone formation and bone loss in older annexin VI^{-/-} mice.

Disclosures: H. Kim, None.

This study received funding from: National Institutes of Health.

T132

PHD1 and PHD3 Are Expressed in Bone Cells but Are Not Essential for Bone Homeostasis. K. Laperre¹, N. Smets¹, R. Bouillon¹, P. Carmeliet², G. Carmeliet¹. ¹Laboratory of Experimental Medicine and Endocrinology, Katholieke Universiteit Leuven, Leuven, Belgium, ²Center for Transgene Technology and Gene Therapy, VIB, Katholieke Universiteit Leuven, Leuven, Belgium.

Hypoxia induces vascular endothelial growth factor (VEGF) expression, an essential factor for angiogenesis. Signalling occurs via stabilization of hypoxia inducible factor (HIF α) that binds to its response element in the VEGF promoter. During normoxia HIF α activity is inhibited by prolyl hydroxylase domain containing proteins (PHD1, PHD2 and PHD3) targeting HIF α for proteasome mediated degradation. Both the 3 VEGF isoforms and HIF α are essential for bone development by affecting angiogenesis and/or bone cell function. The role of PHDs in bone biology is however not yet elucidated.

In this study, we report that PHDs are expressed in primary murine osteoblast, osteoclast and chondrocyte cell cultures as analysed by quantitative PCR. Abundant mRNA levels were observed for PHD1, less expression was detected for PHD2 whereas PHD3 mRNA levels were very low. Exposure of these cultures to hypoxia for 24 hours resulted in a 3 to 4 fold induction of VEGF mRNA expression in all cell types ($p < 0.001$). In addition, PHD2 and mainly PHD3 mRNA levels were highly induced in the 3 cell types ($p < 0.0001$) whereas PHD1 mRNA expression was not affected by hypoxia.

The role of PHD1 and PHD3 in bone homeostasis was investigated by analyzing the bone phenotype of PHD1 and PHD3 knock out (KO) mice. PHD2 KO mice are early embryonic lethal precluding investigation. PHD1 and PHD3 KO mice are viable and show a normal growth curve. Bone modeling and remodeling were investigated in respectively 4 and 14 week old mice. Femur length was not different between PHD1 and PHD3 KO and their respective wild type (WT) littermates. Trabecular parameters of isolated femurs were analysed by peripheral quantitative computed tomography (pQCT). Trabecular density and content were not different between the genotypes. Histomorphometry on Von Kossa stained sections of PHD3 KO and WT mice confirmed these data. In addition, serum osteocalcin levels also revealed no difference between PHD1 and PHD3 KO mice and their respective WT littermates. A possible explanation for the normal bone phenotype is compensation by the other PHDs. Osteoclasts and chondrocytes lacking PHD1 showed an increased expression of PHD2 and PHD3. This compensatory increase was also observed in PHD3 deficient osteoclasts.

In conclusion, the 3 PHDs are expressed in the major bone cell types but lack of PHD1 or PHD3 has no major impact on bone modeling and remodelling.

Disclosures: K. Laperre, None.

T133

The New Surface Modified Demineralized Bone Matrix by rhBMP-2-collagen Hybrid Coating. K. Lee¹, Y. Shim², J. Jang², H. Kim³, Y. Choi², K. Lee², B. Ko², M. Ryu², I. Kim², S. Moon³, H. Lee³. ¹Medical school, Yonsei University, Seoul, Republic of Korea, ²Korea Bone Bank Co., Ltd., Seoul, Republic of Korea, ³Medical School, Yonsei University, Seoul, Republic of Korea.

The use of bone grafts is increasing considerably in orthopaedics and dental practice. Also demineralized bone matrix (DBM) is inherently osteoinductive and it has potential appeal as a bone graft substitute. DBM directly induces new bone formation when implanted subcutaneously or intramuscularly. Allogeneic DBM has intrinsic shortcomings related to procuring, processing and characterizing bone from a human donor pool. Xenogeneic bone represents an unlimited supply of available material if it can be processed to render it safe for transplantation to the human host. Processed xenogeneic DBM still appear a promising alternative to autografts and allografts although several such graft materials were found to be unsatisfactory because of poor histocompatibility which apparently stemmed from the difficulties in manufacturing such a complex material. However, there is lack of consensus about whether DBM from one species can facilitate osteoinduction in a different species, even among lower-order animals. To improve the property of xenogeneic DBM, we modified the surface of DBM by rhBMP-2-collagen hybrid coating. In vitro test, surface modified xenogeneic DBM and human mesenchymal stem cell were cocultured by alginate bead culture. And In vivo test, DBM was implanted in fibular fractured Newzealand white rabbit

Disclosures: K. Lee, Korea Bone Bank Co., Ltd. 3.

This study received funding from: Korea Bone Bank Co., Ltd.

T134

Validation of a Simple Isotope Method for Estimating True Calcium Fractional Absorption in Adolescent Girls. W. Lee¹, G. P. McCabe², M. E. Wastney³, B. R. Martin⁴, C. M. Weaver⁴. ¹Agricultural and Biological Engineering, Purdue University, West Lafayette, IN, USA, ²Statistics, Purdue University, West Lafayette, IN, USA, ³Metabolic Modeling Services, Blenheim, New Zealand, ⁴Foods and Nutrition, Purdue University, West Lafayette, IN, USA.

A 5-hr serum oral isotope method has been validated against a classic double isotope or ratio method for assessing calcium absorption in adults (Heaney and Recker Ann Intern Med 103:516, 1985). A simple approach for calculating absorption has not been developed in children. Our goal was to develop an equation to predict absorption using a single serum measurement of specific activity (SA, expressed as the fraction of dose of single oral tracer per gram calcium) and physiological factors and to also identify the best time points to measure SA. Subjects were 45 adolescent girls aged from 10 to 15 yr participating in metabolic studies. Tracer data following oral (^{44}Ca) and intravenous (^{45}Ca) administration of calcium stable isotopes and SA in serum and urine from various time points up to 4 d were used. Absorption was calculated as the ratio of oral to IV tracer in 24-hr urine. In addition to SA, physiological factors (postmenarcheal age and height) were used as predictors in multiple regression analysis. The 4-hr serum SA showed the highest R^2 value with the 24-hr urine ratio. Measured serum SA values between 2.5 and 12 hr can be used with the same equation to predict the 24-hr urine ratio but with lower precision. A similar approach was used to develop equations for urine sampling following oral stable calcium isotope administration. We conclude that the developed equations can be used with a single blood draw or urine collection to evaluate calcium absorption in adolescents.

Disclosures: W. Lee, None.

T135

Does Increased Local Bone Resorption Result in Increased Cartilage Degradation? D. J. Leeming¹, I. Byrjalsen¹, M. G. Sørensen¹, M. Koizumi², P. Qvist¹, M. Fregerlev³, N. Lynnerup³, C. Christiansen¹, M. A. Karsdal¹. ¹Nordic Bioscience, Herlev, Denmark, ²Cancer Institute Hospital, Tokyo, Japan, ³Institute of Forensic Science, University of Copenhagen, Copenhagen, Denmark.

An association between bone and cartilage degradation in osteoporotic and arthritic patients has previously been reported. Breast and prostate cancer patients often develop lesions of locally high bone turnover, when the primary tumor metastasizes to the bone. The objective of the present study was to determine whether increased bone turnover is associated with an increase in cartilage degradation in an aggressive bone disease such as metastatic cancer.

The study population included 132 cancer patients; 90 breast cancer (45 with bone metastasis (BM)) and 42 prostate cancer (17 with BM). Presence of BM was determined by Tc99 scintigraphy and the skeletal involvement was graded according to the Soloway score 1-4. Urine samples were obtained and bone resorption assessed by CrossLaps ELISA (CTX-I), and cartilage degradation by CartiLaps ELISA (CTX-II). Human cortical bones were collected during autopsies and bone slices were prepared. Human osteoclasts were made by isolated of CD14+ monocytes from human peripheral blood, followed by culturing in the presence of 25ng/ml of M-CSF and RANKL in 2% serum for 28 days. Osteoclastic resorption was investigated by CTXI and CTXII in the conditioned medium. Additionally, bone slices were decalcified using EDTA and treated by cathepsin K in-vitro and markers assessed.

Patients with bone metastases revealed significant increased levels of CTXI at all Soloway scores (p<0.001). In contrast CTXII was not elevated until at Soloway score 3 (p<0.01). The ratio CTXI/CTXII decreased at all Soloway scores (score 1-2: p<0.01; score 3-4: p<0.001). The percentage increase in CTXI was 70 and 903% at score 1 and 4, respectively. CTXII was elevated by 99% at score 3; by 128% at score 4. Human osteoclastic bone resorption on human bone resulted in release of CTXI fragments but not CTXII fragments. In alignment, cathepsin K treatment of human bone released CTXI, but not CTXII fragments. Treatment of cartilage did not result in CTXI or CTXII release. Human osteoclasts and cathepsin K were able to release CTXII fragments from human bone. Cartilage degradation was not elevated at high bone resorption levels until the late stage in the pathology of the cancer invasion involving more than 6 skeletal lesions (score 3). This dissociation of localised bone resorption and cartilage degradation in early stages of cancer patients with bone metastases suggests that other metabolic pathways are responsible for the association of bone resorption and cartilage degradation as is seen in osteoporosis and osteoarthritis

Disclosures: D.J. Leeming, Nordic Bioscience 3.

T136

Biosynthesis of Menaquinone-4 (Vitamin K2) from Phylloquinone (Vitamin K1) and Menadione (Vitamin K3) in Bone. K. Nakagawa*, Y. Shimomura*, Y. Suhara*, T. Okano. Department of Hygienic Sciences, Kobe Pharmaceutical University, Kobe, Japan.

Vitamin K is essential for the modification of glutamic acid residues of specific substrate proteins into γ -carboxyglutamic acid (Gla) residues. In bone, osteocalcin, which has three Gla residues, is thought to be involved in the regulation of mineralization. Vitamin K compounds share a common chemical structure consisting of a naphthoquinone nucleus capable of redox cycling. Vitamin K₁ (phylloquinone; PK) has a long phytyl side-chain, whereas vitamin K₂ has an unsaturated side-chain containing 1-13 isoprene unit. Menaquinone-4 (MK-4), vitamin K₂, possesses a significant pharmacological activity on bone formation and is used as a medication for osteoporosis in Japan. The daily dietary intake of vitamin K is mainly (>90%) in the form of PK. MK-4 may be present in low levels in food products. However, MK-4 is found in most tissues. In general, tissue concentrations of MK-4 exceed those of PK except for liver, where relatively low MK-4 levels are found. Therefore, it has been recognized that PK is converted into MK-4 and accumulates in extrahepatic tissues including bone. Menadione (K₃), commonly added to animal diets, is converted into MK-4 when administered to animals. However, the conclusive scientific evidence for the conversion of PK into MK-4 is exiguous. To elucidate the conversion of PK and K₃ into MK-4, we synthesized deuterium-labeled PK, MK-4 and K₃. PK or K₃ with a deuterium-labeled 2-methyl-1,4-naphthoquinone ring was given orally to mice and bone were collected for LC-APCI-MS/MS analyses. Deuterium labeled-PK (PK-d₇) and deuterium labeled-K₃ (K₃-d₈) administration resulted in the accumulation of MK-4-d₇ in tissues, particularly in liver, brain and bone. This is the first direct evidence using deuterium labeled compounds and LC-APCI-MS/MS analysis that PK and K₃ are converted into MK-4 in bone. Moreover, administration of the anticoagulant warfarin, an inhibitor of vitamin K reductase in vitamin K cycle, significantly blocked the conversion of PK-d₇ and K₃-d₈ to MK-4-d₇ in bone. Interestingly, MK-4 epoxide, an oxidized form of hydroxymenaquinone-4 (a reduced form of MK-4) generated by γ -glutamyl carboxylase during the turn-over of the vitamin K cycle, was found at higher concentrations than PK epoxide. This result suggests that in bone, MK-4 is rapidly and remarkably metabolized to the epoxide form via a hydroquinone form. Our results indicate that MK-4 is the true physiologically active form for bone formation and that it is derived from dietary vitamin K.

Disclosures: K. Nakagawa, None.

T137

Plasminogen Activator Inhibitor-1 Increases Femoral Mineralization Independent of Estrogen Status Through Modulation of Fibronectin Matrix. S. M. Nordstrom, J. W. Covington*, D. E. Vaughan*. Pharmacology, Vanderbilt University, Nashville, TN, USA.

Plasminogen activator inhibitor-1 (PAI-1) is a recognized regulator of matrix remodeling in cardiovascular, renal, and tumor biology, while its role in bone matrix is less well characterized. Previously, we reported a gender-specific and age-dependent increase in femoral strength and mineralization in mice that over-express human PAI-1 (PAI-1.stab). In this study, we investigated the female-specificity of this phenotype and the mechanism by which PAI-1 influences bone remodeling. PAI-1.stab and WT females were ovariectomized (OVX) or SHAM-operated (SHAM) at 16 weeks (n=11-12). Total skeletal (tBMD) and vertebral bone mineral density (vBMD) were measured by DEXA at baseline and at 2-week intervals for 12 weeks. Serum osteocalcin and TRACP5b were determined by EIA. Femora were analyzed for trabecular bone histomorphometry. Primary adherent bone marrow cells were evaluated for fibronectin (Fn) matrix deposition by immunocytochemistry while Fn transcription was determined by real-time RTPCR in primary calvarial osteoblasts. PAI-1.stab mice had increased tBMD (p=0.0014) and a differential pattern of remodeling (p=0.0166) from 16-28 weeks of age under basal conditions (SHAM). This phenotype was maintained in the setting of estrogen-deficiency. PAI-1.stab mice exhibited a trend towards increased vBMD with a significant difference in the remodeling pattern (p=0.0022). Genotype did not influence trabecular architecture of SHAM or OVX femora. However, PAI-1.stab mice had significantly reduced osteoid surface and a 1.7-fold greater mineral apposition rate under both SHAM and OVX conditions (p<0.001). Serum osteocalcin was comparable between genotypes in SHAM and OVX, while TRACP5b levels were decreased in PAI-1.stab OVX mice (p<0.001). PAI-1.stab primary adherent bone marrow cells exhibited increased Fn matrix formation from 2-14 days in culture (p<0.0001) and a greater rate of Fn deposition (p=0.0014) compared to WT cells. Fn mRNA was increased 2-fold in PAI-1.stab osteoblasts compared to WT osteoblasts. Taken together, these studies indicate that PAI-1 over-expression results in increased bone mineralization without alteration of bone architecture. This effect is independent of estrogen and occurs in conditions of basal bone remodeling as well as in accelerated remodeling following OVX. Increased mineralization results, in part, from alterations in the Fn component of bone matrix leading to aberrant osteoblast/osteoclast mineralizing activity. This newly recognized role of PAI-1 in matrix synthesis and mineralization suggests novel targets for the prevention and treatment of bone disorders in humans.

Disclosures: S.M. Nordstrom, None.

T138

The Overexpression of Type III Na-dependent Phosphate Transporter Pit-1 in Rats Develops the Progressive Nephrotic Syndrome. S. Sekiguchi, S. Asano*, K. Nishiwaki-Yasuda*, A. Yokoyama*, K. Inagaki*, H. Kakizawa*, N. Hayakawa*, N. Oda*, A. Suzuki, M. Itoh*. Department of Internal Medicine, Fujita Health University, Aichi, Japan.

Phosphate uptake at the cellular membrane is essential to maintain the cell activity because phosphate has to be supplied for ATP synthesis. Generally, the extracellular signal to stimulate cellular proliferation also induces the enhancement of phosphate uptake, that is, Pi transport activity. On the contrary, accumulating evidence suggests that phosphate overload from the extracellular milieu would be stressful for the cells, because phosphate uptake itself might induce the formation of apoptosome, resulting in the apoptosis of the cells. In the present study, we investigate the effect of overexpression of Pit-1, a type III Pi transporter, on the kidney which is a major phosphate-handling organ in Pit-1 transgenic rats (Tg). Survival was much shorter in Tg rats with death already occurring between the 7 and 9 months of age. The decrease of serum albumin started at the age of 2 months old, and progressively deteriorated. Tg rats developed massive proteinuria at 3 months of age, associated with hyperlipidemia, suggesting the progress of nephrotic syndrome in Tg rats. On the contrary, serum creatinine levels in Tg were not different from those in Wt. At their birth, the difference of electromicroscopic (EM) finding of the glomerulus between Tg and wild type rats (WT) was not apparent, but at 8 weeks after birth, the glomerulus of Tg has started to shrink compared to that of WT. Their glomerular abnormality assessed by EM images were also observed in 8 weeks old Tg rats, that is, glomerulus exhibits diffuse loss of foot processes of visceral epithelial cells (podocytes), thickened basement membrane and the massive deposition of abnormal protein in the glomerulus. These findings suggest that early onset of the development of the damage of glomerulus due to overexpression of Pit-1 phosphate transporter.

In conclusion, Pit-1 overexpression in rats induces the phosphate-dependent cellular stress, which results in the damage of the filtration at glomerulus without affecting renal function itself. This might be a suitable animal model to analyze the pathogenesis of nephrotic syndrome.

Disclosures: S. Sekiguchi, None.

T139

Cementoblast Cultured on Fibrin Induces Fibrinolysis and Its Apoptosis. H. Jung*, Y. Choi*, J. Baek, H. Ryoo, K. Woo. Dept. of Cell and Developmental Biology, Seoul National University, School of Dentistry, Seoul, Republic of Korea.

Cementum is a mineralized tissue covering roots of teeth that provide for the attachment of periodontal ligament to roots and surrounding alveolar bone. During periodontal regeneration after disease or surgery, cementum is thought to play a critical

role in the reparative process. However, it has remained a poorly defined tissue at the cellular and molecular level. We intended to examine effect of fibrin, the natural provisional matrix during wound healing, on cementoblast differentiation. A cementoblast cell line OCCM30 was grown on fibrin matrix and the phenotypes were examined. Unexpectedly, it was observed that the fibrin matrix, on which cementoblasts were cultured, was degraded and the cementoblasts on fibrin underwent apoptosis. In contrast, fibrin matrix promoted expressions of osteoblastic phenotypes in MC4 cells without any observable degradation. The degradation of fibrin was quantified through measuring fluorescence-labeled fibrin released to culture medium. The apoptosis was confirmed by TUNEL staining and activation of caspase 3. Next, we surveyed expression of enzymes responsible for fibrin degradation. Tissue-type plasminogen activator was expressed in cementoblasts grown on fibrin. Aminocaproic acid, an anti-fibrinolytic agent, reduced the fibrin degradation and apoptosis of cementoblast in a dose-dependent manner. Taken together, these results imply that fibrin matrix in periodontal wounds may impair regeneration of cementum.

Disclosures: K. Woo, None.

T140

Analysis of In Vivo Responses to Hydrogen Peroxide Purified PHBV Biomaterial Implanted in a Murine Tibial Defect. A. C. K. Wu^{*1}, S. Toulson^{*2}, A. Pettit^{*3}, L. Grøndahl^{*4}, E. J. Mackie^{*2}, A. I. Cassady^{*3}. ¹School of Biomedical Sciences, University of Queensland, Brisbane, Australia, ²Faculty of Veterinary Science, University of Melbourne, Melbourne, Australia, ³Institute for Molecular Bioscience, University of Queensland, Brisbane, Australia, ⁴School of Molecular and Microbial Sciences, University of Queensland, Brisbane, Australia.

The utilization of biomaterials for the repair of critical bone defects has become an emerging field due to the limitations of current therapeutic options. Optimal bone biomaterial should be able to provide structural support for bone regeneration and elicit minimal inflammatory response and toxic effects when implanted. Poly(3-hydroxybutyrate-co-3-hydroxyvalerate) (PHBV) is a naturally occurring biodegradable polymer that possess properties include slow rate of degradation in biological environments and can be tailored into desired building blocks due to its thermoplastic nature. We have previously reported that PHBV is contaminated with bacterially derived impurities and have developed protocol that can eliminate impurities from the material. The purified PHBV have a much improved biocompatibility as tested by the in vitro tissue culture assays. The aim of the current study was to further validate the biocompatibility of purified PHBV under in vivo conditions. Cylindrical blocks of the materials were implanted into a murine tibial cortical defect, consisting of a hole drilled through the diameter of the tibial diaphysis. The defect was either filled with a material plug or left unfilled as a control. The animals were sacrificed at one week and four weeks after surgery and the extracted tibiae were decalcified and paraffin embedded. Bone sections were examined using standard histological staining as well as immunohistochemical staining to determine the extent of the cellular response surrounding the implant. The PHBV implant induced a mild inflammatory response one week after injury, which persisted at four weeks. Granuloma type tissues were formed at the implant tissue interface at the periosteum encapsulating the implants four weeks post surgery. Our data indicate that solid PHBV biomaterials induce a mild tissue reaction with no evidence of osteointegration into the implant at the tissue interface during the study time frame.

Disclosures: A.C.K. Wu, None.

T141

Using Replication Competent Avian Virus System to Delivery Short Hairpin siRNA to Silence Gene Expression of Wdr5 in Chicken Limb Bud During Embryogenesis. S. Zhu, E. Gori. Endocrine Unit, Massachusetts General Hospital, Harvard Medical School, Boston, MA, USA.

Wdr5, a WD40 protein, is expressed in chondrocytes and osteoblasts in vitro and in vivo. Targeted expression of Wdr5 to osteoblasts, using the 2.3-kb fragment of the mouse type I collagen promoter results in accelerated osteoblast differentiation during skeletal development. A novel finding in these studies was expansion of the hypertrophic chondrocyte layer, suggesting that Wdr5 expression in the bone collar acts in a paracrine fashion to regulate chondrocyte differentiation. In addition, reduction of endogenous Wdr5 protein levels using plasmid-based small interfering RNAs (siRNAs) markedly inhibits osteoblast differentiation of MC3T3-E1 cells, suggesting that Wdr5 is required for osteoblast differentiation in vitro. To address whether Wdr5 is essential for osteoblast and chondrocyte differentiation in vivo during endochondral bone formation, a replication competent avian virus system (RCAN) is being generated to express short hairpin RNA (shRNA) under the control of the U6 RNA polymerase III (U6 pol III) promoter to specifically silence the expression of Wdr5 throughout the developing chicken limb. Four sites targeting the coding sequence of the chicken Wdr5 were chosen using the Ambion web site algorithm. Four RCAN vectors containing the selected Wdr5-shRNA sequences and one RCAN vector containing a scrambled-shRNA (RCAN-control) to use as a control have been generated. To verify the infection efficiency of RCANs, Green Fluorescence Protein (GFP), driven by cytomegalovirus (CMV) promoter, was cloned into the RCAN constructs upstream the U6 Pol III-shRNA cassette. To examine the role of Wdr5 on limb development in vivo, high-titer RCAN-shWdr5 and RCAN-control retroviral inoculates are being injected into the right wing of E3.5 chick embryos, a stage analogous to mouse embryo E12.5. The contralateral wings will serve as control. The effects of the differing degrees of Wdr5 silencing will be investigated histologically and by in situ hybridization analysis. These studies should offer a rapid and efficient method of analyzing the function of

Wdr5 during embryonic skeletal development. Furthermore, they will allow us to dissect the roles of other genes that interact with Wdr5.

Disclosures: S. Zhu, None.

This study received funding from: NIH.

T142

Podocan Affects Cell Proliferation and In Vitro Mineralization Possibly by Inducing Cellular Senescence in MC3T3-E1 Cell. M. Katafuchi¹, Y. Mochida², P. Atsawasuwan^{*2}, M. Sricholpech^{*2}, M. Bahadoran^{*3}, M. Kaku^{*2}, T. Matsuura¹, M. Yamauchi². ¹Department of Oral Rehabilitation, Fukuoka Dental College, Fukuoka, Japan, ²Dental Research Center, University of North Carolina at Chapel Hill, Chapel Hill, NC, USA, ³School of Dentistry, University of North Carolina at Chapel Hill, Chapel Hill, NC, USA.

Recently we have reported that podocan (Podn), a recently identified small leucine-rich proteoglycan/glycoprotein (SLRP), is expressed in preosteoblastic cell line, MC3T3-E1 cells (MC). In this study, to explore the potential function of Podn in bone biology, MC derived clones stably overexpressing Podn (S clone) were generated and partially characterized by comparing with two control groups, MC and a clone transfected with an empty vector (Ev clone). To establish the S clones, MC was transfected with pcDNA3 Podn HA-tag construct using FuGENE6 transfection reagent. After transfection, cells were cultured and exposed to 400 µg/ml of G418 antibiotics for 4 weeks to select stably transfected clones. The overexpression was confirmed by immunoprecipitation followed by western blot analysis with anti-HA antibody. Seven S clones were selected and analyzed for cell proliferation, in vitro mineralization and cellular senescence. The cell proliferation rate evaluated by cell counting at day 5 of culture was significantly decreased in all S clones in comparison to that of controls (25-58 % of the controls). When cells were cultured in α -MEM in the presence of 10 % FBS, 2 mM β -glycerophosphate and 50 µg/ml ascorbic acid for up to 4 weeks, the onset of mineralization evaluated by Alizarin red staining was significantly delayed in 60-70 % of S clones compared to controls. To investigate the potential cause of these phenotypes, cells (10,000 cells/mL) were cultured for 24 hours and evaluated for cellular senescence by staining for senescence-associated- β -galactosidase (SA- β -gal) activity. In S clones, the number of stained cells was significantly increased when compared to controls (by ~6 fold). These results indicate that Podn may induce cellular senescence in MC resulting in decreased cell proliferation and delayed mineralization in vitro.

Disclosures: M. Katafuchi, None.

This study received funding from: NIH grants DE10489 and AR052824.

T143

Abnormal Collagen Type 1 Production by Human Osteoarthritic Osteoblasts. D. Couchourel^{*}, I. Aubry^{*}, A. Delalandre^{*}, D. Lajeunesse. Rhumatology, Centre Hospitalier de l'Université de Montréal (CHUM), Montréal, PQ, Canada.

Osteoarthritis (OA) is characterized by articular cartilage loss, bone sclerosis and synovial inflammation. Bone sclerosis is due to an abundant osteoid matrix that does not mineralize normally. Here, we prepared primary normal and OA osteoblasts (Ob) from subchondral bone of tibial plateaus to study in vitro the mechanisms responsible for this abnormal sclerosis. The expression of collagen type 1 α 1 chain (COL1A1) and α 2 chains (COL1A2) was determined by real-time PCR in parallel with in vitro mineralization evaluated by alizarin red staining. The SaOS-2 cell model, which shows high rates of mineralization, and OA Ob were used to determine the impact of either COL1A1 or COL1A2 overexpression or siRNA inhibition on the mechanism of mineralization. Last, we determined if a putative factor released by OA Ob could inhibit mineralization using conditioned-media (CM) from OA Ob on SaOS-2 cells while SaOS-2 CM was used to determine if this could correct OA Ob mineralization. In vitro alizarin red staining was significantly reduced in OA Ob compared to normal under basal condition and following BMP-2 treatment indicating a reduced mineralization capacity. Mineralization was reduced in OA Ob due to an increase of COL1A1 expression compared to normal with no significant changes in COL1A2. The COL1A1 to COL1A2 ratio was 7.2 ± 0.2 in OA Ob whereas it was 2.5 ± 0.6 in normal Ob at day 30 post-confluence. The COL1A1 to COL1A2 ratio in SaOS-2 cells varied from 7.5 ± 1.5 at day 0 to 1.5 ± 0.2 at day 14 post-confluence whereas the mineralization progressively increased. Overexpressing COL1A1 in SaOS-2 cells reduced whereas COL1A1 siRNA transiently increased mineralization. In OA Ob, overexpressing COL1A2 increased mineralization by 26% whereas the COL1A1 to COL1A2 ratio decreased by 28.8%. Furthermore, siRNA inhibition of COL1A1 expression in OA Ob increased mineralization by 43.62%. Last, SaOS-2 CM increased the mineralization of OA Ob while OA Ob-CM reduced mineralization of SaOS-2 cells but without any significant changes in the COL1A1 to COL1A2 ratio in either cells. This study suggests that the abnormal mineralization of OA bone tissue observed in vivo may be linked, in part, with the abnormal expression of COL1A1 by OA Ob and their incapacity to down-regulate their COL1A1 to COL1A2 ratio. This assessment is illustrated by the fact that when this ratio is altered in primary OA Ob and in SaOS-2 cells mineralization is not optimal. In addition, this could also be linked with the expression of a putative soluble factor that alters mineralization without altering the COL1A1 to COL1A2 ratio.

Disclosures: D. Lajeunesse, None.

T144

An Active Fragment of Secreted Phosphoprotein-24 Enhances but Is Not Indispensable for BMP-Mediated Adult Human Bone Marrow Derived Mesenchymal Stem Cell Differentiation to Osteoblasts. A. Maiti¹, O. Korchynskyi¹, S. C. Ramage², A. P. Pacitti¹, M. J. Beckman². ¹Orthopaedic Surgery, Virginia Commonwealth University, Richmond, VA, USA, ²Biochemistry and Molecular Biology, Virginia Commonwealth University, Richmond, VA, USA.

Mesenchymal stem cells (MSCs) are multipotent cells that can proliferate and differentiate into multiple tissues. The recruitment and differentiation of MSCs into distinct tissues is a precondition for in situ tissue engineering. MSCs play a major role in osteogenesis and their osteogenic potential depends on several factors including BMP/Smad induced transcription and canonical Wnt/ β -catenin signaling. Glucocorticoid signaling is required for normal bone formation, and synthetic glucocorticoids such as dexamethasone (Dex) promote osteoblastic differentiation of MSCs. We examined the osteogenic regulation of secreted phosphoprotein-24 (Spp24), a 24 kDa bone matrix protein hypothesized to possess osteoinductive properties. Adult human bone marrow derived MSCs were isolated by plastic adherence. Both Dex and BMP-2/7 heterodimer accelerated MSC differentiation to osteoblasts (OB) in a 14 day period in the presence of ascorbic acid and β -glycerolphosphate. We used a polyclonal rabbit anti-bovine Spp24 antibody to detect human endogenous Spp24. Gene expression of OB lineage markers were measured by Real-Time RT-PCR and alkaline phosphatase and Alizarin Red staining were performed as measures of an OB-specific marker and OB matrix mineralization, respectively. Western Blot of differentiated MSCs revealed a predominant 18 kDa fragment absent in undifferentiated MSCs. The formation of the 18 kDa fragment of Spp24 in Dex-induced differentiation corresponded with increased gene expression of OB-specific markers (Runx2, Osterix, osteocalcin and collagen I) and alkaline phosphatase staining. Temporal regulation of this putative active form of endogenous human Spp24 was seen at days 7-10 of Dex-induced OB differentiation. To examine the effect of Spp24 on BMP-mediated osteoblastogenesis we replaced Dex with BMP-2/7 as the differentiation mediator and performed adenoviral transduction of Adv5CMV-LacZ control or recombinant Adv5CMV-Spp24 over 12 and 14 day time frames. Expression of full-length mouse Spp24 (mSpp24) enhanced of BMP-mediated matrix mineralization, but without BMP-2/7, Spp24 had only a minor effect at day 12. At day 14 mSpp24 expression induced significant osteoblastogenesis assessed by gene, protein markers and Alizarin Red staining. These results highlight a critical processing step during osteoblastogenesis that produces an activated 18 kDa fragment of Spp24 involved in the enhancement of bone matrix mineralization by its cooperation with BMP.

Disclosures: A. Maiti, None.

T145

Cleavage Products of Amyloid Precursor Protein Regulate Osteoblast Function. J. McLeod¹, N. Curtis², M. Fagan², P. Genever¹. ¹Dept. of Biology, University of York, York, United Kingdom, ²Dept. of Engineering, University of Hull, Hull, United Kingdom.

γ -secretase is an intramembrane protease responsible for the cleavage of numerous molecules which regulate osteoblast activity, such as Notch and EphrinB2. Cleavage of its substrates results in release of a fragment into the extracellular space, and a C-terminal peptide into the cytoplasm. Amyloid precursor protein (APP) is also processed by γ -secretase, though its role in bone is unknown. Amyloid- β (A β) peptides are secreted into the extracellular space as a result of γ -secretase activity on APP, and in the brain can aggregate to form the plaques characteristic of Alzheimer's disease (AD). The amyloid intracellular domain (AICD) binds to the nuclear adaptor protein Fe65 in the cytoplasm, and translocates to the nucleus to form a transcriptionally active AFT complex with Tip60. In this study the expression, cleavage and potential function of APP were investigated during osteogenesis. By qRT-PCR and western blot analysis, expression of all γ -secretase subunits (PS1, PS2, APh-1 α , APh-1 β , Nct, PEN-2) was confirmed. A specific fluorimetric assay showed significant increase in enzyme activity during osteogenic differentiation of human bone marrow stromal cells (MSCs). Using RT-PCR we identified expression of a longer isoform of APP in osteoblasts compared to neuronal APP, which contained an additional Kunitz protease inhibitory domain that promotes aggregation of A β peptides. Western blot analysis confirmed expression and processing of APP throughout osteogenesis, and treatment of samples with γ -secretase inhibitors confirmed that this enzyme specifically cleaves APP within differentiating MSCs. Expression of Fe65 and Tip60 throughout in vitro osteogenesis was confirmed by RT-PCR and western blot analysis. Using confocal microscopy we showed that over-expression of both AICD and Fe65 in C3H10T $\frac{1}{2}$ stromal cells resulted in colocalisation within discrete domains of the nucleus. A specific chemiluminescent immunoassay demonstrated secretion of A β during osteogenesis. MSCs showed a significant increase in adhesion to extracellular matrices containing aged A β plaques compared to non-aged A β peptide controls and A β plaques were localized to the endosteal and periosteal surfaces in sections of adult rat ulna. By μ CT analysis (15 μ m resolution) of vertebrae from a 12 month old AD mouse model, Tg2576, which over-expresses a mutant APP resulting in increased γ -secretase cleavage, we showed a 20% decrease in bone volume compared to wild type controls (10.60mm³ vs. 8.47mm³; wild type vs. transgenic). These findings indicate that APP may function as a novel regulator of osteoblastic activity both in vitro and in vivo, with functions ranging from adhesion to regulation of gene transcription.

Disclosures: J. McLeod, None.

T146

The Effect of IL-6 and sIL-6R on the Expression of Cartilage Matrix Proteins. A. Namba¹, Y. Aida², Y. Watanabe², H. Tanaka³, O. Shimizu¹, N. Suzuki⁴, M. Maeno³. ¹Departments of Oral and Maxillofacial Surgery, Nihon University School of Dentistry, Tokyo, Japan, ²Department of Fixed Prosthodontics, Nihon University School of Dentistry, Tokyo, Japan, ³Department of Oral Health Sciences, Nihon University School of Dentistry, Tokyo, Japan, ⁴Department of Biochemistry, Nihon University School of Dentistry, Tokyo, Japan.

Elevated concentrations of interleukin-6 (IL-6) and soluble IL-6 receptor (sIL-6R α) in the synovial fluid of the temporomandibular joint (TMJ) have been implicated in the joint cartilage destruction associated with TMJ disorders. Recently, we demonstrated that IL-1 β promotes the resolution system of cartilage matrix turnover through an increase in inflammatory cytokine production by chondrocytes and that it also may promote the autocrine action of IL-6 through an increase in IL-6R α expression in human chondrocytes (Life Sci 79, 764-771, 2006). In the present study, we examined the effect of IL-6 and sIL-6R α on cell growth and alkaline phosphatase (ALPase) activity. We also examined the expression of Sox-9, cartilage matrix proteins (including type II collagen, aggrecan core, and link protein), bone morphogenetic protein (BMP)-7, and BMP receptors (BMPR) in human chondrocytes. The cells were cultured with or without 50 ng/mL IL-6 and/or 30 ng/mL sIL-6R α for up to 28 days. The levels of mRNA expression for Sox-9, the cartilage matrix proteins, BMP-7, and BMPR were determined using real-time PCR; protein levels were determined using ELISA. The proteoglycans of the extracellular matrix were stained with Alcian blue. Cell proliferation increased slightly in the presence of both IL-6 and sIL-6R α after 7 days of culture. ALPase activity, a marker enzyme used to differentiate osteoblasts and chondrocytes, decreased markedly in the presence of both IL-6 and sIL-6R α after 10 days of culture. The expression of Sox-9, aggrecan core, and Alcian blue-positive proteoglycans in the extracellular matrix did not change in the presence or absence of IL-6 and sIL-6R α , whereas the expression of type II collagen, link protein, BMP-7, and BMPR increased in the presence of both IL-6 and sIL-6R α after 7 days of culture. These results suggest that IL-6 in the presence of sIL-6R α suppresses the differentiation of chondrocytes and induces the repair of arthrodial cartilage through the increased expression of cartilage matrix proteins, BMP-7, and BMPR.

Disclosures: A. Namba, None.

T147

Histological and Biochemical Characterization of Mandibular Bones in Senile Osteoporotic Mice. K. Tokutomi¹, T. Matsuura¹, Y. Daigo¹, M. Katafuchi¹, K. Toh¹, H. Sato¹, M. Yamauchi². ¹Oral Rehabilitation, Fukuoka Dental College, Fukuoka, Japan, ²Dental Research Center, University of North Carolina at Chapel Hill, Chapel Hill, NC, USA.

The quantity and quality of jaw bone are an important determinant for the outcome of many aspects of dental treatment. However, relatively little is currently known about the age-related changes of jaw bone. In this study, the mandibular bones of SAMP6 mice, a senile osteoporosis mouse model, were partially characterized and compared to those of SAMR1 mice as control. A total of twelve 6 month-old male mice of each strain were used. Static bone morphometric analysis was performed using 6 mice from each strain to assess cortical thickness index (CTI) at the mandibular ramus, bone area (B.Ar / T.Ar), trabecular width (Tb.Wi), trabecular number (Tb.N) and trabecular separation (Tb.Sp) at the interradicular septum between the distal root of the first molar and the mesial root of the second molar. Using other 6 mice from each strain, bilateral condylar necks and mandibular rami were dissected, pulverized, weighed, hydrolyzed with 6N HCl and subjected to amino acid analysis to determine collagen content (μ g/mg bone powder) and the extent of lysine hydroxylation (moles of hydroxylysine/mole of collagen). Statistical analysis was performed by Student t-test. Both CTI and B.Ar/T.Ar values of SAMP6 (20.1 \pm 1.3 % and 62.9 \pm 4.6 %) were significantly lower than those of SAMR1 (21.9 \pm 1.4 % and 77.0 \pm 4.8 %) (p=0.046 and p<0.001). The values of Tb.Wi (75.9 \pm 16.1 μ m) and Tb.N (8.62 \pm 1.79/mm) of SAMP6 showed a trend of decrease but not statistically significant comparing to those of SAMR1 (81.6 \pm 15.1 μ m and 9.72 \pm 1.28/mm, respectively) (p=0.542 and p=0.248). The Tb.Sp value of SAMP6 (45.6 \pm 14.2 μ m) was significantly higher than that of SAMR1 (23.5 \pm 2.8 μ m) (p=0.004). Biochemical analysis revealed that collagen content of SAMP6 (126.4 \pm 9.7 μ g/mg) was significantly lower than that of SAMR1 (149.6 \pm 10.3 μ g/mg) (p<0.001) and that the extent of lysine hydroxylation of SAMP6 (51.10 \pm 0.39) was higher than that of SAMR1 (48.54 \pm 1.42) (p=0.040). These results indicate that the mandible of SAMP6 exhibits not only reduced bone mass but also altered quantity and quality of collagen matrix. The latter may contribute to a mineralization defect seen in osteoporotic patients.

Disclosures: K. Tokutomi, None.

T148

Enamel Phenotype and Sexual Dimorphism in Dentin of dspp-null Mouse Molars. K. Verdelis¹, J. T. Wright², N. Haruyama³, A. Kulkarni³, L. Lukashova¹, A. L. Boskey¹. ¹Research, Mineralized Tissues Laboratory, Hospital for Special Surgery, New York, NY, USA, ²School of Dentistry, University of North Carolina, Chapel Hill, NC, USA, ³NIDCR, NIH, Bethesda, MD, USA.

The dentin phenotype in dentin sialophosphoprotein (dspp) depleted 70 day-old mice resembles that in humans with dentinogenesis imperfecta type III. Our purpose was to quantitatively compare the dentin and enamel mineral density and the amount of dentinal

and enamel tissue formed in normal(WT) and *dsp^{-/-}* (KO) male and female mature molars.

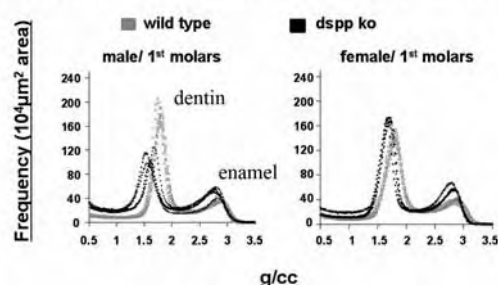
Extracted 1st (m1) and 2nd (m2) lower molars from 8 WT and 9 KO 7-8 mo-old male and female mice (n total=33) were analyzed on a 1172 (Skyscan, Be) μ CT system at 8 μ m isotropic voxel resolution. Parameters calculated from the resulting mineral distributions (1st molars presented in Fig. 1) were: average mineral density (dentin-enamel), mineralized tissue volume (dentin), heterogeneity index (calculated by width at half height of mineral density distribution peaks- dentin).

WT molar crowns had a lower mineral density in both male and female animals (male m1 and m2=-11 to -16%, $p<0.01$, female m1 and m2=-6 to -7%, $p<0.01$). The total volume of dentin was, as initially described, much lower in male KO (-16 to -36%, $p<0.05$), while in female KO this volume was the same (m2) or there was a trend for increased volume ($\pm 8\%$, $p=0.06$ - m1), probably due to enlarged pulp space. Dentin heterogeneity was also sex-dependent, agreeing with the earlier results in KO male (+20 to 28%, $p<0.05$), but lower in female KO animals (-18 to -22%, $p<0.05$). Root dentin showed similar results. Enamel presented phenotypic differences between KO and WT mice that were not sex-dependent, both in mineral density (male=-5%, $p<0.05$, female=-2 to -4%, $p<0.05$) and volume of tissue (male=+21 to 29%, $p<0.05$, female=+22%, $p<0.05$). In KO males only (5 of 8 animals) dystrophic calcification of the pulp and root canals was present.

The results showed that the described dentinogenesis imperfecta III dentin phenotype of the *dsp^{-/-}* mice is sex-dependent, implying possible X-chromosome located protein partners for *dsp^{-/-}* in its signaling function in dentin and possibly in the pulp. They also showed that the final mineral density difference of KO dentin is moderate and that there are some enamel changes as well in the *dsp^{-/-}* mice.

Supported by NIH grants DE 04141 and AR-46121.

Fig.1: Distribution of mineral densities in 1st molars



Disclosures: K. Verdelis, None.

This study received funding from: NIDCR, NIH.

T149

Bone Sialoprotein-Mediated Osteoblast Differentiation and Mineralization Is Principally Dependent on the Intrinsic Characteristics of Responding Cells. J. G. Yost*, Q. Lu*, M. Rodova*, J. Wang. Orthopedic Surgery, The University of Kansas Medical Center, Kansas City, KS, USA.

Bone sialoprotein (BSP) is one of the major non-collagenous phosphoproteins in bone and tooth, which stimulates matrix mineralization and osteogenesis in surgically created rat calvarial defects, but not in rat thoracic subcutaneous tissue (Calcif Tissue Int 2006; 79:179). This has raised an important question of whether BSP-mediated osteogenesis is dependent on local environment and/or cellular conditions. This study tests our hypothesis that the effect of BSP on osteoblast differentiation and function is principally dependent on the characteristics of responding cells. We first examined the origins of BSP-responsive cells at the cranial defect site by using a nitrocellulose membrane to separate BSP-collagen implants from the host bone/periosteum, the dura that is located at the bottom of the defect, and the skin flap covering the defect. The results demonstrated that bone-forming cells observed in the mid-portion of BSP-treated defects are primarily derived from the dura and to a much lesser extent from the host bone and periosteum. Cells derived from the skin flap do not differentiate into osteoblasts or mineralize. To eliminate the effects of local environment on BSP function, primary cells isolated separately from the dura, cranial subcutaneous or thoracic subcutaneous tissues were cultivated in the same conditions of α -MEM media. When the cells reached 75-80% confluence, they were transfected with a BSP expression lentiviral vector with the addition of 10% FBS, 50 μ g/ml ascorbic acid and 5 mM β -glycerolphosphate. Transfection of rat dural cells with a lentiviral BSP expression vector, but not an empty vector, led to the expression of osteocalcin and matrix mineralization at 14 days after transfection; while transfection of rat cranial and thoracic subcutaneous cells with a lentiviral BSP expression vector did not result in osteocalcin expression or mineralization even by 21 days. Quantitative real-time PCR analyses demonstrated that the expression levels of Runx2 and Osterix were significantly higher in normal dura than in normal cranial and thoracic subcutaneous tissues, while there were no significant differences in the expression levels of osteocalcin, BSP and osteopontin between these tissues. These results suggest that the dura-derived cells, at least some of them, are Runx2/Osterix expressing osteoprogenitors or preosteoblasts, which can be further differentiated into functional osteoblasts upon BSP treatment, and that BSP-mediated osteoblast differentiation and mineralization is principally dependent on the intrinsic molecular and cellular characteristics of responding cells.

Disclosures: J. Wang, None.

T150

Focal Bone Loss in Mice with Transient Muscle Paralysis. B. J. Ausk*, P. Huber*, S. Srinivasan, T. S. Gross. Orthopaedics and Sports Medicine, University of Washington, Seattle, WA, USA.

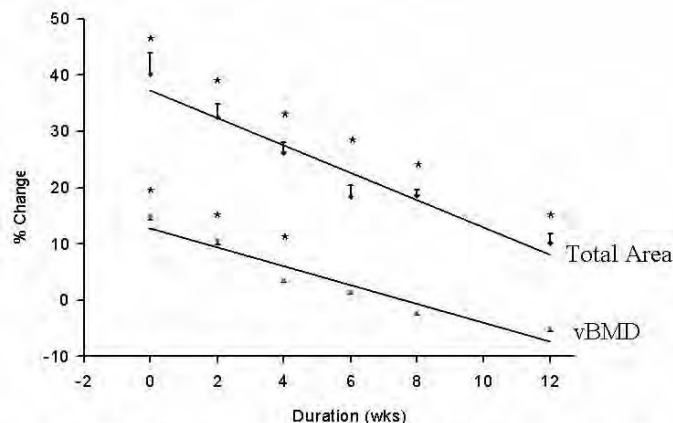
The mechanisms by which muscle function locally mediates bone homeostasis are unclear. We have previously reported that transient muscle paralysis rapidly induces osteoclast mediated trabecular and cortical bone loss in bones nearest the paralyzed muscles. Given this spatial relation, we hypothesized that resorption within a given bone would be focused on the cortex adjacent to the paralyzed muscle. Ten female C57B6 mice (16 wk) received IM injections of Botox (2.0 units/100 g) in the right calf immediately following a μ CT scan of a 2 mm mid-diaphyseal region of the tibia. At 21 d, a second μ CT scan of the same region was obtained. Pre- and post-scans of individual mice were aligned and changes in cross-sectional area determined at three 2-D cross-sections located at the distal (A, 1.4 mm proximal to the tib-fib junction), middle (B, 2.4 mm proximal) and proximal end (C, 3.4 mm proximal) of the scanned volume. Composite 2-D images at each location were partitioned to identify focal bone loss in the posterior third of bone (i.e., adjacent to paralyzed calf muscle; Calf) compared to the remainder of the cross-section (Non-Calf). Mean (\pm s.e.) whole cross-sectional bone area was significantly reduced throughout the scanned volume (A: -0.073 ± 0.009 mm²; B: -0.071 ± 0.012 mm²; C: -0.051 ± 0.009 mm², all $p < 0.001$). Bone loss arose entirely via endocortical expansion and the magnitude of the loss did not differ statistically across the scanned volume ($p > 0.3$). While bone loss at the most distal location (A) was focused in the Calf Sector ($18.8 \pm 2.2\%$ vs $8.3 \pm 1.3\%$, $p = 0.001$), bone loss at the most proximal location (C) was primarily associated with the Non-Calf Sector ($9.4 \pm 1.6\%$ vs $3.1 \pm 0.9\%$, $p = 0.004$). The center of the scanned region (B) demonstrated bone erosion in both cortical sectors ($13.7 \pm 2.4\%$ vs $9.2 \pm 1.9\%$, Calf vs Non-Calf, respectively, $p > 0.15$). These data clearly indicate that the endocortical resorption induced within the bone by transient muscle paralysis, though focal and highly reproducible across mice, was not exclusive to cortical areas adjacent to the paralyzed muscle. As the paralyzed calf spanned the entire scanned bone volume (no muscle insertions within 6 mm of scanned volume), the shift of resorption from anterior predominant to posterior predominant within this region suggests that the dynamics governing focal bone loss have complexities beyond that originally hypothesized. Instead, the data suggest that osteoclast recruitment to bone surfaces is not a random process but is either the result of active osteoclast chemotaxis or focal inhibition of osteoclast attachment.

Disclosures: B.J. Ausk, None.

T151

The Increased vBMD and Bone Area due to Mechanical Loading Gradually Decreased Following Cessation of Loading. C. Kesavan, D. J. Baylink*, P. Gifford*, S. Mohan, MDC, J.L. Pettis VAMC, Loma Linda, CA, USA.

Dynamic loads lead to increases in volumetric (v) BMD and cross sectional area. However, the issue of how long these gains are maintained after cessation of loading has not been fully understood. To address this question, we performed a long term study in which skeletal changes were monitored every 2-4 weeks for a 12 week period following cessation of external loading. A four-point loading device was used to apply external loading (9N at a frequency of 2Hz for 36 cycles once per day for 12 days) to the right tibia of 10-week old female mice. Skeletal changes were monitored by in vivo pQCT. The value of the left non-loaded tibia was subtracted from the value of the right loaded tibia to determine the changes associated with loading at each time point. Two-weeks of four-point loading caused a drastic 40% increase in total area (TA) and 15% increase in total vBMD. However, the increase in size due to external loading did not continue once the external loading was stopped. Furthermore, cessation of loading resulted in a continuous loss of both bone size (TA) and vBMD. The vBMD returned to normal at 12 weeks with a half life of 6 weeks. The TA declined with a half life of 8.5 weeks and was still significantly elevated at 12 weeks. Thus, the decline in elevated TA proceeded at a much slower pace than the loading induced increases in vBMD. Conclusions: 1) External loading-induced increases in bone are lost over a period of time but at a much slower pace than the induction of the increases; 2) While a single burst of external loading provides increased bone mass temporarily, periodic loading may be necessary to maintain long term bone strength.



Values are given as mean \pm SE, * $p<0.05$ vs. non-loaded bones, n = 5

Disclosures: C. Kesavan, None.

T152

Identifying Mechanical Loading QTL by Gene Expression Changes for Alkaline Phosphatase and Bone Sialoprotein in C57BL/6J (B6) X C3H/HeJ (C3H) Intercross. C. Kesavan, D. Baylink*, S. Kapoor*, S. Mohan. MDC, J.L. Pettis VAMC, Loma Linda, CA, USA.

Previous studies have shown that mechanical loading (ML) 1) produces a more robust skeletal anabolic response in B6 mice than C3H mice, which is largely mediated by genetic differences and 2) induces greater expression of bone formation (BF) marker genes in the bones of B6 mice compared with C3H mice. We, therefore, tested the hypothesis that the variation in skeletal anabolic response to ML in the F2 mice of B6 and C3H intercross is largely due to changes in BF response. To examine this, we measured expression changes in two BF markers, namely bone sialoprotein (BSP) and alkaline phosphatase (ALP) in the loaded and non-loaded bones of 10-week F2 female mice (n=241). Loading was performed daily on the right tibia by four-point bending using a 9 Newton at 2Hz, 36 cycles, for 12 days. The left tibiae were used as internal controls. The expression levels of ALP and BSP were quantitated after normalization with two house keeping genes, actin and PPIA. The mean increase in gene expression in the F2 mice, expressed as fold change, ranged from 3.0 ± 2.8 for BSP and 2.7 ± 2.8 for ALP, and showed significant correlation ($r=0.25$ to 0.36 , $p<0.01$) with changes in BMD and bone size. A genome-wide search using 111 microsatellite markers with 15 cM intervals in the

Locus *	β-actin Normalization		PPIA Normalization	
	BSP-LOD	ALP-LOD	BSP-LOD	ALP-LOD
D8Mit88	7.5 ^b	10.5 ^a	8.8 ^b	12.3 ^a
D9Mit151	7.1 ^b	7.4 ^b	5.0 ^c	-
D16Mit153	6.7 ^b	5.1 ^c	7.0 ^b	5.9 ^c
D17Mit51	9.2 ^a	9.3 ^a	12.3 ^a	9.0 ^b
D18Mit144	8.0 ^b	12.6 ^a	-	5.8 ^c
D19Mit68	7.2 ^b	-	10.7 ^a	6.9 ^b

*determined using MapQTL program; ^a $p<0.01$, ^b $p<0.05$, ^c $p<0.1$

F2 mice revealed QTLs on Chrs 8, 9, 17 and 18, which corresponded to ML QTLs we previously identified using changes in BMD and bone size as end points. We identified two new ML QTLs on Chrs 16 and 19 using gene expression data. In conclusion: 1) Identification of several common QTL for BMD, BSP and ALP phenotypes suggests that the skeletal response to ML is largely mediated by increased BF; 2) Identification of genes that are involved in regulating BSP and ALP expression in response to ML will lead to improved understanding of the molecular pathways regulating the bone response to ML.

Disclosures: C. Kesavan, None.

T153

Comparative Analysis of Expression Profile in the Anatomically Separated Parts of Femurs Prepared from Unloading Induced Bone Loss Model of Tail-suspended Mice. J. Nagata, Y. Ezura, M. Noda. Department of Molecular Pharmacology, Medical Research Institute, Tokyo Medical and Dental University, Tokyo, Japan.

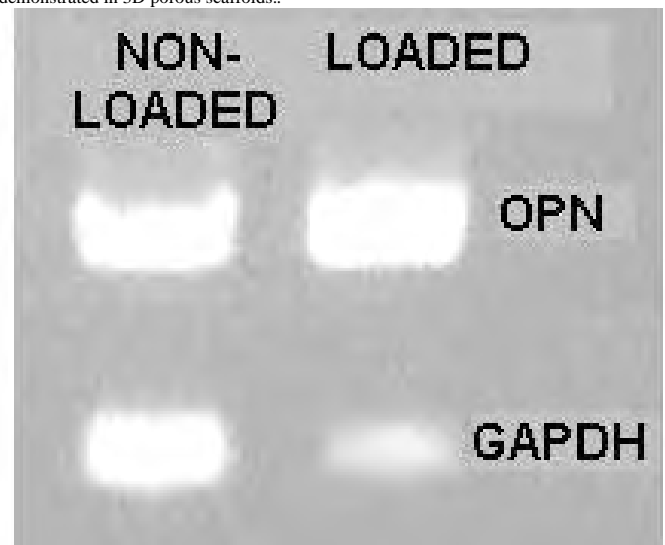
In vivo experimental analysis for disuse osteoporosis has been effectively carried out by rodent experiment of hindlimb unloading obtained by "tail-suspension". Applications of knock-out mice for this experiment unveiled molecular involvement of several genes such as osteopontin, for the unloading induced bone-loss. However, the entire process of the molecular events involved in this phenomenon is largely unknown. To obtain insights into the integrative understandings of the molecular events, we performed DNA microarray analysis on tissues prepared from unloaded femurs of the tail-suspended mice. Tail suspension was carried out using 8-week old C57Bl6 mice (n=5) for 2-weeks, and we compared them with normally loaded mice (n=5). Whole femora were dissected out from left hindlimbs, and separated into three parts; (A) bone marrow flushed out from mid shaft 1/3, (B) mid shaft cortex, and (C) distal and proximal epiphyses and metaphyses. Total RNA was isolated from these samples, and only the quality checked samples were used for expression analyses. Micro-CT analysis on contralateral femora confirmed significant decrease of bone volume in the distal end. Expression profile for up to 39,000 transcripts was analyzed by Affymetrix DNA microarray (Mouse Expression 430_2.0 Array) for three different parts of femurs (A to C). The analyses displayed significantly different patterns. Partial resemblance and reasonable shift observed in the expression pattern of some genes indicated a possibility for analytical reconstruction of changes in proportion of different types of cells and/or changes in expression levels of the gene in specific type of cells in the tissue. For this sake, we first specified significantly up-regulated and down-regulated genes in each type of anatomical site origins (A to C), considering data conceivability regarding flag indication for the spot signal and consistency between the triplicated samples, as well as the statistical significance of the differential expression between loaded and unloaded samples indicated by p-values for Student's t-test. Up-regulated 102 and down-regulated 83 genes were selected from the data for tissue preparation (A). Similarly for preparation (B) and (C), 91 and 46 upregulated and 121 and 50 down-regulated genes were selected. Comparative analysis of these genes among the data obtained from different tissue preparation should clarify the specific cellular events occurring in the unloaded bones in vivo.

Disclosures: J. Nagata, None.

T154

Collagen and Osteopontin Upregulation by Mechanical Loading of Bone Cells in Porous 3D Scaffolds. A. Sittichokechaiwut, L. E. Brown*, G. C. Reilly. Engineering Materials, University of Sheffield, Sheffield, United Kingdom.

Previously, we showed that polyurethane foam scaffolds seeded with osteoblastic cells and loaded in a biodynamic chamber attached to a mechanical testing machine (Bose ElectroForce 3200) provide a good model for analysis of mechanotransduction in 3 dimensions. Under static culture conditions MC3T3-E1 and MLO-A5 cells settled throughout the scaffolds and were shown to be viable up to 15 days of culture. Since MLO-A5s have been demonstrated to be rapid matrix producers (Kato et al. JBMR 2001) we used these cells to investigate the effects of compressive loading in the 3D system. Cell-seeded scaffolds were loaded in compression with a sine wave at 1Hz, 5% strain for 2 hours per day at days 5, 7 and 9 of culture. Collagen content, as assayed by colorimetric analysis of sirius red staining, was significantly ($p<0.05$) higher in loaded scaffolds even if the loading was reduced to days 5 and 7 only. There was no effect of 2 hrs of loading on cell number. However, reducing the length of the loading period to 0.5 or 1 hr eliminated the difference in collagen content but caused an increase in the final number of viable cells in loaded scaffolds. To assess loading induced changes in matrix gene expression 2 types of culture were set up. 1) MLO-A5 cells in polyurethane foams (BritishVita). 2) MC3T3-E1 cells in collagen sponges (BD biosciences). In both experiments cells were cultured until day 5 then subjected to a single bout of 2 hours of loading at 5% strain, 1 Hz. In both experiments an increase in osteopontin mRNA was detectable in loaded samples by PCR. Positive effects of mechanical loading on bone matrix production can clearly be demonstrated in 3D porous scaffolds..



Disclosures: G.C. Reilly, None

This study received funding from: The Royal Society of London.

T155

Continuous Local Infusion of Basic Fibroblast Growth Factor Enhances Consolidation of the Bone Segment Lengthened by Distraction Osteogenesis in Rabbit Experiment. A. Abbaspour, S. Takata, K. Sairoy*, S. Katoh*, K. Yukata*, N. Yasui*. The University of Tokushima, Tokushima, Japan.

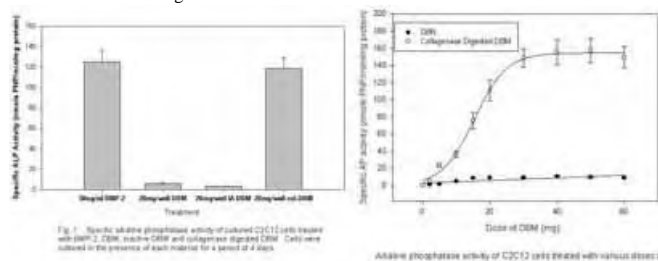
Experimental tibial lengthening was achieved in 52 rabbits to examine the effect of continuous local infusion of recombinant human fibroblast growth factor-2 (rhFGF-2) on bone regeneration during distraction osteogenesis. The tibia was separated by osteotomy and was subjected to slow progressive distraction (rate:0.35 mm/12h) using a monolateral external fixator. The lengthening process consisted of a lag phase for one week after osteotomy, a distraction phase for two weeks, and a consolidation phase for five weeks in this experiment. At various stage of the distraction, rhFGF-2 was infused continuously for two weeks into the lengthened segment [rate:14.28 µg/day(60 µl/day)] using an osmotic pump implanted under the skin. Bone healing was significantly accelerated when rhFGF-2 was infused in the beginning of consolidation phase, but not in the distraction phase nor in the lag phase. Infusion of normal saline (N/S) using the same osmotic pump had no effect. Dual energy X-ray absorptiometry (DXA) and peripheral quantitative computerized tomography (pQCT) studies demonstrated that rhFGF-2-treated tibia had higher bone mineral density (BMD), higher bone mineral content (BMC) and increased cortical bone thickness (CBT) than N/S-treated tibia. In addition, three-point bending test demonstrated that rhFGF-2-treated bone had significantly stronger mechanical properties than N/S-treated bone. Finally, distribution of the infused materials was checked by using Indian ink or Urographin. The dyes distributed widely but exclusively in the lengthened segment. Based on these results we conclude that direct delivery of rhFGF-2 into the lengthened segment can shorten the consolidation phase of limb lengthening and the method is applicable to the clinical treatment.

Disclosures: A. Abbaspour, None.

T156

Limited Collagenase Digestion Increases Solubility and Induction Potential of Human Demineralized Bone Matrix (DBM) In Vitro. H. Tang, L. Shanahan*, M. Diegmann*, N. Forsyth*, D. Knaack*, K. Behnam R&D, Osteotech, Inc., Eatontown, NJ, USA.

When processed in a manner consistent with the preservation of native growth and differentiation factor activity, human demineralized bone matrix has the ability to induce the formation of endochondral bone heterotopically in athymic rodents. Histological demonstration of the formation of ectopic mineralized bone, bone marrow, osteoid, and cartilage is generally considered to be the gold standard for the measurement of osteoinductive activity. While quantitative and semiquantitative histomorphometric methods for defining the osteoinductive potential of DBM have been previously proposed, for the purpose of testing lots of DBM produced from individual donors a predictive in vitro alternative would be desirable. Previously, quantitative in vitro methods for the measurement of the induction of osteoblastic markers in clonal cells have been proposed. We find that a significant limitation of many of these assays is the relative insolubility of the collagenous matrix in the cell culture media. Limited digestion of human demineralized bone matrix with purified bacterial collagenase increases both the solubility of DBM in cell culture media and the ability of the residual matrix to upregulate alkaline phosphatase activity in clonal C2C12 myoblasts. Partial digestion of DBM for 60 minutes increases the ability of the material to induce AP activity in C2C12 cells more than 10 fold 4 days post-treatment but the same treatment has no effect on the activity of guanidine hydrochloride inactivated DBM. The partially digested DBM begins to dissolve into the cell culture medium within 4 to 5 hours, with scant amounts of residual DBM remaining after 48 hours. Complete solubilization of the matrix is dependent on the presence of cells but direct cell contact with the matrix is not required. The capability of DBM to induce alkaline phosphatase activity is dependent both on the dose of the DBM added and the duration collagenase digestion [data not shown]. These results indicate that the solubility of DBM in cell culture media influences the release kinetics of native growth factors which reside within the collagenous matrix.



Disclosures: K. Behnam, Osteotech, Inc. 1, 3.
This study received funding from: Osteotech, Inc.

T157

Continued Enhanced Fgfr2 Function Delayed Fracture Healing in Mice. L. Yin, X. Du, Z. Liu, N. Su, H. Qi, J. Yang, L. Zhao, L. Chen Trauma Center, Research Institute of Surgery, Daping Hospital, Third Military Medical University, chongqing, China.

To evaluate the role of FGFR2 in fracture healing, this study was conducted using twelve-week-old female mice carrying gain-of-function substitution (Ser252Trp) in Fgfr2 or their wild-type littermates. After been anesthetized, mice were subjected to an open mid-diaphyseal fracture of its right femur, a 0.5-mm-diameter metal pin was inserted through the patellar tendon into the medullary canal of the tibia to fix the fracture. Mice were sacrificed at day 5, 7, 10, 14 and 21 after fracture. Digital radiographs of right hind limbs were obtained. After been demineralized, embedded and sectioned, H.E. staining and safranin O/fast green staining were undertaken to show the histological structure of the callus. In situ hybridization using digoxigenin-labeled probes were performed to detect the expression of Fgfr2, Col2(Collagen 2), Ihh(Indian hedgehog) and BMP4(bone morphogenetic protein 4) in callus. The results showed that all the wild-type mice had radiographic evidence of bone union compared with delayed fracture union in mutant-type mice. At 7 days post-fracture, marked chondrogenesis appeared in callus of wild-type mice but not in mutant-type mice. By 21 days, fracture healing was completed in wild-type mice. In contrast, at this time, the fracture healing was not finished in mutant-type mice, with persistence of fibrous scar and cartilage in the fracture gap and bone marrow cavity. The expression of Fgfr2 was present in both wild-type and mutant-type calluses. The initiation of Ihh and Col2 expression in callus was delayed in mutant-type mice than that in wild-type mice. No significant difference in the expression of BMP4 between two groups was observed. Therefore, this study indicated that constitutively activated Fgfr2 function will suppress the endochondral ossification in fracture callus and delay the healing of fracture through the inhibition of the Ihh expression in fracture site.

Disclosures: L. Chen, None.
This study received funding from: 973 Research Projects, No 2005CB522604; National Natural Science Foundation of China, No. 30672121; Opening Project of State Key Laboratory of Trauma, Burn and Combined Injury, No 2006A-4.

T158

FGF-23 Controls NaPiIIa Trafficking via Crosstalk Between the PI-3 kinase and MAP kinase Pathways. M. Khan*, S. M. Jan de Beur Medicine, Johns Hopkins Medical Institute, Baltimore, MD, USA.

Fibroblast Growth Factor 23 (FGF-23) is an important physiological regulator of phosphate homeostasis and its excess or deficiency has been implicated in several human disorders of phosphate homeostasis. FGF-23 exerts its phosphaturic action by promoting internalization of the type IIa and type IIc sodium-phosphate co-transporters (NaPiIIa, NaPiIIc) from the renal brush border membrane and preventing the compensatory increase in 1,25(OH)₂D₃ by reducing renal 1 α hydroxylase expression. FGF-23 can bind several known FGF receptors (FGFR) and activate MAP kinase signaling. However, it is not known which of FGF signaling pathways mediate the diverse actions of FGF-23. We sought to distinguish which FGFR signaling pathway regulates FGF-23-mediated NaPiIIa internalization. Previously, we reported that FGF-23 stimulates ERK1/2 (ERK) phosphorylation and that inhibiting ERK signaling with U0126 abolished FGF-23-mediated NaPiIIa internalization in opossum kidney cells (OK/e). To interrogate other FGFR signaling pathways such as the phosphatidylinositol-3 kinase (PI-3 kinase) pathway, we measured phosphorylation of Akt by immunoblot but observed no increase in pAkt upon stimulation with FGF-23 (0.1 ng/ml-100ng/ml). Yet, surprisingly, inhibition of PI-3 kinase with LY294002 partially blocked FGF-23-mediated NaPiIIa internalization. In tyrosine kinase receptor signaling in general and FGFR signaling specifically, the MAP kinase pathway may be activated by a number of upstream molecules including Ras, phospholipase C γ (PLC γ) via protein kinase C (PKC), and PI-3 kinase via PDK-1. In order, to further dissect the inputs to the MAP kinase pathway, we measured pERK by immunoblot in FGF-23 stimulated OK/e cells treated with the farnesyl transferase inhibitor (FTI-277) that induces accumulation of non-farnesylated cytoplasmic Ras to form inactive Ras/Raf complexes. OK/e cells were preincubated with 2 μ M FTI-277 for 1-24 hrs and then stimulated with FGF-23 (10 ng/ml) or PTH (1-84, 10⁻⁸M). MAP kinase activation was measured by immunoblot of whole cell lysate with a pERK antibody. In OK/e cells treated with FGF-23, FTI-277 did not appreciably reduce pERK compared to untreated FGF-23-stimulated cells. In contrast, PTH-stimulated ERK phosphorylation was completely abolished with FTI-277 treatment. U0126 blocked both FGF-23 and PTH-stimulated ERK phosphorylation. Taken together, these data suggest that the PI3 kinase pathway regulates FGF-23-mediated NaPiIIa internalization through crosstalk with the MAP kinase pathway and that this is a distinct signaling pathway from PTH-mediated NaPiIIa trafficking.

Disclosures: S.M. Jan de Beur, None.
This study received funding from: National Institutes of Health.

T159

Age-Dependent Regulation of FGF23 Production in Murine Bone. T. Masanori¹, B. Yuan², Y. Xing^{2*}, K. Aya¹, T. Morishima¹, M. K. Drezner², H. Tanaka¹ ¹Department of Pediatrics, Okayama Univ., Okayama City, Japan, ²Department of Medicine, Univ of Wisconsin and GRECC, William F. Middleton VAMC, Madison, WI, USA.

The detailed physiological regulation of FGF23 production remains unknown. However, the principal location of the hormone in osteoblasts and variation in the amount present during matrix mineralization suggests FGF23 production may be age-dependent (Bone. 2007 Feb 8 [pub ahead of print]). Thus, in the present study, we examined the influence of age on FGF23 production in mice. Initially, we measured serum FGF23 (s-FGF23) in wild type (WT) C57BL/6J mice at 2, 4 and 12 weeks of age. s-FGF23 was highest at 2 weeks and declined thereafter (516.5 \pm 48.3, 373.3 \pm 56.4 and 106.8 \pm 8.4 pg/ml, respectively; p<0.05). In accord, FGF23 mRNA expression in WT-mice significantly (p<0.05) decreased at 4 (41.5 \pm 9.1%) and 12 (77.9 \pm 8.4%) weeks of age. Interestingly, hypomimetic with a pathological abnormality of FGF23 metabolism, had superimposed on this defect a progressive age-dependent decrease in FGF23 mRNA production, significantly (p<0.05) declining by 42.2 \pm 9.6% at 4 weeks and 89.9 \pm 5.3% at 12 weeks. Accordingly s-FGF23 similarly decreased (4811.8 \pm 184.6, 3391.2 \pm 158.1 and 1367.4 \pm 59.2 pg/ml; p<0.05). To examine if the age-dependent modulation of FGF23 expression is PHEX independent, we established an in vitro system using osteoblasts derived from SV40 Tg mice (SV-Ob). Cells were maintained in α MEM containing 10% FBS, ascorbate and β -glycerolphosphate (VC-GP). The SV-Ob cells proliferated and reached sub-confluence at day 6 of incubation and after 12 days, mineralization of extra-cellular matrix was evident. After 3 days of incubation proliferating cells displayed abundant FGF23 mRNA expression, which decreased with maturity at 6 days (97.4 \pm 1.2%; p<0.05) and 12 days (99.1 \pm 0.2%; p<0.05) of incubation. Incubation of SV-Ob cells in conditioned medium from SV-Ob cells at day 6, but not day 12, of culture significantly elevated FGF23 mRNA expression compared to that in cells incubated with fresh VC-GP medium (4.86 \pm 0.90 fold; p<0.05), indicating that a factor(s) produced by immature osteoblasts plays an important role in regulation of FGF23 production. Interestingly, exposure of SV-Ob cells to d6 medium, containing the phex inhibitor, MH2-64-C, did not modulate the effect on FGF23 expression. Moreover, SV-Ob cells, transfected with pcDNA/phex-WT vector encoding the mouse phex protein, displayed FGF23 mRNA expression no different than that in SV-Ob cells transfected with an empty vector. Our observations clearly indicate that FGF23 production in murine osteoblasts is regulated by an age-dependent mechanism, which results in a PHEX independent decline of FGF23 mRNA with maturity.

Disclosures: T. Masanori, None.

T160

Overexpression of Low Molecular Weight Isoform of FGF2 partly prevents Bone Loss in Ovariectomized Mice. L. Xiao¹, J. D. Coffin², M. M. Hurley¹. ¹University of Connecticut Health Center, Farmington, CT, USA, ²The University of Montana, Missoula, MT, USA.

In humans, there are multiple high molecular weight (HMW, 22, 23, 24kDa) nuclear isoforms of basic fibroblast growth factor (FGF2) and a low molecular weight (LMW, 18kDa) isoform that is exported from cells. We previously reported that targeted over-expression of the LMW FGF2 isoform in preosteoblasts and mature osteoblasts increased bone mass in vivo and in vitro. To determine whether LMWFGF2 protects against ovariectomy induced bone loss, female Col3.6/GFP transgenic mice (VectorTg) and Col3.6/LMWFGF2/GFP transgenic mice (LMWTgFGF2) were ovariectomized (OVX) or sham-operated (sham) at 14 weeks of age and sacrificed 6 weeks post surgery. Six weeks after OVX, there were significant reductions in uterine weight in both VectorTg-OVX and LMWTgFGF2-OVX groups compared to the sham group. Body weight was significantly increased only in the VectorTg-OVX group compared with VectorTg-sham group. DEXA analysis showed a 4.6% and 9% significant reductions in femoral bone mineral density (BMD) and bone mineral content (BMC) in VectorTg-OVX group compared with VectorTg-sham group ($p < 0.05$). There was no significant reduction in BMD and BMC in LMWTgFGF2-OVX group compared with LMWTgFGF2-sham group. Micro-CT analysis revealed that femoral trabecular bone volume/total volume (BV/TV), connective density (Conn-Den) and trabecular number (Tb.N) were significantly decreased by 32%, 38% and 18% respectively in VectorTg-OVX compared with the VectorTg-sham group. However, there were only 24%, 22% and 13% decrease in femoral BV/TV, Conn-Den and Tb.N respectively in LMWTgFGF2-OVX group compared with LMWTgFGF2-sham group. At 2 and 3 weeks mineralized bone nodules were increased in ex vivo bone marrow stromal cell cultures from LMWTgFGF2-sham mice compared with VectorTg-sham and was further increased in cultures from LMWTgFGF2-OVX mice compared with VectorTg-OVX. Northern analysis showed that mRNA for Osteocalcin (OC); a late marker of differentiated osteoblasts; was similar between VectorTg-sham and VectorTg-OVX in 3 week cultures. However there was a 1.75 fold increase in LMWTgFGF2-sham compared with Vector-sham and a 1.91 fold increase in LMWTgFGF2-OVX compared with Vector-OVX group. Similar data was observed in two independent lines of LMWTgFGF2 mice. These data indicate that targeted over-expression of LMW isoform of FGF2 protein in preosteoblasts and osteoblasts partially protected against OVX-induced bone loss in vivo and in vitro.

Disclosures: L. Xiao, None.

T161

Bone Regeneration with Local Controlled Application of Granulocyte Colony-Stimulating Factor (G-CSF) in a Bone Defect of Rabbit Ulna. K. Ishida^{*1}, R. Kuroda^{*1}, K. Sasaki^{*1}, Y. Mifune^{*1}, K. Tei^{*1}, M. Miwa^{*1}, T. Matsumoto^{*1}, Y. Tabata^{*2}, M. Kurosaka^{*1}. ¹Department of Orthopaedic Surgery, Kobe University Graduate School of Medicine, Kobe, Japan, ²Department of Biomaterials, Field of Tissue Engineering, Institute for Frontier Medical Sciences, Kyoto University, Kyoto, Japan.

It is recognized that re-establishment of vascularity is an early event in fracture healing and the appropriate vascularization is emerging as a prerequisite for bone regeneration. G-CSF is a cytokine known to have an angiogenesis-promoting effect by recruitment of bone marrow cells. In this study, we investigated that the local applied G-CSF enhances bone regeneration via revascularization and osteoblast mobilization by controlled release from gelatin hydrogel. Methods: We have designed a biodegradable catonized gelatin (CG) hydrogel as the drug delivery system for G-CSF. All animal procedures were approved by the Animal Research Committee of Kobe University Graduate school of Medicine. 24 Japanese white rabbits were used in this study. A segmental bone defect (20 mm) was created at the diaphysis of rabbit ulna. The defects were treated in two groups as follows: Group G0: defects were filled with CG hydrogel only, Group G5: defects were filled with CG hydrogel with G-CSF (5µg). Every defect of the radiographs was obtained at 2, 4, and 8 weeks after surgery. Semiquantitative radiographic evaluations were performed using Image J and the radiographic healing was graded according to modified Cooks' grading scale. Toluidine blue staining was performed to see endochondral ossification. Histochemical staining for isolectin B4 was performed as an assessment of capillary invasion and immunofluorescent staining for osteocalcin were performed as an osteoblast marker. Results: Radiographic semiquantitative assessment revealed that there were more bone formation in group G5 than in group G0 at every weeks. Radiographic grading also revealed that bone formation was significantly promoted in group G5 at 4 and 8 weeks. Toluidine blue staining revealed that more cartilaginous matrix was seen in group G5 at as early as 2 weeks. Histochemical staining for isolectin B4 showed that capillary density was significantly increased in group G5 at 2 weeks. Osteoblast density was also significantly increased in group G5 at 2 weeks and these results revealed that revascularization and osteoblast mobilization into the bone defects were promoted in group G5. Conclusions: The present study demonstrates that local controlled application of G-CSF promotes rabbit bone regeneration. The reasons seemed that the G-CSF promoted revascularization and osteoblast mobilization. G-CSF had further possibility to apply other situations that needs both bone repair and neovascularization.

Disclosures: K. Ishida, None.

T162

Immunoregulatory Role of RANKL-stimulated Dendritic Cells on Autoimmune Arthritis in MRL/lpr Mice. T. Izawa^{*1}, N. Ishimaru^{*2}, K. Moriyama³, Y. Hayashi^{*2}. ¹Department of Orthodontics and Dentofacial Orthopedics, Institute of Health Biosciences, Tokushima University, Graduate School, Tokushima, Japan, ²Department of Oral Molecular Pathology, Institute of Health Biosciences, Tokushima University, Graduate School, Tokushima, Japan, ³Department of Maxillofacial Orthognathics, Tokyo Medical and Dental University, Graduate School, Tokyo, Japan.

Recent studies have established that receptor activator of NF-κB(RANK)/RANKL signaling plays a key role for maintenance of dendritic cells (DCs) in the periphery. However, the association of the RANKL signaling for DCs with autoimmunity has been obscure. In this study, we investigated the immunoregulatory role of DCs through RANKL signaling on autoimmune arthritis using MRL/lpr mice.

The phenotypes and functions were analyzed using DCs of spleen and lymph nodes, or bone marrow-derived DCs (BMDCs) from MRL/lpr and MRL/+/+ mice. The surface markers on the peripheral DCs and RANKL-stimulated BMDCs were analyzed by flow cytometer. Apoptosis- and cell cycle-related molecules of the DCs were detected by Western blot analysis. In addition, the adaptive transfer of RANKL-stimulated BMDCs was performed into MRL/lpr mice as recipients to modulate the arthritis lesions.

We found that the number of CD11c⁺CD11b⁺CD8a⁺ myeloid DCs in the periphery from MRL/lpr mice was significantly increased comparing with that from control mice, and that the MRL/lpr DCs could survive much longer than control DCs. In addition, the expressions of Bcl-x and Bcl-2 and the nuclear transport of NF-κB of RANKL-stimulated BMDCs from MRL/lpr mice were considerably upregulated compared with those from control mice. On the other hands, Fas expression of normal BMDCs was significantly increased by RANKL stimulation. Moreover, the adoptive transfer of RANKL-stimulated BMDCs resulted in accelerated and severe autoimmune arthritis of MRL/lpr recipients. These findings suggest that the crosstalk between RANKL and Fas signaling in DCs might influence the maintenance of DCs in the periphery and the development of autoimmunity.

Disclosures: T. Izawa, None.

T163

SDF-1/CXCR4 Is Essential for In Vivo Endochondral Bone Repair. T. Kitaori^{*1}, H. Ito¹, E. M. Schwarz², T. Nakamura¹. ¹Orthopaedic Surgery, Graduate School of Medicine, Kyoto University, Kyoto City, Japan, ²The Center for Musculoskeletal Research, University of Rochester, Rochester, NY, USA.

INTRODUCTION A chemokine, SDF-1, and its receptor, CXCR4, have been well known to play a crucial role in homing of hematopoietic stem cells (HSCs) to bone marrow niche. Additionally accumulating data have shown that SDF-1 is highly expressed in some damaged organs, such as myocardial infarction and brain injury, and recruits circulating mesenchymal stem cells (MSCs) to the damaged lesion, allowing them to start normal organ repair. But it is still unknown whether SDF-1 is involved in bone repair. Using murine autograft and allograft models, we tested the hypothesis that SDF-1 is essential in endochondral bone repair. **METHODS** We used in-vivo 4-mm segmental femoral autograft and allograft model of C57Bl/6 mice. For autograft model, the freshly removed bone was transplanted back to the same mouse, and secured by a metal pin. For allograft model, graft bones, which had been harvested from ICR mice and kept frozen for at least 24 hours, were applied to the defects. For a loss of function study in autograft model, mice received anti-SDF-1 neutralizing antibody or control IgG injection peritoneally after the implantation. For a gain of function study in allograft model, rmSDF-1 protein or adeno-SDF-1 was loaded locally around the graft bones. For an in-vivo chemotaxis assay, pre-cultured bone marrow stromal cells (BMSCs) were labeled with BrdU and transplanted through tail vein at the end of the surgery. Bone grafts and surrounding tissue were harvested at days 0.5, 1, 2, and 3 after transplantation for RNA extraction and at days 7, 14, and 28 for histological analysis. The expression of SDF-1 mRNA was measured by RT-PCR. To detect the labeled-BMSCs immunohistostaining using anti-BrdU antibody was examined. **RESULTS & DISCUSSION** In this study we demonstrated the involvement of SDF-1 in endochondral bone repair. The mRNA expression of SDF-1 was increased in autograft at days 2 after transplantation, while no increase was detected in allograft. The transplanted BMSCs were detected around the grafted bones at days 7. Moreover the new bone formation around the autograft was significantly inhibited by the injection of anti-SDF-1 antibody. These data indicated that SDF-1 had an essential role in the acute phase of normal bone repair. The gain of function study, however, showed no remarkable increase in the bone formation, suggesting that SDF-1 may need to collaborate with other molecules to have a successful effect.

Disclosures: T. Kitaori, None.

T164

Intracellular Cytokine Profile of RANKL Expressing Lymphocytes. D. Krenbek, U. Semrad*, M. Rauner*, D. Stupphann*, J. Patsch, M. Willheim*, P. Pietschmann. Department of Pathophysiology, Medical University of Vienna, Vienna, Austria.

Cytokines play an important role in regulation of bone mass by influencing Receptor activator of NF κ B (RANKL). For example, TNF α increases bone resorption by elevating RANKL expression while IFN γ suppresses osteoclastogenesis by inhibiting RANK/RANKL signalling. Lymphocytes are major producers of cytokines and as they express RANKL, they are thought to be involved in bone destruction in a number of diseases including rheumatoid arthritis, parodontitis and possibly osteoporosis. Yet their function in bone metabolism is still poorly understood. Therefore we studied expression of surface and intracellular RANKL in lymphocytes as well as cytokine production by flow cytometry.

Peripheral blood mononuclear cells were isolated from young healthy subjects and stimulated for 4 hours with ionomycin (1.25 μ M), phorbol 12-myristate 13-acetate (10 ng/ml) and brefeldin A (10 μ g/ml). Harvested cells were incubated with an anti human RANKL specific monoclonal antibody followed by saponin treatment and further incubation with antibodies against IFN γ , TNF- α and CD4. To detect intracellular RANKL cells were permeabilised prior to staining.

Data was acquired on a FACSCalibur flow cytometer (Becton Dickinson) and analysed with the CellQuest Pro Software. RANKL positive cells were gated to illustrate their intracellular cytokine pattern.

In most of the cells intracellular RANKL was detected whereas only few cells were positive for surface RANKL. The latter were predominantly negative for IFN γ (80 \pm 7%) but expressed TNF α (47 \pm 26%). By gating on CD4 positive lymphocytes a similar pattern in RANKL and cytokine expression was observed.

Our data suggest that lymphocytes are involved in regulation of bone mass predominantly by the secretion of RANKL, rather than regulatory interaction of surface-expressed RANKL with target cells. Yet a small sub-population of lymphocytes expressing surface RANKL but not IFN γ may act on osteoclasts and their precursors directly via cell-cell contact.

Disclosures: D. Krenbek, None.

T165

TNF-alpha Dependent Redox Signals Upregulate Msx2 Gene Transcription via Stress Activated Protein Kinases in Arterial Myofibroblasts. C. F. Lai-Huang, J. S. Shao, E. Huang*, Z. Al-Aly*, S. L. Cheng, D. A. Towler. Internal Medicine - Bone and Mineral Diseases, Washington University School of Medicine, St. Louis, MO, USA.

Aortofemoral calcification is prevalent in type II diabetes (T2DM), tracking metabolic syndrome parameters and increasing the risk for lower extremity amputation. LDLR $^{-/-}$ mice fed high fat diets (HFD) develop T2DM, and accumulate aortic calcium, mediated via BMP2 and Msx2-Wnt osteogenic mechanisms that resemble craniofacial mineralization. Low-grade inflammation - including elevated serum TNF-alpha -- is characteristic of T2DM. TNF-alpha upregulates myofibroblast BMP2, a potent stimulus for aortic Msx2 expression. We wished to determine if TNF-alpha augmented Msx2 expression in arterial myofibroblasts, potentially via autocrine BMP2 signals. TNF-alpha (10 ng/ml) upregulated both BMP2 and Msx2 mRNA accumulation 4-fold in aortic myofibroblasts following 6 hours of treatment. However, detailed time course reveals that Msx2 induction actually precedes BMP2 expression, with 2-fold Msx2 induction observed within 1 hour of treatment. Moreover, addition of 250 ng/ml recombinant noggin, an inhibitor of BMP2 and BMP4, did not inhibit Msx2 induction, providing further evidence of regulation independent of autocrine BMP2 signals. Msx2 induction was maximal by 3 hours, and dose-response studies revealed an ED50 for TNF-alpha of 2 ng/ml. Induction was completely abrogated by actinomycin treatment, and dose-dependently prevented by DRB, indicating Msx2 induction was transcriptionally regulated by TNF-alpha. Inhibition of the IKK-NF-kappaB pathway with BAY 11-7082 did not inhibit (actually enhanced) Msx2 induction. However, the JNK/SAPK inhibitor SP600125 significantly reduced TNF-alpha actions. JNK/SAPK is a critical component of the oxidative stress signaling cascade downstream of NADPH oxidase. Therefore we examined the effects of apocynin (NADPH oxidase inhibitor), SIN-1 (superoxide and nitric oxide precursor) and H202 on Msx2 expression. Apocynin reduced both basal and TNF-alpha stimulated Msx2 expression, indicating a role for NADPH oxidase redox signaling in aortic myofibroblasts. SIN-1 treatment had no effect. However, H202 dose-dependently upregulated Msx2 mRNA accumulation, phenocopying the response to TNF-alpha. Finally, mice with vascular TNF-alpha augmented by a SM22- TNFalpha transgene exhibit higher levels of aortic Msx2 gene expression vs. non-transgenic sibling cohorts, providing further evidence for a vascular TNFalpha - Msx2 regulatory axis in vivo. Thus, arterial myofibroblast Msx2 gene transcription is directly stimulated by TNF-alpha, entraining vascular Msx2 expression to inflammation via redox-regulated JNK/SAPK signal cascades.

Disclosures: C.F. Lai-Huang, None.

This study received funding from: National Institutes of Health.

T166

The Role of Wnt3A Signaling in Maturation of Rat Osteoblasts. L. Ling*, C. Dombrowski*, L. M. Haupt*, V. Nurcombe*, S. M. Cool. Stem Cells and Tissue Repair, Institute of Molecular and Cell Biology, Singapore, Singapore.

Recent studies have indicated that heparan sulfate (HS) sugar-dependent Wnt signaling is crucial to bone formation. These sugars are manufactured in the Golgi, and are heavily reliant on the HS-synthesizing enzymes glucosaminyl N-deacetylase/N-sulfotransferase-1 (NDST-1) and HS 2-O-sulfotransferase (HS-2-OST). NDSTs and HS-2-OST are responsible for HS N-sulfation and O-sulfation, respectively; NDST1 is also a key enzyme directing further HS modifications including O-sulfation. Recent studies have indicated that HS regulates proliferation and differentiation of osteoblasts and improves bone healing. The work here was designed to investigate the function of Wnt3A during the maturation of primary osteoblasts derived from new-born rat calvaria. Sequential digests of rat calvaria were able to release cells characteristic of the various stages of osteogenic development. Preosteoblasts (fraction 3) were most sensitive to 1,25 α -vitaminD3 and parathyroid hormone, whilst more mature osteoblasts (fraction 5) exhibited the greatest alkaline phosphatase (ALP) activity as well as collagen I α 1 and osteocalcin (OC) expression. The osteogenic potential of F3 and F5 were further demonstrated by Alizarin Red and von Kossa staining. The mRNA level of target genes and the expression of target proteins were determined by RQ-PCR and Western Blot analysis, respectively, and cell proliferation determined by the GUAHA PCA-96 Viacount system. We found that the levels of NDST1 and HS-2-OST were at least 5-fold higher in F3 than F5, suggesting that HS sugars are intimately involved in the maturation of pre-osteoblasts to osteoblasts. We further demonstrated that Wnt3A increased NDST1 expression in F5 (2.7-fold) and F3 (1.4-fold). Wnt3A and LiCl (an activator of Wnt signaling) both inhibited cell proliferation while increasing ALP activity and OC expression in both fractions, inducing a higher ALP activity in F3 (2.1-fold) than F5 (1.5-fold) but a higher OC expression in F5 (5.0-fold) than F3 (1.7-fold). Heparin dose-dependently increased Wnt3A-stimulated ALP activity in F3, but decreased it in F5. We also observed that activation of Wnt signaling dramatically increased noggin expression, a BMP inhibitor, while decreasing RUNX2 expression. In conclusion, Wnt3A signaling regulates the maturation of calvaria osteoblasts by switching the cells from proliferation to differentiation. As Wnt3A is known to interact with BMP2 signaling which is also mediated by HS, the sugar may be orchestrating the availability of these factors to precursor cells.

Disclosures: L. Ling, None.

*This study received funding from: Institute of Molecular and Cell Biology, A*STAR.*

T167

Osteoprotegerin as Cardiovascular Risk Marker in Patients with Type 2 Diabetes Mellitus. P. Rozas-Moreno*, M. Muñoz-Torres, G. Alonso*, D. Fernández-García*, I. Luque-Fernández*, A. Sebastian-Ochoa*, F. Escobar-Jiménez*. Bone Metabolic Unit. Department of Endocrinology, University Hospital San Cecilio, Granada, Spain.

Background: Type 2 diabetes mellitus patients have a high prevalence of cardiovascular disease. The classic cardiovascular risk factors seem not to completely explain such increase in vascular disease in type 2 diabetes mellitus. Hyperhomocysteinemia and enhanced carotid intima-media thickness (CINT) are both predictors of cardiovascular disease in diabetic patients. It has been postulated that osteoprotegerin (OPG) could be the physiopathologic link between osteoporosis and vascular disease. On the other hand, elevated serum levels of OPG, a key cytokine in the bone remodelling process, have been related to an increased mortality due to cardiovascular events in type 2 diabetes mellitus patients.

Objective: To analyze the association between serum OPG and some of the cardiovascular risk factors observed in type 2 diabetes mellitus (Arterial hypertension [HT], hyperlipidemia, obesity, smoking, hyperhomocysteinemia, CINT).

Patients and methods: 72 patients with type 2 diabetes mellitus were studied. All of them attended to the Endocrinology Service of University Hospital "San Cecilio" of Granada, Spain. Arterial hypertension was defined as blood pressure \geq 140/ 90 mmHg and/or actual anti-hypertensive treatment. Serum levels of homocystein, LDLc, HDLc and OPG were measured (OPG ELISA BI-20402, BIO-MEDICA-GRUPPE WIEN, Austria). Hyperlipidemia was defined according to the ATPIII criteria (statins treatment, LDLc \geq 130 mg/dl, HDLc $<$ 40/50 mg/dl in males and females respectively). Obesity was graded using the Body Mass Index (BMI: Kg/m 2). The CINT was determined by means of vascular Eco-doppler (TOSHIBA Vision 6000) of both carotid arteries at the level of 10 mm proximal from the carotid branch off using a mode B, 7.5 MHz probe. A value \geq 0.9 mm was considered as pathologic.

Results: The study population included 41.7% females and 58.3% males, mean age 57.9 \pm 6.3 years-old. Males showed smaller serum levels of OPG than females (4.70 \pm 1.8 vs 5.98 \pm 2.6 pmol/L respectively, p=0.02). Serum levels of OPG were positively related to age in both genders (r=0.31, p=0.01). In female patients OPG levels were not significantly related to none of the studied variables. In males the serum levels of OPG were significantly related to presence of HT (Yes/No: 5.59 \pm 2.3 vs 4.06 \pm 1.5 pmol/L, p=0.01), CINT = 0.9 mm (Yes/No 5.09 \pm 1.6 vs 3.9 \pm 1.9 pmol/L, p= 0.03), presence of carotid plaque (Yes/No: 5.46 \pm 1.6 vs 4.22 \pm 1.8 pmol/L, p= 0.047) and BMI (r= 0.3, p= 0.05).

Conclusion: Our results suggest that the serum levels of OPG could contribute additional information about the cardiovascular risk in males with type 2 diabetes mellitus.

Disclosures: M. Muñoz-Torres, None.

T168

Local CNP Clearance System as a Regulator of CNP-GC-B System for Bone Growth. Y. Nakatsuru*. Endocrinology and Metabolism, Kyoto University, Kyoto, Japan.

Natriuretic peptide family consists of three endogenous ligands, ANP, BNP and CNP. They exert their biological actions by producing intracellular cyclic GMP through two subtypes of membranous guanylyl cyclase (GC), GC-A and GC-B. The third natriuretic peptide receptor is called clearance receptor (C-receptor), which has no GC activity and is involved in the clearance of ligands. ANP and BNP are widely known as regulators of cardiovascular homeostasis through GC-A, whereas recent studies elucidated that CNP plays pivotal roles in the regulation of endochondral bone growth via GC-B. A previous study demonstrated that C-receptor deficient mice exhibit skeletal overgrowth like transgenic mice with targeted overexpression of CNP in cartilage. Here we examined the significance of natriuretic peptide clearance system in the growth plate using fetal mouse tibial organ culture. A specific agonist for C-receptor, C-ANF, increased the production of intracellular cGMP dose-dependently, and accordingly, elongated the tibial explants and their cartilaginous primordium significantly. Histological examination revealed that the width of the growth plate is widened in the C-ANF treated group. On the other hand, C-ANF did not increase the length of tibial explants from CNP depleted mice. These results suggest that C-ANF raised local CNP concentration in the growth plate cartilage. We conclude that local CNP clearance system is essential for the regulation of growth promoting effect of CNP-GC-B system in the growth plate.

Disclosures: Y. Nakatsuru, None.

T169

Involvement of Connexin43 in Interleukin-1 β -induced Osteoarthritis-Associated Changes in Synovial Fibroblasts. C. Nigier, F. D. Howell*, J. P. Stains. Orthopaedics, University of Maryland, Baltimore, MD, USA.

Interleukin-1 beta (IL-1 β), produced by activated synovocytes, has been reported to play a prominent role in the pathology of osteoarthritis (OA). In vivo studies have shown an enhancement in connexin43 (Cx43)-mediated gap junctional intercellular communication between synovial lining cells as one of the changes observed in OA. The purpose of this study is to examine the role that Cx43 plays in the IL-1 β -induced changes in OA-associated gene expression observed in synovial fibroblasts.

We show that treatment of a rabbit synovial fibroblast cell line (HIG-82) with IL-1 β stimulates the synthesis of Cx43 protein in a dose- and time-dependant manner. Additionally, by immunocytochemistry, we observe a large scale redistribution of Cx43 from the cytosol to the plasma membrane, following treatment with 1 ng/ml IL-1 β for 16h. By real time PCR, we detect that IL-1 β treatment or transient transfection of Cx43 in synovial fibroblasts were both effective at increasing gene expression of several OA-associated genes, including matrix metalloproteinases (MMP-1 and -13) and cyclooxygenase-2. Similar results for secreted MMP activity in conditioned media were also observed. Surprisingly, overexpression of Cx43 is as effective, if not more effective, than IL-1 β treatment at inducing the expression and/or activity of OA-associated genes. Thus, it appears that IL-1 β increases Cx43 levels and alters localization, and that this change in Cx43 is sufficient to induce OA-associated gene expression and MMP activity. In order to elaborate on these findings, we examined the signal transduction cascades downstream of IL-1 β treatment. We show that IL-1 β potentially activates the extracellular signal regulated kinase (ERK) cascade. Furthermore, inhibition of the ERK cascade with U0126 abrogates the upregulation of Cx43 expression, the cellular redistribution of Cx43 to the plasma membrane, and the associated changes in gene expression and MMP activity. Importantly, Cx43 overexpression in conjunction with IL-1 β does not synergize to increase transcription of OA-associated genes, nor does Cx43 overexpression potentiate ERK activation by IL-1 β .

Together, our data show that Cx43 is a major target of IL-1 β action on synovial fibroblasts. The data suggest that IL-1 β acts on Cx43 expression and cellular distribution in an ERK-dependent manner, and the subsequent effects of these changes on Cx43 are sufficient to induce OA-associated changes in the phenotype of these cells.

Disclosures: C. Nigier, None.

T170

Role of Interleukin-6 Signalling in c-Src-mediated Osteoblast Differentiation. B. Peruzzi*¹, M. Longo*¹, N. Rucci¹, F. De Benedetti*², A. Teti¹. ¹Experimental Medicine, University of L'Aquila, L'Aquila, Italy, ²Ospedale Pediatrico Bambino Gesù, Rome, Italy.

The non-receptor tyrosine kinase c-Src plays unique roles in the regulation of bone cell activity. In osteoblasts (OBs) c-Src maintains an "immature" state in which cell proliferation is very active and further differentiation is inhibited. In a large-scale transcriptome study of mouse primary OBs treated with the c-Src inhibitor PP1, we noted a ~60% expression decrease of the pro-inflammatory cytokine interleukin-6 (IL-6), confirmed by RT-PCR and ELISA assay. Our previous work had shown that NSE/hIL-6 transgenic mice, which have high levels of circulating IL-6, display reduced OB activity, therefore we hypothesized that c-Src and IL-6 could be functionally associated in regulating OB function and that they could contribute to imbalanced bone remodelling in pathologic situations. In a time-course experiment in which we treated mouse primary OBs with PP1, we investigated IL-6 expression and found a time-dependent reduction of IL-6 mRNA in PP1- vs. vehicle-treated OBs, also confirmed at level of secreted protein by ELISA assay. The same result was also obtained in OBs in which c-Src was inhibited by

siRNA treatment for 48 hours and by retroviral infection with a dominant-negative-Src isoform. In order to explain how c-Src inhibition influenced IL-6 expression, we tested the involvement of "Signal Transducer and Activator of Transcription" (STAT) proteins, among which STAT3 is described to drive the transcription of the IL-6 gene and to be a c-Src substrate. In the PP1 time-course experiment we showed that STAT3-phosphorylation at the tyrosine 705 (a c-Src substrate) was decreased following c-Src inhibition, suggesting involvement of this transcription factor in the c-Src-dependent regulation of IL-6 expression. We then tested a possible role for STAT3 on c-Src signalling. We inhibited STAT3 by siRNA and found a reduced c-Src-activating phosphorylation and increased osteoblast differentiation markers. Consistent with our hypothesized IL-6 role, we observed a time-dependent increase of c-Src activating phosphorylation in primary OBs treated with recombinant human IL-6 (rhIL-6) for 1 week. In conclusion, we have obtained evidence of a relevant interplay between c-Src and IL-6 in OB differentiation, partly based on STAT3-dependent transcription.

Disclosures: B. Peruzzi, None.

T171

Characterization of a New Traumatic Mouse Model of Heterotopic Ossification. B. E. Rapuano*¹, A. Grose*², E. Tomin*¹, J. M. Lane*³, D. Helfet*³. ¹Research, Hospital for Special Surgery, N.Y., NY, USA, ²Orthopedics, Upstate Medical Center, Syracuse, NY, USA, ³Orthopedics, Hospital for Special Surgery, N.Y., NY, USA.

Purpose: To develop a physiologically relevant traumatic model of heterotopic ossification (HO) in the mouse, quantify the amount of ectopic bone which forms in the model, and begin to characterize the molecular regulators that mediate the formation of HO.

Methods: Mice from the C57BL/6J strain underwent a surgical procedure in which the quadriceps in recipient mice were subjected to surgical trauma by clamping and bone marrow cells from donor mice were transplanted into a pouch created surgically in the clamped area in recipient mice. Some recipient mice were sacrificed 42 days following surgery, the femurs with attached quadriceps were removed from the operated hindlimbs, and HO was quantified by microCT analysis. Other recipient mice were sacrificed at 2, 7 and 14 days following surgical induction of HO and femur / muscle samples were removed, fixed, embedded in paraffin and sectioned for histology. The expression of bone morphogenetic protein (BMP) 2, 4 and 7 was analyzed immunohistochemically in deparaffinized sections.

Results: HO (1.47 +/- 0.3 mm³; mean +/- S.E.) formed in the quadriceps of all of the operated limbs (12 of 12). Bone mineral density, tissue mineral density and bone volume fraction were 273 +/- 55 mg/cc, 504 +/- 75 mg/cc and 0.42 +/- 0.02, respectively (N = 12 mean +/- S.E.). BMP positive cells were found at the site of tissue injury several weeks before the development of HO.

Conclusions: By transplanting bone marrow containing stromal cells into a site of muscle injury, traumatic HO can be formed reproducibly in an animal model in which putative molecular regulators of the human disorder are expressed prior to the formation of ectopic bone. Therefore, we have developed a new mouse model of traumatic HO that may be more physiologically relevant than previous models that rely on exogenous BMP's or demineralized bone matrix.

Disclosures: B.E. Rapuano, None.

This study received funding from: AO Foundation.

T172

Connective Tissue Growth Factor Induces NFAT and Osteoblastogenesis In Vitro. A. Smerdel-Ramoya, S. Zanolli, E. Canalis. Research, Saint Francis Hospital and Medical Center, Hartford, CT, USA.

Connective Tissue Growth Factor (CTGF) is a member of the CCN family of secreted proteins that regulates multiple cellular functions. Previously, we demonstrated that osteoblasts express CTGF, but its role in osteoblastic differentiation and function remains unclear. To define the function of CTGF, ST2 stromal cells were transduced with a retroviral vector expressing CTGF under the control of the cytomegalovirus promoter. Overexpression of CTGF induced osteoblastogenesis, increased mineralized nodule formation, alkaline phosphatase activity and osteocalcin mRNA levels. Although, CTGF can interact with BMPs, it did not enhance the effect of BMP-2 on Smad signaling or the effect of Wnt3a on Wnt/ β -catenin signaling. To investigate alternate mechanisms involved in the osteoblastic differentiation induced by CTGF, we examined CTGF activity on the nuclear factor of activated T cells (NFAT), a transcription factor that cooperates with osterix in the formation of bone. CTGF increased the transactivation of a transiently transfected IL-4-9xNFAT-Luc construct, where 9 repeats of NFAT sites direct luciferase expression. The effect was reduced by FK506, an inhibitor of calcineurin, suggesting that CTGF acts on the calcineurin dependent pathway to activate NFAT. In addition, CTGF increased the transcription of Hes-1, a transcription factor known to regulate osteoblastogenesis and NFAT expression. Down regulation of Hes-1 using RNA interference (RNAi) resulted in a decrease of NFAT activation by CTGF, indicating that the induction of Hes-1 by CTGF explains in part its effect on NFAT transactivation. Although, hes-1 is a Notch target gene, its induction by CTGF cannot be explained by activation of the canonical Notch RBPJk/CSL signaling pathway, since CTGF opposed Notch signaling. Down-regulation of CTGF expression by RNAi suppressed NFAT and Hes-1 transactivation confirming that both, NFAT and Hes-1, are dependent on CTGF expression. In conclusion, CTGF overexpression induces osteoblastic differentiation possibly by enhancing NFAT and Hes-1 signaling.

Disclosures: A. Smerdel-Ramoya, None.

T173

NOX Expression in Odontoblasts and Cementoblasts of NOS Knock-out Mice. Y. Sugawara, H. Watanabe, T. Yanagisawa*. Ultrastructural Science, Tokyo Dental College, Chiba, Japan.

Reaction systems of nitric oxide (NO) and reactive oxygen species (ROS) are intricately combined and are involved in the control of many cell functions such as tissue homeostasis, as well as tissue damage and diseases. Oral tissues are sensitive to the effects of their gas environment, but there are a few reports on these effects. In this study, we performed the following experiment to evaluate the protein levels of ROS synthetase, superoxide dismutase (SOD), and nitric oxide synthetase (NOS) in the dental pulp, odontoblasts, periodontal ligament and cementoblasts of normal and NOS1 (n-NOS), NOS2 (i-NOS), and NOS3 (e-NOS) knock-out (KO) mice and to clarify the interrelations of the kinetics of various enzymes in the absence of n-, i-, e-NOS. After anesthetizing 5-week-old normal and NOS1, 2, and 3 KO mice, immunohistochemical evaluation were performed using NOXA, NOXA, NQO, and Mn-SOD antibodies. The expression of NOXA, NOXA, and NQO in odontoblasts and cementoblasts were weakly positive in the control mice and strongly positive in the NOS2KO and NOS3KO mice. The Mn-SOD expression in odontoblasts and cementoblasts were weakly positive in the control mice and strongly positive in the NOS2KO and NOS3KO mice. From these results, ROS were considered to be generated by NOX1 in odontoblasts and cementoblasts, and this ROS generation to be affected by i-NOS and e-NOS. Furthermore, as Mn-SOD and NOX were strongly positive in the same areas, increases in ROS are considered to be accompanied by increases in Mn-SOD.

Disclosures: Y. Sugawara, None.

T174

Adiponectin, Anabolic to Bone In Vitro but Negative Effects In Vivo. G. A. Williams*, K. E. Callon*, J. Lin*, M. Watson*, D. Naot*, Y. Wang*, A. Xu*, J. Cornish*, I. R. Reid*. ¹Medicine, University of Auckland, Auckland, New Zealand, ²Genome Research Center, University of Hong Kong, Hong Kong, Hong Kong, ³Medicine, University of Hong Kong, Hong Kong, Hong Kong.

Adiponectin, the most abundant adipose-specific protein, regulates energy homeostasis as well as glucose and lipid metabolism. Adiponectin is reduced in obesity, insulin resistance and type 2 diabetes, and plasma concentrations are inversely related to body weight.

Body weight is an important risk factor for vertebral and hip fractures, ranking in importance alongside that of age. There is now an accepted positive association of fat mass with the secretion of bone active hormones from the pancreatic beta cell and from the adipocyte.

We have investigated the effect of adiponectin on bone cells in vitro as well as to determine the bone phenotype of adiponectin knockout mice. Adiponectin significantly stimulated osteoclastogenesis by 21% at 0.1 µg/mL, but markedly inhibited this process by 26% and 54% at 1 and 5 µg/mL, respectively. It had no effect on bone resorption in the isolated mature osteoclast assays. Adiponectin was dose-dependently mitogenic to primary osteoblasts (24% increase at 5 µg/mL).

Male adiponectin-deficient (Ad-KO) and wild-type (WT) C57BL/6J mice were examined at 8 and 14-weeks of age. We scanned the left proximal tibia using micro-CT at 5µm resolution and analysed bone micro-architecture by 3D analysis. We found significant increases in trabecular bone volume (BV/TV) (15.92±1.63% in Ad-KO vs 12.19±0.72% in WT, p=0.02) and trabecular number (3.20±0.18mm⁻¹ in Ad-KO vs 2.32±0.12mm⁻¹ in WT, p=0.0009) in 14-week old Ad-KO mice compared to controls. Similar differences between WT and Ad-KO were present in 8-week old animals, but these did not reach statistical significance.

Our results demonstrate that although adiponectin can be anabolic in vitro, adiponectin-deficient animals have increased number and volume of trabeculae, indicating that adiponectin is inhibitory to bone accrual in vivo. The latter data concur with the observations from epidemiological studies in humans that adiponectin negatively correlates with both fat mass and bone mass. Therefore, adiponectin may be a contributor to the link between fat and bone mass.

The actions on bone of novel hormones related to nutrition are an important area of further research. An understanding of this aspect of bone biology may open the way for new treatments of osteoporosis. The role of weight maintenance in the prevention of osteoporosis is an important public health message that needs to be more widely appreciated.

Disclosures: G. A. Williams, None.

This study received funding from: HRC.

T175

EGF-like Ligands Stimulate Osteoclastogenesis by Regulating Expression of Osteoclast Regulatory Factors by Osteoblasts: Implications for Osteolytic Bone Metastases. J. Zhu¹, X. Jia¹, G. Xiao², Y. Kang³, N. C. Partridge¹, L. Qin¹. ¹Physiology and Biophysics, UMDNJ-Robert Wood Johnson Medical School, Piscataway, NJ, USA, ²Medicine, University of Pittsburgh, Pittsburgh, PA, USA, ³Molecular Biology, Princeton University, Princeton, NJ, USA.

Epidermal growth factor (EGF)-like ligands and their receptors constitute one of the most important signaling networks functioning in normal tissue development and cancer biology. In vivo mouse models suggest this signaling network plays an important role in bone metabolism. Previous studies found that EGF stimulates bone resorption in organ cultures but the mechanism was unknown. Here we report that EGF-like ligands stimulate formation of TRAP-positive osteoclastic cells in a coculture system containing bone marrow macrophage and osteoblastic MC3T3-E1 cells. Western blots and [125I]EGF ligand binding experiments revealed that MC3T3-E1 cells express EGF receptor (EGFR) while osteoclasts do not, indicating EGF-like ligands do not function directly on osteoclasts. Conditioned medium from EGF-treated MC3T3-E1 cells generated more multinucleated TRAP-positive osteoclasts in the primary osteoclastic culture than conditioned medium from control-treated MC3T3-E1 cells, suggesting that EGF-like ligands regulate the production of secretory factors from osteoblasts. Using quantitative RT-PCR and ELISA, we identified that EGF-like ligands have no effect on RANKL expression but decrease its decoy receptor osteoprotegerin (OPG) expression and increase monocyte chemoattractant protein 1 (MCP1) expression in both MC3T3-E1 and mouse bone marrow primary osteoblastic cells. MCP1 is a chemokine that recruits osteoclasts and stimulates their fusion. Addition of exogenous OPG completely inhibited osteoclast formation stimulated by EGF-like ligands in the coculture system, while addition of a neutralizing antibody against MCP1 exhibited partial inhibition. Coculture with bone metastatic breast cancer cells, MDA-MB-231, which express significant levels of EGF-like ligands, had similar effects on the expression of OPG and MCP1 in the osteoblastic cells and these effects could be partially abolished by EGFR inhibitor PD153035. In summary, we demonstrate that EGFR signaling stimulates osteoclastogenesis indirectly by regulating OPG and MCP1 expression in osteoblasts. Since a high percentage of human carcinomas express EGF-like ligands, our findings suggest a novel mechanism for osteolytic lesions caused by cancer cells metastasizing to bone.

Disclosures: J. Zhu, None.

This study received funding from: NIDDK.

T176

Glucocorticoid Enhances the Expression of a Wnt Antagonist, Secreted Frizzled-Related Protein 3, in Cultured Human Osteoblasts. K. Ohnaka*, Y. Matsuzaki*, M. Tanabe*, M. Adachi*, H. Kawate*, R. Takayanagi*. ¹Department of Geriatric Medicine, Kyushu University, Fukuoka, Japan, ²Department of Medicine and Bioregulatory Science, Kyushu University, Fukuoka, Japan.

Glucocorticoid-induced osteoporosis (GIO) is one of the most frequent and serious problems of long-term glucocorticoid therapy. Although the major cause of GIO is considered to be impairment of bone formation, detailed mechanism underlying GIO remains to be fully elucidated. Recently, the Wnt signal emerged as a novel key pathway for promoting bone formation. In this study, we investigated the effect of glucocorticoid on a Wnt antagonist, secreted frizzled-related protein (sFRP), in cultured human osteoblasts and an osteosarcoma-derived cell line, MG-63 cells. The expression of mRNA for secreted frizzled-related protein 3 (sFRP3) was markedly induced by dexamethasone among sFRP families. The expression of sFRP3 was also enhanced by hydrocortisone and prednisolone, but not by 17-β estradiol, dehydrotestosterone or 1, 25-dihydroxyvitamin D₃. Similar effect of dexamethasone on sFRP3 expression was observed in MG-63 cells.

To examine the effect of sFRP3 on osteoblast function, we then generated an expression vector containing entire coding region of human sFRP3 cDNA (pcDNA-sFRP3-HA). Transient transfection of pcDNA-sFRP3-HA suppressed the Wnt3a-induced accumulation of cytosolic β-catenin in MG-63 cells. Transfection of sFRP3 also decreased the Tcf/Lef-dependent transcriptional activity in MG-63 cells. Furthermore, sFRP3 suppressed the proliferation of MG-63 cells.

These data suggest that glucocorticoid may impair osteoblast function and bone formation by enhancement of sFRP3 in human osteoblastic cells, which may be involved in the pathogenesis of GIO.

Disclosures: K. Ohnaka, None.

T177

Identification and Functional Involvement of Lipocalin 2 in Glucocorticoid-induced Growth Retardation. H. C. Owen^{*1}, S. F. Ahmed², C. Farquharson¹. ¹Bone Biology Group, Roslin Institute, Edinburgh, United Kingdom, ²Bone and Endocrine Research Group, Royal Hospital for Sick Children, Glasgow, United Kingdom.

Glucocorticoids (GC) are commonly used for immunomodulation and steroid replacement. Long-term use can, however, result in side effects including growth retardation in children. This is thought to be due to their actions on growth plate chondrocytes. To gain an insight into the mechanisms involved in GC-induced growth retardation, we performed Affymetrix microarray analysis of the murine chondrogenic cell line ATDC5, incubated with 10⁻⁶M dexamethasone (Dex) for 24h. Differential expression of selected genes was confirmed by qRT-PCR. Genes confirmed as down-regulated included secreted frizzled-related protein and IGF-I, whilst upregulated genes included serum/GC-regulated kinase, connective tissue growth factor, and lipocalin 2. Lipocalin 2 is an acute phase transport protein which we have shown is expressed in proliferative chondrocytes within the growth plate. In this study, qRT-PCR analysis confirmed that lipocalin 2 gene expression increased in ATDC5 cells by 40-fold after 24h Dex. Expression further increased after 48h (75-fold) and 96h (84-fold) Dex and this response was Dex concentration-dependent. Western blotting confirmed that Dex also increased lipocalin 2 protein expression. The lipocalin 2 response was not blocked by cycloheximide or the p38 inhibitor SB203580, but was blocked by the GC-receptor antagonist RU-486 and the Nuclear-Factor kappa B (NFkB) inhibitor TLCK. The lack of a cycloheximide effect implies a direct action of Dex on lipocalin 2 expression, which is consistent with the presence of a glucocorticoid response-element on the lipocalin 2 promoter. Dex also caused an increase in lipocalin 2 expression in primary murine chondrocytes at 6h (2.5-fold, p<0.05), and this was maintained for up to 72h. Proliferation in ATDC5 cells stably transfected to overexpress lipocalin 2 was slower than control cells (49%, p<0.05) and lipocalin 2 overexpression caused an increase in proteoglycans (66%, p<0.05) and collagen type-X expression (4-fold, p<0.05). Alkaline phosphatase activity and expression was unaffected. The effects of lipocalin 2 overexpression on chondrocyte proliferation (64%, p<0.05) and collagen type-X expression (8-fold, p<0.05) were further exacerbated with the addition of 10⁻⁶M Dex. This synergistic effect may be explained by a further increase in lipocalin 2 expression with 10⁻⁶M Dex in transfected cells (45%, p<0.05). These results suggest that lipocalin 2 may mediate Dex effects on chondrocytes through an NFkB-dependent pathway, and therefore provides a potential novel mechanism for GC-induced growth retardation.

Disclosures: H.C. Owen, None.

This study received funding from: BBSRC.

T178

The Temporal Feature of Bone Marrow Fat Cells in the Process of Steroid-Associated Osteonecrosis Development. H. Sheng^{*1}, G. Zhang^{*1}, L. Qin^{*1}, W. Cheung^{*1}, C. Chan^{*1}, Y. Wang^{*2}, H. Wang^{*3}, K. Lee^{*4}, K. Leung^{*1}. ¹Orthopaedics & Traumatology, the Chinese University of Hong Kong, Hong Kong, Hong Kong, ²Diagnostic Radiology and Organ Imaging, the Chinese University of Hong Kong, Hong Kong, Hong Kong, ³Fudan University, Shanghai, China, ⁴Lee Hysan Clinical Research Laboratory, the Chinese University of Hong Kong, Hong Kong, Hong Kong.

The fat volume of bone marrow in steroid-associated osteonecrosis (ON) increases greatly, but the dynamic change of fat cells in the process of ON development is still unknown. This study aimed to explore the time course change of bone marrow fat cells using our established ON model. Thirty-two rabbits were divided into control (n=16) and steroid-treatment group (n=16). Each of group was further divided into the early (n=8) and late group (n=8) in terms of sacrifice time. The rabbits in steroid-treatment groups were injected with once lipopolysaccharide and three times of methylprednisolone to induce ON. The rabbits in control groups were injected with normal saline accordingly. The blood perfusion function of the femoral heads were measured by dynamic contrast magnetic resonance imaging (MRI) at week 0, week 2 and week 4. The rabbits were sacrificed at week 2 and week 4, the bilateral femurs were harvested and processed for bone marrow fat cell density, fat cell diameter and fat cells area percentage analysis histomorphometrically and ON evaluation histopathologically. The dynamic MRI showed the blood perfusion function decreased continuously in steroid-treatment group, the maximum enhancement decreased from 55% in week 2 to 30% in week 4. The ON incidence increased from 25% (2/8) in week 2 to 87.5% (7/8) in week 4. The fat cells area percentage in steroid-treatment early and late group increased by 44% and 83.4% compared with control group. The fat cells density in early and late group increased by 67.1% and 54.4% than control group, but there is no significant difference between the treatment groups; The fat cells diameter in late group was much larger than control group, but the fat cell diameter in early group was smaller than control group; The fat cells size profile showed most of the increased fat cells were small size cells ranging from 30 to 40µm in diameter in early group, but large size cells ranging from 50 to 60µm in the late group. The marrow fat cells featured increase in number of small size fat cells in the early stage and enlargement in size of fat cells in the late stage in ON development. These imply the active adipogenesis in the early stage and excessive lipogenesis in the late stage in the process of steroid-associated ON development. The forming new hypothesis is inhibiting adipogenesis in early stage and decreasing fat cells lipogenesis in late stage would prevent steroid-associated ON development.

Disclosures: H. Sheng, None.

This study received funding from: RGC(CUHK4503/06M) and IFTF(ITS/012/06).

T179

Transcription Factor E4bp4 Is Induced by Glucocorticoids and Represses Promoter Activity in Osteoblasts. S. M. Woo^{*1}, I. C. Ozkurt^{*2}, S. Tetradis¹. ¹UCLA School of Dentistry, Los Angeles, CA, USA, ²Ankara University, Ankara, Turkey.

Chronic, systemic use of glucocorticoids (GCs) dramatically inhibits bone formation. GCs mediate their effects by binding to and activating the glucocorticoid receptor to regulate downstream gene expression. GCs profoundly repress osteoblastic genes. However, the molecular mechanisms mediating GC repression of osteoblastic gene expression remain largely unknown. E4bp4, a transcription factor acting as a transcriptional repressor in osteoblasts, is induced by GCs in fibroblasts. Thus, we hypothesize that E4bp4 participates in the GC repression of osteoblastic genes. Here, we study GC-induced E4bp4 gene expression and explore E4bp4 involvement in GC regulated promoter activity in osteoblasts. Calvariae-derived murine osteoblasts (MOBs), calvarial cultures, and 6-8 day old CD-1 mice were treated with Dexamethasone (Dex), and E4bp4 expression was measured by Northern and Western blot assays and quantitative real-time PCR. Protein-DNA binding was evaluated by electrophoretic mobility shift assays and promoter activity by luciferase assays. MOBs were infected in vitro with an adenovirus overexpressing E4bp4, and transcriptome profiling was completed using the Affymetrix GeneChip 430A 2.0 Mouse Array and GeneSifter microarray analysis software. Dex increased E4bp4 mRNA and protein expression that peaked at 4-6 h and 1µM Dex, with elevated levels even at 24 h. Pre-treatment with the protein synthesis inhibitor cycloheximide did not prevent E4bp4 induction, showing that E4bp4 is a Dex-induced primary response gene. Nuclear proteins from MOBs treated with Dex specifically bound the E4bp4 response element (EBPRE), but not mutated EBPREs. Co-incubation with E4bp4-specific antibodies showed that the Dex-induced EBPRE-bound nuclear proteins contained E4bp4 protein. Furthermore, Dex treatment attenuated activity of a chimeric promoter containing three tandem repeats of wild-type but not mutant EBPRE, suggesting that E4bp4 protein mediates promoter repression by Dex. Adenoviral-mediated E4bp4 overexpression upregulated 415 and downregulated 337 genes more than 1.8 fold. Gene ontology (GO) grouping summarized the molecular function, biological process, and cellular component of regulated genes. Interesting GO groups with z-score >2 included multicellular organismal development, cell surface receptor linked signal transduction, extracellular space, extracellular matrix, receptor binding, and receptor activity. We are currently investigating direct regulation of individual genes by both GCs and E4bp4. These results support a role of E4bp4 in mediating glucocorticoid-induced gene repression in osteoblasts.

Disclosures: S.M. Woo, None.

This study received funding from: NIDCR R01 DE013316, NIDCR T32 DE007296.

T180

A Novel Mechanism of Glucocorticoid Action-Inhibition of Cox-2 Transcription by Glucocorticoid Induced Leucine Zipper (GILZ). N. Yang^{*}, X. Shi. Institute of Molecular Medicine & Genetics, Medical College of Georgia, Augusta, GA, USA.

Cyclooxygenase-2 (COX-2) plays an important role in rheumatoid arthritis (RA) and therefore, it has been a major target for anti-arthritis therapies. The expression of COX-2 is induced by inflammatory cytokines such as TNF-α and IL-1β, and inhibited by glucocorticoids (GCs). However, the molecular mechanisms underlying the anti-inflammatory and immune suppressive actions of GCs are not well defined. Importantly, long-term GC therapy causes, among other adverse effects, rapid bone loss resulting in osteoporosis, therefore, their use is limited. Here we report that a recently identified GC-inducible protein, GILZ, mimics GC action and inhibits inflammatory cytokine-induced COX-2 expression in bone marrow mesenchymal stem cells (MSCs), the cells that have been recently implicated in the pathogenesis and progression of RA. Using a retrovirus-mediated gene expression approach we demonstrate that overexpression of GILZ inhibits TNF-α and IL-1β-induced COX-2 mRNA and protein expression and knockdown of GILZ by shRNAi abolishes GC inhibition of cytokine-induced COX-2 expression. Consistent to these results, overexpression of GILZ also inhibits NF-κB- and AP-1-mediated COX-2 promoter activity. Finally, we show that GILZ inhibits COX-2 expression by blocking NF-κB nuclear translocation and by inhibiting AP-1 binding to the COX-2 promoter region. Our results suggest that GILZ is a key GC effect mediator and that GILZ may have pharmacotherapeutic value for novel anti-inflammation therapies.

Disclosures: N. Yang, None.

This study received funding from: Arthritis Foundation.

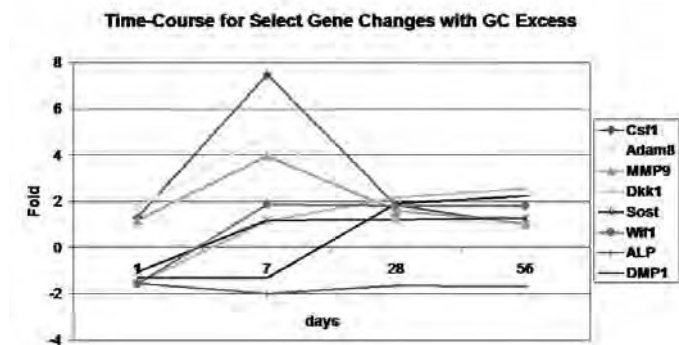
T181

Glucocorticoid Excess in Mice Leads to Early Activation of Osteoclastogenesis and Prolonged Suppression of Osteogenesis Through Gene Expression Profiling. W. Yao, Z. Cheng, C. Busse*, S. Rao*, N. Lane. Center for Healthy Aging, UC Davis Medical Center, Sacramento, CA, USA.

Glucocorticoid (GC) excess induces alterations in bone metabolism that weakens bone structure. We performed genome-wide cDNA microarray on whole bone RNA (Affymetrix Mouse Genome 430 2.0 array) to identify genes associated with bone metabolism in GC-treated mice. Long bones from mice exposed to GC excess were collected at 0, 3, 7, 28 and 56 days (5mg prednisolone 60-day slow release pellet, n=8-12/group). The success of this animal model was confirmed by changes in bone turnover markers as well as bone microarchitecture measured by microCT. Differences in gene expression with time were calculated by unequal-variance ANOVA with a threshold of > 2fold and $p < 0.01$. The significantly expressed 1179 transcripts were then further grouped by Gene Functions using GeneShifter Software. Quantitative real-time PCR was performed on selected genes to confirm microarray results.

Results: Compared to placebo treated mice, GC-treated mice lost trabecular bone volume at the distal femur (16% by d28 and was unchanged at d56). Serum measurements of osteoclast maturation, TRAP5b, increased by 18% at d7 and d28, and increased by 15% at d56; and osteoblast maturation, osteocalcin decreased by 50% from d28-d56. Compared to placebo treated mice, GC excess was associated with increased expression of genes involved with osteoclast activation (csf1, c-fms, c-fos, adam8, Trem2, Oscar, Nfatc1) that peaked at d7; osteoclast cytoskeleton reorganization (β 3, Ibsp, c-src, vav3, ATPase) and genes associated with matrix degradation peaked at d28 (cathepsins, mmps and proteases). At d28 and d56, genes associated with osteoblast activation and function had decreased expression (BMPs 2,5, 8, 12, 13, TGF β 1) and Wnt inhibitors such as Wif1, Dkk1 and Sost had increased expression compared to placebo treated animals. In addition, with GC excess, genes expressed by osteocytes and associated with bone mineralization, DMP1 and PheX, had increased expression at d28 and d56. RT-PCR confirmed our microarray findings in selected genes.

In conclusion, GC excess is associated with early activation of osteoclastogenesis and delayed but prolonged suppression of osteogenesis and matrix mineralization. These rapid and sustained alterations in bone cells maturation and activity help to explain the significant deterioration in bone strength in the presence of GCs.



Disclosures: W. Yao, None.

This study received funding from: R01 AR043052-07, 1K12HD05195801.

T182

Osteoblast-Targeted Disruption of Glucocorticoid Signalling Delays Intramembranous Bone Development In Vivo. H. Zhou, W. Mak, Y. Zheng, C. R. Dunstan, M. J. Seibel. Bone Research Program, ANZAC Research Institute, University of Sydney, Sydney, Australia.

Transgenic (tg) expression of 11 β -hydroxysteroid dehydrogenase type 2 (HSD2), a glucocorticoid (GC) inactivating enzyme, under the control of a 2.3kb collagen type I promoter (Col2.3-HSD2) abrogates intracellular GC signalling in mature osteoblasts. Adult Col2.3-HSD2 tg mice exhibit a mild osteoporotic phenotype but the skeleton otherwise appears normal (1). To investigate the effects of osteoblast-targeted disruption of GC signalling on early skeletal development, calvaria and tibiae of wild-type (WT) and Col2.3-HSD2 tg mice aged 0, 1, 7, 10 and 14 days were analysed.

HSD2 mRNA and protein expression was present in the calvaria and long bones of tg mice but absent in the bones of WT mice. Calvaria from tg mice demonstrated a markedly altered phenotype: compared to their WT littermates, tg mice had poorly formed parietal bones with large amounts of cranial cartilage still present at day 0. A similar picture was seen at day 1, with the extent of parietal bones being reduced by 33% relative to WT mice. The cranial cartilage plate was present in all tg mice but absent in WT mice. In 7-day old mice, the cranial cartilage plate was reduced in size but still present in tg animals, but formation of parietal bones was complete and bone area was similar to WT mice. Calvaria appeared normal at 2 weeks of age. Immunohistochemical analyses showed reduced protein expression of MT1-MMP, an enzyme essential for calvarial cartilage removal in the cranial cartilage of tg mice. TUNEL staining indicated reduced chondrocyte apoptosis. In contrast, no phenotype was observed in the long bones (tibiae) of tg mice.

Our results indicate that osteoblast-targeted disruption of GC signalling results in delayed calvarial (intramembranous) development, without affecting the (endosteal) formation of long bones. These findings further suggest that in neonatal mice, osteoblasts regulate

cranial cartilage removal, a function that appears to be GC-dependent and mediated through activation of chondrocytic MT1-MMP expression. Our studies point to a novel role for both GC and osteoblasts in intramembranous bone development.

(1) Sher et al Endocrinology 145:922-9, 2004.

Disclosures: H. Zhou, None.

This study received funding from: NHMRC #402462.

T183

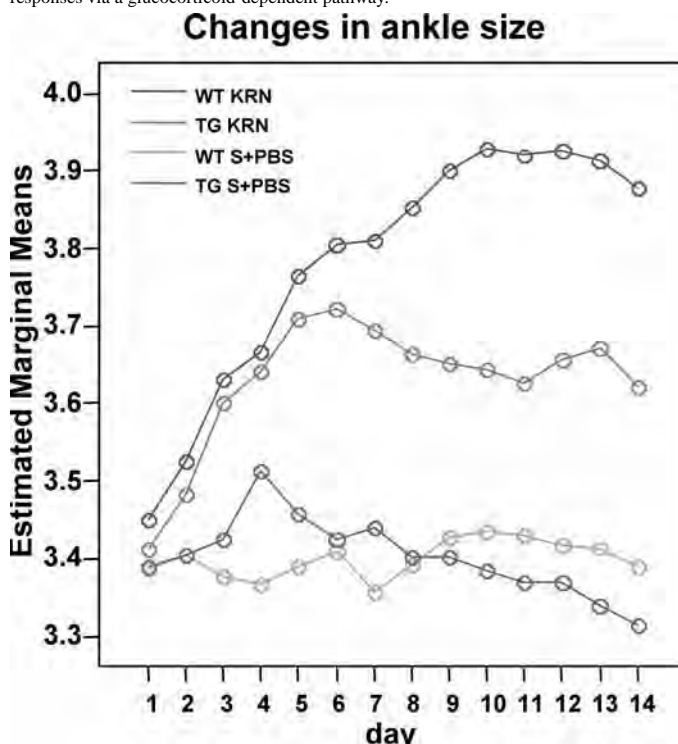
Transgenic Disruption of Glucocorticoid Signalling in Mature Osteoblasts Attenuates KRN Serum-induced Arthritis In Vivo. H. Zhou¹, F. Buttgeriet², T. Gaber², R. Kalak³, R. Dragovic¹, D. Huscher², R. H. Straub³, J. Modzelewski⁴, C. R. Dunstan¹, M. J. Seibel¹. ¹Bone Research Program, ANZAC Research Institute, Sydney, Australia, ²Dept. of Rheumatology & Clinical Immunology, Charité (CCM) and DRFZ, Berlin, Germany, ³Dept. of Internal Medicine I, University Hospital, Regensburg, Germany, ⁴Dept. of Endocrinology & Metabolism, Concord Hospital, Sydney, Australia.

Transgenic (tg) overexpression of 11 β -hydroxysteroid dehydrogenase type 2 (HSD2), a glucocorticoid (GC) inactivating enzyme under the control of a 2.3Kb collagen type I promoter (Col2.3-HSD2), abrogates intracellular GC signalling exclusively in mature osteoblasts. Since GC are important immune modulators, we investigated the impact of osteoblast-targeted disruption of GC signalling on joint inflammation and bone catabolism using the KRN serum transfer model of autoimmune arthritis.

KRN arthritis was induced in 5-week-old male Col2.3-HSD2-tg mice (tg-KRN, n=28) and their wild-type (WT) littermates (WT-KRN, n=27). Twelve tg and 13 WT mice served as controls (CTR) receiving either normal serum or PBS. Body weight and paw swelling (ankle size, clinical arthritis, scored 0-6) were assessed daily from induction (day 0) to day 14. Serum levels of IL-1 β , IL-2, IL-4, IL-6, IL-10, IL-12, TNF- α , IFN- γ , G-CSF, M-CSF and corticosterone (CS) were determined in CTR, and in KRN animals on days 7 and 14. Micro-CT of the tibia and the paw skeleton was employed to assess for morphological changes.

Both tg-KRN and WT-KRN developed acute arthritis. However, the inflammatory response was significantly blunted in tg mice from day 7 onwards (Fig. 1). Compared to CTR, tibia bone volume (BV/TV) was significantly reduced in WT-KRN but not in tg-KRN on day 14. As compared to day 7, mean serum M-CSF levels were significantly lower on day 14 in tg-KRN but not in WT-KRN. Compared to CTR, serum TNF- α , IL-6 and IL-12 levels were significantly lower in tg-KRN on day 14. However, there were no differences in cytokine or CS levels between tg-KRN and WT-KRN at any time point, suggesting that in HSD2-tg mice the inflammatory process was attenuated through local mediators.

We conclude that osteoblasts are able to significantly modulate local inflammatory responses via a glucocorticoid-dependent pathway.



Disclosures: H. Zhou, None.

This study received funding from: NHMRC #402462.

T184

Regulation of Oxidative Stress and Osteoblast Apoptosis by Estrogens Is Preserved in Mice in which the ER Cannot Directly Interact with DNA. M. Almeida, M. Martin-Millan*, L. Han, A. Warren*, V. Lowe*, R. S. Shelton*, A. DeLoose*, R. S. Weinstein, T. Bellido, C. A. O'Brien, R. L. Jilka, S. C. Manolagas. Center for Osteoporosis and Metabolic Bone Diseases, University of Arkansas for Medical Sciences and Central Arkansas Veterans Healthcare System, Little Rock, AR, USA.

To investigate the role of the ER α , and in particular its non-ERE-mediated signaling, in skeletal homeostasis we have crossed knock-in mice in which classical ER α signaling through ERE sites has been selectively eliminated while preserving non-classical signaling (ER $\alpha^{\text{NERK1-/-}}$), with heterozygous mice of the ER α gene, to generate ER $\alpha^{\text{NERK1-/-}}$ mice. We report that 17 β -estradiol (E $_2$) at 10 $^{-8}$ M stimulated apoptosis of mature osteoclasts in bone marrow cultures from ER $\alpha^{\text{NERK1-/-}}$ mice as effectively as in cultures from wild-type control mice. Likewise, E $_2$ prevented etoposide-induced apoptosis in osteoblastic cultures derived from calvaria of either type of mouse. In agreement with the in vitro data, ovariectomy (ovx) upregulated osteoclastogenesis in wild type as well as in ER $\alpha^{\text{NERK1-/-}}$ mice as measured in ex vivo bone marrow cultures. OvX also caused an increase of osteoblast apoptosis in ER $\alpha^{\text{NERK1-/-}}$ and wild-type mice; and E $_2$ replacement prevented the phenomenon in both. Further, ovx led to an increase in reactive oxygen species (ROS) levels and a decrease in glutathione reductase activity in the bone marrow; as well as an increase in the phosphorylation of p66 $^{\text{shc}}$ (a key component of a signaling cascade that is activated by ROS and stimulates apoptosis) in vertebral lysates from both wild-type controls and ER $\alpha^{\text{NERK1-/-}}$ mice. E $_2$ replacement prevented all these changes in both type of mice. Lastly, there was a progressive decrease in baseline BMD in the femur and spine from ER $\alpha^{+/+}$, to ER $\alpha^{+/-}$, to ER $\alpha^{\text{NERK1-/-}}$, to ER $\alpha^{\text{NERK1-/-}}$ mice. Moreover, ER $\alpha^{\text{NERK1-/-}}$ mice exhibited a decrease in bone size and osteoblastogenesis as measured by the number of colony forming units-osteoblasts in ex vivo bone marrow cultures; as well as a decrease in osteocalcin levels in the serum. These results strongly suggest that the antioxidant properties of estrogens, as well as their ability to control osteoblast and osteoclast apoptosis and osteoclastogenesis do not require classical DNA binding of the ER α ; and are consistent with evidence that trabecular (but not cortical) bone mass remains estrogen responsive in the ER $\alpha^{\text{NERK1-/-}}$ mice. The decrease in bone size, BMD and osteoblastogenesis in the ER $\alpha^{\text{NERK1-/-}}$ mice may be explained by evidence presented elsewhere in this meeting that the unliganded wild type ER α (presumably through its ability to bind directly to DNA) is a co-activator of BMP-induced osteoblastogenesis and thereby bone formation and growth during development.

Disclosures: M. Almeida, None.

T185

Estrogens or Androgens Attenuate p66 $^{\text{shc}}$ Phosphorylation via an ERK and PKC β Signaling Cascade: a Critical Mechanism of their Protective Effects Against Oxidative Stress and Bone Loss. M. Almeida, M. Martin-Millan, L. Han, A. Warren*, V. Lowe*, T. Bellido, R. L. Jilka, C. A. O'Brien, S. C. Manolagas. Center for Osteoporosis and Metabolic Bone Diseases, University of Arkansas for Medical Sciences and Central Arkansas Veterans Healthcare System, Little Rock, AR, USA.

Phosphorylation of the adapter protein p66 $^{\text{shc}}$ is not only required for transduction of oxidative stress signals leading to apoptosis but also amplifies such stress by generating reactive oxygen species (ROS) in the mitochondria. Based on this and evidence that ovariectomy (ovx) or orchidectomy of 5 month-old C57BL/6 mice increases the phosphorylation of p66 $^{\text{shc}}$ in vertebral lysates, while replacement with 17 β -estradiol (E $_2$) or DHT prevent this phenomenon as effectively as the antioxidant N-acetyl-L-cysteine (NAC), we have investigated the molecular basis of the effects of sex steroids on p66 $^{\text{shc}}$. We report that exposure of several osteoblastic cell lines as well as primary cultures of calvaria osteoblasts to H $_2$ O $_2$ stimulated the phosphorylation of p66 $^{\text{shc}}$ within 5 min, and that pre-treatment of all these cells for 1 h with either E $_2$ or DHT prevented this effect. Further, overexpression of p66 $^{\text{shc}}$ in C2C12 cells induced apoptosis both under basal condition and in the presence of H $_2$ O $_2$. The suppressive effect of sex steroids on H $_2$ O $_2$ -induced phosphorylation of p66 $^{\text{shc}}$ was inhibited by the ERK-specific inhibitor PD98059 indicating that this is a kinase-mediated action of the ER. Consistent with this finding E $_2$ inhibited the pro-apoptotic effect of H $_2$ O $_2$ as well as p66 $^{\text{shc}}$ phosphorylation in calvaria derived osteoblast cultures from ER $\alpha^{\text{NERK1-/-}}$ mice, a knock-in mouse mutant of the ER α that lacks classical DNA binding on ERE elements. Moreover, the increase in osteoblast apoptosis and p66 phosphorylation in the vertebra following ovx was suppressed by E $_2$ replacement in both wild-type and ER $\alpha^{\text{NERK1-/-}}$ mice. To further dissect the mechanism by which sex steroids antagonize p66 $^{\text{shc}}$ phosphorylation induced by oxidative stress we searched for and found that PKC β activity was required for H $_2$ O $_2$ -induced p66 $^{\text{shc}}$ phosphorylation, as it was blocked by the specific PKC β inhibitor hispidin. Furthermore, activation of PKC by PMA induced p66 $^{\text{shc}}$ phosphorylation and stimulated apoptosis in C2C12 cells; and both effects were prevented by hispidin. Finally, both phosphorylation of p66 $^{\text{shc}}$ as well as apoptosis induced by PMA were prevented by E $_2$ suggesting that modulation of PKC β activity might mediate the anti-apoptotic effects of sex steroids in osteoblastic cells. These results strongly suggest that sex steroids attenuate osteoblast apoptosis induced by oxidative stress by modulating a cascade of cytoplasmic kinases culminating with inhibition of p66 $^{\text{shc}}$ phosphorylation.

Disclosures: M. Almeida, None.

T186

Estrogens Attenuate IL-6, and TNF α Production in Osteoblastic Cells by Decreasing Oxidative Stress and its Effects on NF κ B Activation. M. Almeida, L. Han, M. Martin-Millan, V. Lowe*, A. Warren*, R. L. Jilka, S. C. Manolagas. Center for Osteoporosis and Metabolic Bone Diseases, University of Arkansas for Medical Sciences Central Arkansas Veterans Healthcare System, Little Rock, AR, USA.

Reactive oxygen species (ROS) may play a critical pathogenetic role in osteoporosis, and the anti-osteoporotic effect of estrogens may result from the ability of these hormones to protect against oxidative stress. Indeed both aging and estrogen deficiency increased oxidative stress in the bone of both male and female C57BL/6 mice as well as the number of osteoclast progenitors in the bone marrow. Based on this and the well known relationship among IL-6, TNF α , osteoclastogenesis, and estrogens we tested the hypothesis that estrogens exert their anti-osteoclastogenic effects by enhancing defense against ROS. We report that increasing levels of ROS, decreasing GSR activity, and increasing phosphorylation of p66 $^{\text{shc}}$ between 8 and 31 month of age in C57BL/6 female mice were temporally associated with a progressive increase in the expression of the osteoclastogenic cytokines TNF α and IL-6, as measured by RT-PCR in calvaria. Consistent with the notion that the in vivo changes in oxidative stress and cytokine production were causally related, H $_2$ O $_2$ up-regulated the expression of both TNF α and IL-6 in cultures of the UAMS32 osteoclast supporting stromal cell line. And, 17 β -estradiol (E $_2$) at 10 $^{-8}$ M potentially attenuated the effects of H $_2$ O $_2$ on the production of both cytokines. In line with this finding, H $_2$ O $_2$ strongly activated NF κ B within 1 h, as determined by the phosphorylation of the NF κ B inhibitor kinase I κ B, by Western blot. Consistent with the inhibitory effect of E $_2$ on the expression of IL-6 and TNF α upon H $_2$ O $_2$ stimulation, pre-treatment with E $_2$ for one hour abrogated the effect of H $_2$ O $_2$ on NF κ B activation. Finally, to determine whether the increase in osteoclastogenesis that follows estrogen deficiency is mediated by the anti-oxidant actions of estrogen, we treated ovx mice with E $_2$ or the anti-oxidant N-acetyl-L-cysteine (NAC). NAC was as effective as E $_2$ in preventing the increase in the number of osteoclast progenitors as determined by ex vivo bone marrow cultures. Consistent with this, administration of L-buthionine-(S,R)-sulfoximine (BSO), a specific inhibitor of glutathione synthesis, for 6 weeks, or the oxidant-producing herbicide paraquat for 4 weeks, to 5 month-old C57BL/6 mice increased both ROS levels as well as the number of osteoclast progenitors in the bone marrow. Taken together with evidence that estrogens directly suppress p66 $^{\text{shc}}$ phosphorylation, presented elsewhere in this meeting, these results suggest that estrogens attenuate IL-6 and TNF α production in stromal/osteoblastic cells by decreasing oxidative stress and its effects on NF κ B activation.

Disclosures: M. Almeida, None.

T187

Premenopausal Women with Short Luteal Phase Length Have Reduced vBMD, but Normal Bone Bending Strength at the Tibial Midshaft. B. C. Kaufman*¹, R. J. Wetzsteon¹, M. S. Kurzer*², J. C. Prior*³, M. A. Petit¹. ¹Kinesiology, University of Minnesota, Minneapolis, MN, USA, ²Food Science and Nutrition, University of Minnesota, Minneapolis, MN, USA, ³Vancouver General Hospital, Vancouver, BC, Canada.

Progesterone is hypothesized to have an important influence on bone metabolism, which could influence bone health in women with a shortened luteal phase. The purpose of this cross-sectional study was to explore the relationship between luteal phase length (LPL) and bone parameters in healthy, sedentary, pre-menopausal women. We used baseline data from a subset of women (n = 32, aged 18-30yr; mean BMI = 22.9 \pm 3.1) enrolled in a study of physical activity and ovulation (WISER). Menstrual cycle characteristics were assessed by questionnaire and confirmed with ovulation kits over 5 menstrual cycles. Volumetric bone mineral density (vBMD, mg/mm 3), bone geometry (Total Area), and estimated bone strength (polar strength strain index, SSI) were assessed by pQCT (XCT 3000) at a distal (8%) and midshaft (50%) site of the left tibia. Participants were split into two groups based on average luteal phase length of < 10.9d (short LPL, n = 12) or > 11.0d (normal LPL, n = 20). Groups were similar in age, height, weight, %fat and %lean mass. There were also no differences between groups in physical activity (assessed by questionnaire), total calorie intake (from 3d food records), or average menstrual cycle length (29 and 30d respectively). At the tibial midshaft, total vBMD was significantly lower (-5.9%, p = 0.005) in the women with short LPL, while total bone area was significantly higher (+13%, p = 0.013) resulting in a non-significant difference in SSI between groups (p > 0.05). Similar trends were seen at the distal site, but differences in bone parameters were not significant. Results remained significant after adjusting for tibial length and body weight. These data suggest that sedentary women with shortened luteal phase length may have reduced vBMD that seems to be compensated for by increased bone area, resulting in bone bending strengths similar to sedentary women with normal luteal phase length at the tibial midshaft.

Disclosures: B.C. Kaufman, None.

T188

Identification of Primary Target Cells for the Classical Genomic Effects of Estrogen and Raloxifene in Bone. C. Håkansson^{*1}, P. T. van der Saag^{*2}, J. Å. Gustafsson^{*3}, H. Carlsten^{*1}, C. Ohlsson⁴, M. K. Lagerquist⁴. ¹Dept. of Rheumatology and Inflammation Research, Inst. of Medicine, Gothenburg, Sweden, ²Hubrecht Lab., Netherlands Inst. for Developmental Biology, Utrecht, The Netherlands, ³Dept. of Bioscience at NOVUM, Karolinska Institute, Huddinge, Sweden, ⁴Dept. of Internal Medicine, Inst. of Medicine, Gothenburg, Sweden.

Estrogen, as well as the selective estrogen receptor modulator raloxifene, has bone protective effects, but the mechanism behind these effects is still not completely characterized. Recently, immune cells in the bone marrow have been implicated to be involved in estrogenic effects on bone. The aim of this study was to identify primary target cells in bone marrow for the classical genomic effects of estrogen and raloxifene in an attempt to clarify the mechanism behind the bone protective effects of these compounds. For this purpose we have used a reporter mouse with a luciferase reporter gene under the control of three estrogen-responsive elements (EREs). These mice enable detection of in vivo activation of gene transcription via binding of estrogen receptors (ERs) to ERE-elements. Three-month-old ovariectomized (ovx) mice were given a single dose of 17 β -estradiol (E2) (50 μ g/kg, s.c.) or the raloxifene-analog LY117018 (3mg/kg, s.c.) and the experiment was ended after 10h. The doses were chosen because of their equipotent effects on bone mass.

Bone marrow was flushed from femur and sorting of various cell populations was performed using FACSaria, resulting in cell populations with >95% purity. In total bone marrow, E2 increased luciferase activity to 12000 RLU/10⁶ cells and raloxifene to 700 RLU/10⁶ cells (p<0.01). In the B cell fraction (CD19⁺ cells), E2 increased luciferase activity slightly (1600 RLU/10⁶ cells), while raloxifene had no effect. No effect of either E2 or raloxifene was found in the T lymphocyte or the granulocyte population, while the cell fraction lacking both lymphocytes and granulocytes exhibited the greatest luciferase activity/10⁶ cells (40000 RLU for E2 and 6000 RLU for raloxifene). In conclusion, neither lymphocytes nor granulocytes are primary targets for the classical genomic effects of E2 or raloxifene in bone marrow. Furthermore, raloxifene can activate gene transcription via ER binding to EREs in the bone marrow, but not to the same extent as E2 at doses that give equipotent effects on bone mass.

Disclosures: M.K. Lagerquist, None.

T189

Estrogen Receptors in Adolescent Idiopathic Scoliosis (AIS). D. Leboeuf^{*1}, K. Letellier^{*2}, B. Azeddine^{*2}, G. Grimard^{*3}, S. Parent^{*3}, H. Labelle^{*3}, A. Moreau⁴, F. Moldovan^{*4}. ¹Sciences Biomédicales, Université de Montréal, Montréal, PQ, Canada, ²Biologie Moléculaire, Université de Montréal, Montréal, PQ, Canada, ³Hôpital Sainte Justine, Montréal, PQ, Canada, ⁴Centre de Recherche de l'Hôpital Sainte Justine, Montréal, PQ, Canada.

AIS occurs and progresses during puberty, a period greatly influenced by hormones. This, and the fact that most severe cases of scoliosis affect girls, points to a possible role for estrogens in the onset and the progression of AIS. Estrogen signaling occurs mainly via two nuclear receptors, ER α and ER β . Here we investigate the expression of ER α and ER β in AIS and control (trauma) patients. RNA extracted from osteoblasts of AIS and control patients was investigated by RT-PCR using primers covering all 4 domains of ER α and ER β (protein-protein interaction, hinge, ligand-binding and DNA binding domains). In addition, ER α and ER β were detected by immunohistochemistry on spinal biopsy tissues and on osteoblasts exposed in vitro to 17 β -Estradiol.

All AIS patients (n=10, age=14 \pm 2.02, Cobb=59.37 \pm 20.9) and controls (n=8, age=14.7 \pm 3.0,) show transcripts of many isoforms of ER α . However, the expression of ER β varied between patients and controls, and results suggest the presence of various isoforms in human osteoblasts. We also identified by sequencing an insert specific to isoform h-ER β S1, in 6/10 AIS patients and 8/8 controls. Immunohistochemistry revealed high levels of ER α and low levels of ER β . Finally, osteoblasts of AIS patients exposed to 17 β -Estradiol show increased nuclear expression of ER α , which was not observed in control osteoblasts. It is already known that ER α and ER β have overlapping roles in regulating growth and differentiation of bone tissues. However, ER β is the dominant receptor in many ER-dependent signaling pathways in bone cells, and some isoforms exhibit an antagonistic effect on ER-mediated transcriptional activity. Surprisingly, the level of ER β was very low in AIS cells, compared to ER α . In addition, the lack of the isoform h-ER β S1 in some AIS patients, as well as the altered balance between ER α and ER β , appears to be critical for estrogen-dependent functions of osteoblasts, which could impact bone homeostasis and lead to decreased bone mineral density and osteopenia in AIS.

Disclosures: D. Leboeuf, None.

This study received funding from: La Fondation Yves Cotrel-Institut de France.

T190

The Unliganded ER α or β , but not the AR, Potentiates BMP-induced Transcription and Osteoblastogenesis. M. Martin-Millan, L. Han, A. Warren^{*}, V. Lowe^{*}, C. A. O'Brien, M. Almeida, S. C. Manolagas. Center for Osteoporosis and Metabolic Bone Diseases, University of Arkansas for Medical Sciences and Central Arkansas Veterans Healthcare System, Little Rock, AR, USA.

Whereas estrogens suppress osteoblastogenesis and estrogen loss increases it, female or male mice with ubiquitous ER α deletion (ER α ^{-/-}) exhibit decreased osteoblast number and bone formation rate. Based on this and recent evidence for distinct roles of the unliganded versus liganded ER in the transcriptional repression of the TNF gene, we have tested the hypothesis that the ER may have two opposite effects in osteoblast generation: attenuation in the presence of 17 β -estradiol (E₂) and potentiation in the absence of E₂. We report that E₂ at 10⁻⁷ to 10⁻⁸ M suppressed BMP-2-induced osteoblast progenitor commitment and differentiation in two cell lines, the uncommitted mesenchymal C2C12 and the pre-osteoblasts 2T3, as well as in primary cultures of murine bone marrow, as measured by alkaline phosphatase (AP) activity. Consistent with a suppressive effect on osteoblastogenesis, E₂ also attenuated BMP-2-induced osteocalcin secretion, as well as the expression of the BMP-2 responsive gene Smad6. Importantly, ER α co-immunoprecipitated with Smad1 and Smad4 in all these cell models. Further, treatment of C2C12 or 2T3 cells with ICI182,780 (10⁻⁷ M), an antagonist of ER that promotes its degradation, also attenuated BMP-2-induced AP activity, osteocalcin secretion and the expression of Smad6. In support of the contention that the inhibitory effect of ICI on osteoblastogenesis was indeed due to ER degradation, silencing ER α in C2C12 cells using specific siRNA oligonucleotides abrogated AP activity induced by BMP-2. In agreement with these observations, transfection of C2C12 cells with increasing amounts of plasmids encoding the ER α or the ER β , dose-dependently increased BMP-induced transcription, as measured by a Smad6-luciferase reporter construct. This effect was also evident in cultures not treated with BMP, indicating that the unliganded ER α or β potentiated the effect of both endogenous as well as exogenous BMPs. Transfection with the same amounts of a plasmid expressing the androgen receptor had no effect on basal or BMP-stimulated transcription of the reporter construct. These findings strongly support the hypothesis that the unliganded ER stimulates BMP target genes, perhaps by acting as a co-activator of Smads, and that binding of E₂ antagonizes this effect. Opposite effects of the unliganded versus the liganded ER on osteoblastogenesis can explain why, in spite of the well-known suppressive effect of estrogens on osteoblastogenesis as well as osteoclastogenesis, and thereby on remodeling, bone formation is decreased in mice with ER α deletion.

Disclosures: M. Martin-Millan, None.

T191

Serum Testosterone in Elderly Men Measured by Liquid Chromatography-Tandem Mass Spectrometry and Radioimmunoassay: Concordance and Effect on Epidemiologic Association. T. V. Nguyen¹, C. Meier², D. J. Handelsman^{*3}, M. Kraenzlin², M. M. Kushnir^{*4}, A. L. Rockwood^{*4}, A. W. Meikle^{*5}, J. R. Center⁶, J. A. Eisman⁶, M. J. Seibel². ¹Bone and Mineral Research Program, Garvan Institute of Medical Research, St Vincent's Hospital and UNSW, Darlinghurst, NSW, Australia, ²Bone Research Program, ANZAC Research Institute, Concord, NSW, Australia, ³Andrology, ANZAC Research Institute, Concord, NSW, Australia, ⁴ARUP Institute for Clinical and Experimental Pathology, Salt Lake City, UT, USA, ⁵Department of Medicine and Pathology, University of Utah, Salt Lake City, UT, USA, ⁶Bone and Mineral Research Program, Garvan Institute of Medical Research, St Vincent's Hospital and UNSW, Darlinghurst, NSW, Australia.

Serum testosterone (T) is used as a measure to define androgenic status and its association with health outcomes. Established radioimmunoassays (RIA) have been used to measure T; however, liquid chromatography-tandem mass spectrometry (MS) has increasingly become a reference method for measuring T. The present study assessed the concordance between T measured by RIA and MS, and the effect of this concordance on the association between serum T and fracture risk in men.

T was measured by direct RIA (RIA-T; Delphia, Perkin-Elmer) and liquid chromatography-tandem mass spectrometry (MS-T) in 593 men aged 60+ years, who had participated in the Dubbo Osteoporosis Epidemiology Study between 1989 and 2005. Low-trauma fractures were recorded during the study period. The concordance between the two methods of measurement was assessed by the coefficient of concordance and the limit of agreement method. The association between each measured T and fracture risk was analyzed within the framework of the Cox's proportional hazards model.

The coefficient of concordance between RIA-T and MS-T was 0.67 (p18 pmol/L). RIA-T tended to underestimate MS-T by 25%. In the Cox's model, each SD of log MS-T was significantly associated with fracture risk (hazard ratio [HR] 1.37; 95% CI: 1.15, 1.6), which was slightly higher than the association between log RIA-T and fracture risk (HR: 1.19; 95% CI: 1.02, 1.40).

These data suggest that there was a modest concordance between MS-T and RIA-T, with minor effects on the assessment of associations between serum T and fracture in epidemiologic studies in men.

Disclosures: T.V. Nguyen, None.

T192

Down-Regulation of Klotho Protein Expression by Estrogen. O. K. Oz¹, A. Hajibeigi¹, W. Siyambalapitiyage¹, K. Korach², M. Kuro-o³. ¹Radiology, UT Southwestern Medical Center at Dallas, Dallas, TX, USA, ²NIEHS, NIH, Research Triangle Park, NC, USA, ³Pathology, UT Southwestern Medical Center at Dallas, Dallas, TX, USA.

Klotho is a glycoprotein predominantly expressed in distal tubules cells of kidney. Low klotho gene expression in mice leads to multiple disorders, such as arteriosclerosis, skin atrophy, abnormal calcium homeostasis and shortened life span. More recently klotho has been shown to regulate activity of the calcium channel TRPV5 in the kidney. Estrogens are also regulators of calcium homeostasis. In this study we investigated a potential regulatory role for estradiol in klotho expression. The effect of estradiol treatment on klotho expression in vitro was tested in the renal tubule cell line MDCK grown in estrogen depleted (charcoal stripped) or repleted serum. Lysates of the treated cells were prepared and klotho expression quantified by western blot (WB). To determine the effects of estrogen in vivo, we used wild type (WT), aromatase deficient mice (ArKO), and ArKO mice treated with estradiol (20ug/mouse 3x/week) or vehicle for 3 weeks. RNA and protein were prepared from the kidneys for real time PCR and WB analysis, respectively. MDCK cells grown in charcoal stripped FBS (csFBS) showed higher klotho protein expression than cells grown in 10%FBS. However, klotho expression in cells grown in 10% csFBS supplemented with 10(-5)M and 10(-8)M estradiol was decreased to the same level as cells grown in 10%FBS. Kidneys from ArKO mice showed significantly higher expression of klotho, both at the mRNA and protein levels in ArKO animals compared to WT and estrogen treated ArKO mice. Similarly, protein extracts from estrogen receptor alpha knockout mice kidneys showed higher klotho levels than WT extracts. Based on these observations we conclude that estrogen, acting through ERalpha, down-regulates the klotho protein in the mouse kidney.

Disclosures: O.K. Oz, None.

T193

High Dose Estrodiol Treatment Causes Destruction of Cortical Bone and Is Associated with an Increased Death Rate in Old Wild Type and ERKO Male Mice. Z. Peng¹, P. Härkönen², K. Väänänen³. ¹Pharmatest Services Ltd, Turku, Finland, ²Department of Laboratory Medicine, Tumor Biology, Lund University, Malmö, Sweden, ³Department of Anatomy, University of Turku, Turku, Finland.

Estrogen plays an important role in maintaining bone mass in males as well as in females. The purpose of this study was to learn how estradiol and testosterone treatments influence bone metabolism in very old ERKO male mice. Sham-operated or orchidectomized (ORC) 10-25 mo old ERKO mice and their wild type (WT) littermates were implanted with a pellet of testosterone (Te) (0.21mg/mouse/day), or estradiol (E₂) (3µg/mouse/day or 12µg/mouse/day) and sacrificed after 4 weeks. Bone analysis of the animals showed that ORC decreased the tibial and femoral ash weight of WT mice, which was reversed by Te treatment. The lower dose E₂ treatment increased bone ash weight, TBV, BMD and bending strength of both tibia and femur in wild type but not in ERKO mice. In contrast, a high dose E₂ treatment caused a very high bone turnover rate with enhanced bone formation and an increased number of osteoclasts both in WT and in ERKO mice. TBV was clearly elevated but cortical bone revealed local areas with enhanced bone resorption leading to foci with an almost complete local loss of cortical structures. The mechanical strength of cortical bone was clearly decreased due to the local destruction of cortical bone. T treatment of ORC animals reversed the ORC-induced bone changes both in WT and ERKO mice. However, in intact old animals T treatment did not significantly improve measured bone parameters. Generally, all sham-operated animals, both WT and ERKO, survived the whole 4-week experiment whereas 4 out of 22 ORC WT mice (19.2%) and 16 out of 21 ORC ERKO mice (76.2%) died, and most of them were at 5 to 19 days after operation. However, in Te-treated ORC mouse groups, only 3 out of 21 WT (14.3%) and 2 out of 15 ERKO (13.3%) died. Both low and high dose E₂ treatment of ORC WT and ORC ERKO male mice was associated with an increased death rate. Only 3 out of 39 WT (7.7%) and 5 out of 35 ERKO (14%) survived in E₂-treated groups until the end of the study. Similarly, in E₂-treated intact old WT and ERKO mice groups 5/14 and 4/16 animals died during the experiment, respectively. No deaths occurred in the control or Te-treated groups during the same time period. In conclusion, E₂ treatment was associated with an increased death rate both in intact and ORC old WT and ERKO mice. ORC also increased death rate in old ERKO males which could be decreased by Te treatment of ORC mice. The reason for increased, delayed deaths after ORC or E₂ treatments remains currently unknown since the routine histological examination of major organs did not reveal any obvious cause of death.

Disclosures: Z. Peng, None.

T194

Activation of MAPKs by 17 beta-Estradiol Is Mediated by PKC and c-Src in Skeletal Muscle Cells. A. C. Ronda¹, C. Buitrago¹, E. Roldan², R. Boland¹. ¹Biología, Bioquímica & Farmacia, Universidad Nacional del Sur, Bahía Blanca, Argentina, ²Gador S.A., Buenos Aires, Argentina.

The classical mechanism of action of 17β-estradiol (E2) involves its binding to the intracellular estrogen receptors (ER) α or β. These ligand-activated receptors stimulate mRNA synthesis and de-novo protein expression, for hours to days. Additionally, E2 is also known to exert rapid non-genomic effects on target tissues. Some of these effects involve activation of intracellular signalling pathways. We have previously shown in C2C12 skeletal muscle cells that 10⁻⁸M E2 stimulates ERK1/2 and p38 MAPK at 15 min and that the hormone promotes phosphorylation of CREB and Elk-1 transcription factors in an ERK1/2 and p38-dependent manner. In the present work, we demonstrate that E2 activates c-Src in C2C12 cells within the same time interval as ERK1/2 and p38 MAPK phosphorylation. E2-induced ERK1/2 and p38 activation was abolished by the c-Src specific inhibitor PP2, involving c-Src in hormone stimulation of MAPKs. Treatment of the muscle cells with the specific PKC inhibitor Ro318220 demonstrated that activation of ERK 1/2 and p38 in response to the estrogen is also mediated by PKC. Moreover, E2 modulates Src activation in a PKC-dependent manner, possibly through a Src protein tyrosine phosphatase. The data altogether suggest that the steroid hormone 17β-estradiol triggers upstream at PKC/Src the signalling MAPK cascades leading then to phosphorylation of CREB and Elk-1 transcription factors in the C2C12 skeletal muscle line.

Disclosures: A.C. Ronda, None.

T195

Estrogen Preferentially Suppresses Osteogenic Gene Expression in Mice Lacking Classical ERE Signaling. V. Rudnik^{*}, F. A. Syed, D. G. Fraser^{*}, D. G. Monroe, S. Khosla. Mayo Clinic, Rochester, MN, USA.

Studies with female mice in whom the only functional estrogen receptor α (ERα) is one which cannot bind DNA (ERα-/NERKI) have shown that these mice gained cortical bone mass following ovariectomy (ovx), and E dose-dependently suppressed this increase; these changes were the opposite of those seen in wild type (WT) mice. These paradoxical effects of ovx and E on cortical bone in ERα-/NERKI mice could be due to an alteration of the balance between classical (through EREs) and non-classical (through protein-protein interactions) signaling of ERα in osteoblastic cells. To identify the potential signaling pathways involved in these effects of the NERKI receptor, 3 month old female WT and ERα-/NERKI mice were ovx'd or sham operated (n = 3 per group) for 1 week and then euthanized and the femurs extracted. The metaphyses were removed and bone marrow was flushed in order to isolate RNA purely from cortical bone. Following synthesis of cDNA, QPCR arrays were performed using mouse osteogenesis platforms (SuperArray). Fold differences (following normalization to 5 different housekeeping genes) were compared within the WT and ERα-/NERKI groups between E+ (sham) and ovx (E-) animals. Of particular interest, mRNA levels of TWIST1, which is a known inhibitor of osteoblast differentiation and of runx2 activity, were lower in the cortical bones of E+ as compared to E- WT and ERα-/NERKI mice (by 2 fold for both, P = 0.06 and 0.006, respectively). By contrast, mRNA levels for BMP1, BMP3, and LEF1 (a downstream target gene in the Wnt signaling pathway) were similar in the bones of the E+ and E- WT mice, but were lower (by 2, 2, and 4-fold, respectively, all P < 0.05) in the bones of the E+ as compared to the E- ERα-/NERKI mice. These in vivo data thus demonstrate that (1) TWIST1 may be a novel E-regulated target gene and suggest that suppression of TWIST1 may play a role in the stimulation of osteoblast differentiation by E; and (2) suppression by E of BMP1, BMP3, and Wnt signaling in ERα-/NERKI mice may explain their paradoxical cortical bone response (i.e., gain in bone mass) following ovx.

Disclosures: V. Rudnik, None.

T196

17beta-Estradiol Abrogates Apoptosis in Skeletal Muscle Cells Through Extra-Nuclear Estrogen Receptors. A. Vasconsuelo^{*}, L. Milanese^{*}, A. Russo de Boland^{*}, R. Boland. Biología, Bioquímica & Farmacia, Universidad Nacional del Sur, Bahía Blanca, Argentina.

Although there is evidence showing that estrogens regulate apoptosis in various cellular systems, the underlying molecular mechanism is not well understood. The present study demonstrates that 17β-estradiol, at physiological concentrations, abrogates apoptosis in mouse skeletal muscle C2C12 cells through estrogen receptors (ERs) with non-classical localization. Specific antibodies against ER α or β and silencing of ERs with ER α and β short interference RNAs (siRNAs) inhibited this protective action, which involved PI3K/Akt activation and BAD phosphorylation. Apoptosis inhibition by 17β-estradiol was stronger when ER β was blocked, suggesting that the β isoform mediates to a greater extent than the α isoform the antiapoptotic effects of the steroid hormone. Expression and subcellular distribution of ER α and β in extra nuclear compartments (mitochondria, endoplasmic reticulum and Golgi) of C2C12 cells were confirmed by competitive binding assays, conventional and confocal fluorescence microscopy, silencing of ERs with siRNAs and RT-PCR using specific primers.

These results indicate that 17β-estradiol exerts antiapoptotic effects in skeletal muscle cells mediated by estrogen receptors with extra nuclear localization.

Disclosures: A. Russo de Boland, None.

T197

Bone Formation Is Predicted by Resting Metabolic Rate and Leptin in Exercising Women with Hypothalamic Amenorrhea. J. L. Scheid*, S. L. West*, J. D. Vescovi, S. Awdishu*, M. J. De Souza. Exercise Science, University of Toronto, Toronto, ON, Canada.

The purpose of this study was to assess metabolic factors that impact bone formation and bone resorption in exercising women with hypothalamic amenorrhea. For this observational study, subjects were divided according to menstrual status into one of three groups: 1) Ovulatory (OV, n= 21), 2) Anovulatory (ANOV, n=9), 3) Amenorrheic (AMEN, n=21). Menstrual status was assessed by daily urinary ovarian steroid measurements for 2-3 menstrual cycles, or 30-day monitoring periods if AMEN. Serum was analysed for type I procollagen amino-terminal propeptide (PINP), triiodothyronine (TT3), ghrelin, peptide YY (PYY), leptin, and 24 hour urinary samples for C-terminal telopeptide (CTX). Resting metabolic rate (RMR) was assessed by indirect calorimetry and bone density by dual-energy x-ray absorptiometry. As an indicator of energy deficiency, a measured RMR:Predicted RMR (pRMR) was defined as less than 0.90. All groups were similar (p>0.05) with respect to age (23.3±0.5yr), height (1.65±3.22m), weight (58.0±1.0kg), and BMI (21.2±0.3kg/m²). As expected, Z-scores were lower (p=0.002) in the AMEN (-0.614±0.175) compared to both the OV (0.747±0.352) and ANOV (0.500±0.389) groups at the lumbar spine L2-L4. RMR was suppressed (p=0.023; 28.7±0.7, 31.4±0.8, and 31.1±0.8kcal/day*kg FFM) in the AMEN compared to the OV and ANOV groups, respectively. RMR:pRMR was below 0.90 in the AMEN group, indicative of energy deficiency. Suppressed TT3 (p=0.030), elevated ghrelin (p=0.038) and elevated PYY concentrations (p=0.039) were observed in the AMEN compared to the OV group, but similar to that observed in the ANOV group. Leptin concentrations were similar (p=0.667) among groups (4.83±0.45ng/ml). PINP was similar (p=0.440) among groups (121.5±7.8 ug/L), while CTX was increased (p=0.034) in the AMEN (291.1±39.7ng/ml) compared to the OV (174.8±18.7ng/ml) group, and similar to that observed in the ANOV (224.2±31.4ng/ml) group. Variables in a regression model predicting PINP included RMR:pRMR and leptin which accounted for 28.6% (R²=0.327, p=0.001) of the variance in PINP. However, in the AMEN group, 55.8% (R²=0.626, p=0.004) of the variance in PINP was accounted for by RMR:pRMR and leptin. Variables in a model predicting CTX included the duration of amenorrhea, leptin and PYY concentrations and accounted for 39.9% (R²=0.454, p<0.001) of the variance in CTX. Exercising women with hypothalamic amenorrhea are energy deficient, as depicted by suppressed RMR, RMR:pRMR, TT3, elevated ghrelin, and PYY levels compared to their ovulatory counterparts, and their bone marker profile is predicted by their energy status.

Disclosures: J.L. Scheid, None.

T198

The Role of Androgen Receptor in the Lineage Commitment of Bone Marrow Stromal Cells. C. Shyr¹, T. Meng-Yin^{*2}, H. Ko-En^{*2}, C. Chang^{*3}. ¹Chinese Medicine, Chang-Gung University, Niao-Sung, Taiwan, ²Obstetrics and Gynaecology, Chang-Gung Hospital, Niao-Sung, Taiwan, ³Pathology, University of Rochester, Rochester, NY, USA.

Androgen receptor (AR) mediates androgen action to affect bone, muscle and fat tissue metabolism through controlling cellular events like differentiation process. However, the molecular control by AR on the making of specialized cells such as osteocytes and adipocytes from progenitor cells and more primitive stem cell remain unclear. To determine the role of AR in stem cell fate decision and differentiation, we conducted experiments on bone marrow stromal cells (BMSC) obtained from wild type (WT) and AR knockout (KO) mice, which contain mesenchymal stem cells with pluripotency to give rise all types of cells. We found that ARKO mice had higher numbers of colony formation unit-fibroblast, (cfu-f) and colony formation unit-osteoblast, (cfu-o) than WT mice did. Gene expression profile determined by oligoarray chips revealed that the genes related to osteogenic differentiation decreased, but genes involved in adipogenic differentiation increased in ARKO mice compared to those in wt mice. The Q-RT-PCR results verified the findings obtained from microarray analysis with lower expression of genes linked to osteogenesis and higher expression of adipogenesis-related genes in ARKO mice. Furthermore, cell surface epitope analysis by flow assay demonstrated that ARKO BMSCs exhibited different characteristics to WT BMSCs.

The study on ARKO mice is a direct and evident approach to investigate the role of AR in stem cell fate determination and lineage commitment. Our findings in this study imply that AR may accelerate the use of stem cells from their pool and direct them into differentiation because the loss of AR caused the increased progenitor cell numbers. For stem cell differentiation, we suggest that AR plays a role in promoting the stem cell differentiation decision for osteogenesis other than adipogenesis based on the gene expression profile. By understanding the role of AR on adult stem cell biology, we can find a precise and efficient way to control stem cell self-renewal and differentiation, resulting in a therapeutic application in treating illnesses such as osteoporosis and obesity through the regulatory role of AR on stem cells.

Disclosures: C. Shyr, None.

T199

The UGT2B7 H²⁶⁸Y Polymorphism Is Associated with Serum Sex Steroid Levels and Cortical Bone Size in Young Adult Men. C. Swanson¹, M. Lorentzon¹, L. Vandenput¹, F. Labrie^{*2}, A. Rane^{*3}, J. Jakobsson^{*3}, S. Chouinard^{*2}, A. Belanger^{*2}, C. Ohlsson¹. ¹Center for Bone Research at the Sahlgrenska Academy, Department of Internal Medicine, Gothenburg University, Göteborg, Sweden, ²Laboratory of Molecular Endocrinology and Oncology, Laval University Hospital Research Center and Laval University, Quebec, PQ, Canada, ³Department of Laboratory Medicine, Division of Clinical Pharmacology, Karolinska Institutet at Karolinska University Hospital, Stockholm, Sweden.

Androgens stimulate periosteal bone expansion in males during sexual maturation and the androgen receptor (AR) is required for this effect. The bio-active androgens testosterone (T) and dihydrotestosterone (DHT) can be inactivated directly by conjugation with glucuronic acid. An alternative pathway is the transformation of DHT in two main metabolites, namely androstane-3 α ,17 β -diol (3 α -diol) and androsterone (ADT). Conjugation of 3 α -diol and ADT with polar cofactors, such as glucuronic acid, is an irreversible step, abolishing its affinity for the AR. Conjugation of androgens with glucuronic acid has been suggested to play a role in the regulation of the intracellular levels of unconjugated steroids as well as their biological activities in tissues. It is now well established that UDP glucuronosyltransferase (UGT) 2B7 is one of three major enzymes responsible for the glucuronidation of all androgens and their metabolites in humans. The in vivo role of UGT2B7 for the regulation of circulating, as well as local, levels of androgens, estrogens and their metabolites is unknown. A H²⁶⁸Y polymorphism has been described in the UGT2B7 gene.

Our aim was to determine the impact of the UGT2B7 H²⁶⁸Y polymorphism on serum levels of sex steroids and cortical bone dimensions in the population-based GOOD-study, which includes 1068 young adult men at the age of peak bone mass.

Serum levels (measured by GC-MS) of T (YY 9% over HH, p<0.01), DHT (YY 10% over HH, p<0.01) and estradiol (YY 8% over HH, p<0.01) were associated with the UGT2B7 H²⁶⁸Y polymorphism (genotyping performed by Real-Time PCR). The polymorphism was associated with the metabolites (measured by LC-MS/MS) 3 α -diol-17-glucuronide and 3 α -diol-3-glucuronide (p<0.01) but not with ADT-glucuronide levels in serum. In addition, the UGT2B7 H²⁶⁸Y polymorphism was an independent predictor of cortical bone size (measured by pQCT) as reflected by periosteal circumference and cortical moment of inertia (p<0.01) in both the weight bearing tibia and the non-weight bearing radius.

In conclusion, the UGT2B7 H²⁶⁸Y polymorphism is independently associated with cortical bone size and serum sex steroid levels in young adult men. Subjects homozygous for the Y-allele had higher serum T and larger cortical bone size than subjects homozygous for the H-allele.

Disclosures: C. Swanson, None.

T200

Increased Caloric Intake Is Associated with Reversal of Amenorrhea and Favorable Changes in Metabolic and Bone Markers: A Case Study Report.

S. L. West^{*1}, J. L. Scheid^{*1}, N. I. Williams², J. D. Vescovi¹, S. A. Jamal¹, G. A. Hawker¹, S. Awdishu^{*1}, M. J. De Souza¹. ¹University of Toronto, Toronto, ON, Canada, ²Penn State University, State College, PA, USA.

Physically active women can develop exercise associated menstrual cycle disturbances (EAMD) such as amenorrhea secondary to a chronic energy deficiency. EAMD is frequently associated with low bone mass and stress fractures. Here we report data from an ongoing 12 month randomized controlled trial to determine if increased caloric intake would reverse amenorrhea, and improve energy and bone marker status. Subjects were categorized by ovulatory status into either an ovulatory control or EAMD group. After a one month run in period subjects in the EAMD group were randomly assigned to an EAMD control or EAMD+calories group that was required to increase daily caloric intake (20-30%) above their baseline energy needs. Resting energy expenditure (REE), dietary intake, daily energy expenditure, body composition (by DXA), serum markers of bone formation (PINP) and resorption (CTX), metabolic status (ghrelin and triiodothyronine [TT3]), and daily urinary ovarian steroids (E1G and PdG) were assessed over the study period. Presented is a case study of one participant randomized to the EAMD+calories group who has completed 6 months of the study protocol. The 24 year old subject had been amenorrheic for 2 years. She participated in over 300 minutes of exercise per week (primarily dance and aerobic exercise), and had a V_O max of 43.5 ml/kg/min. At study entry she weighed 54.5 kg, her BMI was 19.8 kg/m² and she had 20% body fat. REE at baseline was 1171 kcal/day and represented 87% of predicted REE, indicative of an energy deficiency. Supplemental caloric intake averaged 300 kcal/day over the study period. After 6 months of increased calories the subject reported resumption of menses, confirmed by daily ovarian steroid profile (E1G cycle area under the curve increased 79.6% from 435.6 to 782.4). There was a 1.9 kg increase in body mass, a 0.7 kg/m² increase in BMI, and endocrine alterations indicative of a move toward energy surplus including a 5.0% increase in REE, a 2.0% increase in TT3, and a 1.7% decrease in ghrelin. PINP increased 26.4% from 73.89 to 93.39 ug/L, while CTX remained unchanged (0.64 ng/ml vs. 0.69 ng/ml). Our data suggest that, in this subject, increased caloric intake results in resumption of menses, as well as more favourable metabolic, energy, and bone marker profiles.

Disclosures: S.L. West, None.

This study received funding from: United States Army Medical Research and Materiel Command Peer Reviewed Medical Research Program (Award Number: PR054531).

T201

Deficiency of the G protein-coupled Estrogen Receptor GPR30 Leads to Reduced Bone Growth and Bone Mineral Density in Female Mice. S. H. Windahl¹, N. Andersson¹, U. E. A. Mårtensson^{2,3}, C. Owman^{2,3}, C. R. Rosen³, M. L. Adamo⁴, B. Olde^{2,3}, F. Leeb-Lundberg^{2,3}, C. Ohlsson¹. ¹Center for Bone Research at the Sahlgrenska Academy, Gothenburg, Sweden, ²Unit of Drug Target Discovery at Lund University, Lund, Sweden, ³The Jackson Laboratory, Bar Harbor, ME, USA, ⁴Department of Biochemistry, The University of Texas Health Science Center, San Antonio, TX, USA.

Estrogens are important regulators of bone growth and adult bone metabolism. There are two known nuclear receptors for estrogen (ER α and ER β). ER α is the most important nuclear ER for bone in both males and females while the role of ER β mainly is to modulate ER α activity in female but not male mice. Recent in vitro studies have suggested that the G-protein-coupled receptor GPR30 is a functional ER but the impact of GPR30 in vivo is unknown. The aim of the present study was to investigate the in vivo role of GPR30 for the skeleton and for reproductive tissues. We therefore developed a mouse model in which the GPR30 gene locus was disrupted. GPR30^{-/-} mice are viable and serum levels of estradiol and testosterone as well as the uterine weight were unchanged in GPR30^{-/-} mice compared with wild type mice. Interestingly, after sexual maturation, the female GPR30^{-/-} mice displayed a reduced body weight (22.6 \pm 0.4g, n=25) compared to WT mice (24.7 \pm 0.6g, n=26; p<0.01). The reduced body weight in female GPR30^{-/-} mice was associated with a reduced skeletal growth, including both the axial skeleton (crown-rump length, p<0.05) and the appendicular skeleton (femur length, p<0.05). The magnitude of the skeletal growth disturbance was similar in the appendicular and the axial skeleton, indicating that it was a proportional skeletal growth disturbance. In contrast, male GPR30^{-/-} mice displayed a normal skeletal growth. Because the growth disturbance became significant after sexual maturation and only was seen in female mice, one may speculate that sex steroid-dependent pubertal growth is affected in female GPR30^{-/-} mice. The GH/IGF-I axis is a major determinant of skeletal growth. Serum IGF-I levels were reduced in female (-11%, p<0.05) but not male GPR30^{-/-} mice, indicating that reduced serum IGF-I levels might be involved in the growth disturbance seen in female GPR30^{-/-} mice. Initial screening of BMD using total body DXA showed that the female but not the male GPR30^{-/-} mice displayed reduced BMD (-3%, p<0.05) compared with wild type mice. In conclusion, deficiency of the proposed novel ER GPR30 results in reduced bone growth and total body BMD associated with reduced serum IGF-I levels in female mice.

Disclosures: S.H. Windahl, None.

T202

DHT Treatment Reverses Gonadectomy-induced Changes in Fat and Lean Mass in Male but Not Female Mice. A. A. Semirale, X. Zhang, K. M. Wiren. VA Medical Center, Oregon Health & Science Univ, Portland, OR, USA.

Androgens have pervasive effects on target tissues including muscle, fat and bone. To characterize the role of androgen receptor (AR) signaling on body composition, an experimental paradigm of protracted hormone ablation followed by steroid replacement was employed. B6D2F2 control mice were sham operated or gonadectomized at 3 months of age. The effect of nonaromatizable dihydrotestosterone (DHT) was determined after an 8 week delay, to provide time for gonadectomy-induced changes in body composition to develop before intervention. The effect of androgen was assessed by dual energy x-ray absorptiometry (DXA) following 6 weeks of treatment with either DHT or placebo pellets. In control males (n = 8-11), lean mass as a % of body weight was significantly reduced (7.7 %, p < 0.001) following orchietomy (ORX) while conversely, % fat mass increased (7.6 %, p < 0.001) vs. sham controls. DHT treatment was beneficial, improving or fully restoring body composition changes induced by ORX compared to placebo. In females (n = 4-10) a similar trend was observed with increased fat (2.2 %) and reduced lean mass (2.3 %) after ovariectomy (OVX). Surprisingly, females were resistant to the effects of DHT to restore body composition. To determine whether changes in bone metabolism contribute to body composition differences, transgenic mice with skeletally-targeted AR overexpression in mature osteoblasts (driven by the 2.3 kb fragment of type I α 1 collagen promoter) were characterized. AR2.3-tg mice demonstrated changes in body composition after gonadectomy that mirrored wild types (n=3-9). Again similar to wild-type controls, DHT improved ORX-induced alterations in % fat and % lean mass in AR2.3-tg males but not females. In contrast to gonadectomized models, DHT treatment in intact wild type mice had a negative impact on body composition in both males and females. Males (n = 14-23) lost 4.4 % lean mass (p < 0.05) and increased fat mass by 4.3 % (p < 0.05) compared to placebo, with similar but less dramatic changes observed in females (n = 14-26). These results show both males and females increase fat and lose lean mass following gonadectomy. In the bone-targeted AR-overexpression model, enhanced androgen signaling does not influence the response to DHT suggesting that circulating factors derived from bone likely do not play a role in the body composition response to androgen therapy. Combined, these data indicate that systemic DHT positively influences body composition changes after a prolonged hypogonadal state in males but is ineffective in females over the same time frame. Furthermore, DHT treatment in the intact animal results in detrimental changes in body composition and should be approached with caution.

Disclosures: K.M. Wiren, None.

This study received funding from: DOD and NIH/NIDDK.

T203

Dissection of Androgen Receptor Signaling: Reconsideration of Direct Anabolic Action in Mature Bone. X. Zhang, A. A. Semirale, K. M. Wiren. VA Medical Center, Oregon Health & Science Univ, Portland, OR, USA.

The effects of androgen on bone remain poorly characterized and understudied. To develop insight into the cell types important in mediating androgen action, we constructed and compared two distinct transgenic lines employing different α 1(I)-collagen promoter fragments to control skeletally-targeted AR overexpression. The col3.6 AR-transgenic (AR3.6-tg) mice demonstrate AR overexpression throughout the osteoblast lineage including the periosteum, while col2.3 (AR2.3-tg) mice have more restricted overexpression in mature osteoblasts and osteocytes. Complex skeletal analysis using morphological characterization by μ CT, dynamic and static histomorphometric analysis, dual-energy x-ray absorptiometry (DXA), biomechanical testing and gene expression studies all indicate that androgen signaling in mature osteoblasts during growth produces a low turnover state, and the consequences are detrimental to overall matrix quality and bone strength. To determine the consequences of androgen treatment in the adult and whether nonaromatizable dihydrotestosterone (DHT) may be effective for treatment of post-menopausal bone loss in an animal model, 3 month old male and female B6D2F2 control mice were gonadectomized. Six weeks of treatment with DHT or placebo pellets was delayed until age 5 months to allow rapid bone turnover to stabilize, thus minimizing the impact of anti-resorptive effects of androgen. DXA demonstrated that systemic DHT administration significantly increased BMD and BMC in both sexes, to reverse loss sustained after a prolonged hypogonadal state (n = 14-26). To test the consequences of enhanced androgen signaling targeted to bone in the adult, male and female AR3.6-tg and AR2.3-tg mice were treated in the same manner. In both AR-tg families and in contrast to wild-type mice, DHT replacement did not improve either measure versus placebo pellet (n = 3-14). Taken together, these results indicate that improvements in bone mass with androgen treatment after gonadectomy in wild-type mice are likely mediated through effects on extra-skeletal tissues, not osteoblasts. Consistent with detrimental effects of enhanced androgen signaling on bone quality, DHT treatment in intact controls significantly reduced bone mass in both males and females. These findings demonstrate that after a sustained hypogonadal period, androgen effectively treats bone loss but that enhanced androgen signaling directly in bone is not anabolic in either male or female adults. The data suggests that targeting androgen response to mature osteoblasts is not beneficial for bone formation, and raise concerns regarding androgen administration or anabolic steroid abuse in healthy individuals in both sexes.

Disclosures: K.M. Wiren, None.

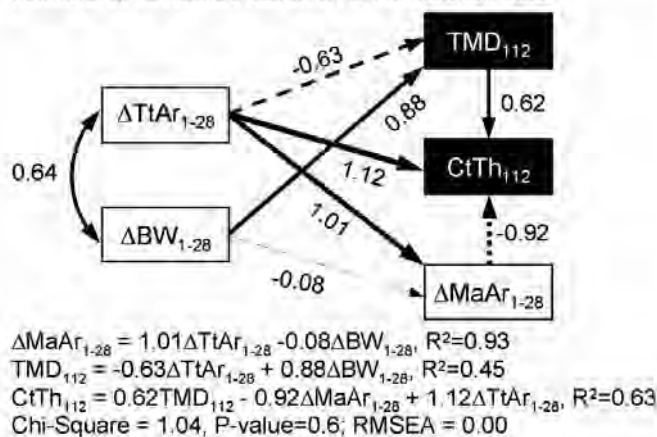
This study received funding from: DOD and NIH/NIDDK.

T204

Genetic Variation in Post-Natal Skeletal Growth Defines Functional Interactions among Adult Bone Traits and Fragility. K. J. Jepsen¹, B. Hu^{*1}, M. A. Cordova^{*1}, S. M. Tommasini², C. Price¹, H. W. Courtland¹, J. H. Nadeau^{*3}. ¹Mt Sinai School of Medicine, NY, NY, USA, ²CUNY Graduate Center, NY, NY, USA, ³Case Western Reserve University, Cleveland, OH, USA.

Prior work revealed that several adult bone traits are functionally related, such that the small cross-sectional size of slender bones was compensated by increased cortical thickness and tissue-mineral density. The set of traits for slender bones, although sufficiently stiff for daily activities, performed poorly under extreme load conditions. Because slenderness is a key determinant of fracture risk, identifying the biological controls responsible for functional interactions among adult traits should advance our understanding of how genetic background influences fracture risk. Femora from 20 female AXB/BXA Recombinant Inbred (RI) mouse strains were analyzed to test the hypothesis that functional interactions among adult traits are determined during early post-natal growth. Femoral mid-diaphyseal traits analyzed at 1 and 28 days of age were compared to adult traits measured at 112 days. Z-transformed data were analyzed using Path Analysis, which uses conditional covariances to establish causal relationships among multiple traits. Path Analysis (Fig 1) revealed a significant correlation between the rate of increase in total area (periosteal expansion) and marrow area (endosteal expansion) from 1 to 28 days, indicating that expansion of the periosteal surface relative to the endosteal surface was biologically controlled. Further, the rate of increase in total area (periosteal expansion) showed a net negative relationship with adult TMD and CtTh, such that variable post-natal periosteal expansion rates defined the degree of matrix mineralization and the relative rate of marrow expansion (and thus cortical thickness). The functional interactions between post-natal surface expansions and the set of adult traits indicated there are adaptive processes, superimposed on allelic variation, that co-adapt traits to match loading demands. These adaptive processes appear to accommodate allelic variation affecting periosteal expansion (i.e., slenderness) by allowing mechanically functional structures to be constructed in different ways. This study provided important new evidence that the set of adult traits which define bone strength and fragility are determined in large part by genetic factors affecting post-natal skeletal growth patterns.

Fig 1. Path Analysis showing causal (straight arrows) and non-causal (curved arrow) relationships among post-natal body weight gain (ΔBW_{1-28}), periosteal expansion ($\Delta TtAr_{1-28}$), marrow expansion ($\Delta MaAr_{1-28}$), and adult tissue-mineral density (TMD_{112}) and cortical thickness ($CtTh_{112}$). Path coefficients calculated based on Z-transformed data.



Disclosures: K.J. Jepsen, None.

This study received funding from: NIH, DOD.

T205

Cells Cultured from Bone Lesions of Patients with Paget's Disease Show No Evidence of Measles Virus RNA or Somatic Mutations in SQSTM1. B. G. Matthews^{*1}, U. Bava^{*1}, K. Callon^{*1}, M. A. Afzal^{*2}, J. Cornish¹, I. R. Reid¹, D. Naot¹. ¹Medicine, University of Auckland, Auckland, New Zealand, ²Division of Virology, National Institute for Biological Standards & Control, Potters Bar, United Kingdom.

Paget's disease is a focal condition of bone of uncertain etiology. The disease appears to be associated with a combination of genetic and environmental factors. SQSTM1 mutations have been identified in familial Paget's and in a minority of sporadic cases, and several groups have suggested long-term infection with a paramyxovirus is associated with the disease. However, the mechanisms for the focal nature of Paget's disease are not understood. In this study, we used cells obtained from pagetic bone lesions to investigate local changes that could possibly account for the characteristic focal pathology.

We have collected RNA from cultured osteoblasts and bone marrow samples taken from both pagetic lesions and unaffected bone from a group of 22 patients with Paget's disease, and from control patients. Differential gene expression, analyzed by real-time PCR, identified several changes in these samples, including increased Dkk1 and IL-6 and a reduced RANKL/OPG ratio in pagetic cells compared with controls.

Somatic mutations within the pagetic lesion have been suggested to be responsible for the focal nature of the disease. In order to investigate the possibility of somatic SQSTM1 mutations, exons 7 and 8 of the SQSTM1 cDNA were sequenced in all the patients with Paget's disease, in some cases using samples from both pagetic and unaffected tissue. The wild-type sequence was found in all but one patient, who was heterozygous for the P392L mutation. DNA from peripheral blood in this subject had an identical sequence of SQSTM1, indicating that this was a germ-line mutation. We conclude that somatic mutations for SQSTM1 are not commonly present in Paget's disease.

The RNA was also used to look for evidence of measles virus involvement in Paget's disease. Nested RT-PCR analysis at the National Institute for Biological Standards and Control in England did not detect measles virus nucleocapsid or matrix genes in any of the pagetic or control samples. This suggests that long term measles virus infection is not commonly present in New Zealand patients with Paget's disease.

The results indicate that pagetic lesions are different from normal bone in terms of gene expression, but do not commonly contain somatic SQSTM1 mutations or measles virus infection.

Disclosures: B.G. Matthews, None.

This study received funding from: Health Research Council of New Zealand.

T206

A Mouse Model for Diabetes-mediated Osteoporosis. Z. Wang^{*1}, K. Ding^{*2}, M. W. Hamrick³, H. He^{*1}, S. Yan^{*4}, L. Zhou^{*1}, C. M. Isles⁵, Q. Mi¹. ¹Center for Biotechnology and Genomic Medicine/Dept. of Pathology, Medical College of Georgia, Augusta, GA, USA, ²Dept. of Medicine, Medical College of Georgia, Augusta, GA, USA, ³Dept. of Cellular Biology and Anatomy, Medical College of Georgia, Augusta, GA, USA, ⁴Dept. of Endocrinology, The Medical School Hospital of Qingdao University, Qingdao, China, ⁵Dept. of Orthopedic Surgery, Medical College of Georgia, Augusta, GA, USA.

Decreased bone mass, osteoporosis, and increased fracture rates are common skeletal complications in patients with type 1 diabetes (T1D). There is a considerable amount of clinical data to link osteoporosis with T1D. However, very little basic research has delved into this phenomenon, and few have directly addressed the influence of diabetes on the skeletal system of mice, an animal model that is amenable to genetic manipulation. Recently, a streptozotocin (STZ)-induced T1D mouse model was used to examine the influence of T1D on bone. However, STZ-induced diabetes causes some diversity among individual animals in terms of the extent of severity and the onset of diabetes. In addition, STZ may directly affect bone function. Here, we employed a novel genetic approach by which T1D would be most stably induced in RIP-iNOS mice as early as 1 week after birth due to the iNOS-mediated selective destruction of insulin-producing pancreatic beta cells. Pixus densitometric analysis showed a significant decrease in bone mineral density of whole bones in 3-month-old male RIP-iNOS mice compared with that of age- and strain-matched wild-type mice. The radiographic analysis also showed a significant lower bone mass in RIP-iNOS mice. However, the body weight was invariant between the two groups during the 3-month observation period. Our study demonstrated that diabetic RIP-iNOS mice can spontaneously develop osteoporosis, and could be served as a novel mouse model for studying T1D-related osteoporosis.

Disclosures: Q. Mi, None.

This study received funding from: Juvenile Diabetes Research Foundation International (19-2006-1065) to W. Mi.

T207

GLP-1 Action on Bone Turnover in Normal and Type 2 Diabetic State. B. Nuche-Berenguer^{*1}, V. Sancho^{*1}, J. Cancelas^{*1}, D. Lozano^{*2}, P. Esbrit², M. L. Villanueva-Peñacarrillo^{*1}. ¹Metabolism, Nutrition & Hormones, Fundación Jiménez Díaz, Madrid, Spain, ²Laboratory of Bone & Mineral Metabolism, Fundación Jiménez Díaz, Madrid, Spain.

An insulin-independent antidiabetic action of GLP-1 (glucagon-like peptide 1) is widely documented, as well as its insulin-like effect upon glucose metabolism in liver, muscle and fat, and neurotrophic and anorectic properties. It was suggested that incretins could participate in bone turnover changes occurring after absorption of nutrients. We have explored the possible in vivo effect of GLP-1 on bone remodeling in normal and diabetic state. Type 2 diabetic model was developed by streptozotocin injection in neonatal Wistar rats (STZ-T2D). Adult rats, normal (n=6) and STZ-T2D (n=6), were treated -3 days through an osmotic pump- with GLP-1 (0.86 nmol/kg/h). In fed conditions, plasma samples were taken before (basal) and by the end of the treatment, when also tibias were collected. MC3T3-E1 osteoblasts were incubated for 24 hours in α -MEM with 5 or 25mM D-glucose (or mannitol), and in absence and presence of 10^{-9} M GLP-1. Measurements: in plasma, osteocalcin (OC), tartrate-resistant acid phosphatase (TRAP) -ELISA-, insulin -RIA- and glucose; in bone and cells, gene expression of OC, osteoprotegerin (OPG) and RANK ligand (RANKL) -RT-PCR-. Untreated rats of both groups (n=6, each) were included as respective controls. In plasma: GLP-1 did not modify normal basal OC (440.5 \pm 6.0 ng/ml), while in STZ-T2D group, initially showing an apparently lower than normal level, GLP-1 induced a reduction (-10.9 \pm 0.9% Δ of basal, p<0.001); TRAP was slightly increased by GLP-1 in normal (2.87 \pm 0.24 U/l vs basal 2.64 \pm 0.27) and also in STZ-T2D (2.88 \pm 0.29 U/l vs basal 2.45 \pm 0.27); glucose and insulin were not significantly affected in either group. In bone: OC mRNA level in STZ-T2D was 1.65 \pm 0.26 times that of normal rats; treatment with GLP-1 induced an increase in normal (2.35 \pm 0.50 times control) and also in STZ-T2D (1.99 \pm 0.44 times control); OPG mRNA was higher in STZ-T2D (4.87 \pm 0.30 times that of normal), but while GLP-1 raised the value in normal (2.73 \pm 0.30 times control, p<0.005), it reduced that in STZ-T2D (0.44 \pm 0.05 times control); RANKL mRNA was slightly higher in STZ-T2D (1.63 \pm 0.19 times that of normal), and was similarly increased by GLP-1 in both groups (normal: 1.97 \pm 0.29 times control; STZ-T2D: 1.38 \pm 0.13 times control). In control STZ-T2D, RANKL/OPG mRNA ratio was 0.326, and GLP-1 treatment raised it to 2.98, similar to the 2.20 value obtained in MC3T3-E1 cells incubated with GLP-1 and high glucose. In conclusion, these novel findings show that GLP-1 directly modulates bone turnover markers in both normal and type 2 diabetic rats, and suggest that this hormone might favor bone resorption.

Disclosures: B. Nuche-Berenguer, None.

This study received funding from: Research Grant from Ministerio de Sanidad y Consumo (FIS:06/0076).

T208

Investigating the Role of Mecp2 in the Epigenetic Regulation of Bone Mineral Density. R. D. O'Connor¹, A. L. Ham^{*1}, A. M. Wolff^{*1}, M. Zayzafoon², N. C. Schanen³, M. C. Farach-Carson¹. ¹Department of Biological Sciences, University of Delaware, Newark, DE, USA, ²Department of Pathology, University of Alabama at Birmingham, Birmingham, AL, USA, ³Laboratory for Human Genetics, Nemours/Al duPont Hospital for Children, Wilmington, DE, USA.

Rett Syndrome (RTT), a neurodevelopmental disorder, is most often caused by inactivating mutations in the X-linked gene encoding a regulator of epigenetic gene expression, methyl CpG binding protein, MeCP2. Clinical data show that, along with neurological defects, females with RTT frequently have marked decrease in Bone Mineral Density (BMD) beyond that expected from disuse atrophy. Preliminary studies with a Mecp2 knock-out mouse model reveal a difference between the wild-type and knock-out mice, with the knock-out mice having a reduced skeletal size and altered bone mineral content compared to their wild type littermates. Histological analyses revealed a noticeable morphological difference in femur and tibia growth plate apparent by 3 weeks of age, prior to the onset of neurological symptoms. We speculate that Mecp2 deficiency leads to a primary dysregulation of genes critical for regulation of bone growth, differentiation and mineral homeostasis. To test this hypothesis, we have utilized a chromatin immunoprecipitation assay (ChIP) on chip strategy to identify specific targets of Mecp2-regulated expression in bone. Several genes essential to proper bone formation and maintenance of bone and calcium homeostasis have been identified as likely targets of Mecp2 in a differentiating osteoblast cell system. Current studies are underway to determine the specific regions of Mecp2 binding, and the functional significance of Mecp2 deficiency on candidate gene expression and function.

Disclosures: R.D. O'Connor, None.
This study received funding from: Nemours.

T209

Dwarfism: Body Composition and Bone Mineral Density Analysis. M. G. B. Pippa^{*1}, D. C. Andrade^{*2}, S. R. Eis³, C. A. Brandao⁴, C. F. Zerbinini¹. ¹Rheumatology, Hospital Heliopolis, Sao Paulo, Brazil, ²Clinical Research, Centro Paulista de Investigação Clínica, Sao Paulo, Brazil, ³Clinical Research, Centro de Diagnóstico e Pesquisa da Osteoporose do Espírito Santo, Vitória, Brazil, ⁴Bone Densitometry, Fleury Medicina e Saude, Sao Paulo, Brazil.

Dwarfism is a medical condition which result in short stature. Characteristically, the arms are shorter than the forearms and the thighs are shorter than the legs. Little is known about bone mass adjusted for body size and body composition (BC) compartments in dwarfism. Our objective was to evaluate bone mineral density (BMD), BC and X-Ray alterations in this population. 24 females and males dwarfs were studied. All of them were submitted to dual-energy X-ray absorptiometry (DXA) in order to analyze BMD of lumbar spine, proximal femur (PF), total body BMD (TBBMD), radio 33% (R33%) and BC as well. Total Lean mass (TLM), Total Fat Mass (TFM), percentage of adiposity (% adp), arms lean mass (ALM), legs lean mass (LLM), and body fat distribution (BFD) were also determined. Areal BMD was measured and reported in g/cm². Adjusted BMD (Adj BMD) was calculated by the relation between bone mineral content (BMC)/height and results were given in g/m². Apparent BMD was calculated according to Bachrach. Sarcopenia was also determined according to Baumgartner classification. AP and lateral Plain X-Ray of dorsal / lumbar spine were performed. Variables were evaluated as descriptive patterns. The adherence to normal curve was evaluated by Kolmogorov Smirnov test. Data were analysed using the statistical computer program Minitab version 15.0%. Twelve male and 12 female dwarfs from 6 to 53 years old were studied. Average age was 34.5 years (SD = 11.9), average weight 18 Kg (SD = 12.1), average BMI 33.9 Kg / m² (SD = 9.2) and average height 1.20 m (SD = 0.12). Areal BMD L1-L4 mean was 0.991 g/cm², App L1-L4 BMD 0.304 g/cm³ and adjusted L1-L4 BMD was 0.0274 g/cm². TBBMD mean was 1.047 (SD = 0.20) BMD, and AdjBMDT mean was 0.616 (SD = 0.52). R33% BMD mean was 0.616 and its Z-score -1.92 (SD = 1.02). According Z-score areal L1-L4 BMD, low bone mass was found in 5 dwarfs (20.8%). When we used Z-score TBBMD no low bone mass was shown. Using Z-score R 33% BMD, low bone mass was present in 52.6%. Five male presented sarcopenia (20.8%) and 3 female (12.5%). Mean age sarcopenic dwarfs was 26.7 (SD = 13.2). All sample had 1 or more X-Ray alterations (scoliosis, scoliosis, hyper lordosis, platyspondyly, narrow AP spinal canal, squared iliac wings, hypoplastic ("bullet nose") T-L vertebrae, mild and severe vertebral crush). Low bone mass was very frequent, particularly when R 33% Z-score was used. We concluded that dwarfism should be submitted to DXA analysis earlier than normal height people.

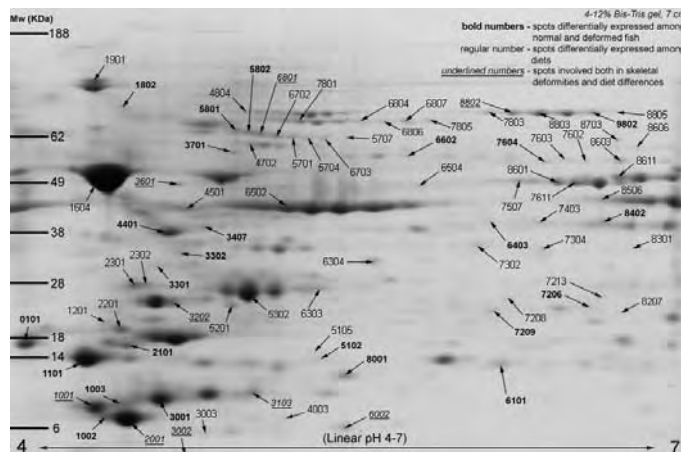
Disclosures: M.G.B. Pippa, None.

T210

Skeletal Development Analysis by Two-Dimensional Electrophoresis (2-DE) in White Bream (Diplodus sargus), Fed with Different Diets. P. M. L. Rodrigues^{*}, O. Cordeiro^{*}, T. S. Silva^{*}, L. E. C. Conceição^{*}. FCMA, Universidade do Algarve, Faro, Portugal.

Although high larval survival rates are commonly observed in aquaculture production of *D. sargus*, skeletal deformities are one of the main constraints. Diets with poor protein content and amino acid deficiencies have been related to the development of skeletal deformities. The central objective of this study is to evaluate the possibility of minimizing the skeletal deformity problems commonly found when *D. sargus* are cultured, through the

use of amino acid supplements. It is also intended to verify how the expression of key proteins involved in skeletal development are affected, in order to better understand the mechanisms present in development of skeletal deformities. The fish used in this study were previously fed since the larval stage with diets containing different amino acid profiles. The effect on skeletal deformities and bone proteins expression of larval *D. sargus* of a well balanced diet in the different indispensable amino acids (group 1 - control), or the same diet supplemented with amino acids involved in skeletal formation (group 2 - trp supplement and group 3 - lys supplement), was studied. Bone and cartilage were removed from *D. sargus* and proteins extracted. Protein expression changes in the three groups for normal and deformed fish were characterized by 2D gels analysis. Triplicates were done for each different condition with a total of eighteen gels. Gels with separated protein spots were analyzed on an imaging densitometer. Qualitative and quantitative analysis was done with PDQuest 2-D analysis software, which enables detection, matching and quantification of protein spots. After spot detection and matching, the intensity volume of each spot was normalized by comparison with a reference set of non-differentially expressed spots. Evaluation of the statistical significance of spot variation between groups was performed using a non-parametric test (Mann-Whitney U test, p < 0.05). The above figure representing the spots differentially expressed shows that the 2-DE technique allows the identification the key proteins involved in skeletal development and deformities. This information may be used for the development of better balanced diets, leading to fewer individuals with skeletal deformities in fish culture.

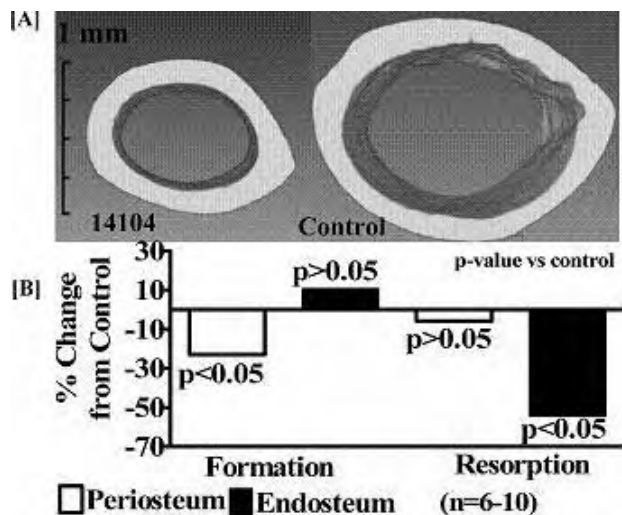


Disclosures: P.M.L. Rodrigues, None.
This study received funding from: Fundação para a Ciência e Tecnologia.

T211

An ENU Mutation Mapped to a Distal Region of Chromosome 11 Is Major Determinant of Bone Size Independent of Body Growth. V. Chest^{*}, S. Mohan, J. E. Wergedal, A. K. Srivastava. JLP VA Medical Center & Loma Linda University, Loma Linda, CA, USA.

Using a phenotype driven N-ethyl-nitrosourea (ENU) screen in growth hormone (GH) deficient mice, we have identified a mutant (named 14104) that exhibited 40% decreased bone size independent of body weight. The mutation is inherited as an autosomal dominant trait in a C57BL/6J background and magnitude of the bone size phenotype is modulated by GHRHR gene (7% lower bone size, p < 0.05 by post Hoc analysis). Measurement of bone size in tibia, femur, and humerus by pQCT, μ CT (Figure-1A), and histology showed 20% low (p < 0.001) periosteal circumference (PC) in mutant mice as compared to control mice. The unique feature of the 14104 mutant mice is that the cortical thickness is not decreased in the same proportion as cross-sectional area due to a greater (40-50%, p < 0.01) decrease in endosteal circumference (EC). This opposing movement of PC and EC is due to 25% decreased bone formation (p < 0.05) at the periosteal surface and a much larger 45% decreased bone resorption (p < 0.05) at the endosteal surface (Figure-1B), determined by histomorphometry. The osteoblasts from 14104 mice showed 40-50% (p < 0.05) reduced proliferation rate and lower induction of ALP activity (p < 0.05) in response to differentiating agents. To identify the chromosomal location of the mutation, we backcrossed the mutant 14104 mice with DBA mice and generated about 140 F2 mice. Employing a selective genotyping and phenotype based DNA pooling method we scanned the genome for linkage using 60 markers. We identified linked markers on chromosome 11 with peak LOD scores of 9.8 and 10.5 (p < 0.000001) for PC and EC, respectively. The 95% confidence interval of the locus involves 52-66 cM region of Chr 11. The allelic distribution of B6 (n = 18) and DBA alleles (n = 15) confirmed that linked locus was contributed by mutant gene because homozygous B6 allele contributed to 21% low PC (p < 0.001) and 53% low EC (p < 0.001) as compared to homozygotes for DBA alleles. In conclusion, we report mutant allele that dramatically reduced bone size independent of bone size by interacting with GH/IGF signaling pathway. The mutation is mapped to a Chr 11 region that includes several important QTLs regulating bone density and size. Since disruption of none of the known genes in this region (GH, Igfbp1, Colla1, Integrin, Noggin) produced phenotype similar to 14104 mutant mice, we believe that mutation is in a novel gene.

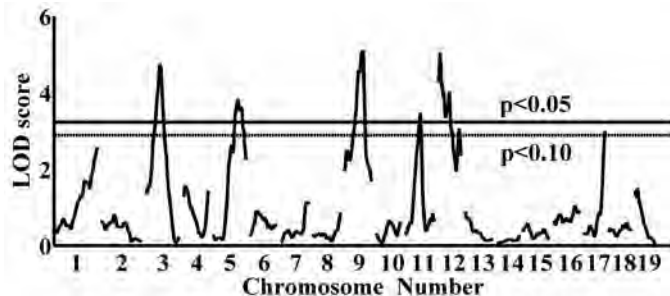


Disclosures: A.K. Srivastava, None.

T212

Serum Alkaline Phosphatase QTLs Provide Evidence that Genes on Chromosome 5 and 11 Regulate Bone Formation and Affect Bone size and Strength. J. E. Wergedal¹, C. L. Ackert-Bicknell², W. G. Beamer², S. Mohan¹, D. J. Baylink³, A. K. Srivastava¹. ¹JLP VA Medical Center & Loma Linda University, Loma Linda, CA, USA, ²The Jackson Laboratory, Bar Harbor, ME, USA, ³Dep. of Med., Loma Linda University, Loma Linda, CA, USA.

We have previously shown that the RF/J (RF) inbred mouse line has a greater femur cross sectional size associated with a higher bone formation rate than the NZB/B1NJ inbred mouse line. We sought to test the hypothesis that genetic loci that regulate bone formation contribute to variation in bone size and strength in the RF and NZB intercross. We analyzed serum alkaline phosphatase (ALP), as a surrogate marker for bone formation phenotype, to obtain evidence for the concordant loci regulating bone strength parameters and bone formation marker. Surprisingly, the mean serum ALP level was higher in the low bone formation mouse strain, NZB (n=8, Mean±SD 151±39 U/L) as compared to RF (n=16, 119±29 U/L, P<0.05 vs NZB). A genome-wide scan was carried out using 94 polymorphic markers and serum from 542 F2 female mice (Fig. 1). Total ALP levels in serum were measured by kinetic assay using a fully automated clinical chemistry analyzer. Interval mapping for co-segregation of genetic marker data with ALP activity revealed five significant QTL on chromosome (Chr) 3 (LOD 4.74, peak location 36 cM), Chr 5 (LOD 3.82, 64 cM), Chr 9 (LOD 5.1, 48 cM), Chr 11 (LOD 3.48, 40 cM), and Chr 12 (LOD 5.04, 4 cM). A suggestive QTL was observed on Chr-17 (LOD 3.00, 56 cM). Combined together, these QTLs explain 29% of the F2 variance in ALP levels. Three of these loci on Chr 5, Chr 9, and Chr 12 represent novel ALP loci that have not been identified in any previously published crosses. The allelic distribution of ALP at the peak marker was compared with values for bone size (periosteal perimeter) and bone bending strength. Two of the ALP QTL (Chr 5 and 11) corresponded with size and strength QTL and had the allele from the RF strain as the high allele. Two additional ALP QTLs corresponded with size or strength QTL but did not have the same strain as the high allele. It is possible that these loci regulate ALP levels by influencing the ALP metabolism. In conclusion, five Chr loci have genes that affect ALP and may affect bone formation. Two Chr loci on 5 and 11 have genes that affect femur size and strength, possibly by regulating bone formation.



Disclosures: A.K. Srivastava, None.

T213

FDPS, GGPS1 and FDFT1 Gene Polymorphisms as Pharmacogenetic Markers for the Response to Bisphosphonates. S. Carbonell Sala¹, V. Martinetti¹, F. Del Monte¹, I. Tognarini¹, S. Silvestri¹, F. Marini¹, L. Masi¹, A. Tanini¹, A. Falchetti², M. Brandi². ¹Internal Medicine, University of Florence, Florence, Italy, ²Internal Medicine, University of Florence, Florence, Italy.

The therapy of metabolic bone diseases is characterized by variability in the response with limited prediction on a patient-by-patient basis. This is relevant in osteoporosis, where therapy is required long-term before outcomes' evaluation. Our aim was to study how genetic traits influence efficacy and acute response to amino-bisphosphonates (N-BPs), key components for the therapy of high turnover metabolic bone diseases. N-BPs can specifically inhibit mevalonate pathway enzymes required for protein prenylation. As the response to N-BPs is highly variable among treated patients, the individual genetic variability could be an explanation.

In this study we analyzed the farnesyl pyrophosphate-synthase (FDPS), the geranylgeranyl pyrophosphate-synthase (GGPS1) and the squalene synthase (FDFT1) gene polymorphisms to assess genetic aspects of N-BPs response. The genotype distribution for FDPS A/C polymorphism (intron 1) in the Italian population corresponded to an A-allele frequency of 0.82, and C-allele frequency is 0.18, with a heterozygosity index of 0.2981 (χ^2 Test: p=0.29). The Polymorphism Information Content of this marker is informative (PIC=0.29). After the evaluation of the PIC value of GGPS1 and FDFT1 selected polymorphisms, our future goal is to perform a cohort study with patients involved in clinical trials with N-BPs, searching for correlations between genotype/haplotype and response to therapy. In a cohort study including a group of 200 Caucasian postmenopausal women was observed no statistically significant association between FDPS polymorphism and baseline-BMD, with a tendency of lowest response to therapy in patients with CC-genotype.

Our final goal is to identify the segregation of clinical response to N-BPs with genetic profile of their targets in chronic metabolic bone syndromes; and to provide models for N-BPs pharmacogenetic functionality studies. Some studies demonstrate the presence of osteoclast precursors in peripheral blood in the mononuclear cell fraction. Future studies will attempt to isolate peripheral human osteoclast precursors obtained from patients with FDPS, GGPS1 and FDFT1 opposite genotypes to perform "in vitro" functionality studies. Altogether these data can contribute to the selection of optimal therapeutic guidelines in patients treated with N-BPs.

Disclosures: S. Carbonell Sala, None.

T214

Genome-wide Haplotype Association Mapping (HAM) in Mice Leads to an Identification of a Genetic Variant in CER1 Associated with Bone Mineral Density in Premenopausal Women. C. L. Cheung¹, P. L. Tang², P. C. Sham³, P. McClurg⁴, S. Chan², D. K. Smith², A. I. Su⁴, K. S. Cheah², A. W. Kung¹, Y. Song². ¹Medicine, The University of Hong Kong, Hong Kong, Hong Kong, ²Biochemistry, The University of Hong Kong, Hong Kong, Hong Kong, ³Genome Research Centre, The University of Hong Kong, Hong Kong, Hong Kong, ⁴Genomics Institute of the Novartis Research Foundation, San Diego, CA, USA.

Bone Mineral Density (BMD) is a complex trait likely determined by multiple genes. We attempted to identify the quantitative trait loci (QTL) for BMD in mouse genome and to replicate the findings in human. Information on single nucleotide polymorphisms (SNPs) (1) and whole body BMD of 18 weeks female mice (2) were gathered from 30 mouse strains. The Haplotype Association Mapping (HAM) program which utilized a sliding window of 3 SNPs in the grouping of a haplotype block was applied (1). A modified F-test was used to query for the existence of some haplotypes structure that can partition mice with high BMD and low BMD. The positional candidate gene was then replicated in 1,083 young southern Chinese women aged 20-40 years having extreme high (BMD Z score > +1 at either the spine or hip) and low BMD (Z score < -1.28, equivalent to the lowest 10th percentile of the population). The association was examined using binary logistic regression with adjustment of age, height and weight. 22 blocks in the female mice genome were identified to contain genes for BMD variation. Chromosome 4, 82.2-87.9 Mb and Chromosome 12, 26.9-28.6 Mb had two peaks in close proximity. No genes can be found in the gap in Chromosome 12, 26.9-28.6 Mb. 27 genes were found in that of Chromosome 4, 82.2-87.9 Mb. Examination of the gene list identified Cer1 as a positional candidate gene in chromosome 4 QTL. Cer1 is a homolog of Cerberus in Xenopus, which belongs to a cysteine knot superfamily containing a cysteine knot motif in a C-terminal cysteine-rich region. Genotyping of 10 SNPs in human CER1 gene in 1,083 high and low BMD subjects revealed a non-synonymous SNP (rs3747532) was associated with an increased risk of low BMD in premenopausal women (odds ratio 2.2; 95% confidence interval: 1.0 - 4.6; p < 0.05). Our successful identification of an association of CER1 with BMD variation in both young mature female mice and humans suggested that CER1 is one of the genes associated with peak bone mass. Our study highlights the utility of publicly available databases for rapidly surveying the genome for QTL.

References:

1. Pletcher, M. T., McClurg, P., Batalov, S., Su, A. I., Barnes, S. W., Lagler, E., et al. (2004). Use of a dense single nucleotide polymorphism map for in silico mapping in the mouse. *PLoS Biol* 2:e393
2. <http://www.jax.org/phenome>

Disclosures: C.L. Cheung, None.

T215

Association Study of CLCN7 Polymorphisms and Areal Bone Mineral Density in White or Black Women or White Men. K. Chu¹, S. Ichikawa¹, D. L. Koller², R. Snyder¹, L. Curry¹, X. Xuei³, H. J. Edenberg³, T. M. Foroud², M. Peacock¹, M. J. Econs¹. ¹Medicine, Medical School of Indiana University, Indianapolis, IN, USA, ²Medical and Molecular Genetics, Medical School of Indiana University, Indianapolis, IN, USA, ³Biochemistry and Molecular Biology, Medical School of Indiana University, Indianapolis, IN, USA.

Mutations in the Chloride Channel 7 (CLCN7) gene result in autosomal dominant osteopetrosis (ADO) or autosomal recessive infantile osteopetrosis. Previously, we found that polymorphisms in CLCN7 were associated with disease severity of ADO. A SNP (single nucleotide polymorphism) in CLCN7 (rs12926089; V418M) was also found to be associated with femoral neck BMD in Scottish women. To determine whether CLCN7 SNPs are associated with normal variation in peak areal BMD we genotyped 6 SNPs distributed throughout CLCN7 in a sample of 1704 premenopausal white women, 517 premenopausal black women or 717 white men. The SNPs were tested for association with lumbar spine and femoral neck BMD in these three samples. We found SNP rs2235579 to be associated with femoral neck BMD ($P=0.03$) in white women; however, only a small proportion (0.52%) of the total variation in femoral neck BMD was explained by rs2235579. No significant association was found in white men or black women. We did not detect significant evidence of association ($P>0.92$) with the SNP rs12926089 (V418M) in our samples. In conclusion, variation in CLCN7 is not a major contributor to the observed variability in peak BMD at either the femoral neck or lumbar spine in white or black women or white men.

Disclosures: K. Chu, None.

This study received funding from: NIH.

T216

Influence of the Gene Polymorphisms of Collagenase-1 in Osteogenesis Imperfecta. P. Román-García¹, C. Gomez¹, M. Rodríguez-García¹, D. Álvarez-Hernández¹, I. Rodríguez-García², M. Muñoz-Torres³, N. Guanyabens-Gay⁴, J. Cannata-Andía¹. ¹Bone and mineral research unit, Hospital Universitario Central de Asturias, Oviedo, Spain, ²Molecular Genetics Laboratory, Hospital Universitario Central de Asturias, Oviedo, Spain, ³Endocrinology, Hospital Universitario San Cecilio de Granada, Granada, Spain, ⁴Rheumatology, Hospital Clinic de Barcelona, Barcelona, Spain.

The osteogenesis imperfecta (OI) is an inheritable disease, characterized by extreme bone fragility, and several extraosseous clinical manifestations. Recent results have revealed that mutations in genes not related with collagen synthesis are the cause of the new OI types. Thus, mechanisms not related to collagen synthesis might explain the different severity of the disease. The matrix metalloproteinases (MMPs) are implicated in the collagen digestion in the bone turnover process.

The aim of this study was to investigate if the functional polymorphism +1519 T/- in the MMP-1 gene (Collagenase I) was associated to the development of the disease and to the number of fractures. We studied the new T/T > T/- polymorphism, at the +1519 position in the MMP-1 gene in 30 patients with clinical diagnosis of OI and healthy controls using PCR-SSCP technique. The OI patients were 10 males and 20 females, 37.08 ± 16.4 years old (8 to 70). As reference population we used 450 people, age and sex matched from a large sample of our community hematological donors.

The frequency of the T/- genotype in OI was 3 fold higher than the observed in control population. Table 1. The clinical picture in patients with OI and T/- genotype was not different with regard T/T patients in mean number of fractures (11.3 ± 5 vs. 11.7 ± 9), presence of blue esclerae. By contrast in T/- patients we did not observed any vertebral fractures whereas in T/T patients, the prevalence of vertebral fractures was 95%. None of T/- patients had familiar history of OI versus 61% in the T/T patients. In terms of BMD we found a trend to have a higher BMD in lumbar spine and total hip in T/- patients.

There is an association between the genotype T/- and the disease. The allele (-) implicates a "frameshit reading" change and the patients with the (-) allele may have a modified collagenolytic activity. These data supports the theory that there are other molecules are affecting the disease or its manifestations or even the possibility of a misclassification in patients with clinical diagnosis.

Table 1 (* $p<0.05$ compared to control)

	T/T	T/-	Total
Controls	450 (97.0%)	14 (3.0%)	464
Osteogenesis Imperfecta	27 (90.%)	3 (10%)*	30
Lumbar-spine (Z-Score)	-3.14 ± 1.21	-1.16 ± 1.24	
Total hip (Z-score)	-1.56 ± 1.04	-0.5 ± 0.21	
Prevalence of lumbar OP	76%	0%	
Prevalence of total hip OP	20%	0%	

Disclosures: C. Gomez, None.

T217

Common Variant of SOSTDC1 Is Associated with Increased Risks of Fractures and Osteoporosis--A Novel Candidate Gene Revealed by Fine Mapping from Anhui Genome-Wide Scan. Y. H. Hsu¹, T. Niu², H. Terwedow², C. Rosen³, X. Xu², J. Brain². ¹Hebrew SeniorLife and Harvard Sch Public Health, Boston, MA, USA, ²Harvard Sch Public Health, Boston, MA, USA, ³Maine Center for Osteoporosis Research and Education, St. Joseph Hospital, Bangor, ME, USA.

Previously, we have revealed three novel QTLs (LOD > 3.65) on Chr 7p21 for femoral neck (FN) BMD, Chr 2q24 for total hip BMD and Chr 5q21 for BMDs combined at different skeletal sites in a genome-wide scan of 3093 adult Chinese siblings selected based on their extreme hip BMD. To narrow down the QTL region, we first genotyped 10-20 microsatellite markers (~2 cM per marker) in each of the QTLs in the same 3093 siblings. Fine mapping of the Chr 7p21 QTL narrowed to a 8 cM region (LOD = 3.72). Among 23 known genes in this region, twist homolog 1 (TWIST1) and sclerostin domain-containing protein 1 (SOSTDC1) have been known functionally relevant to bone metabolism. TWIST1 inactivation reduces the binding ability of CBFA1/RUNX2 to the osteocalcin promoter. SOSTDC1 belongs to a class of bone morphogenetic protein (BMP) antagonists. To test whether polymorphisms in the TWIST1 and SOSTDC1 are associated with BMDs in our cohort, we genotyped tag SNPs in an independent set of 2392 extreme low FN BMD cases (T-score < -1) and extreme high FN BMD controls matched by age and sex, selected from a study of 23,327 Chinese men and women. Tag SNPs were chosen from HapMap dataset (5 tag SNPs with pairwise mean $r^2 = 0.98$ to un-tag SNPs for SOSTDC1; 4 tag SNPs with $r^2 = 0.94$ for TWIST1). Multiple logistic regression with additive genetic model was used, adjusted for age, height, weight, physical activity, smoking, and menopause (women). First, the adjusted odds ratios (ORs) for extreme low FN BMD was associated with three adjacent SNPs located in exon 1 and intron 1 of SOSTDC1 (ORs 1.4-1.6, p -values 0.004- 4×10^{-5} , p -values by permutation test 0.041- 5×10^{-4}) in men. A weak association was found in women for the SNP located in exon 1 of SOSTDC1 ($p=0.017$). No association was found between TWIST1 SNPs and BMD. Second, the ORs (95%CI) for men carrying the polymorphic allele A for the strongest associated SNP (rs16878762, MAF: 28.6%) of SOSTDC1 were 1.7 (1.3-2.4) for osteoporosis, and 2.0 (1.1-3.7) for osteoporotic fractures. Third, men carrying AA genotype had 54 and 80 mg/cm² lower whole body and Lumbar Spine BMD, respectively. Finally, SNP rs16878762 was significantly associated with SOSTDC1 gene expression in men ($p=0.004$) and women ($p=0.049$). Notable, despite the close homologue to sclerostin (SOST), no significant association was found for SOST polymorphism (SRP9) in our study population. In sum, results from linkage, population-based association, and gene expression studies all suggest SOSTDC1 variants may causally reduce BMDs and increase risks of osteoporotic fractures.

Disclosures: Y.H. Hsu, None.

This study received funding from: NIH/NIAMS.

T218

An AluI Polymorphism in ESR2 Is Associated with Reduced Risk of Osteoporotic Fractures. L. B. Husted, N. Gonzalez-Bofill, L. Stenkjær*, M. Carstens*, B. L. Langdahl. Research Lab. C, Aarhus University Hospital, Århus, Denmark.

Estrogen is important for acquisition and maintenance of bone mineral density (BMD) and therefore also for the development of osteoporosis. It acts by binding to estrogen receptors, which are transcription factors belonging to the nuclear receptor hormone superfamily. Two types of estrogen receptors, ERα and ERβ, have been identified. We have previously found that a TA-repeat polymorphism in the gene encoding ERα, ESR1 is associated with osteoporotic fracture risk. In this study we investigated the effect of three polymorphisms in the ERβ gene (ESR2): a synonymous RsaI polymorphism (rs1256049), an AluI polymorphism in the 3'UTR (rs4986938) and a CA-repeat polymorphism (D14S1026) in intron 5 on BMD and risk of vertebral fractures in a case-control study including 466 osteoporotic patients and 336 normal controls.

Prevalence of the CC and CT + TT genotypes of the RsaI polymorphism was 94.5% and 5.5% in patients with vertebral fractures, respectively, and 95.0% and 5.0% in normal controls, respectively, $\chi^2 = 0.071$, ns. BMD at the lumbar spine was 0.844 ± 0.190 g/cm² in carriers of the T allele vs 0.836 ± 0.178 g/cm² in individuals with the CC genotype, ns. Likewise, no differences in BMD between the genotypes were found at any of the hip sites. The AluI polymorphism was associated with reduced risk of vertebral fractures. Distribution of the CC, CT and TT genotypes in patients with vertebral fractures and normal controls was 44.3%, 45.3% and 10.4% and 34.9%, 49.1% and 16%, respectively, $\chi^2 = 7.05$, $p = 0.029$. BMD at the lumbar spine was 0.828 ± 0.179 g/cm², 0.837 ± 0.176 g/cm² and 0.866 ± 0.182 g/cm² in individuals with the CC, CT and TT genotypes, respectively, ns. Similar results were found at the hip. In men, however, the difference in BMD at the total hip between the genotypes was significant ($p = 0.003$).

The distribution of the number of CA-repeats was bimodal and therefore the CA-repeat alleles were divided into a low (≤ 21 repeats) and a high repeat number group (> 22 repeats) for statistical analyses. The prevalence of the CA genotypes was similar between patients with vertebral fractures and normal controls, and there was no difference in BMD between the genotypes.

Because the CA-repeat polymorphism and the RsaI polymorphism were in linkage disequilibrium haplotypes could be estimated. We found no effect of the three common haplotypes on BMD or fracture risk.

By examining the TA-repeat polymorphism in ESR1 and the CA-repeat polymorphism in ESR2 there seemed to be an additive effect of the two polymorphisms on fracture risk.

In conclusion, we found that the AluI polymorphism in ESR2 is associated with reduced risk of osteoporotic fractures.

Disclosures: L.B. Husted, None.

T219

ENPP1 as a Candidate Gene for Femoral Bone Geometry. Y. K. Cho¹, S. Demissie^{*1}, G. Livshits^{*2}, J. B. Meigs^{*3}, L. A. Cupples^{*1}, J. C. Florez^{*3}, J. McAteer^{*3}, D. P. Kiel⁴, D. Karasik⁴. ¹Biostatistics, BU Sch Public Health, Boston, MA, USA, ²Sackler Faculty of Medicine, Tel Aviv University, Tel Aviv, Israel, ³Mass General Hospital and Broad Inst, Boston-Cambridge, MA, USA, ⁴Hebrew SeniorLife and Harvard Med School, Boston, MA, USA.

Secondary mineralization in bone is a controlled process with a tight balance between the levels of extracellular phosphate ions and inorganic pyrophosphate (PPi), which inhibits hydroxyapatite crystal growth and therefore prevents excessive calcification. Ecto-nucleotide pyrophosphatase phosphodiesterase 1 (ENPP1) generates PPi. It is uncertain to what extent ENPP1 may be involved in appendicular skeletal mineralization.

We examined the association of polymorphisms in the ENPP1 gene with femoral geometry measured with Hip Structural Analysis (HSA), in 789 women and 704 men from the Framingham Offspring Cohort (mean age \pm SD: 61.3 \pm 9.1 years), who had DXA and DNA available. HSA measures included femoral neck length (FNL), neck-shaft angle (NSA), and subperiosteal width at the narrowest section of the femoral neck (NN_WID) and shaft (S_WID).

Thirty one single nucleotide polymorphisms (SNPs) were genotyped on an iPLEX Sequenom platform, these SNPs captured 69% of common variants in ENPP1 (minor allele frequency >5%) with an r^2 >0.8. We performed sex-specific ANCOVA using 2 models adjusted for covariates: age (model 1) and age, height, BMI, smoking status, as well as estrogen history in women (model 2).

In men, we found 6 SNPs with nominally significant associations with the age-adjusted bone geometry traits. Intronic SNP (rs775386) was associated with FNL at $p = 0.0009$. Other SNPs (rs9493100, rs1044498, rs9493116, rs7768480, and rs1510) were also associated with bone geometry traits ($p < 0.008$). In women, no nominally significant associations were found. After adjustment for additional covariates, including body size, in general, magnitude and direction of the association did not change. To correct for multiple testing, we performed 10,000 random permutations of phenotypes and covariates while keeping the genotype LD and phenotype correlation information intact. The corrected p -value for rs775386 and FNL was 0.10, suggesting that the observed association may be due to chance.

In conclusion, this is the first study which examined a fairly comprehensive set of common variants in ENPP1 in relation to bone geometry. Nominally significant associations between ENPP1 polymorphisms and femoral geometry in Caucasian males generate the hypothesis that the observed genetic associations are not mediated by body size. These results require improved coverage of ENPP1 polymorphisms and confirmation in larger samples.

Disclosures: D. Karasik, None.

This study received funding from: NHLBI, NIAMS/NIA.

T220

Association of ADIPOR1 and ADIPOR2 Gene Polymorphisms with Bone Mineral Density in Postmenopausal Korean Women. H. Y. Kim¹, B. Oh^{*2}, J. Y. Lee^{*2}, B. L. Park^{*3}, H. D. Shin^{*3}, T. H. Kim^{*4}, E. K. Park^{*4}, S. Y. Kim^{*4}, J. M. Koh⁵, G. S. Kim⁵. ¹Division of Endocrinology and Metabolism, University of Wonkwang College Medicine, Sanbon Medical Center, Gunpo, Republic of Korea, ²National Genome Research Institute, National Institute of Health, Seoul, Republic of Korea, ³Department of Genetic Epidemiology, SNP Genetics, Inc., Seoul, Republic of Korea, ⁴Skeletal Disease Genome Research Center, Kyungpook National University Hospital, Daegu, Republic of Korea, ⁵Division of Endocrinology and Metabolism, University of Ulsan College of Medicine, Asan Medical Center, Seoul, Republic of Korea.

Obesity is associated with both higher fat mass and higher bone mineral density (BMD). Adiponectin is circulating peptide derived from adipose tissue. It mediates its insulin sensitizing and anti-atherogenic effects on target tissue through two known receptors, adiponectin receptor 1 and 2 (ADIPOR1; ADIPOR2). Recently, the expression of both adiponectin and its receptors in the bone forming cells of human was reported. The possibility was suggested that interaction between adiponectin and receptor might have an effect on bone metabolism. Therefore, we examined the associations between ADIPOR1 and ADIPOR2 gene polymorphisms and bone mineral density (BMD) in postmenopausal Korean women.

All exons, their boundaries, and the promoter region (approximately 1.5 kb) of ADIPOR1 and ADIPOR2 were sequenced in 24 individuals. Among identified polymorphisms, three polymorphisms in ADIPOR1 and three polymorphisms in ADIPOR2 were selected based on LDs and frequencies and genotyped in all study participants ($n = 729$). BMD at the lumbar spine and femur neck was measured using dual energy X-ray absorptiometry.

The mean age of the study subjects was 58.7 ± 7.5 years and the mean years since menopause was 9.5 ± 7.8 years. Multivariate analysis showed an association of the +5843 G > A in ADIPOR1 with lumbar spine BMD. Individual with +5843 A allele had lower BMD at the lumbar spine compared with those without A allele (0.90 ± 0.18 vs 0.86 ± 0.16 g/cm², $P = 0.005$) after adjustment age, years since menopause, weight, and height. There was significant association between the -64243T > G in ADIPOR2 with femur neck BMD. Individual with -64243 G allele showed lower BMD at femur neck than those without G allele (0.74 ± 0.12 vs 0.71 ± 0.13 g/cm², $P = 0.005$). However, we did not find any association with fractures.

These finding suggests that the +5843 G > A in ADIPOR1 and -64243T > G in ADIPOR2 gene may be one of the genetic determinants of osteoporosis in Korean postmenopausal women.

Disclosures: H.Y. Kim, None.

T221

Associations of Paraoxonase Gene (PON1) Promoter Polymorphisms with Vertebral Fracture Risk Independently of Bone Mineral Density in Postmenopausal Women. B. Kim^{*1}, S. H. Lee^{*1}, Y. Chung^{*2}, B. Oh^{*3}, J. Lee^{*3}, J. Lee^{*3}, B. L. Park^{*4}, H. D. Shin^{*4}, T. Kim^{*5}, E. K. Park^{*5}, S. Kim^{*5}, J. Koh¹, G. S. Kim¹. ¹Division of Endocrinology and Metabolism, Asan Medical Center, University of Ulsan College of Medicine, Seoul, Republic of Korea, ²Department of Internal Medicine, Seoul Veterans Hospital, Seoul, Republic of Korea, ³National Genome Research Institute, National Institute of Health, Seoul, Republic of Korea, ⁴Department of Genetic Epidemiology, SNP Genetics, Inc., Seoul, Republic of Korea, ⁵Skeletal Diseases Genome Research Center, Kyungpook National University Hospital, Daegu, Republic of Korea.

There is increasing evidence of a biochemical link between oxidative stress and bone metabolism. Paraoxonase (PON1) is associated with high density lipoprotein and has the antioxidant effect by both preventing the formation of oxidized low density lipoprotein (LDL) and inactivating LDL-derived oxidized phospholipids once they are formed. Therefore, PON1 could be an important candidate gene for the modulation of bone metabolism. In order to investigate the effects of PON1 polymorphisms, especially promoter polymorphisms, on the risk of osteoporotic fractures (OFs) and bone mineral density (BMD), we directly sequenced the PON1 gene in 24 Korean individuals, and identified 30 sequence variants. In the present study, we selected 3 promoter polymorphisms of them, and they were genotyped in a larger-scale study of postmenopausal women ($n = 729$). Areal BMD (g/cm²) of the anterior-posterior lumbar spine and the non-dominant proximal femur was measured using dual energy X-ray absorptiometry. Lateral thoracolumbar (T4-L4) radiographs were obtained in all subjects. Multivariate analyses showed that all three promoter polymorphisms were not associated with BMD at the both sites. However, we found that the PON1-1741A > G and -909G > C promoter polymorphisms were associated with vertebral fracture risk independently of BMD before and after adjustment for age, years since menopause, height, weight, and/or BMD. After the adjustments for all covariates, the subjects with the GG homozygote of -1741A > G and the CC homozygote of -909G > C were significantly related with higher vertebral fracture risk (odds ratio = 2.37, 95% CI 1.36-4.15, $P = 0.002$ in the recessive model; and odds ratio = 2.35, 95% CI 1.35-4.07, $P = 0.002$ in the recessive model, respectively). When we categorized the subjects into four levels according to the number of vertebral fractures, we found that the rare alleles of PON1-1741A > G ($P = 0.004$) and -909G > C ($P = 0.006$) increased, as the number of OFs did. These findings suggest that PON1 could be one of the genetic predictive markers for osteoporotic fracture risk and severity in postmenopausal women.

Disclosures: B. Kim, None.

T222

The Association of Bone Mass with SNPs of Frizzled Genes in Wnt System and Circulating Osteoprotegerin (OPG) - Receptor Activator of NF- κ B Ligand (RANKL) System. J. Kim, H. Kim^{*}, S. Chae^{*}, C. Suh^{*}, S. Kim, Y. Choi, S. Moon. Dept. of Obstetrics & Gynecology, Seoul National University Hospital, Seoul, Republic of Korea.

The aim of this study was to investigate the association between single nucleotide polymorphisms (SNPs) in frizzled (FZD)s gene in Wnt signal pathway, and circulating osteoprotegerin (OPG), soluble receptor activator of NF- κ B ligand (sRANKL) levels, bone turnover markers, and bone mineral density (BMD) in postmenopausal Korean women. The SNPs in FZD1 (rs3752146), FZD5 (rs1056614), FZD6 (rs17855053; rs12549394), FZD7 (rs12546413), and FZD9 (rs17852398; rs17856756; rs17856757; rs17852397) gene were analyzed by direct sequencing in 371 Korean postmenopausal women. Levels of serum OPG, sRANKL, osteocalcin (OST), C-telopeptide of type I collagen (CTX), calcium (Ca), phosphorus (P), parathyroid hormone (PTH) and calcitonin, and BMD at the lumbar spine and proximal femur were measured. The SNPs in FZD1, FZD5, FZD7, and FZD9 gene, and in exon 2 of FZD6 gene were not observed. The distributions of C345A SNP (rs17855053) in the exon4 and A664C SNP (rs12549394) in the exon 8 of FZD6 gene were as follows: CC 36.4%, AC 43.7%, AA 19.9%, CC 95.7%, and CA 4.3%. No significant differences in the adjusted BMD of lumbar spine and proximal femur were noted among the genotypes of C345A and A664C SNPs in FZD 6 gene and the distributions of these genotypes were not different according to the status of bone mass. No significant differences in serum levels of OPG, and sRANKL, and their ratios, and bone markers such as OST, CTX, Ca, P, PTH and calcitonin were observed according to these genotypes of FZD 6 gene polymorphisms. In conclusion, the FZDs gene polymorphisms was not associated with BMD of the lumbar spine and proximal femur, bone turnover markers, and circulating OPG-sRANKL levels in Korean women.

Disclosures: J. Kim, None.

This study received funding from: Seoul National University Hospital (#03-2006-0220)

T223

Association Study of Catalase Gene Polymorphisms with an Osteonecrosis of Femoral Head in Korean Population. J. Hong^{*1}, X. Dai^{*1}, T. Kim^{*1}, J. Park^{*1}, J. Jung^{*1}, E. Park^{*2}, S. Kim^{*3}. ¹Skeletal diseases Genome Research Center, Kyungpook National University Hospital, Daegu, Republic of Korea, ²Pathology and Regenerative Medicine, School of Dentistry, Kyungpook National University, Daegu, Republic of Korea, ³Department of Orthopedic Surgery, Kyungpook National University Hospital, Daegu, Republic of Korea.

Osteonecrosis of femoral head (ONFH) frequently leads to progressive collapse of the femoral head followed by a degenerative arthritis of the hip joint. Various theories have been proposed regarding the pathogenic mechanisms of osteonecrosis (ON). Oxidative stress, which has been implicated in many pathological conditions, including vascular injury, has been recently suggested to play a part in the development of ON. In addition, tissue oxidation is known to induce apoptosis, which has also been suggested to be involved ON. Recently, oxidative stress has been also suggested to participate in the development of osteoporosis. Some in vitro and animal studies have suggested that oxidative stress decrease bone formation by modulating the differentiation and survival of osteoblasts and stimulating bone resorption.

Catalase (CAT) is a major antioxidant enzyme that detoxifies hydrogen peroxide by converting it into water and oxygen, thereby preventing cellular injury by oxidative stress. Individuals with reduced catalase activity have an increased incidence of oxidative stress-related disease, such as atherosclerosis, diabetes, and dyslipidaemia. To examine the associations between the CAT gene polymorphisms and ON in Korean population, we selected nine polymorphic sites of CAT from public databases (dbSNP, KSNP and HapMap), and genotyped in 460 ONFH patients and 300 control subjects. The CAT genotype did not deviate from Hardy-Weinberg equilibrium in any of the case or control groups. We classified the patients according to etiology: alcohol-induced, steroid-induced, and idiopathic ONFH subgroup. We found that -89A>T, -20T>C, +14539A>T, and +22348C>T polymorphisms of CAT gene were significantly associated with the risk of ONFH in all alternative analysis model (p range; 0.0003-0.047, OR; 0.56-3.57). However, the minor allele of -89A>T and -20T>C had protective effect on ONFH with significant p-values (p range; 0.004-0.047, OR; 0.56-0.75). Further analysis based on pathological etiology (alcohol-, steroid- or idiopathic) and sex showed that the genotype of -89A>T, -20T>C, +14539A>T, and +22348C>T were also associated with the risk of ONFH in each subgroup with significance. Our results provide, for the first time, evidence supporting the association of CAT gene polymorphisms with the risk of ONFH in Korean population, and suggest that oxidative stress may play an important role in the pathogenesis of ONFH.

Disclosures: S. Kim, None.

T224

Association of Lipoprotein Lipase Hind III Polymorphism with Lumbar Bone Mineral Density in Korean Premenopausal Women. S. Lee¹, O. Kim^{*2}, J. Kim^{*2}, K. Lee^{*2}, H. Baik^{*2}, Y. Jo^{*3}, H. Kim^{*3}, B. Kim^{*3}, K. Park^{*3}, H. Choi^{*4}. ¹Biochemistry-Molecular Biology/Internal Medicine, School of Medicine, Eulji University, Daejeon, Republic of Korea, ²Biochemistry-Molecular Biology, School of Medicine, Eulji University, Daejeon, Republic of Korea, ³Internal Medicine, School of Medicine, Eulji University, Daejeon, Republic of Korea, ⁴Family Medicine, School of Medicine, Eulji University, Daejeon, Republic of Korea.

The association between serum levels of lipid and bone mineral density (BMD) remains debatable. The lipoprotein lipase (LPL) plays a key role in lipid metabolism. Association of LPL Hind III polymorphism with BMD has not been studied. In the present study, we attempted to examine the association between LPL Hind III polymorphism and lumbar BMD in pre- and post-menopausal women, respectively. 201 Korean women (130, premenopausal women; 71, postmenopausal women) were recruited at the Eulji University Hospital, South Korea. We measured lumbar spine L₁-L₄ BMD using DXA. We determined LPL gene polymorphisms affecting Hind III polymorphism site in intron 8 using PCR techniques. The polymorphic allele displaying the restriction site was referred to as (+) and the allele without the site as (-). The (-) allele was less common. We compared the anthropometric parameters, blood lipid levels, and lumbar BMD between women with H(+/+) and H(+/-) genotype in pre- and post-menopausal women, respectively. Frequencies of H(+/+), H(+/-) and H(-/-) genotype were 60.8 %, 33.8 %, and 5.4 %, respectively, in premenopausal women. Frequencies of H(+/+), H(+/-) and H(-/-) genotype were 57.8 %, 39.4 %, and 2.8 %, respectively, in postmenopausal women. There were no differences in total cholesterol levels (184±31 vs 184±37 mg/dL), triglyceride levels (100±56 vs 106±91 mg/dL), HDL-cholesterol levels (54±10 vs 54±11 mg/dL), LDL-cholesterol levels (111±28 vs 109±32 mg/dL), waist circumference (74±7 vs 74±7 cm), and body mass index (22.5±2.5 vs 22.7±2.6 kg/m²) between women with H(+/+) and H(+/-) genotype in premenopausal women. However, there was a difference in lumbar BMD (0.970±0.111 g/cm² vs 1.015±0.108 g/cm²) between women with H(+/+) and H(+/-) genotype in premenopausal women. In postmenopausal women, there were no differences in blood lipid levels, obesity and lumbar BMD between women with H(+/+) and H(+/-) genotype. Our data indicate an association between LPL Hind III polymorphism and lumbar BMD in premenopausal women and suggest that the effect of LPL Hind III polymorphism on lumbar BMD is different between pre- and post-menopausal women at Korea.

Disclosures: S. Lee, None.

This study received funding from: Korea Research Foundation Grant funded by the Korean Government (KRF-2006-331-E00051).

T225

Associations of TSH Receptor Gene (TSHR) Polymorphisms with Bone Mineral Density (BMD) in Postmenopausal Women. S. H. Lee^{*1}, B. Kim^{*1}, W. G. Kim^{*1}, Y. Chung^{*2}, B. Oh^{*3}, J. Lee^{*3}, J. Lee^{*3}, B. L. Park^{*4}, H. D. Shin^{*4}, T. Kim^{*5}, E. K. Park^{*5}, S. Kim^{*5}, J. Koh^{*1}, G. S. Kim^{*1}. ¹Division of Endocrinology and Metabolism, Asan Medical Center, University of Ulsan College of Medicine, Seoul, Republic of Korea, ²Department of Internal Medicine, Seoul Veterans Hospital, Seoul, Republic of Korea, ³National Genome Research Institute, National Institute of Health, Seoul, Republic of Korea, ⁴Department of Genetic Epidemiology, SNP Genetics, Inc., Seoul, Republic of Korea, ⁵Skeletal Diseases Genome Research Center, Kyungpook National University Hospital, Daegu, Republic of Korea.

It is well known that hyperthyroidism is associated with lower bone mass as well as higher fracture risk. Not only high thyroid hormone level but also low thyroid stimulating hormone (TSH), is associated with lower bone mass. We selected TSH receptor gene (TSHR) as a candidate gene and investigated the genetic effects of selected TSHR polymorphisms on the bone mineral density (BMD) in postmenopausal Korean women with normal thyroid function. Four SNPs were selected in the Oriental SNP data, and genotypes for the selected SNPs were determined in 729 healthy postmenopausal women. Areal BMD (g/cm²) of the anterior-posterior lumbar spine and the femoral neck was measured using dual energy X-ray absorptiometry. Serum concentrations of TSH and free thyroxin were measured using immunoluminometry and radioimmunoassay, respectively. Mean age of the studied subjects was 58.7 ± 7.5 year old, and years since menopause was 9.5 ± 7.8 years. We found that TSHR +140974T>C polymorphism was significantly associated with BMDs at the lumbar spine and the femoral neck. After adjustment for age, year since menopause, weight and height, the subjects with the TT homozygotes had lower BMD at the lumbar spine (p = 0.01 and 0.01, respectively) and femoral neck (p = 0.003 and 0.001, respectively) in co-dominant and dominant models. When we divided the subjects into the two groups according to the serum TSH concentrations, the significant associations of the polymorphism with BMDs were persistent at the lumbar spine (p = 0.019) and femoral neck (p = 0.007) in the higher TSH group (1.8-5.0 μU/ml), but not in the lower TSH group (0.4-1.7 μU/ml) (p = 0.491 and 0.667, respectively). These results suggest +140974T>C polymorphism in TSHR is a possible genetic factors for BMD values in the postmenopausal women with normal thyroid function, and the association was more prominent in those with higher serum TSH concentration.

Disclosures: S.H. Lee, None.

T226

Multiplex SNP Genotyping and Data Analysis on 360 Hungarian Postmenopausal Women. G. Speer^{*}, Á. Lazáry, J. Kósa^{*}, B. Tóbiás^{*}, T. Mez^{*}, K. Bácsi^{*}, B. Balla^{*}, I. Takács, Z. Nagy, P. Lakatos. 1st Department of Internal Medicine, Semmelweis University, Budapest, Hungary.

Many single nucleotide polymorphisms were described as risk factors for osteoporosis (OP) but there are only a few reports in the literature about more complex genomic analyses such as haplotypes and gene-gene interactions. The aim of this study was to test the associations between SNPs or haplotypes of OP-related genes and the quantitative and qualitative traits of bone loss in Hungarian postmenopausal women. Thirty-eight SNPs found in OP-related genes were genotyped with GenomeLab SNPstream Genotyping system (Beckman Coulter) from DNA isolated from blood samples of 360 unrelated postmenopausal women. Associations between individual SNPs and traits of OP in three measured skeletal site (hip, spine and radius) were tested by MANOVA adjusted for BMI and years since menopause. We applied Multifactor Dimensionality Reduction (MDR) software for detecting gene-gene interactions and THESIAS software for validating them. Among individual SNPs showing the strongest association with OP were those found in RANKL, OPG and COL1A1 genes, respectively. We could not confirm the association with OP in cases of some previously reported SNPs, however, some new individual relationships have been determined. MDR analysis has shown the best models built by 2, 3, 4 or 5 SNPs for the estimation of OP that have been validated later. "TA" haplotype of RANKL (rs9533156) and VDR (rs1544410) was associated with OP risk on lumbar site (p<0.05) while "AC" haplotype of CYP19 (rs12901187) and IL1B (rs1143634) was associated with total femoral T-score and OP at the femoral site (p<0.05). Two models of three SNPs were determined; the "TAA" haplotype of COL1A1 (rs2857396), IL6 (rs1800797) and VDR (rs1544410) has strong association with the lumbar BMD (p<0.01) and T-score (p<0.05). The "GCA" haplotype of CYP19 (rs12901187), RANKL (rs3742257) and CASR (rs9740) was also associated with OP at the lumbar site (p<0.05). Our results suggest that multiplex SNP analysis can increase the force of genetic studies and can reveal new contexts of the genetic background of OP.

Disclosures: G. Speer, None.

This study received funding from: NKFP-1A/002/2004, NKFP-1A/007/2004, ETT-55059.

T227

Relationship between Variation in the PTH, PTH Related Peptide and the PTH Receptors 1 and 2 Genes and BMD and Fracture in Elderly Women. M. Tenne^{*1}, P. Gerdhem^{*1}, H. Luthman^{*2}, K. Åkesson¹, F. Mc Guigan^{*1}.¹Orthopaedics and Clinical Sciences, Malmö University Hospital, Lund University, Malmö, Sweden, ²Medical Genetics, Clinical Sciences, Malmö University Hospital, Lund University, Malmö, Sweden.

The aim of this study was to evaluate the relationship between genetic variations in 4 key genes of the PTH regulatory pathway and fracture and BMD in 75-year old women. Parathyroid hormone (PTH) plays a key role in calcium homeostasis and skeletal integrity whereas parathyroid hormone related peptide (PTHrP) contributes to skeletal development. Secretion of PTHrP has also been observed in tumors. PTH and PTHrP act through the same receptor, the PTH/PTHrP receptor (PTHrR). In addition, a second receptor, PTHR2 has been identified. We have previously reported on variation in the PTH and PTHrP genes in this cohort. However, we have extended the analyses to also include the receptor genes; PTHR1 and PTHR2.

The study group included 1044 elderly women, all 75-yr old at baseline, from the Malmö Osteoporosis Prospective Risk Assessment study (OPRA). This is an extensively phenotyped cohort which has been followed for up to 9 years. Three single nucleotide polymorphisms (SNPs) at the PTHR1 locus on chromosome 3 and three at the PTHR2 locus on chromosome 2 have been analysed, in addition to six SNPs at the PTH locus on chromosome 11 and three at the PTHrP locus on chromosome 12. Furthermore, for the PTH gene, after verifying LD between the SNPs, we analysed 5 common haplotypes identified using the PHASE program. We found no association between BMD, fracture or serum-PTH and PTHR1 SNPs. Neither did we find any association with PTHR2, a gene relatively unexplored in relation to osteoporosis. There was no association between SNPs in the PTH and PTHrP genes after adjusting for confounders.

Analysis revealed an association between a common haplotype of the PTH gene; Hap 5 occurring in 37% of the population and risk of fracture between age 50 and 75 ($p=0.018$), an association that was strengthened by adding prospectively occurring fractures i.e. from age 75 onwards ($p=0.011$). For Hap 1 (13%) the association was lower ($p=0.02$) for fractures age 50 to 75. In addition, PTH Hap 9 (19%) was associated with risk for any fracture sustained since childhood ($p=0.011$). We did not find any association between PTH haplotypes and BMD. A shift towards increasing PTH levels in the elderly may lead to fracture and genetic variation in the components of the PTH pathway may play a role. The absence of an association with the receptor genes could reflect that they are less important in the elderly. In this study the association between variation in PTH genes and fracture is evaluated for the first time. In our population of elderly women the effect of PTH gene variation, however modest, appears to be independent of BMD.

Disclosures: M. Tenne, None.

T228

No Role for Polymorphisms in the Gene Encoding RANKL in the Development of Sporadic Paget's Disease of Bone in Contrast to Some OPG Polymorphisms. G. Beyens^{*1}, F. de Freitas^{*1}, F. Vanhoenacker^{*2}, L. Verbruggen^{*3}, H. G. Zmierzak^{*4}, R. Westhovens^{*5}, J. Van Offel^{*6}, J. Devogelaer⁷, W. Van Hul¹. ¹Department of Medical Genetics, University of Antwerp, Antwerp, Belgium, ²Department of Radiology, University of Antwerp, Antwerp, Belgium, ³Department of Rheumatology, University Hospital of Brussels, Brussels, Belgium, ⁴Unit of Osteoporosis and Metabolic Bone Diseases, University Hospital of Ghent, Ghent, Belgium, ⁵Department of Rheumatology, Catholic University of Leuven, Leuven, Belgium, ⁶Department of Rheumatology, University of Antwerp, Antwerp, Belgium, ⁷Department of Rheumatology, Saint-Luc University Hospital, Brussels, Belgium.

Paget's disease of bone (PDB) is a metabolic bone disease characterized by focal lesions of increased bone turnover and affects between 1% and 5% of individuals older than 55 years in Western countries. Epidemiological studies have shown that PDB patients can be divided into two groups, a familial patient group and a sporadic group, with at least partially divergent pathogenic mechanisms. In a previous study, we have shown that polymorphisms in the TNFRSF11B gene encoding OPG have a gender-specific influence on the development of sporadic PDB in both Belgian and UK study populations [1]. With the current research we wanted to investigate whether a similar effect could be observed for SNPs in TNFRSF11 encoding RANKL.

Based on HapMap data and using an r^2 -based tagging strategy, we selected 10 SNPs and 2 multi-marker tests that cover all known common (minor allele frequency > 5%) genetic variation in a 44.57kb region surrounding TNFRSF11. These SNPs were genotyped in a population of 159 sporadic Belgian PDB patients and 186 Belgian control individuals. After genotyping one SNP, rs633137, turned out not to be in Hardy-Weinberg equilibrium in controls and was excluded. The remaining 9 SNPs in combination with the 2 multi-marker tests fail to cover 6 informative SNPs in the selected region (resulting in 85.4% coverage). However, these SNPs are all located intronic or at the 3' end of the gene. Genotyping and testing the selected SNPs and multi-marker tests in our Belgian study population indicated that none of them is associated with PDB and no gender-specific effects were observed.

This indicates that in contrast to OPG polymorphisms, RANKL polymorphisms do not play a role in the development of sporadic PDB. Analysis of other populations is necessary to confirm this result.

[1] Beyens et al. JBMR, in press

Disclosures: W. Van Hul, None.

T229

Multifactor Dimensionality Reduction Reveals Antagonistic Epistasis Between ESR1 and ESR2 with BMD Variation in Southern Chinese Women. S. M. Xiao, C. L. Cheung, A. W. C. Kung. The Department of Medicine, The University of Hong Kong, Hong Kong, China.

Osteoporosis is a complex disease, which is affected by both genetic and environmental factors. Epistasis is thought to be a critical genetic architecture underlying complex disease, which allows genetic buffering, i.e. to stabilize the trait through the interaction of polymorphisms in different loci in the gene network. A recent study demonstrated that multifactor dimensionality reduction (MDR) is one of the best ways to study epistasis. In this study, we applied MDR in studying the epistasis between two closely related candidate genes for BMD variation, ESR1 and ESR2.

To study the relation of ESR1 and ESR2 polymorphisms in hip BMD variation in southern Chinese women, 827 subjects with either low BMD (defined by a BMD Z score less than -1.28 at either the femoral neck or total hip) or high BMD (score greater than +1) were studied. A novel CA repeat polymorphism (D6S440) in ESR1 and 8 SNPs in ESR2 were genotyped. We previously reported CA repeat size of 18 was most discriminative for hip BMD in a population cohort. Multifactor dimensionality reduction was applied to test the epistatic effect, with subsequent confirmed by binary logistic regression (at least one allele >18 CA repeats vs <18 repeats) with adjustment of age, height and weight.

Carriers of 18 CA repeats of ESR1 were associated with higher BMD at the femoral neck (OR: 2.4, $p=0.001$) or hip (OR: 3.2, $p<0.001$). Variant allele of T-1213C of ESR2 was associated with lower BMD at the femoral neck (OR: 1.7, $p=0.042$) and variant allele of T-1213C and rs3742641 was associated with low BMD at the total hip (OR: 2.2, $p=0.011$ and OR: 2.2, $p=0.013$ respectively). MDR revealed significant epistasis between 18 CA repeats of ESR1 with several polymorphisms of ESR2 for 2-way, 3-way and 4-way interactions (testing accuracy > 50%). These results were confirmed by binary logistic regression model. Interestingly, when 18 CA repeat interacted with rs944052, rs3742641 and rs928554 of ESR2, the OR resulted from gene-gene interaction was 1.0 ($p=0.038$) at femoral neck and 1.1 ($p=0.004$) at hip.

The epistasis between ESR1 and ESR2 significantly altered the single gene effect of either ESR1 or ESR2. We have demonstrated the epistasis between genes in the same gene network significantly altered the single gene effect. Testing for gene epistasis in association with BMD variation is a powerful approach to understand the pathophysiology of low bone mass in the general population.

Disclosures: S.M. Xiao, None.

This study received funding from: Grants from Hong Kong Research Grant Council, Osteoporosis Research Fund, Matching Grant and University Research Committee/Committee on Research and Conference Grants of the University of Hong Kong.

T230

The Association between Peak Hip Axis Length and Polymorphisms of the Vitamin D Receptor and Estrogen Receptor 1 genes in Chinese Healthy Men. Z. Zhang, J. He*, J. Gu*. The Department of Osteoporosis, Osteoporosis Research Unit, Shanghai Jiao Tong University Affiliated Sixth People's Hospital, Shanghai, China.

To investigate the possible relationship between peak hip axis length (HAL) and polymorphisms of the vitamin D receptor (VDR) and estrogen receptor 1 (ESR1) genes in Chinese healthy men. A total of 252 healthy men aged from 20 to 40 (29.9 ± 5.9 years) of Han nationality in Shanghai were recruited and were measured for hip axis length (HAL, cm) using DXA (Lunar-Prodigy). The VDR Apa I and Fok I genotype and ESR1 Pvu II and Xba I genotype were determined by PCR-RFLP. The distribution of Apa I genotype was as follows: aa 54.4%, Aa 38.5%, AA 7.1%, respectively. Frequencies of Ff, FF, and ff genotype were 52.4%, 25.4%, and 22.2%, respectively. The distribution of Pvu II genotype was as follows: Pp 46.0%, pp 41.3%, PP 12.7%, respectively. Frequencies of xx, Xx and XX genotype were 71.0%, 25.4% and 3.6%, respectively. After phenotypes were adjusted for age, height, and weight, a significant association was found between VDR Apa I genotype and HAL ($P=0.04$). The HAL of subjects with aa genotype (111.5 ± 0.5) were significant higher than that of Aa genotype (109.8 ± 0.5) ($p=0.015$). Moreover, significant association was found between VDR Fok I genotype and HAL ($P=0.002$), and The HAL of subjects with ff genotype (112.6 ± 0.7) were significant higher than that of Ff genotype (110.8 ± 0.5) ($p=0.031$) and that of FF genotype (109.1 ± 0.7) ($p=0.000$). Neither Pvu II genotype nor Xba I genotype was significantly associated with HAL. The study suggested that Apa I and Fok I polymorphism in VDR gene may have influence on variation of peak HAL in Chinese men, but Pvu II and Xba I polymorphism in ESR1 gene is not the quantitative trait loci (QTL) underlying peak HAL variation.

Disclosures: Z. Zhang, None.

T231

Paclitaxel-loaded Hydroxyapatite-alginate Beads for Local Chemotherapy of Metastatic Spine Cancer in Rats. T. Abe^{*1}, M. Sakane¹, T. Ikoma^{*2}, T. Yoshioka^{*3}, J. Tanaka^{*3}, N. Ochiai^{*1}. ¹Orthopedic Surgery, University of Tsukuba, Tsukuba, Japan, ²Biomaterials Center, National Institute for Materials Science, Tsukuba, Japan, ³Metallurgy and Ceramics Science, Tokyo Institute of Technology, Tokyo, Japan.

Breast cancer is one of the most common cancers to develop metastasis to bone. Of these, spine is the most frequent site. As therapy for systemic cancer improves, local control of metastatic site is becoming important. Among patients with breast cancer that had metastasized to bone, 5-10% did not respond to treatment and developed metastatic epidural spinal cord compression. Paralysis caused by spinal cord compression is directly associated with survival and quality of life of breast cancer patients. We have shown successful loading of the Hydroxyapatite (HAP)-alginate carrier with paclitaxel (PTX) previously. This study was made to clarify the effects of the PTX-loaded HAP-alginate beads administered therapeutically in a rat model of metastatic spine cancer. Rat's mammary adenocarcinoma (the CRL-1666 cell line) and female Fischer 344 rats (8 weeks old) weighing 130-150 grams were used. The PTX-loaded HAP-alginate beads were available by the spray-drying method and the gelation of alginate acid. A 7.4 wt% of PTX (0.13 mg) was contained in each HAP-alginate bead with a diameter of 2.2 mm. We made in vivo biocompatibility test by implantation in the paravertebral muscle, performed surgery to obtain metastatic spine cancer model. Thirty rats with metastatic spine cancer were divided into 3 groups. We checked hind-limb motor function and survival time using the BBB scale. The mean time before onset of paralysis of the local-treatment group (n = 12) was 17.45 days, which was significantly longer than 9.0 days of the control group (n = 8). The effect of the systemic-treatment group (n = 10) that administered intravenously was not evident despite 3 times of 6-fold higher dosage of PTX. In addition, the HAP-alginate carrier and local administration of the PTX-loaded HAP-alginate beads showed no toxicity, whereas intravenous administration of PTX showed severe complications including phlebitis of tail vein and sudden death. This report documents that the local administration of the PTX-loaded HAP-alginate beads showed significant delay in the mean time before onset of hind-limb paralysis. The results indicate local chemotherapy offers promise as less invasive treatment for metastatic spine cancer to delay the potential problem of onset of paralysis.

Disclosures: T. Abe, None.

T232

Both N- and C-terminal Fragments of PTHrP exert Pro-Survival Effects on Human Prostate Cancer Cells Through Transcription Factor Runx-2. V. Alonso^{*1}, F. C. Pérez-Martínez^{*2}, F. J. Calahorra^{*2}, P. Esbrit¹. ¹Bone and Mineral Metabolism Laboratory, Fundación Jiménez Díaz, Madrid, Spain, ²Urology Department, Fundación Jiménez Díaz, Madrid, Spain.

The propensity of prostate cancer (PCa) to metastasize to bone seems to be related to the osteomimetic properties of PCa cells. In the present study, we analyzed the putative mechanisms whereby the osteoblast-like features of these cells can promote their survival. Human prostate cancer PC-3 cells were treated with a high dose (50 µM) of the phytoestrogens genistein and daidzein or 17β-estradiol for 24-48 h. Cell death was analyzed by trypan blue exclusion and flow cytometry (propidium iodide staining). Bone-related factors that are expressed by PC-3 cells: parathyroid hormone-related protein (PTHrP) and the PTH1 receptor (PTH1R), osteoprotegerin (OPG), receptor activator of NF-κB ligand (RANKL), and Runx2, as well as apoptosis-related proteins were evaluated by Western blot. Our results show that genistein induces apoptosis (2-fold vs basal) in PC-3 cells; this effect does not appear to be dependent on estrogen receptors, since the same dose of either daidzein or 17β-estradiol failed to affect PC-3 cell death. The pro-apoptotic effect of genistein was unchanged by a neutralizing anti-OPG antibody. However, PTHrP (7-34), a PTH1R antagonist, induced PC-3 cell death in the presence or absence of each phytoestrogen. Moreover, PTH1R protein expression was significantly increased (2-fold vs basal) by both genistein and daidzein in these cells. In addition, pre-treatment (1 h) with 100 nM of either PTHrP (1-36) or PTHrP (107-139) -which does not interact with the PTH1R- abrogated the pro-apoptotic effect of genistein in PC-3 cells. This effect of each PTHrP peptide was associated with an increase in RANKL protein expression. However, blockade with a neutralizing RANKL antibody or stimulation with exogenous RANKL (50 ng/ml) failed to modify genistein-induced PC-3 cell death. We found that each PTHrP fragment triggered Runx-2 nuclear protein internalization, and Bcl-2/Bax ratio (1.5-fold vs basal; at the expense of a Bcl-2 protein increase) in PC-3 cells. Interestingly, PC-3 cells transfected with a dominant negative Runx2 construct abolished these protective effects of both PTHrP peptides.

In conclusion, the present in vitro findings support the anti-apoptotic action of both N- and C-terminal PTHrP fragments in PCa cells. Our data also indicate the pivotal role of Runx-2 on this protective effect of these PTHrP fragments on these cells.

Disclosures: V. Alonso, None.

T233

Progression of Osteonecrosis of the Jaw in Breast Cancer Patients even with Discontinuation of Intravenous Bisphosphonate Therapy. C. Barragan-Adjemian^{*1}, L. Lausten^{*2}, M. L. Johnson¹, J. O. Katz^{*3}, L. F. Bonewald¹. ¹Oral Biology, University of Missouri Kansas City, Kansas City, MO, USA, ²Special Patient Care, University of Missouri Kansas City, Kansas City, MO, USA, ³Oral Pathology, Medicine and Radiology, University of Missouri Kansas City, Kansas City, MO, USA.

Intravenous bisphosphonate (BP) therapy has become the standard of care for the treatment of cancers that metastasize to bone. BPs have been associated with osteonecrosis of the alveolar bones, a condition known as bisphosphonate-related osteonecrosis of the jaw (BRONJ). The incidence or pathogenesis of BRONJ is largely unknown. The lesions are characterized by exposed necrotic bone with no evidence of healing after 8 weeks in the absence of radiation to the head and neck. BRONJ lesions have been recalcitrant to conventional therapies. The current recommendation is to proceed with non invasive dental treatment with patients on BP therapy. If an ONJ lesion has been diagnosed discontinuance of IV infusion of BPs is recommended if systemic conditions permit. We hypothesized that discontinuation of the intravenous BPs in breast cancer patients does not prevent further evolution of the lesions as detected using cone-beam computerized tomography (CBCT), although soft tissue may appear healed. Six subjects with breast cancer in remission that had discontinued BP therapy were followed for at least two years. Dental evaluations and CBCT were performed to follow the progression of the BRONJ lesions. BRONJ lesions were clinically observed and diagnosed during the period of 1 month to 2 years after discontinuation of BP. In all cases, there was exposed, necrotic bone. Two of the BRONJ lesions were associated with an extraction, one lesion was associated with an adjacent periradicular abscess and subsequent root canal and three lesions occurred spontaneously. All of the subjects received the appropriate treatment for the lesions. None of the lesions had completely healed even after discontinuation of BP therapy for up to 2 years. In one subject, the baseline CBCTs revealed a large sequestrum on the mandibular ridge with a surrounding sclerotic area. After vigorous treatment with antibiotics and local surgical debridement of the sequestrum, the gingival tissue healed leaving a small fistula. A CBCT taken one year after diagnosis demonstrating further progression of the diseased state; sclerotic bone and small sequestrums were still present 2 years on CBCT after cessation of the BP therapy. In conclusion, BRONJ lesions can persist for up to 2 years after cessation of BP treatment and CBCT is a technology that can identify and follow the progression of lesions in BRONJ patients allowing better diagnosis and assessment of disease status.

Disclosures: C. Barragan-Adjemian, None.

T234

PTHrP Regulation of Aldo-Keto Reductase 1C3 and Growth in Prostate Cancer Cells. T. M. Downs^{*1}, R. H. Hastings^{*2}, F. Araiza^{*3}, D. Burton^{*4}, A. Stolz^{*5}, L. J. Defos^{*4}. ¹Surgery, Veterans Administration San Diego Healthcare System and University of California, San Diego, CA, USA, ²Anesthesiology, Veterans Administration San Diego Healthcare System and University of California, San Diego, CA, USA, ³Moore's Cancer Center, San Diego, CA, USA, ⁴Medicine, Veterans Administration San Diego Healthcare System and University of California, San Diego, CA, USA, ⁵Medicine, University of Southern California, San Diego, CA, USA.

Parathyroid hormone-related protein is involved in prostate tumor development, growth, progression and metastasis to bone, but the molecular mechanisms that PTHrP uses are not well defined. We previously demonstrated that DU 145 prostate carcinoma cells upregulated aldo-keto reductases (AKR1C1-3) mRNAs when stably transfected to express PTHrP. The goal of this study was to explore the role of PTHrP on prostate cancer growth and its interactions with AKR1C3 and the regulation of androgen and prostaglandin metabolism. We studied the effects of PTHrP on AKR1C3 levels in DU 145 human prostate cancer cells with quantitative PCR, western, and enzymatic studies. We also evaluated the effects of PTHrP, androgens, and prostaglandins on cell proliferation and apoptosis. PTHrP treatment demonstrated significant increases in AKR1C3 mRNA levels in DU 145 cells, increased AKR1C3 protein expression up to 5-fold, and augmented cellular reductase activity. Furthermore, PTHrP promoted prostate cancer cell proliferation and protected the prostate cancer cells against UV and gamma irradiation induced apoptosis. 5α-dihydrotestosterone and 5-androstane-3α-17β-diol had no stimulatory activity on cell proliferation in the androgen receptor-negative cells, but the androgens stimulated the androgen-dependent LNCaP cells. Prostaglandin D2, an AKR1C3 substrate, inhibited prostate cancer cell proliferation, but its metabolite, 9α-11β-prostaglandin F2, had no effect on growth. In summary, PTHrP stimulates the growth, apoptosis, and AKR1C3 expression of androgen-independent prostate cancer cells. These effects could be mediated through AKR1C3-catalyzed reductions in the levels of prostaglandin D2.

Disclosures: D. Burton, None.

This study received funding from: Moore's Cancer Center and the Department of Veterans Affairs.

T235

Wnts Increase Osteoblast Activity in Prostate Cancer Through Bone Morphogenetic Proteins. J. Dai, C. L. Hall*, J. Escara-Wilke*, E. T. Keller. Department of Urology, University of Michigan, Ann Arbor, MI, USA.

Our previous studies have shown that bone morphogenetic proteins (BMPs) promote prostate cancer (PCa) osteoblastic activity, but upstream inducers of BMP expression in PCa are unknown. Wnts are mediators of osteogenesis. In this study, we investigated a potential role of Wnts in PCa osteoblastic lesions.

To investigate whether Wnts regulate the expression of BMPs in PCa cells, C4-2B cells were treated with Wnt3a and Wnt5a. Wnt3a increased BMP4 mRNA and protein expression, whereas Wnt5a increased BMP6 mRNA and protein expression. To investigate whether Wnts activate BMP promoters, C4-2B cells were transfected with BMP4 or BMP6 promoter. Wnt3a increased mainly BMP4 promoter activity, whereas Wnt5a only increased BMP6 promoter activity. DKK-1 and sFRP-1, inhibitors of Wnt binding to Wnt receptors, blocked Wnt3a-induced BMP4 promoter activity. To elucidate whether Wnt canonical pathway or non-canonical JNK-dependent signaling pathway mediate Wnts-induced BMP promoter activity, C4-2B cells transfected with BMP4 or BMP6 promoter were treated with Axin-2, a negative regulator of the canonical Wnt pathway, or a JNK inhibitor. Axin-2 blocked Wnt3a-induced BMP4 promoter activity, and the JNK inhibitor diminished Wnt5a-induced BMP6 promoter activity. To define how Wnts mediate osteoblast activity, MC3T3-E1 cells were treated with Wnt3a or Wnt5a. Wnt3a and Wnt5a increased alkaline phosphatase activity and osteocalcin level. Dkk-1 completely, whereas Noggin, a BMP inhibitor, partially blocked Wnt3a-mediated osteoblast activity, both together did not show further inhibition. DKK-1 and Noggin partially blocked Wnt5a-mediated osteoblast activity and both together showed further inhibition. To investigate whether the secreted proteins from PCa cells mediate osteoblast activity, MC3T3-E1 cells were treated with C4-2B cells or LuCaP23.1 cells conditioned medium (CM). C4-2B cells and LuCaP23.1 CM increased ALP activity and osteocalcin level. Dkk-1 and sFRP-1 partially blocked CM-mediated pro-osteoblast activity. DKK-1 and Noggin together block CM-mediated osteoblast activity. To further elucidate whether C4-2B cells or LuCaP23.1 cells CM-mediated osteoblast activity through BMPs, MC3T3-E1 cells were treated with CM from C4-2B or LuCaP23.1 cells pretreated with DKK-1 and/or Noggin. DKK-1 completely, whereas Noggin partially, blocked CM-mediated pro-osteoblast activity. DKK-1 and Noggin together had no further inhibition on the CM-mediated pro-osteoblast activity. Taken together, we conclude that PCa cells promote osteoblastic activity through both direct Wnt3a and Wnt5a activity on pre-osteoblasts, as well as through induction of BMP4 and BMP6 expression that occurs through both the canonical and non-canonical pathways.

Disclosures: J. Dai, None.

T236

Urinary Excretion of ^{41}Ca in Mice: Application of ^{41}Ca in Cancer-induced Bone Disease. R. L. Fitzgerald¹, D. W. Burton², T. Griffin^{1*}, L. J. Defetos², D. A. Herold^{1*}, D. J. Hillegonds³. ¹Pathology, VAMC/UCSD, San Diego, CA, USA, ²Endocrinology, VAMC/UCSD, San Diego, CA, USA, ³AMS, Lawrence Livermore National Laboratories, Livermore, CA, USA.

Background: ^{41}Ca is novel tracer technique that promises a direct measure of net bone calcium balance in both humans and in animal models.

Purpose: To establish a timeline for the excretion of ^{41}Ca in normal mouse urine and to show the feasibility of monitoring prostate cancer induced bone disease.

Methods: 6 week old male mice were injected i.p. with 10 nCi ^{41}Ca and 24 hour urines were collected once per week for 7 weeks. Feasibility of monitoring prostate cancer induced bone disease was demonstrated by dosing three groups of male immunocompromised mice (1=saline/saline, 2=tumor/saline, and 3=tumor/bisphosphonate) with 10 nCi ^{41}Ca . Three weeks later, the mice were injected i.p. with saline or zoledronate (5 ug/mouse). Four weeks after ^{41}Ca dosing, the mice were injected intra-tibially with saline or 10^6 PC-3-GFP cells. The saline or zoledronate injections were repeated every 4 weeks. Urine and fluorescent images were collected weekly from each mouse for 10 weeks.

Results: Steady-state $^{41}\text{Ca}/\text{Ca}$ ratios were reached at 14 days after ^{41}Ca injection and the $^{41}\text{Ca}/\text{Ca}$ ratios were approximately 10,000-fold above baseline (see Figure 1). In the prostate cancer model, initial results demonstrate that the tumor can be visualized 2 weeks after prostate cancer cell injection and that zoledronate significantly reduces the severity of the bone lesion, as quantitated by x-ray scoring.

Conclusion: Successful implementation of a ^{41}Ca assay in cancer patients with metastatic bone disease could have wide benefits, including improved risk assessment, monitoring treatment, and early detection of metastasis.

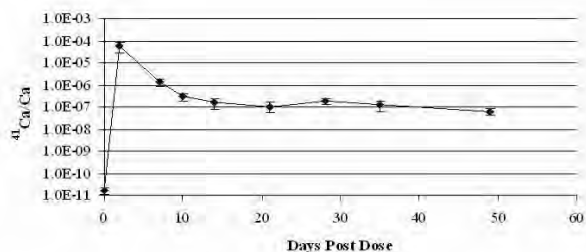


Figure 1. Mean (+/-SEM) of urinary $^{41}\text{Ca}/\text{Ca}$ following a 10 nCi dose of ^{41}Ca (N= 2 or 3). Note y axis is logarithmic.

Disclosures: R.L. Fitzgerald, None.

This study received funding from: NIH.

T237

Breast Cancer Cells Inhibit Osteoblast Differentiation. J. E. Fong^{1*}, D. Le Nihouannen¹, O. Hussein¹, P. M. Siegel², S. V. Komarova¹. ¹Dentistry, McGill University, Montreal, PQ, Canada, ²Medicine, McGill University, Montreal, PQ, Canada.

Skeletal metastasis is a major complication of advanced breast cancer which results in bone fractures and considerable pain burden. Osteoclasts recruited to the site of metastasis lead to the destruction of bone and formation of osteolytic lesions. Osteoblasts are known to contribute to osteoclast activation by producing a key pro-resorptive cytokine RANKL, however the effects of cancer cells on osteoblasts are not fully understood. We have studied the effects of MDA-MB-231 human breast carcinoma cells on proliferation and differentiation of primary osteoblast precursors. MDA-MB-231 cells were cultured until 80% confluent, and conditioned medium was collected after 24h of culturing. Bone marrow cells were isolated from the long bones of C57BL/6J mice, and treated for 5 days with ascorbic acid (50 µg/ml) in the presence or absence of MDA-MB-231 conditioned medium (10%). As a control, we used medium conditioned by MC3T3-E1 cells. Cell numbers were assessed in samples labeled with nuclear stain DAPI, and processed using image analysis. Treatment with ascorbic acid alone led to formation of 390 +/- 90 cells/mm². Addition of MDA-MB-231 conditioned medium to osteoblastic cultures led to a 2-3 fold increase in cell number, whereas treatment of cultures with MC3T3 conditioned medium had no effect, indicating that MDA-MB-231 cells produce factors that stimulate proliferation of osteoblastic cells. To assess osteoblast differentiation, the cultures were stained for alkaline phosphatase (ALP) and the labeled area was quantified using image analysis. Even at this early cultures, treatment with ascorbic acid alone led to significant increase in APL-positive cells, compared to untreated cultures. Addition of MDA-MB-231 conditioned medium to ascorbic acid-treated cultures resulted in a 5-fold decrease in ALP expression. Thus, our data indicate that soluble factors produced by breast cancer cells stimulate proliferation and inhibit differentiation of native osteoblasts. Since it has been previously shown that immature osteoblast precursors represent a major source of RANKL, compared to mature osteoblasts, our findings suggest a novel mechanism for osteoblast-mediated stimulation of osteoclasts that potentially contributes to the establishment and progression of metastatic lesions in bone.

Disclosures: J.E. Fong, None.

This study received funding from: CIHR/IMHA/TAS and NSERC.

T238

TGF- β Increases Osteolytic Prostate Cancer Bone Metastases and Expression of Pro-metastatic Genes. P. G. J. Fournier, G. A. Clines, J. M. Chirgwin, T. A. Guise. Internal Medicine, University of Virginia, Charlottesville, VA, USA.

Prostate cancers commonly metastasize to bone, where high concentrations of TGF- β are released by osteoclastic resorption. TGF- β stimulates production of PTHrP, IL-11 and CTGF, which are central factors in bone metastases due to breast cancer and melanoma. We hypothesized that TGF- β would also promote prostate cancer bone metastases.

First, we showed that a specific inhibitor of the TGF- β type I receptor (T β RI) kinase, SD-208, inhibited TGF- β -dependent Smad2 phosphorylation in PC-3 prostate cancer cells in vitro. Mice were inoculated with PC-3 cells via the left cardiac ventricle. In both prevention and treatment protocols, SD-208 (50mg/kg/d) decreased osteolytic metastases and increased survival. To determine downstream targets of TGF- β in prostate cancer, we analyzed PC-3 cells treated with TGF- β (24h, 5ng/mL) by Affymetrix gene array with DMT and dCHIP data analyses. Significantly upregulated genes included known TGF- β targets PTHrP, CTGF, MMP-13, TSP-1 and ADAM19, which function in bone remodeling or are dysregulated in cancer.

The most increased gene was PMEPA1 (23.2-fold, P<0.03), a protein highly expressed in breast, colon and prostate cancers. Using real-time qPCR of RNA from PC-3 cells treated with TGF- β (5ng/mL, for 0 to 48h), we confirmed that PMEPA1 mRNA was rapidly induced and peaked at 24h (16.7-fold, P<0.05). TGF- β also increased PMEPA1 mRNA in prostate, breast and lung cancer lines. PC-3 cells were treated with SD-208, the transcription inhibitor actinomycin D, or the translation inhibitor cycloheximide; the results showed that TGF- β directly activates PMEPA1 transcription. TGF- β also increased PMEPA1 protein production in PC-3 by Western blot; the induction was prevented by SD-208. We cloned and made deletion mutants in 3.7kb of the PMEPA1 promoter, which contains 5 putative Smad binding elements. Dual-luciferase assays and overexpression of Smad2, -3 and -4, indicated that PMEPA1 transcription is regulated by TGF- β via both Smad-dependent and independent pathways.

PMEPA1 interacts with the E3 ubiquitin ligase Nedd4, which is related to the Smurfs. These proteins inhibit TGF- β signaling by targeting Smads and T β RI for proteasomal degradation. PMEPA1 could prevent proteasomal inhibition of the TGF- β pathway by suppressing Nedd4/Smurf activity, leading to sustained TGF- β signaling in bone metastases. Our data indicate that TGF- β promotes osteolytic bone metastases by stimulating known prometastatic factors, as well as novel factors that may enhance TGF- β signaling in the tumor cell. Thus, TGF- β inhibitors should be effective treatments for osteolytic prostate cancer bone metastases.

Disclosures: P.G.J. Fournier, None.

This study received funding from: Department of Defense - Prostate Cancer Research Program.

T239

Serum TRACP 5b Increases with Advancement of Osteolysis in a Nude Mouse Model of Breast Cancer Bone Metastasis. M. I. Suominen, R. Käkönen*, J. P. Rissanen, S. Ylönen*, J. M. Halleen. Pharmatest Services Ltd, Turku, Finland.

Serum tartrate-resistant acid phosphatase isoform 5b (TRACP 5b), a marker of osteoclast number, is significantly elevated in breast cancer patients with bone metastases. We investigated if elevated TRACP 5b values would indicate the development of bone lesions in a mouse model of breast cancer bone metastasis. MDA-MB-231(SA) breast cancer cells (n=19) or PBS (n=11) were inoculated into the left cardiac ventricle of five-week-old female nude mice. Serum samples were collected before the inoculation (day 0), at days 6, 9, 13, 16, and at sacrifice (day 23). Bone lesions were quantitated by radiography at days 16 and 23. Bone samples were collected for histomorphometric analysis at day 23, and osteoclasts were counted from TRACP-stained sagittal sections. Statistical analysis was performed using Student's t-test with necessary transformations after checking the assumptions for normality and homogeneity of variances. A p-value <0.05 was considered statistically significant. Pearson's correlation coefficients were calculated for cancer-inoculated mice. Body weight of the tumor-bearing animals was significantly lower compared with the PBS-controls at sacrifice due to tumor-induced cachexia. Osteolytic foci were found in 47.4% of the cancer cell-inoculated mice already at day 16, and all animals had lesions at sacrifice. Because the animals were growing rapidly during the study, their TRACP 5b values decreased in both groups during the first two weeks. At day 16, the TRACP 5b values reached a plateau in the control mice inoculated with PBS. However, in the cancer cell-inoculated mice, TRACP 5b values were elevated on day 16, and a sharp increase was observed between days 16 and 23. The changes in TRACP 5b values were significantly different in the cancer cell-inoculated mice than in the control mice on days 16 and 23. The TRACP 5b values correlated with osteolytic area determined by radiography on day 23. Furthermore, the TRACP 5b values correlated reversibly with body weight in tumor-bearing mice at sacrifice, whereas no correlation was observed in control mice. The histomorphometrically determined number of osteoclasts was radically increased, as expected based on the increased TRACP 5b values, and bone volume was decreased in the cancer cell-inoculated mice. Of note, large numbers of osteoclasts were found residing inside the tumor, with no bone surface nearby. These results demonstrate that TRACP 5b correlates with osteolysis and tumor-induced cachexia and is therefore a useful marker in the nude mouse model of breast cancer bone metastasis.

Disclosures: J.M. Halleen, SBA-Sciences 5, 7.

T240

Calcium Enhances Anti-tumor Effects of Ibandronate in Breast Cancer Cells. F. Journe¹, N. Kheddoumi*¹, C. Chaboteaux*¹, G. Laurent*², J. J. Body¹. ¹Institut Bordet, Brussels, Belgium, ²Université de Mons-Hainaut, Mons, Belgium.

Bisphosphonates now constitute standard therapy for the management of breast cancer-induced skeletal complications. Although their therapeutic effects mainly result from an inhibition of osteoclastic bone resorption, in vitro data indicate that bisphosphonates may also act directly on breast cancer cells by inhibiting their proliferation and inducing their apoptosis. This study examined the effects of Ca++ on the growth inhibitory activity of ibandronate in MDA-MB-231 and MCF-7 breast cancer cell lines. In presence of 0.6 mM Ca++, 30 µM ibandronate had no effect on MDA-MB-231 cell growth, and only a borderline effect on MCF-7 cell growth (13.6±6.6% inhibition). By contrast, in presence of 2 mM Ca++, ibandronate dramatically inhibited cell culture growth by 55.5±7.8% and 76.1±4.6% (p<0.01) in MDA-MB-231 and MCF-7 cells, respectively. Moreover, dose-response curves revealed that increasing Ca++ concentrations from 0.6 to 1.6 mM decreased ibandronate IC50 values of from 100 to 30 µM in MDA-MB-231 cells and from 60 to 10 µM in MCF-7 cells. In addition, whereas 30 µM ibandronate did not markedly induce cell apoptosis in presence of 0.6 mM Ca++, it significantly increased the percentage of apoptotic cells (annexin V-PE-positive) in presence of 1.6 mM Ca++ (11.4 and 32.9% in MDA-MB-231 and MCF-7 cells, respectively). Of note, Ca++ chelation by EGTA at a concentration which did not affect cell growth (0.5 mM) significantly reduced the growth inhibitory effect of 30 µM ibandronate in culture medium containing 1.6 mM Ca++. To address the effects of Ca++ on cell drug accumulation, cells were cultured in medium containing 0.6 or 1.6 mM Ca++ and were exposed to [14C]-ibandronate for 4 hours. In presence of 1.6 mM Ca++, cells accumulated much more [14C]-ibandronate than cells cultured in presence of 0.6 mM Ca++ (about 4.6 and 11.4-fold increases in MDA-MB-231 and MCF-7 cells, respectively). Finally, when evaluating the inhibition of protein prenylation, we found that high Ca++ level increased the intracellular activity of ibandronate. Thus, in both cell lines, 10 µM ibandronate were sufficient to produce a detectable inhibition of Rap1A prenylation in presence of 2 mM Ca++, while 100 µM ibandronate were required to achieve a similar effect in presence of 0.6 mM Ca++. In conclusion, our data indicate that extracellular Ca++, likely through its binding to ibandronate, modifies its cellular pharmacokinetics and increases its inhibitory activity on tumor cells. Thus, Ca++ released during the process of tumor-induced osteolysis could enhance the anti-tumor effects of bisphosphonates.

Disclosures: F. Journe, Hoffmann-LaRoche, Basel, Switzerland 2.

T241

Heparin-like Polysaccharides Markedly Reduce Osteolytic Bone Destruction and Tumor Growth in a Mouse Model of Breast Cancer Bone Metastasis. R. S. Kakonen*¹, S. Kakonen², K. S. Mohammad*³, J. P. Rissanen¹, J. M. Halleen¹, A. Warri*⁴, L. Nissinen*⁴, M. Pihlavisto*⁴, J. M. Chirgwin³, M. Salmivirta*⁵, A. Marjamäki*⁴, T. A. Guise³. ¹Pharmatest Services Ltd, Turku, Finland, ²Department of Anatomy, University of Turku, Turku, Finland, ³University of Virginia, Charlottesville, VA, USA, ⁴BioTie Therapies Corp, Turku, Finland, ⁵Turku Centre for Biotechnology, Turku, Finland.

Heparin treatment effectively prevents venous thromboembolism, but may also prolong survival in patients with malignant disease. Experimental studies support the hypothesis that cancer progression can be influenced by heparin and heparin-like glycosaminoglycans (HLGAGs), but their widespread use is hindered by their high anticoagulant activity. We have evaluated the therapeutic potential of two HLGAGs with low anti-coagulant activity, a low-molecular-weight synthetic heparin (fragmin), and a high-molecular-weight K5-derived heparin-like polysaccharide (K5-NSOS), to inhibit osteolytic bone destruction and tumor growth in an experimental mouse model of breast cancer bone metastasis. MDA-MB-231 breast cancer cells were inoculated into the left cardiac ventricle of athymic nude mice, which were then administered with Fragmin, K5-NSOS or vehicle once daily for 4 weeks. HLGAG-treated animals had significantly increased body weight when compared to vehicle. In addition, osteolytic lesion area as measured by radiography was significantly decreased by both HLGAGs. Histomorphometric examination revealed that both HLGAGs significantly reduced tumor burden in bone. In vitro studies showed that both HLGAGs inhibited significantly cancer cell adhesion, and K5-NSOS inhibited significantly bone resorption activity of human osteoclasts. Our data demonstrate that HLGAGs can efficiently reduce osteolytic lesion area and tumor burden in bone. K5-NSOS HMW is a potential antimetastatic and antiresorptive agent with low anticoagulant activity, and it could be further optimized as an anti-tumor agent.

Disclosures: R.S. Kakonen, Pharmatest Services Ltd 3, 4.

T242

Human Breast Stem Cell Transformation and Invasiveness Is Mediated Upregulation of IL-8 by TWIST Interactions with NFκB. S. E. Kendall*¹, K. S. Aboody*², S. D. Flanagan*³, C. A. Glackin¹. ¹Molecular Medicine, City of Hope/Beckman Research Institute, Duarte, CA, USA, ²Hematopoietic Cell Transplantation/Neurosciences, City of Hope/Beckman Research Institute, Duarte, CA, USA, ³Neurosciences, City of Hope/Beckman Research Institute, Duarte, CA, USA.

Interleukin (IL-8), a prototypical chemokine has been shown to play an important role in tumor growth, angiogenesis and metastasis. Transcriptional activation of IL-8 is critically dependent on NFκB, but can be modulated by several transcription factors, i.e. AP-1, C/EBP and NRE. TWIST, a basic helix-loop-helix transcription factor has been shown to bind to NFκB and transcriptionally repress two pro-inflammatory cytokines, IL-1β and TNFα at E-box consensus sites on their respective promoters. We have previously demonstrated that TWIST over-expression in benign human breast cancer cells (MCF-7) significantly enhances their growth and invasiveness through an epithelial to mesenchymal transition (EMT) process. In our current studies, designed to delineate these early transformation events, we over-expressed TWIST in the MCF10A human breast luminal epithelial cell line. Results display a phenotypic change in their cell surface marker expression (ESA, Muc1, CD49f), reminiscent of breast stem cells. Affymetrix microarray analysis confirmed EMT associated differential gene expression where epithelial markers such as Keratins and E-cadherins were down regulated and mesenchymal markers such as vimentin were upregulated. Western blot analysis also reflected EMT related changes, such as the E- to N-cadherin switch. However, elevated levels of cytokines (IL-1α, IL-8, uPAR?) and their target genes (NFκB, MMP9, uPA) were observed, indicating that alterations in these inflammatory signaling pathways were being affected by TWIST overexpression. Protein array screening of conditioned media from TWIST over-expressing cells confirmed significantly elevated levels of IL-8. Moreover, TWIST and NFκB form a transcription factor complex that interacts to enhance IL-8 expression through the NFκB consensus site on the IL-8 promoter. The signals produced through CXCR1 and CXCR2 binding activate MMP9 gene expression. Importantly, TWIST over-expressing cells show a significant level of MMP9 activity that facilitates their invasion towards osteocytes. Collectively our results suggest that TWIST over-expression in breast epithelial cells promotes their transformation to a stem cell-like state and enhances their invasive capabilities through the creation of an IL-8 feedback loop. Thus, TWIST may play a significant role in the transformation of normal/benign breast cells towards malignancy.

Disclosures: S.E. Kendall, None.

This study received funding from: NIH/NCI.

T243

Zoledronic Acid Delayed the Wound Healing of Tooth Extraction Socket but Failed to Cause Osteonecrosis of the Jaw in Mice. Y. Kobayashi^{*1}, T. Hiraga^{*2}, A. Ueda¹, R. Nishimura¹, H. Yatani^{*3}, T. Yoneda¹. ¹Biochem, Osaka Univ Grad Dent, Suita, Japan, ²Oral Anat, Matsumoto Dent Univ, Matsumoto, Japan, ³Fixed Prosth, Osaka Univ Grad Dent, Suita, Japan.

Bisphosphonates (BPs), particularly nitrogen-containing BP such as zoledronic acid (ZOL) and pamidronate, have been widely- and beneficially-used for the treatment of cancer patients with bone metastases and/or hypercalcemia. However, observations are accumulating that cancer patients who have received these BPs occasionally show osteonecrosis of the jaw (ONJ) following dental treatments, especially tooth extraction. To understand the underlying mechanism of ONJ, we examined the effects of ZOL on the wound healing of tooth extraction socket. C57BL/J mice (6 week-old, male) were given ZOL (5µg/mouse, ip) once a day. After 7 days, the upper right first molar was extracted under anesthesia. Administration of ZOL was continued until 5 days after the tooth extraction. There was no marked histological difference in the wound healing of extraction sockets between control and ZOL-treated group until day 3. At day 5, histomorphometrical analysis revealed active new bone formation and substantial numbers of CD3-positive blood vessels in control mice. In contrast, the amount of new bones and the numbers of TRAP-positive osteoclasts and CD31-positive blood vessels were significantly decreased in ZOL-treated mice, indicating the delay of the socket healing. The non-nitrogen-containing BP etidronate (ETI, 5µg/mouse, ip) showed no effects on the healing. In the dorsal air sac (DAS) assay in which Millipore chambers containing VEGF and/or ZOL were implanted in the skin at the back of mice, ZOL significantly inhibited the angiogenesis promoted by VEGF. Moreover, ZOL (5-50µM), but not ETI, inhibited the proliferation of bone marrow endothelial cells and human endothelial-like cells in monolayer and collagen gel in a dose-dependent manner. ZOL also inhibited the capillary tube formation of human umbilical vessel endothelial cells on matrigel. Finally, we examined the effects of ZOL combined with doxorubicin (100µg/mouse, ip) and/or dexamethazone (400µg/mouse, ip) as a clinically-relevant setting. Contrary to our expectation, however, combination of these agents did not further delay the healing than ZOL alone. Of note, we did not observe ONJ following the treatment with each or combination of these agents. In conclusion, our results suggest that ZOL delays the wound healing of tooth extraction sockets through inhibiting new bone formation and angiogenesis. However, ZOL alone or combined with steroid and/or anti-cancer agent failed to cause ONJ in our model. Additional unknown factors may be involved in the pathogenesis of ONJ seen in cancer patients who have been treated with BPs.

Disclosures: Y. Kobayashi, None.

T244

Osteoblast - Prostate Cancer Cell Signaling: Role of Hedgehog Pathway. M. L. G. Lamm, T. Douglas^{*}. Pediatrics, Northwestern University Feinberg School of Medicine, and Children's Memorial Research Center, Chicago, IL, USA.

The key to understanding the proclivity of metastatic prostate carcinoma to bone lies in unraveling unique interactions between invading prostate cancer cells and host bone stroma including bone cells and extracellular matrix. The purpose of the present study is to test the hypothesis that Sonic hedgehog signaling between prostate cancer cells and osteoblasts promotes osteoblast differentiation, a requisite step toward metastatic prostate tumor formation in bone. Sonic hedgehog (Shh) is a secreted ligand that mediates epithelial-mesenchymal interactions critical to normal morphogenesis of many developing organs including the prostate. Shh signaling activates the expression of genes for the transcription factor Gli1 and the Shh receptor Ptc1 in target cells. The genes for Shh, Gli1, and Ptc1 are expressed in human prostate cancer specimens including prostate metastatic carcinoma. We have previously shown that human prostate cancer cells, LNCaP, which are genetically-engineered to express high levels of Shh (designated LNCaP-Shh cells) upregulate Gli1 and Ptc1 expression in stromal cells and promote xenograft prostate tumor growth in a mouse model.

In the present study, LNCaP-Shh cells and vector-transfected control LNCaP cells were co-cultured with mouse calvaria-derived non-transformed osteoblast precursor cells MC3T3-E1. Cells were co-cultured for varying periods of time either as mixed populations within the same culture chamber or separate populations in two chambers that share the same culture medium. Gene expression analysis was performed by real time quantitative RT-PCR using species-specific primers to differentiate gene expression between human and mouse cells. Staining for alkaline phosphatase activity was used as a marker of osteoblast differentiation.

Data show that Shh-expressing prostate cancer cells upregulate Gli1 and Ptc1 expression in osteoblasts and, this effect is inhibited by cyclopamine and dependent upon Gli transcriptional activity. Shh signaling in osteoblasts increases alkaline phosphatase activity and upregulates expression of osteopontin indicative of osteoblast differentiation. These results demonstrate that Shh signaling between prostate cancer cells and osteoblasts promotes osteoblast differentiation, and implicate the hedgehog signaling pathway in the development of osteoblastic prostate cancer metastasis.

Disclosures: M.L.G. Lamm, None.

This study received funding from: National Cancer Institute.

T245

Non-isomerized C-telopeptides of Type I Collagen (ALPHA CTX) for Early Detection and Treatment Monitoring of Bone Metastases Secondary to Prostate Cancer. D. J. Leeming¹, A. Hegele^{*2}, M. A. Karsdal¹, P. Qvist¹, P. Olbert^{*2}, C. Christiansen^{*1}, I. Byrjalsen¹. ¹Nordic Bioscience, Herlev, Denmark, ²Department of Urology, Philipps University, Medical School, Marburg, Germany.

Skeletal spread of metastasis represents a devastating event, which should be detected as early as possible prior to that of traditional imaging techniques. The objective of this study was to compare a novel biochemical marker of cancer mediated bone resorption, ALPHA CTX, to that of prostate specific antigen (PSA) and total alkaline phosphates (tALP) in patients with prostate cancer.

Two studies were performed. 1) Cross-sectional study of 170 prostate cancer patients without bone metastases (-BM) prior to radical prostatectomy, including 24 patients with lymph node metastases (+LN), compared to 68 controls. 2) Prospective study of 40 hormone refractory stage prostate cancer patients including 20 with bone metastases (+BM). Patients received four treatment cycles during four months of 35mg/m2 docetaxel in week 1, 2, and 3 (all patients) and 4mg zoledronate in week 1 (only +BM). Urine samples were collected at 0, 1, 2, 3 and 4 months and assessed in ALPHA CrossLaps (ααCTX) (Nordic Bioscience), PSA and tALP (Roche Diagnostics). Presence of bone metastases was determined by bone scans and verified by X-ray. Adjacent bone metastases sections from prostate cancer patients were stained for the presence of tumor cells (anti-cytokeratin antibody), osteoclasts (TRAP activity) and αCTX (anti-αCTX antibody).

PSA was elevated in both -LN and +LN patients compared to controls (p<0.001), ααCTX was only elevated in +LN patients (p<0.01); in contrast no difference in tALP was detected. In the prospective study, only ααCTX decreased significantly, -52% (p<0.05) and 62% (p<0.01) in the combined zoledronate/docetaxel group at week 4 and 16, respectively. The suppression of PSA and tALP in the +BM group was similar to the suppression induced by docetaxel in the -BM group. Immunohistochemistry revealed accumulation of TRAP+ osteoclasts and intense staining for αCTX epitopes in the proximity of tumor cells.

ααCTX was increased in +LN, indicating that these patients already had sustained skeletal spread as detected prior to that of imaging techniques, representing a high-risk group that need to be closely monitored. ααCTX in these patients predicts presence of skeletal spread of the malignancy, presently undetected by bone scans, and may thus be of great benefit for early detection of metastasis. In the prospective study, ααCTX decreased in zoledronate/docetaxel treated +BM patients to levels below docetaxel-treated -BM patients, emphasizing the skeletal specificity of this markers in contrast to PSA and tALP.

Disclosures: D.J. Leeming, Nordic Bioscience 3.

T246

The α_vβ₃ Integrin Inhibitor MK-0429 Is Generally Safe and Decreases Bone Turnover in Men with Hormone-Refractory Prostate Cancer (HRPC) and Bone Metastases (MBD). M. Rosenthal^{*1}, P. Davidson^{*2}, F. Rolland^{*3}, A. Lombardi⁴, Y. Berd^{*4}, W. He^{*4}, L. Wehren⁴. ¹Melbourne Comprehensive Cancer Centre, Parkville, Australia, ²CURT Medical Trials Trust, Christchurch, New Zealand, ³Centre Gauducheau Medecine Oncologie, Saint Herblain, France, ⁴Merck & Co., Inc., Rahway, NJ, USA.

Background: Osteoclast adhesion to bone surface, essential for bone resorption, is mediated by α_vβ₃ integrin. Inhibition of this activity might slow the development or progression of MBD. MK-0429 is an oral α_vβ₃ inhibitor being evaluated in MBD in patients (pts) with HRPC.

Materials and methods: This multicenter Phase 1 study enrolled 21 pts with HRPC and MBD. Pts were randomized to receive either 200 mg (n=5) or 1600 mg (n=16) b.i.d. of MK-0429 for 4 weeks, with an optional open-label extension of 48 weeks. The study examined the toxicity and pharmacokinetics of MK-0429 in this population, as well as its effect on markers of bone turnover, urinary cross-linked N-telopeptides of type I collagen to creatinine ratio (uNTx), and bone-specific alkaline phosphatase (BSAP).

Results: Eighteen pts (86%) completed 4 weeks of treatment. All pts in the 200-mg group and 8 pts (50%) in the 1600-mg group subsequently entered the extension study. Nausea (Grade 1 or less commonly Grade 2) occurred in 11 pts in the 1600-mg group, and 1 pt in the 200-mg group. Only 1 Grade 3 event (anemia) occurred. Two pts in the 1600-mg group discontinued treatment (1 due to spinal cord compression, the other to nausea), and an additional pt withdrew consent. At 4 weeks, the mean AUC_{0-12hr} and C_{max} values were 210 µM•hr and 42 µM in the 200-mg group and 673 µM•hr and 154 µM in the 1600-mg group, respectively. Baseline and end-of-treatment values of the biochemical markers are displayed in the table.

Conclusions: In this Phase I study, MK-0429 was generally safe in pts with HRPC and MBD, with the most common side effect being nausea. There was evidence of an early reduction in biochemical markers of bone turnover.

Biochemical Marker*	200 mg b.i.d.		1600 mg b.i.d.	
	Baseline	% Change from Baseline	Baseline	% Change from Baseline
uNTx (pmol/µmol)	175.0 (173.2)	-43.4 (4.6)	295.8 (264.0)	-34.1 (4.2)
BSAP (IU/L)	187.7 (214.3)	-3.5 (6.3)	159.1 (112.4)	-10.2 (7.0)

*Presented as mean (standard deviation) at baseline; geometric mean % change from baseline (standard error) after treatment.

Disclosures: A. Lombardi, Merck & Co., Inc. 1, 3.

This study received funding from: Merck & Co., Inc.

T247

PTHrP-induced MCP-1 Production by Human Bone Marrow Endothelial Cells and Osteoblasts Promotes Osteoclast Differentiation In Vitro: A Novel Role in Prostate Cancer Bone Metastasis. Y. Lu¹, G. Xiao¹, Z. Cai^{*1}, X. Chen^{*1}, D. L. Galson¹, Y. Nishio^{*2}, A. Mizokami^{*3}, J. Zhang¹. ¹Medicine, University of Pittsburgh, Pittsburgh, PA, USA, ²Medicine, Shiga University of Medical Science, Shiga, Japan, ³Urology, Kanazawa University, Kanazawa, Japan.

Prostate cancer (PCa) preferentially metastasizes to bone resulting in osteolytic lesions with underlying osteolytic activities. The mechanisms by which PCa cells promote osteolytic activities and subsequent osteoblastic bone formation remain poorly understood. Parathyroid hormone-related protein (PTHrP), produced by bone cells and PCa, binds to receptors on osteoblasts and stimulates bone formation and resorption. We have previously reported that MCP-1 acts as a paracrine and autocrine factor for PCa progression. However, the role of PTHrP in regulating MCP-1 expression in bone microenvironment, specifically by human bone marrow endothelial cells (HBME) and osteoblasts (hFOB), as well as by PCa cells, has not been studied. Accordingly, we determined the effect of PTHrP on MCP-1 expression by bone cells and PCa cells. PTHrP induced both MCP-1 protein and mRNA expression by HBME and hFOB cells, but not by PCa LNCaP and PC3 cells. To further determine the mechanisms of PTHrP-induced MCP-1 transcription, analysis of the MCP-1 promoter was performed. MCP-1 promoter activity was induced by PTHrP. Both C/EBP β and NF- κ B binding elements are required for PTHrP-induced MCP-1 transcription. Finally, when a constitutively-active PTH receptor construct was transfected into HBME and hFOB cells, MCP-1 production was increased. The conditioned media collected from these cells induced osteoclast differentiation and PC3 proliferation and invasion in vitro. These effects were partially inhibited by MCP-1 neutralizing antibody. We conclude that PTHrP-induced MCP-1 production by HBME and hFOB cells promotes osteoclast differentiation in vitro and such induction may play a critical role in PCa development in the bone microenvironment.

Disclosures: Y. Lu, None.

T248

Activation of MCP-1/CCR2 Axis Promotes Prostate Cancer Invasion and the Tumor-induced Osteoclast Activity In Vitro. Y. Lu¹, Z. Cai^{*1}, X. Chen^{*1}, G. Xiao¹, A. Mizokami^{*2}, G. D. Roodman¹, J. Zhang¹. ¹Medicine, University of Pittsburgh, Pittsburgh, PA, USA, ²Urology, Kanazawa University, Kanazawa, Japan.

When prostate cancer (PCa) metastasizes to the skeleton, bidirectional interactions between tumor cells and the bone microenvironment occur. Both the tumor cells and cells from the bone microenvironment produce growth factors, angiogenic factors, and chemotactic factors which enhance tumor growth. These factors may account for the increased frequency of bone metastasis in PCa. Monocyte chemotactic protein-1 (MCP-1) is a member of the CC chemokine superfamily that plays a critical role in recruitment and activation of monocytes during acute inflammation and angiogenesis. We previously showed that MCP-1, produced by PCa epithelial cells, stroma/osteoblasts, and bone marrow endothelial cells, is chemotactic for PCa cells. More recently, we reported that CCR2 expression correlates with Gleason score and clinical pathological stages as determined by immunohistochemistry. We hypothesized that the MCP-1/CCR2 axis plays a critical role in PCa invasion and the tumor-induced osteoclast activity. Accordingly, to determine whether the expression of CCR2 on PCa cells play a fundamental role in PCa invasion and proliferation, CCR2 or control shRNAs were transfected into human C4-2B or PC3 cells using lipofectamine reagents and individual clones were selected and evaluated. CCR2 knockdown in both C4-2B and PC3 cells significantly diminished the MCP-1-induced cell invasion in matrigel assays. Furthermore, to determine whether MCP-1 knockdown in PCa cells alters the PCa conditioned media (CM)-induced osteoclast formation, MCP-1 or control shRNA were generated and transfected into C4-2B or PC3 cells. CM were collected from 4 clones and evaluated for their capacity to induce osteoclast formation. Non-adherent mouse bone marrow cells were cultured for 7 days with M-CSF (10ng/ml) and/or RANKL (50ng/ml) or 10% CM collected from the stable clones. We found that MCP-1 knockdown significantly diminished the capacity of PCa CM to induce osteoclast formation. Taken together, we have demonstrated that activation of MCP-1/CCR2 axis promotes prostate cancer invasion and the tumor-induced osteoclast activity in vitro. Our data suggest that MCP-1/CCR2 axis may serve as a therapeutic target.

Disclosures: Y. Lu, None.

T249

The Constitutive Activity of the NF- κ B p65/p50 Transcriptional Complex is Critical for Bone Metastasis in Breast Cancer. C. Menaa^{*1}, A. Moscovitz^{*2}, S. Kim^{*1}, C. J. Froelich^{*1}, S. M. Sprague¹. ¹Department of Medicine, Evanston Northwestern Healthcare, Northwestern University Feinberg School of Medicine, Evanston, IL, USA, ²Department of Medicine, Hadassah University Medical Center, Jerusalem, Israel.

Long-term breast cancer (BC) survival decreases dramatically in patients with bone metastases and represents a major challenge for treatment. This is due in large part to the capacity of tumor cells to induce osteoclastogenesis. How tumor cells acquire this capacity and the mechanism(s) involved are not yet defined. We previously reported that NF- κ B is a

key pathway for bone metastasis. Here we demonstrate that the NF- κ B p65/p50 transcriptional complex controls the capacity of BC cells (MDA and MCF7) to support OC formation in vitro and tumor growth and bone metastasis in vivo. The over-expression of p65 DN significantly reduced the production of osteoclastogenic factors (OF), including PTHrP expression in vitro. Furthermore, the p50 subunit is necessary to form the active transcriptional complex with the p65 subunit in BC. The transdominant negative form of p50, where the DNA binding capacity has been disrupted, significantly reduced the constitutive activation of NF- κ B in BC and the transcriptional activity of the p65 as measured by gel shift and reporter gene assays. Moreover, stable BC cells expressing p50 mutants where (A56/L-F57/A) or (Y59/A-V60/S) are unable to support osteoclastogenesis and PTHrP production in vitro. The intra-cardiac injection of the wild type cells into nude mice results in diffuse bone metastasis, whereas the injection of the p50 mutant cells do not lead to osteolytic lesions as assessed by X-Rays and histological analyses. This effect was not due to a reduction in cell viability and/or proliferation, since p50 mutant cells form tumors similarly to the WT cells when injected subcutaneously, but lack the ability to induce osteoclastogenesis. In addition, BC p50 mutant cells are less invasive and aggressive compared to the WT. We specifically found that the transcriptional factor snail is down-regulated in non-bone metastatic BC (MCF7) as well as MDA-p50 mutant cells compared to MDA WT cells. These data suggest that snail could be the down stream factor for NF- κ B that is responsible for bone metastases.

In summary, we found that the NF- κ B p65/p50 transcriptional complex is essential for the NF- κ B constitutive activation and the capacity of BC to form osteolytic metastasis by controlling expression and secretion of osteoclastogenic factors such as PTHrP which could be mediated by snail transcription factor. In conclusion, these data further highlight the role of NF- κ B in bone metastasis in breast cancer. Thus, NF- κ B (p65/p50 complex) could be a suitable therapeutic target for bone destruction in breast cancer.

Disclosures: C. Menaa, None.

This study received funding from: NIH.

T250

High Extracellular Calcium Directly Stimulates MDA-MB 231 Human Breast Cancer Cell by a Mechanism Involving the Calcium Sensing Receptor. R. Mentaverri^{*}, R. Abdoune^{*}, J. Lion^{*}, M. Brazier^{*}, S. Kamel^{*}. Pharmacy, INSERM, ERI-12, Amiens, France.

Bone is the most common site of breast cancer metastasis and skeletal metastases greatly contribute to the morbidity and mortality associated to the disease. Over the past several years, significant effort has been focused on elucidating the molecular mechanisms that govern bone metastasis. However, so far, the factors that regulate the preferential metastasis of breast cancer cells in bone are not well identified. Recently, it has been demonstrated that cancer cells invade preferentially the bone microenvironment subjected to high bone remodeling suggesting that some factors released during high bone turnover can accelerate the development of cancer cell in bone. Here we show that high extracellular calcium concentrations ([Ca]_e) can trigger migration of human MDA-MB 231 breast cancer cells, in Boyden's chambers. Thus, when breast cancer cells were exposed to different concentrations of calcium (from 1.8 to 7.5 mM) the mobility of the cells was dose-dependently stimulated. The maximum effect was obtained at 5mM where the cell mobility was approximately three fold increased compared to cell submitted to control medium ([Ca]_e = 1.8 mM). Using pharmacological inhibitors known to selectively block the ERK1/2 and phospholipase C pathway (i.e. U-0126 and U-73122), we completely abrogated the [Ca]_e-induced effect, suggesting the implication of a G Protein Coupled Receptor. Because these two pathways are known to be triggered by the calcium sensing receptor (CaR), we first confirmed that breast cancer cell expressed both at transcriptional and at protein level the CaR. Finally, confirming the role played by the CaR in this process, we demonstrated that small interfering RNA (siRNA) targeting of the CaR almost completely reversed the effects of calcium on cancer cell mobility. Taken together, these data demonstrate that high [Ca]_e, such as those seen in the bone microenvironment, can directly stimulate the breast cancer cell mobility by a mechanism involving the CaR. From these results, it can be hypothesized, that high [Ca]_e may participate to processes allowing tumor cells which express the CaR to invade and proliferate into the bone.

Disclosures: R. Mentaverri, None.

T251

Skeletal Effects of 2-Methoxyestradiol in Combination with other Prostate Cancer Therapies. K. S. Mohammad¹, V. Duong^{*1}, L. Kingsley¹, C. R. McKenna^{*1}, H. Walton^{*1}, X. Peng^{*1}, L. J. Suva², T. A. Guise¹, J. M. Chirgwin¹. ¹Internal Medicine, University of Virginia, Charlottesville, VA, USA, ²Orthopaedic surgery, University of Arkansas for Medical Sciences, Little Rock, AR, USA.

The majority of patients with hormone-refractory advanced prostate cancer develop bone metastases, in which the characteristic disorganized new bone formation results from the paracrine stimulation of osteoblasts by tumor cells. Many of the secreted proteins that activate osteoblasts are regulated by the hypoxic response pathway via induction of HIF-1 α . We hypothesized that anti-hypoxic therapy would be effective against bone metastases and tested this idea with 2-methoxyestradiol (2ME2), an inhibitor of microtubule polymerization and the Hif-1 α pathway that is currently in phase II clinical trials in cancer patients.

2ME2 was used alone and in combination with two established treatments for bone metastases: zoledronic acid (ZA), and the endothelin A receptor antagonist, atrasentan. We assessed the skeletal effects of treatments on tumor-free bones in 8 groups of nude mice: vehicle control, 3 single-treatment groups, 3 double-treatment groups and 1 triple-

treatment group. Mice were treated for 20wks, followed by X-ray and Piximus for bone mineral density and analyzed after euthanasia by histomorphometry and micro-CT of selected bones. Atrasentan (20mg/kg/d) had no substantial effect on bone parameters when used alone or in combination with ZA or 2ME2 as determined by X-ray, histomorphometry and micro-CT. Histomorphometric analysis of mice treated with ZA (5ug/kg/3x/wk sc) showed an increase in trabecular bone volume fraction (BV/TV%). Micro-CT revealed a similar increase in BV/TV, with a parallel increase in trabecular number and a reduction in trabecular separation. Across all single, double and triple treatment groups, we observed that 2ME2 (150mg/kg ip) increased bone mass. Histomorphometric analysis showed increased BV/TV and more osteoclasts in 2ME2-treated mice. Micro-CT demonstrated a similar increase in BV/TV and a parallel increase in trabecular thickness and reduction in trabecular separation. The groups in which 2ME2 and ZA were combined showed significant additive effects on bone mass, with even greater increases in BV/TV and trabecular thickness and decreased trabecular separation and osteoclast number. The data demonstrate that 2ME2 increased bone mass and osteoclast number. Inhibition of osteoclasts with ZA further increased bone mass. Preclinical studies are underway to see if these additive therapeutic effects also reduce prostate cancer tumor burden in bone. The experiments will test if 2ME2 is selectively active against bone metastases and if it is more effective in combination with ZA than either agent alone.

Disclosures: K.S. Mohammad, None.

T252

Tissue Engineered Bone: Components of Native Bone Environment Involved in Breast Cancer Metastasis. J. E. Moreau¹, K. Anderson^{*1}, M. Reagan^{*2}, D. L. Kaplan^{*2}, M. Rosenblatt¹. ¹Physiology, Tufts University School of Medicine, Boston, MA, USA, ²Biomedical Engineering, Tufts University, Medford, MA, USA.

Challenges in breast cancer (BrCa) treatment are due to the migration of primary tumor cells to the skeleton, initiating osteolysis, formation of metastases, and the entry of the disease into an incurable phase. Tissue engineered bone constructs afford a controllable microenvironment and have been confirmed as efficacious targets for metastatic spread using a mouse model of metastasis originating from the orthotopic site. We continued assessment of the contribution of individual components of engineered bone present upon initiation of metastasis cells, scaffold, and protein to begin characterizing the metastatic bone environment. Specimens of porous silk-based tissue engineered bone and native human bone (controls) were prepared for subcutaneous implantation in immunodeficient (NOD/SCID) mice. Orthotopic injection of the luciferin-expressing human epithelial breast cancer cell line, SUM1315, for assessment of cell migration was subsequently performed one month following implantation. Four groups of scaffolds untreated silk, bone morphogenic protein 2 (BMP2) coupled, bone marrow stromal cell (BMSC) seeded, and BMP2/BMSC treated were prepared and implanted subcutaneously over the left shoulder, with native human bone controls cored from discarded femoral heads over the right. BMSC were administered to scaffolds one day prior to implantation in their respective treatment groups. One month following implantation, SUM1315 cells were injected into mouse mammary fat pads and monitored over the course of 12 weeks. Luminescent imaging of implants at final harvest revealed the presence of metastases in 0 of 6 untreated scaffolds, 4 of 4 with BMSC treatment, 4 of 4 with BMP2 treatment, and 1 of 6 with BMP2/BMSC treatment. Metastatic spread to engineered scaffolds and the progression of bone remodeling was further confirmed through immunohistochemistry, labeling cytokeratin 5/6 for BrCa identification, trichrome for collagen I and early bone development, and von Kossa staining of calcium deposit. All metastatic spread was exclusive to the implants, with no invasion of the mouse skeleton, as confirmed via luminescent imaging. These findings provide impetus for continued research to explore the roles of bone proteins in breast cancer recruitment, the nature of the developing bone scaffold as a homing site, and the differentiation/influence of adult stem cells in creating a niche for metastatic spread.

Disclosures: J.E. Moreau, None.

T253

Metastasis-Associated Protein 1 (MTA1) was Highly Expressed and Localized in Nucleus in Prostate Cancer Bone Metastasis. J. Wang, A. Levenson*, J. Jarrett*, W. Laskin*, R. Satcher*. Northwestern University, Chicago, IL, USA.

Bone is the most frequent target site for prostate cancer metastasis. The preferential metastasis to bone suggests that bone microenvironment provides suitable conditions for tumor growth and survival. Bone marrow stromal cells (BMSC) play an active role in regulating colonization and progression of metastatic malignant epithelial cells through diffusible factors and cell-cell contact. The molecular mechanism responsible for stromal-epithelial crosstalk in bone microenvironment remains largely unknown.

We established a novel co-culture system with direct heterotypic cell-cell contact. Five different prostate cancer cell lines (PC3, DU145, LNCaP, C4-2, MDA-PCa2b) were labeled with fluorescence and co-cultured with BMSC respectively. Two types of cells were then separated by fluorescence-activated cell sorting. Gene expression profiles were analyzed using cDNA microarray. Among the most significantly modified genes, metastasis-associated protein 1 (MTA1) was found to be highly up-regulated in multiple prostate cancer cell lines during the co-culture. The expression of MTA1 was further studied in normal prostate tissue, primary prostate tumor, and bone metastasis tissue using tissue microarray and immunohistochemistry. The results showed that in normal prostate tissue (n=15) there was weak staining in cytoplasm (Intensity=0.8±0.4, Frequency=1.1±0.7) but no staining in nucleus. In contrast, in primary prostate cancer tissue (n=72) there was moderate staining both in cytoplasm (I=1.8±0.7, F=3.3±1.2,

P=0.00002 vs normal tissue) and in nucleus (I=2.1±0.6, F=3.6±0.8). There was no significant correlation between MTA1 expression level with Gleason score, TNM grade or PSA level. In bone metastasis tissue (n=8), there was no staining in cytoplasm, but strong staining in nucleus (I=2.6±0.5, F=3.4±0.5, P=0.04 vs primary tumor).

We concluded that MTA1 was differentially expressed in normal prostate tissue, primary tumor and bone metastasis tissue. The differential localization in cytoplasm and nucleus of MTA1 may indicate the degree of metastasis potential. As a member of nucleosome remodeling complex, the translocation of MTA1 between cytoplasm and nucleus in primary tumor and bone metastasis may conduct different function on transcription regulation and signaling transduction.

Disclosures: J. Wang, None.

T254

Regulation of Protein Synthesis Factors in Estrogen Metabolite-Mediated Inhibitions of Osteosarcoma Cells. K. L. Shogren^{*1}, M. J. Yaszemski¹, T. E. Hefferan¹, M. C. Charlesworth^{*2}, B. J. Madden^{*2}, R. T. Turner³, A. Maran¹. ¹Orthopedic Research, Mayo Clinic, Rochester, MN, USA, ²Proteomics Research Center, Mayo Clinic, Rochester, MN, USA, ³Nutrition and Exercise Sciences, Oregon State University, Corvallis, OR, USA.

Protein biosynthesis is one of the fundamental processes involved in both the regulation of normal eukaryotic cell growth and tumorigenesis. Previous studies show that a natural metabolite of 17 β -estradiol, 2-Methoxyestradiol (2-ME) can induce growth inhibition and cell death in human osteosarcoma cells. 2-ME treatment leads to the induction of apoptosis and the activation of RNA dependent protein kinase (PKR). Here, we have further investigated the molecular mechanisms associated with 2-ME-dependent cell death in human osteosarcoma cells. We employed 2-dimensional gel electrophoresis followed by trypsin digestion of the 2D spots. Subsequent analysis of the peptides by nano-LC-ESI tandem mass spectrometry combined with the Swiss-Prot database identified several proteins that participate in the mammalian protein synthesis. Western blot analysis using MG63, KHOS and SAOS2 osteosarcoma cells, further validated the proteomic results and revealed a significant down-regulation of proteins involved in translational regulation. Another protein synthesis initiation factor, EIF5A-2, which has been implicated in tumorigenesis was down-regulated by 2.5-fold within 24hrs of 2-ME treatment. These findings are consistent with the studies showing that 2-ME treatment results in the activation of PKR and subsequent phosphorylation of the initiation factor EIF-2. Taken together, these studies suggest that multiple translational control pathways are modulated by 2-ME treatment and the deregulation of factors catalyzing the various steps of polypeptide chain synthesis contributes to apoptosis and anti-osteosarcoma effects of 2-ME.

Disclosures: A. Maran, None.

This study received funding from: National Institutes of Health and the Mayo Clinic.

T255

Tyrosine Kinase Inhibitors Slow Motility of Osteosarcoma Cells In Vitro. P. J. Messerschmitt*, E. M. Greenfield. Orthopaedics, CWRU, Cleveland, OH, USA.

We determined whether tyrosine kinases regulate osteosarcoma cell motility, a critical component of metastasis. Three genetically-related human osteosarcoma cell lines were used: TE85: non-tumorigenic and non-metastatic; MNNG: tumorigenic, non-metastatic; and 143B: tumorigenic, highly metastatic. Motility assays measured migration distance, the width between two converging cell fronts, in a scrape created in confluent cultures. All tyrosine kinase inhibitors were tested at maximally effective concentrations based on the literature. In vitro motility correlated with metastatic ability as the 143B cells migrated 65% (p<0.001) faster than the non-metastatic cells. These differences are not due to proliferation, since aphidicolin, a DNA polymerase inhibitor, did not affect migration, but completely blocked proliferation.

Inhibitors of HER-2, NGF-R, PDGF-R, and JAK had little effect on the motility of all cell lines. In contrast, the EGF-R inhibitor (Calbiochem #324674) slowed motility of all cell lines by 50-75% (p<0.001). The met inhibitor (SU11274) slowed motility of MNNG cells by 80% (p<0.001), while only slowing motility of the 143B and TE85 cells by 20% (p<0.001). This is consistent with the finding that tumorigenesis in the MNNG cells is due to a chromosomal translocation resulting in overexpression of met. Suramin slowed motility of the MNNG and TE85 cells by 60% (p<0.001) and 41% (p<0.001), but only slowed motility of the 143B cells by 11% (p=0.012). Suramin prevents growth factor binding and thereby inhibits activation of many receptor tyrosine kinases, including activation of met by Hepatocyte Growth Factor (HGF). The preferential inhibition of MNNG motility suggests that met-dependent motility in these cells is due to autocrine production of HGF. The molecular basis for inhibition of TE85 motility remains to be identified. 3,4-Methylenedioxy- β -nitrostyrene (MNS), a newly identified tyrosine kinase inhibitor, preferentially slowed motility of the metastatic 143B cells by 53% (p<0.001), while only slowing motility of the MNNG cells by 25% (p<0.001) and not detectably affecting motility of the TE85 cells. MNS inhibits the tyrosine kinase activity of both Syk and Src. However, other inhibitors of Syk and Src, either alone or in combination, had no detectable effect on 143B motility. Thus, it is likely that MNS slows motility by inhibiting another, as yet unidentified, tyrosine kinase. Nonetheless, MNS is an attractive, potential therapeutic agent for further study as it preferentially slowed motility of the metastatic cell line. Our results also show that inhibitors of EGF-R and met are attractive therapeutic agents for patients with osteosarcoma that overexpress those receptors.

Disclosures: P.J. Messerschmitt, None.

T256

Fracture Risk Is Increased in Danish Men with Prostate Cancer. A Nationwide Register Study. M. F. Nielsen¹, K. Brixen², S. Walter^{3,4}, J. Andersen⁴, P. Eskildsen⁵, B. Abrahamsen⁶. ¹Dept. of Endocrinology, Odense University Hospital, Odense, Denmark, ²Dept of Endocrinology, Odense University Hospital, Odense, Denmark, ³Urology, Odense University Hospital, Odense, Denmark, ⁴Dept. of Urology, Roskilde Hospital, Roskilde, Denmark, ⁵Dept. of Internal Medicine, Koege Hospital, Koege, Denmark, ⁶Dept. of Medicine, Copenhagen University Hospital Gentofte, Copenhagen, Denmark.

The purpose of this study was to examine the effect of prostate cancer on fracture risk and calculate the national impact of prostate cancer on hip fracture incidence, while taking into account any modifying effects of orchiectomy and androgen deprivation therapy (ADT). Data from the National Hospital Discharge Register, the National Bureau of Statistics, and the National Prescriptions Database were merged. The analysis covered 15,716 men aged 50+ years presenting with a fracture at any hospital in the country in the year 2000 and 47,149 age-matched controls. A prior diagnosis of prostate cancer had been recorded in 1.3% of controls and 2.5% of fracture cases, with a median time span between the first consultation for prostate cancer and the index fracture of three years. In 75 percent of the patients, the time span was less than five years. Prostate cancer was associated with significant increase in all-fracture risk, OR 1.8 (95% CI 1.6-2.1), and hip fracture risk, OR 3.7 (3.1-4.4) whereas no impact on vertebral fracture risk was found, OR 1.0 (0.7-1.5). The effects were undiminished by adjustment for age, prior fracture, living circumstances and income. In men aged 50-65 years, prostate cancer increased the risk of hip fracture by as much as nine-fold, OR 9.2 (4.8 - 17.5).

After adjustment for previous fracture, cancer diagnosis, and age, both ADT and orchiectomy significantly increased overall fracture risk, OR 1.7 (1.2-2.5, $p < 0.01$) and 1.7 (1.2-2.4, $p < 0.01$), respectively. ADT also increased hip-fracture risk (OR 1.9, 1.2-3.0, $p < 0.05$), but prostate cancer therapy was not associated with demonstrable increases in vertebral fracture risk.

In conclusion, prostate cancer was associated with an increase in all-fracture risk as well as hip-fracture. The increased fracture risk became apparent early after diagnosis and remained pronounced even in long-term survivors. In total, 3.1% of hip fractures in men aged 50+ were attributable to prostate cancer. The risk of hip fracture was not confined to the very old, neither was fracture risk made negligible by the excess mortality in patients with advanced prostate cancer.

Disclosures: M.F. Nielsen, None.

This study received funding from: Cancer Foundation.

T257

Role of CXCL13 Chemokine Ligand 13 in Squamous Cell Carcinoma Associated Osteolysis in Athymic Mice. S. N. M. Pandravad¹, X. Liu², J. S. Norris², K. Sundaram¹, S. Shanmugarajan¹, W. L. Ries¹, S. D. London³, S. V. Reddy¹. ¹Charles P. Darby Children's Research Institute, Charleston, SC, USA, ²Department of Microbiology and Immunology, Medical University of South Carolina, Charleston, SC, USA, ³College of Dental Medicine, Medical University of South Carolina, Charleston, SC, USA.

Head and neck squamous cell carcinoma is the most common malignant neoplasm estimated to be more than 40,000 cases per year in the US. These malignant tumors are known to have a potent activity of local bone invasion; however the molecular mechanisms of SCC associated osteolysis are unknown. In this study, we identified high level expression of chemokine ligand, CXCL13 and RANK ligand (RANKL) in squamous cell carcinoma (SCC) derived cell lines. SCC 14a cell conditioned media (20%) induced osteoclast differentiation which was inhibited by addition of OPG in human peripheral blood derived monocyte cultures indicating that SCC cells produce soluble RANKL. In addition, recombinant CXCL13 (10 ng/ml) significantly enhanced RANKL stimulated osteoclast differentiation in these cultures. Trans-well migration assay further identified that CXCL13 induces (7-fold) chemotaxis of peripheral blood monocytes in vitro which was inhibited by addition of anti-CXCR5 receptor antibody. Zymogram analysis of conditioned media obtained from RAW 264.7 macrophage cells stimulated with CXCL13 for 48 hr demonstrated a significant increase (4.0-fold) in the level of MMP-9 expression. Real-time PCR analysis of total RNA isolated from human bone marrow derived stromal cells stimulated with CXCL13 for 48 hr showed a significant increase (4-fold) in RANKL mRNA expression. Interestingly, CXCL13 treatment to SCC 14a cells induced CXCR5 receptor and MMP-9 expression suggesting an autocrine regulatory function in SCC cells. To further examine the molecular mechanisms associated with SCC tumor cell invasion and osteolysis of bone, we established an in vivo model for SCC by subcutaneous injection of SCC 14a cells (7×10^6 cells in PBS) onto the surface of calvaria in NCr-nu/nu athymic mice, which developed tumors in 4-5 weeks. Immunohistochemical analysis confirmed CXCL13 and MMP-9 expression in the tumor cells and invasion of bone/osteolysis in vivo. Histochemical staining further demonstrated a significant increase in the numbers of multinucleated TRAP positive osteoclasts at the tumor bone interface. Thus, our data implicate a functional role for CXCL13 in SCC tumor cells invasion/osteolysis of bone and may be a potential therapeutic target to prevent osteolysis associated with SCC in vivo.

Disclosures: S.N.M. Pandravad, None.

T258

Balloon Kyphoplasty in the Treatment of Osteolytic Lesions in the Thoracic and Lumbar Spine Due to Cancer - 2 Years Prospective Follow-up. R. Pflugmacher*. Centrum für Muskuloskeletale Chirurgie, Charité - Universitätsmedizin Berlin, Berlin, Germany.

Purpose: Balloon Kyphoplasty is a minimally invasive stabilization procedure for osteoporotic and osteolytic vertebral fractures. The purpose of this prospective study was to evaluate this operative procedure in the treatment of osteolytic vertebral fractures in reduction of pain and functional improvement of these patients and further to evaluate the restoration of vertebral height postoperatively and over a time period of 24 months.

Materials and methods: In this prospective study, 96 patients (45 patients with multiple myeloma, 51 patients with metastatic disease) with osteolytic vertebral fractures (176 vertebrae) were treated with Balloon Kyphoplasty. We were able to collect 2 year follow up data for 82 patients. 38 patients (30 male, 8 female) with 83 osteolytic vertebral fractures due to multiple myeloma and 44 patients (26 male, 18 female) with 78 osteolytic vertebral fractures due to metastatic disease. Preoperatively conventional radiographs in lateral and a.p. view, CT and / or MRI were performed. Pre- and postoperatively, pain (Visual Analogue Scale) and disability (Oswestry disability index) were evaluated. Radiographs were performed pre- and postoperatively and after 3, 6, 12 and 24 months. Vertebral height and endplate angles were measured.

Results: Clinical results for the patients with multiple myeloma and metastatic disease improved significantly. The median pain scores (VAS) decreased significant from pre- to post-treatment ($p < 0.001$) as well as the Oswestry disability index ($p < 0.001$). Balloon Kyphoplasty led to a significant and sustained reduction of pain resulting in a significant functional improvement of the patients. In the radiological evaluation a significant restoration of vertebral height ($p < 0.05$) and reduction of the kyphotic angle ($p < 0.05$) could be achieved in the patients with multiple myeloma. In patients with metastatic disease only a slight restoration of vertebral height and reduction of the kyphotic angle was achieved. Balloon Kyphoplasty was able to stabilize the vertebral height and avoid a further kyphotic deformity in the long term for both patient groups. Radiation therapy and / or chemotherapy could be performed without any loss of time.

Conclusion: In the treatment of osteolytic vertebral fractures Balloon Kyphoplasty led to a quick and sustained reduction of pain and functional improvement. Balloon Kyphoplasty was able to stabilize the fractured vertebrae in the long-term and was able to prevent an increase of kyphotic deformity. Balloon Kyphoplasty is an outstanding alternative in comparison to the established therapeutic concepts in the treatment of osteolytic vertebral fractures.

Disclosures: R. Pflugmacher, None.

T259

Chondrostatin: A New Inhibitor of Angiogenesis, Tumor Invasion and Osteoclast Activity. L. J. Sandell¹, Z. Wang¹, C. Franz¹, N. Havioglu², J. Bryan³, B. El³, A. Rapraeger³. ¹Orthopaedic Surgery, Washington University, St. Louis, MO, USA, ²Pathology, St. Louis University, St. Louis, MO, USA, ³Pathology and Laboratory Medicine, University of Wisconsin, Madison, WI, USA.

Cartilage tissue is avascular and resistant to tumor invasion: the molecule mechanism of is unknown. We have recently shown that a normally produced fragment of the predominant cartilage collagen, called chondrostatin, is responsible for exquisite targeting of inhibition of cell migration and for cell death. The cells targeted are endothelial cells, osteoclasts and tumor cells. The targeting is based on the specific binding of the chondrostatin to integrins $\alpha_v\beta_3$ and $\alpha_v\beta_5$, expressed on osteoclasts, endothelial and tumor cells but not on normal chondrocytes. The chondrosarcoma cell line, Ch-1 and the breast cancer cell line MDA-MB 231 were used to establish the proof of concept. First, we demonstrated that Ch-1 cells adhere to chondrostatin dependent on binding to an RGD sequence. Next, we established that Ch-1 and MDA cells express the $\alpha_v\beta_3$ and $\alpha_v\beta_5$ integrins and that these integrins are responsible for adhesion. Confocal microscopy studies showed that chondrostatin is internalized into the cells. Inside the cells, it is able to induce cell death in a dose and time-dependent manner. Inhibition of α_v integrin by RNA interference eliminated adhesion and cell killing. In further studies, we examined the ability of chondrostatin to inhibit angiogenesis. Two well accepted assays were used: formation of tubes from HUVEC endothelial cells, and outgrowth of endothelial cells from explants of aorta. Chondrostatin inhibited angiogenesis in both of these assays reducing angiogenesis by 50% at a concentration of 100 nM. In conclusion, naturally occurring chondrostatin inhibits angiogenesis and kills tumor cells mediated by the $\alpha_v\beta_3$ and $\alpha_v\beta_5$ integrins. This molecule may be useful in the treatment of neo-vascular disease, cancers and osteoporosis.

Disclosures: L.J. Sandell, None.

This study received funding from: NIH.

T260

Development of Small Molecule Adrenomedullin Antagonists for Treatment of Bone Metastases. V. A. Siclari¹, K. S. Mohammad², A. Martinez^{*3}, C. Gineste^{*4}, H. M. Geysen^{*4}, T. A. Guise², J. M. Chirgwin².

¹Biochemistry and Molecular Genetics, University of Virginia, Charlottesville, VA, USA, ²Internal Medicine, University of Virginia, Charlottesville, VA, USA, ³Instituto Cajal, Madrid, Spain, ⁴Chemistry, University of Virginia, Charlottesville, VA, USA.

Adrenomedullin (AM) is a 52 amino acid peptide of the calcitonin/CGRP gene family secreted by cancers such as breast, lung, and prostate, where it can stimulate angiogenesis and autocrine signaling and may cause cancer-associated pain. AM also dose-dependently stimulates new bone formation at picomolar concentrations, by binding to the calcitonin-receptor-like receptor plus RAMP2 or 3 and stimulating adenylyl cyclase. It stimulates osteoblast proliferation, although the molecular pathways activated in bone cells by AM are poorly understood. When we treated primary mouse osteoblasts with AM, the mRNAs encoding bone matrix proteins (bone sialoprotein, type I collagen, osteocalcin, and osteopontin) were not increased. However, AM stimulated IL-6 mRNA expression by primary osteoblasts. We previously reported increased or decreased bone metastases due to AM overexpression and siRNA knockdown in prostate and lung cancer models respectively. These observations identify AM as a significant target for therapeutic intervention against bone metastasis.

Small molecules have been identified that function as agonists or antagonists of the action of AM to increase cAMP, by binding to the AM ligand rather than the receptor. One of the antagonists, NCI 16311, binds with $K_d = 8\text{ nM}$ to AM without altering ligand:receptor binding affinity. We added 100nM 16311 to neonatal mouse calvarial organ cultures. Increases in new bone and osteoblast number caused by 1nM AM were completely blocked by 16311, without cellular toxicity or blockade of new bone formation due to IGF1 receptor activation. Two additional antagonists were tested in the same assays. NCI 28086 was ineffective, but the methylene-bis- benzoic acid derivative NCI 37133 was as effective as NCI 16311 at blocking AM-induced new bone formation. The two lead compounds may be effective bone-selective antagonists of tumor-secreted AM. NCI 16311 and 37133 are aromatic carboxylic acid derivatives that act extracellularly, offering attractive pharmacological properties without needing to be cell-permeant. Further development of these compounds into higher affinity, second-generation derivatives should be possible. Small molecule AM antagonists may provide improved treatment for osteoblastic bone metastasis and associated cancer bone pain.

Disclosures: V.A. Siclari, None.

T261

Synthesis and Biological Evaluation of Vitamin K₂ Metabolites. Y. Suhara^{*}, A. Murakami^{*}, M. Kamao^{*}, S. Mimitsu^{*}, K. Nakagawa^{*}, N. Tsugawa^{*}, T. Okano. Department of Hygienic Sciences, Kobe Pharmaceutical University, Kobe, Japan.

Vitamin K is an essential nutrient and a cofactor for the carboxylation of specific glutamyl residues of proteins to gamma-glutamyl residues, which activates osteocalcin related to the bone formation. Recently, the metabolism of vitamin K has been studied in humans and rats, and urinary metabolites as glucuronides of K acid I, II, and omega-carboxylic acid have been detected. However, their biological activities have hardly been evaluated so far. We anticipated that if those metabolites were studied in detail, they would provide insight into the biological significance of vitamin K and valuable information for the development of new drugs. In this study, we synthesized six kinds of "predictable" vitamin K metabolites. They were introduced vitamin K₂ (menaquinone-2, 3, and 4) molecule to omega-hydroxyl group or omega-aldehyde group instead of omega-carboxylic acid because the metabolites including omega-carboxylic acid were unstable and unable to use for assay. The requisite analogues were synthesized by coupling the naphthoquinone derivative and side-chain moiety. For the synthesis of side-chain part, we chose geraniol, farnesol and geranylgeraniol as the starting material. While the naphthoquinone part was prepared from 1,4-diacetoxy-2-methylnaphthoquinone. After coupling reaction, deprotection of protective group gave omega-hydroxyl derivative, and additional oxidative reaction yielded omega-aldehyde derivative. To investigate the biological activities of those analogues, we focused on the apoptosis-inducing activity against HL-60 cells (human leukemia cells). Samples of 5 and 10 μM analogues were successively added to HL-60 cells. After 72 h, the cells were collected and treated with propidium iodide, and then apoptosis activity was determined with a fluorescence-activated cell sorter (FACS). As a result of biological evaluation, omega-hydroxylation of the side-chain part of menaquinone-4 increased apoptosis-inducing activity for HL-60 cells compared to menaquinone-4. Our results indicated that metabolites of vitamin K might have potential as biologically active compounds and can provide useful information to develop new drugs based on vitamin K with modification of the terminal alkyl group. A more detailed examination is currently undergoing based on these findings.

Disclosures: Y. Suhara, None.

T262

Benign and Malignant Bone Tumors Express the Melatonin Receptor Isoform 1 (MT1). M. Svoboda^{*1}, C. D. Toma^{*2}, F. Arrich^{*2}, C. Ekmekcioglu^{*3}, O. Assadian^{*4}, T. Thalhammer^{*1}. ¹Department of Pathophysiology, Medical University Vienna, Vienna, Austria, ²Department of Orthopaedic Surgery, Medical University Vienna, Vienna, Austria, ³Department of Physiology, Medical University Vienna, Vienna, Austria, ⁴Clinical Department of Hygiene and Medical Microbiology, Medical University Vienna, Vienna, Austria.

The indolamine melatonin is synthesized and secreted by the pineal gland during night time and is well known for its role in the regulation of circadian rhythms. Recent studies showed that melatonin exhibits potent anti-tumor activity in vitro as well as in vivo and it is produced in extrapineal tissues, e.g. the bone marrow. Melatonin acts by receptor independent and dependent pathways. The latter is mediated through high-affinity G-protein receptors (MT1 and MT2) signaling.

To account for a possible role of MT1/MT2 in bone homeostasis, we investigated whether MT1/MT2 are expressed in malignant and non-malignant human bone lesions and osteosarcoma cell lines (HOS, MG-63). By RT-PCR, Western blot and immunofluorescence we found that MT1, but not MT2 was detectable in the tumor cell lines. By TaqManPCR, we analyzed 30 specimens from osteosarcoma and 11 from benign bone tumors for MT1-mRNA expression and determined mRNA expression (relative to a control specimen) of the osteoclast activity stimulating receptor activator of nuclear factor- κ B ligand (RANKL) and its opponent osteoprotegerin (OPG).

We found that MT1 was similarly expressed in malignant (4.39 ± 4.98 -fold) and benign samples (4.64 ± 6.81 -fold). Also, mean RANKL- and OPG-mRNA levels were comparable in malignant and benign samples (RANKL: 7.38 ± 9.61 -fold vs. 3.57 ± 3.11 -fold, $p=0.207$; OPG: 23.45 ± 32.76 vs. 8.07 ± 7.23 -fold, $p=0.13$). Expression of MT1-mRNA was also found in normal human osteoblasts (hOB), and bone marrow stromal cells (BMSC). High expression levels of MT1-mRNA together with low OPG-mRNA were found in both cancer cell lines, while in normal hOB and BMSC, high OPG-mRNA levels were associated with low MT1-mRNA levels.

In summary, we found that MT1-mRNA is abundantly expressed in human malignant and benign bone tumors and in osteosarcoma cells lines. Despite our finding that the relative expression levels of MT1 mRNA in malignant and non-malignant bone tumors did not differ significantly, the highest MT1 levels were detected in individual osteosarcoma specimens, i.e., in two specimens from patients with a local recurrence of the tumor. Whether this may be a prognostic parameter remains to be established in further work.

Disclosures: M. Svoboda, None.

T263

TGF-beta Inhibition Suppresses Myeloma Cell Growth via Enhancement of Osteoblast Differentiation. K. Takeuchi^{*1}, M. Abe¹, A. Oda^{*1}, H. Amou^{*1}, M. Hiasa^{*2}, O. Tanaka^{*1}, S. Fujii^{*1}, S. Nakamura^{*1}, A. Mihara^{*1}, H. Miki^{*1}, J. Asano^{*1}, K. Kagawa^{*1}, K. Kitazoe^{*1}, K. Yata^{*1}, T. Hashimoto^{*1}, S. Ozaki^{*1}, S. Kido¹, T. Matsumoto¹. ¹Dept of Medicine and Bioregulatory Sciences, Univ of Tokushima Graduate Sch of Med Sci, Tokushima, Japan, ²Dept of Orthodontics and Dentofacial Orthopedics, Univ of Tokushima Graduate Sch of Dent Sci, Tokushima, Japan.

Multiple myeloma (MM) enhances osteoclast formation and suppresses stromal cell differentiation into osteoblasts (OBs). Because both osteoclasts and undifferentiated stromal cells enhance MM cell growth and survival, such effects of MM create a microenvironment suitable for MM expansion in the bone marrow, which can be called as myeloma niche. TGF-beta, an inhibitor of terminal OB differentiation, is released from the bone matrix through enhanced bone resorption by MM. We previously demonstrated that TGF-beta inhibition is able to restore OB differentiation suppressed by MM. However, it is not known whether the restoration of OB differentiation by TGF-beta inhibition affects MM growth. We therefore aimed to clarify the role of TGF-beta inhibition on MM growth in relation to the induction of OB differentiation. Terminally differentiated MC3T3-E1 osteoblastic cells with mineralized nodules secreted a factor(s) with potent apoptosis-inducing activity in 5TGM1 and RPMI8226 MM cells. The anti-MM activity was elaborated exclusively by terminally differentiated MC3T3-E1 cells with mineralized nodule formation, whereas untreated MC3T3-E1 cells with pre-osteoblastic phenotypes enhanced MM growth. SB431542, a TGF-beta type 1 receptor kinase inhibitor, facilitated OB differentiation as well as the production of MM cell growth inhibitory activity in MC3T3-E1 cells. Although interaction of MM cells with stromal cells/undifferentiated OBs gives rise to drug resistance in MM cells, terminally differentiated OBs potentiated the cytotoxic effects of doxorubicin on MM cells. These results demonstrate that, in contrast to stromal cells/undifferentiated OBs, terminally differentiated OBs inhibit MM cell growth and survival, and that inhibition of TGF-beta actions enhances OB differentiation, suppresses MM cell growth and potentiates responsiveness to cytotoxic agents. It is suggested that suppression of OB differentiation by MM not only accelerates bone destruction but also enhances MM growth to create myeloma niche, and that induction of OB differentiation by TGF-beta inhibition may provide a novel approach to disrupt myeloma niche.

Disclosures: K. Takeuchi, None.

T264

Surgical Treatment for Benign Bone Tumors with Fully Interconnected Porous Hydroxyapatite Ceramics. N. Tamai*, A. Myoui*, T. Ueda*, H. Yopshikawa*. Dep. of Orthopaedics, Osaka University Graduated School of Medicine, Osaka, Japan.

PURPOSE: Large bone defects remaining after curettage of benign bone tumors should be filled with a substitute to restore mechanical strength. We have utilized several kinds of CHAs available in Japan for massive bone defect after curettage of benign bone tumors and have reported our follow-up study. In 2000, we have developed a fully interconnected porous calcium hydroxyapatite ceramics (NEOBONE) and have utilized them as bone substitute. The purpose of this study is to evaluate the clinical outcomes with the use of NEOBONE as bone substitute after curettage of benign bone tumors.

METHODS: We reviewed the results of 27 patients with benign bone tumors sequentially treated by curettage followed by implantation of NEOBONE™ between 2000 and 2004. There were 8 women and 19 men, with the mean age of 29 years. The locations were as follows: phalanx (11patients), femur (6), pelvis (3), tibia (2), radius (1), calcaneus (1), humerus (1), talus (1). The histological diagnoses included enchondroma (9patients), solitary bone cyst (6), chondroblastoma (4), giant cell tumor of bone (3), fibrous dysplasia (3), intraosseous ganglion (2). The mean follow-up period was 30 months. Assessment was based on plain radiography at the final follow-up. Radiographic findings were classified into four grades: Grade1, slight bone formation in NEOBONE; Grade2, moderate bone formation in NEOBONE and their openings; Grade3, consolidation phase; Grade4, absorption phase.

RESULTS: Radiographs at the final follow-up were graded as follows; Grade1 in 6 patients; Grade2 in 4; Grade3 in 13; Grade4 in 4. The mean periods required to reach each grade were as follows; Grade1 in 2.5 months (2-9 months); Grade2 in 6 months (2-12 months); Grade3 in 18 months (6-31 months); Grade4 in 41 months (27-55 months). There were two local recurrences, observed in each one case of solitary bone cyst and giant cell tumor of bone.

CONCLUSIONS: NEOBONE (pore size: 150-300µm, porosity: 75%) has a finely-organized, 3-dimensional interconnecting pore structure. The large interconnecting channels (average diameter: 40 µm) permit the easy penetration of tissue into the deep pores and, therefore, NEOBONE can itself induce local bone repair processes. In the present study, we utilized NEOBONE as a bone substitute after curettage of benign bone tumors, and demonstrated its superior osteoconductivity. We conclude that NEOBONE is an excellent next generational bone substitute in surgery for benign bone tumors.

Disclosures: N. Tamai, None.

T265

Mediation of Cell Proliferation and Tumorigenicity of Musculoskeletal Tumor Cells by an Interferon Inducible IFI16 Protein. Y. Zhang*, R. D. Howell*, L. Kong*, C. Liu. Orthopaedic Surgery, New York University, New York, NY, USA.

IFI 16, a member of an interferon-inducible p200-protein family, modulates cell proliferation, differentiation, apoptosis and cellular senescence. It has also been implicated in the pathophysiology of autoimmune diseases and antitumor activity of several kinds of cancer cells. In this study we showed that the level of IFI 16 was dramatically reduced in the primary human osteosarcoma compared to normal bone. Overexpression of functional IFI 16 in human osteosarcoma and chondrosarcoma cell lines significantly inhibited cell growth. This IFI16-mediated inhibition on musculoskeletal tumor cells is overcome by a siRNA that specifically knockdown the expression of IFI16, suggesting that certain level of IFI16 is critical for controlling musculoskeletal tumor growth. In addition, ectopic expression of IFI 16 in musculoskeletal tumor cell lines markedly inhibited colony formation and was associated with a senescence-like phenotype, production of senescence-associated beta-galactosidase. Further, upregulation of p21 and inhibition of cyclin E, cyclin D1, c-Myc and Ras accompanied inhibition of cell growth by IFI 16 in musculoskeletal tumor cell lines. Taken together, our observations provide insight into the process of musculoskeletal tumors regulated by IFI16, and more importantly, our findings also provide evidence indicating that IFI16 has great potential to be employed as a therapeutic target for treating musculoskeletal tumors, including both osteosarcoma and chondrosarcoma.

Disclosures: Y. Zhang, None.

T266

Longitudinal Changes in Bone Density and Management in Men with Osteopenia. R. A. Adler, X. Samaropoulos*, M. I. Williams*, V. I. Petkov*. Endocrinology, McGuire VAMC, Richmond, VA, USA.

Until 10 year fracture risk can be easily calculated from DXA and clinical factors, patients with osteopenia (low bone mass but not osteoporosis) by DXA usually receive recommendations to take calcium, vitamin D, exercise and repeat DXA in two years. We identified 78 men who had participated in a screening program based on the OST (Osteoporosis Self-Assessment Tool) equation, which identifies risk for osteoporosis by DXA based on age and weight only. The men had at least 1 T-score in spine, total hip, femoral neck, total forearm, or distal 1/3 forearm between -1 and -2.5, except for 4 men who had a T-score of ≤ -2.5 but not given pharmacologic treatment. The men had a second DXA at least 2 years after the first. At first DXA, mean age was 70.7 yrs, mean weight 76.4 kg, mean OST score 1 (moderate risk). Low bone mass was found in 33% of spine, 46% of total hip, 78% femoral neck, 51% total forearm, and 40% distal 1/3 forearm DXA measurements. 37/78 men were prescribed calcium and 21/78 Vitamin D (beyond a

multivitamin). After an average of 998 days, weight was down an average of 1.2 kg. The overall diagnosis worsened to osteoporosis in 3 men, but in only one man was the change in DXA statistically significant. Interestingly, after the second DXA, calcium and/or vitamin D supplementation was started in 17 men. Thus, while the second DXA only identified 3 more men with osteoporosis, an additional group had conservative treatment of osteopenia started for the first time. In conclusion, a second bone density test for men at risk of osteoporosis seldom changes the diagnosis. However, the second DXA may spur providers to start preventive methods.

Disclosures: R.A. Adler, None.

T267

Solid-State ^{31}P MRI Quantifies Decreased Mineralization Density in OVX Rat Bone. S. Anumula*, S. L. Wehrli*, J. Magland*, F. W. Wehrli*. ¹Radiology, University of Pennsylvania, Philadelphia, PA, USA, ²NMR Core Facility, Children's Hospital of Philadelphia, Philadelphia, PA, USA.

Osteoporosis is characterized by rapid bone turnover resulting in decreased mineralization density of bone (MDB), a parameter that cannot currently be measured in vivo. Here we examine the hypothesis that 3D ^{31}P solid-state magnetic resonance imaging (SS-PH) is able to quantify cortical bone phosphorus content in situ in a rat model of osteoporosis in view of possible future application of the technique to humans in vivo. The study involved six ovariectomized rats (4 months old, OVX) compared to six sham-operated rats of the same age (NO). After the surgery all the animals were given standard chow and water ad libitum for 50 days after which they were euthanized and cortical bones extracted from the right and left femurs. In order to optimize the imaging parameters, the spin lattice relaxation time T_1 was measured in the specimens using inversion-recovery sequence. 3D SS-PH was performed at 9.4 Tesla (~162 MHz) using a sequence with non-selective excitation followed by sampling of the free induction decay in the presence of a readout gradient whose K-space data were reconstructed off-line yielding an isotropic resolution of 177 µm (Fig. 1). Specimens were co-imaged with a reference phantom of 2M K_2HPO_4 in order to quantify the mineral phosphorus. The sequence was implemented on a vertical-bore superconducting system (DMX-400, Bruker Instruments, USA) in conjunction with a home-built solenoid coil. Quantitative MRI results were compared with micro-CT derived MDB values using calibration samples made of various concentrations of K_2HPO_4 . Phosphorus concentration obtained by SS-PH was lower in the OVX than in the NO group (6.7 ± 0.9 vs $7.5 \pm 0.7\%$; $p=0.01$) (Fig. 2a). This result was paralleled by lower MDB measured by $\mu\text{-CT}$ in the OVX group (1199 ± 24 vs 1225 ± 10 ; $p=0.02$) (Fig. 2b). In conclusion our data suggest that ^{31}P SS-PH may have potential for studying changes in mineral metabolism nondestructively and noninvasively, i.e. without the use of ionizing radiation.

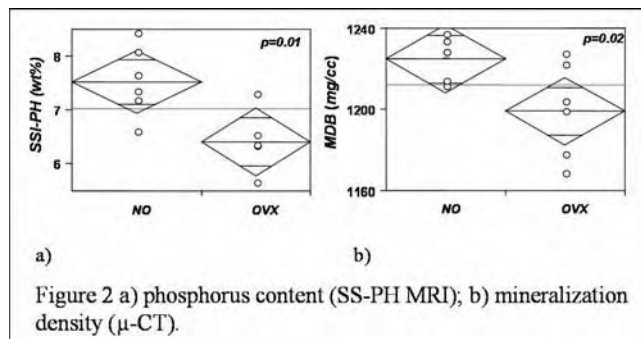


Figure 2 a) phosphorus content (SS-PH MRI); b) mineralization density ($\mu\text{-CT}$).

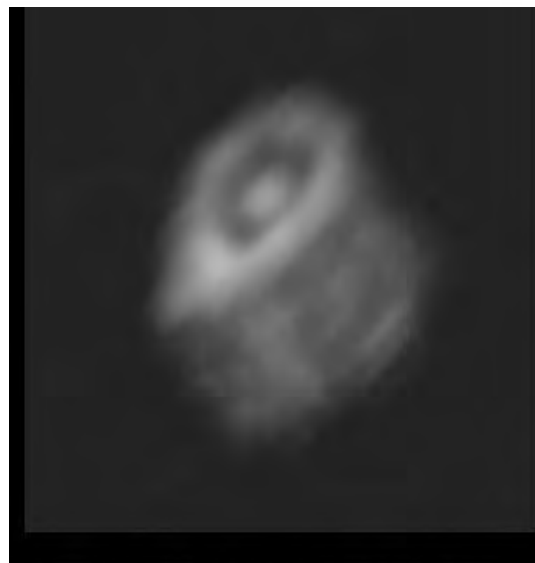


Figure 1. Volume-rendered ^{31}P MR image of the rat femur with central reference sample.

Disclosures: S. Anumula, None.

T268

Accuracy and Precision of Adipose Tissue Cross-sectional Area Measured Using Peripheral Quantitative Computed Tomography (pQCT). C. Gordon¹, D. Inglis^{2*}, L. Giangregorio³, J. M. Zmuda⁴. ¹Radiology, McMaster University, Hamilton, ON, Canada, ²Civil Engineering, McMaster University, Hamilton, ON, Canada, ³Kinesiology, University of Waterloo, Waterloo, ON, Canada, ⁴Epidemiology, University of Pittsburgh, Pittsburgh, PA, USA.

Purpose: Using magnetic resonance images (MRI) as the gold standard to quantify adipose tissue cross-sectional area (CSA), this study assessed the accuracy of quantifying sub-cutaneous fat, marrow fat, and fat in and around muscle from pQCT images of the calf. The precision errors for each of the fat components were also determined.

Methods: Twenty-five subjects participated in this study. Ten subjects were scanned with MRI and pQCT at a calf location corresponding to 66% of the distance up from the medial malleolus to the medial condyle of the tibia. pQCT scans were acquired with a STRATEC XCT 2000L scanner (Orthometrix Inc., White Plains, NY) at a voxel size of 0.4 mm³ and scan speed of 10 mm/sec. The MRI images were acquired on a 1.0 T peripheral magnet (ONI Corp, Wilmington, MA) using a fast spin echo sequence that acquired 10 contiguous 2 mm slices around the 66% location. CSAs of the adipose tissue components in the pQCT image were determined using various edge tracking and threshold steps available within the pQCT analysis software. To reduce noise, median filtering was applied before segmentation. Custom software was used to extract the CSA of the adipose tissue components in the MRI calf images. Least squares analysis was used to compare pQCT and MRI fat areas. To assess precision, 15 subjects had pQCT scans done on the same day, with repositioning between scans. Precision error was calculated as percent coefficient of variation.

Results: There was good agreement between pQCT and MRI derived areas for total fat ($R^2=0.98$, $p<0.0001$), subcutaneous fat ($R^2=0.96$, $p<0.0001$) and marrow fat ($R^2=0.61$, $p<0.03$). CSA of the fat in and around the calf muscles was not well defined with pQCT ($R^2=0.12$, $p=0.8$). pQCT defined adipose tissue at the calf with precision errors of 10% for total fat, 4% for subcutaneous fat, and 16% for marrow fat. The precision error for the area of fat in and around the calf muscle exceeded 100%.

Conclusion: Adipose tissue CSAs in the calf can be accurately derived from pQCT images. The fatty infiltration between and within the calf muscles may have to exceed a threshold to be accurately detected with pQCT or be best characterized by an index such as muscle density.

Disclosures: C. Gordon, Orthometrix Inc. 5.

T269

Comparison of QCT and DXA Derived Areal Bone Mineral Density. B. C. C. Khoo^{1*}, S. Henzell^{2*}, S. Gustafsson^{2*}, K. Zhu², R. I. Price¹, R. L. Prince³. ¹Medical Technology and Physics, Sir Charles Gairdner Hospital, Nedlands, Australia, ²Department of Endocrinology and Diabetes, Sir Charles Gairdner Hospital, Nedlands, Australia, ³School of Medicine and Pharmacology, University of Western Australia, Crawley, Australia.

WHO guidelines, promulgated in 1994, considered that a gold standard for diagnosis of bone fragility in the clinical setting should be areal bone mineral density (aBMD, gcm²) measurements of the proximal femur using DXA. Recently there has been a return to the use of quantitative computed tomography (QCT) in clinical diagnosis to facilitate the understanding of bone fragility and structural analysis in individuals. aBMD is one of many variables that can be generated in such QCT studies. A critical question arises is how similar are the aBMD measurements derived from QCT and DXA?

This study compared the aBMD and T scores of 91 elderly female subjects aged 82.8 (2.5) years [mean (SD)], height 157.4 (6.0) cm, weight 63.6 (12.4) kg. All subjects were scanned on a Hologic Discovery DXA and a Phillips Brilliance CT scanner. The DXA aBMD was measured using Hologic software version 12.6 and QCT aBMD using Mindways software version 4.1.3. Using the QCT data aBMD data a "Hologic aBMD equivalent" can be calculated using manufacturer data which then allows calculation of an NHANES equivalent T score. The data was compared using linear regression and Bland-Altman (B-A) plots.

In linear regression the R^2 for total hip (TH), femoral neck (FN), inter-trochanter (IT) and trochanter (T) aBMD comparisons were 0.88, 0.84, 0.84 and 0.85 respectively, the regression coefficients were 0.87, 0.83, 0.90 and 0.83 respectively. The B-A plots showed that the QCT aBMD measurement under estimated the DXA aBMD (TH 0.13 (0.05) g/cm², FN 0.09 (0.04) g/cm², IT 0.14 (0.07) g/cm² and T 0.10 (0.05) g/cm²) with no bias as the mean increased.

These data confirm that QCT hip areal structural values are highly correlated with DXA aBMD. However there is an offset which needs further consideration.

Disclosures: B.C.C. Khoo, None.

T270

A New CUSUM Method for Simultaneous Quality Control of BMD, BMC, and Area for DXA Scanners. Y. Lu, S. Zhao*, B. Fan, J. Shephard. Department of Radiology, University of California, San Francisco, San Francisco, CA, USA.

CUSUM method has been used in longitudinal quality control (QC) of bone mineral density (BMD) by dual X-ray absorptiometry (DXA) scanners. It identifies significant deviations from the baseline as breakpoints for further investigations. With an increase of pediatric and whole body studies, a new QC method is necessary to monitor BMD, bone mineral contents, and area simultaneously. In this paper, we presented a new multivariate CUSUM method. After a log-transformation of variables ($\ln(BMD)=\ln(BMC)-\ln(Area)$), we normalized and rotated variables $\ln(BMD)$ and $\ln(BMC)$ into two linearly unassociated variables X and Y based on their observed covariance matrix. A modified univariate CUSUM was then performed on X and Y separately in both increasing and decreasing directions. Multivariate (2-D) CUSUM parameters were selected to assure a false alarm rate similar to the univariate CUSUM of one variable. Simulation studies were conducted to evaluate performance comparing to our previously proposed 2-D Shewhart. $\ln(BMD)$, $\ln(BMC)$, and $\ln(Area)$ were generated by multivariate normal distribution using mean and covariance matrix derived from a whole body QC study. We simulated the in-control condition with 365 scans. We then generated 365 off-control data in the following conditions: (1) Case 1: both log BMD and BMC increased 1 SD and Area was relative stable; (2) Case 2: BMC increased in 1SD but not BMD, and area increased accordingly; and (3) Case 3: BMC increased 1 SD but BMD decreased 1SD. Each condition was repeated for 2000 times. Table 1 showed simulation results. When a scanner was in control, the median running length for the 1st false alarm was 213 and 31 scans, respectively, for the 2-D CUSUM and Shewhart methods. When a scanner was out of control, CUSUM identified the breakpoints within 5 to 20 scans on average similar to Shewhart. In conclusion, multivariate CUSUM method can be used for QC of BMD, BMC, and Area simultaneously for whole body phantom data with satisfactory false and true positive rates.

Table 1: Simulation Results for Bivariate QC Methods (n=2000)

Case	Median # of Scans	for the 1st Alarm	% Simulations Alarmed	Within the 1st 100 scans
Case Control	Shewhart	CUSUM	Shewhart	CUSUM
In Control	31	213	92%	42%
Case 1	6	8	98%	98%
Case 2	9	20	98%	95%
Case 3	7	5	98%	99%

Disclosures: Y. Lu, NIH R01EB004079 2.

This study received funding from: R01EB004079.

T271

Vitamin D Status/insufficiency May Predict Physical Performance in a Group of Osteopenic/osteoporotic Women. Preliminary Study. S. R. Mastaglia*, M. Seijo*, D. M. Muzio*, B. Oliveri. Sección Osteopatías Médicas, Hospital de Clínicas. Universidad de Buenos Aires, Buenos Aires, Argentina.

Hypovitaminosis D is frequent in population over 65 years of age, producing a secondary hyperparathyroidism, increase of bone remodeling, bone loss and osteoporotic fractures, loss of the muscle force function. The aim of this study was to assess the vitamin D (25OHD) nutritional state in osteopenic/osteoporotic women >65 and the relationship with muscle force and function. To date, forty women were assessed, with an average age ($X \pm DS$) 71.2 \pm 5.3, body mass index (BMI) 27.5 \pm 4.2, with a bone mineral density (BMD) (DXA-LUNAR) of femoral neck (FN) 0.752 \pm 0.71 (T-1.9). The exclusion criteria applied were: having received vitamin D during the year preceding the study, pathology or medication affecting mineral metabolism, neurological and/or motor-function disease. The physical performance of lower limbs (walking speed, balance, standing-up and sitting-down) and the hip force with a dynamometer was assessed. The population sample was divided into two groups, taking as cut point 20ng/ml of 25OHD (Lips P Endocr Rev 2001): Group 1 (G1): > 20 ng/ml, Group 2: (G2) \leq 20 ng/ml. The results obtained are shown in the table. A lower score in the physical performance and a tendency to a lesser left hip abduction in women with 25OHD \leq 20ng/ml was observed.

Preliminary data show that the levels of insufficient vitamin D could predict physical performance in osteopenic/osteoporotic women >65.

Table

	25OHD (ng/ml)	Left Hip Flexion	Left Hip Abduction	Physical Performance
G1 (n=20)	31.85 \pm 6.4	13.8 \pm 1.8	7.33 \pm 1.66	11.1
G2 (n=20)	12.9 \pm 3.9	14.01 \pm 2.4	6.74 \pm 2.09	9.6
p	0.000	NS	0.1>p>0.05	0.02

Disclosures: S.R. Mastaglia, None.

T272

In Vivo and In Vitro Comparison of DXA Scanners. T. K. Omsland^{1*}, N. Emaus^{2*}, C. G. Gjesdal^{1*}, J. A. Falch^{3*}, G. S. Tell^{3*}, L. Forsen^{4*}, G. Berntsen^{2*}, H. E. Meyer¹. ¹University of Oslo, Oslo, Norway, ²University of Tromsø, Tromsø, Norway, ³University of Bergen, Bergen, Norway, ⁴Aker University Hospital, Oslo, Norway, ⁵Norwegian Institute of Public Health, Oslo, Norway.

When comparing BMD measured by different DXA scanners in multi-centre studies, the agreement between scanners is essential for the quality of the data obtained. In-vivo calibration is considered the "gold standard" when assessing agreement, but phantoms are frequently used instead. The European Spine Phantom (ESP) is an imitation of human vertebrae developed for comparison between scanners. The aim of this study was [1] to assess the agreement between in-vivo measurements (total femur) on three scanners (one GE Lunar DPX-IQ and two GE Lunar Prodigy scanners) and [2] to determine whether the ESP was able to reproduce the in-vivo variability in hip measurements on the different scanners.

The data were collected as part of the Norwegian Epidemiological Osteoporosis Studies (NOREPOS). The scanners compared in this study were located in three different cities, and the study subjects travelled between the cities. 6 men and 10 women aged 28-66 years had three repeated scans (with repositioning) on each machine. Body weight ranged from 58 to 100 kg. The ESP was scanned at least 40 times on each machine. Bland & Altman plots and multilevel linear regression analyses were used to analyse the data.

Mean difference between hip measurements on the two Prodigy scanners was small (<0.001 g/cm²) and insignificant ($p=0.97$). The differences between the scanners were not dependent on BMD level. The ESP was able to reproduce the in-vivo findings.

Mean difference between hip measurements on Prodigy and DPX-IQ was also small (0.007 g/cm²) and insignificant ($p=0.10$). However, the differences between the scanners changed over the range of BMD. The ESP did not fully reproduce the in-vivo difference between the scanners. The mean difference between ESP and measurements in humans was 0.010 g/cm² ($p=0.02$).

In conclusion, there were little overall differences between the in-vivo measurements. The ESP is a valid substitute when assessing agreement between Prodigy scanners. However, when assessing agreement between Prodigy and DPX-IQ, substitution of in-vivo with in-vitro measurements should be made with caution.

Disclosures: T.K. Omsland, None.

T273

The Effect of Bone Mineral Density (BMD) Measurement of Hip Bilateral in Clinical Practice. J. B. Lopes*, C. F. Danilevicius*, Y. F. Caparbo*, L. Takayama*, R. M. Pereira. Rheumatology Division (Bone Metabolism Laboratory), University of São Paulo, São Paulo, Brazil.

The aim of this study was to determine the effect of adding BMD measurement of contralateral hip on osteoporosis (OP) treatment based on NOF (National Osteoporosis Foundation) criteria. Sixty hundred and five consecutive elderly people community-dwelling (374 women/ 231 men) with 65 years-old or more (73.28 ± 5.40 yr) were evaluated. Subjects with a stroke causing hemiplegia, confined to a wheelchair, or with conditions resulting in immobilization of one limb were also excluded from the study. Densitometry of both hips and lumbar spine was evaluated using dual-energy X-ray absorptiometry (DXA) with HOLOGIC Discovery scanner. Precision errors and least significant change (LSC) were determined for each site: left/right hip (femoral neck and total femur) and lumbar spine. Clinical and anthropometric data were obtained by specific questionnaire and physical examination. The lowest T-score analyzed by DXA was considered in three distinct circumstances: lumbar spine+right hip; only hips and lumbar spine+hips. The risk factors were associated to the lowest T-score in these 3 situations and NOF criteria were applied to point out pharmacological treatment. Person's coefficient was used to assess the correlation between the 2 hips and McNemar's test to assess the differences using the NOF treatment criteria adding BMD measurement of contralateral hip.

There was a highly significant correlation between BMD of the two hips at femoral neck and total femur ($r = 0.93$ and 0.95 , respectively; $p < 0.0001$). Using the lowest T-score in the sites (lumbar spine, right/left femoral neck, right/left total femur) and WHO classification, osteoporosis was found in: 48.6% ($n=294$) analyzing lumbar spine+right hip; 31.2% ($n=189$) analyzing only hips and 49.75% ($n=301$) analyzing lumbar spine+hips. Similarly, pharmacological treatment using NOF criteria differed compare all analysis situations. Treatment indication occurred in 65.4% (396) analyzing lumbar spine+right hip versus 55.0% (333) analyzing only hips with a significant discordance treatment ($p < 0.0001$). Comparing lumbar spine+right hip BMD analysis and lumbar spine+hips analysis, the pharmacological therapy was indicated in 65.4% vs. 69.3% respectively with a significant discordance in treatment suggestion ($p=0.028$). This study indicate that the added of the both hips at the lumbar spine scan; can expand the number of people with the osteoporosis diagnosis and treatment indication. Furthermore, although of the artifacts such as osteoarthritis and osteophytic calcification influence in the lumbar spine BMD in elderly people, this site should be consider in the OP diagnosis and treatment.

Disclosures: R.M. Pereira, FAPESP # 03/09313-0 2.

T274

The Relationship Between the Knowledge on Osteoporosis in Females and Bone Mineral Density at Hip, Spine and Forearm. W. Pluskiewicz*, B. Drozdowska*, A. Grodzki*. ¹Metabolic Bone Diseases Unit, Silesian School of Medicine, Zabrze, Poland, ²Silesian School of Medicine, Zabrze, Poland, ³Central Clinical Hospital, Medical University in Warsaw, Warsaw, Poland.

The study assessed the thesis that better knowledge on osteoporosis ought to be related with better results of bone mineral density (BMD) measurements.

The study group included 859 females (aged 18-88 y.) without prior treatment for osteoporosis and fractures. The knowledge of osteoporosis and attitude towards methods for preventing the disease were assessed using a questionnaire consisting of ten questions. BMD was measured at femoral neck, spine or forearm.

The level of knowledge and its duration did not influence BMD of spine, femoral neck and forearm either in the whole group and in subgroups divided according to the level of education. Mean number of correct answers was 7.25 ± 1.73 , and was significantly higher in better than in less educated women (7.93 ± 1.06 versus 6.39 ± 2.01 , $p < 0.0001$). In the whole group, the majority of women (63.7%) declared an increase in calcium intake (Chi-square test=74.5, $df=3$, $p < 0.00001$), and only 44.5% declared modification of physical activity (Chi-square test=44.3, $df=3$, $p < 0.00001$).

In less educated women an increase in calcium intake declared 54.7% versus 71.3% for better educated women (Chi-square test=15.0, $df=1$, $p < 0.001$). An increase in physical activity declared 37.6% versus 50.4%, respectively (Chi-square test=8.34, $df=1$, $p < 0.01$). Concluding, the level of knowledge on osteoporosis is not related with skeletal status in female population.

Level of knowledge (Number of correct answers)	Z-score spine L1-L4	Z-score femoral neck	Z-score forearm
0-5 (poor)	-0.11 +/- 1.49	-0.12 +/- 0.9	-0.77 +/- 0.96**
6-7 (moderate)	-0.52 +/- 1.41*	-0.22 +/- 1.1	-1.09 +/- 0.88**
8 (good)	-0.58 +/- 1.17*	-0.03 +/- 0.93	-1.52 +/- 0.98
9-10 (very good)	-0.34 +/- 1.26	0.05 +/- 0.76	-1.33 +/- 0.87

*significantly lower than poor result, $p < 0.05$

**significantly higher than good result, $p < 0.05$

no significant differences between Z-score values for femoral neck

Z-score values in whole group in regard to an increase (answer A) or no change (B) in calcium intake			
Answer	Spine Z-score	Femoral neck Z-score	Forearm Z-score
A	-0.65 +/- 1.37*	-0.06 +/- 0.99	-1.32 +/- 0.90
B	-0.30 +/- 1.53	-0.18 +/- 0.96	-1.06 +/- 0.92

* even significantly lower than in subgroup B ($p < 0.05$)

Z-score values in regard to an increase (answer A) or no change (B) in physical activity.			
Answer	Spine Z-score	Femoral neck Z-score	Forearm Z-score
A	-0.60 +/- 1.15	0.03 +/- 0.89	-1.37 +/- 0.84*
B	-0.41 +/- 1.60	-0.18 +/- 0.99	-1.09 +/- 0.98

* even significantly lower than in subgroup B ($p < 0.05$)

Disclosures: W. Pluskiewicz, None.

T275

The Qualitative Method and the Method Based on the Concept of 10 Years Probability of Bone Fracture in Qualifying Patients for Pharmacological Treatment of Osteoporosis. J. Przedlacki, K. Ksiezopolska-Orlowska*, A. Grodzki*, T. Bartuszek*, D. Bartuszek*, A. Swirski*, J. Musiał*, E. Luczak*, E. Loth*, P. Teter*, A. Lasiewicki*, A. Walkiewicz*, I. Drozdowska-Rusinowicz*. Krajowe Centrum Osteoporozy, Warsaw, Poland.

Introduction: The lack of generally accepted guidelines for osteoporosis in Poland obliges the specialist centers to perform free diagnostic procedures for each referred patient. The one worked out and used in Krajowe Centrum Osteoporozy (KCO) is a qualitative method based on the data from the specialist literature. It combines the assessment of the clinical risk factors with the results of DXA test. Another method, which considered for introduction to Poland, is that worked out by the Canadian authors derived from the concept of 10 years probability of bone fracture.

Purpose of study: The aim of the study was to compare both methods in terms of qualifying patients for the pharmacological treatment of osteoporosis.

Material and methods: The diagnostic tests were done on 908 patients (108 men and 800 women) aged over 50 years (64.7 +/- 8.3 years). They were referred to KCO mainly by GPs, for the diagnosis and treatment of osteoporosis from 21.03.2006 to 20.03.2007. The tests leading to the diagnosis were conducted separately according to each method.

Results: According to the method used in KCO 250 patients were qualified for pharmacological treatment of osteoporosis (27.5% of all, 16 men and 234 women). According to the Canadian authors' method 334 patients would have been qualified for the pharmacological treatment (risk of bone fracture >20%). The decision to introduce pharmacological treatment was unanimous in both methods in the case of 243 patients. In the group of women <65 years old and men <70 years old according to the Canadian authors' method there would have been qualified 95 patients out of 483 (19.7%), and

according to the KCO method 44 patients (9,1%) - conformity 46,3%. In the group of 55 patients that were not qualified for the pharmacological treatment 41 (74,5%) didn't have an indication for DXA test. In the group of men and women in older age according to the Canadian authors' method there would have been 239 patients out of 425 (56,2%) qualified for treatment, and according to KCO method 205 (48,6%) - conformity 84,5%. In the group of 37 patients not qualified for treatment 18 had a T-score > -2,0.

Conclusion: There was a moderate general agreement of implication for treatment in both methods, significant in older patients, smaller in younger ones. The authors think that the method currently used in KCO can be continued with. Interpretation of the differences in both methods is not explicit. The obtained results will be taken into account in preparing a periodical actualisation of our method.

Disclosures: J. Przedlacki, None.

T276

Evaluation of Bone Area in the BMIL QA/QC Phantom on the Norland System. T. V. Sanchez¹, J. M. Wang², G. Ekker^{*3}, K. M. Dudzek^{*4}. ¹Research and Development, Norland--a CooperSurgical Company, Socorro, NM, USA, ²Research and Development, Norland--a CooperSurgical Company, Beijing, China, ³Engineering, Norland--a CooperSurgical Company, Fort Atkinson, WI, USA, ⁴Customer Service, Norland--a CooperSurgical Company, Fort Atkinson, WI, USA.

Bone area assessment using DXA varies with bone edge detection algorithms and equipment. Phantoms offer a tool by which to evaluate equipment performance when examining bone area. The current study evaluated DXA-based measurement of bone area on the BMIL QA/QC Phantom using AP Spine, Research and Small Subject Software to determine instrument response.

The commercially available BMIL QA/QC Phantom was evaluated on the Norland XR-46 using AP Spine Software at 1.5 x 1.5 mm and scan speeds of 65mm/s or 130mm/s and both Research and Small Subject Software at 1.0 x 1.0 mm with a scan speed of 15mm/s. The Phantom was scanned 25 times on each setting and operator set region of interest were analyzed for the total individual vertebrae (L1, L2, L3 and L4) on each scan. Regression analysis evaluated instrument performance.

When analyzed the studies done using AP Spine at 130 mm/s resulted in Bone Area for L1, L2, L3 and L4 of 13.526 cm², 17.484 cm², 21.648 cm² and 26.668 cm², respectively. Regression analysis between AP Spine mode at 130 mm/s and AP Spine mode at 65 mm/s ($y = 0.9928x + 0.3621$, $r = 0.9815$), Research mode ($y = 1.0812x - 6.399$, $r = 0.9909$) or Small Subject mode ($y = 0.9777x - 4.4908$, $r = 0.9991$) indicated strong relationships.

In summary, this study demonstrates that the Norland scanning system is able to assess the four segments of the BMIL QA/QC Phantom and that the operating software modes produce similar bone area results. Phantoms, like the BMIL QA/QC Phantom, can prove to be powerful tools for evaluating the performance of a DXA system.

Disclosures: T.V. Sanchez, None.

T277

Limits for Exclusion of Individual Vertebra from the L2-L4 AP Spine Assessment. J. M. Wang¹, T. V. Sanchez². ¹Research and Development, Norland--a CooperSurgical Company, Beijing, China, ²Research and Development, Norland--a CooperSurgical Company, Socorro, NM, USA.

Evaluation of the AP Spine L2-L4 region assumes that the individual vertebrae are free of defects that will skew the L2-L4 result. When evaluating the Norland AP Spine study, methodology calls for examining the individual vertebrae for a spread of less than 10% to insure that group value is not skewed. The current study examines the effect of spread on the L2-L4 result to establish if the criteria are valid.

A population of 424 AP Spine studies were pulled from clinical achieves. T-score results of studies were divided into four groups based on the spread of the L2, L3 and L4 percent young normal value_Group 1 (n = 115) with ≤5% variation, Group 2 (n = 167) with variation over 5% to 10%, Group 3 (n = 78) with variation over 10% to 15% and Group 4 (n = 64) with variation over 15%. To assess the effect of variation on the clinical findings, we examined discordance in T-score based diagnosis obtained from individual vertebrae and the L2-L4 region. The number of discordant diagnosis moved from 21% and 27.5% in Group 1 and Group 2 to a substantial 49% and 59% in Group 3 and Group 4.

The study demonstrates that as spread of the percent young normal increases in individual vertebrae beyond ten percent the population experiences a substantial increase in the number of discordant diagnosis. A limit in spread of ten percent or less among individual vertebrae is justified.

Disclosures: T.V. Sanchez, None.

T278

Reliability of Two Consecutive Prodigy Densitometers. M. C. Schoeller^{*1}, S. Mehle^{*2}, C. Simonelli¹. ¹Internal Medicine, HealthEast Osteoporosis Care, Woodbury, MN, USA, ²HealthEast Research and Education, HealthEast Medical Research Institute, Woodbury, MN, USA.

Evaluation of long-term stability of DXA devices is important for assessing precision and maintaining quality control of bone mineral density measurements in longitudinal studies. Quality control procedures generally use spine phantoms with known values provided by manufacturer. We evaluated long-term precision over a 4-year and 9-month period of

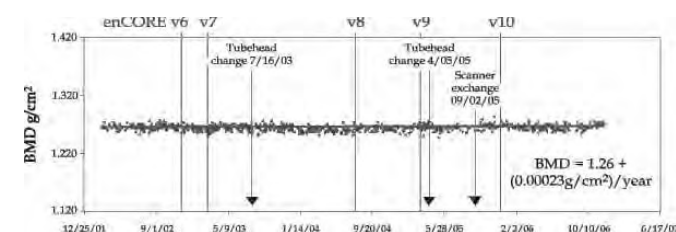
measurement of a single Lunar spine phantom on two consecutive Lunar Prodigy (GE Healthcare) scanners located in an osteoporosis clinic.

The phantom consisted of an aluminum spine with increasing density from L2 to L4 embedded in a plastic that mimics human tissue (%fat=30%). The original Prodigy scanner was replaced 3.5 years into the study with a Prodigy Advance scanner. Six versions of enCORE operating software were used during the study. In addition to routine service on both scanners, two service interventions (tube head replacement) occurred on the first scanner. Both Prodigy scanners were used heavily (more than 160 scans/week on average). A total of 785 measurements of the spine phantom (L2-L4) were analyzed.

Long-term BMD precision was 0.4% and a regression of BMD on date showed no significant trend ($p(t)=0.08$, $R^2=0.004$). The average individual measurement change from baseline (first 5 measurements) was -0.31%. Minitab run chart evaluations of BMD for trends and oscillation around the mean were not significant ($p=0.20$ and 0.80 , respectively). The average change seen in phantom BMD measurements was insignificant at 0.0002 g/cm^2 per year and there were no significant trends.

We conclude that spine phantom measurements over a 4-year 9-month period on Lunar densitometers involving service interventions, multiple software versions, and a complete scanner exchange revealed highly stable values with average BMD shifts of -0.31%. The excellent BMD precision error of 0.4% for these densitometers demonstrated reliable system performance, long-term stability of results, and enhanced confidence in longitudinal studies.

	Prodigy Long-term Precision Error Measured with Phantom	
	BMD (g/cm ²)	BMC (g)
Mean	1.265	52.52
SD	0.005	0.323
CV	0.40%	0.67%



Disclosures: M.C. Schoeller, None.

T279

Phalangeal BMD Assessment Using Radiographic Absorptiometry From Hand X-rays Taken With Digital Mammography. S. L. Silverman¹, X. Bi^{*2}, L. Al-Dayeh^{*2}. ¹Cedars-Sinai/UCLA, Beverly Hills, CA, USA, ²CompuMed, Inc, Los Angeles, CA, USA.

Osteoporosis is under diagnosed and under treated. Recent guidelines from the US Preventive Systems Task Force recommend bone density screening for women over age 65 or women above age 60 with risk factors. Yet only 22.9% of Medicare recipients have had a BMD test in the 3 years after Medicare reimbursement for osteoporosis screening began¹. Breast cancer risk increases steadily with age. Mammography is recommended yearly for women over age 50.

We hypothesized that the availability of software to measure phalangeal BMD with digital mammography equipment would allow at risk postmenopausal women to have their BMD assessed when a routine mammogram is performed.

Radiographic Absorptiometry (RA) measures volumetric BMD of the middle phalanges from a standard AP x-ray of the non-dominant hand (with an aluminum reference wedge placed near the hand). We conducted a feasibility study to validate the use of Full Field Digital Mammography (FFDM) system to acquire the required hand x-ray for RA analysis, and to assess the accuracy of the results from the mammography system as compared to the results from standard x-ray films.

A customized module of the OsteoGram® (CompuMed Inc., Los Angeles, CA) which uses RA, has been developed to accept digital images from a Hologic - LORAD Selenia digital mammography system. The module accounted for normalizing the radiographic optical density response of the mammography system to the standard radiographic response of standard x-ray equipment.

50 volunteers, age between 40 to 78 seen for routine mammography at University of California, San Diego (UCSD) Medical Center were recruited to assess their phalangeal BMD by taking two hand x-rays. One x-ray was taken with the Hologic FFDM system with the settings at 35 kVp, 5 mAs; and another using standard x-ray equipment with mammography films. The exclusion criterion was a history of diagnosed osteoporosis.

To analyze the two data sets of radiographs, the customized module was used for the FFDM data and a standard OsteoGram system was used for standard film data (using standard flatbed scanner). Regression analysis of the results showed a significant ($p<0.001$) Pearson correlation coefficient of 0.94 between the two methods validating the results from FFDM.

Of the 50 volunteers, 16 had a phalangeal BMD T-score of less than -1.0 and 4 had a T-score below -2.5 (T-score calculated using OsteoGram's normative database). This finding calls for assessing the prevalence of low bone density amongst females scheduled for mammogram.

We conclude that the availability of phalangeal BMD testing during breast cancer screening with FFDM may provide an opportunity for BMD screening for osteoporosis.

1. J Am Geriatr Soc. 2006 Mar;54(3):485-9.

Disclosures: S.L. Silverman, CompuMed 6.

This study received funding from: CompuMed.

T280

Clinical Evaluation of Jaw Bone Density with a Newly Developed “Jaw Bone Density Evaluation System” - Relationship with Osteoporosis Evaluation. Y. Takaishi¹, A. Kamada², T. Ikeo², T. Miki³. ¹Takaishi Dental Clinic, Himeji-city, Japan, ²Biochemistry, Osaka Dental University, Osaka, Japan, ³Geriatric medicine, Osaka City University, Osaka, Japan.

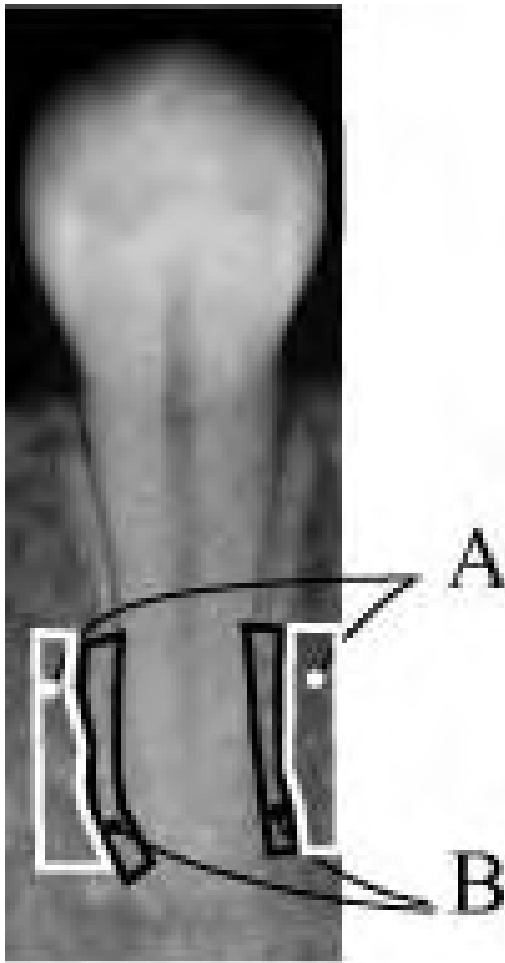
<Background> The relationship between osteoporosis and changes in alveolar bone has become a target of interest, as the formation and resorption processes of the bone structure and periodontal structure are analogous. The number of osteoporosis patients increases in accordance with age. The same trend is observed in patients with periodontal diseases or with teeth loss. Therefore, osteoporosis may be one of the risk factors of the teeth loss due to reduction of the alveolar bone. Unfortunately clinical methods to evaluate alveolar bone have yet to be established and medical proofs are still insufficient.

<Objective> We estimated alveolar bone density using a new “mandibular bone density evaluation system” and examined the relationship with osteoporosis to determine whether jaw bone evaluation is clinically useful in assessing osteoporosis.

<Method> Thirty four postmenopausal female subjects (age: 50-69, average age: 59.9) participated in the experiment. In a simple X-ray scan of mandibular bone, standard substance (aluminum step wedge) was also scanned. The bone density was estimated based on the difference in their rates of transmittance. The correlations among bone mineral density (BMD) by DXA, cortical bone of proper alveolar bone portion and cancellous bone of support alveolar bone portion in mandibular bone were examined.

<Results> Cancellous bone density of support alveolar bone (A) and cortical bone density of proper alveolar bone (B) were 87.0 ± 18.1 (SD) and 89.9 ± 26.7 , respectively. Significant correlation between (A) and (B) was observed ($r=0.736, p<0.01$). The correlations of lumbar BMD by DXA and BMD (A) and (B) were significant, respectively ($r=0.638, p<0.01$, $0.414, p<0.05$).

<Conclusion> Both cancellous bone density of support alveolar bone (A) and cortical bone density of proper alveolar bone (B) correlated with lumbar BMD; however, the correlation with (A) was greater. These results suggest alveolar bone BMD by the jaw bone density evaluation system can be utilized as one of the screening tools for osteoporosis. This system may also utilized in a large scale screening of osteoporosis in the dental fields because of low cost and short period for the evaluation. This system may provide great contributions for osteoporosis patients.



Disclosures: Y. Takaishi, None.

T281

Body Composition Measurements with Lunar iDXA: Precision Evaluation. E. Toussiot^{*1}, C. Semon^{*2}, F. Penfornis^{*2}, D. Wendling¹. ¹Rheumatology, University Hospital, Besancon, France, ²Endocrinology, University Hospital, Besancon, France.

Dual-energy x-ray absorptiometry (DXA), widely used for osteoporosis assessment, is increasingly used for measurement of body composition. Body composition is an important issue in metabolic diseases, pediatric patients but also in rheumatological conditions such as inflammatory rheumatic diseases, osteoarthritis and osteoporosis.

Precision error is a measure of the ability of a DXA system to detect small changes in a patient's body composition and bone mineral density (BMD). Lower precision error reduces the least significant change (LSC), allowing a smaller change in BMD or fat and lean mass to be identified as biological rather than related to instrument variability. Precision error is related to technology as well as the subject population; precision may degrade in thicker subjects due to decreased x-ray flux and the effect of thicker tissue on edge detection.

We evaluated precision error of total body BMD, bone mineral content (BMC), %fat, fat mass, and lean mass.

We scanned 24 women and 7 men for a total of 31 subjects (mean age 56.9 yrs, SD 13.1; mean BMI 28.4, range 17.3 - 39.6). 13 subjects had BMI values in the obese category (above 30), with a mean total %fat of 38% for the entire group. Each subject's total body was scanned two times, with repositioning between scans. Precision (%CV) was calculated as the root-mean-square standard deviation.

Precision values for Lunar iDXA total body BMD and BMC were 0.56% and 0.57% respectively. Body composition precision values were 0.63% for %fat, 0.59% for fat mass, and 0.45% for lean mass.

We conclude that the Lunar iDXA provided excellent precision for total body measurements, including BMD, BMC and body composition.

n=31	IDXA	Mean	CV
	BMD (g/cm ²)	1.065	0.56%
	BMC (g)	2318	0.57%
	%Fat	38%	0.63%
Total Body	Fat (g)	28779	0.59%
	Lean (g)	42783	0.45%

Disclosures: E. Toussiot, None.

T282

An Evaluation of Forearm BMD Measurement for Diagnosis and Treatment Monitoring in Men. N. Vallarta-Ast, D. Krueger, N. Binkley. University of Wisconsin, Madison, WI, USA.

Degenerative disease commonly confounds lumbar spine (LS) DXA assessment in older men, as such, forearm measurements are often appropriate. The ISCD recommends that the 1/3rd or “mid” radius site be utilized as the forearm region of interest (ROI) for diagnosing osteoporosis. It is therefore logical that this site would also be utilized for monitoring therapy. However, as the 1/3rd radius ROI is small and comprised primarily of cortical bone, it is plausible that use of the “total” radius ROI, which contains a higher proportion of cancellous bone, would be preferable for monitoring response to therapy. This report investigates the utility of routine forearm measurement in men and explores the utility of using the 1/3rd vs. the total radius ROI in monitoring BMD change over time in men. Between November 2003 and September 2006, 1599 men had clinically-indicated DXA scans performed at the Middleton VAMC. LS, proximal femur and non-dominant forearm images were obtained in all. Thirty-two percent (516/1599) of these predominately white men (97%, 2% Black), of mean age 68 years and mean BMI 28.3 kg/m², were osteoporotic by lowest T-score. The 1/3rd radius was equal to the spine ($p = 0.9$) in ability to detect low BMD in the group as a whole. However, in men age 80 and over, the 1/3rd radius was superior in low BMD detection ($p = 0.007$). Moreover, in men age 70+, osteoporosis was uniquely identified at the lumbar spine in only 2%, but at the 1/3rd radius in 14%.

From November 2003 to September 2006, 141 men had a repeat DXA scan performed, of whom 49 had initiated bisphosphonate (BP) therapy. As such, evaluation of non-response to BP therapy (defined here as a BMD decline greater than the LSC) is feasible. As might be expected, a BMD increase greater than the LSC was observed in 43%, 27%, 12% and 14% at the L1-4 spine, total femur, 1/3rd and total radius respectively. However, significant BMD declines were observed in none of these men at the LS, 4% at the total femur, 6% at the 1/3rd radius and 16% at the total radius.

In conclusion, the 1/3 radius is useful in identifying men with osteoporosis. However, “non-response” to BP therapy will be more common at the total radius than the 1/3rd radius, total femur or LS. DXA interpreters should be aware of this phenomenon when utilizing the total radius as a site to monitor therapy. Evaluation of the clinical significance, if any, of this “non-response” is indicated.

Disclosures: N. Vallarta-Ast, None.

T283

Skeletal Health between Two Different Groups of Hispanic American Women. J. Vargas-Jerez*, M. D. Walker, C. Gagel*, D. J. McMahon, R. A. Lantigua*, J. P. Bilezikian. College of Physicians and Surgeons, Columbia University, New York, NY, USA.

Osteoporosis is common in non-Caucasian women, particularly Hispanic Americans. Multiple studies suggest obvious racial differences in bone mineral density (BMD) and fracture risk. It is unclear whether fracture risk in non-Caucasian individuals should be assessed using race-specific referent BMD databases. A Hispanic referent BMD database for the hip, comprised of BMD values from Mexican Americans, is available from the third National Health and Nutrition Examination Survey (NHANES III). It is not known if this Mexican American database is applicable to other Hispanic groups. The purpose of this study is (1) to develop a local referent BMD database for Dominican American women who make up the majority of our local Hispanic population; and (2) to compare these data to referent values for Mexican and Caucasian American women.

560 women, 80 per decade from 20 to 90, are being recruited. Along with DXA of the total hip (TH), femoral neck (FN) lumbar spine (LS) and forearm, demographic, familial, medical, nutritional and behavioral information is being obtained. To date, 332 women have been recruited. Preliminary data suggest that Dominican American women have significantly higher mean BMD values at the TH for the decades beginning at age 50 (0.927 ± 0.113 vs. 0.859 ± 0.134 g/cm²; $p < 0.001$), 60 (0.876 ± 0.131 vs. 0.815 ± 0.134 g/cm²; $p = 0.04$), and 70 (0.830 ± 0.109 vs. 0.720 ± 0.134 g/cm²; $p < 0.001$) but not at the younger decades up to 40, or over 80 as compared with the NHANES III database for Mexican Americans. Femoral neck (FN) values were similar between the Dominican and Mexican American groups.

Dominican American women have higher bone density at the TH compared to Caucasian women for the decades beginning at age 40 (0.985 ± 0.125 vs. 0.922 ± 0.122 ; $p < 0.001$), 50 (0.927 ± 0.113 vs. 0.886 ± 0.122 g/cm²; $p = 0.04$), 60 (0.876 ± 0.131 vs. 0.827 ± 0.122 g/cm²; $p = 0.07$), 70 (0.830 ± 0.109 vs. 0.759 ± 0.122 g/cm²; $p < 0.001$), & 80 (0.780 ± 0.081 vs. 0.691 ± 0.122 g/cm²; $p = 0.04$) but not for the 2 younger decades (20-40). Mean FN values were also greater in the Dominican American group compared to Caucasians across most age ranges. Mean LS BMD values were similar between groups.

These data suggest major differences in BMD between two Hispanic American subgroups and in comparison to the standard Caucasian database. The data also suggest that a single Hispanic American referent database may not be applicable to all Hispanic American women. How these differences relate to fracture risk among different Hispanic American groups is an important next investigative step.

Disclosures: M.D. Walker, None.

T284

Comparison of pQCT-based Measures of Radial Bone Geometry and Apparent Trabecular Structure Acquired Using Different Algorithms. N. J. MacIntyre*, D. Inglis². ¹School of Rehabilitation Science, McMaster University, Hamilton, ON, Canada, ²Department of Civil Engineering, McMaster University, Hamilton, ON, Canada.

The purpose of this study was to compare methods of analyzing peripheral quantitative computed tomography (pQCT) images using different software and/or algorithms aimed at evaluating similar bone characteristics in the distal radius. The sensitivity of variables to changes in positioning in the region of the 4% site was also assessed.

Seven left cadaveric forearms (mean age (SD) 74.13 (7.09) y) were imaged at 0.5 mm intervals around the 4% site using pQCT (10 slices, 0.2 mm × 0.2 mm, 2.5 mm thick; Stratec XCT2000L). We analyzed the images for total and cortical cross-sectional areas (B.Ar, Ct.Ar), mean cortical thickness (Ct.Th) and its variation in terms of SD using both commercial software (Stratec v6.00 B) and an in-house developed program (pQCT Pro). pQCT Pro not only quantifies a variety of bone geometry variables, but also provides estimates of apparent trabecular structure, including number (App.Tb.N), thickness (App.Tb.Th) and spacing (App.Tb.Sp) using two different stereological approaches: the parallel plate model and mean intercept length (MIL) analysis. Measures of similar bone characteristics (mean values for 10 slices) were compared using Bland Altman plots and the absolute mean differences were expressed as percentages. We assessed the effect of slice position using one-way repeated measures ANOVA ($p < 0.05$).

The percent difference in measures varied from 3.5% (B.Ar) to 64.7% (App.Tb.Sp). As the mean value for App.Tb.Sp increased, the difference between the measures increased. The other measures did not differ systematically. Comparable methods produced mean values that ranked the seven specimens similarly with few exceptions (Ct.Th, specimen 3; App.Tb.Th, specimen 7; App.Tb.N, specimens 1, 3, 5, 6).

Measurements of B.Ar at the 4% site differed from those acquired more than 0.5 mm proximal and all more distal positions ($p < 0.001$). Ct.Ar at the 4% site differed only from positions that were at least 2 mm more proximal or distal ($p < 0.001$). Parallel plate model measurements of App.Tb.Sp at the 4% site differed from those 2 mm more proximal ($p < 0.02$). For the other variables, positioning did not have a significant effect.

Excellent agreement in B.Ar measures was observed. Differences between the other measures reflect differences in the algorithms used to derive them and these differences need to be considered when selecting outcome measures. Parallel plate derived measures are more influenced by anatomic variation than MIL based measures of apparent structure which makes the latter measure more desirable for cross sectional study designs. With the exception of B.Ar, measures acquired within 2 mm of the 4% site are consistent.

Disclosures: D. Inglis, None.

This study received funding from: NSERC RGPIN (NJM).

T285

Longitudinal Change in Bone Strength Indices: The Framingham Study. S. Menn, Y. H. Hsu, D. P. Kiel, D. Karasik. IFAR, Hebrew SeniorLife, Boston, MA, USA.

Bone strength is a valid predictor of bone's ability to resist fracture. Metacarpal bones have been routinely measured in previous research studies to predict fractures and quantify bone loss. Since change in metacarpal bones geometry over time may characterize the other long bones in the body, we evaluated effect of age, height and weight, as well as change in height and weight over a time interval of 22.5 ± 0.8 yrs on change in radiographic metacarpal Bone Strength Indices (BSIs).

Convenience sample of digitized hand x-rays (208 out of ~800) participants of the Framingham Study Original cohort (54±5 yrs old at baseline, BL), was used. At both BL (1967-1970) and follow-up, FU (1992-1994), the following indices as well as changes in them, Δ, were measured at the midshaft: Metacarpal Cortical Index (MCI), Cortical Thickness (MCT), and Section Modulus (MZ). Second (Met2) and third (Met3) metacarpals were studied.

All analyses were done by gender. We calculated correlation coefficients between ΔBSIs and BL age, height, weight, Δheight, and Δweight. Subsequently, we performed regression analysis to estimate effect of the above variables on ΔBSIs over time.

In final analysis, 79 men and 129 women were included. Changes in Met2 and Met3 BSIs were normally distributed and evident in both sexes, ranging from -45.6 to 38.5% in men and -63.6 to 42.4% in women.

In Met2, age at BL significantly negatively correlated with ΔMCI and ΔMCT in women only ($r = -0.25$ to -0.29 , $p < 0.005$). Height on BL significantly negatively correlated with ΔMCI and ΔMCT in men, while weight on BL and Δheight correlated with ΔMZ in women. Δweight positively correlated with ΔMCI, ΔMCT, and ΔMZ of both Met2 and Met3 in women ($r = 0.17$ to 0.24 , $p < 0.05$).

In regression analyses of Δheight and Δweight (with BL age, height, and weight in the same model), BL weight and Δheight were marginally significant predictors of Met2 ΔMCI in men, whereas in women, BL weight, height and Δheight predicted Met2 ΔMZ (beta = -1.17, 8.74 and 26.20, $p < 0.05$). In women, Δweight was significant predictor of both Met2 and Met3 ΔMCI and ΔMCT (beta = 0.07 to 0.11, $p < 0.05$).

In conclusion, in this pilot study, change in metacarpal bone geometry and strength was observed over an interval of 22 yrs, mostly in women. There was a wide range of changes with age, from loss to gain of bone strength indices. Weight and height at baseline, as well as change in weight and height, predicted the longitudinal change in BSIs in women, less strongly in men. Age-related change in metacarpal bone strength indices may reflect general behavior of long bones.

Disclosures: D. Karasik, None.

This study received funding from: NIAMS/NIA.

T286

Correlations Between HR-pQCT & High-Field MR In Vivo Bone Imaging. G. J. Kazakia¹, B. Hyun¹, A. Burghardt¹, R. Krug¹, D. Newitt¹, A. DePapp², T. Link¹, S. Majumdar¹. ¹Radiology, UC San Francisco, San Francisco, CA, USA, ²Merck & Co., Inc., Bryn Mawr, PA, USA.

The purpose of this study was to compare bone structural measures obtained via high-resolution peripheral QCT (HR-pQCT) to those obtained by high-field MRI in a cohort of post-menopausal females enrolled in a longitudinal pilot study comparing the effects of alendronate to placebo on bone microarchitecture.

Fifty-two early post-menopausal women classified as osteopenic by lumbar and/or hip DXA T-score underwent HR-pQCT (XtremeCT, Scanco Medical AG) and MR imaging of the distal radius and tibia. For HR-pQCT imaging a 9 mm axial length was imaged, with isotropic 82 micron voxels. Bone volume fraction (BV/TV) was derived assuming a density of 1200 mg HA/cc for mineralized bone. The 3D distance transform (DT) method was used to assess trabecular number (Tb.N). Following cortical segmentation using a Gaussian blur and a fixed intensity threshold, cortical thickness (Ct.Th) was calculated as the cortical volume divided by the periosteal area.

MR imaging was performed at 3 Tesla (GE Medical) using a balanced steady state free precession sequence. Spatial resolution of the resulting images was 156 x 156 x 500 micron. Regions of interest corresponding to the HR-pQCT regions were used to calculate structural parameters. Each image was binarized using a global threshold, and BV/TV, apparent Tb.N and other structural parameters were calculated using 2D histomorphometric methods. Cortical boundaries were defined manually and Ct.Th was derived using the DT method.

Despite the distinct differences between analysis techniques, significant correlations between HR-pQCT and MR parameters were found. The correlation was strongest for Tb.N ($R^2 = 0.52$) and Ct.Th ($R^2 = 0.43$) and weaker for all other parameters. However, MR and HR-pQCT provide statistically different measures of structure parameters. BV/TV was significantly higher in the MR analyses (mean MR/pQCT = 3.2 radius; 3.9 tibia) while Tb.N was lower (mean MR/pQCT = 0.9 radius & tibia). Tb.Th and Tb.Sp values were therefore higher and lower, respectively, as calculated by MRI. MR analysis resulted in higher values of Ct.Th (mean MR/pQCT = 2.0 radius; 1.3 tibia). In terms of correlations with DXA measurements, significant relationships were found only between HR-pQCT parameters at the distal radius and radius T-score ($R^2 = 0.19-0.58$).

The XtremeCT system uses a unique density derived analysis technique, necessitating the careful investigation of relationships between HR-pQCT and MR measures. Our results demonstrate discrepancies in absolute values and moderate correlations between modalities, suggesting that differences in the analysis techniques must be taken into account when comparing and interpreting the results of these imaging modalities.

Disclosures: G.J. Kazakia, Merck & Co., Inc. 2.

This study received funding from: Merck & Co., Inc.

T287

High-Resolution CT Images Yield Accurate Microstructural Information if Processed by 3-D Extensions of Standard Histomorphometric Analysis or Fuzzy Segmentation Approaches. A. Krebs¹, C. Graeff¹, I. Frieling^{2,3}, B. Kurz³, W. Timm⁴, C. C. Glüer¹. ¹Med. Phys., Diagn. Radiology, UKSH, Kiel, Germany, ²Osteoporose-Praxis Neuer Wall, Hamburg, Germany, ³Anatomisches Institut, CAU, Kiel, Germany, ⁴Synarc, Hamburg, Germany.

In vivo assessment of trabecular bone microstructure is limited by image quality and radiation exposure. We investigated whether microstructural information can be accurately extracted from High Resolution CT (HRCT) images of human vertebrae.

Microstructural variables can be defined by 3-D adaptation of 2-D stereological methods used in histomorphometry. However, binarization of bone structures is affected by image resolution and image noise. Fuzzy segmentation approaches may overcome these limitations. For bone voxels exceeding a minimum gray level, a minimal weighted distance to the bone marrow background, named fuzzy distance, is calculated as measure of local thickness. A complementary process based on the marrow phase yields a measure of trabecular separation. Both the stereologic and the fuzzy methods were implemented on StructuralInsight, our imaging software developed in house and yield estimates of microstructural variables, defined analogously to histomorphometry, including bone volume fraction (BV/TV), trabecular thickness (Tb.Th), and trabecular separation (Tb.Sp).

16 vertebral biopsies of 8mm diameter (Set 1, training) and 8 whole vertebrae (Set 2, validation) embedded in PMMA were measured by HRCT (Siemens Somatom 16, 120 kV, 360 mAs, pixel size 156 x 156 μm^2 , slice thickness 400 μm) inside a CIRS abdomen phantom to emulate in vivo conditions. Reference measurements on micro-CT systems were obtained on a Scanco $\mu\text{CT}40$ (voxel size 24 μm^3) for Set 1 and a Scanco Xtreme CT (voxel size 82 μm^3) for Set 2.

The table lists residual root-means-square (RMS) errors (in% of the reference mean) and coefficients of determination for regression of reference systems against HRCT.

Reference results [mean \pm SD(in mm, %)]		BV/TV 0.08 \pm 0.02 (26%)	Tb.Th 0.12 \pm 0.02 (17%)	Tb.Sp 0.94 \pm 0.13 (14%)
Set 1	Stereol.	19%, $r^2=0.48$	13%, $r^2=0.45$	13%, $r^2=0.20$
	Fuzzy	16%, $r^2=0.61$	11%, $r^2=0.63$	9%, $r^2=0.61$
Reference results [mean \pm SD(in mm, %)]		BV/TV 0.33 \pm 0.08 (25%)	Tb.Th 0.37 \pm 0.04 (12%)	Tb.Sp 0.79 \pm 0.21 (27%)
Set 2	Stereol.	17%, $r^2=0.58$	8%, $r^2=0.66$	20%, $r^2=0.55$
	Fuzzy	21%, $r^2=0.40$	5%, $r^2=0.88$	21%, $r^2=0.49$

Both methods estimate structural variables with RMS-errors substantially smaller than the sample SD, demonstrating that microstructural information could be extracted from the HRCT images with acceptable residual accuracy errors of 5-21% under in vivo like conditions. HRCT has value for the assessment of vertebral microstructure in patients.

Disclosures: A. Krebs, None.

This study received funding from: Synarc.

T288

Hip Structural Geometry and Incidence of Osteoporotic Fractures in the Women's Health Initiative-Bone Mineral Density (WHI-BMD) Cohort. A. Z. LaCroix¹, Z. Chen², D. Sherrill^{3,4}, T. Beck³, J. Cauley⁴, C. E. Lewis⁵, R. Jackson⁶. ¹Public Health Sciences, Fred Hutchinson Cancer Research Center, Seattle, WA, USA, ²University of Arizona, Tucson, AZ, USA, ³Johns Hopkins University, Baltimore, MD, USA, ⁴University of Pittsburgh, Pittsburgh, PA, USA, ⁵University of Alabama, Birmingham, AL, USA, ⁶Ohio State University, Columbus, OH, USA.

While the relationship between bone mineral density (BMD) as measured by dual-energy x-ray absorptiometry (DXA) and risk of hip and osteoporotic fractures is well established, much less is known about how the amount and distribution of underlying bone tissue relate to fracture. We studied 10,432 postmenopausal women ages 50-79 at baseline enrolled in the WHI Observational Study or Clinical Trial who had a hip BMD scan by DXA at baseline at one of three WHI clinical centers in Pittsburgh, PA, Tucson, AZ, or Birmingham, AL. The hip DXA scans were analyzed using a validated program developed by T. Beck which yielded the following measurements for this analysis: section moduli at the narrow neck and proximal shaft (cm^3); Buckling ratios at the narrow neck; and shaft (dimensionless). For each of these parameters measured at baseline, time to first fracture was studied using Cox Proportional Hazards models adjusting for age, ethnicity, history of falls, hip BMD and hormone therapy intervention. All fractures were physician-adjudicated at the local clinical centers and hip fractures were also centrally reviewed and adjudicated. During an average follow-up time of 8 years, 1599 clinical fractures occurred with 161 of these at the hip. Hazard ratios (HRs) are expressed for a 1 standard deviation change in each parameter. HRs for all four parameters indicated associations with increased risk of hip fracture, which were statistically significant for three out of four measurements. The strongest association was seen for section modulus at the shaft (HR=1.79; 95% CI 1.43-2.24), whereas the other HRs were in the range of 1.2-1.3. Hazard ratios were lower for prediction of total fracture, ranging from 1.0-1.2, but still statistically significant for all except for the section modulus at the narrow neck. These results show that geometric measurements of hip bone strength predict future hip fracture even after adjustment for hip BMD. An interesting result is that the direction of the effect of section modulus is reversed after adjustment for hip BMD, such that a higher bending resistance is associated with greater fracture risk for a given BMD level. The theoretical reasons for the change in the direction of the effect on risk will be presented.

Disclosures: A.Z. LaCroix, None.

T289

The Spinal Curvature Irregularity Index Discriminates Hip Fractures: Comparison with Femur BMD. G. Maalouf¹, R. Zebaze², N. Maalouf³, S. Maalouf⁴, A. Nehme⁵, Z. Tannous⁶, J. Wehbe⁷, G. Adib⁸, M. Gannagé-Yared⁹, E. Seeman². ¹St George Hospital, Beirut, Lebanon, ²Austin Hospital, U. Melbourne, Melbourne, Australia, ³U Texas Southwestern Medical Center, Dallas, TX, USA, ⁴General Company for Technical Services, Beirut, Lebanon, ⁵Italian Hospital, Damascus, Syrian Arab Republic, ⁶Hotel Dieu de France, Beirut, Lebanon.

Vertebral and hip fractures (fx) are common consequences of osteoporosis. The Spinal Curvature Irregularity Index (SCII) gives a quantitative estimate of the regularity of spinal curvature that is a robust, simple, and independent indicator of the presence of vertebral fx. SCII is calculated by comparing the ratio of the anterior to the posterior vertebral heights of one vertebra to that of adjacent vertebrae throughout the thoracolumbar spine (T4-L4). SCII is the integrated average of these calculations for all pairs of adjacent vertebrae in an individual. A perfectly regular spine has an SCII of zero percent.

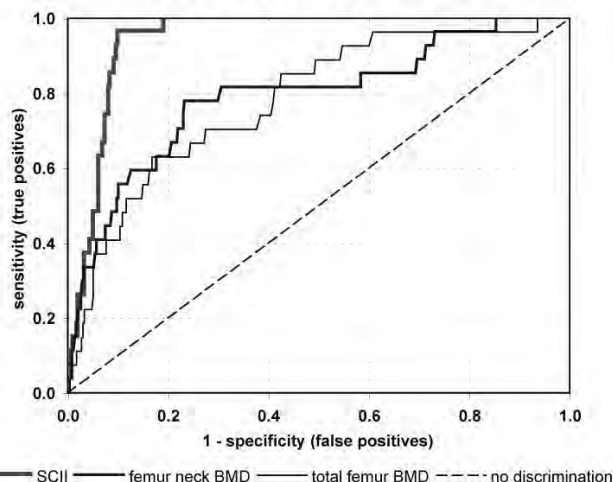
We compared the ability of SCII to discriminate between patients with and without hip fx. Vertebral heights from the Vertebral Fracture Assessment application, and spine and femur bone mineral density (BMD) values, were measured with a Lunar Prodigy (GE Healthcare) in 420 Lebanese women (age 22 - 89 years, total femur (TF) BMD 0.446 - 1.305 g/cm^2). 27 subjects had previous hip fx; 393 subjects without hip fx served as controls. The average SCII was 14.6% (SD=4.1%) for hip fx cases and 7.5% (SD=3.4%) in controls. ROC analysis tested the ability of SCII, L1-L4 spine BMD, TF BMD, femur neck (FN) BMD, hip axis length (HAL) and Femur Strength Index (FSI) to discriminate between hip fx and control subjects. SCII was the strongest discriminator (AUC=0.941) and was superior to FN BMD ($p=0.0023$). An SCII cut-point of 11.2 yielded 90% sensitivity and specificity in identification of hip fx subjects. We conclude that SCII in this population discriminated between subjects with and without hip fx better than FN and TF BMD.

References: Zebaze RM, JBMR 2004 19(7); Zebaze RM, Bone 2004 35(2); Maalouf G, Osteoporos Int 2007 8(3)

ROC Analysis: Area under the curve (AUC)

Predictor	AUC	SE	95% CI	P-value
SCII	0.941	0.0121	0.918-0.965	<0.0001
FN BMD	0.789	0.0504	0.690-0.887	<0.0001
TF BMD	0.780	0.0455	0.691-0.870	<0.0001
FSI	0.676	0.0477	0.583-0.770	0.0001
HAL	0.635	0.0504	0.536-0.734	0.0037
Spine BMD	0.557	0.0606	0.438-0.676	0.17

ROC for Hip Fracture Discrimination



Disclosures: G. Maalouf, None.

T290

Model Effects in the Ovariectomized Rhesus Monkey as Measured with pQCT. P. J. McCracken¹, R. Y. Jayakar¹, L. T. Duong², R. Hargreaves³, T. N. Hangartner³, D. S. Williams¹. ¹Imaging Department, Merck Research Laboratories, West Point, PA, USA, ²Department of Molecular Endocrinology, Merck Research Laboratories, West Point, PA, USA, ³Department of Biomedical, Industrial and Human Factors Engineering, Wright State University, Dayton, OH, USA.

Preclinical evaluation of disease burden and treatment efficacy is critical to the development of new therapies for osteoporosis. Clinically translatable imaging modalities beyond DEXA, such as pQCT and hrMRI, give us the advantage of studying in-vivo macro- and micro-architectural parameters relevant to bone strength. We have quantified pQCT endpoints of the ovariectomized (OVX) rhesus monkey as compared to intact

animals to examine potential technological and model-based measurement limitations. pQCT (XtremeCT, Scanco Medical) of the distal radius, one-third radius, distal tibia, and one-third tibia in OVX and intact monkeys (n = 10/group, aged 14-20 years) was performed at 12 months post-OVX to assess cortical and cancellous bone at the distal bone sites. BMD was also measured using a Hologic QDR Discovery DXA. With the midpoint of the distal endplate as reference, scanning started proximally at a distance of 2mm, 3mm, and 50-70mm for the distal radius, distal tibia, and one-third proximal locations, respectively, with the slice pack for 1/3 locations chosen according to the length of the shaft. Both model-derived and direct measurements in each relevant site included Cortical Thickness (CtTh), Bone Volume Fraction (BVf), Trabecular Number (TbN), Trabecular Thickness (TbTh), Trabecular Separation (TbSp), Structure Model Index (SMI), Total Density (D100) and Cortical Density (Dcomp). After precalibration and scout imaging at each location, anesthetized animals were scanned using: 9mm slice pack, 220 slices, 1500 projections, 3072 points per projection, 3000x3000 matrix, 200 ms integration time, 40 μ m voxel size, 8.3 min measurement time. Total imaging time was under 40 minutes. The data were reconstructed at a 100 μ m voxel size and processed using the manufacturer's 'clinical' and 'research' analysis protocols. One animal was scanned ten times per site to quantify test-retest variability. Results showed significant differences in radial and tibial BVf (-8%, -13%), 1/3 CtTh (-25%, -37%), and Dcomp (-4.5%, -6%) between the OVX and intact groups. There were trends in measures of TbTh, CtTh, TbSp and TbN consistent with the estrogen deficient model, and test-retest variability estimates indicated adequate precision for monitoring longitudinal changes. Density measurements by DEXA correlated with comparable XCT measurements. Our quantification of the results of OVX in rhesus monkeys as measured with pQCT encourages its further investigation in disease-modifying therapies.

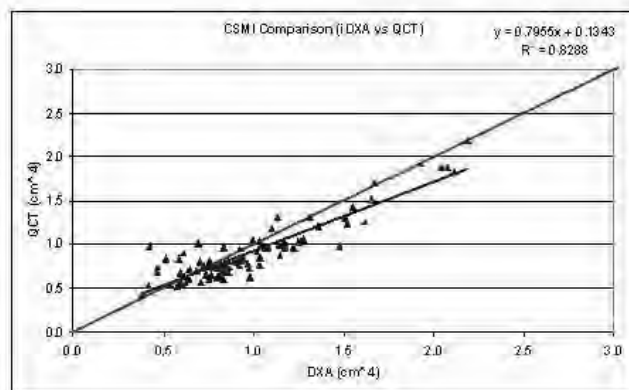
Disclosures: P.J. McCracken, Merck Research Laboratories 3.

T291

DXA and QCT Geometric Structural Measurements of Proximal Femoral Strength. C. Muschitz¹, L. Milassin^{*1}, T. Pirker^{*1}, R. Waneck^{*2}, H. Resch^{*1}.

¹Medical Department II, St. Vincent Hospital, Vienna, Austria, ²Department of Radiology, St. Vincent Hospital, Vienna, Austria.

Hip fracture results mainly from loss of femoral strength associated with aging. Femoral strength is a function of bone mineral density (BMD) and distribution of bone mass in the proximal femur. Geometric measurements known to relate to femoral strength and fracture risk include cross-sectional moment of inertia (CSMI), cross-sectional area (CSA) and hip axis length (HAL). BMD contributes only half the variation in strength estimated by CSMI, indicating that CSMI contributes additional information (Yoshikawa 1994). These variables are measured with both dual-energy X-ray absorptiometry and quantitative computed tomography (QCT). We measured 93 Caucasian clinic patients from 37-91 years of age (mean 67.6 yrs; SD 11.97) with femur BMD 0.452-1.171 g/cm² (mean 0.795 g/cm²). We compared DXA (Lunar iDXA, software version 11.2, GE Healthcare) measurements with CT (Phillips MX8000 4-slice CT, 3.2mm slices). The iDXA automatically measures CSMI as the minimum CSMI in the neck region of interest (ROI), and CSA of the minimum CSMI line in the neck ROI. These are often found in narrowest section of the neck, but may occur further up the neck due to individual variation in location of center of mass. We used a commercial QCT application (QCT PRO version 4.1, Mindways Software Inc) that generated measurements from cross-sectional images at the narrowest portion of the femoral neck to most closely duplicate the DXA measurement site. QCT values were adjusted by the ratio of DXA/QCT reference for average density of bone (1.85/1.05 g/cm³). Results showed high correlations for CSMI (r 0.91) and CSA (r 0.87), although the reported values were not equal, possibly due to different measurement location. HAL was highly correlated (r=0.94) with a slope not significantly different from identity. Femoral neck BMD values were also highly correlated (r=0.91). We conclude that structural measurements made at the femoral neck with DXA were highly correlated with similar QCT measurements.



CSMI DXA vs QCT

CSMI (cm ⁴)	CSMI (QCT) = 0.7955 CSMI (DXA) + 0.1343	0.1414	0.91
CSA (cm ²)	CSA (QCT) = 0.8032 CSA (DXA) + 0.0790	0.1210	0.87
HAL (mm)	HAL (QCT) = 0.9957 HAL (DXA) + 4.1492	2.8522	0.94
Femur Neck BMD (g/cm ³)	BMD (QCT) = 0.8551 BMD (DXA) - 0.0837	0.0486	0.91

Disclosures: C. Muschitz, None.

T292

MRI-based Measurement of Vertebral Shape in Japanese Women. T. Nakano^{*1}, A. Harada², H. Hagino³. ¹Department of Orthopaedic Surgery, Tamana Central Hospital, Kumamoto, Japan, ²Department of Restorative Medicine, National Center for Geriatrics and Gerontology, Aichi, Japan, ³Rehabilitation Division, Tottori University Hospital Faculty of Medicine, Tottori University, Tottori, Japan.

We propose the cutoff values for diagnosing a previous vertebral fracture by determining the dimensions of the normal vertebral body, as expressed by the anterior-posterior (A/P) ratio, central-posterior (C/P) ratio, and other indices. The subjects were 56 female volunteers, and their age distribution was as follows: 20-29 years (n=13), 30-39 years (n=14), 40-49 years (n=15), and 50-59 years (n=14). T1-weighted magnetic resonance imaging (MRI) scan of 14 vertebral bodies from T4 to L5 revealed that measured values of L4 and L5 were remarkably different from those of the remaining vertebral bodies. No age-related tendency was observed. The A/P ratios obtained from images of the thoracic and upper lumbar spine were below 1.00, showing a slight wedge or rectangular deformity. The A/P ratios obtained from images of the lower lumbar spine exceed 1.0 with an inverse wedge deformity. Few differences were found in C/P ratios obtained from images of the parts from the upper thoracic spine to the upper lumbar spine. The levels of -3.0 SD of the A/P and C/P ratios of the parts from T4 to L3 were 0.82 and 0.79, respectively, therefore it is reasonable that the A/P ratio below 80% and the C/P ratio below 75% are considered as the cutoff values for diagnosing a vertebral fracture based on vertebral body measurement from T4 to L3.

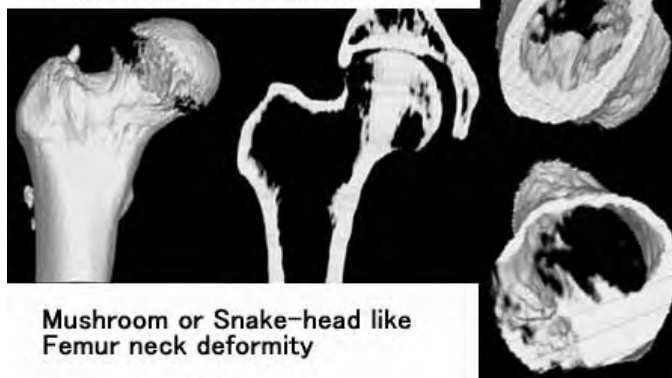
Disclosures: T. Nakano, None.

T293

Sclerosis of the Principal Medial Compressive Trabeculae in the Osteoporotic Femur May Mask The Bone Mineral Loss of the Femoral Cortex. S. Okamoto¹, H. Noguchi^{*2}, H. Suzuki^{*3}, N. Ohtsu^{*1}, T. Okamoto^{*1}, S. Okamoto^{*4}, A. Itabashi⁵. ¹SORF Okamoto Clinic, Oita, Japan, ²Noguchi Thyroid Clinic and Hospital Foundation, Beppu, Japan, ³Suzuki Orthodontic Office, Nagasaki, Japan, ⁴KS Okamoto Clinic, Shimabara, Japan, ⁵Saitama Center of Bone Research, Saitama, Japan.

We have examined three dimensional CT of the osteoporotic femurs and found substantial mineral loss in the femur cortex in the neck region. Meanwhile, there was significant sclerosis in the principal medial compressive trabeculae extending from the femoral head to the medial cortex of the femur. This gross rearrangement of bone structure may be a risk factor for femur fracture and may serve to explain the lack of correlation between femur neck BMD and bone fracture frequency. Femur neck BMD is said to be the parameter of osteoporosis most responsive to therapy, yet is more variable than trochanter or total femur BMD. In some cases, neck BMD rises or drops in ways that conflict with the direction of the systemic bone mineral loss or gain. This paradoxical behavior may in part be explained by the increasing sclerosis of the principal compression trabeculae of the femur that progresses in tandem with the thinning of the femoral cortex. Radiological measurements may pick up the increased density of the principal compression trabeculae and present a falsely high value of the weakened femur. To test this theory, TV-X ray fluoroscopy with the postural adjustment was performed in 134 normal volunteers and 2600 female osteoporosis patients. Lumbar and Femur BMD were measured (QDR 4500 or Discovery, Hologic) and PQCT of the radius (Stratec) was assessed in all patients. 3-D figures of bilateral femurs were performed by Helical CT (Asteion Super 4 edition Toshiba) analysis in 55 cases. We found a number of cases where femur neck BMD did not correlate with trochanter and total femur BMD and observed gross increase in the density of the principle compression trabeculae. This change in bone structure may be the result of adaptation of the trabeculae to increased load due to the weakened cortex. A collection of cases will be presented.

Over-adaptation of principal compressive trabeculae.



Disclosures: S. Okamoto, None.

T294

Regional Thinning of Cortical Bone in the Femoral Neck with Age: Interim Analysis of a Study of Women from the Second to the Eighth Decade. K. Poole¹, C. Rose²*, S. Kaptoge¹, K. Brown², N. Loveridge¹, P. Bearcroft²*, J. Reeve¹. ¹Clinical School, University of Cambridge, Cambridge, United Kingdom, ²Mindways Software, Austin, TX, USA.

In the superoposterior (SP) region of the female femoral neck, cortical thinning occurred at 10% per decade in a post mortem study (Mayhew et al Lancet 366:129 2005). This may be sufficient that elderly hips fracture in a sideways fall through local cortical buckling, when SP suffers the hip's maximal loading. Improved estimation of risk would then require estimation of cortical thickness (C.Th), measurable with whole body Computed Tomography (WCT) but not DXA. Women were recruited aged 20 to 80 (IQR 39-65) to investigate C.Th using Siemens 64 WCT and Mindways software (v4.1.3). They were a sample of 56 healthy volunteers attending for routine clinical WCT scans including the pelvis (exclusions; corticosteroid use, carcinomatosis), and they consented to a slightly caudal extension to include both hips (1mm slice thickness, 0.59 mm pixel size). Bone architecture was assessed using a contour-tracking algorithm after automatic calibration of greyscale CT images to BMD equivalents (using a K2HPO4 phantom). A single cross-section of the femoral neck was automatically extracted at a reproducible location (ratio of 1.4:1 'in plane' to 'out of plane' diameter) for analysis of regional C.Th. in octants defined using the centre of mineral mass and principle axes. Combining octants resulted in four anatomical quadrants; SP, supero-anterior, infero-posterior and infero-anterior. Overall intra-operator CV (6 subjects measured twice) was 5.85% and was independent of subject age (p=0.1), octant (p=0.6) and any interaction between the two (p=0.6). There were no differences in C.Th between right and left hips so the data were measured for the analysis. Longitudinal drift by phantom measurement was <2%. In the SP quadrant, there was a marked decline with advancing age, amounting to loss in thickness of nearly 60% between the age of 20 and 80. The superior quadrants were better fitted log-linearly and age accounted for 60% of the variance in cortical thickness at SP. The exponential rate was highest at SP, more than two-fold more than that in the inferior quadrants. Ageing was associated with relatively much faster thinning of the SP cortex of the femoral neck than BMD decline, confirming Mayhew's results. Local femoral neck cortical thickness can be quite reliably estimated in vivo by WCT. Better-than-DXA estimation of hip fracture risk might be achievable using whole body CT and calibrated measurement of proximal femur geometry.

Disclosures: K. Poole, None.

This study received funding from: UK Medical Research Council plus provision of reduced price software and free upgrades from Mindways.

T295

Laws' Masks Descriptors Applied to Bone Texture Analysis: An Innovative and Discriminant Tool. M. Rachidi¹*, A. Marchadier¹*, C. Gadois²*, E. Lespessailles³, C. Benhamou¹, C. Chappard¹. ¹Inserm u 658, CHR Orleans, Orleans, France, ²D3A, Orleans, France, ³CHR Orleans, Orleans, France.

Bone micro-architecture evaluation in vivo is not largely available at present. A few techniques of texture analysis were developed to assess trabecular bone micro-architecture. Laws' masks are known as one of the best methods for texture analysis in image processing, and are used in various applications, but not in bone tissue characterization. This method is based on masks aiming to filter image. From each mask, five parameters can be calculated namely Mean, Standard Deviation, Skewness, Kurtosis and Energy. The objective of this study was to explore a new method of texture analysis to characterize bone micro-architecture.

This study was performed on 182 healthy post menopausal women with no fracture and 114 age-matched women with fractures (26 Hip fractures (HF), 29 vertebrae (VF), 29 wrist (WF) and 30 other fractures (OF)). For all subjects the radiographs were obtained on calcaneus using a new high resolution X-ray device with direct digitisation (BMATM, D3A[®] France). The lumbar spine, femoral neck, and total hip BMD were assessed by DXA.

In terms of reproducibility, the best results were obtained with E5E5 mask especially for two parameters: "Mean" and "Standard Deviation" with respectively in vitro RMSCV%=1.0 and 1.5%, in vivo short term RMSCV%= 2.0 and 3.6, and mid term RMSCV%= 1.8 and 4.2. The Mean parameter had a better reproducibility but Standard Deviation had a better discriminant power (cf table).

After multivariate analysis with adjustment for age and total hip BMD, for "Standard Deviation" parameter the difference remained statistically significant between Control group versus HF and VF groups (p<5.10⁻³, and p=4.10⁻² respectively).

No significant correlation between these two Laws' masks parameters and BMD measured at different sites was obtained. The data suggest that this analysis can be useful for assessing fracture risk independently from BMD. Thus, Laws' masks may constitute one of the best methods for bone texture analysis.

Mask E5E5 Controls	Parameter "Mean" 0.693 ± 0.102	Parameter "Standard Deviation" 0.112 ± 0.016
HF	0.629 ± 0.115 (p=0.003)	0.095 ± 0.017 (p<10 ⁻³)
VF	0.669 ± 0.122 NS	0.105 ± 0.017 (p=0.02)
WF	0.702 ± 0.097 NS	0.113 ± 0.017 NS
OF	0.670 ± 0.111 NS	0.105 ± 0.018 (p<10 ⁻³)

Disclosures: M. Rachidi, None.

T296

Iliac Cortical Bone Structure in Osteoporotic Women. S. Bare¹*, K. McCon²*, R. Recker¹, D. B. Kimmel². ¹Osteoporosis Research Center, Creighton University, Omaha, NE, USA, ²Molecular Endo and Bone Biology, Merck Research Laboratories, West Point, PA, USA.

Evaluation of small features in cortical bone of living humans is limited by the available biopsy sites. An intact transiliac biopsy specimen (TIBx) has two cortices around a trabecular area. Our purpose is to use TIBxs to study cortical thickness (Ct.Th), cortical porosity (Ct.Po), and pore diameter (Po.D) of osteoporotic women.

TIBxs (7.5mm diameter) were obtained via a lateral approach from 42 untreated post-menopausal osteoporotic women (T-score<-1.8; age 69±6yrs, range 60-85yrs). 6µm sections from plastic-embedded TIBxs were stained with toluidine blue.

For each cortex, the endocortical surface (ES) was the boundary between trabecular and cortical bone. The distance from the ES to the periosteal surface (PS) was measured (6-7 sites) to find Ct.Th. Total cortical area (Ct.Ar) and pore area (Po.Ar) were measured. Pores were non-marrow containing voids in bone tissue between the ES and PS, with area >500µm². Ct.Po was Po.Ar/Ct.Ar. Po.D was calculated from Po.Ar and pore number.

32 TIBxs had two cortices. Cortices of each TIBx were grouped as "thick" or "thin." Thickness of the single cortex from the other ten was equal to the thick cortex from the 32; the ten were deemed "thick." Differences between the two cortices for Ct.Po and Po.D were tested (Mann-Whitney U). Pearson's correlation coefficient (r) was calculated among age, Ct.Po, Ct.Th, and Po.D.

Summary: The thick cortex is more porous with pores of larger diameter than the thin cortex (P<0.0001). More porous cortices have larger pores, rather than greater pore number. Cortices exhibit age-related thinning.

Conclusion: The interrelationships of cortical porosity with age and cortical thickness revealed in untreated post-menopausal osteoporotic women suggest that cortical porosity in the ilium, and perhaps at all anatomic sites, is a complex issue. Thick cortices are more porous than thin cortices, regardless of age. Techniques with resolution of 85-100µm may miss 30-50% of cortical pores. Approximately 70 additional TIBxs are under analysis.

Endpoint	Mean±SD	Range
Thick Cortex (mm)	0.82±0.31	0.32-1.48
Thin Cortex (mm)	0.46±0.19	0.20-1.01
Ct.Po (Thick) (mm)	5.38±3.39	1.40-12.84
Ct.Po (Thin) (mm)	2.67±1.48&	0.17-5.70
Po.D (Thick) (µm)	110±36	57-177
Po.D (Thin) (µm)	79±25&	39-142

&P<.0001 vs. Thick Cortex

Endpoint	Pearson's R		
	Age	Ct.Th	Ct.Po
Ct.Th	-0.399*	-	-
Ct.Po	0.013	0.385**	-
Po.D	0.049	0.248*	0.824&

*P<.05; **P<.001; &P<.0001 (N=74)

Disclosures: R. Recker, Merck 5; Roche 5.

This study received funding from: Merck.

T297

A Newly Developed Quantitative Ultrasound Scanner for the Proximal Femur: First Data of Hip Fracture Discrimination. R. Barkmann¹, S. Dencks¹*, P. Laugier²*, F. Padilla²*, C. Glüer¹. ¹Medizinische Physik, Diagnostische Radiologie, UKSH, Kiel, Germany, ²Laboratoire d'Imagerie Paramétrique, Université Paris, Paris, France.

Calcaneal Quantitative Ultrasound (QUS) has similar power as DXA for the prediction of osteoporotic fracture risk. However, femur DXA shows best performance in the prediction of hip fractures. We developed a QUS scanner for the proximal femur (femur ultrasound scanner, "FEMUS") and present first results of the power of this new method to discriminate between women with and without hip fractures.

Patients who had visited the traumatology for surgery after osteoporotic hip fracture within the last half year were asked to participate in the study. Controls without hip fractures were recruited from the OPUS study. The study was approved by the local ethical committee and informed consent was given. Fracture patients were older (78 ± 6 vs. 72 ± 10 years) and had lower weight (62 ± 7 vs. 68 ± 17 kg), however, differences were not significant. Height did not differ between groups (1.60 ± 0.05 m). All participants were measured using DXA and the FEMUS. QUS signal transmission through the center of the greater trochanter was evaluated and QUS variables SOS and BUA were calculated. SOS was adjusted for variations in hip width using transit times of signals reflected from both anterior and posterior surfaces of the hip. Correlations of QUS variables with trochanteric and total hip BMD were calculated. The ability of discriminating between women with recently fractured hips and controls without fractures was calculated for QUS and DXA using logistic regression analysis and expressed as standardized odd's ratios, per one SD decrease of population variance, adjusted for age (confidence intervals in brackets).

Both SOS and BUA correlated significantly with trochanteric BMD (SOS: R²=0.66, p<0.0001, BUA: R²=0.54, p<0.001) and total BMD (SOS: R²=0.59, p<0.0001, BUA: R²=0.36, p<0.01). Odd's ratios were 3.9 (2.0 - 7.6) for trochanteric BMD, 7.8 (2.9 - 20.7) for total BMD, 8.7 (3.3 - 22.8) for SOS and 2.2 (1.3 - 3.7) for BUA. Weight and height did not contribute significantly to any of these associations.

First measurements on patients using our new FEMUS device demonstrated similar power of QUS and BMD in the discrimination between women with and without fractures. Total hip BMD and SOS showed best performance. Femoral QUS might become an additional tool for osteoporosis assessment.

Disclosures: R. Barkmann, None.

T298

Associations Between Bone Mineral Density and Speed of Sound: Canadian Multicentre Osteoporosis Study. K. S. Davison¹, J. D. Adachi², D. A. Hanley³, J. P. Brown¹, W. P. Olszynski⁴, ¹U. of Laval, Quebec, PQ, Canada, ²McMaster U., Hamilton, ON, Canada, ³U. of Calgary, Calgary, AB, Canada, ⁴Saskatoon Osteo. Centre, Saskatoon, SK, Canada.

The objective of this investigation was to compare bone mineral density (BMD) attained from dual-energy x-ray absorptiometry (DXA) with speed of sound (SOS) data attained from a Sunlight Omnisense quantitative ultrasound (QUS) in a large sample of randomly-selected community-based individuals from the Canadian Multicentre Osteoporosis Study (CaMOS). In year 5 of CaMOS 4124 men and women were assessed by both DXA and QUS in one of six centres from CaMOS equipped with both instruments. BMD (g/cm²) was assessed at the lumbar spine (L1-4; LS), femoral neck (FN), total hip (TH), Ward's triangle (WT) and the greater trochanter (GT) by DXA. The DXAs were cross-calibrated among centres using a common phantom and a calibrated BMD was used for all analyses. SOS (m/s) was assessed at the distal radius (DR), tibia (TIB) and phalanx (PX) sites by Sunlight Omnisense QUS. Pearson product-moment correlations were performed between measures of BMD and SOS for men and women separately. Alpha was set at $p < 0.05$ for all analyses. In this subset of CaMOS data there were 2948 women and 1176 men included with a mean (SD) age of 66.5 (11.49) and 63.7 (13.04) years, respectively, and a range of 30-96 years of age. For the women, DR SOS was significantly ($p < 0.0001$) positively correlated with LS ($r = 0.24$), FN ($r = 0.29$), TH ($r = 0.28$), WT ($r = 0.36$), and GT ($r = 0.24$) BMD. TIB SOS was significantly ($p < 0.0001$) positively correlated with LS ($r = 0.21$), FN ($r = 0.20$), TH ($r = 0.20$), WT ($r = 0.25$), and GT ($r = 0.19$) BMD, and PX SOS was significantly ($p < 0.0001$) positively correlated with LS ($r = 0.24$), FN ($r = 0.29$), TH ($r = 0.27$), WT ($r = 0.31$), and GT ($r = 0.21$). For the men, DR SOS was significantly ($p < 0.05$) positively correlated with FN ($r = 0.08$), TH ($r = 0.07$), WT ($r = 0.14$), and GT ($r = 0.07$), but not LS ($r = 0.05$) BMD. TIB SOS was significantly ($p < 0.05$) positively correlated with BMD only at the LS ($r = 0.07$), FN ($r = 0.04$), TH ($r = 0.03$), WT ($r = 0.05$), and GT ($r = 0.03$). PX SOS was only significantly ($p < 0.05$) positively correlated with BMD at the FN ($r = 0.07$), TH ($r = 0.06$), and WT ($r = 0.09$); LS (0.003) and GT (0.02). Despite the differences in significance between the men and women for a number of comparisons, the greatest r^2 attained indicates that there is at best 13% of the variance shared between the measures; most associations were far weaker. While the power of this sample allowed for statistically significant results to be found between the methods it can be safely assumed that they are measuring different attributes of bone which may have important implications for fracture prediction that need to be further assessed with prospective trials, particularly with QUS.

Disclosures: K.S. Davison, None.

T299

Ultrasound and Dual-energy X-ray Absorptiometry Comparisons at the Distal Radius. S. Grzybowski¹, K. S. Davison², D. Hein¹, W. P. Olszynski¹. ¹Saskatoon Osteo. Centre, Saskatoon, SK, Canada, ²U. of Laval, Quebec, PQ, Canada.

The primary objective of this study was to determine how the speed of sound (SOS) at the distal radius using the Sunlight Omnisense Quantitative Ultrasound (QUS) correlates to the bone mineral density (BMD) of the distal radius using dual-energy x-ray absorptiometry (DXA). Sixty women were enrolled into the study in three different stratum levels with twenty participants in each strata: ages 20-40, 41-60 and 61-80 years. DXA BMD (g/cm²) measurements were performed at the ultra-distal (UD), mid-shaft (MID), one-third (OT) radius using the Hologic Delphi W. A composite total radius (TOT) BMD was also calculated for the three regions. QUS (m/s) measurements of the distal radius were performed using the Sunlight Omnisense. Measurements were performed on the left radius, however, if a patient had a previous fracture of the left radius, then the measurements were performed on the right. T-scores and z-scores were provided from both machines using manufacturer-specific databases. Pearson product-moment correlations were performed between DXA BMD and QUS SOS measures. Alpha was set at $p < 0.05$. The mean (SD) age of the women was 50.4 (17.2) years. Mean BMDs were 0.394 (0.08), 0.564 (0.08), 0.658 (0.11) and 0.543 (0.08) g/cm² at the UD, MID, OT and TOT sites, respectively. The mean SOS was 4113.2 (148.2) m/s. The mean t- and z-scores ranged from -0.38 to -0.57 and 0.22 to 0.62 for the DXA assessed-sites and -0.55 and 0.41 for QUS-assessed radius, respectively. SOS was significantly ($p < 0.01$) correlated with BMD measures from all four sites: UD $r = 0.40$, MID $r = 0.63$, OT $r = 0.62$, TOT $r = 0.63$. The correlations between SOS and BMD T-scores were also all significant ($p < 0.001$): UD $r = 0.53$, MID $r = 0.68$, OT $r = 0.73$ and TOT $r = 0.68$. Similar, yet weaker, correlations were seen with z-scores. These results suggest that at the distal radius 16-40% of the variance in SOS and BMD is shared. While this is a significant relationship the inverse needs to be also stressed in that 60-82% of the variance is not shared between these measures indicating that the majority of bone characteristics each machine is measuring are unique to one another.

Disclosures: S. Grzybowski, None.

T300

Bone Health of Vegans. H. J. Hinkley*, I. P. Drysdale. British College of Osteopathic Medicine, London, United Kingdom.

Public health strategies aimed at preventing osteoporosis through modifiable factors such as diet are currently under review. Vegans usually have a substantially lower calcium intake due to their lack of consumption of dairy products, unless they consume calcium-rich plant foods, which may result in lower bone mineral density and greater risk of osteoporosis. However, optimal acid/base balance may be a beneficial consequence of the

absence of dietary meat and fish protein due to the reduction in acid load, which results in decreased mobilization of bone mineral, which lowers excretion of calcium in the urine and preserves the integrity of bone despite lower calcium intakes. Therefore, it is unclear as to whether or not the bone health of vegans is better or worse than that of comparable omnivores. A pilot study recruited age-matched females (20 to 44 years) to assess calcaneal Broadband Ultrasound Attenuation (BUA; McCue CubaClinical), a measure of bone mineral density and structure of cancellous bone, in 60 vegans of mean body mass index (BMI) 23.1 (sd 5.9) kg/m² and compared this group with 110 female omnivores of mean BMI 22.0 (sd 2.7) kg/m². The hypothesis tested was that the vegan diet was not detrimental to bone health as assessed by calcaneal BUA. Data were analysed using t-test and multiple regression analysis. Despite the slightly lower mean BUA of the vegans, no significant difference was observed in BUA between vegans (78.3 (sd 16.5) db/MHz) and omnivores (82.2 (sd 16.8) db/MHz). However, these preliminary findings were potentially confounded by large inter-individual variability in both BUA and weight, found previously to influence BUA, and weight was also observed to be slightly higher (non-significant) in the vegans (vegans, 63.0 (sd 15.8) kg; omnivores, 60.1 (sd 8.1) kg). Therefore, BUA was adjusted for weight. However, no significant difference was observed between the groups. The mutually exclusive variables of vegan and non-vegan were entered stepwise with weight, height and age into a multiple regression model. The vegan category was found to be an independent significant predictor of BUA along with weight, but not height or age. In conclusion, the hypothesis that the vegan diet does not adversely affect bone health is supported in part, although slightly confounded, by the results of this cross-sectional study, possibly due to the large extent of biological variability (BUA measurement variability, in house CV 2.3%). This indicates that further work would be of value to establish potential longitudinal effects of the vegan diet and any mechanisms involved in maintaining a healthy balance in bone metabolism. On the basis of this pilot study, a larger study is currently being undertaken in which a number of indices of bone mineral density are assessed along with other measures of health in general.

Disclosures: H.J. Hinkley, None.

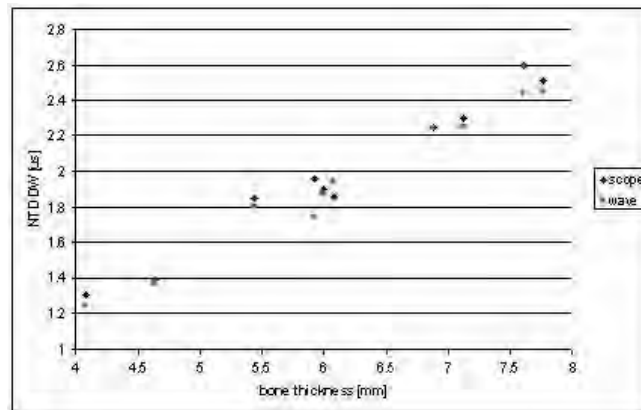
T301

A New Through-Transmission Approach for Ultrasonic Assessment of the Radius. J. J. Kaufman¹, G. Luo², R. S. Siffert². ¹CyberLogic, Inc., New York, NY, USA, ²Orthopedics, The Mount Sinai School of Medicine, New York, NY, USA.

The overall objective of this study was to develop a new ultrasonic system for estimating bone mineral density (BMD) at the forearm. Estimation of BMD is an important component in diagnosis and managing osteoporosis. The use of BMD is based on the well-established thesis that bone strength is strongly related to the amount of bone material present and that a stronger bone in a given individual is associated generally with a lower fracture risk. Radiological densitometry (e.g., DXA), which measures the BMD at a given site is currently the accepted indicator of fracture risk. Because of its expense, inconvenience, and associated x-ray exposure, ultrasound has been proposed as an alternative to DXA.

This study used both empirical ultrasound measurements and data generated in computer simulations. In vitro measurements were conducted on a set of 6 plastic rods, 7 plastic tubes, and 20 human radii. A 3.5 MHz source and receiver in a through-transmission configuration were used within a water tank, between which the plastic or bone samples were placed. The received waveform was stored for subsequent processing. A set of ultrasound simulations of analogous models was also carried out using a commercial software package (Wave2000 Pro, CyberLogic, Inc., NY).

The ultrasound data obtained from both the bench-top experiments and the computer simulations were processed to obtain an ultrasound parameter known as net time delay (NTD), associated with each sample. Results obtained show extremely close correspondence between the simulated and empirical results, validating the use of the software for further development. Moreover, the results obtained show correlations of NTD with overall rod, wall, or cortical thicknesses, respectively, of 0.99, 0.99, and 0.97. The figure below displays the results for ten of the radial bone specimens.



In conclusion, this study suggests that ultrasonic transmission measurements at the forearm may be a useful, simple, and radiation-free alternative to DXA for assessing bone mass and fracture risk.

Disclosures: J.J. Kaufman, CyberLogic, Inc. 3, 4, 5, 6.
This study received funding from: NIAMS of the NIH.

T302

Calcaneal Broadband Ultrasound Attenuation and Risk Factors for Osteoporotic Fractures in Postmenopausal South Asian and Caucasian Women. S. R. Mitra¹, P. Foster^{*1}, P. Judd^{*2}, B. Ellahi^{*3}, I. Bhojani^{*4}, J. F. McCann^{*5}, N. Lowe^{*1}. ¹Biological Sciences, University of Central Lancashire, Preston, United Kingdom, ²Lancashire School of Health and Postgraduate Medicine, University of Central Lancashire, Preston, United Kingdom, ³Biological Sciences, University of Chester, Chester, United Kingdom, ⁴Bangor Street Health Centre, Blackburn, Blackburn, United Kingdom, ⁵Medical Rehabilitation Centre, Royal Preston Hospital, Preston, United Kingdom.

Managing postmenopausal osteoporosis involves measuring bone mineral status and assessing clinical risk factors for osteoporotic fractures. Early onset of menopause, personal history of fracture after 50 and sedentary lifestyle are among the key risk factors. The purpose of this study was to investigate risk factors for osteoporotic fractures in postmenopausal South Asian compared to Caucasian women living in Blackburn, U.K.; using calcaneal broadband ultrasound attenuation (BUA) measurements and known or suspected risk factors.

BUA of the calcaneus was determined by contact ultrasound sonometry (McCue CUBA Clinical Ultrasonometer) in 76 South Asian women and 47 Caucasian women. Relevant life-style factors, including physical activity level were assessed in all the participants using an interviewer administered structured questionnaire.

The mean age of the South Asian and Caucasian participants was (mean±SEM) 55.9 y (±0.50) and 59.9 y (±0.53) respectively, with a BMI of 31.1 kg/m² (±0.63) for South Asians, significantly higher than the Caucasians at 28.0 kg/m² (±0.78) (p=0.002). The mean age of menopause was not significantly different in the two groups, 48.0y (±0.61) and 48.6y (±0.86), (p=0.55) respectively.

There was no significant difference in BUA measurements between the South Asian and Caucasian women (68.5 dB/MHz (±1.8) and 66.8 dB/MHz (±2.0) respectively). We classified 38.3% of Caucasians and 31.6% of the South Asians as 'at risk' for the development of osteoporosis (BUA T score ≤ -1.7) and 29.8% Caucasians and 26.3% South Asians as osteoporotic (BUA T score ≤ -2). A significant difference was observed in 'personal history of fracture above the age of 50', 12.8% of the Caucasians with this risk factor as compared to 2.6% of South Asians (p=0.05). There was significant positive correlation between current body weight and BUA in both groups, r=0.44, p=0.002 (Caucasian); r=0.31, p=0.006 (South Asian).

Analysis of our study data reveals that, South Asian and Caucasian women in this population have comparable calcaneal BUA scores. High BMI may have contributed to the maintenance of a healthy bone mass in both groups of women. We are currently investigating the role of vitamin D status and secondary hyperparathyroidism in the skeletal status of this population.

Disclosures: S.R. Mitra, None.

This study received funding from: The Lancashire Teaching Hospitals NHS Trust, Research Directorate, Seedcorn Funding.

T303

Canadian Normative Data for Sunlight Omnisense Quantitative Ultrasound: Canadian Multicentre Osteoporosis Study. W. P. Olszynski¹, J. P. Brown², J. D. Adachi³, D. A. Hanley⁴, K. S. Davison². ¹Saskatoon Osteo. Centre, Saskatoon, SK, Canada, ²U. of Laval, Quebec, PQ, Canada, ³McMaster U., Hamilton, ON, Canada, ⁴U. of Calgary, Calgary, AB, Canada.

The objective of this investigation was to generate a normative database of speed of sound (SOS) measures for Canadians as provided from Sunlight Omnisense quantitative ultrasound (QUS) in a large sample of randomly-selected community-based individuals from the Canadian Multicentre Osteoporosis Study (CaMOS). In year 5 of CaMOS 4124 men and women were assessed by QUS in one of six centres from CaMOS equipped with a Sunlight Omnisense QUS (Calgary, Halifax, Hamilton, Saskatoon, Ste-Foy, St. John's). SOS (m/s) was assessed at the distal radius (DR), tibia (TIB) and phalanx (PX) sites by Sunlight Omnisense QUS. For the normative data creation, data was separated for men and women and into age groups from 30-39y, 40-49y, 50-59y, 60-69y, 70-79y and 80+y and reported for each of the three sites investigated. The mean and standard deviation (SD) from both the men's and women's 30-39y group was used as the reference point and assigned a t-score of 0. The means of all other groups were then reported as a t-score based on these sex-specific reference values ((sex-specific 30-39y mean - mean for age group)/SD for 30-39y group)). In this subset of CaMOS data there were 2948 women and 1176 men included with a mean (SD) age of 66.5 (11.49) and 63.7 (13.04) years, respectively, and a range of 30-96 years of age. The mean (SD) SOS for the women at 30-39y of age was 4192 (111), 3877 (163), and 4005 (200) m/s at the DR, TIB and PX, respectively (n=87). The mean (SD) SOS for the men at 30-39y of age was 4137 (113), 3949 (135), and 3949 (181) m/s at the DR, TIB and PX, respectively (n=70).

T-scores for mean SOS of each age group (women:men)

Age Group (n)	DR t-score	TIB t-score	PX t-score
40-49 y (119:94)	-0.28:-0.47	0.29:0.01	-0.07:-0.12
50-59y (611:277)	-0.80:-0.36	-0.01:-0.10	-0.48:0.00
60-69 y (853:303)	-1.35:-0.54	-0.21:0.00	-0.98:-0.30
70-79y (981:334)	-1.98:-0.81	-0.43:-0.21	-1.54:-0.64
80+y (297:98)	-2.52:-0.98	-0.66:-0.43	-1.90:-1.03

The t-scores showed that there was a steady decline in SOS m/s for women with age at the DR and PX, with a slower decline at the TIB. A similar, yet smaller magnitude, trend was observed in the men. This relative preservation in TIB may be a consequence of greater

maintenance of load bearing on the legs as compared to the arms with aging. While there was a large overall pool of data to study the change of SOS in three sites over time, the sample size for the reference group needs to be larger to allow for a greater determination of the mean and particularly the SD, which has a large impact on t-scores.

Disclosures: W.P. Olszynski, None.

T304

Improved Standardization of Calcaneal Speed-of-Sound Measurements: Results in 73 Women. K. A. Wear^{*}. Center for Devices and Radiological Health, US Food and Drug Administration, Silver Spring, MD, USA.

Although calcaneal speed of sound (SOS) is an effective predictor of osteoporotic fracture risk, the SOS measurement exhibits substantial dependence on measurement system hardware and analysis algorithm software. Accordingly, improvement in standardization methods will be required before quantitative ultrasound can play a major role in clinical practice (C. C. Gluer, "Quantitative ultrasound: It is time to focus research efforts," Bone, 40, 9-13, 2006).

The purpose of this study was to develop and validate a method for reducing variability in calcaneal SOS measurements.

A compensation formula that corrects for the dependence of SOS measurements on center frequency, bandwidth, broadband ultrasound attenuation (BUA), and transit-time marker (e.g. zero-crossing) was derived. The formula predicts that variations in SOS measurements (i.e. deviations from group velocity) are approximately proportional to 1) BUA, and 2) the square of the fractional bandwidth of the ultrasound data acquisition system. To test the formula, SOS data from 73 women and from a bone-mimicking phantom were acquired using a GE Lunar Achilles Insight bone sonometer.

Compensation of SOS measurements using the formula reduced 1) average transit-time-marker-related SOS variability by 75% in 73 women and 2) bandwidth-related SOS variability by 80% in the bone-mimicking phantom. Transit-time-marker-related variations in SOS were found to decrease as the transit-time marker was moved toward the pulse center. Therefore, compared with other time-domain measures of SOS, group velocity (which is measured using the pulse center as a transit-time marker) exhibited the minimum system dependence.

This new method of compensating SOS measurements will enable a substantial improvement in consistency in bone sonometry.

The mention of commercial products, their sources, or their use in connection with material reported herein is not to be construed as either an actual or implied endorsement of such products by the Department of Health and Human Services.

Disclosures: K.A. Wear, None.

This study received funding from: FDA Office of Women's Health.

T305

Improved Accuracy of Broadband Ultrasound Attenuation Measurement Using Phase Insensitive Detection: Results in 73 Women. K. A. Wear^{*}. Center for Devices and Radiological Health, US Food and Drug Administration, Silver Spring, MD, USA.

Although calcaneal broadband ultrasound attenuation (BUA) is an effective predictor of osteoporotic fracture risk, the BUA measurement exhibits substantial inter-system variability. As Gluer recently emphasized, improvement in standardization methods will be required before quantitative ultrasound can play a major role in clinical practice (C. C. Gluer, "Quantitative ultrasound: It is time to focus research efforts," Bone, 40, 9-13, 2006). Typical clinical BUA measurements are performed with phase sensitive (PS) receivers and therefore can be corrupted by phase cancellation artifacts. In bone sonometry, phase cancellation results from the ultrasound beam propagating through cortical plates. Cortical plates have a relatively high speed of sound and uneven thickness. Therefore, the lateral phase profile of the ultrasound beam becomes distorted as it propagates through cortical plates. This produces phase cancellation artifact when the beam is converted to an electrical signal by the piezoelectric receiver.

The purpose of this study was to investigate phase insensitive (PI) detection, which suppresses phase cancellation artifacts, as an alternative to conventional PS detection for the measurement of BUA.

Through-transmission data from 73 women and from phantoms with acrylic wedge phase aberrators were acquired using a GE Lunar Achilles Insight bone sonometer with a two-dimensional receiver array. Radio frequency data from 52 central elements of the receiver array were digitized and stored individually. Radio frequency data were processed off-line using both PI and PS algorithms. Calcaneal bone mineral density (BMD) was measured on all 73 women using a GE PIXI dual-energy x-ray absorptiometer. Their x-ray T-scores ranged from -3.2 to 2.5 (mean: -0.4, standard deviation: 1.1).

PI BUA measurements on phantoms with acrylic wedge phase aberrators were found to be far more resistant to phase cancellation artifact than PS BUA measurements. In data from 73 women, the means (standard deviations) for BUA measurements were 81.4 (21.4) dB/MHz (PS) and 67.2 (9.7) dB/MHz (PI).

This study is the first investigation of PI BUA on a clinically-relevant population with a commercial bone sonometer. On the average, phase cancellation artifacts accounted for at least 17% of clinical PS BUA values. Because of superior accuracy and lower coefficient of variation, PI BUA is a promising alternative to PS BUA for diagnosis of osteoporosis. The mention of commercial products, their sources, or their use in connection with material reported herein is not to be construed as either an actual or implied endorsement of such products by the Department of Health and Human Services.

Disclosures: K.A. Wear, None.

This study received funding from: FDA Office of Women's Health.

T306

Precision Study of Quantitative Ultrasound(QUS) and DXA in Korean Female. S. Yang¹, D. Kim², Y. Chung³, Y. Lee⁴. ¹Radiology, Eulji University Hospital, Daejeon, Republic of Korea, ²Nuclear Medicine, Kyunghee University Hospital, Seoul, Republic of Korea, ³Internal Medicine, Ajou University Hospital, Suwon, Republic of Korea, ⁴Internal Medicine, Yonsei University Hospital, Seoul, Republic of Korea.

Quantitative ultrasound(QUS) is one of the major tools for evaluating osteoporosis. The appropriate role of QUS in osteoporosis is not clear and diagnostic cut-off value for the specific QUS devices are not determined, so confusion is existing to diagnose using QUS compared with DXA(dual energy x-ray absorptiometry) results. Purpose of this study is to establish the precision data among five different QUS devices and DXA, and correlation coefficients between QUS parameters and DXA results of the L-spine.

Precision of QUS devices was taken by duplication of the test in 30 examinees or triplication of the test in 15 examinees according to the hospital. All the precision for DXA was made using European Spine Phantom(ESP) which is made up of water equivalent plastics and epoxy resins and bone-equivalent tissues are simulated by adding calcium hydroxyapatite to the water-equivalent materials. It is composed of three vertebrae which vary in mineral density and cortical thickness.

Results are as follows:

1. Precisions of DXA using ESP among the four University Hospitals varied from 0.44 to 1.10%.
2. Precisions of speed of sound(SOS) in five QUS devices in-vivo varied 0.20 to 2.76%.
3. Precisions of broadband ultrasound attenuation(BUA) in three QUS devices in-vivo varied 1.71 to 3.51%.
4. Correlation coefficients between L-spine BMD and SOS varied 0.194 to 0.526.
5. Correlation coefficients between L-spine BMD and BUA varied 0.242 to 0.516.

Certain QUS device showed very low correlation and poor precision, so accurate assessment of the device quality is mandatory to enhance the accuracy of osteoporosis diagnosis. Clinical role of QUS and diagnostic criteria should be determined after including more normal volunteers and patients with osteoporosis by nationwide prospective study.

Disclosures: S. Yang, None.

T307

Intake of Calcium and Other Minerals Through Water: Health Implications. À. Martínez-Ferrer*, P. Peris, R. Reyes*, N. Guàrdia. Rheumatology, Hospital Clínic de Barcelona, Barcelona, Spain.

Calcium (Ca) intake through diet is mainly obtained from dairy products. However, there are other sources of Ca, like water, which can significantly contribute to this intake. Moreover, water also contains other minerals, such as magnesium (Mg) and sodium (Na), with potential implications for health. Thus, Mg has been associated with a reduction of sudden death, whereas Na contributes to the occurrence of hypertension. The rise in the consumption of bottled water in the general population clearly indicates the necessity of knowing the possible effects on health. Indeed, there is a great variation in the content of these minerals depending on the type of water.

Methods: We obtained the mineral content of Ca, Mg y Na from tap water of 475 Spanish towns and cities (through data given by autonomous communities, city/town halls or municipal water companies) and from 128 commercially available bottled waters (108 available in Spain, 20 available in Europe). The results were compared with the recommended dietary allowances of these minerals (minimum daily required intake for Ca of 800 mg, and for Mg of 350 mg; and maximum intake of 2400 mg for Na).

Results: There is a great variation in the mineral content among the different bottled water and also among tap waters. Thus, among bottled waters in our country the Ca concentration ranges between 0.5-367 mg/l; 16% of these waters had a concentration > 100 mg/l and only one > 300 mg/l; some European waters showed high concentrations of Ca (459-546 mg/l); Na concentrations ranged between 0.1-1138 mg/l, and Mg between 0.1-70.5mg/l. In tap water Ca concentrations ranged between 0-440 mg/l, Na between 1.0-240mg/L, and Mg between 0.3-200mg/L. 34% of the analysed tap water the Ca concentration was > 100 mg/l, in 3 of them it was > 200 mg/l. One village (Albox [Almería]) showed a marked increase of Ca and Mg concentrations, 440 mg/l and 200 mg/l, respectively.

Conclusion: Water, even bottled water or tap water, has a great variability in the concentrations of Ca, Mg and Na. In some occasions, water may even supply the minimum recommended allowances of Ca and Mg and can exceed the Na content. These data should be considered when selecting one for consumption.

Disclosures: À. Martínez-Ferrer, None.

T308

Bone Mineral Density in Japanese Adolescent Girls with Anorexia Nervosa. K. Matsuzaki¹, T. Hasegawa², H. Takaishi³, Y. Toyama³. ¹Dept. of Orthopedic Surgery, National Hospital Organization Tokyo Medical Center, Tokyo, Japan, ²Dept. of Pediatrics, Keio University, Tokyo, Japan, ³Dept. of Orthopedic Surgery, Keio University, Tokyo, Japan.

Anorexia nervosa (AN) present with severe body weight loss and amenorrhea caused by decrease in food intake with psychological problem. Malnutrition, low body weight, decrease in gonadal steroid followed by insufficiency of ovary and high cortisolemia are considered to be the cause of low BMD. Osteoporosis or osteomalacia in young onset cases have been increasing and getting big issue because they should attain peak bone mass in their adolescent. However, data about BMD in young onset AN in Japan is insufficient, although there are a few report about BMD in adult onset AN. We report here the effect of nutritional status and gonadal steroid on BMD in young onset AN in Japan.

We studied 22 Japanese girls (12-17 years old) who admitted to Keio Univ. Hospital for the treatment of incipient AN prospectively. Dual energy x-ray absorptiometry (DEXA) was performed to determine lumbar spine (L2-4) BMD. The effects of nutritional status and gonadal steroid on BMD were evaluated. We used obesity index, BMI and serum IGF-1 level for the index of nutritional status and the duration of amenorrhea for the index of gonadal steroid effect.

12 cases (55 %) showed BMD lower than -1SD and 10 cases (45 %) showed BMD lower than -2SD. Their obesity index were -51.3~ -21.6% (median: -34.4). Their BMIs were 9.7~ 15.9kg/m² (median: 12.9). Serum IGF-1 level were -5.17~ 0.986 SD (median: -2.694). 9 girls had not started their menstrual periods. In 11 girls with their menstrual periods, age at menarche were 10~ 13 (median: 11) and duration of amenorrhea were 1~ 15 months (median: 5). A significant correlation was found between obesity index and BMD. A significant correlation was also found between BMI and BMD. On the other hand, the correlation between serum IGF-1 and BMD approached, but did not reach, significance. There was not a correlation between duration of amenorrhea and BMD.

These results suggest that nutrition status may have stronger contribution on BMD than the effects of gonadal steroid. Therefore increasing body weight may be the most effective way of prevention and treatment for AN in Japanese adolescent girl.

Disclosures: K. Matsuzaki, None.

T309

Net Endogenous Acid Production (NEAP) and Bone Mineral Density in Men and Women: The Framingham Offspring Study. R. R. McLean¹, C. E. McLennan², N. Qiao³, K. E. Broe², K. L. Tucker³, L. A. Cupples⁴, M. T. Hannan¹. ¹Hebrew SeniorLife & Harv Med Sch, Boston, MA, USA, ²Hebrew SeniorLife, Boston, MA, USA, ³USDA HNRC, Tufts Univ, Boston, MA, USA, ⁴BU Sch of Public Health, Boston, MA, USA.

In the short term, bone may buffer excess acid by releasing calcium. It has been proposed that diets high in protein, which have high potential renal acid load, may contribute to low BMD. In contrast, some evidence indicates higher protein intake may be beneficial for bone health, possibly by enhancing calcium absorption. NEAP is the daily amount of net acid produced by the metabolic system and can be estimated using the ratio of average dietary intakes of protein to potassium. We hypothesized that NEAP is directly associated with BMD, but only among individuals with dietary calcium intakes <800 mg/day. We examined the cross-sectional relation between NEAP and BMD among 1287 men and 1581 women (mean age 61 yrs, range 29-86) of the Framingham Offspring Study who completed the Willett food frequency questionnaire between 1996-2001. We also determined whether the association between NEAP and BMD differed by dietary calcium intake. Estimated NEAP (mEq/day) was calculated as [62.1 x protein / potassium(mEq)] - 17.9, standardized to 10.46 MJ and adjusted for energy using the residual method. BMDs (g/cm²) of the proximal femur (neck, trochanter) and lumbar spine (L2-L4) were measured using a Lunar DPX-L. Multivariable linear regression was used to calculate the association between NEAP and BMD for men and women separately and within dietary calcium intake groups (<800 mg/day: y/n). Analyses were adjusted for age (yrs), height (in), weight (lbs), smoking (c/t/n), physical activity, daily intakes of alcohol (g), caffeine (mg), dietary vitamin D (IU), dietary calcium (<800 mg: y/n) and total calories (MJ), vitamin D supplement use (y/n), calcium supplement use (y/n), and in women, estrogen use (c/t/n) and menopause status (y/n). Mean NEAP (±SD) was 47.4 (14.9) for men and 45.2 (14.5) for women. For both men and women, NEAP was not associated with BMD at the femoral neck (p≥0.7), trochanter (p≥0.4) or lumbar spine (p≥0.1). 65% of men and 61% of women had dietary calcium intake <800 mg/day. NEAP was not associated with BMD at any site among men with calcium intake ≥800 mg/day (p≥0.5). Among men with calcium intake <800 mg/day, higher NEAP tended to be associated with increased lumbar spine BMD (p=0.06), but not with femoral neck or trochanter BMD (p≥0.3). NEAP was not associated with BMD among women regardless of dietary calcium intake. Although these cross-sectional results suggest diets with high potential acid load, such as those high in protein, may not contribute to low BMD in community-dwelling men and women, further studies of longitudinal bone loss are needed.

Disclosures: R.R. McLean, None.

T310

Physical Activity in Young Adulthood Is an Independent Predictor of Bone Mineral Density in Elderly Swedish Men. M. Nilsson^{*1}, C. Ohlsson¹, M. Karlsson^{*2}, Ö. Ljunggren^{*3}, D. Mellström¹, M. Lorentzon¹. ¹Center for Bone Research at the Sahlgrenska Academy, Dept. of Internal Medicine, Gothenburg University, Sweden, Gothenburg, Sweden, ²Clinical and Molecular Osteoporosis Research Unit, Dept. of Clinical Sciences, Lund University, Dept. of Orthopaedics, Malmö University Hospital, Sweden, Malmö, Sweden, ³Dept. of Medical Sciences, University of Uppsala, Sweden, Uppsala, Sweden.

Physical activity (PA) is believed to have a positive influence on bone mineral density (BMD) accrual, especially during the attainment of peak bone mass. However, whether or not the positive effects of PA on BMD during young adulthood remain at old age is still unclear. The purpose of this study was to investigate if previous PA was associated with present BMD in elderly Swedish men. The 498 subjects, with a mean age of 75.2 ± 3.3 (mean \pm SD), included in the present study were randomly selected from the population based Mr OS Göteborg study. BMD of the total body, femur trochanter, femoral neck, and lumbar spine (L1-L4) was assessed using Dual X-ray Absorptiometry (Hologic). Data concerning patterns of PA, including both competition (CS) and recreational sports (RS), and occupational physical load in a lifetime perspective (divided into years of age: 10-20, 21-35, 36-50, 51-65, and 66-) were collected at interview.

Subjects training with the highest intensity (n=81) of CS during ages 10-20, had 3.3% higher BMD of the total body (p=0.01) and 6.5% higher BMD of the trochanter (p<0.01) than subjects not participating in CS during this time period (n=319).

In order to determine the independent role of current and previous PA as well as of occupational physical load on present BMD, a stepwise linear regression analysis was used. In this regression model, present age, height, weight, calcium intake, smoking status (yes/no), present PA (daily walking distance), and CS and RS as well as occupational physical load for all the investigated time periods were included. Intensity of CS between ages 10-20 was an independent positive predictor of present BMD at the total body ($\beta=0.11$, p=0.01) and trochanter ($\beta=0.09$, p=0.03), while intensity of CS between ages 21-35 predicted present BMD at the femoral neck ($\beta=0.09$, p=0.03) and lumbar spine ($\beta=0.11$, p=0.01).

Neither current PA, intensity of CS in any of the later time periods (51-65 and 66-), nor intensity of RS, or occupational physical load for any time period investigated, independently predicted BMD at any bone site measured.

In conclusion, our results demonstrate that PA in CS during adolescence and in young adulthood is associated with areal bone mineral density in 75-year-old Swedish men, suggesting that high intensity PA early in life could aid in preventing osteoporosis in elderly men.

Disclosures: M. Nilsson, None.

T311

A Nutrition Survey about the Status of Fat-soluble Vitamins in Japanese Women. T. Okano¹, M. Kamano^{*1}, N. Tsugawa^{*1}, Y. Suhara^{*1}, K. Tanaka^{*2}, K. Uenishi³, H. Ishida⁴. ¹Department of Hygienic Sciences, Kobe Pharmaceutical University, Kobe, Japan, ²Department of Nutrition, Kyoto Women's University, Kyoto, Japan, ³Laboratory of Administrative Dietetics, Kagawa Nutrition University, Tokyo, Japan, ⁴Laboratory of Physiological Nutrition, Kagawa Nutrition University, Tokyo, Japan.

Dietary habits are an important risk factor for lifestyle-related diseases. To carry out a nutrition survey of fat-soluble vitamins, we developed novel determination methods for fat-soluble vitamins using liquid chromatography-atmospheric pressure chemical ionization/tandem mass spectrometry or high-performance liquid chromatography with fluorescence detection. In these methods, stable isotope-labeled compounds or vitamin K analogues with a saturated side-chain were used as internal standards. These methods have high sensitivity and sufficient accuracy. We applied them in a nutrition survey about the status of fat-soluble vitamins in Japanese healthy women. Plasma concentrations of 25-hydroxyvitamin D₃ [25(OH)D₃] and 25-hydroxyvitamin D₂ [25(OH)D₂] in healthy postmenopausal women (n=98) were 20.5 ± 7.9 and 0.4 ± 1.4 ng/ml, respectively. A significant negative correlation in plasma levels between 25-hydroxyvitamin D [25(OH)D] and parathyroid hormone was observed. For vitamin K homologues, plasma levels of phyloquinone, menaquinone-4 and menaquinone-7 in Japanese women of various ages (n=1409) were 1.03 ± 0.90 ng/ml, 0.12 ± 0.28 ng/ml and 6.71 ± 13.6 ng/ml, respectively. The mean total vitamin K intake of Japanese young women was about 130 µg/day, and 94% of participants met the Adequate Intake of vitamin K for women aged 18-29 years in Japan, 60µg/day. Moreover, we determined fat-soluble vitamins in breast milk collected from Japanese lactating women and revealed that the contents of all-trans-retinol, vitamin D₃, 25(OH)D₃, α-tocopherol, phyloquinone and menaquinone-4 in breast milk were 0.39 ± 0.14 ng/ml, 0.10 ± 0.15 ng/ml, 0.08 ± 0.04 ng/ml, 3.96 ± 1.84 ng/ml, 3.56 ± 2.19 ng/ml and 1.77 ± 0.68 ng/ml, respectively. Those levels except for vitamin D₃ and 25(OH)D₃ were within reference values set for breast-fed infants in Japan. In contrast, Daily intake of vitamin D calculated from an infant's consumption of breast milk, 780 ml/day was 0.47 µg/day, which did not meet current Japanese Adequate Intake of 2.5 µg/day.

Disclosures: T. Okano, None.

T312

Nutrient Intakes Related to Bone Mineral Density in Brazilian Men and Women- The BRAZILIAN Osteoporosis Study (BRAZOS). M. M. Pinheiro¹, N. O. Jacques^{*2}, P. S. Genaro^{*2}, R. M. Ciconelli^{*3}, M. B. Ferraz^{*3}, L. A. Martini². ¹Reumatology, UNIFESP, Sao Paulo, Brazil, ²Nutrition, USP, Sao Paulo, Brazil, ³Paulista Center of Economy in Health, CPES, UNIFESP, Sao Paulo, Brazil.

Dietary calcium, vitamin D and K, phosphorus and magnesium are important determinants of bone mineral density. The purpose of the present study was to evaluate mean dietary intakes of Brazilian men and women older than 40 y. A total of 2392 subjects (1693 women) were enrolled in the nutritional evaluation at the BRAZILIAN Osteoporosis Study - BRAZOS, undertaken in 120 cities across 5 regions (North, Northeast, Central, Southeast and South) of the country, and included people from five categories of economical level (from A to E). The sampling was based in the census data from IBGE (Brazilian Institute of Statistics and Geographic) 2000 and PNAD (National Research of Home Sampling) 2003 and it was calculated accordingly with to the probabilistic and representative sample of Brazilian population. The coefficient of variation is 2.2% with 95% confidence interval. Dietary intakes were evaluated by a 24h Food Record. For the nutrient analysis the Nutrition Data System software (Minneapolis, MN 2005) was used. Statistical analysis was performed by SAS (SAS Institute Inc, Cary, NC, USA, v 8.02). Student T test was used for gender comparison and One way ANOVA for comparisons between regions and economical level. Three was ANCOVA was used for interactions between gender, economical level and regions. Significance was considered as p<0.05. The mean calcium intake in the entire population was 411 (249) mg/d, vitamin D 2.2 (1.9) µg/d, vitamin K 69 (117) µg/d, phosphorus 759 (397) mg/d and magnesium 197 (111) mg/d. A significant difference was observed between genders for calcium (F_{1,2333}=15.19, p<0.001), vitamin K (F_{1,2333}=18.65, p<0.001), phosphorus (F_{1,2333}=44.85, p<0.001) and magnesium (F_{1,2333}=67.44, p<0.001), being men higher than women. Mean vitamin D intake (F_{4,2333}=8.15, p<0.001) and phosphorus (F_{4,2333}=7.29, p<0.001) was significantly higher in the North region. Magnesium was similar in North and Central regions, instead higher than other ones (F_{3,2333}=7.77, p<0.001). Significant differences were observed between economical levels, being higher in people from level A, for all nutrients evaluated. Calcium, vitamin D, K and magnesium was under recommended levels for age in all regions and economical levels. The present data suggests that an improvement in nutrients related to bone mineral density should be recommended in Brazilian population.

Disclosures: M.M. Pinheiro, Wyeth Health Consumer 2.

This study received funding from: Wyeth Health Consumer.

T313

The Association of Dietary Calcium, Bone Mineral Density and Biochemical Markers of Bone Turnover Among Rural Thai Women. C. Pongchaiyakul¹, V. Kosulwat^{*2}, N. Rojroonwasinkul^{*2}, S. Charoenkiatukul^{*2}, L. Chailurkit^{*3}, R. Rajatanavin^{*3}. ¹Division of Endocrinology and Metabolism, Department of Medicine, Faculty of Medicine, Khon Kaen University, Thailand, ²Institute of Nutrition, Salaya campus, Mahidol University, Bangkok, Thailand, ³Division of Endocrinology, Department of Medicine, Faculty of Medicine, Mahidol University, Bangkok, Thailand.

Objective: To investigate the relative contribution of dietary calcium intake on biochemical bone turnover markers and bone mineral density (BMD) in Thai women.

Materials and Methods: A cross-sectional investigation was designed in 255 rural Thai women. Usual dietary calcium intake was determined by quantitative food frequency questionnaire. BMD were measured by DXA. Three markers for bone turnover: type I collagen C-telopeptide, serum N-mid osteocalcin, serum total alkaline phosphatase including serum calcium were determined.

Results: An average daily calcium intake in this study was 265 mg/day. Of 233 (87%) women consumed dietary calcium less than half of the recommended value and only 3% of women (n = 7) had calcium intake >800 mg/day. After controlling for age and body mass index, women who consumed higher amount of dietary calcium had significantly higher BMD at all sites. Moreover, marked increasing of bone turnover markers was observed in those who were in lowest quartile of calcium intake. Women with osteopenia and osteoporosis were older, lighter weight, consumed less calcium and had significantly higher values of all biochemical markers for bone turnover than those who had normal BMD.

Conclusion: This study indicated that habitual diet of the northeastern population might not provide enough calcium needed for bone retention and for prevention of bone loss during the later years. Modification of eating pattern by promotion of increased consumption of locally available calcium rich food together with adopting other protective healthy lifestyle may be beneficial in prevention of osteoporosis among this population.

Disclosures: C. Pongchaiyakul, None.

This study received funding from: Thailand Research Fund.

T314

Gender Related Differences in Bone Mineral Quality. D. Porter^{*1}, M. Faugere^{*2}, D. Pienkowski³, H. H. Malluche^{*2}. ¹Biomedical Engineering, University of Kentucky, Lexington, KY, USA, ²Nephrolog, Bone and Mineral Metabolism, University of Kentucky, Lexington, KY, USA, ³Orthopaedic Surgery, University of Kentucky, Lexington, KY, USA.

Gender related differences in adult fracture risk are well known, but the etiology of this differential remains unclear. To identify the contributing variables, most studies have focused on extrinsic factors, e.g. fall risk, bone shape, etc. Except for bone mineral density, few studies have addressed the relationship between gender and the intrinsic material properties of bone. Therefore, this study sought to determine if gender is related to bone mineralization or bone mineral perfection.

Bone specimens were obtained in this IRB approved study from 23 males (56.7 ± 8.0 yrs) and 21 females (55.9 ± 7.7 yrs) that had iliac crest biopsies for workup of renal bone disease. Subjects treated with medications known to affect bone metabolism, or those with stable bone aluminum, diabetes, or a kidney transplant were excluded. Bone specimens were sectioned and analyzed by Fourier Transform Infrared Spectroscopy to quantify the mineral-to-matrix and carbonate-to-phosphate ratios. These measures of bone mineral quality were analyzed for gender differences.

The mean relative mineral content of bone (mineral/matrix ratio) was 7.5% greater (p<0.05) in males than in females. No difference was detected in the carbonate/phosphate ratio (a measure of the degree of mineral perfection), but the diminutive values of this parameter (>2 orders of magnitude less than the mineral/matrix ratio) may have obscured detection of true differences.

Given that a 6% increase in density can produce a 3-fold increase in fatigue life [2] and that fracture toughness peaks when the mineral/matrix ratio is within ± 1% of the peak value (i.e., 65%) [3], the observed 7.5% greater mineral/matrix ratio may be clinically significant. This finding extends our knowledge of gender related differences in bone and advances our understanding of bone mineral beyond that available from BMD. We conclude that gender has a role in determining the relative mineral content of bone; this in turn merits further study to determine its role in fracture risk.

Mineral Quality vs Gender			
	Male	Female	p - value
Mineral/matrix	3.88 ± 0.32	3.61 ± 0.39	< 0.05
Carbonate/phosphate	0.010 ± 0.001	0.010 ± 0.002	NS

± std. dev

1. Boskey et al., Osteoporosis Int, 2031-8: 16, 2005

2. Carter and Hayes, Science 194, 1174-6, 1976

3. Wainwright, S., et al., Mechanical Design in Organisms. 1976

Disclosures: D. Porter, None.

T315

Vitamin D Status in Postmenopausal Japanese-American Women Living in Hawaii: A Population-Based Study. P. Pramyothin^{*1}, S. Techarurongkul^{*1}, J. Lin^{*2}, H. Wang^{*2}, A. Shah^{*2}, P. D. Ross², R. Puapong^{*1}, R. D. Wasnich¹. ¹Hawaii Osteoporosis Center, Honolulu, HI, USA, ²Merck Research Laboratories, Rahway, NJ, USA.

Apart from its role in calcium metabolism, vitamin D has also been shown to have a beneficial role in neuromuscular function and fall prevention. Fall and hip fracture rates in native Japanese and Japanese-American females in Hawaii have been reported to be half of those of Caucasians living in both Hawaii and other parts of the United States. Differences in the vitamin D status and the seasonal variation in serum vitamin D levels among these populations may contribute to this finding. Contributors to vitamin D status include both cutaneous synthesis of vitamin D from sunlight exposure and dietary vitamin D intake. In this study, we examine serum 25(OH)D levels and their seasonal variation in a cohort of community-dwelling postmenopausal Japanese females living in Hawaii. Data for these analyses came from 495 women of Japanese ancestry living in Hawaii who participated in the 8th examination of the Hawaii Osteoporosis Study (HOS) conducted from January 1992 through September 1994. All participants gave signed informed consent, and the study was reviewed and approved by an Institutional Review Board. Serum specimens were collected and preserved at -70 degrees. Serum 25(OH)D assays were performed at the Nichols Institute using liquid chromatography tandem mass spectrometry. The mean age of the subjects was 74±5 years. The mean serum total 25(OH)D was (mean ± SD) 79.9±23.7nmol/L (31.9±9.5ng/mL); 43% of women (n=216) had values <75nmol/L (30ng/mL), 8% (n=41) <50 nmol/L (20ng/mL), 0.60% (n=3) <30 nmol/L (12ng/mL), and none had <25 nmol/L (10ng/mL). There was little evidence of seasonal variation, with mean serum 25(OH)D levels of ~28 ng/mL during January and February, and 31 to 34 ng/mL during most other months. The current study has several limitations. Analyses were cross-sectional in design, and vitamin D levels were measured at a single point in time. When compared to published data for ambulatory Caucasians in the US and Europe, as well as other populations, low serum 25(OH)D level in our cohort was somewhat less prevalent. For example, the prevalence of 25(OH)D <20ng/mL in one US study of women with osteoporosis was 18%, compared to 8% in our study. In contrast to studies conducted at more northerly latitudes, there was little evidence of seasonal serum 25(OH)D variation in Hawaii. Although the prevalence of very low vitamin D was lower in Hawaii than in other parts of the world, a substantial proportion (43%) had serum 25(OH)D values less than the 75nmol/L (30ng/mL) considered optimal by some experts, despite the abundant sunshine in this tropical latitude.

Disclosures: P. Pramyothin, Merck Research Laboratories 2.

This study received funding from: NIH and Merck Research Laboratories.

T316

Low Calcium Intake and Insufficient Serum Vitamin D Status in Treated and Non-Treated Postmenopausal Osteoporotic Women in Spain: The Previcad Study. J. M. Quesada Gómez¹, J. M. Mata Granados^{*1}, J. Delgadillo^{*2}, E. Ramírez^{*3}. ¹Unidad de Metabolismo Mineral, Servicio de Endocrinología, Hospital Universitario Reina Sofía, Córdoba, Spain, ²Medical Department, Procter & Gamble Pharmaceuticals Iberia, Barcelona, Spain, ³Medical Writing, Infocencia, Barcelona, Spain.

The purpose of the present study was to assess the calcium intake and serum vitamin D level in postmenopausal women treated and non-treated for osteoporosis, and to evaluate the influence of sunlight exposure on vitamin D status.

This observational epidemiologic and cross-sectional study was conducted at Spanish hospitals and primary care centres, which were categorized on basis of their sunlight exposure (above or below 2500 sunlight hours/year). The participant investigators collected demographic and clinical data from postmenopausal women diagnosed of osteoporosis, including their history of prior fractures, pharmacological treatment, and dietary calcium intake. In addition, measures of 25OHD and other bone metabolism markers were determined from a blood sample. All the patients gave their written signed informed consent to participate in the study, which followed the Declaration of Helsinki principles and was approved by the local institutional human research committee.

A total of 336 postmenopausal women aged 71.2 ± 4.9 were enrolled, 190 of which were under osteoporosis treatment. Among them, the bisphosphonate drugs were the first choice therapy (69.5%), followed by the use of selective estrogen receptor modulators (11.1%), while only 1.6% received a combination of both. A high percentage of insufficient dietary calcium intake (<1500 mg/day) was observed, with an average value of 1018.6 mg/day in the whole sample and without differences between treated and untreated.

Mean serum 25OHD concentration was 25.5 ng/ml, and a 68.9% exhibited vitamin D insufficiency (<30 ng/ml), 76.4% in non-treated and 63.2% in treated women. In contrast, no significant benefit of the sunlight exposure was found when patients from areas receiving more or less than 2500 sunlight hours/year were compared. Furthermore, the calcium intake did not appear to influence either 25OHD or PTH levels.

In conclusion, strikingly even in a sunny country such as Spain, there is a large prevalence of vitamin D insufficiency amongst untreated osteoporotic women, regardless of the sun hour's availability. Moreover, 63.2% of Spanish women under osteoporosis therapy have vitamin D insufficiency and a low calcium intake. Hence, it is important to highlight the need for improving physician and patient's knowledge about the optimization of vitamin D status and calcium intake in this population segment in order to improve the therapeutic response.

Disclosures: J.M. Quesada Gómez, None.

This study received funding from: P&G

T317

Lack of Association of Carotenoid Intake with Bone Mineral Density (BMD) in Older Adults: The Framingham Osteoporosis Study. S. Sahni¹, M. T. Hannan², J. Blumberg^{*1}, L. A. Cupples³, D. P. Kiel², K. L. Tucker¹. ¹JM USDA HNRCA, Tufts Univ., Boston, MA, USA, ²Hebrew SeniorLife, Boston, MA, USA, ³Boston Univ. SPH, Boston, MA, USA.

In vitro and in vivo studies suggest that carotenoids may inhibit bone resorption and stimulate bone formation. One study of BMD showed positive and negative associations for specific carotenoids, and a fracture study showed interaction by smoking. Thus, we evaluated intakes of total and individual carotenoids (α -carotene, β -carotene, β -cryptoxanthin, lycopene, lutein+zeaxanthin) and BMDs at hip, spine and radius in the Framingham Osteoporosis Study.

277 men and 476 women had hip and spine BMDs (g/cm², Lunar DP3), radius BMD (Lunar SP2) and food frequency questionnaires (FFQ), all obtained in 1988-89. Carotenoid intakes were estimated with Willett FFQ and adjusted for total energy (residual method). Least squares mean BMDs were estimated for men and women separately by quartile of carotenoid. Linear regression models were adjusted for age, BMI, height, total energy, physical activity, alcohol, smoking, calcium, vitamin D, caffeine, & estrogen (women). We tested interaction with pack-years of smoking (male mean: 26.2 ± 3.9; female mean 12.7 ± 19.0).

Mean age was 75y ± 5.0. For women, no associations were seen between total carotenoids, α -carotene, β -carotene, β -cryptoxanthin and BMD at any site. Men had similar results except β -carotene showed borderline positive association with radius BMD (P for trend=0.08). Women in lowest quartile (Q1) of lycopene had significantly lower trochanteric BMD compared to Q2, Q3, Q4 (adjusted mean BMD=0.62±0.01 in Q1 vs 0.66±0.01, 0.66±0.02 and 0.67±0.02 g/cm² in Q2-4, P<0.05, P for trend=0.009). For men, lycopene and BMD was modified by smoking (P for interaction term =0.003 for femoral neck; P=0.002 for trochanter). Male smokers (not non-smokers), in Q1 of lycopene had significantly higher trochanteric BMD compared to other quartiles (adjusted mean BMD=0.89±0.01 in Q1 vs 0.82±0.01, 0.82±0.01 and 0.80±0.01 g/cm² in Q2-4, P<0.05, P for trend=0.005). No associations were seen with lycopene and other BMD sites. Women in Q1 of lutein+zeaxanthin intake had significantly lower trochanteric BMD compared to Q4 (adjusted mean BMD=0.63±0.01 in Q1 vs 0.66±0.02 g/cm² in Q4, P<0.05, P for trend=0.062), while no associations were seen in men.

In sum, few associations were seen between carotenoids and BMDs in our study: none for total carotenoids, α -carotene or β -cryptoxanthin, and marginal results for β -carotene, lycopene and lutein+zeaxanthin. As these results were inconsistent across BMD sites and gender and no results were sufficiently strong to rule out chance, we believe our findings indicate lack of association between carotenoids and BMD in this elderly population.

Disclosures: S. Sahni, None.

This study received funding from: NIH-NIAMS #AR/AG41398.

T318

The Single Nucleotide Polymorphism R325Q in the Vitamin K-Dependent Gamma-Glutamyl Carboxylase Gene Has Effects on the Correlation Between Dietary Vitamin K Intake and Gamma-Carboxylation of Serum Osteocalcin in Young Males. N. Sogabe^{*1}, N. Tsugawa^{*2}, R. Maruyama^{*1}, M. Kamao^{*2}, T. Okano², T. Hosoi³, M. Goseki-Sone¹. ¹Department of Food and Nutrition, Japan Women's University, Tokyo, Japan, ²Department of Hygienic Sciences, Kobe Pharmaceutical University, Kobe, Japan, ³Department of advanced Medicine, National Center for Geriatrics and Gerontology, Aichi, Japan.

Vitamin K is a cofactor for gamma-glutamyl carboxylase (GGCX), which is an essential enzyme for the gamma-carboxylation of vitamin K-dependent proteins such as osteocalcin (OC). Associations among dietary vitamin K intake, vitamin K status, and bone metabolism have not been thoroughly investigated. Recently, it has been reported that single nucleotide polymorphisms (SNPs) of GGCX (R325Q, 974G>A) were associated with age-related bone loss. We investigated the associations among dietary vitamin K intake, the level of serum vitamin K, and the ratio of undercarboxylated OC (ucOC) to intact OC. The subjects were 60 healthy young male volunteers (mean age, 22.6 y; standard deviation, 1.7). Dietary nutrient intake was assessed by consecutive, individual 3-day food records before the day of blood examinations. Serum concentrations of vitamin K (phylloquinone: PK, menaquinone 4: MK-4, and menaquinone 7: MK-7), ucOC, intact OC, calcium, phosphorus, and bone-specific alkaline phosphatase were measured. All subjects were genotyped for polymorphism (R325Q). Dietary vitamin K intake from vegetables was significantly correlated with the level of serum PK ($p=0.009$), and vitamin K intake from fermented beans, natto, was also significantly correlated with the level of serum MK-7 ($p<0.001$). The ratio of ucOC to intact OC showed a negative association with the total vitamin K intake or MK-7 intake from natto. Interestingly, grouped by the GGCX genotype, a significant interaction between the ratio of ucOC to intact OC with serum MK-7 was observed in 325R homozygotes ($p=0.003$), but not in heterozygotes, nor in 325Q homozygotes. In the present study, we revealed that the single nucleotide polymorphism R325Q in the GGCX gene had effects on the correlation between dietary vitamin K intake and gamma-carboxylation of serum osteocalcin in young males. Our data may be useful for planning nutritional strategies for preventing osteoporosis.

Disclosures: N. Sogabe, None.

T319

Effects of Weight Reduction on Bone Mass and Structure in Obese Women. K. Uusi-Rasi, H. Sievänen, P. Kannus*, M. Pasanen*, K. Kukkonen-Harjula*, M. Fogelholm*. The UKK Institute for Health Promotion Research, Tampere, Finland.

Obesity is associated with obvious health risks, such as hypertension, type 2 diabetes, atherosclerosis and osteoarthritis, while it is also connected with greater bone mass. Therefore, one deleterious consequence of weight loss may be bone loss and increased bone fragility.

This pilot study was a non-controlled, prospective 3-mo study of women treated in weight loss groups by the general primary health care. The groups used conservative energy restrictive diet or VLED products (Cambridge Diet) in reducing body weight. Totally 54 of 60 recruited women completed the study. All assessments were done at baseline (0 month) and after 12 weeks' weight reduction.

Waist circumference, body composition by DXA-based and bone mineral content (BMC) of the right proximal femur were assessed. Cortical (shaft CoD) and trabecular bone density (distal TrD) of the radius and tibia was measured with pQCT. As markers of bone turnover, serum tartrate-resistant acid phosphatase isoform 5b (S-TRACP 5b), serum C-telopeptide of collagen cross-links (S-CTX) and serum amino-terminal propeptide of type I procollagen (S-PINP) were determined. Linear regression analysis was used to analyze associations of weight loss with bone characteristics.

At baseline, mean age (SD) was 45 (7) years, and mean BMI 34.4 (4.8). The mean weight loss was 4.0 (4.1) kg ranging from -14.8 kg to +2.1 kg. Waist circumference decreased by 4.0 (4.2) cm. The change in S-CTX was negatively associated with weight change ($r = -0.314$; $p=0.022$), while changes in S-TRACP5b and S-PINP were not associated with weight change. There were correlations of borderline statistical significance between changes in biomarkers and bone mass. S-PINP and S-CXT correlated negatively with trochanter BMC ($r=-0.262$; $p=0.058$ and $r=-0.262$; $p=0.058$), respectively.

The correlation between weight change and change in femoral neck BMC was negative ($r=-0.280$; $p=0.042$), the β -coefficient of weight change being -0.009 for femoral neck BMC. There was also a negative correlation between weight change and radial CoD ($r=-0.291$; $p=0.036$) and radial TrD ($r=-0.247$; $p=0.077$) suggesting increased bone loss at the radius. For radial bone changes, change in body fat mass was a better predictor than change in lean mass (significant for CoD only). A 1 kg change in fat mass was associated with 0.001 mg/cm³ mean decline in the radial CoD ($p=0.004$). As the radius is a nonweight-bearing bone, changes in bone loading due to reduced body weight cannot explain this association.

These findings suggested that changes in body mass influence bone metabolism to some extent, apparently in a complex fashion. Therefore the possibility of harmful effects of weight loss on bone cannot be ruled out. Further research is definitely needed.

Disclosures: K. Uusi-Rasi, None.

T320

Serum 25(OH)D Levels and Falls, Frailty, and Fractures among Postmenopausal Women in the Hawaii Osteoporosis Study. S. Techaturunkul^{*1}, P. Pramyothin^{*1}, J. Lin^{*2}, H. Wang^{*2}, A. Shah^{*2}, P. D. Ross², R. Puaopong^{*1}, R. D. Wasnich¹. ¹Hawaii Osteoporosis Center, Honolulu, HI, USA, ²Merck Research Laboratories, Rahway, NJ, USA.

In this study we investigate the relationship of serum 25-hydroxyvitamin D (25(OH)D) levels to measures of physical performance and muscle strength, and to subsequent falls and fractures in the Hawaii Osteoporosis Study (HOS). Using liquid chromatography tandem mass spectrometry, 25(OH)D levels (D3 and total) were measured in serum stored at -70 degrees that had been collected from 495 postmenopausal women during the 8th examination of the HOS cohort in 1992-94. In the primary analyses, the relationship of total 25(OH)D to performance-based measurements (walking speed, timed get-up-and-go, chair stand, hand & foot reaction time, functional reach), and muscle strength (grip, triceps, and quadriceps) was explored using multivariate regression models, adjusted for age, height, and weight. Logistic regression analyses adjusted for age, height, and weight were also performed to evaluate the relationship of total 25(OH)D to falls and to the incidence of vertebral and non vertebral fractures during a mean 2.7 year follow-up. Secondary analyses were performed: 1) using vitamin D3 as the predictor variable, 2) using vitamin D (D3 and total) with adjustment only for age, and 3) including quadriceps strength as an additional covariate in models of falling. The mean serum 25(OH)D level was 79.9 (SD=23.7 nmol/L; n=495). After adjustment for age, height, and weight, only quadriceps strength had a significant association ($p=0.0002$) with 25(OH)D. No significant association of 25(OH)D was found with either vertebral or non-vertebral fractures, or with the incidence of one or more falls. There was a borderline significant ($p = 0.05$) association of total 25(OH)D with two or more falls after adjustment for age alone, but there was no association in the model adjusted for age, height, weight, and quadriceps strength, suggesting that an effect on falls may be partly mediated by quadriceps strength. The current study has several limitations. Analyses were of cross-sectional design, and vitamin D levels were measured at a single point in time. Although prospective data were available for falls and fractures, the numbers of fracture events were relatively small. Also, the interpretation of tests for statistical significance are less straightforward due to the large number of endpoints studied. The lack of association with fractures and falls, or with most physical performance measures, might be related to the fact that very low levels of 25OHD are less common in this population than in other studies.

Disclosures: R.D. Wasnich, Merck Research Laboratories 2.

This study received funding from: NIH and Merck Research Laboratories.

T321

Association between Urinary Potassium and Hip Bone Mass in a Prospective Cohort Study of Elderly Postmenopausal Women. K. Zhu¹, A. Devine^{*2}, J. Beilby^{*3}, R. L. Prince⁴. ¹Department of Endocrinology and Diabetes, Sir Charles Gairdner Hospital, Nedlands, Australia, ²School of Exercise, Biomedical and Health Science, Edith Cowan University, Perth, Australia, ³Pathcentre, Sir Charles Gairdner Hospital, Nedlands, Australia, ⁴School of Medicine and Pharmacology, University of Western Australia, Nedlands, Australia.

Dietary potassium intake, best evaluated by potassium output in the urine, has been suggested to be beneficial for bone structure perhaps because of its relationship to fruit and vegetable intake.

The association between urinary potassium and hip bone mass was evaluated in 266 elderly postmenopausal women selected from the population who participated in a 5-year calcium intervention study in which subjects were randomised to calcium 1.2 g or placebo (the CAIFOS study). Twenty-four hour urine samples were collected at baseline and urinary potassium (Urine K) measured by autoanalyzer (Roche Diagnostics Hitachi 917). Dietary intake was assessed by a validated food frequency questionnaire (Victorian Anti Cancer Council) and Net Endogenous non carbonic Acid Production (NEAP) calculated. One year later total hip DXA BMD was assessed (Hologic 4500A).

At baseline subjects mean age was 75.0 ± 2.7 years and mean calcium intake was 959 ± 338 mg/day. In correlation analysis there was a positive relationship between the urine K and total hip BMD ($r = 0.188$, $P = 0.002$). Subjects in the highest quartile of urine K had a total hip BMD 5% higher of those in the lowest three quartiles after adjustment for age, weight, height and calcium treatment group. There were no significant differences between the four groups in intakes of calcium and protein or NEAP. The effects remained after further adjustment for these variables.

	24 hour Urine Potassium (mM/day)			
	1 st quartile <41	2 nd quartile 42 - 57	3 rd quartile 58-76	4 th quartile >76
Total hip BMD mg/cm ²	789 ± 142 (0.02)*	794 ± 127 (0.03)*	805 ± 126 (NS)	857 ± 112
Hip BMD % df from 4 th quartile	-9.0 ± 2.8 (0.002)*	-8.0 ± 2.8 (0.004)*	-6.6 ± 2.8 (0.020)*	-
Hip BMD adjusted % df from 4 th quartile	-5.1 ± 2.4 (0.037)**	-5.0 ± 2.4 (0.038)**	-5.1 ± 2.4 (0.035)**	-
Calcium intake mg/day	947 ± 382	955 ± 308	984 ± 317	950 ± 351
Protein intake g/day	80 ± 29	78 ± 23	86 ± 32	83 ± 29
NEAP mEq/day	51 ± 17	50 ± 11	53 ± 20	52 ± 17

Results mean \pm SD, % results mean \pm SEM, * P value of 4th quartile ** P value of 4th quartile adjusted for age, weight, height and treatment. These findings suggested that increase the intake of food rich in potassium, such as fresh fruit and vegetables may have a substantial beneficial effect on the maintenance of bone mass at the hip.

Disclosures: K. Zhu, None.

This study received funding from: Australian NHMRC.

T322

Secondary Causes of Osteoporosis in Fracture Patients. E. R. Bogoch¹, V. I. M. Elliot-Gibson^{*2}, R. Wang^{*3}, R. G. Josse⁴. ¹Department of Surgery, St. Michael's Hospital, Toronto, ON, Canada, ²Mobility Program Clinical Research Unit, St. Michael's Hospital, Toronto, ON, Canada, ³Orthopaedic Resident, Department of Surgery, St. Michael's Hospital, Toronto, ON, Canada, ⁴Department of Medicine, St. Michael's Hospital, Toronto, ON, Canada.

This analysis was performed to report the prevalence of vitamin D deficiency and other secondary causes of osteoporosis (OP) in patients with fragility fracture. A chart audit of 399 patients referred from an inner city orthopaedic unit to the Metabolic Bone Disease Clinic (MBDC) over a three year period was conducted. A total of 117 males, average age 64.6 (SD 12.8) and 282 females, average age 63.5 (SD 14.6) were reviewed. Fracture locations and etiology: 90 hip (76 fragility), 161 wrist (135 fragility), 8 vertebral (6 fragility), 77 shoulder (62 fragility) and 62 other sites (45 fragility) and one with both hip and shoulder (fragility). Thirty percent (42 males and 78 females) of patients had a total of 149 secondary causes of OP recorded in their MBDC note. Secondary causes included medication use (oral steroids, anti-seizure), rheumatic, gastrointestinal and endocrine conditions (RA, IBD, Graves disease, Type 1 DM, hyperparathyroidism), hypogonadal states (premature ovarian failure, hypogonadism), genetic conditions (hypophosphatasia), hematological conditions (thalassemia) and miscellaneous causes (smoking, renal impairment). A total of 308 patients completed blood work, including 269 patients who had a 25-OH vitamin D measurement: seven patients were deficient at ≤ 25 nmol/L, 137 were insufficient at 26 to 74 nmol/L and 125 were sufficient at ≥ 75 nmol/L. There were no differences between males and females ($p=0.457$), or among fracture locations ($p=0.246$). Over 75% of the blood/urine analyses were within the normal range for: 1,25 vitamin D ($n=18$), ALP ($n=266$), ALT ($n=75$), AST ($n=105$), bilirubin ($n=19$), creatinine ($n=247$), T3 ($n=173$), T4 ($n=229$), homocysteine ($n=3$), magnesium ($n=74$), phosphorus ($n=249$), platelets ($n=220$), serum calcium ($n=269$), protein ($n=282$), albumin ($n=282$), globulin ($n=281$), TSH ($n=254$), tissue transglutaminase ($n=49$), Vit B12 ($n=17$), WBC ($n=220$), and 24 hour urine calcium ($n=52$) and phosphorus ($n=34$). Between 50 and 74% of the blood/urine analyses were within the normal range for: CRP ($n=30$; 30% elevated), ESR ($n=173$; 43% elevated), testosterone ($n=53$; 25% of men below normal), bioavailable testosterone ($n=52$; 40% of men below normal), N-telopeptide ($n=5$; 30% of women elevated), PTH ($n=130$; 19% elevated), RBC folate ($n=12$; 33% elevated), 24 hour urine creatinine ($n=51$; 27% below normal). A standardized blood test protocol for all fracture patients is now being used.

Disclosures: V.I.M. Elliot-Gibson, None.

T323

Osteoporosis Post-Fracture Screening Program. V. I. M. Elliot-Gibson^{*1}, R. Jain^{*2}, F. Jiwa^{*2}, D. E. Beaton¹, E. R. Bogoch³, S. Richie^{*4}, F. Samji^{*5}. ¹Mobility Program Clinical Research Unit, St. Michael's Hospital, Toronto, ON, Canada, ²Osteoporosis Canada, Toronto, ON, Canada, ³Department of Surgery, St. Michael's Hospital, Toronto, ON, Canada, ⁴Department of Surgery, McMaster University and Brantford General Hospital and Ontario Orthopaedic Association, Hamilton, ON, Canada, ⁵Ministry of Health and Long-Term Care, Government of Ontario, Toronto, ON, Canada.

In 2005, the Ontario Government, committed up to \$5 million per year towards an Osteoporosis (OP) Strategy with the primary goal to prevent OP through early detection and education. One of the five main components of this program is the creation of a province-wide fracture clinic program with the goals to improve OP diagnosis and treatment in this population, prevent future fractures, improve OP knowledge among health professionals and patients and increase collaboration between orthopaedic surgeons and family physicians. The Ministry of Health and Long-Term Care (MOHLTC) has commissioned Osteoporosis Canada (OC) to develop, implement and evaluate this program. The Post-Fracture OP Program has been designed as a multifaceted intervention program aimed at orthopaedic surgeons, health care professionals, administration and staff at the hospital level, family physicians, and individuals who have sustained a fragility fracture. For this program, OC will deploy 14 OP Screening Coordinators (OSCs) in 35 medium to high volume fracture clinics across the province of Ontario. In these clinics, the OSCs will screen and identify fragility fracture patients, educate them on OP and their risks and recommend follow up with the family physician for further investigation and treatment of the patients bone health. Family physicians will also receive a standardized form letter recommending follow up with their patients. Quality assurance self-report data is collected on all patients. This includes OP risk factors, prior OP treatment and adherence, prior bone mineral density (DXA) testing, OP knowledge and beliefs and socio-demographics characteristics. Patient review at three months will evaluate their follow-up with their family physician, DXA testing and self-report of these results, new OP diagnosis, treatment and adherence to treatment and assessment of OP knowledge and beliefs. This data will be collected using touchscreen technology. A website is being developed to support the ongoing training of the OSCs. The Ontario Orthopaedic Association (OOA) will identify an 'Orthopaedic Osteoporosis Champion' in each hospital to support the deployment of these coordinators and promote the program strategy. Educational materials for patients have been developed for this program by OC.

Disclosures: V.I.M. Elliot-Gibson, None.

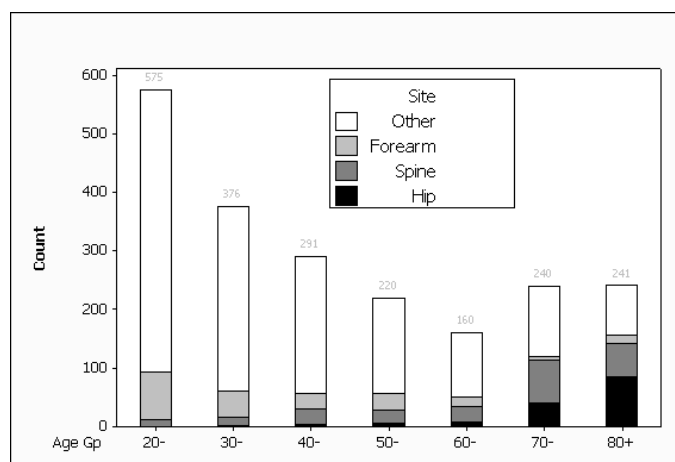
T324

The Pattern of Fractures in Men: Geelong Osteoporosis Study. S. Korn^{*}, J. Pasco, M. Henry^{*}, M. Kotowicz, G. Nicholson. Department of Clinical and Biomedical Sciences: Barwon Health, University of Melbourne, Geelong, Australia.

Using radiology reports at the Geelong Hospital, all men aged 20+yr with incident fracture in 2005-6 were identified; approximately 90% of fractures in the region can be ascertained by this method. We aimed to describe fracture epidemiology by age, fracture site and trauma. Low trauma fracture included spontaneous fracture and those resulting from falls <standing height or unspecified, overexertion or strenuous movement. We identified 2,103 men aged 20-97yr sustaining at least one incident fracture (Figure). Trauma level was determined for 1088 cases: 401 low and 687 high. Among men aged <60yr, 80% (599/748) of fractures were attributable to high trauma whereas among men aged >60yr only 26% (88/340) were high trauma.

In a subset of 217 fracture cases, total-hip BMD (Lunar Prodigy) for high trauma ($n=130$, median age 46yr IQR 34-59) and low trauma ($n=87$, median age 56yr IQR 38-73) was compared with controls from a random population-based sample ($n=879$, 54yr IQR 33-75). Mean age- and weight- adjusted BMD was statistically lower according to trauma level (mean \pm SE: low trauma 0.995 ± 0.015 vs high trauma 1.040 ± 0.012 vs controls 1.068 ± 0.004 g/cm², all $p<0.05$).

One-third of the fracture burden arose from men aged >60yr, with age-related increases in traditional osteoporotic fractures (forearm, spine and hip) and relatively few high trauma. In contrast, high trauma fractures at non-osteoporotic sites predominated in younger men. Despite differences in trauma patterns between younger and older men with fracture, BMD was consistently lower for fracture cases compared with controls across all ages.



Disclosures: S. Korn, None.

T325

Chronic Kidney Disease Stages Classified by Serum Cystatin-C and Incidence of Hip Fracture in the Women's Health Initiative Observational Study (WHI-OS). A. Z. LaCroix¹, J. Lee², L. Wu^{1*}, J. Cauley³, M. G. Shlipak^{4*}, S. M. Ott⁴, J. Robbins⁵, J. D. Curb^{6*}, M. LeBoff⁷, R. Jackson⁸, C. Kooperberg^{4*}, D. C. Bauer², S. R. Cummings². ¹Public Health Sciences, Fred Hutchinson Cancer Research Center, Seattle, WA, USA, ²University of California at San Francisco, San Francisco, CA, USA, ³University of Pittsburgh, Pittsburgh, PA, USA, ⁴University of Washington, Seattle, WA, USA, ⁵University of California at Davis, Irvine, CA, USA, ⁶University of Hawaii, Honolulu, HI, USA, ⁷Harvard University, Boston, MA, USA, ⁸Ohio State University, Columbus, OH, USA.

Recent epidemiological studies have investigated associations between impaired renal function and hip fracture with inconsistent results. None have evaluated the recently defined KDIGO Chronic Kidney Disease (CKD) Stages using serum cystatin-C, a measure of renal function that is not dependent on lean body mass. We conducted a nested case-control study within the WHI-OS among 400 cases of incident adjudicated hip fracture and 400 controls matched on baseline age, race/ethnicity and date of blood draw (average follow-up time=7.1 years). Subjects were selected from 39,795 eligible postmenopausal women without previous hip fracture, not using estrogen, androgens or osteoporosis treatments and not on kidney dialysis. Cystatin-C levels were measured on baseline serum using the Dade Behring BN-II nephelometer with a particle-enhanced immunonephelometric assay (interassay co-efficient of variation=5.7%, sensitivity=0.02 mg/L). Estimated glomerular filtration rates (eGFR) were calculated with a validated equation ($76.7 \times \text{cystatin-C}^{-1.18}$) and categorized into CKD Stages of 0-1 (eGFR>90 ml/min/1.73 m²; n=133), 2 (60-90; n=517), or 3-4 (30-59; n=138; <30; n=6). Compared to women with CKD Stages 0-1, conditional logistic regression models adjusting for body mass index, parental hip fracture, smoking, alcohol, and physical function revealed an odds ratio (OR) of 2.50 (95% confidence interval (CI) 1.32-4.72) for Stages 3-4 CKD, but no association was seen for Stage 2 CKD (OR=1.04; CI 0.66-1.64). These associations were not affected by adjustment for other indicators of poor health status (frailty score, # of chronic conditions); hemoglobin level; or serum 25 hydroxy vitamin D level. Recent experimental data show that eGFR by cystatin-C is an important determinant of homocysteine level independent of vitamin B12 and folate status. Adjustment for plasma homocysteine levels ($r=0.45$ for cystatin-C & homocysteine) reduced the OR for Stages 3-4 CKD to 1.83 (CI 0.93-3.61) suggesting that reduced renal function may increase hip fracture risk partly through raising homocysteine levels. These results indicate that women with cystatin-C eGFR levels <60 have a substantially increased risk of hip fracture.

Disclosures: A.Z. LaCroix, None.

T326

Low Levels of 25 hydroxyvitamin D Associated with Moderate/Severe Vertebral Fractures. J. B. Lopes^{1*}, C. F. Danilevicius^{1*}, L. Takayama^{1*}, E. Bonfá^{1*}, V. F. Caparbo^{1*}, P. R. Menezes^{2*}, R. M. Pereira¹. ¹Rheumatology Division, University of São Paulo, São Paulo, Brazil, ²Preventive Medicine Department, University of São Paulo, São Paulo, Brazil.

The aim of this study was to determine the possible relevance of serum vitamin D levels as a parameter for the presence of vertebral fracture. Eighty-five women with moderate/severe vertebral fracture and 85 women without vertebral fractures were consecutively selected in a well established elderly community in the city of São Paulo, a subtropical area, located at 23°34'S. All of them collected 25-hydroxyvitamin D (25-OHD) during the same period of the year. None had received vitamin D supplementation. Clinical and anthropometric data were obtained by specific questionnaire and physical examination. Vertebral fractures were evaluated by thoracic and lumbar X-ray using a semi-quantitative assessment (Genant et al.). The levels of serum 25-OHD [immunoradiometric assay (DiaSorin, Stillwater, MN, USA)], intact parathyroid hormone (intact PTH), serum calcium and estimated glomerular filtration rate (Cockcroft-Gault equation), were examined in both groups. Patients with vertebral fractures compared to those without fractures had a higher mean age (73.4 ± 4.9 vs. 71.8 ± 4.4 years, $p=0.032$), and lower weight (62.51 ± 12.47 vs. 68.01 ± 12.84 Kg, $p=0.005$) and height (1.49 ± 6.36 vs. 1.51 ± 6.22 m, $p=0.029$). Of interest, serum levels of 25-OHD in the group with fractures were significantly lower compared to the other group (17.6 ± 7.5 vs. 24.9 ± 13.3 ng/ml, $p<0.0001$). Reinforcing this finding, hypovitaminosis D (25-OHD<20 ng/ml) was more frequently observed in patients with fractures than in those without this complication (67 vs. 42.5%, $p=0.001$). Accordingly, intact PTH were significantly higher in the group with fractures compared to those without vertebral fractures (50.21 ± 36.23 vs. 40.27 ± 17.25 pg/ml, $p<0.024$). Serum calcium and glomerular filtration rate were comparable in both groups ($p>0.05$). Logistic regression analysis, using 25-OHD, age, weight, height, intact PTH revealed that only 25-OHD remains a significant factor for the presence of moderate/severe vertebral fracture. In our study, serum levels of vitamin D have an emerged promising index of vertebral fracture in elderly community-dwelling women.

Disclosures: J.B. Lopes, None.
This study received funding from: FAPESP.

T327

Prevalence of Asymptomatic Vertebral Fractures in Postmenopausal Women with Osteoporosis in Buenos Aires. Z. Man, M. S. Larroude^{*}, M. P. D. Yantorno^{*}, M. S. Moggia^{*}, R. D. Diaz^{*}, M. G. Torres Cerino^{*}, G. A. Macías^{*}, J. C. Morgenstern^{*}, M. Pérez Sáinz^{*}. Centro TIEMPO, C.A.Buenos Aires, Argentina.

Introduction: Underdiagnosis of vertebral fractures (VFX) is a common problem. The semiquantitative evaluation provided by the Genant Method is a very useful tool in the assessment of these fractures, by means of plain lateral thoracic and the lumbar radiographs.

Objective: To determine the prevalence of asymptomatic VFX in the postmenopausal women (PMW) with the osteoporosis diagnosed by the DXA scans performed at our center, located in Buenos Aires, Argentina, who attended for control. Material and method: After ruling out history of VFX through medical interrogatory, 337 PMW [mean age, 67 years (range, 51-85)] with at least five years postmenopausal, had plain lateral thoracic and lumbar X-rays done. A reduction >20% of the vertebral body height was considered for the diagnosis of VFX.

Results: We found 146 VFX, of which 103 VFX (70%) and 43 VFX (30%) were located in the thoracic and lumbar spine, respectively. 94 PMW with osteoporosis (27.89% of the total sample) had VFX; 31 of these (33%) had more than one VFX.

Conclusion: It is well known that the presence of a VFX is a predisposing factor for the future fractures. Their diagnosis represents a useful tool for the establishing risk groups. Plain radiographs of the spine are accessible and inexpensive imaging methods, whose benefits are important in terms of public and the individuals health.

Disclosures: Z. Man, None.

T328

A Novel, Integrated Approach to the Management of Patients Following Hip Fracture: The Hip Fracture Integrated Intervention Program (HIIP). V. Nanci^{1*}, G. Berry^{2*}, E. Harvey^{3*}, D. Goltzman³, S. N. Morin³. ¹McGill University, Montreal, PQ, Canada, ²Orthopedics, McGill University Health Center, Montreal, PQ, Canada, ³Medicine, McGill University Health Center, Montreal, PQ, Canada.

Clinical guidelines recommend that patients having sustained a fragility fracture be considered for osteoporosis treatment to reduce the risk of recurrent events. Because of their frailty and inability to comply with follow-up appointments, patients with hip fractures receive therapy less than 30% of the time.

The purpose of this study was to evaluate the feasibility of implementing an integrated approach to the delivery of care to patients having sustained a hip fracture. Specific objectives were to describe the characteristics and current care of patients who survive to hospital discharge, to characterize patients lost to follow-up and to evaluate the applicability of evaluation tools.

Patients admitted to our institution for a hip fracture from November 15th 2005 to October 21st 2006 were scheduled for a bone mineral density and pertinent blood tests while in hospital. Upon discharge, patients were given a 6 week follow-up conjoint appointment with the treating surgeon and a bone metabolism specialist, at which time a comprehensive treatment plan was elaborated. A summary letter was sent to the patient's primary care physician, who was asked to follow-up on the recommendations.

154 patients with hip fractures were admitted during the study period. 74 patients were seen in follow up (78% women, age = 80.0 years [SD=3.1], 22% men, age = 76.8 [SD=10.6]). Amongst the patients seen in clinic, 30% had sustained a previous fracture, 45 % were receiving some calcium or vitamin D and 19% were on an antiresorptive agent at the time of the fracture. 79% underwent BMD and blood tests while in hospital; of those, 67% had a Femoral Neck T score of -2.5 or less and 34% had evidence of secondary hyperparathyroidism. Factors associated with inability to undergo the prescribed tests were: short hospital stay and medical deterioration. Failure to return to clinic was related with dementia and travelling distance. All patients who returned for follow-up received recommendations on fall prevention and appropriate prescriptions for calcium, vitamin D and pharmacological therapy. Patients' satisfaction level with this approach was high.

We conclude that this novel, integrated program is well suited for the hip fracture population and fosters collaboration between health care professionals. We propose to address the following questions: 1) evaluation of the impact of our interventions on adherence to therapy at 6 and 12 months, 2) development of a treatment pathway for patients who do not return to clinic for the initial follow-up and 3) development and validation of fracture-reduction strategies.

Disclosures: S.N. Morin, None.

T329

Using a Case-Manager to Improve Osteoporosis Treatment after Hip Fracture: Results of a Randomized Controlled Trial. D. W. Morrish^{*1}, S. R. Majumdar^{*1}, L. A. Beaupre^{*2}, N. R. Bell^{*3}, J. G. Cinats^{*4}, D. A. Hanley^{*5}, C. H. Harley^{*1}, A. G. Juby^{*1}, D. A. Lier^{*6}, W. P. Maksymowych^{*1}. ¹Medicine, University of Alberta, Edmonton, AB, Canada, ²Rehabilitation Medicine, University of Alberta, Edmonton, AB, Canada, ³Family Medicine, University of Alberta, Edmonton, AB, Canada, ⁴Surgery, University of Alberta, Edmonton, AB, Canada, ⁵Medicine, University of Calgary, Calgary, AB, Canada, ⁶Institute of Health Economics, University of Alberta, Edmonton, AB, Canada.

Purpose: Patients having hip fracture frequently have osteoporosis, yet osteoporosis diagnosis and treatment rates remain inappropriately low at 10-20%. Therefore, we designed a randomized controlled trial to determine the cost and effectiveness of using a case manager to achieve diagnosis and appropriate treatment for this patient group.

Methods: The protocol was approved by the institutional Health Research Ethics Board. We recruited patients from all hospitals in Capital Health, Edmonton. Inclusion criteria were age over 50 years, not receiving active osteoporosis treatment other than calcium/vitamin D, and not living in long-term care facilities. The intervention consisted of a case manager who educated, arranged bone mineral density (BMD) testing by DEXA, provided bisphosphonate prescriptions to patients with low bone mass and communicated with primary care physicians. The control arm was "usual care", which did not include these measures.

Results: We screened 2219 patients and allocated 110 patients randomly to each of control or intervention. 88 intervention patients (80%) versus 32 (29%) controls had BMD performed ($p<0.001$). Of the 120 patients who had a BMD, 27 (23%) had normal bone mass. At 6 months, 56 (51%) of intervention patients versus 24 (22%) of controls were treated with bisphosphonates (adjusted odds 4.7, 95% CI 2.4-8.9, $p<0.001$). Intervention patients were more likely to receive appropriate care (defined as prescribed bisphosphonate therapy if BMD was <-1.5 SD t-score) than controls (67% versus 26%, adjusted $p<0.001$). The intervention cost was \$52 CDN per patient.

Conclusions: We conclude that a case manager substantially increases rates of osteoporosis testing and treatment in hip fracture patients for a modest cost.

Disclosures: D.W. Morrish, sanofi-aventis 2.

This study received funding from: Alberta Heritage Foundation for Medical Research.

T330

Vertebral Fractures in Patients with Chronic Obstructive Pulmonary Disease Patients: The EOLO Study. R. Nuti¹, S. Maggi^{*2}, G. Guglielmi^{*3}, G. Martini¹, C. Caffarelli^{*1}, S. Batucci^{*4}, T. De Feo^{*4}, G. Crepaldi², S. Gonnelli¹. ¹Institute of Internal Medicine, University of Siena, Siena, Italy, ²CNR Aging Branch, University of Padua, Italy, ³Institute of Internal Medicine, Department of Radiology, Scientific Institute Hospital, Casa Solievo della Sofferenza, San Giovanni Rotondo, Italy, ⁴Procter & Gamble, Roma, Italy.

Osteoporosis has been recognized as one of the systemic effects associated with chronic obstructive pulmonary disease (COPD). In particular there is a growing concern about the risk of vertebral fractures (VFs) which in COPD patients lead to a notable worsening of the respiratory condition. The aetiology of osteoporosis in COPD is complex and many factors may contribute to its pathogenesis, in particular the role of glucocorticoids (GCs) is still being debated.

The E.O.L.O. (Evaluation of Obstructive Lung disease and Osteoporosis) is a national study aimed to evaluate the prevalence of osteopenia, osteoporosis and VFs in a large sample of patients affected by COPD. Moreover E.O.L.O. study aimed to evaluate the impact of the use of oral and inhaled GCs and the severity of COPD on VFs. A total of 3030 ambulatory COPD patients (1768 men and 1262 women) aged 50+ yrs were enrolled. The patients underwent an evaluation of bone status by using a Quantitative Ultrasound device (Achilles, GE-Lunar) and a lateral chest X-ray for thoracic spine evaluation. X-ray films were locally and centrally digitized and morphometry software (MorphoXpress) was used for measuring vertebral heights.

Both in men and in women VFs are more frequent ($p<0.001$) in osteoporosis patients (72.8% and 78.3%) than in osteopenics (52.2% and 62.9%) or in normals (50.1% and 55.8%). The number of patients with osteoporosis or osteopenia is significantly influenced by COPD severity but not by COPD duration or GCs. The logistic regression model showed that the frequency of VFs is associated to the COPD severity and higher rates of VFs are observed in patients treated with oral or inhaled GCs. (see below)

LOGISTIC REGRESSION MODEL FOR VERTEBRAL FRACTURES

$n=2934$ (no fractures =1072, one or more fractures = 1862)

	OR	95% C.I.	
GENDER (Men)	0.547	0.464	0.644
AGE (yrs) *	1.034	1.024	1.044
BMI (<26.7)	1.448	1.239	1.692
COPD	1.000		
Mild	1.307	1.070	1.595
Moderate	1.426	1.137	1.790
Severe + Very Severe			
GC	1.000		
No TR.	1.350	1.028	1.774
No CS	1.593	1.029	2.466
O-CS	1.418	1.145	1.756
I-CS	2.018	1.449	2.810
O-CS + I-CS			

* 5 years increase in age

Variables in the model: gender, age, BMI, smoke, GCs, COPD severity

In conclusion the E.O.L.O. study confirms that COPD patients are at higher risk of having osteoporosis and of developing VFs. COPD severity and the use of GCs (both oral and inhaled) seem to play a crucial role in determining VFs.

Disclosures: R. Nuti, None.

T331

The Chaos Clinic - A Randomized Controlled Trial of a Falls Clinic for Prevention of Falls and Related Fractures. M. Palvanen^{*1}, P. Kannus^{*1}, J. Parkkari^{*2}, J. Rintala^{*3}, M. Järvinen^{*4}, M. Fogelholm^{*1}. ¹UKK Institute, Tampere, Finland, ²The Sports Medicine Centre of Tampere, Tampere, Finland, ³Suomen Terveystalo, Tampere, Finland, ⁴Tampere University Medical School and University Hospital, Tampere, Finland.

The purpose of this preliminary report of a falls clinic is to determine the number of falls and fall-related injuries (fractures) among our Finnish Chaos Clinic participants.

The Chaos Clinic is a falls clinic for prevention of falls and related injuries among elderly people. All persons aged 70 years or more with high-risk for falling and fractures are first interviewed and examined carefully at the Chaos Clinic to evaluate all individual intrinsic and extrinsic risk factors for falls and fall-induced injuries such as fractures. After the comprehensive and individual assessment of the risk factors for falling, the participants are randomized to the intervention group and control group. Thereafter, the personnel of the Chaos Clinic decide, on individual basis, the falls prevention measures needed and supervise their execution in the intervention group (a multifactorial preventive approach). All the participants are then followed-up for 12 months (in three months intervals) for falls and related injuries. Our hypothesis is that persons in the intervention group will have 30% less falls and related injuries than their counterparts in the control group.

The trial started in January 2005 and is still in process. So far, 400 participants have been followed for 12 months. At the one-year follow-up, 202/400 (51%) of the participants had fallen at least once having altogether 490 falls. These falls caused 262 injuries, 15 of them (5.7%) being fractures. The mean age of the participants was 76 years at baseline and 87% of them were women.

The randomized study evaluating the effect of the Chaos Clinic in falls prevention of older adults has started well and the number of falls and related injuries have been at expected level. The coming years will show the true efficacy of the falls prevention intervention of the Clinic.

Disclosures: M. Palvanen, None.

T332

X-ray Ordering Improves in Patients with Height Loss or Kyphosis Following an Osteoporosis Educational Intervention: Canadian Quality Circle (CQC) National Project. A. Papaioannou¹, G. Ioannidis¹, B. Kvern^{*2}, A. Hodsman³, L. Thabane^{*1}, A. Gafni^{*1}, D. Johnstone^{*4}, L. Salach^{*5}, F. Jiwa^{*6}, J. D. Adachi¹. ¹McMaster University, Hamilton, ON, Canada, ²University of Manitoba, Winnipeg, MB, Canada, ³University of Western Ontario, London, ON, Canada, ⁴Procter and Gamble Pharmaceuticals, Toronto, ON, Canada, ⁵Ontario College of Family Physicians, Toronto, ON, Canada, ⁶Osteoporosis Canada, Toronto, ON, Canada.

The CQC National Project is an integrated disease management study designed to improve family physicians' (FPs) adherence with the Osteoporosis Canada 2002 guidelines. The project consists of five phases: wave I data collection, 1st educational intervention, wave II data collection, 2nd educational intervention, and wave III data collection. During the educational intervention QC's met to discuss physician profiles on how they managed osteoporosis and to participate in an osteoporosis workshop. This interim analysis (wave I & II) examined the change in x-ray ordering in patients with kyphosis or height loss. The guidelines recommend that x-rays should be ordered in all patients with kyphosis or height loss. A total of 340 (wave I) and 301 (wave II) PCPs formed 34 QCs. For each wave, PCPs collected data from different patients via chart reviews and a standardized collection form. There were 8376 (wave I) and 7354 (wave II) patient records selected at random and analyzed. All patients were women 55 years and older. The generalized estimating equations (GEE) technique was used to evaluate differences in x-ray ordering in patients with kyphosis or height loss before and after the educational intervention. The cluster variable for the GEE model was physician and the analysis was adjusted for other clinical risk factors. An exchangeable correlation matrix was used for the analysis. Odds ratios (OR) and 95% confidence intervals (CI) were calculated. A total of 54.3% (662/1220), 56.2% (654/1163) and 53.1% (958/1804) of patients with kyphosis, height loss, or either kyphosis or height loss during wave I and 63.9% (726/1136), 61.0% (834/1367) and 60.2% (1130/1877) of patients with kyphosis, height loss, or either during wave II had a x-ray ordered, respectively. The likelihood of x-ray ordering increased following the educational intervention for patients with kyphosis (OR: 1.35; 95% CI: 1.07, 1.70), height loss (OR: 1.28; 95% CI: 1.04, 1.57) or either (OR: 1.32; 95% CI: 1.12, 1.55). In conclusion, more patients with kyphosis or height loss had x-rays done following the educational intervention. Appropriate x-ray ordering may result in a greater number of vertebral fractures detected. Patients with vertebral fractures may benefit with osteoporosis therapies.

Disclosures: A. Papaioannou, Alliance for Better Bone Health 2, 5; Eli Lilly and company 2, 5; Merck Frosst 2, 5; Novartis 2, 5.

This study received funding from: Alliance for Better Both Health.

T333

A Five Year Longitudinal Study of Health Related Quality of Life in Individuals with and without Incident Fractures: The Canadian Multicentre Osteoporosis Study (CaMos). A. Papaioannou¹, G. Ioannidis¹, C. Kennedy¹, L. Pickard¹, A. Tenenhouse², J. P. Brown³, R. Josse⁴, A. M. Sawka⁵, S. M. Kaiser⁶, T. Anastassiades⁷, W. Hopman⁸, J. D. Adachi¹. ¹McMaster University, Hamilton, ON, Canada, ²McGill University, Montreal, ON, Canada, ³Laval University, Sainte-Foy, PQ, Canada, ⁴University of Toronto, ON, Canada, ⁵University of Toronto, Toronto, ON, Canada, ⁶Dalhousie University, Halifax, NS, Canada, ⁷Queen's University, Kingston, ON, Canada.

CaMos, is a nation-wide, random sample of Canadian that provides a unique longitudinal opportunity to determine the relationship between incident fractures on health related quality of life (HRQL) over a 5 year period. A total of 4820 women and 1783 men 50 years of age and older were examined. The Health Utilities Index (HUI) Mark II and III systems were used to assess HRQL. The Mark II and III consist of a multi-attribute utility function score; Mark II has 6 attributes (sensation, mobility, emotion, cognition, self-care, and pain), and Mark III, 8 attributes (vision, hearing, speech, ambulation, dexterity, emotion, cognition, and pain). Multivariable linear regression analyses were conducted to examine changes in utility functions in patients with incident fractures versus those without fractures during a 5 year period. The analyses were adjusted for baseline covariates and were conducted for men and women separately. Parameter estimates and 95% confidence intervals (CI) were calculated. During the course of the study 8.0% (141/1766) of men and 11.8% (556/4773) of women had at least one incident fracture. For women, the differences between those with and without incident fractures for the Mark II were -0.06 (95% CI: -0.10, -0.02), -0.04 (95% CI: -0.07, -0.004), -0.04 (95% CI: -0.07, -0.01) and -0.10 (95% CI: -0.15, -0.04) for the multi-attribute utility function; and mobility, self-care, and pain attributes, respectively. For the Mark III, the differences were -0.07 (95% CI: -0.13, -0.01), -0.05 (95% CI: -0.09, -0.01) and -0.12 (95% CI: -0.18, -0.06) for the multi-attribute utility function; and ambulation and pain attributes, respectively. For men, the differences between those with and without incident fractures were -0.06 (95% CI: -0.11, -0.02) for the sensation domain of the Mark II; and -0.09 (95% CI: -0.16, -0.02), -0.03 (95% CI: -0.06, -0.001), -0.05 (95% CI: -0.10, -0.01), and -0.06 (-0.12, -0.01) for the multi-attribute utility function, vision, ambulation, and pain attributes of the Mark III. In conclusion, incident fractures are associated with reduced HRQL in both men and women. These impairments should be addressed to improve patient outcomes.

Disclosures: A. Papaioannou, Alliance for Better Bone Health 2, 5; Eli Lilly and Company 2, 5; Merck Frost 2, 5; Novartis 2, 5.
This study received funding from: Government of Canada, Pharmaceutical Industry.

T334

A Randomized Controlled Assessment for Effectiveness of an Evidence-based Guideline for Osteoporosis and Osteoporotic Fracture Prevention: Design and Pre-intervention Assessment. M. Iki¹, Y. Nakatani², M. Komatsu³, J. Tamaki¹, E. Kajita³. ¹Public Health, Kinki University School of Medicine, Osaka-Sayama, Japan, ²Community Nursing, Hamamatsu University School of Medicine, Hamamatsu, Japan, ³Public Health and Home Nursing, Nagoya University School of Health Sciences, Nagoya, Japan.

Background: Many evidence-based clinical guidelines have been published for the treatment of patients with osteoporosis and for its prevention. However, only a little evidence for the effectiveness of such guidelines has been obtained.

Aim: To assess whether an evidence-based guideline helps public health professionals improve their preventive programs for osteoporosis better than other information.

Setting: Nation-wide study for community health centers in Japan.

Design: Randomized controlled trial with allocation concealed from evaluators.

Subjects: 100 municipal health centers were selected randomly from all the centers in Japan which responded to our screening questionnaire for this study and had a plan of revising the preventive programs for osteoporosis.

Primary outcome: Change in a score for the concordance of the programs provided by the centers to corresponding evidence before and after the intervention.

Intervention: Use of an evidence-based practice guideline which was compiled by the authors for public health practitioners to prevent community-dwelling people from osteoporosis and osteoporotic fracture. The guideline was approved with the AGREE instrument to have good quality. After the pre-intervention assessment of the concordance score, the independent controller of the trial allocated the centers randomly to one of the intervention and the control groups. The controller sent several copies of the guideline to each center of the intervention group and asked to revise the programs by using the guideline. He also asked each center of the control group to revise their program with any information other than the guideline.

Results: The screening questionnaires were sent to 1,978 community health centers throughout Japan and 1319 centers (66.7%) responded. 100 random samples were obtained and random allocation was successfully performed. The revised programs are being implemented in both groups. A post-intervention assessment will be conducted to know the change in the concordance score of the programs to the evidence through the intervention. **Conclusions:** The first half process of the present trial has been successfully performed. We will soon conduct a post-intervention assessment of the revised programs. The effectiveness of the guideline for osteoporosis prevention will be clarified on the outcome basis next year.

Disclosures: M. Iki, None.

This study received funding from: Grant-in-aid from the Japanese Ministry of Health, Labour and Welfare.

T335

Poverty Is a Risk Factor for Osteoporotic Fractures. M. Sosa¹, M. Navarro², P. Saavedra³, P. Lainez², M. Torres², M. Marerro², C. Medina². ¹Ciencias Médicas y Quirúrgicas, University of Las Palmas de Gran Canaria, Hospital University Insular, Spain, Spain, ²Enfermería, University of Las Palmas de Gran Canaria, Grupo de Trabajo Promoción y Educación de la Salud, Spain, ³Mathematics, University of Las Palmas de Gran Canaria, Spain, Spain.

Background: Some life-styles are related to the development of osteoporosis and osteoporotic fractures. Indeed, poverty is closely related to some life-styles. There are few studies about the possible relationship between poverty and osteoporotic fractures.

Objective: To study in a population of postmenopausal women the possible association between poverty and the presence of osteoporosis, determined by Dual X-Ray Absorptiometry (DXA) and the association between poverty and vertebral and non-vertebral fractures.

Method: Cross-sectional study, performed on 1,139 postmenopausal Canarian women. They completed a questionnaire about risk factors for osteoporosis. A complete medical examination and a detailed assessment of their socioeconomic status was also performed. An X-ray of the lateral spine was also performed. We measured bone mineral density by DXA in the lumbar spine and proximal femur. Finally, we estimated ultrasound parameters at the calcaneus (QUS).

Results: Group I (Poverty Group) was composed by 474 women. Group II (Controls), was composed by 665 women without poverty. Poverty Group had lower values of BMD in the lumbar spine than controls ($0.86 \pm 0.18 \text{ g/cm}^2$ vs $0.89 \pm 0.16 \text{ g/cm}^2$, $p = 0.001$). There were no statistical significant differences at the proximal neck. Indeed, Group I had lower values of some QUS parameters, (SOS and QUI). There were at least an osteoporotic fracture in 37.8% of women with poverty while controls had a fracture in 27.5% ($p < 0.001$). Vertebral fractures were also more prevalent on Group I (poverty), than in controls (24.7% vs 13.4%, $p < 0.001$). There were no statistical differences in non-vertebral fractures between the two groups.

Conclusions: Postmenopausal women with poverty showed lower BMD values in the lumbar spine than controls. Indeed, they had lower values of QUS at the calcaneus and a higher prevalence of vertebral fractures. In postmenopausal women with poverty, the risk of osteoporosis and fragility fractures should be taken into account to establish adequate preventive programs.

Type of fractures	Prevalence of fractures.		p value
	Group I Poverty n= 474	Group II. Controls n= 665	
Total	37.8	27.5	< 0.001
Vertebral	24.7	13.4	< 0.001
Non-vertebral	17.5	17.1	0.872

Disclosures: M. Sosa, None.

T336

Positive Association of Physical Exercise and Coffee Consumption with BMD in Postmenopausal Women: The Fukuoka Cohort Study. R. Takayanagi¹, M. Adachi², K. Ohnaka², H. Kawate², S. Kono³. ¹Department of Medicine and Bioregulatory Science, Graduate School of Medical Sciences, Kyushu University, Fukuoka, Japan, ²Department of Geriatric Medicine, Graduate School of Medical Sciences, Kyushu University, Fukuoka, Japan, ³Department of Preventive Medicine, Graduate School of Medical Sciences, Kyushu University, Fukuoka, Japan.

The etiology of osteoporosis is multifactorial, and lifestyle factors seem to play an important role in the occurrence and progression of osteoporosis. We have recruited 1294 women (50-74 years of age) in The Fukuoka Cohort Study, interviewed about lifestyle, and measured body composition, blood chemistry and BMD of hip and spine using DXA measurements. We examined the relationship between the BMD values adjusted for age and these lifestyle parameters.

Both hip and spine BMD values were associated positively with body mass index, abdominal circumference, and hip circumference, and inversely with the duration after menopause. The spine BMD was higher in diabetic subjects than in non-diabetic subjects. HbA1c values were also positively associated with both hip and spine BMD. Physical exercise levels were positively associated with the hip BMD ($p=0.047$). Although no clear association was observed for green tea and milk consumption, coffee consumption was associated with higher BMD values of the hip and spine.

Multivariate analysis showed that age, BMI, hip circumference and duration after menopause was associated with both hip and spine BMD independently. Furthermore, positive associations with HbA1c values and coffee consumption remained after adjustment for age, BMI, hip circumference and duration after menopause. This present study firstly supports that coffee consumption may be protective against osteoporosis in postmenopausal women.

Disclosures: R. Takayanagi, None.

T337

Long Term Retention of Knowledge from an Osteoporosis Education Program. P. S. Via*, V. I. Petkov*, R. A. Adler. Endocrinology Section, McGuire Veterans Administration Medical Center, Richmond, VA, USA.

The study objective was to evaluate the effects of education on knowledge gain and retention in a population of high-risk veterans attending an osteoporosis education class. Methods: Veterans with low bone mass were scheduled for an Osteoporosis Education Seminar. Attendees were invited to complete a 15-question anonymous test with content about osteoporosis (risk factors, sources of Ca and Vit D, use of glucocorticoids) prior to the seminar and again at the conclusion of the seminar. The same test was mailed at 6 and 12 months after the education seminar.

Results: During the study period of 14 months, a total of 318 patients attended the Osteoporosis Education Seminar. Of them, 226 agreed to participate in our study and 209 completed both pre and posttests and were included in the analysis. The mean age of study participants was 70.4 (± 9.4) years, 67.3 % were Caucasian, and 94.3% were men. There was a significant increase in osteoporosis knowledge evaluated by the total score of the administered test (paired t-test p-value < 0.0001). The response rate at 6 months was 63% and at 12 months 52%. Responders did not differ significantly from non-responders in any of the examined characteristics. Compared to pre-tests scores, the participants still had significantly higher scores at 6 and 12 months post education 10.1 (2.4) and 10.2 (2.5) vs. 7.6 (2.7), paired t-test p-value < 0.0001. There was a significant decrease in the mean scores at 6 and 12 months post education compared to the post-test scores immediately after the education class (10.2 vs. 12.2).

Conclusions: The knowledge about osteoporosis gained in 2-hour educational seminar was retained over 1 year.

Disclosures: P.S. Via, None.

T338

The Influence of Prior and Current Weight Change on Forearm Bone Loss in Menopausal Women, a 15 Year Longitudinal Population-Based Study. The Nord-Trøndelag Health Study, Norway. S. Forsmo, A. Langhammer*. Dept. of Public Health and General Practice, Norwegian University of Science and Technology, Trondheim, Norway.

Low body weight and weight loss has detrimental effects on bone. The purpose of this study was to investigate the effect on forearm bone mineral density (BMD) of weight change 11 years prior to, and during, a five years follow-up study in peri- and postmenopausal women.

In 1984-86, a total of 8,856 women aged 45-60 years, virtually all Caucasians, attended the first Nord-Trøndelag Health Study (HUNT I). Among these women, a random sample of 2,795 was invited to distal forearm densitometry (SXA technology) in 1995-97 (HUNT II), and 2,188 women (mean age: 65.1 years) attended. In 2001, 2,098 women were invited for subsequent forearm BMD, weight and height measurement and 1,421 (67.8%) attended. After exclusion of women reporting hyper- or hypothyroidism or with missing weight data, a total of 1,302 women were eligible for analyses. Weight change was defined as a more than 1 kg increase or loss. The influence of weight change on BMD was assessed by linear and logistic regression and in general linear models, adjusting for body weight, smoking and oestrogen use at HUNT II.

During the 11.3 years between HUNT I and HUNT II, a total of 17.3% had lost and 68.8% had gained more than 1 kg. During the next 4.6 years, weight loss was observed in 40.1% and weight gain in 32.6% of the women. A total of 85 (6.5%) had lost and 284 (21.8%) had gained weight during both periods of observation. Mean annual loss in BMD was 1.03 %, highest in the youngest and oldest age groups. In linear regression models, with either prior or current weight change as independent variables, a statistically significant positive relationship between changes in weight and BMD was found. Women with previous weight loss experienced increased bone loss compared to women with previous weight gain, also when current body weight was stable or increasing. A significant reduction in bone loss was only seen in women who had gained more than 3.5 kg after a history of prior weight loss. In a logistic regression model with prior and current weight change (gain, stable and loss) as independent variables, the adjusted odds ratio (OR) for bone loss in the highest age-specific quartile (most bone loss) was 1.42 (p<0.05) for the category of prior weight loss and 1.37 (p<0.05) for current weight loss, with weight gain as reference categories. There was no interaction between previous and current weight change. The study shows that both prior and current weight loss, independently of each other, are associated with increased bone loss at the distal forearm in middle-aged and elderly women. Weight gain reduces bone loss.

Disclosures: S. Forsmo, None.

T339

Change of Bone Mineral Density and Biochemical Markers of Bone Turnover in Patients on Suppressive L-thyroxine Therapy for Differentiated Thyroid Carcinoma. S. Hong, W. Park*, S. Kim*, M. Nam*, Y. Kim*. Internal Medicine, Inha University, Incheon, Republic of Korea.

Untreated hyperthyroidism and high dose of thyroid hormone are associated with osteoporosis. Bone mineral density (BMD) has been shown to be increased in postmenopausal females with postthyroidectomy hypoparathyroidism. However, their effect on the BMD and biochemical markers of bone turnover in patients on long-term suppressive L thyroxine therapy for differentiated thyroid carcinoma. In this study, we measured BMD of lumbar spine and femur and bone turnover markers in 7 premenopausal, 22 postmenopausal women with thyroid carcinoma at the baseline and during the follow-up period (12th-48th month) using dual-energy x-ray absorptiometry. Biochemical marker of bone resorption was measured by urine deoxypyridinoline and bone formation by serum osteocalcin. None of the women gave a medical history that could possibly affect bone metabolism. All of them had undergone a total thyroidectomy and subsequent thyroxine therapy. Their age ranged from 39-76 years old, with a mean of 51.7 year. TSH was suppressed during the study. The results showed that BMD of femur and lumbar were not changed significantly in pre, postmenopausal women. Postoperative hypoparathyroidism occurred in 4 premenopausal women and 12 postmenopausal women. BMD of femur neck was changed 0.003 ± 0.066 g/cm² (p>0.05). Patients with hypoparathyroidism had higher BMD gain than those without hypoparathyroidism in femur (-2.14 vs 3.65 %, p<0.05). Biochemical markers of bone turnover, serum osteocalcin and urine deoxypyridinoline were not changed significantly. For all patients enrolled in this study TSH exhibited a significant negative correlation with osteocalcin ($r=-0.50$; p-value <0.01) but not with deoxypyridinoline ($r=-0.03$; p-value=0.9) levels. Baseline TSH was negative correlation with baseline lumbar spine BMD($r=-0.47$, p-value <0.05), follow up lumbar spine($r=-0.46$, p-value <0.05) and trochanter BMD($r=-0.44$, p-value<0.05). In conclusion, patients with well differentiated thyroid carcinoma are not at great risk of bone loss. The state of chronic hypoparathyroidism is associated with increased BMD, especially at the femur neck.

Disclosures: S. Hong, None.

T340

Effects of Daily Muscle Trainings on Falls and Vertebral Fractures in the Elderly Osteoporotic Women. T. Horiuchi¹, A. Kanemaru², T. Katoh², H. Tobimatsu¹. ¹Endocrinology, Tokyo Metropolitan Geriatric Hospital, Tokyo, Japan, ²Rehabilitation, Tokyo Metropolitan Geriatric Hospital, Tokyo, Japan.

Objective: We conducted a randomized case control study for one year to examine the effects of the home daily exercises to prevent osteoporotic women from falling and suffering fracture. Subjects & Methods: Ninety-three osteoporotic elderly women were recruited to participate in this study and they were divided into two groups: one is the control whose physical strength we only estimate, whereas the other group were intervened by exercise. The exercise group were instructed to repeat daily muscle training at home. The exercise instruction include muscle training to increase the strength of abdominal, back, quadriceps, gastrocnemius, soleus and plantaris muscles. In order to evaluate muscle strength we measured grasp power (GP), knee flexion strength (KNS), maximal walk velocity (MAW) and 3m timed up and go test (TUGT), lumbar and femoral bone mineral density and bone metabolic markers before and after one-year training, checking the reproducibility and QOL with SF36 every six months. Falls frequencies and vertebral fractures incidences were also examined. Statistics were done using a two-way ANOVA and stepwise multiple regression analysis. The medications for osteoporotics have not been altered in all participants during this study. Results: LBMD were significantly increased in both groups for one year (p<0.05). In exercise group GP, MAW and KNS were significantly increased, and TUGT were significantly decreased (p<0.05). There was a graph interaction between control and intervention group in left KNS, which means that a significant difference between two groups disappeared in one year (p=0.006). Physical component score and mental component score in SF36 were not changed in both groups. Falls frequencies were decreased in two groups, showing a trend of steep reduction in a training group. There was no significant difference in vertebral fracture incidence between two groups. In multivariate regression analysis TUGT was significantly associated with Falls frequencies (p<0.0001). Conclusion: Exercise for the elderly women are effective to increase the strengths of muscles. Exercises might be effective to prevent elderly osteoporotics from falling. We should furthermore continue to perform exercise instruction as an intervention using TUGT.

Disclosures: T. Horiuchi, None.

T341

Back Extensor Strength, Lumbar Spine Mobility and Spinal Inclination as Related Factors for Falls in Osteoporotic Patients. Y. Kasukawa, N. Miyakoshi, M. Hongo, Y. Ishikawa, H. Noguchi, K. Kamo, H. Sasaki, Y. Shimada*. Department of Orthopedic Surgery, Akita University, Akita, Japan.

We have previously reported that mobility of the lumbar spine and back extensor strength (BES) are decreased in osteoporotic patients with a history of falls or fear of falling. However, factors related to the history of falls or tendency for falling remain unclear. The purpose of this study was to clarify possible factors including spinal deformity, mobility and BES related to history of falls or fear of falling in osteoporotic patients. Subjects comprised 92 elderly patients with osteoporosis (mean age, 74 years; range, 60-96 years) who had no neurological or metabolic disorders other than osteoporosis. Subjects were divided into 2 groups: subjects with a history of falls, fear of falling, or need for support when walking (Fall group, n=52; 11 men, 41 women); and subjects with no such history (Non-fall group, n=40; 12 men, 28 women). Angles of thoracic or lumbar kyphosis and mobility of the thoracic or lumbar spine were measured in the upright position and at maximum flexion/extension using a computer-assisted device (SpinalMouse). Spinal inclination reflecting spinal sagittal alignment was also evaluated using SpinalMouse. Bilateral grip strengths were measured using a handgrip dynamometer. Isometric BES was measured using a strain-gauge dynamometer. No significant differences between groups were observed in age, gender, height, bodyweight, or body mass index. Mean grip strength and BES were 24% (p<0.01) and 30% (p<0.05) lower in the Fall group than in the Non-fall group. Angle of lumbar kyphosis and mobility of lumbar spine were 81% (p<0.01) and 31% (p<0.01) lower in the Fall group than in the Non-fall group. However, no significant differences were observed between groups in angle of thoracic kyphosis or mobility of the thoracic spine. Logistic regression analysis was performed to clarify risk factors for falling in these osteoporotic patients. BES, mobility of the lumbar spine and spinal inclination were identified as significant contributors to falls. These results suggest that decreased back extensor strength, decreased mobility of lumbar spine, and increased spinal inclination could represent risk factors for falls in patients with osteoporosis.

Disclosures: Y. Kasukawa, None.

T342

Risk Factors for Osteoporosis and Bone Mineral Density in Late Postpartum Women. C. A. M. Kulak¹, A. A. Franke^{*1}, B. M. Filippetto^{*2}, A. A. Urbanetz^{*2}, V. Z. C. Borba¹. ¹Endocrinology, UFPR, Curitiba, Brazil, ²Gynecology and Obstetrics, UFPR, Curitiba, Brazil.

Calcium and bone metabolism is altered during pregnancy and lactation, some adaptive changes occur during pregnancy to preserve the mother's bone mass. In breast-feeding period these compensatory alterations do not exist. Our purpose was to determine the existence of known risk factors for low bone mass in a group of women in the late postpartum period, evaluate the bone mass in these women and correlate bone mass to the presence of risk factors. We did an observational, transversal study in 81 women in the postpartum period recruited from the Maternity Outpatient Clinic of the Hospital de Clinicas da Universidade Federal do Paraná, during a routine return visit after 40 days of child birth. Patients who had agreed to participate had been submitted to a questionnaire approaching known risk factors for decreasing bone mass and to a DXA bone densitometry measurement in lumbar spine and hip. Blood sample for posterior evaluation of laboratorial parameters was harvested. We analyzed 81 women with an average age of 28.7 ± 7.7 years at 43.4 ± 9.2 days after childbirth. We observed that 91.4% were Caucasian. We demonstrated an average bone density in lumbar spine of 0.989 ± 0.137 g/cm² and hip of 0.931 ± 0.128 g/cm². In accordance with the ISCD criteria, 8 patients (9.8%) had presented a low bone mass for their age in lumbar spine (Z score less than -2.0). These patients were younger, with an average age of 26.4 ± 8.9 years old (RR 0.22; p<0.05), and average BMI of 23.11 ± 3.77 kg/m² against 25.8 ± 4.9 kg/m² of the general group (RR 0.36; p<0.05). This group also showed a greater smoking index, physical inactivity, personal history of previous bone fractures and familiar history of osteoporosis (compared to all of them p>0.05). We did not observe in this group differences in calcium consumption, parity, age in a first gestation, or duration of breast-feeding. Our study group data suggest that general risk factors were more related to low bone mass than the factors related to the gestation and breast-feeding.

Disclosures: C.A.M. Kulak, None.

T343

High Cholesterol, Smoking and Coffee Consumption but Low BMI Are Risk factors for Fractures - a 20-Year Follow-up of Men and Women. K. L. L. Landin-Wilhelmsen¹, P. Trimpou^{*2}, A. Odén^{*2}, L. W. Wilhelmsen^{*2}. ¹Sahlgrenska University Hospital, Section for Endocrinology, Göteborg, Sweden, ²Sahlgrenska University Hospital, Institution of Medicine, Göteborg, Sweden.

According to some studies there is a link between osteoporosis and cardiovascular disease. The purpose was to study this possible link with access to risk factors for fractures. The study comprised a random population sample of men and women aged 25-64 years, N=1396 (52% women), from the 1985 World Health Organisation (WHO), MONITORing of trends and determinants in Cardiovascular disease (MONICA) study in Gothenburg, Sweden.

The baseline examination in 1985 included history of fractures, physical activity at work and during leisure time graded low (1) to high (4), psychological stress, smoking habits graded non-smoker (1) to >24 cigs./day (5), coffee consumption in cups/day, BMI kg/m², waist/hip ratio, blood pressure mmHg, total cholesterol, HDL-cholesterol, triglycerides all in mmol/L and fibrinogen g/L.

Osteoporotic fractures during 20 years follow-up (n=140) were retrieved from the hospital registers of the city.

Out of the measured factors increasing age, previous fractures, higher smoking habits, higher coffee consumption (Hazard rate [HR] =1.07), higher total cholesterol (HR=1.15) and lower BMI (HR=0.96) significantly increased the risk for fractures.

The gradient of risk for fractures per 1.0 standard deviation (SD) towards higher HR was for total cholesterol 1.22 and for BMI 1.21 (lower) when they were included in the same model. There was a positive correlation between the two variables with a partial correlation coefficient with gender taken into account being 0.153 (p<0.001). For comparison it can be mentioned that when all types of osteoporotic fractures were considered the gradient of risk per 1.0 SD for bone mineral density varied between 1.4 and 1.6 depending on location. In summary, there was an equal importance of BMI and cholesterol for osteoporotic fracture risk, but the association had different directions. As for cardiovascular disease smoking and high cholesterol increased risk for fractures. Coffee consumption increased the risk for osteoporotic fractures, but coffee has not been a risk factor for myocardial infarction according to our experience.

Disclosures: K.L.L. Landin-Wilhelmsen, None.

T344

Clinical Factors Associated with Osteoporotic Fractures in a Representative Population of French Women. E. Lespessailles¹, P. Fardellone², C. Roux³, F. Cotte^{*4}, A. Gaudin^{*4}. ¹Rheumatology, CHR Orleans, Orléans, France, ²Rheumatology, CHU Hôpital Nord, Amiens, France, ³Rheumatology, Université René Descartes, Hôpital Cochin, Paris, France, ⁴Health Outcomes Studies, GlaxoSmithKline, France, Marly le Roi, France.

Background: Post-menopausal osteoporosis represents a major socio-economic problem. Bone fracture is the main clinical consequence in this population.

Objectives: The aim of the study was to identify risk and protective factors for fracture in French women aged 45 or more years with osteoporosis

Methods: This study was a cross-sectional observational epidemiological survey carried out in a representative sample of the population of women aged 45 or more years, constituted according to the quota method, a stratified random sampling method. The risk factors of fractures were analyzed in women with osteoporosis confirmed by DXA. The investigation was conducted by face-to-face home interviews between September and December 2006.

Results: Among the 2,613 interviewed women (mean age: 65.8 +/- 11.2 years), the prevalence of osteoporosis diagnosed by DXA was 9.7%. Fractures were reported by 101 (39.8%) subjects identified with osteoporosis (n=254). The odds-ratios of fractures were significantly associated with age (OR=1.03, per year increase; P=0.031) and the following factors (univariate analysis)(table).

Hormonal replacement therapy, osteoporosis treatment, vitamin D and/or calcium supplementation, smoking, alcohol intake and diabetes were not associated with a risk of fracture.

Conclusion: Several risk factors of fractures in osteoporotic women have been confirmed. This study highlighted the role of fall-related factors in osteoporotic fracture.

Main factors associated with a risk of fracture			
Factors	P	OR	95 % CI
History of cardiovascular problems	<0.001	3.27	1.73 - 6.19
Fracture before 40 years	0.001	2.46	1.44 - 4.19
Reduced mobility	0.001	2.42	1.44 - 4.06
PMO history (> 5 y)	0.01	2.33	1.10 - 4.91
Diagnosed rheumatoid arthritis	0.045	1.96	1.02 - 3.75
Intake of sleeping pills	0.031	1.79	1.09 - 3.58
Well-corrected vision	0.003	0.42	0.20 - 0.75

Disclosures: E. Lespessailles, Novartis 2.

This study received funding from: GlaxoSmithKline.

T345

Chemotherapy Is Associated with Increased Risk of Fracture in Elderly Patients with Non-Hodgkin's Lymphoma. H. Lu^{*1}, M. Cabanillas², S. Fang^{*3}, X. L. Du^{*4}. ¹General Internal Medicine, Section of Rheumatology, UT MD Anderson Cancer Center, Houston, TX, USA, ²General Internal Medicine and Leukemia, UT MD Anderson Cancer Center, Houston, TX, USA, ³Division of Epidemiology, School of Public Health, The University of Texas Health Science Center, Houston, TX, USA, ⁴Division of Epidemiology, School of Public Health, University of Texas Health Science Center, Houston, TX, USA.

Background: With advancements in treatment, patients with non-Hodgkin's lymphoma (NHL) can now survive longer. Early detection and supportive care for long term complications from cancer and its treatment is needed. The incidence of osteoporosis increases with age and prolonged corticosteroid use. Corticosteroids are often part of the chemotherapy treatment for NHL. Untreated osteoporosis can lead to fracture, causing significant morbidity and mortality.

Objective: To determine whether chemotherapy is associated with increased risk of

fracture in elderly patients with NHL.

Methods: Retrospective cohort study using the population-based SEER (Surveillance, Epidemiology, and End Results)-Medicare linked data. Cases reported by the SEER cancer registries from 1992-1999 were matched against Medicare master enrollment files. The study population consisted of patients ≥ 65 years with NHL. We searched for any diagnosis of fracture 1 year prior to and thereafter the diagnosis during 11 years of follow-up.

Results: Of the 13,570 patients identified with NHL, approximately 60% received chemotherapy. African-Americans and patients with stage I disease were less likely to receive chemotherapy. Younger patients and those with lower comorbidity scores were more likely to receive chemotherapy. The prevalence of fracture prior to the diagnosis was significantly lower in patients who were to receive chemotherapy (7.9%) than those who did not (11.1%) ($P < 0.001$). Although fracture rate in both groups increased with follow-up, the rate of fractures after the diagnosis of NHL was significantly higher in patients who received chemotherapy (31.1%) compared to those who did not (18.5%, $p < 0.001$). After adjusting for age, race/ethnicity, tumor stage, comorbidity and radiation therapy in the multivariate logistic regression analyses, patients who received chemotherapy had more than double the risk of fracture compared to patients who did not receive chemotherapy. Other risk factors included more advanced age, female gender and non-African American origin.

Conclusions: This population-based retrospective cohort study demonstrates for the first time that chemotherapy for NHL is associated with a significantly increased risk of fracture in elderly patients. Further prospective studies may be needed to confirm this finding in different populations.

Disclosures: H. Lu, None.

T346

Gold Standard Measurement of Physical Activity Energy Expenditure and Bone Mineral Density in Older Adults: The Health ABC Study. D. C. Mackey¹, T. B. Harris^{*2}, T. M. Manini^{*3}, L. Ferrucci^{*2}, S. E. Hardy^{*4}, E. S. Strotmeyer⁴, F. A. Tykavsky⁵, S. R. Cummings, for the Health ABC Study¹. ¹San Francisco Coordinating Center, California Pacific Medical Center, San Francisco, CA, USA, ²National Institute on Aging, Bethesda/Baltimore, MD, USA, ³University of Florida, Gainesville, FL, USA, ⁴University of Pittsburgh, Pittsburgh, PA, USA, ⁵University of Tennessee, Memphis, TN, USA.

Self-reported physical activity has been associated with bone mineral density (BMD) and rate of change in BMD in older adults, but the effects of objectively measured physical activity on bone have not been well characterized. Doubly labeled water is the gold standard method for assessing physical activity energy expenditure (AEE). Our aims were to determine whether AEE is associated with hip BMD and rate of change in hip BMD among older adults.

We measured AEE over 2 weeks using doubly labeled water in 119 participants (51% women, 45% white, 55% black, mean \pm SD age: 75.7 \pm 2.7 yrs, mean \pm SD weight: 76.3 \pm 15.6 kg) from the prospective Health ABC Study. At the time of the doubly labeled water dosing, we measured hip and whole body BMD with dual energy x-ray absorptiometry (Hologic QDR 4500A). We repeated hip BMD measures two (n=102) and five (n=76) years later. We used general linear models to compare mean baseline BMD and change in BMD across levels of AEE.

AEE was not associated with total hip or femoral neck BMD at baseline (Table). The overall rate of change in total hip BMD over two years was -1.44% (95%CI: -0.87 to -2.02%), equivalent to a loss of 13.0 mg/cm² (8.1 to 18.0 mg/cm²), and over five years was -3.31% (-2.26 to -4.37%), equivalent to a loss of 30.1 mg/cm² (20.6 to 39.6 mg/cm²). There were no differences in 2-year ($p=0.335$) or 5-year ($p=0.422$) percentage rate of change in total hip BMD across tertiles of AEE, controlling for age, gender, race, total bone-free lean mass, total fat mass, weight change, and clinical site. Similar results were observed for the femoral neck.

Table. Mean BMD (g/cm²) and 95% confidence intervals by tertile of AEE, adjusted for age, gender, race, total bone-free lean mass, total fat mass, and clinical site.

Activity energy expenditure (AEE), kcal/d	Total Hip BMD (n=119)	Femoral Neck BMD (n=119)
Tertile 1 (94 to < 522)	0.891 (0.849-0.933)	0.741 (0.703-0.779)
Tertile 2 (522 to < 761)	0.907 (0.868-0.946)	0.759 (0.724-0.794)
Tertile 3 (761-2050)	0.864 (0.827-0.901)	0.723 (0.690-0.756)
P for trend	0.304	0.360

Energy expenditure from physical activity measured with the gold standard technique was not associated with hip BMD or rate of change in hip BMD in older women and men. Exercise prescriptions based on simple energy expenditure goals may not influence bone density in older populations.

Disclosures: D.C. Mackey, None.

T347

C-reactive Protein (CRP), Bone Mineral Density (BMD) and Hip Fracture Risk in Elderly Men and Women: The Framingham Study. R. R. McLean¹, R. Roubenoff^{*2}, M. T. Hannan¹, L. A. Cupples^{*3}, D. P. Kiel¹. ¹Hebrew SeniorLife & Harv Med Sch, Boston, MA, USA, ²Biogen Idec, Cambridge, MA, USA, ³BU Sch of Public Health, Boston, MA, USA.

Several of the pro-inflammatory cytokines that regulate immune response also mediate bone metabolism. Many inflammatory diseases are associated with osteoporosis, and previous studies suggest that otherwise healthy individuals with elevated CRP, an indicator

of systemic inflammation, are at increased risk of low bone mass and fractures. We examined the association of CRP with BMD and hip fracture risk in men and women in the now elderly Framingham Study Original Cohort. Non-fasting blood samples were drawn from 310 men and 502 women (mean age 78 yr, range 72-94) in 1992-94 (baseline) and serum CRP was measured to the nearest mg/L by an immunoprecipitation assay. Participants were classified into undetectable (0 mg/L), medium (1 to 2 mg/L) and high (≥ 3 mg/L) CRP groups. BMDs of the proximal femur (neck, trochanter) and lumbar spine (g/cm²) were measured at baseline using a Lunar DPX-L. Incident hip fractures were ascertained from baseline through December 2003. Analysis of covariance was used to compare mean BMD among CRP groups. Cox proportional hazards regression was used to calculate the hazard ratios (HR) and 95% confidence intervals (CI) estimating the relative risk of hip fracture for the medium and high CRP groups versus the undetectable group. All analyses were adjusted for sex and baseline measures: age (yrs), weight (lbs), height (in), current smoker (y/n), caffeine intake (>2 cup/d: y/n), alcohol intake (oz/wk), and current estrogen use (y/n) among women. The proportions (%) of participants with undetectable, medium and high CRP were 68, 13, and 19, respectively.

	Least-squares mean (\pm SE) BMD (g/cm ²) for CRP groups		
	Undetectable	Medium	High
Femoral neck	0.767 (0.005)	0.771 (0.012)	0.777 (0.010)
Trochanter	0.695 (0.005)	0.702 (0.012)	0.713 (0.010)
Lumbar spine	1.147 (0.010)	1.149 (0.022)	1.130 (0.019)

There were no significant differences in baseline BMD among CRP groups for either femur site or for the lumbar spine (all $p > 0.1$). Median hip fracture follow-up was 9.5 yr with 66 hip fractures (men 12, women 54) occurring over follow-up. Participants in the both the medium (HR 0.95; 95%CI 0.49, 1.95) and high (HR 0.99; 95%CI 0.48, 2.05) CRP groups had similar hip fracture risk to those with undetectable CRP. There was a similar lack of association with hip fracture risk when only the women were examined. In contrast to previous findings, these results suggest that low-grade systemic inflammation may not be a risk factor for low bone mass or increased fracture risk among community-dwelling elders.

Disclosures: R.R. McLean, None.

T348

Risk Factors for Osteoporosis and Fragility Fractures in Postmenopausal Women and Men Older than 50 Attended in a Primary Care Center of Spain: The Camargo Cohort Study. J. M. Olmos¹, C. Ramos^{*2}, J. L. Hernández^{*1}, P. García^{*2}, J. Martínez^{*1}, J. de Juan^{*2}, D. Nan^{*1}, C. Valero^{*1}, J. González-Macías¹. ¹Medicina Interna, Hospital Universitario M. Valdecilla. Universidad de Cantabria, Santander, Spain, ²Centro de Salud "José Barros". Camargo. Universidad de Cantabria. Santander, Spain, Santander, Spain.

The purpose of the study was to determine the prevalence of several risk factors for osteoporosis and fragility fractures in a population of postmenopausal women and men older than 50. We present preliminary results of the first 756 subjects (604 women, and 152 men) included in the Camargo Cohort Study, a community-based study designed to evaluate the prevalence of metabolic bone diseases and disorders of mineral metabolism, as well as the prevalence of fractures and risk factors for osteoporosis and fragility fractures, in postmenopausal women and men older than 50 attended in a primary care center of Northern Spain. Studied women and men were 63 \pm 9 and 65 \pm 8 years old, respectively. Demographic, anthropometrics, and clinical variables were collected, and subjects were evaluated with a questionnaire of risk factors for osteoporosis and fragility fractures. The prevalence of main osteoporosis risk factors in women and men was as follows: familial history of fragility fractures: 18% and 9%; fracture after 40 years: 17% and 16%; tobacco and alcohol consumption: 13% / 17%, and 10% / 38%, respectively. Reduced mobility was present in four percent of women and one percent of men. Early menopause (< 40 years) and low body weight (< 57 kg) was present in 15% of women and 11% of men. Thirty two per cent of women and fourteen of men were treated with benzodiazepines, 22% and 11% reported at least one fall during the previous year, and 13% and 18% had hypoaesthesia. Seven percent of women and nine percent of men were taking inhaled or systemic glucocorticoids, respectively. Six percent of women and two percent of men were receiving thyroid hormone treatment. Mean calcium intake in dairy products was 661 \pm 316 mg in women and 563 \pm 337 mg in men. Besides age, the most prevalent risk factors for osteoporosis and fragility fractures in our series were a history of fragility fractures, benzodiazepine use and previous fall. Early menopause, familial history of fragility fractures, low body weight, previous fall and treatment with benzodiazepines were more relevant in women, whereas tobacco and alcohol consumption were more frequent in men.

This study was supported by a grant from the "Fondo de Investigación Sanitaria", Ministerio de Sanidad y Consumo, Spain (FIS: PI05 0125)

Disclosures: J.M. Olmos, None.

T349

The Effect of Anti-epileptic Medications on Bone Mineral Density- A Twin and Sibling Study. S. J. Petty^{*1}, L. M. Paton^{*1}, T. Fedorova^{*2}, S. F. Berkovic^{*1}, P. Sambrook², T. O'Brien^{*3}, J. D. Wark¹. ¹Department of Medicine, RMH, The University of Melbourne, Melbourne, Australia, ²Department of Rheumatology, Institute of Bone and Joint Research, Royal North Shore Hospital, Sydney, Australia, ³Department of Neurosciences, The Royal Melbourne Hospital, Melbourne, Australia.

Patients with epilepsy taking anti-epileptic medications (AED) have an increased fracture risk. There are also increasing numbers of patients taking AED for indications other than epilepsy. We investigated the effects of AED on bone mineral density (BMD) using a twin/sibling matched-pair design, and examined subgroups including current AED users, users of polytherapy (more than one AED concurrently) and the indication for use of AED for effects on BMD compared with non-AED using co-twins or siblings.

Methods: We identified AED-discordant pairs from our twin and sibling research databases and clinical practices. BMD was measured at the lumbar spine (LS), total hip (TH), femoral neck (FN) and total forearm (FA). Total body bone mineral content (TB BMC) also was determined (Hologic 4500A or 1000W). Lifetime duration (LDT) and number (LNM) of AEDs were calculated. Results were expressed as the within-pair percentage difference (paired t test) relative to the non-user. All data were adjusted for age, height and weight.

Results: Fifty-six pairs discordant for AED use were identified (46 current, 10 past AED users; 47 female, 9 male; 21 MZ, 21 DZ twins, 14 sib pairs matched within 3 years of age) with mean (SD) age 45.6 (15.3)y, height 164.7(9.8)cm and weight 70.6 (16.2)kg. Overall group: no significant within-pair difference in age, height, weight, total fat or total lean mass. Within-pair differences were seen at: TH -4.2% (p=0.017), LS -4.0% (p=0.0318); Among current users: TH-5.4% (p=0.01), FN-4.3% (p=0.045), LS -4.8% (p=0.029). Significant within-pair differences were seen related to: polytherapy [FA -3.4% (p=0.049), TH -8.9% (p=0.043), FN -9.7% (p=0.030) (n=14); mean (SD) LMN 3.3(1.9), mean LDT 20.8y (10.3); AED indication epilepsy [TH -5.4% (p=0.011), FN -4.3% (p=0.046), LS -4.8% (p=0.029) (n=41), LDT (SD) 20.8 (13.7)y]. No significant within-pair differences were seen with non-epilepsy indications for AEDs, mean LDT 4.7(6.3)y (n=14).

We conclude that patients taking AEDs, particularly for epilepsy, and taking polytherapy have reduced BMD compared to their non-AED-using siblings. This may reflect severity of epilepsy or duration and number of AEDs used and requires further investigation. Further study is required for patients taking AED for other indications.

Disclosures: S.J. Petty, NHMRC postgraduate medical research scholarship 2. This study received funding from: NHMRC Project Grant.

T350

Incidence of Osteoporotic Fractures and Vitamin D Status in Hip-fracture Patients. M. Sakuma^{*1}, T. Oinuma^{*1}, N. Endo², E. Endo^{*3}. ¹Orthopedic Surgery, Sado General Hospital, Sado, Japan, ²Orthopedic Surgery, Niigata University Graduate School of Medical and Dental Sciences, Niigata, Japan, ³Orthopedic Surgery, Nagaoka Chuo General Hospital, Nagaoka, Japan.

Osteoporotic fracture among elderly populations has been increasing in worldwide, and the prevalence of hypovitaminosis D in patients with acute hip fracture was pointed out recently.

The purpose of this study was to determine the incidence of osteoporotic fractures and to examine whether osteoporotic patients with hip fracture have lower levels of serum 25-hydroxyvitamin D (25-OHD) compared to non-osteoporotic cases in a particular geographical area: Sado City, Niigata Prefecture, Japan.

From January to December 2004 osteoporotic fractures of vertebra, hip, distal radius and proximal humerus occurred in Sado City was checked. The incidence, age, gender, were checked in each fracture. The levels of serum 25-hydroxyvitamin D (25-OHD), intact parathyroid hormone (intact PTH), alkaline phosphatase (ALP), albumin, and the number of remaining teeth were examined in both hip-fracture and control groups. In the hip-fracture group, serum calcium, serum phosphorus, urine N-terminal crosslinking telopeptide of type I collagen (NTx), bone mineral density (BMD) of the non-fractured hip, the presence of a vertebral fracture on X-ray, severity of dementia, and physical activity level were also examined.

The incidence per 100,000 population was 232.8 in vertebra, 121.4 in hip, 108.6 in distal radius and 37.1 in proximal humerus, respectively. The total incidence of these four kinds of fracture was 499.9 per 100,000 person year. The average injury age was 81.4 in hip, 77.7 years old in vertebra, 75.7 in proximal humerus and 60.2 in distal radius, respectively. 81% of hip fracture patients had vertebral fracture (more than one fracture).

Both the serum 25-OHD and serum albumin levels were significantly lower in patients with hip fracture than in controls, and the intact PTH level was significantly higher in patients with hip fracture. In the hip-fracture group, 62% of the subjects had hypovitaminosis D (25-OHD < 20 ng/mL) and one-fifth of cases with hypovitaminosis D showed elevated PTH levels (> 65 pg/mL). On the other hand, in the control group, hypovitaminosis D occurred in 18.9% of the subjects. The serum 25-OHD level showed a decrease as the severity of dementia progressed and the activity level decreased.

Our results indicate that about two-thirds (62%) of hip-fracture patients had vitamin D insufficiency, suggesting that this condition is closely associated with hip fracture in elderly people. Therefore, a decrease in serum 25-OHD level is a useful index for the risk of hip fracture in elderly people.

Disclosures: M. Sakuma, None.

T351

Does Oral Contraceptive Use Adversely Impact Bone Density in Young Women? D. Scholes¹, L. E. Ichikawa^{*1}, A. Z. LaCroix², L. Spangler¹, S. M. Ott³. ¹Center for Health Studies, Group Health, Seattle, WA, USA, ²Fred Hutchinson Cancer Research Ctr, Seattle, WA, USA, ³U of WA, Seattle, WA, USA.

Emerging evidence suggests that contemporary oral contraceptive (OC) formulations may act to suppress bone mass accrual in young women who are gaining bone. We report on a cross-sectional evaluation of OC use and bone mineral density (BMD) in adolescent and young adult women, ages 14-30 years. Participants were enrollees of Group Health Cooperative, a Washington State HMO, who were selected from the health plan computerized databases based on prescriptions for OC use and age. We enrolled 606 women: 389 OC users (42% new and 58% prevalent OC users; OCs contained ≤ 35 mcg ethinyl estradiol, EE); and 217 OC age-similar non-users. BMD (DXA) was measured at the hip, spine, and whole body. Data on OC use and other factors related to bone health were collected via interview and survey. Overall, 51% of the cohort was 14-18 years of age. Relative to non-users, OC users were more likely to be White, to currently smoke, and consume less calcium. Women who reported current OC use for >12 months had lower mean hip BMD than non-users (p=0.10) after adjusting for age, race, BMI, physical activity, calcium intake, and current smoking status, with smaller differences at the spine and whole body. Among 14-18 year olds, adjusted BMD values for OC users (mean current use 6 months, range <1-37 months) did not differ from non-users at any anatomic site (Table). Among 19-30 year-old women (mean current OC use 13 months, range <1-135 months), adjusted mean BMD at the spine was significantly lower with increasing duration of current OC use (p, trend=0.01), with a similar trend for the hip (p, trend=0.31). In this group, mean spine BMD was 4.8% lower for women with >24 months' OC use vs. non-users. Evaluation of cumulative lifetime OC use attenuated these trends (p, trend=n.s.), suggesting there may be some BMD recovery after OC discontinuation. The data from this sizeable study group provide evidence that current prolonged use of OCs containing ≤ 35 mcg EE may adversely impact bone density in young women.

Mean BMD by Duration of Current OC Use and Age Group					
Duration of current OC use (months)	N	Age 14-18 years		Age 19-30 years	
		Adj [†] mean BMD (g/cm ²)	Adj [†] mean BMD (g/cm ²)	Adj [†] mean BMD (g/cm ²)	Adj [†] mean BMD (g/cm ²)
		Hip (s.e.); Spine (s.e.)	Hip (s.e.); Spine (s.e.)	Hip (s.e.); Spine (s.e.)	Hip (s.e.); Spine (s.e.)
0 (non-users) [*]	111	0.992 (0.01); 1.003 (0.01)	1.006 (0.01); 1.017 (0.01)	0.985 (0.01); 1.040 (0.01)	0.985 (0.01); 1.036 (0.01)
>0-12	163	0.993 (0.02); 1.015 (0.02)	1.006 (0.01); 1.017 (0.01)	0.967 (0.01); 1.025 (0.02)	0.954 (0.02); 0.990 (0.02)
>12-24	47	0.971 (0.02); 0.999 (0.02)	0.971 (0.02); 0.999 (0.02)	0.954 (0.02); 0.990 (0.02)	0.954 (0.02); 0.990 (0.02)
>24	9	0.971 (0.02); 0.999 (0.02)	0.971 (0.02); 0.999 (0.02)	0.954 (0.02); 0.990 (0.02)	0.954 (0.02); 0.990 (0.02)
p-value for trend		0.56 (hip); 0.88 (spine)	0.29 (hip); 0.01 (spine)		

^{*} Adjusted for age, race, BMI, physical activity, calcium intake, current smoking.

^{*} Non-users had no OC use in the past 2 yrs and no more than 8 yrs lifetime use.

Disclosures: D. Scholes, None.

This study received funding from: US National Institutes of Health (NICHD).

T352

Does Low Bone Mass Predict Carotid Atherosclerosis in Postmenopausal Women? The Japanese Population-based Osteoporosis (JPOS) Cohort Study. J. Tamaki¹, M. Iki², Y. Hirano^{*3}, Y. Sato^{*4}, E. Kagita^{*5}, S. Kagamirori^{*6}, Y. Kagawa^{*7}, H. Yoneshima^{*8}. ¹Public Health, Kinki Univ. School of Med., OsakaSayama, Japan, ²Public Health, Kinki Univ. School of Med., OsakaSayama, Japan, ³Internal Medicine, Division of Cardiology, Kinki Univ. School of Med., OsakaSayama, Japan, ⁴Domestic Science, Jin-ai Women's College, Fukui, Japan, ⁵Public Health & Home Nursing, Nagoya Univ. School of Health Sciences, Nagoya, Japan, ⁶Welfare Promotion & Epidemiology, Univ. of Toyama, Toyama, Japan, ⁷Kagawa Nutrition Univ., Tokyo, Japan, ⁸Shuuwa General Hospital, Kasukabe, Japan.

The present retrospective study was conducted as a part of the Japanese Population-based Osteoporosis (JPOS) Study to clarify whether low bone mass predicts the increase of carotid intima-media thickness (IMT) in women. In 2006, the JPOS study followed 1040 women aged 15-79 years in 1996 selected randomly from three areas in Japan (follow-up rate: 68.6%). We analyzed 271 postmenopausal women aged 50 or older in 2006, after excluding the subjects with a history of cardiovascular disease, or any disease or medication affecting bone metabolism. The lumbar spine BMD measured with dual x-ray absorptiometry at baseline was used. McCloskey-Kanis criteria was used for diagnosis of vertebral fractures at baseline. The maximum IMT of carotid bifurcation was measured by B-mode ultrasonography in 2006. The intraobserver test-retest reliability of the IMT measurement was 12.4%. Information of present illnesses was interviewed with a questionnaire. Age-adjusted IMT values among normal, osteopenia, osteoporosis or presence of vertebral fracture were 1.15mm, 1.36mm, and 1.38mm among the women with less than 10 years since menopause (YSM<10) (n=123, mean age at baseline: 55.6±4.1 y), respectively (p<0.05 for trend), 1.30mm, 1.37mm, 1.53mm, respectively (p=0.083) among the women with 10 years or more since menopause (10≤YSM) (n=148, mean age: 66.6±5.9 y). T-score of spine BMD and presence of vertebral fracture were significantly associated with the IMT values with multivariate analysis adjusted for factors shown in the table among the women with YSM<10. Adjusted IMT values by lumbar bone status are

also shown in the table. Low lumbar bone mass or the presence of vertebral fracture may predict the subclinical carotid atherosclerosis in women with less than 10 years since menopause, and in postmenopausal women who have no risk factors of cardiovascular disease.

	Adjusted carotid intima-media thickness values, mean(95%CI)mm, by lumbar bone status		
	Normal -1≤T-score	Osteopenia -2.5≤Tscore<-1	Osteoporosis /Vertebral fracture
YSM<10 (n=123)a,*	1.14 (1.04,1.24)	1.37 (1.27,1.48)	1.39 (1.20,1.57)
10≤YSM (n=148)a	1.36 (1.17,1.16)	1.36 (1.25,1.47)	1.50 (1.37,1.63)
YSM<10 w/o CVD RFs(n=53)b,c	1.08 (0.95,1.22)	1.32 (1.17,1.47)	1.36 (1.05,1.66)
10≤YSM w/o CVD RFs (n=57)c,*	1.11 (0.74,1.47)	1.31 (1.14,1.48)	1.59 (1.40,1.78)

YSM: Years since menopause, w/o CVD RFs: Total cholesterol(TCH) <5.7mmol/L, w/o hypertension (HT) at baseline, or hyperlipidemia or diabetes mellitus (DM) at follow-up. *P<0.05, b P=0.059 for trend test.

a Adjusted for age, TCH, HT at baseline, BMI, SBP, hyperlipidemia, DM, medication use affecting IMT values, smoking & drinking habits at follow-up.

c Adjusted for the same variables as above, except for hyperlipidemia or DM.

Disclosures: J. Tamaki, Japan Society for the Promotion of Science, the Ministry of Education, Culture, Sports, Science and Technology, Japan 2.

This study received funding from: Japan Society for the Promotion of Science, The Ministry of Education, Culture, Sports, Science and Technology, Japan.

T353

Trabecular Bone Structure in Men of African Heritage: Age Patterns and Familial Resemblance. X. Wang¹, D. Inglis², C. L. Gordon³, Y. Sheu⁴, C. M. Kammerer¹, C. H. Bunker⁴, V. W. Wheeler⁵, A. L. Patrick⁵, J. A. Cauley⁴, J. M. Zmuda⁴. ¹Dept of Human Genetics, University of Pittsburgh, Pittsburgh, PA, USA, ²Dept of Civil Engineering, McMaster University, Hamilton, ON, Canada, ³Dept of Radiology, McMaster University, Hamilton, ON, Canada, ⁴Dept of Epidemiology, University of Pittsburgh, Pittsburgh, PA, USA, ⁵The Tobago Health Studies Office, Scarborough, Trinidad and Tobago.

Changes in trabecular structure with aging may influence bone strength independent of bone mass. We investigated the age-related patterns and, for the first time, the familial resemblance of trabecular architectural parameters in 803 Afro-Caribbean men (33 full-sib and 7 half-sib pairs) aged 40 to 92 years (mean±SD: 58±10 yr) who were recruited from the population of Tobago. All men underwent peripheral quantitative computed tomography (pQCT) measures of the distal radius and tibia. The pQCT images were acquired with an in-plane pixel size of 0.2 mm x 0.2 mm and a slice thickness of 2.2 mm. Specialized segmentation and analysis software (pQCT Pro) was used to assess indices of apparent trabecular structure including: trabecular bone volume/tissue volume (BV/TV, %), average thickness (Th_{AVE}, mm), average marrow hole size (Hole_{AVE}, mm²), number (Num., 1/mm) and connectivity index (CI, %). We determined the % difference between middle aged (40-49 yr; n=206) and older (>70 yr; n=126) men. Familial correlation was estimated among the subset of 33 brother pairs. BV/TV, Num., Th. and CI decreased whereas Hole increased with age with greater differences at non-weight (radius) than weight bearing (tibia) sites (Table). Although the sample size was small, we found statistically significant (P<0.05) familial correlations for BV/TV (r=0.47) at the radius and Th. (r=0.53) and CI (r=0.41) at the tibia, suggesting a genetic contribution to these traits. Further studies are needed to understand the natural history and genetic and environmental determinants of trabecular architectural changes with aging. A better understanding of the factors contributing to trabecular architecture may lead to new ways to preserve bone strength with aging.

Table. Percent difference in trabecular structure between middle-aged (40-49 yr) and older (>70 yr) Afro-Caribbean men.

Skeletal Site	BV/TV (%)	Thick _{AVE} (mm)	Number (1/mm)	CI (%)	Hole _{AVE} (mm ²)
Radius	-10%***	-10%***	-9%***	-56%***	78%***
Tibia	-6%**	-9%***	-7%(P=0.06)	-30%*	49%**

*P<0.05, **P<0.01, *P<0.0001; P value for differences between middle aged and older men.

Disclosures: X. Wang, None.

This study received funding from: NIAMD R01-AR049747.

T354

The Association Between Psychiatric Illness and Falls: Geelong Osteoporosis Study. L. J. Williams*, M. J. Henry*, F. N. Jacka*, M. Berk*, S. Dodd*, M. A. Kotowicz, G. C. Nicholson, J. A. Pasco. Clinical and Biomedical Science: Barwon Health, The University of Melbourne, Geelong, Australia.

Agents used in the treatment of depressive and anxiety disorders are known to cause sedation and have been associated with falls. However it is not clear whether psychiatric illness itself contributes to the increased risk of falling. This study investigated the association between depressive and anxiety disorders and the risk of falls in a population-based sample of women living in the community. Depressive and anxiety disorders for the preceding 12-month period were ascertained by clinical interview (SCID-I/NP); current medication use and falling history were self-reported. Participants were classified as fallers if they had fallen to the ground at least twice during the same 12-month period. Current users of antipsychotic medication and

mood stabilisers were excluded (n=12) resulting in a sample of 961 women aged 20-93yr (median 53yr, IQR 38-67).

Fifty-one women (5%) were classified as fallers. Fallers were older [61 (IQR 51-73) vs. 52 (37-66) yr, p=0.001] and more likely to use antidepressants (27% vs.11%, p<0.001) or benzodiazepines (12% vs. 4%, p = 0.005) than non-fallers. Those with depression (n=110) were younger [48 (36-60) vs. 53 (38-68) yr, p=0.01] and yet more likely to fall (10% vs. 5%, p=0.02). Age-adjusted odds for falling were 2.7-fold greater for women with depression (OR=2.7, 95% CI 1.3-5.5, p=0.007) and this relationship was attenuated after adjusting for antidepressant and benzodiazepine use (OR=2.0, 95% CI 0.9-4.1, p=0.07). In contrast, anxiety disorders were not associated with falls, even after adjustment for age, medication use or depression.

Depression itself contributed independently to the risk of falling. A similar relationship was not observed in those with anxiety disorders. Further research into the mechanistic factors is warranted.

Disclosures: L.J. Williams, None.

T355

BMD Changes in Male Veterans with Type 2 Diabetes. S. Yaturu¹, S. Humphrey². ¹Endocrinology, Overton Brooks VAMC/ LSUHSC, Shreveport, LA, USA, ²Nursing, Overton Brooks VAMC, Shreveport, LA, USA.

Prevention of osteoporosis requires not only recognition of population at risk, but also screening programs targeting those populations. Subjects with diabetes said to have a higher risk of non traumatic fractures even after adjustment for their bone mineral density (BMD). In a cross sectional study, we compared the clinical and BMD data of 735 men with type 2 diabetes to 3458 men with out diabetes (table 1).

	Subjects with diabetes (735)	Subjects without diabetes (3458)	P value
Age	67.5 ± 0.38	66.2 ± 0.12	0.06
BMI	30.08 ± 0.2	27.8 ± 0.12	< 0.0001
BMD AP spine	1.223 ± 0.008	1.149 ± 0.003	< 0.0001
BMD Hip	0.892 ± 0.009	0.930 ± 0.003	< 0.0001

Most of the subjects with diabetes have metabolic syndrome. Then we compared the BMD data of subjects with diabetes to age, BMI matched population (table 2).

	With diabetes (735)	BMI matched without diabetes (715)	P value
Age	67.5 ± 0.38	67.5 ± 0.39	NS
BMI	30.08 ± 0.2	30.10 ± 0.11	NS
BMD AP spine	1.223 ± 0.008	1.216 ± 0.003	NS
BMD Hip	0.892 ± 0.009	0.942 ± 0.08	<0.01

Interestingly, we noted that there was no significant difference between the two groups at spine. Subjects with diabetes had decreased BMD at hip. We conclude that it would be interesting to look into the area of metabolic syndrome in relation to bone mineral metabolism.

Disclosures: S. Yaturu, None.

T356

Development of Novel Mini-Tetrapod Bone Fillers. K. Igawa*, K. Yamamoto*, S. Ohba, T. Ogasawara, F. Kugimiya, D. Chikazu, K. Nakamura, H. Kawaguchi, T. Takato*, K. Tomizuka*, U. Chung. Sensory & Motor System Medicine, and Biochemistry & Molecular Biology, University of Tokyo, Tokyo, Japan.

The use of injectable biomaterials is of interest in osteoporotic patients to locally restore bone mass in sites at risk of fracture. Currently available granular type bone fillers are being produced by pulverizing porous calcium phosphate blocks. Because of the irregular size and shape of granules, dead space is often formed and connectivity of pores is not guaranteed. In contrast, the size and shape of the tetrapod is uniform, which can be designed in such a way that connecting pores of the ideal size for cell and blood vessel invasion are formed when the tetrapods are assembled. Four protrusions of each tetrapod help stabilize assembled structure. In addition, by changing sintering temperature and other conditions, alpha-tricalcium phosphate, beta-tricalcium phosphate, hydroxyapatite and octacalcium phosphate can be formed, which have distinct mechanical strength and remodeling speed. We fabricated new small tetrapod-shape artificial bone elements by injection molding of micro particles of alpha-tricalcium phosphate. Maxillary first molar teeth were extracted from 4 mature (5 years old) beagle dogs with preservation of the alveolar bone. Thereafter, left mesial sockets were filled with tetrapods-shape bone fillers. As a control, the right mesial sockets were filled with Osferion® and the left distal sockets were left unfilled. The surface shape of the tetrapod bone fillers was homogeneous in SEM images and they filled space uniformly in CT image. In contrast, the surface shape of Osferion® was heterogeneous and they filled space nonuniformly. The ink absorption test and cell culture test revealed that the tetrapod bone fillers have a good affinity for fluid and cells. In animal test, the dogs were euthanized at 1, 2 months. No side effects related to the fillers were observed. CT analysis showed that the substantial osteogenesis occurred around the tetrapod bone fillers. Histological analysis revealed that substantial bone formation occurred around the tetrapod fillers with osteoclasts resorbing them. These data suggest that the tetrapod bone fillers were safe and effective. We plan to apply these fillers to preventing the alveolar ridge resorption after tooth extraction.

Disclosures: K. Igawa, None.

T357

Non-pharmaceutical Strontium and Calcium Supplements Have Inconsistent Mineral Analyses and DXA Imaging Analyses. D. L. Kendler¹, E. M. Lewiecki², R. Hage-Moussa^{*1}, S. T. Robertson^{*1}, J. Zhang^{*3}.

¹Osteoporosis Center of British Columbia, Vancouver, BC, Canada, ²New Mexico Clinical Research & Osteoporosis Center, New Mexico, NM, USA, ³Tang Shan Workers' Hospital, Tang Shan, China.

Strontium (Sr) ranelate is a novel osteoporosis therapy proven effective in the prevention of fractures with postmenopausal osteoporosis. Substitution of Sr for calcium (Ca) in bone may increase bone mineral density (BMD) due to the higher molecular weight of Sr (87.62) than Ca (40.08). These changes are additive to the BMD effects of Sr ranelate associated with its antiresorptive and anabolic activity. Other (non-ranelate) Sr salts can be obtained as nutritional supplements at health food stores or over the internet. These have unknown composition, bioavailability and toxicity. We have previously analyzed by DXA, the bone mineral content (BMC) of 13 Ca and Sr supplements and reported a poor correlation of DXA BMC with the stated Ca or Sr content on the labels.

In the current study we analyzed the 13 supplements for Ca and Sr by Inductively Coupled Plasma Atomic Emission Spectrometry (ICP/AES). Samples were subjected to acid digestion and dilution to determine mineral content.

We observed good agreement between analysis of Ca and label Ca in 5 of 7 tablets; however, agreement was poorer between analysis of Sr and label Sr with only 3 of 6 showing accurate labeling. In all discrepant cases, the stated amount of mineral was higher than the analyzed amount of mineral. DXA analysis of the tablets indicates a good correlation of the DXA BMC determination with the chemical analysis for all samples but as expected, a poor correlation with the label amount.

We conclude that the mineral content of Sr and Ca supplements as measured by ICP/AES correlates poorly with the label amount. DXA-measured BMC of the supplements correlated well with the values obtained by chemical analysis. DXA may be a useful clinical tool for determining the Sr content of supplements. In addition, the DXA image may be useful in identifying artifact due to radiodense Sr-containing tablets that could be a confounding factor in BMD measurement.

Supplement Name	Ca or Sr label per tablet (mg)	Weight of element per tablet by ICP/AES (mg)
Natures Harmony Coral Ca: Ca hydroxyapatite	120	123.0
Genuine Health Bone builder: Ca citrate-malate/bisglycinate	500	167.0
New Roots Strong Bones: Ca	930	143.0
Oscal: Ca carbonate	500	513.5
Citricid-D: Ca citrate	315	316.5
Osteoporosis Naturally: Ca	250	225.0
OsteoSupport: various Ca salts	250	260.5
AOR Sr Support: Sr citrate	227	215.0
Neutraceutical Science Institute: Sr citrate	680	368.0
Osteovalin: Sr carbonate	600*	476.0
Stontium Bone Maker: Sr citrate	340	361.0
Sr Citrate	227	225.5
Strontium Osteo Complex: Sr carbonate	1000**	0.0***

* Value not shown on label, provided by manufacturer

** In powder form: Sr label is for 3 teaspoons (10.5 g)

*** Per mg of powder: weight of powder analyzed = 100 mg

Disclosures: D.L. Kendler, None.

T358

Absence of Toxicity Despite High Dietary Vitamin D and Calcium Intake in Non-Human Primates. R. J. Colman^{*}, D. Krueger, N. Binkley. University of Wisconsin, Madison, WI, USA.

Old world primates are widely recognized as an outstanding model of human skeletal physiology. However, laboratory monkey chow contains amounts of vitamin D3 (cholecalciferol) that lead to dietary vitamin D intakes which are much higher on a per kg body weight basis than amounts currently recommended for humans. Despite this, vitamin D toxicity is not recognized in laboratory non-human primates. As such, the purpose of this report is to describe the vitamin D and calcium status of rhesus monkeys (*Macaca mulatta*) for which long-term dietary intake has been closely monitored and explore potential unappreciated vitamin D toxicity. These animals are part of a long-term study on the effects of dietary restriction (DR) and aging. Prior to study initiation, these laboratory-born animals had been on standard Purina monkey chow containing high amounts of calcium and vitamin since birth. In their young adult life, a purified diet was instituted on which males (n=14) have been maintained for 17 years and females (n = 20) for 12 years. Currently, the males are 25.4-31.3 years of age (mean \pm sem: 26.6 \pm 0.4) and the females are 20.7-26.9 years of age (mean \pm sem: 23.4 \pm 0.5). Serum chemistries and 25-hydroxyvitamin D [25(OH)D] were measured and urine calcium/creatinine ratios determined. Serum/urine chemistry determinations were performed by autoanalyzer at a regional medical laboratory; 25(OH)D was measured by HPLC. Control animals (n = 15, age 24.2 \pm 0.7 years) weighed more (10.7 \pm 0.6 kg, p < 0.01) than the DR animals (n = 19, age 25.2 \pm 0.5 years; 8.8 \pm 0.3 kg). For the six months prior to blood collection, dietary vitamin D and calcium intake ranged from 214-447 (mean/SEM 324 \pm 10) IU/day and 772-1608 (mean/SEM 1167 \pm 34) mg/day. If these mean values are extrapolated to humans, a

70 kg human would be ingesting ~2400 IU of vitamin D and ~8500 mg of calcium daily. The mean serum 25(OH)D was positively correlated (p = 0.05) with recent dietary vitamin D intake and was higher among DR animals than control (91 vs. 75 ng/ml, p < 0.01), but did not differ by sex. In the entire cohort the mean serum calcium was 9.8 \pm 0.1 mg/dl and urine Ca/Cr ratio was 0.76 \pm 0.07. The highest individual serum calcium and creatinine values were 10.9 mg/dl and 1.3 mg/dl respectively. Nephrolithiasis has not been appreciated clinically and no nephrocalcinosis or nephrolithiasis was evident upon review of spine radiographs. In conclusion, despite life-long intakes of calcium and vitamin D that many would consider toxic for humans, no evidence of vitamin D intoxication was observed in male or female rhesus monkeys.

Disclosures: D. Krueger, None.

T359

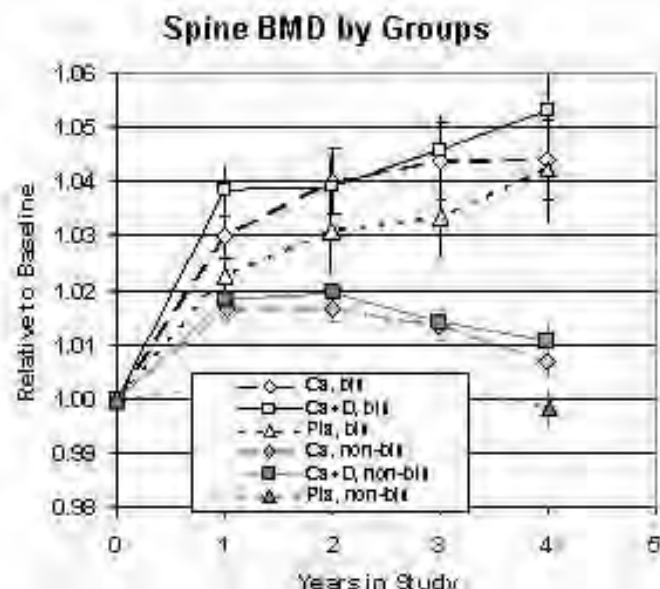
Calcium and Vitamin D Supplementation Improves Bone Health in a Population-based Sample of Postmenopausal Women. J. Lappe, K. Davies^{*}, D. Travers-Gustafson^{*}, G. Haynatzki^{*}, R. Heaney, R. Recker. Creighton University, Omaha, NE, USA.

The efficacy of calcium and vitamin supplementation (supp) for improving bone health of populations continues to be debated though strong evidence of a positive effect exists. Thus, we randomly sampled a population of healthy postmenopausal women \geq 55 yrs from 9 rural counties and enrolled 1179 into a double-blind, placebo-controlled, 4-yr study of calcium and vitamin D supp. Specific aims were to determine: 1) the anti-fracture efficacy of calcium (Ca) or calcium and vitamin D (Ca+D) supp; and 2) the comparative effects of Ca+D vs Ca on BMD.

Subjects were randomly assigned to 3 groups: calcium 1400 mg/d (Ca); calcium and vitamin D₃ 1000 IU/d (Ca+D); and placebo (Pla). Baseline measurements were: DXA, spine (sp) x-ray, diet recall, and serum 25(OH)D. At 6-mo visits, fracture (fx) incidence, supp adherence and medical history were assessed. Annually, DXA and serum 25(OH)D were repeated. Women with a t-score <2.5 or a sp fx at any visit were referred to their physician but kept on study.

Mean baseline Ca intake was 1150 mg/day and mean serum 25(OH)D was 72 nmol/L, indicating that most of these women were Ca replete with 25(OH)D levels nearly replete (80 nmol/L). Over 4 yrs, 18 % of the women took bisphosphonates (bis) for \geq 0.5 yrs; they were equally distributed among the 3 grps. 145 women had incident low-trauma fx; the incidence did not differ significantly among the 3 supp groups. However, both Ca and Ca+D increased sp BMD more than Pla (P<0.025). Changes in sp BMD over 4 yrs for subjects on bis were greater than for the non-bis grp (P < 0.005). See Figure. Supp did not result in greater increases in sp BMD in the bis grp. However, in the non-bis, supp resulted in greater increases than in Pla (P<0.05). There was no difference in mean increase between the Ca and Ca+D subgrps. The greatest effect of supp on sp BMD was in non-bis in the lowest tertile of Ca intake at baseline: Ca and Ca+D 2.0%, and Pla 0.0% (P=0.02). Analyses indicate that in the non-bis, increases in sp BMD peak at about 2 yrs (when the remodeling space would be filled in) and then age-related loss resumes.

Anti-fx effects of Ca and D supp are not seen in this population who are nearly Ca and D replete with 18% taking bis. However, in the Ca deplete non-bis grp, supp raises BMD to a new higher steady state. These findings suggest that Ca and D may prevent fx in Ca deplete individuals; studies have not targeted this population.



Disclosures: J. Lappe, GlaxoSmithKline 8.

T360

Diet Effects on Bone Mechanical and Molecular Markers. C. Lorincz*, M. E. Blaauw*, J. Klinck*, R. Reimer*, R. F. Zernicke. Kinesiology, University of Calgary, Calgary, AB, Canada.

The recent changeover of disease etiology has brought to the forefront the need to examine the environmental factors that have influenced the epidemic of chronic disease affecting our society. For bone, fracture associated with osteoporosis can lead to severe morbidity or mortality and is increasing faster than demographic changes in the population. Concurrently, an increase in the consumption of saturated fats and refined carbohydrates have been documented. Emerging data suggest diets high in saturated fat and sucrose (HFS) have a negative effect on skeletal structural integrity and should be investigated to substantiate this risk factor to bone health. The purpose of this study was to investigate the effects of consuming a HFS diet on mechanical, molecular, and blood markers of bone turnover.

Female C57BL/6 mice (aged 9 wk) were randomly assigned to one of two dietary cohorts: high-fat-sucrose (HFS, n=36) or adjusted starch (n=36). Mice were fed their respective diets for 10 weeks. Prior to sacrifice, blood was extracted by way of cardiac puncture and used to test serum levels of vitamin D, parathyroid hormone (PTH), osteocalcin (OC), and tartrate resistant acid phosphatase (TRAP). Upon sacrifice, tibiae were dissected and randomly assigned to group A or group B. Group A tibiae underwent mechanical testing and morphological analysis. Group B tibiae were used to measure the expression of two genes, osteoprotegerin (OPG) and receptor activator for nuclear factor κ B ligand (RANKL).

For blood markers of bone homeostasis, no significant differences were observed between dietary cohorts for vitamin D, PTH, or OC. In contrast, TRAP levels were significantly increased (30%) in the HFS cohort when compared to the starch cohort ($p < 0.05$). HFS mice were significantly heavier than the starch mice ($p < 0.05$). After normalizing for body mass, the mice fed a HFS diet had 23% reduced load at max, 25% smaller cross-sectional area, and 28% thinner cortex when compared to their starch-fed counterparts ($p < 0.05$). Pilot data for gene analysis indicated an 8% decrease in OPG and a 7% increase in RANKL for mice fed a HFS diet. Gene results were not statistically significantly different, however, likely due to low sample number.

Elevated levels of serum TRAP, a marker for bone resorption, alongside unchanged levels of OC, a marker of bone formation, would suggest a negative imbalance in bone remodeling, potentially compromising skeletal structure. Pilot gene analysis indicated an elevation in RANKL expression with a concurrent decrease in OPG expression. Both an increase in RANKL and a decrease in OPG expression have been closely linked with activation of osteoclasts, are consistent with the TRAP results, and are congruent with the observed changes in mechanical properties.

Disclosures: C. Lorincz, None.

T361

Restricting Dietary Protein may Improve Skeletal Integrity in Exercising Female Rats. S. N. Miller*, K. Baek*, M. I. Nilsson*, J. L. Stallone*, J. Lemmon*, H. A. Hogan*, S. A. Bloomfield*. ¹Health & Kinesiology and Nutrition, Texas A&M University, College Station, TX, USA, ²Health & Kinesiology, Texas A&M University, College Station, TX, USA, ³Mechanical Engineering, Texas A&M University, College Station, TX, USA.

We sought to elucidate which nutrient (calcium, protein, or energy) when restricted by 40% had the greatest negative effects on the structural and mechanical properties of bone in exercising female rats. Sixty Sprague-Dawley virgin female rats aged 4 mos. were acclimated to AIN-93M purified diet for 8 weeks prior to the 12-week protocol. Rats were randomly assigned to 5 groups (n=10/group). The control group (CON) ate AIN-93M ad libitum. The protein- (PR), calcium- (CR), and energy-restriction (ER) groups were fed custom diets providing 40% less protein, calcium, or energy, respectively; a global food restriction group (FR) was fed 40% less of all nutrients. All rats performed moderate intensity treadmill training 3 d/wk, 45 min/d. After euthanization peripheral quantitative tomography (pQCT) scans were performed on excised femoral neck (FN) and femoral midshaft prior to 3-point bending and FN compression tests on an Instron 1125. Only FR and ER rats lost body weight (-27% and -26% respectively) over 12 weeks vs. CON. In ER rats, FN total area was maintained, but marrow area was much larger (+75%) vs. CON, suggesting endocortical resorption. Midshaft femur cortical bone mineral content (BMC) and cortical area were lower for both CR and ER versus CON. PR outcomes were not different from those of CON for any variables at midshaft femur. The femoral neck total volumetric bone mineral density (vBMD) for PR was higher than both ER and FR; ER was lower versus CON; FR was not different versus CON. PR exhibited a larger ultimate load (non-significant) at the femoral neck (+8%) and a larger ultimate load at the midshaft femur (+9%) vs. CON. In addition, PR had higher (non-significant) values for stiffness (+15%), elastic modulus (+6%), and ultimate stress (+3%) at the midshaft femur than CON. Restricting only energy produced more negative effects on bone health than global FR, even though FR were fed 40% less of all other nutrients than ER. Unexpectedly, restricting protein intake by 40% resulted in several improved mechanical properties of midshaft femur and increased vBMD at the femoral neck. These are the first data, to our knowledge, to examine the impact of ER, PR, and CR in exercising rodents, offering a possible explanation for the novel results. It remains to be confirmed if reduced protein intake improves acid-base balance, impacting on resorptive activity.

Disclosures: S.N. Miller, None.

This study received funding from: American College of Sports Medicine.

T362

Additive and Synergistic Effects of 17 β -estradiol and Docosahexaenoic Acid on Bone Post-Ovariectomy in Rats. R. C. Poulsen, M. C. Kruger*. IFNHH, Massey University, Palmerston North, New Zealand.

A possible additive or synergistic effect of long chain polyunsaturated fatty acid (LCPUFA) supplementation in conjunction with 17 β -estradiol treatment on maintaining bone mass post-ovariectomy in rats has previously been reported. More recently, the n-3 LCPUFA docosahexaenoic acid (DHA, 22:6n-3) has been found to be particularly bone-protective. The aim of the present study was to determine if combined treatment with DHA and 17 β -estradiol would have greater bone-protective effects than either treatment alone. Six-month old rats were randomised into 5 groups and either sham-operated ("SHAM", n=10) or ovariectomised (ovx) (n=46). A slow-release 17 β -estradiol pellet (providing 1 μ g/day) was inserted subcutaneously into two groups of ovx animals (n=12 per group). All other groups received a placebo pellet. One group of estradiol-treated ovx animals ("OES", n=12), one group of placebo-treated ovx animals ("OVX", n=10) and the SHAM group were fed a balanced diet containing 4% corn oil and 0.5% calcium. The remaining estradiol-treated ("OESDHA", n=12) and placebo-treated ("DHA", n=12) ovx groups were fed the same base diet however a portion of corn oil was substituted for DHA (0.5g/kg body weight/day). Study duration was 18 weeks. BMC, BA and BMD were measured by DEXA at baseline and study completion. Trabecular and cortical BMC, BMD and BA were measured by pQCT; plasma IL-6 by immunoassay and red blood cell (RBC) fatty acid composition by GC at study completion.

Both DHA and estradiol treatment significantly protected against OVX-induced bone loss at the lumbar spine (LS) and femur (F). Combined treatment had an additive effect and final F BMC and LS BMC were greater in OESDHA compared to OES ($p=0.01$ and $p=0.07$ respectively). Cortical BMC and periosteal circumference were significantly higher in OESDHA compared to OES ($p=0.05$ and $p=0.02$ respectively) and a significant interaction between estradiol and DHA was evident for periosteal circumference ($p=0.05$). Both estradiol and DHA treatment were associated with increased levels of n-3 LCPUFAs in RBCs. Combined estradiol and DHA treatment further increased both the percentage of DHA and percentage of total n-3 LCPUFAs in RBCs. Neither estradiol nor DHA treatment alone had any significant effect on plasma IL-6 concentration however plasma IL-6 concentration was significantly lower in OESDHA compared to OES or DHA ($p=0.02$). Combined treatment with 17 β -estradiol and DHA is more effective than either treatment alone in preventing ovx-induced bone loss in rats due to both additive and synergistic interactions between the two treatments.

Disclosures: R.C. Poulsen, None.

This study received funding from: Palmerston North Hospital Medical Research Fund.

T363

Dried Plum Polyphenols Stimulate Osteoblast Activity and Attenuate Detrimental Effects of TNF- α on Runx2, Osterix and IGF-I in MC3T3-E1 Cells. S. Bu¹, T. S. Hunt^{*2}, B. J. Smith^{*2}. ¹Department of Nutritional Sciences, Oklahoma State University, Stillwater, OK, USA, ²Department of Surgery, University of Oklahoma Health Sciences Center, Oklahoma City, OK, USA.

Previous studies have demonstrated that supplementation with dried plum, a rich source of polyphenols, can restore bone mass and structure, and increase indices of bone formation (e.g. ALP & IGF-I). The purpose of this study was to determine how dried plum polyphenols influence osteoblast activity and function under normal and inflammatory conditions. MC3T3-E1 cells were plated and treated with polyphenols extracted from dried plums (0, 2.5, 5, 10 and 20 μ g/ml) and 24 hrs later stimulated with TNF- α (0 or 1.0 ng/ml). Alkaline phosphatase (ALP) activity was assessed as an indicator of osteoblast activity, Alizarin red S was used to determine nodule formation, and real-time PCR was used to evaluate alterations in gene expression. All doses of dried plum polyphenols significantly increased intracellular ALP activity under normal conditions at 14 days and restored the TNF- α -induced suppression of ALP ($p<0.001$) to the level of controls. After 28 days of treatment, the 5 μ g/ml dose of polyphenols increased mineralized nodules under normal conditions as evidenced by increased Alizarin red S staining density and number of mineralized nodules. All doses of polyphenols enhanced ($p<0.05$) nodule formation under inflammatory conditions. In the absence of TNF- α , 5 μ g/ml of polyphenols significantly up-regulated IGF-I mRNA levels compared to controls, while the 5 and 10 μ g/ml doses increased lysyl oxidase expression. Increases in Runx2 and Osterix expression induced by polyphenols under normal conditions did not reach statistical significance. TNF- α decreased the expression of Runx2, Osterix, and IGF-I, and polyphenols restored their mRNA levels to that of the controls. Although TNF- α failed to alter lysyl oxidase, dried plum polyphenols up-regulated ($p<0.05$) its expression in the presence of TNF- α . In the absence of TNF- α , the lowest dose of polyphenols down-regulated the expression of RANKL. As expected, TNF- α up-regulated RANKL mRNA and the 5, 10 and 20 μ g/ml doses of polyphenols decreased RANKL expression without altering OPG. We conclude that dried plum polyphenols enhance osteoblast activity and function under normal and inflammatory conditions by up-regulating growth and transcription factors, increasing the expression of an enzyme involved in extracellular matrix synthesis, as well as attenuating the inflammatory response.

Disclosures: B.J. Smith, None.

T364

The Effect of Onion on Ovariectomy-induced Osteopenia: A Histomorphometric Study in Rats. R. Yang¹, T. Huang^{*2}, R. C. Mühlbauer^{*3}, H. Chen^{*4}, H. Lin^{*2}, Y. Huang^{*5}, Y. Lai^{*5}. ¹Department of Orthopaedics, National Taiwan University Hospital, Taipei, Taiwan, ²Institute of Physical Education, Health and Leisure Studies, National Cheng-kung University, Tainan, Taiwan, ³Bone Biology Group, Department Clinical Research, University of Bern, Bern, Switzerland, ⁴Institute of Physiology, National Cheng-kung University, Tainan, Taiwan, ⁵Department of Life Science, National Cheng-kung University, Tainan, Taiwan.

Fruits and vegetables enriched diets have been suggested to benefit bone health. Among those natural foods, onion has been well proved about its effect on reduced bone resorption in animal study. The purpose of this study is to investigate the potential protective effects of an onion-enriched diet on the ovariectomy-induced bone loss.

Experimental Design: Animals with sham operation or ovariectomy were assigned into six groups: The CON group, sham operated control group (n=8); the OVX group, ovariectomized group (n=11); the ALN group, ovariectomized rats oral treated with alendronate (1mg/kg body weight/day) (n=11); the 3%ON, 7%ON and 14%ON groups, ovariectomized rats fed with diets containing 3%, 7% and 14% (w/w) onion, respectively (n=11 for each group). Animals were sacrificed after a six-week treatment course.

Results: The ALN group, which served as a positive control group, showed significantly higher in bone volume ratio (BV/TV) as compared to the OVX, 3%ON and 7%ON groups in cancellous bone of the proximal metaphysis of tibiae ($p < .05$). In addition, onion-enriched food decreased bone loss in a dose dependent manner (BV/TV, 3-45% higher than the OVX rats) and the 14%ON group was significantly higher than the OVX and 3%ON groups ($p < .05$). Further structural analysis of the proximal tibiae showed that both the ALN and 14%ON groups had significantly higher trabecular number (Tb. N.), less separation of trabeculae (Tb. Sp.), and less osteoclast per tissue area (N. Oc./T.A.). Thus, onion as well as alendronate showed efficacious inhibition of bone resorption.

Conclusions: Onion-enriched diet was demonstrated further to protect bone from ovariectomy-induced osteopenia. Further investigations would be of worth in clarifying the molecular mechanisms of onion on bone homeostasis.

Disclosures: R. Yang, None.

This study received funding from: National Science Council.

T365

Biochemical and Histological Assessment of the Effects of Alkali Therapy on Bone During High Animal Protein Intake. J. E. Zerwekh, L. Zou*, K. Sakhaee, C. Y. C. Pak, O. W. Moe*, P. A. Presig*. Center for Mineral Metabolism and Clinical Research, University of Texas Southwestern Medical Center at Dallas, Dallas, TX, USA.

The Westernized diet is acidogenic due to a high content of sulfur-containing amino acids. Chronic acid loads can result in hypercalciuria and negative calcium balance often attributed to loss of bone mineral. Alkali therapy has been shown to reverse hypercalciuria but little is known regarding its effect on bone turnover. We utilized dynamic bone histomorphometry to evaluate the effects of alkali therapy on acid-induced high bone turnover. We performed serum, urine, and bone histomorphometry in 4 groups of rats (n=9 per group) after 2 months of either neutral potassium salt as potassium chloride (KCl) or alkaline potassium salt as potassium citrate (KCit) administration (4 mEq K/d for each salt) while placed on either a low casein (LC) or high casein (HC) diet.

Compared to animals on LC-KCl diet, HC-KCl diet delivered a substantial acid load as shown by a significant increase in urinary sulfate, lower urinary pH and citrate, increased urinary ammonium and net acid excretion. Acid load also increased urinary calcium (3.5 ± 2.6 vs 6.0 ± 2.0 mmol/L, $p=0.039$) without detectable changes in serum parameters. Dynamic and static bone histomorphometry (Table 1) disclosed a significant reduction (as assessed by ANOVA) in cancellous bone volume associated with a 2.5-fold increase in eroded surfaces and a 3.5-fold increase in osteoclastic surfaces. There was also a near 2-fold increase in bone formation rate for rats on HC-KCl diet. When animals were given KCit in place of KCl, all of the aforementioned changes in urine biochemistry and bone turnover were prevented or attenuated (HC-KCIt vs. LC-KCIt). These findings clearly underscore the deleterious effects of high animal protein intake in promoting hypercalciuria and reducing bone mass through an increase in bone resorption. In contrast, co-administration of potassium alkali as KCit prevented or attenuated these changes and preserved bone mass. Thus, in this animal model of high protein intake, the major effect of alkali therapy on bone was to reduce bone resorption with little or no direct effect on bone formation. These findings may offer an explanation for epidemiological studies that have observed increased BMD in subjects with the greatest intakes of dietary alkali.

The effect of alkali on cancellous bone histomorphometry during low and high protein intake.				
Parameter	LC-KCl	HC-KCl	LC-KCIt	HC-KCIt
BV/TV $p=0.019$	19.3 ± 8.8	10.1 ± 5.2	13.3 ± 4.6	18.4 ± 6.8
Tb.Th	49 ± 10	44 ± 5	48 ± 5	48 ± 6
Ob.S/BS	4.3 ± 2.1	3.0 ± 1.6	2.7 ± 1.4	3.3 ± 1.1
ES/BS $p<0.0001$	6.0 ± 2.2	14.9 ± 4.0	9.1 ± 2.1	9.5 ± 2.9
Oc.S/BS $p<0.0001$	1.2 ± 0.8	4.2 ± 1.8	1.9 ± 0.6	2.3 ± 0.9
MS/BS $p=0.010$	17.5 ± 5.1	26.6 ± 4.6	22.8 ± 6.6	23.3 ± 4.5
BFR $p=0.024$	50 ± 22	91 ± 22	80 ± 35	69 ± 30

Disclosures: J.E. Zerwekh, None.

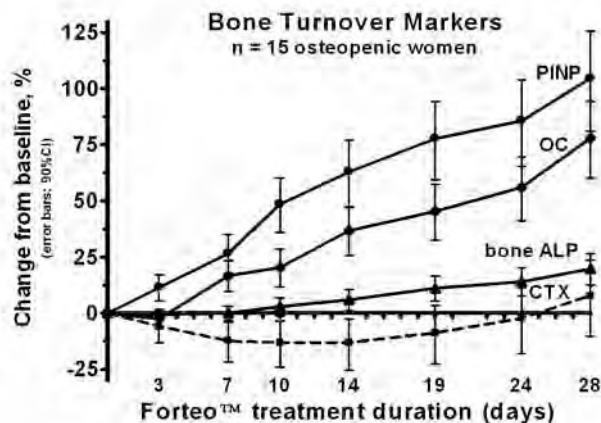
This study received funding from: NIH P01-DK20543.

T366

Rapid and Robust Biochemical Response to Teriparatide Therapy for Osteoporosis. R. Eastell¹, E. V. McCloskey¹, S. Glover¹, A. Rogers¹, P. Garnero², J. Lowery^{*3}, R. Belleli^{*3}, T. M. Wright^{*3}, M. R. John³. ¹University of Sheffield, Sheffield, United Kingdom, ²INSERM U 664 and Synarc, Lyon, France, ³Translational Medicine, Novartis Pharma AG, Basel, Switzerland.

Teriparatide is a potent anabolic treatment option for postmenopausal osteoporosis. Studies have shown that teriparatide induced large increases in biochemical markers of bone formation after one month of therapy onwards and a later increase in resorption markers. The aim of this study was to establish the very early biochemical response to teriparatide.

We recruited 15 postmenopausal women (ages 55 to 69 years, mean 62) with a BMD T-score less than -1 at the lumbar spine or total hip (mean T-scores at spine and hip, -1.8 and -0.8, respectively) and normal 25-hydroxy vitamin D levels. The treatment regimen was teriparatide 20 micrograms s.c. /day for 28 days. Serum levels of type I collagen N-terminal propeptide (PINP), type I collagen C-terminal propeptide (PICP), osteocalcin (OC), bone alkaline phosphatase (bone ALP), crosslinked C-telopeptide of type I collagen (CTX), and tartrate resistant acid phosphatase type 5b (TRACP5b) were measured on 11 occasions: baseline (an average value derived from 3 samples each taken two days apart immediately before treatment initiation), after 3, 7, 10, 14, 19, 24 and 28 days of treatment and at 56 days i.e. 28 days after teriparatide was stopped. The mean percent-changes from the average baseline and the 90% confidence intervals are shown in the figure.



The changes in PINP are early and large, differing significantly from baseline by day 3. A similar pattern was observed for PICP (not shown). The increase in OC showed a similar timecourse, but the increase was of smaller magnitude. The increase in bone ALP was delayed and smaller than the other formation markers. Interestingly, CTX decreased significantly between days 7 and 14, but TRACP5b did not (data not shown). In conclusion, the anabolic biochemical markers serum PINP and PICP show a robust response to teriparatide within the first week of therapy. These findings have implications for designing and interpreting studies of new anabolic agents for osteoporosis and for monitoring individual patients treated with teriparatide.

Disclosures: R. Eastell, Novartis 2, 5, 8; Lilly 2, 5, 8.

This study received funding from: Novartis Pharma AG

T367

BMD Response to Teriparatide in Treatment Naïve Patients Versus Patients Previously Treated with a Bisphosphonate. E. A. File^{*1}, C. L. Deal¹, R. S. Butler^{*2}. ¹Rheumatology, Cleveland Clinic Foundation, Cleveland, OH, USA; ²Biostatistician, Cleveland Clinic Foundation, Cleveland, OH, USA.

rh PTH 1-34 (teriparatide) (TPTD) is approved for the treatment of patients at high risk for fracture. Pretreatment with a bisphosphonate has been shown to blunt the bone density response to TPTD in some but not all studies. This study evaluated whether prior exposure to a bisphosphonate would blunt the skeletal response to TPTD. A retrospective analysis of patients given a prescription for TPTD at the Cleveland Clinic from 1/2003 to 7/2006 was performed. Patients were stratified into two TPTD treatment arms: bisphosphonate naïve and those previously treated with a bisphosphonate. Inclusion criteria for primary outcome analysis were the following: BMD < 12 months prior to initiation of TPTD, follow up BMD ≥ 12 months after therapy with TPTD, and bone turnover markers drawn before and after initiation of TPTD therapy. Primary outcome was absolute change in lumbar spine, total hip, and femoral neck BMD after ≥ 12 months of TPTD therapy. Secondary outcomes included the percent change in markers of bone turnover (urinary NTX, osteocalcin, and alkaline phosphatase). We evaluated the percent of patients who developed significant hypercalcemia, defined as a calcium level ≥ 11.0 on one occasion or > 10.5 on two or more occasions.

Sixty-six (66) patients met criteria for primary outcome analysis, 30 patients were bisphosphonate naïve and 36 patients received a bisphosphonate prior to initiation of TPTD. There was no significant difference between the two groups in the mean absolute change in the lumbar spine, total hip, or femoral neck BMD after ≥ 12 months of therapy with TPTD (see table). Both treatment arms had significant increases in NTX and osteocalcin with no significant difference in the percent change of response. In the entire cohort, which included 96 patients, significant hypercalcemia occurred in 21% (20/96) receiving TPTD. Patients with hypercalcemia had higher mean baseline calcium (10.0 vs. 9.6, $p = 0.0013$). Only 1 patient discontinued TPTD due to hypercalcemia. In our cohort, prior exposure to a bisphosphonate did not blunt the anabolic effect of TPTD. There was no significant difference in the percent change in bone turnover markers in the two groups. Calcium elevations were frequent in patients on TPTD, but discontinuation of therapy was rare.

Location	Absolute Change in BMD after ≥ 12 months of therapy with TPTD		P-Value [‡]
	Prior BP [†] Mean BMD Change (g/cm ²) n=36	BP Naïve Mean BMD Change (g/cm ²) n=30	
Spine (SD)	+0.084 (0.61)	+0.096 (0.56)	0.31
Total Hip (SD)	+0.034 (0.27)	+0.037 (0.35)	0.86

[†] Bisphosphonate

[‡] Wilcoxon Two Sample Test

Disclosures: E.A. File, None.

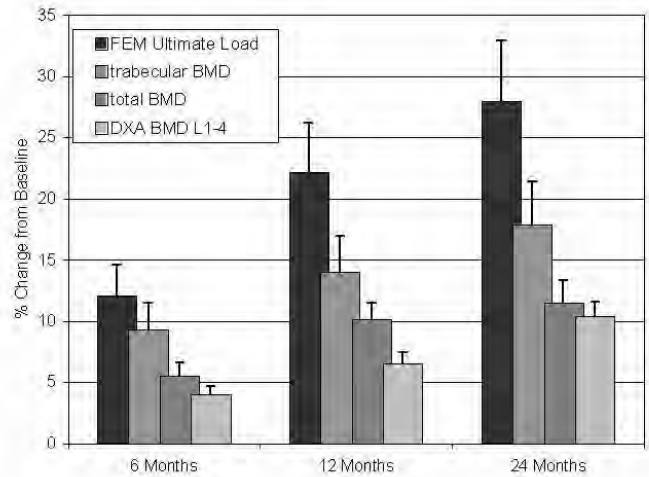
T368

Effects of 2 Years of Teriparatide Treatment on Bone Strength Assessed by High Resolution CT Based Finite Element Analysis of Human Vertebrae In Vivo: Results from the EUROFOR Study. C. Graeff¹, C. C. Glüer¹, J. Borggrefe¹, M. Charlebois^{*2}, Y. Chevalier^{*2}, P. Varga^{*2}, D. Pahr^{*2}, T. N. Nickelsen³, E. Marin^{*4}, J. Farrerons^{*5}, P. Zysset^{*2}. ¹Medical Physics, Department of Radiology, UKSH, Kiel, Germany; ²Institute for Lightweight Design and Structural Biomechanics, Vienna University of Technology, Vienna, Austria; ³Medical Research, Lilly, Europe, Bad Homburg, Germany; ⁴Medical Research, Lilly, Europe, Madrid, Spain; ⁵Hospital de Santa Creu I Sant Pau, Barcelona, Spain.

A digital finite element (FE) analysis method validated ex vivo (see abstract this meeting) was applied to assess vertebral strength changes in vivo induced by 2 years of teriparatide treatment.

For 43 patients aged 68 ± 7 years taking part in the high resolution computed tomography (HRCT) addendum of the EUROFOR study, HRCT scans of T12 and DXA scans of L1-4 were performed at 0, 6, 12, and 24 months. The patients differed by pre-treatment status: treatment naïve (7 patients), pre-treated with antiresorptives (11), or inadequate response to antiresorptives (25). The HRCT scans of the T12 vertebrae were segmented semi-automatically including the entire vertebral body except for the manually removed processes. A trabecular VOI was defined by peeling off the outer 3 mm of the total volume. Volumetric BMD was calculated in the trabecular VOI and the whole vertebra. For FE analysis the entire segmented vertebrae were converted into digital finite element models with 1.3 mm isotropic voxel size. Material properties were assigned according to a transverse isotropic elastic plastic damage model for bone following a power law based on BMD. The ultimate load under axial compression of the vertebral endplates was determined.

Figure 1 shows percent changes from baseline (all significant: $p < 0.0001$). Increases in bone strength were significantly larger volumetric or DXA-based BMD changes (after 6 months only vs DXA: $p < 0.01$; later: $p < 0.4$)



In vivo HRCT-based FE analysis allows monitoring of teriparatide treatment over two years with an increased sensitivity compared to DXA. Two years of teriparatide treatment are associated with a substantial 28% increase in FE analysis derived bone strength.

Disclosures: C. Graeff, None.

This study received funding from: Eli Lilly & Company

T369

GH Treatment Increases Cortical Thickness by Stimulating Endosteal Bone Growth in Young Adults with Childhood Onset GH-Deficiency. L. Hyldstrup^{*}. Dept. of Endocrinology, Hvidovre Hospital, Dk-2650 Hvidovre, Denmark.

Patients with childhood-onset growth hormone deficiency (CO GHD) are usually treated with GH until final height is reached, but the treatment is stopped long before peak bone mass is obtained. Since GH has well known effects on bone growth and bone mineral accretions, it might be useful to prolong GH treatment in CO GHD beyond final height. To evaluate the potential benefit of GH-treatment on cortical bone in this patient-group a randomized controlled, open-label study of young adults with CO GHD was performed. Material and methods: In a group of 160 patients with CO GHD, 109 were randomized to Norditropin® SimpleXx® and 51 patients were randomized to receive no treatment. Male/female ratio was 61/99, with a mean age of 21.2 (2.2) years. Mean (SD) height for males / females was 171.7 (7.5) / 157.5 (8.1) cm, mean weight was 69.0 (13.4) kg / 56.2 (11.1) kg, corresponding to BMI 22.5 (3.4) / 23.3 (3.5). Patients were treated for 2 years, with a maintenance dose of 1.0 / 1.4 mg daily for males and females, respectively. For all individuals hand x-rays were obtained at 0, 6, 12, 18 and 24 months and sent to a central reading facility where they were analyzed in a blinded manner, using digital x-ray radiogrammetry (DXR) of metacarpal 2-4. From this reading information on cortical thickness, bone width, endosteal diameter and metacarpal index was obtained. In the GH-treated group a significant increase in cortical thickness and metacarpal index was seen. The main cause of the increase in cortical thickness is a significant reduction of the endosteal diameter. In the control group the endosteal diameter did not change, leading to a much smaller increase in cortical thickness.

Conclusion: Treatment with Norditropin® SimpleXx® for 2 years in young adults with CO GHD led to a substantial endosteal bone growth with a reduction of the marrow space diameter and consequently an increase in the cortical thickness. Since cortical bone loss later in life is mainly caused by endosteal bone resorption, the effects of 2 years treatment with growth hormone (Norditropin®) before peak bone mass is reached may prove useful in preventing osteoporosis later in life.

	Results after 24 months			
	Cortical thickness	Bone Width	Inner Diameter	Metacarpal Index
Norditropin	1.10	1.02	0.96	1.08
Untreated	1.04	1.02	1.01	1.01
Effect (%)	6.43	0.68	-4.64	6.14
P-values	<0.0001	0.472	0.0006	<0.0001

Disclosures: L. Hyldstrup, Eli-Lilly, Nycomed, MSD 5, 8; Eli-Lilly, Nycomed, Novo-Nordisk 2.

This study received funding from: Novo-Nordisk.

T370

Teriparatide Treatment in Osteoporotic Patients Treated with Glucocorticoids for Chronic Inflammatory/Autoimmune Rheumatic Diseases. R. La Corte*, G. Limpido*, S. Volpinari*, F. Trotta*. Departement of clinical and experimental medicine, Rheumatology Unit, Ferrara, Italy.

Among osteoporotic patients, with multiple prevalent and/or incident vertebral/femoral fractures, treated with teriparatide all cases with concomitant rheumatic inflammatory/autoimmune diseases treated with glucocorticoids (GC) have been selected to evaluate the analgesic and antifracturative effects of the drug.

Of the 25 selected patients, 9 had connective tissue diseases (2 PM, 5 SLE, 2 UCTD), 3 had vasculitis (2 Behcet's disease and 1 Wegener's granulomatosis); 10 had RA and 2 had seronegative spondyloarthropathies. During teriparatide treatment, all the patients continued GC therapy (prednisone doses between 5 to 12.5 mg/d), in 8 cases as sole therapy, in the remaining associated with anti TNF α -therapy (4), DMARDs (12), and cyclophosphamide (1). In all patients pain was evaluated with a visual analogue scale (VAS) and the quality of life (QoL) with the Italian version of mini osteoporosis quality of life questionnaire (mini-qualleffo) at T0, and after T1, T3, T6, T12 months. Vertebral fractures by radiographic morphometry was performed before starting teriparatide and at 6 and 12 months or when considered necessary. Statistical analysis was performed using non parametric paired Wilcoxon test and analysis of variance (ANOVA) using Bonferroni as post hoc test.

An improvement of VAS $\geq 20\%$ and $\geq 50\%$ was seen at T1 in 13/26 and 2/26 respectively; at T3 in 11/20 and 2/20; at T6 in 5/14 and 6/14; at T12 in 1/7 and 6/7. The next statistical analysis do not consider T12 for the low number of patients. VAS was at T0: $73.5 \pm 4.17_{SEM}$; T1: $60.2 \pm 3.9_{SEM}$; T3: $55.3 \pm 4.8_{SEM}$; T6: $48.3 \pm 5.5_{SEM}$; T12: $31.4 \pm 5.7_{SEM}$ with differences statistically significant (T0 vs T1, $p < 0.0001$; T0 vs T3: $p < 0.0002$; T0 vs T6: $p < 0.003$ and between 4 groups (T0,T1,T3,T6): $F: 14.6$; $p < 0.001$; post hoc test showed a significant improvement from T0 to T3 and a stability between T3 and T6. Mini qualleffo analysis revealed a progressive improvement of QoL but the differences were not significant probably for the disability due to the underlying disease. Five patients withdrew the treatment: in 3 cases for increasing arthralgias (2 at T3; 1 at T6); 1 for inefficacy (T6) and 1 for hepatic replication of lung cancer (T3). Only a patient had a hip fracture and no vertebral fractures were detected. Two patients had a progressive asymptomatic reduction of PTH and 1 had mild hyperuricaemia. These preliminary data show and evident analgesic effect of teriparatide already presents during the first month of therapy in patients treated with GC therapy

Disclosures: R. La Corte, None.

T371

Transdermally-Delivered hPTH (1-34) - A New Treatment for Osteoporotic Patients: Results of Phase I Studies. G. Levin¹, C. Mazouz². ¹R&D, TransPharma-Medical, Lod, Israel, ²Clinical affairs, TransPharma-Medical, Lod, Israel.

TransPharma Medical is developing a novel transdermal hPTH (1-34) product designed to help people manage their osteoporosis by eliminating the need for daily injections. TransPharma's ViaDerm Micro delivery system for hPTH (1-34) consists of a reusable, handheld device, used to create microscopic pores which penetrate the outer skin layer, a 1 cm² disposable microelectrode array and a compatible patch containing the hPTH (1-34) formulation.

The company has performed two clinical studies on PTH-ViaDerm system: a proof of concept, single administration study using a 90 mcg patch and a 7-day recurrent administration study with patch doses of 50, 70 or 90 mcg. The single dose administration study was performed in India, while the seven day study was performed in The Netherlands. Both studies were performed in accordance to the Declaration of Helsinki and approved by the appropriate regulatory authorities.

A total of 44 healthy post-menopausal women, age 60-75, were treated with the PTH-ViaDerm system on the upper arm or thigh. The resulting PK profiles of plasma hPTH (1-34) were determined by a specific hPTH (1-34) ELISA for up to 22-24 hours following patch application. Total and ionized calcium in the serum was measured as indicative of treatment safety, and compared to that of a subcutaneous (SC) FORTEO injection (20 mcg). The studies were successfully completed with no serious adverse events and with a favorable systemic and dermal safety and tolerability profiles. All safety data, including serum total or ionized calcium, were well within the acceptable range for clinical use.

Transdermal delivery of hPTH (1-34) through ViaDerm-generated MCs resulted in the attainment of therapeutic levels of hPTH systemic concentrations. The transdermal delivery resulted in a peak hPTH plasma profile with a smaller inter-subject variability than that of SC injection. Relative bioavailability was calculated by comparing the area under the curve of transdermal delivery to that of SC injection, and was found to range from 30%-60%, depending on the dose and delivery site.

These safety and delivery results of the single and recurrent 7-day administration are very encouraging. hPTH (1-34) was delivered via the PTH-ViaDerm system with extremely high bioavailability relative to the therapeutic dose of SC injection. The transient and reversible changes in blood calcium following transdermal delivery of hPTH (1-34), which were similar to those observed in FORTEO, indicate safety of the delivered dose and peptide bioactivity in-vivo. Furthermore, the small variability achieved indicates high reproducibility and reliability. We plan to continue our development process in-house, bringing this high-potential product to an advanced clinical stage.

Disclosures: G. Levin, TransPharma-Medical LTD 3.

This study received funding from: TransPharma-Medical.

T372

Teriparatide Treatment Following Bisphosphonate-resistant Osteoporosis. 6 Months Clinical Data of the 'BBB-Study'. B. Mucche¹, B. Jobke², J. Semler². ¹Osteology, Immanuel-Krankenhaus Rheumaklinik, Berlin, Germany, ²MQIR-Dept. of Radiology, UCSF, San Francisco, CA, USA.

BACKGROUND: There are patients with relevant progression (fractures, continuous BMD loss) of their osteoporosis (OPO) despite of good compliance to at least 1 year of bisphosphonate (BIS) treatment. Teriparatide (recombinant human parathyroid hormone 1-34 = rhPTH) is a good option, but due to the high cost, it is only used in a minority of the target patients and only limited experience exists about the effects of previous treatments on bone markers, BMD, QoL and bone structural parameters. In this prospective single center study, clinical data were collected and paired iliac crest biopsies were performed. Data of the first 6 months are presented. **PATIENTS/METHODS:** 25 women (age 69 ± 9 years) with progression of severe OPO during BIS (mean treatment duration 3.5 (1...7) years; 12 ALN/13 RIS; new fragility fractures (n=14), BMD decline $>3.5\%$ (n=11)) were recruited for 18 months teriparatide treatment (plus daily 500 mg Ca & 400 IU Vit.D3 supplementation). DEXA scans of the lumbar spine (LS), femoral neck (FN) and total-hip (TH) were conducted every 6 months on a GE Lunar Prodigy, lab (serum-calcium, Bone ALP and crosslaps) and QoL questionnaire (with VAS for pain) performed at months 0, 1, 3 and 6. Paired bone biopsies by Jamshidi technique at the dorsal iliac crest were taken at M 0 and 6 (data presented by Jobke et al.). **RESULTS:** Consent withdrawal (n=1), compliance $< 75\%$ after 6 months (due to side effects; n=2) were excluded from the analysis. BMD T-scores M0/M6: LS -2.96/-2.20 (p=0.05), FN -2.21/-2.08 (NS), TH -1.94/-1.73 (NS). Lab M0/M1/M3/M6: s-calcium 2.32/2.36/2.46/2.36 (p<0.001 for M3 vs. M0; normal 2.05...2.65 mmol/l; observation of hypercalcaemia at any time, n=4); Bone ALP 14.4/20.5/20.3/28.4 (p<0.001; ULN=21.4 mg/l); crosslaps 239/350/553/850 $\mu\text{g/l}$ (p<0.001; ULN=573 $\mu\text{g/l}$). VAS for pain 48/45/39/48% (p=0.02 only for M3 vs. M0) did not show relevant clinical changes in this cohort. Duration of BIS $> 3.5\text{y}$ delayed changes of crosslaps until M3 (despite trend also at M1). Neither use of ALN or RIS, nor fracture vs. BMD decline had influence on any of the observed results. **CONCLUSIONS:** Early (M1) and continuous (M3, M6) increases of Bone ALP and crosslaps were observed as well as significant increase of LS-BMD at M6. No influence of duration or type of previous BIS treatment could be detected. Our patients seem to represent "real" BIS failures (in contrast to Ettinger et al., JBMR 2004; 19(5):745-51). Mean increases of s-calcium were moderate, but 4 of 22 patients had (intermittent and asymptomatic) hypercalcaemia. No clinically relevant change of VAS for pain was seen.

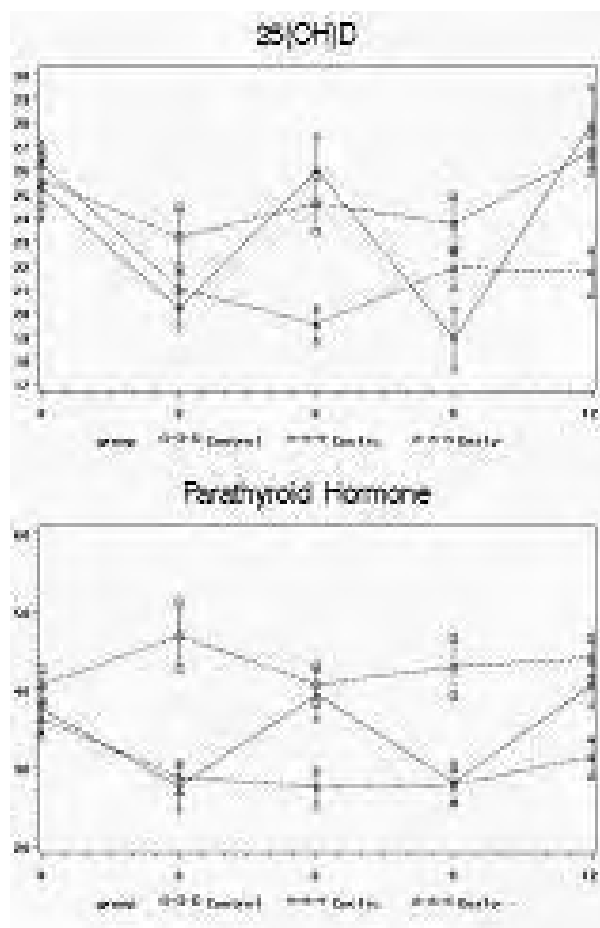
Disclosures: B. Mucche, None.

This study received funding from: Lilly Deutschland.

T373

Reduction in Serum 25(OH)D During PTH Treatment. J. W. Nieves, E. Cosman, M. Zion*, D. W. Dempster, R. Lindsay. Clinical Research Center, Helen Hayes Hospital, West Haverstraw, NY, USA.

Treatment with 1-34PTH (hPTH) is well known to increase serum calcium levels transiently, however, effects on vitamin D metabolites and endogenous parathyroid hormone (PTH) levels have not yet been described. We report data here on calcium homeostasis variables in two clinical trials, one trial involving patients on prior raloxifene (RLX; n=42) randomized to daily hPTH or RLX alone and one trial involving patients on prior alendronate (ALN; n=126) randomized to daily hPTH, cyclic hPTH (3 months on and 3 months off) or ALN alone. All subjects were supplemented with vitamin D to achieve levels above 20 ng/ml prior to entry into the trial. Serum was measured for intact PTH, 25(OH)D, 1,25(OH)₂D and ionized calcium every 3 months for one year. Intact PTH was measured by radioimmunoassay (Nichols), 25(OH)D and 1,25(OH)₂D were measured by radioimmunoassay (Diasorin). Changes in biochemical variables were similar across the trials; therefore data were grouped for analyses (RLX and ALN control groups were pooled and daily hPTH groups were pooled). In the control group there were no significant changes in any variables. Ionized calcium increased in the hPTH groups within 3 months (all levels stayed within normal range). Levels remained significantly elevated in the daily hPTH group at all subsequent time points, compared to the cyclic hPTH group. PTH levels declined by 15-25% in both hPTH groups within 3 months and remained below baseline (Figure). In the cyclic group, PTH returned to baseline during off-cycles and declined again during on-cycles. 25(OH)D declined by 15-17% within 3 months in the hPTH groups and remained below baseline in the daily hPTH group (Figure). In the cyclic group levels increased during off-cycles and declined again during the on-cycles. 1,25(OH)₂D levels increased 25-30% within 3 months and remained above baseline throughout the study in the daily hPTH group. In the cyclic group, there was a similar pattern with increments and decrements related to on and off cycles. In conclusion, reductions in 25(OH)D are consistently seen with PTH treatment, along with increases in 1,25(OH)₂D, modest increases in serum calcium and decreases in PTH. Given the dramatic differences in their half lives (days versus hours) it is possible that the reduction in 25(OH)D results from exogenous hPTH stimulation of 25(OH)D conversion to 1,25(OH)₂D.



Disclosures: J.W. Nieves, None.

T374

Comparison of Alendronate and Strontium Ranelate in Men with Established Primary Osteoporosis. J. D. Ringe, A. Dorst*, H. Faber*, P. Farahmand*. Medical Clinic 4, Klinikum Leverkusen, University of Cologne, Leverkusen, Germany.

Background: Strontium ranelate is a new therapeutic option for osteoporosis. Due to a simultaneous anabolic effect on osteoblasts and catabolic effect on osteoclasts it is different from all previous treatments. In two large pivotal trials on postmenopausal women a significant risk reduction was demonstrated for both vertebral and non-vertebral fractures. Therapeutic experience in men with osteoporosis has not been reported so far.

Purpose of the study: To study the effect of strontium ranelate on lumbar spine and total hip bone mineral density (BMD) in men with established primary osteoporosis. Secondary endpoints include fractures, height loss, back pain and use of analgetic therapies.

Patients and methods: In this single center, open label, controlled, prospective one year trial we enrolled 68 men with T-score values of lower than -3.0 SD at lumbar spine (LS) and lower than -2.5 SD at the total hip (TH) with one or more prevalent vertebral fractures (vert-fx). Patients in group A (n=34) received 2g strontium ranelate plus 1200 mg calcium and 800 IU Vitamin D daily. The 34 patients of group B were treated with 70mg alendronate once weekly and the same amounts of calcium and vitamin D daily. BMD measurements and x-rays were performed at baseline and month 12.

Results: The increase in LS-BMD after 12 months amounted to 5.1% and 4.1% resp. in strontium ranelate and alendronate patients. The respective mean changes at the total hip site were 3.2% and 2.6%. The mean increases in BMD were significant higher with strontium ranelate as compared to alendronate. The average increase rates at the two skeletal sites of group A are consistent with the respective one year results in postmenopausal women treated with strontium ranelate. In group A we observed 2 vert-fx and 2 non-vert-fx, in group B 2 vert-fx and 4 non-vert-fx (ns). For both treatments a significant decrease in the average back pain and analgetic therapy score was documented with a stronger tendency for strontium ranelate.

Conclusion: Strontium ranelate seems to be at least as potent in men with established osteoporosis than alendronate, which is approved for this indication. These data are encouraging to study further male patients.

Disclosures: J.D. Ringe, None.

T375

Monitoring Bone Mineral Density During the Course of Teriparatide Therapy in a Community Setting. G. Valenzuela*, P. Miller*, A. Rana*, M. Wong*, K. Taylor*, K. Krohn*. ¹West Broward Pulmonary, Plantation, FL, USA, ²Colorado Center for Bone Research, Lakewood, CO, USA, ³Eli Lilly and Company, Indianapolis, IN, USA.

Experts have suggested monitoring patients' BMD at 12 months after initiating teriparatide 20µg/d (TPTD) therapy [Endo Pract (2004)10:139-48]. Medicare provides reimbursement for BMD 1 yr after starting an FDA-approved osteoporosis (OP) therapy. However, clinicians may choose to monitor patients' BMD at other time points. This analysis examines the time from baseline to the first follow-up LS-BMD assessment during the course of TPTD therapy in a "real world" OP patient population in the ongoing, observational DANCE trial. The study design specified investigators to prescribe TPTD for ≤24 months, with 24 months' follow-up after cessation of therapy, and to make all patient-care decisions. In 794 patients with a baseline and ≥1 follow-up BMD measurement (Table), the LS-BMD increase was 5.7% ± 0.3% after 16.6 ± 0.3 months (mean ± SE) to the first follow-up BMD measurement.

Of the 794 patients, 161 were treatment-naïve and 633 had previously used OP therapy, of which 566 had used bisphosphonates (BP) and 67 used other antiresorptives. Patients who had taken both BP and another antiresorptive were included in the BP group. Previous BP patients had their first follow-up BMD measurement at 16.2 ± 0.4 months, which differed (P=0.008) from naïve patients (18.1 ± 0.6 months), but not from those who took other therapies (16.8 ± 0.9 months). Previous BP patients had a 5.0% ± 0.4% increase in LS-BMD, which was lower than naïve patients (7.1% ± 0.7%, P=0.009) and those who took other therapies (8.3% ± 1.2%, P=0.006). Time to first follow-up BMD measurement and LS-BMD increase did not significantly differ between naïve patients and those who used other therapies. These data suggest that physicians in community practice generally adhere to recommended guidelines for monitoring BMD in TPTD patients, but previous BP patients may have follow-up BMD measured earlier than naïve patients. It is not known whether the lower LS-BMD increases in previous BP patients result from BP actions on bone or the earlier BMD follow-up.

Interval from Baseline to First Follow-Up BMD Measurement (Months)			
Interval from Baseline to First Follow-Up BMD Measurement (months)	Patients (n)	Patients (% of total)	Percent Change in LS-BMD from Baseline (mean ± SE)
0 to ≤3	21	2.6	4.7 ± 3.6
>3 to ≤6	103	13.0	3.3 ± 0.7*
>6 to ≤9	136	17.1	4.8 ± 0.8*
>9 to ≤12	225	28.3	5.4 ± 0.5*
>12 to ≤18	193	24.3	7.4 ± 0.8*
>18 to ≤24	65	8.1	6.8 ± 1.1*
>24	51	6.4	6.9 ± 1.3*

Disclosures: G. Valenzuela, Eli Lilly and Company 2.

This study received funding from: Eli Lilly and Company.

T376

The Effects of Intravenous Zoledronate on Bone Turnover and Bone Density Persist For At Least 24 Months. M. J. Bolland*, A. Grey¹, A. Horne*, S. Briggs*, M. Thomas*, R. Ellis-Pegler*, A. Woodhouse*, G. Gamble*, I. R. Reid¹. ¹Department of Medicine, University of Auckland, Auckland, New Zealand, ²Department of Infectious Diseases, Auckland City Hospital, Auckland, New Zealand.

Recently, we have shown that annual administration of intravenous zoledronate increases bone mineral density (BMD) in HIV-infected men for at least 24 months. We set out to determine the duration of effect of zoledronate after 2 annual doses.

We performed a randomized, placebo-controlled trial in HIV-infected men with BMD T score at hip or spine < -0.5 who had taken highly active antiretroviral therapy for >3 months. Zoledronate 4mg infusion or placebo was administered at baseline and 1 year and follow-up continued to 24 months following the last dose.

In the zoledronate group (n=15), lumbar spine BMD increased from baseline by 8.8% at 12m post second zoledronate dose and by 9.2% at 24m compared to an increase of 3.4% at 12m and 4.1% at 24m in the controls (n=17). In the zoledronate group, total hip BMD increased by 3.7% at 12m and 3.8% at 24m compared to an increase of 0.9% at 12m and 1.0% at 24m in the controls. In the zoledronate group, total body BMD increased by 2.2% at 12m and 2.0% at 24m compared to an increase of 0.35% at 12m and a decrease of 0.07% at 24m in the controls. At both 12m and 24m, the between-groups differences at all sites were significant (P<0.01).

CTX levels were 0.14 (0.07) ng/ml at 12m post second zoledronate dose and 0.17 (0.10) at 24m in the zoledronate group, and 0.36 (0.12) at 12m and 0.39 (0.15) at 36m in the control group. Osteocalcin levels were 9.7 (2.8) µg/L at 12m and 11.6 (2.7) at 24m in the zoledronate group, and 17.0 (4.9) at 12m and 19.7 (7.6) at 24m in the controls. For both osteocalcin and CTx, the between-groups differences at both time points were significant (P<0.01). CTx did not change significantly in either group between 12m and 24m, whereas osteocalcin increased significantly from 12m to 24m in both groups but there were no between-groups differences in these increases.

In summary, 2 annual doses of 4mg zoledronate suppress bone turnover for at least 24 months after the second dose of zoledronate, and BMD remains stable between 12 and 24 months after the second dose of zoledronate. This suggests that the antiresorptive effects of zoledronate last longer than 12 months, and raises the possibility that it could be administered less frequently than on an annual basis.

Disclosures: M.J. Bolland, None.

This study received funding from: Health Research Council of New Zealand.

T377

Similar Improvements in Hip Bone Mineral Density with Monthly Oral Ibandronate (150mg) Versus Weekly Oral Alendronate (70mg) in Postmenopausal Osteoporosis. J. L. C. Borges¹, M. Bolognese², S. Epstein³, F. Sedarati⁴, C. Neate⁵, P. D. Miller⁶. ¹Universidade Catolica de Brasilia, Brasilia, Brazil, ²Bethesda Health Research, Bethesda, MD, USA, ³Mt Sinai School of Medicine New York and Doylestown Hospital, Doylestown, PA, USA, ⁴Hoffmann-La Roche Inc., Nutley, NJ, USA, ⁵Roche Products Ltd, Welwyn Garden City, United Kingdom, ⁶Colorado Center for Bone Research, Lakewood, CO, USA.

The purpose of the MOTION (Monthly Oral Therapy with Ibandronate for Osteoporosis Intervention) study was to compare the efficacy of monthly oral ibandronate 150mg with weekly oral alendronate 70mg in improving bone mineral density (BMD) in women with postmenopausal osteoporosis. Here we present BMD data from hip sites.

MOTION was a randomized, multinational, double-blind, double-dummy, parallel-group, non-inferiority study. A total of 1,760 postmenopausal women with osteoporosis were enrolled. Patients were aged 55-84 years, ≥ 5 years since menopause, and had a mean lumbar spine BMD T-score (L2-L4) < -2.5 and ≥ -5.0 SD. Randomization was to either monthly oral ibandronate 150mg plus weekly placebo (n=887), or to weekly oral alendronate 70mg plus monthly placebo (n=873). All patients also received vitamin D (400IU/day) and calcium (500mg/day) supplements. The co-primary efficacy endpoints were the relative change (%) from baseline at 12 months in mean lumbar spine (reported separately) and total hip BMD. Monthly ibandronate would be proven clinically comparable to weekly alendronate if the lower boundary of the one-sided 97.5% CI was ≥ 0.87 percentage points for total hip. Secondary efficacy endpoints included the relative change (%) from baseline at 12 months in mean trochanter BMD and additionally as an exploratory analysis, femoral neck BMD.

Per-protocol (PP) analyses (ibandronate n=725, alendronate n=720) found that the change from baseline in mean total hip BMD was 2.94% with ibandronate and 3.03% with alendronate (95% CI, -0.38, 0.18; non-inferiority met at ≥ 0.87). The change from baseline in mean trochanter BMD was 4.20% in both treatment groups (95% CI, -0.49, 0.43) and in mean femoral neck BMD was 2.07% with ibandronate and 2.30% with alendronate (95% CI, -0.61, 0.13). These data show that monthly oral ibandronate is essentially similar to weekly oral alendronate in terms of improvements in total hip BMD and that the two regimens also produced similar improvements in trochanter and femoral neck BMD after 12 months.

Disclosures: J.L.C. Borges, F. Hoffmann-La Roche Ltd/GlaxoSmithKline 5.
This study received funding from: F. Hoffmann-La Roche Ltd/GlaxoSmithKline.

T378

Improved Tendency in Esophageal-Gastrointestinal Mucosal Effect of Enterocoating Alendronate Combined with Calcitriol Drug (Maxmarvil®) Compared with Alendronate Only in Korean Postmenopausal Women. D. Byun¹, J. Mok², H. Park³, K. Lee³, Y. Kim⁴, S. Kim⁵, C. Kim⁶, K. Suh¹, M. Yoo¹, M. Rho¹, H. Park⁵. ¹Endocrinology, Soonchunhyang University Hospital, Seoul, Republic of Korea, ²Endocrinology, Soonchunhyang University Hospital, Bucheon, Republic of Korea, ³Endocrinology, Soonchunhyang University Hospital, Cheon-Ahn, Republic of Korea, ⁴Endocrinology, Soonchunhyang University Hospital, Cheon-ahn, Republic of Korea, ⁵Obstetrics & Gynecology, Chung Ang University Hospital, Seoul, Republic of Korea.

Background: Bisphosphonates (BPs) are widely used for postmenopausal osteoporosis but sometimes their medications are restricted because of gastrointestinal (GI) symptoms which associated with injury to the upper GI tract. Previous studies had tried to reduce the damaging effect on the gastric mucosa by developing new drugs or coating the drugs etc. So we compared endoscopic findings after use of alendronate (5 mg/day) only and recently developed Maxmarvil® drug (enterocoating drug of 5mg alendronate combined with 0.5µg calcitriol).

Methods: Healthy 24 postmenopausal volunteers (50-70 years old) without GI symptoms with normal baseline endoscopy findings were participated. Esophagogastroduodenoscopy (EGD) was taken at the time of the baseline and again at 2 weeks later after daily intake of Maxmarvil (9 subjects) or alendronate (15 subjects). Mucosal injury scores were reported by a blinded endoscopist on day 14 of treatment.

Results: Esophageal and gastric mucosal injury showed reduced tendency in Maxmarvil group but did not significantly different between 2 groups. Esophageal mucosal injury developed 2 subjects out of 15 alendronate only group (mucosal damage score; 4) while none of 9 Maxmarvil group. Gastric mucosal injury developed in 7 out of 15 subjects with alendronate group (mucosal damage score; 18) while 4 out of 9 Maxmarvil group (mucosal damage score; 8). These data showed no significant differences.

	No. of Maxmarvil group (mucosal damage score)	No. of Alendronate group (mucosal damage score)
Esophagus	0/9	2(4)/15
Stomach	4 (8)/9	7 (18)/15
Total	4 (8)/9	9 (22)/15

Conclusion: The mucosal damage scores for the alendronate group (total score; 22) exceeded those for the maxmarvil group (total score; 8) in the esophagus and stomach. But this was not significant between 2 groups. (Fisher exact test, p-value=0.253)

Disclosures: D. Byun, None.

T379

The Change of Bone Markers after Once-weekly Low Dose Alendronate in Postmenopausal Women with Moderate Bone Loss. H. Choi, S. Kim*. Family Medicine, Eulji University Hospital, Daejeon, Republic of Korea.

Introduction: High bone turnover with the bone resorption exceeding bone formation is a major mechanism of postmenopausal osteoporosis. Therefore, inhibition of bone resorption is a rational approach for the prevention. The Objective of the current study was to determine the short-term efficacy of once-weekly low dose alendronate in the prevention of bone loss in early postmenopausal Korean women with moderate bone loss via bone turnover markers.

Methods: This study was a 12-week, randomized, double-blind clinical trial compared the effects of placebo with alendronate 20 mg once weekly. All subjects received supplemental calcium 600 mg and vitamin D 400 IU daily. Fifty two postmenopausal women (the ages between 50-65 year) with lumbar spine BMD at least 2.0 SD below the peak young adult mean were recruited at Eulji University Hospital, Daejeon, Korea. BMD was measured by DXA at baseline and serum alkaline phosphatase, osteocalcin and C-terminal telopeptide of type I collagen was measured at baseline and 12 weeks after treatment.

Results: Fifty two women were randomly assigned either to placebo or alendronate 20 mg once a week for 3 months. Among the fifty two women who participated in baseline, thirty nine continued and completed all 3 months. After 3 months, significantly greater decreases in bone resorption markers in the alendronate group vs. placebo occurred: C-terminal telopeptide of type I collagen $-0.252 \pm 0.200\%$ vs. $0.078 \pm 0.196\%$ ($P < 0.001$), alkaline phosphatase $2.7 \pm 18.6\%$ vs. $17.7 \pm 19.5\%$ ($P < 0.021$), osteocalcin $-8.0 \pm 6.4\%$ vs. $-4.0 \pm 6.8\%$ ($P < 0.071$). Women receiving alendronate had adverse experience incidences similar to those receiving placebo.

Conclusion: Once-weekly low dose alendronate was effective, cost saving and had a good safety profile in suppression of bone turnover in early postmenopausal women with moderate bone loss.

Disclosures: H. Choi, None.

This study received funding from: Eulji University, School of Medicine.

T380

How Quickly Do Oral Bisphosphonates Work, and Are There Differences Between Them? J. R. Curtis, A. Westfall*, H. Cheng, E. Delzell*, K. G. Saag. University of Alabama at Birmingham, Birmingham, AL, USA.

Background: The time necessary for bisphosphonates (BPs) to maximally reduce non-vertebral fracture (fx) risk is uncertain; there is controversy regarding effectiveness differences between BPs.

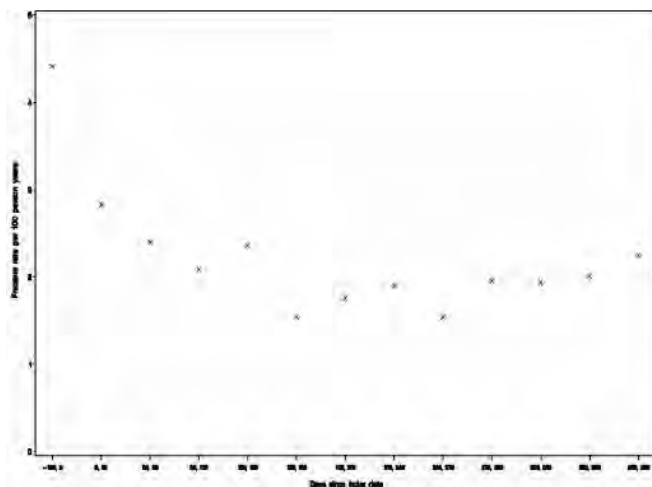
Methods: Using claims data from a large national U.S. health care organization, we identified persons initiating alendronate or risendronate (no prior use in 6 months). Date of first BP use defined the 'index date'. Claims data identified all non-vertebral and hip fxs before and after the index date. To exclude follow-up visits for prior fx, claims for fx within 90 days after the index date among persons who also had fxs in the 6 months prior to the index date were excluded. Post-index fx rates were computed at 30 day intervals. Because we focused on efficacy, we required eligible persons to be at least 80% adherent (quantified using medication possession ratio, MPR) at 6 months after the index date.

A subset analysis among persons initiating weekly BPs with MPR $\geq 80\%$ was performed and compared 1-year hip and non-vertebral fx risk between new risendronate users and new alendronate users.

Results: Among 46,805 new BP users adherent at 6 months, mean \pm SD age was 61.6 ± 7.9 y. We identified 1,022 non-vertebral fxs and 250 hip fxs that occurred in the first year after the index date. The rate of non-vertebral fx reached a nadir between 3 and 6 months after the index date and remained low thereafter. Results were similar for hip fx. Comparing pre and post-treatment non-vertebral fx rates, there was an absolute fx rate difference of approximately 2.7 fractures per 100 py (number needed to treat = 37).

In the subgroup analysis of new weekly BP users, unadjusted time to hip fx among new alendronate users was significantly lower ($p = 0.004$) than among new risendronate users; the absolute rate difference at 1 year was approximately -0.2% (number needed to treat = 500). The difference in non-vertebral fx rates between alendronate and risendronate users was significant ($p = 0.03$) although rate differences were of smaller magnitude.

Conclusions: Oral BPs appear to achieve maximal non-vertebral fx rate reduction between 3 and 6 months. In unadjusted analyses, we found minimal differences in the absolute fx rate between weekly BPs. Ongoing work will determine if channeling higher risk patients may explain some risk differences between BPs. However, even small differences between specific BPs are likely overshadowed by the larger effect size seen with use of any BP.



Disclosures: J.R. Curtis, Merck 2, 5, 8; Procter & Gamble 5; Amgen 2, 8; Roche 5, 8.

T381

Effect of Various Substances on the Reduction of Fractures. M. A. Dambacher¹, K. Articus², M. Neff³, J. Gasser³, A. Kreiss², H. Radspieler¹, L. Quin¹. ¹ZORG International, Zurich Osteoporosis Research Group, Zurich, Switzerland, ²Novartis Pharma, Nuremberg, Germany, ³Novartis Pharma, Basel, Switzerland.

The purpose of this analysis is to give an overview about the published data on fracture risk reduction.

The intervention threshold for the treatment of osteoporosis has changed within the last years. Whereas bone mineral density (BMD) alone was used in the past to determine, whether a patient should be treated or not, nowadays the whole situation of the patient (incl. e.g. age, BMI, previous fractures, family history) has to be considered. These factors combined with the BMD allow to calculate the height of the individual fracture risk, upon which the physician can base his treatment decision. In addition three dimensional assessment of bone structure will gain further importance in the future (fig 1).

We analysed published results of randomized controlled trials of various bisphosphonates, parathormone and strontium ranelate and calculated the absolute and relative risk reduction (ARR and RRR) and "number needed to treat" (NNT).

Whereas all analysed substances were able to reduce the risk of vertebral fractures, only Risedronat (RRR=28%, p=0,02), Alendronat (RRR=50%, p=0,047) and Zoledronic acid (RRR=41%, p=0,002) have been able to demonstrate an additional reduction of hip fractures.

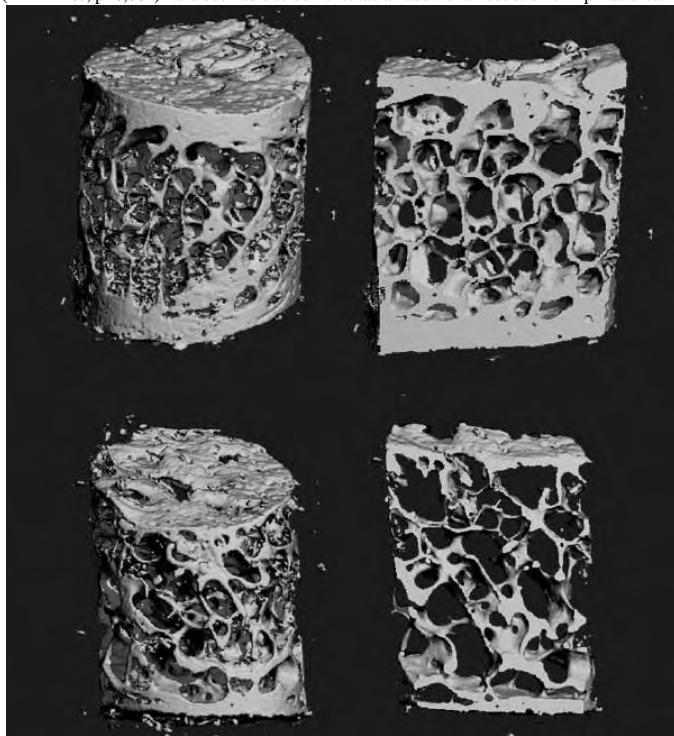


Figure 1: Bone biopsy of patients who took either zoledronic acid (top images) or placebo (bottom images), Xtreme CT, Scanco Medical AG Zurich

Disclosures: M.A. Dambacher, None.

T382

The Efficacy and Tolerability of a Once-A-Month Dosing Regimen of 150 Mg Risedronate for the Treatment of Postmenopausal Osteoporosis - The Merit-OP Study. P. D. Delmas¹, M. R. McClung², J. R. Zanchetta³, A. Racewicz⁴, C. Roux⁵, C. L. Benhamou⁶, Z. Man⁷, R. Eusebio⁸, J. F. Beary⁸, D. E. Burgio⁸, S. Boonen⁹. ¹INSERM, Research Unit 403, Lyon, France, ²Oregon Osteoporosis Center & Providence Medical Center, Portland, OR, USA, ³Instituto de Investigaciones (IDIM), Buenos Aires, Argentina, ⁴Centrum Medyczne Specjalistyczny Gabinet Lekarski, Bialystok, Poland, ⁵Cochin Hospital, Rene Descartes University, Paris, France, ⁶Inserm, Research Unit U658, Orléans, France, ⁷Centro Médico TIEMPO, Buenos Aires, Argentina, ⁸Procter & Gamble Pharmaceuticals, Mason, OH, USA, ⁹Leuven University Center for Metabolic Bone Diseases & Division of Geriatric Medicine, Katholieke Universiteit Leuven, Leuven, Belgium.

The MERIT-OP (Monthly Evaluation of Risedronate Trial in Osteoporosis) study is a multinational, 2-year, randomized, double-blind, active-control (5 mg daily risedronate) clinical trial designed to evaluate a 150 mg risedronate once-a-month (OAM) dose for the treatment of osteoporosis in postmenopausal women. Patients were postmenopausal, 50 years of age or older with a lumbar spine (LS) BMD T-score ≤ -2.5 or a LS BMD T-score ≤ -2.0 and at least one prevalent vertebral fracture. Risedronate was given per-label 30 minutes before breakfast. All patients received daily supplemental calcium 1000 mg and vitamin D 400-1000 IU. The primary efficacy endpoint is to demonstrate non-inferiority of the OAM regimen to the daily regimen as assessed by percent change from baseline in LS BMD at Month 12 using the last observation carried forward. Secondary efficacy endpoints include: percent change in biochemical markers of bone metabolism, in BMD at total proximal femur, femoral trochanter, and femoral neck. Safety endpoints include evaluation of adverse events, clinical laboratory measurements, and bone histology by histomorphometry (at Month 24 only).

A total of 1292 women (94% Caucasian) between 50 and 88 years old, mean age 64.9, were randomized to 150 mg risedronate OAM or 5 mg daily from 47 clinical centers in 13 countries. The mean LS BMD T-score and years since menopause at baseline were -3.2 and 18 years, respectively, across both treatment groups. The study remains blinded at the writing of this abstract. The last patient completed the Month 12 primary endpoint visit in March of 2007. The full Month 12 efficacy and safety results related to the primary and secondary endpoints will be available and presented at the time of the meeting.

Disclosures: P.D. Delmas, Procter & Gamble Pharmaceuticals 5.

T383

The MOTION Study: Tolerability of Monthly Ibandronate and Weekly Alendronate in Women with Postmenopausal Osteoporosis. P. D. Delmas¹, E. M. Lewiecki², S. Ragi-Eis³, F. Sedarati⁴, C. Leigh⁵, F. Cosman⁶. ¹Université de Lyon and INSERM Research Unit 831, Lyon, France, ²New Mexico Clinical Research & Osteoporosis Center, Albuquerque, NM, USA, ³CEDOES Diagnóstico e Pesquisa, Vitoria, Brazil, ⁴Hoffmann-La Roche Inc., Nutley, NJ, USA, ⁵Roche Products Ltd, Welwyn Garden City, United Kingdom, ⁶Helen Hayes Hospital, West Haverstraw, NY, USA.

The MOTION (Monthly Oral Therapy with Ibandronate for Osteoporosis Intervention) study is the first head-to-head comparison of monthly oral ibandronate and weekly oral alendronate for the treatment of postmenopausal osteoporosis. The study compared efficacy (bone mineral density [BMD] at spine and hip and bone turnover markers) and tolerability and safety of the regimens.

Women aged 55-84 years and ≥ 5 years since menopause with a mean lumbar spine BMD T-score (L2-L4) < -2.5 and ≥ 5.0 were randomly allocated to 12 months of double-blind, double-dummy treatment with oral ibandronate (IBN) 150mg once monthly (plus weekly placebo) or oral alendronate (ALN) 70mg once weekly (plus monthly placebo). Treatments were taken in the morning after an overnight fast. Patients also received vitamin D 400IU/day and calcium 500mg/day. Safety was monitored during the study by assessment of adverse events (AEs) and laboratory tests. We present here the AE data.

A total of 1,733 (IBN, 874; ALN, 859) patients were included in the safety analysis population (patients who took at least 1 active treatment dose). The overall incidence of AEs, including those considered related to treatment or leading to withdrawal, was similar across both treatment groups (Table). Of the serious AEs reported (IBN: 4.5%; ALN: 6.4%), very few were considered treatment related ($< 1\%$ per group; Table). There was one death with IBN and four with ALN. The incidence of upper gastrointestinal (GI) AEs was similar in the two treatment groups (Table) but more patients in the ALN group (15; 1.7%) withdrew after drug-related upper GI events than patients in the IBN group (9; 1.0%). In conclusion, monthly ibandronate and weekly alendronate were shown to have very similar tolerability profiles in women with postmenopausal osteoporosis.

Incidence (n, %)	IBN (n=874)	ALN (n=859)
Any AE	659 (75.4)	632 (73.6)
Any drug-related AE	232 (26.5)	176 (20.5)
Any drug-related AE leading to withdrawal	29 (3.3)	26 (3.0)
Any drug-related serious AE	1 (0.1)	5 (0.6)
Upper GI AEs	153 (17.5)	143 (17.2)
Perforations, ulcers and bleeding	4 (0.5)	8 (1.0)
Any drug-related serious upper GI disorders	0	3 (0.3)

Disclosures: P.D. Delmas, F. Hoffmann-La Roche Ltd/GlaxoSmithKline 5.
This study received funding from: F. Hoffmann-La Roche Ltd/GlaxoSmithKline.

T384

Bisphosphonate Therapy and Hip Fractures Within the Risedronate and Alendronate (REAL) Cohort Study: A Comparison to Patients with Minimal Bisphosphonate Exposure. P. D. Delmas¹, S. L. Silverman^{2*}, N. B. Watts³, J. L. Lange^{4*}, R. Lindsay^{5*}. ¹INSERM Unit 403, University of Lyon, Lyon, France, ²Cedars-Sinai Medical Center, Beverly Hills, CA, USA, ³Bone Health and Osteoporosis Center, Cincinnati, OH, USA, ⁴P&G, Mason, OH, USA, ⁵Helen Hayes Hospital, West Haverstraw, NY, USA.

In the published REAL cohort study,¹ we observed that patients on risedronate had a lower incidence of hip fractures during the first year of therapy, but not in the year before therapy, compared with patients on alendronate. That study design did not include a comparison to an untreated control group. Here we present an approach to utilize patients with minimal bisphosphonate exposure as a control group for the REAL study. The original study population was identified within records of health services utilization and included new users of once-a-week dosing of risedronate or alendronate. These bisphosphonate users were followed until a 15 day gap occurred between the completion of a 30-day prescription and any subsequent prescription. To identify the control group within the same data source, we selected patients who filled only a single prescription of alendronate or risedronate over one year. Hip fracture in the first year after the initial prescription was the primary outcome. Cox proportional hazard modeling was used to compare the incidence of hip fractures between patient populations.

In the control group of patients receiving a single bisphosphonate prescription, the one year incidence of hip fractures in patients who were prescribed alendronate (0.81% of 1850 patients) or risedronate (0.78% of 1152 patients) was similar (relative risk 1.0, 95% CI 0.4 - 2.2). Compared to this control group with minimal bisphosphonate exposure, patients on risedronate had a significantly lower incidence of hip fractures, while patients on alendronate were not significantly (table).

Patients with minimal bisphosphonate exposure to either risedronate or alendronate were at similar risk for hip fracture and can be pooled to serve as a control group. Patients on risedronate had significantly fewer hip fractures than this control group, patients on alendronate did not.

¹Silverman et al. Effectiveness of bisphosphonates on nonvertebral and hip fractures in the first year of therapy: the risedronate and alendronate (REAL) cohort study. *OJ* 2007 18:25

Incidence of hip fractures in the initial year of therapy by cohort						
Cohort	Cohort size	Number women with hip fracture	Percent* women with hip fracture	Adjusted** rate ratio vs control	95% confidence interval	p-value
Minimal exposure (control)	3,002	24	0.80	referent		
Alendronate	21,615	80	0.58	0.90	0.56 - 1.44	0.66
Risedronate	12,215	29	0.37	0.50	0.28 - 0.87	0.01

*based on Kaplan-Meier estimate

**adjusted for differences in history of co-morbidities and concomitant medications, which may relate to fracture risk

Disclosures: P.D. Delmas, Procter & Gamble Pharmaceuticals 5.

T385

Reduction of Bone Turnover Markers With Annual Infusion of Zoledronic Acid 5 mg in Postmenopausal Osteoporosis: Influence of Age, Renal Function, Concomitant Therapy, and Duration of Treatment. P. Delmas¹, D. M. Black², S. Boonen³, D. C. Bauer², F. Cosman⁴, C. Mautalen⁵, I. A. Skripnikova^{6*}, E. F. Eriksen⁷, P. Mesenbrink^{8*}, H. Hu^{8*}, R. Eastell⁹. ¹INSERM Research Unit 831, Univ of Lyon, Lyon, France, ²Univ of California, San Francisco, CA, USA, ³Univ Ziekenhuizen K.U. Leuven, Leuven, Belgium, ⁴Helen Hayes Hospital, West Haverstraw, NY, USA, ⁵Hospital de Clinicas University of Buenos Aires, Buenos Aires, Argentina, ⁶Russian Ministry of Health, Moscow, Russian Federation, ⁷Novartis Pharma AG, Basel, Switzerland, ⁸Novartis Pharmaceuticals Corp, East Hanover, NJ, USA, ⁹Univ of Sheffield, Sheffield, United Kingdom.

Annual infusions of zoledronic acid (ZOL) 5 mg have been shown to reduce vertebral and hip fractures by 70% and 40% respectively (Black et al, *NEJM* 2007) in postmenopausal women w/ osteoporosis compared w/ placebo. Serum C-telopeptide of collagen-1 (CTX-1) and bone alkaline phosphatase (ALP) were measured in a subgroup of 605 women (300 ZOL, 305 placebo). Mean decreases at 6 mos relative to placebo for CTX and bone ALP were 69% (95% CI: 67,72) and 33% (95% CI: 31,35) respectively, both P < .0001. Our objective was to analyze the influence of age, renal function, concomitant therapy (Stratum II: pts taking raloxifene, tibolone, hormone replacement therapy, or nasal calcitonin in addition to study drug) and duration of therapy on magnitude of bone turnover marker (BTM) decrease. In women ≥75 yrs mean decreases (95% CI) at 6 mos w/ ZOL compared w/ placebo for CTX and bone ALP were 70% (95% CI: 65,74) and 33% (30,36) respectively, comparable to women <70 yrs, for whom they were 69% (62,75) and 35% (30,40) respectively. In women w/ creatinine clearance <60 mL/min mean decreases (95% CI) at 6 mos w/ ZOL compared w/ placebo for CTX and bone ALP were 69% (64,73) and 33% (30,37) respectively, comparable to women w/ creatinine clearance >60 mL/min, for whom they were 70% (66,73) and 33% (30,36) respectively. In Stratum II pts mean decreases (95% CI) at 6 mos w/ ZOL relative to placebo for CTX were 67% (62,72) and for bone ALP were 29% (25,32), both P < .0001, as compared to women in Stratum I, for

whom they were 71% (68,74) for CTX and 36% (33,39) for bone ALP, both P < .0001. BTM reduction differences across strata were accounted for by lower baseline levels in Stratum II. CTX mean decrease (95% CI) from pre-infusion to 10 days after the 3rd ZOL infusion relative to placebo was 77% (72,80) (P < .0001). In summary, ZOL 5 mg reduced BTM independently of age and creatinine clearance, and to a greater magnitude in naive pts than in those receiving concomitant therapy, and CTX-1 levels following the 3rd annual infusion showed rapid and transient decrease, indicating ongoing bone remodeling. The data suggest ZOL reduces BTM values to safe levels in a wide range of osteoporotic women.

Disclosures: P. Delmas, Novartis 5.

This study received funding from: Novartis Pharma AG, Basel, Switzerland.

T386

Comparison of Bone Architecture via Micro-CT after Long-term Treatment with Risedronate and Alendronate: A Cross-sectional Study in Women with Postmenopausal Osteoporosis. T. E. Dufresne^{1*}, P. A. Chmielewski^{1*}, J. H. Nurre^{1*}, B. Borah¹, X. Zhou^{1*}, R. Phipps¹, G. Woodson², P. D. Miller³. ¹Procter & Gamble Pharmaceuticals, Mason, OH, USA, ²Atlanta Research Center, Decatur, GA, USA, ³Colorado Center for Bone Research, Lakewood, CO, USA.

To compare the effects of risedronate and alendronate on trabecular and cortical bone architecture we analyzed transiliac crest biopsies collected from a sample of 100 women with postmenopausal osteoporosis. Subjects were at least 5 yr postmenopause and had been treated for 3 or more yr with daily or weekly alendronate (n=68, mean age 69.7 yr) or risedronate (n=32, mean age 70.2 yr). Complete biopsies were scanned at 8 µm resolution using a Scanco MicroCT40 scanner. After thresholding and masking, trabecular and cortical bone measurements were derived from these 3-D data sets. In addition, the grey level images were calibrated against hydroxyapatite standards to allow for accurate measurement of mineralization in the cortical and trabecular envelopes.

There were no significant differences in patient demographics either prior to treatment initiation or at time of biopsy, including age, lumbar spine and total hip T-scores, and previous fractures. There were no significant differences in trabecular architecture, cortical porosity or cortical thickness between risedronate and alendronate. The low: high mineralization ratio in both trabecular and cortical bone was significantly higher in biopsies from risedronate-treated subjects than in alendronate-treated subjects, consistent with the higher bone turnover in risedronate-treated subjects seen by histomorphometry (MS/BS 2.55% vs 1.32%, P<0.01).

These results support that long-term treatment with risedronate provided equivalent preservation of trabecular and cortical bone architecture compared with alendronate, despite producing significantly lower suppression of bone remodeling.

Parameter	Alendronate (Median)	Risedronate (Median)	P-value (Wilcoxon Rank Sum Test)
Trabecular bone volume (%)	15.59	16.02	0.57
Trabecular number (n)	1.26	1.31	0.21
Trabecular thickness (µm)	148	151	0.74
Low:high mineralization ratio - trabecular	0.26	0.41	0.01
Low:high mineralization ratio - cortical	0.22	0.30	0.02
Cortical porosity (%)	3.21	3.57	0.41
Cortical thickness (µm)	460	479	0.70

Disclosures: T.E. Dufresne, Procter & Gamble 3.

This study received funding from: The Alliance for Better Bone Health.

T387

Determinants of Femoral Neck Bone Loss in the HORIZON-PFT Study: Impact of Zoledronic Acid Therapy. R. Eastell¹, D. Black², S. Boonen³, S. Cummings², P. Delmas⁴, L. Palermo^{2*}, E. Eriksen⁵, P. Mesenbrink^{6*}, K. Lippuner⁷, C. Zerbinì⁸, A. Skag^{9*}, P. J. Cauley¹⁰. ¹Univ. of Sheffield, Sheffield, United Kingdom, ²Univ. of California, San Francisco, CA, USA, ³Univ. Ziekenhuizen K.U., Leuven, Belgium, ⁴Univ. of Lyon, INSERM Research Unit 831, Lyon, France, ⁵Novartis Pharma AG, Basel, Switzerland, ⁶Novartis Pharmaceuticals Corp, East Hanover, NJ, USA, ⁷Poliklinik für Osteoporose der Medizinischen Fak. und des Inselspitals der Univ., Bern, Switzerland, ⁸Hosp. Heliópolis, São Paulo, Brazil, ⁹Senter for kliniske studier AS, Bergen, Norway, ¹⁰Univ. of Pittsburgh, Pittsburgh, PA, USA.

The HORIZON-PFT is a multinational, 3-year, randomised, double-blind, placebo (PLB)-controlled trial evaluating the effect of once-yearly zoledronic acid (ZOL) 5 mg, on vertebral and hip fracture risk in 7736 postmenopausal osteoporotic women (65-89 yrs). Femoral neck BMD was measured annually in all participants. In this post-hoc analysis, we examined the determinants of bone loss in the PLB group and whether ZOL is effective in preventing bone loss across all subgroups. Specifically, we examined the effect of ZOL on femoral neck BMD in women stratified by age (<70, 70-79, ≥80 years), weight (<55, 55-64, >64 kg), current smoking status, race (Caucasian, Asian, other) and region (Europe, Asia, Americas), see table. We found bone loss was greater in women ≥80 yr (-1.14/3-yr) vs women <70 yr (-0.76%/3-yr) in the PLB group. This difference was maintained in the ZOL group for older and younger women, respectively (3.90 and 4.33%/3-yr). Bone loss was greater in lighter (-1.29/3-yr) vs heavier women (-0.50%/3-yr) and this was maintained in the ZOL group for lighter and heavier women (3.92 and 4.43%/3-yr). Bone

loss was greater in smokers (-1.42%/3-yr) vs non-smokers (-0.92%/3-yr) and this difference was greater in the ZOL group for smoking and non-smoking women (3.35 and 4.17%/3-yr). We found bone loss was greater in Caucasian (-0.96%/3-yr) vs Asian women (-0.49%/3-yr) and this was maintained in the ZOL group for Caucasian and Asian women (4.08 and 4.37%/3-yr). Bone loss was greater in women from the Americas (-1.47%/3-yr) vs those from Asia (-0.48%/3-yr) and this was maintained in the ZOL group for women from the Americas and Asia (3.50 and 4.44%/3-yr). We conclude that older age, lighter weight, smoking, being Caucasian or from the Americas are risk factors for hip bone loss, and that ZOL is equally effective on hip BMD in each of these groups.\

Factor	Category	ZOL	PLB	p, Rx	p, CAT
Age	<70	4.33	-0.76	<0.0001	0.01
	70-79	4.08	-0.95		
	80+	3.52	-1.55		
Race	Asian	4.37	-0.49	<0.0001	0.01
	Caucasian	4.08	-0.96		
	Other	3.71	-1.97		
Region	Americas	3.5	-1.47	<0.0001	<0.0001
	Asia	4.34	-0.48		
	Europe	4.44	-0.73		
Smoking	No	4.17	-0.92	<0.0001	0.02
	Yes	3.35	-1.42		
Weight	<55 kg	3.92	-1.29	<0.0001	0.001
	55-64 kg	3.97	-1.1		
	>64 kg	4.43	-0.5		

Disclosures: R. Eastell, Novartis Pharma AG 2, 5, 8.

This study received funding from: Novartis Pharma AG

T388

In Case of Gastrointestinal Side Effects or Contraindications for Oral Bisphosphonates Treatment with Intravenous Pamidronate Is a Good Alternative. D. A. Eekman^{*1}, M. Vis², I. E. M. Bultink^{*1}, H. J. G. M. Derikx^{*2}, B. A. C. Dijkman¹, W. F. Lems¹. ¹Rheumatology, VU University Medical Center, Amsterdam, The Netherlands, ²Rheumatology, Slotervaart Hospital, Amsterdam, The Netherlands.

Background: oral bisphosphonates (OB) are the preferred treatment for osteoporosis (OP), however they may cause gastrointestinal side effects. In patients with side effects or contraindications it is possible to administer pamidronate intravenously (APD). In a previous 1 year prospective study in 2 groups of each 20 patients, we have shown that the effects on BMD of APD and OB are comparable.¹

Objectives: to compare the effect on change in BMD of the lumbar spine and total hip of long term treatment (≥ 2 years) with APD (60mg intravenously every 3 months) in comparison to alendronate 70mg or risedronate 35mg weekly in patients with OP.

Methods: all consecutive patients receiving OP treatment for at least two years at the Slotervaart Hospital OP clinic were enrolled. Most patients started with an OB according to protocol. In case of intolerance (within 3 months of start of treatment) of an OB or in case of contraindications for an OB, APD 60mg was started. BMD was measured on a Hologic 4500 at the lumbar spine (L1-L4) and the total hip before the start of treatment and at the end of follow-up. Changes in BMD between the groups were compared by an independent student t-test.

Results: 67 patients were enrolled, 34 in the OB group (17 alendronate and 17 risedronate) and 33 in the APD group. Mean follow-up duration (SD) was 4.3 (1.3) years. There were no differences in baseline characteristics or baseline T scores of hip and spine between both groups. There was no significant difference in BMD change between the OB and APD group. (see table)

	Oral Bisphosphonates (n=34)	APD (n=33)
Duration of treatment	4.3 (1.37)	4.2 (1.29) (ns)
Mean (SD) years		
BMD lumbar spine baseline	0.787 (0.17)	0.778 (0.092) (ns)
mean (SD) g/cm ²		
BMD lumbar spine follow-up	0.851 (0.136)	0.844 (0.123) (ns)
mean (SD) g/cm ²		
% change of lumbar spine BMD per year	2.47	2.33 (ns)
BMD Hip baseline	0.721 (0.137)	0.745 (0.126) (ns)
mean (SD) g/cm ²		
BMD Hip follow-up	0.736 (0.142)	0.763 (0.119) (ns)
mean (SD) g/cm ²		
% change of hip BMD mean (SD)	0.31	0.62 (ns)

Conclusion: after 4 years of treatment, the change of BMD of the lumbar spine and hip is not significantly different between patients treated with intravenous pamidronate versus oral bisphosphonates. BMD of the hip remained stable, whereas BMD of the lumbar spine improved with 2% per year in both groups. We therefore conclude that intravenous administration of pamidronate is an alternative for oral bisphosphonates in the treatment of OP. References: ¹ M. Vis et al. Osteoporos Int. 2005 Nov;16(11):1432-5

Disclosures: D.A. Eekman, None.

T389

Benefits of Oral Ibandronate on Non-Vertebral Fracture Risk in Postmenopausal Osteoporosis: Further Analyses From a Pivotal Phase III Study. R. Emkey¹, C. H. Chesnut^{*2}, R. C. Schimmer^{*3}, C. Neate^{*4}, R. R. Recker⁵. ¹Radiant Research, Wyomissing, PA, USA, ²University of Washington, Osteoporosis Research Group, Seattle, WA, USA, ³F. Hoffmann-La Roche Ltd, Basel, Switzerland, ⁴Roche Products Ltd, Welwyn Garden City, United Kingdom, ⁵Creighton University, Osteoporosis Research Center, Omaha, NE, USA.

Ibandronate is a potent, nitrogen-containing bisphosphonate that has shown efficacy and tolerability for the treatment of postmenopausal osteoporosis (PMO) in a number of clinical trials. In the BONE (Bonviva Osteoporosis Trial in North America and Europe) study, 2,946 women (aged 55-80 years, menopause onset ≥5 years) with PMO (1-4 prevalent vertebral fractures, lumbar spine BMD T-score <-2.0 SD) were randomized to receive oral ibandronate either daily (2.5mg) or intermittently (20mg every other day for 12 doses every 3 months), or placebo for 3 years. All patients received daily oral calcium (500mg) and vitamin D (400IU). Daily ibandronate reduced vertebral fracture risk (primary endpoint) by 52% (US; p=0.0003)¹ and 62% (Europe; p=0.0001).² The population was relatively low risk for non-vertebral fractures, with a minority of women (30.5%) having low femoral neck BMD at baseline (T-score ≤-2.5 SD), and >30% having a femoral neck BMD T-score >-1.6 SD. Consequently, no statistically significant effect was seen on non-vertebral fractures in the overall study population. Without appropriate fracture risk and a sufficient number of events, it is not possible to detect a true reduction in fracture risk. Therefore, we carried out a subanalysis in women at higher risk for non-vertebral fractures; women (n=278) with lumbar spine BMD T-score <-2.5 and a history of clinical fractures in the previous 5 years. The incidence of non-vertebral fracture in women from the higher-risk subgroup was reduced to 6.28% with daily ibandronate (n=152) vs 14.9% with placebo (n=126). This corresponds to a significant reduction in the risk of non-vertebral fractures of 60% (p=0.0371) for daily ibandronate vs placebo. This risk reduction is consistent with a previously reported subgroup analysis of the BONE study,² which showed a 69% (p=0.013) reduction in the risk of non-vertebral fractures in a group of patients with similar fracture risk.

In conclusion, daily oral ibandronate significantly reduced the risk of non-vertebral fractures in a higher-risk subgroup, even though the overall population was at relatively low risk for non-vertebral fractures. Importantly, the sub-population analyzed represents the majority of patients typically treated for postmenopausal osteoporosis.

1. Chesnut CH et al. Curr Med Res Opin 2005;21:391-401.

2. Chesnut CH et al. J Bone Miner Res 2004;19:1241-9.

Disclosures: R. Emkey, F. Hoffmann-La Roche Ltd/GlaxoSmithKline 5.

This study received funding from: F. Hoffman-La Roche Ltd/GlaxoSmithKline.

T390

Pamidronate Is Effective for Children with Severe Glucocorticoid-induced Osteoporosis. I. Fujiwara, A. Saito^{*}, K. Ishii^{*}, J. Kanno^{*}, S. Tsuchiya^{*}. Pediatrics, Tohoku University School of Medicine, Sendai, Japan.

Glucocorticoid-induced osteoporosis (GIO) is a dose- and duration-dependent side-effect of glucocorticoid treatment, and in severe GIO patients, fractures and deformities of bone may be seen even during childhood. Bisphosphonates are effective for adult GIO patients, but reports of its use in children are limited. We report efficacy of pamidronate infusion in severe GIO children who experienced spinal fracture.

Five GIO patients (age 3 to 21y, median 8y) received monthly pamidronate infusion (1mg/kgBW) for 3 to 27 months after the diagnosis of vertebral fracture. They had been treated with glucocorticoid due to hematological (Diamond-Blackfan anemia, idiopathic thrombocytopenic purpura), inflammatory (Weber-Christian disease), or respiratory (bronchiolitis obliterans after bone marrow transplantation) diseases, respectively.

Relief from pain was particularly notable, which was obtained one or two days after the first infusion in all the patients. Although not significant, the average Z score of lumbar BMD increased after pamidronate (-4.06 SD at the beginning to -2.96 SD at 12months), but in one, BMD continued to decrease probably because of the immobilization of the patient. No apparent adverse events were seen during and after pamidronate. In conclusion, monthly pamidronate infusion is an effective treatment for children with severe GIO.

Disclosures: I. Fujiwara, None.

T391

The Impact of Bonemarker Feedback on Adherence to Once Monthly Ibandronate Treatment for Postmenopausal Osteoporosis (PMO) in Mexican and Chilean Patients (BOHEMIA Study). P. A. Garcia-Hernández^{*1}, S. Carranza-Lira^{*2}, A. G. Garcia-Sevillano^{*3}, E. Motta-Hernandez^{*4}, P. De la Pena⁵.

¹Endocrinology, Hospital Universitario Nuevo Leon, Monterrey NL, Mexico, ²Gynecology, HGO Luis Castelazo Ayala IMSS, Mexico City, Mexico, ³Metabolism, Roche, Mexico City, Mexico, ⁴Gynecology, COM, Mexico City, Mexico, ⁵Endocrinology, Centro de Osteoporosis, Guadalajara, Jal, Mexico.

The impact of bonemarker feedback on adherence to once monthly ibandronate treatment for postmenopausal osteoporosis (PMO) in Mexican and Chilean patients (BOHEMIA Study)

Poor adherence is a common cause of reduced patient benefit from bisphosphonates therapies used in the clinical area. An open-label, prospective, randomized, multi-center clinical study to investigate the impact of bonemarker feedback on adherence to once monthly ibandronate treatment for postmenopausal osteoporosis (PMO) in Mexican and Chilean patients (BOHEMIA Study) were performed. All patients received oral ibandronate 150 mg once-monthly during 6 months of treatment. A total of 781 patients were enrolled into the study across 25 centers in Mexico (700 patients) and 24 centers in Chile (81 patients), and they were divided in 2 arms at baseline either to receive bonemarker feedback or not to receive it, who were either naïve to bisphosphonate treatment, lapsed bisphosphonate users, or current BP users. We found statistical differences among patients who received bonemarker feedback versus those patients who did not, according results in treatment adherence ($p < 0.001$). It can be observed that patients who use bonemarker feedback had a 95% IC range from 98.8% to 99.8%, while the no user patients had a range from 95.5% to 97.5% ($p < 0.001$). We also found significant differences among patients with bonemarker feedback versus no users in the percentage of change of CTX in basal conditions compared with 3 and 6 months ibandronate treatment. According ibandronate safety, 247 (31.6%) patients had at least one adverse event (AE), while 534 (68.40%) patients did not have any AE. In order of frequency, bone pain was the most common AE (65 cases; 13.8%). According with our results, bonemarker feedback is recommended in order to have benefits in the osteoporosis therapy, supported by the physician opinion, where 49% percent of them recommend bonemarker feedback every 6 months in order to improve the adherence of the patients. The reduction in CTX observed in the patients after ibandronate therapy and the results in terms of adherence to treatment were a good signal for supporting the use of the oral monthly ibandronate in order to improve the persistence in the treatment.

Disclosures: P.A. Garcia-Hernández, None.

This study received funding from: Roche Mexico.

T392

Prevention of Bone Loss in Acute Spinal Cord Patients over One Year with Alendronate: Randomized Double-blind Placebo Controlled Study. N. L. Gilchrist¹, C. P. Frampton^{*2}, R. R. Acland^{*3}, R. L. March^{*1}, P. Maguire^{*1}, A. Heard^{*1}, P. Reilly^{*1}, K. Marshall^{*3}.

¹Canterbury Geriatric Medical Research Trust, Christchurch, New Zealand, ²Department of Medicine, Christchurch School of Medicine, Christchurch, New Zealand, ³Spinal Unit, Burwood Hospital, Christchurch, New Zealand.

The aim of the study was to document the effect on bone mass loss in acute spinal cord injury patients using oral alendronate 70mg once weekly having commenced within 10 days of acute spinal cord injury and administered for a period of 12 months. The study enrolled patients between March 2001 and February 2004, males and females, 18 - 55 years presenting to the Burwood Hospital, Spinal Injury Unit, Christchurch, New Zealand with acute spinal cord injury (C4 - L2, ASIA scores A - D) were randomly assigned to enter a prospective double blind placebo controlled study to compare the safety and efficacy of oral alendronate with 70mg once weekly. The treatment was begun as inpatients. No additional calcium or vitamin D was administered. Vitamin D deficiency at baseline was corrected. Data was collected at baseline 3, 6, 12 and 18 months (bone mineral density, total body and regional areas, hip, lumbar spine and ultrasound at calcaneus). Weight body mass index and adverse events were collected. Bone mineral density loss was prevented at the total body site ($>7\%$ and at the regional site, pelvis $>15\%$, trunk $>4\%$, legs $>7\%$, arms $>3\%$). No significant loss was observed at the spine. All areas at the hip demonstrated prevention of bone loss, total $>16\%$, femoral neck $>16\%$, trochanter $>20\%$, femoral shaft $>15\%$. No significant treatment related side effects were noted. In conclusion this is the first study to use once weekly oral alendronate in patients with acute spinal cord injury soon after the acute event. Bone loss was prevented in most bone sites measured and occurred over 12 months with oral alendronate 70mg per week. There were no significant treatment related adverse events.

Disclosures: N.L. Gilchrist, None.

This study received funding from: Merck Sharp & Dohme.

T393

Nothing works without Calcium and Vitamin D. C. Guenther^{*1}, A. Kapner^{*1}, H. Schultis^{*2}, C. Spanier^{*1}, D. Arnold-Dahmen^{*1}, V. Schäfer^{*1}.

¹Deutsches Zentrum für Osteoporose, Johannesbad Reha-Kliniken AG&Co.KG, Bad Füssing, Germany, ²Gemeinschaftspraxis für Laboratoriumsmedizin und Mikrobiologie, Weiden, Germany.

Aim: To show in a case report that antiresorptive therapy of osteoporosis is not effective without calcium and vitamin D.

Method: The 75 year old woman with a new L-1 fracture were treated by the family doctor only with one tablette Fosamax 70mg per week. In our clinic we added the basic therapy with calcium and vitamine and investigated different laboratory values including bone markers.

Results: A nine days later occurring laboratory analysis showed an increase of calcium in serum by 2.3%, a decrease of alkaline phosphatase by 15%, an increase of 25-OH-D3 by 53% and a decrease of β -crosslaps by 45%. Simultaneous balneophysical therapy and pain therapy improved the patients condition additional, so that she could continue the care of her husband after being discharged.

Summary and Conclusion: This case report shows that only treatment with highly active antiresorptive agents (in this case Fosamax, but other cases with Actonel 35, Evista, Bonviva, Protelos also regarding bone markers prove this statement too) do not lead to sufficient reduction of bonecatabolism, if the basic therapy with calcium and vitamin D is neglected. Therefore in all bisphosphonate studies calcium and vitamin D have been given as "placebo". Furthermore it can be proved that the bone markers (in this case the high sensible catabolism marker β -CTx of Roche) show therapy effects already after a short time (here after nine days). This case confirms Köster J.C. et al. (Eur J Clin, Pharmacol, 1996; 51:145-147) that under sole Editronat-therapy without vitamin D- supplementation of postmenopausal patients with osteoporosis only 0.4% increase of bone density at the spine and 0.5% at the neck of the femur could be reached while the other group with calcium and vitamin D supplementation noted an increase of 1.9% respectively 5.2%.

Therefore in any kind of osteoporosis therapy with antiresorptive or osteoanabolic (like Forsteo, Preotact or Protelos) drugs basic therapy with calcium and vitamin D should never be forgotten.

Disclosures: C. Guenther, None.

T394

Persistence with Risedronate Therapy Is Already High and Further Improved by a Patient Educational Program. P. Hadji. Gyn. Endocrinology, Reproductive Medicine and Osteology, University Hospital Marburg, Marburg, Germany.

Objective: There is concern that persistence with therapy for chronic, asymptomatic diseases, i.e. postmenopausal osteoporosis is suboptimal and this may affect clinical efficacy. Recent analyses, however, show a satisfactory 1-year persistence as high as 68% for weekly bisphosphonates. To further improve persistence with risedronate therapy a patient educational program was introduced in 2000 in Germany by the Alliance for Better Bone Health. Patients can enrol into the program sending in a reply card. They receive reminder letters together with leaflets informing them about osteoporosis in regular intervals over the first 7-month period. In this study we evaluated whether persistence with risedronate therapy improved in patients enrolled into the program versus a control group. **Methods:** Telephone interviews were conducted with postmenopausal women with osteoporosis enrolled into the program ($n = 204$) and a control group of patients that was recruited from physicians in private practice who were not enrolled into the program ($n = 204$). Treatment start was equally distributed between February 2003 and February 2005. Survival analyses were used to determine persistence at 12, 24, and 29 months. Log rank test was used to statistically compare the two groups. **Results:** Average age in both groups was similar (69 years). The majority of patients were taking weekly risedronate. Persistence with risedronate therapy in the patient group enrolled into the program was significantly higher than in the control group ($p < 0.03$). Persistence at 12 months was 91.6% for the group enrolled in the program versus 84.7% in the control group. After 24 months persistence was 84.6% versus 75.7%, and at 29 months persistence was 79.1% versus 75.7%. **Conclusion:** Persistence with risedronate therapy is high in Germany. These data suggest that enrolling patients in a mailed education program can further improve persistence.

Disclosures: P. Hadji, Procter&Gamble Pharmaceuticals-Germany GmbH, Weiterstadt, Germany 2.

This study received funding from: Procter & Gamble Pharmaceuticals-Germany GmbH, Weiterstadt, Germany.

T395

Comparison of the Effect of Daily 1mg Minodronate with 5 mg Alendronate in Japanese Women with Postmenopausal Osteoporosis: A Randomized Double-Blind Study. H. Hagino¹, Y. Nishizawa², T. Sone³, H. Morii², Y. Taketani⁴, T. Nakamura⁵, A. Itabashi⁶, H. Mizunuma⁷, Y. Ohashi⁴, M. Shiraki⁸, T. Minamide⁹, T. Matsumoto¹⁰. ¹Tottori University, Yonago, Japan, ²Osaka City University, Osaka, Japan, ³Kawasaki Medical School, Okayama, Japan, ⁴University of Tokyo, Tokyo, Japan, ⁵University of Occupational and Environmental Health, Kitakyushu, Japan, ⁶Saitama Center for Bone Research, Saitama, Japan, ⁷Hirosaki University, Hirosaki, Japan, ⁸Research Institute and Practice for Involuntional Diseases, Nagano, Japan, ⁹ONO Pharmaceutical CO.,LTD., Osaka, Japan, ¹⁰University of Tokushima Graduate School of Health Biosciences, Tokushima, Japan.

The efficacy and safety of minodronate, a new bisphosphonate, were examined in Japanese patients with postmenopausal osteoporosis by a double-blinded, randomized, active-controlled, multicenter study to compare with alendronate.

A total of 270 postmenopausal women ≥ 45 years of age with osteoporosis were randomized into minodronate group (N=135) or alendronate group (N=135). Patients for each group received minodronate 1mg or alendronate 5mg once a day for 12 months.

The changes in lumbar spine BMD in both treatment groups were very similar to each other over the course of study until 12 months. The lumbar spine BMD after 12 months of treatment increased 5.86 and 6.29% from the baseline in minodronate and alendronate group, respectively (treatment difference [95% CI]: -0.43% [-1.29, 0.43; $p=0.0002$]). As for the effect on BMD of minodronate at 12 months, non-inferiority to alendronate was shown. Total hip BMD increased from baseline by 3.47 and 3.27% after 12 months in minodronate and alendronate groups, respectively. The bone turnover markers were rapidly reduced within 1 month in both treatment groups and there was no significant difference between the two groups, except for an earlier reduction in urinary type I collagen N-telopeptide in minodronate group than in alendronate group. The completion rates for 12 months of the study were similar in the two treatment groups (minodronate, 91.8%; alendronate, 89.6%). The overall incidence and severity of clinical adverse events was almost similar between the two groups, including gastrointestinal events (39.6% and 37.0% in minodronate and alendronate group, respectively), and most of gastrointestinal events were mild in the two groups.

The effects of 12-month treatment with 1mg minodronate on lumbar and hip BMD were similar to those of 5 mg alendronate. Minodronate was generally well tolerated and the safety profile was comparable to that of alendronate.

Disclosures: H. Hagino, ONO Pharmaceutical CO.,LTD. 5; Astellas Pharma Inc. 5.

T396

Bisphosphonate use Increases in Patients with Osteopenia and Prior Fractures Following a Multifaceted Osteoporosis Educational Intervention: Canadian Quality Circle (CQC) National Project. G. Ioannidis¹, L. Thabane², A. Gafni³, A. Papaioannou¹, B. Kvern⁴, A. Hodsmann⁵, D. Johnstone⁶, L. Salach⁷, F. Jiwa⁸, J. D. Adachi¹. ¹McMaster University, Hamilton, ON, Canada, ²University of Manitoba, Winnipeg, MB, Canada, ³University of Western Ontario, London, ON, Canada, ⁴Procter and Gamble Pharmaceuticals, Toronto, ON, Canada, ⁵Ontario College of Family Physicians, Toronto, ON, Canada, ⁶Osteoporosis Canada, Toronto, ON, Canada.

The Quality Circles (QCs) project is a disease management process that involves a small group of people who identify and analyze work related problems and recommend solutions. The project was developed to improve primary care physicians' (PCPs) management of osteoporosis in accordance with the Osteoporosis Canada (OC) 2002 Guidelines. The study consisted of five phases: wave I data collection, 1st educational intervention, wave II data collection, 2nd educational intervention, and wave III data collection. During the educational intervention QCs met to discuss physician profiles (snapshots of how they managed osteoporosis) and to participate in an osteoporosis workshop. This interim analysis (wave I & II) evaluated the change in treatment administration in high risk patients with BMD t-scores in the osteopenia range and prior fragility fracture at the hip, wrist or spine. None of the patients had BMD t-scores in the osteoporotic range (defined as a BMD t-score < -2.5). A total of 340 (wave I) and 301 (wave II) PCPs formed 34 QCs. For each wave, PCPs collected data from different patients via chart reviews and a standardized collection form. A total of 8376 (wave I) and 7354 (wave II) patient records were selected. All patients were women 55 years and older. The generalized estimating equations (GEE) method was used to evaluate differences in bisphosphonate use in high risk patients pre and post educational intervention. The cluster variable for the GEE model was physician and the analysis was adjusted for other clinical risk factors for fracture. An exchangeable correlation matrix was used for the analysis. Odds ratios (OR) and 95% confidence intervals (CI) were calculated. A total of 21, 82, 74 and 169 patients during wave I and 45, 144, 133 and 290 patients during wave II had hip, spine, wrist or any (hip, spine or wrist) fractures, respectively. The likelihood of bisphosphonate use increased following the educational intervention for patients with spine (OR: 1.74; 95% CI: 0.104, 2.91) wrist (OR: 2.56; 95% CI: 1.34, 4.90) and any fracture (OR: 2.19; 95% CI: 1.47, 3.26). No change in bisphosphonate use was observed for hip fractures (OR: 1.0; 95% CI: 0.99, 1.01). The use of QCs is an effective knowledge translation approach that increases PCPs bisphosphonate utilization in high risk patients with osteopenia and fracture.

Disclosures: G. Ioannidis, None.

This study received funding from: Alliance for Better Bone Health.

T397

Comparative Efficacy of Osteoporosis Treatment in Postmenopausal Women. Y. Ishida, T. Taguchi*. Department of Orthopaedic Surgery, Yamaguchi University Graduate School of Medicine, Yamaguchi, Japan.

This study was conducted to assess the comparative effectiveness of several medications on bone mineral density, biochemical bone markers, and the incidence of vertebral fractures in postmenopausal women with osteoporosis. We also investigated the difference in the efficacy of several medications according to the age and the bone turnover. The analysis was based on combined data from two randomized controlled trials. A total of 596 postmenopausal women, aged 50 to 85 years, were analyzed on an intention-to-treat basis. Treatment groups were 1) alendronate, 2) risendronate, 3) etidronate, 4) hormone replacement therapy, 5) eel calcitonin, 6) alfacalcidol, 7) vitamin K2, and 8) control (no treatment). Thoracic and lumbar spine radiographs, bone mineral density at the distal radius, and markers of bone turnover were assessed at baseline and at 3, 6, 12, 18, and 24 months of treatment during the 2-year study. Compared with baseline, the 2-year mean changes in bone mineral density were 2.3% for alendronate, 1.9% for risendronate, -0.5% for etidronate, 2.0% for hormone replacement therapy, 1.6% for calcitonin, -3.6% for alfacalcidol, -1.9% for vitamin K, and -3.3% for control. Seventeen (25.6%) of the control patients developed new vertebral fractures. Compared with controls, the fracture incidence was reduced by 69% ($P=0.02$) in alendronate, 66% ($P=0.01$) in risendronate, 56% ($P=0.04$) in etidronate, 65% ($P=0.02$) in hormone replacement therapy, 59% ($P=0.03$) in calcitonin, 44% ($P=0.13$) in alfacalcidol, and 56% ($P=0.049$) in vitamin K. We observed significant reductions in the incidence of vertebral fractures with alendronate, risendronate, etidronate, hormone replacement therapy, and calcitonin, and significant improvements in bone mineral density with alendronate, risendronate, and hormone replacement therapy. With regard to the magnitude of increase in BMD and the magnitude of the reduction in the risk of vertebral fractures, alendronate, risendronate, and hormone replacement therapy have shown significantly stronger efficacy than that in other medications.

Disclosures: Y. Ishida, None.

T398

Comparison of Effects of Alendronate and Raloxifene on the Lumbar Bone Mineral Density, Bone Turnover, and Lipid Metabolism in Elderly Women with Osteoporosis. J. Iwamoto¹, T. Takeda², M. Uzawa². ¹Department of Sports Medicine, Keio University, Tokyo, Japan, ²Department of Orthopaedic Surgery, Keiyo Orthopaedic Hospital, Gunma, Japan.

The purpose of the present open-labeled prospective study was to compare the treatment effects of alendronate and raloxifene on the lumbar bone mineral density (BMD), bone turnover, and lipid metabolism in elderly women with osteoporosis. One hundred twenty-two postmenopausal women with osteoporosis (mean age: 69.4 years) were randomly divided into two groups of 61 patients each: the alendronate group (5 mg daily) and the raloxifene group (60 mg daily). The BMD of the lumbar spine (L1-L4), urinary level of cross-linked N-terminal telopeptides of type I collagen (NTX), and serum levels of alkaline phosphatase (ALP), total cholesterol (TC), high and low density lipoprotein cholesterol (LDL-C and HDL-C, respectively), and triglycerides (TG) were measured during the 12-month-treatment period. There were no significant differences in the baseline characteristics between the two treatment groups. The trial could be completed in 50 patients in the alendronate group and 52 patients in the raloxifene group. Both alendronate and raloxifene increased the lumbar BMD (+8.0% and +2.4% at 12 months, respectively) following reductions of the urinary level of NTX (-44.6% and -34.5% at 3 months, respectively) and serum level of ALP (-17.7% and -9.6% at 12 months, respectively), with the effects of alendronate, however, being more pronounced than those of raloxifene. Only raloxifene reduced the serum levels of TC and LDL-C (-3.9% and -7.7% at 12 months, respectively) without any significantly effect on the serum HDL-C and TG levels. No serious adverse events were observed in either group. The present study confirmed the greater efficacy of alendronate than raloxifene in increasing the lumbar BMD, through its effect of causing more marked reduction of the bone turnover than that by raloxifene, and some beneficial effects of raloxifene on lipid metabolism in elderly women with osteoporosis.

Disclosures: J. Iwamoto, None.

T399

Comparison of Changes in Bone Mineral Density and Bone Turnover Marker with Alendronate Once-weekly and bi-weekly in Postmenopausal Korean Women. H. Oh^{*1}, I. Joo^{*1}, B. Yu^{*2}, S. Lee^{*3}, H. Lee^{*3}. ¹Family Medicine, Cheil General Hospital, Kwandong University, Seoul, Republic of Korea, ²Family Medicine, Konyang University Hospital, Daejeon, Republic of Korea, ³Family Medicine, Ewha Womens University Hospital, Seoul, Republic of Korea.

Objectives: A pilot study in Japan indicates that alendronate 2.5mg daily dose is as effective as a 10mg dose in increasing the bone mineral density because of the differences of genetic, dietary and environmental factors between Asian and Caucasian populations. And for the convenience of patients and cost-effectiveness, increasing the dosing interval should be also considered. Therefore, we designed the comparative studies which measuring the changes of bone mineral density and bone turnover marker between alendronate 70mg weekly administration and alendronate 70mg bi-weekly administration for the postmenopausal women in the one of the Women's Health Care Centers in Seoul, Korea.

Design: We retrospectively evaluated the postmenopausal women with T score<-2.0 treated with alendronate 70mg weekly or biweekly and compared the changes of bone mineral density and bone turnover marker.

Results: Lumbar bone mineral density was increased by 4.3%, and femoral bone mineral density was also increased by 2.3% in alendronate 70mg weekly group with statistical significance. However, in the group with alendronate 70mg bi-weekly administration, lumbar bone mineral density was decreased by 0.3%, femoral bone mineral density was increased by 1.0% without the statistical differences.(p<0.05) Bone turnover markers showed decreasing pattern, but not statistically significant.

Conclusions: Our study suggested alendronate 70mg bi-weekly administration also has preventive effect on bone loss, even though not strongly, but below the physiologic decrease rate of bone mass.

Table 1. Changes of bone mineral density of the subjects with once weekly and bi-weekly alendronate 70mg administration

	ALN-weekly (N=34)	P value	ALN-bi-weekly (N=27)	P value
L-BMD %change	4.3 ± 0.4	0.000	-0.3 ± 0.1	0.581
F-BMD %change	2.3 ± 0.6	0.000	1.0 ± 0.1	0.631

Table 2. Changes of bone turnover marker of the subjects with once weekly and bi-weekly alendronate 70mg administration

	ALN-weekly (N=34)	P value	ALN-bi-weekly (N=27)	P value
ALP %change	-19.2 ± 2.1	0.096	-47.8 ± 12.1	0.459
DPYD %change	3.0 ± 14.1	0.133	3.2 ± 3.2	0.766

Disclosures: I. Joo, None.

T400

Lipid Profile and BMD Changes in Postmenopausal Korean Women Treated with alendronate (10mg) for 2 Years. I. Joo^{*1}, H. Oh^{*2}, B. Yu^{*3}, K. Kim^{*4}. ¹Family Medicine, Cheil General Hospital, Seoul, Republic of Korea, ²Family Medicine, Cheil General Hospital, Kwandong University, Seoul, Republic of Korea, ³Family Medicine, Konyang University Hospital, Daejeon, Republic of Korea, ⁴Family Medicine, Catholic University Hospital, Seoul, Republic of Korea.

Background: Recently, it is known that bisphosphonate which has been used for prevention and treatment of osteoporosis with the mechanism of inhibiting bone resorption also has an association with cholesterol synthetic process. However, few reports to reveal the relationship between the action of bisphosphonate and lipid metabolism with BMD changes in postmenopausal Korean women. We planned this study to recognize the effect of alendronate(10mg) on serum lipid level in postmenopausal Korean women.

Subjects and Methods: We evaluated postmenopausal Korean women aged over 50 who visited the Osteoporosis clinic in the Health Care Center in Seoul from March of 2003 to October of 2005 retrospectively. The changes of serum lipid levels including total cholesterol, triglyceride, HDL were evaluated.

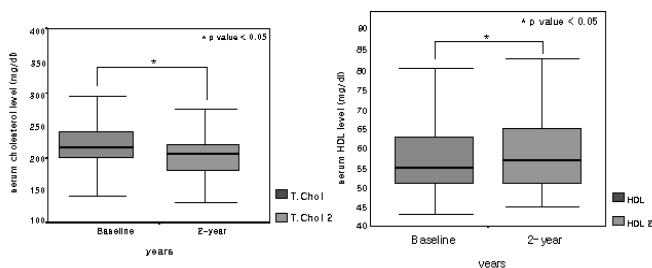
Results: After 2-year alendronate(10mg) administration, total cholesterol level was decreased by 11.8±3.7mg/dl, and HDL level was increased by 5.2±1.4mg/dl with compared to the baseline lipid level. Both of the results showed the statistical significances. Changes of triglyceride and fasting blood sugar levels also showed a declined pattern by 15.4±9.8mg/dl and 6.0±1.4mg/dl, but not statistically significant.

Conclusions: Alendronate might have a beneficial effect on lipid metabolism to decrease cholesterol and increase HDL. With the concern about the postmenopausal natural increase in cholesterol level, alendronate is recommended for prevention of hyperlipidemia in postmenopausal women in addition to prevent and treatment of osteoporosis.

Table 1. Changes in lumbar and femoral BMD after 2-year alendronate(10mg) administration

	baseline	2-year	p
L-BMD (gm/cm ²)	0.876±0.123	0.932±0.075	0.000 [*]
F-BMD (gm/cm ²)	0.717±0.103	0.752±0.080	0.000 [*]

Figure 1. Serum cholesterol and HDL level after 2-year alendronate(10mg) administration



Disclosures: I. Joo, None.

T401

Patient's Satisfaction and Compliance for Risedronate, Once-Weekly Versus Once-Daily: A Multicenter, Prospective, Randomized, 2-way Crossover, Open-Label Study in Postmenopausal Women with Osteoporosis in Korea and Taiwan. H. Kim^{*1}, I. Park^{*2}, I. Lee^{*2}, J. Kim^{*2}, H. Shon^{*3}, J. Choe^{*3}, U. Kim^{*4}, H. Lee^{*5}, Y. Soong^{*6}, S. Tu^{*7}, M. Kim^{*1}. ¹Keimyung University, Daegu, Republic of Korea, ²Kyungbook University, Daegu, Republic of Korea, ³Daegu Catholic University, Daegu, Republic of Korea, ⁴Fatima hospital, Daegu, Republic of Korea, ⁵Yongnam University, Daegu, Republic of Korea, ⁶Chang Gung Memorial Hospital, Taipei, Taiwan, ⁷Changhua Christian Hospital, Taipei, Taiwan.

Postmenopausal osteoporosis(PMO) is characterized by a reduction in bone mass leading to an increased risk of fracture. The Medication for PMO requires long-term persistence with high compliance. The purpose of this study was to determine whether dosing frequency affects compliance and persistence with risedronate, one of the bisphosphonates, in Korea and Taiwan. The study was a multicenter, prospective, randomized, open-label, 2-way crossover (daily to weekly versus weekly to daily) study in postmenopausal women with osteoporosis, who received 24 weeks of treatment (12 weeks with 35 mg risedronate once-weekly and 12 weeks with 5 mg risedronate once-daily dosing). The primary objective was to compare patient's satisfaction of once weekly regimen to once daily regimen using a questionnaire administered to the subjects at 12 and 24 weeks. The secondary objective was to measure compliance (defined as more than 50% of drug taken by tablet count) and persistence (continuing study medication at 12 and 24 weeks). A total of 262 patients were enrolled. 199 patients were included in analysis of the intention to treat (ITT) group, and 185 patients were included in the per protocol evaluation group. Total number of patients included in the safety analysis was 216. The preference of once-weekly dosing regimen was 2 times greater than that of once-daily dosing regimen (52.8% and 25.1% respectively, P-value<0.0001). However, the overall compliance and persistence did not show statistical difference between the two types of dosing regimen (only one patient in each of the dosing regimens was not compliant). Adverse events were reported in 22.8% of patients during the once-daily dosing regimen and in 20.2% of patients during the once-week dosing regimen. There was no statistically significant. The results showed that the patient's preference of once-week dosing regimen was greater. However, compliance and persistence were not different, which can suggest that although preference was higher in longer interval dosing regimen, it did not necessarily lead to the same extent of higher compliance and persistence. Meanwhile, although there were differences in preference, the lack of a difference in compliance may have been because this was a controlled study, and that this may not happen in "real life"

Disclosures: H. Kim, None.

T402

Risedronate Preserves Bone Turn Over as Measured by Biochemical Markers after 5 Years Treatment in Postmenopausal Greek Women. I. C. Koulouris, G. Skarantavos*, T. Kaplanoglou*, P. Katsibri*, P. Soukakos*. First Orthopaedic Clinic, Attiko University General Hospital, Athens, Greece.

Aim of study was to investigate turnover 5-years administration Risedronate in early PO Greek women. Forty early PO women between 48-53 years old(mean 50 years)6 months -1year after the menopause with T score <2SD on lumbar spine DEXA and without any prior metabolic disorders or fractures were separated into 2 groups. Group A (n=30)received 5mg Risedronate 1mcg Alfacalcidol and 1000 mg Calcium carbonate daily for 12 months and 0,5 mg Alfacalcidol and calcium for the rest of the study period while group B(n=10) received the same doses of Alfacalcidol and calcium for the 1st year and only 1000 mg calcium carbonate thereafter.Serum and urine bone turnover markers were measured at 0,6,12,24,36,48,60 month intervals by automated electrochemiluminescence assay.No premenopausal values were available for comparison.Two patients in group A discontinued treatment after 24 months so to investigate the effect of daily administration of Risedronate to early PO Greek women for 5years by measuring sCTX changes uNTX urine Pyrilinks serum BGP.PTHi and 25(OH)D. A questionnaire including VASscore and PPI score concerning quality of life indexes was completed and reevaluated by all patients at the above intervals.1)Group A showed a statistically significant decrease in uNTX(16,15%,p<0.0005)as early as 6 months after treatment whilst there were no statistically significant changes after the 12month period.In group B uNTX was increased(10,9 %,p<0.0005)while the rest of the markers showed a statistically significant decrease for the same period.No values fell below the normal range.2) Group A showed a statistically significant decrease in sCTX(11,69%,p<0.0005) as early as 6 months after treatment whilst there were no statistically sign changes after the 12month period.In group B sCTX was increased (13,32%, p<0.0005)while the rest of the markers showed a statistically significant decrease for the same period.No values fell below the normal range.3)PTHi changes both of groups is not sign.A showed improved indexes in the quality of life scores.Changes in the measured markers especially sCTX uNTX demonstrate that Risedronate effectively decreases the turnover as early as 6 months after treatment and the effect is maintained without further changes from the 6 of the 1st year until end of the 5-years period provided that vitD is sufficient.The fact that no values fell below normal during the 1st year of treatment and bone markers continued to keep these values during the following years of treatment excludes the untoward presence of frozen bone.Quality of life was also improved in the Risedronate group without any untoward GI.effects from upper tract and musculoskeletal system.

Disclosures: I.C. Koulouris, None.

T403

Effect of Bisphosphonates on Bone Mineral Density in Subjects with Normocalcaemic Primary Hyperparathyroidism. A. W. C. Kung, K. K. Lee*. Department of Medicine, The University of Hong Kong, Hong Kong, Hong Kong.

Normocalcaemic primary hyperparathyroidism (NPHPT) as a disease entity is increasingly recognised in the general population. Whether NPHPT is associated with increased bone loss is not well studied, and whether bisphosphonates are effective in preventing bone loss, if present, is unclear. To determine the rate of change of BMD in subjects with NPHPT and to study the effect of bisphosphonates on BMD changes in these subjects. Subjects with elevated PTH on 2 occasions after exclusion of renal impairment, vitamin D insufficiency (<20ng/ml) and other secondary causes of elevated PTH were diagnosed as having NPHPT. BMD, serum albumin-adjusted calcium, PTH, 25(OH)D, ALP and C-Telopeptide, urinary calcium excretion were monitored at yearly intervals. Subjects were randomized to receive either risedronate 35mg once weekly. 24(0.4%) subjects (female/male=21/3, mean age 71±10 years) were diagnosed to have NPHPT from a cohort of 5,600 healthy community dwelling adults aged >50 years. The mean serum calcium and PTH was 2.39±0.10nmol/l and 69±17pg/ml respectively. 19subjects had BMD T score <-2.5 at anyone site, 5 were osteopenia and none had normal BMD. 13 had osteoporotic fractures. The rate of change of BMD after one year was -1.68%, -0.63% and -1.99% respectively at the spine, total hip and forearm. 14 subjects were randomized to risedronate while 10 received calcium and vitamin D alone. BMD was similar between the 2 groups. At 2 years of treatment, BMD increased by 8.5%, 1.8% and 0.7% at the spine, total hip and forearm in the risedronate group, while the calcium and vitamin D group had bone loss of 1.5%, 0.6% and 0.8% at the respective sites (p all <0.05).None of the subjects had elevation of serum calcium during observation. Subjects with NPHPT had a high prevalence of osteoporosis and fractures. The increased bone loss in these subjects can be controlled with bisphosphonates.

Disclosures: A.W.C. Kung, None.

T404

Effect of Anti-Resorptive Agents on Fracture Rates in Subjects Selected for Therapy on the Basis of Clinical Risk Factors or Low Bone Mineral Density. A. W. C. Kung, K. K. Lee*. Department of Medicine, The University of Hong Kong, Hong Kong, Hong Kong.

BMD measurement has been the standard used to diagnose and initiate intervention in osteoporosis. However increasing evidence suggests that BMD alone is inadequate to detect all at-risk individuals and clinical risk factors (CRF) evaluation is recognised as an important element for fracture risk assessment. Whether anti-osteoporosis drug treatment would actually prevent fractures in women selected for therapy on the basis of CRFs alone is unclear. To determine the fracture rate in subjects treated with anti-resorptive agents selected on the basis of low BMD or CRFs. Postmenopausal community dwelling Southern Chinese women (n=2,315) were evaluated for CRFs for fractures (previous low trauma fracture, age>65years, BMI<19Kg/ m², family history of hip fracture) and low BMD (T score<-2.5 at any site). Anti-resorptive agents (HRT or bisphosphonates) were given to subjects with any CRF or low BMD. Subjects were followed prospectively for outcomes of incident low trauma fracture. The fracture rate of subjects who had received any form of treatment was compared to those with one or more CRFs or low BMD but received no treatment and those without risk factors. The mean age of the subjects was 64 ± 8 years.The median follow-up was 5(range 1-10) years. Cox regression analysis also revealed reduced odds of fractures with anti-resorptive therapy in subjects selected on the basis of low BMD but not CRFs. Clinical trials are needed to prove that anti-osteoporosis drug treatment would actually prevent fractures in women selected for therapy on the basis of these CRFs alone.

Patient groups	Any anti-osteoporosis Treatment	Fracture rates
No CRF and BMD T score > -2.5	No	4.0%
Any CRF	No	7.5% ^a
BMD T score < -2.5	No	8.9% ^a
Any CRF+ BMD T score < -2.5	No	10.1% ^a
Any CRF with treatment	Yes	6.1% ^a
BMD T score < -2.5	Yes	6.8% ^{a,b}
Any CRF+ BMD T score < -2.5	Yes	8.6% ^{a,c}
Chi-square tests:		
a, vs No CRF and BMD T score > -2.5 and no treatment, p<0.001		
b, vs BMD T score < -2.5 and no treatment, p<0.03		
c, vs Any CRF+ BMD T score < -2.5, p<0.05		

Disclosures: A.W.C. Kung, None.

T405

Monthly Oral Ibandronate Is Well Tolerated and Efficacious in Japanese Osteoporotic Subjects. T. Nakamura¹, H. Mizunuma², A. Itabashi³, H. Yamane⁴, T. Hannita⁴, M. Karube⁴, K. Takeuchi⁴, R. Ikegami⁴, S. Okamoto⁴, T. Hasunuma⁴, Y. Kumagai⁴. ¹University of Occupational and Environmental Health, Kita-kyushu, Japan, ²Hirosaki University, Hirosaki, Japan, ³Saitama Center for Bone Research, Kumagaya, Japan, ⁴The Ibandronate Clinical Study Group, Tokyo, Japan.

The efficacy and safety of orally administered ibandronate, given once monthly, have been demonstrated in Caucasian women with postmenopausal osteoporosis. However, responses in Japanese women with osteoporosis were yet to be demonstrated. A multi-centre, double-blind, randomized, placebo-controlled study was performed to examine the efficacy and safety profile of ibandronate which was orally administered for four months in this patient group. In total, 137 osteoporotic subjects, aged 55 to 84 years, were randomly assigned to treat by placebo (n=28), 20 mg (n=27), 50 mg (n=27), 100 mg (n=26) and 150 mg (n=26) ibandronate by oral administration 4 times for 4 months. All patients were supplemented by daily calcium (305 mg) and vitamin D (200 IU). At 4 months, urinary CTX (uCTX) concentrations were reduced by 28.9%, 35.7%, 43.0%, 70.9% and 81.7%, respectively (median change from baseline). The decrease relative to the placebo was statistically significant at 50, 100 and 150 mg, but not at 20 mg group. The dose-dependently reduction in uCTX was maintained throughout the treatment period. Other bone turnover markers also showed the dose-dependent suppression throughout the treatment period. At 4 months, mean increases in lumbar spine bone mineral density of 0.7%, 1.4%, 3.1%, 4.0% and 3.2% were observed in the placebo, 20 mg, 50 mg, 100 mg and 150 mg group, respectively. No serious drug-related adverse events were reported. These results first demonstrate that monthly oral ibandronate effectively reduces bone turnover and increases lumbar spine bone mineral density in Japanese with osteoporosis, without serious side effects.

Disclosures: T. Nakamura, Chugai Pharmaceutical Co. Ltd. 2.
This study received funding from: Chugai Pharmaceutical Co. Ltd.

T406

Study Subjects and Ordinary Patients in Treatment of Osteoporosis. A Prospective Observational Study on 106 Consecutive Patients. R. J. Forestier*, D. Briançon, A. Françon*. Rheumatologic and thermal research centre, Aix Les Bains, France.

The purpose of this study is to measure evolution of bone density (BD) and fracture incidence in a routine population and to compare it with published randomised clinical trial. Material and method: We analyzed 302 consecutive patients coming in our hospital for bone mineral density (BD) measurement between June 2005 and December 2006. 106 had a previous measurement, 2 years or more, with the same Hologic QDR 4500. We also collected number and type of fracture, drug intake and some prognosis factors. BD variations were compared with Mann Whitney U test and fracture rate by Chi².

Results: Evolution of bone density is more favorable for patients under active treatment (risedronate, alendronate, raloxifene and hormonal supplementation) than for patients taking no treatment. For patients with calcium vitamin D supplementation and patient changing or stopping treatment, there is not significant difference with no treatment.

Commentary / Conclusions: Bone density increase more under active treatment than without treatment but variations seems smaller than those observed in experimental studies. Fracture rate is similar in both group but higher than in experimental studies groups.

Real effect of osteoporosis treatment could be lower than their potential effect reported in large randomized clinical trial and meta-analysis. Further investigation are needed, with greater sample size, to measure it in "real life"

Treatment	Number of Follow up	p fracture (comparison with no treatment)	Bone Density Variation [CI 95%] in %/year	p bone density (comparison with no treatment)
Active treatment (alendronate, risedronate, raloxifene, hormonal supplementation)	3/33 4,3 years +/-1,4	0.90	+0.30% [- 0.24;+0.85]	<0,001
Calcium +/- vitamin D	0/11 4,01 years +/-1,9	0.85	-2.77% [- 9,05;+3,46]	0,281
Changing or stopping treatment	1/20 4,6 years +/- 1,6	0.81	-0.41% [- 1.00;+0.18]	0,320
No treatment	3/42 4,3 years +/-1,5		-0.74% [- 1.07;-0.41]	

Disclosures: R.J. Forestier, None.

T407

Osteoporosis Care Pathways for Hospital Patients with Fragility Fractures: A Paradigm Shift. J. Glowacki¹, M. B. Harris^{*1}, J. B. Simon^{*1}, N. S. Kolatkar^{*2}, T. S. Thornhill^{*1}, M. S. LeBoff². ¹Orthopedic Surgery, Brigham and Women's Hospital, Boston, MA, USA, ²Medicine, Brigham and Women's Hospital, Boston, MA, USA.

The 2004 Health Plan Employer Data and Information Set (HEDIS) State of Healthcare Quality Report found that only 18% of patients received post-fracture evaluation/therapy. We had reported that only 10% of our hip fracture (Fx) patients were vitamin D-sufficient [25-hydroxyvitamin D (25OHD) >32 ng/mL]. We therefore designed, implemented, and revised multidisciplinary pathways to improve care of Fx patients.

The 2004 Admission Pathway (AP) trained the surgeons to obtain serum calcium, albumin, and 25OHD, to start calcium carbonate (600 mg elemental calcium/100 IU cholecalciferol, bid) and multivitamin (400 IU cholecalciferol), and to order an Endocrinology consult. The amended 2005 AP implemented a computer-assisted pop-up reminder and added administration of a single dose of ergocalciferol (50,000 IU). The Discharge Pathway (DP) (implemented in 2003 as computer-based directives) prompts the surgeon to discharge on daily calcium with vitamin D, a multivitamin, additional vitamin D (400 IU cholecalciferol), and outpatient osteoporosis evaluation. We reviewed the medical records of 3 cohorts [from Aug through Dec in 2004 (n=57), 2005 (n=41), and 2006 (n=40)] of consecutive patients ≥ 50 years of age who were admitted with a fragility hip or femur Fx. Effectiveness of AP was defined as measurement of 25OHD during hospitalization, and effectiveness of DP, as a prescription for calcium/vitamin D.

Adherence with the surgeon-driven 2004 AP (33%) was half that for the computerized DP (67%, p<0.001). According to the 2005 AP amendment, 29% received 50,000 IU ergocalciferol; AP effectiveness (41%) was not significantly improved. With retraining of surgeons, AP effectiveness was significantly greater in 2006. The older computer-based DP was more effective (88%) than the computer-assisted AP (60%, p=0.010). These findings led to recent launching of a computer-based AP. The high prevalence of vitamin D insufficiency observed in this study (78%) corresponds with prior reports and reaffirms the importance of incorporating vitamin D recommendations in Fx care pathways. This ongoing work shows increasing effectiveness of computer-based directives and of retraining the multidisciplinary team of caregivers. These pathways represent a much-needed paradigm shift in the care of Fx patients.

EFFECTIVENESS OF PATHWAYS					
ADMISSION (Order for 25OH)	ADMISSION (Order for 25OH)	DISCHARGE (Order for Ca/D)	DISCHARGE (Order for Ca/D)		
2004	2005	2006	2004	2005	2006
33%	41%	60%	67%	82%	88%
p=0.013			p=0.030		

Disclosures: J. Glowacki, None.

This study received funding from: Internal Funds.

T408

Proportion of Clinical Vertebral and Nonvertebral Fractures among Women in a Managed Care Population. R. Lindsay*¹, N. N. Borisov^{*2}, M. Steinbuch^{*2}. ¹Helen Hayes, West Haverstraw, NY, USA, ²Procter & Gamble Pharmaceuticals, Mason, OH, USA.

This study used two integrated administrative medical claims databases (Ingenix Lab/RxTM and Medstat MarketScan[®]) to estimate the proportion of fractures that are clinical vertebral or nonvertebral occurring in a managed care setting among women ages 65 and over.

A retrospective cohort study was conducted among women with a new non-traumatic closed vertebral or nonvertebral fracture between July 1, 2000 and December 31, 2003. Fracture rates by 10-year age groups were calculated for 9 anatomical sites: hip, femur, tibia/fibula, humerus, clavicle, pelvis, forearm, wrist, and spine.

As expected, fracture rates increased with age, from 68.6 to 210.7 per 10,000 women per year between 65-74 and 85+ age groups. Hip and pelvis fractures contributed the most to this increase. Overall, the most common fractures were those of hip, wrist, and spine (table). Nonvertebral fractures represented 77% of all fragility fractures among women ages 65 and over. Eleven percent of women experiencing a fracture had a record of an additional fragility fracture within a year of the initial fracture. Women with an initial nonvertebral fracture were more likely to experience a subsequent nonvertebral fracture than vertebral fracture (9% vs. 2%, respectively, p<0.0001). Women with an initial vertebral fracture were more likely to experience a subsequent vertebral fracture than nonvertebral fracture (8% vs. 6%, respectively, p<0.0001). Overall, the majority (70%) of subsequent fractures were nonvertebral.

Rates (per 10,000/year) of vertebral and nonvertebral fractures among women in managed care population by age groups

Age groups	65-74	75-84	85+	Total
Total eligible women population*, 2000-2003	223,774	168,777	56,218	448,769
Nonvertebral Fractures	54.0	97.0	160.4	83.5
Hip	7.9	29.2	68.4	23.5
Femur	2.3	5.4	10.2	4.5
Tibia/Fibula	4.5	4.6	6.0	4.7
Humerus	11.9	18.8	23.9	16.0
Clavicle	1.5	2.4	3.8	2.1
Pelvis	3.2	8.2	17.3	6.8
Forearm	5.5	5.4	5.3	5.5
Wrist	17.3	23.0	25.6	20.5
Vertebral Fractures	14.5	31.6	50.3	25.4
Total Fragility Fractures	68.6	128.6	210.7	108.9
% Fragility Fractures that are Nonvertebral	78.7%	75.4%	76.1%	76.7%

* Data from Ingenix Lab/RxTM and Medstat MarketScan[®] databases

Due to the relative magnitude of nonvertebral fractures, it is imperative that a therapy for osteoporosis in this high risk population demonstrates proven efficacy beyond the spine to provide a clinical benefit for patients and to be cost-effective in the managed care setting.

Disclosures: R. Lindsay, Procter & Gamble Pharmaceuticals 5.

T409

The Socioeconomic Burden of Osteoporotic Fractures in Korea. I. Park¹, S. Baek^{*1}, K. Yang^{*2}, S. Moon^{*2}, J. Kim^{*3}, J. Kong^{*2}. ¹Department of Orthopedic Surgery, Kyungpook National University Hospital, Daegu, Republic of Korea, ²Department of Orthopedic Surgery, Yonsei University Hospital, Seoul, Republic of Korea, ³Department of Health Administration, Inje University, Seoul, Republic of Korea.

In contrast to western countries, few literatures have been reported on the economic burden of osteoporotic fracture in Asian countries including Korea. The purpose of this study is to reveal the national burden of osteoporotic fractures in Korea.

From the database of National Health Insurance, the incidence of three osteoporotic fractures was extracted in female and male patients 50 years or older during 2003; the spine (ICD-10 code: S32.0), wrist (S52.6) and hip fracture (S72.0). Health professional and orthopedic surgeons specialized in osteoporosis were cooperated to analyze resource utilization. Costs per unit of identified resources were estimated based on the collected information from multicenters throughout the country. Direct costs includes fee for hospitalization, diagnostic modalities, surgery, care giver, pharmacotherapy, outpatient care, and public transportation while indirect cost includes loss of productivity.

Incidence and socioeconomic burden of hip, spine and wrist fractures in the year 2003 were estimated as shown in the following table.

	Hip	Spine	Wrist	total
Incidence (No. of Cases)	23,280	29,419	25,037	77,736
Cost of treatment (USD)				
Direct cost	7,626	6,827	3,682	
Indirect cost	7,114	8,093	10,008	
Total	14,740	14,920	13,690	
National burden of treatment (USD)				
Indirect cost - Excluded	177,533,280	200,843,513	92,186,234	470,563,027
Indirect cost - Included	343,147,200	438,931,480	342,756,530	1,124,835,210

Korea with increasing proportion of elderly population is currently facing a heavy socioeconomic burden from osteoporotic fractures. This study was conducted first in

Korea using nationwide database to estimate cost and medical resource utilization. These findings suggest a compelling need to establish and implement an efficient health care policy which in the long-term mitigates the national burden of osteoporotic fractures through active prevention.

Disclosures: 1. Park, Merck Korea 2.

This study received funding from: Merck Korea.

T410

High Dose Vitamin E Prevents the Formation Atherosclerotic Lesions but Does Not Reverse Loss of Bone Due to Orchidectomy in Rats. S. C. Chai¹, E. A. Lucas^{*2}, B. J. Smith³, M. R. Lerner^{*3}, D. J. Brackett^{*3}, C. Wei^{*4}, L. Devareddy^{*1}, B. H. Arjmandi¹. ¹Nutrition, Food and Exercise Sciences, Florida State University, Tallahassee, FL, USA, ²Nutritional Sciences, Oklahoma State University, Stillwater, OK, USA, ³Department of Surgery, University of Oklahoma Health Sciences Center, Oklahoma City, OK, USA, ⁴College of Agriculture, University of Maryland, College Park, MD, USA.

Previously, we have reported that supplemental vitamin E was effective in improving bone strength in mice as well as preventing loss of bone mineral density in hindlimb-unloaded rat model. In this study, the dose-dependent effects of vitamin E in reversal of orchidectomy (ORX)-induced bone loss was examined. Forty 12-mo old male Sprague-Dawley rats were either sham-operated (Sham, one group) or ORX (three groups) and fed a control diet for 120 days to induce bone loss. Thereafter, rats were assigned to various treatment groups (n=10): Sham+75 IU vit E; ORX +75 IU vit E, ORX+ 250 IU vit E, ORX+500 IU vit E per kg diet. After 90 days of treatment, rats were necropsied and tissues were collected for analyses. Although vitamin E supplementation at any dose was incapable of exerting positive effects on bone, it was able to favorably alter serum total- and HDL-cholesterol and superoxide dismutase, an enzyme that plays a crucial role in the detoxification of products resulting from oxidative stress. Additionally, vitamin E at the highest dose (500 IU) significantly reduced the development of atherosclerotic lesions as well as aortic fatty streak area due to ORX. Hence, we conclude that vitamin E is beneficial in improving lipid profile and prevention of atherosclerotic lesion formation, but unable to restore bone mass once the loss has occurred at least in an ORX rat model.

Disclosures: S.C. Chai, None.

T411

Improved Strontium Bioavailability in a New Tablet Formulated Strontium Salt. S. Christgau¹, M. Weis^{*1}, K. Krogsgård^{*2}. ¹Osteologix, Copenhagen, Denmark, ²PhaseOneTrials, Hvidovre, Denmark.

AIM: Preclinical and clinical studies have suggested that strontium is useful as a therapy in osteoporosis due to a mild anabolic effect on bone formation concomitant with an anti-resorptive effect. One strontium salt, strontium ranelate (SR), is approved in Europe for treatment of postmenopausal osteoporosis. SR is available in a sachet formulation. Our aim was to assess pharmacokinetic properties of another strontium salt, strontium malonate (NB-S101) formulated in tablets and to compare the strontium bioavailability from a single oral dose of this salt with that of SR.

METHODS: 60 healthy male volunteers were randomized into five groups to receive either NB S101 in doses of 0.6, 1.2 and 2.4 g (containing 277, 554 and 1108 mg ionic strontium) or 2 g SR in sachets, containing 680 mg ionic strontium or placebo. Subjects were fasting from 1PM and given a single oral dose at 7PM. They had frequent blood samples drawn for strontium determinations in the following 24 h, and at 1, 3 and 5 weeks post dosing. Bone turnover was measured at baseline 2, 4 and 24 h using s-CTX (resorption) and osteocalcin (formation).

RESULTS: Pharmacokinetic profiles of strontium uptake from the four treated groups were similar, but SR had a lower T_{max} (3.75±0.37 h) than NB-S101 (5.92±0.53; 5.00±0.55; 5.67±0.41 h respectively for the three NB S101 groups, p<0.05). Strontium uptake assessed by Area Under the Curve (AUC) analysis, revealed a good bioavailability of strontium from NB S101 tablets. The SR group had an AUC_{0-24h} of 356.3±24.4 µg*h/ml compared with 275.3±24.3; 386.9±39.5; 654.6±63.7 µg*h/ml in the three NB S101 groups. Elimination rates were similar for both strontium salts, with T_{1/2} for SR of 116.1±8.3 h compared with 140.4±11.7; 125.2±6.6, 130.7±5.3 h for the three NB S101 groups. A 0.99 g dose of NB S101 was estimated to give theoretical bioequivalence to 2 g SR. NB S101 appeared to induce a dose dependent suppression in the nocturnal elevation in bone resorption measured by CTX. Only for the high dose group did this reach statistical significance at 4 h (29.0% vs 86.3% increase from baseline in the 2.4 g group and placebo, p<0.05). Bone formation was not changed in the strontium treated groups compared to placebo.

CONCLUSIONS: This pharmacokinetic study shows that NB S101 (strontium malonate) tablets containing less than 555 mg ionic strontium delivers more bioavailable strontium ions than a 2 g strontium ranelate sachet formulation containing 680 mg ionic strontium. This suggests that the tablet formulated NB S101 provides better bioavailability. Bone turnover analysis indicates a dose dependent antiresorptive effect of NB S101. Phase II studies are ongoing to assess the effect of NB-S101 on bone turnover and BMD in postmenopausal women.

Disclosures: S. Christgau, Osteologix Inc. 1, 3.

This study received funding from: Osteologix.

T412

Strontium Ranelate Reduces the Risk of Vertebral Fracture in Young Postmenopausal Women with Severe Osteoporosis. J. P. Devogelaer¹, C. Roux², G. Isaia³, J. B. Cannata Andia⁴. ¹Service de rhumatologie, Université catholique de Louvain, Bruxelles, Belgium, ²Department of rheumatology, Cochin Hospital, René Descartes University, Paris, France, ³I Divisione Universitaria di Medicina Generale, Torino, Italy, ⁴Servicio de Metabolismo Osseo y Mineral, Hospital central de Asturias, Oviedo, Spain.

Strontium ranelate is an anti-osteoporotic treatment which decreases vertebral and hip fracture risks with a unique mode of action, both reducing bone resorption while promoting continued bone formation. Early fractures occurring within the first 10 years after menopause have a great impact on the further progression of the disease, as it has been shown that the first osteoporotic fracture is a major risk factor for further additional fractures. Subsequently, the assessment of antifracture efficacy of antioosteoporotic treatments in this younger female population aged less than 65 years appears of utmost interest.

Materials and methods. The phase III SOTI study was an international, double-blind, placebo-controlled trial, supporting the efficacy and safety of strontium ranelate 2g/day orally in reducing the risk of vertebral fractures in postmenopausal women with osteoporosis and a prevalent vertebral fracture. An analysis of the data from SOTI was performed to investigate the efficacy of strontium ranelate in women aged between 50 and 65 years (n=353; 168 in the strontium ranelate treated group versus 185 in the placebo treated group).

Results. The baseline characteristics of patients were similar in both groups (mean value ±SD data: age 60.0±3.5 years; lumbar BMD T-score -3.6±1.1; femoral neck BMD T-score -2.5±0.8) with 80.5% of patients having a prevalent vertebral fracture and 23.0% of patients having a prevalent non-vertebral fracture. Over 3 years of treatment, in the intent-to-treat population, strontium ranelate significantly reduced the risk of vertebral fracture by 47% (RR=0.53; 95%CI[0.33;0.85], p=0.006). The incidence of vertebral fractures over 3 years was 16.9% in the strontium ranelate treated group versus 29.6% in the placebo treated group. The reduction in the risk of vertebral fracture is paralleled by a significant increase after 3 years by 13.7% in the relative change from baseline of lumbar BMD (95%CI[11.54;15.87], p<0.001) and by 7.5% in the relative change from baseline of femoral neck BMD as compared to placebo. These changes are in accordance with those of the whole Phase III population.

Conclusion. These data demonstrate a significant vertebral antifracture efficacy of strontium ranelate in young postmenopausal women aged less than 65 years with severe osteoporosis and confirms the efficacy of this anti-osteoporotic treatment, whatever the age of the patients.

Disclosures: J.P. Devogelaer, None.

T413

Action Seniors!: An RCT of the Otago Home Exercise Program to Ameliorate Fall Risk Factor Profile in Patients at High Risk of Falls. M. G. Donaldson^{*1}, K. M. Khan², B. Sobolev^{*1}, P. A. Janssen^{*1}, W. L. Cook^{*3}, H. A. McKay⁴. ¹Health Care and Epidemiology, University of British Columbia, Vancouver, BC, Canada, ²Department of Family Practice, University of British Columbia, Vancouver, BC, Canada, ³Geriatric Medicine, University of British Columbia, Vancouver, BC, Canada, ⁴Orthopaedics, University of British Columbia, Vancouver, BC, Canada.

Fall prevention is an important element of fracture prevention strategies. Although strength and balance training reduces falls among community-dwelling seniors, we know of no RCTs testing the effectiveness of a strength and balance training program among very frail seniors with low bone mass who attended a dedicated falls clinic. We aimed to determine the effect of the Otago Exercise Program (OEP), a physiotherapist-initiated, home-based, progressive strength and balance retraining program in older men and women who attended a falls clinic. The primary outcome was fall risk factor profile over a 6-month period; secondary outcome was occurrence of falls over a 12-month period.

We enrolled 74 participants aged 70 years and older from two falls clinics in Vancouver, British Columbia. Participants were randomly allocated to the OEP group (n=36) and standard care (SC) group respectively (n=38). Fall risk factor profile was assessed using Lord's Physiological Profile Assessment (PPA) tool which measures vision, reaction time, strength, proprioception and balance. Participants documented falls on monthly calendars for 12 months. We used linear regression to model the relationship between group and change in PPA from baseline to 6-months. We used negative binomial regression to model the relationship between group and the occurrence of falls. We used the Mean Cumulative Function to report the average number of falls per participant by 12-months.

At 6-months 34 and 32 in the OEP group and SC group respectively returned for follow-up. The OEP group was associated with a 9% improvement in PPA z-score from baseline to 6-months (2.3 (1.3) to 2.1 (1.3)) compared to the SC group which remained stable (2.0 (1.3) to 2.0 (1.2)), p=0.55. The OEP group was associated with a 38% reduction in the rate of falls (IRR 0.62, 95% confidence interval 0.3 to 1.4). The average number of falls per participant by 12-months in the OEP and SC group was 1.1 and 3.1 respectively.

This study demonstrated that the OEP did not significantly reduce PPA z-score over a 6-month period. However the reduction in the rate of falls over a 12-month period is consistent with the literature and provides encouraging pilot data for a larger study powered to measure falls as the primary outcome. This is the first study to investigate the effectiveness of strength and balance training delivered within a falls clinic setting among frail seniors at high risk of falls.

Disclosures: M.G. Donaldson, None.

T414

The Effects of Strontium Ranelate on Biochemical Bone Markers in Elderly Women and Men with Reduced Bone Mineral Density. B. H. Durham¹, A. A. Joshi^{*2}, A. M. Ahmad^{*2}, J. P. Vora^{*2}, W. D. Fraser¹. ¹Clinical Chemistry, Royal Liverpool University Hospital, Liverpool, United Kingdom, ²Clinical Endocrinology, Royal Liverpool University Hospital, Liverpool, United Kingdom.

We have investigated the effect that 3 months of strontium ranelate therapy [StR], a bone agent that increases bone formation, has on a panel of biochemical markers of bone formation and bone resorption. We recruited 26 elderly subjects [15F, 11M] average age 64 ± 3yr with low bone mineral density who were assigned into one of two groups. Group A [8F, 5M] received 2 g of StR/day whilst group B [7F, 6M] received growth hormone supplementation [GH] in addition to StR. Fasting serum samples were collected prior to and after 3m of StR and stored at -70°C until analysed. The biochemical markers used to study bone formation were bone alkaline phosphatase [BalP], osteocalcin [OstC] and the amino terminal extension peptide of type 1 collagen [PINP] and for resorption carboxy terminal telopeptide of type 1 collagen [beta CTX] and tartrate resistant acid phosphatase 5B [TRACP], we also measured osteoprotegerin [OPG].

For group A there was no significant change in the means of OPG [2.6 vs 2.5 pmol/L], TRACP [2.3 vs 2.3 U/L], BalP [17 vs 18 U/L]. The mean OstC increased by 6% from 23.8 to 25.1 mcg/L whereas beta CTX decreased by 14% from a mean of 0.49 to 0.42 mcg/L and PINP by 10% from 55 to 50 mcg/L. In group B there were significant increases in the means of all parameters [p<0.05], PINP 68 to 88 mcg/L [29%], OstC 26.5 to 35.8 mcg/L [35%], BalP 22 to 32 U/L [45%], TRACP 2.8 to 3.7 U/L [32%], beta CTX 0.54 to 0.66 mcg/L [22%], the increase in the mean of OPG from 2.3 to 2.6 pmol/L [10%] was not significant. In group B the increase in the rate of bone turnover as demonstrated by the increases in formation and resorption markers was probably due to the GH supplementation. In group A there was no significant change in either formation or resorption markers; it may be that 3m was too short a period for StR to have an influence on bone metabolism and a longer period of treatment would result in a different outcome.

Disclosures: B.H. Durham, None.

T415

Exercise Prevents Falls and Maintains Bone Mineral Density in Elderly Postmenopausal Women. Preliminary Data of the Erlangen Senior Fitness and Prevention (SEFIP) Study. W. Kemmler^{*}, S. von Stengel^{*}, W. A. Kalender^{*}, K. Engelke. Institute of Medical Physics, University of Erlangen, Erlangen, Germany.

The aim of the study was to demonstrate that an intensive aerobic and strength training can maintain BMD at the spine and the hip and can prevent falls in elderly community-living women.

Via population registers we recruited 246 community-living women of 65 years and older. Exclusion criteria were medication or diseases related to bone metabolism, low aerobic capacity (<75 W on ergometry), and medication potentially increasing the likelihood of falls. There were no inclusion or exclusion conditions based on BMD or prevalent fractures. Subjects were randomly assigned to an exercise intervention group (EG: 2-3 sessions/week) or to a wellness control group (WCG: 1 session/week for three 10 week blocks). The exercise training consisted of 20 min of intense aerobic dancing (70-85% HF_{max}), 5 min of specific balance exercises and 35 min of isometric and dynamic (60-70% 1RM) strength training. No machines were used for the strength training part. All subjects were individually supplemented with calcium and cholecalciferol up to a maximum of 1500 mg/d and 500 IU/d. Bone mineral density at the lumbar spine and the hip was measured with DXA and QCT. Falls as defined by the PROFANE workgroup were counted using daily protocols conducted by all participants. Here we present initial 12 month DXA and fall results for 182 participants (EG: n=90; WCG: n=92).

After 12 months there were significant differences between exercise and wellness control group of BMD of the spine (EG: +1.4% vs. WCG: -0.3%) and of the hip (EG: -0.2% vs. WCG: -1.3%). The number of falls was significantly higher in the WCG (n=124) than in the EG (n=72). The same was true for injurious falls (EG: n=28 vs. WCG: n=42). In the exercise group 5 and in the wellness control group 8 fractures occurred but the power of the subset of patients included in this preliminary analysis was too low for the difference to be significant.

In conclusion preliminary results of our randomized exercise trial show that exercise training positively impact BMD at the hip and spine as well as fall frequency and may prevent fall related fractures in elderly subjects. The training scheme used in the study can easily be transferred into rehabilitation programs as no special equipment was used.

Disclosures: K. Engelke, Synarc 3.

T416

3-Year Outcome After Kyphoplasty in a Prospective Controlled Trial Role of Initial Bone Edema and Selection of Cement Type (PMMA vs. Calciumphosphate Cement). I. Grafe^{*1}, G. Nöldge^{*2}, M. Baier^{*3}, K. Da Fonseca^{*3}, J. Hillmeier^{*3}, U. Sommer^{*1}, U. Wolf^{*1}, M. Libicher^{*2}, P. J. Meeder^{*3}, P. Nawroth^{*1}, C. Kasperk¹. ¹Internal Medicine I, Endocrinology, University of Heidelberg, Heidelberg, Germany, ²Radiology, University of Heidelberg, Heidelberg, Germany, ³Orthopedic Surgery, University of Heidelberg, Heidelberg, Germany.

Introduction: Kyphoplasty (KP) is a safe and effective method for reducing pain and improving quality of life in patients with painful osteoporotic vertebral fractures in prospective controlled and randomized trials. We sought to investigate how beneficial short term effects of KP on pain and mobility will affect long term outcome and fracture incidence, and if (a) selection of PMMA or CaP cement for vertebral stabilization and how (b) an initial bone edema of the fractured vertebrae before KP impact on long term outcome after KP

Methods: KP was performed in 40/60 patients with primary osteoporosis and painful vertebral fractures, 20 patients received PMMA- and 20 CaP cement (Calcibon), 20 served as non-KP controls (Con). In another cohort 45 KP-patients received pre-OP MRI of the fractured painful vertebrae to visualize bone edema and were analyzed with regards to VAS score after 12 months (bone edema 27 pat., no edema 18 pat). All patients received pharmacological treatment (oral aminobisphosphonate, 1000 mg calcium + 1000 IE vitaminD3) and physiotherapy. Pain (VAS [100=most severe pain]), mobility (EVOS score[100=full mobility]) and radiomorphology were determined after 6, 12 and 36 months.

Results:

	Pre-KP PMMA/CaP Con	6 mo. PMMA/CaP Con	12 mo. PMMA/CaP Con	36 mo. PMMA/CaP Con
Pain	74.5 / 73.1 66.4	53.1 / 58.5 64.4	53.7 / 57.6 65.7	52.7 / 55.2 64.0
Mobility	40.1 / 47.5 39.8	55.7 / 53.1 43.8	54.5 / 54.6 44.3	53.6 / 56.0 43.6

Number of total new vertebral fractures after 3 years:

KP 21 # (in 14 of 34 patients)

Con 18 # (in 10 of 14 patients) p=0.0341

VAS Pain scores

Pre-KP: Edema 72.2, No edema 70.7

Post-KP: Edema 46.8, No edema 60.3

12 mo.: Edema 48.0, No edema 50.1

Conclusion: KP is superior to conservative treatment of painful osteoporotic vertebral fractures for at least 3 years after intervention and reduces fracture incidence. There was no significant difference between the outcome in patients after KP using either PMMA or CaP-cement for the internal stabilization of the fractured vertebrae. Patients with and without bone edema of painful vertebral fractures benefit from kyphoplasty.

Disclosures: I. Grafe, None.

T417

Comparison of the Effects of Calcium as Carbonate or Citrate on Bone Resorption Markers in Early Post Menopausal Women. S. D. C. Grasby^{*}, A. G. Need, B. E. C. Nordin. Clinical Biochemistry, Institute of Medical and Veterinary Science, Adelaide, Australia.

It has been reported that calcium citrate is better absorbed and more effective than calcium carbonate in suppression of parathyroid hormone (PTH). The implication has been that less calcium as the citrate than calcium as the carbonate is required to achieve the same effect.

A double blind cross over study was undertaken to compare the effects of these two calcium salts on a bone resorption marker in women within 5 years of the menopause. Fasting baseline serum biochemistry, PTH, 25 hydroxyvitamin D and beta crosslaps were measured in 20 women. Subjects were assigned to receive either calcium as the carbonate (1000mg oral) or as the citrate (500mg oral) using a random number generator. The serum measures were repeated 12 hours after the Ca salt taken at 9 pm the previous night. After a washout period of at least 1 week, the process was repeated, but the subjects who received the carbonate form previously now received the citrate preparation and vice versa.

The mean baseline values for serum biochemistry, PTH and 25 hydroxy vitamin D were all within the normal range.

The mean changes from baseline in selected variables after 1000mg Ca as the carbonate and 500mg Ca as the citrate are shown in the table.

Variable	Serum total Ca Ca type	Serum ionised Ca Calculated (mmol/L)	Serum PO4 (mmol/L)	Serum PTH (pmol/L)	Serum cross laps (ng/L)
carbonate	0.068*	0.024	0.137*	-0.572*	-76.65**
citrate	0.033	0.015	0.063	-0.25	-71.25**
P#	0.187	0.418	0.213	0.3.7	0.791

#For difference between the 2 calcium preparations; P calculated using 2 tailed paired T test.

Significance of change from baseline (P<0.05 = *; P<0.005 = **)

In conclusion, total serum calcium and phosphate rose and PTH fell significantly following 1000mg of Ca as the carbonate but not following Ca 500 mg as the citrate. However the bone resorption marker fell significantly and to the same degree on both salts. We conclude that in terms of the primary end point, 500mg Ca as the citrate was equivalent to 1000mg of Ca as the carbonate.

Disclosures: S.D.C. Grasby, None.

T418

Testing of Mechanical Properties of Hip Protectors Using High Tech Materials. G. Holzer, L. A. Holzer*. Department of Orthopaedics, Medical University of Vienna, Vienna, Austria.

Purpose: To test the mechanical properties of hip protectors using high tech materials compared to conventional hip protectors according to a European Standard.

Methods: Two hip protectors using new high tech materials and five conventional hip protectors (AHIP protector, Astrosorb; AHF Hip pant, Hips, KPH, Safehip, Safety Pants) were mechanically tested using an mechanical testing machine (impact testing with 50 Joule) according to a European Standard (EN 1621-1). Results are peak (max) expressed in kiloNewton.

Results: The results of impact testing of two hip protectors using high tech materials were superior (AHIP protector 9.10 kN, Astrosorb 12.65 kN) to conventional hip protectors (21.97 - 50.62 kN), which differ in performance to mechanical testing. **Conclusions:** The results of this study show that new high tech materials with improved mechanical properties are superior to currently available hip protectors from the mechanical point of view. Utilizing these materials allow designing new hip protectors with increased compliance and adherence. AHIP protector, a hip protector using high tech material, implements modern design, improved wearing comfort and best mechanical properties.

Disclosures: G. Holzer, None.

T419

Vertebral Compression Fractures in Patients with Poor Bone Quality: When and Which Osteoplasty? The Need for a Global Approach. R. Iundusi*, G. Cannata*, D. Lecce*, I. Cerocchi*, M. Celi*, U. Tarantino*. ¹Orthopaedics and Traumatology, University of Rome "Tor Vergata", Rome, Italy, ²Orthopaedics and Traumatology, University of Rome, Rome, Italy.

INTRODUCTION: Osteoporosis (OP) is estimated to afflict 200 million women worldwide. About 1.7 million vertebral compression fractures (VCFs) occur every year in Europe and in the US. Vertebral fractures are the most common type of fragility fractures due to alterations in bone quality, quantity and microarchitecture. Usually they occur with low energy trauma and result in pain about the fracture site, loss of vertebral body height, and kyphotic deformity. Only few patients gain benefits using conservative treatments. The aim of our study is to establish when there are the conditions to perform a vertebral osteoplasty and which technique, based on personal experiences and on omogeneous datas from the international literature, is suitable for each patient.

MATERIALS AND METHODS: Vertebroplasty and balloon kyphoplasty are two minimally invasive surgery approaches developed for the management of symptomatic VCFs. Vesselplasty is a new minimally invasive surgical technique which provide pain relief, stabilization of the vertebral body, and it has the ability to provide some correction of deformity with partial restoration of vertebral body height. During vesselplasty procedure an artificial "vessel" system, the Vessel-X[®], is introduced into the vertebral body to achieve augmentation after which low-viscosity bone cement mixed with calcium phosphate is injected into the vertebral body: the Vessel-X[®] are expanded to their predetermined configuration and a few bone void filler material penetrates through the "vessels" interdigitating the vertebral body, reducing one of the most common adverse effects of other minimally invasive techniques such as cement leakage.

DISCUSSION: Treatment of OP has made enormous advances in the past years, resulting in a wide range of options. We remind the importance of a global approach to the osteoporotic patients: the best treatment remains early diagnosis evaluating bone remodelling markers, lumbar and femoral Dual-energy X-ray absorptiometry (DEXA), thoracic and lumbar x-rays imaging and risks fracture assessment to ensure an individual and best appropriated therapy as specific as possible. Vesselplasty is a safe and effective minimally invasive procedure for relief of pain associated with VCFs, and improves mobility decreasing the potential risks associated with immobility. Future trials evidence should investigate if the association of vertebral osteoplasties with specific drugs acting on bone quality and rehabilitation could improve clinical outcomes reducing comorbidities and restoring a good and reasonable quality of life.

Disclosures: R. Iundusi, None.

T420

Organic Nitrate Use, Bone Loss and Fractures in Older Men. S. A. Jamal¹, D. C. Bauer², J. A. Cauley³, S. R. Cummings². ¹Medicine, University of Toronto, Toronto, ON, Canada, ²San Francisco Coordinating Center, CPMC Research Institute and University of California, San Francisco, CA, USA, ³Epidemiology, University of Pittsburgh, Pittsburgh, PA, USA.

Observational studies report positive associations between organic nitrate use, increased BMD, and decreased fractures among postmenopausal women. To determine the association between self-reported nitrate use, bone loss and fracture incidence in men we used data from the Osteoporotic Fractures in Men (MrOS) study, a large cohort of older men.

Men who reported use of nitroglycerin, isosorbide mononitrate or isosorbide dinitrate (either on an "as needed" or regular basis) in the 2 weeks preceding the baseline visit were classified as nitrate users. BMD at the hip and lumbar spine was measured with a Hologic QDR4500 at study entry and about 4.5 years later. Low trauma non-spine fractures were centrally adjudicated, and 331 men suffered one or more fracture during a mean follow-up of 5.4 years.

We used multiply adjusted linear regression models to determine the association between

nitrate use and % change in BMD, and Cox proportional hazards models to determine the association between nitrate use and fracture. There were 248 nitrate users and 5455 nonusers at the baseline visit. Nitrate users were significantly older than nonusers (76.5 yrs vs. 73.6) but there was no significant difference in body weight (82.7 kg vs. 83.1). Compared with nonusers, users were more likely to have had a fall in the past year, had poorer self-rated health, reported greater impairment of activities of daily living, were less physically active and had weaker grip strength. More nitrate users than nonusers reported use of statins and thiazides. After adjusting for these differences, and clinic site, there was no difference in the change in BMD over 4.5 years of follow up at the total hip among nitrate users -1.9% (95% Confidence Interval [CI] CI: -2.6 to -1.3) compared to nonusers -1.8% (95% CI: -1.9 to -1.7). There was no difference in the % change in spine BMD among users 5.1% (95% CI: 3.1 to 7.2) compared to nonusers 4.6% (95% CI: 4.2 to 4.9). There was no difference in the incidence of fractures among nitrate users compared to nonusers (Relative Hazard: 0.9; 95% CI: 0.5 to 1.5).

Contrary to previous studies in older women, we found that use of nitrates was not associated with increased BMD or decreased in fracture risk among men participating in the MrOS study. The lack of association may be due to limitations of observational data, differences in dose or frequency of nitrate administration, or biological differences in organic nitrate effects by gender. Further research is required to definitively determine the effects of nitrates on bone in men.

Disclosures: S.A. Jamal, None.

T421

TENS (Transcutaneous Electrical Nerve Stimulation) in the Management of Osteoporosis-related Pain. S. Kalra*, A. Sharma*, B. Kalra*, N. Kumar*. ¹Endocrinology, Bharti Hospital, Karnal, India, ²Gynaecology, Bharti Hospital, Karnal, India, ³Physiotherapy, Bharti Hospital, Karnal, India.

Pain is a disabling symptom in persons with osteoporosis, and it often reduces the quality of life. This paper studies the effect of TENS in subjects with osteoporosis, complaining of pain.

30 adult osteoporosis patients with lower limb pain, receiving five sittings of TENS on daily or alternate day basis, were compared with 30 age-matched, disease-matched patients who were administered daily diclofenac and five sittings with sham electrodes.

Pain scores, measured by visual analog score, reduced significantly in both groups, but much more so in the TENS group (from 4.60 ± 0.54 to 1.60 ± 0.54) than the sham electrodes + diclofenac group (from 4.40 ± 0.54 to 3.60 ± 0.54). This difference was maintained after 3 weeks, even though the TENS sittings had stopped. Best improvement was obtained in patients with burning (3.28 ± 0.64) and lancinating (3.12 ± 0.64) pain. Least benefit was in patients with deep pain (2.15 ± 0.35) and restless legs syndrome (2.16 ± 0.56).

The dose of TENS used varied from 5.5 to 9.0 Hz on the initial day to 3.5 to 5.5 Hz on the last sitting. The dose varied insignificantly for different symptoms.

Validated health-related questionnaires were used to assess the effect of physiotherapy sessions in the subjects. Physician communication score improved from 1.43 ± 1.19 to 3.93 ± 0.86 over one month of therapy in all subjects. Time spent by them in stretching/strengthening exercise increased from 0.0 ± 0.0 to 15.0 ± 0.0 minutes per week. The social/role activities limitation due to the disease reduced from 2.25 ± 0.63 to 1.08 ± 0.39 . Cognitive symptom management improved from 1.30 ± 0.63 to 2.00 ± 0.67 .

The health distress score fell from 3.20 ± 0.82 to 1.35 ± 0.47 while energy/fatigue scores raised from 2.25 ± 0.51 to 3.30 ± 0.50 in all subjects. No difference was noted in these scores between the two groups.

This paper demonstrates the beneficial effect of TENS on pain related to osteoporosis, and the advantageous effects of regular physiotherapy on various health-related parameters in persons with osteoporosis.

Disclosures: S. Kalra, None.

T422

Withdrawn

T423

The Effects of Black Cohosh Root Extract on the Vasomotor Symptom and Bone Metabolism of Menopausal Women. H. Kim^{*1}, H. Choi^{*2}, H. Park^{*3}, B. Kang^{*4}, B. Lee^{*5}, B. Yoon^{*6}, T. Kim^{*7}. ¹Dept. of OB & GYN, College of Medicine, Koin University, Busan, Republic of Korea, ²Dept. of OB & GYN, College of Medicine, Inje University, Seoul, Republic of Korea, ³Dept. of OB & GYN, College of Medicine, Chungang University, Seoul, Republic of Korea, ⁴Dept. of OB & GYN, College of Medicine, Ulsan University, Seoul, Republic of Korea, ⁵Dept. of OB & GYN, College of Medicine, Yonsei University, Seoul, Republic of Korea, ⁶Dept. of OB & GYN, College of Medicine, Sungkyunkwan University, Seoul, Republic of Korea, ⁷Dept. of OB & GYN, College of Medicine, Korea University, Seoul, Republic of Korea.

Introduction: Extract of the rootstock of *Cimicifuga racemosa* (black cohosh) have a traditional reputation as herbal remedies. For the last 4 decades case reports and clinical research with the socially manufactured *C. racemosa* extract have shown a good therapeutic efficacy and safe profile in the treatment of neuroprotective climacteric complaints. Safety concerns associating 6 month use with climacteric complaints and prevention of bone loss, have prompted the search for the effect of BCRE.

Objective: To evaluate the effect of black cohosh root extract (BCRE) on vasomotor symptoms, BMD and bone metabolism in postmenopausal women

Method: This prospective randomized clinical trial examined the effects of BCRE on vasomotor symptom, bone mineral density, and biochemical markers of bone turnover in 90 postmenopausal women. Treatment included BCRE (group I, n=30) or 0.625mg CEE (group II, n=30), control group (group III, n=30) for 6 months. Kupperman index, BMD and biochemical bone marker were measured at 0, 3 and 6 months.

Results: Kupperman index decreased significantly at 3 months and 6 months of the treatment in group I and group II (P<0.05). BMD of lumbar spine increased significantly during the treatment in group I and group II (P<0.05). Urinary deoxypyridinoline decreased significantly at 3 months and 6 months of the treatment in group I and group II (P<0.05).

Conclusion: BCRE appears to be a safe and effective alternate to hormone therapy for vasomotor symptom and prevention of bone loss. It may be especially useful in women with intolerance or contraindication to traditional hormone therapy.

Disclosures: H. Kim, None.

T424

The Effect of Vitamin K2 in Addition to Risedronate on the Patients with Postmenopausal Osteoporosis. H. Kwak, S. Kim. Rehabilitation, Dong-A University, College of Medicine, Busan, Republic of Korea.

Objective: To assess the effect of vitamin K2 in addition to risedronate on postmenopausal osteoporosis

Method: We enrolled 21 postmenopausal osteoporosis women (age: 65.2±7.8 years). Ten subjects received risedronate (35 mg, weekly) and vitamin K2 (45 mg, daily) and eleven subjects only received risedronate. They all received calcium citrate 2,130 mg and vitamin D 600 IU daily. The duration of treatment was 7.7±1.4 months. Bone mineral density (BMD) of lumbar spine and both femurs, serum osteocalcin and urine deoxypyridinoline were examined at baseline and after treatment.

Results: After treatment, BMD, serum osteocalcin and urine deoxypyridinoline were improved in each group but there was no statistical difference between the groups.

Conclusion: There was no evidence of the benefit of vitamin K2 in addition to risedronate in bone metabolism on postmenopausal osteoporosis.

Disclosures: H. Kwak, None.

T425

Baseline Characteristics of Participants in the Soy Phytoestrogens as Replacement Estrogen (SPARE) Study. S. Levis¹, N. Strickman-Stein^{*2}, J. P. Krischer^{*3}. ¹Medicine, University of Miami Miller School of Medicine, Miami Veterans Healthcare System, and University of South Florida, Miami, Tampa, FL, USA, ²Medicine, University of Miami Miller School of Medicine, Miami, FL, USA, ³University of South Florida, Tampa, FL, USA.

After the early termination of the Women's Health Initiative, an increasing number of menopausal women stopped hormone replacement (HRT) and began to self-medicate with over-the-counter products. Soy is particularly popular because of its phytoestrogen content. The aims of this study are to establish the long-term effectiveness of soy phytoestrogens, or isoflavones, in (1) preventing the rapid bone loss seen in the first years of menopause and (2) improving general health-related quality of life and emotional health in menopausal women. This is a 5-year, ongoing, randomized, double-blind, placebo-controlled clinical trial that concluded its recruitment phase in March 2007. Of the 524 women who were screened, 283 met eligibility criteria: age 45-60 years, menopausal for ≥ 6 months but < 5 years, non-obese, no current HRT, and no history of osteoporosis, treatment with bone-active drugs, or cancer. The study randomized 247 women to either soy isoflavone tablets 200 mg/day or placebo tablets (50/50). Each participant will be followed for 2 years during 10 clinic visits, receiving serial measurements of lumbar spine and hip bone mineral density (BMD) and urinary N-telopeptide of type I bone collagen (NTx). The primary outcome variable is change in BMD at 2 years. The mean age of participants at screening was 52.44 years (35.8% of women were ages 52-54); 75% of participants are Hispanic and 90% are White. Nearly 90% of enrolled women reported a high school education and

41.5% are college graduates. At time of randomization, the mean BMD (L1-L4) was 1.130 g/cm² ± 0.125 and the mean total hip BMD was 0.981 g/cm² ± 0.102. In addition, mean lumbar spine (L1-L4) T-score was -0.383 ± 1.04 and mean total hip T-score was 0.981 ± 0.102. No differences in BMD were found between Hispanics and non-Hispanics, or between African American and White women. Comparisons between the two study groups were made by the study biostatistician. They demonstrate that the randomization process produced two equivalent groups with respect to baseline demographic and key clinical parameters. The results of this trial will provide new information on the safety and long-term efficacy of soy phytoestrogens in preventing bone loss and menopausal symptoms. These results will enable women to make informed decisions at the time of menopause. Choices made at the time of menopause will impact rates of bone loss and future incidence of osteoporosis and fractures when these menopausal women become older adults.

Disclosures: S. Levis, None.

T426

Low Magnitude Mechanical Signals Reduce Risk-Factors for Fracture During 90-Day Bed Rest. J. W. Muir^{*1}, Y. Xia¹, N. Holguin^{*1}, S. Judex¹, Y. Qin¹, H. Evans^{*2}, T. Lang³, C. Rubin¹. ¹Biomedical Engineering, SUNY Stony Brook, Stony Brook, NY, USA, ²Johnson Space Center, NASA, Houston, TX, USA, ³Dept of Radiology, University of California, San Francisco, San Francisco, CA, USA.

Long duration spaceflight leads to multiple deleterious changes to the musculoskeletal system, where loss of bone density, an order of magnitude more severe than that which follows the menopause, combined with increased instability, conspire to elevate the risk of bone fracture due to falls on return to gravitational fields. Here, a ground-based analog for spaceflight is used to evaluate the efficacy of a low-magnitude mechanical intervention, VIBE (Vibrational Inhibition of Bone Erosion), as a potential countermeasure to preserve musculoskeletal integrity in the face of disuse. Twenty-six subjects consented to ninety days of six-degree head-down tilt bed-rest. 18 completed the 90d protocol, 8 of which received daily 10-minute exposure to 30 Hz, 0.3g VIBE, applied in the supine position using a vest elastically coupled to the vibrating platform. The shoulder harness induced a load of 60% of the subjects' body weight. At baseline and 90d, Qualitative Ultrasound Scans (QUS) of the calcaneus and CT-scans of the hip and spine were performed to measure changes in bone density. Postural control (PC) was assessed through center of pressure (COP) recordings while subjects stood on a force platform for 4 minutes of quiet stance with eyes closed, and again with eyes opened. As compared to control bedrest subjects, CT indicated a trend that VIBE reduced the loss of BMD in the proximal femur, including integral (0.9 ± s.e. 0.3% vs. 1.17 ± 0.5%; 15% dif; p=0.38), trabecular (1.5 ± 0.4% vs. 2.2 ± 0.5%; 28%; p=0.20), and cortical region (0.4 ± 0.4% vs. 0.7 ± 0.4%; 37%; p=0.28). QUS showed a 0.9% loss in ultrasound velocity for control subjects, as compared to a 0.3% gain for VIBE (p=0.05). The increase in postural instability suffered by control subjects was diminished by VIBE, with a per month increase in maximal forward sway angle (35.4 ± 8.3% reduced to 20.2 ± 6.2%; 43%; p=0.08), root-mean-square (RMS) of anterior-posterior COP displacement (30.1 ± 9.5% reduced to 15.9 ± 5.5%; 47% decrease; p=0.11), and maximal forward sway velocity (53.1 ± 12.0% reduced to 16.2 ± 7.2%; 70%; p=0.01), maximal total velocity (53.8 ± 17.4 reduced to 20.6 ± 6.9; 64%; p = 0.05), mean velocity of sway (43.3 ± 9.7 reduced to 27.3 ± 7.3; 37%; p = 0.1), and RMS velocity (48.0 ± 9.1% reduced to 27.8 ± 7.0; 42%; p = 0.06). These data provide early evidence that low-level mechanical signals can ameliorate the damage of non-weight bearing to several aspects of the musculoskeletal system. Certainly, the preservation of both bone quality and postural control during extended disuse will ultimately reduce the risk of both falls and fracture.

Disclosures: J.W. Muir, None.

This study received funding from: NASA NRA-03-OBEP-06.

T427

Teriparatide in Clinical Practice - Experience with 158 Patients Beyond Randomized Controlled Trials. C. Muschitz¹, L. Milassin^{*1}, T. Pirker^{*1}, J. Patsch^{*2}, G. Nimberger^{*3}, H. Resch¹. ¹Medical Department II, St. Vincent Hospital, Vienna, Austria, ²Department of Pathophysiology, Medical University Vienna, Vienna, Austria, ³Bioconsult Ltd, Perchtoldsdorf, Austria.

We established a prospective single-center open-label database evaluate response to 9 & 18 month teriparatide treatment (rhPTH [1-34] 20µg/d; 1000mg calcium & 800IU vitamin D/d) for patients with progressive osteoporosis who are not subject to randomized controlled trials.

We included 158 consecutive Caucasian patients (141 females, 17 males). 78.4% were considered as bisphosphonate non-responder and 9.6% as bisphosphonate incompatibility. 1.2% had steroid induced osteoporosis. At 10.8% we performed a bone biopsy due to uncertain diagnostic findings. All patients were subject to standardised diagnostic examinations (iDXA hip and spine - GE Lunar, QCT spine Mindways, serum parameters, vertebral X-ray, medication, side effects). Statistical calculation was performed by rank tests and by an ANCOVA and regression model.

Mean age was 71.94 ± 9.97 years. 86 % presented more than 1 vertebral fracture (mean: 3.6 fractured vertebrae). Serum parameters of bone metabolism were within normal range at baseline.

After nine months alkaline phosphatase increased from 68.87 ± 87 to 93.77 ± 38.36 U/l (p < 0.001), S-OC (ng/ml) changed from 17.21 ± 12.82 at baseline to 71.70 ± 34.90 (p < 0.001), S-CTX (ng/ml) increased from 0.25 ± 0.14 to 0.80 ± 0.49 (p < 0.001), P1NP (ng/ml) increased from 39.12 ± 25.76 to 144.87 ± 22.18 (p < 0.05) and PTH (pg/ml) decreased from 41.65 ± 14.56 to 28.83 ± 12.87 (p < 0.001), respectively. Serum and 24 hour excretion of calcium and phosphorus remained within normal range.

BMD of spine measured by DXA increased from 0.85 ± 0.15 g/cm² at baseline to 0.92 ± 0.16 g/cm² at month 9 (p=0.0004) and to 0.95 ± 0.17 g/cm² at month 18 (p=0.0006). At hip was no

significant increase of BMD (0.75 vs 0.76 g/cm²). BMD of lumbar spine measured by QCT increased from 48.25 ± 29.58 to 52.96 ± 35.31 g/cm³ (n.s.). Concomitant oral medication like proton pump inhibitors, statins, antidiabetics or antithrombotics had no significant influence on BMD or parameters of bone metabolism after nine months. Only one patient had one new vertebral fracture during treatment.

Teriparatide treatment in clinical practice is safe and effective for patients with progressive osteoporosis who are not subject to randomized controlled trials.

Disclosures: C. Muschitz, None.

T428

Effect of Treatment with Depot GH on Bone Remodeling and Heel Ultrasonometry in Dwarfism Due to Mutation in the GHRH-R Gene. F. J. A. Paula¹, M. B. Gois Jr.^{*1}, F. A. Pereira¹, R. C. Pereira^{*2}, C. R. P. Oliveira^{*3}, C. Farias^{*3}, J. A. Barreto-Filho^{*3}, C. M. Santos^{*4}, T. Vicente^{*4}, M. H. Aguiar-Oliveira^{*3}, R. Salvatori^{*5}. ¹Internal Medicine, School of Medicine of Ribeirão Preto, University of São Paulo, Ribeirão Preto, Brazil, ²Internal Medicine, School of Medicine of Federal University of Sergipe, Aracaju, Brazil, ³Internal Medicine, School of Medicine of Federal University of Sergipe, Aracaju, Brazil, ⁴Internal Medicine, School of Medicine of Federal University of Sergipe, Ribeirão Preto, Brazil, ⁵Internal Medicine, School of Medicine of Johns Hopkins University, Baltimore, MD, USA.

GH treatment of individuals with isolated chronic GH deficit (GHD) probably has beneficial effects that exceed the risks. We had evaluated heel ultrasonometry and bone remodeling in individuals with GHD at baseline, after 6 months of treatment with depot GH, and 6 and 12 months after the end of treatment. Subjects with GHD (20) due to mutation of the GHRH-R gene and a control group (CO=20) were evaluated. The groups were matched for age (GHD= 46.1 ± 14.5 vs CO= 46.4 ± 15.9 years), sex (GHD and CO = 10M/10F) and BMI (GHD= 23.8 ± 3.9 vs CO= 23.9 ± 3.6 Kg/m²). The GHD group presented lower weight (GHD= 36.8 ± 3.9 vs CO= 67.2 ± 14.7 Kg) and height (GHD= 1.24 ± 0.07 vs CO= 1.67 ± 0.05 m) ($p < 0.01$). The GHD received depot Nutropin administered every 15 days for 6 months. The initial and final doses were 0.33 ± 0.33 and 0.38 ± 0.08 mg/kg for women and 0.25 ± 0.01 and 0.38 ± 0.04 mg/kg for men. QUS was performed with the Achilles in Sight apparatus. The QUS parameters used were stiffness and T score, which were compared to the values of a normal South American population. Serum osteocalcin, ICTP and IGF-1 were determined. T-score ($p < 0.01$) and stiffness ($p < 0.04$) values were significantly lower in the GHD group. GH induced elevation of the T score, which persisted after the end of treatment, with a significant difference compared to baseline being observed at 6 months and 12 months ($p < 0.04$) after GH discontinuation. The GHD group presented elevation of osteocalcin during treatment ($p < 0.01$), which remained elevated for 6 months after the end of treatment ($p < 0.01$). ICTP showed elevation only during treatment ($p < 0.01$). IGF-1 levels were low in GHD group at baseline (< 10 ng/ml) and increased significantly during treatment. Our results show that depot GH induced a significant improvement in QUS and in bone remodeling parameters in individuals with GHD. The beneficial effect on bone ultrasonometry was maintained for 12 months after the discontinuation of treatment. These results are encouraging and indicate that other studies should be conducted in order to establish the ideal periodicity of treatment with GH, and that data obtained by bone densitometry should be compared to those obtained by QUS in individuals with GHD.

Disclosures: F.J.A. Paula, None.

This study received funding from: NIH, FAPESP, CAPES, FAPESP.

T429

A Theoretical Analysis of Current Density to Increase Bone Mass with Low-Frequency Interferential Electrical Stimulation. M. Shih¹, R. Kamondetdacha^{*2}, J. A. Nyenhuis^{*2}, W. J. Carroll^{*1}. ¹RS Medical, Vancouver, WA, USA, ²Purdue University, West Lafayette, IN, USA.

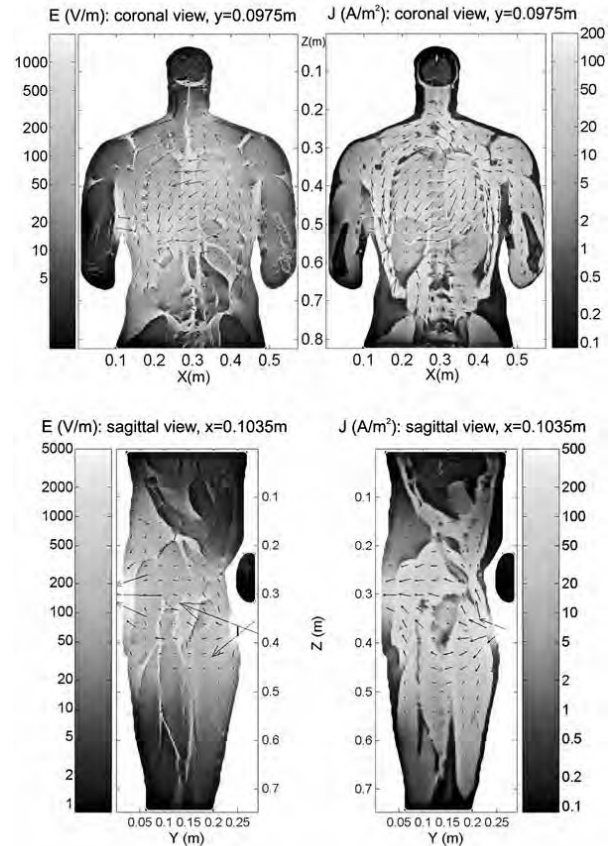
Low-frequency electrical fields have been shown to enhance bone tissues repair when specific frequencies are applied at appropriate current levels. Repeated studies using interferential stimulation (IS) in neonatal rat calvaria cultures confirmed a positive effect of such electrical fields from interferential current on osteoblastic proliferation and bone matrix production. Creation of a therapeutic device capable of strengthening bone in the lower back or hip has awaited a robust frequency-based human body conductivity model. The present work theoretically models the IS to the targeted tissue, i.e., human vertebrae and femoral head and calculates the electric field strengths.

Using a mathematical model of conductivity within the human body (Hugo), the electrical fields and current densities for particular electrical potentials passing through electrodes applied to specific surfaces of the body were calculated. By use of an impedance technique and by applying quasi-static approximation, the current density from electrodes was calculated for a 3-mm resolution with local sub-gridding at a resolution of 1 mm. Electrode pairs were placed on the back at the approximate longitudinal locations of T5 and T11 and also T3 and L3 of the human model; electrodes were also placed over the femur at the front and back of the modeled body (Fig.1).

For an electrode current of 1 A, the predicted electric field amplitude (EFA) in a vertebral body would be approximately 130 V/m. EFA in the vertebral bodies and discs are similar, but the current density is much greater in the discs due to their larger conductivities. The EFA in the femur is predicted to be about 300 V/m for the chosen electrode locations. Waveforms of IS were calculated for different frequency currents applied to electrode pairs.

The experimentally determined therapeutic current would be 27 mA for delivery of 20mV/cm to bone in human. The data, compared with the values reported by Carter (IEEE Trans.

Biomedical Engineering, 1990) with consideration of approximations in the two models, are felt to be in good agreement. Using the same modeling methodology, estimates of EFA closely matched values measured in a Petri dish culture of neonatal rat calvaria in which osteoblastic cell number and matrix production were successfully stimulated.



Disclosures: M. Shih, RS Medical 3.

This study received funding from: RS Medical.

T430

Results of the 'e-Bone Study': Bone Density Changes with Pulsing Electromagnetic Field Treatment of the Forearm after Disuse. J. A. Spadaro, W. H. Short^{*}, P. R. Sheehee^{*}, D. H. Feiglin^{*}, J. C. Calabrese^{*}, R. M. Hickman^{*}. Upstate Medical University, Syracuse, NY, USA.

A feasibility and dosing study was undertaken to determine if pulsing electromagnetic field (PEMF) treatment, typically used for treating non-union fractures, could moderate the osteopenia that occurs following forearm disuse. This was a randomized, double blind, sham controlled and age and gender balanced trial approved by the IRBPHS at SUNY Upstate Medical University. Entry and baseline was 6-8 weeks after a distal radius fracture or carpal surgery and 99 subjects were randomized to wear a distal forearm PEMF transducer for either 1, 2, or 4 hours per day during the 8 weeks following their baseline visit. 25% of the subjects were randomly assigned (double blinded) to receive identical but inactive sham transducers. Bone mineral density (BMD) and geometry at several sites in the forearm were measured by dual energy x-ray absorptiometry (DXA) and peripheral quantitative CT (pQCT) at baseline, 8, 16, and 24 weeks. Serum markers of bone formation (BSAP) and resorption (CTX) were measured at baseline and 8 weeks. Analyses of the % change from baseline for BMD and other variables was performed using multiple regression and analysis of co-variance based on the general linear model, with means adjusted for the effects of age, gender and baseline BMD. 82 subjects completed all four visits with an average hourly treatment compliance of 88%. Based on previous work, the typical BMD loss at baseline is of the order of 3-5 %. In this study we measured a subsequent average loss of 5-7% for the ultra-distal radius and 3-4 % for the radial shaft. An 'intent to treat' analysis (n= 99) on a composite 'grand mean' of % loss of BMD by DXA or pQCT at six forearm sites from 8-24 weeks showed no evidence of a positive effect of active vs. sham PEMF treatment on the loss after baseline. This was true also for subjects completing all visits (n=82) either on the 'grand mean' BMD loss or at each individual site. Model-adjusted standard errors in BMD change were in the 0.5-3% range. Interestingly, the pQCT data suggested a rapid increase in cortical cross-sectional area and strength index in the distal forearm during the study period. Serum BSAP was unchanged after treatment but serum CTX was clearly decreased in all treatment groups (but unaffected by PEMF). Even with the large between subject variability, the results suggest that the chosen timing and PEMF used here were not sufficient to substantially moderate the rapid bone loss and slow recovery induced by the injury and immobilization.

Disclosures: J.A. Spadaro, None.

This study received funding from: NIH-NIAMS.

T431

Establishment of Vascular Calcification Model Using High Dose of Vitamin D in Mice. J. Jin*, H. Jin*, M. Han*, H. Kim*, Y. Jung*, Y. Park*, M. Park*, W. Lee*, J. Choi. Biochemistry & Cell Biology, Kyungpook Natl. Univ. School of Medicine, Skeletal Diseases Genome Research Center, Daegu, Republic of Korea.

Vascular calcification represents an important risk factor for high mortality of cardiovascular diseases. High dose of vitamin D has been used to induce vascular calcification mostly in rats, however, it has not been determined whether it is applicable to mice. Here, mice (n=7 in each group) were injected with various doses of vitamin D (0, 10, 30, 50, 100 x 10⁴ IU/kg) in subcutaneous tissue one time per day for 3 days and mice were sacrificed at day 9 after last injection. Blood chemistry and histological analysis such as Alizarin Red S and von Kossa staining were performed. Vitamin D injected mice were more lethargy and sluggish according to the time. Their body weights were nearly a half compared to control group and their hair appeared no glossiness. Blood calcium, creatine and alkaline phosphatase activity were increased according to the dose of vitamin D. In bone tissues, vitamin D increased TRAP positive staining in trabecular bone area. In soft tissues, calcification was observed in aorta, kidney, and lung, but it was not observed in heart, spleen and brain. Calcification was prominent especially kidney and lung around proximal tubule and alveoli, respectively. Interestingly, calcification in medial layer of aorta was more severe than intimal layer. Collectively, these results indicate that high dose of vitamin D is a good mouse model for medial calcification which is frequently shown in diabetes mellitus and uremic conditions

Disclosures: J. Choi, None.

T432

Fosamax® (alendronate sodium) and Cholecalciferol (Vitamin D₃) in the Treatment of Men and Postmenopausal Women with Osteoporosis. F. Chouha¹, M. Shulman^{*1}, C. Liao^{*2}, T. Koulis^{*2}, J. S. Sampalis^{*3}, A. C. Karaplis⁴. ¹Merck Frosst Canada, Kirkland, PQ, Canada, ²JSS Medical Research, Westmount, PQ, Canada, ³Dept. of Surgery, McGill Univ., Montreal, PQ, Canada, ⁴Dept. of Medicine, McGill Univ., Montreal, PQ, Canada.

Background: Osteoporosis is a debilitating disease associated with significant morbidity and mortality. It is recommended that patients on antiresorptive medication receive supplemental calcium and vitamin D.

Objective: To describe the distribution of serum 25-hydroxyvitamin D [25-(OH) D] in Canadian men and postmenopausal women with osteoporosis and to evaluate the impact, safety, and tolerability of vitamin D₃ supplementation taken as 400 IU daily concurrently with alendronate 70 mg weekly.

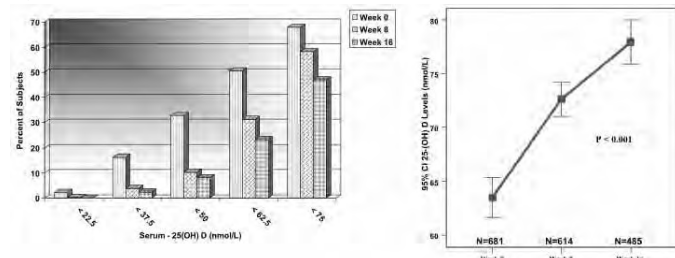
Methods: A 16 week, open-label, multi-center, observational study. Eligible patients with osteoporosis were either men or community dwelling ambulatory women, postmenopausal for ≥ 6 months. Outcomes were changes in serum 25-(OH) D levels, adherence, and incidence of adverse events attributed to treatment.

Results: 728 patients were enrolled, comprising 684 with 25-(OH) D evaluation at baseline; 614 (84.3%) and 485 (66.6%) completed week 8 and 16, respectively. The majority of discontinuations were lost to follow-up, 131 (18.0%). The mean (SD) age of the patients was 67.7 (10.3) years old. There were 605 (83.1%) female and 593 (81.5%) Caucasian. The figures illustrate the prevalence of serum vitamin D inadequacy (<75 nmol/L) by cut-off points and statistically significant increases of serum 25-(OH) D with P < 0.001 (between visits 1, 2 and 3)

The mean (SD) change in 25-(OH) D value (nmol/L); 8.6 (22.8) for week 8 vs. baseline (P < 0.001); 13.7 (25.3) for week 16 vs. baseline (P < 0.001); and 5.2 (19.9) for week 16 vs. week 8 (P < 0.001). Adherence (<20% missed dose) at week 8 was 96.7% with Fosamax® and 96.3% with vitamin D. At week 16, adherence was 98.6% and 97.1%, respectively.

103 non-serious adverse events reported by 70 (9.6%) subjects were attributed to treatment, among which gastrointestinal disorders were the majority observed by 50 (6.9%) subjects.

Conclusion: A significant proportion (68.0%) of the study population has vitamin D inadequacy at baseline. Daily vitamin D₃ supplementation taken concurrently with alendronate weekly was effective in significantly improving the 25-(OH) D levels of subjects. Treatment was safe, well tolerated with a low incidence of adverse events and a high adherence.



Disclosures: F. Chouha, Merck Frosst Canada Ltd. 1, 3.
This study received funding from: Merck Frosst Canada Ltd.

T433

The Combination of Calcitriol Shows more Bone Sparing Effect by Suppressing Secondary Increment of Parathyroid Hormone in Raloxifene Therapy than when Laloxifene Is Used Alone in Postmenopausal Japanese Women with Osteoporosis and Osteopenia. I. Gorai¹, Y. Tanaka^{*1}, Y. Iwaoki^{*2}. ¹Obstetrics and Gynecology, International University of Health and Welfare Atami Hospital, Atami, Japan, ²Obstetrics and Gynecology, Hiroshima-ken JA Yoshida General Hospital, Takada-gun, Japan.

It has been reported that vitamin D insufficiency is prevalent in osteopenic and osteoporotic postmenopausal women. Secondary hyperparathyroidism decreases the beneficial effects of antiresorptive therapy on bone mineral density (BMD) in osteoporotic women. We aimed to see the effects of raloxifene, 1α(OH)vitamin D₃ and a combination of both on bone density and turnover in postmenopausal Japanese women with osteoporosis or osteopenia (<2.0SD). A total of 153 subjects aged 49 to 81 years [64.8±6.9 years, 16.2±8.5 years since menopause (YSM)] were randomly assigned to 60mg raloxifene (R), 1μg 1α(OH)vitamin D₃ (D) or a combination of both (R+D) daily for 1 year. Lumbar spine (L-) BMD, biochemical indices, and intact (i-)PTH were monitored over 1 year. Baseline 25(OH)D levels were measured at the start of the study. There were no significant differences in the background characteristics among the three groups. Baseline 25(OH)D levels were 24.3ng/ml in D-group, 22.9ng/ml in R-group and 24.2 ng/ml in D+R-group (P=0.3980). PPS analysis was used for statistical analysis. In the combination-treated group there was a significant increase in L-BMD (+3.6% in 6 mo. and +4.4% in 1 yr, P<0.001) and the increases were significant as compared with those in D-treated group (vs.+0.7% and 0.9%, P<0.05). At 6 mo. i-PTH showed significant decrease in D-group (-17.7%, P<0.01), significant increase in R-group (+19.2%, P<0.05) and non-significant change in combination-group (-4.8%) and the change in D-group was significantly different from that in R-group (P<0.05). We found significant decreases in corrected serum calcium in R-group (-4.5% and -3.8%, P<0.01) at 6 mo. and 1 yr. Bone-specific alkaline phosphatase (BAP), urinary cross-linked N-telopeptides of type I collagen (u-NTX) and urinary type I collagen C-telopeptide breakdown products (u-CTX) in combination-group showed significant decreases at 1 mo., 3 mo., 6 mo. and 1 yr (-17.1%--36.7%, -13.5%--34.0% and -28.3%--47.4%, respectively) except for BAP at 1 mo., whereas BAP and u-NTX after 6 mo. (-13.4%--16.7% and -22.3%--28.0%) and u-CTX after 1 mo. (-14.8%--32.3%) significantly decreased in R-group. We conclude that the combination of calcitriol shows more bone sparing effect by suppressing secondary increment of parathyroid hormone and lowering bone turnover more greatly in raloxifene therapy than when raloxifene was used alone in postmenopausal Japanese women with osteoporosis and osteopenia.

Disclosures: I. Gorai, None.

T434

A Combination Therapy of Alendronate and Calcitriol Increases in Bone Mineral Density by Keeping Intact Ca Metabolism for the Treatment of Osteoporosis. M. Yamanaka^{*1}, Y. Sakamoto^{*1}, A. Tokita², K. Kitahara³, M. Ishijima¹, H. Kurosawa^{*1}. ¹Orthopaedics, Juntendo University School of Medicine, Tokyo, Japan, ²Pediatrics, Juntendo University School of Medicine, Tokyo, Japan, ³Orthopaedics, Juntendo Tokyo Koto Geriatric Medical Center, Tokyo, Japan.

A combination therapy of alendronate (ALN) and calcitriol (a-D) is widely accepted as one of the best approaches for the management of osteoporosis in Japan. The purpose of this study was to compare the efficacy of a combination of ALN and a-D with that of ALN alone for the treatment of osteoporosis. The subjects were post-menopausal women with primary osteoporosis (20 cases), who were treated with ALN alone for one year. At the beginning of the second year, they were divided into two treatment groups: patients treated with ALN alone for one more year (ALN group) and patients treated with a combination of ALN and a-D (0.5ug/day) (ALN+D group) for a year. The primary outcome was assessed by lumbar spine mineral density (BMD), and secondary outcomes were assessed by biochemical makers for bone metabolism. BMD and biochemical makers were measured at the beginning of treatment and after one and two years. No significant difference in serum 25(OH)D was detected between the ALN group and ALN+D group at the beginning of treatment (23.9±9.4 ng/ml, 20.6±9.9 ng/ml respectively). In addition, no significant difference between the groups in the median increase of BMD was detected in the first year (8.0±4.4%, 6.9±6.7% respectively). The median increase of BMD in the second year was -0.61% in ALN group and +1.77% in ALN+D group (p=0.07). In the second year, the median increase in serum intact parathyroid hormone (i-PTH) of the ALN+D group was significantly lower (p=0.025) than that of the ALN group, while the median increase of urine Ca/Creatinine in the ALN+D group was significantly higher (p=0.033) than that of the ALN group. These results suggest that, similar to treatment with a-D alone, a combination therapy using active ALN and a-D promotes absorption of Ca and inhibits hyperparathyroidism. Our results demonstrate that the combination therapy with ALN and a-D is superior to gain BMD with intact Ca metabolism over ALN alone for the treatment of osteoporosis.

Disclosures: M. Ishijima, None.

T435

Lasofloxifene Preserves Lumbar Vertebral Strength by Preventing Bone Loss and the Deterioration of Bone Architecture and Geometry in Ovariectomized Rats. M. Li¹, H. Qi^{1*}, Y. Li^{1*}, H. A. Simmons¹, D. T. Crawford^{1*}, D. R. Healy^{1*}, T. A. Brown¹, H. Z. Ke², D. D. Thompson¹. ¹Cardiovascular and Metabolic Diseases, Pfizer Global Research and Development, Groton, CT, USA, ²Amgen, Thousand Oaks, CA, USA.

We have previously demonstrated that lasofloxifene, a selective estrogen receptor modulator, prevented cancellous bone loss and preserved bone strength in ovariectomized (OVX) rats. In this study, we further characterized the effects of lasofloxifene on bone architecture and geometry and their contribution to the preservation of bone strength in the lumbar vertebra of OVX rats. Female rats at 13 weeks of age were OVX and treated orally with vehicle or lasofloxifene at 10 µg/kg/d or 17α-ethynylestradiol (EE) at 30 µg/kg/d for 8 weeks. The vehicle-treated OVX rats exhibited bone loss and compromised bone strength as demonstrated by a significant decrease in total bone density, cortical bone content, and cancellous bone volume and ultimate strength. Deterioration of cancellous and cortical architecture and cortical geometry was also seen in these animals as evident by a significant decrease in trabecular number, trabecular thickness, cortical area and cortical thickness, and an increase in trabecular separation and endocortical circumference. In contrast, lasofloxifene treatment completely abolished the changes induced by estrogen deficiency in total bone density, cancellous bone volume, trabecular number and separation, cortical area, cortical content, and ultimate strength. In addition, the OVX rats treated with lasofloxifene had significantly increased trabecular thickness and decreased endocortical circumference compared with the vehicle-treated OVX controls. The aforementioned effects of lasofloxifene on bone mass, architecture, geometry and strength were similar to those observed in the OVX rats treated with EE. Significant positive correlations were found between ultimate strength and total bone content, total bone density, cortical content, cortical area, cortical thickness, endocortical circumference, cancellous bone volume, trabecular number and trabecular separation with *r* values ranging from 0.338 to 0.571 and *p* values ranging from 0.0351 to 0.0002. The strongest correlation observed was between the ultimate strength and cancellous bone volume followed by trabecular number and cortical thickness. In summary, lasofloxifene protected against estrogen deficiency induced bone loss and the deterioration of bone architecture/geometry, and preserved bone strength at lumbar vertebra of rats. In addition to bone mass, trabecular and cortical architecture as well as geometric properties contributed to the preservation of bone strength by lasofloxifene treatment.

Disclosures: M. Li, Pfizer Inc. 3.

T436

Prevalence of Hypovitaminosis D and Male Hypogonadism in Prednisone-treated Rheumatic Disease Patients. H. B. Lindsley^{1*}, D. Walia^{1*}, H. Singh^{1*}, K. Jennings^{1*}, F. Wolfe^{2*}, D. D. Smith^{1*}, B. P. Lukert¹. ¹Dept Medicine, Univ Kansas Medical Center, Kansas City, KS, USA, ²Dept Medicine, Univ Kansas School of Medicine--Wichita, Wichita, KS, USA.

Inadequate vitamin D nutritional status is an underappreciated health problem in adults at risk for osteoporosis. Serum levels of 25-hydroxy vitamin D [25(OH)D] are rarely ordered as there are no specific symptoms to suggest this deficiency. Serum PTH levels rise as 25(OH)D levels decrease, contributing to osteoporosis. The purpose of this prospective observational study was to identify patients at high risk for osteoporosis, who had insufficient levels of vitamin D (either gender) or testosterone (males). We enrolled 175 patients, 40 years of age or older, on ≥5 mg prednisone daily for a least one month. Blood was obtained for measurement of 25(OH)D (DiaSorin method), PTH, osteocalcin, and free testosterone.

Using 30 ng/mL as a minimum threshold for adequacy of vitamin D, 71% of all subjects had insufficient levels of 25(OH)D, and 23% of all subjects had vitamin D deficiency (<15 ng/mL). 21% were taking at least 100 IU of Vitamin D daily (median=400) and 3% were taking weekly Vit D (≥25,000 IU). Median prednisone dosage was 10 mg daily.

Vit D Grp (ng/ml)	N	25(OH)D level (ng/ml, median±SEM)	PTH (pg/ml)	Osteocalcin (ng/ml)
<15	40	12±2	45±5	3.0±0.5
15-29	84	24±1	32±3	3.2±0.4
30-45	47	34±1	25±4	2.8±0.2
>45	4	89±25	23±4	2.2±0.9

Ethnic differences were apparent: African-Americans (N=19) had distinctly lower 25(OH)D levels, 15±1, compared to Caucasians (N=142), 25±1; whereas PTH levels were higher, 40±8 versus 30±2. There was an inverse correlation between 25(OH)D and PTH levels (Pearson correlation = -0.23). Osteocalcin levels were independent of 25(OH)D levels.

For males 30 of 59 (51%) had low free testosterone levels (<1 ng/mL), 0.79±0.04 (median±SEM), whereas the remaining 29 subjects had normal levels, 1.40±0.14. Median prednisone usage in the low group was 7.5 (±2.0) mg daily, whereas the group with normal levels took 10.0 (±0.6) mg daily.

In summary, there was an unexpected high frequency of 25(OH)D insufficiency and male testosterone deficiency in prednisone-treated patients at increased risk for osteoporosis. Furthermore, OTC Vitamin D supplementation was uncommon and inadequate.

Disclosures: H.B. Lindsley, Procter & Gamble 2.

This study received funding from: Procter & Gamble.

T437

Vitamin D Deficiency in Osteogenesis Imperfecta: Recommendations for Supplementation. E. N. Martin^{1*}, A. Khosravi^{1*}, K. BrintzenhofeSzoc^{2*}, J. R. Shapiro¹. ¹The Kennedy Krieger Institute, Baltimore, MD, USA, ²Catholic University of America, Washington, DC, USA.

The contribution of vitamin D deficiency to BMD and fracture risk is undefined in adult OI. This report presents baseline and 2-year 25(OH) vitamin D concentrations in 50 adults, 18-65 years, and preliminary data for 10 children, 3-18 years, with types I, III, and IV OI. Types V, VI, and VII OI were not included. Values were examined with respect to OI type, BMD, serum PTH, alkaline phosphatase and urine NTX.

Patients received supplements of 400 IU vitamin D/day following then current RDA recommendations, now recognized to be insufficient. Serum levels measured at baseline and 2 year values in adults below 32ng/mL were: type I 79% and 42%, type III 84% and 50%, type IV 100% and 75% (Table 1). In children, preliminary data showed 6 type I patients with baseline and 2 year serum values 38ng/mL and 30 ng/mL, 2 type III patients 23ng/mL and 16ng/mL, and 2 type IV patients 24ng/mL and 13ng/mL.

PTH levels showed the expected inverse relationship to 25(OH)D level. No significant relationship between alkaline phosphatase or NTX and vitamin D levels was found. In adults, there was a non-significant trend for increasing BMD over a 2 year period when patients received 400 IU/day.

As RDA recommendations of 400-600 IU (RDA, 1989) are not adequate to produce serum levels above 32 ng/mL in OI, we propose the following guidelines based on patient weight rather than age because of marked size variation within the OI population (Table 2). Individual monitoring of serum levels as patients alter vitamin D intake is essential. In conclusion, people with OI demonstrate a significant incidence of vitamin D deficiency, which may be due to lack of sun exposure and deficient oral intake. Also, compliance in this population may limit adequate D supplementation. Maximizing calcium absorption and minimizing bone resorption in OI is particularly critical, and so adequate serum vitamin D levels should be maintained. At this time we have not assessed effects of these supplements on parameters of BMD or biomarkers in adults or children with OI.

Table 1: Baseline Serum Levels in Adults

Serum 25(OH) vitamin D level	<10 ng/mL	<20 ng/mL	<32 ng/mL
Type I OI	7%	56%	79%
Type III OI	4%	40%	84%
Type IV OI	17%	50%	100%
Healthy Canadian Adults (1)	6%	34%	N/A
Healthy US Adults age 18-29 years and 49-83 years (2)	N/A	36% and 41%	53.3%
US Adult Inpatients (3)	22%	57%	N/A

Table 2: Recommended Vitamin D Daily Intake

Age (RDA)	Weight (Recommended)	
0-50 years	200 IU/day	50 lbs/ 20 kg
51-70 years	400 IU/day	90 lbs/ 40 kg
70+ years	600 IU/day	110 lbs/ 50 kg
		150 lbs/ 70 kg +
		2000-2800 IU/day

Disclosures: E.N. Martin, None.

T438

Antifracture Efficacy of Combined Treatment with Alendronate and Alfacalcidol for Osteoporosis in Early-phase Treatment. N. Miyakoshi¹, Y. Kasukawa¹, H. Kodama^{2*}, H. Noguchi^{1*}, H. Sasaki^{1*}, K. Kamo^{1*}, Y. Shimada^{1*}. ¹Orthopedic Surgery, Akita University School of Medicine, Akita, Japan, ²Minamiakita Orthopedic Clinic, Katagami, Japan.

Alendronate, a bisphosphonate, decreases the incidence of vertebral fractures by increasing bone mineral density (BMD). However, because the effects on bone are exerted in an indirect manner by reducing the remodeling space and prolonging the duration of mineralization, several months are required to increase bone strength. Previous reports have shown significant antifracture effects can be expected after 6 months of treatment. Alfacalcidol also displays preventive effects against osteoporotic fractures, despite a small effect on bone mass. We thus conducted a 6-month, prospective, randomized trial of postmenopausal women with osteoporosis to evaluate the possibility of early-phase superiority using combined treatment with alendronate and alfacalcidol compared to either alone, with radiographically diagnosed vertebral fracture as the primary endpoint. Subjects comprised 363 postmenopausal women >60-years-old (mean age, 74 years) and with osteoporosis. Subjects were randomly divided into 3 groups: ALN group (n=119), treated with daily oral administration of 5 mg of alendronate; D group (n=122), treated with daily oral administration of 1 µg of alfacalcidol; and ALN+D group (n=122), treated with daily oral administration of 5 mg of alendronate plus 1 µg of alfacalcidol. Demographic data including age, baseline BMD of distal radius, and number of vertebral fractures did not differ significantly between groups. The number of vertebral fractures at baseline and follow-up were evaluated using spinal radiography. During the 6-month treatment period, new vertebral fractures comprised 11 fractures in 9 ALN group patients (7.6%), 9 fractures in 9 D group patients (7.4%), and 3 fractures in 3 ALN+D group patients (2.5%). In conclusion, combination therapy with alendronate and alfacalcidol exhibited superiority in terms of preventing vertebral fracture over either treatment alone in early-phase treatment (≤6 months). However, as several other risk factors such as spinal hyperkyphosis, lower BMD, and higher bone resorption markers also affect incidence of vertebral fractures, further studies including these factors will be needed to reconfirm the present findings and clarify the antifracture efficacy of combination therapy using alendronate and alfacalcidol in early-phase treatment.

Disclosures: N. Miyakoshi, None.

T439

Vitamin D Status, Bone Mass, and Bone Metabolism in Postmenopausal Japanese Women. K. Nakamura¹, N. Tsugawa^{*2}, T. Saito^{*3}, Y. Tsuchiya^{*1}, A. Yoshihara^{*4}, T. Okano^{*2}, M. Yamamoto^{*1}. ¹Department of Community Preventive Medicine, Niigata University Graduate School of Medical and Dental Sciences, Niigata, Japan, ²Kobe Pharmaceutical University, Kobe, Japan, ³Niigata University of Health and Welfare, Niigata, Japan, ⁴Department of Oral Health Science, Niigata University Graduate School of Medical and Dental Sciences, Niigata, Japan.

The purpose of this study was to identify how the serum 25(OH)D concentration is associated with bone mineral density (BMD) of the lumbar spine and femoral neck, and with bone metabolism in postmenopausal Japanese women. This cross-sectional, community-based epidemiologic study design was conducted among 600 ambulatory postmenopausal women. The serum 25-hydroxyvitamin D (25[OH]D) concentration was measured with radioimmunoassay. Other blood biochemical measurements were intact parathyroid hormone and markers of bone turnover, including osteocalcin and type I collagen cross-linked N-telopeptides. BMD of the lumbar spine and right femoral neck were measured with the dual-energy X-ray absorptiometry method using a QDR4500a. The protocol of this study was approved by the Ethics Committee of Niigata University School of Medicine. The mean serum 25(OH)D concentration was 55.6 nmol/L (SD 14.6). The serum 25(OH)D concentration was non-linearly associated with BMD of the lumbar spine, i.e., mean BMDs of the lumbar spine between two groups with and without vitamin D insufficiency (cutoff value 50 nmol/L of serum 25[OH]D) were significantly different. On the other hand, the serum 25(OH)D concentration was linearly associated with BMD of the femoral neck ($R^2=0.020$, $P=0.002$). While mean serum intact PTH concentrations for serum 25(OH)D < 50 nmol/L were significantly higher than those for serum 25(OH)D ≥ 50 nmol/L, markers of bone turnover were not significantly associated with serum 25(OH)D concentrations. This study showed that the serum 25(OH)D concentration should be maintained at a minimum of 50 nmol/L for high BMD, and that the pattern of an association between the serum 25(OH)D concentration and BMD of the femoral neck are different from that of the lumbar spine, suggesting vitamin D status affects cortical bone more than spongy bone.

Disclosures: K. Nakamura, None.

T440

Prevalence of Vitamin D and Calcium Supplementation Following Low Impact Hip Fracture: A Three Year Retrospective Analysis of Acute Care and Rehabilitation Facility Prescribing Practices. H. Nasr^{*}, J. Semel^{*}. Department of Physical Medicine and Rehabilitation, St. Charles Hospital / SUNY at Stony Brook, Port Jefferson, NY, USA.

Background: In the United States more than 300,000 individuals sustain a hip fracture each year and this number is expected to increase. In recent years there has been much discussion on the role of both vitamin D and Calcium in osteoporotic fracture prevention. While some literature questions the benefit of these supplements in fracture prevention, there is growing evidence that hypovitaminosis D is common in individuals who sustain low impact hip fractures. This study looks at the patterns of Vitamin D and Calcium supplementation following low impact hip fractures.

Methods: Data was collected through a retrospective chart review of hip fracture patients discharged from the acute inpatient rehabilitation service at a large acute Inpatient Rehabilitation Facility (IRF) from 1/1/2003 through 12/31/2005. The abstracted data was entered into a database worksheet. Key data elements collected include: Demographics (Age, Gender, Weight, Height), Past History (Smoking, Alcohol, Medical history, Medications & Vitamin Supplementation, prior level of independence and living situation), Referring Hospital (RH) information (Lab results, Osteoporosis diagnosis, Osteoporosis medications, Vitamins and high risks medications for falls), IRF Information (Lab results, Osteoporosis diagnosis & Medications, Vitamins and High risk medications for falls), Functional Independence Measure (FIM) Scores and Discharge Status.

Results: A total of 498 hip fracture admissions were reviewed. Eighty-nine (89) charts were excluded for high impact trauma or hip fracture as a secondary diagnosis (e.g. stroke with a hip fracture). Data was abstracted for the remaining 409 low impact hip fracture admissions. The majority of admissions were female (307, 75.1%) vs. male (102, 24.9 %) and the average age was 76.1 years (female) and 75.1 years (male). A review of charts revealed that both Calcium and Vitamin D were prescribed in 25 (6.1%) and 43 (10.5%) of cases by the RH and IRF respectively. Calcium only was prescribed in 3 (0.7%) and 8 (2.0%) of cases by the RH and IRF respectively. Vitamin D only was prescribed in 24 (5.9%) and 114 (27.9%) of cases by the RH and IRF respectively. Neither Vitamin D nor Calcium was prescribed in 357 (87.3%) and 244 (59.7%) of cases by the RH and IRF respectively.

CONCLUSION: Our data indicate that the majority of individuals admitted for inpatient rehabilitation following a low impact hip fracture were not prescribed supplemental vitamin D nor Calcium by either the referring or treating hospital. Continued effort is needed to ensure that this population receives adequate Vitamin D and Calcium.

Disclosures: H. Nasr, None.

This study received funding from: Novartis.

T441

Prevalence of Vitamin D Deficiency in Women Age 45 and Older in a Small Michigan Community and the Effect of Vitamin D Supplementation on Myalgia. R. B. Reddy^{*1}, E. W. Busdicker^{*1}, S. Reddy². ¹Port Huron Northern High School, Port Huron, MI, USA, ²Endocrinology & Diabetes Center, Fort Gratiot, MI, USA.

Vitamin D deficiency is a common secondary cause of osteoporosis, for which perimenopausal women are at risk. The purpose of this study was to determine the prevalence of vitamin D deficiency in women age 45 and older in a small Michigan community which lies at a latitude of 42°. This study also evaluated differences in the 25-OHD levels of these women based on three factors known to affect vitamin D: age, BMI, and season. Additionally, this study observed the effects of vitamin D supplementation on a subset of vitamin D deficient women who experienced myalgia.

A total of 200 women had 25-OHD levels measured from July 2006 to January 2007. The age, BMI, and month during which the level was measured were noted for each subject. Data was analyzed using a Difference of Means Independent Assortment Test. The prevalence of vitamin D deficiency in the entire study population was 49% using a 25-OHD cutoff point of < 30 ng/mL and 25% using a cutoff point of < 20 ng/mL.

Of the 200 women, 62 were age 70 and older and 138 were age 45 to 69. There was no significant difference in 25-OHD levels in women age 45 to 69 versus women age 70 and older (30.4 ± 13.7 vs. 28.8 ± 11.9 , respectively).

Of the 200 women, 82 had 25-OHD levels measured from July to September (summer) and 74 had levels measured from November to January (winter). 25-OHD levels measured in October were not used as it was considered a transitional month. There was no significant difference in subjects' 25-OHD levels in summer months versus winter months (30.2 ± 13.4 vs. 27.7 ± 13.7).

Of the 200 women, 87 were obese ($BMI \geq 30 \text{ kg/m}^2$) and 113 were not obese. Women who were obese had significantly lower 25-OHD levels than women who were not obese (27.1 ± 12.1 vs. 32.2 ± 13.6 ; $P=0.0076$).

Seventeen vitamin D deficient women were questioned about the number and severity of their myalgia episodes before and after taking 50,000 I.U. of vitamin D weekly for four to eight weeks. Data was analyzed using a paired one-tailed student t test. There was a significant decrease in both the number (5.96 ± 5.47 vs. 1.13 ± 2.13 ; $P=0.003$) and the severity (7.17 ± 1.59 vs. 3.13 ± 2.6 ; $P=0.0005$) of myalgia episodes after supplementation. These results show that vitamin D deficiency is a widespread problem among women age 45 and older not limited to the elderly or to winter months with lower levels in obese women. Supplementation of vitamin D improves myalgia. Women who experience myalgia should be evaluated for vitamin D deficiency. The high prevalence of vitamin D deficiency should be communicated to physicians and the general public.

Disclosures: R.B. Reddy, None.

T442

Prevention of Falls and Fractures: What Is the Evidence for Plain Vitamin D and Active D-hormone Analogs? J. D. Ringe¹, E. Schacht², P. Farahmand^{*1}. ¹Med. Klinik 4, Klinikum Leverkusen, Univ. of Cologne, Leverkusen, Germany, ²ZORG (Zürich Osteoporosis Res. Group), Munich - Hong-Kong - Zurich, Switzerland.

Frequent falling is an increasing problem in the elderly with deleterious consequences. Falls break bone, fear of further falling reduces self-esteem, physical activity, social contacts and quality of life. Fractures are the clinically most relevant outcome of osteoporosis and the majority of the non-vertebral fractures are fall-related.

D-Hormone (1,25(OH)₂D; calcitriol), the active vitamin D metabolite, and its receptor (VDR) play an important role in muscle development and function. Older age is significantly associated with decreased VDR expression in skeletal muscle tissue and femoral muscle power and function. These parameters are closely related to D-Hormone serum levels in the elderly suggesting that the age-related increase of falls is at least partly explained by a decrease of D-Hormone and of VDR's.

A significant decrease in the fall rate after 3 years treatment with 0.5 µg calcitriol daily in osteopenic women without vitamin D deficiency has been described. For alfacalcidol (1 µg daily), a pharmacologically advantageous pro-drug of calcitriol, a significant reduction of falls of 50-70% was proved after 9 months in elderly women and men (normal vitamin D levels at onset, > 500 mg daily calcium from diet, creatinine clearance < 65 ml/min). From a meta-analysis it was concluded that both plain vitamin D and active D-hormone analogs reduce the risk of falls. Subgroup analyses however prove that the effect on falls is mainly triggered by the trials with active D-analogs.

Four recently published clinical studies in elderly with or without previous osteoporotic fractures cast doubt on the role of either an annual injection (300,000 IU) or of daily orally given vitamin D (400-800 IU) plus calcium (1 g) on the prevention of falls or fractures. On the other hand newer meta-analyses proved the reducing potency of active D-analogs on vertebral and non-vertebral fractures in postmenopausal osteoporosis and found a clear superiority of active D-analogs over plain vitamin D. In an own head-to-head study the superiority of alfacalcidol versus plain vitamin D has been shown in glucocorticoid-induced osteoporosis. A combination therapy of alendronate plus alfacalcidol was superior in terms of BMD, rate of falls, overall fractures and back pain over alendronate plus plain vitamin D.

Our concept on the advantage of active D-analogs is that these drugs are acting without the physiologically controlled activation in the kidney. This results in significantly higher concentrations in the target tissues and in an increased local expression of VDR's. Plain vitamin D however, can only be active in vitamin D deficient patients with normal kidney function.

Disclosures: J.D. Ringe, TEVA Pharmaceuticals Ltd. 5.

T443

Vitamin D Insufficiency in the Adult, Low-Energy Fracture Population. G. J. Roehrig*, C. P. DiPaola*, S. V. Bukata. Orthopaedic Surgery, University of Rochester, Rochester, NY, USA.

This study investigated the prevalence of vitamin D insufficiency in adults 50 years and older presenting with operative low-energy fractures, to determine whether routine high-dose vitamin D supplementation is warranted.

In an 8 month period, data were collected on patients at our Level 1 trauma center and affiliated community hospital, cared for by the study authors. All patients were tested on hospital admission for serum calcium, 25-(OH) vitamin D, and intact PTH levels. Inclusion criteria: age ≥ 50 , low-energy mechanism of injury, and fracture of the axial or appendicular skeleton. Exclusion criteria: pre-existing high-dose vitamin D therapy or 1-34 PTH therapy. The prevalence of hypocalcemia (serum calcium < 8.6 mg/dL), vitamin D insufficiency (serum 25-(OH) Vit D < 32 ng/mL) and deficiency (< 15 ng/mL), and secondary hyperparathyroidism (serum iPTH > 72 pg/mL) were calculated. The means, median, and ranges serum calcium, 25-(OH) Vit D, and intact PTH were determined as well.

Ninety patients were included during an 8 month collection period. Two patients did not have a serum 25-(OH) vitamin D drawn, and two patients did not have an intact PTH level drawn. The average age was 79.9 years. There were 22 (24.4%) males and 68 (75.6%) females. The prevalence of hypocalcemia was 40/90 (44.4%). The mean serum calcium = 8.8 mg/dL, the median = 8.6 mg/dL, and the range = 7.4-10.5 mg/dL. The prevalence of vitamin D insufficiency was 39/88 (44.3%). The prevalence of vitamin D deficiency was 18/88 (20.5%). The mean 25-(OH) Vit D = 26.6 ng/mL, the median = 27 ng/mL, and the range = 7.0-63.0 ng/mL. The prevalence of secondary hyperparathyroidism was 37/88 (42.0%). The mean iPTH = 73.3 pg/mL, the median = 59.9 pg/mL, and the range = 17.3-358.4 pg/mL. The average age of patients with vitamin D insufficiency was 84.1 years. The average age of patients with vitamin D deficiency was 77 years. The ratios of males to females with vitamin D insufficiency and vitamin D deficiency were 10/29 and 7/11, respectively.

Our study demonstrates that hypovitaminosis D and secondary hyperparathyroidism are not uncommon in this high-risk population. Further work is necessary to determine whether restoration of vitamin D stores aids fracture healing, but it is clear that adequate levels contribute to bone health and fracture prevention.

This raises the question of vitamin D supplementation as a standard component of the discharge plan. In addition, given that the cost of high-dose vitamin D therapy is less than one tenth that of the laboratory testing costs, prophylactic supplementation in this high-risk population should be considered. Larger epidemiologic studies are warranted to compare vitamin D levels in this population to age-matched controls.

Disclosures: G.J. Roehrig, None.

T444

Increased Markers of Bone Formation Seen Following Bariatric Surgery in Morbidly Obese Patients. N. Sinha¹, E. Stein¹, D. Ortiz¹, A. Schulman¹, G. Strain², M. Gagner², A. Pomp², G. Dakin², C. Sison¹, R. Bockman³.

¹Endocrinology, NY Presbyterian Hospital-Weill Medical College, New York, NY, USA, ²Surgery, NY Presbyterian Hospital-Weill Medical College, New York, NY, USA, ³Endocrinology, Hospital for Special Surgery, New York, NY, USA.

Bariatric surgery has been associated with an increase in markers of bone resorption and a decrease in bone mineral density.

In an on-going prospective study, alterations in bone metabolism were followed in morbidly obese patients after bariatric surgery (Roux-en-Y gastric bypass or biliopancreatic diversion with duodenal switch). Markers of bone turnover, calcitropic hormones and bone density are followed from baseline to 18 months post-operatively. All patients are followed by a nutritionist and vitamin D & calcium are replaced as needed.

Baseline data have been obtained in 105 subjects, 66 women (mean age 36 \pm 8 years, BMI 47.4 \pm 6.3 kg/m²) and 39 men (mean age 44 \pm 9 years, BMI 50.2 \pm 8.7 kg/m²). 38 patients have had surgery and their postoperative data (given as means \pm SD) are summarized in the table below.

TABLE 1: Bone Parameters at Timepoints After Surgery

	Baseline (n=105)	1 mo (n=39)	3 mo (n=24)	6 mo (n=18)	9 mo (n=14)	12 mo (n=10)
BMI kg/m ²	48.45 \pm 7.4	44.1 \pm 5.7	39.4 \pm 5.1	38.2 \pm 5.2	37.0 \pm 6.3	31.9 \pm 5.2
Calcium (8.5-10.1 mg/dL)	9.3 \pm 0.4	9.3 \pm 0.4	9.4 \pm 0.3	9.3 \pm 0.4	9.1 \pm 0.3	9.1 \pm 0.3
25-OH VitD (9-54ng/mL)	20 \pm 10	32 \pm 13	34 \pm 14	31 \pm 12	27 \pm 8	36 \pm 21
1,25-OH VitD (15-75pg/mL)	122 \pm 50	176 \pm 79	204 \pm 92	195 \pm 53	179 \pm 117	243 \pm 72
PTH,intact (9-44pg/mL)	83 \pm 48	72 \pm 32	63 \pm 28	71 \pm 41	63 \pm 35	66 \pm 31
Osteocalcin (5-30ng/mL)	4.5 \pm 2.4	3.9 \pm 1.4	5.4 \pm 1.0	6.9 \pm 0.5	5.0	7.5 \pm 1.9
BSAP (4.5-20.1ug/L)	11.2 \pm 5.1	8.3 \pm 2.5	6.8 \pm 1.8	7.5 \pm 1.7	7.1	8.0
PINP (20-76ng/mL)	43.5 \pm 15.0	53.3 \pm 20.1	65.8 \pm 22.8	89.0 \pm 32.8	68.9 \pm 8.4	77.9 \pm 7.0
Leptin (0.98-17.4ng/mL)	35.9 \pm 24.7	33.1 \pm 22.9	16.3 \pm 9.0	11.2 \pm 8.0	10.9 \pm 0.4	8.7 \pm 5.0
u-Ntx (nMBCE/nMCR)	31 \pm 13	40 \pm 14	62 \pm 19	59 \pm 28	52 \pm 6	69 \pm 34

Bariatric surgery results in significant changes in BMI at all timepoints following surgery ($p<0.0001$).

Preoperatively, Vit D insufficiency (<30 ng/mL) was found in 85% of patients. The mean PTH was two times the upper limit of normal, associated with low mean 25-OH VitD levels and elevated 1,25-OH VitD levels.

Postoperatively PTH levels remained elevated at all timepoints with the suggestion of a declining trend. There was a significant elevation in 1,25OH Vit D levels at months 1 and 12. There was a significant elevation in PINP at 1, 6 and 12 months ($p<0.01$). All other bone turnover markers did not significantly change.

Procollagen Type I N-terminal propeptide (PINP) is a sensitive marker of bone formation: levels are proportional to the amount of new collagen produced by osteoblasts. The elevation of PINP seen postoperatively and the lack of change in resorption markers suggests an uncoupling of resorption and formation. The mechanism of increased anabolic osteoblastic activity may be related to changes in PTH activity or the correction of vitamin D insufficiency.

Disclosures: N. Sinha, None.

T445

The Relative Efficacy of Vitamin D2 or D3 Treatment for D-insufficiency in Morbidly Obese Subjects. E. Stein¹, N. Sinha¹, D. Ortiz¹, G. Strain², M. Gagner², A. Pomp², G. Dakin², R. Singh³, C. Sison⁴, R. Bockman⁵.

¹Medicine/ Endocrinology, New York Presbyterian Hospital, New York, NY, USA,

²Surgery, New York Presbyterian Hospital, New York, NY, USA,

³Laboratory Medicine and Pathology, Mayo Clinic, Rochester, MN, USA,

⁴Biostatistics, North Shore-LIJ Health System, Manhasset, NY, USA,

⁵Endocrinology, Hospital for Special Surgery, New York, NY, USA.

Vitamin D insufficiency is an increasingly recognized problem among obese persons. This prospective study of morbidly obese (BMI > 35 kg/m²) subjects compared levels of vitamin D and PTH using different techniques (vitamin D: DiaSorin radioimmunoassay (RIA) and High Performance Liquid Chromatography (HPLC); PTH: "intact" IRMA assay (iPTH) and Scantibodies third generation IRMA (PTH1-84). Fifty-four subjects (ages 19-63, mean BMI 48 kg/m²) were enrolled in this ongoing trial. Thirty-nine subjects with 25OHD less than 25 ng/ml were randomized to weekly ergocalciferol (D2) 50,000 IU or cholecalciferol (D3) 8,000 IU for 8 weeks. Baseline (Wk 0) data on 15 vitamin D sufficient subjects are provided for initial comparison. Dietary calcium and vitamin D and sun exposure were assessed in all subjects.

Time-point	D-Sufficient (>25 ng/ml)	D2 Treatment		D3 Treatment	
	Wk 0 n=15	Wk 0 n=19	Wk 8 n=11	Wk 0 n=20	Wk 8 n=11
iPTH					
9-44 pg/ml	53.6 (28.6) ^a	76.1 (32.8)	72.2 (22.4)	98.8 (68.8)	76.1 (20.7)
PTH 1-84					
5-39 pg/ml	19.1 (9.1) ^a	26.8 (9.4)	23.0 (6.5)	36.1 (26.1)	24.9 (6.0) ^c
RIA					
25OHD					
20-57 ng/ml	34.7 (8.9) ^a	14.6 (3.4)	41.1 (17.7) ^b	15.9 (3.7)	26.1 (6.0) ^b
HPLC 25OHD Total					
25-80 ng/ml	25.5 (9.1) ^a	15.4 (5.1)	28.1 (4.7) ^b	16.3 (6.8)	21.5 (3.4) ^b
HPLC 25OHD2	<4.0 (0.12)	<4.0 (0.0)	21.3 (3.5) ^b	<4.0 (0.11)	<4.0 (0.0)
HPLC 25OHD3	25.1 (8.4) ^a	15.4 (5.1)	6.9 (1.9) ^b	16.1 (7.0)	21.5 (3.4) ^b

Table values are mean (S.D.)

^a vs D-insufficient ($p<0.03$)

^b vs wk 0 ($p<0.01$)

^c vs wk 0 ($p<0.05$)

Our findings showed elevated mean levels of iPTH in morbidly obese subjects, consistent with prior studies, but normal levels of PTH (1-84). 25OHD levels increased in both groups by both assays at 8 weeks ($p<0.01$), with a greater change in the D2 group ($p<0.03$). PTH 1-84 levels decreased in the D3 group ($p<0.04$) with a trend in iPTH ($p<0.09$). At these doses, D3 may be more suppressive of parathyroid function.

Disclosures: E. Stein, None.

This study received funding from: WMC GCRC M01 RR00047 and Clinical Research Feasibility Funds (CreFF) Award (awarded to young investigators by Weill Medical College GCRC).

T446

The Prevalence of Osteoporosis and Vitamin D Deficiency/Insufficiency Among Elderly People with Falls in Denmark. A. B. Vind, H. E. Andersen*, P. Schwarz. Geriatric Department, Glostrup University Hospital, Glostrup, Denmark.

Insufficiency of Vitamin D is a risk factor for falls and osteoporosis among elderly people, and osteoporosis is a risk factor for injury related to falls. We present data on the prevalence of osteoporosis and deficiency/insufficiency of Vitamin D among elderly Danish patients with falls.

In a randomized controlled intervention study on multifactorial fall prevention, including 392 patients above the age of 65 years, who have had an injurious fall, participants in the intervention group are offered a measurement of Vitamin D and a BMD-measurement.

Data are available for 169 participants, mean age 74, range 65-90, 73 % women. Among women 40 % and among men 39 % are insufficient of Vitamin D ($25\text{-OHD} < 50\text{nmol/l}$), 2.4% and 6.5 % respectively are deficient ($25\text{-OHD} \leq 25\text{nmol/l}$). 34 % of women and 15 % of men are supplemented with calcium and Vitamin D at inclusion, and are more likely to be sufficient ($\chi^2=10.67$, $p<0.001$). 29 % of women and 33 % of men suffer from osteoporosis (T-score < 2.5 at hip or spine), 41 % of women and 24 % of men had a fracture at the fall leading to entering the intervention. The proportions of fractures are similar among patients later diagnosed with osteoporosis and those not.

When comparing subjects insufficient of Vitamin D with sufficient subjects, there is no difference between the groups with regard to sex and fracture at latest fall and osteoporosis is more common among sufficient subjects ($\chi^2=5.41$, $p<0.02$).

We conclude, that although less common than in prior studies, the prevalence of insufficiency of Vitamin D is still high in a sample of elderly Danes with falls. Osteoporosis is common, especially among men, and also among those not suffering from fractures at latest fall. Screening for osteoporosis is relevant, as is securing a sufficient supply of Vitamin D.

Disclosures: A.B. Vind, None.

T447

Patient and Physician Attitudes Toward Vitamin D in Osteoporosis Treatment. S. P. Chan*, J. A. West², L. E. Wehren³, S. S. Sen³. ¹University of Malaya, Malaya, Malaysia, ²Merck, Rahway, NJ, USA, ³Merck, Rahway, NJ, USA.

BACKGROUND: Vitamin D is essential for calcium absorption and bone health, and most osteoporosis treatment guidelines recommend vitamin D supplementation. This study explored the knowledge and attitudes of physicians and patients towards supplement use in osteoporosis treatment.

METHODS: Randomly selected Physicians from Malaysia, Taiwan, Philippines, Korea, and Singapore and their postmenopausal women patients with osteoporosis were surveyed. Physicians rated the importance of vitamin D and calcium in osteoporosis management on a scale of 1(not important) to 10 (extremely important) and estimated supplement use by their patients. Patients reported their use of vitamin D and calcium and their perceptions regarding these supplements.

RESULTS: 237 physicians (37 from Malaysia, and 50 each from Taiwan, Philippines, Korea, and Singapore), and 1463 patients (251, 218, 194, 400, and 400 from Malaysia, Taiwan, Philippines, Korea, and Singapore respectively) completed the survey. 84% of patients in Malaysia, 46% in Taiwan, 16% in the Philippines, and 55% each in Singapore and Korea reported never having discussed Vitamin D supplementation with their Physician. Physicians and patients in all countries reported that calcium was discussed more frequently than Vitamin D. Physicians reported that their patients have little knowledge of the relationship between vitamin D and calcium, and this was confirmed by patient responses.

CONCLUSION: Most osteoporosis patients recognize the importance of calcium, but have less awareness of that of Vitamin D. Lack of understanding about the role of Vitamin D and numerous concomitant medications can reduce compliance with Vitamin D supplementation.

Disclosures: J.A. West, Merck 3.

This study received funding from: Merck.

T448

Hyponatremia Induces Bone Loss and Prevents Fat Accumulation in Aged F344 Brown Norway Rats. J. Barsony¹, M. B. Manigrasso*, H. Tam*, A. H. Doshi*, J. G. Verbalis*. ¹Office of the Director, NIH/NIDDK, Bethesda, MD, USA, ²Division of Endocrinology and Metabolism, Georgetown University, Washington, DC, USA.

Chronic hyponatremia is a common abnormality in older people, but long-term pathological effects of this disorder are not well understood. Our recent studies on young rats indicated that hyponatremia is associated with severe osteoporosis. No change in serum parameters of calcium homeostasis and calcium regulating hormones accounted for the bone loss, but the mechanisms involved increased osteoclastogenesis and bone resorption. To better approximate the age of the population most affected by hyponatremia, this study evaluated male F344 Brown Norway hybrid rats (F344BN), a well-known model of aging. We induced hyponatremia for 4.5 months by infusing desmopressin via minipumps (5ng/h) in 22-month-old F344BN rats who were fed a liquid diet enriched with vitamin D and calcium; high dose vitamin D was added during the last 6 weeks to maximize calcium balance. Normonatremic control aged F344BN rats also received

desmopressin, but were fed a solid diet of equivalent composition to the liquid diet. Caloric intake was equalized daily between pairs of hyponatremic and normonatremic rats to allow monitoring the effects of hyponatremia on body composition. Previous reports have shown an inverse relationship between bone mineral density (BMD) and bone marrow fat (BMF) in old rodents and humans and an effect of vitamin D to decrease BMF. We evaluated how hyponatremia changes this relationship via biweekly measurements of BMD, BMF and abdominal fat by DXA. Body weight was similar in both groups before and at the end of the study. As expected, in control aged rats BMD decreased (AP spine -3%, total femur -2%, and proximal tibia -0.7% per month) and BMF increased (AP spine 15%, total femur 8%, and proximal tibia 11% per month) progressively. In hyponatremic rats, BMD decreased at a much higher rate than in the controls during the first 3 months (AP spine -20%, total femur -17.5%, and proximal tibia -20% per month), and BMF remained unchanged at the AP spine, increased only by 8% per month at the total femur and 5% per month at the proximal tibia. During the final 6 weeks on vitamin D injections, BMD did not recover and BMF did not increase in the hyponatremic rats. Abdominal fat increased in the normonatremic group but remained unchanged in the hyponatremic group over the entire study. These findings confirm that hyponatremia induces osteoporosis in aged as well as young rats. Hyponatremia also prevented fat accumulation in aged rats, and eliminated the inverse relationship between BMD and BMF, likely due to induction of Wnt signaling by chronic hyponatremia.

Disclosures: J. Barsony, None.

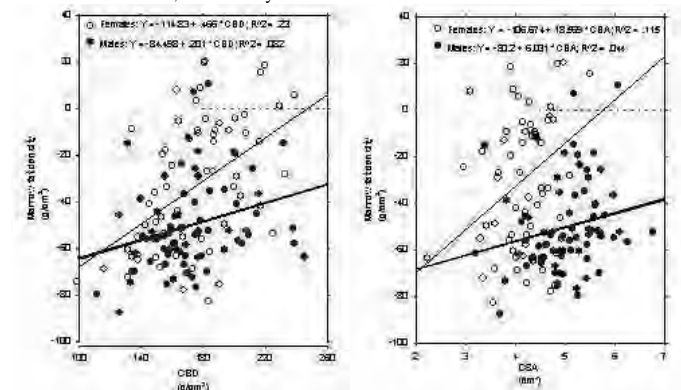
T449

Marrow Fat and Peak Bone Mass. N. Di Iorgi*, F. J. Perez*, D. Lee, T. Wren, V. Gilsanz. Radiology, University of Southern California, Los Angeles, CA, USA.

Recent data suggest that osteoblasts and adipocytes originate from the same mesenchymal stem cells. Our aim was to determine whether there is a reciprocal relation between bone marrow fat and cancellous bone in the axial, and cortical bone in the appendicular, skeleton. To this end, we examined vertebral cancellous bone density (CBD), femoral cortical bone area (CBA), and the density of adipose tissue in the marrow canal at the midshaft of the femurs in 138 young, healthy men and women, 16-25 years of age, using computed tomography (CT) and a reference phantom for calibration. Males were heavier, and had greater values for CBA and marrow fat than females ($P<0.001$). Marrow fat density had strong significant negative relations with cancellous and cortical bone in both males and females; the associations were stronger in females (see diagrams). There was no association between marrow fat and age, weight, BMI and the cross sectional dimensions of vertebral and femoral bone. Our results suggest a link between marrow adiposity and cortical and cancellous bone at or around the time of peak bone mass, supporting the concept that stem cells differentiate into either cell lineage in a mutually exclusive way.

	Males (n=74)	Females (n=64)
Age (yrs)	19.0 ± 1.8	18.9 ± 2.0
Weight (kg)	71.0 ± 12.4	62.0 ± 11.2
BMI	23.8 ± 3.4	23.9 ± 4.2
CBD (mg/cm ³)	172 ± 27	177 ± 29
CBA (cm ²)	5.02 ± .65	4.02 ± .53
Marrow fat (mg/cm ³)*	-50.4 ± 19	-32.0 ± 28

*Values for fat are <0; the arbitrary CT reference ascribed to water.



Disclosures: N. Di Iorgi, None.

This study received funding from: University of Southern California.

T450

Influence of Exercise and Low Dose Oral Contraceptives on Vertebral and Femoral Bone Mass in Young Adult Women. M. Hartard¹, C. Kleinmond^{2*}, M. Wiseman³, D. Felsenberg⁴, R. Erben⁵, E. R. Weissenbacher^{*1}, K. Friesse^{*1}.

¹Department of Gynecology and Obstetrics, Ludwig Maximilians Universität, Munich, Germany, ²Institute of Preventive and Rehabilitative Sports Medicine, Technische Universität München, Munich, Germany, ³Leibniz Data Processing Center, Bavarian Academy of Sciences, Munich, Germany, ⁴Department of Radiology, Freie Universität Berlin, Berlin, Germany, ⁵Department of Natural Sciences, University of Veterinary Medicine, Vienna, Austria.

It was the aim of the present study to explore further the relationship between oral contraceptive (OC) use and exercise in a controlled, open, non-randomized 24-month trial in a group of 71 women aged 25 - 35 years (mean age 28.5 ± 2.7). After discontinuation of OCs for at least 4 months, physical work capacity (PWC), nutrition, exercise history, bone density, bone markers, and hormones were determined on admission and after 24 months. In addition, bone markers were measured 6 months after start of the trial. Women were classified as exercisers (EX) or non-exercisers (NEX) by measurement of relative PWC at a heart rate of 170/min (PWC170/kg) using bicycle ergometry and additionally by a self-report questionnaire. With-out changing exercise behavior, the women had to decide whether or not to use a low dose monophasic OC preparation (30 µg ethinylestradiol and 75 µg gestodene) during the 24-month study period. Thirty-five women decided to use the OC preparation (16 EX and 19 NEX), 36 women served as controls (20 EX and 16 NEX). At baseline, we found no significant differences between the groups in terms of anthropometry, nutrition, BMD, or biochemical bone markers. After 24 months data from 52 women could be analyzed. OC use was associated with increases in serum triglycerides, sex hormone binding globulin, and cortisol, while it decreased serum FSH, estradiol, and progesterone. Serum osteocalcin was lower in OC users at 6 months after start of the trial, while serum bone-specific alkaline phosphatase and urinary deoxypyridinoline excretion remained unchanged. In both the EX control and the EX OC groups spine BMD decreased during our 24-month trial. OC use did not influence hip or spine BMD in non-exercisers. However, OC use induced a 1.8% loss of anterior-posterior vertebral BMD, a 2.6% loss of lateral vertebral BMD, and a 1.4% loss of hip BMD in exercising women over the 24-month study period. Although the latter BMD changes were not significant compared with baseline values, our data add further evidence to the notion that the combination of OC use and exercise may have negative effects on bone mass in young women.

Disclosures: M. Hartard, None.

This study received funding from: Federal Institute of Sports Science of Federal Ministry of the Interior's, VF 0407/01/14/97/98.

T451

Addition of Phosphorous to Cadmium Exacerbate the Compromised BMD Gain in Ovariectomized Rats. S. Hooshmand¹, D. Y. Soung², S. C. Chai¹, E. A. Lucas³, L. Devareddy^{*1}, B. H. Arjmandi¹. ¹Nutrition, Food and Exercise Sciences, Florida State University, Tallahassee, FL, USA, ²Center of Musculoskeletal Research, University of Rochester, Rochester, NY, USA, ³Nutritional Sciences, Oklahoma State University, Stillwater, OK, USA.

Ovariectomized (OVX) rats have been extensively used as a model of postmenopausal bone loss because it is generally believed that rats lose bone mineral density (BMD) as a result of OVX. This decrease in BMD has been linked to the hypothesis that ovarian hormone deficiency causes hypercalcemic suppression of the parathyroids which lead to a decrease in vitamin D synthesis and gut malabsorption of calcium. Data from a number of studies from our laboratory contraindicate this hypothesis and showed that OVX animals not only do not lose bone but rather gain, albeit, to a lesser extent in compression with intact animals. The findings of the present study clearly demonstrate this fact. We used five groups of 3-month old OVX Sprague Dawley rats to examine the time- and dose-dependent deleterious effects of cadmium (Cd) on BMD of whole body and as well as the final femoral and fourth lumbar vertebrae BMD. OVX gained 3.9 and 9.8 % BMD in compression with baseline BMD value after three and six months, respectively. High dose of Cd (200 ppm) completely prevented the gain in BMD. When phosphorous (P) was added to Cd, the harmful effect of Cd on bone was pronouncedly exacerbated. The results indicated that Cd+ 1.2 % P had the most deleterious effect on BMD of these animals and caused 7% bone loss (see table). Accumulation of trace elements such as Cd in soils may be transferred via the food chain to consumers and it may become a public concern. However, their effects on bone have hardly been studied. The results of this study demonstrate that Cd at higher doses completely prevents gain in bone mass and addition of P to Cd causes significant bone loss. Since phosphate fertilizer is a significant source of trace element, especially for Cd, overtime repeated application of fertilizer may lead to a gradual buildup of these elements in agricultural products grown in such a soil and become a public health issue. Hence, this study should be considered an early warning as how big of an issue this problem is.

Disclosures: S. Hooshmand, None.

T452

Bone Mineral Density Declines with Age in Zebrafish (Danio rerio). J. M. Keller, J. F. Escara-Wilke, C. Yu*, E. T. Keller. Urology, University of Michigan, Ann Arbor, MI, USA.

Old age in humans is associated with a decline in bone mineral density (BMD). This age-related decline in bone mass may be associated with pathological conditions such as osteoporosis, frailty, and fractures. We are currently developing the zebrafish (Danio rerio) as a model for study of aging and age-related diseases. As such, we maintain a large colony of approximately 3500 aging zebrafish. The oldest fish in our colony to date are approximately 45 months of age, and the average age of natural death thus far is 32.1 ± 5.6 months. In the course of our studies, we observed various skeletal abnormalities in our fish as they aged. We sought to characterize these changes in our population of zebrafish. Radiographic analysis of young (1 year or less) and old (3 or more years) fish showed marked skeletal changes in the spine of old fish compared to young fish, including scoliosis and kyphosis. Changes in radiodensity of the bones were also seen, suggestive of a change in bone density. This was confirmed by micro-CT analysis, which revealed a marked decrease in BMD in old fish compared to young fish. This decrease was seen in trabecular, cortical, and subcortical bone. The average total BMD in old fish was 74 ± 9 mg/cc compared to 360 ± 48 mg/cc in young fish. To evaluate these changes at the tissue level, we stained for mineral in the bone using von Kossa stain on histological sections from these fish. We found a decrease in bone mineral staining in old compared to young fish. These results suggest that the aging zebrafish may represent a potential model for study of osteoporosis and age-related changes in bone in humans. The zebrafish provides an extensive wealth of resources including informational databases, husbandry methods, and genetic tools, and its genome has recently been sequenced. In addition, there are many similarities between human and zebrafish bones. Like humans, zebrafish bone remodeling involves osteoblasts and osteoclasts and shares many of the same signaling pathways, including BMPs, Runx2, and Wnt pathways. These proteins in zebrafish are orthologous to those in humans and are highly conserved. Many zebrafish skeletal mutants are also being discovered. We therefore propose the zebrafish as a potential model for bone diseases and age-related changes in skeletal structure in humans.

Disclosures: J.M. Keller, None.

T453

Parathyroid Response to Vitamin D Insufficiency: Relations to Bone and Body Composition and to Life Style Characteristics. L. Rejnmark¹, P. Vestergaard¹, C. Brot^{*2}, L. Mosekilde¹. ¹Dept. of Endocrinology and Metabolism C, Aarhus University Hospital, Aarhus, Denmark, ²Osteoporosis Research Centre, Hvidovre Hospital, Copenhagen, Denmark.

Vitamin D insufficiency is very common and is known to cause secondary hyperparathyroidism (SHPT). However, in some subjects the PTH response to low vitamin D levels is blunted, which has been termed functional hypoparathyroidism (FHPT). We studied whether differential PTH responses in women with vitamin D insufficiency are associated with indices of bone metabolism, and body composition.

We studied 1097 recent postmenopausal women recruited from the local background population and identified women with vitamin D insufficiency defined as plasma 25-hydroxyvitamin D (P-25OHD) < 50 nmol/l. Among studied subjects 405 (37%) had vitamin D insufficiency. In women with vitamin D insufficiency, we compared levels of bone turnover markers, bone mineral density (BMD), body composition, body weight, and life style characteristics between subjects with SHPT and FHPT.

P-25OHD levels were slightly higher in SHPT compared with FHPT (p<0.05). SHPT was associated with higher levels of osteocalcin and bone-specific alkaline phosphatase, whereas whole body BMD and hip- and lumbar spine-BMD were significantly reduced (p<0.01). Compared with FHPT, subjects with SHPT had a 7% (p<0.01) higher body weight and a 23% higher fat mass (p<0.01), whereas lean tissue mass did not differ between groups. In SHPT, fat mass was increased by 14% (p < 0.001) at the upper and lower extremities and by 33% (p < 0.001) at the trunk. Lifestyle characteristics differed significantly between groups, as women with SHPT smoked less and consumed less alcohol than those with FHPT. In addition, women with SHPT use of loop diuretics more often than those with FHPT. However, physical activity as well as total energy intake and dietary intake of calcium, magnesium, phosphate, and vitamin D did not differ between groups.

The effects of vitamin D insufficiency on bone seem to be highly dependent on the PTH responses to low vitamin D levels. In patients with primary hyperparathyroidism, an increased body weight has been reported. Similarly, the increased body weight and fat mass in SHPT compared with FHPT during vitamin D insufficiency may suggest that PTH excess contributes to fat accumulation.

Disclosures: L. Rejnmark, None.

T454

Changes in Adiponectin and Leptin Serum Levels in Osteoporotic Postmenopausal Women After Treatment with Raloxifene or Alendronate.

A. Sebastian Ochoa^{*1}, D. Fernández-García^{*1}, R. Reyes García^{*1}, G. Alonso^{*1}, P. Rozas^{*1}, I. Luque^{*1}, B. Torres^{*2}, M. Ruiz-Requena^{*2}, M. Muñoz-Torres¹.

¹Bone Metabolic Unit. Department of Endocrinology, University Hospital San Cecilio, Granada, Spain, ²Biochemist Department, University Hospital San Cecilio, Granada, Spain.

Adipose tissue is considered to be an endocrine organ. Recently, the relation between adiponectin and leptin with bone has been investigated. However, the effect of antiresorptive drugs on these adipokines and their relation with osteoclastogenesis markers have not been studied before.

The aims were to evaluate serum adiponectin and leptin in osteoporotic postmenopausal women and their relation with bone mineral density (BMD) and osteoclastogenesis markers and analyze changes on adiponectin and leptin levels after treatment with raloxifene or alendronate, and their relation with changes in BMD.

We selected fifty-three untreated women (63±7 years) with postmenopausal osteoporosis divided into two groups: women treated with raloxifene (60mg/day; n=20) or alendronate (70 mg/week; n= 33) for one year. We determined at baseline and after 12 months of treatment: anthropometric data, osteoprotegerin (OPG) ultrasensible estradiol (E2), insulin-like growth factor I (IGF-I), adiponectin (HADK1-61K-A, LINCplex), leptin (HADK2-61K-B, LINCplex) and BMD by DEXA (DXA-Hologic QDR 4500) in lumbar spine (LS), femoral neck (FN) and total hip (TH).

At baseline, leptin and adiponectin serum levels of our patients were 1371.4±822.4 pM/ml and 41.47±26.42 µg/ml, respectively. Circulating leptin was related significantly with weight (r:0.42; p<0.01), BMI (r:0.47; p<0.01) and waist (r:0.38, p<0.01), but not with OPG, IGF-1, E2 and BMD in LS, FN and TH. Adiponectin was significantly correlated with age (r:0.38; p:0.012) and OPG levels (r: 0.28; p: 0.04), but not with weight, height, body mass index (BMI), leptin, IGF-1, E2 and BMD in LS, FN and TH. After 12 months, no changes were observed in leptin (p:0.46) and adiponectin (p:0.55) in alendronate group; however, a significant increase in leptin levels (973.47±637.37 pM/ml vs 1305.7±793.4 pM/ml; p:0.031) was detected in the raloxifene group, whereas adiponectin levels showed no significant changes (p:0.46). Moreover, the percentage changes of adiponectin levels did not differ between the two groups (p:0.79); while the percentage changes in leptin levels was different but not significantly, between the two groups (p:0.07).

In conclusion, adiponectin and leptin concentrations do not seem to be consistently related to BMD and osteoclastogenesis markers in patients with postmenopausal osteoporosis. The increase in leptin levels after one year of treatment with raloxifene could be indirectly implicated in raloxifene bone effects.

Disclosures: A. Sebastian Ochoa, None.

T455

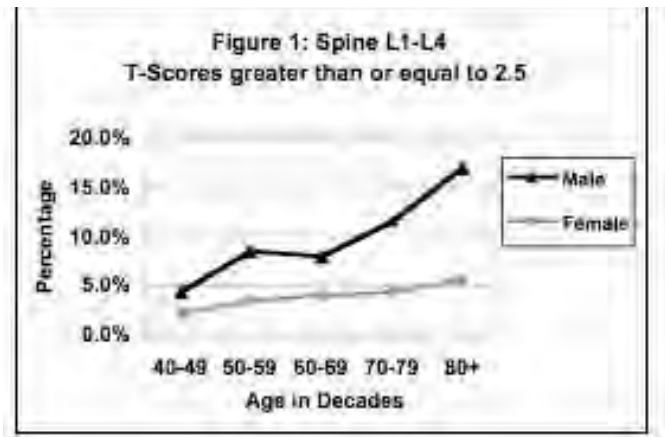
Prevalence of High Bone Mineral Density T-scores in a Community Population. C. Simonelli¹, P. J. Sinner^{*2}, M. C. Schoeller^{*1}. ¹Osteoporosis Care, HealthEast Clinics, Woodbury, MN, USA, ²Research and Education, HealthEast Medical Research Institute, St. Paul, MN, USA.

There is no designated upper limit of normal for bone mineral density (BMD) testing results with DXA, although a number of pathological disease states may be associated with a high BMD and may potentially increase fracture risk. Diseases associated with high BMD include osteopetrosis, Paget's bone disease, hypervitaminosis A or D and fluorosis among others. Genetic causes for high BMD are often diagnosed before adulthood. The purpose of this study was to determine the incidence of BMD T-scores +2.5 or greater (high BMD) in adults by gender, age in decades from 40-80+ and by site of BMD measurement: lumbar spine (LS), femoral neck (FN) and total proximal femur.

BMD testing using the GE Lunar Prodigy densitometer was performed between November 1999 and January 2007 on 8110 females and 549 males referred to an osteoporosis center for BMD testing. Fracture history of the hip, spine and non-hip/non-spine was recorded at the time of the scan. For individuals who may have had multiple scans, the results of the most recent scan were used in this analysis.

High BMD T-scores increased with age at the LS (figure 1), most notably for men, from 4.4% at age 40-49 to 16.9% at age 80+ and in women from 2.2% at age 40-49 to 5.5% at age 80+ consistent with progressive degenerative sclerotic changes artifactually elevating the BMD. Increased BMD T-scores with aging was not seen at the total femur or FN sites for men or women and the incidence of BMD T-scores +2.5 or greater was rare ranging from 0% to 2.2% depending on site and age. Finally, patients with high BMD scores reported fewer fractures at non-hip/non-spine sites compared to patients with a normal T-score of -1.0 to +1.0 (1.3% vs. 6.7%, p-value = 0.06) and patients with high BMD reported fewer fractures at the spine and non-hip/non-spine sites compared to patients with osteoporosis, BMD T-score -2.5 or lower (0% vs. 11.1%, p-value < 0.001 for spine fractures and 1.3% vs. 24.7%, p-value < 0.001 for non-hip/spine sites). There was no difference in hip fracture rates between patients with high, normal or osteoporotic BMD values.

BMD T-score +2.5 or greater at the femur sites is rare, does not increase with aging and appeared to be associated with a decrease in fracture history at non-hip/non-spine sites. Further study of the significance of potentially high BMD and associated disease states is warranted



Disclosures: C. Simonelli, Merck 2, 5, 8; Eli Lilly 2, 8; Novartis 2; Roche/GSK 2, 5, 8.

T456

Osteoarthritis of Knee Decreases Regional and Total Bone Mineral Density in Japanese Women. S. Takata, A. Abbaspour^{*}, S. Nakano^{*}, Y. Kawasaki^{*}, K. Yukata^{*}, N. Yasui^{*}. Orthopedics, Institute of Health Biosciences, The University of Tokushima, Tokushima, Japan.

We studied the effects of osteoarthritis (OA) of knee on total and regional bone mineral density (BMD) in Japanese women. Two hundred and fifteen patients were divided into four groups: patients with knee OA group (knee OA group, n=37), group of normal level of mean BMD of the 2nd and 4th lumbar vertebrae (L2-4BMD) group (normal group, n=53), group of osteopenia level of L2-4BMD (osteopenia group, n=63), group of osteoporosis level of L2-4BMD (osteoporosis group, n=62). No significant differences were found between the four groups with regard to age, height, weight and BMI. Regional and total BMD were measured by dual energy X-ray absorptiometry using a Hologic QDR 2000 (Waltham, MA, USA). The regional BMD were measured in the head, arms, legs, ribs, thoracic vertebrae, lumbar vertebrae and pelvis. BMD was statistically compared among four groups. L2-4BMD of knee OA group was significantly smaller than that of normal group (p=0.0006). L2-4BMD of knee OA group was significantly greater than that of osteopenia group (p=0.0001). Total BMD of knee OA group was significantly smaller than that of normal group (p=0.0058). There was no significant difference of total BMD between knee OA and osteopenia groups (p=0.1778). Leg BMD of knee OA group was significantly smaller than that of normal group (p=0.0002). There was no significant difference of leg BMD between knee OA and osteopenia groups (p=0.2536). The results showed that L2-4BMD, leg and total BMD of knee OA group were significantly smaller than those of normal group, and suggest that knee OA affects bone mineral metabolism to decrease regional and total BMD.

Disclosures: S. Takata, None.

T457

A Negative Impact of Caloric Restriction on the Bone Mineral Density: An Involvement of Suppression of Growth Hormone-IGF-1 Signaling. M. Tomita¹, S. Motokawa^{*2}, H. Shindo^{*1}, I. Shimokawa^{*3}. ¹Orthopedic Surgery, Nagasaki University Graduate School of Biomedical Sciences, Nagasaki, Japan, ²Orthopedic Surgery, National Nagasaki Medical Center, Ohmura, Japan, ³Investigative Pathology, Nagasaki University Graduate School of Biomedical Sciences, Nagasaki, Japan.

Objective: Bone mineral density (BMD) decreases with age. Caloric restriction (CR) suppresses several aging-dependent changes and diseases, and expands the longevity of the rodent. Growth hormone (GH) and insulin-like growth factor 1 (IGF-1) secretions decrease with age; however, the suppressed GH-IGF-1 signaling also leads to increased lifespan. In this study, we investigated the effects of CR and suppression of GH secretion on the aging change of BMD.

Materials and Methods: We used wild type (WT) male Wistar rats and the transgenic rat strain (mini), in which GH secretion was suppressed by overexpression of anti-sense GH gene. F1 hybrid rats (F1), which showed intermediate phenotypes in the GH-IGF-1 level and body weight between WT and mini rats, were also used. From 6 weeks of age, rats were divided into two groups: group AL rats continued to receive food ad libitum, whereas group CR rats were restricted food intake 70% of those for group AL. Rats were sacrificed at 6, 15, and 24 months of age (mo). Femoral BMD's were measured by pQCT.

Results: 1) The BMD of cortical bone did not differ among WT, F1, and mini rats.

2) The BMD of cancellous bone decreased with age in all groups. The cancellous bone BMD in CR group was lower than AL group in WT, F1, and mini rats at any age. The cancellous bone BMD was lower in the following order; mini, F1, and WT rats respectively.

3) F1-AL and WT-CR showed similar cancellous bone BMD on 6, 15, and 24 mo.

Discussion: CR exhibited a negative impact on the cancellous bone BMD. Similarity of phenotypes between CR and the transgenic rats suggest an involvement of GH-IGF-1 signaling in the impact of CR. It should be, therefore, cautious when we apply CR or suppression of GH-IGF-1 signaling as an anti-aging intervention in human.

Disclosures: M. Tomita, None.

T458

Relative Contribution of Body Composition to Bone Mineral Density in Young Chinese and Caucasians. X. Wang*, Y. Duan*, A. Evans*, E. Seeman. Endocrine Centre, Austin Health, University of Melbourne, West Heidelberg, VIC, Australia.

To investigate the racial differences in the relationship of body composition and bone mineral density we studied 258 healthy Chinese (182 females) and 391 Caucasians (282 females) aged 18-45 years living in Melbourne. Body mass index (BMI) was calculated using weight/height². Total body bone mineral density (TBBMD), total fat mass, and lean body mass (LBM) were measured by dual energy X-ray absorptiometry (DXA, Lunar, DPX-L) total body scan.

At peak, Chinese had a 4.7-6.5% lower BMI, 14.9-22.9% lower total fat mass and 10.2-12.2% lower LBM than Caucasians in both sexes. There was no racial difference in TBBMD between Chinese and Caucasian women, while TBBMD was 3.1% lesser in Chinese than Caucasians men. Using Pearson correlation test, BMI, total fat mass and LBM had a positive correlation with TBBMD in both races. Moreover, in women, BMI ($r_{\text{Chinese}} = 0.54$ vs. $r_{\text{Caucasian}} = 0.29$, $p < 0.01$) and total fat mass ($r_{\text{Chinese}} = 0.50$ vs. $r_{\text{Caucasian}} = 0.26$, $p < 0.01$) were more highly correlated with TBBMD in Chinese than Caucasians. There was no racial difference in the correlation of LBM and TBBMD between Chinese and Caucasian women ($r_{\text{Chinese}} = 0.38$ vs. $r_{\text{Caucasian}} = 0.23$, $p = 0.08$). For men, there were no racial differences in the correlation of BMI ($r_{\text{Chinese men}} = 0.50$ vs. $r_{\text{Caucasian men}} = 0.31$, $p = 0.12$), total fat mass, and LBM with TBBMD between Chinese and Caucasians. Partial correlation was used to further explore independent correlations between total fat mass or LBM and TBBMD. The correlation coefficient for BMI and TBBMD diminished controlling for total fat mass and age more than controlling for LBM and age in Chinese and Caucasian women. In men, the partial correlation decreased further controlling for LBM and age than controlling for total fat mass and age in both races.

In conclusion, TBBMD was related to BMI, total fat mass and LBM in young women and men in both Chinese and Caucasians. The racial differences in the correlation of BMI, total fat mass and TBBMD was found in women only. In both races, fat mass had more influence on the TBBMD in young women. However, LBM was more related to TBBMD in young men in both races.

Disclosures: X. Wang, None.

This study received funding from: Australia NHMRC.

T459

Age-related Changes in Vertebral Trabecular Architecture in Female Japanese Macaques. S. C. Agarwal¹, P. Beauchesne*, A. Burghardt², Y. Hamada*, S. Majumdar². ¹Anthropology, University of California, Berkeley, CA, USA, ²Musculoskeletal Quantitative Imaging Research Group, University of California San Francisco, San Francisco, CA, USA, ³Primate Research Institute, Kyoto University, Inuyama, Japan.

There have been few studies of age and sex-related changes in trabecular microarchitecture in nonhuman primates. This study investigates age-related patterns in vertebral trabecular architecture in female Japanese macaques. A total of 30 seventh lumbar vertebrae were selected from adult (age 8-32 yrs.) female Macaca fuscata skeletons with known age and life history variables (such as parity, diet, activity) housed at the Primate Research Institute, Kyoto University, Japan, for a pilot investigation of trabecular microarchitecture using High Resolution Peripheral Quantitative Computed Tomography (HR-pQCT) (XtremeCT, Scanco Medical AG, Bassersdorf, Switzerland). Individuals were categorized into three broad age groups: young (8-13 yrs), middle (14-19 yrs), and old (20+ years), and a mid-coronal area of the vertebral body was scanned to examine bone mineral density, bone connectivity, anisotropy, and classic histomorphometric parameters (bone volume BV/TV, trabecular number Tb.N, thickness Tb.Th, separation Tb.Sp) (scan parameters are as follows: 41µm isotropic voxels, 220 slices spanning 9.02mm, 200ms integration time per angle, 1000 angles over 180degrees, source: 60kVp, 900µA). Significant differences in female connectivity density, and related trabecular histomorphometric parameters (Tb.N, Tb.Th, Tb.Sp) were found between the oldest and younger age groups (ANOVA, $p < 0.05$), while no significant differences in age groups is seen with bone mineral density or bone volume. Further, age related-patterns in trabecular architecture also seem to be related to life history variables, and we hypothesize that reproductive variables such as parity may also be playing a role in age-related bone changes. The age-related patterns seen in the female macaque are similar to those seen in human females and offer a valuable model to examine the effect of age, as well life history variables on the female skeleton.

Disclosures: S.C. Agarwal, None.

This study received funding from: COR UC Berkeley Grant, Stahl Fund ARF UC Berkeley.

T460

Differences in Regional Femoral Neck Cortical Thickness with Aging: Implications for Hip Fracture Risk. S. Amin, E. J. Atkinson*, J. Camp*, R. Robb*, L. J. Melton, B. L. Riggs, S. Khosla. Mayo Clinic, Rochester, MN, USA.

Cadaveric studies suggest there are age-related differences in regional femoral neck [FN] cortical thickness [CTH], reflecting an adaptive effect of habitual loading, yet which may be maladaptive to loads during a fall, contributing to fracture susceptibility. Regional FN CTH in an in vivo aging cohort has not been described. In an age- and sex-stratified

random sample of the population, we determined the CTH at four quadrants of the FN (posterior [P], superior [S], anterior [A], inferior [I]), assessed by QCT. We examined for regional differences in CTH by age and explored how observations could be explained by physical activity level (a surrogate for habitual loading) or serum bioavailable estradiol [bio E₂].

Following exclusion of individuals on bisphosphonates or hormone replacement, we studied 304 men (age range: 23-93 y) and 260 women (range: 21-97 y) and created 3 age-groups: young (20-39 y), mid-age (40-59 y) and old (≥ 60 y). In a linear mixed effects model, accounting for correlations from having multiple measurements per subject, we examined the differences in CTH for each quadrant, relative to the [I] quadrant, among age groups. Men and women were analyzed separately.

Age Groups	Men			Women		
	Young	Mid	Old	Young	Mid	Old
N	75	96	133	71	83	106
Age (y)	32	50	75	32	49	74
Bio E ₂ (pg/ml)	15.0	12.5	9.1	25.7	18.6	4.5
Phys Act (kcal x 10 ⁻²)	422	385	313	308	299	254
Total FN CTH (mm)	2.97	2.89	2.72*	2.99	2.91	2.68*
P CTH	2.77	2.76	2.51*	2.80	2.70	2.40*
S CTH	3.00	2.66*	2.49*	2.90	2.58*	2.19*
A CTH	2.77	2.65	2.42*	2.63	2.61	2.39*
I CTH	3.32	3.48	3.45	3.62	3.74	3.78
FN CTH Differences:						
P-I	-0.55	-0.73	-0.94*	-0.83	-1.04	-1.38*
S-I	-0.33	-0.83*	-0.96*	-0.72	-1.16*	-1.59*
A-I	-0.55	-0.83*	-1.03*	-0.99	-1.13	-1.39*

* $p < 0.05$ relative to young age-group; mean values reported in table

In both sexes, FN CTH was thickest inferiorly and did not change with age. In other quadrants, CTH decreased with age, especially superiorly, and more so in women (see table). In both sexes, within the mid-age group only, greater activity was associated with greater CTH in all quadrants ($r = 0.24$ to 0.45 , $p < 0.05$). In the oldest group, lower bio E₂ was associated with decreased CTH in both sexes, but not significantly at [I] FN (for P, S, A and I, respectively: $r = 0.26^*$, 0.24^* , 0.27^* , 0.11 , for men; and $r = 0.44^*$, 0.18 , 0.24^* , 0.15 , for women; $*p < 0.05$). In this group, greater activity was associated with greater [I] CTH in men ($r = 0.26$, $p < 0.05$), but not women ($r = 0.10$).

Physical activity may help to maintain FN CTH in all quadrants with aging, however, with advancing age, low bio E₂ may have a dominant effect at thinning the FN cortex, likely through enhanced endocortical resorption. We hypothesize that the [I] quadrant may be relatively spared from this effect due to the compressive loads related to habitual activity, but requires further exploration. High compressive loads acting on [S] FN at fall impact may be more likely to cause fracture when there is greater relative thinning of [S] to [I] FN cortex, as is seen with aging, and especially women.

Disclosures: S. Amin, Merck&Co. 5.

This study received funding from: NIH.

T461

Increased Age and a Rod-Like Trabecular Architecture Are Independently Associated with Accumulation of Microdamage in Human Vertebral Trabecular Bone. M. E. Arlot¹, B. Burt-Pichat*, J. P. Roux*, D. Vashishth¹, M. L. Bouxsein², P. D. Delmas¹. ¹INSERM Unit 831, Université de Lyon, Lyon Cedex 08, France, ²Beth Israel Deaconess Medical Center, Boston, MA, USA.

It has been hypothesized that age-related accumulation of unrepaired microdamage may contribute to skeletal fragility. However, limited information is available on microdamage accumulation in human vertebral bone and its relationship with architecture - a key index of bone quality. We studied 23 human L2 vertebral bodies from cadaveric donors (53 to 93 yrs; 15 females and 8 males; Mean = 76 ± 12 yrs). After bulk-staining with xylenol, cores, oriented in the supero-inferior direction, were obtained from the anterior region of the vertebrae and subjected to 3D microCT analyses (μ CT40, Scanco Medical). Measured parameters included bone volume/tissue volume (BV/TV; %), trabecular number (Tb.N), thickness and separation (Tb.Sp), structure model index (SMI), connectivity density and degree of anisotropy. Three 100-micron thick longitudinal sections, obtained from the cores, were used to quantify microdamage. Crack density (Cr Dens) (#/mm²), length (mm) and diffuse damage area (mm²) were measured under UV light and confirmed with confocal laser microscopy. Mean Cr Dens and length were 1.01 ± 0.76 mm² and 70 ± 20 microns, respectively, whereas the mean diffuse damage area was 1267 ± 996 microns². There was no significant difference between sexes, but women tended to have a higher Cr Dens than men (1.21 ± 0.08 vs. 0.65 ± 0.54 , respectively). Cr Dens increased exponentially with age ($r = 0.64$; $p < 0.001$). Cr Dens was negatively associated with BV/TV ($r = -0.55$; $p < 0.01$), Tb.N ($r = -0.56$ $p = 0.008$), SMI ($r = -0.59$; $p = 0.005$) and positively associated with Tb.Sp ($r = 0.59$; $p < 0.009$). As expected all architecture parameters were strongly correlated with each other, and with BV/TV, in particular SMI vs BV/TV ($r = -0.80$; $p < 0.0001$). Stepwise regression demonstrated that SMI, a measure of the relative prevalence of rods vs plates in trabecular bone, was the only parameter predicting Cr dens independent of BV/TV, BMD, BMC and all other architectural parameters. SMI explained 35% of the variance of Cr Dens ($p < 0.005$), independently of age. In conclusion, our study demonstrated that Cr Dens exponentially increased with age in the trabecular bone of elderly human L2 vertebrae, and that the major architectural risk factor for the accumulation of microcracks was the presence of rod-like structures, as estimated by μ CT-based SMI measurements.

Disclosures: M.E. Arlot, Eli Lilly 2.

T462

Comparison of Early-stage Immobilization and Estrogen-deficiency Induced Bone Loss in Rats Assessed by In Vivo Micro-CT. J. Brouwers*, E. Lambers*, B. van Rietbergen, R. Huiskes*. Technische Universiteit Eindhoven, Eindhoven, The Netherlands.

Osteoporosis can be caused by estrogen-deficiency and by long-term immobilization. While cross-sectional studies have investigated both types of bone loss, the exact pathway of bone loss has not been compared. Therefore, our purpose was to compare early-stage bone loss in immobilization and estrogen-deficiency induced osteoporosis assessed by in vivo micro-CT. 6-month old virgin Wistar rats were divided into an ovariectomy (OVX, n=8) and a sciatic neurectomy (NX, n=8) group. Proximal tibiae were scanned (Scanco vivaCT 40) with a 15 µm resolution at week 0, 1, 2, 3. Bone structural parameters (bone volume fraction (BV/TV), connectivity density (Conn.D), structure model index (SMI), trabecular number, thickness and spacing (Tb.N, Tb.Th, Tb.Sp)) were determined in the metaphysis. A student t-test was performed at week 3 to compare the structural parameters. Also, a repeated measures was done on all measurements to determine differences in response over time between the two treatments. Both the NX and OVX group already showed significant reductions in BV/TV, Conn.D and Tb.Th and an increase in SMI one week post-operatively. The OVX group also showed a reduced Tb.N at week 1, while in the NX group, it had significantly decreased at week 2. Tb.Sp was significantly increased in both groups at week 2. Bone loss was similar in both groups at week 1, while after that, bone loss became more severe in the NX groups at week 2 and 3. After three weeks, BV/TV, Conn.D and Tb.Th were significantly lower and SMI was significantly lower in the NX compared to the OVX group, based on a repeated measures ANOVA done on all measurements and a student t-test done at week 3. Both ovariectomy and immobilization led to rapid, significant changes in all structural parameters within three weeks. The loss of bone and microstructure was similar at week 1 in both groups while the immobilized rats showed a more deteriorated bone microstructure at week 3 than the ovariectomized rats, indicating that the extent and time-course in early-stage bone loss may vary slightly in both osteoporosis types.

Disclosures: J. Brouwers, None.

This study received funding from: Netherlands Organisation for Scientific Research.

T463

Influence of Menarcheal Age on Microstructural Constituents of Distal Tibia in 20 Years Old Women and their Middle-aged Mothers. T. Chevalley¹, S. Ferrari¹, D. Hans², J. P. Bonjour¹, R. Rizzoli¹. ¹Service of Bone Diseases, Department of Rehabilitation and Geriatrics, Geneva University Hospitals, Switzerland, ²Service of Nuclear Medicine, Department of Radiology, Geneva University Hospitals, Switzerland.

Late menarche is a risk factor for fragility fractures, probably by permanently affecting bone structural components so that pubertal-timing dependent alterations persist from peak bone mass to menopause time attainment. We have studied the influence of menarcheal age (MENA) on areal bone mineral density (aBMD) and bone microstructure in healthy young adult daughters (YAD, 20.4±0.6 (±SD), yrs n=124) and, simultaneously, in their middle-aged mothers (MAM, 50.7±4.1 yrs, n=102). We measured aBMD by DXA at femoral neck (FN) and volumetric bone density and microstructure at distal tibia by non-invasive high resolution peripheral computerized tomography (XtremeCT, Scanco medical AG[®], CH) including: total (Dtot), cortical (Dcort) and trabecular (Dtrab) bone density; trabecular bone volume fraction (BV/TV), trabecular number (TbN), mean cortical thickness (Cth) and cross-sectional area (CSA). Mother-daughters MENA were significantly correlated (R=0.30, p<0.01). Median of MENA, were 12.9 and 13.3 yrs, in YAD and MAM, respectively. FN aBMD was inversely related to MENA in both YAD (R=-0.20, p=0.027) and MAM (R=-0.27, p=0.007). In distal tibia a significant inverse relationship was observed in both YAD and MAM between MENA and Dtot (R=-0.26, p=0.004 and R=-0.22, 0.030, respectively), Dcort (R=-0.21, p=0.023 and R=-0.21, p=0.034), and Cth (R=-0.21, p=0.022 and R=-0.19, p=0.058). In contrast, there was a positive relationship between MENA and CSA (mm², R=0.25, p=0.011) in MAM and a trend in YAD. In MAM these significant relationships were independent of years since menopause. The values below and above the median of MENA in YAD and MAM were as follows:

	Mean(SD). *p<0.0001, #p=0.002, \$p=0.016 by Anova			
	YAD Early	YAD Late	MAM Early	MAM Late
FN aBMD (mg/cm ³)	878(97)	838(116)	799(128)	744(89)*
Dtot (mgHA/cm ³)	334(46)	314(51)	308(50)	276(56)*
Dcort (mgHA/cm ³)	934(29)	924(32)	924(43)	904(54)#
Dtrab (mgHA/cm ³)	185(32)	176(31)	161(39)	142(36)*
BV/TV (%)	15.4(2.7)	14.6(2.6)	13.4(3.3)	11.9(3.0)*
TbN (mm ⁻¹)	1.94(0.28)	1.85(0.30)	1.80(0.38)	1.71(0.30)#
Cth (µm)	1214(203)	1163(231)	1165(174)	1082(241)\$

In conclusion, late menarcheal age has a negative influence not only on femoral neck aBMD, but also on several microstructural elements at distal tibia. This influence of pubertal timing on both bone mass and microstructure, as already observed at 20 yrs of age is clearly expressed 30 yrs later at the time of menopause attainment. Alterations in both bone mass and microstructural components could explain the increased risk of fragility fractures associated with menarcheal age.

Disclosures: T. Chevalley, None.

T464

The Effect of Age on Bone Mass and Bone Material Properties in C57BL/6 Mice. J. G. Hofstaetter¹, D. C. Jones^{*2}, M. Wein^{*2}, M. J. Glimcher³, L. H. Glimcher^{*2}, K. Klaushofer⁴, P. Roschger⁴. ¹Ludwig Boltzmann Institute of Osteology at the Hanusch Hospital of WGKK and AUVA Trauma Centre Meidling and Department of Orthopaedics, Medical University of Vienna, Vienna, Austria, ²Department of Immunology and Infectious Diseases, Harvard School of Public Health, Boston, MA, USA, ³Laboratory for the Study of Skeletal Disorders and Rehabilitation, Department of Orthopaedic Surgery, Harvard Medical School and Children's Hospital, Boston, MA, USA, ⁴Ludwig Boltzmann Institute of Osteology at the Hanusch Hospital of WGKK and AUVA Trauma Centre Meidling, 4th Medical Dept., Hanusch Hospital, Vienna, Austria.

Little is known about the effects of age on material properties of normal bone. The purpose of this study was to study bone material quality in young and aged normal mice. We used quantitative backscattered electron imaging (qBEI) to determine Bone Mineral Density Distribution (BMDD) as well as histomorphometry of the metaphyseal trabecular and compact cortical bone of the distal femur in 6-week, 4 and 18 months old male and female (n = 6, each) C57BL/6 mice. At 4 and 18 months of age a significant loss of bone mass was observed in the metaphyseal region (-57.1%, p<0.005 and -62.5%, p<0.005, respectively) when compared to 6 week old animals with significantly altered microarchitecture. However, BMDD parameters such as the degree of mineralization (CaMean and CaPeak), the heterogeneity of mineralization (CaWidth) as well as the amount of low mineralized bone (CaLow) remained constant with age. In contrast, in cortical bone the peak values for cortical width and cross-sectional area were seen at the age of 4 months. Interestingly, an age-dependent increase in the degree of mineralization of cortical bone was seen (+4.84%, p<0.05 and +6.77%, p<0.05) at 4 and 18 months when compared to 6 weeks, while CaWidth and CaLow did not show significant changes. Our data showed that despite a significant loss of trabecular bone mass in the metaphyseal region with age in C57BL/6 mice, the intrinsic bone material properties as determined by qBEI remain constant with age. However, cortical bone showed an age-associated increase in the degree of mineralization with altered bone geometry. This may indicate that ageing has differential effects on average cortical and trabecular tissue age and thus on bone material properties.

Disclosures: J.G. Hofstaetter, None.

T465

Three-dimensional In Vivo Trabecular Microstructure Analysis of Spine, Calcaneus, and Femoral Head/Neck/Trochanter in Japanese Postmenopausal Women. M. Ito, M. Uetani*. Radiology, Nagasaki University, Nagasaki, Japan.

Several animal studies using micro-CT have demonstrated that analysis of trabecular microstructure is useful for the assessment of bone strength and efficacy of anti-osteoporotic agents. We have successfully applied multi-slice CT for the clinical assessment of trabecular microstructure in axial skeleton, and demonstrated its potential utility (JBMR 2005). In this study we investigated trabecular microstructure in five different bone sites and their age-related changes for future clinical application. The femoral head (HEAD)/neck (NECK)/trochanter (TROCH), spine (SPINE) and calcaneus (HEEL) were scanned by CT (Aquilion, Toshiba) at spatial resolutions of approximately 200 microns. The calculated 3D microstructure indices included apparent BV/TV (appBV/TV), appTb.Th, appTb.N, appTb.Sp, fractal dimension (FD), Euler number (E), trabecular bone pattern factor (TbPF), structure model index (SMI), and degree of anisotropy (DA). BMD was measured by DXA and QCT. Data for femur and spine/heel were obtained from 67 (50-83 years old) and 65 post-menopausal women (47-82), respectively. For each site, 17 (75.3±6.5) and 32 women (68.1±4.7) with vertebral fracture and their respective age-matched controls without fracture were compared. The study protocol was approved by the ethical committee of Nagasaki University. The results indicate the microstructure parameters in NECK significantly correlated with QCT at the same bone sites, but not with DXA. Those in SPINE had significant correlations with spine QCT/DXA, and FD, E, and SMI with heel DXA. QCT/DXA had no significant correlation with age, except for spine QCT, whereas most microstructural parameters in NECK, TROCH, SPINE (appBV/TV, Tb.N, Tb.Sp and E in all 3 sites, FD in NECK and SPINE, SMI in SPINE, and appTb.Th in TROCH) had significant correlations with age. HEAD microstructure was well constructed with minimal age-related changes, whereas that in TROCH was poorly constructed with clear-cut age-related declines and large variations among individuals. Plate-to-plate transformation was mainly observed in HEAD, rod-to-rod in TROCH, and plate-to-rod in NECK and SPINE. Measurement reproducibility was poor in TROCH and HEEL. In addition to BMD, significant differences were observed between fracture and non-fracture cases in most microstructure indices in SPINE, appTb.N and Tb.Sp in NECK, BV/TV, FD and SMI in TROCH. In conclusion, using CT, much greater age-related changes in microstructure than BMD have been documented, especially appBV/TV, Tb.N and Tb.Sp. Substantial site-dependent variations in microstructure are found, and the spine and femoral neck are recommended sites for microstructural analysis to assess fracture risk and drug efficacy.

Disclosures: M. Ito, None.

T466

Long-Distance Runners Have Greater Cortical Thickness of Distal Tibia but not of Distal Radius. X. Martin^{*1}, N. Farpour-Lambert^{*2}, T. Chevalley¹, R. E. Rizzoli¹. ¹Rehabilitation & Geriatrics, University Hospital, Geneva, Switzerland, ²Pediatrics, University Hospital, Geneva, Switzerland.

Bone repeated loading, such as in long distance runners, is associated with increased bone mineral density. Whether bone structure is altered in runners, in relation to weight bearing skeletal site and sex, is not well established. We investigated femoral neck (FN) and total hip (Hip) areal BMD, using DXA, as well as cross-sectional area (CSA), cortical thickness (CTh) and density, relative cancellous bone volume (BV/TV), trabecular number, thickness and spacing, using high resolution computerized tomography (Xtrem-CT, Scanco, Switzerland) at the level of distal tibia and distal radius, weight bearing and non-weight bearing skeletal sites, respectively, in long distance runners (> 5 hours per week, quantified by accelerometry (MTI/CSA Actigraph)) of both sexes. We recruited 76 young women (15 runners and 61 sedentary controls, mean age \pm SD 25.1 \pm 7.6 and 20.9 \pm 2.0 years, respectively), and 56 men (31 runners and 25 controls, 26.5 \pm 3.7 and 26.9 \pm 3.8 years, respectively). Despite similar levels of physical activity as recorded with an accelerometer, in the runners of both sexes, FN and Hip areal BMD was significantly higher in males runners than in sedentary controls (FN: 1.105 \pm 0.124 vs 0.915 \pm 0.138, $p < 0.05$; Hip: 1.117 \pm 0.120 vs 1.043 \pm 0.122, $p < 0.05$), but there was no difference in females. Adjusted for the sex differences, distal tibia CTh was higher in runners than in controls ($p = 0.013$). For CSA and BV/TV, the significance was $p = 0.074$ and $p = 0.067$, respectively. At the distal radius, all structural variables were higher in males than in females, irrespective of running, which did not influence at all the values of this non weight bearing site. CTh was not anymore different between runners and controls when adjusted for sex, FN or Hip BMD. In conclusion, repeated loading, like in long distance runners, was associated with higher proximal femur areal BMD in males, and higher sex-adjusted distal tibia cortical thickness. The latter difference disappeared after adjustment for BMD variables, suggesting that running-modified cortical thickness is a component captured in the measurement of areal BMD.

Disclosures: R.E. Rizzoli, None.

This study received funding from: Swiss Federal Office for Education and Sciences.

T467

Association between FSH and Bone Mass in Postmenopausal Women. K. H. Baek^{*1}, M. I. Kang¹, K. W. Oh^{*2}, J. H. Han¹, S. S. Lee^{*1}, H. S. Kim^{*1}. ¹The Catholic University of Korea, College of Medicine, Seoul, Republic of Korea, ²Sungkyunkwan University, School of Medicine, Seoul, Republic of Korea.

Diminished ovarian function and drop in estrogen levels have long been considered the cause of bone loss. Recently, it has been reported that the pituitary hormone follicle stimulating hormone (FSH), previously thought to target only the gonads, also acts on osteoclasts to activate bone resorption. In conjunction with genetic studies, these data raise the possibility that FSH, independent of estrogen, causes hypogonadal bone loss.

In this cross-sectional study, we investigated the association between the serum levels of FSH and either the bone turnover markers or bone mineral density (BMD) in 160 postmenopausal women (68.6 \pm 5.4 years, 57 to 84 years, BMI 24.4 \pm 2.8 kg/m²). Mean \pm SD years since menopause (YSM) was 18.9 \pm 7.0 years and fragility fracture was noted in 39 subjects (24.4%). Inclusion criteria were cessation of menses for at least 5 years, and no previous hormone replacement therapy. Women with liver or renal disease or endocrine or metabolic abnormalities or inflammatory diseases and/or receiving medicine known to influence bone mineralization were excluded. The FSH and biochemical markers of bone turnover (bone ALP, ICTP) were measured from the serum collected at morning. Areal BMD of lumbar spine, total hip, femoral neck, and trochanter were measured by dual energy X-ray absorptiometry.

The mean \pm SD concentrations of bone ALP and ICTP were 36.1 \pm 16.5 U/L (11.9 - 83.9) and 4.6 \pm 0.9 ng/ml (2.8 - 7.7), respectively. The median FSH concentration was 61.3 IU/L with the 25th and 75th percentiles being 42.9 and 75.2 IU/L, respectively. Partial correlation analysis after adjustment for age, BMI, and YSM revealed that FSH concentrations were not correlated with levels of bone turnover markers or BMD at any site. When categorized the subjects into four levels, we also did not find any statistically significant differences in age, BMI, YSM, prevalence of fracture, mean levels of bone turnover markers and BMD at four sites in the FSH quartiles. These findings suggest that FSH is not associated with increased bone resorption and low bone mass in healthy postmenopausal women.

Disclosures: K.H. Baek, None.

T468

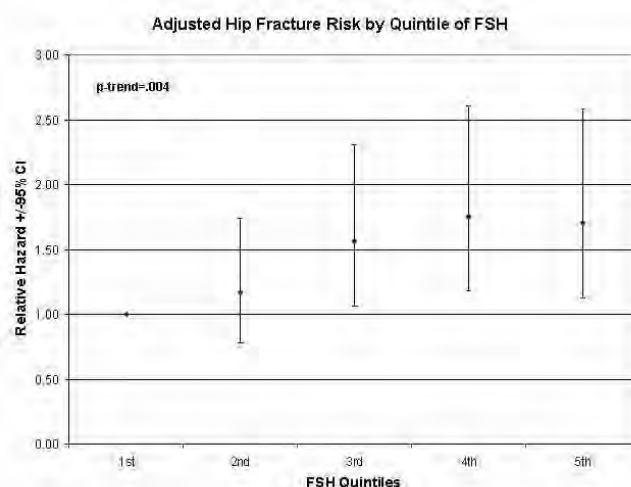
Elevated FSH Predicts Increased Hip Fracture Risk: The Study of Osteoporotic Fractures. D. C. Bauer¹, S. L. Harrison², P. Garnero³, K. E. Ensrud⁴, J. A. Cauley⁵. ¹UCSF, San Francisco, CA, USA, ²CPMC Research Institute, San Francisco, CA, USA, ³Synarc, Lyon, France, ⁴University of Minnesota, Minneapolis, MN, USA, ⁵University of Pittsburgh, Pittsburgh, PA, USA.

Levels of follicle-stimulating hormone (FSH) increase among postmenopausal women in response to estrogen deficiency, and recent rodent studies suggest FSH may regulate bone mass via a direct effect on osteoclasts. The relationship between FSH and fracture risk is unknown.

We performed a nested case-cohort analysis within the Study of Osteoporotic Fractures (SOF) to determine if FSH levels were associated with bone turnover, bone loss or hip fracture risk. At the 2nd SOF visit (V2), hip DXA (Hologic QDR2000) was measured and non-fasting serum was archived at -190C (N = 8070). Repeat hip DXA was obtained at the 4th visit after a mean follow-up of 3.5 yr. 726 women had documented hip fractures after V2 (mean follow-up of 10.0 yr). After excluding women who reported hormone replacement therapy, we used V2 serum to measure FSH (Beckman Coulter) and PINP (Roche Diagnostics) in 706 women with hip fracture and 607 randomly selected women. Bone loss (in the randomly selected women) and fracture outcomes were examined in multivariate regression and hazard models adjusted for age, BMI, total hip BMD, prior fracture and chair stands.

Compared to women without fracture, those with hip fracture were significantly older (75.7 yr vs. 73.3), lighter (63.4 kg vs. 66.5), performed 5 chair stands more slowly (13.0 sec vs. 12.4) and had lower total hip BMD (0.68 gm/cm² vs. 0.75). Mean (\pm SD) FSH was higher among women with hip fracture (90.7 \pm 33.1 IU/L vs. 80.7 \pm 32.0, $p < 0.001$), but PINP levels were similar (56.3 ng/mL vs. 55.4, $p = 0.57$). After full adjustment, each SD increase in FSH was associated with a 26% increase (95% CI: 10, 45) in hip fracture risk, and fracture risk was nearly 2-fold higher (Figure) among those in the two highest quintiles of FSH (>89 IU/L) compared to those in the lowest quintile (<60.3 IU/L). PINP and FSH were weakly correlated ($r = 0.06$, $p = 0.03$) and further adjustment for PINP did not alter the relationship between FSH and hip fracture. FSH was not associated with bone loss ($p = 0.27$).

We conclude that higher levels of FSH are associated with increased hip fracture risk in older women. FSH is not strongly associated with bone turnover or bone loss in this cohort. Ongoing analyses will determine if the effect of FSH on hip fracture risk is independent of sex hormone levels.



Disclosures: D.C. Bauer, None.

This study received funding from: NIAMS.

T469

Angiotensin Converting Enzyme (ACE) Inhibitor Use Is Not Associated with Serum Concentrations of Bone Related Hormones in Older Men. T. Kwok¹, C. Ho^{*2}, P. Leung^{*3}. ¹Medicine & Therapeutics, The Chinese University of Hong Kong, New Territories, Hong Kong, ²Chemical Pathology, The Chinese University of Hong Kong, New Territories, Hong Kong, ³Jockey Club Centre for Osteoporosis Care and Control, The Chinese University of Hong Kong, New Territories, Hong Kong.

Purpose - Intake of ACE inhibitors has been found to be associated with greater bone mineral density (BMD) in older Chinese men. The underlying mechanism is unclear. The potential associations of intake of ACE inhibitors with serum concentrations of bone related hormones and metabolic bone markers were examined.

Method - 400 out of 2,000 of the older Chinese men aged 65 years or older in the Mr. Os (Hong Kong) cohort study had fasting serum analyzed for Collagen C-telopeptide, bone specific alkaline phosphatase, total testosterone (T) and estradiol (E), sex hormone binding globulin, insulin-like growth factor 1 (IGF), IGF binding globulin and intact parathyroid hormone. Bioavailable T and E were calculated by published formulae.

Results - 179 subjects (45%) were taking antihypertensive drugs. Out of these, 62 subjects were taking ACE inhibitors. When compared with remaining subjects, subjects on ACE inhibitors were older (72.9 versus 71.5 years) and had higher body mass index (BMI, 24.7 versus 23.4 kg/m²). They had significantly lower total T (16.0 versus 18.1 nmol/L, $P = 0.019$) and lower Collagen C-telopeptide (0.26 versus 0.31 ug/L, $P = 0.048$). However, after adjustment for age and BMI, these differences became non-significant. There was no significant group difference in the other hormonal variables.

Conclusion - Use of ACE inhibitors is not associated with serum concentrations of hormones related to bone metabolism in older men.

Disclosures: T. Kwok, None.

This study received funding from: Research Grant Council of Hong Kong and NIH Grant (US).

T470

A Microdeletion Involving TNK Alters the Phenotype of Dup(3q) Syndrome. J. D. Akunowicz^{*1}, M. P. Sciaudone^{*1}, X. Reveles^{*2}, A. M. Deshpande^{*1}, T. Davis^{*2}, J. A. Aragon-Martin^{*3}, M. Sarfarazi^{*3}, R. J. Leach², M. F. Hansen¹. ¹Center for Molecular Medicine, University of Connecticut Health Center, Farmington, CT, USA, ²Cellular and Structural Biology, University of Texas Health Science Center, San Antonio, TX, USA, ³Department of Surgery, University of Connecticut Health Center, Farmington, CT, USA.

Dup(3q) syndrome is a congenital developmental disorder resulting from a duplication of the distal portion of the long arm of chromosome 3. Symptoms typically include craniofacial abnormalities like cleft palate and craniosynostosis, clinodactyly and other mild upper limb and digital anomalies, delayed skeletal maturation, and mild mental retardation. However, one well characterized patient had an unbalanced 3;22 translocation leading to a chromosomal duplication from 3q25.3 to 3qter. Surprisingly, this patient had a more severe phenotype with microbrachycephaly, high arched palate, micrognathia, and profound mental retardation. FISH analysis using BACs from the chromosome 3q25-3q27 region revealed that the patient had a microdeletion within the region of 3q duplication. FISH analysis using subclones of the BACs within the region confirmed and narrowed the microdeletion to the boundary of 3q26-q27. Quantitative analysis of copy number by primer extension at specific SNP locations (SNuPE) within the region revealed that the microdeletion involved only the TRAF2 and NCK-interacting Kinase (TNK) locus on chromosome 3q26-q27. The microdeletion generated an imbalance in copy number between TNK (2 copies) and the remaining chromosome 3q25.3-qter region (3 copies). This microdeletion was not present in Dup(3q) syndrome patients with the milder phenotype. Our conclusion is that duplication of TNK normally modulates the effect of duplication of other genes within the Dup(3q) syndrome region and that an imbalance in copy number between TNK and the rest of chromosome 3q leads to a more severe Dup(3q) syndrome phenotype.

Disclosures: J.D. Akunowicz, None.

T471

Carrier Frequency of Recurring Mutation Causing Severe/Lethal Recessive Type VIII Osteogenesis Imperfecta in African-Americans. W. A. Cabral^{*1}, A. M. Barnes^{*1}, F. D. Porter^{*2}, J. C. Marini¹. ¹Bone and Extracellular Matrix Branch, NICHD, NIH, Bethesda, MD, USA, ²Heritable Disorders Branch, NICHD, NIH, Bethesda, MD, USA.

The majority of cases of Osteogenesis imperfecta (OI) are caused by dominant mutations in either of the two genes encoding type I collagen, COL1A1 and COL1A2, with an incidence of 1/20,000 births. Two recessive forms of OI have recently been shown to be caused by defects in the genes encoding cartilage-associated protein (CRTAP) or prolyl 3-hydroxylase 1 (LEPRE1). Although recessive OI accounts for approximately 5% of OI cases overall, we have identified a recurring mutation in the LEPRE1 gene, IVS5+1G>T. The common mutation occurs in a compound heterozygous or homozygous state in 6 of 8 probands (9 of 16 alleles) with severe/lethal recessive type VIII OI (Cabral and Chang et al, Nat Genet (2007) 39:359-365). All six probands with the IVS5+1G>T mutation were born to carrier parents of West-African descent, suggesting the existence of a stable mutant allele in this population. In order to determine the carrier frequency of the IVS5+1G>T mutation in African-Americans, we screened genomic DNA extracted from 1149 random African-American newborn metabolic screening cards from the state of Pennsylvania. Four carriers were identified, predicting a carrier frequency of 1 in 287 newborns (0.35%) in African-Americans. Our results predict a 1 in 330,000 rate of occurrence of lethal type VIII OI in African-Americans due to homozygosity for the LEPRE1 IVS5+1G>T mutation. In addition, screening of this population has identified a previously reported SNP, g.IVS5+115A→G occurring with an allele frequency of 2.2%. This polymorphism is not linked to the mutant allele, but may be useful for haplotype analysis of the African-American population.

Disclosures: W.A. Cabral, None.

T472

Correlation Between Cortical Bone Structure and Biomechanics and Metabolic Indicators in Spontaneously Diabetic, eSS Rats. G. Cointry^{*1}, S. M. Daniele^{*1}, R. Capozza^{*1}, S. Montenegro^{*1}, M. Tarés^{*1}, S. Martinez^{*1}, M. R. Ulla¹, L. Morisoli^{*1}, J. L. Ferretti. Centro de Estudios de Metabolismo Fosfocálcico, Faculty of Medicine, UNR, Rosario, Argentina.

Mechanical and tomographic (pQCT) data of the femur diaphyses and metabolic data were obtained from 9 type-II diabetic adult male eSS rats weighing 400-450g and 10 unaffected, age-paired "e" controls to define their pathogenetic relationships.

Body weight was similar between groups. eSS rats showed a. excessive cortical tissue vBMD and stiffness (vCtD, E) and diaphyseal stiffness, with low resilience and toughness (resistance to crack generation and progress), b. impaired bone mass-geometry indicators (BMC, cortical area, moment of inertia -MI-) with respect to body weight, and c. low diaphyseal strength (fracture load), with respect to controls (ANOVA, always p<0.001). A Bone Strength Index (BSI=MI.vCtD) which disregards mineralization-unrelated microstructural factors, underestimated the actual bone strength. eSS rats were hypercalciuric, and serum PTH varied directly with blood glucose, fructosamine and P and inversely with plasma Ca. Despite their

generally low values in eSS, bone mass and geometry indicators improved as a function of blood PTH, glucose and fructosamine (not Ca or P). Bone "material" or strength indicators did not vary with metabolic indicators in eSS but they did when analyzed together with controls.

Results suggest that skeletal alterations in eSS rats might result from 1. delayed bone growth with respect to body growth; 2. bone matrix hypermineralization and altered microstructural properties, associated to altered glycosylation indicators; 3. excessive stiffness of bone tissue and bones with impaired resilience and toughness (associated to 2); 4. inadequate bone geometry because the reduced bone strain by customary usage reduced bone mechanostat stimulation (associated to 3); and 5. bone weakness (associated to 3-4). An enhanced PTH activity, secondary either or both to hypercalciuria or to the diabetic condition, would be anabolic on bone formation but not enough to compensate for the primary delay of bone growth.

Disclosures: J.L. Ferretti, None.

T473

Bone Formation in Atherosclerotic Vessels: A Physiologic Mechanism to Understanding Heterotopic Ossification. F. H. Gannon^{*1}, Z. Lazard^{*2}, C. Foulletier-Dilling^{*2}, E. Davis², M. Heggeness³, A. Davis². ¹Pathology and Orthopedic Surgery, Baylor College of Medicine, Houston, TX, USA, ²Center for Cell and Gene Therapy, Baylor College of Medicine, Houston, TX, USA, ³Orthopedic Surgery, Baylor College of Medicine, Houston, TX, USA.

Heterotopic ossification (HO) is a process of bone formation that spans several diseases. Our lab has recently published a proposed mechanism of HO in a mouse using BMP2 introduced through a viral vector. Atherosclerosis is a widespread condition with bone formation noted in many of the plaques however this bone formation has not been extensively investigated. We sought a means to understand our proposed mechanism of HO in a human physiologic condition and chose bone formation in atherosclerosis as a means to do so. 10 consecutive vascular specimens obtained from surgical procedures performed on patients with known moderate to severe atherosclerosis were analyzed in a prospective manner. The segments of the vessels most severely affected by plaque were decalcified, serially sectioned, and submitted entirely. H and E sections were analyzed and sections were stained immunohistochemically for HIF, MAC1, SMA, CD 44, and CD68. We found bone formation in both distal extremity and cardiac vessels in 9 of 10 prospective specimens on H and E examination. The bone formation demonstrated evidence of active remodeling with osteoclasts, active osteoblasts, and viable osteocytes. Examination with polarized light demonstrated lamellar bone formation. Immunohistochemical staining revealed the presence of stem cells, smooth muscle cells, and brown fat cells. These result correlated with our previous findings and similar indication of microenvironment regulations were present in both systems. The histologic features of the atherosclerotic plaque containing bone have several characteristics in common to the heterotopic bone formed in animals using a BMP2 model of heterotopic ossification. The presence of HO may be the result of the microenvironment regulation by the brown fat cells enabling the recruited stem cells to differentiate along the vascular and osteoblastic lineages with resultant bone formation and remodeling. Further examination of this disease process will shed additional light on all of the steps necessary to form HO in a number of other clinical conditions.

Disclosures: F.H. Gannon, None.

T474

Possible Hypophosphatasia in a Man With Hypophosphatasemia, Spinal Ankylosis, and Recurrent Fractures. F. N. Hant^{*1}, K. Hermayer^{*2}, M. P. Whyte^{*3}, M. B. Bolster^{*1}. ¹Rheumatology and Immunology, Medical University of South Carolina, Charleston, SC, USA, ²Endocrinology, Medical University of South Carolina, Charleston, SC, USA, ³Research Center, Shriners Hospitals for Children, St. Louis, MO, USA.

We report a 69-year-old man with a 30-year history of ankylosing spondylitis (AS) treated with NSAID therapy. He never received glucocorticoids, and was being considered for anti-tumor necrosis factor (TNF)α treatment. His medical history included multiple dental extractions during adolescence for "soft teeth", and multiple recurrent fractures including a heel while walking at age 44, spontaneous fracture of his right hip at age 55 requiring pinning, left elbow fracture at age 58 (atraumatic), fracture below the plate (atraumatic) at age 61, left hip fracture at age 63, and hip re-fracture at age 68 years requiring surgery. He had taken alendronate 70 mg weekly for four years, but perioperatively this bisphosphonate was held due to concern for bone healing. Radiographs (2006) revealed fusion of the SI joints bilaterally, and ankylosis of the lumbar spine. DXA (2006) of his spine and left hip revealed T-scores of +3.0 and +0.6, respectively. Laboratory studies revealed serum total alkaline phosphatase (ALP) activity < 10 IU/L (normal: 25-100), and low bone-specific ALP activity of 10 U/L (15-41 normal). Serum calcium, vitamin D, and PTH levels were normal, but creatinine was 2.0 mg/dl. Based on his fracture and dental histories, as well as hypophosphatasemia, hypophosphatasia (HPP) seemed possible. HPP, a rare inborn-error-of-metabolism caused by loss-of-function mutation in the gene encoding the tissue-nonspecific isoenzyme of ALP (TNSALP), leads to skeletal hypomineralization and premature loss of dentition. One literature report associates HPP with AS (ZFR 50: 387, 1991). AS features new bone formation at sites of ongoing inflammation, as well as increased fracture risk due to reduced bone mass. Further biochemical and genetic studies are underway. His osteopathy is now being treated with teriparatide (JCEM 92:1203, 2007). TNFα has been shown to stimulate bone resorption, and as a class of medications to treat AS, TNFα inhibitors may delay or change the phenotype of osteoporosis in AS patients. Our patient's response to both anti-TNFα therapy for AS, and teriparatide for his hypophosphatasemia and recurrent fractures, will be closely monitored.

Disclosures: F.N. Hant, None.

T475

Molecular Exclusion of Mutations in EXT1 and EXT2 as the Cause of Metachondromatosis. S. Mumm¹, M. Huskey^{*1}, W. H. McAlister^{*2}, M. P. Whyte³. ¹Div Bone & Mineral Diseases, Washington Univ School Medicine, St. Louis, MO, USA, ²Mallinckrodt Inst Radiol, Washington Univ School Medicine, St. Louis, MO, USA, ³Research Center, Shriners Hospt Children, St. Louis, MO, USA.

Metachondromatosis (OMIM# 156250) is a rare, autosomal dominant, skeletal dysplasia featuring multiple metaphyseal juxtaepiphyseal exostoses (characteristically pointing toward the adjacent joint, and often involving the bones of the hands and feet), metaphyseal striated enchondromas (see figure), periarticular ossification, and femoral head deformities resembling avascular necrosis. These result in pain and deformities, and often require surgical removal. At least 22 cases have been reported, although lack of large families has precluded identification of the genetic defect through linkage analysis. We have clinically evaluated two families with multigenerational metachondromatosis.

Metachondromatosis shares clinical similarities with hereditary multiple exostoses (HME, OMIM #133700 & #133701), which is also an autosomal dominant disorder; HME is caused by loss-of-function mutations in the EXT1 and EXT2 genes. Like metachondromatosis, HME has cartilage-capped exostoses, primarily in the juxtaepiphyseal region of the long bones. However, in HME, the exostoses point away from the adjacent joint. Accordingly, we examined EXT1 and EXT2 for mutations in our 2 families with metachondromatosis. One proband from each was studied using genomic DNA isolated from blood leukocytes. All 11 exons for EXT1 and 15 exons for EXT2, including the entire coding region and adjacent mRNA splice sites, were amplified by PCR and sequenced in both directions. DNA sequence was examined using VectorNTI-AlignX software. No mutations in EXT1 or EXT2, that would explain metachondromatosis, were found (approximately 95% of this analysis is complete).

The metachondromatosis gene encodes a protein necessary for endochondral bone development, including shaping (defects result in exostoses) and ossification (defects result in enchondromas). We hypothesize that the metachondromatosis protein plays a role in the regulation of the critical pathways, including PTHrP and IHH, essential in chondrocyte differentiation and endochondral bone formation.

Figure Legend

The left knee of this boy at age 2 years shows enchondromas in the tibia and fibula, and exostoses that point toward the knee joint in keeping with metachondromatosis



Disclosures: S. Mumm, None.

This study received funding from: Shriners Hospitals for Children, The Clark and Mildred Cox Inherited Metabolic Bone Disease Research Fund, The Barnes-Jewish Hospital Foundation, and The Hypophostasia Research Fund.

T476

Testosterone Therapy Increases Vertebral and Hip Strength via Complex Changes in Bone Mass and Structure: A Longitudinal Study Using QCT and Finite Element Analysis in Costello Syndrome. S. Prevhal¹, T. M. Keaveny^{*2}, J. Reeder^{*3}, P. F. Hoffman^{*4}, E. S. Orwoll³. ¹Radiology, UCSF, San Francisco, CA, USA, ²Mechanical Engineering, UC Berkeley, Berkeley, CA, USA, ³Medicine, Oregon Health and Sciences University, Portland, OR, USA, ⁴O.N. Dianostics, Berkeley, CA, USA.

Costello's Syndrome is often associated with hypogonadism, delayed skeletal growth and low bone density. In this case study, a 19 year old prepubertal man with Costello's syndrome was treated with testosterone for 30 months. Therapy was associated with marked increases in areal measurements of bone mineral content, area and density at the proximal femur and lumbar spine. However, QCT analyses showed these changes in areal density were the result of complex alterations in bone mass and structure. Therapy induced increases in bone size (Lumbar Spine +12%, Femoral Neck +14%) and volumetric bone mineral density (LS +25%, FN +2.5%). Finite-element analysis of the femur revealed similarly marked increases in vertebral and hip strength. Vertebral compressive strength increased by 17%, primarily as a result of increased vertebral size and the accumulation of bone mass in the outer shell. Compressive strength of the proximal femur increased (24%) via increased size as well as added cortical and trabecular bone, which was associated with an increase of 40% total mass. Thus, therapy with testosterone in hypogonadal men with Costello Syndrome may have skeletal benefits. Moreover, QCT analyses reveal that testosterone treatment is associated with pleiotropic changes in bone structure, including increased bone size and increased cortical and trabecular mass.

Disclosures: S. Prevhal, None.

T477

Bone Growth, Adipocytokines and Physical Training in Obese Children. E. Rocher^{*}, C. Chappard, C. Jaffre^{*}, C. Benhamou. U 658, Inserm, Orleans, France.

Childhood obesity is now classified as a pandemic. Very few studies emphasised the effect of physical activity on bone growth and biological factors in obese children. The aim of our study was to investigate the effect of a physical training on bone and biological status in obese children. Subjects, 7-11 yr of age, were randomised to engage in physical training (n=16; 10.5 ± 1.3 years old) or control (n=21; 10.9 ± 1.3 years old) groups. All baseline subjects' characteristics were similar between groups. Trained group underwent a 6-month physical training (90 min. 2d/wk) doing individualized and group aerobic exercises (cycling, rowing, jumping, games, hip-hop...). Whole-Body composition and Bone Mineral Density (BMD) were measured by DXA. Usual sites (lumbar spine (L2-L4) and total hip) were also measured by DXA. Pubertal status, energy output and diet were assessed by validated questionnaire. Lipid metabolism markers such as leptin, adiponectin, glucose, insulin, and bone markers such as osteocalcin and crosslaps were dosed. The mean baseline leptin ± SD were 22.5 ± 22 and 14.1 ± 8.1 respectively for trained and control groups. The mean baseline adiponectin ± SD were 10.1 ± 3.0 and 10.4 ± 2.5 respectively for trained and control groups. The variables mean changes after training are indicated in Table 1. The 6-month physical training did not result in significant mean group differences in body composition, DXA and biological parameters. However, the interindividual variability of the response for the subjects was quite high (for example variation of plasma leptin ranging from -40.5 to 32.2 µg/L). We found correlations between plasma leptin and adiponectin with fat mass after training (respectively r = 0.53 and r = -0.33; p<0.05). Moreover, we found a correlation between plasma adiponectin and osteocalcin after training (r = -0.39; p<0.05). Finally, these findings suggest that leptin and adiponectin are probably involved in the regulation of the body composition and might play a role in bone metabolism in obese children. Nevertheless in our study, BMD and lipid metabolism markers were not influenced by a 6-month physical training in a population of obese children.

Table 1 Baseline and mean changes after physical training in trained group compared to control group

		Trained group	Control group
Body composition	Δ Total mass (kg)	4.30 ± 2.6	3.16 ± 2.6
	Δ Fat mass (%)	0.25 ± 8.2	-1.73 ± 5.7
BMD results	Δ BMD _{whole-body} (g/cm ²)	2.60 ± 1.84	2.64 ± 1.93
	Δ BMD _{L2-L4} (g/cm ²)	0.035 ± 0.03	0.023 ± 0.03
	Δ BMD _{total hip} (g/cm ²)	0.036 ± 0.03	0.025 ± 0.04
Biological factors	Δ Leptin (µg/L)	1.21 ± 21.82	6.28 ± 9.96
	Δ Adiponectin (µg/L)	-1.11 ± 2.86	-0.15 ± 5.01
	Δ Glucose (mmol/L)	-0.14 ± 0.27	-0.24 ± 0.43
	Δ Insulin (mmol/L)	0.55 ± 1.76	0.60 ± 1.74
	Δ Osteocalcin (µg/L)	-4.43 ± 10.42	-4.00 ± 10.71
	Δ Cross laps (ng/L)	238.9 ± 496	167.10 ± 291.7

Disclosures: E. Rocher, None.

T478

Diagnosis of Fibrodysplasia Ossificans Progressiva (FOP) Prior to the Onset of Heterotopic Ossification. M. Xu^{*1}, A. Ganguly^{*2}, F. S. Kaplan¹, E. M. Shore¹. ¹Orthopaedics, University of Pennsylvania, Philadelphia, PA, USA, ²Genetics, University of Pennsylvania, Philadelphia, PA, USA.

Fibrodysplasia ossificans progressiva (FOP) is a rare and disabling genetic condition characterized by congenital malformation of the great toes and by progressive heterotopic ossification in specific anatomic patterns. Most patients with FOP are misdiagnosed early in life prior to the appearance of heterotopic ossification and undergo diagnostic procedures that can cause lifelong disability. The genetic cause of FOP was recently identified and genetic testing for FOP is now available. We recently evaluated seven children for diagnosis of FOP prior to the onset of heterotopic ossification. A medical history, physical examination, and skeletal survey were obtained on all patients, as well as clinical genetic testing for the canonical FOP mutation. All seven children (four females, three males; ages three months to six years) had congenital malformations of the great toes, but none had radiographic evidence of heterotopic ossification at the time of evaluation. Five of the seven children had soft tissue lesions of the neck and back suggestive of early FOP flareups, three of whom had undergone invasive diagnostic procedures that exacerbated their condition. Two children had no history or signs of soft tissue swelling or flareups. DNA sequence analysis found that all seven children had the recurrent FOP missense mutation, a single nucleotide substitution (c.617G>A) at codon 206 in the glycine-serine activation domain of activin receptor IA (ACVR1), a bone morphogenetic protein (BMP) type I receptor. This study demonstrates that clinical suspicion of FOP early in life on the basis of malformed great toes can lead to early clinical diagnosis, confirmatory diagnostic genetic testing, and the avoidance of further harmful diagnostic and treatment procedures.

Disclosures: E.M. Shore, None.

T479

Teriparatide Therapy in Hajdu-Cheney Syndrome. P. J. Tebben, R. D. Tiegs, B. L. Clarke. Endocrinology, Mayo Clinic, Rochester, MN, USA.

To describe the response of two patients with Hajdu-Cheney Syndrome (HCS) to therapy with teriparatide.

The clinical, biochemical, and radiographic data of two patients with HCS are provided.

Case 1: A 55 year-old female was referred for evaluation and management of osteoporosis and HCS. Clinical findings included progressive acro-osteolysis, short stature, delayed closure of several cranial sutures, enlarged sella turcica, premature loss of teeth, low bone density, and fractures. During a 2 year course of conjugated equine estrogen (0.625 mg/day) and alendronate (70 mg/week) her bone mineral density (BMD) at the spine (L2-L4) declined by 8.2% and at the left hip declined by 3.5%. Serum calcium, phosphorus, creatinine, PTH, and alkaline phosphatase were within the reference range.

Due to declining BMD and vertebral fractures, teriparatide 20 mcg daily for 2 years was substituted for the alendronate. A 12.4% and 4.2% improvement was seen in the spine and left hip, respectively, over the initial 6 months of treatment followed by subsequent decrements in BMD at both sites. She also sustained a left tibial fracture after one year of teriparatide. Acro-osteolysis in her hands progressed while on teriparatide, a process that continued after substituting intravenous zoledronic acid (ZA) for teriparatide. Her BMD continued to decline on ZA.

Case 2: A 50 year old male was referred for evaluation of progressive acro-osteolysis affecting his left hand that was first apparent as a teenager. Although the disease was quiescent for several years, he developed similar findings in his right hand at age 35 while working as an artist. Features consistent with HCS included progressive acro-osteolysis, low BMD, and fractures. Teriparatide therapy had been initiated prior to his referral and after three years of alendronate. Serum calcium and total alkaline phosphatase were mildly elevated presumably due to teriparatide. Serum phosphorus and creatinine were within the reference range.

BMD increased by 7.3% and 10.2% at the spine and left hip, respectively, while on alendronate. BMD increased by 5% at the spine, but declined by 6.2% at the hip while on teriparatide. It was also felt that the rate of progression of acro-osteolysis had increased while on teriparatide.

HCS is an autosomal dominant condition characterized by a slowly progressive skeletal dysplasia including acro-osteolysis. Low BMD, fractures, short stature, and typical facial features are frequently described. The molecular pathogenesis is unknown. Beneficial effects of bisphosphonates have been reported in patients with HCS. Our two cases suggest that teriparatide does not effectively improve bone density or slow acro-osteolysis and that bisphosphonate therapy may be superior.

Disclosures: P.J. Tebben, None.

T480

Expression of GCMB, the Master Switch for Parathyroid Development, Is Normal in Parathyroid Neoplasia. A. Hoschar^{*1}, C. Ding², M. Milas^{*3}, A. Siperstein^{*3}, M. A. Levine². ¹Anatomic Pathology, Cleveland Clinic, Cleveland, OH, USA, ²Pediatric Endocrinology, Cleveland Clinic Children's Hospital, Cleveland, OH, USA, ³General Surgery, Cleveland Clinic, Cleveland, OH, USA.

Parathyroid cell development requires the expression of the GCMB gene (6p24.2) in specific cells of the third and fourth branchial pouches during early embryogenesis. GCMB encodes a member of a small family of conserved transcription factors that share a unique DNA binding motif, and is expressed exclusively in parathyroid glands. Although mice and humans that lack functional GCMB fail to develop parathyroid glands, it is unclear whether GCMB is required postnatally to maintain PTH expression and to allow physiological proliferation and neoplastic expansion of parathyroid glands. We therefore studied expression of GCMB in normal (n=9) and neoplastic parathyroid tissue from subjects with a single parathyroid adenoma who were less than 26 years (n=9), between 26-79 years (n=23), and over 80 years (n=6) as well as from patients with parathyroid carcinoma (n=5) or multi-gland disease due to MEN1 (n=4) or non-MEN (n=9). Formalin-fixed, paraffin-embedded tissue sections were stained with affinity-purified anti-human GCMB rabbit antiserum using an automated Ventana BenchMark XT staining system. Antibody binding was detected by biotin-streptavidin immunoperoxidase with the iVIEW DAB kit. Slides were examined by light microscopy and 400-cell count was performed on each case. Each cell was categorized with respect to the intensity of nuclear reactivity, and percentages of each of the four categories were then multiplied by a number as follows: "none" x 0, "weak" x 1, "moderate" x 2, and "strong" x 3. This generates a score that ranges from 0 to 300. All staining was nuclear and GCMB staining was detected in all samples. Scores ranged from 120 for MEN1 to 169 for normal glands, with no significant differences detected between any of the groups by ANOVA. In addition, we isolated genomic DNA from 10 solitary parathyroid adenomas and analyzed the nucleotide sequence of the GCMB genes. No mutations were identified but 3 adenomas were heterozygous (C/T) at SNP rs16870746 located -44 from ATG. Because neoplastic parathyroid tissue often exhibits fractional allelic loss or gene silencing, we conclude that the robust expression of GCMB in normal and all neoplastic parathyroid glands is consistent with an important post-natal role for this protein in maintaining the parathyroid phenotype.

Disclosures: M.A. Levine, None.

This study received funding from: Lerner Research Institute.

T481

Screening for Asymptomatic Normocalcemic Hyperparathyroidism in the United States. B. Misra^{*}, S. J. Silverberg, J. P. Bilezikian. Dept. of Endocrinology, College of Physicians and Surgeons, Columbia University, New York, NY, USA.

Little is known about the epidemiology of normocalcemic hyperparathyroidism (NPHPT) in the United States. Most of the published data come from referral centers in which a selection bias identifies individuals who already have signs or symptoms of primary hyperparathyroidism (PHPT). A better way to establish the incidence of asymptomatic NPHPT is to screen an asymptomatic population that represents "normal" free living individuals by measuring both the calcium and parathyroid hormone (PTH) concentration. In 2003-2004, the National Health and Nutrition Examination Survey (NHANES), which provides epidemiologic data to monitor health trends in the civilian, non-institutionalized US population, measured PTH and calcium levels in over 6000 individuals. Sample weighting to correct for over- or under- sampling permits calculation of national average estimates. Using a sampled NHANES database of 1909 people age ≥45 with a creatinine clearance of ≥60cc/min (to eliminate those with renal-based secondary HPT), we screened for an elevated PTH (≥65pg/mL) and a mid-range, normal, corrected serum calcium (9-10mg/dL). Using these screening criteria, 248 individuals were identified (60% female) representing 15% of women and 11% of men. The mean PTH in this group was 83±20pg/mL. Most subjects in this sample were 45-54 years old and Caucasian. National estimates using sample weighting confirm the above demographic data, and suggest that 11% of the American population age ≥45 with creatinine clearance ≥60 cc/min fit the above criteria. Clearly, this figure overestimates the incidence of NPHPT, because the calcium and PTH levels were not verified by repeat testing, and the incidence of vitamin D deficiency (40-57% in NHANES III, data available soon for NHANES 2003-2004) and other causes of secondary HPT are not known. Significant adjustments consistent with lower percentages of the population with NPHPT are likely. Nevertheless, this initial analysis demonstrates a method whereby using available unselected free-living cohorts, it will be possible to verify initial normocalcemic and elevated PTH values, rule out vitamin D deficiency and other causes of secondary HPT, and thus gain accurate estimates of the prevalence of NPHPT. Future studies will yield more certain estimates and allow a direct test of the hypothesis that these individuals represent the true forerunner of asymptomatic PHPT.

Disclosures: B. Misra, None.

T482

PTH(7-84) Inhibits PTH(1-34)-induced Production of 1,25-(OH)₂D₃ in Primary Cultured Murine Renal Tubules. K. Nakajima^{*1}, K. Nohtomi^{*2}, K. Takano^{*1}, K. Sato^{*1}. ¹Institute of Clinical Endocrinology, Tokyo Women's Medical University, Tokyo, Japan, ²Department of Internal Medicine, Showa University, Tokyo, Japan.

The serum level of 1,25-(OH)₂D₃ is generally increased in patients with primary hyperparathyroidism, but is occasionally not increased, or even decreased, when hypercalcemia is very severe. Recently, we have seen a 65-year-old male patient with primary hyperparathyroidism accompanied by markedly increased serum levels of intact PTH (4085 pg/ml; normal range 10-65 pg/ml) and whole PTH (842 pg/ml; normal range 9.0-39.0 pg/ml). Serum levels of calcium (12.3 mg/dl) and creatinine (3.5 mg/dl) were moderately increased. Despite the markedly increased PTH level, serum 1,25-(OH)₂D₃ was undetectable (<3 pg/ml). After resection of a huge right parathyroid adenoma (37x20x50 mm), the serum calcium level was normalized. To clarify whether PTH(7-84), a degradation product of whole PTH (1-84) that inhibits bone resorption in skeletal tissue, also exerts an antagonistic effect on the kidney, we studied the effect of PTH(7-84) on PTH(1-34)-induced 1 α -hydroxylase activity in renal tubules.

Neonatal mouse renal tubules were cultured in DMEM/F-12(1:1) supplemented with 0.2% BSA, insulin (5 μ g/ml) and transferrin (5 μ g/ml) for 7 days in the presence or absence of PTH(1-34) and/or PTH(7-84). After changing the medium, 25-OHD₃ was added to a final concentration of 10⁻⁶ M, and 1,25-(OH)₂D₃ was determined after 3 h of culture. Furthermore, effects of PTH(1-34) and/or PTH(7-84) on mRNA expression were investigated by real-time RT-PCR.

PTH(1-34) dose-dependently increased the level of 1,25-(OH)₂D₃ in the conditioned medium, and this PTH(1-34)-induced production of 1,25-(OH)₂D₃ at 10 ng/ml was dose-dependently inhibited by PTH(7-84). Real-time RT-PCR analysis also confirmed that PTH(1-34) increased the expression of 1 α -hydroxylase mRNA. Effect of PTH(7-84) on 1 α - and 24-hydroxylase mRNA in the presence of 25-OHD₃ was not constant and is under investigation in the absence of 25-OHD₃.

These in vitro findings suggest that PTH(7-84) inhibits not only bone resorption in skeletal tissue but also 1 α -hydroxylase in renal tubules. Although hypercalcemia per se inhibits 1 α -hydroxylase activity, non-N-terminal PTH fragments may be also partly involved in the normal or decreased serum level of 1,25-(OH)₂D₃ in severely hypercalcemic patients with primary hyperparathyroidism. This in vitro observation may also account for the decreased serum level of 1,25-(OH)₂D₃ in patients with secondary hyperparathyroidism, in whom the ratio of whole PTH/intact PTH is decreased.

Disclosures: K. Nakajima, None.

T483

In Multiple Endocrine Neoplasia Type 1 (MEN1) the Estimated Ratio of Mutated p27 Versus Mutated MEN1 Genes Is Below 1:100. A. Ozawa^{*1}, S. K. Agarwal^{*1}, C. M. Mateo^{*1}, A. L. Burns^{*1}, T. S. Rice^{*1}, P. A. Kennedy^{*1}, C. M. Quigley^{*1}, W. F. Simonds¹, L. S. Weinstein¹, S. C. Chandrasekharappa^{*2}, E. S. Collins^{*2}, A. M. Spiegel¹, S. J. Marx¹. ¹NIDDK, National Institutes of Health, Bethesda, MD, USA, ²NHGRI, National Institutes of Health, Bethesda, MD, USA.

p27 (CDKN1B, cyclin-dependent kinase inhibitor 1B; the alternate name for p27 is KIP1) belongs to one of two classes of cyclin dependent kinase inhibitor. Mice with homozygous knockout of p27 develop endocrine tumors but only in the pituitary intermediate lobe. Rats with a homozygous inactivating mutation of p27 have tumors with features of MEN1 and MEN2.

One variant of MEN1 shows sporadic tumors of both the parathyroids and pituitary. The prevalence of identified MEN1 gene mutations in this variant is far lower than in familial MEN1 (7% versus 90%, p<0.0001), suggesting different causes. Recently one index case of this variant had a germline mutation of p27 (Pellegata et al; PNAS 2006).

Our purpose was to estimate the frequency of p27 mutations in MEN1 and MEN1-like states. We sequenced germline DNA from 34 cases and control cases for the p27 gene by PCR of the protein coding exons and intron/exon boundaries. No identifiable MEN1 mutation was a required criterion for inclusion.

We tested 16 MEN1 cases with sporadic tumor of both parathyroid and pituitary. In these 16 cases, parathyroid tumors were single in 2 cases and multiple in 14. Six pituitary tumors over-secreted GH, 6 over-secreted PRL, 2 over-secreted ACTH, and 2 were non-functioning. Eighteen additional index cases with closely related familial tumor phenotypes were also evaluated. There were 11 index cases for families with tumors of the parathyroids and pituitary, 5 index cases of familial isolated tumors of pituitary and 2 index cases of familial hyperparathyroidism with renal angiomyolipoma. One p27 germline single nucleotide change was identified. This predicted a silent substitution of Thr142Thr. Furthermore, there was a normal prevalence of heterozygosity (35%) for a common p27 polymorphism (Val109Gly; GTC to GGC), making a large p27 deletion unlikely in all or most of these cases. Thus there was no pathologic p27 mutation in any of 34 cases. We can estimate the frequency of p27 mutations in MEN1. Assume 1000 cases of MEN1 and MEN1-like variants, about 700 will have MEN1 mutations. Of the remaining 300, we estimate less than 6 p27 mutations. The estimated ratio of p27 versus MEN1 mutation in MEN1 is therefore below 1 to 100. p27 is thus a rare cause of MEN1, but it has implications for understanding endocrine tumors that are disproportionate to its rarity.

Disclosures: A. Ozawa, None.

T484

Long Term Morbidity & Mortality in Untreated Mild Primary Hyperparathyroidism. J. Iskander^{*}, D. Rao. Bone & Mineral Metabolism, Henry Ford Health System, Detroit, MI, USA.

Optimal management of mild asymptomatic primary hyperparathyroidism (PHPT) continues to be debated despite recent revised guidelines. A small number of prospective studies of untreated PHPT suggested very few disease specific complications, but others differ. Therefore, it is unclear if untreated PHPT is associated with significant longer term morbidity and mortality. Accordingly, we determined long term outcomes in carefully followed patients with untreated PHPT.

We prospectively studied 50 patients (8 men and 42 women, and 21 white and 29 black, with a mean age of 66 \pm 8y), with mild PHPT to determine longer term effects of chronic PTH excess in the absence of parathyroidectomy (PTX). Patients were evaluated every 6-12 months for up to 18y.

There was a small significant rise in serum creatinine, but none of the values were > 1.5 mg/dl during the first 10y of follow up. Serum PTH and calcium did not change. There was a small but significant decline in forearm absolute BMD with consequent decline in T-score but not in Z-scores. Absolute BMDs and T- and Z-scores did not change either at the spine or at the hip. Quality of life scores, by SF-36, generally remained stable over time. Relevant morbidity and mortality data are in Table.

During follow-up, 2 patients started hemodialysis (one 10y after PTX), most likely related to diabetes and hypertension, and 2 patients had kidney stones, one of whom had PTX before the kidney stone incident.

Eleven patients sustained 14 fractures: one each of humerus, ischium, glenoid cavity and femur, 3 - 7y after PTX. Fractures 1-4y before PTX were: 3 foot, 2 finger, and one each of fibula, forearm, femur, ankle, and tibia due to trauma or automobile accident. None of the fractures were considered due to PHPT. Eight patients died at a mean age of 76.3 \pm 7.2y from causes unrelated to PHPT (2 cancers, 3 cardiac, one each in hospice, ruptured aneurysm, and unknown; all unrelated to PHPT). Seven of the 9 patients had PTX because of the formal conclusion of the study in concert with existing guidelines.

We conclude that mild untreated PHPT is not associated with continued bone loss or worsening disease severity. There were the usual age and lifestyle related morbidity and mortality, but no disease specific complications.

Incidents	Pre-PTX (y)	Post-PTX (y)
Fractures (n)	3 (1,2,&12y)	4 (3,4,4,&7y)
Kidney Stones (n)	2 (1&7y)	0
Renal Failure (n)	1	1 (10y)
Deaths (n)	7	1 (6y)

Disclosures: D. Rao, None.

T485

Use of Parathyroid Hormone in Hypoparathyroidism. M. R. Rubin, S. J. Silverberg, J. Sliney^{*}, J. P. Bilezikian. Columbia University College of P&S, New York, NY, USA.

Hypoparathyroidism (HypoPT) is a disorder in which PTH is absent from the circulation. Without PTH, calcium homeostasis is abnormal and bone mineral density (BMD) by DXA is markedly elevated. Calcium and vitamin D supplementation are required but control can be a clinical challenge. PTH seems to be an ideal agent because it replaces what is missing in these individuals. Accordingly, we studied the effects of PTH replacement therapy in HypoPT on biochemical and densitometric abnormalities. We studied 30 subjects (48.9 \pm 13 yr; 21 female) with HypoPT (duration 18 \pm 13 yrs; 17 postsurgical, 11 autoimmune, 2 DiGeorge). Baseline biochemistries were: serum calcium, 8.7 \pm 1 mg/dl (nl 8.5-10.4); PTH, 7.1 \pm 6 pg/ml (nl 10-65); urinary calcium, 261 \pm 123 mg/l; serum phosphorus, 4.4 \pm 0.8 mg/dl (nl 2.5-4.5); total alkaline phosphatase, 66 \pm 20 IU/l (nl 33-96); 25-hydroxyvitamin D, 63 \pm 76 ng/ml (nl 9-52); 1,25-dihydroxyvitamin D, 33 \pm 15 pg/ml (nl 15-60). Baseline calcium supplementation ranged from 0-9 g/d (av.3 g/d); baseline calcitriol doses ranged from 0 to 3 ug/d (av. 0.75 ug/d); baseline parent vitamin D doses (n=9) ranged from 4000-100,000 IU/d (av. 10,000 IU). Baseline DXA-based BMD was by T-scores at the lumbar spine, +1.7 \pm 2.3 (cohort range: -1.60 to +7.90), total hip, +0.57 \pm 1.3 (cohort range: -2.10 to +4.30) and 1/3 distal radius, -0.34 \pm 1.06 (cohort range: -2.6 to +1.5). PTH(1-84) was administered at 100 ug every other day for up to 24 months (range of time: 1-24 months). Calcium supplementation decreased by 33% at 1 month (p<0.01); calcitriol supplementation decreased by 27% at 3 months (p<0.05); parent vitamin D supplementation trended downwards by 31% at 3 months. Serum calcium remained within the normal range, with the greatest increase occurring at 2 months, to 9.3 \pm 1 mg/dl (p<0.01). Urinary calcium decreased at 12 months to 164 \pm 102 mg/dl (p=0.02). BMD decreased at the distal 1/3 radius (-2.9 \pm 2% at 18 months; p=0.02), but increased at the lumbar spine (2.9 \pm 4% at 12 months; p=0.02) and did not change at the total hip. We conclude that the administration of PTH improves calcium homeostasis in HypoPT and allows serum calcium levels to be maintained while permitting a reduction in the calcium and vitamin D regimen. It appears that there are differential effects of PTH replacement on BMD by DXA, as a function of skeletal site and composition. Whether other changes in bone quality occur with PTH replacement are currently under investigation.

Disclosures: M.R. Rubin, None.

T486

Bone Quality in Mild Primary Hyperparathyroidism. R. Zoehrer^{*1}, D. W. Dempster², J. P. Bilezikian², H. Zhou³, S. J. Silverberg⁴, E. Shane⁴, P. Fratzl^{*5}, E. Paschalis¹, P. Roschger¹, K. Klaushofer¹. ¹Ludwig Boltzmann Institute of Osteology, Hanusch Hospital of WGKK and AUVA Trauma Centre Meidling, 4th Med. Dept. Hanusch Hospital, Vienna, Austria, ²Regional Bone Center, Helen Hayes Hospital, & College of Phys & Surg, Columbia University, New York, NY, USA, ³Regional Bone Center, Helen Hayes Hospital, New York, NY, USA, ⁴College of Phys & Surg, Columbia University, New York, NY, USA, ⁵Department of Biomaterials, Max Planck Institute of Colloids and Interfaces, Potsdam, Germany.

Mild primary hyperparathyroidism (PHPT) is a common endocrine disorder characterized by excessive secretion of parathyroid hormone (PTH) and hypercalcemia. The present study examines bone quality in PHPT by applying two imaging technologies: quantitative backscattered electron imaging (qBEI) and Fourier transform infrared imaging analysis (FTIRI). qBEI permits determination of bone mineral density distribution (BMDD), expressed as CaMean, CaPeak, CaWidth and CaLow, and FTIRI describes the extent of collagen maturity expressed as the ratio of 2 of the major bone type I collagen cross-links (pyridinoline/dehydro-dihydroxylysinonorleucine;collx). Percutaneous transiliac bone biopsies were obtained from 51 unselected subjects with mild PHPT (16 men, aged 28-68; 35 women, aged 26-74). Forty of the biopsies were from untreated patients. Seven biopsies were from subjects biopsied after an average of 6 years after parathyroidectomy (PTX). All biopsies were fixed and dehydrated in ethanol, and embedded in polymethylmethacrylate. By qBEI analysis, PHPT differed from healthy controls in that they had markedly higher CaWidth (+15.7%, p<0.0001) and CaLow (+44.7%, p<0.0001), and somewhat lower CaMean (-2.5%, p<0.0001). These differences were reversed in the 7 patients who underwent PTX. For FTIRI analysis, spectral images were acquired of 3 areas (each 400 µm x 400 µm) on separate trabeculae devoid of resorption pits and with primary mineralization evident on at least one surface (based on qBEI images). The collx in the PHPT patients was significantly lower than in normal controls (p<0.001), while those studied after PTX was normal. The difference in collx in PHPT was age-independent but gender-dependent: with women exhibiting a lower ratio than men. Both qBEI and FTIRI outcomes were strongly correlated with bone formation rate and mineralizing surface parameters as determined by histomorphometry. These results are consistent with previous observations of increased bone turnover in this disease, and consequently, reduced mean age of bone tissue. Reduced mineralization density and collx in patients with PHPT would be expected to reduce the stiffness of bone tissue. These observations are relevant to considerations of fracture risk in PHPT.

Disclosures: R. Zoehrer, None.

T487

The Relationship between iPTH and Bone Metabolic Markers. Y. Kodama^{*}, Y. Kato^{*}, K. Kanaya^{*}, K. Wada^{*}, S. Shimamoto^{*}, C. Ishi^{*}. Orthopedics, Tokyo Women's Medical University, Tokyo, Japan.

Introduction: Currently, instead of a bone biopsy, bone metabolic markers are often used to evaluate bone quality, since this is non-invasive test. However, in HD patients, the diagnosis and prognosis based on bone metabolic marker levels were sometimes difficult. The pathological histology of renal osteodystrophy (ROD) is well-known to be related to the level of iPTH. We investigated the relationship between iPTH and bone metabolic markers to evaluate bone quality in HD patients.

Patients: iPTH and bone metabolic markers had been measured in our department. The data from 1200 patients, whose background characteristics were available, was analyzed in this study. The patients were categorized into the following 10 groups, HD group, metastatic bone tumor (meta) group and so on.

Methods: 1. In each disease group, iPTH and bone metabolic markers were assessed using multiple comparisons. 2. In HD group, the correlations between iPTH and bone metabolic markers were examined. 3. For each marker, the patients were divided into two groups based on their iPTH levels: low, iPTH <65 pg/mL; and high, iPTH ≥65 pg/mL. Their correlations were then examined.

Results: 1. HD group showed higher iPTH than other groups. ICTP, NTX, and OC had a similar distribution to iPTH. The meta group showed a significantly higher BAP than other groups. 2. sNTX, OC and BAP had statistically significant correlation with iPTH, but ICTP had none. 3. In "high" group, all bone metabolic markers were strongly correlated with iPTH. In "low" group, however, none of the bone metabolic markers were correlated with iPTH.

Discussion: 1. Two hypotheses could explain the results of multiple comparisons. Bone metabolic markers may simply accumulate due to impaired kidney function and due to the differences in the dialyzer membrane's permeability. Alternatively, the bone metabolic markers truly reflect accelerated bone turnover due to secondary hyperparathyroidism. To confirm these hypotheses, we investigated the correlations between iPTH and the various bone metabolic markers. 2. OC had the highest correlation coefficient with iPTH. In HD patients, OC appears to have the best contribution ratio to iPTH. 3. When iPTH is lower than 65 pg/mL, the histopathology of ROD shows aplastic bone disease (ABD) with 100% specificity. To exclude the influence of ABD, the patients were divided into two groups based on their iPTH levels. In this study, all bone metabolic markers were correlated with iPTH in "high" group. Therefore bone metabolic markers can be used to evaluate the bone quality of ROD in patients without ABD.

Conclusions: ICTP, OC, and NTX had similar distribution to iPTH. In HD group, OC had the highest correlation coefficient with iPTH. In HD patients with iPTH ≥ 65 pg/mL, all bone metabolic markers were correlated with iPTH.

Disclosures: Y. kodama, None.

T488

Non-invasive Study of Bone and Cardiovascular Disease in Chronic Hemodialysis Subjects. L. Kooienga^{*1}, A. Furniss^{*2}, A. Bellasi^{*3}, P. Raggi^{*4}, G. Block². ¹Division of Renal Disease and Hypertension, University of Colorado Health Sciences Center, Denver, CO, USA, ²Clinical Research Division, Denver Nephrology, Denver, CO, USA, ³Nephrology, University of Milano, San Paolo Hospital, Milan, Italy, ⁴Division of Cardiology, Emory University, Atlanta, GA, USA.

To assess the relationship between interval changes in bone mineral density (BMD) with changes in arterial health as determined by changes in aortic and coronary artery calcification scores (CACS) and arterial stiffness over a 12 to 18 month follow-up period. This is a single center study of subjects on chronic hemodialysis who underwent medical interviewing, dual energy x-ray absorptiometry, electron beam computed tomography, and pulse wave velocity (PWV) assessment at baseline and at follow-up. In addition, subjects had time-averaged laboratory values obtained from routine dialysis monitoring throughout the follow-up period. Medication exposure was defined as > 3 months of the study period.

59 subjects completed baseline and follow-up evaluations. 3 subjects with a parathyroidectomy during the study were excluded. The mean age was 58.8 (15.2) years, mean vintage was 45.9 (41.9) months, and mean follow-up was 13.6 (1.6) months. 54% of subjects were female, 63% were Caucasian, and 30% were African American. ESRD etiology was from diabetes mellitus in 34% and hypertension in 30%. Mean hip BMD at baseline was 0.813 (0.148) g/cm² and decreased by a mean of -2.6 (4.6) % at follow-up. 17 subjects had an improvement or no change in BMD and 37 subjects had a decrease in BMD. In subjects with improvement/no change in hip BMD vs. those that had a decrease there was no significant difference at follow-up in time-averaged albumin, adjusted calcium, adjusted Ca x P product, LDL cholesterol, PTH, or the % with mean PTH between 150-300 pg/mL. Those with a decrease in hip BMD had a higher % of aspirin use (81 vs 47%; p=0.02), lower Cinacalcet use (27 vs 65%; p=0.02), and a trend towards lower calcium binder use (57 vs 88%; p=0.07) and lower serum phosphorus [4.8 (0.8) md/dL vs. 5.2 (0.7) mg/dL; p=0.09]. They also had a greater change in mean PWV [1.4 (3.6) m/s vs. -0.8 (1.8) m/s; p=0.01] with a concomitant higher median aortic artery calcium score [2496 (47,927) vs. 784 (9514); p=0.05]. However, there was no significant difference in CACS, cardiovascular events, or fractures between the groups.

69% of prevalent HD patients experienced a dramatic loss of hip BMD over a mean 13.6 month follow-up. This loss of BMD was independent of the typical parameters of bone mineral metabolism, time on dialysis, or age. Subjects who lost hip BMD had higher median aortic artery calcification scores and demonstrated significant worsening of arterial PWV supporting the proposed hypothesis linking loss of bone mineral with vascular pathology.

Disclosures: L. Kooienga, None.

This study received funding from: Shire Pharmaceutical Inc.

T489

The Mechanism of Skeletal Involvement in Cardiovascular Mortality in Chronic Kidney Disease (CKD). S. Mathew^{*1}, R. Lund^{*2}, K. A. Hruska¹. ¹Pediatrics, Washington University, St. Louis, MO, USA, ²Medicine, Creighton University, Omaha, NE, USA.

CKD is complicated by high mortality rates due to cardiovascular events. Hyperphosphatemia and vascular calcification (VC) have been determined in observational studies to be risk factors. In animal models with CKD, we have demonstrated that renal injury impairs osteoblast function and decreases bone formation rates without suppressing osteoclastic resorption, i.e. produces the adynamic bone disorder. In an animal model of type 2 diabetes with atherosclerosis, induction of the adynamic bone disorder by CKD contributes to hyperphosphatemia by excess skeletal resorption, and stimulates vascular calcification. Control of the serum phosphorus by stimulation of bone formation or phosphate binding inhibited VC. These results have been confirmed in dialysis patients treated with phosphate binders, and improved patient survival was found. In atherosclerotic vascular smooth muscle cells, the mechanism of phosphorus action in VC was sought and found to be stimulation of a heterotopic BMP-2 and RUNX2 directed osteoblastic transcription program. Despite the expression of these osteoblastic determinants in basal conditions, matrix mineralization by atherosclerotic aortic smooth muscle cell cultures was not observed until media phosphorus was increased. The action of phosphorus on mineralization was due to stimulated expression of osterix, a critical osteoblast transcription factor. Phosphorus stimulated mineralization in vitro was silenced by inhibition of osterix through BMP-7, and by inhibition of BMP-2 action through addition of a BMP antagonist, noggin.

In our animal model of CKD stimulated VC, we found the BMP-2/MSX2 program including RUNX2 expression to be present in the atherosclerotic aorta prior to CKD and unaffected by induction of CKD, analogous to the atherosclerotic cell cultures. CKD stimulated aortic osterix expression. Stimulation of bone formation and control of hyperphosphatemia using BMP-7 or phosphate binding agents, decreased aortic osterix expression, osteocalcin expression and aortic mineralization. These studies demonstrate a multiorgan system of the kidney, skeleton, and the cardiovascular system, that fails due to CKD involving loss of skeletal anabolism, hyperphosphatemia and heterotopic mineralization representing kidney-bone and bone-vascular signaling.

Disclosures: S. Mathew, Genzyme 2; Shire 2.

This study received funding from: NIH.

T490

Bone Microarchitecture As Assessed by High Resolution Quantitative CT (HRpQCT) in Chronic Kidney Disease. T. L. Nickolas¹, D. J. McMahon¹, H. Eisenberg^{*1}, S. Cabral^{*1}, C. Go^{*1}, M. Leonard², E. Shane¹. ¹Medicine, Columbia University, New York, NY, USA, ²Pediatrics, University of Pennsylvania, Philadelphia, PA, USA.

Moderate chronic kidney disease (CKD) and end-stage kidney disease (ESKD) are associated with increased susceptibility to fracture, due in part to the catabolic effects of secondary hyperparathyroidism on cortical bone. However, the effects of moderate CKD on trabecular (Tb) and cortical (Ct) microarchitecture have not been addressed. High resolution quantitative CT (HRpQCT) (XtremeCT, Scanco Medical AG) is a new imaging technology (resolution <100 microns) that distinguishes Ct from Tb bone and yields noninvasive measurements of Tb and Ct architecture that are more sensitive markers of bone fragility. To assess effects of impaired kidney function on bone architecture, we performed HRpQCT scans in 31 subjects (18 men), aged 51-88 yr, across a range of kidney function. The MDRD formula was used to estimate GFR. Overall, 5 subjects were on dialysis and 9 had normal eGFR. Of the remainder, the median (range) eGFR was 40 ml/min (11-64). HRpQCT variables that were not normally distributed were log-transformed. Univariate analyses demonstrated that Tb deficits were significantly associated with lower eGFR and female gender. Ct deficits were significantly associated with lower eGFR and older age. Linear regression was used to investigate the relationship between HRpQCT microarchitectural parameters and eGFR, adjusted for age and gender. Ct density, but not thickness, was directly related to eGFR. Similarly, Tb parameters were worse in patients with lower eGFR, with decreased Tb density, BV/TV and TbN, increased TbSp and heterogeneity of the Tb network (TbSpSD). By multivariate regression analysis adjusted for gender and age, Tb changes were independently associated with eGFR (Table 1). This preliminary investigation confirms that lower eGFR was associated with both Ct and Tb deterioration that was independent of gender and age. These alterations in Ct and Tb microstructure may contribute to the increased risk of fracture in patients with CKD and ESKD. Further studies are required to elucidate the pathogenesis of the microarchitectural deterioration and its relationship to bone mechanical competence.

Multivariate Linear Regression of Bone Microarchitecture
Against eGFR, Gender and Age

	B	SE	p-value
Ct Density	1.4	0.6	0.03
Ct Thickness	0.002	0.001	NS
Tb Density	0.5	0.25	0.04
Tb Bone Volume (BV/TV)	0.0005	0.0002	0.03
Tb Thickness (TbTh)	0.00006	0.00007	NS
Log (Tb Number, TbN)	0.004	0.002	0.03
Log (Tb Separation, TbSp)	-0.004	0.002	0.03
Log (TbSp SD)	-0.01	0.003	0.01

*Gender and Age were not significantly associated either with cortical or trabecular parameters in multivariate linear regression

Disclosures: T.L. Nickolas, Hoffman-La Roche 5; Abbott 8; Gilead 8.

T491

Etidronate Inhibits Progression of Vascular Calcification and Decrease in Bone Mineral Density in Chronic Dialysis Patients. Y. Okada, O. Hashimoto*, T. Tanikawa*, Y. Tanaka. First Department of Internal Medicine, University of Occupational and Environmental Health Japan, Kitakyushu, Japan.

Severe atherosclerosis/calcinosis is common in patients on long-term dialysis. No therapy is currently available to suppress the progression of vascular calcification. In the present study, we determined the effect of etidronate (EHDP), a first generation bisphosphonate, on vascular calcification in chronic dialysis patients. 81 patients undergoing chronic hemodialysis were divided into EHDP-treated group (n=37) and control group (n=44). EHDP was administered in a single dose (400 mg/day) just before sleep each day for two weeks followed by suspension for 10 weeks, and a repeat of the cycle every 12 weeks for one year. The area of calcification affecting the abdominal aorta (ACA) was measured with X-ray computed tomography. ACA was measured by an image analysis device and the mean ACA of six slices was calculated. ACA was measured at the start and end of the study (12 months) in each patient. Bone mineral density (BMD) was measured by DXA at the start and end of the study (12 months). Scans were performed for the forearm, at one-third radius without A-V fistula. In the EHDP-treated group, no significant changes in BMD were noted throughout the study. However, BMD decreased significantly in the control group from 0.57 ± 0.17 (mean \pm SD) at enrolment to 0.55 ± 0.18 g/cm² at 12 months (P<0.01). ACA increased significantly in the control group from 71.3 ± 58.6 at enrolment to 83.1 ± 63.6 mm² at 12 months (P<0.01). In contrast, ACA changed in the EHDP-treated group from 71.3 ± 63.3 at enrolment to 73.2 ± 63.5 mm² at 12 months statistically insignificant. The delta increase in ACA in EHDP-treated group was 1.9 ± 18.6 mm² (95% CI 1.33-5.60) which was significantly lower than that of the control group (11.8 ± 19.2 mm², 95% CI 8.19-14.55). The independent association between changes in ACA and various parameters in multivariate linear regression analysis indicated that EHDP was an independent factor for the observed changes in ACA. Our findings suggest that EHDP is potentially useful for prevention of vascular calcification and might improve the prognosis of chronic dialysis patients.

Disclosures: Y. Okada, None.

T492

TRAP5b Profiles in Children with Chronic Kidney Disease (CKD). H. E. Price, C. B. Langman*. Pediatric Kidney Diseases, Northwestern University, Childrens Memorial Hospital, Chicago, IL, USA.

Serum tartrate-resistant acid phosphatase 5b (TRAP5b) is derived from osteoclast activity. Levels of TRAP5b rise during growth spurts in children, associated with bone modeling. The osteodystrophy of CKD in children is associated with high-turnover disease from 2^o hyperparathyroidism (SHPTH), resulting in increased remodeling. The purpose of this cross-sectional study was to measure serum TRAP5b in children with CKD, and we asked whether modeling was reflected by its levels. 36 children (23 males (M) 13 females (F)) with CKD stages 1-4 (NKF classification using eGFR) had measures made of hormones and factors related to their osteodystrophy. These included iPTH, 25(OH)D, 1,25(OH)₂D, in addition to TRAP5b (TRAP5b levels were made using an ELISA, Quidel Corporation, San Diego, CA.). Values were compared to 65 healthy children of the same age distribution. As eGFR decreased in CKD, serum TRAP5b increased. There were correlations with iPTH (r=-0.5) and 1,25(OH)₂D (r=-0.5) in children with CKD, but not in healthy children. There was no correlation between TRAP5b & 25(OH)D. When compared to healthy children matched for age and gender, children with CKD had increased levels of TRAP5b in childhood (pre-pubertal) years (F CKD: 19.7 ± 6.3 vs. healthy: 8.1 ± 3.8 U/L, p<0.001; M CKD: 12.2 ± 4.6 vs. healthy: 6.6 ± 3.6 , p<0.01). In early adolescence, healthy children had an increase in TRAP5b, followed by a decrease as they approached late adolescence into adulthood. However, children with CKD had a decrease of TRAP5b in early adolescence followed by a steady decline into adulthood. Thus, the values of TRAP5b in early adolescence were lower when compared to healthy children (F CKD: 13 ± 8.2 vs. healthy: 10 ± 2.7 ; M CKD: 7.9 ± 5 vs. healthy: 9.9 ± 3.3). In conclusion, as kidney function decreases in the childhood years, TRAP5b increases, indicating accelerated bone turnover from SHPTH. However, during a period of expected increased bone modeling, and despite SHPTH, TRAP5b values declined, consistent with reduced linear growth in adolescent CKD. Additional prospective studies underway will further clarify these relationships. Thus, TRAP5b may be an important corollary marker to profile bone modeling, since bone biopsy is not clinically available, and SHPTH reflects bone remodeling. The osteodystrophy of pediatric CKD thus may be able to be better separated into abnormalities of bone modeling, and bone remodeling, with a multi-faceted measurement approach that includes TRAP5b.

Disclosures: H.E. Price, None.

T493

Hyperphosphatemia Mediates Oxidative Stress in Bovine Aortic Endothelial Cells. E. Shuto*, Y. Taketani¹, R. Tanaka*, A. Tanimura*, M. Isshiki*, N. Harada*, H. Yamamoto*, E. Takeda*. ¹Department of Clinical Nutrition, University of Tokushima Graduate School, Tokushima, Japan, ²Department of Nephrology and Endocrinology, University of Tokyo, Tokyo, Japan, ³Department of Nutrition and Metabolism, University of Tokushima Graduate School, Tokushima, Japan.

Hyperphosphatemia causes calcification of vascular smooth muscle cells. The calcification is closely associated with progress of cardiovascular disease and mortality in end-stage renal disease (ESRD) patients. We hypothesized that hyperphosphatemia may also contribute the progress of atherosclerosis in early-stage chronic kidney disease by involving endothelial dysfunction. To prove the hypothesis, we investigate the effect of high inorganic phosphate (Pi) loading on the endothelial function using bovine aortic endothelial cells (BAECs). First, we examined production of reactive oxygen species (ROS) by fluorescence ROS indicator (APF: aminophenyl fluorescein), and found that high Pi (1.5-3mM) increased production of reactive oxygen species in a dose-dependent manner compared with control (0.9 mM Pi). The increase in ROS was inhibited by diphenylene iodonium (DPI; NAD(P)H oxidase inhibitor) and phosphonoformic acid (PFA; Na/Pi co-transporter inhibitor). Therefore, both Pi influx and NAD(P)H oxidase activation play an important role in the ROS production in response to high Pi loading in endothelial cells. In second, we examined effect of high Pi on the nitric oxide (NO) production in response to bradykinin in the BAECs, and found that pretreatment with high Pi (2 mM) for 3 days decreased the hormone-dependent NO production. One possible mechanism of the inhibition of NO production was due to phosphorylation of endothelial NO synthase (eNOS) by conventional PKC activated by high Pi loading. These results suggest that increase in Pi influx can mediate intracellular signal such as PKC activation and ROS production, and would be involved in oxidative stress and some adverse effect on endothelial function. Oxidative stress caused by hyperphosphatemia in endothelium may be a novel patho-mechanism for atherosclerosis and cardiovascular diseases in ESRD patients.

Disclosures: E. Shuto, None.

This study received funding from: Grants-in-Aid for Young Scientist and Exploratory Research from Ministry of Education, Culture, Sports, Science, and Technology in Japan, Uehara Memorial Foundation, and 21st Century COE Program.

T494

Prospective Controlled Study assessing the Clinical Benefit of Evening Administration of Vitamin D in Hemodialysis Patients. K. Takasawa^{*1}, C. Takaeda^{*1}, Y. Takeshita^{*2}, K. Kawai^{*2}. ¹Renal Division, Public Central Hospital of Matto-Ishikawa, Hakusan, Japan, ²Internal Medicine, Public Central Hospital of Matto-Ishikawa, Hakusan, Japan.

Control of serum calcium (sCa) and phosphorus (P) levels is important in improving the survival of hemodialysis patients. We assessed whether sCa is decreased in hemodialysis patients by administering a Vitamin D (VitD) at evening instead of in the morning. We selected 24 patients having a serum Ca level of ≥ 9.5 mg/dl (A1b-adjusted) from 72 hemodialysis patients at our institution. Concerning the 24 patients above, an informed consent was obtained based on the Helsinki declaration. The 24 patients (the average age is 63.4 ± 14.8 years, the mean duration of dialysis is 10.6 ± 8.4 years), who were undergoing oral VitD administration in the morning, were randomized into two groups for morning administration and evening administration of VitD (n=12 per group) and were prospectively followed-up for 6 months. During the follow-up period, the patients were monitored for the sCa levels, iPTH, osteocalcin, bone alkaline phosphatase and the serum P while receiving a fixed dose of VitD as a rule. However, the dose of iPTH was adjusted as appropriate in compliance with the Japanese guidelines and K/DOQI that recommend a dose of iPTH not exceed 180 pg/mL. Out of the 12 patients treated in the morning, one who suffered from cerebral hemorrhage and 5 who received a reduced dose of VitD were excluded, and the remaining 6 patients (2 treated with alfacalcidol and 4 with falecalcitriol) were evaluated. I have excluded the 5 patients in the evening group because that one had renal transplantation, one died of infection and 3 whose VitD dosage had been reduced, and the remaining 7 patients (4 treated with alfacalcidol and 3 with falecalcitriol) were evaluated. The sCa levels were no difference between two groups at the beginning. In the morning group, the sCa level was 10.3 ± 1.0 mg/dl at baseline and 10.4 ± 0.8 mg/dl after 6 months. In the evening group, the sCa level was 9.9 ± 0.6 mg/dl at baseline and was significantly decreased to 9.4 ± 0.6 mg/dl after 6 months ($p < 0.05$). The serum iPTH level was 181.7 ± 133.5 pg/ml at baseline and 208.5 ± 165.4 pg/ml after 6 months in the morning group versus 121.4 ± 139.6 pg/ml at baseline and 142.1 ± 94.9 pg/ml after 6 months in the evening group, showing no pronounced change in the both groups. The osteocalcin levels of the evening group were reduced from 46.6 ± 45.3 to 29.5 ± 22.3 ng/ml, significantly. These data suggest that oral VitD was administered at evening in patients on hemodialysis to address the diurnal rhythm of bone metabolism, and the serum Ca level was decreased as a result in these patients. Evening administration of VitD is more beneficial effect for patients on hemodialysis.

Disclosures: K. Takasawa, None.

T495

Impact of Cinacalcet HCL on Bone Remodeling and Minimodeling in Patients with Secondary Hyperparathyroidism. A. Yajima¹, H. E. Takahashi², T. Akizawa^{*3}, K. Study Group^{*4}. ¹Nephrology, Towa Hospital, Tokyo, Japan, ²Niigata University of Health and Welfare, Niigata, Japan, ³Nephrology, Showa University, School of Medicine, Tokyo, Japan, ⁴KRN 1493 Study Group, Tokyo, Japan.

Purpose: Impact of cinacalcet HCL on hyperparathyroid bone disease was investigated. Methods: Iliac bone biopsy was taken before and after the treatment with cinacalcet HCL for one year in the three hemodialysis patients with secondary hyperparathyroidism, and histomorphometric parameters including remodeling parameters and minimodeling volume were measured in cancellous bone.

Results: Serum intact PTH was decreased from 747.7 ± 391.1 to 140.3 ± 80.5 pg/ml, respectively. Oc.S/BS decreased from (8.5, 6.2, 6.2) to (1.2, 0.2, 1.0) %, Fb.V/TV decreased from (2.1, 0.3, 0.2) to (0, 0, 0) %, Ob.S/BS decreased from (45.5, 20.0, 22.5) to (7.8, 1.5, 1.0) %, OS/BS decreased from (58.1, 44.7, 37.3) to (17.1, 8.2, 13.5) %, BFR/BS also decreased from (0.069, 0.023, 0.044) to (0.004, 0.003, 0.004) $\text{mm}^3/\text{mm}^2/\text{year}$. Minimodeling volume (MLV/BV) increased from (0.49, 0.45, 1.73) to (5.18, 4.95, 4.41) %. In addition, MAR of remodeling sites were decreased from (0.89, 0.79, 0.65) to (0.4, 0.41, 0.39) mcm/day after the treatment of cinacalcet HCL. And MAR of minimodeling sites were decreased from (0.94, 0.84, 0.64) to (0.44, 0.48, 0.40) mcm/day after the treatment. As a result, MAR values were generally greater in minimodeling sites than in remodeling sites.

Conclusions: Cinacalcet HCL well suppressed bone remodeling and turnover, but effectively increased bone formation due to minimodeling in cancellous bone in these patients.

Disclosures: A. Yajima, None.

T496

Minimodeling Reduces the Rate of Cortical Bone Loss in Patients with Secondary Hyperparathyroidism. A. Yajima¹, M. Mitobe^{*1}, I. Takahashi^{*1}, T. Nakayama^{*2}, O. Otsubo^{*1}, M. Inaba^{*3}, Y. Tominaga^{*4}, A. Ito^{*5}. ¹Nephrology, Towa Hospital, Tokyo, Japan, ²Orthopedic Surgery, Towa Hospital, Tokyo, Japan, ³Metabolism, Endocrinology, and Molecular Medicine, Osaka City University Graduate School of Medicine, Osaka, Japan, ⁴Transplant Surgery, Nagoya Second Red Cross Hospital, Nagoya, Japan, ⁵Ito Bone Histomorphometry Institute, Niigata, Japan.

Purpose: Secondary hyperparathyroidism causes progressive cortical thinning due to increased bone resorption at the endocortical surface, and increases cortical porosity due to increased resorption at the intracortical surface. However, patients with severe hyperparathyroidism do not always suffer from bone fractures, perhaps because of the increased

minimodeling occurring in cortical bone. Because bone formation by minimodeling has not yet been reported in cortical bone, we investigated the effects of cortical minimodeling on the reduction of the rate of bone loss.

Methods: Thirty-five patients with secondary hyperparathyroidism were enrolled. Remodeling and minimodeling parameters at the endocortical and periosteal surfaces as well as at the intracortical surface were measured. The relationships between remodeling parameters and minimodeling parameters at each surface were investigated by linear regression analysis. Cortical bone specimens were classified into three groups according to the values of cortical width and cortical porosity. The relationships of minimodeling parameters at the endocortical surface with cortical width and at the intracortical surface with cortical porosity were investigated.

Results: Some minimodeling parameters showed positive correlations with serum parathyroid hormone levels and remodeling parameters. Minimodeling bone volume at the endocortical surface was greater in the narrow cortical width group than in the wide cortical width group, possibly slowing the progression of cortical thinning. Minimodeling volume at the intracortical surface was greater in the high porosity group than in the low porosity group, possibly slowing the progression of enlargement of the intracortical resorption spaces. Minimodeling of the periosteal surface was found in one specimen.

Conclusions: The results revealed enhanced cortical minimodeling in patients with secondary hyperparathyroidism, possibly representing the reduction of the rate of cortical bone loss.

Disclosures: A. Yajima, None.

T497

Bone Loss Following Small Bowel Transplantation. K. S. Awan^{*1}, J. M. Wagner^{*1}, D. Martin^{*2}, D. L. Medich^{*1}, S. Perera^{*3}, K. Abu Elmagd^{*2}, S. L. Greenspan¹. ¹Medicine, University of Pittsburgh, Pittsburgh, PA, USA, ²Department of Surgery, UPMC Thomas E. Starzl Transplantation Institute, University of Pittsburgh, Pittsburgh, PA, USA, ³Medicine/ Biostatistics, University of Pittsburgh, Pittsburgh, PA, USA.

Little is known about the impact of small bowel transplantation (SBTx) on skeletal integrity. We compared bone mineral density (BMD, Hologic Discovery A) in 81 patients who had undergone SBTx (43 \pm 2 years old, average SBTx 2.2 years before, 65% women) with 51 small bowel controls (SBCon), with similar small bowel diseases (47 \pm 13 years old) awaiting transplantation matched for age and gender. In addition to SBTx, surgery could include transplantation of the liver, pancreas, and stomach. Following SBTx, patients receive tacrolimus, supplementary calcium and vitamin D and bisphosphonates if appropriate. BMI was similar for the 2 groups (SBTx 22.7 ± 0.5 kg/m² vs. SBCon 23.1 ± 0.8 kg/m²). Compared with the SBCon, the SBTx group had significantly lower absolute BMD and Z-scores at the hip and femoral neck without differences noted at the spine (Table). 25 hydroxy vitamin D levels were similar in SBTx patients compared to SBCon (17.4 ± 1.5 vs. 21.1 ± 1.9 ng/dl) as were levels of serum calcium (8.9 ± 0.1 vs. 8.9 ± 0.1 mg/dl) and parathyroid hormone (60.5 ± 9.5 vs. 81.6 ± 11.0 pg/ml). Twenty three patients were followed with BMD's prospectively; nine patients before and after transplantation (Pre to Post: mean 1.3 years follow-up); fourteen patients after transplant (Post: mean 1.8 years average follow-up). Bone loss (percent change in g/cm²) was greatest in the patients who were followed through transplantation surgery (Pre to Post), with an average bone loss of 15% at the hip, compared to patients followed after transplantation (Post). There were no significant changes in levels of 25 hydroxy vitamin D, calcium, or parathyroid hormone. We conclude that patients undergoing SBTx have significant bone loss, primarily at the hip, occurring within the first year post transplant despite preventive measures with calcium, vitamin D and bisphosphonates.

Bone Mineral Density in SBTx and SBCon Patients (Table as Mean \pm SEM.)

	Lumbar Spine	Total Hip	Femoral Neck
Cross-sectional			
SBTx Z-score (SD)	-1.3 \pm 0.2**	-1.5 \pm 0.1**	-1.4 \pm 0.1**
SBCon Z-score (SD)	-0.5 \pm 0.3	-0.7 \pm 0.2**	-0.7 \pm 0.2**
P-value SBTx vs. SBCon	0.02	<0.01	<0.01
SBTx (gm/cm ²)	0.876 \pm 0.018	0.742 \pm 0.019	0.654 \pm 0.018
SBCon (gm/cm ²)	0.940 \pm 0.031	0.834 \pm 0.028	0.721 \pm 0.024
P-value SBTx vs. SBCon	0.08	<0.01	0.02
Longitudinal			
SBTx Pre to Post (% change)	-2.6 \pm 3.1	-15.9 \pm 4.3**	-15.3 \pm 3.4**
SBTx Post (% change)	0.5 \pm 1.9	-0.6 \pm 1.7	-1.1 \pm 3.0
P-value Pre to Post vs. Post	0.37	0.01	0.01

*p<0.05, **p<0.01 difference from zero for cross-sectional, change from baseline for longitudinal

Disclosures: K.S. Awan, None.

This study received funding from: NIH/K24.

T498

Interest of Platelet-derived Products for Bone Repair. L. Begot^{*1}, C. Doucet^{*2}, I. Ernou^{*2}, F. X. Gunepin^{*3}, C. Laplace-buihle^{*4}, J. J. Lataillade^{*2}, X. Holy¹. ¹Histology and Tissue Repair, IMASSA, Brétigny sur Orge, France, ²Département Recherches, CTSA, Clamart, France, ³Service de Chirurgie Orthopédique, HIA Percy, Clamart, France, ⁴Imagerie, Généthon, Evry, France.

The French Army Hospitals have to treat a high number of patients presenting lesions with large loss of bone substance. The size of defects, rendering the bone auto graft strategy unsuitable, suggests a stem cell therapy approach. Progress in tissue engineering make it possible to conceive the development of macroporous ceramic bone substitutes combined to Mesenchymal Stem Cells (MSC) for filling in bone defects. This approach needs cell cultures and implantation in clinical conditions. As platelets are a source of growth factors, Platelet-rich plasma (PRP) could be used as substitute for Foetal Calf Serum (FCS) in cultures and to prepare a platelet-derived Glue (PG) mixture interesting for its properties of adhesiveness, malleability and haemostasis. In this work, we studied the effect of the proliferation and differentiation of MCS in presence of PRP products.

PRP was obtained by apheresis collection and processed for platelet activation to stimulate growth factor release. First, human marrow-derived MSC were isolated and expanded in a medium with 10% FCS or 10% PRP through a process of subculturing. The ability of PRP to enhance MSC proliferation was investigated by measuring cell numbers at consecutive passages, by characterizing MSC phenotype (CD45⁺, CD90⁺, CD105⁺, CD73⁺, CD13⁺) and by performing in vitro osteogenic evaluation (alkaline phosphatase activity, Von Kossa staining, osteocalcin detection). Second, proliferation, survival differentiation were evaluated in glue. Finally, we compared the biocompatibility and functionality of MSC or osteoblastic precursors loaded on bio-ceramics in a mice orthotopic implantation model in presence or not of PG.

Our results showed that PRP medium was considerably more effective in stimulating MSC proliferation than FCS one without affecting their phenotype. Furthermore, MSC cultured with PRP maintained their differentiation properties. MSC and osteoprogenitors were able to proliferate at the surface and within the bio-ceramic in presence of glue. In vitro and in vivo experiments demonstrated that osteogenic differentiation of MSC was improved when PG was associated with the hybrid implant. Osteoblastic precursors appeared to be better candidates than MSC regarding their long term in vivo survival in mice.

In conclusion, our data show that for ex vivo expansion of human MSC prior to transplantation, PRP could efficiently replace FCS and that the PG could be a powerful tool in bone repair. We suggest that PRP biotechnology should be useful in combination with MSC for bone reconstructive cellular therapy.

Disclosures: L. Begot, None.

This study received funding from: DGA (Direction Générale pour l'Armement).

T499

Long-term Follow up of Bone Mineral Density, Bone Turnover Markers and 25-hydroxyvitamin D in Bone Marrow Transplant Survivors. B. Buehring^{*1}, D. Krueger¹, W. Longo^{*2}, B. Flynn^{*2}, N. Binkley¹. ¹University of Wisconsin Osteoporosis Clinical Research Program, Madison, WI, USA, ²University of Wisconsin Blood and Marrow Transplant Program, Madison, WI, USA.

Increasing data are available showing that long-term bone marrow transplantation (BMT) survivors have deficits in bone mineral density (BMD) with consequent increased fracture risk. As the numbers of BMT recipients are increasing and survival rates improve, the impact of decreased BMD and increased fracture risk on morbidity and mortality also rises. Data defining the skeletal effects of BMT beyond six months post transplantation are limited. As such we report twelve month BMD data as well as six month bone metabolism parameters and 25OH vitamin D [25(OH)D] levels in BMT survivors.

A subset of 15 long-term BMT survivors with hematologic malignancies from a prospective trial documenting BMT effects on skeletal status were used to obtain these data. This sample of eight women and seven men, mean age 40.8 ± 1.6 years, had BMD measured at the lumbar spine (LS), total proximal femur (TF), and femur neck (FN) on a Lunar Expert (Madison, WI) densitometer at baseline, 100 days, six months and one year post transplant. 25(OH)D, osteocalcin (Oc), bone specific alkaline phosphatase (BSAP) and n-telopeptide of type 1 collagen (NTx) were measured at similar time points.

BMD decreased (p<0.01) in all measured regions. TF and FN declined by 10% and 8% respectively at three months and were reduced 12% and 9% at one year. LS BMD was 9% lower than baseline after 12 months. At time of BMT bone turnover was elevated, and subsequently at 30 days Oc was numerically but not statistically lower. At six months both BSAP and Oc were increased from baseline. NTx trended upwards (p=0.07) by 30 days and was not different from baseline after half a year.

Low vitamin D status was extremely common prior to BMT being present in 87% (13/15) and remained suboptimal at 6 months in 67%. No clinical fractures were reported within the first 12 months.

In conclusion, following BMT, despite elevation of bone formation, rapid and pronounced bone loss occurs which persists at one year. 25(OH)D levels were low before transplantation and remained low. Femur BMD results are comparable to other studies, however only minimal loss in LS BMD has been reported elsewhere. Although no clinical fractures were reported in the first year post transplantation, these data suggest BMT patients are likely at increased fracture risk. As such, skeletal status and quality of life assessments in these individuals now 5-7 years post transplantation is planned.

Disclosures: B. Buehring, None.

T500

Severe Hypovitaminosis D, Associated with Hyperparathyroidism and Osteopenia/Osteoporosis in a Cohort of Long-Term Kidney Transplant Recipients with Excellent Kidney Function. R. Hayashi^{*1}, M. Stratilova^{*2}, M. Markell^{*1}. ¹Renal Diseases, SUNY Downstate Medical Center, Brooklyn, NY, USA, ²Renal Diseases, Westchester County Medical Center, Valhalla, NY, USA.

Vitamin D deficiency, manifested as decreased 25-OH vitamin D levels, is highly prevalent in hemodialysis patients, and may contribute to hyperparathyroidism and renal osteodystrophy. It is widely believed that successful kidney transplantation, which presumably restores the kidney's ability to activate vitamin D by 1-hydroxylase, will result in restoration of Vitamin D homeostasis, and Vitamin D supplementation is not routinely recommended. We measured 25-OH vitamin D levels in 24 long-term (mean time since transplant - 59.6±11.4 mos) kidney transplant recipients (KTR) with excellent function, mean creat 1.6±0.1 mg/dl. There were 14 women (51%), 80% Black or Hispanic, mean age 48.9±1.8 yrs. 60% were receiving tacrolimus and the rest cyclosporine, 80% were taking prednisolone. The mean 25-OH vitamin D level was 12.9±1.3 ng/ml (range 5-28, normal value >40 ng/ml). Only 1 pt had a value >25 ng/ml and 11 pts (46%) had values <12 ng/ml (severe deficiency). Mean intact PTH level was also elevated (150.6±28.4, range 20-624), with 12 pts (50%) having values >300. There was no relationship between 25-OH Vitamin D level and PTH level. Neither Vitamin D level nor PTH value were related to age, gender, race, time since transplant, creatinine, current calcium or phosphate value, hematocrit, albumin or use of activated vitamin D supplements (8 pts). Bone density scans were available for 6 patients with mean T scores of -2.33 in the L-spine and -1.54 in the femoral neck. We conclude, in our population of primarily minority race KTRs: 1. Vitamin D deficiency is universally prevalent, with severe deficiency occurring in 46% of pts. 2. Persistent hyperparathyroidism is present in over 50% of pts despite the long time since transplant, and excellent kidney function. 3. The degree to which vitamin D deficiency contributes to persistent hyperparathyroidism and osteoporosis, in this population with multiple risk factors, is not known. 4. Hypovitaminosis D is prevalent in a Blacks and Hispanics, in general, and whether this degree of deficiency exists in a Caucasian population of KTR's should be studied. 5. The appropriate dose of Vit D remains to be established, as pts on maintenance active vitamin D preparations in this population had PTH levels that were similar to those not receiving it. It is possible that patients should receive 25-OH Vitamin D as well as the active form is. 6. Long term studies examining repletion of Vitamin D and its effect on the accelerated cardiovascular disease & chronic kidney fibrosis that affects the KTR population are suggested.

Disclosures: R. Hayashi, None.

T501

Effect of Risedronate on Bone Loss Associated with Liver Transplantation. S. Guadalix^{*1}, M. Gomez-Juaristi^{*1}, G. Martinez¹, C. Vargas^{*2}, J. Meneu^{*3}, A. de Lozar^{*2}, S. Azriel^{*1}, E. Jodar^{*1}, E. Moreno^{*3}, F. Hawkins¹. ¹Endocrinology Service, University Hospital 12 de Octubre, Madrid, Spain, ²Biochemistry Service, University Hospital 12 de Octubre, Madrid, Spain, ³Digestive Surgery, University Hospital 12 de Octubre, Madrid, Spain.

Background: Liver transplantation (LTx) increases the risk of osteoporosis and osteoporotic fractures. Most of the bone loss usually occurs in the first 6 months after transplantation, but many patients remains with low bone mass in the long term. The best preventive measure in this setting is being investigated. Objective: To analyse the effect of weekly risedronate on bone loss in patients with low bone mass after LTx. Patients and Methods: we show preliminary results of a randomized open-label single center prospective study. Forty-three patients (32 males, 11 females; mean age 54.2 ± 11.2 years) with LTx and low bone mass (lumbar and/or femoral T-score <-1) have been included so far. After transplantation (mean time 31.4 ± 15.4 days) patients were randomly assigned to one of two treatment arms: Group 1 (n=21) received risedronate (35 mg orally, once weekly) plus calcium (1000 mg/day) and vitamin D (800 IU); Group 2 (n=22) received calcium and vitamin D at same doses. Primary endpoint is BMD change at lumbar spine (L1-L4) and femoral regions (measured at baseline, 6 and 12 months after LTx; Hologic QDR 4500 densitometer); secondary endpoints include biochemical markers of bone turnover (serum β-CTX and PINP, urinary D-Pyr), and calcitropic hormones (PTH, 25-OH vitamin D) measured at baseline, 3, 6 and 12 months after LTx. Baseline spine X-rays were obtained in all patients. Results: No differences were found in baseline characteristics between groups. At baseline 46.6% of patients had densitometric criteria of osteoporosis, and 16.2% had prevalent vertebral fractures. At 6 months, spine BMD increased in Group 1 (+2.1 ± 6.8 %), and decreased in Group 2 (-0.6 ± 4.6%). Changes were similar at femoral neck and total hip in both groups. Baseline bone resorption markers were increased in 40.5% (β-CTX) and 56% (D-Pyr) of patients. Ninety-three of patients showed vitamin D insufficiency at entry in the study. In Group 1, a significant decrease of serum β-CTX was observed after 3 months (p=0.032) and 6 months (p=0.007). Treatment was well tolerated in both groups. Conclusions: Preliminary data of this prospective trial suggest that risedronate could be effective in preventing the natural course of bone loss associated with liver transplantation.

Disclosures: G. Martinez, None.

This study received funding from: Fundacion Mutua Madrileña (2005-072).

T502

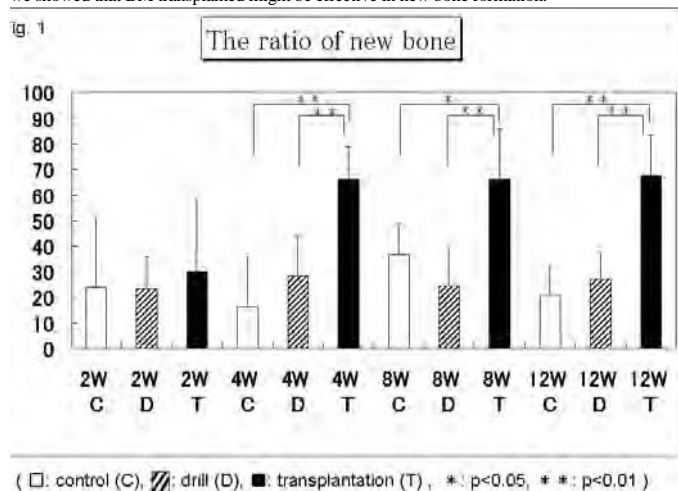
An Experimental Rabbit Model of Lunate-like Osteonecrosis: Is Transplantation of Bone Marrow Effective for Remodeling of Necrotic Bone. T. Ogawa*, T. Ishii*, H. Mishima, N. Ochiai*. Orthopaedic Surgery, University of Tsukuba, Tsukuba, Japan.

Introduction Lunate malacia (Kienbock disease) is a progressive wrist disorder characterized by osteonecrosis of the lunate. We decided to investigate whether transplantation of bone marrow (BM), a less invasive procedure, would be an effective treatment. There was no animal Kienbock disease model; so, we have developed an experimental rabbit model of lunate-like osteonecrosis using a rabbit's 4th tarsal bone. We investigated the validity of the model and the usefulness of BM transplantation for remodeling of necrotic bone.

Material and Method Thirty six adult Japanese white rabbits were used. The bilateral 4th tarsal bones were removed and soaked in liquid nitrogen for 5 minutes. After the freezing, the bone was inserted in subcutaneous of the back of the rabbit. The total number of the necrotic bone was seventy two. They were divided into three groups, BM transplantation (T), drilling (D) and control (C). In the group T, three drill holes were made cortical surface of the tarsal bone with Kirschner wire, cartilage surface were remained intact, and after subcutaneous insertion they were filled with BM from iliac crest. In the group D, three drill holes were also made but no BM transplantation. In the group C, the tarsal bones were only soaked in liquid nitrogen. Fluorochrome label (Calcein) was injected subcutaneously at 8 days and 2 days before sacrifice. We sacrificed nine rabbits (three from each group), obtaining six specimens of necrotic bone from each group, at 2, 4, 8 and 12 weeks. Bone morphological study (Toluidine-blue), ALP staining and TRAP staining were made, using the undecalcified sections.

Results We compared histological finding of the ratio of the fluorochrome-labeled trabecular bone surface in each group. Group C and D had poor new bone formation from 2 to 12 weeks. In group T, new bone formation, were significantly higher than in the other groups at 4, 8 and 12 weeks (Fig.1). TRAP-positive multinucleated cells were found in group T at 8 and 12 weeks more than another groups. Qualitative analysis, there were found ALP-positive osteoblast-like cells in group T at 4, 8 and 12 weeks more than another groups.

Discussion This study established a new animal necrosis model similar to human lunette, in terms of avascular necrosis and surrounding with cartilage and cortical bone. Using this model we showed that BM transplanted might be effective in new bone formation.



Disclosures: T. Ogawa, None.

T503

Effects of Immunosuppressants on Bone Metabolism (Bone Mineral Density, Bone Vitamin K Analogs, and Serum Osteocalcin and Calcium) in Rats. H. Wakabayashi¹, J. Kanda¹, A. Takahashi², K. Onodera³. ¹Clinical Pharmacotherapy, Niigata University of Pharmacy and Applied Life Sciences, Niigata, Japan, ²The Clinics of Dentistry for the Disabled, Tohoku University Dental Hospital, Sendai, Japan, ³Dental Pharmacology, Okayama University Graduate School of Medicine and Dentistry, Okayama, Japan.

This study was carried out to evaluate the effects of short-term administration of corticosteroids (hydrocortisone, prednisolone and dexamethasone) on bone metabolism. Growing rats were administered daily with the equiactive dose of corticosteroid (hydrocortisone: 20 mg/kg; prednisolone: 4 mg/kg; dexamethasone: 0.8 mg/kg) at 9 am for two weeks. No significant differences in bone vitamin K analogs (VKs), bone mineral density (BMD) and serum osteocalcin (OC) were observed both in the hydrocortisone-treated group and prednisolone-treated group compared with the control group, whereas significant decreases were observed in MK-4 (one of the VKs), BMD and serum OC of the dexamethasone-treated group compared with those in the control group. Furthermore, we also investigated about a preventative effect against bone loss caused by short-term injection of dexamethasone, using combined administration of alfacalcidol, risenedronate, and menatrenone with dexamethasone. Combined administration of risenedronate and menatrenone with dexamethasone for two weeks prevented the reduction of BMD induced by dexamethasone, especially the administration of risenedronate and menatrenone at 5 pm was more effective to prevent the bone loss than the administration at 9 am. The degree of bone loss induced by drugs has been considered to be dependent on drug type

(corticosteroid type) and dose, duration of treatment, age and sex of recipients. Additionally, the present results suggest that the degree of bone loss induced by drug is dependent on the drug administration time.

Disclosures: H. Wakabayashi, None.

T504

$\alpha 5$ Integrin Association with Cx43 Regulates the Function of Osteocyte Hemichannels in Response to Shear Stress. A. J. Siller-Jackson¹, S. Burra¹, S. E. Harris², L. F. Bonewald³, E. Sprague⁴, J. X. Jiang¹. ¹Biochemistry, University of Texas Health Science Center, San Antonio, TX, USA, ²Periodontics, University of Texas Health Science Center, San Antonio, TX, USA, ³Oral Biology, School of Dentistry, University of Missouri, Kansas City, MO, USA, ⁴Radiology, University of Texas Health Science Center, San Antonio, TX, USA.

Primary osteocytes and MLO-Y4 osteocyte-like cells express large amounts of connexin 43 (Cx43) which forms gap junctions and hemichannels. Our previous studies have shown that fluid flow shear stress (FFSS) induces the opening of hemichannels in MLO-Y4 cells. Analysis by gene microarray of MLO-Y4 cells showed elevation of $\alpha 5$ integrin with FFSS and inhibition with a gap junction/hemichannel inhibitor, a result further confirmed by Northern blot assay. $\alpha 5$ integrin blocking antibody significantly decreased FFSS induced dye uptake mediated by Cx43 hemichannels, suggesting a role for $\alpha 5$ integrin in FFSS regulation of Cx43 hemichannels. Immunostaining showed co-localization of $\alpha 5$ integrin with Cx43 not only on the cell surface but throughout the cell body and processes, becoming more pronounced when exposed to FFSS. Cx43 and $\alpha 5$ integrin were not co-localized with vinculin or paxillin, components of focal adhesions, suggesting that the association between Cx43 and $\alpha 5$ integrin is unrelated to the function of integrins in focal adhesions. Co-immunoprecipitation analysis showed the association of $\alpha 5$ integrin with Cx43. To determine the involvement of $\alpha 5$ integrin in Cx43 hemichannel function, $\alpha 5$ integrin siRNA was transfected into MLO-Y4 cells, which leads to a 90% reduction of $\alpha 5$ integrin levels. Interestingly, cellular localization was significantly altered in $\alpha 5$ integrin siRNA-treated cells with the disappearance of punctate expression of Cx43 on the cell surface. In fact, Cx43 was found outlining the entire cell surface border. FFSS applied to $\alpha 5$ integrin siRNA transfected MLO-Y4 cells resulted in the localization of Cx43 in punctate spots on the surface, although less prominent than in untransfected cells. More importantly, $\alpha 5$ integrin siRNA completely abolished hemichannel-mediated dye uptake induced by FFSS. Together, these results suggest that $\alpha 5$ integrin plays an essential role in the function of Cx43-hemichannels and is a likely mechanical sensor or tether that transmits mechanical stress to Cx43 hemichannels.

Disclosures: J.X. Jiang, None.

This study received funding from: National Institutes of Health.

T505

Mechanical Activation of β -catenin Is Enhanced After Caveolin-1 Knock-down. M. Ma¹, B. Sen¹, N. Case¹, Z. Xie¹, H. Jo², T. Gross³, J. Rubin¹. ¹Medicine, UNC, Chapel Hill, NC, USA, ²Emory/GaTech, Atlanta, GA, USA, ³Orthopaedics, U.Washington, Seattle, WA, USA.

Mechanical loading of bone initiates an anabolic, anti-catabolic pattern of gene response; some of this response may be attributed to induction of β -catenin responsive genes. Caveolin-1, a structural membrane protein, can sequester β -catenin. The skeletal phenotype of the caveolin-1 knock-out mouse is of increased trabecular and cortical bone. This suggested to us that the presence of caveolin-1 might limit the process of osteogenesis; indeed we have shown that delivery of siRNA targeting caveolin-1 (siCav) to stromal cells causes upregulation of Runx2 and osteix and suppression of RANKL. We therefore asked if an interaction of caveolin-1 with β -catenin might constrain mechanical stimulation of the osteoblast phenotype. For these experiments we plated CIMC-4 preosteoblast cells expressing caveolin-1 on BioFlex collagen plates. Application of 2%, 0.17 Hz substrate strain for 2 h followed by 2 h incubation induced a β -catenin gene response: WISP-1 rose to 1.86 ± 0.06 fold ($p < 0.05$), returning to baseline 6 h later. Other β -catenin target genes, Runx2 and osteoprotegerin, were not increased at 4 h after the strain protocol. Delivery of siCav (50 nM) caused an 80% reduction in cav-1 mRNA and >75% reduction in caveolin-1 protein compared to control siRNA (siSCR). After strain, at 4 h, +siCav cells showed not only an enhanced WISP-1 response, but also significant elevation of osteoprotegerin (+siCav+strain 1.7 ± 0.4 fold above +siCav-unstrained) and Runx2 (1.4 ± 0.15 fold increased). RANKL expression was repressed to < 0.4 that of unstrained controls, and was unaltered by siCav, indicating that RANKL repression did not involve caveolin-1. We next explored means of measuring β -catenin activation after mechanical stimulation. Strain caused an increase in cytoplasmic β -catenin levels as assayed by Western after 3 h. Though the TopFlash β -catenin reporter was activated by LiCl in CIMC-4 cells (3.1 ± 1.7 fold above untreated cells), we have not yet shown that strain induces TopFlash activity. However, siCav treated cells showed increases in basal cytoplasmic β -catenin, and basal and strain stimulated TopFlash activity were increased by 2.14 and 2.5 fold respectively. Our data indicates that a reduction in caveolin-1 is accompanied by an increase in the β -catenin pool accessible to exogenous stimuli. This suggests that not only can caveolin-1 limit incoming mechanical signals by sequestering the actionable β -catenin pool, but also that mechanical activation of β -catenin may involve its release from the membrane.

Disclosures: M. Ma, None.

This study received funding from: NIAMS/NIH.

T506

Nmp4/CIZ Contributes to Fluid Shear Stress Induced MMP-13 Gene Induction in Osteoblasts. K. Panyayong¹, J. Yang², F. M. Pavalko³, R. Gerard-O'Riley³, J. P. Bidwell¹. ¹Department of Oral Biology and Occlusion, Faculty of Dentistry, Prince of Songkla University, Hatyai, Songkhla, Thailand, ²Department of Anatomy and Cell Biology, Indiana University School of Medicine, Indianapolis, IN, USA, ³Department of Cellular and Integrative Physiology, Indiana University School of Medicine, Indianapolis, IN, USA.

Mechanical force or load impacts bone remodeling. The expression of matrix metalloproteinase-13 (MMP-13), involved in bone turnover, is elevated in stretched MC3T3-E1 osteoblast-like cells. Strain-mediated forces on bone move fluid through the canalicular-lacunar network resulting in fluid shear stress (FSS) on the membranes of bone cells initiating remodeling. Although the nuclear events mediating putative FSS-induced changes in osteoblast MMP-13 transcription are unknown, previous studies with osteoblasts suggest an overlap between osteoblast FSS- and PTH-induced signal response pathways. MMP-13 PTH response is regulated by a 110 bp 5' regulatory region, conserved across the mouse, rat, and human genes, that supports the binding of numerous transcription factors including Runx2, c-fos/c-jun, Ets-1, and nuclear matrix protein 4/cas interacting zinc finger protein (Nmp4/CIZ), a nucleocytoplasmic shuttling trans-acting protein that attenuates PTH-driven transcription. Nmp4/CIZ also binds p130^{cas}, an adaptor protein implicated in mechanotransduction. Our objective was to determine whether Nmp4/CIZ contributes to FSS-induced changes in MMP-13 transcription. MC3T3-E1 cells were transfected with MMP-13 promoter-reporter or Nmp4/CIZ promoter-reporter constructs, then exposed to FSS (12 dynes/cm², 1-5 hr). MMP-13 mRNA levels and Nmp4/CIZ-DNA binding activity were analyzed by real-time PCR and gel shift assays, respectively. Western analysis of nuclear, membrane, and cytoplasmic fractions was used to assess FSS-induced changes in p130^{cas} subcellular distribution. We observed that FSS (3-5 hr) increased MMP-13 promoter-reporter activity approximately 2-fold in MC3T3-E1 cells attended by a comparable increase in mRNA expression. This was accompanied by a decrease in Nmp4/CIZ binding to its cis-element within the PTH response region, the mutation of which abrogated FSS response. Interestingly, FSS enhanced Nmp4/CIZ promoter activity. FSS also induced p130^{cas} nuclear translocation. We conclude that the PTH regulatory region of MMP-13 also contributes to FSS response and that Nmp4/CIZ plays similar but distinct roles in mediating hormone- and FSS-driven induction of MMP-13 in bone cells.

Disclosures: K. Panyayong, None.

T507

The Presence of p120-Catenin in Osteocytes and Other Bone Cells. H. W. Sampson, A. R. Parrish*, A. C. Dearman*, W. E. Zimmer*. Systems Biology and Translational Medicine, TAMHSC_College of Medicine, College Station, TX, USA.

P120 is a member of the armadillo supergene family which has been reported to bind cadherins at a juxtamembrane domain and regulate their cell surface trafficking. It can become cytoplasmic regulating activities of Rac, Rho and Cdc42; thus functioning in maintenance of cell shape and enhanced cell motility. It can also enter the nucleus where it is considered to possibly modulate Wnt/ β -catenin/TCF signaling in a synergistic manner in the nucleus to activate matrilysin expression. The purpose of this study was to document the presence of p120-catenin in bone cells. We used conventional RT-PCR, Western blot, immunohistochemical and fluorescent immunohistochemistry in conjunction with light and fluorescent microscopy and confocal microscopy to study in situ bone cells and also MLO-Y4 osteocyte-like cells in culture (a generous gift from Dr. Lynda Bonewald, University of Missouri-Kansas City). The p120-catenin antibody used was a monoclonal antibody at 1:100 dilution and the biotinylated secondary antibody, was incubated in conjugated streptavidin horseradish peroxidase followed by Betazoid 3, 3' Diaminobenzidine. In the case of the fluorescent studies the secondary antibody was Alexa Fluor 488 goat anti-mouse IgG (molecular probes, OR). The in vivo studies were conducted on mouse tibia and all experimental procedures were in compliance with the guiding principles in the "Care and Use of Animals" as published in the Am. J. Physiol., and were approved by the TAMU animal care and oversight committee. All methods used indicated a high concentration of p120 RNA and protein in osteocytes, both in situ and in culture, in osteoblasts, and in chondrocytes of the resting zones and hypertrophic zones of the mouse growth plate. All studies indicated a cytoplasmic or sub-membrane localization. We have demonstrated, for the first time, the presence of p120-catenin in osteocytes and other bone cells. This is an adhesion molecule whose importance in cell signaling is becoming more and more apparent with time and with its ability to move from the plasma membrane, to the microtubule system of the cytoplasm and to the nucleus is positioned to play an important role in cell development and possibly in mechanotransduction.

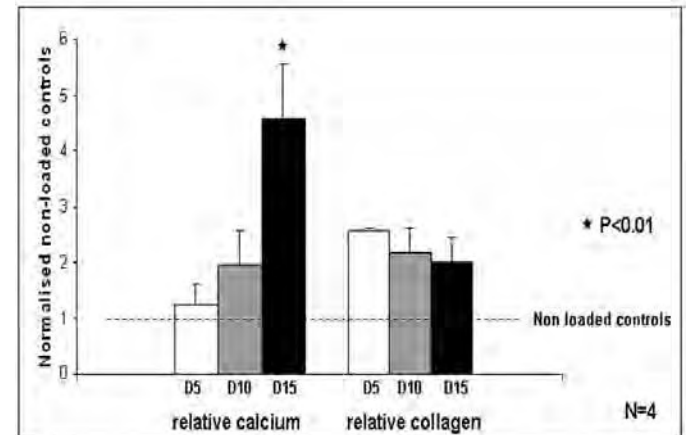
Disclosures: H.W. Sampson, None.

T508

The Effects of Compressive Loading on Matrix Production by Osteoblastic Cells Cultured in Polyurethane Scaffolds. A. Sittichokechaiwut, A. Scutt, G. C. Reilly. Engineering Materials, University of Sheffield, Sheffield, United Kingdom.

Bone tissue engineering constructs are composed of scaffold materials and matrix synthesizing cells. It is likely that mechanical stimulation of tissue engineered bone will enhance matrix synthesis, however, the underlying mechanisms by which osteoblasts respond to their mechanical environment in 3-D are poorly understood. The aims of this

study are to examine the effects of cyclic compressive loading on bone matrix production in 3-D scaffolds over 20 days of culture. 3-D polyurethane scaffolds with an average pore size 150 micrometres were cut into cylinders of 10 mm diameter and 10 mm height. Scaffolds were seeded with MLO-A5 osteoblastic cells (Kato et al. JBMR 2001), kindly donated by Dr. L. Bonewald, at densities of 2.5×10^5 per scaffold. Cell-seeded scaffolds were dynamically loaded in compression at 1Hz, 5% strain in a biodynamic chamber (BOSE/Electroforce3200). Loading was applied for 2 hours per day at day 5, 10 and 15 of culture. Between loading, scaffolds were cultured in an incubator in standard conditions for up to 20 days. Cell-seeded scaffolds were assayed on days 10, 15 and 20 of culture for scaffold stiffness (Young's modulus of elasticity), cell viability by MTS assay, calcium by alizarin red staining and collagen content by sirius red staining. Cells survived in all loaded samples, final relative cell number was increased at day 10 but slightly lower at days 15 and 20. Calcium content increased in all loaded samples and was significantly higher on day 20 ($p < 0.01$, t-test) compared with non loaded samples. Total collagen also increased significantly at day 15 and 20 in loaded samples compared with non loaded samples ($p < 0.02$). Scaffold stiffness was higher in loaded samples at the end of experiment (~ 39 vs 62 Pa, $p < 0.01$). In conclusion, although the number of viable cells was lower in loaded samples after 10 days, the amount of calcium, collagen and scaffold stiffness was greater, indicating the formation of new extracellular matrix within the constructs. Therefore, cyclic compressive loading at 5% strain for 2 hours every 5 days has the potential to produce more bone matrix than static culture conditions.



Disclosures: A. Sittichokechaiwut, None.

This study received funding from: The Royal Society of London.

T509

Calibration of the ZETOS Bone Loading System. S. Garcia^{*1}, H. L. Ploeg^{*1}, E. L. Smith². ¹Mechanical Engineering, University of Wisconsin, Madison, WI, USA, ²Population Health Sciences, University of Wisconsin, Madison, WI, USA.

An ex vivo bone culture and loading system, ZETOS, has been developed to study morphological and physiological responses of trabecular bone (10 mm diam., 5 mm ht.). A piezoelectric actuator (PZA) expands, compressing the specimen while measuring expansion and load. Calibration was performed when manufactured, but the system's compliance changes with time, requiring recalibration. The purpose of this study was to develop and validate a recalibration protocol for the ZETOS bone loading system. Ten aluminum (alloy 7075-T6) reference bodies (RBs) of known stiffness (40 to 2000 MPa, trabecular bone stiffness range) were designed using finite element analysis (FEA) and manufactured. Geometry was verified using a coordinate measuring machine, at 72 points throughout the RB, showing uniform surfaces (SD = 2.34 μ m). Calibration of the unloaded PZA expansion transducer was performed with a fiberoptic sensor. All RBs were tested in ZETOS, recording force and expansion. A FEA model duplicated the physical compression setup of the RBs in ZETOS. Stiffness was found for each RB by dividing total reaction force by displacement. FEA was validated with physical testing in an Instron by compressing six RBs on a setup replicating the ZETOS system. RB deformation was measured using a 10x microscope and calibrated digital camera. Percent differences of FEA-determined stiffness were found with respect to stiffness from Instron testing. ZETOS force and expansion, and compression from FEA were integrated in a calibration table. For verification of the calibration table, all RBs were tested in ZETOS, as well as 3 metal springs of unknown stiffness, comparing these results to those from the FEA. FEA results had a mean percent difference with respect to Instron testing of 5.08%. The results from the Instron measurements were used to validate the FEA. Verification of RB stiffness determined by ZETOS after calibration resulted in an overall mean difference from the FEA of 1.10%. Results from testing of the 3 metal springs found a mean percent difference in stiffness, compared to their FE models, of 2.25%.

Calibration of the ZETOS loading system is important to assure stiffness measurement accuracy. FEA was an essential tool for RB design and calculated stiffness. The combination of physical testing and FEA enabled a precise determination of RB stiffness. Test results validated the FEA, which provided results that could not be physically measured to generate the calibration table. The successful development of a recalibration protocol of the ZETOS assures accuracy of trabecular bone stiffness measurements. Jones, D.B. et al. European Cells and Materials, 2003, 5, 48-60 Smith, E.L. et al. J. Bone and Mineral Research, 2001, 16(Suppl 1), S481

Disclosures: E.L. Smith, None.

This study received funding from: University of WI Graduate School.

T510

Identification of Genes that May Modulate the Musculoskeletal System's Early Response to Unloading. M. E. Squire¹, M. Monaghan^{*2}, L. R. Donahue³, A. Dhundale^{*2}, C. T. Rubin⁴, S. Judex⁴. ¹Biology, University of Scranton, Scranton, PA, USA, ²Center for Biotechnology, Stony Brook, NY, USA, ³Jackson Laboratories, Bar Harbor, ME, USA, ⁴Biomedical Engineering, Stony Brook University, Stony Brook, NY, USA.

Bone and skeletal muscle are both capable of remodeling their structures to accommodate altered levels of mechanical loading. In the absence of functional loading, musculoskeletal tissue is lost at rates that can exceed 2% per month. Based on the functional relationship between bone and muscle, it is plausible that similar molecular mechanisms may be involved in the early stages of their responses to altered mechanical loading. In this study, we examined gene expression in bone and muscle following short-term hindlimb unloading, with a particular interest in genes that were differentially regulated in both tissues. Total RNA was extracted from the whole proximal tibia and soleus of adult (4 mo) female F1 crossbred (BALB/cByJ x C3H/HeJ) mice following 4d of normal cage activity (control) or tail suspension (disuse) (n=5 each). Reference samples were hybridized with either a control or disuse sample onto custom oligonucleotide arrays (n=5 per group) containing 16,442 ESTs (70mer oligos) from the Operon mouse genome library (v2). Following normalization and filtering, 164 (tibia) and 115 (soleus) differentially regulated genes were identified (p<0.05), with only 3 genes common to both lists. Further classification of affected genes based on their "biological function" annotations revealed 17 genes (tibia; 7 up- and 10 down-regulated) and 14 genes (soleus; 6 up- and 8 down-regulated) that belonged to the "cell communication" category. Some of these identified genes have known roles in classic signaling pathways or are known intracellular signal transducers in bone or skeletal muscle. In the "response to stimulus" category, 14 genes (tibia; 6 up- and 8 down-regulated) and 8 genes (soleus; 2 up- and 6 down-regulated) were significantly affected. This list included one gene that was down-regulated 1.2 and 2.0 fold in the tibia and soleus, respectively, following unloading. In addition, one significantly down-regulated gene in the tibia (-1.4 fold) encodes for a receptor protein that has been identified previously as a responder to mechanical stimuli in osteoblasts and osteocytes. Current qPCR studies will validate these findings. Taken together, the results suggest that although some genes may mediate the early response of both tissues to mechanical unloading, the vast majority of genes involved are likely distinct across tissues. Future analyses will be needed to examine whether the lack of common genes is due a difference in molecular mechanisms or a difference in the temporal response in bone vs. muscle.

Disclosures: M.E. Squire, None.

T511

Ultrasound Induces Hypoxia-Inducible Factor-1 Activation and iNOS Expression Through Integrin/ILK/Akt Pathway in Cultured Osteoblasts. C. Tang¹, W. Fu^{*2}, D. Lu^{*3}, T. Tan^{*1}, R. Yang⁴. ¹Pharmacology, China Medical University, Taichung, Taiwan, ²Pharmacology, National Taiwan University, Taiwan, Taiwan, ³Pharmacology, National Taiwan University, Taipei, Taiwan, ⁴Orthopaedics, National Taiwan University & Hospital, Taipei, Taiwan.

It has been shown that ultrasound (US) stimulation accelerates fracture healing in the animal models and in clinical studies. Nitric oxide (NO) is a crucial early mediator in mechanically induced bone formation. Here we found that US stimulation increased nitric oxide (NO) formation and the protein level of inducible nitric oxide synthase (iNOS). US-mediated iNOS expression was attenuated by anti-integrin $\alpha 5 \beta 1$ or $\beta 1$ antibodies but not anti-integrin $\alpha v \beta 3$ or $\beta 3$ antibodies or focal adhesion kinase mutant. Integrin-linked kinase (ILK) inhibitor (KP-392), Akt inhibitor or mammalian target of rapamycin (mTOR) inhibitor (rapamycin) also inhibited the potentiating action of US. US stimulation increased the kinase activity of ILK and phosphorylation of Akt and mTOR. Furthermore, US stimulation also increased the stability and activity of HIF-1 protein. The binding of HIF-1 α to the HRE elements on the iNOS promoter was enhanced by US stimulation. Moreover, the use of pharmacological inhibitors or genetic inhibition revealed that both ILK/Akt and mTOR signaling pathway were potentially required for US-induced HIF-1 α activation and subsequent iNOS up-regulation. Taken together, our results provide evidence that US stimulation up-regulates iNOS expression in osteoblasts cells by a HIF-1 α -dependent mechanism involving that activation of ILK/Akt and mTOR pathways via integrin receptor.

Disclosures: C. Tang, None.

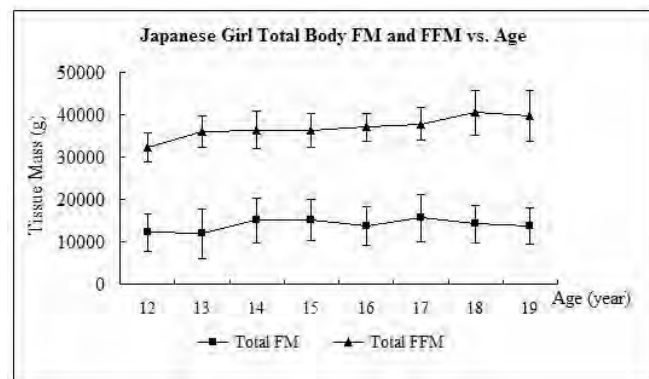
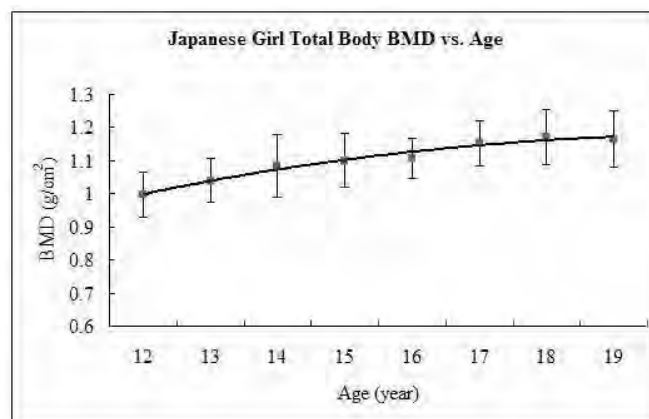
T512

Bone Density and Body Composition Values in Healthy Japanese Girls. T. Aizawa^{*1}, M. Konishi^{*2}, Q. Zhou². ¹Dept of Health and Sport Sciences, Mukogawa Women's University of Letters, Nishinomiya, Kyoto, Japan, ²GE Healthcare Asia, Shanghai, China.

Reference values for bone mineral density (BMD) and soft tissue assessment with dual-energy X-ray absorptiometry (DXA) provide valuable clinical information to help physicians evaluate children with growth disorders and metabolic diseases. As reference values can vary among populations in different geographic regions, it may be advisable to establish region-specific reference values. We measured the total body BMD and body composition in 557 Japanese healthy girls (ages 12 to 19 yrs) with a Lunar DPX-NT (GE Healthcare) densitometer. BMD increased rapidly (4%/year) as did height, bone area (BA),

and fat free mass (FFM) between ages 12 and 14 years, presumably approximating the end of puberty. Another period of rapid increase was found at from ages 16 to age 17 years, when both BMD and BA increased at 4%/year, although height remained stable. On average, BMD values increase from age 12 to 18 at 3%/year, while BA and FFM increased by about 3%/year and 4%/year respectively. There was a strong correlation between bone mineral content (BMC) and lean mass (LM) ($r=0.734$, $p<0.01$), as well as between bone area and height ($r=0.786$, $p<0.01$) over the entire age range. Between the ages of 12 and 19, BMD, bone area and FFM increased rapidly in this population. BMD values at age 18 and 19 for these Japanese girls were slightly higher values previously reported for Caucasian girls of that age.

Age group	N	Height (cm)	Weight (kg)	BMD (g/cm ²)	BA (cm ²)	FM (g)	FFM (g)
12	13	150.7	42.9	0.996	1714	12166	32249
13	44	155.8	48.5	1.040	1885	11920	35971
14	41	157.5	52.4	1.084	1957	15025	36407
15	52	158.1	52.1	1.100	1958	15190	36265
16	40	159.4	51.7	1.106	1989	13752	37013
17	66	159.7	54.3	1.154	2063	15614	37852
18	129	160.6	55.2	1.172	2081	14158	40435
19	172	160.9	54.0	1.165	2074	13676	39703



Disclosures: T. Aizawa, None.

T513

Bone Mineral Density, Body Composition, Body Mass Index and Height in Children Treated for Acute Lymphoblastic Leukemia. M. Ansari^{*1}, N. Alos², A. Moghrabi^{*1}. ¹Pediatrics-Hematology-oncology service, CHU Ste-Justine and University of Montreal, Montreal, PQ, Canada, ²Pediatrics-Endocrinology service, CHU Ste-Justine and University of Montreal, Montreal, PQ, Canada.

Short stature, obesity and bone morbidity are commonly reported as late effects of therapy for childhood with acute lymphoblastic leukemia (ALL). We evaluated height, body mass index, body composition and lumbar bone mineral density in children after treatment for ALL.

Patients and Methods: Between January 1997 and August 2002, a cross-sectional study was done in children in remission treatment for ALL, using the Dana-Farber-Cancer-Institute (DFCI) consortium protocol 95-01. Lumbar bone mineral density (BMD) and body composition were measured by dual energy X-ray absorptiometry (DEXA). Height, body mass index (BMI), lumbar BMD (areal and volumetric) and body composition (fat mass and lean mass) were converted to z scores, adjusting for age and sex.

Results: 132 patients were enrolled; 99 were evaluated using DEXA. Median age at diagnosis was 3.8 years (0.5 - 12.6 years). Mean follow-up from end of therapy was 3.2 years (0.6 to 7.1 yrs). There was no significant difference in population characteristics between risk groups (Standard and High Risk, SR/HR), including age, height, BMI,

percentage Body Fat (% Fat) and Lean Body Mass (LMB) Z score. The mean Z score for % Fat was -0.715 ± 1.25 SD and the mean Z score for LMB was 1.36 ± 1.06 SD. There was no bone fracture or back pain reported. The mean volumetric lumbar spine BMD Z-score was 0.31 ± 0.97 SD for all patients; 0.36 ± 1.0 SD for HR (n=39) and 0.28 ± 0.95 SD for SR patients (n=60) (p=0.69). No patients had a volumetric lumbar spine BMD (g/cm³) Z-score of less than -2 SD.

Conclusions: Children with ALL treated with DFCl protocol 95-01 in our institution have little side effects related to growth, body composition and BMD, at a median interval of 3.2 years post end of therapy. Longer follow up is needed to confirm these results as well as comparison to cohorts using different protocol therapies.

Disclosures: N. Alos, None.

T514

Bone Ultrasonography in the Longitudinal Monitoring of Bone Status in Patient with Rett's Syndrome. S. Gonnelli¹, C. Caffarelli¹, J. Hayek², A. Montagnani¹, A. Cadirni¹, L. Tanzilli¹, B. Franci¹, B. Lucani¹, R. Nuti¹.

¹Institute of Internal Medicine, University of Siena, Siena, Italy, ²Department of Child Neurology and Psychiatry, University of Siena, Siena, Italy.

Rett syndrome, an X-linked neurodevelopmental disorder primarily affecting girls, is frequently characterized by osteopenia with a consequent increased risk of fragility fractures.

The aim of the study was to evaluate the usefulness of Quantitative Ultrasound (QUS) at phalanges in the assessment and monitoring of bone status in Rett patients.

In 109 Rett girls (10.1 ± 6.1 yrs) and in 101 age-matched controls, serum calcium, bone alkaline phosphatase, parathyroid hormone (PTH), 25-hydroxyvitamin D (25OHD) and QUS parameters at phalanges by Bone Profiler-IGEA (amplitude dependent speed of sound: AD-SoS and bone transmission time: BTT) were measured at baseline and then yearly for 3 years.

At baseline both QUS parameters and 25OHD levels were significantly lower in Rett patients than in controls. Serum 25OHD was inversely correlated with serum PTH ($r = -0.38$; $p < 0.05$) and BTT Z-score ($r = 0.37$ $p < 0.01$). BTT Z-score was significantly lower ($p < 0.05$) in the patients with 25OHD serum levels ≤ 9 ng/ml (-2.49 vs -1.58). Multiple regression analysis showed that BTT was significantly influenced by 25OHD levels. Eighty-two Rett patients completed the 36 month longitudinal study. During the longitudinal study the patients who at baseline were non-ambulatory presented a worsening of their bone status, and BTT and AD-SoS Z-score presented the tendency to markedly decrease. In contrast the BTT and AD-SoS of patients with severe or mild-moderate ambulatory impairment showed mild changes. At years 2 and 3 the difference in Z-score between the non-ambulatory group and the mild-moderate group was significant for both AD-SoS and BTT. At the end of the study period no significant differences in AD-SoS or BTT Z-scores were observed between Rett patients of the non-ambulatory group and those with severe ambulatory impairment. The AD-SoS Z-score at the end of the study period resulted significantly influenced by the changes in ambulatory performance and the use of anticonvulsant therapy.

In conclusion this prospective study suggests the usefulness of QUS parameters at phalanges, namely AD-SoS and BTT, in the monitoring of bone status in Rett patients. More specifically we found that in Rett patients QUS parameters are markedly decreased and that ambulatory impairment and low levels of 25OHD play a key role in the progressive deterioration of bone status.

Disclosures: S. Gonnelli, None.

T515

Prevalence of Osteopenia in Children with Early Juvenile Chronic Arthritis (JCA). L. Kroger¹, H. Kroger². ¹Paediatrics, Kuopio University Hospital, Kuopio, Finland, ²Orthopaedics, Kuopio University Hospital, Kuopio, Finland.

Children suffering from juvenile chronic arthritis (JCA) are at risk of developing osteoporosis due to inflammation, reduced/ limited physical activity and use of corticosteroids.

Because these children may have been suffering from inflammation a long time before seeking medical advice, we wanted to study whether bone mineral density (BMD) is already decreased at the time of diagnosis of JCA.

The material consisted of 52 consecutive patients, aged 5-15 yrs, admitted to the paediatric outpatient clinic in Kuopio University Hospital, Finland between 2004-6 and fulfilling the criteria of JCA. A total of 40 girls (77%) and 12 boys (23%) were included in the study. BMD was measured using dual X-ray absorptiometry (Lunar DPX-IQ). Results were expressed as bone mineral content (BMC; g) and BMD (BMC/ projected area; g/cm). To minimise the effect of bone size on BMD, apparent volumetric BMD (BMDvol, g/cm³) was calculated using a cylindrical model published earlier by Kroger et al.

The mean age was 10.8 yr for boys and 11.8 yr for girls (p= ns). Thirty-three children (69 %) suffered from polyarthritis (PA) and 16 (31%) from oligoarthritis (OA). There were no differences in weight or height between sexes or between different JCA type. BMDvol at the femoral neck was lower in boys as compared to girls (p=0.025). The girls with PA showed significantly lower volumetric spinal Z-scores (-0.46 vs. $+0.52$, $p = 0.01$) and volumetric femoral neck Z-scores (-0.21 vs. $+0.44$, $p = 0.04$) than girls with OA. In all, 29% of children (PA=11, OA=4) showed volumetric BMD Z-score values lower than -1 SD either in lumbar spine or femoral neck. If only areal BMD Z-scores were considered, 13.4 % of patients were found osteopenic. Low BMD values were found both in PA and OA cases.

In conclusion, measuring BMD is important in all children suffering from JCA, since BMD is decreased in substantial number of patients already at the time of diagnosis. This

group of patients needs special attention, eg. supplementation of calcium and vitamin D, and repeated BMD measurements in the follow-up.

Disclosures: L. Kroger, None.

T516

Evaluation of the Muscle-bone Relationship in the Midthigh of Children with Cerebral Palsy. C. M. Modlesky¹, A. Meyers¹, E. Hoffmann¹, J. J. Smith¹, F. Miller². ¹Health, Nutrition and Exercise Sciences, University of Delaware, Newark, DE, USA, ²Orthopaedics, A.I duPont Hospital for Children, Wilmington, DE, USA.

The strong relationship between muscle and bone has led to the proposal of a muscle-bone index in which a measure of bone that reflects its resistance to fracture, such as cortical volume or section modulus (Z), is divided by a measure that reflects muscle strength, such as muscle mass. Understanding the muscle-bone relationship may give us further insight into the mechanisms underlying poor bone development in children. Children with cerebral palsy (CP) who are unable to ambulate independently have poor muscle and bone development in the thigh and a high rate of fracture in the femoral shaft. However, the muscle-bone relationship is poorly studied in children with CP. The purpose of this study was to determine if the muscle-bone relationship in the midthigh is different in children with CP than typically developing children. Nine nonambulatory children with CP (8 to 14 years) and 9 typically developing children within the 10th and 90th age-based percentiles for height, weight and BMI were studied. Magnetic resonance images of the thigh (1 cm thick and 0.5 cm apart) were collected along the entire length of the more involved femur using a torso PA coil (GE 1.5 T; TR = 750, TE = 14, FOV = 16, 1 NEX, Phase = 512; Frequency = 512). Images at the level of the middle third of the femur were identified and measures of bone size, composition and strength [i.e., total and cortical volume, and anterior-posterior and medial-lateral section modulus (Z_{ap} and Z_{ml}, respectively)] and muscle mass were estimated using custom software developed with Interactive Data Language (IDL; Research Systems, Inc, Boulder CO). Indexes that reflect the muscle-bone relationship were determined by dividing total bone volume, cortical bone volume, Z_{ap} and Z_{ml} by muscle mass. There were no group differences in age, Tanner stage or BMI; however, height (1.26 ± 0.12 vs. 1.44 ± 0.08 m) and weight (27.9 ± 10.8 vs. 36.3 ± 4.5 kg) were lower in children with CP than controls ($P < 0.05$). Children with CP also had 55 % lower total bone volume (19.8 ± 6.5 vs. 44.4 ± 11.2 cm³), 55 % lower cortical volume (12.1 ± 4.2 vs. 27.6 ± 7.3 cm³) 61 % lower Z_{ap} (0.31 ± 0.11 vs. 0.80 ± 0.23 cm³) and 60 % lower Z_{ml} (0.29 ± 0.10 vs. 0.73 ± 0.21 cm³) in the midfemur and 58 % lower muscle mass (0.436 ± 0.144 vs. 1.030 ± 0.175 kg) in the midthigh ($P < 0.001$) than controls. However, none of the indexes that reflect the muscle-bone relationship were different between groups ($P > 0.05$). The findings suggest that children with CP who are unable to ambulate independently have a muscle-bone relationship in the midthigh that is not different from typically developing children.

Disclosures: C.M. Modlesky, None.

This study received funding from: National Institutes of Health and the National Osteoporosis Foundation.

T517

Poor Bone Growth in Children with Cerebral Palsy Is Underestimated by Dual-energy X-ray Absorptiometry. J. J. Smith¹, F. Miller², C. M. Modlesky¹. ¹Health, Nutrition and Exercise Sciences, University of Delaware, Newark, DE, USA, ²Orthopaedics, A.I. duPont Hospital for Children, Wilmington, DE, USA.

Femoral fracture incidence is elevated in children with cerebral palsy (CP). Prior fracture occurrence increases subsequent fracture risk which increases treatment costs and decreases their quality of life. Therefore, decreasing fracture incidence in this population is important. Size is a major determinant of a bone's resistance to fracture as wider bones are more resistant to fracture than thinner bones. There is evidence that children with CP have considerably thinner bones at the femoral shaft compared to typically developing children; however, the size of the distal femur, a primary fracture site, has not been evaluated. The purpose of this study was to determine if the distal femur is smaller in children with CP who are unable to ambulate independently compared to typically developing children. Nine nonambulatory children with CP (8-14 years) and 9 typically developing children between the 10th and 90th age-based percentiles for height, weight and BMI participated in the study. Bone area of the distal femur (1.4 cm region above the growth plate) was determined using dual-energy X-ray absorptiometry (DXA; Delphi W, Hologic Inc.). Trabecular bone cross-sectional area of the lateral side of the distal femur (approximating the region evaluated using DXA) was determined using magnetic resonance imaging (MRI; GE 1.5 T, 3D fast gradient echo sequence, reconstructed spatial resolution = $175 \times 175 \times 700$ μ m³). There were no group differences in age, pubertal status or BMI; however, children with CP had lower height (1.25 ± 0.04 vs. 1.43 ± 0.03 m) and weight (26.7 ± 3.7 vs. 35.6 ± 1.2 kg) compared to controls ($P < 0.05$). Although bone area determined by DXA was ~ 13% lower in children with CP than controls, this difference was not statistically significant ($P = 0.07$). On the other hand, trabecular bone cross-sectional area determined by MRI was ~ 36% lower in children with CP than controls and the difference was statistically significant ($P < 0.01$). The findings suggest that the distal femur is substantially smaller in nonambulatory children with CP than typically developing children and the degree of the discrepancy is underestimated by DXA.

Disclosures: J.J. Smith, None.

This study received funding from: NIH and National Osteoporosis Foundation.

T518

Bone Age Measurements by Ultrasound Are Equivalent to Radiological Assessments. C. Wuester, M. Hartmann*, W. Omran*, U. Cordes*. Clinic for Endocrinology, Mainz, Germany.

The purpose of the study was to show that the measurements of bone age (BA) by ultrasound at the wrist correlates with radiological BA measurements on conventional hand X-rays.

103 patients (age range 9.5 - 22.5 years, mean 14.4) were included. Thirty-one patients had delayed puberty, 17 patients had constitutional short stature, 5 patients GH deficiency and the other were normals. The ultrasound method to determine bone age at the wrist (BonAge™, Sunlight Medical Ltd., Tel Aviv, Israel; arewus, Mainz, Germany) evaluates the relationship between the velocity of the wave (speed of sound) passing thorough the distal radial and ulna epiphysis and growth, using gender- and ethnicity-based algorithms. Three experienced investigators (one radiologist, two endocrinologists) analysed conventional X-rays of the left hand and assigned bone age scores according to the Greulich & Pyle atlas (G&P). The investigators were blinded to the chronological age (CA) and the BonAge™ results. DXA was measured at the spine and hip using Osteocore 3 by MediLink/arewus, Mainz/Germany.

Correlation coefficients of BA ultrasound with the 3 X-ray investigators were $r = 0.80, 0.82$ and 0.88 respectively. The correlation between the three X-ray investigators were $r = 0.92, 0.92$ and 0.96 respectively among each others and not significant different from the correlation with the ultrasound results. BMC rather than BMD correlated best with ultrasonic BA.

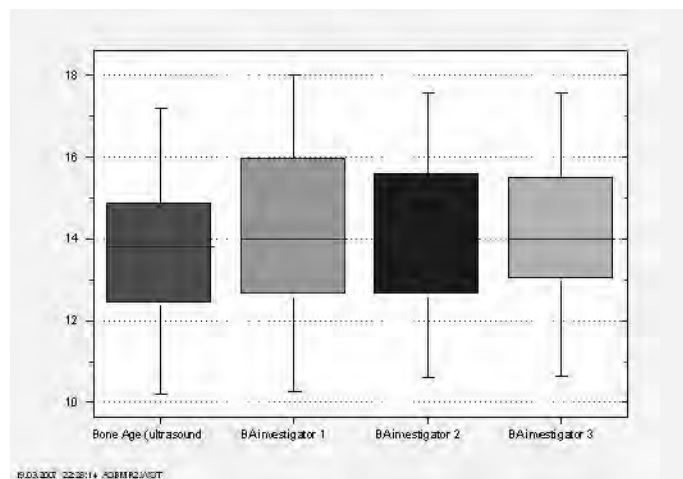


Figure 1 shows the mean BA of the ultrasound-based system and the three radiological investigations. There was no statistical significant difference between the four evaluations. We conclude from the data that BonAge™ ultrasound system to measure bone age is precise and accurate. The results show high correlation with radiological assessments. The system has the advantage of being radiation-free which is important in a target group of still growing patients.

Disclosures: C. Wuester, None.

T519

Low Doses of Pamidronate for Children with Metabolic and Genetic Diseases. C. Bowles*, R. Kreikemeier*, S. Coughlin*, H. Plotkin*. ¹Pediatrics, UNMC, Omaha, NE, USA, ²Metabolics, Children's Hospital, Omaha, NE, USA.

Retention of calcified cartilage is a well-known dose-related side effect of pamidronate treatment in children and adolescents with OI. Low doses of pamidronate are effective to treat pediatric patients with cerebral palsy and osteogenesis imperfecta.

IV pamidronate (0.75 mg/kg/day for two days) was administered every 4 months to 13 non-ambulatory children and adolescents (age range 1.5 - 12 y.o) with metabolic and genetic diseases. Diagnosis included mitochondrial complex I deficiency, fumarate deficiency, pediatric neurotransmitter disease, myotonic dystrophy, Micro syndrome, Rett syndrome, and undefined genetic syndromes. On the first day of treatment patients received half dose to minimize the acute phase reaction, and acetaminophen was administered every 6 hours during the first 2-day infusion. Lumbar spine (LS) and femoral neck (FN) BMD (DEXA, Hologic Delphi) Z-scores were assessed at baseline, 4, 12 and 24 months. Calcium, phosphorus, magnesium, alkaline phosphatase, osteocalcin, NTx, 25 and 1,25 vitamin D levels in serum, were also assessed. All patients had adequate calcium and vitamin D intakes for age. The study was approved by Children's Hospital IRB.

BMD measurement z-scores at the femoral neck (FN) (N=11) and the lumbar spine (LS) (N=13) showed statistical evidence of an increase in bone mineral density at both the femoral neck and the lumbar spine with pamidronate treatment at 24 months. The rate of increase appears to have been initially less at the femoral neck than the lumbar spine (increases at 4 months: FN: 0.38; LS: 0.85. The increase at 1 year of follow-up at the two sites was similar (FN: 1.08; LS: 1.18). Further improvement in BMD was not seen at the 2 year follow-up.

	Baseline Mean(SD)	4 mo Mean(SD)	12 mo Mean(SD)	24 mo Mean(SD)
LS BMD	0.32 (0.09)	0.38 (0.062)	0.40 (0.059)	0.38 (0.17)
LS Z-score	-3.65 (1.37)	-2.83 (0.92)	-2.63 (1.22)	-2.35 (1.20)
FN BMD	0.25 (0.084)	0.28 (0.081)	0.35 (0.089)	0.36 (0.098)
FN Z-score	-4.62 (0.98)	-4.36 (0.72)	-3.55 (1.27)	-3.80 (0.86)
Serum NTx	62.68 (41.14)	43.16 (16.12)	46.29 (9.56)	35.33 (9.22)
Osteocalcin	25.17 (8.75)	19.2 (8.51)	19.00 (10.43)	35.75 (24.60)

With low doses of pamidronate, there is no significant change over 2-year for serum 1,25 vitamin D, 25 vitamin D, total calcium, ionized calcium, sNTx, or osteocalcin measures. BMD in both LS and FN increase for the first year and remains stable during the second year of treatment.

Disclosures: C. Bowles, None.

T520

Effects of Risedronate on Bone Change at Children with Osteogenesis Imperfecta. C. Galesanu¹, C. Ciubotariu^{*1}, M. R. Galesanu^{*2}, D. Raileanu^{*1}, C. Tache^{*1}, T. Bostaca^{*3}. ¹Endocrinology, University of Medicine and Pharmacy, IASI, Romania, ²Osteodensitometry, Centre of Imaging and Radiologic Diagnosis, IASI, Romania, ³Radiology, University of Medicine and Pharmacy, IASI, Romania.

Osteogenesis imperfecta (OI) is a disturbance in the synthesis of type I collagen, predominant protein of the extracellular matrix of most tissues. In bone, this defect causes osteoporosis, which leads to an increased tendency to fracture. Type I collagen is also a constituent of dentin, sclerae, blood vessels, ligaments and skin; individuals with OI may have also abnormalities of these structures. OI type IA is without dentinogenesis imperfecta. The OI type IB is a rare form with tooth abnormalities. The major signs of OI type I include blue sclerae, hearing loss, mild bone fragility.

The aim of our study was to verify the efficacy and safety of risedronate treatment in children with OI type IA.

Eight children, six girls and two boys were treated 12 months with risedronate. The children weighing under 30 kg received 35 mg risedronate at 14 days and children weighing more 30 kg received 35 mg risedronate weekly.

Three girls were declared with history of fractures (between 8 and 16). BMD was assessed at lumbar spine (LS) using Hologic DXA scanning at time 0 and 12 months. The results at time 0 by DXA-BMD were compared with reference data for bone density published by I.M. von der Sluis in 2002 (Children's Bone Health) Z-score at time 0 (DXA-BMD) was in all cases more -2.5.

At baseline mean BMD at LS was 0.562 g/cm² for girls vs. mean BMD reference data which is 0.896 g/cm²; it was a deficit on 38%. After a year of risedronate therapy the mean BMD at LS was 0.619 g/cm², a gain of 10%. For the boys the baseline mean BMD at LS was 0.790 g/cm² vs. mean BMD reference data which is 1.096 g/cm²; it was a deficit on 28%. After a year of risedronate, the mean BMD at LS was 0.916 g/cm², which is a gain of 15%. No adverse effects regarding gastrointestinal tract under risedronate therapy. No new fractures. The treatment and the following of children going on.

Risedronate therapy is accompanied by an important increase of LS-BMD after a year. Children with OI type IA respond to oral bisphosphonates at standard doses for osteoporosis. Risedronate 35 mg weekly seems to be safe and effective in children with OI.

Disclosures: C. Galesanu, None.

T521

Vitamin D Status of Apparently Healthy Schoolgirls from two Different Socioeconomic Strata in Delhi: Relation to Nutrition and Lifestyle. R. Marwaha*. Department of Endocrinology and Thyroid research Centre, Institute of Nuclear Medicine and Allied Sciences, Delhi, India.

Forty to fifty percent of total skeletal mass is accumulated during childhood and adolescence, which is influenced, by sunlight exposure, physical activity, lifestyle, endocrine status, nutrition and gender. In view of scarce data on the association of nutrition and lifestyle with hypovitaminosis D in Indian children and adolescents, an in-depth study on 3127 apparently healthy (6-18 years) schoolgirls from the lower (LSES =1477) and upper socioeconomic strata (USES=1650) in Delhi was carried out. These girls were subjected to anthropometry and clinical examination for hypovitaminosis D. Randomly selected 404 (LSES =193, USES =211) girls from the two strata underwent detailed lifestyle, dietary, biochemical and hormonal assessment. Clinical features of vitamin D deficiency were noted in 11.5% girls (12.4% LSES and 10.7% USES.). USES girls had significantly higher Body Mass Index (BMI) than LSES counterparts. Prevalence of biochemical hypovitaminosis D (serum 25-OHD <50nmol/l) was seen in 90.8% girls (LSES=89.6% and USES= 91.9%). Mean intake of energy, protein, fat and calcium, as well as milk intake of USES girls was significantly higher across all ages. Among the LSES group, the intake of carbohydrate, fibre, phytate was higher. Physical activity and sun exposure in terms of duration and percentage of body surface area exposed was significantly greater in LSES. In conclusion, in the absence of fortification of food products with vitamin D in India, diet alone appears to have an insignificant role; however lifestyle factors may contribute to the vitamin D status of apparently healthy school subjects.

Disclosures: R. Marwaha, None.

W001

Effect of Energy Restriction on Bone Turnover in Physically Active Females. C. Sale¹, J. P. Greeves¹, J. P. R. Scott¹, W. D. Fraser². ¹QinetiQ, Farnborough, United Kingdom, ²University of Liverpool, Liverpool, United Kingdom.

Initial military training can result in a negative energy balance in female recruits, which may alter bone turnover and potentially increase the risk of stress fracture injury. The aim of the present study was to investigate the acute effect of reduced energy intake on bone turnover in females and to examine the interaction with daily training.

Seven habitually active females (mean (SD) age: 26 (5) y; height: 1.67 (0.30) m; body mass: 66.7 (9.5) kg) completed all aspects of the study. This study was approved by the QinetiQ Research Ethics Committee. Subjects completed two conditions in a counterbalanced crossover design. Each condition comprised 5 d of energy restriction (50% of normal daily intake), which were separated by a minimum of 7 d. In one condition, subjects completed a 1.5-mile self-paced run on the afternoon of each day (EX) and in the other condition subjects remained sedentary (SED). Energy intake on the exercising days was increased to compensate for increased energy expenditure so that the level of energy restriction was the same in both conditions. Blood and second-void urine samples were obtained after an overnight fast on days 0 (baseline, [B]), 3 (mid-restriction, [D3]), 6 (post-restriction, [D6]) and 7 (recovery, following 24 h with no restriction, [D7]). Blood was assayed for markers of bone resorption (β -CTx), bone formation (P1NP, Bone ALP) and regulatory hormone concentrations (T_3 , IGF-1, leptin and cortisol). Urine was assayed for markers of bone resorption (UfPYD and UfDPD).

Five days of energy restriction resulted in a significant ($p < 0.01$) loss of body mass in both EX (66.4 (9.8) kg to 65.1 (9.5) kg) and SED (66.8 (9.2) kg to 65.0 (8.8) kg). P1NP concentrations declined significantly ($p < 0.05$) from B (44.29 (11.88) $\mu\text{g}\cdot\text{L}^{-1}$) to D3 (39.43 (12.49) $\mu\text{g}\cdot\text{L}^{-1}$) and D6 (38.71 (12.22) $\mu\text{g}\cdot\text{L}^{-1}$) in EX, and from baseline (46.14 (15.91) $\mu\text{g}\cdot\text{L}^{-1}$) to D6 (37.43 (11.33) $\mu\text{g}\cdot\text{L}^{-1}$) in SED. P1NP concentrations remained significantly lower than B ($p < 0.05$) on D7 in SED (40.29 (12.65) $\mu\text{g}\cdot\text{L}^{-1}$). Bone ALP and markers of bone resorption (β -CTx, UfPYD and UfDPD) remained unchanged in both EX and SED conditions. There were no differences in markers of bone turnover between EX and SED. Energy restriction resulted in a significant ($p < 0.05$) reduction in leptin concentrations in both EX (between B and D6 and D7) and SED (between B and D3, D6 and D7), whilst IGF-1 and T_3 concentrations were reduced in EX only (IGF-1 between B and D6 and D7; T_3 between B and D3). No changes in cortisol concentrations were observed. Short-term energy restriction resulted in a reduction in bone formation, as shown by a decrease in P1NP, which occurred independently of moderate exercise training.

Disclosures: C. Sale, None.

This study received funding from: The Human Capability Domain of the UK Ministry of Defence Scientific Research Programme.

W002

Osteoblast Response to Titanium Microtopography Is Dependent on Integrin Alpha-2. R. Olivares-Navarrete¹, P. Raz^{*1}, R. A. Chaudhri^{*1}, J. Chen^{*1}, M. Wieland^{*2}, B. D. Boyan¹, Z. Schwartz¹. ¹Petit Institute of Bioengineering and Bioscience, Georgia Institute of Technology, Atlanta, GA, USA, ²Institut Straumann AG, Basel, Switzerland.

Titanium surface microtopography modulates phenotypic maturation of osteoblast-like cells, production of local regulatory factors, and response of osteoblasts to bone anabolic agents such as 1,25 dihydroxyvitamin D₃ [1,25(OH)₂D₃]. Changes in cell morphology suggest that integrin-mediated signaling may play a role. Alpha-2 and beta-1 integrins are increased in osteoblasts grown on Ti surfaces with rough microtopographies and 1,25(OH)₂D₃ modulates expression of beta-1 on these same substrates, but alpha-5 is not affected. We showed that silencing beta-1 alters osteoblast response to substrate microtopography and 1,25(OH)₂D₃. Here we determined if integrin alpha-2 was specifically responsible for the surface-dependent changes in osteoblast response. Alpha-2 siRNA targeted 21 bases starting at base-3406 of the alpha-2 gene (NM-002203.3). Double-strand oligonucleotides were constructed in a pSuppressorNeo vector containing a U6 promoter. A permanent MG63 cell line exhibiting 70% reduction in alpha-2 protein was established. Normal and silenced MG63 cells were grown on tissue culture polystyrene (plastic) or on Ti substrates with different surface microtopographies and surface energy. Confluent cultures were treated with 1,25(OH)₂D₃ for 24h. Real-time PCR showed that alpha-2 and beta-1, but not alpha-5, alpha-v, or beta-3 integrin subunits were increased on surfaces with rough microtopographies and further enhanced on surfaces with high surface energy, as were mRNAs for alkaline phosphatase, osteocalcin, OPG and TGF- β 1. Alpha-2 siRNA did not alter levels of alpha-5 or beta-1 protein. However, effects of surface topography and surface energy on alkaline phosphatase activity, osteocalcin, and levels of PGE₂, OPG and TGF- β 1 in the conditioned media were abolished. Moreover, response to 1,25(OH)₂D₃ was reduced, even when cells were cultured on plastic or smooth Ti substrates. The results indicate that the stimulatory effects of surface microtopography and surface energy on osteoblastic differentiation depend on alpha-2 and suggest that alpha-2 signaling is involved in osteoblast-dependent regulation of bone remodeling. Silencing also reduced effects of 1,25(OH)₂D₃ supporting our previous studies showing that the synergistic effect of surface roughness and 1,25(OH)₂D₃ is mediated by the same signaling pathways. Silenced MG63 cells responded to microrough surfaces in a comparable manner, whether or not surface energy was high, suggesting that the role of alpha-2/beta-1 is to detect surface structure rather than surface chemistry.

Disclosures: Z. Schwartz, None.

This study received funding from: Children's Healthcare of Atlanta, NIH AR052102, NSF 9731642, ITI Foundation, Institut Straumann AG.

W003

Local Transplantation of Human Multipotent Adipose-Derived Stem Cells Improve Fracture Healing. T. Shoji^{*1}, Y. Mifune^{*1}, M. Li^{*2}, M. Kurosaka^{*3}, T. Asada^{*4}, T. Asahara^{*1}. ¹Laboratory for Stem Cell Translational Research, Riken Kobe Institute, Kobe, Japan, ²Foundation for Biomedical Research and Innovation, Kobe, Japan, ³Department of Orthopaedic Surgery, Kobe University Graduate School of Medicine, Kobe, Japan, ⁴Stem Cell Sciences KK, Kobe, Japan.

It's well known that human adipose tissue is one of the sources of multipotent stem cells called "adipose-derived stromal cells"¹. Among them, human multipotent adipose-derived stem (hMADS) cells obtained from young donor demonstrating fast adherent characteristics in culture, have extensive expansion capacity ex vivo, multilineage differentiation potential and long-term engraftment and tissue regeneration capacity. It has already reported hMADS may have therapeutic potential for muscle diseases². Based on these evidences, we test the hypothesis that hMADS contributes to fracture healing in a rat femur nonunion fracture model.

We separated crude SVF from adipose tissue in human young donors. We selected fast-adherent cells and expanded them. They were treated as hMADS cells. A reproducible model of femoral fracture was created in nude rat (F344/nude rat) with cauterized periosteum which leads to nonunion 8 weeks post-fracture³. The hMADS cells (1×10^5 /rat) or PBS was transplanted locally with atelocollagen gel after fracture creation.

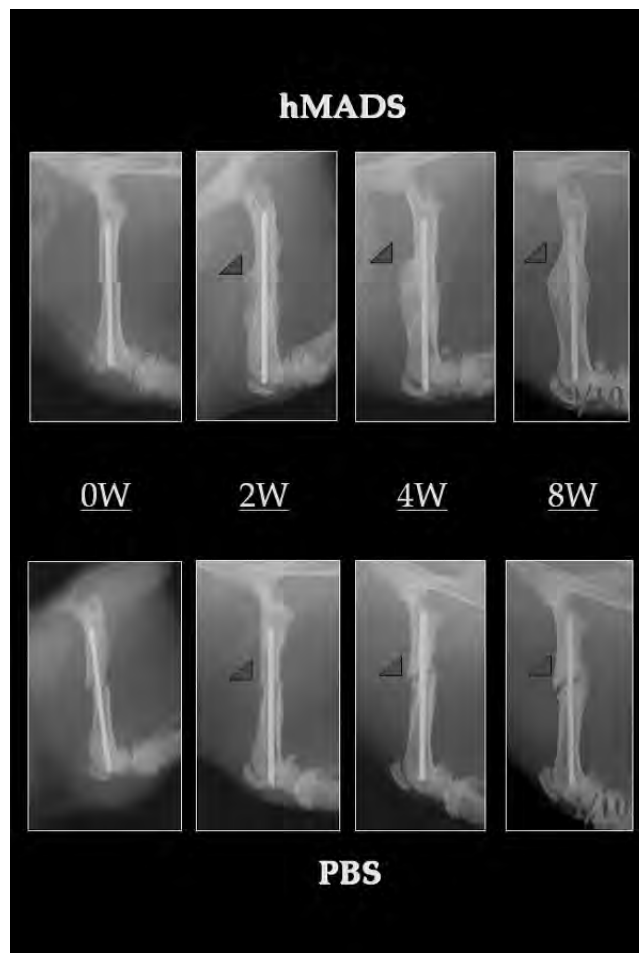
Human-specific osteoblast (OB) and endothelial cell (EC) related genes were detected by RT-PCR of tissue RNA isolated from peri-fracture site in the hMADS group at week 2. Differentiated human OBs and ECs were identified in the hMADS group by immunohistochemical staining. They also demonstrated human cell-derived osteogenesis and angiogenesis. Capillary density at peri-fracture site scaled by vascular staining was higher in the hMADS group than the PBS group. Moreover, mean flux ratio of laser doppler perfusion imaging was significantly greater in the hMADS group. 9 of 10 fractures were healed radiographically and histologically at week 8 in the hMADS group. On the other hand, 1 of 10 in the PBS group was observed (Fig.).

hMADS cells transplanted to the fracture site contribute to fracture healing via osteogenesis and angiogenesis in rat non-union fracture model. hMADS the small amount of an easily available tissue source may have a therapeutic potential for fracture healing.

1. Zuk, P.A. et al. Tissue Eng., 7:2, 2001.

2. Anne-Marie, R. et al. J.Exp.Med., 201:9, 2005

3. Kokubu, T. et al. J.Orthop.Res., 21:3, 2003



Disclosures: T. Shoji, None.

This study received funding from: Stem Cell Sciences KK.

W004

Vitamin A Deficiency Delays Healing Process After Cortical Bone and Bone Marrow Injury. K. Tanaka^{*1}, S. Tanaka¹, A. Sakai¹, Y. Katae^{*1}, H. Hirasawa^{*1}, N. Nakura^{*1}, K. Sabanai^{*1}, K. Menuki^{*1}, H. Yamane^{*1}, Y. Shimizu^{*1}, Y. Arai^{*2}, T. Nakamura¹. ¹Orthopaedic surgery, University of Occupational and Environmental Health, Kitakyusyu, Japan, ²Division of Hard Tissue Research, Institute for Oral Science, Matsumoto Dental University, Matsumoto, Japan.

The necessity of vitamin A in chondrogenesis and generation of limbs has been reported. The role of vitamin A in bone regeneration has not been elucidated. Using three groups of 10-week-old male C57BL/6J mice, we investigated the effects of vitamin A deficiency on healing process after cortical bone and bone marrow injury. One group was vitamin A deficiency (VAD) mice, which were fed the diet without vitamin A from 10 day of gestation to the end of the experiments. Another group was deficiency-sufficiency (VADS) mice, which were fed the diet without vitamin A from 10 day of gestation until weaned and thereafter fed the standard diet. The other was sufficiency (VAS) mice, which were fed only the standard diet. We made drill-hole injury, 1mm in diameter, at the anterior portion of the diaphysis of bilateral femurs. One group was used for sequential analysis of the amount of regenerating bone using in vivo micro CT. The femurs of each group were also harvested at 7, 14, 21 days after operation to do histomorphometry and quantitative mRNA analysis.

Regenerating bone was observed from 7 day in VAS and VADS mice, and appeared to be almost healed until 28 day, while cortical bone defect was still apparent in VAD mice at 28 day. In histomorphometrical analysis, the volume of medullary callus tended to decrease in VAD mice throughout the experimental period and regenerated cortical bone volume of the drill-hole area in the VAD mice was lower than that in the VAS at day 7, 14 and 21. Osteocalcin mRNA expression in VAD mice apparently decreased compared with VAS mice at day 7.

These results clearly demonstrated that vitamin A deficiency suppressed medullary callus formation and cortical bone healing in association with the impairment of osteoblast maturation after cortical bone and bone marrow injury.

Disclosures: K. Tanaka, None.

W005

Interaction of galectin-9 with Lipid Rafts Induces Osteoblast Proliferation Through the c-Src/ERK Signaling Pathway. R. Tanikawa¹, Y. Okada¹, K. Nakano^{*1}, T. Tanikawa¹, R. Hosokawa^{*2}, Y. Tanaka¹. ¹First Department of Internal Medicine, University of Occupational and Environmental Health, Kitakyusyu, Japan, ²Department of Oral Reconstruction and Rehabilitation, Kyushu Denrai College, Kitakyusyu, Japan.

Galectin-9 is a β -galactoside-binding lectin that modulates many biological functions by interacting with particular carbohydrates attached to proteins and lipids. The role of galectin-9 in bone metabolism remains unclear. This study investigated galectin-9 in osteoblasts with respect to proliferation and lipid raft-dependent regulatory mechanisms. We used human osteoblasts purified from metaphyseal trabecular bone in the proximal femur. The effect of galectin-9 on osteoblast proliferation was tested using WST-8 (consists of tetrazolium salt). Protein phosphorylation was assayed by western blotting and confocal microscopy was used to localize lipid rafts. Galectin-9 induced osteoblast proliferation in a dose- and time-dependent manner. Galectin-9 induced the activated form of c-Src and ERK phosphorylation, and PP2, a Src-family tyrosine kinase inhibitor, inhibited both osteoblast proliferation and ERK phosphorylation. And c-Src si RNA transfection inhibited galectin-9 induced osteoblast proliferation. Furthermore, galectin-9 induced clustering of lipid rafts in osteoblasts. Disruption of lipid rafts by β -methylcyclodextrin inhibited galectin-9-induced proliferation, as well as the galectin-9-induced activation of c-Src. Our results indicated that galectin-9 interacts with lipid rafts and induces osteoblast proliferation through the c-Src/ERK signaling pathway. We propose that clustering of lipid rafts induced by galectin-9 might be an important trigger of the c-Src/ERK signaling cascade for osteoblast proliferation.

Disclosures: R. Tanikawa, None.

W006

The Effects of Chlorobenzenes on Bone Formation. Z. Valkusz¹, G. Nagyri^{*1}, M. Radács^{*1}, B. Hegedus^{*2}, A. Juhász^{*3}, A. Petri^{*4}, J. Julesz^{*1}, M. Galfi^{*2}. ¹Endocrine Unit, University of Szeged, Szeged, Hungary, ²Environmental Protection Group, University of Szeged, Szeged, Hungary, ³Department of Psychiatry, University of Szeged, Szeged, Hungary, ⁴Department of Surgery, University of Szeged, Szeged, Hungary.

Several chemicals used in the agriculture, industry and community as pesticides and fungicides may induce environmental damages and alterations in the homeostasis of biological organisms. It is known that these pollutants such as chlorobenzenes (CIB) have toxic effects on liver, immune-, nervous- and endocrine systems due to their chemical properties. Our aim was to investigate the effects of chronic exposures to discrete doses (0.1 or 1 μ g/kg/day) of CIB on bone structure and activity of liver enzymes in rats.

Wistar male rats (150-250 g) were given tri- and hexachlorobenzenes (1:1) dissolved in ethanol (0.05%) through gastric tube for 1 and 3 months. Control animals were untreated rats (absolute control, n= 10), rats treated with tap water (negative control, n= 10 and

treated with ethanol (positive control, n= 10). At the end of the experimental period the animal's body weight and organ weight were measured (by gravimetric method); serum and femoral samples were taken. Serum liver enzymes (γ GT, SGOT, SGPT) were measured (with colorimetric methods). Electrically-mobilized Ca^{2+} and bone mineral content (BMC) of femur were determined. The bone structure was investigated by histological methods. Data were analyzed with SPSS software.

The activity of liver enzymes, the weight of animals and the main organs did not change significantly applying exposures due to their subtoxic characteristic. Both of the doses, but particularly the 1 μ g/kg/day dose could modulate the electrically mobilized Ca^{2+} and BMC of the femur in a dose- and time-dependent manner. The histology of femur was altered only with 1 μ g/kg/day doses of CIB.

Our data suggest that 1 μ g/bw.kg/day doses of CIB, which is permanently present in our environment may be a risk factor for alteration of bone formation. However, a minimal dose (0.1 μ g/bw.kg/day) CIB is not likely to disturb the bone structure.

Disclosures: Z. Valkusz, None.

W007

Osteoblast-Mediated Bone Formation Is Suppressed at Sites of Focal Bone Erosion in Inflammatory Arthritis. N. C. Walsh¹, C. A. Manning^{*1}, K. W. Condon^{*2}, J. Ratliff^{*2}, K. Iwata^{*2}, D. B. Burr², E. M. Gravalles^{*1}.

¹Department of Medicine, University of Massachusetts Medical School, Worcester, MA, USA, ²Department of Anatomy and Cell Biology, Indiana University School of Medicine, Indianapolis, IN, USA.

Osteoclast (OC)-mediated focal articular bone erosion is a common feature of rheumatoid arthritis (RA). Despite treatment for RA with attenuation of focal bone erosion, most patients do not repair erosive lesions. Therefore osteoblast (OB)-mediated bone formation may be impaired at these sites. We have used the K/BxN serum transfer arthritis (STA) model to determine the impact of inflammatory arthritis on OB-lineage cells at sites of focal bone erosion. In prior studies we determined that differentiation of OB-lineage cells is compromised at sites of erosion, with a paucity of mature OB-lineage cells at these sites. We now confirm by in situ hybridization that OB-lineage cells expressing mRNA for markers of mature OB-lineage cells (alkaline phosphatase and osteocalcin) are absent from sites of erosion, but are present at sites remote from erosion. In addition, the capacity of OB-lineage cells to form bone at sites of erosion was determined by dynamic bone histomorphometry. STA was induced in 12 week-old male C57BL/6J mice and the fluorochromes, alizarin and calcein, were administered with a 10 day interval. The navicular bone was assessed as a predictable site of erosion. Fluorochrome labeling, indicating newly mineralized bone, was observed at sites remote from invading inflammatory tissue (pannus). In contrast, minimal label incorporation was observed at sites where pannus was in contact with the bone surface. Quantitation of mineralized surface/total bone surface (MS/BS, %) confirmed this observation, with a reduction in the MS/BS (%) at the pannus-bone interface compared to bone surfaces remote from the pannus, and non-arthritis navicular bones. Bone formation parameters quantified in the distal femur (a site remote from inflammation) showed no differences between arthritic and non-arthritis mice. Together our results indicate that OB differentiation and bone formation activity is suppressed at sites of erosion in inflammatory arthritis, contributing to net loss of bone at these sites. Previously we have shown that antagonists of the Wnt signaling pathway, DKK1 and sFRP1, are expressed at erosion sites and in this study, qRT-PCR analysis confirms the induction of DKK1 and sFRP1 mRNA at sites of erosion over time. These factors are candidates for inhibiting OB function at these sites in this model of inflammatory arthritis. As proof of principle, a recent study published by Diarra et al., showed that DKK1 blockade in inflammatory arthritis models resulted in protection from focal bone erosion.

Diarra, D., et al (2007) Nature Med. 13(2):156-63

Disclosures: N.C. Walsh, None.

W008

A Locus on Mouse Distal Chromosome (Chr) 4 Exerts Genetic Control of Bone Size by Regulating the Differentiated Function of Periosteal Cells. J. E. Wergedal¹, M. H. C. Sheng¹, K. L. Shultz², D. J. Baylink³, S. Mohan¹, W. G. Beamer².

¹Musculoskeletal Disease Center, Jerry L. Pettis VA Medical Center, Loma Linda, CA, USA, ²The Jackson Laboratory, Bar Harbor, ME, USA, ³Medicine, Loma Linda University, Loma Linda, CA, USA.

Genes that regulate bone cross sectional size and strength are important to identify because they are potential therapeutic targets for increasing bone strength in osteoporotics. QTL studies using multiple inbred strain crosses including C3H/HeJ (C3H) X C57BL/6J (B6) have revealed that Chr 4 contains an important locus that regulates bone size. Based on the findings that a region of Chr 4 in C3H, when transferred to B6, increases bone size (Table 1) and that C3H osteoblasts exhibit higher activity than B6 osteoblasts both in vivo and in vitro, we proposed the hypothesis that Chr 4 QTL contains a gene that increases bone size by regulating osteoblast activity. To evaluate this hypothesis, we characterized the processes that contribute to increased bone size by histomorphometry in a B6 congenic strain, B6.C3H-4T. Both periosteal and endosteal bone formation were elevated in the congenic line (Table 1). Furthermore, the increased bone formation was due to increased mineral apposition rate (MAR) rather than increased forming surface (Md.S). These increases in bone formation are consistent with our previous study showing higher osteoblastic activity in C3H mice than in B6 mice and suggest that the genes responsible at least in part reside on Chr 4. To further narrow down the region of the Chr 4 containing the gene of interest, sublines from the B6.C3H-4T have been produced. The subline (B6.C3H-4T-3) demonstrating the largest difference in cross sectional area (19+/-3% difference, p<.001; Mean+/-SE) from the B6 background strain (B6.C3H-4T-3) covered the region between 50 cM and 80 cM. Summary: 1) This study confirms that the congenic line B6.C3H-4T has increased periosteal bone formation due to osteoblast with increased activity. 2)

A subline of the B6.C3H-4T with a smaller segment of Chr 4 from the C3H strain also has increased cross sectional size. These observations are consistent with the presence of a gene(s) on the distal portion of mouse chromosome 4 regulating the differentiated function of periosteal cells.

Table 1. Femur midshaft MAR, bone formation rates (BFR), and mineralizing (forming) surface (MS) at periosteum and endosteum in B6.C3H-4T and B6 control mice (mean±SE).

Parameter	B6	B6.C3H-4T	p<
Periosteal Perimeter, mm	4.44±0.04	4.87±0.08	.001
Periosteal MAR (um/day)	4.65±0.34	5.98±0.48	.05
Periosteal BFR (mm ³ /year)	10.7±1.5	16.0±1.5	.03
Periosteal Md.S (%)	50.8±4.5	55.3±2.8	NS
Endocortical MAR (um/day)	3.64±0.27	4.62±0.15	.05
Endocortical BFR (mm ³ /year)	5.49±0.65	8.64±1.34	.05
Endocortical MS (%)	44.4±3.2	48.4±5.4	NS

Disclosures: J.E. Wergedal, None.

W009

Attachment of Osteoblast-like Cell on ALD-derived Hydroxyapatite Surface. L. Xu¹, P. Rahkila^{*1}, T. Sajavaara^{*2}, M. Putkonen^{*3}, H. J. Whitlow^{*2}, S. Cheng¹. ¹Department of Health Sciences, University of Jyväskylä, Jyväskylä, Finland, ²Department of Physics, University of Jyväskylä, Jyväskylä, Finland, ³Beneq Ltd., Vantaa, Finland.

Focal adhesions contain structural and secondary signaling molecules crucial to cell function. The attachment, adhesion and spreading of osteoblasts are essential events when studying their proliferation and differentiation on biomaterial surfaces. Different techniques have been utilized for the deposition of hydroxyapatite (HA) which offers an interesting selection of biomimetic surface coating material. Here we have used a novel Atomic Layer Deposition (ALD) method to produce thin HA films for osteoblast culture experiments. ALD is a highly controlled and conformal method for thin film deposition especially suitable for preparation of microelectronic and nanoscale materials and coating of three dimensional structures. In this study, ALD was used to obtain stable and biocompatible nanocrystalline HA films on Si (100) substrate. The topography of the films was analyzed by AFM. Heavy ion elastic recoil detection analysis (HI-ERDA) was utilized for the determination of Ca, P, O and H contents in the films. Crystalline films were obtained when amorphous as-deposited films were annealed at 800°C. AFM showed a quite uniform nanocrystalline HA layer interspersed with macrocrystalline HA. MC3T3-E1 cells were used to test the bioactivity of ALD-derived HA films (ALD-HA). 1×10⁵ cells in serum-free α-MEM medium were seeded onto UV sterilized silicon plates (10×10mm²) coated with annealed ALD-HA and unannealed amorphous films. Cells were cultured for 1 hour and 3 hours. Thereafter the cells were fixed in 4% paraformaldehyde. Vinculin was immunostained by alaxa-546 labeled antibody. F-actin was stained by alaxa-488 labeled phalloidin. Hoechst staining was used to show the cell nucleus. Cell behavior on ALD-HA surface was examined under inverted confocal fluorescence microscope. Osteoblasts adhered to ALD-HA surface after 1 hour incubation, presenting numerous filopodia and some focal adhesion sites. But the cells did not spread well and F-actin was not clearly organized. Vinculin appeared as diffuse perinuclear staining. Well-organized cytoskeleton was noticed in the cells incubated for 3 hours. Forming focal adhesion sites were clearly seen at the colocalization of vinculin and actin filaments. When comparing the amorphous and annealed crystalline surfaces the adhesion of the cells as well as the formation of focal adhesion sites are faster on the latter surface. These results suggested that crystalline ALD-HA is a promising surface coating material for the study of osteoblast/osteoclast biology.

Disclosures: L. Xu, None.

This study received funding from: Academy of Finland and Finnish Ministry of Education.

W010

Mechanosensitivity of Osteoblasts Is Regulated by Actin Polymerization Through Activation of RhoA. W. Yang, M. Malik*, K. L. van Golen*, K. Czymmek*, E. Adams*, G. Madden*, A. Kronbergs*, R. L. Duncan. Biological Sciences, University of Delaware, Newark, DE, USA.

While the skeleton is exquisitely sensitive to mechanical stimulation, bone becomes quickly desensitized to continued mechanical loads. We have previously reported that fluid shear rapidly increases the formation of actin stress fibers in osteoblasts and that depolymerization of the actin cytoskeleton increases the activity of the mechanosensitive, cation selective channel and the intracellular calcium response to fluid shear in osteoblasts. Numerous studies from cells derived from a variety of tissues indicate that activation of small GTPases can alter the cellular cytoskeletal integrity. Here, we postulated fluid shear rapidly activates RhoA to increase actin polymerization, thereby regulating the mechanosensitivity of osteoblasts. We found that RhoA was activated within 15 min of application of 12 dynes/cm² fluid shear to MC3T3-E1 osteoblasts. Confocal microscopy demonstrated that this shear-induced activation resulted in phosphorylation of the actin severing protein, cofilin, by LIM kinase II. Cofilin was rapidly translocated to the nucleus. Inhibition of this pathway with Y27623 or C3 transferase prevented shear-induced cofilin phosphorylation and translocation, as well as actin stress fiber formation in osteoblasts. Using Atomic Force Microscopy to determine changes in the elastic modulus of MC3T3 osteoblasts in response to shear, we found that fluid shear produced an 8-fold increase in cellular stiffness that was completely abrogated by inhibition of the RhoA pathway. Using intracellular calcium imaging, we found that inhibition of RhoA did not change the peak calcium response to shear, but did significantly increase the number of cells responding to shear. We have previously observed that MC3T3 osteoblasts rarely respond to a second

bout of shear with an increase in intracellular calcium if that challenge was administered within 30 min of the first onset of shear. However with RhoA inhibition, 50% of the cells that responded to the initial application of fluid shear responded to a second shear challenge. These data indicate that RhoA plays an important role in the loss of mechanosensitivity of osteoblasts to continued loading by increasing the actin cytoskeletal organization and stress fiber formation. This change in actin integrity increases cellular stiffness that may reduce the ability of the cellular membrane to deform to additional shear.

Disclosures: W. Yang, NIH/NIANS (Adaptation of osteoblasts to mechanical stimulation, R01 AR043222) 2.

This study received funding from: NIH/NIANS.

W011

Studies on Improving Bone Bonding Ability of Titanium by Hydrothermal Treatment with CaCl₂. L. Zhang^{*1}, M. Nakagawa^{*1}, Y. Ayukawa^{*2}, R. Z. LeGeros³, S. Matsuya^{*1}, K. Koyano^{*2}, K. Ishikawa^{*1}. ¹Department of Biomaterials, Faculty of Dental Science, Kyushu University, Fukuoka, Japan, ²Department of Removable Prosthodontics, Faculty of Dental Science, Kyushu University, Fukuoka, Japan, ³Department of Biomaterials & Biomimetics, New York University College of Dentistry, New York, NY, USA.

Titanium has been used extensively as an implant material in dentistry and orthopedics. However, the bone bonding ability of Ti is much lower than those of osteoconductive materials such as hydroxyapatite, characterized by delayed bone formation and fibrous tissue interposition at Ti-bone interface. Alkali treatment is reported to be effective in improving the osteoconductivity of Ti. After such kind of treatment, Ti can bond calcium ions to its surface in vivo and this enhances bone formation. We hypothesized if calcium ions are bonded on Ti surface before it is implanted into the bone, the period of bone formation might be shortened. Therefore the purpose of this study is to find a method to fabricate Ca-bonded Ti and thus to improve the bone bonding ability of Ti implant materials.

In order to attain Ca-bonded Ti (Ca-Ti), we investigated hydrothermal treatment with CaCl₂ solution. From the results of X-ray photoelectron spectroscopy analysis, the Ca-Ti was successfully fabricated by using hydrothermal treatment with 10 mmol/L CaCl₂ at 200°C for 24 h. To reveal the bone cell responses to Ca-Ti, rat bone marrow cell experiments were performed. Results showed that Ca-Ti promoted cell adhesion and proliferation, accelerated the production of osteocalcin and the mineralization of the extracellular matrix. A rodent tibia model was applied to determine the in vivo bone response to Ca-Ti surface. Ca-Ti implant showed osteoblasts adhesion and new bone formation within 1 week. When compared with untreated or alkali treated Ti, Ca-Ti showed higher bone contact ratio from the early stage: 1 week 55%, 2 weeks 88%, 4 weeks 96%. The early, direct bone bonding of Ca-Ti forms a striking contrast to untreated Ti which showed late, fibrous tissue-intervened bone formation [Figure].

We concluded that through hydrothermal treatment with CaCl₂, Ti can be altered into the osteoconductive material. Such surface treatment is a promising alternative for modifying Ti (or Ti alloy) implant surfaces for accelerated osteointegration and skeletal fixation.

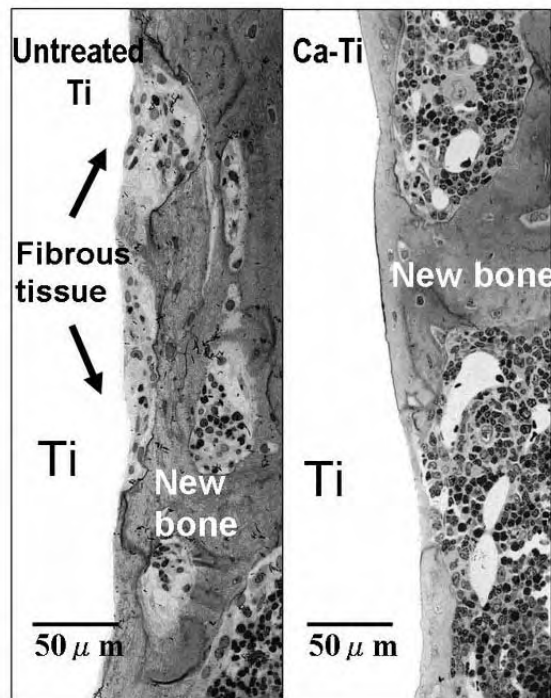


Figure. Different tissue responses to untreated Ti and Ca-Ti after 2 weeks in rat tibia

Disclosures: L. Zhang, None.

W012

Ciz, a Nucleo-cytoplasmic Shuttling Protein Interacts with Extracellular Matrix Proteins. T. Hayata¹, T. Nakamoto^{*2}, Y. Ezura¹, H. Hirai^{*3}, M. Noda¹.

¹Molecular Pharmacology, Medical Research Institute, Tokyo Medical & Dental University, Tokyo, Japan, ²Medicine and Rheumatology, Tokyo Medical & Dental University, Tokyo, Japan, ³Hematology and Oncology, University of Tokyo, Tokyo, Japan.

Ciz is a zinc finger transcription factor with nucleocytoplasmic shuttling activity. We previously showed that Ciz-null mice show high bone mass phenotype, suggesting that Ciz is a negative regulator of bone formation *in vivo*. However, how Ciz suppresses bone formation through protein-protein interaction remains unclear. In the present study, to better understand molecular mechanism of Ciz function in bone formation, we wished to identify the binding partners of Ciz. We performed a yeast two-hybrid screening for Ciz-interacting protein, after constructing a cDNA library from neonatal mouse calvaria. An N-terminal fragment of Ciz (Ciz-deltaZF, amino acid 1-279) that lacks zinc finger domain and contains a proline-rich domain was used as a bait. The proline-rich domain is thought to bind to SH3 domains of signaling proteins. After the screening of 4.2×10^5 clones, 150 positive clones were sequenced. While Ciz is an intracellular protein, 47% of the clones encoded genes for extracellular matrix proteins (ECM), including collagen type 1 alpha 2 (Col1a2), 57%; Col1a1, 10%; Fibulin 2 (Fbln2), 7%; laminin receptor 1 (Rpsa), 7%. Coimmunoprecipitation experiments using *in vitro* translated proteins confirmed binding of Ciz-deltaZF to the fibrillar collagens C-terminal domain of Col1a1 and Col1a2. Association of the transfected Ciz and C-terminal domain of Col1a1 was also confirmed in Cos-7 cells by immunoprecipitation experiments. Although the physiological significance of the interactions is currently under investigation, these results revealed that Ciz interacts with fragments of extracellular matrix proteins at least under the tested condition.

Disclosures: T. Hayata, None.

W013

Hypoxia Accelerates the Transformation of Osteoblasts to Osteocytes. M. Hirao, J. Hashimoto, N. Yamasaki^{*}, W. Ando, H. Tsuboi^{*}, A. Myoui, H. Yoshikawa, Orthopaedics, Osaka University Graduate School of Medicine, Suita, Japan.

Osteocytes are derived from osteoblasts, but reside in the mineralized bone matrix without direct blood flow. It has been reported that MLO-Y4, osteocyte-like cells show much higher expression of ORP150, which is induced by hypoxia, than osteoblast-like cells (27th, 28th ASBMR). Accordingly, we hypothesized that the oxygen tension may regulate the transformation of osteoblasts to osteocytes. MC3T3-E1 cells and calvariae from 4-day-old mice were cultured under normoxic (20% O₂) or hypoxic conditions (5% O₂). To investigate osteoblastic differentiation and transformation to osteocytes, alkaline phosphatase (ALP) staining and alizarin red staining were done and expression of various factors (osteocalcin, DMP1, MEPE, FGF23, Cx43, ORP150) was assessed by real time RT-PCR, ELISA analysis, western blot analysis, immunocytochemical analysis, and immunohistochemical analysis. Hypoxic culture promoted the increased synthesis of mineralized matrix by MC3T3-E1 cells. ALP activity was increased initially during hypoxic culture, but decreased during osteogenesis. Osteocalcin production was also increased by hypoxic culture, but decreased after mineralization. Hypoxia accelerated the change of ALP activity and osteocalcin production in cultured MC3T3-E1 cells. Furthermore, expression of DMP1, MEPE, and FGF23, and Cx43 which are osteocyte-specific or osteocyte-predominant proteins, by MC3T3-E1 cells was greater under hypoxic than normoxic conditions. In mouse calvarial organ cultures, the number of cells in the bone matrix and cells expressing DMP1 and MEPE were increased by hypoxia. In MC3T3-E1 cell cultures, ORP150 expression was only detected in the mineralizing nodules under normoxic conditions, while its expression was diffuse under hypoxic conditions, suggesting that the nodules were hypoxic zones even in normoxic cultures. Collectively, these findings suggest that a low oxygen tension promotes osteoblast maturation and subsequent transformation to osteocytes.

Disclosures: M. Hirao, None.

W014

Adiponectin Action Influences Osteoblast Related Gene Expression. T. Ikeo¹, A. Kamada¹, I. Tamura^{*1}, S. Goda^{*1}, Y. Yoshikawa¹, E. Domae^{*1}, Y. Takaiishi¹, T. Miki². ¹Biochemistry, Osaka Dental University, Hirakata, Japan, ²Geriatric Medicine, Osaka City University, Osaka, Japan.

Adiponectin, which is one of the adipocyte-derived biologically active molecules, is abundantly present as a plasma protein, and exhibits various biological functions, such as regulating energy homeostasis, increasing insulin sensitivity in the liver and skeletal muscle, and protecting the vascular walls from atherosclerosis. Low plasma adiponectin levels are known to cause insulin resistance and metabolic syndrome. Recently, receptors of adiponectin (AdipoR1 and AdipoR2) were cloned and found to be expressed ubiquitously. We previously demonstrated gene expression of the receptors in osteoblast, indicating that adiponectin may affect bone metabolism. In this study, we investigated the expression of osteoblast differentiation markers in osteoblasts which showed suppressed receptor expression due to small interfering RNA (siRNA), to elucidate the influences of the failure of adiponectin action on bone metabolism.

Murine pro-osteoblastic cell line, MC3T3-E1 cells were cultured in alpha-MEM with 10% FBS. Two days after transfecting siRNA against adiponectin receptors (siRNA-AR), the cells were stimulated by ascorbic acid (VC) and beta-glycerolphosphate (BGP) to induce osteoblast

differentiation. The mRNA expression level was measured using real-time quantitative RT-PCR two days after the addition of VC and BGP.

VC and BGP-dependent induction of bone morphogenetic protein-2 (BMP-2) and osteocalcin were significantly suppressed by siRNA-AR compared with non-silencing siRNA controls ($p < 0.01$). Both mRNA expression levels of BMP-2 and osteocalcin were correlated with that of AdipoR2 ($r = 0.895$ and $r = 0.893$, respectively, $p < 0.001$), while there was no correlation of osteoblast differentiation markers with AdipoR1. Suppression of the gene expression of adiponectin receptor in osteoblasts inhibited the induction of BMP-2 and osteocalcin. Hence failure of adiponectin action may suppress the progression of osteoblast differentiation and bone formation.

Disclosures: T. Ikeo, None.

This study received funding from: Grant-in-Aid for Scientific Research (C)(16591877).

W015

Estrogen Receptor-Related Receptor Gamma (ERR γ) Negatively Regulates Osteoblast Differentiation and Mineralization Through Runx2- and Smad-Dependent Pathway. B. Jeong^{*1}, I. Bae^{*1}, I. Kim^{*1}, H. Choi^{*2}, J. Koh¹. ¹Dental Science Research Institution and Brain Korea 21 project, School of Dentistry, Chonnam National University, Gwangju, Republic of Korea, ²Hormone Research Center, School of Biological Sciences and Technology, Chonnam National University, Gwangju, Republic of Korea.

Recently the orphan nuclear Estrogen receptor-Related Receptors (ERR α , β , γ) have been cloned and described their expressions in bone development. This study was undertaken to elucidate roles of ERR γ in osteoblast differentiation. Mouse myoblast C2C12 and pre-osteoblast MC3T3-E1 cells were infected with adenovirus ERR γ (AdERR γ) or siERR γ (AdsiERR γ), in the presence or absence of BMP2. Osteoblast differentiation was determined by alkaline phosphatase (ALP) activity and osteocalcin (OC) production. Mineralization was measured by Alizarin Red staining. For the transcriptional regulation of ERR γ , co-immunoprecipitation, glutathione S-transferase (GST)-pull down, GST-competition and reporter gene assays were done. ERR γ was ubiquitously expressed in various mesenchymal cells, and increased by BMP2 treatment in C2C12 cells. Overexpression of ERR γ significantly inhibited BMP2-induced ALP activity, OC production and mineralization with decreases in BMP2 induction of ALP and OC mRNA expression. AdsiERR γ enhanced ALP activity and OC production in C2C12. Transient transfection of ERR γ significantly inhibited both Runx2-dependent stimulation of OC promoter activity and Smad-dependent modulation of SBE promoter activity. Co-immunoprecipitation and GST pull-down assay showed physical interactions between ERR γ and Runx2-p300 complex or Smad-1 and -5. These results suggest that orphan nuclear ERR γ should be a novel negative regulator of osteoblast differentiation through interfering with Runx2 and Smad signaling.

Disclosures: B. Jeong, None.

This study received funding from: Brain Korea 21 Project for Dental School.

W016

Downstream Signal Transactivation by FGF-4/Osterix Transgene Partially Imitates Changes of BMP-2 Induced Osteogenic Transcription Factors in NIH3T3 Cells. S. Kuroda, M. Samee^{*}, H. Kondo, S. Kasugai. Oral Implantology and Regenerative Dental Medicine, Tokyo Medical and Dental University, Tokyo, Japan.

Bone morphogenetic proteins (BMPs) are well known potent inducers of osteogenesis. In the process of bone formation, BMP-2 stimulates the three osteogenic master transcription factors: Dlx5, Runx2 and Osterix, mediated by the Smad pathways. Fibroblast growth factors (FGFs) are important signal molecules involved in both intramembranous and endochondral ossification. The transactivation of downstream genes such as Runx2 but not Osterix by FGF/FGF receptor signalings is one of the target initial events for osteoblastic differentiation mediated by the PKC pathway. FGF-4 plays important roles in bone development during embryogenesis, and systemic or local application of the recombinant protein demonstrated increase of bone formation in our previous studies. Furthermore, an additional treatment of FGF-4 over BMP-2 enhanced ectopic mineralization in our implant study. However, the mechanisms by which FGF-4 or BMP-2 signaling for osteogenesis are not well understood. In this study, we profiled the signal transactivation of osteogenic transcription factors including Dlx5, Runx2 and Osterix, activated by transgenes in an NIH3T3 cell culture. NIH3T3 cells were seeded in 24-well plates. Each well harbored 1×10^5 cells in 500 μ l D-MEM with 10% FBS. The experimental periods were scheduled as day 3, 7 and 14. The cells were given a transfection using a plasmid vector encoding for FGF-4, Osterix, FGF-4/Osterix or BMP-2. A vehicle vector was also applied for control. At each time point, the samples were subjected for RT-PCR, alkaline phosphatase (ALP) activity, and histological stainings for ALP positive cells and mineralized nodules. BMP-2 gene transfer was followed by elevation of Dlx5, Osterix and Smad1. On the other hand, FGF-4 transgene did not affect the changes of these gene expressions. However, the combination of FGF-4/Osterix overcame weak effects of FGF-4 or Osterix alone, resulting in up-regulation of Dlx5 mRNA as high as in the BMP-2 transfection. Increase of ALP activity per DNA, which was prominent in the FGF-4/Osterix and the BMP-2 transgenes, was not seen in the FGF-4 transgene. The histological works did not elicit nodule apposition in any of the treatments. Conclusively, the current study demonstrated that not FGF-4 alone but FGF-4/Osterix combination partially mimicked BMP-2 in this fibroblastic cell culture, regarding the signal transactivation of two osteogenic transcription factors, Dlx5 and Osterix, although Runx2 mRNA expression was weak over time. Further studies remain to explore the downstream signal pathways of FGF-4 and BMP-2 using other techniques and different cell cultures.

Disclosures: S. Kuroda, None.

This study received funding from: Japan Society for the Promotion of Science.

W017

Gene Networks in Osteoblasts that Are Regulated by the Dlx Gene Family: Requirement for Dlx Transcription Factors in Mesenchymal Commitment to the Osteoblast Lineage. H. Li¹, W. Yang², A. C. Lichtler¹, S. E. Harris².¹Genetics and Developmental Biology, University of Connecticut Health Center, Farmington, CT, USA, ²Periodontics, University of Texas Health Science CTR, San Antonio, TX, USA.

Previous studies demonstrated that Dlx genes promote osteoblast differentiation, are expressed very early in the osteoblast lineage and are stimulated dramatically by BMPs. However, evidence suggests that Dlx genes are functionally redundant, making the study of Dlx genes in regulating osteoblast function difficult. We used a dominant negative Dlx homeodomain-engrailed repressor fusion protein (DNDlx) to inhibit Dlx protein induction of target genes. Co-transfection of DNDlx inhibited Dlx2, 3, 5, and 6 induction of a Dlx reporter construct, and infection of osteoblast cell lines with DNDlx suppresses BMP induced genes. Mouse marrow stromal cells (MSC) expressing DNDlx produced fewer alkaline phosphatase positive colonies and mineralized nodules than control cultures. For comparison, we also expressed Dlx5 which greatly accelerated osteogenesis. Full genome expression microarray analysis of the RNA from these cultures at 11 and 16 days was carried out to discover new and altered pathways regulated by Dlx genes. At 11 days, mineralization had just begun and by 16 days, mineralization is almost complete. Affymetrix array data from 430 2.0 with 41,000 probe sets were analyzed with the Limma program, and genes with a 2.6 or more fold change and $P < 0.01$ were analyzed for functional classification changes using the David program and compared to other gene sets from Gene Expression Omnibus at NCBI. In the 11 day cultures, over 500 genes were specifically inhibited by DNDlx; by Gene Ontology (GO) classification, these included ribosomal proteins, genes associated with osteoblast mineralization and differentiation, such as Osterix and with primary metabolism and mitochondrial function, extracellular matrix and collagen production. Over 120 GO classes are regulated. 398 significant genes were increased at least 2.6 fold by DNDlx, indicating that DNDlx promoted the differentiation of the MSC towards chondrocyte and immunological like phenotypes, probably because DNDlx specifically suppresses the osteoblast lineage. 497 genes were positively regulated by Dlx5 overexpression and many were in the skeletal development and mineralization classes determined by functional clustering with David. We identified 32 poorly annotated genes showing a strong correlation with many osteoblast markers, some induced 10 to 50 fold. Of the 1042 genes downregulated by overexpression of Dlx5, many were characteristic of chondrocytes and immune cells also suggesting that Dlx genes are critical for driving mesenchymal precursors to the osteoblast lineage.

Disclosures: H. Li, None.

This study received funding from: NIH.

W018

Pyrrolidine Dithiocarbamate Inhibits SOD1 Gene and Cell Growth by Activating JNK Pathway in Human Osteosarcoma Cells (U2OS). G. Ngouala*, V. Afonso*, H. Riera*, P. Collin*, A. Lomri. Lariboisiere Hosp., INSERM U-606 & University Paris VII, Paris 10, France.

It has recently been shown that the alteration of the cell-redox status affects the transcription factor expression and activity. Pyrrolidine dithiocarbamate (PDTC) is a potent antioxidant agent that can switch the expression of genes dependent on the activation of the transcription factors AP-1 and NF B. PDTC is also a metal-chelating compound that acts as antioxidant or pro-oxidant and is widely used to study redox regulation of cell function. In the present study, we investigated effects of PDTC on the antioxidant gene SOD1 and cell growth in human osteosarcoma cells (U2OS), using transfection and cell growth assays. We have previously reported that treatment of cells with TNF-alpha repressed SOD1 gene and protein expression. We now show that PDTC treatment does not protect SOD1 from TNF inhibition, but induced further repression. PDTC effects are not linked to NF-kappaB repression. Transfection experiments of U2OS cells with reporter constructs harboring different promoter regions of SOD1 gene indicated the presence of a functional PDTC-responsive region located between positions -157 and +17 of the promoter. Furthermore, transfection studies of JNK-/- cells with SOD1 promoter did not show any repression by PDTC, indicating that JNK pathway is important for PDTC action on SOD1 gene. In contrast, when JNK pathway was restored in these cells, PDTC was able to repress again SOD1 promoter activity. Furthermore, PDTC induced significant inhibition of osteosarcoma cell growth, probably through SOD1 repression and this effect was not linked to cell toxicity. These results indicate that PDTC-dependent repression of SOD1 and cell growth in U2OS osteosarcoma cells is tightly regulated by JNK pathway and point-out SOD1 as a target gene in the anti-proliferative effects of PDTC in cancer cells

Disclosures: A. Lomri, None.

W019

Endogenous Hesr/Hey Genes Redundantly Support Osteoblast Differentiation. S. Maeda¹, H. Kokubo², H. Aburatani³, S. Nomura⁴, S. Komiya⁵, K. Miyazono⁶, T. Imamura⁷. ¹Department of Biochemistry, The Cancer Institute of the Japanese Foundation for Cancer Research, Tokyo, Japan, ²Division of Mammalian Development, National Institute of Genetics, Mishima, Japan, ³Genome Science Division, Research Center for Advanced Science and Technology, University of Tokyo, Tokyo, Japan, ⁴Department of Pathology, Graduate School of Medicine and Frontier Biosciences, Osaka University, Osaka, Japan, ⁵Department of Neuromusculoskeletal Disorder, Orthopaedic Surgery, Graduate School of Medicine and Dentistry, Kagoshima University, Kagoshima, Japan, ⁶Department of Molecular Pathology, Graduate School of Medicine, University of Tokyo, Tokyo, Japan, ⁷Department of Biochemistry, The Cancer Institute of The Japanese Foundation for Cancer Research, Tokyo, Japan.

Bone morphogenetic proteins (BMP) induce osteoblast differentiation of mesenchymal progenitor cells, which event is governed by two master regulators, Runx2 and Osterix. In addition to these transcription factors, other nuclear proteins are also induced by BMP, which roles in osteoblast differentiation are obscure. It has been reported that Hesr1/Hey1 is induced synergistically by BMP and Notch signaling in vitro, and osteoblasts express Hesr1/Hey1 in vivo. Other group showed in the last ASBMR, that ubiquitous overexpression of Hesr1/Hey1 in vivo induced progressive osteopenia in the transgenic mice due to decreased osteoblast differentiation. However, it is still not clear whether endogenous level of Hesr1/Hey1 also acts inhibitory to bone formation or not. To answer this question, we analyzed bones of Hey1/Hesr1 knockout mice. Unexpectedly, the bone mineral density and bone morphometric analysis of Hesr1/Hey1 -/- mice showed no overt phenotype. We considered this result might be due to redundancy between Hesr/Hey genes. Indeed, we found that Hesr3/HeyL gene is also expressed in bone in vivo. So we generated Hesr1/Hey1:Hesr3/HeyL double knockout (Hesr1-/-:3-/-) mice. Some of Hesr1-/-:3-/- mice died before weaning as recently reported by other group. However, survivors of double null mice showed normal growth, which could be subjected to bone analysis. Contrary to our expectations, the bone mineral density of four-allele mutants was decreased. Analysis of mRNA extracted from bones of these mice revealed that osteocalcin was elevated. As we found in vitro, that Hesr1/Hey1 interacts with Runx2 and inhibits its function, this interaction may be, at least in part, responsible for the phenotypes. These data suggest that endogenous expression level of Hesr/Hey genes plays a supportive role in regulating adult bone formation.

Disclosures: S. Maeda, None.

W020

Osterix Functions as Downstream of Runx2 and Msx2 During BMP2-Regulated Osteoblastogenesis. T. Matsubara¹, K. Kumiko^{*1}, K. Hata^{*1}, A. Yamaguchi², H. Aburatani³, R. Nishimura¹, T. Yoneda¹. ¹Biochemistry, Osaka University graduate school of dentistry, Osaka, Japan, ²Oral Pathol, Tokyo Med Dent Univ, Tokyo, Japan, ³Res Cent Adv Sci Tech, Univ Tokyo, Tokyo, Japan.

Complete absence of bone formation and osteoblasts in null mice indicates an Sp1 family transcription factor Osterix/Sp7 is necessary for bone development. Osterix expression is known to be associated with BMP2 actions. However, the precise mechanism that controls the expression and function of Osterix during BMP2-induced osteoblastogenesis remains elusive. In this study, we attempted to study this. Since a previous study suggests that Osterix is a downstream of Runx2, we first examined the effects of Runx2 overexpression on Osterix expression. We found that overexpression of Runx2 induced Osterix expression in mesenchymal cell lines, C2C12 and C3H10T1/2, and primary mesenchymal cells isolated from Runx2-deficient mice along with an up-regulation of ALP and osteocalcin expression, demonstrating that Osterix functions as a downstream of Runx2. However, of interest, BMP2 treatment induced ALP activity and Osterix expression in the Runx2-deficient cells. These results suggest that expression and function of Osterix is regulated by Runx2-independent mechanism in addition to Runx2-dependent mechanism. To verify this possibility, we examined whether Smad signaling is involved in this process. Overexpression of Smad1 and Smad4 up-regulated Osterix expression in the Runx2-deficient cells. In contrast, an inhibitory Smad, Smad6 markedly suppressed BMP2-induced Osterix expression in these cells, indicating that Smad signaling is required for Runx2-independent induction of Osterix. Because Msx2 has been shown to regulate BMP2-induced osteoblastogenesis independent of Runx2, we tested whether Msx2 is involved in the Runx2-independent regulation of Osterix. In the Runx2-deficient cells, treatment with BMP2 induced Msx2 expression and overexpression of Msx2 markedly up-regulated Osterix expression and ALP activity. These data indicate an important role of Msx2 in regulating Osterix expression and suggest that Osterix may have distinct roles from Runx2 during osteoblast differentiation. To test this idea, we performed microarray analyses using Runx2-deficient cells introduced with either Runx2 or Osterix, and found that Osterix up-regulated several genes that are distinct from Runx2. In conclusion, our results suggest that BMP2 regulates Osterix expression through Msx2 but independent of Runx2 and that Osterix controls osteoblast differentiation of mesenchymal cells in Runx2-dependent and independent fashions.

Disclosures: T. Matsubara, None.

W021

Retinoblastoma Binding Protein-1 (RBP1), a Novel Factor Critical For Runx2 Expression and Transcriptional Activation. D. G. Monroe¹, J. R. Hawse¹, M. Subramaniam¹, F. J. Secreto¹, S. Khosla², T. C. Spelsberg¹.¹Biochemistry and Molecular Biology, Mayo Clinic, Rochester, MN, USA,²Endocrine Research Unit, Mayo Clinic, Rochester, MN, USA.

The retinoblastoma binding protein-1 (RBP1) is a broadly expressed transcription factor involved in the suppression of proliferation mediated through the retinoblastoma protein (pRb), a major pathway implicated in the pathogenesis of numerous cancers including osteosarcoma. We have previously demonstrated an estrogen receptor- α -dominant regulation of RBP1 in osteoblasts (OBs), suggesting an important role of RBP1 in OB function. Here we present evidence that RBP1 is involved in Runx2 expression as well as Runx2-dependent transcriptional activation, therefore potentially playing a broader role in general skeletal biology. Overexpression of wild-type RBP1 in the U2OS human osteosarcoma significantly enhances Runx2-dependent activation of a synthetic Runx2-dependent reporter construct (pOSE2-Luc), whereas a mutant RBP1 construct, containing a deletion of the LxCxE motif necessary for RBP1 binding to pRb, fails to enhance Runx2 activity. Similar experiments were conducted in the SAOS2 human osteosarcoma, which lacks pRb activity. Overexpression of Runx2 and/or RBP1 in SAOS2 cells resulted in comparatively weak activation of the pOSE2-Luc, suggesting that an intact pRb/RBP1 system is necessary for maximal regulation of Runx2-dependent transcription. To further characterize the importance of RBP1 in the transcriptional regulation of bone marker genes, we utilized siRNA against RBP1 in mouse calvarial cell cultures. Reduction of RBP1 resulted in a significant transcriptional inhibition of important bone marker genes such as Runx2, osterix, BMP2, osteocalcin, osteopontin, TIEG and BMP2. Similar siRNA experiments targeting both RBP1 and pRb expression were conducted in the mouse MC3T3-E1 osteoblast cell line. Reduction in the expression level of either RBP1 and/or pRb resulted in an inhibition of Runx2-dependent transcriptional activation of these bone marker genes. These results suggest a transcriptional system where both RBP1 and pRb are necessary for maximal Runx2-dependent transcriptional activation in osteoblasts. These data are consistent with previous studies showing that BMP2-treated Rb^{-/-} mouse embryo fibroblasts fail to form bone in vitro and that the Rb knockout mice are not viable. Current experiments are focused on deciphering the long-term effects of RBP1 depletion using both stable shRNA osteoblast cell lines and examining the skeletal phenotype of RBP1 knockout mouse models.

Disclosures: D.G. Monroe, None.

W022

Identification of Osteoblast-specific Co-Regulator Complex for Vitamin D Receptor (VDR). E. Ochiai¹*, H. Kitagawa²*, I. Takada²*, Y. Tushima³*, S. Fujiyama⁴*, S. Sawatsubashi⁴*, M. Kim⁴*, Y. Mezaki²*, K. Takagi³*, K. Takeyama²*, K. Yamaoka⁵*, S. Kato⁶, T. Kamimura³*, ¹Teijin Institute for Bio-Medical Research/ Laboratory of Nuclear Signaling, Institute of Molecular and Cellular Biosciences, The University of Tokyo, Tokyo, Japan, ²Laboratory of Nuclear Signaling, Institute of Molecular and Cellular Biosciences, The University of Tokyo, Tokyo, Japan, ³Teijin Institute for Bio-Medical Research, Tokyo, Japan, ⁴ERATO, Japan Science and Technology Agency, Saitama, Japan, ⁵ERATO, Japan Science and Technology Agency, Saitama/ Teijin Institute for Bio-medical Research, Tokyo, Japan, ⁶Laboratory of Nuclear Signaling, Institute of Molecular and Cellular Biosciences, The University of Tokyo, Tokyo/ ERATO, Japan Science and Technology Agency, Saitama, Japan.

Vitamin D actions in regulating bone metabolism and calcium homeostasis have been well described. Such actions of vitamin D are believed through nuclear vitamin D receptor (VDR), and gene disruption of VDR in mice caused severe rachitic phenotype. And the benefit of vitamin D for bone formation has been shown. Indeed several VDR ligands are applied for clinical use but are expected to reduce side effects like hypercalcemia. Such actions of vitamin D on bone were well known, but the molecular bases of the skeletal vitamin D action are not elucidated in that VDR cofactor complexes formed in osteoblasts. To address this issue, we used biological approach to identify the osteoblast specific co-regulator complex interacting with VDR. Using GST-fused VDR ligand binding domain (LBD) as a bait, nuclear complexes associated with liganded VDR-LBD were purified from nuclear extract of HOS osteoblastic cell line and HeLa as a control cell line. Together with well-reported DRIP/TRAP complex components, CDP (CCAAT Displacement Protein, also known as CUTL1, a homeodomain transcription factor) has identified as a novel ligand-dependent and osteoblast-specific VDR interactant by MALDI-TOF/MS. Furthermore using glycerol density gradient centrifugation, the CDP complex was distinct from the DRIP/ TRAP complex by their molecular weights. By a GST-pull down and co-immunoprecipitation assay, CDP exhibited ligand-dependent interaction with VDR. In a transient expression assay with GAL4-VDR-LBD in HOS cells, CDP co-activated ligand-induced transactivation of VDR. Ectopic CDP expression by adenovirus vector potentiated the expression of the VDR target gene expression in HOS cells and induced osteoblastic differentiation in human osteoblastic SaM-1 cells. From the present findings, it is likely that CDP serves as an osteoblast-specific co-activator complex component for VDR. Currently, recruitment of CDP on the VDR target gene promoters are under investigation and will be presented.

Disclosures: E. Ochiai, None.

W023

Activation of Liver X Receptor Inhibits Hedgehog Signaling and Osteogenic Differentiation of Marrow Stromal Cells. W. Kim, K. Mouillesseaux*, V. Meliton*, C. M. Amantea*, F. Parhami. Medicine, UCLA, Los Angeles, CA, USA.

Liver X receptors (LXRs) are members of the family of nuclear hormone receptors that are activated by specific oxysterols and pharmacological agents such as TO901317 (TO) and GW3965 (GW). LXRs are involved in a variety of physiologic processes including lipid and glucose metabolism, cholesterol homeostasis, and inflammatory signaling. We previously reported that treatment of bone marrow stromal cells (MSC) with TO and GW inhibits spontaneous osteogenic differentiation of these cells, and therefore speculated that LXR activation may inhibit osteoblast differentiation and bone formation. Recently LXRs were found to influence osteoclast differentiation and activation, with LXR^{-/-} mice demonstrating an improved cortical bone phenotype. We also reported that specific osteogenic oxysterols, including 20S-hydroxycholesterol (20S), induce the osteogenic differentiation of MSC by activating the hedgehog (Hh) signaling pathway. In addition, we found that TO and GW blocked oxysterol-induced osteogenic differentiation of MSC, and therefore hypothesized that LXR activation may interfere with osteogenic differentiation induced by the activation of Hh signaling. In order to test this hypothesis, we examined the effects of TO and GW on sonic hedgehog (Shh)-induced osteogenic differentiation of MSC line, M2-10B4 (M2). Results showed that both TO and GW (1-10 μ M) caused a significant inhibition of Shh-induced alkaline phosphatase (ALP) activity and osteocalcin mRNA expression after 3 and 8 days, respectively. Furthermore, treatment of M2 cells with LXR ligands inhibited Shh-induced mRNA expression of Hh target genes, Gli1 and Patched. siRNA to LXR α and LXR β caused an 80-90% inhibition of mRNA expression for these genes, as well as inhibition of ligand-induced expression of LXR target genes, ATP-binding cassette (ABC) transporter proteins ABCA1 and ABCG1. The ability of TO and GW to inhibit Shh-induced signaling and ALP activity was blocked in cells transfected with LXR α and LXR β siRNA, but not in cells transfected with control scrambled siRNA. These results demonstrate for the first time that LXR activation inhibits Hh signaling and osteogenic differentiation of MSC, suggesting a negative role for LXR in bone metabolism. Modulation of Hh signaling through LXR activation may be a novel therapeutic strategy relevant to a variety of indications including age-related osteoporosis and tumorigenesis that is caused by aberrant Hh signaling.

Disclosures: F. Parhami, None.

This study received funding from: NIH/NIAMS.

W024

Expression of Osteoblast-Specific Transcription Factors in Aged Mice. J. M. Patsch¹, M. Rauner¹*, D. Stupphann¹*, K. Tragl¹*, P. Pietschmann¹.

¹Institute of Pathophysiology, Medical University of Vienna, Vienna, Austria,²Ludwig-Boltzmann Institute of Aging Research, Vienna, Austria.

Bone mass and bone stability decline during aging. Impaired osteoblast function is an important mechanism of age-related bone loss. The cellular and molecular mechanisms, which mediate age-dependent changes in osteoblast function, are poorly characterized. Therefore, the first aim of our study was to determine the gene expression pattern of the osteoblast-specific transcription factors runx2 and osterix in aged mice. Secondly, we analysed the gene expression of the osteoblast proteins alkaline phosphatase (ALP), receptor activator of NF κ B ligand (RANKL) and osteoprotegerin (OPG). Bone marrow stromal cells were isolated from 18-months old and 6-weeks old mice. Osteoblast differentiation was induced by adding 5 mM β -glycerophosphate and 50 μ M ascorbic acid to the culture medium. After 7, 14, 21 and 28 days total RNA was isolated, and quantitative real-time PCR analysis was performed. The marrow-free bones were homogenized in liquid nitrogen and also analyzed by real-time PCR. In bone marrow cultures from old mice, the mRNA level of ALP was significantly lower at all time points when compared to young mice. Runx2 mRNA levels also decreased during the first 28 days of culture. We did not detect an age-dependent alteration of ex-vivo gene expression of osterix, RANKL or OPG. mRNA levels of ALP were significantly lower in the bone tissue samples of old mice ($p < 0.05$). In direct correlation with our results obtained from cultured cells, the tissue mRNA levels of osterix, RANKL and OPG remained unaffected by age.

Our results demonstrate that not all osteoblast-specific markers decline with aging. In particular, the expression levels of ALP and runx2 mRNA were downregulated in bone tissue and osteoblast cultures from aged mice. As ALP and runx2 are early markers in osteoblast differentiation, we conclude that aging mainly affects early steps of osteoblasts differentiation.

Disclosures: J.M. Patsch, None.

W025

Interactions Between PTH and the gp130 Cytokine Pathway in Differentiating Osteoblasts. J. M. Quach, E. H. Allan, K. D. Hausler*, M. T. Gillespie, T. J. Martin. St. Vincent's Institute, Melbourne, Australia.

Signaling through gp130 is required for normal osteoblast function, and PTH for accrual of maximal bone mass, yet the crosstalk between these pathways is not well understood. This work is aimed at understanding how PTH interacts with the gp130 cytokines in osteoblasts and precursors, by identifying transcriptional regulators responding to both classes of ligand. A gene array was performed on mouse marrow stromal cells, Kusa 4b10, which were differentiated through 16 days of culture to the time the cells developed functional PTH receptor. The cells were treated with PTH (1-34) or with PTHrP (1-141), and RNA used to probe Affymetrix whole mouse genome microarrays. Several genes known to be regulated through PTHrP (e.g., RANKL, RGS-2, VDR, LIF, IL-6) were used to validate responses on independent Kusa 4b10 RNA samples. Notably, several of the genes enhanced by PTH or PTHrP were involved in the gp130 pathway. These were IL-6, IL-11, LIF and CLCF, as well as the signal-transducing proteins for these cytokines gp130, LIFR, OSMR, and the signaling molecules STAT3, JAK3, SOCS2 and SOCS3. Each of these genes was validated on independent Kusa 4b10 RNA samples. From twelve transcriptional regulators differentially expressed in response to PTH and PTHrP and confirmed by real time-PCR on independent RNA samples, two were chosen for further investigation because pathway analysis indicated links to the gp130 signaling pathway. These were Btg2 (B-cell translocation gene 2) and Zinc-finger protein-36 (Zfp36), both of which have been implicated in bone cell function. Btg2 mRNA was increased 4-fold by PTH at 1 hr, 70-fold with Oncostatin M (OsM), 5-fold with LIF and 3-fold with cardiotrophin-1. Zfp36, which has been shown to bind to AU-rich elements in mRNA and to decrease mRNA stability, was increased 3-fold by PTH, 70-fold by OsM, 2.5-fold by both LIF and cardiotrophin-1. Additionally, both Btg2 and Zfp36 mRNA were rapidly induced by 3 to 4-fold with PTH and 16 to 25-fold with OsM in primary mouse calvarial osteoblasts. Analysis of these interactions between PTH/PTHrP and gp130 cytokine production and action provides new information on local communicating processes in bone.

Disclosures: J.M. Quach, None.

W026

Identification and Characterization of Runx2 Phosphorylation Sites involved in Matrix Metalloproteinase-13 Promoter Activation. N. Selvamurugan, E. Shimizu, N. C. Partridge. Physiology and Biophysics, UMDNJ-Robert Wood Johnson Medical School, Piscataway, NJ, USA.

Parathyroid hormone (PTH) plays a central role in regulation of calcium metabolism. It acts through its G-protein-coupled receptor on the osteoblast to elicit enhanced bone resorption by the osteoclast. Matrix metalloproteinase-13 (MMP-13; collagenase-3) plays a critical role in PTH-induced bone resorption and endochondral bone formation. Our earlier studies showed that PTH induced MMP-13 gene transcription in the rat osteoblastic cell line, UMR 106-01. We identified the PTH-response elements in the regulatory region of the MMP-13 gene and the proteins (Runx2 and Fos/Jun) binding to them. PTH acts via protein kinase A (PKA) to phosphorylate and stimulate the transactivation of Runx2 through a PKA consensus site. To further identify PTH-stimulation of Runx2 phosphorylation in vivo, immunoprecipitation of Runx2 and Western blot analysis were performed. We found that PTH stimulated Runx2 phosphorylation mostly on serine residues with a small amount at threonine and tyrosine residues in UMR 106-01 cells. To determine Runx2 phosphorylation residues in vivo, Runx2 protein was metabolically labeled in COS-7 cells and subjected to immunoprecipitation, acid hydrolysis and thin layer chromatography. Runx2 phosphorylation was increased at serine residues after 8-Br-cAMP treatment. Further, the Runx2 phosphorylation sites in vivo were identified by transient transfection of a c-myc-tagged Runx2 construct into COS-7 cells, followed by 8-Br-cAMP treatment, immunoprecipitation and matrix-assisted laser desorption/ionization MS analysis. Runx2 was identified to be phosphorylated on serines 14 and 332, and threonine 325 after 8-Br-cAMP treatment. To determine the role of Runx2 phosphorylation sites for MMP-13 promoter activation, the wild type Runx2 and Runx2 mutated at these phosphorylation sites (at single, double or triple sites) were transiently transfected into either COS-7 or C3H10T1/2 cells along with the MMP-13 promoter construct. In the presence of 8-Br-cAMP, the wild type Runx2 construct stimulated MMP-13 promoter activity; while the Runx2 construct having mutations at all three phosphorylation sites was unable to stimulate MMP-13 promoter activity in these cells. Thus, we have identified for the first time Runx2 phosphorylation sites necessary for PKA stimulated MMP-13 promoter activation and this event may be critical for bone remodeling.

Disclosures: N. Selvamurugan, None.

W027

Connexin43 Amplifies FGF2-Responsiveness in a Runx2/Protein Kinase C delta- dependent Manner. F. Lima, C. Niger, J. P. Stains. Orthopaedics, University of Maryland, Baltimore, MD, USA.

We examined the molecular and biochemical role of the gap junction protein, connexin43 [Cx43], in the transcriptional response of osteocalcin to fibroblast growth factor 2 [FGF-2]. By luciferase reporter assays, we identified that the osteocalcin transcriptional response to FGF2 in MC3T3 cells is markedly increased by overexpression of Cx43. The transcriptional synergy between Cx43 and FGF2 on osteocalcin transcription is dependent on the dose of FGF2, affecting at 5, 10 and 25 ng/ml. The amplification of FGF2 responsive osteocalcin transcription by Cx43 is mediated by runx2, via its OSE2 cognate element, but not by a previously identified connexin-responsive Sp1/Sp3 binding element. Disruption of Cx43 function with siRNA against Cx43 markedly attenuated the response of MC3T3 cells to FGF2 treatment. Similarly, overexpression of connexin45 - a gap junction protein with "dominant negative" properties with respect to Cx43 function - diminished FGF2 induced osteocalcin transcription. To assess the signal transduction machinery responsible for the Cx43-dependent enhanced FGF2 responsiveness, we used chemical inhibitors and/or siRNA to block ERK, p38 and JNK cascades, as well as, protein kinase C delta [PKC δ] activity. FGF2 was able to induce the phosphorylation of all of these cascades, as shown by immunoblotting with phospho-specific antibodies. Despite the activation of multiple signal transduction pathways, only the PKC δ inhibitor, rottlerin, was able to abrogate the Cx43-dependent enhancement of osteocalcin transcription in response to FGF2. In order to illuminate how Cx43, PKC δ and runx2 mediate the osteoblast response to FGF2, we examined the biochemical changes occurring in FGF2 treated cells. We identified by immunoprecipitation that PKC δ and Cx43 physically interact. Further, we show by immunocytochemistry that upon treatment with FGF2, PKC δ is translocated to the nucleus. By immunoblotting, we show that PKC δ and runx2 are phosphorylated in response to FGF2 treatment. The abundance of phosphorylated protein is increased by overexpression of Cx43, suggesting that the degree of activation is enhanced by increased Cx43 levels. In total, these data show that the gap junction protein Cx43 plays a critical role in regulating osteoblast response to FGF2, as both gain and loss of Cx43 function impact the FGF2-induced osteocalcin transcription. This effect is mediated by PKC δ , which can physically "dock" with Cx43, and, when activated, translocate to the nucleus where it enhances runx2 transcriptional activity.

Disclosures: J.P. Stains, None.

This study received funding from: NIH grant AR052719.

W028

TGF β Inducible Early Gene-1 Directly Binds to, and Represses, the OPG Promoter in Osteoblasts Resulting in Decreased Support of Osteoclast Differentiation. M. Subramaniam¹, J. R. Hawse¹, D. G. Monroe¹, A. Sanyal², M. Cicek², M. J. Oursler¹, T. C. Spelsberg¹. ¹Biochemistry and Molecular Biology, Mayo Clinic, Rochester, MN, USA, ²Endocrine Research Unit, Mayo Clinic, Rochester, MN, USA.

TGF β Inducible Early Gene-1 (TIEG) is a member of the Krüppel-like family of transcription factors that plays an important role in TGF β mediated Smad signaling. To understand the physiological role of TIEG, we generated TIEG-null (TIEG^{-/-}) mice. Calvarial osteoblasts isolated from these mice have a reduced ability to support osteoclast differentiation in vitro. Gene expression studies revealed decreased RANKL and increased OPG expression in TIEG^{-/-} osteoblasts suggesting a role for TIEG in regulating the expression of these genes. Since OPG is one of the most important regulators of osteoclast differentiation, and since TIEG^{-/-} osteoblasts have decreased levels of OPG expression, we sought to determine if TIEG directly regulates OPG expression. A luciferase construct, containing an approximately 1.6 kb fragment of the mouse OPG promoter, was cloned into a pGL3 reporter vector and transiently transfected into TIEG^{-/-} calvarial osteoblasts with and without a TIEG expression vector. The OPG promoter activity was completely abolished in the presence of TIEG suggesting that TIEG directly regulates the expression of OPG in osteoblasts. In order to determine the region of this promoter through which TIEG acts, sequential 5'-deletion constructs were created. Transient transfection of these constructs revealed that the TIEG binding site(s) resides within a 200 bp region of the OPG promoter. To determine if TIEG protein directly interacts with this region, transient ChIP analyses were performed using a TIEG-specific antibody. The results of these studies revealed that TIEG does bind to this region of the OPG promoter. As a confirmation, real-time PCR analysis of these ChIP assays demonstrated that this 200 bp region is enriched by approximately 8-fold in the presence of TIEG protein relative to vector transfected cells. These studies confirm that TIEG interacts with this specific region of the OPG promoter to inhibit its activity. Since we have previously shown that TIEG regulates target gene expression through Sp-1 sites, we scanned this region of the OPG promoter for potential TIEG binding elements. Interestingly, this sequence analysis identified 4 Sp1 binding sites and suggests that TIEG could be acting through these DNA elements to regulate the expression of the OPG gene. Taken together, these results confirm that TIEG directly binds to and inhibits OPG promoter activity and as expected, TIEG^{-/-} mouse osteoblasts display a significant inability to support osteoclast differentiation.

Disclosures: M. Subramaniam, None.

W029

C/EBP β Is a Crucial Partner of ATF4 in Osteoblast Differentiation. H. Tominaga^{*1}, S. Maeda¹, M. Hayashi^{*1}, S. Akira^{*2}, T. Komori^{*3}, S. Komiya^{*4}, T. Imamura¹. ¹Department of Biochemistry, The Cancer Institute of the Japanese Foundation for Cancer Research, Tokyo, Japan, ²Exploratory Research for Advanced Technology, Japan Science and Technology Agency, Department of Host Defense, and The 21st Century COE, Combined Program on Microbiology and Immunology, Research Institute for Microbial Diseases, Osaka University, Osaka, Japan, ³Department of Developmental and Reconstructive Medicine, Division of Cell Biology, Nagasaki University Graduate School of Biomedical Sciences, Nagasaki, Japan, ⁴Department of Neuromusculoskeletal Disorder, Orthopaedic Surgery, Graduate School of Medicine and Dentistry, Kagoshima University, Kagoshima, Japan.

ATF4 is a member of CREB/ATF family basic leucine zipper (bZIP) transcription factors, and plays a crucial role in osteoblast differentiation in cooperation with Runx2. ATF4 binds to DNA element OSE1, which sequence exists in osteocalcin gene promoter, to enhance the differentiation. We and other groups have reported that another bZIP protein C/EBP β also enhance osteoblast differentiation with Runx2 synergistically, through interacting to CEBP-binding element. ATF4 and C/EBP β are reported to be able to form stable heterodimers. Moreover, OSE1 resembles reported DNA binding sequence for ATF4-C/EBP β heterodimers. Thus we hypothesized that the heterodimers could act on OSE1. First we confirmed interaction of endogenous ATF4 and C/EBP β in primary calvarial osteoblasts. We next tested the question by gel shift and luciferase assays. ATF4-C/EBP β heterodimers bound OSE1 with more strong affinity than homodimers of ATF4. The heterodimers induced more intense signals from luciferase constructs of OSE1 and OC promoter than ATF4-homodimers, which activity was elevated to maximum level with Runx2. We finally studied function of C/EBP β on bone formation in vivo by analyzing C/EBP β knockout mice, which phenotype regarding bone has not been studied. C/EBP β null mice showed delayed bone formation like ATF4 null mice. These results suggest that C/EBP β plays an indispensable role in forming active complex with ATF4 and Runx2 on OSE1, in addition to CEBP-binding element, during osteoblast differentiation.

Disclosures: H. Tominaga, None.

W030

Osr1 Gene Expression Is Regulated by Runx2 and Ikaros Transcription Factors. M. Yamauchi¹, S. Kawai², A. Amano^{*2}, T. Ooshima^{*1}. ¹Department of Pediatric dentistry, Osaka university Graduate School of Dentistry, Suita-Osaka, Japan, ²Department of Oral Frontier Biology, Osaka university Graduate School of Dentistry, Suita-Osaka, Japan.

Odd-skipped gene is one of the pair-rule genes which contribute to Drosophila somite formation. Two mammalian homologues, Odd-skipped related 1 (Osr1) and Osr2, has been shown to be expressed in limb, branchial arches, kidney, eye, and dermis. Osr1 is known to play a critical role in the heart and urogenital development. While, the function of Osr1 in bone formation as well as the regulation of Osr1 gene expression are still unclear. To understand regulatory mechanism of Osr1 gene expression, we cloned mouse Osr1 promoter (4.7kb) and analyzed the promoter activity. We constructed 7 deleted promoters and cloned them into pGL-3 basic vector. As a result, two regulatory regions which consisted of positive regulatory region (-741bp~-144bp) and negative regulatory region (-1651bp~-742bp) were found in Osr1 promoter. GATA1, CP-2, Ikaros, Nkx-2.5, Runx1, and Runx2 binding sites existed around these regulatory regions. Osr1 promoter-luciferase reporter construct and various transcription factors were co-transfected and luciferase activity was measured. As a result, Ikaros and Runx2 decreased Osr1 promoter activity, and it was also found that Osr1 gene expression was dose-dependently downregulated by these factors. Furthermore, point mutation at transcription factor binding site for Ikaros or Runx2 prevented the downregulatory effects by them. We also confirmed the binding of transcription factors to Osr1 promoter with chromatin immunoprecipitation and electrophoretic mobility shift assay. These data indicates that Osr1 gene expression is negatively regulated by at least two transcription factors, Ikaros and Runx2. Ikaros is one of the important regulators of lymphocyte differentiation. Runx2 is a crucial regulator of bone formation. Osr1 is regulated by these transcription factors, suggesting that Osr1 has a functional role in lymphocyte differentiation and bone formation.

Disclosures: M. Yamauchi, None.

W031

Age-Related Intrinsic Changes in Human Bone Marrow-Derived Mesenchymal Stem Cells and Their Differentiation to Osteoblasts. J. Glowacki¹, S. Zhou¹, J. S. Greenberger², M. W. Epperly^{*2}, J. P. Goff^{*2}, C. Adler^{*1}, M. S. LeBoff³. ¹Orthopedic Surgery, Brigham and Women's Hospital, Boston, MA, USA, ²Radiation Oncology, University of Pittsburgh Medical Center, Pittsburgh, PA, USA, ³Medicine, Brigham and Women's Hospital, Boston, MA, USA.

A sub-population of marrow-derived stromal cells (MSCs, a.k.a. mesenchymal stem cells) has potential to differentiate into multiple cell types, including osteoblasts. We tested the hypotheses that there are intrinsic effects of age on human MSCs. We measured the

effect of age on proliferation, cell cycling, apoptosis, p53 pathway genes, senescence-associated β -galactosidase (SA- β -gal), and osteoblast differentiation in hMSCs that were obtained from marrow discarded from men and women (17-90 years) undergoing orthopedic surgery. Low density mononuclear cells were isolated by centrifugation on Ficoll/Histopaque 1077 and hMSCs were established in monolayer culture with phenol red-free α -MEM, 10% Fetal Bovine Serum-Heat Inactivated, 100 U/ml penicillin, and 100 μ g/ml streptomycin. For some experiments, the low-density mononuclear cell suspensions were sorted with FITC-labeled STRO-1 antibody. Viable hMSCs at passage 2 were counted every other day with a hemocytometer. Cell cycle was assessed by FACS. SA- β -gal-positive cells were enumerated cytochemically. Osteoblast differentiation was assayed in basal medium with osteogenic supplements (10 nM dexamethasone, 5 mM β -glycerophosphate, and 170 μ M ascorbic phosphate). For most analyses, nonparametric statistical tools were used.

Doubling time of hMSCs was 1.6-fold longer in cells from the older (78.8 ± 13.5 hrs, $n=13$) than the younger subjects (48.8 ± 0.7 hrs, $n=3$) and was positively correlated with age ($r = 0.60$, $p=0.0137$, $n=16$). With age, there was uniform prolongation of the duration of all phases of the cell cycle, but with age, more cells were apoptotic ($r=0.723$, $p=0.0248$, $n=9$). Further, there were age-related increases in expression of p53 and its pathway gene p21 and BAX (RT-PCR). There were 4-fold more hMSCs positive for SA- β -gal in samples from older (8.9 ± 2.4 , $n=12$) than younger subjects (2.3 ± 1.8 , $n=5$, $p<0.001$). With age, there was a significant decrease in generation of osteoblasts both in the STRO-1⁺ cells ($r = -0.714$, $p=0.047$, $n=8$) and in adherent MSCs ($r = -0.81$, $p=0.010$, $n=8$). In sum, there are age-dependent decreases in proliferation and osteoblast differentiation and increases in p53 and its pathway genes, SA- β -gal, and apoptosis in hMSCs. The p53 pathway may have a critical role in age-related changes of hMSCs, in light of recent murine data that p53 is a negative regulator of osteoblast differentiation. These findings support the view that there are intrinsic alterations in human MSCs with aging that may contribute to the process of skeletal aging.

Disclosures: J. Glowacki, None.

This study received funding from: NIH.

W032

Wdr5 Is Essential for Osteoblast Differentiation. F. Gori, E. Zhu^{*}, M. B. Demay. Endocrine Unit, Massachusetts General Hospital/Harvard Medical School, Boston, MA, USA.

Wdr5, a BMP-2 induced gene, is developmentally expressed in osteoblasts and accelerates osteoblast differentiation in vitro. Transgenic mice overexpressing Wdr5 in maturing osteoblasts display accelerated endochondral bone formation during embryonic development, associated with earlier activation of the canonical Wnt signaling pathway. To address whether Wdr5 is essential for osteoblast differentiation, plasmid-based small interfering RNAs (siRNAs) were used to stably suppress endogenous Wdr5 protein levels in MC3T3E-1 cells. Levels of endogenous Wdr5 protein were assessed by Western analyses after 7 days in culture, when Wdr5 protein levels are maximally expressed. Clones expressing two of the selected siRNAs targeting Wdr5 demonstrated a significant decrease in endogenous Wdr5 protein levels relative to that of the scrambled (siRNA-S) clone. This reduction of endogenous Wdr5 levels markedly inhibited osteoblast differentiation, resulting in a significant decrease in alkaline phosphatase activity, impaired expression of Runx-2 and osteocalcin mRNAs and absence of mineralized matrix formation. Based on the observation that overexpression of Wdr5 enhances canonical Wnt signaling in osteoblasts, the effects of Wdr5 silencing on a key mediator of this pathway, β -catenin, was examined. A decrease in nuclear β -catenin protein levels was observed with Wdr5 knockdown, suggesting that inhibition of canonical Wnt signaling may, in part, underlie the impaired osteoblast differentiation observed when Wdr5 protein levels are suppressed. Analysis of Wnt target genes demonstrated that suppression of Wdr5 expression resulted in a significant decrease in the levels of c-myc, the expression of which is increased by canonical Wnt signaling. Furthermore, the expression of SFRP-2, which is repressed in response to Wnt signaling, was increased in association with Wdr5 knockdown. Although suppression of Wdr5 protein levels decreased the antiapoptotic protein Bcl-2 and increased caspase 9 activation, only a minimal increase in apoptosis was observed in these cells (from 3.2% to 5%). Thus, our investigations demonstrate that Wdr5 not only accelerates osteoblast differentiation when it is overexpressed, but is also essential for osteoblast differentiation. In addition, our findings suggest that Wdr5 is required for optimal canonical Wnt signaling in MC3T3E-1 cells.

Disclosures: F. Gori, None.

W033

The Role of EphB/ephrin-B Interactions in Cell Attachment and Spreading of Mesenchymal Precursors Derived from Human Bone Marrow and Dental Pulp Tissues. A. Arthur^{*1}, S. Koblar^{*2}, S. Gronthos¹. ¹Division of Haematology, Institute of Medical and Veterinary Science, Adelaide, Australia, ²Faculty of Health Sciences, University of Adelaide, Adelaide, Australia.

The Eph family of receptor tyrosine kinases and their ligands, the ephrin molecules, appear to play an important role in skeletal development during embryogenesis. Our study examined the expression pattern and function of EphB/ephrin-B molecules on mesenchymal stem/precursor cells derived from human bone marrow and dental pulp tissues. Multiple receptors and ligands were identified on dental pulp stem cells (DPSC) and bone marrow stromal stem cells (BMSSC) by real time PCR and immunohistochemistry. The function of EphB/ephrin-B molecules during BMSSC and DPSC attachment and spreading was assessed in the presence of different Eph/ephrin-Fc fusion proteins using an established in vitro cell-spreading assay. In response to either

EphB2-Fc or ephrin-B1-Fc, the stem cells formed rounder and smaller cell bodies demonstrated by F-actin distribution, and restricted their ability to spread. Additionally, immature focal adhesions were identified at the edge of the cell membrane, reminiscent of spreading initiation centres (SIC), which have only been observed at early stages of cell spreading. In the presence of Inhibitors, Eph forward signaling through the mitogen activated protein kinase (MAPK) pathway restricted cellular spreading, while reverse signaling through the ephrin ligand was mediated via the phosphorylation of the Src homology (SH2) domain activating downstream signaling cascade. Collectively, these studies indicated that EphB/ephrin-B molecules provide an inhibitory environment for mesenchymal stem/precursor cell attachment, consequently resulting in the lack of spreading and detachment. These results may have implications for calcified skeletal/dental tissue development and regeneration.

Disclosures: S. Gronthos, None.

This study received funding from: NHMRC

W034

PTEN and Osteoblastogenesis. A. R. Guntur¹, M. C. Naski². ¹Biochemistry, UTHSCSA, San Antonio, TX, USA, ²Biochemistry & Pathology, UTHSCSA, San Antonio, TX, USA.

Osteoblastogenesis is marked by increased expression of PTEN, the chief inhibitor of phosphatidylinositol 3-kinase (PI3K) signaling. Based on this observation we hypothesized that PTEN/PI3K signaling regulates osteoblast differentiation. To test this hypothesis we conditionally inactivated PTEN in osteoblast precursors. This caused a dramatic increase in osteoblast differentiation and bone formation. Moreover, precocious differentiation ensued, indicating loss of physiological restraints. Increased numbers of osteoblasts were in part accounted for by enhanced cell proliferation and diminished pathways of feedback inhibition. Accelerated differentiation coincided with increased levels of the hedgehog-dependent transcription factor Gli2. Increased hedgehog signaling was evidenced by up-regulation of patched, a transcriptional target of hedgehog. We conclude that PTEN is required to restrict osteoblast replication and halt precocious differentiation. The results demonstrate that the PI3K signaling pathway is an attractive target for pharmacological regulation to enhance bone mass.

Disclosures: A.R. Guntur, None.

W035

Role of Type III NaPi Transporter(s) in Osteoblastic Differentiation. C. Haldrup^{*1}, L. B. Nielsen^{*2}, J. Lykke^{*3}, L. Pedersen¹. ¹Dept of Molecular Biology and Inst of Clinical Medicine, Aarhus University, Aarhus, Denmark, ²Dept. of Paediatrics, Glostrup University Hospital, Glostrup, Denmark, ³Dept. of Medical Biochemistry and Genetics, University of Copenhagen, Copenhagen, Denmark.

The role of the type III sodium-dependent inorganic phosphate (Pi) transporters in osteoblastic differentiation and mineralization was addressed using the murine preosteoblastic cell line, MC3T3-E1. These cells differentiate over time into mature mineralizing osteoblasts upon addition of ascorbic acid and β -glycerophosphate. To impair the function of the 2 type III transporters, Pit1 and Pit2, cells were infected with retroviruses, which employ Pit1 and/or Pit2 as receptors for infection and thus inhibit their function. Blocking of Pit1 and Pit2 protein function was confirmed by virus interference studies. Mineralization was analyzed with Alizarin red. Expression of Pit1 and osteocalcin were followed by Northern blotting. Pi uptake was analyzed using 32Pi.

We found that infecting MC3T3-E1 cells with a virus impairing both Pit1 and Pit2 severely reduced their ability to mineralize. Infection with this virus only reduced Pi uptake with about 30 % suggesting that the 2 type III transporters are not responsible for the bulk Pi uptake in the cells. However, Pit1 has previously been shown to be upregulated during osteoblastic differentiation implying that at least Pit1 has a specialized function in osteoblasts. To further analyze the role of Pit1, we investigated Pi uptake in undifferentiated MC3T3-E1 cells overexpressing epsilon-tagged human Pit1 or Pit2. These results surprisingly showed that although human Pit1 was present in the cell membrane, it did not facilitate an increased Pi uptake compared to wt cells. In contrast, Pi uptake was more than tripled when Pit2 was overexpressed. Thus, Pi transport does not seem to be Pit1's primary function in undifferentiated MC3T3-E1 cells. Moreover, while osteocalcin could still be upregulated in cells infected with a virus impairing Pit2 function, its expression was undetectable in cells infected with a virus impairing both Pit1 and Pit2 function suggesting that Pit1 has a direct effect on osteoblastic differentiation. In conclusion, the results strongly suggest that Pit1 is necessary for osteoblastic differentiation and, possibly as a consequence of this, also for mineralization. The data do not reveal the exact role of Pit1 in differentiation, however, since overexpressed Pit1 does not appear to facilitate an increase in Pi uptake in undifferentiated MC3T3-E1 cells, we speculate that 1) Pit1 Pi transport function is differently regulated in the membrane in differentiated osteoblasts compared to undifferentiated cells and/or 2) Pit1 may function in signaling.

Disclosures: C. Haldrup, None.

This study received funding from: Danish Medical Research Council.

W036

Heparan Sulfate Proteoglycan (HSPG) Aulfation During In Vitro Osteogenesis. L. M. Haupt^{*1}, A. van Wijnen², G. S. Stein³, V. Nurcombe^{*1}, S. M. Cool¹. ¹Stem cell and tissue repair laboratory, IMCB, Singapore, Singapore, ²Department of Medicine, University of Massachusetts, Worcester, MA, USA, ³Medical School, University of Massachusetts, Worcester, MA, USA.

The heparan sulfate proteoglycans (HSPGs) are a family of extracellular matrix (ECM) and cell membrane-associated complexes that mediate a host of soluble, cell-cell, and ECM interactions. They are composed of a core protein to which highly variable glycosaminoglycan (GAG) sugar chains of the heparan sulfate class are attached, and they are capable of interacting with multiple morphogens, including the fibroblast growth factors (FGFs), Wnts, and the bone morphogenic proteins (BMPs), based upon their side chain sulfation patterns. Structural heterogeneity within the HS chain is generated during chain initiation and polymerisation, with the key modifications performed by the specific, coordinated actions of the glycosyltransferases (Ext-1 and -2), the N-deacetylase/N-sulfotransferases (NDST1-4), as well as 2-O-sulfotransferase and 6-O-sulfotransferase enzymes. Under osteogenic conditions in vitro, MC3T3 cells reach confluence between days 6 and 8, exit the cell cycle and commit toward the osteogenic lineage. We have compared the expression profile of the glycosyltransferase and sulfotransferase enzymes under non-osteogenic and maintenance media culture conditions between the proliferative (Day 6) and differentiative (Day 14) phases of cell culture to determine a role for HSPG sulfation activity during in vitro osteogenesis. Under osteogenic conditions, MC3T3 cells demonstrated increased gene expression of osteogenic markers with a coincident decreased gene expression of Ext-1 and -2 genes but increased expression of NDST-3. Significantly, the osteogenic driven cells dramatically increased their syndecan-1 and glypican-3 gene expression profiles as compared to their non-osteogenic counterparts. In addition, these cells alter their FGFR profile, increasing FGFR2, FGFR3 and FGFR4 gene expression levels. Combined this data implicates the production of shorter, highly sulfated HSPGs during in vitro osteogenesis. In particular, glypican-3 and syndecan-1 appear to be central to the in vitro differentiation of MC3T3 pre-osteoblast cells by the mediating growth factor response of the cells.

Disclosures: L.M. Haupt, None.

This study received funding from: AStar Singapore.

W037

Continuous Treatment with PTH Is Anabolic in Cultured Osteoblasts from COX-2 Knockout Mice. H. Huang^{*}, S. Choudhary, L. Raisz, C. Pilbeam. Endocrinology Division, University of Connecticut Health Center, Farmington, CT, USA.

PTH is a potent anabolic agent in vivo, but its anabolic effects in vitro are difficult to demonstrate. Since PTH induces cyclooxygenase (COX)-2 and PGE₂ production in osteoblasts and PGE₂ is anabolic in vitro, we hypothesized that whatever anabolic effects PTH might have in vitro would be diminished in cells from COX-2 knockout (KO) mice compared to cells from wild type (WT) mice. Marrow stromal cells (MSCs) and primary calvarial osteoblasts (POBs) from 6-8 wk old COX-2 KO and WT mice in a CD-1 background were treated with PTH (10⁻⁸ M) or vehicle (control) for up to 21 d. Alkaline phosphatase (ALP) and osteocalcin (OCN) mRNA levels were determined at d 14 and 21, respectively, by real-time PCR and mineralization at d 21 by alizarin red staining. In both MSC and POB cultures, ALP and OCN mRNA expression were 35%-50% lower in KO control cultures than in WT control cultures. PTH had no effect on ALP and OCN mRNA expression in either MSC or POB WT cultures but did increase expression in KO cultures relative to controls. PTH increased ALP and OCN expression 6.5-fold (p < 0.01) and 4.4-fold (p < 0.01), respectively, in KO MSC cultures and 2.1-fold (p < 0.05) and 7.0-fold (p < 0.01), respectively, in KO POB cultures. PTH had no effect on mineralization in WT MSC or POB cultures but increased mineralization in both KO MSC and POB cultures. Basal cAMP levels in POB cultures, in the presence of the phosphodiesterase inhibitor IBMX, were 2-fold higher in WT compared to KO cells (p < 0.05). PTH treatment for 15 min increased cAMP 70-fold in WT and only 40-fold in KO cells. Hence, the increased anabolic effects of PTH in KO cells do not appear to be associated with increased cAMP production. To screen for other factors that might be responsible for the differences in PTH-mediated anabolic effects, POBs from WT and KO mice were cultured for 1 wk and treated with and without PTH for 1, 3 and 24 h and mRNA expression measured by real-time PCR. No change in BMP-2 mRNA expression was observed with PTH. PTH increased Runx-2 mRNA by 2-fold in both WT and KO cultures at 3 h (p < 0.01). PTH increased IGF-1 by 1.7-fold in KO cultures at 24 h (p < 0.01) but had no effect in WT cultures. In contrast to the increased anabolic effects of PTH in KO cells, the PTH stimulation of osteoclast differentiation in marrow cultures, measured by counting TRAP positive multinucleated cells at d 7 of culture, was decreased 70% (p < 0.01) in COX-2 KO cultures compared to WT cultures as reported previously. We conclude that absence of COX-2 increases the stimulatory effects of PTH on osteoblastic differentiation in vitro but decreases the stimulatory effects of PTH on osteoclastic differentiation in vitro. These data are consistent with the observation that intermittent PTH has greater anabolic effects in COX-2 KO mice than in WT mice.

Disclosures: H. Huang, None.

This study received funding from: NIH DK-48361 and AR-47673.

W038

Bioactive Tripeptides Enhance Osteoblast Function In Vitro. M. M. Huttunen*, M. Pekkinen*, M. E. Ahlström*, C. J. Lamberg-Allardt. Dept. of applied chemistry and microbiology/Nutrition, University of Helsinki, Helsinki, Finland.

The purpose of this in vitro study was to elucidate the short- and long-term effects of bioactive tripeptides Ile-Pro-Pro (IPP), Val-Pro-Pro (VPP) and Leu-Lys-Pro (LKP) on osteoblast proliferation, differentiation and bone formation. Preliminary screening of the peptides on osteoblast proliferation was carried out on rat osteosarcoma UMR-106 cells. Further studies were carried out on human mesenchymal stem cells (Poietics, Cambrex Bio Science) purified from bone marrow and osteoblasts differentiated from them. Cell proliferation experiment was carried out with 5, 50 and 500 µM peptide concentrations and 6-, 24- or 48-h treatment time. DNA synthesis activity was assessed by a Cell Proliferation ELISA kit (Roche Diagnostics GmbH, Germany). The expression profiles of osteoblasts were compared after a 24-h treatment with 50 µM IPP, VPP or LKP with a Hum16-K protocol, consisting of 16 000 human gene probes. Microarray results were confirmed by qRT-PCR (Mx3000P, Stratagene) according to the manufacturer's instructions using a Brilliant SYBRGreen qPCR Master mix kit. IPP's long-term effects on nine genes in hMSC-differentiated osteoblasts was analysed by qPCR on days 13, 17 and 20. Total protein content and bALP activity were assessed on days 3, 7, 12, 14, 17, 21 and 34 of culture. Cell culture mineralization was assessed by Alizarin Red S staining. The results show increased UMR-106 and hMSC proliferation. Microarray data analysis revealed IPP to upregulate 270 genes and downregulate 100 genes. The respective numbers for VPP were 25 and 10 and for LKP 16 and 14. IPP regulated genes associated with cell differentiation, cell growth and cell signal transcription. The upregulation of these genes indicates that IPP enhances osteoblast proliferation and differentiation. Long-term treatment with IPP enhanced osteoblast gene expression in favour of bone formation and increased mineralization, but did not influence bALP activity. Apoptosis related caspase-8 and PTHrP were downregulated. Our results show that bioactive peptides stimulate pathways resulting to increased osteoblast function and bone formation. Agents that increase the number and function of osteoblasts can improve bone mass and structure and decrease fracture risk. Bioactive peptides such as IPP may well conduct some of the positive effects dietary protein has on bone.

Disclosures: M.M. Huttunen, None.

W039

Progenitor Cells in Traumatically Injured Muscle Have Characteristic Similarities to Bone Marrow-Derived Stem Cells. W. M. Jackson*¹, S. M. Koehler*¹, J. R. Giuliani*², R. S. Tuan¹, L. J. Nesti². ¹Cartilage Biology and Orthopaedics Branch, National Institute of Arthritis and Musculoskeletal and Skin Diseases, Bethesda, MD, USA, ²Department of Orthopaedics and Rehabilitation, Walter Reed Army Medical Center, Washington, DC, USA.

Heterotopic ossification (HO), or the formation of mature bone in soft tissues, is prevalent in patients with severe time-of-war extremity wounds. Although the cellular mechanisms of HO pathogenesis are unclear, it is likely that mesenchymal progenitor cells in the traumatized muscle (tmMPCs) are responsible for HO formation. The relationship between these MPCs and bone marrow-derived mesenchymal stem cells (bmMSCs) is unknown; therefore, the objective of this study was to compare the phenotype and differentiation potential of tmMPCs in traumatically injured muscle to bmMSCs. With IRB approval at Walter Reed Army Medical Center, muscle debridements were obtained from patients sustaining traumatic orthopaedic injury, and bone marrow was obtained from total hip arthroplasties. The tmMPCs were isolated from the muscle after extensive mincing, collagenase digestion and direct plating onto tissue culture plastic (TCP). bmMSCs were isolated from the marrow by direct plating onto TCP. After culture expansion, the expression of characteristic cell surface markers for MSCs was assayed by flow cytometry. Both groups of cells were cultured in defined differentiation media for osteogenesis, chondrogenesis, adipogenesis and myogenesis. The differentiation potential was assayed with histology (osteogenesis: alizarin red; adipogenesis: oil red O; chondrogenesis: alcian blue; myogenesis: hematoxylin) and by expression of lineage dependent genes (osteogenesis: ALP, Col I, and Runx2; adipogenesis: LPL and PPARγ; chondrogenesis: Col II, Col IX, AGN and Sox 9; myogenesis: MyoD and myosin heavy chain).

Although there were slight morphological differences between tmMPCs and bmMSCs, both populations expressed cell surface markers characteristic for MSCs (CD 73, CD 90 and CD105), and did not express markers absent on MSCs (CD14, CD34 and CD45). After 21 days in differentiation media, the histological staining and genetic expression of tmMPCs and bmMSCs was characteristic for differentiation into osteoblasts, chondrocytes and adipocytes but not into myoblasts.

This study demonstrates that MPCs in traumatized muscle have similar phenotype and differentiation potential as bmMSCs. The tmMPCs appear to be distinct from myogenic progenitors since they do not readily differentiate into myoblasts or form myotubes. Our findings suggest that dysregulation of the tmMPCs by inflammatory and wound response signals associated with trauma would be sufficient to induce ectopic osteogenesis.

Disclosures: W.M. Jackson, None.

This study received funding from: The Military Amputee Research Program, Walter Reed Army Medical Center.

W040

Temporal Regulation of Histogenesis by Mesenchyme During Craniofacial Bone Development. A. H. Jheon*, B. F. Eames*, R. A. Schneider*. Orthopaedic Surgery, UCSF, San Francisco, CA, USA.

Development of bones involves a vast array of molecular and cellular interactions. Although, the roles of mesenchyme and epithelium in the patterning of facial bones have been studied extensively, little is known about their roles in the temporal control of bone histogenesis, which involves distinct and sequential modules including pre-osteoblast specification, osteogenic condensations, osteoid deposition, and mineralization. In the present study, we exploit the different developmental rates between quail and duck (quail hatch in 17 days whereas duck hatch in 28 days) to test the extent to which mesenchyme and epithelium control the initiation and progression of these modules during intramembranous bone development. By transplanting faster-developing quail mesenchyme adjacent to slower-developing duck epithelium (to generate chimeric quack), or conversely, slower-developing duck mesenchyme adjacent to faster-developing quail epithelium (to generate dual), the contribution of mesenchyme or epithelium can be determined. We show that mineralization of intramembranous bones occurs concordant with the developmental times of the donor. Thus, in quack, the first trace of facial bone mineralization occurs 36 hours earlier on the quail-donor side compared to the duck-host side, whereas in dual, mineralization occurs approximately 36 hours later on the duck-donor side. Further observations in quack show that deposition of osteoid and appearance of osteogenic condensations also occur according to the donor time line. These histological observations correlate with the molecular expression profiles of various genes necessary in osteoblast differentiation and mineralization. Preosteoblast-specification, measured by Runx2 expression, arises at a stage far before any evidence of bone and its expression is concomitant with a decrease in cell proliferation and an increase in cell differentiation. Thus, by utilizing the quail-duck chimeric system, we conclude that the temporal control of the various modules of intramembranous bone development is determined by mesenchyme, whereas epithelium appears to play a permissive role.

Disclosures: A.H. Jheon, None.

This study received funding from: CIHR, NIH.

W041

Flow Cytometric Immunophenotyping of Human Periodontal Ligament Cells. N. Kawanabe, K. Murakami*, S. Murata*, T. Yamashiro*. Department of Orthodontics and Dentofacial Orthopedics, Okayama University, Graduate School of Medicine, Dentistry and Pharmaceutical Sciences, Okayama, Japan.

To characterize its primitive phenotypes analogous to mesenchymal stem cells, we investigated cell surface antigens' expression in cultured human periodontal ligament (PDL) cells. After obtaining approval from the Ethical Committee, intact permanent teeth were collected from healthy patients who were undergoing orthodontic treatment at Okayama University Hospital. The PDL cells isolated from these teeth were cultured. The cells were incubated with antibodies, then subjected to flow cytometric analysis. Primary human PDL cells used in this study showed fibroblastic spindle shape and capillary network formation. Flow cytometric studies demonstrated that PDL cells express mesenchymal stem cell markers, including CD9, CD13, CD29, CD44, CD73, CD90, CD105 and CD166, while they are negative for many hematopoietic markers (CD2, CD3, CD4, CD8a, CD14, CD16, CD19, CD20, CD24, CD33, CD34, CD38, CD41a, CD45, CD66b, CD117, CD133 and CD235a), endothelial cell markers (Flt-1, Flk-1 and von Willebrand factor), and an epithelial cell marker (cytokeratin 5/8). Integrins positive for PDL cells were CD29 (β1), CD41a (α1) and CD51 (αv). Positive cytokine receptors were CD71 (Transferrin R), CD105 (endoglin), CD119 (IFNγ R) and CD120a (TNF RI), and negative were CD117 (c-kit), CD121a (IL-1 R) and CD124 (IL-4 R). PDL cells expressed matrix receptors such as CD54 (ICAM-1) and CD166 (ALCAM), but lacked CD31 (PECAM-1), CD56 (NCAM) and CD106 (VCAM-1). Human leukocyte antigen (HLA) expressed in PDL cells was HLA-ABC, however, HLA-DR expression was not detected. No reactions of STRO-1 and CDPC-1 (CUB-domain-containing protein 1) were observed in PDL cells. Thus, the antigens expressed in PDL cells were basically identified with that of bone marrow stromal precursors, suggesting that PDL cells possess primitive characteristics as mesenchymal stem cells.

Disclosures: N. Kawanabe, None.

W042

Effects of BHH9, an Ethanol Extract from Herbs, on Expression of Vascular Endothelial Growth Factor and Their Receptors During Human Osteoblasts Differentiation. D. Kim¹, J. Huh^{*2}, Y. Baek^{*2}, D. Choi^{*2}, D. Park^{*2}, J. Lee^{*2}. ¹Internal Medicine, Kyung Hee University Hospital, SEOUL, Republic of Korea, ²Acupuncture & Moxibustion, College of Oriental Medicine, Kyung Hee University, SEOUL, Republic of Korea.

Endochondral bone formation is regulated by systemically and locally acting growth factors. Vascular endothelial growth factor (VEGF) is an important regulator of bone formation and osteoblast differentiation. The aim of this study was to identify the BHH9 that may induce the angiogenic factor VEGF and its receptors (VEGFR) in osteoblast from human subchondral bone.

BrdU assay was used to determine the proliferation of human osteoblast cells. RT-PCR and ELISA assay were used to demonstrate the message and protein expression of VEGF, and extracellular matrix proteins including alkaline phosphatase (ALP), osteocalcin (OCN), osteopontin (OPN) and collagen I (ColI). Flow cytometry analysis (FACS) was used to confirm the expression of VEGF, VEGFR-1 and VEGFR-2.

BHH9 slightly increased cell proliferation, and dramatically increased ALP activity in human

osteoblast cells. Also, the expression of OCN, OPN, and Col I mRNA did not affected by treatment with BHH9 at 3 days and 7 days, but BHH9 was markedly enhanced at 14 days of culture. In addition to, BHH9 stimulated message and protein expression of VEGF and VEGFR-2 expression at 7 days of culture.

These results suggest that BHH9 plays an important role in bone remodeling by stimulating osteoblast differentiation via up-regulation of VEGF expression and possibly lead to the development of bone-forming drug.

Disclosures: D. Kim, Oriental Medicine R&D Project, Ministry of Health & Welfare, Republic of Korea 2.

This study received funding from: Grant of the Oriental Medicine R&D Project, Ministry of Health & Welfare, Republic of Korea.

W043

Hairy Enhancer of Split 1 (HES-1) Is an Anti-adipogenic Mediator of Osteogenic Oxysterols and Hedgehog Signaling. W. Kim¹, V. Meliton^{*1}, C. M. Amantea^{*1}, T. J. Hahn², F. Parhami¹. ¹David Geffen School of Medicine, UCLA, Los Angeles, CA, USA, ²VA Greater Los Angeles Healthcare System and Geriatric Research, Education, and Clinical Center, Los Angeles, CA, USA.

Age-related bone loss is associated with a progressive decrease in bone formation and an increase in adipogenesis in the bone marrow. An increase in adipose tissue volume and a decrease in trabecular bone volume in bone marrow have been observed with aging and in patients with osteoporosis. Growing evidence indicates that PPAR γ plays an important role in the regulation of bone metabolism. It has been shown that hedgehog signaling pathway, activated by sonic hedgehog protein, inhibits adipogenic differentiation. Previously, our lab reported that osteogenic oxysterols inhibit PPAR γ expression and adipogenic differentiation of pluripotent bone marrow stromal cells (MSC) by activating hedgehog signaling. The present report identifies the molecular mechanism(s) by which oxysterols and hedgehog signaling inhibit PPAR γ expression and adipogenic differentiation. Microarray-based gene expression analysis revealed that osteogenic oxysterols caused a 2 fold induction of HES-1 mRNA expression in the pluripotent M2-10B4 (M2) MSC after 48 hours of treatment. Q-RT-PCR analysis of M2 cells showed that HES-1 expression was induced by the osteogenic oxysterol 20S-hydroxycholesterol (20S) and sonic hedgehog (Shh) in a time-dependent manner. HES-1, a target of notch signaling, is a basic helix-loop-helix DNA binding protein that is down-regulated during adipogenesis, and notch signaling profoundly inhibits adipogenesis through HES-1. After 48 hours, 20S (5 μ M) or Shh (200ng/mL) completely blocked PPAR γ mRNA expression in M2 cells treated with the PPAR γ ligand, troglitazone. 20S- and Shh-induced HES-1 expression was completely blocked by the inhibitor of hedgehog signaling pathway, cyclopamine (4 μ M), suggesting that HES-1 is a downstream target of hedgehog signaling. We also found a HES-1 binding site in the mouse Gli1 promoter using a Genomatix software, suggesting a potential feedback loop between Gli1 and HES-1. To demonstrate that HES-1 is a repressor of adipogenesis in MSC, we transfected M2 cells with 0.5, 1, 2, and 4 μ g of pCMV-HES-1 overexpression vector, and the effect of HES-1 overexpression on PPAR γ expression was assessed by Q-RT-PCR. Results showed that troglitazone-induced PPAR γ expression was inhibited by HES-1 overexpression in a dose-dependant manner. Altogether, the present study suggests that the anti-adipogenic effects of osteogenic oxysterols and Shh are mediated by a HES-1 dependent mechanism.

Disclosures: W. Kim, None.

This study received funding from: NIH/NIAMS.

W044

Proinflammatory Control of BMP-Smad-driven Transcription and Osteogenesis. O. Korchynskyi¹, P. ten Dijke^{*2}, D. D. Patel^{*3}, S. S. Makarov^{*4}. ¹Orthopedic Surgery, Virginia Commonwealth University, Richmond, VA, USA, ²Leiden University Medical Center, Leiden, The Netherlands, ³Thurston Arthritis Research Center, University of North Carolina at Chapel Hill, Chapel Hill, NC, USA, ⁴Thurston Arthritis Research Center, University of North Carolina at Chapel Hill, Chapel Hill, NC, USA.

Impaired bone homeostasis contributes to development of osteopenia, osteolysis and joint erosions during the rheumatoid arthritis (RA). Bone morphogenetic proteins (BMP) are crucially important regulators of osteogenesis. Activation of specific BMP receptors (BMPR) leads to activation of the major BMP signaling pathway, namely intracellular Smad proteins, as well as other, Smad-independent, pathways that transduce BMP signals to the nucleus. Using in vitro tissue culture approaches we show that activation of NF- κ B pathway with proinflammatory cytokines IL-1 β and TNF α inhibits osteogenic differentiation of pluripotent mesenchymal precursor cells through Smad7-independent inhibition of Smad1/5 transcriptional activity. Immunoblot and EMSA experiments show that correspondingly neither Smad1/5 phosphorylation by BMPR-Is, nor direct Smad1/5 binding to DNA into BMP target genes promoters are affected by the activation of NF- κ B pathway with TNF α , or by the overexpression of NF- κ B signaling components. Nevertheless, Smad1/5 transactivation and, consequently, transcription of BMP target genes is greatly reduced upon activation of NF- κ B signaling. Neither ectopic expression of Smad1/5, nor CBP/p300 can rescue the negative effect of NF- κ B pathway activation. We used Real time PCR to analyse BMP and TNF α target genes mRNA induction in the presence of protein synthesis cycloheximide and found that negative effect of NF- κ B activation requires new protein synthesis due to the induction of BMP signaling inhibitor expression. Furthermore, we found two distinct TNF α /NF- κ B target genes (T/NTG) that are novel potent inhibitors of BMP signaling. Interestingly, overexpression of T/NTG1 induces apoptotic death of osteoblasts. shRNA-mediated knockdown of the expression of each T/NTG results in partial rescue of BMP-Smad-driven transcription from inhibition by TNF α . Thus, our data suggest these T/NTGs as possible central candidates responsible for the

development of osteolysis and joint erosions during the RA. We are validating this current hypothesis in vivo using BMP reporter mice and ectopic bone formation in SCID mice models.

Disclosures: O. Korchynskyi, None.

W045

BK Channels in Human Osteoblast-like Cells - Properties and Function. B. Li^{*1}, N. C. Henney^{*1}, B. A. J. Evans², P. Reviriego^{*1}, A. K. Campbell^{*3}, K. T. Wann^{*1}. ¹Welsh School of Pharmacy, Cardiff University, Cardiff, United Kingdom, ²Child Health, School of Medicine, Cardiff University, Cardiff, United Kingdom, ³Medical Biochemistry & Immunology, Cardiff University, Cardiff, United Kingdom.

Ion channels which are normally associated with excitable cells are also emerging players in the life and death decisions of many other cells. We have focussed on large conductance Ca²⁺-activated K⁺ channels (BK channels) in osteoblast-like cells. BK channels exist as a tetramer of 4 α subunits associated with β subunits, and the type of β subunit, modifies both the voltage- and Ca²⁺-sensitivity and the pharmacological fingerprint of BK channels¹. Here we attempt a pharmacology of the channel, test its role in proliferation and try to specify the subunit composition of BK channels in MG63 cells.

Single channel activity was measured using patch-clamp methods. Determination of numbers of osteoblast-like cells was achieved by use of the MTS assay. RT-PCR was carried out to investigate the expression of α (KCNA) and β (KCNMB) subunits of the BK channel.

BK channels were observed in cell-attached patches at potentials close to rest. In excised outside-out patches external tetraethylammonium chloride (TEA, 500 μ M) reduced the open probability, producing reversible flickery block. Intriguingly, both BK-selective blockers, iberiotoxin (IbTX- 5-60nM) and tetrandrine (5-30 μ M) also blocked the channel in outside-out patches. Internal paxilline (10 μ M) blocked reversibly. The BK channel opener, isopimaric acid (10 μ M), also increased channel activity. RT-PCR showed that the α (KCNA) subunit and the β 1-4 (KCNMB1-4) subunits were present. Some blockers had a dual effect on cell numbers. Thus TEA and tetrandrine increased cell numbers at low (1mM and 3 μ M respectively), and reduced cell numbers at high concentration (>10mM and >10 μ M). In contrast, IbTX (10 - 300nM) was inactive.

These data are the first systematic description of the pharmacology of the BK channel in bone cells and it turns out to be novel. This has implications for both the subunit composition of the channel and its use in therapeutic intervention. The data also show that BK may have a role in modulating MG63 cell numbers and future investigations are focusing on characterising further the pharmacology of the channel and defining the native subunit composition, and the role of the channel in mineralization and secretion in osteoblast-like cells.

1.Wang YW, Ding JP, Xia XM, Lingle CJ. (2002) Consequences of the stoichiometry of Slo1 α and auxiliary β subunits on functional properties of large-conductance Ca²⁺-activated K⁺ Channels. J Neurosci, 22(5): 1550-61.

Disclosures: B. Li, None.

W046

Application of Bioluminescence in Stem Cell-Based Bone Formation. K. E. de Rooij¹, G. van der Horst^{*1}, H. C. M. Sips^{*1}, I. Que^{*1}, L. J. A. van der Wee-Pals^{*1}, C. H. F. Bloys^{*1}, J. Hoogendam^{*2}, C. W. G. M. Löwik¹, M. Karperien¹. ¹Endocrinology, LUMC, Leiden, The Netherlands, ²Pediatrics, LUMC, Leiden, The Netherlands.

Current treatments for osteoporosis suppress bone resorption, thereby blocking further deterioration, but do not restore bone. Therefore, therapies stimulating bone formation would greatly enhance treatment of osteoporosis.

The bone forming osteoblasts originate from the multipotent mesenchymal stem cells (MSCs). MSCs have great potential for application in tissue engineering of bone and cartilage. However, differentiation of MSCs in vitro or in vivo as well as interactions with other cells or biomaterials in vivo is poorly understood. Therefore, we have created a stem cell model which, in combination with bioluminescent imaging, allows us to study these processes in intact mice over time.

The murine mesenchymal progenitor cell-like KS483 cell line was genetically modified enabling efficient generation of isogenic stable cell clones by Flp-mediated recombination by integrating 1 copy of a FRT-target site into the cell's genome. After we had tested the efficacy of the FRT-site by the overexpression or knock-down of the RunX2 gene, it was used to insert a luciferase2 gene containing a His tag enabling us to follow cell fate in vivo by bioluminescence after implantation in nude mice and the detection of cells ex vivo by immunohistochemistry using antibodies against the His tag. KSfrt HisLuc2 cells were used to perform a bone marrow ablation assay in which the cells were injected in the marrow cavity. Cell fate was followed by non-invasive bioluminescent imaging. At several time points, mice were sacrificed and both tibias were isolated for analysis. Using an antibody against the His tag, we could identify KSfrt HisLuc2 cells in the callus which was formed following bone marrow ablation. In addition, to study their fate outside the bone forming environment and to study possible adverse effects, cells were also transplanted subcutaneously. We have followed cell fate non-invasively for 20 weeks and afterwards isolated the luciferase expressing tissue for immunohistochemical analysis.

Finally, we used the genomic FRT site for the insertion of gene reporter constructs, which respond to Wnt- or BMP-signaling. Isogenic stable cell lines were obtained that were highly sensitive for Wnt and BMP, respectively, and retained multipotency. In conclusion, genetically modified KSfrt cells provide a simple and fast model to study MSC function. In combination with bioluminescent imaging, we will use this model to evaluate the effects of biomaterials on stem cell function in vitro and in vivo as a first step towards a bone replacement therapy for osteoporosis.

Disclosures: C.W.G.M. Löwik, None.

This study received funding from: Dutch Program for Tissue Engineering (DPTE).

W047

The LIM Protein, LMD1, Modulates Osteoblast Differentiation and Function. H. F. Luderer¹, S. Bai^{*2}, G. Longmore^{*3}. ¹Cell Biology, Washington University in St. Louis School of Medicine, St. Louis, MO, USA, ²Pathology, Washington University in St. Louis School of Medicine, St. Louis, MO, USA, ³Cell Biology and Medicine, Washington University in St. Louis School of Medicine, St. Louis, MO, USA.

Recent studies have shown that LMD1 contributes to osteoclast (OC) differentiation in vivo, suggesting LMD1 may be involved in maintaining normal bone homeostasis. To test this hypothesis, bone density measurements of Wild Type (Wt) and Lmd1^{-/-} mice were compared. In addition, the capability of primary calvarial cells isolated from Lmd1^{-/-} and Wt mice to differentiate, mineralize, and regulate OC differentiation was analyzed to determine if LMD1 affected osteoblast (OB) function. While Lmd1^{-/-} mice lack any gross skeletal abnormalities at steady state, defects in both differentiation and function of primary calvarial cells in culture were found. Lmd1^{-/-} calvarial cells display increased mineralization and accelerated differentiation compared to Wt controls despite equivalent rates of proliferation. More specifically, RT-PCR analysis of differentiating calvarial cells demonstrated that Runx2 regulated genes are expressed earlier in Lmd1^{-/-} calvarial cells compared to Wt. Intriguingly, LMD1 interacts with Runx2 by co-immunoprecipitation, suggesting a potential mechanism explaining the observed defects. Furthermore, RT-PCR analysis showed decreased expression of RANKL, a potent inducer of OC differentiation, and increased expression of osteopontin, the inhibitor of RANKL, in Lmd1^{-/-} calvarial cells. In agreement with this observation, when co-cultured with Wt primary bone marrow derived macrophages, Lmd1^{-/-} calvarial cells supported differentiation of fewer OCs than Wt controls. Since LMD1 was clearly important for OB differentiation in vitro, mice were treated with an anabolic stimulus to determine if LMD1 contributed to stress response. Wt and Lmd1^{-/-} mice were treated daily with parathyroid hormone (PTH) or vehicle for four weeks. Analysis by both micro-CT and histomorphometry showed no differences in bone density or bone growth between PTH treated groups. Interestingly, Lmd1^{-/-} PTH treated mice exhibited increased OB numbers compared to Wt. To determine if this was due to differing osteoprogenitor numbers, total marrow flushed from the long bones of Wt and Lmd1^{-/-} mice was cultured under normal, adipogenic or osteogenic conditions. Interestingly, loss of Lmd1 resulted in an increased number of osteoprogenitor cells while the number of adipogenic and fibroblastic colonies was unchanged. In conclusion, LMD1 affects OB differentiation, OB function and contributes to maintaining mesenchymal stem cell lineages.

Disclosures: H.F. Luderer, None.

W048

Local Transplantation of G-CSF Mobilized CD34-positive Cells Contributes to Fracture Healing. Y. Mifune¹, T. Matsumoto², A. Kawamoto^{*1}, R. Kuroda^{*2}, T. Shoji^{*1}, M. Miwa^{*2}, K. Masahiro^{*2}, T. Asahara^{*1}. ¹Stem Cell Translational Research, Kobe Institute of Biomedical Research and Innovation / RIKEN Center for Developmental Biology, Kobe, Japan, ²Department of Orthopedic Surgery, Kobe University Graduate School of Medicine, Kobe, Japan.

We recently reported that human peripheral blood (PB) CD34⁺ cells, an endothelial/hematopoietic progenitor enriched cell population, contribute to fracture healing via vasculogenesis and osteogenesis in intravenous transplantation (IT) method. In addition to a confirmation of human PB CD34⁺ cell differentiation into osteoblasts (OBs) in vitro, we performed next experiments to prove a hypothesis that granulocyte colony stimulating factor mobilized peripheral blood (GM-PB) CD34⁺ cells, transplanted locally to the non-healing fracture model of immunodeficient rat, dose-dependently contribute to fracture healing. In vitro study, GM-PB CD34⁺ cells proved their capacity to differentiate into OBs by alizarin red staining and RT-PCR. In vivo study, as a proof of a therapeutic superiority of local transplantation (LT) to IT, the immunostaining for HLA-ABC at the peri-fracture site showed the significantly massive recruitment of the human cells in rats receiving LT compared to IT. RT-PCR and immunohistochemistry demonstrated significantly higher expression of human specific markers for endothelial cells and OBs in animals receiving high (10⁵) compared to middle (10⁴) and low (10³) dose of CD34⁺ cells and PBS at week 2. As enhancement of intrinsic vascularization and osteogenesis at the peri-fracture site, capillary density was significantly greater in high group compared with the other groups, as well as in middle group than low and PBS groups, and OB density was significantly greater in high group compared with the other groups. The Laser Doppler Perfusion Imager estimating a blood flow at the fracture site indicated the high and middle groups had a significantly higher perfusion value than the other groups at week 1 and 2. Radiographic assessment showed all of the high group and half the middle group obtained union at week 8, while all fractures in the other groups failed to union. The degree of fracture healing assessed by Allen's histological classification was significantly higher in high group than the other groups at week 8, as well as middle group than low and PBS groups (high, 3.8±0.13; middle, 2.1±0.16; low, 0.4±0.48; PBS, 0.0±0.00, respectively, P<0.01 for high vs other groups and middle vs low or PBS group). In this study, we suggested GM-PB CD34⁺ cells have a potential for vasculogenesis and osteogenesis with fracture healing, and more than 1x10⁴ CD34⁺ cells per rat were necessary and effective for fracture healing in LT method. These findings must be a help to close up to the feasibility for clinical application.

Disclosures: Y. Mifune, None.

W049

In Vitro and In Vivo Effects of sFRP3 Overexpressed by Phi 31 Integrase Strategy. D. Han^{*1}, S. Park^{*1}, S. Kim^{*1}, Y. Kim², Y. Rhee^{*1}, Y. Chung^{*3}, S. Lim¹. ¹Internal Medicine, Yonsei University, Seoul, Republic of Korea, ²Internal Medicine, NHIC Ilsan Hospital, Seoul, Republic of Korea, ³Internal Medicine, Ajou University, Seoul, Republic of Korea.

Wnt signaling increases bone mass through a number of mechanism. Secreted frizzled related proteins (sFRPs) do not have transmembrane and cytosolic domains, thus they bind and act as decoy receptors for Wnt proteins and antagonize the Wnt/frizzled signaling pathway. However, previous studies reported that sFRP3 decreased osteoblast proliferation and increased osteoblast differentiation. Because Tg or KO models regulating Wnt signaling may alter bone development, it is more desirable to evaluate the effects of sFRP3 in skeletally mature animals with pharmacological activators or inhibitors. In this study, we overexpressed sFRP3 by Phi 31 integrase strategy in 7-20 weeks old ICR mouse (male) to demonstrate the effects of sFRP3 in bone. sFRP3 expression in liver was documented by PCR and confocal microscopy analysis. Serum sFRP3 was detected at ~ ug range by ELISA. In sFRP3 overexpressed mice, femur BMD measured by PIXImus was increased. Both BV/TV and Trabecular number measured by μ CT were also increased, and Tb.Sp (trabecular separation) was decreased. Furthermore, three point bending test revealed increased load max and slope of femurs. To clarify the mechanism of sFRP3 induced positive effects on bone, sFRP3 was overexpressed in MC3T3E1 preosteoblast cells. Overexpression of sFRP3 reduced Wnt3a mediated proliferation, and real time PCR analysis revealed that colla1a1 expression was increased. In addition, the luciferase assay presented that Wnt-responsive gene activation were increased in sFRP3 treated group. Based on our findings, we propose that constitutive overexpression of sFRP3 increases BMD and bone strength. Furthermore, continuous over activation of Wnt signal might not be beneficial to bone, and coordinated regulated activation of Wnt signal should be necessary for optimal bone remodeling and bone strength.

Disclosures: D. Han, None.

W050

Osteocyte Specific DMP1 and MEPE Expression after Mechanical Stimulation in the Mouse Ulnae Loading Model: Correlation to Strain Fields, Dynamic Bone Formation, and Potential Role in Bone Mineral Quality. S. E. Harris¹, J. Gluhak-Heinrich^{*2}, M. A. Harris¹, W. Yang¹, L. F. Bonewald³, D. Riha^{*4}, D. P. Nicoletta⁴, P. S. N. Rowe⁵, A. G. Robling^{*6}, C. H. Turner⁶. ¹Periodontics, U, Texas Health Sci Ctr San Antonio, San Antonio, TX, USA, ²Orthodontics, U, Texas Health Sci Ctr San Antonio, San Antonio, TX, USA, ³Oral Biology, U, of Missouri at Kansas City, Kansas City, MO, USA, ⁴Southwest Research Institute, San Antonio, TX, USA, ⁵Periodontics, Kansas University Medical Center, Kansas City, KS, USA, ⁶Indiana University School of Medicine, Indianapolis, IN, USA.

DMP1 and MEPE are involved in local effects on bone mineralization as well as systemic phosphate metabolism. These two genes are highly expressed in osteocytes and suggest that the osteocyte can alter its local environment as well as act as an endocrine cell. We previously have shown preliminary data that DMP1 and MEPE increased at 24hrs after a single 2.4N load for 30 sec at 2 Hz. We now show a direct highly statistically significant correlation between gene expression and strain field determinations from finite element analysis. This correlation shows osteocyte specific DMP1 and MEPE expression is highest in areas of maximal compressive and tensile strains in cortical bone. DMP1 is an early response gene and its expression is first stimulated at 1hr after loading and continues to increase up to 24hrs. Load induced MEPE expression is a late response gene and does not increase with load until 24hrs. Using a 3D model relating the 3 dimensional strain field with both DMP1 and MEPE expression, the gene expression threshold (Get) for both genes is approximately 1500 μ strain. MEPE protein is cleaved by a cathepsin like protease to a highly phosphorylated C-terminal ASARM peptide. We know that overproduction of MEPE and the ASARM peptide are associated with hypophosphatemia and osteomalacia. DMP1 affects local mineralization by proper maintenance of canaliculi and lacunar walls and, if deleted, may result in the osteocyte being overstimulated. As we previously showed, MEPE and the ASARM peptide are overexpressed in the DMP1 knock-out model, supporting that osteocytes in this model are experiencing higher local strain than control mice under normal cage conditions. The normal role of MEPE and its response to load may be related to the capacity of MEPE and the ASARM peptide to alter local mineral to matrix properties.

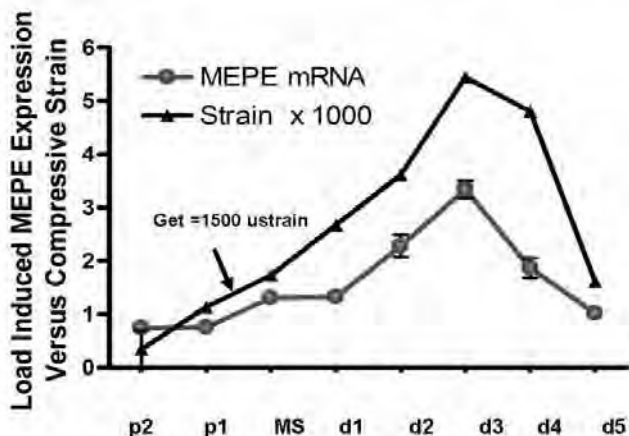


Figure 1. Correlation of Load Induced MEPE Expression(24hrs) with maximum surface Compressive Strain Determined by Finite Element Model. MS is the midshaft and d1 to d5 are 1mm intervals distal to MS and p1 and p2 are 1mm intervals proximal to midshaft

Disclosures: S.E. Harris, None.

This study received funding from: NIH.2

W051

Cell-Cell Communication in Living Bone and Its Regulation Factor. Y. Ishihara¹, H. Kamioka^{*1}, T. Takano-Yamamoto², T. Yamashiro^{*1}. ¹Department of Orthodontics and Dentofacial Orthopedics, Okayama University Graduate School of Medicine, Dentistry, and Pharmaceutical Sciences, Okayama, Japan, ²Division of Orthodontics and Dentofacial Orthopedics, Tohoku University Graduate School of Dentistry, Sendai, Japan.

Intercellular network among osteocytes consists of gap junctions. Gap junctional intercellular communication (GJIC) is thought to play an important role in integration and synchronization in bone remodeling. We hypothesized that extracellular pH (pH_e) and extracellular calcium ion ([Ca²⁺]_e), which were dynamically changed by osteoclast while bone remodeling, would affect GJIC among osteocytes. GJIC among osteocytes in chick calvaria was analyzed by using Fluorescence Replacement After Photobleaching (FRAP) analysis. Simultaneously, we examined the effect of PTH on GJIC in osteocytes. Anti-Connexin43 (Cx43) immunolabelling was used to identify gap junction localization in chick calvaria. FRAP analysis was performed to osteocytes in chick calvariae which were exposed to 5.0 μM Calcein-AM. We assessed subsequent recovery of fluorescence intensity into the photobleached cell by the fluorescence replacement from surrounding cells. In each experiment, bone fragments were precultured with conditioned medium before FRAP analysis. Cx43 immunoreactivity was detected in most of osteocyte processes without any specific distribution. FRAP analysis showed dye-coupling among osteocytes in chick calvariae. Fluorescence intensity recovered to 43.7 ± 2.2% within 5 min after photobleaching. Pretreatment of 18 α-GA, a reversible inhibitor of GJIC, significantly decreased replacement of the fluorescence to 10.7 ± 2.2% in a bleached osteocyte. When pH_e was decreased from 7.4 to 6.9, replacement of the fluorescence in a bleached osteocyte was significantly decreased from 43.3 ± 2.9% to 19.7 ± 2.3%. Conversely when pH_e was increased from 7.4 to 8.0, it was significantly increased up to 61.9 ± 4.5%. When [Ca²⁺]_e was altered from 1 mM up to 25 mM, replacement of the fluorescence in a bleached osteocyte was significantly decreased from 47.0 ± 6.1% to 16.1 ± 2.1%. In addition, when bone fragments were exposed from 1 nM to 10 nM rPTH, replacement of the fluorescence in a bleached osteocyte was significantly increased up to 60.7 ± 7.2% after 3 h. These results indicated GJIC among osteocytes in bone are regulated by extracellular environment and hormonal stimulation in bone remodeling.

Disclosures: Y. Ishihara, None.

W052

Greater Sensitivity of Osteocytes to Shear Stress as Compared to Osteoblasts: PGE₂ Production and Wnt/β-catenin Signaling. M. L. Johnson, M. A. Kamel, N. A. Kim-Weroha^{*}, B. Holladay^{*}, S. Kotha. Oral Biology, UMKC School of Dentistry, Kansas City, MO, USA.

The osteocyte is widely held to be the primary cell in bone responsible for sensing mechanical loads due to its location in bone and it has been shown that primary osteocytes are more sensitive to shear stress than primary osteoblasts. Ironically, the majority of in vitro studies examining mechanoresponsiveness have used primary osteoblast cultures and/or osteoblastic cell lines as surrogates for osteocytes. We compared the sensitivity of osteocyte MLO-Y4 cells to osteoblast 2T3 cells using fluid flow at 2 and 16 dynes/cm². Media was sampled at 5, 15, 30, 60 and 120 minutes for PGE₂ production and at 120 min for nuclear translocation of β-catenin. At 2 dynes/cm², PGE₂ was not detectable in the media from the 2T3 cells (<10 pg/ml). At 16 dynes/cm², PGE₂ was first detectable 15 min after initiation of fluid flow and increased to 90 pg/ml by 2 hours. In contrast, at 2 dynes/cm², MLO-Y4 cells produced 450 pg/ml PGE₂ by 5 minutes which continued to increase for the 2 hours of shear stress to a maximum of 1400 pg/ml. At 16 dynes/cm², PGE₂ production was 500 pg/ml at 5 minutes and reached >2000 pg/ml at 2 hours. At 2 dynes/cm², β-catenin nuclear translocation was detected by immunostaining in MLO-Y4 cells, but not in 2T3 cells. At 16 dynes/cm² both cell lines showed nuclear translocation. We further examined the sensitivity of osteocytes versus osteoblasts in vivo using ulna loading of the TOPGAL mouse. Nuclear translocation of β-catenin, assayed by lacZ activity, was initially observed in osteocytes within bone at 1 hour post load but not until 24 hrs in cells on the bone surface. At 4 hours post loading immunostaining for sclerostin, which binds to Lrp5 and acts as an inhibitor of β-catenin signaling; demonstrated high levels of sclerostin in most osteocytes, except those with active β-catenin signaling, implying a reciprocal relationship. We hypothesize that this initial activation of β-catenin signaling is PGE₂ dependent and thereby able to bypass the inhibitory effects of sclerostin on the Lrp5 co-receptor that regulates Wnt/β-catenin signaling. These observations support the hypothesis that osteocytes are first cells in bone to sense and respond to mechanical load.

cm², β-catenin nuclear translocation was detected by immunostaining in MLO-Y4 cells, but not in 2T3 cells. At 16 dynes/cm² both cell lines showed nuclear translocation. We further examined the sensitivity of osteocytes versus osteoblasts in vivo using ulna loading of the TOPGAL mouse. Nuclear translocation of β-catenin, assayed by lacZ activity, was initially observed in osteocytes within bone at 1 hour post load but not until 24 hrs in cells on the bone surface. At 4 hours post loading immunostaining for sclerostin, which binds to Lrp5 and acts as an inhibitor of β-catenin signaling; demonstrated high levels of sclerostin in most osteocytes, except those with active β-catenin signaling, implying a reciprocal relationship. We hypothesize that this initial activation of β-catenin signaling is PGE₂ dependent and thereby able to bypass the inhibitory effects of sclerostin on the Lrp5 co-receptor that regulates Wnt/β-catenin signaling. These observations support the hypothesis that osteocytes are first cells in bone to sense and respond to mechanical load.

Disclosures: M.L. Johnson, None.

W053

Fluid Flow Shear Stress and Prostaglandin E2 Activates β-catenin Signaling in MLO-Y4 Osteocytic and 2T3 Osteoblastic Cells. M. A. Kamel, Y. Kitase, N. A. Kim-Weroha^{*}, B. Holladay^{*}, S. Kotha, L. F. Bonewald, M. L. Johnson. Oral Biology, UMKC School of Dentistry, Kansas City, MO, USA.

The low-density lipoprotein receptor-related protein 5 (Lrp5) and the Wnt/β-catenin signaling pathway that it regulates are known to be required for new bone formation in response to mechanical loading. Prostaglandins are also known to be rapidly released from bone cells in response to mechanical loading. We have proposed a model in which Prostaglandin E₂ (PGE₂) released by osteocytes and/or osteoblasts, in response to mechanical loading activates β-catenin signaling through a mechanism that is independent of Lrp5 co-receptor regulation of the Wnt/β-catenin pathway. This model accounts for the activation of β-catenin signaling in the presence of inhibitory proteins such as sclerostin that is produced by osteocytes. We hypothesized that this activation occurs through a PGE₂ mediated inhibition of Glycogen Synthase Kinase-3β (GSK-3β), a key regulator of intracellular levels of β-catenin. To test this hypothesis we treated MLO-Y4 osteocytic and 2T3 osteoblastic with 5 × 10⁻⁶ M PGE₂ for 2 hours. We observed a significant increase in phosphorylation of GSK-3β as determined by western blot compared to untreated cells. Interestingly we also observed parallel changes in GSK-3α phosphorylation, which can also regulate intracellular β-catenin levels. Immunostaining of PGE₂ treated cells demonstrated nuclear accumulation of β-catenin compared to non-treated cells. 2T3 osteoblastic and MLO-Y4 osteocytic cells were subjected to 16 dynes/cm² of fluid flow for 2 hours. Fluid flow significantly increased the phosphorylation of GSK-3β and α, and increased nuclear translocation of β-catenin. These data support our hypothesis that PGE₂ released in response to mechanical loading/fluid flow shear stress leads to inhibition of GSK-3β and nuclear translocation of β-catenin. Our data also suggests a possible, previously unsuspected role for GSK-3α in the regulation of β-catenin signaling in bone cells. We propose that this initial activation of β-catenin signaling leads to changes in key target genes, such as sclerostin and Wnts creating a permissive environment for further amplification of the Wnt/β-catenin signaling at the level of Lrp5. Loss of Lrp5 prevents this amplification step, which is required for new bone formation.

Disclosures: M.A. Kamel, None.

W054

The Effects of Mechanical Strain on Osteocytes - Induced Bone Cell Proliferation and Recruitment. S. Ko, J. Lee^{*}, S. Kim^{*}. Dept. of Pharmacology & Dental Therapeutics, Kangnung National University, Gangneung, Republic of Korea.

There are several evidences that osteocyte plays a critical role in bone remodeling. Healthy or apoptotic osteocytes can send signals to other bone surface cells like osteoblasts, osteoclasts, osteoclast precursors and bone lining cells through their networking in canaliculi. And osteocyte which responds to mechanical strain may send signal to other cells. Therefore, to determine the role for osteocytes and mechanical strain in bone remodeling, we examined the effect of mechanical strain and apoptosis of osteocytes on osteoclast precursors and osteoblasts proliferation and recruitment. We used the MLO-Y4 cells as in vitro model for osteocytes, RAW 264.7 cells and MOC-P5 cells as osteoclast precursor, and 2T3 cells as osteoblasts. MLO-Y4 cells conditioned medium (Y4-CM) was collected after 24h culture. For fluid flow experiments, MLO-Y4 cells were exposed to 2 hrs of pulsatile fluid flow(PFF) at 2, 4, 8, 16 ± 0.6 dynes/cm² using Flexcell Streamer™ system. For induction of MLO-Y4 cell apoptosis, MLO-Y4 cells were treated with 100 μM etoposide and apoptosis was determined with increase of casapase-3 activity and ratio of trypan blue staining cells. We did proliferation assay of RAW 264.7 and 2T3 cells with control media or 10% Y4-CM at specific time. The migration of RAW 264.7 and 2T3 cells was assayed using transwells with control media or 10, 20, 50, 100% Y4-CM. MLO-Y4-CM increased osteoclast precursor proliferation and migration. Y4-CM decreased 2T3 cell proliferation and migration. After MLO-Y4 cells were exposed to PFF, Y4-CM decreased RAW 267.4 cell proliferation, migration and 2T3 migration compared to control CM (Y4-CM without strain). However Y4-CM exposed PFF had no effect on 2T3 osteoblastic cell proliferation. Apoptotic Y4-CM induced by etoposide increased the proliferation of 2T3 cells compared to control Y4-CM. These results suggest that osteocytes can regulate the bone remodeling by communication with osteoclast precursors and osteoblasts and that osteocytes can communicate mechanical signals and their apoptosis to other cells.

Disclosures: S. Ko, None.

This study received funding from: Korean Research Foundation Grant funded by the Korean Government (R04-2004-000-10146-0).

W055

Ex Vivo Model of Stress Shielding and Osteocyte Viability in Human Trabecular Bone. H. Kroger¹, V. Mann², B. Noble². ¹MTEC and Dept. of Orthopaedics, University of Edinburgh and University of Kuopio, Kuopio, Finland, ²MTEC, University of Edinburgh, Edinburgh, United Kingdom.

Stress shielding associated periprosthetic bone loss is common after total hip and knee arthroplasty (THA, TKA). However the cell/molecular mechanism that drives this bone loss is unknown. Osteocyte death has been hypothesised to initiate localised bone remodelling. Here we test the hypothesis that mechanical unloading of specific regions of human trabecular bone will engender osteocyte death in a site and mechanical strain specific manner. Excised femoral head material was obtained from an individual patient undergoing THA. Trabecular bone cores 10mm diameter were prepared plan parallel to a height of 5mm (+/-2µm) within 2 hours post surgery under sterile conditions. Regional stress shielding (SS) was accomplished in bone cores (n = 3) through the removal of a portion of load-transmitting bone, such that mechanical stimulation below this area was disrupted. The bone cores were then randomly assigned into 4 groups: Time Zero (T0, immediately flash frozen n=4), loaded control (LC, n=3), unloaded control (UC, n=3) and stress shielded (SS n=3). These samples were maintained within a bioreactor system for 7 days under conditions of either no mechanical stimulation (UC) or mechanically stimulated (LC, SS). Mechanical stimulation was carried out for 5 minutes on a daily basis using a maximum of 3000 µstrain in a waveform corresponding to physiological jumping exercise. Osteocyte viability was analysed in unfixed/undecalcified bone sections using in situ histochemical analysis of Lactate Dehydrogenase (LDH) activity. Total cell number was determined using DAPI nuclear stain. The results are expressed as the ratio of LDH positive osteocytes to total number of osteocytes corrected for bone area (Viability Index). In the SS samples the viability index was determined separately in the region of bone which experienced mechanical loading (SSLR) and the unloaded region (SSUR) within the same sample. The viability index of bone maintained in the bioreactor in the absence of mechanical stimulation decreased relative to T0 samples (1.54 UC vs. 7.47 T0, p<0.001). Application of mechanical stimulation increased viability relative to unloaded samples (3.10 LC vs. 1.54 UC, p<0.001). In the stress shielded samples the viability was reduced in the stress shielded region relative to the loaded region within the same sample (0.96 SSUR vs. 2.74 SSLR, p<0.001). There was no significant difference between the loaded region in the stress shielded sample and the loaded control (2.74 SSLR vs. 3.10 LC, p = 0.857). In conclusion unloading is associated with a decrease in osteocyte viability. Decreased osteocyte viability may play a significant role in stress shielding induced bone resorption and bone loss.

Disclosures: H. Kroger, None.

W056

Bone Biomarker Responses to Short-Term Training: Influence of Exercise Mode vs. Osteogenic Index. M. E. Lester^{*1}, R. K. Evans^{*1}, W. J. Kraemer^{*2}, J. S. Staab^{*1}, J. R. Pierce^{*1}, D. E. Catrambone^{*1}, H. M. Isome^{*1}, M. L. Urso^{*1}, B. A. Spiering^{*2}, D. L. Hatfield^{*2}, C. M. Maresh^{*2}, B. C. Nindl^{*1}. ¹Military Performance Division, US Army Research Institute of Environmental Medicine, Natick, MA, USA, ²Dept of Kinesiology, University of Connecticut, Storrs, CT, USA.

The value of monitoring bone turnover biomarkers during short-term exercise training is not established. Further, it is not clear whether these biomarkers are influenced by either exercise mode or the osteogenic index (OI = I * LN(N+1)), where I = mean weekly intensity of activity in bodymass units, and N = number of loading cycles per wk (Robbling and Turner, ESSR 2003). This study examined the influence of three, 9-wk exercise regimens (exercise performed 3 d/wk) on bone turnover responses. Fifty-seven women (21.7 yr) were randomly assigned to a control (CON), aerobic (AER), resistance (RES), or combined aerobic and resistance (COMB) training group. Serum markers of bone formation [BAP and Osteocalcin (OC)] and bone resorption (TRAP5b and CTx) were assessed after 0, 4, and 9 weeks of the exercise training via immunoassays. Changes were analyzed using a 4x3 repeated measures ANOVA with a Fisher's LSD post-hoc where appropriate, and significance was accepted at P<0.05. The average weekly OI for the groups were: RES group=14.1, AER=22.2, and COMB=40.1. Results for BAP and OC appear below:

Group	BAP (U/L)			OC (ng/mL)		
	Wk 0	Wk 4	Wk 9	Wk 0	Wk 4	Wk 9
COMB (n=17)	18.7 ± 1.4	20.7 ± 1.7*	22.2 ± 1.5*‡#	10.8 ± 0.9	10.5 ± 0.8	11.8 ± 0.8‡#
RES (n=17)	19.6 ± 1.4	21.4 ± 1.6*	23.4 ± 1.5*‡#	10.6 ± 0.9	10.9 ± 0.8	13.2 ± 0.8*‡#
AER (n=13)	18.9 ± 1.6	20.8 ± 1.9*	20.5 ± 1.7#	10.6 ± 0.9	10.3 ± 0.9	10.4 ± 0.9
CON (n=9)	16.5 ± 1.9	6.1 ± 2.2	14.6 ± 2.1	9.6 ± 1.2	9.0 ± 1.1	8.8 ± 1.1

Values are mean±SE; *P<0.05 vs. week 0; ‡P<0.05 vs. week 6; #P<0.05 vs. CON group. For BAP, interaction effects revealed increases at 4 weeks for all exercise groups, while further increases at 9 weeks were only evident for the RES and COMB groups. For OC concentrations, only RES and COMB increased over the training period. There were no significant changes in CTx during training; however there was a significant decrease in TRAP5b over time (wk 0: 3.7±0.1 > wk4: 3.4±0.1 = wk9: 3.3±0.1 U/L). The greatest increase in biomarkers of bone formation was observed for the RES group, which had the lowest OI. Our results demonstrate 1) biomarkers of bone formation are more responsive to short-term exercise training than are biomarkers of bone resorption, 2) exercise modes that incorporate resistance training increase biomarkers of bone formation independent of OI. While the OI was developed and validated upon structural increases in bone strength, our data indicate that exercise programs with higher OIs do not necessarily contribute to a biochemical milieu reflective of increased bone formation.

Disclosures: M.E. Lester, None.

W057

Nanoprobng Osteocytic Subcellular Compartments by Surface-Enhanced Raman Spectroscopy. I. Pavel^{*1}, M. Mahmood^{*1}, K. Vyas^{*2}, M. Whitlow^{*1}, L. I. Plotkin², S. C. Manolagas², A. S. Biris^{*1}, T. Bellido². ¹Nanotechnology Center / Applied Science Department, Univ Arkansas at Little Rock, Little Rock, AR, USA, ²Center for Osteoporosis and Metabolic Bone Diseases, Univ Arkansas for Medical Sciences and Central Arkansas Veterans Healthcare System, Little Rock, AR, USA.

The optical fields provided by single nanoparticles (NPs) or NP aggregates of noble metals can enhance by up to 15 orders of magnitude the Raman spectroscopic signals of neighboring molecules. This technique, called surface-enhanced Raman spectroscopy (SERS), was used herein to study the molecular composition of the nanometer-scaled environment of NPs delivered into living MLO-Y4 osteocytic cells. Gold or silver NPs of 10-20 nm diameter were prepared by citrate- or borohydride-mediated reduction of chloroauric acid or silver nitrate, respectively. Cells were exposed to growing medium without or containing NPs (10⁻¹² or 0.5x10⁻⁹ M) for 5 min to 12 h. Medium containing NPs was then removed; and cells cultured in fresh medium for a total of 12 h for all conditions and fixed. NP uptake was followed by light microscopy and their subcellular localization was visualized by transmission electron microscopy. NPs were detected in different subcellular compartments depending on their concentration and time of exposure. In cells exposed to 10⁻¹² M, NPs were detected only in the cytoplasm irrespective of the time of exposure. On the other hand, in cells exposed to 0.5x10⁻⁹ M, NPs were found near the plasma membrane and in the cytoplasm after 10 to 30 min; and in cellular organelles and the nucleus after 12 h. SERS spectra were recorded from 1 µm diameter areas of different subcellular compartments using a confocal Raman microscope in a back-scattering geometry. A He-Ne laser of 632.8 nm wavelength and 2 mW power at the sample level was used for excitation. Acquisition time was 20 sec. No signal was detected in cells not exposed to NPs. Moreover, in cells incubated with NPs, SERS signals were detected only in areas near NPs or NP aggregates. The SERS spectra indicate that distinct chemical compositions characterize different subcellular compartments. Thus, spectra recorded from cytoplasmic areas exhibited mostly vibrational modes characteristic of proteins, lipids and carbohydrates; whereas, spectra obtained from nuclear, chromatin-rich areas revealed vibrational modes typical of DNA as well as proteins. To our knowledge, this is the first demonstration that NPs serve as nanosensors by providing SERS signatures of different subcellular compartments, including the nucleus, in bone cells. This approach might be used for detecting with high sensitivity subcellular changes associated with biological processes such as cell replication or apoptosis.

Disclosures: I. Pavel, None.

This study received funding from: NIH and Arkansas Nanotechnology Center.

W058

Estimation of Osteocyte Density from Total Lacunar Population. S. Qiu, S. Palnitkar^{*}, D. Rao. Bone and Mineral, Henry Ford hospital, Detroit, MI, USA.

Many investigators estimate osteocyte density based on measurement of osteocyte lacunae. The prerequisite for this estimation is that the empty lacunae remaining after osteocyte death should disappear subsequently, leading to a decrease in total lacunae. There is evidence for such disappearance of empty lacunae. However, the relationship between osteocyte and total lacunar densities remains unclear. This study attempted to determine whether the decreased total lacunar density can be used to estimate the loss of osteocytes.

From our archived iliac biopsy sections, the cancellous bone in 136 white women (92 healthy and 44 with osteoporotic vertebral fracture) were examined. Ten unbroken areas were randomly selected in each section stained with Goldner's trichrome for determining the numbers of osteocytes (Ot.N), empty lacunae (EL.N) and total lacunae (Tt.L.N) per bone area. Table 1 shows the correlations of osteocyte density with densities of empty lacunae and total lacunae (Pearson test). The correlation between osteocyte and total lacunar densities was excellent in superficial, deep and whole bone (SB, DB and WB) in all subject groups (Table 1). The correlation between osteocyte and empty lacunar densities was significantly weaker in both fracture patients and normal women.

In conclusion, bone biopsy specimens contained well preserved osteocytes, so the iliac biopsy sections were used to estimate the relationship between osteocyte and total lacunar densities. The results indicate that, regardless of the location in bone, >80% variation in osteocyte density can be explained by total lacunar density in either normal subjects or patients with fragility fracture. Therefore, the decrease in total lacunar density can represent the loss of osteocyte, although the rate of osteocyte death will be underestimated due to the time lag needed for lacunar obliteration.

Table 1. Correlation between Ot.N, ELN and Tt.LN

			ELN	Tt.LN
SB	Ot.N	A	0.013 (0.491)	0.970 (<0.001)
		B	0.042 (0.129)	0.978 (<0.001)
		C	0.010 (0.534)	0.964 (<0.001)
DB	Ot.N	A	0.010 (0.559)	0.899 (<0.001)
		B	0.011 (0.432)	0.813 (<0.001)
		C	-0.174 (0.005)	0.904 (<0.001)
WB	Ot.N	A	-0.146 (0.018)	0.960 (<0.001)
		B	0.004 (0.635)	0.949 (<0.001)
		C	-0.261 (<0.001)	0.976 (<0.001)

A: 38 premenopausal women; B: 54 postmenopausal women;
C: 44 postmenopausal women with fragility vertebral fracture
Data expressed as r^2 (p value)

Disclosures: S. Qiu, None.

W059

Histochemical Assessments on the Distribution of Osteocyte-Lacunar Canalicular System. U. Sobhan¹, M. Li², K. Oda³, T. Maeda⁴, R. Takagi⁵, N. Amizuka². ¹Oral Maxillofacial Surgery 2, Niigata University, Niigata, Japan, ²Center for Transdisciplinary Research, Niigata University, Niigata, Japan, ³Biochemistry, Niigata University, Niigata, Japan, ⁴Oral Anatomy, Niigata University, Niigata, Japan, ⁵Oral maxillofacial surgery 2, Niigata University, Niigata, Japan.

The purpose of this study is to histochemically evaluate the arrangement of osteocyte-lacunar canalicular system (OLCS) associated with bone remodeling, i.e., OLCS in sites of rapidly and slowly remodeled bone. Twelve-week-old female ICR mice were fixed with aldehyde solution, and the femora and tibiae were extracted. They were then decalcified with 10% EDTA solution prior to paraffin embedding. In order to envision the distribution of OLCS and the localization of osteoclasts and/or osteoblasts on regular paraffin sections, we performed double and triple stainings of silver impregnation (modified Schoen's method), alkaline phosphatase (ALP) immunohistochemistry and/or tartrate resistant acid phosphatase (TRAP) by Azo dye method. In addition, paraffin sections were also stained for detection of osteopontin or DMP-1 (dentin matrix protein-1) with silver impregnation. When analyzing the double and triple stainings, the bone matrix with ALP-positive plump osteoblasts, indicative of active form of osteoblasts, and TRAP-positive osteoclasts showed an irregularly arranged OLCS. In contrast, the region covered by ALP-positive bone lining cells, which are less active osteoblasts, demonstrated well arranged OLCS. Osteopontin-positive cement lines divided different bone matrices: one showed well-arranged lacunar canaliculi and the other figured haphazardly arranged canaliculi, thereby indicating the possibility that bone remodeling reconstructs the distribution of OLCS. Although DMP-1, specifically expressed in osteocytes, has been postulated to be involved with mechanotransduction in bone, DMP-1-immunoreactive osteocytes were unevenly distributed throughout the cortical bone that showed the regular arrangement of OLCS; the distribution of DMP-1 did not seem to be related to the distribution patterns of OLCS. Statistical analysis showed a higher number of canaliculi for each osteocyte in the areas that has been remodeled, compared to the area with ongoing remodeling. Our findings suggest that bone remodeling would reorganize the OLCS into regularly-arrangement.

Disclosures: U. Sobhan, None.

W060

Modulation of Site Specific Bone Adaptation by Signaling in Osteocytic Networks. B. J. Ausk^{*}, T. S. Gross, S. Srinivasan. Orthopaedics, University of Washington, Seattle, WA, USA.

The osteocytic network in vivo is characterized by non-uniform cellular distributions and heterogeneity in cell-cell connectivity. While the mechanosensory role of osteocytic cells is broadly posited, the functional significance of the cellular network and its complex architecture remains opaque due to its current inaccessibility. In part to explore this process, we previously developed an agent based model (ABM) that simulates how real-time Ca^{2+} signaling induced in osteocytic networks by mechanical stimuli influences osteoid secretion by osteoblastic cells. The ABM accurately simulated whole tissue bone formation induced by cyclic (1-Hz) and 10-s rest-inserted loading protocols at 3 different strain magnitudes and at 2 different loading cycle numbers (error < 15%). Using this ABM, we examined the hypothesis that cell-cell signaling within the osteocytic network influences site-specific bone adaptation induced by mechanical stimuli. The osteocytic network topology was determined via imaging of thin sections obtained from the tibia mid-shaft of C57BL/6J mice (5 μ m, n = 6, 16-wk) and the ABM was used to simulate focal osteoblastic activity around the mid-shaft for baseline loading protocols that were previously found to be osteogenic in vivo. We explored the general hypothesis by examining 3 conditions in which osteoblastic activity was: 1) linearly related to local tissue strains, 2) further modulated by strain related thresholds, or 3) further modulated by signaling within the underlying osteocytic network. We found that activation of osteoblastic cells solely by local tissue strains was poorly correlated with site specific adaptation observed in vivo ($r^2 = 0.17 \pm 0.04$). Unexpectedly, when strain thresholds further modulated osteoblast activation, the relation was only minimally improved ($r^2 = 0.23 \pm 0.05$, $p = 0.3$ vs strain magnitude only). Interestingly, when cell-cell signaling in the osteocytic network activated individual osteoblastic cells, the relation between ABM simulations and site specific osteoblastic activity observed in vivo was significantly improved ($r^2 = 0.41 \pm 0.06$, $p = 0.01$ and 0.05 vs conditions 1, 2). This dramatic improvement in ABM predictions when cell-cell signaling is included (2.4 and 1.8 fold, respectively) suggests that interactions between osteoblasts and the osteocytic network are more important in influencing focal osteoblast activity compared with just the distribution of mechanical strains. This study, for the first time to our knowledge, begins to quantify the functional significance of the bone cell network in vivo. Given this relation, knowledge of the cellular topology within a bone is likely to be critical if osteoblastic activity is to be targeted to structural sites most in need of bone accretion.

Disclosures: S. Srinivasan, NIH 2.

This study received funding from: NIH.

W061

The Elastic Modulus of Osteoblasts and Osteocytes. Y. Sugawara¹, H. Kamioka², R. Ando³, Y. Ishihara⁴, S. A. Murshid², K. Hashimoto³, N. Kataoka⁴, K. Tsujioka³, F. Kajiyama⁴, T. Yamashiro¹, T. Takano-Yamamoto².

¹Department of Orthodontics and Dentofacial Orthopedics, Okayama University Graduate School of Medicine, Dentistry, and Pharmaceutical Sciences, Okayama, Japan, ²Department of Orthodontics and Dentofacial Orthopedics, Tohoku University Graduate School of Dentistry, Sendai, Japan, ³Department of Physiology, Kawasaki Medical School, Okayama, Japan, ⁴Department of Medical Engineering, Kawasaki Medical School, Okayama, Japan.

In general, growth, cell cycle progression, gene expression, and other cell behaviors are sensitive to changes in the mechanical force. Therefore, modulations of cellular mechanical properties exerted by mechanical force are intimately related to physiologically important processes. To understand the various functions of osteoblasts and osteocytes, a physical portrait of the mechanical properties of the osteoblasts and osteocytes is necessary. However, it has been difficult to study their mechanical properties because they are in mineralized tissue. In this study, we analyzed the elastic modulus of isolated osteoblasts and osteocytes. On the other hand, the cellular tension was created by the cytoskeletal components based on focal adhesion sites. Therefore, we also examine the relationship between focal adhesion and the elastic modulus. In order to isolate osteoblasts and osteocytes from embryonic chick calvariae, serial treatment was performed with collagenase type I and EDTA. The elastic modulus of living cells was analyzed with Atomic Force Microscopy. We analyzed the elastic modulus of living cells both on peripheral region of the cell body and nucleus region. Osteoblasts and osteocytes were identified by alkaline phosphatase substrate and by OB 7.3, which was a chick osteocyte-specific antibody, respectively. To examine the implication of focal adhesion formation on the elastic modulus, GRGDS, which is the inhibitor of focal adhesion, was pretreated in the culture and we analyzed elastic modulus of the cells. Elastic modulus of peripheral region was higher than that of nucleus region in both osteoblasts and osteocytes. Furthermore, the elastic modulus of peripheral and nucleus region in osteoblasts were higher than those in osteocytes. After treatment with GRGDS, the elastic modulus of osteoblasts was decreased. On the contrary, osteocyte didn't change their elastic modulus. In summary, the elastic modulus of osteoblasts was higher than that of osteocytes. Osteoblast elastic modulus might be influenced by the cytoskeleton based on cell adhesion.

Disclosures: Y. Sugawara, None.

W062

Effects of 3 Months of Aerobic Exercise on Bone Turnover in Premenopausal Non-obese Women. N. I. Williams^{*1}, J. J. Sanders^{*2}, M. De Souza³. ¹Kinesiology, Penn State University, University Park, PA, USA, ²Physiology, Penn State University, University Park, PA, USA, ³Physical Education and Health, University of Toronto, Toronto, ON, Canada.

Exercise is generally believed to represent an osteogenic stimulus, especially when high impact forces are experienced. Few studies have addressed whether moderate impact aerobic activity representing a significant cardiorespiratory stimulus can favorably impact bone turnover in premenopausal non-obese women. To begin to elucidate whether moderate impact aerobic activity (treadmill running, cycling, and elliptical) can alter bone turnover we assessed the effects of 3 months of aerobic exercise and controlled diet on bone formation (PINP) and bone resorption (serum NTX) in 17 premenopausal eumenorrheic women (age = 21 +/- 1 yrs; weight = 57.7 +/- 5.6 kg). Subjects were randomly assigned to either non-exercise (n = 10) or exercising (n = 7) groups. Food intake kcals in both groups was prescribed and adjusted throughout the intervention such that subjects maintained body weight. For both groups, dietary composition was 55% CHO, 15% PRO, and 30% FAT, and a multivitamin with calcium (40 mg) was provided. Supervised exercise training was 5 days per week 30-90 minutes at 70-85% of maximal heart rate. Daily urine samples for estrone-1-glucuronide (E1G) and pregnanediol glucuronide were collected during a baseline menstrual cycle and each day during the intervention. VO2max (ml/kg/min), increased in both groups, but the increase in exercising subjects was greater (ANOVA time effect $P < 0.001$; time X group $P = 0.07$); Non-exercise, Pre = 32.4 +/- 3.1, Post = 36.9 +/- 5.1, Exercise, Pre = 36.5 +/- 4.2, Post = 44.3 +/- 4.7. A significant decrease in bone formation over time was observed when both groups were considered together (ANOVA time effect $P = 0.004$). Exercise produced a trend toward a greater decrease in bone formation (ANOVA time X group effect $P = 0.099$). Means +/- sd for PINP ($\mu\text{g/l}$) were non-exercise, Pre = 143 +/- 36, Post = 129 +/- 27; Exercise, Pre = 185 +/- 79, Post = 140 +/- 48. A significant overall increase in bone resorption was observed when both groups are considered (ANOVA time effect; $P = 0.013$), but no significant effect of exercise was revealed (ANOVA time X group; $P = 0.484$). Means +/- sd for NTX (nmol/l) were Non-exercise, Pre = 12.8 +/- 0.9, Post = 14.9 +/- 2.8; Exercise, Pre = 14.9 +/- 2.2, Post = 16.1 +/- 2.7. Overall decreases in bone formation, and increases in bone resorption are surprising and may be attributable to changes in diet or other factors. These data do not support favorable changes in bone turnover in response to moderate impact aerobic exercise in previously sedentary premenopausal non-obese women.

Disclosures: N.I. Williams, None.

This study received funding from: NIH-R01 HD 39245-01A1 and M01RR10732.

W063

Knockout of Cathepsin K in Adult Mice Does Not Result in Bone Fragility. S. J. Hoffman¹, V. Shen², X. Liang¹, C. A. Capriotti^{*1}, G. B. Stroup³, S. Kumar¹. ¹Musculoskeletal Diseases, GlaxoSmithKline, Collegeville, PA, USA, ²MDS Pharma Services, Bothell, WA, USA, ³GlaxoSmithKline, King of Prussia, PA, USA.

Cathepsin K (Cat K) plays an essential role in osteoclast-mediated degradation of the organic matrix of bone. Knockout of the enzyme in mice as well as lack of functional enzyme in the human condition, pycnodysostosis, results in osteopetrosis. However, there is controversial data over the bone fragility of Cat K knockout mice. In the current study, histomorphometry as well as bone mass and strength of the mid-femur were evaluated in Cat K knockout (KO) and wild-type (WT) adult female mice.

WT and KO female mice were sacrificed at 4 and 6 months of age. The left femur was excised and underwent pQCT imaging as well as biomechanical testing of the mid-femur. Histomorphometric analysis was performed on the mid-femur of a different set of mice of the same age and genetic background.

KO mice had greater total and cortical area and moment of inertia (MI) of the mid-femur when compared to WT. In addition, total and cortical bone mineral content (BMC) and density (BMD) were greater for the KO mice at both ages. The increases in area measurements resulted from a combination of greater cortical thickness and periosteal surfaces in the KO mice. In the KO mice, cortical area, BMC, BMD, thickness and MI significantly increased from 4 to 6 months of age whereas these changes were not observed in the WT mice.

Histomorphometric analysis showed that the KO had greater total area and reduced marrow area which resulted in greater cortical area and width compared to WT mice. No difference in periosteal bone formation rate (BFR) was observed between mice but decreased with age for both genotypes. On the endosteal surface, BFR was increased and eroded perimeter decreased in the KO mice compared to WT at 6 months of age. Intracortical remodeling spaces were observed only in a small percentage of KO mice and very little woven bone was observed.

The bending test determined that maximum load and stiffness were increased 27% and 56%, respectively, in the 6 month old KO mice compared to the WT. Energy (work to failure) increased with age in both genotypes, however, no difference was detected between the KO and WT mice at either age. Post-yield displacement tended to decrease (39 and 24 % reductions in the 4 and 6 month mice, respectively) in the KO compared to the WT mouse. When the size and geometry of the bone is taken into account, no differences in ultimate strength and elastic modulus between WT and KO were observed.

These data suggest that KO mice have different bone content and geometry than WT mice and it changes with age. These data suggest that the material present in bones of both genotypes is of similar quality although this may be due to different contributing factors.

Disclosures: S.J. Hoffman, GlaxoSmithKline 3.

W064

Conditional Inactivation of the Cathepsin K (Ctsk) Gene in Adult Mice Results in Osteopetrosis without Activation of Compensatory Mechanisms for Impaired Bone Resorption. R. Kiviranta¹, I. Koskivirta^{*1}, J. Morko^{*1}, J. Heikkinen^{*1}, E. Bergman^{*1}, S. L. Alatalo^{*2}, J. Risteli^{*3}, E. Vuorio^{*1}. ¹Dept. of Medical Biochemistry and Molecular Biology, University of Turku, Turku, Finland, ²Dept. of Anatomy, University of Turku, Turku, Finland, ³Dept. of Clinical Chemistry, University of Oulu, Oulu, Finland.

Cathepsin K is the major protease responsible for matrix degradation in osteoclasts. We recently reported that Ctsk-deficient mice are osteopetrotic but retain some degree of bone turnover due to several compensatory mechanisms for the impaired bone resorption, including enhanced osteoclastogenesis and elevated expression of other proteases (MMP-9, MMP-13, MMP-14). The purpose of this study was to investigate the effects of inactivation of the Ctsk gene in adult mice and to determine whether the same compensatory mechanisms would arise when the gene is inactivated after development.

For this purpose, we generated mice harboring a modified Ctsk allele where exon 5 was flanked by loxP sites and transgenic mice with ubiquitous expression of tamoxifen-controlled Cre recombinase, which were crossed to produce mice homozygous for the floxed Ctsk allele and heterozygous for the tamoxifen-controlled Cre (CKLP^{loxP/loxP}Cre⁺). Animals were treated with either tamoxifen or vehicle at the age of 2 months and given booster injections at 3 months. Samples were collected at the age of 4 months.

Northern and pQCT analyses verified that CKLP^{loxP/loxP} mice were normal. Treatment of CKLP^{loxP/loxP}Cre⁺ mice with tamoxifen for 7 days efficiently induced recombination in the Ctsk allele and thus production of truncated Ctsk mRNA. pQCT measurements revealed that inactivation of the Ctsk gene at the age of 2 months resulted in osteopetrosis by 4 months of age. The phenotype appeared more striking than in conventional Ctsk knockout mice. Furthermore, the tamoxifen-treated animals exhibited some features of pycnodysostosis, such as decreased bone size, that we did not observe in our conventional Ctsk knockout animals. Decreased levels of serum resorption markers CTX and ICTP verified the impaired bone resorption in the tamoxifen-treated animals. Serum TRACP activity was not changed, suggesting no significant change in osteoclast numbers. Molecular biological analyses of bone samples demonstrated decreased expression of MMP-14 and cathepsin L in tamoxifen-treated mice, but no changes in the expression of TRACP, MMP-9 or MMP-13, all of which were upregulated in our conventional knockout mice. In conclusion, inactivation of the Ctsk gene in adult mice results in osteopetrosis that appears more pronounced than in conventional Ctsk knockouts. This may be due to the lack of compensatory mechanisms observed in conventional Ctsk knockout mice.

Disclosures: R. Kiviranta, None.

W065

Regulation of Osteoclast Activity by Cathepsin K-Generated Type I Collagen Fragments. S. R. Wilson^{*1}, C. Peters^{*2}, P. Saftig^{*3}, D. Bromme^{*1}. ¹Faculty of Dentistry, University of British Columbia, Vancouver, BC, Canada, ²Albert-Ludwigs-Universitaet Freiburg, Freiburg, Germany, ³Christian-Albrechts-Universitaet Kiel, Kiel, Germany.

Cathepsin K (catK) is responsible for the degradation of type I collagen in osteoclast mediated bone resorption. As collagen fragments are known to be biologically active, this study investigates their potential regulatory effect on mature murine osteoclasts.

Soluble type I collagen, type II collagen, and murine long bone powder were subject to degradation reactions by 200-400nM catK, L and 50nM MMP-1. Soluble collagen degradation products or a GRGDS peptide were added to isolated neonatal mature murine osteoclasts seeded on type I collagen substrate. Alternatively, the collagen I substrate was predigested with catK and L. Wild type, catK and catL deficient osteoclasts were also treated with cysteine proteinase inhibitor LHSV (5 μM) and MMP inhibitor GM6001 (5 μM). After 24h osteoclasts were stained with FITC-phalloidin and actin rings were counted as a percentage of total osteoclast number.

Mature murine osteoclasts seeded on type I collagen substrate treated with catK degraded type I collagen or bone demonstrated a lower percentage of actin rings. This was demonstrated in wild type, catK deficient and catL deficient osteoclasts. However, this was shown with neither undegraded collagen, nor collagen degraded by MMP-1 or catL. This inhibition could be partially abrogated by the presence of a vitronectin receptor blocking antibody. CatK deficient osteoclasts and wild type osteoclasts treated with LHSV were found to have a lower basal level of active osteoclasts compared to untreated wild type cells. The number of actin rings was increased by seeding catK deficient osteoclasts on catK pre-digested type I collagen but not catL pre-digested type I collagen. MMP inhibition had no effect on actin ring percentage on any cell type studied.

CatK is known to be the most efficient mammalian collagenase. These studies suggest it may release collagen fragments containing RGD sequences, which are not normally exposed. These soluble fragments may then interact with osteoclast integrin receptors disrupting the actin ring. This is a novel regulatory role for catK and collagen fragments in bone resorption.

Disclosures: S.R. Wilson, None.

W066

PIAS3 Modulates Osteoclastogenesis by Down-Regulation of NFATc1 and OSCAR. K. Kim*, J. Lee*, J. Kim*, H. Jin*, N. Kim, Research Institute of Medical Sciences and Medical Research Center for Gene Regulation, Chonnam National University Medical School, Gwangju, Republic of Korea.

Protein inhibitor of activated STAT3 (PIAS3) has been shown to regulate the activity of various transcription factors. Here, we show that overexpression of PIAS3 in bone marrow-derived monocyte/macrophage lineage cells attenuates osteoclast formation and down-regulates the expression of NFATc1 and osteoclast-associated receptor (OSCAR), which are important modulators in osteoclastogenesis. PIAS3 has been shown to associate with histone deacetylase 1 (HDAC1) as well as with transcription factors, including microphthalmia transcription factor, NFATc1, and c-Fos. Moreover, overexpression of PIAS3 inhibits transactivation of target genes such as NFATc1 and OSCAR. This inhibitory effect of PIAS3 is possibly mediated by HDAC1 recruitment to the promoter regions of NFATc1 and OSCAR. Furthermore, silencing of PIAS3 by RNA interference in osteoclast precursors enhances osteoclast formation as well as gene expression of NFATc1 and OSCAR. Taken together, our results reveal that PIAS3 acts as a modulator in osteoclastogenesis.

Disclosures: K. Kim, None.

W067

The POZ-Zn Transcriptional Regulator OCZF/LRF Is Induced by RANKL and Increases c-Fos Expression in Osteoclastogenesis. A. Kukita¹, T. Shobuike^{*1}, M. Asagiri^{*2}, H. Takayanagi², F. Pessler^{*3}, K. Matsuo⁴, T. Kukita⁵. ¹Pathology and Biodefense Medicine, Saga University, Saga, Japan, ²Cell Signaling and COE program, Tokyo Medical and Dental University, Tokyo, Japan, ³Rheumatology Pediatrics, The Children's Hospital of Philadelphia, Philadelphia, PA, USA, ⁴Keio University School of Medicine, Tokyo, Japan, ⁵Oral Biological Sciences, Kyushu University, Fukuoka, Japan.

Osteoclast-derived zinc finger (OCZF, also known as ZBTB7, FBI-1, LRF and Pokemon) is a member of the BTB/POZ zinc finger family of transcriptional regulators that have been implicated in cell differentiation and oncogenesis. We have reported that OCZF is highly expressed in rat osteoclasts in vivo and plays a role in osteoclastogenesis in bone marrow culture. In the present study, we investigated the role of OCZF and its mouse homologue LRF in RANKL-induced osteoclastogenesis. Expression of LRF mRNA and protein was specifically induced by RANKL and M-CSF but not M-CSF alone in mouse bone marrow macrophages and the macrophage cell line, RAW-D. LRF protein was localized in the nuclei of osteoclast precursor cells and multinucleated osteoclasts. Targeted inhibition of LRF by small interfering RNAs markedly suppressed the formation of TRAP-positive multinucleated osteoclasts but not mononuclear osteoclast precursor cells in the differentiation from RAW-D cells. We then expressed OCZF under the control of the cathepsin K promoter (Ctsk-OCZF) in RAW-D cell. Expression of OCZF from the cathepsin K promoter did not induce osteoclast differentiation in the absence of RANKL, but stimulated RANKL-induced osteoclastogenesis. In addition, Ctsk-OCZF expression markedly increased the protein levels rather than mRNA levels of c-Fos and NFATc1 in the presence of RANKL. Importantly, Ctsk-OCZF induced c-Fos protein in the absence of RANKL. Furthermore, immunofluorescence studies by using confocal microscopy demonstrated that LRF is co-localized with c-Fos in the nuclei of osteoclasts. Moreover, retroviral expression of OCZF did not rescue the osteoclastogenesis of c-Fos KO mice, while LRF protein levels were extremely low in the coculture of osteoblasts and spleen of c-Fos KO mice. Together, these data suggest that OCZF/LRF promotes osteoclastogenesis by positively cooperating with c-Fos protein in the presence of RANKL.

Disclosures: A. Kukita, None.

W068

Annexin VIII Is a Critical Bone Matrix-dependent Osteoclast Gene Transcriptionally Regulated by RANKL and NFATc1. K. P. McHugh¹, Z. Shen¹, R. P. O'Sullivan^{*1}, T. N. Crotti¹, M. R. Flannery^{*1}, S. R. Goldring².

¹Rheumatology, Beth Israel Deaconess Medical Center, Boston, MA, USA, ²Hospital for Special Surgery, New York, NY, USA.

Analysis of tissues from sites of bone erosion in rheumatoid arthritis (RA) and periprosthetic osteolysis revealed that cells expressing the full morphological and functional properties of mature osteoclasts (Ocs) are restricted to the immediate bone surface. Therefore, in addition to cytokines, we hypothesize that adhesion to bone matrix plays a role in determining the genetic profile and functional properties of fully differentiated resorbing Ocs. Through expression profiling of mouse Oc cells differentiated on bone surfaces vs plastic, we have previously identified a cluster of bone matrix-dependent Oc genes, with annexin VIII (Anx8) as a prominent member. The annexins are a family of calcium-dependent phospholipid binding proteins, some members of which bind F-actin. Annexin family members perform diverse cellular functions with many mediating vesicular trafficking and targeting. Anx8 message was found, by QPCR, to increase temporally during Oc formation with kinetics similar to that of CTR and the beta-3 integrin. Anx8 expression was confirmed at the protein level in bone-adherent Ocs in peri-implant tissues and at sites of bone erosions in RA. siRNA-mediated gene knockdown in RAW264.7 cells was utilized to determine the function and requirement for Anx8 in Ocs. Consistent with a key role in Oc formation, siRNA knockdown blocked Oc spreading and actin ring formation, and was shown to result in a >50% inhibition of resorption of mineralized matrix.

We have further characterized transcriptional regulation of the Anx8 gene in Ocs by cloning the mouse Anx8 promoter and generating deletion reporter constructs. The mouse Anx8 promoter displays significant homology with its human homologue in a proximal region and in a separate region near -4kb. RANKL induced the Anx8 promoter up to 10 fold following transient transfection into RAW264.7 cells. We next tested for NFATc1 trans-activation since the Anx8 promoter responds to RANKL and the evolutionarily conserved regions contain consensus NFAT binding sites. Consistent with an Oc-specific and Ca⁺⁺ regulated gene, we find that the mouse Anx8 promoter is trans-activated by NFATc1. Using an in vitro model of bone-matrix-dependent Oc differentiation, we have identified a novel matrix-dependent and required Oc gene. We show here that the promoter region contains functional Oc regulatory elements. The Anx8 gene plays a key role in Oc formation and we speculate that Anx8 represents a potential new target for anti-Oc therapy in osteolytic and metabolic bone diseases.

Disclosures: K.P. McHugh, None.

This study received funding from: NIH; NIAMS.

W069

Myosin IIA Regulates Precursor Cell Fusion and Osteoclast Motility. B. K. McMichael¹, R. B. Wysolmerski^{*2}, B. S. Lee¹. ¹Physiology and Cell Biology, The Ohio State University, Columbus, OH, USA, ²Neurobiology and Anatomy, West Virginia University, Morgantown, WV, USA.

Osteoclasts, large multinucleated cells formed by fusion of monocyte/macrophage precursors, differentiate by stimulation of precursors with macrophage colony stimulating factor (M-CSF) and receptor for activation of nuclear factor kappa B ligand (RANKL). M-CSF and RANKL stimulation leads to altered expression of many genes. In this work, expression of the nonmuscle myosin IIA (myoIIA) during osteoclastogenesis was examined, as was its role in regulating cell differentiation and osteoclast activity. Class II nonmuscle myosins are ATP-driven motors that contain a motor domain that binds actin and a tail that forms a coiled-coil structure. Myosin IIA has been implicated in many cellular functions including cytokinesis, maintenance of cortical tension, and cell spreading. However, its role in osteoclast function has not yet been well examined.

Our previous studies showed nonmuscle myoIIA to be distributed within podosomes and the actin ring of polarized osteoclasts, suggesting that myoIIA may play a role in osteoclast motility and bone resorption. During a normal seven day differentiation period of both mouse RAW 264.7 and primary marrow cells, myoIIA protein levels temporarily diminished on days 3-4, corresponding to the time at which fusion of osteoclast precursors is initiated. During this same time course, myoIIA mRNA levels did not change indicating the loss of expression to be a post-transcriptionally mediated process. Pulse-chase analyses demonstrated that this temporary loss of myoIIA expression was due to increased degradation of the protein during days 3-4. The timing of this alteration in expression suggests a potential role for myoIIA in osteoclast differentiation. Therefore, RNA interference was used to suppress expression of the myoIIA heavy chain during the latter stages of osteoclastogenesis in both RAW 264.7 and mouse marrow cells. This suppression led to the generation of very large osteoclasts that were a result of increased precursor fusion, as demonstrated by elevated numbers of nuclei per cell. These large osteoclasts showed decreased cell motility in addition to a failure to reattach to substrate following dissociation. On bone, these cells formed either very large actin rings or multiple rings per cell. While the large cells were capable of resorbing bone to a similar extent as normal-sized controls, their diminished motility was apparent from a clustered patterning of resorption pits. These results suggest that nonmuscle myosin IIA is required during osteoclastogenesis to limit the extent of precursor fusion and to promote osteoclast motility.

Disclosures: B.K. McMichael, None.

W070

Diverging Pathways of Calmodulin Regulation of Osteoclastogenesis. K. J. Micoli, A. Zayzafoon*, S. Singhal*, J. M. McDonald. Pathology, UAB, Birmingham, AL, USA.

Osteoporosis results from an imbalance in bone remodeling that favors resorption, and increased osteoclastogenesis is one mechanism important in development of low bone mass.

The purpose of these studies was to determine the role of calmodulin (CaM) in regulating osteoclastogenesis via calcineurin (CaN)/NFAT and CaMKII. The studies utilized in vitro differentiation of RAW 264.7 cells, Western blotting, TRAcP staining, IF, CaN and CaMKII assays, PCR, and siRNA or shRNA transfection to determine the CaM/CaMKII-dependent events in the RANK pathway.

RANKL treatment of RAW 264.7 cells induces rapid phosphorylation of numerous signaling molecules, including ERK, JNK, p38, and Akt, and upregulation of c-fos. Inhibition of CaMKII with 5 μ M KN93 prevented RANKL-induced phosphorylation of ERK, JNK and Akt, c-fos upregulation, and blocked osteoclast formation without preventing NFAT nuclear translocation. CaMKII is a complex holoenzyme, composed of α , β , γ and δ isoforms, all of which are expressed in RAW cells during differentiation. RAW cells expressing CaMKII α shRNA did not form osteoclasts in response to RANKL treatment, and siRNA constructs against β , γ and δ also resulted in marked inhibition of osteoclastogenesis. Interestingly, RAW cells were also found to express a non-kinase form of CaMKII α , α KAP, which is upregulated during osteoclastogenesis and may play a role in redistributing CaMKII during later stages of differentiation. We show that CaMKII activity increases rapidly (peaking at 10-15 min) following RANKL treatment, and peaks again after 72 h, consistent with a role in regulating both early and late RANK signaling.

RANKL is known to induce nuclear translocation of NFAT, presumably through activation of calcineurin. Our data show that, in fact, RANKL activation leads to an approximate two-fold increase in CaN activity after 10-15 min, but activity drops to 50% of basal after 72h, which is when peak nuclear NFAT is detected. This apparent paradox is partly explained by data showing that RANKL treatment downregulates casein kinase 1 α , which phosphorylates NFAT. Thus, despite low levels of CaN activity, NFAT remains in the nucleus because the phosphorylation pathway is shut down to an equal extent.

These data are the first to describe actual enzyme activity for CaMKII and CaN in this system and are consistent with a model in which RANK signaling leads to rapid increases in intracellular calcium, activation of calmodulin, and CaMKII, which regulate osteoclastogenesis at early and late time points.

Together, these studies provide evidence that CaMKII is the primary target of CaM signaling in the RANK pathway, and represents a novel NFAT-independent target for inhibiting osteoclastogenesis.

Disclosures: K.J. Micoli, None.

W071

Osteoclasts Generated in Ectopic Bone Are Derived from Postmitotic Osteoclast Precursors (pOCPs). A. Muto*¹, T. Mizoguchi*², T. Noguchi*¹, N. Udagawa*³, N. Takahashi*². ¹Department of Periodontology, Aichi-gakuin University school of Dentistry, Nagoya, Japan, ²Institute for Oral Science, Matsumoto Dental University, Shiojiri, Japan, ³Department of Biochemistry, Matsumoto Dental University, Shiojiri, Japan.

We have reported that when collagen pellets containing BMP-2 (BMP-pellets) were implanted into mice, osteoclasts as well as osteoblasts appeared simultaneously in the BMP-pellets (Endocrinology 147:3366, 2006). We also showed that cell cycle progression and subsequent cell cycle arrest in osteoclast precursors are required for their differentiation into osteoclasts. The quiescent osteoclast precursor cells were named "postmitotic osteoclast precursors" (pOCPs) (JBMR 20 Suppl 1: M244, 2005). Here, we examined whether pOCPs are present in the blood, using a system of the BMP-induced ectopic bone formation. BMP-pellets were implanted into dorsal muscular pouches of mice. To discriminate between proliferating and quiescent cells, mice were given 5'-bromo-2'-deoxyuridine (BrdU) in drinking water during an implantation period of 2 weeks. Then, BMP-pellets and tibiae were recovered from the mice, and subjected to TRAP and BrdU staining. The results obtained from this work are as follows: (1) In tibial sections, BrdU-positive nuclei were detected in bone marrow cells, osteoblasts, chondrocytes and mesenchymal cells. In contrast, none of the nuclei in TRAP-positive osteoclasts incorporated BrdU. (2) In BMP-pellet sections, many TRAP-positive osteoclasts were found to be in close contact with ALP-positive osteoblasts. A large number of mesenchymal cells including osteoblasts possessed BrdU-positive nuclei. Some of the macrophage-like cells also had BrdU-positive nuclei. In contrast, all the nuclei in TRAP-positive osteoclasts observed in the BMP-pellets were negative for BrdU. We have reported that osteoblasts prepare the osteoclast niche, which supports a long-term survival of pOCP. Osteoclasts were differentiated from pOCPs in the osteoclast niche in response to several stimuli including the intraperitoneal administration of RANKL. In the present study, osteoclasts in ectopic bone are also differentiated from pOCPs without cell proliferation. These results suggest that pOCPs are present in the blood flow and osteoblasts may play a role in specific homing of pOCPs to the precise sites of action of osteoclasts.

Disclosures: A. Muto, None.

W072

M-CSF Independent Mechanisms for Osteoclastogenesis. Y. Nakamichi¹, N. Udagawa², H. Yasuda³, M. Nakamura², Y. Kobayashi*¹, N. Takahashi*¹. ¹Institute for Oral Science, Matsumoto Dental Univ., Shiojiri, Japan, ²Dept. of Biochemistry, Matsumoto Dental Univ., Shiojiri, Japan, ³Nagahama Institute for Biochemical Science, Oriental Yeast Co., Ltd., Nagahama, Japan.

M-CSF and RANKL are osteoblast-derived cytokines essential for differentiation of monocytes (MOs)/macrophages (MΦs) into osteoclasts (OCs). M-CSF-deficient op/op mice exhibit severe osteopetrosis due to deficiencies of OCs. It is known that the defect is prominent especially in young op/op mice and OCs gradually appear with aging. However, the molecular mechanisms for OC formation in the absence of M-CSF have remained elusive. To elucidate M-CSF independent mechanisms for OC formation, we performed four experiments as follows: (1) We tried to induce OC formation by administering an 1 α ,25(OH)₂-vitamin D₃ analog (2MD) or GST-RANKL (kindly provided by Oriental Yeast Co., Ltd.) intraperitoneally in young (3-week-old) op/op mice in which OCs are totally absent. When op/op mice were administered 2MD (30 pmol /day) for 2 days, many TRAP-positive OCs were formed at the surface of trabecular bone. Similarly, when GST-RANKL (40 μ g/ day) or M-CSF (10⁵ IU/day) was administered into op/op mice for 4 days, many OCs appeared in bone tissues as if they had existed in WT mice. Concomitantly, serum TRAP5b activity, an indicator of osteoclastic bone resorption, was increased by the administration of these agents. (2) To assess the requirement of M-CSF for OC formation in normal animal, WT mice were pretreated with M-CSFR (c-Fms)-neutralizing antibody (AFS98) for a month and followed by simultaneous treatment with both 2MD and AFS98 for 4 days. 2MD effectively induced TRAP-positive cells and hypercalcemia under the conditions where the c-Fms signal was suppressed. (3) To find a substitute for M-CSF, we examined whether M-CSF-related growth factors (PDGF, SCF, VEGF, FLT3L) could replace M-CSF in the in vitro differentiation of MΦs into OCs. None of these factors supported in vitro OC formation. (4) To investigate whether cell adhesion molecules such as N-cadherin and ICAM can support OC differentiation, we tested in vitro OC formation on the plates pre-coated with adhesion molecules. N-cadherin but not ICAM induced mononuclear TRAP-positive cells even in the absence of M-CSF. These findings suggest that M-CSF is not absolutely required for in vivo OC formation in WT mice as well as op/op mice. In culture conditions, TRAP-positive cells were induced in N-cadherin-coated plates in the absence of M-CSF, suggesting that the adhesion-mediated signal may play a role in OC differentiation in vivo.

Disclosures: Y. Nakamichi, None.

W073

Expression of Angiotensin II Receptor in Osteoclasts and Its Roles on Differentiation and Survival. C. Nakamura¹, S. Kamiya*², T. Fukawa*², N. Nimura*¹, S. Wada*². ¹Bio-Analytical Chemistry, Josai International University, Chiba, Japan, ²Clinical Sciences, Josai International University, Chiba, Japan.

Angiotensin (Ang) II is well known for its action on vasoconstriction, vascular cell proliferation, and remodeling of myocardium. In this study, we examined whether Ang II could be involved in bone remodeling process, since it was found recently that bone marrow cells expressed high levels of Ang II receptor.

Bone marrow macrophages (BMMs) were prepared from bone marrow cells (BMCs) through incubating with M-CSF, and then treated with M-CSF/sRANKL. Ang II receptor (AT_{1A}, AT_{1B} and AT₂) expression was examined by RT-PCR and Western blot analysis through osteoclasts (OCs) development from precursors.

AT_{1A} mRNA was highly expressed and was stable throughout culture period in BMCs, BMMs and OCs, whereas AT_{1B} mRNA was increased parallel to OC differentiation. Expression of AT₁ which could not be discriminated as protein levels of AT_{1A} and AT_{1B} was not changed in these cells. AT₂ mRNA and protein expression was much lower than AT₁ but the levels were increased in either BMMs or OCs. To examine possible roles of Ang II on OC development, we studied the effects of AT₁ agonist (L-162,313, 10⁻⁵M) in the cells. Treatment with AT₁ agonist completely suppressed OC formation at the early culture period (day 0-3) and even late culture period (day 3-7). Treatment with AT₁ agonist on mature OCs 24-48h reduced the number of viable OCs. AT₁ antagonist (Losartan), AT₂ agonist (CGP42112A) and AT₂ antagonist (PD123319), however, did not affect OCs differentiation and their survival. The mechanism of these inhibitory effects of AT₁ agonist remains to be clarified, but we are currently focusing on down-stream signaling and changeable cytokine expression related to OC differentiation.

In this study, we found that AT_{1B} and AT₂ receptor expression are increased parallel to OC differentiation and that AT₁ agonist inhibits OC differentiation and survival, which may indicate possible roles of Ang II-AT₁ pathway on OC formation and bone remodeling process.

Disclosures: C. Nakamura, None.

W074

The TREM2 Pathway Is Involved in Osteoclastogenesis Induced By Nucleoside Reverse Transcriptase Inhibitors in AIDS. G. Pan*, J. M. McDonald, Pathology, University of Alabama at Birmingham, Birmingham, AL, USA.

An increased incidence of osteopenia and osteoporosis in HIV infected patients receiving antiretroviral therapy has now been reported in several studies. Our previous studies show that antiviral nucleoside reverse transcriptase inhibitors (NRTIs) stimulate osteoclast differentiation in vitro and produce osteopenia in mice. Moreover, NRTI-enhanced osteoclastogenesis is mediated through the RANK pathway. The underlying molecular mechanisms responsible for activating the RANK pathway by NRTIs have not been elucidated.

We analyzed osteoclastogenesis-associated gene expression in nucleoside-stimulated osteoclastogenesis and found that antiviral NRTIs up-regulated the expression of triggering receptor expressed on myeloid cells 2 (TREM2) in RAW264.7 cells and mouse bone marrow macrophages. To further determine the role of TREM2 in NRTI-stimulated osteoclastogenesis, antibodies against TREM2 were used to determine whether NRTI-stimulated osteoclastogenesis can be inhibited. The elevated osteoclastogenesis (TRACP) induced by RANKL plus AZT was reduced by TREM2 antibody approximately to the level of RANKL treatment alone, whereas antagonists of the purinergic receptor failed to inhibit NRTI-stimulated osteoclastogenesis. Then, we determined whether NRTI-enhanced RANKL-mediated osteoclastogenesis is associated with TREM2 expression. Our results indicated that RAW264.7 cells with high TREM2 expression were sensitive, whereas cells with low TREM2 expression were resistant to NRTI-stimulated differentiation of osteoclasts. Finally, we determined the function of the TREM2 pathway in NRTI-stimulated osteoclastogenesis. NRTIs stimulated the promoter activity of NFATc1, increased the translocation of NFATc1 into nuclei, and accelerated actin formation, all down-stream events of TREM2 signaling. In conclusion, osteoclast differentiation induced by NRTI not only requires RANK signaling, but also requires the costimulatory TREM2 pathway. NRTIs activate the TREM2 pathway, which interact with the RANK pathway enhancing osteoclastogenesis. The TREM2 pathway is largely responsible for increased osteoclastogenesis induced by NRTIs during treatment of AIDS which induces osteopenia/osteoporosis.

Disclosures: G. Pan, None.

W075

Cobalt Incorporation into Calcium Phosphate Layers Stimulates Osteoclast Differentiation and Activation via Hypoxia Inducible Factor Pathway. S. Patnirapong*, P. Habibovic*, P. V. Hauschka*. ¹Orthopaedic Surgery, Children's Hospital, Boston, MA, USA, ²Tissue Regeneration, University of Twente, Enschede, Netherlands Antilles.

One of the major etiologies of implant failure is activation of macrophages by particulate wear debris, resulting in inflammatory stimulation of osteolysis. Recent studies have shown an increase of metal ions released from wear particles and metallic prostheses due to mechanical stress. Furthermore, these metal ions seem to accumulate in body fluids, peri-implant soft tissues, and bone mineral. We hypothesized that metallic ions could directly activate osteolysis, particularly cobalt (II), which is a known "hypoxia mimic" activator of hypoxic gene expression and a component of alloys used for prostheses. To address this question, we prepared calcium phosphate (CaP) coatings with traces of cobalt ions to examine the effects on osteoclast formation and resorptive activation. Treatments were divided into 2 conditions with various cobalt concentrations either incorporated into the CaP layer, or added to culture media. Scanning electron microscopy (SEM) and inductively coupled plasma mass spectrometry (ICP-MS) were used to visualize the CaP crystallization, and to measure Co²⁺ concentrations in the CaP and in the culture medium, respectively. SEM demonstrated that incorporated Co²⁺ did not modify the nucleation and growth mechanism of the CaP crystallizing system. Measurement of Co²⁺ by ICP-MS indicated the release of Co²⁺ from the CaP layers during equilibration with culture medium. Low concentrations of cobalt delivered to developing osteoclast precursors by both routes increased osteoclast differentiation as well as resorptive function. A 1.7 to 1.75-fold increase in osteoclast numbers and a 2.3 to 2.7-fold more resorptive activity of the CaP layer were observed for 0.1 - 20 µM Co²⁺, which is within the range found in peri-implant tissues in vivo. In addition, we investigated the stabilization of hypoxia inducible factor alpha (HIF-α), an important transcription factor of the hypoxic pathway, and its target genes. Immunoblotting showed that HIF-1α and HIF-2α were stabilized in osteoclastic cells exposed to Co²⁺. Quantitative RT-PCR demonstrates upregulated mRNA levels of glucose transporter-1 (Glut-1), phosphofructokinase muscle (Pfkfb) and vascular endothelial growth factor (Vegf) by Co²⁺ treatment, indicating the osteoclastic switch to glycolytic metabolism. This direct effect of Co²⁺ on osteoclasts through the HIF pathway may contribute to osteolysis and aseptic implant loosening independently of the inflammation-mediated pathways.

Disclosures: S. Patnirapong, None.

This study received funding from: DOD grants BC044721 and BC045539.

W076

Inhibition of Osteoclastogenesis by Prosthetic Wear Debris Involves Suppression of RANK Expression. E. Purdue*, K. Ly*, L. Ivashkiv*, B. Nestor*, T. Sculco*, S. Goldring. Osteolysis Research Laboratory, Hospital for Special Surgery, New York, NY, USA.

Osteoclasts, multinucleated foreign body giant cells, and mononuclear phagocytic macrophages are derived from a common myeloid precursor. Multiple factors control the commitment of these precursors to each of the cell types, including cytokines, cell-cell and cell-matrix interactions. There remains controversy, however, regarding the effect of activation of phagocytic pathways on myeloid cell fate. The present studies were undertaken to define the effect of phagocytic activation on osteoclast differentiation in order to gain insight into the mechanisms associated with prosthetic wear debris-induced osteolysis, the major cause of implant failure after total joint replacement. Human monocytes were cultured with MCSF in the presence or absence of polymethylmethacrylate (PMMA) bone cement or titanium wear particles followed by treatment with or without RANKL. Osteoclastogenesis was assessed by identification of TRAP-positive multinucleated cells. Real-time RT-PCR and Microarray analysis were used to determine the effects of PMMA and titanium particles on the pattern of gene expression. At doses of 30 particles per cell, both PMMA and titanium completely inhibited RANKL-induced osteoclast formation. At lower numbers, osteoclastogenesis was reduced but not obliterated. Interestingly, the osteoclasts formed in the presence of reduced particle number appeared largely devoid of particles. PMMA and titanium also inhibited RANKL-induced expression of the osteoclast markers cathepsin K and TRAP. Most strikingly, PMMA and titanium very strongly inhibited expression of RANK, both in the presence or absence of RANKL. Our data suggest a molecular explanation for the observation, first recorded over fifteen years ago, that osteoclasts within the osteolytic tissues associated with periprosthetic osteolysis do not contain particles (Willert et al, Clin Orthop Relat Res. 1990 258:108-21). Although it has been reported that PMMA can induce osteoclastogenesis and that particle-laden macrophages can differentiate into osteoclasts, our results indicate that phagocytic activation inhibits RANKL-induced osteoclast formation, and that this affect can be attributed to suppression of RANK, which is essential for RANKL-induced osteoclast formation. Taken together with the well-known ability of wear debris to activate pro-inflammatory cytokine signaling in myeloid cells, and the more recent observations that wear debris can promote alternative, non-inflammatory, macrophage activation, these results highlight the multiple ways in which wear debris can influence myeloid cell fate in periprosthetic osteolysis.

Disclosures: E. Purdue, None.

W077

Functional Role for Spinal Muscular Atrophy (SMA) Gene Expression in Bone Remodeling. S. Shanmugarajan¹, K. J. Swoboda*, S. T. Iannaccone*, W. L. Ries¹, B. L. Maria*, S. V. Reddy¹. ¹Charles P. Darby Children's Research Institute, Medical University of South Carolina, Charleston, SC, USA, ²University of Utah School of Medicine, Salt Lake City, UT, USA, ³University of Texas Southwestern Medical Center, Dallas, TX, USA.

Spinal muscular atrophy (SMA) is the second most common fatal childhood disorder which occurs 1 in 8000 newborns. Although the core clinical features of SMA include muscle weakness caused by degenerating lower motor neurons, patients also have a high incidence of bone fractures. SMA determining gene encoding protein, SMN levels are significantly reduced due to deletions/mutations in the telomeric SMN1 gene in these patients. However, a centromeric SMN2 gene copy can not compensate for the deficiency due to an aberrant splicing of the exon 7 region. SMN expression is ubiquitous. We have recently reported SMN expression and differential splicing in bone resorbing osteoclasts. Also, we have shown SMN interaction with the osteoclast stimulatory factor (OSF). It is our hypothesis that SMN plays an important role in the osteoclast (OCL) formation/bone resorption activity. SMA bone disease involves OCL development/abnormalities due to SMN deficiency which leads to bone fractures. In the present study, we utilized the *Smn*^{-/-} - SMN2 mouse model of SMA to determine the functional role for SMN in bone remodeling. DEXA analysis demonstrated a significant decrease in total bone area and poorly developed caudal vertebra in *Smn*^{-/-}; SMN2 mice. Interestingly, these mice also showed pelvic bone fractures similar to patients with SMA. Histological analysis demonstrated a thin porous cortex of cortical bone and thin trabeculae at the proximal end of the growth plate in the caudal vertebrae of *Smn* deficient mice compared to wild-type mice. Further, histochemical staining of caudal vertebra in the *Smn*^{-/-}; SMN2 mice portrays the presence of activated osteoclasts on the sparse trabeculae and in the inner endosteal surface of the thin cortex. In contrast, OCL are mostly confined to the base of the growth plate region in wild-type mice. Histomorphometric analysis further confirmed an increased OCL number and a decreased number of osteoblast cells on bone surfaces in *Smn* deficient mice. Also, urine N-telopeptides of type I collagen (NTx) levels are significantly increased (13.6 fold) in these mice indicating excess bone resorption by osteoclasts. Furthermore, *Smn* deficient mouse bone marrow cultures demonstrated a significant increase (54%) in OCL formation and bone resorption capacity compared to wild-type mice. Taken together, our results implicate SMN function in bone remodeling. Therefore, understanding bone remodeling in SMA may lead to novel therapeutic approaches to prevent bone fractures and enhancing the quality of life in SMA children.

Disclosures: S. Shanmugarajan, None.

W078

Adenosine Receptors in the Osteoclast. S. Stephens^{*1}, J. Auchampach^{*2}, A. Blangy³, R. Rose-Meyer^{*1}, J. Headricks^{*1}, N. Morrison¹. ¹Medical Sciences, Griffith University, Gold Coast, Australia, ²Pharmacology and Toxicology, Medical College of Wisconsin, Milwaukee, WI, USA, ³CRBM-CNRS, Montpellier, France.

The osteoclast is a cAMP-sensitive cell whose formation is stimulated by the decrease in cAMP via follicle-stimulating hormone but whose function is inhibited by the increase in cAMP via the calcitonin receptor. Adenosine receptors (ARs) are P1 G-protein-coupled receptors composed of four subtypes AR₁, AR_{2A}, AR_{2B} and AR₃. These receptors have diverse effectors but all regulate the levels of intracellular cAMP via modulation of adenylyl cyclase (AR₁/AR₃ decreases cAMP and AR_{2A}/AR_{2B} increases cAMP). We found all four ARs expressed in human osteoclasts with AR₁ being the most abundant and upregulated (~15 fold compared to non-RANKL-treated control). Later experiments confirmed the presence of all four ARs in murine osteoclasts with AR₁ being the only osteoclast-specific AR, albeit the least expressed. In this study, we set out to establish whether ARs when stimulated, could affect RANKL-induced osteoclast differentiation. Using adenosine (1-10µM), the endogenous agonist for all adenosine receptors, we showed a significant increase in osteoclastogenesis. This effect was not blocked by P2 receptor antagonists confirming that this effect is P1-selective and not via the ATP-specific P2 receptors whose role in augmenting osteoclastogenesis is already confirmed. Next, to evaluate which receptor(s) is/are responsible for increased osteoclast formation, the agonists CCPA, CGS1280, NECA and CI-IB MECA were used in place of adenosine for the specific activation of AR₁, AR_{2A}, AR_{2B} and AR₃ respectively. At specific concentrations (1-10nM), the agonists showed that all ARs can mediate an increase in osteoclast formation with up to 7 times more osteoclasts compared to RANKL-only treated cells. Moreover, the combination of all agonists did not further increase osteoclastogenesis (ie non additive actions) implying that the four ARs signal through the same pathway or converge through a common signalling gateway. A common pathway is possible through the IP₃ signalling cascade but not via cAMP. IP₃ signalling is directly linked to Ca²⁺ extrusion from the endoplasmic reticulum which can activate NFATc via calmodulin/calcineurin and potentially explains the pathway exploited by ARs in the osteoclast.

Disclosures: S. Stephens, None.

This study received funding from: Griffith University.

W079

RANKL Is Produced by Adipocytes and Stimulates Osteoclastogenesis. S. Takeshita, K. Ikeda. Bone and Joint Disease, National Center for Geriatrics and Gerontology, Obu, Japan.

RANKL is an osteoclastogenic cytokine that is induced on osteoblastic/stromal cells in response to osteotropic hormones, such as 1α,25(OH)₂D₃ or PTH. However, it remains to be determined which cell types actually express RANKL in vivo in response to types of cues. We have found that long-term cultures of mouse whole bone marrow cells, under adipogenic induction with Dexamethasone and IBMX, exhibit strongly induced osteoclastogenesis without the addition of any osteotropic hormones or RANKL. In fact, RANKL expression was induced in marrow stromal cell lines, ST2 and MC3T3-G2/PA6, following adipogenic induction. RANKL was induced transiently during adipogenesis, with concomitant down-regulation of OPG, but not at a later stage with the accumulation of lipid droplets, suggesting that adipocytes at a certain stage of differentiation express RANKL and support osteoclastogenesis. In order to test this hypothesis, we used an aged model in which bone marrow is full of adipose cells. Bone marrow cells from 2-year-old C57BL/6 male mice cultured under osteogenic conditions (β-glycerolphosphate and ascorbic acid), without the addition of any stimulator, gave rise to "osteoclast colonies" (i.e. ALP-positive osteoblastic colonies containing TRAP-positive osteoclasts) that exceeded 30% of total CFU-F, whereas those from younger mice produced very few osteoclast colonies. Adipogenic cultures of bone marrow cells from the aged mice yielded even more osteoclasts than did osteogenic cultures, and RT-PCR analysis revealed RANKL was up-regulated in adipogenic cultures of bone marrow stromal cells. These results suggest that bone marrow cells in aged animals have a potent capacity for generating osteoclast colonies under adipogenic conditions without the need of any osteotropic hormones, and that adipogenic cells in bone marrow may contribute to accelerated osteoclastogenesis in senile or steroid-induced osteoporosis by producing RANKL as an adipokine.

Disclosures: S. Takeshita, None.

W080

The Matrix PRoline/arginine-rich End Leucine-rich Repeat Protein (PRELP) Inhibits Osteoclastogenesis Inactivating the NF-kappaB Signal. M. Alamanou^{*1}, N. Rucci¹, A. Rufo^{*1}, D. Heinegård^{*2}, A. Teti¹. ¹Experimental Medicine, University of L'Aquila, L'Aquila, Italy, ²Experimental Medical Science, Lund University, Lund, Sweden.

PRELP originally found in cartilage is also found at certain basement membranes where it may serve as an anchor by binding to heparan sulfate side chains of perlecan and concomitantly to collagens type I/II collagens. Loss of function mutations of PRELP are involved in the pathogenesis of Hutchinson-Gilford progeria, characterized, among other symptoms, by severe osteoporosis. PRELP is highly expressed in cartilage and developing bone. Herein we demonstrate that a peptide corresponding to the entire heparin-binding domain of PRELP inhibits mouse osteoclast formation. Treatment with the PRELP-peptide decreased osteoclastogenesis by 80% in non-fractionated mouse bone marrow cultures

exposed to 1,25(OH)₂VitD₃, and in purified bone marrow macrophages treated with M-CSF and RANKL (IC₅₀=7.3 microM). Pre-treatment of mature osteoclasts with the PRELP-peptide decreased adhesion to fetal calf serum protein substrate by 60%. In contrast, the peptide showed no activity with osteoclast precursors and neither their number, nor TRAcP activity and adhesion were affected by the treatment. Consistently, the PRELP-peptide inhibited osteoclastogenesis when added at the 4th day of culture, suggesting a late effect on pre-fusion osteoclast precursors. Although a terminally-tagged PRELP-peptide co-localized with heparan sulphate proteoglycans (HSPGs), they did not appear to physically interact. Consistently, treatment with heparinase to remove the heparan sulfate chains, failed to prevent PRELP from inhibiting osteoclastogenesis. In contrast, the peptide activity was shown to depend on binding to the chondroitin sulphate chains of cell surface proteoglycans, and the effect was abolished by treatment with chondroitinase. Tagged PRELP was internalised by osteoclast precursors by an annexin II-dependent mechanism. It translocated to the nucleus where it bound NF-kappaB reducing its transcriptional activity by 50%. Finally, the PRELP-peptide was found to affect osteoclastogenesis and bone resorption only by a direct mechanism as real-time RT-PCR failed to detect any change in expression of cytokines promoting osteoclastogenesis in mouse calvarial osteoblasts. Accordingly, the PRELP-peptide showed no effect on their alkaline phosphatase activity, nodule mineralization, gene expression nor intracellular signalling protein phosphorylations. We conclude that PRELP is a direct negative regulator of osteoclast formation, which blocks NF-kappa B signaling in late stage pre-fusion committed osteoclast precursors, with no apparent effect on the osteoblast lineage.

Disclosures: A. Teti, None.

This study received funding from: EU project OSTEOGENE LSHM-CT-2003-502941.

W081

Comparative Analysis of Osteoclast Bone Resorption Activity and Apoptosis in Young and Old Mice. S. J. Wimalawansa, X. Wang, J. Ghosh^{*}, F. Azeez^{*}. Medicine, Robert Wood Johnson Medical School, New Brunswick, NJ, USA.

Osteoporosis is a systemic skeletal disease characterized by low bone mass and micro-architectural deterioration of bone tissue with consequent increase in bone fragility and susceptibility to fracture. Besides the effects of hormone, environmental factors and other secondary causes on bone, aging itself is believed to be a major cause of bone loss in the elderly.

In the present study, we compared the osteoclasts bone-resorbing activity and life span of old and young mice. Five, 4-6 week old (young) female mice and five, 20-24 months old (aged) female mice were utilized to obtain osteoclast progenitors and osteoclasts. The osteoclast progenitor cells were obtained from mice bone marrow of long bones in simultaneously, and cultured in 10% FBS α-MEM with 5ng/ml MCSF for two days. The non-adherent cells were further cultured for 11 days in vitro with OC medium contained 30 ng/ml MCSF and 60 ng/ml RANK. 200,000 cells were seeded on each calcium phosphate coated disc (BD Biosciences Discovery Labware, Canada) for pit resorption assay; and 200,000 cells were seeded on each pre-treated cover slip for TRAP stain and apoptosis assay. The pit area is measured using the Metavue Software version 6.0 on the Nikon 2000U confocal microscope. TRAP stain was used to quantify matured osteoclasts (>3 nuclei). The Image-iT LIVE Green Poly Caspases Detection Kit, Molecular Probes Invitrogen Technologies was used for apoptosis assay. The protocol of molecular Probes was adopted and the number of mature osteoclasts with three or more nuclei were counted using ACT-1 Software, Nikon 2000U confocal microscope. The fluorescence intensity indicated the apoptotic status of the cells.

The osteoclasts from aged mice showed more bone resorbing activity than those from young mice; the resorption area of age osteoclasts are 11.6 ± 1.2 %, while the resorption area from young osteoclast are 5.1 ± 2.5 % ($p=0.02$). Trap stain results indicated that the matured osteoclasts from aged mice are almost twice as much as those from young mice (122 vs. 69). Furthermore, the apoptotic mature osteoclasts in young were more than those in old mice (90% vs. 81%).

The etiology of age-related bone loss is complicated, and although some mechanisms involving osteoblast and osteoclast dysfunction have been reported, the process remains elusive. Our data indicate that matured osteoclast from old mice A). Survived longer, B). Less apoptotic, and thus, C). Absorbed more bone than osteoclast from young mice. Osteoclastic apoptotic-induction agents should help to combat osteoporosis in the elderly.

Disclosures: S.J. Wimalawansa, None.

W082

High D(+)-glucose Concentration Inhibits RANKL-induced Osteoclastogenesis. Y. Wittrant^{*1}, Y. Gorin^{*2}, K. Woodruff^{ff*1}, D. Horn^{*1}, S. Mohan^{*1}, H. E. Abboud^{*2}, S. Werner¹. ¹Pathology, University of Texas Health Science Center San Antonio and Audie Murphy VA Hospital, San Antonio, TX, USA, ²Nephrology, University of Texas Health Science Center San Antonio, San Antonio, TX, USA.

Diabetes is associated with altered bone metabolism that may lead to increased risk of osteoporosis and fracture. Hyperglycemia has been implicated in the pathogenesis of diabetic bone disease; however, the biologic effect of glucose on osteoclastogenesis is unclear. Although glucose is a source of energy for osteoclast resorption, effect of sustained high glucose levels on osteoclast (OC) differentiation and function have not been explored. We examined the effect of high D(+)-glucose and L(-)-glucose (osmotic control) on RANKL-induced osteoclastogenesis using RAW264.7 cells and Bone Marrow Macrophages as models. OC formation was analyzed using TRAP assay, expression of CTR and cathepsin K mRNAs. Since reactive oxygen species (ROS), caspase-3 and NF-

kB are crucial for RANKL-induced osteoclastogenesis, the effect of glucose on these factors was examined. Intracellular ROS generation was determined by measuring fluorescence intensity in cultures incubated with 2',7'-dichlorofluorescein diacetate (DCF-DA). Caspase-3 activity was quantified in cell lysates and NF- κ B-dependent luciferase activity was analyzed following transient transfection with a vector containing NF- κ B response elements linked to the luciferase reporter gene. The effect of glucose on cellular function was assessed using a migration assay. Results showed that high D-Glc, but not L-Glc, caused a profound decrease in RANKL-induced TRAP-positive OC and led to a predominance of mononuclear cells; this effect correlated with reduced expression of CTR and Cathepsin K. Compared to cultures incubated with RANKL alone, high D-Glc markedly reduced ROS levels by 90%, decreased caspase-3 activity and inhibited NF- κ B transcriptional activity, whereas high L-Glc had little or no effect. In separate experiments, incubation of cells with H₂O₂ in the absence of RANKL induced NF- κ B luciferase activity, indicating the ability of ROS to directly affect NF- κ B activity. In migration assays, fewer cells migrated into and covered the wounded site in high D-Glc-treated cultures compared to control cultures. These findings indicate, for the first time, that high D-Glc inhibits OC formation, ROS production, caspase-3 activity and migration in response to RANKL through a metabolic pathway. High D-Glc may alter RANKL-induced OC formation by inhibiting NF- κ B activity via a ROS-dependent mechanism. Our data suggest that high glucose may prevent excessive osteoclast-mediated bone loss in diabetes and provide new insight into the biologic effects of glucose on osteoclastogenesis.

Disclosures: Y. Wittrant, None.

This study received funding from: NIH (AR-42306) and VA's Merit Award.

W083

The Role of Bcl2 in Osteoclastogenesis Ex Vivo. D. Yang, F. Liu, L. K. McCauley, J. Yamashita. University of Michigan School of Dentistry, Ann Arbor, MI, USA.

Activation of B-cell leukemia/lymphoma 2 (Bcl2) suppresses programmed cell death in many cell types. It has been reported that forced expression of Bcl2 in M-CSF deficient monocytes partially rescued osteopetrosis of op/op mice. We recently reported that Bcl2 homozygous mutant mice had increased bone mass and that such skeletal phenotype was at least partially attributed to osteoclast defects. These findings suggest an important role of Bcl2 in osteoclastogenesis. However, the function of Bcl2 in osteoclast differentiation and survival has not been well investigated. In this study the impact of Bcl2 on osteoclastogenesis was studied using bone marrow cells. Mononuclear cells were obtained from freshly isolated bone marrow of Bcl2 wild type (+/+) and knockout (-/-) mice and cultured. Osteoclastogenesis was induced using M-CSF and RANKL. Cell enumeration and morphometric analysis of TRAP-stained osteoclasts revealed substantial differences in a course of osteoclastogenesis between Bcl2 +/+ and -/- cultures. At day-5 a more vigorous osteoclastogenesis was observed in Bcl2 -/- cultures compared to those in +/+ (p<0.01). Not only were numbers increased in Bcl2 -/- cultures at day-5, but the average size of Bcl2 -/- osteoclasts was approximately twice that of +/+ (p<0.001). However, at day-7 and -9, Bcl2 -/- osteoclasts were no longer large and no difference was detected between genotypes. To determine the mechanism of vigorous Bcl2 -/- osteoclastogenesis, M-CSF dependent bone marrow macrophages were stimulated with RANKL and M-CSF and the expression of NFATc1, TRAP, and DC-STAMP at the RNA level was quantitatively analyzed with real-time PCR. It was revealed that the expression of DC-STAMP and TRAP was more rapid and considerably stronger in Bcl2 -/- than that in +/+ preosteoclasts. Higher expression of NFATc1 was also noted in Bcl2 -/- than +/+ preosteoclasts. The early expression of osteoclast markers fits the results of cell enumeration and morphometric analysis. These data suggest that Bcl2 plays a role in regulation of RANK signaling in myeloid cells. In summary, Bcl2 -/- osteoclastogenesis was rapid and robust, and vanished quickly thereafter, while +/+ osteoclastogenesis occurred more gently. Such vigorous Bcl2 -/- osteoclastogenesis was associated with early and elevated expression of DC-STAMP and TRAP.

Disclosures: J. Yamashita, None.

W084

Lysine-Specific Gingipain (Kgp) and Lipopolysaccharide (LPS) Synergistically Induces Osteoclast Differentiation. R. Yasuhara^{*1}, Y. Miyamoto^{*1}, M. Takami¹, T. Imamura^{*2}, R. Kamijo¹. ¹Department of Biochemistry, Showa University School of Dentistry, Tokyo, Japan, ²Department of Neuroscience and Immunology, Kumamoto University Graduate School of Medical Sciences, Kumamoto, Japan.

Porphyromonas gingivalis is known as a major pathogen of periodontitis associated with alveolar bone loss due to excessive bone resorption by osteoclasts. *P. gingivalis* produces cysteine proteases called gingipain divided into two types, Lys-gingipain (Kgp) and Arg-gingipain (Rgps), according to their cleavage-sites. In this study we examined the effects of gingipains on osteoclast differentiation. In cocultures of mouse bone marrow cells and osteoblasts, the addition of Kgp but not Rgp induced the formation of multinucleated osteoclasts (Kgp: 23 +/- 3.5 cells/well, Rgp: 0 cells/well). On the other hand, LPS, a constituent of gram-negative bacteria including *P. gingivalis*, induced mononuclear osteoclasts and small number of multinucleated osteoclasts (0-1 cells/well). Interestingly, simultaneous addition of Kgp and LPS to the cocultures induced significantly larger number of multinucleated osteoclasts (97 +/- 4.5 cells/well) than that induced by Kgp or LPS alone. Numerous resorption pits were developed on the surface of dentin slices on which cells were cocultured in the presence of Kgp and LPS together. However, LPS alone did not induce any resorption pits. Not only LPS but also the other bacterial constituents such as CpG ODN, poly(I:C) RNA and peptidoglycan, synergistically induced osteoclast differentiation in the combination with Kgp. We further examined the mechanisms of osteoclast differentiation by Kgp. Inactivated Kgp by Z-FK-cmk, a specific inhibitor for Kgp, completely inhibited osteoclast differentiation induced

by Kgp in the cocultures, indicating that the specific enzymatic activity of Kgp was essential for the induction of osteoclasts. Kgp did not induce the expression level of mRNAs for the receptor activator of NF- κ B ligand (RANKL) in osteoblasts, whereas Kgp significantly reduced the protein level of OPG in coculture media. In an in-vitro study, Kgp cleaved recombinant OPG protein suggesting that degradation of OPG by Kgp caused the enhancement of osteoclast differentiation in cocultures. These results suggest that Kgp exhibits synergistic virulence with LPS resulting in the inflammatory bone resorption characteristically seen in periodontitis. Therefore, we propose here that Kgp is a new target for the prevention and treatment of periodontitis.

Disclosures: R. Yasuhara, None.

W085

Analysis of Matrix Vesicle Poteins from Long Bone Growth Plates. J. Jeong^{*1}, H. Kim^{*1}, H. Kim^{*1}, E. Park¹, J. Cho¹, R. Garimella², N. N. Nahar², H. C. Anderson², J. Lim^{*1}, S. Kim¹, J. Choi¹. ¹Biochemistry & Cell Biology, Kyungpook Natl. Univ. School of Medicine, Skeletal Diseases Genome Research Center, Daegu, Republic of Korea, ²Pathology, Kansas University Medical Center, Kansas, KS, USA.

Initiation of bone mineralization is a key step to make a proper bone formation. Matrix vesicles (MVs) have been known as an initiation site for mineralization. Thus, identification of proteins from MV will provide fundamental clues to access the mechanism of the initiation step in bone mineralization. Although many components of MV have been identified by tedious single protein confirmation approach, comprehensive protein component analysis from MV has not been studied. In this study, we isolated MVs from growth plates of rachitic rat bones. Proteins from MVs were separated by SDS-PAGE and the gels were cut into 15 pieces from top to bottom. After in-gel digestion with trypsin, eluted peptides were extracted for LC-MS/MS analysis. Identified proteins from MVs were various including previously known proteins such as annexins and peptidases, along with other variety of enzymes, extracellular matrix, growth factors, and signal molecules. The systematic proteomic analysis of MVs gives an important opportunity to understand the molecular mechanism of initiation step of bone mineralization.

Disclosures: J. Choi, None.

W086

Comparison of In Vivo Model of Functional Bone Adaptation to the Calculated Mechanical Environment. C. J. MacKay^{*1}, G. C. Goulet^{*2}, D. Coombe^{*3}, R. F. Zernicke^{*1}. ¹Faculty of Medicine, University of Calgary, Calgary, AB, Canada, ²Faculty of Engineering, University of Calgary, Calgary, AB, Canada, ³Computer Modeling Group, Ltd., Calgary, AB, Canada.

Interest in functional adaptation of bone has led to the development of numerous experimental models [1,2,3,4]. Animal models provide insights into the molecular signaling pathways by which bone senses and adapts to changes in functional demand, but ambiguity persists about the mechanical components contributing to the principal determinants of skeletal morphology. Here, experimental results from an in vivo model of functional bone adaptation, using 12 adult female Sprague-Dawley rats, were compared to a finite element model (FEM). Animals were subjected to 28 day, daily lateral-medial cantilever tibial loading regime, consisting of 1 s pulses of a 1 Hz trapezoidal wave followed by 9 s of rest to a maximal strain magnitude of 1000 μ e, for a total duration of 120 s. Bone-targeted fluorochromes, calcein AM (days 6 and 18) and xylenol orange (days 13 and 27) were administered to estimate relative bone formation rates and localize osteogenic mineralization in response to exogenous loading. Histology and comparison of tibial cross-sections, obtained from experimental and contralateral limbs, indicated increases in bone mineralization rates on several ossification fronts across the tibial cross-section. These results were compared to the FEM model. The model calculated areas of maximal compression and tension across the experimental region of interest during loading, and estimates fluid flow vectors and pressure gradients, thereby quantifying the mechanical milieu during experimental loading. The comparison of the resultant osteogenic responses in this model with previously calculated results provided insight into the specific mechanical signals that may influence dynamic skeletal morphology. [1] Judex et al. (1997). J. Bone Min. Res. 12, 1737-1745. [2] Judex & Zernicke (2000). J. Appl. Physiol. 88, 2183-2191. [3] Gross et al. (1992). J. Biomech. 25, 1081-1087. [4] Rubin & Lanyon (1987). J. Orthop. Res. 5, 300-310.

Disclosures: C.J. MacKay, None.

W087

Temporal Expression of PHOSPHO1 During Chick Limb Bud Mesenchymal Cell Differentiation and Mineralization. V. E. MacRae^{*1}, M. G. Davey^{*1}, J. L. Milan², C. Farquharson¹. ¹Gene Function and Development, Roslin Institute, Midlothian, United Kingdom, ²Burnham Institute for Medical Research, La Jolla, CA, USA.

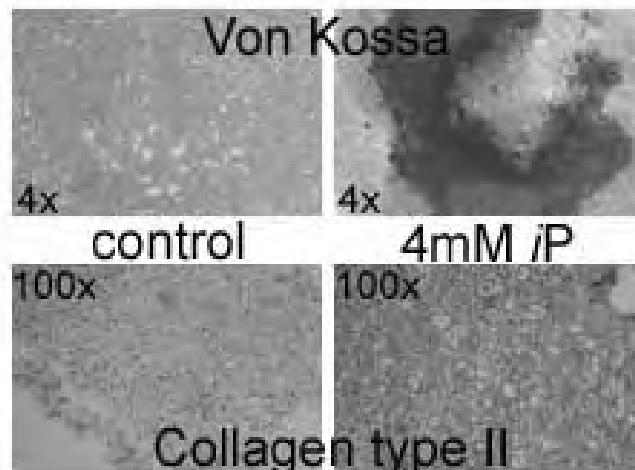
PHOSPHO1 is a phosphatase with up-regulated expression in growth plate chondrocytes and osteoblasts, and is implicated in the initiation of inorganic phosphate generation for matrix mineralization. This study has established the temporal expression of PHOSPHO1 during chondrogenesis and endochondral ossification within the developing chick limb bud. This model permits the monitoring of PHOSPHO1 expression during mesenchymal cell differentiation into mineral producing chondrocytes. Micromasses were prepared from stage 24 limb bud mesenchymal cells which were cultured for 0, 3, 7 and 10d. Alcian blue (proteoglycan synthesis) and alizarin red (mineral formation) staining was negligible at 0d, with a marked increase in staining intensity at 7d and 10d. This confirmed that the mesenchymal cultures had differentiated into chondrocytes with subsequent mineralization. mRNA expression of phospho1, tissue non-specific alkaline phosphatase (Akp2) and collagen II was also determined. Phospho1 expression was observed at all time points, however a notable increase in expression was seen by 7d. Interestingly, phospho1 expression decreased between 7d and 10d, which is in agreement with previous studies that have suggested that PHOSPHO1 is involved in the initial events of mineral formation. Akp2 was expressed at 0d and 3d, with a marked decrease at 7d and 10d. A comparable pattern has previously been reported for alkaline phosphatase activity in chick limb bud cultures. Collagen II was absent at 0d and was upregulated at 3d onwards. Further studies using chick limb tissue at E3.5 (stage 24), E5.5 (stage 28), E6.5 (stage 30) and E10.5 (stage 36) were undertaken. A marked increase in PHOSPHO1 protein expression was seen at E6.5 and E10.5. These data were complemented by increased phospho1 mRNA expression in E6.5 and E10.5 compared to E3.5 and E5.5. TNAP protein expression was noted at all developmental stages, with no obvious differences in expression levels. Collagen II gene expression was present from E5.5 onwards. Using whole-mount in-situ hybridisation, Phospho1 mRNA expression was observed in chick metatarsi (E6.5) around the mid-shaft of the bone. Immunohistochemical staining of tibia sections (E6.5) revealed that PHOSPHO1 staining was localized to the osteoid (bone collar) and associated periosteal osteoblasts within the mid-diaphyseal region. Some chondrocytes within the rudiment also stained positively for PHOSPHO1. These studies concur with our hypothesis that PHOSPHO1 has a pivotal role in the first phase of the mineralization process.

Disclosures: V.E. MacRae, None.

W088

Mineralization of Murine Mesenchymal C3H10T1/2 Cells in Micromass Culture. R. Roy¹, I. Binderman^{*2}, S. Doty^{*1}, V. Kudryashov^{*1}, A. Boskey¹. ¹Hospital for Special Surgery, New York, NY, USA, ²Ichilov Hospital, Tel Aviv, Israel.

Chick limb bud mesenchymal cells have been shown to undergo mineralization in micromass culture with the addition of inorganic phosphate (iP) (J Cell Biochem. 84(3):509-19). The murine multipotential mesenchymal cell line C3H10T1/2 undergoes chondrogenic differentiation in micromass cultures when stimulated by bone morphogenic protein-2 (Differentiation. Jan;64(2):67-76). These murine cells were used in micromass culture to determine whether they mineralize similar to the chick system. Cells were expanded in monolayer culture with DMEM supplemented with 10% FBS and 1% antibiotics/antimycotics (AB/AM). For micromass cultures cells were trypsinized, counted, and resuspended in Ca free DMEM supplemented with 10% FBS and 1% AB/AM. Cells were plated at a density of 100,000 cells per 10µl spot at the center of 35mm poly-L-lysine coated cell culture dishes to aid in attachment. Cells were allowed to attach at 37°C for 2 hours. Dishes were then flooded with 2mL of Ca free DMEM with 10% FBS and 1% AB/AM along with 100ng/mL of BMP-2. Media was changed 3X/wk and on day 2 of micromass cultures L-glutamine, 25µg/ml ascorbic acid, and 1mM Ca were added to all cultures, while 4mM iP was added to some cultures to promote mineralization. Alizarin red (AR), and von Kossa (VK) stains were performed on whole mount cultures and sections to visualize mineralization. Type I and type II collagen immunohistochemistry was used to determine whether these cultures form calcified cartilage or mineralized bone. VK and AR stains showed mineralization on day 28 in 4mM (iP) cultures, while control cultures showed no mineralization (Fig). In all cultures both type I and type II collagen was present at day 16, 21, and 28. At early time points there was more type II collagen in mineralizing cultures than in control cultures. These results indicate that this murine cell line does mineralize in the presence of exogenous phosphate which has been supported by previous ⁴⁵Ca uptake data, although mineralization may be delayed relative to the chick cultures. This murine culture system is comparable to the chick system and may be more useful for study of gene expression and signaling.



Disclosures: R. Roy, None.

This study received funding from: NIH AR037661.

W089

Alterations in Collagen Structure and Mineral Composition in Calcified Cartilage and Subchondral Bone in a Monkey Model of OA. M. E. Ruppel¹, C. S. Carlson², L. M. Miller³. ¹Biomedical Engineering, SUNY Stony Brook, Stony Brook, NY, USA, ²Dept. of Veterinary Population Medicine, College of Veterinary Medicine, University of Minnesota, St. Paul, MN, USA, ³National Synchrotron Light Source, Brookhaven National Laboratory, Upton, NY, USA.

Osteoarthritis (OA) can be a debilitating disease which is characterized by disorganization and calcification of the collagen matrix in the cartilage and increased turnover and thickening of the subchondral bone. In the present study, collagen structure and chemical composition were studied in the calcified cartilage and subchondral bone in plastic-embedded mid-coronal sections of proximal tibia from cynomolgus monkeys (n=26 animals; ages 6-30 yrs). These sites contained a range of histological OA lesions, from normal morphology to severe OA. Synchrotron-assisted Fourier transform infrared microscopy (FTIRM) was used to determine the level of mineralization (mineral/protein ratio), carbonate accumulation (carbonate/phosphate ratio), and collagen structure (protein amide band ratio) as a function of tissue compartment and OA severity. Preliminary results showed that the protein amide band ratios were significantly different between subchondral bone and calcified cartilage, suggesting differences in collagen organization between the two tissue compartments; however, the differences were not affected by OA severity. Both the level of mineralization (p=0.0431) and carbonate accumulation (p<0.0001) were significantly higher in subchondral bone when compared to calcified cartilage. Although the mineralization level of the calcified cartilage increased (p=0.0037) with increasing OA severity, the subchondral bone remained unchanged. Carbonate accumulation increased significantly in both tissue compartments as a function of OA severity. These compositional changes that are observed as a function of OA severity are consistent with the progression of a "mineralization front" where endochondral ossification occurs and calcified cartilage is replaced by subchondral bone. These findings indicate that calcified cartilage and subchondral bone have distinctly different collagen structure and mineral compositions that are affected by OA severity and could increase stress on the afflicted joints.

Disclosures: M.E. Ruppel, None.

This study received funding from: The Department of Energy (contract DE-AC02-98CH10886) and National Institutes of Health Grant RR14099.

W090

Distribution and Localization of Aluminum in Bone Tissues of Aluminum Osteopathy. Y. Teraki¹, H. Sasakabe^{*2}. ¹Internal Medicine, Shinjo Tokushukai Hospital, Mitaka, Japan, ²Internal Medicine, Shinjo Tokushukai Hospital, Shinjo, Japan.

The pathophysiology of the so-called aluminum (Al) osteopathy is yet to be fully clarified. To investigate the dynamic behavior of Al in bone tissues, we have examined aluminum in bone tissue sections by laser scanning confocal microscopy using the staining with lumogal, a new chelating reagent we have developed. On account of the reported finding that Al is not excreted in urine in the presence of impaired renal function, this study was performed in 20 5/6-nephrectomized rats which were dosed orally or parenterally with an Al preparation for 3-6 months, followed by sacrifice and preparation of bone tissue slides. Thanks to the high detection sensitivity of Al-lumogal complex, the technique allowed Al identification with a lower detection limit of 19.0 µg/g. Results: The study showed diffuse or dense granular Al deposits in osteoids rather than in the generally believed calcification front. No Al was detected in calcified bone tissues. Furthermore, Z-scans of the stained bone tissues enabled observation of a three-dimensional Al deposition status. The results indicate potential usefulness of the lumogal stain technique in the diagnosis of Al osteopathy.

Disclosures: Y. Teraki, None.

W091

Role of Cell Death and Osteogenic Activity in Injury-induced Calcification from TNF- α Receptor p55 $^{-/-}$ p75 $^{-/-}$ Mice. Y. Zhao¹, A. L. Urganus^{*1}, Y. Chen^{*2}, P. H. Stern³, A. L. Boskey⁴, L. M. Pachman^{*5}. ¹Childrens Memorial Research Center, Northwestern University, Chicago, IL, USA, ²Research Center for Genetic Medicine, Children's National Medical Center, Washington D.C., DC, USA, ³Department of Molecular Pharmacology and Biological Chemistry, Northwestern University Feinberg School of Medicine, Chicago, IL, USA, ⁴Hospital for Special Surgery, Cornell University-Weill Medical College, New York, NY, USA, ⁵Department of Pediatrics, Northwestern University Feinberg School of Medicine, Chicago, IL, USA.

Background: TNF- α receptor (p55 $^{-/-}$, p75 $^{-/-}$) null mice develop calcifications along with increased inflammation after an injection with cardiotoxin (CTX), a snake venom component. While TNF- α inhibits osteoblast differentiation in vitro and promotes osteoclast formation the mechanism of the pathological mineralization in this mouse model remains unknown.

Objective: To elucidate the potential roles of cell death and formation of osteoblasts and osteoclasts in CTX-induced calcifications.

Materials and Methods: Four-week-old wild type C57B6 mice and TNF- α receptor null mice were injected with CTX into the skeletal muscle (Tibialis anterior) and sacrificed after 3, 7, 14 and 28 days. The muscles were stained for calcifications by von Kossa or calcein pre-labeling. The osteoblast markers, core binding factor alpha 1 (Cbfa1), osteocalcin and the osteoclast marker, tartrate-resistant acid phosphatase (TRAP) were stained in the injured tissues after 3, 7 and 14 day treatment. Total RNA was extracted from the muscle for microarray analysis and realtime PCR analysis of Cbfa1 and Receptor Activator for Nuclear Factor κ B Ligand (RANKL) from the 3 day group.

Results: Calcifications were apparent in all of the TNF- α receptor null mice at day 3 and day 7 after CTX administration whereas they were observed in only 29% of wild type mice at day 3 and 7. By day 14, no calcifications were observed in either strain. Microarray result indicated that the anti-apoptotic genes (BCL2A1(+1.51), BCL2L1(+1.8)), pro-apoptotic genes (CASP7(+1.22), BID(+1.8)), Cbfa1(+1.7) and TRAP(+1.3) were marginally up-regulated in TNF- α receptor null mice compared to wild type mice. Realtime PCR failed to show difference of Cbfa1 and RANKL in the injured muscles between the mutant and control mice. Osteocalcin was expressed in mineralized muscle in both strains. TRAP staining was positive in TNF- α receptor null mice at day 7 but was much less at day 14. We speculate that the formation of osteoclasts contribute to the resorption of the minerals.

Conclusion: Cell death and osteoblastic differentiation may lead to muscle calcifications following CTX administration to TNF- α receptor null mice. Osteoclastic resorption may account for the transient nature of the calcifications.

Disclosures: Y. Zhao, None.

This study received funding from: Cure JM.

W092

Mx2 Promotes Late Stages of Chondrocyte Differentiation by Up-regulating Ihh Expression. K. Amano^{*1}, F. Ichida^{*2}, A. Sugita^{*2}, K. Hata^{*2}, M. Kogo^{*1}, R. Nishimura², T. Yoneda². ¹Oral and Maxillofac, Osaka Univ Grad Dent, Suita City, Osaka, Japan, ²Biochem, Osaka Univ Grad Dent, Suita City, Osaka, Japan.

A homeobox gene, Mx2 (muscle segment homeobox 2), plays important roles in the development, growth and differentiation of various types of cells and tissues including ectodermal organs, teeth, vascular cells and cancer. Accumulating data also suggest that Mx2 regulates the skeletal development by controlling endochondral ossification and/or membranous ossification. Mice deficient in Mx2 gene exhibit disturbed chondrogenesis with reduced bone formation. However, little is known about the molecular basis by which Mx2 modulates chondrogenesis. In the present study, we investigated the role of Mx2 using murine primary rib chondrocytes. Treatment of chondrocytes with BMP2 up-regulated the expression of Mx2 mRNA along with the differentiation. Overexpression of Mx2 stimulated calcification of primary chondrocytes in the presence of BMP2, whereas Mx2 alone had no effects. We also found that constitutively-active Mx2 (caMx2; Mx2P148H) more strongly enhanced BMP2-stimulated calcification than wild-type Mx2. Consistent with this, caMx2 overexpression up-regulated the expression of alkaline phosphatase and type X collagen that were stimulated by BMP2. However, caMx2 had no effects on type II collagen expression. Furthermore, organ culture experiments using mouse embryonic metatarsals showed that caMx2 markedly stimulated the differentiation of chondrocytes into the prehypertrophic and hypertrophic stages in the presence of BMP2. The stimulatory effects of Mx2 on chondrocyte differentiation were enhanced by co-overexpression of Smad1 and Smad4, but inhibited by Smad6, an inhibitory Smad of BMP2 signaling. Of note, caMx2 overexpression enhanced BMP2-induced indian hedgehog (Ihh) expression in mouse primary chondrocytes and Ihh overexpression promoted calcification of primary chondrocytes. Importantly, cyclopamine, a specific inhibitor of hedgehogs, blocked Mx2- or Ihh-induced calcification of primary chondrocytes. In conclusion, our results suggest that Mx2 plays important roles in the regulation of late, but not early, stages of chondrocyte differentiation by up-regulating Ihh expression in collaboration with BMP2/Smad signaling.

Disclosures: K. Amano, None.

W093

Effects of Pro-inflammatory Cytokines on Suppressor of Cytokine Signalling-2 (SOCS-2) Expression in the Growth Plate. V. E. MacRae^{*1}, S. Pells^{*1}, S. F. Ahmed², C. Farquharson¹. ¹Gene Function and Development, Roslin Institute, Midlothian, United Kingdom, ²Child Health, Royal Hospital for Sick Children, Glasgow, United Kingdom.

Abnormal growth patterns are commonly observed in children suffering from chronic inflammatory diseases, which are associated with the increased production of pro-inflammatory cytokines. Suppressor of Cytokine Signalling-2 (SOCS-2) negatively regulates the signal transduction of several cytokines and this study examined the role of SOCS2 in regulating bone growth, and the response of growth plate chondrocytes to pro-inflammatory cytokines. Initial studies indicated that SOCS2 was expressed by both murine primary chondrocytes and the ATDC5 chondrogenic cell line. Foetal (E14-E18) and neonatal (1 and 9-day-old) primary murine chondrocyte expressed SOCS-2 mRNA at similar levels whereas SOCS-2 protein expression was greater (78%) during chondrogenesis than terminal differentiation. IL-1 β and TNF α (both 10ng/ml) exposure for 48h increased SOCS-2 protein expression in primary 1-day-old murine chondrocytes (79% and 65% increase respectively). 7-week-old female mice lacking SOCS-2 (SOCS2 $^{-/-}$) expression were significantly heavier (26%; P<0.0001) and longer (6%; P<0.001) compared to wild-type (WT) mice. The tibiae of the null mice were longer (8%; P<0.001), wider (18%; P<0.001) and had wider growth plates (24%; P<0.001) than WT mice. Proliferative and hypertrophic zones were significantly wider in SOCS2 $^{-/-}$ mice compared to WT mice (10% and 14% respectively; P<0.001). The growth of metatarsals from 1-day-old female SOCS2 $^{-/-}$ and WT mice over 8-days was inhibited by TNF α (47% and 33% respectively; both p<0.001) and IL-1 β (71% and 86% respectively; both p<0.001) by comparable amounts. No effect of genotype was observed. In contrast, matrix gene expression by primary chondrocytes exposed to pro-inflammatory cytokines over 48h was dependent upon the genotype of the host animal. RT-PCR studies revealed that aggrecan expression was notably reduced only in chondrocytes from SOCS2 $^{-/-}$ exposed to IL-1 β and TNF α . Collagen Type X expression was markedly reduced in chondrocytes from both SOCS2 $^{-/-}$ and WT mice whereas collagen Type II expression was not altered by cytokine exposure. This is the first study to show the expression of SOCS-2 in growth plate chondrocytes and its dramatic effect on suppressing skeletal growth. IL-1 β and TNF α may mediate their effects through SOCS-2, influencing the growth of children with inflammatory diseases through a local effect at the growth plate.

Disclosures: V.E. MacRae, None.

W094

Hormonal Regulation of Hypertrophic Chondrocyte Apoptosis. S. U. Miedlich^{*}, M. B. Demay. Endocrine Unit, MGH, Boston, MA, USA.

In vivo studies in genetically modified (Npt2a knockout, VDR knockout and hyp) and dietary manipulated mouse models have demonstrated that hypophosphatemia leads to impaired apoptosis of hypertrophic chondrocytes in the growth plate and plays a critical role in the development of rickets. However, studies in the Npt2a knockout mice demonstrate that the expansion of the growth plate and impaired apoptosis observed at 16 days of age, has reverted to normal by 35 days of age, despite the presence of persistent hypophosphatemia. The transient nature of these findings in the Npt2a null mice strongly suggests the presence of additional factors that modulate the response of hypertrophic chondrocytes to circulating phosphate levels. Thus, we are undertaking investigations in an in vitro model of chondrocyte maturation in order to investigate whether 1,25-dihydroxyvitamin D or parathyroid hormone modulate the effects of phosphate on hypertrophic chondrocyte apoptosis.

The clonal chondrocytic cell line (RCJ3.1C5.18) has been shown to recapitulate the program of chondrocytic differentiation in culture, including acquisition of markers of hypertrophic differentiation and formation of mineralized matrix nodules. To address whether these cells were susceptible to phosphate-mediated hypertrophic chondrocyte apoptosis, they were subjected to 7mM sodium phosphate or 7mM sodium chloride (control) for 18 to 72 hours. The Guava Nexin assay was employed to measure plasma membrane changes associated with apoptosis (Annexin V-PE) and to identify dead cells (7-AAD). An MTT based assay was also used to evaluate mitochondrial activity, a surrogate for cellular viability.

Western analyses were performed to insure that collagen X, a marker of hypertrophic chondrocyte differentiation, was observed in RCJ3.1C5.18 cells after 7-10 days of culture in the presence of ascorbic acid. Treatment of hypertrophic chondrocytes with phosphate (7 mM) resulted in a significant increase in apoptotic as well as dead cells after > 24 hours of treatment. Studies are underway to evaluate whether 1,25-dihydroxyvitamin D enhances the susceptibility of hypertrophic chondrocytes to phosphate-mediated apoptosis in this model. Investigations will also examine the effects of parathyroid hormone on phosphate-induced apoptosis in hypertrophic RCJ3.1C5.18 cells.

These investigations demonstrate that the RCJ3.1C5.18 cell model is an appropriate system in which to investigate the effect of hormones on phosphate-induced apoptosis. Studies of these potential regulatory factors will not only further our understanding of the pathophysiological mechanisms underlying rickets but may also provide insights into the universal regulation of cellular apoptosis.

Disclosures: S.U. Miedlich, None.

This study received funding from: NIH.

W095

A-Raf and B-Raf Are Dispensable for Endochondral Bone Development and PTHrP Suppresses ERK Activation in Hypertrophic Chondrocytes. S. Provot¹, G. Nachtrab^{*2}, J. Paruch^{*2}, A. P. Chen^{*3}, A. Silva^{*3}, H. M. Kronenberg². ¹Anatomy, UCSF, San Francisco, CA, USA, ²Endocrine Unit, MGH - Harvard Medical School, Boston, MA, USA, ³Neurobiology, UCLA, Los Angeles, CA, USA.

Parathyroid hormone-related peptide (PTHrP) and its PTHrP receptor (PPR) increase chondrocyte proliferation and delay chondrocyte maturation in endochondral bone development, at least partly through cAMP-dependent signaling pathways. Because some data suggest that the ability of cAMP to stimulate cell proliferation involves the MAPKKK B-Raf, we hypothesized that PTHrP's proliferative action in chondrocytes might be mediated by B-Raf. While B-raf gene expression is detected by *in situ* hybridization (ISH) in proliferative chondrocytes, its conditional removal in cartilage using a type II collagen promoter-driven cre (col2-cre) and a floxed B-raf allele does not affect chondrocyte proliferation and maturation, as indicated by histologic analyses, BrdU assays, and ISH with various chondrogenic markers on embryonic and postnatal samples. Lack of B-raf does not alter either PTHrP-induced increased chondrocyte proliferation and delayed maturation, both *in vivo* in mice expressing a constitutively active PPR in cartilage (col2-caPPR), and *in vitro* in metatarsal explants treated acutely with PTHrP. Similar results were obtained by conditionally removing B-Raf from osteoblasts using Osterix- and col1-cre mice. Because A-raf expression detected by ISH is identical to that of B-raf in cartilage, whereas that of C-raf is restricted to hypertrophic chondrocytes, we speculated that A-Raf might play a redundant function with B-Raf in this tissue. Surprisingly, mice deficient for both A-Raf (universal A-raf knockout) and B-Raf in chondrocytes exhibit normal endochondral bone development, suggesting that the Raf-ERK pathway is not critical for chondrocyte proliferation. Consistent with this idea, the presence of activated ERK detected by immunohistochemistry is essentially restricted to hypertrophic chondrocytes. Notably, acute treatment of bone explants with PTHrP or prolong activation of PPR in col2-caPPR mice suppress ERK activation in these cells, while ERK activation is increased in PTHrP KO mice. Thus, PTHrP signals suppress ERK activation in normal conditions. Taken together, these results demonstrate that B-raf and A-Raf are dispensable for endochondral bone development, and they suggest that ERK might regulate hypertrophic differentiation rather than proliferation in cartilage, possibly through its activation by C-Raf in hypertrophic chondrocytes.

Disclosures: S. Provot, None.

This study received funding from: NIH.

W096

Cell Death and Cell Proliferation of Cartilage Layer in Human Anterior Cruciate Ligament Tibial Insertion after Rupture. H. Mutsuzaki¹, M. Sakane², K. Honda^{*3}, K. Ikeda^{*4}, S. Hattori^{*5}, N. Ochiai^{*2}. ¹Department of Orthopaedic Surgery, Tsukuba Central Hospital, Utsunomiya, Japan, ²Department of Orthopaedic Surgery, Institute of Clinical Medicine, Graduate School of Comprehensive Human Sciences, University of Tsukuba, Tsukuba, Japan, ³Department of Legal Medicine, Doctoral Program in Social and Environmental Medicine, Graduate School of Comprehensive Human Sciences, University of Tsukuba, Tsukuba, Japan, ⁴Department of Orthopaedic Surgery, Ichiyama Hospital, Tsukuba, Japan, ⁵Department of Agriculture, Ibaraki University, Ami, Japan.

The purpose of this study is to investigate cellular responses of cartilaginous layers in human anterior cruciate ligament (ACL) tibial insertions compared with normal ones. Sixteen tibial insertions of ruptured ACLs were obtained during primary ACL reconstructions. We also obtained sixteen normal ACL tibial insertions from cadavers. A terminal deoxynucleotidyl transferase-mediated deoxyuridine triphosphate-biotin nick end labeling (TUNEL) staining assay to detect apoptosis, proliferating cell nuclear antigen (PCNA) staining and a histological examination was performed. The percentage of TUNEL-positive chondrocytes in ruptured ACL insertions ($43.6 \pm 14.8\%$) was higher than that of normal ones ($9.6 \pm 5.8\%$). The percentage of PCNA-positive chondrocytes was not significant difference between ruptured ACL insertions ($23.1 \pm 26.3\%$) and normal ones ($12.3 \pm 7.3\%$). The average thickness of the cartilage layer, the glycosaminoglycan-stained area and the number of chondrocytes per millimeter in ruptured ACL insertions were lower than that of normal ones. The decrease of chondrocytes because of imbalance of the cell death and the cell proliferation in the ACL insertions after rupture compared with those in normal could lead to histological changes of the cartilage layer in the insertions. The results may help elucidate the etiology of the histological changes, the function and the significance of existence of the ACL insertion.

Disclosures: M. Sakane, None.

W097

Intra-articular Osteoclastogenesis Inhibitory Factor/Osteoprotegerin Prevents Cartilage Degeneration in a Murine Model of Osteoarthritis. S. Shimizu^{*1}, Y. Asou², S. Itoh^{*3}, U. Chung⁴, H. Kawaguchi¹, K. Shinomiya^{*2}, T. Muneta^{*1}. ¹Section of Orthopaedic Surgery, Graduate School, Tokyo Medical and Dental University, Tokyo, Japan, ²Department of Orthopaedic Surgery, Tokyo Medical and Dental University, Tokyo, Japan, ³Human Gene and Science Center, Tokyo Medical and Dental University, Tokyo, Japan, ⁴Department of Orthopaedic Surgery, University of Tokyo, Tokyo, Japan.

Osteoarthritis (OA) is a chronic degenerative joint disorder characterized by articular cartilage destruction and osteophyte formation. RANK, RANKL, and Osteoclastogenesis Inhibitory Factor (OCIF)/Osteoprotegerin (OPG) mRNAs and proteins are expressed in normal cartilage. Cartilage from patients with OA contains increased levels of OPG mRNA. However, the functions of OPG expressed during OA pathogenesis are poorly understood. The purpose of this study was to investigate the effect of endogenous and exogenous OPG on chondrocytes during OA pathogenesis *in vivo*. First, OA was surgically induced in young adult OPG^{-/-} mice and wild-type (WT) littermates to investigate the effect of chondrocyte-derived OPG deficiency. Four weeks after surgical induction of OA, histological evaluation of tibial cartilage demonstrated typical features of cartilage degeneration both in WT and OPG^{-/-} mice. The degenerative changes in the articular cartilage, however, were significantly enhanced in OPG^{-/-} mice compared to WT littermates. Cartilage thickness was significantly reduced in OA-induced OPG^{-/-} mice. The morphology of subchondral bone structures was not affected by OPG haploinsufficiency. Next, we investigated the effect of exogenously administered rhOPG by daily intra-articular injections following surgical induction of OA. Histological evaluation indicated that OA-induced mice in rhOPG treated group were protected from cartilage degeneration compared to vehicle group four weeks after the operation. Cartilage thickness was significantly preserved in rhOPG administered mice. Subchondral bone volume was not affected by rhOPG treatment, indicating that chondro-protective effect of rhOPG was independent of subchondral bone metabolism. TUNEL assay indicated that rhOPG administration prevented chondrocyte apoptosis in an experimental model of OA. Pro-apoptotic ligand TRAIL, one of the ligands for OPG, was co-expressed with OPG in articular chondrocytes irrespective of OPG administration. These data indicated that endogenous OPG had a protective effect against the mechanical stress-induced cartilage degeneration. Furthermore, direct administration of rhOPG to articular chondrocytes prevented cartilage degeneration via prevention of chondrocyte apoptosis.

Disclosures: S. Shimizu, None.

W098

Mechanisms of Osterix Control of Endochondral Ossification. D. Y. Soung, L. A. Kaback^{*}, A. Naik^{*}, N. Smith^{*}, E. M. Schwarz, R. J. O'Keefe, H. Drissi. Orthopaedics, University of Rochester, Rochester, NY, USA.

We investigated the expression and regulation of the zinc finger protein Osterix (Ox) during endochondral ossification in the developing embryo. Our *in situ* hybridization and immunohistochemical analyses of Ox expression showed a restricted expression of Ox transcript and protein to the immature chondro/osteoprogenitor cells and mature osteoblasts but excluded from hypertrophic chondrocytes. Using a fracture injury model we show consistent expression of Ox protein in mesenchymal progenitor cells in the periosteum and immature chondrocytes and osteoblasts embedded in the fracture callus while hypertrophic chondrocytes, vessels and fibrous tissue remain devoid of Ox expression. Additionally, using RNAs isolated from fracture calluses throughout the healing process and achievement of bony unions, we observe that Ox transcripts parallel that of Runx2 and differentially overlap both cartilage and bone phenotypic markers. Furthermore, using the limb bud-derived MLB13MYC Clone 17 cells, we show that PTHrP inhibited chondrocyte maturation while it enhanced mRNA levels of Ox in these chondro/osteoprogenitor cells. Our viral over-expression studies, complemented with siRNA mediated loss of Ox function experiments indicate that Ox serves as an inhibitor of chondrogenesis and chondrocyte terminal differentiation while it promotes osteoblast maturation. Together, our findings provide novel evidence for the molecular mechanisms underlying Ox inhibition of chondrocyte differentiation, and further suggest a role for this transcription factor in promoting endochondral ossification during bone repair.

Disclosures: D.Y. Soung, None.

This study received funding from: HIAMS/NIH.

W099

Epigenetic Modulatory Agents Suppress the Chondrocytic Phenotype. M. Stewart¹, E. Caporali^{*1}, A. Stewart^{*1}, P. Jones^{*2}. ¹Veterinary Clinical Medicine, University of Illinois at Urbana-Champaign, Urbana, IL, USA, ²Cell and Developmental Biology, University of Illinois at Urbana-Champaign, Urbana, IL, USA.

Epigenetic processes impact gene transcription by directly altering DNA/chromatin structure, resulting in transcriptional repression. There is increasing recognition that genes active in chondrocyte differentiation, proliferation and arthritis are subject to epigenetic control, however epigenetic regulatory processes can have global impacts on cellular transcriptional activity. This study was carried out to assess the effects of epigenetic-modifying agents on the articular chondrocytic (AC) phenotype. Cartilage was collected from equine articular joints and murine epiphyses. Chondrocytes

were cultured as explants or isolated by collagenase digestion and cultured as non-adherent aggregates. 5-azacytidine (5AZA) and zebularine (ZEB) were administered to inhibit DNA methylation, while valproic acid (VA) and Trichostatin A (TSA) was used to block histone deacetylation. The phenotypic effects on these epigenetic modifying reagents on the chondrocytic phenotype were assessed by Northern blot analyses of Coll II and aggrecan mRNAs, DMMB measurement of sulfated GAG secretion and Col II ELISA assays.

Treatment of chondrocyte aggregate cultures with epigenetic modulating reagents resulted in profound suppression of Coll II and aggrecan mRNA levels, reduced sulfated GAG secretion and Col II deposition. Similar effects were noted in cartilage explants. Consequent experiments showed these profound effects were reversible, with return to control levels within 3 days of 5AZA or VA removal. In contrast, chondrocytes treated continuously for 10 days of the experiments showed persistent transcriptional suppression of chondrocyte-specific genes. In contrast to previous reports, no Coll X mRNA was detected in articular chondrocytes treated with 5AZA or co-treated BMP-2.

These data show that epigenetic-modifying agents have profound but reversible effects on the chondrocytic phenotype. The conventional effect of these reagents is to 'de-repress' genes normally silenced epigenetically. Inhibition of AC-specific genes could follow unmasking of repressive elements in the gene promoters or by activation of genes that repress the AC phenotype. The effects might also result from non-epigenetic pharmacological actions; however multiple epigenetic reagents induce similar effects on two distinct AC-specific genes, arguing against this possibility.

Disclosures: M. Stewart, None.

This study received funding from: Arthritis Foundation.

W100

Runx2 Haploinsufficiency Ameliorates the Ectopic Calcification in a Mouse Model of Ossification of the Posterior Longitudinal Ligament (OPLL). S. Takeda¹, M. Iwasaki², S. Sato¹, A. Kimura¹, H. Inose¹, K. Shinomiya¹. ¹Department of Orthopedics and ²COE, Tokyo Medical and Dental University, Tokyo, Japan, ²Department of Orthopedics, Tokyo Medical and Dental University, Tokyo, Japan.

Ossification of the Posterior Longitudinal Ligament (OPLL) is a disease characterized by the ectopic calcification of the ligament, but its pathogenesis remains to be addressed. Histologically, calcification in OPLL is characterized by the existence of chondrocytes and bone marrow, suggesting that it is caused by endochondral bone formation-like mechanism. In an effort to elucidate the molecular pathogenesis of OPLL, we focused on Runx2. Runx2 is an essential transcription factor for osteoblastogenesis, whose deficiency causes the complete lack of endochondral bone formation. Induction of Runx2 expression was demonstrated in the ectopically-calcified ligaments of *ttw* mice, a mice model of OPLL, by monitoring the lacZ activity inserted into the Runx2 genomic locus. To address the functional role of Runx2 in the promotion of OPLL, we crossed Runx2 heterozygote-deficient mice with *ttw* mice. Analyzing the area of calcification in the posterior longitudinal ligament by micro-computed tomography revealed that *ttw* mice with Runx2 haploinsufficiency carry less calcification than *ttw* mice without Runx2 haploinsufficiency. Histologically, reduction of mineralized bony structures and bone marrow stroma was observed in *ttw* mice with Runx2 haploinsufficiency; Runx2 haploinsufficiency ameliorated the ectopic calcification in *ttw* mice. Taken together, our results demonstrated that Runx2 is intimately involved in the cause of OPLL *in vivo*.

Disclosures: S. Takeda, None.

W101

Transcriptional Induction of SOX9 by NF- κ B Subunit p65 During Chondrogenesis. M. Ushita, T. Ikeda, T. Saito, A. Kan, K. Nakamura, U. Chung, H. Kawaguchi. Sensory and Motor System Medicine, University of Tokyo, Tokyo, Japan.

Although SOX9 is an essential molecule for chondrogenic differentiation from mesenchymal cells, little is known about the upstream signaling. The present study attempted to identify transcription factors to induce SOX9 expression and examined the mechanism. By exhaustive comparison of the genomic sequences between human and mouse SOX9 proximal promoters, we identified several highly conserved regions within which NF- κ B, NFAT, and CREB/ATF motifs were found as putative transcription factor binding sites. We then created expression vectors of transcription factors and co-factors for these sites: 11 for NF- κ B, 5 for NFAT, and 11 for CREB/ATF, and transfected them in mouse chondrogenic ATDC5 cells and non-chondrogenic HeLa cells with a luciferase-reporter construct containing a human 1,000 bp SOX9 promoter. Among them, an NF- κ B subunit p65 most strongly activated the luciferase activity. Deletion analysis using a series of 5'-deletion constructs of the SOX9 promoter confirmed that the core responsive element to p65 included the estimated NF- κ B motifs located around -250 bp relative to the transcriptional start site. The transcriptional activity of p65 was decreased by a site-directed mutagenesis in the NF- κ B motif, and the tandem-repeat constructs responded to p65 depending on its repeat number. Electrophoretic mobility shift assay revealed specific binding of the *in vitro*-translated p65 protein with the wild-type NF- κ B motif oligonucleotide probe, but not with the mutated probe. Cold competition with an excess of the unlabelled probe, but not with the unlabelled mutated probe, cancelled the complex formation. In addition, the complex underwent supershift by the antibody to p65, confirming the specific binding of p65 and the NF- κ B motif. *In vivo* expression of p65 was shown by immunohistochemistry to be co-localized with SOX9 in the resting and proliferative chondrocytes of the mouse growth plate. To further investigate the functional relevance of p65 to chondrogenic differentiation, we established HeLa cells or mouse primary costal chondrocytes overexpressing p65. Expressions of type II collagen and

SOX9 were markedly increased in both cells by the overexpression as compared with respective GFP-transfected control cells. In conclusion, we identified NF- κ B / p65 as a potent transcriptional signaling for SOX9 promoter activation and chondrogenic differentiation. Elucidation of the molecular network related to the SOX9 - NF- κ B / p65 axis will greatly benefit development of the regenerative medicine of cartilage.

Disclosures: M. Ushita, None.

W102

Tissue Specific Expression of Murine Aggrecan Is Regulated Through Both Regulatory Enhancer and Repressor Elements. N. A. Wigner, T. A. Einhorn, L. C. Gerstenfeld. Orthopaedics, Boston University School of Medicine, Boston, MA, USA.

Aggrecan deposition is a hallmark of the mature chondrocyte. Thus the analysis of aggrecan's unique temporal and spatial expression regulation can extend current understanding of cartilage specific transcriptional control. Previous studies, using collagen type II as a model gene, have identified a complex transcription network during skeletal tissue development. As a result, transcription factors such as Sox9, Runx2, and Snail1 have been shown to regulate collagen type II expression and have been implicated in chondrogenesis. However, few studies have explored the cis-acting elements and the interacting transcriptional regulators of other cartilage extracellular matrix proteins such as aggrecan. The goal of these experiments was to characterize the cis-transcriptional regulatory motifs that mediate aggrecan expression during chondrogenic differentiation and to identify the temporal interaction of transcription factors that impart cartilage specific expression. The 5' proximal region of the aggrecan gene and various permutations of its promoter and 5'UTR were cloned into luciferase reporter vectors and assessed by transient transfection into both chondrogenic and non chondrogenic cell lines and C3H10T1/2 stems cells induced to undergo chondrogenic differentiation. The temporal and functional nature of specific cis-elements was further assessed by electromobility shift analysis. During the sequential pattern of chondrogenic differentiation, an increased expression of Sox9 was accompanied with a decrease in Runx2 and Snail1. Concomitant with this, was an increase in aggrecan mRNA. We have identified regulatory regions within the aggrecan promoter and 5'UTR that mediate its tissue specific regulation. This study has shown aggrecan's 5'UTR to be a robust tissue-specific regulator of expression. In undifferentiated chondrocytes, placing this 5'UTR immediately downstream of both its own proximal promoter and the promoter of collagen type II, enhanced reporter activity by 5.6-fold and 3.4-fold relative to their respective basal promoters alone. In addition, the presence of the 5'UTR was necessary to maintain observable reporter activity in differentiated chondrocytes. Co-transfection of the aggrecan reporters with Sox9 resulted in an enhanced reporter activity by 1.6-fold relative to controls, although the presence of the 5'UTR did not mediate this effect. Thus, the potential identification of both cis and trans acting factors involved in the regulation of aggrecan can provide insight into the regulation of cartilage as a whole and identify key molecular switches mediating cell differentiation.

Disclosures: N.A. Wigner, None.

W103

Cartilage Extracellular Matrix Homeostasis Is Regulated by RAR γ Repression Function. J. A. Williams¹, N. Kondo¹, N. Takeshita², T. Okabe¹, M. Enomoto-Iwamoto¹, M. Pacifici¹, M. Iwamoto¹. ¹Orthopaedic Surgery, Thomas Jefferson University, Philadelphia, PA, USA, ²Orthopaedic Surgery, Tohoku University, Sendai, Japan.

Cartilage extracellular matrix is maintained at homeostasis in the upper regions of growth plate and is rapidly degraded in hypertrophic zone, but the mechanisms underlying such critical metabolic shift are not fully understood. We previously showed that transcription factor RAR γ is strongly expressed in the upper growth plate zones and mice lacking RAR γ and another family member exhibit dwarfism and low cartilage matrix content. RARs are known to serve as transcriptional repressors and activators depending on absence or presence of ligands, respectively. Given that the upper growth plate zones contain scanty endogenous retinoid levels if any, we asked whether RAR γ exerts ligand-independent repressor function and contributes to matrix homeostasis. Primary rib chondrocytes in monolayer culture were treated with a retinoid pan-agonist or pan-antagonist. As expected, agonist treatment markedly increased matrix catabolism and MMP gene expression compared to untreated control cultures. However, treatment with antagonist inhibited endogenous matrix catabolism and MMP expression to levels below control. The same was seen when RARE reporter activity was measured; the agonist increased it above control levels, whereas the antagonist reduced it to below control levels. To determine whether these responses were attributable to RAR function, we compared double-floxed and double-null RAR β /RAR γ chondrocytes. The former behaved just as wild type cells, whereas the double-null chondrocytes failed to respond to either agonist or antagonist. The zinc finger transcription factor Zac1 modulates nuclear hormone receptor function and is co-expressed with RAR γ in cartilage. We found that Zac1 over-expression enhanced RAR γ repressor activity in RAR α /RAR β double-null chondrocytes that express RAR γ only. Mammalian two hybrid tests showed that Zac1 physically associates with RAR γ and such association is lost when the LxxLL motif of Zac1 is mutated. The results of our study provide the first evidence that RAR γ acts as a ligand-independent repressor in cartilage matrix homeostasis and may do so in strict cooperation with Zac1.

Disclosures: J.A. Williams, None.

W104

Phosphate Regulates Chondrocyte Differentiation in a model of Embryonic Endochondral Bone Formation. A. A. Zalutskaya, M. Cox*, M. B. Demay. Endocrine Unit, MGH, Boston, MA, USA.

Phosphate is required for terminal differentiation of hypertrophic chondrocytes during postnatal growth plate maturation. To investigate whether extracellular phosphate plays a role during embryonic endochondral bone formation, we performed investigations in the mouse metatarsal culture model. This model recapitulates *in vivo* bone development in culture and circumvents the homeostatic changes that occur in the intact animal. Metatarsals were isolated from day 15.5 C57BL/6J embryos and cultured in phosphate-free high glucose DMEM, 1% Pen/Strep, 0.05mg/ml ascorbic acid and 0.25% heat-inactivated FBS. The estimated phosphate content of this basal medium is 0.3 μ M. Three culture conditions were used to address the effect of extracellular phosphate on chondrocyte differentiation: 0 mM added phosphate, 1.25 mM added phosphate (control) and 7 mM added phosphate. Metatarsals were cultured for 4, 8 and 12 days at 37°C, 5% CO₂. The length of each metatarsal was measured at the time of isolation, as well as at the end of the 12 day culture period. At the end of the culture period, frozen sections were obtained to permit *in situ* hybridization analyses with digoxigenin-UTP labeled probes. Metatarsals cultured in 1.25mM phosphatic demonstrated a 120 \pm 6.66 % increase in length over 12 days. While the absence of supplemental phosphate impaired growth, as did 7mM added phosphate, there was still a significant increase in the length of the metatarsals cultured under these conditions over a 12 day period (90 \pm 10.18 % and 70 \pm 2.59 % increase respectively). *In situ* hybridization analyses did not reveal a significant change in the expression of Sox 5 or Sox 6, early markers of chondrocyte differentiation, among the three phosphate concentrations. However, analyses of later markers of chondrocyte differentiation, including Col II, Col X and osteopontin demonstrated an attenuation of chondrocyte differentiation in metatarsal elements cultured under hyper- or hypophosphatemic conditions, relative to that observed in those cultured under normophosphatemic conditions. While, von Kossa staining demonstrated significant mineralized matrix formation in the metatarsals cultured under control phosphate conditions, there was marked impairment in mineral deposition in the elements cultured without added phosphate and with 7mM phosphate. Thus, extracellular phosphate has a significant effect on the differentiation of chondrocytes in the metatarsal culture system. The effects of phosphate are biphasic: both high and low phosphate attenuate growth and impair chondrocyte differentiation. Studies are underway to determine the molecular basis for these effects.

Disclosures: A.A. Zalutskaya, None.

W105

The Role of Nkx3.2 in Muscle/Cartilage Cell Fate Determination. D. Cairns*, L. Zeng*. Anatomy and Cell Biology, Tufts University School of Medicine, Boston, MA, USA.

Significance. Bone and muscle are distinct tissues that are situated adjacent to each other in vertebrates. Failure to establish and maintain their identities may lead to serious genetic diseases such as fibrodysplasia ossificans progressiva (FAP), where a mutation in the BMP receptor causes the muscle tissue to be transformed into cartilage and bone. The mechanism of how BMP signaling leads to this transformation is not fully understood. Results. In the embryo, BMP pathway is crucial for inhibiting muscle cell fate and promotes cartilage cell fate determination. Nkx3.2 is a BMP-induced transcription factor that is expressed exclusively in cartilage progenitors and is absent in the muscle progenitors. Prior work has demonstrated that Nkx3.2 promotes Sox9 expression and chondrocyte differentiation and survival. Here we show that *in vivo* Nkx3.2 ectopic expression in the progenitors of the back muscle (via electroporation of the somite) prevents the expression of Pax3, Pax7 and terminal muscle marker myosin. In addition, virally-expressed Nkx3.2 prevents muscle marker expression in the chicken limb micromass culture. Furthermore, C2C12 cells that are transfected with Nkx3.2 fail to differentiate into myotubes upon serum deprivation. Conclusion. Our work demonstrates that BMP-induced factor Nkx3.2 plays a critical role in muscle/cartilage cell fate decision in the embryo.

Disclosures: L. Zeng, None.

This study received funding from: Arthritis National Research Foundation.

W106

Localization of the Cis-enhancer Element for Mouse Col10a1 Expression in Hypertrophic Chondrocytes *In Vivo*. Q. Zheng¹, B. Keller^{*1}, G. Zhou^{*2}, D. Napierala^{*1}, Y. Chen^{*1}, B. Zabel^{*3}, A. Parker^{*4}, B. Lee⁵. ¹Molecular and Human Genetics, Baylor College of Medicine, Houston, TX, USA, ²Orthopedics, Case Western Reserve University, Cleveland, OH, USA, ³Center of Pediatrics and Adolescence Medicine, University Hospital of Freiburg, D-79106, Germany, ⁴Respiratory and Inflammation Research Area, AstraZeneca, Cheshire, United Kingdom, ⁵Howard Hughes Medical Institute, Baylor College of Medicine, Houston, TX, USA.

We and others had previously shown that 4kb or 4.6kb Col10a1 promoter containing Runx2 or AP-1 (Activator Protein-1) elements contribute to its hypertrophic chondrocyte-specific expression *in vivo* (Zheng et al., 2003; Gebhard et al., 2004). These data suggest that the Col10a1 distal promoter (-4.4 to -3.8 kb) harbors a critical enhancer that mediates its tissue specificity. To further localize the tissue-specific enhancer element, we have generated series of transgenic reporter constructs containing 600, 300 or 150 bp of fragments derived from this region upstream of the Col10a1 basal promoter driving LacZ

gene. The results demonstrated that 150bp Col10a1 promoter element (-4.3 to -4.15 kb) is sufficient to direct its tissue-specific expression *in vivo*. *In silico* analysis of this region identified several transcription factor binding sites including two potential AP-1 sites within 5'- and 3'- end respectively. Interestingly, transgenic mice using reporter construct without the two putative AP-1 elements showed tissue-specific reporter activity. We have also performed EMSA studies and specific DNA/Protein complexes were observed when oligos derived from this region were incubated with the MCT cell nuclear extracts. *In vitro* transfection studies using reporter constructs derived from these oligos showed up-regulated reporter activity. These data together with previous observations suggest that there are transacting factors in addition to Runx2 or AP-1 that may bind the cis-elements within this Col10a1 distal promoter and mediate its tissue-specific expression *in vivo*.

Disclosures: Q. Zheng, None.

This study received funding from: NIH, Arthritis Foundation.

W107

The Diverge Effects of Noggin on BMP-2-induced Osteogenesis. T. Engstrand^{*1}, C. Aulin^{*2}, J. Hilborn^{*2}. ¹Department of Reconstructive Plastic Surgery, Karolinska Institute, Stockholm, Sweden, ²Department of Materials Chemistry, Uppsala University, Uppsala, Sweden.

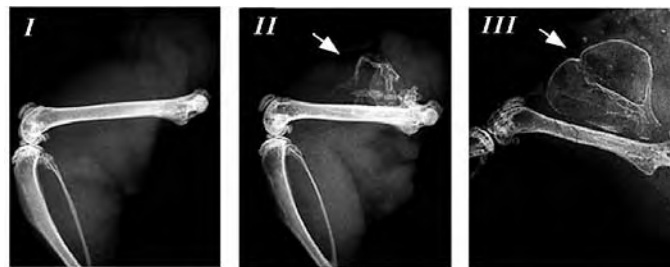
The purpose of the study was to evaluate the *in vitro*-effects of noggin on BMP-2 in mesenchymal cells and the *in vivo*-effects of transplanted mesenchymal cells co-expressing noggin and BMP-2.

The W20-17 murine mesenchymal celline was retrovirally infected with either BMP-2 cDNA or co-infected with BMP-2 and noggin cDNAs. The expression and production of BMP-2 and noggin was determined by mRNA dot blot and western blot, respectively. The *in vitro* effect was measured by alkaline phosphatase activity. Ectopic bone formation induced by transplanted BMP-2- or bmp-2/noggin- overexpressing cells was visualised by radiography and histology.

The amounts of secreted BMP-2 in culture medium was dramatically enhanced in BMP-2/noggin co-expressing cells as compared to cells expressing BMP-2 alone (control). The co-expressing cells induced a 5-fold increase in ALP activity as compared to the control *in vitro*. The enhanced effects in co-expressing cells was verified *in vivo* where transplanted BMP-2/noggin cells induced abundant bone formation. However, the enhanced osteoinductive effect of BMP-2/noggin co-expressing cells was found to be concentration-dependent since noggin exerted an inhibitory effect on BMP-2 when expressed at higher rate. Using added recombinant BMP-2 and noggin we demonstrate that noggin had a stabilizing effect on BMP-2 as determined by ALP-activity in long-term cell cultures.

Noggin exerts an inhibitory effect by direct binding to BMP-2. Unexpectedly, we have found that noggin enhances the secreted amounts of BMP-2 in osteoprogenitor cells co-expressing noggin and BMP-2. These cells also demonstrate an increased osteoinduction *in vitro* and *in vivo* as compared to cells expressing BMP-2 alone. The positive effects of noggin on BMP-2 osteoinduction was dependent on the relative concentrations of BMP-2 and noggin since higher noggin expression completely inhibited BMP-2 action. Our results suggest that noggin stabilizes BMP-2 and functions as a BMP-carrier. The mechanisms of the dissociation of BMP-2 from noggin still remain to be solved.

Figure legend: Transplanted noggin/BMP-2-overexpressing cells induced abundant bone formation when implanted ectopically in rats (III) as compared to cells expressing BMP-2 alone (II). Cells transduced with vector alone had no activity in this assay (I).



Disclosures: T. Engstrand, None.

This study received funding from: Vinnova/SSF.

W108

***In vitro* Characterization of Bidirectional Tet-inducible Expression Systems for Bone Tissue Engineering.** G. Feichtinger*, B. Klösch*, M. van Griensven*, H. Redl*. Austrian Cluster of Tissue Regeneration, Ludwig Boltzmann Institute for exp. and clin. Traumatology, Vienna, Austria.

Gene medicine approaches for osteoinduction could provide potent alternatives to current growth factor or stem-cell based approaches being cheaper and safer. The additional employment of inducible promoters could maximize safety of these approaches. Furthermore inducible systems that express more than 1 therapeutic gene can be useful regarding differentiation processes in which more than 1 gene is required to generate a sufficient impulse. Therefore, the aim of this study was to characterize a Tet-inducible system for bidirectional expression of hBMP2 and 7, hBMP4 and 7 or Runx2 and Osterix. The TetON-system (TRETight-BI) was modified to express the reverse tet-transactivator (rtTA) on the response vector making it a single vector system. This new system mediates inducible expression of 2 different genes of interest and constitutive expression of the rtTA in only 1 plasmid making it more convenient for practical use. *In vitro* characterization was

carried out in C2C12 cells transfected with the described TetON systems at different doxycycline (doxy) concentrations (0; 50-1000ng/ml). Osteogenic differentiation was detected by alkaline phosphatase, RT-PCR and von Kossa staining (day 10). Time and dose dependent kinetics were studied for 14 days using EYFP and dsRED. Reportergene expression levels were detected by fluorescence microscopy and RT-PCR compared to constitutive promoters (CMV, human ubiquitin C promoter).

Osteogenic differentiation was confirmed for all therapeutic expression systems. These new single vector systems did not exhibit lower expression capacity as the original double vector system. The maximal level of expression was comparable to constitutive promoters. No expression was detectable at 0ng/ml doxy. There was initial expression activation 12 hours after doxy application in a dose dependent manner decreasing within 14 days.

Our in vitro data strongly supports the potential of expression systems to induce differentiation in targeted cells. We conclude from our in vitro results that the constructed single vector, bidirectional inducible expression systems provide a promising alternative to currently employed growth factor therapies in bone tissue engineering. Furthermore expression of two therapeutic genes generates more potent responses compared to single gene approaches. The TRE element together with the rtTA is a reliable and stringent inducible expression system. The major concerns for future in vivo application of the described systems are efficient non-viral in vivo transfection methods and nephrotoxic features at certain doxy concentrations.

Disclosures: G. Feichtinger, None.

W109

Identification of Novel Factors Associated with Osteoblast Differentiation.

M. S. Friedman¹, W. Luo^{*2}, S. M. Oyserman^{*1}, H. Shitaye^{*3}, P. J. Woolf^{*2}, K. D. Hankenson¹. ¹Animal Biology, University of Pennsylvania, Philadelphia, PA, USA, ²Biomedical Engineering, University of Michigan, Ann Arbor, MI, USA, ³University of Michigan, Ann Arbor, MI, USA.

A variety of signaling molecules, transcription factors, and extracellular matrix (ECM) proteins are known to be involved in osteoblast differentiation. How these factors interact in human mesenchymal stem cells (hMSC) to yield functional osteoblasts is poorly understood. We hypothesized that by using high-throughput expression analysis of hMSC we could identify individual genes, gene expression patterns, and transcriptional networks associated with osteoblast differentiation and function. We examined how BMP treatment duration correlated with osterix and Dlx-5 expression. hMSC treated with BMP6 (20 nM) for one hour and cultured for 4 days without BMP6 show increased DLX5 and osterix expression (6 and 100 fold, respectively). However, only MSC treated with BMP for a minimum of 24 hours and cultured for 14 days without BMP, demonstrate terminal osteoblast differentiation and function (mineralization). Using this preliminary expression and function data, we designed a novel growth factor induction strategy coupled with microarray analysis. RNA was harvested following treatment, or cells were further cultured without BMP for 24h, 96h, or 10d and RNA harvested (13 Affymetrix U133+ microarrays). Genes were sorted into 20 clusters based on BMP treatment duration, gene expression levels, and gene expression patterns. The transcription factors DLX2, 3, 5, ID1, 3, and 4, and SMAD5, and 6 clustered together and were highly elevated with only 8 hours of BMP treatment and remained elevated for 10 days without additional BMP. However, expression of these genes did not correlate with osteoblast function (increased expression with increased BMP treatment). In contrast, expression of Osterix and the Notch associated transcription factors HEY1 and HEY2 correlated with osteoblast function. Osteopontin, BSP, aggrecan 1, syndecan 1, osteomodulin, and GPM6B, clustered with these transcription factors, showing expression patterns associated with osteoblast function. Results for select genes were validated by Q-PCR. To evaluate if genes in these clusters were involved in osteoblast function, we performed overexpression and loss of function studies. Importantly, antagonism of Notch signaling by gamma secretase inhibitors (L685,458) greatly inhibits BMP induced mineralization, suggesting a role for Notch signaling in BMP induced osteoblast differentiation. In contrast, neither osterix nor osteomodulin are sufficient for osteoblast induction. In conclusion, by using a novel functional microarray analysis, we identified novel factors that may be critical to osteoblast differentiation and function.

Disclosures: M.S. Friedman, None.

W110

Bone Morphogenetic Protein-4 and -6 Are Over-Expressed in the Multiple Myeloma Bone Marrow Samples.

D. Grcevic^{*1}, R. Kusec^{*2}, A. Luki^{*1}, I. K. Lukic³, N. Kovacic³, D. Nemet^{*4}, A. Marusic^{*3}. ¹Department of Physiology and Immunology, Zagreb University School of Medicine, Zagreb, Croatia, ²Department of Hematology, Clinical Hospital "Dubrava", Zagreb University School of Medicine, Zagreb, Croatia, ³Department of Anatomy, Zagreb University School of Medicine, Zagreb, Croatia, ⁴Department of Hematology, Clinical Hospital "Zagreb", Zagreb University School of Medicine, Zagreb, Croatia.

Multiple myeloma (MM) is a B-lymphocyte neoplasia characterized by the slow proliferation of plasma-cells in bone marrow (BM) and bone destruction. Although several bone morphogenetic proteins (BMP) have been shown to elicit apoptosis of myeloma cells in vitro, we proposed that BMPs may have other non-apoptotic and pro-survival effects. BM was obtained from MM patients (n = 25) and control subjects (n = 14) after the informed consent and approval of the Ethical Board. Selected BM MM samples were magnetically separated for CD138 positive cells. Primary MM samples and myeloma lines (NCI H-929 and Thiell) were cultured for 48 hours and treated by recombinant human

(rh)BMP-2 or -6 (500 ng/mL for both) with or without BMP inhibitor rhNoggin. cDNA was extracted from mononuclear BM cells or cell lines, amplified by quantitative PCR using TaqMan assays for BMPs, corresponding receptors and downstream regulatory molecules, and normalized to GPDH. For detection of apoptotic and dead cells, we used flow cytometric annexin V/propidium iodide staining. ELISA assays for p53, Bax and Bcl-2 were performed on cultured cell lysates.

Expression of BMP-4, -6 and Alk-2 was significantly higher in MM BM samples compared with control BM (around 10-fold for BMP-4, 35-fold for BMP-6, 2-fold for Alk-2), with significant positive correlation of BMP-6 expression and plasma-cell percentage in MM samples (p<0.01). Upon in vitro BMP-2 or -6 treatment, insignificant changes in the percentage of death/apoptotic cells were observed paralleled by down-regulation of pro-apoptotic Bax and p21 (up to 2-fold and 5-fold respectively), and up-regulation of inhibitors of differentiation ID-1 and -2 (up to 200-fold and 5-fold respectively). Changes induced by BMPs were blocked by the addition of Noggin. ELISA confirmed the involvement of p53 pathway and decrease in the expression of Bax. Selected CD138 positive myeloma cells showed relatively higher endogenous expression of BMPs/receptors compared with corresponding full BM samples and CD138 negative population, providing a basis for autocrine action.

We found that BMP-4 and -6 are over-expressed in MM BM samples and selected CD138 positive myeloma cells, indicating the role of BMPs as proliferative and survival autocrine factors in MM. Our study opened the possibility to further test clinical application of BMP inhibitors in MM treatment.

Disclosures: D. Grcevic, None.

W111

Similar Effects of Proteasome Inhibition on Osteoblast Differentiation and Anagen Induction.

G. E. Gutierrez¹, I. R. Garrett², W. Gallwitz^{*2}, G. Rossini^{*2}, C. Christiansen³, G. R. Mundy¹. ¹Bone Center and Dept of Medicine/Clinical Pharmacology, Vanderbilt University and Medical Center, Nashville, TN, USA, ²OsteoScreen, LTD, San Antonio, TX, USA, ³Center for Clinical and Basic Research, Ballerup, Denmark.

We have noticed that the mammalian bone remodeling process shares many features in common with the hair cycle. In both, there are phases of growth, resorption or regression, and rest. Moreover, the regulatory controls of both involve many of the same extracellular and intracellular factors. For example, both anagen (growth phase of the hair cycle) and the bone formation phase of the bone remodeling cycle are controlled by the BMP-2 ligand-signal transduction pathway and downstream molecules such as Wnt and beta-catenin. Therefore, we hypothesized that manipulation of specific molecules in this pathway should increase both bone formation and anagen induction. Accordingly, we examined the effects of compounds that stimulated transcription of the BMP-2 gene for their effects on osteoblasts and the hair follicle. We have shown that inhibitors of the proteasome stimulate osteoblast differentiation and bone formation via this mechanism. During studies to determine the effects of proteasome inhibition on bone growth in vivo, we injected proteasome inhibitors (PI) into the subcutaneous tissue over murine calvaria. There was increase in bone formation and marked morphologic changes in hair follicles, with an increase in size, in the inner and outer root sheath diameters and extension into the dermal adipose tissue, all characteristic features of the anagen phase of the hair cycle. All PI tested had similar effects, independent of their chemical structure. Other non-proteasome anti-proteolytic agents had no effect. To confirm that the PI were stimulating hair growth, we examined the effects of the PI PSI on hair on the right dorsal trunk after depilation. There was a rapid increase in hair growth in the treated mice. We next examined PI on hair follicles in explants of murine skin, assessed by changes in hair follicle diameter and hair elongation. rhBMP-2 (100ng/ml) increased follicle area in these cultures. We found that increase in follicle area stimulated by both PSI and epoxomicin was inhibited by noggin, indicating that these effects are BMP-dependent. We then determined the effects of proteasome inhibition on anagen induction in subjects with male pattern baldness. Topical administration of the proteasome inhibitor PSI led to a 40% increase in anagen induction in 8 subjects over a two week treatment period.

These results point to the similarities between the bone remodeling process and the cycling of the hair follicle and suggest both processes are responsive to proteasome inhibition and are dependent on the BMP-2 ligand-signal transduction pathway.

Disclosures: G.E. Gutierrez, Neosil I.

W112

Increased Expression of BMP Antagonists During Distraction Osteogenesis in a Mouse Model. T. Haque^{*1}, F. Hamadeh^{*1}, N. Alam^{*1}, M. Kotsioprifitis^{*2}, D. Lauzier^{*1}, R. St-Arnaud^{*1}, V. Rosen^{*3}, R. C. Hamdy¹.

¹Orthopaedics, Shriners Hospital for Children, Montreal, PQ, Canada, ²Orthopaedics, Montreal Childrens Hospital, Montreal, PQ, Canada, ³Oral and Developmental Biology, Harvard School of Dental Medicine, Boston, MA, USA.

Distraction osteogenesis (DO) is a widely used technique for limb lengthening and replacement of bone loss due to trauma, infection or malignancies. The procedure involves gradually applying controlled distraction of two bony segments post osteotomy resulting in the generation of new bone within the distracted gap. Although the technique is widely used, one of its limitations is the long period of time required for the newly formed bone to consolidate. It has previously been shown that the application of bone morphogenetic proteins (BMPs) can increase bone formation during DO, however, exogenous BMPs have many drawbacks. An alternative method for accelerating the rate of bone formation may be to modulate the intrinsic BMP signaling pathway. The aim of this study was to identify BMP antagonists involved in distraction osteogenesis in order to determine if targeting BMP antagonists can be used for increasing BMP signaling and hence the rate of bone consolidation during DO.

DO was applied to the right tibia of 60 adult wild type mice. The surgery involved applying a mini ilizarov fixator and performing an osteotomy in the centre of the tibia. Distraction began after a latency period of 5 days at a rate of 0.2mm/12hrs for 2 weeks. Mice were sacrificed in groups of 12 during the following times post surgery: day 5 (latency), days 11 and 17 (distraction) and days 34 and 51 (consolidation). Specimens were examined using x-rays, µCT, histology, real-time PCR and immunohistochemistry. The expression of the extracellular BMP inhibitors: BMP3, Noggin, Gremlin and Chordin; intracellular BMP inhibitors: Smad 6, 7, Smurf 1, 2; as well as the receptor level inhibitor: BAMBI was analyzed. In addition, the expression of the BMP ligands 2, 4, 6 and 7 and their receptors were also monitored.

Results revealed an increase in BMP 2, 4 and 6 during the distraction phase. Most interestingly, a significant increase in the expression of BMP3, noggin, chordin, BAMBI, Smad 7 and Smurf 1 were observed. Activin receptor expression was also upregulated in the distraction and consolidation phases. Altogether, our results suggests that regulation of BMP signaling through noggin as well as BMP3 and Activin receptors may be important in the distraction system.

The current study provides a clearer understanding of the genes involved in DO. According to the results, future studies should be targeted at blocking specific intrinsic BMP inhibitors as a means for accelerating the rate of bone formation during DO.

Disclosures: T. Haque, None.

W113

Regulation of Mouse BAMBI Gene Expression. T. Kondo, R. Kitazawa, K. Mori, S. Kitazawa. Division of Pathology, Kobe University Graduate School of Medicine, Kobe, Japan.

BMP and activin membrane-bound inhibitor (BAMBI) is a transmembrane glycoprotein structurally similar to the transforming growth factor (TGF)- β family type I receptor, except that it lacks an intracellular kinase domain. As a pseudoreceptor, BAMBI interacts with many of the type I and II TGF- β receptors and functions as a negative regulator of TGF- β signaling. To elucidate the role of BAMBI during skeletogenesis and osteoblastic differentiation, we first immunohistochemically analyzed the localization of mouse BAMBI expression in mouse bone tissue. BAMBI expression was seen in some of periosteal osteoblasts, in chondrocytes in articular cartilage and in hypertrophic chondrocytes in the growth plate. Most of the osteocytes embedded in trabecular bone were, however, negative for BAMBI. In vitro studies revealed that BAMBI mRNA expression increased 95-fold in recombinant human bone morphogenetic protein 2 (rhBMP-2)-treated C2C12 myoblastic cells induced into the osteoblastic lineage. Furthermore, BAMBI knockdown by siRNA increased alkaline phosphatase and Runx2 expression in ST2, suggesting that BAMBI expression plays an important role as part of the negative feedback loop system in TGF- β /BMP signaling during osteoblastic differentiation. Additionally, transient transfection studies with the use of the mouse BAMBI promoter reporter construct showed that BAMBI promoter activity in ST2 increased 1.8-fold by TGF- β treatment, 1.2-fold by rhBMP-2 treatment, and 1.9-fold by treatment with lithium chloride, an agonist of the β -catenin signaling pathway. Since both BMP responsive elements and TCF-1 binding sites are conserved in mouse and human BAMBI promoters, BAMBI gene expression is regulated by both TGF- β /BMP and Wnt/ β -catenin signaling pathways. We then assessed the methylation status of the BAMBI promoter region by Southern blot analysis and found tissue-specific distribution of promoter hypermethylation. Sodium bisulfite mapping, however, revealed no CpG locus methylation around the transcription start site in primary cultured osteoblasts or osteocytes. We therefore speculate that the epigenetic regulation of BAMBI gene expression by CpG hypermethylation is physiologically involved in tissue- and development-specific BAMBI expression, and that decreased BAMBI expression in terminally-differentiated osteocytes is due not to epigenetic gene silencing but passively to decreased β -catenin and/or BMP signaling in osteocytes. Thus, BAMBI is a target gene of both BMP and Wnt/ β -catenin signaling and may be involved in preventing some of the osteoblast precursors and chondrocytes from terminal differentiation.

Disclosures: T. Kondo, None.

W114

Type III TGF β Receptor Regulates BMP Signaling in Differentiating Osteoblasts In Vitro and In Vivo. M. Ni^{*1}, G. R. Mundy², R. L. Caldwell³.

¹Department of Pharmacology, Vanderbilt University School of Medicine, Nashville, TN, USA, ²Department of Medicine/Clinical Pharmacology, Vanderbilt University School of Medicine, Nashville, TN, USA, ³Department of Orthopaedics and Rehabilitation, Vanderbilt University School of Medicine, Nashville, TN, USA.

Several cell surface receptors for TGF- β are now well established. Type I and II receptors (TRI and TRII) express intracellular kinase domains responsible for receptor activation and signaling. The type III TGF- β receptor (TRIII) is an 849-amino acid transmembrane proteoglycan that exists as a co-receptor for TGF- β , yet maintains biological functions distinct from TRI and TRII. TRII has a short, highly conserved 43-amino acid cytoplasmic domain (CD). TRII regulates TGF- β signaling by recruiting TGF- β ligand to TRII, driving endocytosis of the signaling complex, and guiding regiospecificity of cellular differentiation. BMPs are necessary for osteogenesis from early embryonic tissue patterning to postnatal skeletal development. BMPs promote bone development by stimulating proliferation and differentiation of osteoblasts, and recent work has suggested that non-union of bone may be the result of decreased levels of BMP activity. Due to signaling homology shared between TGF- β and BMP, we hypothesized that BMP-induced bone formation is regulated by TRII from early embryogenesis through development of mature skeleton, and that the TRII CD is central to these functions. Our hypothesis was tested by phenotypic analysis of TRII knockout mice, immunohistochemical (IHC) localization of TRII in developing and mature bone, and transfection assays using 2T3 osteoblasts. We observed TRII null mice exhibit a shorter skeletal phenotype (<10%) than WT mice. IHC analysis of femoral bone from WT 2-month old mice revealed enhanced TRII expression in bone marrow as well as the growth plate, while IHC analyses for TRII in adult mice reveal little TRII expression in mature bone. In committed bone cells, TRII attenuates BMP signaling. We found that forced TRII expression down-regulates SMAD 1, 5 and 8 phosphorylation after BMP2 stimulation, and deletion of the TRII CD further decreases SMAD phosphorylation. Bone cells demonstrate decreased alk phos activity upon TRII forced expression. TRII up-regulates SMAD6 after BMP2 stimulation, and represses BMPRII promoter activity via the TRII CD. We conclude that TRII plays a dual role in regulating BMP signaling throughout bone development. Furthering our understanding of TRII in bone biology will give insights into the control of normal bone formation and provide better understanding of disorders of bone formation.

Disclosures: M. Ni, None.

This study received funding from: Developmental Funds from the Dept. of Orthopaedics and Rehabilitation and the Vanderbilt University Tumor Microenvironment Network.

W115

Protein Related to DAN and Cerberus (PRDC) Is Expressed in Skeletogenesis and Prevents Osteoblastic Differentiation. A. Nifuji¹, H. Ideno^{*2}, R. Takanabe^{*2}, A. Shimada^{*1}, R. Araki^{*2}, M. Abe^{*2}.

¹Department of Pharmacology, Tsurumi University of Dental Medicine, Yokohama, Japan, ²National Institute of Radiological Sciences, Chiba, Japan.

Protein related to DAN and cerberus (PRDC) is a secreted protein with a cysteine knot structure that binds bone morphogenetic proteins (BMPs) and inhibits BMP actions. In this study we investigated PRDC expression and regulation in skeletogenesis and examined if PRDC functions during skeletal cell differentiation. First we examined mRNA expression of PRDC by real-time PCR using RNA extracted from primary calvaria derived osteoblastic (pOB) cells and MC3T3-E1 (MC) cells. We observed constitutive expression of PRDC mRNA in those osteoblastic cells. By in situ hybridization analysis for embryonic day 18 calvaria in mice, we found that PRDC mRNA was localized in calvarial osteoblast-like cells adjacent to osteopontin and osteocalcin expressing cells. In both of pOB cells and MC cells, PRDC mRNA expression level is significantly elevated in treatment with recombinant BMP2. Next to investigate PRDC functions, we constructed an adenovirus expressing PRDC. We infected PRDC expressing adenoviruses into pOB, MC and C1 mesodermal stem (C1) cells and analyzed their effects on those cells. PRDC infection did not alter cell numbers when compared with cells infected with LacZ expressing control adenoviruses in pOB cells. Expression of mRNAs for osteoblastic markers, alkaline phosphatase and osteocalcin, as well as a BMP target gene, Id1, were suppressed in pOB, MC and C1 cells infected with PRDC expressing adenoviruses. Furthermore, forced expression of PRDC inhibited alkaline phosphatase activity and mineralized nodule formation during pOB cell differentiation. Finally, we blocked PRDC expression by using siRNA against PRDC mRNA. We found that transfection of siRNA against PRDC mRNA resulted in elevation of alkaline phosphatase activity when compared with control siRNA. These results suggest that PRDC is expressed in skeletogenesis and prevents osteoblastic differentiation possibly through inhibition of BMP action.

Disclosures: A. Nifuji, None.

This study received funding from: JSPS.

W116

Membrane Domain Dynamics During Osteoblast Differentiation. K. Young^{*1}, B. Bragdon^{*1}, L. G. Horton^{*2}, W. G. Beamer², A. Nohe¹. ¹Chemical and Biological Engineering, University of Maine, Orono, ME, USA, ²The Jackson Laboratory, Bar Harbor, ME, USA.

Bone Morphogenetic Proteins (BMPs) belong to a subgroup of the TGF-beta superfamily of receptor ligands. BMP levels influence multipotent mesenchymal cells to differentiate into chondrocytes, osteoblasts, myocytes, and adipocytes. They are crucial during skeletal development and homeostasis, affecting osteoblast and osteoclast differentiation. Defects in BMP signaling are linked to several bone diseases. The bone marrow of osteoporotic patients show high levels of adipocytes suggesting the differentiation of bone marrow stromal cells (BMSCs) markedly favors adipocytes. The initiation of the BMP signaling involves binding of the cognate ligand to a combination of BMP receptors (BMPR) on the plasma membrane. Using the Family of Image Correlation Spectroscopy (FICS) methodology combined with molecular biological approaches current research indicates that not only do BMP type-I (BRIa) and type-II (BRII) receptors aggregate and cluster in specific domains on the cell surface, but that these receptors must shuttle between distinct membrane rafts in order to transduce their signals. Interdomain shuttling influences BMP signaling and regulates the early steps of osteoblast differentiation. Using a cell culture model our data further suggest that the aggregation status of BMP receptors with membrane domains was crucial in prevention of heterotopic ossification. Additionally, using these techniques we showed that membrane domain organization was disturbed in mice displaying an osteoporotic phenotype. These results point to the importance of membrane domains in regulating osteogenesis. Moreover, we identified casein kinase-2 (CK2) as a key protein that mediates osteoblast differentiation. Utilizing FICS and Fluorescence Energy Transfer methods, our data showed that CK2 was not only involved in the regulation of receptor re-shuttling and signal silencing on the cell surface but also in osteoblast differentiation. In detail peptides derived against the CK2 binding domains of BRIa led to enhanced mineralization of bone marrow stromal cells (BMSCs). These data indicated that membrane and receptor dynamics are crucial during osteoblast differentiation and that CK2 was a key player in regulating these dynamics.

Disclosures: A. Nohe, None.

W117

Smad1 and Smad4 Differentially Regulate Osteoblast Differentiation and Myogenesis in Myoblasts. J. Nojima¹, T. Fukuda¹, K. Kanomata^{*1}, T. Yoda^{*2}, T. Katagiri¹. ¹Division of Pathophysiology, Saitama Medical University, Research Center for Genomic Medicine, Hidaka-shi, Saitama, Japan, ²Oral and Maxillofacial Surgery, Saitama Medical University, Moroyama, Saitama, Japan.

BMPs inhibit terminal differentiation of myoblasts and convert them into osteoblast lineage cells. Fibrodysplasia ossificans progressiva (FOP) is a genetic disorder of skeletal malformation and undergoing ectopic bone formation in muscle. Recently, a mutation of BMP type I receptor was identified in FOP patients, suggesting that BMP signaling is involved in both pathological and physiological bone formation. In the present study, we examined a role of Smad pathway, how to inhibit myogenesis prior to induce bone formation. We previously reported a constitutively activated form of Smad1 (caSmad1), which induced osteoblast differentiation in C2C12 myoblasts even in the absence of BMPs. Co-expression of Smad4, a partner of Smad1, synergistically enhanced the osteoblast differentiation induced by caSmad1, although Smad4 alone failed to induce any markers of osteoblast differentiation. Over-expression of Smad1 and Smad4 suppressed myogenic differentiation induced by MyoD. To examine roles of translocation of Smad proteins from cytoplasm to nucleus on osteoblast differentiation and myogenesis, we further generated NLS-Smad1 and NLS-Smad4, in which a nuclear localization signal derived from SV40 was fused to each Smad. NLS-Smad1 neither induced osteoblast differentiation nor inhibited myogenesis. In contrast, targeted expression of NLS-Smad4 markedly suppressed myogenesis, but it did not induce osteoblast differentiation. Deletion of MH1 or MH2 from NLS-Smad4 destroyed the inhibitory activity on myogenesis. Taken together, these results clearly indicate that both the induction of osteoblast differentiation and the inhibition of myogenesis are dependent on Smad proteins. A complex formation between Smad1 and Smad4 seems to be essential for the transactivation of downstream targets required for the osteoblast differentiation. In contrast, translocation of Smad4 to nuclei, even in the absence of Smad1, was the critical event for suppression of myogenesis. It was suggested that Smad4 moved into nuclei as a part of the Smad complex inhibits myogenesis, then it induces osteoblast differentiation cooperate with Smad1.

Disclosures: J. Nojima, None.

W118

Endogenous Cyclic Adenosine 3', 5'-Monophosphate Response Element-Binding Protein (CREB) Signaling Enhances Smad-Mediated Bone Morphogenetic Protein (BMP) Signaling. Y. Ohta^{*1}, K. Nakagawa¹, Y. Imai¹, T. Katagiri², T. Koike¹, K. Takaoka¹. ¹Department of Orthopaedic Surgery, Osaka City University Graduate School of Medicine, Osaka City, Japan, ²Division of Pathophysiology, Research Center for Genomic Medicine, Saitama Medical School, Saitama, Japan.

It has been reported that increase in intracellular cyclic adenosine 3',5'-monophosphate (cAMP) accumulation by pentoxifylline, a nonspecific inhibitor of phosphodiesterase and rolipram, a phosphodiesterase-4 specific inhibitor and prostaglandin E2 EP4 receptor selective agonist can enhance BMP-induced osteoblastic differentiation of mesenchymal cells both in vivo and in vitro. However, the mechanism by which cAMP enhances BMP-induced osteoblastic differentiation remains unclear in detail. To further clarify the mechanism of enhancement of BMP signaling by cAMP, we examined the BMP signaling pathway at the transcriptional level in C2C12, muscle-derived mesenchymal cells expressing BMPR1 and BMPR2.

In the present study, we examined the relationship between cAMP and BMP signaling at the transcriptional level, using the promoter of the Id1 gene, an early response gene to BMPs which includes both BMP responsive element (BRE) and cAMP response element (CRE), and performed luciferase activity assay. In the cells transfected with wild-type Id1 promoter, treatment with BMP-4 increased relative luciferase activity (RLA), which was further enhanced by the addition of dibutyryl cAMP (dbcAMP), a cell membrane-permeable analogue of cAMP. Interestingly, RLA levels which were increased by treatment with both BMP-4 and dbcAMP or BMP-4 alone were decreased when the CRE site was inactivated (with wild-type BRE present). We also examined the effects of down-regulation of endogenous CREB on the transcriptional activity mediated by Smads using an Id1 promoter construct. Cells were transfected with CREB RNAi and wild-type Id1 promoter construct and treated with or without BMP-4 or dbcAMP. Inhibition of BMP signaling was observed when endogenous CREB was knocked down using RNAi technology. Similar findings were obtained when cells were co-transfected with reporter plasmid containing the wild-type Id1 promoter and A-CREB, a dominant-negative inhibitor of CREB plasmid.

In this study, we showed that cAMP/CREB signaling enhances the BMP-induced transcriptional activity of the BRE in the Id1 gene promoter by activating the CRE close to the BRE in this promoter. We also confirmed that endogenous CREB/CRE signaling plays an important role in Smad-mediated BMP signaling.

Disclosures: Y. Ohta, None.

W119

Bone Metabolism After Posterolateral Lumbar Fusion Using Osteogenic Protein-1. K. Shigenobu^{*}, T. Hashimoto^{*}, M. Kanayama^{*}, F. Oha^{*}. Orthop. Surgery, Hakodate Central General Hosp., Hakodate, Hokkaido, Japan.

INTRODUCTION: Bone morphogenetic proteins are being used clinically for spinal fusion. Numerous pre-clinical investigations have demonstrated efficacy of osteoinductive proteins in spinal fusion, but the metabolism of the BMP induced fusion process has not been well studied in human clinical setting. This study compares the expression of bone metabolic makers following posterolateral lumbar fusion using Osteogenic Protein-1 (rhBMP-7) to fusion with HA / TCP granules and local autograft. **METHODS:** Nineteen patients with symptomatic degenerative spondylolisthesis underwent a single-level (L3-4 or L4-5) posterolateral fusion using pedicular screw fixation. The patients were randomly divided into two groups: 10 cases with HA/TCP granules and local autograft (HA/TCP group), and 9 cases with OP-1 putty [3.5mg OP-1/g collagen matrix] (OP-1 group&). The mean age was 59 years in the HA/TCP group, and 70 years in the OP-1 group. Two bone formation markers were measured; serum bone-specific alkaline phosphatase (BAP) and type I pro-collagen C-terminal propeptide (PICP). Three bone resorption markers were measured; serum type I collagen C-terminal telopeptide, urinary deoxypyridinoline and cross-linked N-telopeptides of type I collagen. Samples were obtained preoperatively and 1 day, 1, 2, 4, 12, and 24 weeks postoperatively. **RESULTS:** The bone resorption marker levels peaked at 4 weeks and decreased to preoperative levels by 24 weeks. There were no significant differences between the study groups. The bone formation marker levels exhibited a different pattern in each study group. BAP rapidly increased over 2 weeks in both groups; however, the level peaked earlier in the OP-1 group. PICP gradually increased after surgery in both groups, however it elevated earlier in OP-1 group. **DISCUSSION:** PICP increases in the early stages of osteogenesis influencing the synthesis of collagen fibrils. BAP is a specific marker for the function of osteoblasts. Both of these markers were elevated earlier in OP-1 group despite the older patient population. These results suggest that OP-1 has the potential to enhance earlier bone formation in posterolateral fusions.

Disclosures: K. Shigenobu, None.

W120

Assessing BMP-2 Activated Osteoblast Differentiation with Nanopatterned Surfaces. K. H. Szymczyk*, J. P. Spatz*, E. A. Cavalcanti-Adam. Biophysical Chemistry, University of Heidelberg, Heidelberg, Germany.

Bone morphogenetic proteins (BMPs), found in bone extracellular space in soluble and bound form, are necessary for osteogenesis during embryonic development, and in post-natal mammals for bone growth, remodeling, and repair. Elucidating the structural and molecular mechanisms behind BMP signaling will augment current knowledge of bone formation and contribute to advancements in skeletal defect repair. One new approach to assessing ligand clustering and signaling is by the use of nanopatterned-surfaces presenting a regular, repeating pattern of proteins. Consequently, the local density of these molecules can be varied and the ligand/receptor activation can be evaluated. Thus, the purpose of this study was 1) to create a surface with nanopatterned BMP-2 and 2) to characterize the effects of nanoscale variations in spacing and density of BMP-2 ligands on osteoblast cell adhesion and differentiation.

We used a well-established method of nanopatterning to create a BMP-2 coated glass surface. Surfaces were decorated with various nanospaced gold-dots (100nm), and a homogeneously gold-coated surface was used as a control. Scanning electron microscopy confirmed that the surfaces were composed of a regular repeating pattern. BMP-2 protein was deposited onto the surface in anticipation that the terminal cysteine residue covalently linked to the gold-dots. Characterization of the homogenous surface was performed by immunohistochemical and X-ray photoelectron spectroscopy (XPS) analysis. These methods indicated that BMP-2 was deposited on to the surface.

To study cell behavior and differentiation, C2C12 cells were plated on the homogenous surfaces and allowed to adhere overnight. Proliferation and viability was then determined using the MTS assay. Viability was not compromised on the BMP-2 functionalized surface however, proliferation was decreased. Cell adhesion behavior was assessed using phase contrast time-lapse microscopy. These results indicated that cell motility was reduced on the BMP-2 coated nanosurface in comparison to tissue culture plastic. Differentiation was evaluated by measuring alkaline phosphatase enzyme activity after 21 days. C2C12 cells grown on the BMP-2 surface had increased AP expression.

Well-defined nanopatterns of peptides are a unique tool to investigate the relevant ligand densities necessary in cell differentiation, with a resolution as small as single proteins. On going investigations will determine whether osteoblasts can distinguish between different surface densities of BMP-2 proteins and respond with altered attachment, spreading, migration, and differentiation.

Disclosures: K.H. Szymczyk, None.

This study received funding from: Alexander von Humboldt Foundation.

W121

Noggin Short Interfering RNA Gene Transfer Enhances the In Vivo Ectopic Bone Formation Induced by Bone Morphogenetic Protein-2. K. Takayama*, A. Suzuki*, T. Manaka*, S. Taguchi*, Y. Hashimoto, K. Takaoka. Department of Orthopaedic Surgery, Osaka City University Graduate School of Medicine, Osaka, Japan.

Noggin is one of major extracellular antagonists of bone morphogenetic proteins (BMPs). It is reported that noggin is upregulated in undifferentiated mesenchymal cells and myoblasts in response to BMPs, and this may cause diminish the performance of BMPs in bone formation. In this study, we investigated the effect of noggin silencing by short interfering RNA in osteogenic differentiation in vitro, and the ectopic bone formation in vivo.

Noggin expression induced by BMP-4 in C2C12 cells, a myoblastic cell line, was confirmed by real-time RT-PCR. Noggin mRNA expression was elevated by BMP-4 stimulation in dose- and time- dependent manner. We designed six double-stranded short interfering RNAs (siRNAs) for targeting noggin. Plasmid vectors expressing noggin and siRNAs were co-transfected into C2C12 cells, and successful specific suppression of noggin protein expression was confirmed in one of six siRNAs by Western blot. Transfection of the noggin siRNA into C2C12 cell also suppressed the endogenous noggin mRNA expression induced by BMP-4, and enhanced BMP-4 induced alkaline phosphatase activity up to two fold.

In vivo effect of noggin siRNA gene transfer on rhBMP-2 induced bone formation was examined by ectopic bone formation assay in mice. Noggin siRNA plasmid (10 µg) was injected into the dorsal muscle and electroporation procedures was applied to the left paravertebral muscle, and then collagen sponge disk (6mm diameter) containing 5 µg of rhBMP-2 was implanted into the muscle. On days 4 after surgery, total RNA was extracted from muscle tissue around the collagen disk for real time RT-PCR analysis. Electroporation-mediated transfer of noggin siRNA markedly decreased expression of noggin mRNA, which increased after implantation of the collagen disk containing rhBMP-2. At 3 weeks after surgery, the implants were harvested and radiographed with a soft X-ray apparatus, and bone mineral content (BMC) of each ossicle was measured by dual-energy X-ray absorptiometry. The size of new bone induced by rhBMP-2 and the mean BMC were significantly increased by noggin siRNA gene transfer.

Conclusively, these findings suggest that noggin siRNA gene transfer enhances the osteoblast differentiation induced by BMP-4 in vitro and the bone formation induced by BMP-2 in vivo. While further study is needed, this approach may be useful tool in clinical application.

Disclosures: K. Takayama, None.

W122

Gremlin Induces Mitogen Activated Protein (MAP) Kinase Signaling in Osteoblasts. S. Zanotti, A. Smerdel-Ramoya, E. Canalis. Research, Saint Francis Hospital and Medical Center, Hartford, CT, USA.

Gremlin, the product of gremlin, is a 20 kDa secreted glycoprotein that binds bone morphogenetic proteins (BMPs) -2, -4 and -7, and antagonizes BMP actions. Gremlin plays a central role in limb bud patterning and development, and in skeletal homeostasis. Targeted over expression of gremlin in the bone environment in mice leads to osteopenia and the in-vivo conditional deletion of gremlin in bone tissue causes an increase in bone formation and trabecular bone volume. Furthermore, down regulation of gremlin expression by RNA interference (RNAi) sensitizes osteoblasts to BMP signaling and activity. These observations suggest that the skeletal effects of gremlin can be explained by its ability to bind and oppose BMP activity. However, activities independent of BMP binding have been postulated. To determine whether gremlin has direct effects in osteoblasts, we examined its ability to induce signaling through Smad2/3 (Smad) or MAP kinase activity in ST-2 stromal cells and calvarial mouse osteoblasts. Gremlin did not stimulate Smad signaling, and suppressed the BMP-2 induced Smad 1/5/8 phosphorylation. In contrast, gremlin as well as BMP-2 induced extracellular regulated kinase (ERK) -1/-2 phosphorylation. To determine whether the effects of gremlin and BMP on ERK 1/2 phosphorylation were interdependent, we tested the effects of gremlin in the presence of the BMP antagonist noggin in excess and the effects of BMP-2 under conditions of gremlin down regulation by RNAi. Noggin prevented the effect of gremlin on ERK signaling indicating that endogenous BMPs were required for the gremlin effect. Down regulation of gremlin decreased the effect of BMP-2 on ERK phosphorylation, confirming that gremlin is necessary for this BMP activity. These results indicate that BMP and gremlin effects on ERK phosphorylation are interdependent. To determine whether ERK activation is used as a mechanism to modulate BMP effects on Smad signaling, the effect of the ERK inhibitor U0126 was tested. Inhibition of ERK caused an increase in BMP-2/Smad signaling in the absence and presence of gremlin. In conclusion, gremlin and BMP-2 have interdependent activities to enhance ERK signaling, possibly by conformational changes that favor specific BMP receptor interactions. ERK activation may be a mechanism to temper BMP/Smad signaling and activity.

Disclosures: S. Zanotti, None.

W123

Treatment of XLH with Calcitriol and Phosphate Increases FGF23 Concentration. E. A. Imel¹, L. A. DiMeglio¹, S. L. Hui^{1*}, T. O. Carpenter^{2*}, M. J. Econs¹. ¹Indiana University School of Medicine, Indianapolis, IN, USA, ²Yale University, New Haven, CT, USA.

X-Linked hypophosphatemic rickets (XLH), due to mutations in PHEX, causes rickets and osteomalacia due to renal phosphate wasting, with inappropriately low or normal 1,25-dihydroxyvitamin D concentrations. The PHEX mutation results in increased expression of fibroblast growth factor 23 (FGF23) in bone cells, and elevated circulating FGF23 concentrations are reported. XLH is treated with high dose phosphate and calcitriol, both of which could further increase FGF23 concentrations.

We measured FGF23 concentrations in 8 subjects, age 2 to 30 years, using an ELISA that detects only full-length FGF23. FGF23 concentrations were determined before treatment and following initiation of treatment with phosphate and calcitriol. Pretreatment, 1-3 samples were obtained. Post-treatment, 1-5 samples were obtained over 0.5 to 3.5 years.

Because doses of phosphate and calcitriol were generally changed together, there was high correlation between treatment doses with these two agents. All pretreatment FGF23 concentrations were elevated (compared to a normal control range of <71pg/ml). Average pretreatment FGF23 ranged from 127 to 1353 pg/ml (mean 349 ± 408 pg/ml). During the course of therapy, post-treatment FGF23 concentrations ranged from 136 to 3270 pg/ml (mean 807 ± 839 pg/ml). Most subjects had an increase in FGF23 concentrations after treatment, but the degree of elevation varied in extent and timing. FGF23 increased > 20% in 5/8 and >100% in 3/8 subjects during treatment. FGF23 did not decrease in any subject with treatment. FGF23 concentrations correlated with both phosphate (p = 0.03) and calcitriol doses (p = 0.004). When controlling for combined treatment, calcitriol dose remained a significant predictor of FGF23 concentrations (p = 0.01), while phosphate dose was no longer significant.

Although our sample size was small, treatment of XLH with phosphate and calcitriol was associated with concurrent increase in FGF23 concentrations. This effect is more strongly associated with the calcitriol dose. Previous studies indicated that current therapy improves the bone disease. However, increasing FGF23 concentrations may make the disease more difficult to manage, or contribute to complications of therapy and is an undesirable consequence. Although more study is needed, it may be preferable to adjust therapy to minimize the effect on FGF23 concentrations.

	FGF23 concentrations			
	Average pretreatment FGF23 (pg/ml)	FGF23 concentration at highest calcitriol dose for each subject	Calcitriol dose (ng/kg/day)	Phosphate dose (mg/kg/day)
Case A	145	229	14	7
Case B	219	235	16	24
Case C	224	226	17	25
Case D	225	1136	22	14
Case E	223	271	29	28
Case F	277	1826	30	22
Case G	127	136	31	27
Case H	1353	3270	31	31

Disclosures: E.A. Imel, None.

W124

Regulatory Mechanism of Production and Circulatory Level of FGF23 in Human. N. Ito*, S. Fukumoto, H. Suzuki*, T. Fujita*. Division of Nephrology & Endocrinology, Department of Medicine, University of Tokyo Hospital, Tokyo, Japan.

FGF23 has been identified as a phosphaturic factor which plays important roles in the development of hypophosphatemic rickets/osteomalacia. Because FGF23-null mice show hyperphosphatemia and high 1,25-dihydroxyvitamin D [$1,25(\text{OH})_2\text{D}$] levels, and deficient action of FGF23 results in familial hyperphosphatemic tumoral calcinosis, FGF23 seems to be a physiological regulator of serum phosphate and $1,25(\text{OH})_2\text{D}$. Previous studies indicated that high phosphate diet increases and phosphate restriction decreases FGF23 levels both in human and rodents. It has been also shown that $1,25(\text{OH})_2\text{D}_3$ increases FGF23 level and enhances promoter activity of FGF23 gene in rodents. However, it remains largely unknown how circulatory FGF23 level and production of FGF23 are controlled in human. Especially, it has not been shown whether phosphate directly regulate production and serum level of FGF23. Therefore, we first examined whether acute changes of serum phosphate modify FGF23 levels in vivo. Serum phosphate levels were modulated by infusion of dibasic potassium phosphate or ingestion of partially hydrolyzed starch in 4 volunteers. While serum phosphate significantly increased by phosphate infusion and conversely decreased by ingestion of carbohydrate, these maneuvers did not change serum FGF23 levels within 6 hours. These results indicate that acute changes of serum phosphate do not modify FGF23 secretion in human. We then investigated whether phosphate regulates FGF23 production in vitro by reporter assay with human FGF23 gene in osteoblast-like HOS-TE85 cells. We have cloned promoter region of human FGF23 gene with various length. Relative luciferase activity of -3990 bp promoter was 5.7 times, and -1826 bp promoter was 13.8 times higher than that of pGL3 basic. Shorter promoters (-1384 bp to -446 bp) showed lower activities. Changes of phosphate concentrations in culture media did not affect either promoter activity of FGF23 gene. These results suggest that phosphate does not directly modify expression of human FGF23 gene although it is also possible that HOS-TE85 cells do not have a mechanism to sense extracellular phosphate level. Together with the in vivo study, our results suggest that the regulation of FGF23 by phosphate in vivo is indirect and some other factor(s) is necessary for changing production and serum level of FGF23 in human.

Disclosures: N. Ito, None.

W125

FGF23 Is an Independent Predictor of BMD in a Population-based Cohort of Elderly Men: MrOS Sweden. R. Marsell*, E. Grundberg*, T. Krajsnik*, H. Mallmin*, M. Karlsson*, D. Mellstrom*, E. Orwall*, C. Ohlsson*, K. B. Jonsson*, O. Ljunggren*, T. E. Larsson*. ¹Department of Surgical Sciences, Uppsala University Hospital, Uppsala, Sweden, ²Department of Medical Sciences, Uppsala University Hospital, Uppsala, Sweden, ³Uppsala University Hospital, Uppsala, Sweden, ⁴Department of Surgical Sciences, Malmö University Hospital, Malmö, Sweden, ⁵Sahlgrenska University Hospital, Gothenburg, Sweden, ⁶Oregon Health and Science University, Portland, OR, USA, ⁷Department of Medical Sciences, Uppsala University Hospital, Uppsala, Sweden.

Fibroblast Growth Factor-23 (FGF23) is a circulating factor that regulates serum levels of phosphate (Pi) and $1,25(\text{OH})_2\text{D}_3$. Increased FGF23 levels are central in the pathogenesis of several hypophosphatemic disorders with rickets/osteomalacia, such as ADHR, XLH and TIO. Since both Fgf23 null mice and FGF23 transgenic mice harbor skeletal phenotypes, the objective of the current study was to investigate the association between intact serum FGF23 and BMD. We used a population-based epidemiological prospective study; the Swedish MrOS Study in Uppsala. In total, 1000 men aged 70-80 years were randomly selected from population registries. BMD was measured with dual x-ray absorptiometry (DXA) at the femoral neck, total hip, lumbar spine and total body. In addition, serum levels of intact FGF23, Pi, calcium, albumin, PTH, $25(\text{OH})_2\text{D}_3$ and glomerular filtration rate (GFR, calculated from cystatin C), were analyzed. Mean FGF23 levels were 44.1 ± 54.1 pg/mL; femoral neck BMD 0.919 ± 0.138 g/cm²; total hip BMD 0.998 ± 0.152 g/cm²; lumbar spine BMD 1.231 ± 0.219 g/cm²; total body BMD 1.194 ± 0.109 g/cm². Univariate linear regression analysis revealed that FGF23 positively correlated to BMD in femoral neck ($r=0.080$, $p=0.018$), total hip ($r=0.082$, $p=0.015$), lumbar spine ($r=0.080$, $p=0.016$) and total body ($r=0.096$, $p=0.004$). In parallel, multi-regression analysis including FGF23, PTH, GFR, calcium, Pi, $25(\text{OH})_2\text{D}_3$, age and weight as independent variables, revealed that FGF23 and PTH were the only significant explanatory variables for femoral neck (FGF23: $\beta=0.104$, $p=0.004$; PTH: $\beta=-0.073$, $p=0.042$) and total hip BMD (FGF23: $\beta=0.117$, $p=0.001$; PTH: $\beta=-0.081$, $p=0.023$). In addition, FGF23 and calcium were independently associated with lumbar spine BMD (FGF23: $\beta=0.089$, $p=0.013$; Calcium: $\beta=-0.074$, $p=0.045$) as well as total body BMD, where age also showed an independent association (FGF23: $\beta=0.121$, $p<0.001$; Calcium: $\beta=-0.071$, $p=0.049$; age: $\beta=-0.074$, $p=0.035$).

In conclusion, our study indicates that FGF23 is an independent and positive predictor of BMD in elderly men, further supporting an important role of FGF23 in bone and mineral metabolism.

Disclosures: R. Marsell, None.

W126

Possible Direct Regulatory Role of Active Vitamin D Increased by Ultraviolet B on Fibroblast-growth factor 23 in Healthy Adults. Y. Rhee¹, J. Lee², H. Choi¹, S. Kim¹, K. Lee², Y. Park², S. Lim¹. ¹Internal Medicine, College of Medicine, Yonsei Univ., Seoul, Republic of Korea, ²Dermatology, College of Medicine, Yonsei Univ., Seoul, Republic of Korea.

Fibroblast growth factor (FGF) 23 is known as a phosphaturic factor regulating phosphate homeostasis. FGF23 acts negatively on the NaPi2a cotransporter and 1α -hydroxylase with a resultant decrease in renal phosphate reabsorption. Its expression is up-regulated by $1,25$ -dihydroxyvitamin D₃ ($1,25(\text{OH})_2\text{D}_3$). It is thought that there exists a novel vitamin D-FGF23 feedback system affecting phosphate homeostasis and biomineralization. Several studies suggest that dietary phosphate, serum phosphate and $1,25(\text{OH})_2\text{D}_3$ are candidates as the regulators. While the human studies which modulated the dietary phosphate showed in rather controversial results, manipulation of the active vitamin D in animals definitely affected FGF23. Therefore, we tried to elucidate the relationship between active vitamin D directly stimulated by UVB exposure on FGF23 level in human. Ten healthy young adult (28-38 y.o., female 3) were recruited to get the UVB exposure thrice a week at sub-minimal erythral dose (MED)[20-50 sec/session] with gradual increment by 10% for 4 weeks. Blood tests for calcium, inorganic phosphorus (P), mineral-related hormones [$25(\text{OH})_2\text{D}$ (VD), $1,25(\text{OH})_2\text{D}_3$ (AVD), parathyroid hormone (PTH), FGF23], and bone markers were checked before, during and after the exposure. Surprisingly, vitamin D insufficient group comprised about 90%. VD increased by 215% (19.8 ng/mL to 40.5 ng/mL, $p<0.001$) after 4 weeks of UVB exposure. While AVD increased by 175% (49.9 pg/mL to 64.4 pg/mL, $p<0.001$) then both level decreased to 141%, 130% respectively after 4 weeks of withdrawal. No significant changes in iP or PTH were noticed. C-telopeptide rised early as 2nd week then decreased, while osteocalcin gradually increased. FGF23 gradually went up then, significant increase was detected at 4th weeks after withdrawal of UVB by 194% (27.8 pg/mL to 41.4 pg/mL, $p=0.025$). In conclusion, AVD and VD were effectively increased by sub-MED UVB exposure for 4 weeks with interesting stimulatory effect on FGF23. We could presume that FGF23 in human body might be directly affected by the AVD even with P in normal range.

Disclosures: Y. Rhee, None.

W127

Treatment of Mice with Antiresorptive Agents Increases Circulating FGF23, Decreases Renal mRNA Expression of 25-hydroxyvitamin D 1α -hydroxylase, and Reduces Circulating 1,25 Dihydroxyvitamin D. R. Samadfam*, C. Richard*, Q. Xia*, D. Goltzman. Department of Medicine, McGill University, Montreal, PQ, Canada.

We examined the effect of two anti-resorptive agents, alendronate (ALN) and osteoprotegerin (OPG), on the hormones regulating calcium (Ca) and phosphorus (P) homeostasis. Four month old ovariectomized (OVX) mice were treated with either vehicle, ALN (100 µg/Kg/week), or OPG (2.5 mg/kg twice a week), for 2 months. After sacrificing the animals, blood was collected for determination of serum Ca, P, $1,25$ dihydroxyvitamin D [$1,25(\text{OH})_2\text{D}$], PTH, the phosphaturic factor FGF23 and the bone turnover markers TRAP-5b and osteocalcin. The tibia, and lumbar spine were collected for histology and histomorphometry, and the kidney was collected for RT-PCR analysis. Our results indicate that, at the doses used, OPG, and to a lesser extent ALN produced decreases in circulating $1,25(\text{OH})_2\text{D}$ but increases in circulating FGF23. The decreased $1,25(\text{OH})_2\text{D}$ was associated with down-regulation of gene expression of 25-hydroxyvitamin D 1α hydroxylase (1OHase) in kidney. Bone turnover was markedly decreased with OPG and to a lesser extent with ALN at the doses used. The levels of TRAP-5 b and osteoclast numbers correlated positively with levels of $1,25(\text{OH})_2\text{D}$ and negatively with FGF23. No statistically significant changes were observed in circulating Ca, P or PTH. The experiment was repeated in 3 month old male mice with a shorter treatment period (20 days). The effects of OPG treatment on reducing gene expression of renal 1OHase, decreasing circulating $1,25(\text{OH})_2\text{D}$, and increasing serum FGF23, and the marked reduction of serum TRAP5b and osteoclast number were similar to the results obtained in older OVX females. However in male mice, ALN, a less potent antiresorptive agent compared to OPG, had no significant effects on serum $1,25(\text{OH})_2\text{D}$ or FGF23. With the shorter treatment period employed, serum P was decreased in OPG treated animals compared to controls. The reduction in serum P was associated with decreased protein expression of the sodium phosphate co-transporter NaPi2 in renal tubules as assessed by immunohistochemistry. Serum Ca and PTH were not significantly changed after treatment with either OPG or ALN. In conclusion, our results demonstrate that antiresorptive agents decrease the expression of renal 1OHase and consequently the levels of serum $1,25(\text{OH})_2\text{D}$ by increasing the levels of FGF23. The magnitude of these effects correlates with their antiresorptive potency. Furthermore, the effect of antiresorptives on serum P is normalized after long term treatment with these agents suggesting the existence of other regulatory mechanisms, in P homeostasis.

Disclosures: R. Samadfam, None.

W128

Effects of Pit-1 Type III Sodium-dependent Phosphate Transporter Overexpression on Calcium Phosphate and Bone Metabolism. A. Suzuki¹, P. Amman², S. Sekiguchi¹, S. Asano^{*1}, K. Nishiwaki-Yasuda^{*1}, S. Nagao^{*3}, H. Takahashi^{*3}, M. Hirabayashi^{*4}, M. Itoh^{*1}. ¹Department of Internal Medicine, Fujita Health University, Aichi, Japan, ²Service of Bone Diseases, Department of Rehabilitation and Geriatrics, University of Geneva, Geneva, Switzerland, ³Education and Research Center of Animal Models for Human Diseases, Fujita Health University, Aichi, Japan, ⁴National Institute of Physiological Sciences, Aichi, Japan.

The Pit-1 type III Pi transporter, initially thought to be a house keeping gene, was previously found to be preferentially expressed in developing long bones. Several studies also described a regulation of its expression in cultured bone cells by osteotropic factors suggesting a role of this transporter in bone metabolism. In the present study, we investigated the effects of Pit-1 overexpression in Wistar rats on calcium phosphate and bone metabolism. Skeletal development was not affected by the transgene. In four months old adult transgenic rats, serum Pi was significantly increased in both females and males compared with WT littermates. Enhanced serum Pi was associated with a significantly increased renal Pi transport. In males, elevated serum Pi was associated with a slight decrease in calcium and increased in PTH serum levels. Variations in serum Pi in WT and Pit-1 Tg rats were negatively correlated with serum FGF-23 whereas 1,25-dihydroxyvitamin D₃ was not affected by Pit-1 overexpression. Analysis of bone by DXA indicated that the bones of transgenic rats were significantly smaller, had less mineral and a significantly decreased BMD due to alteration in both trabecular and cortical bone compared with WT littermates. Volume densitometric analysis by μ CT indicated that the bones of females was more affected than those of males by Pit-1 overexpression.

In conclusion, Pit-1 overexpression in rats was associated with enhanced serum Pi and renal Pi transport without influencing skeletal development. Changes in serum Pi correlated negatively with circulating FGF-23, suggesting that Pi is not a direct in vivo regulator of FGF-23 synthesis. Excess serum Pi concentration was rather deleterious for the integrity of bone and was associated with decreased bone mass at several sites.

Disclosures: A. Suzuki, None.

W129

Analysis and Importance of Glycosylation Status in FGF23 Protein. H. Suzuki^{*}, S. Fukumoto, N. Ito^{*}, T. Fujita^{*}. Division of Nephrology & Endocrinology, Department of Medicine, University of Tokyo Hospital, Tokyo, Japan.

Previous studies have indicated that a part of FGF23 protein is cleaved between Arg¹⁷⁹ and Ser¹⁸⁰ into inactive fragments. Familial hyperphosphatemic tumoral calcinosis is characterized by hyperphosphatemia from enhanced tubular phosphate reabsorption. Two genes, FGF23 and GALNT3, were shown to be responsible for this disease and patients with mutations in these genes have extremely high C-terminal fragment of FGF23 with rather low full-length FGF23. These results suggest that the processing and production of FGF23 protein is enhanced in these patients. GALNT3 gene product is involved in the synthesis of O-linked glycans indicating that O-linked glycosylation affects the cleavage of FGF23. However, it has been unclear which amino acids are actually glycosylated and how mutations of FGF23 gene affect the processing. In order to clarify these issues, we have analyzed various mutant FGF23 proteins by Western blotting. The processing-resistant FGF23 mutant protein (FGF23RQ) was created by substitution of Arg¹⁷⁶ and Arg¹⁷⁹ by Gln. When FGF23RQ was expressed, three proteins around 32 kDa were observed. We have previously shown that these three proteins were FGF23 with one, two and three O-linked glycans between amino acids Asn¹⁶² and Arg²²⁸, respectively. There are 10 Ser or Thr residues as potential sites for glycosylation in this region. Therefore, we first changed each of these 10 Ser or Thr residues into Ala in processing-resistant FGF23RQ. When Thr¹⁷¹, Thr¹⁷⁸ or Thr²⁰⁰ was substituted by Ala, the protein with the highest molecular weight disappeared. Substitutions of other Ser or Thr residues did not affect the three protein bands indicating that O-linked glycans attach to Thr¹⁷¹, Thr¹⁷⁸ and Thr²⁰⁰. Substitution of Thr¹⁷¹, Thr¹⁷⁸ or Thr²⁰⁰ by Ala in wild-type FGF23 virtually vanished the full-length FGF23 protein indicating that only FGF23 with three O-linked glycans is resistant to the processing. Substitution of Ser⁷¹ by Gly or Ser¹²⁹ by Phe in FGF23RQ that was reported in patients with familial hyperphosphatemic tumoral calcinosis did not modify three protein bands around 32 kDa indicating that these mutant proteins have three O-linked glycans. These results indicate that FGF23 has three O-linked glycans at Thr¹⁷¹, Thr¹⁷⁸ and Thr²⁰⁰, and these three glycans are essential for the maintenance of full-length FGF23. Finally, mutations in FGF23 gene enhance the processing by other mechanisms than inhibiting O-linked glycosylation.

Disclosures: H. Suzuki, None.

W130

The Calcium Phosphate Regulating Hormone Stanniocalcin 2 Is Positively and Negatively Regulated by 1,25(OH)₂D₃ and PTH in Renal Proximal Tubular Cells. H. Yamamoto, Y. Takei^{*}, M. Masuda^{*}, T. Sato, Y. Taketani, E. Takeda. Clinical Nutrition, University of Tokushima School of Medicine, Tokushima, Japan.

Stanniocalcin (STC) is a hormone that was originally identified in fish, where it inhibits calcium (Ca) uptake by the gills and gut and stimulates phosphate (Pi) adsorption by the kidney. We previously have been identified human (h) STC-2 by its primary amino acid sequence identity to the hormone STC-1, and observed the inhibition of phosphate uptake and Npt2 gene promoter activity by hSTC-2 in opossum kidney (OK) cells. It has been also reported that mice deficient in klothe expression (klothe mice) have hypervitaminosis D, hypercalcemia and hyperphosphatemia, and increased renal gene expression of STC-2 compared with wild-type mice. However, the regulation mechanism of renal STC-2 gene expression is not well known. In this study, we addressed the mechanisms by which 1,25-dihydroxyvitamin D₃ [1,25(OH)₂D₃] and parathyroid hormone (PTH) modulates STC-2 gene expression in renal proximal tubular cells. We first examined the effects of 1,25(OH)₂D₃ on the secretion of STC-2 from opossum kidney (OK) cells. Western blot analysis of media conditioned by untreated OK cells revealed no detectable levels of STC-2, but the levels of STC-2 in the media increased markedly after exposure of cells to 1,25(OH)₂D₃ and its analogues. Surprisingly, PTH inhibited the 1,25(OH)₂D₃ induced STC-2 secretion. We also observed that the injection of PTH to rat decreased the levels of STC-2 protein and mRNA expression in kidney compared with control animals. Real-time PCR analysis revealed the mRNA levels of STC-2 in OK cells was increased by 1,25(OH)₂D₃ and rapidly decreased by PTH. In contrast, PTH increased the STC-1 mRNA levels. Moreover, the experiments using activator or inhibitor of PKC indicated that PKC signaling pathway is involved in the down-regulation of STC-2 gene expression by PTH. In summary, STC-2 gene expression is positively and negatively regulated by 1,25(OH)₂D₃ and PTH in proximal tubular cells. Such regulation suggests a link between Ca, Pi and vitamin D homeostasis in the kidney.

Disclosures: H. Yamamoto, None.

W131

Extracellular Inorganic Phosphate Induces ERK1/2 Phosphorylation and Up-regulates a Target Gene of FGF23 in Renal Proximal Tubule Cells via Type IIa Sodium-Phosphate Co-transporter. M. Yamazaki^{*}, M. Kimata^{*}, K. Tachikawa^{*}, K. Ozono, T. Michigami. Department of Bone and Mineral Research, Osaka Medical Center and Research Institute for Maternal and Child Health, Osaka, Japan.

It has been recently established that extracellular inorganic phosphate (Pi) functions as a signaling molecule and regulates gene expression in mineralizing bone cells such as osteoblasts and mature chondrocytes. Pi exerts various biological functions besides mineralization of bone, and renal proximal tubule plays a central role in Pi homeostasis. Therefore, we hypothesized that alteration in extracellular Pi concentration might trigger the signal transduction in proximal tubular cells as well as bone cells. In the current study, using HEK293 human embryonic kidney cells and LLC-PK1 porcine proximal tubular cells, we examined the effects of altered extracellular Pi (0-10 mM) on signal transduction and gene expression. Treatment with increased extracellular Pi induced ERK1/2 phosphorylation within 15 min in a dose-dependent manner. Phosphorylation of c-Raf at Ser338 was also induced by increased extracellular Pi, indicating that the extracellular Pi signals through c-Raf/MEK/ERK pathway. Since it is reported that phosphaturic hormone FGF23 induces the expression of early growth response-1 (Egr-1) through ERK1/2 phosphorylation, we examined the effect of altered extracellular Pi on the expression of Egr-1. Interestingly, the expression of Egr-1 was up-regulated by increase in extracellular Pi, suggesting the commonality between extracellular Pi and FGF23 in terms of the downstream signaling networks. Next, we examined whether type IIa sodium-phosphate co-transporter (NaPi-IIa) is involved in Pi-induced ERK1/2 phosphorylation and increased expression of Egr-1. Treatment with phosphonoformic acid, an inhibitor of sodium-phosphate co-transporter, inhibited the Pi-induced phosphorylation of ERK1/2 and cancelled the up-regulation of Egr-1. In addition, transfection of the expression vector encoding NaPi-IIa enhanced both the Pi-induced phosphorylation of ERK1/2 and up-regulation of Egr-1 expression. These results suggest the involvement of NaPi-IIa in the signaling triggered by alteration in extracellular Pi. In conclusion, in proximal tubular cells, extracellular Pi induces the phosphorylation of ERK1/2 and regulates gene expression in a NaPi-IIa-mediated pathway. Since the expression of Egr-1, a target of FGF23, was regulated by extracellular Pi, extracellular Pi might share the downstream signaling network with FGF23.

Disclosures: M. Yamazaki, None.

W132

CREB Phosphorylation and DNA Binding Along with Demethylation and Deacetylation Are Required for Ultimate Activation of CYP27B1 Promoter by PTH. M. N. Forster^{*1}, A. Maiti¹, M. J. Beckman². ¹Orthopaedic Surgery, Virginia Commonwealth University, Richmond, VA, USA, ²Biochemistry and Molecular Biology, Virginia Commonwealth University, Richmond, VA, USA.

1,25-Dihydroxyvitamin D₃ is synthesized by the mitochondrial P450 enzyme 1- α -hydroxylase (CYP27B1) expressed in the renal proximal tubule. Low serum Ca²⁺ increases parathyroid hormone (PTH), the main regulator of CYP27B1. The signaling pathway of PTH to increase CYP27B1 involves PKA activation and recruitment of p300 to the CYP27B1 promoter, but the molecular mechanisms that alternately stimulate and repress CYP27B1 are not fully solved. Our hypothesis is that PTH transmits signaling through the PKA/CREB pathway in order to up-regulate CYP27B1. A mouse proximal tubule epithelial cell (MPCT) model stably transfected with human PTH receptor type 1 was used to study the temporal regulation of phospho-CREB at 0, 2, 6, 8, 12, 16, and 24 hrs. In order to study the regulation of CYP27B1 promoter (-1500/+74 bp), mRNA, and protein levels RT-PCR, western blots, and luciferase assays were used. A 50nM PTH treatment to MPCT cells showed that all of these components were optimally and significantly activated at the 12 hour time point. The next several studies involved both low and normal Ca²⁺ medium with and without PTH treatment. A forskolin (10 μ M) treatment similarly increased CYP27B1 promoter activity at 12 hrs demonstrating involvement of cAMP, and the PKA inhibitor H89 (100 μ M) blocked CYP27B1 promoter activity indicating the involvement of PKA. To test the role of CREB phosphorylation and binding on CYP27B1 promoter activation two approaches were used; the dominant negatives CREB133 and KCREB were transfected into MPCT cells, significantly blocking CYP27B1 promoter activation by PTH. However, transfection of wild-type CREB further enhanced CYP27B1 promoter activity in the presence of PTH. In addition, treatment with the histone deacetylase inhibitors trichostatin A (10 μ M) and apicidin (1 μ M) suppressed CYP27B1 promoter at the 12 hr time point, suggesting that deacetylase activity is a required determinant of phospho-CREB-mediated activation of CYP27B1. Finally, a treatment with a methylation inhibitor, 5' Aza-cytidine, increased the expression of CYP27B1 thus illustrating that methylation is a second important component of phospho-CREB mediated activation of CYP27B1. This study provides evidence for the key involvement of PTH-mediated CREB phosphorylation and DNA binding for ultimate activation of CYP27B1 promoter in MPCT cells, and demonstrates a requirement of reversing basal repression of CYP27B1 in MPCT cells by DNA demethylation and histone deacetylation at the promoter level.

Disclosures: M.N. Forster, None.

W133

Endogenous PTH Measurements in Cynomolgus Monkey Serum: Wide Immunoassay Kit-to-Kit Variation. T. Greutzner^{*}, J. Reeves^{*}, P. Oldfield. Charles River Laboratories, Preclinical Services Montreal, Senneville, PQ, Canada.

This study was conducted to identify an immunoradiometric assay (IRMA) for parathyroid hormone (PTH) equivalent to the discontinued Diagnostic Products Corporation's (DPC) Coat-a-Count IRMA.

The DPC assay was compared with two alternative IRMAs: the Diagnostic Systems Laboratories (DSL) Active Intact PTH assay, and Scantibodies Total Intact PTH coated bead method. Duplicate assays were performed according to the manufacturer's instructions and applied to the serum of 20 naive Cynomolgus monkeys. Inter-method comparisons used the Bland Altman method.

Table 1: Descriptive statistics

Method (assay range)	Mean PTH concentration	PTH concentration range
DPC (15-3000 pg/mL)	69.2 pg/mL	15.2-211.9 pg/mL
DSL (10-2000 pg/mL)	98.8 pg/mL	22.4-268.4 pg/mL
Scantibodies (10-2500 pg/mL)	55.3 pg/mL	9.9-188.2 pg/mL

Table 2: Inter-method comparisons

Comparison	Mean ratio (95% CI)*	+/- 1.96 SD of ratios**
DPC/DSL	0.78 (0.72-0.85)	0.50-1.07 (63-137% of mean ratio)
DPC/Scantibodies	1.30 (1.21-1.38)	0.94-1.65 (72-127% of mean ratio)
Scantibodies/DSL	0.61 (0.56-0.67)	0.38-0.84 (62-138% of mean ratio)

* Mean ratio represents bias from one method to the other. ** The standard deviation of the ratios x 1.96 represents the range where 95% of samples are predicted to fall when one method is used in place of another.

The three methods produced different results, with significant bias ($p < 0.001$) between each justifying the use of correction factors to bring one method into the range of another. The Scantibodies results x 1.30 produce PTH values that are predicted to be within 27% of the DPC values in 95% of samples in the concentration range tested. The DSL values x 0.78, give PTH results that are likely to be within 37% of the DPC values in 95% of samples. The results from the Scantibodies assay more closely resemble the DPC data than do the results from the DSL assay. Of concern is the wide range in absolute values given by the three IRMAs which have been designed to measure the same analyte. This may be the result of different kit calibrators or due to the use of antibodies with differing specificities for the various PTH truncation fragments.

In a parallel study, a non-radioactive alternative method requiring low sample volume (Immutopics, Human PTH ELISA) was validated according to current regulatory guidelines with acceptable selectivity, sample stability, dilution linearity and precision and accuracy in the range of 13-426 pg/mL.

Disclosures: T. Greutzner, None.

W134

Biomarker Effect of Daily Dosing of Human PTH1-34 on Intact Cynomolgus Monkeys for Twelve Days. L. C. Dare^{*1}, J. A. Vasko^{*1}, G. B. Stroup², S. Kumar¹, V. R. Vaden^{*2}, S. J. Hoffman¹. ¹Musculoskeletal Diseases, GlaxoSmithKline, Collegeville, PA, USA, ²GlaxoSmithKline, King of Prussia, PA, USA.

Parathyroid hormone (PTH) is known to stimulate bone formation when administered intermittently to animals and humans. In cynomolgus monkeys, increases in bone mass and strength have been observed with 6 months of PTH treatment. In addition, biochemical markers of bone resorption and formation have been used to assess the effects of PTH on bone in the longer term. The purpose of this study was to determine if daily injection of PTH for twelve days is sufficient to see biomarker changes and to determine how long the biomarker effect remains once dosing is discontinued.

Fourteen female cynomolgus macaques were divided into two treatment groups (n=7/group) and treated daily by SC injection for 12 days with either vehicle (saline, 0.1% BSA) or human PTH1-34 at 1 μ g/kg. Serum was collected on fasted animals prior to dosing on days 1, 5, 8, 12, and at the same time on days 15, 19, and 22. The bone formation biomarkers, osteocalcin (OC), bone specific alkaline phosphatase (BALP), and amino-terminal propeptide of type I procollagen (PINP) as well as the bone resorption biomarker, serum N-terminal telopeptide of type I collagen (NTx), were determined. All procedures were approved by the Institutional Animal Care and Use Committee.

Daily transient elevations of plasma PTH1-34 (C_{max} 215 pg/mL) were seen following SC injection. This resulted in significant increases compared to vehicle treatment in the bone formation markers OC and PINP but not BALP. These elevations were first noted after 7 consecutive days of PTH administration and remained elevated compared to vehicle treatment throughout the duration of the dosing period. Osteocalcin levels continued to be elevated compared to vehicle 7 days after the last injection (day 19; $p < 0.075$). PINP levels were significantly elevated compared to vehicle on days 8 and 12 and returned to vehicle levels by day 19. BALP levels, although not significantly different than vehicle treatment group at anytime, did appear to increase slowly in response to the daily injection of PTH (in comparison to the daily fluctuations of the vehicle treatment group). The BALP levels continued to increase until 3 days after the last injection (day 15). Interestingly, significant reductions in NTx were detected 4 days after the first PTH injection and remained reduced throughout the duration of the study. The reduction in NTx levels were significant compared to vehicle treatment on days 5, 8, 12, and 22.

This study demonstrates that daily injection of PTH1-34 results in significant changes in bone biomarkers as early as 5 days after the first daily administration in the monkey and the biomarker effect is maintained for up to 10 days post-dosing.

Disclosures: S.J. Hoffman, GlaxoSmithKline 3.

W135

Serum Parathyroid Hormone Is Associated with Cortical Bone Dimensions in Young Men - The GOOD Study. M. Lorentzon, D. Mellström, C. Ohlsson. Center for Bone Research at the Sahlgrenska Academy (CBS), Dept. of Internal Medicine, Gothenburg University, 413 45 Gothenburg, Sweden, Gothenburg, Sweden.

An excess of parathyroid hormone (PTH) as seen in primary hyperparathyroidism has been associated with low bone mass, but PTH administered intermittently has bone anabolic effects. The role of physiological levels of parathyroid hormone (PTH) on trabecular and cortical volumetric bone mineral density (vBMD) or cortical bone dimensions has not previously been investigated in young men.

The aim of the present study was to determine if PTH was associated with volumetric BMD (vBMD) and/or bone geometry of the trabecular and cortical bone compartments in a large cohort of young men.

The Gothenburg Osteoporosis and Obesity Determinants (GOOD) study is a population-based study that consists of 1068 young men, age 18.9 \pm 0.6 yrs (mean \pm SD). Serum levels of intact PTH were measured using an immunoluminometric assay while 25(OH)D level were measured using a competitive RIA. vBMD and bone size of the trabecular and cortical bone of the radius and tibia were measured using peripheral quantitative computerized tomography (pQCT).

PTH levels were correlated to adult stature ($r=0.06$, $p<0.05$) and to length of the long bones (radius: $r=0.09$, $p<0.01$; tibia: $r=0.07$, $p=0.03$), but not to the sitting height ($r=0.00$, $p=0.89$).

Regression models including age, height, weight, smoking status, amount of physical activity, calcium intake, serum levels of 25(OH)D, cystatin C, month of measurement, as well as PTH, demonstrated that PTH was an independent positive predictor of cortical periosteal circumference (radius: $\beta=0.07$, $p=0.02$; tibia $\beta=0.07$, $p<0.01$), and endosteal circumference (radius: $\beta=0.08$, $p<0.01$; tibia $\beta=0.07$, $p=0.01$) of the long bones. Using the same regression model, PTH negatively predicted cortical vBMD of the tibia ($\beta=-0.09$, $p<0.01$), but not of the radius ($\beta=-0.05$, $p=0.09$). PTH was not associated with trabecular vBMD of either the radius or tibia.

Our results demonstrate that PTH levels are associated with adult stature due to affected length of the long bones. Furthermore, PTH levels are clear independent predictors of both periosteal and endosteal circumference, suggesting that physiological levels of PTH play a significant role in the determining cortical bone dimensions in young men.

Disclosures: M. Lorentzon, None.

W136

Effect of Ovariectomy and Low Calcium Diet on Bone Properties in Female Mice. A. Minematsu. Physical Therapy, Health Science, Nara, Japan.

Aim: This study was investigated the effects of ovariectomy (OVX) and low calcium (Ca) diet on bone properties in female mice.

Subjects and Methods: Forty female ICR mice aged 3 months divided into 4 groups randomly. Two groups were sham-operated, and remain of two were ovariectomized. They were fed standard laboratory diet (Ca: 1.1g/100g) or special low Ca diet at libitum for 100 days. After this experiment, maximum load (ML) of the femur and tibia were measured by the three-point bending test, and calculated maximum stress (MS), elastic modulus (EM), and energy absorption (EA). The bones were measured bone length (BL) and bone width (BW), weighted dry bone mass (BM), and burned to ash, and measured ash contents (AC). Data were analyzed by two-way ANOVA and Scheffé's procedure to find the effects of OVX and low Ca diet on bone properties. A significance level of $p=0.05$ was set. This study was carried out in accordance with the Guide for Animal Experimentation, Hiroshima University and the Committee of Research Facilities of Laboratory Animal Science, Hiroshima University school of Medicine.

Results: OVX decreased EM, EA, BM, and AC of the femur and tibia significantly. BL was longer by OVX. Low Ca diet significantly influenced all bone properties of the both bones except for EM and BM of tibia. Bone properties were reduced by OVX and low Ca diet, and those of combined these factors showed the lowest. Alterations were found BW of both bones. **Conclusions:** OVX and low Ca diet decreased bone properties and combination of these factors affected bone properties further. It was considered that OVX influenced EM and bone shape (BL), and low Ca diet influenced structural and material properties (ML, MS, EA), especially.

Group	Results of Bone Properties of Femur and Tibia			
	SHAM (Femur / Tibia)	OVX (Femur / Tibia)	SHAM+L.Ca (Femur / Tibia)	OVX+L.Ca (Femur / Tibia)
Maximum Load (N)	20.84±1.90 / 15.46±1.55	18.98±2.98 / 14.62±1.80	18.72±2.26 / 14.52±0.90	16.80±3.12 / 13.68±0.67
Maximum Stress (MPa)	72.06±7.94 / 49.07±5.41	69.45±8.12 / 47.89±4.14	62.76±7.85 / 47.38±2.81	58.44±4.79 / 44.27±2.21
Elastic Modulus (GPa)	17.17±1.83 / 5.24±0.50	15.00±1.49 / 4.65±0.75	16.52±1.76 / 5.10±0.71	12.68±1.14 / 4.02±0.72
Energy Absorption (Nmm)	6.92±0.98 / 6.16±0.97	5.83±0.70 / 5.68±0.98	6.70±0.95 / 4.68±0.91	4.51±0.85 / 3.79±0.90
Bone Mass (mg)	71.4±3.3 / 56.3±4.1	67.0±3.6 / 51.7±3.5	65.1±3.0 / 49.6±3.9	57.8±3.3 / 47.0±3.9
Ash Content (mg)	37.5±1.8 / 29.4±2.2	34.8±2.7 / 26.4±2.1	33.8±2.4 / 25.6±1.4	29.2±1.8 / 24.2±2.6
Bone Length (mm)	16.92±0.45 / 19.92±0.44	17.48±0.56 / 20.66±0.56	16.73±0.48 / 19.91±0.29	16.95±0.40 / 20.37±0.60

Disclosures: A. Minematsu, None.

W137

PTH Upregulates Placental Calcium Transfer in Response to Fetal Hypocalcemia While PTHrP Does Not. C. S. Noseworthy^{*1}, G. Karsenty², A. C. Karaplis³, C. S. Kovacs¹. ¹Memorial University of Newfoundland, St. John's, NF, Canada, ²Columbia University, New York, NY, USA, ³McGill University, Montreal, PQ, Canada.

Previous studies in mice and sheep have shown that PTHrP stimulates placental 45Ca transfer but PTH does not. Specifically in Pthrp null fetuses, placental 45Ca transfer was reduced by ~25% vs. WT but was stimulated by exogenous PTHrP 1-86 or 67-86, while PTH 1-34 and 1-84 were without effect. However, endogenous PTH levels were upregulated 7-fold in Pthrp null mice, which may have obliterated a detectable response to exogenous PTH.

We have been examining the role of fetal PTH with two models, Pth null (which lack PTH), and Gcm2 null (which lack parathyroids but retain thymic PTH). We have previously found that Pth and Gcm2 null fetuses are hypocalcemic compared to respective WTs (~1.30 vs 1.75 mmol/l), and that placental 45Ca transfer was normal in Pth null but increased to 119% of normal in Gcm2 nulls. As well, PTH was reduced to 5.03 pg/ml in Gcm2 null, but was undetectable (<1.6 pg/ml) in Pth null fetuses.

We now report that the presence of PTH, and not upregulation of PTHrP, may explain the increased placental 45Ca transfer in Gcm2 nulls v. Pth nulls.

Plasma PTHrP was assessed using a rodent PTHrP 1-34 RIA and (in pmol/l) was 8.1±0.4 in Pth null and 7.8±0.4 in Gcm2 null, no different than corresponding WTs (8.4±0.4 and 7.8±0.4, respectively). RNA was extracted from anterior neck sections (to include parathyroids) and intact placentas, and no difference in PTHrP expression (by quantitative real time RT-PCR) was observed in Pth or Gcm2 nulls versus respective WTs (placental values 0.98±0.07 in Pth null and 0.95±0.07 in Gcm2 null versus 1.00±0.07 in respective WT).

The effect of exogenous PTH 1-84 was then tested with 1 nmol of PTH 1-84, which is equimolar to the amount of PTHrP 1-86 that was effective in Pthrp nulls. On day 17.5 pc, all fetuses were injected in utero with either PTH 1-84 or saline, 85 minutes prior to administration of 45Ca/51Cr-EDTA to the mother. Accumulation of isotopes in the fetuses was measured after 5 minutes. By this standard method, placental 45Ca transfer was increased to 124±6.4 vs 106±7.9% in PTH-injected vs. saline-injected Pth nulls ($p<0.04$), while WT and Pth+/− fetuses showed no response.

Thus, we have demonstrated that PTH was detectable in Gcm2 nulls (in which placental 45Ca transfer was upregulated) but not Pth nulls, that placental and circulating PTHrP was not upregulated in either Pth or Gcm2 nulls, and that exogenous PTH administration increased placental 45Ca transfer in Pth nulls. We conclude that PTH likely stimulated placental 45Ca transfer in response to fetal hypocalcemia (Gcm2 nulls) while PTHrP was not upregulated in response to hypocalcemia; the factors that regulate PTHrP remain undetermined.

Disclosures: C.S. Noseworthy, None.

W138

The PTH/PTHrP Receptor Modulates the Pool of Bone Marrow Stromal Cells: Implications for the Anabolic Action of PTH. M. Ohishi¹, L. E. Purton^{*2}, W. L. Stanford^{*3}, D. T. Scadden^{*2}, H. M. Kronenberg¹, E. Schipani¹.

¹Endocrine unit, Massachusetts General Hospital, Boston, MA, USA, ²Center for Regenerative Medicine, Massachusetts General Hospital, Boston, MA, USA, ³Institute of Biomaterials and Biomedical Engineering, University of Toronto, Toronto, ON, Canada.

Transgenic mice expressing constitutively active PTH/PTHrP receptors (PPR) in osteoblasts (Tg) show an increase in trabecular bone with a concomitant expansion of the bone marrow (BM) stromal cell population, and increased number of osteoblasts and hematopoietic stem cells. The goal of this study was to investigate whether PPR signaling in osteoblasts has an effect on mesenchymal stem cells (MSCs)/progenitors. It has been previously reported that the BM pool of Scf1(+) CD45(-) CD31(-) cells is enriched in MSCs/progenitors. In addition, Scf1 deficient mice (Scf1-/- mice) show an osteoporotic phenotype by 7 months of age, which is due to a decrease of MSCs/progenitors. Flow cytometry analysis of BM cells revealed that the percentage of Scf1(+) CD45(-)CD31(-) cells is at least 50% higher in Tg BM than in wild-type (Wt). Immunohistochemistry for Scf1 showed that osteoblasts do not express Scf1, which indicates that the pool of Scf1(+) CD45(-)CD31(-) cells does not contain osteoblasts. Collectively, our data thus suggest that the number of MSCs/progenitors could be indeed expanded in Tg mice. Interestingly, in vitro colony forming unit fibroblast (CFU-F) assay did not confirm this increase of MSCs/progenitors. We believe that the discrepancy is secondary, at least in part, to the high degree of heterogeneity of the CFU-F cultures. To investigate whether the MSCs/progenitors contribute to the phenotype of the Tg mice, we have then generated Tg mice lacking Scf1 (TgScf1-/- mice). Preliminary data showed a partial attenuation of the Tg phenotype in TgScf1-/- mice at an age when there is no observed osteoporosis in Scf1-/- mice. We are also investigating whether intermittent PTH treatment expands the pool of MSCs/progenitors in vivo. For this purpose, we are treating Wt mice with intermittent PTH(1-34) daily for 4 weeks; flow cytometry analysis of BM cells will be performed at the end of the treatment. Finally, in order to investigate whether the anabolic action of intermittent PTH is preserved in mice that are depleted of MSCs/progenitors, Scf1-/- mice are being injected with intermittent PTH (1-34) daily for 4 weeks. Bone density will be measured at the end of the treatment and presented together with the histological findings. To study whether intermittent PTH modulates the pool of MSCs/progenitors and whether the anabolic action of PTH is affected in a setting in which the pool of MSCs/progenitors is depleted could have important therapeutic implications for the treatment of osteoporosis.

Disclosures: M. Ohishi, None.

W139

Targeted Overexpression of Parathyroid Hormone Type 2 Receptor in Chondrocytes Impairs Cartilage Differentiation and Trabecular Bone Growth. D. K. Panda^{*}, H. Su^{*}, D. Goltzman, A. C. Karaplis. Department of Medicine, McGill University, Montreal, PQ, Canada.

Members of the parathyroid hormone (PTH) family of ligands and receptors play a pivotal role in the maintenance of calcium and phosphorus homeostasis as well as in the regulation of skeletal growth and development. TIP39 is the newest member of the family and exerts its function by binding and activating its cognate receptor, the PTH type 2 receptor (PTH2R). Experimental evidence suggests that TIP39 and PTH2R form a neuromodulator system in the CNS. However, there is very little indication that this signaling pathway partakes in the regulation of skeletal development. Using CFK2 chondrocytic cells stably transfected with human PTH2R cDNA, we have reported that treatment with TIP39 inhibited both the proliferation and differentiation of these cells and was associated with down regulation of the expression of the cartilage-associated transcription factor Sox9.

In the present study, we investigated in vivo the potential role of TIP39/PTH2R signaling in chondrocyte biology. First, using immunohistochemistry, we determined that PTH2R is highly expressed in growth plate chondrocytes in long bones from young mice but restricted to cells in the subarticular region. On the other hand, immunostaining for the ligand TIP39 was localized in hypertrophic chondrocytes.

To further explore the role of TIP39/PTH2R signaling in the growth plate, we generated transgenic mice expressing PTH2R under the control of the rat type II collagen promoter/enhancer. In mice expressing the transgene, there was a marked reduction of type II collagen expression in differentiating growth plate chondrocytes. Moreover, trabecular bone content was diminished. Employing quantitative microcomputed tomography analysis we confirmed the reduction of trabecular bone meshwork in 5 week-old PTH2R transgenic mice compared to control litter mates. Bone volume/total volume (11.55 vs. 9.34 %), trabecular number (1.86 vs. 1.54 per mm), trabecular separation (0.35 vs 0.31 mm), and degree of anisotropy (2.94 vs. 2.68) were decreased while structure model index (2.04 vs. 2.19) was increased in bones from PTH2R transgenic mice compared to wild type controls.

In summary, we have investigated in vivo the potential physiologic role of PTH2R in chondrocyte biology. In conformity with our in vitro findings, studies with PTH2R transgenic mice indicate that overexpression of the receptor impairs chondrocyte differentiation and impacts negatively on subsequent trabecular bone development.

Disclosures: D.K. Panda, None.

W140

Identification of Distinct, Functional Domains in the Hyperplastic Rat Parathyroid Gland. C. S. Ritter*, J. L. Finch*, E. Slatopolsky, A. J. Brown. Internal Medicine, Washington University School of Medicine, St Louis, MO, USA.

Secondary hyperparathyroidism (2°HPT) due to chronic kidney disease is characterized by hypersecretion of parathyroid hormone and enlargement of the parathyroid gland (PTG). We have previously shown that heterogeneous growth in uremic rat PTGs is associated with differential expression of the calcium-sensing receptor (CaR) (Kidney Int, vol 55:1282, 1999). To better understand the nature of this heterogeneity, we examined PTGs of rats in response to 5/6 nephrectomy and a high phosphate (HP) diet. Immunostaining was used to examine expression of CaR, vitamin D receptor (VDR), 1 α -hydroxylase (1 α -OHase), parathyroid hormone (PTH), glial cells missing 2 (Gcm2), E-cadherin, N-cadherin, β -catenin, p120, and proliferating cell nuclear antigen (PCNA). 2°HPT produced a heterogeneous growth of parathyroid tissue consisting of at least three functionally distinct domains. 1) Normal, non-proliferating areas, in which cells express cytoplasmic VDR and high levels of plasma membrane localized CaR, E-cadherin, β -catenin and p120, comparable to that observed in non-uremic control rats. 2) Areas of proliferating cells (PCNA positive) which express nuclear VDR, possibly attributable to local 1,25(OH) $_2$ D $_3$ produced by the elevated 1 α -OHase found in the same areas. Also found in the areas of proliferation were increased levels of PTH and Gcm2, and decreased levels of CaR. Proteins important for cell:cell adhesion, E-cadherin, β -catenin and p120, were also decreased in areas of proliferation. 3) A unique subset of cells exhibiting a distinct morphology. These nests of cells form whorl-like structures (~20-50 cells each), and are located within the proliferating areas of the gland, although the whorls themselves contain no PCNA. Cells in the whorls have smaller, darker nuclei than the surrounding proliferating cells. The whorls are readily identified by their exceptionally low levels of VDR, 1 α -OHase, Gcm2 and PTH. In addition, the whorls express N-cadherin, as well as aberrant (non-membranous) forms of β -catenin, E-cadherin and CaR. Surprisingly, the whorls appeared as early as 1 day after uremic rats were placed on a HP diet, indicating a rapid transformation of normal cells. In some glands, the whorls comprised ~25% of the tissue section. In conclusion, the uremic rat hyperplastic PTG is composed of at least three distinct functional domains, each identifiable by specific protein expression. Of particular interest is the finding of aberrant β -catenin in a previously unreported subset of whorl-like cells, suggesting the involvement of Wnt signaling. The role of these non-proliferating whorls in the progression of the hyperplasia is under investigation.

Disclosures: C.S. Ritter, None.

W141

Phosphate Stimulates Greater PTH Release and Parathyroid Cell Proliferation in Organ Cultures of Parathyroid Tissue from Patients with Secondary Hyperparathyroidism than with Primary Hyperparathyroidism: Microarray Analyses of Phosphate-induced Genes. K. Sato*, K. Nakajima*, K. Takano*, S. Kosaka*, T. Obara*, K. Umino*, Y. Azuma*. ¹Institute of Clinical Endocrinology, Tokyo Women's Medical University, Tokyo, Japan, ²Central Research Laboratory, Tokyo Women's Medical University, Tokyo, Japan, ³Institute of Clinical Endocrinology, Department of Surgery, Tokyo Women's Medical University, Tokyo, Japan, ⁴Teijin Institute for Bio-medical Research, Teijin Ltd., Tokyo, Japan.

To elucidate the mechanism by which hyperphosphatemia stimulates parathyroid cell proliferation, we developed a method for organ culture of parathyroid tissues obtained from patients with primary (I-HPT) and secondary hyperparathyroidism (II-HPT), and studied the effects of calcium and phosphate on cell proliferation and PTH release, using oligo-DNA microarray. When parathyroid cells were cultured in a monolayer, calcium and phosphate elicited no significant effects on cell proliferation or PTH release. However, when parathyroid tissue was cultured in small pieces on a collagen-coated membrane, calcium decreased the release of PTH in a concentration-dependent manner but did not modulate cell proliferation during short (for 1 day) or prolonged culture (for 1-3 weeks). When parathyroid tissues were cultured in high phosphate medium (8-10 mg/dl), cell proliferation and PTH release were significantly increased (for up to 4 weeks) compared with those cultured in low phosphate medium (3 mg/dl). Both PTH-induced effects were significantly greater in tissue from patients with II-HPT than in those from patients with I-HPT. Microarray analyses capable of analyzing the whole human genome in a single run (Agilent) revealed that humanin, DRD4, BBC3, prion, and PTH were expressed most abundantly and that high calcium decreased the mRNA levels of PTH and chromogranin A, whereas high phosphate increased constantly the mRNA levels of PTH. Growth factors reported to be involved in parathyroid cell proliferation, such as the TGF- α /EGFR, TGF- β , EGF, and FGF-1&2 were expressed to the same level as those in human thyroid follicles. Although mRNA expression levels of PRKAR1A, FGF-3, and TGFBI (beta IGH3) were much increased in II-HPT (compared to those in cultured human thyroid follicles), they were not responsive to phosphate. In summary, using organ culture of hyperplastic or adenomatous parathyroid tissues, we have demonstrated that parathyroid cells from patients with II-HPT are more responsive to high phosphate concentration. Furthermore, our microarray analyses revealed that there may be unknown pathway(s) through which phosphate stimulates parathyroid cell proliferation.

Disclosures: K. Sato, None.

W142

Dynamic Bone Changes in PTH(1-34) Treated Ovariectomized Rats, Evaluated by In-Vivo Micro-CT Scanning. O. P. Van der Jagt*, J. H. Waarsing*, J. A. N. Verhaar*, J. C. Van der Linden*, H. Weinans. Orthopaedic Research Lab, Erasmus Medical Center, Rotterdam, The Netherlands.

PTH and Teriparatide have strong anabolic effects on bone. Whether new bone is formed by thickening of trabeculae and later will transform, or new bone can also arise in the marrow is under debate. With in vivo uCT-scanning we can follow bone changes of a single rat in time in a very detailed manner (spatial resolution 18 μ m). By a registration procedure we can match the 3-dimensional scans of different time points and in this way evaluate the exact trabecular and cortical bone changes of a single rat. Morphological bone parameters of the cortex and cancellous bone were also calculated. Female Wistar rats were ovariectomized at 20 weeks of age. Ten weeks of bone depletion was allowed, thereafter subcutaneous injections with PTH(1-34); Teriparatide, 30 μ g/kg were given 5 times a week for ten weeks. At 0, 3, 6 and 10 weeks after ovariectomy and after 3, and 6 weeks after start of the treatment in-vivo micro-CT scans were made. Trabecular volume fraction increased as a consequence of Teriparatide with more than 50% at 3 weeks, but after 6 weeks trabecular resorption had occurred. Connectivity showed the same pattern. Trabecular thickness was increased but between 3 and 6 weeks it decreased in all rats with 1-3%. Trabecular structures changed from rod-like to plate-like but after 6 weeks there was a shift towards rod-like again. Cortical bone volume did not increase the first 3 weeks of treatment, between 3 and 6 weeks cortical volume increased with more than 10%. New bone formation was seen only at already existing bone structures. Trabecular thickening but also loss of trabeculae was seen. At start of the treatment there were no trabecular structures in the central proximal metaphysis, but during treatment trabeculae tended to migrate towards it. Remarkable is the different effect of PTH(1-34) between cortical and trabecular bone. A large increase in trabecular volume occurred the first 3 weeks of treatment whereas the cortical volume did not change. Between 3 and 6 weeks on the other hand trabecular bone resorption had occurred whereas cortical bone volume increased. We hypothesize that this is due to the large difference in available surface between cancellous and cortical bone. Once the cortical bone becomes thicker it can take a higher portion of the loading and thereby stress-shields the cancellous bone that as consequence becomes resorbed again. Longer follow up studies with in-vivo micro-CT scanning are needed to evaluate if migration of trabeculae are the result of resorption and transformation or the result of repetitive thickening and osteoclastic tunneling of trabecular structures.

Disclosures: O.P. Van der Jagt, None.

W143

Rapid Site-Specific Bone Growth by a Combination of Bone Marrow Ablation, PTH and Biphosphonate Therapy. Q. Zhang¹, J. Carlson^{*1}, E. Cuartas^{*1}, M. Kim^{*1}, N. Mehta², J. Gilligan², M. Kotas^{*1}, M. Ma^{*3}, S. Rajan^{*3}, M. W. Saltzman^{*3}, C. Chalouhi^{*1}, A. Vignery¹. ¹Yale School of Medicine, New Haven, CT, USA, ²Unigene Laboratories, Inc., Fairfield, NJ, USA, ³Yale University, New Haven, CT, USA.

During development and repair of bone, two distinct yet complementary mechanisms, intramembranous and endochondral, mediate new bone formation via osteoblasts. Mechanical bone marrow ablation leads to differentiation of osteoblasts, and formation of cancellous bone. The intramembranous bone-formation phase that follows bone marrow ablation is complete by day 7 at which time osteoclasts differentiate in synchrony and resorb the newly formed bone to re-create the marrow cavity into which bone marrow cells return. This transient induction of bone formation in response to marrow ablation has been used as an in vivo model to discover new genes, and to investigate the role of known genes, in the process of bone formation. We initially questioned whether parathyroid hormone (PTH) could promote the formation of new bone that occurs after marrow ablation. We subjected the left femur of rats to marrow ablation, and injected the animals daily with the PTH analog PTH(1-34)NH $_2$ for one, two or three weeks. Both femurs from each rat were analyzed by soft X-ray, pQCT, microCT and histology, and serum osteocalcin concentration was determined. Bone progressively filled the marrow cavity of the ablated femoral shafts in animals treated with PTH. The newly formed bone endowed femoral shafts with improved biomechanical properties when compared to those of contra lateral femurs as well as left femurs from control, sham operated and vehicle-treated rats. To ask whether this new bone could be maintained for extended times, we subjected the left femurs of rats to marrow ablation, and injected the animals daily with PTH(1-34)NH $_2$ for three weeks followed by treatment with alendronate or PBS for two months. Both femurs from each rat were analyzed as before. The bone that had formed in response to marrow ablation and daily PTH for 3 weeks was resorbed after two months in the PBS treated controls. By contrast, bone was maintained in the ablated marrow cavity following daily alendronate treatment for two months. These findings might potentially be useful for investigations on the molecular mechanisms of intramembranous bone formation, and for preferential site-directed bone growth in areas of high bone loss, for fracture repair, and for reinforcing the implantation of prosthetic devices.

Disclosures: A. Vignery, Unigene Laboratories, Inc. 2, 5.

This study received funding from: Unigene Laboratories, Inc.

W144

Fluorescence Resonance Energy Transfer Analysis Reveals Selective Binding of Long- and Short-Acting PTH(1-28) Analogs to Distinct PTH Receptor Conformations. S. Férrandon^{*1}, M. Castro^{*2}, M. Okasaki^{*2}, J. T. Potts¹, T. J. Gardella², J. Vilardaga^{*2}. ¹Massachusetts General Hospital and Harvard Medical School, Boston, MA, USA, ²Endocrine Unit, Massachusetts General Hospital and Harvard Medical School, Boston, MA, USA.

Fluorescence resonance energy transfer (FRET) technology can now be used to monitor with high temporal resolution conformational changes that occur in a receptor upon ligand binding. The binding of a PTH ligand to the PTH/PTHrP receptor (PTHrP) and the subsequent activation of the bimolecular complex is likely to involve a cascade of conformational changes that occur in both the ligand and receptor. Furthermore, different PTH or PTHrP ligands may bind via different mechanisms so as to induce or stabilize distinct receptor conformations. We tested these hypotheses using the FRET approach to record kinetics of ligand association and dissociation, as well as kinetics of receptor activation and deactivation. Our data show that ligand binding, studied with PTH, occurs as a biphasic process and that the second phase co-incides with a conformational change in the PTH-receptor. This conformational change, reflecting transition into an active receptor signaling conformation, is dependent on the nature of the ligand; we showed that PTH and PTHrP as well as long- and short-acting PTH(1-28) analogs stabilize distinct PTH receptor conformations.

Disclosures: J. Vilardaga, None.

W145

Parathyroid Hormone Levels Are Associated with Carotid Plaque Thickness and Number. M. D. Walker, J. Fleischer, D. J. McMahon, T. Rundek^{*}, J. DeRosa^{*}, J. Udesky^{*}, A. Tineo^{*}, R. Sacco^{*}, S. J. Silverberg. Columbia University, New York, NY, USA.

Elevated serum calcium concentrations are associated with vascular calcification and cardiovascular (CV) disease. We have previously published that serum calcium levels in a multi-ethnic population of older men and women were positively associated with mean carotid plaque thickness (MCPT), a powerful early predictor of clinical coronary and cerebrovascular events. This study was designed to pursue this observation. In particular, we assessed whether such relationships can be explained by the calcium-phosphate product (Ca x PO₄), as in renal disease, or by calciotropic hormones that may affect the vascular system.

To date, we have enrolled 113 consecutive community-dwelling stroke free adults from the Northern Manhattan Stroke Study (NOMAS; age: 68±10 SD, 50-93 yrs). Carotid ultrasound determined the presence/absence and number of plaques (plaque #), MCPT and intima-medial thickness (IMT), another marker of CV disease. As expected, these variables were highly correlated with age (IMT R= .435 P<.0001; plaque # R= .425 P<.001; MCPT R= .408 P<.0001). In a mixed model including demographic and known CV risk factors, age and male sex emerged as the strongest predictors of increased IMT, while age and diabetes emerged in the model of MCPT. No association was found between plaque #, MCPT or IMT and serum calcium or Ca x PO₄ product. 63 subjects had measurable plaque (56%). Carotid plaque # and plaque thickness were associated with PTH levels (plaque # R=0.331 P= .008; MCPT R=0.225 P=.076). There was no association between PTH and IMT. Conversely, an inverse relationship was found between IMT and levels of 25(OH)-vitamin D (R= -.217 P= .08). When controlling for age and sex, only the relationship between PTH and carotid plaque persisted. Calcitriol levels did not correlate with any CV measure.

In summary, in a small group of older adults, PTH levels were associated with carotid plaque and 25(OH)-vitamin D levels inversely related to IMT. PTH has known CV effects, including vasodilation and alterations in heart rate, coronary blood flow, peak pressure, and rate of rise of left ventricular pressure. Vascular calcification may also be accelerated in vitamin D deficiency states. If confirmed, these preliminary data suggest an association between circulating levels of calciotropic hormones and subclinical markers of CV disease, and support the hypothesis that the complex effect of mineral metabolism on vascular biology varies in different parts of the vasculature.

Disclosures: M.D. Walker, None.

W146

Neurocognitive Changes in Mild Primary Hyperparathyroidism. M. D. Walker¹, S. B. Vardy^{*2}, W. B. Inabnet^{*1}, A. Tineo^{*1}, D. J. McMahon¹, F. Cosman², S. J. Silverberg¹. ¹College of Physicians and Surgeons, Columbia University, New York, NY, USA, ²Helen Hayes Hospital, West Haverstraw, NY, USA.

Although patients with primary hyperparathyroidism (PHPT) often report non-specific neuropsychiatric symptoms, these symptoms are not considered an indication for parathyroidectomy (PTX) because of conflicting data on their nature and reversibility. To date, most studies have investigated psychiatric but not cognitive defects. We examine both in this prospective study of mild PHPT. 29 postmenopausal women with PHPT and 95 healthy age-matched women (CTL) have been studied to date, using 10 standardized, validated cognitive and psychiatric tests, at baseline and 5-6 months later (or post-PTX). Differences between PHPT and controls, and association between cognitive dysfunction and serum calcium, parathyroid hormone, and vitamin D levels were investigated. PHPT and CTL subjects were similar in IQ (115 ± 8 vs. 112 ± 8), but those with PHPT were slightly older (62 ± 6 vs. 56 ± 4 yrs; p<0.05) and better educated (17 ± 2 vs. 15 ± 3 yrs; p<0.05) than controls. There were no differences between PHPT and CTL on tests

measuring anxiety (Spielberger State-Trait Anxiety Inventory: 49.9 ± 13.3 vs. 46.2 ± 11.3), visual learning (Rey Visual Design Learning test) or non-verbal abstraction (Booklet Category Test - Victoria Revision). PHPT subjects had more symptoms of depression (Beck Depression Inventory: 8.38 ± 5.9 vs. 5.2 ± 6.7; p=0.03) although both groups measured in the non-depressed range (0-13). Those with PHPT performed worse on tests of verbal memory (Wechsler Memory Scale: Z-score -0.92 ± 0.71 vs. -0.34 ± 0.94; p<0.01) and tended to have worse auditory memory (Bushke Selective Reminding Test: Z-score -0.47 ± 1.27 vs. -0.07 ± 1.20; p=0.09). PHPT subjects also did less well in tests measuring attention & response speed [Rosen Target Detection (RTD) test (47.5 ± 15.6 vs. 39.0 ± 8.9; p<0.01) & Wechsler Adult Intelligence Scale - Revised Digit Symbol (WAIS-R DSY) subtest (12.7 ± 2.1 vs. 12.8 ± 2.2; NS)]. Depressive symptoms and verbal memory improved with PTX, while RTD performance did not. PHPT patients performed better than CTL on tests of mental manipulation (WAIS-R digit span). Decreased attention and response speed was related to serum calcium level (r=0.35; p=0.05).

In summary, in addition to having more symptoms of depression, these PHPT patients performed less well on tests of attention, response speed and verbal memory than did age-matched healthy women. Some cognitive alterations improved with PTX, but those involving attention and response speed did not. While previous investigation has focused on psychiatric features of the disease, this prospective study suggests that neurocognitive function may be altered in mild PHPT.

Disclosures: M.D. Walker, None.

W147

Distance Restraints and Resolution Limit in Molecular Modeling of G Protein-coupled Receptor-Peptide Ligand Interactions. A. Wittelsberger¹, D. F. Mierke², M. Rosenblatt¹. ¹Physiology, Tufts University School of Medicine, Boston, MA, USA, ²Chemistry and Molecular Pharmacology, Brown University, Providence, RI, USA.

Photoaffinity crosslinking studies in combination with molecular modeling are often the only means of gaining insight into the three-dimensional structure of a G protein-coupled receptor-peptide ligand complex. Typically, a contact site identified by photoaffinity crosslinking is used as a distance restraint in molecular dynamics simulations. A ligand analog containing a photoreactive group (e.g. p-benzoylphenylalanine, Bpa) is used in the crosslinking experiment, whereas the simulations are carried out with the native ligand sequence.

We compare models of the parathyroid hormone ligand-receptor complex obtained using distance restraints of different lengths. Our study suggests that a Bpa residue in position 11 of PTH-(1-34) precludes the mid-region of the hormone from entering its binding groove on top of the seven helical bundle, resulting in a crosslinking site outside the bundle at the C-terminal end of the N-terminal extracellular domain. We conclude that a distance around 14 Å corresponds to the resolution limit obtainable with the Bpa-based photoaffinity crosslinking methodology.

Disclosures: A. Wittelsberger, None.

W148

The Nuclear Interactions of the VDR and Lef1 Are Ligand Independent. C. Luisella, M. B. Demay. Endocrine Unit, Massachusetts General Hospital Harvard Medical School, Boston, MA, USA.

Studies investigating the molecular basis for alopecia in VDR null mice have demonstrated that the expression of the VDR in keratinocytes is essential for postmorphogenic hair cycling and that the actions of the VDR that mediate these effects are ligand independent. Vitamin D receptor ablation leads to a gradual decrease in keratinocyte stem cells, associated with an increase in sebaceous differentiation analogous to the differentiation defect seen in the skin of mice with impaired Lef1-βcatenin interactions. Investigations in primary keratinocytes demonstrate that the absence of the VDR impairs the cooperative transcriptional effects of βcatenin and Lef1, however, the nuclear localization of βcatenin in the hair follicle stem cells is not impaired by the absence of the VDR. Studies were, therefore, performed to address whether the VDR could participate in the formation of a complex with βcatenin and/or Lef1 in the absence or presence of ligand. COS-7 cells were transfected with expression vectors for βcatenin, HA-tagged Lef1 and the VDR. Cells were treated with 10⁻⁸M 1,25(OH)₂D₃ or vehicle in charcoal-stripped serum 16 hours prior to harvesting. Nuclei were obtained by mechanical separation and homogenized in lysis buffer containing 0.5% NP-40 and 1% Triton. Immunoprecipitation was performed using a mouse α-HA antibody and protein G sepharose beads. Immunoprecipitated proteins were subjected to Western analyses. Immunoprecipitation of Lef1 resulted in coimmunoprecipitation of the VDR and of βcatenin, both in the presence and the absence of ligand. Thus, in the nuclei of intact cells, the interactions of the VDR with these effectors of the canonical Wnt signaling pathway are not dependent upon the presence of ligand. These results suggest that the ligand-independent interactions of the VDR with one or both of these key effectors of the canonical Wnt signaling are essential for the maintenance of post-morphogenetic hair cycling.

Disclosures: C. Luisella, None.

W149

Prevalence of Hypovitaminosis D and its Correlation with Different PTH Values in a Sample of Postmenopausal Women in Buenos Aires. Z. Man, M. S. Larroude*, M. S. Moggia*, R. D. Diaz*, J. C. Morgenstern*, M. P. D. Yantorno*, M. G. Torres Cerino*, G. A. Macías*, M. Pérez Sáinz*, Centro TIEMPO, C.A. Buenos Aires, Argentina.

Vitamin D (VD) has multiple biological effects, as it plays a key role in the serum calcium homeostasis. The definition of normal values was based on Gaussian distributions of the concentrations seen in apparently healthy subjects, but it did not take into account race, age, latitude, poor dietary VD intake, use of sunscreens. The optimal value would be the one that, below that point, PTH levels starts to increase.

Objective: To evaluate the levels of 25-hydroxyvitamin D [25(OH)D] in a sample of postmenopausal women and its correlation with four groups of PTH levels using two different 25(OH)D cutoff values considered as desirable by two different classifications.

Material and method: 196 postmenopausal women from Buenos Aires and its metropolitan area (Lat: 35°S), mean age: 65 y.(51-85), were evaluated between October and December 2005. Women with thyroid, liver or renal diseases or those treated with corticosteroids, antiepileptic and anticoagulants were excluded. 25(OH)D levels were measured by a RIA assay using the Diasorin® kit, and PTH levels by chemiluminescence. VD status was sorted using the Hollis and McKenna classifications and were correlated with different cut off points for PTH values. The prevalence of secondary hyperparathyroidism (PTH levels > 65pg/ml) was evaluated.

Bruce Hollis classification: 25(OH)D deficiency <10ng/ml; insufficiency 10-20ng/ml; hypovitaminosis 20-30ng/ml; desirable >30ng/ml.

McKenna classification: 25(OH)D deficiency <10ng/ml; insufficiency 10-20ng/ml; hypovitaminosis 20-40ng/ml; desirable >40ng/ml.

We divided PTH values into four categories > 65 pg/ml, > 60 pg/ml, > 55pg/ml, and > 50 pg/ml. **Results:** No VD deficiency was detected. With Hollis classification: 70 women (35.7%) had VD insufficiency; 90 (46%) had hypovitaminosis D; and only 36 (18.3%) had desirable values. And with McKenna classification: 121 women (61.8%) had hypovitaminosis D, and 2,6% had desirable values.

Valor de PTH N=196	VD Hollis < 10 ng/ml	10-20 ng/ml	20-30 ng/ml	> 30 ng/ml
> 65 pg/ml	0	19 (9,7%)	15 (7,7%)	3 (1,5%)
> 60 pg/ml	0	27 (13,8%)	22 (11,22%)	4 (2%)
> 55 pg/ml	0	32 (16,3%)	31 (15,8%)	5 (2,55%)
> 50 pg/ml	0	36 (18,3%)	37 (18,9%)	7 (3,6%)
Valor de PTH N=196	VD McKenna < 10 ng/ml	10-20 ng/ml	20-40 ng/ml	> 40 ng/ml
> 65 pg/ml	0	19 (9,7%)	18 (9,2%)	0
> 60 pg/ml	0	27 (13,8%)	26 (13,2%)	0
> 55 pg/ml	0	32 (16,3%)	36 (18,3%)	0
> 50 pg/ml	0	36 (18,3%)	44 (22,4%)	0

Conclusions: We found that the prevalence of secondary hyperparathyroidism was 1.5% and 0% by using a cut off value for sufficiency of 30 ng/ml and 40 ng/ml. Using values > 40 ng/ml of vitamin D doesn't registered PTH values > 50 pg/ml. Therefore, we recommend a 25 (OH) D cut off value higher than 40 ng/ml.

Disclosures: Z. Man, None.

W150

Calcium-Independent and 1,25-Dihydroxyvitamin D₃-Dependent Regulation of the Renin-Angiotension System in 25(OH)D 1 α -Hydroxylase Knockout Mice. C. Zhou*¹, F. Lu*², D. Goltzman³, D. Miao¹. ¹The Research Center for Bone and Stem Cells, Nanjing Medical University, Nanjing, China, ²Department of Cardiology, Nanjing Medical University, Nanjing, China, ³Department of Medicine, McGill University, Montreal, PQ, Canada.

Previous studies have demonstrated that genetic disruption of the VDR results in overstimulation of the renin-angiotension system (RAS), leading to high blood pressure and cardiac hypertrophy. We employed mice with targeted deletion of the 25(OH)D 1 α -hydroxylase [1 α (OH)ase^{-/-}] gene to determine whether the effect of 1,25(OH)₂D₃ is calcium-dependent or independent. At 6 weeks of age, sex-matched wild-type and 1 α (OH)ase^{-/-} mice were fed a normal diet or a "rescue diet" diet containing 2% calcium, 1.25% phosphorus, and 20% lactose. For 4 subsequent weeks, animals on the normal diet received vehicle or 62.5ng 1,25(OH)₂D₃, intraperitoneally daily while animals on the rescue diet received vehicle, 100mg/Kg captopril, an inhibitor of angiotensin converting enzyme, or 30mg/Kg losartan, an angiotensin II (Ang II) type I receptor antagonist. At the end of this time period, in vehicle-treated 1 α (OH)ase^{-/-} mice, plasma levels of renin, Ang II and aldosterone were raised, and renal renin mRNA and protein levels and renal Ang II mRNA levels were up-regulated. Heart weight relative to body weight (BW), interventricular septum thickness diastolic (IVSD) and left ventricular mass (LVM)/BW were increased, however, indices of cardiac systolic function including fractional shortening (FS) and ejection fraction (EF) were reduced in vehicle-treated 1 α (OH)ase^{-/-} mice compared with their wild-type mice. Although the serum calcium and phosphorus levels were normalized in 1 α (OH)ase^{-/-} mice on the "rescue diet", alterations in blood pressure, RAS and cardiac hypertrophy remained abnormal. In contrast, 1,25(OH)₂D₃ administration not only normalized serum calcium and phosphorus levels, but also normalized the blood pressure, RAS, and cardiac hypertrophy. After administration of either captopril and losartan to 1 α (OH)ase^{-/-} mice, although renin expression remained up-regulated, the blood pressure, cardiac histology and function all normalized. This study demonstrates that 1,25(OH)₂D₃ plays a protective role on the cardiovascular system through repression of RAS and that this action is calcium-independent.

Disclosures: D. Miao, None.

W151

Postpartum Vitamin D Insufficiency and Secondary Hyperparathyroidism in Healthy Danish Women. U. Möller Liendgaard*¹, C. H. Ramlau-Hansen*², L. Rejnmark*³, L. Heickendorff*⁴, T. Brink Henriksen*⁵, L. Mosekilde*¹.

¹Department of Endocrinology and Metabolism C, Aarhus University Hospital, Aarhus, Denmark, ²Department of Occupational medicine, Aarhus University Hospital, Aarhus, Denmark, ³Department of Endocrinology and Metabolism C., Aarhus University Hospital, Aarhus, Denmark, ⁴Department of Clinical Biochemistry, Aarhus University Hospital, Aarhus, Denmark, ⁵Perinatal Epidemiology Research Unit, Department of Obstetrics and Paediatrics, Aarhus University Hospital, Aarhus, Denmark.

Objective: To examine vitamin D status and parathyroid function in normal Danish women postpartum.

Design: Three cross sectional measures during follow-up of 89 women postpartum.

Subjects and intervention: We assessed vitamin D status by measuring plasma 25-hydroxyvitamin D (P-25OHD) and the degree of secondary hyperparathyroidism by measuring plasma parathyroid hormone (P-PTH) in 89 Caucasian women at three consecutive visits: (mean (range)) 23 (10-37) days (spring), 117 (95-140) days (late summer) and 274 (254-323) days (winter) postpartum.

Results: P-25OHD showed seasonal variations with higher values in late summer than in the other periods (p<0.001). At the first visit 65% received vitamin D supplements. At the following visits almost 50% were supplemented. Vitamin D insufficiency (P-25OHD<50 nmol/l) occurred more often during winter (28%) than in spring (14%) (Fishers exact test, p=0.02) or late summer (7%) (p=0.0001). Irrespective of season, vitamin D insufficiency occurred most frequent in women who did not take vitamin D supplements (Fishers exact test, p<0.02). Frank vitamin D deficiency (P-25OHD<25 nmol/l) was observed during winter in 6%. At all three periods P-25OHD correlated inversely with P-PTH indicating secondary hyperparathyroidism at deficient vitamin D status. During spring, late summer and winter three, one, and four females, respectively, had elevated plasma PTH.

Conclusion: Vitamin D-insufficiency with secondary hyperparathyroidism is a frequent finding in healthy Danish women postpartum and especially during winter. Vitamin D supplements reduced the risk of vitamin D insufficiency, especially during winter. Our results support the importance of increased alertness regarding information of pregnant and lactating women about vitamin D supplements. Furthermore, it has to be studied whether the present recommendations of an intake of 5-10 µg vitamin D per day are sufficient, especially during winter months.

Disclosures: U. Möller Liendgaard, None.

W152

Changes in VDR Coregulator Recruitment Result in 1 α ,25(OH)₂D₃ Hypersensitivity in MVNP Expressing Cells. A. Hidalgo*¹, J. Florea*¹, G. D. Roodman², N. Kurihara³, S. Onate*⁴. ¹Urologic Oncology, Roswell Park Cancer Institute, Buffalo, NY, USA, ²Medicine, University of Pittsburgh and VA Pittsburgh Healthcare System, Pittsburgh, PA, USA, ³Medicine, University of Pittsburgh, Pittsburgh, PA, USA, ⁴Pharmacology & Therapeutic, Roswell Park Cancer Institute, Buffalo, NY, USA.

Osteoclast precursors (OCLP) in Paget's disease (PD) are characterized by expression of measles virus nucleocapsid protein (MVNP) and changes in the 1 α ,25(OH)₂D₃ signaling axis that result in their hypersensitivity to 1 α ,25(OH)₂D₃ and abnormal bone remodeling. The effects of 1 α ,25(OH)₂D₃ are mediated by the intracellular 1 α ,25(OH)₂D₃ receptor (VDR). In the absence of ligand, VDR is in the nucleus bound to chromatin loci and associated with the corepressors SMRT and NCoR. This complex represses the transcriptional activity of 1 α ,25(OH)₂D₃ regulated genes by recruitment of histone deacetylases (HDACs) through the corepressors. Ligand activates transcription through recruitment of coactivators SRC-1/p160, CBP/p300, and the DRIP/TRAP mediator complex. Consequently, changes in the VDR coregulator profile may be a mechanism for 1 α ,25(OH)₂D₃ hypersensitivity of PD OCLP. In support of this hypothesis, we reported that TAFII-17, a VDR coactivator, is increased in PD OCLP. To test this hypothesis, 1 α ,25(OH)₂D₃-mediated gene transcription in MVNP transduced cells was analyzed using adenoviral luciferase expression reporter assays linked to the 25-hydroxyvitamin D₃-24-hydroxylase (CYP24) gene promoter. MVNP transduced cells contained similar levels of functional VDR, as control cells. However, 1 α ,25(OH)₂D₃ was much more efficient in promoting VDR-mediated reporter activity in MVNP cells than in controls. Chromatin immunoprecipitation (ChIP) assays showed that the VDR corepressor, SMRT, was released from the CYP24 promoter when MVNP was expressed in the absence of 1 α ,25(OH)₂D₃. Further, immunohistochemistry and confocal analyses showed that the SMRT corepressor was excluded from the nucleus and translocated to the cytosol in MVNP transduced cells, while VDR continued to translocate to the nuclei in the absence or presence of ligand. These results indicate that MVNP alters 1 α ,25(OH)₂D₃ cellular signaling by changing the cellular localization of the SMRT corepressor and decreasing its recruitment to the promoter of VDR regulated genes, thereby increasing their sensitivity to ligand. Taken together, these results suggest that transactivation of 1 α ,25(OH)₂D₃ regulated genes is increased in PD OCLP, in part, due to altered recruitment of coregulators required for VDR-mediated gene transcription.

Disclosures: S. Onate, None.

W153

Vitamin D Status and Infection Frequency in Diabetic Patients. J. Park, S. Jung*, J. Rho*, M. Kim*, H. Jin*, T. Park*, H. Baek*. Division of Endocrinology and Metabolism, Department of Internal Medicine, Chonbuk National University Medical School, Jeonju, Chonbuk, Republic of Korea.

The active metabolite of vitamin D, 1,25-dihydroxyvitamin D₃, is an important immunomodulatory hormone which enhances phagocytosis via the activation of macrophages and influences immune response. Serum 25-hydroxyvitamin D₃ [25(OH)D₃] is a good indicator of vitamin D nutritional status. Increasing susceptibility to infection in diabetes mellitus is support by altered immunity. Polymorphonuclear leukocyte function is depressed, particularly when acidosis is also present. The aim of this study is to determine that 25(OH)D₃ status is associated with infectious disease frequency, together with quantification of factors related to vitamin D status in diabetic patients. Subjects were selected among diabetic patients living in their own homes and spending at least 3 hours per week outdoors. 296 diabetes subjects including 149 case and 147 controls, aged 20 to 80 years were enrolled. Subjects who experience at least one acute infectious disease from 1998 to 2006 were used for cases. We divided the participants into five groups depending in their infectious disease incidences. 25(OH)D₃ was analyzed for the infectious disease frequency and parathyroid hormone, corrected calcium, phosphorus. Subjects with medication that could interfere with vitamin D metabolism or bone mineralization and autoimmune disease as multiple sclerosis, SLE, RA, inflammatory bowel disease, Psoriasis were excluded from study. The mean concentration of 25(OH)D₃ and PTH and corrected calcium were 63.35 ± 35.67 nmol/L and 29.92 ± 31 pg/mL and 2.28 ± 0.17 mmol/L, respectively. The overall prevalence of vitamin D insufficiency (25(OH)D₃ < 80 nmol/L) was 73.3%. In one-way anova analyses, there were significant differences 25(OH)D₃ and corrected calcium by infectious disease frequency. 25(OH)D₃ levels of subjects with at least four recurrent infections were below 50 nmol/L. In multiple linear regression analyses 25(OH)D was negatively and independently associated with PTH levels ($p=0.04$). Serum 25(OH)D concentration at baseline varied cyclically with season, with the solar cycle ($p<0.05$). Approximately 70% of diabetes patients fell below 80 nmol/L, a value considered to be the lower end of the optimal range. Serum 25(OH)D₃ concentration was association with the frequency of infectious diseases in diabetic patients. Experimentally, vitamin D deficiency and host resistance to infectious diseases have not been studied extensively. Further studies are needed to explain the association of the vitamin D status and infection frequency in diabetic patients.

Disclosures: J. Park, None.

W154

Transgenic Expression of the Human Vitamin D Receptor (VDR) in the Proximal Small Intestine of VDR-Null Mice Improves the Utilization of Calcium- and Lactose-Rich (Rescue) Diet in Young Mice. S. Peleg, H. D. Marks*. Endocrine Neoplasia & Hormonal Disorders, M. D. Anderson Cancer Center, Houston, TX, USA.

The hormone 1,25(OH)₂D₃ (1,25D₃) regulates active calcium absorption in the proximal small intestine through binding to its nuclear receptor (VDR). The inactivation of VDR in humans or its ablation in mice causes severe hypocalcaemia and rickets. We have previously shown that transgenic expression of the human VDR (hVDR) in the proximal small intestine of VDR-null mice (hVDR+/mVDR-/-) was insufficient to restore calcium homeostasis and bone mineralization if the mice were fed a normal rodent diet (containing 1% calcium and 0.65% phosphorus). However when 3 months old rachitic mice were fed a rescue diet (2% calcium, 1.25% phosphorus, 20% lactose), the hVDR+/mVDR-/- responded by normalizing bone mineralization and serum calcium, whereas the mVDR-/- mice did not respond. In the present study we investigated whether the hVDR in the proximal small intestine had an effect on mineral utilization even in young mice. To that end, mVDR-/- and hVDR+/mVDR-/- mice were fed a rescue diet starting at weaning (21 day-old) and calcium homeostasis was assessed when they were 60-days old. We found that total serum calcium was normalized in both groups of mice and its levels were not distinguishable from serum calcium in WT mice. In contrast, serum levels of intact PTH were normalized in the hVDR+/mVDR-/- mice but not in the mVDR-/- mice. When femurs were analyzed, we found that bone mineralization improved in the mVDR-/- mice on rescue diet compared to mVDR-/- on normal diet. However, bone mineral density and bone mineral content in these mice were slightly but significantly lower than these values in hVDR+/mVDR-/- mice on rescue diet or WT mice. Furthermore, significant structural abnormalities (thinner cortical bone, and high trabecular density) were detected in the mVDR-/- mice but not in the hVDR+/mVDR-/- mice. We propose that transgenic expression of the hVDR in the proximal small intestine improves calcium homeostasis by correcting fluxes in ionized serum calcium, which prevents excess PTH secretion and abnormal bone mineralization.

Disclosures: S. Peleg, None.

W155

Combination of Vitamin D and BADGE Potentiates their Pharmacological Inhibition of PPARgamma and Increases Osteogenic Differentiation of Adipocyte Precursors. D. Rivas¹, G. Duque². ¹Lady Davis Institute for Medical Research, Montreal, PQ, Canada, ²Medicine/Geriatrics, McGill University, Montreal, PQ, Canada.

Peroxisome proliferator activator gamma 2 (PPARγ2) is one of the main factors involved in the pathogenesis of age-related bone marrow adipogenesis. Although knock out mice for PPARγ2 have shown increased bone mass and lower adipogenesis the pharmacological inhibition of PPARγ2 has shown contradictory results. Studies in diabetic rodents have shown that pharmacological inhibition of PPARγ with bisphenol-A-diglycidyl ether (BADGE) prevents bone marrow adiposity but not bone loss. In this study, we hypothesize that the combination of 1,25(OH)₂D₃ and BADGE would revert the inhibitory effect of BADGE on osteoblastogenesis and therefore facilitate the differentiation of adipocyte precursors into osteoblasts. Human mesenchymal stem cells (MSC) were induced to differentiate into adipocytes for one week. Subsequently, the media was replaced with osteogenesis induction media with either BADGE (5-10 μM), 1,25(OH)₂D₃ (10⁻⁸ M) or both. Untreated cells were used as a control. Cells were treated for two weeks and then stained with alizarin red and alkaline phosphatase (ALP). Additionally, changes in the expression of PPARγ2, cbfa1 and osteocalcin were determined by RT-PCR and western blot. We found that expression of cbfa1 and osteocalcin was significantly affected by BADGE alone while addition of 1,25(OH)₂D₃ reverted this effect. In addition, the reduction in mineralization and ALP activity seen after treatment with BADGE was reverted by 1,25(OH)₂D₃ inducing significantly higher mineralization and ALP activity than untreated cells ($p<0.01$). To further examine the mechanism involved, changes in both PPARγ2 and cbfa1 nuclear complex activation were assessed using ELISA TransAM kit. We found that whereas BADGE inhibited both nuclear complexes activation, addition of 1,25(OH)₂D₃ reverted its inhibitory effect on the cbfa1 complex and potentiate its inhibitory effect on the PPARγ2 nuclear complex. In summary, although the pharmacological inhibition of PPARγ2 could become an alternative for the treatment of age-related bone loss, the combination of an inhibitor plus vitamin D would be required in order to inhibit adipogenesis and stimulate osteoblastogenesis.

Disclosures: D. Rivas, None.

This study received funding from: Canadian Institutes for Health Research.

W156

Development of an Assay for 25-Hydroxyvitamin-D on the Abbott ARCHITECT Analyzer. M. Martens^{*1}, C. van Duren^{*1}, S. Peters-Gdanitz^{*1}, F. Rosmalen¹, W. Krack^{*2}, J. Dhein^{*2}, J. Schultess^{*2}, M. Eppinger^{*2}, M. Hausmann^{*2}. ¹R&D, Future Diagnostics, Wijchen, The Netherlands, ²R&D, Abbott Diagnostics, Delkenheim, Germany.

Background and objective. The concentration of 25-Hydroxyvitamin-D (25-OH Vitamin D), in serum, is considered to be the most reliable determination of the overall vitamin D status.

The purpose of our study was to evaluate a prototype assay for the measurement of 25-OH Vitamin D on the Abbott ARCHITECT instrument.

Methods and results. The ARCHITECT 25-OH Vitamin D assay is a delayed one-step competitive immunoassay that utilizes direct, chemiluminescence technology in combination with paramagnetic particles. The assay utilizes a sheep polyclonal antibody specific for 25-OH-D in combination with biotinylated 25-OH Vitamin D and an anti-biotin monoclonal conjugate. The assay has a reportable range of up to 400 nmol/L (160 ng/mL), and has a time to first result of 36 minutes. Analytical sensitivity for the assay (95% confidence method) was < 3.5 nmol/L. Functional sensitivity (inter-assay imprecision <20%) was < 10 nmol/L. Preliminary assay imprecision, with serum panels, was evaluated based on guidance from CLSI, testing different levels on 1 reagent lot and 1 instrument at 2 separate times per day over 5 days. Imprecision at approximate levels of 25, 150 and 225 nmol/L were < 6%, < 4% and < 6%, respectively. A preliminary method comparison, on a relative small number of samples (n = 21), versus another commercially available diagnostic kit gave a correlation coefficient of 0.97 (Pearson).

Conclusions. Based on our data, we conclude that the ARCHITECT 25-OH Vitamin D assay is a rapid, accurate, and precise automated method for the measurement of 25-Hydroxyvitamin-D.

Disclosures: F. Rosmalen, None.

W157

Calcitriol and its Analog Successfully Elongate Survival Period and Improve the Skeletal Growth via Independent Pathway of Vitamin D Receptor. K. Shiizaki¹, I. Hatamura², T. Sakaguchi³, I. Imazeki⁴, S. Kato⁵, T. Akizawa⁶, E. Kusano¹. ¹Division of Nephrology, Department of Internal Medicine, Jichi Medical University, Shimotsuke, Japan, ²The First Department of Pathology, Wakayama Medical University, Wakayama, Japan, ³Division of Nephrology and Blood Purification Medicine, Wakayama Medical University, Wakayama, Japan, ⁴Product Research Department, Chugai Pharmaceutical Co., Ltd, Gotemba, Japan, ⁵Institute of Molecular and Cellular Biosciences, The University of Tokyo, Tokyo, Japan, ⁶Department of Nephrology, Showa University School of Medicine, Tokyo, Japan.

It is well known that vitamin D plays a major role in skeletal and mineral homeostasis through the interaction with nuclear vitamin D receptor (VDR) of target cell. For the investigation of VDR-independent effects of calcitriol (CAL) and maxacalcitol (OCT) on these, VDR knockout (VDR^{-/-}) mice treated by the high dose of CAL and OCT were analyzed.

VDR^{-/-} mice were fed normal or high calcium diet containing 20% lactose (rescue diet) immediately after weaning. These rats were intraperitoneally administered by CAL (20 µg/kg), OCT (20 µg/kg) or control solution (CONT) at three times a week for eight weeks. The differences in survival status among these treatments were investigated in mice fed normal diet. The measurements of serum ionized Ca (iCa), phosphorus (P) and intact-PTH levels and histopathological examinations of femur were performed 24 hours after the final administration in mice fed rescue diet.

The survival periods of mice administered by both CAL and OCT were significantly longer than that with control treatment (about three and two folds in mice treated by CAL and OCT, respectively). The significant differences in serum iCa, P, and intact-PTH levels among the treatments in mice fed rescue diet were not observed. However, the enlarged and distorted cartilaginous growth plates and the irregular disposition of chondrocytes were observed in mice administered by CONT, and the treatments with CAL and OCT normalized these deformities.

These results suggest that CAL and OCT elongate the survival period and improve skeletal growth via independent pathway of VDR without significant changes in serum iCa, P, and intact-PTH levels. Vitamin D may exert discreet effects on survival, skeletal growth and mineral metabolism via VDR-dependent or -independent manner.

Disclosures: K. Shiizaki, None.

W158

The Vitamin D Receptor, Hedgehog Signaling and Epidermal Carcinogenesis. A. E. Teichert¹, J. J. Welsh², D. D. Bikle¹. ¹Endocrine Unit, UCSF-NCIRE, San Francisco, CA, USA, ²Department of Biological Sciences, University of Notre Dame, Notre Dame, IN, USA.

Over 1 million skin cancers occur annually in the United States, 80% of which are basal cell carcinomas (BCC) (16% squamous cell carcinomas, 4% melanomas), making it by far the most common cancer. Extensive epidemiologic data support the concept that the incidence of a number of epithelial malignancies (e.g. breast, prostate, colon) is reduced by increasing 25OHD levels. 1,25(OH)₂D₃, produced by the kidney from 25OHD or locally produced, reduces proliferation and enhances differentiation and thus has been investigated for a role in preventing or treating cancer. However, UVB exposure, which increases 1,25(OH)₂D₃ production in the keratinocyte, causes skin cancer. Conceivably, the 1,25(OH)₂D₃ produced by the skin provides at least partial protection from UVB induced skin cancer such that lack of 1,25(OH)₂D₃ or its receptor would make the skin even more sensitive to UVB induced malignancy.

We have chosen UVB epidermal carcinogenesis as a model to directly address the issue of the balance between the increased risk of UVB exposure as an inducer of carcinogenesis with the benefit of promoting vitamin D and thus 1,25(OH)₂D₃ production in the epidermis as a chemopreventive measure.

Mice deficient for the vitamin D receptor (VDR null mice), for which 1,25(OH)₂D₃ is a ligand, have a marked hyperproliferative response in the hair follicle and epidermis and decreased epidermal differentiation. These mice, when treated with 7,12 dimethylbenzanthracene (DMBA), unlike their wildtype littermates, develop skin tumors containing hair follicle elements and/or are of basal cell origin, tumors characteristic of overexpression of the hedgehog (HH) signaling pathway in keratinocytes. We found that the epidermis and hair follicles of the VDR null animals, as well as the DMBA induced tumors in VDR null mice, overexpress elements of the HH signaling pathway [Sonic Hedgehog (Shh), Patched 1 (Ptc1), Smoothened (Smoh), Gli 1, and Gli 2]. Moreover, keratinocytes in which the VDR has been knocked down with siRNA directed against the VDR show increased expression of Shh.

Interestingly, mice overexpressing Gli1, Gli2, or Shh in their basal keratinocytes or grafted with human keratinocytes overexpressing Shh develop BCC like lesions. Furthermore, BCC show overexpression of Ptc1, Smoh, Gli1 and Gli2, raising the question of a link between the vitamin D system, HH signaling and skin cancer predisposition.

These results suggest then that increased expression of Shh in the keratinocytes of the VDR null animal activates the HH signaling pathway, predisposing the skin to the development of BCC.

Disclosures: A.E. Teichert, None.

This study received funding from: NIH.

W159

Effect of Plasma 1,25-Dihydroxyvitamin D Concentration or Calcium Intake on Negative Correlation between Plasma 25-Hydroxyvitamin D and PTH Concentrations in Japanese Adolescents. N. Tsugawa¹, K. Uenishi², H. Ishida³, R. Ozaki¹, M. Kamao¹, Y. Suhara¹, T. Okano¹. ¹Hygienic Sciences, Kobe Pharmaceutical University, Kobe, Japan, ²Laboratory of Administrative Dietetics, Kagawa Nutrition University, Sakado, Japan, ³Laboratory of Physiological Nutrition, Kagawa Nutrition University, Sakado, Japan.

It is known that vitamin D insufficiency leads to secondary hyperparathyroidism, which has a negative effect on bone metabolism in the elderly. However, little is known about the effect of the vitamin D status on PTH concentration in Japanese adolescents. Plasma PTH concentration is also known to be regulated by dietary calcium (Ca) intake or 1,25-dihydroxyvitamin D (1,25D). The aim of this study is to examine the association between vitamin D status and PTH concentration in healthy Japanese adolescents and the effect of dietary Ca intake and plasma 1,25D concentration on the negative correlation between 25D and PTH concentrations. A total of 324 healthy Japanese adolescents aged 12-18 years (boys: 158, girls: 166) had enrolled in this study. Plasma PTH concentration was negatively correlated with 25D concentration or dietary Ca intake, and positively correlated with 1,25D. If 25D and 1,25D concentrations and dietary Ca and vitamin D intakes were included in the original model of stepwise multiple linear regression analyses, 25D and 1,25D concentrations and dietary Ca intake were independently associated with plasma PTH concentration. When subjects were divided into two groups (high and low Ca groups) by median of dietary Ca intake (462 mg/d), slope and intercept of equation obtained from negative correlation between 25D and PTH concentrations in low Ca group were higher than those in high Ca group. On the other hand, when subjects were divided into two groups (high and low 25D groups) by 20 ng/mL of plasma 25D concentration, slope and intercept of equation obtained from negative correlation between dietary Ca intake and PTH concentrations in low 25D group were higher than those in high 25D group. Plasma 1,25D concentration associated with only PTH concentration. However, when subjects were divided into high and low 25D groups, slope of equation obtained from positive correlation between PTH and 1,25D concentrations in high 25D group were higher than those in low 25D group. These results suggest that increases of 25D concentration and dietary Ca intake could independently decrease plasma PTH concentration. Moreover, although plasma 1,25D concentration did not directly associate with plasma 25D concentration, it was confirmed that the increase rate of 1,25D concentration which depends on PTH concentration was associated with plasma 25D concentration in adolescents.

Disclosures: N. Tsugawa, None.

W160

Global Vitamin D Levels in Relation to Age, Gender, Ethnicity, and Latitude: an Ecologic Metaregression Analysis. T. Hagenau¹, R. Vest¹, T. Gissel¹, C. S. Poulsen¹, M. Erlandsen², L. Mosekilde³, P. Vestergaard¹. ¹The Osteoporosis Clinic, Aarhus Amtssygehus, Aarhus, Denmark, ²Department of Biostatistics, Aarhus University, Aarhus, Denmark, ³Department of Endocrinology and Metabolism C, Aarhus Amtssygehus, Aarhus, Denmark.

Aim: To study vitamin D status (serum 25-hydroxy-vitamin D (25OHD)) in native subjects in all regions to assess deficiency by latitude.

Subjects and methods: We retrieved 5,855 papers from January 1, 1970 to November 1, 2004 by searching PubMed, Embase, and Web of Science using terms: "serum", "25-hydroxy-vitamin D", "cholecalciferol", and "human". Inclusion criteria were studies on serum 25OHD levels in healthy subjects around the world.

Results: A total of 393 studies including 33,332 subjects from all over the world were included in the study. The mean serum 25OHD level was 54 nmol/l (95% CI: 51-57 nmol/l). Women had significantly higher 25OHD levels than men (p=0.02), and Caucasians had higher levels than non-Caucasians (p<0.01). Serum 25-OHD levels were higher in subjects aged >15 years than in younger subjects (p<0.01).

Unadjusted there was a small non-significant decrease in serum 25OHD with latitude (-0.11±0.10 nmol/l per degree latitude north or south of equator, p=0.27). There was a significant decline with latitude for Caucasians (-0.69±0.30 nmol/l per degree, p=0.02), but not for non-Caucasians (0.03±0.39 nmol/l per degree, p=0.94). After adjustment for age, gender, and ethnicity, no overall correlation was present between serum 25OHD and latitude (-0.29±0.24 nmol/l per degree, p=0.23).

Conclusion: The present analysis has shown that vitamin D status globally depend on age, gender, and ethnicity. There was no overall influence of latitude. However, in separate analyses plasma 25-OHD decreased with latitude in Caucasians but not in non-Caucasians. The study indicates a widespread global vitamin D insufficiency compared with proposed threshold levels.

Disclosures: P. Vestergaard, None.

W161

Identification of cEts1 and STAT1 as Potential Primary Targets in the Secondary Gene Regulation of the Human Fibroblast Growth Factor-23 Gene by 1,25-dihydroxyvitamin D₃. A. Hsieh^{*1}, M. Gurevich^{*1}, D. Mathern^{*1}, M. J. Kaczmarek^{*1}, C. A. Haussler², G. K. Whitfield², M. R. Haussler². ¹Biochemistry & Molecular Biophysics, University of Arizona College of Medicine, Tucson, AZ, USA, ²Basic Medical Sciences, University of Arizona College of Medicine, Phoenix, AZ, USA.

The mammalian fibroblast growth factor-23 (FGF23) gene encodes a protein hormone, produced in osteoblasts, that serves as a potent inhibitor of kidney phosphate reabsorption. The hormonal form of vitamin D, 1,25-dihydroxyvitamin D₃ (1,25D), has a reciprocal role to that of FGF23, promoting both kidney reabsorption and intestinal absorption of phosphate. Recent findings have revealed that FGF23 and 1,25D form an endocrine loop, with 1,25D upregulating FGF23 and the resulting FGF23 inhibiting production of 1,25D to close the loop. The stimulatory effect of 1,25D was previously shown in rat osteoblast-like UMR-106 cells to involve a substantial increase in FGF23 mRNA. Transactivation by 1,25D is typically mediated by the vitamin D receptor (VDR), which binds to vitamin D response elements (VDREs) in the vicinity of regulated genes. However, conserved VDREs of the DR3 or ER6 type have not been found near the FGF23 locus; also, previous cycloheximide experiments indicated that 1,25D regulates FGF23 likely via a secondary mechanism. Utilizing a bioinformatics approach to seek potential secondary regulators, we first located segments of sequence conservation within 130 kb upstream and 20 kb downstream of the FGF23 gene using the UC Santa Cruz genomic browser, which compares sequences among 14 vertebrate genomes. Within these conserved sequences, we then sought consensus binding sites for known transcriptional regulators. This search yielded several candidates, notably members of the STAT and GATA families, as well as cEts1. As an initial screen, regulation of the relevant mRNAs by 1,25D was examined in rat UMR-106 cells. Two nuclear factors, cEts1 and STAT1, were found to be both well expressed in UMR-106 cells and also reproducibly (~2-fold) upregulated by 1,25D. Examination of the cEts1 promoter revealed two conserved VDREs of the DR3 type located at -24 and -26 kb upstream of the rat cEts1 promoter. These two VDREs were shown to bind VDR in a gel mobility shift and are currently being evaluated for their ability to confer 1,25D responsiveness onto a heterologous luciferase reporter gene. We will also evaluate if VDR binding to these sequences actually takes place in vivo via a chromatin immunoprecipitation assay. Elucidation of the molecular details whereby 1,25D regulates FGF23 will significantly enhance our overall understanding of bone mineral homeostasis in mammals.

Disclosures: G.K. Whitfield, None.

W162

Co-stimulation of 1,25-(OH)₂D₃ and BMP-2 Enhances the Expression of VDR and RANKL mRNA in Osteoblasts. Y. Yoshikawa, A. Kamada, E. Domae*, S. Goda*, I. Tamura*, A. Kawamoto*, J. Okazaki*, Y. Komasa*, T. Ikeo. Osaka Dental University, Hirakata, Japan.

1,25-(OH)₂D₃ (1,25-(OH)₂D₃) appears to indirectly induce osteoclast formation by up-regulating RANKL expression and down-regulating OPG expression in marrow stromal cells. A recent study has shown that BMP-2 enhances the induction of osteoclast formation by 1,25-(OH)₂D₃, but little is known about the mechanism of the promoting effect of 1,25-(OH)₂D₃ and BMP-2 co-stimulation on osteoblast-osteoclast interaction. In this study, we investigated the time-dependent expression of RANKL, OPG and vitamin D receptor (VDR) mRNA in osteoblasts co-stimulated with 1,25-(OH)₂D₃ and BMP-2.

Osteoblastic MC3T3-E1 cells were grown in culture medium with 1,25-(OH)₂D₃ and BMP-2 for 3, 6, 12 and 24 hours. Total RNA was extracted from cells and first-strand cDNA was synthesized from total RNA using reverse transcriptase. The mRNA expression level was assessed using real-time PCR.

The mRNA expression of VDR in osteoblasts increased significantly 3 hours after co-stimulation with 1,25-(OH)₂D₃ and BMP-2 compared with that stimulated with 1,25-(OH)₂D₃ only ($p < 0.01$). RANKL mRNA expression also increased significantly 6 hours after co-stimulation ($p < 0.01$), while OPG mRNA expression showed no significant difference at any time course.

These results suggested that BMP-2 may accelerate the 1,25-(OH)₂D₃-induced osteoclast formation by through enhance the expression of VDR and following RANKL in osteoblast.

Disclosures: Y. Yoshikawa, None.

W163

Plasminogen Activator Inhibitor (PAI-1) Deficiency Enhances Fracture Callus Size but Reduces Cartilage Remodeling During Fracture Repair. C. H. Rundle, X. Wang*, R. M. Porte*, J. E. Wergedal, S. Mohan, K. H. W. Lau. Research (151), J.L. Pettis VAMC, Loma Linda, CA, USA.

The plasmin system, which functions in extracellular matrix remodeling, plays a critical role in tissue healing, including bone repair. Plasminogen activators (PAs), key activators of the plasmin system, are regulated by plasminogen activator inhibitors (PAIs). Consistent with a regulatory role of PAI-1 in bone, we have found that femur size parameters of adult male PAI-1 knockout (KO) mice [C57BL/6 (B6) background] were reduced relative to adult male B6 mice (periosteal circumference: 14 % less, 4.51 ± 0.13 vs 5.23 ± 0.14 mm, $p < 0.0001$; endosteal circumference: 19% less, 3.10 ± 0.12 vs 3.82 ± 0.15 mm, $p < 0.0001$; femur length: 4% less, 15.3 ± 0.31 vs 16.01 ± 0.47 mm, $p < 0.02$). Because we have also found PAI-1 gene expression to be reduced during fracture healing, we evaluated fracture healing in PAI-1 KO mice to determine

its functional role in bone repair. Adult male PAI-1 KO mice and B6 mice (12 weeks, $n=6$ per group) underwent femoral fracture, and fracture healing was followed by pQCT and histomorphometry at 7, 10, 14, 21 and 28 days post-fracture. When compared with B6 mice, PAI-1 KO fractures displayed increased woven bone area at 10 days (1.66 ± 0.11 vs 1.30 ± 0.36 mm², $p < 0.05$) and 14 days healing (4.77 ± 1.34 vs 2.48 ± 0.86 mm², $p < 0.002$) and increased bone mineral content (BMC) at 10 days (0.43 ± 0.03 vs 0.28 ± 0.13 mg, $p < 0.03$), 14 days (1.27 ± 0.37 vs 0.54 ± 0.29 mg, $p < 0.001$) and 28 days healing (0.57 ± 0.18 vs 0.35 ± 0.08 mg, $p < 0.04$). These results are consistent with increased callus size and bone. Histomorphometry ($n=3$ to 5 mice per group) at 7, 14 and 21 days healing showed that the relative cartilage area:total callus area at 14 days healing was greater in PAI-1 KO mice than in B6 mice ($38 \pm 8\%$ vs $11 \pm 4\%$, respectively, $p < 0.0003$). The augmented callus cartilage and bone were even greater in PAI-1 KO mice than in B6 mice when normalized for the smaller femur size in PAI-1 KO mice. At 28 days, the callus bone remained elevated in PAI-1 KO mice, but was remodeled to cortical bone in B6 mice, suggesting that callus remodeling in PAI-1 KO mice was less effective than in B6 mice. Histology revealed that PAI-1 deficiency not only failed to accelerate bony union of the fracture, but also yielded an abnormal pattern of callus remodeling by 14 days healing in which the surface of the fracture callus cartilage ossified prior to its interior. Conclusions: 1) PAI-1 is an important regulator of bone, since PAI-1 deficiency reduced bone size and marrow space and reduced bone length in KO mice, 2) PAI-1 deficiency may impede fracture cartilage remodeling, resulting in an enlarged callus, and 3) because PAI-1 deficiency yielded an abnormal pattern of bony bridging, the PAI/PA system may have a regulatory role in bony union of the fracture.

Disclosures: C.H. Rundle, None.

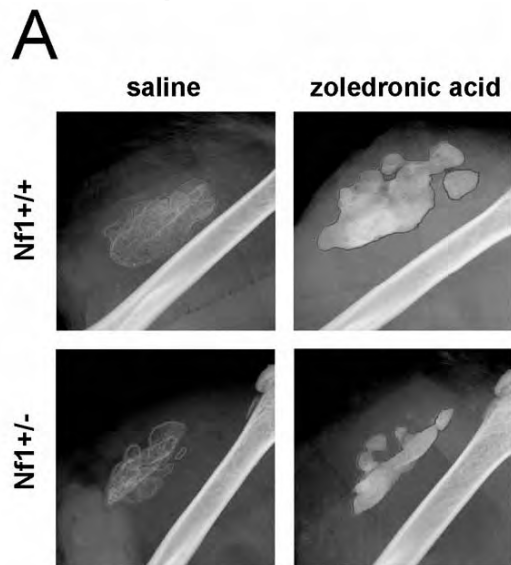
W164

Modeling Bone Morphogenetic Protein and Bisphosphonate Combination Therapy in Wild Type and Nf1 Haploinsufficient Mice. A. Schindeler*, M. Ramachandran*, C. Godfrey*, A. Morse*, M. M. McDonald*, K. Mikulec*, D. G. Little*. Orthopaedic Research & Biotechnology, The Children's Hospital at Westmead, Westmead, Australia.

Recombinant bone morphogenetic proteins (BMPs) show promise in treating the orthopaedic complications associated with neurofibromatosis type 1 (NF1), such as congenital pseudarthrosis of the tibia. Minimal scientific data is available regarding the effects of BMPs in the context of NF1. We hypothesized that as abnormalities in both bone formation and resorption have been documented in Nf1-deficient mice, co-treatment with the bisphosphonate zoledronic acid (ZA) could be used to augment the effects of BMP-induced bone formation.

First, primary osteoblasts isolated from wild type (Nf1^{+/+}) and Nf1-deficient (Nf1^{-/-}) mice were cultured in the presence and absence of BMP-2. While Nf1^{-/-} cells exhibited significantly less alkaline phosphatase (ALP) expression than Nf1^{+/+} cells ($P < 0.01$), addition of 100ng/ml BMP-2 for 1 week increased ALP by 2-fold in cells of both genotypes ($P < 0.01$). Analogous results were obtained for matrix mineralization at 3 weeks. To model this response in vivo, 20µg BMP-2 was implanted intramuscularly into the quadriceps of 12 week old mice to induce heterotopic bone. When examined radiographically, less heterotopic bone was present in Nf1^{-/-} mice than in Nf1^{+/+} controls at both 3 weeks ($P < 0.03$) and 6 weeks ($P < 0.01$). Mice of an Nf1^{-/-} genotype also showed an increase in osteoclast number relative to bone surface (Oc.N/BS) suggesting a greater potential for the resorption of BMP-2 induced bone.

To test the effect of an anti-resorptive agent, BMP-2 implanted mice were co-treated twice weekly for 3 weeks with 0.02mg/kg ZA or with saline. ZA treatment led to a synergistic increase in the amount of heterotopic bone in both Nf1^{+/+} and Nf1^{-/-} mice compared with saline controls, as measured by dual-energy X-ray absorptiometry ($P < 0.03$) and histomorphometry (BV/TV, $P < 0.01$). However, significantly less net bone was still observed in Nf1^{-/-} mice ($P < 0.03$) indicating that despite suppressing bone catabolism with ZA, bone anabolism remained impaired.



BMP-2 induced heterotopic bone

Thus, the anabolic deficiency noted in *Nf1*^{+/−} mice is amenable to stimulation by BMP-2, but mineralized tissue formation remains below that of *Nf1*^{+/+} controls in vitro and in vivo. Bisphosphonate combination therapy is superior to BMP therapy alone in terms of net bone production in vivo in both wild type and *Nf1*-deficient mice.

Disclosures: A. Schindeler, None.

This study received funding from: The Australian Orthopaedic Association, The Neurofibromatosis Association of Australia.

W165

Identification of Novel Dentin Matrix Protein-1 (DMP1) Mutations in Two Unrelated Kindreds with Autosomal Recessive Hypophosphatemia. S. Turan¹, M. Bastepe¹, A. Bereket^{*2}, T. Akcay^{*2}, T. Güran^{*2}, O. Mäkitie^{*3}, H. Jüppner¹. ¹Endocrine Unit, Massachusetts General Hospital and Harvard Medical School, Boston, MA, USA, ²Pediatric Endocrinology, Marmara University, Istanbul, Turkey, ³Hospital for Children and Adolescents, University of Helsinki, Helsinki, Finland.

DMP1, a non-collagenous bone matrix protein, is thought to play an important role in bone mineralization. Homozygous DMP1 mutations have recently been identified as a cause of an autosomal recessive form of hypophosphatemia (ARHP). Here, we report two new unrelated ARHP kindreds in whom the affected individuals carry novel homozygous DMP1 mutations. The index case in the first kindred was 3 years old when he presented with short stature and bowing of the legs that had become apparent during late infancy after he started to walk. Laboratory investigations revealed hypophosphatemia (2.8 mg/dl) due to renal phosphate-wasting, elevated serum alkaline phosphatase activity (964 U/L) and normal serum PTH levels (47.6 pg/ml). Similar clinical and biochemical findings were observed for his 16 month-old brother and his 12.5 year-old female cousin; the parents of all three affected children are first-degree cousins. In the second family, the index case and his sister are now 78 and 66 years old respectively. Both patients presented in early childhood with bone pain and bowing of their legs, and later in life, developed severe joint pain and contractures, calcifications of paraspinal ligaments leading to complete immobilization of the cervical, thoracic and lumbar spine, and significant cranial hyperostosis. Laboratory studies revealed hypophosphatemia due to renal phosphate-wasting as well as increased markers of bone turnover. Nucleotide sequence analysis of the PCR-amplified exons encoding DMP1 and the flanking intronic regions lead, in the first kindred, to the identification of a novel homozygous frame-shift mutation (485Tdel) in exon 6 resulting in a premature stop codon. The parents and available unaffected siblings were heterozygous for 485Tdel. In the second kindred, a novel homozygous missense mutation was identified that changes a conserved serine located in exon 6 to cysteine (S69C). The identified genetic mutations underscore the importance of DMP1 in the pathogenesis of ARHP and for the normal regulation of phosphate homeostasis.

Disclosures: S. Turan, None.

This study received funding from: National Institutes of Health (R21 DK075856-01).

W166

Bone Formation Rate Falls After Puberty in *Brtl* OI Mouse Due to Cellular Uncoupling. T. E. Uveges^{*1}, W. A. Cabral^{*1}, C. Bergwitz^{*2}, F. Legard^{*3}, P. Collin-Osdoby^{*4}, A. Forlino^{*5}, P. Osdoby^{*4}, G. A. Gronowicz^{*3}, J. C. Marini¹. ¹BEMB, NIH/NICHD, Bethesda, MD, USA, ²Endo Unit, Mass Gen/Harvard Med, Boston, MA, USA, ³U Conn Health Ctr, Farmington, CT, USA, ⁴Dept Biology/Bone&Min Metab, Washington U, St. Louis, MO, USA, ⁵Dept Biochem, U of Pavia, Pavia, Italy.

The *Brtl* mouse is a knock-in model for moderately severe (type IV) osteogenesis imperfecta (OI); it carries a mutation causing a classical glycine substitution on one *col1a1* allele (Gly349Cys) and models the molecular, biochemical and phenotypic changes (small size, reduced BMD) of OI. We have previously shown that 2-month *Brtl* femurs have reduced cortical thickness and cross-sectional area and fracture at a lower maximum load. Geometric parameters remain reduced while load to fracture normalizes after puberty, implying that *Brtl* pubertal adaptation increases material strength and elastic modulus.

We have now examined *Brtl* long bone histomorphometry, cellular function and bone formation and resorption at 2 and 6 months of age to further understand the pathophysiology of OI. Both cortical and trabecular bone are reduced in *Brtl* before and after puberty; *Brtl* BV/TV is reduced 40-45%. An uncoupling of cellular number develops after puberty, favoring osteoclast number and function. *Brtl* ObS/BS is comparable to that of wt littermates at both ages. ObS decreases about 40% in both genotypes with age, although *Brtl* marrow can replenish osteoblasts as efficiently as wt marrow, as demonstrated by normal numbers of CFU at both ages. In contrast, OcS/BS is increased in *Brtl* compared to wt at both ages (35-45%), as are the number of TRAP positive cells (50-35%). Interestingly, OcS falls only modestly (~ 1/5) after puberty. Noc is stable and TRAP positive cells decline substantially (~ 4/5). *Brtl* MAR and BFR are comparable to wt at 2 months of age, declining to half of wt values only at 6 months. These data suggest that both (1) uncoupling of cellular numbers, with a greater decline in ObS than OcS at 6 months, and (2) a decline in production of bone matrix by *Brtl* osteoblasts occur as *Brtl* mice age. Normal levels of urinary DPD crosslinks were detected in *Brtl*, as in many OI patients with structural defects of collagen; the lack of elevation of bone resorption in spite of increased osteoclasts may reflect the matrix insufficiency of *Brtl* or resistance of abnormal matrix to resorption. Finally, although *Brtl* osteoblasts in culture deposit normal amounts of mineral, as detected by alizarin red staining, mineralized *Brtl* bone has reduced levels and organization of birefringence under polarized light, suggesting that mineral deposited on the abnormal *Brtl* matrix is improperly aligned. Changes in the composition of bone matrix or mineral may underlie the improved mechanical properties of post-pubertal *Brtl* bone.

Disclosures: T.E. Uveges, None.

W167

Double KO of the Huntingtin Interacting Protein-1 (HIP1) Family Members, HIP1 and HIP1r, Lead to an Osteopenic Phenotype with Severe Spinal Defects. E. I. Waldorff^{*1}, T. S. Hyun^{*2}, K. I. Oravec-Wilson^{*2}, T. S. Ross^{*2}, S. A. Goldstein¹. ¹Orthopaedic Surgery, University of Michigan, Ann Arbor, MI, USA, ²Internal Medicine, University of Michigan, Ann Arbor, MI, USA.

Endocytic protein HIP1 has been shown to be over-expressed in a variety of cancers and both HIP1 and HIP1-related (HIP1r) prolong the half-life of multiple growth factor receptors. Previously generated double HIP1/HIP1r KO (DKO) mice surprisingly demonstrated a dramatic skeletal phenotype distinguished by dwarfism and severe kypholordosis. Single HIP1 KO mice have less severe kypholordosis while HIP1r KO mice have no spinal defects.

To investigate the effect of the HIP1 family on skeletal development; closed, internally-stabilized transverse fractures were created in left tibiae of 3 WT, 7 Het (HIP1r^{-/-};HIP1^{+/+}), and 3 DKO female 3.5 month old mice. Fractures were examined 4 wks post-fracture using microCT and histology. The spine and right tibiae were examined using microCT, while marrow from both femora was used for protein analysis using Western blots.

Compared to Het and WT, DKO mice have smaller spine angle; larger vertebral bodies, smaller vertebral foramen and smaller posterior spinous processes; a trend for decreased TMD of the vertebral body; increased vascularity in the thoracic vertebrae; shorter tibiae, lower tibial cortical and trabecular TMD; smaller cortical thickness; a trend toward decreased BVF of tibial trabecular bone and thinner trabeculae, while trabecular number were similar.

RANK expression of the femoral marrow was similar between groups, but the transcription factor, NFATc1, which acts downstream of RANK, was more highly expressed for DKO mice. Previous studies have shown no change in osteoclast numbers or differentiation, and normal TRAP5b serum levels for DKO mice.

DKO fracture callus was smaller than the other groups, with a trend toward higher BMD within the callus. Histological examinations showed that DKO mice had higher cartilage to callus ratio, and higher ratio of TRAP positive surface to total surface within the callus. Red blood cell numbers in the callus were increased for DKO mice, indicating a possible increase in vascularity.

The interpretation of the data suggests several possible underlying mechanisms that might explain the skeletal phenotype of the DKO mouse. Deletion of the HIP1 family may affect primary bone formation in the long bones through the influence on cartilage matrix formation, or direct bone matrix formation. Results from the fracture study in combination with the vertebral defects, suggest that progenitor cell availability, tissue maintenance and remodeling might also be compromised in this phenotype. Further longitudinal studies will examine the fracture repair over time.

Disclosures: E.I. Waldorff, None.

W168

Aromatase Deficiency in an Adult Chinese Male Caused by Heterozygote for Two New Point Mutations in the CYP19 Gene. O. Wang^{*}, X. Xing^{*}, X. Meng^{*}, M. Nie^{*}, Z. Chen^{*}, M. Li^{*}, W. Xia^{*}, Y. Jiang^{*}. Endocrinology, Peking Union Medical College Hospital, Beijing, China.

The aromatase enzyme encoded by CYP19 gene catalyzes the conversion of androgens to estrogens. Deficiency of aromatase causes estrogen deficiency which may affect bone growth and metabolism. The purpose of this study was to report the first Chinese male with aromatase deficiency and the genetic mutations in his CYP19 gene.

The 24-year-old male was admitted in Peking Union Medical College Hospital for continuing linear growth for 24 years and malformation in his legs for 2 years. He had no growth spurt. Sexual function was normal. When he was 22-year-old he got genua valga which deteriorated gradually. His parents and brother were phenotypically normal. His mother was 165cm, father 172cm and brother 175cm in height. The patient was 182.5cm and the ratio of the upper segment to the lower segment was 0.92. Physical examinations showed genua valga, acanthosis nigricans and enlarged liver. The secondary male characteristics and testicular size were normal. The biochemical markers and BMD were measured. Genomic DNA was extracted from WBC of peripheral blood from the patient and his family members. Ten exons of CYP19 gene were amplified by PCR and sequenced directly.

His serum testosterone levels were 14.6 to 20.5nmol/l while estrogen level was undetectable. FSH and LH levels were elevated. Bone age was 16 years old. Epiphyses were unfused in lower extremities, phalange and wings of iliac bones. BMD was reduced at lumbar spine (Z score = -2.9) and femoral neck (Z score = -0.9). Semen analysis was normal. OGTT suggested type 2 diabetes mellitus. Serum cholesterol level was elevated with increased ALT levels and severe liver steatohepatitis identified by ultrasound. Genetic analysis showed two heterozygous point mutations in CYP19 gene, one was Tyr81Cys in exon 3 (from his mother), the other was Leu451Pro in exon 10 (from his father). This new case of aromatase deficiency confirmed previous studies that estrogen plays an important role on bone growth and gain of peak bone mass in males. Estrogen may also affect glucose and lipid metabolism in males. In this patient, two new point mutations in CYP 19 gene are likely to be the molecular basis of his estrogen deficiency.

Disclosures: O. Wang, None.

W169

Osteoprotegerin Deficiency (Juvenile Paget's Disease): Responses to Oral and IV Bisphosphonates in 3 Children. D. Wenkert¹, M. Natter^{2*}, M. Otsuka^{3*}, N. Fish^{4*}, J. Lopez-Benitez^{5*}, M. Markowitz^{6*}, W. McAlister^{7*}, S. Mumm⁸, M. Whyte⁵. ¹Shriners Hospt Children, St Louis, MO, USA, ²Tufts-New Eng Med Ctr, Boston, MA, USA, ³N. Navajo Med Ctr, Shiprock, NM, USA, ⁴Montefiore Hospt, Bronx, NY, USA, ⁵Wash U Sch Med, St Louis, MO, USA.

Osteoprotegerin (OPG) deficiency, the principal variant of juvenile Paget's disease, is a rare, autosomal recessive osteopathy featuring markedly accelerated bone turnover. Here, we assess responses of 3 affected, unrelated children to bisphosphonate (BP) therapy (Table).

Pt #1: A 4 yr old boy of Cypriot descent suffered leg swelling, periosteal elevation, and ESR=74 from "Caffey disease" diagnosed at age 1 mo. Alkaline phosphatase (ALP) reached 2470 U/L. Hearing (normal at birth) was lost by 21 mo (cochleas absent on CT). Three fxs and warm, bony expansions deformed all limbs. Growth, except head size (OFC), was stunted. On referral, he had weakness, torticollis, chest and limb deformity, could not sit, and cried when moving. X-rays showed markedly expanded bones, "bowtie" vertebrae, thickened diploic space, and marked coxa vara.

One wk after 1/3 mg/kg pamidronate (PAM), he sat; 3 weeks after the first 3-dose cycle (total ~2 mg/kg), he crawled. After 3 cycles, he stood. Stamina, appetite, mood, torticollis, and mobility remarkably improved.

Pt #2: A 7 yr old girl of Puerto Rican descent seemed well until an atraumatic femoral fx at age 2. X-rays showed limb deformities from "Engelmann disease" (ALP 1963 U/L). By referral, she had 4 fxs (25% ht, 20% wt, 5% arm span, <5% sitting ht, and >95% OFC), mild deafness, and arm pain; leg pain limited walking. Femurs and tibias were bowed. X-rays showed periosteal elevation, osteopenia, and expanded bones. At age 10, after 1.5 yrs of alendronate, knee pain was minimal.

Pt #3: An 11 yr old, dwarfed, deaf, Navajo boy (NEJM 2002; 347:175) had macrocephaly, and chest and limb deformity. He became poorly compliant for calcitonin, and declined risedronate. At age 7, PAM was begun (ALP max 2716) with symptom and x-ray improvement.

Pt 1 and 2 had different, homozygous, loss-of-function defects in exon 2 of TNFRSF11B encoding OPG. Pt #1 had a frame-shift, single base deletion (c.278delT), likely forming no functional protein, consistent with severe disease. Pt #2 had a missense mutation (c.T349C, p.Phe117Leu) causing a less severe phenotype. Pt #3 is deleted for OPG.

Children with OPG deficiency show varying responsivity to BPs, reflecting the underlying OPG mutation.

Biochemical and DXA response to Bisphosphonates in 3 children with OPG deficiency

	Pt 1		Pt 2		Pt 3	
	Pamidronate (i.v.) (6 mo of 8 mg/kg/6 mo)		Alendronate (p.o.) (1.5 yr of 35 mg twice/wk)		Pamidronate (i.v.) (3.5 yr of ~8 mg/kg/yr)	
	Before	After	Before	After	Before	After
ALP (IU/L)	720	247 (nl)	1232	303 (nl)	1927	436 (nl)
Osteocalcin (mg/g)	31	79	53	97	197	142
Urine Ca/Cr (mg/g)	488	615	373	85	489	715
ESR (mm/hr)	61	17	37	11	57	15
CRP (mg/dL)	2.5	<0.5	<0.8	<0.5	<0.1	-
L1-L4 DXA (Z-score)	-6.8	-2.7	-3.1	+0.1	-3.1	+0.4

Disclosures: D. Wenkert, None.

This study received funding from: Shriners Hospitals for Children, The Clark and Mildred Cox Inherited Metabolic Bone Disease Research Fund, The Barnes-Jewish Hospital Foundation, and The Hypophostasia Research Fund.

W170

Three Novel Mutations of the PheX in Three Chinese Families with X-linked Hypophosphatemic Rickets. W. Xia^{1*}, X. Meng¹, Y. Jiang^{1*}, X. Xing^{1*}, M. Li^{1*}, O. Wang^{1*}, Y. Pei^{2*}, L. Yu^{1*}, L. Pang^{1*}, Y. Sun^{1*}, Y. Hu^{1*}, X. Zhou^{1*}. ¹Endocrinology, Peking Union Medical College Hospital, Beijing, China, ²Endocrinology, Second Artillery Forces General Hospital, Beijing, China.

X-linked hypophosphatemia (XLH), the most prevalent form of inherited rickets in humans, is a dominant disorder of phosphate homeostasis characterized by growth retardation, rachitic and osteomalacic bone disease, hypophosphatemia, and renal phosphate wasting. The gene responsible for XLH was identified by positional cloning and designated PHEX (formerly PEX) to depict a phosphate regulating gene with homology to endopeptidases on the X chromosome. Recently, extensive mutation analysis of the PHEX gene has revealed a wide variety of gene defects in XLH. The ethnic distribution of the mutations is very broad. Only a few mutations in Chinese were reported previously. To analyze the molecular basis of three unrelated Chinese families with XLH, we determined the nucleotide sequence of the PHEX gene and fibroblast growth factor 23 (FGF-23) gene of affected members. The serum FGF-23 concentrations of these patients with XLH were also measured. Three different types of novel mutations were observed in three families respectively from our study: one deletion mutation c.264delG causing p.W88 X; one missense mutation c.1673C>G causing p.P558A; one non-sense mutation c.1809G>A causing p.W603 X. Serum concentration of FGF-23 in XLH patients of these three families was significantly higher than normal range. These results suggest that PHEX gene mutations were responsible for XLH in these Chinese patients. And these mutations may contribute to higher serum FGF-23 level.

Disclosures: W. Xia, None.

W171

Identification of Sex-specific QTL for Femoral Neck Density and Strength in Inbred COP and DA Rats. I. Alam¹, Q. Sun¹, L. Liu^{2*}, D. L. Koller², L. G. Carr^{3*}, M. J. Econs³, T. Foroud², C. H. Turner¹. ¹Biomedical Engineering, Indiana University Purdue University Indianapolis, Indianapolis, IN, USA, ²Medical and Molecular Genetics, Indiana University Purdue University Indianapolis, Indianapolis, IN, USA, ³Medicine, Indiana University Purdue University Indianapolis, Indianapolis, IN, USA.

Hip fracture is one of the most common osteoporotic fractures with significant morbidity and mortality. Several studies in humans identified potential chromosomal regions linked to hip size and bone mass. Animal models, particularly the inbred rat, serve as a potential complementary model for studying the genetic influences on hip fragility. Previously we demonstrated that, despite similar body size, Copenhagen 2331 (COP) rats had greater femoral neck biomechanical properties compared with Dark Agouti (DA) rats. To identify genes regulating fracture risk at the femoral neck, we mapped quantitative trait loci (QTL) for femoral neck density, structure and strength phenotypes using 828 (405 males and 423 females) F2 progeny derived from the inbred COP and DA rats. Skeletal phenotypes were measured by peripheral quantitative computed tomography (pQCT) and biomechanical testing. Femoral neck phenotypes included volumetric bone mineral density (vBMD), cross-sectional area, polar moment of inertia (Ip), neck width, ultimate force, and energy to break. We performed a whole-genome screen using 93 microsatellite markers with an average intermarker distance of 20 cM. Genetic marker maps were generated using MAPMAKER/EXP from the COP x DA F2 data and compared with published Rat Genome Database (RGD) maps. These recombination based maps were then employed for genome-wide linkage analyses to detect sex-specific and sex-independent QTLs. Permutation testing was employed to obtain the thresholds for genome-wide significance (p<0.01). Strong evidence of linkage for femoral neck vBMD QTLs was observed on chromosomes (Chrs) 1, 2, 10, 17 and 18 when both males and females F2 were included in the analyses. In addition, QTLs affecting femoral neck structure were found on Chrs 7, 10 and 17 and QTLs for biomechanical properties were detected on Chrs 1, 4, and 15. Sex-specific QTL analyses revealed several QTLs that have male-specific effects: total vBMD on Chrs 2 and 18, cortical vBMD on Chr 2, trabecular vBMD on Chr 17 and biomechanics on Chr 15. Female-specific QTLs were found on Chr 10 for total and cortical vBMD, and on Chr 1 for trabecular vBMD and biomechanics. Several QTL regions identified in this study are homologous to human chromosomal regions previously linked to QTLs contributing to femoral neck and related phenotypes. In summary, we detected evidence that sex-specific QTL contribute to hip fragility in the rat.

Disclosures: I. Alam, None.

W172

Heritability of the Principal Components of a Statistical Shape Model Describing Baboon Midshaft Femur Geometry. T. L. Bredbenner¹, L. M. Havill², M. C. Mahaney², D. P. Nicoletta¹. ¹Materials Engineering, Southwest Research Institute, San Antonio, TX, USA, ²Genetics, Southwest Foundation for Biomedical Research, San Antonio, TX, USA.

Cross-sectional geometry is an important contributor to bone strength. Studies in humans and inbred rodents suggest that bone shape is under partial genetic control. It is less clear, however, that genes contribute substantially to normal population-level variation in bone geometry. Using the pedigreed baboon, an established nonhuman primate model for the genetics of bone strength-related traits, we previously established that geometric properties of the midshaft femur are significantly heritable. In the present study, we developed a statistical shape model to efficiently describe the complex geometry of a set of midshaft transverse sections from 110 pedigreed baboons (30 male, 80 female; 5-33 yrs) and investigated the heritability of principal components of the statistical shape model. Midshaft sections were digitized, the images were segmented, and cubic splines were fit to inner and outer cortical boundaries. Parameter vectors were defined for each section using spline point coordinates and a statistical shape model (SSM) representation of all cross-sections was developed using the minimum description length (MDL) method. A Principal Component Analysis of the statistical shape model showed that 90% of the variability in bone cross-section geometry can be described using 6 independent components (Table 1). Shape component scores were determined to reconstruct individual cross-sectional boundaries from the statistical shape model. Maximum likelihood-based variance decomposition methods were used to estimate the mean effects of age and sex covariates and the additive effects of genes on the variability of the first 6 shape factors (Table 1). Covariate effects accounted for ~10-55% of the variability in shape factor values (p_{age} , p_{sex} , and/or $p_{age \times sex}$ < 0.005). The additive effects of genes significantly influence ($p < 0.1$) the normal variation in the 2 dominant shape factors that described 77% of the variability in baboon midshaft femur geometry. The statistical shape model retains significant dependence on the additive effects of genes and potentially can be used to efficiently quantify the contribution of bone geometry to an individual's risk of fracture.

Factor	Results of Principal Component Analysis and Variance Decomposition		
	Principal Component Analysis	Heritability	Covariate Effects
	% SSM Variability Explained	$h^2 \pm \text{Std.Err. (p value)}$	% Factor Variability Explained
b ₁	41.9	0.24 \pm 0.20 (0.07)	55.2
b ₂	35.0	0.41 \pm 0.28 (0.036)	27.7
b ₃	5.4	0 (0.5)	36.4
b ₄	3.2	0.13 \pm 0.21 (0.245)	9.5
b ₅	2.5	0 (0.5)	32.3
b ₆	2.0	0.25 \pm 0.28 (0.157)	22.3

Disclosures: T.L. Bredbenner, None.

This study received funding from: Southwest Research Institute Advisory Committee for Research.

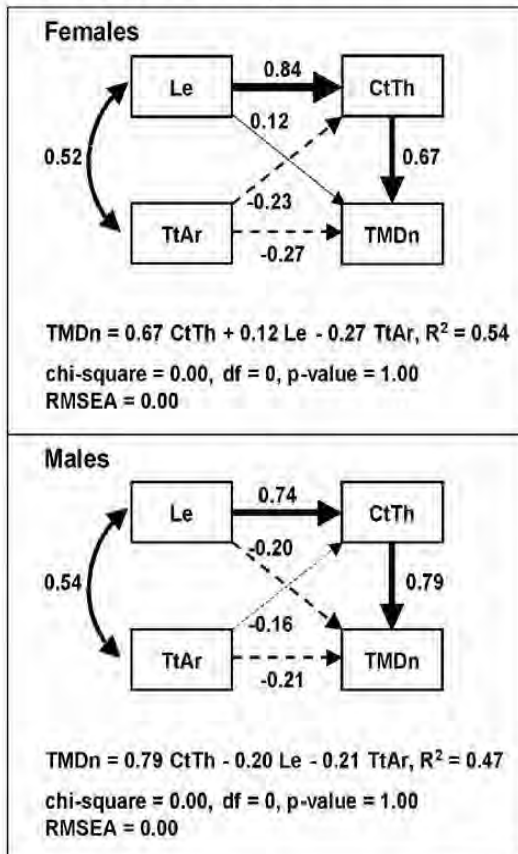
W173

Single Chromosome Substitutions Alter Functional Interactions Among Femoral Morphological Traits and Mineral Density in Inbred Mice. H. C. Courtland¹, B. Hu^{*1}, A. Hill^{*2}, J. B. Singer^{*3}, E. S. Lander^{*3}, J. H. Nadeau^{*2}, K. J. Jepsen¹. ¹Orthopaedics, Mount Sinai School of Medicine, New York, NY, USA, ²Case Western Reserve University, Cleveland, OH, USA, ³The Broad Institute of MIT and Harvard University, Cambridge, MA, USA.

Prior work established a hierarchical relationship between heritable whole bone traits (morphology, ash content) and mechanical properties that define fracture susceptibility in inbred mice. Functional interactions among these traits were then determined using Path Analysis on a panel of adult AXB/BXA Recombinant Inbred (RI) strains (Fig. 1)[1]. To test if genetic manipulation can perturb these functional interactions, we examined whole chromosome substitutions of 21 B6-Chr^A strains (C57BL/6J background with one chromosome replaced by the corresponding A/J chromosome), many of which demonstrate a significant alteration of whole bone traits. 16 week B6-Chr^A femoral length (Le), total area (TtAr), cortical thickness (CtTh) and tissue mineral density (TMDn) values were measured. The expected TMDn value for each B6-Chr^A strain was calculated using the AXB/BXA RI structural equation for TMDn. Significant differences between the expected TMDn and actual TMDn were calculated using genome-wide corrected t-tests ($p \leq 0.003$). Results showed that four female B6-Chr^A (2, 6, 16, and X) and male B6-Chr^A (2, 3, 4, and 18) strains had observed TMDn values significantly different than expected. For both female and male B6-Chr² mice and male B6-Chr² mice, TMDn was significantly lower than expected based on values for Le, CtTh, and TtAr which were similar to B6. Female B6-Chr^{6,16,X} mice had Le, CtTh, and TtAr values significantly larger than B6 and yet their observed TMDn values were not different than B6. The observed decrease in TMDn in male B6-Chr⁴ mice was not expected based on an increase in CtTh and in male B6-Chr¹⁸ mice a large increase in TMDn was not expected with a small increase in femoral length. Thus, eight chromosomes alter the functional relationship between femoral morphology and TMDn in inbred mice, suggesting that one or more genes present have a role in maintaining the biological control mechanisms that establish mechanically functional combinations of femoral TMDn, Le, CtTh, and TtAr. Future studies are needed to determine if these chromosomes disrupt functional interactions during growth.

[1] Jepsen et al. Mamm. Gen. 2007 In Press

Figure 1. Path diagrams detailing functional interactions among femoral bone traits in female and male RI mice. Straight arrows and path coefficients indicate functionally related bone traits with directionality (causality). Structural equations are listed below each Path diagram.



Disclosures: H.C. Courtland, None.

W174

Genome-wide Scan for QTL Influencing Bone Mineral Density: The Southwest Ohio Family Study. S. A. Czerwinski^{*1}, M. Lee¹, A. C. Choh^{*1}, E. W. Demerath^{*1}, B. Towne^{*1}, R. J. Sherwood^{*1}, D. L. Duren^{*1}, J. Blangero^{*2}, S. A. Cole^{*2}, R. M. Siervogel¹. ¹Community Health, Wright State University Boonshoft School of Medicine, Kettering, OH, USA, ²Genetics, Southwest Foundation for Biomedical Research, San Antonio, TX, USA.

In order to identify QTL influencing susceptibility to osteoporosis, we performed genome-wide quantitative trait linkage analysis on bone mineral density (BMD) phenotypes collected in a sample of individuals from five large extended families participating in the Southwest Ohio Family Study. A total of 581 (265 males, 316 females) individuals ranging in age from 8-86 years had at least one BMD phenotype and genetic marker data. These individuals were genotyped for 395 autosomal markers spaced approximately every 10 cM along the genome. Our analyses focused on three BMD phenotypes- total body, femoral neck and lumbar spine collected using the Hologic QDR 4500 bone densitometer (Hologic, Inc., Waltham, MA). Using a variance-components based maximum likelihood method (SOLAR) for pedigree data, we calculated initial heritability estimates (h^2) and identified quantitative trait loci (QTL) influencing variation in the three BMD phenotypes. In this sample, each of the BMD traits measured was highly heritable ranging from $h^2 = 0.31$ to 0.56 ($p < 0.000001$) after adjusting for the effects of age, sex, age², age-by-sex, age²-by-sex, ethnicity, and height. Preliminary results of the quantitative trait linkage screen revealed significant evidence for linkage on chromosome 3 (82cM) near marker D3S1300 with a maximum LOD of 3.6. Evidence of suggestive linkage was also found on chromosome 6 (165 cM) near marker D6S441 with a maximum LOD of 2.8, and on chromosome 2 (51 cM) near marker D2S165 with a maximum LOD of 2.0. These results provide preliminary evidence of replication of linkage signals between our study and other previous studies.

Disclosures: S.A. Czerwinski, None.

W175

Positional Cloning Identified ESR2, ESRRB, BMP4 and LTBP2 as the Candidate Genes for the Quantitative Trait Locus in Chromosome 14 for BMD Variation. Z. J. Dai¹, C. L. Cheung¹, P. C. Sham^{*2}, V. Chan^{*1}, K. D. K. Luk^{*3}, A. Paterson^{*4}, A. W. C. Kung¹. ¹Department of Medicine, The University of Hong Kong, Hong Kong, China, ²Genome Research Centre, The University of Hong Kong, Hong Kong, China, ³Department of Orthopaedics and Traumatology, The University of Hong Kong, Hong Kong, China, ⁴Hospital for Sick Children, University of Toronto, Toronto, ON, Canada.

Chromosome 14 has previously been linked to BMD variation in several genome-wide linkage studies. To replicate and fine-map the quantitative trait locus (QTL) influencing BMD in southern Chinese, a high-density linkage and association screen of chromosome 14q13-32 was performed using high-density microsatellite markers in 306 extended southern Chinese families having a proband with BMD Z score < -1.28 (equivalent to lowest 10th percentile of the population) at either hip or spine. Candidate genes were identified within the QTL with gene prioritization using the Endeavour programme. Genotyping of the candidate genes was performed with Tag SNPs in another cohort of 600 pairs of unrelated high (Z score $> +1$) and low BMD (Z score < -1.28) subjects. Maximum LOD score of 1.89 was detected at 69.2cM (14q23) for total hip BMD. LOD scores greater than 1.2 were detected at 14q21 for femoral neck BMD, 14q12-13 and 14q23 for trochanter BMD. Five candidate genes were identified within these regions, namely estrogen receptor β (ESR2), bone morphometric protein 4 (BMP4), estrogen-related receptor β (ESRRB), latent transforming growth factor beta binding protein 2 (LTBP2), and transforming growth factor beta 3 (TGFB3). Significant association was detected with the following SNPs: T1213C, A110732G of ESR2, rs762642 and rs2071047 of BMP4, rs2980896, rs4903413 and rs12436385 of ESR2, rs2359141, rs3825709, rs2286411, rs2043948 and rs7569 of LTBP2, rs3917201 of TGFB3. Epistasis revealed significant gene-gene interaction between these genes which may be the underlying mechanism explaining the linkage peak. Our results identified multiple genes within the QTL in chromosome 14 that contribute to BMD variation in the general population. These results help in understanding the pathophysiology of low bone mass and osteoporosis.

Disclosures: Z.J. Dai, None.

This study received funding from: Grants from Hong Kong Research Grant Council, Osteoporosis Research Fund, Matching Grant, University Research Committee/Committee of Research and Conference Grants of the University of Hong Kong.

W176

Heritability of Lumbar Trabecular Bone Mechanical Properties in Baboons. L. M. Havill¹, M. R. Allen², T. L. Bredbenner³, D. P. Nicoletta³, D. B. Burr², C. H. Turner⁴, M. C. Mahaney¹. ¹Southwest Foundation for Biomedical Research, San Antonio, TX, USA, ²Indiana University School of Medicine, Indianapolis, IN, USA, ³Southwest Research Institute, San Antonio, TX, USA, ⁴Indiana University Purdue University, Indianapolis, IN, USA.

Mechanical properties of bone provide a direct and inclusive measure of bone's fracture resistance. Genetic effects on these properties have been demonstrated in rodents but not in primates, and the degree to which these genes contribute to population level normal variation in mechanical properties is unknown. In this study we 1) characterize normal variation, including age and sex effects, on vertebral trabecular bone mechanical properties in a non-human primate model, and 2) detect and quantify the proportion of variation in these properties that is due to the additive effects of genes (heritability (h^2)). Cranio-caudally oriented trabecular bone cores (6 mm x 8 mm) were obtained from the L3 vertebral body of 156 baboons (110 females, 46 males; 6-32 years) from a single extended pedigree. Cross-sectional area and bone volume/tissue volume for each core were obtained via microCT (uCT-20; SCANCO USA, Inc.). Each core was then tested to failure in monotonic compression (0.5 mm/min) using a servohydraulic testing machine (Model 858 Mini Bionix II, MTS Corp.). Ultimate stress, modulus, and toughness were determined from load vs displacement data (10Hz). Age, sex, and additive genetic effects were assessed using maximum likelihood-based variance components methods. After accounting for relatively small but significant age and sex effects, a substantial amount of the residual variation in ultimate stress (0.58 ± 0.20 ($p=0.0005$)), modulus (0.29 ± 0.24 ($p=0.0855$)) and toughness (0.64 ± 0.22 ($p=0.0003$)) is attributable to genes. Subsequent analyses in which bone volume ($h^2=0.55 \pm 0.20$ ($p=0.0009$)) is accounted for yield non-significant heritability estimates for ultimate stress (0.15 ± 0.14 ($p=0.1042$)) and modulus (0.02 ± 0.13 ($p=0.4413$)), suggesting that much of the genetic effect detected in the first analyses acts through bone volume. Interestingly, the results for toughness differ. When bone volume is accounted for, a significant genetic effect on toughness (0.29 ± 0.23 ($p=0.0389$)) remains. This indicates that variation in toughness is due, in part, to genes that affect bone volume, but also to genetic effects that are independent of bone volume. These results clearly demonstrate that mechanical properties of vertebral trabecular bone are strongly heritable in the baboon and that these genetic effects are largely, but not entirely, due to genetic effects on bone volume.

Disclosures: L.M. Havill, None.

W177

A Genome-Wide Scan of Metacarpal Bone Geometric Strength Indices in the Framingham Study. N. Shimabuku¹, S. Menn², S. Demissie³, L. A. Cupples³, D. P. Kiel², D. Karasik². ¹Creighton U Med Sch, Omaha, NE, USA, ²IFAR, Hebrew SeniorLife, Boston, MA, USA, ³Biostatistics, BU Sch Public Health, Boston, MA, USA.

Bone geometry, which has a substantial genetic component, contributes to a bone's ability to resist fracture. Metacarpal bones have the same characteristic geometry of other long bones in the body and have been routinely measured in previous research studies to predict fractures and quantify bone loss. Thus, to identify chromosomal regions governing bone geometry and strength, we performed linkage analysis of metacarpal bone geometry indices.

In this study, a genome-wide scan (with a set of 615 markers with an average spacing of 5.7 cM) was performed on 1,702 individuals from 330 extended families of the Framingham study. Metacarpal strength indices, namely Metacarpal Cortical Thickness (MCT), Cortical Index (MCI), and Section Modulus (MZ), were obtained at the midshaft, from the digitized x-rays of 1,412 men and women (mean age, 56.6 yrs parents ($n=638$), 47.3 yrs offspring ($n=774$)). Data for metacarpals 2, 3 and 4 were averaged. All indices were adjusted for age and age² in each sex. Two-point and multipoint linkage analysis was performed using SOLAR, to determine regions of excess chromosomal sharing.

Heritability (h^2) was significant for all indices, ranging from 0.53 and 0.62 (Table). Both two-point and multipoint linkage identified several chromosomal regions with the maximum log10 of the odds ratio (LOD) scores >2.0. Thus, MCI and MCT were linked to chr. 7 (149 cM) with multipoint LOD>2.0. MZ was linked with chr. 9 (49 cM) (multipoint LOD=2.4). Highest LOD scores (both two- and multipoint) were obtained at chr. 11 (between 101 and 106 cM) with MZ. Additional adjustment for height and weight did not change h^2 but generally reduced the LOD scores, especially multipoint.

In conclusion, in this preliminary study, we have identified excess allelic sharing at the genomic markers D11S2000 and D11S1986 on chr.11q21-q22, as demonstrated by the section modulus, which reflects bending resistance. Linkage to this and other regions may be in some part due to effects on body size. Identification and subsequent characterization of loci for bone strength of the appendicular skeleton can further elucidate the genetic contributions to bone geometry and resistance to stress.

		MCT	MCI	MZ
Chrom.	Heritability	0.53 +/- .06	0.62 +/- .05	0.60 +/- .05
	marker (position, cM)	LOD scores: two-point (multipoint)		
7	D7S3061 (149)	1.24 (2.11)	2.10 (2.43)	0 (0)
9	D9S1121 (49)	0 (0)	0 (0)	1.22 (2.40)
11	D11S2000 (101)			3.29 (1.97)
	D11S1986 (106)	0 (0)	0 (0)	2.46 (2.95)

* two-point (multipoint)

Disclosures: D. Karasik, None.

This study received funding from: NIAMS/NIA, NHLBI.

W178

Linkage Screen for Bone Mineral Density Phenotypes in Male and Female COP and DA Rat Strains. D. L. Koller¹, I. Alam², Q. Sun², L. Liu³, M. J. Econs³, T. Foroud⁴, C. H. Turner⁴. ¹Medical and Molecular Genetics, Indiana University School of Medicine, Indianapolis, IN, USA, ²Biomedical Engineering, Indiana University School of Medicine, Indianapolis, IN, USA, ³Medicine, Indiana University School of Medicine, Indianapolis, IN, USA, ⁴Orthopaedic Surgery, Indiana University School of Medicine, Indianapolis, IN, USA.

Studies attempting to localize and identify genes contributing to variation in BMD in both humans and model organisms have demonstrated that multiple genes of modest effect may be involved. Since inbred strains of experimental animals may be informative for only a subset of these genes, we undertook a genome screen to identify BMD QTLs in F2 progeny derived from the inbred Copenhagen 2331 (COP) and dark agouti (DA) strains of rats to complement our previous study in inbred Fisher 344 and Lewis rats. Phenotyping of areal BMD (aBMD) and volumetric BMD (vBMD) at the lumbar spine and femur was completed in 828 animals (405 male and 423 female). Microsatellite marker typing was performed using 93 markers at an average density of 20 cM. Skeletal phenotypes were measured by peripheral quantitative computed tomography (pQCT) and DEXA. Genetic marker maps were generated using Mapmaker/EXP from the genotype data and compared with published maps (RGD). These genotype, phenotype, and mapping data were then employed in the R/qtl software package to perform genome-wide linkage analyses to detect QTLs acting in both sexes as well as those that have sex-specific effects. Permutation tests were conducted to determine genome-wide significance thresholds. A major QTL was detected in both sexes on chromosome 18 for vBMD at midfemur (genome-wide $p<0.01$). On distal chromosome 1, a QTL was found in both sexes affecting femur and lumbar aBMD as well as vBMD at distal femur, and this QTL appears distinct from the proximal chromosome 1 QTL impacting BMD in our previous Fisher 344xLewis F2 cross. Additional aBMD and vBMD QTLs on chromosomes 2, 6, and 10 were also detected in both sexes of the COPxDA F2. Several sex-specific QTL were also detected, notably for the distal femur vBMD phenotype. These included a male-specific QTL ($p<0.01$) on chromosome 8 and female-specific QTL on chromosomes 7 and 14 ($p<0.01$). Interestingly, few of the QTL identified demonstrated overlap with the significant QTLs from the Fisher/Lewis cross. These results confirm the presence of QTL which act in both sexes, as well as some which are gender specific. In addition, unique QTL appear to influence different measures of BMD. Thus, the genetic architecture of BMD in the rat model is quite complex and would appear to be influenced by a number of different genes.

Disclosures: D.L. Koller, None.

W179

Evidence for QTL Underlying Normal Variation in Calcaneal Quantitative Ultrasound Measures: The Southwest Ohio Family Study. M. Lee¹, A. C. Choh², E. W. Demerath¹, B. Towne¹, R. J. Sherwood¹, D. L. Duren¹, J. Blangero², R. M. Siervogel¹, S. A. Cole², S. A. Czerwinski¹. ¹Community Health, Wright State University Boonshoft School of Medicine, Kettering, OH, USA, ²Genetics, Southwest Foundation for Biomedical Research, San Antonio, TX, USA.

Research in the the genetics of osteoporosis has steadily increased in recent years, but the identification of specific genes that influence osteoporosis risk factors such as calcaneal quantitative ultrasound (QUS) measures is still not well established. Quantitative ultrasound traits are correlated with bone mineral density (BMD), but are useful independently from BMD, as they predict risk for future fracture. The purpose of this study is to conduct a whole genome scan to search for quantitative trait loci influencing normal variation in QUS traits. QUS measures were collected from a subset of 555 individuals (255 males and 300 females) from the Southwest Ohio Family Study who were genotyped and had at least one QUS measurement. Participants ranged in age from 8 to 86 years and were distributed across 5 large extended families. Using the Sahara @ bone sonometer (Hologic, Inc., Waltham, MA), speed of sound (SOS), broadband ultrasound attenuation (BUA), and quantitative ultrasound index (QUI) were collected in each heel (right and left). Variance components based linkage analysis was performed on all six traits using 395 polymorphic genetic markers spaced approximately 10 cM apart across the whole genome to identify quantitative trait loci (QTL) influencing the QUS traits. Age, sex, race and weight effects were simultaneously estimated in all models. Initial heritability estimates (h^2) for the 6 QUS traits ranged from 0.54 to 0.68. Suggestive evidence for a QTL influencing SOS was found on chromosome 5p15 (LOD = 2.00) near marker D5S1953, while a suggestive QTL on chromosome 5q32 (LOD = 2.23) near marker D5S436 was found for QUI. An additional suggestive linkage was observed on chromosome 15q21 for both SOS (LOD = 2.27) and QUI (LOD=2.23) near marker D15S978. Additionally, QTL with LOD scores > 1.5 were observed on chromosomes 1, 3, and 16.

Disclosures: M. Lee, None.

W180

A Quantitative Trait Locus Mapping to Chromosome 2p Influences Variation in Bending Resistance of Bone: The Framingham Osteoporosis Study. M. C. Mahaney¹, L. M. Havill¹, S. Demissie², L. A. Cupples², D. P. Kiel³, D. Karasik³. ¹Genetics, Southwest Foundation for Biomedical Research, San Antonio, TX, USA, ²School of Public Health, Boston University, Boston, MA, USA, ³Hebrew SeniorLife, Institute for Aging Research, Boston, MA, USA.

Genes influencing geometric bone indices at the hip have not been clearly identified in previous studies. Thus we used maximum likelihood based variance decomposition methods to detect, characterize, and localize to specific chromosomal regions the effects of genes influencing variation in average buckling ratio (ABR), cross sectional moment of inertia (CSMI), and section modulus (Z) at the femoral neck (FN) and proximal femoral shaft (FS) measured in more than 1350 Framingham Osteoporosis Study participants from 323 nuclear and small extended families. Initial analyses of age- and sex-adjusted residuals following inverse-Gaussian normalization detected significant ($P \leq 1.72 \times 10^{-15}$) additive genetic effects; with heritability estimates (h^2) ranging from $h^2 = 0.34$ (FN-ABR) to $h^2 = 0.61$ (FS-Z). Univariate whole genome linkage screens detected genome-wide significant evidence (at $\alpha = 0.05$, LOD=3.01) for a quantitative trait locus (QTL) for two bending resistance traits (FS-CSMI and FS-Z) at the same genomic location: 80 cM from 2pter. Bivariate statistical genetic analyses revealed that nearly all (94%; $\rho_G = 0.97$, $P < 5.23 \times 10^{-37}$) additive genetic variance in these two measures was due to the shared effects of the same gene(s). Follow-up bivariate linkage analyses focusing on chromosome 2 supported a pleiotropic QTL at this same location (QTL-specific genetic correlation, $\rho_Q = 1.0$, $P < 0.0001$). Although univariate evidence for an FS-ABR QTL on 2p was only suggestive, a subsequent trivariate linkage analysis that included this measure in addition to FS-CSMI and FS-Z found significant ($P < 0.0001$), complete ($\rho_Q^2 = 1$), and negative (i.e., $\rho_Q = -1$) QTL-specific pleiotropy between it and both FS-CSMI and FS-Z. These observations are consistent with known differences in the relationships of the variables to fracture resistance: i.e., both CSMI and Z are positively correlated with bone strength while increased ABR is associated with higher fracture risk. Additionally, bivariate whole genome linkage screens localized pleiotropic QTLs influencing CSMI and Z at both the FS and FN sites (respectively, maximum bivariate LOD=3.19 and LOD=2.81) at this same location on 2p. Peak evidence places all the QTLs detected in this study just qter of the midpoint of a 16.4 mb region bounded by D2S1352 and D2S1772 and within which no bone related QTLs or obvious candidate genes have been mapped previously. We conclude that this QTL contributes to variation in bending resistance-related traits at both proximal femur sites.

Disclosures: M.C. Mahaney, None.

W181

QTL on Chr 11 Regulates Bone Shape in SAMP6 Mice. B. Otsuki¹, M. Shimizu², M. Mori³, S. Okudaira², R. Nakanishi², K. Higuchi³, T. Tsuboyama², T. Nakamura². ¹Orthopaedic Surgery, Kishiwada City Hospital, Kishiwada, Japan, ²Orthopaedic Surgery, Kyoto University, Kyoto, Japan, ³Aging Angiology, Shinsyu University, Matsumoto, Japan.

In our previous study using SAM strains, we reported a QTL (Pbd1) on Chr11 with significant linkage to cortical thickness index (CTI, Fig. 1A). The aim of this study was to clarify the effects of Pbd1 and narrow the QTL region. All mice were handled according to the Guideline for Animal Experiments of Kyoto University.

We first generated a congenic strain named P6.P2-Pbd1b that carried a 39 cM SAMP2-derived Chr11 interval onto a SAMP6 background, and the CTI of P6.P2-Pbd1b was significantly higher than that of SAMP6 (Fig. 2). To narrow the interval, sixteen sub-congenic strains that have smaller overlapping intervals were generated (Fig. 2). From the CTI or BA/TA values, the Pbd1 locus should be seated on the region between D11Mit10 and D11Mit184.

In the morphological analyses of femora using μ CT at 16 weeks (Fig.1B and 1C), the cross-sectional shape of S5 at midshaft was more compressed than that of SAMP6 in the anteroposterior direction (Fig.1D). We then examined the time-course change of OBL between SAMP6 and S5 (Fig.1E). OBL was not different at 5 days of age. However, the difference in OBL became remarkable as they grew, indicating that the difference was formed in the process of bone modeling. The shape of epiphyseal growth plate of SAMP6 and S5 was not different; however, dynamic histomorphometrical analysis at 8 weeks revealed that rates of endocortical and periosteal bone formation were different between SAMP6 and S5 (Table 1).

In conclusion, the Pbd1 locus that was seated between D11Mit10 and D11Mit184 alters the cross-sectional shape of the femur.

Dynamic histomorphometrical parameters at the midshaft (n=9).			
Parameters	SAMP6	S5	p
Ps.MAR (μ m/day)	4.07 (1.35)	2.39 (0.59)	0.0058
Ps.BFR/BS (μ m/day)	1.83 (0.67)	1.60 (0.28)	0.38
Ec.MAR (μ m/day)	3.16 (0.76)	5.25 (1.02)	0.0002
Ec.BFR/BS (μ m/day)	1.62 (0.51)	2.34 (0.68)	0.025

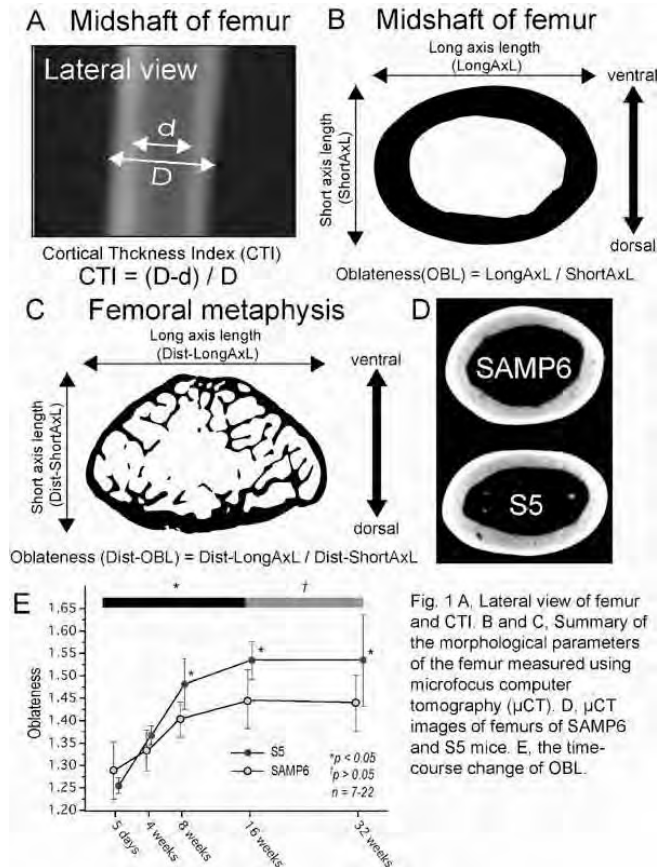


Fig. 1 A, Lateral view of femur and CTI. B and C, Summary of the morphological parameters of the femur measured using microfocus computer tomography (μ CT). D, μ CT images of femurs of SAMP6 and S5 mice. E, the time-course change of OBL.

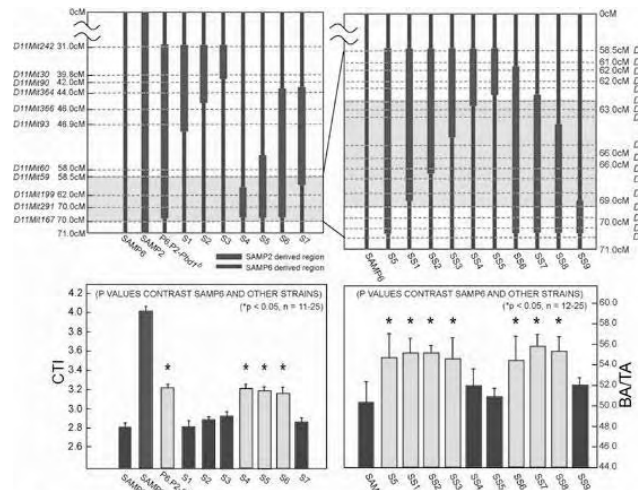


Fig. 2 Characteristics of initial seven subcongenic strains and second-generation nine-subcongenic strains. We used CTI and BA/TA for the index of relative bone mass because these values are quite well correlated ($R = 0.929$, $p < 0.0001$).

Disclosures: B. Otsuki, None.

W182

QTLs for Femoral BMD Identified in Two Separate Chicken Intercrosses Are Syntenic to Loci Controlling Human BMD. C. Rubin^{*1}, D. Wright^{*2}, A. Sahlqvist^{*1}, S. Kerje^{*1}, P. Jensen^{*3}, C. Ohlsson⁴, H. Mallmin⁵, S. Larsson^{*5}, O. Ekval^{*1}, O. Kämpe^{*1}, K. Johnsson⁶, L. Andersson^{*2}, A. Kindmark¹. ¹Dept. Med. Sciences, Uppsala University, Uppsala, Sweden, ²Dept. of Medical Biochemistry and Microbiology, Uppsala University, Uppsala, Sweden, ³IFM Biology, Linköping University, Linköping, Sweden, ⁴Dept. of Internal Medicine, The Sahlgrenska University Hospital, Gothenburg, Sweden, ⁵Department of Surgical Sciences, Uppsala University Hospital, Uppsala, Sweden, ⁶Department of Surgical Sciences, Uppsala University, Uppsala, Sweden.

We have previously conducted QTL-analysis for femoral bone traits in an intercross between the Red Junglefowl (RJ), the wild ancestor of domestic chicken, and White Leghorn (WL) strain L13 (L13), a breed heavily selected for egg-production. We have now performed QTL-analyses in a replicate intercross where RJ was intercrossed to another strain of White Leghorn (the OS-strain). The two WL-strains have been reproductively separated for approximately 50 years, during which genetic recombination has taken place within each strain. QTL-analyses in the OS/RJ-intercross may therefore considerably confine confidence intervals for shared QTLs.

From the RJ/L13-intercross, 337 F2-individuals were genotyped for 548 informative genetic markers and pQCT and DXA were used to measure femoral BMD and bone structure. From the RJ/OS-intercross, 700 F2-individuals were genotyped for 384 informative SNP-markers and were subjected to femoral bone phenotyping by pQCT. QTLs were mapped in the software QTL-express using forward selection for loci with significant marginal effects with bodyweight included as a covariate.

In the RJ/L13 intercross eight QTLs were identified as significant on the 5% genome-wide level. Six QTLs were identified in the RJ/OS intercross, three of whose confidence intervals overlap with RJ/L13 QTLs. The three QTLs which overlap are situated on chicken chromosomes 1, 2 and 3 and affect total and cortical BMD (chr. 1), BMD (chr. 2) and bone size as well as BMD (chr. 3). The three overlapping QTL-regions are syntenic to human Xp22 (chr. 1), 18p11 and 18q11-q12 (chr. 2), and 6q21-q26 (chr. 3). A QTL for BMD on human Xp22 has previously been reported, as have murine QTLs in the region syntenic to Xp22. Similarly, a human QTL for BMD of lumbar spine has previously been identified on 18p11. A QTL affecting BMD and biomechanical strength in mice is located in a region syntenic to human 6p22-23. The three chicken loci will be fine-mapped, mapped further for interspecies synteny to mouse and man and will be searched for presence of selective sweeps, the latter of which could help confine QTL-intervals greatly. Furthermore, 500 femoral bone RNA-samples collected from RJ/OS F2-individuals will be used for upcoming eQTL-studies.

Disclosures: C. Rubin, None.

W183

Mouse Chromosome 4 Homologous with Human 1p36: Fine Mapping Femoral vBMD and Trabecular Microstructure. K. L. Shultz, L. G. Horton, H. F. Coombs^{*}, V. E. DeMambro, C. J. Rosen, W. G. Beamer. The Jackson Laboratory, Bar Harbor, ME, USA.

We previously reported (28th ASBMR Mtng) that B6.C3H-4-7 congenic mice carried 15 Mb of C3H alleles from Chr 4 that regulate femoral volumetric (v)BMD and trabecular BV/TV. Ten sublines were developed from B6.C3H-4-7 mice to fine map this bone genetic regulation. Isolated femurs from groups (4 mo old) of female and male mice (B6 controls + new sublines) were phenotyped by pQCT for total femoral vBMD and by Micro CT40 for distal trabecular microstructure (BV/TV, trabecular no., thickness). A haplotype map with 11 chromosomal markers made from genotyping the 10 sublines revealed C3H Chr 4 segments of 0.8 to 12 Mb in size. This genetic map was correlated with bone phenotypes to find patterns of segregation indicative of C3H alleles with bone regulation.

vBMD increased in females from 6 sublines that share a region from 135.00-136.42 Mb, while 4 sublines were B6-like. Males from these 6 sublines also increased vBMD, indicating the presence of a gene(s) that regulates vBMD in both sexes. Males of two sublines with C3H alleles in the 126.86-132.69 Mb region also increased vBMD in male but not female femurs, indicating a second region with male-specific regulation.

Data for female distal trabecular microstructure did not reveal a clear segregation pattern indicative of BV/TV, trabecular number, or thickness regulation. However, B6.C3H-4-19 subline females showed a consistent negative effect for all three phenotypes when compared to B6 controls, suggesting C3H alleles in this subline represent a third regulatory locus. Males carrying C3H alleles in the 126.86-132.69 Mb region showed increased BV/TV and trabecular thickness, while males carrying C3H alleles in the 135.00-136.42 Mb region had increased BV/TV and trabecular number.

The Chr 4 region from 135.00-136.42 Mb carries ~28 known or predicted genes. Examination of the Novartis gene expression database for tissue specific expression showed strong expression of 3 genes (Cnr2, E2f2, Zbtb40) and weak expression for 2 genes (Luxp1, Aof2) in bone/bone marrow. Cnr2 ^{-/-} mice have reduced osteoclast activity and low bone mass (Ofek et al 2006). Akp2 (Klein et al, 27th ASBMR Mtng) reported as a candidate for B6.DBA/2 congenic is distal to this region identified by our B6.C3H-4 congenic sublines. The larger proximal region is 5.85 Mbp and contains ~100 known or predicted genes.

In summary, 1) congenic sublines partitioned a major QTL into components affecting bone density and microstructure; 2) Chr 4 has at least two distinct bone QTLs: A, 1.41 Mb, females & males, vBMD & trabeculae; B, 5.85 Mb, males, vBMD & trabeculae; and 3) gene expression databases suggest several candidate genes in region A; while the male-specific region, B, requires further mapping.

Disclosures: K.L. Shultz, None.

This study received funding from: NIAMS 45433.

W184

Heritability of Serum 25-hydroxyvitamin D Suggests Genetic Factors Contribute to Endogenous Vitamin D Production. E. A. Streeten, K. Hairston^{*}, K. A. Ryan^{*}, B. D. Mitchell, A. R. Shuldiner^{*}. Endocrinology, Diabetes and Nutrition, University of Maryland School of Medicine, Baltimore, MD, USA.

Vitamin D deficiency is an important contributor to poor bone health and fractures. The main source of Vitamin D is skin production responding to UVB sunlight, converting 7-dehydrocholesterol precursors to Vitamin D3. With similar occupational sun exposure in the summer, individual serum 25(OH)D levels have been shown to vary widely. Possible explanations for this variability include genetic factors. We hypothesize that genetic factors play a role in endogenous production of Vitamin D and its metabolites.

In 1151 participants of the Amish Family Osteoporosis Study (AFOS), 25(OH)D was measured by Diasorin RIA, intact PTH (iPTH) was measured by RIA and serum calcium (Ca), phosphorus (P), alkaline phosphatase (AP) were measured by multichannel analysis. BMD was measured at the hip, spine, forearm and whole body by DXA (Hologic). Clinical information collected included over-the-counter supplements. All participants had normal values of serum calcium (8.5-10 mg/dl) and creatinine (<1.3 mg/dl) and were not on chronic glucocorticoids. The heritability (h²) of these measures was estimated using a pedigree-based likelihood approach. Associations of BMD (corrected for age, sex and BMI) with 25(OH)D and iPTH (both corrected for season) was estimated by regression analysis.

The mean age (±SD) of AFOS participants was 50.5 ± 15.6 (range 18-91); 481 men and 680 women. The mean 25(OH)D was 22.4 ± 7.3 ng/ml (range <5 to 51.2); higher in summer (June-Aug) 25.5 ± 6.9, than in winter (Dec-Feb), 18.9 ± 6.3 (p<0.0001). PTH was higher in winter (58.7 ± 18.1 pg/ml) than in summer (53.9 ± 18.5) (p=0.01). 25(OH)D levels were in the deficiency range (<15 ng/ml) in 17%, insufficiency range (16-29 ng/ml) in 69% and sufficiency range (>30 ng/ml) in 14%. Of those with 25(OH)D<30 ng/ml, 24% had secondary hyperparathyroidism (iPTH >65 pg/ml). Heritability (h²) was 0.35 ± 0.06 for 25(OH)D, 0.32 ± 0.06 for iPTH, 0.34 ± 0.06 for Ca, 0.25 ± 0.06 for P, 0.35 ± 0.06 for AP and 0.22 ± 0.06 for ln PTH/25(OH)D. BMD (corrected for age, sex, BMI) at total hip (but not other sites) was correlated with 25(OH)D (corrected for season), but only in those with 25(OH)D >30 ng/ml (p=0.03). BMD (corrected for age, BMI) was correlated with iPTH (corrected for season) for spine and hip in women (p=0.04, 0.02) but not in men (p=0.78, 0.48). Vitamin D supplements were taken in 41% (136/329); daily dose mean 398 IU, median 400 IU).

Vitamin D insufficiency and deficiency are common in the Amish and the serum level of 25(OH)D is heritable. The moderate heritability of 25(OH)D and other factors involved in Vitamin D homeostasis (Ca, P, iPTH) suggest that genetic factors may be important to endogenous Vitamin D production.

Disclosures: E.A. Streeten, None.

W185

Genetic Loci for Bone Structure and Strength Identified in Inbred COP and DA Rats. Q. Sun¹, I. Alam¹, L. Liu^{*2}, D. L. Koller², L. G. Carr^{*3}, M. J. Econs³, T. M. Foroud², C. H. Turner¹. ¹Biomedical Engineering, Indiana University, Indianapolis, IN, USA, ²Medical and Molecular Genetics, Indiana University, Indianapolis, IN, USA, ³Medicine, Indiana University, Indianapolis, IN, USA.

Bone strength and structure are major determinants of osteoporotic fracture. These two phenotypes are under substantial genetic regulation and the identification of the genes contributing to their observed phenotypic variation may provide important insight regarding the genetics of osteoporosis and fracture risk. Previous studies have shown that the Copenhagen 2331 (COP) and Dark Agouti (DA) rats have significant differences in bone strength despite their similar body mass. Thus, these inbred rat strains may provide a unique resource to identify the genetics underlying the phenotypic variation in bone strength and structure. A sample of 828 (405 males and 423 females) COP x DA F2 progeny had extensive phenotyping for bone structure measures including cortical bone area and polar moment of inertia at the femur midshaft and total, cortical and trabecular bone areas at the distal femur, and lumbar vertebra 5 (LV5). Bone strength phenotypes included ultimate force of femur and LV5. These skeletal phenotypes were measured using peripheral quantitative computed tomography (pQCT) and mechanical testing. A whole-genome 20 cM screen was conducted in the F2 rats. Genetic marker maps were generated using MARMAKER/EXP from the F2 data and compared with maps from the Rat Genome Database (RGD). The recombination-based maps were then used for genome-wide linkage analyses to detect linkage to the bone structure and strength phenotypes. Permutation testing was employed to obtain the thresholds for genome-wide significance (p<0.01). A very significant QTL for femur midshaft cortical structure and strength was identified on the distal part of chromosome (Chr) 1 with a LOD score of 33; evidence of linkage was found with both the male and female F2. In addition, Chrs 6, 7, 10, 13, and 15 were linked to femur midshaft structure. Linkage for femur trabecular structure was detected on the proximal part of Chr 1 and Chr 14. Additional QTL for femur strength were identified on Chrs 6 and 15. For LV5, Chrs 2, 16, and 18 harbored QTL for cortical structure. Trabecular structure for LV5 was linked to Chrs 1, 7, 12, and 18. Our study demonstrates genetic linkage for bone structure and strength on several rat chromosomes. The strongest linkage was discovered for several femoral phenotypes on chromosome 1 harboring two distinct QTLs, one at each end.

Disclosures: Q. Sun, None.

W186

Oral Bisphosphonate Treatment Prevents the Changes of Bone Mineral Density and Bone Biomarkers in Postmenopausal Japanese Women with Early Breast Cancer Treated with Aromatase Inhibitor. O. Chaki, K. Kurasawa*, T. Ishikawa*, Y. Nomura*, H. Yoshikata*, R. Kikuchi, F. Hirahara*. Yokohama City University, School of Medicine, Yokohama, Japan.

Many clinical trials have demonstrated the efficacy and safety of long-term adjuvant treatment with aromatase inhibitors (AIs) in women with breast cancer. Whereas aromatase inhibitors are generally well tolerated and, compared with tamoxifen, offer superior efficacy and safety, in certain other respects they are associated with the loss of bone mineral density and an increased risk of fracture. Bisphosphonates are effective inhibitors of osteoclast activity and bone resorption, and are standard treatments for osteoporosis. Bisphosphonates are now being incorporated into breast cancer treatment regimens in order to combat osteoporosis caused by ovarian suppression, chemotherapy treatment, aromatase inhibitors and the postmenopausal state itself.

The aim of our study was to investigate changes in bone loss and bone turnover associated with aromatase inhibitor treatment and the effectiveness of oral bisphosphonate treatment. We conducted an open prospective study in 34 postmenopausal women treated with anastrozole for an early breast cancer. Fourteen patients were treated with alendronate (5mg/day). Bone mineral density (BMD) was measured using DXA at baseline and one year later. The bone turnover markers bone alkaline phosphatase (BAP) and urinary NTX were measured at baseline and 1,3 and 6 months later. In the aromatase inhibitor group, there was a marked bone loss at the lumbar spine by -2.8% ($p < 0.001$) and hip by -1.3% ($p < 0.05$), but there was no significant increase in bone turnover (+16.4% for BAP and +5.3% for uNTX). BMD of bisphosphonate treatment group was increased at the lumbar spine by 2.3% and hip by 7.8%.

In conclusion, anastrozole treatment of breast cancer induces an accelerated bone loss but doesn't induce an increased bone turnover in Japanese postmenopausal women with breast cancer. This bone loss is suppressed by oral bisphosphonate treatment completely.

Disclosures: O. Chaki, None.

W187

Dynamic Genomic and Proteomic Patterns of Osteosarcoma Metastasis to Lung: Implication of Macrophage Migration Inhibitory Factor and Tumor Necrosis Factor for Lung Metastasis. B. White¹*, C. Wilburn²*, G. Holt¹*, H. Schwartz¹*, R. Caprioli³*, L. Gerstenfeld⁴, R. Caldwell¹. ¹Department of Orthopaedics and Rehabilitation, Vanderbilt University School of Medicine, Nashville, TN, USA, ²Department of Medicine/Clinical Pharmacology, Vanderbilt University School of Medicine, Nashville, TN, USA, ³Department of Biochemistry, Mass Spectrometry Research Center, Vanderbilt University School of Medicine, Nashville, TN, USA, ⁴Department of Orthopaedic Surgery, Boston University Medical Center, Boston, MA, USA.

Despite successful treatment of osteosarcoma (OSA), death from lung metastasis occurs in >30% of patients. Novel molecules permissive for OSA metastasis to lung may improve treatment outcome by existing as prognostic markers or therapeutic targets. The rationale of this study was to examine differences in common osteoblastic gene expression between high and low metastatic OSA and mine the proteome for differences in protein expression. We focused on transcript and protein profiles from an established OSA model using northern blotting analyses, 2-dimensional difference gel electrophoresis (2D-DIGE) and MALDI-TOF mass spectrometry. This balb/c murine model of OSA is characterized by orthotopic primary tumor growth, a period of minimal residual disease, spontaneous pulmonary metastasis, and clonally related variants (K7M2 and K12). K7M2 cells are aggressive and highly metastatic, whereas K12 cells are less aggressive with infrequent pulmonary metastases. Analysis of gene expression during mineralization assays revealed dynamic differences in mRNA levels of COLA1, APase, and OC between the K7M2 and K12 OSA cells in both the proliferative and extracellular matrix deposition stages. 2D-DIGE and MALDI protein profiling demonstrated a comprehensive proteomic evaluation between the K12 and K7M2 OSA cells, revealing several differentially expressed proteins such as macrophage migration inhibitory factor (MIF), ubiquitin, and thymosin beta-4. Computer modeling algorithms further implicated VEGF, TNF, and IL-1B as key mediators in OSA metastasis to lung. Western blotting and IHC validated these findings as we observed increased TNF and MIF expression in the metastatic cells. Taken together, decreased levels of osteoblast markers in K7M2 cells demonstrate dedifferentiation, while up-regulation of MIF and TNF in highly invasive K7M2 cells represent molecular mechanisms to compromise host immunosurveillance during metastasis. These studies are among the first to implicate MIF and TNF as potential biomarkers and therapeutic targets for OSA lung metastasis. These data also represent a rational, comprehensive approach to evaluate the cellular proteome to identify proteins that may be causally associated with metastasis.

Disclosures: R. Caldwell, None.

This study received funding from: Brooks Fund.

W188

Melanoma Bone Metastasis: Osteoclasts Cannot Be Excluded. L. C. Dumitrescu, J. R. Edwards, J. A. Sterling, G. R. Mundy. Center for Bone Biology, Vanderbilt University Medical Center, Nashville, TN, USA.

Recently, there has been much controversy on the role of osteoclasts in bone metastasis in melanoma. Jones et al (2006) have suggested that melanoma bone metastases are not mediated by osteoclasts. Since we have been unable to find convincing evidence that bone osteolysis in cancer ever occurs independent of osteoclasts, we employed the melanoma cell lines B16F10 and Mel A along with primary bone marrow-derived cells to investigate and characterize the effect of this aggressive tumor on osteoclast formation and function, using bone resorption assays, enzymatic and immunohistochemical analysis and RT-PCR for melanoma-derived osteolytic factors. Treatment of primary bone marrow-derived osteoclast-precursors with M-CSF (30ng/ml), RANKL (50ng/ml) and media conditioned by B16F10 or Mel A cells showed a significant dose-dependent increase in the formation of TRAP+ multinucleated cells. These cells were also vitronectin receptor and calcitonin receptor positive. Addition of only 5% B16F10 conditioned media to bone marrow cultures stimulated the formation of 47 ± 1 TRAP+ cells/well, compared to 5.5 ± 2.5 in control treated cultures ($p < 0.05$). A similar significant response was observed with media conditioned by Mel A cells, with 49.5 ± 10.5 TRAP+ cells/well seen in treated cultures compared to 8.5 ± 0.5 in control cultures ($p < 0.01$). The quantity of TRAP+ cells formed correlated with a dose-dependent increase in bone resorption and lacunae pit formation on dentine discs. RT-PCR analysis showed clear expression of PTHrP on B16F10 and Mel A cells, although RANKL was not expressed in either cell type. These studies demonstrate a clear interaction between melanoma cells and osteoclast precursors through the release of potent soluble factors, and indicate that melanoma cells are capable of stimulating osteoclast activity. These findings are consistent with a central role for osteoclasts in the extensive osteolysis observed in melanoma bone metastases.

Disclosures: J.R. Edwards, None.

W189

A Phase II Pilot Study of Safety and Effects on Bone Resorption of AZD0530 in Prostate or Breast Cancer Patients with Bone Metastases. R. D. Finkelman¹, F. M. Torti²*, A. Lipton³*, R. A. Hannon⁴, A. Hussain⁵*, C. Evans⁶*, M. Akilu²*, R. Iacona¹*, A. Swaisland⁷*, M. Stuart⁷*. ¹AstraZeneca, Wilmington, DE, USA, ²Wake Forest University Comprehensive Cancer Center, Winston Salem, NC, USA, ³Hershey Medical Center, Hershey, PA, USA, ⁴Academic Unit of Bone Metabolism, University of Sheffield, Sheffield, United Kingdom, ⁵Greenebaum Cancer Center, University of Maryland School of Medicine, Baltimore, MD, USA, ⁶University of California, Davis, Sacramento, CA, USA, ⁷AstraZeneca, Alderley Park, Macclesfield, United Kingdom.

We have reported previously that once daily dosing for 14 days with AZD0530, a highly selective and orally available Src kinase inhibitor with Bcr-Abl activity, resulted in a dose-dependent reduction of bone resorption markers β CTx and NTx in healthy male volunteers (Hannon et al, ASBMR 2005). A similar outcome was evident in preliminary, unvalidated data from cancer patients with advanced disease. The present study is the first to investigate AZD0530 in cancer patients specifically with metastatic bone disease, and is due to start enrollment in September 2007. Patients with prostate or breast cancer and at least one radiographically confirmed metastatic bone lesion will be randomized to one of two treatment arms: (1) AZD0530, 175 mg once daily; or (2) zoledronic acid, 4 mg iv infusion, every 4 weeks. Patients must have been on stable therapy for their cancer for at least 8 weeks with no anticipated change of therapy for 4 weeks after randomization. Patients will continue on their present therapy during the study. Patients must have had no previous exposure to bisphosphonates. Concomitant chemotherapy with cytotoxic or novel molecularly targeted agents is not allowed on study or within 4 weeks prior to study entry. Concomitant therapy with bisphosphonates is not allowed on study for patients randomized to the AZD0530 treatment arm. Fasted serum and urine samples for assessment of bone turnover biomarkers β CTx, NTx, bone ALP, PINP, ICTP, and TRAP 5b will be collected at baseline and at 1, 2, and 4 weeks. PTH, PTHrP, calcium, phosphate, and total ALP will also be assessed in serum at the same timepoints. Serum PSA will be assessed in patients with prostate cancer at baseline and at 4 weeks. Changes from baseline will be compared between treatment arms. Data from this study will be used to determine the future development of AZD0530 in the treatment of metastatic bone disease.

Disclosures: R.D. Finkelman, AstraZeneca 3.

This study received funding from: AstraZeneca.

W190

Zoledronic Acid Decreases Serum Low-density Lipoprotein Cholesterol in Multiple Myeloma Patients. G. Martini¹, A. Gozzetti^{*2}, L. Gennari¹, S. Salvadori^{*1}, D. Merlotti¹, A. Avanzati^{*1}, B. Franci^{*1}, M. Campagna^{*1}, E. Lauria^{*2}, R. Nuti¹. ¹Metabolic Disease Unit, University of Siena, Siena, Italy, ²Hematology and Transplants Division, University of Siena, Siena, Italy.

Nitrogen-containing bisphosphonates (N-BPs) have been designed to inhibit osteoclast-mediated bone resorption and therefore they are the most widely used and effective anti-resorptive agent for the treatment of diseases in which there is an increase of osteoclastic resorption as postmenopausal osteoporosis, Paget's disease and tumor-associated osteolysis. The mechanism of action of these drugs has not been completely clarified but it has been observed that N-BPs may inhibit squalene synthase, as ibandronate, or farnesyl pyrophosphate synthase, as alendronate or pamidronate, inducing also a reduction of cholesterol biosynthesis. Zoledronic acid (ZA) represents a novel N-BPs which has also antitumor activity. "In vitro" studies suggest that ZA can inhibit cholesterol production, but 90% of the biosynthesis was rescued after 48 hours.

To explore the effects of ZA on serum lipids "in vivo", we studied 26 patients with smoldering myeloma at diagnosis. Sixteen patients were treated with ZA (4 mg ev) at baseline and at months 1, 2, 4 and 6. The remaining 10 served as controls. At baseline and after 1, 3 and 6 months, a blood sample was drawn from each patient to evaluate total cholesterol (TC), triglycerides (TG), high-density lipoprotein cholesterol (HDL-C), low-density lipoprotein cholesterol (LDL-C) and C-terminal telopeptide of Type I collagen (CTX). In the control group no significant changes were observed throughout the study period for any of the biochemical variables. As expected, CTX decreased significantly by 40-50% after ZA administration. In treated patients, we observed a progressive and significant reduction of TC with a maximum decrease of 13% at 6 months; moreover LDL-C decreased by 21% at 6 months while no significant differences were appreciated as regards HDL-C and TG. Also the indexes of cardiovascular risk improved after ZA administration: TC/HDL-C ratio progressively decreased by 18% and HDL-C/LDL-C ratio increased by 35% showing an effect that appears to be cumulative.

In conclusion we demonstrated that ZA, a third class of N-BPs, is able to alter lipid profile more than older N-BPs as pamidronate or neridronate. This effect can be due to the potency of ZA to inhibit FPP synthase that is about 70-fold than pamidronate.

Disclosures: L. Gennari, None.

W191

Characterization of Leupaxin as a Focal Adhesion-associated Protein in Prostate Cancer Cells. A. Gupta. Biomedical Sciences, Dental School, University of Maryland, Baltimore, Baltimore, MD, USA.

We have identified the presence of leupaxin (LPXN), which belongs to the paxillin extended family of focal adhesion-associated adaptor proteins, in prostate cancer (PC) cells. Previous studies have demonstrated that LPXN is a component of the podosomal signaling complex found in osteoclasts, where LPXN was found to associate with the protein tyrosine kinases Pyk2 and c-Src, and the protein-tyrosine phosphatase-PEST (PTP-PEST). In the current study, LPXN was detectable as a 50 kDa protein in PC-3 cells, a bone-derived metastatic androgen-independent prostate cancer cell line. Second, we demonstrate that the subcellular localization of LPXN is both cytoplasmic and nuclear, suggesting the possibility of nucleo-cytoplasmic shuttling in PC-3 cells. Third, in PC-3 cells, LPXN was also found to associate with Pyk2, c-Src, and PTP-PEST. Fourth, a siRNA-mediated inhibition of LPXN expression resulted in decreased in vitro PC-3 cell migration. Fifth, a recombinant adenoviral-mediated overexpression of LPXN resulted in an increased association of Pyk2 with LPXN, whereas a similar adenoviral-mediated overexpression of PTP-PEST resulted in decreased association of Pyk2 and c-Src with LPXN. Sixth, the overexpression of LPXN in PC-3 cells resulted in increased migration, as assessed by in vitro Transwell migration assays. On the contrary, the overexpression of PTP-PEST in PC-3 cells resulted in decreased migration. Finally, overexpression of LPXN resulted in increased activity of Rho GTPase, which was decreased in PTP-PEST-overexpressing cells. Our data demonstrates that LPXN forms a signaling complex that may play a role in PC-3 cell function.

Disclosures: A. Gupta, None.

This study received funding from: AR-47942.

W192

Effects on Bone Turnover of the Potent, Once-Daily, Oral Src Inhibitor AZD0530 in Patients with Advanced Solid Malignancies. R. A. Hannon¹, R. D. Finkelman², G. Clack³, R. B. Iacona^{*2}, P. Baker^{*3}, M. Rimmer^{*3}, F. Gossiel^{*1}, I. C. Smith^{*3}, A. Robinson^{*3}, R. Eastell^{*1}. ¹Academic Unit of Bone Metabolism, University of Sheffield, Sheffield, United Kingdom, ²AstraZeneca, Wilmington, DE, USA, ³AstraZeneca, Alderley Park, Macclesfield, United Kingdom.

AZD0530 is a potent, orally active, once-daily Src inhibitor with Bcr-Abl activity that modulates multiple key signaling pathways in cancer and has potential activity in many different tumor types. We have previously demonstrated significant AZD0530 dose-dependent reduction in bone resorption in healthy males. In the present Phase I study, we assessed the effect of AZD0530 on bone resorption in adult patients with advanced solid malignancies resistant to standard therapy.

Patients were randomized into three parallel groups to receive AZD0530 50, 125, or 175 mg/day. After a single dose on day 1 followed by 6 days washout, patients received once-daily doses for 21 consecutive days. Fasted serum and second-morning void urine were collected on

day 1 predose and on days 2, 3, 17, and 28. Serum cross-linked C-terminal telopeptide of type I collagen (sCTX) and urinary cross-linked N-terminal telopeptide expressed as a ratio to urinary creatinine (uNTX) were assessed as markers of bone resorption. An analysis of covariance model was fitted to the log-transformed baseline-scaled ratio data at day 28, with treatment as a fixed-effect factor and log-transformed baseline (predose day 1) as a covariate.

There were significant reductions in sCTX in all treatment groups and in uNTX at 125 and 175 mg. Percent changes from baseline at day 28, derived from the adjusted geometric mean baseline-scaled ratios, were 36.3% (95% CI 57.6%, 4.4%; P=0.030; n=12), 61.7% (95% CI 73.6%, 44.5%; P<0.001; n=14), and 74.5% (95% CI 83.3%, 61.3%; P<0.001; n=11) for sCTX in the 50, 125, and 175 mg treatment groups, respectively; and 12.7% (95% CI 32.6%, 13.1%; P=0.293; n=12), 48.3% (95% CI 59.2%, 34.4%; P<0.001; n=14), and 50.1% (95% CI 61.8%, 34.7%; P<0.001; n=11) for uNTX, respectively. There was a dose-response trend for reductions in biomarkers.

The significant reductions in the biomarkers are in accordance with inhibition of osteoclast-mediated bone resorption by suppression of Src activity. The reduction (>60%) in sCTX at 125 and 175 mg of AZD0530 is similar to reductions reported with bisphosphonate therapy. These data suggest that AZD0530 may have therapeutic benefit in osteoclast-driven metastatic bone disease in addition to its inhibitory activity on Src in tumor cells. The trend for dose-dependent changes in biomarkers indicates that the maximum tolerated dose should be taken forward in further development.

Disclosures: R.A. Hannon, AstraZeneca 2.

This study received funding from: AstraZeneca.

W193

A New Urine Assay for Sensitive Detection and Assessment of Cancer-induced Skeletal Perturbations. D. J. Hillegonds¹, D. W. Burton^{*2}, J. S. Vogel¹, E. Denk^{*3}, T. R. Walczyk³, M. Yang^{*4}, S. Vijayakumar^{*5}, D. A. Herold^{*2}, L. J. Deftos², R. L. Fitzgerald². ¹Center for Accelerator Mass Spectrometry, Lawrence Livermore National Laboratory, Livermore, CA, USA, ²University of California, San Diego, San Diego, CA, USA, ³Laboratory of Human Nutrition, ETH Zurich, Zurich, Switzerland, ⁴Anticancer, Inc., San Diego, CA, USA, ⁵Davis Cancer Center, University of California, Davis, Sacramento, CA, USA.

The need for earlier detection and improved management of metastatic bone disease has driven the search for new bone remodeling biomarkers, but existing techniques are insufficiently sensitive for reliable use in individuals. We report on a novel tracer technology for bone health wherein one calcium-41 (41Ca) dose fully equilibrates with the living skeleton and remains measurable in urine and blood for many years. Urinary 41Ca/Ca is dominated by tracer incorporation and re-release from mineralized bone. In healthy humans, intra-individual urinary variability averaged 3.3+/-0.2% diurnally and 6+/-3% over 200 days. In a preclinical prostate cancer metastasis model, serum 41Ca/Ca directly and significantly correlated with bone disruption, tumor size, serum calcium, osteoprotegerin, and parathyroid hormone-related protein. We posit that longitudinal urinary 41Ca/Ca measurements may sensitively reveal skeletal perturbations, enabling improved clinical management through rapid identification of therapeutic success and non-invasive detection of the earliest stages of cancer growth in bone.

Disclosures: D.J. Hillegonds, None.

W194

Five Years Results of Bisphosphonate Treatment in Long-term Survivors of Highly-Malignant Osteosarcoma. G. Holzer, M. Dominkus^{*}, R. Kotz^{*}. Department of Orthopaedics, Medical University of Vienna, Vienna, Austria.

Purpose: Two thirds of long-term survivors of highly-malignant osteosarcoma treated with chemotherapy protocols including high-dose methotrexate (MTX) have low bone mineral density (BMD) and one third report about fractures after completion of chemotherapy.

Methods: Ten patients with BMD < 2.5 STD (6 male, 4 female; mean age: 33 {plusmn} 1.4 years) participated in this study. Patients received risendronate orally once daily (5 mg) or weekly (35 mg) plus a calcium / vitamin D combination daily. BMD of lumbar spine (LS) and proximal femur of the non-operated side (PF) were measured by dual energy X-ray absorptiometry at twelve months after beginning of the treatment (mean time after chemotherapy at beginning of oral bisphosphonate treatment: 13.8 {plusmn} 2.3 years).

Results: After five years of oral bisphosphonate treatment BMD increased at a mean by 2.28 % in the LS, whereas in the PF no changes were seen. No fracture occurred during the study time. Conclusions: It was shown that even in long-term survivors of highly-malignant osteosarcoma treated with chemotherapy protocols including MTX increases in BMD values are possible.

Disclosures: G. Holzer, None.

W195

Activity of the Akt Inhibitor Perifosine and Heat Shock Protein (HSP)-90 Inhibitor 17-(Dimethylaminoethylamino)-17-Demethoxygeldanamycin (17-DMAG) in Modulating Osteoclastogenesis and the Bone Marrow Microenvironment (BMM) in Multiple Myeloma (MM). A. Huston¹, X. Leleu², X. Jia², J. Anderson³, S. Vallet², A. Roccaro², A. Moreau², J. Runnels², H. Ngo², E. Hatjiharissi², G. D. Roodman³, Y. Tai², P. Sportelli⁴, T. Hideshima², P. Richardson², K. Anderson², I. Ghobrial². ¹Hematology/Oncology, James P. Wilmot Cancer Center, Rochester, NY, USA, ²Medical Oncology, Dana-Farber Cancer Institute, Boston, MA, USA, ³Medicine-Hematology/Oncology, University of Pittsburgh, Pittsburgh, PA, USA, ⁴Keryx Biopharmaceuticals, New York, NY, USA.

Alterations in the BMM are thought to be critical to MM pathogenesis. The PI3K/Akt and HSP-90 pathways have previously been shown to be dysregulated in MM. We hypothesize that combining two agents that interact at the level of Akt will lead to synergistic cytotoxic activity among MM cells, osteoclastogenesis and the BMM. Effects of treatment with perifosine (5-10µM; Keryx, NY) and 17-DMAG (50nM; NCI) upon the BMM were evaluated through osteoclastogenesis and osteoclast (OCL) precursor development assays, co-culture of MM cells with bone marrow stromal cell (BMSC) and endothelial cells, in vitro capillary formation, and migration/adhesion assays in the presence/absence of stromal derived factor-1 (SDF-1) and vascular endothelial growth factor (VEGF).

Perifosine and 17-DMAG induced a near complete inhibition of OCL formation. Effects were observed regardless of perifosine treatment timing (100% inhibition first vs. final week), vs. 17-DMAG (100% inhibition first vs. 60% final week). CFC assays for CFU-GM development resulted in significant inhibition after 17-DMAG treatment, as compared to perifosine or control (mean 2 ± 0.5 colonies/well vs. 18 ± 3 vs. 20 ± 3 ; $p=0.01$ 17-DMAG vs. control). Treatment with perifosine, 17-DMAG and the combination resulted in significant inhibition in MM cell growth following co-culture with BMSCs ($p<0.001$). Addition of IL-6 or IGF-1 resulted in MM cell proliferation, which was blocked by perifosine, 17-DMAG or the combination ($p=0.013$). Co-culture of HUVEC endothelial cells with MM cells or addition of VEGF to MM cells resulted in increased proliferation, which was blocked by the combination of agents ($p=0.02$ in HUVEC co-culture system; $p=0.024$ with VEGF). Similarly, perifosine, 17-DMAG and the combination significantly inhibited MM.1S cell migration (2.5-fold inhibition) and adhesion in the presence of SDF-1 or VEGF.

The PI3K/Akt and HSP-90 pathways play a critical role in regulating the BMM in MM, including OCL formation, angiogenesis and MM cell migration and adhesion. Targeting these pathways with perifosine and 17-DMAG represents an attractive approach for modulating the BMM in MM.

Disclosures: A. Huston, Amgen Oncology Institute Hematology/Oncology Fellowship Grant (6/2005-6/2006) 2.

W196

Prostaglandin E2 (PGE2) Receptor EP4 Antagonist Attenuates Osteolysis Due to Cancer Metastasis. M. Takita¹, M. Inada¹, M. Hirata¹, T. Maruyama², C. Miyaure¹. ¹Department of Biotechnology and Life Science, Tokyo University of Agriculture and Technology, Koganei, Tokyo, Japan, ²Discovery Research Laboratory, Minase Research Institute, Ono Pharmaceutical, Co., Ltd., Osaka, Japan.

Bone metastasis of cancer is accompanied by severe bone destruction with increased bone resorption. We recently identified that prostaglandin E2 (PGE2)-induced osteoclast formation was mediated by RANKL expression in osteoblasts, EP4 is the major PGE receptor than in the other EP subtypes (EP1-EP3). Recent studies suggest a possible role of EP4 receptor on cancer growth, but the roles of PGE2 and EP4 on host osteoblast in bone metastasis is still unclear. Here we examine the effects of EP4 antagonist, a selective inhibitor of EP4 signaling in bone destruction due to malignant melanoma. When mice were injected with B16 cells from the left heart ventricle, metastasis was detected as black spots in distal femurs on day12 after injection. In the B16 injected group, RANKL and cyclooxygenase-2 mRNA expression was elevated in the femur associated with B16 metastasis. PGE2 production was also elevated in B16 metastatic femur. Bone mineral density (BMD) measured by DEXA showed significant decrease of BMD in femur with B16 metastasis. Histomorphometry indicated that increased bone resorption at the site of B16 metastatic region, BV/TV and Tb.Th were significantly reduced, whereas Tb.Sp and ES/BS were increased, that was compared with femur of control mice. When EP4 antagonist was orally administered to mice injected with B16 cells, the osteolysis due to bone metastasis in femurs was suppressed, and the morphometric parameters were restored to the levels of femur of control mice. To know further mechanisms of B16 induced bone resorption, B16 cells were cultured with bone marrow cells and osteoblasts to evaluate the capacities of osteoclast formation. Contact with un-viable B16 cells fixed with formalin induced RANKL expression and PGE2 production in osteoblasts in the absence of bone-resorbing factors, and RANKL-dependent osteoclast formation was seen in the co-culture of bone marrow cells, fixed-B16 and osteoblasts. In the co-culture, EP4 antagonist completely inhibited osteoclast formation. These results suggest that cell-to-cell interaction between B16 and osteoblasts elicits PGE2 production by osteoblasts, and EP4 signaling induces RANKL expression in osteoblasts to form osteoclasts. Therefore, EP4 antagonist may be a possible candidate for the therapy of bone metastasis due to cancers.

Disclosures: M. Inada, None.

W197

Vitamin D Deficiency in Oncologic Patients - an Ignored and Potentially Life Threatening Condition, Possible Role of Increased Osteoblastic Activity in Induction of Hypocalcemia. S. Ish-Shalom¹, E. Segal^{*1}, S. Felder^{*2}, H. Yoffe⁻ Sheinman^{*2}, M. Volner^{*2}, E. Gez^{*2}, B. Raz^{*3}, Z. Shen-Or^{*3}, N. Haim^{*3}. ¹Bone and Mineral Metabolism Unit, Rambam Medical Center, Haifa, Israel, ²Department of Oncology, Rambam Medical Center, Haifa, Israel, ³Endocrine Laboratory, Rambam Medical Center, Haifa, Israel.

Introduction: Monthly administration of bisphosphonates to oncologic patients with skeletal involvement decreases bone turnover and in combination with poor vitamin D status and consequent decrease in calcium absorption may lead to life threatening hypocalcemia.

Routine or sporadic (based on medical history) evaluation of vitamin D status and subsequent vitamin D supplementation is not included in the national or international guidelines for bisphosphonate treatment for metastatic bone diseases.

The aim of this study was to assess vitamin D status and bone turnover in oncologic patients and their impact on the risk of hypocalcemia

Patients / Methods: Following IRB approval, we have assessed serum calcium, phosphate, albumin, 25(OH)D3, alkaline phosphatase and plasma PTH, procollagen type1 nitrogenous propeptide (PINP), C-terminal telopeptide of collagen (CTX) in 41 consecutive patients with metastatic bone disease, aged 58.2 ± 12.4 years, range 39- 86. The patients were treated with intravenous bisphosphonates, pamidronate or zoledronate, every 3-4 weeks.

Results: Serum albumin corrected calcium was $9.26 \text{ mg/dl} \pm 0.66$, range 6.7- 10.72. 25(OH)D3 serum concentration was $12.3 \pm 7.04 \text{ ng/ml}$ (max. value 27.6) ; vitamin D deficiency 25(OH)D3 $< 10 \text{ ng/ml}$ was observed in 17 pt (41.5%); vitamin D insufficiency 10 - 15 ng/ml in 10 pt (24.5%), vitamin D inadequacy $< 30 \text{ ng/ml}$ in 14 pt (35%). Plasma PINP was $115.686 \pm 192.6 \text{ ng/ml}$

Albumin corrected calcium strongly negatively correlated with PINP (R(- 0.517) ;P = 0.001) and with serum alkaline phosphatase (R(- 0.562), P< 0.001). Plasma CTX level was 0.265 ± 0.3 (within premenopausal range of 0.14 - 0.299 ng/ml) and has not correlated with albumin corrected calcium.

Conclusions: Vitamin D deficiency is common in oncologic patients; they are prone to hypocalcemia due to bisphosphonate treatment and absence of supplementation with calcium and vitamin D, especially in presence of increased osteoblastic activity.

Hypocalcemia and vitamin D deficiency are a preventable conditions; evaluation of vitamin D status and adequate calcium and vitamin D supplementation should be part of management of oncologic patients.

Disclosures: S. Ish-Shalom, MSD 2; Novartis 2; Lilly 2.

W198

Microarray Analysis of Craniofacial and Appendicular Osteosarcoma. C. Kong^{*}, M. F. Hansen. Center For Molecular Medicine, University of Connecticut, Farmington, CT, USA.

Although both primary craniofacial and appendicular osteosarcoma are classified under the rubric of osteosarcoma, their clinical phenotypes are actually quite distinct. Most significantly, chemotherapy treatment leads to vastly different morbidity outcomes; craniofacial patients have a 40% survival rate compared to an 80% survival rate for appendicular osteosarcoma. Given the differences in outcome with conventional chemotherapeutic agents for this disease, there is a clear need to identify differentially expressed genes in these two tumor types as potential new targets for therapy. We have used the Illumina Human Cancer Panel microarray platform to compare craniofacial and appendicular osteosarcoma tumor cell lines to identify quantitative and qualitative alterations in gene expression that distinguish these two diseases. Our comparison of seven osteosarcoma tumor cell lines (1 craniofacial OS tumor cell line, USAC1, and 6 appendicular OS tumor cell lines: SAOS2, U2OS, MG63, HOS, SJSA1, OHS50) revealed distinct differences in gene expression with a bias towards alteration of expression of genes involved in cell DNA damage response and repair and bone signaling. Genes known to be involved in bone signaling such as FGF8, WNT2, WNT1, BMP4, WNT8B, and WNT5A were significantly overexpressed in the craniofacial osteosarcoma cell line when compared to the appendicular osteosarcoma cell lines. In contrast, genes involved in DNA repair such as MSH6, WRN, MSH3, FANCA, RECQL, XPA, PCNA, and BRCA2 were significantly underexpressed in the craniofacial osteosarcoma cell line when compared to the appendicular osteosarcoma cell lines. It is possible that at least some of the differences in phenotype between craniofacial and appendicular osteosarcomas are the result of the developmental pathways by which the bones of craniofacial and appendicular skeleton arise; the craniofacial bones arise from cranial neural crest cells while the appendicular skeleton arises from mesenchymal-derived cells. Our results indicate that craniofacial and appendicular osteosarcoma tumor cell lines show distinct patterns of gene expression. These patterns may provide insight into the molecular basis of these two diseases and possible targets for chemotherapeutic intervention.

Disclosures: C. Kong, None.

W199

A Comparative Study of Anti-resorptive and Anti-cancer Treatments in the Geometrical and Biomechanical Properties of Rat Femurs with Tumor-induced Osteolysis. T. Lee*, X. Wang*, L. Li*, K. Si-hoe*. Division of Bioengineering, National University of Singapore, Singapore, Singapore.

While much has been learned about the mechanisms of metastatic spread of cancer to bone, there has been little headway in establishing guidelines for monitoring the response of metastases to treatment. The objective of this study was to investigate the efficacy of two different treatments (Anti-Resorptive:Ibandronate and Anti-Cancer:Paclitaxel) of tumor induced osteolysis in terms of geometrical and biomechanical parameters.

A rat femur model for tumor-induced osteolysis using W256 cancer cells was adapted from a previous study. Of the 30 rats implanted with cancer cells, 12 were untreated (CANCER), 9 received Ibandronate (IBAN), and 9 received Paclitaxel (PAC). Another 12 underwent a sham operation (CONTROL). Micro-computer tomography (μ CT) scans of the femurs extracted post-mortem were used to quantify standard geometrical parameters such as bone volume (BV) and cross-sectional area (CSA). A 3-point bending test was used to assess the femurs' mechanical stiffness. Finally, serum levels of deoxypyridinoline (Dpd) were measured to obtain the degree of bone resorption, which in turn gave an indication of cancer activity.

A summary of the data recorded 30 days post-surgery (20 days for PAC group) are shown in Table 1. CSA data - taken at 25% of the total femur length from the distal end - from the CANCER group had the largest % difference between the left and right femurs (corresponding with a 13.4% increase in Dpd levels). IBAN rats showed the least % difference in CSA (38.1% drop in Dpd levels), followed by PAC rats. This pattern is repeated in the % differences in BV. The anti-cancer effect of PAC can be inferred from the lower Dpd levels of the PAC group (8.86% increase) as compared to the CANCER group. Both IBAN (2.85%) and PAC (-3.86%) maintained the stiffness properties of the operated femurs, with PAC being marginally more effective.

The initial results suggest the viability of this rat model for bone metastasis, and that IBAN was most effective in maintaining skeletal geometry. Interestingly, PAC seemed to be more capable of preserving the biomechanical properties of the femur, despite deterioration in its geometrical properties. A subsequent full scale study, with additional bone mineral content and histomorphological analysis, is in progress to confirm these results.

Group	Summary of Geometrical data and Dpd levels after 30 days			
	CSA Group %	BV Group %	Stiffness Group %	Dpd levels Group %
	Differences between Left (INTACT) and Right (TUMOR) Femurs	Differences between Left (INTACT) and Right (TUMOR) Femurs	Differences between Left (INTACT) and Right (TUMOR) Femurs	Differences between 0 and 30 day levels
CONTRO L	10.19	0.08	2.68	-13.9
CANCER	16.18	10.80	10.27	13.4
IBAN	3.63	-0.13	2.85	-38.1
PAC	12.54	5.35	-3.86	8.86

Disclosures: T. Lee, None.

This study received funding from: National Medical Research Council, Ministry of Health, Singapore.

W200

Wwox Knockout Mice Reveal Impaired Steroidogenesis, Defects in Bone Metabolism, and Formation of Osteosarcomas. R. I. Aqeilan*, M. Q. Hassan*, A. de Bruin*, S. Hussain*, S. Lee*, J. P. Hagan*, S. Volinia*, G. S. Stein*, J. B. Lian*, C. M. Croce*. ¹Department of Molecular Virology, Immunology and Medical Genetics, Comprehensive Cancer Center, Ohio State University, Columbus, OH, USA, ²Department of Cell Biology and Cancer Center, University of Massachusetts Medical School, Worcester, MA, USA.

The WW domain-containing oxidoreductase (WWOX) gene encodes a 46kDa tumor suppressor that is not present in the majority of cancer cell lines. The bona fide *in vivo* tumor suppressor activity was recently reported (Proc.Natl.Acad.Sci. 104:3949, 2007). Loss of both alleles of Wwox resulted in the formation of frequent juvenile osteosarcomas, while loss of one allele increased the incidence of spontaneous and chemically-induced tumors. In the present study we investigated WWOX function *in vivo* by examining Wwox deficient (Wwox^{-/-}) mice for phenotypical abnormalities. Wwox^{-/-} mice are significantly reduced in size and die between 3 and 4 weeks. Mutant homozygous mice are born with gonadal abnormalities, displayed impaired steroidogenesis and suffer of a metabolic disorder. Wwox^{-/-} mice exhibit a delay in bone formation and develop metabolic bone disease. LacZ staining of whole embryos revealed Wwox expression in the axial skeleton, craniofacial bones and limbs. An osteopenic phenotype was observed histologically and by μ CT, suggesting a high rate of bone resorption, particularly given the serum values of 50% lower calcium and 20% increased phosphate in the KO mouse. Higher acid phosphatase activity was observed in femur bone sections of KO mice compared to the WT, indicating increased osteoclast activity in KO mice. Gene expression in calvaria and femur bone was examined. A 30-40% reduction in Runx2 and alkaline phosphatase (Alkp) suggested a decrease in cells recruited into the osteoblast lineage. The mechanism for these findings was addressed. WWOX protein, via its first WW domain, interacts with several transcriptional activators containing proline-tyrosine motifs and suppresses their function. We find WWOX physically associates with Runx2, the principal transcriptional regulator of osteoblast differentiation, and functionally suppresses Runx2 transactivation ability in osteoblasts. Expression of Wwox in MDA-MB-231 breast cancer cells reduces the mRNA

levels of all Runx2 target genes related to metastasis to bone including MMP9, VEGF, and osteocalcin. These results reveal a vital requirement for WWOX in postnatal survival, steroidogenesis and suggest a central role of WWOX in bone metabolism and repression of tumor growth in bone in part coupled to regulation of Runx2 transcriptional activity.

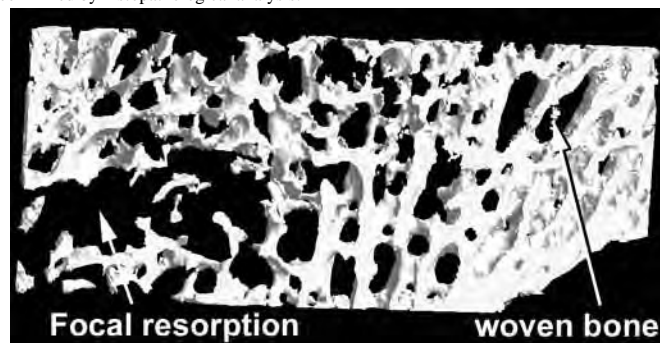
Disclosures: J.B. Lian, None.

W201

Computed Microtomography of Bone Specimens in the Diagnosis of Bone Metastases. H. Libouban*, M. Audran*, E. Legrand*, N. Ifrah*, M. F. Basle*, D. Chappard*. ¹Faculté de Médecine, INSERM EMI 0335 - LHEA, Angers, France, ²CHU d'Angers, INSERM EMI 0335 - Service de Rhumatologie, Angers, France, ³CHU d'Angers, Service d'Hématologie, Angers, France.

Bone metastases occur in more than half the patients with advanced cancer. Breast and prostate cancers are specially metastasizing to bone. When anchored in the bone marrow, malignant cells release soluble factors which interact with bone cell metabolism. Bone metastases from breast or lung cancer usually exhibit a mixed osteolytic and osteosclerotic, with osteolysis usually predominating. Osteosclerosis is a common finding in prostatic cancer although lytic areas can be identified by computed tomography within the sclerotic lesions. Pathological examination of bone biopsies performed in metastatic areas plays a key role in the diagnosis of malignancies. However, histological analysis often needs several days. The recent development of microCT has allowed non-destructive and fast examination of bones.

118 patients who presented at least one bone metastasis (identified by scintigraphy), an overt myeloma or lymphoma or a monoclonal gammopathy of undetermined significance (MGUS) were studied. All patients had a bone biopsy studied by histomorphometry for the diagnosis of the malignant invasion. During the fixation time, the bone cores (7mm in diameter) were analyzed on a Skyscan microCT (resolution 11 μ m/pixel). On the 3D reconstructed models, signs of metastasis were searched: excess of bone resorption, focal disorganization of microarchitecture, plexiform bone apposition (woven bone), osteosclerosis. Results were compared with data obtained by histomorphometry using kappa test. Excellent agreement was obtained for bone metastases and overt myeloma or lymphoma. MicroCT identified excess bone resorption on trabecular surfaces when ES/BS were >11%. MicroCT failed to identify patients with smoldering myeloma (with little tumor mass) or some lymphomas with microresorption. MicroCT data are rapidly obtained (< one day) and can confirm the malignant invasion of bone marrow when excess of bone resorption/formation is obtained. However, these signs are not specific and must be confirmed by histopathological analysis.



Disclosures: H. Libouban, None.

W202

Development of a Highly Sensitive High-throughput Mass Spectrometry-based Assay for Rat Procollagen Type I Propeptide (PINP). J. E. Hale*, B. Han*, L. V. Hale*, M. Sato*, J. You*, M. Copeland*. ¹Lilly Research Laboratories, Greenfield, IN, USA, ²Lilly Research Laboratories, Indianapolis, IN, USA, ³Indiana Center for Applied Protein Sciences, Indianapolis, IN, USA.

Type I procollagen aminoterminal propeptide (PINP) is a reliable marker of osteoblastic bone formation activity, and is routinely used in clinical trials. PINP has also recently been shown to be a reliable early bone formation marker in the rat. PINP is proteolytically derived from the type I procollagen molecule. Thus, serum level of PINP reflects new collagen matrix synthesis, the majority of which subsequently become newly mineralized bone. Currently the only commercially available assay for PINP is a radioimmunoassay for human PINP, which may not cross react with PINP from other species. It is important to have PINP assay for non-primate species to investigate the mechanism of bone formation and for preclinical development of drugs that can enhance bone formation.

We developed a highly sensitive, high-throughput mass spectrometry-based assay for PINP in rat plasma or serum that does not rely on antibody reagents. Cysteine sulphydryl groups in plasma or serum proteins were reduced and alkylated then digested with trypsin. The resulting peptides were separated by HPLC and the N-terminal tryptic fragment of the PINP was detected and quantified using tandem mass spectrometry by monitoring selected ion transitions upon high-energy fragmentation. The N-terminal glutamine residue was found to have quantitatively converted to pyroglutamate and an internal Asn residue was found to be deamidated to Asp.

Enrichment of PINP prior to HPLC-MS was necessary due to low levels of PINP in adult rats. This was achieved by combining reduction-alkylation of the serum proteins with a one-step precipitation of the majority of the serum proteins using acetonitrile. By optimizing the sample preparation method and HPLC conditions, up to 1000 samples could be processed in duplicates by a single person in one week. Circulating levels of PINP showed an age-dependent decrease in concentration. While PINP concentration in the 5 week-old rats was 200-250 nM, it dropped to 10-20 nM in the 9 month-old rats. Ovariectomy of adult female rats initially increased PINP, consistent with increased remodeling of the bone, which includes increased formation and resorption activities. Daily treatment of rats with parathyroid hormone (PTH) showed a statistically significant increase in PINP as has been observed in humans.

Disclosures: J.E. Hale, Eli Lilly & Co 3.

W203

C-Reactive Protein, a Marker of Inflammation, in Patients with Osteoporotic Non-Traumatic Fractures. L. A. Holzer^{*1}, U. Willinger^{*2}, G. Holzer¹. ¹Department of Orthopaedics, Medical University of Vienna, Vienna, Austria, ²ENT Clinic, Medical University of Vienna, Vienna, Austria.

Purpose: Inflammation could be partially responsible for the aetiology of osteoporosis. C-reactive protein (CRP) is a sensitive marker of inflammation, tissue damage, and infection. The purpose of this study was to investigate the inflammatory status expressed by levels of high-sensitive CRP in patients with osteoporosis to assess a possible role of inflammation in the development of osteoporosis.

Methods: Eight hundred twenty-four individuals (495 female and 329 male, mean age: 63.2 ± 14.0 years) were examined at our institution. All individuals answered a questionnaire concerning history, had x-ray and densitometry of the lumbar spine, and, if possible, of the proximal femur. Individuals were classified semi-quantitatively due to the spine fracture status and due to the bone mineral density (BMD) (t-score) of the lumbar spine (LS) and the proximal femur (PF). Laboratory examinations, sexual and thyroid hormone levels and, more specifically, bone turn-over markers were done routinely. Serum high-sensitive CRP was measured using an ultrasensitive immuno-nephelometry (N Latex CRP mono, Behringwerke AG, Marburg, Germany) on a BNA Behring nephelometer. Statistical analysis was done using Pearson correlation, t-tests (unpaired), discriminant analysis, and analysis of variance (ONEWAY). For data handling and analyses SPSS for Windows, Version 10.0 was used.

Results: Group differences between individuals without fractures (mean: 0.32 ± 0.38) and such with multiple non-traumatic fractures (mean: 0.56 ± 0.70) in respect to CRP were statistically significant (t=-2.3, df=100, p=0.026), as were group differences between controls (mean: 0.25 ± 0.18) and patients with osteoporosis (mean: 0.47 ± 0.57) (t=-2.8, df=53.5, p<0.0008).

Conclusions: The relationship between high-sensitive CRP serum levels and low BMD and multiple non-traumatic fractures in otherwise healthy individuals, is confirming the possible role of inflammation in the development of osteoporosis.

Disclosures: L.A. Holzer, None.

W204

Optimum Testing Strategy for Urinary N-Telopeptide. S. R. Johnson, I. Gioni^{*}, K. Lehan^{*}, J. Ellis^{*}. R&D, Unipath, Bedford, United Kingdom.

Effective therapies exist to treat osteoporosis, such as bisphosphonates. However, non-compliance and persistence mean that many women do not receive the full benefit of their treatment. Bone markers, such as urinary N-Telopeptide (uNTx) can be used to track response to therapy. This can help improve compliance and enable clinicians to identify poor or non-responders, so therapies can be optimised. The aim of this study was to ascertain the best testing strategy for uNTx to enable an accurate determination of levels, whilst providing a method that is practicable for both patients and clinicians.

Twenty women were recruited into each of three age-related cohorts, 31-40, 41-50, 51-60 years. The volunteers provided a second morning void urine sample following an overnight fast, for 30 consecutive days. The Osteomark uNTx ELISA was then used to measure NTx, adjusted for creatinine.

The effect of using 1, 2, 3, 4, 5 or 6 days worth of tests to provide a summary level for uNTx was compared to the weekly mean. Using only 1 or 2 tests produced uNTx estimates that could be greater than 20% different from the weekly mean. However, using 3 or more days worth of testing provided a good estimate of uNTx level, with more tests providing increased accuracy. A 3 day strategy was selected for further analysis because it provided sufficient accuracy, with less effort than 4+ day testing.

The effect of testing on consecutive days, testing every other day and random testing over a week was examined to determine the best 3 test regime. Testing strategies beginning at the start of the week produced the lowest variability, with consecutive measurements providing the most accurate result. Although random testing produced standard deviations higher than testing strategies starting on a Monday, it was no worse than consecutive or alternate measurements made later in the week.

As the influence of testing strategies on providing an accurate level was so small, the recommended testing strategy would be to use any 3 samples within a week. With no rigidity on providing a sample on particular days, more emphasis can be placed on ensuring the sample is second void after fasting. This relaxed strategy also enables sampling to fit in with clinic visits and is more achievable by the patients.

	Std. Mean	Std. Median
Consecutive Days (All start days)	12.4	11.9
Consecutive Days (Monday start)	11.5	11.8
Alternate Days (All start days)	12.8	12.1
Alternate Days (Monday start)	11.3	11.4
Random Testing	12.2	12.3

Disclosures: S.R. Johnson, Unipath 3.

This study received funding from: Unipath.

W205

Some but not all Estrogen-Like Molecules Have Both Bone and Cartilage Protective Effects: Evidence for Complete Uncoupling of Bone and Cartilage Effects. M. A. Karsdal, I. Byrjalsen, D. Leeming, P. Qvist, C. Christiansen. Nordic Bioscience, Herlev, Denmark.

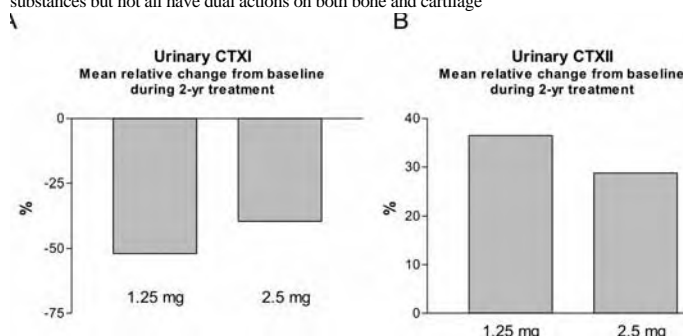
Postmenopausal osteoporosis is associated with increased bone resorption and increased cartilage degradation. Previous investigators have found chondroprotective effects of compounds with estrogenic properties in both preclinical and clinical settings, in which bone and cartilage degradation seemed to be closely coupled.

The objective of the present study was to determine whether Tibolone, a synthetic steroid with estrogenic, androgenic, and progestogenic properties, would have similar dual actions on both bone and cartilage turnover.

Methods: Ninety-one healthy postmenopausal women aged 52-75 yrs entered a 2-yr double blind, randomized, placebo-controlled study of treatment with either 1.25 mg/day (n=36), or 2.5 mg/day Tibolone (n=35), or placebo (n=20). Second void morning urine samples were collected at baseline, and at 3, 6, 12, and 24 months. The biochemical markers CTX-I and CTX-II were measured in Urine CrossLaps™ ELISA and Urine CartiLaps™ ELISA (Nordic Bioscience A/S) as markers of bone resorption and cartilage degradation, respectively.

Results: Bone and cartilage turnover was evaluated as the mean relative change from baseline during the 2-yr study period, corrected for placebo. Tibolone strongly and highly significantly (P<0.001) suppressed bone resorption as measured by CTX-I, figure 1A. In contrast, an increase rather than a decrease on cartilage degradation was observed, figure 1B.

Discussion: Previous studies have demonstrated positive effects of estrogens and various SERMs on both cartilage and bone degradation. In the present study we demonstrate a complete uncoupling of the bone and cartilage effects of the synthetic steroid, Tibolone. Bone resorption was highly significantly decreased as expected, whereas cartilage degradation was elevated. These effects are in direct contrast to those observed and published for other SERMs e.g. raloxifene and levormeloxifene decreasing both bone and cartilage degradation. In conclusion, these results may have important implications for the development of improved SERMs with additional effects on cartilage health supplementary to that of the primary endpoint, bone health. Interestingly these data clearly demonstrate that only some estrogen-like substances but not all have dual actions on both bone and cartilage



Disclosures: M.A. Karsdal, None.

W206

Development of Multiplex Immunoassay Panels for Simultaneous Quantification of Bone Metabolism Markers using Luminex xMAP Technology. W. Lie*, H. Hwang*, J. Wang*, J. Mistry*. MILLIPORE, St Charles, MO, USA.

Biochemical markers of bone metabolism play an important role in the assessment of bone diseases such as osteoporosis, arthritis, chronic inflammatory disorders, and bone metastasis with cancers. Millipore has developed various multiplexed immunoassay panels for the simultaneous measurement of multiple bone metabolism markers in mouse, rat, and human, using the Luminex xMAP platform. These bead-based sandwich assays are rapid, sensitive, and reproducible and require $\leq 25 \mu\text{L}$ of serum/plasma sample or tissue culture supernatants per well in 96-well plates. The mouse bone panels allow simultaneous quantitation of the following biomarkers in any combinations in the same sample well: Mouse Panel 1 - OPG, Osteocalcin, ACTH, Insulin, Leptin, TNF α , IL-6, and IL-1 β and Mouse Panel 2 - RANKL, Osteocalcin, ACTH, Insulin, Leptin, TNF α , IL-6, and IL-1 β . The dynamic ranges for the mouse analytes are 10-40,000 pg/mL (OPG, Osteocalcin, RANKL, and Leptin), 24-100,000 pg/mL (Insulin), and 2-10,000 pg/mL (ACTH, TNF α , IL-6, and IL-1 β). The rat bone panels allow simultaneous measurement of the following biomarkers: Rat Panel 1 - OPG, ACTH, Insulin, and Leptin, Rat Panel 2 - RANKL, ACTH, Insulin, and Leptin, and Rat Panel 3 - Osteocalcin and PTH. The dynamic ranges for the rat analytes are 10-40,000 pg/mL (OPG, PTH, Leptin), 5-20,000 pg/mL (Osteocalcin), 4-15,000 pg/mL (RANKL), 24-100,000 pg/mL (Insulin), and 2-10,000 pg/mL (ACTH). The human bone metabolism panels allow for simultaneous measurement of the following biomarkers in any combinations: Human Panel A (serum samples) - OPG, Osteocalcin, Osteopontin, and PTH and Human Panel B (tissue culture samples) - OPG, Osteocalcin, Osteopontin, PTH, Leptin, Adiponectin, Insulin, ACTH, TNF α , IL-6, IL-1 β , and VEGF. We have also developed a sensitive immunoassay for measuring the serum levels of human RANKL. The dynamic range for this Human RANKL Single-plex assay is 5-20,000 pg/mL. The above bone metabolism panels exhibited acceptable analytical performance characteristics in terms of sensitivity, intra- and inter-assay precision, linearity of dilution, spike recovery, and antibody pair specificity. In conclusion, various multiplexed assay panels were developed and validated for the measurement of multiple bone metabolism markers in mouse, rat, and human samples. The availability of these multiplexed Bone Metabolism Panels and the RANKL, OPG, and Osteocalcin Single-plex assays may provide a powerful tool in studying biological functions of these biomarkers as well as the pathological roles of these molecules.

Disclosures: W. Lie, None.

W207

Increased Bone Resorption in Knee Osteoarthritis with Severe Joint Surface Wear. T. Mashiba, S. Mori, Y. Kaji*, K. Iwata*, S. Komatsubara*, T. Manabe*, T. Yamamoto*. Orthopedic Surgery, Kagawa University Faculty of Medicine, Kagawa, Japan.

It has been known that the patients with knee osteoarthritis (OA) have little higher bone mineral density (BMD) when compared with normal controls. Recently, however, it has been suggested that subchondral bone metabolism is associated with the progression of osteoarthritis of the knee. The objective of this study is to examine the relationship of bone mineral density and bone metabolic markers to radiological progression of knee OA. One hundred sixty-six postmenopausal women (55-89 y.o.) with radiographic knee OA were enrolled in this study. Weight-bearing antero-posterior knee radiograph with the patellae in central position were taken in all women. They were divided into 5 groups based on Koshino's grading system of knee OA (Grade1: sclerosis or osteophyte formation, Grade2: joint space narrowing $< 3\text{mm}$, Grade 3: joint space disappearance, Grade 4: subchondral bony wear $< 5\text{mm}$, Grade 5: subchondral bony wear $> 5\text{mm}$). All women underwent bone mineral density (BMD) measurements of lumbar spine and hip. Serum osteocalcin (OC) and urinary deoxypyridinoline (DPD) were measured. There were no significant differences among groups in body mass index or BMD at any site. DPD was significantly higher in grade 5 group than in others, and Spearman's rank correlation analysis showed significant association between elevated OA grade and increased DPD value. However, no significant differences were found in OC among all groups. In this study, bone resorption expressed by DPD was elevated especially in women knee OA with the severest joint surface wear. Our results indicate that increased bone resorption was associated with the progression of subchondral bony wear in knee OA although it is not clear whether increased bone resorption is cause or results of joint surface wear.

Disclosures: T. Mashiba, None.

W208

Fluctuation of the Normal Values of the Biochemical Markers of Bone Turnover in Greek Premenopausal Women. E. Metania*¹, P. Dimou*², P. Katsimbri*¹, T. Kaplanoglou*¹, I. Koulouris*¹, P. N. Soucacos*¹, G. Skarantavos*¹. ¹1st Department of Orthopaedic Surgery, Metabolic Bone Diseases Unit, General University Hospital 'ATTIKON', Athens, Greece, ²Biochemical Department, Asclepion Hospital, Voulas, Athens, Greece.

Aim: In clinical practice, normal values of the biochemical markers of bone turnover are considered the values defined by the manufactory companies of the various reagent kits used universally. The fact that the abnormal rate of bone turnover in Greek women is based on normal values of the biochemical bone markers of women of a different nationality, has led to the need to create a data base based in normal values in Greek premenopausal women. Material-Methods: A detailed medical history was recorded and blood samples were collected from 100 healthy, Greek premenopausal women, between 30 to 54 years, with normal physical

activity. Women in pregnancy, or women who had diseases, or taking pharmacological agents affecting bone metabolism were excluded. In all participants detailed information was given regarding the purpose of the study, and written consent was obtained. Blood samples were collected and, after centrifuging, the values of 3 bone formation markers [osteocalcin, bone alkaline phosphatase, PINP], and 2 bone resorption markers [serum NTX and CTX] were determined. Osteocalcin, PINP (Roche Diagnostics GmbH Mannheim) and serum CTX (Roche Diagnostics GmbH Mannheim) was measured with an electrochemiluminescence immunoassay. Bone alkaline phosphatase (Quidel Corporation, San Diego, CA USA) and serum NTX (Osteomark NTx Serum, Wampole Laboratories, NJ USA) was measured with an ELISA. The participants were categorized in three groups according to their age and statistical analysis of the results was performed.

Results: According to our study the normal values for premenopausal Greek women are: 1) Osteocalcin: 3,56 to 33,8 ng/ml (Mean: 18,68, SD:7,56. 2) Bone Alkaline Phosphatase: 4,52 to 27,08 U/L (Mean: 15,80, SD:5,64). 3) PINP: 12,01 to 58,49 $\mu\text{g/L}$ (Mean: 35,25, SD:11,62). 4) NTX: 5,18 to 21,98 ng/ml (Mean: 13,58, SD:4,20). 5) CTX: $< 0,531\text{ng/ml}$, (Mean: 0,265, SD:0,133). The reproducibility of our measurements was 5-8%.

Conclusion: 1. The present study reflects the reference values for the biochemical bone markers that determine the normal rate of bone turnover in the Greek women. 2. Thereby, it is feasible to more accurately determine high or low bone turnover in postmenopausal Greek women. 3. In all bone markers that were examined, we observed difference in the values of the Greek population compared with the reference values, especially for osteocalcin and bone alkaline phosphatase. 4. Our results suggest that, during the premenopausal period, the biochemical bone markers show no age variability.

Disclosures: E. Metania, None.

W209

Comparison of Serum Tartrate-resistant Acid Phosphatase Type 5b Assays and Other Bone Resorption Markers for Monitoring Raloxifene Therapy. Y. Mochizuki*¹, A. Oishi*¹, Y. Igarashi*², N. Inaba*¹. ¹Department of Obstetrics and Gynecology, Dokkyo Medical University, Tochigi, Japan,

²Department of Basic Medicine, Dokkyo Medical University, Tochigi, Japan.

Objectives: Tartrate-resistant acid phosphatase type 5b (TRACP 5b) is a reliable bone marker derived specifically from osteoclasts and its serum levels are not affected by feeding, renal or hepatic function. The purpose of this study was to compare the clinical performance of two different TRACP 5b assays and other markers of bone resorption for monitoring raloxifene therapy. Methods: Twenty five postmenopausal women with osteoporosis/osteopenia were treated raloxifene 60mg daily. Serum TRACP 5b, serum and urinary N-terminal telopeptides of type I collagen (S-NTX and U-NTX), urinary deoxypyridinoline (DPD) were measured at baseline and 1, 3 and 6 months after treatment. Lumbar bone mineral density (LBMD) was determined at baseline and six months. The TRACP 5b assays and other markers were as follows: A novel assay system for TRACP 5b called fragments absorbed immunocapture enzymatic assay (FAICEA) (Nitto Boseki Co., Ltd., Fukushima, Japan), A pH-selective immunoassay measuring TRACP 5b activity (BoneTRAP[®] Assay, IDS Ltd., NE, UK), S-NTX and U-NTX (Mochida Pharmaceutical Co., Ltd., Osaka, Japan) and DPD (DS Pharma Biomedical Co., Ltd., Osaka, Japan). Results: Serum TRACP 5b values were reduced significantly by raloxifene on 1 month using 2 assay kits. The reduction rates on 1, 3 and 6 months were 22.7%, 26.9% and 28.3% (FAICEA), 13.7%, 18.6% and 22.7% (BoneTRAP[®]), respectively. On the other hand, the reduction rates of other markers on 1, 3 and 6 months were 16.9%, 14.3% and 17.2% (S-NTX), 18.7%, 31.0% and 25.8% (U-NTX), 15.6%, 22.6% and 18.9% (DPD), respectively. Serum TRACP 5b change exceeded the least significant change (LSC) on 6 month in 66.7% (FAICEA; LSC 31.6%) and 33.3% (Bone TRAP[®]; LSC 29.5%) of the subjects. The changes of LBMD at 6 months only correlated significantly with the changes of TRACP 5b with FAICEA ($r^2=0.190$, $p<0.05$) at 3 months. Conclusions: These results suggest that serum TRACP 5b with FAICEA is an excellent bone resorption marker for monitoring raloxifene treatment.

Disclosures: Y. Mochizuki, None.

W210

Serum PINP Is a Useful Marker of Bone Formation in Rat Ovariectomy

Model. J. Morko*¹, J. P. Rissanen*¹, M. I. Suominen*¹, Z. Peng*¹, S. Rasi*², J. Risteli*³, J. M. Halleen*¹. ¹Pharmatest Services Ltd, Turku, Finland, ²SBA-Sciences, Oulu, Finland, ³Department of Clinical Chemistry, University of Oulu, Oulu, Finland.

Serum procollagen I N-terminal propeptide (PINP) is a useful marker of bone formation in humans. We report here the development and characterization of a non-radioactive immunoassay for rat PINP, and the use of PINP as a bone formation marker in rat ovariectomy (OVX) model. A polyclonal PINP antiserum was developed in rabbits using a synthetic peptide QEDIPEVS as antigen, corresponding to the first amino acids of the N-terminal propeptide of rat type I procollagen $\alpha 1$ chain. Intra- and inter-assay coefficients of variation (CVs) were calculated from a panel of rat serum samples in three different PINP levels ($n=10$ in each level). Two OVX studies were performed, both with 3-month old rats. A pilot 14-day study contained a sham-operated control group and an OVX group, and included measurement of serum PINP and other bone turnover markers before the operation and at days 2, 4, 7, 10 and 14. An extensive 8-week study included a sham-operated control group, an OVX group receiving vehicle, and an OVX group receiving 17 β -estradiol (E2, 10 $\mu\text{g/kg/day}$ s.c.). PINP and other bone turnover markers, including serum osteocalcin, C-terminal cross-linked telopeptides of type I collagen (CTX) and tartrate-resistant acid phosphatase 5b (TRACP 5b), were measured before the operations and at 2 and 8 weeks. Trabecular bone parameters were determined from tibial metaphysis using pQCT analysis and histomorphometry at 8 weeks. The PINP immunoassay had an intra-assay CV of 2.8%, inter-assay CV of 7.5%, dilution linearity of 95%

and recovery of 107%. PINP increased during the first 2 weeks after OVX, and returned to sham-level at 8 weeks. Osteocalcin and CTX were increased at 2 weeks, but they were also increased at 8 weeks. TRACP 5b was decreased at 2 and 8 weeks, and the values at 8 weeks correlated strongly with the histomorphometrically determined absolute number of osteoclasts (N.Oc/T.Ar). E2 prevented the increase of PINP, as well as the changes of the other bone turnover markers caused by OVX. Changes in PINP showed a strong correlation with changes in other bone turnover markers at 2 weeks, and PINP values at 2 weeks correlated significantly with trabecular bone parameters at 8 weeks. These results demonstrate that rat serum PINP is a useful marker of bone formation, and short-term changes in PINP predict long-term changes in trabecular bone parameters in rat OVX model. Osteocalcin behaved similarly than CTX and differently than PINP at 8 weeks, suggesting that a substantial amount of rat serum osteocalcin may be derived from bone resorption rather than bone formation.

Disclosures: J. Morko, None.

W211

Automated Measurement of 1,25 Dihydroxyvitamin D on the LIAISON® Analyzer. D. M. Heldman*, D. L. Ersfeld*, C. L. Ross*, P. J. Krohn*, G. T. Olson, J. A. Schmidt, Research & Development, DiaSorin Inc, Stillwater, MN, USA.

1,25-dihydroxyvitamin D (1,25-Vit-D) is the metabolically active, most potent form of vitamin D. Its production in the kidneys is tightly regulated by serum calcium, phosphorus, and PTH concentrations. However, numerous disorders exist that can disrupt this carefully controlled system. These include renal failure, type I and II vitamin D dependent rickets, as well as extra-renal disorders such as sarcoidosis and rheumatoid arthritis. Because of these and similar conditions it is becoming increasingly important to have an accurate measurement of 1,25-Vit-D. Therefore, we have developed a sensitive and precise automated assay for the measurement of 1,25-Vit-D on the LIAISON® Analyzer. Using a competitive inhibition, chemiluminescent immunoassay and a solvent based C-18 column extraction, we were able to demonstrate the following performance parameters over a range of 4-200 pg/mL. Analytical and functional sensitivity were <4 pg/mL and <15 pg/mL respectively. Recovery ranged from 96-112%, with an average of 103%. The coefficient of variance (CV) for intra-assay precision was <13% and inter-assay precision was <15%. Linear regression for dilution linearity yielded a slope of 0.95 and r-value of 0.99. Linear regression for the method comparison of 51 patient samples compared to the DiaSorin 1,25 Dihydroxyvitamin D RIA kit was LIAISON® = 0.91(RIA) + 2.1, r = 0.94. Results obtained during development demonstrate that the LIAISON® 1,25 Dihydroxyvitamin D Assay is an accurate and precise means of measuring serum 1,25-Vit-D levels. This product significantly enhances the expanding DiaSorin LIAISON® bone and mineral product line.

Product availability subject to required regulatory approvals.

Disclosures: G.T. Olson, DiaSorin Inc. 3.
This study received funding from: Diasorin, Inc.

W212

Analytical and Clinical Performance of an Automated Assay for the Measurement of Osteocalcin on the LIAISON® Analyzer. A. L. Podgorski*, D. L. Vaught*, J. J. Body*, F. Vertongen*, G. T. Olson, F. A. Blocki, J. A. Schmidt. ¹Research and Development, DiaSorin Inc., Stillwater, MN, USA, ²Department of Medicine, Institut J. Bordet, Université Libre de Bruxelles, Brussels, Belgium, ³CHU Saint Pierre, Université Libre de Bruxelles, Brussels, Belgium.

Osteocalcin (OC) is a small bone matrix protein (Mr 5800) produced by osteoblasts (OB). Three of OC's 49 amino acids are calcium binding gamma-carboxyglutamic acids. OC comprises nearly 1% of bone's organic matrix: smaller amounts are synthesized in dentine by odontoblasts. Expression of OC is vitamin K-dependent and under the control of 1,25-dihydroxyvitamin D. OC is a marker of bone formation reflecting increased or decreased bone turnover in patients with altered bone metabolism. Although OC serum levels are broadly accepted as reflecting increased OB activity, intact OC and OC fragments from the resorption of bone matrix have recently been reported as contributing to serum OC levels.

The LIAISON® Osteocalcin Assay utilizes a 25 µL serum sample, 20 µL magnetic particles coated with a monoclonal anti-OC (directed to residues 20-43) and 175 µL tracer, a second Mab anti-OC (directed to residues 1-19) labeled with an isoluminol derivative. Following a 10-min incubation, wash, and chemical trigger addition, light is measured that is proportionate to the amount of OC in the sample. Results are available in 20 minutes with a throughput of 180 tests/hour. Performance was established following standard CLSI protocols. Analytical and functional sensitivities are ≤0.3 ng/mL and ≤3 ng/mL, respectively. Intra- and inter-assay imprecision with samples throughout the range is ≤9%, following a 20 day precision protocol. Mean recovery is 93% and dilution linearity is (observed) = 1.05(expected) + 0.12, R = 1.00. A correlation using 249 serum samples across the range is: LIAISON = 0.99(commercial assay) - 1.01, R = 0.98.

In a clinical laboratory samples from patients with osteoporosis or metastatic breast cancer were tested using the LIAISON® Osteocalcin Assay to demonstrate the clinical utility of this assay for treatment evaluation. The results of the LIAISON® Osteocalcin assay corresponded well with another approved automated assay.

The accurate, precise LIAISON® Osteocalcin Assay enhances the expanding LIAISON® bone and mineral product line.

Product availability is subject to required regulatory approvals.

Disclosures: A.L. Podgorski, DiaSorin Inc. 3.
This study received funding from: Diasorin Inc.

W213

A Comparison Between Gene Expression in Skeletal Muscle and Bone of Postmenopausal Osteoporotic Females and Their Controls. S. Reppe*, O. K. Olstad*, V. T. Gautvik*, S. Nygård*, L. S. Nissen-Meyer*, P. I. Høvring*, R. Jemtland*, K. M. Gautvik*. ¹Medical Biochemistry, University of Oslo, Oslo, Norway, ²Dept. of Clinical Chemistry, Ullevaal University Hospital, Oslo, Norway, ³Mathematics, University of Oslo, Oslo, Norway, ⁴Section of Endocrinology, Rikshospitalet University Hospital, Oslo, Norway.

It is well known that patients with osteoporosis also have reduced muscle strength and show increased tendency to falls, thereby increasing the fracture risk. There is a question whether the entire musculo-skeletal system is affected in postmenopausal osteoporosis or only the skeleton. Maximum bone density and muscle mass are both 60 % - 80 % genetically determined. In this study we have assessed the global gene expression patterns in trans-iliac bone and in muscle biopsies from the same individuals from osteoporotic females (n=12,) and healthy controls (n=12), using total RNA (pooled two by two) and Affymetrix HG U133 Plus 2.0 arrays. The osteoporotic group had T-scores < -2.5 in vertebrae and hips and low impact fractures. The MAS 5.0 software was used to identify and filter out absent genes, while signal values were obtained using PLIER. Students t-test were used for significant differences (p<0.05). 310 mRNAs (genes) showed significantly changed expression between healthy and osteoporotic women in the bone biopsies while the corresponding number in muscle biopsies were 130 at the level of significance of p < 0.05. Using Ingenuity Pathway Analysis we found that the top canonical pathways involving more than 5 genes associated with the altered gene expression in bone were: calcium signaling (p<0.000), Cardiac β-adrenergic signaling (p<0.000) and actin cytoskeletal signaling (p < 0.001), represented by 12, 9 and 9 genes, respectively. In muscle no pathway with more than 3 genes was found to be affected in osteoporotic women as compared to healthy controls. The major physiological systems and functions affected in bone were "skeletal and muscular system development and function" and "tissue morphology" involving 62 and 42 genes, respectively, while the corresponding top systems in muscle were "hematological system development and function" and "Immune response" both with 4 genes. Thus, the osteoporotic phenotype is reflected by altered gene expression in bone. The present study also indicate abnormal gene expression in skeletal muscle, in support of the hypothesis of musculo-skeletal disorder in female osteoporosis.

The EU project LSHM-CT-2003-50294 is acknowledged for financial support.

Disclosures: S. Reppe, None.

W214

A Non-radioactive Immunoassay for Mouse PINP. J. P. Rissanen¹, M. I. Suominen¹, J. Morko¹, S. Rasi², J. Risteli³, J. M. Hallee¹. ¹Pharmatest Services Ltd, Turku, Finland, ²SBA-Sciences, Oulu, Finland, ³Department of Clinical Chemistry, University of Oulu, Oulu, Finland.

Serum procollagen I N-terminal propeptide (PINP) is a useful marker of bone formation in humans. We have reported the development and characterization of a non-radioactive immunoassay for rat PINP. Here we demonstrate that the assay can also be used for measuring PINP from mouse serum samples. We used the PINP immunoassay to study the use of PINP as a bone formation marker in a mouse model of glucocorticoid-induced osteoporosis. PINP was measured from mouse serum samples with a polyclonal PINP antiserum developed in rabbits using a synthetic peptide QEDIPEVS as antigen, corresponding to the first amino acids of the N-terminal propeptide of rat type I procollagen α1 chain. Twelve weeks old Balb/c male mice (n=8/group) were given either vehicle (control group) or 3, 10 or 30 mg/kg/d of prednisolone orally for 4 weeks. Serum osteocalcin and PINP were measured from fasting blood samples before the start of treatment, and at 2 and 4 weeks. For dynamic histomorphometry, tetracycline labelling was performed at day 10 and calcein labelling at day 2 before termination. Parameters of dynamic histomorphometry were determined from trabecular bone and cortical bone at the end of the study. Statistical analysis was performed with ANCOVA for follow-up measurements and either ANOVA or Kruskal-Wallis test for end-point measurements after checking the assumptions for normality and homogeneity of variances. Linear contrasts of means or Mann-Whitney test were utilized for pairwise comparisons. Parameters of dynamic histomorphometry were dramatically decreased by prednisolone. The decrease was dose-dependent in trabecular bone parameters, whereas maximal reduction was observed already with the lowest dose of prednisolone in cortical bone parameters. PINP values were dose-dependently decreased by prednisolone treatment at both 2 and 4 weeks. The values were decreased by more than 50% already with the lowest dose of prednisolone at 2 weeks. Similar, although not as dramatic changes were observed for serum osteocalcin values. These results demonstrate that PINP is a useful marker of bone formation in this mouse model of glucocorticoid-induced osteoporosis. Prednisolone changes PINP values in a similar pattern than it changes parameters of dynamic histomorphometry, particularly in trabecular bone.

Disclosures: J.P. Rissanen, None.

W215

Reproducibility of Biochemical Markers of Bone Turnover in Clinical Practice. A. L. Schafer^{*1}, E. Vittinghoff^{*2}, R. Ramachandran^{*3}, N. Mahmoudi^{*4}, D. C. Bauer¹. ¹Medicine, University of California, San Francisco, San Francisco, CA, USA, ²Epidemiology and Biostatistics, University of California, San Francisco, San Francisco, CA, USA, ³Laboratory Medicine, University of California, San Francisco, San Francisco, CA, USA, ⁴Hospital Medicine, Kaiser Permanente, Oakland, CA, USA.

Recent investigation has shown that biochemical markers of bone turnover may be useful to predict fracture risk and to assess response to osteoporosis therapy. Although several bone turnover markers are FDA-approved, there is little information about reproducibility of marker measurements in clinical practice. This study aimed to determine the laboratory reproducibility of two markers: urine N-telopeptide (NTX) and serum bone-specific alkaline phosphatase (BSAP). Fasting morning serum and urine were collected from 5 postmenopausal women (mean \pm SD age 65 \pm 6.3 years) not taking osteoporosis therapy. The serum and the urine were pooled, divided into identical aliquots, and stored at -80°C. An identical specimen was sent to each of 6 high-volume US commercial labs on 5 dates over an 8-month period. On the fifth date, 5 identical specimens were sent to each lab. Fictional identifiers were used, and specimens were sent by the authors' institutional lab, so that the commercial labs were unaware of the investigation. Means, SDs, and coefficients of variation (CVs) with 95% confidence intervals (CIs) were calculated. Longitudinal reproducibility was evaluated as one specimen was sent to each lab on each of 5 dates. For urine NTX (Table), CVs varied from 5.4% to 37.6%. Longitudinal variation was significantly higher for labs using the Osteomark assay (CV 40.2%, CI 26.6-86.9) than for those using the Vitros ECI assay (CV 7.0%, CI 5.3-10.4). For BSAP, CVs ranged from 3.1% (CI 1.9-9.1) for Esoterix to 23.6% (CI 13.9-77.2) for LabCorp.

Lab (Assay)	Longitudinal Reproducibility for NTX			Within-Run Reproducibility for NTX		
	Mean \pm SD	CV, % (95% CI)		Mean \pm SD	CV, % (95% CI)	
ARUP (Vitros ECI)	35.8 \pm 1.9	5.4 (3.2-15.5)		36.4 \pm 0.5	1.5 (0.9-4.3)	
Quest (Vitros ECI)	34.0 \pm 2.2	6.6 (3.9-19.1)		34.0 \pm 1.2	3.6 (2.2-10.4)	
Esoterix (Vitros ECI)	35.8 \pm 2.9	8.0 (4.5-30.4)		34.0 \pm 1.4	4.2 (2.5-12.0)	
Mayo (Vitros ECI)	35.0 \pm 3.0	8.6 (5.1-25.0)		40.0 \pm 1.6	4.0 (2.4-11.4)	
LabCorp (Osteomark)	74.2 \pm 19.3	25.9 (15.2-87.9)		59.0 \pm 4.2	7.1 (4.2-20.6)	
Specialty (Osteomark)	42.8 \pm 16.0	37.6 (21.6-168.0)		52.8 \pm 9.1	17.2 (10.2-52.9)	
Units for means and SDs: nM BCE/mM Cr						

Within-run reproducibility was evaluated as each lab was sent 5 identical specimens on one date. For urine NTX, see Table. For BSAP, Esoterix produced 5 identical measurements, and CVs for the other labs ranged from 2.2% (CI 1.3-6.3) for Quest to 15.5% (CI 9.2-47.1) for LabCorp.

We conclude that the reproducibility of urine NTX and serum BSAP is highly variable at US commercial labs. Poor reproducibility is a barrier to the use of biochemical markers of bone turnover in clinical practice, particularly if clinicians do not consistently use the same assay and laboratory.

Disclosures: A.L. Schafer, None.

This study received funding from: Procter & Gamble Pharmaceuticals.

W216

Measurement of 25-OH Vitamin D₂ by the LIAISON[®] 25 OH Vitamin D TOTAL Assay. J. A. Schmidt, E. M. Frenzel*, M. A. Friedberg*, A. L. Podgorski*, J. S. Fenske*. Research & Development, DiaSorin Inc, Stillwater, MN, USA.

The role of vitamin D in bone and mineral metabolism was recognized from its first identification as a factor that could cure rickets. However, vitamin D is now recognized as a prohormone with multiple roles in maintaining optimal health. Vitamin D₃ (cholecalciferol) is the form of vitamin D that occurs naturally in humans, but vitamin D deficiency is commonly treated in the United States with vitamin D₂ (ergocalciferol). Fortified foods or supplements may contain either form. Thus, it is important that an assay for use world-wide measure both D₂ and D₃ forms of 25 OH vitamin D.

We compared the results obtained for 25 OH vitamin D in 110 serum samples by a validated liquid chromatography-tandem mass spectrometry (LC-TMS) method and by LIAISON[®] 25 OH Vitamin D TOTAL, a chemiluminescent immunoassay. LC-TMS gives separate results for 25OH D₂ and 25OH D₃, but there is no clinical utility in separate values; the LIAISON[®] assay gives a single result. Of 110 samples tested, 46 were found to contain detectable amounts of 25OH D₂. Actual values were 4-45 ng/mL 25OH D₂ and 6-53 ng/mL total 25OH D. Regression equations were similar:

LIAISON[®] = 0.83(LC-TMS) + 2.7; R = 0.87 for all samples; and

LIAISON[®] = 0.80(LC-TMS) + 3.6; R = 0.78 for samples containing 25OH D₂.

Furthermore, there was no trend to higher or lower bias with increasing 25OH D₂.

These results demonstrate that the LIAISON[®] 25 OH Vitamin D TOTAL assay measures both the D₃ and D₂ forms of the vitamin equally.

Product availability subject to required regulatory approvals.

Disclosures: J.A. Schmidt, DiaSorin Inc. 3.

This study received funding from: Diasorin, Inc.

W217

Development of a Bone Specific Alkaline Phosphatase Assay for the LIAISON[®] Analyzer. K. E. Paulsen, C. M. Klatt*, F. A. Blocki, P. J. Krohn*, G. T. Olson, M. A. Friedberg*, J. A. Schmidt. R&D, DiaSorin Inc, Stillwater, MN, USA.

Bone Specific Alkaline Phosphatase (BAP) is a serum marker for osteoblastic bone formation. Measurement of BAP is useful in diagnosing Paget's disease and osteoporosis and in monitoring the response to antiresorptive therapy in these patients, and for assessing bone turnover in patients with chronic kidney disease - mineral and bone disorders (CKD-MBD). BAP is also an emerging marker of bone formation within the context of reversing adynamic bone disease. We report here the development of a chemiluminescent immunoassay for BAP on the LIAISON[®] Analyzer.

Approximately 95% of total alkaline phosphatase activity in normal human serum is due to the presence of the liver and bone isoforms present in approximately equal quantities. BAP and Liver Alkaline Phosphatase (LAP), alternatively known as TNALP, tissue non-specific alkaline phosphatase, share a common primary sequence and differ structurally solely due to post-translational glycosylation. Antibody with specificity toward the carbohydrate portion of the BAP enzyme is needed in order to minimize cross reactivity to the LAP isoform in the assay.

The BAP assay uses 50 μ L of serum sample mixed with paramagnetic particles coated with monoclonal antibody to BAP in a 20 minute incubation. A tracer of a second monoclonal antibody labeled with an isoluminol derivative is then added followed by a 15 minute incubation. Particles are washed and a chemiluminescent reaction produces a signal proportionate to the quantity of BAP in the sample.

The LIAISON[®] Bone Specific Alkaline Phosphatase assay measures in the range of 0.1 to 120 ng/mL with analytical sensitivity < 0.1 ng/mL, functional sensitivity < 0.4 ng/mL, and inter-assay imprecision \leq 8%. The assay demonstrates good correlation to a predicate device, LIAISON[®] = 0.94x + 1.78 ng/mL, R = 0.90. Dilution Linearity yields a regression equation of y = 1.04 (expected) - 4.0, R = 0.98. Cross reactivity to the LAP isoform in this two-site mass based assay is comparable to or better than other methods which use phosphatase activity for detection.

The LIAISON[®] Bone Specific Alkaline Phosphatase assay is an accurate and precise assay, with minimal cross reactivity toward liver alkaline phosphatase, significantly enhancing DiaSorin's expanding bone and mineral product line. Product availability subject to required regulatory approvals.

Disclosures: J.A. Schmidt, DiaSorin Inc 3.

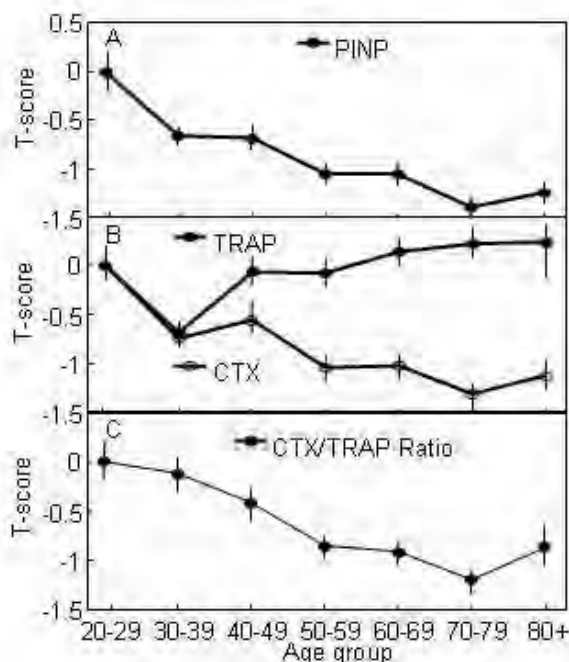
This study received funding from: Diasorin, Inc.

W218

Age-Related Changes in Bone Turnover in Men: Evidence for Impairments in Both Osteoblast and Osteoclast Function. B. Srinivasan, B. L. Riggs, E. J. Atkinson*, L. J. Melton III, S. Khosla. Mayo Clinic, Rochester, MN, USA.

While bone turnover generally increases after menopause and with aging in women, age-related changes in bone remodeling in men have been less clearly defined. Most studies have found decreases in biochemical markers of bone formation with age in men, consistent with an age-related defect in bone formation. Results with bone resorption markers have been more variable; some studies have found an increase and others report no clear changes. Serum CTx is a well established marker of bone resorption, reflecting the net effects of osteoclast number and activity on bone. By contrast, data from in vitro, animal, and human studies indicate that measurement of serum tartrate-resistant acid phosphatase (TRAP) 5b (which is specific for TRAP derived from osteoclasts) principally reflects osteoclast numbers. To dissociate possible age-related changes in osteoclast numbers versus activity, we measured serum CTx and TRAP 5b levels using highly sensitive and specific immunoassays in a large, population-based sample of men (n = 313) age 22 to 91 yrs. We also calculated the ratio of CTx:TRAP 5b as an index of resorptive activity per osteoclast. As a measure of bone formation, we assessed serum PINP levels. Panel A shows the age-related changes (mean \pm SE, expressed as T-scores relative to men age 20-29 yrs) in serum PINP levels, demonstrating a 45% decrease in bone formation between age 20 to 90 yrs (P < 0.0001). Panel B shows the changes in serum CTx and TRAP 5b; as is evident, while serum CTx decreased over life by 40% (P < 0.001), serum TRAP 5b levels increased by 32% (P < 0.001), suggesting that despite an apparent age-related increase in osteoclast numbers, net bone resorption decreased with age in men. Panel C shows the ratio of CTx: TRAP 5b, representing an index of activity per osteoclast, which decreased in men over life by 36% (P < 0.001).

These findings thus demonstrate that bone formation clearly decreases with age in men. While TRAP 5b (an index of osteoclast numbers) increases, CTx (an index of net bone resorption) decreases with age in men, consistent with an age-related defect in osteoclast function. Since there is increasing evidence that osteoclasts directly regulate osteoblastic activity, the observed deficit in osteoclast function with aging in men may contribute to the age-related impairment in bone formation in men.



Disclosures: B. Srinivasan, None.

This study received funding from: NIH/NIA - AR27065.

W219

Utilize of s-RANKL, s-FREE RANKL and Osteoprotegerin Serum Levels for Prediction of Bone Density. D. Stejskal^{1*}, M. Karpisek^{2*}, P. Solichova^{1*}, R. Ochmanova^{3*}. ¹Department of Laboratory Medicine, Sternberk hospital, Sternberk, Czech Republic, ²Department of Toxicology, University of Veterinary and Pharmacology Sciences, Brno, Brno, Czech Republic, ³Department of Internal Medicine, Sternberk hospital, Sternberk, Czech Republic.

Background: RANKL and its inhibitor OPG are decisive for osteoclast differentiation and osteoresorption function so that they became the aim of an intensive research. Recently, there are some informations about importance of free RANKL for BMD prediction.

Aim: to determine OPG, s-RANKL, s-RANKL free concentrations in persons with various degree of reduced bone density and to find correlations between BMD and listed markers. **Methods:** We examined 69 patients who under the follow-up for osteopathy. All individuals were examined for OPG (Biovendor), s-RANKL (Biovendor), s-RANKL free (Immunodiagnostic), osteocalcin, b-ALP, DPD/creatinine index. We performed DXA of the skeleton. Patients were divided into the subgroup of persons with normal bone density (T score>-1 "N") and individuals with reduced bone density (T score<-1, "OP"). **Results:** 27 patients had normal bone density and 42 probands had osteopenia or osteoporosis. OPG: individuals "N" had median values 2.9 vs 3.7 pmol/l in probands "OP" (p<0.05). S-RANKL-free: values didn't differ significantly in "OP" versus "N" patients (0.1 vs 0.09 pmol/l). S-RANKL: individuals "N" had median 311 vs 127 pmol/l in probands "OP" (p<0.05). OPG strongly correlated with s-RANKL (r = -0.35; p<0.01) and BMD (r = -0.4; p<0.01). Index s-RANKL/OPG had sufficient efficacy for reduced BMD. Discrimination analysis revealed that the known s-RANKL/OPG index allows a correct prediction into given groups in 83 % of cases.

Conclusions: The negative correlation between OPG and s-RANKL was detected. S-RANKL/OPG index discriminates probands with significant BMD decrease. S-RANKL-free cannot be used for mathematical assessment of bone density.

Disclosures: D. Stejskal, None.

W220

Clinical Significance of Pentsidine in Glucocorticoid-induced Osteoporosis (GIO). I. Tanaka¹, H. Oshima². ¹Department of Laboratory Medicine, Fujita Health University School of Medicine, Toyoake, Japan, ²Department of Internal Medicine, National Hospital Organization Tokyo Medical Center, Tokyo, Japan.

[Objective] In GIO, bone fractures are often seen even at high bone mineral density. This suggests bone quality is an important factor in GIO for bone strength. Recently, it is reported that Pentsidine(PEN) reflects bone quality. In this study, we tried to clarify the clinical usefulness of PEN in predicting the bone quality in GIO. **[Subjects & Methods]** Fifty nine patients (47 females and 12 males) with collagen diseases under glucocorticoid treatment were enrolled in this prospective study. An incidence of the vertebral

compression fracture in two years after the start of glucocorticoid therapy was evaluated in 37 patients among those. The mean of age, daily glucocorticoid dosage (prednisolone equivalent), and total glucocorticoid dosage were 46 years old, 20.3mg/day, and 6.3g, respectively. NTX in the urine (uNTX) and Pentosidine (PEN) were measured by the ELISA methods. Vertebral compression fractures were evaluated with X-ray photography. **[Results]** 1) After the start of glucocorticoid therapy, PEN increased significantly. 2) Doses of glucocorticoids, were significantly correlated with PEN positively. 3) PEN were significantly correlated with uNTX positively. 4) PEN was lower in patients without incident fractures in 2 years than in those with the fractures. 5) Incident fractures in 2 years was high in patients over 180ug/mgCr. **[Conclusion]** 1) These results suggested that PEN was an important risk factor for incident fracture in patients with glucocorticoid-induced osteoporosis. 2) Fracture risk in patients over 180ug/mgCr of PEN was high.

Disclosures: I. Tanaka, None.

W221

Effect of Food Intake on Bone Resorption in Cynomolgus Monkeys: A Preliminary Study. F. Vlasseros^{1*}, A. Varella¹, S. Y. Smith¹, D. Henriksen². ¹Charles River Laboratories, Preclinical Services Montreal, Senneville, PQ, Canada, ²Sanos Bioscience A/S, Roedovne, Denmark.

The objective of this preliminary study was to monitor the effect of food intake on biochemical markers of bone turnover in young adult cynomolgus monkeys. Food (Rhesus liquid diet) was provided via oral gavage in the morning (approximately 8 to 10 a.m.) following a minimum period of 12 hours fasting and blood samples collected (n=2 to 4 per time-point) prior to feeding and at 10, 15, 20, 30 and 60 minutes, and 4, 6 and 8 hours post feeding. Samples were analyzed for serum N-telopeptide, TRAP5b, osteocalcin and GLP-2. GLP-2 (glucagon-like-peptide-2) is a gut hormone released following food intake, and has been associated with significant decreases in bone resorption markers with no effect on bone formation markers in humans (Henriksen D.B, et al. 2003, JBMR 18 (12):2180-89).

Relative to baseline levels (pre-feeding), NTx showed postprandial decreases of approximately 52% and 25% at 4 and 6 hours, respectively. NTx levels showed no meaningful changes up to 60 minutes following food intake. At 8 hours post feeding NTx was similar to pre-prandial fasting levels. There were no consistent changes in TRAP5b or osteocalcin levels. Relative to baseline levels, GLP-2 plasma levels showed increases 20 to 30 minutes following food ingestion for all animals, although the magnitude of the response was variable and ranged from 20% to 3-fold.

These preliminary data suggest bone resorption activity as measured by serum NTx levels may be decreased 1 to 4 hours following food intake with values rising to fasting levels >8 hours later. This may be related to transient increases in GLP-2 levels 20 to 30 minutes following food intake. A similar spatial and causal relationship has been reported in humans. Importantly, these data suggest measurement of bone resorption activity in samples collected 1 to 8 hours after feeding may be lower than at any other timepoints. Samples can be collected early morning following overnight fasting and later the same day more than 8 hours after feeding. These preliminary data warrant further investigation into the effects of food intake on biochemical markers of bone turnover and the possible role of gastrointestinal hormones in Cynomolgus monkeys.

Disclosures: F. Vlasseros, None.

W222

Specificity of Mouse and Rat Circulating Serological Osteocalcin Values Using a Novel Immunoassay. C. D. Wisherd^{1*}, N. E. Nasser^{1*}. Specialty Products Group (SPG), Quidel Corporation, San Diego, CA, USA.

Osteocalcin (OC) or BGP (bone gla protein) is a 5800 molecular weight extrahepatic vitamin K dependent protein produced by osteoblasts found exclusively in bone tissue. It contains three gamma-carboxyglutamic acid residues that are thought to be involved in calcium ion and hydroxyapatite binding and accounts for 10-20% of the noncollagenous protein in bone. While the in vivo function of osteocalcin is unknown, its affinity for bone mineral constituents implies a role in bone turnover.

Many current enzyme immunoassay (EIA) methods used to detect intact human osteocalcin (hOC) show negligible cross reactivity with mouse osteocalcin (mOC) and rat osteocalcin (rOC). This can be explained by current anti-human osteocalcin antibodies' inability to recognize mouse and rat proteins. Development was performed to establish an EIA with the ability to recognize these proteins while maintaining intact hOC detection. Monoclonal antibodies were developed to capture mOC and rOC in addition to hOC. EIA detection is achieved using hOC-coated plates competing with hOC calibrators and neat serum samples to capture a horseradish peroxidase (HRP) conjugated monoclonal antibody. Tetramethylbenzidine (TMB) substrate is subsequently used to detect the enzyme. The reaction is quenched with 2N H₂SO₄ and read at an absorbance wavelength of 450 nm. The total assay time is 45 minutes.

Specificity studies were run using purified mOC and rOC. mOC was prepared via extraction from mouse bone and purification via G75 gel filtration, DEAE 52 and HPLC. rOC was prepared with rat bone utilizing the mOC extraction method. Balb-C, C57BL6 and CD-1 mouse sera were spiked with 6.7 ng/mL of mOC and tested in the EIA. Average spike recovery of mouse sera was 116% (n=13, range: 86 - 135%). Sprague-Dawley and Wistar rat sera were spiked with 34.3 ng/mL of rOC. Average spike recovery of rat sera was 109% (n=7, range: 102 - 115%).

The results of this study indicate that this novel osteocalcin EIA overcomes shortcomings of the previous methods including: limited species cross reactivity, additional secondary antibody steps, and provides improved sensitivity and short overall assay time.

Disclosures: C.D. Wisherd, None.

W223

Comparison of alpha CTX Levels in Healthy Prepubertal Children, Adolescent, Pre And Postmenopausal Women. S. N. Zeni¹, G. G. Pellegrini^{*1}, M. Linari^{*2}, N. Piazza^{*2}, J. Somoza^{*1}, M. E. Rio^{*3}. ¹Sección Osteopatías Médicas, Hospital de Clínicas, Universidad de Buenos Aires, Buenos Aires, Argentina, ²Public Health Secretary of Vicente López, Epidemiology. Infantil Nutrition., Buenos Aires, Argentina, ³National Council of Scientific and Technical Research, School of Pharmacy and Biochemistry, UBA., Buenos Aires, Argentina.

Collagen type I fragments are formed by osteoclasts and some of them can be determined using a specific immunoassays. The CTX epitope EKAHDGGR comprises a DG-motif susceptible to post-translational modifications. In newly synthesised collagen this motif is in the α -CTX form, but during aging of bone it is isomerized to β -CTX form. The α -CTX form can be determined in urine using a new sandwich ELISA. The aim of the present study was to assess the ability of this marker to discriminate the degradation of new bone in different stage of aging. A total of 243 healthy subjects were included. The distribution of the subjects were: 173 prepubertal children (70 girls and 103 boys) and 30 adolescent (12 girls and 18 boys) attending public schools of Vicente Lopez, Buenos Aires and 20 premenopausal and 20 postmenopausal women. The α -CTX (Alpha CTX ELISA; Nordic Bioscience) was assessed in the second void urine. Results of α -CTX/creatinine levels (ug/mCreatinine) as mean \pm SD were: Prepubertal children: 20 ± 7.2 (6 to <7 years); 15.7 ± 4.5 (7 to <8 years); 14.9 ± 6.7 (8 to <9 years) and 15.3 ± 6.3 (9 to <10 years); adolescents: 4.2 ± 1.9 (11-12 years); premenopausal women: 0.61 ± 0.26 (36.9 \pm 7.5) and postmenopausal women: 0.93 ± 0.58 (58.0 \pm 5.3 years). There was a significant differences among all groups however the levels of significance between postmenopausal vs. premenopausal women ($p < 0.05$) was the lowest. The present results suggest that α -CTX marker reflects well the increase of bone resorption associated with bone modeling at childhood and with high bone turnover after menopause.

Disclosures: S.N. Zeni, None.

This study received funding from: UBACyT, B703. SU Project.

W224

Hip Geometry and Density Parameters Derived from Volumetric DXA (VXA) Correlate Strongly with 3D QCT. O. M. Ahmad^{*1}, K. Ramamurthi^{*2}, E. Thrall^{*3}, D. Karasik³, M. Boussein³, K. E. Wilson², K. Engelke⁴, R. H. Taylor^{*1}. ¹CISST, Johns Hopkins University, Baltimore, MD, USA, ²Hologic, Inc., Bedford, MA, USA, ³Orthopaedic Biomechanics Laboratory, BIDMC, Boston, MA, USA, ⁴Institute of Medical Physics, University of Erlangen, Erlangen, Germany.

3D assessment of hip geometry and density using volumetric DXA (VXA) may improve assessment of skeletal fragility. In this study we tested the correlation between structural parameters and volumetric density of the proximal femur derived from VXA and those derived from 3D QCT.

Methods: Male and female statistical models of the proximal femur, capturing both the 3D geometry and density variation, were created using in vivo CT scans from 62 Caucasian men and 57 Caucasian women. Each statistical model comprises a mean-shape and a set of modes of variation. The mean-shape represents the average 3D geometry and density, and consists of a tetrahedral mesh with density functions for each tetrahedron in the mesh. The modes of variation are vectors, derived from principal component analysis on the set of femurs which comprise the statistical models. The modes of variation allow the mean-shape to geometrically vary to match a particular subject's femur. A particular instance of the statistical model can be transformed into a voxel-volume and projections can be calculated to simulate DXA scans. To achieve a 3D model from DXA, 4 DXA scans are acquired at different projection angles (chosen to minimize pelvic overlap in vivo), and an iterative process is performed wherein the DXA projections are compared to projections of the statistical model and the modes of variation are varied to minimize the error between these simulated DXA projections of the model and the actual DXA images acquired. To test the fidelity of this approach, we performed 3D QCT (1 mm slice thickness, GE Lightspeed) and VXA in 20 human cadaveric femora (11 F, 9 M, age 62 to 95). Each resulting model was then voxelized and aligned to the QCT. We examined the association between VXA and QCT-derived femoral neck length (FNL), volumetric density of the total proximal femur (vBMD), as well as the area of bone mineral in the cross section (CSA_b), the mass-weighted polar moment of inertia (CSMI_p) computed at a corresponding VXA and QCT slice at the mid-neck, perpendicular to the neck axis.

Results: We found very strong linear correlation between VXA and QCT for all parameters: FNL ($r=0.97$), vBMD ($r=0.96$), CSA_b ($r=0.94$), and CSMI_p ($r=0.96$). In conclusion, reconstructions that contain both volumetric shape and density information can be made from four DXA views that can be obtained readily in vivo with limited radiation exposure. These VXA reconstructions are highly correlated with structural parameters and volumetric density measured with 3D QCT.

Disclosures: O.M. Ahmad, Hologic Inc. 2.

This study received funding from: Hologic, Inc.

W225

A Technique for Calculating Area Moment of Inertia of Long Bones Using Computed Tomography (CT) Data. A. K. Aiyangar^{*}, H. Ploeg^{*}. Mechanical Engineering, University of Wisconsin, Madison, Madison, WI, USA.

A technique to compute the Area Moment of Inertia (MI) of long bones is presented. In problems related to bending of beams and beam-like structures, there are two main parameters that are indicative of the resistance of the structure to bending: Young's Modulus (E), and MI. While Young's Modulus is a material property, MI is, essentially, a geometrical property of the long bone and depends on a reference axis and the distribution of the material around that axis at every cross-section along the bone. There is not yet a significant appreciation of the effect of ignoring the deviations from standard symmetric beam bending theories as applied to homogeneous materials, while interpreting data from bending tests. As a consequence, there is a strong requirement for a standard method to accurately compute the MI, taking into account the heterogeneities in the bone structure and irregular geometrical shape. Accurate calculation of MI for bone is further complicated as a composite materials model needs to be employed, wherein the different constituent materials are given weighting factors according to their respective elastic moduli. This can be accomplished by using the grayscale variations in computed tomography (CT) images, which is linearly dependent on the density distribution in the bone. The density distribution, in turn, correlates with the elastic modulus. Segmented CT data of a porcine femur bone was used for the study. A porcine femur bone was scanned in a CT scanner (GE Lightspeed. 120kV, 0.352mm pixel size, 0.625mm slice thickness, bone algorithm). The images from the scanning procedure were processed and segmented using Mimics 10.0 software (Materialise, Ann Arbor MI) to obtain the density distribution of the bone. The data for each cross-section was digitized and mapped in the form of pixels (0.125mm²). A custom-written MATLAB function using a composite materials model was used to compute the MI. The equations are shown below.

Where:

x, y = x and y coordinates of centroid respectively

I_{xx}, I_{yy} = MI about the x - and y - axes respectively

R = density ratio for each material

r = constant correlating density to the stiffness

gr = density given as hounsfield units

x_i, y_i = x and y coordinates respectively of pixel "i" in a given cross-sectional slice

The weighted and un-weighted moments of inertia (the difference between a homogeneous versus a composite materials model) differed by 20%. Details of the technique will be presented.

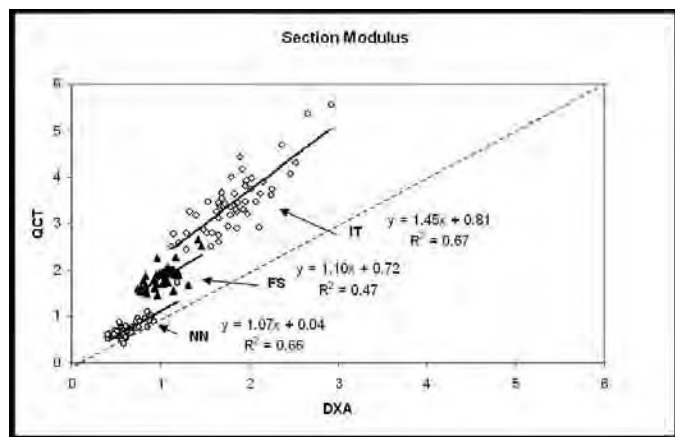
Disclosures: A.K. Aiyangar, None.

This study received funding from: Ali Seireg Memorial Fellowship.

W226

In Vivo Comparison of CT and DXA Methods of Proximal Femur Cross-sectional Geometry Measurement Using HSA. T. J. Beck¹, J. K. Brown², S. Gustafsson^{*3}, K. Zhu³, I. Dick⁴, S. Hentzell^{*5}, V. H. Low⁶, K. E. Wilson⁷, R. L. Prince³. ¹Radiology, Johns Hopkins University, Baltimore, MD, USA, ²Mindways Software Inc., Austin, TX, USA, ³Endocrinology and Diabetes, University of Western Australia, Perth, Australia, ⁴Medicine, University of Western Australia, Nedlands, Australia, ⁵Endocrinology and Diabetes, University of Western Australia, Baltimore, Australia, ⁶Radiology, Sir Charles Gairdner Hospital, Nedlands, Australia, ⁷Hologic Inc., Bedford, MA, USA.

The Hip Structure Analysis (HSA) method for measuring femur geometry from 2D DXA scans needs in vivo 3D validation, but methods for comparison with QCT are lacking. In this ongoing study 54 elderly post-menopausal women from the longitudinal CAIFOS/CARES study of ageing, had standard hip DXA (Hologic Discovery A) and CT scans (Phillips 64 slice) of the pelvis/hips. CT axial images were acquired with 0.78 mm pixels and 1 mm slices at 1 mm intervals. Results were analyzed with CTHSA, a collaborative development between Mindways Software Inc. and Johns Hopkins University. The software extracts cross-sections at DXA HSA femur locations: narrow neck (NN), intertrochanter (IT) and femur shaft (FS) and reformatted them to 0.78 mm pixel spacing. The method then measures the geometry for ultimate use in an automated 3D engineering analysis under development. For the present work, we compared CTHSA geometry and bending properties corresponding to frontal plane DXA with those from DXA HSA. In pooled comparisons of all three regions, bone cross sectional area, outer diameter, cross-sectional moment of inertia, section moduli and buckling ratio showed R^2 values of 0.91, 0.81, 0.95, 0.93 and 0.49, respectively. Within HSA regions, section moduli R^2 values for FN, IT and FS regions were 0.66, 0.67 and 0.47 respectively. Neck values corresponded to the line of identity but shaft and intertrochanter values were shifted upward (Fig). Overall, results correlate well between frontal plane geometry measurements measured by DXA and QCT in elderly women and with prior ex vivo studies. These preliminary results show a small dimensional error in CTHSA integrals which appear to explain the shift and should be correctable. Although work remains, results show that CTHSA may provide an in vivo geometry gold standard for DXA as well as a stand-alone method for automated engineering analysis of the hip for use with recent generation multi-slice CT scan data.



Disclosures: T.J. Beck, Hologic Inc. 7.
This study received funding from: Hologic Inc.

W227

Automated Assessment of Vertebral Shape by Statistical Shape Modelling on Lateral Radiographs. A. D. Brett^{*1}, J. Krasnow^{*2}, C. Miller³, J. Haslam^{*1}, T. Ozanian^{*1}, C. van Kuijk^{*4}, K. Abrams^{*5}, R. Cope^{*3}, M. Beke^{*5}, C. Hayes^{*6}.

¹Optasia Medical Ltd, Manchester, United Kingdom, ²Roche Pharmaceuticals, Nutley, NJ, USA, ³Bio-Imaging Technologies Inc, Newtown, PA, USA, ⁴VU University Medical Center, Amsterdam, The Netherlands, ⁵Novartis Pharmaceuticals, East Hanover, NJ, USA, ⁶VCU Medical Center, Medical College of Virginia, VA, USA.

We describe the construction methodology, accuracy and reproducibility of a statistical model for the automated annotation and characterisation of vertebral shape from lateral radiographs.

Prevalent vertebral fractures are important predictors of future osteoporotic fractures in the spine and hip. Accurate computerized vertebral fracture detection and classification may benefit from capture of vertebral shape information beyond standard 6-point morphometry, similar to the visual cues that characterize semi-quantitative vertebral assessment. Accurate and reproducible acquisition of vertebral shape may also enhance the prediction of subsequent osteoporotic fractures.

Using a statistical learning technique, a vertebral model that can be altered in its shape and appearance was constructed from lateral radiographs. The model was trained on a set of manually-annotated radiographs (165 subjects from the Canadian Multicentre Osteoporosis Study [CaMos], enriched for prevalent deformities). Each vertebra, from T4-L4, was described using 95 points representing the circumferential vertebral borders, including right/left/central endplate margins, anterior/posterior margins, and osteophytes when present. Radiographs of 100 randomly chosen subjects were used to build the model; the remaining 65 subjects were used for accuracy and reproducibility testing. The resulting model may be used in the annotation of a previously unseen image; vertebral landmarks are searched for automatically after manual initialisation.

Accuracy was assessed by measuring the mean absolute distance between manually placed vertebral contours and automatically fitted points on the 65 test subjects. 79895 points were assessed on 841 individual vertebrae. The mean accuracy calculated over each vertebra in each test image was 1.11 +/- 0.94 mm. Inter-operator reproducibility was simulated by varying the placement of model initialisation points by adding random offsets of up to 4 mm and running 10 searches on each test image. The observed mean standard deviation per vertebra of the resulting annotations is 0.31 +/- 0.24 mm.

These results indicate that statistical modelling can provide a robust tool for the accurate and reproducible automated annotation of vertebral body shape. This method may prove useful as a workflow tool to aid the physician in vertebral fracture assessment.

Disclosures: A.D. Brett, None.
This study received funding from: Novartis Pharmaceuticals.

W228

HR-pQCT Assessment of Cortical Bone: Correlations to FE Derived Mechanical Properties. A. J. Burghardt, K. Davis*, T. M. Link, S. Majumdar. Radiology, University of California, San Francisco, San Francisco, CA, USA.

High-resolution peripheral quantitative computed tomography (HR-pQCT) is a promising new tool for longitudinal evaluation of bone quality. Cortical bone geometry is known to be an important factor in whole bone strength. Various methods, which rely on specific assumptions of cortical structure, exist to quantify cortical thickness. In this study, two common definitions of cortical thickness were evaluated using correlations to micro Finite Element (μFE) derived mechanical properties as a measure of significance.

The distal radius and tibia (n=28 and n=24, respectively) from normal volunteers (age 23-76) were imaged using HR-pQCT (Scanco XtremeCT, 82 μm isotropic nominal resolution). The cortical bone compartment was segmented using the standard clinical routines provided by the manufacturer: a strong Gaussian blurring filter (σ=1.5, kernel=7) to wash out the trabecular structure, followed by a fixed global threshold to define the

cortical bone phase. Ct.Th was calculated in 2 ways: 1) as the ratio of the cortical area to the perimeter of a semi-automatically defined periosteal contour, and 2) using a direct 3D sphere filling technique. As a standard of reference, a 1% uniaxial compressive strain (in the direction of the long axis of the radius) was simulated in the complete structure using a voxel based finite element technique. The total reaction force and the estimated failure load were determined [1].

Visually, the use of a large blurring filter clearly eliminated thinner cortical components, particularly in the ultra-distal radius. The area-to-perimeter estimate of cortical thickness included these regions as segments with zero thickness. In contrast, the direct 3D measure only considered the cortical volume that survives the segmentation step. No significant difference in tibial cortical thickness was found between methods. In the radius, the direct 3D method yielded thickness values that, on average, were 0.2 mm larger than the area-to-perimeter method (p < 0.0001). Both methods were positively correlated to μFE derived reaction force (R²=0.72 and R²=0.48 respectively) and to the estimated failure load (R²=0.70 and R²=0.46 respectively).

In conclusion, the results suggest that there is significant site dependence in the agreement between different definitions of cortical thickness in limited resolution scenarios. The μFE results indicate that, for HR-pQCT, the area-to-perimeter definition is a better predictor of mechanical competence, likely due to its inherent incorporation of thin segments lost during the segmentation process.

[1] Pistoia, W. Bone 2002

Disclosures: A.J. Burghardt, None.

W229

Topological Analysis and Spatial Distribution of Apparent Trabecular Bone in Radiographs Correlate to Biomechanical Bone Properties: An In Vitro Study of the Proximal Femur. J. Carballido-Gamio^{*1}, M. B. Huber^{*1}, K. Fritscher^{*2}, R. Schubert^{*2}, M. Haenni^{*3}, C. Hengg^{*4}, S. Majumdar¹, T. M. Link¹.

¹University of California, San Francisco, San Francisco, CA, USA, ²University of Health Sciences, Medical Informatics and Technology, Innsbruck, Austria, ³AO Development Institute, Davos Platz, Switzerland, ⁴Medical University Innsbruck, Innsbruck, Austria.

Analysis of the trabecular bone (Tb) pattern observed in radiographs has recently received more attention as significant correlations to different biomechanical bone properties have been found. Most of the analyses however have been based on Fourier, fractal, or morphological approaches trying to characterize texture.

The purpose of this study was therefore to develop an image analysis technique to characterize the apparent (App) Tb architecture observed in radiographs and evaluate it based on biomechanical bone properties.

Radiographs of 13 specimens of the proximal femur were obtained and digitized. Bone mineral density values (BMD) were measured at the femoral neck, and biomechanical testing was performed based on failure load (FL). Five regions of interest (ROI) were automatically positioned in each specimen (head, upper and lower neck, and trochanteric and inter-trochanteric compartment). Regions were normalized for contrast variations and an App Tb map was computed automatically by using soft fuzzy c-means clustering. The skeletons of these maps were computed and their junctions and terminations automatically identified. Voronoi diagrams were constructed using the junctions as nodes, and 1st and 2nd order moments of area of the cell polygons, as well as the distribution of App Tb based on the Voronoi cells were computed and correlated to FL.

Significant correlations were found for the lower neck and inter-trochanteric ROI for different moments of area and App Tb distributions. Correlation values to FL went from 0.577 (p<0.039) for the mean area of the polygons normalized by the mean distance of the nodes of the polygons to their corresponding centroids, up to -0.866 (p<0.0001) for the standard deviation of the distributions of App Tb normalized in a similar manner. When significant correlations were found to FL, no significant correlations were found to BMD. However, the mean elongations of the cell polygons of the upper neck ROI showed significant correlations to BMD (r = -0.568; p<0.042). Similar analysis was performed for the terminations of the skeletons yielding additional significant correlations. The correlation between BMD and FL was 0.695 (p<0.008).

Results suggest that the topology of the App Tb architecture and the distribution of the App Tb observed in radiographs can be quantified and that they are closely related to the biomechanical properties of the Tb in the proximal femur.

Disclosures: J. Carballido-Gamio, None.
This study received funding from: AO Foundation.

W230

Influence of A1330V LRP5 Gene Polymorphism on Volumetric BMD and Structural Parameters of Bone in Men and Women. C. Cepollaro¹, F. Lauretani², A. Gozzini¹, L. Masi¹, A. Falchetti¹, F. Del Monte¹, S. Carbonell Sala¹, G. Leoncini¹, A. Tanini¹, A. Corsi², S. Bandinelli³, M. Brandi¹.
¹Department of Internal Medicine, University of Florence, Florence, Italy, ²Tuscany Health Regional Agency, Florence, Italy, ³Azienda Sanitaria di Firenze, Geriatric Rehabilitation, Florence, Italy.

Hereditability studies show that genetic factors may contribute to the variability in bone mineral density (BMD), metabolism and microarchitectural deterioration leading to bone fragility. Several candidate genes, identified since their mutations cause severe Mendelian bone phenotypes, exhibit nucleotide sequence variants with modest effects on bone structure and remodeling. Mutations in the LRP5 gene have been associated with rare inherited syndromes characterized by extremely low (loss of function) or high (gain of function) BMD; but little is known about the contribution of this gene to the development of osteoporosis and determination of BMD in a normal population. A recent large population-based study showed that distinct genetic polymorphisms of LRP5 are associated to BMD and to fracture risk namely in elderly men. No data have been published on the relationships between LRP5 polymorphisms and structural parameters of bone as assessed by pQCT. The aim of the present study was to investigate the possible association of Ala1330Val polymorphism in LRP5 gene with volumetric BMD and structural parameters of bone in men and women. We studied 959 subjects (451 men and 508 women), participating to the InCHIANTI study. In all subjects we performed pQCT (XCT 2000, Stratec, Germany) at the tibia level obtaining the following parameters: trabecular vBMD (vBMDt, mg/cm³), cortical vBMD (vBMDc, mg/cm³), cortical bone area (tCSA mm²) and cortical thickness (Ct.Th, mm). Ala1330Val genotypes were determined by polymerase chain reaction-restriction fragment length polymorphism (PCR-RFLP).

In men and women, the LRP5 1330-valine variant was associated with decreased values of all pQCT parameters, reaching the statistical significance ($p < 0.05$) for vBMDt in men and in women and for Ct.Th and tCSA in women. These results show that Ala1330Val polymorphism may contribute to the determination of BMD and geometric parameters of bone in the male and female populations.

Disclosures: C. Cepollaro, None.

W231

Texture Analysis and Geometry Measurements on Plain Radiographic Femurs: Correlation with Ultimate Load. C. Chappard¹, V. Bousson², C. Bergot³, A. Marchadier¹, T. Moser³, D. Mitton⁴, C. Benhamou¹, J. Larédo³.
¹U 658 Inserm, Inserm, Orleans, France, ²Laboratoire Radiologie Expérimentale, Université Paris VII, Paris, France, ³Laboratoire Radiologie Expérimentale, Université Paris VII, Paris, France, ⁴Laboratoire Biomécanique UMR 8005, ENSAM CNRS, Paris, France.

Osteoporosis diagnosis and fracture risk at the upper femur are usually assessed by Bone Mineral Density (BMD) measurements with Dual X-ray Absorptiometry (DXA). We propose a new method combining texture analysis and geometrical measurements, obtained from plain femur radiographs. Forty pairs of excised femurs were obtained in 18 males and 22 females (mean age: 81.5±12.3 years). Total femur BMD was measured by DXA. Film radiographs (GE Prestilix 1600x) were digitized with a Fonction Transfert Modulation of 166 µm. We selected 3 square Regions of Interest (ROIs) of 3.2*3.2cm in Femoral Neck (FN), Greater Trochanter (GT) and in Inter-Trochanteric regions (IntT) and finally a ROI of 3.6*3.6 cm in the Femoral Head (FH). We calculated texture parameters derived from the cooccurrence matrix such as Correlation (COR), Contrast (CON), Entropy (ENT), Homogeneity (HOM), Dissymmetry (DIS), Inverse of Differential Moment (IDM), Angular Second Moment (ASM) and Maximum (MAX). Geometrical parameters were directly measured on the radiographs: the total length of femoral neck (FNL), from the base of the greater trochanter to the medial limit of the femoral head, and the neck-shaft angle. All femurs were randomly assigned for axial or lateral compression testing to measure ultimate load (N), axial compression mimicking femoral neck fracture and lateral compression peritrochanteric fracture. All textural parameters were significantly correlated with total femur BMD at FH and GT and few of them were marginally significant at FN and IntT. After checking Gaussian distribution, we combined textural and geometrical parameters to obtain the best fit with ultimate load. The best results were obtained with 3 parameters, more parameters in the regression calculation did not improve the results.

	Axial Compression	r ²	Lateral Compression	r ²
Total Femur	BMD	0.74	BMD	0.78
FN	ENT+ASM	0.55	ENT+MAX	0.55
	FNL+ENT+ASM	0.66	FNL+ENT+MAX	0.70
GT	FNL+ENT	0.64	FNL+ENT	0.67
	FLN+ENT+HOM	0.67	FNL+ENT+MAX	0.69
IntT	FLN+ENT	0.49	FNL+ENT	0.48
	FLN+ENT+HOM	0.67	FNL+ENT+HOM	0.64
FH	HOM+MAX	0.76	HOM+MAX	0.76
	FLN+HOM+MAX	0.77	FNL+HOM+MAX	0.77

In term of prediction of ultimate load, the combination of textural parameters with geometry was close to BMD alone. Except for Femoral head ROI, the addition of FNL measurements in the model substantially improved the prediction of ultimate load. These results show the potential of measurements on plain radiographs to predict bone strength at the upper femur.

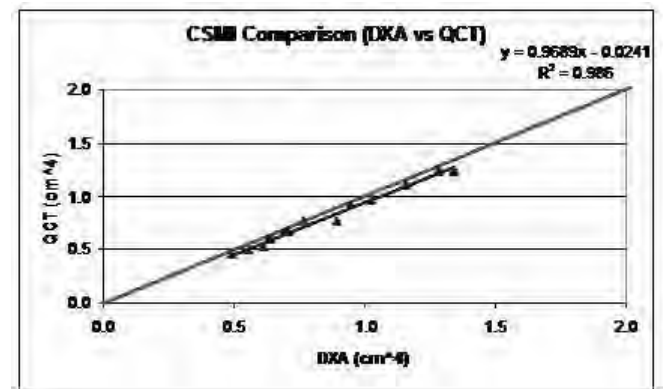
Disclosures: C. Chappard, None.

W232

Comparison of Femur Structure Measurements Derived from DXA and QCT. X. Cheng¹, H. Barden², J. K. Brown³, Q. Zhou⁴.
¹Radiology Department, Beijing University Beijing Jishuitan Hospital, Beijing, China, ²GE Healthcare, Madison, WI, USA, ³Mindways Software Inc., Austin, TX, USA, ⁴GE Healthcare Asia, Shanghai, China.

The strength of the proximal femur is a function of both bone mineral density (BMD) and spatial distribution of bone mass determined from structural measurements such as cross-sectional moment of inertia (CSMI), cross-sectional area (CSA) and hip axis length (HAL). These measurements, which assist in estimating hip fracture risk, are made by both dual-energy X-ray absorptiometry (DXA) and quantitative computed tomography (QCT). Because of the ability to control the projection plane, three-dimensional measurement of femur geometry with QCT can be used for evaluating accuracy of other techniques. We compared CSMI, CSA and HAL measured with DXA (Prodigy, GE Healthcare, software version 10.5) and CT (Toshiba 64-slice, 1.0 mm slices). We measured the left femur in 14 healthy subjects, aged 35 to 78 years (64.7 ± 3.01 yrs) with total femur DXA BMD from 0.729 to 1.179 g/cm³ (0.921 ± 0.126 g/cm³). The DXA automatically measures CSMI (mm⁴) as the minimum CSMI within the neck region of interest (ROI), and CSA of the minimum CSMI section within the neck ROI. These DXA measurements usually occur in the section with the minimal neck diameter. A commercial QCT application (QCT PRO version 4.1, Mindways Software Inc.) was used to generate CSMI, CSA and HAL values from the QCT data. The QCT cross-sectional image at the narrowest portion of the femoral neck that most closely approximated the DXA CSMI measurement site was chosen for comparison purposes. QCT values were adjusted by the ratio of the DXA/QCT reference for average physical density of bone (1.85/1.05 g/cm³). Results showed very high correlations for CSMI (r=0.99), CSA (r=0.98), and HAL (r=0.86), with regression slopes not significantly different from identity. We also found high correlations (r=0.95) between DXA and QCT BMD values at the hip. We conclude that DXA structural measurements at the proximal femur had very high correlation and agreement with similar QCT measurements.

Comparison of DXA and QCT measurements of proximal femur structure and BMD				
Measurement	Regression Equation	SEE	r	
CSMI (cm ⁴)	CSMI (QCT) = 0.9689 CSMI (DXA) - 0.0241	0.0329	0.99	
CSA (cm ²)	CSA (QCT) = 0.9475 (DXA) - 0.0503	0.0555	0.98	
HAL (mm)	HAL (QCT) = 0.8278 HAL (DXA) + 23.8343	3.2308	0.86	
Femur Neck BMD	BMD (QCT) = 0.8306 BMD (DXA) - 0.0338	0.0381	0.96	
Total Femur BMD	BMD (QCT) = 0.9740 BMD (DXA) - 0.1204	0.0395	0.95	



Disclosures: X. Cheng, None.

W233

Trends in Femur Structural Strength with Aging in Canadian Adults: Canadian Multicentre Osteoporosis Study. K. S. Davison¹, T. J. Beck², J. D. Adachi³, D. Goltzman⁴, J. P. Brown¹.
¹U. of Laval, Quebec, PQ, Canada, ²Johns Hopkins U., Baltimore, MD, USA, ³McMaster U., Hamilton, ON, Canada, ⁴McGill U., Montreal, PQ, Canada.

This study details changes in hip structural strength parameters during aging in a large sample of randomly-selected community-based individuals from the Canadian Multicentre Osteoporosis Study (CaMos). Hip Structural Analysis (HSA) was performed on all CaMos baseline DXA hip scans at sites with HSA calibration data. A total of 5334 scans, 3724 women, and 1610 men were used. At the narrow neck (NN), inter-trochanter (IT), and shaft (FS) regions, BMD, outer diameter (OD), bone cross-sectional area (CSA), section modulus (SM) and estimates of cortical thickness (CT) and buckling ratio (BR) were computed. All eligible CaMos participants were separated by sex and grouped according to age: <30y, 30-39 y, 40-49y, 50-59y, 60-69y, 70-79y, and 80+y. Percent differences relative to the <30y group were used to approximate the age trend. The mean (SD, range) age was 61.0y (12.44, 25-92) for women and 57.6y (14.30, 25-90) for men. Structural and strength values provided in parentheses below represent the range in the parameter between men and women from the 80+y age group, unless otherwise noted. At the NN structural trends were similar in men and women with small almost linear increases in OD (3-9%) and large decreases in CSA and CW (21-28%). At the NN there were large

near-linear decreases in SM (12-18%) and exponential increases in BR (44-59%) with aging in both sexes. The structural changes with aging at the IT region were similar to the NN for both sexes. The IT region showed an exponential increase in BR for both sexes (30-50%) while the SM increased moderately at the 60-69y group (6-12%) and then slowly decreased in the oldest group of women. At the FS, there were small increases in OD (8-9%), moderate decreases in CSA (4-13%), and large decreases in CT (13-24%) with aging in both sexes. The FS strength changes were similar to those of the IT region. The BR for the FS region increased exponentially with aging (31-49%). In general, with age there was a slow transformation toward a wider, thin-walled bone. With regards to strength, there were relatively steady losses of CSMI and SM at the NN with aging after 40-49y; however, at the other regions there were small to moderate increases in CSMI and SM during a large portion of adulthood and generally small losses later in life resulting in a preservation of strength in comparison with the reference group. For all regions and for both sexes there was an exponential increase in BR with age which may suggest this as being one of the mechanisms of fracture in old age.

Disclosures: K.S. Davison, None.
This study received funding from: CIHR.

W234

Association Between DXA-Assessed Muscle-Bone Proportionality and Fractures in Pre- and Post-Menopausal Women. R. Capozza^{*1}, C. Cure Cure^{*2}, G. Cointry^{*1}, M. Meta³, P. Cure Ramirez^{*2}, L. Plantalech⁴, J. Rittweger^{*5}, J. L. Ferretti¹. ¹Centro de Estudios de Metabolismo Fosfocálcico, Faculty of Medicine, UNR, Rosario, Argentina, ²Universidad de Barranquilla, Barranquilla, Colombia, ³UCSF, San Francisco, CA, USA, ⁴Hospital Italiano, Buenos Aires, Argentina, ⁵Manchester Metropolitan University, Manchester, United Kingdom.

This study aimed to evaluate the DXA-assessed bone mass (BMC) / muscle mass (lean mass, LM) relationship as an indicator of nonmechanical (i.e. "systemic") disturbances of the bone-muscle relationships in women in relation with the presence of fractures in different sites. Graphs of the BMC(y)/LM(x) proportionality showing CIs for ± 1 , 2, and 3 SDs from the regression line were obtained from the whole body and lower limbs (HB,LL) of 1,035 pre-MP and 1,556 post-MP healthy women as normal references (No-Fx group). Other 614 pre-MP and post-MP women with fractures in "osteoporotic" sites (hip, spine, long-bone metaphyses; Type-II Fx, n=386) or in other sites (Type-I Fx, n=228) were studied the same way. Individual SD-scores of the BMC/LM relationship (BMC/LM SD-scores) were calculated for all pre- and post-MP women as per the determined CIs of the regression curves of the healthy controls. The BMC/LM SD-scores of all Type-I-Fx women and of the pre-MP women with Type-II Fx were similar to those of their normal references, but lower than that in the post-MP women with Type-II Fx, especially in those with hip fractures. While the BMC-LBM curves were linear and similar in all the other groups, Type-II-Fx post-MP women showed nonlinear relationships, with progressively decreasing BMC and BMC/LBM SD-score values as their LBM decreased. Results were similar in WB and LL. Age and body weight and height were discarded as significant sources of variation for the studied relationships. Results show that the BMC/LM relationship may predispose somehow to Type-II Fx in post-MP women. They also suggest that both LBM and BMC/LBM SD-score determinations, either in the WB or in the LL, can help to differentiate between osteopenias/osteoporoses that ought to receive different treatments. Low BMC/LM SD-scores would define "metabolic" osteopenias which should be treated pharmacologically. Normal BMC/LM SD-scores would indicate a "mechanical" nature of the osteopenia for which only a physical or perhaps no other treatment should be indicated. The SD-scores would allow also to optimize monitoring following biomechanical criteria at low cost

Disclosures: J.L. Ferretti, None.
This study received funding from: FONCyT (Argentina).

W235

Reference Graphs of Age-Related Changes in Bone Mass, Volumetric Density, Design and Strength and of Muscle-Bone Interactions in Normal Men and Women. S. Feldman^{*}, R. F. Capozza^{*}, G. R. Cointry^{*}, S. E. Ferretti^{*}, P. S. Reina^{*}, B. Homse^{*}, M. Zapata^{*}, J. L. Mansur, J. L. Ferretti. Centro de Estudios de Metabolismo Fosfocálcico, Faculty of Medicine, UNR, Rosario, Argentina.

Tomographic scans of forearms and legs (pQCT, 6 different sites) of normal, unfractured men and pre- and post-MP women (n = 60, 80, 120) aged 25-85 yr were performed to describe the variations and interrelationships of indicators of bone "mass" (BMC, cortical area, trabecular vBMD), bone material "quality" (cortical vBMD, vCtD), and bone design (moments of inertia, MIs), and of muscle strength (muscle cross-sectional area, mCSA). Three different patterns of variation were shown: 1. Bone "mass" indicators were higher in males than females and decayed slightly after MP. 2. Bone material "quality" (as assessed by vCtD) was higher in pre-MP women than men and decayed dramatically after MP. 3. Bone design was better in men than women but did not decay after MP. Calculated Bone Strength Indices (BSIs = MIs . vCtD) varied similarly to bone mass indicators. Bone mass, design and strength indicators (not so the vCtD) were linearly correlated with mCSA in all 3 groups, with parallel slopes for men and pre-MP women and lower slopes for post-MP women. The SD-scoring of the relationships between bone mass, design or strength indicators and the mCSA for men and pre-MP women allowed calculation of individual SD-scores of every relationship for post-MP women. The SD-scores for the relationships between bone mass and strength (not MIs or vCtD) and mCSA correlated negatively with time since MP (TSMP). Results show that

women would tend conveniently to maintain bone design after MP, with an independent variation of bone mass, material quality, design and strength. From a practical point of view, 1. the SD-score charts of the correlations between the different bone indicators, and of these with TSMP, provided normal references suitable for evaluation of the two true determinants of "bone quality", namely, bone material quality and design, and 2. the reference charts of the bone-muscle relationships allowed a non-invasive distinction between "disuse" and "systemic" osteopenias (with normal or reduced bone-muscle SD-scores, respectively) requiring substantially different treatments

Disclosures: J.L. Ferretti, None.
This study received funding from: FONCyT.

W236

Relationships Between Diaphyseal Geometry and Cortical Mineral Density as Assessed by pQCT in the Human Tibia. R. Capozza^{*1}, P. Reina^{*1}, G. Cointry^{*1}, S. Feldman^{*1}, S. Castellini^{*1}, J. Rittweger^{*2}, J. L. Ferretti¹. ¹Centro de Estudios de Metabolismo Fosfocálcico, Faculty of Medicine, UNR, Rosario, Argentina, ²Manchester Metropolitan University, Manchester, United Kingdom.

Indicators of tibial cortical bone "mass" (cortical BMC, CtC, g), mineral density (cortical vBMD adjusted for the partial-volume effect, Rho-vCtD, g/cm³) and design (cross-sectional moments of inertia, CSMIs, mm⁴) were determined in calf pQCT scans of normal men, and pre- and post-MP women (n = 60, 80, 120) aged 25-85 yr to evaluate the mechanical efficiency of the distribution of the available compact tissue as a function of its intrinsic properties.

The CSMIs (y) and Rho-vCtD (x) values correlated negatively ("distribution/quality", d/q hyperboles) showing high-CSMI / low-Rho-vCtD values for men; low-CSMI / high-Rho-vCtD values for pre-MP women, and low-CSMI / low-Rho-vCtD values for post-MP women. Parallel, linear correlations between the CSMIs and the CtCs of the same scans from every group ("distribution/mass" curves) were observed, with a common slope (b = 11,796 mm⁴/gm.cm⁻¹, p<0.001). Statistical adjustment of all CSMI values (Adj-CSMIs) to a common CtC value (3.5 mg/cm) according to that slope allowed expression of the mechanical ability of the diaphyseal design (CSMIs) achieved as a function of the available mineralized mass in every individual. Re-built d/q graphs after substituting Adj-CSMIs for the raw CSMI values showed a substantially reduced but still significant difference between curves for men and pre-MP women, and similar curves for pre- and post-MP women.

Results suggest that cortical density has an effect upon the geometrical design of the tibia diaphysis. As far as the reduced density may reflect a reduced Young's modulus of the tissue, the d/q curves can be regarded as expressing the bone ability to self-distribute the available cortical tissue (as assessed by the CSMIs) as a function of its intrinsic stiffness (as approached by its Rho-vCtD) according to the "Mechanostat" Theory. The gender-related differences between curves can be attributed to sex-hormone influences on that system.

Disclosures: J.L. Ferretti, None.
This study received funding from: FONCyT (Argentina).

W237

Trabecular Bone Mass Evaluation as Related to Cortical Mass in the Human Leg: A pQCT Study. G. R. Cointry^{*}, R. F. Capozza^{*}, S. Feldman^{*}, P. Mortarino^{*}, L. Maffei, A. Alvarisqueta, J. L. Ferretti. Centro de Estudios de Metabolismo Fosfocálcico, Faculty of Medicine, UNR, Rosario, Argentina.

In uniaxial compression, the relevant factors to bone strength are the amount and material properties rather than the distribution of bone mass, and the nature of bone structure.

The distal 38% of the tibial length undergoes chiefly uniaxial compression. Toward the mid-diaphysis, an increasing proportion of bending and torsion is combined. At 4% of bone length from the heel, tibial structure is mostly trabecular. At 14% distal, almost exclusively cortical, the diameter is minimal and the section is closely rounded, with a fairly homogeneous cortical thickness. At 38% distal the shape departs from circularity.

We have determined the total BMC (TC) by pQCT at the 4%, 14% and 38% sites in the leg in normal men and pre- and post-MP women (n = 60,80,120) in order to determine 1. the proportion between total bone mass at the 4%, 14% and 38% sites in the different groups; 2. the functions describing those relationships[3], and 3. whether gender and estrogen status have any impact on these associations.

The TC at the 4% site (y) correlated linearly with that at the 14% site in all men, pre-MP and post-MP women, either separately or taken together (whole group, y = -0.45 + 1.54 x; r=0.938, R²=0.881, p<0.001, SEE=0.25) and at the 38% site (whole group, y = -0.31 + 1.08 x, r=0.903, R²=0.815, p<0.001, SEE=0.33) with similar intercepts for each group.

Results indicate that 1. the mechanical efficiency of the combined bone structure at the 4% site in compression would approximate 66% of that of the cortical structure at the 14% site, and 2. the mechanical solicitations of cortical structure at the 38% site would require the same amount of cortical mass than that of the combined structure at the 4% site, regardless of gender and reproductive status. SD-scored graphs of both relationships studied might provide normal references of the biomechanical proportionality between trabecular and cortical masses. As far as trabecular bone mass is usually more sensitive than cortical mass to metabolic changes, this may provide a diagnosis of metabolic bone diseases as based on data from the same individuals, obviating any comparison with references taken from different populations.

Disclosures: J.L. Ferretti, None.
This study received funding from: FONCyT (Argentina)

W238

Evaluation of Bone Microarchitecture with High Resolution-pQCT in Patients with Thalassemia. I. M. Frieling^{*1}, R. Grosse^{*2}, E. B. Fung^{*3}, R. Fischer^{*2}, H. Kruse^{*1}, G. E. Janka^{*2}. ¹Osteoporosis Center, Hamburg, Germany, ²Pediatric Hematology, University Medical Center, Hamburg, Germany, ³Children's Hospital & Research Center, Oakland, CA, USA.

Thalassemia is a genetic disorder of hemoglobin synthesis. Due to improved blood transfusion and chelation therapy, survival has been increased with the consequence of complications like osteoporosis not seen during childhood and adolescence. The obvious shortcomings of conventional BMD methods like dual energy x-ray absorptiometry (DXA), can be overcome by simultaneously assessing the microarchitecture of the bone using high-resolution peripheral quantitative computed tomography (HR-pQCT), which may improve the estimation of the fracture risk in patients with thalassemia. In 17 regularly transfused patients (age: 13 - 43 y, 9/17 female) with beta-thalassemia major (n = 10), -intermedia (n = 6), and CDA-II (n = 1), the BMD of lumbar spine (LS) and total hip was measured by DXA (Hologic QDR1000+, Bedford, USA). Age, gender and ethnic specific BMD Z-scores were calculated. In addition, we assessed the volumetric BMD and the trabecular architecture of the non-dominant distal radius and tibia by HR-pQCT (XtremeCT[®], SCANCO Medical AG, Bassersdorf, Schweiz). Liver iron concentration and endocrinological parameters were also determined. In 15/17 patients low BMD values (LS Z-score range: -1.1 to -3.1) measured by DXA were significantly correlated with total volumetric density (range: 91 - 388 mg/cm³, p = 0.002) measured by HR-pQCT at the distal radius. In 6/17 patients (> 28 y), all with latent hypogonadism, the spongiosa was porous or nearly dissolved. Patients with hypogonadism (n = 9) were significantly different from normals with respect to radial trabecular inhomogeneity parameter TbSp SD (p = 0.02), but not to LS Z-score. Patients with fractures (n = 5) had lower total densities (p = 0.02) and trabecular TbSp SD (p = 0.02) at the tibia and started blood transfusions at a higher age (p = 0.023). However, Z-scores did not reflect the fracture risk in this patient group (p = 0.11). Liver iron was mainly correlated with tibial TbSp SD (Rs = 0.54, p = 0.025).

In patients with thalassemia BMD Z-scores seem to underestimate fracture risk because a normal cortical thickness and density may conceal a porous trabecular structure. Endocrinological failures, especially hypogonadism, were responsible for the pathological microarchitecture of distal radius and tibia, while bone marrow expansion as in thalassemia intermedia and liver iron concentration seem to play a minor role. These initial results from bone microarchitecture measurements in thalassemia should be confirmed in a larger sample of patients with greater age range.

Disclosures: I.M. Frieling, None.

W239

Trabecular Microarchitecture Assessed by MicroMRI in Postmenopausal Women with Osteoporosis on Therapy. P. Greeley^{*1}, J. M. Wagner^{*1}, P. Seaman^{*2}, S. Perera^{*3}, B. R. Gomberg^{*2}, O. Ganel^{*2}, M. Kleerekoper², S. L. Greenspan¹. ¹Medicine, University of Pittsburgh, Pittsburgh, PA, USA, ²MicroMRI Inc., Philadelphia, PA, USA, ³Medicine/ Biostatistics, University of Pittsburgh, Pittsburgh, PA, USA.

Although bone mineral density (BMD) is the gold standard to diagnose patients with osteoporosis prior to fracture, and to follow response to therapy, changes in BMD may only account for 30% of the reduction in fracture risk following therapy. Other factors such as trabecular micro-architecture contribute to fracture risk. A novel, noninvasive technique based on high resolution MRI (MicroMRI), examines trabecular microstructure and provides an index of the trabecular rods and plates. In order to examine the associations between standard measures of BMD by DXA at the wrist, hip and spine and distal radius micro-architecture by MRI in women on treatment, we recruited 20 postmenopausal women (mean age 70 years). Ten women had previously been on a bisphosphonate and 10 women, previously on a bisphosphonate short term, had just initiated treatment with teriparatide. Outcomes included bone mineral density by DXA (Hologic Discovery A) of the right wrist, PA spine, and hip (total, femoral neck,). MicroMRI was examined using a right bird cage wrist coil with a Sigma 1.5 Tesla MRI scanner and analyzed by MicroMRI Inc. (Philadelphia, PA). MicroMRI indices included: BV/TV (bone volume/total volume), Surf (topological surface density), Curv (topological curve density), Surf/Curv (surface to curve ratio, number of platelike to rodlike trabeculae, higher values indicate intact trabeculae); Erosion Index =(ratio of parameters that increase with deterioration). Table Pearson Correlation Coefficients, *p<0.05, ** p<0.01

	BV/TV	Surf	Curv	Surf/Curv	Erosion Index
Age	-.763*	-.719**	.242	-.601**	.574**
Femoral Neck	.446*	.476*	-.211	.396	-.458*
Spine	.036	.044	-.005	.022	-.029
Ultra Distal Radius	.838**	.800**	-.569**	.785**	-.744**
1/3 Distal Radius	.552*	.522*	-.200	.460*	-.456*

Indices of MRI micro-architecture at the radius had the greatest association with BMD at the ultra distal radius but was also associated with BMD at the 1/3 distal radius and femoral neck sites. Correlation at the spine was poor. Older age was associated with fewer plates, lower plate to rod ratio and greater deterioration as assessed by the erosion index.

We conclude that measures of microMRI at the wrist are associated with the wrist and hip BMD and demonstrate a deterioration in architecture in postmenopausal women with osteoporosis on therapy. Additional studies are needed to examine these changes prospectively.

Disclosures: P. Greeley, None.

This study received funding from: NIH/NCRR.

W240

Bone Strength and Toughness Are Reduced by Loss of Architecture - A Non-linear FE Analysis. G. J. Gross^{*}, H. Hong^{*}, B. Borah^{*}, R. J. Phipps, T. E. Dufresne^{*}. Procter & Gamble Pharmaceuticals, Mason, OH, USA.

Reductions in bone volume and deterioration in bone architecture occur in osteoporosis. We performed non-linear computational modeling to understand the effect of architectural changes and bone loss on bone strength and toughness.

MicroCT scanning was performed on iliac crest biopsies collected from a placebo-controlled clinical study in postmenopausal osteoporosis. Finite element models were created directly from these microCT data over a wide range of bone volumes (11-29% BV). The volume of interest was maximized to include the largest number of bone elements possible. A custom program was written to simulate bone loss, which used a 3D Euclidian distance map for each sample to randomly select bone erosion sites. A 26% loss of BV was used to match the 3-yr placebo-treated results from the clinical study. This 26% simulated bone loss resulted in architectural changes comparable to those observed experimentally in clinical biopsies. The plasticity of bone was represented using a non-linear constitutive model with apparent properties measured by compression loading each FE model.

With a 26% loss of BV, reductions in bone strength and toughness were similar, but depended on initial bone volumes.

	Sample (% BV)		
	29	19	11
% Change from baseline			
Bone Strength	-57	-61	-82
Toughness	-56	-73	-81

To understand the "dose response" of strength and toughness to bone loss better, a single sample (19% BV) was analyzed at five levels of bone loss (10, 15, 20, 26 and 35%). Both strength and toughness were reduced across all bone loss levels even after only 10% loss. Strength and toughness reductions followed similar trends.

	% of Bone Loss in 19% BV Sample				
	10	15	20	26	35
% Change from baseline:					
Bone Strength	-25	-38	-40	-55	-67
Toughness	-23	-35	-44	-52	-65

Use of non-linear tissue properties made these predictions in bone toughness possible and is a valuable technique in assessing bone fragility. Our results show that deterioration of trabecular architecture directly effects both strength and bone toughness. Toughness, the ability to absorb energy and prevent crack propagation, is important in bone fragility and will be further investigated in larger sample groups.

Disclosures: G.J. Gross, Procter & Gamble Pharmaceuticals 3.

W241

Trabecular Bone Microstructure Assessments of the Distal Radius Using a Compact MRI. S. Handa^{*1}, B. R. Gomberg^{*2}, T. Haishi^{*3}, K. Kose^{*1}. ¹Institute of Applied Physics, Tsukuba, Japan, ²MicroMRI Inc., Philadelphia, PA, USA, ³MRTechnology Inc., Tsukuba, Japan.

Trabecular bone (TB) microstructure measurements have shown promise for estimation of bone strength and evaluation of drug therapies for osteoporosis. Up to now, several groups have studied this extensively using whole body MRI (wbMRI) system, however the wbMRI systems are expensive and heavily utilized for other clinical indications. A compact peripheral MRI (cpMRI) system dedicated to measure TB microstructure would offer a solution to overcome these disadvantages.

In this study, we have evaluated a cpMRI system (MRTechnology Inc. Tsukuba, Ibaraki, Japan) for TB microstructure measurements of the distal radius.

The cpMRI consists of a 1.0 T permanent magnet (100 mm gap, homogeneous volume: 60 mm diameter sphere), gradient coil set, radio frequency probes, and an MRI console[1]. To acquired data, we developed 3D driven equilibrium spin-echo pulse sequence (matrix size: 512 X 384 X 32, voxel size: 150 X 150 X 500 micron cube, data-acquisition time: 17 minutes) for the distal radius imaging of five healthy male volunteers.

Ages ranged from 21 to 25 years (mean 22.4 years) and volunteers were scanned three times independently over two weeks.

Image data processing and analysis was performed semi-automatically using digital topological analysis (DTA - MicroMRI Inc., Philadelphia, PA, USA). Table 1 shows the reproducibility of BV/TV and selected DTA structural parameters in the distal radius. The root mean square CV (RMS-CV) values range from 2.9 % to 14 %. These values are close to those previously reported for the distal radius and tibia using a wbMRI system[2].

In conclusion, the 1.0 T permanent magnet cpMRI system was found to be capable of performing trabecular bone micro-architectural assessment of the distal radius consistent with the results from wbMRI systems, showing great promise of our system for evaluating bone quality in clinical settings.

References

- Haishi, T., et al., Magn Reson Imaging. 2001. 19(6): p. 875-80.
- Gomberg, B.R., et al., Bone 2004. 35(1): p266-76.

Table 1. DTA parameter averages ,CVs and their RMS-CVs from five volunteers (S1-S5). T_THICK: trabecular bone thickness, SCR : surface-to-curve ratio, TEI : topological erosion index. All parameters except T_THICK are unitless.

		BV/TV	T_THICK(μ m)	SCR	TEI
Average, (CV%)	S1	0.145(7.7)	97.6(2.5)	9.259(14.0)	0.872(10.6)
	S2	0.128(4.9)	88.8(3.3)	7.355(6.6)	0.926(4.5)
	S3	0.175(7.7)	114.6(4.1)	16.041(23.4)	0.604(14.0)
	S4	0.120(1.4)	92.8(0.4)	6.759(0.8)	1.039(2.4)
	S5	0.118(8.1)	87.8(3.0)	6.132(18.1)	1.162(11.1)
RMS-CV (%)		6.5	2.9	14.0	9.6

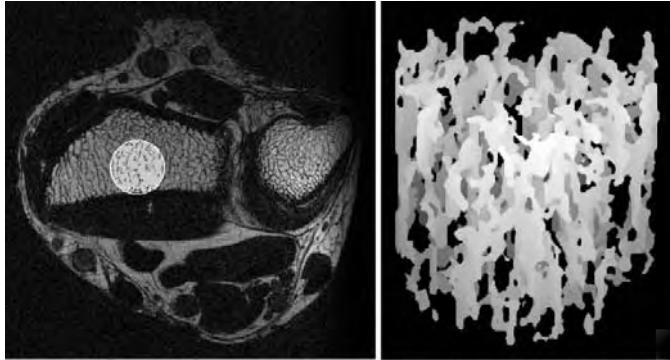


Figure 1. Cross-sectional image and projection image of microscopic TB structure in the distal radius.

Disclosures: S. Handa, None.

W242

Vertebral Fracture Risk: Is Size More Important than BMD. A. Hoiseth*. Sentrum Røntgeninstitute, Oslo, Norway.

Size is a major (bio)mechanical parameter, strongly associated to structural strength; compressive strength thus being associated to radius² and bending strength to radius⁴. BMD, often defined as a gold standard for fracture risk assessment, was constructed to eliminate the size factor, being the best approximation to bone density as measured by a two-dimensional projection. A dimension-less parameter, however, may not adequately reflect structure and thus strength. By DXA, however, also assessment of size as projectional area and bone mass (BMC) are derived. PURPOSE: To report the association for DXA parameters with fractures and with clinical and social consequences of fractures. MATERIAL: DXA parameters were measured in a total of 41,217 women aged >40 years. Fracture history was obtained in two cohorts of these, respectively 8,584 and 5,138 large. METHOD: After correcting for age, using the total material, the DXA parameters were ranked from high to low values into 10 equally large groups. Identical, but separate fracture analyses were then performed in the two cohorts. Fractures were classified as a) those having at least one vertebral fracture but without femoral fractures and b) those having at least one femoral fracture. Risk ratio (RR) was calculated for each tenth using the average number of fractures in the cohorts as RR=1. Only consistent results between the two cohorts were considered as "significant". RESULTS: For the femoral fracture group there was an exponential increase in RR from high to low BMC and BMD in "total femur". RR for the lower tenths being respectively 2.5 and 2.8. For area there was no difference in RR between the tenths. For the vertebral fracture group there was a linear increase in RR from high to low vertebral BMC and BMD, RR in the lowest tenth being respectively 1.5 and 1.4. For spine area there was an exponential increase in RR to 1.8 in the lowest tenth. The RR for having fractures with clinical or social consequences also increased exponentially with lower BMD and BMC in the femur, and with spine area. DISCUSSION: The results indicate a need for giving attention to bone as a structure, not merely as a material. Exploring different mechanically relevant parameters may help us to more correct predictions of the risk of vertebral fractures, a fracture that to a large degree is independent of BMD.

Disclosures: A. Hoiseth, None.

W243

Age, Gender and Region Related Changes in Bone Mineral Density of Korean Adult. W. Choi, S. Hong*. Internal Medicine, Hanyang University, College of Medicine, Seoul, Korea, Seoul, Republic of Korea.

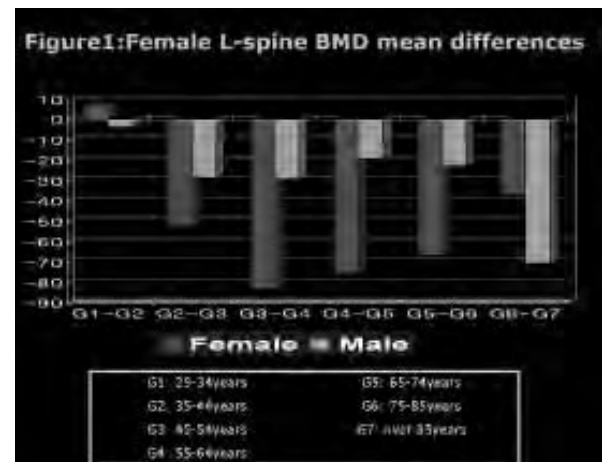
Background: Early diagnosis by measurement of bone mineral density(BMD) and treatment can reduce osteoporosis complications. But we had no large population data & Korean specific reference value in diagnosis of osteoporosis.

Method: we performed cross sectional study involving 50208 people(lumbar BMD / M:4,810, F:45,398), and 50026 people (femur neck BMD /M:4745, F:44,700) from Seoul, Gyeonggi,

Daegu, jeonbuk. BMD was measured by using DEXA (HOLOGIC, QDR 4500 system) Result: Female peak BMD was obtained at 35-45 years (lumbar: n=2224, 0.985±0.129 and femur: n=6800, 0.864±0.114 mg/cm2). Male peak BMD was obtained at 25-35years (lumbar: n=458, 1.010±0.118, femur: n=489 0.960±0.113 mg/cm2). And BMD was decreased with age. But decrease of BMD was more prominent with female and other regions than with male and Seoul. Especially female lumbar and femur wards BMD decrease was accentuated at menopause period.(figure1) The reference value in diagnosis of osteoporosis from our data was lower than the previous used reference data (Japanese data) except female femur.(figure2) Conclusion: Korea is racially homogeneous and not large nation. But there was regional difference in the BMD change. Also the diagnosis of osteoporosis may be overestimated. So further research is needed considering with social factors and fractures.

Figure2: T-score in this study

	Mean±SD	1.0 SD	2.0 SD	3.0 SD	4.0 SD
Female(35-45, n=2735)	0.992±0.124	0.868	0.744	0.620	0.715
Male(25-34, n=458)	1.008±0.127	0.881	0.754	0.631	0.729
Female(35-44, n=5500)	0.853±0.117	0.748	0.631	0.515	0.589
Male(25-35, n=489)	0.961±0.113	0.827	0.694	0.568	0.540



Disclosures: W. Choi, None.

W244

In Vivo Proteomic Analysis of Circulating Monocytes in Chinese Pre-menopausal Females with Extremely Discordant Bone Mineral Density. E. Y. Deng*, Y. Z. Liu*, C. Jiang*, L. M. Li*, S. Wu*, Y. Chen*, H. Jiang*, F. Yang*, P. Xiao*, S. M. Xiao*, L. J. Tan*, X. Sun*, J. X. Xiong*, X. Z. Zhu*, M. Y. Liu*, S. F. Lei*, X. D. Chen*, J. Y. Xie*, G. G. Xiao*, S. P. Liang*, H. W. Deng*. ¹Departments of Basic Medical Science and Orthopaedic Surgery, University of Missouri - Kansas City, Kansas City, MO, USA, ²Hunan Normal University, Changsha, China, ³Osteoporosis Research Center, Creighton University, Omaha, NE, USA, ⁴Department of Pediatrics, Harbor University of California, Los Angeles, Torrance, CA, USA.

Osteoporosis (OP) is a major public health problem and bone mineral density (BMD) is an important determinant of OP. Circulating monocytes (CMCs) may serve as progenitors of osteoclasts and produce a wide variety of factors important to bone metabolism. However, little is known about the specific roles of CMCs in the pathogenesis of OP. Using proteomics techniques of 2-Dimensional Gel Electrophoresis (2-DE) coupled with Matrix Assisted Laser Desorption and Ionization Time-of-Flight/ Time-of-Flight Mass Spectrometry (MALDI-TOF/TOF-MS), we performed a comparative protein expression profiling study of CMCs in Chinese pre-menopausal females with extremely high or low BMD. A total of 38 differentially expressed proteins on 2-DE gels were identified. We confirmed with western blotting five proteins that potentially might have important roles in osteoclastogenesis: up-regulation of ras suppressor protein 1 (RSU1), gelsolin (GSN), and manganese-containing superoxide dismutase (SOD2), and down-regulation of glutathione peroxidase 1 (GPX1) and prolyl 4-hydroxylase beta subunit (P4HB) in low vs. high BMD group. RSU1, GSN, SOD2 and GPX1 might affect monocyte trans-endothelium (via regulating its adhesion, morphological changes, or locomotion), differentiation, and/or downstream osteoclast function (via regulating osteoclast podosome formation, adhesion, motility, or activity). Thus, these proteins may contribute to differential osteoclastogenesis and finally lead to BMD variation. This is the first in vivo proteomics study of OP in humans and the five identified proteins may serve as biomarkers for early prevention and novel targets for clinical intervention of this debilitating disease.

Disclosures: H.W. Deng, None.

This study received funding from: Natural Science Foundation of China, NIH.

W245

The Loss of Follow up After Fragility Hip Fractures in Some Regions in Czech Republic. T. Hala¹, F. Senk^{*2}, P. Zivny^{*3}, B. Skyvarova^{*4}, M. Carda^{*5}, T. Dedek^{*6}. ¹SYNARC/CCBR Czech, Pardubice, Czech Republic, ²Osteocentre, Hospital Havlickuv Brod, Czech Republic, ³Osteocentre, Teaching Hospital Hradec Králové, Czech Republic, ⁴Osteocentre, Hospital Jablonec nad Nisou, Czech Republic, ⁵Traumatology, Regional Hospital Pardubice, Czech Republic, ⁶Traumatology, Teaching Hospital Hradec Kralove, Czech Republic.

Fragility fracture is a major risk for osteoporosis and has been identified as the only clinically relevant marker of bone quality. It is important to identify whether patients who experienced fragility fractures are being assessed and treated for osteoporosis in order to reduce the risk of future fracture. The patients with fractures should be managed in accordance with evidence-based clinical guidelines for osteoporosis.

Objective: The main objective of this study was to establish the BMD testing rate in osteoporosis management for people over 50 years of age who had already suffered a hip fracture. This is the first study in Czech Republic conducted for this purpose.

Methods: We conducted a retrospective cohort study using data from 5 fracture clinics and bone disease centres. Study population consisted of all individuals over 50 years of age who sustained hip fracture between January 1, 2004 and December 31, 2005 from regional hospitals where one fracture clinic and one bone disease centre are in house, for accurate data analysis. We used Czech classification system for fractures: hip (S 72.0), pertrochanteric fracture (S 72.1) and subtrochanteric fracture (S 72.2). We included patients with osteoporotic fractures and with DXA measurements of L1-L4 and hip. We excluded those with high-energy trauma fractures.

Results: We analyzed data from 1465 patients, 1054 (71.95%) women and 411 (28.05%) men with proximal femur fractures. We have documented that 99 patients (6.75%) with fractures underwent densitometric evaluation. The number of women and men was 86 (5.87%) and 13 (0.88%), respectively. Out of those 99 patients, 67.3% were over 70 years of age.

Patients	women	men	assessed by DXA	women	men
1465	1054	411	99	86	13
%	71,95	28,05	6,75	5,87	0,88

Conclusions: There is evidence of a care gap between the occurrence of fragility fractures and the diagnosis of osteoporosis in some regions in Czech Republic. This study provides evidence that many Czechs who experienced fragility fracture are not being diagnosed and treated for prevention of future fractures. The prevalence of bone mass measurements or physician follow-up is enormously low.

Disclosures: T. Hala, None.

W246

Skeletal and Vitamin D Status in Two Indigenous North American Populations. I. V. Haller¹, W. D. Leslie², J. Jaakola^{*3}, H. A. Weiler^{*4}, D. Krueger⁵, N. Binkley⁵. ¹Education and Research, SMDC Health System, Duluth, MN, USA, ²Faculty of Medicine, University of Manitoba, Winnipeg, MB, Canada, ³Human Services Division, Fond du Lac Band of Lake Superior Chippewa, Cloquet, MN, USA, ⁴School of Dietetics and Human Nutrition, McGill University, Montreal, PQ, Canada, ⁵Osteoporosis Clinical Research Program, University of Wisconsin, Madison, WI, USA.

Bone health and vitamin D status have received only limited study among North American indigenous populations. To explore potential geographic differences in peripheral BMD and wintertime 25OHD levels, we conducted a secondary analysis of data from studies of two indigenous North American populations of women: First Nations (FN) in Canada and American Indian/Alaska Native (AI/AN) in the US. The FN group was comprised of 96 women from the First Nations Bone Health Study (FNBHS); the second group included 78 AI/AN women from the Great Lakes region. All participants had weight, height, and calcaneal BMD measurements (Lunar PIXI) performed. Serum calcium, PTH, and 25OHD were evaluated during winter months (January-March). In the FNBHS study, the Diasorin RIA and DPC EIA were used to measure 25OHD and PTH, respectively, while in the AI/AN cohort, HPLC and the DPC IRMA were utilized for these measurements.

In this analysis, the FN women were on average younger than their AI/AN counterparts (42.4±11.3SD vs. 50.3±9.9SD years old). There were no differences between the two groups in weight (82.7±18.9SD vs. 86.4±18.7SD kg) or BMI (30.8±6.3SD vs. 32.2±6.6SD kg/m²). Due to the effects of age and weight on peripheral BMD, we used general linear modeling (GLM) to test the difference in absolute values of calcaneal BMD between the two groups adjusted for weight and age. Adjusted BMD values in FN and AI/AN women did not differ (0.515±0.009SEM vs. 0.542±0.010SEM g/cm², respectively, P=0.052).

In bivariate analysis, the FN group had lower serum calcium (9.0±0.4SD vs. 9.4±0.3SD mg/dl, P<0.001), higher PTH (55.1±22.2SD vs. 42.5±23.6SD pg/ml, P<0.001) and higher 25OHD (21.2±10.0SD vs. 18.1±8.9SD ng/ml, P=0.032). Serum 25OHD was negatively correlated with PTH in the overall sample (r=-0.19, P=0.014); no correlation between 25OHD and BMI was observed. Similar proportions of women in both groups had serum 25OHD concentrations below 30 ng/ml (82.1% in FN vs. 89.7% in AI/AN group). There was a significant effect of group on serum 25OHD concentrations after adjustment for age, BMI and PTH levels using GLM: 22.0±1.0SEM ng/ml in FN group vs. 17.1±1.2SEM ng/ml in AI/AN group (P<0.001). In conclusion, low vitamin D status is common in these two populations of indigenous North American women. Investigation of approaches to optimize vitamin D status in FN and AI/AN women is indicated.

Disclosures: I.V. Haller, None.

W247

Low Bone Mass Is Common in Premenopausal Black Women with Systemic Lupus Erythematosus on Prednisone: High BMI Is Protective. J. K. Jenkins, I. Srivastava-Hadley*, K. Demoruelle*. Division of Rheumatology, University of Mississippi Medical Center, Jackson, MS, USA.

The purpose of this study was to examine a premenopausal black female systemic lupus erythematosus (SLE) population on prednisone to determine the prevalence of low bone density (LBD) and osteoporosis (OP) and identify modifying clinical factors.

We performed a retrospective chart evaluation to examine factors affecting bone mass in premenopausal black women with SLE on steroids. Protected by ethnicity, this population has a higher SLE disease burden that may affect the development of low bone mass (LBM, i.e., LBD and OP). We identified patients from our lupus specialty clinic in 2004-2006 who also had a bone density assessment in the Division of Rheumatology. All patients were on daily prednisone >2 mg/d. Clinical information was collected from the DXA records and clinic charts. ACR criteria were used for the classification of SLE.

Sixty-one women met our criteria. Nine others were excluded because of incomplete data. Average age at the time of the DXA scan was 32.9 yrs. Average disease duration was 7.1 yr. Prednisone was first used 7.1 yrs prior to DXA. Average prednisone dose was 11.9 mg/d at the time of DXA. Patients took: 0.7 other medications that may be associated with LBM (anticonvulsants, furosemide, anti-ulcer drugs, warfarin); 1.2 steroid sparing drugs (hydroxychloroquine, azathioprine, methotrexate, and mycophenolate); and 0.7 drugs that were potentially protective (calcium, HCTZ, bisphosphonates). Average BMI was 30.3. There were 3 non-vertebral fractures including one hip fracture.

DXA results were (WHO classification): 41% normal, 39% LBD, 20% OP. Regression analysis was performed to identify modifying factors. Duration of steroids, number of steroid sparing drugs, and the number of LBM-associated drugs or -protective drugs used were not associated with LBM. Bone density was strongly positively correlated (p<0.01, r=0.7) with BMI at all sites. Frank obesity (BMI>30, n=32) was protective, and was associated with a higher BMD (p<0.003) at all sites by 12-17%. In contrast to one report in which non-white SLE patients had a higher prevalence of hip OP, we find the usual higher prevalence of vertebral OP (20%, vs. 3% hip) with steroids in the black SLE population. This is a large study of black women with SLE on prednisone examining multiple factors affecting the development of low bone mass. Low bone density and osteoporosis appear to be as common in young premenopausal black women with SLE on steroids as in white women in previous reports (23%). This may be due to a greater disease burden and steroid use. Obesity is a significant protective factor against prednisone-associated osteoporosis in SLE in black women.

Disclosures: J.K. Jenkins, None.

W248

What Are the Characteristics of Postmenopausal Women with the T-score of the Total Hip that Is Lower than that of the Lumbar Spine? M. Kang*, M. Kim*, D. Lim*, S. Lee*, K. Baek*, J. Han*, H. Kim*, K. Lee*. Department of Internal Medicine, The Catholic University of Korea, College of Medicine, Seoul, Republic of Korea.

Background. Generally, T-score of the lumbar spine is lower than that of the total hip in postmenopausal women because of an accelerated loss of trabecular bone after menopause. However, some women had the reversed T-score which meant that the T-score of the total hip was lower than that of the lumbar spine. It is well known that PTH and thyroid hormone preferentially involve cortical bone rather than trabecular bone. Thus, we aimed to investigate the characteristics of postmenopausal women with T-score of the total hip that is lower than that of lumbar spine.

Methods. We enrolled 246 postmenopausal women (mean age: 55.87±6.99 years) in our study. Serum levels of TSH, free T4, PTH, FSH, Estradiol, Alkaline phosphatase, Calcium, Phosphorus were measured by the standard methods. BMD at the lumbar spine and femur were measured by dual energy X-ray absorptiometry.

Results. Among 246 postmenopausal women, there were 25 cases in which the T-score of the total hip were lower than that of the lumbar spine (low hip T-score group). Body weight and BMI were significantly lower in the low hip T-score group, when compared to group that had similar lumbar BMD (55.41±6.13 vs. 60.51±7.84, p=0.011, 22.83±2.63 vs. 24.57±3.17, p=0.034). Age, YSM (years since menopause), free T4, TSH, PTH, FSH and Estradiol showed no differences between the two groups.

Conclusions. We have found that postmenopausal women, having the lower T-score of the total hip than that of the lumbar spine, have low body weight and low BMI. But, we could not detect any statistically significant differences in PTH and thyroid hormone levels. Additional studies are required to find the characteristics of postmenopausal women having the lower T-score of the total hip than that of the lumbar spine.

Disclosures: M. Kang, None.

W249

The Effect of Home Parenteral Nutrition on Bone Mineral Density. H. Karakelides*, J. L. Burnes*, J. M. Nadeau*, D. G. Kelly*, D. L. Hurley*, K. A. Kennel*. ¹Endocrinology, Mayo Clinic College of Medicine, Rochester, MN, USA, ²Gastroenterology, Mayo Clinic College of Medicine, Rochester, MN, USA.

Home parenteral nutrition (HPN) or long-term parenteral nutrition has been associated with poor bone health. Altered nutrition, components of parenteral nutrition formulations (e.g., aluminum) and underlying gastrointestinal (GI) disorders have been suggested as reasons for reduced bone density in this population. In addition to changing nutrition

support practices, there have been advances in pharmacotherapies for metabolic bone disorders. However, there is little data on the effects of bone active drugs in patients who are on long-term parenteral nutrition. We conducted a retrospective study of patients on HPN to assess risk factors for bone loss and effects of bone active drugs on bone mineral density (BMD). Subjects studied had been treated by the Mayo Clinic Rochester HPN team since 1994 and had been on HPN for at least 1 year and had at least 2 BMD measurements performed at least 1 year apart. 52 subjects were included with a mean age 59.8 ± 2.0 years, mean duration of HPN 115.1 ± 14.2 months, mean body mass index (BMI) 23.0 ± 0.5 kg/m². There was no association between gender, age, BMI, duration of HPN or underlying GI pathology (inflammatory vs non-inflammatory disorders) and change in BMD during follow-up. The subjects were then divided into those who had been treated (tx, n=31) with bone active drugs versus those who had not been treated (untx, n=21). There was no difference in time on HPN, time between BMDs, underlying GI pathology, BMI or age between the two groups. As may have been expected, subjects in the tx group had a lower baseline BMD of the lumbar spine (LS) (0.92 ± 0.03 in tx vs 1.03 ± 0.04 g/cm² in untx, $p < 0.05$) and femoral neck (FN) (0.76 ± 0.03 in tx vs 0.87 ± 0.03 g/cm² in untx, $p = 0.01$). However, there was no significant impact of treatment with bone active drugs on the change in LS or FN BMD from baseline to final observation. In conclusion, in subjects on HPN, gender, age, BMI, duration on HPN and underlying GI disorder were not good predictors of BMD. Subjects with lower BMD were more likely to be treated with bone active medications.

Disclosures: H. Karakelides, None.

W250

Gonadotropins Associated with Bone Mineral Density in Males. A. Kåss*, H. Gulseth*. Department of Rheumatology, Betanien Hospital, Skien, Norway.

It has been recently suggested that FSH regulates bone mass (1,2) independent of the action of oestrogen. FSH was shown to stimulate osteoclastogenesis and bone resorption by acting on $G_{i\alpha}$ -coupled FSH receptors, which are localised on the surface of mouse and human osteoclasts and their precursors. We wanted to examine the levels of FSH, LH in men and explore their relationship to bone mineral density (BMD). One hundred and eighteen males (age range 49-90 years) with low impact forearm fractures were included. Lumbar spine BMD was measured according to standard procedures with Lunar DXA equipment. Serum FSH, luteinizing hormone (LH) and testosterone were measured using fluoroimmunoassay. Multiple linear regression was used to assess the relationship between BMD and these hormones controlling for age and BMI. Of males with established osteoporosis (defined as a T score below 2.5 SD), 28.6% had above normal (>12.0 IE/L) FSH levels, 21.4% had above normal (>12.0 IE/L) LH levels and 33.3% had below normal (<8.0 IE/L) testosterone levels. FSH and LH were significantly associated ($\beta = -0.775$, $p = 0.021$, $\beta = -0.751$, $p = 0.013$ respectively) with BMD after controlling for age and BMI. To our knowledge this association has only been previously reported in women (3). Further studies are required to assess the oestrogen-independent role of FSH in osteoclastogenesis. It is unknown whether the associations observed between LH and BMD are confounded by FSH or gonadal hormones, or whether LH itself might have oestrogen-independent effects on bone mass; this remains to be studied. References: (1) Sun L, Peng Y, Sharrow AC, Iqbal J, Zhang Z, Papachristou DJ, Zaidi S et al. FSH directly regulates bone mass. *Cell* 2006; 125: 247-260. (2) Martin TJ, Gaddy D. Bone loss goes beyond estrogens. *Nat Med* 2006; 12: 612-613. (3) Sowers MR, Greendale GA, Bondarenko I, Finkelstein JS, Cauley JA, Neer RM, Ettinger B. Endogenous hormones and bone turnover markers in pre- and perimenopausal women: SWAN. *Osteoporos. Int* 2003; 14:191-197.

Disclosures: A. Kåss, None.

W251

Spine Bone Mineral Density Predicted Incident New Vertebral Fractures in Postmenopausal Korean Women. S. Kim¹, Y. Rhee¹, H. Choi^{*1}, Y. Kim², E. Kang^{*1}, B. Cha^{*1}, E. Lee^{*1}, H. Lee^{*1}, S. Lim¹. ¹Internal Medicine, Yonsei University, Seoul, Republic of Korea, ²Internal Medicine, NHIC Ilsan Hospital, Goyang, Republic of Korea.

The identification of individuals at risk for osteoporotic fracture is essential for prevention. Low bone mineral density has been shown to be an important predictor of increased fracture risk. However, it is not known whether bone mineral density (BMD) in the axial skeleton is related to fractures in postmenopausal Korean women. We examined the relationship between BMD measured by dual energy x-ray absorptiometry (DXA) and incident vertebral fractures in postmenopausal Korean women. Baseline data collected from 2000 to 2002 (670 Korean women aged 49-87 years) at Severance Hospital, Seoul, Korea; mean follow-up of 3.2 years. Of the 670 subjects included in the study, 514 had no vertebral fractures and 156 had at least one. The women with vertebral fractures were older, smaller, and lower BMD compared to those without. In a binary logistic regression model with multivariate adjustment, age ($p < 0.001$), spine BMD ($p < 0.01$), and total hip BMD ($p = 0.001$) were independent risk factor for prevalent vertebral fractures. During follow up period, 77 women (34 in 156 women with prevalent vertebral fractures and 43 in 514 women without) developed new incident vertebral fractures. In women without prevalent vertebral fractures, age (OR=1.070; 95% CI, 1.005-1.140) and spine BMD (OR=0.559; 95% CI, 0.332-0.940) were independent risk factor for incident new vertebral fractures in a binary logistic regression model with multivariate adjustment. In models adjusted for age, Spine BMD was associated with increased risk of incident new vertebral fractures ($p < 0.05$) in women with baseline vertebral fractures. Decreased spine BMD was associated with an increased risk of incident new vertebral fractures in postmenopausal Korean women.

Disclosures: S. Kim, None.

W252

Longitudinal Study of Changes in Bone Mineral Density in Women Undergoing Screening for Osteoporosis. K. Kurasawa*, K. Katayama*, Y. Nomura*, R. Kikuchi, O. Chaki, F. Hirahara*. Obstetrics and Gynecology, Yokohama City University, Yokohama, Japan.

Objective: Measurements of bone mineral density (BMD) are an important tool for the diagnosis and treatment of osteoporosis. Low BMD is an independent risk factor for fracture. However, longitudinal studies of BMD are few. Longitudinal studies and analyses of the time course of BMD are essential. **Methods:** The study group comprised 69 women free of diseases potentially affecting bone metabolism who presented at our department from 1993 through 2006 to undergo measurement of BMD. Their mean age was 58.8 years (range, 43 to 71). The subjects were classified into 3 groups according to status: perimenopausal women, early postmenopausal women, and late postmenopausal women. Height, body weight, lumbar-spine bone mineral density, and femoral BMD were measured over time. The percent changes in these values were compared. Lumbar-spine radiography was performed in 1998 and 2006. The presence or absence of new fractures was examined. **Results:** At the beginning of the study, lumbar-spine bone mineral density (0.954 ± 0.04 mg/cm²), femoral BMD (total, 0.710 ± 0.05 mg/cm²; neck, 0.801 ± 0.06 mg/cm²), radial bone mineral density (0.447 ± 0.04 mg/cm²), and calcaneal bone mineral density ($91.54\% \pm 13.42\%$) were significantly higher in perimenopausal women than in early and late postmenopausal women ($p < 0.01$). In perimenopausal women, lumbar-spine BMD significantly decreased by 7.71% at 5 years, by 10.29% at 7 years, and by 13.49% at 13 years. BMD at all other sites also significantly decreased during follow-up. In early and late postmenopausal women, lumbar-spine and femoral BMD did not decrease significantly. In contrast, calcaneal BMD significantly decreased in all groups, suggesting that calcaneal BMD may not reflect the estrogen-deficiency-related decrease in BMD after menopause. Height did not significantly decrease in any group, and there were no new fractures. **Conclusions:** The age-related decrease in BMD seen in women differs depending on the site examined. Early after menopause, BMD decreases rapidly at all sites. Subsequently, longitudinal monitoring confirmed that the percent decreases in BMD gradually converged. When screening for osteoporosis, the BMD of sites other than the calcaneus should be measured mainly during the perimenopausal period. In women with no decrease in height, bone density can be measured at intervals of 1 year or longer.

Disclosures: K. Kurasawa, None.

W253

No-vertebral Fracture Rates Are Lower in Hong Kong Chinese Men than American Caucasians but Bone Mineral Density Predicts Fracture Risk Similarly in the 2 groups-Results from Mr Os International. E. M. C. Lau¹, J. Lapidus², P. C. Leung³, T. Kwok³, D. Bauer⁴, J. Cauley⁵, S. R. Cummings⁶, E. S. Orwoll, for the Mr Os Study group⁷. ¹Hong Kong Orthopaedic and Osteoporosis Center, Hong Kong, China, ²Oregon Health and Science University, Portland, OR, USA, ³Chinese University of Hong Kong, Hong Kong, China, ⁴California Medical Center, San Francisco, CA, USA, ⁵University of Pittsburgh, Pittsburgh, PA, USA, ⁶San Francisco Co-ordinating Center, California Pacific Medical Center, San Francisco, CA, USA, ⁷Oregon Health and Science University, Portland, OR, USA.

The purpose of this study is to compare fracture rates in Hong Kong (HK) Chinese and American (US) Caucasian men and to study the relationship between BMD and fracture risk in these 2 groups by a cohort method.

The Mr Os cohort consists of 5,995 ambulatory men recruited from 6 communities in the US, plus 2000 men recruited from a single site in Hong Kong. Protocols in the two countries are comparable. BMD was measured with DXA, and standardized to account for equipment differences. Age and body mass index (BMI) were collected at baseline examination. Fractures were ascertained using standardized country-specific protocols, and all were confirmed by physician adjudication. Numbers and rates of fracture were compiled for each country individually. Data from the two countries were pooled, and Cox regression models used to compare associations with fracture in HK vs. US. Regression models were adjusted for age, BMI and clinical site in US.

There were 70 non-spine fractures in 69 Hong Kong participants; 500 fractures in 413 US participants. Rates of all non-spine fractures were significantly lower among HK Chinese (967.1 per 100,000) than among US Caucasians (1818.3 per 100,000) (RR = 0.53, 95% CI for RR 0.41 - 0.68). Rates of hip fractures were also lower (218.5 per 100,000) in Hong Kong than in US (281.3 per 100,000), but not significantly so (RR=0.78, 95% CI: 0.45 - 1.33).

Hong Kong participants, on average, were younger (72.4 vs. 73.8 years), had lower BMI (23.4 vs. 27.4), and lower femoral neck BMD (0.79 vs. 0.84) (all $p < 0.0001$). We adjusted for age and BMI. The relative hazard of non-spine fracture per 0.1 gm/cm² decrease in femoral neck BMD did not significantly differ in Hong Kong, 1.39 (95% CI: 1.10 - 1.76) and US, 1.48 (95% CI: 1.36 - 1.62), $p = 0.63$. The relative hazard of hip fracture per 0.1 gm/cm² also did not differ between the countries (Hong Kong RH: 2.23, 95% CI 1.30 - 3.85; US RH: 2.76, 95% CI 2.13 - 3.59), $p = 0.49$.

In conclusion, the rates of non-spine fracture were lower among HK Chinese than among US Caucasians, but the relationship between femoral neck BMD, and fracture was similar in the two countries.

Disclosures: E.M.C. Lau, None.

This study received funding from: The National Institute on Aging (NIA) and the National Cancer Institute, under the following grant nos: U01 AG 18197, U01 AR45614, U01 AR45632, U01 AR45647, U01 AR45654, U01 AR45583, AG18197, M01 RR000334.

W254

Bone Mineral Density in Hispanic Lupus Patients. I. Moldovan. Loma Linda University, Loma Linda, CA, USA.

The purpose of this study is to examine the bone mineral density (BMD) and its clinical determinants in a cohort of Hispanic women with systemic lupus erythematosus (SLE). The charts of one hundred consecutive Hispanic SLE patients were reviewed and twenty women who had BMD assessment by dual X-ray absorptiometry (DXA) were identified. Ten patients were premenopausal and ten were postmenopausal. The student t-test was used to assess statistical differences between the two groups. Clinical determinants of BMD were evaluated, including age, height, weight, body mass index (BMI), smoking and alcohol use, duration of SLE, steroid treatment, SLE disease activity index (SLEDAI) at the time of the DXA scan, SLE damage index (SLICC), as well as use of immunosuppressives and osteoporosis medications. The mean age was 34.3 in the premenopausal group and 52.6 in the postmenopausal group. The mean duration of SLE was 6.55 years in the premenopausal women and 19.1 years in the postmenopausal group. The disease activity score trended towards more active disease in the younger patients, however, the average doses of prednisone were comparable. BMI results were also comparable in both groups and were in the range of overweight. Four patients in the younger group and five in the postmenopausal ones had a BMI consistent with obesity. Overall, seventeen patients (85%) were taking glucocorticoids, but only five (25%) were taking medications for osteoporosis, including bisphosphonates, calcium and vitamin D. None of them were drinking alcohol and only one was an active smoker. The results showed that 35% of patients had osteopenia at the spine, 40% at the femoral neck and 10% at the total hip. Osteoporosis was present in 10% of the patients at both femoral neck and spine. One patient had a vertebral compression fracture. When comparing BMD in the pre- and postmenopausal groups, there was a trend towards lower BMD at the spine in the postmenopausal patients, and no statistical significant difference was detected for the total hip and the femoral neck. In conclusion, this study is one of the first ones looking at Hispanic lupus patients in terms of the prevalence of low BMD. In this small retrospective study, the prevalence of low BMD in the studied Hispanic SLE patients was comparable to reports from the literature in other ethnic groups. The small number of patients taking osteoporosis medications, despite widespread use of glucocorticoids underscores the importance of educating both physicians and patients regarding this matter. Somewhat surprising was the fact that there was no statistical difference in BMD, regardless of menopausal status. One explanation can be the small sample of patients analyzed. Another possibility could be that the higher BMI of the patients analyzed confers a protection against bone loss. Further, larger, prospective studies in this ethnic group are needed.

Disclosures: I. Moldovan, None.

W255

Lower Hip BMD Among Ethnically Diverse Postmenopausal Women with Anemia--Results from a Subgroup of the Women's Health Initiative. J. S. Nicholas, T. Bassford*, Z. Chen. University of Arizona, Tucson, AZ, USA.

Previously, we reported a significantly increased risk for hip fracture but not total fracture among anemic women in the Women's Health Initiative (WHI) Observational Study (OS). Additionally, a relationship between anemia and bone density was reported in a population of older community-dwelling anemic Italians, as well as among a variety of groups with specific conditions (thalassemia, hemodialysis, sickle cell anemia). Our aim was to investigate whether this relationship was evident among an ethnically diverse subcohort (n = 5,874) of postmenopausal women, age 50-79 at baseline from three clinical centers that performed bone density assessments in the WHI observational study. Questionnaires were used to collect demographic, medical, and lifestyle information. Bone mineral density (BMD) was measured by dual-energy x-ray absorptiometry. Anemia was defined using the WHO criteria of hemoglobin <12 g/dl in women using baseline measurements. Multivariate regression analysis was used to assess the relationship between whole body and total hip BMD with anemia after adjusting for age, ethnicity, body mass index (BMI), physical activity, total calcium (Ca) intake, and hormone use. Participants were 63.7 (SD=7.4) years old at baseline, 22.4% non-White minority and had a mean hemoglobin level of 13.5 (SD1.1) g/dl. There were 393 (6.7%) participants with anemia (mean hemoglobin level 11.3 g/dl SD=1.02) of whom 47.8% were non-White minority. No statistically significant (at a p=0.1 level) ethnic interactions with anemia on BMD were found with one exception for the Native American group in which only 6 women were anemic. The ethnic stratified results were similar across all the ethnic groups in the direction of the association, so the combined results for the relationship between anemia and BMD are presented in Table 1. Results from this analysis suggest that anemia is associated with a reduced hip BMD, which may explain the increased hip fracture risk we found previously among anemic women in the entire WHI-OS cohort. The relationship between whole body BMD and anemia is much weaker, which is also inline with our previous findings of no statistical significant association between total fracture and anemia.

	Hip BMD (g/cm ²)		Whole body BMD (g/cm ²)	
	β (SE)	P	β (SE)	P
Model 1 ^a	-0.02 (0.01)	<0.001	-0.004 (0.01)	0.5
Model 2 ^b	-0.01 (0.01)	0.03	-0.001 (0.01)	0.8

^a adjusted for age & ethnicity

^b adjusted for age, BMI, physical activity, total Ca intake, hormone use

Disclosures: J.S. Nicholas, None.

This study received funding from: NIH.

W256

Impact of Birth Weight and Age at Menarche on Skeletal Growth in Young Women. H. Ohta, T. Kuroda*, S. Orito*, Y. Onoe, Y. Miyabara*, R. Yoshikata*, M. Ohara*, K. Ishitani*, H. Okano. Dept. of Obstetrics and Gynecology, Tokyo Women's Medical University, Tokyo, Japan.

Objectives: Skeletal growth is assumed to occur under the influence of congenital genetic as well as acquired environmental factors. In recent years, fetal programming as developmental origins of health and disease (DOHaD) has drawn attention as a factor affecting lifestyle related disease.

However, it has also been suggested that birth weight and age at menarche, as well as lifestyle factors such as nutritional intake and physical activity, may affect skeletal growth. In this study, therefore, we investigated how these factors might affect skeletal growth in young women.

Subjects and Methods: Following approval of the study protocol by the institutional ethics committee at Tokyo Women's Medical University, birth weight and age at menarche, as well as lifestyle habits were surveyed in a total of 315 healthy young female volunteers aged 19 to 29 years old who were nursing school students at the institution and who gave informed consent to participate in the current study.

Results: The subjects' mean age was 22.1 \pm 3.0 (mean \pm SD); their mean birth weight, 3,143 \pm 45 g; their birth week, 39.3 \pm 1.8 weeks; their age at menarche, 12.0 \pm 1.2 years of age; their height, 158.8 \pm 4.8 cm; their body weight, 53.4 \pm 7.3 kg; and their BMI, 21.1 \pm 2.6 kg/m².

Birth weight was found to be significantly positively correlated with current BMI and BMD, and current BMI and L₂₋₄ BMD were found to be significantly higher in those who weighed 3,500 g or greater at birth, while there was no correlation seen between birth week and current BMI or L₂₋₄ BMD.

In those with normal menarche occurring between 10 to 15 years of age, age at menarche was found to be negatively correlated with current BMI and L₂₋₄ BMD, and positively correlated with body height.

Conclusions: The study results demonstrated that the greater the birth weight, the greater the current BMI and L₂₋₄ BMD, thus suggesting a role for birth weight in skeletal growth.

It was also suggested that the earlier the age at menarche, the shorter the body height, likely due to the resulting early closure of the epiphyseal space, and, as a consequence, the greater the BMI and the BMD in these young women.

It was therefore concluded that birth weight and age at menarche are independent factors affecting skeletal growth.

Disclosures: H. Ohta, None.

W257

Association Study of IL-15 Polymorphisms with Bone Mineral Density and Fracture Risk in Postmenopausal Korean Women. J. Koh*¹, B. Oh*², J. Lee*², J. Lee*¹, K. Kimm*³, J. Kim*⁴, J. Lim*⁴, T. Kim*³, J. Hong*⁵, G. Kim*¹, S. Kim*⁶, E. Park*⁴. ¹University of Ulsan College of Medicine, Seoul, Republic of Korea, ²National Genome Research Institute, Seoul, Republic of Korea, ³Eulgi University School of Medicine, Daejeon, Republic of Korea, ⁴School of Dentistry, BK21, Kyungpook National University, Daegu, Republic of Korea, ⁵Skeletal Diseases Genome Research Center, Kyungpook National University Hospital, Daegu, Republic of Korea, ⁶Kyungpook National University Hospital, Daegu, Republic of Korea.

Interleukin-15 (IL-15) has been implicated in both inflammation and bone destruction. In the present study, we investigated the genetic effect of IL-15 polymorphism on bone mineral density (BMD) in postmenopausal women. IL-15 polymorphisms were genotyped in study participants (n = 728). BMD at the lumbar spine and proximal femur was measured using dual-energy X-ray absorptiometry. We found that IL-15+13815A>T polymorphism was significantly associated with BMD of various bone sites. IL-15+13815A>T polymorphism was associated with high BMD of the lumbar spine (p=0.006-0.01), femoral neck (p=0.001-0.02), trochanter (p=0.009-0.05), femoral shaft (p=0.008-0.009), and total femur (p=0.008-0.04). Haplotype (ht) analyses showed that ht1 and ht2 were also significantly associated with high BMD at various sites (p=0.001-0.05). Moreover, IL-15+13815A>T polymorphism, ht1, and ht2 showed an association with risk of fracture (OR (95%CI) = 0.62(0.39-0.99), P = 0.04). These findings indicate that the +13815A>T polymorphism, ht1, and ht2 of IL-15 may be useful genetic markers for bone metabolism and risk of vertebral fracture.

Disclosures: E. Park, None.

W258

Percutaneous Injection of Allantoin Accelerates Fracture Repair. A. A. Selim*¹, K. Mezghani*², A. Abou-Samra*³, D. Al-Tamimi*⁴. ¹Biotechnology Center, KFUPM, Dhahran, Saudi Arabia, ²Mechanical Engineering, KFUPM, Dhahran, Saudi Arabia, ³Wayne State University School of Medicine, Detroit, MI, USA, ⁴Pathology Department, College of Medicine, King Faisal University, Al-Khobar, Saudi Arabia.

Allantoin is a botanical extract of the comfrey plant and is used for its healing, soothing, and anti-irritating properties. Allantoin helps to heal wounds and skin irritations and stimulate growth of healthy tissue. Its chemical formula is C₄H₆N₄O₃. It is also called 5-ureidohydantoin or glyoxyldiureide. In this study, we examined the effects of allantoin on the proliferation of the osteoblastic cell lines, MC3T3 and ROS17/2.8, in vitro; and on fracture repair in vivo. Cell cultures were treated with allantoin (1, 10 and 100 nM) for seven days (From Day 1 of culture to Day 7). On day 7, MTT (3-(4,5-dimethylthiazol-2-yl)-2,5-diphenyl tetrazolium bromide) and cell counting assays were performed to examine the effect of

allantoin on osteoblast proliferation. Allantoin significantly induced osteoblast proliferation in a dose dependent manner as compared to control cultures (35% and 56% increase for 10 and 100 nM, respectively, $p < 0.05$). It is important to mention that Carcinogenic Potency Project (CPP) studies demonstrated that allantoin has no carcinogenic effects on male or female rats and mice. We further examined the effect of allantoin on fracture repair. Experimental fractures were performed on 8-week Sprague-Dawley rats under anesthesia as follows: from an anterior incision we performed a transverse osteotomy at the mid tibia with a bone saw. The animals were then treated with vehicle or allantoin (weekly percutaneous injections; 10 mg/kg) for up to 4 weeks. Torsional biomechanical testing indicated that the stiffness of the allantoin-treated fractures was 2 fold higher than that of control groups at the two, three, and four-week time-points. The strength of the allantoin-treated fractures was 34%, 60% and 77% greater than that of controls at 2 ($p < 0.05$), 3 ($p < 0.005$) and 4 weeks ($p < 0.005$), respectively. At 4 weeks, the stiffness and strength of the allantoin-treated fractures were equal to those of the intact contralateral tibia, whereas the buffer-treated and untreated fractures were significantly weaker than the intact tibiae. These data demonstrate that percutaneous injections of allantoin accelerate fracture repair in this fracture repair model. Our data on osteoblastic cell lines in-vitro suggest the possibility that the beneficial effects of allantoin on bone may result from increasing osteoblast proliferation and thereby bone formation at the fracture site.

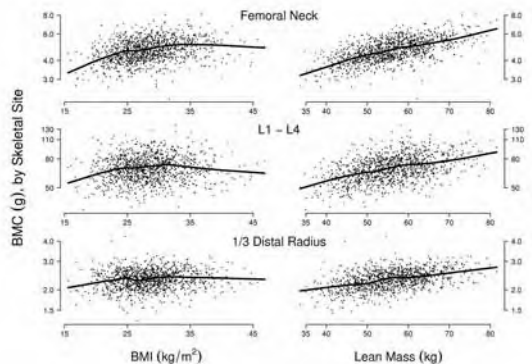
Disclosures: A.A. Selim, None.

This study received funding from: KFUPM and KFU.

W259

Threshold Associations between Aspects of Body Composition and Bone Mineral Mass. T. G. Travison, A. B. Araujo, G. R. Esche*, J. B. McKinlay. New England Research Institutes, Watertown, MA, USA.

Reduced weight is associated with decreased bone mineral content and density (BMC and BMD). It is unclear, however, whether lean mass (LM), fat mass (FM), or the combination of both (expressed through weight or BMI) is most important in stimulating osteogenesis and therefore bone strength. Using data from a racially/ethnically diverse sample of 1,209 men enrolled in the Boston Area Community Health / Bone study, we examined BMC and BMD at the hip, spine and forearm as a function of weight, body mass index (BMI), waist circumference, total body FM, and total body LM. Data were obtained on 363 non-Hispanic black, 397 Hispanic, and 449 non-Hispanic white randomly-chosen male residents of Boston, MA, USA. Subjects' ages ranged from 30 to 79 y. BMC and BMD were determined by dual x-ray absorptiometry. Analyses indicated that weight, BMI, waist circumference and FM displayed strong positive associations with BMC or BMD up to certain threshold values, beyond which associations were attenuated. LM, by contrast, displayed a strong and consistent association over all values (Figure); for instance, models controlling for fat mass and other covariates indicated a 12.8% and 9.2% increase in femoral neck BMC and BMD, respectively, per 10 kg unit in LM ($p < 0.001$). Once the effect of LM was accounted for, the magnitude and significance of associations between other parameters and BMC or BMD were sharply reduced. Percent increases in BMC or BMD corresponding to increased body size were greater in magnitude at load-bearing sites (hip and spine) than at the wrist; for instance, percent difference in BMD per 10kg difference in LM was significantly ($p < 0.001$) greater at the lumbar spine (6.9%) than the wrist (3.4%). Results were similar for all race/ethnicity groups. These results indicate that decreased body size parameters are strongly associated with decreased BMD, conferring increased risk of fracture at all sites and among all race/ethnicity groups. However, the protective effect of increased weight, BMI, waist circumference or fat mass on BMC and BMD manifests only within certain ranges of body size, beyond which the effect is diminished. On the other hand, it appears that increased LM is positively associated with BMD over the entire range of values, indicating that the protective influence of body composition on BMC or BMD is largely mediated by total lean mass.



Disclosures: T.G. Travison, None.

W260

Correlations Between Bone and Body Composition in Post-pubertal Daughters and Their Premenopausal Mothers. K. Uenishi¹, H. Ishida², M. Konishi³, Q. Zhou³. ¹Kagawa Nutrition University, Laboratory of Physiological Nutrition, Saitama, Japan, ²Kagawa Nutrition University, Laboratory of Administrative Diets, Saitama, Japan, ³GE Healthcare Asia, Shanghai, China.

Evidence suggests that both environmental and genetic factors play important roles in the development of osteoporosis. A strong correlation between lean mass (LM) and bone

mineral density (BMD) as well as bone mineral content (BMC) has been repeatedly demonstrated in individuals. However, studies of the relationships of bone and body composition values in families are lacking. Dual-energy X-ray absorptiometry (DXA) provides accurate, precise measurements of regional and total body composition. We measured total body BMD, BMC, LM, fat mass (FM), and %fat in 104 post-pubertal healthy Japanese girls (aged 19.6±1.3 years) and their healthy premenopausal mothers (aged 48.0±2.5 years) with DXA (Lunar DPX-IQ, GE-Healthcare). Pearson's correlation coefficients were calculated to examine the relationship between mothers and daughters. Weight, height, BMI, BMD, BMC, FM, LM, and %Fat showed low-to-moderate similarity between the girls and their mothers ($r = 0.23-0.47$, $p < 0.01$). Significant heritability ($h^2 \pm SE$) was detected for BMD (0.506 ± 0.03 , $P < 0.001$) and BMC measured with DXA (0.658 ± 0.04 , $P < 0.001$). Among the girls, BMD was moderately correlated with weight, BMI, FM and LM ($r = 0.34-0.49$, $p < 0.01$). While among their mother, correlations of BMD with weight, BMI and FM were slightly lower ($r = 0.26-0.31$, $p < 0.01$), and there was no significant relationship between BMD and LM ($p > 0.05$). We conclude that the bone and body composition values of these post-pubertal daughters are significantly related to their premenopausal mothers. The relationship between BMD and LM in these Japanese girls was stronger than in their mothers.

Table 1. Correlations between bone mineral and body composition in daughters

	BMD Correlation	P value	BMC Correlation	P value
FM	0.41	<0.001	0.553	<0.001
LM	0.392	<0.001	0.729	<0.001
%Fat	0.336	<0.001	0.39	<0.001
Height	0.162	0.1	0.522	<0.001
Weight	0.489	<0.001	0.737	<0.001
BMI	0.447	<0.001	0.524	<0.001

Table 2. Correlations between bone mineral and body composition in Mothers

	BMD Correlation	P value	BMC Correlation	P value
FM	0.312	0.001	0.411	<0.001
LM	0.17	0.084	0.552	<0.001
%Fat	0.268	0.006	0.261	0.007
Height	0.12	0.227	0.498	<0.001
Weight	0.302	0.002	0.525	<0.001
BMI	0.262	0.007	0.359	<0.001

Disclosures: K. Uenishi, None.

W261

Racial Differences in Skeletal Health. M. D. Walker¹, R. Babbar^{2*}, J. Vargas-Jerez¹, J. Udesky¹, C. Gagel¹, D. J. McMahon¹, R. Lantigua¹, G. Liu^{2*}, J. P. Bilezikian¹. ¹College of Physicians and Surgeons, Columbia University, New York, NY, USA, ²New York Downtown Hospital, New York, NY, USA.

Although there are racial differences in bone mineral density (BMD) and fracture risk, little data are available regarding racial differences in bone mass accrual, peak bone mass (PBMD) achieved and bone loss. We compared changes in BMD between Chinese American, Hispanic and Caucasian women across all decades of adult life. In this cross-sectional study, 1120 Chinese American and Hispanic American women, 80 per decade from age 20 to 90 in each racial group, are being recruited. Along with DXA of the total hip (TH), femoral neck (FN) lumbar spine (LS) and forearm, demographic, familial, medical, nutritional and behavioral information is being obtained. To date, 743 subjects (411 Chinese American and 332 Hispanic women) have been recruited. BMD data for these cohorts were compared to Caucasian referent values. BMD means and standard deviations for each decade were calculated. Decade means were used to approximate longitudinal changes in bone density. These preliminary data suggest that Chinese American women achieve peak bone at the LS later (age 40-49) than Caucasian or Hispanic women (age 30-39). Chinese American women achieved 96.7% of the Caucasian PBMD at the LS ($p = 0.1$), while the Hispanic group reached 99.3% of the Caucasian PBMD ($p = 0.74$). Elderly Caucasian women (age 80-89) lost 28.2% of their bone mass at the LS from peak BMD compared to 22.2% ($p < 0.01$) for Chinese American and 25.8% for Hispanic American women ($p = 0.2$). Chinese and Hispanic American women achieved peak TH BMD later (age 40-49) than Caucasian women (30-39). TH peak BMD for Chinese American women was 96.2% of the Caucasian TH PBMD value ($p = 0.1$) while TH peak BMD for Hispanic women was 104.5% of the Caucasian TH PBMD ($p = 0.04$). Aged Caucasian women (age 80-89) lost 26.6% of their bone mass at the TH from peak BMD compared to 20.7% for Chinese American ($p < 0.01$) and 20.5% for Hispanic American women ($p < 0.01$). Hispanic American women achieve peak FN BMD later (age 40-49) than Caucasian and Chinese American women (age 30-39). Chinese American women reached 93.8% of the Caucasian PBMD at the FN ($P = 0.01$). Hispanic American peak FN BMD was similar to that of Caucasian women (101.8% of Caucasian PBMD; $p = 0.51$). Elderly Caucasian women (age 80-89) lost 32.9% of their bone mass at the FN from peak BMD compared to 25.8% for Chinese American and 27.5% for Hispanic American women ($p < 0.01$). The differences we have shown in the rate of bone mass accrual and decline among these 3 groups may contribute to racial and ethnic disparities in fracture rate.

Disclosures: M.D. Walker, None.

W262

Peak Spine and Hip Bone Mass in Korean Women. Y. Won¹, H. Kim^{*1}, Y. Shin^{*2}. ¹Endocrinology and Metabolism, Kwandong University College of Medicine, Goyang, Republic of Korea, ²Clinical Nutrition Research Center, Kwandong University College of Medicine, Goyang, Republic of Korea.

The achievement of maximal peak bone mass early on in life is one of the most important strategies for prevention of osteoporosis in women. The aim of this study was to clarify the correlation between body morphometry and bone mineral density. Bone mineral density (BMD) of the spine, femoral neck, total hip, and bone mineral content (BMC) of spine, femoral neck, total hip were assessed by dual energy x-ray absorptiometry in 322 healthy women (age 20-84 years).

The peak lumbar spine BMC was gained during fifth decades (40s) of life. However, peak BMD in lumbar spine was gained during fourth decades (30s) of life. The femur neck and total hip peak BMC were gained during third decades (20s) of life. However, peak BMD of femur neck and total hip were gained during fourth decades (30s). The age was all negative significant correlation of all these bone measurements. The weight and height were all positive significant correlation of all these bone measurements. In multiple stepwise regression analysis, age and weight were independent variable on spine BMD ($R^2 = 0.305$), femur neck BMD ($R^2 = 0.294$), total hip BMD ($R^2 = 0.283$). The weight was a stronger predictor than height for all sites.

We conclude that age of attaining peak bone mass at the hip is younger than at the spine, and age and weight were most important predictor on achievement of peak bone mass in Korean women.

Disclosures: Y. Won, None.

W263

In Vivo Genome-wide Expression Study of Human Blood B Cells Suggests a Novel ESR1 and MAPK3 Network for Postmenopausal Osteoporosis. P. Xiao¹, Y. Chen^{*1}, H. Jiang^{*1}, T. L. Yang^{*1}, F. Pan^{*1}, Z. H. Tang^{*1}, Y. Z. Liu², R. R. Recker¹, H. W. Deng². ¹Osteoporosis Research Center, Creighton University, Omaha, NE, USA, ²Department of Orthopedic Surgery and Basic Medical Sciences, University of Missouri-Kansas City, Kansas City, MO, USA.

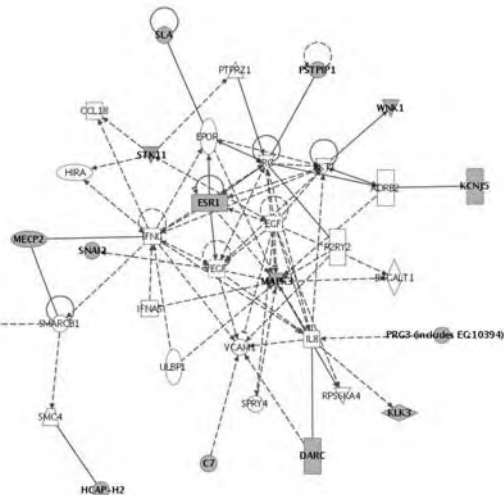
Osteoporosis is characterized by low BMD resulting from bone resorption (by osteoclasts) exceeding bone formation (by osteoblasts). Estrogen deficiency evokes increased osteoclastic activity and bone loss.

Studies showed that B cells may participate in osteoclastogenesis via expression of osteoclast-related factors, such as NF-kappaB ligand (RANKL), transforming growth factor beta (TGFB), and osteoprotegerin (OPG). However, the role of B cells in bone metabolism and osteoporosis is still largely unknown, particularly at the systematic expression level in vivo.

In this study, we recruited 20 unrelated postmenopausal Caucasian females aged 54 - 60, 10 with high (spine or hip Z-score > 0.84) and 10 with low BMD (spine or hip Z-score < -0.84). Total RNA of the freshly isolated blood B cells from those subjects were extracted and hybridized individually to Affymetrix HG-U133A GeneChip[®] arrays to identify genes differentially expressed between low and high BMD subjects. Significance of differential expression was tested by t-test and adjusted with Benjamini and Hochberg (BH) procedure for multiple-testing.

Twenty-nine genes were down-regulated in the low vs. high BMD group. Those genes were further analyzed using Ingenuity Pathways Analysis (Ingenuity[®] Systems, www.ingenuity.com) and a network involving estrogen receptor 1 (ESR1) and mitogen-activated protein kinase 3 (MAPK3) was identified (Fig. 1). Real-time RT-PCR confirmed the differential expression of 8 genes, including ESR1 ($p = 0.044$) and MAPK3 ($p = 0.002$).

This is the first in vivo genome-wide expression study on human B cells for osteoporosis. Our results suggest a novel mechanism for postmenopausal bone loss that downregulation of ESR1 and MAPK3 in B cells further regulates the secretion of factors leading to increased osteoclastogenesis or decreased osteoblastogenesis.



Disclosures: P. Xiao, None.

This study received funding from: State of Nebraska LB595 and NIH.

W264

Sarcopenia in Ageing Men with Osteopenia, Osteoporosis and Normal Bone Mineral Density. C. A. Zerbini, M. G. Pippa*. Rheumatology, Hospital Heliopolis, Sao Paulo, Brazil.

Ageing men is accompanied by a loss of muscle mass. Sarcopenia, the decrease of muscle mass with age has been widely studied because of its relation to impaired gait, disability and falls. Aimed to evaluate sarcopenia, we measured body composition (BC) in 220 men at 50 years and older by dual X-ray absorptiometry (DXA). Sarcopenia was defined as a relative skeletal muscle index (RSMI) (appendicular skeletal muscle mass divided by height) below 7.26 kg/m², according to Baumgartner classification. Osteoporosis and Osteopenia prevalence were studied as well as its occurrence in sarcopenic subjects. L1-L4 bone mineral density (BMD), femoral (FNBMD) and total body BMD (TBBMD) were also measured by DXA. Total Lean mass (TLM), Total Fat Mass (TFM), percentage of adiposity (% adp), arms lean mass (ALM), legs lean mass (LLM), and body fat distribution (BFD) were also determined. Sample was gathered in different groups according to age: 50-60y, 61-70y and 71 or older. The adherence to normal curve was evaluated by Kolmogorov Smirnov test. Cochran-Armitage Trend Test was used to test proportion linear trend. To compare the difference of quantitative variables the Student t test was used. The effective P value to be considered significant was < 0.05. Data were analysed using the statistical computer program Minitab version 15.0% and SAS version 9.1.3. The average age was 61.8 years (SD = 8.15), average weight 72.9 Kg (SD = 12.0), average L1-L4 BMD 1.146 g/cm² (SD = 0.17), FNBMD 1.366 g/cm² (SD = 0.10) and TBBMD was 1.145 g/cm² (SD = 0.10). A hundred ninety five men were not sarcopenic (88.6%) and 25 men presented sarcopenia (11.36%). Sarcopenia prevalence presented a linear decrease according to BMI increase ($p < 0.0001$). Ageing showed a linear increase in sarcopenia prevalence ($p = 0.0305$). According to FNBMD T-score, 38.8% of sarcopenic showed osteoporosis (OP); 10.5% osteopenia and 9.58% normal BMD. Using L1-L4 BMD T - score 31.5% had OP, 12.7% osteopenia and 13.12% had normal BMD. According to TBBMD T - score, 40.9% had OP, 10.5% osteopenia and 12.1% normal BMD. There was a statistic significant difference between sarcopenic group (SG) and non sarcopenic group (NSG) second these variables: age (66.3 ± 9.50 SG), (61.24 ± 7.80 NSG), p value = 0.016; BMI (21.7 ± 2.0 SG), (27.3 NSG), p value < 0.0001; TBBMD (1.041 g/cm² SG), (1.158 g/cm² NSG) $p < 0.0001$; T - score L1-L4 BMD (-1.5 SG), (-0.5 NSG), p value = 0.001; T-score FNBMD (-1.8 SG), (-1.0 NSG), $p = 0.000$. Our data confirm higher prevalence of OP in Sarcopenic as well as negative influence of ageing and lower BMI in muscle mass loss.

Disclosures: C.A. Zerbini, None.

W265

Measures of Fitness and Body Composition in Childhood Are associated with Calcaneal Quantitative Ultrasound in Adulthood: A 20 Year Prospective Study. S. J. Foley¹, S. Quinn^{*1}, T. Dwyer^{*2}, A. Venn^{*1}, G. Jones¹. ¹Menzies Research Institute, Hobart, Australia, ²Murdoch Children's Research Institute, Melbourne, Australia.

Peak bone mass is a major determinant of fracture risk later in life. Weight-bearing exercise during growth is generally accepted as one factor that can influence bone mass, however the long-term effects of childhood exercise and body composition on bone mass remain uncertain as many studies have been retrospective in design. The aim of this inception cohort study was to describe the associations between childhood physical performance measures and body mass index (BMI), and adult bone mass. We measured an Australia wide representative random sample of 1,434 children, aged 7 to 15 yrs, originally included as part of the Australian Schools Health and Fitness Survey in 1985 and approximately 20 yrs later (mean age 31). Measures included 1.6 km run and 50 meter sprint (childhood only) and leg strength, standing long jump and physical work capacity at 170 beats/min (PWC₁₇₀) (in both childhood and adulthood). Body composition was assessed at both time points by BMI. A single Sahara bone ultrasound densitometer was used at follow-up to determine heel bone mass (CV = 1%). In females, there were modest but significant beneficial relationships between physical measures and adult bone mass (1.6 km run: $r = +0.08$ to $+0.10$, $p = 0.02-0.049$; 50 m sprint: $r = +0.08$ to $+0.11$, $p = 0.03-0.10$; standing long jump: $r = +0.06$ to $+0.08$, $p = 0.20-0.33$; PWC₁₇₀: $r = +0.12$ to $+0.21$, $p = 0.004-0.09$), of which the last was independent of adult performance ($R^2 = 1-4\%$). In males, childhood BMI (but no performance measures) was positively associated with all adult QUS parameters after adjustment for adult BMI ($r = +0.11$ to $+0.12$, $p = 0.001-0.003$) ($R^2 = 1-2\%$). An age-PWC₁₇₀ interaction was documented with PWC₁₇₀ at age nine, in both sexes, having a greater influence on adult bone mass ($r = +0.25$ to $+0.32$, $p = 0.002-0.01$) ($R^2 = 5-8\%$) than it did at ages 12 and 15 ($r = -0.01$ to $+0.02$, $p = 0.80-0.97$). On further examination, a sex-PWC₁₇₀ interaction was also observed in the 12 yr olds, with childhood PWC₁₇₀ also having a positive effect on female adult bone mass ($r = +0.19$ to $+0.25$, $p = 0.045-0.13$), but not male adult bone mass ($r = -0.19$ to -0.24 , $p = 0.06-0.13$). In conclusion, childhood fitness levels, particularly in females and in the prepubertal years, are predictive of adult skeletal status as measured by QUS, explaining up to 8% of the variation in adult bone mass. Furthermore, childhood BMI in males was predictive of all adult QUS parameters. These results strongly suggest that increased skeletal loading in childhood (especially in the prepubertal years) leads to an increase in peak bone mass which is maintained many years later independent of current fitness or body mass index.

Disclosures: S.J. Foley, None.

This study received funding from: National Health and Medical Research Council of Australia, Heart Foundation of Australia, Tasmanian Community Fund.

W266

Dietary Protein and Bone Mineral Density (BMD) in the Presence of Low vs High Calcium in Men and Women of the Framingham Study. C. E. McLennan^{*1}, K. B. Broe^{*1}, K. L. Tucker^{*2}, R. R. McLean^{*1}, D. P. Kiel¹, L. A. Cupples³, M. T. Hannan¹. ¹HSL, Boston, MA, USA, ²HNRC-Tufts, Boston, MA, USA, ³BUSPH, Boston, MA, USA.

Short-term metabolic studies show that increasing dietary protein creates negative calcium balance, yet epidemiologic studies support a beneficial effect of protein on bone. However, long-term influences of typical protein intake may rely upon concurrent calcium. We examined the cross-sectional association of dietary protein on BMD in presence of low calcium in Framingham Offspring and Original Cohort members. We hypothesized that protein intake would be positively associated with BMD only in those with low calcium.

3,988 participants (2919 Offspring members with BMD obtained in 1996-2000, and 1069 Original Cohort members with BMD from 1988-89 or 1992-93) had BMD obtained at femoral neck (FN), trochanter (TR) and lumbar spine (LS). Dietary protein and calcium intakes were estimated via 126-item Willett food frequency questionnaire. At each BMD site, by sex and by cohort, we used multivariable linear regression to examine the association of BMD with %protein (% of total energy from protein) adjusted for calcium intake (mg/d), indicator of calcium < 800 mg/d, total energy, age, weight, height, current smoking, vitamin D, supplement use of calcium or vitamin D, and in women menopause and estrogen use. Further models adjusted for physical activity, caffeine and alcohol. We then stratified by low calcium (< 800 mg/d) adjusting for calcium intake within strata.

Mean age of Original Cohort members was 75 (SD 5) and of Offspring cohort was 60 (SD 9). Mean %protein intake was 16% and 17% respectively. Over 60% of both groups had calcium intake < 800 mg/d. No associations were seen between protein and BMD in either men or women of elderly Original Cohort (all p>0.30). In Offspring cohort, no associations were seen in men but there was positive effect between protein and all 3 BMD sites in 1639 women. Adjusting for physical activity, caffeine or alcohol did not change results. Upon stratifying (table), similar though not significant results were seen for 1006 women with low calcium while no association was seen for 633 women with calcium ≥ 800.

Calcium intake modified the cross-sectional effect of dietary protein on BMD but only for middle-aged Offspring cohort women. Our findings suggest that protein and BMD studies may also need to consider concurrent calcium intake.

Table: Framingham Offspring Women, Protein coefficient

	All Women Beta (SE), p-value	Calcium<800mg/d Beta (SE), p-value	Calcium>800mg/d Beta (SE), p-value
FN	.00194 (.0009), 0.03	.00173 (.0011), 0.11	.00133 (.0017), 0.44
TR	.00199 (.0008), 0.01	.00187 (.0008), 0.057	.00120 (.0016), 0.45
LS	.00272 (.0014), 0.05	.00256 (.0016), 0.107	.00153 (.0026), 0.56

Disclosures: M.T. Hannan, None.

This study received funding from: NIH.

W267

Clusters of Dietary Protein and Relation to Bone Mineral Density (BMD) in Men and Women of the Framingham Offspring Study. K. L. Tucker^{*1}, N. Qiao^{*1}, C. E. McLennan^{*2}, K. E. Broe^{*2}, R. R. McLean^{*2}, D. P. Kiel², L. A. Cupples^{*3}, M. T. Hannan². ¹HNRC, Tufts University, JM USDA, Boston, MA, USA, ²HSL Institute for Aging Research, Boston, MA, USA, ³BUSPH, Boston, MA, USA.

Several studies have shown that dietary protein intake may be protective of BMD rather than contributing to calcium loss. We have previously shown a positive relation between BMD and protein in the elderly Framingham Original Cohort. As protein-rich foods are also rich sources of other nutrients, we now further examined this relation by food source of dietary protein in the primarily middle-aged members of the Framingham Offspring cohort.

We evaluated the cross-sectional relation between food sources of protein and BMD in 2919 Framingham Offspring Study participants (mean age 61y) with BMD at femoral neck (FN), trochanter (TR) and lumbar spine (LS) obtained by Lunar DPX-L in 1996-2000. Dietary intakes were estimated using the Willett 126-item food frequency questionnaire and we used cluster analysis to classify individuals into 5 groups determined by major source of protein (table). Multivariable linear regression was used to compare least-squares adjusted mean BMD among protein clusters, adjusting for: total energy, sex, age, weight, height, smoking, total protein intake, calcium, vitamin D, physical activity, caffeine, alcohol and in women, menopause status and estrogen use. We further adjusted for fruit and vegetable servings, an indicator of overall healthy diet also associated with higher BMD.

The dietary cluster for which the primary source of protein was low-fat milk had significantly greater FN and TR BMD than the other clusters (this cluster also tended to have greater LS BMD, p<0.10). Associations remained after further adjustment for fruit and vegetable servings.

In summary, increased protein intake continues to be associated with higher BMD, but a dietary pattern with primary protein sources of low-fat milk and breakfast cereal appears to have the greatest effect, even after adjusting for calcium, vitamin D and fruit and vegetable intakes. These findings show that the beneficial effect of protein on BMD may depend upon the source from which protein is obtained.

Least Squares Mean BMD ± SE across protein clusters for Framingham Offspring Participants					
	Cluster 1: Low-fat milk cereal, etc. (N=337)	Cluster 2: Fish, beans, rice, other grain, etc. (N=561)	Cluster 3: Poultry (N=551)	Cluster 4: Meat, whole milk, etc. (N=690)	Cluster 5: Bread, egg, other dairy, processed meat, pasta, etc. (N=598)
FN BMD	0.9519±0.009	0.9238±0.008*	0.9261±0.008*	0.9180±0.007*	0.9300±0.008*
TR BMD	0.8252±0.009	0.8066±0.007	0.8013±0.008*	0.7976±0.007*	0.8062±0.008
LS BMD	1.2841±0.014	1.2501±0.012†	1.2621±0.012	1.2496±0.011†	1.2627±0.012

*Significantly different from cluster 1 at p<0.05

†Significantly different from cluster 1 at p<0.10

Disclosures: M.T. Hannan, None.

This study received funding from: NIH.

W268

Withdrawn

W269

Vitamin D status and Bone Health in Adolescents: The Northern Ireland Young Heart's Project. T. R. Hill^{*1}, J. Wallace^{*2}, P. J. Robson^{*2}, W. Dubitzky^{*2}, L. Murray^{*3}, J. Strain^{*2}, A. Flynn^{*1}, M. Kiely^{*1}, K. D. Cashman¹.

¹Department of Food and Nutritional Sciences, University College Cork, Cork, Ireland, ²Northern Ireland Centre for Food and Health, University of Ulster, Coleraine, United Kingdom, ³Department of Epidemiology and Public Health, Queens University, Belfast, United Kingdom.

Our objective was to investigate the relationship between vitamin D status {as measured by serum 25-hydroxyvitamin D [25(OH)D]} and adolescent bone health.

The present cross-sectional study used data from the Northern Ireland Young Heart's Project cohort of adolescents, which included 468 girls and 458 boys, aged either 12 or 15 yr who were sampled throughout the year. Bone mineral density (BMD) was measured by DXA at the non-dominant forearm and dominant heel. Stored serums were analysed for 25(OH)D, parathyroid hormone (PTH), osteocalcin (OC) and C-telopeptide of collagen metabolism (CTX) using enzyme-immunoassays. Multivariate models were used to examine the relationship between bone parameters and tertiles of serum 25(OH)D.

Significant age × gender interactions (p<0.05) were evident in the bone parameters, which justified analysing each age-gender group separately. After adjustment for physical, lifestyle and dietary variables, there was no significant association between tertiles of serum 25(OH)D on heel BMD in any of the age-gender groups. In addition, no significant associations were observed between tertiles of serum 25(OH)D and forearm BMD in boys. However, after adjustment for physical, lifestyle and dietary variables, girls in the highest tertile of serum 25(OH)D had significantly (p<0.05) higher forearm BMD than did the girls in the lowest tertile (β = 0.018; 95% CI: 0.003, 0.033; and β = 0.018; 95% CI: 0.001, 0.034, for 12 and 15-y old girls, respectively). Mean serum 25(OH)D levels for the lowest, middle and highest tertile of serum 25(OH)D in girls were 35.1, 58.7 and 94.6 nmol/l. In general, biochemical bone indices (PTH, OC, CTX), after adjustment for covariates, were significantly (p<0.001-0.082) higher in girls (aged 12 and 15-y olds) in the lowest tertile compared to those in the highest tertile of serum 25(OH)D. When limiting the female subjects to only those sampled in winter (December to February), when vitamin D status is at its lowest, girls in the lowest tertile of serum 25(OH)D (mean: 33.5 nmol/l) had significantly (p = 0.05) lower forearm BMD (β = 0.016; 95% CI: -0.00005, 0.033) compared to those in the highest tertile (mean: 81.0 nmol/l). In conclusion, low vitamin D status appeared to be related to lower bone mass and higher bone turnover in adolescent girls, but not in boys. This may have an impact on peak bone mass development in girls.

Disclosures: T.R. Hill, None.

This study received funding from: Higher Education Authority, Ireland.

W270

Higher Dietary Calcium Intake along with Higher Vitamin D Status Could Suppress Bone Turnover and BMD Decrease in Asian Osteoporotic Patients. T. Hirota¹, H. Ikeda^{*1}, K. Hirota^{*2}. ¹Research Laboratory, Tsuji Academy of Nutrition, Osaka, Japan, ²Department of Obstetrics and Gynecology, Nissay Hospital, Osaka, Japan.

Recently some data failed to prove that calcium and vitamin D supplementation reduces the risk of fractures in Caucasian population. The purpose of this study was to evaluate the effects of dietary calcium intake and vitamin D status on bone turnover and BMD in osteoporotic Asian women whose habitual intake of calcium is thought to be much lower and vitamin D is higher than that of Western people.

We evaluated 215 postmenopausal Japanese women (aged 49-87 yrs, median 67 yrs) diagnosed as osteoporotic by L2-4 BMD or vertebral fractures. They had not taken any medicines affecting endocrine systems and bone turnover for 2 months nor bisphosphonates for a year. Subjects could walk and visit the physicians as out patients. Their calcium intakes were evaluated by food frequency questionnaires and vitamin D status was determined from serum 25-hydroxyvitamin D [25(OH)D] measured by RIA. Markers of bone turnover, including serum bone-specific alkaline phosphatase (BAP), osteocalcin (OC), procollagen type I N-propeptide (PINP) for bone formation, and urinary deoxypyridinoline (DPD), type I collagen N-telopeptide (NTX) for bone resorption, along with serum PTH and 1,25(OH)₂D were determined. The BMD of the lumbar spine and the total hip was measured by DXA.

The mean calcium intake in the patients was 814±307 mg/day, which was much higher than non-osteoporotic postmenopausal controls (548±257 mg/day, n=158 aged 45-74 yrs), probably due to an improvement in diet following awareness of a previous calcium shortage. However, their mean serum 25(OH)D was 43±13 nM, which was still low compared with that reported for healthy, elderly, Japanese women. Calcium intakes in patients were negatively associated with all bone turnover markers (BAP, OC, PINP, DPD and NTX). Serum 25(OH)D was negatively associated with OC and DPD, as well as PTH. The association of 25(OH)D with bone resorption markers (DPD, NTX) was clearly observed in younger patients (aged 49-66 yrs). These associations were independently observed after adjustment for 25(OH)D and calcium intake. Higher calcium intake (more than 800 mg/day), together with higher 25(OH)D status (more than 50 nM) showed not only a significant additive decrease in NTX and BAP, but also a significantly higher hip BMD.

We suggested that many osteoporotic patients could improve their diets and succeed in calcium intake but not vitamin D. Higher dietary calcium intake and vitamin D status could suppress bone turnover and BMD decrease in Asian osteoporotic patients. We recommend therapy for osteoporotic patients should include dietary calcium intake greater than 800 mg/day and serum 25(OH)D status of more than 50 nM.

Disclosures: T. Hirota, None.

W271

Differential Accumulation of Lead and Zinc in the Tidemark of Normal and Osteoarthritic Human Articular Cartilage and Subchondral Bone. N. Zoeger^{*1}, J. G. Hofstaetter², P. Roschger³, C. Jokubonis^{*1}, G. Pepponi^{*4}, G. Falkenberg^{*5}, R. Simon^{*6}, P. Fratzl^{*7}, A. Berzlanovich^{*8}, C. Strelti^{*1}, P. Wobraschek^{*1}. ¹Vienna University of Technology, Atomintstitut, Vienna, Austria, ²Ludwig Boltzmann Institute of Osteology at the Hanusch Hospital of WGKK and AUA Trauma Centre Meidling and Department of Orthopaedics, Medical University of Vienna, Vienna, Austria, ³Ludwig Boltzmann Institute of Osteology at the Hanusch Hospital of WGKK and AUA Trauma Centre Meidling, 4th Medical Dept., Hanusch Hospital, Vienna, Austria, ⁴ITC-irst, Centro per la Ricerca Scientifica e Tecnologica, Trento, Italy, ⁵Hamburger Synchrotronstrahlungslabor HASYLAB am Deutschen Elektronen- Synchrotron, Hamburg, Germany, ⁶Institut für Synchrotronstrahlung, Forschungszentrum Karlsruhe, Karlsruhe, Germany, ⁷Max-Planck Institute of Colloids and Interfaces, Dept. of Biomaterials, Potsdam, Germany, ⁸Department of Forensic Medicine, Medical University of Vienna, Vienna, Austria & University of Munich, Munich, Germany.

Little is known about the spatial distribution of the toxic element lead (Pb) and other trace elements in normal and osteoarthritic articular cartilage and subchondral bone. We assessed the elemental distribution of lead (Pb), zinc (Zn), strontium (Sr) and calcium (Ca) using synchrotron radiation induced micro X-ray fluorescence (SR μ -XRF) in the chondral and subchondral bone region of 4 normal, 4 osteoarthritic femoral heads and 3 normal patellae from adults with no history of work-related exposure to Pb. SR μ -XRF line and area scans in confocal geometry were correlated to backscattered electron images visualizing mineralized tissue. We found a highly specific accumulation of Pb in the tidemark, the transition zone between calcified and non-calcified articular cartilage. Pb fluorescence intensities in single tidemarks of normal samples were 13-fold higher when compared to subchondral bone and were strongly correlated with Zn, but were distinctly different from Ca and Sr. However, in the double tidemarks of osteoarthritic samples, Pb fluorescence intensities in the inner tidemark were 3-fold higher than in the outer and were approximately 36.1-fold higher when compared to subchondral bone. Interestingly, Zn-intensities did not correlate with Pb-intensities in double tidemarks. Zn-intensities were approximately 5-fold higher in both, the inner and outer tidemark, when compared to subchondral bone. Our data showed a very specific spatial accumulation of Pb in the tidemark of articular cartilage in normal and osteoarthritic samples. Temporal differences in the accumulation of Zn and Pb in the mineralization front of calcified articular cartilage suggest different mechanisms in Pb and Zn accumulation in the mineralization front.

Disclosures: J.G. Hofstaetter, None.

W272

Effect of Four Weeks of Vitamin D3 Supplementation During Late Winter on Markers of the Vitamin D Endocrine System and Bone Turnover. K. Holvik¹, A. A. Madar^{*1}, H. E. Meyer¹, C. M. Lofthus^{*2}, L. C. Stene^{*3}. ¹Institute of General Practice and Community Medicine, University of Oslo, Oslo, Norway, ²The Hormone Laboratory, Center of Endocrinology, Aker University Hospital, Oslo, Norway, ³Division of Epidemiology, Norwegian Institute of Public Health, Oslo, Norway.

A seasonal variation in vitamin D status is commonly observed at northern latitudes with a drop in serum 25(OH)D and a corresponding increase in serum PTH and bone turnover during late winter, which is most evident in non-supplement users. We investigated the effect of four weeks' daily supplementation with 10 μ g (400 IU) vitamin D3 on vitamin D metabolites, PTH, and bone turnover in healthy young adults during late winter.

In a trial designed to compare the effect of two common types of vitamin D supplement on vitamin D status⁽¹⁾, 55 men and women aged 19-48 y recruited in the community received a daily dose of 10 μ g vitamin D3 during a 4-week period in late winter 2005. Venous serum samples were drawn at baseline and after 28 days for the analysis of serum concentration of 25-hydroxyvitamin D (s-25(OH)D), 1,25-dihydroxyvitamin D (s-1,25(OH)₂D), intact parathyroid hormone (s-iPTH), and osteoclast-specific tartrate-resistant acid phosphatase (s-TRAP). As previously reported, mean s-25(OH)D increased from 44 (95% CI 38, 51) nmol/l to 78 (95% CI 72, 85) nmol/l during the period (p<0.001), and the increase did not differ according to type of vitamin D3 supplement.⁽¹⁾ Mean s-iPTH decreased from 5.85 (95% CI 5.14, 6.57) pmol/l to 4.70 (95% CI 4.14, 5.26) pmol/l; p=0.001. Mean s-1,25(OH)₂D increased slightly during the period; from 120 (95% CI 109, 131) pmol/l to 134 (95% CI 124, 144) pmol/l; p=0.057. Mean s-TRAP was 2.65 (95% CI 2.46, 2.84) U/l at baseline, and it increased to 3.03 (95% CI 2.84, 3.21) U/l; p<0.001.

We conclude that four weeks of supplementation with 10 μ g vitamin D3 led to a decrease in s-iPTH, a tendency to an increase in s-1,25(OH)₂D, and an increase in s-TRAP concentration. The suggested increase in osteoclast activity in spite of the improvement in vitamin D status and corresponding PTH suppression is surprising.

(1) Holvik K, Madar AA, Meyer HE, Lofthus CM, Stene LC. A randomised comparison of increase in serum 25-hydroxyvitamin D concentration after four weeks of daily oral intake of 10 μ g cholecalciferol from multivitamin tablets or fish oil capsules in healthy young adults. *Br J Nutr* 2007 [in press]

Disclosures: K. Holvik, None.

This study received funding from: Peter Möller (now MöllerCollett AS).

W273

Comparison of iDXA Measurements of Mid-Body Fat Mass and Tape-Measured Circumferences in Overweight Women. P. Liu^{*}, H. Shin^{*}, S. Pounds^{*}, J. Folkert^{*}, A. P. Crombie^{*}, J. Z. Ilich. Nutrition, Food and Exercise Sciences, Florida State University, Tallahassee, FL, USA.

Studies show mid-body fat is more predictive of cardiovascular risk factors than total body fat. New bone densitometers have ability to measure body fat in android (abdominal) and gynoid (hip) regions utilizing total body scans. The data comparing those values obtained by iDXA series (GE Healthcare, Madison, WI) with tape-measured circumferences in overweight women are not available. Our objective was to compare android and gynoid measurements from iDXA with tape-measured circumferences in abdominal and hip regions. Tape measurements were performed according to the USDHHS guidelines (PHS, NHANES III, 1996). Participants were 37 postmenopausal women aged 56.3±3.7 y, BMI 31.7±4.8 kg/m² (mean±SD). Results showed high correlation (Pearson's r ranging from 0.7 to 0.9) between corresponding tape-measured and iDXA-analyzed regions, all p's<0.0001. In multiple regression models with android fat (g) as dependent variable and controlled for weight and age, tape-measured abdominal circumference remained significant predictor, t-ratio=2.55, p<0.05. In models with gynoid fat (g), controlled for weight and age, tape-measured hip circumference remained significant predictor t-ratio=2.23, p<0.05. We conclude that fat mass measured by iDXA in android and gynoid regions corresponds well with tape-measured circumference values and could be utilized during the total body scan and particularly rendered useful if there is no trained personnel to perform tape measurements in overweight women.

Disclosures: J.Z. Ilich, None.

This study received funding from: USDA/CSREES/NRI #2004-05287.

W274

Influence of Overweight/Obesity on BMD of Various Skeletal Sites in Early-Postmenopausal Women. P. Liu^{*}, J. Folkert^{*}, S. Pounds^{*}, H. Shin^{*}, A. Crombie^{*}, J. Z. Ilich. Nutrition, Food and Exercise Sciences, Florida State University, Tallahassee, FL, USA.

We reported earlier that higher body weight was associated with higher BMD in women of wide age range. However, excess weight beyond BMI of 30 kg/m² was not associated with additional increase in BMD. The objective of this study was to examine closer the relationship between weight and BMD in either overweight or obese postmenopausal women. Participants included 37 early (from 2-10y) postmenopausal women aged 56.3±3.7 y who were classified according to their BMI as either overweight (BMI=25-29 kg/m², n=17), or obese (BMI>30 kg/m², n=20). BMD of the whole body, femur (neck, Ward's triangle, shaft, trochanter and total femur), lumbar spine and forearm were measured with iDXA (GE Healthcare, Madison, WI). Non-parametric statistics was used

and based on Mann-Whitney tests, obese women did have statistically higher BMD at radius, total forearm, Ward's, trochanter, shaft and total femur (all $p < 0.05$). There was no statistical difference in spine, femoral neck and total body BMD between overweight and obese women. Based on this preliminary study focused on overweight/obese postmenopausal women only, it appears that weight status classified as obesity might lead to higher BMD in some skeletal sites compared to just overweight. More studies with larger sample size are necessary to gain better understanding of the influence of overweight/obesity on BMD.

Disclosures: J.Z. Ilich, None.

This study received funding from: USDA/CSREES/NRI #2004-05287.

W275

Isoflavone and Soya Foods Intakes in Brazilian Population: Data from the BRAZOS Study. N. O. Jacques^{*1}, J. P. Roque^{*1}, M. M. Pinheiro², R. M. Ciconelli^{*3}, M. B. Ferraz^{*3}, L. A. Martini¹. ¹Nutrition, Universidade de Sao Paulo, Sao Paulo, Brazil, ²Reumatology, UNIFESP, Sao Paulo, Brazil, ³Paulista Center of Economy in Health, CPES, UNIFESP, Sao Paulo, Brazil.

Epidemiological studies have been demonstrated a positive association between dietary isoflavones and/or soy foods and bone mineral density. The purpose of present study was to evaluate the mean isoflavone and soy foods intake in men and women older than 40 years. This study was part of the Brazilian Osteoporosis Study (BRAZOS). A total of 2392 subjects (1693 women) were enrolled in the nutritional evaluation at the BRAZOS Osteoporosis Study - BRAZOS, undertaken in 120 cities across 5 regions (North, Northeast, Central, Southeast and South) of the country, and included people from five categories of economical level (from A to E). The sampling was based in the census data from IBGE (Brazilian Institute of Statistics and Geographic) 2000 and PNAD (National Research of Home Sampling) 2003 and it was calculated accordingly with the probabilistic and representative sample of Brazilian population. Dietary intakes were evaluated by a 24h Food Record. For the nutrient analysis the Nutrition Data System software (Minneapolis, MN 2005) was used. The use of supplements was not considered in the present analysis. Statistical analysis was performed by SPSS (v 12.0). Student T test was used for gender comparison and One way ANOVA for comparisons between regions and economical level. Data was log-transformed since there are no normal distribution in isoflavone intakes. Significance was considered as $p < 0.05$. Data is presented as median (min-max). The isoflavone/soy intake in the population evaluated was very low, only 1% of the sample presented an isoflavone intake higher than 1 mg/day. Considering the isoflavone intake in all participants, the mean daidzein was 0.08 mg/d (0.01-69.5) and the mean genistein was 0.03 mg/d (0.01-64.8). The mean genistein intake in men was 0.02 mg/d (0.01-15.78) and in women was 0.13 mg/d (0.01-69.54). For daidzein the mean intake in men was 0.03 mg/d (0.01-11.93) and in women 0.03 mg/d (0.01-69.54). No significant differences were observed between gender and between regions of the country. The major contributors to isoflavone intake were soy milk and soy grains, 52% and 28%, respectively. Besides soy milk and soy-grains, there was others foods that contributed to isoflavones intake, as such as: wholemeal bread, meat-substitute foods containing textured vegetable protein, soy protein isolate and toasted soy beans. Considering the benefits of isoflavones intake for bone health, the nutritional advice for osteoporosis patients, besides calcium and vitamin D, should include an increase in soy products.

Disclosures: N.O. Jacques, Wyeth Health Consumer 2.

This study received funding from: Wyeth Health Consumer.

W276

Low-Level Radiation Can Enhance Trabecular Bone Quantity and Architecture. L. Karim^{*1}, M. Vazquez^{*2}, S. Judex¹. ¹Stony Brook University, Stony Brook, NY, USA, ²NSRL, Upton, NY, USA.

Detrimental effects of high-level radiation exposure to the skeleton range from cell death to cancer and may be strongly catabolic to the skeleton, in particular to trabecular bone. Charged particle radiation such as iron ions and its secondary fragmentation products are of particular concern due to their high charge and energy deposition. However, little is known about the long-term effects of these particles, applied at relatively low-levels, on trabecular and cortical bone morphology. Here, it was hypothesized that even low-level charged particle radiation can deteriorate bone quantity and architecture. Adult male C57BL/6J mice were exposed to full-head FE ion radiation (56-Fe, 1 GeV/n) with only 14% exposure for the appendicular skeleton at 120 cGy (16.8 cGy to the extremities), 60 cGy (8.4 cGy to the extremities), or 0.0 cGy (age-matched controls) for 11.5 months (n=11 per group). The metaphysis, epiphysis, and mid-diaphysis of the femurs were analyzed for differences in bone quantity and architecture by microCT. Three-point bending tests evaluated cortical bone mechanical properties. In the metaphysis, 8.4 cGy radiated femurs had significantly greater ($p < 0.05$) bone volume fraction (+61%) and trabecular number (+17%) than controls. In the epiphysis, the same mice showed a 31% greater bone volume fraction and a 31% smaller structural model index (a smaller structural model index is typically associated with greater bone strength). Bones radiated at 16.8 cGy showed a similar trend as 8.4 cGy mice but morphological indices were not significantly different from controls. There were no significant differences in cortical bone morphology between any radiated group and control mice. The mechanical tests revealed that bone's material properties did not deteriorate upon radiation at either level. In contrast to our original hypothesis, this data indicated that low-level iron radiation may enhance, rather than deteriorate, trabecular bone in the femoral metaphysis and epiphysis of mice. Mice receiving the smallest dosage showed the greatest beneficial response. The mechanisms by which these anabolic and/or anti-catabolic effects were induced remain to be determined but may be related to processes involving cell differentiation and proliferation, in particular for cells of the more radio-sensitive osteoclast lineage.

Disclosures: S. Judex, None.

W277

Does Pre- or Post-menopausal Soy Consumption Affect Postmenopausal Bone Loss? C. J. Lees, H. Chen^{*}, J. R. Kaplan^{*}. Wake Forest University School of Medicine, Winston-Salem, NC, USA.

Chronic soy consumption has been associated with a decreased incidence of hip fracture in Asian women, an effect often attributed to the estrogen-like compounds (isoflavones) found in soy. However, it is not known whether pre- or post-menopausal soy exposure initiated in fully adult individuals will affect postmenopausal bone loss.

Ninety-six female *Macaca fascicularis* were randomized into 2 dietary treatments that differed only in major protein source, casein/lactalbumin or isoflavone-enriched soy. The animals consumed these diets for 30 months and then all were ovariectomized (OVX). Post-OVX, one half of monkeys in each diet treatment switched to the opposing diet while the remainder continued to consume their original diet, resulting in 4 pre and postmenopausal treatment conditions (casein-casein [CC], casein-soy [CS], soy-casein [SC], soy-soy [SS]). Bone mass was determined throughout the pre-menopausal phase and six months after OVX. Percent change was calculated from 30 month pre-menopausal and 6 postmenopausal measurements.

All groups had a significant decrease in whole body (WB, $p < 0.04$) and lumbar vertebral bone mineral content (LVBMC, $p < 0.03$).

	% Change in WBBMC	% Change in LVBMC
CC	-11.9	-9.1
CS	-5.2	-4.2
SC	-9.9	-10.7
SS	-9.9	-7.5

In the immediate postmenopausal period, consumption of soy significantly slowed the rate of bone loss, but only in animals that had consumed casein diet in the pre-menopausal period. Pre-menopausal consumption of soy did not affect the rate of bone loss during the first 6 months after OVX.

Disclosures: C.J. Lees, None.

This study received funding from: NIH.

W278

Use of a Web-Based Fracture Risk Assessment Tool. B. Ettinger¹, C. Gross¹, K. Cody^{*2}, R. Walker^{*3}. ¹Medicine, University of California, San Francisco, CA, USA, ²Foundation for Osteoporosis Research and Education, Oakland, CA, USA, ³Walker Associates, Long Beach, CA, USA.

Current methods for interpretation of bone densitometry results are inadequate. Reporting of T-score has been the standard for many years, but experts throughout the world have called for a more accurate and clinically useful report format. We modified an existing fracture risk model that was developed at Kaiser Permanente's Division of Research* and made it available to providers through the Foundation for Osteoporosis Research and Education (FORE) website. The model calculates 10-year fracture risk and portrays patient risk graphically, categorized into 3 zones: "low-green" 20%. The interactive model will be available at the poster site for ASBMR attendees and for general use at <http://riskcalculator.fore.org>.

Physicians who had referred at least one patient to FORE's densitometry service during 2004-2006 were mailed invitations to use the fracture assessment tool on a special FORE-sponsored password-protected website. We assessed the percentages of invitees who logged on to the site and who performed a patient calculation using the tool.

Of 241 providers who received the mailed invitation 11 (4.9%) logged on to the fracture risk assessment website within 8 weeks. Of those logging on, 10 (91%) completed the necessary quantitative data entry fields (age, height, weight, total hip Z-score, spine Z-score), answered 7 yes/no clinical questions (prior osteoporotic fracture, mother/sister with hip fracture, current smoking, alcohol intake >2 drinks/day, exposure to glucocorticoids, rheumatoid arthritis), and submitted these data for risk calculation. The median usage of the risk calculator among those with any usage was 3 times. When invitees were categorized into 4 quartiles based on number of prior DXA referrals, there was a trend for greater likelihood of using the tool with greater prior referral: 1 referral (n=60) 3.3% use; 2-5 (n=69) 1.4%; 6-20 (n=56) 5.4%; >20 (n=56) 7.1%.

We conclude that, based on a mailed outreach and web-based practicum, only a small percentage of providers referring patients to a well-recognized center of bone densitometry excellence appear to be interested in learning about fracture risk assessment. In the near future, fracture risk assessment is expected to become a key element of densitometry reporting and would likely become the standard method for osteoporosis counseling/decision-making. More efforts will be necessary to reach providers and teach them how to interpret and use fracture risk assessment.

* Ettinger B, Hillier TA, Pressman AR, Che M, Hanley DA. Computer model for calculating fracture risk. J Women's Health 2005; 14:158-172.

Disclosures: B. Ettinger, None.

This study received funding from: Procter & Gamble.

W279

Progression of Vertebral Deformities but no Change in Bone Mineral Density in Patients with Sarcoidosis: A 4 Year Follow-up Study. A. Heijckmann¹, M. Drent^{*2}, A. Nieuwenhuijzen Kruseman^{*3}, P. Geusens³, M. Huijberts^{*3}. ¹Internal Medicine, Hospital Bernhoven, Veghel/Oss, The Netherlands, ²Sarcoidosis Management Center, University Hospital, Maastricht, The Netherlands, ³Internal Medicine, University Hospital, Maastricht, The Netherlands.

Introduction: Several disease related factors may influence bone mineral density (BMD) and bone quality in sarcoidosis. We have previously demonstrated in a cross-sectional study that BMD is unaffected in a large cohort of individuals with sarcoidosis. Nevertheless, increased bone turnover and a high prevalence of vertebral deformities (20%) were found in these patients. This may imply that bone strength rather than BMD is decreased in sarcoidosis. The aim of this study was to determine whether this may have consequences for the incidence of new or progressive vertebral deformities during follow up.

Methods: BMD of the hip (DXA) and vertebral fracture assessment (VFA) with a lateral single energy densitometry was performed at baseline and follow-up (45 months, range 35-49) in 66 patients with sarcoidosis. In addition, clinical risk factors and glucocorticoid use were assessed. Potential predictors of new or progressive vertebral deformities were assessed using logistic regression analysis.

Results: The BMD of the total group was unchanged after follow up, even in the groups with current or previous glucocorticoid use. The prevalence of vertebral deformities increased from 20 to 32% of all subjects, and in 17 subjects one or more new or progressive vertebral deformities were diagnosed (26%). 84% of the subjects with a new or progressive deformity had a BMD in the low normal range (T-score \leq -0.5). Logistic regression analysis revealed that a lower T-score of the femoral neck at baseline (OR=2.5 (CI: 1.0-5.9), p=0.04) and a mother with a hip fracture (OR=14.1 (CI: 1.4-142.6), p=0.02) were determinants for new or progressive vertebral deformities.

Conclusions: Our study shows that in subjects with sarcoidosis the number of vertebral deformities increases in the course of this disease, despite unchanged BMD. The combination of a low normal bone mass in combination with a family history of fragility fractures contributes to an increased risk of the incidence of these deformities.

Disclosures: A. Heijckmann, None.

W280

To What Extent do Vertebral Fractures, Disc Height Loss, Low Bone Density, and Poor Muscle Strength Contribute to Hyperkyphosis in Older Women? D. M. Kado¹, K. Prenovost^{*1}, L. Palermo², K. Stone³, T. A. Hillier⁴, S. R. Cummings³. ¹Medicine, UCLA, Los Angeles, CA, USA, ²UCSF, San Francisco, CA, USA, ³California Pacific Medical Center Research Institute, San Francisco, CA, USA, ⁴Center for Health Research, Kaiser Permanente, Portland, OR, USA.

Thoracic hyperkyphosis has been traditionally attributed to underlying fractures of the thoracic spine, but only 36-38% of those with the worst kyphosis have underlying fractures. Since thoracic hyperkyphosis is associated with adverse health outcomes including poor pulmonary and physical function, and increased mortality, we sought to determine other important, and possibly modifiable causes. Using baseline data from the Study of Osteoporotic Fractures, we randomly sampled 1196 women, aged 65 or older who had baseline radiographs available to measure Cobb angle kyphosis (T4-T12), disc heights (T4-T12), and prevalent vertebral deformities (3SD definition, from T4-L5). Participants also underwent baseline calcaneal bone mineral density and hip abduction strength testing, and answered questions regarding their medical history and health behaviors. Because vertebral fractures represent a continuous rather than discrete break in bone, we examined both a dichotomous vertebral fracture index and anterior to posterior vertebral height ratios from T4 to T12. We hypothesized that even if not classifiable as a vertebral fracture, vertebral wedging may substantially contribute to degree of kyphosis. In multivariable regression, the vertebral height ratio (averaged over T4-T12) independently explained 60% (consistent with previous literature), average disc height ratio explained 22%, and a paternal history of stooped posture explained 0.2% of Cobb angle variance. All reported values are squared semi-partial correlations that factor out inter-correlations among predictors, that in this case also included prevalent vertebral fractures, calcaneal bone mineral density, and hip abduction strength (each explaining less than 0.1% of Cobb angle variance). The overall total adjusted R² for this model was 74.2%. Whether osteoporosis treatments can decrease vertebral wedging and improve kyphosis is unknown.

Disclosures: D.M. Kado, None.

This study received funding from: NIH/NIAMS and NIA AG24246.

W281

5 Year Incidence of Fractures in Patients with Severe Osteoporosis: The Canadian Multicentre Osteoporosis Study (CaMos). S. M. Kaiser¹, G. Ioannidis², J. Lorraine³, W. P. Olszynski⁴, J. C. Prior⁵, D. A. Hanley⁶, J. P. Brown⁷, A. Papaioannou², R. G. Josse⁸, T. Anastassiades⁹, K. Siminoski¹⁰, S. Kirkland¹, C. Joyce^{*11}, D. Goltzman¹², J. D. Adachi². ¹Dalhousie University, Halifax, NS, Canada, ²McMaster University, Hamilton, ON, Canada, ³Eli Lilly and Company, Toronto, ON, Canada, ⁴University of Saskatchewan, Saskatoon, SK, Canada, ⁵University of British Columbia, Vancouver, BC, Canada, ⁶University of Calgary, Calgary, AB, Canada, ⁷Laval University, Sainte-Foy, PQ, Canada, ⁸University of Toronto, Toronto, ON, Canada, ⁹Queen's University, Kingston, ON, Canada, ¹⁰University of Alberta, Edmonton, AB, Canada, ¹¹Memorial University, St. John's, NF, Canada, ¹²McGill University, Montreal, PQ, Canada.

WHO defines patients with severe osteoporosis as those with a bone mineral density (BMD) T-score of < -2.5 and one or more fragility fractures. Patients with multiple fragility fractures also have severe bone disease. To assess future fracture risk, we classified CaMos participants 50 years and older, into two "severe" groups, and two comparator groups, according to their prevalent fracture status and BMD T-scores: (1) Severe Group 1: patients defined by the WHO classification (SG1, n=372, 91.4% women); (2) Severe Group 2: patients with 2 or more prevalent fragility fractures irrespective of their BMD T-score (SG2, n=390, 78.5% women); (3) Low BMD group (LG): patients with BMD T-scores ≥ -2.5 and no prevalent fragility fractures (n=3498, 67.7% women); and (4) Normal BMD group (NG): patients with T-scores > -1 and no prevalent fragility fractures (n=1437, 58.7% women). Multivariable logistic regression analyses were conducted to examine differences between the "severe" groups, and the two comparator groups, in the likelihood of developing a new fracture. Subclinical vertebral fractures were not examined, and fractures of the fingers, toes and face were excluded. Odds ratios (OR) and 95% confidence intervals (CI) were calculated. Over the 5 year period, 25.7% (80/331), 24.2% (80/315), 7.1% (221/3096), and 5.2% (66/1272) of the SG1, SG2, LG and NG developed new fractures. The likelihoods of developing a new fracture are summarized in the table below.

Group	OR vs NG (95% CI)	OR vs LG (95% CI)
SG1 men and women	3.86 (1.12,13.35)	2.47 (1.05, 5.85)
SG1 women only	7.53 (0.80, 70.7)	2.58 (0.81, 8.22)
SG2 men and women	3.35 (1.12, 10.08)	2.49 (1.06, 5.84)
SG2 women only	15.69 (1.87, 131.60)	4.00 (1.26, 12.70)

Subjects with severe osteoporosis, either as defined by WHO or as defined by having 2 or more fragility fractures, are more likely to develop a new fracture as compared with participants with no prevalent fragility fractures and normal or osteopenic BMD T-scores.

Disclosures: S.M. Kaiser, Alliance for Better Bone Health 5; Servier 5; Novartis 5; Eli Lilly and Company 5.

This study received funding from: Government of Canada, Pharmaceutical Industries.

W282

An Epidemiological Study of Hip Fractures in Korean Women: Estimated from a National Health Insurance Claims Database. H. Kang^{*1}, K. Yang^{*2}, S. Moon³, S. Kwon^{*4}, J. Park^{*5}, D. Kang^{*6}, S. Park^{*7}. ¹School of Public Health, Yonsei University, Seoul, Republic of Korea, ²Orthopaedics, Yonsei University, Seoul, Republic of Korea, ³Orthopedics, Yonsei University, Seoul, Republic of Korea, ⁴Orthopaedics, Catholic University, Seoul, Republic of Korea, ⁵Orthopedics, Konkuk University, Seoul, Republic of Korea, ⁶Severance Hospital Clinical Trial Center, Yonsei University, Seoul, Republic of Korea, ⁷Health Insurance Review Agency, Seoul, Republic of Korea.

Purpose: Previous epidemiologic studies in Korea were limited because the incidence rate was derived from the population in a single region and they require extrapolation from small populations to the national level. Thus, this study was conducted to provide a national estimate of population incidence rates of hip fracture in Korean women over the age of 50 using the Korean National Health Insurance (NHI) claims database. **Methods:** All claims records of visits or admissions of female patients aged 50 or older, containing a diagnosis of hip fracture (fracture of femur (ICD-10 code: S72), fracture of neck of femur (S72.0, S72.00), perthrochanteric fracture (S72.1, S72.10), fracture of pubis (S32.5, S32.50), osteoporosis with pathological fracture (M80.05, M80.55, M80.85, M80.95)) from 2002 to 2004 were identified from the NHI claims database. The first 6-month period (January - June, 2002) was set to be a 'window period,' such that patients were defined as incident cases only if their first records of fracture visit or admission was observed after June 30, 2002. Among the incidence cases identified, we excluded traumatic fractures and those with multi-fracture. **Results:** Average annual incidence was 17,826 fractures. Age-standardized annual incidence rates adjusted to Korean population of 2000 and to US non-Hispanic population of 1990 were 305.0 and 459.2 per 100,000 women, respectively. The incidence rate of hip fracture increased with age, ranging from 22.0 per 100,000 for 50-54 years old to 1,988.5 for 85 or older. Mortality rate within 1 year following hip fracture was 177.3 per 1,000 patients, with an increase in an exponential fashion after age 65. **Conclusion:** Our results support a high incidence rate of hip fracture for women living in Korea. The high incidence rate is a sentinel signal of the impact of hip fracture in Korea, in terms of high mortality, morbidity, and health care costs to treat hip fracture. It is hoped that this national epidemiological study contributes to raising the awareness of hip fractures among elderly population and to motivating the adoption of effective treatment options for osteoporosis needed to prevent the increase in hip fracture.

Disclosures: H. Kang, Sanofi-Aventis 2.

This study received funding from: Sanofi-Aventis.

W283

Risk Factors for Osteoporotic Fractures in Brazilian Men and Women - The Brazilian Osteoporosis Study (BRAZOS). M. M. Pinheiro¹, R. M. Ciconelli^{*1}, L. A. Martini², M. B. Ferraz^{*1}. ¹Rheumatology, Unifesp, Escola Paulista de Medicina, Sao Paulo, Brazil, ²Nutrition, Faculdade de Saude Publica, Universidade de Sao Paulo, Sao Paulo, Brazil.

Background/ Aims: Osteoporotic fractures are an important public health problem in worldwide. Several European, North American and Asian studies have demonstrated that the identification of risk factors for osteoporosis has a relevant role to early diagnosis and for treating people at high risk. The BRAZOS is the first epidemiological study performed in a representative sampling of the Brazilian population. The purpose of the present study was to evaluate the risk factors for osteoporotic fractures in Brazilian men and women older than 40 years. **Patients and Methods:** A total of 2420 subjects (1695 women) were enrolled in the BRAZOS study - BRAZOS, undertaken in 120 cities across 5 regions (North, Northeast, Central, Southeast and South) of the country, and included people from five categories of economical level (from A to E). This study evaluated aspects on lifestyle, fractures, dietary intake, physical activity, falls, quality of life, willingness to pay and knowledge on osteoporosis by quantitative and personal research that was applied in a face-to-face way. The sampling was based in the census data from IBGE (Brazilian Institute of Statistics and Geographic) 2000 and PNAD (National Research of Home Sampling) 2003 and it was calculated accordingly with to the probabilistic and representative sample of Brazilian population. The coefficient of variation is 2.2% with 95% confidence interval. After that, the data were slanted to total Brazilian population. **Results:** Subjects were classified as White (50%), Mixed Race (35%), Black (13%), Asian (1%) and Indian (1%) race. Mean age, height and weight for men and women were 58.4±12.8 and 60.1±13.7 years, 1.67±0.08 and 1.56±0.07 m and 73.3±14.7 and 64.7±13.7 kg, respectively. Men (56%) and women (51%) had BMI > 25.1 kg/ m2. Menopause's mean age was 47 years and 39% of them were at postmenopausal and 15% was currently taking hormone therapy. Osteoporotic fracture was reported by 5.29% of the subjects and the main skeletal sites were forearm, femur, ribs, spine and humerus. Osteoporosis was observed in 6% of this population. **Conclusions:** Our results have demonstrated that main risk factors for osteoporotic fractures in Brazilian men and women were age, sedentary, familial history of hip fracture, smoking and low intake of calcium and vitamin D. This study suggests that a better comprehension of clinical risk factors in our population could be an important tool to identify men and women with higher risk for osteoporotic fractures.

Disclosures: M.M. Pinheiro, Grants from Wyeth Health Consumer 2.
This study received funding from: Wyeth Health Consumer.

W284

National Differences in the Risk for Falls and Fractures. L. Dukas^{*1}, M. Runge^{*2}, E. Schacht³. ¹Acute Geriatric University Clinic, Kantonsspital Basel, Basel, Switzerland, ²Center for Muscle and Bone Research, Aerpah Klinikum, Esslingen, Germany, ³Zurich Osteoporosis Research Group ZORG, Zurich, Switzerland.

A Creatinine clearance (CrCl) of <65ml/min. was described in multiple national studies from Germany, Switzerland and the USA as a significant risk factor for falls and fractures. In a multinational study in 7 different European countries including Russia we investigated this association. We also investigated if there are national differences in the risk for falls and fractures. For this cross-sectional study data we included 1190 women and 127 men aged 60 years and older with a mean BMI of 27.2kg/m2 and a mean CrCl of 58.6ml/min., newly diagnosed and therefore untreated osteoporosis. Patients with a CrCl of <65ml/min. had in multivariate controlled analyses a 72% significantly increased risk for falls (RR 1.72, 95%CI 1.30-2.29, p<.001) and a 47% significantly increased risk for fractures (RR 1.47, 95%CI 1.05-2.07, p=.02) compared to patients with a CrCl of >65ml/min. Interestingly we found a multivariate-controlled significant difference in fall incidence according to the country of origin: Within the past 12 months we found in patients from Russia, Lithuania, Hungary, Romania and Slovenia a 40-70% higher incidence of falls and fractures compared to patients from the Czech Republic and Latvia (p=0.04 res. p<.0001). In this study we found that a CrCl of <65ml/min is a significant risk factor for falls and fractures and are thereby inline with the results of other studies. We also found that the country of origin is also a significant risk factor for falls and fractures in elderly people. This result might be explained by the well-known national differences in the health and nutritional status of elderly people.

Disclosures: E. Schacht, Teva Pharmaceutical Industries 3.
This study received funding from: TEVA Pharmaceutical Industries.

W285

Detection of Prevalent Vertebral Fractures Using a Combination of Physical Examination Maneuvers. K. Siminoski¹, K. Lee^{*2}, H. Jen^{*2}, R. Warshawski^{*2}. ¹Radiology and Internal Medicine, University of Alberta, Edmonton, AB, Canada, ²Radiology, University of Alberta, Edmonton, AB, Canada.

Studies of several physical examination maneuvers have shown that they can be used to detect prevalent vertebral fractures when used individually. In this study, we have assessed the accuracy of vertebral fracture detection when the results of three such maneuvers are combined into a single spinal evaluation. Subjects were women referred for specialist assessment of osteoporosis (n=241; average age 53.5 yrs; range: 18-92 years). Vertebral morphometry was performed on all subjects from T4 to L4. Prevalent vertebral fracture was defined as a vertebral height ratio < 0.80. One or more fractures were present in 24.7%; the average number of fractures among those with fractures was 2.2. Three physical parameters were determined: HHL (historical height loss, tallest recalled height minus current measured height using a wall-mounted stadiometer), WOD (wall-occiput distance, the distance between the back of the head and the wall, with the patient standing erect and with feet and buttocks touching the wall, facing forward in the Frankfort plane, quantified using a tape measure); and RPD (rib-pelvis distance, the distance between the top of the pelvis and the lowest rib in the mid-axillary line, in fingerbreadths). Points were assigned to each of the physical findings as follows: HHL: ≤ 2.0 cm = 0 points, 2.1 to 4 cm = 1 point, 4.1 to 6.0 cm = 2 points, 6.1 to 8.0 cm = 3 points, > 8 cm = 4 points; WOD: ≤ 3 cm = 1 point, 3.1 to 6.0 cm = 2 points, ≥ 6 cm = 3 points; RPD: 0 fb = 4 points, 1 fb = 3 points, 2 fb = 2 points, 3 fb = 1 point, 4 fb = 0 points. The values for the three maneuvers were added to produce a score for each patient (referred to as the Combined Score) and the accuracy of the Combined Score for vertebral fracture detection was assessed. The area under the receiver operating characteristics curve was 0.78 (95% confidence interval, 0.72-0.85; p<0.001). Accuracy results are shown in the table. A Combined Score < 3 rules out the presence of vertebral fracture with moderate accuracy (negative predictive value of 84% in this population) while a Combined Score ≥ 6 rules in the presence of vertebral fracture with moderate accuracy (positive predictive value of 82%). Combining physical exam maneuvers that assess spinal deformity may lead to enhanced detection of prevalent vertebral fractures.

Score	Accuracy of Combined Physical Exam Score			
	LR	OR	Sens	Spec
>7	15.4	55.0	19	99
6-7	7.0	24.9	41	96
4-5	1.3	4.8	62	80
3	0.9	3.1	73	67
2	0.6	2.1	89	41
0-1	0.3	1.0	100	0

LR= likelihood ratio; OR = odds ratio; Sens = sensitivity; Spec = specificity

Disclosures: K. Siminoski, None.

W286

Prognostic Factor on MRI Findings Inducing Prolonged Intractable Pain due to Pseudoarthrosis Following Osteoporotic Vertebral Fracture. T. Tsujio^{*1}, H. Nakamura^{*2}, H. Terai^{*1}, A. Matsumura^{*1}, M. Hoshino^{*1}, A. Suzuki^{*1}, K. Takayama^{*1}, K. Takaoka¹. ¹Orthopaedic Surgery, Osaka City University Medical School, Osaka, Japan, ²Orthopaedic Surgery, Osaka City General Hospital, Osaka, Japan.

Severe pain following osteoporotic vertebral fracture usually subsides in accordance with bony union of the fracture. In some cases, however, severe pain continues due to delayed union of the fracture site in the vertebral body. The purpose of this study was to evaluate the prognostic factor of osteoporotic vertebral fracture on MRI in the early stage after the injury.

Fifty-eight patients, 62 vertebrae, with fresh osteoporotic vertebral fracture were enrolled in the study. Seven were men and 51 were women. The age at the time of injury was 73.7 years in average. Those cases were followed for six months prospectively and were judged whether bony union was obtained based on vertebral cleft within the vertebral body. In those cases, MRI findings at the time of injury both on T1 and T2 weighted image were evaluated.

Bony union was obtained in 52 cases and pseudoarthrosis was observed in 10 cases. On plain X-ray, the collapsing ratio of vertebral body at the time of injury was not different each other, but the posterior wall of vertebral body was frequently involved in the pseudoarthrosis group. Cases showing wide low intensity change in the vertebral body both on T1 and T2 weighted MRI tended to become pseudoarthrosis. Also cases having local high intensity change on T2-weighted MRI had a tendency to become pseudoarthrosis.

Recently vertebroplasty has been a treatment option for pseudoarthrosis following osteoporotic vertebral fracture. If we can estimate the prognosis of the fracture at the time of injury, we can utilize this procedure in the early stage following the fracture and prevent the prolonged pain and disability of the patients. Based on the present study, involvement of posterior wall of vertebral body, large low intensity change both on T1- and T2-weighted MRI and partial high intensity change on T2-weighted MRI seems to be prognostic factors for pseudoarthrosis.

Disclosures: T. Tsujio, None.

W287

Osteoporotic Fragility Fractures in Older Adults Admitted in a French Primary Care Department: A Prospective Population-based Study. M. Rancier^{*1}, S. Petit^{*1}, A. Bellou^{*2}, V. Pascal-Vigneron^{*1}, N. de Talancé^{*1}, I. Chary-Valckenaire^{*3}, H. Coudane^{*4}, D. Mainard^{*5}, G. Weryha¹. ¹Department of Endocrinology, CHU de Nancy, Vandoeuvre, France, ²Department of Endocrinology, Service d'Accueil des Urgences, Nancy, France, ³Department of Rheumatology, CHU de Nancy, Vandoeuvre, France, ⁴Department of Endocrinology, ATOL-Orthopedy, Nancy, France, ⁵Department of Endocrinology, COT- Orthopedy, Nancy, France

Primary care units diagnose most osteoporotic fractures. During one year we have recorded all low energy fractures in patients attending the primary care department of the University Hospital of Nancy (France). Patients are 45 years old and over.

Population: 929 women (73.8 years \pm 13.5), 365 men (65.4 years \pm 14.3).

28 died in the first month; 100 patients were already followed by a rheumatologist.

Complete exploration of osteoporosis was performed in 170 women and 72 men.

Fractures:

Women: 150 wrist; 283 femoral neck; 52 vertebra; 120 humerus; 19 pelvis; 302 other.

Men: 32 wrist; 99 femoral neck; 20 vertebra; 46 humerus; 14 pelvis; 133 other.

Fourteen double fractures; 2 triple fractures.

72% of patients experienced their first osteoporotic fracture.

Age distribution of fractures: Data are summarized in table 2. In men, fracture distribution has a bimodal shape with higher incidence in younger and older patients. In all age groups, only femoral neck fractures show the expected sharp increase in elderly.

DEXA (Z-score \pm SD): Performed in 170 women and 72 men.

Conclusion: Less than 8% of our patients are usually followed by a medical specialist of osteoporosis. Primary care units are the best place to record and patients with a recent osteoporotic fracture. The population profile is different from patient detected by DEXA in primary prevention. This assessment strongly supports the necessity of a multidisciplinary cooperation

		DEXA distribution by age		
Age		45 to 65 years	65 to 80 years	80 years and over
Femoral neck	Women	-1.266 \pm 1.013	-1.936 \pm 1.089	-2.237 \pm 1.241
	Men	-1.163 \pm 0.993	-1.338 \pm 1.328	-3.425 \pm 0.460
Lumbar spine	Women	-1.536 \pm 1.313	-2.160 \pm 1.193	-1.832 \pm 1.398
	Men	-1.660 \pm 1.517	-1.318 \pm 1.026	-2.850 \pm 0.948

		Fracture site distribution by age and sex		
Age		45 to 65 years; n=466	65 to 80 years; n=406	80 years and over; n=421
Femoral neck	M 20		M 38	M 41
	W 21		W 75	W 187
Vertebra	M 11		M 4	M 5
	W 14		W 21	W 17
Humerus	M 21		M 16	M 9
	W 34		W 38	W 48
Pelvis	M 8		M 4	M 2
	W 2		W 5	W 12
Wrist	M 19		M 12	M 1
	W 63		W 62	W 24
Other fractures	M 98		M 24	M 11
	W 126		W 107	W 69

Disclosures: G. Weryha, None.

W288

High Leisure Time Physical Activity and High BMI Protect Against Fractures, but Heavy Work and Smoking Increase Risk - A 30-Year Follow-up of 7202 Men. L. W. Wilhelmsen^{*1}, K. L. L. Landin-Wilhelmsen², P. Timpou^{*1}, A. Odén^{*1}. ¹Department of Medicine, Sahlgrenska University Hospital, Institution of Medicine, Göteborg, Sweden, ²Department of Medicine, Sahlgrenska University Hospital, Section for Endocrinology, Göteborg, Sweden.

The purpose was to study life style factors for fracture risk in a random population of 7202 men aged 46-56 years at start and followed for > 30 years (203 051 person-years). Physical activity graded from low (1) to heavy work or regular training (4). Stress was coded from never experienced stress (1) to continuous stress during last year (5) or last 5 years (6). Never smoked was coded (1), stopped smoking (2), smoking 1-14 cig:s/day (3), 15-24 cig:s/day (4) and 25 or more (5). Coffee in cups/day.

Osteoporotic fractures, n=1031, were retrieved from the hospital registers.

All variables were of significant importance for fractures except stress and coffee consumption. Fracture risk decreased with higher level of physical activity during leisure time, but increased with higher level at work (unexpected) and with increasing age. By use of Poisson regression, which included interaction between the predictor and follow up time, we could estimate how the importance of the predictor changed by time (age not included)

Variable	Hazard rate for 1 unit increase (95% CI)		
	Mean of entire follow-up period	At start	At 10 years
BMI (continuous)	0.96 (0.94-0.99)	0.94 (0.88-1.01)	0.96 (0.93-0.98)
Physical activity, leisure	0.85 (0.78-0.93)	0.67 (0.49-0.92)	0.81 (0.72-0.91)
Physical activity, work	1.08 (1.01-1.15)	1.24 (1.00-1.53)	1.11 (1.03-1.20)
Smoking	1.09 (1.03-1.15)	1.14 (0.96-1.36)	1.10 (1.03-1.17)

The effect of changes for the entire population was calculated. At the beginning of follow-up the hazard rate (HR) for previous smokers versus never smoked was 1.05, and after 15 years 1.0. Thus the 15-year horizon was selected. 49.7% were smokers, and the calculated reduction of HR after 15 years if all smokers stopped smoking was 6.9%. Low physical activity was reported by 84.2%, and if they were assumed to train regularly the estimated reduction of HR after 15 years was 6.9%. Men with BMI lower than the three cut offs 24, 25 and 26 kg/m², were 43.0%, 57.3% and 70.0%. The calculated reductions after 15 years if they instead had BMI = 24, 25 and 26 kg/m² would be 3.1%, 4.9% and 7.3%, respectively.

In summary, leisure time physical activity and high BMI protect against fractures, but heavy work activity and smoking increase fracture risk among men between age 50 and 80 years.

Disclosures: L.W. Wilhelmsen, None.

W289

Physical Impact of Morphometric Vertebral Fractures in Men: Geelong Osteoporosis Study. J. A. Pasco, M. J. Henry^{*}, S. Korn^{*}, G. C. Nicholson, M. A. Kotowicz. Clinical & Biomedical Sciences, Barwon Health, The University of Melbourne, Geelong, Australia.

This cross-sectional study compared physical functioning in elderly men with and without morphometric vertebral fractures (MVFs). Using vertebral morphometry from lateral scans of the spine (Lunar Prodigy Pro, T10-12 and L1-4), moderate and severe wedge, biconcave or compression deformities (>25% reduction in any height and accompanying area) were identified in a population-based, age-stratified, random sample of 556 men (median age 75.0yr, range 60-93; 99% white) enrolled in the Geelong Osteoporosis Study.

The timed 'Up-&Go'¹ and functional reach² tests were performed as clinical measures of functional mobility and balance, respectively. Physical activity scores, incorporating household, sport and leisure activities, were determined by questionnaire³ and categorised into tertiles representing high, medium and low levels. All statistical analyses were age-adjusted.

Fifty-five men had MVFs, 26 lumbar and 35 thoracic. Age-stratified prevalence was 4.7% for 60-69yr, 10.0% for 70-79yr, 14.6% for 80+yr and prevalence for the entire group was 8.1% (age-standardised, Australia 2001). Ninety-three percent were unaware of their vertebral deformity. MVFs were associated with longer 'Up-&Go' times (10.0 (95%CI 9.3, 10.7) vs 9.2 (9.0, 9.5) secs, P=0.03) and lower height-adjusted functional reach on the non-dominant side (31.0 (28.8, 33.2) vs 34.1 (33.4, 34.7) cm, P=0.008). No difference was detected on the dominant side. Using high physical activity scores as the referent group, there were increased odds for MVF in the medium [OR=2.45 (95%CI 1.04, 5.77)] and low [OR=2.69 (1.16, 6.27)] groups.

Despite most men being unaware of their condition, MVFs were associated with compromised functional mobility, balance and reduced levels of physical activity.

¹Podsiadlo D et al. JAGS 1991;39:142. ²Duncan P, et al. J Gerontology 1990;45:192 ³Voorrips L, et al. Med Sci Sports Exerc 1991;23:974

Disclosures: J.A. Pasco, None.

W290

Fracture and Sway Analyzed by Computed Posturography. T. Fujita¹, M. Ohue^{*2}, Y. Fujii³, A. Miyauchi³, Y. Takagi⁴, T. Sugishita^{*3}. ¹Medicine, Calcium Research Institute, Katsturagi Hospital, Kishiwada, Japan, ²Orthopedic Surgery, Katsturagi Hospital, Osaka, Japan, ³Medicine, Calcium Research Institute, Kishiwada, Japan, ⁴Medicine, National Hospital System Hyogo Chuo Hospital, Hyogo, Japan, ⁵First Division, The Tazuke Kofukai Medical Research Institute, Osaka, Japan.

In a preliminary study comparing spinal and non-spinal fracture in 723 patients consulting Osteoporosis and Osteoarthritis Clinic of Katsuragi Hospital, augmented sway was suggested in spinal but not in non-spinal fracture patients. In order to define the role of sway in each sway factor more precisely, fracture state in 420 patients with complete BMD and sway analysis were classified into 4 groups; 271 (64 %) had no fracture (O), 63 (15 %) only non-spinal fracture, 58 (14 %) only spinal fracture, and 288 (7%) both spinal and non-spinal fracture. Lumbar bone mineral density (LBMD) was measured by DXA (DPX) and distal radial trabecular bone density (t), midradial cortical bone density (c) and midradial cortical bone volume relative to the whole bone (cv) by pQCT (Norland-Stratec). Sway parameters; total length of gravity center track (LNG), track density per unit area indicating postural controlling efficiency (LNGA) and rectangular area covered by the track (REC) were measured by computed posturography (Anima) with eyes open and then closed. The difference among each group was analyzed by analysis of variance followed by multiple comparison using PLSD, Scheffe and Bonferroni-Dunn method. LMD was found to be significantly lower in B 0.810 \pm 0.03 gm/cm² (p=0.0075 and 0.0005) and S 0.851 \pm 0.02 gm/cm² (p=0.0075 and 0.0007) than in O 0.953 \pm 0.01 gm/cm² (Scheffe and Bonferroni-Dunn). LNG expressing the degree of sway was also significantly larger in B 105 \pm 11 (p=0.0046) than O, but not significantly different from O in S, 88 \pm 5 (p=0.1973), suggesting a close association of the increase of sway with spinal fracture. On eye closure, insufficient postural control efficiency in the group with spinal fracture alone became

clearer, compared with the group with both spinal and non-spinal fracture. Persistently significant negative regression was noted on pQCT-measured bone factors LNG, REC and LNG on eye closure suggesting sway aggravation on decrease of these pQCT-measured factors, whereas no significant regression of sway factors except for REC on eye closure suggesting a decreases sway on decreasing LBMD was noted, indicating different influence on sway. Computed posturography appears to be useful in evaluating sway as a risk factor for fall and fracture.

Disclosures: T. Fujita, None.

W291

Does Low Subjective Well-Being Predict Falls and Fractures in Postmenopausal Women? R. J. Honkanen¹, H. T. Koivumaa-Honkanen^{*2}, M. T. Tuppurainen¹, H. P. Kröger³. ¹BCRU, Clinical Research Center, University of Kuopio, Kuopio, Finland, ²Psychiatry, Kuopio University Hospital, Kuopio, Finland, ³Surgery, Kuopio University Hospital, Kuopio, Finland.

Some studies suggest that depression might be associated with osteoporosis. A 4-item life satisfaction (LS) scale is strongly correlated with depressive symptoms ($r=0.7$). It is associated with and predicts morbidity, mortality and health behaviour. The purpose was to examine if subjective well-being as measured with LS scale predicts falls and fractures in postmenopausal women.

The study population was formed of the 9403 OSTPRE cohort women (born in 1932-41) who responded to all the four OSTPRE enquiries in 1989, 1994, 1999 and 2004. The follow-up time was 5 years: 1999-2004. Self-reported follow-up fractures were validated by perusal of patient records: the number of women with fractures was 835, including 322 women with distal forearm fracture (DFF) and 28 women with hip fracture. A total of 3312 women reported a fall during the past 12 months in 2004. LS scale (range 4-20, mean 7.95 (SD 2.7) categorized as satisfied 4-6, intermediate 7-11, dissatisfied 12-20) was formed with four questions about happiness, interest in life, loneliness and ease of living. Logistic regression was used as the statistical method.

At baseline, the strongest correlate of LS was self-rated health ($r=0.336$ ($p<0.001$)). Also work disability and number of health disorders were associated with LS ($p<0.001$). Old fractures before year 1989 were a correlate of dissatisfaction ($r=0.035$, $p=0.001$), whereas fractures in 1989-99 were not and former DFF correlated with satisfaction $r=-0.024$, $p=0.022$.

Life dissatisfaction predicted falls: falling risk was 19 % higher in the intermediate group and 56 % higher in the dissatisfied than in the satisfied ($p<0.001$). After adjusting for weight, height, calcium intake, fracture history, time of menopause, HRT and number of health disorder (or self-rated health) these risk estimates were only slightly reduced. Life dissatisfaction did not predict fractures in general or any specific fracture type except hip fracture. As a continuous (but not categorized) variable it predicted hip fracture ($p=0.005$) with a 16.5 % increase in risk for a unit increment of LS scale. This prediction weakened but did not vanish after adjusting for weight, height, fracture and falling history, HRT, time of menopause, calcium intake and number of health disorders. Adding self-rated health to the model changed the association non-significant ($p=0.119$).

The results suggest that low subjective well-being (as an indicator of depression) predicts falls and hip fracture but not fractures in general in late postmenopausal women before old age.

Disclosures: R.J. Honkanen, None.

W292

Low-Dose Estrogen Oral Contraceptive Use and Bone Mineral Density in Adolescents and Young Adult Women. L. Ichikawa^{*1}, D. Scholes¹, A. Z. LaCroix², S. M. Ott³. ¹Group Health Cooperative, Seattle, WA, USA, ²Fred Hutchinson Cancer Research Ctr, Seattle, WA, USA, ³Univ of WA, Seattle, WA, USA.

Oral contraceptive (OC) use may adversely impact bone mineral density (BMD) in young women. Use of low-estrogen dose OC has recently been increasing, but few studies have examined the association of these OC formulations and BMD in young women. We report results from a cross-sectional study of OC use and BMD, comparing adolescents 14-18 years old and young adult women 19-30 years old. Study invitation letters were sent to potential study participants who were selected from the computerized databases of Group Health, a Washington state HMO, based on age and OC prescriptions. We enrolled 606 women who were 20 mcg ethinyl estradiol (EE) OC users ($n=148$), 30-35 mcg EE OC users ($n=241$), or OC non-users ($n=217$) at the time of their visit. OC non-users may have had some past OC use but it was limited to no use in the last 2 years and less than 8 years lifetime use. BMD (DEXA) was measured at the hip, spine, and whole body. Women were asked about their contraceptive history and OC brand and start and stop dates were collected. Data on factors related to bone health were collected using health and food frequency questionnaires. OC users were more likely to be White and smokers. Young adult women had less calcium intake and physical activity and more smokers compared to adolescent women. Average current, continuous OC use was 6 months (range 0.1-37) among adolescents and 13 months (range 0.1-135) among young adults. OC use is often intermittent and life-time exposure was 8 months (range 0.3-53) in adolescents and 42 months (range 0.3-172) in young adults. We found no association between OC group and BMD at any anatomic site among adolescents after adjusting for age, race, BMI, calcium intake, physical activity, period regularity, and current smoking status. For young adults, the adjusted mean spine BMD by OC group was significantly different with the 20 mcg EE OC users 3.5% lower compared to 30-35 mcg EE OC users ($p=0.03$) and 3.3% lower compared to OC non-users ($p=0.04$) (Table). Patterns were similar but non-significant for the hip and whole body. Results did not differ when OC non-users were restricted to those who never used in the past and the amount of past OC use of a different formulation was restricted to less than one year. Our data suggest the use of 20 mcg EE OC may suppress

bone mass accrual in young adult women.

Age Group (years)	Adjusted Mean BMD by Age Group and OC Group			
	OC Group (n)	Total hip BMD, g/cm ² (s.e.)	Spine BMD, g/cm ² (s.e.)	Whole body BMD, g/cm ² (s.e.)
Age 14-18, Adolescent women	20 mcg EE OC (n=74)	1.012 (0.012)	1.016 (0.011)	1.094 (0.009)
	30-35 mcg EE OC (n=124)	0.997 (0.010)	1.016 (0.008)	1.089 (0.007)
	OC Non-user (n=111)	0.992 (0.010)	1.003 (0.009)	1.084 (0.007)
Age 19-30, Young adult women	20 mcg EE OC (n=74)	0.960 (0.013)	1.005 (0.013)	1.098 (0.010)
	30-35 mcg EE OC (n=117)	0.988 (0.010)	1.041 (0.010)	1.120 (0.008)
	OC Non-user (n=106)	0.985 (0.011)	1.039 (0.011)	1.108 (0.008)

Disclosures: L. Ichikawa, None.

This study received funding from: US National Institutes of Health (NICHD).

W293

The Association of Pulse Wave Velocity and Bone Mineral Density. Y. Kim, Y. Kim^{*}, S. Lee^{*}. Family Medicine, Pusan National University Hospital, Busan, Republic of Korea.

Background: Increased arterial stiffness and decreased bone mass is age-related disease. So we investigated association of arterial pulse wave velocity (PWV) and bone mineral density (BMD).

Subjects and Methods: In this study, 304 postmenopausal women who underwent annual physical health check-ups recruited. Brachial-ankle PWV were measured using automated device. The BMD was measured using dual-energy X-ray absorptiometry.

Results: The mean age of the subjects was 57.3 ± 6.0 years. 202 subjects who have normal BMD and 102 subjects who have osteopenic and osteoporotic BMD. There were no significant difference of PWV between subjects with normal BMD and with osteopenic and osteoporotic BMD ($P>0.05$, 1452.6 ± 228.0 cm/sec, 1495.3 ± 247.1 cm/sec). But after adjusting for age, subjects with osteopenic and osteoporotic BMD had a significantly higher PWV ($R = 0.270$, $P<0.01$).

Conclusions: Postmenopausal women with normal BMD had a lower arterial stiffness than with osteopenic and osteoporotic BMD. This result suggest normal BMD postmenopausal women may have a lower cardiovascular disease with osteopenic and osteoporotic BMD.

Key words: postmenopausal women, BMD, PWV

Disclosures: Y. Kim, None.

W294

Clinical Risk Factors for Fracture Are Additive in Postmenopausal Women Who Are at Risk for Fracture in a Primary Care Setting. J. LaFleur^{*1}, C. McAdam-Marx^{*1}, C. V. Asche^{*1}, S. Alder^{*2}, X. Sheng^{*2}, D. I. Brixner^{*1}, S. Silverman^{*3}. ¹Department of Pharmacotherapy, University of Utah, Salt Lake City, UT, USA, ²Department of Family and Preventive Medicine, University of Utah, Salt Lake City, UT, USA, ³Cedars-Sinai/University of California, Los Angeles, CA, USA.

Background: Increasing number of clinical risk factors (CRFs) has been linked to higher fracture risk in postmenopausal (PM) patients. We characterized hip fracture (HF) risk associated with combining multiple CRFs among at-risk patients in a primary care setting.

Methods: A historical cohort study of primary care health records from 1995-2005 was conducted to identify PM patients at risk of fracture. Patients had a 395-day run-in period and an average follow-up of 29 months. CRFs of interest during run-in were age, body mass index (BMI), bone mineral density (BMD), fracture since age 50, and maternal osteoporosis history. Other CRFs including race, drug exposures, and comorbid diseases were also evaluated. Cox models were used to estimate the risks of HF over time for each CRF in univariate and multivariable models. Risks for patients with combined CRFs were calculated.

Results: We identified 50,783 patients. Mean age was 66.8 years (SD 8.6). BMD T-scores were present in 6.8% of which 52.4% and 25.9% had T-scores in the osteopenia and osteoporosis ranges, respectively. Most patients were overweight or obese (55.8% with BMI ≥ 25); 2.8% of the population was underweight (BMI < 18.5). A prior fracture since age 50 was identified in 3.5% of which 41.9% and 21.1% had a prior vertebral fracture (VF) and HF, respectively. Maternal history was not available. Race was identified for 30.9% of which 82.8% were Caucasian.

Incident HFs occurred in 0.76% with a mean time-to-event of 23 months. In univariate analyses, increasing 5-year age increments, lower BMI, prior fracture, and race were statistically significant predictors of HF risk. BMD was not significant, but the number of patients with BMD data was small. Of the primary CRFs, only age, BMI, and prior fracture were used in the multivariable models due to a lack of univariate significance or missing data.

Risks for HF were markedly higher for older patients with both low BMI and prior fractures versus younger patients with higher BMI and no fracture. Underweight patients age 70-74 with no prior fracture, a prior VF, or a prior HF had 42, 143, and 155 times the risk, respectively, compared to a younger obese woman with no fracture. These risks increased to 86, 290, and 315 for patients age 80 and above.

Conclusion: We studied the utility of CRFs for predicting HF risk in a primary care setting using historical data. CRFs for HF included age, BMI, and prior fragility fracture. The CRFs were additive, thus combinations of CRFs could be useful for identifying PM women at high risk for HF.

Disclosures: J. LaFleur, NPS Pharmaceuticals, Inc. 2.

This study received funding from: NPS Pharmaceuticals, Inc.

W295

Factors Associated with Lack of Osteoporosis Care at the Time of Fragility Fracture. J. J. Laughren*, B. G. Escott, S. E. Ward*, V. Elliot-Gibson*, D. E. Beaton*, E. R. Bogoch. Mobility Research, St. Michael's Hospital, Toronto, ON, Canada.

Purpose: Previous work has identified low rates of preventive OP care when people arrive for treatment of an OP related fracture. Identification of those least likely to be on care could help streamline or prioritize care in a busy fracture clinic. The purpose of this study is to identify the factors associated with not being on OP care at the time of presentation with a fragility fracture.

Methods: Cross sectional survey of women >40 years and men >50 years presenting to fracture clinic with a fragility fracture. Data collected at baseline via a self-reported survey included socio-demographics, previous osteoporosis diagnosis, treatment and risk factors as well as self-reported osteoporosis awareness and health beliefs. A patient was identified as receiving treatment for osteoporosis if they were taking any anti-resorptive or anabolic bone agent at the time of presentation. Potential predictors were evaluated first at a univariate, unadjusted odd-ratios of being on care and then in a multivariable logistic regression. The data was randomly split in two prior to analysis, and with the modeling rerun in a the validation set of data. Results were compared for stability between multivariable models. Adjusted odds ratios are reported from the validation model.

Results: 508 people participated in this study. The average age was 68.5 years and there were 111 (21.9%) males. 165 patients (32.5%) were on care for OP at the time of presentation. Multivariable analysis revealed that being male (adjusted OR: 3.39; 95% CI: 1.22-9.43), not perceiving that OP could have caused the fracture (adjusted OR: 6.39; 95% CI: 2.96-13.81) and not perceiving that one has low bone mass (adjusted OR: 10.78; 95% CI: 4.10-28.36) were predictive of a lack of osteoporosis care in both design and validation multivariable models. While the effect of age <60 and previous history of a fracture were not stable in both design and validation models, their effect was in the same direction. After multivariable modeling, fracture site was not predictive of being on osteoporosis care.

Conclusions: Male patients and patients with poor awareness of osteoporosis and its risks are less likely to be receiving treatment for osteoporosis at the time of fracture. While men are at lower risk of osteoporosis than women, our findings may suggest that care should be exercised not to overlook these patients should be screened at time of presentation. Patients' poor awareness of OP and its risks may be both a cause and effect of their lower rates of treatment. While patients already on treatment may be more aware of OP and its risks as a result of exposure and education, patients with poor beliefs may render them less willing to accept treatment if offered by GP or professional.

Disclosures: J.J. Laughren, None.

W296

Age Increases the Risk of Subsequent Fractures Following an Initial Fracture among Women in Managed Care Population. R. Lindsay¹, N. N. Borisov², M. Steinbuch². ¹Helen Hayes Hospital, West Haverstraw, NY, USA, ²Procter & Gamble Pharmaceuticals, Mason, OH, USA.

The study objective was to assess the risk of subsequent fracture with age among women 65 years and older utilizing integrated administrative medical claims databases (Ingenix Lab/Rx™ and Medstat MarketScan®).

A retrospective cohort study was conducted among women who presented with a new fracture between July 1, 2000 and December 31, 2003. The study included non-traumatic closed fractures at nine sites: hip, femur, tibia/fibula, humerus, clavicle, pelvis, forearm, wrist, and spine. The cohort was followed for at least 12 months after the initial fracture to identify subsequent fractures and to evaluate the proportion of women who received treatment for osteoporosis (nasal calcitonin, raloxifene, alendronate, or risendronate). From a total of 448,769 eligible women, 19,554 women were identified with a new fragility fracture during the study period. Nonvertebral fractures represented 77% of the all index fragility fractures in this population. The average follow-up time after the index fracture was 24 months (range 12 months to 54 months). During this period, 72% did not receive any treatment for osteoporosis. The occurrence of subsequent fragility fractures increased from the youngest to oldest age cohorts, peaking at 4% vertebral and 10% nonvertebral fractures.

Subsequent fractures and treatment pattern after a fragility fracture by age groups

Age groups	65-74	75-84	85+	Total
Women, N	6,138	8,679	4,737	19,554
Nonvertebral Fractures, n (%)	4,836 (79)	6,549 (75)	3,607 (76)	14,992 (77)
Subsequent Fractures, n (%)	590 (10)	991 (11)*	650 (14)**	2,231 (11)
Nonvertebral	414 (7)	697 (8)*	457 (10)**	1,568 (8)
Vertebral	180 (3)	296 (3)	196 (4)**	672 (3)
Women who did not receive osteoporosis treatment, n (%)	4,449 (72)	6,221 (72)	3,499 (74)**	14,169 (72)

*significantly different from age group 65-74 at p < 0.05

**significantly different from age groups 65-74 and 75-84 at p < 0.05

In this study, age was observed to have a significant effect on risk of a subsequent fracture after the initial fracture. The risk of subsequent fractures (vertebral and nonvertebral) increased with age. The majority of women remained untreated after their initial fracture.

Disclosures: R. Lindsay, Procter & Gamble Pharmaceuticals 5.

W297

Association of Self-Reported Frailty with Bone Mineral Density (BMD) and Incident Fractures in an Elderly Population. S. Ma, J. Oyler*, T. J. Vokes. Medicine, University of Chicago, Chicago, IL, USA.

Although BMD declines with chronological age, little is known about the association between BMD and "biological age" or frailty. The Vulnerable Elders Survey (VES-13) measures self-reported functional impairment and is widely used to assess frailty. We examined whether the VES-13 can predict low calcaneal BMD and incident fractures in the elderly.

207 elderly community subjects (age 65-95 yrs, mean 77±7 yrs, 170 women, 37 men, 127 African-Americans[AA], 80 Caucasians[CA]) had calcaneal BMD measured by the PIXI densitometer, and frailty assessed by the VES-13. Besides the VES-13 score (range 0-10), a modified score was developed that excluded age, a known strong predictor of BMD. The modified total score (range 12-60) was the sum of the points for general health, 6 functional activities and 5 activities of daily living (ADL), with higher scores reflecting greater impairment. Functional and ADL subscores were created by adding the points for the respective functional and ADL items. The two subscores were added to create a Physical subscore reflecting physical impairment without age or general health. Six years after the initial assessment, each subject or relative was contacted by phone to ascertain incident fractures and/or death. 114 of the 207 subjects completed the follow-up.

At the initial evaluation, BMD significantly correlated with age (r=-0.32), weight (r=0.56) and height (r=0.42), was higher in men and in AA. In multivariate linear regression with BMD as the outcome, only the modified total score (p=0.013) and subscores (p=0.007 for Physical) remained significant after controlling for age, weight, sex and race. Based on the model, the difference in BMD between subjects with the lowest and highest Physical subscores was 0.102 g/cm², corresponding to 1.275 T-score units and a doubling of the fracture risk.

At the follow-up evaluation, 13 of 114 subjects were deceased and 17 had incident fractures. Death was associated with higher baseline frailty using the VES-13 score (p=0.01) and even more significantly with the Physical subscore (p=0.001), providing validation for both scoring methods. Fractures were associated with lower baseline heel BMD (OR=1.65 for fracture per 1 unit T-score decrease, p=0.02). The positive association between fractures and Physical subscore was not statistically significant (p=0.06), likely due to small numbers.

We conclude that frail elderly subjects have lower calcaneal BMD than expected for their age, sex, race and weight. Assessing frailty with an easily-obtained, self-reported measure like the VES-13 can identify elderly community subjects with lower BMD who would benefit most from an aggressive approach to the diagnosis and treatment of osteoporosis.

Disclosures: S. Ma, None.

W298

Epidemiology of Chronic Obstructive Pulmonary Disease and Osteoporosis: The E.O.L.O. Study. S. Maggi¹, P. Siviore¹, S. Gonnelli², S. Battucci³, D. De Feo³, G. Guglielmi⁴, L. Sartori⁵, R. Nuti², G. Crepaldi².

¹Aging, National Research Council, Padova, Italy, ²Internal Medicine, University of Siena, Siena, Italy, ³Procter & Gamble, Rome, Italy, ⁴Department of Radiology and Division of Endocrinology, Scientific Institute Hospital "Casa Sollievo della Sofferenza, San Giovanni Rotondo, Italy, ⁵Internal Medicine, University of Padua, Padova, Italy.

Chronic obstructive pulmonary disease (COPD) is a complex disease and a major cause of morbidity and mortality worldwide. In the last few years a link has been identified between COPD and other systemic diseases, such as cardiovascular disease, diabetes and osteoporosis. Several factors contribute to the development of osteoporosis in COPD patients, such as smoking, Vit. D deficiency, low BMI, decreased free fatty mass, hypogonadism, immobility, use of glucocorticoids. (Iqbal et al., Chest 1999)

E.O.L.O. (Evaluation of Obstructive Lung disease and Osteoporosis) is a study aimed at evaluating the prevalence of osteopenia, osteoporosis and vertebral fractures in a sample of patients affected by COPD treated or not with GCs. Fifty-nine Teaching and General Hospitals in Italy participated in the study. A total of 3030 outpatients with COPD, aged 50+ yrs, were enrolled. All subjects had undergone a BMD evaluation (QUS) and a latero-lateral chest X-ray for thoracic spine evaluation.

The results of this study showed:

- The prevalence rates of osteopenia and osteoporosis in COPD patients are higher than in the general population of same age and sex (Figure)

- The frequency of osteoporosis is associated with COPD severity, even after adjusting for age, sex, BMI, smoking and GCs use (Table)

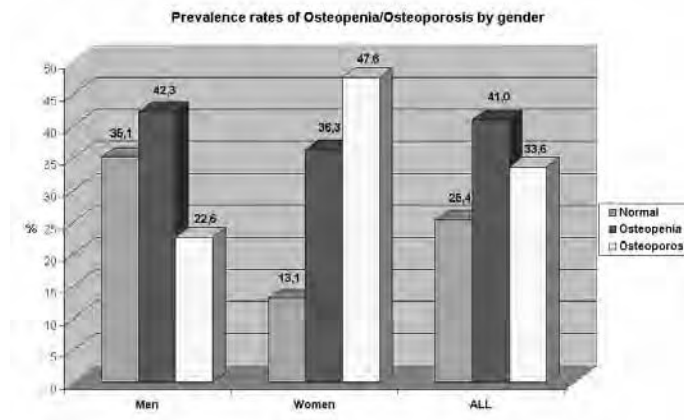
Sex-specific multivariate analyses did not show differences between men and women in the association of predictors and outcomes.

This study confirms that COPD patients are at higher risk of osteoporosis compared to the general population.

Logistic Regression Model for Osteopenia/Osteoporosis (N=2106: normal=538, osteopenia=857, osteoporosis=711)*

	OSTEOPENIA vs NO			OSTEOPOROSIS vs NO		
	OR	95% C.I.		OR	95% C.I.	
GENDER (Men)	0,395	0,307	0,508	0,136	0,103	0,178
AGE (year)	1,013	0,999	1,027	1,062	1,046	1,078
BMI (<26.6)	1,189	0,952	1,484	1,483	1,163	1,892
COPD (Severe+Much Severe)	0,851	0,667	1,087	1,405	1,079	1,830

* Variables in the model: gender, age, BMI, smoking, GCs use, COPD



Disclosures: S. Maggi, None.

W299

Effects of Doxorubicin on Bone Mineral Content and Density in Rats. M. A. McNulty^{*1}, L. C. Sharkey^{*1}, C. C. Curran^{*2}, C. S. Carlson^{*1}. ¹Veterinary Population Medicine, University of Minnesota, Saint Paul, MN, USA, ²Biostatistics Design and Analysis Center, University of Minnesota, Minneapolis, MN, USA.

Doxorubicin (DOX) is a chemotherapeutic agent commonly used to treat a variety of cancers. This agent has known cardiotoxic effects and DOX treatment has been reported to be toxic to osteoblasts in vitro; however, little work has examined its effects on bone in vivo. The purposes of this study were 1) to evaluate the effects of 6 or 8 weeks of treatment with DOX on bone mineral content (BMC) and density (BMD) in rats; and 2) to determine if these effects were influenced by strain or gender. Six- to eight-week old male and female rats of 3 different strains (SHHF, SHR, and WKY) were treated with saline (Controls) or were injected subcutaneously with 2mg/kg of DOX once per week for 6 (DOX6) or 8 (DOX8) weeks. Each group contained 6 or 7 rats for a total of 120 animals. The rats were euthanized 12 weeks after the end of the treatment period and post-mortem dorsoventral whole body bone scans were taken using a GE Lunar Prodigy Densitometer. The spine of each animal (T2-L6) was analyzed using the GE Small Animal software to determine BMC & BMD values for this site. BMC and BMD data for treatment and strain were evaluated by ANOVA, and for gender, strain, and treatment after adjusting for pretreatment body weight using ANCOVA. BMC and BMD were significantly decreased by treatment in a dose dependent manner ($P < 0.001$ for both BMC & BMD) and also were significantly affected by strain ($P < 0.001$ for both BMC & BMD). The SHHF strain had significantly higher BMC & BMD values than both the SHR & WKY strains, and the SHR strain had slightly higher BMC values and significantly higher BMD values than the WKY strain. After adjusting for all other factors, the following were observed: 1) There was a significant effect of DOX treatment on BMC & BMD ($p < 0.001$). The control group had a significantly higher mean BMC & BMD than the DOX6 group ($P < 0.05$), but not the DOX8 group; 2) There was a significant association between strain and mean BMC & BMD ($P < 0.001$), with SHHF & SHR strains having higher mean values for both than the WKY strain ($P < 0.001$); and 3) There was a significant gender by strain interaction ($P < 0.001$). Specifically, males had on average significantly higher mean BMC & BMD values than females within strains SHHF ($P < 0.001$ for both BMC & BMD) and SHR ($P = 0.001$ for BMC, $P < 0.001$ for BMD). Within strain WKY, males had slightly lower mean BMC & BMD values, but these differences were not significant ($P = 0.316$ for BMC, $P = 0.05$ for BMD). These results demonstrate that DOX treatment in young rats results in significant reductions in BMC and BMD compared with saline-treated control rats and that the choice of rat strain and gender are important considerations.

Disclosures: M.A. McNulty, None.

This study received funding from: University of Minnesota Grant-in-Aid.

W300

Long-term Use of Oral Anticoagulants and Risk for Osteoporosis. E. Stenova^{*1}, J. Payer², Z. Killinger^{*2}, L. Baqi^{*2}. ¹1st Department of Internal Medicine, University Hospital In Bratislava, Bratislava, Slovakia, ²5th Department of Internal Medicine, University Hospital In Bratislava, Bratislava, Slovakia.

Introduction: Vitamin K allows for gamma-carboxylation of glutamyl residues, a conversion that activates clotting factors and bone proteins, including osteocalcin, which is a marker of osteoblastic activity. Vitamin K antagonists such as warfarin inhibit this process. Studies of oral anticoagulant use and BMD have produced conflicting results. There were usually retrospective, limited by small sample sizes with very short follow-up period and no control group.

Aim: The presented prospective study was conducted to demonstrate the effect of long-term oral anticoagulation therapy on bone mass.

Material and Methods: 54 patients / postmenopausal female 23, male 31/ of age 50 years or older treated with warfarin of mean dosage 4,5mg per day were enrolled in this study. The

mean INR was 2-2, 5. 62 age- and sex-matched volunteers were also randomized according to same exclusion and inclusion criteria as healthy controls, without warfarin treatment. Hip and spine bone density was measured by dual X-ray absorptiometry with Hologic Delphi scanner. Sera were analyzed for osteocalcin /OSC-S/, C-terminal cross-linking telopeptide of type I collagen /CTx-S/, alkaline phosphatase /ALP-S/ and calcium /Ca-S/. 24-hour urine samples were collected for detection of urinary calcium loss /Ca-dU/. The BMD and the concentrations of laboratory markers were measured at baseline and after 12 months.

Results: No differences between warfarin-treated and control groups in markers of calcium metabolism /Ca-S, Ca-dU/, ALP-S and BMD at baseline were observed. After 12 month there was also no significant difference of these markers between treated and untreated groups. The concentrations of CTx-S / $p < 0,05$ / and OSC-S / $p < 0,001$ / were significantly lower in warfarin-treated group. We determined a significant elevation of Ca-S / $p < 0,05$ / and Ca-dU / $p < 0,05$ / after 12 month in warfarin-group. These results were not recognized in controls. There were no significant changes of BMD after 12 month in either group.

Conclusion: There were no changes of bone mineral density in both warfarin-treated and control group after 12 month. The significantly lower OSC and CTx serum levels suggest that vitamin K has an influence on bone turnover, but this effect is probably modest. The long-term anticoagulant treatment is associated with higher urinary calcium loss and elevation of calcium serum level. The mechanism of these laboratory findings is unclear and should be confirmed by other investigations including determination of vitamin D level.

Disclosures: J. Payer, None.

W301

The Osteoporosis Self-Assessment Tool vs. Alternative Triage Tests: a Comparative Systematic Review of Accuracy. B. Rud¹, J. Hilden^{*2}, L. Hyldstrup¹, A. Hróbjartsson^{*3}. ¹Osteoporosis Unit 545, Hvidovre University Hospital, Copenhagen, Denmark, ²Department of Biostatistics, Faculty of Health Sciences, University of Copenhagen, Copenhagen, Denmark, ³The Nordic Cochrane Centre, Rigshospitalet, Copenhagen, Denmark.

Previous studies have suggested that the Osteoporosis Self-Assessment Tool (OST), which is an index based on age and weight, may be as accurate as alternative triage tests in selecting postmenopausal women with low BMD for assessment by DXA. Our aim was to systematically compare the accuracy of OST and alternative triage tests in postmenopausal women.

We searched PubMed, Embase, Web of Science, citation lists and conference proceedings for studies that compare the accuracy of OST and alternative triage tests using a paired design. Our main measure of accuracy was the diagnostic odds ratio (DOR). By using the Moses-Littenberg method we summarised DOR in pair wise meta-analyses for OST and alternative triage tests when three or more studies were available, otherwise we performed qualitative summaries. We evaluated methodological quality by using the QUADAS checklist.

We identified 21 relevant studies of which 16 provided data for the pair wise meta-analyses. In whites, regardless of measurement regions and threshold for low BMD, summary estimates of DOR (sDOR) for OST were consistently at least as high as sDOR for the clinical decision rules SCORE, ORAI and SOFSURF (p -values > 0.02). By contrast, sDOR was almost twice as high for Stiffness Index assessed by quantitative ultrasonography using Achilles devices (GE-lunar) than for OST with respect to lumbar spine T-score ≤ -2.5 ($p = 0.005$). Similar results were found across measurement regions and thresholds for low BMD, although meta-analyses were unfeasible because studies were few. A few studies in whites suggested that weight is only slightly less accurate than OST regardless of how low BMD is defined. Between-study heterogeneity in estimates of DOR varied considerably between triage tests, measurement regions and thresholds for low BMD. Studies were few in Asian and black women and meta-analyses were unfeasible, but OST and alternative triage test were in general equally accurate. Methodological quality was generally low; no studies compared the accuracy of the triage tests prospectively as used by clinicians in settings where decisions about DXA referral are common.

Only the QUS variable Stiffness Index was consistently more accurate than OST in white women; however the transferability of our findings to clinical settings is uncertain due to low methodological study quality.

Disclosures: B. Rud, None.

W302

Dental Status, Low Bone Mass, and other Osteoporosis-related Conditions as Predictors of Adverse Outcomes in an Elderly Population. E. Musacchio^{*1}, E. Perissinotto^{*2}, P. Binotto^{*2}, F. Silva-Netto^{*1}, M. C. Corti^{*3}, G. Baggio^{*4}, S. Zambon^{*1}, E. Manzato^{*1}, G. Crepaldi⁵, L. Sartori¹. ¹Clinica Medica 1, Dpt of Medical and Surgical Sciences, University of Padova, Padova, Italy, ²Dpt of Environmental Medicine and Public Health, University of Padova, Padova, Italy, ³Direzione Sanitaria, ULSS 16, Padova, Italy, ⁴Azienda Ospedaliera, Padova, Italy, ⁵Institute of Neurosciences, CNR, Padova, Italy.

We have previously reported that, in an aging (65+ years old) Italian population of both sexes cross-sectionally evaluated (ProVA Study cohort), the condition of low remaining number of teeth alone identified a larger proportion of impaired subjects as compared to the presence of osteoporosis alone. We now further investigated this issue through the data resulting from the longitudinal phase of ProVA consisting of two follow up at 5 (F1) and 7 (F2) years. The prevalence of edentulism in our population was 43.7% at baseline (n=3058), 46.2% at F1 (n=2176), and 44.9% at F2 (n=160), while the prevalence of subjects with 20+ teeth was 15.8%, 13.0% and 13.1% respectively. Logistic regression analyses with stepwise forward selection were performed in order to estimate the independent contribution of number of teeth, low bone mass and other osteoporosis-related conditions - after adjustment for confounders and including in the model variables hypothesized to be in the causal pathway - at baseline, in predicting physical impairment (PI), mortality, femoral fracture and institutionalization at follow up. With respect to PI, a low basal T-score was not critical, while edentulism appeared to be an independent risk factor with an OR=1.65 (CI 95%: 1.19-2.27). A stronger significant association (OR=3.38) was found considering separately edentulous subjects that did not wear prosthesis. Interestingly, analysis at F2, which was in general consistent with that F1, revealed an effect of low vitamin D levels (OR=3.69) not present at F1. With respect to mortality, low T-score and vitamin D levels had OR=1.38 and 1.99 respectively, while for low functional remaining teeth, OR was 1.45. Incident femoral fractures were associated with low T-score (OR=2.35) and previous femoral fracture (OR=3.39), but not with the number of teeth. Institutionalization was associated with previous falls (OR=2.85). Our data support the hypothesis that, in the elderly, oral status is a more reliable tool than osteoporosis in predicting impaired physical activity and mortality. Oral condition assessment could then have a role in the daily clinical practice for the identification of subjects at risk.

Disclosures: L. Sartori, None.

W303

The Direct Assessment of Non-vertebral Fracture in Community Experience (DANCE) Study: Baseline Demographics and Reasons for Initiating Teriparatide Therapy. A. Sebba^{*1}, R. Sierra-Zorita^{*2}, P. Miller^{*3}, P. Chen^{*4}, K. Taylor^{*4}, M. Wong^{*4}, K. Krohn^{*4}. ¹Arthritis Associates, Palm Harbor, FL, USA, ²Univ of Puerto Rico School of Medicine, Hato Rey, PR, USA, ³Colorado Center for Bone Research, Lakewood, CO, USA, ⁴Eli Lilly and Company, Indianapolis, IN, USA.

Randomized, placebo-controlled clinical trials have shown the efficacy of teriparatide (TPTD) in treating osteoporosis (OP) and preventing fractures, but therapeutic decisions may differ in community practice. The ongoing, prospective, observational DANCE study examines the long-term effectiveness, safety, and tolerability of TPTD in a heterogeneous "real world" population of patients with co-morbidities, severe OP, and/or prior OP therapy, in a community setting. Study investigators prescribe TPTD 20 µg/d for up to 24 months to patients, and follow them for another 24 months. For the 4057 patients enrolled in DANCE, baseline demographics (Table) and reasons for initiating TPTD are described here.

Physicians cited reasons for initiating TPTD therapy in 4010 patients, of which 3335 (83.2%) had ≥1 fracture risk factors. The most frequent reasons included very low BMD (61.2%), previous self-reported osteoporotic fracture (33.8%), general frailty (20.7%), advanced age (18.8%), propensity to fall (17.7%), and family history of OP fractures (17.3%). In 2938 patients who previously used OP therapies, 596 patients (20.3%) had intolerance, and 2041 (69.5%) had an inadequate response, which included a decline (44.5%) or no change (10.9%) in BMD, or occurrence of new fractures (20.8%). It appears that in addition to BMD, several other clinical risk factors are important in the physicians' decisions to initiate TPTD therapy. Data from DANCE may clarify the rationale used by physicians in the community for assessing antiresorptive therapy and initiating TPTD therapy, to facilitate an evidence-based method of patient management.

Table. Baseline Demographics of DANCE Study Cohort (Mean ± SD)

Characteristic (*P<0.05 between genders)	Women (N=3653)	Men (N=404)	Overall (N=4057)
Age (years)*	68.2 ± 11.6	64.9 ± 13.3	67.9 ± 11.8
Caucasian (%)*	88.1	92.1	88.5
Lumbar Spine Bone Mineral Density (BMD) T-score*	-2.50 ± 1.40	-2.25 ± 1.48	-2.48 ± 1.41
Femoral Neck BMD T-score	-2.46 ± 0.95	-2.36 ± 0.95	-2.45 ± 0.95
% with Fragility Fractures	37.2	38.6	37.4
% with Previous OP Therapy*	87.7	60.2	85.0
% with ≥1 Active Medical Conditions	82.6	83.3	82.7

Disclosures: A. Sebba, Eli Lilly and Company 2.

This study received funding from: Eli Lilly and Company.

W304

Peripheral Artery Disease and Osteoporosis in Older Adults. D. von Mühlen^{*}, M. A. Allison^{*}, S. K. Jassal^{*}, E. Barrett-Connor. Family and Preventive Medicine, UCSD, La Jolla, CA, USA.

Increased rates of bone loss, osteoporosis and osteoporotic fractures have been reported in patients with cardiovascular disease, suggesting a relationship between osteoporosis and atherosclerosis. Limited information is available on whether low bone mass is associated with vascular disease. We examined the cross-sectional and longitudinal association between peripheral artery disease (PAD) and bone health in a sample of community-dwelling older adults. We studied 525 men and 806 women, aged 30 to 97 (mean age=73.8, SD=9.2) who attended a baseline clinic visit in 1992-1996, when ankle-brachial index (ABI) and BMD were measured, and spine x-rays were taken. In 1999-2002, 321 men and 517 women attended a follow-up visit, when BMD was re-assessed and incident OP fractures were queried. PAD defined by an ABI ≤ 0.90 was present in 15.4% of the women and 13.3% of the men. Compared to those without PAD, participants with PAD were older (77 vs. 73 years old, p<0.001), leaner (BMI = 24.5 vs. 25.3, p=0.02), and more likely to have hypertension (77% vs. 70% p=0.05), diabetes (12% vs. 7%, p=0.02) and to be current smokers (12% vs. 6%, p=0.002). They were also more sedentary (38% vs. 25%, p<0.001) and reported less frequent alcohol intake (38% vs. 47%, p=0.01) than participants without PAD. Among those with PAD, the prevalence of osteoporosis by T score at the femoral neck and hip was significantly higher in women (59% vs. 49% and 25% vs. 17% respectively, p<0.05), but not men. Women with PAD also had a significantly higher rate of bone loss at the hip (-0.85%/year vs. -0.52%/year, p=0.05). However, the associations between PAD and bone mass did not persist after adjusting analyses for age and/or body mass index. At baseline more women than men had a vertebral and/or non-vertebral osteoporotic fractures (13% vs. 8% and 12% vs. 7% respectively, all p's<0.01). After a mean follow up of 3.7 (SD=0.9) years there were no sex differences in the incidence of non-vertebral fractures (8.3% in women and 8.9% in men). PAD was not associated with prevalent or incident osteoporotic fractures in either men or women. In conclusion, we found an association between PAD with osteoporosis and bone loss in women, but not men. However, the associations were not independent of age, body weight or other confounders.

Disclosures: D. von Mühlen, None.

W305

High Prevalence of Abnormal Lumbar Spinal DXA Scans in Men Receiving Methadone Maintenance Therapy for Opiate Dependence. K. M. Wesa^{*1}, L. S. Hafner^{*2}, D. P. McGuire^{*3}, C. L. Smith¹, J. J. Monk^{*4}, G. A. Carlson^{*1}, K. E. Ensrud^{*5}, R. H. Grimm^{*1}. ¹Department of Medicine, Hennepin County Medical Center, Minneapolis, MN, USA, ²Department of Experimental and Clinical Pharmacology, University of Minnesota, Minneapolis, MN, USA, ³Thomson West, Eagan, MN, USA, ⁴Bone & Mineral Metabolism, Davita, Minneapolis, MN, USA, ⁵VA Medical Center & University of Minnesota, Minneapolis, MN, USA.

One area of chronic opiate use that has not been extensively examined is the correlation between narcotic-induced hypogonadism and associated side effects such as osteoporosis in men receiving methadone maintenance therapy (MMT). This is a case-control study comparing lumbar spine densitometry by DXA scan and sex-hormone levels in 29 men receiving MMT for opiate dependence and 28 age-matched controls not on MMT.

Serum testosterone (T), estradiol (E), luteinizing hormone (LH), sex-hormone binding globulin, albumin, 25(OH)vitamin D, 1,25(OH)²vitamin D and lumbar spinal bone mineral density (BMD) were measured in all participants. Serum samples were obtained 24 hours post methadone dosing for those on MMT.

Both groups were similar regarding age, physical activity, calcium intake and BMI. Mean length of time on MMT was 5.4 years (1 - 25, ± 5.6) with a mean daily methadone dose of 92 mg (13 - 150, ± 29).

Test	Cases mean (SD)	Controls mean (SD)	p value
Total Testosterone	339.45 (164.79)	556.71 (204.89)	0.000
Estradiol	16.86 (7.68)	27.21 (10.53)	0.000
25(OH)vit D	20.93 (12.23)	17.32(10.21)	0.232
DXA L2-4 BMD	1.159 (0.143)	1.261 (0.195)	0.029
DXA L2-4 T score	-0.679 (1.186)	0.175 (1.635)	0.029
Tobacco pack-yr	19.6 (10.57)	10.8 (15.17)	0.014
Alcohol #drinks/wk	0.62 (1.9)	8.11 (13.7)	0.008

For the cases length of time receiving MMT was negatively correlated with serum T (p=0.035). Across all subjects there was a significant negative correlation between T level and both length of time receiving MMT (p=0.001) and daily methadone dose (p=0.001). Serum T was positively correlated with E (p=0.003) across all subjects as was E level and L2-4 BMD (p=0.014). The cases had 9% lower BMD compared with the controls (p=0.029). Vitamin D deficiency was present in 25 (86%) of the cases and 25 (89%) of the controls. Controlling for tobacco exposure, daily methadone dose strongly predicts E (p=0.001) but not T (p=0.092) or BMD (p=0.068); and years of MMT strongly predicts T (p=0.000) but not E (0.261) or BMD (0.446). Controlling for alcohol use, daily methadone dose strongly predicts E (p=0.001) but not T (p=0.065) or BMD (p=0.198); and years of MMT strongly predicts T (p=0.000) but not E (p=0.339) or BMD (p=0.668).

There are many osteoporosis risk factors which are amenable to modification in the MMT population. Routine screening of sex-hormone levels, Vitamin D status and bone densitometry should be strongly considered and smoking cessation encouraged.

Disclosures: K.M. Wesa, None.

This study received funding from: Minneapolis Medical Research Foundation.

W306

Hip Geometry and Bone Fragility Among Postmenopausal Women with Rheumatoid Arthritis. N. C. Wright¹, J. Lisse^{*1}, T. J. Beck², T. Bassford^{*1}, A. Z. LaCroix^{*3}, J. A. Cauley⁴, C. E. Lewis⁵, S. B. Going^{*1}, Z. Chen¹. ¹Univ. of Arizona, Tucson, AZ, USA, ²Johns Hopkins University, Baltimore, MD, USA, ³Fred Hutchinson Cancer Research Center, Seattle, WA, USA, ⁴Univ. of Pittsburgh, Pittsburgh, PA, USA, ⁵Univ. of Alabama-Birmingham, Birmingham, AL, USA.

Bone strength, comprised of bone mineral properties and bone geometry, is one of the primary determinants of osteoporotic fractures. Rheumatoid Arthritis (RA) has also been shown to be an independent risk factor for osteoporotic fractures. The overall goal of this analysis is to investigate the impact of hip geometry on bone fragility of postmenopausal women with RA. Participants of the Women's Health Initiative Observational Study (WHI-OS) from the BMD clinical centers were included in the analysis. Arthritis status was self-reported at baseline, identifying 335 (5.8%) women with RA and 2,701 (47.1%) women without any form of arthritis. BMD and hip geometry parameters (cross sectional area (CSA), outer diameter, section modulus (SM), cortical thickness, and buckling ratio (BR)) at three hip regions (narrow neck, intertrochanter, and shaft) were derived from baseline and follow-up dual energy x-ray absorptiometry scans using hip structural analysis programs developed by Beck and colleagues. After adjusting for age, height, and weight, white women with RA (n=220) had significantly higher mean CSA, outer diameter, and SM at the narrow neck, and higher mean CSA and SM at the shaft compared to white women without arthritis (n=2,105) at baseline. No statistically significant differences by RA status were seen in African American women at baseline (RA n=69, non n=310), although having RA was associated with lower mean BMD, CSA, and SM in the narrow neck and intertrochanter, and higher means at the shaft. After adjusting for age, height, weight, and the baseline parameter, RA was associated with decreases in hip strength from baseline to year 3 in African American but not white women (Table 1: coefficients and 95% confidence intervals (CI)). Though decreases were seen in both groups, the findings suggest that RA may play a larger role in hip strength in African American women. Further investigation is needed to examine how variables such as hormone use, physical activity, and medication usage affect the relationships between hip geometry and RA.

Table 1: Associations between RA and changes in narrow neck hip strength from baseline to year 3

	White		African American	
	Coeff.	(95% CI)	Coeff.	(95% CI)
BMD	-0.005	(-0.013, 0.004)	-0.023	(-0.045, 0.000)**
Cross Sectional Area	-0.012	(-0.035, 0.012)	-0.065	(-0.135, 0.005)*
Section Modulus	0.001	(-0.015, 0.016)	-0.027	(-0.071, 0.017)
Cortical Thickness	-0.001	(-0.003, 0.001)	-0.005	(-0.009, -0.000)**
Buckling Ratio	0.151	(-0.066, 0.367)	0.250	(-0.091, 0.591)

(year 3 - baseline hip geometry) = β_1 RA + β_2 baseline hip geometry + β_3 age + β_4 height + β_5 weight + ϵ

* p<0.10; ** p<0.05

Disclosures: N.C. Wright, None.

This study received funding from: NIAMS R01-AR049411.

W307

Is Osteoporosis Related to Future Incidence of Osteoarthritis Over 10 Years, or Vice-Versa? N. Yoshimura, S. Muraki, H. Oka*, A. Mabuchi*, H. Kawaguchi, K. Nakamura. 22nd Century Medical Center, Univ. of Tokyo, Tokyo, Japan.

To learn the contribution of the presence of osteoporosis (OP) or osteoarthritis (OA), two major disorders causing disability of the elderly, to future incidence of the other disorder, a 10-year population-based epidemiological study was conducted in a cohort of a mountain area. Among the entire 1,543 participants (716 men, 827 women), 400 subjects (200 men, 200 women) were selected randomly but evenly from each generation, and evaluations of OP and OA were performed by BMD and X-ray examinations, respectively, in 1990 as the baseline study. BMD measurement was performed by DXA (Lunar DPX) at the antero-posterior projection of lumbar vertebrae (L2-4) and the proximal femur, and was repeated after 3, 7, and 10 years. The presence of OP was diagnosed by the WHO criteria. X-ray examination was performed on antero-posterior and lateral images of thoracolumbar vertebrae (Th5-L5), and was repeated after 10 years. The presence of OA was determined according to the Kellgren/Lawrence (KL) grade (0-4) at intervertebral spaces from Th5/6 to L5/S1, and those with at least one space of KL \geq 3 were diagnosed as OA. The cumulative incidences of OA at intervertebral spaces during 10 years for the subjects without OA at the baseline in their 40s, 50s, 60s and 70s were 15.6%, 24.1%, 24.2% and 34.4% for men, and 27.1%, 32.6%, 38.5% and 58.3% for women, respectively. A logistic regression analysis was carried out utilizing the incidence of OA (1: Yes, 0: No) as an objective factor and the presence of OP at the lumbar spine or the femoral neck (1: OP, 0: osteopenia or normal range) as an explanatory factor after adjustment for age. There was no significant relationship between the presence of OP at the baseline and the incidence of OA in men or women (OP at the lumbar spine; men: odds ratio [OR]=2.52, 95% confidential interval [CI]=0.57-11.3, P=0.22; women: OR=0.56, 95% CI=0.23-1.35, P=0.19), (OP at the femoral neck; men: OR=0.72, 95% CI=0.29-1.79, P=0.48; women: OR=0.95, 95% CI=0.37-2.41, P=0.91). Similarly, the presence of OA at the baseline was not significantly related to the incidence of OP during a 10 year period. In conclusion, based on the observation over 10 years of a population-based cohort, the presence of OP did not predict the future incidence of OA, or vice-versa, suggesting that these disorders have independent backgrounds.

Disclosures: N. Yoshimura, None.

W308

Effects of Treatment of Ovariectomized Adult Rhesus Monkeys with Parathyroid Hormone 1-84 on Trabecular and Cortical Bone Structure and Biomechanical Properties of the Proximal Femur. J. Fox¹, M. A. Miller¹, R. R. Recker², C. H. Turner³, S. Y. Smith⁴. ¹NPS Pharmaceuticals, Salt Lake City, UT, USA, ²Creighton University, Omaha, NE, USA, ³Indiana-Purdue University, Indianapolis, IN, USA, ⁴Charles River Laboratories, Montreal, PQ, Canada.

Treatment of monkeys and humans with parathyroid hormone 1-84 (PTH) stimulates skeletal remodeling which increases trabecular (Tb) BMD and decreases cortical (Ct) BMD at locations where these bone types predominate. We have also previously reported that daily PTH treatment (5, 10 or 25 μ g/kg) of ovariectomized (OVX) rhesus monkeys for 16 months increased bone stiffness at a lumbar vertebra, and decreased stiffness at the femoral diaphysis which led to increased work-to-failure (the energy required to fracture). We now report the effects of PTH treatment on bone structure and biomechanical properties at the proximal femur, a mixed trabecular and cortical bone site, in these monkeys. PTH reversed the OVX-induced decrease in DXA BMD within 3 to 7 months at the proximal femur, femoral neck, and distal femur. pQCT confirmed a significant dose-related decrease in Ct.BMD and increase in Tb.BMD at the total proximal femur, and proximal and distal femoral metaphyses of PTH-treated monkeys. The decrease in Ct.BMD resulted primarily from increased cortical area, because cortical bone mineral content was unaffected by PTH. Histomorphometry revealed significant dose-related increases in trabecular bone formation rate, volume, and number at the proximal femur. Trabecular thickness was unaffected by PTH. Osteoblast and osteoid surface were increased by PTH, but osteoid thickness was unaffected. Activation frequency and eroded surface were increased significantly by PTH, but osteoclast surface was unchanged. PTH did not affect periosteal or Haversian BFR at the femoral neck; however, cortical porosity was slightly, but statistically significantly higher in the 25 μ g/kg group (2.7% vs 1.5% in OVX controls). PTH treatment had no significant effects on stiffness or peak load measured using a shear test, but work-to-failure was significantly higher. Thus, PTH 1-84 treatment induced changes in trabecular and cortical bone at the proximal femur that were similar to those that occur at skeletal sites where each bone type predominates and ultimately increased the total energy required to break the proximal femur.

Disclosures: J. Fox, NPS Pharmaceuticals 1, 3.

This study received funding from: NPS Pharmaceuticals.

W309

Pharmacokinetics and Pharmacodynamics of Human Parathyroid Hormone 1-84 in Adult Ovariectomized Rhesus Monkeys. J. Fox¹, S. Y. Smith², D. S. Wells^{*1}. ¹NPS Pharmaceuticals, Salt Lake City, UT, USA, ²Charles River Laboratories, Montreal, PQ, Canada.

When administered by daily injection, human parathyroid hormone 1-84 (PTH) acts as a potent anabolic agent in bone of animals and humans, and also markedly decreases the incidence of vertebral fractures in postmenopausal women with osteoporosis. We have previously reported that daily PTH administration (5, 10 or 25 μ g/kg) for 16 months increases bone formation and BMD and improves the biomechanical properties of vertebral bodies of ovariectomized adult rhesus monkeys. We now report the pharmacokinetics of PTH and the pharmacodynamic responses that result from PTH exposure in these animals. Blood samples were collected before and for 24 hours after PTH injection on day 1, and again during months 3, 6, 12, and 16 of the study, and analyzed for PTH and Ca levels. Predose serum 25(OH)D and 1,25(OH)₂D levels and urine Ca (normalized to creatinine levels) were also measured. A dose-related linear increase in PTH C_{max} and exposure (area under the concentration-time curve) occurred. PTH doses of 5, 10 or 25 μ g/kg produced plasma PTH exposures that were 2.1-, 4.1- and 13.2-fold greater than occurred in women given a 100 μ g dose. T_{max} occurred later with the high dose (1.1 vs. 0.6 hr). Predose PTH levels were restored by \leq 6 hr with the 5 and 10 μ g/kg doses but remained elevated at 6 hr with the 25 μ g/kg dose. Serum Ca levels increased acutely in a dose-related and consistent manner following PTH administration at each time point throughout the study. When averaged across all time points, the serum Ca T_{max} occurred at 3.7, 4.8, and 7.3 hr after dosing, with a C_{max} increase of 0.6, 1.0 and 1.8 mg/dL with the 5, 10, and 25 μ g/kg doses, respectively. No sustained increases in predose Ca occurred with the 5 and 10 μ g/kg doses whereas an increase of \sim 0.6 mg/dL occurred with the 25 μ g/kg dose. Serum 25(OH)D levels were variable but tended to be lower in PTH-treated animals; the decrease was significant with the 25 μ g/kg dose at months 6 and 12. Serum 1,25(OH)₂D levels were also variable but tended to be higher in PTH-treated animals, particularly with the 25 μ g/kg dose at month 6. There were no increases in fasting predose urine Ca levels with the 5 and 10 μ g/kg PTH doses, but sustained increases occurred with the 25 μ g/kg dose. In summary, PTH exposures 4-fold those observed in women did not result in sustained increases in serum or urinary Ca in adult rhesus monkeys.

Disclosures: J. Fox, NPS Pharmaceuticals 1, 3.

This study received funding from: NPS Pharmaceuticals.

W310

Intrabone Tunneling Increases Trabecular Number at Multiple Skeletal Locations in Ovariectomized Rhesus Monkeys Treated with Parathyroid Hormone 1-84. M. A. Miller¹, S. P. Bare^{*2}, R. R. Recker², S. Y. Smith³, J. Fox¹. ¹NPS Pharmaceuticals, Salt Lake City, UT, USA, ²Creighton University, Omaha, NE, USA, ³Charles River Laboratories, Montreal, PQ, Canada.

We have reported that daily treatment of ovariectomized (OVX) adult rhesus monkeys with human parathyroid hormone 1-84 (PTH) (5, 10, or 25 µg/kg) for 16 months increased trabecular bone volume (BV/TV), number (Tb.N) and connectivity at lumbar vertebra-3 (L3) and thoracic vertebra-10. We proposed that the increased Tb.N and connectivity was achieved by stimulation of intrabone tunneling, a remodeling event orientated parallel to the long axis of a trabecula at a non-nodal location. Bone formation followed resorption thus maintaining normal trabecular thickness (Tb.Th). Collectively, these features are important determinants of bone strength. Using histomorphometry to determine frequency of events, we have now quantified intrabone tunneling at L3 and extended it to investigate the effects of PTH treatment on trabecular bone at the proximal femur, distal radius and iliac crest of these animals. At L3, tunneling frequency was low in control sham and OVX animals (~0.05/mm²) but increased significantly in PTH-treated animals (0.27, 0.49 and 0.95/mm² with 5, 10 and 25 µg/kg doses, respectively). Very similar tunneling frequencies were observed at the other 3 trabecular bone sites in all treatment groups. Iliac crest biopsies were also collected at baseline and after 6 months of treatment and showed significant time- and dose-related increases in tunnels. For example, in the 10 µg/kg PTH dose group the tunneling frequency was 0.03, 0.36 and 0.64/mm² at baseline, month 6 and month 16, respectively. Although the pattern and magnitude of response varied slightly from site to site, the PTH-induced intrabone tunneling significantly increased Tb.N, as well as BV/TV and bone formation rate at all sites. A modest but statistically significant increase in Tb.Th occurred only at the iliac crest. In summary, intrabone tunneling is rare in control monkeys, but increased substantially with PTH 1-84 treatment. This phenomenon provides a plausible explanation for the PTH-induced increase in Tb.N observed at all trabecular bone locations in OVX monkeys.

Disclosures: J. Fox, NPS Pharmaceuticals 1, 3.

This study received funding from: NPS Pharmaceuticals.

W311

The Skeletal Effects of Teriparatide in Glucocorticoid-Treated Mice. K. S. Howe¹, J. H. Long^{*1}, T. J. Wronski², U. T. Iwaniec³, R. T. Turner³, R. W. Braith^{*1}. ¹Applied Physiology and Kinesiology, University of Florida, Gainesville, FL, USA, ²Department of Physiological Sciences, University of Florida, Gainesville, FL, USA, ³Nutrition and Exercise Sciences, Oregon State University, Corvallis, OR, USA.

Synthetic analogs of glucocorticoids (GC) are widely used in treating many inflammatory diseases. However, they result in serious side effects, including osteoporosis. The purpose of this study was to determine whether treatment with teriparatide (PTH 1-34) can prevent or reverse the detrimental effects of GC on bone. Seven month old male Swiss-Webster mice were randomized by weight into 4 groups: (1) vehicle only (8 w CNTL); (2) GC for 8 w (GC8); (3) simultaneous GC and teriparatide administration for 8 w (GC+PTH8); or (4) GC for 4 w followed by GC+ teriparatide for 4 w (GC4/GC+PTH4). Either vehicle, prednisolone (2.1 mg/kg/d), or prednisolone and teriparatide (40µg/kg/d) were administered subcutaneously 6 d/w. Fluorochrome markers, demeclocycline (15 mg/kg) and calcein (15 mg/kg), were injected prior to sacrifice to label mineralizing bone. Femurs and lumbar vertebrae were harvested at the end of the 8-week study and processed for cancellous bone histomorphometry. Data were analyzed using the Kruskal-Wallis test followed by a non-parametric posthoc test.

GC treatment did not induce cancellous bone loss in adult male mice. However, GC inhibited and teriparatide increased osteoblast surface (Ob. S) and mineralizing surface (MS). Teriparatide prevented bone changes associated with GC exposure (Table). Although 8 weeks of teriparatide treatment increased BV/TV in the distal femur and lumbar vertebrae (data not shown), the relative effects were greater in the distal femur (+100%, p = 0.02) than in the lumbar spine (+42%, p = 0.01). Four and 8 w of teriparatide significantly increased Ob. S, MS, mineral apposition rate (MAR), and bone formation rate/bone surface (BFR/BS). In conclusion, teriparatide effectively prevented the inhibitory effects of GC on cancellous bone formation in the distal femur.

Changes in Distal Femur Cancellous Bone Parameters Based on Treatment with Vehicle, GC, or GC-PTH

	8 w CNTL	GC8	GC4/GC-PTH4	GC-PTH8
BV/TV	2.6 ± 1.9	3.1 ± 1.6	4.5 ± 1.7	5.2 ± 2.9 a
Ob. S	1.1 ± 1.1	0.9 ± 0.7	0.8 ± 0.6	1.7 ± 1.2 c
Ob. S	7.2 ± 3.5	2.1 ± 1.5 a	13.6 ± 12.0 b	20.0 ± 7.8 a,b,c
MS	3.1 ± 3.3	1.6 ± 1.8 a	14.2 ± 5.3 a,b	16.8 ± 8.7 a,b
MAR	0.6 ± 0.2	0.6 ± 0.2	0.9 ± 0.1 a,b	0.8 ± 0.2 a
BFR/BS	2.2 ± 3.0	1.0 ± 1.1	10.8 ± 5.7 a,b	14.8 ± 12.8 a,b

Data are reported as mean ± standard deviation. a = p ≤ 0.05 versus 8 w CNTL; b = p ≤ 0.05 versus GC8; c = p ≤ 0.05 versus GC4/GC-PTH4.

Disclosures: K.S. Howe, None.

W312

RAP-011 (a Soluble Activin Receptor Type IIA) Increases Bone Mineral Density in Combination with Prior Antiresorptive Therapy. M. Mangini^{*}, M. Cornwall-Brady^{*}, A. Pullen^{*}, K. Halley^{*}, T. Monnell^{*}, J. Milling^{*}, B. Haigis^{*}, R. Kumar^{*}, K. Underwood^{*}, R. S. Pearsall. Acceleron Pharma, Cambridge, MA, USA.

RAP-011 is a soluble activin receptor type IIA (ActRIIA) fused to a murine IgG1-Fc region. Previously, we demonstrated that treatment with RAP-011, an activin antagonist, reversed bone loss in ovariectomized mice (Pearsall et al, J Bone Min. Res. 21(S1) 2006). We have further investigated the use of RAP-011 in combination with bisphosphonate treatment in ovariectomized mice.

To investigate the bone effects of RAP-011, 8 week old female C57BL/6 mice (N=40) were ovariectomized and allowed to lose bone for 8 weeks prior to treatment. When the mice were 16 weeks old half the mice were given a single dose of zoledronic acid (ZOL, IP, 20 µg/kg). Three days later, mice began RAP-011 (IP, 1 or 10 mg/kg, biw) treatment for 8 weeks either individually or after the initial ZOL injection. Whole body DXA and pQCT scanning was performed at baseline, 4 weeks and at the conclusion of the study.

In the ovariectomized mice, treatment with RAP-011 showed a significant (p≤0.01) increase in BMD (+11%) than either ZOL (+5%) or PBS treated mice (+1%). In addition, pre-treatment with ZOL followed by RAP-011 increased BMD to a greater extent than either treatment by itself (+15%).

This data show that RAP-011 able to act as a bone anabolic agent regardless of the presence of a previously administered bisphosphonate. The data provide support for the use of soluble ActRIIA fusion proteins for the treatment of skeletal fragility regardless of prior treatment history.

Disclosures: R.S. Pearsall, Acceleron Pharma 1, 3.

W313

Protective Role of Green Tea Polyphenols in Bone Microarchitecture in Aged Female Rats. C. Shen¹, P. Wang^{*2}, J. Guerrieri^{*1}, J. Hoefler^{*3}, J. K. Yeh⁴, B. J. Stoecker³, J. Wang^{*2}. ¹Pathology, Texas Tech University Health Sciences Center, Lubbock, TX, USA, ²The Institute of Environmental and Human Health, Texas Tech University, Lubbock, TX, USA, ³Nutritional Sciences, Oklahoma State University, Stillwater, OK, USA, ⁴Medicine, Winthrop-University Hospital, Mineola, NY, USA.

Human epidemiological and laboratory studies strongly suggested that green tea polyphenols (GTP), extracted from green tea, are promising agents for preventing bone loss in women due to currently unclear mechanisms. This study was to explore the bioavailability, molecular mechanism, and efficacy of GTP in preventing bone loss in aged rats with and without ovariectomy (OVX). A 2 (Sham vs. OVX) × 3 (no GTP, 0.1% GTP, and 0.5% GTP in drinking water) factorial design using 60 aged female rats (14-mo-old) assigned to 6 groups (n=10/group): Sham, Sham+0.1% GTP, Sham+0.5% GTP, OVX, OVX+0.1% GTP, and OVX+0.5% GTP for 16 wks. Concentrations of urinary GTP ingredients and 8-hydroxydeoxyguanosine were determined by high-pressure liquid chromatography-coularray detection. Efficacy was evaluated in tibia and lumbar vertebra microarchitecture by histomorphometric and µCT analysis, respectively. GTP supplementation in drinking water increased concentrations of epigallocatechin and epicatechin in urine of rats (0, 27.8, and 46.9 µg/mg creatinine for no GTP, 0.1% and 0.5% GTP, respectively), but decreased urinary 8-hydroxydeoxyguanosine level (32.5, 27.3, and 21.8 µg/mg creatinine for no GTP, 0.1%, and 0.5% GTP, respectively). OVX resulted in lower values for trabecular bone volume, number and thickness in proximal tibia, and stiffness and force for compression of lumbar vertebra, but higher values for bone formation rates in cancellous proximal tibia as well as periosteum and endocortical tibial shaft. The results of two-way ANOVA show that GTP treatment resulted in significantly increased trabecular bone volume (F value=7.5, P<0.001), thickness (F value = 9.4, P<0.001), and bone formation rates in both proximal tibia (F value=5.4, P=0.008) and endocortical tibial shaft (F value=9.9, P<0.001), but lower values for eroded surface in both proximal tibia (F value=10.4, P<0.001) and endocortical tibial shaft (F value=20.3, P<0.001). This study demonstrates that GTP administered in drinking water for 16 weeks prevents trabecular bone loss through increasing bone formation while suppressing bone resorption. Such a protective role of GTP may, in part, be attributed to a decrease in oxidative stress DNA damage. The results merit investigation of a potentially significant prophylactic role of green tea in bone health of premenopausal and postmenopausal women.

Disclosures: C. Shen, None.

W314

Low Serum IGF-I Levels Results in Cortical Osteopenia but Increased Life Span in Elderly Mice. J. Svensson^{*}, K. Sjögren^{*}, N. Andersson^{*}, J. Jansson^{*}, O. Isaksson^{*}, C. Ohlsson^{*}. Department of Internal Medicine, Center for Bone Research, Göteborg, Sweden.

Background. It is unknown whether circulating IGF-I regulates cortical bone mass and life span in old mice.

Methods. Transgenic mice with adult, liver-specific IGF-I inactivation (LI-IGF-I^{-/-} mice) were used. These mice have an approximately 80 % reduction in serum IGF-I level. Body composition was measured using dual energy X-ray absorptiometry (DEXA). Bone mass and density was measured using peripheral quantitative computed tomography (pQCT). In addition, the life span was determined.

Results: Two-year old female mice with inactivation of liver derived IGF-I at one month of

age displayed a 25% reduction in femur cortical cross-sectional bone area at the middiaphyseal level ($p<0.05$ vs. control using pQCT). This was mainly due to a decrease in the periosteal circumference ($p<0.001$) whereas there was no significant difference in femur length. Experiments in 18-month old male LI-IGF-I^{-/-} mice with inactivation of liver derived IGF-I at one year of age demonstrated reduced body weight ($p<0.01$ vs. control) due to decreased fat mass ($p<0.01$) as measured using DEXA. In addition, in the 18-month old male LI-IGF-I^{-/-} mice, there was a 13% reduction femur cortical cross-sectional bone area at the middiaphyseal level ($p<0.05$ vs. control using pQCT), confirming that liver-derived circulating IGF-I is of importance for cortical bone mass in late life. The trabecular volumetric BMD was unaffected in all experiments. Importantly, the life span was increased in the LI-IGF-I^{-/-} mice (LI-IGF-I^{-/-} mice (n=84): 24.2 months vs. control (n=137): 22.5 months, $p<0.05$). This was mainly due to increased life span in the female LI-IGF-I^{-/-} mice (LI-IGF-I^{-/-} mice 26.7 vs. control 23.0 months, $p<0.001$). Conclusion. Deficiency of liver derived, circulating IGF-I in old mice results in decreased body weight due to decreased fat mass and markedly reduced cortical bone mass but increased life span. Thus, low serum IGF-I levels results in cortical osteopenia but increased life span in elderly mice.

Disclosures: J. Svensson, None.

W315

Dual-Action Cathepsin K Inhibitors: Regulation of Human Mesenchymal Stem Cell (MSC) Lineage Commitment. T. Twomey*, D. Chagnovich, J. Zielinski*, M. W. Long. Velcura Therapeutics, Inc., Ann Arbor, MI, USA.

Cathepsin K (CTSK), a cysteine protease secreted by osteoclasts (OC), is an attractive target for therapies aimed at osteoporosis and other bone diseases. Moreover, the recent demonstration of CTSK's expression in osteoblasts (OB) suggests that other functions exist for this enzyme. VEL-0230 is a dual-action, orally available CTSK inhibitor that has an anabolic effect on OBs (stimulation of ex vivo and in vivo bone formation) while also inhibiting osteoclast bone resorption. The effects of VEL-0230 on MSC Lineage commitment and differentiation were investigated and compared to TGF- β and BMP-6. Culture of human MSC in serum-free media containing TGF- β (200 pM), BMP-6 (2 nM), or Vel-0230 (1uM) results in OB lineage commitment and differentiation. In particular, cells so-treated undergo a process of ex vivo bone formation (a process previously described by us (Nat. Biotech 18, 954, 2000)) in which growth factor-induced OBs form tissue-like aggregates and produce microcrystalline bone. We next used transcriptional analysis to discover the molecular events underlying MSC cell-fate determination. Interestingly, comparison of induced cells to uninduced indicate a very small number of genes (60 -150) are significantly ($p<0.05$) modulated during this process. Non-supervised hierarchical clustering of TGF- β , BMP-6 and VEL-0230 expression profiles show distinct but related patterns of gene modulation suggesting different, but convergent, cellular pathways regulate OB commitment and/or differentiation. This also was illustrated in analysis of individual genes, e.g., TGF- β induction up-regulates collagen X and COMP, but down-regulates BSP; BMP-6 up-regulates the expression of Collagen X, COMP, and BSP, but Vel-0230 up-regulates BSP, and down-regulates COMP. None of these three regulators modulate myogenic or adipogenic markers. Cell pathway-mapping reveals that the canonical Wnt, BMP, and TGF- β signaling pathways play a role in MCS fate decision and that the TGF- β , BMP-6, and VEL-0230 pathways converge at Smad 2. However, siRNA-mediated knockdown of SMAD2 does not block osteoblastic commitment or differentiation of human MSC. We conclude that VEL-0230 functions in a similar fashion to the biological regulators TGF- β and BMP-6 and that these molecules function through an as yet unknown final common pathway. Importantly, they seemingly signal via a SMAD2- independent pathway suggesting either redundant or novel signaling molecules translocate osteogenic signals to the nucleus. Finally, VEL-0230 may serve as a useful therapeutic by promoting both OB recruitment from MSC, as well as OB differentiation into bone-forming cells.

Disclosures: T. Twomey, Velcura Therapeutics, Inc 1, 3.

W316

Recombinant Human Platelet-Derived Growth Factor BB (rhPDGF-BB) and Beta-Tricalcium Phosphate (β TCP) Accelerate Fracture Healing in Aged-Osteoporotic Rats. J. O. Hollinger*, A. O. Onikepe*, J. MacKrell*, T. Einhorn*, G. Bradica*, C. S. Young*, S. E. Lynch*, C. E. Hart*. ¹Carnegie Mellon University, Pittsburgh, PA, USA, ²Boston University, Boston, MA, USA, ³Kensley-Nash Corporation, Exton, PA, USA, ⁴BioMimetic Therapeutics Inc., Franklin, TN, USA.

Aged individuals with osteoporosis exhibit impaired fracture healing, and rhPDGF-BB may provide therapeutic benefit for these people. PDGF-BB released from platelets initiates wound healing by supporting neovascularization, and stimulating chemotaxis and mitosis in mesenchymal progenitor cells that differentiate to osteoblasts, chondrocytes, and vascular smooth muscle cells. The clinical efficacy of rhPDGF-BB in wound healing has been underscored in patients for periodontal applications (GEM 21S[®]) and rhPDGF-BB (GEM OS[™]) is currently in clinical trials for orthopaedic indications. The goal of this study was to demonstrate that rhPDGF-BB delivered in a collagen/ β TCP matrix accelerates fracture healing in an osteoporotic, geriatric rat model. Eighty six-week old virgin female Sprague Dawley rats were ovariectomized and placed on a 30% caloric reduced diet for 4 months to ensure osteopenia and then housed for 2 years. Transverse, mid-diaphyseal tibial osteotomies were surgically prepared and stabilized with a K-wire. Ten animals were included per treatment group as follows: fracture alone, fracture + buffer + collagen/ β TCP, fracture + 0.3 mg/ml rhPDGF-BB + collagen/ β TCP, and fracture + 1.0 mg/ml rhPDGF-BB + collagen/ β TCP and the time of sacrifice was either 3 or 5 weeks post-surgery. At each time, treated and contralateral untreated tibiae were harvested, and the bones were processed for analyses by torsional biomechanics, or microCT and

histology. MicroCT analysis indicated that β TCP particles remained around the fracture sites at both 3 and 5 weeks, but there was less material at 5 weeks compared to 3 weeks. For both rhPDGF-BB-treated groups, histology demonstrated that fracture healing was accelerated compared to either non-treated fractures or fractures treated with collagen/ β TCP alone. Torsional biomechanical testing indicated that at 5 weeks in both groups of rhPDGF-BB-treated animals there was no significant difference in torsional strength between rhPDGF-BB-treated and contralateral unfractured tibiae. In contrast, the torsional strength of the untreated and buffer-treated fractures were statistically weaker than the contralateral unfractured tibiae. In conclusion, the combination of rhPDGF-BB and a collagen/ β TCP matrix significantly accelerated fracture healing versus untreated fractures and the effect was a time-dependent increase in torsional strength.

Disclosures: C.S. Young, BioMimetic Therapeutics Inc 1, 3.
This study received funding from: Biomimetic Therapeutics Inc.

W317

Patients Treated with Risedronate Have a Fracture Risk Similar to Patients 20 Years Younger in Age. S. Boonen¹, A. Klemes², X. Zhou^{*2}, S. Pack^{*3}, P. D. Delmas⁴. ¹Universiteit Leuven, Leuven, Belgium, ²Procter & Gamble Pharmaceuticals, Mason, OH, USA, ³Procter & Gamble Pharmaceuticals, Egham, United Kingdom, ⁴INSERM Unit 403, Lyon, France.

Age is a well recognized independent risk factor for fracture. Generally, older patients have lower BMD T-scores and greater risks for fracture. It has been recently reported that, for every 1 decade increase in age, osteoporotic fracture risk for an untreated patient increases by 46% (Klemes et al. 2007 IBMS abstract). In this research, the objective was to examine the effect of risedronate on fracture risk as patients' age. 3229 osteoporotic PMO women in clinical trials (VERT, RON & ROE) who took at least one dose of placebo or risedronate 5mg pill were included in the analysis. Patients ranged from 38 to 85 years in age and had a mean FN T-score of -2.2 SD. The fracture endpoint was the incidence of a new morphometric vertebral fracture over a three year period, as previously described. The impact of age on fracture risk was examined using Cox regression models with age and treatment as explanatory variables. Both treatment and age had a statistically significant impact on fracture risk. The interaction between treatment and age was included in the initial model but removed from the final model as it was not statistically significant ($p>0.05$). The association of the increased risk for fracture and age did not differ significantly by treatment groups ($p>0.05$ for the interaction term). Regardless of treatment group, for every 1 decade increase in age, patient risk for any osteoporotic fracture increased by 37% on average. It also suggested that the magnitude of the treatment benefit was consistent regardless of age, i.e. risedronate reduced the fracture risk by 46% with $p<0.001$ after adjusting for age. When comparing 3-year fracture risk between risedronate and placebo patients, we found that fracture risk for patients who had been treated with risedronate 5 mg was estimated to be similar to the placebo patients who were 19.8 (95% CI: 10.8, 42.7) years younger in age. 70-year-old patients in the risedronate 5 mg group had a risk of fracture similar to 50-year-old patients in the placebo group. In conclusion, fracture risk increases with age. Patients who had been treated with risedronate had a similar osteoporotic fracture risk to the patients in the placebo group who were 20 years younger in age.

Disclosures: S. Boonen, Procter & Gamble Pharmaceuticals 5.

W318

Evaluation of Cell Apoptosis and Cox-2 expression in Glucocorticoid-induced Osteoporosis in Rats Treated with Risedronate. L. Dalle Carbonare^{*1}, M. T. Valenti^{*1}, F. Bertoldo^{*1}, L. Donatelli^{*1}, S. Sella^{*2}, S. Giannini², G. Realdi^{*2}, V. Lo Cascio¹. ¹Dpt. of Biomedical and Surgical Sciences, Medicina Interna D, Verona, Italy, ²Dpt. of Medical and Surgical Sciences, Clinica Medica I, Padova, Italy.

Osteoporosis is a severe complication of the glucocorticoid (GC) treatment and bisphosphonates are a powerful therapeutic option to prevent osteoporotic fractures by inhibiting bone resorption. Recent findings demonstrated that bisphosphonates are also able to prevent osteoblastic and osteocytic apoptosis induced by glucocorticoids. More recently, it has been suggested that endogenous prostaglandins are involved in modulation of bone formation in vivo by COX-2 modulated BMP synthesis.

To confirm the effects of bisphosphonates, in particular risedronate (Ris), in the prevention of apoptosis of osteoblasts and osteocytes induced by GC and to explore a possible role of COX-2 in this pattern, we evaluate apoptosis and COX-2 expression in 40 female Sprague-Dawley rats randomly divided into 4 groups of treatment, and administered 3 times a week subcutaneously as follows:

1. Control: vehicle of methylprednisolone (GC) + vehicle of risedronate (Ris); 2. Ris: Ris 5 μ g/Kg body weight vehicle of GC; 3. GC: GC 7 mg/Kg + vehicle of Ris; 4. GC+Ris: GC 7 mg/Kg, Ris 5 μ g/Kg. Animals were treated for 30 days and then were sacrificed.

The apoptosis was quantified by TUNEL method, whereas the COX-2 expression was performed by immunohistochemistry and the data were expressed by German Immunoreactive score (IHS).

Preliminary results confirm that GC induces apoptosis of osteocytes (88%, $p<0.0001$ vs controls). This effect is reduced by risedronate (44%, $p<0.0001$ vs GC). Concerning COX-2, Ris seems to increase their expression in osteocyte with respect to controls (IHS: 8.75 vs 1.00, $p<0.0001$). The last suggests a possible positive effect of Ris in bone formation, by enhancing COX-2 expression.

Disclosures: L. Dalle Carbonare, None.
This study received funding from: Procter & Gamble.

W319

Daily and Monthly Ibandronate Restores Bone Loss in Androgen Deficient Male Rats. M. Montero^{*1}, I. Quiroga^{*2}, M. Rubert^{*1}, M. Diaz-Curiel³, F. Bausa⁴, C. De la Piedra¹. ¹Biochemistry, Osteoarticular Pathology Laboratory, Fundacion Jimenez Diaz, Madrid, Spain, ²Endocrinology, Hospital Puerta de Hierro, Madrid, Spain, ³Internal Medicine, Fundacion Jimenez Diaz, Madrid, Spain, ⁴Pharma Research Penzberg, Roche Diagnostics GmbH, Penzberg, Germany.

Ibandronate (IBN) is a highly potent bisphosphonate which is approved in many countries for the treatment of postmenopausal osteoporosis and metastatic bone disease. However, little is known about the effect of IBN in male osteoporosis due to androgen deficiency. In particular, the clinically attractive mode of intermittent administration of IBN has not yet been investigated in male osteoporosis.

The aim of this work was to study the ability of IBN, administered daily (d) or monthly (m), to revert the deleterious effects on bone produced by orchidectomy. Forty, 9 month-old, male Wistar rats were sham-operated (SHAM) or orchidectomized (OQX). All animals were left untreated for 6 months after surgery, and subsequently submitted to 4 groups, which were administered subcutaneously over a duration of 20 weeks with either placebo (SHAM; n=10) and (OQX; n=10) or with two regimens of ibandronate (Roche Diagnostics GmbH, Germany): 1 microg/Kg/day (OQX+IBNd (n=10) or 28 microg/Kg/28 days (OQX+IBNm (n=10)).

After sacrifice, bone mineral density (BMD) was determined in the lumbar spine and in the whole left femur by DEXA in situ. Also, the following biochemical markers of bone remodelling were determined by ELISA at the end of the study: rat 5b isoenzyme of serum tartrate resistant acid phosphatase (IDS, UK) and rat osteocalcin (BGP, Nordic Bioscience, Denmark).

When compared to the sham group, lumbar spine and femoral BMD were significantly lower in the OQX-controls (p=0.07 and p<0.01 respectively). Both treatment regimens, IBNd and IBNm restored the BMD levels observed in orchidectomized rats to those of the SHAM group, with equivalent data for both regimens. OQX rats presented significantly higher levels of BGP than those in the SHAM group (p<0.01), while no difference was observed for TRAP. IBNd or IBNm treatment decreased BGP and TRAP levels in OQX rats to levels significantly lower than those of the SHAM group (p<0.01). The above results in androgen-deficient rat suggest that daily treatment with ibandronate is as effective as monthly treatment to revert the changes in bone mass and remodelling, provided the same cumulative total dose per animal is administered. Any numerical difference in any parameter between the two regimens did not reach statistical significance.

Disclosures: C. De la Piedra, F Hoffmann LaRoche 2.

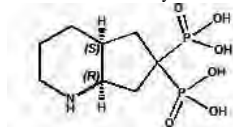
This study received funding from: Roche Diagnostics GmbH.

W320

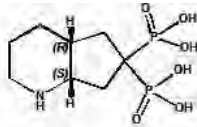
The Mode of Binding of Nitrogen Containing Bisphosphonates in Farnesyl Pyrophosphate Synthase. F. H. Ebetino^{*1}, J. E. Dunford^{*2}, M. W. Lundy^{*1}, X. Dao^{*2}, R. Dobson^{*1}, J. T. Triffitt^{*2}, M. Quijano^{*1}, X. Song^{*3}, R. K. Boeckman^{*3}, R. G. G. Russell^{*2}, B. L. Barnett^{*4}. ¹Procter & Gamble Pharmaceuticals, Mason, OH, USA, ²Oxford Univ., Oxford, United Kingdom, ³Chemistry, Univ. of Rochester, Rochester, NY, USA, ⁴Chemistry, Univ. of Cincinnati, Cincinnati, OH, USA.

Enzyme inhibitory potency of Farnesyl Pyrophosphate Synthase (FPPS) is one of the key components of the mechanism of antiresorptive action of nitrogen containing bisphosphonates (NBPs). In vivo, subsequent to binding at the bone surface, NBPs are taken up by osteoclasts where they inhibit FPPS & interfere with multiple cellular functions. Each NBP possesses a different combination of these properties, which may lead to differences in clinical performance. From crystal structures of human FPPS ligated with NBPs, it is clear that differences in inhibitory potency are based on key interactions of the NBPs within the geranyl pyrophosphate (GPP) binding site. The most potent FPPS inhibitors seem to form strong hydrogen bonds between the BP nitrogen & the hydroxyl of T 201-OH and the backbone carbonyl (C=O) of K 200. Following this concept, we used protein crystallography to study a mirror image pair of conformationally restricted NBPs within the GPP binding site of FPPS & noted that only one, the IR 6S version of cis-2-azabicyclo[4.3.0]nonane-8,8-diphosphonic (PG-1014491) could orient its nitrogen in the region of the binding site necessary for such hydrogen bonding.

Previously, the racemic mixture demonstrated good antiresorptive activity in acute models in vivo. PG-1014491 should be the more potent inhibitor of FPPS and resorption. Using a unique chemical synthesis, stereochemically pure versions of each enantiomer were prepared. Enzyme inhibition studies with hFPPS confirmed that PG-1014491 was the more potent inhibitor with an IC₅₀ of 15 nM vs. 359 nM for the poorly oriented enantiomer PG-1014493. The IC₅₀ of the racemic mixture was consistent with a 50:50 mixture of these two isomers (42 nM). In vivo studies to further relate this IC₅₀ difference to overall antiresorptive performance have also shown that in growing rats, BMD increases of 20% vis-à-vis controls occur at lower doses with PG-1014491 (9 µg P/kg) than with PG-1014493 (600 µg P/kg). These results confirm the key role of the Lys 201 & Thr 200 hydrogen bonding site in NBP inhibition of FPPS & further confirms the role of FPPS as the key biochemical target in the bisphosphonate mechanism of action on bone.



PG-1014491



PG-1014493

Disclosures: F.H. Ebetino, Procter & Gamble Pharmaceuticals 3.

W321

Novel Effects of High Doses of Olpadronate on Cortical Bone and Mechanism of Fracture in Young-Rat Femurs. G. R. Cointy^{*1}, R. F. Capozza^{*1}, M. Meta², N. Mondelo^{*3}, E. Piccini^{*3}, J. L. Ferretti¹. ¹Centro de Estudios de Metabolismo Fosforológico, Faculty of Medicine, UNR, Rosario, Argentina, ²David Geffen Med Sch, UCSF, San Francisco, CA, USA, ³Gador S.A., Buenos Aires, Argentina.

This study aimed to determine whether the administration of high doses of OPD affect bone mass, design and mineralization, simultaneously impairing, maintaining or improving bone pre- and post-yield properties of young rat femurs (an almost only-modeling model). Twenty male and 22 female 4-5-week-old rats received orally 45 or 90 mg/kg/d olpadronate (dimethyl-pamidronate) over 3 months (8/9 male/female controls). Periosteal perimeter, cortical vBMD, cross-sectional area (CSA), moment of inertia (xCSMI), cortical bone elastic modulus (E), stiffness and strength of femur diaphyses were determined by pQCT and bending tests.

Treatment proportionally enhanced periosteal perimeter, CSA and xCSMI with no change in vBMD and E. While yielding stiffness and strength were mildly improved, post-yield strength was strikingly increased (males +385%; females +80%). Ultimate strength was enhanced mainly as a consequence of post-yield properties rather than pre-yield or geometric properties. No dose-related effects were observed. The expected improvement in pre-yield properties suggests a mild anabolic effect. The large effect on post-yield properties (bone toughness) suggests a role for microstructural factors unrelated to mineralization. Sex-related differences were attributed to a better bioavailability of the drug and a much larger body weight in males, perhaps in connection with the mechanical stimulation of bone structure. Results reveal novel effects of OPD on bone strength and mechanism of fracture unrelated to tissue mineralization and stiffness, possibly associated with a positive interaction on the bone mechanostat, with little or no involvement of bone remodeling. No deterioration of any material, geometric or mechanical property was observed, despite the high doses employed.

Disclosures: J.L. Ferretti, None.

This study received funding from: Gador S.A.

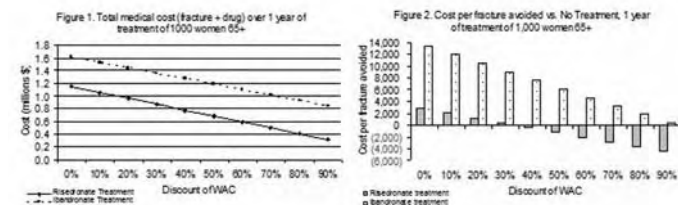
W322

Cost-Effectiveness of Risedronate vs. Ibandronate: Impact of Discounts. D. Grima^{*1}, N. N. Borisov^{*2}. ¹Cornerstone Research Group Inc, Burlington, ON, Canada, ²Procter & Gamble Pharmaceuticals, Mason, OH, USA.

This study uses a Markov model of postmenopausal osteoporosis (PMO) to compare the clinical- and cost-effectiveness of risedronate and ibandronate at a range of rebate discounts of wholesale acquisition cost (WAC). The Markov model simulated a cohort of women aged 65+, with previous vertebral fracture and BMD T-score <-2.5, under a one-year time horizon. Fracture rates were derived from US clinical studies. Vertebral and nonvertebral risk reduction measures are 58% and 0% for ibandronate respectively (Chesnut, Skag, Christiansen, et al., 2004), and 65% and 74% for risedronate, respectively (Harris, Watts, Genant, et al., 1999 and Harrington JT, Ste-Marie LG, Brandt ML, et al., 2004). Annual WAC before rebate discounts was \$924.69 for risedronate and \$853.56 for ibandronate.

At equal levels of discounts, treatment with risedronate results in lower fracture costs and lower total costs of treating fractures than treatment with ibandronate. Total medical costs for risedronate at 0% discount were still lower than total costs for ibandronate up to 60% discount (figure 1).

The costs per fracture avoided versus no treatment were consistently lower for risedronate than for ibandronate. Discount at 40% or above for risedronate resulted in cost savings compared to no treatment (figure 2). The cost per fracture avoided for ibandronate at 80% rebate discount approaches the cost per fracture avoided for risedronate at 0% discount. Ibandronate treatment did not achieve any savings even with 90% discount. In this analysis, overall cost-effectiveness is more dependent on efficacy than rebate discounts.



Disclosures: D. Grima, Cornerstone Research Group Inc 3; Procter & Gamble Pharmaceuticals 5.

W323

The Efficacy and Safety of Intravenous Ibandronate for Chinese Primary Osteoporotic Women. M. Li^{*1}, X. Xing^{*1}, X. Meng^{*1}, Z. Zhang^{*2}, J. Liu^{*3}, W. Xia^{*1}, D. Liu^{*1}. ¹Endocrinology, Peking Union Medical College Hospital, Beijing, China, ²Endocrinology, 6th People Hospital of Shanghai, Shanghai, China, ³Obstetrics and Gynecology Endocrinology, General Hospital of Chinese PLA, Beijing, China.

Objective Antiresorptive agents are widely used to treat osteoporosis. We observe a new kind of bisphosphonate, ibandronate in a multicenter randomized, positive controlled open study, to evaluate its efficacy and safety on postmenopausal osteoporosis women in China. Methods 158 postmenopausal osteoporosis women, aged 49 to 75 years, were randomized as two groups in this one year phase study. Women in ibandronate group intravenously received 2mg Ibandronate every three months. Women in control group took 70mg alendronate weekly. All women also received supplemental calcium (500 mg) and vitamin D (200 IU) daily. The primary end point was mean relative change from baseline in lumbar spine, femoral neck, trochanter BMD after one year. The secondary end points were relative changes in biochemical bone turnover markers (AKP, a bone formation marker; CTX, a bone resorption marker) and stature after one year. Safety was suggested by adverse events, new fractures liver and kidney function.

Results 151 cases completed the observation. Treatment with ibandronate for 1 years produced mean increases in BMD of 4.27% at the lumbar spine (95 %CI, 12.0 to 15.5 percent), 3.48% at the femoral neck (95 %CI, 8.1 to 12.4 percent), 2.03% at the trochanter (95 %CI, 3.5 to 7.4 percent) as compared with baseline values. Mean increases in BMD of 4.24% at the lumbar spine (95 %CI, 12.0 to 15.5 percent), 2.72% at the femoral neck (95 %CI, 8.1 to 12.4 percent), 2.99% at the trochanter (95 %CI, 3.5 to 7.4 percent) as compared with baseline values were observed in alendronate group. No difference of mean relative change from baseline was found between two groups. Significant decrease in serum CTX value and ALP level were found in two groups after one and three month of treatment respectively, then they were maintained in low level during the whole study. Decrease of ALP was significantly less and later than that of CTX. No change of stature was found in two groups. Except ibandronate group had more cases with mild muscle pain in the first month of treatment than alendronate group ($P < 0.001$), ibandronate and alendronate also had good tolerance and compliance.

Conclusions Treatment with Ibandronate 2mg once three-monthly intravenous dosing significantly reduced bone resorption and increased bone mineral density with good tolerance in Chinese postmenopausal osteoporotic women, therefore it had potency to improve adherence and avoid peptic side effects of oral bisphosphonate.

Key words: postmenopausal osteoporosis, ibandronate, alendronate

Disclosures: M. Li, None.

This study received funding from: Bio-med Center, Hebei Medical University, China.

W324

Osteotropic Cyclodextrins as Novel Bone Anabolic Agents. X. Liu¹, J. Rutledge^{*2}, A. Wiswall^{*2}, R. A. Reinhardt^{*2}, D. Wang¹. ¹Department of Pharmaceutical Sciences, University of Nebraska Medical Center, Omaha, NE, USA, ²Department of Surgical Specialties, University of Nebraska Medical Center, Lincoln, NE, USA.

Alendronate-cyclodextrin conjugate (ALN-CD) was evaluated as an osteotropic delivery system for prostaglandin E1 (PGE1).

A bilateral rat mandible local injection model was used for this study. Mandibles were isolated 24 days post injection of the drug formulations and analyzed histomorphometrically.

Initial study with ALN-CD/PGE1 complex shows that it generates significantly higher amount of new bone than the non-osteotropic cyclodextrin (CD)/PGE1 complex. Surprisingly, as a control, ALN-CD was found with strong bone anabolic effect (Table 1). To investigate this observation, following groups were added: ALN-CD/PGE1 vs. ALN-CD; PGE1 in ethanol vs. ethanol; ALN in saline vs. saline and saline vs. no treatment. The histomorphometry data show that ALN-CD generates more bone than ALN-CD/PGE1 complex (equivalent dose to ALN-CD). ALN stimulates moderate bone formation, but mostly on the opposite side of the injection (Figure 1). All other formulations show minimal anabolic effect.

Evidently, the anabolic effect of ALN-CD is independent of the effects of PGE1 and ALN. Since the cyclodextrins could form strong inclusion complexes with many lipophilic compounds, such as PGEs, lipids, steroids, etc., one may speculate that the immobilization of ALN-CD on bone surface would cause local enrichment of the certain endogenous anabolic factors and lead to the observed bone anabolic effect.

Table 1. Histomorphometry analysis of rat mandibles 24 days post single injection of different formulations. New Bone Width-1, injection site; New Bone Width-3, non-injection site.

Groups	New Bone Area (mm ² ± SEM)	New Bone Width-1 (mm ± SEM)	New Bone Width-3 (mm ± SEM)
ALN-CD/PGE ₁	0.97 ± 0.23	0.50 ± 0.14	0.17 ± 0.06
CD/PGE ₁	0.18 ± 0.09	0.14 ± 0.06	0.16 ± 0.06
p	0.00001	0.00001	NS
ALN-CD	0.78 ± 0.10	0.36 ± 0.07	0.18 ± 0.03
CD	0.25 ± 0.08	0.05 ± 0.02	0.19 ± 0.11
p	0.003	0.0002	NS

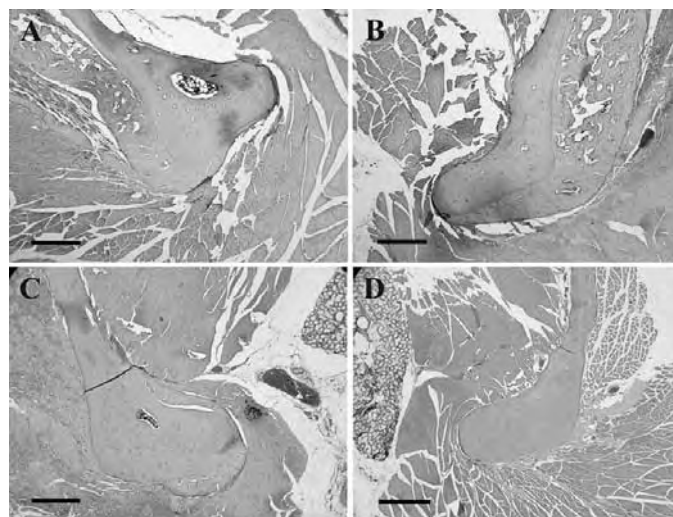


Figure 1. New bone formation on mandibles with different formulations. (A) ALN-CD/PGE1; (B) ALN-CD; (C) ALN; (D) Saline. Bar size = 0.5 mm.

Disclosures: X. Liu, None.

This study received funding from: University of Nebraska Medical Center.

W325

Bisphosphonate Affinity to Hydroxyapatite and Farnesyl Pyrophosphate Inhibitory Potency, Together, Drive In Vivo Efficacy. M. W. Lundy¹, F. H. Ebetino¹, L. Fei^{*1}, Z. Xia^{*1}, M. Pozzi^{*1}, D. Trokhan^{*1}, R. Phipps¹, J. Dunford^{*2}, J. T. Triffitt^{*2}, R. G. G. Russell². ¹Procter & Gamble Pharmaceuticals, Mason, OH, USA, ²Oxford University, Oxford, United Kingdom.

The nitrogen containing bisphosphonates (N-BPs) are believed to exert their clinical antiresorptive effects via two fundamental mechanistic properties, bone mineral affinity and enzyme inhibitory potency. In vivo, N-BPs are targeted to the bone surface and site of osteoclastic activity due to binding of the 2 phosphonate groups to hydroxyapatite (HAP). Subsequently, N-BPs are taken up by osteoclasts where they diminish osteoclastic activity by inhibiting farnesyl pyrophosphate synthase (FPPS). It is well documented in vitro that the relative mineral affinity and FPPS inhibitory potencies among N-BPs can vary broadly over a range from weak to strong. To determine the relative influence of mineral binding and enzyme inhibitory potency on efficacy in vivo, we used the growing rat model (Schenk model) to investigate N-BPs with a range of mineral affinities and FPPS inhibitory potencies.

Male Sprague-Dawley rats 6 weeks old were treated for 7 days, over a range of doses, with 17 N-BPs. BMD of the proximal tibial metaphysis was measured ex vivo using a Hologic QDR-4500 densitometer, with the effect of each dose expressed as a percent change from the vehicle control. The efficacy of each compound was identified as the dose which increased BMD 20 percent higher than control (D20). The relationship between in vivo efficacy, FPPS IC₅₀ (inhibition of isolated human enzyme) and HAP affinity (minutes to elution from an HAP column) was determined using multiple regression analysis, with FPPS and D20 log transformed.

Bisphosphonate inhibition of hFPPS correlated poorly with HAP affinity ($r^2 = 0.03$). Bisphosphonate inhibition of FPPS predicted in vivo efficacy expressed as D20 with an $r^2 = 0.66$. HAP affinity also correlated poorly with D20 ($r^2 = 0.12$). However when antiresorptive potency was predicted using both HAP affinity and hFPPS inhibition; the combination improved the prediction of D20 ($r^2 = 0.91$).

The in vivo efficacy predicted by inhibition of FPPS can be increased or decreased by how avidly the N-BP binds to bone mineral as measured by HAP affinity. A better correlation of in vivo anti-resorptive activity is therefore derived from measurements that include both FPPS inhibition and bone affinity than data from either alone. These results also illustrate that each N-BP has a unique combination of these two properties, which may help explain clinical differences such as onset of efficacy, relative efficacy at different skeletal sites, and the rate at which their inhibitory activity recovers after stopping treatment.

Disclosures: M.W. Lundy, Procter & Gamble Pharmaceuticals 3.

This study received funding from: Procter & Gamble Pharmaceuticals.

W326

Statins Decrease Bone Turnover Markers in Postmenopausal Women. J. Martínez^{*1}, J. L. Hernández^{*1}, J. M. Olmos¹, E. Pariente^{*2}, C. Valero^{*1}, P. García^{*2}, D. Nan^{*1}, G. Pinedo^{*2}, J. González-Macías¹. ¹Medicina Interna, Hospital Universitario M. Valdecilla. Universidad de Cantabria, Santander, Spain, ²Centro de Salud "José Barros". Camargo. Universidad de Cantabria, Santander, Spain.

The aim of the present study was to evaluate the effects of treatment with statins on calcium homeostasis, bone turnover and bone mineral density in a population of postmenopausal women from Cantabria, Spain. We present preliminary results of the first 258 women included in the Camargo Cohort Study, a community-based study designed to evaluate the prevalence of metabolic bone diseases and disorders of mineral metabolism, as well as the prevalence of fractures and risk factors for osteoporosis and fragility fractures, in postmenopausal women and men older than 50 attended in a primary care centre from Northern Spain. Serum levels of aminoterminal propeptide of type I collagen (PINP), C-terminal telopeptide of type I collagen (β -CrossLaps, CTX), parathyroid hormone (iPTH), bone mineral density at the lumbar spine and hip by DXA (BDM) and quantitative ultrasound at the calcaneus (QUS), were measured in 49 postmenopausal women who had been treated with statins for more than one year, and compared with 209 age- and gender-matched controls. Women who were receiving treatment with bisphosphonates, oestrogen, raloxifene, or glucocorticoids were excluded. The mean (\pm SD) age of subjects was 65 \pm 8 years in treated women and 62 \pm 8 in controls. The statin-treated subjects had lower plasma levels of PINP (38.9 \pm 14.8 vs. 46.8 \pm 20.5 ng/ml; $p=0.03$) and CTX (0.298 \pm 0.162 vs. 0.374 \pm 0.194 ng/ml; $p=0.01$). However, serum iPTH levels (57 \pm 16 vs. 53 \pm 17 pg/ml), BMD at lumbar spine (0.916 \pm 0.13 vs. 0.919 \pm 0.132 g/cm²), femoral neck (0.722 \pm 0.098 vs. 0.726 \pm 0.120 g/cm²), and total hip (0.870 \pm 0.119 vs. 0.870 \pm 0.125 g/cm²), and QUS did not differ between groups. Once adjusted by age, BMI, serum cholesterol levels and presence of diabetes, this association remain statistically significant only for serum CTX ($p=0.04$) but not for PINP. This fact was confirmed in a stepwise multiple regression analysis. Treatment with statins was associated with a reduction in serum markers of bone resorption. However, no changes were observed in either BMD or QUS.

This study was supported by a grant from the "Fondo de Investigación Sanitaria", Ministerio de Sanidad y Consumo, Spain (FIS: PI05 0125)

Disclosures: J. Martínez, None.

W327

Essential Mechanistic Studies of the Esophagogastric Transit of Oral Bisphosphonates. A. C. Perkins^{*1}, P. E. Blacckshaw^{*1}, R. J. Dansereau^{*2}. ¹Academic Medical Physics Medical School University of Nottingham, Nottingham, United Kingdom, ²Procter & Gamble Pharmaceuticals, Mason, OH, USA.

The incomplete swallowing of oral bisphosphonate tablets has potential iatrogenic implications for patients on long-term treatment. The major risk factors for "pill-induced esophagitis" are tablet size, shape and coating, esophageal dysmotility factors, patient posture and water volume for dosing. The pharmaceutical design of oral formulations influences the site of drug release, rate of dispersal and absorption within the gastrointestinal tract. We have extensive in vivo evidence of the swallowing of tablets and capsules labeled with ^{99m}Tc and ¹⁵³Sm. In general, these studies have shown more rapid transit of tablets compared with similar sized capsules. We have observed the slow esophageal release of contents from a lodged capsule over a period of 90min with the subject not aware of any dysmotility.

Our studies have shown short transit times of commercially available, film-coated 35 mg risedronate tablets ingested with 2 separate water volumes (50 ml and 120 ml) in elderly patients with postmenopausal osteoporosis, gastroesophageal reflux disease and postural kyphosis where mean transit times of 12 and 16s were measured for 50ml and 120ml water respectively. The severity of kyphosis did not affect the esophageal transit time. We have also examined the effect of posture on tablet swallowing, this being important for bed-ridden patients in long term care facilities.

There is now increased worldwide availability of generic alendronate formulations that have yet to show proven gastrointestinal acceptability. A previous report of in vitro disintegration times of generic 70mg alendronate formulations ranged between 7 seconds to 31 minutes indicating quite different pharmaceutical properties¹. It is therefore important to demonstrate the swallowing exposure and esophageal exposure of these generic tablets is minimal if equivalent safety is to be assumed. Our current work is examining the transit of generic formulations and data will be presented.

Scintigraphic studies have proven value in the design and selection of oral pharmaceutical dosage forms and in assessing their physiological characteristics. Such studies provide essential data for the physician prescribing to osteoporotic patients.

¹Epstein S, et al. Current Medical Research and Opinion. 2003;19:781-789

Disclosures: A.C. Perkins, Procter & Gamble Pharmaceuticals S.

W328

Effect of Combined Treatment of Alendronate and Vitamin K₂ on Bone Mineral Density and Strength in Ovariectomized Mice. H. Sasaki, N. Miyakoshi, Y. Kasukawa, S. Maekawa, H. Noguchi, K. Kamo, Y. Shimada. Orthopedic surgery, Akita University School of Medicine, Akita, Japan.

Bisphosphonates increase bone mineral density (BMD) in an indirect manner by reducing the remodeling space and by prolonging the duration of mineralization; however, the effects of bisphosphonates on bone quality have not been fully evaluated. On the other hand, menatetrenone (vitamin K₂) has been considered to reduce the incidence of fractures by improving bone quality more than BMD in patients with osteoporosis. The purpose of this study was therefore to investigate the effects of combined treatment of menatetrenone and alendronate (ALN) on BMD and bone strength in ovariectomized (OVX) mice. OVX was performed at 16 weeks of age, and treatment was started 4 weeks after surgery. OVX mice were randomized into following four groups: 1) OVX-control group, treated with normal diet and administered with the vehicle of ALN; 2) K₂ group, treated with menatetrenone (30mg/kg p.o., daily); 3) ALN group, treated with ALN (56µg/kg s.c., once a week); and 4) K₂ + ALN group, treated with menatetrenone plus ALN. At the end of the 8-week treatment period, the femur was harvested, and BMD and mechanical strength of distal metaphysis were evaluated. BMD was measured by peripheral quantitative computed tomography (pQCT), and mechanical strength was evaluated by failure energy of the compression test. Total-BMD at the distal metaphysis of the femur in the K₂ group showed no significant difference from that in the OVX-control group. The total BMD in the ALN group and K₂+ALN group was significantly higher than that in the OVX-control group (20% and 15% respectively, $p<0.0001$). No significant difference was observed in failure energy of the distal femur between the ALN and OVX-control groups; however, failure energy was significantly higher in the K₂+ALN group compared to the OVX-control group (25%, $p<0.01$). These results suggest that ALN alone or in combination with menatetrenone showed significant improvement on BMD but combined treatment of ALN and menatetrenone was more effective than ALN alone for improving bone strength in OVX mice. Using menatetrenone with bisphosphonates might have a more positive effect on bone quality in patients with osteoporosis.

Disclosures: H. Sasaki, None.

W329

VDR, ESR1, and COL1A1 Associations with Osteoporosis Phenotypes at Baseline and after Risedronate Treatment in the IMPACT Trial. A. Uitterlinden¹, J. van Meurs¹, D. Contopoulos-Ioannidis^{*2}, R. Eastell³, P. Delmas⁴, H. Pols¹, L. van de Langerijt⁵, J. Ioannidis^{*2}. ¹Internal Medicine, Erasmus MC, Rotterdam, The Netherlands, ²Hygiene & Epidemiology, University of Ioannina, Ioannina, Greece, ³Metabolic Bone Centre, Sheffield University, Sheffield, United Kingdom, ⁴Internal Medicine, Université de Lyon & INSERM unit 831, Lyon, France, ⁵Sanofi-Aventis, Gouda, The Netherlands.

Purpose: To examine the association of 6 single nucleotide polymorphisms (SNPs) of the COL1A1 (-1997 promoter G/T and Sp1 G/T), ESR1 (XbaI and PvuII), and VDR (308 and 464 3'UTR SNPs) genes, with bone mineral density (BMD) at hip and lumbar spine and bone turnover markers (N- and C-terminal telopeptides of type I collagen (NTx, CTx), and with changes of BMD and bone turnover markers during therapy with risedronate for osteoporosis.

Methods: We performed genotyping (Taqman) on DNA from a large cohort of 5412 women participating in the IMPACT trial for COL1A1 SNPs; 3742 (69%) women were also evaluated for the ESR1 and VDR SNPs. Changes in indices upon treatment were evaluated in women who had additional follow-up data during their participation in the trial ($n=2048$; 38%).

Results: Genotype and allele frequencies were consistent with previous data and followed Hardy-Weinberg equilibrium.

For both hip and spine BMD, allele-based models showed no nominally statistically significant effects with any SNP, for baseline values and changes during treatment: all p -values were >0.05 except for one $p=0.036$ unadjusted for multiple comparisons. No associations were seen for haplotype analyses of both SNPs at each gene.

Similarly, no associations were seen for any SNP with bone turnover markers, except for VDR 464 and change in CTx during follow-up ($p=0.003$), also seen in VDR haplotype analyses ($p=0.013$). However, the recessive effect was limited to 26 and 17 subjects, respectively, and the meaning of this isolated finding is unclear given the multiplicity of performed analyses. Other genetic contrasts and adjusted analysis did not yield more significant results.

Point estimates were entirely consistent with prior large-scale evidence (in GENOMOS) on the impact of these genetic markers on BMD, e.g., COL1A1 Sp1 TT had 0.15 SD lower BMD on a standardized scale, although this was far from being nominally statistically significant.

Conclusions: COL1A1, ESR1 and VDR SNPs do not have a major impact on BMD and bone turnover markers at baseline, and no genotype-dependent response to risedronate treatment was observed. We cannot exclude small effects of these polymorphisms by these data. Our results support the requirement of large databases and genome-wide approaches to delineate the genetics of osteoporosis, including response to treatment.

Disclosures: A. Uitterlinden, None.

This study received funding from: Sanofi-Aventis.

W330

Effects of Alendronate-induced Bone Matrix Changes on Resorption and Turnover. D. Vashishth¹, B. Merle², E. Gineyts², G. Boivin², M. Allen³, D. B. Burr³, P. D. Delmas². ¹INSERM Unite 831 Université de Lyon, France & Rensselaer Polytechnic Institute, Troy, NY, USA, ²INSERM Unite 831 Université de Lyon, Lyon, France, ³Anatomy & Cell Biology, Indiana University School of Medicine, Indianapolis, IN, USA.

Bisphosphonates (BP) including alendronate (ALN), used for treatment of osteoporosis, increase osteoclast apoptosis and reduce bone turnover. The reduction in bone turnover preserves bone mass but alters bone matrix. At the bone matrix level, the mean degree of tissue mineralization (DMB) increases [1] and the collagen accumulates crosslinks by non-enzymatic glycation (NEG) [2]. Because mineralization increases resorption and NEG-crosslinks decrease resorption [3], matrix changes may alter resorption and the efficacy of drug therapy. Here, using an in vitro cell-tissue culture approach, we have investigated the role of ALN-induced bone matrix changes on bone resorption. 100 ± 5 µm thick bone sections were obtained from ribs of 12 skeletally mature female beagles treated either with ALN at the clinical dose of osteoporosis (0.20 mg/kg/day) or vehicle (1 mL/kg/day of saline) for 1 year. The sections were microradiographed for the measurement of DMB and subjected to in vitro bone resorption caused by rabbit osteoclasts for 8 days under standard cell culture conditions. Additional sections from the same anatomical site were harvested to measure enzymatic (mmol pyridinoline or deypyridinoline /mol of collagen) and non-enzymatic crosslink content (mmol pentosidine /mol of collagen). The frequency and area of resorption pits were compared between groups and tested for correlation with DMB and crosslink content. Similar to in vivo reports, this in vitro model showed that the resorption pit area was smaller in ALN-treated than in the vehicle-treated group (p<0.01) and there were no differences in the pit frequency between the groups (p=0.52). NEG-crosslinks were significantly higher in ALN-treated than in vehicle-treated controls (p<0.05) and were inversely correlated with the mean resorption area ($r = -0.9$; p<0.05). Enzymatic crosslinks were not different between the groups but pyridinoline showed an inverse trend with resorption pit frequency ($r = -0.9$; p = 0.08). DMB was not different between the groups and showed a weak and non-significant correlation with resorption parameters. In conclusion, this study demonstrates for the first time that bone matrix changes, particularly the accumulation of NEG crosslinks with BP therapy, reduce bone resorption and may consequently affect bone quality by a further reduction in turnover. References: [1] Boivin et al. Bone. 2000 5: 687-94. [2] Gineyts et al. ASBMR Sept. 2006. [3] Valcourt et al. JBC 282:5691-5703.

Disclosures: D. Vashishth, Merck 5.

This study received funding from: INSERM France & NIH Grants AR49635, AG20618, AR047838, AR007581, C04RR10701.

W331

PTH and Risedronate Prevented Glucocorticoid Induced Reduction in Bone Mineralization Through Different Mechanisms. W. Yao, C. Busse*, Z. Cheng, S. Rao*, N. Lane. Center for Healthy Aging, UC Davis Medical Center, Sacramento, CA, USA.

Glucocorticoids (GC) excess inhibits bone mineralization which leads to reduced bone strength. Both anabolic (PTH) and anti-resorptive agents (Risedronate) are used to prevent and treat GC induced bone loss. The purpose of this study was to further evaluate how PTH and Risedronate (Ris) may modulate GC induced bone loss through alteration of bone mineralization in vivo and at the transcriptional levels. Five-month-old Swiss-Webster male mice were treated with prednisolone [2 mg/kg 28-day slow-release pellet (GC), or placebo (PL)] or with GC+ Vehicle, GC+PTH (20µg/kg, 5x/wk) or GC+Ris (5µg/kg, 3x/wk) for 28 days. X-ray tomography microscopy (XTM) was used to determine the DBM in lumbar vertebral body, and real-time PCR were used to monitor the expression of several key genes regulating bone mineralization, including Dmp1, Phex, OPN, Akp2, Enpp1 and Ank. In addition, microCT and biochemistry were used to determine bone microarchitecture and bone turnover. Results. Compared to the placebo treated mice, 28 days of GC treatment decreased trabecular bone volume (BV/TV) by 20%, osteocalcin (OSC) by 60% and increased TRAP5b by 18% (p<0.05). On the other hand, GC+PTH and GC+Ris increased BV/TV by 15% and 7%, respectively with OSC and TRAP5b similar to the PL levels. Average DBM was lowered after GC treatment (-15%). Both PTH and Ris treatments maintained DBM while PTH increased (+18%) and Ris decreased (-10%) the heterogeneity of mineral distribution (half maximum width of the mineral distribution). At day 28, whole bone gene expression by RT-PCR done in triplicate revealed that continuous exposure to GCs increased the expression of gene that inhibit bone mineralization (Spp1, Enpp1, Dmp1). GC+PTH further increased OPN and Dmp1 gene expressions while GC+Ris decrease their expression (Table) compared to the PL group. These results suggest that GC induced inhibition of bone mineralization is in part through the expression of gene that inhibit mineralization. Both GC+PTH and GC+Ris increase the global degree of bone mineralization (DBM) but PTH increases heterogeneity of mineral distribution while Ris improves mineral homogeneity. Differential expression of genes regulating mineralization (phosphate metabolism) may explain the in vivo changes in degree of mineralization observed with GC treatment.

Table: Fold changes from placebo

Treatment Groups	Ank	Enpp1	Spp1	Dmp1	Phex
PL + Vehicle	1	1	1	1	1
GC + Vehicle	1.71*	1.56*	3.01*	1.89*	1.05
GC+PTH	1.10	-2.14*	3.84*	2.21*	-2.65*
GC+Ris	1.33	-2.70*	1.23	1.25	-1.89*

Note: Fold changes = 2^{-ΔΔCt}; *, p < 0.01 vs. PL.

Disclosures: W. Yao, None.

This study received funding from: Ro1 AR043052-07, 1K12HD05195801.

W332

One Week Evaluation of Pharmaceuticals in sRANKL-injected Osteopenia Model Mice. H. Yasuda¹, K. Mori¹, Y. Nakamichi², M. Koide³, N. Udagawa³, Y. Tomimori¹. ¹Nagahama Institute for Biochemical Science, Oriental Yeast Co., Ltd., Shiga, Japan, ²Institute for Oral Science, Matsumoto Dental University, Shiojiri, Japan, ³Department of Biochemistry, Matsumoto Dental University, Shiojiri, Japan.

There are several osteopenia or osteoporosis models such as OVX, tail-suspension and low Ca diet. However, they require skills in animal testing and it takes at least a couple of weeks for the models to establish. Here we report the establishment of a novel and rapid osteopenia model mice and the evaluation of pharmaceuticals using this model. Receptor activator of NF-κB ligand (RANKL) is the membrane-bound protein essential for osteoclast development. We prepared a fusion protein of Gultathione S-transferase and extracellular domain of RANKL (GST-RANKL) for this study. GST-RANKL showed much higher activity than commercially available sRANKLs in in vitro osteoclastogenesis assay. GST-RANKL (10ug, 20ug and 40ug/ mouse) was injected intraperitoneally every 24 hours for 3 days into 7 week-old female C57/B6 mice. One and half hours later the third injection, mice were sacrificed and the blood and tissue samples were taken. Bone resorption markers (serum Ca, CTx and TRAP-5b) were increased in GST-RANKL-injected groups in a dose dependent manner. In contrast, bone synthetic markers (serum osteocalcin and ALP) were not changed. BMD of femurs was measured by pQCT and their 3D-images were made by µCT. Compared with the control group, bone mass of the GST-RANKL injected mice was decreased in a dose dependent manner. Especially the mice injected with the highest dose of GST-RANKL showed 43% decrease in BMD compared with the control mice. These results suggested that severity of osteopenia could be controlled by selecting the dose of GST-RANKL. Next, we tested whether sRANKL-injected model mice were useful for evaluation of pharmaceuticals. Risedronate (Actonel) was injected subcutaneously (0.01mg/kg/day) for 3 days before RANKL injection and was further injected for 3 days with GST-RANKL injections as described above. CTx and TRAP-5b were increased in GST-RANKL-injected mice, but the treatment of RANKL-injected mice with risedronate completely inhibited the increases of bone resorption makers. Bone synthetic markers were decreased in risedronate/RANKL injected mice. The risedronate treatment also completely inhibited the decrease of BMD of femurs in RANKL-injected mice. The in vivo evaluation of risedronate was successfully done within a week. In conclusion, we established the 50 hour-osteopenia model. This model would be useful for and applicable to the rapid evaluation of drugs for osteopenia and osteoporosis. Evaluation of bone anabolic factors in this model is underway.

Disclosures: H. Yasuda, Oriental Yeast Co., Ltd. 3.

W333

Role of Prostaglandins in Strontium Ranelate Effects on Osteoblastic Differentiation and Growth Factor Production. S. Choudhary¹, P. Halbout², C. Alander¹, C. Pilbeam¹, L. Raisz¹. ¹Musculoskeletal Institute, University of Connecticut Health Center, Farmington, CT, USA, ²Institute De Recherches Internationales Servier, Coubevoise, Cedex, France.

Strontium ranelate is a new treatment for osteoporosis that has both antiresorptive and anabolic effects. Strontium ranelate increases osteoblastic differentiation and induces cyclooxygenase (COX-2) and prostaglandin E₂ (PGE₂) production in murine marrow stromal cells (MSCs), and differentiation is diminished in cultures treated with COX-2 inhibitors or derived from COX-2 knockout animals. To further investigate the hypothesis that strontium ranelate exerts some of its anabolic effects on osteoblasts via prostaglandin production, we examined the ability of strontium ranelate to stimulate gene expression of growth factors in MSCs cultured from COX-2 knockout (KO) and wild type (WT) mice. A dose-dependent increase in PGE₂ production was seen after treatment of cells from COX-2 WT mice with 1 or 3 mM strontium ranelate for 7 days. COX-2 KO MSCs showed minimal PGE₂ production. MSCs from COX-2 WT and KO mice were cultured up to 21 days. Gene expression was determined by real time PCR. After 14 and 21 days of culture, strontium ranelate (1 or 3 mM) significantly and dose-dependently increased alkaline phosphatase (ALP) and osteocalcin (OCN) mRNA expression in WT cultures. These effects were associated with an increase insulin-like growth factor 1 (IGF-1) and vascular endothelial growth factor (VEGF) mRNA expression by 1.4-1.5 fold (p<0.01) and 1.4-1.7 fold (p<0.01), respectively. In COX-2 KO cultures, ALP and OCN mRNA levels were decreased 50% (p<0.05) and 60% (p<0.01), respectively, compared to WT cultures, and there was no increase in ALP and OCN mRNA expression or in IGF-1 and VEGF mRNA expression with strontium ranelate. In summary, strontium ranelate increased osteoblastic differentiation and IGF-1 and VEGF mRNA expression in a COX-2 dependent manner in murine MSCs. Coupled with previous data, this study indicates that strontium ranelate effects on bone formation may involve the local production and action of prostaglandins on osteoblasts, and that strontium ranelate-induced prostaglandin synthesis may increase production of growth factors that are implicated in stimulation of bone formation.

Disclosures: S. Choudhary, Institute De Recherches Internationales Servier, Coubevoise, Cedex, France 2.

This study received funding from: 5R01AR018063-31, NIH DK 48361.

W334

MK-0822 Is a Potent and Selective Cathepsin K Inhibitor that Maintains Its High Selectivity in Whole Cell Assays. W. C. Black^{*1}, S. Desmarais^{*1}, L. T. Duong², J. Falgoutyret^{*1}, J. Gauthier^{*1}, S. Lamontagne^{*1}, C. Li^{*1}, F. Masse^{*1}, V. Truong^{*1}, G. Wesolowski², M. Percival^{*1}. ¹Merck Research Laboratories, Pointe-Claire-Dorval, PQ, Canada, ²Merck Research Laboratories, West Point, PA, USA.

Cathepsin K (Cat K) is a lysosomal cysteine protease that is highly expressed in osteoclasts and plays a critical role in the degradation of bone collagen. It has been demonstrated that Cat K inhibitors are effective anti-resorptive agents for the treatment of osteoporosis. Several inhibitors of Cat K, including balicatib and L-006235, contain a basic substituent that results in lysosomotropism - the physical property in which the drug accumulates in the acidic lysosomes of the cell. Since off-target cathepsins reside in lysosomes, this resulted in a dramatic loss of selectivity of these inhibitors when tested in whole cell assays.

To address this problem, we have identified a neutral Cat K inhibitor, MK-0822, which has an IC₅₀ of 0.2 nM against human Cat K and is 300-fold selective versus Cat S and >5000-fold selective versus Cat B and Cat L. The potency and selectivity of MK-0822 against isolated enzymes are similar to those of the basic inhibitors, but its high selectivity is maintained in whole cell assays.

	Cat K		Cat B		Cat L		Cat S	
	IC ₅₀ (nM)	enzyme	IC ₅₀ (nM)	enzyme	IC ₅₀ (nM)	enzyme	IC ₅₀ (nM)	enzyme
balicatib	0.6	4800	61	503	48	65000	2900	
MK-0822	0.2	1034	1050	2995	4843	60	45	

In a functional bone resorption assay using rabbit osteoclasts, MK-0822 has an IC₅₀ of 23 ± 14 nM as compared to balicatib with an IC₅₀ of 89 ± 29 nM. Since MK-0822 is 5-fold less potent against rabbit Cat K compared to human Cat K, this value likely under represents its true potency.

MK-0822 has an excellent pharmacokinetic profile in preclinical species with terminal half-lives of 6h in rat, 57h in dog and 18h in monkey. The observed volumes of distribution are near unity, distinguishing this compound from analogous basic inhibitors, which have large volumes of distribution. In conclusion, MK-0822 is a potent and selective Cat K inhibitor that is non-lysosomotropic and maintains its high selectivity in whole cell assays.

Disclosures: L.T. Duong, Merck & Co. 3.

W335

Cathepsin K Inhibitors Prevent Matrix-Derived Growth Factor Degradation by Human Osteoclasts. K. Fuller¹, K. M. Lawrence^{*1}, J. L. Ross^{*1}, U. B. Grabowska^{*2}, M. Shiroo^{*2}, B. Samuelsson^{*2}, T. J. Chambers¹. ¹St George's, University of London, London, United Kingdom, ²Medivir UK, Little Chesterford, United Kingdom.

Under normal circumstances, bone resorption and bone formation are coupled in such a way that, if bone resorption is inhibited, then so is bone formation. This coupling between bone formation and resorption creates therapeutic difficulties in osteoporosis: further bone loss can be prevented using antiresorptive therapy, but because suppression of resorption also inhibits bone formation, the condition is not reversed. Surprisingly, inhibition of resorption by cathepsin K inhibitors has recently been found to augment bone formation. Uniquely amongst resorption-inhibitors, inhibitors of cathepsin K suppress degradation of the organic matrix while allowing demineralisation. We hypothesised that these characteristics might explain the unexpected capacity of cathepsin K inhibitors to enhance bone formation: they might prevent degradation not only of matrix collagen, but also other matrix-embedded proteins, including the growth factors that are known to be embedded in bone matrix. We tested this hypothesis using osteocalcin and IGF-I as examples of matrix-embedded proteins. We found that, when osteoclasts were incubated on bone, inhibitors of cathepsin K dramatically increased the concentrations of these matrix-derived proteins in supernatants. Other resorption-inhibitors did not do this. Inhibition of cathepsin K appeared to act by protecting the proteins against intracellular degradation, rather than against their degradation in supernatant. We also found that protons are both necessary and sufficient to release IGF-I from bone matrix, and that recombinant cathepsin K is capable of the degradation of both marker proteins. In the presence of a cathepsin K-inhibitor, the amount of IGF-I released from matrix by osteoclasts substantially exceeded the amount they secreted. Cathepsin K-inhibition similarly augmented release of bone morphogenetic protein (BMP)-2. Moreover, the numbers of osteoblastic MC3T3-E1 were greater after co-culture with osteoclasts on bone with versus without cathepsin K-inhibitor, showing that osteoclasts release biologically-significant quantities of growth factors from bone, and that the biological activity of the released growth factors is preserved by inhibition of cathepsin K. These results suggest a model in which cathepsin K inhibitors prevent degradation of growth factors released from bone matrix by osteoclast-derived protons, thus augmenting the anabolic component of the coupling between bone resorption and bone formation.

Disclosures: K. Fuller, None.

W336

Elcatonin Injections after Drill-hole Injury in Mice Inhibits Osteoclast Differentiation and Prevents the Decrease of Bone Mineral Density in Non-injured Bones with Promotion of Repair in the Cortical Bone Defect. Y. Katae^{*1}, S. Tanaka¹, A. Sakai¹, M. Nagashima^{*2}, H. Hirasawa^{*1}, N. Nakura^{*1}, K. Sabanai^{*1}, K. Menuki^{*1}, H. Yamane^{*1}, K. Tanaka^{*1}, Y. Shimizu^{*1}, T. Nakamura¹. ¹Orthopaedic Surgery, School of Medicine, University of Occupational and Environmental Health, Kitakyushu, Japan, ²Orthopaedic Surgery, Moji Rosai Hospital, Kitakyushu, Japan.

We evaluated the effects of elcatonin on the bone repair of drilled bones and non-injured bones in mice. Twelve-week-old male C57BL/6J mice were treated with a subcutaneous injection of elcatonin 3 times a week in three doses (0.2mg/kg body weight (BW); ELL, 2.0mg/kg BW; ELM, and 20mg/kg BW; ELH), or the vehicle (VC) from 12 weeks of age until sacrifice. Base-control animals at 12 weeks of age were sacrificed before drilling (day 0), and the specimens were obtained. At 12 weeks of age (day 0), a drill-hole was made in the diaphysis of the left femur and tibia. Twelve-week-old sham operated mice were used as the Control. Specimens were obtained at days 0, 5, 7, 9, 14, 21 and 28 after surgery.

The mean bone mineral density (BMD) values of the vertebral bodies in the VC group decreased at days 7, 14 and 21, and those of one-third of the non-injured distal femoral in the VC group decreased at day 28. Elcatonin injection inhibited the reduction of those values. In the non-injured femur of the VC group, the values of the osteoclast surface of the distal metaphysis and the number of osteoclasts derived from bone marrow increased, but did not increase in the ELM and ELH groups at day 14. In the elcatonin-treated groups, regenerating bone was filled up earlier than in the VC group. The BFR values of the regenerating bone at the drill-hole in the ELM and ELH groups tended to increase compared with those in the VC group at day 21, but did not at day 28. In the ELH group, the number of alkaline phosphatase-positive colony forming unit-fibroblasts in the bone marrow cell culture was higher than in the VC group at day 7. In the elcatonin-treated groups, the osteoblastic mRNAs expression levels of bmp2, osterix, colla1, and osteocalcin were significantly increased compared to those in the VC group at day 5. The expression levels of rankl/opg and trapc mRNA were similar among all groups.

These data indicate that injection of elcatonin after a drill-hole injury in mice inhibited osteoclast differentiation and prevented the decrease of BMD in non-injured bone without retardation of the filling up with regenerating bone in the drill-hole.

Disclosures: Y. Katae, None.

W337

Icariin, an Active Ingredient in Herba Epimedii, Exerts Bone Protective Effects In Vivo and In Vitro. W. P. Lai^{*1}, S. K. Mok^{*1}, W. Y. Pang^{*1}, X. L. Wang^{*2}, X. S. Yao^{*2}, M. J. Favus³, M. S. Wong¹. ¹Applied Biology and Chemical Technology, The Hong Kong Polytechnic University, Hong Kong, China, ²School of Pharmacy, Shenyang Pharmaceutical University, Shenyang, China, ³Pritzker School of Medicine, The University of Chicago, Chicago, IL, USA.

Icariin is an active compound identified in Herba Epimedii (HEP), a Chinese medicinal herb frequently used for treatment of osteoporosis. The present study aims to determine the osteoprotective effect of Icariin in vivo and in vitro.

Four-week-old sham-operated or ovariectomized C57BL/6J mice were pair-fed and treated with icariin (300ug/g/day), E₂ (4ug/g/day) or its vehicle by tube-feeding for 6 weeks. Body weight and uterus weight were recorded. Blood sample were collected for Ca and P detection, while bone tissues were for BMD measurement by pQCT. Icariin treatment did not alter serum Ca and P in OVX mice. Unlike E₂ treatment (OVX vs. E₂, p<0.01), icariin feeding did not alter the uterus to body weight ratio (OVX vs. Icariin, p=NS) in OVX mice. Six weeks of icariin treatment increased trabecular BMD (Icariin vs. OVX, p<0.05) in distal end of femur and cortical BMD (Icariin vs. OVX, p<0.05) in mid-shaft of tibia as well as its cortical thickness (Icariin vs. OVX, p<0.05) significantly. The results indicated that icariin is effective in maintaining BMD in OVX mice.

The in vitro effect of icariin (10⁻¹⁴ to 10⁻⁶M) on bone cell proliferation and differentiation were determined by MTS and alkaline phosphatase (ALP) activity assay using rat osteoblast-like UMR 106 cells, respectively. In addition, the effects of icariin on osteoprotegerin (OPG) and RANKL mRNA expression were determined by real time reverse-transcriptase polymerase chain reaction (RT-PCR). Icariin could increase proliferation (at 10⁻¹⁰M to 10⁻⁶M, p<0.05) and differentiation (at 10⁻¹⁴M to 10⁻⁶M, p<0.05; maximal at 10⁻¹²M) of UMR-106 cell. OPG and RANKL mRNA expression in UMR 106 cells increased significantly in response to treatment with icariin. However, the degree of up-regulation was generally higher for OPG than RANKL at all dosages, resulting in a higher OPG to RANKL gene expression ratio in all icariin treated groups, suggesting that icariin might inhibit the process of osteoclastogenesis.

The results clearly demonstrated that icariin, a major active ingredient in Herba Epimedii, could exert bone protective both in vivo and in vitro. The study provides the mechanistic basis for the use of Herba Epimedii in treatment of postmenopausal osteoporosis.

Disclosures: W.P. Lai, None.

This study received funding from: The National Natural Science Foundation of China and the Research Grants Council of Hong Kong Joint Research Scheme (N PolyU536/.094).

W338

The Approach for Screening Natural Plant Ingredients for Development of Nutraceutical Supplements to Support Bone Health. Y. Lin^{*1}, M. A. Murray^{*1}, D. Krempin^{*1}, K. Gellenbeck^{*1}, H. Roh-Schmidt^{*1}, L. Wilkins^{*2}, J. F. Rehman^{*1}, R. K. Randolph^{*1}. ¹Nutrilit Health Institute, Buena Park, CA, USA, ²Interleukin Genetics Incorporated, Waltham, MA, USA.

Preformulation research towards development of efficacious nutraceutical supplements was conducted to identify natural plant ingredients that have positive effects on reducing bone resorption and stimulating bone formation. A systematic screening strategy included mechanism of action specific bio-assays and neonatal murine calvarial organ culture systems. Natural ingredient extracts were first screened for the ability to inhibit the receptor activator of NFκB ligand (RANKL) expression via inhibition of IL-1 production by T cells. The ingredients that exhibited the best inhibition of RANKL expression were further assessed for their ability to reduce 45Ca release in a murine calvarial organ culture system. A similar screening strategy was also conducted for identifying bone formation ingredients where ingredients were first assessed for their ability to trigger osteoblast cell differentiation by the activation of bone morphogenic protein (BMP) expression by BMP-2 gene expression. Ingredients with positive outcome were also screened for their ability to induce BMP-2 promoter activity and BMP-2 protein expression. The ingredients that exhibited the best induction in BMP-2 assays were further assessed for their ability to increase new bone formation in a neonatal murine calvaria organ culture system. More than 50 natural ingredients screened by RANKL assay and BMP-2 gene expression assay. Nine ingredients found to inhibit RANKL expression were evaluated for inhibition of bone resorption in the calvarial system. Pomegranate extract was found to be the most efficacious ingredient to reduce bone resorption and compared favorably to alendronate in the calvarial system. Grape seed extract also exhibited a reduction in bone resorption similar to alendronate in the calvarial system. Eight of 50 natural ingredients were found to induce BMP-2 gene expression, and further screened for induction of BMP-2 promoter activity, BMP-2 protein expression, and bone formation in the calvarial system. Natural quercetin was found to be the most effective to induce both BMP-2 activity, and was comparable to drug control in increasing new bone formation in the calvarial system. Ethanolic licorice extract also exhibited a positive effect on bone formation in both BMP-2 assays and the calvarial system. This screening strategy was successful in preliminary identification of potentially efficacious ingredients towards the development of nutraceutical formulas to support bone health.

Disclosures: Y. Lin, Nutrilit 3.

This study received funding from: Access Business Group, LLC.

W339

Role of Nitric Oxide in the Preventive Effects of Electrical Stimulation on Ovariectomy-induced Bone Loss in Rats. A. P. R. Lirani-Galvão^{*1}, C. Bergamaschi^{*2}, O. L. Silva^{*3}, N. Portero-Muzy^{*4}, A. B. Carvalho^{*5}, V. Jorgetti^{*5}, P. Chavassieux^{*4}, M. Lazaretti-Castro^{*1}, P. D. Delmas^{*4}. ¹Departamento de Medicina, Universidade Federal de São Paulo, São Paulo, Brazil, ²Departamento de Ciências da Saúde, Universidade Federal de São Paulo, Santos, Brazil, ³Bioengenharia, Universidade de São Paulo, São Carlos, Brazil, ⁴INSERM Unité 831, Université de Lyon, Lyon, France, ⁵Departamento de Medicina, Universidade de São Paulo, São Paulo, Brazil.

Electrical stimulation (ES) is able to stimulate osteogenesis probably through the production of nitric oxide (NO). The aim of the present study was to evaluate the effects of ES and the potential role of NO on bone structure, microarchitecture and remodelling in ovariectomized (OVX) rats. Sixty rats (200-220g) were divided into 6 groups: sham; treated with 6mg/d of L-NAME, an inhibitor of NO synthase (sham-L); ovariectomized (OVX); treated with L-NAME (OVX-L) or subjected to an electrical stimulation (OVX-ES) or both (OVX-L-ES) for 12 weeks. After double tetracycline labelling, rats were sacrificed and the tibias were collected for histomorphometric analysis. The decreased bone mass and increased remodeling with an augmentation of eroded surface (ES/BS) induced by OVX were prevented by ES. In sham-L, the significant increases in bone volume (BV/TV), trabecular number (TbN) and node number (NdN/TV) associated with decreases of mineralizing surface (MS/BS) and bone formation rate (BFR/BS) suggested a possible biphasic effect of L-NAME on the bone formation with a possible initial stimulation followed by a diminution of the osteoblast activity. In contrast, in OVX-L, this initial increased formation was not observed. In presence of L-NAME, ES did not induce significant increases in BV/TV and TbN. But ES seemed to partly prevent the negative effect of L-NAME on bone formation after 12 weeks.

Groups	BV/TV (%)	TbN (/mm ²)	NdN/TV (/mm ²)	ES/BS (%)	MS/BS (%)	BFR/BS (μm ² /μm/d)
sham	24.8±8	3.9±0.9	9.6±4	3.2±1.8	7.7±2.9	0.15±0.1
OVX	10.2±2 ^{ab}	1.7±0.3 ^{ab}	3.65±1 ^{ab}	4.7±1.7 ^a	15.9±7.9 ^{ab}	0.47±0.4 ^{ab}
OVX-ES	22±11	3.69±1.8	4.27±2	3.3±2	7.7±6	0.12±0.1
sham-L	37±7 ^{ad}	5.8±0.6 ^{ad}	19.1±3 ^{ad}	4.14±1.8	3.80±2 ^a	0.04±0.03 ^a
OVX-L	14±7	2.3±1	3.52±2	6.24±2	5.8±3.7	0.06±0.05
OVX-L-ES	15.8±9 ^c	2.4±1 ^c	6.84±7 ^c	2.65±1.4 ^{cd}	12.1±3.7 ^c	0.205±0.1 ^c

P<0.05^a vs sham; ^b vs OVX-ES; ^c vs sham-L; ^d vs OVX-L

In conclusion, ES may prevent OVX-induced bone loss. These effects may be mediated through NO. However, L-NAME appeared to directly modulate bone formation. The initial increase in bone formation under L-NAME may be due to the augmented blood pressure which may act as a mechanical stimulation on osteoblasts (Turner et al., Bone 1997, 21:487-90) but after long-term, L-NAME inhibited osteoblastic activity.

Disclosures: A.P.R. Lirani-Galvão, None.

This study received funding from: CAPES, CNPq.

W340

Knowledge of Osteoporosis Among Tertiary Students in Vietnam. H. T. T. Nguyen^{*1}, N. D. Nguyen^{*2}, T. T. H. Ha^{*3}, C. K. T. Nguyen^{*3}, B. H. Nguyen^{*3}, T. V. Nguyen^{*2}. ¹Medical University, Karolinska Institute, Stockholm, Sweden, ²Bone and Mineral Research Program, Garvan Institute of Medical Research, Sydney, Australia, ³Hanoi Medical University, Hanoi, Viet Nam.

Osteoporosis has emerged as one of the most significant public health problems in the world, especially in developing countries. Prevention is recognized as an ideal approach to reduce the burden of osteoporosis. Knowledge is considered as important component in any preventative program; however, assessment of osteoporosis knowledge has not been well studied. The aim of this study was to assess the knowledge about osteoporosis among tertiary students in Vietnam.

Three hundred and five students were randomly invited from 5 universities/colleges (Medicine, 40%; Pharmacy, 12%; Poly-techniques, 17%; Journalism, 17%; and Pedagogy, 14%). The median age of the students was 23y. Each student was administered a Vietnamese version of the OPQ questionnaire, which consists of 20 items with four components: general knowledge (GK), risk factors (RF), nutrition and exercise (N&E) and treatment (T). Each question was scored as 1 for correct answer and 0 for incorrect answer. Therefore, the maximum score for a participant was 20 and the minimum score was 0. The proportion of correct answers was then estimated for each participant. A log-binomial regression was used to estimate the association between factors and the likelihood of correct answers.

The median proportion of correct answers (for 20 items) was 65% (inter-quartile range, IQR: 45-75). The median of proportion of correct answers for GK was 80% (IQR: 60-100), RF 63% (IQR: 50-75), N&E 75% (IQR: 50-100) and T 33% (IQR: 0-67%). Results from a multivariable analysis suggested that medical and pharmacy students were more knowledgeable than other students, with the proportion of >75% correct answers being 55% vs. 7%. The multivariable log-binomial regression analysis suggested that the degree of osteoporosis knowledge among medical and pharmacy students was 7.3 times (95% CI: 3.7-14.6) higher than non-medical and pharmacy students. Moreover, students spending more than 2 hours in reading and listening to radio were 1.41 times (95% CI: 1.1-1.9) more likely to answer >75% correct questions compared to those with limited time (< 2hrs).

In summary, university/college students in Vietnam had good knowledge of osteoporosis, including general knowledge, nutrition and exercise and risk factors for osteoporosis. However, they had poor knowledge of treatment. These findings imply that there is a need for educational program via newspapers and radio to impart the osteoporosis knowledge in the general public and university students.

Disclosures: H.T.T. Nguyen, None.

W341

Local Delivery of Lovastatin by a Biodegradable Polymer Increases Callus Strength in Rats. J. S. Nyman¹, G. Gutierrez², I. R. Garret^{*3}, G. Rossini^{*3}, G. R. Mundy². ¹Orthopaedics, Vanderbilt University, Nashville, TN, USA, ²Medicine, Vanderbilt University, Nashville, TN, USA, ³Osteoscreen, San Antonio, TX, USA.

The one-time administration of BMP-2 at the site of a recent fracture has been found to enhance the strength of the callus and thus hasten fracture repair. However, BMP-2 is expensive to manufacture, and delivery of peptides to fracture sites can be problematic. Therefore, we have been investigating fracture repair with lovastatin, a small molecule that stimulates BMP-2 transcription when it reaches the bone microenvironment. Being insoluble, its release into the fracture site must be controlled in order to be effective. Therefore, we encapsulated the drug into nano-sized beads made of a biodegradable polymer (nanobeads in PGLA). Upon establishing the release kinetics and osteoinductive potential of lovastatin nanobeads, we investigated their effect on fracture repair. Mixing poly-DL-lactide (DURECT Corp.) with lovastatin in acetone produced nanobeads after dripping 1% PVA under continuous stirring. Following centrifugation, the encapsulated lovastatin was re-suspended in saline. An in vitro release assay determined the concentrations in which nanobeads could deliver doses of 0, 0.2, 1, 1.5, or 7.5 μg of lovastatin per day. These doses were assessed in a closed-pin, transverse fracture model involving male Sprague Dawley rats. Weight matched rats were divided into 5 groups, one for each nanobead dose. A single injection of 50 μl was administered directly into the fracture site immediately following the femoral break. After four weeks of healing, rats were sacrificed, and then the fractured femur was excised for micro-CT analysis (at 36 micron resolution) and biomechanical testing. The former involved measuring the fracture gap in sagittal images of the callus, while the latter involved three point bending at 3 mm/min about the medial-lateral plane. Results showed that when compared to vehicle-treated rats, the local delivery of lovastatin using biodegradable nanobeads reduced the fracture gap between the cortices by 125%, 160%, 219%, and 207% in a dose-dependent manner. Likewise, structural strength improved as the release rate increased, peaking at 1.5 μg/day. At this dose, there was a 39% and 94% increase in strength and work-to-fracture of the callus, respectively. For comparison, a single injection of rhBMP-2 has been found to increase the torsional strength of the callus by 60% at 4 weeks using similar rat model (Einhorn et al. JBJS 2003). Thus, a single injection of lovastatin that is released into the fracture in a controlled-manner also significantly increased the structural strength of the callus. Creating a stronger callus increases the likelihood that the fractured femur returns to functionality sooner than without treatment.

Disclosures: J.S. Nyman, None.

This study received funding from: Osteoscreen.

W342

Total Flavonoid Fraction of Rhizoma Drynaria and Its Active Ingredient, Naringin, Exert Bone Protective Effect In Vivo and In Vitro. W. Pang^{*1}, X. Wang^{*2}, S. Mok^{*1}, W. Lai^{*1}, X. Yao^{*2}, M. Wong¹. ¹Applied Biology and Chemical Technology, The Hong Kong Polytechnic University, Hong Kong, Hong Kong, ²School of Pharmacy, Shenyang Pharmaceutical University, Shenyang, China.

Rhizoma Drynaria (RD) is a Chinese medicinal herb commonly used for treatment of bone fracture in China. Naringin, a major flavonoid isolated from RD, was previously reported to stimulate bone cell proliferation and thus might be useful for treatment of osteoporosis. The present study aims to determine if the total flavonoid fractions of RD as well as naringin could exert bone protective effects in vivo and in vitro, respectively. Six-weeks old sham-operated or ovariectomized young C57 BL/6J mice were orally administered with either the total flavonoid fractions (ex-low: 0.03875, low: 0.0775, mid: 0.155, high: 0.31 mg/g/day) of RD, 17 β -estradiol (4 μ g/g/day) or its vehicle for 6 weeks. Serum and urine were collected for biochemical marker determination while femur were collected bone mineral density (BMD) determination using peripheral quantitative computed tomography (pQCT). Total flavonoid fractions of RD did not alter serum Ca, P and uterus weight in OVX mice. The increase in urinary Ca excretion by OVX was reduced in rats treated with RD fractions. Treatment of OVX-mice with RD flavonoids increased trabecular BMD in femur in a dose-dependent manner with the optimal dosage at 0.155 mg/g/day. The in vitro effects of total flavonoid fraction (0.02 to 200 μ g/ml) and naringin (10^{-8} to 10^{-5} M) on bone cell proliferation and differentiation were determined by MTS and alkaline phosphatase activity assay using rat osteoblastic-like cell, UMR 106 cells, respectively. Total flavonoid fraction of RD increased cell proliferation in dose-dependent manner. At 2 μ g/ml, it significantly increased cell proliferation by 79% ($p < 0.001$). Naringin also increased cell proliferation and differentiation in a dose-dependent manner. At 10^{-8} M, it significantly increased cell proliferation by 50% ($p < 0.001$) and differentiation by 60% ($p < 0.001$). Our studies demonstrated that total flavonoid fraction of RD and its isolated flavonoid compound, naringin, could exert bone protective effects in vivo and in vitro. Our results suggest that RD and naringin might be an effective therapeutic agent for treatment of osteoporosis.

Disclosures: W. Pang, None.

This study received funding from: The National Natural Science Foundation of China and the Research Grants Council of Hong Kong Joint Research Scheme (N PolyU536/04).

W343

Interactive Effects of Milk Basic Protein Supplementation and Habitual Physical Activity on Bone Health in Older Women: A 1-Year Randomized Controlled Trial from the Nakanojo Study. H. Park¹, A. Yasunaga^{*1}, E. Watanabe^{*1}, F. Togo^{*1}, S. Park^{*1}, K. Yoshiuchi^{*2}, H. Kikuchi^{*2}, H. Kawakami^{*3}, Y. Morita^{*3}, A. Ono^{*3}, R. J. Shephard^{*4}, Y. Aoyagi^{*1}. ¹Exercise Sciences Research Group, Tokyo Metropolitan Institute of Gerontology, Tokyo, Japan, ²Department of Psychosomatic Medicine, The University of Tokyo, Tokyo, Japan, ³Technology and Research Institute, Snow Brand Milk Products Co., Ltd., Saitama, Japan, ⁴Faculty of Physical Education and Health, University of Toronto, Toronto, ON, Canada.

Milk basic protein (MBP) has been reported as improving bone health in healthy adults (aged <50 years). However, findings were not controlled for possible differences of habitual physical activity between control and experimental subjects. Thus, we examined possible interactive effects of MBP and habitual physical activity in the elderly. 79 Japanese female volunteers aged 65-86 years completed a randomized controlled study. Serum and urinary indices of bone metabolism, a forearm dual X-ray absorptiometric measure of bone mineral density (BMD), and a calcaneal osteosonic index (OSI) were measured at 0, 6, and 12 months. Step count and activity intensity (metabolic equivalents, METs) were measured by accelerometer every 4 s throughout one year. MBP (40 mg/day) had no effects on serum osteocalcin (OC) or bone-specific alkaline phosphatase (BALP). Urinary deoxypridinoline (Dpd) and cross-linked N-telopeptides of type-I collagen (NTx) also showed no MBP effect at 6 months, but at 12 months excretion was significantly less than in controls. Forearm BMD and calcaneal OSI scores tended to decrease in controls, but experimental subjects maintained BMD and had a statistically significant 1.5% increase of OSI at 12 months. After adjustments for age and baseline values of bone-related parameters, OC, NTx, Dpd, and/or OSI at 12 months were significantly related to step count and/or activity >3 METs, with no significant treatment x activity interactions for other parameters (BALP and BMD). MBP supplementation appears to prevent bone loss in older women, particularly in the lower extremities. However, a longer trial is needed to establish the clinical significance of the observed changes. Reduced resorption of bone is favored by moderate habitual physical activity.

Disclosures: H. Park, None.

This study received funding from: Grant-in-Aid for Scientific Research (C): 1500503.

W344

The Long Term Effect of 2-Arachidonoyl Glyceryl (AG) Ether on Body Weight and Bone Mass. S. Park, C. Hwang^{*}, H. Kwak^{*}, M. Jung^{*}, Y. Kang^{*}, H. Yoon, C. Yim^{*}, K. Han^{*}. Division of Endocrinology, Department of Internal Medicine, Cheil General Hospital & Women's Healthcare Center, Kwandong University College of Medicine, Seoul, Republic of Korea.

The CB1 cannabinoid receptor, one of the cannabinoid receptors has been known to regulate appetite, bone remodeling and bone mass. CB1 receptor-related researches have revealed discrepancies for body weight and bone mass according to murine phenotype and methodology. We investigated the effect of prolonged use of CB1 receptor agonist on body weight, behavioral activity and bone mass in mice. 6-week female Balb/c mice were received noladin ether (2-AG ether) known as a CB1 specific agonist or placebo intraperitoneally with ad libitum food for 10 weeks and injections were performed 6 times per week. There was a significant increase in body weight following administration of noladin ether (0.1 and 1 mg/kg), which was pronounced since 5-week treatments with noladin ether. The examinations for pharmacological activity of noladin ether showed a significant dose-dependent decrease in intestinal motility reflected by rate of defecation, however, showed no specific change in other tests for locomotor activity and antinociception. For bone mass, 0.1 mg/kg of noladin ether resulted in increased bone mineral density in femur. In conclusion, the chronic study with CB1 receptor agonist suggests that the body weight enhancement effect of 2-AG ether could be maintained throughout prolonged use for a long period and additional bone-protective effect might be obtained with 2-AG ether. Further study to delineate mechanism of noladin ether on bone would be needed.

Disclosures: S. Park, None.

W345

P2X₇ Agonist Reduce Ovariectomy-induced Bone Loss in a Murine Model. S. Syberg^{*1}, S. Petersen^{*1}, J. Teilmann^{*1}, J. B. Jensen¹, P. Schwarz², N. R. Jørgensen¹. ¹Endocrinology and Clinical Biochemistry, Copenhagen University Hospital Hvidovre, Hvidovre, Denmark, ²Research Center of Aging and Osteoporosis, Copenhagen University Hospital Glostrup, Glostrup, Denmark.

The purinergic P2X₇ receptor mediates intercellular signaling between osteoblasts and osteoclasts, and it is involved in the regulation of osteoclast activity. Knockout models for this receptor have been established, but conflicting results have been reported for the different models. We have reported earlier, that deletion of the P2X₇ receptor in C57BL/6N.CrlBR mice results in increasing BMD. BzATP is a P2X₇ agonist that has been reported to increase mineralization in osteoblasts in vitro. In this study ovariectomized BALB/cJ mice were treated with BzATP for a month, to investigate the effect of the agonist in vivo. Female mice were, at the age of 4 months, DEXA scanned on a Piximus scanner (Lunar Corp.) to determine bone mineral density (BMD) and bone mineral content (BMC). One group were sham operated, the rest were ovariectomized. After a period of 4 weeks to resituate, the animals were again DEXA scanned, and treatment were initiated. 85 ovariectomized mice were treated with BzATP in two concentrations or positive (PTH) and negative controls (vehicle) for 4 weeks. At sacrifice serum was collected from animals to measure in vivo markers of bone formation and resorption (Osteocalcin, C-telopeptide collagen and Alkaline phosphatase). All animal procedures were approved by the Danish Animalcare Society. The ability of the femurs to resist mechanical forces ex vivo was quantified. After treatment lumbar spine, femur and tibia were collected for histomorphometric analysis and the other femur and tibia was saved for bone strength measurements and μ CT scanning respectively. Four weeks after the ovariectomy the animals had lost 9% of their bone mineral density (BMD). Subcutaneous injection of low doses of BzATP every other day reduced the loss of BMD to 5%. Compared to the positive control group, that were treated with PTH, the BzATP treated animals had higher BMDs. In the femur region the PTH treated group did not differ significantly from the vehicle treated group, but the effect of BzATP were maintained. In this study we have shown that BzATP in vivo is capable of increasing BMD in animals that have lost BMD in response to estrogen depletion by ovariectomy, further results will be presented to confirm the results.

Disclosures: S. Syberg, None.

W346

Unfocused Extracorporeal Shockwave Therapy Diminishes Bone Loss in Ovariectomized Rats. O. P. Van der Jagt^{*1}, W. Schaden^{*2}, H. T. Van Schie^{*1}, T. M. Piscoer^{*1}, J. A. N. Verhaar^{*1}, J. C. Van der Linden^{*1}, H. Weinans¹. ¹Orthopaedic research lab, Erasmus MC, Rotterdam, The Netherlands, ²Orthopaedics, Unfallkrankenhaus Meidling, Vienna, Austria.

Extracorporeal Shockwave (ESW) therapy has shown to be effective in the treatment of non-unions and fracture healing. Other studies also show enhanced proliferation and differentiation of osteoprogenitor cells in rats after a single ESW treatment. Therefore ESW therapy might play a role in the treatment of osteoporosis. We evaluated if unfocused electro-hydraulically driven ESW could influence the bone architecture and the fracture healing in ovariectomized rats.

To induce bone depletion ovariectomy was performed, 3 or 10 weeks before the first ESW treatment. To evaluate the effects on fracture healing in the same animals a bilateral fibula osteotomy was performed two days before the first treatment. Also a sham-ovariectomy

with fibula-osteotomy was treated, to evaluate architectural changes in healthy bone. A control group to exclude influences of the osteotomy and ovariectomy was also evaluated. N=6 for all groups.

ESW therapy was given to the right leg, 3 or 10 weeks after OVX. Two treatments regimes were evaluated: a single treatment with 2000 pulses, 0.13 mJ/mm², or two treatments with three weeks in between with 1000 pulses, 0.13 mJ/mm².

In vivo micro-CT scans of the treated and non-treated leg were made before ESW treatment as well as 3, 6 and 10 weeks thereafter.

With in vivo micro-CT scanning we can longitudinally evaluate the bone architecture of a single rat in a highly detailed manner (voxelsize of 18 microns). The proximal metaphysis of the tibia and the osteotomy site of the fibula were analyzed. Bone morphologic parameters of both the cortex and cancellous bone were calculated.

3 Weeks after ESW treatment of shamOVX rats, 10% higher trabecular volume fraction (TBV), 8% higher connectivity and 3% higher trabecular thickness was seen. Cortical volume and thickness were 3 % lower in all treated legs. TBV of the treated legs of rats ovariectomized 3 weeks prior to treatment was 5% more than contralateral non-ESW legs and mean trabecular thickness was lower in all treated legs (3%). Also effects on cortical bone of OVX were diminished. These effects but smaller were also seen in rats ovariectomized 10 weeks prior to treatment but only in the group which received 2000 pulses.

These data suggest that electro-hydraulically driven unfocused shockwaves can influence bone architecture in healthy and osteoporotic bone. The number of shocks seems to be important in more progressed bone loss. How long a single treatment has its anabolic effect on the bone must be further investigated. Because these unfocused shockwaves are not painful, ESW can become a clinically relevant treatment for osteoporosis.

Disclosures: O.P. Van der Jagt, None.

W347

Extracorporeal Shockwave Therapy Stimulates Bone Remodeling in the Rat, Evaluated with In-vivo Micro-SPECT Scanning. O. P. Van der Jagt^{*1}, T. M. Piscoer^{*1}, M. Bijster^{*2}, W. Schaden^{*3}, J. A. N. Verhaar^{*1}, J. C. Van der Linden^{*1}, M. De Jong^{*2}, H. Weinans¹. ¹Orthopaedic Research Lab, Erasmus MC, Rotterdam, The Netherlands, ²Nuclear Medicine, Erasmus MC, Rotterdam, The Netherlands, ³Orthopaedics, Unfallkrankenhaus Meidling, Vienna, Austria.

It is known that Extracorporeal Shockwave therapy (ESWT) can stimulate fresh fracture repair and healing of non-union, in animal models as well as in humans. There are indications that ESWT may stimulate normal bone remodeling as well. By labeling the radioisotope 99m-Tc-methylene diphosphonate (Tc-99m-MDP) we can image bone remodeling with in vivo multi pinhole micro-SPECT scanning of a single rat in a longitudinal manner. In this way we can observe effects of the treatment on bone remodeling and evaluate these in time with a resolution of less than 0.5 mm.

Male Wistar rats 13 weeks of age received one ESW treatment on the tibia with 1000 pulses of 0.13 mJ/mm² or 1000 pulses with 0.30 mJ/mm², both with n=6. Only the right tibia was treated, the contra-lateral left tibia served as control. At 48 hours and 1 week after treatment micro-SPECT scanning was performed. 6 hours before scanning rats got an injection with Technetium-99m-MDP. Both lower legs were scanned in the same session, using gas anesthesia.

Follow-up scans of the rats treated with 0.13 mJ/mm² did not show an enhancement of the bone remodeling of the treated leg compared to the control leg at both 48 hours and 1 week.

The higher dose of 0.30 mJ/mm² on the other hand did show a 20% higher activity in the treated leg compared to the non-treated contralateral left leg at after 1 week after shockwave therapy.

Unfocused electro-hydraulic generated shockwave therapy can alter bone remodeling in rats, but this is highly dependent on the energy level of the shockwaves. It is likely that this alteration will influence the bone architecture, but how long the enhanced effects remain after a single treatment is not known yet. An explanation for the enhanced turnover cannot be concluded from these data, though the dependency of energy level and the resemblance with fracture healing may suggest that micro damage can be the trigger for enhanced bone remodeling. More work (e.g. histology for microdamage) is needed to reveal the underlying mechanisms of the described phenomena.

Disclosures: O.P. Van der Jagt, None.

W348

Restoration of Regenerative Osteoblastogenesis in Aged Mice: Modulation of TNF. E. C. Wahl^{*1}, J. Aronson^{*1}, L. Liu^{*1}, R. A. Skinner^{*1}, M. J. Miller^{*1}, J. L. Fowlkes¹, K. M. Thraill¹, T. M. Badger^{*1}, M. J. J. Ronis^{*1}, J. Sims^{*2}, C. K. Lumpkin¹. ¹University of Arkansas for Medical Sciences, Little Rock, AR, USA, ²Amgen, Seattle, WA, USA.

Studies have demonstrated that skeletal changes accompanying aging (type 2 osteoporosis) are associated with decreased bone mass, increased risk of fractures, impaired fracture healing, and increased serum levels of pro-inflammatory cytokines: tumor necrosis factor alpha (TNF) and interleukin 6 (IL-6). Previous studies utilizing a mouse distraction osteogenesis (DO, tibial lengthening) model demonstrate that aging is associated with elevated serum TNF levels and inhibition of direct bone formation and that treatment of young mice with recombinant mouse tumor necrosis factor α (rmTNF) inhibits bone formation. Here we report the results of studies on aged mice undergoing DO and treatment with TNF blockers (Pegsunercept-soluble TNF receptor 1 derivative [sTNFR1] or Enbrel-soluble TNF receptor 2 derivative [sTNFR2]).

1) To study the effects of a TNF antagonist on direct bone formation 24 (22 month old) male C57BL/6 mice underwent the DO protocol. After the three day latency period, half the mice were treated (sq injection) with either vehicle or sTNFR1 (8 mg/kg/every two days) over the 14 day distraction period. Histological analysis demonstrated an increase in bone formation (also observed in the radiographs) of the treated mice (76.1% \pm 7.6) versus the vehicle controls (31.2% \pm 12.4; P<0.01). In fact, 86% of the treated mice "bridged" (osteoid from both cortices meet and overlap) the gap during distraction, while none of the controls exhibited bridging. Serum analyses confirmed high levels of sTNFR1 in treated mice only and further demonstrated increased serum levels of TNF α , IL -6, and insulin in 22 month old mice as compared to 3 month old male C57BL/6 mice from a contemporary study. No differences were noted in serum mIGF-1 levels in aged mice.

2) A study comparing the effects of sTNFR1 and Enbrel (FDA approved derivative of sTNFR2) in 21 month old mice was performed. Mice were divided into three equal groups: vehicle, sTNF-R2, and sTNF-R1 treated. The mice received subcutaneous injections of vehicle (PBS pH 7.4), Enbrel (8.0 mg/kg), or sTNF-R1 (8.0 mg/kg) every other day for the 14 day distraction period. Histological analysis demonstrated an increase in bone formation in the treated aged mice (sTNFR1:70.5% \pm 4.9; sTNFR2:75.7% \pm 6.3) versus the aged vehicle controls (45.7% \pm 12.8; P<0.05).

These studies provide proof of concept that age-related deficits in direct bone repair are reversible.

Disclosures: E.C. Wahl, None.

W349

Turmeric Extracts for Postmenopausal Osteoporosis Treatment: An Initial Evaluation. L. E. Wright^{*1}, J. B. Frye^{*1}, T. Henderson^{*1}, M. L. Bouxsein^{*2}, S. L. Marion^{*1}, P. Hoyer^{*1}, J. L. Funk¹. ¹Physiological Sciences Graduate Program, University of Arizona, Tucson, AZ, USA, ²Beth Israel Deaconess Medical Center and Harvard Medical School, Boston, MA, USA.

In previous studies, curcuminoid-containing turmeric extracts were remarkably protective in preventing bone loss in an animal model of rheumatoid arthritis (RA), preventing up to 50% of bone resorption as measured by increases in bone mineral density (BMD), normalization of the local ratio of RANK/OPG, and inhibition of osteoclast formation in the distal femur. To determine whether turmeric might also prevent bone resorption in postmenopausal osteoporosis, its effects on bone were examined in ovariectomized (OVX) rats. In prevention (daily turmeric begun 4 days after OVX) or treatment studies (turmeric begun 1 month after OVX), 3 month old female Sprague Dawley rats were placed in the following treatment groups: (1) sham operated + vehicle; (2) OVX + vehicle; (3) OVX + turmeric extract (purified curcuminoid extract, 25 mg/kg/d ip); (4) OVX + turmeric extract (purified curcuminoids, 50 mg/kg/d ip). Effects of 2 months of in vivo extract treatment on bone were monitored by BMD analysis of the distal femur using dual-energy x-ray absorptiometry (DXA), serum markers for bone turnover, and assessment of bone microarchitecture of the distal femur by microCT. In the prevention study, OVX animals treated with vehicle lost bone mass relative to sham animals, had an 40% increase in serum C-telopeptide fragments of type I collagen (CTX-1), and had decreased trabecular number and increased structure model index (SMI) by microCT. Turmeric-treated OVX animals maintained on average higher BMD than OVX animals treated with vehicle, however this trend was not statistically significant. Trabecular microarchitecture in OVX animals was not changed after 2 months of turmeric extract treatment relative to vehicle-treated OVX animals, except for a decrease in trabecular thickness in animals treated with high dose turmeric. Turmeric treatment also did not alter serum markers of bone resorption except at day 10 with high dose turmeric treatment where levels were actually higher than in the OVX/vehicle group. In contrast, in the treatment study, turmeric-treated rats maintained significantly higher BMD relative to OVX animals treated with vehicle that continued to lose bone. However, at the end of treatment, serum CTX-1 levels in OVX animals remained increased relative to sham animals and were unchanged by turmeric treatment. From these studies we can conclude that despite similarities in the pathway of bone loss in RA and postmenopausal osteoporosis, the active components of turmeric extract may act differently on bone resorption in each disease.

Disclosures: L.E. Wright, None.

This study received funding from: The National Institutes of Health [P50 A500474].

W350

Phenotypic Variations of Fluoride Responses Between Inbred Strains of Mice. D. Yan^{*1}, X. Gu², E. Everett³. ¹Dental Research, University of North Carolina at Chapel Hill, Chapel Hill, NC, USA, ²Oral Biology Curriculum, University of North Carolina at Chapel Hill, Chapel Hill, NC, USA, ³Pediatric Dentistry, University of North Carolina at Chapel Hill, Chapel Hill, NC, USA.

Excessive exposure to fluoride (F) can lead to disturbances of bone homeostasis and tooth enamel development. We have previously shown (J Dent Res. 2002 Nov;81(11):794-8.) differences in dental fluorosis (DF) susceptibility between inbred strains of mice. The current study was undertaken to investigate F responsive variations in bone metabolism and to determine possible relationships with DF susceptibility. Seven-week-old male mice (n=6 for each strain and treatment/control group) from FVB/NJ, C57BL/6J, C3H/HeJ, A/J, 129S1/SvImJ, AKR/J, DBA/2J and BALB/cByJ strains were exposed to F (0 or 50ppm as F ion) in their drinking water for 60 days. Sera were collected for Ca, Mg, P04 and ALP levels. Bone marrow cells were harvested for ex vivo osteoclast potential, hematopoietic colony-forming cell (CFC), and fibroblast-colony-forming unit (CFU-f) assays. The DF severity in mandibular incisors was evaluated by quantitative light-induced fluorescence (QLF) and clinical criteria. Strain specific responses to fluoride were observed for DF, serum chemistries and ex vivo cell culture studies. For each strain examined total serum Ca was not significantly affected. Serum P04 was elevated in A/J mice (34%, p=0.001) and decreased in C57BL/6J (12%, p=0.008). Serum Mg was elevated in FVB/NJ (13%, p=0.004) and decreased in AKR/J and DBA/2J (12%, p=0.003 and 19%, p=0.006, respectively). Total ALKP increased in AKR/J (13%, p=0.032), C3H/HeJ (16%, p=0.005), FVB/NJ (40%, p=0.007) and 129S1/SvImJ (43%, p=0.002), whereas ALKP decreased in A/J (38%, p=0.008). Osteoclast potential increased in A/J (13%, p=0.003) and 129S1/SvImJ (84%, p<0.001). CFU-f (AKLP positive) colonies increased only in FVB/NJ (48%, p=0.026). DF severity (QLF) showed the greatest increase in A/J (417%, p<0.001) and C57BL/6J (157%, p<0.001); modest increase in FVB/NJ (76%, p<0.001), DBA/2J (62%, p=0.001), and C3H/HeJ (47%, p=0.017); and no significant changes in 129S1/SvImJ, AKR/J, and BALB/cByJ. Among the strains investigated there were no patterns or significant correlations between DF severity and any of the serum chemistries or ex vivo assays. Prolonged fluoride exposure lead to variable phenotypic responses between inbred strains involving bone metabolism, osteoclast potential and osteoprogenitor potential. Supported by the NIH/NIDCR R01DE014853.

Disclosures: D. Yan, None.

This study received funding from: NIH/NIDCR R01DE014853.

W351

Risedronate Efficacy for Non-vertebral Fractures Is Consistent Across Age Groups. J. P. Bilezikian¹, X. Zhou^{*2}, A. B. Klemes², S. Boonen^{*3}. ¹Columbia University, New York, NY, USA, ²Procter & Gamble Pharmaceuticals, Mason, OH, USA, ³University Hospital Leuven, Leuven, Belgium.

Age is one of the most important risk factors for fracture among untreated patients. With age, fracture risk increases. In this study, we examined relationships between age and fracture risk using data from randomized, placebo-controlled clinical trials. Risedronate anti-fracture efficacy (5 mg daily vs. placebo) was examined among and across a wide range of age groups.

The analysis population included 3229 post-menopausal women from 4 risedronate phase III randomized placebo-controlled clinical trials. Average age was 68 yrs and Femoral Neck (FN) T-score was -2.2. Fracture was defined as any osteoporosis-related radiographically confirmed non-vertebral fracture.

The impact of age was estimated using a Cox regression model, adjusted for FN T-score and treatment group and stratified by clinical trial in order to take into account different underlying hazard functions. Interactions among treatment, age and FN T-score were included in the initial model but then removed because it was not statistically significant (p>0.05).

The association between increased fracture risk and age did not differ significantly by treatment groups (p>0.05, for the interaction terms). For every decade increase in age, patient risk for any osteoporotic fracture increased by 49% (95% CI: 21%, 88%) among patients in the same treatment group with similar baseline FN T-score.

Overall, risedronate reduced non-vertebral fracture risk by 43% (33%, 58%) relative to placebo after adjusting for age and BMD. The relative risk reductions for patients with age <=65, 66-75 and >=76 were 51%, 39% and 45% with p-values < 0.03. The therapy is well tolerated in the treatment of women with established postmenopausal osteoporosis (Harris et al. JAMA 1999).

Age is an important risk factor for fracture. Risedronate demonstrated consistent efficacy for non-vertebral fractures across a wide range of age groups.

Osteoporotic Non-vertebral Fracture Incidence Over 0-3 Years by Age Group				
	<=65	66-75	>=76	OVERALL
Number of Patients	1197	1480	552	3229
Non-vertebral Fracture incidence				
Placebo	7.5%	9.4%	19.5%	10.5%
Ris 5 mg	3.8%	6.3%	11.3%	6.4%
RR (95% CI)	0.49 (0.26, 0.92)	0.61 (0.39, 0.96)	0.54 (0.31, 0.94)	0.57 (0.42, 0.77)
p-value	0.026	0.031	0.028	<0.001

Disclosures: J.P. Bilezikian, Procter & Gamble Pharmaceuticals S.

W352

Tolerability of Once-Monthly Ibandronate Across Different Age Groups of Women Switched From Once-Weekly Bisphosphonates. N. Binkley¹, M. G. Martens^{*2}, J. D. Kohles³, R. Civitelli⁴. ¹University of Wisconsin, Madison, WI, USA, ²Oklahoma University, Tulsa, OK, USA, ³Roche, Nutley, NJ, USA, ⁴Washington University, St Louis, MO, USA.

CURRENT, an open-label, 6-month, multicenter study, was designed to identify satisfaction levels and tolerability with once-monthly oral ibandronate in women switched from once-weekly bisphosphonates (BPs). Since drug tolerability is often a concern for older adults, tolerance to ibandronate was compared between women in younger and older age groups.

Postmenopausal women currently taking a weekly BP for ≥3 months for the treatment or prevention of osteoporosis or osteopenia were eligible to participate. Enrolled participants received 150-mg monthly oral ibandronate for 6 months. Adverse events (AEs) were monitored throughout the study.

The intent-to-treat population (n=1678) was grouped by age: <60 years of age (n=496); ≥60 to <70 (n=574); ≥70 to <80 (n=459); and ≥80 (n=149). The prevalence of osteoporosis in each age group was 49.2%, 66.7%, 73.2%, and 80.5%, respectively. AEs in the safety population (defined as participants who had received ≥1 dose of ibandronate and had ≥1 postbaseline safety measurement) are presented in the Table. In general, numerical differences in the percentage of participants with ≥1 AE between the <60 years group and the older groups were small. Infections/infestations were the most common class of AEs followed by gastrointestinal (GI) disorders. The percentage of participants experiencing GI AEs was 9.8% in the <60 group, 14.2% in the ≥60 to <70 group, 13.3% in the ≥70 to <80 group, and 12.8% in the ≥80 group. Four women (0.8%) in the <60 group experienced a renal and urinary AE. In the older groups, the range was 0.5% (≥60 to <70 group) to 1.5% (≥70 to <80 group). Women in the <60 group had the highest rate of fracture-related AEs among all the age groups. The incidence of participants withdrawing from treatment because of an AE was low and comparable between the <60 and older groups. GI disorders were the most common class of AEs leading to withdrawal in all the age groups. One patient, in the <60 group, experienced a renal AE leading to withdrawal; the AE was considered unrelated to medication.

No clinically meaningful differences were evident in the tolerability profile of once-monthly ibandronate for women of different age groups switched from weekly BPs.

Table. Adverse events in women across different age groups in the safety population

	<60 years n=491 n (%)	≥60 to <70 years (n=570) n (%)	≥70 to <80 years (n=459) n (%)	≥80 years (n=149) n (%)
Study participants with:				
≥1 AE	180 (36.7)	234 (41.1)	210 (45.8)	65 (43.6)
≥1 serious AE	9 (1.8)	12 (2.1)	24 (5.2)	9 (6.0)
≥1 fracture-related AE	15 (3.1)	10 (1.8)	11 (2.4)	4 (2.7)
≥1 AE resulting in withdrawal	13 (2.6)	21 (3.7)	29 (6.3)	5 (3.4)

AE, adverse event.

Disclosures: N. Binkley, Roche Laboratories, Inc. 2, 5, 8; GlaxoSmithKline 2, 8; Merck 2, 5, 8; Novartis 2, 5.

This study received funding from: Roche Laboratories, Inc.

W353

Monthly Ibandronate Is Associated with Reduced Risk of Serious GI Events Compared with Weekly Bisphosphonates: Results of an Observational Analysis. W. A. Blumentals^{*1}, S. T. Harris². ¹Roche Laboratories, Inc, Nutley, NJ, USA, ²University of California, San Francisco, CA, USA.

The use of oral bisphosphonates (BPs) has been associated with the occurrence of gastrointestinal (GI) symptoms. The objective of this study was to investigate the incidence of clinically severe GI events (including acute, bleeding, or perforation events) among patients receiving monthly ibandronate therapy compared to patients receiving weekly BPs.

Data were collected from the Medstat MarketScan® database. Eligible women were ≥45 years of age, filled a new (index) prescription for monthly ibandronate or weekly alendronate or risedronate from April 1, 2005 to December 31, 2005, and had continuous enrollment for at least 6 months prior to the index date (pre-index period). Exclusion criteria included Paget's disease and the use of any BPs during the 6 month pre-index period. Patients on weekly BPs were propensity-score matched to monthly ibandronate patients using baseline characteristics, including age and history of GI events, to ensure a well-matched patient population and reduce selection bias. Severe GI events were identified via ICD-9 and CPT codes. Incidence rates of GI events were calculated and logistic regression was used to compare odds of experiencing a serious GI event in patients receiving monthly ibandronate versus those receiving weekly BPs. Additionally, GI-related healthcare utilization rates, which included GI medication use, visits to GI specialists, and procedures such as endoscopies, were compared.

A total of 17216 patients (mean age of 63 years) were eligible for inclusion in this analysis, with 8608 patients per group. During the 6 month pre-index period, 106 (1.2%) patients in the monthly ibandronate group and 113 (1.3%) patients in the weekly BP group experienced a GI event. During the follow-up period (average of 93 days), 45 (0.52%) monthly ibandronate patients and 70 (0.81%) weekly BP patients experienced a GI event. Monthly ibandronate patients had a 36% reduction in the risk of serious GI events compared to weekly BP users (OR = 0.64, 95% CI = 0.44-0.93). In general, monthly ibandronate patients appeared to have lower GI-related healthcare service utilization but

these differences did not reach statistical significance.

Despite the low incidence of serious GI events that occurred in either group, we observed a statistically significant reduction in the risk of serious GI events for monthly ibandronate patients. Results of this analysis suggest that monthly ibandronate may be associated with a lower incidence of serious GI events compared with weekly BPs.

Disclosures: W.A. Blumentals, Roche 3.

This study received funding from: Roche Laboratories.

W354

Clinical Comparison in BMD Gains with Monthly Oral Ibandronate (150mg) and Weekly Oral Alendronate (70mg): Results From the MOTION Study. P. D. Miller¹, C. A. F. Zerbin², R. R. Recker³, F. Sedarati⁴, C. Neate⁵, J. Y. Reginster⁶. ¹Colorado Center for Bone Research, Lakewood, CO, USA, ²Hospital Heliopolis, Sao Paulo, Brazil, ³Creighton University, Osteoporosis Research Center, Omaha, NE, USA, ⁴Hoffmann-La Roche Inc., Nutley, NJ, USA, ⁵Roche Products Ltd, Welwyn Garden City, United Kingdom, ⁶University of Liège, Liège, Belgium.

The efficacy of monthly oral ibandronate and weekly oral alendronate for the treatment of postmenopausal osteoporosis has been directly compared for the first time in the MOTION (Monthly Oral Therapy with Ibandronate for Osteoporosis INtervention) study. The primary aim was to show non-inferiority for monthly ibandronate versus weekly alendronate in increasing bone mineral density (BMD) at both the lumbar spine and total hip over 12 months.

This was a randomized, multinational, multicenter, double-blind, double-dummy, parallel-group, non-inferiority study. The study enrolled 1,760 postmenopausal women with osteoporosis (age 55-84 years, time since menopause ≥ 5 years), with mean lumbar spine BMD T-score (L2-L4) < -2.5 and ≥ -5.0 SD. Patients were randomized to receive either 150mg monthly oral ibandronate and weekly placebo (n=887), or 70mg weekly oral alendronate and monthly placebo (n=873). All patients also received supplemental vitamin D 400IU/day and calcium 500mg/day. The primary efficacy endpoint was to show non-inferiority between ibandronate and alendronate in the relative change (%) from baseline at 12 months in mean BMD of the lumbar spine (L2-L4) and total hip. Monthly ibandronate would be proven clinically comparable to weekly alendronate if the lower boundary of the one-sided 97.5% CI was ≥ -1.41 percentage points for lumbar spine and ≥ -0.87 percentage points for total hip.

The intent-to-treat (ITT) population comprised 836 patients in the ibandronate arm and 822 in the alendronate arm. The per-protocol (PP) population comprised 725 patients treated with ibandronate and 720 with alendronate. The relative change in mean lumbar spine BMD (PP) was 5.10% with ibandronate and 5.78% with alendronate (95% CI for difference, -1.13, -0.23; non-inferiority met at ≥ -1.41). The relative change in mean total hip BMD (PP) was 2.94% with ibandronate and 3.03% with alendronate (95% CI for difference, -0.38, 0.18; non-inferiority met at ≥ -0.87). The PP analyses were confirmed in the ITT population. In conclusion, the primary endpoint was met with monthly oral ibandronate shown to have essentially similar increases from baseline to weekly oral alendronate at 12 months in both lumbar spine and total hip BMD.

Disclosures: P.D. Miller, F. Hoffmann-La Roche Ltd/GlaxoSmithKline 5.

This study received funding from: F. Hoffmann-La Roche Ltd/GlaxoSmithKline.

W355

Clinical and Nonvertebral Fracture Risk Is Reduced with the Use of Ibandronate in Women with Postmenopausal Osteoporosis. P. D. Miller¹, S. T. Harris², W. A. Blumentals³. ¹Department of Medicine, Colorado Center for Bone Research, PC, Lakewood, CO, USA, ²Osteoporosis Clinic, University of California, San Francisco, San Francisco, CA, USA, ³Roche Laboratories, Inc, Nutley, NJ, USA.

The purpose of this study was to assess fracture efficacy of ibandronate (IBN) at increasing doses and levels of annual cumulative exposure (ACE) in women with postmenopausal osteoporosis by pooling and analyzing data from the 4 pivotal phase III clinical trials.

Patients in the intent-to-treat (ITT) population who received oral or IV doses of IBN or placebo (PBO) in 4 studies (IV dose fracture study, BONE, MOBILE, and DIVA) were included in this pooled analysis.

BONE and the IV dose fracture study were 3-year PBO-controlled fracture trials. MOBILE and DIVA were 2-year BMD active-controlled studies that examined fractures as secondary endpoints. Doses were grouped by ACE, ie, high (≥ 10.8 mg includes 150mg oral monthly, 3mg IV quarterly, and 2mg IV every 2 months [q2mo]), mid (5.5-7.2mg), and low (≤ 4.0 mg) annual doses. ACE was defined as the drug strength (mg) multiplied by the number of annual doses and an absorption factor (0.6% for oral and 100% for IV). Fracture risk with IBN vs PBO was estimated using Cox hazards models, which controlled for age, baseline BMD T-score, and clinical fracture history. Due to confounding with ACE, the analysis was not stratified by study. All clinical fractures (both vertebral and nonvertebral), nonvertebral fractures (NVFs), and a subgroup of the 6 major NVFs (clavicle, humerus, wrist, pelvis, hip, leg) were examined. Time-to-fracture for different ACE groups was compared using log-rank tests.

A total of 1924 patients received PBO, 1911 received 2.0- ≤ 4.0 mg ACE, 3585 received 5.5-7.2mg ACE, and 1290 received ≥ 10.8 mg ACE in this pooled analysis. The group that received the highest annual doses of IBN (≥ 10.8 mg) had a reduction in relative risk of 28.8% for all clinical fractures, 29.9% for NVFs, and 34.4% for the subgroup of 6 NVFs compared with PBO (Table). The high ACE group had a longer time-to-fracture vs PBO

for all clinical fractures (P=0.002), and NVFs (P=0.025) at 2 years as determined by a log-rank test.

In this pooled analysis, we observed that the risk of clinical fractures and NVFs was significantly reduced for doses of ibandronate resulting in ACEs of ≥ 10.8 mg—which includes the marketed doses of 150mg monthly oral and 3mg IV quarterly.

Table. Adjusted hazard ratios for fractures at varying dose levels relative to placebo (ITT)

Fracture type ACE group (mg)	Adjusted hazard ratio	95% CI	P value
All clinical (vertebral + nonvertebral)			
High* (≥ 10.8)	0.712	0.55-0.92	0.010 [†]
Mid [‡] (between 5.5 and 7.2)	0.881	0.74-1.05	0.148
Low [§] (≤ 4.0)	0.887	0.73-1.07	0.211
Nonvertebral (all sites)			
High* (≥ 10.8)	0.701	0.50-0.99	0.041 [†]
Mid [‡] (between 5.5 and 7.2)	1.04	0.83-1.30	0.722
Low [§] (≤ 4.0)	0.893	0.69-1.15	0.383
Key nonvertebral sites (clavicle, humerus, wrist, pelvis, hip, and leg)			
High* (≥ 10.8)	0.656	0.45-0.96	0.032 [†]
Mid [‡] (between 5.5 and 7.2)	1.15	0.90-1.46	0.270
Low [§] (≤ 4.0)	0.871	0.66-1.15	0.334

*includes 150mg oral monthly, 3mg IV quarterly, and 2mg IV q2mo; [†]Significance defined as P<0.05 (unadjusted for multiple comparisons); [‡]include 2.5mg daily oral, 20mg oral intermittent, 2 x 50mg monthly oral, 100mg monthly oral; [§]includes 0.5mg IV q3mo and 1.0mg IV q3mo;
ACE, annual cumulative exposure

Disclosures: P.D. Miller, Roche Laboratories, Inc. 2, 5, 8; GlaxoSmithKline 5, 8; Proctor and Gamble 2, 5, 8; Sanofi-Aventis 2, 5, 8.

This study received funding from: Roche Laboratories, Inc.

W356

An Open Label Study on the Effects of Alendronate in Osteoporotic Patients Affected by Monoclonal Gammopathy of Undetermined Significance. S. Minisola¹, J. Pepe², C. Cipriani¹, M. T. Petrucci², M. L. Mascia¹, E. Romagnoli¹. ¹Department of Clinical Sciences, University of Rome, Rome, Italy, ²Department of Cellular Biotechnology and Haematology, University of Rome, Rome, Italy.

Patients with monoclonal gammopathy of undetermined significance (MGUS) should be considered at risk of fracture; the pathophysiological mechanism could be ascribed to the raised bone turnover rate, probably due to an altered relationship of the RANKL/OPG balance. Therefore, it seems rational that these patients could benefit by the use of drugs able to normalize the negative balance at the level of the single remodelling units.

We studied 100 patients (65 females and 35 males), divided in two groups according to the presence of vertebral fractures and/or osteoporosis. The group with skeletal fragility (group A, 50 patients) was treated with alendronate (70mg/weekly) plus calcium and cholecalciferol for 18 months. The group without skeletal fragility (group B) was treated with calcium and cholecalciferol. In each patient, BMD at lumbar and hip level together with bone turnover markers were evaluated every 6 months.

Thirty patients in group A and 29 in group B completed the study. After 18 months, the mean BMD of the lumbar spine had increased by 6.1 percent in group A and by 1.24 % in group B, an absolute difference between the two groups of 4.8 percent (p ≤ 0.001). The mean BMD of the total femur had increased by 1.5 percent in the alendronate group and decreased by 1.2 % in group B, an absolute difference between the two groups of 2.7 percent (p ≤ 0.01). After starting therapy with alendronate, there was a marked decrease in mean serum β CTX that persisted throughout the treatment period in osteoporotic MGUS patients; smaller mean decreases were observed concerning the other markers investigated. In MGUS patients without osteoporosis, we observed significant decreases of bone remodelling markers (the only exception being mean bone sialoprotein-BSP) following therapy with cholecalciferol and calcium. At 18 months, the absolute percent difference between the groups was -23.2 (p ≤ 0.01) for serum isoenzyme of bone alkaline phosphatase, -23.6 for serum osteocalcin (p ≤ 0.01), -35.1 for serum β CTX (p ≤ 0.001) and -0.47 (p = ns) for serum BSP.

These data suggest that the increase in vertebral BMD together with the reduction of bone turnover markers could lead to a significant reduction in fracture risk in MGUS patients with skeletal fragility.

Disclosures: S. Minisola, None.

W357

Therapeutic Effects of Risedronate for Two Years, on Bone Metabolic Markers, Especially on TRACP-5b. H. Naka^{*1}, H. Masaki^{*1}, Y. Imanishi^{*2}, T. Miki¹, Y. Nishizawa². ¹Geriatric Medicine, Osaka City University Graduate School of Medicine, Osaka, Japan, ²Department of Metabolism, Endocrinology and Molecular Medicine, Osaka City University Graduate School of Medicine, Osaka, Japan.

The prevention of treatment cessation for osteoporosis patients is important for providing protection against fractures. Assessing bone resorption in the early stage of treatment by evaluating various bone metabolic markers over time in risedronate therapy is considered useful in preventing cessation of treatment. Therefore, we conducted prospective study on the extent to which the therapeutic effect on the patient can be assessed by evaluating bone metabolic markers over time, including the new bone resorption marker TRACP-5b.

Risedronate was administered to 36 postmenopausal osteoporosis patients (mean age 66.3 years) for 2 year and the therapeutic effects on bone density and bone metabolic markers were evaluated. As a control, 8 people received Ca and were evaluated in the same manner. When bone metabolic markers (BAP, uNTX, uCTX, sNTX, TRACP-5b) were measured before treatment and in Months 1, 3 and 6, some of the bone resorption markers were significantly inhibited from Month 1 and by Month 6 mean inhibition was 15-60%. Bone formation markers were suppressed 25-35% in Months 3-6, and lumbar BMD had increased 3.7% in 6 months, 4.2% in 12 months and 4.5% in 24 months. The proportion of patients who showed an inhibition rate (S/N ratio) against the least significant change of 1 or more in Month 1 was 83.3% for TRACP-5b, 52.8% for sNTX, 66.7% for uNTX and 44.4% for uCTX. In Month 3 they were 81.1%, 70.3%, 75.7% and 51.4%, respectively. In the Ca administration controls, no long-term significant changes in TRACP-5b were observed, but fluctuations in the collagen degradation products NTX and CTX were observed. Significant correlation ($p < 0.05$) between the rate of TRACP-5b inhibition and the rate of increase in lumbar bone density in Month 12 was observed at -0.386 in Month 1 and -0.513 in Month 3. In contrast, correlation between the rate of change in BMD and the rate of uCTX inhibition was -0.335 and -0.425, respectively. There was no significant correlation between the rate of increase in BMD and uNTX, sNTX or DPD. Correlation with the rate of BAP inhibition in Months 3 and 6 was -0.492 and -0.633. Furthermore, about 28 patients who could be measured BMD in 24 months, Significant correlation ($p < 0.05$) between the rate of TRACP-5b inhibition and the rate of increase in BMD in Month 24 was observed at -0.419 in Month 6, but other bone resorption marker were not. Correlation with the rate of BAP inhibition in Months 6 was -0.536.

Some bone metabolic markers can predict the therapeutic effect for short periods like a year after. However, only fewer markers can predict the therapeutic effect for long periods.

Disclosures: H. Naka, None.

W358

Three-Year Effects of Bisphosphonates on Treatment of Osteoporosis and on Reducing the Risk for Vertebral Fractures of Rheumatoid Arthritis Patients.(Fracture Intervention Trial). H. Nakayama¹, F. Hagiwara^{*2}, K. Shimada^{*1}, T. Matsui^{*1}, T. Tohma^{*2}. ¹Department of Rheumatology, National Hospital Organization, Sagami-hara National Hospital, Sagami-hara-City, Kanagawa Pref., Japan, ²Department of Rheumatology, Clinical Research Center for Allergy and Rheumatology, National Hospital Organization, Sagami-hara National Hospital, Sagami-hara-City, Kanagawa Pref., Japan.

[PURPOSE]To evaluate the efficacy of alendronate, risedronate and etidronate in the change of bone mineral density (BMD), bone metabolic markers and, reducing the risk for vertebral fractures of rheumatoid arthritis(RA) patients.[METHODS]We carried out 36-month, randomized, intervention trial of five groups in 400 patients with RA(366 women and 34 men). GroupA (n=77): alendronate(ALN) 5mg, GroupR(n=80): risedronate (RIS) 2.5mg, GroupE4 (n=77): cyclical (every 3 month) etidronate (EHDP)400mg, GroupE2(n=72): cyclical EHDP200mg, and GroupD(n=90): not treated with any bisphosphonate(BP). All patients received supplemental calcium and alfacalcidol(VD) 0.5µg. Every dose of BPs was licensed in Japan. BMD was measured at lumbar spine(LS), femoral neck(FN) total hip(TH) by dual energy X-ray absorptiometry technique, and we checked thoracic and lumbar vertebral fractures by X-ray at baseline, 6, and 12 month later. BAP and urine NTX(uNTX) were measured at baseline, 3, 6, and 12 month.[RESULTS]Mean age of the patients of every group was 61-63 years. The mean percent change from baseline to 36 month in LS/FN/TH BMD was +3.7/+3.5% in GroupA, +3.3/-0.7% in GroupR, +2.0/-2.2% in GroupE4, +0.7/-1.9% in GroupE2, and +0.5/2.4% in GroupD. The mean percent change in BAP/uNTX was -25.7/-37.9% in GroupA, -23.2/-23.8% in GroupR, -8.2/-26.7% in GroupE4, -13.1/-11.2% in GroupE2, and +3.9/-7.7% in GroupD. The frequency of incidental vertebral fracture (per 100 person-year) for latter 30 months was 1.8 in GroupA, 1.9 in GroupR, 7.3 in GroupE4, 8.7 in GroupE2, and 16.8 in GroupD. Reductions in risk of vertebral fractures were 89% in GroupA, 88% in GroupR, 56% in GroupE4, 48% in GroupE2[CONCLUSIONS]ALN increased both LS and FN BMD significantly, and RIS also increased LS BMD. ALN and RIS decreased both BAP and uNTX significantly, cyclic EHDP400mg also decreased uNTX. ALN, RIS and cyclic EHDP400mg reduced the risk of vertebral fractures by less than half. These effects were superior to that with cyclic EHDP200mg or VD alone.

Disclosures: H. Nakayama, None.

W359

Prevalence of Severe Suppression of Bone Turnover Among Patients with Atypical Osteoporotic Fractures. N. Napoli¹, D. Novack¹, K. M. Diemer^{*1}, M. Watkins¹, S. L. Teitelbaum², R. C. Armamento-Villareal¹. ¹Div. of Bone and Mineral Diseases, Washington University in St Louis, St Louis, MO, USA, ²Department of Pathology, Washington University in St Louis, St Louis, MO, USA.

Recent reports of patients on long-term bisphosphonates (BPs) developing fragility fractures in sites that are not typical for osteoporosis with bone biopsy findings suggestive of severe suppression of bone turnover (SSBT), have raised important safety concerns on the prolonged use of the drug. This study is a retrospective analysis of the patients (14 women and 6 men) at the Bone Health Program at Washington University School of Medicine who underwent bone biopsy because of unusual osteoporotic fractures (femoral shaft, pelvis, rib, metatarsal, shoulder) from November 2004 to January 2007. Ten of 15 patients were found to have biopsy findings consistent with SSBT, defined as total absence of double tetracycline labels in trabecular bone. There were no significant differences in bone mineral density by DEXA, clinical and biochemical data (age, BMI, serum Ca, alkaline phosphatase, PTH, Vitamin D) between the 2 groups, except for the duration of therapy. On the average, SSBT cases took BPs for a significantly longer period of time than non-SSBT (6.1 ± 0.58 vs 3.9 ± 0.83 , $P = 0.05$). Histomorphometric analysis also demonstrated significantly lower Ob.S/BS (0.57 ± 0.28 vs 2.23 ± 0.42 , $P < 0.01$), but no difference in Oc.S/BS, in cases of SSBT. Our findings suggest that a majority of patients treated with BPs who develop fractures at sites not typical of osteoporosis have SSBT, and that duration of BP therapy is a risk factor. Further studies are needed to determine whether patients at risk for SSBT and atypical fracture can be identified clinically, without biopsy. Given the large numbers of patients who have been treated with BPs for >5 years without atypical fractures, and reports of normal turnover in a random sample of treated patients (Black DM et al., JAMA, 2006 Dec 27;296(24):2927-38) the overall risk for SSBT in all patients taking BPs is low. However, it is important to define the subpopulation at risk for these atypical fractures.

Disclosures: N. Napoli, None.

W360

CFOS Trial: Alendronate Once Weekly for the Prevention and Treatment of Osteoporosis in Canadian Adult Cystic Fibrosis Patients. A. Papaioannou¹, C. C. Kennedy¹, G. Ioannidis¹, J. O'Neill^{*2}, C. Webber², M. Pui^{*2}, A. Freitag^{*1}, R. Josse^{*3}, A. Cheung^{*3}, Y. Berthiaume^{*4}, H. Rabin^{*5}, N. Paterson^{*6}, A. Jeanneret^{*4}, E. Matouk^{*7}, J. Villeneuve^{*8}, R. McCallum^{*1}, M. Nixon^{*1}, J. D. Adachi¹. ¹Medicine, McMaster University, Hamilton, ON, Canada, ²Radiology, McMaster University, Hamilton, ON, Canada, ³Medicine, University of Toronto, Toronto, ON, Canada, ⁴Medicine, Centre hospitalier de l'Université de Montréal, Montreal, PQ, Canada, ⁵Medicine, University of Calgary, Calgary, AB, Canada, ⁶Medicine, London Health Science Centre, London, ON, Canada, ⁷Medicine, Montreal Chest Institute, Montreal, PQ, Canada, ⁸Medicine, Le Centre hospitalier universitaire de Québec, Quebec City, PQ, Canada.

Introduction: A multicentre, randomized controlled trial (RCT) was conducted in adults with cystic fibrosis to assess the efficacy and safety of oral alendronate (FOSAMAX®). This is the only Canadian RCT to examine a bisphosphonate in this patient population. **Methods:** Patients received placebo or alendronate 70 mg once weekly for 12-months. All patients received 800 IU Vitamin D and 1000 mg calcium (500 mg supplementation, 500 mg from diet) daily. Patients age 18 years and older with cystic fibrosis (confirmed by positive sweat test or DNA analysis) with a bone mineral density (BMD) T-score <-1.0 were eligible for inclusion. Patients with a prior organ transplantation; endoscopy-proven esophagitis, gastritis, ulceration; metabolic bone disorders; severe renal disease; or using systemic corticosteroids (dose of 7.5 mg/day or greater) in previous 6-months, were excluded. The primary measure was percent change in lumbar spine (LS) BMD after 12-months. Secondary measures were percent change in total hip BMD, proximal femur (PF) BMD, and N-telopeptide after 12-months. **Results:** A total of 56 patients (34 males, 22 females) were enrolled in the study. The mean age was 29.1 (SD=8.78) years. Mean baseline 25-OHD was 60.3 (SD=27.9) nmol/L. Five patients (4 Placebo, 1 Alendronate) had a new vertebral fracture (all Grade 1) during the study. The number of withdrawals was equal between the treatment groups (4 Alendronate, 4 Placebo). Over 12-months, the active treatment group had a 4.99% (95% CI: 2.40, 7.59) greater increase in LS BMD and a 3.50% (95% CI: 1.37, 5.63) greater increase in PF BMD compared with the placebo group (adjusted for age, body mass index, baseline BMD, number of baseline vertebral fractures).

Conclusion: Patients with cystic fibrosis are at risk for early bone loss due to several factors including delayed pubertal maturation, glucocorticoid therapy, malabsorption of vitamin D, poor nutritional status, inactivity, and hypogonadism. Alendronate was well tolerated and produced a significantly greater increase in BMD over 12-months compared with placebo.

Disclosures: A. Papaioannou, Merck Frosst 2, 5.

This study received funding from: Merck Frosst Canada.

W361

The Bisphosphonates Cause Inflammatory Response In Vivo and in Human Peripheral Blood Mononuclear and Polymorphonuclear Cells In Vitro. W. Park¹, M. Lim¹, S. Kwon¹, S. Hong¹, S. Lee². ¹Medicine/Rheumatology, IN-HA University Hospital, Incheon, Republic of Korea, ²Medicine/Rheumatology, Konkuk University Hospital, Seoul, Republic of Korea.

Bisphosphonates (BPs) are currently mainstay therapy for various clinical conditions including osteoporosis, Paget's disease, multiple myeloma, and metastatic bone disease. However BP associated osteonecrosis of jaw (ONJ) and influenza-like illness were reported mainly in patients who received intravenous (IV) BPs. Therefore we speculated that high blood concentration of BP after IV or intermittent large oral dose would cause inflammatory reaction and the reaction would be related to those side effects.

Five patients with idiopathic osteoporosis without recent bisphosphonate, glucocorticoid, or the immunosuppressant use were selected. They were given 30 mg of IV pamidronate. Acute phase reactants such as erythrocyte sedimentation rate (ESR) and C-reactive protein (CRP) were measured for 3 days. The in vitro effects of BP on the mRNA expression of the pro-inflammatory cytokines was measured using the human peripheral blood mononuclear (PBMC) and polymorphonuclear (PBMNCs) cells isolated by centrifugation over Histopaque-1077 and Histopaque-1119 (Sigma, 1119-1, St. Louis, MO, USA). The isolated PBMCs and PBMNCs were incubated in RPMI-1640 containing alendronate 0, 1, 5, 25, 125 μ M for 18 hours. One million cells were harvested to extract RNA. The real-time RT-PCR quantified the expression of the interferon (IFN)- γ , TGF- β , interleukin (IL)-1 β , IL-10, IL-6, RANKL, TNF- α , TRAP, cathepsin-K (CTK).

At baseline, serum CRP level was normal but the level rose 24-72 hours after pamidronate IV infusion (0.08 \pm 0.074 vs. 0.23 \pm 0.240 mg/dL, $p=0.042$, paired T-test). The ESR at the concurrent time did not rise significantly (13.4 \pm 18.02 vs. 15.6 \pm 15.13 mm/hr). Most of the inflammatory cytokines increased after alendronate pulse dose-dependently. The expression of IFN- γ , IL-6, and TNF- α were most prominent in the PBMCs and those of IFN- γ , IL-6, and IL-1 β in the PBMNCs. (Table 1) RANKL and CTK expression were not detectable in PBMNCs.

Acute inflammation caused by BP may be due to its high blood level after intravenous infusion or large intermittent oral dose. The clinical study concerning whether the very slow IV infusion or small dose daily oral therapy would minimize those inflammatory side effects is warranted

Expression of cytokines in human PBMCs after alendronate pulse measured by real time PCR

Alendronate (μ M)	1	5	25	125
IFN- γ	2.7	17.1	73.2	818.1
TGF- β	2.4	3.0	2.2	14.7
IL-1 β	7.4	7.8	10.9	13.8
IL-6	473.8	303.5	1943.6	13934.7
RANKL	13.2	14.2	23.1	26.1
TNF- α	37.4	18.4	119.0	76.2
CTK	0.5	0.1	0.3	0.3

Disclosures: W. Park, None.

W362

Comparable Adherence and Improvement in Gastrointestinal (GI) Tolerability with Monthly Oral and Quarterly Intravenous Ibandronate in Patients Who Discontinued Previous Bisphosphonates Because of GI Intolerance. V. K. Pizlak¹, A. M. Babbitt², J. D. Kohles³, E. M. Lewiecki⁴. ¹The Children's Hospital at Scott & White, Temple, TX, USA, ²Greater Portland Bone & Joint Specialists, South Portland, ME, USA, ³Roche Laboratories, Inc, Nutley, NJ, USA, ⁴NM Clin Res & Osteoporosis Center, Albuquerque, NM, USA.

The PRIOR study evaluated adherence and gastrointestinal (GI) tolerance to monthly oral (PO) ibandronate 150 mg and quarterly intravenous (IV) ibandronate 3 mg in patients who discontinued previous daily or weekly bisphosphonate (BP) therapy because of GI intolerance.

PRIOR was a 12-month, prospective, open-label, multicenter, noninferiority study in postmenopausal women with osteoporosis or osteopenia. Patients chose either PO or IV ibandronate and could switch formulations once because of side effects. Patients were considered adherent to therapy if adherence (ratio of the actual duration of trial medication intake over the maximum duration of the trial medication intake) was $\geq 75\%$. In comparing the IV and PO groups, the between-group difference in adherence rates was adjusted by propensity score and a 2-sided 90% confidence interval (CI) was constructed. If the upper limit of the CI was $<20\%$, then noninferiority of the adherence of the PO group compared with the IV group was concluded. Patients reported GI symptoms by completing a self-administered GI Experience Survey at screening, and Months 1, 4, 7, and 10.

Of 543 patients in the intent-to-treat population, 147 (27.1%) chose PO and 396 (72.9%) chose IV as the initial therapy. Twenty-seven patients switched administration route; 11 switched to IV ibandronate because of GI intolerance (all completed the study), and 16 patients switched to PO therapy for various reasons, including bone or joint pain (n=4), influenza-like symptoms (n=3), and injection-site reactions (n=3) (5 withdrew prior to study completion). Within the per-protocol (PP) population, 69.7% of patients in the PO group and 82.9% in the IV group were adherent to their originally chosen therapy at study end. Based on the adjusted difference in adherence rates in the PP population, adherence to PO therapy was noninferior to adherence to IV therapy (12.4% difference; 90% CI, 5.1%

to 19.7%). Overall mean GI tolerance scores improved significantly from baseline to all postbaseline assessments for both the PO and IV treatment groups ($P<0.0001$ for both). Both dosing regimens were generally well tolerated.

In this population of patients who had discontinued daily or weekly BP treatment because of GI symptoms, adherence rates were similar between patients on monthly PO and quarterly IV ibandronate. Patients reported improvement of GI symptoms compared with baseline while receiving either form of ibandronate.

Disclosures: V.K. Pizlak, Proctor and Gamble 2, 8; Roche 8; Lilly 2; GlaxoSmithKline 8. This study received funding from: Roche Laboratories, Inc.

W363

Quarterly Intravenous Ibandronate Injections Provide Continuing Benefits in Women with Postmenopausal Osteoporosis: DIVA Study Long-Term Extension. C. Recknor¹, M. Lilliestol², R. Grant³, C. Neate⁴, R. R. Recker⁵. ¹United Osteoporosis Centers, Gainesville, GA, USA, ²Internal Medicine Associates, Fargo, GA, USA, ³Hoffmann-La Roche Inc., Nutley, NJ, USA, ⁴Roche Products Ltd, Welwyn Garden City, United Kingdom, ⁵Creighton University, Osteoporosis Research Center, Omaha, NE, USA.

Oral and intravenous (i.v.) ibandronate are available for treatment of postmenopausal osteoporosis. The daily oral regimen (2.5mg) has proven antifracture efficacy,¹ and in the DIVA trial, i.v. injections of 2mg every 2 months (q2mo) or 3mg every 3 months (q3mo) were shown to be superior to daily oral.^{2,3} After 2 years, patients in the i.v. arms had superior gains in lumbar spine (LS) BMD (q2mo 6.4%, q3mo 6.3%) compared with daily oral (4.8%; $p<0.001$). Gains in total hip (TH) BMD were also superior ($p<0.001$) and reductions in serum CTX were comparable (53.4-59.9%).³

After completion of the 2-year, double-blind DIVA study, patients could be enrolled in a long-term extension (LTE). Eligible patients from the i.v. arms continued to receive open-label i.v. ibandronate at the same dose for a further 3 years (q2mo, n=253; q3mo, n=263), those in the oral arm were re-randomized to receive q2mo (n=128) or q3mo (n=137) i.v. according to whether they had received 2- or 3-monthly i.v. placebo during DIVA. Here we present the LTE first year results.

Further increases were seen after 1 year in LS BMD (q2mo 0.92%; q3mo 0.95%) and TH BMD (q2mo 0.48%; q3mo 0.13%). A pooled analysis evaluating only those patients who remained on the same treatment for 3 years showed 3-year gains in LS BMD of 7.6% (q2mo; $p<0.0001$) and 7.0% (q3mo; $p<0.0001$). 3-year increases in TH BMD were 3.7% (q2mo; $p<0.0001$) and 3.3% (q3mo; $p<0.0001$). The reduction of serum CTX seen in the first 2 years of DIVA was maintained in the LTE. In the pooled analysis, median reductions in peak (30 months) and trough (36 months) serum CTX were 89.0% (q2mo), 92.4% (q3mo), and 40.2% (q2mo), 41.4% (q3mo), respectively. Both i.v. regimens continued to be well tolerated, with a similar incidence of adverse events (AEs) to those seen during the 2 years of DIVA and no evidence of late or cumulative toxicity. Treatment-related AEs were reported in 14% (q2mo) and 9% (q3mo) of patients, with serious AEs in 8% (q2mo) and 9% (q3mo), of which two were considered treatment related (both GI disorders in the q2mo group). Five patients (all q2mo) were withdrawn for AEs. The continuing efficacy benefits and good tolerability seen here show that i.v. ibandronate is a valuable long-term treatment option for postmenopausal osteoporosis.

1. Chesnut CH, et al. J Bone Miner Res 2004;19:1241-9.

2. Delmas PD, et al. Arthritis Rheum 2006;54:1838-46.

3. Emkey R, et al. Arthritis Rheum 2005;52:4060.

Disclosures: C. Recknor, F. Hoffmann-La Roche Ltd/GlaxoSmithKline 5.

This study received funding from: F. Hoffmann-La Roche Ltd/GlaxoSmithKline.

W364

The Efficacy of Fosamax 35mg a Week for the Treatment of Osteoporosis in Postmenopausal Women with Subclinical Hyperthyroidism. L. Y. Rozhinskaya*, G. A. Melnichenko*, Z. E. Belaya*, G. S. Kolesnikova*, A. V. Iijin*, N. I. Sazonova*. Neuroendocrinology and Osteoporosis, The National Research Centre for Endocrinology, Moscow, Russian Federation.

The aim was to estimate the effects of treatment with alendronate (Fosamax 35 mg) in postmenopausal women with osteoporosis and subclinical hyperthyroidism. Thirty postmenopausal women (64 (60-69) years old) with osteoporosis and subclinical hyperthyroidism (77% with endogenous subclinical hyperthyroidism and 23% on L-thyroxine suppressive therapy after thyroidectomy due to differentiated thyroid cancer) were randomly assigned into two groups: (1) 14 women received Fosamax 35 mg a week in combination with 500 mg of calcium and 400 UI of Vitamin D3 (VD) daily; (2) 16 women received 1000 mg of calcium and 800 UI of VD daily. Euthyroidism was achieved in all women with endogenous subclinical hyperthyroidism. An increase in physical activity was recommended to all patients and a hypolipidemic diet was given to those who had had high cholesterol level. Calcium (Ca), phosphorous (P), creatinine (Cre), alkaline phosphatase (ALP), cholesterol, low density lipoprotein (LDL), high density lipoprotein (HDL), triglycerides (TG), cholesterol/HDL ratio) in fasting serum as well as calcium/creatinine ratio in fasting urine (U-Ca/U-Cre); osteocalcin (OC) and C-terminal telopeptide of type I collagen (b-CTX) serum, BMD (DXA; Prodigy, Lunar) at the lumbar spine (L1-L4), femoral neck (FN), total hip (TH) and radius total (RT) were measured at the baseline visit and after 1 year of treatment. At the baseline visit there were not found any differences between the (1) and the (2) groups. After 12 months of treatment the markers of bone metabolism as well as ALP decreased significantly in both groups, though the decreases were significantly greater ($p < 0.001$ for both OC and b-CTX) in the (1) versus the (2) group. BMD in the (1) group increased by 7.6% at L1-L4 ($p = 0.003$), 2.8% at FN ($p = 0.013$), 3.3% at TH ($p = 0.012$) and 3.2% at RT ($p = 0.047$). There was not detected any BMD loss in the (2) group. The changes were not significant between the two groups. The levels of Ca, P, Cre, U-Ca/U-Cre did not change in both groups. Significant improvements in lipid levels were found: HDL increased ($p = 0.035$ (1) $p = 0.034$ (2)), cholesterol/HDL ratio decreased ($p = 0.011$ (1); $p = 0.004$ (2)). In addition, cholesterol ($p = 0.003$); TG ($p = 0.016$) and LDL ($p = 0.006$) decreased for patients from the (1) group. Conclusion: The achievement of euthyroidism and Fosamax 35 mg a week increase BMD in all regions of the skeleton in postmenopausal women with osteoporosis and subclinical hyperthyroidism and reduce bone resorption significantly more than Calcium and VD supplementation.

Disclosures: L.Y. Rozhinskaya, None.

W365

Relationship Between Increasing Annual Cumulative Exposure to Ibandronate, Increases in BMD and Reductions in Clinical Fractures. A. Sebban*, R. D. Emkey*, W. A. Blumentals*, P. N. Sambrook*. ¹University of South Florida, Tampa, Palm Harbor, FL, USA, ²Emkey Arthritis and Osteoporosis Clinic, Wyomissing, PA, USA, ³Roche Laboratories, Inc, Nutley, NJ, USA, ⁴Institute of Bone & Joint Research, University of Sydney, Sydney, Australia.

Analyses of the relationship between changes in bone mineral density (BMD) and fracture reduction with bisphosphonate therapy have produced varying results, but only a limited range of doses has been examined. Data from 4 pivotal phase III clinical trials of ibandronate (2 oral and 2 intravenous [IV]) were pooled and analyzed to examine increases in BMD at various annual cumulative exposures (ACEs) in women with postmenopausal osteoporosis.

Data from the intent-to-treat populations, comprising patients who received oral or IV ibandronate or placebo in 4 studies (Study 4380 [IV fracture study], BONE, MOBILE, and DIVA), were pooled. BONE and the IV fracture study were 3-year placebo-controlled fracture trials, and MOBILE and DIVA were 2-year BMD studies that examined fractures as secondary endpoints. Oral doses included 2.5 mg daily, 20 mg intermittent, 100 mg monthly, 2x50 mg monthly, and 150 mg monthly. IV doses included 0.5 mg quarterly, 1 mg quarterly, 2 mg every 2 months, and 3 mg quarterly. ACE was computed by multiplying the drug strength in milligrams by the number of annual doses and by an absorption factor (0.6% for oral and 100% for IV). Rates of BMD increases at the lumbar spine (LS) and total hip (TH) and rates of all clinical fractures over 2 years were calculated. Linear models, weighted by the sample sizes of the trials, were constructed to examine the clinical fracture rate as a function of increases in LS BMD.

This analysis included a total of 8710 patients. Plots constructed to visually observe any potential association between clinical fractures and ACE showed a trend to decreased clinical fractures with increasing ACE. Plots of change in LS BMD vs ACE showed an increase in percentage change in LS BMD with increasing ACE. The same relationship was seen for TH BMD. There was a statistically significant inverse linear relationship between clinical fracture rates and gains in LS BMD (Figure: $\beta = -0.397$, $P = 0.0046$; $R^2 = 0.65$).

Increasing gains in BMD at the LS correlated with decreasing rate of clinical fractures. Higher ibandronate doses were associated with the highest level of BMD gain and lowest rate of clinical fracture.

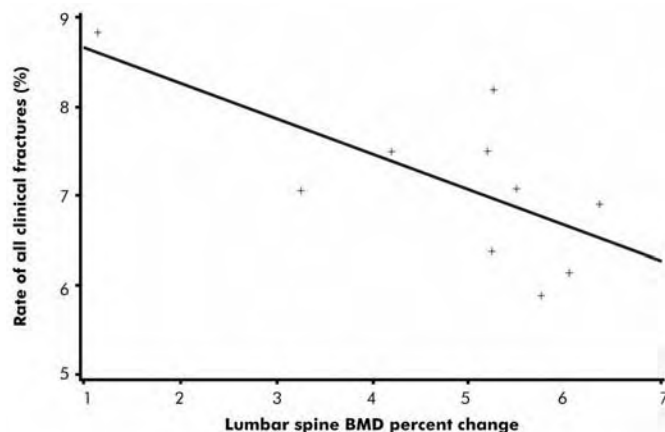


Figure. Clinical fracture rates vs percent change in lumbar spine BMD at 2 years

Disclosures: A. Sebban, Roche Laboratories, Inc. 2, 8; Eli Lilly 2, 8; Merck 2, 8; Amgen 2. This study received funding from: Roche Laboratories, Inc.

W366

Women Are More Persistent with Monthly Bisphosphonate Therapy Compared to Weekly Bisphosphonates: 12 Month Results from Two Retrospective Databases. S. L. Silverman¹, J. A. Cramer^{2*}, J. A. Sunycz^{3*}, C. Sarawate^{4*}, C. Harley^{5*}, W. A. Blumentals^{6*}, S. Poston^{7*}, E. M. Lewiecki⁸. ¹Cedars-Sinai Medical Center, Beverly Hills, CA, USA, ²Yale University, West Haven, CT, USA, ³Laurel Highlands Ob/Gyn, Hopwood, PA, USA, ⁴HealthCore, Inc., Wilmington, DE, USA, ⁵i3 Innovus, Eden Prairie, MN, USA, ⁶Roche, Nutley, NJ, USA, ⁷US Health Outcomes, GlaxoSmithKline, Research Triangle Park, NC, USA, ⁸NM Clin Res & Osteoporosis Ctr, Albuquerque, NM, USA.

This study evaluated medication persistence among patients receiving monthly ibandronate versus weekly bisphosphonates. The 12-month results of 2 retrospective database analyses are presented here.

Deidentified patient data were obtained from 2 large managed care claims databases (provided by i3 Innovus and HealthCore Integrated Research Network™) in parallel studies. The combined databases represent over 30 million covered lives. In both studies, eligible women were ≥ 45 years of age and filled ≥ 1 pharmacy claim(s) for a weekly or monthly bisphosphonate from April 1, 2005 to November 30, 2006 (i3 Innovus) or October 31, 2006 (HealthCore). Baseline data were collected for 6 months prior to the index date (date of first prescription filled). Persistence, defined as continuous use, was evaluated at 12 months based on a refill gap of 30 days for weekly bisphosphonates; a gap of 45 days was used for monthly ibandronate because of its longer dosing window. Persistence was assessed using Cox proportional hazard models to control for baseline characteristics and potential confounders such as patient age, co-pay amount, comorbidities, long-term prescriptions, concomitant medications, fracture history, and prior DXA scans.

The i3 Innovus database provided claims data from 3,512 women prescribed monthly ibandronate and 13,967 prescribed weekly bisphosphonates. The HealthCore database included 1,006 women receiving monthly ibandronate and 10,658 receiving weekly bisphosphonates. The analyses determined that women on monthly therapy demonstrated higher persistence than women receiving weekly therapy (Table). After adjusting for age, co-pay and comorbidities, monthly users were 25.1% and 37.7% less likely to discontinue therapy versus weekly users in the i3 Innovus and HealthCore analyses, respectively (Table).

	Monthly ibandronate (unadjusted rate)	Persistence at 12 months		Adjusted hazard ratio (95% CI)	P value
		Weekly bisphosphonates (unadjusted rate)	P value		
i3 Innovus	35.7%	24.8%	<0.0001	0.749 (0.702-0.796)	<0.0001
HealthCore	36.3%	26.9%	<0.0001	0.623 (0.575-0.676)	<0.0001

The 12 month results of these analyses suggest that women prescribed monthly ibandronate are more persistent than women on weekly bisphosphonates.

Disclosures: S.L. Silverman, Roche Laboratories, Inc. 2, 5, 8; Merck 2, 5, 8; Procter and Gamble 2, 5, 8; Wyeth 2, 5.

This study received funding from: Roche Laboratories, Inc

W367

Oral Monthly Ibandronate Is Associated with Rapid Suppression of Serum CTX Within Three Days of Treatment Initiation. S. L. Silverman¹, E. Barrett-Connor^{*2}, C. Simonelli³, J. D. Kohles^{*4}, G. Dasic⁵, N. C. Binkley⁶.

¹Cedars-Sinai Medical Center/UCLA, Beverly Hills, CA, USA, ²University of California at San Diego, La Jolla, CA, USA, ³Health East Osteoporosis Care, Woodbury, MN, USA, ⁴Roche Laboratories, Inc, Nutley, NJ, USA, ⁵GlaxoSmithKline, King of Prussia, PA, USA, ⁶University of Wisconsin, Madison, WI, USA.

The purpose of the Rapid Onset study was to examine the speed of onset and pattern of suppression of the bone resorption marker serum C-terminal telopeptide of type 1 collagen (sCTX) in postmenopausal women with osteoporosis treated for 6 months with monthly ibandronate.

Rapid Onset was a randomized, double blind, placebo-controlled study of women diagnosed with postmenopausal osteoporosis within the past 12 months and with no more than 3 months exposure to daily or weekly bisphosphonate therapy for the 5 years before screening. Participants received once monthly oral ibandronate (150 mg) or placebo for 6 months. Levels of sCTX were measured at baseline and Day 3 (first month only), as well as on Day 7, 14, 21, and 28 after the doses were administered. The primary study endpoint was the relative change in median sCTX from baseline to Day 3. Responder analyses (defined as $\geq 50\%$ and $\geq 70\%$ sCTX decreases) were also performed.

An Independent Data Monitoring Committee performed the analyses. Sixty-seven women participated in this study; 1 did not take any study drug, 49 received ibandronate and 17 received placebo. Mean baseline sCTX measurements levels were the same (0.63 ng/mL) for patients receiving ibandronate and placebo. Rapid suppression of sCTX occurred in those receiving ibandronate; median sCTX was reduced by almost 70% within 3 days of ibandronate administration ($P < 0.0001$ vs placebo) and remained suppressed at day 28 (median decrease of 43% from baseline, [$P = 0.0014$ vs placebo]). In contrast, in the placebo group, the median sCTX was reduced by almost 6% on Day 3 and the maximum median percent change in sCTX from baseline was 22% on Day 14. A high proportion of women responded to ibandronate; at Day 3, 71% of patients receiving ibandronate had $\geq 50\%$ decreases in sCTX and 47% had $\geq 70\%$ decreases in sCTX. No patients receiving placebo were considered to be responders at Day 3. This study demonstrated that ibandronate treatment rapidly decreases sCTX levels within 3 days of treatment initiation.

Disclosures: S.L. Silverman, Lilly 2, 8; Merck 2, 5, 8; Procter & Gamble 2, 5, 8; Roche 2, 5, 8.

This study received funding from: Roche Laboratories, Inc.

W368

Daily or Intermittent Oral Ibandronate Preserves Trabecular Microarchitecture: Micro-Computed Tomography Analysis of Patients in the 3-Year BONE Study. L. G. Ste-Marie¹, B. Langdahl^{*2}, D. Masanaukaite^{*3}, D. Ethgen^{*4}, R. R. Recker⁵.

¹CHUM Université de Montreal, Montreal, PQ, Canada, ²Aarhus University Hospital, Aarhus, Denmark, ³F. Hoffmann-La Roche Ltd, Basel, Switzerland, ⁴GlaxoSmithKline, Collegeville, PA, USA, ⁵Creighton University, Osteoporosis Research Center, Omaha, NE, USA.

In postmenopausal osteoporosis, trabecular bone microarchitecture contributes significantly to overall bone strength. Micro-computed tomography (microCT) is a quantitative 3D scanning procedure used to assess trabecular architecture. In the 3-year BONE study, oral ibandronate (IBN) administered daily (2.5mg) or intermittently (20mg every other day for 12 doses every 3 months) significantly reduced vertebral fracture risk (primary endpoint) by 62% ($p=0.001$) and 50% ($p=0.006$) respectively; significantly increased lumbar spine and proximal hip bone mineral density (BMD) and reduced markers of bone turnover, vs placebo (PBO).¹ 2D histomorphometric analysis of biopsies taken at months 22 and 34 of the study indicated that newly formed bone was of normal quality.² In the current analysis, biopsies have been analyzed by microCT to assess 3D trabecular microarchitecture. Biopsies were analyzed at Creighton University with a Scanco microCT 40 scanner (Scanco Medical, Bassersdorf, Switzerland) and rod and plate distribution quantified by differential analysis of the triangulated bone surface. The structural model index (SMI), was then calculated, with a lower SMI indicating an increased ratio of plates to rods and thus improved trabecular microarchitecture. Biopsies were obtained from 110 patients, with 84 evaluable by microCT (28 PBO, 56 IBN [both arms]). Median SMI was 1.001 with IBN vs 1.365 with PBO (90% CI for difference in medians: -0.626, -0.033) and connectivity density was higher in IBN-treated patients (median 3.904 vs 3.112/mm³, 90% CI for difference in medians: 0.159, 1.517). This indicates that trabecular microarchitecture was better preserved in patients receiving IBN than PBO. Additional measurements showed that IBN is consistently beneficial on multiple parameters of bone structure and architecture vs PBO. Taken together with previous results from the BONE study showing reduced fracture risk, improved BMD and decreased bone turnover as well as histomorphometric and hip structural analyses,³ these findings indicate that treatment with ibandronate preserves bone strength by maintaining good quality trabecular microarchitecture in women with postmenopausal osteoporosis.

1. Chesnut CH, et al. J Bone Miner Res 2004;19:1241-9.

2. Recker RR, et al. Osteoporos Int 2004;15:231-7.

3. Fuerst T, et al. J Bone Miner Res 2006;21(Suppl. 1):S287 (Abst SU323).

Disclosures: L.G. Ste-Marie, F. Hoffmann-La Roche Ltd/GlaxoSmithKline 5.

This study received funding from: F. Hoffmann-La Roche Ltd/GlaxoSmithKline.

W369

10-Years-Follow-Up of a Pregnancy-associated Osteoporosis (PAO). A Clinical Case Report. U. C. Stumpf¹, J. Windolf^{*1}, W. J. Fassbender².

¹Department of Traumatology and Handsurgery, University Hospital, Duesseldorf, Germany, ²Department of Internal Medicine, Hospital z. Hl. Geist, Kempen, Germany.

Pregnancy-associated osteoporosis (PAO) is an uncommon condition characterized by the occurrence of painful fractures during late pregnancy or lactation. The pathophysiology of this disease is uncertain, and its therapeutical management is poorly defined. At the moment exist no guidelines for the therapy. Although rare, diagnosis of pregnancy-associated osteoporosis should be suspected when lumbar or thoracic spine pain occur during pregnancy or in the post-partum period as it can lead to multiple vertebral fractures. Case report: A 41-years-old, premenopausal, slim (BMI= 19) woman is accompanied by pain of the whole spine and the bone in general since 10 years. Within her adolescence she got traumatic fractures of the jaw, metatarsus and toes. She had two pregnancies 10 and 8 years ago. Since the first pregnancy a PAO was known, which impaired after the second one. A secondary cause is the treatment for asthma bronchiale over 12 years with inhalative, intermittent oral, corticosteroids (CS) in the range between 5-16 mg /die. Seven years ago, the first DXA-scan was performed and showed a t-score (L2-L4): -2,1 (z-score:-2,0); medication started with etidronate, calcitonin and supplementation of calcium and vitamin D3. In the DXA-scan after 1 year, a consolidation of the PAO could be observed (t-score L2-L4: -1,7; z-score:-1,6). With this medication back pain got under control. 5 years ago, the patient had a horse-riding accident with an instable burstfracture of L1, which was stabilised by internal fixator from Th12 to L2. In the actual DXA-scan an increase of bone mineral density up to a t-score L2-L4 of -1,3 (z-score:-1,3) was observed. In the first laboratory investigation an overall low turnover of bone was seen, due to CS therapy without accelerated bone resorption, PTH and vitamin D3 in normal range. Furthermore a low estradiol (24 pg/ml range: 0.0 - 270.00 female) despite regular menstrual cycle was noticed. We started a combined osteoporosis (ibandronate 3 mg iv /12 weeks) and pain treatment (level I WHO) with supplementation of 1000 mg calcium and 800 IU vitamin D3 per die.

Conclusion: As we can observe in this long time follow up the PAO accompanies the patient their whole life and should not be underestimated. We conclude that it is necessary to avoid a long course of pain and fractures in these young women in order to treat the PAO initially adequate with antiresorptive or even osteoanabolic substances to obtain a fast consolidation of BMD and to lower the risk of further fractures and chronification of pain.

Disclosures: U.C. Stumpf, None.

W370

The Effects of Risedronate and Raloxifene on Serum Lipid Levels in Postmenopausal Women. H. Suh^{*}, K. Lee^{*}. Family Medicine, Gachon Medical School, Gil Medical Center, Incheon, Republic of Korea.

Purpose: Some studies in other countries have reported that the intravenous injection of bisphosphonate and the oral administration of raloxifene, which are used in the prevention and treatment of osteoporosis, have the effect of lowering lipid levels. However, there have been no studies on the effect of the oral administration of bisphosphonate. Furthermore, there have been no studies on the effect of raloxifene in Korea. Thus, we studied the effect of typical bisphosphonate medication, risedronate and raloxifene, classified as SERM(Selective Estrogen Receptor Modulator) on the serum lipid levels of post-menopausal Korean women.

Methods: At a certain university hospital, each 199 postmenopausal women who had either taken 35mg of risedronate per week or 60mg of raloxifene daily for at least 1 year were selected. We followed them up and compared their baseline serum lipid levels with that of 1 year after.

Results: The risedronate group showed a valid decrease in the level of total cholesterol, LDL cholesterol, non-HDL cholesterol($P<0.05$). The raloxifene group showed a valid decrease in the level of total cholesterol, LDL cholesterol, non-HDL cholesterol($P<0.05$) and showed a valid increase in HDL cholesterol levels($P<0.05$). The raloxifene group showed a valid decrease in the level of total cholesterol, LDL cholesterol, non-HDL cholesterol compared to the risedronate group($P<0.05$)

Conclusions: In post-menopausal Korean women, the oral administration of risedronate and raloxifene reduced total cholesterol, LDL cholesterol and non-HDL cholesterol levels. As well, raloxifene showed superior effects to risedronate.

Disclosures: H. Suh, None.

W371

Efficacy and Safety of Alendronate for the Treatment of Glucocorticoid-induced Osteoporosis in Children: A Prospective Multicenter Study in Japan. H. Tanaka¹, Y. Seino². ¹Pediatrics, Okayama University, Okayama, Japan, ²Pediatrics, Osaka Koseinenkin Hospital, Osaka, Japan.

OBJECTIVE: Glucocorticoid-induced Osteoporosis (GIOP) is being increasingly reported even in children. And efficacy and safety of the use of oral bisphosphonate treatment have been established in adult area. But few randomized control trials have been published and its efficacy and safety are still controversial in growing children. In this preliminary study, we evaluated the effect of an oral bisphosphonate (alendronate) on bone mass in children under long-term glucocorticoid treatment. **METHODS:** Fifty six children under long-term (over 6months) glucocorticoid treatment were randomly assigned into 2 groups; 30 children (Group A) were treated with alfacalcidol and alendronate, and 26 (Group B) were treated with only alfacalcidol as a control for 2 years. We measured lumbar bone mineral density (LBMD) and metabolic bone markers (NTx and Bone specific ALP) every 6months. **RESULTS:** Mean LBMD at the start of the trial was 88.7% and 86% of the healthy Japanese children in group A and B respectively. In group A, Mean LBMD increased to 93.6 % (6 months), 98.5 % (12 months) and maintained until the end of the trial, while it decreased to 83.3 % (6 months) and 80.5 % (12 months) and then continued to decreased slowly in group B. Urinary excretion of NTx decreased by 33.7 % at 6 month while it increased by 9.6 % in group B. Considering their condition, increases in the height of all patients but one enrolled in this trial was satisfactory. No new fractures were observed in group A, but multiple vertebral fractures were observed in one case of group B. **CONCLUSION:** Bisphosphonates can be considered essential components of the treatment of GIOP, not only in adults, but also in pediatric patients. Alendronate has a positive effect on GIOP in children.

Disclosures: H. Tanaka, None.

W372

Identifying the Treatment Care Gap in Postmenopausal Women at the Southlake Regional Health Centre: The Role of a "Shared Care" Model. C. Thorne¹, G. Ioannidis², L. Fraser^{*1}, E. Ng^{*1}, J. D. Adachi². ¹Southlake Regional Health Centre, Newmarket, ON, Canada, ²McMaster University, Hamilton, ON, Canada.

Inadequate osteoporosis management in patients with fragility fractures has been well documented in Canada. We performed a patient chart audit to examine the treatment care gap in postmenopausal women 50 years of age and older with at least one fragility fracture and who were admitted to the acute musculoskeletal inpatient nursing unit in the Southlake Regional Health Centre (Newmarket, ON, CAN) in 1999 (T1), 2003 (T2) and 2005 (T3). During this time period, a "Shared Care" program was developed where by all patients with fragility fractures admitted by orthopedic surgeons were seen by one of two rheumatologists. The program began in 1999 and was fully implemented in 2005. The treatment care gap was defined as any fracture patient who was not on therapy at the time of discharge (potential therapies included bisphosphonates, calcitonin, raloxifene and parathyroid hormone). Exact multivariable logistic regression analysis was performed to determine how the treatment care gap changed from T1 to T3. Covariates included in the analysis were patients' history of osteoporosis (yes/no), past osteoporosis medications (yes/no), age of patient (years), length of hospital stay (days), and most responsible physician (orthopedic surgeon, rheumatologist, or general internal medicine physicians alone). Odds ratios (OR) and 95% confidence intervals (95% CI) were calculated. A total of 27, 43 and 44 patients with fragility fractures were evaluated at T1, T2, and T3, respectively. Of these patients, 90, 86 and 96% had a hip fracture. The mean (standard deviation) age, and length of hospital stay of the patients were 81.1 (7.7) years and 8.2 (5.8) days at T1, 79.0 (9.6) years and 10.5 (14.0) days at T2, and 84.8 (7.9) years and 9.6 (7.9) days at T3. The number (%) of patients with a history of osteoporosis and past osteoporosis drug use were 2 (7.4) and 0 (0.0) at T1, 20 (46.5) and 10 (23.3) at T2, and 26 (59.1) and 25 (56.8) at T3. A large number (%) of responsible physicians were orthopedic surgeons (T1=27 (100%), T2=36 (83.7%), T3=34 (77.3%)). The number (%) of patients on therapy at the time of discharge was 0 (0.0), 13 (30.2) and 35 (79.6) at T1, T2, and T3 respectively. As compared with treated patients at T1, the OR of patients treated in T2 and T3 was 1.6 (95% CI: 0.166,∞), and 20.3 95% CI: (2.6,∞). A patient's history of osteoporosis (OR= 12.5, 95% CI: 2.4, 128.2) and past osteoporosis medications (OR= 6.2, 95% CI: 1.2, 45.5) was associated with higher treatment rates. In conclusion, the treatment gap at the health centre has decrease from 1999 to 2005. The development of the "Shared Care" program has resulted in improved management of patients with fragility fractures.

Disclosures: C. Thorne, Alliance of Better Bone Health 2.

This study received funding from: Alliance for Better Bone Health.

W373

Two-Consecutive Days-a-Month Risedronate 75 Mg (2Cd) Reduces Vertebral Fracture Risk at One Year. N. Watts¹, J. Brown^{*2}, G. Cline^{*3}, P. D. Delmas⁴. ¹University of Cincinnati, Cincinnati, OH, USA, ²Laval University, Quebec City, PQ, Canada, ³Procter & Gamble Pharmaceuticals, Mason, OH, USA, ⁴INSERM Research Unit 403, Lyon, France.

The antifracture efficacy of new osteoporosis therapies is usually based on placebo-controlled trials, but inclusion of a placebo arm in subsequent clinical trials may be limited by practical or ethical considerations. In these cases, use of historical controls can be explored as an interesting alternative. To assess the anti-fracture efficacy of this new regimen, we analyzed fracture data in an active-controlled study of risedronate dosing regimens (the 2CD study) using matched historical controls from previous placebo-controlled trials. Women in the 2CD study were matched for age, years since menopause, BMD and prevalent vertebral fractures, with placebo patients in the Vertebral Efficacy of Risedronate Therapy (VERT) trials, forming an historical placebo group. We also constructed an historical active-treatment group from the risedronate 5 mg daily arm of the VERT trials for comparison with the 5 mg daily (n=613) and 2CD (n=616) treatment groups in the 2CD study; historical control groups consisted of daily placebo patients (n=99, matched from 993) and risedronate 5 mg daily patients (n=96; matched from 990) in the VERT studies. Over 1 year of treatment, risk of new vertebral fractures in the 2CD group (1.1%) was reduced by 79% relative to the historical placebo group (5.1%) (OR 0.21; 95% CI, 0.05 to 0.88, P=0.016), similar to the 1-year risk reduction observed in the VERT trials of risedronate 5 mg daily (61-65%). The incidence of new vertebral fractures, assessed for internal validation, was similar in the three treatment groups: 1.0% in the historical risedronate 5 mg group, 1.5% in the risedronate 5 mg daily group from the 2CD study, and 1.1% in the 2CD group. The use of appropriate historical control data provides an approach to the assessment of fracture effects in osteoporosis trials for which placebo-controlled data are not available. Risedronate 75 mg for 2 consecutive days each month appears as effective as the 5 mg daily dose in reducing the risk of new vertebral fractures in the first year of treatment.

Disclosures: N. Watts, Procter & Gamble Pharmaceuticals 5.

W374

Vertebral Fracture Efficacy with Risedronate Is Apparent Early and Is Sustained. N. B. Watts¹, C. Roux^{*2}, X. Zhou^{*3}, A. Grauer³. ¹University of Cincinnati, Cincinnati, OH, USA, ²Cochin Hospital, Rene Descartes University, Paris, France, ³Procter & Gamble Pharmaceuticals, Mason, OH, USA.

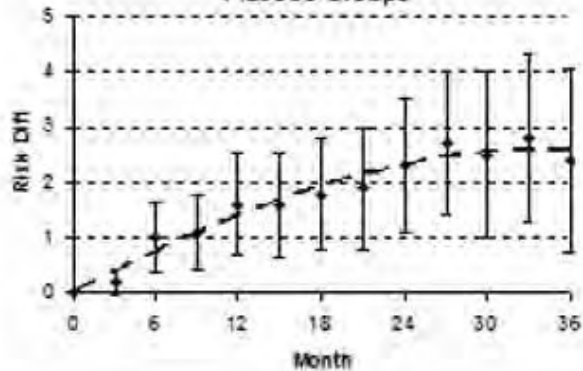
Treatment with an agent that provides both early and sustained fracture protection can benefit patients. Superficial examination of published studies suggests that the early effect of treatment on vertebral fracture (as reflected in relative risk reduction) may lessen over time. In this study, absolute vertebral fracture risk reduction was examined in the Vertebral Efficacy with Risedronate Trials (VERT).

The population included 2442 patients from VERT-NA and VERT-MN who were treated with at least 1 dose of either placebo or risedronate (RIS) 5 mg daily. The mean age was 69 and the mean spine T-score was -2.5. Treatment groups were balanced with respect to key baseline characteristics. Fracture endpoints included clinical vertebral fracture and radiographic vertebral fractures. Difference in risk of vertebral fractures between placebo and RIS 5 mg groups was estimated using the difference of the Kaplan-Meier (KM) estimators at months 3, 6, ... and 36.

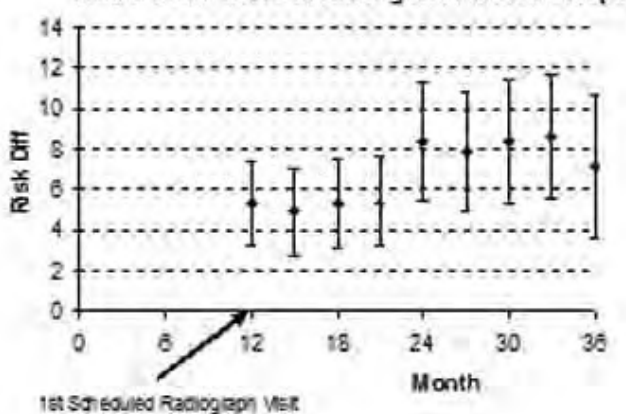
The findings for clinical vertebral fracture were consistent with the rapid onset of risk reduction with risedronate treatment; relative to placebo, RIS significantly reduced the risk for clinical vertebral fracture starting from Month 6, with significant absolute risk reduction of 1.0% (95% CI: 0.3%, 1.6%). The magnitude of the difference in fracture risk between the placebo and risedronate 5 mg groups increased over time (Figure). Relative to placebo, RIS significantly reduced the risk for radiographic vertebral fracture starting from the first scheduled radiographic visit at one year. In general, the mean magnitude of the difference in the fracture risk between the placebo and risedronate 5 mg groups increased over time (from 5.3 % at 12 months up to 8.6%, (95% CI: 5.5%, 11.6%).

In summary, the results confirmed the risedronate rapid protection against clinical vertebral fracture as early as Month 6. Further, risedronate anti-vertebral fracture efficacy as reflected in absolute fracture risk reduction increased over 3 years for both clinical and radiographic vertebral fractures

Difference and 95% CI Of Clinical Vertebral Fracture Risk Between Risedronate and Placebo Groups



Difference and 95% CI Of Radiographic Vertebral Fracture Risk Between Ris 5mg and Placebo Groups



Disclosures: N.B. Watts, Procter & Gamble Pharmaceuticals 5.

W375

Long-term Bisphosphonates Therapy and Increase Fracture Risks. S. J. Wimalawansa. Medicine, Div. Endocrinology, UMDNJ-RWJMS, New Brunswick, NJ, USA.

Bisphosphonate have been in the market for over 2 decades. However, no credible evidence available on fracture benefits of continuation of bisphosphonate therapy >5 years. The terminal half-life of alendronate is similar to bone mineral, ~10 years, while risedronate is ~2 years. The skeletal effects of these two bisphosphonates last for years after stopping therapy. Studies with alendronate show 5 years after discontinuation of therapy, patients bone marker levels remain below the pretreatment levels.

The patients on long-term bisphosphonate therapy continue to maintain their BMD with reduced bone remodeling markers. Once bisphosphonate therapy is discontinued, BMD is stable for about 1 to 2 years depending on bisphosphonate used. Increase in bone remodeling, as indicated by markers of bone turnover will occur before reduction of BMD begins. Therefore, bone markers are much sensitive indicators than BMD to consider starting bisphosphonate or another therapy following discontinuation of bisphosphonate.

Current data suggest that discontinuation of bisphosphonate after 4 to 5 years of therapy does not increase fracture risks, but may in fact be beneficial to patients. Whereas, patients who continue to have fractures while on therapy are non-compliant, or likely to have an underlying secondary cause of bone loss. After several years' therapy with bisphosphonates, stable BMD (with suppressed bone turnover markers) or demonstration of normal histology by biopsy does not signify that the drug protects against fractures. Not only biopsies can miss generalize trends, but also the very small sample sizes used in these studies give false sense of security of the safety of long-term bisphosphonate use. Although the optimal duration of treatment with bisphosphonate (or any therapy) for osteoporosis is uncertain. Data accumulating to suggest that there are no benefits to patients by continuation of therapy beyond five years. The only useful therapy to be continued in the long-term is calcium and vitamin D supplementation. To-date, no independent data available on fracture efficacy of long term anti-osteoporosis medications; this need to be critically evaluated. Prospective clinical trial addressing this issue is underway at this institute. It is now a decade since the first FDA approval of bisphosphonates for osteoporosis. It is time now to examine this issue seriously and to develop clinical practice guidelines (and cost-benefit analysis) for minimizing complications of long-term use of bisphosphonates. This pro-active measure may save millions of tax payer dollars and other health costs (i.e., cost of unnecessary drug therapy, management of complications, and the potential for increased fractures incidence).

Disclosures: S.J. Wimalawansa, None.

W376

Bringing Bone Health to Seniors' Communities: A Unique Approach to Help Manage Osteoporosis. M. Kloseck^{*1}, M. van Zandvoort^{*2}, R. Crilly³, M. Speechley^{*4}. ¹Faculty of Health Sciences, University of Western Ontario, London, ON, Canada, ²Department of Health and Rehabilitation Sciences, Faculty of Health Sciences, University of Western Ontario, London, ON, Canada, ³Department of Medicine, University of Western Ontario, London, ON, Canada, ⁴Department of Epidemiology and Biostatistics, University of Western Ontario, London, ON, Canada.

Osteoporosis is preventable and treatable, yet there is a significant care gap in Canada. We hypothesized that engaging seniors in raising awareness, identifying neighbours and others in their community at risk and a peer-led senior-friendly education program would increase diagnosis and treatment of osteoporosis, and that ongoing peer support would encourage compliance and persistence with medication and lifestyle change. This hypothesis is being tested in a randomized controlled trial (RCT). In Phase 1 (completed) community capacity building and participatory action research methodology was used to train seniors in a local community to act as peer educators and mentors within their community. Ten seniors (mean age=82 yrs. \pm 6.74 yrs. SD, range=71-90) participated in a 2-week training program containing 5 osteoporosis education modules and 1 session on public presentation skills delivered by local experts. Once trained, these seniors formed the Community Osteoporosis Advisory Committee which collaboratively developed a peer advisor training manual, designed a community information and recruiting program, and developed a senior-friendly education and support program which they practiced until all were comfortable. Pre- and post-knowledge surveys showed a statistically significant change ($p=.04$) in knowledge from project start to end of Phase 1. Confidence by seniors in their role as osteoporosis advisors increased significantly ($p=.02$), as did confidence in their ability to deliver information to their neighbours through community presentations ($p=.02$). Overall confidence in their role as peer educators and mentors increased significantly from project start to end of Phase 1 ($p=.01$). In Phase 2 (in progress) the senior-led education and support program is being tested in a RCT ($n=100$) in a local community of seniors ($n=2500$, mean age=79 \pm 9.53 SD). Outcomes include BMDs performed, treatments begun, appropriateness of treatment and persistence. Preliminary baseline knowledge surveys ($n=33$, mean age=81 \pm 7.18 yrs. SD, range 67-91 yrs., 97% female, 3% male) show a substantial gap in knowledge. On the 19-item osteoporosis questionnaire the mean correct minus incorrect score=6.15 \pm 4.79 SD. Scores ranged from -4 to 16 out of 19. Forty-one percent reported having fallen in the past year. This unique approach to diagnosing and treating osteoporosis may be a useful model for other communities of seniors.

Disclosures: R. Crilly, Alliance for Better Bone Health 2.

This study received funding from: Alliance for Better Bone Health.

W377

Compliance with Osteoporosis Treatment and Incidence of Hip and Wrist Fracture after Forearm BMD Screening. M. W. J. Davie, T. Jones*, N. Dugard*. Charles Salt Research Centre, Robert Jones & Agnes Hunt Orthopaedic Hospital NHS Trust, Oswestry, United Kingdom.

Treatment compliance in osteoporosis may affect fracture outcome. To investigate compliance and fracture after a screening programme, we revisited 1299 women aged 50-97y screened by forearm scanning after a minimum of 3 years. Women were scanned at the request of their doctor (GP) and treatment advised if BMD values were $<0.34\text{g/cm}^2$ (osteoporosis (OP)). Treatment was decided by the woman's GP. No follow up was arranged. Women completed a detailed questionnaire at the scanning visit and again when revisited. Women lost to follow up were traced through health records and treatment details between scanning and revisit obtained from the women's own GP. 74% of women returned their questionnaires with no difference between those osteoporotic and those not. Fractures were validated with a 10% sample (and were correct within 5%).

All but 98.5% were traced of whom 14.4% had died. 254 women had osteoporosis at the first visit (aged 50-9, 2.4% had OP, 60-9 15.8%, and >69 54.3%). Of these 37.4% had never started any treatment (excluding Ca and Vit D only) - with no difference across ages. 1.3% had HRT and 98.7% Bisphosphonate (BP) of which 38% used Didronel, 43% Fosamax and 19% had had >1 BP. Compliance with BP dropped to 73.8% after 1yr (no difference across ages) with 22.9% only collecting 1 script. Fewer women with OP in institutions had ever had treatment (28%, $p<0.01$) and were also more likely to stop treatment (28.6% had only 1 script). Excluding women who were no longer available compliance at 2yr was 68.3%, 3yr 58.6%, 4yr 50% and 49.6% at 5yr. Hip fracture occurred in 1 woman with OP out of 38 (age 76.6 \pm 8.1y) who were never treated and in 7 of 55 women (73.2 \pm 7.3y (age $p<0.05$)) fully compliant for 5yr. The excess in women fully compliant occurred after >3y treatment (2 had used Didronel, 2 Fosamax, 3 both). Wrist fractures occurred in 3 women in each group.

Compliance declined early suggesting early follow up is indicated. Treatment in institutions may be overlooked. Compliance is not necessarily associated with hip fracture reduction. However the age of patients with hip fracture (75% were >80y) is consistent with BP efficacy being less in this age group. Moreover most of the hip fractures occurred >3y after treatment started when BP may be less effective at preventing hip fracture.

Disclosures: M.W.J. Davie, None.

W378

An Outreach Program Improved Osteoporosis Management after a Fracture. A. C. Feldstein¹, W. M. Vollmer^{*1}, D. H. Smith^{*1}, A. Petrick^{*1}, J. Schneider^{*1}, H. Glauber^{*2}, M. Herson^{*2}. ¹Center for Health Research, Kaiser Permanente Northwest, Portland, OR, USA, ²Northwest Permanente, Portland, OR, USA.

This longitudinal retrospective cohort study evaluated implementation of a 2-phase intervention to improve management of osteoporosis after a fracture. Stakeholder barriers and facilitators of osteoporosis management were also determined. The study setting was a nonprofit group model HMO in the U.S. Pacific Northwest with 15 clinics, 480,000 members, and comprehensive electronic medical record data. Study participants were women members aged 67 or older who sustained a qualifying clinical fracture(s) and who had not received a bone mineral density (BMD) measurement or osteoporosis treatment in the 12 months prior to the fracture (n=3588) and their 255 primary care providers (PCPs). Interviews/focus groups were conducted with 58 patients, health care managers, PCPs, and orthopedic clinicians. Phase 1 included outreach to clinicians and patients; Phase 2 added clinician/staff incentives. The primary outcome was "osteoporosis management" receipt of a BMD measurement or osteoporosis medication in the 6 months after an index fracture. Prior to the intervention, 13.4% (95% confidence interval [CI] = 12.0%-14.8%) of fracture patients had received osteoporosis management; the pre-intervention time trend was not significant. After the intervention, the unadjusted probability of osteoporosis management increased on average by 3.1% (95% CI = 2.6%-3.5%) every 2 months throughout both study phases. There was no significant added improvement in Phase 2. Overall, the probability of osteoporosis management increased from the baseline level to 44.0% (95% CI = 40.0%-48.0%) by the end of the study period (20 months post intervention). Adjusted models revealed that osteoporosis management was less likely in older patients and in those with dementia and was more likely in those with fractures more highly associated with osteoporosis. Improvement varied by clinic and was less likely for patients with dementia. Patient knowledge gaps and fatalism were common, especially among older patients. Common clinician barriers were lack of time, difficulty interpreting all relevant results, patient management concerns in the transition from specialty to primary care, and frustration with the side effects of and poor patient adherence to osteoporosis medications. This study found that an outreach program to clinicians and patients improved the management of osteoporosis after a fracture. More-tailored interventions may be necessary for high-risk subgroups. There is also a need for more effective patient and clinician education and a stronger role for specialists.

Disclosures: A. C. Feldstein, None.

This study received funding from: Merck & Co., Inc.

W379

Adherence to Raloxifene Therapy: Assessment Methods and Relationship with Efficacy. J. Finigan¹, J. A. Clowes², M. A. Paggiosi^{*1}, D. K. Swindell^{*1}, K. E. Naylor^{*1}, N. F. A. Peel¹, R. Eastell¹. ¹Academic Unit of Bone Metabolism, University of Sheffield, Sheffield, United Kingdom, ²Mayo Clinic School of Medicine, Rochester, MN, USA.

Adherence to study medication is usually estimated by counting returned tablets. This method relies on subjects' honesty and may be inaccurate.

We aimed to assess adherence more accurately, and examine its effect on measures of bone response, by using monitoring caps on the medication bottles in two 2-year studies of osteopenic women, ages 50 to 80. Study 1: 75 women took 60 mg Raloxifene. Study 2: 50 were randomised to take 60 mg Raloxifene (n=25) or no treatment (n=25). Electronic caps (MEMS, Aardex) recorded the date and time whenever the bottle was opened. Returned tablets were also counted. We measured bone mineral density (BMD) by DXA at the lumbar spine (LS) and total hip (TH) twice, a week apart, at baseline and 2 years. Percentage changes from mean baseline to mean 2-year BMD were calculated. We measured urinary NTX from samples taken while fasting on 4 consecutive mornings at baseline, 1 and 2 years. We calculated the mean NTX for baseline and the mean for years 1 and 2 combined, and hence the mean percentage change since baseline.

Combining data from both studies, 100 women took Raloxifene, of whom 29 withdrew during the 2 years. Adherence was assessed by both methods for 71 subjects as a percentage of the total study days. The two methods correlated significantly ($p < 0.001$, Spearman's $\rho = 0.73$) but the tablet count showed a higher mean adherence than the MEMS caps (91.4% v 79.8%, $p < 0.001$), with greater divergence at lower adherence levels. Using the MEMS results for 65 subjects with complete data, adherence correlated with NTX response ($p < 0.01$, $\rho = -0.33$) but not BMD response (LS $p = 0.087$, $\rho = 0.21$, TH $p = 0.25$, $\rho = 0.15$). However there was a threshold effect, with adherence in the lowest quartile associated with poorer BMD response at LS (+0.61% v +2.10%, $p = 0.040$) and at TH (-0.66% v +0.91%, $p = 0.012$).

Monitoring caps may assess adherence more accurately than tablet counts. The degree of adherence is associated with both bone turnover and BMD responses.

Disclosures: J. Finigan, None.

W380

Adherence and Persistence with Teriparatide Therapy in Commercial Insurance Plans and Managed Medicare. S. A. Foster¹, K. A. Foley^{*2}, E. S. Meadows^{*1}, J. A. Johnston^{*1}, S. Wang^{*2}, G. M. Pohl^{*1}, S. R. Long^{*2}. ¹Eli Lilly and Company, Indianapolis, IN, USA, ²Thomson Medstat, Ann Arbor, MI, USA.

The purpose of this study was to evaluate adherence to teriparatide (TPTD) therapy and to identify the factors that impact persistence. Beneficiaries (45 years and older) with at least one claim for teriparatide in 2003 or 2004 and continuous enrollment in the previous 12 months and subsequent 6 months were identified in a large (7.6 million covered lives) national commercial and Medicare administrative claims database (MarketScan). Adherence was assessed through the calculation of the medication possession ratio (MPR) at 6 months and 12 months. The MPR was calculated as the sum of days supply dispensed between the start of the observation period and the end of the observation period and divides that number by the total number of days being examined. Persistence was calculated as the time (days) to discontinuation (meaning the last prescription for the index drug regardless of gaps in fills - with at least 2 months remaining enrollment without the script). In addition, factors associated with time to discontinuation in treatment were assessed using Cox proportional hazards models. The average age of patients in this analysis was 70.3 and 89.7% were female. In the 12 months prior to initiating TPTD, 38% of patients had experienced a fracture. The average MPR at 6 months was 0.74 (N=2218) and 12 months was 0.66 (N=1303). At 6 months (N=2218), 64.6% of patients remained on TPTD therapy and at 12 months (N=1303), 56.7% of patients remained on TPTD. Prior use of an antiresorptive therapy, having BMD screening within the 12 months prior to starting TPTD, and lower patient copayments were associated with longer times until discontinuation. Overall, despite being an injectable, TPTD adherence was comparable with adherence rates found with other osteoporosis medications in the literature. Understanding the factors that impact persistence with therapy may allow clinicians to make informed decisions about patient selection that may improve persistence.

Disclosures: S.A. Foster, Eli Lilly and Company 3.

This study received funding from: Eli Lilly and Company.

W381

Patient Perceptions and Reasons for Discontinuing Teriparatide Treatment: Initial Results from the DANCE Observational Study Addendum. D. T. Gold¹, D. L. Weinstein^{*2}, G. Pohl^{*3}, K. D. Krohn³, E. Meadows^{*3}. ¹Psychiatry & Behavioral Sciences, Sociology, and Psychology, Duke University, Durham, NC, USA, ²Medicine, Washington University, St. Louis, MO, USA, ³Outcomes Research, Eli Lilly, Indianapolis, IN, USA.

Purpose: To determine the perceptions of patients who initiate and persist on treatment with teriparatide (Forteo) for osteoporosis.

Methods: The Direct Assessment of Non-vertebral Fractures in the Community Experience (DANCE) is a multi-center, prospective, observational study. The DANCE addendum includes questionnaires (Q1 and Q2) completed by the teriparatide patients. Administered at initiation of therapy, Q1 includes items related to the patient's experience with self-injection drugs, perceptions about the severity of their osteoporosis, relationships with their prescribing physician and staff, and concerns about starting treatment. The Q2 instrument (completed 2 to 6 months after initiating therapy) includes items regarding training or other support offered at therapy initiation, the patient's early experience with teriparatide treatment (including problems, adverse events, and concerns), and whether the patient is still taking treatment. If the patient has stopped teriparatide treatment when Q2 is completed, the patient is asked to choose one of 6 pre-specified reasons why they stopped treatment.

Results: As of January 2007, 700 patients had completed both Q1 and Q2. The DANCE Addendum patients were relatively homogeneous in their perceptions at initiation of teriparatide treatment. Fewer than 1 out of 4 (n=150, 22%) patients reported that they had previous experience with self-injectable medications. Many (n=409, 59%) patients believed their osteoporosis was severe or very severe. Nearly all (n=662, 95%) believed that it was extremely or very important to treat their osteoporosis. Additionally, some (n=167, 24%) patients were extremely or very concerned about their ability to pay for teriparatide. Few patients (n=50, 7%) reported discontinuing teriparatide treatment by the time Q2 was administered. The reasons for discontinuation are shown below.

Reasons for discontinuation of teriparatide therapy	n	%
concerns about treatment outweighed the benefits	18	2.6
cost issues - difficulty paying for it	14	2.0
taken as long as physician prescribed	7	1.0
problems with injecting	3	0.4
did not believe it was beneficial	2	0.3
too hard to follow all the steps necessary to use Forteo	2	0.3
unspecified	4	0.6
total	50	7.1

Conclusions: Few patients have discontinued teriparatide treatment in the DANCE Addendum before the first follow-up visit 2-6 months after initiation. The 2 most common reasons for discontinuation were (1) that treatment concerns outweighed the benefits of teriparatide and (2) concern about paying for teriparatide.

Disclosures: D.T. Gold, Eli Lilly and Company 5; Procter and Gamble, sanofi-aventis, GlaxoSmithKline, Roche, and Amgen 5, 8.

This study received funding from: Eli Lilly & Company.

W382

A Group-based Patient-Education Program Increases Knowledge of Osteoporosis and Adherence to Pharmacological Treatment - A Randomised Trial. D. Nielsen¹, J. Ryg^{*1}, W. Nielsen^{*2}, B. Knold^{*1}, N. Nissen^{*1}, L. Stilgren¹, A. Riis Madsen^{*1}, K. Brixen¹. ¹Endocrinology, Odense University Hospital, Odense, Denmark, ²Physiotherapy, Odense University Hospital, Odense, Denmark.

Purpose: A large number of studies have demonstrated that pharmacological therapy of osteoporosis is effective; however non-adherence to such therapy is a well recognized problem. Few studies, have examined the effect of particular patient education programs on knowledge and adherence to therapy. We hypothesised that group-based, multi-disciplinary, education program increases the patients' knowledge of osteoporosis and adherence with pharmacological therapy. **Methods:** A total of 300 patients (32 men aged 65 ± 9 yrs and 268 women aged 63 ± 8 yrs), recently diagnosed with osteoporosis and started on specific treatment, were randomised to either the "school" (n=150) or "control" (n=150) group. In the school-group, patients attended four classes with 8-12 participants during four weeks (a total of 12 hours). Teaching was performed by nurses, physiotherapists, dieticians, and doctors and was based on dialogs and situated learning. The classes covered "facts on osteoporosis", "fractures and pain", "diet", "preventive measures", "balance and exercise", and "medical treatment". Teaching was designed to increase empowerment. We assessed the patients' knowledge about osteoporosis and compliance to pharmacological treatment, using validated questionnaires. **Results:** At baseline, no significant difference was seen between the groups regarding knowledge score (20.1 ± 5.6 versus 21.0 ± 4.7). The change in knowledge at 3 months was significantly higher in the school group (3.43 ± 4.0) compared with the control group (0.33 ± 2.48) (p<0.001). Adherence with pharmacological therapy at 2 years was significantly higher in the school group (99%) compared to controls (84%) (p<0.001, Log Rank test). Neither baseline knowledge score, nor change in knowledge score, however, was significantly associated with compliance. **Conclusion:** A multidisciplinary patient education program leads to increased knowledge of osteoporosis and increased adherence to treatment. Knowledge, however, did not predict adherence. There are more issues important when it comes to adherence to treatment.

Disclosures: D. Nielsen, Eli Lilly 2, 8; Nycomed 2; Servier 2, 8; Pharma Vinci 2, 8. This study received funding from: Danish Osteoporosis Society, Augustinus Foundation, Frimondt-Heineke Foundation, Sygekassernes Helse Foundation, Medical Industries: Novo Nordisk, Aventis, Eli Lilly, MSD and Pharma Vinci, Nycomed and Servier.

W383

Convenience and Preference Perceptions After 1 Year of Oral Bisphosphonate Treatment in a Group of Brazilian Women. S. Ragi-Eis¹, I. F. Francischetto^{*2}, B. Albergaria^{*2}, A. A. Oliveira^{*2}, F. V. Simões^{*2}, K. Milagre^{*2}, C. Bonomo^{*2}. ¹Clinical Research Department, CEDOES, Vitoria - ES, Brazil, ²Clinical Research, CEDOES, Vitoria - ES, Brazil.

Once monthly dosing (OM) of ibandronate has been shown to provide similar efficacy in increasing BMD to once weekly dosing (OW) of alendronate for treatment of osteoporosis in postmenopausal women. Whether patients will prefer monthly dosing to weekly dosing for a chronic condition such as osteoporosis has not been well documented in a Latin American population. The aim of this study was to assess the preference as well as their perception of convenience for monthly versus weekly dosing regimens among sample of Brazilian osteoporotic postmenopausal women.

One hundred and eighty one postmenopausal women with osteoporosis were originally randomized in the Motion Study, to receive treatment with either (1) alendronate 70 mg once weekly plus once monthly placebo tablet or (2) ibandronate 150 mg once monthly plus once weekly placebo for 12 months. From this subset, 145 (One hundred and forty five) women (80.1%) were interviewed during the follow-up visits, after completion of the study. The patients were asked about the convenience as well as their preference about treatment regimens to continue their treatment.

Among those expressing preference (n=115), 69 % (79) pointed the once monthly dosing regimen as the preferred regimen to continue their treatment from that moment on. The main reasons to justify their option were "better to remember" (30 subject for the OM vs 22 for the OW) and "more favorable time interval" (22 subjects for the OM vs 0). In addition, from the patients expressing opinion about convenience (n=81) the once monthly regimen was considered by 73% (59) to be the more convenient one. The key factor to justify their opinion was "fits better in my lifestyle" (56 subjects for the OM vs 16).

After having the opportunity to try both weekly and monthly regimens for a 12 month period, the majority of the patients preferred the OM one to continue their treatment. They also considered this option the more convenient one. In conclusion, patient preference and convenience perceptions about dosing regimen should also be taken into consideration when taking the decision to prescribe an oral bisphosphonate for Brazilian Women. This could have a favorable impact on treatment compliance.

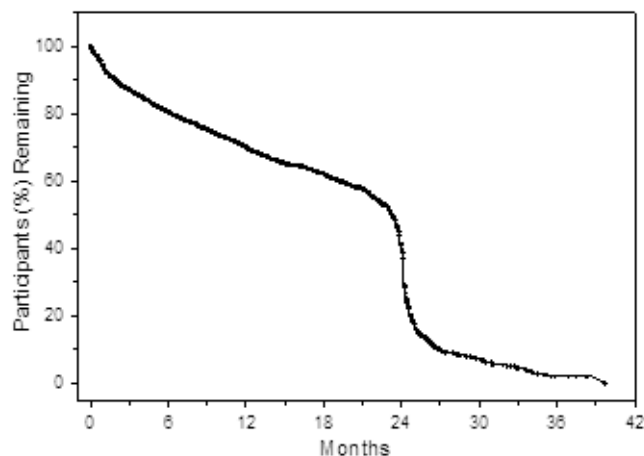
Disclosures: S. Ragi-Eis, Sanofi-Aventis, Eli Lilly, GE 2; Merck, Roche, Sanofi-Aventis, Eli Lilly 8.

W384

Persistence with Teriparatide Therapy Among Participants in the DANCE Trial. K. Taylor^{*1}, D. Gold^{*2}, S. Silverman^{*3}, P. Chen^{*1}, M. Wong¹, K. Krohn^{*1}. ¹Eli Lilly and Company, Indianapolis, IN, USA, ²Duke University, Durham, NC, USA, ³OMC Research, Beverly Hills, CA, USA.

Despite the benefits of osteoporosis (OP) therapies shown in clinical trials, poor persistence is a common cause of reduced patient benefit in a "real world" setting [Mayo Clin Proc 2006;81:1013-22]. Overall persistence with OP therapies has been reported to be between 25-45% at 1 yr [Maturitas 2004;48:271-87; Arch Int Med 2005;165:2414-9]. Few, if any, US studies have assessed persistency with teriparatide (TPTD) in community settings. A prescription tracking database [IMS Health LRxTM] estimated persistency with TPTD (20 µg/d) to be about 30% at 12 months (Lilly data on file). The ongoing, observational DANCE study captures data on persistence with TPTD therapy. A survival model (Figure) assesses the rate of patients persisting with therapy at defined time points after their start date. This analysis included 2474 patients who were eligible to have had 12 months of TPTD therapy. The model estimated ~70% of patients persisted with therapy at 12 months.

Persistence was not significantly affected by age, co-morbidity, or baseline severity of OP, as assessed by BMD T-score, prevalent fracture status, or clinical risk factors for fracture. Of these 2474 patients, 419 completed 18-24 months of therapy, 852 discontinued therapy before completing the 18-24 month course, and 1203 remained in the study. Reasons for discontinuation were categorized as patient decision (422, 49.5%), physician decision (136 patients, 16%), serious adverse event (57, 6.7%), sponsor decision (2, 0.2%) and other unstated reasons (172, 20.2%), and 63 patients (7.4%) had no data available. For the 422 patients who listed "patient decision" as the reason for discontinuation, additional comments about their discontinuation were collected, and included insurance reimbursement, inconvenience, and concerns about injection. Persistence with TPTD in DANCE subjects at 12 months may be higher than that measured using a prescription tracking database. Different methodologies used to measure persistence may reflect some of this disparity. Further analysis of the DANCE cohort may elucidate factors affecting persistence to TPTD therapy and offer new approaches to optimize TPTD use in the community.



Disclosures: K. Taylor, K. Taylor, P. Chen, M. Wong, K. Krohn 1, 3; D. Gold 2; S. Silverman 2.

This study received funding from: Eli Lilly and Company.

W385

Safety and Tolerability of Bazedoxifene in Postmenopausal Women with Osteoporosis: Results from a 3-Year, Randomized, Placebo- and Active-Controlled Clinical Trial. J. D. Adachi¹, C. H. Chesnut², J. P. Brown³, C. Christiansen⁴, L. A. Russo⁵, C. E. Fernandes⁶, J. C. Menegoci⁷, A. Kung⁸, A. A. Chines⁹, L. Bessac⁹, D. Chakrabarti⁹. ¹St. Joseph's Hospital - McMaster University, Hamilton, ON, Canada, ²University of Washington, Seattle, WA, USA, ³CHUL Research Center, Laval University, Quebec, PQ, Canada, ⁴Center for Clinical and Basic Research (CCBR), Ballerup, Denmark, ⁵CCBR, Rio de Janeiro, Brazil, ⁶Women's Health and Wellness Institute (ISBEM), São Paulo, Brazil, ⁷San Francisco Clinic, São Paulo, Brazil, ⁸The University of Hong Kong, Hong Kong, China, ⁹Wyeth Pharmaceuticals, Collegeville, PA, USA.

Bazedoxifene (BZA) is a novel selective estrogen receptor modulator selected for clinical development based on preclinical evidence of tissue-selective estrogen agonist activity on the skeletal system and lipid metabolism and estrogen antagonist activity on breast and uterine tissues. A total of 7492 postmenopausal women with osteoporosis (mean age \pm SD, 66.4 \pm 6.7 years) were randomized to receive BZA 20 mg, BZA 40 mg, raloxifene (RLX) 60 mg, or placebo (PBO) daily and received \geq dose of study medication. At 36 months, BZA exhibited a statistically significant decrease in new vertebral fracture compared with placebo (primary efficacy endpoint to be reported elsewhere). We report here the 3-year safety and tolerability data from this study. After 3 years of treatment, BZA was overall well tolerated and exhibited a favorable safety profile. Findings of selected safety/tolerability analyses are shown below.

	No. of Women (%)			
	BZA 20 mg (n=1886)	BZA 40 mg (n=1872)	RLX 60 mg (n=1849)	PBO (n=1885)
Discontinuations	632 (33.5)	643 (34.3)	598 (32.3)	629 (33.4)
Discontinuations due to adverse events	269 (14.3)	270 (14.4)	262 (14.2)	240 (12.7)
Myocardial infarctions	8 (0.4)	8 (0.4)	6 (0.3)	8 (0.4)
Ischemic stroke	13 (0.7)	18 (1.0)	11 (0.6)	13 (0.7)
Hemorrhagic stroke	1 (0.1)	1 (0.1)	1 (0.1)	5 (0.3)
Deep vein thrombosis (DVT)	7 (0.4)	11 (0.6)	8 (0.4)	1 (0.1)
Hot flushes	238 (12.6)	243 (13.0)	222 (12.0)	118 (6.3)
Leg cramps	205 (10.9)	204 (10.9)	216 (11.7)	155 (8.2)
Breast cancer	5 (0.3)	4 (0.2)	7 (0.4)	8 (0.4)
Breast cysts/fibrocystic breast	14 (0.7)	13 (0.7)	32 (1.7)	20 (1.1)

No safety concerns related to the cardiovascular and reproductive systems, including breast, were observed in the BZA treatment groups. There was a higher incidence of DVT in the BZA groups compared with the PBO group. The incidence of breast cancer and cystic/fibrocystic breast disease was lower in women receiving BZA than in those receiving PBO. Transvaginal ultrasonography examinations revealed that BZA had no significant effects on the endometrium or ovaries.

In conclusion, BZA has a favorable safety and tolerability profile in postmenopausal women with osteoporosis. The safety and tolerability profile was similar between BZA 20 and 40 mg groups. BZA is a promising new SERM for the prevention and treatment of postmenopausal osteoporosis.

Disclosures: J.D. Adachi, Amgen, Astra Zeneca, Eli Lilly, GlaxoSmithKline, Merck, Novartis, Pfizer, Procter & Gamble, Roche, Servier 5, 8; Amgen, Astra Zeneca, Eli Lilly, GlaxoSmithKline, Merck, Novartis, Pfizer, Procter & Gamble, Roche 2.
This study received funding from: Wyeth Pharmaceuticals.

W386

Postmenopausal Osteoporosis and Weight Gain. A. Bazarra-Fernandez*. ObGyn, Juan Canalejo University Hospital Trust. La Coruña. Spain, La Coruña, Spain.

Background: Recent studies have found weight gained during menopause increase the risk of high blood pressure, the diabetes, heart disease, and has been strongly linked to increased incidence of breast and other hormone-related postmenopausal malignancies. These healthcare concerns have led to the conception of specific products that target menopausal weight gain.

Aim: Looking over weight gain and osteoporosis treatment in climacteric. Material and methods: 20 women who were 44 to 58 years old have been recruited. BMI was increased to age. Those with an intact uterus have moderate to severe vasomotor symptoms associated with the menopause, moderate to severe symptoms of vulvar and vaginal atrophy and risk of postmenopausal osteoporosis. They were ascribed to equal two 10 women groups. One group was assigned to 2 mg drospirenone /1 mg 17 beta- estradiol hemihydrate. The other group treated with 40 mg soy bean.

Results: in the women on 2 mg drospirenone /1 mg 17 beta- estradiol hemihydrate medication decreased, moderate to severe symptoms of vulvar and vaginal atrophy vasomotor symptoms associated with the menopause in regard to the other group treated with 40 mg soy bean. They had weight main loss of 3 kg in one year, (P < 0.05).

Conclusions: Human HRT is in relation to decrease osteoporosis. Nobody noted 17 beta-estradiol is in relation to breast cancer. Estradiol is the same oestrogen produced by the ovaries before menopause. Drospirenone has the unique property of reducing water retention often associated with the use of oestrogen and other synthetic progestin hormones. The impact of obesity on hormone replacement therapy is due to many women associate hormones with weight gain. This late medication formula can be beneficial in minimizing uncomfortable symptoms, such as weight gain, hot flashes, night sweats, and

mood swings, associated with the natural progression of a woman's life cycle. So, it is due to conduct one great try to make clear and more comprehensible these points.

Disclosures: A. Bazarra-Fernandez, None.

W387

Safety and Tolerability of Bazedoxifene for the Prevention of Postmenopausal Osteoporosis. C. H. Chesnut¹, C. Christiansen², H. C. Hoec², H. Genant³, D. van Duren⁴, A. B. Levine⁵, A. A. Chines⁵, G. Constantine⁵. ¹University of Washington, Seattle, WA, USA, ²Center for Clinical and Basic Research, Ballerup, Denmark, ³University of California San Francisco, San Francisco, CA, USA, ⁴Menox BV, Nijmegen, The Netherlands, ⁵Wyeth Pharmaceuticals, Collegeville, PA, USA.

Bazedoxifene (BZA) is a novel selective estrogen receptor modulator (SERM) selected for its antagonist activity on endometrial and breast tissues. Here we report on the safety and tolerability of BZA for the prevention of postmenopausal osteoporosis in a randomized, double-blind, placebo- and raloxifene-controlled phase III trial. Healthy postmenopausal women (aged \geq 45 years) with lumbar spine or femoral neck bone mineral density T-scores no less than -2.5 (mean, -1.2) were enrolled if they did not have vasomotor symptoms requiring treatment, bone diseases (other than osteoporosis), previous vertebral fractures, or endometrial hyperplasia at baseline. Subjects were randomized to take BZA 10, 20, or 40 mg; raloxifene 60 mg; or placebo daily for 2 years. Efficacy assessments (bone mineral density, bone markers, and lipids) are presented in detail elsewhere. Safety was evaluated based on adverse event (AE) reporting, laboratory analyses, and physical examination. Endometrial and ovarian safety were assessed by periodic transvaginal ultrasound and endometrial biopsy. Of 1,583 women (mean age \pm standard deviation, 57.6 \pm 6.5 years) included in the safety population; 1,113 (70.3%) completed the 2-year study. The rates of treatment-emergent AEs, serious AEs, and discontinuations due to AEs were similar among treatment groups. Vasodilatation was more common with BZA 20 and 40 mg (19.9% and 22.6%, respectively) than with placebo (13.2%; P < 0.05 for both), but similar to raloxifene (18.3%). The incidence of leg cramps was similar across treatment groups (range, 9.3%-11.6%). The incidence of venous thrombotic events with BZA was low (<1%) and similar to that with RLX or placebo. No cases of endometrial hyperplasia or malignancy were diagnosed in women treated with BZA. In conclusion, BZA was well tolerated and had a safety profile similar to placebo in a population of relatively young postmenopausal women. BZA is a new promising SERM that could become an important addition to the available therapies for the prevention of postmenopausal osteoporosis.

Disclosures: C.H. Chesnut, Roche 8.

This study received funding from: Wyeth Research.

W388

Methods of Transition from Hormone Therapy to Raloxifene or Other Regimens Administered to Postmenopausal Women for the Prevention or Treatment of Osteoporosis: The HORTHON Study. G. Christodoulakos¹, V. Drossinos², C. Barker³, E. Korelis², G. Kreatsas¹, & the Hellenic HORTHON Study Group¹. ¹2nd Dpt of Obstetrics & Gynecology, University of Athens, Aretaion Athens Hospital, Greece, ²Dpt of Medical Research, Pharmaserve-Lilly, Athens, Greece, ³EuMIS Statistics, Eli Lilly & Company, Erl Wood, United Kingdom.

HORTHON is a Hellenic prospective observational study designed to investigate the preferred method of transition from hormone therapy (HT) to Raloxifene or other pharmaceutical agents for the prevention or treatment of osteoporosis.

The study design was non-interventional. Patients were asked to sign an informed consent document before entering the study. Inclusion criteria were a postmenopausal status for at least 2 years and continuous treatment with HT for at least 6 months prior to inclusion.

494 patients were included in the study, enrolled by 39 investigative sites. Mean age (SD) was 52.2 (5.12) years, mean (SD) age at start of menopause was 47.1 (4.94), mean (SD) time since menopause was 5.2 (4.13) and mean (SD) duration of HT was 4.0 (2.85) years. 49.0% had a history of osteoporosis in mother and 7.7% had a family history of breast cancer. 62.2% of enrolled patients were diagnosed with Osteopenia and 14.8% with Osteoporosis.

83.0% of patients received Raloxifene either as monotherapy (Raloxifene only) or combined mainly with calcium and vitamin D (Raloxifene plus Other), 11.6% received other treatment (Other Therapy) while 5.3% were not administered any therapy, as chosen in the course of normal clinical practice. The primary reason of choice was safety in the "Raloxifene only" (52.8%) and "Raloxifene plus other" (41.0%), while in the "Other therapies" was efficacy (34.5%).

Transition methods included "no wash out and no taper", "wash out only", "wash out and taper" and "taper only" (45.2%, 45.2%, 7.6% and 1.9% of patients respectively). For "Raloxifene only" group, "no wash out and no taper" method applied to 55.9% of patients. "For Raloxifene plus Other" and "Other" new therapies "wash out only" method was chosen for the majority of patients (46.0% and 49.1% respectively). Mean (SD) satisfaction from transition method (taper and/or wash out), estimated by a visual analogue scale, was 32.9 (19.30).

The main reason for discontinuation of HT was prolonged use (42.3% of patients). Mean (SD) satisfaction to previous HT treatment was 30.8 (20.16) while for patients who received no new therapy, satisfaction (SD) was 22.7 (15.48). In this study, patients who discontinue HT, mainly for prolonged use, were more likely to transition to Raloxifene rather than another pharmaceutical agent. Safety is the major reason for choosing the new

therapy. The most frequent transition methods were "no wash out and no taper" and "wash out only".

Disclosures: G. Christodoulakos, None.

This study received funding from: Pharmaserve - Lilly S.A.C.I.

W389

Possible Role of Equol Status in the Effects of Isoflavone on Bone and Fat Mass in Postmenopausal Japanese Women: A Double-Blind Randomized Controlled Trial. Y. Ishimi¹, J. Oka², S. Uchiyama³, T. Ueno⁴, T. Toda⁴, M. Uehara⁵, J. Ezaki¹, J. Wu⁶. ¹Nutritional Epidemiology Program, National Institute of Health and Nutrition, Tokyo, Japan, ²Home Economy, Tokyo Kasei University, Tokyo, Japan, ³Saga Nutraceuticals Research Institute, Otsuka Pharmaceutical Co. Ltd., Saga, Japan, ⁴Fujico Co. Ltd., Kobe, Japan, ⁵Nutritional Science, Tokyo University of Agriculture, Tokyo, Japan, ⁶Central Research Laboratory, Nisshin Oillio Group, Ltd., Yokosuka, Japan.

Introduction: Equol is more biologically active than its precursor daidzein, which is the principal isoflavone found in soybean. There are inter-individual differences in the ability to produce equol; this may lead to differences in the effects of isoflavone intervention on human health. This study aims to investigate whether the effects of soy isoflavones on bone and fat mass are related to an individual's equol status.

Methods: We performed a 1-year double-blind randomized trial to compare the effects of isoflavone (75 mg of isoflavone conjugates/day; equivalent to 47 mg/day of aglycone form) with those of placebo on bone mineral density (BMD), fat mass, and serum isoflavone concentrations in early postmenopausal Japanese women who were classified based on their equol-producer phenotype.

Results: After 1-year, the isoflavone intervention significantly increased serum equol concentration in the equol producers but not in the nonproducers. In the isoflavone group, the annualized changes in the BMD of the total hip and inter-trochanteric regions were -0.46% and -0.04%, respectively, in the equol producers and -2.28% and -2.61%, respectively, in the nonproducers; these values were significantly different ($p < 0.05$ for both the regions). Significant differences were observed between the equol producers and nonproducers in the isoflavone group with regard to the annualized changes in the fat mass. No significant difference in the annualized changes in the BMD and fat mass was observed between the equol producers and nonproducers in the placebo group.

Conclusions: Our data suggest that the preventive effects of isoflavones on bone loss and fat accumulation in early postmenopausal women depend on an individual's equol-producing capacity.

Disclosures: Y. Ishimi, None.

This study received funding from: Japan Health Science Foundation.

W390

Success and Complication Rate of Percutaneous Vertebroplasty (PVP) in Patients with Osteoporosis (OP). M. Gaugg¹, F. Kanel², P. Breiter², W. Kump², B. Kutil¹, L. Erlacher¹. ¹Internal Medicine, Division of Rheumatology and Osteology, SMZ Süd, Vienna, Austria, ²Radiology, SMZ Süd, Vienna, Austria.

Background: Percutaneous vertebroplasty (PVP) is an evidence-based, minimally-invasive procedure to manage pain and vertebral spine deformation after vertebral compression fracture (VCF) in patients with OP^{1,2}. **Objective:** To describe success and complication rates in patients affected by VCF and treated by PVP in specialized clinical care, to evaluate their clinical and treatment characteristics. **Materials and Methods:** Data were collected retrospectively by review of examination reports. PVP was performed by two interventionists. CT fluoroscopy guided PVP with additional guidance by conventional C-arm fluoroscopy was performed as described previously^{3,4}, between October 2003 and February 2007. **Results:** A total of $n = 133$ procedures were available for analysis. PVP was performed in $n = 85$ patients [71 females/14 males, mean age 75.5 ± 9.5 a; (53-93a)]. Post-interventional cement leakage was found in 44/85 patients (51.7%) or 50/133 vertebrae (37.6%). The location of the leakage was distributed as follows: 9.7% ($n = 13$) to basivertebral veins, 5 % ($n = 7$) to paravertebral structures including paravertebral veins, 15 % ($n = 20$) to adjacent vertebral disc (upper or lower end plate), and 7% ($n = 10$) to epidural venous system. All PVP's were completed successfully with conscious sedation and local anesthesia. During treatment of 133 vertebrae (TH4-L5), no clinically evident neurologic or embolic events occurred. There was no procedure related mortality. **Conclusion:** PVP can be performed safely and effectively in patients with OP and VCF. Post-interventional cement leakage is found frequently by combination of CT and conventional fluoroscopy. However, clinically relevant neurologic and/or thromboembolic complications may be rare with careful patient selection by clinicians and appropriate radiologic imaging.

References:

- 1) Interventional Techniques: Evidence-based Practice Guidelines in the Management of Chronic Spinal Pain. Mark V. Boswell, et al. Pain Physician 2007 Jan;10(1):7-111.
- 2) Balloon kyphoplasty and vertebroplasty for vertebral compression fractures: a comparative systematic review of efficacy and safety. RS Taylor et al. Spine 2006 Nov 1;31(23):2747-55
- 3) Percutaneous vertebroplasty guided by a combination of CT and fluoroscopy. A Gangi, et al. AJNR Am J Neuroradiol. 1994 Jan; 15(1): 83-6
- 4) Evaluation of percutaneous vertebroplasty in osteoporotic vertebral fractures using a combination of CT fluoroscopy and conventional lateral fluoroscopy. MB Pitton et al. Rofo. 2004 Jul;176(7):1005-12

Disclosures: M. Gaugg, None.

W391

Health-related Quality Of Life 7 Years After Hip Or Vertebral Fractures. I. Hallberg¹, M. Bachrach-Lindström¹, G. Toss², A. C. Ek¹. ¹Dept of Medicine and Care, Div of Nursing Science, Faculty of Health Sciences, Linköping University, SE-581 85 Linköping, Sweden, ²Dept of Medicine and Care, Div of Internal medicine, Faculty of Health Sciences, Linköping University, SE-581 85 Linköping, Sweden.

In a previous paper we reported that women with vertebral fracture had severe reduction of health-related quality of life two years after a fracture. In order to estimate the long-term impact of osteoporotic fractures on HRQOL we examined 67 women, 7 years after a hip or vertebral fracture. Patients were otherwise attending routine primary health care. HRQOL was evaluated by the SF-36 questionnaire and compared with a local age-matched reference material ($n = 804$). High scores in SF-36 indicate better HRQOL. Bone mineral density (BMD) was measured with Hologic 4500A. Physical function was assessed by handgrip strength (Jamar dynamometer) and static balance on dominant leg with eyes open. The number of the vertebral fractures was evaluated by lateral radiographs of the spine and calculation of spinal deformity index (SDI, range 0-39), according to the Genant visual semiquantitative criteria.

At the 7 year investigation 51 women had one or more vertebral fractures (9 of which also had a hip fracture). Mean SDI was 5.7 (range 1-25). Of the women with a hip fracture 16 were without vertebral fractures. Mean age (SD) was in vertebral fracture group 76.0 (4.7) and in hip fracture group 73.6 (4.2) years ($p = 0.07$). Bisphosphonate treatment was used by 23 of 67 women (17/51 and 6/16 respectively, n.s.).

HRQOL (SF-36) was reduced in the vertebral fracture group regarding physical function ($p = 0.005$), role-physical ($p < 0.001$), bodily pain ($p < 0.001$), role-emotional ($p = 0.046$), vitality and social function ($p = 0.06$). Women with hip fracture ($n = 16$) but no vertebral fracture did not differ from the reference material.

In the total fracture group ($n = 67$) static balance showed a significant positive correlation ($p < 0.05$) to SF-36 regarding all 8 domains (range $r_s = 0.268-0.549$). Also handgrip strength correlated in all domains except role-emotional (range $r_s = 0.261-0.387$). SDI showed negative correlation to all domains except physical function, general health and mental health (range $r_s = -0.269-0.346$). Age showed negative correlation to vitality and mental health (range $r_s = -0.246-0.292$). BMD in hip or lumbar spine did not correlate with any domain in SF-36.

In conclusion women with vertebral fractures still had pronounced reduction of most HRQOL domains 7 years after fracture and treatment in routine health care. The long-term reduction of HRQOL and its correlation to static balance and handgrip strength raise questions for further investigation.

Disclosures: I. Hallberg, None.

W392

Importance of Balloon Kyphoplasty in the Management of Vertebral Fractures. J. Hamon^{*}, P. Longis^{*}. Orthopedie, Hospital, Saint-Nazaire, France.

Objectives: To show the importance of balloon kyphoplasty, in the management of vertebral compression fractures of the elderly and vertebral fractures secondary to cancer. This minimally invasive procedure is designed to reduce the fracture, correct the deformity, stabilize the lesion by injection of cement, decrease the pain, limit the hospitalization time and improve the patients' quality of life.

Methods: Retrospective study from Dec 2005 to Apr 2007. All patients older than 40 years and presenting with a vertebral compression fracture or a metastatic vertebral fracture, localized between T6 and S4 without neurological complication, were included. The procedure is performed under general anesthesia and is characterized by controlled inflation of 2 small balloons under fluoroscopic control in order to correct the vertebral deformity before injection of the cement. **Results:** 44 patients, 26 women and 18 men were included in the study, 51 vertebrae were treated. The average age is 64 years. 35 vertebral compression fractures (from T7 to L4) and 16 metastatic vertebral lesions (from T6 to S4) were treated (2 prostate, 3 pulmonary, 3 hematologic, 5 gastro-intestinal, 1 gynecologic and 2 neuro-endocrine primary cancer). For traumatic fractures, mean fracture age is 67 days. Pre-operative use of analgesics, according to the classification of the W.H.O., is of level 1 in 8 patients, level 2 in 11 patients and level 3 in 25 patients. The mean cement volume injected per vertebra is 5 cc. For the trauma lesions, height restoration of the anterior vertebral body wall is on average 15% lost height restored and the correction of the local kyphosis is 5°. Cement leakages in the adjacent discs are found in 9 patients without any clinical consequences. No post-operative complications were seen. Post-operative mobilization is on average on day 1. Hospital discharge is on average on day 2. Post-operatively prescribed analgesics, according to the classification of the W.H.O., are of level 1 in 29 patients, level 2 in 9 patients and level 3 in 6 patients. 38 patients returned home, 6 patients needed revalidation (1 because of associated traumatic lesions and 5 patients needed specialized care for their primary tumor).

Discussion: The usual treatments of this type of vertebral lesions as well as their frequent adverse events are known. The interest of Kyphoplasty is thus highlighted. The review of the literature also highlights the advantages of this technique compared to vertebroplasty. **Conclusion:** Balloon kyphoplasty is an alternative with reduced surgery time, good safety profile, early mobilization and without need for bracing. Balloon kyphoplasty allows reduction in analgesics consumption, an early hospital discharge and improvement of the patients' quality of life.

Disclosures: J. Hamon, None.

W393

Significant Reduction of Vertebral Fractures: Comparison of Rehabilitation of Osteoporosis Program-Exercise (ROPE) versus No-ROPE, With or Without Pharmacotherapy. D. A. Kurmen Figueroa*, M. Sinaki. Physical Medicine and Rehabilitation, Mayo Clinic, Rochester, MN, USA.

The objective of this study was to determine whether patients with osteoporosis who received the Rehabilitation of Osteoporosis Program-Exercise (ROPE) had reduced risk of vertebral fracture as compared with those who did not (No-ROPE). To avoid bias in choice of treatment, none of the subjects or evaluators had knowledge of group assignment. We reviewed the medical records of 200 patients. One hundred and twelve patients with osteoporosis met the inclusion criteria, i.e. women older than age 40 with the diagnosis of osteoporosis, baseline and follow-up radiographs of spine. Patients with steroid-induced bone loss and active malignancy were excluded. Two groups were formed: 71 subjects in the ROPE group and 41 subjects in the No-ROPE group met the enrollment criteria. Follow up was the date of follow up x-rays or recurrence of fracture/back pain. The duration of follow up ranged from 3 months to 118 months with an average of 45.5 months. The results showed that fifty-six of the 71 ROPE subjects (78.9%) and 20 of the 41 No-ROPE subjects (48.8%) had no new fracture at the time of final follow up. Interestingly, 56 subjects (78.9%) of the 71 ROPE subjects had received pharmacotherapy whereas all 41 (100%) of the No-ROPE subjects had received pharmacotherapy for bone loss. The 79% of the ROPE population without new fracture were distributed as: 29.6% combination therapy, 26.8% bisphosphonates only, 9.9% calcium only, and 12.7% no pharmacotherapy. The 49% of the No-ROPE population without new fracture were distributed as: 26.8% combination therapy, 17.1% bisphosphonates only, and 4.9% calcium only. In the population taking some kind of pharmacotherapy, 21.1% had new fractures during the time to follow up in the ROPE group versus 51.2% in the No-ROPE group. The No-ROPE group was four times more susceptible to fracture during the time to follow up ($P = 0.001$), Pearson Chi Sq test. The group with the lowest incidence of fractures was the ROPE group with combination pharmacotherapy. To prevent vertebral osteoporosis fractures, we enthusiastically suggest that ROPE be mandatory for management of every woman with osteoporosis, regardless of choice of pharmacotherapy.

Disclosures: D.A. Kurmen Figueroa, None.

W394

Relationship Between Serum 25-hydroxyvitamin D₃ Concentration and Walking Ability, Leg Strength, or Balance in Community-Dwelling Japanese Frail Elderlies. J. Okuno*, S. Tomura*, H. Yanagi*, N. Yabushita*, T. Okura*, K. Tanaka*. Graduate school of Comprehensive Human Sciences, University of Tsukuba, Tsukuba City, Japan.

The aim of this study was to evaluate the relationship between serum 25-hydroxyvitamin D₃ (25OHD) concentration and walking ability, muscle strength, or balance in community-dwelling Japanese frail elderly. The study was a longitudinal study conducted in a town near Tsukuba city (latitude 36° north) from June to September, in 2005 and 2006. Forty-five participants were community dwelling elderly aged 65 years and over who required minimum support or nursing care to maintain their ADL. Their mean age was 76.5±5.9 years (mean±SD, range: 65-90). Of the participants, 32 attended a 3-month exercise program for nursing care prevention once per week (exercise group). The remaining 13 received only advice for nursing care prevention (control group). The Ethics Committee of University of Tsukuba approved the study. An interview was conducted based on a questionnaire including score of functional capacity of ADL (Tokyo Metropolitan Institute of Gerontology (TMIG) score), experiences of fall, stumbling and body sway during the past one year, walking ability, and the frequency of going outside of the home. The serum levels of 25OHD, intact parathyroid hormone (iPTH) and calcium were measured. The following physical tests were performed at baseline and 3 months: Timed Up & Go (TUG) and a 5-meter walk for walking ability, functional reach and foot balance with open eyes for balance, trunk flexion for flexibility, and ankle strength and grip strength for muscle strength. Among 45 patients who underwent the tests, 66.7% and 40% had difficulties in standing up and in walking, respectively. 54.3% experienced falls, 73.8% experienced stumbling and body sway more than once during the past one year. The mean level of 25OHD was 62.1±13.7 nmol/L (mean±SD, range: 27.5-87.5). At baseline, the rate of 25OHD levels less than 50 nmol/L that is the cut-off point of 25OHD resulting from the significant difference of intact PTH level was 18.0%. At baseline and 3 months there were no significant differences in physical tests between the control group and the exercise group. The subjects with 25OHD levels more than 50 nmol/L at baseline improved their walking ability and ankle strength for a period of three months in both groups. On the other hand, the subjects with 25OHD levels less than 50 nmol/L did not improve their physical performance even in the exercise group. It is suggested that serum 25OHD level is related to walking ability and muscle strength in Japanese frail elderly, and that serum 25OHD level more than 50 nmol/L may be needed for maintaining their mobility or balance.

Disclosures: J. Okuno, None.

W395

Treatment of Osteoporotic Vertebral Body Fractures by Means of Percutaneous Balloon Kyphoplasty. Long Term Results of a Prospective, Clinical Trial. T. R. Blatter*, Trauma & Reconstructive Surgery, Leipzig University, Leipzig, Germany.

Introduction: Balloon kyphoplasty is a minimally-invasive, percutaneous surgical technique for reduction and stabilization of osteoporotic vertebral body fractures. However, there is no prospective, clinical trial on long term results concerning the safety and efficacy of the method so far.

Patients and Methods: This prospective, clinical trial investigated both safety and efficacy of percutaneous Balloon kyphoplasty. All vertebrae were stabilized with Polymethylmethacrylate (PMMA). Pre- and postoperatively, the following data were acquired: subjective rating of pain (Visual Analog Scale, VAS), bisegmental endplate-angle (EA2), anterior and posterior height of vertebra. Inclusion criteria were osteoporotic fractures of vertebral bodies in the thoracolumbar spine, patient age ≥ 65 years, fracture age ≤ 4 months, and t-score ≤ -2.5 (DEXA). Exclusion criteria were tumor lesions and additional posterior instrumentation.

Results: 352 vertebrae of 314 patients suffering from acute pain could be included with a minimum-follow up of two years. The average patient age was 74 years (57-92). Average t-score was -2.7. (-3.1 to -2.5). 262 patients suffered from pain for three weeks on average, whereas 52 patients were not able to recall the onset of pain. Fractures were only localized within the thoracolumbar spine with only A type of injuries occurring. 309 of 314 patients experienced marked pain-relief as expressed on the VAS (2.1 ± 1.9 to 8.2 ± 1.5 ; 0 "worst" to 10 "best"). Average correction of EA2 was 6.2°. The anterior vertebral height could be restored by 7.4 mm on average, posterior height by 3.0 mm. There were no neurological complications. In 32 (9.1%) vertebrae, we saw intraoperative leakage of cement (6 (1.7%) out of these with epidural leakage), however, no clinical consequences had to be noted. There were 6 (1.7%) cases of intraoperative balloon-perforation, and 11 (3.1%) cases of subsequent vertebral body fractures in the adjacent level.

Conclusion: Balloon-kyphoplasty is an efficient, and minimally-invasive therapeutic option for the treatment of painful vertebral body fractures having its focus on cases with underlying osteoporosis. Depending on the age and type of fracture, this treatment can obtain a significant rate of fracture reduction that is being maintained over the course of two years minimum. Compared to current literature on vertebroplasty, this technique presents fewer leakage complications at equal long term success in reducing pain.

Disclosures: T.R. Blatter, Kyphon Europe 5.

W396

Life Quality in Patients with Surgically Treated Vertebral Stenosis and the Relation with Bone Quality. I. D. A. Nemes*, D. V. Poenaru*, H. Vermesan*, R. Prejbeanu*, D. Vermesan*, I. Branea*, M. Dragoi*, O. Bereteu*, R. Onofrei*, E. Amarica*, D. Popa*, I. Ilia*, C. Nemes*. ¹Timisoara City University and Emergency Hospital - Rehabilitation and Rheumatology Department, Timisoara "Victor Babes" University of Medicine and Pharmacology, Timisoara, Romania, ²Timis County University and Emergency Hospital - Orthopaedic and Traumatology Department, Timisoara "Victor Babes" University of Medicine and Pharmacology, Timisoara, Romania, ³Medical Lab, Timisoara City University and Emergency Hospital, Timisoara, Romania.

Purpose: To establish the ratio of real vertebral stenosis versus those supposed to be and to assess life quality of patients with surgically treated vertebral stenosis and to the relation with bone quality.

Methods: In 3 years period from 380 patients considered to have vertebral stenosis, only 130 had the real disease. They were divided in 3 therapy groups: 25 patients with mild to moderate symptoms and a conservative treatment; 46 patients with more severe symptoms and surgically treated with decompressive laminectomy ± chypophoveroplasty; 59 patients with severe symptoms and surgically treated with decompressive laminectomy + instrumented fusion.

All patients benefit from diet, pain management, antiosteoporotic drugs in group II and III and physical therapy (local analgetic electrotherapy, biofeed-back training of the local muscle and Williams programme in group I/ biofeed-back training of the local muscle and Florida Spine Institute post-operative protocol in group II and III). All patients were evaluated, regarding their life quality, according to WOMAC scale at baseline, day 21 and at 3 month and DXA bone densitometry and lab parameters of bone metabolism were performed at 40 patients of group III.

Results: In group I and II the three months evaluation showed a clinical and functional improvement. The clinical and functional status of the third group patients was significantly improved at 3 month assessment. A "slow" evolution was seen at 40 patients after six months, despite the fact that DXA scores and lab parameters had an improvement.

Conclusion: The ratio of vertebral stenosis/ vertebral hernia is almost 1/3 in our area. If the conservative therapy applied in moderate forms has no significant result in 3 month we should consider the surgical therapy as the appropriate therapy. As a result of the protocol's applying a better life quality, related with DXA scores and lab parameters, was seen. The difference in outcomes between the post surgical evaluations in group III may be due to the type or intensity of the rehabilitation programme followed after the hospitalization period or cultural issues, patients having greater expectation from the surgical treatment than this is meant to realise.

Disclosures: I.D.A. Nemes, None.

W397

Adjacent Fractures in the Thoracic and Lumbar Spine after the Treatment with Balloon-Kyphoplasty - 2 Years Prospective Follow-up. R. Pflugmacher*. Centrum für Muskuloskeletale Chirurgie, Charité - Universitätsmedizin Berlin, Berlin, Germany.

Purpose: To evaluate the long-term outcomes of 57 patients with 87 osteoporotic vertebral fractures, located in the thoracic and lumbar spine, treated with Balloon Kyphoplasty.

Material and Methods: 63 patients (20 males and 43 females) with 96 osteoporotic vertebral fractures were treated with Balloon Kyphoplasty. We were able to have a 2 year follow up in 57 patients with 87 vertebrae treated. Symptomatic levels were identified by correlating the clinical presentation with conventional radiographs, CT and / or MRI. During the 2 year follow-up reduction in pain was determined. The effects on pain symptoms were measured on a self-reported Visual analog Scale (VAS) and the Oswestry score was documented to assess disability. Radiographic scans were performed pre- and postoperatively and after 3, 6, 12 and 24 months. The vertebral height and kyphosis angle were measured to assess the restoration of the sagittal alignment.

Results: The median pain scores (VAS) improved significantly from pre- to post-treatment as did the Oswestry Disability Score ($p < 0.001$). This improvement was maintained at 2 year follow up. In 9 patients (15.8%) (6 female, 3 male) an adjacent fracture occurred in 12 vertebrae (13.8 %) within 2 weeks to 22 months follow-up. In four patients the adjacent fractures were asymptomatic. Five patients with symptomatic adjacent fractures were treated again with Balloon Kyphoplasty. Clinically asymptomatic cement leakage occurred in 12 of 96 vertebral bodies (12.5 %). During 2 year follow-up this surgical technique demonstrated restoration and stabilization of the height of the vertebral body.

Conclusion: Balloon Kyphoplasty is an effective minimal invasive procedure for the stabilization of osteoporotic vertebral fractures leading to a statistically significant reduction of pain status.

Disclosures: R. Pflugmacher, None.

W398

Improving Trunk Strength and Endurance in Older Women with Vertebral Fractures. K. M. Shipp, D. T. Gold, C. F. Pieper*, K. W. Lyles. Duke University, Durham, NC, USA.

The trunk musculature is important for people with osteoporosis. First, strong, fatigue-resistant trunk muscles are necessary for erect postural alignment. Second, strong trunk extensors may prevent vertebral fractures. An observational study associated trunk extension strengthening over 2 years with decreased incidence of vertebral fractures in the next 8 years [Sinaki M et al. Bone 2002;836-841]. The relationships between trunk alignment, strength, and endurance; functional status; and fracture risk are complex and not yet fully understood.

Results will be presented from a randomized clinical trial of a group exercise intervention (3X/week for 6 months) in older women ($n=122$, mean age 81 years) with vertebral fractures (mean # 2.3) [Gold DT et al. J Am Geriatr Soc 2004;52:1471-1478]. Randomization was by site: 3 trunk exercise intervention sites ($n=53$) and 3 control sites ($n=69$). The trial was a modified cross-over design: the control sites received the exercise intervention after 6 months of health education sessions. The exercises included 1) stretches to increase trunk extension flexibility and 2) progressive resistive strengthening exercises for trunk extensors, abdominals, and posterior scapular groups.

Using mixed-model ANCOVA (intention-to-treat), we found a significant difference between groups for trunk extension strength at 6 months ($p=0.0001$; +6.6 ft-lbs. [up 24%] exercisers, -4.6 ft-lbs. controls). When the control subjects received the exercise intervention, there was a mean increase of 15.0 ft-lbs [up 45%].

An ancillary study examined the effect of the intervention on Timed Loaded Standing (TLS), a measure of combined trunk and arm endurance [Shipp KM et al. Osteoporos Int 2000;11:914-922]. Using mixed-model ANCOVA (intention-to-treat), we found a trend for difference between groups for TLS time at 6 months ($p=0.0542$; +8.8 sec exercisers, -8.9 sec controls). Among compliers (those attending 2/3s of sessions), group was significant ($p=0.035$; +14.9 sec exercisers, -10.3 sec controls). Change in TLS time, but not change in trunk extensor strength, over 6 months was significantly correlated ($p < 0.05$) with change in psychological symptoms and functional status.

These results demonstrated that trunk extension strength and combined trunk and arm endurance could be increased, in older women with vertebral fractures, by 6 months of group, physical therapist-led, trunk-specific exercise classes. Improved trunk endurance was associated with fewer psychological symptoms and better functional status.

Disclosures: K.M. Shipp, None.

This study received funding from: NIH (NIA and NICHD).

W399

Peak Vertical Impact Forces During Backward Falls onto the Buttocks and the Influence of Compliant Flooring. M. M. Sran, S. N. Robinovitch*. Simon Fraser University, Burnaby, BC, Canada.

Fall-related vertebral fractures are common and backward falls result in impact to the buttocks and pelvis. Compliant flooring is a promising technique for reducing impact force and risk for vertebral fracture during a fall. However, we have little knowledge of the peak forces applied to the body during a backward fall, or how floor stiffness affects this force. Our goal was to measure the peak vertical force applied to the buttocks in a backward fall from standing, and to determine whether this force is lowered by reductions in floor

stiffness. Participants included 11 males mean age 25 ± 5 (SD) yrs and body mass mean 81 ± 16 (SD) kg. A tether and electromagnet suddenly released the participant from a backward lean of 15° , causing him to fall backward onto the ground, which was covered with a layer of ethylene-vinyl acetate (EVA) foam rubber. We conducted 5 trials for each of 3 foam thicknesses [4.5 cm (Firm), 7.5 cm (Medium), and 10.5 cm (Soft)]. Participants were instructed to avoid contacting the ground with their hands until their buttocks had contacted the ground, not to squat or step. We measured peak vertical impact forces applied to the buttocks at 960 Hz with a force plate (model 4060H, Bertec Corp.). An 8-camera, 240 Hz motion measurement system (EVA-RT 4.6, Motion Analysis Corp.) was used to track peak velocity (m/s) of a skin surface marker on the sacrum. We also modeled peak vertical force for falls onto a rigid (bare) floor. We used repeated measures ANOVA and post-hoc t-tests to compare peak forces between the 3 conditions ($p = 0.016$). There was a significant difference in peak normalized vertical force (N/kg) between falls onto the Soft foam condition compared with the Medium ($p = 0.002$) and Firm ($p < 0.001$) conditions. Peak normalized vertical force (N/kg) was (mean \pm SD) 63.6 ± 6.2 , 59.9 ± 6.2 , and 56.9 ± 5.9 for Firm, Medium, and Soft respectively. Estimated peak normalized vertical force (N/kg) for the rigid (bare floor) condition was 75.3 ± 7.6 . In comparison to the rigid floor, falling onto the Firm, Medium and Soft floors provided, on average, 15, 20 and 24% force attenuation. This novel data improves our understanding of this mechanism of vertebral injury and is essential if we are to design techniques for the prevention of vertebral fractures, such as protective equipment and safe movement environments. Peak vertical forces were $5099 \text{ N} \pm 868$ (SD) for the thinnest foam condition. Studies report the compressive force required to cause fracture of elderly lumbar vertebrae to be between (mean \pm SD) 3009 ± 1505^1 and $6910 \pm 2480 \text{ N}^2$, similar to the peak loads measured in this study. A thin (4.5cm) layer of foam overlying the floor can provide 15% force attenuation during a fall onto the buttocks. ¹Burklein D et al. J Biomech 2001 ²Cheng XG et al. J Bone Miner Res 1998.

Disclosures: M.M. Sran, None.

W400

A Community-Based Program to Minimize Osteoporosis and Fractures Risks. S. J. Wimalawansa*, M. Bartello*², K. Morgan*³, M. Wagner*⁴, K. Hodapp*⁵, S. Lachenmayr*⁶. ¹Medicine, UMDNJ-RWJMS, New Brunswick, NJ, USA, ²Memorial Hospital, Morristown, NJ, USA, ³Rutgers University, New Brunswick, NJ, USA, ⁴Rutgers University, Milltown, NJ, USA, ⁵Morristown Memorial Hospital, Morristown, NJ, USA, ⁶NJ Dept. of Health, Trenton, NJ, USA.

In New Jersey (NJ), ~1 million residents have low bone mass and ~8,000 individuals over 65 fractures a hip annually. The NJ Interagency Council on Osteoporosis (ICO) oversees osteoporosis (OP) education & prevention initiatives in the state. Since 1997, Project Healthy Bones, a 24-week, comprehensive, peer-led OP exercise & education program provides a public health approach to healthy behaviors improving BMD, dietary calcium intake, balance & strength, and minimize falls and associated fracture risk.

In 2004, reduced funding resulted in creating new training at local level for community class leaders, establish program sites for local program demand, provision of resources / technical assistance and provide program oversight. This model utilizes regional, trainers-training program with community-based partnerships. ICO provides 2-day training program in volunteer Peer Leader training, evaluation protocols and oversight accountability.

Our data demonstrated improved balance, increased strength & higher bone density through this program. The impact of Project Healthy Bones was evaluated through exercise tracking forms, pre-post- knowledge tests and food diaries. With the new program, 90% of participants increased weight lifting and exercise tolerance, and 68% increased their calcium intake (~500 mg per day).

From March 05 to December 06, a network of 82 agency staff and 318 volunteer peer leaders provided >two-hundred 24-week programs to nearly 2,000 participants in every county in NJ (over 15,000 volunteer hour contributions). This is in addition to continuing of 80% regular classes beyond the initial 24-weeks. A statewide ICO listserv also provides a forum answers questions/challenges, disseminates current research and OP news, and coordinates local program offerings. Many physicians and HMOs are referring patients directly to the program based on improved DXA results (pre- and post-class) and decrease falls.

The Project Healthy Bones maintain existing community programs; create new programs based on local demand; and oversight to assure program integrity. The program is on CD-ROM, which is designed to use locally by peer leaders. Program demonstrated improve balance and nutrition; prevent falls, increased strength, morale and social well-being among participants. Despite lack of state funding, the modeled program has been strengthened and expanded with extensive community partnerships, fostered volunteerism, and has shown a positive impact in the health and quality of individuals' lives.

Disclosures: S.J. Wimalawansa, None.

W401

Overexpression of Osteoblast IGF-I Blunts the Deleterious Effects of Low Protein Intake on Bone Strength. P. Ammann¹, B. Kream², C. Rosen³, R. Rizzoli¹. ¹Department of Rehabilitation and Geriatrics, Division of Bone Diseases, Geneva, Switzerland, ²University of Connecticut Health Center, Farmington, CT, USA, ³St Josephs Hospital Maine Center for Osteoporosis Research, Bangor, ME, USA.

Isocaloric low protein intake decreases bone mass and bone strength. These alterations are associated with decreased circulating IGF-I levels. Osteoblast IGF-I expression is decreased by low amino-acids concentration. Whether circulating and/or bone locally produced IGF-I are responsible for low protein diet-induced bone damages is not established yet. We investigated 6-month adult transgenic male mice overexpressing IGF-I in osteoblasts under the control of collagen type-1 promoter (TG-IGF) and wild type mice (WT), fed a normal or an isocaloric low protein diet, for 8 weeks. After sacrifice, tibia were tested for biomechanics, size, microstructure using microcomputerized tomography, cortical histomorphometry and bony tissue nano-indentation. Blood was also collected. In WT on low protein diet, compression strength was significantly decreased and resistance to bending displays similar trend, whereas they were not changed in TG-IGF. Data in the table show a cortex thinning, and also alterations of intrinsic bone tissue quality in WT but not in TG-IGF. Outer bone diameter was higher in TG-IGF-I, irrespective of the protein intake. Endosteal BFR was reduced in WT on a low protein diet, but not in TG-IGF. Trabecular bone mass was significantly decreased in WT only. Plasma IGF-I was similar in WT and TG-IGF, and equally decreased by the low protein diet. These results in adult male mice indicate that bone local overexpression of IGF-I blunts the deleterious effects of a low protein diet, even in the presence of lower IGF-I circulating levels.

	WT Control	WT low prot	TG-IGF control	TG-IGF low prot
Maximal load	48.5±6.5	35.6±3.9*	40.3±3.4	41.2±3.2
Cortical thickness	0.288±0.009	0.250±0.010*	0.285±0.006	0.271±0.010
Diameter	1.24±0.02	1.27±0.02	1.31±0.02*	1.34±0.02*
Hardness nano	719±31	601±29*	709±27	704±30
IGF-I	567±29	344±34*	614±31	369±29

Disclosures: P. Ammann, None.

This study received funding from: Swiss National Research Foundation.

W402

Sub-Optimal 25(OH)D₃ Levels Causes Increased Osteoclastogenesis and Bone Loss. P. H. Anderson^{*1}, R. K. Sawyer^{*1}, A. J. More^{*1}, A. Muliabrahimovic^{*1}, B. K. May^{*1}, P. D. O'Loughlin^{*1}, H. A. Morris². ¹Endocrine Bone Research, Institute of Medical and Veterinary Science, Adelaide, Australia, ²Hanson Institute, Institute of Medical and Veterinary Science, Adelaide, Australia.

The association between increased risk of hip fracture and a low vitamin D status has long been recognised. However, the level of circulating vitamin D required to maintain bone strength is controversial. To determine the circulating 25-hydroxyvitamin D (25D) level required for the maintenance of bone, we generated 6 groups of Sprague-Dawley rats with stable, mean 25D level ranging from 11 nmol/L to 118 nmol/L. Vitamin D depleted animals were fed various levels of vitamin D (0ng-500ng/d) with 0.4% Ca for 4 months before being killed at 7 months of age for serum biochemistry and bone histomorphometry analyses. Proximal femora structure was analysed by µCT and distal femora histomorphometry was analysed using sagittal 5µm undecalcified sections. Fasting serum calcium, PTH and phosphate levels were normal in animals with low 25D levels. Evidence of osteomalacia was seen only in animals with 11(±0.7) nmol/L 25D, with elevated serum ALP and cross-laps, increased osteoid surface and delayed osteoid maturation time (OMT) compared to animals fed higher levels of vitamin D. OMT was constant in animals fed between 50 and 500ng/d vitamin D and trabecular bone volume (BV/TV) was positively related to circulating 25D ($R^2=0.51$, $P<0.001$), but not to 1,25(OH)₂D₃ levels, nor PTH levels. Animals fed between 50 and 100ng/d vitamin D (mean 25D <80nmol/L) had lower BV/TV (Fig 1) and both osteoid surface and osteoclast surface (Fig 2) were elevated compared to animals fed higher vitamin D. In summary, while osteomalacia occurs at extremely low 25D levels, less severe depletion of vitamin D was associated with increased osteoclast numbers, and significant bone loss. The molecular mechanism for the changes in cellular activity due to vitamin D insufficiency are currently under investigation. In conclusion, for animals fed adequate dietary Ca, a circulating 25D above 80nmol/L is required to prevent bone loss.



Figure 1: Trabecular bone volume with changes in vitamin D intake

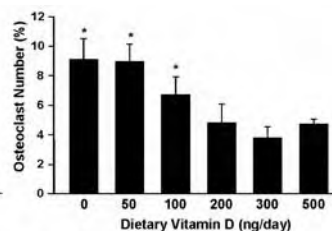


Figure 2: Osteoclast Numbers with changes in vitamin D intake

Disclosures: P.H. Anderson, None.

This study received funding from: NH&MRC of Australia.

W403

A More Alkaline Diet May Enhance the Favorable Impact of Dietary Protein on Lean Tissue Mass in Older Adults. B. Dawson-Hughes, S. S. Harris*, L. Ceglia*. Bone Metabolism Laboratory, The Jean Mayer Human Nutrition Research Center on Aging at Tufts University, Boston, MA, USA.

Maintaining muscle mass in aging is important to prevent falls and fractures. Dietary protein is required to preserve muscle mass, however the acid load from diets rich in acidogenic protein foods and cereal grains relative to alkaline fruits and vegetables may contribute to loss of lean tissue mass in older adults.

This analysis was conducted to determine whether for a given protein intake, a more alkaline diet has a more favorable effect on lean body mass (LBM). Subjects were 384 men and women age 65+ who participated in a 3-yr calcium and vitamin D versus placebo trial. All subjects gave written informed consent.

Urinary nitrogen (N), an indicator of protein intake, and potassium (K) were measured at baseline in 24-hr collections. N was measured by the Dumas combustion method and K by direct-current emission spectroscopy. The N:K ratio, reflecting the ratio of acidic protein foods to alkaline fruit/vegetable intake, was calculated. LBM, defined as total body non-fat, non-bone tissue mass, was measured by DXA at baseline and 3 years. Physical activity, measured by Physical Activity Score for the Elderly (PASE) questionnaire, height, and weight were assessed at baseline and 3 years.

At baseline, the mean N:K was 5.98 ± 1.70 (SD) mmol/mmol. The N:K was inversely associated with baseline LBM (regression coefficient = -0.245, $P = 0.011$, adjusted for sex, age, weight, physical activity score, and nitrogen excretion) and with 3-yr change in LBM (regression coefficient -0.105, $P = 0.046$, adjusted in addition for treatment group and baseline LBM).

These results suggest that the effect of protein on muscle may be enhanced when the overall diet is less acidic, that is, higher in fruit and vegetable content.

Disclosures: B. Dawson-Hughes, None.

This study received funding from: NIH.

W404

Propensity to Accumulate Bone Microdamages Is Increased in Adult Female Rats Fed an Isocaloric Low Protein Diet. V. Dubois-Ferrière*, R. Rizzoli, P. Ammann, Division of Bone Diseases, Geneva, Switzerland.

Low protein intake decreases bone strength through a change in bone mass, bone microstructure and intrinsic bony tissue quality. Whether the low protein diet-induced alterations of bony tissue could favor the accumulation of bone microdamages is not known. We investigated the effects of repeated loading on humerus bone strength in 6-month-old female rats pair-fed a control (15% casein, n=10) or an isocaloric low-protein (2.5%, n=10) diet for 10 weeks. The humeri were cyclically loaded in three-point bending under load control for 2000 cycles. The peak load selected corresponded to 60% of the maximal load of the controlateral humerus. The humeri were then loaded to failure. We compared the load/displacement curve of the cyclically loaded humerus to the controlateral non-cyclically loaded humerus.

Whereas cyclic loading did not induce any deterioration in rats fed a normal protein diet, this cyclic loading regimen negatively influenced the post-yield behaviour of humerus in rats fed a low protein diet, as indicated by the significant decrease of post-yield load and plastic deflection. This suggests that bone microdamages could be more prominent in rats fed a low protein diet than in control bones submitted to the same loading regimen.

Results are mean±SEM; * p<0.05 as evaluated by a Student's t-test				
Casein Diet	15%	15% controlateral loaded	2.5%	2.5% controlateral loaded
Maximal Load (N)	92.3±2.9	90.8±2.8	87.1±2.5	77.8±4.8
Stiffness (N/mm)	236.6±16.5	272.8±17.9	237.5±12.4	218.6±22.5
Yield Point (N)	71.8±3.6	71.4±1.6	64.4±2.7	67.1±3.3
Post-yield load(N)	20.5±1.7	19.4±2.7	22.7±1.6	10.7±2.0*
Elastic deflection (mm)	0.35±0.04	0.32±0.02	0.29±0.01	0.35±0.03
Plastic deflection (mm)	0.14±0.01	0.12±0.01	0.15±0.01	0.08±0.01*

Disclosures: V. Dubois-Ferrière, None.

W405

Thin Healthy Women Have a Similar Low Bone Mass as Women with Anorexia Nervosa. D. Fernandez-García^{*1}, J. García-Aleman^{*1}, A. Sebastian Ochoa^{*2}, M. Muñoz-Torres², F. Tinahones^{*1}. ¹Department of Endocrinology, University Hospital Virgen de la Victoria, Malaga, Spain, ²Department of Endocrinology, University Hospital San Cecilio, Granada, Spain.

Association between anorexia nervosa (AN) and low bone mass has been demonstrated. Bone loss associated with AN involve hormonal and nutritional impairments, though their exact contribution is not clearly established. The aim: of our study was to compare bone mass in AN patients with women of similar weight with no criteria for anorexia nervosa, and a third group of healthy, normal-weight, age-matched women.

We studied 48 patients with AN (DSM-IV criteria), 22 healthy eumenorrheic women with low weight (LW Group; BMI <18.5 kg/m²) and 20 healthy women with BMI >18.5 kg/m² (Control Group), all of similar age. We measured by DEXA lean body mass, percentage of fat mass, total bone mineral content (tBMC) and bone mineral density in lumbar spine (BMD LS) and total (BMD T). We measured anthropometric parameters, leptin and GH.

The control group had greater BMD T and BMD LS than the other groups, with no differences between the AN and LW groups. No differences were found in BMD T, BMD LS and t BMC between the restrictive (n=25) and binge-purge type (n=23) in AN patients. In AN, minimum weight ($p=0.002$) and percent of fat mass ($p=0.02$) explained BMD LS variation ($r^2:0.48$) and minimum weight ($r^2:0.42$; $p=0.002$) for BMD T in stepwise regression analyses. In LW group, BMI explained BMD LS ($r^2:0.72$; $p=0.01$) and BMD T ($r^2:0.57$; $p=0.04$).

Conclusions: Patients with AN had similar BMD as healthy thin women. Anthropometric parameters could contribute more significantly than estrogen deficiency in achievement of peak bone mass in AN patients.

Disclosures: D. Fernandez-García, None.

W406

Vitamin D Insufficiency and Normal Parathyroid Function: Disease or No Disease? K. E. Hansen¹, J. Riggert^{*1}, A. N. Jones^{*1}, J. Engelke^{*1}, M. Shafer^{*2}.

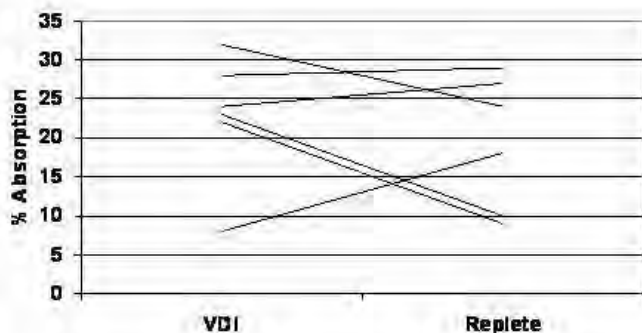
¹Medicine, University of Wisconsin, Madison, WI, USA, ²Wisconsin State Lab of Hygiene, Madison, WI, USA.

Vitamin D insufficiency (VDI) is allegedly widespread. In patients with normal parathyroid hormone (PTH), the diagnosis rests upon an increase in calcium absorption (CA) following increments in serum 25(OH)D to levels >30 ng/ml. However, estimates of increased CA with correction of VDI vary dramatically, depending on methods used to measure CA. Using the increment for serum calcium as an index of CA, correction of VDI reportedly increases CA by 65% (J Am Coll Nutr 2003;22(2):142). Of concern, estimates of CA using serum calcium levels correlate poorly with estimates using calcium isotopes ($r=0.42$, Calcif Tissue Int, 1983;35(6):819). We initiated a dual stable calcium isotope study to clarify the impact of vitamin D repletion on CA in postmenopausal women with VDI and normal PTH.

Eligible women were ≥ 5 years postmenopausal with a serum 25(OH)D of 16-24 ng/ml by HPLC assay, normal PTH and an estimated calcium intake $\leq 1,100$ mg daily. Exclusion criteria included hypercalcemia, hypercalciuria, chronic intestinal disorders, use of medications known to interfere with vitamin D or calcium metabolism, osteomalacia, prior adult fragility fracture or a T-scores below -3.0 (spine or femur).

Each woman underwent inpatient dual calcium isotope studies when vitamin D insufficient and subsequently when vitamin D replete (25(OH)D > 35 ng/ml after ergocalciferol 50,000 IU/daily for 15 days). During each CA study, women consumed 18 mg of ^{44}Ca orally with breakfast and received 3 mg of ^{42}Ca intravenously. Each woman's typical diet was replicated during each CA study using 7-day diet records and Food Processor software. Urine was collected for 24 hours and analyzed for its calcium isotope content by mass spectrometry. We calculated CA using the formula by Eastell (JBMR 1989;4(4):463-468). Thus far, 6 of 22 women have completed the study. All had normal PTH at baseline (46 (9) pg/ml). Basal serum 25(OH)D was 20 (4) ng/ml, increasing to 73 (22) ng/ml with ergocalciferol. CA was 23% (8%) initially and 20% (8%) following vitamin D repletion ($p>0.05$, Wilcoxon signed-rank test).

Our observations suggest that calcium absorption does not increase in women with VDI who achieve unequivocal vitamin D repletion with ergocalciferol. Although preliminary, our data raise significant questions about whether VDI is a true disorder in patients with normal parathyroid function.



Disclosures: K.E. Hansen, None.

This study received funding from: CReFF, WI Partnership Program, Jackson Foundation.

W407

Effect of Citrus Flavanones on Bone Metabolism in Old Male Rats. V. Habauzit^{*1}, A. Trzeciakiewicz^{*1}, J. Mardon^{*1}, J. Mardon^{*1}, P. Lebecque^{*1}, M. Davicco^{*1}, C. Morand^{*1}, E. Offord^{*2}, V. Coxam¹, M. Horcajada^{*1}.

¹Human Nutrition, INRA, Saint Genès Champanelle, France, ²Nutrition and Health, NESTLE, Lausanne, Switzerland.

Currently, there is an increasing interest in fruit and vegetables as their consumption appears to be related to lower risk of metabolic disorders occurring during ageing. Polyphenols could be involved in these benefits. In this study we investigated the potency of hesperidin and naringin, their two major citrus flavonoids (flavanones), in regulating bone metabolism in senescent male rats.

Forty-eight 20-m-old male Wistar rats were divided into 4 groups. Control group received

a casein-based diet. The others were fed, for 90 days, the same diet but added with either 0.5 % hesperidin (Hp), 0.5 % naringin (Nar) or a mix of both flavanones (0.25%Hp + 0.25%Nar). Femoral mineral density and strength, bone biomarkers (deoxypyridinoline and osteocalcin) were measured. Plasma and serum analyses (leptin, cholesterol, triglycerides, insulin, glucose, IGF-1, IL-6, FRAP, NO) were performed.

During the experiment, body weights were steady in each group and flavanones intake did not affect this parameter. Besides, plasma leptin was significantly decreased in Hp and Hp+Nar groups, suggesting an effect on body composition. At necropsy, daily Hp intake improved bone mineral density compared with control group, whatever bone sites considered ($p<0.05$). While the same pattern for the animals fed with the mix of flavanones was observed, only metaphyseal density was affected by Nar consumption ($p<0.05$). However bone strength was not modified by flavanones. Bone resorption was slowed down by Hp and Nar whereas accretion remained unchanged. Flavanones induced a decrease in plasma triglycerides and total cholesterol and no changes in blood glucose and plasma insulin were detected.

The consumption of flavanones appeared to prevent serum IL-6 from increasing during aging-related inflammation. Oxidative status seemed also to be improved in animals consuming flavanones as shown by FRAP assay and decreased NO production. Finally, circulating flavanones were only detected in rat plasma receiving Hp and/or Nar.

These results suggest that both hesperidin and naringin were able to affect bone metabolism in senescent male rats, hesperidin being apparently the more efficient. This effect could be partly due to the ability of flavanones in slowing down bone resorption rate. Bone sparing effect of hesperidin and naringin observed in senescent intact male rats, a model of ageing, should also be linked with anti-inflammatory, antioxidant and also hypolipidemic capacities of these compounds.

Disclosures: M. Horcajada, None.

W408

Influence of Moderate Energy Restriction and Seafood Consumption on Bone Turnover in Overweight Young Adults. A. J. Lucey^{*1}, G. Paschos^{*1}, K. D. Cashman², J. A. Martínez^{*3}, N. Bandarra^{*4}, I. Thorsdottir^{*5}, M. Kiely^{*1}.

¹Department of Food & Nutritional Sciences, University College Cork, Cork, Ireland, ²Department of Food & Nutritional Sciences & Department of Food & Medicine, University College Cork, Cork, Ireland, ³Department of Physiology & Nutrition, University of Navarra, Pamplona, Spain, ⁴National Institute on Agriculture and Fisheries Research, Lisbon, Portugal, ⁵Unit for Nutrition Research, Landspítali University Hospital, Reykjavik, Iceland.

While weight loss may increase bone turnover, increased intakes of n-3 fatty acids (FA) may maintain skeletal health by reducing bone resorption. This study examined relationships between weight loss, changes in FA in red blood cell (RBC) membrane phospholipids (%) and bone turnover biomarkers, induced by an 8-week dietary intervention, which included fish or fish oil as part of an energy restricted diet (-30%) in 20-40 year old adults (BMI 27.5-32.5 kg/m²). Participants (n 276) were randomised to 1 of 4 groups: placebo (sunflower oil capsules; 3g/day); cod (3 x 150g/week); salmon (3 x 150g/week); fish oil capsules (3g/day). At baseline and endpoint serum levels of the biomarkers of bone formation (osteocalcin (OC) and bone specific alkaline phosphatase (BAP)) and resorption (serum crosslaps (CTx) and N-telopeptide of Type I collagen (NTx)) were measured by enzyme linked immunosorbent assay (ELISA) and the FA composition of RBC membrane phospholipids (%) was measured by gas chromatography. Using repeated measures analysis of variance, before adjusting for confounding factors, serum levels of CTx ($P < 0.001$) and NTx ($P < 0.05$) increased, BAP showed little response, while levels of OC ($P < 0.05$) decreased from baseline to end point, however, these changes were no longer present after adjusting for country, gender, sampling month, age, smoking status and % weight loss. Mean weight loss was 5.8% (range 0 to 15) over the 8-week intervention and was similar across the 4 study groups. Weight loss and changes in body composition were the main factors influencing the increases in CTx ($P < 0.001$) and NTx ($P < 0.05$), while OC was unrelated to weight loss. Increased n-3 FA consumption in the salmon and fish oil groups resulted in increases in n-3 FA in RBC membranes and decreases in n-6 FA ($P < 0.05$). After adjusting for confounding, OC was positively correlated with the % RBC n-3 FA at baseline and endpoint. However, the overall inclusion of fish or fish oil in the diet had no significant effect on bone turnover. We conclude that a nutritionally adequate energy-restricted diet over 8 weeks, which resulted in modest weight loss and changes in body composition influenced biomarkers of bone resorption in young overweight adults.

Disclosures: A.J. Lucey, None.

This study received funding from: The YOUNG study (co-ordinator Prof. Inga Thorsdottir) is part of the SEAFOODplus Integrated Project (co-ordinator Prof. Torger Borresen), which is funded by the EC through the 6th Framework Programme Contract No FOOD-CT-2004-506359.

W409

Effects of Calcium Sources and Soluble Silicate on Bone Metabolism and the Related Gene Expression in Mice. F. Maehira¹, I. Miyagi¹, Y. Eguchi².

¹Lab. Metabolic Chemistry, Faculty of Medicine, University of the Ryukyus, Okinawa, Japan, ²Research Laboratory Center, Faculty of Medicine, University of the Ryukyus, Okinawa, Japan.

Silicon has been known as an essential element for the formation of collagen and glycosaminoglycans in bone and cartilage. The effects of five calcium (Ca) sources were compared on bone biochemical and mechanical properties and the related gene expression using the control strain of senescence-accelerated mice (SAMR1), from a viewpoint of their soluble silicon (Si) content. The experimental protocols of this study were approved by our Institutional Animal Studies Committee. Weanling male SAMR1 were fed the diets containing 1% Ca supplemented with CaCO₃ as the control (CT), coral sand (CS), fossil stony coral (FSC), fish (FC), egg-shell (EC) powders, and 50 ppm Si in the CT diet for 6 months. The mRNA expression of Runx2, BMP-2, IL-11, COL1A1, PPAR- γ , OPG, RANKL, TGF- β was quantified by a real-time PCR. Soluble Si content was 9.83, 7.17, 2.48, 0.29, and 0.20 ppm for CS, FC, FSC, EC, and Ca-deficient basal diet, respectively. In bone biochemical properties, Si, CS, and FSC in order increased ($P < 0.05$) dry and ash weights, Ca and hydroxyproline (OHP) contents, and alkaline phosphatase and decreased ($P < 0.05$) tartrate resistant acid phosphatase, urinary excretion of OHP comparing with the CT group. In bone mechanical properties, Si increased ($P < 0.05$) and FC decreased ($P < 0.05$) strength and stiffness. In the mRNA expression related to osteoblastogenesis, Si increased ($P < 0.05$) Runx2, Si, CS, and FSC in order decreased ($P < 0.05$) and FC, EC increased ($P < 0.05$) PPAR- γ . In the mRNA expression related to osteoclastogenesis, Si, CS increased ($P < 0.05$) and FC, EC decreased ($P < 0.05$) OPG/RANKL ratio whereas Si, CS decreased ($P < 0.05$) TGF- β . FC in spite of its high Si content showed worst effects on bone, probably due to its high phosphorus content. The results indicated that soluble silicate and coral sand with highest soluble Si content among Ca sources improved bone biochemical and mechanical properties through stimulation of gene expression related to osteoblastogenesis and suppression of that related to osteoclastogenesis.

Disclosures: F. Maehira, None.

W410

The Effect of a High Protein Diet on Bone and Body Composition in Young Female Rats. K. M. Pye¹, A. Wakefield², H. Aukema², J. House², M. Ogborn², H. Weiler¹. ¹School of Dietetics and Human Nutrition, McGill University, Ste-Anne de Bellevue, PQ, Canada, ²Department of Human Nutritional Sciences, University of Manitoba, Winnipeg, MB, Canada.

Long-term, high protein diets at 35% of energy may have implications in bone biology. Increased consumption of protein lowers blood pH levels which may interfere with blood calcium homeostasis leading to an increased stimulation of osteoclasts and elevated calcium losses. However, inconsistencies within the literature make it impossible to state whether this level of bone resorption, over long periods, has a negative impact on bone health. No one study within the eighty years of high protein diet research has examined all the biochemical, physical, and largely the biomechanical markers of bone health. This study will be the first to give a complete analysis and examine whether a high protein diet at the 35% energy level can be deemed safe with respect to long-term bone health. The objective of this research is to examine the effect a high protein diet at 35% of energy has on bone mass and strength in the rat model.

Eighty female Sprague-Dawley rats were randomized to receive 4, 8, 12, or 17 months of a control diet (15% of energy as protein) or the high protein diet (35% energy). Weekly food intake and weight was documented. Whole body composition and regional bone mass were measured in vivo using dual-energy x-ray absorptiometry (DXA; Hologic QDR version 11.2, Hologic, Inc.). Following termination, femurs and tibias were excised. Ex vivo, femur and tibia bone mass were measured using DXA and right femurs were tested for mechanical strength using designed 3-point bending tests (INSTRON 5544, Instron Inc.). Main effects of diet and time were detected using factorial ANOVA ($p < 0.05$). The high protein diet increased BMC (g/kg) in femur, tibia, and vertebrae as illustrated in the table below. High protein consumption also decreased whole body fat (normal diet: 165.17 ± 87.92 g, high diet: 110.60 ± 70.92 g, $p < 0.0001$), increased lean mass (normal diet: 634.68 ± 99.95 g/kg, high diet: 717.11 ± 92.75 g/kg, $p < 0.0001$), and decreased abdominal fat (normal diet: 44.56 ± 22.32 g, high diet: 31.55 ± 19.18 g, $p = 0.0006$). Diet had no effect on the biomechanical strength of femurs. Thus preliminary results suggest that high protein diets at the current upper limit of 35% of energy increase mineral content, decrease body fat content, but does not hinder the mechanical and weight bearing abilities of bone.

	Normal Protein BMC (g/kg)	High Protein BMC (g/kg)	p values
Femur	1.4555 ± 0.324	1.6125 ± 0.347	0.0046
Tibia	0.9172 ± 0.233	1.0535 ± 0.333	0.0178
Vertebrae	1.5751 ± 0.344	1.7365 ± 0.366	0.0076

Disclosures: K.M. Pye, None.

This study received funding from: Canadian Institutes for Health Research.

W411

Low Calcium Diet Accelerates Alveolar Bone Resorption in Rat Experimental Periodontitis. K. Tokunaga¹, C. Wada¹, H. Ohba¹, H. Seto¹, E. Takeda², T. Nagata¹. ¹Periodontology and Endodontology, Health Bioscience,

Tokushima, Japan, ²Clinical Nutrition, Health Bioscience, Tokushima, Japan.

Periodontitis is characterized by the inflammatory destruction of periodontal tissues including alveolar bone, periodontal ligament, and gingiva. Alveolar bone resorption is a major cause of tooth loss. It is possible that a decrease of general bone density may affect the pathogenesis of periodontitis. Estrogen deficiency by menopause and lack of Ca ingestion is known to be a risk factor for osteoporosis. However, it is not clear whether the lack of Ca ingestion influences alveolar bone resorption in periodontitis. In this study, we examined the effect of low Ca diet on alveolar bone resorption in rat experimental periodontitis. Male Wistar rats, 8 weeks old, were firstly divided into 2 groups: rats with low Ca diet (Ca: 0.18%), and the control (Ca: 1.08%). The diets were given for 5-20 days. Nylon ligature was placed around the cervix of maxillary lateral second molars to induce periodontitis with bone resorption. Then ligature-treated group and ligature-treated low Ca group were prepared. On days 5 and 20, maxillae was extracted and analysed using micro CT. Samples were decalcified and the thin sections were stained by tartrate-resistant acid phosphatase (TRAP). Multinuclear osteoclast-like cells were visualized under light microscopy. Micro CT images of maxillae showed that there was no change in the non-ligature group and that alveolar bone resorption was strongly induced around the second molar from days 5 to 20 in the ligature-treated groups. The ligature-treated sites in low Ca group showed a greater bone resorption than the ligature-treated control. Histological examination showed that TRAP positive cells appeared at the top of alveolar bone on day 5 in the ligature-treated groups. The number of osteoclasts in the ligature-treated low Ca group was more than that in the ligature-treated control. These osteoclast-like cells disappeared on day 20 in both groups. Taken together, low Ca diet may increase the number of osteoclasts at the top of alveolar bone and induce the greater resorption of alveolar bone in the experimental periodontitis. These findings suggest that the lack of Ca ingestion in daily life may accelerate alveolar bone resorption in periodontitis.

Disclosures: K. Tokunaga, None.

W412

A Marked Abnormality in Myeloid and Mesenchymal Somatic Stem Cells Explains the Skeletal Defect in Glucagon-Like Polypeptide-2 Receptor KO Mice. J. Xiao¹, D. J. Drucker², J. A. Clowes¹. ¹Mayo Clinic, Rochester, MN, USA, ²Department of Medicine, University of Toronto, Toronto, MN, USA.

Clinical studies have established nutritional intake as a key factor regulating the marked circadian rhythm in bone turnover. In addition, at pharmacological concentrations the intestinal hormone, glucagon like peptide 2 (GLP2) which is released in response to nutrient intake acutely decreases bone resorption. Furthermore, we have established that there is a marked skeletal deficit during growth in GLP2 receptor knockout (GLP2R -/-) mice.

In addition, previous studies have established that CD11b+ myeloid precursors differentiate into mature osteoclasts (OCs) and express key surface receptors, including c-Fms (the receptor for MCSF) and RANK (the receptor for RANKL). Furthermore, cells expressing stro1 a mesenchymal stem cell (MSC) marker differentiate into osteoblast (OB) precursors following co-expression with RANKL. Finally CD133 is a marker of the most primitive somatic stem cell (SSC).

Although the importance of nutrition in bone biology has been clearly established the mechanism(s) for how GLP2 regulates bone metabolism in vivo at physiological concentrations has not yet been determined. We determined this in 6 week old GLP2R -/- mice (n = 4) compared to their wild type (WT) C57BL/6 littermates (n = 5) by examining the percentage of cells (as a fraction of bone marrow MNCs) expressing the various receptors using flow cytometry.

As shown in the Table, a defect in the GLP2R resulted in a significant increase in the % of total cells expressing RANK+ and the % of RANK+/CD34- and RANK+/cFms- cells. Furthermore, there was a significant increase in the % of total cells expressing the MSC marker stro1, the % of stro1+/CD133- and stro1+/RANKL+ cells.

	Percent positive cells			
	RANK+	Stro-1+	Stro-1+/CD133-	Stro-1+/RANKL+
WT	-0.22 ± -0.22	-0.07 ± -0.07	-0.02 ± 0.17	0.06 ± 0.09
GLP2R-/-	1.03 ± 1.04	0.13 ± 0.18	0.26 ± 0.18	0.33 ± 0.19

Data are mean \pm SD; * $P < 0.05$

These studies thus represent the first systematic examination of the effects of a nutrient-regulated hormone at physiological concentrations on OC and OB precursor populations in vivo. Collectively, these data indicate that the absence of GLP2 signaling increases the differentiation of myeloid cells towards mature osteoclasts. Since there is a profound defect in OB differentiation and mineralization in vitro it suggests the increase in MSC differentiation towards mature OBs may either represent a compensatory mechanism or an increase in OB precursors due to a distal block in OB differentiation.

Disclosures: J. Xiao, None.

This study received funding from: Arthritis Research Campaign, IUK.

W413

Comprehensive Analysis of Bone-related Genes Expression Induced by Acute Oxidative Stress. K. Mori¹, R. Kitazawa¹, T. Kondo¹, Y. Hamada², S. Kitazawa¹. ¹Division of Pathology, Kobe University Graduate School of Medicine, Kobe, Japan, ²Division of Nephrology and Kidney Center, Kobe University Hospital, Kobe, Japan.

In the diabetic condition, accumulation of methylglyoxal (MG), an intermediate metabolite of glucose formed through glycolysis, precedes formation of advanced glycation end products (AGE), which then cause oxidative stress in various cells and organs. This oxidative stress is now regarded as a major cause of diabetic complications such as diabetic nephropathy, retinopathy, angiopathy and bone loss. In this study, we comprehensively analyzed gene expression by the DNA microarray system to identify genes in osteoblastic/ stromal cells modulated by oxidative stress. Mouse bone marrow stromal cells, ST2, were treated with MG (100 μ M) for 48hr, and RNA extracted from ST2 cells cultured with or without MG was examined. DNA microarray analysis revealed that the expression of osteoprotegerin (OPG), a decoy receptor of receptor activator of nuclear factor- κ B ligand (RANKL), was markedly reduced by MG treatment. In contrast, the expression of soluble Frizzled-related protein 4 (sFRP-4), a decoy receptor for Wnt proteins, increased by MG treatment. This reciprocal gene expression between OPG and sFRP-4 was also reproduced and confirmed by quantitative real-time RT-PCR. Since the canonical Wnt/ β -catenin signaling pathway contributes to OPG gene expression in osteoblastic cells through the transactivation of the gene, the rapid and marked decrease of OPG gene expression after MG-induced acute oxidative stress may be due to reduced Wnt/ β -catenin signaling by the upregulated expression of its antagonist, sFRP-4. Furthermore, the expression of several target genes of the Wnt/ β -catenin signaling pathway (e.g. cyclin D1, Wnt1 inducible signaling pathway protein 1 (WISP1), WISP2) also decreased in MG-treated ST2 cells. On the other hand, the expression of mesenchymal cell differentiation regulating transcription factors, such as Runx2 for osteoblasts and peroxisome proliferators-activated receptor γ (PPAR- γ) for adipocytes, did not change significantly by short-term MG treatment. In conclusion, oxidative stress induces a rapid reduction of Wnt/ β -catenin signaling and expression of its target genes. We speculate therefore that diabetic bone loss is ultimately caused by decreased Wnt/ β -catenin signaling, and that the early bone-resorption-dominant phase attributed to rapid and marked decrease of OPG gene expression may precede final low turnover osteoporosis as a late complication of diabetes.

Disclosures: K. Mori, None.

W414

Poor Long Term Glycemic Control Is Not Associated with Decreased Bone Mineral Density in Typ 1 Diabetes. T. Neumann¹, A. Saemann², S. Lodes¹, B. Kaestner¹, S. Franke¹, C. Hemmelmann³, U. A. Mueller², G. Hein¹, G. Wolf⁴. ¹Department of Medicine III, Rheumatology/ Osteology, Friedrich-Schiller-University of Jena, Jena, Germany, ²Department of Medicine III, Endocrinology, Friedrich-Schiller-University of Jena, Jena, Germany, ³Institute of Medical Statistics, Computer Sciences and Documentation, Friedrich-Schiller-University of Jena, Jena, Germany, ⁴Department of Medicine III, Nephrology, Friedrich-Schiller-University of Jena, Jena, Germany.

It is assumed that type 1 diabetes is associated with lower bone mineral density (BMD) and increased fractures risk. The impact of duration of diabetes on BMD is controversial. In a cross-sectional study design we investigated the influence of long term glycemic control on BMD in type 1 diabetes. We studied 126 unselected patients with diabetes mellitus type 1 from our outpatient clinic, 63 premenopausal women (41 \pm 8 years) and 63 men (45 \pm 10 years), duration of diabetes was 22 \pm 10.5 years. All patients received standard questionnaire on diabetic history and risk factors for osteoporosis. History of HbA1c was obtained from medical records (mean HbA1c for each year of diabetes duration). 15 patients (10 women and 5 men) were excluded from analysis of long term glycemic control because of missing HbA1c data. BMD was measured using DXA (Lunar Prodigy Advance) at lumbar spine (LS), right femoral neck (FN) and total hip (TH). Osteoporosis (T-score $<$ -2.5 SD) at the LS (FN; TH) was found in 5 (4; 2) %. Osteopenia (T-score between -1 and -2.5 SD) at the LS (FN; TH) was found in 33 (34; 26) %. BMD was not associated with cigarette smoking or a familial history of osteoporotic fracture. Neither diabetes duration nor quartile of duration (1st, 2 to $<$ 14 years; 2nd, 14 to $<$ 21 years; 3rd, 21 to $<$ 31 years; 4th, 31-48 years) were associated with BMD. Quartiles of median HbA1c (1st, 5.4 to $<$ 6.8 %; 2nd, 6.8 to $<$ 7.4 %; 3rd, 7.4 to $<$ 8.1 %; 4th, 8.1-10.8 %) over the time of diabetes were not associated with BMD. No association was found for markers of bone turnover and median HbA1c by measuring serum C-terminal telopeptide of type I collagen (CTX).

Our data suggest that osteoporosis is a clinical significant and commonly underestimated problem in type 1 diabetes. However, the quality of long term glycemic control as well as the duration of diabetes type 1 has no impact on BMD of lumbar spine, femoral neck and total hip.

Disclosures: T. Neumann, None.

W415

Antiepileptic Drugs Affect Bone Loss Via Reproductive Hormones. A. Pack¹, E. Shane², D. McMahon², A. Randall¹, M. Morrell³. ¹Neurology, Columbia University, New York, NY, USA, ²Medicine, Columbia University, New York, NY, USA, ³Neurology, Stanford University, Palo Alto, CA, USA.

The antiepileptic drugs (AEDs), phenytoin (PHT) and carbamazepine (CBZ), are commonly associated with low bone density (BMD) and high bone turnover markers (BTM). Traditionally they are thought to affect bone metabolism by inducing the hepatic cytochrome P450 enzyme CYP3A4 which in turn increases catabolism of vitamin D to inactive metabolites, causing lower serum calcium (SCa) and higher parathyroid hormone (PTH) secretion. Notably, however, CYP3A4 also increases metabolism of estradiol (E2) to inactive 2-OH-estradiol. Moreover, CYP enzyme inducing AEDs (EIAEDs) are associated with increased oral contraceptive failure rates, decreased serum E2 and androgens, and increased serum sex hormone binding globulin (SHBG), thus decreasing free, biologically active hormone. These effects of EIAEDs on E metabolism may also compromise bone health. We hypothesized that women with epilepsy (WWE) treated with EIAEDs have lower E levels, higher bone turnover and lower BMD than WWE treated with lamotrigine (LTG), an AED with no effect on CYP450.

WWE aged 18-40 on monotherapy with EIAEDs CBZ or PHT (n=18) or LTG (n=13) were studied during the follicular phase of the menstrual cycle. E2, estrone (E1), testosterone (T), and SHBG were measured. Free E2 and T were calculated. BMD was measured by DXA. SCa, 25-OHD, 1,25(OH)₂D, PTH, osteocalcin (OC), bone alkaline phosphatase (BSAP) and urine N-telopeptide (UNTX) were assessed.

E1, % free E2, and % free T were lower and SHBG was higher in women on EIAEDs compared to LTG. SCa was lower and UNTX was higher in women on EIAEDs, although there was no correlation between BTMs and reproductive hormones. In contrast, vitamin D metabolites and PTH did not differ. BMD did not differ between groups at any site. In the EIAED group, spine BMD correlated positively with E2 (r=0.58; p=0.02) but femoral neck BMD correlated negatively with % free E2 (r=-0.54; p=0.03). There was no relationship between BMD and calciotropic hormones or SCa in either group.

In summary, women on PHT or CBZ had lower levels of gonadal hormones and higher SHBG than those on LTG, while calciotropic hormones did not differ. Although BMD was not lower in the EIAED group, lower E exposure may lead to higher rates of bone loss over time. We conclude that adverse effects of EIAEDs on bone health may be mediated in part through effects on gonadal hormone status.

	EIAEDS		LTG		p-value
	Mean	SD	Mean	SD	
E1 (pg/ml)	22	8	34	10	0.002
E2 (pg/ml)	30	10	33	17	0.51
% free E2	0.8	0.3	1.1	0.4	0.02
T (pg/ml)	24	12	27	10	0.52
% free T	0.6	0.3	1.0	0.4	0.008
SHBG (nmol/l)	175	80	103	49	0.008
SCa (mg/dl)	9.2	1.2	10.1	0.7	0.03
PTH (pg/ml)	27.4	10.8	29.0	13.7	0.73
25-OHD (ng/ml)	22.2	7.5	22.4	7.6	0.93
1,25(OH) ₂ D (pg/ml)	43.6	9.4	40.5	16.6	0.52
BSAP (μ g/l)	24.4	7.5	20.2	4.2	0.08
OC (ng/ml)	9.2	3.5	8.6	3.4	0.56
UNTX (nMBCE/nMCR)	13.7	3.7	13.0	3.4	0.06

Disclosures: A. Pack, GlaxoSmithKline 2, 5, 8; Novartis 8; Abbott 8.
This study received funding from: GlaxoSmithKline.

W416

Hepatic Osteodystrophy: Expression of IGF-1 and GH Receptor (GHR) and Biomechanical Studies in Experimental Model of Cholestatic Liver. E. A. Pereira¹, I. Facincani^{*1}, L. N. Z. Ramalho^{*2}, J. B. Volpon^{*3}, F. J. A. Paula¹.

¹Internal Medicine, School of Medicine of Ribeirão Preto, University of São Paulo, Ribeirão Preto, Brazil, ²Pathology, School of Medicine of Ribeirão Preto, University of São Paulo, Ribeirão Preto, Brazil, ³Biomechanical and Rehabilitation of the Locomotor System, School of Medicine of Ribeirão Preto, University of São Paulo, Ribeirão Preto, Brazil.

Hepatic osteodystrophy is an important co-morbidity of chronic liver disease. In the present study we assessed the impact of chronic cholestasis on the expression of IGF-1 and GHR in liver and in growth plate and bone resistance in rats submitted to bile-duct obstruction (BDO). Male Wistar rats were divided into two groups: Sham (n=15) and Cirrhotic (n = 15). On day 30 post-surgery, the rats were sacrificed and blood was withdrawn to determine serum liver enzymes and bilirubin. Liver and left tibia were used for immunohistochemistry and right femur for biomechanical study. Liver histology was evaluated. Immunohistochemistry semi-quantitative expression was performed according to the following criteria: (-) no stained cells; (+) less than 10% positive cells; (++) 10% -50% positive cells; (+++) more than 50% positive cells. Bilirubin (Sham =0.08 ± 0.01 mg/dl vs Cirrhotic 6.6 ± 0.1 mg/dl p<0.001), alkaline phosphatase (Sham =68.3 ± 0.3 U/L vs Cirrhotic 1864 ± 0.6 U/L p<0.001), γ GT (Sham =5.8 ± 0.2 U/L vs Cirrhotic 66.5 ± 0.2 U/L p<0.001) levels were significantly higher in Cirrhotic group. In this group, all animals showed histological evidence of cholestatic cirrhosis. Also, in liver tissue, the levels of IGF-1 expression were significantly higher in Cirrhotic group in comparison with Sham group (p<0.01), and the level of GHR expression were significantly lower in cirrhotic group (p<0.01). In growth plate cartilage the levels of IGF-1 expression was significantly lower in cirrhotic group (all animal showed no stained cells or less than 10% of positive cells) in comparison with Sham group (the majority of animals showed more than 50% IGF-1 positive cells) (p<0.01). The same pattern was observed in the growth plate cartilage in relation to GHR expression (p<0.01). The applied forces at the fracture moment were: Sham = 82.5 ± 8.6 N vs Cirrhotic = 57.1 ± 12.1 N p<0.001). Our results indicate that the bone quality is significantly impaired on chronic liver cholestasis in rats and probably the reduction of expression of growth factors on bone microenvironment is involved in this process.

Disclosures: F.A. Pereira, None.

W417

An Integrated Model for Evaluation and Simulation of Therapeutic Responses to Bone-Related Therapies. M. C. Peterson¹, M. M. Riggs^{*2}.

¹Amgen Inc., Thousand Oaks, CA, USA, ²Metrum Research Group, LLC, Tariffville, CT, USA.

Calcium (Ca) homeostasis and bone remodeling are complexly integrated, highly regulated processes involving multiple organs and endocrine pathways. Published generalized models have failed to provide adequate platforms for describing multiple therapeutic class effects on the system. Our aim was to develop a model that predicts longitudinal Ca homeostasis and co-factor levels (including phosphate, PTH, and calcitriol), as well as expected rates of bone turnover due to natural progression, therapeutic intervention, or disease states.

Our approach is based on physiologic requirements to maintain Ca balance, with the general model predicated on 3 manuscripts [Raposo et. al, J Clin Endocrin Metab, 2002; Lemaire et. al, J Theor Biol, 2004; Bellido et. al, J Biological Chem, 2003]. Based on literature and Amgen clinical data, significant modifications and additional feedback mechanisms have been added to appropriately integrate the model. The model includes the RANK-RANKL-OPG system to enable characterization of osteoclast (OC) and osteoblast (OB) genesis and survival, PTH-mediated anti-apoptotic signaling in OB to allow description of anabolic and catabolic effects of PTH on bone remodeling, and TGF β -mediated feedback mechanisms to capture homeostatic observations.

The model has enabled evaluation of various affecting mechanisms, ramifications of therapeutic interventions, and disease state sequelae, including the following: (1) administration of the RANKL inhibitor, denosumab, (2) intermittent- and (3) constant-PTH infusion, and (4) progressive renal insufficiency. The integrated model appears to provide a generalizable structure with known or plausible cell signaling concepts and physiologically consistent parameters. Model predictions under conditions (1) - (4) provide results consistent with clinical observations.

In conclusion, a robust physiologic model that provides continuous descriptions of biomarkers and electrolytes including calcium, phosphate, PTH, and markers of bone turnover consistent with literature and Amgen internal data has been developed. This model may facilitate characterization of therapeutics under development, enable predictions of cytokine mediators of bone homeostasis, and provide a platform for hypothesis testing prior to clinical investigations.

Disclosures: M.C. Peterson, Amgen Inc. 1, 3.

This study received funding from: Amgen, Inc.

W418

Effects of Estrogen on Circulating dlk1/pref-1/FA1 Levels in Postmenopausal Women and Correlations with Bone Turnover and Volumetric BMD. B. Srinivasan¹, B. M. Abdallah^{*2}, S. Khosla¹, M. Kassem².

¹Mayo Clinic, Rochester, MN, USA, ²Odense University Hospital, Odense, Denmark.

dlk1/FA1 (Delta-like 1/fetal antigen1), also known as Pref-1, (Pre-adipocyte factor 1), is a member of the epidermal growth factor-like protein family, known to modulate differentiation of mesenchymal and hematopoietic stem cells in bone marrow in a paracrine/endocrine fashion. Studies in mice have shown that dlk1/FA1 inhibits adipogenesis and is a marker for pre-adipocytes. Recently, Dlk1/FA1 was identified as a novel paracrine/endocrine inhibitor of human bone marrow stromal (hMSC) cell differentiation. Since estrogen (E) is known to enhance osteoblast differentiation and inhibit adipocytic differentiation, we measured circulating FA1 levels by immunoassay in untreated and E-treated postmenopausal women (n = 83 per group, mean age, 63 yrs) who were matched for age and BMI. Circulating FA1 levels were significantly higher in the untreated women (mean ± SEM, 41.5 ± 1.8 ng/ml) as compared to E-treated women (29.9 ± 1.4 ng/ml, P < 0.001). Serum FA1 levels were correlated with serum osteocalcin levels in untreated (age and BMI adjusted correlation coefficient, R^{age,BMI} = 0.26, P = 0.02) and E-treated women (R^{age,BMI} = 0.27, P = 0.02), with femur neck cortical volumetric BMD (vBMD) measured by QCT in both groups (R^{age,BMI} = 0.24 and 0.26, respectively, P < 0.05), and with trabecular vBMD at the distal radius in the E-treated women (R^{age,BMI} = 0.24, P = 0.03). No significant associations with other bone turnover markers (PINP or CTx) or vertebral vBMD were noted. Collectively, these findings indicate that E suppresses circulating FA1 levels in postmenopausal women, perhaps reflecting the known effects of E in inhibiting differentiation of bone marrow stromal cells to pre-adipocytes. The positive associations with serum osteocalcin levels and with vBMD that were noted raise the possibility that higher dlk1/FA1 levels, whether in untreated or E-treated women, may suppress adipocyte differentiation of bone marrow stromal cells to a greater extent than osteoblastic differentiation, leading to a net positive effect of dlk1/FA1 on bone. Further studies are needed to test this hypothesis and to better understand the endocrine role of dlk1/FA1 in regulating bone turnover and bone mass.

Disclosures: B. Srinivasan, None.

This study received funding from: NIH/NIA - AR27065.

W419

To Detamine Serum Fluoride Levels in Patients with Osteoporosis Is Quite Useful for the Judgment of Effectiveness of Osteoporosis Treatment. K. Tanno^{*1}, K. Itai^{*1}, M. Ohsawa^{*1}, T. Onoda^{*1}, Y. Yaegashi^{*1}, T. Sato^{*1}, K. Sakata^{*1}, G. Murooka^{*2}, T. Shimamura^{*2}, A. Okayama^{*3}.

¹Department of Hygiene and Preventive Medicine, Iwate Medical University, Morioka, Japan, ²Department of Orthopedic Surgery, Iwate Medical University, Morioka, Japan, ³Department of Preventive Cardiology, National Cardiovascular Center, Suita, Japan.

Endogenous fluoride is mostly stored within the bone and vividly released into blood circulation along with bone resorption, therefore, serum fluoride levels may faithfully reflect resorption rates of bone metabolism. Purpose of this study is to determine serum fluoride levels in postmenopausal women with osteoporosis before and after treatment of antiresorptive agents and to examine whether serum fluoride levels faithfully reflect resorption rates represented as changes in bone mineral density (BMD) and changes in biochemical markers of bone turn over. A total of 55 postmenopausal women with osteoporosis were enrolled (mean age 69.4 years). BMD (measured by Dual energy X-ray absorptiometry), serum levels of bone alkaline phosphatase (BAP), serum levels of type I collagen cross-linked N-telopeptide (NTX), urinary levels of deoxypyridinoline (DPD), and serum fluoride levels (measured by flow injection method with ion selective electrode) were determined and compared before and after treatment with antiresorptive agents (Alendronate, Risedronate). Mean treatment period was 6.2 months (3.8 - 7.6 months). Serum fluoride levels, as well as serum BAP levels, serum NTX levels, and urinary DPD levels significantly decreased along with increases in BMD in patients with osteoporosis after antiresorptive treatment (see table). In conclusion, markedly decreased serum fluoride levels indicated attenuated resorption rates of bone metabolism, and serum fluoride should be a useful marker that faithfully reflects bone metabolism. To determine serum fluoride levels in patients with osteoporosis should become increasingly essential for the judgment of disease severity and effectiveness of osteoporosis treatment.

Levels of measurements in postmenopausal women with osteoporosis before and after treatment

Measurement	Before Tx	After Tx	p - value
BMD (g/cm ²)	0.62±0.06	0.66±0.06	p < 0.001
serum fluoride (ng/mL)	11.0±3.69	6.5±2.20	p < 0.001
serum BAP (U/L)	33.4±10.0	20.5±6.4	p < 0.001
serum NTX (nmol/BCE/L)	22.1±6.8	14.2±3.3	p < 0.001
urinary DPD (nmol/mmol Cr)	8.5±2.8	4.8±1.7	p < 0.001

Disclosures: K. Tanno, None.

W420

Case Series: Osteomalacia Following Gastric Bypass and Biliopancreatic Diversion Surgery. A. Al-Shoha¹, R. Lakhdar^{*1}, D. S. Rao². ¹Internal Medicine, Henry Ford Hospital, Detroit, MI, USA, ²Bone & Mineral Metabolism, Henry Ford Hospital, Detroit, MI, USA.

Gastric bypass surgery (GBS) and Biliopancreatic diversion (BPD) are the most common procedures for management of morbid obesity, a disorder that is increasing in epidemic proportions in the US and world wide. Metabolic bone disease after GBS has been reported. However, to our knowledge, only two cases of post-GBS osteomalacia (OM) have been reported, but the diagnosis of OM in both cases was based solely on biochemical findings. We report 4 patients with bone biopsy confirmed OM after GBS. Three women and one man (age range 29-53y) were seen for evaluation of metabolic bone disease not responding to "usual" therapy. Two of the 4 patients had BPD; one of those 2 had gastric stapling (GS) about 9y before BPD (Case 2). The other 2 patients had Roux-en-Y GBS; one of those had GS at the time of GBS (Case 3) and the other had jejunoileal bypass 26y before GBS (Case 4). Clinical features included generalized bone pain and tenderness, muscle weakness, difficulty walking, and waddling gait, stooping posture, and fractures. Two patients (Cases 2 and 4) had history of kidney stones at presentation. Diagnoses prior to referral were varied including arthritis, gout, vitamin D deficiency and osteoporosis. Serum chemistry (Table) and radiological findings were suggestive of OM in all the 4 cases, and the diagnosis was confirmed by bone biopsies. Following high doses of Vitamin D and calcium therapy there was significant improvement in the symptoms and functional status and biochemical variables. Our experience suggests that GBS may predispose to severe vitamin D depletion and OM in the absence of high dose vitamin D and calcium supplements. The current "usual" supplements are grossly inadequate in this population and the presentation may be non-specific and misleading. Prospective long-term studies are needed to determine the appropriate vitamin D dose to prevent metabolic bone disease in this uniquely susceptible population.

	Pertinent Laboratory Data			
	Case 1	Case 2	Case 3	Case 4
Time to presentation (years)	5	2	5	5
25-hydroxyvitamin D (ng/mL)	9	6	5	7
Corrected Calcium (mg/dL)	9.5	8.8	8.9	7.3
Alkaline Phosphatase (IU/L)	249	227	1246	178
PTH (pg/mL)	297	324	504	498

Disclosures: A. Al-Shoha, None.

W421

Rickets Is Associated with Failure of Epiphyseal/Metaphyseal Bone Tether Formation. J. Chen^{*1}, C. H. Lohmann^{*2}, R. Coleman^{*1}, R. E. Guldberg^{*1}, Z. Schwartz¹, B. D. Boyan¹. ¹Petit Institute of Bioengineering and Bioscience, Georgia Institute of Technology, Atlanta, GA, USA, ²University of Hamburg-Eppendorf, Hamburg, Germany.

Recently, we showed that bone bridges (tethers) connect the metaphyseal and epiphyseal trabecular bone through the rat tibial growth plate (GP); altered tether formation was highly correlated to growth disruption. We hypothesized that altered chondro-osseous morphology typical of rickets might involve changes in tether number, distribution, or structure. To test this, we imaged the GP via micro-CT and histology to assess if 8-week old VDR^{-/-} mice have changes in tether parameters compared to VDR^{+/+} littermates. GPs were isolated from micro-CT scans (resolution = 16 μ m) of right distal femurs from 15 VDR^{-/-} and 15 VDR^{+/+} mice and average thickness and volume were calculated. To define the tether area, GPs were marked with ellipses using Adobe Photoshop. The "tether probability index" was set as the fraction of samples with tethers in each area. Randomly selected GPs were processed for decalcified (8) and undecalcified (1) histomorphometry; serial sagittal sections were stained with H&E or silver nitrate, respectively. GP and tether vertical height (GP width), horizontal width and area were measured (Image-Pro Plus) and GP volume, GP projection area, tether volume and tether occupancy rate calculated; tether number was determined by reconstruction the consecutive histological images. For reconstructed 3D micro-CT images, tether number was counted directly, GP and tether projection area were measured with Image-Pro Plus software, tether volume was calculated from tether area and average GP thickness. Tethers occurred in all VDR^{+/+} femurs; in contrast, only 20% of VDR^{-/-} femurs had tethers, and their area and distribution were different. Although VDR^{-/-} GPs had greater area and thickness, tether number, area, occupancy rate and volume fraction were dramatically reduced. This was confirmed by histology of non-decalcified femurs. Statistical analysis showed that the histological results correlated with micro-CT for all tether parameters except tether volume. This study demonstrates the utility of the micro-CT method for assessing GP morphology and pathology. Tethers did form at specific sites in some VDR^{-/-} animals, suggesting that rickets does not affect all regions of the GP equally. The results indicate that failure of the GP to develop properly has consequences for establishing the appropriate interface between two mechanically dissimilar tissues.

Disclosures: B.D. Boyan, None.

This study received funding from: Children's Healthcare of Atlanta, Price Gilbert, Jr. Foundation, NSF 9731643.

W422

Minimally Invasive Treatment of Oncogenic Osteomalacia by Radiofrequency Ablation. E. Hesse¹, H. Rosenthal^{*2}, G. Brabant^{*3}, F. Langer^{*4}, K. F. Gratz^{*5}, L. Bastian^{*6}. ¹Orthopaedics and Cell Biology, Yale University School of Medicine, New Haven, CT, USA, ²Diagnostic Radiology, Hannover Medical School, Hannover, Germany, ³Endocrinology, Christie's Hospital, Manchester, United Kingdom, ⁴Pathology, Hannover Medical School, Hannover, Germany, ⁵Nuclear Medicine, Hannover Medical School, Hannover, Germany, ⁶Trauma Surgery, Klinikum Leverkusen, Leverkusen, Germany.

Oncogenic osteomalacia (OOM) is a rare disorder characterized by hyperphosphaturia, hypophosphatemia, and osteomalacia. OOM is treated by surgical excision, which rapidly and permanently abrogates all symptoms. However, tumor removal can be complicated because the lesion is usually small and difficult to distinguish from the surrounding tissue. Complete excision is necessary, however, because the syndrome typically persists if any tumor tissue remains. To ensure complete excision, surgery may require wide resection margins, causing iatrogenic tissue damage that is disproportional to tumor size and to the almost always benign nature of the tumor. We report for the first time the use of minimally invasive radiofrequency ablation (RFA) to completely destroy a tumor causing OOM and thereby avoid arthroplasty. A 40-year-old woman was diagnosed for an acquired hypophosphatemic vitamin D-resistant osteomalacia due to a tumor in her right femoral head that was detected as recently described (JBMR, 2007 Jan;22(1):158-62). Laboratory analyses revealed hypophosphatemia and a diminished TmP/GFR. A complete tumor removal by an open surgical procedure would have required total hip arthroplasty. Because of her young age, we attempted to preserve the hip joint, which was healthy and not affected by the tumor. Histology revealed a benign mesenchymal tumor. We performed CT-guided RFA to destroy the lesion, thereby avoiding arthroplasty. Complete tumor ablation was achieved six days later after a second round of RFA and confirmed on the following day by magnetic resonance imaging (MRI). A few weeks after RFA, biochemical markers returned to normal and all symptoms resolved. A one year clinical follow-up was unremarkable. RFA is a well-established procedure for selectively removing small tissue volumes. In bone, RFA is an effective palliative method for treating skeletal metastases. RFA of benign primary bone tumors has been primarily used to treat osteoid osteoma. This case demonstrates that CT-guided RFA can successfully treat a tumor causing OOM. We believe that RFA may broaden the scope of treatment options in OOM and may offer an effective, less invasive technique that would be a very attractive alternative to classical surgery.

Disclosures: E. Hesse, None.

W423

Severe Vitamin D Depletion in Arab-American Women Living in Dearborn, MI, USA. R. D. Hobbs^{*1}, Z. Habib^{*1}, D. Alromaihi^{*1}, L. Ida^{*2}, N. Parikh^{*2}, J. Schmidt^{*3}, J. Kordosky^{*3}, D. S. Rao². ¹Internal Medicine, Henry Ford Hospital, Detroit, MI, USA, ²Bone & Mineral Research Laboratory, Henry Ford Hospital, Detroit, MI, USA, ³DiaSorin, Inc, Stillwater, MN, USA.

Although vitamin supplements and dairy intake are important determinants of vitamin D nutrition, most individuals can maintain sufficient 25-OHD levels with adequate sun exposure. Secular habits, geographic location (latitudes <40°) or diminished sun exposure may lead to vitamin D depletion. European studies have documented vitamin D depletion in veiled Muslim women living in areas with decreased ambient sunlight, but no such data exist for this ethnic group living in the US. Accordingly we assessed vitamin D nutritional status by serum 25-OHD in Arab-American women living in Dearborn, MI, the largest, most concentrated Arab settlement in the US.

Serum 25-OHD and PTH were measured in 87 Arab-American women who attended an ethnic market on either April 7 or 14, 2007. Demographic variables, dress, medication use, medical history, vitamin supplementation and a food analysis were performed on each subject. A cross sectional approach with analysis using MANOVA or Fischer's exact test was used.

Three groups were formed as follows: unveiled (UV; n=22), veiled with supplementation (VS; n=45), and veiled non-supplemented (VNS; n=20).

Mean 25-OHD levels were lowest and mean PTH levels highest in the veiled non-supplemented group, and differed significantly from the other two groups and from each other (p=0.004, p=0.003 respectively). Although mean age and location did not differ, the mean time in the US was significantly different between the groups (p=0.002). Vitamin D supplementation between the veiled/supplemented (1250 \pm 1243 IU/week) and unveiled groups (1000 \pm 1276 IU/week) did not differ (p=.45).

Vitamin D depletion, as assessed by 25-OHD, is highly prevalent in a sample of Muslim women living in Dearborn, MI and probably the highest among any demographic groups studied thus far. Similar to European studies the findings are at least in part attributable to conservative dress in an area with decreased sun exposure. With increasing time spent in the United States vitamin D levels increase across all tested groups although most (61/87) had levels \leq 10 ng/ml. These findings potentially identify a problem in the largest, most concentrated Arab-American population in the United States.

Variable	Comparison Between Arab-American Women in Terms of Clothing and Vitamin Supplementation		
	UV	VS	VNS
Mean Age (yrs)	36.4 \pm 13.4	37.2 \pm 14.1	37.6 \pm 7.1
Time in the US (yrs)	18.9 \pm 14.2	9.8 \pm 9.1	9.5 \pm 7.3
25-OHD (ng/dl)	11.1 \pm 8.8	8.6 \pm 4.9	4.9 \pm 3.5
PTH (pg/ml)	72 \pm 27	62 \pm 23	88 \pm 35

Disclosures: R.D. Hobbs, None.

W424

Lack of Efficacy of Octreotide in the Treatment of Tumor-induced Osteomalacia. M. H. Kelly^{*1}, B. Brillante^{*1}, A. Khosravi^{*2}, M. T. Collins¹.

¹National Institute of Dental and Craniofacial Research, National Institutes of Health, Bethesda, MD, USA, ²Neurorehabilitation Department, Kennedy Krieger Institute, Johns Hopkins University, Baltimore, MD, USA.

The purpose of this study was to test the efficacy of the somatostatin analogue, octreotide, in the treatment of tumor-induced osteomalacia (TIO).

TIO is a rare, acquired disease characterized by low serum phosphate and 1,25-dihydroxyvitamin D₃ (1,25-D), and osteomalacia. It is due to mesenchymal tumors that produce the phosphate and vitamin D-regulating hormone, FGF-23. Removal of the tumor is curative, but the tumors sometimes cannot be located and medical treatment is required. Octreotide has been reported to be an effective medical therapy. We sought to confirm the efficacy of octreotide by treating six patients with TIO.

Six patients with TIO who were off phosphate and calcitriol replacement were studied. Five of the six subjects had FGF-23 secreting tumors that were localized on Indium-111-pentetreotide scans (a radiolabeled analogue of octreotide). Subjects were treated with octreotide (Sandostatin, Novartis) 100 mcg by subcutaneous injection every 8 hours for three days. Serum phosphorus, 1,25-D, and FGF-23 were measured serially for 3 days. Repeated measures ANOVA was performed to test for significant changes in serum measurements.

None of the subjects responded to the octreotide. The mean changes in serum values over the 3 day period were: phosphorus 4% (range -3 to 13), 1,25-D 10% (-5 to 14), and FGF-23 -1% (-11 to 8). There was no significant change in serum phosphorus, 1,25-D, or FGF-23 in response to treatment with octreotide.

During 3 days of treatment with relatively high doses of octreotide, there was no effect on serum phosphorus, 1,25-D, or serum FGF-23 in patients with FGF-23 secreting tumors, in spite of the fact that 5/6 tumors took up pentetreotide.

Disclosures: M.H. Kelly, None.

W425

Skeletal Fluorosis from Instant Tea: A Second Case. M. P. Whyte¹, W. G. Totty^{*2}, G. M. Whitford^{*3}. ¹Division of Bone and Mineral Diseases, Washington University School of Medicine, St. Louis, MO, USA, ²Mallinckrodt Institute of Radiology, Washington University School of Medicine, St. Louis, MO, USA, ³School of Dentistry, Medical College of Georgia, Augusta, GA, USA.

Skeletal fluorosis (SF) usually results from prolonged consumption of well water with > 4 parts per million (ppm) fluoride ion (F⁻); i.e., > 4 mg/L. Black and green teas can contain significant amounts of F⁻. In 2005, SF due to drinking 1 - 2 gallons of double-strength instant tea daily throughout adult life was reported in a 52-year-old woman (Am J Med 118:78).

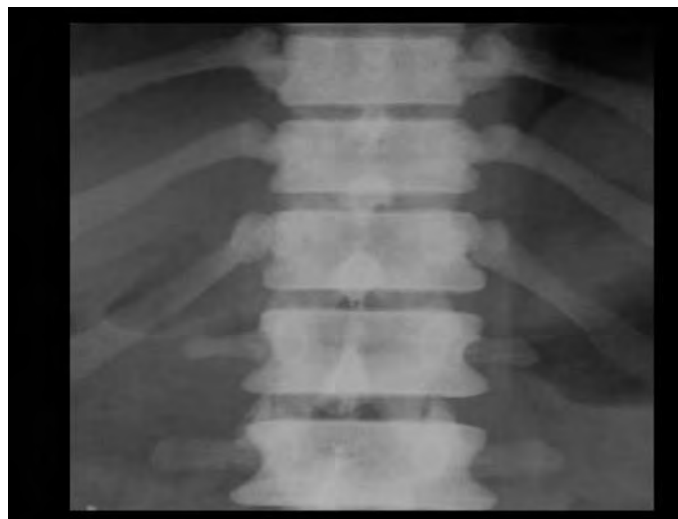
A 49-year-old woman developed widespread musculoskeletal pains, considered fibromyalgia, in her mid-30's. Additionally, there was unexplained, increasing, axial osteosclerosis. She reported drinking 2 gallons (7.56 liters) of instant tea each day since age 12 years, and took fluoxetine intermittently for 5 years. Ion-selective electrode methodology quantitated F⁻ in her blood, urine, municipal tap water, beverage, and extracts of fingernail and toenail clippings.

Radiographs showed uniform osteosclerosis involving the axial skeleton, but enthesopathy was consistent with her age. DXA Z-scores were + 10.3 in the lumbar spine, and + 2.8 in the total hip. Serum F⁻ concentration was 120 µg/L (20 - 80, reference range), and a 24-hour urine specimen contained 18 mg F⁻/gm creatinine (< 3, reference range). Mean F⁻ levels were 2.2 and 2.8 times greater than for 3 age-matched controls in fingernails and toenails, respectively (p < 0.001). Her instant tea beverage, prepared extra-strength as usual and using tap water with ~ 1.14 ppm F⁻, contained 5.8 ppm F⁻. In the U.S.A., this F⁻ level exceeds the Environmental Protection Agency limit of 4.0 ppm for primary drinking water, the Food and Drug Administration limit of 1.4 - 2.4 ppm for bottled water or beverages, and the Public Health Service optimum fluoridation level in community water ranging from 0.7 - 1.2 ppm. The tea product contributed ~35 of the 44 mg daily F⁻ exposure from her beverage. Fluoxetine could have added as much as 3.3 mg F⁻ daily.

A second case of SF from habitual consumption of large volumes of extra-strength instant tea calls for recognition and better understanding of a skeletal safety limit for this modern preparation of the world's most popular beverage.

Legend to Figure:

Anteroposterior radiograph of the lower thoracic and upper lumbar spine at age 48 years shows uniformly dense, but properly shaped, vertebrae.



Disclosures: M.P. Whyte, None.

This study received funding from: Shriners Hospitals for Children, The Clark and Mildred Cox Inherited Metabolic Bone Disease Research Fund, and the Barnes-Jewish Hospital Foundation.

W426

The Relationship between Bone Formation Rate and Bone Marrow Adipocytes in Pediatric Metabolic Bone Diseases. M. S. Cheung^{*}, F. H. Glorieux, L. M. Ward, R. Travers^{*}, F. Rauch. Genetics Unit, Shriners Hospital for Children, Montreal, PQ, Canada.

Adipocytes are derived from the same mesenchymal stem cells as osteoblasts. If mesenchymal stem cells differentiate into either adipocytes or osteoblasts depending on functional requirements, there should be an inverse relationship between the number of adipocytes in the bone marrow and bone formation rate on adjoining bone surfaces. Indeed, histomorphometric studies in adults seem to confirm this hypothesis. In the present study we examined whether a similar relationship between adipocyte numbers and bone formation rate is present in a range of pediatric metabolic bone disorders. Iliac bone samples from 71 children and adolescents with osteogenesis imperfecta (OI) -before medical treatment and after two years of pamidronate therapy (OI-PAM) - idiopathic juvenile osteoporosis (IJO), Crohn's disease and pseudohypoparathyroidism (PHP) were assessed for cancellous bone formation rate per bone surface (BFR/BS) and the presence of adipocytes. Results were compared to those of 58 controls who were individually age-matched to each disease cohort.

	N	Age (yr)	BFR/BS (µm ³ *µm ⁻² *y ⁻¹)	Samples with Adipocytes (N)
OI	24	11.4 (4.2)	71 (33)*	6*
OI-PAM	24	11.5 (3.9)	19 (17)	7*
Controls	24	11.3 (5.0)	42 (17)	0
Crohn's	8	15.5 (2.7)	46 (25)	8***
Controls	8	15.7 (3.2)	34 (11)	0
PHP	8	16.5 (3.2)	86 (43)**	8***
Controls	8	16.4 (3.0)	30 (18)	1
IJO	7	10.9 (0.9)	23 (14)*	0
Controls	7	11.1 (1.1)	57 (14)	1

*p<0.05; **p<0.01;***p<0.001 compared to controls

In untreated OI, both BFR/BS and the proportion of samples containing adipocytes were higher than in controls. Pamidronate treatment led to lower BFR/BS, but had no effect on the number of samples with adipocytes. In Crohn's disease and PHP, adipocytes were more prevalent than in controls, even though average BFR/BS was similar or higher. When all biopsy samples were examined, there was no difference in BFR/BS between samples with adipocytes present compared to those without adipocytes (p=0.40). In conclusion, no evidence for an inverse relationship between bone formation and the presence of adipocytes was found in the disease groups studied here. Factors other than bone formation rate seem to be more important determinants of adipogenesis in these conditions.

Disclosures: M.S. Cheung, None.

W427

Exostoses After Pediatric Stem Cell Transplant Are Associated with Growth Hormone Treatment. K. J. Dilley¹, K. Danner-Koptik². ¹Pediatric Hematology-Oncology-Transplant, Children's Memorial Hospital, Feinberg School of Medicine, Chicago, IL, USA, ²Pediatric Hematology-Oncology-Transplant, Children's Memorial Hospital, Chicago, IL, USA.

Allogeneic hematopoietic stem cell transplant (SCT) is a curative therapy for pediatric patients with both malignant and non-malignant diseases. Single or multiple benign exostoses or osteochondromas have been reported following total body irradiation (TBI) as well as focal irradiation. Patients exposed to TBI at a young age are at highest risk of developing exostoses. The objective of this study was to look at potential factors besides radiation that may play a role in development of exostoses. All patients who have undergone SCT at a single institution between March 1992 and October 1998 and who have had an exostosis identified by clinical findings or as an incidental finding on a radiologic study were included. A case-control design matched patients with controls who had the same stem cell source. 11/13 cases were matched to controls within the same age group at SCT of <4 yrs or ≥4 yrs but 2 others were not able to be so closely matched to unique controls. Treatment-related variables as well as physical and laboratory findings were collected from medical record reviews. Of 110 eligible patients, 13 (12%) were found to have exostoses at the time of data collection, 7 male and 6 female. All but two were transplanted for malignancy. All but one received TBI, that case did receive radiation but to a site remote from the exostosis. Multiple exostoses were noted in 62% (8/13). Treatment with growth hormone was more likely in cases (n=6) than in controls (n=2), p=0.046. Also, cases had a nonsignificant trend toward more negatively skewed height Z scores (mean -2.1 vs -1.5, p=0.056) and weight Z scores (mean -1.4 vs -0.2, p=0.097) at most recent follow-up than did controls. Patients available for use as controls tended to be older than cases, anecdotally supporting other studies that have reported younger age to be a risk factor for exostoses. No other SCT treatment factors such as HLA-mismatch or the occurrence of GVHD were associated with exostosis risk. Calcium (9.8 vs 9.9, p=0.75) and IGF-1 (382 vs 331, p=0.60) values were not significantly different at latest follow-up (cases at mean age 14.6 yrs vs controls at mean age 13.5 yrs), but IGF-BP3 approached significance with a mean of 5.0 in cases compared to 3.7 in controls (p=0.066). In conclusion, allogeneic SCT patients with the most extreme growth disruption and subsequent treatment with growth hormone appear to be at highest risk for development of exostoses. All reported samples to date have been small, use of multi-institution data to further examine risk factors is warranted.

Disclosures: K.J. Dilley, None.

W428

Postnatal Vitamin D Supplementation Normalized Neonatal Bone and Lean Mass Following Maternal Dietary Vitamin D Deficiency in the Guinea Pig. S. L. Finch, H. A. Weiler. School of Dietetics and Human Nutrition, McGill, Ste. Anne-de-Bellevue, PQ, Canada.

While vitamin D deficiency is common at birth, the consequences to growth and bone mass by weaning are unclear. This study was designed to determine if maternal dietary vitamin D deficiency in pregnancy has a negative impact on mineralization of full term infants and if postnatal supplementation would recover the limited bone mass using a 2-by-2 design. Forty pregnant guinea pigs were randomized to receive a diet with or without 1 IU vitamin D3/g diet. Blood was sampled in sows before mating at the start of the 3rd trimester (d42) to coincide with fetal mineralization and postpartum to measure 25(OH)D as the marker for vitamin D status. At birth pups were randomized to receive 10 IU of cholecalciferol or a placebo of equal volume until weaning at d28. Diets and supplements were blinded using letter coding. Dual energy x-ray absorptiometry (DXA) was used to measure body composition, as well as bone mineral density (BMD), bone area and bone mineral content (BMC) of the whole body, tibia, femur and lumbar spine at birth and d28 of life. Main and interaction effects were detected using factorial ANOVA and post-hoc testing using Bonferroni tests. Weight of the pups was lower in the vitamin D deficient group at birth and d28 (Birth: 169.59±97.94 vs 155.34±97.89 g, P=0.042; d28: 279.13±47.43 vs 255.91±44.19 g, P=0.024). Main effects of the maternal diet showed vitamin D deficient offspring had lower whole body BMC (5.58±2.69 vs 5.24±2.52 g, P=0.012) and lower tibia BMC (0.15±0.07 vs 0.14±0.07 g, P=0.012) than the control group. Interaction effects showed that the deficient group were lower than the control group in whole body BMD (P=0.045) and lean mass (P=0.024) unless they received supplemental vitamin D. Additionally, femur BMC was lower at d 28 in the deficient males unless they received the supplement (P=0.012). Weight and whole body BMC increased 2.5 to 3 times from birth to weaning demonstrating the magnitude of growth that this novel model is capable of in a short period of time. In summary, postnatal vitamin D supplementation normalized neonatal bone and lean mass following maternal dietary vitamin D deficiency in the guinea pig.

Disclosures: S.L. Finch, None.

This study received funding from: Dairy Farmers of Canada and The Natural Sciences and Engineering Council of Canada.

W429

Hyperparathyroid Bone Disease in Two Sisters with Parathyroid Hormone Resistance (pseudohypoparathyroidism 1b). R. C. Gensure¹, M. Bastepe². ¹Pediatrics, Ochsner Clinic Foundation, New Orleans, LA, USA, ²Endocrine Unit, Massachusetts General Hospital and Harvard Medical School, Boston, MA, USA.

Pseudohypoparathyroidism (PHP) is a disorder of hypocalcemia and elevated serum parathyroid hormone (PTH) levels caused by defective signaling via the stimulatory G protein α subunit (G α). PHP type-1a results from mutations in G α -coding GNAS exons, and is characterized by multi-hormone resistance and a bone dysplasia syndrome called Albright's hereditary osteodystrophy (AHO). PHP-1b is caused by mutations that disrupt the imprinting of GNAS and is characterized by resistance to PTH (and occasionally to TSH) with no bone dysplasia. In each subtype, hormone resistance develops only after maternal inheritance of the genetic defect, consistent with the predominantly maternal expression of G α in some tissues, including the renal proximal tubule. We report on two sisters with PHP-1b, demonstrating both PTH- and TSH-resistance in the absence of AHO, seen in consultation because of increased fractures. The genetic defect in this family, a 4.4-kb deletion in STX16, has been reported previously (Am J Hum Genet. 2005 May;76(5):804-14). The elder sister (patient A, 15 9/12 y.o.) had one pathological fracture and was found to have a low lumbar bone mineral density (BMD) (Z-score -1.7). Importantly, the BMD did not show the expected increase with age, but rather decreased 12.6% over the past year. The younger sister (patient B, 14 0/12 y.o.) had two recent fractures and had a BMD closer to the normal range (Z-score -0.7), with a slight increase (2.6%) over the past year. Each had been managed with calcium and calcitriol according to the standard practice to maintain low-normal serum calcium levels to reduce risk of kidney stones; the PTH levels were elevated in both patients (272 pg/ml for patient A, 320 pg/ml for patient B). G α is not imprinted in bone; hence, while patients with PHP-1a have a 50 percent reduction in G α signaling leading to partial PTH resistance in bone, patients with PHP-1b are predicted to have normal G α signaling in bone and could therefore develop hyperparathyroid bone disease. The patients' medications were adjusted to lower PTH levels to the normal range (57 pg/ml and 35 pg/ml, respectively). After 8 months, their bone mineral densities improved to Z=-0.9 and Z=-0.3, respectively (increased by ~0.5 S.D. in each case), and they did not have any additional fractures. Neither patient developed hypercalcaemia, likely because of the lack of imprinting of GNAS in the renal distal tubule. Given that bone is not resistant to PTH in PHP-1b, we recommend that these patients' serum PTH levels be maintained in the normal range to prevent hyperparathyroid bone disease.

Disclosures: R.C. Gensure, None.

W430

Physal Closure from Chronic Vitamin A Intoxication. D. Wenkert¹, W. H. McAlister², M. P. Whyte³. ¹Res Ctr, Shriners Hospt Children, St. Louis, MO, USA, ²Mallinckrodt Inst Radiol, Wash Univ Sch Med, St. Louis, MO, USA, ³Div Bone & Miner Dis, Wash Univ Sch Med, St. Louis, MO, USA.

Vitamin A excess causes periosteal calcification, diffuse idiopathic skeletal hyperostosis, and fractures. In pediatric patients, skeletal growth, modeling, and remodeling can be disrupted. Premature growth plate fusion from vitamin A and D toxicity was first reported in animal hind limbs ("hyena disease"). Subsequently, in 1962, 3 of 7 children with growth retardation from vitamin A toxicity had early lower limb physal closure (JAMA; 182:980). Further reports concerned vitamin A derivatives used in severe pediatric dermatoses or cancers.

A 6-yr-old boy with a history of hypervitaminosis A, associated with liver fibrosis, was referred for "epimetaphyseal disease". Birth weight was 10 lbs, and he walked at 10 mo. At that time, gastroenteritis was reportedly treated by a chiropractor with a dose of 3 million units (U) of vitamin A over 16 days, followed by 60,000 U/d except when intercurrent illness prompted ~20 additional 3 million U, 16-day courses.

By age 2 ½ yrs, fingernails reportedly "bubbled up and fell off", speech regressed, and gross motor skills were lost. Hospitalization elsewhere revealed a critically ill, anorexic child with shiny, hairless, jaundiced skin, icterus, mouth sores, mucosal bleeding, pseudotumor cerebri, ataxia, and marked hepatosplenomegaly. Laboratory studies revealed a coagulopathy, hepatitis, anemia, and thrombocytopenia, but normal serum Ca, P, and Mg levels. Alkaline phosphatase was elevated at 827 IU/L. Hypervitaminosis A was diagnosed. After vitamins were stopped, he resumed walking and eating within 9 mo. Nevertheless, leg bowing, noted at age 3, worsened. Radiographs at age 5 showed physal closure within distal femurs and proximal and distal tibias.

Upon referral, he had dysphagia, dyspnea, anemia, bleeding tendency, morning stiffness, knee and ankle pain, but took only vitamin K. Height was 5%, weight 75%, sitting height 50%, arm span 75%, and head circumference >>95%. He had petechia, bruises, telangiectasias, hypertelorism, cupped optic discs, and splenomegaly (17 cm) without hepatomegaly, 30° knee contractures, enlarged warm ankles and knees, and bowed tibias. Radiographs revealed the physal closure, now with relative overgrowth of fibulae, and 1/2 yr later, closure of the proximal fibular physes. Physes elsewhere remained open.

Long-term follow-up of physal fusion from vitamin A toxicity (eg. 12 yrs: JBJS[AmJ] 1974;56:1283) suggests disproportionate, asymmetric shortening of lower limbs. Narrowing of physes from isotretinoin can resolve (Am J Dis Child 1988;142:316-8). Experience with our patient suggests that reversal of physal fusion is not possible if vitamin A toxicity has been severe and prolonged.

Disclosures: D. Wenkert, None.

This study received funding from: Shriners Hospitals for Children, The Clark and Mildred Cox Inherited Metabolic Bone Disease Research Fund, and the Barnes-Jewish Hospital Foundation.

W431

The Importance of Biochemical Markers of Bone and Cartilage Turnover as the Predictors of Radiographic Progression in Patients with Early Rheumatoid Arthritis. J. Hashimoto¹, P. Garnero², N. Miyasaka³, K. Yamamoto⁴, S. Kawai⁵, T. Takeuchi⁶, N. Murata⁷, H. Yoshikawa¹, N. Nishimoto⁸. ¹Orthopaedic Surgery, Osaka University Graduate School of Medicine, Suita, Japan, ²INSERM Research Unit 664 and Synarc, Lyon, France, ³Tokyo Medical and Dental University, Tokyo, Japan, ⁴The University of Tokyo, Tokyo, Japan, ⁵Toho University Omori Medical Center, Tokyo, Japan, ⁶Saitama Medical Center/School, Saitama, Japan, ⁷Orthopaedic Surgery, Kyowakai Hospital, Suita, Japan, ⁸Osaka University Graduate School of Medicine, Suita, Japan.

Background: Rheumatoid arthritis (RA) is characterized by chronic arthritis leading to joint damage due to bone and cartilage destruction. Although early intervention of RA could prevent the progression of joint damages, it is difficult to predict the radiological progression in patients with early RA.

Objectives: To evaluate the predictive value of biological, radiological and clinical parameters for the prognosis of radiographic joint damage in RA patients treated with conventional DMARDs.

Methods: Among 302 patients with active RA of less than five years duration who participated in the prospective 1-year randomized controlled trial of tocilizumab monotherapy, termed SAMURAI study, the control arms (n=145), in which the dose regimens of the conventional DMARDs therapy excluding any biologics, were analyzed. Biochemical markers (bone turnover, cartilage turnover and inflammation), clinical score (number of swollen joint, tender joint, DAS score) and body mass index were measured at baseline and radiographic joint damage were scored at baseline, week 28 and 52 by two independent blinded readers according to the van der Heijde modified Sharp method.

Results: At baseline, mean age, disease duration, DAS28 score, total Sharp score and CRP were 53 years, 2.3 years, 6.5, 29.4 and 4.8 mg/dl, respectively. Increased urinary C-terminal crosslinking telopeptide (CTX-II) levels, higher urinary pyridinoline/deoxypyridinoline ratio (PYD/DPD), higher JSN score and low BMI at baseline were associated with increased radiological progression at 1 year both for erosion and the JSN score. When categorized into two or three groups of baseline risk factors (cut-off values: 500 and 1000 ng/mmol/creatinine for CTX-II, median for PYD/DPD, 0 unit or more for JSN, 18.5 and 25 for BMI), logistic regression analysis showed that these four variables were significant independent predictors of radiological progression (+0.5 unit increase of erosion or JSN score at week 52).

Conclusion: High baseline levels of biomarkers of bone and cartilage turnover including CTX-II and PYD/DPD, JSN score and low BMI are significantly and independently associated with 1-year progression of joint destruction in early RA.

Disclosures: J. Hashimoto, None.

W432

Tartrate-Resistant Acid Phosphatase Isoform 5a as a Marker of Disease Severity in Rheumatoid Arthritis. A. J. Janckila¹, D. H. Neustadt², L. T. Yam¹. ¹Medicine, VA Medical Center, Louisville, KY, USA, ²Medicine, University of Louisville, Louisville, KY, USA.

Objective: This study was undertaken to determine the clinical significance of tartrate-resistant acid phosphatase (TRACP) isoforms 5a and 5b as markers of chronic inflammation and cartilage/bone destruction in rheumatoid arthritis (RA).

Methods: 118 patients were recruited including 50 with RA (25 with subcutaneous nodules), 26 with osteoarthritis (OA) and 42 with other rheumatic diseases. 26 healthy adults served as controls. Serum TRACP-5a activity, TRACP-5a protein and TRACP-5b activity were determined by in-house immunoassays. C-reactive protein (CRP) was determined by in-house immunoassay using commercial antibodies and CRP. Other commercial markers included bone-specific alkaline phosphatase (bALP), C-telopeptides of type-I collagen (ICTP), cartilage glycoprotein-39 (YKL-40), and IgM rheumatoid factors (IgM-RF).

Results: TRACP-5a protein was elevated in RA and correlated only with IgM-RF. Amongst RA patients, TRACP-5a protein and IgM-RF were higher in those with nodules. TRACP-5a protein and IgM-RF tended to decline with disease duration, but not age in RA patients with nodules. In contrast, TRACP-5b activity was slightly elevated in RA and correlated with bALP and ICTP, but not with IgM-RF or CRP. TRACP-5b activity was not related to presence of nodules, however it increased with age and disease duration in RA.

Conclusion: TRACP isoforms may be useful disease markers in RA. TRACP-5a protein may be a measure of systemic inflammatory macrophage burden and a marker for disease severity. TRACP-5b activity is a marker for osteoclast number and may be useful to monitor local or systemic bone destruction in early RA.

Disclosures: A.J. Janckila, None.

W433

Association of tri-nucleotide (CAG and GGC) Repeat Polymorphism of androgen Receptor Gene in Taiwanese Women with Refractory or Remission Rheumatoid Arthritis. H. Kang¹, S. Yu¹, Y. Hsu², C. Chang³.

¹Graduate Institute of Clinical Medical Sciences, Chang Gung University, Kaohsiung, Taiwan, ²Program for Population Genetics, Harvard School of Public Health, Boston, MA, USA, ³Departments of Pathology, Urology, Radiation Oncology, Rochester University, Rochester, NY, USA.

To investigate the relationship between CAG and GGC repeat polymorphism of the androgen receptor (AR) gene and rheumatoid arthritis (RA) in female patients with different disease subtypes. This case-control study enrolled 215 females in three groups: RA patients refractory to standardized therapy (n=51); RA patients at complete remission phase (n=60); and healthy controls (n=104). CAG and GGC repeat lengths were determined by automated fluorescence-based DNA fragment-sizing method. Demographic data, allele lengths, allele distribution, and zygosity status of CAG/GGC repeats were assessed for the three group. Refractory RA patients tend to have a significantly younger onset age of RA and more elevated erythrocyte sedimentation rates than do remission RA patients. Mean and median values of CAG and GGC repeat lengths are similar in both RA and control patients. However, RA patients harboring any long CAG alleles with more than 23 repeats had an increased risk of a refractory course, whereas differences in risk were not observed between these patients and RA subtypes harboring any long GGC alleles with more than 16 repeats. In addition, the homozygous frequency of CAG but not GGC alleles was lower in refractory RA than in remission RA patients or in controls (p=0.042). Neither CAG nor GGC repeat lengths had a significant relationship with rheumatoid factor reactivity. Our observations indicate that short CAG repeats of the AR gene with higher transactivation activity may have protective effects against refractory course of RA development and that homozygous frequency of CAG alleles may be involved in the disease remission subtype. In contrast, lack of association of GGC polymorphism and RA was also observed. Together, these data imply that CAG but not GGC alleles in the AR polymorphism may play an important role in modulating the disease pattern of RA among Taiwanese women.

Disclosures: H. Kang, None.

This study received funding from: Chang Gung Memorial Hospital and University.

W434

The Effect of Etanercept on Bone Metabolism in Patients with Rheumatoid Arthritis. D. Kida^{*}, Y. Eto^{*}, M. Tsukamoto^{*}, T. Sato^{*}, A. Kaneko^{*}, G. Ishihara^{*}, H. Sugishita^{*}, K. Saito^{*}. Department of Orthopedic surgery and Rheumatology, National Hospital Organization Nagoya Medical Center, Nagoya, Japan.

Background: Recently, the discovery of the RANKL-RANK-OPG pathway contributed to a better understanding of bone diseases such as RA, osteoporosis, and bone metastasis. On the other hand, TNF has been shown to increase the expression of RANKL and act directly on osteoclasts by enhancing their resorpting activity. Furthermore, TNF enhances bone loss in RA by inducing osteoblast apoptosis. Therefore, the imbalance between bone resorption and bone formation leads to focal and systemic bone loss in RA. Although the most recent data suggest that infliximab therapy may inhibit generalized bone loss in patients with RA, it has not been studied in etanercept (ETN).

Purpose: The aim of this study was to evaluate urinary N-telopeptide of type-I collagen / creatinine (NTx) and serum bone specific alkaline phosphatase (BAP) in RA before and after treated with ETN.

Methods: Sixty postmenopausal females (mean age 62 yr; mean disease duration 14 yr) with RA who had not been treated for osteoporosis were divided into three groups: Twenty treated with bisphosphonate (BP), twenty treated without BP and twenty treated with ETN alone. To evaluate disease activity, ESR, CRP, DAS28ESR-4, modified Stanford Health Assessment Questionnaire (mHAQ) score, NTx, and BAP were measured in all patients at baseline, and after 6 months.

Results: However, ESR (p<0.01), CRP (p<0.001), DAS28ESR-4 (p<0.001), and mHAQ score (p<0.05) had decreased significantly, NTx levels did not differ significantly in 6 months after initial treatment with ETN. BAP levels (p<0.01) were significantly increased, and higher (p<0.01) in patients treated with ETN compared to others.

Conclusion: ETN therapy may not inhibit bone resorption but stimulate bone formation in patients with RA. This effect may be due to a beneficial roll of TNF-alpha blockade on bone turnover. Studies of longer duration are needed to assess the effect of ETN on bone metabolism.

Disclosures: D. Kida, None.

W435

Human Rheumatoid Synovial Fibroblasts Promote Osteoclastogenic Activity by Activating RANKL via TLR-2 and TLR-4 Activation. H. Kim¹, S. Lee¹, K. Kim², M. Cho², W. Park³, H. Kim². ¹Internal Medicine, Konkuk University Hospital, Seoul, Republic of Korea, ²Internal Medicine, Catholic University of Korea, Seoul, Republic of Korea, ³Internal Medicine, INHA University Hospital, Seoul, Republic of Korea.

Objective: The interplay between the innate immune system and inflammatory bone destruction in the joints of individuals with rheumatoid arthritis (RA) remains unclear. This study was undertaken to explore the effect of toll-like receptor (TLR) signaling in fibroblast-like synoviocytes (FLS) on the expression of RANKL and induction of

osteoclastogenic activity.

Methods: The levels of RANKL mRNA and protein were measured using RT-PCR, real-time PCR, and immunostaining. Monocytes were cocultured with RA-FLS that had been stimulated with TLR ligands in fresh media and subsequently stained for tartrate-resistant acid phosphatase (TRAP) activity. Osteoclast molecule markers were measured using real-time PCR.

Results: Expression of TLR-2 and TLR-4 was higher in RA-FLS than in OA-FLS and normal skin fibroblasts. TLR-2 and TLR-4 ligands induced RANKL expression in RA-FLS. TLR stimulation of RA-FLS also induced the production of IL-1 β and TNF- α to a lesser extent; however, it had no effect on IL-17 production. Inhibition of TLR induced IL-1 β production, which partially reversed the upregulation of RANKL induced by TLR ligands. RA-FLS stimulated by TLR-2 and TLR-4 ligands and cocultured with human monocytes induced high levels of expression of TRAP, RANK, cathepsin K, calcitonin receptor, and matrix metalloproteinase-9, suggesting that RA-FLS promote osteoclast differentiation. Our results suggest that the TLR signaling pathway, through TLR-2 and TLR-4, induces RANKL expression in RA-FLS and the expression of RANKL promotes the differentiation of osteoclasts in RA synovium.

Conclusion: Targeting specific TLRs may be a promising approach to prevent inflammatory bone destruction in the pathogenesis of RA.

Disclosures: S. Lee, None.

W436

Alpha Lipoic Acid Attenuates Vascular Smooth Muscle Calcification via the Expressional Regulation of Genes Related to Apoptosis and Oxidative Stress. E. Kim^{*1}, I. Lee^{*1}, H. Kim^{*2}, W. Jang^{*1}, I. Park¹. ¹Kyungbook National University, Daegu, Republic of Korea, ²Keimyung University, Daegu, Republic of Korea.

Vascular smooth muscle cell (VSMC) calcification is an important risk factor for cardiovascular diseases. It is reported that alpha lipoic acid (ALA) has many beneficial effects on vascular cells in atherosclerosis. The present study was designed to investigate whether ALA can prevent VSMC calcification. We explored the effects of ALA on human VSMC calcification in vitro and found that ALA attenuates VSMC calcification induced by high phosphate conditions as quantified by the o-cresolphthalein complexone method. ALA also inhibits vitamin D3-induced aortic calcification in vivo. Using DNA microarray analysis and secretome analysis using LC/MS/MS, we identified genes and proteins whose expression was changed by high phosphate conditions and ALA. Proteins up-regulated by high phosphate condition that were subsequently down-regulated in the presence of ALA were related to apoptosis and oxidative stress. Gene expression analysis using DNA microarray tools confirmed the up-regulation or down-regulation of some, but not all, of the proteins observed in ALA challenged, in high phosphate condition. The present data suggest that vascular calcification is inhibited by ALA through modulation of apoptosis and oxidative stress pathway and provide valuable information about the underlying mechanisms of atherosclerosis.

Disclosures: I. Lee, None.

W437

Survey on the Effect of Immunomodulatory Therapy on Bone in Multiple Sclerosis. M. J. McKenna¹, M. Shuhaiber^{*2}, K. Foy^{*2}, R. Lonergan^{*2}, M. Au-Yeong^{*1}, J. Brady^{*3}, B. Murray^{*3}, J. M. T. Redmond^{*2}. ¹DXA Unit, St. Vincent's University Hospital, Dublin 4, Ireland, ²Neurology Department, St. James' Hospital, Dublin 8, Ireland, ³Metabolism Laboratory, St. Vincent's University Hospital, Dublin 4, Ireland.

Osteoporosis is a complication of multiple sclerosis (MS) especially if corticosteroid therapy is given. Little is known about the effect on bone of immunomodulatory therapy for MS. We sought to evaluate bone mass in patients with MS on immunomodulators. We performed a cross-sectional survey and a follow-up survey.

At baseline, we studied bone mineral density (BMD) by dual energy X-ray absorptiometry (DXA) in 37 patients with MS who received immunomodulators. The BMD was measured at two sites: the lumbar spine (L1 to L4) and the left total femur site, using a Hologic QDR4000 Elite Densitometer (Bedford, MA). In our DXA unit, the least significant change at the 95% level is 3.2% at the spine and 2.5% at the femur.

Different immunomodulators were administered: Interferon beta-1a in 70%, Interferon beta-1b in 27% and Glatiramer in 3%. High-dose pulse steroid therapy (intravenous methylprednisolone 500 mg) was given to 81% ranging from one course to 17 courses. The mean age was age 38.8 \pm 8.9 years, the mean duration of MS was 5.8 \pm 3.7 years; the mean number of relapses was 4.0 \pm 0.7; and the mean disability score (EDSS) was 3.1 \pm 1.9. Both mean BMD Z-score at spine of 0.53 (CI: 0.15-0.92; p<0.001) and mean BMD Z-score at femur of 0.72 (CI: 0.42-1.01; p<0.0001) were significantly greater than zero.

A follow-up survey after nearly 4 years of continuous immunomodulatory therapy is now being conducted. BMD is being remeasured. In addition, biochemical studies are being performed including: vitamin D status; parathyroid status; and bone turnover markers (serum bone specific alkaline phosphatase, intact osteocalcin, procollagen type I aminopeptide, beta-carboxyterminal telopeptide of type I collagen; and, urine aminoterminal telopeptide of type I collagen, and deoxypyridinoline crosslinks). Preliminary analysis of DXA in 7 subjects shows no change in BMD at the spine (1.046 \pm 0.16 g/cm² vs 1.051 \pm g/cm²; p=0.58) and at the femur (1.024 \pm 0.20 g/cm² vs 1.02 \pm 0.20 g/cm²; p=0.46).

In conclusion, immunomodulatory therapy in MS does not appear to have an adverse effect on bone.

Disclosures: M.J. McKenna, None.

W438

Prevalence of Radiographic Osteoarthritis of Knee and Lumbar Spine and Its Association with Pain: The Research on Osteoarthritis Against Disability (ROAD) Study. S. Muraki¹, N. Yoshimura¹, H. Oka^{*1}, A. Mabuchi^{*1}, Y. En-yo^{*2}, M. Yoshida^{*2}, T. Suzuki³, H. Yoshida³, H. Ishibashi^{*3}, S. Yamamoto³, H. Kawaguchi¹, K. Nakamura¹. ¹22nd Century Medical Ctr., Univ. of Tokyo, Tokyo, Japan, ²Wakayama Medical Univ., Wakayama, Japan, ³Tokyo Metropolitan Institute of Gerontology, Tokyo, Japan.

Although osteoarthritis (OA) of knee and lumbar spine is a major cause of disability in the elderly, few epidemiologic studies have been performed. We established a large-scale nationwide clinical study called ROAD (Research on Osteoarthritis Against Disability) in 2005, and created a comprehensive and systemic database including clinical and genetic information in three cohorts of urban, mountainous and seacoast areas. We recruited 3,040 participants in total, from which 2,288 subjects older than 60 years (818 men & 1,470 women; mean age=74.3 yrs.) were enrolled for investigation of the prevalence of radiographic OA of knee and lumbar spine, as well as its association with the respective local pain. The radiographic severity of OA was determined according to the Kellgren/Lawrence (KL) grade (0-4) at femoral-tibial joints of bilateral knees and at intervertebral spaces from L1/2 to L5/S1 of the lumbar spine. Prevalence of radiographic OA (KL> or = 2) in either knee joint was 47.0% in men and 70.2% in women, while that in either intervertebral space was 84.1% in men and 70.7% in women. Prevalence of radiographic knee OA was higher in the female sex (odds ratio [OR]=3.28, 95% confidential interval [CI]=2.71-3.97) and mountainous residents (OR=1.62, 95%CI=1.44-1.83 compared to urban residents), whereas that of lumbar OA was higher in the male sex (OR=2.06, 95%CI=1.63-2.61) and urban residents (OR=1.43, 95%CI=1.13-1.83 compared to mountainous residents). We next compared the association between radiographic severity and local pain by logistic regression analysis after adjustment for age and BMI. The radiographic severity of knee OA was positively associated with knee pain (OR=6.7, 95%CI=4.10-11.2 in men; OR=4.3, 95%CI=3.07-6.02 in women; for KL3/4 compared to KL0/1), while that of lumbar OA was weakly associated with low back pain at all spaces in women (OR=1.6-2.1 for KL3/4 compared to KL0/1), but not in men. The initial investigation in the ROAD study using the baseline data revealed a high prevalence of radiographic OA in knee and lumbar spine among elderly people, and found that gender and community differences were distinctly associated with the knee and lumbar OA. Furthermore, the radiographic knee OA showed a strong association with knee pain in both genders. Contrarily, the radiographic lumbar OA had a moderate association with low back pain only in women. With the progress of the ROAD study, the underlying environmental and genetic backgrounds will be elucidated.

Disclosures: S. Muraki, None.

W439

Treatment with Anti-TNF- α Antibody Recovers Osteoclast Maturation Deviated from Bone Remodeling Cycle in RA Joint Destruction. M. Nawata^{*}, Y. Okada^{*}, K. Saito^{*}, Y. Tanaka^{*}. The First Department of Internal Medicine, School of Medicine, University of Occupational and Environmental Health, Japan, Kitakyusyu, Japan.

Rheumatoid arthritis (RA) is characterized by inflammatory synovitis, erosive arthritis and joint destruction. Recent evidence indicates that TNF- α plays a pathological role in joint destruction and that infliximab (anti-TNF- α antibody) provides significant protection against the destructive process, even in patients who show no clinical improvement, suggesting the dissociation of these two disease processes. However, the mechanism of bone destruction in RA remains unknown. Here we assessed bone metabolism in RA patients before and after infliximab treatment. RA patients (n=100, mean age, 53.6 \pm 12.1 years, \pm SD) were treated with either methotrexate (MTX) or infliximab+MTX. We evaluated DAS (Disease Activity Score)-28, bone metabolism markers and bone mineral density (BMD) at 0, 6, 12 and 24 months after treatment. At enrollment, BMD was within the normal aged-adjusted level (L2-4; 0.89 \pm 0.18 g/cm², left hip; 0.67 \pm 0.14 g/cm²), as was serum bone alkaline phosphatase (BAP; 26.9 \pm 10.5 U/l), a bone formation marker, but urinary crosslinked N-telopeptide of type I collagen (u-NTx), a bone resorption marker, was notably high (76.4 \pm 37.7 nmol/mmol CRE). Treatment with infliximab resulted in the following: i) No change in BMD for 2 years (L2-4 BMD 0.90 \pm 0.22, left hip 0.68 \pm 0.11 g/cm²). ii) Decrease in u-NTx to 61.3 \pm 32.1 (p<0.05), 48.8 \pm 27.0 (p<0.01) and 42.3 \pm 18.3 nmol/mmol CRE (p<0.01) at 6, 12 and 24 months, respectively. iii) Increase in BAP to 31.6 \pm 11.5 (p<0.05), 31.9 \pm 11.7 (p<0.05) and 29.2 \pm 11.2 U/l at 6, 12 and 24 months, respectively. iv) These changes were independent of the dose of steroids or disease activity. v) Improvement of bone erosion was noticeable on the joint X-p after 24 months. BAP and u-NTx did not change in patients treated with MTX alone. Bone metabolism is normally maintained by bone remodeling, bone resorption by osteoclast and formation by osteoblasts, respectively. In contrast, we here propose that joint destruction in RA is induced by osteoclast maturation in "deviation" from the remodeling cycle in a TNF-dependent manner, based on the followings: i) increase in u-NTx with normal BMD and BAP levels, ii) TNF- α and/or sRANKL induce osteoclast maturation in the absence of osteoblasts in RA synovium, iii) joint erosion is observed within 10 weeks in TNF- α transgenic mice. Furthermore, infliximab treatment allowed recovery from the "deviation" into the remodeling cycle as evident by the decrease in u-NTx and increase in BAP. These results imply the dissociated efficacy of infliximab for joint destruction from clinical improvement, which leads to repair of RA bone erosion.

Disclosures: M. Nawata, None.

W440

Evaluation of the Bone Mineral Density and Body Composition in Early Rheumatoid Arthritis - The Osteoporosis and Early Rheumatoid Arthritis (OPERA) Study. A. C. Azevedo^{*1}, M. M. Pinheiro¹, K. S. Sarkis^{*2}, E. T. Reis Neto^{*1}, L. A. Martini², V. L. Szejnfeld¹. ¹Rheumatology, Unifesp, Escola Paulista de Medicina, Sao Paulo, Brazil, ²Nutrition, Faculdade de Saude Publica, Universidade de Sao Paulo, Sao Paulo, Brazil.

BACKGROUND: Traditional and not traditional risk factors for osteoporotic fractures have been described in patients with rheumatoid arthritis (RA), like menopause, smoking, glucocorticoids, immobilization and bone mineral density (BMD). Recently, some authors have showed that aspects related to body composition could also be associated with bone loss. **OBJECTIVES:** To evaluate bone mineral density (BMD) and body composition in patients with early rheumatoid arthritis (ERA) before and after the treatment. **PATIENTS AND METHODS:** Thirty-two RA patients (ACR, 1987) with time of symptoms less 15 months and without previous treatment with DMARDs (disease-modifying anti-rheumatic drugs) were enrolled in this study. Patients using medications that interfered on bone mass were excluded. Details on lifestyle, demographic data, fractures, dietary intake, physical activity, quality of life were evaluated by a specific questionnaire. Disease's characteristics and activity (DAS28) and current treatment of RA were also evaluated. Moreover, it was applied SF-36 and HAQ (Health Assessment Questionnaire). All the patients underwent bone densitometry (spine and femur BMD) by DXA (GE-Lunar, DPX MD+). Body composition was measured by DXA (lean, fat and bone mass). Descriptive statistical analysis, chi-squared test and logistic regression were used. $P < 0.05$ was adopted. After 12 months, the questionnaires and DXA measurements were repeated. **RESULTS:** Mean age and BMI were 43.4 ± 11.8 years and 24.7 ± 6.5 kg/m², respectively. Women were 26 (83.9%) and mixed race were 13 (41.9%). At baseline, disease duration, DAS28 and HAQ was 7.97 ± 4.5 months, 5.41 ± 1.45 and 0.896 ± 0.605 , respectively. Corticosteroids were referred by 21 patients (67.7%) with mean dosage 7 ± 8.9 mg/day. Spine and total femur BMD was 1.068 ± 0.15 and 0.987 ± 0.12 g/cm², respectively. Total and skeletal lean mass was 37.180 ± 6.4 kg and 6.34 ± 0.9 kg/m², respectively. Fat mass was $36.8 \pm 6.9\%$. After 12 months of follow-up, we did not verify significant bone or lean loss. On the other hand, there were significant reduction of the disease's activity and significant increase of functional ability and fat mass. **CONCLUSIONS:** We observed low prevalence of osteopenia/osteoporosis and sarcopenia in patients with ERA at baseline. Although the patients were considered as euthrophic by BMI, there was higher percentage of fat mass than lean mass between 2 visits. Thus, our data suggest that health interventions may emphasize more prevention of fat mass increase than lean or bone mass loss in ERA patients.

Disclosures: M.M. Pinheiro, None.

W441

Bone Metabolism in an Animal Model of Ankylosing Spondylitis. M. Rauner^{*1}, D. Stupphann^{*1}, J. Patsch^{*1}, M. Haas^{*2}, M. Breban^{*3}, I. Fert^{*3}, S. Glatigny^{*3}, P. Pietschmann¹. ¹Institute of Pathophysiology, Medical University of Vienna, Vienna, Austria, ²Department of Internal Medicine III, Medical University of Vienna, Vienna, Austria, ³Institut Cochin, Hôpital Cochin, Paris, France.

Ankylosing Spondylitis (AS) is a chronic inflammatory disease characterized by the main involvement of axial joints and bilateral sacroiliitis. Besides the formation of new bone leading to syndesmophytes and ankylosis, osteoporosis is a reported feature as well. Thus, AS raises the paradox of new bone formation at sites of inflammation and the association of reduced bone mass and high fracture risk. The major histocompatibility complex class I allele HLA-B27 has been found to be strongly associated with AS. HLA-B27 transgenic (tg) rats spontaneously develop a multisystemic disease with the appearance of spondylitis and syndesmophytes. However, there is no information about bone metabolism in this animal model. Hence, the aim of our study was to investigate the suitability of the HLA-B27 tg rat as a model for the bone-related alteration in AS. Therefore, bone histomorphometry was conducted for the femur, tibia and fourth vertebral body from six control rats, six healthy HLA-B27 tg rats and six HLA-B27 tg rats exhibiting the phenotype of spondyloarthropathies. Each group consisted of two male and four female rats aged between seven and ten months. Sections, stained with Goldner's trichrome, were analyzed using the Osteomeasure Software (Osteometrics, USA). Femur, tibia and the fourth vertebral body of the diseased HLA-B27 tg rats exhibited a significant reduction of bone volume over total volume compared with control rats and healthy tg rats. Moreover, trabecular thickness and trabecular number of the diseased rats were significantly reduced. The trabecular separation was significantly increased. The number of osteoblasts and osteoid volume did not show any alterations, however, the number of osteoblasts as well as osteoid volume were higher in femur and tibia than in the vertebral body. Osteoclasts tended to be more abundant in the diseased HLA-B27 tg rats. The decrease in bone volume, trabecular number and thickness as well as the increase of trabecular separation in the diseased HLA-B27 tg rats indicate an enhanced bone resorption, possibly mediated by the increased number of osteoclasts. Moreover, the indices of osteoid volume show, that the mineralization process in the diseased rats was not disturbed. Our results demonstrate that HLA-B27 tg rats is an appropriate model for the study of bone loss in AS. In further experiments, we will analyze markers of bone formation and resorption in the serum and bone of HLA-B27 tg rats to assess bone turnover on a systemic level.

Disclosures: M. Rauner, None.

W442

Osteoporosis and Rheumatoid Arthritis, Which Nutritional Factors Are Associated? K. S. Sarkis^{*1}, R. G. Silva^{*2}, C. F. Zerbin^{*2}, M. M. Pinheiro³, L. A. Martini¹. ¹Nutrition, Universidade de Sao Paulo, Sao Paulo, Brazil, ²School of Medicine, Universidade de Sao Paulo, Sao Paulo, Brazil, ³Reumatology, UNIFESP, Sao Paulo, Brazil.

The aim of this study was investigate the association between diet, body composition and Bone Mineral Density (BMD) in women with Rheumatoid Arthritis (RA). This is a cross-sectional study performed at RA outpatient clinic and included forty-five (45) patients who fulfilled the ACR criteria for RA and agreed to participate. Mean age was 55 ± 10 y and the mean duration of disease was 7.5 ± 5.6 y. The patients were divided in two groups according to BMD status: group 1 - normal BMD ($n=24$); group 2 - patients with osteoporosis ($n=21$) (WHO 1994). Standardized questionnaires were used to ascertain demographic characteristics, medical history and use of oral glucocorticosteroids. Functional status was assessed using the Health Assessment Questionnaire (HAQ) score and the disease activity by the Disease Activity Score (DAS28). A validated food frequency questionnaire was used to assess the dietary intake. Mean daily intake, including total energy (kcal/day) and all others macronutrients, calcium, phosphorus and vitamin D was calculated and adjusted for energy. Percentage Body Fat (%BF), Total Fat Free Mass (TFFM), Appendicular Lean Mass (ALM), Relative Skeletal Muscle Index (REMI) and BMD was measured at the total femoral, femoral neck and lumbar spine (L1-L4) in g/cm² by using DXA (GE Lunar Radiation Corporation, DPX IQ, Madison, WI, USA). Statistical analysis included Student T test, Pearson correlation and multiple linear regression. BMD was considered dependent variable. Significance was adopted as $p < 0.05$. There were no significant difference in HAQ, DAS 28 and use of oral glucocorticosteroids between groups. Also no differences were observed in total energy, protein, carbohydrate, calcium, phosphorus and vitamin D intake. However both groups presented mean calcium and vitamin D intake lower than recommended values (597.3 ± 281.7 mg/day vs 692.2 ± 217.1 mg/day and 60.7 ± 56.9 vs 88.1 ± 89.6 UI/day, group 1 and 2 for calcium and vitamin D, respectively). Patients with lumbar or femoral osteoporosis were significantly older ($p < 0.01$), had a lower %BF ($p < 0.05$), FFM ($p < 0.01$), ALM ($p < 0.01$), RSMI ($p < 0.01$), longer disease duration ($p < 0.05$) and a higher lipid intake ($p < 0.05$). In the regression linear model, being older with more than 7.5 years with AR, lower %BF, fat free mass, appendicular lean mass together with higher lipid intake, were negatively associated with BMD [Femoral total = $0.637 - 0.008$ (age) - 0.009 (disease duration) + 0.073 (RSMI) + 0.006 (%BF), with $R^2=66.8$; $p < 0.001$]. The present study indicated two important modifiable factors that could improve BMD in patients with RA; the body composition and a reduction in fat intake.

Disclosures: K.S. Sarkis, None.

W443

Vitamin D Receptor Deficiency Aggravates TNF-Mediated Arthritis. K. Polzer^{*1}, J. Zwerina^{*1}, K. Redlich^{*2}, J. Smolen^{*2}, G. Schett^{*1}. ¹University of Erlangen-Nuremberg, Erlangen, Germany, ²Medical University of Vienna, Vienna, Austria.

Background: Vitamin D is an important hormone for calcium homeostasis and bone metabolism and may have immunomodulatory effects. The aim of this study was to investigate the role of the Vitamin D Receptors (VDR) in inflammatory arthritis.

Methods: To determine the role of the Vitamin D in TNF-mediated joint disease, we crossed mice deficient for the VDR with arthritic human TNF transgenic (hTNFtg) mice. Offsprings were analysed for clinical signs of arthritis as well as the histological degree of synovitis, cartilage damage and bone erosion. Systemic mineral bone density was evaluated by bone histomorphometry. Furthermore, serum levels of cytokines and other inflammatory mediators were determined by ELISA.

Results: hTNFtg mice with VDR deficiency showed pronounced weight loss, increased paw swelling and decreased grip strength compared to hTNFtg mice. In addition, VDR-/-hTNFtg mice showed lower bone mineral density compared to hTNFtg mice. In line, serum levels of TNF were significantly increased in VDR-/-hTNFtg mice compared to hTNFtg mice. Consequently, histological analysis showed an increase in synovial inflammation in VDR-/-hTNFtg mice compared to hTNFtg mice. The VDR-/-hTNFtg mice showed a dramatic increase in osteoclast number compared to hTNFtg mice, accompanied with strengthened bone erosions in the joints. These data were verified in osteoclast assays of the four genotypes in vitro. Cartilage proteoglycan loss was also enhanced in VDR-/-hTNFtg mice compared to hTNFtg mice.

Conclusion: These findings suggest that deficiency of the VDR leads to an increase in inflammation, cartilage destruction and bone erosion with enhanced recruitment of osteoclasts. This leads to the assumption that additional treatment with active metabolites of Vitamin D may have potentially positive effects as an additive therapy in RA.

Disclosures: G. Schett, None.

W444

Bone Microarchitecture as Assessed by High Resolution Peripheral Quantitative CT (HRpQCT) in HIV+ Postmenopausal Women. A. D. Shu^{*1}, M. T. Yin¹, D. J. McMahon^{*1}, S. Cabral^{*1}, H. Eisenberg^{*1}, D. Ferris^{*2}, E. Shane¹. ¹Columbia University, NY, NY, USA, ²Bronx-Lebanon, Bronx, NY, USA.

As a result of effective antiretroviral therapy (ART), more HIV+ women are surviving beyond menopause and are at increased risk for osteoporosis (OP). We previously reported lower BMD but similar rates of bone loss in HIV+ PM Hispanic women compared to HIV-controls. There are no studies on bone microarchitecture and limited fracture data in HIV+ individuals. We hypothesized that lower BMD in HIV+ women is associated with microarchitectural deterioration. Xtreme CT (Scanco Medical AG) is a new HRpQCT system with sufficiently high resolution (<100µm) to permit in vivo assessment of trabecular (Tb) architecture at the radius (RAD) and tibia (TIB). DXA and HRpQCT were performed in 32 HIV+ (75% on ART) and 38 HIV- Hispanic and African American PM women from outpatient clinics, excluding women with known OP, metabolic bone disease and serum Cr >2.5 mg/dL. HIV+ and HIV- groups were similar with regard to age (mean 60 y), prevalence of hypertension, diabetes, thyroid disease, and use of HRT, glucocorticoids and antiepileptics. HIV+ women were more likely to use tobacco. BMI was higher in HIV- women (31 v 28, p = 0.04). In contrast to our previous findings in Hispanics, mean BMD did not differ at any site. Similarly, HRpQCT measurements of 13 cortical (Cort) or Tb microstructural parameters did not differ between groups (Table). Analyses stratified by HIV status and race and adjusted for covariates of age, BMI and tobacco use were compared by repeated measures ANCOVA. No differences between HIV and race-defined groups were observed at the TIB. At the RAD, Hispanics had higher D100 (average bone density) (p<0.003) and Cort thickness (p<0.03); however, HIV status was not associated with any differences. In summary, DXA and HRpQCT parameters did not differ between HIV+ and HIV- PM women. The groups may be similar because the controls are drawn from a clinic population and many have chronic illnesses common in older minority women. The similarities in microarchitecture may also explain why retrospective studies of HIV+ patients on ART have not found that fracture rates are higher than expected.

Table: Mean HRpQCT and DXA values (± SD) with reference values^{*}

	Study		p-value	Reference values		
	HIV+ N = 32	HIV- N = 38		PreM [†]	LBM [†]	OP [†]
DXA hip BMD (g/cm ³)	0.852 (0.17)	0.901 (0.12)	0.17	0.942	0.820	0.637
RAD Bone vol/Total vol (%)	9.5 (3.1)	9.2 (2.9)	0.71	13.4	10.3	8.5
Tb number (1/mm)	1.6 (0.4)	1.6 (0.4)	0.70	1.7	1.4	1.3
Tb thickness (µm)	58 (13)	58 (13)	0.86	78	71	63
Cort thickness (µm)	699 (178)	731 (219)	0.51	804	571	487
TIB Bone vol/Total vol (%)	10.5 (3.4)	10.2 (2.6)	0.68	14.1	11.4	9.7
Tb number (1/mm)	1.5 (0.4)	1.4 (0.3)	0.17	1.6	1.4	1.3
Tb thickness (µm)	67 (15)	72 (16)	0.21	89	82	77
Cort thickness (µm)	979 (242)	1056 (234)	0.18	1232	882	722

^{*} DXA reference NHANES/Hologic. HRpQCT reference in Caucasian women from Boutroy et al. JCEM 90:6508-6515. [†]PreM, premenopausal or T ≥ 1.0; LBM, low bone mass or T-score < 1.0; OP, T-score ≤ -2.5.

Disclosures: A.D. Shu, None.

This study received funding from: R01A1065200.

W445

OPG Prevents Osteopenia in Arthritic Rats Via Different Mechanisms than Bisphosphonate Therapy. M. Stolina, D. Dwyer^{*}, S. Middleton^{*}, S. Adamu^{*}, M. S. Ominsky, D. Zack^{*}, P. J. Kostenuik. Amgen Inc., Thousand Oaks, CA, USA.

RANKL was recently suggested to be a mediator of systemic bone loss in arthritic rats (Stolina et al, JBMR 2005). The catabolic effects of RANKL are inhibited by osteoprotegerin (OPG), and the RANKL:OPG ratio may be an important determinant of bone resorption. Skeletal catabolism can also be prevented by bisphosphonates, which can exert modest changes in OPG levels in patients and in osteoblast cultures. However, local and systemic changes to the RANKL:OPG ratio have not been described with BP treatment in an osteopenia model. We therefore compared the effects of OPG versus zoledronic acid (ZA) on serum and bone proteins and BMD in a rat arthritis model.

Adjuvant arthritis (AIA) was induced in rats by heat-killed mycobacteria. AIA rats were treated with human OPG-Fc (1 mg/kg), ZA (0.1 mg/kg), or PBS (Veh) at the clinical onset of arthritis (day 0), day 3, and day 6. Non-arthritic (NA) controls were treated with Veh. BMD was assessed at the lumbar vertebrae (LV) by DXA on day 9 when serum was collected and total protein was extracted from LV for evaluation of OPG, RANKL, and the resorption marker TRAP-5b.

AIA-Veh rats had lower LV BMD compared to NA controls (P < 0.05). Histology showed no evidence of inflammation in the LV of AIA-Veh rats, so osteopenia may have been related to an 80% increase in serum RANKL (P < 0.05 vs NA controls). Osteopenia was fully prevented by OPG or ZA treatment. Whereas OPG treatment prevented the AIA-related increase in serum RANKL, ZA treatment led to a further non-significant RANKL increase (vs AIA-Veh) and had no effect on serum OPG levels. The serum RANKL:OPG ratio was markedly reduced by OPG treatment (P < 0.05, vs AIA-Veh), and non-significantly increased by ZA (vs AIA-Veh). Serum TRAP-5b was significantly reduced by both treatments (P < 0.05 vs. AIA-Veh), more so with OPG (P < 0.05 vs ZA). The RANKL:OPG ratio in LV protein extracts was significantly increased in AIA-Veh rats (P < 0.05 vs NA controls). This increase was primarily related to local suppression of OPG.

OPG treatment significantly reduced LV RANKL, whereas ZA caused a 2-fold increase in LV RANKL (P < 0.05 vs AIA-Veh). OPG treatment markedly increased LV OPG levels, while ZA caused a modest reduction in LV OPG (vs AIA-Veh). The RANKL:OPG ratio was thereby reduced with OPG treatment, while ZA led to a 5-fold increase (both P < 0.05 vs AIA-Veh). LV TRAP-5b was significantly reduced by both treatments, to a greater extent with OPG (P < 0.05 vs ZA).

In summary, two potent agents of different therapeutic classes fully prevented systemic bone loss in arthritic rats. RANKL inhibition by OPG reduced the RANKL:OPG ratio in bone whereas ZA increased this ratio, highlighting the different mechanisms of action of these therapeutics.

Disclosures: M. Stolina, Amgen Inc. 1, 3.

This study received funding from: Amgen, Inc.

W446

Increased Expression of Receptor Activator of NF-kappaB Ligand (RANKL) in Stimulated T-cells from Patients with Ankylosing Spondylitis.

D. Stupphann^{*1}, M. Rauner^{*1}, D. Krenbek^{*1}, J. Patsch^{*1}, T. Pirker^{*2}, C. Muschitz^{*2}, H. Resch^{*2}, P. Pietschmann¹. ¹Medical University of Vienna, Vienna, Austria, ²St. Vincent Hospital, Medical Department II, Vienna, Austria.

Ankylosing spondylitis (AS) is a chronic, disabling rheumatic disease, which initially mainly involves the sacroiliac joints and in later stages affects the vertebral column. Besides new bone formation leading to syndesmophytes and ankylosis, osteoporosis is a reported feature as well. Based on the hypothesis, that activated T cells are the major source of RANKL in inflammatory bone-resorptive diseases, we investigated the presence of intracellular (ic) and membrane bound (mb) RANKL on activated T cells from patients with ankylosing spondylitis (AS). Further we determined their relationship to bone mineral density (BMD), disease activity and bone metabolism markers. T-cell surface and intracellular expression of RANKL was analyzed by flow cytometry. BMD at the lumbar spine and total hip was measured by dual-energy x-ray absorptiometry (DXA) and quantitative computed tomography (QCT). Serum OPG levels were determined by ELISA. Expression of icRANKL was statistically significantly increased in patients with AS compared to the healthy volunteers (p < 0.05). In contrast expression of mbRANKL was significantly lower in the group of patients compared to the controls (p < 0.01). The cytokine expression was not associated with bone loss that was found with DXA at the total hip in 45% of all cases, and with QCT at the lumbar spine in 48 % of all cases. Spinal BMD values measured by QCT were positively correlated with age (r = - 0.630; p = 0.003) and negatively correlated with serum OPG levels (r = - 0.571; p = 0.025). We conclude that intracellular RANKL in T cells is overexpressed in patients with AS, indicating that these cells may act as a storage for soluble RANKL which rapidly can be mobilized and secreted into the circulatory system after an inflammatory stimulus. In contrast, the expression of mbRANKL is significantly decreased in the AS patients, that might be due to a different activity or prevalence of the enzymes, responsible for the ectodomain shedding of RANKL.

Disclosures: D. Stupphann, None.

W447

Advanced Glycation-end-products Induce Vascular Calcification Through the RAGE/p38 MAPK Signaling Pathway. T. Tanikawa, R. Tanikawa, Y. Okada, Y. Tanaka.

First Department of Internal Medicine, University of Occupational and Environmental Health, Japan, Kitakyushu, Japan.

Mönckeberg's calcification in type 2 diabetes, known as medial artery calcification is a strong independent predictor of cardiovascular mortality. However, the mechanism of vascular calcification in diabetes remains to be elucidated. Advanced glycation-end-products (AGEs), long-term products of the Maillard reaction, are formed at an accelerated rate in diabetes. They are thought to contribute to the development of diabetic complications, including atherosclerosis and microvascular diseases. In our in vitro studies, AGEs induced calcification of cultured vascular smooth muscle cells by von kossa staining and also induced the expression of Runx2 mRNA by RT-PCR, known as a transcription factor in osteoblast differentiation. Furthermore, AGEs increased alkaline phosphatase (ALP) activity and osteocalcin secretion, two osteoblast differentiation markers. Finally, AGEs induced phosphorylation of p38 MAPK and the phosphorylation was inhibited by anti-RAGE blocking antibody, which was assayed by western blotting. Increased ALP activity was inhibited by a p38 MAPK inhibitor. Our findings indicate that AGEs induce vascular calcification by osteoblast-like differentiation of smooth muscle cells and through the RAGE/p38 MAPK signaling pathway and suggest that inhibition of the AGE/RAGE pathway could be potentially effective therapeutically for prevention of vascular calcification in diabetic patients.

Disclosures: T. Tanikawa, None.

W448

Type 2 Diabetic Patients with Charcot Arthropathy Display Reduced Calcaneal Stiffness Despite Normal Foot BMD. K. A. Witzke¹, H. K. Parson^{*2}, A. I. Vinik^{*2}, ¹Kinesiology, California State University, San Marcos, San Marcos, CA, USA, ²Internal Medicine, Eastern Virginia Medical School, Norfolk, VA, USA.

Because bone is innervated it is subject to degradation when the nerves that innervate it lose their function. Charcot neuroarthropathy is a complication of diabetes associated with severe nerve dysfunction that often leads to unusual fractures that collapse the ankle and/or midfoot. These fractures may be caused by declines in bone mineral density (BMD), although BMD of the feet is not a common evaluation site. We believe that Charcot probably compromises the quality of bone, specifically its microarchitecture, crystallinity, and collagen properties, and these changes may not be completely explained by BMD alone. Calcaneal stiffness, measured by Quantitative Ultrasound (QUS), is a simple method of determining the stiffness of bone, an important biomechanical property related to bone quality and fracture. The purpose of this preliminary study was to determine if poor nerve function is related to reduced calcaneal stiffness and/or reduced BMD of the feet, and whether type 2 diabetics with Charcot display significantly different bone stiffness and BMD than either controls or type 2 diabetics without Charcot. We measured BMD of the whole body, hips, and feet (BMD, GE Lunar Prodigy), Calcaneal stiffness (QUS, GE Achilles Express), peroneal nerve conduction velocity (NCV), vibration detection threshold (VDT), and pressure perception (PRES), in 56 male subjects (n=22 controls; n=31 type 2 diabetic; n=3 diabetic patients with Charcot) aged 56.1 +/- 8.4 y. Diabetics averaged 127.4 +/- 80.4 months of diabetes. As expected, all nerve function measures were significantly worse in Charcot patients than the other two groups. For bone measures, Charcot patients displayed significantly lower calcaneal stiffness but similar BMD measures at all sites including the feet, compared to the diabetic and control groups. This may suggest a direct relationship between motor nerve dysfunction and the structural properties of bone in Charcot neuroarthropathy. Although the Charcot patients in this study were fairly homogeneous, these assumptions need to be tested in more patients, and a more direct measure of bone collagen would also be useful.

Nerve Function, Bone Density, and Stiffness Across Groups [mean (SD)]			
	Control (n=22)	Diabetic (n=31)	Charcot (n=3)
Foot BMD (g/cm ²)	0.757 (0.084)	0.790 (0.111)	0.786 (0.053)
QUS (Stiffness Index)	106.0 (15.2)	104.5 (18.9)	79.7 (19.5) *
VDT (u)	2.99 (0.33)	3.09 (0.39)	5.00 (1.48) *
PRES (g)	5.40 (2.25)	7.34 (5.92)	18.97 (13.29) *
NCV (m/s)	12.13 (2.19)	12.78 (3.00)	7.95 (9.12) *

* p < 0.05 for Charcot compared to Control and Diabetic

Disclosures: K.A. Witzke, None.

This study received funding from: Commonwealth Health Research Board.

W449

Morphological Texture Analysis of Radiographs of the Proximal Femur: In Vitro Study Using Biomechanical Strength as a Standard of Reference. M. B. Huber^{*1}, J. Carballido-Gamio^{*1}, K. Fritscher^{*2}, R. Schubert^{*2}, M. Haenni^{*3}, C. Hengge^{*4}, S. Majumdar^{*1}, T. M. Link^{*1}. ¹University of California, San Francisco, San Francisco, CA, USA, ²University of Health Sciences, Medical Informatics and Technology, Innsbruck, Austria, ³AO Development Institute, Davos Platz, Switzerland, ⁴Medical University Innsbruck, Innsbruck, Austria.

Texture analysis of femur radiographs may serve as a potential low cost technique to predict osteoporotic fracture risk and has received considerable attention in the last years. The goal of this in vitro study was to use automatically placed regions of interest (ROI) and morphological texture analysis methods in radiographs of proximal femur specimens to investigate their biomechanical strength.

Radiographs were obtained from 14 femoral specimens and bone mineral density (BMD) was measured in the femoral neck. Biomechanical testing in terms of failure load (FL), breakaway torque (BT) and number of cycles (NC) was performed. Five ROIs were placed automatically in the head, upper and lower neck, trochanteric and intertrochanteric compartment. In each ROI, we obtained isotropic and anisotropic morphological gradients (MG) and Minkowski Dimensions (MD), and three Minkowski Functionals [Area (MFA), Perimeter (MFP), Euler number (MFE)] and calculated coefficient of determination with parameters of biomechanical strength. In a stepwise multiregression analysis, we identified the most predictive parameters in different models.

A moderate correlation between neck BMD and FL of $R^2=0.40$ ($p<0.05$) was found and a high correlation $R^2=0.78$ ($p<0.01$) between BMD and BT. For isotropic MG-filters, correlations with FL up to $R^2=0.64$ ($p<0.001$) and with BMD, BT and NC up to $R^2=0.62$ were found. Using anisotropic MGs even higher correlations were obtained ($R^2=0.70$) for FL and NC, but no significant correlations were found with BMD. Correlations between MDs and FL were in the range $R^2=0.37$ - 0.61 *. MFA and MFP correlated significantly with FL and NC ($R^2=0.55$), and were independent of BMD. All these correlations were based on femoral head and lower neck ROIs. Our multiregression analysis showed, that BMD was not able to improve the prediction of FL using a model with three MGs ($R^2=0.85$). The model testing all parameters resulted in a high prediction of $R^2=0.97$ and included MGs, MD and MFP, however, not BMD. In conclusion morphological texture features were highly correlated with biomechanical strength and were partially independent from BMD. We showed that femoral head and lower neck ROI were best suited to estimate bone strength. Morphological information contained in trabecular bone structure visualized on radiographs may provide osteoporotic fracture risk prediction as a low-cost modality.

Disclosures: M.B. Huber, None.

This study received funding from: AO Foundation.

W450

Micro-architectural Changes of Developing Bone in Male and Female Rats. R. J. Arends^{*1}, M. V. Beuningen - Vaan^{*1}, M. V. Boven - Nunen^{*1}, M. T. Brok - Bardoel^{*1}, D. V. Dobbela^{*2}, G. B. Janssen^{*2}, T. V. Klundert^{*1}, P. E. Langerwerf^{*1}, T. J. Robben^{*1}, M. G. Scheepers^{*1}, J. V. Vliet^{*2}, A. G. Ederveen^{*1}. ¹Pharmacology, N.V. Organon, Oss, The Netherlands, ²Toxicology & Drug Disposition, N.V. Organon, Schaijk, The Netherlands.

MicroCT measurements are extensively applied in pre-clinical research on bone and are well validated to study micro architecture in adult and aged animals. However, the number of studies on the growing skeleton is limited. In this report, we have combined the metaphyseal trabecular bone and mid-diaphyseal bone μ CT data of a number control groups of male and female Wistar rats at the age of 5, 8, 11 and 14 weeks to obtain a reference dataset of μ CT parameters in growing animals.

From week 5 to 14 bodyweight increased from 107 to 424 gram in male and from 97-228 in female rats. Cortical BMD decreased rapidly between 5 and 8 weeks in males (1441 to 1148 mg/cm³) and in females (1459 to 1187) and thereafter remained constant until week 14. Moreover, between week 5 and 14 cortical thickness increased gradually; more in males (0.30 to 0.6 mm) than in females (0.31-0.51 mm). As a result of this, polar moment of inertia increased; more pronounced in males (4.2 to 19.6 mm⁴) than in females (3.6 to 8.4).

Trabecular BMD gradually decreased between week 5 and 14 in males (283-239 mg/cm³), however it increased in females (321-378). BV/TV increased steadily in females from 26.7 to 52.8% between 5 and 14 weeks and only slightly in males (24.8-31.8). Trabecular number decreased rapidly between 5 and 8 weeks in both males and females (3.1 to 1.8 1/mm and 3.3 to 2.7 1/mm, resp.) and this was accompanied by an increase in trabecular thickness (0.079 to 0.170 mm in males, 0.082 to 0.190 in females). As a net effect of these changes, trabecular separation strongly increased between 5 and 14 weeks in males (0.19-0.54 mm) and only slightly in female rats (0.18-0.23). Between 5 and 14 weeks, the degree of anisotropy decreased gradually in both males (3.29 to 2.15) and females (3.04 to 1.80), furthermore a modest decrease in structure model index was detected in males (1.49-1.12), while in females a strong decrease was measured (1.38-0.31).

In conclusion, the cortical femur is still growing in both sexes up to 14 weeks of age; males grow more than females. In femur of growing male rats, cortical thickness and diameter are the major parameters that determine bone strength as is predicted by a high polar moment of inertia. However, the cancellous compartment showed a different profile. In female rats, during skeletal growth trabecular bone volume and trabecular thickness increase in the femur, resulting in a gain of trabecular bone and an architectural change from a rod like structure to a more plate like structure, whereas in males trabecular bone is partially lost before it reaches a plateau phase.

Disclosures: R.J. Arends, N.V. Organon 3.

W451

Correlation Between the Mechanical Properties of Trabecular Bone Assessed by Finite Element Analysis and Experimental Test. Y. Won¹, B. Min^{*2}, Y. Chung³, M. Baek^{*1}, W. Cui^{*1}, M. Hahn^{*4}. ¹Orthopaedics, Ajou University School of Medicine, Suwon, Republic of Korea, ²Orthopaedics, Keimyung University School of Medicine, Daegu, Republic of Korea, ³Endocrinology and Metabolism, Ajou University School of Medicine, Suwon, Republic of Korea, ⁴Orthopaedics, Kwandong University School of Medicine, Gangneung, Republic of Korea.

Introduction: Following development of imaging technology, image-based finite element analysis has been commonly used to assess the mechanical properties of bone as a surrogate of experimental test. The aim of this study was to investigate the correlation between the mechanical properties of trabecular bone from the primary compressive trabecular system of human femoral head assessed by micro- finite element analysis and the experimental test.

Materials and Methods: Twenty-one human femoral heads were obtained from 11 patients undergoing total hip arthroplasty and 10 cadavers. Cylindrical trabecular bone was cored from the primary compressive trabecular system of the femoral head. The sample size was diameter of 19 mm, height of 15 mm. All samples were scanned with a high-resolution micro-computed tomography system at a spatial resolution of 21.31 μ m. Based on the serial micro-CT images, a volume of interest (VOI) was selected to be 9.50 mm of diameter and 7.50 mm of side length. Based on these micro-images of trabecular bone, the finite element model was created, and the finite element analysis and the compressive test were performed sequentially. The yield stress and Young's modulus were calculated from two methods.

Results: The average yield stress and Young's modulus from FEA and Instron system were 13.04 MPa and 1.30 GPa, 13.06 MPa and 0.11 GPa, respectively. The correlations between the yield calculated from FEA and Instron were significant ($p = 0.001$), but not for the Young's modulus ($p=0.055$).

Conclusion: The mechanical properties of trabecular bone calculated from FEA are well correlated with those from the mechanical test, suggesting that the micro-image-based finite element analysis as a substitute of the mechanical test can be a useful tool to evaluate the mechanical properties of trabecular bone, further to predict the fracture risk.

Disclosures: M. Baek, None.

W452

A Methodology for Bone Strength Prediction using Parametric Statistical Shape and Density Finite Element Modeling. T. L. Bredbenner*, D. P. Nicoletta. Materials Engineering, Southwest Research Institute, San Antonio, TX, USA.

Bone strength is the result of the complex combination of traits related to bone shape and bone density distribution. The use of finite element (FE) modeling methods improve the estimation of bone strength over predictions based on clinical image data alone since FE models can explicitly incorporate detailed descriptions of bone geometry and bone density distribution. However, the efficient construction of finite element models that accurately represent the complex morphology of skeletal structures is a major challenge thereby limiting their clinical use in diagnosing fracture risk. In the present study, methodology based on statistical shape modeling was developed and implemented to parametrically describe the complex geometry and bone density distribution using clinical imaging data for a set of 7 human female proximal femurs. The femurs were scanned using a clinical CT scanner (Lightspeed Ultra, GE Healthcare) along with a density calibration phantom (Mindways Software). Triangulated surfaces were created to describe the outer geometry for each femur (Amira, Mercury Computing) and a volumetric finite element mesh was mapped onto each femur using optimal point-to-point correspondence methods. Apparent ash density was estimated at each node for all femur models using the calibrated CT image data. Statistical shape and density modeling methods were then used to develop a parametric finite element model describing the set of cadaver femurs. Principal Component Analysis of the statistical shape and density FE model showed that 78% of the variability in bone geometry and density can be described using only 3 independent components. Reconstructing the FE model using each component independently and predicting bone strength under simulated fall conditions estimated the contribution of each component to proximal femur strength. Finally, individual finite element models of femurs within the training set could be accurately reconstructed, and a leave one out analysis demonstrated that a volumetric finite element model of a previously unseen femur could be reconstructed with a maximum geometry error of 1.25 mm and an average error of 0.04 mm.

Disclosures: T.L. Bredbenner, None.

This study received funding from: Southwest Research Institute Advisory Committee for Research.

W453

Assessment of Vertebral Fracture Threshold and Alendronate Therapeutic Effects by a QCT-based Nonlinear Finite Element Model in Postmenopausal Women. K. Imai¹, I. Ohnishi^{*2}, S. Yamamoto¹, K. Nakamura². ¹Orthopaedic Surgery, Tokyo Metropolitan Geriatric Medical Center, Tokyo, Japan, ²Orthopaedic Surgery, Tokyo University, Tokyo, Japan.

A QCT-based nonlinear finite element model (CT/FEM) accurately predicts vertebral strength, fracture sites and distribution of minimum principal strain (Spine 2006; 31:1789-94). This study aimed to assess the risk of vertebral fracture and the therapeutic effects of alendronate on osteoporosis using a CT/FEM. We performed a cross-sectional analysis of L2 vertebral strength for 104 postmenopausal Japanese women (mean age, 71.3 yrs; range, 49-85; mean height, 149.7 cm; mean weight, 50.5 kg) with no history of previous L2 fracture, traumatic vertebral fracture or osteoporosis medication. Subjects comprised 75 women without vertebral fracture and 29 women with non-traumatic vertebral fracture. The optimal point on the ROC curve that was used as vertebral fracture threshold was 1950 N with 75.9% sensitivity and 73.3% specificity. We also prospectively assessed the biomechanical effects of alendronate in 33 patients (mean age, 76.5 yrs) who were treated with alendronate at a dose of 5 mg/day for 1 year. QCT scans of the L2 were obtained at baseline and 3, 6 and 12 months, and the vertebral strength and mechanical parameters for each patient were analyzed using the CT/FEM. BMD of the L2-4 was measured by DXA at baseline and 6 and 12 months. BMD tended to increase from baseline at 6 months (3.7%; $p=0.0451$), and was significantly increased at 12 months (7.5%; $p<0.0001$). Vertebral strength from the CT/FEM significantly increased by 10.2% from baseline at 3 months ($p<0.0001$), 16.7% at 6 months, and 26.9% at 12 months. The CT/FEM also revealed that the area with large negative value of minimum principal strain before medication, where a high risk of fracture exists, decreased after medication. After 1 year of medication, the density of the inner cancellous bone with a distance of more than 2 mm from the outer surface increased by 8.3% ($p=0.0013$), while the density of the peri-cortical bone with a thickness of 2mm increased by 13.6% ($p=0.0004$). The CT/FEM could assess the vertebral fracture threshold with higher sensitivity and specificity, and also assess the therapeutic effects of alendronate with higher sensitivity and earlier (at 3 months) than BMD. The increase in the vertebral strength might be attributed to the alterations in the distribution of bone density, stress, and strain within the vertebra. The alendronate treatment was more effective in the peri-cortical and cortical areas compared to the inner trabecular compartment. The CT/FEM allows us to analyze quantitatively vertebral strength and biomechanical characteristics and is useful to assess the risk of vertebral fracture and therapeutic effects on osteoporosis.

Disclosures: K. Imai, None.

W454

Radiographic Analysis of Trabecular Bone Structure and Bone Geometry in the Prediction of Hip Fracture Load. T. J. Jämsä^{*1}, P. Pulkkinen^{*1}, E. Lochmüller^{*2}, V. Kuhn^{*3}, M. Nieminen^{*4}, E. Eckstein^{*5}. ¹Department of Medical Technology, University of Oulu, Oulu, Finland, ²1st Gynecology Hospital, Ludwig-Maximilians-University, Munich, Germany, ³Department of Trauma Surgery, Medical University Innsbruck, Innsbruck, Germany, ⁴Department of Radiology, Oulu University Hospital, Oulu, Finland, ⁵Institute of Anatomy and Musculoskeletal Research, Paracelsus Medical Private University, Salzburg, Germany.

The clinical diagnosis of osteoporosis is typically based on measuring bone mineral density (BMD) with dual-energy X-ray absorptiometry (DXA). However, access to DXA is limited in many regions, while radiography is widely available. Here, we used an image processing method for assessment of trabecular structure, density and geometry from radiographs, to estimate the mechanical strength of femur.

The sample consisted of 62 femoral cadaver specimens (34 females, 81.6±10.7 yrs, and 28 males, 77.8±11.1 yrs). After radiography and DXA, the femora were mechanically tested in a side impact configuration. The fracture patterns were classified as being cervical or trochanteric. Computerized image analysis was applied to obtain several structure-related trabecular parameters, and a set of geometrical variables was also defined. Multiple linear regression analysis was performed to identify the variables that best explain variation in BMD and failure load between subjects.

In the cervical fracture cases, trabecular bone area (TBA) and calcar femoral cortex thickness (CFC) explained 68% of the variability in DXA-based femoral neck BMD ($p<0.001$). TBA and femoral neck axis length (FNAL) explained 64% of the variability in failure loads ($p<0.001$), while femoral neck BMD also explained 64%. In the trochanteric fracture cases, trabecular homogeneity index (HI) and femoral shaft cortex thickness explained as much as 87% of the variation in trochanteric BMD ($p<0.001$). Euler number (EN) and calcar femoral cortex thickness (CFC) explained 66% of the variability in failure load ($p=0.001$), while trochanteric BMD explained 72% ($p<0.001$).

In conclusion, trabecular bone structure, as determined from conventional radiographs, reflects a substantial proportion of the variability in DXA-based BMD. Structural parameters of trabecular bone and bone geometry predict in vitro failure loads of the proximal femur with quite similar accuracy as DXA, when using appropriate image analysis technology.

Disclosures: T.J. Jämsä, None.

This study received funding from: Finnish Funding Agency for Technology and Innovation.

W455

Evolution of the Crack-Growth Resistance and Toughening Mechanisms of Human Cortical Bone via In-Situ Electron Microscopy. K. J. Koester^{*1}, J. W. Ager^{*2}, R. O. Ritchie^{*1}. ¹Materials Science and Engineering, University of California, Berkeley, Berkeley, CA, USA, ²Lawrence Berkeley National Laboratory, Berkeley, CA, USA.

Mammalian bone has evolved to support a variety of physiologically relevant loads and also to resist fracture, which, in many cases, can have life endangering consequences. It is imperative to understand the toughening mechanisms in human bone to characterize influence of age, disease, and drug treatments on the fracture properties of bone. Previous works have established that bone "toughens" to resist crack growth. However, without looking at the fracture of human bone in situ, these studies lack the potency to elucidate the phenomenon taking place during the fracture process. Here, in-situ crack propagation measurements performed in an environmental scanning electron microscope have allowed simultaneous measurement of the crack-growth resistance curve and real-time visualization of the toughening mechanisms. This work is the first study of the evolution of toughness in the transverse and longitudinal orientations in human cortical bone (humerus). The dominant toughening mechanisms were found to be crack deflection in the transverse direction and uncracked ligament bridging in the longitudinal direction.

Disclosures: K.J. Koester, None.

W456

Compromised Fracture Healing in Lrp5 Null Mice. D. E. Komatsu¹, A. G. Robling², C. H. Turner³, S. J. Warden¹. ¹Physical Therapy, Indiana University, Indianapolis, IN, USA, ²Anatomy & Cell Biology, Indiana University, Indianapolis, IN, USA, ³Biomedical Engineering and Orthopaedic Surgery, Indiana University, Indianapolis, IN, USA.

The importance of Wnt signaling in skeletal development and regulation has been unequivocally demonstrated in recent years. However, the role of this pathway in fracture repair has been the subject to far less attention. At the cellular level, Wnt pathway activation is initiated by the binding of Wnt ligands to the Wnt co-receptor Low-Density Lipoprotein Receptor-Related Protein 5 (Lrp5). Mice with homozygous null Lrp5 mutations (Lrp5^{-/-}) demonstrate a low bone mass phenotype, concomitant with decreased mechanical properties. As Lrp5 is also known to be up-regulated during fracture repair, we hypothesized that fracture repair in Lrp5^{-/-} mice would be compromised compared to wild-type littermates (Lrp5^{+/+}). To test this hypothesis, closed fixed femoral fractures were generated in the left femurs of 4 month old male Lrp5^{-/-} (N=7) and Lrp5^{+/+} (N=6) mice. Fracture repair was qualitatively assessed by radiography, performed post-surgery and weekly until sacrifice at day 28 post-fracture. The fractured and contralateral intact femurs were harvested and quantitatively analyzed by peripheral quantitative computed tomography (pQCT), dual energy X-ray absorptiometry (DXA) and biomechanical testing (4-point bending). To correct for baseline phenotypic differences, the results obtained for the fractured femurs were normalized to those of their contralateral intact femurs. No apparent differences in callus development were seen in the weekly radiographs. Similarly, analysis by DXA showed no differences in area or BMD, though a 15% reduction in BMC was observed in fractured femurs from Lrp5^{-/-} mice, compared to Lrp5^{+/+} mice ($p < 0.02$). Likewise, the pQCT results also failed to identify substantial changes in callus morphology, with the sole significant difference being a 32% reduction in cross-sectional mature bone area in Lrp5^{-/-} fracture calluses, as compared to Lrp5^{+/+} calluses ($p < 0.05$). However, biomechanical testing revealed a gross hindrance in the mechanical properties of fractured femurs from Lrp5^{-/-} mice, compared to Lrp5^{+/+} mice, with reductions of 64-76% seen for ultimate load, stiffness, yield force, energy to yield and energy to ultimate force (all $p < 0.05$). The striking mechanical impairment in Lrp5^{-/-} calluses, combined with minimal radiographic differences, indicates that the newly formed bone is biomechanically unsound despite the fact that these calluses appear to undergo almost normal development and mineralization. We conclude that signaling through Lrp5 is critical for the establishment of biomechanical integrity in healing bone.

Disclosures: D.E. Komatsu, None.

W457

Biomechanical Testing in Experimental Bone Interventions - May the Power Be with You. O. Leppänen¹, H. Sievänen², T. L. N. Järvinen¹. ¹Department of Trauma, Musculoskeletal Surgery and Rehabilitation, University of Tampere, Tampere, Finland, ²Bone Research Group, UKK Institute, Tampere, Finland.

Total variation in any measured variable, in conjunction with the expected treatment effect, dictate the minimum sample size (minSS) required to detect the expected effect with statistical confidence should the effect truly exist. The objective of this study was to introduce a practical algorithm for calculating the minimum sample size needed to detect a statistically significant treatment effect in biomechanical parameters. A comprehensive literature survey comprising all 3472 original studies published in four major bone journals during 1999-2003 was carried out to identify studies in which biomechanical testing of whole bones was applied. The total variation in most commonly used biomechanical tests of various bones was statistically estimated. In addition, the average intervention effects were calculated for most common settings (ovariectomy, increased and decreased loading) in rats. Employing this data, the adequately-powered sample size for common biomechanical testing procedures was determined. According to our literature survey, the total variation in different biomechanical tests of bones from different species was similar, justifying the use of rat femur as a model for detailed calculations. Due to poorer repeatability in terms of total variation, minSS in the femoral neck compression test is considerably larger compared to the midshaft bending test. Similarly, the use of stiffness and energy absorption required substantially larger sample size than the use of breaking load. For example, minSS to show a 10% treatment effect in the femoral shaft breaking load with 80% power was 11 rats/group, while the respective minSSs for the stiffness and energy absorption were 23 and 53, respectively. For the femoral neck compression, these numbers were 16, 51, and 134, respectively. Of note, a typical ovariectomy experiment in rats resulted in ~5% decrease in femoral shaft breaking load, thus requiring a sample size of 42 rats. The present analysis underscores the need for considerably larger sample sizes in experimental bone interventions using mechanical parameters as primary outcome variables. In particular, the poor repeatability in terms of total variation and the generally small expected treatment effects appear to compromise the general utility of stiffness and energy absorption results in typically small experimental bone interventions.

Disclosures: O. Leppänen, None.

W458

Prednisolone Induces Osteocyte's Death and Erosion of Osteocytic Lacunae Walls. M. Li¹, K. Hara², Y. Akiyama², N. Amizuka¹. ¹Center for Transdisciplinary Research, Niigata University, Niigata, Japan, ²Pharmacological Evaluation Section, Eisai Co., Ltd., Tokyo, Japan.

We have examined the abnormalities in the bones of Wistar rats that received prednisolone (20mg/kg) three times per week. Four, 8 and 12 weeks after beginning the steroid administration, rats were perfused with 4% paraformaldehyde in 0.1M phosphate buffer (pH 7.4), and their femora and tibiae were processed for paraffin and epoxy-resin embedding. Bone abnormalities in prednisolone-administered rats were assessed by performing alkaline phosphatase (ALP), acid phosphatase (ACP), tartrate resistant acid phosphate (TRAP) histochemistry, TUNEL assay and transmission electron microscope (TEM) imaging. Peripheral quantitative computed tomography (pQCT) was performed for evaluating bone mineral density (BMD) and bone mineral content at the metaphyseal and diaphyseal regions of prednisolone-administered and control rats. Three-point bending test was employed for estimating bone strength. BMD and mineral contents at metaphyseal and diaphyseal regions, as well as values of maximum loading were reduced as early as 4 weeks in prednisolone-administered rats. Ratio of maximum load divided by bone mineral content was much lower in prednisolone-treated rats, so that the reduced maximum load-bearing values appear to relate not only with a decreased BMD, but also with diminished bone quality in prednisolone-administered bones. ALP and TRAP assessments did not reveal obvious difference between control and prednisolone-treated bones. When examining cortical bones, however, several empty osteocytic lacunae were seen in prednisolone-administered rats, and a statistical analysis on the number of empty lacunae showed a significant increase in the prednisolone group. TUNEL assay unveiled increased osteocytic apoptosis in prednisolone bones. However, empty lacunae seem not to be a result of apoptosis only, as the number of apoptotic cells was lower than the number of such lacunae. TEM images demonstrated disrupted osteocytes in relatively enlarged osteocytic lacunae, as well as irregularly shaped osteocytes that were embedded in lacunae featuring eroded peripheral walls. In addition, osteocytes distant from bone-resorbing osteoclasts tended to show ACP-positive granules, indicative of activated lysosomal enzymes in prednisolone-treated rats. Thus, in our study, prednisolone appears to target osteocytes, inducing their cell death and erosion of the surrounding walls of their lacunae, which might influence overall bone quality.

Disclosures: M. Li, None.

W459

New Method to Determine Variation of the Elasticity of Single Trabeculae. S. Lorenzetti*, E. Stüssi. Institute for Biomechanics, ETHZ, Zürich, Switzerland.

By comparing the deflection of an experimental 3 point bending test with FE calculation, the Young's modulus of single trabeculae can be determined.

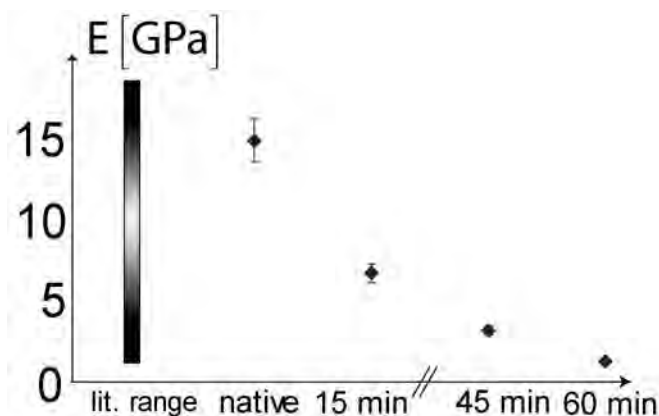
With DXA and QCT the bone mineral density (BMD) is measured. Due to this technique, variations of the calcium apatite are detectable, but changes of the collagen mesh are not visible. With the presented new method, variations of the elastic behavior of single trabeculae are accessible.

A special micro-positioning device enables sample rotation around the trabecular axis. The force was applied normal to the optical axis and the trabecular with a nylon thread, and the deflection could be measured with the microscope. Based on the image stack from microscopy, a CAD body of the trabecula can be built using Amira™ and Geomagic™. FE calculations were performed with ANSYS™. By comparing the FE modeling with the deflection of the experimental 3 point bending test, the Young's modulus can be determined.

To obtain the accuracy of the method, two types of error calculations were performed: First, a straight forward estimation according to Gauss which includes the length, the force and the deflection, and second, FE calculations with variation of the volume. The expected resulting error for the Young's modulus is <10 %.

To test the new method the collagen was removed from a set of samples. Samples from the femur of an adult sheep were treated with sodium hypochlorite (NaOCl). The treatment with NaOCl is a standard method to deproteinize bone, and therefore, to alter the Young's modulus without changing the geometric properties or the inorganic part of the bone. The analysis of a native (untreated) femoral sample resulted in a Young's modulus of 15.0 ± 1.4 GPa. This is in the upper range of the published data in the literature of 1 up to 19 GPa. The treated samples showed a reduction of the Young's modulus by a factor of 15. Broz et al (1997) observed a decrease at macroscopic samples by a factor of 2.7.

Using DXA, no variation of the BMD would have been observed in this type of samples. With the new method, changes of the organic part (collagen) of the bone become visible.



It is concluded that the new method including sample preparation, experimental 3 point bending test with optical control, determination of the volume and FE modeling is suitable to determine the Young's modulus of single trabeculae in the natural boundary conditions of the sponiosa.

Broz et al. (1997) J. mat. Sci. 8:395-401

The technical support of C. Hauser is gratefully appreciated.

Disclosures: S. Lorenzetti, None.

W460

Fracture Strength of the Distal Radius Can Be Estimated by Non-linear Finite Element Analysis Using 3D High Resolution Peripheral Computed Tomography. J. A. M. MacNeil*, S. K. Boyd. Mechanical Engineering, University of Calgary, Calgary, AB, Canada.

Finite element (FE) modeling based on micro-computed tomography data has the potential to provide significant insight into disease- and treatment-related bone quality changes through estimation of fracture strength. The goals of this study were to determine if linear finite element models of bone stiffness can predict bone strength, and determine if non-linear finite element models provide an improvement over linear finite element models, through a direct assessment of strength. It was also investigated whether a non-homogeneous tissue Young's modulus scaled according to attenuation values can improve bone stiffness and strength measurements.

Fresh human cadaver forearms (5 male and 5 female) with ages ranging from 55 to 93 were obtained from the Gross Anatomy Lab at the University of Calgary. The distal radius was dissected free from each forearm and four 9.1 mm sections were cut beginning at the subchondral plate. The sections were scanned with high resolution peripheral quantitative computed tomography (HR-pQCT) (XtremeCT, Scanco Medical, Switzerland; voxel size 82 μm) in saline solution. These forty samples were mechanically tested and used to determine appropriate homogeneous and non-homogeneous tissue Young's moduli for finite element analyses. Ten samples corresponding to the standard clinical measurement location for in vivo HR-pQCT measurements were used for non-linear finite element evaluation.

Bone stiffness measurements by linear FE analysis using a non-homogeneous tissue Young's modulus had a significantly higher correlation to bone ultimate strength than the homogeneous tissue Young's modulus models, likely due to implicit correction for partial volume effects ($R^2=0.983$ vs. $R^2=0.960$; $p<0.05$). For the clinical measurement samples, the non-linear FE analysis predicted the experimentally determined ultimate strength better than correlations based on apparent stiffness estimates from linear FE. This trend was true for homogeneous tissue Young's modulus models ($R^2=0.937$ vs. $R^2=0.868$) and was statistically significant for non-homogeneous tissue Young's modulus models ($R^2=0.951$ vs. $R^2=0.928$; $p>0.05$).

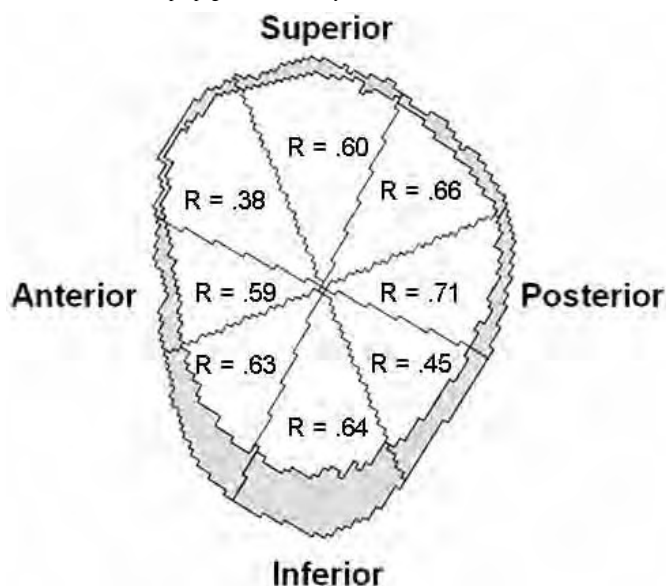
It was concluded that for estimation of bone strength using in vivo HR-pQCT measurements, non-homogeneous tissue Young's modulus improves estimations, and that linear finite element measurements were highly predictive of bone ultimate strength, albeit based on correlations rather than direct measurements. A non-linear finite element measurement directly estimated bone strength, and can provide improved accuracy when the increased computation is justified.

Disclosures: J.A.M. MacNeil, None.

W461

Posterior Cortical BMC in the Femoral Neck Predicts Proximal Femur Failure Load. S. L. Manske*, D. M. L. Cooper*, T. Liu-Ambrose*, P. Guy*, H. A. McKay*. ¹University of Calgary, Calgary, AB, Canada, ²University of British Columbia, Vancouver, BC, Canada.

Region-specific deterioration of the femoral neck (e.g. superoposterior) may play a key role in hip fractures. We aimed to determine the region of the femoral neck where cortical bone mineral content (CoBMC) best predicted failure load. We obtained 36 unembalmed, previously frozen human cadaveric femora (36 - 92 years), and scanned each with a 16-slice helical QCT scanner (GE LightSpeed Ultra). QCT scans were acquired axially and images ($0.5 \times 0.5 \times 0.63$ mm) were reconstructed perpendicular to the femoral neck axis ($0.5 \times 0.5 \times 2.5$ mm). We assessed total area (mm^2) and CoBMC (g) in the femoral neck cross-section with the lowest total area (i.e., narrowest-neck). We also measured cortical BMC regionally within 8 sectors (octants) radially defined about the centroid of the cross-section (Figure). The femora were then loaded to failure in an apparatus that simulated a sideways fall at a rate of 100 mm/s. Femora that fractured outside of the neck or intertrochanteric regions ($n=7$) were excluded from analyses. We performed hierarchical linear regression with failure load (N) as the dependent variable. In the regression model, we entered total area at the first level to account for differences in bone size and then utilized stepwise selection of the sector-based CoBMC values at the second level. Two additional specimens were excluded as outliers based on Cook's distance. The highest correlations between CoBMC and failure load were along the anteroinferior to superoposterior axis (R ranged from 0.63 to 0.71, Figure). The stepwise regression selected CoBMC from the posterior sector based on its association with failure load. CoBMC in the posterior region explained 65% of the variance (R^2) in failure load after accounting for total area. Our results agree with the predictions of Mayhew et al. (2005) and Lotz et al. (1995) who suggest that the superoposterior region may be critical to the strength of the femoral neck. We extend their findings by providing measurements of proximal femur strength in ex vivo specimens. Our quantitative results further correspond with our observation that most of the fracture lines propagated through the superoposterior region. We conclude that the superoposterior region requires further investigation as a key site of fracture initiation and propagation in sideways falls.



Disclosures: S.L. Manske, None.

W462

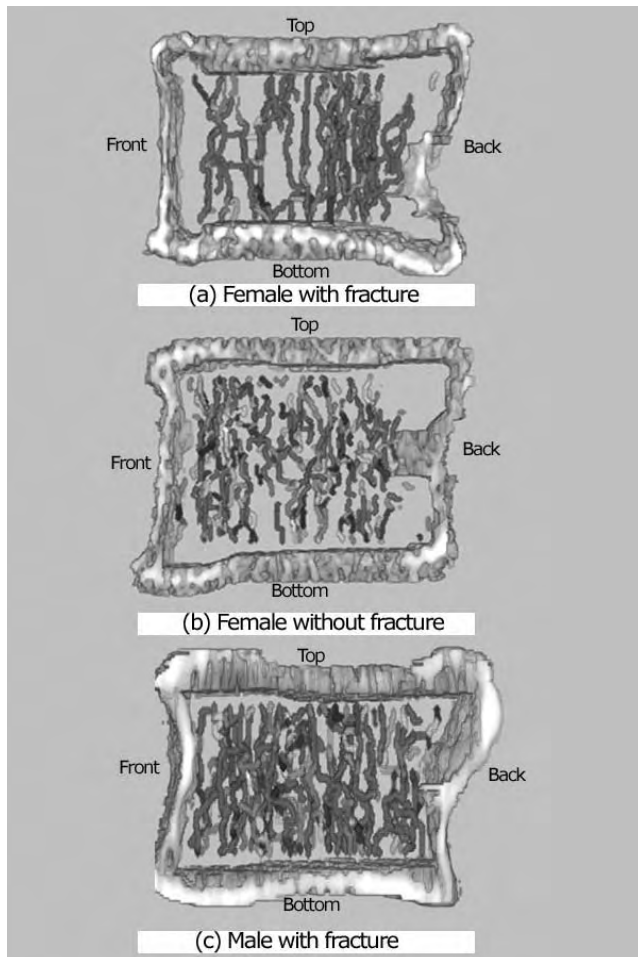
Evaluation of Vertebrae Fragility by Osteoporosis. N. Nango¹, N. Endo^{2*}, T. Yamamoto^{3*}, H. Takahashi⁴, M. Machida^{5*}, Y. Suga^{6*}, T. Asai^{6*}. ¹Ratoc System Engineering Co., Ltd., Tokyo, Japan, ²Niigata University, Niigata, Japan, ³Niigata Bone Science Institute, Niigata, Japan, ⁴Niigata University of Health and Welfare, Niigata, Japan, ⁵Murayama Medecal Center, Tokyo, Japan, ⁶Kawaguchi Municipal Medical Center, Saitama, Japan.

We developed a method to quantify the trabecula path that connects between the two endplates of the vertebrae. We consider this connecting path primarily prevent the vertebral deformation. We used in-vivo Multi Detector CT images of females aged 70 with lumbar stress fracture (a), females aged 86 without fracture(b), and males aged 57 without fracture (c). Based on the CT values of these bone images, we determined the trabecula bone (TRI/3D-BON software by RATOC), and measured the length (L) and cross section (S) of each trabecula. We define the trabecula elasticity coefficient (k) as $k \propto S/L$, and the resistance force (f) as $f = k \cdot d$ for deformation distance (d). We define the simulation model as follows: loaded surface, fixed surface and trabecula network connecting both surfaces. Using given external deformation (D), deformation (d) for each trabecula was obtained: each trabecula path connecting the two surfaces satisfy $D = \sum d$; we also calculated the resistance force (fe) of each trabecula composing the network. The resistance force of vertebrae (Fe) was calculated as the sum of (fe) of the trabeculae contacting loaded surface $Fe = \sum fe$.

This calculated Fe is the simulation of resistance force generated in vertebrae when stress deformation is applied to the loaded surface. The figure shows the results, of the connecting trabecula paths between upper and lower endplates which resistance force greater than the specified threshold. The value of the resistance force decreased in the order of young male(c), old female(b), female with stress fracture(a). The resistance force in females with stress fracture was half of that in the male.

As the images show, in the female with stress fracture, the density of trabecula bone connecting the endplates is low at the front of the vertebrae and there are few straight connecting paths, instead the paths are connected by many detours. The paths of the old female without fracture have many fragmented disconnections. The trabecula bone network of the female with stress fracture has disappeared locally and is regarded as the cause of the fragility.

This model shows the mechanical strength of vertebrae trabecula bones but also demonstrates the fragility.



Disclosures: N. Nango, None.

W463

Improved Analysis of Bone Nano-mechanical Properties Using a Novel Nanoindentation Technique. S. Pathak^{1*}, S. R. Kalidindi^{1*}, H. W. Courtland², K. J. Jepsen², H. M. Goldman³. ¹Materials Science and Engineering, Drexel University, Philadelphia, PA, USA, ²Orthopedics, Mount Sinai School of Medicine, New York, NY, USA, ³Neurobiology and Anatomy, Drexel University College of Medicine, Philadelphia, PA, USA.

Currently, there exists a critical need to develop better techniques to understand the relationship between bone matrix composition and organization and tissue-level mechanical properties, thereby improving our ability to predict fracture risk. To address this gap, we have developed a new technique for extracting mechanical property information at the nano-scale in bone, by translating nanoindentation generated load-displacement curves into indentation stress-strain (ISS) curves for a better representation of material deformation at the lamellar level. We applied this method to a sample of femora obtained from strains of inbred mice known to have varying whole-bone mechanical properties.

Femora from A/J, C3H/HeJ (C3H), and C57BL/6J (B6) mice (16 wks of age, n=3 each) were embedded in PMMA, sectioned transversely below the third-trochanter and surface polished to 0.05µm. Backscattered electron microscopy (BSE-SEM) was used to assess mineralization density across the postero-lateral (PL) cortex of each sample. Nanoindentations (20µm apart) were carried out across this same cortex using a nanoindenter (MTS XP[®]) with a 13.5 µm radius spherical diamond tip, and corresponding ISS curves were computed. Examination of the ISS curves taken at a 40µm distance from the actively forming periosteal surface of each strain demonstrate that all three have similar slopes during (elastic) loading, but vary in post yield behavior; A/J demonstrates the highest hardening slope, while B6 demonstrates the lowest. Obtaining the elastic modulus values from the loading portion of these ISS curves rather than the unloading portion of the load-displacement curve also helps us more readily discern the differences in modulus between bone of lower and higher mineralization density.

Our results demonstrate that this method can be used to elucidate trends in yield and post-yield behavior at the lamellar level that are consistent with findings found in macro-mechanical testing of these mouse strains. This represents a significant advancement in the characterization of mechanical behavior of bone under indentation pressure beyond the regimes of elastic limit to which it has been restricted to thus far. The additional local property information provided by our nanoindentation technique, in conjunction with compositional analyses, will help us tremendously in developing an understanding of the complex interactions between bone quality, composition and mechanical properties.

Disclosures: S. Pathak, None.

This study received funding from: NIH AR44927.

W464

Osteoblast-specific Knockout of IGF Receptor Gene in Mice Alters Mechanical Properties of Cortical Bone. G. Ramaswamy^{1*}, X. Cao^{2*}, S. Chowdhury^{3*}, C. Wan², G. McGwin^{4*}, J. E. Lemons^{5*}, T. L. Clemens^{2*}, A. W. Eberhardt^{1*}. ¹Department of Biomedical Engineering, University of Alabama at Birmingham, Birmingham, AL, USA, ²Department of Pathology, University of Alabama at Birmingham, Birmingham, AL, USA, ³Department of Physics, University of Alabama at Birmingham, Birmingham, AL, USA, ⁴Department of Epidemiology, University of Alabama at Birmingham, Birmingham, AL, USA, ⁵Department of Prosthodontics and Biomaterials, University of Alabama at Birmingham, Birmingham, AL, USA.

Insulin-like growth factor-1 is essential for normal embryonic and postnatal growth. Previous studies have shown that selective disruption of the IGF receptor gene (Igflr) in mouse osteoblasts decreased bone formation and mineral apposition rates over the pubertal period.¹ The present study compared the geometric and mechanical properties of cortical bone at the mid-diaphysis of tibiae in 3 week old Igflr knockout and control mice (n = 14 per group) at the whole bone level by microCT and three-point bending and at the microstructural level using nanoindentation. MicroCT data revealed a decrease in cortical thickness (p < 0.05) which translated into a dramatic reduction in bone area (p < 0.05) and bone volume fraction (p < 0.0001) in the knockouts. Elastic modulus and toughness obtained from bending showed significant reductions (p < 0.05) in the knockouts as compared to controls while overall bending stiffness was only mildly affected. These bones showed geometric adaptation with increased mediolateral radii (p < 0.05) and moments of inertia similar to controls, which partially counteracted for the material degradation to maintain their structural integrity. Microstructural properties from nanoindentation did not show any genotype effect, which was consistent with bone mineral density measurements from microCT that were similar between controls and knockouts. Gender specific comparison demonstrated females to be smaller in size with structural properties more severely reduced following ablation of IGF signaling. In conclusion, the current study suggests that local IGF signaling in murine osteoblasts is essential for normal appositional growth of cortical bone during diaphyseal modeling and its disruption affects the mechanical properties, more severely in females, at the prepubertal stage in mice.

1. Zhang M, et al. Endocrinology 2002;277:44005-44012.

Disclosures: G. Ramaswamy, None.

W465

Txnp Deficient HcB/19 Mice Have Decreased BMD and Femoral Strength. N. Saless¹, J. Chen^{*2}, A. Shalev^{*2}, R. D. Blank². ¹Cellular and Molecular Biology, University of Wisconsin, Madison, WI, USA, ²Medicine, University of Wisconsin, Madison, WI, USA.

Thioredoxin interacting protein (Txnp) mediates the oxidative stress response. Txnp-thioredoxin interaction reduces thioredoxin activity, so that in vitro Txnp overexpression leads to increased apoptosis and decreased proliferation following exposure to oxidative stress. HcB/19 recombinant congenic mice harbor a nonsense mutation of Txnp, resulting in a metabolic profile similar to human familial combined hyperlipidemia. Mice harboring the Txnp mutation also display an increase in fat mass relative to wild-type. Hypothesizing that the observed increase in fat mass is accompanied by a concomitant decrease in bone mass, we compared bone density and biomechanical performance in HcB/19 mice and C3H/DiSn mice, their recipient progenitor, which harbor the normal Txnp allele.

Mice were studied at 4 months of age, examining BMD by DXA (PIXIMus, GE-Lunar) and femoral biomechanics by 3-point bend testing. The latter was performed under displacement control at a rate of 0.3 mm/second and post spacing of 3.75 mm. Data were analyzed for total displacement, structural stiffness, maximum load, and energy to failure. Data from the right and left femora were averaged for each individual. Data were analyzed by 2 way ANOVA with $\alpha = 0.05$.

We found that HcB/19 mice display decreased total body BMD, and decreased maximum load and stiffness, in spite of similar body mass (see table). Although energy to failure tended to be lower in HcB/19, the difference did not reach significance. There were no interactions between strain and sex. Biomechanical performance was greater in females than males.

Our data show that Txnp deficiency reduces peak bone mass and bone strength. Txnp is known to be induced by 1, 25 di-OH D and repressed by mechanical loading. Our data do not address the question of whether either of these mechanisms contributes to the observed biomechanical phenotype. Our data also do not allow us to determine whether the Txnp mutation alters the balance between the osteoblastic and adipocytic lineages during development. Our experiment is limited in that other loci also segregate between the strains. Nevertheless, the epidemiological association between atherosclerosis and osteoporosis and our biomechanical data justify further investigation of Txnp

	C3H/DiSn		HcB/19	
	F (N = 8)	M (N = 6)	F (N = 9)	M (N = 8)
BMD (mg/cm ³) *†	56.4 ± 1.1	52.4 ± 1.2	52.4 ± 1.0	51.2 ± 0.9
Displacement (mm)	0.53 ± 0.03	0.53 ± 0.04	0.53 ± 0.03	0.56 ± 0.03
Stiffness (N/mm) *†	130 ± 4	115 ± 5	120 ± 4	100 ± 4
Max Load (N) *†	19.1 ± 0.6	17.5 ± 0.6	17.0 ± 0.5	15.5 ± 0.6
Energy to Failure (N*mm)	6.6 ± 0.4	6.8 ± 0.5	6.0 ± 0.4	6.0 ± 0.4

Data shown as mean ± SEM, NS = not significant, * = significant strain difference, † = significant sex difference

Disclosures: N. Saless, None.

W466

Biomechanics and Body Size Quantitative Trait Loci in HcB/8 x HcB/23 F2 Mice. N. Saless¹, G. E. Lopez Franco^{*2}, S. J. Litscher^{*2}, K. Abdul Raheem^{*3}, K. Kozarek^{*3}, S. Sudhakaran^{*3}, M. J. Houlihan^{*3}, A. S. Ahmed^{*3}, T. K. O'Neill^{*3}, S. J. Han^{*3}, R. D. Blank². ¹Cellular and Molecular Biology, University of Wisconsin, Madison, WI, USA, ²Medicine, University of Wisconsin, Madison, WI, USA, ³University of Wisconsin, Madison, WI, USA.

Recombinant congenic mouse strains HcB/8 and HcB/23 differ in biomechanical performance in spite of similar ash percentages. To identify quantitative trait loci contributing to the differences in biomechanical performance between these strains, we performed a reciprocal F2 intercross to map the responsible QTLs. Below, the female progenitor is listed first, in accordance with convention.

F2 mice were kept to 17 ± 1 weeks under standard husbandry conditions. Following sacrifice, we performed microsatellite genotyping and measured femoral whole bone biomechanics and BMD by DXA. From 3-point bend testing performed under displacement control, post separation of 3.5 mm, and a deflection rate of 0.3 mm/sec, we extracted total and post-yield displacement, stiffness, maximum load, and energy to failure. We analyzed the data with QTL Cartographer and established experiment-wide significance levels by permutation testing. We studied 124 8x23 females, 163 23x8 females, 169 8x23 males and 147 23x8 males.

Significance thresholds ranged between LOD scores of 1.9 for stiffness to 3.7 for post-yield displacement, reflecting the reproducibility of the trait assays. In the entire F2 population, the only significant QTL is for body mass at 27 cM on chromosome 2. In the 8 x 23 arm, there is a significant QTL at 68 cM on chromosome 3 for total displacement and post-yield deflection (LOD = 4.9 and 5.7, respectively). On chromosome 10, there is a stiffness QTL (LOD = 2.6) at 28 cM. In the 23x8 arm, there are a pair of chromosome 3 QTLs for length centered at 12 cM (LOD = 3.0) and 68 cM (LOD = 3.2). Among males of both arms, there is a broad body mass QTL (LOD = 3.3) located between 18 and 72 cM on chromosome 3. Among females of both arms, there is a body mass QTL (LOD = 3.2) at 79 cM on chromosome 3. Arm and sex specific subgroups display some of these QTLs and also display additional significant QTLs not listed above. Comparison of the overall phenotypic distributions also revealed evidence of one or more X-linked QTLs.

The data show that there are both cross and sex effects, as others have found in previous bone linkage studies. Epistatic interactions between pairs of genes, genomic imprinting, and mitochondrial inheritance are all possible mechanisms underlying the observations. Future work to isolate the genes responsible for the QTLs found in this cross will be facilitated by the fact that the donor segments in the parental strains have already

undergone multiple recombination events, limiting their length and providing physical landmarks for fine structure genetic mapping.

Disclosures: N. Saless, None.

This study received funding from: Veterans Administration Biomedical Research and Development Service.

W467

Interrelation Between Dietary Fatty Acids and Fibers in Modulating Bone Quantity and Quality During Skeletal Growth. A. Schirmer^{*1}, S. Ferreri^{*1}, L. M. Miller^{*2}, Y. Qin^{*1}, N. Turner^{*3}, J. Lupton^{*3}, S. Judex¹. ¹Biomedical Engineering, Stony Brook University, Stony Brook, NY, USA, ²Biomedical Engineering, Brookhaven National Laboratory, Upton, NY, USA, ³Texas A&M University, College Station, TX, USA.

Dietary factors can influence the levels of bone formation, bone resorption and impact bone quantity and quality. Increased quantities of dietary lipids may have detrimental effects on bone mass but emphasizing specific lipid sources, while maintaining the total amount of dietary fat, can be beneficial. Little is known about the interaction between dietary lipid and fiber source. The objective of this study two different lipid sources were factorially combined with two different fiber sources to investigate their skeletal impact in rapidly growing rats. Forty-nine 4wk old male rats were randomly divided and fed one of four dietary combinations for 4wk (fish oil/cellulose, fish oil/pectin, corn oil/cellulose, corn oil/pectin). At completion of the protocol, micro-computed tomography determined differences in trabecular and cortical bone morphology of the distal and diaphyseal femur. Mechanical and chemical properties of the femoral diaphysis were determined by 3-point bending and Fourier transform infrared spectroscopy. There were no significant differences between the four dietary groups for any morphological or micro-architectural parameter in the distal femoral metaphysis. In contrast, middiaphyseal cortical bone was sensitive to differences in dietary components. Rats fed a fish oil rather than a corn oil diet had a 5% (p<0.02) greater cortical bone area, a 5% (p<0.005) greater periosteal area, and a 6% (p<0.02) greater endocortical envelope area. Conversely, bones from rats on the corn oil diet showed a 26% (p<0.002) higher energy to failure. There were no significant differences in collagen structure between groups but rats fed the corn oil diet had a 16% (p<0.02) higher level of mineralization compared to rats on the fish oil diet. When comparing rats on cellulose versus pectin diets, no differences were found for any morphological, mechanical, or chemical properties. These data indicate that dietary fish oil, compared to corn oil, can moderately promote cortical, but not trabecular, bone growth but, at the same time, may decrease measures of bone quality. In the absence of effects, or interactions, of pectin and cellulose, any skeletal differences observed in this study could be attributed to differences in fatty acid content. Whether the only modest differences in bone quantity and quality are related to the relatively short experimental protocol or the genetically modulated high levels of cellular activity in the rapidly growing rat remains to be determined.

Disclosures: A. Schirmer, None.

W468

Vitamin D Deficiency: A Common Occurrence in Both High and Low Energy Fractures. B. Schreck^{*1}, A. Serota^{*1}, D. Helfet^{*1}, M. G. E. Peterson^{*1}, N. Sinha², J. M. Lane¹. ¹Hospital for Special Surgery, New York, NY, USA, ²New York Presbyterian Hospital, New York, NY, USA.

Vitamin D insufficiency is an under-recognized problem in adults in the United States. Vitamin D influences Ca homeostasis, bone mineral density, muscle strength, and bone strength and healing. This retrospective study tests the hypothesis that vitamin D deficiency is prevalent among fracture patients, regardless of high vs. low energy fracture etiology.

A retrospective analysis of the medical records for 44 in-patients with non-vertebral fractures on the orthopedic trauma service at the Hospital for Special Surgery was conducted from June 1, 2006 to February 1, 2007. The obtained data included a 25-hydroxyvitamin D level, age, gender, and reason for admission; high energy fracture vs. low energy fracture (a fall from standing height or less).

Vitamin D deficiency, 25(OH)D<32 ng/ml, was found in 59.1% of the patients and the mean 25(OH)D was 30 ng/ml ± 13. Significantly more women (75%) than men (40%) were vitamin D deficient. Significantly more women than men with high energy fractures were vitamin D deficient (p=0.01). In women, both high and low energy fractures present with vitamin D deficiency (80% of high energy fractures and 71.4% of low energy fractures). In men, the mean vitamin D level was lower for low energy fractures (16 ng/ml) compared to high energy fractures (32 ng/ml), p=0.007. In addition, men with low energy fractures were significantly older than men with high energy fractures, p=0.02, but this age difference was not significant among women, p=0.053. The mean age for women (66 years) was higher than the mean age for men (51 years), p=0.02. Women showed a significant correlation of age vs. 25(OH)D as older women actually had higher values of 25(OH)D than younger women, rho=0.46 (p=0.02). For men, there was no significant correlation of age vs. 25(OH)D, rho=-0.2 (p=0.2).

A high prevalence (59%) of vitamin D deficiency is seen among in-patients on the orthopedic trauma service. Statistically more vitamin D deficiency is seen in women and our results are consistent with the gender difference seen in the general population. The higher values of 25(OH)D in older women compared to younger women may be due to the fact that older women are more likely to be treated with calcium and vitamin D. Even among younger men who sustain a high energy fracture, 25% are vitamin D deficient. Women regardless of age or energy level causing fracture have low vitamin D levels. 25(OH)D levels should be measured in all orthopedic trauma patients and deficient patients should be treated.

Disclosures: B. Schreck, None.

W469

Variation of the Young's Modulus of Single Trabeculae in a Sheep Femur. E. Stüssi, S. Lorenzetti*. Institute for Biomechanics, Ethz, Zürich, Switzerland.

In this work, first results of a study of the variation of the Young's modulus of single trabeculae within a femur are presented.

The fracture risk of bone is influenced by several parameters. The important factors are age, gender, mobility, type of bone, the bone mineral density (BMD) and the material properties. The mechanical properties are influenced by the architecture, the structure and the quality of the bone forming material. One of the major parameters of the material properties is the Young's (elastic) modulus E. This value describes the linear deformation under loading.

Various standard methods are known to measure the stiffness of the entire spongiosa or bone at macroscopic scale. Furthermore, indentation tests are available to determine the elastic behavior of microscopic spongiosa samples. In this work, the first results of a new method to determine the Young's modulus of single trabecula using experimental and FE simulation of a 3 point bending test are presented.

This method takes the exact 3D geometry and the behavior under loading into account. Stacks of images were taken using a laser scanning microscope (LSM) and a near infrared laser. Based on the image stack from microscopy, a CAD body of the trabecula can be built using Amira™ and Geomagic™. FE calculations were performed with ANSYS™. The experimental 3 point bending test was performed with the boundary conditions of the natural trabecular network. The force was applied normal to the optical axis with a thread, and the deflection could be measured with the microscope. By fitting the FE modeling to the deflection of the experimental 3 point bending test, the Young's modulus can be determined. The experimental error estimated by Gaussian error calculation and variation of the input parameters of the FE calculations is < 10 %.

The spongiosa samples were taken from the femur of a healthy 2.5 y old sheep. The bone was cut into cubic samples using a band saw. The bone marrow was extracted using ultrasound wave bath and pressure air.

The presented data shows variation of the Young's modulus within one femur by a factor of about 4. This is a similar range as summarized by Bayraktar et al. 2004.

Bayraktar et al. J. of Biomech. 37(11):27-35

The technical support of C. Hauser is gratefully appreciated.

Results	
Sample site	Young's modulus E [GPa]
Trochanter major	10.3
Trochanter minor	27.8
Epikondylus medialis	6.6
Epikondylus lateralis	12.0

Disclosures: E. Stüssi, None.

W470

Bone Fragility May Be Caused by Mechanostress Inequality in Transitional Period from a Steady-state Bone Metabolism to Another State. Y. Tamura, K. Nakayama, S. Katayama*. Saitama Medical University, Saitama Pref., Japan.

We have presented a computer simulation program of bone metabolism in a past ASBMR meeting. In this meeting, we want to show unloading model of bone on this program.

At first, we made a two-dimensional square bone model in computer and loaded 10 units of mechanical force to the initial bone. After dozens of simulation time, this bone became a structure like trabecular bone and reached steady-state bone metabolism. Then we reduced this force from 10 to 5 units to simulate mechanical unloading. BV/TV decreased promptly, but Tb.N decreased slowly. Dozens of simulation time later, this bone reached new steady state.

We postulated that the phase between fast and slow convergence of BV/TV and Tb.N was transient period for bone to adapt to change of external load. So we examined local mechanical stress, bone formation and resorption in this period.

Before and after transient period, local mechanical stresses were uniform and steady, and bone formation and resorption were also stable. However, during transient period, local stresses varied from place to place, causing increased and fluctuated bone metabolism. Trabecular perforation caused stress concentration to parts of residual trabecula and the places became very weak transiently.

These results suggest that bone fragility with increased bone metabolic marker may occur in transitional period from a steady state bone metabolism to another one, as shown in this unloading simulation model. If so, fractures in osteoporosis may be caused by mechanostress inequality in transient and unstable structures during adaptation processes to another environment of external load and hormones. And it may be very important that this unstable state continued for a long time after bone mass had changed. This condition may mean poor bone quality in osteoporosis.

Disclosures: Y. Tamura, None.

W471

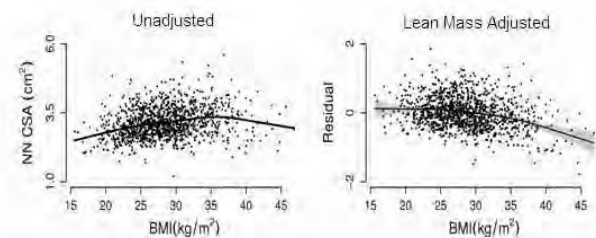
Lean and Not Fat Mass Is Associated with Male Proximal Femur Strength. T. G. Travison¹, A. B. Araujo¹, G. R. Esche^{*1}, T. J. Beck², J. B. McKinlay¹. ¹New England Research Institutes, Watertown, MA, USA, ²Johns Hopkins University School of Medicine, Baltimore, MD, USA.

Obesity is thought to confer protection against fracture, but the mechanism driving this association is poorly understood. We hypothesized that the effect of increased weight or BMI on bone structure would be accounted for by total and/or appendicular lean mass (LM), and that once these trends were removed, fat mass (FM) would demonstrate no protective influence. To test this hypothesis, we examined body composition and geometric indices of proximal femur strength in a diverse sample of randomly-selected men, ages 30-79 y.

Data were obtained from N=1,171 community-dwelling men randomly selected for inclusion in the cross-sectional Boston Area Community Health / Bone study. Body composition was obtained by dual X-ray absorptiometry (DXA). Hip geometry parameters at the narrow neck (NN), intertrochanter, and shaft regions of the proximal femur were obtained via Hip Structural Analysis of DXA images. These measures included bone mineral density (BMD), bone material in cross sections (cross-sectional area, CSA), bending strength (section modulus, Z) and propensity to buckle under compression (average buckling ratio, ABR). Analyses controlled for age, race/ethnicity (black, Hispanic, white), height, and physical activity.

When considered individually, BMI, LM and FM were each positively associated with hip strength. However, controlling for LM removed the positive, and induced a negative, association for BMI or FM (the Figure depicts results for BMI and NN CSA). In joint models including LM, FM and covariates, NN CSA and Z increased by an estimated 12.4 percent (95% CI: 10.2, 14.6) and 15.1 percent (95% CI: 12.2, 17.9), respectively, per 10 kg increase in LM, while FM had no positive effect. Finally, LM alone was sufficient to account for a substantial proportion of racial difference in hip strength measures (≥ 50% for the majority of comparisons), while FM exhibited no explanatory power. Findings were similar whether total or appendicular mass was considered.

These results indicate that the positive association between relative weight and proximal femur strength is accounted for by lean mass, and suggest that the protective effects of BMI in preventing fracture risk is mediated not by adipose tissue but by the influence of increased muscle mass accompanying elevated BMI.



Disclosures: T.G. Travison, None.

W472

Development of a High-Resolution 3D Micro-CT Based Model to Predict Fracture Callus Histological Architecture. J. A. Weis^{*1}, F. Granero-Molto¹, L. D. O'Rear^{*1}, M. I. Miga^{*2}, A. Spagnoli¹. ¹Pediatrics, Vanderbilt University, Nashville, TN, USA, ²Biomedical Engineering, Vanderbilt University, Nashville, TN, USA.

Annually ~600,000 people in the US suffer from fracture healing failure. There is a compelling need for studies that define the dynamic mechanisms underlying the fracture healing process and predict when it fails. The purpose of this study is to determine appropriate microCT thresholds that can predict callus bone/cartilage architecture. A stabilized tibia fracture was created in FVB mice by three-point bending. The tibia was harvested after 14 days and subjected to microCT scanning at 6 micron voxel resolution for 7.4 mm length around the callus (Scanco µCT 40). The tibia was sectioned at 6 micron for 5.2 mm length around the callus. Sections were placed on 288 slides with 3 sections per slide. In-situ hybridization for collagen 1 and collagen 10 was performed for 210 sections for each probe. The collagen 1 and 10 stained sections were quantified and labeled with a defined color value and spatially reconstructed by a custom built image registration code (MATLAB). Each section was centered and rotated to align with the previous section. The reconstructions were then overlaid to produce a bone/cartilage 3-D model based on collagen 1 and 10 expressions. The 3-D model was then compared to the 3-D reconstruction from microCT. As shown in Figure 1, callus volumetric analysis demonstrated that the CT voxel based 3-D reconstruction well predicted the 3-D bone/cartilage model based of collagen 1 (A) and 10 (B) expressions. Figure 2 depicts representative sections of collagen 1 (A), collagen 10 (B), voxel based CT image (C), and predicted 3-D bone/cartilage model (D) clearly indicating the high resolution predictability of the CT model. This study provides basic information for developing a CT voxel based 3-D model that correlates with histological structure of a fractured callus. This model can potentially overcome the limitation of histological studies that can only be based on a limited number of tissue sectional analysis.

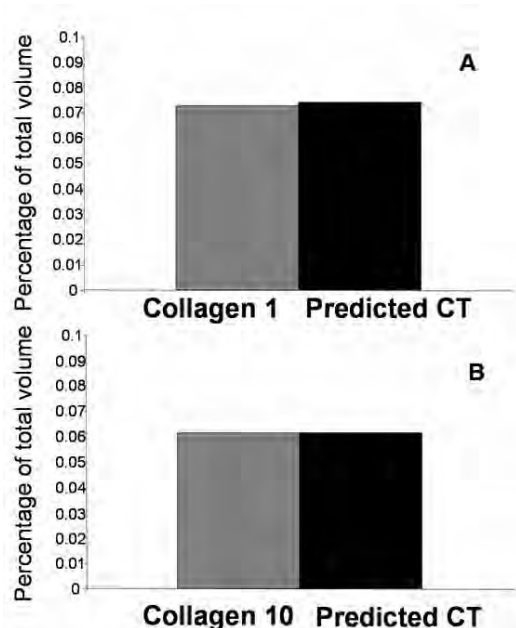


Figure 1. Volumetric analysis of bone/cartilage model vs the predicted voxel-based CT reconstruction.

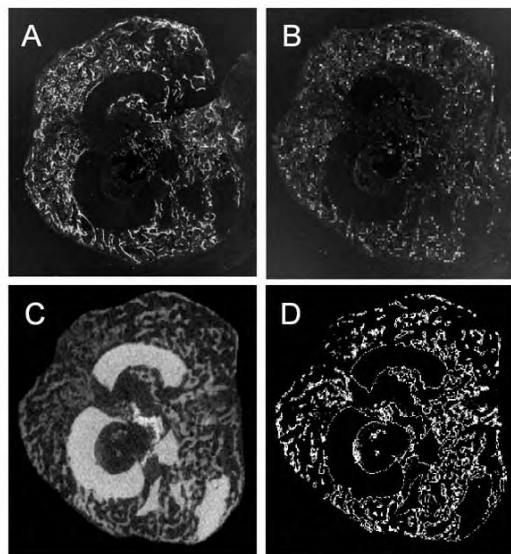


Figure 2. Representative callus sections of Col 1 (A) Col 10 (B) in situ hybridization, CT imaging (C), and predicted model (D)

Disclosures: J.A. Weis, None.
This study received funding from: NIH-NIDDK.

W473

Unilateral Osteoarthritic Hips Have Lower Trochanteric BMD and Higher Femoral Neck BMD Compared with the Unaffected Side - An Explanation Why Trochanteric Fractures Are More Frequent Than Femoral Neck Fractures in Osteoarthritic Hips. O. Wolf*, J. Milbrink*, S. Larsson*, H. Mallmin. Surgical Sciences, Uppsala, Sweden.

Patients with osteoarthritis of the hip, OAH, are subject to trochanteric hip fractures but very seldom to femoral neck fractures. One reason might be differences in bone strength due to altered bone composition in the proximal femora. In OAH there might be a problem using DXA, as external contracture is common and this might affect BMD compared to the recommended slight inward rotation. Our aim was to compare BMD at the proximal femur and heel in OAH-affected and healthy legs as well as body composition in the lower extremities. In addition we measured the effect of differences in rotation on DXA values in patients with no hip disease.

41 patients (20 women, 54 ± 8.8 years) with unilateral OAH scheduled for arthroplasty were included. Before surgery DXA was done bilaterally at the proximal femora and heels, as well as total body. Three regions of interest (ROI) for the proximal femur (femoral neck-FN, trochanter-TR and total hip-TH) were investigated. Preoperative weight bearing (WB) was measured with the F Scan system and hip abductor strength with a dynamometer (MS). Differences in rotation on DXA images between OAH and control side were thoroughly assessed. In 21 hip-healthy patients (64.1 ± 11.5 years; 42 hips) DXA was done with the foot in a vertical position as well as the recommended inward rotation to assess the effect of rotation. OAH had 5% higher BMD_{FN} ($p < 0.007$), 8% lower BMD_{TR} ($p < 0.000002$) and 5% lower BMD_{TH} ($p < 0.001$) compared with the control side. 21/38 had no differences in rotation whereas 16 had an increased outward rotation of the OAH side. Regional analyses of the total body measurement showed significantly lower BMC and fat mass, 5% and 2%, respectively, in OAH legs but no difference in lean mass ($p < 0.67$). However, when calculated as ratios these differences did not remain significant. We found no significant differences in BMD_{HEEL} , WB or MS between OAH and controls. For the hip-healthy patients there was a significant increase in BMD_{TR} (2.5%, $p < 0.00001$) but no significant influence on BMD_{FN} and BMD_{TH} with the foot in vertical position compared with slight inward rotation.

Higher BMD_{FN} and lower BMD_{TR} in OAH compared with controls, indicates that the trochanteric region is the weakest part of the proximal femur in patients with OAH. This finding can not be explained as false low values due to external contracture. On the contrary, neutral position seems to provide higher BMD_{TR} values. In conclusion, low BMD_{TR} offers a potential explanation why OAH-patients are far more likely to suffer a trochanteric rather than a femoral neck fracture.

Disclosures: O. Wolf, None.

W474

The Effect of Collagen Degradation on the Stiffness of Bone in an Emu Model. C. Wynnckijy^{*1}, S. Omelon^{*2}, M. D. Grynbas². ¹Materials Science Engineering, University of Toronto, Toronto, ON, Canada, ²Samuel Lunenfeld Research Institute, Mount Sinai Hospital, Toronto, ON, Canada.

Current methods of bone quality assessment, such as Dual energy X-ray Absorptiometry (DXA) and Quantitative Ultrasound (QUS) measure bone mineral content and density, while less emphasis has been devoted to collagen's role in fracture risk assessment. Neither DXA nor QUS provide a direct measurement of the mechanical properties of bone. DXA measures bone mineral density (BMD) and QUS measures speed of sound (SOS) transmitted through bone. Although these surrogate measurements are related to fracture risk, they are not sufficient to adequately predict bone fragility. Consequently, there is a need for a technique that can provide more information related to fracture than the data from DXA or QUS. A promising candidate is the Mechanical Response Tissue Analyzer (MRTA), a radiation free, non-invasive instrument developed by NASA to investigate the effect of space travel on bones. The MRTA directly measures a mechanical property of bone, the cross-sectional bending stiffness, which describes the ability of bone to resist deformation.

In order to assess the contribution of collagen on the mechanical properties of bone, the emu tibia was selected as a model due to its size and approximate cylindrical shape, making it ideal for devices designed to accommodate human long bones. The effect of deproteinization in ex-vivo emu bone was explored using DXA, QUS and MRTA. Four groups ($n=7-10$) of female emu tibiae were endocortically deproteinized in 1M KOH solution for 1, 3, 7 and 14 days, resulting in negligible mass loss (0.5%). Hydroxyproline assays were used to confirm minimal loss in collagen content. Statistical analysis of results over time and between techniques was performed. The negligible mass loss resulted in significant changes in modulus of elasticity between all time points (except between 3 and 7 days), as determined by 3-point bending and MRTA. The change in SOS and BMD varied by less than 2%. This is not surprising as both techniques measure changes in bone mineral content, which is not affected by KOH. In contrast, the MRTA reflected changes in the modulus caused by deproteinization of bone more significantly. No significant differences were seen between 3-point bending and MRTA. The significant reduction in modulus caused by the small amount of bone mass removal may be due to in situ collagen degradation rather than collagen loss.

	1 day	3 day	7 day	14 day
3-point bending - % Change Modulus	5.3±1.4	9.7±1.8	11.6±1.1	16.8±3.1
MRTA - % Change Modulus	4.8±1.4	10.9±1.5	13.2±2.8	18.3±3.3
DXA - % Change BMD	1.1±0.5	1.7±0.8	0.8±0.3	1.2±0.2
QUS - % Change SOS	0.9±0.2	1.4±0.4	0.9±0.4	1.0±0.2

Disclosures: C. Wynnckijy, None.

W475

A Novel Patient-Specific Finite Element Model to Predict Damage Accumulation in Vertebral Bodies under Axial Compression. Y. Chevalier*, M. Charlebois*, P. Varga*, D. Pahr*, P. K. Zysset. Institute of Lightweight Design and Structural Biomechanics, Vienna University of Technology, Vienna, Austria.

In the past years, QCT-based finite element (FE) approaches were applied to monitor the effect of anti-resorptive or anabolic treatments on vertebral body stiffness under axial compression or bending.

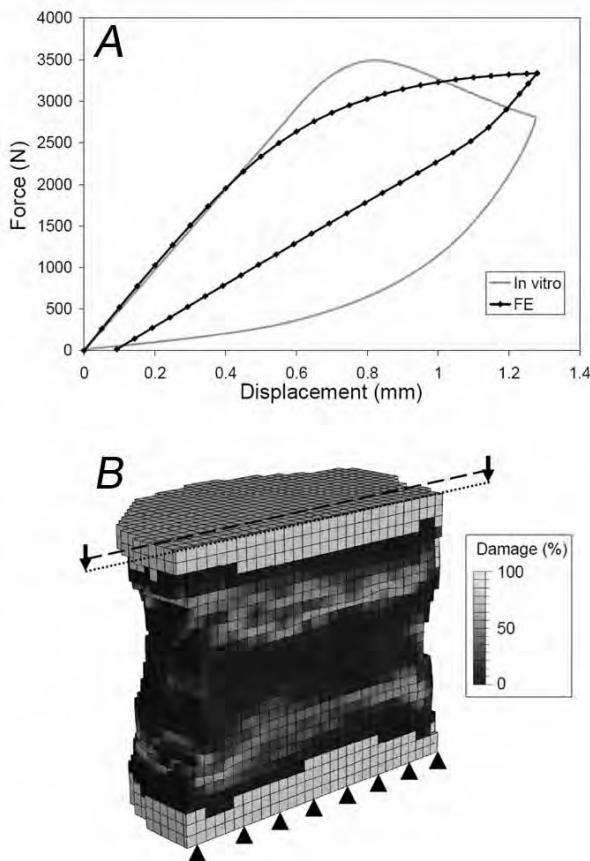
However, these FE analyses were either elastic, that is they excluded any representation of damage accumulation, or utilized constitutive laws based on metal plasticity which have limited accuracy in simulating irreversible strain and damage in bone tissue.

In this work, a novel constitutive law specifically designed for trabecular bone elasticity, plasticity and damage was applied to a collection of 12 cadaveric human vertebral bodies (L1-L5, age 47 to 83) in the framework of an automated finite element model generation software.

The vertebral bodies were scanned by pQCT at 80 microns, segmented and coarsened into 1.3mm isotropic voxels. Mineral density was converted into bone volume fraction (BV/TV) on which the elastic, yield and ultimate properties of the developed transverse isotropic constitutive law were based. Superior and inferior endplates in PMMA were added to transmit load to the vertebral bodies. Axial compression was applied to the digital meshes in the form of axial displacements on the superior endplate. Generation of the mesh and application of the boundary conditions were fully automated and a typical FE simulation took approximately 240 minutes of CPU time on 3GHz Xeon processors with 16GB RAM.

Beyond the usual compression stiffness, the yield and ultimate loads as well as the irreversible deformation of the vertebral bodies were computed. A typical force versus displacement curve is shown in Fig. 1A. While a map of the induced damage is visualized in Fig. 1B. Both vertebral stiffness and ultimate force predicted by the finite element models were linearly related to the experimental values ($r^2=0.64$ and $r^2=0.76$ respectively). The slopes and intercepts of these regressions were not significantly different from 1 and 0 respectively.

This novel finite element model of the human vertebral body was therefore properly validated by experimental data, computationally efficient and could be applied to investigate the effect of 2 years teriparatide treatment within the Eurofors study (see abstract this meeting).



Disclosures: P.K. Zysset, None.

This study received funding from: Lilly Deutschland GmbH.

W476

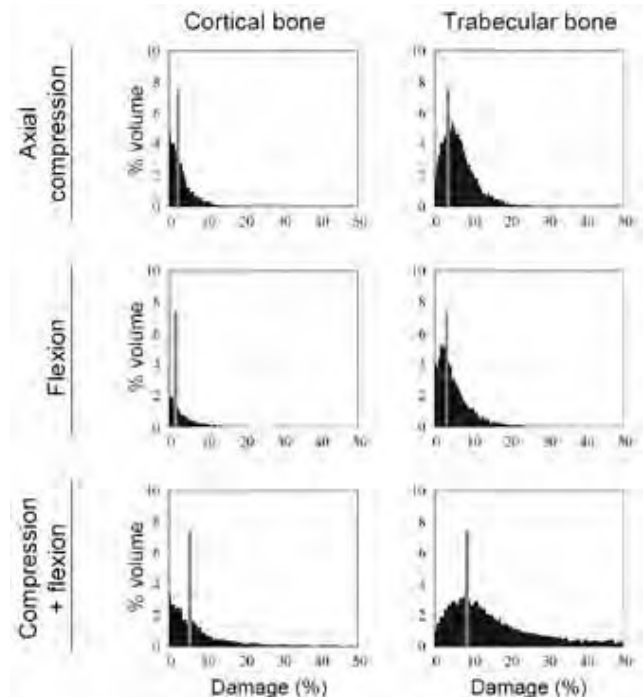
A Combined Axial Compression and Flexion Loading Mode to Evaluate Strength of Vertebral Bodies using a Voxel-Based Finite Element Method. M. Charlebois*, Y. Chevalier*, P. Varga*, D. Pahr*, P. K. Zysset. Institute of Lightweight Design and Structural Biomechanics, Vienna University of Technology, Vienna, Austria.

The effect of pharmacological treatment on the mechanical properties of bone relies increasingly on finite element models. For human vertebral bodies, axial compression is the loading mode of choice to investigate stiffness or nonlinear characteristics such as yield or ultimate force. However, in daily activities, the human lumbar spine is subjected to a variety of loading modes and vertebral fractures also exhibit different morphologies. In this context, the goal of this study was to compare stiffness and ultimate mechanical properties of human vertebral bodies under axial compression, antero-posterior flexion and a combination of these two loading modes.

A group of 12 human lumbar vertebrae (age 47-83) were scanned with high-resolution pQCT and digitized to 1.3mm voxels. A novel transverse isotropic constitutive law for bone including elasticity, plasticity and damage accumulation was used for all loading cases. Superior and inferior endplates in PMMA were added to the vertebral models to apply loads in the form of axial displacements on the superior endplate and flexion angles about a transverse axis located at the most posterior voxel of the superior endplate. A combined proportional loading mode was then applied using the axial displacement and flexion angle obtained at the yield point of the individual loading modes.

Beyond the independent axial and flexion stiffnesses, the full stiffness matrix of the sagittal motion was computed. Ultimate load and moment were calculated as the maximum force and torque resisted by each vertebrae.

As a first result, the axial and flexion stiffnesses as well as their respective ultimate properties were linearly related ($r^2=0.87$, $r^2=0.74$). In all loading modes, the level of damage was substantially lower in the cortical than in the trabecular compartment where damage localization occurred preferentially (Fig. 1). As expected, the amount of damage was increased for the combined loading mode and was higher than the sum of the damage produced by the individual compression and flexion modes. In conclusion, the combined loading mode applied in voxel-based finite element analyses provides a refined insight into the damage mechanisms leading to failure of vertebral bodies.



Disclosures: P.K. Zysset, None.

This study received funding from: Project 05Z26 of the AO Research Fund, AO Foundation; Lilly Deutschland GmbH.

W477

Effects of Strontium Ranelate Therapy after Long Term Bisphosphonate Treatment. Histomorphometric and μ XRF/EDX Analysis of Paired Iliac Crest Bone Biopsies in 15 Patients. B. Busse*, M. Priemel¹, B. Jobke², M. Hahn³, J. Zustin³, J. Semler⁴, M. Amling¹. ¹Center for Biomechanics & Trauma Surgery, Univ. Med. Center Hamburg, Hamburg, Germany, ²MQIR, Radiology, UCSF, San Francisco, CA, USA, ³Bone Pathology, Univ. Med. Center, Hamburg, Germany, ⁴Internal Medicine, Immanuel Hospital, Berlin, Germany.

Several medications have proved effective in reducing the fracture risk in patients with osteoporosis. However, the optimal duration of use of these medications and the effects of changes between treatment strategies remain to be established. The latter are of special clinical

interest in patients who have been on bisphosphonate (BP) therapy for years and present with persistent high fracture risk. To gain insights into the effects of strontium ranelate (SR) therapy after long term BP treatment we studied paired transiliac crest biopsies from 15 patients. All patients had previous BP therapy (Ø 32 months) and were subjected to bone biopsy at baseline. Patients were treated with 2g SR/d and subjected to a second biopsy after 6 months (group I, n=5) and 12 months (group II, n=10), respectively. Biopsies were undecalcified histologically processed. The bone mineral density distribution was evaluated by the gray level allocation (mean GL) of backscattered signal intensities. Energy dispersive x-ray analysis (EDX) combined with μ -x-ray fluorescence analysis (μ XRF) was used to monitor Sr concentration (Sr/(Sr+Ca), Wt%). Static analysis was performed using the Osteomeasure system according to ASBMR standard and included the quantification of bone volume (BV/TV, %), trabecular interconnection (TbPF, mm-1), trabecular thickness (Tb.Th, μ m), osteoid volume (OV/BV, %), osteoid surface (OS/BS, %), as well as osteoclast number (NOC/BPm, mm-1). In group I there was an increase in Sr content while all other indices did not show significant changes as compared to baseline. In sharp contrast in group II there was not only a further increase in Sr content of bone and mean GL but also a significant increase in BV/TV (11.12 ± 3.78 vs. 8.53 ± 2.14) with an improved TbPF (0.69 ± 0.52 vs. 1.35 ± 0.63) and increased Tb.Th (99.39 ± 9.89 vs. 89.99 ± 10.96). These structural changes were explained by activated bone formation indicated by increased OS/BS (12.04 ± 6.81 vs. 7.97 ± 5.6) and OV/BV in face of persistent suppression of bone resorption and unchanged low NOC/BPm (0.011 ± 0.016 vs. 0.035 ± 0.065). These data show that Sr is present in bone in patients that have been on BP treatment previously and that one year after SR therapy active bone formation sites are increased while osteoclasts are still repressed with beneficial effects on bone quality. Therefore SR might be considered as an alternative therapeutic option in patients that have been on long term BP treatment.

Disclosures: B. Busse, None.

W478

Bone Turnover and Quality: How Discrepancies in BMD Changes and Fracture Risk May Be Explained. M. A. Karsdal, I. Byrjalsen, D. Leeming, P. Qvist, C. Christiansen. Nordic Bioscience, Herlev, Denmark.

Introduction: Bone matrix quality may be important for anti-fracture efficacy as the reduction in risk is only partly explained by a concomitant increase in BMD during anti-resorptive therapy. Some of these discrepancies may in part be explained by careful investigation of novel bone turnover markers.

The main protein component of the extracellular bone matrix is collagen type I of which the C-telopeptide motif is released during osteoclastic bone resorption (CTX). Newly synthesized bone matrix contains the α -form of CTX, but with aging the motif spontaneously isomerizes to the β -form. Thereby index of alpha/ beta fragments released during osteoclastic of bone resorption may be a representative for endogenous bone age, which may be related to bone quality and affected differently by different treatments regimes.

The aim of the present study was to evaluate the effect of different anti-resorptive treatments (bisphosphonates, HRT, SERMs and calcitonin) on the age profile of bone collagen degradation measured as the ratio between the degradation products of newly synthesized and mature isomerized C-telopeptides of type I collagen.

Methods: Participants were from cohorts of healthy postmenopausal women participating in double blind, placebo-controlled 2-year studies of alendronate, ibandronate, intranasal hormone replacement therapy (HRT), oral HRT, transdermal HRT, oral calcitonin or raloxifene (n = 487). The non-isomerized $\alpha\alpha$ CTX and isomerized $\beta\beta$ CTX were assessed by ALPHA CrossLaps and BETA CrossLaps ELISAs, respectively, in urine samples obtained at baseline, and after 6, 12, and 24 months of therapy. Presently only 3 months data are available for calcitonin.

Results: Bone collagen age measured as the ratio between $\alpha\alpha$ CTX and $\beta\beta$ CTX showed that bisphosphonate treatment induced a pronouncedly older age profile with a 52% (alendronate) and 38% (ibandronate) reduction in the ratio between the two CTX isoforms in face of 3% and 15% with HRT or raloxifene. Calcitonin treatment resulted in an increase of 10%, rather than a decrease.

Conclusions: The different responses of $\alpha\alpha$ CTX to $\beta\beta$ CTX ratio by the various anti-resorptive therapies reflect a treatment-dependent effect on the endogenous age profile of bone collagen. These data highlight that even though the treatments have comparable effects on BMD, the endogenous bone composition, which may be associated to bone quality, is strongly affected by the type of intervention.

Disclosures: M.A. Karsdal, None.

W479

Quality and Strength of Cortical Bone in Both Ovariectomized and Sham-operated Rats Are Lowered by Limiting Physical Activity. Y. Mikuni-Takagaki¹, K. Miyagawa^{*1}, Y. Kozai^{*2}, Y. Ito^{*3}, K. Naruse^{*4}, Y. Nagai^{*5}, H. Yamato⁵, I. Kashima^{*2}, K. Ohya⁶, K. Aoki⁷. ¹Functional Biology, Kanagawa Dental College, Yokosuka, Japan, ²Maxillofacial Diagnostic Science, Kanagawa Dental College, Yokosuka, Japan, ³Yokohama Training Center, Kanagawa Dental College, Yokohama, Japan, ⁴Department of Orthopedic Surgery, Kitasato University School of Medicine, Sagami-hara, Japan, ⁵Kureha Special Laboratory Co., Ltd, Tokyo, Japan, ⁶Hard Tissue Engineering, Graduate School, Tokyo Medical and Dental University, Tokyo, Japan, ⁷Department of Hard Tissue Engineering, Department of Hard Tissue Engineering, Section of Pharmacology, Tokyo, Japan.

Lack of estrogen after menopause and reduced activity (hypokinesia) are both important factors in the pathogenesis of osteoporosis in the elderly women. To compare the contribution of these two factors independently, we developed an animal model comparing

ovariectomized (OVX) or sham-operated rats, which were housed in cages with limited space or in regular institutional cages. The experimental cages restricted standing and walking, while allowing other activities such as eating, drinking and changes in position. Thirty-two Wistar rats, 14 weeks of age, were assigned to four groups of OVX-Restricted, OVX-Walking, Sham-Walking and Sham-Restricted rats. Serum samples were collected during postoperative weeks 1, 4, 8 and 12 to study metabolic bone markers. After sacrificing rats at week 12, femora and tibia were examined with peripheral quantitative computed tomography (pQCT), laser Raman spectroscopy, three point bending, and histopathology. Although significantly elevated levels of metabolic markers, CTx, and osteocalcin were recorded in OVX groups compared to the Sham groups, results of bone strength as well as structural parameters revealed significant differences only between Sham and Restricted groups. In the Restricted rat tibial cortices, both the number of empty osteocytic lacunae and lacuno-canalicular sclerostin staining were significantly increased. Osteoclast activity was not necessarily associated with the osteoporotic pathology in restrained rat bones, suggesting a predominant role of osteocytic control of osteolysis in the bone loss of individuals with restricted activity.

Disclosures: Y. Mikuni-Takagaki, None.

This study received funding from: Ministry of Science, Education, and Culture of Japan to YM-T.

W480

Changes in Dental Enamel Crystals by Bleaching. M. Ogiwara, Y. Miake*, T. Yanagisawa*. Ultrastructural Science, Tokyo Dental College, Masago 1-2-2, Mihama-ku, Chiba -city, Japan.

Recently, the number of requests for dental bleaching has been rapidly increasing for aesthetic reasons. Clinically, dental bleaching is widely performed. Bleaching is considered to occur by the decomposition of organic substances, without affecting inorganic substances. However, there have been only a few number of basic morphological studies, and no study has been conducted on changes in the crystal structure examined by ultrahigh-resolution transmission electron microscopy. We considered that crystal-morphological evaluation of the effects of dental bleaching on enamel crystals was necessary.

We observed the structural changes in the superficial layer of extracted teeth that agreed with patient and approved ethics committee, after trimming and bleaching by scanning electron microscopy (SEM,3D-SEM), and examined the radiolucency by contact microradiography (CMR). Furthermore, trabecular and crystallographic changes in the enamel were analyzed by ultrahigh-resolution transmission electron microscopy (HR-TEM).

SEM and 3D-SEM revealed trabecular capsules, indicating a change caused by bleaching. Furthermore, HR-TEM demonstrated the decalcification of enamel crystals in some samples.

It has been considered that since bleaching occurs through the action of generated reactive oxygen species (ROS) on organic substances, it does not affect inorganic substances. However, the results of this study suggested that bleaching had considerable effects on inorganic substances. The pH is reduced by a bleaching agent, suggesting that the decalcification of enamel crystals caused by bleaching was related to the pH reduction.

Disclosures: M. Ogiwara, None.

W481

Image Processing for Three Dimensional Dynamic Histomorphometry. C. R. Slyfield^{*1}, R. E. Tomlinson^{*2}, E. V. Tkachenko^{*1}, G. J. Steyer^{*2}, C. G. Patthanacharoenphon^{*1}, G. J. Kazakia^{*3}, D. L. Wilson^{*2}, C. J. Hernandez¹.

¹Mechanical and Aerospace Engineering, Case Western Reserve University, Cleveland, OH, USA, ²Biomedical Engineering, Case Western Reserve University, Cleveland, OH, USA, ³Radiology, University of California, San Francisco, San Francisco, CA, USA.

Bone remodeling has been implicated as an indicator of bone quality. The manner in which bone remodeling influences bone strength independent of bone mass is not yet well understood but is believed to be influenced by cavities formed during remodeling. Cavity number and size may therefore influence bone quality and strength. Two dimensional (2D) histomorphometry is currently the only way to examine local bone remodeling. Unfortunately, 2D histomorphometry cannot quantify the number and size of remodeling events. In addition, 2D histomorphometry is very labor intensive and requires special training. Here we present methods for performing automated three dimensional dynamic histomorphometry which enable the measurement of remodeling cavity number and size. 3D images of bone and two different fluorescent formation markers are obtained using a automated serial milling technique at a resolution of five microns (Kazakia et al., 2007). A 3D model is created using an automated image pre-processing technique. Subsurface fluorescence is removed and an adaptive threshold automatically labels mineralizing bone. While 2D histomorphometry requires manual labeling of five or more bone surface traits (labeled surface, bone surface, osteoid surface, etc.), the 3D histomorphometry technique only requires eroded surfaces to be traced manually. Just as micro computed tomography led to improved precision and accuracy in trabecular microarchitecture measures, 3D dynamic histomorphometry is expected to be more precise and accurate than 2D methods. This is the first image processing technique to allow precise 3D measures of bone and fluorescent markers in cancellous bone. This technique will enable investigations of the effect of remodeling size and number on bone biomechanics and help to identify differences among osteoporosis therapies.

Disclosures: C.R. Slyfield, None.

This study received funding from: Case Western Reserve University.

W482

The Role of Dynamic Muscle Contractions on Inhibition of Bone loss and Muscle Atrophy in a Functional Disuse Mouse Model. A. M. Ali*, Y. Qin. Biomedical Engineering, SUNY Stony Brook, Stony Brook, NY, USA.

It is proposed that musculoskeletal disorder may be counterbalanced by understanding the relationship between muscle function and bone adaptation. Skeletal muscle dynamics and its related mechanotransduction function have been suggested as a modulator of intramedullary pressure, and may play a role in bone adaptation. The objective of this study was to evaluate optimized dynamic muscle stimulation in the therapeutic potentials in prevention of bone loss and muscle atrophy. The aims of this study were to test the role of varying the frequency and duration of repetitive muscle contractions at 1 Hz, 20 Hz, and 50 Hz on muscle mass and bone morphology in a functional hind limb disuse mouse model. Forty-four adult female BALB/c mice were randomized into 6 groups: baseline control (n=6), age-matched control (n=6), hind limb suspension non-stimulated (HLS-NS) (n=8), HLS with electrically stimulated muscle contractions at 1 Hz (n=8), 20 Hz (n=8), and 50 Hz (n=8). Pulsatile signal was delivered to the quadriceps muscle with stainless steel needle electrodes for 2 seconds, followed by a 3 second rest period, for total of 10 minutes per day, for 3 weeks. Upon sacrifice, soleus, gastrocnemius, quadriceps, and whole hind limb weights were recorded. Femoral trabecular bone was quantified using micro-CT (SCANCO) at 8 micron resolution for a 1-mm region of interest at the distal metaphysis. HLS-NS showed a decrease in the weight of soleus (-21%), gastrocnemius (-26%, p<0.01), quadriceps (-20%, p<0.01), and the whole hind limb (-15%, p<0.05). Electrically stimulated muscle contractions at all frequencies showed increasing trends in soleus (+6% to +21%), gastrocnemius (+7% to +18%), quadriceps (+3% to +12%), and the whole hind limb (+7 to +13%, p<0.05). Micro-CT revealed that HLS-NS reduced bone volume fraction (-62%, p<0.01), connectivity density (-40%, p<0.01), trabecular number (-19%, p<0.01), and increased trabecular separation (+22%, p<0.01). Muscle contractions at 1 Hz, 20 Hz, and 50 Hz significantly recovered bone volume fraction (+34% p<0.05; +47% p<0.01; +48% p<0.01), connectivity density (+50% p<0.01; +59% p<0.001; +65% p<0.001), trabecular number (+10% p<0.05; 15% p<0.001; 15% p<0.001), and decreased trabecular separation (-10% p<0.01; -14% p<0.001; -14% p<0.001), respectively. The significant recovery of muscle mass and bone structural parameters in the treatment animals suggests that the dynamic muscle contraction is a valid potential therapeutic signal for musculoskeletal disuse. Among all the applied signals, 50 Hz contraction generated the greatest response in bone morphology. These data suggest that an optimized range of physiologic signals can be responsible for prevention of bone loss and muscle atrophy noninvasively and at low magnitude.

Disclosures: A.M. Ali, None.

W483

The Long Term Macro-architectural Benefits of High Impact Exercise During Growth: A Study of Retired Gymnasts. P. Eser*, B. Hill*, S. Bass. Centre for Physical Activity and Nutrition Research, Deakin University, Burwood, Australia.

The greatest skeletal benefits from exercise occur during growth; for these benefits to be important in the primary prevention of osteoporosis they must be maintained into adulthood. Little is known however about the macro-architectural structure of bone changes in response to exercise during growth and how these changes may be maintained when exercise is ceased.

The objective of this study was to determine if retired gymnasts have greater bone strength (i.e. bigger bone size, mass and density) at both cortical and trabecular sites compared to age-matched controls. In this study we compared 30 female gymnasts (age: 23.0 ± 4.4 years, training duration: 10.5 years) who had been retired for 6.1 years, with 20 age, height and weight-matched controls (less than 2 hours of exercise per week). Volumetric BMD and bone cross-sectional area (CSA) were assessed by peripheral quantitative computed tomography (pQCT) at the epiphyses and diaphyses of the radius, humerus, tibia and femur. Polar bone strength strain index (SSIpol) and muscle CSA were assessed at the mid-shaft of each limb.

Upper Limb: At the radial and humeral shafts, cortical CSA, total CSA, BMC and SSIpol were significantly greater (15%-40%) in the retired gymnasts (p<0.01). Muscle CSA at the arm and forearm was also increased by 14% and 16%, respectively (p<0.05). At the distal radius, cortical CSA, BMC and trabecular vBMD was 19%-23% greater in the retired gymnasts (p<0.001). Lower Limb: At the tibial shaft, cortical CSA and BMC was 10% greater (p<0.05). At the femoral shaft BMC was 10% greater (p<0.08). At the distal tibia and femur, trabecular vBMD was greater by 8% and 7%, respectively (p<0.05). Muscle CSA at the upper and lower leg was not different between groups. At the lower extremity, the magnitude of the differences were approximately half that observed in the upper extremity. Between-group differences in bone geometry and vBMD paralleled the differences in muscle CSA. No significant linear relationship was found between years of retirement and any of the bone or muscle parameters.

Despite a greatly reduced level of physical activity (less than 2 hrs/week) and at least 6 years of retirement gymnasts maintained benefits that were site and region specific; at the diaphysis the macro-architectural changes were due to greater bone size and cortical CSA at the upper limb but only a greater cortical CSA at the lower limb. At the epiphysis the benefit was predominantly due to a greater trabecular vBMD at both upper and lower limbs. In conclusion, greater bone strength is maintained in gymnasts retired for up to 6 years. The macro-architectural basis of these benefits varies depending on the skeletal site and region.

Disclosures: S. Bass, None.

This study received funding from: Victorian Golf Association.

W484

The Effect of Vibration Resistance Exercise During 56 Days of Bed Rest on Different Muscle Properties. B. Buehring*, U. Gast*, I. Michaelis*, D. Belavy*, D. Felsenberg*, J. Rittweger*. ¹Internal Medicine, University of Wisconsin Hospital and Clinics, Madison, WI, USA, ²Center for Muscle and Bone Research - Charite Berlin, Berlin, Germany, ³Institute for Biophysical and Clinical Research into Human Movement, Manchester Metropolitan University, Alsager, United Kingdom.

Multiple studies have examined the effect of microgravity on muscle function. There is ongoing debate whether the observed loss of muscle function is solely correlated to loss of muscle mass. Finding the causes of muscular function loss in microgravity is important not only for future space flight missions but also for immobilized patients on earth.

Maximal voluntary contraction force (MVC) and dynamic muscle power during counter-movement jumps were examined in a 56 day bed rest setting. The effect of vibration resistance exercise (VRE) on the two tasks was also assessed. VRE, consists of a combination low frequency vibration applied to the feet and resistance training. 20 healthy male subjects participated and were divided into an exercise and a control group (CTRL). Mean MVC and surface electromyography (EMG) was measured in the plantarflexors with a dynamometer. Muscle power and jump height were used to evaluate counter-movement jumps.

After bed rest, MVC in CTRL was decreased by 17% (p<0.01), but remained unchanged in the VRE group. Maximal EMG amplitude was unaffected in both groups. Neuromuscular drive (ND) did not change in the VRE group but a trend in the decline of ND was found (p=0.052) in CTRL. Counter-movement jumps revealed a loss in peak power in both groups. Jumping ability decreased by 13% (p<0.001) in the VRE group whereas the CTRL lost 26% (p<0.001).

This study showed that bed rest without any countermeasures lead to a significant loss of MVC and a decrease in neuromuscular drive of 21% which was on the border of statistical significance. It proved that VRE was able to preserve MVC in the plantarflexors, maintain neuromuscular properties but could not prevent a decrease in the ability to perform counter-movement jumps. Mulder et al report a 14.1% loss of total quadriceps cross sectional area (CSA) in the same control group. The VRE group had a significantly smaller loss of 3.5%. We conclude that besides muscle atrophy, other factors like coordination, neuromuscular drive and changes in muscle cell function contribute to loss of certain muscle functions. VRE can preserve MVC, however it can only alleviate the loss of function in more complex tasks. Therefore it is important to add training methods like VRE to astronauts in space or immobilized patients on earth. However more research is needed to examine the effects of microgravity and immobilization on muscular functions besides maximal force.

Disclosures: B. Buehring, None.

W485

Exercise Induced Changes in the Macro-Architectural Parameters of Cortical Bone as Boys Progress Through Puberty: A Large Window of Opportunity? G. Ducher*, J. Black*, L. Saxon*, R. Daly*, C. Turner*, S. Bass*. ¹Centre for Physical Activity and Nutrition Research, Deakin University, Burwood, Australia, ²Musculoskeletal Research Centre, La Trobe University, Heidelberg, Australia, ³Basic Sciences, The Royal Veterinary College, London, United Kingdom, ⁴Department of Orthopaedic Surgery, Indiana University School of Medicine, Indianapolis, IN, USA.

Very little is known about the macro-architectural changes in cortical bone in response to exercise during different stages of growth. In this study we compared the side-to-side differences in cortical bone parameters in pre- (n=6), peri- (n=16) and post- (n=16) pubertal boys who played tennis to determine the site- and maturation-specific changes in cortical bone parameters in response to loading. Humeral BMC was assessed by DXA and bone geometry of the mid (40-50%) and distal (60-70%) humeral diaphyses was assessed by magnetic resonance imaging. The pre-, peri, and late or post-pubertal players were aged 11.2±0.5, 12.9±0.3, and 15.3±0.3 yrs and were currently training for 9.1±1.8, 15.4±1.7, 13.0±1.7 hr/wk respectively. Relative side-to-side differences in total and cortical areas ranged from 6.9% to 33.6% at both sites for all pubertal groups (p ranging <0.09 to 0.001). The absolute side-to-side difference in cortical CSA was greater in the peri- and post pubertal boys compared with the pre-pubertal boys (p<0.05). Medullary contraction was detected at the distal site (ranging from 7.9 to 14%) in all pubertal groups. In contrast, expansion in the medullary cavity was observed at the mid site (~5%) in pre- and peripubertal boys.

Table 1. Absolute side-to-side differences in humeral bone parameters in the young male tennis players according to their pubertal status (mean ± SE).

Pubertal status	Pre-	Peri-	Post-
Humeral BMC (g)	5.1 ± 1.2*	10.9 ± 1.0*	15.3 ± 1.7*†
Mid periosteal area (mm ²)	15.6 ± 7.4*	33.4 ± 4.5*	41.9 ± 5.3*†
Mid medullary area (mm ²)	5.5 ± 2.5*	3.7 ± 1.9*	3.1 ± 2.9
Mid cortical area (mm ²)	10.2 ± 5.0*	29.8 ± 4.0*‡	38.8 ± 4.3*†
Distal periosteal area (mm ²)	12.8 ± 4.4*	30.1 ± 3.7*	41.6 ± 5.0*†
Distal medullary area (mm ²)	-7.8 ± 2.2*	-10.6 ± 1.2*	-7.4 ± 3.0*
Distal cortical area (mm ²)	20.6 ± 5.4*	40.2 ± 3.5*‡	49.0 ± 4.6*†

* Playing vs non-playing significant at p<0.09-0.001

Between groups comparison: ‡ Pre < Peri at p<0.05; † Pre < Post at p<0.01

Large absolute and relative side-to-side differences in total and cortical cross-sectional areas were detected in prepubertal boys; these differences were greater in the peri and postpubertal boys. These findings are in contrast to our previous work in girls where we report an initial response in the prepubertal players but no further increase in peri and postpubertal girls despite a longer duration of loading. These findings together suggest that males may have a larger

window of opportunity to optimize the osteogenic response to loading.

Disclosures: G. Ducher, None.

This study received funding from: National Health and Medical Research Council.

W486

Optimising Bone Health in Pre-Pubertal Children: The Importance of Muscle Strength. R. English^{*1}, P. Eser^{*1}, A. Patchett^{*1}, R. Daly¹, G. Naughton², M. Seibel³, R. Telford^{*4}, S. Bass¹. ¹Centre for Physical Activity and Nutrition Research, Deakin University, Burwood, Australia, ²Centre of Physical Activity Across the Lifespan, Australian Catholic University, Sydney, Australia, ³ANZAC Research Institute, University of Sydney, Sydney, Australia, ⁴Australian Institute of Sport, Australian National University, Belconnen, Australia.

Peak muscle force is a determinant of bone strength; however its contribution to sex-specific differences in skeletal development remains uncertain. We investigated the role of muscle cross-sectional area (MCSA); a surrogate measure of peak muscle force on bone mineral content (BMC), geometry and strength at different skeletal sites (weight bearing and non-weight bearing) and bone compartments (trabecular versus cortical). Peripheral QCT was used to assess non-dominant tibia and radius (distal 4% and mid-shaft 66%) BMC, total and cortical CSA and MCSA in 598 pre-pubertal boys (n=302) and girls (n=296) aged 8-9 years.

No sex differences were detected in age, weight or tibial length. Compared to girls, boys were taller (1.4 cm), had greater radial length (0.4 cm) (p<0.001) and greater MCSA at the lower leg (3.5%) and arm (7.9%) (p<0.001). At the tibia and radius metaphyses boys had greater BMC (~10%) and total CSA (7%) (p<0.0001). These differences remained after adjusting for MCSA. At the diaphysis total and cortical CSA, and polar strength strain indices were 2-10% greater in boys (p<0.05). These differences were not maintained after adjusting for MCSA, which accounted for 10 to 40% of the variance in bone parameters. All results were maintained after adjusting for bone length. In conclusion, MCSA accounted for the greater bone strength at the diaphyses in boys compared to girls. Factors other than MCSA contributed to the sex-specific differences in skeletal parameters at the metaphyses. These findings highlight the importance of developing MCSA for improved bone health at the diaphysis in children.

Disclosures: R. English, None.

This study received funding from: Commonwealth Institute of Australia.

W487

Bone Turnover Response of Men and Women to a Strenuous Gender-Integrated Recruit Training Regimen. R. K. Evans¹, A. J. Antczak^{*1}, M. E. Lester^{*1}, R. Yanovich^{*2}, E. Israeli^{*2}, D. S. Moran^{*2}. ¹Military Performance Division, US Army Research Institute of Environmental Medicine, Natick, MA, USA, ²Sheba Medical Center, Heller Institute of Medical Research, Tel Hashomer, Israel.

Rapid onset of strenuous exercise training can lead to stress fracture, a bone overuse injury. Stress fracture susceptibility is hypothesized to result from accelerated bone remodeling and changes in bone turnover that favor resorption. Whether the bone metabolism response is different in women, who present with a five-fold greater risk for stress fracture than men, has not been studied. The purpose of this study was to assess gender disparity and changes in biomarkers of bone metabolism during a four-month recruit training program. Healthy age-matched men (n=58) and women (n=199) (19.0 ± 1.0 yr) entering a four-month gender integrated basic combat training program in the Israeli Defense Forces volunteered for this study. Blood was collected at baseline and at 2 and 4 months. Serum was analyzed for biomarkers reflecting bone formation (BAP and PINP), bone resorption (CTX and TRAP5b), nutrition (PTH, calcium, and 25-OH-D), and the cytokine response (IL-1, IL-6 and TNFalpha). A repeated measures ANOVA was used to analyze changes over time and between genders for each variable. Bone formation and resorption markers were higher in men than women (p<0.001) over the training period, though there were no gender differences in the response to training. For men and women combined, an increase in bone turnover was evident from 0 to 2 months as reflected by significant increases in BAP, PINP, CTX, and TRAP5b (see table), which decreased or stabilized from 2 to 4 months.

	Baseline		2 mos		4 mos	
	Men	Women	Men	Women	Men	Women
BAPhos (ug/L)	32.0±13.3	17.8±6.9	35.3±15.7*	21.7±8.2*	36.0±17.2	20.8±7.8
PINP (ug/L)	120.6±59.0	65.4±22.5	126.8±58.6*	78.8±32.6*	124.0±58.5*	73.6±31.5*
CTX (ng/mL)	1.3±0.5	0.9±0.4	1.4±0.6*	1.0±0.4*	1.3±0.6**	0.9±0.4**
TRAP (U/L)	4.1±1.6	3.0±0.6	4.1±1.6*	3.2±0.7*	4.2±1.7	3.1±0.8

*denotes increase for both genders 0-2 mos (p<0.001); **denotes decrease for both genders 2-4 mos (p<0.01)

Serum calcium and PTH decreased similarly in both genders from 0-2 months, returning to baseline by 4 months. 25(OH)D decreased over the study period in men, but not women. IL-1B, IL-6, and TNFalpha values did not differ between genders, and did not change over the training period. Our results show that a four-month strenuous recruit training regimen increased markers of bone formation and resorption in both men and women during the first two months of training. These data suggest that rapid onset of strenuous training initially results in acceleration of bone turnover. Whether this is related to changes in bone that predispose women to stress fracture warrants further examination.

Disclosures: R.K. Evans, None.

W488

The Functional Muscle-Bone Unit in Young Active Women. P. C. Fehling, L. Ishkanian*, K. Hawkins*, A. Lange*. Exercise Science, Skidmore College, Saratoga Springs, NY, USA.

Several authors have proposed a functional bone to muscle unit (FBMU) defined as the ratio of bone mineral content (BMC) to muscle (BMC/muscle)^{1,2,3} to characterize the relationship between bone and muscle. However, which measure of bone and muscle to use in calculating FBMU remains unclear. Therefore, this study investigated FBMU in young, healthy women, using various measures of bone and muscle to calculate FBMU.

Participants in the study were 39 women (20.1 yr ± 1.1); categorized as advanced dancers (DN; n=15), Division III volleyball players (VB; n=9) or non-athletic controls (CN; n=15). A total body (TB) DXA scan was acquired to assess total BMC and leg BMC (Lunar DPX-IQ, V4.5). A 1 RM leg press (LP; kg) and squat (kg) were used to assess leg strength. The muscle portion of FBMU (denominator) was calculated using TB fat free mass (FFM; kg), TB weight (TBW; kg), leg FFM (kg), leg mass (kg) or strength (leg press & squat; kg). Differences among groups were assessed with a 1-way ANOVA with a Tukey Post Hoc analysis. An ANCOVA was used to adjust for height and weight group differences. Significance level was set at p < .05.

The VB were significantly taller (172.2 vs. 163.3 and 163.1 cm) and heavier (65.8 vs. 59.5 and 59.0 kg) than the DN and CN groups, respectively. After adjusting for height and weight the DN and VB had significantly greater BMC than the CN in the legs; had greater TB and leg FFM; and were stronger (all measures). However, when FBMU was calculated using various measures of bone and muscle (mass or strength), no consistent FBMU pattern emerged (Table 1). For example, when FBMU was expressed as TB BMC/squat, CN had significantly greater FBMU than DN & VB. However, when FBMU was expressed as leg BMC/squat CN were significantly lower than VB. It appears that depicting the physiological relationship between bone tissue and muscle tissue using FBMU is problematic due to functional, theoretical and practical measurement issues. Several questions about FBMU remain unanswered, including, what does this variable tell us and how should it be calculated?

¹ Rittweger, J et al. Bone. 2000; 27: 319-326

² Sumnik, Z et al. J Musculoskelet Neuronal Interact. 2006; 6: 195-200

³ Dowthwaite, J et al. J Clin Densitom. 2007; 10:65-75

FBMU*	Dancers	Volleyball	Control
TB BMC/TB FFM	60.3 ± 1.5	60.5 ± 2.2	62.1 ± 1.4
TB BMC/TBW	41.8 ± 0.9	42.8 ± 1.3	40.3 ± 0.9
TB BMC/squat	13.5 ± 0.7	12.7 ± 1.0	15.6 ± 0.6 ^a
TB BMC/LP	19.0 ± 1.7	18.7 ± 2.4	25.1 ± 1.6 ^b
Leg BMC/TB FFM	22.2 ± 0.5	22.8 ± 0.8	22.1 ± 0.5
Leg BMC/TBW	15.4 ± 0.3	16.1 ± 0.5	14.3 ± 0.3 ^c
Leg BMC/Leg FFM	65.3 ± 1.4	67.5 ± 2.0	66.3 ± 1.3
Leg BMC/Leg W	45.4 ± 0.9	48.4 ± 1.3	42.9 ± .09 ^d
Leg BMC/squat	193.3 ± 10.0	213.3 ± 14.3	160.0 ± 9.2 ^d
Leg BMC/LP	7.03 ± 0.6	7.01 ± 0.9	8.9 ± 0.7 ^b

*FBMU (g/kg), x ± se

^a CN > VB & DN; ^b CN > DN; ^c DN & VB > CN; ^d VB > CN; p < .05

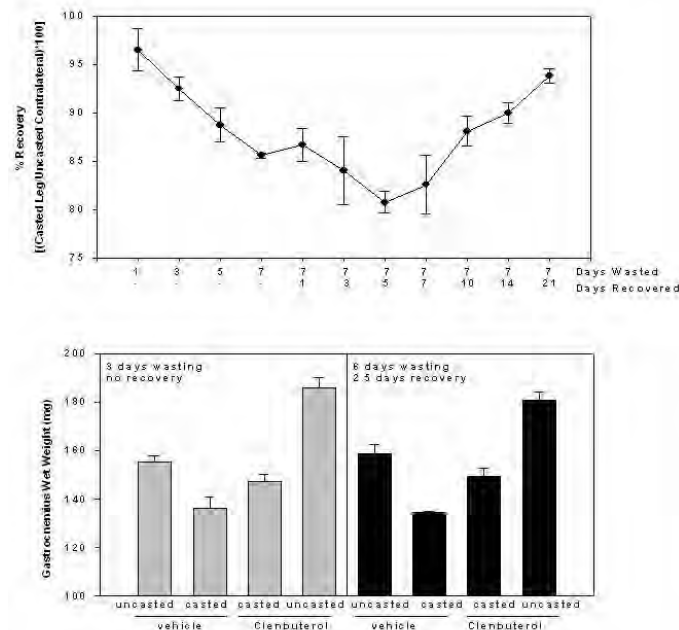
Disclosures: P.C. Fehling, None.

This study received funding from: Skidmore College Opportunity Funds.

W489

Characterization of Muscle Disuse Atrophy and Recovery in Mice Using an In Vivo Casting Model. L. V. Hale*, B. C. Yaden*, J. L. Andrews*, L. M. Helvering*, S. T. Estrem*, F. Lawrence*, S. Li*, S. McAhren*, G. Field*, H. A. Bullock*, V. Krishnan. Musculoskeletal, Lilly Research Laboratories, Indianapolis, IN, USA.

Atrophy of skeletal muscle is characteristic of sarcopenia, cancer cachexia, and disuse in both humans and rodents. Treatment of muscle atrophy is an unmet therapeutic need in these conditions and several preclinical models have been previously described. We have developed and characterized an in vivo model of disuse muscle atrophy in mice by immobilizing one hindlimb in the plantar flexion position by means of a cast. This model is very well-tolerated by the animals and results in no body weight changes with casting. Muscle loss is observed as a decrease in wet weight in both the gastrocnemius and soleus within one day of immobilization with an increasing gradual loss (15-20%) over a 7 day period. This loss is largely reversed after 3 weeks following removal of the cast and reloading of the hindlimb by the animal. Upon reloading, there is edema and some additional loss in gastrocnemius wet weight before noticeable improvement in muscle mass is observed. Atrophied and control gastrocnemius muscles were also subjected to microarray analysis and compared histologically. The beta-adrenergic agonist, Clenbuterol (2mg/kg/day), is able to diminish the extent to which the gastrocnemius atrophies during casting. IGF-1 mRNA is elevated in both the Clenbuterol casted and contralateral legs. We conclude that this in vivo model allows for consistent and characteristic muscle wasting and is useful for the evaluation of pharmacological agents which may prevent atrophy and/or enhance the recovery of muscles which are atrophied from disuse.



Disclosures: L.V. Hale, None.

W490

Electrically Stimulated Eccentric Muscle Contraction Benefits Bone in the Tibia of Hindlimb Unloaded Rats at Both the Mid-Diaphysis and Proximal Metaphysis. L. R. Sumner*, M. L. Nilsson*, J. M. Swift*, J. M. Jeffery*, C. J. Walthall*, J. L. Stallone*, S. A. Bloomfield*, H. A. Hogan*. ¹Mechanical Engineering, Texas A&M University, College Station, TX, USA, ²Health and Kinesiology, Texas A&M University, College Station, TX, USA.

The objective of this study was to investigate controlled electrical muscle stimulation as a countermeasure for bone degradation due to hindlimb unloading in adult male rats. The stimulation protocol uses fine wire electrodes to stimulate the sciatic nerve and induce contractions of the muscles of the lower left hindlimb. The ankle is dorsiflexed during stimulation to create eccentric contractions of the posterior muscles below the knee. In the current study, each session of this simulated resistance training (SRT) consisted of 4 sets of 5 contractions (1000ms) with ankle torques equal to 100% of peak isometric torque. Six-month old male Sprague Dawley rats were divided into 3 groups of 12 each: CC (cage control) animals were allowed normal ambulation; HU animals were hindlimb unloaded using standard protocols for 28 days; HU+RT animals were hindlimb unloaded for 28 days with SRT (every other day). The mid-diaphysis and proximal metaphysis of the tibia were assessed by peripheral computed tomography (pQCT). In addition, reduced platen compression (RPC) testing was used to evaluate the mechanical properties of the cancellous bone of the proximal metaphysis. On a separate group of animals, strain gauges were applied to the anteromedial surface of the tibial metaphysis. Values ranged from 800 to 1200 microstrain, which are levels generally expected to be osteogenic. The SRT protocol was highly effective as a countermeasure at both sites in the tibia. At mid-

diaphysis, total BMD was significantly higher for HU+RT than both CC (7.2%) and HU (7.0%). Total BMC was similarly higher in HU+RT (7.8% vs. CC; 14.2% vs. HU). Mid-diaphysis cross-sectional area was also higher in HU+RT (6.6% vs. CC; 13.2% vs. HU). Beneficial effects of SRT were even more dramatic at the proximal metaphysis. Total BMD was higher in HU+RT (13.4% vs. CC; 16.8% vs. HU), as was total BMC (2.4% vs. CC; 21.9% vs. HU). Ultimate stress of the cancellous bone of the metaphysis was 175% higher for HU+RT compared to CC and 268% higher compared to HU. To our knowledge, these data (along with those first presented by our laboratory last year; JBMR 2006 21(S1): S171) are the first to demonstrate not only effective mitigation of bone loss but absolute gains in bone mass during a simulated microgravity exposure with a physiological exercise intervention. In the earlier study, each exercise session consisted of 4 sets of 10 contractions (500ms) with ankle torques of 120% of peak isometric torque.

Disclosures: H.A. Hogan, None.

This study received funding from: NASA Cooperative Agreement NCC-948 with the National Space Biomedical Research Institute.

W491

The Effects of Endurance Running Training on Bone Quality in Growing Rats. T. Huang¹, R. Yang², F. Chang³, S. Lin⁴, S. Liu⁴, S. S. Hsieh⁵.

¹Institute of Physical Education, Health and Leisure Studies, National Cheng-kung University, Tainan, Taiwan, ²Department of Orthopaedics, National Taiwan University, Taipei, Taiwan, ³Department of Physical Education, National Taiwan Normal University, Taipei, Taiwan, ⁴Institute of Toxicology, National Taiwan University, Taipei, Taiwan, ⁵Institute of Sports Science, National Taiwan Normal University, Taipei, Taiwan.

To investigate the effects of two different endurance-running modes on bone quality in the growing rats. Thirty-one male Wistar rats were randomly assigned into three groups: the END group (n=10), undergoing continuous endurance treadmill running; the INT group (n=11), undergoing intermittent endurance treadmill running; the CON group, served as sedentary control group (n=10). For equalizing the training volume, the daily training distance was set equal for both exercise groups through out the eight-week training period. Intensity and distance of the two training programs were progressively increased. Both exercise groups showed decreased body weight gain after 8 weeks of running training. Regarding the effects of training on aerobic capacity, both exercise groups showed significantly higher levels in citrate synthase of soleus and heart muscle ($p < .05$) after eight-week training. Densitometric analysis of femur showed a significantly lower areal bone mineral density (aBMD) in both exercise groups as compared with CON group ($p < .05$). A three-point bending test was used to measure the biomaterial properties of bone. In extrinsic biomechanical analysis, both the END and INT groups showed significantly higher energy to maximal load and fracture load ($p < .05$), whereas significantly lower in bending stiffness as compared to the CON group. In intrinsic biomechanical analysis, both exercise groups showed a significantly higher bending stress, bending toughness and Young's modulus ($p < .05$). Additionally, the INT group was even better than the END group in some of the intrinsic biomechanical parameters. In conclusion, either continuous or intermittent endurance training did benefit the biomaterial bone properties but seemed not to be necessarily associated with aBMD. In addition to conventional geometric and densitometric measurements, further study would be important to investigate the contribution of exercise-enhanced micro-architecture on bone quality.

Disclosures: T. Huang, None.

This study received funding from: National Science Council.

W492

Hypergravity Prevents Bone Loss in Rats Following Ovariectomy. A.

Kawaguchi*, T. Ninomiya*, Y. Nakamichi*, M. Nakamura*, N. Udagawa*, N. Takahashi*, H. Kato*, K. Takaoka*, S. Wakitani*. ¹Department of Orthopedic Surgery, Shinsyu University of Medicine, Matsumoto, Japan, ²Division of Hard Tissue Research, Institute for Oral Science, Matsumoto Dental University, Shiojiri, Japan, ³Department of Biochemistry, Matsumoto Dental University, Shiojiri, Japan, ⁴Department of Orthopedic Surgery, Osaka City University Graduate School of Medicine, Osaka, Japan.

There are a lot of reports that characterize the negative effects of microgravity environment on the bone. However, little is known about the effects of hypergravity on bone loss, such as after ovariectomy in rats. Therefore, the purposes of this study were to examine whether hypergravity prevents bone loss after ovariectomy, and to elucidate the mechanisms of hypergravity effects on bone formation and bone resorption. Adult sixteen female Sprague-Dawley rats were randomized to four groups of four rats (sham or ovariectomized, and control or hypergravity exposed). Rats were performed ovariectomy or sham operation at 20 weeks of age, and the gravity treatment was started at the next day of operation. Hypergravity group were subjected to about 3G by centrifugation in accelerated gravity loading machine. The control group at 1G in an identical compartment on the floor of the centrifuge room experienced the same noise, temperature, and light environment as the hypergravity groups. The centrifuge was run continuously for 28 days, except for one hour stops each day for rat care. All animals were triple labeled with tetracycline hydrochloride and calcein injection. After 28 day of centrifugation, femur bones were excised and used for structural analysis by micro computed tomography, measurement of bone mineral density (BMD) by pQCT, and histomorphometric analysis. Micro computed tomography images showed that cancellous bone was greatly decreased in OVX control group, but the bone loss was prevented in OVX with hypergravity group. As a result of pQCT analysis, sham and OVX treated with hypergravity had significantly higher BMD of trabecular bone in distal femur metaphysis compared to control.

groups. In histomorphometric analysis, OVX decreased BV/TV as a result of increased bone turnover, but OVX with hypergravity group had significantly higher BV/TV, and significantly lower Ob.S/BS, BFR/BS, MAR, N.Oc/BS, OcS/BS. Sham groups had same tendency as OVX groups. These results demonstrate for the first time that hypergravity can suppress high bone turnover following Ovariectomy, and resulting in prevention of bone loss in aged OVX rats.

Disclosures: A. Kawaguchi, None.

W493

Association of Body Weight and Daily Walking Steps with QUS Parameters and Urinary DPD in Elderly Japanese Women. J. Kitagawa¹, Y. Nakahara². ¹Human System Science, Tokyo Institute of Technology, Tokyo, Japan, ²Health and Nutrition, Wayo Women's University, Chiba, Japan.

High levels of physical activity (PA) have positive effects on quantitative ultrasound (QUS) parameters of the calcaneus and bone resorption markers. However, it remains unclear whether the effects of PA are similar between elderly women with a high body weight and a low body weight. The aim of this study was to investigate the association of body weight and daily walking steps, as an outcome measure of PA, with QUS parameters and urinary DPD in elderly Japanese women.

The subjects were 114 elderly women aged 60 to 85 years (71.4±4.8 years). They were members of a senior citizen's club. Subjects with a history of disease known to affect bone metabolism were excluded. QUS parameters (SOS, BUA and Stiffness) in the right calcaneus were measured with an A-1000 (Lunar, USA). A pedometer (HJ-005, Omron, Japan) was given to each subject. The subjects were instructed to wear the pedometer during waking hours for 7 consecutive days.

There were significant decreases in body weight and daily walking steps with age in the simple regression analysis. Then, the subjects plotted on the upper part and lower part of the regression line were defined as a high body weight group (BW⁺) and a low body weight group (BW⁻) respectively. Similarly, the subjects were divided into a high walking steps group (WS⁺) and a low walking steps group (WS⁻) according to the regression line for daily walking steps plotted against age. Finally, the subjects were assigned to one of four groups (BW⁺WS⁺; n=17, BW⁺WS⁻; n=35, BW⁻WS⁺; n=33, BW⁻WS⁻; n=29). The associations of body weight and walking steps with QUS parameters and DPD were analyzed by two-way ANOVA in which body weight and walking steps were used as factor variables. There were no significant differences in age among the groups.

The main effects of body weight and walking steps on Stiffness were significant (p<0.001, p<0.05, respectively). Although there was no significant body weight x walking steps interaction for Stiffness (p=0.16), BW⁺WS⁺ had a significantly (p<0.05) greater Stiffness compared with BW⁺WS⁻, whereas there was no significant difference in Stiffness between BW⁻WS⁺ and BW⁻WS⁻. The main effect of walking steps on DPD was significant (p<0.05), whereas that of body weight was not significant. The body weight x walking steps interaction for DPD was not significant. BW⁺WS⁺ showed significantly (p<0.05) lower DPD compared with BW⁺WS⁻. BW⁺WS⁺ showed non-significant 16% lower DPD compared with BW⁻WS⁻. These results indicate that there may be additive effects of walking steps on QUS parameters for elderly women with a high body weight. On the other hand, higher levels of walking steps may be effective in reducing DPD irrespective of the body weight levels.

Disclosures: J. Kitagawa, None.

W494

Role of the L-Type Voltage-gated Calcium Channel Cav1.3 in Bone Mechanotransduction. J. Li¹, C. H. Turner². ¹Department of Biology, Indiana University Purdue University Indianapolis, Indianapolis, IN, USA, ²Department of Orthopedic Surgery, Indiana University School of Medicine, Indianapolis, IN, USA.

Osteoblasts respond to mechanical stimulation with a rapid increase in intracellular calcium ion that is dependent on both extracellular calcium entry and release of calcium ion from intracellular stores. Previous studies have demonstrated that extracellular calcium entry via L-type voltage sensitive calcium channels (L-VSCC) is important in osteoblast proliferation. An alpha 1 subunit forms the pore of the channel and contains the sequences for the dihydropyridine receptor and the voltage sensor. Cav1.3 (alpha 1D) is one of the four different genes that code for the L-VSCC alpha 1 subunit and has been found in osteoblastic cells. We hypothesized that Cav1.3 plays a role in bone growth and mediates mechanically induced bone formation. In order to test this hypothesis, we measured the bone length and bone mineral content in Cav1.3 knockout (KO) mice (obtained from D James Surmeier, Northwestern University, Chicago, USA). We also investigated the skeletal response to loading in Cav1.3 KO mice. The body weight of male KO mice was significant lower than the wildtype male mice (p < 0.05). There was no difference in femur length and bone mineral content of femur and tibia between KO and WT control mice. Axial loading of the ulna with a peak force of 2.5 N (2 Hz for 120 cycles) for 3 days induced new lamellar bone formation on the periosteal surface at midshaft in both KO and normal control mice. There was no difference in mechanically induced mineralizing surface and bone formation rate between KO and WT mice (p = 0.12 and p = 0.17). Others have shown that L-VSCCs are important for osteoblast signaling after mechanical loading. However, our data suggest that Cav1.3 is not necessary for bone growth and skeletal response to mechanical loading. We conclude that the Cav1.3 subtype of L-VSCC is not primarily responsible for the role of L-VSCC in bone development and mechanotransduction in osteoblasts.

Disclosures: J. Li, None.

This study received funding from: NASA.

W495

Mechanical Enhancement of Bone Quality Is Paralleled by Suppression of Fat Production: Can Osteoporosis and Obesity be Countered Through the Same Mechanism? Y. K. Luu¹, E. Capilla², B. J. Lee¹, J. E. Pessin², S. Judex¹, C. T. Rubin¹. ¹Biomedical Engineering, Stony Brook University, Stony Brook, NY, USA, ²Pharmacology, Stony Brook University, Stony Brook, NY, USA.

An inverse yet interdependent relationship between osteoblasts and adipocytes in the marrow cavity has been identified, emphasizing that both bone and fat stem from a common precursor - the mesenchymal stem cell. We posit that the introduction of a low magnitude mechanical signal that is anabolic to bone can in effect alter the balance of bone and fat development at the tissue level, and while improving bone quality could also serve as an effective preventative measure towards the onset of obesity. Twenty four C57/BL6 male mice, 7wks of age, were randomly split into two groups, VIB: 12 wks of whole body vibration (0.2g, 90Hz, 15min/d, 5d/wk), and PL: an equal number of placebo sham controls. To promote adiposity, all animals were fed a high fat diet (45 kcal % fat) through the study duration. Body mass gains and the average food intake/wk were similar for both vibrated and control groups. In vivo microCT scans at 12 wks were used to quantify bone and fat (subcutaneous and visceral) of the entire torso of each animal. Normalized to body mass, VIB showed a 6.6% increase (p = 0.015) in lean volume and 5.3% increase (p = 0.098) in bone volume over PL. Post-sacrifice, high resolution (12 µm) microCT scans of the left tibia of VIB indicated a 13.8% (p = 0.058) increase in trabecular bone volume over PL. Additionally, connectivity density (+27.1%, p = 0.058) and trabecular number (+12.1%, p = 0.060) in VIB were increased over PL, while trabecular spacing (-12.5%, p = 0.051) decreased.

In contrast to the increase in bone quantity and quality measured in VIB, these animals also had 28.5% less fat volume (p=0.030) as compared to PL. Weights of epididymal fat pads harvested at sacrifice correlated strongly with CT data (R² = 0.80), and also demonstrated a reduction in VIB animals. That the anabolic effect to bone is achieved at the "cost" of a significant reduction in adiposity, achieved without a metabolic challenge (i.e., the signal is low and the duration is short), suggests that these mechanical signals influence the skeletal and fat phenotype by preferentially driving the lineage commitment and subsequent differentiation of the mesenchymal stem cells towards bone.

Disclosures: Y.K. Luu, None.

This study received funding from: NIH (AR 43498), NASA (NAG 9-1499), and a Wallace H. Coulter Early Career Translational Research Award.

W496

Using pQCT to Assess Regional Bone Changes Resulting from Short-Term Exercise Interventions. C. H. Negus¹, R. K. Evans², W. Shen¹, H. M. Isome², M. L. Lester², D. E. Catrambone², B. A. Spiering³, D. L. Hatfield³, W. J. Kraemer³, B. C. Nindl². ¹L-3 Jaycor, San Diego, CA, USA, ²U.S. Army Research Institute of Environmental Medicine, Natick, MA, USA, ³University of Connecticut, Storrs, CT, USA.

The purpose of this randomized controlled trial was to evaluate the effect of several short term exercise interventions over 13 weeks on regional bone strength parameters of the tibia using peripheral quantitative computed tomography (pQCT). Fifty-seven female volunteers (age 20.4 ± 1.8) were assigned to one of four groups: a sedentary control group, a resistance training group, an aerobic group, or a combined aerobic-resistance group. pQCT scans were taken at sites 4%, 38% and 66% from the distal end plate of the tibia at baseline and at the end of the 13-week training period. Cross-sectional images were divided into six 60° sectors centered on the intramedullary canal. Matlab was used to register and align images and to assess geometry (4%: trabecular area; 38%, 66%: cortical area, periosteal diameter, cortical thickness, & cross-sectional moment of inertia), density (4%: trabecular density; 38%, 66%: cortical density) and overall bone strength (38%, 66%: bone strength index, Slenderness Index). A repeated-measures ANOVA compared the four training groups over time; Fisher's LSD was used to analyze significant interactions. Trabecular density increased significantly at the 4% site with exercise intervention, while the control group exhibited no change. Changes were most pronounced in the groups incorporating impact exercise, and were evident on the medial aspect of the tibia. Measures derived from the 38% and 66% site did not change significantly.

Region	Control (N=10)		Resistance (N=16)		Aerobic (N=14)		Combined (N=17)	
	Pre	Post	Pre	Post	Pre	Post	Pre	Post
Lateral- Anterior	290.2 15.9	289.2 14.0	296.6 39.9	295.5 39.1	281.6 48.1	283.4 45.8	284.6 31.2	284.8 29.7
Anterior	278.1 16.3	278.0 17.0	279.5 37.9	280.7 37.4	267.5 48.2	270.7 48.9	269.5 27.8	270.9 27.5
Medial- Anterior	272.0 22.0	269.4 18.3	264.9 37.6	265.1 37.7	255.6 37.1	260.0* 37.5	258.6 22.4	260.9 19.6
Medial- Posterior	297.0 25.3	297.6 27.1	290.7 45.1	295.4* 44.7	279.2 30.5	288.0* 31.8	282.9 33.0	288.7* 31.0
Posterior	299.9 25.0	299.7 27.6	302.9 46.2	302.1 46.1	280.0 40.7	282.1 41.0	291.6 32.4	293.8 30.5
Lateral- Posterior	301.9 33.1	304.6 31.2	312.4 52.3	311.9 52.7	286.5 51.5	287.9 49.4	297.2 36.1	299.2 34.6
ALL	289.9 13.4	289.7 13.6	291.2 39.8	291.8 39.4	275.1 39.6	278.7* 38.8	280.7 26.3	283.0* 24.5

Trabecular density (mg/cm³) at the 4% site. Values expressed as mean ± SD. * significance at p<0.01

These results indicate that a subtle regional increase in trabecular density may be the earliest manifestation of improvements in bone strength resulting from exercise intervention.

Disclosures: C.H. Negus, None.

W497

Load-specific Differences in Femoral Neck Cortical Geometry: Preliminary data from 3-D MRI Study of Proximal Femur of Athletes. R. Nikander¹, H. Sievänen¹, P. Dastidar^{*2}, A. Heinonen³, P. Kannus^{*4}. ¹Bone Research, UKK Institute for Health Promotion Research, Tampere, Finland, ²Department of Radiology, University Hospital, Tampere, Finland, ³Department of Health Science, University of Jyväskylä, Jyväskylä, Finland, ⁴Department of Trauma, Musculoskeletal Surgery and Rehabilitation, University and University Hospital, Tampere, Finland.

During normal walking, femoral neck (FN) is subjected to a large number of consecutive, low magnitude impacts from typical directions. In contrast, during sport performance, power-lifters' femoral neck experiences very high magnitude, low rate loading from unusual direction, while swimmers' femoral neck is subjected to high rate muscle activity lacking virtually the weight-bearing component. We aimed to investigate the differences in the femoral neck cortical geometry among world-class power-lifters, national level swimmers and normal exercisers serving as referents.

In this preliminary analysis of accumulating bone data from five power-lifters, five swimmers and five referents were compared. In all groups, the femoral neck cortical structure was assessed with DXA and 3-D MRI of the proximal femur. ANCOVA (age, weight and height as covariates) were used for statistical analysis.

The femoral neck BMC and BMD were 35% and 31% higher in power-lifters, but 11% and 13% lower in swimmers compared with controls ($0.02 < p < 0.07$). Interestingly, the shape of power-lifters' femoral neck appeared to be round at the narrowest section, while swimmers' and controls' FN seemed to be oval being wider in the superior-inferior direction.

Although the inter-group differences in the femoral neck cortical thickness did not reach statistical significance, a clear trend suggesting substantially thicker cortices in power-lifters in all anatomic directions (anterior 22%, posterior 52%, superior 12% and inferior 45%) was found, while the cortices between swimmers and referents were similar.

The strong femoral neck structure (more mass, denser bone, round shape and thick cortices) seemed to be characteristic of power-lifting performance. High magnitude loading produced at low rate seemed to account for strong femoral neck, while non-weight bearing, low-magnitude loading, despite large number of repetitions at relatively high rate, seems not benefit to bone structure at all.

Disclosures: R. Nikander, None.

W498

The Effect of Resistance Exercise on In Vivo-Derived Tomography Measures and Mechanical Properties of Rodent Bone: Is More Load Always Better? M. Nilsson^{*1}, J. M. Swift^{*1}, C. J. Walthall^{*2}, J. L. Stallone^{*1}, H. A. Hogan², J. D. Fluckey^{*1}, S. A. Bloomfield¹. ¹Department of Health and Kinesiology, Texas A&M University, College Station, TX, USA, ²Department of Mechanical Engineering, Texas A&M University, College Station, TX, USA.

Weight-bearing resistance exercise and high-impact jump training have previously been shown to be particularly beneficial to skeletal growth compared to other modes of exercise. Exercising against an increased resistance, such as traditional strength training, would theoretically yield higher bone strains compared to exercise with just your own bodyweight (BW), and is expected to produce a greater anabolic response in bone. The purpose of this study was to compare the osteogenic effects of a 5-week progressive resistance exercise paradigm with a BW exercise protocol in rats. Mature male Sprague-Dawleys (mean BW of 407 ± 26.5 g) were operantly conditioned to perform a full leg extension to reach an illuminated lever (mimicking a traditional squat), and thereafter assigned to a resistance exercise group (RT; n=16), a BW exercise group (BW-EX; n=15), or a cage-control group (CC; n=7). Three training sessions were performed per week and resistance was progressively increased from 80 g during session 1 to 410 g during session 15 in the RE group. The BW-EX completed the same number squats per session as the RT group, but without added weights, resulting in many rats being able to jump off the cage floor. In vivo peripheral quantitative computed tomography scans (pQCT) of midshaft and proximal tibiae were done at baseline and after 5 weeks of training. Strength, stiffness, and toughness of mid-diaphyseal tibial bone were assessed with 3-point bending tests to failure post sacrifice. Ex vivo pQCT scans and bending/compression tests of the femoral neck were also performed. RE and BW-EX resulted in similar increases in tibial total bone mineral content (BMC) at the metaphysis (+10% and +11%, respectively) and midshaft (+19% and +18%, respectively). Diaphyseal bone area, cortical shell thickness, and polar moment of inertia increased significantly in RT (+14%, +9%, and 29%, respectively) and BW-EX (+13%, +9%, and +26%, respectively), and both groups had significantly stronger, stiffer, and tougher bone compared to CC ($p < 0.05$). Femoral neck total BMC ($p < 0.001$) and max force ($p < 0.01$) were significantly higher in exercise groups compared to CC, but there were no differences between RT and BW-EX. In summary, increasing load magnitude by up to ~100% of the animal's bodyweight in this voluntary resistance exercise paradigm did not produce additional gains in BMC, bone geometry, or mechanical properties. We speculate that the additional impact provided by jumping in the BW-EX group may account for the similar benefits.

Disclosures: M. Nilsson, None.

This study received funding from: Huffine's Institute, Texas A&M University.

W499

Musculoskeletal Response to Altered Mechanical Demand Is Tissue Specific and Influenced by Genetic Make-up. E. Ozcivici¹, S. Lublinsky^{*1}, C. Rubin¹, L. Donahue², S. Judex¹. ¹Biomedical Engineering, SUNY Stony Brook, Stony Brook, NY, USA, ²Bone Biology Group, Jackson Labs, Bar Harbor, ME, USA.

The degree of musculoskeletal devastation by the loss of functional weightbearing is heavily influenced by genetic variations. Here, we subjected genetically heterogeneous mice to 3wk of disuse (hindlimb unloading) and 3wk of subsequent reambulation to investigate: (a) if the degree of mechanosensitivity of cortical bone, trabecular bone and muscle are similar, (b) whether the amount of tissue at baseline is associated with disuse induced changes in morphology (c) to what extent the loss in tissue morphology can be recovered upon reambulation. In vivo μ CT quantified longitudinal changes in metaphyseal trabecular bone, middiaphyseal cortical bone, and muscle surrounding cortex in the femur of adult (4mo) F2 female progeny of BALB and C3H (high and low mechanosensitivity) mice (n=450). During disuse and reambulation, changes in cortical area amounted to $-1(\pm 4)\%$ and $4(\pm 4)\%$, respectively. Age-matched controls (n=29) added $3(\pm 1)\%$ and $4(\pm 1)\%$ of cortical bone in an identical time frame indicating that appositional growth was retarded with disuse. Muscle loss during disuse was $9(\pm 11)\%$, 82% of which was recovered upon reambulation. Trabecular bone was devastated during disuse as characterized by a $44(\pm 17)\%$ smaller volume fraction and a $18(\pm 8)\%$ drop in both trabecular number and thickness. Recovery of trabecular volume fraction upon reambulation reached only to 10% of the loss during disuse. Even worse, trabecular number was reduced by an additional $8(\pm 9)\%$ upon reambulation while 71% of the loss was recovered in trabecular thickness. Baseline trabecular volume fraction and muscle area were inversely related to the loss during disuse ($R^2=34\%$ and 16% , respectively), while changes in cortical area were not associated with baseline morphology ($R^2<1\%$). The relation between the loss of skeletal tissue during disuse and gain upon reambulation was weak ($R^2<10\%$) for both trabecular and cortical bone, while in muscle, a moderate correlation ($R^2=32\%$) was observed. In summary, changes in mechanical demand resulted in a very tissue- and compartment-specific response with large differences between muscle, cortical bone, and trabecular bone. The data also suggest a genetically regulated protective effect of the quantity of trabecular and muscle tissue at baseline on the preservation of tissue during disuse. In contrast to muscle that recovered most of its losses upon reambulation, the recovery of trabecular bone was minimal with some architectural aspects even continuing to deteriorate. The large variations between individuals emphasizes that the identification of the underlying molecular basis will be invaluable for the future development of tailored treatments.

Disclosures: E. Ozcivici, None.

This study received funding from: NASA.

W500

Males Have an Enhanced Osteogenic Responsiveness to Loading vs. Females - A Consequence of Higher Mechanical Competence of Female Bones Relative to Locomotive Loading. I. Pajamäki^{*1}, O. Leppänen^{*1}, J. Jokihaara^{*1}, H. Sievänen^{*2}, P. Kannus^{*2}, T. L. N. Järvinen¹. ¹Orthopaedics and Traumatology, University of Tampere, Tampere, Finland, ²UKK Institute, Tampere, Finland.

Sex is considered one of the primary factors modulating the responsiveness of bone to mechanical loading. The purpose of this study was to assess whether the loading-induced bone gain (mechanoresponsiveness) differs between young male and female rats.

A total of 40 three-week old male (M) and female (F) rats were used. At entry, unilateral sciatic neurectomy was performed to remove loading from left limb (L-) while the contralateral right limb remained intact (subjected to normal physiological loading, L+). After a 6-month study period, a comprehensive structural analysis of the femoral midshaft was carried out utilizing peripheral quantitative computed tomography (pQCT) and mechanical testing. Total cross-sectional area (tCSA), cortical cross-sectional area (cCSA), cortical bone mineral content (cBMC) and fracture load (Fmax) were determined. To eliminate the inherent bias arising from comparisons between animals differing in body weight and size, all data pertaining to bone mechanical competence was equalized in terms of the animal's apparent loading environment by using the body weight and femoral length as covariates.

A clear sex-difference was observed in the mechanoresponsiveness, males exhibiting significantly higher loading-induced responses than females (Figure). However, it should be noted that the non-loaded (L-) bones of females displayed clearly higher mechanical competence relative to the animal's apparent loading. Thus, it is quite plausible that there is no need for these already "overstrengthened" female bones to adapt to mechanical loading with the same magnitude as the male bones.

In conjunction with our previous findings (Järvinen et al. Bone 2003 and JBMR 2003), the reduced mechanoresponsiveness of female bones seems to be explained by the difference in the mechanical (locomotive) competence of bones between sexes. Thus, our results emphasize the importance of acknowledging the locomotive context (existing bone characteristics) in studies evaluating the mechanoresponsiveness of bones.

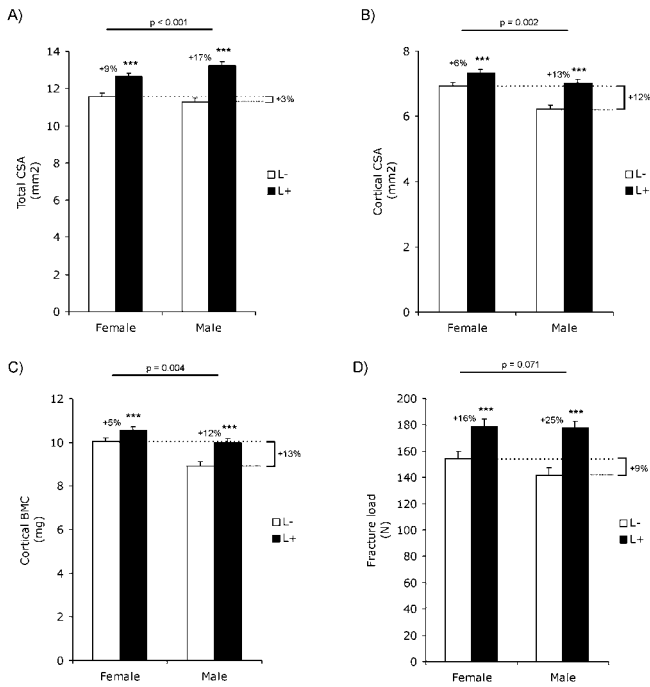


Figure. The mechanoresponsiveness of female and male bones. Bars represent mean \pm standard error of mean (SEM). Significant differences between L+ vs. L- are indicated as follows: *** p < 0.001. The p-value for interaction (sex and loading) is presented on top of each figure. □ denote the difference in the normal (control) bones between females and males.

Disclosures: I. Pajamäki, None.

W501

Effects of Vibration Plus Resistance Training on Bone Metabolism in Postmenopausal Women. I. J. Palmer*, M. G. Bemben*, D. A. Bemben. Health and Exercise Science, University of Oklahoma, Norman, OK, USA.

Whole body vibration has been shown to be osteogenic in animal models, however the efficacy of vibration as an intervention for the prevention of osteoporosis in humans is not clear. The purpose of this study was to examine the effect a vibration stimulus preceding resistance exercise on bone mineral density (BMD) and bone biomarkers in healthy estrogen-deficient postmenopausal women, 55 to 75 years of age. Subjects were assigned to a control group (C, n=12), resistance training group (R, n=22), or a vibration plus resistance training group (VR, n=21). R and VR trained 3 days/week for 8 months, with 3 sets of 10 reps (80% of 1RM) on 8 exercises. VR received vibration in three different positions beginning with 1 set of 15 sec (30Hz, 2.16g) and progressing to 2 sets of 60 seconds (40Hz, 2.8g). Training loads were adjusted every 5 weeks. Daily calcium intake was estimated by a food frequency questionnaire. Bone-specific alkaline phosphatase (BAP) and C-terminal telopeptides of Type-1 collagen (CTX) were measured as indicators of bone turnover. BMD and bone mineral content (BMC) of the AP lumbar spine, dual proximal femur, radius 33%, and total body were measured by DXA (GE Lunar Prodigy, enCORE version 8.80.001). At baseline, there were no significant (p>.05) group differences in age, height, weight, strength, calcium intake, BMD, or BMC. Two-way repeated measures ANOVA (group x time) did not detect significant group or time effects for BAP, CTX, or BMD or BMC at any site. VR had significantly (p<.05) higher relative strength increases in 5 of the eight exercises, compared with R. Multiple regression analyses were used to determine significant (p<.05) predictors of absolute changes in BMD and BMC in response to training for VR and R groups. Total BMD was predicted by upper body strength change ($R^2=0.089$ p=0.031). Right and left trochanter BMD was predicted by fat mass change ($R^2=0.083$ and 0.127 , p<.05). Right femoral neck BMD was predicted by change in BAP ($R^2=0.113$, p=0.019), by fat mass change ($R^2=0.108$, p=0.021), and by weight change and calcium intake change ($R^2=0.203$, p=0.005). Right total hip BMD was predicted by change in calcium intake ($R^2=0.12$, p=0.015). Spine (L2-L4) BMD was predicted by change in lean mass ($R^2=0.079$, p=0.042). Radius 33% BMD was predicted by change in fat mass ($R^2=0.091$, p=0.028) and by group ($R^2=0.074$, p=0.045). In conclusion, the vibration plus resistance training protocol did not result in significant alterations in bone biomarkers, BMD, or BMC. Although the addition of the vibration stimulus to a traditional resistance training program significantly enhanced muscle strength, no benefits for skeletal health were evident.

Disclosures: I.J. Palmer, None.

This study received funding from: Graduate College, University of Oklahoma.

W502

Flexible Multibody Simulation Approach in The Analysis of Tibial Strains During Walking. T. Rantalainen*, R. Al Nazer*, A. Heinonen*, H. Sievänen*, A. Mikkola*. ¹Department of Biology of Physical Activity, University of Jyväskylä, Jyväskylä, Finland, ²Department of Mechanical engineering, University of Lappeenranta, Lappeenranta, Finland, ³Department of Health sciences, University of Jyväskylä, Jyväskylä, Finland, ⁴UKK-Institute, Tampere, Finland.

Strains within the bone play a major role in bone remodeling. These small deformations can be determined using experimental strain gage measurements which are challenging and invasive tasks. Further, the strain measurements are, in practise, limited to certain regions of superficial bones only, e.g. the anterior surface of tibia. In this study, tibial strains occurring during walking were estimated using a numerical approach based on the flexible multibody dynamics. A written informed consent was obtained from healthy male volunteer (25 years, 184 cm, 89 kg), who served as a subject. The study was approved by the local ethical committee. The subject was asked to walk on a level surface at a natural cadence and at a constant velocity (1.47 m/s). The walking performance was recorded using four digital video cameras (COHU High Performance CCD Camera, San Diego CA, USA). A detailed lower body musculoskeletal model was developed by employing motion analysis data obtained from the walking test. The motion analysis data was used in inverse dynamic simulation to train the muscles to replicate the motion in forward dynamics simulation using a commercial human movement modeling software (BRGLifeMOD Biomechanics Modeler®, Biomechanics Research Group, Inc, USA). The tibial strains were then estimated by applying the forward dynamic simulation to a lower body model with a flexible tibia. The maximum and minimum principal strains predicted by the model were 376 and -472 microstrains, respectively, which are in line with literature values from in vivo measurements. It is concluded that the non-invasive flexible multibody simulation approach may be used as a surrogate for experimental bone strain measurements and be of use in the detailed strain analyses of bones.

Disclosures: T. Rantalainen, None.

This study received funding from: European Regional Development Fund.

W503

The Relationship Between Serum 25-hydroxyvitamin D and Bone Markers in the Professional Football Players. Y. Saita, H. Nakajima*, H. Ikeda*, H. Kurosawa*. Department of Orthopaedic Surgery and Sports medicine, Juntendo University, Tokyo, Japan.

Stress fractures are one of the most common types of overuse injuries in top athletes. A recent report suggested a relationship between the incidence of stress fractures and low 25-hydroxyvitamin D (25OH(D)) concentration in military recruits. However, relationships between 25OH(D) and bone markers in top athletes are not well known. Therefore, serum levels of 25OH(D) and bone markers were measured in the professional football (soccer) players in Japan (n = 32, mean age 24 years). The average values of 25OH(D) and bone markers were as follows; 25OH(D): 25.9 ± 2.8 ng/ml (mean \pm SD), bone-specific alkaline phosphatase (BAP): 31.3 ± 9.1 U/L, cross-linked N-telopeptides of type I collagen (NTX): 18.8 ± 5.2 nmolBCE/l. The levels of BAP and NTX were elevated above normal range in 28.1% and 62.5% in all players, respectively. There are significant positive correlations between BAP and NTX values ($r = 0.37$, p<.05). Then, we assessed the correlations between 25OH(D) and bone markers. The players were divided into two groups according to their 25OH(D) levels (low-vitD group: less than mean value of 25OH(D), n=15; high-vitD group; n=17), and bone markers were compared. Interestingly, low-vitD group showed higher levels of BAP compared to high-vitD group (p<.05). Similarly, low-vitD group showed relatively higher levels of NTX, though it was not statistically significant. The levels of 25OH(D) and BAP showed negative correlations ($r = -0.25$), yet it was not statistically significant. These findings indicate that football (soccer) players tend to be in a high turnover state in bone remodeling and the serum 25OH(D) concentration would negatively correlate with it. Further study may reveal whether 25OH(D) level could be a biomarker to predict the occurrence of stress fractures in athletes.

Disclosures: Y. Saita, None.

W504

Bone Mineral Density and Bone Quality in Unilateral Lower Limb Amputees. V. D. Sherk*, M. G. Bemben*, J. T. Cramer*, D. A. Bemben. Health and Exercise Science, University of Oklahoma, Norman, OK, USA.

Bone(s) in a residual limb undergo prolonged unloading after amputation, potentially causing significant bone loss in the hip and distal bony end of the residual limb. The purpose of this study was to examine the effect of amputation on bone geometry, volumetric bone mineral density (vBMD) and areal bone mineral density (aBMD) by comparing the intact and residual limbs in unilateral transfemoral and transtibial amputees. Five above-knee and four below-knee amputee subjects (23-50 years of age) who had been ambulatory with a prosthesis for at least 6 months gave informed consent to participate in this study. Bone geometry and vBMD were assessed at the distal end of the residual limb and comparable cross-sectional slice of the intact limb using pQCT (Stratec XCT 3000). aBMD of the proximal femurs was assessed using DXA (GE Lunar Prodigy, enCORE version 8.80.001). Paired t-tests were used to determine differences in bone variables between the amputated and intact limbs. There were significant differences in the hip BMD sites ($p < .05$) with total hip aBMD for the amputated side being 32% lower than that of the intact side. Femoral neck and trochanter aBMD were 27% and 37% lower in the amputated hip, respectively. Forty-four percent of amputees had hip T-scores < -2.5 . As shown in the table below, total and cortical areas and densities were significantly lower at the end of the residual limb compared to the midshaft of the intact limb ($p < .05$), but there were no significant differences in the trabecular area and density. In conclusion, amputees had significant decrements in total bone area and density in the residual limb compared to the intact limb, which was attributed to concomitant changes in the cortical bone variables. Based on the aBMD for the hip sites, these individuals are at increased risk for osteoporosis.

Table 1. Bone Area (A) and Density (D) pQCT Variables (Means \pm SE)

Limb	Cortical A (mm ²)	Cortical D (mg/cm ³)	Trabecular A (mm ²)	Trabecular D (mg/cm ³)	Total A (mm ²)	Total D (mg/cm ³)
Intact	400.46 \pm 36.14*	1156.67 \pm 48.96*	222.81 \pm 53.09	151.74 \pm 12.31	657.87 \pm 42.12*	796.51 \pm 64.63*
Residual	139.02 \pm 29.46	970.66 \pm 27.05	238.93 \pm 38.53	209.92 \pm 51.80	465.19 \pm 61.34	489.70 \pm 61.74

* $p < .01$

Disclosures: V.D. Sherk, None.

This study received funding from: College of Arts and Sciences, University of Oklahoma.

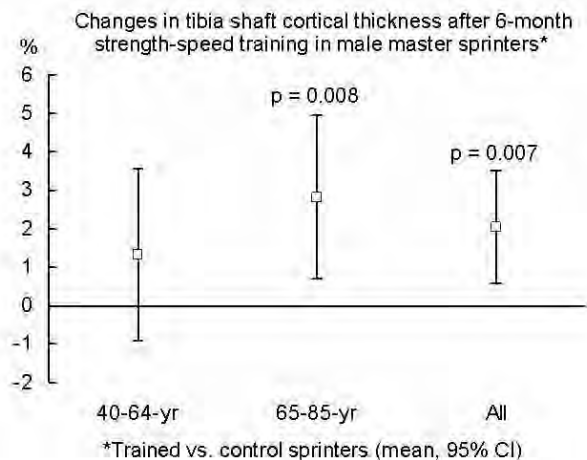
W505

Effect of Combined Strength and Speed Training on Cortical Bone Geometry and Mass Distribution in Master Athletes. H. Suominen¹, M. Korhonen¹, J. Hautakangas¹, T. Suominen¹, M. Alen¹, A. Mero².

¹Department of Health Sciences, University of Jyväskylä, Jyväskylä, Finland,

²Department of Biology of Physical Activity, University of Jyväskylä, Jyväskylä, Finland.

Cross-sectional and longitudinal observational studies have shown that athletes competing in strength and power events have superior bone mineral mass and cross-sectional geometry of long bones compared with their non-athletic counterparts. The purpose of the present study was to investigate the effects of intensive physical training on cortical bone geometry and mass distribution in master sprinters. Seventy-three male athletes aged 40-85 years with long-term experience and success in sprint events were randomly assigned into two groups. The men in the experimental group ($n=40$) participated in a periodized strength and speed training program for 6 months while the controls ($n=32$) continued their accustomed training routines. Volumetric bone mineral density (vBMD), cortical thickness (CTh), and polar mass distribution were assessed in the tibia shaft by pQCT (XCT 2000) using a Geanie 2.1. software. No significant interaction of group by time was observed in vBMD, while the mean change in CTh was 2-3% greater in the experimental group compared to controls, particularly among the older sprinters (Fig.). According to polar mass distribution, the changes were more evident in the medioanterior region of the tibia shaft. The results indicate that high-load and high-speed exercise training may improve cortical bone geometry even in elderly athletes with long-term training background.



Disclosures: H. Suominen, None.

W506

Association of Serum Osteocalcin with Bone Gain in Pubertal Girls and Bone Loss in Postmenopausal Women. S. M. Cheng¹, K. M. Fagerlund², P. Rahkila¹, E. Helkala¹, F. Tyllavsky³, F. Tyllavsky³, H. K. Väänänen⁴, S. Cheng¹.

¹Department of Health Sciences, University of Jyväskylä, Jyväskylä, Finland, ²Department of Medicine, University of Turku, Turku, Finland, ³Department of Preventive Medicine, University of Tennessee, Memphis, TN, USA, ⁴Department of Preventive Medicine, University of Turku, Turku, Finland.

Serum osteocalcin (OC) has been proposed as a specific and sensitive marker for bone formation because it is present exclusively in bone tissue and increases significantly when skeletal growth becomes boosted. Furthermore, since OC is incorporated into the bone matrix it may be released even during bone resorption. In this study we evaluate whether OC reflects bone modeling in pubertal girls, and bone loss in a group of their mothers and grandmothers. The study subjects consisted of 258 girls (mean age at baseline 11.2 yrs, menarche age 13 yrs), and 80 pre-menopausal mothers (PreM, mean age 43yrs), and 100 post-menopausal mothers and grandmothers (PostM, mean age 63yrs). Serum total OC was assessed by an in-house immunofluorometric assay. Bone mineral content (BMC) and density (BMD) of whole body (WB), total femur (TF) and lumbar spine (L2-4) were assessed by DXA (Prodigy, GE Lunar). Data for the girls were collected at baseline and 12, 24, 36, 48 and 84 months intervals. Mother and grandmother participated in the study twice at 36 and 84 months time points. The correlation between OC (not measured at 84 months) and BMC, BMD and the annual changes of BMC and BMD were calculated for successive measurement interval. In girls the mean OC concentration decreased from 45.5 \pm 12.5 ng/ml at baseline to 44.4 \pm 11.9 (12m), 42.5 \pm 12.9 (24m), 35.1 \pm 12.6 (36m), and 25.6 \pm 10.4 ng/ml (48m). The decrease was significant from 36 to 48 months. In PreM the OC concentration was lower than in PostM (6.9 \pm 2.3 vs 8.5 \pm 4.4 ng/ml $p=0.023$). In girls the OC concentrations between different time points were highly correlated ($r=0.387-0.827$). In girls a significant positive correlation was found between OC and BMC or BMD of WB, TF, and L2-4 at baseline, but significant negative correlations at 24 months and 36 months. In PostM the OC concentration was negatively correlated with BMC or BMD of the WB. Further, we found that in girls the initial OC value is associated with a positive annual BMC or BMD change during the following measurement interval. For all measured bone sites this positive relationship was strongest during 24-36 months ($r=0.447-0.595$) and 36-84 months ($r=0.701-0.771$) intervals. In PostM, the association of OC and the annual change of BMC was negative (TF $r=-0.427$, $p=0.037$ and WB $r=-0.551$, $p=0.005$). Our results indicate that in pubertal girls serum OC concentration reflects the bone gain during the bone modeling period, and bone loss by resorption in postmenopausal women.

Disclosures: S.M. Cheng, None.

This study received funding from: ASBMR Bridge Funding, Academy of Finland and Finnish Ministry of Education.

W507

Sexual Dimorphism in the Relationship Between Serum Leptin and Skeletal Health in Healthy Adolescents. J. Maalouf¹, N. Hwalla², Z. Mahfoud³, O. Obeid², G. El-Hajj Fuleihan¹.

¹Calcium Metabolism and Osteoporosis Program, American University of Beirut-Medical Center, Internal Medicine, Beirut, Lebanon, ²American University of Beirut, Nutrition & Food Sciences, Beirut, Lebanon, ³American University of Beirut, Epidemiology & Population Health, Beirut, Lebanon.

Serum leptin and bone mass are concordant in several respects and both increase at the initiation of puberty. Few studies have investigated the relationship between serum leptin concentrations and bone mineral in both genders in the context of other mediators of bone mineral accretion.

The purpose of this cross-sectional study is to determine the relationship between leptin and bone mass in 363 healthy adolescents (184 boys and 179 girls), 10-17 years old. Height (Ht), weight, Tanner stages (TS), dietary calcium and exercise were evaluated. Bone mineral density (BMD), content (BMC) and body composition were measured by DEXA. Serum leptin, 25-hydroxyvitamin and IGF1 were also measured.

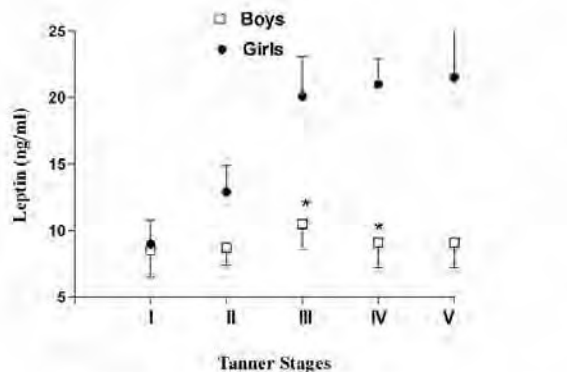
Girls had higher leptin levels than boys at all TS and reached significance at TS3 ($p=0.025$) and TS4 ($p=0.012$). In girls, leptin levels increased substantially across TS and were two-fold higher in post-pubertal girls than pre-pubertal, while in boys the increments were negligible ($p=0.87$) (Figure). This significant sexual dimorphism persisted ($\beta = 4.75$ ng/ml, $p<0.001$) after controlling for fat mass (FM) and TS.

There was a correlation between leptin and BMD at the lumbar spine, total hip (TH), femoral neck (FN), radius and subtalar body (TB) and at FNBM in boys ($r=0.17-0.26$, $p<0.05$) and at all skeletal sites for BMD and BMC in girls ($r=0.28-0.38$, $p<0.001$). Serum leptin was correlated with lean mass (LM) in boys ($r=0.31$ $p<0.001$) and girls ($r=0.48$, $p<0.001$). It was highly correlated with FM ($r=0.78$, $p<0.001$) in boys and ($r=0.67$, $p<0.001$) in girls.

There was no independent effect of serum leptin on BMD or BMC in boys after adjusting for TS, LM, FM, Ht, exercise, dietary calcium, IGF1 and serum vitamin D. Conversely, in girls, after adjustment, leptin was a consistent predictor of BMD but not BMC at cortical sites i.e. at the TH, FN, trochanter, and TB explaining 4-4.5% of variability in BMD.

Leptin correlates with BMD in girls independent of fat and other classical bone mass predictors. The basis for the sexual dimorphism in the relationship between leptin and bone mass is unclear and deserves further investigation

Plasma leptin concentrations by gender and Tanner stages



*p<0.05 between boys and girls at the same Tanner Stage by independent T-test

Disclosures: G. El-Hajj Fuleihan, Nestle 2; Merck KGaA 2.
This study received funding from: Nestle/KGaA.

W508

Analysis and Quantification of Spontaneous Bone Regeneration. T. P. Fairbanks^{*1}, T. M. Link^{*2}, D. Ellis^{*1}, J. S. Lee¹. ¹Oral & Maxillofacial Surgery, UCSF, San Francisco, CA, USA, ²Radiology, UCSF, San Francisco, CA, USA.

Rib grafts are commonly used for reconstruction in the craniofacial region. Despite the size of the defect at the donor site, the rib will regenerate completely and can be harvested a second time. Little is known about this spontaneous regeneration. This unique ability provides an opportunity to study bone regeneration in the only known site to spontaneously and completely form bone in the postnatal setting. The purpose of this study is to use quantitative CT to analyze in vivo rib regeneration at the costochondral bone graft site. This data will provide further understanding of spontaneous bone regeneration and the effects of age on bone formation.

8 Subjects (3 Female, 5 Male) were enrolled at the UCSF Oral and Maxillofacial Surgery Clinic. IRB approved consent was obtained from each participant for CT imaging at 3 intervals: immediately post-operative (T0), 3- and 6- months follow-up (T1, T2 respectively). A standard imaging protocol based on height/weight was used for each patient in a 16 row multi-slice CT scanner (Lightspeed, GE, Milwaukee, Wisconsin). The CT scans were analyzed at PACS workstations (AGFA, Somerville, New Jersey). Using image analysis software, the CT images were analyzed and quantified for densitometric and volumetric data of the regenerated osseous tissue. Using known values of bone mineral density from the calibration phantom, the computed density was converted from Hounsfield Units to mg/mL hydroxy-apatite. The area of the outlined form was given in units of cm²; volume was calculated by multiplying the computed area in the region of interest by the thickness of the axial CT slice and represented in units of mm³.

To compare regenerative capacity as a function of age, the subjects were assigned to the adult (>16 years) or pediatric (≤ 16 years) group. The adult group: 3 subjects (2 Female, 1 Male); each subject demonstrated incomplete regeneration at T2. The average volume of regenerated bone was 2049.45 mm³, with an average density of 323.76 mg/ml hydroxy-apatite. The pediatric group: 5 subjects (1 Female, 4 Male) exhibited complete rib regeneration, typically by T1. The average final volume of the young group was 4511.45 mm³, and a density of 305.45 mg/ml hydroxy-apatite.

Despite evidence of bone regeneration in all of the subjects enrolled in the study, the pediatric group exhibited substantial and complete regeneration of osseous tissue compared to the adult group.

Disclosures: T.P. Fairbanks, None.

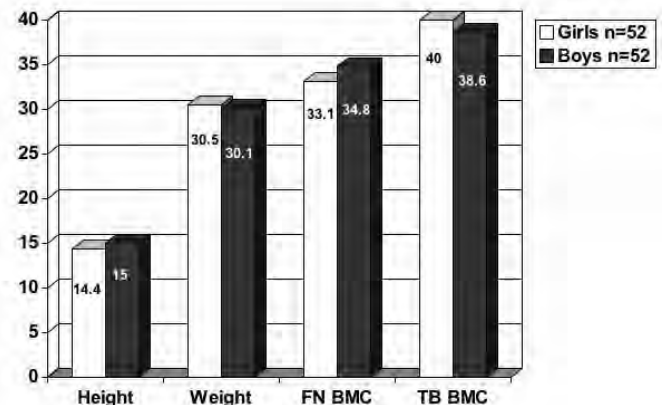
This study received funding from: UCSF School of Dentistry, Dean's Creativity Fund.

W509

Tempo and Timing of Bone Mineral Accrual During the Pre, Peri and Post Adolescent Growth Periods. M. R. Forwood¹, A. D. G. Baxter-Jones^{*2}, R. A. Faulkner², R. L. Mirwald^{*2}, D. A. Bailey². ¹School of Biomedical Sciences, The University of Queensland, Brisbane, Australia, ²College of Kinesiology, University of Saskatchewan, Saskatoon, SK, Canada.

Existing data on bone mineral acquisition during growth is limited because most studies have been cross-sectional in design or have failed to adequately control for maturational differences in growing children. Starting in 1991 we have been monitoring bone mineral accrual and bone strength in a sample of children who are now in their mid-twenties. From our original sample we present data on 52 boys and 52 girls who have been measured annually for seven consecutive years across the adolescent growth spurt years and again for up to three years as adults. Bone mineral content of the lumbar spine, femoral neck and total body was measured by DXA (Hologic 2000 QDR in the array mode). To control for maturational differences in children of the same chronological age a cubic spline curve was

applied to each subject's longitudinal height data and an age of peak linear growth (PHV) for each subject was determined. Pre-adolescence was then defined as the stage of growth up to 2 years before the age of PHV; Peri-adolescence from 2 years before the age of PHV until two years after PHV. Post adolescence was defined as the stage of growth from PHV +2 until adult status (PHV + 10 years). The purpose of the study was to describe bone mineral accrual at the three bone sites during these three developmental time periods; pre-adolescence, peri-adolescence and post-adolescence. The following graph shows the percent of adult accrual during the four year growth period surrounding PHV (Defined as Peri-adolescence = PHV ±2yr). At all sites, for both sexes, over 98% of bone mineral has been laid down by 4 years beyond the age of PHV.



Disclosures: M.R. Forwood, None.

This study received funding from: National Health Research Development Program, Health Canada.

W510

A Model of Secondary Amenorrhea in the Adolescent Female Rat. R. Joshi¹, V. R. Yingling². ¹Kinesiology, Temple University, Philadelphia, PA, USA, ²Kinesiology & Anatomy and Cell Biology, Temple University, Philadelphia, PA, USA.

Optimizing peak bone mass during late adolescence may be effective in reducing the effects of osteoporosis. Osteopenia, osteoporosis, stress fracture as well as a failure to achieve peak bone strength are all observed in young women with secondary amenorrhea. Multiple factors contribute to bone deficits in secondary amenorrhea including increased bone resorption through suppressed estrogen levels and suppressed bone formation resulting from decreased insulin-like growth factor-1 (IGF-1) levels. Therefore it is important to develop an animal model to reproduce a milieu similar to that of secondary amenorrhea in humans to study the effects of this devastating condition on bone structure. The purpose of this study was to access the effects of secondary amenorrhea induced by gonadotropin releasing hormone antagonist (GnRH-a) injections on serum levels of estradiol and IGF-1. At 23 days of age, 40 female Sprague Dawley rats were randomly assigned into a baseline group (BL) (n=6) sacrificed on day 25, a baseline 65 group (BL65) (n=10) sacrificed on day 65, an aged-match control group (C) (n=15) sacrificed on day 90, and an experimental group (Ex) (n=9) that received daily injections (2.5 mg/kg/dose) intraperitoneally for a 25 day period from day 65 to day 90. The study was approved by the IACUC. Differences in body weights and serum levels of estradiol and IGF-1 were detected using a One-way ANOVA (p < 0.05). Body weights were similar on day 65 prior to the injection protocol however on day 90, Ex group weights were significantly greater than C. Estradiol levels were suppressed by 36% in Ex compared to C and 26% compared to BL65. IGF-1 levels were 19% higher compared to C and similar to BL65 levels, IGF-1 values typically decrease as animals mature. The decrease in estradiol levels following GnRH suppression resulted from decreased pulsatile secretion of GnRH from the hypothalamus which then resulted in decreased LH and FSH secretion from the pituitary. The increase in IGF-1 levels is not similar to the clinical condition of secondary amenorrhea which results in suppressed IGF-1 levels. These data suggest that secondary amenorrhea is not only a suppression of the reproductive axis (Hypothalamic-Pituitary-Gonadal) but also results from a suppressed somatic axis (GH-IGF-1). In conclusion, modeling secondary amenorrhea using a GnRH-a may model a subset of the clinical condition.

Estradiol and IGF-1 mean (SD) * p<0.05				
	BL	BL65	C	Ex
Estradiol (pg/ml)	13.44* (1.65)	20.83 (5.08)	24.08 (4.7)	15.49* (1.99)
IGF-1 (ng/ml)	827.6 (94.8)	1256.3* (212.1)	966.1 (217.5)	1195.1* (110.7)

Disclosures: R. Joshi, None.

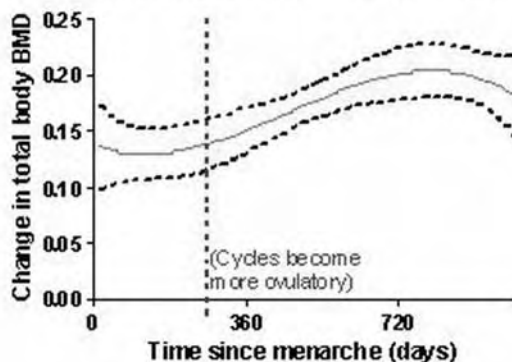
This study received funding from: NIH Grant AG19654, PSC-CUNY Grant 64293-00-33.

W511

Is Development of Ovulatory Cycles in Adolescence Important for Peak Bone Mass? S. Kalyan*, S. I. Barr*, R. Alamoudi*, J. C. Prior. Medicine, University of British Columbia, Vancouver, BC, Canada.

The purpose of this study was to investigate the potential importance of establishing ovulatory cycles following menarche in bone mineral accretion in peripubescent girls. Healthy premenarcheal Caucasian girls were recruited to this 3-year prospective study of bone development (SI Barr, JBM, 2001). The mean enrollment age of the 38 girls who completed the study was 10.6 ± 0.6 years. Body mass index (BMI, kg^2/m^2) and bone mineral density (BMD) by DXA of the total body (TB) and lumbar spine (LS) were measured every 12 months for 36 months. Participants reported when and if menarche occurred. 33 experienced menarche and 5 did not. Progesterone was measured in saliva 3-weeks after flow and weekly thereafter until the next flow by 13 of the menstruating girls; levels > 40 nmol indicated ovulation. Nine of the 13 girls had at least one ovulatory cycle. The earliest following menarche that ovulation occurred was 10 ± 5 months. The 4 girls who did not ovulate were only sampled in cycles occurring < 8 months post-menarche. BMI at baseline (18.31 ± 2.6) or 36 months (21.21 ± 3.5) did not relate to change in BMD ($r = 0.017$ and 0.163 , respectively). However, there was a significant positive correlation between the change in both LS and TB BMD and time since menarche ($r^2 = 0.14$, $p < 0.05$; $r^2 = 0.40$, $p < 0.0001$, respectively). Regression analysis (Figure 1) with the 95% confidence interval suggests that greater gains in BMD are noted at the time following menarche when cycles are more likely to become ovulatory. Although the effect of menarche on bone accrual is already appreciated, the influence of ovulatory cycles in peripubertal girls as a determinant of bone gain has not been investigated. Results of this study provide preliminary evidence to suggest that attaining ovulatory cycles contributes to optimal peak bone mass. This hypothesis is line with previous work showing that ovulatory disturbances accounted for 24% of the variance seen in changes of cancellous-bone density in regularly cycling premenopausal women (JC Prior, NEJM, 1990).

Figure 1: Regression analysis of the change in BMD over 3 years in relation to time since menarche.



Disclosures: S. Kalyan, None.

This study received funding from: British Columbia Health Care Research Foundation and the British Columbia Children's Hospital Foundation.

W512

5-Year Follow-up of Bone Mineral Distribution and Bending Strength Changes Across Puberty: Comparison Between Biological Age-Aligned Boys and Girls. S. Kontulainen¹, H. Macdonald², J. Johnston², H. McKay². ¹University of Saskatchewan, Saskatoon, SK, Canada, ²University of British Columbia, Vancouver, BC, Canada.

The greater incidence of fragility fractures in older women compared to men may be related to sex-specific patterns of bone strength development during growth [1]. Thus, the aim of this 5-year follow-up was to assess changes in bone bending strength to the smallest (Imin) and greatest (Imax) direction of rigidity, and polar distribution of bone mineral content (PDBMC) at the tibial diaphysis in boys and girls at the same maturational stage. Biological age was defined as years from age at peak height velocity for 98 participants (52 girls) in the Healthy Bones II Study. A single slice at the 50% site of the tibial diaphysis was acquired using the Norland/Stratec XCT 2000. Bonalyse 2.1 was used to assess cortical bone Imax and Imin, the polar distribution of bone mineral content (PDBMC) and muscle cross-sectional area (MCSA). K-mode with an outer threshold of $200 \text{ mg}/\text{cm}^2$ was used to define the periosteal bone surface and an inner threshold of $480 \text{ mg}/\text{cm}^2$ was used to separate cortical bone from trabecular bone. PDBMC defines the angular distribution of bone around the centre of mass. The distance from the centre represents the mass (in grams) in a 1 cm thick section. Data were analyzed using a hierarchical (random effects) modelling approach. During and after rapid skeletal growth boys distributed their bone mass further from the neutral axis, especially towards the anterior and posterior directions of the tibial diaphysis, when compared with girls at the same biological age (Fig 1). This resulted in a greater magnitude of the sex-difference in the direction of greatest bending rigidity (Imax). When biological age, tibial length and MCSA were controlled for, boys had a statistically significant greater increase in bending strength in both directions. These results are in accordance with evidence from anthropological samples suggesting that

lower limb bones of adult males are more adapted for anterior-posterior (A-P) bending and common loading direction compared with females [2]. However, this phenomenon may be site-specific and further research at other bone sites is warranted.

References:

1. Seeman E, Delmas PD. N Engl J Med. 2006;354:2250-612.
2. Ruff CB, Hayes WC. Am J Phys Anthropol. 1983;60:383-400.

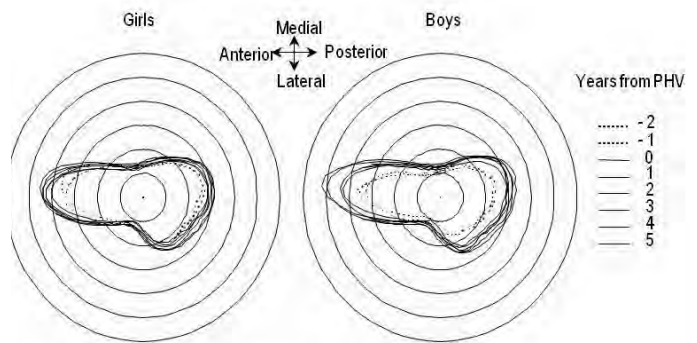


Figure 1. Change in PD_{BMC} in both sexes aligned with biological age

Disclosures: S. Kontulainen, None.

W513

Age-Related Distribution of Bone and Skeletal Parameters in 1,322 Young Women. T. Kuroda¹, Y. Onoe¹, S. Orito¹, M. Ohara¹, M. Sakai¹, K. Ishitani¹, H. Okano¹, A. Uyama², M. Kume², H. Ohta¹. ¹Dept. of Obstetrics and Gynecology, Tokyo Women's Medical University, Tokyo, Japan, ²School of Nursing, Tokyo Women's Medical University, Tokyo, Japan.

Objective: The age-related distribution of bone and skeletal parameters was examined in young female subjects to establish methodologies for prophylaxis of osteoporosis through acquisition of high bone mineral density (BMD) in younger years as well as to identify interventional measures aimed at acquisition of high BMD in these women.

Subjects and Methods: All students attending School of Nursing at Tokyo Women's Medical University, and Toho Girls Junior and Senior High Schools during August 2004 and August 2006 were enrolled in the study with the exclusion of those who were receiving treatments that could affect bone. The subjects were inquired about their date of birth, birth weight, weeks at birth, and age at menarche using a questionnaire, and their body height and weight were also measured. As relevant bone-related parameters, BMD, bone mineral content (BMC), and bone area (BA) in the lumbar spine (L2-4) as well as in the total proximal femur (hip) were measured in these subjects using QDR-4500; (Hologic Inc., USA). In addition, blood samples were drawn from the subjects to measure their calcium (Ca), phosphorus (P), bone-specific alkaline phosphatase (BAP), and urinary N telopeptide of type I collagen (NTX) levels.

Results: 1,322 students comprised our study subjects who ranged in age from 12 to 30 years of age. Their mean birth weight was $3,101 \pm 431.3$ g, and their mean age at menarche was 12.0 ± 1.2 years old. Their body height peaked at the age of 14 years, and their body weight peaked at the age of 21 years of age. Their BMD peaked at the age of 18 years of age but their L2-4 BMD gradually increased thereafter. In contrast, their total hip BMD peaked at the age of 18 years but decreased thereafter. Their L2-4 BA showed a rapid increase until the age of 14 years, while their total hip BA continued to increase gradually beyond the age of 14 years. Their L2-4 BMC exhibited a rapid increase until the age of 18 years and continued to increase gradually with increasing weight, while their total hip BMC remained constant between the ages of 18 and 23 years old and then decreased thereafter. Additionally, their BAP and NTX values were shown to decrease by about 80% between the ages of 12 and 18 years. **Conclusions:** Of all constituents of BMD examined, BMC was associated with increases in body weight and changes in bone metabolic markers. In contrast, BA was associated with increases in body height until the age of 14 years, although it appeared to be influenced by body weight beyond that age. Study results pointed to a need for lifestyle intervention by the age of 18 and increasing body weight beyond that age to ensure acquisition of high BMD in young women.

Disclosures: T. Kuroda, None.

W514

Correcting DXA Pediatric Bone Mineral Density Measurements to Account for Fat Inhomogeneity. D. C. Lee, T. A. L. Wren, V. Gilsanz. Departments of Orthopaedic Surgery & Radiology, Childrens Hospital Los Angeles, Los Angeles, CA, USA.

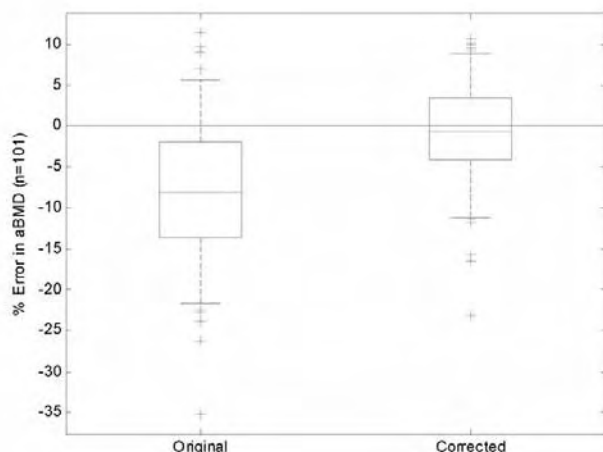
Dual energy x-ray absorptiometry (DXA) assumes that the soft-tissue anterior/posterior (AP) to the vertebrae (bone region) has the same attenuation properties as soft tissue adjacent/lateral to the bone (soft tissue region). DXA areal bone mineral density (aBMD) measurements are therefore subject to error when there is an inhomogeneous distribution of soft-tissue. The purpose of this study was to use computed tomography (CT) to calculate the error in vertebral aBMD due to inhomogeneous fat distribution and to develop an equation to correct for this error using easily obtained clinical parameters.

CT (General Electric CT-T 9800) scans were performed on the lumbar vertebrae of 700

children (350 boys, 350 girls), age 5-24 yr. Based on CT axial slices through L3, fat percent was determined in the bone and soft tissue regions. The error in vertebral aBMD was then calculated and correlated with anthropometric parameters including age, height, weight, body mass index (BMI), and trunk width (laterally), thickness (AP), and circumference. A correction equation was generated using stepwise regression. This equation was tested on a separate validation group of 101 subjects (46 boys, 55 girls) to determine the extent to which the soft tissue error was reduced.

Fat percentage was higher in the bone region than in the soft tissue region in 599 out of 700 subjects (85.5%), with an average difference of $6.0 \pm 5.7\%$ ($p < 0.001$). This inhomogeneity resulted in an average error of $-7.2 \pm 7.4\%$ in aBMD measurements (range: -21.6% to 5.5%). Stepwise regression analysis indicated that weight and trunk width had the strongest influence on the measured error ($p < 0.001$). The correction equation derived from the stepwise regression was (Corrected aBMD [g/cm^2] = aBMD [g/cm^2] - $0.1144 + 0.0011 \times \text{Weight [kg]} + 0.0004 \times \text{Body Width [mm]}$). When this equation was applied to the validation group, the range of error decreased by 25.7% and the average was reduced from $-7.7 \pm 8.3\%$ to $-0.9 \pm 6.3\%$ (Figure).

Our findings show that soft-tissue AP to the vertebrae contains more fat than soft-tissue lateral to the vertebrae, resulting in erroneously low aBMD values. Using a correction equation based on weight and trunk width, this error can be reduced significantly. Further correction may be obtained by developing equations tailored for specific subgroups such as by age, gender, sexual or skeletal maturity, or measures of body composition.



Disclosures: D.C. Lee, None.

This study received funding from: NIH & Army.

W515

Body Composition - Bone Relationship in Females Is Hormonal Stage Dependent: A Longitudinal Study. A. E. Lyytikäinen¹, F. Tylavsky², Q. Wang¹, H. Suominen¹, M. Alén¹, V. Ristimäki¹, E. Völgyi¹, S. M. Cheng¹, P. Rahkila¹, U. M. Kujala¹, E. Seeman³, S. Cheng¹. ¹Department of Health Sciences, University of Jyväskylä, Jyväskylä, Finland, ²Department of Preventive Medicine, University of Tennessee, Memphis, TN, USA, ³Department of Medicine, University of Melbourne, Melbourne, Australia.

The relationships of bone mass to lean and fat mass are controversial. We hypothesized that 1) the associations of bone mass (BM) with lean tissue mass (LM) and fat mass (FM) will change during puberty and 2) the loss of BM in premenopausal and postmenopausal females is accompanied by the loss of LM. We followed the growth of 10-13-year (y) old girls ($n=258$) 84 months (mo). In addition 80 pre-menopause (PreM, mean age 43y) and 28 peri-menopause (PeriM, mean age 49y) mothers, and 72 post-menopause grandmothers (PostGM, mean age 67y) of these girls were measured twice at a 42 mo interval. Whole body BM, LM, and FM were assessed by DXA (Prodigy, GE Lunar). Hierarchical linear model was used to evaluate the changes in BM, LM, and FM relative to menarche for the girls and annual change in the mothers and grandmothers. The mean menarche age for the girls was 13.0 ± 0.9 y. The girls' BM accrual was accompanied by LM accrual until 3y after menarche. Thereafter, growth of LM ceased, but FM continued to increase (0.96 kg/y) and was the main contributor of body weight change (1.12 kg/y) near peak HT [164.5 cm (48mo), 164.8 cm (84mo)]. The annual changes of BM were associated with those of LM ($r^2=0.327$ for 0-24mo, $r^2=0.277$ for 24-36mo and $r^2=0.404$ for 36-84mo) and FM ($r^2=0.165$ for 0-24mo; $r^2=0.185$ for 24-36mo; and $r^2=0.313$ for 36-84mo). In PreM, no changes in BM and FM were observed, but LM decreased 0.4 kg , $0.94\%/y$. LM decreased both in PeriM (0.53 kg , $1.3\%/y$) and PostGM (0.63 kg , $1.5\%/y$). This decrease was the factor that accounted for the loss of BM (PeriM= 33 g , $1.3\%/y$, and PostGM= 20 g , $0.9\%/y$). In summary, the changes in BM and LM are synchronized during rapid growth period in early puberty. In late puberty LM ceases to increase, and the fat accumulation is associated with bone accrual. The small increase in LM has higher impact than that of fat during postpuberty to early adulthood. In premenopausal women, although LM decreases, its effect on BM is minor. However, in both peri- and postmenopausal females, the loss of LM is of great importance in the loss of BM. In conclusion, the influence of body composition on bone mass gain or loss is stage-dependent from prepuberty to late postmenopausal years.

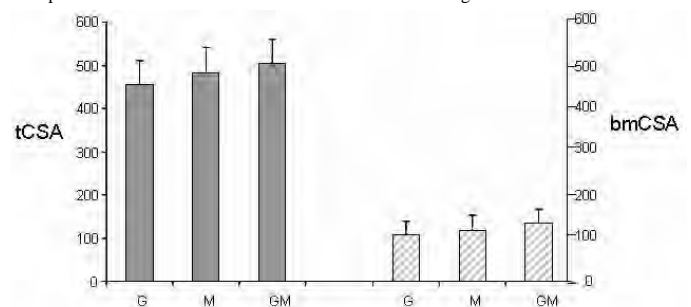
Disclosures: A.E. Lyytikäinen, None.

This study received funding from: Finnish Ministry of Education, Academy of Finland, Juho Vainio Foundation Finland, ASBMR Bridge Funding.

W516

Tibial Bone Mineral Density and Geometric Properties in Females of Three Generations. H. Q. Ma, E. Völgyi, H. Suominen, Q. Wang, P. Rahkila*, S. M. Cheng, A. Lyytikäinen, M. Alén*, S. Cheng. Department of Health Sciences, University of Jyväskylä, Jyväskylä, Finland.

The evolution of bone mineral density (BMD) and geometric properties throughout life is not well understood. In this study we investigated the volumetric BMD and geometric properties of the tibial shaft in female of three generations. Altogether 82 girls (G, mean age 17.9 ± 1.0 yrs), 76 mothers (M, 47 ± 4.8 yrs) and 47 grandmothers (GM, 71 ± 5.0 yrs) were measured using peripheral quantitative computed tomography. Total tibial cross-section area (tCSA), total bone mineral density (tBMD), cortical cross-section area (cCSA), cortical bone mineral density (cBMD), cortical thickness (cTh), bone marrow cross-section area (bmCSA), and muscle cross-section area (mCSA) were determined. Analysis of variance was used to compare the differences between generation groups. The girls had smaller tCSA than mothers and grandmothers showing the unaccomplished bone periosteal expansion. However, the tBMD of the GM group was 10% lower than either in the G or M groups due to the age related bone loss. The cCSA and cBMD were highest in the M group. The G group also had significantly higher cBMD than the GM group. The GM group had the thinnest cTh and largest bmCSA. Our results showed that the periosteal apposition may continue throughout life and endocortical resorption occurs in adult, but to a similar degree to the periosteal apposition in young adults keeping their cortical thickness unchanged. In older female, the periosteal apposition is less than the endocortical resorption thus cortex become thinner and bones become fragile.



Disclosures: H.Q. Ma, None.

This study received funding from: ASBMR Bridge Funding, Academy of Finland and Finnish Ministry of Education.

W517

Effect of the Dietary Habit of Skipping Breakfast on Bone Metabolism, Skeleton and Nutritional Status in Young Japanese Women. Y. Onoe¹, T. Kuroda¹, Y. Miyabara¹, M. Sakai¹, R. Yoshikata¹, M. Ohara¹, S. Orito¹, H. Okano¹, M. Kume², S. Sasaki³, H. Ohta¹. ¹Dpt. of Obstetrics and Gynecology, Tokyo Women's Medical University, Tokyo, Japan, ²Faculty of Nursing, Tokyo Women's Medical University, Tokyo, Japan, ³School of Public Health, the University of Tokyo, Tokyo, Japan.

The dietary habit of skipping meals not only affects systemic nutritional status but also influences intake of nutrients that are related to bone metabolism. However, it is unclear what effect such dietary habit may have on bone metabolism and skeleton. In our previous study, we have reported that ensuring appropriate physical activity, BMI, and serum 25(OH) D levels are crucial to acquisition of high bone volume during younger years. In this study, we examined the effect of skipping breakfast on nutritional status, intake of nutrients related to bone, and bone metabolism. Two hundred seventy-five healthy female volunteers aged 19 to 25 years old were enrolled in our study. All subjects were interviewed about their background information, and their height and body weight were measured. Their sera were tested for bone metabolic markers, such as BAP and NTX. Bone mineral density (BMD) was measured in these subjects using DXA (QDR 4500). The subjects were also asked about their current physical activity using a questionnaire as well as about their current diet using the self-administered Diet History Questionnaire (DHQ). The number of meals each subject skipped for breakfast, lunch and dinner during 1 week was obtained from the DHQ. Eighteen subjects (6.5%) had no breakfast during the week, while 131 subjects (45%) had breakfast every day of the week. The subjects were divided into two groups: those who had breakfast every day (group I) and those who skipped breakfast (group II). Significant differences were noted between groups in total energy intake and intake of three major nutrients (carbohydrate, protein and fat), with total energy intake and intake of the major nutrients becoming significantly lower with the increasing frequency of breakfast skipped. Oral intake of bone metabolism-related nutrients (Vit D, Vit K, Ca, P, Mg and K) was highest in group I with intake of each nutrient becoming significantly lower with the increasing number of meals skipped. Group I showed significantly higher BMD than group II in both the hip and L2-4. However, the habit of skipping breakfast had no significant effect on BMI. The habit of skipping meals had no significant effect on BAP, while it was significantly negatively correlated with NTX. Our data demonstrates that the habit of skipping breakfast leads to a decrease in systemic nutritional status, intake of nutrients, and bone metabolic and skeletal indices, thus suggesting that the habit of skipping breakfast hinders acquisition of high bone volume.

Disclosures: Y. Onoe, None.

W518

Correlation of Isokinetic Knee and Trunk Muscular Strength with Bone Mineral Content in Female Soccer Players. M. F. Saccol^{*1}, N. C. Oliveira^{*1}, A. S. Pinto^{*1}, R. M. Pereira¹, L. Takayama^{*1}, J. D. Greve^{*2}, F. R. Lima^{*1}.

¹Rheumatology Division (Bone Metabolism Laboratory), University of São Paulo, São Paulo, Brazil, ²Orthopedic Institute, University of São Paulo, São Paulo, Brazil.

The purpose of this study was to assess the correlation between knee and trunk muscle strength and bone mineral values in female junior soccer players. Twenty-two consecutive female soccer players with at least 15 h.wk⁻¹ of training during the previous year were compared with 20 females not engaged in regular exercise. Bone mineral density (BMD) and bone mineral content (BMC) were measured in lumbar spine (L1-L4), femoral neck and total femur of dominant hip, dominant leg and whole body by dual-energy X-ray absorptiometry (DXA). Fat mass and lean mass were also determined using whole body scan by DXA. Isokinetic muscle measurements were performed using the Biodex System 3 dynamometer with knee or trunk attachment on. Knee and trunk flexors and extensors strength were evaluated with 5 repetitions (concentric and eccentric modes) for the following variables: peak torque (PT), total work (TW) and set total work (STW). Statistical analysis was performed using Student t-test and Pearson's correlation. The two groups were alike regarding age, height, weight and calcium intake ($p>0.05$). Female soccer players had higher percentage of lean body mass (72.45 ± 3.52 vs. $66.75\pm5.45\%$, $p<0.001$) and lower percentage of body fat (23.7 ± 3.67 vs. $29.94\pm5.75\%$, $p<0.001$) compared to controls. For bone mineral values, the athletes demonstrated significant higher BMD and BMC compared to control group, in all sites evaluated ($p<0.05$). Dominant knee strength were also significantly higher for soccer group (concentric extension PT 150.46 ± 31.08 vs. 129.47 ± 21.72 Nm, $p=0.016$; eccentric extension PT 127.21 ± 27.15 vs. 104.85 ± 25.46 Nm, $p=0.009$). Related to trunk strength, only concentric mode had higher performance in the soccer group (concentric extension PT 214.23 ± 52.24 vs. 146.12 ± 49.72 Nm, $p<0.001$). All knee strength extension variables demonstrated positive correlation to BMC of leg, femoral neck and total femur of dominant hip ($0.46<r<0.70$). This correlation was also found for flexion knee strength, but only with PT variable ($0.42<r<0.64$). On trunk evaluation, only flexors strength performance were correlated with BMC of total trunk at variables TW ($r=0.525$) e STW ($r=0.513$). These findings of positive correlation between muscle strength and bone mineral values in a specific site reinforces that there is a direct role of muscle function on the accretion of the regional bone mineral mass.

Disclosures: R.M. Pereira, None.

W519

Weight Bearing Bones Are More Sensitive to Physical Exercise in Boys than in Girls During Pre- and Early Puberty. S. Kriemler^{*1}, L. Zahner^{*1}, J. Puder^{*2}, C. Braun-Fahrlander^{*3}, C. Schindler^{*3}, M. Kraenzlin⁴, R. E. Rizzoli⁵.

¹Institute Sport & Health, Basel, Switzerland, ²Division Endocrinology, Diabetes & Clinical Nutrition, Basel, Switzerland, ³Institute Social & Preventive Medicine, Basel, Switzerland, ⁴Endocrinology, Diabetes and Clinical Nutrition, Basel, Switzerland, ⁵Rehabilitation & Geriatrics, University Hospital, Geneva, Switzerland.

Background: Physical activity (PA) positively influences bone mineral accrual. However, little is known whether there are gender differences in bone sensitivity to loading and to what extent spontaneous objectively recorded PA influences bone mineral mass independently from muscle mass. We investigated gender differences in the association between bone mineral density/content (BMD/BMC) and measures of PA, during pre- and early puberty.

Methods: We measured BMD/BMC and fat-free mass in 374 6-13-year-old children from randomly selected schools at the hip, lumbar spine and total body by DXA. PA was evaluated by accelerometers, and lower extremity strength by a jump&reach test.

Results: Boys had higher hip and total body BMD than girls at all ages. Boys had higher fat-free mass, greater lower extremity muscle strength and were more physically active than girls at all ages. Total hip BMD was positively associated with time spent in total and vigorous PA in boys ($r=0.33$ and 0.27 , respectively, $p<0.01$), but not in girls ($r=0.02$ and 0.04 , $p=ns$), even after adjusting for fat-free mass and lower extremity strength. While boys and girls in the lowest tertile of vigorous PA (22 min per day) had similar hip BMD (0.668 vs 0.679 g*cm⁻²), those boys in the highest tertile (72 min per day) had significantly higher values than the corresponding girls (0.730 vs. 0.692 g*cm⁻², $p<0.05$). In multiple logistic regression analyses, a low hip BMD in boys was best predicted by fat-free mass (OR 0.55 [95%CI 0.38, 0.78] per 1 kg) and total PA (OR 0.69 [95%CI 0.49, 0.98] per 106 counts), while in girls predictors included fat-free mass (OR 0.63 [95%CI 0.50, 0.79] per 1 kg) and jump&reach (OR 0.90 [95%CI 0.84, 0.98] per 1 cm). Similar data were obtained for femoral neck BMD/BMC. There was no influence of PA on lumbar spine BMD in either gender.

Conclusion: Though at low physical activity during pre- and early puberty, hip BMD is similar in both genders, it increases proportionally to PA, and differences in bone mineral mass between genders appears, likely related to a different sensitivity of bone to physical loading, independently from muscle mass.

Disclosures: R.E. Rizzoli, None.

W520

Accrual of Lean Mass Has More Impact Than the Accrual of Fat Mass on BMC During Growth. F. A. Tylavsky¹, G. Somes^{*1}, M. Alen², A. Lyytikäinen³, V. Ristimäa^{*3}, S. M. Cheng³, H. Suominen³, U. M. Kujala^{*3}, S. Cheng³.

¹Preventive Medicine, University of Tennessee, Memphis, TN, USA,

²Health Sciences, University of Jyväskylä, Jyväskylä, Finland, ³University of Jyväskylä, Jyväskylä, Finland.

Many reports have focused on the role lean (LM) and fat mass (FM) plays in the accrual of bone mass. The objective of this study was to examine the relationship between FM and LM and bone mineral content (BMC), bone mineral density (BMD) as girls transition through puberty.

The study subjects consisted of 258 10-13-year old girls at the baseline. They were followed on average of 6.5 years and their results reflect the entire follow-up period ($n=217$). Whole body BMC, LM and FM were assessed by DXA (Prodigy, GE Lunar). Height, weight, Tanner stage and menarche status was obtained at baseline, 6, 12, 24, 36, and 84 months. 218 participants provided 1160 observations with a minimum of 2 and a maximum of 8 observations. 206 participants provided observations before menarche with a range of 1 to 6 observations from 51.6 months before menarche. 193 subjects provided observations after menarche with a range of 1 to 7 observations to 95.6 months after menarche.

	Mean \pm SD, kg			
	Weight	Fat Mass	Lean Mass	BMC
Before Menarche	43 \pm 8	11.4 \pm 6	30.0 \pm 4	1.6 \pm 0.3
After Menarche	54.1 \pm 9	15.4 \pm 7	36.3 \pm 4	2.1 \pm 0.3

Using random coefficients modeling in the MIXED procedure of SAS we found that subjects gained about 0.49 kg/month before menarche (BM) and 0.17 kg/month after menarche.

The weight gain was respectively portioned into 124 g/mo of fat and 355 g/mo of lean mass before menarche; and 108 g/mo of fat mass and 59 g/mo of lean mass after menarche. Regardless of menarche status, the effect of gains in lean and fat on BMC is that for every kg of fat mass there is a 16 g gain of BMC during puberty; for every kg of lean mass there is a gain of 47 grams of BMC; indicating the important effect of lean mass on the bone mass. We also found that the relative position within a cohort, LM, and BMC is already established by early puberty with fat mass being subject to environmental and pubertal changes. These findings provide evidence and implications for prevention of fat mass gain in those children who are at risk of overweight or obesity.

Disclosures: F.A. Tylavsky, None.

This study received funding from: ASBMR Bridge Funding, Academy of Finland and Finnish Ministry of Education.

W521

Determinants of Change in Bone Volumetric Density and Geometry Differ Between Boys and Girls in a Multiethnic Population. R. J. Wetzsteon, B. C. Kaufman^{*}, J. M. Hughes^{*}, S. Stovitz^{*}, M. A. Petit. Kinesiology, University of Minnesota, Minneapolis, MN, USA.

The purpose of this study was to explore determinants of change in bone volumetric density (vBMD, mg/mm³), bone area and estimated bone strength in a multi-ethnic population of boys and girls. A total of 116 (60 boys, 56 girls) children aged 10.9 ± 0.8 years at baseline participated. Ethnicity was based on CDC categories (17% Caucasian, 27% African American, 24% Hispanic, 10% Asian, 22% Other). Measurements of height, weight, and tibia length were taken by standard techniques; daily calcium intake and physical activity (PA score) were assessed by questionnaire; and dynamic power estimated by a vertical jump test. Peripheral quantitative computed tomography (pQCT) was used to assess the 50% site of the tibia for cortical volumetric density (CoD), area (CoA), polar strength-strain index (SSI_p), muscle cross-sectional area (MCSA), and total fat area (FatA). All measurements were taken at baseline and after 5-months. At baseline, boys and girls were similar in age, weight, calcium intake, PAscore, and vertical jump ($p < 0.10$ for all). Girls were significantly taller ($p = 0.04$). Baseline CoA and SSI_p did not differ between the boys and girls, but girls had greater CoD ($+2.2\%$, $p = .001$) which remained significant after adjusting for height. All bone values increased significantly over 5 months, but the magnitude of the change did not differ between boys and girls. Stepwise regression analyses were run to determine predictors of change with change in tibia length entered in the first step, and other predictors (change in MCSA, change in FatA, age, ethnicity, PAscore, average daily calcium, and change in vertical jump) entered in a stepwise manner if $p < 0.05$. Separate models were run for boys and girls. For both boys and girls, change in tibia length explained ~20% of the variance for change in SSI_p. For girls, change in MCSA explained an additional 31%, with daily calcium and change in vertical jump explaining and additional 10% of the variance. For boys, only change in MCSA entered the model explaining an additional 23% of the variance for change in SSI_p. These data are consistent with recently published data showing higher bone vBMD in girls. They also suggest that MCSA may be a reasonable surrogate of muscle force in boys, but for girls other factors (muscle power and calcium) may be important predictors of change in bone strength.

Disclosures: R.J. Wetzsteon, None.

VITAMIN D WORKING GROUP

WG1

Deletion of the 25 Hydroxy Vitamin D 1 α Hydroxylase from Mice Expressing the Null Mutation for the Calcium Sensing Receptor Converts a Hypercalcemic to a Hypocalcemic Hyperparathyroid Phenotype. C. Richard^{*1}, D. Miao², R. Samadfar^{*1}, Y. Wang^{*1}, G. N. Hendy¹, D. Goltzman¹.¹Dept of Medicine, Calcium Laboratory, McGill University, Royal Victoria Hospital, Montreal, PQ, Canada; ²Department of Human Anatomy, Nanjing Medical University, Nanjing, China, China.

The calcium sensing receptor (CaSR) is functional mainly in the parathyroid gland and kidney, but likely as well in other tissues such as the gastrointestinal tract and the skeleton. These tissues are also target sites for the action of 1,25-dihydroxyvitamin D [1,25(OH)₂D]. Mice which are heterozygous or homozygous for the calcium sensing receptor null mutation (CaSR^{-/-} and CaSR^{-/-} respectively) develop hypercalcemia and hyperparathyroidism to a moderate or severe degree, respectively. Mice which are homozygous for targeted deletion of the 25 hydroxyvitamin-D 1 α -hydroxylase [1 α (OH)ase^{-/-}] which synthesizes 1,25(OH)₂D develop hypocalcemia, hyperparathyroidism and rickets but survive long term. To assess the interactions between the important calcium regulating molecules, CaSR and 1,25(OH)₂D, we created compound mutants of the CaSR and 1 α (OH)ase mutants and assessed their growth, biochemistry and skeletal morphology. CaSR ^{+/+};1 α (OH)ase^{+/+} mice grew normally and exhibited normal longevity. CaSR ^{+/+};1 α (OH)ase^{-/-} mice developed severe rickets and osteomalacia as assessed by faxitron x-ray analysis and von Kossa staining of the skeleton but survived at least 2 months. CaSR ^{-/-};1 α (OH)ase^{-/-} mice developed even more severe rickets, osteomalacia and growth retardation but also survived long term. BMD, assessed by PIXIMUS, was reduced by 68% in the lumbar spine and by 49% in the femur compared to wild type mice, but only by 58% and 38% in the lumbar spine and femur respectively of the CaSR ^{+/+};1 α (OH)ase^{-/-} mice. Although CaSR^{-/-};1 α (OH)ase^{+/+} mice develop severe hypercalcemia and most die before or shortly after weaning, deletion of the 1 α (OH)ase in CaSR^{-/-};1 α (OH)ase^{-/-} mice facilitated survival for at least 2 months although these animals exhibited the most severe growth retardation, rickets and osteomalacia of all mutants. All mutant animals showed evidence of hyperparathyroidism with CaSR^{+/+};1 α (OH)ase^{+/+} and CaSR^{-/-};1 α (OH)ase^{+/+} mice displaying hypercalcemia. In contrast, CaSR^{+/+};1 α (OH)ase^{-/-} mice and CaSR^{-/-};1 α (OH)ase^{-/-} mice were severely hypocalcemic (serum calcium 1.28 and 1.27mM respectively). The results indicate that the phenotypic manifestations of hyperparathyroidism may be markedly influenced by the vitamin D status of animals with CaSR mutations, confirm that elimination of hypercalcemia sustains longevity in mice homozygous for the CaSR null mutation, and suggest that mutations in the CaSR contribute to worsening of skeletal mineralization.

Disclosures: C. Richard, None.

WG2

Targeted Inactivation of the Vitamin D Receptor by Caspase-3. P. J. Malloy^{*}, D. Feldman. Department of Medicine, Stanford University, Stanford, CA, USA.

Calcitriol inhibits the growth of many cells including breast, colon, ovarian, pancreatic, and prostate cancer cells by causing cell cycle arrest and in some cells by inducing apoptosis. In breast cancer cells, calcitriol induces apoptosis by a caspase independent mechanism. On the other hand, in prostate cancer cells, calcitriol induction of apoptosis involves activation of caspase activity. Calcitriol actions are mediated by the vitamin D receptor (VDR) a member of the steroid-thyroid-retinoid receptor superfamily of nuclear transcription factors. In LNCaP prostate cancer cells induction of apoptosis by staurosporine abolished [³H]1,25(OH)₂D₃ binding and VDR protein suggesting to us that the VDR might be targeted for inactivation by caspases, a family of cysteine proteases that are activated during apoptosis. We identified a potential caspase-3 cleavage site (DxxDS) in helix H2n (D₁₉₅MMDS₁₉₉) in the VDR ligand-binding domain. Mutations (D195A, D198A and S199A) were generated in the putative caspase-3 cleavage site and their effects on caspase cleavage of VDR examined. In reporter gene assays, all of the VDR mutants exhibited transactivation activity similar to the WT VDR. COS-7 cells transfected with WT and mutant VDR cDNA expression vectors were then treated with staurosporine and VDR examined by western blot. A 22 kDa cleavage fragment was detected on western blot from cleavage of the WT VDR and the S199A mutant VDR but not the D195A or D198A mutant VDRs. Addition of the caspase-3 specific inhibitor z-DEVD-FMK prevented cleavage of the WT VDR *in vivo*. Treatment of transfected COS-7 cells with calcitriol also resulted in cleavage of the WT VDR but not the D198A mutant VDR. Calcitriol-induced cleavage of the WT VDR was blocked with z-DEVD-FMK demonstrating that calcitriol activates caspase-3 in these cells. *In vitro* treatment with caspase-3 resulted in the cleavage of WT VDR and S199A but not D195A or D198A mutant VDRs. WT VDR was also cleaved by caspase-6, and -7 but not caspase-8 *in vitro*. In conclusion, our results demonstrate that the VDR is cleaved by caspase-3 *in vivo*. We further demonstrate that calcitriol induces caspase-3 activity that results in the cleavage of the VDR. Our results suggest that activation of caspase-3 by calcitriol, while contributing to apoptosis may also may limit the apoptotic effects of calcitriol in cells that express caspase-3. Since caspases also regulate the activity of many proteins under non-apoptotic conditions, the inactivation of VDR by caspases may be of general importance as a mechanism to limit calcitriol activity.

Disclosures: P.J. Malloy, None.

WG3

The Vitamin D Receptor, Hedgehog Signaling and Epidermal Carcinogenesis. A. E. Teichert^{*1}, J. J. Welsh^{*2}, D. D. Bikle¹. ¹Endocrine Unit, UCSF-NCIRE, San Francisco, CA, USA; ²Department of Biological Sciences, University of Notre Dame, Notre Dame, IN, USA.

Over 1 million skin cancers occur annually in the United States, 80% of which are basal cell carcinomas (BCC) (16% squamous cell carcinomas, 4% melanomas), making it by far the most common cancer. Extensive epidemiologic data support the concept that the incidence of a number of epithelial malignancies (e.g. breast, prostate, colon) is reduced by increasing 25OHD levels. 1,25(OH)₂D₃, produced by the kidney from 25OHD or locally produced, reduces proliferation and enhances differentiation and thus has been investigated for a role in preventing or treating cancer. However, UVB exposure, which increases 1,25(OH)₂D₃ production in the keratinocyte, causes skin cancer. Conceivably, the 1,25(OH)₂D₃ produced by the skin provides at least partial protection from UVB induced skin cancer such that lack of 1,25(OH)₂D₃ or its receptor would make the skin even more sensitive to UVB induced malignancy.

We have chosen UVB epidermal carcinogenesis as a model to directly address the issue of the balance between the increased risk of UVB exposure as an inducer of carcinogenesis with the benefit of promoting vitamin D and thus 1,25(OH)₂D₃ production in the epidermis as a chemopreventive measure.

Mice deficient for the vitamin D receptor (VDR null mice), for which 1,25(OH)₂D₃ is a ligand, have a marked hyperproliferative response in the hair follicle and epidermis and decreased epidermal differentiation. These mice, when treated with 7,12 dimethylbenzanthracene (DMBA), unlike their wildtype littermates, develop skin tumors containing hair follicle elements and/or are of basal cell origin, tumors characteristic of overexpression of the hedgehog (HH) signaling pathway in keratinocytes. We found that the epidermis and hair follicles of the VDR null animals, as well as the DMBA induced tumors in VDR null mice, overexpress elements of the HH signaling pathway [Sonic Hedgehog (Shh), Patched 1 (Ptc1), Smoothened (Smoh), Gli 1, and Gli 2]. Moreover, keratinocytes in which the VDR has been knocked down with siRNA directed against the VDR show increased expression of Shh.

Interestingly, mice overexpressing Gli1, Gli2, or Shh in their basal keratinocytes or grafted with human keratinocytes overexpressing Shh develop BCC like lesions. Furthermore, BCC show overexpression of Ptc1, Smoh, Gli1 and Gli2, raising the question of a link between the vitamin D system, HH signaling and skin cancer predisposition.

These results suggest then that increased expression of Shh in the keratinocytes of the VDR null animal activates the HH signaling pathway, predisposing the skin to the development of BCC.

Disclosures: A.E. Teichert, None.

This study received funding from NIH.

PEDIATRIC BONE AND MINERAL WORKING GROUP

WG4

Childhood Hyperparathyroidism with Bilateral Slipped Femoral Epiphysis, Severe Bone Disease and Vitamin D Deficiency. R.N. Mehrotra¹, J. Pingle², U K Nayak³. ¹Department of Endocrinology, ²Orthopedics, and ³Head & Neck Surgery, Apollo Hospitals, Jubilee Hills, Hyderabad, India.

Primary Hyperparathyroidism (PHPT) in children is an uncommon disease. It constitutes less than 5% of all cases of PHPT. PHPT causing slipped epiphyses has been described, but is an uncommon manifestation. In contrast to asymptomatic disease seen in the west PHPT in Asians presents with more severe bone disease, large glands and are associated with low Vitamin D levels. This report is about a child with PHPT from India who presented with B/L slipped epiphyses and had associated severe bone disease. 12 year old girl had onset of pain in both the hip joints five years. She had associated symptoms of proximal weakness. As X-rays showed B/L slipped epiphyses she underwent fixation by screws. Repeat X-rays showed no healing. There has been gradually increasing valgus deformity at the knee. Her proximal weakness has increased. So much so that at presentation she was bed ridden because of severe deformity. During admission during transport she suffered a fracture of right fore arm. Initial calcium done previously was 8.2 mg/dl. At our hospital it was 11.9, with Phosphorus of 3 mg/dl. Alkaline phosphatase was 4050 u/l. Intact PTH levels was 2867 picogm/ml and 25 Hydroxy Vitamin D was 6.6 nanogm/ml. The X-rays showed subperiosteal re-absorption, Brown tumors, and severe deformities. U/S neck revealed parathyroid lesion of 2x3 cm. This was confirmed on Sestamibi scan. She underwent removal of parathyroid tumor. During surgery both neck sides were explored, but there was no evidence of second adenoma. Biopsy from second gland was normal. Immediate post op she had hypocalcaemia because of hungry bone disease. Histopathology showed parathyroid adenoma. She has been on Vitamin D and calcium supplements since then. At last follow up calcium was 9.0 mg/dl, PTH and alkaline phosphatase had declined. Repeat X-rays showed healing of Slipped epiphysis. Due to persistent deformities she underwent corrective osteotomies, and now she is able to walk.

Vitamin D deficiency and poor calcium intake modifies the disease presentation of PHPT in Indians. Slipped epiphysis seems to be due to changes in the metaphyseal spongiosa which leads to un locking of interdigitations due to increased PTH levels.

WG5

Tissue-specific Knockout of CaRs in Parathyroid Cells: A Model of Primary Hyperparathyroidism. W. Chang, C. Tu, T-H. Chen, D. Bikle, D. Shoback. Endocrine Research Unit, University of California, Department of Veterans Affairs Medical Center, San Francisco, CA, USA.

Serum ionized $[Ca^{2+}]$ is tightly maintained by the steep inverse relationship between $[Ca^{2+}]$ and the level of parathyroid hormone (PTH) secretion. Increases in the extracellular $[Ca^{2+}]$ ($[Ca^{2+}]_e$) activate signaling pathways that inhibit PTH secretion by ligating the extracellular Ca^{2+} receptor (CaR) expressed on parathyroid cells. Heterozygous and homozygous loss-of-function mutations in the CaR gene cause familial benign hypocalciuric hyperparathyroidism (FBHH) and neonatal severe hyperparathyroidism (NSHPT), respectively. Patients with these disorders demonstrate both hyperparathyroidism (HPT) and hypocalciuria depending on gene dosage effects. The deletion of both parathyroid and renal CaRs is thought to be necessary for the development of this phenotype. Mutations in the CaRs in FBHH and NSHPT cause reduced responsiveness and/or expression of the receptor in both parathyroid (PT) and kidney cells. To determine the contribution of parathyroid vs renal CaRs to the metabolic disturbances in NSHPT and FBHH and to discern the role of CaRs in tissues beyond the parathyroid and kidney, we generated a floxed CaR mouse ($CaR^{lox/lox}$) by inserting loxP sites flanking exon 7 of the CaR, which encodes the transmembrane and intracellular loops of the CaR. We bred parathyroid (PT)-specific CaR knockout ($^{PT}CaR^{-/-}$) mice using this $CaR^{lox/lox}$ mouse crossed to a transgenic PTH promoter Cre mouse line. The resulting heterozygous knockout ($^{PT}CaR^{-/-}$) mice were backcrossed to the $CaR^{lox/lox}$ mice to generate heterozygous and homozygous ($^{PT}CaR^{-/-}$) knockout mice and their wild-type (WT) littermates for analyses. $^{PT}CaR^{+/+}$ and $^{PT}CaR^{-/-}$ mice were born alive in normal Mendelian ratios. Serum total $[Ca^{2+}]$ were significantly elevated in the $^{PT}CaR^{-/-}$ (12.75 \pm 0.12 mg/dl) and $^{PT}CaR^{-/-}$ (15.60 \pm 0.19 mg/dl) mice, compared to WT controls (11.58 \pm 0.34 mg/dl), consistent with the phenotype of HPT and a gene-dosage effect. Urine $[Ca^{2+}]$ were also increased by \approx 60 and 80% in $^{PT}CaR^{+/+}$ and $^{PT}CaR^{-/-}$ mice, respectively, vs controls, supporting a compensatory hypercalciuria in $^{PT}CaR^{+/+}$ and $^{PT}CaR^{-/-}$ mice. While the $^{PT}CaR^{+/+}$ mice developed normally, the body weight of the $^{PT}CaR^{-/-}$ mice was \approx 25% of their WT and heterozygous littermates. The bones of $^{PT}CaR^{-/-}$ mice were significantly smaller and severely undermineralized as indicated by micro-computed tomography (μ CT) scans. This work confirms that decrements in parathyroid cell CaR expression are sufficient to induce HPT, growth retardation, and skeletal demineralization after birth. This floxed CaR mouse model will provide the opportunity to understand the role of CaRs in other tissues unhampered by the global metabolic disturbances of the generalized CaR knockout.

WG6

Bone Mass in Adults and Children with Hypoparathyroidism. MT Collins^{1,4}, JE McKie^{1,4}, JC Reynolds², KK Winer³. ¹Skeletal Clinical Studies Unit, CSDB, NIDCR; ²Nuclear Medicine Department; ³NICHD, NIH, Bethesda, MD, USA; ⁴Authors Contributed Equally.

Hypoparathyroidism is a rare condition that is associated with high bone mass. The mechanism of the development of high bone mass is unknown. Since adults and children differ in the cellular processes by which they maintain their bone mass, adults by remodeling and children primarily by modeling, differences between adults and children may shed light on the mechanism by which high bone mass is achieved in hypoparathyroidism. Seventy-five subjects were studied. There were 30 children (18/12 M/F, ages 4-19, median 11, length of disease 3mo.-15y, median 6.5y), and 45 adults (13/32 M/F, ages 20-75, median 45, length of disease 3mo.-35y, median 10y). Bone mineral density (BMD) was measured by Hologic DXA and Z-scores were calculated using the manufacturer's most recent reference database.

BMD at the PA spine (PASp) and femoral neck (FN) were increased in adults (mean Z-score = 1.8 \pm 2.0 and 0.98 \pm 1.1, respectively), but normal in children (0.36 \pm 1.3 and 0 \pm 1.4, respectively, for PASp adult to child comparison p=0.0008, and FN p=0.0017). To assess whether or not differences in BMD between adults and children were the result of length of hypoparathyroidism, adults and children were grouped and matched by length of disease (\leq 5 y, and 6-15 y). When there was \leq 5 y of hypoparathyroidism, there was no difference between adults and children in BMD Z-score at either the PASp or the FN (PASp: 0.95 \pm 0.89 vs 0.62 \pm 1.3, p=0.41, FN: 0.56 \pm 0.87 vs 0.37 \pm 1.6, p=0.69). However, when adults and children with 6-15 y of hypoparathyroidism were compared, adults had increased mean BMD Z-score at the PASp and FN (1.9 \pm 0.86 and 0.20 \pm 1.3, respectively, vs 1.0 \pm .93 and -0.25 \pm 1.3, respectively, for PASp adult to child comparison p=0.002, and FN p=0.016). When subjects with hypoparathyroidism due to autoimmune polyglandular syndrome (who often have malabsorption, gonadal failure, and/or are on glucocorticoid treatment for adrenal insufficiency) were excluded from the analysis, there was a significant positive correlation between length of disease and BMD in adults (PASp: R=0.41, p=0.0066, FN: R=0.35, p=0.03), but not in children (PASp R=-0.24, p=0.33, FN R=-0.25, p=0.30). Hypoparathyroidism did not have an effect on growth, as height was normal in children (height Z-score = -0.21 \pm 1.2).

From these data, it appears that normal skeletal modeling is not dependent on PTH, and the elevated BMD seen in hypoparathyroidism occurs only in the adult (remodeling) skeleton. These observations create novel perspectives from which to assess the role of PTH in the formation of the skeleton and the accrual of bone mass.

WG7

Genetic Mosaicism for *de novo* Mutations of the Calcium Sensing Receptor (CASR) Gene: Implications for Recurrence Risks in Autosomal Dominant Hypoparathyroidism. DEC Cole, BYL Wong, L Canaff, GN Hendy. Depts. of Laboratory Medicine & Pathobiology, Medicine, and Paediatrics (Genetics), University of Toronto, Toronto ON and Depts. of Medicine, Physiology and Human Genetics, McGill University, Montreal QC Canada.

In sporadic cases of autosomal dominant hypoparathyroidism (ADH) and familial hypocalciuric hypercalcemia (FHH), *de novo* mutations of the calcium sensing receptor gene (CASR) are not uncommon. Previously, we described somatic mosaicism in the healthy mother of two siblings with severe ADH due to an activating F788L mutation of CASR (JCEM 2003;88:3674). Here we report on the analysis of nine more parent/proband triads – five with *de novo* ADH and four with *de novo* FHH. Analysis of heterozygosity by denaturing high performance liquid chromatography (dHPLC) revealed that CASR exon 4 amplified from leukocyte DNA of the mother of one ADH proband (E228K mutation) had an abnormal melting profile suggestive of mosaicism. This was confirmed by allele-specific amplification for the 228K variant and inspection of the sequencing capillary electrophoretograms as well as sequence analysis of multiple subclones of the exon 4 amplicon. The degree of heterozygosity was estimated at \sim 10%, like the mother of the F788L proband, and is similar to that found in other *de novo* dominant disorders. In the eight remaining cases, dHPLC profiles were all normal, indicating that if somatic mosaicism was present, the proportion of the mutant allele in peripheral leukocytes was less than 1%. Our second mosaic family emphasizes that *de novo* mutations in offspring cannot be regarded as eliminating all risk for recurrence. Mosaicism should be factored into the *a priori* risk estimate and appropriate testing offered as part of the counseling process. Whether there is some significance to the fact that maternal activating mutations account for both instances of mosaicism remains to be seen. Similarly, the absence of any evidence for mosaicism in the other eight cases (ADH or FHH) may well be associated with reduced risk of recurrence, a supposition that can be addressed when a larger case cohort is evaluated.

WG8

Rett Syndrome: Bone Mass Determination in Girls and Mice. J. Shapiro, A. Boskey, G. Bibat, S. Doty, M. Blue, B. Metcalf, A. Khosravi, S. Naidu. Kennedy Krieger Institute, Baltimore, MD, Hospital for Special Surgery, NYC, NY, USA.

The purpose of this study was to evaluate osteoporosis in Rett (RTT) syndrome and the RTT murine model. RTT is an X-linked disorder caused by mutations in the Methyl-CpG-Binding Protein (MeCP2) located at Xq28. Some patients with severe seizures and RTT-like features have mutations in cyclin-dependent kinase-like 5 (CDKL5). Features of RTT include deceleration of head growth, early onset cognitive defects, and a movement disorder with stereotypic hand movements. Decreased bone mass on x-rays and an increase in fractures has been observed in RTT children unrelated to their ambulatory status.

Diagnosis was confirmed by mutational analysis in 25 RTT girls ages 1-14. Hologic DXA (n=19) scans were performed. Additionally, 6 MeCP2 deleted (heterozygote-/-) females and (knockout -/-) males were compared to 6 wks control C57BL/6 male and female mice by Faxitron and micro-computed analyses (GE-EVS), histology, and Fourier transform infrared imaging spectroscopy of mineral and matrix. For the girls, 8 of 17 subjects had lumbar spine Z-scores -2.0 or less; Z-scores were within reference range in 9 children. DXA values low for age occurred as early as 6 years. Four children were post pubertal. DXA hip scans could not be obtained because of anatomic variation and motion. Mean BMI ages 1-14 was 16.9 ± 2.1 , 15/24 used anticonvulsant drugs.

Micro CT Analysis of wild type (wt) and mutant mice (females (het) and male ko) are shown in the table as means with n=2/group.

	BMD(mg/cc)	Cortical			BMD	Trabecular		
		BVF	Imin*	Imax*		BVF	TbN	TbSp
M wt	1025.3	0.33	0.062	0.053	568.6	0.187	12.3	0.060
M ko	931.3	0.21	0.034	0.027	502.9	0.121	9.2	0.098
F wt	977.3	0.23	0.0313	0.026	477	0.126	8.52	0.105
F het	1024.	0.30	0.046	0.037	511	0.099	7.02	0.129

BVF Fractional bone volume; * Areal moment of inertia; TbN: trabecular number TbS: trabecular separation

Based on the 2 samples/group analyzed to date (-/-) bone has lower BMD and BVF, smaller moments of inertia, lower TbN and greater trabecular separation. The male (-/-) has decreased BMD, BVF, lower TbN and greater TbS. The (+/-) bone did not have altered BMD, but had greater BVF, but lower TbN and increased TbSp. The increased Imin and Imax suggests bone are stronger in the (+/-) females. Histochemical stains indicate a more intense procollagen presence in the (+/+) female compared to the (+/-) female. The intensity of stain was similar in (+/+) vs (-/-) males (n=4).

In conclusion, the low bone mass observed in 50 % of Rett children parallels the preliminary data that the MeCP2 murine models provide as models for RTT syndrome.

PHYSICAL ACTIVITY AND FALLS WORKING GROUP

WG9

Bone Adaptation to Impact Loading - Significance of Loading Intensity. A. Vainionpää*¹, R. Korpelainen*², J. Leppäluoto*³, T. Jämsä*¹. ¹Department of Medical Technology, University of Oulu, Oulu, Finland, ²Department of Sports Medicine, Oulu Deaconess Institute, Oulu, Finland, ³Department of Physiology, University of Oulu, Oulu, Finland.

It is important to find efficient strategies for prevention of osteoporosis and fragility fractures as the prevention with medication is impossible at the population level. Exercise is one of the major prevention strategies even though the optimal loading patterns of bone have not yet been clearly defined in terms of bone loading forces in clinical settings. Our aim was to study the effects of impact loading on bone and assess the intensity and amount of efficient impact loading.

We conducted a 12 month population-based exercise intervention in 120 premenopausal women aged 35 to 40 years. The women were randomized equally to exercise (EG) and control groups (CG). The exercise regimen consisted of supervised, progressive high-impact exercises three times per week and an additional home program. Bone mineral density (BMD) in the proximal femur was measured by dual x-ray absorptiometry and bone geometry in the mid-femur was quantified by computed tomography (QCT). Also bone turnover was examined by using biochemical markers (TRACP-5b, PINP and Uncoupling Index). Daily impact loading was continuously recorded with a novel accelerometer-based measurement device and analyzed as the daily number of impacts within five acceleration ranges between 0.3 g to 9.2 g (g=acceleration of gravity, 9.81 m/s²).

Regular impact exercise increased the femoral neck BMD by 1.5 % (p=0.003) and led to geometric adaptations by increasing the mid-femur periosteal circumference by 0.2 % (p=0.03) when compared to controls. It also altered bone turnover balance in favour of bone formation. The women with the highest number of impacts at the intensity level above 4 g had the greatest increment in proximal femur BMD. The number of impacts needed exceeding this level was 60 impacts per day. Impacts exceeding 2.5 g were associated with increased periosteal circumference and enhanced bone turnover favouring bone formation.

According to our results, impact loading has significant dose- and intensity dependent effect on weight-bearing bones. The threshold for improving BMD in the hip is 60 impacts per day exceeding 4 g, while geometric adaptation and bone turnover activation can be achieved with lower intensity levels. Impacts required for osteogenic effects can be obtained during habitual exercise training. These thresholds for osteogenic exercise give tools to promote efficient exercise patterns to be included in everyday routines and personal activities, thus increasing the potential to affect in community level.

Disclosures: A. Vainionpää, None.

WG10

Timing of Peak Bone Mass and Bone Mineral Density Are Influenced by High-Level Physical Activity in Young Adults of Both Sexes. S. Breban*, C. Chappard, C. Jaffre*, C. Benhamou. Chr Orleans, INSERM Unit U658, Orleans, France.

Optimization of Peak Bone Mass may help to prevent osteoporosis and sport is known to be beneficial for bone tissue by increasing Bone Mineral Density (BMD). No study has reported effects of physical activity on Peak Bone Mass. Thus, the aim of this cross-sectional study was to analyse the influence of physical activity on timing and level of Peak Bone Mass.

70 girls and 90 boys aged 17-28 years participated in this study. The sample included 40 athlete-girls and 60 athlete-boys participating in weightlifting, ball collective sports or judo for more than 6 hours per week (9.6±3.5 hours per week for women and 10.4±3.7 for men). They were age and sex matched with control girls (n=30) and boys (n=30). Bone Mineral Content (BMC, g) and BMD (g/cm²) were measured by DXA (Delphi, Hologic®, Waltham, MA), at lumbar spine (LS) and non dominant femur (total and femoral neck (FN)). We also evaluated whole body (WB) BMC and BMD, with derived analysis of trunk, lower and upper limbs. Height, weight and body composition were derived from these DXA measurements. The timing of Peak Bone Mass was analysed by the inflexions of the age/BMD curves at all bone sites. Our variables were best fitted by second order polynomial regression equations. Thus, the model was expressed as $y=ax^2+bx+c$. The age of maximal bone mass was determined as the maximum of the curve, i.e. when $x = -b/2a$. Athletes had higher BMD measurements than controls in both sexes at all bone sites (p<0.05). Consequently all the Peak Bone Mass levels were significantly higher in athletes than controls. BMD peaks were achieved around 21.5 (FN), 22 years (LS), and 24-25 years (WB, upper and lower limbs) in athlete girls; BMD peaks were reached before 17 years for all bone sites except for LS (21.8 years) in control girls. In athlete boys, BMD peaks were reached before 17 years for upper and lower limbs, and ranged from 21.0 years (FN) to 25.5 and 26.0 years respectively for WB and LS. Finally, in control boys, BMD peaks were reached before 17 years at all bone sites. Timing of Peak Bone Mass was different according to bone sites, sex and athletic or non athletic status. Thus, those results confirm that weight-bearing physical activity lead to a better bone status compared to non athletes, in both sexes and even after puberty. Moreover, our data suggest that the Peak Bone Mass was not reached at all bone sites before 17 years: thus, it is yet possible to optimize BMD and Peak Bone Mass in young adults between 17 and 28 years. High level weight-bearing physical activity seemed to induce a delayed and higher Peak Bone Mass compared to controls.

Disclosures: S. Breban, None.

WG11

Exercise Prevents Falls and Maintains Bone Mineral Density in Elderly Postmenopausal Women. Preliminary data of the Erlangen Senior Fitness and Prevention (SEFIP) Study. W. Kemmler*, S. von Stengel*, W. A. Kalender*, K. Engelke. Institute of Medical Physics, University of Erlangen, Erlangen, Germany.

The aim of the study was to demonstrate that an intensive aerobic and strength training can maintain BMD at the spine and the hip and can prevent falls in elderly community-living women.

Via population registers we recruited 246 community-living women of 65 years and older. Exclusion criteria were medication or diseases related to bone metabolism, low aerobic capacity (<75 W on ergometry), and medication potentially increasing the likelihood of falls. There were no inclusion or exclusion conditions based on BMD or prevalent fractures. Subjects were randomly assigned to an exercise intervention group (EG: 2-3 sessions/week) or to a wellness control group (WCG: 1 session/week for three 10 week blocks). The exercise training consisted of 20 min of intense aerobic dancing (70-85% HF_{max}), 5 min of specific balance exercises and 35 min of isometric and dynamic (60-70% 1RM) strength training. No machines were used for the strength training part. All subjects were individually supplemented with calcium and cholecalciferol up to a maximum of 1500 mg/d and 500 IU/d. Bone mineral density at the lumbar spine and the hip was measured with DXA and QCT. Falls as defined by the PROFANE workgroup were counted using daily protocols conducted by all participants. Here we present initial 12 month DXA and fall results for 182 participants (EG: n=90; WCG: n=92).

After 12 months there were significant differences between exercise and wellness control group of BMD of the spine (EG: +1.4% vs. WCG: -0.3%) and of the hip (EG: -0.2% vs. WCG: -1.3%). The number of falls was significantly higher in the WCG (n=124) than in the EG (n=72). The same was true for injurious falls (EG: n=28 vs. WCG: n=42). In the exercise group 5 and in the wellness control group 8 fractures occurred but the power of the subset of patients included in this preliminary analysis was too low for the difference to be significant.

In conclusion preliminary results of our randomized exercise trial show that exercise training positively impact BMD at the hip and spine as well as fall frequency and may prevent fall related fractures in elderly subjects. The training scheme used in the study can easily be transferred into rehabilitation programs as no special equipment was used.

Disclosures: K. Engelke, Synarc 3.

WG12

Relationship Between Serum 25-hydroxyvitamin D₃ Concentration and Walking Ability, Leg Strength, or Balance in Community-Dwelling Japanese Frail Elderlies. J. Okuno*, S. Tomura*, H. Yanagi*, N. Yabushita*, T. Okura*, K. Tanaka*. Graduate school of Comprehensive Human Sciences, University of Tsukuba, Tsukuba City, Japan.

The aim of this study was to evaluate the relationship between serum 25-hydroxyvitamin D₃ (25OHD) concentration and walking ability, muscle strength, or balance in community-dwelling Japanese frail elderlies. The study was a longitudinal study conducted in a town near Tsukuba city (latitude 36°north) from June to September, in 2005 and 2006. Forty-five participants were community dwelling elderlies aged 65 years and over who required minimum support or nursing care to maintain their ADL. Their mean age was 76.5±5.9 years (mean±SD, range: 65-90). Of the participants, 32 attended a 3-month exercise program for nursing care prevention once per week (exercise group). The remaining 13 received only advice for nursing care prevention (control group). The Ethics Committee of University of Tsukuba approved the study. An interview was conducted based on a questionnaire including score of functional capacity of ADL (Tokyo Metropolitan Institute of Gerontology (TMIG) score), experiences of fall, stumbling and body sway during the past one year, walking ability, and the frequency of going outside of the home. The serum levels of 25OHD, intact parathyroid hormone (iPTH) and calcium were measured. The following physical tests were performed at baseline and 3 months: Timed Up & Go (TUG) and a 5-meter walk for walking ability, functional reach and foot balance with open eyes for balance, trunk flexion for flexibility, and ankle strength and grip strength for muscle strength. Among 45 patients who underwent the tests, 66.7% and 40% had difficulties in standing up and in walking, respectively. 54.3% experienced falls, 73.8% experienced stumbling and body sway more than once during the past one year. The mean level of 25OHD was 62.1±13.7 nmol/L (mean±SD, range: 27.5-87.5). At baseline, the rate of 25OHD levels less than 50 nmol/L that is the cut-off point of 25OHD resulting from the significant difference of intact PTH level was 18.0%. At baseline and 3 months there were no significant differences in physical tests between the control group and the exercise group. The subjects with 25OHD levels more than 50 nmol/L at baseline improved their walking ability and ankle strength for a period of three months in both groups. On the other hand, the subjects with 25OHD levels less than 50 nmol/L did not improve their physical performance even in the exercise group. It is suggested that serum 25OHD level is related to walking ability and muscle strength in Japanese frail elderlies, and that serum 25OHD level more than 50 nmol/L may be needed for maintaining their mobility or balance.

Disclosures: J. Okuno, None.

ADULT BONE AND MINERAL WORKING GROUP

WG13

Sclerotic Bone Changes Found on Densitometry Testing in a Patient with a Remote History of Breast Cancer. L. Eck, R. Bhattacharya, B. Lukert. University of Kansas Medical Center, Kansas City, KS, USA.

Background: Sclerosing bone disorders presenting with increased skeletal mass are caused by many rare, often hereditary dysplastic conditions, as well as by dietary, metabolic, endocrine, hematologic, infectious, and neoplastic processes.

Case Report: A 53 year old white female with a remote history of breast cancer on aromatase inhibition therapy presented for routine osteoporosis evaluation. Her only subjective complaint was mild, intermittent left sided back discomfort of six months duration. Densitometry findings were significant for substantial increases in bone mineral density since testing two years prior. The lumbar spine density was 1.684g/cm² which was increased from 1.115g/cm², resulting in a 51% upward trend. The hip density was 1.241g/cm² which was increased from 0.980g/cm², resulting in a 28% upward trend. Concomitant laboratory testing was significant for normal renal function, recent onset normocytic anemia, serum calcium of 8.7mg/dL (8.5-10.4mg/dL), PTH of 92 pg/mL (10-65pg/mL), elevated phosphorous of 4.4mg/dL (2-4mg/dL), significantly elevated alkaline phosphatase of 361U/L (25-110U/L) and bone specific alkaline phosphatase of 129.0mcg/L (5-18.2mcg/L), elevated AST at 103U/L (7-40), normal 25-hydroxy vitamin D at 35ng/dL, and a normal TSH.

Due to substantially increased bone mass on densitometry, an evaluation for a pathologic etiology of osteosclerosis was undertaken. Hepatitis C serology was negative. Heavy metal screening was normal. Vitamin A intoxication was ruled out. Serum and urine protein electrophoresis were unremarkable. An ACE level was found to be within normal limits. Plain films of the hip and spine revealed diffuse osteosclerotic changes. A technetium bone scan revealed mild to moderately increased activity in bilateral humeral heads and calcanei. CT scans of the chest and abdomen showed trabecular sclerosis without evidence of lytic lesions. A bone marrow biopsy and aspirate was performed and was significant for carcinoma cells with positive histochemical staining for pan-cytokeratin consistent with metastatic breast cancer. An increased number of osteoblasts were seen on the bone marrow touch preps. A bone biopsy was performed. The specimen was suboptimal but did show evidence of increased bone turnover.

Discussion: This case highlights the finding of osteosclerotic breast cancer metastases in a patient greater than ten years out from her initial breast cancer diagnosis. Sclerosing bone disorders can be identified with routine bone densitometry. The differential diagnosis of non-hereditary sclerosing bone disorders includes fluorosis, heavy metal poisoning, hepatitis C, hypervitaminosis A and D, hyper-, hypo-, and pseudohypoparathyroidism, renal osteodystrophy, leukemia, lymphomas, mastocytosis, multiple myeloma, sarcoidosis, and skeletal metastases.

Bone metastases in breast cancer may be osteolytic, osteosclerotic, or a mixture of the two. Osteoblastic metastases are lesions having both increased bone formation and resorption. The metastatic lesion is radiodense/sclerotic in appearance when bone formation is greater than resorption. Osteoblastic metastases begin in the marrow cavity. Most prostate cancer metastases and few breast cancer metastases are osteoblastic. The tumor-related factors that induce new bone formation may include endothelin-1, prostate specific antigen, bone morphogenic proteins, urokinase, insulin-like growth factors, osteoprotegerin, or other substances.

It is imperative that we are cognizant of osteosclerotic findings on dual energy densitometry as well as unusual increases in density on serial testing in order to avoid missing underlying pathologic conditions.

WG14

Osteomalacia Following Gastric Bypass and Biliopancreatic Diversion Surgery. A.O. Al-Shoha, R. Lakhdar, D. S. Rao. Internal Medicine and Bone & Mineral Metabolism, Henry Ford Hospital, Detroit, MI, USA

Gastric bypass surgery (GBS) and Biliopancreatic diversion (BPD) are the two most common procedures for morbid obesity, a disorder that is increasing in epidemic proportions in the US and world wide. There have been reports of metabolic bone disease after GBS. However, to our knowledge, only two cases of post-GBS osteomalacia (OM) have been reported. The diagnosis of OM in both cases was based solely on biochemical findings. We report 4 patients with bone biopsy confirmed OM after GBS.

Four patients (3 women and 1 man; age range 29-53y) were seen for evaluation of metabolic bone disease not responding to "usual" therapy. Two of the 4 patients had BPD; one of those 2 had gastric stapling (GS) about 9y before BPD (Case 2). The other 2 patients had Roux en-Y GBS (GBS); one of those had GS at the time of GBS (Case 3) and the other had jejunoileal bypass 26y before GBS (Case 4). Clinical features included generalized bone pain and tenderness, muscle weakness, difficulty walking, and waddling gait, stooping posture, and fractures. Two patients (Cases 2 and 4) had history of kidney stones at presentation. Diagnoses prior to referral were varied including arthritis, gout, vitamin D deficiency and osteoporosis. Serum chemistry (Table) and radiological findings were suggestive of OM in all the 4 cases, and the diagnosis was confirmed by bone biopsies. Following high doses of Vitamin D and calcium therapy there was significant improvement in the symptoms and functional status and biochemical variables.

	Case 1	Case 2	Case 3	Case 4
Time to presentation (years)	5	2	5	5
25-hydroxyvitamin D (ng/mL)	9	6	5	7
Corrected Calcium (mg/dL)	9.5	8.8	8.9	7.3
Alkaline Phosphatase (IU/L)	249	227	1246	178
PTH (pg/mL)	297	324	504	498

Our experience suggests that GBS may predispose to severe Vitamin D depletion and OM in the absence of high dose vitamin D and calcium supplements. The current "usual" recommendations are grossly inadequate in this population and the presentation may be non-specific and misleading. Prospective long-term studies are needed to determine the appropriate vitamin D dose to prevent metabolic bone disease in this uniquely susceptible population.

WG15

Unusual Presentation of Severe Vitamin D Deficiency Osteomalacia in a Patient with Congenital Hypophosphatemia. M. Cardenas, M. Honasoge. Henry Ford Hospital, Detroit, MI, USA.

Introduction: Congenital hypophosphatemic osteomalacia (HPOM) is generally not associated with secondary hyperparathyroidism (SHPT) in the absence of phosphate therapy. We present a patient with HPOM diagnosed in adulthood with severe vitamin D deficiency and SHPT.

Case Report: Thirty year old man was referred for evaluation of multiple low trauma fractures and muscle weakness. He has a history of intractable seizure disorder and mental retardation since age 18 months. No gait abnormalities, pain or deformities were noted during childhood. Progressive weakness and severe kyphosis developed over the past 8 years to the point that he was unable to walk without assistance. He has been on multiple medications for seizure disorder including phenobarbital, phenytoin, carbamazepine and more recently levetiracetam, and topiramate. Hypophosphatemia was noted 5 years ago and calcitriol 0.25mcg/d and ergocalciferol 50,000 IU/monthly were started by a neurologist. No family history of hypophosphatemia or rickets. Mother and sister are short but their serum phosphate levels are normal.

He was short (height 154cm, length of the legs 79cm), with severe kyphosis and proximal muscle weakness. Serum phosphate was 1.9 mg/dl and calcium 8.4 mg/dl, 25-OHD was 9ng/ml, and alkaline phosphatase and PTH were high (538 IU/L & 267 pg/ml respectively). His renal function was normal, but with mild metabolic acidosis. BMD by QCT was high in the spine (T score +8.2 and Z score of +8.1) and normal in the hip (T score of -0.9 and Z score of -0.9). X-rays showed osteosclerosis in the axial and marked osteopenia in the appendicular skeleton. Multiple healing pseudofractures were seen in the forearms, femur and fibula along with enthesiopathy around the pelvic bones.

Calcitriol and ergocalciferol doses were increased to 0.5mcg bid and 50,000 IU twice a week respectively. Therapy with sodium phosphate 500mg tid and calcium carbonate 600mg tid was started and topiramate discontinued. Hypophosphatemia and metabolic acidosis improved but SHPT continues despite vitamin D and calcium repletion. Proximal muscle weakness has improved.

Discussion: The patient has rather unique clinical, radiological and biochemical features of congenital HPOM complicated by severe vitamin D depletion and SHPT. Diagnosis was delayed until fractures and muscle weakness related to vitamin D deficiency complicated the clinical picture. Numerous healing pseudofractures in the forearm, an unusual finding in vitamin D depletion, are most likely due to trauma related to wheelchair use. Prior use of phenobarbital, phenytoin and carbamazepine may have aggravated vitamin D deficiency.

Conclusion: Diagnosis of HPOM may be complicated by severe vitamin D depletion and SHPT especially in patients on anticonvulsant therapy. Topiramate may aggravate metabolic acidosis related to SHPT.

WG16

Use of Teriparatide in Hajdu-Cheney Syndrome. P.J. Tebben, R.D. Tiegs, B.L. Clarke. Endocrinology and Metabolism, Mayo Clinic, Rochester, MN, USA.

To describe the response of two patients with Hajdu-Cheney Syndrome (HCS) to therapy with teriparatide.

The clinical, biochemical, and radiographic data of two patients with HCS are provided.

Case 1: A 55 year-old female was referred for evaluation and management of osteoporosis and HCS. Clinical findings included progressive acro-osteolysis, short stature, delayed closure of several cranial sutures, enlarged sella turcica, premature loss of teeth, low bone density, and fractures. During a 2 year course of conjugated equine estrogen (0.625 mg/day) and alendronate (70 mg/week) her bone mineral density (BMD) at the spine (L2-L4) declined by 8.2% and at the left hip declined by 3.5%. Serum calcium, phosphorus, creatinine, PTH, and alkaline phosphatase were within the reference range.

Due to declining BMD and vertebral fractures, teriparatide 20 mcg daily for 2 years was substituted for the alendronate. A 12.4% and 4.2% improvement was seen in the spine and left hip, respectively, over the initial 6 months of treatment followed by subsequent decrements in BMD at both sites. She also sustained a left tibial fracture after one year of teriparatide. Acro-osteolysis in her hands progressed while on teriparatide, a process that continued after substituting intravenous zoledronic acid (ZA) for teriparatide. Her BMD continued to decline on ZA.

Case 2: A 50 year old male was referred for evaluation of progressive acro-osteolysis affecting his left hand that was first apparent as a teenager. Although the disease was quiescent for several years, he developed similar findings in his right hand at age 35 while working as an artist. Features consistent with HCS included progressive acro-osteolysis, low BMD, and fractures. Teriparatide therapy had been initiated prior to his referral and after three years of alendronate. Serum calcium and total alkaline phosphatase were mildly elevated presumably due to teriparatide. Serum phosphorus and creatinine were within the reference range.

BMD increased by 7.3% and 10.2% at the spine and left hip, respectively, while on alendronate. BMD increased by 5% at the spine, but declined by 6.2% at the hip while on teriparatide. It was also felt that the rate of progression of acro-osteolysis had increased while on teriparatide.

HCS is an autosomal dominant condition characterized by a slowly progressive skeletal dysplasia including acro-osteolysis. Low BMD, fractures, short stature, and typical facial features are frequently described. The molecular pathogenesis is unknown. Beneficial effects of bisphosphonates have been reported in patients with HCS. Our two cases suggest that teriparatide does not effectively improve bone density or slow acro-osteolysis and that bisphosphonate therapy may be superior.

WG17

Very Low or Undetectable Intact Parathyroid Hormone Levels in Patients with Surgically Verified Parathyroid Adenomas. S. Bhadada¹, M. Cardenas², A. Bhansali¹, BR Mittal², A. Behra³, G.V. Chanukya¹, U. Nahar⁴, D. Sudhaker Rao⁵. ¹Departments of Endocrinology, ²General Surgery, ³Nuclear Medicine, ⁴Pathology, Postgraduate Institute of Medical Education & Research, Chandigarh, India; ⁵Bone & Mineral Research Laboratory, Henry Ford Health System, Detroit, MI, USA.

Background: In patients with primary hyperparathyroidism (PHPT), serum PTH levels are either within the upper half of the reference range or clearly elevated in most patients. However, a few case reports have appeared with very low or undetectable PTH levels in patients with PHPT. We report 3 such patients and explore potential reasons for undetectable or low serum PTH levels in patients with surgically verified PHPT, review the relevant literature, offer suggestions for management of such patients occasionally encountered in clinical practice and for future research to help understand mechanisms underlying "undetectable" or inappropriately low PTH levels. Material & Methods: Serum intact PTH level was measured pre and postoperatively by immunochemiluminometric assay and the results were confirmed by at least two repeated measurements on different occasions. The 3 unusual patients with PHPT had typical biochemical and/or clinical features of the disease (pancreatitis and kidney stones). However, the serum PTH levels were either very low or undetectable in the context of hypercalcemia in two patients and normal serum calcium in the third. All patients had ^{99m}Tc sestamibi scan showing increased uptake in one of the parathyroid glands. The patients underwent surgery with the removal of a parathyroid adenoma.

Results: The mean serum Ca was 10.4 ± 1.3 mg/dl and 11.8 ± 0.29 mg/dl in the two patients with hypercalcemia and 8.6 ± 1.3 mg/dl in the third, but serum PTH levels were either very low or suppressed in all (2; 10 and 12.3 pg/ml respectively). Post-operatively, serum calcium levels normalized in the two hypercalcemic patients. In contrast, serum intact PTH levels, which were either suppressed or very low before surgery, rose and remained within the reference range in all the 3 patients.

Conclusions: In the context of a high degree of clinical suspicion, the diagnosis of PHPT should be pursued despite suppressed or low normal serum PTH levels after careful and thorough exclusion of other rare causes of hypercalcemia. However, secretion of PTHrP remains a possibility. Further research on various PTH molecular species secreted by parathyroid adenomas and potential post-translational changes in PTH molecule that might interfere with in vitro measurements should be pursued to understand the precise reason(s) for such anomalous findings.

WG18

Novel Algorithm Using ^{99m}Tc-MIBI Scintigraphy, Sequential Whole Body Magnetic Resonance Imaging and Venous Sampling for Fibroblast Growth Factor -23 for Tumor Localization in Tumor Induced Osteomalacia. Sushil Kumar Gupta¹, Srikanth Kongara^{1*}, Sanjay Gambhir², Amit Agarwal³, RV Phadke⁴, Sunil Jain⁴, Manoj Kathuria⁴, Rakesh Pandey⁵, V. Ramesh⁵, Amit Rawat⁵, Isha Tyagi⁶, Rajan Syal⁶, Raman Boddula¹, Gangadhar Taduri⁷, Madan M Godbole¹, Gunter Path⁸, Luitgard Kraus⁸, Jochen Seufert⁸. ¹Department of Endocrinology, ²Nuclear Medicine, ³Endocrine Surgery, ⁴Radiodiagnosis, ⁵Pathology and ⁶Neurosurgery (Neuro-otology unit). Sanjay Gandhi Post Graduate Institute of Medical Sciences, Raebareli Road, Lucknow, India; ⁷Department of Nephrology, Nizams Institute of Medical Sciences, Hyderabad, India; ⁸Division of Endocrinology and Diabetology, Department of Internal Medicine-2, University Hospital of Freiburg, Freiburg, Germany.

Background: Localization of mesenchymal tumors causing tumor induced osteomalacia (TIO) is often difficult, delaying surgical cure by several years. No standardized protocol exists for rapid tumor localization. We have evaluated the role of whole body ^{99m}Tc-MIBI scintigraphy, sequential whole body magnetic resonance imaging (MRI), and venous sampling for fibroblast growth factor-23 (FGF-23) in tumor localization in suspected cases of TIO.

Methods: Six patients of adult onset hypophosphatemic osteomalacia were subjected to ^{99m}Tc-MIBI scintigraphy. Focused MRI was done for MIBI positive regions in five patients. Sequential whole body MRI was performed in a systematic manner starting from areas of highest regional prevalence to lowest regional prevalence (pelvis and thighs, legs and foot, head and neck, upper limbs, thorax and abdomen) in MIBI negative case. Selective or systemic venous sampling for serum FGF-23 was performed in five patients. FGF-23 mRNA expression analysis of tumor tissue was done post operatively in all. Serial estimations for serum calcium, phosphorus, and FGF-23 were performed postoperatively.

Results: Whole body ^{99m}Tc-MIBI scintigraphy revealed enhancing lesions in five patients which were subsequently confirmed as tumors by focused MRI. In one MIBI negative patient, sequential whole body MRI localized the tumor. Baseline serum FGF23 levels were elevated in all patients (range: 91.5-3863 RU/ml, normal range: 11-30). Venous sampling identified higher FGF-23 concentration in the major draining vein of tumor as compared to contralateral/distant vein in four patients. Surgical cure was achieved in 4 patients while 2 patients had incomplete excision of tumor. Tumor tissue from all the patients abundantly expressed FGF-23 mRNA. Postoperatively, serum FGF-23 declined to normal or marginally above the normal range in surgically cured patients.

Conclusion: Whole body ^{99m}Tc-MIBI scintigraphy, sequential whole body MRI and venous sampling for FGF-23 facilitate early localization of phosphaturic tumors in suspected TIO patients. Serum FGF-23 monitoring improves postoperative management.

WG19

Risedronate Preserves Bone Turn Over as Measured by Biochemical Markers After 5 Years Treatment in Postmenopausal Greek Women. I.C. Koulouris, G. Skarantavos, Th. Kaplanoglou, P. Katsimbri, E. Metania, G. Antipas, E. Konstantellou, P.N. Soukakos. 1st University Orthopaedic Clinic, Attikon University Hospital, Athens, Greece, and Agios Panteleimon General Hospital, Pireaus, Greece.

Increased rates of bone turn over, as observe in many PO women, are associated with loss of bone mass, determination of trabecular architecture and a decrease in mineralization of bone tissue.

The aim of this study was to investigate the effect on uNTX, sCTX and PTHi following daily continuous administration of Risedronate for 60 months in early postmenopausal Greek women.

Material and Methods: Forty early postmenopausal women between 48-53 years old (mean 50 years), 6 months -1year after the menopause, with T score <2SD on lumbar spine DEXA and without any prior metabolic disorders or fractures were separated into 2 groups: Group A (n=30) received 5mg Risedronate, 1mcg Alfacalcidol and 1000 mg Calcium carbonate daily for 12 months and 0.5 mg Alfacalcidol and calcium for the rest of the study period, while group B(n=10) received the same doses of Alfacalcidol and calcium for the first 12 months and only 1000 mg calcium carbonate thereafter. From 36 months Risedronate was given as 35mg once weekly. Serum and urine bone turnover markers were measured at 0,6,12,24,36,48 and 60 month intervals by automated electrochemiluminescence assay. No premenopausal values were available for comparison. Two patients in group A discontinued treatment after 24 months was to investigate the effect of daily administration of Risedronate to early postmenopausal Greek women for 5years by measuring sCTX changes, uNTX, urine PTHrP, serum osteocalcin, PTHi and 25(OH) D. A questionnaire including VAS score and PPI score concerning quality of life indexes was completed and reevaluated by all patients at the above intervals. Results:: 1)Group A showed a statistically significant decrease in uNTX (16,15%,p<0.0005) as early as 6 months after treatment whilst there were no statistically significant changes after the 12month period. In group B uNTX was increased (10,9 %, p<0.0005) while the rest of the markers showed a statistically significant decrease for the same period. No values fell below the normal range Group 2)A showed a statistically significant decrease in sCTX(11,69%,p<0.0005) as early as 6 months after treatment whilst there were no statistically significant changes after the 12month period. In group B sCTX was increased (13.32%, p<0.0005) while the rest of the markers showed a statistically significant decrease for the same period. No values fell below the normal range.3) PTHi changes both of groups its not significant.A showed improved indexes in the quality of life scores.

Conclusion: Changes in the measured markers, especially sCTX, uNTX, demonstrate that Risedronate effectively decreases the turnover as early as 6 months after treatment and the effect is maintained without further changes from the end of the first year until the end of the 60 months period provided that vitD is sufficient. The fact that no values fell below normal, during the first year of treatment and bone markers continued to keep this values during the following years of treatment, excludes the untoward presence of frozen bone. Quality of life was also improved in the Risedronate group without any untoward effects from upper gastrointestinal tract and musculoskeletal system. No values fell below normal, during the first year of treatment and bone markers continued to keep this value during the following 5 years of treatment.

WG20

Old Before His Time: A 16 Y/O Male with Idiopathic Juvenile Osteoporosis. Vollbrecht, Jill E., and Rao, D. Sudhaker. Bone & Mineral Metabolism, Henry Ford Health System, Detroit, MI, USA.

Idiopathic juvenile osteoporosis (IJO) is a self-limited phenomenon causing reduced trabecular bone formation, which leads to vertebral and metaphyseal fractures during early puberty. While the disease course follows a typical clinical pattern, the diagnosis is often made well after it has resolved, leaving the clinician with many questions regarding the appropriate treatment. We present a case of a 16 y/o male with recurrent fractures and IJO.

This patient is a 16 and 5/12 months' y/o Caucasian male who was referred for evaluation of recurrent fractures. The patient had been diagnosed with skull and rib fractures at ages 3 and 6 years, respectively, after two traumatic accidents. He remained fracture-free until age 10, when he sustained distal radius, metacarpal, and fibula fractures while playing sports. At age 11, he fractured his right mid-femur after falling from standing height during a soccer game; its repair required retrograde intramedullary flexible nailing. Later that year, spine radiographs, obtained to evaluate complaints of back pain, showed symmetric, biconcave compression deformities of most thoracic and lumbar vertebrae. Shortly thereafter, he developed a transverse fracture of the left scapula while rollerblading.

The patient has no family history of recurrent fractures, and has had no other medical problems. His height has historically placed him between the 5th and 10th percentiles for gender and age, and his weight has remained at the 50th percentile. His physical exam at age 11 was notable for Tanner I virilization. His initial laboratory evaluation, performed in 2003, was unremarkable except for an abnormality in growth hormone: post-dexamethasone cortisol 1 ug/dL (0-5 ug/dL); 25(OH)-vitamin D 61 ng/mL (15-80 ng/mL); iPTH 31 pg/mL (10-75 pg/mL); calcium 10.2 mg/dL (8.2-10.2 mg/dL); P 5.3 mg/dL (2.5-4.5 mg/dL) BSAP 157.2 U/L (20-166 U/L for age); alkaline phosphatase 252 U/L (38-126 U/L for age); IGF-I 63 ng/mL (109-485 ng/mL for a Tanner I male).

He was treated with daily growth hormone injections for one year based on his low IGF-I, but demonstrated no significant change in height. A skin biopsy was obtained for evaluation of possible osteogenesis imperfecta, was normal. After his evaluation was complete, no diagnosis was made and no treatment offered. At age 15, he re-fractured his right mid-femur and again required intramedullary nailing; his orthopedic surgeon noted atypical "softening" and "widening" of the bone during the procedure.

One year after his second femur fracture, he presented for a second opinion on his fractures. His physical exam at age 16 demonstrated a visible limp and marked thoracic kyphosis, as well as Tanner III virilization. His IGF-I had normalized (IGF-I 166 ng/mL (94-765 ng/mL)), and all other labs were essentially unchanged. Total testosterone was slightly low: 203 ng/dL (241-827 ng/dL).

Given that the locations of his fractures were predominantly metaphyseal and vertebral, and that they occurred during early puberty, a presumptive diagnosis of IJO is made. IJO has been described in fewer than 200 cases in the medical literature, and is generally associated with a return to normal bone density by adulthood. The dilemma in managing these patients involves determining the appropriate treatment within the appropriate timeframe, which is often difficult to assess. It is unclear whether or not treatment with anabolic or antiresorptive therapy is beneficial once the patient's bone density begins to recover, as is likely the case in this patient.

WORKING GROUP ON OSTEOPOROSIS AND RHEUMATIC DISEASES

WG21

Glucocorticoid Enhances the Expression of a Wnt Antagonist, Secreted Frizzled-Related Protein 3, in Cultured Human Osteoblasts. K. Ohnaka^{*1}, Y. Matsuzaki^{*1}, M. Tanabe^{*1}, M. Adachi^{*1}, H. Kawate^{*1}, R. Takayanagi².

¹Department of Geriatric Medicine, Kyushu University, Fukuoka, Japan;

²Department of Medicine and Bioregulatory Science, Kyushu University, Fukuoka, Japan.

Glucocorticoid-induced osteoporosis (GIO) is one of the most frequent and serious problems of long-term glucocorticoid therapy. Although the major cause of GIO is considered to be impairment of bone formation, detailed mechanism underlying GIO remains to be fully elucidated. Recently, the Wnt signal emerged as a novel key pathway for promoting bone formation. In this study, we investigated the effect of glucocorticoid on a Wnt antagonist, secreted frizzled-related protein (sFRP), in cultured human osteoblasts and an osteosarcoma-derived cell line, MG-63 cells. The expression of mRNA for secreted frizzled-related protein 3 (sFRP3) was markedly induced by dexamethasone among sFRP families. The expression of sFRP3 was also enhanced by hydrocortisone and prednisolone, but not by 17- β estradiol, dehydrotestosterone or 1, 25-dihydroxyvitamin D3. Similar effect of dexamethasone on sFRP3 expression was observed in MG-63 cells. To examine the effect of sFRP3 on osteoblast function, we then generated an expression vector containing entire coding region of human sFRP3 cDNA (pcDNA-sFRP3-HA). Transient transfection of pcDNA-sFRP3-HA suppressed the Wnt3a-induced the accumulation of cytosolic β -catenin in MG-63 cells. Transfection of sFRP3 also decreased the Tcf/Lef-dependent transcriptional activity in MG-63 cells. Furthermore, sFRP3 suppressed the proliferation of MG-63 cells. These data suggest that glucocorticoid may impair osteoblast function and bone formation by enhancement of sFRP3 in human osteoblastic cells, which may be involved in the pathogenesis of GIO.

Disclosures: K. Ohnaka, None.

WG22

Regulation of RANKL Expression by Glucocorticoid in Human Osteoblast-like Cells. F. Hirano, N. Maruyama^{*}, K. Komura^{*}, K. Okamoto^{*}, Y. Makino^{*}, M. Haneda^{*}. Medicine, Asahikawa Medical College, Asahikawa, Japan.

Glucocorticoid-induced osteoporosis remains the most common secondary form of metabolic bone diseases. The soluble and transmembrane cytokines, RANKL, are produced by the osteoblast under hormonal and cytokine control and are essential for osteoclastogenesis and bone resorption. In contrast, osteoprotegerin is known to bind to RANKL and to block the interaction between RANKL and its receptor RANK. Glucocorticoid has been reported to induce RANKL mRNA expression in osteoblasts, although circulating soluble RANKL is reduced by glucocorticoid. The reasons of this discrepancy are still unknown. The purpose of this study was to clarify the regulation of RANKL expression by glucocorticoid in human osteoblast-like cells. We used human osteoblast-like cell line MG-63 and examined effect of glucocorticoid on RANKL expression. Quantitative real-time RT-PCR and ELISA methods revealed that 100 nM dexamethasone (DEX) significantly increased RANKL mRNA expression (15-fold, $p < 0.05$) in MG-63 cells for a time-dependent manner and decreased soluble RANKL protein in supernatant, as expected. In addition, we found that DEX did not influence RANKL transcriptional activity by reporter gene assay using human RANKL promoter. Moreover, Treatment with actinomycin D and DEX markedly prolonged the half-life of RANKL mRNA in MG-63 cells, as compared to treatment with actinomycin D alone ($T_{1/2}$ = over 24h v.s. 10h), presumably indicating that DEX-induced RANKL mRNA expression is due to the stabilization of RANKL mRNA. Next, we investigated effect of glucocorticoid on the expression of TNF converting enzyme (TACE), a known RANKL sheddase. The activity of TACE was dose-dependently reduced by DEX. Moreover, 100 nM DEX significantly decreased both mRNA- and protein-expression of TACE by quantitative real-time RT-PCR and ELISA, respectively. Furthermore, 100 nM DEX clearly induced transmembrane RANKL protein in MG-63 cells by flow cytometry and Western blot analysis, suggesting that DEX-reduced soluble RANKL protein expression in supernatant is associated with the decreases of TACE activity and protein expression in MG-63 cells. In conclusion, we presented glucocorticoid up-regulated RANKL mRNA expression via the stabilization of RANKL mRNA and reduced soluble RANKL expression via the decrease of TACE expression, possibly indicating that glucocorticoid-induced transmembrane RANKL expression in osteoblasts mainly played a pivotal role in osteoclastogenesis.

Disclosures: F. Hirano, None.

WG23

Periarticular Bone Loss in Arthritis: Role of Synovial Glucocorticoid Generation. M. S. Cooper¹, R. Hardy^{*1}, E. H. Rabbitt^{*1}, N. J. Gittos¹, M. Hewison², C. D. Buckley^{*1}, K. Raza^{*1}, P. M. Stewart^{*1}. ¹University of Birmingham, Birmingham, United Kingdom; ²Cedars-Sinai Medical Centre, Los Angeles, CA, USA.

Periarticular osteoporosis is a common feature of inflammatory arthritis. This feature is related to disease activity and is associated with uncoupling of bone resorption from formation. We previously hypothesised that local glucocorticoid generation within osteoblasts in response to inflammation may underlie this bone loss. An alternative possibility is that excess glucocorticoids are generated from other joint tissues. Primary synovial fibroblasts express the 11 β -hydroxysteroid dehydrogenase type 1 (11 β -HSD1) enzyme that generates the active glucocorticoids cortisol and prednisolone from their inactive counterparts cortisone and prednisone suggesting that synovium might generate glucocorticoids. We have now explored this hypothesis by characterizing glucocorticoid metabolism in synovial tissue explants from patients with rheumatoid arthritis (RA) and osteoarthritis (OA). Glucocorticoid metabolism was examined in synovial tissue taken from subjects with OA (n=8) or RA (n=12) during orthopedic surgery using radiolabelled steroids and TLC. Immunohistochemistry was used to identify the cellular distribution of enzymes. The functional consequences of enzyme activity on IL-6 production were examined by ELISA. All synovial biopsies had substantial capacity to activate glucocorticoids (cortisone to cortisol and prednisone to prednisolone) which was blocked by a specific 11 β -HSD1 inhibitor confirming 11 β -HSD1 expression. No difference in steroid metabolism was seen between samples from RA and OA subjects. In patients with RA, synovial cortisol generation increased with the ESR of the tissue donor ($R^2=0.4$, $p < 0.05$). 11 β -HSD1 activity had functional consequences with cortisone able to decrease synovial IL-6 production in tissue from patients with RA or OA (31+15% for RA, 36+9% for OA, both $p < 0.05$). Steroid inactivation was also apparent in synovium and was not blocked by inhibition of 11 β -HSD1. Using immunohistochemistry 11 β -HSD2 expressing cells were identified in RA synovium and expression colocalized with the monocyte marker CD68. This pattern was distinct from 11 β -HSD1 which was expressed in fibroblasts. Synovial tissue metabolises glucocorticoids with the predominant effect being glucocorticoid activation and this increases with inflammation. Endogenous glucocorticoid production in the joint is likely to regulate tissue inflammation but in excess might detrimentally impact on periarticular bone integrity. Additionally, a subset of immune cells expressing 11 β -HSD2 within synovium will be resistant to cortisol/prednisolone through steroid inactivation and this could perpetuate synovial inflammation.

Disclosures: M.S. Cooper, None.

WORKING GROUP ON MUSCULOSKELETAL REHABILITATION

WG24

Associations of Osteoporotic Spinal Deformity with Back Strength Among Elderly Women in Japan and the United States. M. Hongo¹, M. Sinaki², N. Miyakoshi¹, Y. Shimada¹, E. Itoi³. ¹Dept. of Orthopedic Surgery, Akita University, Akita, Japan; ²Dept. of Physical Medicine and Rehabilitation, Mayo Clinic, Rochester, MN, USA; ³Dept. of Orthopedic Surgery, Tohoku University, Sendai, Japan.

Kyphosis is associated with diminished daily physical function, increased risk of falls, and increased mortality risk. Back extensor strength (BES) is an important factor in maintaining the sagittal alignment of spine and preventing vertebral fractures. When back exercises are prescribed, it is important to know the associations of the sagittal alignment with BES. However, there is a controversy in the literature regarding the influence of the thoracic and lumbar spinal curvatures on BES or quality of life. We hypothesized that the regional or ethnic factor may influence the relationship between thoracic and lumbar sagittal curve, BES and other factors. The purpose of this cross-sectional study was to assess the associations of osteoporotic spinal deformity with back strength in elderly women in Japan and the United States. Using the same inclusion criteria, 104 Asian women residing in Akita, Japan and 102 Caucasian women residing in Minnesota with postmenopausal osteoporosis were selected for this study. Kyphosis angle of the thoracic and lumbar spine were measured with lateral radiographs. Isometric BES was evaluated using a custom-made dynamometer. Correlations between the kyphosis angle, isometric BES, bone mineral density, physical activity score or quality of life score, the number of vertebral fractures, and grip strengths were analyzed. No significant difference was found in thoracic kyphosis between Akita and Minnesota (43.1° and 44.1°, respectively), whereas lumbar kyphosis angle in Akita was significantly larger than in Minnesota (-15.4° and -54.0° p<0.0001). In Akita, BES showed significant negative correlation with lumbar kyphosis angle (r=-0.492, p<0.0001), but no correlation with thoracic kyphosis angle (r=-0.004, p=0.97). In Minnesota, BES showed significant negative correlation with thoracic kyphosis angle (r=-0.372, p<0.0001), but no correlation was found with lumbar kyphosis angle (r=-0.087, p=0.362). In addition, quality of life score in Akita demonstrated significant correlation with lumbar kyphosis, but not with thoracic kyphosis. Physical activity score in Minnesota showed significant negative correlation with thoracic kyphosis, but not with lumbar kyphosis. In conclusion, there was a significant difference in lumbar kyphosis angle between the two countries. Lumbar kyphosis angle has more significant influences in maintaining BES and quality of life among women in Akita, Japan compared with those in Minnesota.

Disclosures: M. Hongo, None.

WG25

Significant Reduction of Vertebral Fractures: Comparison of Rehabilitation of Osteoporosis Program-Exercise (ROPE) versus No-ROPE, with or without Pharmacotherapy. Diana A. Kurmen, Mehrsheed Sinaki. Department of Physical Medicine and Rehabilitation, Mayo Clinic, Rochester, MN, USA

The objective of this study was to determine whether patients with osteoporosis who received the Rehabilitation of Osteoporosis Program-Exercise (ROPE) had reduced risk of vertebral fracture as compared with those who did not (No-ROPE). To avoid bias in choice of treatment, none of the subjects or evaluators had knowledge of group assignment.

We reviewed the medical records of 200 patients. One hundred and twelve patients with osteoporosis met the inclusion criteria, i.e. women older than age 40 with the diagnosis of osteoporosis, baseline and follow-up radiographs of spine. Patients with steroid-induced bone loss and active malignancy were excluded. Two groups were formed: 71 subjects in the ROPE group and 41 subjects in the No-ROPE group met the enrollment criteria. Follow up was the date of follow up x-rays or recurrence of fracture/back pain. The duration of follow up ranged from 3 months to 118 months with an average of 45.5 months.

The results showed that 56 of the 71 ROPE subjects (78.9%) and 20 of the 41 No-ROPE subjects (48.8%) had no new fracture at the time of final follow up. Interestingly, 56 subjects (78.9%) of the 71 ROPE subjects had received pharmacotherapy whereas all 41 (100%) of the No-ROPE subjects had received pharmacotherapy for bone loss.

The 79% of the ROPE population without new fracture were distributed as: 29.6% combination therapy, 26.8% bisphosphonates only, 9.9% calcium only, and 12.7 % no pharmacotherapy. The 49% of the No-ROPE population without new fracture were distributed as: 26.8% combination therapy, 17.1% bisphosphonates only, and 4.9% calcium only.

In the population taking some kind of pharmacotherapy, 21.1% had new fractures during the time to follow up in the ROPE group versus 51.2% in the No-ROPE group.

The No-ROPE group was four times more susceptible to fracture during the time to follow up (P = 0.001), Pearson Chi Sq test. The group with the lowest incidence of fractures was the ROPE group with combination pharmacotherapy.

To prevent vertebral osteoporosis fractures, we enthusiastically suggest that ROPE be mandatory for management of every woman with osteoporosis, regardless of choice of pharmacotherapy.

Disclosures: D.A. Kurmen Figueroa, None.

WG26

An Interdisciplinary Approach to Improve Pain and Mobility in Patients with Osteoporosis and Painful Vertebral Fractures by Kyphoplasty. C. Kasperk¹, M. Baier², G. Nöldge³. ¹University Clinic of Heidelberg, Dept. of Endocrinology and Metabolism, Heidelberg, Germany; ²University Clinic of Heidelberg, Dept. of Trauma Surgery, Heidelberg, Germany; ³University Clinic of Heidelberg, Dept. of Radiology, Heidelberg, Germany.

Osteoporosis and arteriosclerosis are associated diseases heavily impacting on the patients lifespan and quality of life (QoL) whereby the lifespan is shortened by an increased cardiovascular mortality of osteoporotic patients and the QoL is worsened by the occurrence of painful vertebral fractures, related disabilities and immobility. Immobility is a crucial risk factor for further bone loss and arteriosclerotic complications (e.g. stroke, hypertension). A prerequisite for an improved mobility of patients with osteoporosis/arteriosclerosis is a reduction of pain induced impairments of the musculoskeletal activity. Despite the accomplished pharmacological progress in the treatment of the osteoporotic disorder of bone metabolism painful vertebral fractures (VF) are still occurring during under any available antiresorptive or osteoanabolic treatment. Analgetic treatment of bone pain associated with 50 % of incident vertebral fractures does not improve the cause of the pain. Internal stabilization of painfully fractured vertebral bodies terminates the permanently ongoing microfracturing in VF and thus the irritation of pain fibres which are present in bone, even in the Haversian canals.

In this trial we sought to investigate how beneficial short term effects of KP on pain and mobility will affect long term outcome and fracture incidence. The selection of patients was done by an interdisciplinary team of endocrinologists, orthopaedic surgeons and radiologists on the basis of the precise knowledge of the complaints and X-rays, CT- and MRI scans of every patient to exclude other causes of pain than vertebral fracture associated pain.

KP was performed in 40 of 60 patients with primary osteoporosis and painful vertebral fractures, 40 patients received vertebral stabilization by balloon kyphoplasty, 20 served as non-KP controls (Con). All patients received pharmacological treatment (oral aminobisphosphonate, 1000 mg calcium + 1000 IE vitaminD3) and physiotherapy. Pain (VAS scale [100=most severe pain]), mobility (EVOS score [100=full mobility]) and radiomorphology were determined after 6, 12 and 36 months.

	PRE-KP KP Con	6 mo. KP Con	12 mo. KP Con	36 mo KP Con
Pain	74.5 66.4 40.1	53.1 64.4 55.7	53.7 65.7 54.5	52.7 64.0 53.6
297	39.8	43.8	44.3	43.6

Number of total new vertebral fractures after 3 years:

KP21 # (in 14 of 34 patients)

Con18 # (in 10 of 14 patients)p=0.0341

In a selected group of patients with painful vertebral fractures KP is superior to conservative treatment of painful osteoporotic vertebral fractures for at least 3 years after intervention. KP has long term beneficial effects on pain reduction, improved mobility and fracture incidence provided that an interdisciplinary team of endocrinologists, orthopaedic surgeons and radiologists select those patients whose pain truly originates from the fractured vertebral body and not from spondylitis, spondylarthrosis or destruction of the intervertebral disc.

WG27

Improving Trunk Strength and Endurance in Older Women with Vertebral Fractures. K. M. Shipp, D. T. Gold, C. F. Pieper*, K. W. Lyles. Duke University, Durham, NC, USA.

The trunk musculature is important for people with osteoporosis. First, strong, fatigue-resistant trunk muscles are necessary for erect postural alignment. Second, strong trunk extensors may prevent vertebral fractures. An observational study associated trunk extension strengthening over 2 years with decreased incidence of vertebral fractures in the next 8 years [1]. This presentation will review the evidence for the relationships between trunk alignment, strength, and endurance; functional status; and fracture risk. Time will be allotted for discussion, with the goal of identifying important, unanswered research questions regarding these parameters.

Our work at Duke University Medical Center with patients with vertebral fractures will be described. Particularly, results will be presented from a randomized clinical trial of a group exercise intervention (3X/week for 6 months) in older women (n=122, mean age 81 years) with vertebral fractures (mean # 2.3) [2]. Randomization was by site: 3 trunk exercise intervention sites (n=53) and 3 control sites (n=69). The trial was a modified cross-over design: the control sites received the exercise intervention after 6 months of health education sessions. The exercises included 1) stretches to increase trunk extension flexibility and 2) progressive resistive strengthening exercises for trunk extensors, abdominals, and posterior scapular groups.

Using mixed-model ANCOVA (intention-to-treat), we found a significant difference between groups for trunk extension strength at 6 months ($p=0.0001$; +6.6 ft-lbs. [up 24%] exercisers, -4.6 ft-lbs. controls). When the control subjects received the exercise intervention, there was a mean increase of 15.0 ft-lbs [up 45%].

The outcome of an ancillary study was the effect of the intervention on Timed Loaded Standing (TLS), a measure of combined trunk and arm endurance [3]. Using mixed-model ANCOVA (intention-to-treat), we found a trend for difference between groups for TLS time at 6 months ($p=0.0542$; +8.8 s exercisers, -8.9 s controls). Among compliers (those attending 2/3s of sessions), group was significant ($p=0.035$; +14.9 s exercisers, -10.3 s controls). Change in TLS time over 6 months was significantly correlated ($p<0.05$) with psychological symptoms and functional status.

These results showed that trunk extension strength and combined trunk and arm endurance could be increased, in older women with vertebral fractures, by 6 months of group, physical therapist-led, trunk-specific exercise classes.

References: 1. Sinaki M, Itoi E, Wanner HW, et al. Bone 2002;836-841.
2. Gold DT, Shipp KM, Pieper CF, et al. J Am Geriatr Soc 2004;52:1471-1478.
3. Shipp KM, Purser JL, Gold DT, et al. Osteoporos Int 2000;11:914-922.

Disclosures: K.M. Shipp, None.

This study received funding from NIH (NIA and NICHD).

WG28

Looking Beyond the Fracture: Women and Men with a Recent Clinical Fracture Have Bone and Fall Related Fracture Risks Far Beyond the Presence of Low Bone Mineral Density. Piet P. Geusens. University Hospital Maastricht, Department of Internal Medicine, Maastricht, The Netherlands.

Introduction: Fractures are associated with bone and fall related risk factors. Both have additive effects in predicting fractures. However, no data are available on the relative prevalence of these risk factors in patients with a recent clinical fracture.

We therefore systematically analysed these risk factors in subjects with a recent clinical fracture.

Methods: All women and men older than 50 years, admitted during a one-year period because of a recent fracture, were offered an evidence-based bone and fall related risk factor assessment and bone densitometry.

Results: Of the 941 consecutive patients, 798 (85%) were eligible for this study and 568 (60%) approved to participate. Fall-related risk factors (n= 425, 75% (95%CI: 71 % - 78 %)) and bone related risk factors (n=299, 53% (95%CI: 49% - 57%)) were more frequently present at the time of fracture than osteoporosis (DXA T score < -2.5 in spine and/or hip (n=201, 35% (95%CI: 31% - 39%)), and were irrespective of the fracture location, the age categories included, and gender. Overlap between bone and fall related risk factors were found in 50% of the patients. The 406 women in this study were compared with 492 postmenopausal women without a fracture history of another cohort study. Adjusted for age, weight, and height the patients with fractures had more osteoporosis (OR 2.9; 95%CI 2.0 - 4.1) and more had a history of falls (OR 4.0; 95%CI 2.7 - 5.9). Based on available osteoporosis guidelines many women with a fracture would not have been detected if screened for an increased fracture risk.

Conclusions: Women and men of 50 years and older with a recent clinical fracture have, at the time of fracture, bone and fall related risk factors far beyond the presence of osteoporosis. Together with the heterogeneity, multiple combinations and overlap of risk factors irrespective of age, fracture location and gender, this may implicate that an integrated bone and fall related risk factor assessment is to be preferred to trace subjects at risk for fracture. Integrated bone and fall related risk assessment and treatment studies are needed to document this.

WG29

Jump Starting Skeletal Health: Bone Increases from Jumping Exercise Persist Seven Years Post Intervention. K. B. Gunter*, A. Baxter-Jones*, R. Mirwald*, H. C. Almstedt*, S. Durski*, A. A. Fuller-Hayes*, C. M. Snow*.

¹Department of Nutrition and Exercise Sciences, Oregon State University, Corvallis, OR, USA; ²College of Kinesiology, University of Saskatchewan, Saskatoon, SK, Canada; ³Department of Natural Science, Loyola Marymount University, Los Angeles, CA, USA.

Evidence suggests that bone mineral increases attributable to exercise training prior to puberty may confer a significant advantage into adulthood. However, there is a dearth of supportive prospective longitudinal data. We assessed the change in bone mineral content (BMC) at the left proximal femur over eight years in children who participated in a seven-month jumping intervention and who were pre-pubertal at study onset.

We hypothesized that jumpers would accrue and retain more BMC compared to controls and therefore be at a considerable advantage in optimizing peak bone mass accrual. Subjects were drawn from the BUGSY study (Building Growing Skeletons in Youth), an ongoing mixed longitudinal study of bone mineral accretion in growing children initiated in the fall of 1997. Participants were recruited from local elementary schools in Corvallis, Oregon and were randomly assigned within classrooms to either an intervention (jumping) or control (stretching) group. Subjects were assessed at baseline, at the end of the intervention (7 months) and at approximately 19 months. Participants were reassessed at 31, 43, 55, 67, 79 and 91 months from study entry for a total of nine measurement occasions over approximately 8 years. Bone mineral content was assessed by dual-energy X-ray absorptiometry. Multi-level random effects models were constructed and used to predict change from study entry in BMC at each measurement occasion. We were able to utilize data from a total of 421 DXA scans on 57 individuals who were measured on 3 or more occasions. At 7 months, the intervention group had 3.6% more total hip bone accrual than the non-intervention group ($p<0.05$), once the effects of change in age, height and weight were accounted for. The effects of the intervention, in terms of percentage contribution to total hip BMC, decreased at each measurement occasion thereafter. After an average of 7.6 years, the intervention group had 1.4% more total hip bone accrual than the non-intervention group, once the effects of change in age, height and weight were accounted for ($p<0.05$). This provides the first evidence that changes in BMC attributable to short-term exercise undertaken prior to puberty persist more than 7 years following exercise cessation in growing children. If the benefits are sustained into adulthood, effectively increasing peak bone mass, this could have substantial effects on fracture risk.

Disclosures: K.B. Gunter, None.

WG30

Weight Bearing Bones Are More Sensitive to Physical Exercise in Boys than in Girls During Pre- and Early Puberty. S. Kriemler*, L. Zahner*, J. Puder*, C. Braun-Fahrlander*, C. Schindler*, M. Kraenzlin*, R. E. Rizzoli*.

¹Institute Sport & Health, Basel, Switzerland; ²Division Endocrinology, Diabetes & Clinical Nutrition, Basel, Switzerland; ³Institute Social & Preventive Medicine, Basel, Switzerland; ⁴Endocrinology, Diabetes and Clinical Nutrition, Basel, Switzerland; ⁵Rehabilitation & Geriatrics, University Hospital, Geneva, Switzerland.

Background: Physical activity (PA) positively influences bone mineral accrual. However, little is known whether there are gender differences in bone sensitivity to loading and to what extent spontaneous objectively recorded PA influences bone mineral mass independently from muscle mass. We investigated gender differences in the association between bone mineral density/content (BMD/BMC) and measures of PA, during preand early puberty. Methods: We measured BMD/BMC and fat-free mass in 374 6-13-year-old children from randomly selected schools at the hip, lumbar spine and total body by DXA. PA was evaluated by accelerometers, and lower extremity strength by a jump&reach test.

Results: Boys had higher hip and total body BMD than girls at all ages. Boys had higher fat-free mass, greater lower extremity muscle strength and were more physically active than girls at all ages. Total hip BMD was positively associated with time spent in total and vigorous PA in boys ($r=0.33$ and 0.27 , respectively, $p<0.01$), but not in girls ($r=0.02$ and 0.04 , $p=ns$), even after adjusting for fat-free mass and lower extremity strength. While boys and girls in the lowest tertile of vigorous PA (22 min per day) had similar hip BMD (0.668 vs 0.679 g*cm⁻²), those boys in the highest tertile (72 min per day) had significantly higher values than the corresponding girls (0.730 vs 0.692 g*cm⁻², $p<0.05$). In multiple logistic regression analyses, a low hip BMD in boys was best predicted by fat-free mass (OR 0.55 [95%CI 0.38, 0.78] per 1 kg) and total PA (OR 0.69 [95%CI 0.49, 0.98] per 106 counts), while in girls predictors included fat-free mass (OR 0.63 [95%CI 0.50, 0.79] per 1 kg) and jump&reach (OR 0.90 [95%CI 0.84, 0.98] per 1 cm). Similar data were obtained for femoral neck BMD/BMC. There was no influence of PA on lumbar spine BMD in either gender.

Conclusion: Though at low physical activity during pre- and early puberty, hip BMD is similar in both genders, it increases proportionally to PA, and differences in bone mineral mass between genders appears, likely related to a different sensitivity of bone to physical loading, independently from muscle mass.

Disclosures: R.E. Rizzoli, None.

WG31

Effects of Daily Muscle Trainings on Falls and Vertebral Fractures in the Elderly Osteoporotic Women. T. Horiuchi¹, A. Kanemaru^{*2}, T. Katoh^{*2}, H. Tobimatsu^{*1}. ¹Endocrinology, Tokyo Metropolitan Geriatric Hospital, Tokyo, Japan; ²Rehabilitation, Tokyo Metropolitan Geriatric Hospital, Tokyo, Japan.

Objective: We conducted a randomized case control study for one year to examine the effects of the home daily exercises to prevent osteoporotic women from falling and suffering of fracture.

Subjects & Methods: Ninety-three osteoporotic elderly women were recruited to participate in this study and they were divided into two groups: one is the control whose physical strength we only estimate, whereas the other group were intervened by exercise. The exercise group were instructed to repeat daily muscle training at home. The exercise instruction include muscle training to increase the strength of abdominal, back, quadriceps, gastrocnemius, soleus and plantaris muscles. In order to evaluate muscle strength we measured grasp power (GP), knee flexion strength (KNS), maximal walk velocity (MAW) and 3m timed up and go test (TUGT), lumbar and femoral bone mineral density and bone metabolic markers before and after one-year training, checking the reproducibility and QOL with SF36 every six months. Falls frequencies and vertebral fractures incidences were also examined. Statistics were done using a two-way ANOVA and stepwise multiple regression analysis. The medications for osteoporotics have not been altered in all participants during this study.

Results: LBMD were significantly increased in both groups for one year ($p < 0.05$). In exercise group GP, MAW and KNS were significantly increased, and TUGT were significantly decreased ($p < 0.05$). There was a graph interaction between control and intervention group in left KNS, which means that a significant difference between two groups disappeared in one year ($p = 0.006$). Physical component score and mental component score in SF36 were not changed in both groups. Falls frequencies were decreased in two groups, showing a trend of steep reduction in a training group. There was no significant difference in vertebral fracture incidence between two groups. In multivariate regression analysis TUGT was significantly associated with Falls frequencies ($p < 0.0001$).

Conclusion: Exercise for the elderly women are effective to increase the strengths of muscles. Exercises might be effective to prevent elderly osteoporotics from falling. We should furthermore continue to perform exercise instruction as an intervention using TUGT.

Disclosures: T. Horiuchi, None.

WG32

Load-specific Differences in Femoral Neck Cortical Geometry: Preliminary data from 3-D MRI Study of Proximal Femur of Athletes. R. Nikander¹, H. Sievänen¹, P. Dastidar^{*2}, A. Heinonen³, P. Kannus^{*4}. ¹Bone Research, UKK Institute for Health Promotion Research, Tampere, Finland; ²Department of Radiology, University Hospital, Tampere, Finland; ³Department of Health Science, University of Jyväskylä, Jyväskylä, Finland; ⁴Department of Trauma, Musculoskeletal Surgery and Rehabilitation, University and University Hospital, Tampere, Finland.

During normal walking, femoral neck (FN) is subjected to a large number of consecutive, low magnitude impacts from typical directions. In contrast, during sport performance, power-lifters' femoral neck experiences very high magnitude, low rate loading from unusual direction, while swimmers' femoral neck is subjected to high rate muscle activity lacking virtually the weight-bearing component. We aimed to investigate the differences in the femoral neck cortical geometry among world-class power-lifters, national level swimmers and normal exercisers serving as referents. In this preliminary analysis of accumulating bone data from five power-lifters, five swimmers and five referents were compared. In all groups, the femoral neck cortical structure was assessed with DXA and 3-D MRI of the proximal femur. ANCOVA (age, weight and height as covariates) were used for statistical analysis. The femoral neck BMC and BMD were 35% and 31% higher in power-lifters, but 11% and 13% lower in swimmers compared with controls ($0.02 < p < 0.07$). Interestingly, the shape of power-lifters' femoral neck appeared to be round at the narrowest section, while swimmers' and controls' FN seemed to be oval being wider in the superior-inferior direction. Although the inter-group differences in the femoral neck cortical thickness did not reach statistical significance, a clear trend suggesting substantially thicker cortices in power-lifters in all anatomic directions (anterior 22%, posterior 52%, superior 12% and inferior 45%) was found, while the cortices between swimmers and referents were similar. The strong femoral neck structure (more mass, denser bone, round shape and thick cortices) seemed to be characteristic of power-lifting performance. High magnitude loading produced at low rate seemed to account for strong femoral neck, while non-weight bearing, low-magnitude loading, despite large number of repetitions at relatively high rate, seems not benefit to bone structure at all.

Disclosures: R. Nikander, None.

WG33

TENS (Transcutaneous Electrical Nerve Stimulation) in the Management of Osteoporosis-related Pain. S. Kalra^{*1}, A. Sharma^{*1}, B. Kalra^{*2}, N. Kumar^{*3}. ¹Endocrinology, Bharti Hospital, Karnal, India; ²Gynaecology, Bharti Hospital, Karnal, India; ³Physiotherapy, Bharti Hospital, Karnal, India.

Pain is a disabling symptom in persons with osteoporosis, and it often reduces the quality of life. This paper studies the effect of TENS in subjects with osteoporosis, complaining of pain.

30 adult osteoporosis patients with lower limb pain, receiving five sittings of TENS on daily or alternate day basis, were compared with 30 age-matched, disease-matched patients who were administered daily diclofenac and five sittings with sham electrodes.

Pain scores, measured by visual analog score, reduced significantly in both groups, but much more so in the TENS group (from 4.60 ± 0.54 to 1.60 ± 0.54) than the sham electrodes + diclofenac group (from 4.40 ± 0.54 to 3.60 ± 0.54). This difference was maintained after 3 weeks, even though the TENS sittings had stopped. Best improvement was obtained in patients with burning (3.28 ± 0.64) and lancinating (3.12 ± 0.64) pain.

Least benefit was in patients with deep pain (2.15 ± 0.35) and restless legs syndrome (2.16 ± 0.56).

The dose of TENS used varied from 5.5 to 9.0 Hz on the initial day to 3.5 to 5.5 Hz on the last sitting. The dose varied insignificantly for different symptoms.

Validated health-related questionnaires were used to assess the effect of physiotherapy sessions in the subjects. Physician communication score improved from 1.43 ± 1.19 to 3.93 ± 0.86 over one month of therapy in all subjects. Time spent by them in stretching/strengthening exercise increased from 0.0 ± 0.0 to 15.0 ± 0.0 minutes per week. The social/role activities limitation due to the disease reduced from 2.25 ± 0.63 to 1.08 ± 0.39 . Cognitive symptom management improved from 1.30 ± 0.63 to 2.00 ± 0.67 .

The health distress score fell from 3.20 ± 0.82 to 1.35 ± 0.47 while energy/fatigue scores raised from 2.25 ± 0.51 to 3.30 ± 0.50 in all subjects. No difference was noted in these scores between the two groups.

This paper demonstrates the beneficial effect of TENS on pain related to osteoporosis, and the advantageous effects of regular physiotherapy on various health-related parameters in persons with osteoporosis.

Disclosures: S. Kalra, None.

WORKING GROUP ON PATIENT EDUCATION AND ADHERENCE TO TREATMENT

WG34

Patient and Physician Attitudes Toward Vitamin D in Osteoporosis Treatment. S. P. Chan^{*1}, J. A. West², L. E. Wehren², S. S. Sen^{*2}. ¹University of Malaya, Malaya, Malaysia, ²Merck, Rahway, NJ, USA.

BACKGROUND: Vitamin D is essential for calcium absorption and bone health, and most osteoporosis treatment guidelines recommend vitamin D supplementation. This study explored the knowledge and attitudes of physicians and patients towards supplement use in osteoporosis treatment.

METHODS: Randomly selected Physicians from Malaysia, Taiwan, Philippines, Korea, and Singapore and their postmenopausal women patients with osteoporosis were surveyed. Physicians rated the importance of vitamin D and calcium in osteoporosis management on a scale of 1(not important) to 10 (extremely important) and estimated supplement use by their patients. Patients reported their use of vitamin D and calcium and their perceptions regarding these supplements.

RESULTS: 237 physicians (37 from Malaysia, and 50 each from Taiwan, Philippines, Korea, and Singapore), and 1463 patients (251, 218, 194, 400, and 400 from Malaysia, Taiwan, Philippines, Korea, and Singapore respectively) completed the survey. 84% of patients in Malaysia, 46% in Taiwan, 16% in the Philippines, and 55% each in Singapore and Korea reported never having discussed Vitamin D supplementation with their Physician. Physicians and patients in all countries reported that calcium was discussed more frequently than Vitamin D. Physicians reported that their patients have little knowledge of the relationship between vitamin D and calcium, and this was confirmed by patient responses.

CONCLUSION: Most osteoporosis patients recognize the importance of calcium, but have less awareness of that of Vitamin D. Lack of understanding about the role of Vitamin D and numerous concomitant medications can reduce compliance with Vitamin D supplementation.

Disclosures: J.A. West, Merck 3.

This study received funding from Merck & Co., Inc.

WG35

So How Was It? Patient Opinions on Osteoporosis Interventions in the Fracture Clinic Setting. D. E. Beaton, E. R. Bogoch, R. Sujic*, V. Elliot-Gibson*. Mobility Program, St. Michael's Hospital, Toronto, ON, Canada.

Our study aims to understand factors that influence fragility fracture patient's adherence with St. Michael's Hospital Osteoporosis Exemplary Care Program's recommendations for further osteoporosis testing and treatment. Our previous research indicates that coordinator-based interventions are an effective way of preventing future fractures. The results of this study will help identify key variables to consider when evaluating the Ontario Osteoporosis Strategy's Fracture Clinic Screening Program which is based on the coordinator model.

This is a qualitative study using focus-group methodology. Out of 45 patients who were eligible based on the study criteria, 24 patients participated in five focus groups. Transcripts of the five focus groups were transferred to N-Vivo for storing and sorting the data. Transcripts were coded for content and links between descriptive labels were made. By using qualitative method, we are hoping to explore the impact of the Osteoporosis Exemplary Care Program in a much more contextualized fashion.

Emerging results support Anderson's behavioural model of health care utilization. Perceived need and susceptibility were associated with osteoporosis prevention efforts and treatment adherence as reported by the patients involved in the focus groups. The most frequent barriers that patients identified in diagnosis and treatment of osteoporosis included the perceived lack of clear and reliable information regarding the nature of BMD testing and proper treatment as well as the lack of general practitioner's recommendations about osteoporosis care and prevention. Most often cited facilitators of osteoporosis testing and treatment included thorough follow up by an osteoporosis coordinator, accessibility and ease of BMD testing and general practitioners' recommendations for treatment and testing.

General practitioners were named as key influence over the initiation of prevention and treatment of osteoporosis.

Disclosures: D.E. Beaton, None.

WG36

Improvement of the Persistence with Teriparatide in Postmenopausal Osteoporosis: The French Experience of an Education Program. K. Briot¹, P. Ravaud^{*2}, S. Liu-Léage^{*3}, C. Roux¹. ¹Rheumatology, Cochin Hospital, Paris, France, ²Biostatistics and Epidemiology, Bichat Hospital, Paris, France, ³Lilly France, Suresnes, France.

Several anti-osteoporotic treatments have been proved effective in decreasing the risk of fractures but available data suggest low adherence and persistence rates in patients taking medications for osteoporosis. This can result in failure in treatment efficacy. Several strategies have been developed to improve adherence and persistence. Teriparatide, prescribed 20 µg/day injected subcutaneously, is an anabolic treatment licensed for established postmenopausal osteoporosis. Education program has been developed after its launch, to help elderly women to deal with the pen take and consequently better follow the

prescribed treatment. The objective is to assess the efficacy of an education program to improve the persistence with teriparatide in postmenopausal osteoporotic women. This education program has been created by the promotor of teriparatide since its launch of teriparatide in France in September 2004 and it is proposed to each woman who begins the teriparatide. The program includes injection technique learning, osteoporosis education, observance and persistence assessment. Women are interviewed by regular calling of a nurse, each month the first year and every 3 months the 6 following months. Data about persistence and side-effects are available for the period September 2004 to December 2006. Persistence is defined as the percentage of patients still on treatment at the end of the 18-month course. Since the launch of teriparatide in France in September 2004, 4518 postmenopausal women (mean age 73.6 ± 11.4 years) with osteoporosis (lumbar spine and/or femoral T score ≤ -2.5) and vertebral fractures (4 fractures on average) have participated to the program. At the end of the year 2006, 1951 women have been followed at least 18 months. Of these 1951 women, persistence at 18 months was 82.6%. Main reasons for discontinuation, as declared by the patients, were side-effects (43.8%), wish of the patient (23.8%), physicians' decisions (17%) and deaths (5.3%). Persistence has been compared to the data of the French universal health insurance system; and it has been estimated that persistence at 18 months was closed to 0% for women who have been prescribed teriparatide without any education program. This study shows that an education program can highly improve the persistence with teriparatide at 18 months. Persistence is greater than that of existing oral therapies for osteoporosis, and this high persistence should improve the effectiveness of this therapy.

Disclosures: K. Briot, None.

WG37

Compliance with Osteoporosis Treatment and Incidence of Hip and Wrist Fracture after Forearm BMD Screening. M. W. J. Davie, T. Jones*, N. Dugard*. Charles Salt Research Centre, Robert Jones & Agnes Hunt Orthopaedic Hospital NHS Trust, Oswestry, United Kingdom.

Treatment compliance in osteoporosis may affect fracture outcome. To investigate compliance and fracture after a screening programme, we revisited 1299 women aged 50-97y screened by forearm scanning after a minimum of 3 years. Women were scanned at the request of their doctor (GP) and treatment advised if BMD values were <0.34g/cm² (osteoporosis (OP)). Treatment was decided by the woman's GP. No follow up was arranged. Women completed a detailed questionnaire at the scanning visit and again when revisited. Women lost to follow up were traced through health records and treatment details between scanning and revisit obtained from the women's own GP. 74% of women returned their questionnaires with no difference between those osteoporotic and those not. Fractures were validated with a 10% sample (and were correct within 5%).

All but 98.5% were traced of whom 14.4% had died. 254 women had osteoporosis at the first visit (aged 50-9, 2.4% had OP, 60-9 15.8%, and >69 54.3%). Of these 37.4% had never started any treatment (excluding Ca and Vit D only) - with no difference across ages. 1.3% had HRT and 98.7% Bisphosphonate (BP) of which 38% used Didronel, 43% Fosamax and 19% had had >1 BP. Compliance with BP dropped to 73.8% after 1yr (no difference across ages) with 22.9% only collecting 1 script. Fewer women with OP in institutions had ever had treatment (28%, p<0.01) and were also more likely to stop treatment (28.6% had only 1 script). Excluding women who were no longer available compliance at 2yr was 68.3%, 3yr 58.6%, 4yr 50% and 49.6% at 5yr. Hip fracture occurred in 1 woman with OP out of 38 (age 76.6±8.1y) who were never treated and in 7 of 55 women (73.2±7.3y (age p<0.05)) fully compliant for 5yr. The excess in women fully compliant occurred after >3y treatment (2 had used Didronel, 2 Fosamax, 3 both). Wrist fractures occurred in 3 women in each group.

Compliance declined early suggesting early follow up is indicated. Treatment in institutions may be overlooked. Compliance is not necessarily associated with hip fracture reduction. However the age of patients with hip fracture (75% were >80y) is consistent with BP efficacy being less in this age group. Moreover most of the hip fractures occurred >3y after treatment started when BP may be less effective at preventing hip fracture.

Disclosures: M.W.J. Davie, None.

WG38

An Outreach Program Improved Osteoporosis Management after a Fracture. A. C. Feldstein¹, W. M. Vollmer^{*1}, D. H. Smith^{*1}, A. Petrick^{*1}, J. Schneider^{*1}, H. Glauber^{*2}, M. Herson^{*2}. ¹Center for Health Research, Kaiser Permanente Northwest, Portland, OR, USA, ²Northwest Permanente, Portland, OR, USA.

This longitudinal retrospective cohort study evaluated implementation of a 2-phase intervention to improve management of osteoporosis after a fracture. Stakeholder barriers and facilitators of osteoporosis management were also determined. The study setting was a nonprofit group model HMO in the U.S. Pacific Northwest with 15 clinics, 480,000 members, and comprehensive electronic medical record data. Study participants were women members aged 67 or older who sustained a qualifying clinical fracture(s) and who had not received a bone mineral density (BMD) measurement or osteoporosis treatment in the 12 months prior to the fracture (n=3588) and their 255 primary care providers (PCPs). Interviews/focus groups were conducted with 58 patients, health care managers, PCPs, and

orthopedic clinicians. Phase 1 included outreach to clinicians and patients; Phase 2 added clinician/staff incentives. The primary outcome was "osteoporosis management" receipt of a BMD measurement or osteoporosis medication in the 6 months after an index fracture. Prior to the intervention, 13.4% (95% confidence interval [CI] = 12.0%-14.8%) of fracture patients had received osteoporosis management; the pre-intervention time trend was not significant. After the intervention, the unadjusted probability of osteoporosis management increased on average by 3.1% (95% CI = 2.6%-3.5%) every 2 months throughout both study phases. There was no significant added improvement in Phase 2. Overall, the probability of osteoporosis management increased from the baseline level to 44.0% (95% CI = 40.0%-48.0%) by the end of the study period (20 months post intervention). Adjusted models revealed that osteoporosis management was less likely in older patients and in those with dementia and was more likely in those with fractures more highly associated with osteoporosis. Improvement varied by clinic and was less likely for patients with dementia. Patient knowledge gaps and fatalism were common, especially among older patients. Common clinician barriers were lack of time, difficulty interpreting all relevant results, patient management concerns in the transition from specialty to primary care, and frustration with the side effects of and poor patient adherence to osteoporosis medications. This study found that an outreach program to clinicians and patients improved the management of osteoporosis after a fracture. More-tailored interventions may be necessary for high-risk subgroups. There is also a need for more effective patient and clinician education and a stronger role for specialists.

Disclosures: A.C. Feldstein, None.

This study received funding from Merck & Co., Inc.

WG39

Bringing Bone Health to Seniors' Communities: A Unique Approach to Help Manage Osteoporosis. M. Kloseck^{*1}, M. van Zandvoort^{*2}, R. Crilly³, M. Speechley^{*4}.

¹Faculty of Health Sciences, University of Western Ontario, London, ON, Canada, ²Department of Health and Rehabilitation Sciences, Faculty of Health Sciences, University of Western Ontario, London, ON, Canada, ³Department of Medicine, University of Western Ontario, London, ON, Canada, ⁴Department of Epidemiology and Biostatistics, University of Western Ontario, London, ON, Canada.

Osteoporosis is preventable and treatable, yet there is a significant care gap in Canada. We hypothesized that engaging seniors in raising awareness, identifying neighbours and others in their community at risk and a peer-led senior-friendly education program would increase diagnosis and treatment of osteoporosis, and that ongoing peer support would encourage compliance and persistence with medication and lifestyle change. This hypothesis is being tested in a randomized controlled trial (RCT). In Phase 1 (completed) community capacity building and participatory action research methodology was used to train seniors in a local community to act as peer educators and mentors within their community. Ten seniors (mean age=82 yrs. + 6.74 yrs. SD, range=71-90) participated in a 2-week training program containing 5 osteoporosis education modules and 1 session on public presentation skills delivered by local experts. Once trained, these seniors formed the Community Osteoporosis Advisory Committee which collaboratively developed a peer advisor training manual, designed a community information and recruiting program, and developed a senior-friendly education and support program which they practiced until all were comfortable. Pre- and post-knowledge surveys showed a statistically significant change ($p=.04$) in knowledge from project start to end of Phase 1. Confidence by seniors in their role as osteoporosis advisors increased significantly ($p=.02$), as did confidence in their ability to deliver information to their neighbours through community presentations ($p=.02$). Overall confidence in their role as peer educators and mentors increased significantly from project start to end of Phase 1 ($p=.01$). In Phase 2 (in progress) the senior-led education and support program is being tested in a RCT ($n=100$) in a local community of seniors ($n=2500$, mean age=79 + 9.53 SD). Outcomes include BMDs performed, treatments begun, appropriateness of treatment and persistence. Preliminary baseline knowledge surveys ($n=33$, mean age=81 + 7.18 yrs. SD, range 67-91 yrs., 97% female, 3% male) show a substantial gap in knowledge. On the 19-item osteoporosis questionnaire the mean correct minus incorrect score=6.15 + 4.79 SD. Scores ranged from -4 to 16 out of 19. Forty-one percent reported having fallen in the past year. This unique approach to diagnosing and treating osteoporosis may be a useful model for other communities of seniors.

Disclosures: R. Crilly, Alliance for Better Bone Health 2.

This study received funding from Alliance for Better Bone Health

MUSCLE AND BONE WORKING GROUP

WG40

Fracture Risk Assessment in Dialysis Patients. S. Jamal, University of Toronto, Canada.

After one year, over half of the men and women with stage 5 chronic kidney disease (CKD) will have a fracture. Dual energy x-ray absorptiometry (DXA) is inconsistently associated with fracture these patients. For example, we recently published a meta analysis of cross-sectional, observational studies which reported on the unadjusted association between BMD and fracture. While we found that BMD was lower in patients with stage 5 CKD who have fractures we also noted that there were important limitations of all the studies included in our meta analysis and our results should be interpreted with caution.

One reason for the lack of association between DXA and fracture may be due to underlying metabolic bone disease, one of the most common being osteitis fibrosa from secondary hyperparathyroidism. Hyperparathyroid bone disease has preferential effects on cortical components of bone and measures such as DXA, which do distinguish between trabecular and cortical components, may not detect cortical abnormalities in HD patients.

In contrast to DXA, peripheral quantitative computed tomography (pQCT) discriminates between trabecular and cortical components, allows assessment of volumetric density, and can be used to derive indices of bone strength. pQCT studies in HD patients consistently demonstrate a selective decrease in cortical measures due to elevated levels of PTH. However, the associations between pQCT measures and fractures are not known.

This session will review the relative contributions of pQCT (trabecular and cortical) and DXA measurements to fracture risk among hemodialysis (HD) patients. Specifically, we will report on the cross sectional associations between cortical and trabecular measures and fractures in 36 men and 16 women, 50 years and older, on HD for at least one year. Low trauma non-spine fractures since starting HD were identified by self report and confirmed by review of radiographs or radiology reports. Prevalent vertebral fractures were identified by morphometry of lateral spine X-rays. pQCT measurements of the non-dominant radius included trabecular density, cortical density, total area, cortical area, and cortical thickness. We also obtained DXA measurements of the hip and lumbar spine. We used logistic regression models, adjusted for age, weight, and gender to examine the association between fracture (vertebral and/or self-reported non-spine) and each pQCT measure.

The mean (SD) age was 65.8 (9.0) years, the mean weight was 72.3 (15.6) kg, most (32 of 52) subjects were Caucasian, and there were 32 fractures in 27 subjects (prevalent vertebral fracture or low trauma fracture) since starting dialysis. A decrease in cortical density was associated with fractures (OR = 16.7; 95% CI: 2.9 to 83.3), as was a decrease in cortical area (OR = 3.0; 95% CI: 1.3 to 7.3), and a decrease in cortical thickness (OR = 3.3; 95% CI: 1.4 to 7.9). Fractures were not associated with pQCT trabecular density (OR = 1.2; 95% CI: 0.6 to 2.3), total area (OR = 1.1; 95% CI: 0.59 to 1.7) or DXA measurements of the hip and spine.

Our findings suggest that cortical parameters of the radius were associated with fractures in HD patients. If confirmed in prospective studies, these findings may explain the lack of association between fracture and DXA measurements and raise the possibility that pQCT could be used to identify HD patients at high risk of fracture.

WG41

Bone-muscle Disconnect During Pubertal-driven Skeletal Growth in Type 1 Diabetes. (T1DM). MA Murray¹, H Slater², KK Clarke², JL Quick², and L Moyer-Mileur² ¹Division of Pediatric Endocrinology and ²Center for Pediatric Nutrition Research, Department of Pediatrics, University of Utah, Salt Lake City, Utah.

Purpose: To compare bone characteristics in adolescents with T1DM to healthy reference and examine associations between T1DM-related factors and bone-muscle characteristics during pubertal-driven skeletal growth. **Methods:** Measures of tibia bone characteristics by pQCT (XCT-2000, Stratec) and whole body, hip, and spine by DXA (4500A, Hologic) were performed in adolescents with T1DM ages 12-17 y (n=42; 26 girls) at baseline and 12 months later. Results were compared to a regional reference (n=199). Height, weight, diet and health histories, Tanner stage, disease duration, insulin regimen, and glucose control (average glycosylated hemoglobin (HbA1c) were recorded. Glucose control, bone biomarkers, and bone characteristics were compared in a separate cohort of T1DM adolescent girls (n=11) age 12-15y with good glucose control (HbA1c <8.0%) and matched controls (n=11). **Results:** T1DM adolescents had lower baseline and 12-month gains for tibia trabecular volumetric density (vBMD, mg/cm³) and cortical bone mineral content (BMC, mg) and whole body BMC relative to lean body mass (Figure 1, p<0.05). Disease duration (6.1 ± 3.8 y) was inversely related to tibia cortical bone cross-sectional area (CSA, mm²) and whole body BMC (R²=0.25-0.34, p<0.05) while average HbA1c (8.5 ± 1.0%) was a negative predictor of height-adjusted whole body BMC gains (R²=0.32, p<0.01). In the cohort study, height-adjusted whole body BMC/bone area (BA, cm²) and FN areal BMD (aBMD, gm/cm²) and bone apparent density (BMAD, gm/cm³) values were significantly lower in T1DM girls despite good to moderate glucose control when compared to healthy controls (p<0.05). The evaluation of tibia bone geometry and density revealed T1DM girls had significantly lower cortical BMC and cortical BMC/muscle CSA (Figure 2; p<0.05) with a trend toward thinner cortical bone thickness (p=0.07). Higher urine magnesium excretion was predictive of a greater height deficit, lighter bones, decreased FN BMAD, and lower tibia cortical bone area, thickness, and BMC (R=0.51 to 0.84, p<0.05) accounting for 26% to 60% of the variance. Higher fasting serum glucose was the single significant predictor of greater bone resorption (R=0.69, p<0.01) and urine magnesium excretion (R=0.77, p<0.001) accounting for 48% and 61% of the variability observed in urine deoxypyridinoline and magnesium levels, respectively. **Conclusions:** These findings provide further support for compromised bone mineral acquisition associated with poor glucose control leading to a bone-muscle disconnect during pubertal-driven skeletal growth in adolescents with T1DM.

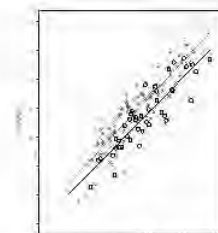


Figure 1. Lower whole body BMC/Muscle in T1DM boys and girls vs. Reference (p<0.05)

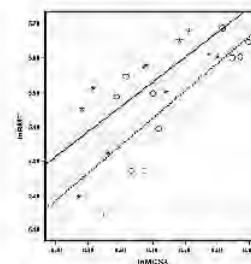


Figure 2. Decreased Tibia BMC/Muscle in T1DM girls vs. Controls (p<0.05)

A		Akhter, M. P.	M155, M279, M511, M512, M521, S279, S512	Amedei, A.	T118	Articus, K.	T381
				Ames, R.	M449	Asaba, Y.	1238
Abbaspour, A.	M188, T155, T456	Akhter, N.	M370	Amin, S.	T460	Asada, T.	W003
Abboud, H.	T039	Akilu, M.	W189	Amizuka, N.	1115, M116, M239, S239, W059, W458	Asagiri, M.	O099, M099, S099, W067
Abboud, H. Emile	W082	Akira, S.	W029	Amling, M.	1300, M298, S298, W477	Asahara, H.	M089
Abdallah, B. M.	W418	Akiyama, H.	M010, S010	Amman, P.	W128	Asahara, T.	T013, W003, W048
Abdelmagid, S.	1023	Akiyama, T.	1098, 1181, 1290, T102	Ammann, P.	W401, W404	Asai, T.	W462
Abdoune, R.	T250	Akiyama, Y.	W458	Amou, H.	M302, T263	Asano, J.	T263
Abdul Raheem, K.	W466	Akiyoshi, K.	M101	Amoui, M.	1081, O112, M112, S112	Asano, S.	T138, W128
Abe, E.	1153, T071	Akizawa, T.	T495, W157	Anastassiades, T.	T333, W281	Ascanio, L. Jose Lunar	M433
Abe, M.	M302, T263, W115	Akter, R.	M038	Ancoli-Israel, S.	1157	Asche, C. V.	W294
Abe, T.	T231	Akunowicz, J. Dawn	T470	Andersen, H. Elkjaer	T446	Ashley, J.	M102
Abe, Y.	M346	Al Mukaddam, M.	M216	Andersen, J.	T256	Ashley, L. A.	M018
Aboody, K. S.	T242	Al Nazer, R.	W502	Anderson, M.	M286, M467	Asou, Y.	W097
Abou Samra, H.	M532	Al-Aly, Z.	O185, M185, S185, T165	Anderson, T. L.	1005	Aspelund, T.	1278
Abou-Samra, A.	W258	Al-Dayeh, L.	T279	Anderson, A.	M427, S427	Assadian, O.	T262
Abrahamsen, B.	1162, M286, T256	Al-hawagri, M.	1294	Anderson, H. Clarke	W085	Asuncion, F. J.	1088
Abrams, K.	W227	Al-qallaf, M.	M055	Anderson, J.	1099, W195	Athanasou, N. A.	T092
Abu Elmagd, K.	T497	Al-Shoha, A.	W420, WG14	Anderson, K.	T252, W195	Atkins, G. J.	M009
Abu-Amer, Y.	1294, T098	Al-Tamimi, D.	W258	Anderson, P. H.	W402	Atkinson, E. J.	1160, 1239, T460, W218
Aburatani, H.	M097, T021, W019, W020	Alam, I.	W171, W178, W185	Anderson, R.	1130, M421, S421	Atkinson, J. E.	1082, O409, M409, S409
Achenbach, S.	M369, S369	Alam, N.	W112	Anderson, L.	W182	Atkinson, S.	M489, S489
Achten, J.	T002	Alamanou, M.	W080	Andersson, R.	1218, T201, W314	Atsawasuwan, P.	M011, M203, T142
Ackert-Bicknell, C. L.	1228, O021, M021, M285, S021, T212	Alamoudi, R.	W511	Andersson, N.	W061	Attalah, H. Lynda	M117
Acland, R. R.	T392	Alander, C.	W333	Ando, R.	W013	Au, B.	M271
Adachi, J. D.	1055, M328, M371, M428, M429, M436, M438, S371, T298, T303, T332, T333, T396, W233, W281, W360, W372, W385	Alander, C. B.	M180	Ando, W.	W274, T209	Au-Yeong, M.	W437
Adachi, M.	T176, T336, WG21	Alaql, Z. S.	1065	Andrews, J. L.	W489	Aubin, J. E.	M160, M210, S160, S210
Adamo, M. L.	T201	Alatalo, S. L.	W064	Ang, E.	M103, S103	Aubry, I.	T143
Adams, D. J.	M027, M235, S027, S235	Albain, K. S.	M312	Ansari, M.	T513	Auchampach, J.	W078
Adams, E.	W010	Albany, C.	M216	Antczak, A. J.	W487	Audran, M.	W201
Adams, J.	M510	Albergaria, B.	W383	Antipas, G.	WG19	Aukema, H.	W410
Adams, J. S.	1028, 1029, 1221, 1222, M252, M253, S253	Albert, C.	M287	Anthony, M. S.	M34, S349	Aulin, C.	W107
Adamu, S.	W445	Alder, S.	W294	Anton, I.	1001	Ausk, B. J.	T150, W060
Adib, G.	T289	Alekel, D. L.	M183	Anumula, S.	T267	Auxier, A. J.	M018
Adler, C.	W031	Alén, M.	1083, M533, S533, W505, W515, W516, W520	Aoki, K.	M101, M110, M114, S114, T094, T095, W479	Avanzati, A.	M478, W190
Adler, R. A.	T266, T337	Alexander, K. A.	1186	Aoyagi, K.	M346	Avila-Campos, M. J.	M181
Afghani, A.	M335	Alexandersen, P.	1127	Apffelstaedt, J. on behalf of the SABRE investigators	M300, S300	Awan, K. S.	T497
Afonso, V.	W018	Alhava, E.	1270, M344, M452, S344, S452	Aoyagi, Y.	W343	Awdishu, S.	T197, T200
Afzal, M. A.	T205	Ali, A. M.	W482	Appelt, D. M.	M128	Aya, K.	T159
Agarwal, A.	WG18	Ali, J. Tahir	M514, S514	Applegate, L.	T041	Aydin, C.	M218
Agarwal, M.	M312	Ali, T.	T092	Aqeilan, R. I.	W200	Ayers, D.	1258
Agarwal, S. C.	T459	Allaert, F. Andre	M372	Arabi, A.	1153, 1194, M283, T071	Aymar, I.	M288, S288
Agarwal, S. K.	T483	Allan, E. Hilary	T012, W025	Aragaki, A. K.	1274	Ayukawa, Y.	W011
Ager, J. W.	W455	Allen, M.	W330	Aragon-Martin, J. Antonio	T470	Azadfar, M. R.	M292
Agueda, L.	M288, M289, S288	Allen, M. J.	M304	Arai, Y.	W004	Azeddine, B.	1035, T189
Aguiar-Oliveira, M. Hermínio	T428	Allen, M. R.	1084, W176	Araiza, F.	T234	Azeez, F.	W081
Aguila, L. H.	1215	Allen, S.	1213	Araki, R.	W115	Azevedo, A. C.	W440
Aguirre, J. Ignacio	1265, M385	Alles, C. N. R.	M101, T094	Aranami, F.	1115	Azizi, N.	M087
Aguirre, J. I.	M393	Alles, N.	M110, S110	Arango-Hisijara, I.	1023, M008	Azriel, S.	M496, T501
Ah Kioon, M.	M134	Allison, M. A.	W304	Araujo, A. B.	M337, M338, W259, W471	Azuma, Y.	W141
Ahamed, Y.	M527	Allison, S.	1134	Arendell, L.	M377, S377		
Ahlström, M. E. B.	T046, W038	Almeida, E. A. C.	M462	Arendell, L. A.	1274		
Ahmad, A. M.	T414	Almeida, M.	M002, M052, M174, S002, S052, T184, T185, T186, T190	Arends, R. J.	W450	Babbar, R.	W261
Ahmad, K.	M352	Almstedt, H. C.	M530, S530, WG29	Arikawa-Hirasawa, E.	1064	Babbitt, A. M.	W362
Ahmad, O. Mian	W224	Alnaeeli, M.	M080	Arita, S.	M431	Bachrach-Lindström, M.	W391
Ahmed, A. Saeed	W466	Alonso, G.	T167, T454	Arjmandi, B. H.	M445, T410, T451	Bacon, C. Jane	M415, S415
Ahmed, O.	M340	Alos, N.	M489, S489, T513	Arlot, M. E.	T461	Bácsi, K.	M138, M284, T124, T226
Ahmed, S. Faisal	T177, W093	Alromaihi, D.	W423	Armamento-Villareal, R. C.	M292, W359	Badger, T. M.	W348
Ahmed, Y.	M120	Alt, F.	1097	Armas, L. A. G.	1210, M450	Badiei, A.	M505
Ahn, J. Hyun	M209	Altman, M. K.	1265, M385	Armstrong, S.	M109	Bae, I.	T024, W015
Ahn, J. Mok	M519	Alvarez, G. K.	M511, M521	Armstrong, V. J.	O064, M064, S064, T067	Bae, M.	M387
Ahn, K.	M343	Alvarez-Hernández, D.	T216	Arnander, C.	M170	Baek, H.	W153
Ahuja, A. T.	1133	Alvarisqueta, A.	W237	Arnold, A.	M485	Baek, J.	M020, T139
Aida, Y.	T146	Amagasa, T.	M086, S086	Arnold-Dahmen, D.	T393	Baek, K.	1110, T361, W248
Aisaka, K.	M431	Amano, A.	M003, W030	Arnott, J. A.	1287, M158	Baek, K. Hyun	T467
Aiyangar, A. K.	W225	Amano, H.	T071	Aronson, J.	W348	Baek, M.	M503, W451
Aizawa, T.	T512	Amano, K.	W092	Aropuu, S.	1060	Baek, S.	T409
Akamine, A.	M108	Amantea, C. M.	W023, W043	Arrich, F.	T262	Baek, W.	M010, S010
Akay, T.	W165	Amaricai, E.	W396	Arrington, S. A.	M304	Baek, Y.	M135, W042
Akerstrom, G.	1191	Amasaki, H.	T083	Arterburn, L. B.	1154	Baggio, G.	W302
Åkesson, K.	1073, T227	Ambrogini, E.	M052, M174, S052	Arthur, A.	W033	Bahadoran, M.	T142
		Amcheslavsky, A.	M081			Bai, L.	1104
		Amédée, J.	M041, S041			Bai, S.	W047

(Key: 1001-1300 = Oral, O = Oral Poster, S = Sunday Plenary poster, M = Monday poster, T = Tuesday Poster, W = Wednesday Poster, WG = Working Group Abstract)

Bai, X.	M208, S208	Baxter-Jones, A.	M530, M531, S530, W509, WG29	Berthiaume, Y.	W360	Block, G.	T488
Baidoo, C.	I131			Bertin, T.	1184, 1212, 1261, M202, S202	Blocki, F. A.	W212, W217
Baier, M.	T416, WG26	Baylink, D. J.	1081, T151, T152, T212, W008	Bertoldo, F.	M147, W318	Bloomfield, S. A.	1110, M514, S514, T361, W490, W498
Baik, H.	T224	Bazarra-Fernandez, A.	M012, M401, M446, W386	Bertrand, G.	1031	Bloys, C. Henny F.	W046
Bail, H.	M193	Bazille, C.	M134	Berzlanovich, A.	W271	Blue, M.	WG8
Bailey, D. A.	W509	Beamer, W. G.	1228, 1253, M269, M285, T212, W008, W116, W183	Bessac, L.	W385	Blumberg, J.	T317
Bain, S. D.	M153	Bearcroft, P.	T294	Bessant, J.	M350, M364, S364	Blumentals, W. A.	W353, W355, W365, W366
Baker, P.	W192	Beard, H.	T113	Bessette, L.	M350, M364, S364	Bock, O.	M453
Bala, Y.	O504, M504, S504	Beary, J. F.	T382	Beuningen - Vaan, M. van	W450	Bockman, R.	T444, T445
Balcells, S.	M288, M289, S288	Beaton, D. E.	M382, M439, T323, W295, WG35	Bevelock, L. M.	M197	Boddula, R.	WG18
Baldock, P. A.	I134	Beauchesne, P.	T459	Beyens, G.	T228	Boden, S. D.	T038
Baldrige, D.	I261	Beaudet, A. L.	M202, S202	Bhadada, S.	WG17	Bodine, P. V. N.	1010, 1048, 1258, M045, M404, S045
Balla, B.	M138, M284, T124, T226	Beaulieu, M.	M350, M364, S364	Bhansali, A.	WG17	Body, J. Jacques	M249, T240, W212
Ballock, R. T.	M118, M119, S118	Beaupre, L. A.	T329	Bhat, B. M.	1048	Boeckman, R. K.	W320
Balogh, A.	M341	Beck, B. R.	M524	Bhat, R. A.	1010	Boerst, H.	M453
Balooch, M.	M392, S392	Beck, G. R.	1143, M030	Bhatnagar, P.	1131, O386, M386, M427, S386, S427	Boghossian, S.	M148, S148
Bamford, S.	M442	Beck, T.	M377, S377, T288	Bhatt, R.	M412	Bogoch, E. R.	M382, M439, T322, T323, W295, WG35
Bandarra, N.	W408	Beck, T. J.	1052, 1207, 1240, O373, M348, M373, M381, S373, S381	Bhattacharya, A.	1135, M397, S397	Boguzewski, C. Luiz	M454
Bandinelli, S.	W230	Beckman, M. John	W226, W233, W306, W471	Bhattacharya, R.	1017, WG13	Bohren, K. M.	I016
Bandstra, E. R.	M145			Bhattoa, H. P.	M341	Bohte, A.	M333, M334
Banerjee, S.	M068, S068			Bhojani, I.	T302	Boileau, G.	I259
Banu, J.	I135, M397, S397			Bi, L. X.	M040	Boivin, G.	O435, O504, M435, M504, S435, S504, W330
Baqi, L.	W300			Bi, X.	T279	Boland, R.	T064, T194, T196
Baranci, M.	M350, M364, S364			Bi, Y.	O157, M157, S157	Bolland, M. J.	M449, T376
Barazza, M.	I230	Beeson, C.	I103	Bianchi, E. N.	1121, M455	Bolognese, M.	I205, T377
Barbe, M. Francis.	M008, T020	Begot, L.	T498	Bianchi, G.	M379, S379	Bolster, M. B.	T474
Barber, A.	M449	Behnam, K.	T156	Biano, P.	M178	Bonafede, B.	T080
Barbosa, D.	M394, S394	Behonick, D. J.	M163, S163	Bibat, G.	WG8	Bone, H. G.	I128, I130, M420
Barbosa, M. Adolfo	M041, S041	Behra, A.	WG17	Bick, T.	M042, T009	Bonewald, L. F.	I043, I044, I045, I296, M066, M237, M520, T233, T504, W050, W053
Barbuto, N.	I096, M388, S388	Behringer, R. R.	M171, S171	Bidwell, J. P.	T506	Bonfá, E.	T326
Barclay, C. Lynn	I130, M421, S421	Beilby, J.	T321	Bijster, M.	W347	Bonivitch, A. Rath	M066
Barden, H. S.	M320, W232	Beke, M.	W227	Bikle, D. D.	I109, I176, 1284, O223, M223, M241, S223, S241, W158, WG3, WG4	Bonjour, J. P.	I041, I243, T463
Bare, S. P.	T296, W310	Belanger, A.	T199			Bonnet, N.	I126
Bareille, R.	M041, S041	Belavy, D.	W484			Bonomo, C.	W383
Barengolts, E.	M370	Belaya, Z. Evgenjevna	W364			Boone, L. I.	I012
Barger-Lux, M. J.	M450	Belcher, J. Y.	I023, M158	Bilezikian, J. P.	I090, I091, I092, I094, I164, M060, M420, S060, T044, T283, T481, T485, T486, W261, W351	Boonen, S.	I055, I168, M192, M244, M432, M434, S244, S432, S434, T382, T385, T387, W317, W351
Bargouti, M.	T038	Bell, N. R.	T329			Borah, B.	M508, S508, T386, W240
Barker, C.	W388	Bellasi, A.	T488	Billiard, J.	I010, M045, S045	Borba, V. Zeghibi C.	M454, T342
Barkmann, R.	I075, T297	Belleli, R.	T366	Binderman, I.	W088	Borges, J. L. C.	T377
Barlogie, B.	I173	Beller, G.	M453	Bingham, S.	I281, O360, M360, S360	Borggreffe, J.	I269, T368
Barnes, A. M.	T471	Bellido, T.	I011, M233, S233, T184, T185, W057			Borisov, N. N.	M429, T408, W296, W322
Barnes, B. McRae	M515	Bellou, A.	W287	Binkley, N.	M451, T282, T358, T499, W246, W352	Borsy, A.	T124
Barnett, B. L.	W320	Bemben, D. A.	W501, W504	Binkley, N. C.	W367	Boskey, A.	I124, M501, T109, T148, W088, W091, WG8
Baron, R.	I069, I248, I250	Bemben, M. George	W501, W504	Binkley, T.	M532	Bostaca, T.	T520
Barone, A.	M379, S379	Ben-Dov, I. Zeev	M217, S217	Binotto, P.	W302	Bostrom, M.	I096, M388, S388
Barr, A. E.	T020	Bencsik, M.	I021	Biris, A. S.	W057	Boudignon, B. M.	I019, M189, M513
Barr, R. J.	I012	Benedikt, M.	M306	Bischoff, D. S.	M276, T051	Bouillon, R.	I101, I169, M192, M244, M266, S244, T132
Barr, S. I.	W511	Benhamou, C.	M534, T295, T382, T477, W231, WG10	Bishop, J.	M421, S421	Boumier, P.	M500
Barragan-Adjemian, C.	T233	Benjamin, E. J.	I240	Biswas, P.	I030	Bourget, C.	M041, S041
Barrero, M.	I088	Benn, B. S.	I026	Bito, H.	M114, S114	Boussou, V.	W231
Barreto-Filho, J. Augusto	T428	Bennet, B.	M340	Bjorklund, P.	I191	Boutroy, S.	I280
Barrett-Connor, E.	I074, I158, I161, M335, M495, W304, W367	Bennett, C.	I108	Blaauboer, M. E.	T360	Bouxsein, M. L.	I119, I138, I230, I233, I253, I280, O021, M021, M269, M418, M508, M516, S021, S508, T461, W224, W349
Barsony, J.	T448	Bensamoun, S. F.	M152, S152	Blacakshaw, P. E.	W327	Bouzegaou, N.	M357
Bartello, M.	W400	Benscik, M.	I019	Black, D.	T387	Boven - Nunen, M. van	W450
Bartholin, L.	I286	Bentmann, A.	I179, T007	Black, D. M.	I056, I057, I090, I094, I168, M418, T385	Bowles, C.	T519
Bartik, L.	M25, S2555	Berd, Y.	T246			Boyan, B. D.	M187, W002, W421
Bartuszek, D.	T275	Bereket, A.	W165	Black, J.	W485	Boyce, B.	I100, I148, I212
Bartuszek, T.	T275	Bereteu, O.	W396	Black, W.	M291, S291	Boyd, S. Kyle	W460
Baslé, M. Felix	M067, W201	Bergamaschi, C.	W339	Black, W. C.	W334	Boyesen, P.	M497
Basler, L.	M459, S459	Bergemann, C.	T049	Blackwell, K. A.	M168	Boykin, C.	I099
Bass, S.	W483, W485, W486	Berger, C.	M336, S336	Blackwell, T.	I157	Brabant, G.	W422
Bassford, T.	I052, I207, I274, O373, M373, M377, M381, S373, S377, S381, W255, W306	Bergman, E.	W064	Blackwell, T. L.	I158	Brackett, D. J.	T410
Bastepe, M.	M218, W165, W429	Bergot, C.	W231	Blackwell, T. S.	I097, I147	Bradica, G.	W316
Bastian, L.	W422	Bergstralh, E.	M207	Blair, H. C.	I153		
Bateman, T. A.	M145, M464	Bergström, U.	I051, M361	Blair, J. M.	I006		
Bates, A. L.	O309, M309, M310, S309	Bergwitz, C.	I114, I264, W166	Blake, G. M.	M448		
		Berk, M.	T354	Blanck, H. M.	M483		
Bathum, L.	M286	Berkovic, S. F.	T349	Blanger, J.	W174, W179		
Battie, M. Crites	M313	Berlanga, E.	M376	Blangy, A.	M073, S073, W078		
Battucci, S.	T330, W298	Berndt, T.	M207, M212, S212	Blank, R. D.	W465		
Bauer, D. C.	I057, I074, I090, I157, I161, I202, M471, S471, T325, T385, T420, T468, W215, W253	Berntsen, G.	T272	Blank, R. Daniel	W466		
Bauss, F.	W319	Berry, G.	T328	Blattert, T. R.	W395		
Bava, U.	T205	Berry, J.	M001	Blenk, T.	I075, M359		
		Berry, S.	M362, S362	Bliuc, D.	I050		
		Berryhill, S. B.	I086	Blizotes, M. Michael	I159, M013		

(Key: 1001-1300 = Oral, O = Oral Poster, S = Sunday Plenary poster, M = Monday poster, T = Tuesday Poster, W = Wednesday Poster, WG = Working Group Abstract)

Bradley, A.	1063	Buehring, B.	T499, W484	Cann, C. E.	1054	Chalberg, C.	M308
Bradley, E. W.	M111	Buford, W. Jr.	M040	Cannata, G.	T419	Chalouni, C.	W143
Brady, J.	W437	Buitrago, C.	T194	Cannata-Andía, J.	T216, T412	Chambers, T. John	M408, T104, W335
Bragdon, B.	M190, W116	Bukata, S. V.	M023, S023, T443	Cao, X.	1032, 1065, 1072, 1256, 1297, M205, W464	Chambers, T. M.	1058, 1086
Brain, J.	T217	Bullock, H. A.	W489	Caparbo, V. F.	T273, T326	Chambon, P.	1220, 1235
Braith, R. W.	W311	Bulnheim, U.	T049	Capilla, E.	W495	Chami, H.	M287
Brandao, C. A.	M274, T209	Bultink, I. E. M.	M314, M315, T388	Caporali, E.	W099	Chamoux, E.	M474, M475, T001
Brandi, M.	T028, T053, T118, T213, W230	Bunker, C. H.	T353	Capozza, R. F.	T472, W234, W235, W236, W237, W321	Chan, B.	1158
Brändström, H.	1196	Burghardt, A. J.	M419, S419, T107, T110, T286, T459, W228	Caprioli, R.	W187	Chan, C.	T178
Branea, I.	W396	Burgio, D. E.	T382	Capriotti, C. A.	W063	Chan, E. K.	M094
Branski, L. K.	M487, S487	Burnes, J. L.	W249	Carballido-Gamio, J.	W229, W449	Chan, M.	M228
Brasen, C. L.	M286	Burnett, K.	M405, S405	Carbone, L. D.	M324, M352	Chan, S.	T214
Braun-Fahrlaender, C.	W519, WG30	Burns, A. L.	T483	Carbonell Sala, S.	T028, T053, T118, T213, W230	Chan, S. P.	T447, WG34
Brazier, H.	M073, S073	Burns, T. L.	M528, M529, S528	Carda, M.	W245	Chan, V.	M282, W175
Brazier, M.	M500, T250	Burr, D. B.	1093, 1095, W007, W176, W330	Cardenas, M.	WG15, WG17	Chan, W. W.	M442
Breban, M.	W441	Burra, S.	M520, T504	Cardoso, C. Ribeiro B.	M181	Chandler, R. L.	1257
Breban, S.	M534, WG10	Burrell, H. E.	M065	Carle, G.	M287	Chandrasekhar, S.	1277
Brebene, A.	T071	Burrows, M.	M531	Carlos, A. S.	1237	Chandrasekharappa, S. C.	T483
Bredbenner, T. L.	W172, W176, W452	Burshell, A. L.	M425, S425	Carlson, C. S.	W089, W299	Chang, C.	1297
Breitner, P.	W390	Burt-Pichat, B.	T461	Carlson, G. Alan	W305	Chang, C.	M430, S430
Brennan, T. C.	M014, T006	Burton, D. W.	M238, M308, T234, T236, W193	Carlson, J.	W143	Chang, C.	T198
Brett, A. D.	W227	Busdicker, E. Wells	T441	Carlsten, H.	T188	Chang, E.	W433
Breuil, V.	M287, M372	Bushinsky, D. A.	M063, M267	Carmeliet, G.	1101, 1169, M266, T132	Chang, F.	M083, M088
Brian, S.	M220	Busquets, N.	M470	Carmeliet, P.	1169, T132	Chang, M.	W491
Briançon, D.	T406	Busse, B.	W477	Carossino, A.	T053	Chang, M. K.	M015
Briggs, S.	T376	Busse, C.	T181, W331	Carpenter, T. O.	1264, W123	Chang, P. Wei	1186
Brigitte, M.	M067	Bustamante, M.	M288, M289, S288	Carr, L. G.	W171, W185	Chang, S.	1019
Brillante, B.	W424	Butler, J. S.	M057, M469	Carranza-Lira, S.	T391	Chang, W.	M499
Bringham, F. R.	1047, 1119, M068, S068, S142, O142, M142	Butler, R. S.	T367	Carroll, A.	1293, M104	Chang, W.	1109, 1176, 1284, O223, M223, M241, S223, S241, WG5
Brink Henriksen, T.	W151	Butters, R.	M224, M227, M230, S227	Carroll, W. J.	T429	Chang, W. Y.	M405, S405
Brinton, B. T.	M228	Buttgereit, F.	T183	Carsten, S.	T218	Chang, Y.	M129
BrintzenhofeSzoc, K.	T437	Byers, P. H.	1261	Cartmell, S.	M151, T003	Chanukya, G. V.	WG17
Briot, K.	1077, M441, WG36	Byon, C.	1216	Carvalho, A. Barbosa	W339	Chappard, C.	M534, T295, T477, W231, WG10
Brixen, K.	1162, M286, M467, T256, W382	Byrjalsen, I.	1127, M264, T135, T245, W205, W478	Carver, A.	1286	Chappard, D.	M067, W201
Brixner, D. I.	W294	Byun, D.	T378	Casado, A.	T050	Charlebois, M.	T368, W475, W476
Brocq, O.	M287	Byun, J.	T033	Casado, E.	M376	Charlesworth, M. Cristine	T254
Brodie, A.	M261, M263	C		Case, N.	M517, T505	Charnay, P.	M025, S025
Brodt, M. D.	M51, S5188	Cabanillas, M. E.	M374, T345	Cashman, K. D.	W269, W408	Charoenkiatkul, S.	M396, T313
Broe, K.	M362, S362	Cabral, S.	T490, W444	Cassady, A. I.	T140	Chary-Valckenaire, I.	W287
Broe, K. B.	W266	Cabral, W. A.	T471, W166	Castellini, S.	W236	Chassande, O.	M160, S160
Broe, K. E.	1240, M347, S347, T309, W267	Cadaval, A.	M275, S275	Castillo, A. B.	1084	Chatila, T. A.	M114, S114
Brok - Bardeel, M. ten	W450	Cadiri, A.	T514	Castro, M.	W144	Chau, J. F. L.	M017
Bromme, D.	W065	Caffarelli, C.	T330, T514	Catrabone, D. E.	W056, W496	Chaudhri, R. A.	W002
Bronson, S. K.	1285	Cahall, D.	1092	Cauley, J. A.	1052, 1053, 1057, 1074, 1157, 1159, 1168, 1202, 1207, 1271, 1273, O373, M373, M377, M381, M471, S373, S377, S381, S471, T288, T325, T353, T420, T468, W253, W306	Chaudhuri, J.	M151
Brot, C.	T453	Cai, J.	O185, M185, S185	Cauley, P. J.	T387	Chavassieux, P.	O435, M435, S435, W339
Brouwers, J.	T462	Cai, Z.	T247, T248	Cavalcanti-Adam, E. A.	W120	Cheah, K. S. E.	T214
Browett, P.	T018	Caira, F. C.	1154	Cavener, D. R.	1022	Checa, M. Angel	M288, S288
Brown, A. J.	M226, W140	Cairns, D.	W105	Cawthon, P. M.	1158	Chellaiah, M. A.	M113
Brown, E. M.	M224, M227, M230, S227	Calabrese, J. C.	T430	Cazer, P. Elizabeth	1067	Chen, A. Pin	W095
Brown, J.	M336, S336	Calahorra, F. J.	T232	Ceglia, L.	M221, W403	Chen, D.	1180
Brown, J.	W373	Caldwell, R. L.	M297, M310, W114, W187	Celi, M.	T419	Chen, D.	T114
Brown, J. K.	1054, W226, W232	Callahan, J. F.	O386, M386, M427, S386, S427	Celil Aydemir, A. B.	M519	Chen, F.	M175
Brown, J. P.	1130, 1152, M350, M364, M371, M474, M475, M479, S364, S371, T298, T303, T333, W233, W281	Callewaert, F.	M192, M244, S244	Center, J. R.	1050, 1079, 1166, 1201, O358, M358, S358, T191	Chen, H.	1221, 1222
Brown, K.	T294	Callon, K.	T018, T174, T205	Cepollaro, C.	W230	Chen, H.	T364
Brown, L. E.	T154	Calton, E. F.	M501	Cerocchi, I.	T419	Chen, H.	W277
Brown, M. J.	T096	Calvet, J. P.	1142	Cersosimo, S.	M178	Chen, H. H.	T099
Brown, R. J.	M149	Calvi, L. M.	M039, S039	Cha, B.	W251	Chen, H. Yan	M417
Brown, T. A.	1014, T435	Camacho, N. Pleshko	M155	Chaboteaux, C.	M249, T240	Chen, I.	M268, S268
Bruening, J.	1070	Camacho, P. M.	M312	Chadwick, R. B.	M246, S246	Chen, J.	1256
Brufsky, A.	1017	Cameron, M. Ann	M383, S383	Chae, S.	T222	Chen, J.	M356, S356
Brummel-Smith, K.	M445	Camp, J.	T460	Chagin, A. S.	M121, S121	Chen, J.	W002, W421
Brune, K. A.	1277	Campagna, M.	W190	Chagnovich, D.	M389, W315	Chen, J.	W465
Brunner, R.	1272	Campagna, S.	M275, S275	Chahine, C. J.	1198	Chen, J. Sheng	1279
Bryan, J.	T259	Campanelli, A. Paula	M181	Chai, S. Ching	M445, T410, T451	Chen, K.	M120
Bryant, H. U.	1012, 1277	Campbell, A. K.	T022, W045	Chailurkit, L.	T313	Chen, L.	T157
Bu, S.	T363	Campone, M.	M300, S300	Chaisson-Blake, M.	M307, S307	Chen, M.	1020
Buchbinder, L.	1014	Canaff, L.	1187, WG7	Chaki, O.	W186, W252	Chen, P.	M371, S371
Buck, K. B.	1023, 1287, M158	Canalis, E.	1178, 1233, 1253, O021, M021, S021, T172, W122	Chakrabarti, D.	W385	Chen, P.	M424, M425, S425
Buckley, C. D.	M232, WG23	Cancelas, J.	T207			Chen, P.	W303

(Key: 1001-1300 = Oral, O = Oral Poster, S = Sunday Plenary poster, M = Monday poster, T = Tuesday Poster, W = Wednesday Poster, WG = Working Group Abstract)

Chen, T.	M102	Cho, Y. Kelly	T219	Cline, G.	W373	Covington, J. W.	T137
Chen, T.	M223, O223, S223	Choe, J.	T401	Clines, G. A.	1286, M197, T238	Cowan, C. M.	1105
Chen, T-H.	WG5	Choh, A. C.	W174, W179	Clines, K. L.	M197	Cowell, C. T.	1038
Chen, T. C.	M338	Choi, C.	1248	Clowes, J. A.	M332, S332, W379, W412	Cox, M.	W104
Chen, X.	M052, S052	Choi, D.	M135, W042	Cody, K.	W278	Cox, T. M.	T004
Chen, X.	T247, T248	Choi, H.	M115	Coenegrachts, L.	1169	Coxam, V.	W407
Chen, X. Ding	W244	Choi, H.	T224, T379	Coffin, J. Douglas	T160	Craig, T.	M207, M254
Chen, Y.	1104	Choi, H.	T423	Cogan, J.	T026	Cramer, J. A.	W366
Chen, Y.	1104	Choi, H.	W015	Cohen, A.	1164, M327	Cramer, J. Timothy	W504
Chen, Y.	1212	Choi, H. Jin	W126, W251	Cohen, S.	1208	Crandall, C. Janet	M368, S368
Chen, Y.	1216	Choi, J.	M209	Cohen-Solal, M. E.	M134	Cranney, A. for the SCIENCE Meta-analysis Group	M428
Chen, Y. M150, M202, S150, S202		Choi, K. C.	M022, M143, T431, W085	Cohn, D. H.	1261	Crawford, D. T.	1014, T435
Chen, Y.	M357	Choi, O. K.	1133	Cointry, G. R.	T472, W234, W235, W236, W237, W321	Crawford, S.	M368, S368
Chen, Y.	W091	Choi, S.	M044	Cole, D. E. C.	WG7	Cream, B.	M140
Chen, Y.	W106	Choi, W.	M322	Cole, J. H.	M502, T108	Crenshaw, T. D.	M400
Chen, Y.	W244, W263	Choi, Y.	W243	Cole, S. A.	W174, W179	Crepaldi, G.	T330, W298, W302
Chen, Z.	1052, 1207, 1274, O373, M348, M373, M377, M381, S373, S377, S381, T288	Choi, Y.	T133	Coleburn, V. E.	1048	Crilly, R.	M413, W376, WG39
Chen, Z.	W168	Choi, Y.	T139	Coleman, R.	W421	Crine, P.	1259
Chen, Z.	W255, W306	Chon, S.	T222	Collette, N. M.	1046, O179, M179, S179	Croce, C. M.	W200
Cheney, R. E.	M076	Choucair, M.	M343	Collin, P.	W018	Crombie, A. P.	W273, W274
Cheng, H.	M324, M378, M440, M444, S440, T380	Choudhary, S.	1194, M283	Collin-Osdoby, P.	W166	Cronier, L.	M054
Cheng, S.	1083	Chouha, F.	T432	Collins, F. S.	T483	Cronstein, B. N.	1124
Cheng, S.	1140	Chouinard, S.	T199	Collins, M. T.	W424, WG6	Crook, M. K.	1286
Cheng, S.	1197, M533, S533	Chow, J. Ting-Chun	1160	Collins, R. J.	T358	Cross, J.	M352
Cheng, S.	T114	Chowdhury, S.	W464	Colman, R. J.	M163, S163	Crossland, R.	T004
Cheng, S.	W009, W506, W515, W516, W520	Chrishti, W.	M352	Colnot, C.	1055	Crotti, T. N.	M071, W068
Cheng, S. Li	O185, M185, S185, T036, T165	Chrisler, W. B.	M058, S058	Colon-Emeric, C.	1010	Crouch, P.	M004, S004
Cheng, S. Mei	M533, S533, W506, W515, W516	Christakos, S.	1026, 1027	Commons, T. J.	T210	Cuarteras, E.	W143
Cheng, S. M.	W520	Christensen, S. Engkjaer	M222	Conceição, L. Eugénio C.	1132	Cui, L.	M234
Cheng, T.	M103, M104, S103	Christgau, S.	T411	Condon, C.	W007	Cui, W.	M503, W451
Cheng, X.	1282	Christiansen, C.	1127, 1206, 1209, O272, M264, M272, M356, S272, S356, T005, T093, T135, T245, W111, W205, W385, W387, W478	Conen, K. L.	M122	Cullen, D. M.	M279, M511, M512, M521, S279, S512
Cheng, X.	W232	Christodoulakos, G.	M286	Conigrave, A. D.	M014, M225	Cummings, E.	M489, S489
Cheng, Z.	M392, S392, T181, W331	Christopher, T. A.	W388	Conklin, B.	1019, 1021	Cummings, L.	M151
Cheon, H.	M387	Chrysis, D.	1277	Connelly, L.	1097, 1147	Cummings, S.	1202, M471, S471, T387
Cherniack, E. Paul	M414	Chrysovergis, K.	M121, S121	Conrads, T. P.	1143	Cummings, S. R.	1053, 1056, 1057, 1161, 1271, M363, M380, T325, T420, W253, W280
Chesnut, C. H.	T389, W385, W387	Chu, K.	M167	Cons-Molina, F.	M380	Cummings, S. R. for the Health ABC Study.	T346
Chest, V.	T211	Chun, K.	T215	Constantine, G.	1206, 1209, W387	Cuomo, A. V.	M046
Cheung, A.	W360	Chun, H.	M075	Contopoulos-Ioannidis, D.	W329	Cupples, L. Adrienne	M277, T219, T309, T317, T347, S277, W177, W180, W266, W267
Cheung, A. M.	M399, S399	Chun, J.	M139, T120, T122, T123	Cook, W. L.	T413	Curtis, N.	T145
Cheung, C. Lung	M282, T214, T229, W175	Chun, R. F.	1029, M252, M253, S253	Cool, S. M.	T166, W036	Curtis, J. R.	M324, M354, M378, M440, M444, S440, T380
Cheung, M.	1198	Chung, D.	M456	Coombe, D.	M069, W086	Czermanski, S. A.	W174, W179
Cheung, M. S.	W426	Chung, H.	M343	Coombs, H. F.	M269, W183	Czymmek, K.	T061, W010
Cheung, W.	1263, T178	Chung, J.	M456	Cooper, A.	M092		
Cheung, W. M. W.	M019	Chung, M.	M456	Cooper, D. M. L.	1040, M069, M527, W461		
Chevalier, Y.	T368, W475, W476	Chung, U.	1112, 1175, 1182, 1185, 1211, 1247, M127, S127, T356, W097, W101	Cooper, M. S.	M232, WG23		
Chevalley, T.	1041, 1243, T463, T466	Chung, Y.	M398, M503	Cope, A.	M053		
Chiang, C.	1217	Chung, Y.	T221, T225	Cope, R.	W227		
Chiba, K.	M251	Chung, Y.	T306	Copeland, M.	W202		
Chidiac, P.	T063	Chung, Y.	W049	Corbin, T. J.	1088		
Chikazu, D.	T356	Chung, Y.	W451	Cordeiro, O.	T210		
Chin, H.	M028	Ciccomancini, M.	T005	Cordes, U.	T518		
Chines, A. A.	1206, 1209, W385, W387	Cicek, M.	M070, W028	Cordova, M. A.	T204		
Chintalacharuvu, S. R.	1012	Ciconelli, R. M.	T312, W275, W283	Cornish, J.	T018, T174, T205		
Chirgwin, J. M.	1003, M197, T238, T241, T251, T260	Ciesielska, M.	1209	Cornwall-Brady, M.	M394, S394, W312		
Chiu, M.	1217	Cinats, J. G.	T329	Corradini, C. F.	M422		
Chlebowski, R. T.	1274	Cipriani, C.	W356	Correa, D.	1069		
Chmielewski, P. A.	M508, S508, T386	Ciubotariu, C.	T520	Correa-Rotter, R.	M425, S425		
Cho, D.	M456	Ciuffi, S.	T053	Corsi, A.	W230		
Cho, H. Y.	M044	Civitelli, R.	M518, S518, W352	Cortet, B.	M372, M465		
Cho, H. Young	M209	Clack, G.	M300, S300, W192	Corti, M. Chiara	W302		
Cho, J.	M199	Clark, O. H.	M485	Cory, E.	1233		
Cho, J.	T122	Clark, P.	M380	Cosman, F.	1096, 1125, O423, M388, M423, M424, S388, S423, T373, T383, T385, W146		
Cho, J.	W085	Clarke, B. L.	T479, WG16	Cote, G. J.	1120		
Cho, K.	M285	Clarke, K. K.	WG41	Cotte, F.	M345, M372, T344		
Cho, M.	W435	Clarson, C.	M489, S489	Couch, R.	M489, S489		
Cho, S.	M499	Claus, H.	M467	Couchourel, D.	T143		
Cho, S. W.	M044	Clemens, T. L.	1284, W464, 1013, 1065, 1070, 1216, 1217, 1283, M241, S241	Coudane, H.	W287		
Cho, S. Wook	M209	Clement, J. G.	M069	Coughlin, S.	T519		
Cho, T.	M352	Clements, D.	M102	Courtland, H. C.	W173		
Cho, Y. K.	M277, S277	Clemmons, D.	1253	Courtland, H. W.	1242, T204, W463		
		Clifton, K. B.	M024	Coutant, D. E.	1012		
				Couture, J. N.	M474, M475		

(Key: 1001-1300 = Oral, O = Oral Poster, S = Sunday Plenary poster, M = Monday poster, T = Tuesday Poster, W = Wednesday Poster, WG = Working Group Abstract)

Dam, T.	1161	Dearman, A. C.	T507	Dillon, J. P.	M065	Dudzek, K. M.	T276
Dambacher, M. A.	M330, S330, T381	Deblois, D.	M117	DiMeglio, L. A.	W123	Dufresne, T. E.	M508, S508, T386, W240
Daniele, S. M.	T472	Dedek, T.	W245	Dimou, P.	W208	Dugard, N.	W377, WG37
Daniels, S. R.	M536	Defamie, N.	M054	Dinant, G.	1276	Dukas, L. C.	M256, M278, W284
Danielson, K. K.	M457	Deftos, L. J.	M238, M308, T234, T236, W193	Ding, B.	1205	Dumas, A.	M067
Danielson, M.	1202	Del Carpio-Cano, F.	M158	Ding, C.	T480	Dumitrescu, L. Caneel	1147, W188
Danilevicius, C. F.	T273, T326	Del Monte, F.	T213, W230	Ding, K.	T206	Duncan, R. L.	T061, W010
Danks, L.	T097	del Pino, J.	1269	DiPaola, C. P.	T443	Duneas, N.	M172, M173
Dann, P.	M220	Del Prete, D.	1099	Dishmon, D.	M352	Dunford, J. E.	W320, W325
Danner-Koptik, K.	W427	DeLa Cadena, R. A.	M158	Divieti, P.	1047, M068, S068	Dunlop, D.	1273
Danoff, T.	M427, S427	DeLahunty, K. M.	M269	Dixon, L.	M340	Dunstan, C. R.	1006, 1018, T062, T182, T183
Dansereau, R. J.	W327	Delaisse, J.	1005	Dixon, S. Jeffrey	M109, T099	Duong, L. T.	M290, M291, S291, T290, W334
Dao, X.	W320	Delalandre, A.	T143	Dobbelsteen, D. van den	W450	Duong, V.	T251
Daragon, A.	M500	Delgadillo, J.	T316	Dobnig, H.	1093, 1095	Duque, G.	M038, M048, M243, W155
Darah, G.	M442	Delling, G.	M419, S419	Dobson, R.	M295, S295	Duquesnoy, B.	M465
Dare, L. C.	W134	Delmas, P. D.	1091, 1092, 1168, 1209, 1280, O435, O504, M434, M435, M468, M504, S434, S435, S468, S504, T382, T383, T384, T385, T387, T461, W317, W329, W330, W339, W373	Docherty Skogh, A.	M170	Durbecq, V.	M249
Darling, M.	1129	DeLong, W. G.	M008	Dodd, S.	T354	Duren, D. L.	W174, W179
Daroszewska, A.	1036	DeLoose, A.	T184	Dodge, J. A.	1012	Durham, B. H.	T414
Darwech, I.	T098	Delzell, E.	M324, M378, M440, M444, S440, T380	Doecke, J.	1033	Durosier, C.	1167
Dasic, G.	W367	DeMambro, V. E.	1228, 1253, O021, M021, S021, W183	Doherty, J.	1033	Durrani, A.	M124, M125, M126
DaSilva, C.	1128	Demay, M. B.	W032, W094, W104, W148	Dolehide, C. P.	1154	Durski, S.	M530, S530, WG29
Dastidar, P.	W497, WG32	Demer, L. L.	1117	Dolios, G.	T071	Dvorak, M.	1284, O223, M223, S223
Datta, H. K.	M105	Demerath, E. W.	W174, W179	Domae, E.	M144, W014, W162	Dworakowski, E.	M060, S060, T044
Datta, N. S.	M001	Demissie, S.	1240, M277, M285, S277, T219, W177, W180	Dombrowski, C.	T166	Dwyer, D.	1088, 1122, 1126, W445
Daveau, R.	M500	Demoruelle, K.	W247	Domingo, C.	M376	Dwyer, T.	W265
Davey, M. G.	W087	DeMoss, D. L.	M018	Dominkus, M.	W194	Dyson, J.	M050
Davey, R. A.	1217	Dempster, D. W.	1096, 1125, 1164, M388, M477, S388, S477, T373, T486	Donahue, H. J.	1285, T060		
Davico, M.	W407	Dencks, S.	T297	Donahue, L.	M146, S146, T510, W499		
David, V.	1118, 1155, 1226	Deng, F. Yan	W244	Donaldson, M. G.	T413		
Davidson, P.	T246	Deng, H. Wen	W244, W263	Donatelli, L.	W318		
Davie, M. W. J.	W377, WG37	Deng, L.	1013, 1065	Donescu, O. S.	M313		
Davies, K.	T359	Denk, E.	W193	Dong, Y.	M038, M129, T116, T117		
Davies, M.	1230	DePapp, A.	T286	Donley, D. W.	1089		
Davies, T. F.	1153	Derfoul, A.	T048	Dorad, G.	T108		
Davis, A.	T473	Derikx, H. J. G. M.	M314, M315, T388	Dorado, G.	T050		
Davis, A. R.	1071, M169, S169	DeRosa, J.	W145	Doran, P. P.	M057, M469		
Davis, E.	T473	Desai, M. P.	M458	Dore, R. K.	1208		
Davis, K.	T107, W228	Deshpande, A. M.	T470	Dorschner, R. A.	M238		
Davis, M. W.	M460	Desmarais, S.	W334	Dorst, A.	T374		
Davis, S. I.	1116	Desrochers, C.	T087	Doshi, A. H.	T448		
Davis, T.	T470	Devareddy, L.	M445, T410, T451	Doty, S.	1124, W088, WG8		
Davison, A.	1285	Devine, A.	T321	Doucet, C.	T498		
Davison, K. Shawn	M350, M364, S364, T298, T299, T303, W233	Devogelaer, J.	T228	Doucet, R.	T087		
Dawson-Hughes, B.	M221, M424, W403	Devogelaer, J. Pierre	T412	Dougall, W.	M307, M311, S307, S311		
Day, A. J.	T092	Dewailly, D.	M465		M449		
Day, C. J.	T073, T074	Dewailly, J.	M465	Doughty, R.	T244		
Dayal, A.	M312	Dhawan, P.	1026	Douglas, T.	1217		
Dazzi, F.	M053	Dhawan, S.	M352	Doust, E.	1217		
De Souza, M.	W062	Dhein, J.	W156	Dow, T.	M442		
De Benedetti, F.	T170	Dhundale, A.	T510	Dowd, T. L.	M159		
de Bruijine, M.	M356, S356	Di, L.	1104	Downs, T. M.	T234		
de Bruin, A.	W200	Di Iorgi, N.	T449	Dowthwaite, J. Noelle	1037		
de Brum-Fernandes, A. J.	T001	Diaz, J.	M312	Doyle, J. M.	1084		
de Crombrughe, B.	1249, M010, S010	Diaz, R. D.	T327, W149	Dragann, B. N.	M128		
De Feo, D.	W298	Diaz-Curiel, M.	M426, W319	Dragoi, M.	W396		
De Feo, T.	T330	Diaz-Doran, V.	1234	Dragovic, R.	T183		
de Freitas, F.	T228	Dick, I.	W226	Drake, B.	M510		
De Gendt, K.	M244, S244	Dick, I. M.	1203	Drake, M.	1268		
De Jong, M.	W347	Dickinson, M. E.	1071	Drent, M.	W279		
de Juan, J.	T348	Diegmann, M.	T156	Dreyfuss, E.	M042		
De la Pena, P.	T391	Diem, S. J.	1159	Drezner, M. K.	1225, M451, T159		
De la Piedra, C.	W319	Diemer, K. M.	W359	Drissi, H.	M023, M038, M100, M129, S023, T029, W098		
De Las Rivas, J.	1001	Diez-Perez, A.	M288, M289, S288	Drossinos, V.	W388		
De Laurentiis, B.	M236	Dijkmans, B. A. C.	T388	Drozdowska-Rusinowicz, I.	T275		
de Lozar, A.	T501	Dilley, K. J.	W427	Drozdowska, B.	T274		
De Paola, V.	M275, M478, S275			Drucker, D. J.	W412		
De Remigis, A.	M236			Drysdale, I. P.	T300		
De Remigis, P.	M236			Du, X.	T157		
de Rooij, K. E.	W046			Du, X. L.	M374, T345		
De Souza, M. Jane	T197, T200			Du, X. Qin	1038		
de Talancé, N.	W287			Duan, Y.	T458		
De Vernejoul, M.	M162			Dubitzky, W.	W269		
de Villiers, T. J.	1206			Dubois-Ferrière, V.	W404		
Deal, C. L.	T367			Ducher, G.	W485		
Dean, T.	1190			Dudbridge, F.	1203		

(Key: 1001-1300 = Oral, O = Oral Poster, S = Sunday Plenary poster, M = Monday poster, T = Tuesday Poster, W = Wednesday Poster, WG = Working Group Abstract)

Gaber, T.	T183	Gerdhem, P.	1073, T227	Goltzman, D.	1266, M116, M208,	Grimm, R. H.	W305
Gacad, M.	M252	Gerstenfeld, L. C.	1065, T111, W102,	M231, M336, M371, S208, S336,	Grimston, S. K.	M518, S419	
Gadois, C.	T295		W187	S371, T058, T328, W127, W139,	Grinberg, A.	1230	
Gafni, A.	M436, T332, T396	Gertz, E. R.	M183	W150, W233, W281, WG1	Grinberg, D.	M288, M289, S288	
Gagel, C.	T283, W261	Geusens, P.	1276, W279, WG28	Golub, L.	M412	Grisanti, M.	1088, 1122, 1231, 1232
Gagel, R. F.	1120	Geysen, H. M.	T260	Gomberg, B. R.	W239, W241	Grisot, C.	M287
Gagner, M.	T444, T445	Gez, E.	W197	Gomes, P.	M454	Grodzki, A.	T274, T275
Galesanu, C.	T520	Ghasem-Zadeh, A.	M334	Gomez, C.	T216	Gröndahl, L.	T140
Galesanu, M. Romeo	T520	Ghérardi, R. K.	M067	Gomez-Juaristi, M.	T501	Gronowitz, G. A.	W166
Galfi, M.	W006	Ghobrial, I.	W195	Gómez-Vaquero, C.	M470	Gronthos, S.	W033
Galindo, M.	M047, S047	Ghosh, J.	W081	Gong, W. Yan.	M034	Grose, A.	T171
Gall, M.	1168	Ghosh-Choudhury, G.	M100, T029	Gonnelli, S.	T330, T514, W298	Grosse, C.	W278
Gallagher, C.	1130	Ghosh-Choudhury, N.	M100, T029	Gonzalez-Bofill, N.	T218	Gross, G. J.	W240
Gallagher, J. A.	M065	Giangregorio, L.	M328, T268	González-Macías, J.	T348, W326	Gross, T.	T505
Gallant, M. A.	T001	Giannini, S.	W318	Goodship, A.	1213	Gross, T. S.	M153, T150, W060
Gallego, M.	M376	Gifford, P.	T151	Gooi, J.	T012	Grosse, R.	W238
Galley, S.	1136, 1298	Giger, M.	M331	Gopalsamy, A.	1010	Grothaus, L. C.	M339, S339
Galli, C.	1067	Gigliotti, B. J.	M039, S039	Gorai, I.	T433	Grubbs, B.	M311, S311
Galli, G.	T028, T053	Gilbert, L. C.	1143	Gordon, C.	M328, T268, T353	Grubbs, B. G.	M296
Gallo, R. L.	M238	Gilbert, S. R.	1065	Gordon, J. A. R.	T099	Gruber, H. E.	M276
Gallwitz, W.	W111	Gilchrist, N. Leslie	T392	Gori, F.	T141, W032	Grubisic, V.	M004, S004
Galson, D. L.	M479, T247	Gilcrest, N.	M476	Gorin, Y.	T039, W082	Grundberg, E.	W125
Gambhir, S.	WG18	Gillespie, M. T.	1068, 1150, T005,	Goseki-Sone, M.	M342, S342, T318	Gruntmans, U.	M491
Gamble, G.	M415, M449, S415,		T012, T081, W025	Gosselin, K. C.	M516	Grynepas, M. D.	M267, W474
	T018, T376	Gilligan, J.	W143	Gossiel, F.	W192	Grzybowski, S.	T299
Ganel, O.	W239	Gilmore, J. M. E.	M528, M529, S528	Gössl, M.	1262	Gu, J.	T230
Ganguly, A.	T478	Gilsanz, V.	T449, W514	Goulet, G. C.	M069, W086	Gu, W.	M280
Gannagé-Yared, M.	T289	Gineste, C.	T260	Gourion-Arsiquaud, S.	T109	Gu, X.	W350
Gannon, F. H.	1071, M169, S169,	Gineyts, E.	W330	Govoni, K. E.	1107, M005, M246,	Gu, Y.	T060
	T473	Gioni, I.	W204		S246	Guadalix, S.	M496, T501
Gao, Q.	1234, M180	Giovanazzi, B.	M147	Govoni, K. Elizabeth	T034	Guan, K.	1108
Gao, Y.	1136, 1298	Girasole, G.	M379, S379	Gowen, M.	1131, O386, M386,	Guañabens, N.	T307
Garabedian, M.	1195	Gissel, T.	W160		M427, S386, S427	Guanyabens-Gay, N.	T216
Garces, J.	M289	Gitter, B.	1277	Gozzetti, A.	W190	Guarente, L.	1097
Garces, J. Maria	M288, S288	Gittings, J.	M151	Gozzini, A.	T053, T118, W230	Guadnason, V.	1278
Garcia, P.	M434, S434, T348, W326	Gittoes, N. J.	M232, WG23	Graber, J.	M285	Guenther, C.	T393
Garcia, S.	T509	Giuliani, J. R.	W039	Grabowska, U. B.	M408, W335	Guerrieri, J.	W313
García-Aleman, J.	W405	Giusti, A.	M379, S379	Graeff, C.	1075, 1165, 1267, 1269,	Guglielmi, G.	T330, W298
Garcia-Giralt, N.	M288, M289, S288	Gjesdal, C. Gram	T272		M359, T287, T368	Guise, T. A.	1003, 1137, 1169, 1286,
Garcia-Hernández, P. A.	T391	Glackin, C. A.	T242	Grafe, I.	M459, S459, T416		M197, M305, S305, T238, T241,
Garcia-Palacios, V.	1099	Glantschnig, H.	M175, T042	Gramoun, A.	M087, T105		T251, T260
Garcia-Sevillano, A. G.	T391	Glass, E. V.	1089, O423, M423, S423	Grandchamp, B.	1031	Gulberg, R. E.	W421
Garcia-Tunon, I.	1001	Glatigny, S.	W441	Granero-Molto, F.	M191, S191, W472	Gulseth, H.	W250
Gardella, T. J.	1189, 1190, W144	Glatt, V.	1233	Granfar, R. M. S.	T073, T074	Gulberg, C. M.	M159
Gardiner, E. Margaret	T056	Glauber, H.	W378, WG38	Granja, P. Lopes	M041, S041	Gundersen, R.	M190
Gardner, T. R.	M519	Glendenning, P.	M264	Grant, R.	M489, S489, W363	Gunepin, F. Xavier	T498
Garimella, R.	W085	Glimcher, L. H.	T464	Grasby, S. D. C.	T417	Gunter, K. B.	M530, S530, WG29
Garlet, G. P.	M181	Glimcher, M. J.	T464	Grassi, F.	1136	Guntur, A. R.	W034
Garnero, P.	1074, 1168, M319, T366,	Glise, H.	1129	Gratacòs, J.	M376	Guo, D.	1043, 1106, M140
	T468, W431	Globus, R. K.	M462	Gratz, K. F.	W422	Guo, H.	M030
Garrett, I. R.	W111, W341	Glorieux, F. H.	1198, W426	Grauer, A.	M432, M438, S432, W374	Guo, J.	1119, O142, M142, S142
Gartland, A.	M065	Glover, S. J.	1168, T366	Gravallese, E. M.	W007	Guo, R.	1100
Gary, L. C.	M378	Glowacki, J.	T407, W031	Grcevic, D.	M004, s004W110	Guo, X. Edward	1164, M327
Garza de Leon, F.	M510	Glüer, C. C.	1075, 1077, 1165, 1267,	Greeley, P.	W239	Gupta, A.	W191
Gasser, J. A.	M434, S434, T381		1269, M359, T287, T297, T368	Green, A.	1261	Gupta, M.	M352
Gast, U.	W484	Glüer, M. G.	M359	Green, T.	1248	Gupta, S. K.	WG18
Gaudin, A.	M345, M372, T344	Gluhak-Heinrich, J.	1106, M140,	Greenberger, J. S.	W031	Güran, T.	W165
Gaudreau, P.	M048		W050	Greendale, G.	M368, S368	Gurevich, M.	W161
Gaugg, M.	W390	Go, C.	T490	Greene, J.	M187	Gustafson, Y.	1051
Gaur, T.	1258	Goda, S.	M144, W014, W162	Greenfield, E. M.	T255	Gustafsson, J. Åke	T188
Gauthier, J.	W334	Godbole, M. M.	WG18	Greenfield, H.	1038	Gustafsson, S.	T269, W226
Gautvik, K. Morten	W213	Godfrey, C.	T088, W164	Greenspan, S. L.	1017, 1090, 1094,	Gutierrez, G. E.	T115, W111, W341
Gautvik, V. Teig	W213	Goellner, J.	1011, 1086		1130, M420, T497, W239	Guy, P.	W461
Gayet, A.	M500	Goetz, R.	1113	Greer, P. Alan	1024		
Gehin, M.	1235	Goff, J. P.	W031	Greeves, J. Patricia	T002, W001	H	
Gellenbeck, K.	W338	Goh, S. Lii	M460	Grellier, M.	M041, S041	Ha, H.	T100
Gemar, D.	M451	Going, S. B.	1052, M348, M377,	Greutzner, T.	W133	Ha, J.	M083
Genant, H.	W387		S377, W306	Greve, J. D.	W518	Ha, T. T. H.	W340
Genant, H. K.	1206, M325, M357	Goins, B.	M311, S311	Grey, A.	M449, T018, T376	Haas, M.	W441
Genaro, P. S.	T312	Gois Jr., M. Bolivar	T428	Gridley, D. S.	M464	Haavardsholm, E.	M497
Geneau, G.	M054	Gold, D. T.	M429, W381, W384,	Grieshaber, S. S.	M092	Habauzit, V.	W407
Genever, P.	M050, T145		W398, WG27	Griffin, A. Charles	O157, M157, S157	Habib, Z.	W423
Genever, P. G.	1139, 1214, M051	Gold, E.	M368, S368	Griffin, T.	T236	Habibovic, P.	W075
Gennari, L.	M275, M478, S275,	Goldberg, H. A.	T099	Griffith, J. F.	1133	Hackfort, B. T.	M511, M521
	W190	Goldman, H. M.	W463	Griffiths, K. N.	M405, S405	Hackl, N.	T007
Gensure, R. C.	1229, W429	Goldring, S. R.	M071, W068, W076	Griffiths, S.	T003	Haddock, L.	M380
Geoffroy, V.	M162	Goldstein, S. A.	T108, W167	Grima, D.	W322	Hadji, P.	T394
Gerard-O'Riley, R.	T506			Grimard, G.	T189		

(Key: 1001-1300 = Oral, O = Oral Poster, S = Sunday Plenary poster, M = Monday poster, T = Tuesday Poster, W = Wednesday Poster, WG = Working Group Abstract)

Haenni, M.	W229, W449	Hanson, L. N.	M183	Hayashibara, T.	1224	Higgins, L. S.	M305, S305
Haenscheid, H.	M367	Hant, F. N.	T474	Hayata, T.	1015, 1292, M390, M141, O390, S390, T030, W012	Higuchi, K.	W181
Hafner, L. S.	W305	Hanyu, R.	M390, O390, S390	Hayek, J.	T514	Hikita, T.	M089
Haga, M.	T127	Haque, T.	W112	Hayes, B.	M324	Hikim, A.	1018
Hagan, J. P.	W200	Hara, K.	W458	Hayes, C.	W227	Hikita, A.	M186
Hage-Moussa, R.	T357	Harada, A.	T292	Hayman, A. R.	T004	Hilborn, J.	W107
Hagen, C.	M286	Harada, H.	M176, S176	Haynatzki, G.	T359	Hilden, J.	W301
Hagenau, T.	W160	Harada, N.	T493	Haynes, D. R.	M009	Hill, A.	W173
Hagino, H.	1059, T292, T395	Harada, S.	1048, M416	Hayton, M. J.	M065	Hill, B.	W483
Hagiwara, F.	W358	Hardy, R.	M232, WG23	He, H.	T206	Hill, T. R.	W269
Hagiwara, H.	M131	Hardy, S. E.	T346	He, J.	T230	Hillegonds, D. J.	T236, W193
Hagström, E.	M213	Harfe, B.	T292	He, Q.	M356, S356	Hillier, T. A.	1271, W280
Hahn, M.	W451, W477	Hargreaves, R.	T290	He, W.	T246	Hillmeier, J.	T416
Hahn, T. J.	W043	Härkönen, P.	T193	He, Y.	1104	Himeno, M.	M365
Haigis, B.	M394, S394, W312	Harland, R. M.	M179, O179, S179	Head, T. W.	1198	Hinkley, H. J.	T300
Haim, N.	W197	Harley, C. H.	T329, W366	Headricks, J.	W078	Hirabayashi, M.	W128
Hairston, K.	W184	Harmon, M. J.	M018	Healy, D. R.	1014, T435	Hiraga, T.	1170, M293, O293, S293, T243
Haishi, T.	W241	Harris, M.	1043, M140	Heaney, R. P.	1210, M450, T359	Hirahara, F.	W186, W252
Hajibeigi, A.	T192	Harris, M. A.	1106, W050	Heard, A.	T392	Hirai, H.	M486, W012
Hajj-Shahine, C.	M216	Harris, M. B.	T407	Hedge, A.	1118, 1155, 1226	Hirano, F.	T068, WG22
Hajjar, A.	M352	Harris, S.	1129, M140	Hediger, M.	1026	Hirano, Y.	T352
Håkansson, C.	T188	Harris, S. E.	1047, 1106, M068, S068, T504, W017, W050	Hedström, E. M.	M361	Hirao, M.	W013
Hakimi, M.	T051	Harris, S. S.	M221, W403	Heeren, J.	T015	Hirasawa, H.	W004, W336
Hala, T.	W245	Harris, S. T.	W353, W355, 1278, 1282	Heersche, J. N. M.	T105, T106	Hirata, M.	1247, M161, M262, O262, S262, W196
Halade, G.	1135, M397, S397	Harris, T.	1278, 1282	Hefferan, T. E.	T254	Hirota, K.	W270
Halbout, P.	M014, W333	Harris, T. B.	T346	Hegedus, B.	W006	Hirota, T.	W270
Haldrup, C.	W035	Harrison, J. R.	M235, S235	Hegele, A.	T245	Hiruma, Y.	1152, M477, M479, S477
Hale, J. E.	1277, W202	Harrison, S.	M263	Heggeness, M. H.	1071, M169, S169	Hiyama, S.	M091
Hale, L. V.	W202, W489	Harrison, S. L.	1074, T468	Heickendorff, L.	M222, W151	Ho, C.	T469
Haley, H.	O386, M386, S3886	Hart, C. E.	W316	Heijckmann, A.	W279	Hobbs, R. D.	W423
Hall, C. L.	T235	Hartard, M.	T450	Heikkinen, J.	W064	Hochberg, M. C.	1057, 1271
Hallberg, I.	W391	Hartl, F.	M434, S434	Hein, D.	T299	Hock, C.	M023, S023
Halleen, J. M.	M317, M407, T239, T241, W210, W214	Hartmann, B.	1127	Hein, G.	W414	Hodapp, K.	W400
Haller, I. V.	W246	Hartmann, M.	T518	Heinegård, D.	W080	Hodge, J. M.	T075
Halley, K.	W312	Haruyama, N.	T148	Heinonen, A.	1204, W497, W502, WG32	Hodor, P.	T042
Halloran, B.	1019, 1284, M189, M513	Harvey, A.	1277	Heldman, D. M.	W211	Hodsman, A.	1130, M436, T332, T396
Halse, J.	M434, S434	Harvey, E.	T328	Helfet, D.	T171, W468	Hoeck, H. C.	1209, W387
Ham, A. L.	T208	Hasegawa, T.	T032, T043, T308	Helfrich, M.	1036	Hoefler, J.	W313
Hama, H.	T017	Hashimoto, J.	M453, W013, W431	Helkala, E.	W506	Hoepfner, L. H.	T023
Hamada, Y.	O498, M498, S498, T459, W413	Hashimoto, K.	M184, W061	Helm, J.	T048	Hoey, K.	1239
Hamadeh, F.	W112	Hashimoto, N.	M131	Helmering, L. M.	W489	Hofbauer, L. C.	1009
Hamano, T.	M215	Hashimoto, O.	T491	Hemmelmann, C.	W414	Hoff, A. O.	1120
Hamdy, R. C.	W112	Hashimoto, Y.	W121	Hemmi, H.	1015, 1292, M390, M141, O390, S390	Hoffman, A. R.	1161
Hamilton, M.	1176	Haskin, A.	M352	Henderson, T.	W349	Hoffman, E. A.	M326
Hamon, J.	W392	Haslam, J.	W227	Hendy, G. N.	1187, M231, WG1, WG7	Hoffman, P. F.	T476
Hamrick, M. W.	T206	Hassan, M. Q.	W200	Hengg, C.	W229, W449	Hoffman, S. J.	M386, O386, S386, W063, W134
Han, B.	1277, W202	Hastings, R. H.	M240, T234	Hennighausen, L.	1181	Hoffmann, E.	T516
Han, D.	W049	Hasunuma, T.	T405	Henney, N. C.	T022, W045	Hoffmann, P. F.	1089
Han, J.	M499, W248	Hata, K.	T055, W020, W092	Hennighausen, L.	1181	Hoffmeister, B.	M298, S298
Han, J. Ho	T467	Hata, Y.	T043	Henriksen, D.	1127, M264, W221	Hofstaetter, J. G.	T464, W271
Han, K.	M247, W344	Hatamura, I.	W157	Henriksen, K.	M272, O272, S272, T005, T093	Hogan, E. A.	1058, 1086
Han, L.	M002, M052, S002, S052, M174, T184, T185, T186, T190	Hatfield, D. L.	W056, W496	Henriksen, Z.	M248, S248	Hogan, H. A.	M514, S514, T361, W490, W498
Han, M.	M022, T431	Hatjiharissi, E.	W195	Henry, M. J.	T324, T354, W289	Hogue, A.	M405, S405
Han, S. Jun	W466	Hattori, S.	W096	Hentzell, S.	W226	Hoiseth, A.	W242
Han, S. W.	1147	Haugeberg, G.	M497	Henzell, S.	T269	Holding, C.	M009
Hanada, R.	1061	Haupt, L. M.	T166, W036	Heo, J.	M387	Holts, M.	1085, 1193
Handa, S.	W241	Hauschka, P. V.	W075	Her, S. J.	M044	Holguin, N.	T426
Handelsman, D. J.	1018, M358, O358, S358, T191	Hausler, K. D.	T005, T012, W025	Hermayer, K.	T474	Holick, M. F.	M338
Haneda, M.	T068, WG22	Hausmann, M.	W156	Hernandez, C. J.	W481	Holladay, B.	W052, W053
Haney, E.	1157, 1159	Hausssler, C. A.	M255, M259, S255, S259, W161	Hernández, J. L.	T348, W326	Holliday, L. S.	M092, M094, M393
Hanfland-Schmidt, M.	M211	Hausssler, M. R.	M255, M259, S255, S259, W161	Herndon, D. N.	M487, S487	Hollinger, J. O.	W316
Hangartner, T. N.	M509, T290	Hautakangas, J.	W505	Herold, D. A.	M308, T236, W193	Holmbeck, K.	M165, M167, O165
Hankenson, K. D.	W109, 1007	Havill, L. M.	T109, W172, W176, W180	Herrera, I.	T050	Holmberg, A.	1200
Hanley, D. A.	1266, M336, S336, T298, T303, T329, W281	Havioglu, N.	T259	Herson, M.	W378, WG38	Holst, J. Juul	1127
Hannan, M. T.	M347, S347, T309, T317, T347, W266, W267	Hawker, G.	1275, M399, S399, T200	Herzog, H.	1134	Holt, G.	W187
Hannita, T.	T405	Hawkins, F.	M496, T501	Hesse, E.	1250, W422	Holvik, K.	W272
Hannon, R. A.	M300, S300, W189, W192	Hawkins, K.	W488	Hewison, M.	1028, 1029, 1221, 1222, M232, M252, M253, S253, WG23	Holy, X.	T498
Hans, D.	1167, T463	Hawse, J. R.	1144, M035, M152, S152, W021, W028	Hiasa, M.	M302, T263	Holzer, G.	T418, W194, W203
Hansen, K. E.	W406	Hayakawa, N.	T066, T138	Hick, J.	M202, S202	Holzer, L. A.	T418, W203
Hansen, M. F.	T470, W198	Hayashi, K.	M059	Hickman, R. M.	1037, T430	Homma, S.	M481
Hansma, P. K.	M510	Hayashi, M.	M206, T021, W029	Hidalgo, A.	W152	Homse, B.	W235
		Hayashi, R.	T500	Hideshima, T.	W195	Honasoge, M.	WG15
		Hayashi, Y.	T162	Higashikawa, A.	1175, M127, S127	Honda, K.	W096

(Key: 1001-1300 = Oral, O = Oral Poster, S = Sunday Plenary poster, M = Monday poster, T = Tuesday Poster, W = Wednesday Poster, WG = Working Group Abstract)

(Key: 1001-1300 = Oral, O = Oral Poster, S = Sunday Plenary poster, M = Monday poster, T = Tuesday Poster, W = Wednesday Poster, WG = Working Group Abstract)

Javed, A.	M047, S047	Jorgetti, V.	W339	Kamitani, T.	M375, S375	Kasukawa, Y.	T341, T438, W328
Javelaud, D.	M305, S305	Joseph, L.	M336, S336	Kamiya, N.	M270, S270	Katae, Y.	W004, W336
Jayakar, R. Y.	T290	Joshi, A. A.	T414	Kamiya, S.	T076, T083, W073	Katafuchi, M.	M203, T142, T147
Jean, S.	M350, M364, S364	Joshi, R.	W510	Kamizono, J.	1034	Katagiri, T.	1034, W117, W118
Jeanneret, A.	W360	Josse, R. G.	1266, M371, M399, S371, S399, T322, T333, W281, W360	Kammerer, C. M.	T353	Kataoka, N.	W061
Jee, W. S. S.	M417			Kamo, K.	T341, T438, W328	Kataovic, V.	M004, S004
Jeffery, J. M.	W490	Journe, F.	M249, T240	Kamondetdacha, R.	T429	Katayama, K.	W252
Jehan, F.	1195	Joyce, C.	W281	Kämpe, O.	W182	Katayama, S.	W470
Jemtland, R.	W213	Ju, J.	T078	Kan, A.	1175, 1182, 1185, W101	Kathiresan, S.	1240
Jen, H.	W285	Juanola, X.	M470	Kanaley, J. A.	1037	Kathuria, M.	WG18
Jenkins, J. K.	W247	Juby, A. G.	T329	Kanatani, N.	1066, M123, S123	Kato, H.	W492
Jennings, K.	T436	Judd, P.	T302	Kanaya, K.	T487	Kato, M.	M251
Jensen, E. D.	T023	Judd, S. E.	M483	Kanayama, M.	W119	Kato, S.	1098, 1220, 1292, M260, W022, W157
Jensen, J. Beck	M248, S248, W345	Judex, S.	M145, T112, T426, T510, W276, W467, W495, W499	Kanazawa, I.	M056, S056	Kato, Y.	T487
Jensen, P.	W182	Juhász, A.	W006	Kanda, J.	T503	Katoh, S.	M188, T155
Jentsch, T. J.	O272, M272, S272	Jules, J.	M084, S084	Kaneko, A.	W434	Katoh, T.	T340, WG31
Jeong, B.	T024, W015	Julesz, J.	W006	Kaneko, I.	1115	Katono, T.	T084
Jeong, I.	M343	Jung, H.	T139	Kanemaru, A.	T340, WG31	Katsibiri, P.	T402, WG19
Jeong, J.	M143, W085	Jung, J.	T223	Kanemaru, K.	M273	Katsimbri, P.	W208
Jepsen, K. J.	1241, 1242, T204, W173, W463	Jung, M.	M247, W344	Kanemoto, S.	M029, S029	Katz, J. O.	T233
Jeschke, M. G.	M487, S487	Jung, S.	W153	Kang, B.	T423	Katz, M. S.	M026
Jeukendrup, A.	T002	Jung, T. I.	M298, S298	Kang, C.	M046	Katz, S.	T064
Jheon, A. H.	W040	Jung, Y.	M143, T431	Kang, D.	M410, W282	Kaufman, B. C.	T187, W521
Jia, X.	T175, W195	Jüppner, H.	1031, 1114, 1189, 1264, W165	Kang, E.	W251	Kaufman, J. J.	T301
Jiang, B.	1062	Jurado, S.	M288, M289, S288	Kang, H.	M098, W282, W433	Kauppinen, M.	1204
Jiang, C.	W244	Jurutka, P. W.	M255, S255	Kang, K.	T078	Kawaguchi, A.	W492
Jiang, D.	1007			Kang, M.	W248	Kawaguchi, H.	1112, 1123, 1175, 1182, 1185, 1211, 1247, M127, M136, S127, S136, T356, W097, W101, W307, W438
Jiang, H.	W244, W263			Kang, M. II	T467	Kawai, K.	T494
Jiang, J. X.	M520, T504			Kang, Y.	M247, T175, W344	Kawai, N.	M365
Jiang, M.	1212, M150, M202, S150, S202			Kangawa, K.	1061	Kawai, S.	1224, M003, W030, W431
Jiang, X.	1215, M027, S027	K		Kanis, J.	1060, 1167	Kawakami, H.	W343
Jiang, Y.	M007, M023, M037, S023, T059, W168, W170	Kaback, L. A.	M023, S023, W098	Kanno, J.	1220, T390	Kawamata, A.	M086, S086
Jiao, Y.	M280	Kaczmarzka, M. J.	M255, S255, W161	Kannus, P.	1087, T319, T331, W497, W500, WG32	Kawamoto, A.	T013, W048, W162
Jilka, R. L.	M002, M052, M174, S002, S052, T184, T185, T186	Kado, D. M.	M363, W280	Kanomata, K.	1034, W117	Kawamura, N.	1211, 1247
Jimi, E.	1034, M085, T094	Kadono, Y.	1098, 1290	Kantham, L.	M224, M227, M230, S227	Kawana, H.	1102
Jin, H.	T431, W066, W153	Kadowaki, T.	1211	Kaplan, D. L.	T252	Kawanabe, N.	W041
Jin, J.	T431	Kadri, A.	M134	Kaplan, F. S.	1151, 1156, T478	Kawano, T.	1008
Jin, R.	M412	Kaestner, B.	W414	Kaplanoglou, T.	T402, W208, WG19	Kawano, Y.	M028, T129
Jiwa, F.	M436, T323, T332, T396	Kagasmirori, S.	T352	Kapner, A.	T393	Kawasaki, Y.	1175, 1182, T456
Jo, H.	M517, T505	Kagawa, K.	M302, T263	Kapoor, A.	1107	Kawashima, Y.	1138
Jo, Y.	T224	Kagawa, Y.	T352	Kapoor, S.	T152	Kawata, K.	T125
Jobke, B.	M419, S419, T372, W477	Kagita, E.	T352	Kaprio, J.	1204	Kawate, H.	T176, T336, WG21
Jódar, E.	M496, T501	Kahan, S.	M167	Kaptoge, S.	M360, O360, S360, T294	Kawato, T.	T084
Johansson, H.	1060	Kahler, K. H.	M442	Kapur, S.	1081	Kawelke, N.	1179, T007
John, M. R.	T366	Kaiser, S. M.	T333, W281	Kara, F. M.	1124	Kazakia, G. J.	T110, T286, W481
Johnsen, S. A.	M035	Kaji, H.	M484, S484	Karagiosis, S. A.	M058, M182, S058, S182	Ke, H. Zhu	1122, 1231, 1232
Johnson, J. F.	1146	Kaji, Y.	W207	Karakelides, H.	W249	Ke, H. Z.	T435
Johnson, K.	1236, 1259	Kajita, E.	T334	Karaplis, A. C.	1295, M116, M208, S208, T432, W137, W139	Kearns, A. E.	1160
Johnson, M. L.	M237, T233, W052, W053	Kajiya, F.	W061	Karasik, D.	1240, M277, S277, T219, T285, W177, W180, W224	Keaveny, T. M.	1089, M506, T476
Johnson, S. R.	W204	Kakehi, S.	M077	Karim, L.	W276	Keene, D. R.	M150, S150
Johnsson, K.	W182	Kakizawa, H.	T066, T138	Karin, N. J.	M058, M182, S058, S182	Kekow, J.	1269
Johnston, J.	M368, S368, W512	Käkönen, R.	T239, T241	Kärkkäinen, M.	1270, M452, M344, S452, S344	Keller, B.	M202, S202, W106
Johnston, J. A.	W380	Kakonen, S.	T241	Karl, I.	1008	Keller, E. T.	1188, T235, T452
Johnston, S.	1125	Kaku, M.	M203, T142	Karl, T.	1134	Keller, H.	1046
Johnstone, D.	M436, T332, T396	Kaku, T.	M154	Karlsson, M.	1200, M177, T310, W125	Keller, J. M.	T452
Jokihaara, J.	1087, W500	Kakuru, S.	M150, S150	Karnel, F.	W390	Kelly, C.	1230
Jokubonis, C.	W271	Kalajzic, I.	1044, 1045, 1215	Karperien, M.	W046	Kelly, D. G.	W249
Jolette, J.	O409, M406, M409, S409	Kalak, R.	1006, 1018, T183	Karpisek, M.	W219	Kelly, K.	M301
Jones, A.	M333, M334	Kalender, W. A.	T415, G11	Karsdal, M. A.	M272, O272, S272, T005, T018, T093, T135, T245, W205, W478	Kelly, M. H.	W424
Jones, A. N.	W406	Kalidindi, S. R.	W463	Karsenty, G.	W137	Kemmler, W.	T415, WG11
Jones, C. E.	M493, S493	Kalinowski, J.	1254	Karube, M.	T405	Kemp, B. E.	1150
Jones, D. C.	T464	Kallio, P. J.	M407	Kashima, I.	W479	Kendall, S. E.	T242
Jones, G.	1042, M366, S366, W265	Kalra, B.	T421, WG33	Kashiwagi, H.	M416	Kendler, D. L.	1130, 1209, T357
Jones, J.	M307, S307	Kalra, S.	T421, WG33	Kashiwaguchi, S.	M375, S375	Kennedy, C. C.	T333, W360
Jones, J. B.	M461, M463	Kalra, S. P.	M148, S148	Kasperk, C.	M459, S459, T416, WG26	Kennedy, P. A.	T483
Jones, M. R.	1203	Kalyan, S.	W511	Kass, A.	W250	Kennel, K. A.	W249
Jones, P.	W099	Kamada, A.	M144, T280, W014, W162	Kassem, M.	W418	Kerje, S.	W182
Jones, T.	W377, WG37	Kamao, M.	T261, T311, T318, W159	Kasugai, S.	W016	Kern, J. C.	1010
Jonsson, B.	1278	Kamekura, S.	M127, S127			Kern, M. J.	1143
Jonsson, H.	1051	Kamel, M. A.	W052, W053			Kesavan, C.	1081, T151, T152
Jonsson, K. B.	1191, W125	Kamel, S.	T250			Kessler, S.	1300
Joo, I.	T399, T400	Kamijo, R.	1145, M201, T121, W084			Khan, B.	M352
Jordan, C. T.	M039, S039	Kamimura, T.	W022			Khan, K. M.	T413
Jorgensen, N. R.	M248, S248, W345	Kamioka, H.	W051, W061			Khan, M.	M352, T158
						Khanal, R. C.	M258

(Key: 1001-1300 = Oral, O = Oral Poster, S = Sunday Plenary poster, M = Monday poster, T = Tuesday Poster, W = Wednesday Poster, WG = Working Group Abstract)

Khanzode, D.	1230	Kim, H. Y.	T220	Kinosita-Kawano, S.	T129	Kolattkar, N. S.	T407
Khatkhatay, M.	M458	Kim, I.	T024	Kinugawa, S.	1149, M106	Kolesnikova, G. Sergeevna	W364
Khaw, K. Tee	1281, M360, O360,	Kim, I.	T078	Kirkland, M. A.	T075	Koller, D. L.	T215, W171, W178,
	S360	Kim, I.	T133	Kirkland, S.	W281		W185
Kheddoumi, N.	T240	Kim, I.	W015	Kirman, S.	1085, 1193, 1268	Kolta, S.	1075, 1077
Khoo, B. C. C.	T269	Kim, J.	M010, S010	Kirsch, T.	1111, M043, S043, T131	Komarova, S. V.	1244, T237
Khosla, S.	1085, 1160, 1193, 1235,	Kim, J.	M199	Kirschke, C. P.	M183	Komasa, Y.	W162
	1239, 1262, 1268, M024, M250,	Kim, J.	M343	Kirschner, L.	T045	Komatsu, D. E.	W456
	M369, S250, S369, T040, T054,	Kim, J.	M410	Kishimoto, M.	M365	Komatsu, M.	T334
	T195, T460, W021, W218, W418	Kim, J.	M499	Kishiya, M.	M273	Komatsu, T.	M375, S375
Khosravi, A.	T437, W424, WG8	Kim, J.	T130	Kiss, J.	T124	Komatsubara, S.	W207
Khoury, P. R.	M536	Kim, J.	T222	Kitagawa, H.	W022	Komiyama, S.	M303, S303, W019
Khousam, R.	M352	Kim, J.	T224	Kitagawa, J.	W493	Komiyama, S.	W029
Kida, D.	W434	Kim, J.	T401	Kitahara, K.	T434	Komm, B. S.	1010, M404
Kidd, B. D.	M018	Kim, J.	T409	Kitaoka, T.	M486	Komori, T.	1066, M116, M123,
Kidd, E. J.	M055	Kim, J.	W066	Kitao, T.	T163		S123, W029
Kidd, L. J.	1246	Kim, J.	W257	Kitase, Y.	M237, W053	Komura, K.	T068, WG22
Kido, S.	M302, M365, T263, M362	Kim, K.	T400	Kitaura, H.	M107	Kondo, H.	M462, W016
Kiel, D. P.	1076, 1240, M277, M285,	Kim, K.	W066	Kitazawa, R.	1219, O498, M095,	Kondo, N.	W103
	M347, M362, S277, S347, S362,	Kim, K.	W435		M498, S498, W113, W413	Kondo, S.	M029, S029
	T219, T285, T317, T347,	Kim, M.	M247	Kitazawa, S.	1219, O498, M095,	Kondo, T.	1219, M095, W113, W413
	W177, W180, W266, W267	Kim, M.	M260		M498, S498, W113, W413	Kong, C.	W198
Kiely, M.	W269, W408	Kim, M.	T401	Kitazoe, K.	M302, T263	Kong, J.	T409
Kikuchi, H.	W343	Kim, M.	W022	Kitchen, V. S.	1131	Kong, L.	1062, M166, T265
Kikuchi, R.	W186, W252	Kim, M.	W143	Kitterman, R. T.	M461, M463	Kongara, S.	WG18
Kikuchi, T.	M251	Kim, M.	W153	Kiviranta, R.	1069, W064	Konish, M.	T512
Kilgore, M. L.	M378	Kim, M.	W248	Kladde, T.	1300	Konishi, M.	W260
Killinger, Z.	W300	Kim, N.	W066	Klatt, C. M.	W217	Kono, S.	T336
Kilts, T. M.	1174, M157, O157, S157	Kim, O.	T224	Klaushofer, K.	M437, M447, S437,	Konstantellou, E.	WG19
Kim, B.	M199	Kim, S.	1114		S447, T464, T486	Kontulainen, S.	W512
Kim, B.	M322	Kim, S.	M343	Kleerekoper, M.	W239	Kontulainen, S. A.	1040
Kim, B.	T221	Kim, S.	M410, M410	Klein, G. L.	M487, S487	Koo, H.	M199
Kim, B.	T224	Kim, S.	M499	Klein, R.	1237, 1263	Kooienga, L.	T488
Kim, B.	T225	Kim, S.	T221	Kleinman, S. J.	1288, T037	Kooperberg, C.	M471, S471, T325
Kim, C.	T378	Kim, S.	T222	Kleinmond, C.	T450	Kopperdahl, D. L.	1089
Kim, D.	M135	Kim, S.	T223, T225	Klemes, A. B.	W317, W351	Korach, K.	T192
Kim, D.	M343	Kim, S.	T249	Klinck, J.	T360	Korchynskyi, O.	M156, T144, W044
Kim, D.	T306	Kim, S.	T339	Klösch, B.	W108	Kordosky, J.	W423
Kim, D.	W042	Kim, S.	T378	Kloseck, M.	M413, W376, WG39	Korelis, E.	W388
Kim, E.	M343	Kim, S.	T379	Klundert, T. van de	W450	Korhonen, M.	W505
Kim, E.	W436	Kim, S.	T424	Knaack, D.	T156	Korn, S.	T324, W289
Kim, G.	M020	Kim, S.	W049	Knackstedt, M.	M333, M334	Korpelainen, R.	M525, S525, WG9
Kim, G.	W257	Kim, S.	W054	Kneissel, M.	1046	Kósa, J.	M138, T124, T226
Kim, G. S.	T220	Kim, S.	W085	Knold, B.	W382	Kósa, J. Péter	M284
Kim, G. Su	T221, T225	Kim, S.	W126, W251	Ko, A.	M240	Kosaka, S.	W141
Kim, H.	1111	Kim, S.	W257	Ko, B.	T133	Kosaki, K.	1064
Kim, H.	M022	Kim, S. W.	M044	Ko, J.	M088	Kose, K.	W241
Kim, H.	M043, S043	Kim, S. Wan	M209	Ko, S.	M410, M499, W054	Koshimizu, T.	M137
Kim, H.	M075	Kim, S. Yeon	M209	Ko-En, H.	T198	Koskenvuo, M.	1204
Kim, H.	M075	Kim, S. Y.	T220	Kobayashi, H.	M154	Koskivirta, I.	W064
Kim, H.	M075	Kim, T.	T221, T223, T225	Kobayashi, M.	M161, M201	Kostenuik, P.	1126
Kim, H.	M083	Kim, T.	T423	Kobayashi, T.	1047, 1062, M270,	Kostenuik, P. J.	1009, 1082, 1088,
Kim, H.	M083, M088	Kim, T.	W257		S270		1117, 1122, 1231, 1232, O409,
Kim, H.	M088	Kim, T. H.	T220	Kobayashi, Y.	1149, M082, M106,		M409, S409, W445
Kim, H.	M088	Kim, U.	T401		S082, T085, T243, W072	Kosulwat, V.	T313
Kim, H.	M387	Kim, W.	W023, W043	Koblar, S.	W033	Kotadiya, P.	M074
Kim, H.	M499	Kim, W. Gu	T225	Kodama, H.	T438	Kotas, M.	W143
Kim, H.	M503	Kim, Y.	M343	Kodama, Y.	T487	Kotha, S.	W052, W053
Kim, H.	T008	Kim, Y.	M354	Koehler, S. M.	W039	Kotowicz, M. A.	T324, T354, W289
Kim, H.	T008	Kim, Y.	T339	Koester, K. J.	M392, S392, W455	Kotsioprifitis, M.	W112
Kim, H.	T008	Kim, Y.	T378	Koga, T.	1289	Kotz, R.	W194
Kim, H.	T078	Kim, Y.	W049	Kogo, M.	W092	Koulis, T.	T432
Kim, H.	T100	Kim, Y.	W251	Koh, J.	T024, T221, T225, W015,	Koulouris, I. Ch	T402, W208, WG19
Kim, H.	T130	Kim, Y.	W293		W257	Kousteni, S.	M060, S060, T044
Kim, H.	T131	Kim, Y.	W293	Koh, J. M.	T220	Kovacic, N.	M004, S004, W110
Kim, H.	T133	Kim-Weroha, N. A.	W052, W053	Kohara, H.	M107	Kovacs, C. S.	W137
Kim, H.	T222	Kimata, M.	M137, W131	Kohda, K.	M431	Koyama, A.	1282
Kim, H.	T224	Kimlin, M. G.	M261, M263	Kohda, M.	1034	Koyano, K.	W011
Kim, H.	T401	Kimm, K.	W257	Kohles, J. D.	W352, W362, W367	Kozai, K.	M210, S210
Kim, H.	T423	Kimmel, D. B.	M175, M411, M437,	Koide, M.	M106, W332	Kozai, Y.	W479
Kim, H.	T431, W085		S411, S437, T296	Koike, T.	W118	Kozarek, K.	W466
Kim, H.	W085	Kimura, A.	1061, 1112, M049, M133,	Koinuma, D.	M206	Kozlow, W. M.	1137
Kim, H.	W248		S049, S0133, W100	Koivumaa-Honkanen, H. Tuulie	W291	Krack, W.	W156
Kim, H.	W262	Kimura, T.	M136, S136	Koizumi, M.	T135	Kraemer, W. J.	W056, W496
Kim, H.	W435	Kindmark, A.	1196, W182	Kojima, M.	1061	Kraenzlin, M.	T191, W519, WG30
Kim, H.	W435	Kingsley, L. A.	1003, M305, S305,	Kokubo, H.	W019	Krajisnik, T.	1191, W125
Kim, H.	W436		T251	Kokubun, S.	M184	Krakow, D.	1261
Kim, H. Soo	T467	Kingston, H.	M032	Kolailat, R.	M001	Kramer, I.	1046

(Key: 1001-1300 = Oral, O = Oral Poster, S = Sunday Plenary poster, M = Monday poster, T = Tuesday Poster, W = Wednesday Poster, WG = Working Group Abstract)

Kramer, W.	1132	Kung, A. W. C.	T214, M019, T229,	Lane, J. M.	M430, T171, W468, S430	Lee, B. J.	W495
Krasnow, J.	W227		T403, T404, W175	Lane, N.	1208, 1291, M392, S392,	Lee, B. S.	M074, M076, W069
Kraus, L.	WG18	Kurasawa, K.	W186, W252		T181, W331	Lee, C.	M075, T008
Krause, D.	M421, S421	Kurihara, N.	1152, M477, M479,	Lang, C. A.	M261, M263	Lee, D.	T449
Kream, B.	1106, 1284, O223, M223,		S477, W152	Lang, T.	1091, 1094, 1278, 1282,	Lee, D. Choen	W514
	M235, S223, S235, W401	Kurimoto, P.	M513		T426	Lee, E.	T033, W251
Kreatsas, G.	W388	Kurmen Figueroa, D. A.	W393,	Langdahl, B.	T218, W368	Lee, F. Y.	M519
Krebs, A.	T287		WG25	Lange, A.	W488	Lee, H.	1105
Krebs, L. J.	M485	Kuro-o, M.	T192	Lange, J. L.	T384	Lee, H.	M020
Krege, J. H.	O423, M371, M423,	Kuroda, R.	T013, T043, T161, W048	Lange, P.	M272, O272, S272	Lee, H.	M075, T008, T133
	M424, S371, S423	Kuroda, S.	1105, W016	Länger, F.	W422	Lee, H.	T399
Krege, J. Henry	M425, S425	Kuroda, T.	W256, W513, W517	Langerwerf, P. E.	W450	Lee, H.	T401
Kreiger, N.	M371, S371	Kurosaka, M.	T013, T043, T161,	Langhammer, A.	T338	Lee, H.	W251
Kreikemeier, R.	T519		W003	Langman, C. B.	T492	Lee, I.	T401, W436
Kreiss, A.	T381	Kurosawa, H.	1015, O390, M390,	Langsetmo, L.	M336, S336	Lee, J.	1202
Kreiter, M. L.	1113		S390, T434, W503	Lanier, L. L.	1291	Lee, J.	M075
Kremer, R.	1295, M257	Kurz, B.	T287	Lanske, B.	1114, T011	Lee, J.	M135
Krempin, D.	W338	Kurzer, M. S.	T187	Lantigua, R. A.	T283, W261	Lee, J.	M199
Krenbek, D.	T164, W446	Kusano, E.	W157	Lanyon, L. E.	1213, O064, M036,	Lee, J.	M387
Krieg, M.	1167	Kusec, R.	W110		M064, M523, S036, S064,	Lee, J.	M471, S471
Krieger, N. S.	M063	Kushnir, M. M.	O358, M358, S358,		S523, T067	Lee, J.	T008
Kriegl, J. M.	T108		T191	Laperre, K.	T132	Lee, J.	T100
Kriemler, S.	W519, WG30	Kutil, B.	W390	Lapidus, J.	W253	Lee, J.	T221
Kriegsinyos, W.	M396	Kuwabara, A.	M365	Laplace-Buihle, C.	T498	Lee, J.	T221, T225
Krischer, J. P.	T425	Kuwahara, S.	1115	LaPlante Strutz, K.	M063	Lee, J.	T225
Krishnamurthy, G.	1010	Kuwahata, M.	1115, M214, S214	Lapointe, D.	M047, S047	Lee, J.	T325
Krishnan, V.	W489	Kuzutani, K.	M402	Lappe, J.	M327, T359	Lee, J.	W042
Kröger, H.	1083, 1270, M344, M452,	Kvern, B.	M436, T332, T396	Larédo, J.	W231	Lee, J.	W054
	M533, S344, S452, S533, T515,	Kvien, T.	M497	Larrosa, M.	M376	Lee, J.	W066
	W055, W291	Kwak, H.	M247, T424, W344	Larroude, M. Silvia	T327, W149	Lee, J.	W126
Kroger, L.	T515	Kwak, H. Bok	T100	Larsimont, D.	M249	Lee, J.	W257
Krogsgård, K.	T411	Kwok, T.	1133, T469, W253	Larson, E. A.	1237	Lee, J.	W257
Krohn, K.	1089, T375, W303, W381,	Kwon, M.	M343	Larsson, S.	W182, W473	Lee, J. S.	W508
	W384	Kwon, S.	W282, W361	Larsson, T. E.	1191, M213, W125	Lee, J. Y.	T220
Krohn, P. J.	W211, W217	Kwon, T.	T091	Lasiewicki, A.	T275	Lee, K.	M143
Kronbergs, A.	W010			Laskin, W.	T253	Lee, K.	T008
Kronenberg, H. M.	1020, 1062, 1119,	L		Lassar, A. B.	M164	Lee, K.	T133
	M122, M270, S270, W095, W138	La Corte, R.	T370	Laster, A.	M324	Lee, K.	T133
Kronenberg, M. S.	M027, S027	Labelle, H.	T189	Lataillade, J. Jacques	T498	Lee, K.	T178
Krueger, D.	M451, T282, T358,	Labrie, F.	1200, M245, T199	Lattanzio, M.	M236	Lee, K.	T224
	T499, W246	Lachenmayr, S.	W400	Lau, E. M. C.	W253	Lee, K.	T378
Krug, R.	T286	LaCroix, A. Z.	1202, 1207, 1272,	Lau, K. H. W.	1081, 1223, O112,	Lee, K.	W126
Kruger, M. C.	T362		O373, M339, M373, M377,		M112, S112, W163	Lee, K.	W248
Kruse, H.	W238		M381, M471, M535, S377,	Laudier, D.	M403, S403	Lee, K.	W285
Ksiezopolska-Orlowska, K.	T275		S339, S373, S381, S471,	Laughren, J. J. J. J. J.	W295	Lee, K.	W370
Kuboki, Y.	M154		S535, T288, T325, T351,	Laughier, P.	T297	Lee, K. Kui	T403, T404
Kubota, S.	T125		W292, W306	Launer, L.	1278	Lee, M.	M010, S010
Kubota, T.	M486			Laurence, J.	1155	Lee, M.	M139
Kudo, H.	M273			Laurent, G.	M249, T240	Lee, M.	M199
Kudryashov, V.	W088	Ladefoged, M.	T018	Lauretani, F.	W230	Lee, M.	T130
Kugimiya, F.	1112, 1211, 1247, T356	LaFleur, J.	W294	Lauria, F.	W190	Lee, M.	W174, W179
Kuhn, V.	W454	Lafontaine-Lacasse, M.	M048	Lausten, L.	T233	Lee, S.	M115
Kuiper, N.	M151	Lagerquist, M. K.	T188	Lauter, K. B.	M485	Lee, S.	M199
Kujala, U. M.	1083, M533, S533,	Lago, A. M.	O386, M386, M427,	Lauzier, D.	W112	Lee, S.	M247
	W515, W520		S386, S427	Lavecchia, C.	1055	Lee, S.	M398
Kukita, A.	O099, M099, M108, S099,	Lai, C. Fang	M185, O185, S185	Lawrence, F.	W489	Lee, S.	M398
	W067	Lai, W.	W342	Lawrence, K. M.	T104, W335	Lee, S.	M499
Kukita, T.	O099, M099, M108, S099,	Lai, W. Ping	W337	Layfield, R.	1036	Lee, S.	M519
	W067	Lai, Y.	T364	Lazard, Z.	1071, M169, S169, T473	Lee, S.	T224
Kukkonen-Harjula, K.	T319	Lai-Huang, C. F.	T165	Lazaretti-Castro, M.	W339	Lee, S.	T399
Kukreja, S.	M370	Laine, C. M.	M281, S281	Lazáry, Á.	M138, M284, T124, T226	Lee, S.	W200
Kulak, C. A. M.	M454, T342	Lainez, P.	T335	Le Loët, X.	M500	Lee, S.	W248
Kulick, E. R.	M008	Laitala-Leinonen, T.	T091	Le Nihouannen, D.	T237	Lee, S.	W293
Kuliwaba, J. S.	1186, 1246, M505,	Lajeunesse, D.	T143	Le-Capling, T.	M228	Lee, S.	W361
	T113	Lakatos, P.	M138, M284, T124, T226	Leach, R. J.	T470	Lee, S.	W435
Kulkarni, A.	T148	Lakhdar, R.	W420, WG14	Leal, M. E.	1265, M393	Lee, S. Hun	T221, T225
Kulkarni, N. H.	1277	Lamberg-Allardt, C. J. E.	T046, W038	Lebecque, P.	W407	Lee, S. Kyeong	1254
Kumagai, Y.	T405	Lambers, F.	T462	Leboeuf, D.	T189	Lee, S. Soo	T467
Kumar, N.	T421, WG33	Lambert, D.	1261	LeBoff, M. S.	1052, 1202, 1207,	Lee, T.	W199
Kumar, R.	1132, 1230, M207, M212,	Lamm, M. L. G.	T244		M471, S471, T325, T407, W031	Lee, W.	T134
	M254, M394, S212, S394, W312	Lamontagne, S.	W334	Lecanda, F.	1001	Lee, W.	T431
Kumar, S.	1131, O386, M386, M427,	Lamothe, K.	1215	Lecce, D.	T419	Lee, Y.	M088
	S386, S427, W063, W134	LaMotta, A.	M437, S437	Leclerc, N.	T026	Lee, Y.	M399, S399
Kume, M.	W513, W517	Lampe, J. W.	M339, S339	Leder, B. Z.	M337	Lee, Y.	T306
Kumiko, K.	W020	Lander, E. S.	W173	Lederer, E.	M494	Lee, Z.	M083, M088
Kumpan, W.	W390	Landin-Wilhelmsen, K. L. L.	M194,	Lee, B.	1180, 1184, 1212, 1261,	Lee, Z. Hee	T100
Kung, A.	M282		T343, W288		M032, M150, M202, S150, S202	Leeb-Lundberg, F.	T201
Kung, A.	W385	Landreth, G.	1141	Lee, B.	T423	Leeming, D. J.	T135, T245, W205,
		Landsittel, D. P.	1053	Lee, B.	W106		W478

(Key: 1001-1300 = Oral, O = Oral Poster, S = Sunday Plenary poster, M = Monday poster, T = Tuesday Poster, W = Wednesday Poster, WG = Working Group Abstract)

Leena, P. Sagaya, T.	M204	Li, K.	T106	Link, T. M.	M419, S419, W228, W229, W449, W508	Lopez, A. Maria	1274
Lees, C. J.	W277	Li, L.	M159	Linkhart, T. A.	1288, T034, T037	López, F. Jose	M405, S405
Legard, F.	W166	Li, L.	W199	Lion, J.	T250	Lopez Franco, G. Estella	W466
LeGeros, R. Z.	W011	Li, L. Ming	W244	Liote, F.	M134	Lopez-Benitez, J.	W169
Legrand, E.	W201	Li, M.	1014	Lippuner, K.	T387	Lorentzon, M.	1200, M177, M245, T199, T310, W135
Legroux-Gerot, I.	M465	Li, M.	M116, M239, S239	Lipton, A.	W189	Lorenzetti, S.	W459, W469
Lehane, K.	W204	Li, M.	M417, T435	Lirani-Galvao, A. Paula R.	W339	Lorenzo, J.	1254
Lehesjoki, A.	M281, S281	Li, M.	W059	Lisse, J.	W306	Lorich, D. G.	M430, S430
Lehtonen-Veromaa, M.	M317	Li, M.	W168, W170, W323	Litscher, S. J.	W466	Lorincz, C.	T360
Lei, S. Feng	W244	Li, M.	W458	Little, D.	T088	Lorraine, J.	W281
Lei, W.	1032	Li, S.	W489	Little, D. G.	T056, T089, W164	Loth, E.	T275
Leigh, C.	T383	Li, T.	T116, T117	Little, S. C.	1151	Lotinun, S.	M482, S482
Leino, A.	M317	Li, X.	1088, 1122	Litvin, J.	T020	Loveridge, N.	T294
Leleu, X.	W195	Li, X.	1172, 1173	Liu, B.	1176, 1284, M223, O223, S223	Low, V. H. S.	W226
LeLujian, J.	M510	Li, X.	1231, 1232	Liu, C.	1062, M166, T265	Lowe, N.	T302
Lembersky, B. C.	1017	Li, X.	M207	Liu, D.	M146, S146	Lowe, V.	M174, T184, T185, T186, T190
Lemenchick, B. G.	M474	Li, X.	M412	Liu, D.	M412	Lowery, J.	T366
Lemire, I.	1259	Li, Y.	1014	Liu, D.	T010	Löwik, C. W. G. M.	W046
Lemmon, J.	T361	Li, Y.	M093, S093	Liu, D.	W323	Lowry, M. B.	M482, S482
Lemons, J. E.	W464	Li, Y.	M108	Liu, F.	W083	Lozano, D.	T207
Lems, W. F.	M314, M315, T388	Li, Y.	T435	Liu, G.	W261	Lu, C.	1297
Lenart, B.	M430, S430	Lian, J. B.	1144, 1258, M022, M047, M143, M295, S047, S295, W200	Liu, H.	T027	Lu, D.	T511
Lennington, J.	1261, M150, S150	Lian, N.	T027	Liu, J.	1104	Lu, F.	W150
Leonard, M.	M493, T490, S493	Liang, B.	1180	Liu, J.	1257	Lu, G.	1099
Leonard, P.	1259	Liang, S. Ping	W244	Liu, J.	W323	Lu, H.	M202, M374, T345, S202
Leoncini, G.	W230	Liang, X.	M386, O386, S386, W063	Liu, J.	W171, W178, W185	Lu, Q.	T149
Leong, W.	M271	Liang, Y.	M412	Liu, L.	W348	Lu, S. S.	M200
Leppäluoto, J.	M525, S525, WG9	Liao, C.	T432	Liu, M.	1119	Lu, W.	1021
Leppänen, O.	W457, W500	Liao, L.	M192	Liu, M. Yuan	W244	Lu, X.	1143
Lerman, A.	1262	Liard, F.	M372	Liu, P.	1028	Lu, Y.	1100
Lerner, M. R.	T410	Libanati, C.	M325	Liu, P.	W273, W274	Lu, Y.	1282
Lerner, U.	M177	Libicher, M.	T416	Liu, P. Y.	1018	Lu, Y.	1296
Leslie, W. D.	1078, 1080, 1163, M321, M351, S321, S351, W246	Libouban, H.	W201	Liu, R.	M481	Lu, Y.	M007, M037, T247, T248
Lespessailles, E.	M345, T295, T344	Lichtler, A.	1106, M027, M028, M140, S027, W017	Liu, S.	1227, 1296	Lu, Y.	T270
Lester, M. E.	W056, W487	Lie, W.	W206	Liu, S.	W491	Luan, Y.	M166
Lester, M. L.	W496	Lieben, L.	M266	Liu, W.	M084, S084	Luben, R. N.	1281, M360, O360, S360
Letellier, K.	T189	Lieberman, J. R.	M046	Liu, X.	1013	Lublinsky, S.	W499
Letuchy, E.	M528, M529, S528	Liebold, A.	T049	Liu, X.	T257	Lucani, B.	M275, S275, T514
Leung, A.	M476	Liegibel, U.	M459, S459	Liu, X. Qing	M417	Lucas, E. A.	T410, T451
Leung, K.	T178	Lier, D. A.	T329	Liu, Y.	1205	Lucey, A. J.	W408
Leung, K. S.	1133	Lieu, S.	M163, S163	Liu, Y.	M034	Luczak, E.	T275
Leung, P.	M291, S291, T469	Lillestol, M.	W363	Liu, Y.	M045, S045	Luderer, H. F.	W047
Leung, P. C.	1133, W253	Lim, D.	W248	Liu, Y. Zhong	W244, W263	Lue, Y.	1018
Leung, S.	M351, S351	Lim, J.	W085	Liu, Z.	1070	Luis-Ravelo, D.	1001
Leupin, O.	1046	Lim, J.	W257	Liu, Z.	T157	Luisella, C.	W148
Levenson, A.	T253	Lim, K.	W022	Liu-Ambrose, T.	W461	Luiz de Freitas, P. Henrique	M239, S239
Levin, G.	T371	Lim, M.	W361	Liu-Léage, S.	M441, WG36	Luk, K. D. K.	W175
Levine, A. B.	W387	Lim, S.	M499	Livshits, G.	T219	Lukashova, L.	T148
Levine, M. A.	T480	Lim, S.	T033	Lix, L. M.	1078, 1080, 1163, M321, M351, S321, S351	Lukert, B. P.	T436, WG13
Levis, S.	M414, T425	Lim, S.	W049	Ljunggren, Ö.	1191, 1196, 1200, M177, M213, T310, W125	Luki, A.	W110
Levy, E.	T087	Lima, F.	W027	Lo Cascio, V.	M147, W318	Lumpkin, C. K.	W348
Levy, S. M.	M528, M529, S528	Lima, F. R.	W518	Lochmüller, E.	W454	Lund, R.	M450, T489
Lewiecki, E. M.	1205, 1209, T357, T383, W362, W366	Limoli, C.	M462	Lodes, S.	W414	Lundy, M. W.	M508, S508, W320, W325
Lewiecki, M.	M434, S434	Limpido, G.	T370	Lofthus, C. M.	W272	Luo, G.	T301
Lewinson, D.	M042, T009	Lin, D.	1134	Loftus, D. J.	M462	Luo, M.	1007, M007, M037
Lewis, B.	M377, S377	Lin, H.	T364	Lohman, T.	M377, S377	Luo, Q.	M229
Lewis, C. E.	1052, 1207, O373, M373, M381, S373, S381, T288, W306	Lin, J.	T174	Loisel, T. P.	1259	Luo, T.	1013
Lhoste, Y.	M319	Lin, J.	T315, T320	Lombardi, A.	1057, M437, S437, T246	Luo, W.	W109
Li, B.	M017	Lin, L.	M297	Lombardini, D.	T019	Lupton, J.	W467
Li, B.	M264	Lin, S.	W491	Lomri, A.	W018	Luque, I.	T454
Li, B.	M271	Lin, S. Qing	M034	London, S. D.	T257	Luque-Fernández, I.	T167
Li, B.	W045	Lin, Y.	W338	Loneragan, R.	W437	Luthman, H.	T227
Li, C.	1282	Linares, G. R.	M005, T034	Long, J. H.	W311	Luu, Y. Kim	W495
Li, C.	M447, S447	Linari, M.	W223	Long, M. W.	M389, W315	Luzi, E.	T028, T118
Li, C.	W334	Lindahl, K.	1196	Long, S. R.	W380	Ly, K.	W076
Li, C. Yang	M403, S403	Lindhe, T.	M213	Longis, P.	W392	Lykke, J.	W035
Li, H.	M027, S027, W017	Lindner, T.	M193	Longmore, G.	W047	Lyles, K.	1055, M440, M444, S440, W398, WG27
Li, H. Tao	M028	Lindsay, R.	1091, 1092, 1096, 1125, M388, M438, S388, T373, T384, T408, W296	Longo, M.	T170	Lymperi, S.	M053
Li, J.	1093	Lindsley, H. Benzinger	T436	Longo, W.	T499	Lynch, S. E.	W316
Li, J.	1095	Lindstrand, S.	M194	Loots, G. G.	1046, M179, O179, S179	Lynnerup, N.	T135
Li, J.	1295	Lindvall, C.	1108	Lopes, J. B.	T273, T326	Lyons, J.	1249
Li, J.	M228	Ling, L.	T166				
Li, J.	W494	Link, T.	T286				
Li, K.	M202, S202						

Lyons, K. M.	M171, S171	Majumdar, S.	M418, M419, S419, T061, T107, T110, T286, T329, T459, W228, W229, W449	Martin, E. N.	T437	May, B. K.	W402
Lyytikäinen, A.	1083, M533, S533, W515, W516, W520	Mak, R.	1263	Martin, T. J.	1068, 1220, 1277, T005, T012, T081, W025	Mayfield, J. D.	M515
M		Mak, W.	M282, T062, T182	Martin, X.	T466	Mazouz, C.	T371
		Makarov, S. S.	W044	Martin-Millan, M.	M174, T184, T185, T186, T190	Mazzola, L.	M394, S394
		Makhijani, N. S.	M276	Martineti, V.	T213	Mc Guigan, F.	T227
		Makino, Y.	T068, WG22	Martinez, A.	M275, S275, T260	McAdam-Marx, C.	W294
		Mäkitie, O.	M281, S281, W165	Martínez, G.	M496, T501	McAhren, S.	W489
		Maksymowycz, W. P.	T329	Martínez, J.	T348, W326	McAlinden, A.	M132
		Malaval, L.	M160, S160	Martínez, J. Alfredo	W408	McAlister, W.	T475, W169, W430
		Malik, M.	W010	Martínez, S.	1001, T472	McAteer, J.	T219
		Malleson, P.	M490	Martínez-Ferrer, À.	T307	McCabe, G. P.	T134
		Mallmin, H.	1200, W125, W182, W473	Martínez, L.	M140	McCallum, R.	W360
		Malloy, P. J.	M265, S265, WG2	Martini, G.	M275, M478, S275, T330, W190	McCann, J. F.	T302
		Malluche, H. H.	T314	Martini, L. A.	T312, W275, W283, W440, W442	McCauley, L. K.	1188, M001, W083
		Man, Z.	T327, T382, W149	Martus, P.	M453	McCloskey, E. V.	1060, 1076, M332, S332, T366
		Manabe, S.	M365	Marty, C.	M162	McClung, M.	1128, 1205, M432, S432, T382
		Manabe, T.	W207	Marumo, K.	1149	McClurg, P.	T214
		Manacu, C. Alexandra	M117	Maruno, H.	M395	McCon, K.	T296
		Manaka, T.	W121	Marusic, A.	M004, S004, W110	McCracken, P. J.	T290
		Manalac, C.	1019	Maruyama, N.	T068, WG22	McCrea, P.	1249
		Mandal, C. Charan	M100, T029	Maruyama, R.	T318	McCready, L.	1193, 1239
		Manduca, P.	T019	Maruyama, T.	W196	McDonald, J. M.	1104, 1216, 1283, T052, W070, W074
		Mangine, A.	1010	Marvell, T.	M394, S394	McDonald, M. M.	T088, T089, W164
		Mangini, M.	M394, S394, W312	Masahiro, K.	W048	McGonnell, I. M.	1213
		Manigrasso, M. B.	T448	Masaki, H.	W357	McGrath, B.	1022
		Manini, T. M.	T346	Masanauskaite, D.	W368	McGregor, N. E.	1068, 1150
		Manjubala, I.	M447, S447	Masanori, T.	T159	McGuckin, B.	M511, M521
		Mann, R.	M403, S403	Masarchia, P.	M411, S411	McGuire, D. P.	W305
		Mann, V.	W055	Mascia, M. Lucia	W356	McGwin, G.	W464
		Manning, C. A.	W007	Mashiba, T.	W207	McHugh, K. P.	M071, M095, W068
		Mannstadt, M.	1031	Masi, L.	T118, T213, W230	McKay, H. A.	1040, M527, M531, T413, W461, W512
		Manolagas, S. C.	1011, 1058, 1067, 1086, M002, M052, M174, M233, S002, S052, S233, T184, T185, T186, T190, W057	Mason, B.	M449	McKee, M. D.	1155, 1259
		Manolson, M. F.	M087, T105, T106	Mason, M.	M413	McKenna, C. R.	1137, 1286, M305, S305, T251
		Manske, S. L.	W461	Mason, R.	M014	McKenna, M. J.	W437
		Mansur, J. L.	W235	Mason, R. Sarah	T006	McKie, J. E.	W66
		Manzato, E.	W302	Massaro, J.	1240	McKinlay, J. B.	M337, M338, W259, W471
		Maran, A.	M306, T254	Masse, F.	W334	McLaughlin, E. John	T061
		March, L. M.	1279	Mastaglia, S. R.	T271	McLean, J. E.	T111
		March, R. L.	T392	Masuda, M.	W130	McLean, R. R.	M347, S347, T309, T347, W266, W267
		Marchadier, A.	T295, W231	Masuda, Y. Murakami	T121	McLennan, C. E.	T309, W266, W267
		Marchandise, X.	M465	Masunari, N.	M318	McLeod, J.	T145
		Marcucio, R.	M163, S163	Masuyama, R.	1101	McMahon, A. P.	1020, 1024
		Marden, C.	M146, S146	Mata Granados, J. M.	T316	McMahon, D. J.	1164, M327, M481, T283, T490, W145, W146, W261, W415, W444
		Mardon, J.	W407	Mateo, C. M.	T483	McMichael, B. K.	M074, M076, W069
		Marerro, M.	T335	Matheny, C.	1131	McNulty, M. A.	W299
		Maresch, C. M.	W056	Mathern, D.	M259, S259, W161	Meadows, E.	W380, W381
		Margarita, D.	M380	Mathew, S.	T489	Medich, D. L.	T497
		Margulies, B. S.	M304	Mathieu, L.	T041	Medina, C.	T335
		Maria, B. L.	W077	Matouk, E.	W360	Meeder, P. Jürgen	M459, S459, T416
		Maricic, M.	1274	Matsubara, T.	1002, T055, W020	Meeves, S.	1091
		Marin, F.	1267, 1269, T368	Matsui, T.	W358	Mehle, S.	T278
		Marini, F.	T028, T213	Matsui, Y.	M188	Mehrota, R. N.	WG4
		Marini, J. C.	T471, W166	Matsumoto, K.	T121	Mehta, N.	W143
		Marion, S. L.	W349	Matsumoto, M.	1115, M089, M251	Mei, L.	M079
		Marjamaki, A.	T241	Matsumoto, T.	1059, 1220, M302, T013, T161, T263, T395, W048	Meier, C.	M358, O358, S358, T191
		Markell, M.	T500	Matsumura, A.	W286	Meigs, J. B.	T219
		Markowitz, M.	W169	Matsunobu, T.	1064	Meikle, A. W.	T191
		Marks, H. D.	W154	Matsuo, K.	W067	Meikle, W. A.	M358, O358, S358
		Marks, L. D.	M442	Matsuoka, R.	M431	Mejia, W.	1138
		Marley, K.	M482, S482	Matsushita, O.	1229, M204	Mejjad, O.	M500
		Marquis, R.	1131	Matsushita, T.	1141	Melhuish, T.	1286
		Marschke, K.	M405, S405	Matsuura, T.	T142, T147	Melton, V.	W023, W043
		Marsell, R.	1191, W125	Matsuya, S.	W011	Mellibovsky, L.	M288, M289, S288
		Marshall, K.	T392	Matsuzaki, K.	M136, S136, T308	Mellström, D.	1200, M177, T310, W125, W135
		Marshall, L. M.	1161	Matsuzaki, Y.	T176, WG21	Melnichenko, G. Afanasjevna	W364
		Marshall, T.	M528, M529, S528	Matthews, B. G.	T205	Melton, L. Joseph	1160, 1193, M369, S369, T460, W218
		Martel-Pelletier, J.	1035	Matthews, R.	M324, M378	Melville, J.	1272
		Martens, M.	W156	Mattioli, P. M.	M128		
		Martens, M. G.	W352	Matzinger, F.	M489, S489		
		Mårtensson, U. E. A.	T201	Mauck, K. F.	O423, M423, S243		
		Martin, A.	1118, 1155, 1226	Mautalen, C.	1055, T385		
		Martin, B. R.	T134	Mauviel, A.	M305, S305		
		Martin, D.	T497				

(Key: 1001-1300 = Oral, O = Oral Poster, S = Sunday Plenary poster, M = Monday poster, T = Tuesday Poster, W = Wednesday Poster, WG = Working Group Abstract)

Mena, C.	T249	Miller, P.	1091, 1092, 1205, 1209,	Moggia, M. Susana	T327, W149	Morris, M. D.	T108
Menagh, P. J.	M196		M432, M434, S432, S434, T375,	Moghrabi, A.	T513	Morris, S.	M420
Mendenhall, S. D.	M461, M463		T377, T386, W303, W354, W355	Mohammad, K. S.	1137, 1286, M305,	Morrisey, M. A.	M378
Mendoza-Londono, R.	M202, S202	Miller, R.	M307, S307	S305, T241, T251, T260		Morrish, D. W.	T329
Menegoci, J. C.	W385	Miller, S. N.	T361	Mohammadi, M.	1113	Morrison, N.	1033, T073, T074,
Meneu, J.	T501	Miller, T. A.	T051	Mohan, S.	1081, 1107, 1223, M005,		W078
Menezes, P. R.	T326	Milling, J.	M394, S394, W312	M246, S246, T039, T080, T151,		Morse, A.	T088, T089, W164
Meng, X.	W168, W170, W323	Mill, E.	M102	T152, T211, T212, W008, W082,		Mortarino, P.	W237
Meng-Yin, T.	T198	Milner, C. M.	T092		W163	Mortlock, D. P.	1257
Menn, S.	T285	Mimatsu, S.	T261	Mohangi, G. Udaibhan	M173	Moscovitz, A.	T249
Menn, S.	W177	Min, B.	M503, W451	Mojarrab, R.	M462	Mosekilde, L.	1049, M222, T453,
Mentaverri, R.	T250	Minamida, A.	M096, S096	Mok, J.	T378		W151, W160
Mentzer, B. M.	M128	Minamide, T.	T395	Mok, S.	W342	Moser, T.	W231
Menuki, K.	W004, W336	Minamizaki, T.	M210, S210	Mok, S. Keng	W337	Moss, S. E.	T131
Merkel, M.	T015	Minamizato, T.	T070	Moldovan, F.	1035, M117, T189	Motohashi, M.	T084
Merle, B.	W330	Minck, D. R.	M404	Moldovan, I.	W254	Motokawa, S.	T457
Merlotti, D.	M275, M478, S275,	Minematsu, A.	W136	Møller Liendgaard, U.	W151	Motomura, S.	M273
	W190	Minisola, S.	W356	Monaghan, M.	T510	Motta-Hernandez, E.	T391
Mero, A.	W505	Mirams, M.	M120	Monaghan, P.	1299	Möttönen, T.	M317
Mesenbrink, P.	1055, 1056, M434,	Mirwald, R.	M530, M531, S530,	Monde, N.	W321	Mouillesseaux, K.	W023
	S434, T385, T387		WG29	Monfoulet, L.	M160, S160	Mount, J. G.	1213
Mesnil, M.	M054	Mirwald, R. L.	W509	Monk, J. J.	W305	Mouton, C. P.	1274
Messerschmitt, P. J.	T255	Miseki, A.	M365	Monnell, T.	1230, W312	Móvère-Skrtic, S.	1218
Messina, D.	M380	Mishima, H.	T502	Monroe, D. G.	1144, T195, W021,	Moyer-Mileur, L.	WG41
Meta, M.	W234, W321	Mishina, Y.	1043, 1106, M270, S270		W028	Mroczek, R.	1252
Metania, E.	W208, WG19	Misra, B.	T481	Montagnani, A.	T514	Mroueh, Z.	M287
Metcalfe, B.	WG8	Mistry, J.	W206	Montenegro, S.	T472	Muche, B.	M419, S419, T372
Metge, C. J.	M351, S351	Mitchell, B. D.	W184	Montero, M.	W319	Mudano, A.	M354
Metz-Estrella, D.	1252	Mitchell, P. G.	1277	Montjovent, M.	T041	Mueller, R.	1164
Meudt, J. J.	1225	Mitlak, B. H.	1089	Moon, E.	M075	Mueller, U. Alfons	W414
Meunier, P. J.	M504, O504, S504	Mitobe, M.	T496	Moon, R. T.	M057, M469	Mühlbauer, R. C.	T364
Meyer, H. E.	T272, W272	Mitra, S. R.	T302	Moon, S.	M075, T008, T133, T222,	Muir, J. W.	T426
Meyers, A.	T516	Mittal, B. R.	WG17		T409, W282	Muir, M. Mary	T006
Mez, T.	T226	Mitton, D.	W231	Moonga, B. S.	1153	Mukkananchery, A.	M357
Mezaki, Y.	W022	Miura, K.	M486	Moore, A. J.	1217	Mukudai, Y.	T125
Mezghani, K.	W258	Miwa, M.	T013, T043, T161, W048	Moore, K.	1055	Muliabrahimovic, A.	W402
Mi, Q.	T206	Miyabara, Y.	W256, W517	Moore, W. J.	1010	Mullarney, T.	1095
Miake, Y.	W480	Miyagawa, K.	W479	Moran, D. S.	W487	Muller, P.	T049
Mian, M. H.	M101, M110, S110	Miyagi, I.	W409	Moran, E.	M030	Muller, W.	1295
Miao, D.	M231, T058, W150, WG1	Miyahara, H.	M132	Moran, R. A.	1010	Mullin, B. H.	1203
Miard, S.	M048	Miyai, K.	T030	Morand, C.	W407	Mullins, M. C.	1151
Michael, V.	M151	Miyakoshi, N.	M472, T341, T438,	Morasso, M. M.	M027, S027	Mulpuri, K.	M490
Michaelis, I.	W484		W328, WG24	More, A. Jane	W402	Mumm, S.	T475, W169
Michalenka, A. C.	M063	Miyamoto, K.	1115, M214, S214	Moreau, A.	1035, M117, T087, T189	Mundlos, S.	M298, S298
Michienzi, S.	M178	Miyamoto, T.	1102, 1290, M016,	Moreau, A.	W195	Mundy, G Robert	1004, 1097, 1147,
Michigami, T.	M137, M488, W131		S016, T016	Moreau, J. E.	T252		T115, W111, W188
Michno, P.	M361	Miyamoto, Y.	W084	Moreau, M. Françoise	M067	Mundy, G R.	1106, 1257, O309,
Miclau, T.	M163, S163	Miyasaka, N.	1292, W431	Morelli, G.	M421, S421		M294, M296, M297, M309, M310,
Micoli, K. James	W070	Miyata, T.	M154	Morello, R.	1016, 1184, 1261,		M311, S309, S311, W114, W341
Middleton, S.	W445	Miyauchi, A.	W290		M150, S150	Muneta, T.	T126, W097
Miedlich, S. U.	W094	Miyaura, C.	O262, M161, M262,	Moreno, E.	T501	Munns, C.	T089
Mierke, D. F.	1299, W147		S262, W196	Morey-Holton, E.	M462	Munoz, F.	1280
Mifune, Y.	T013, T161, W003, W048	Miyazaki, K.	M161	Morgan, E.	M046	Munoz, S. Anthony.	T115
Miga, M. I.	M191, S191, W472	Miyazaki, T.	1098	Morgan, K.	W400	Muñoz-Torres, M.	T167, T216, T454,
Mihara, A.	T263	Miyazawa, K.	M206	Morgenstern, J. Carlos	T327, W149		W405
Mihovilovic, K.	M004, S004	Miyazono, A.	M201	Mori, K.	1219, M095, W113, W332,	Murai, J.	M130, S130, T119
Mikami, S.	M215	Miyazono, K.	1034, T021, W019		W413, W181	Murakami, A.	T261
Mikecz, K.	T092	Mizobuchi, M.	M226	Mori, S.	W207	Murakami, K.	W041
Miki, H.	T263	Mizoguchi, F.	1292, T030	Möricke, R.	1269, M425, S425	Murakami, M.	T101
Miki, T.	M144, T280, W014, W357	Mizoguchi, T.	1149, M082, S082,	Morii, H.	1059, T395	Murakami, S.	1141
Mikkola, A.	W502		T085, W071	Morikawa, K.	M416	Murakami, T.	M029, S029
Mikkola, T.	1204	Mizokami, A.	T247, T248	Morikyu, T.	M402	Muraki, S.	W307, W438
Mikulec, K.	T088, T089, W164	Mizuno, A.	1002	Morimura, N.	M201	Murata, N.	W431
Mikuni-Takagaki, Y.	W479	Mizunuma, H.	T395, T405	Morin, S. N.	T328	Murata, S.	W041
Milagre, K.	W383	Mlcak, R. P.	M487, S487	Morishima, T.	T159	Murooka, G.	W419
Milan, J. L.	W087	Moayyeri, A.	1281, M360, O360,	Morisoni, L.	T472	Murray, B.	W437
Milanesi, L.	T196		S360	Morissette, J.	1152, M475	Murray, L.	W269
Milas, M.	T480	Mochida, Y.	M011, M203, M270,	Morita, I.	M077, M078	Murray, M. A.	W338, WG41
Milassin, L.	T291, T427		S270, T142	Morita, Y.	W343	Murshid, S. A.	W061
Milbrink, J.	W473	Mochizuki, Y.	W209	Moriwaki, S.	T090	Murthy, S. M.	1245
Mildner, K.	M466, S466	Modlesky, C. M.	T516, T517	Moriyama, K.	T162	Musacchio, E.	W302
Millan, J. Luis	1236, 1259	Modlin, R. L.	1028	Moriyama, Y.	T085	Muschitz, C.	T291, T427, W446
Millard, S. M.	1021	Modzelewski, J.	1006, T183	Morko, J.	M407, W064, W210,	Musial, J.	T275
Miller, C.	W227	Moe, O. W.	T365		W214	Muto, A.	M082, S082, W071
Miller, F.	T516, T517	Moedder, U.	1235, 1262, 1268, T040,	Morley, P.	1130, M421, S421	Muto, K.	M365
Miller, L. M.	T112, W089, W467		T054	Morony, S.	1117	Mutoh, Y.	M375, S375
Miller, M. A.	W308, W310	Moermans, K.	1101	Morrell, M.	W415	Mutsuzaki, H.	W096
Miller, M. J.	W348	Mogensen, B.	1278	Morris, H. A.	1217, W402	Muzio, D. María	T271

(Key: 1001-1300 = Oral, O = Oral Poster, S = Sunday Plenary poster, M = Monday poster, T = Tuesday Poster, W = Wednesday Poster, WG = Working Group Abstract)

Muzylak, M.	1213, O064, M036, M064, S036, S064, T067	Nakayama, T.	T496	Nguyen, T. V.	1050, 1079, 1166, 1201, M358, O358, S358, T191, W340	Nolla, J. M.	M470
Myers, E. R.	M502	Nakchbandi, I.	1179, T007			Nomura, R.	M484, S484
Myoui, A.	T264, W013	Nakura, N.	W004, W336	Nguyen-Yamamoto, L.	M257	Nomura, S.	T127, W019
Myung, D.	M456	Nam, M.	T339	Ni, M.	M297, W114	Nomura, Y.	W186, W252
N							
Nabhan, F.	M312	Namba, A.	T084, T146	Nichol, M. B.	M442	Norbury, W. B.	M487, S487
Nabulsi, M.	1194, M283	Namba, N.	M486	Nicholas, J. Skye	W255	Nordheim, A.	M025, S025
Nachtrab, G.	W095	Nan, D.	T348, W326	Nicholson, G.	1033, T324	Nordin, B. E. C.	T417
Nadeau, J. H.	1241, T204, W173	Nan, M.	M075, T008	Nicholson, G. C.	T075, T354, W289	Nordstrom, S. M.	T137
Nadeau, J. M.	W249	Nanci, V.	T328	Nickel, E. D.	M018	Nork, S. E.	M153
Nadella, K.	T045	Nanes, M. S.	1143, M483	Nickelsen, T. N.	1165, 1260, 1269, T368	Norrudin, R. W.	M464
Nagai, S.	1189, 1190	Nango, N.	W462	Nickolas, T. L.	T490	Norris, J. S.	T257
Nagai, Y.	W479	Nantermet, P. V.	T042	Nicolella, D. P.	1045, M066, W050, W172, W176, W452	Norton, J.	M312
Nagamune, K.	T043	Naot, D.	T018, T174, T205	Nie, M.	W168	Noseworthy, C. S.	W137
Nagao, M.	1015	Napierala, D.	1184, W106	Niedzielska, D.	T015	Novack, D.	W359
Nagao, S.	W128	Napoli, N.	M292, W359	Nielsen, D.	W382	Nozaki, D.	M375, S375
Nagasaka, K.	M431	Narisawa, S.	1236, 1259	Nielsen, L. B.	W035	Nozawa-Inoue, K.	T127, T129
Nagasawa, K.	M262, O262, S262	Naruse, K.	W479	Nielsen, M. F.	T256	Ntougou Assoumou Hourfil, G.	M522
Nagase, Y.	1098, 1181, 1290	Narweker, R.	M471, S471	Nielsen, S.	T091	Nuche-Berenguer, B.	T207
Nagashima, M.	W336	Nashimoto, M.	M031, S031	Nielsen, T. Leo	M286, M467	Nuglozeh, E.	1287
Nagata, J.	1015, O390, M141, M390, S390, T153	Naski, M. C.	W034	Nielsen, W.	W382	Numasawa, T.	M273
Nagata, K.	O099, M099, M108, S099	Nasr, H.	T440	Niemeier, A.	T015	Nunn, C.	T063
Nagata, T.	T017, W411	Nasser, N. Edward	W222	Niemenen, M.	W454	Nurcombe, V.	T166, W036
Nagl, N. G.	M030	Nasser, W.	M352	Nieuwenhuijzen Kruseman, A.	W279	Nurre, J.	M508, S508, T386
Nagy, T. R.	1032	Natt, F.	1046	Nieves, J. W.	1096, M388, S388, T373	Nuti, R.	M275, M478, S275, T330, T514, W190, W298
Nagy, Z.	M138, M284, T124, T226	Natter, M.	W169	Niewolna, M.	1137, 1286, M305, S305	Nyenhuis, J. A.	T429
Nagyver, G.	W006	Naughton, G.	W486	Nifuji, A.	W115	Nygård, S.	W213
Nahar, N. N.	W085	Navarro, M.	T335	Nigam, N.	1244	Nyman, J. S.	W341
Naidu, S.	WG8	Naveh-Many, T.	M217, S217	Niger, C.	M054, T169, W027	O	
Naik, A.	1251, M023, S023, W098	Nawata, M.	W439	Nihtianova, S. A.	M493, S493	O'Brien, C. A.	1067, T184, T185, T190
Nail, L.	M299	Nawroth, P.	M459, S459, T416	Niida, S.	T090	O'Brien, T.	T349
Naka, H.	W357	Nayak, U. K.	WG4	Nikander, R.	W497, WG32	O'Byrne, J. M.	M057, M469
Nakagawa, K.	T136, T261, W118	Naylor, K. E.	W379	Nilius, B.	1101	O'Connor, R. D.	T208
Nakagawa, M.	W011	Neate, C.	T377, T389, W354, W363	Nilsson, A. G.	M194	O'Donnell, C. J.	1240
Nakagawa, T.	1102	Nechama, M.	M217, S217	Nilsson, M.	T310, W498	O'Keefe, R. J.	1251, M023, M039, M129, S023, S039, W098
Nakahama, K.	M077, M078	Need, A. Geoffrey	T417	Nilsson, M. I.	T361	O'Loughlin, P.	T171, W402
Nakahara, Y.	W493	Neff, L.	1069, 1248, 1250	Nilsson, M. L.	W490	O'Malley, B. W.	1235
Nakajima, H.	W503	Neff, M.	M330, S330, T381	Nilsson, S.	M245	O'Neil, T. Karla	W466
Nakajima, K.	T482, W141	Negus, C. Hugh	W496	Nilsson-Ehle, H.	M177	O'Neill, J.	W360
Nakajima, S.	M486	Nehme, A.	T289	Nimura, N.	W073	O'Rear, L. D.	M191, S191, W472
Nakamichi, Y.	1149, M082, S082, W072, W332, W492	Nelson, D. A.	1052	Nimura, Y.	1238	O'Sullivan, R. P.	W068
Nakamoto, T.	W012	Nelson, M.	M366, S366	Nindl, B. C.	W056, W496	O'Sullivan, S.	T018
Nakamura, C.	T076, W073	Nemere, I.	M258	Ninomiya, K.	M016, S016, T016	Oates, M. K.	M320
Nakamura, E.	1109	Nemes, C.	W396	Ninomiya, T.	M082, M106, M239, S082, S239, T085, W492	Oballa, R.	M291, S291
Nakamura, H.	1170, M106, M342, S342, W286	Nemes, I. D. A.	W396	Nirnberger, G.	T427	Obara, T.	W141
Nakamura, K.	1098, 1112, 1123, 1175, 1181, 1182, 1211, 1247, 1290, M127, S127, T102, T356, T439, W101, W307, W438, W453	Nemet, D.	W110	Nishimori, S.	M122	Obeid, O.	W507
Nakamura, M.	1098, 1290, M239, S239, T085, T102, T121, W072, W492	Nemeth, E. F.	O386, M228, M386, S386	Nishimoto, N.	W431	Obrant, K. J.	1073
Nakamura, M. C.	1291	Nemoto, K.	M154	Nishimura, H.	T013	Ochiai, E.	W022
Nakamura, S.	T070, T263	Nesheiwat, J.	M352	Nishimura, R.	M176, S176, T055, T243, W020, W092	Ochiai, H.	T031, T069
Nakamura, T.	1059, 1098, 1220, 1292, T163, T395, T405, W004, W181, W336	Nesti, L. J.	W039	Nishio, Y.	T247	Ochiai, N.	T128, T231, T502, W096
Nakanishi, R.	W181	Nestler, E.	1248	Nishizawa, Y.	T395, W357	Ochmanova, R.	W219
Nakano, K.	W005	Nestor, B.	W076	Nissen, N.	W382	Ochoa, L.	M434, S434
Nakano, S.	T456	Neumann, T.	W414	Nissen, P. H.	M222	Oda, A.	M302, T263
Nakano, T.	1059, T292	Neusch, G.	M290, M291, S291	Nissen-Meyer, L. Sofie	W213	Oda, H.	1034
Nakao, A.	M085, T077, T103	Neustadt, D. H.	W432	Nissenson, R. A.	1019, 1021	Oda, K.	M116, M239, M342, S239, S342, W059
Nakao, K.	1145	Neutsky-Wulff, A. V.	M272, O272, S272, T005, T093	Nissinen, L.	T241	Oda, N.	T066, T138
Nakashima, A.	M031, S031	Neviaser, A.	M430, S430	Niu, Q.	1088, 1122, 1231, 1232	Oden, A.	1060, 1200, M194, T343, W288
Nakashima, K.	1015, 1292, O390, M086, M141, M390, S086, 390, T030	Nevitt, M. C.	1053, 1271	Niu, T.	T217	Odgren, P. Rae	M146, S146
Nakashima, T.	M114, S114	Newhouse, M.	M421, S421	Nixon, M.	W360	Odvin, C. V.	M491
Nakatani, Y.	T334	Newitt, D.	T286	Niziolek, P. J.	1245	Oe, K.	T043
Nakatsuru, Y.	T168	Newman, N.	M117	Noble, B.	W055	Oerlemans, F.	M083
Nakayama, H.	W358	Newmark, R.	1208	Noda, M.	1015, 1292, O390, M086, M141, M390, S086, S390, T030, T126, T153, W012	Offermanns, S.	1123
Nakayama, K.	1034, W470	Newton, K.	1272, M339, S339	Noguchi, H.	M353, S353, T293, T341, T438, W328	Offord, E.	W407
		Ng, A.	M267	Noguchi, T.	W071	Ogasawara, T.	T356
		Ng, E.	W372	Nogues, X.	M288, M289, S288	Ogata, E.	M416
		Ng, M.	M282	Noh, T.	T026	Ogata, N.	1112, 1123
		Ngo, H.	W195	Nohe, A.	M190, W116	Ogawa, T.	T502
		Ngouala, G.	W018	Nohtomi, K.	T482	Ogawa, Y.	M365
		Nguyen, B. H.	W340	Nojima, J.	1034, W117	Ogborn, M.	W410
		Nguyen, C. K. T.	W340	Nöldge, G.	T416, WG26	Ogita, M.	M060, S060, T044
		Nguyen, H. T. T.	W340			Ogiwara, M.	W480
		Nguyen, L.	1028, 1029, 1222, M252			Oh, B.	T220, T221, T225, W257
		Nguyen, M.	1109, 1195				
		Nguyen, M. P.	M294, M296				
		Nguyen, N.	1050				
		Nguyen, N. D.	1079, 1166, 1201, W340				
		Nguyen, T. T.	M005				

(Key: 1001-1300 = Oral, O = Oral Poster, S = Sunday Plenary poster, M = Monday poster, T = Tuesday Poster, W = Wednesday Poster, WG = Working Group Abstract)

Oh, G.	1026	Olszynski, W. P.	M336, M371, S336, S371, T298, T299, T303, W281	P	Pachman, L. M.	W091	Park, S.	M075
Oh, H.	M139, T399, T400	Omelson, S.	W474	Pacicca, D. M.	1177	Park, S.	M247	
Oh, J.	T130	Ominsky, M. S.	1082, 1088, 1122, 1232, O409, M409, S409	Pacifici, M.	T082, W103	Park, S.	T033	
Oh, K. Won	T467	Ominsky, M. S.	W445	Pacifici, R.	1136, 1298	Park, S.	T078	
Oh, S.	M343	Omran, W.	T518	Pacitti, A. Peter	T144	Park, S.	W049	
Oha, F.	W119	Omsland, T. K.	T272	Pack, A.	W415	Park, S.	W282	
Ohara, M.	W256, W513, W517	Onate, S.	W152	Pack, S.	W317	Park, S.	W343	
Ohashi, Y.	1059, T395	Onikepe, A. O.	W316	Padalecki, S. S.	M296, M311, S311	Park, S.	W344	
Ohata, Y.	M488	Onitsuka, A.	1115	Padhi, D.	1129	Park, T.	W153	
Ohba, H.	T017, W411	Ono, A.	W343	Padilla, F.	T297	Park, W.	T339, W361, W435	
Ohba, S.	1112, 1175, 1247, M127, S127, T356	Onoda, T.	W419	Page, K.	1136, 1298	Park, Y.	T431	
Ohgawara, T.	T125	Onodera, K.	T503	Pagel, C. Neil	M120	Park, Y.	W126	
Ohishi, M.	W138	Onoe, Y.	W256, W513, W517	Paggiosi, M. A.	W379	Park-Min, K.	T079	
Ohishi, W.	M318	Onofrei, R.	W396	Pahr, D.	T368, W475, W476	Parker, A.	W106	
Ohlsson, C.	1200, 1218, M177, M245, T188, T199, T201, T310, W125, W135, W182, W314	Onyia, J. E.	1277, T012	Pajamäki, I.	1087, W500	Parker, R.	M310	
Ohnaka, K.	T176, T336, WG21	Oohata, T.	M395	Pak, C. Y. C.	T365	Parkinson, I. H.	M505	
Ohnishi, I.	W453	Ooshima, T.	W030	Palermo, L.	1057, 1090, 1094, 1161, M363, M418, T387, W280	Parkkari, J.	T331	
Ohno, T.	M131	Opresko, L. K.	M058, S058	Palmer, I. James	W501	Parrish, A. R.	T507	
Ohnuma, T.	M072	Oravec-Wilson, K. I.	W167	Palmer, W.	1208	Parson, H. K.	W448	
Ohsawa, M.	W419	Ordovas, J.	M285	Palmieri, D.	T019	Partridge, N. C.	T175, W026	
Ohta, H.	W256, W513, W517	Orellana, C.	M376	Palnitkar, S.	W058	Paruch, J.	W095	
Ohta, J.	M365	Orimo, H.	M342, S342	Palta, M.	M457	Pasanen, M.	T319	
Ohta, Y.	W118	Orito, S.	W256, W513, W517	Palummeri, E.	M379, S379	Pascal-Vigneron, V.	W287	
Ohtake, A.	1034	Orosz, L.	T124	Palvanen, M.	T331	Paschalis, E. P.	M447, S447, T486	
Ohtsu, N.	T293	Ortiz, D.	T444, T445	Pan, F.	W263	Paschos, G.	W408	
Ohue, M.	W290	Orwall, E.	M177, W125	Pan, G.	T052, W074	Pasco, J.	T324, T354, W289	
Ohya, K.	M101, M110, M114, S110, S114, T094, T095, W479	Orwoll, B.	M513	Pancheri, S.	M147	Pasparakis, M.	1294	
Ohyabu, Y.	M402	Orwoll, E.	1157, 1200	Panda, D. K.	W139	Paszty, C.	1122, 1231, 1232	
Oinuma, T.	T350	Orwoll, E. S.	1074, 1158, 1159, 1161, T476	Pandey, R.	WG18	Patchett, A.	W486	
Oishi, A.	W209	Orwoll, E. S. for the Mr Os Study group	W253	Pandruvada, S. N. M.	T257	Patel, D. D.	W044	
Oka, H.	W307, W438	Ory, S.	M073, S073	Pang, J.	M224, M227, M230, S227	Patel, M.	M490	
Oka, J.	W389	Osaki, M.	M473	Pang, L.	W170	Paterson, A.	W175	
Okabe, K.	M085, T077, T103	Osato, M.	1033	Pang, W.	W342	Paterson, N.	W360	
Okabe, T.	W103	Osato, M.	1033	Pang, W. Yin	W337	Path, G.	WG18	
Okada, C.	M375, S375	Osdoby, P.	W166	Panupinthu, N.	M062, S062	Pathak, S.	W463	
Okada, Y.	M136, T491, S136, W005, W439, W447	Oshima, H.	W220	Panyayong, K.	T506	Pathmanathan, D.	1105	
Okamoto, F.	M085, T077, T103	Oshima, Y.	1098, 1181, 1290	Pao, V.	M323, S323	Patntirapong, S.	W075	
Okamoto, K.	1289, T068, WG22	Ostrov, D. A.	M393	Papadimitropoulos, M.	M371, S371	Paton, L. M.	T349	
Okamoto, M.	T119	Ota, N.	M136, S136	Papaioannou, A.	1266, M328, M436, T332, T333, T396, W281, W360	Patrene, K.	1007, 1099	
Okamoto, S.	M353, S353, T293, T293, T405	Otero, J. E.	1294	Papapoulos, S. E.	M428	Patrick, A. L.	T353	
Okamoto, T.	M353, S353, T293	Otsu, N.	M353, S353	Papavasiliou, V.	1295	Patsch, J.	T164, T427, W441, W446	
Okano, H.	W256, W513, W517	Otsubo, O.	T496	Parent, J.	T001	Patsch, J. M.	W024	
Okano, T.	T136, T261, T311, T318, T439, W159	Otsuka, M.	W169	Parent, S.	T189	Patthanacharoenphon, C. G.	W481	
Okasaki, M.	W144	Otsuki, B.	W181	Parhami, F.	W023, W043	Paul, E. M.	1285	
Okayama, A.	W419	Ott, S. M.	M535, S535, T325, T351, W292	Pariente, E.	W326	Paula, F. J. A.	T428, W416	
Okazaki, J.	W162	Ottanelli, S.	T118	Parikh, N.	W423	Pauley, K. M.	M094	
Okazaki, M.	1189, 1190	Ou, Z.	T010	Parimi, N.	1159, M355	Paulsen, K. E.	W217	
Okazaki, R.	T069	Oursler, M. J.	1144, 1239, M024, M035, M070, M111, M152, M250, S152, S250, W028	Parise, C.	M442	Pavalko, F. M.	T506	
Okazaki, Y.	1034	Ouyang, H.	1108	Parisuthiman, D.	M203	Pavel, E.	T045	
Okudaira, S.	W181	Owan, I.	1034	Park, B. L.	T220	Pavel, I.	W057	
Okumura, H.	M131	Owen, H. C.	T177	Park, B. Lae	T221, T225	Pavlos, N.	M103, S103	
Okumura, S.	M479	Owman, C.	T201	Park, D.	M135, W042	Pavlos, N. John	1293, M104	
Okuno, J.	W394, WG12	Oxford, J. R. T.	M149	Park, E.	T223, W085, W257	Pavo, I.	1093, 1095	
Okura, T.	W394, WG12	Oyajobi, B. O.	M296	Park, E. K.	T220	Pawlak, G.	M073, S073	
Olbert, P.	T245	Oyamada, A.	T013	Park, E. Kyun	T221, T225	Payer, J.	W300	
Olde, B.	T201	Oyler, J.	W297	Park, H.	M199	Peacock, M.	T215	
Oldfield, P.	W133	Oyserman, S. M.	W109	Park, H.	M375, S375	Pearsall, A.	1132, 1230	
Olivares-Navarrete, R.	W002	Oz, O. K.	T032, T192	Park, H.	T378, T423	Pearsall, R. Scott	1132, 1230, 1233, M394, S394, W312	
Oliveira, A. A.	W383	Ozaki, R.	W159	Park, H.	W343	Pecaut, M. J.	M464	
Oliveira, C. Raquel P.	T428	Ozaki, S.	M302, T263	Park, I.	T401	Pedersen, L.	W035	
Oliveira, N. C.	W518	Ozanian, T.	W227	Park, I.	T409	Pedram, B.	M405, S405	
Oliveri, B.	T271	Ozato, K.	1145	Park, J.	W436	Pedrazzoni, M.	M379, S379	
Olivier, E.	M172, M173	Ozawa, A.	T483	Park, J.	M075	Pedula, K. L.	1271	
Olmos, J. M.	T348, W326	Ozcivici, E.	W499	Park, J.	M080	Peel, N.	M332, S332, W379	
Olmsted-Davis, E. A.	1071, M169, S169	Ozeki, S.	T077	Park, J.	M499	Pei, Y.	W170	
Olson, D. A.	1237	Ozkurt, I. C.	T179	Park, J.	T008	Pekkinen, M.	T046, W038	
Olson, G. T.	W211, W212, W217	Ozono, K. M137, M486, M488, W131	M218	Park, J.	T223	Pela, I.	T118	
Olson, M.	M443, S443	Ozturk, D.	M218	Park, J.	W153	Peleg, S.	W154	
Olstad, O. Kristoffer	W213			Park, J.	W282	Pellegrini, G. G.	W223	
				Park, K.	T224	Pells, S.	W093	
				Park, M.	T431	Pena, M. Jesus	M288, S288	
				Park, N.	M143	Penformis, F.	T281	
						Peng, J.	1019, 1021, 1026	
						Peng, X.	1026, 1072, M305, S305, T251	
						Peng, Z.	T193, W210	
						Penninger, J. M.	M096, S096	

Pennisi, A.	1172, 1173	Pippa, M. G.	M274, T209, W264	Pun, S.	M175, M411, S411	Rancier, M.	W287
Pennypacker, B.	M175	Pirker, T.	T291, T427, W446	Purdue, E.	W076	Randall, A.	W415
Pepe, J.	W356	Pirngruber, J.	M035	Purple, C. R.	M429	Randolph, R. K.	W338
Pepponi, G.	W271	Piscaer, T. M.	W346, W347	Purton, L. Elizabeth	W138	Rane, A.	T199
Percival, M.	M291, S291, W334	Pitts, K.	1010	Püschel, K.	1300	Rani, S.	T020
Pereira, F. Assis	T428	Piziak, V. K.	W362	Putkonen, M.	W009	Ranieri, P.	M236
Pereira, F. A.	W416	Plantalech, L.	W234	Puzas, J.	1252	Rantalainen, T.	W502
Pereira, R. C.	T428	Platt, I. D.	T047	Pye, K. Maura	W410	Rantanen, T.	1204
Pereira, R. M.	T273, W518	Pleshko Camacho, N.	1236, 1259			Rao, D. Sudhaker	M370, M480,
Pereira, R. M. R.	T326	Plesner, T.	1005				T484, W058, W420, W423,
Perera, S.	1017, T497, W239	Ploeg, H.	T509, W225				WG14, WG17, WG20
Pereverzev, A.	M109, T099	Plotkin, H.	T519			Rao, L. G.	T047
Perez, F. Javier	T449	Plotkin, L. I.	1011, M233, S233,			Rao, S.	T181, W331
Pérez Sáinz, M.	T327, W149		W057			Rapraeger, A.	T259
Pérez-Casellas, L. Angélica	T034	Pluskiewicz, W.	T274			Rapuano, B. E.	T171
Perez-Edo, L.	M288, S288	Podani, J.	T124			Raschke, M.	M193
Pérez-Martínez, F. C.	T232	Podgorski, A. L.	W212, W216			Rascon, Y.	M240
Peris, P.	T307	Poenaru, D. V.	W396			Rasheed, N.	M017
Perissinotto, E.	W302	Pohl, G.	W380, W381			Rasi, S.	W210, W214
Perkins, A. C.	W327	Poliachik, S. L.	M153			Rasmussen, H.	M221
Peruzzi, B.	T170	Pollak, M. M224, M227, M230, S227				Rastelli, A.	M292
Pessin, J. E.	W495	Pols, H.	W329			Ratajczak, T.	M225
Pessler, F.	W067	Polzer, K.	W443			Ratliff, J.	W007
Peters, C.	W065	Pomp, A.	T444, T445			Rauch, F.	1198, M489, S489, W426
Peters, K. D.	M152, S152	Ponce-de-Leon, H.	1010			Rauner, M.	T164, W024, W441,
Peters-Gdanitz, S.	W156	Pongchaiyakul, C.	T313				W446
Petersen, S.	M248, S248, W345	Ponnappakkam, T.	1229			Ravanti, L.	M407
Peterson, J.	1239	Poole, K.	T294			Ravaud, P.	M441, WG36
Peterson, J.	1268	Popa, D.	W396			Rawat, A.	WG18
Peterson, J.	M369, S369	Popoff, S. N.	1023, 1287, M008,			Ray, M.	1043
Peterson, M. C.	W417		M158			Raz, B.	W197
Peterson, M. G.	M430, S430	Porta, A.	1026			Raz, P.	W002
Peterson, M. G. E.	W468	Porte, R. M.	1223, W163			Raza, K.	M232, WG23
Petit, M. A.	T187, W521	Porter, D.	1156, T314			Raza, S.	M352
Petit, S.	W287	Porter, F. D.	T471			Reagan, M.	T252
Petkov, V. I.	T266, T337	Portero-Muzy, N.	W339			Realdi, G.	W318
Petri, A.	W006	Possmayer, F.	M062, S062			Rebhun, J. F.	W338
Petrick, A.	W378, WG38	Poston, S.	W366			Recker, R. R.	1164, M279, M327,
Petrigliano, F.	M046	Posvar, E.	1129				M434, M512, S279, S434, S512,
Petrucci, M. Teresa	W356	Potts, J. T.	1189, 1190, W144				T296, T359, T389, W263, W308,
Pettersen, P. C.	M356, S356	Poulsen, C. Søndergaard	W160				W310, W354, W363, W368
Pettersson, U.	1051	Poulsen, R. C.	T362			Recknor, C.	1055, M423, O423,
Pettit, A. R.	1186, M015, T140	Poulton, I. J.	1020, 1068, 1150				S423, W363
Pettway, G.	M001	Pounds, S.	W273, W274			Reddy, R. Beeravolu	T441
Petty, S. J.	T349	Pourfathi, S.	M357			Reddy, S. V.	1103, M480, T257,
Pflugmacher, R.	T258, W397	Powderly, W. G.	M469				T441, W077
Phadke, R. V.	WG18	Powell, W. F.	1047			Redl, H.	W108
Phang, D.	T080	Pozzi, M.	W325			Redlich, K.	W443
Phillips, J.	1131, M462	Pramyothin, P.	T315, T320			Redline, S.	1157
Phipps, R.	M505, M508, S508, T386,	Pratap, J.	M047, M295, S047, S295			Redmond, J. M. T.	W437
	W325	Prejbeanu, R.	W396			Reed, I. R.	M476
Phipps, R. J.	W240	Prenovost, K.	W280			Reed, S.	1272
Pi, M.	M229	Presig, P. A.	T365			Reed, S. D.	M339, S339
Piazza, N.	W223	Prevhal, S.	T476			Reeder, J.	T476
Picard, C.	1035	Price, B.	M494			Reeve, J.	M360, O360, S360, T294
Picard, F.	M048	Price, C.	1242, T204			Reeves, J.	W133
Piccini, E.	W321	Price, H. Elizabeth	T492			Reginster, J. Y.	W354
Pick, A.	M326	Price, J.	M523, S523			Rehage, M.	T080
Pickard, L.	T333	Price, J. S. 1213, O064, M036, M064,				Rehman, S.	M008
Pickarski, M.	M290, M291, S291		S036, S064, T067			Reichenberger, E. J.	M26, S2688
Pienkowski, D.	T314	Price, R. I.	T269			Reid, D. M.	1075, 1077, M359
Pieper, C.	1055, W398, WG27	Priemel, M.	1300, W477			Reid, I. R.	M415, M434, M449,
Pierce, J. R.	W056	Prince, R.	1033				S415, S434, T174, T205, T376
Pierroz, D.	1126, 1134	Prince, R. L. 1054, 1203, T269, T321,				Reilly, G. C.	T154, T508
Pietschmann, P.	T164, W024, W441,		W226			Reilly, P.	T392
	W446	Prior, H. J.	M351, S351			Reimer, R.	T360
Pignolo, R. J.	1156	Prior, J.	M336, S336			Reina, P.	W236
Pihlavisto, M.	T241	Prior, J. C. 1266, M371, S371, T187,				Reina, P. S.	W235
Pike, J. Wesley	1067		W281, W511			Reiners, C.	M367
Pilbeam, C.	1234, M168, M180,	Proctor, A.	M510			Reinhardt, R. A.	W324
	W037, W333	Prouillet, C.	M162			Reis Neto, E. Torres	W440
Pinedo, G.	W326	Provot, S.	M122, W095			Rejnmark, L.	1049, T453, W151
Pingle, J.	WG4	Prueksaritanont, T.	M290			Ren, S.	1028, 1029, M253, S253
Pinheiro, M. M.	T312, W275, W283,	Przedlacki, J.	T275			Renn, K. E.	T096
	W440, W442	Puapong, R.	T315, T320			Rensen, P. C.	T015
Pintar, J.	M189	Puder, J.	W519, WG30			Repeke, C. Eduardo P.	M181
Pinto, A. S.	W518	Pui, M.	W360			Reppe, S.	W213
Pioletti, D.	T041	Pulkkinen, P.	W454			Requejo, H.	M496
Pioli, G.	M379, S379	Pullen, A.	W312			Resch, H.	T291, T427, W446

Q

Qi, H.	1014, T157, T435
Qi, J.	1013
Qiao, N.	T309, W267
Qin, L.	T175, T178
Qin, M.	M189
Qin, X.	T080
Qin, Y.	T426, W467, W482
Qiu, D.	M208, S208
Qiu, G. Xing	M034
Qiu, S.	W058
Qiu, T.	1256, M205
Quach, J. M.	W025
Quarles, L. Darryl	1142, 1227, 1296,
	M229
Que, I.	W046
Quesada, J. Manuel	T050
Quesada Gómez, J. M.	T316
Quick, J. L.	WG41
Quigley, C. M.	T483
Quijano, M.	W320
Quin, L.	T381
Quincey, D.	M287
Quinn, J. M. W.	1150, T012, T081
Quinn, S.	M224, M227, M230, S227,
	W265
Quintana, R.	M240
Quiroga, I.	W319
Qvist, P.	M264, T135, T245, W205,
	W478

R

Rabbitt, E. H.	M232, WG23
Rabin, H.	W360
Racewicz, A.	T382
Rachidi, M.	T295
Radács, M.	W006
Radominski, S. Cesar	M454
Radspieler, H.	M330, S330, T381
Raggatt, L.	1186, M015
Raggi, P.	T488
Raghow, S.	M406
Ragi-Eis, S.	M380, T383, W383
Rahkila, P.	1083, W009, W506,
	W515, W516
Rahman, M.	1135, M397, S397
Raileanu, D.	T520
Raisz, L.	1234, M168, M180, W037,
	W333
Rajamannan, N. M.	1154, M035,
	M152, S152
Rajan, S.	W143
Rajatanavin, R.	T313
Ralston, S.	1033, 1036, 1199
Ramachandran, M.	W164
Ramachandran, R.	W215
Ramage, S. Cowan	M156, T144
Ramalho, L. Naira Z.	W416
Ramamurthi, K.	W224
Ramamurthy, R.	M451
Ramaswamy, G.	1065, W464
Ramesh, V.	WG18
Ramírez, E.	T316
Ramlau-Hansen, C. Høst	W151
Ramos, C.	T348
Rana, A.	T375

(Key: 1001-1300 = Oral, O = Oral Poster, S = Sunday Plenary poster, M = Monday poster, T = Tuesday Poster, W = Wednesday Poster, WG = Working Group Abstract)

Retting, K. N.	M171, S171	Roehrig, G. J.	T443	Rufo, A.	W080	Salovaara, K.	M344, M452, S344,
Reveles, X.	T470	Rogers, A.	T366	Ruiz-Requena, M.	T454		S452
Reviriego, P.	W045	Rogers, C.	T038	Rundek, T.	M481, W145	Salovaara, K. T. J.	1270
Reyes, R.	T307	Rogers, J. T.	M062, S062	Rundle, C. H.	1223, W163	Saltzman, M. W.	W143
Reyes García, R.	T454	Roh-Schmidt, H.	W338	Runge, M.	M256, M278, M453,	Salvadori, S.	W190
Reynolds, J. C.	WG6	Rojas, J. A.	I036		W284	Salvatori, R.	T428
Rhee, S.	M343	Rojroonwasinkul, N.	T313	Runnels, J.	W195	Salzmänn, G.	M476
Rhee, Y. T033, W049, W126, W251		Rokutanda, S.	M123, S123	Ruppel, M. E.	W089	Sam, K.	1184
Rho, J.	W153	Roldan, E.	T194	Russell, R. G. G.	W320, W325	Samadfam, R.	M231, W127, WG1
Rho, M.	T378	Rolland, F.	T246	Russo, L. A.	W385	Samarawickrama, D. B.	T026
Rice, T. S.	T483	Romagnoli, E.	W356	Russo de Boland, A.	T064, T196	Samaropoulos, X.	T266
Richard, C.	M231, W127, WG1	Román-García, P.	T216	Rutledge, J.	W324	Sambrook, P.	1033, 1279, T349,
Richardson, P.	W195	Romera, M.	M470	Ryan, K. A.	W184		W365
Richie, S.	T323	Ronda, A. Carolina	T194	Ryan, M. R.	I136	Samee, M.	W016
Rico, M. C.	I023	Ronis, M. J. J.	W348	Ryan, P.	M366, S366	Samelson, E. J.	1240
Ricofort, R.	M092	Roodman, G. David	I007, I099,	Rybak-Feiglin, A.	I128	Samji, F.	T323
Riehle, U.	T046		I152, M007, M037, M477, M479,	Rybchyn, M. S.	M014	Sampalis, J. Sotirios	T432
Riera, H.	W018		S477, T248, W152, W195	Rychly, J.	T049	Sampson, H. W.	T507
Ries, W. L.	T257, W077	Roos, B. A.	M414	Ryg, J.	W382	Samuelsson, B.	M408, W335
Rietbrock, S.	M443, S443	Roque, J. P.	W275	Ryoo, H.	M020, M199, T033, T139	San Martin, J.	1205
Rifkin, D. B.	M202, S202	Roschger, P.	M437, M447, S437,	Ryser, M. D.	I244	Sanchez, T. V.	T276, T277
Riggert, J.	W406		S447, T464, T486, W271	Ryu, J.	M088, M398	Sancho, V.	T207
Riggs, B. L.	I193, M369, S369,	Rose, C.	T294	Ryu, M.	T133	Sandell, L. J.	M132, T259
	T460, W218	Rose Meyer, R.	W078			Sanders, J. J.	W062
Riggs, M. M.	W417	Rosen, C. J.	I090, I094, I138, I228,			Sanderson, R.	I171
Riha, D.	W050		I235, I253, O021, M021, M190,			Sanjay, A.	I023
Riihonen, R.	T091		M269, M285, M418, S021, T201,			Santiago, R.	T050
Riis Madsen, A.	W382		T217, W183, W401			Santiago-Parton, S.	M528, S528
Rikkonen, T.	I270, M452, S452	Rosen, E.	I233			Santillán, G.	T064
Riminucci, M.	M178	Rosen, V.	W112			Santora, A. C.	I128
Rimmer, M.	W192	Rosenblatt, M.	I299, T252, W147			Santos, C. Marques	T428
Rimoin, D. L.	I261	Rosenthal, H.	W422			Sanyal, A.	I235, I239, W028
Ringe, J. D.	I260, T374, T442	Rosenthal, M.	T246			Saran, M. J.	T051
Ringertz, H.	M195	Roshak, A.	I131			Sarawate, C.	W366
Rintala, J.	T331	Rosmalen, F.	W156			Sarfarazi, M.	T470
Rio, M. Esther	W223	Ross, C. L.	W211			Sarkar, G.	M306
Ripoll, V. M.	M015	Ross, F. Patrick	I146			Sarkis, K. S.	W440, W442
Rissanen, J. P.	M407, T239, T241,	Ross, J. L.	T104, W335			Sarmasik, A.	M479
	W210, W214	Ross, P. D.	T315, T320			Sartori, L.	W298, W302
Risteli, J.	W064, W210, W214	Ross, T. S.	W167			Sasakabe, H.	W090
Ristimaa, V.	W515, W520	Rossignol, M.	M372			Sasaki, A.	T082
Ritchie, R. O.	M392, S392, W455	Rossini, G.	W111, W341			Sasaki, H.	T341, T438, W328
Ritter, C. S.	M226, W140	Rothman, B.	M172, M173			Sasaki, K.	T161
Rittling, S. R.	T086	Roubenoff, R.	T347			Sasaki, S.	W517
Rittweger, J.	W234, W236, W484	Roudier, M.	M307, S307			Sasisekharan, R.	I171
Rivadeneira, F.	I199	Rousche, K. T.	T048			Sasonova, N. Ivanovna	W364
Rivas, D.	M038, M048, M243, W155	Rousseau, C.	I152			Satcher, R.	T253
Rivera, M. F.	M385	Routson, S. M.	M128			Sato, H.	T147
Rizzo, J. H.	I271	Roux, C.	I075, I077, M345, M359,			Sato, K.	M114, S114, T482, W141
Rizzoli, R.	I041, I121, I243, M455,		M438, M441, T344, T382,			Sato, M.	I012, I093, I095, M031,
	T463, W401, W404		T412, W374, WG36				S031, W202
Rizzoli, R. E.	T466, W519, WG30	Roux, C. H.	M287			Sato, S.	I061, M049, M133, S049,
Roach, H. Isolde	M184	Roux, J. Paul	T461				S133, W100
Robb, R.	T460	Roux, S.	M474, M475, T001			Sato, T.	W130, W419, W434
Robben, T. J.	W450	Rowe, D. W.	I044, I045, I215			Sato, Y.	T352
Robbins, J.	I272, T325	Rowe, G. Cameron	I248, I250			Satomi, K.	M395
Roberts, A.	M297, M310	Rowe, P. S. N.	I118, I155, I226,			Satomura, K.	M488
Roberts, A. J.	M294, M296		W050			Saukkonen, T.	M281, S281
Roberts, H. C.	T004	Roy, R.	W088			Sävendahl, L.	M121, S121
Robertson, S. T.	T357	Rozas, P.	T454			Sawatsubashi, S.	W022
Robinovitch, S. N.	W399	Rozas-Moreno, P.	T167			Sawka, A. M.	T333
Robinson, A.	W192	Rozen, N.	M042, T009			Sawyer, R. Kay	W402
Robinson, M.	I129, I232	Rozhinskaya, L. Y.	W364			Saxena, R.	T052
Robinson, P.	M312	Ruan, M. M.	M111			Saxon, L. K.	M036, M064, M523,
Robling, A. G.	I245, W050, W456	Rubert, M.	W319				S036, O064, S064, S523, W485
Robson, P. J.	W269	Rubin, B.	M045, S045			Sbaiz, F.	T053
Roccaro, A.	W195	Rubin, C.	W182			Scadden, D. T.	W138
Rocher, E.	T477	Rubin, C. T.	M493, S493, T426,			Scalletta, C.	T041
Rockwood, A. L.	M358, O358, S358,		T510, W495, W499			Scerpella, T. Ann	I037
	T191	Rubin, J.	M517, T505			Schacht, E.	M256, M278, M453,
Rodd, C.	M489, S489	Rubin, M. R.	I164, M485				T442, W284
Rodda, S.	I020	Rubin, M. Ruth	T485			Schaden, W.	W346, W347
Rodova, M.	T149	Rubio, R.	M496			Schafer, A. L.	W215
Rodrigues, P. M. L.	T210	Rucci, N.	T170, W080			Schäfer, V.	T393
Rodriguez, S.	M054	Ruckle, J.	I132			Schaffler, M. B.	M403, S403
Rodríguez-García, I.	T216	Rud, B.	W301			Schanen, N. C.	T208
Rodríguez-García, M.	T216	Rudkin, G. H.	T051			Schauber, J.	M238
Rodríguez-Moreno, J.	M470	Rudnik, V.	T195			Scheepers, M. G.	W450

S

Saadat, R. L.	M445		
Säaf, M.	M195		
Saag, K. G.	M324, M354, M378,		
	M440, M444, S281, T380		
Saarinén, A.	M281., S281		
Saavedra, P.	T335		
Saba, O. I.	M326		
Sabanai, K.	W004, W336		
Sabokbar, A.	T092		
Sacchetti, B.	M178		
Sacco, R.	M481, W145		
Saccol, M. F.	W518		
Sadrzadeh, N.	M421, S421		
Saemann, A.	W414		
Safadi, F. F.	I023, I287, M008, M158		
Saftig, P.	W065		
Saha, P. K.	M326		
Sahlqvist, A.	W182		
Sahni, S.	T317		
Sainsbury, A.	I134		
Sairyo, K.	T155		
Saita, Y.	I015, M390, O390, S390,		
	W503		
Saito, A.	T390		
Saito, H.	I248, M101, M110, S110		
Saito, K.	W434, W439		
Saito, T.	I112, I175, I182, I185,		
	M12, S1277		
Saito, T.	T439, W101		
Sajavaara, T.	W009		
Sakaguchi, T.	W157		
Sakai, A.	W004, W336		
Sakai, M.	W513, W517		
Sakai, S.	T072		
Sakai, Y.	T043		
Sakamoto, K.	T035, T070		
Sakamoto, T.	M276		
Sakamoto, Y.	T434		
Sakane, M.	T128, T231, W096		
Sakata, K.	W419		
Sakhaee, K.	M383, M491, S383,		
	T365		
Sakon, J.	I229, M204		
Sakuma, M.	T350		
Salach, L.	M436, T332, T396		
Sale, C.	W001		
Saleh, H.	I150, T081		
Saleess, N.	W465, W466		
Salihoglu, S.	I023		
Salminen, H. S.	M195		
Salmivirta, M.	T241		
Salo, G.	M288, S288		

(Key: 1001-1300 = Oral, O = Oral Poster, S = Sunday Plenary poster, M = Monday poster, T = Tuesday Poster, W = Wednesday Poster, WG = Working Group Abstract)

Scheid, J. L.	T197, T200	Seim, H. B.	M200	Shi, Z.	1072, M084, M102, S084	Sigurdsson, S.	1278
Scheinfeld, V. L.	M128	Seino, Y.	W371	Shibanuma, N.	T043	Silkman, L. J.	T111
Scher, J.	M399, S399	Seitz, S.	1300	Shigenobu, K.	W119	Siller-Jackson, A. J.	M520, T504
Schett, G.	W443	Sekiguchi, S.	T066, T138, W128	Shih, M.	T429	Silva, A.	W095
Schilling, A.	T015	Sekiya, I.	T126	Shiizaki, K.	W157	Silva, J. Santana	M181
Schiltz, C.	M162	Selby, P.	M476	Shim, S.	M410	Silva, M. J.	M518, S518
Schimmer, R. C.	T389	Selim, A. A.	W258	Shim, S.	M499	Silva, O. Lopes da	W339
Schindeler, A.	W164	Selim, A. H.	M128	Shim, Y.	T133	Silva, R. G.	W442
Schindler, C.	M358, O358, S359, W519, WG30	Sella, S.	W318	Shimabuku, N.	W177	Silva, T. S.	T210
Schinke, T.	1300	Sellmeyer, D. E.	1161, M323, S323	Shimada, A.	W115	Silva-Netto, F.	W302
Schipani, E.	1024, 1119, T011, W138	Selvamurugan, N.	W026	Shimada, K.	T065, W358	Silve, C.	1031
Schirmer, A.	T112, W467	Semel, J.	T440	Shimada, M.	1024	Silver, J.	M217, S217
Schmidt, A.	1012	Semirale, A. A.	T202, T203	Shimada, Y.	M472, T341, T438, W328, WG24	Silverberg, S. J.	M481, M485, T481, T485, T486, W145, W146
Schmidt, J. A.	W211, W212, W216, W217, W423	Semon, C.	T281	Shimamoto, S.	T487	Silverman, N.	M183
Schneider, D. K.	M400	Semrad, U.	T164	Shimamura, T.	W419	Silverman, S.	W294, W384
Schneider, J.	W378, WG38	Sen, B.	M517, T505	Shimizu, E.	W026	Silverman, S. L.	1206, T279, T384, W366, W367
Schneider, P.	M367	Sen, S. S.	T447, WG34	Shimizu, M.	W181	Silvestri, S.	T213
Schneider, R. A.	W040	Senger, C.	M490	Shimizu, O.	T146	Simanainen, U.	1018
Schoeller, M. C.	T278, T455	Senk, F.	W245	Shimizu, S.	W097	Simi, C.	M504, O504, S504
Schoenborn-Kellenberger, O.	1168	Senn, J.	M480	Shimizu, Y.	W004, W336	Siminoski, K.	W281, W285
Scholes, D.	1272, M535, S535, T351, W292	Senoh, S.	T085	Shimo, T.	T082	Simmons, H. A.	1014, T435
Schoppet, M.	1009	Sepanski, R.	M324, M352	Shimohata, N.	M097	Simões, F. V.	W383
Schorr, K.	1187	Serota, A.	W468	Shimokawa, H.	T095	Simon, J. B.	T407
Schott, A.	1167	Serrano, E.	M092	Shimokawa, I.	T457	Simon, L.	M275, S275
Schousboe, J. T.	1076, M355	Seto, H.	T017, W411	Shimomura, Y.	T136	Simon, R.	W271
Schreck, B.	M430, S430, W468	Setoguchi, T.	M303, S303	Shin, C. S.	M044	Simonds, W. F.	T483
Schreiweis, M. A.	1277	Setterberg, R. B.	M417	Shin, C. Soo	M209	Simonelli, C.	T278, T455, W367
Schroder, K.	M015	Seufert, J.	WG18	Shin, H.	W273, W274	Simonet, W. S.	1122, 1231, 1232
Schroeder, J.	1082, M409, O409, S409	Sh, Q.	T116	Shin, H. Doo	T220, T221, T225	Simpson, J. M.	1279
Schubert, R.	W229, W449	Shafer, M.	W406	Shin, J.	M115	Sims, J.	W348
Schüler, C.	M466, S466	Shah, A.	T315, T320	Shin, S.	T120	Sims, N. A.	1020, 1068, 1150, T012
Schulman, A.	T444	Shah, E.	1136, 1298	Shin, Y.	M398, W262	Sims, S. M.	M062, M109, S062, T099
Schulmerich, M. V.	T108	Shaheen, S.	M068, S068	Shindo, H.	M473, T457	Sinaki, M.	M472, W393, WG24, WG25
Schultess, J.	W156	Shaikh, A.	M212, S212	Shinoda, Y.	1123	Sinding, C.	1195
Schultis, H.	T393	Shalev, A.	W465	Shinoff, C. W.	M349, S349	Singer, J. B.	W173
Schultz, M.	M427, S427	Sham, P.	M282, T214, W175	Shinohara, M.	1289	Singer, M. V.	T007
Schwartz, A.	M299	Shanahan, I.	T156	Shinomiya, K.	1061, M049, W097, W100	Singh, H.	M400, T436
Schwartz, A. V.	1057, 1161	Shane, E.	1164, M327, T486, T490, W415, W444	Shipp, K. M.	W398, WG27	Singh, R.	M369, S369, T445
Schwartz, E. N.	M242	Shanmugarajan, S.	1103, T257, W077	Shirai, Y.	T128	Singh, T.	M074
Schwartz, H.	W187	Shao, J. Su	O185, M185, S185, T165	Shiraki, M.	1059, T395	Singha, U. K.	M007
Schwartz, S.	1198	Shao, Y. Y.	M118, M119, S118	Shiroo, M.	M408, W335	Singhal, S.	W070
Schwartz, Z.	M187, W002, W421	Shapiro, J.	T437, WG8	Shitaye, H.	W109	Sinha, K.	1249
Schwarz, E.	1251, M129	Sharkey, L. C.	W299	Shivdasani, R.	1184	Sinha, N.	T444, T445, W468
Schwarz, E. M.	1100, M023, S023, T163, W098	Sharma, A.	T421, WG33	Shlipak, M. G.	T325	Sinner, P. J.	T455
Schwarz, P.	M248, S248, T446, W345	Shaughnessy, J.	1171	Shoback, D.	1176, 1284, M223, O223, S223, WG5	Sinnott, B.	M370
Schwarze, U.	1261	Sheeche, P. R.	T430	Shobuike, T.	M099, O099, S099, W067	Sinomiya, K.	M133, S133
Sciaudone, M. P.	T470	Shelton, R. S.	1011, 1086, T184	Shogo, A.	T066	Siperstein, A.	T480
Scodelaro Bilbao, P.	T064	Shemian, B.	T009	Shogren, K. L.	M306, T254	Sipilä, S.	1204
Scott, G.	1043	Shen, C.	W313	Shoji, T.	T013, W003, W048	Sipos, A.	1093, 1095
Scott, J. Paul R.	W001	Shen, Q.	1151	Shon, H.	T401	Sips, H. C. M.	W046
Sculco, T.	W076	Shen, V.	1125, W063	Shore, E. M.	1151, 1156, T478	Sirola, J.	1270, M452, S452
Scutt, A.	T508	Shen, W.	W496	Short, W. H.	T430	Sison, C.	T444, T445
Seaman, P.	W239	Shen, X.	1065	Shriver, Z.	1171	Sitara, D.	1114
Searby, N. D.	M462	Shen, Y.	M405, S405	Shu, A. D.	W444	Sittichokechaiwut, A.	T154, T508
Sebastian-Ochoa, A.	T454, W405, T167	Shen, Z.	W068	Shuhaiber, M.	W437	Siviero, P.	W298
Sebba, A.	W303, W365	Shen-Or, Z.	W197	Shuldiner, A. R.	W184	Siyambalapitiyage, W.	T192
Secer, R.	T015	Sheng, H.	T178	Shulman, G.	1248	Sjögren, K.	1218, W314
Secreto, F. J.	W021	Sheng, M. H. C.	1223, M112, O112, S112, W008	Shulman, M.	T432	Skag, A.	T387
Sedarati, F.	T377, T383, W354	Sheng, X.	1022, W294	Shultz, K. L.	W008, W183	Skalicky, M.	1009, M466, S466
Seeber, R.	M104	Shenouda, N.	M489, S489	Shuto, E.	T493	Skarantavos, G.	T402, W208, WG19
Seehra, J.	1132	Shephard, J.	T270	Shyr, C.	T198	Skedros, J. G.	M461, M463
Seeman, E.	1039, 1083, 1197, M333, M334, M508, S508, T289, T458, W515	Shephard, R. J.	W343	Si, J.	1256	Skinner, C. M.	M052, S052
Seestaller-Wehr, L. M.	1010	Shergy, W.	1208	Si-hoe, K.	W199	Skinner, R. A.	W348
Segal, E.	W197	Sherk, V. Dawn	W504	Sibai, T.	1184	Skrpnikova, I. A.	T385
Segawa, H.	1115, M214, S214	Sherman, M. L.	1132	Sicard, G.	M226	Skyvarova, B.	W245
Segre, G. V.	1123	Sherrill, D.	T288	Siclari, V. A.	T260	Slater, H.	WG41
Seibel, M. J.	1018, T062, 1006, 1279, O358, M298, M358, S298, S358, T182, T183, T191, W486	Sherwood, R. J.	W174, W179	Siegel, P.	1295, T237	Slater, S. A.	M259, S259
Seijo, M.	T271	Sheu, T.	1252	Sierra, O. L.	1140, T036	Slatopolsky, E.	M226, W140
		Sheu, Y.	T353	Sierra-Zorita, R.	W303	Sliney, J.	T485
		Shi, J.	M167	Siervogel, R. M.	W174, W179	Slyfield, C. R.	W481
		Shi, M.	1010	Sievänen, H.	1087, 1204, T319, W457, W497, W500, W502, WG32	Smerdel-Ramoya, A.	1178, T172, W122
		Shi, Q.	T114, T117	Siffert, R. S.	T301	Smets, N.	T132
		Shi, W.	1256	Siggeirsdottir, K.	1278	Smith, B. J.	T363, T410
		Shi, X.	T057, T180	Sigurdsson, G.	1278	Smith, C. L.	W305
		Shi, Y.	T056				

(Key: 1001-1300 = Oral, O = Oral Poster, S = Sunday Plenary poster, M = Monday poster, T = Tuesday Poster, W = Wednesday Poster, WG = Working Group Abstract)

Smith, D. D.	T436	Sprague, S. M.	T249	Strivers, C.	1288	Svensson, O.	1051, M361
Smith, D. H.	W378, WG38	Squire, M. E.	T510	Strohbach, C. A.	T034, T037	Svoboda, M.	T262
Smith, D. K.	T214	Sran, M. M.	W399	Strong, D. D.	1288, T034, T037	Swaissland, A.	W189
Smith, E.	T026	Sriarj, W.	T095	Strotmeyer, E. S.	1161, T346	Swaminathan, S.	M378
Smith, E. A.	1014	Sricholpech, M.	T142	Stroup, G. B.	1131, O386, M386, M427, S386, S427, W063, W134	Swanson, C.	1218, T199
Smith, E. J.	T056	Srikusalanukul, W.	M460	Stuart, M.	W189	Swerdlloff, R.	1018
Smith, E. L.	T509	Srinivasan, B.	W218, W418	Studenski, S. A.	1053	Swift, J. M.	M514, S514, W490, W498
Smith, I. C.	W192	Srinivasan, S.	T150, W060	Study Group K	T495	Swindell, D. K.	W379
Smith, J. Jermaine	T516, T517	Srivastava, A. K.	O112, M112, S112, T211, T212	Stumpf, U. C.	M211, W369	Swirski, A.	T275
Smith, K. C.	M308	St-Adaud, R.	M033, S033, W112	Stupphann, D.	T164, W024, W441, W446	Swoboda, K. J.	W077
Smith, N.	W098	Staab, J. S.	W056	Stüssi, E.	W459, W469	Syal, R.	WG18
Smith, N. M.	M258	Stadmeyer, L.	1178, 1233	Su, A. I.	T214	Syberg, S.	M248, S248, W345
Smith, P. N.	M460	Stains, J. P.	T169, W027	Su, H.	W139	Syed, F. A.	M250, S250, T195
Smith, R. J.	T112	Stallone, J. L.	1110, M514, S514, T361, W490, W498	Su, N.	T157	Szabo-Davenport, K. A.	M328
Smith, S. Y.	1082, O409, M406, M409, S409, W221, W308, W310	Stampa, B.	M325	Su, Q.	M175	Szabova, L.	O165, M165, S165, M167
Smith, T. F.	T111	Stanford, W. L.	W138	Subler, M. A.	M477, S477	Szatkowski, J. P.	M306
Smith, U.	M177	Stauffer, B.	1010	Subramaniam, M.	1144, 1154, M035, M070, M152, S152, W021, W028	Szejnfeld, V. L.	W440
Smolen, J.	W443	Ste-Marie, L.	M350, M364, S364, W368	Suda, R. K.	1156	Szulc, P.	M468, S468
Snel, A.	M272, O272, S272	Stebbins, E. G.	M305, S305	Suda, T.	1102, M016, S016, T016	Szymczyk, K. H.	W120
Snow, C. M.	M530, S530, WG29	Stefanick, M. L.	M355	Sudhakar, S.	M026		
Snyder, R.	T215	Stein, E.	T444, T445	Sudhakaran, S.	W466		
Sobhan, U.	W059	Stein, G. S.	1144, 1258, M022, M047, M143, M295, S047, S295, W036, W200	Suematsu, A.	M114, S114		
Sobolev, B.	T413	Stein, J. L.	M022, M047, M143, M295, S047, S295	Suetsugu, Y.	T128		
Sodek, J.	M087	Steinberg, D. Michelle	M242	Suga, Y.	W462		
Søe, K.	1005	Steinbuch, M.	T408, W296	Sugatani, T.	M090, S090		
Soeta, S.	T083	Steinhoff, G.	T049	Sugawara, Y.	M006, T173, W061		
Sogabe, N.	M342, S342, T318	Stejskal, D.	W219	Sugimoto, T.	M056, M059, M316, M484, S056, S316, S484		
Soldano, S.	T019	Stene, L. C.	W272	Sugino, S.	M214, S214		
Solichova, P.	W219	Stenkjær, L.	T218	Sugishita, H.	W434		
Solomon, D. H.	M354	Stenova, E.	W300	Sugishita, T.	W290		
Somer, M.	M281, S281	Stenström, M.	1200	Sugita, A.	1224, M416, W092		
Somes, G.	W520	Stepan, J. J.	1093, 1095	Sugiyama, T.	M523, S523		
Sommer, S.	M207	Stephens, A.	1033, 1246	Suh, C.	T222		
Sommer, U.	M459, S459, T416	Stephens, A. S.	T073	Suh, H.	W370		
Somoza, J.	W223	Stephens, S.	M073, S073, W078	Suh, K.	T378		
Son, M.	M167	Stephens, S. R. J.	T073	Suhara, Y.	T136, T261, T311, W159		
Sondergaard, T. Esben	1005	Stephure, D.	M489, S489	Sujic, R.	M439, WG35		
Sone, T.	T395	Sterchi, D. L.	1277	Sukhija, K. B.	1245		
Song, H. Kwon	M329	Sterling, J. A.	M294, M296, M297, W188	Summer, L. R.	W490		
Song, I.	T091	Sterling, T. M.	M258	Sun, B.	1008		
Song, J.	1016, 1273	Stern, D.	M079	Sun, H.	1138		
Song, N.	M398	Stern, P. H.	1192, W091	Sun, H. J.	M044, M209		
Song, X.	W320	Stevens, D.	M532	Sun, H. Min	T100		
Song, Y.	T214	Stevens, K. T.	M515	Sun, L.	1153, M198		
Soo, C.	1105, M200	Stewart, A.	1075	Sun, Q.	M526, W171, W178, W185		
Soong, Y.	T401	Stewart, A.	W099	Sun, X.	W244		
Sorace, S.	T053	Stewart, J. W.	M183	Sun, Y.	W170		
Sorensen, M. G.	T093, T135	Stewart, M.	W099	Sundaram, K.	M480, T257		
Sorensen, O. Helmer	M248, S248	Stewart, P. M.	M232, WG23	Sung, H.	M499		
Sorenson, A. H.	1113	Steyer, G. J.	W481	Sunters, A.	O064, M064, S064, T067		
Sornay-Rendu, E.	1280	Stilgren, L.	W382	Sunycz, J. A.	W366		
Sosa, M.	T335	Stockmans, I.	1169	Suominen, H.	1083, 1204, M533, S533, W505, W515, W516, W520		
Soucasos, P. N.	W208	Stoecker, B. J.	W313	Suominen, M. I.	M407, T239, W210, W214		
Soudry, M.	M042, T009	Stolina, M.	1009, 1088, 1122, 1126, W445	Suominen, T.	W505		
Soukakos, P.	T402, WG19	Stolz, A.	T234	Supervia, A.	M288, S288		
Soundarajan, A.	S311, M311	Stone, K.	1157, M363, W280	Supronik, J.	M434, S434		
Soung, D. Y.	M129, T451, W098	Storer, A.	1021	Surmak, A.	M167		
Southcott, E. K.	M460	Stouch, B.	1129	Suthutvoravut, U.	M396		
Soysa, N. S.	M101, T094	Stovitz, S.	W521	Sutton-Smith, P.	M505, T113		
Spadaro, J. A.	1037, T430	Strader, C.	M349, S349	Suva, L. J.	1171, 1286, T251		
Spagnoli, A.	M191, S191, W472	Strain, G.	T444, T445	Suzawa, T.	T121		
Spangler, L.	1272, M535, S535, T351	Strain, J.	W269	Suzuki, A.	T066, T129, T138, W121, W128, W286		
Spanier, C.	T393	Stranczyk, F.	1202	Suzuki, D.	M201		
Spatz, J. P.	W120	Stratilatova, M.	T500	Suzuki, H.	M353, S353, T293, W124, W129		
Specker, B. L.	M532	Straub, R. H.	T183	Suzuki, M.	1002		
Spector, T. D.	1203	Straub, E. A.	W184	Suzuki, N.	1064, T065, T084, T146		
Speechley, M.	W376, WG39	Streiten, E. A.	W271	Suzuki, R.	M186		
Speer, G.	M138, M284, T124, T226	Strel, C.	M195	Suzuki, S.	M210, S210		
Spelsberg, T. C.	1144, 1154, 1235, M035, M070, M152, S152, W021, W028	Strender, L.	M195	Suzuki, T.	M016, S016, T016, W438		
Spencer, G. J.	1139, 1214	Strickman-Stein, N.	T425	Svensson, J.	W314		
Spiegel, A. M.	T483						
Spiering, B. A.	W056, W496						
Sportelli, P.	W195						
Sprague, E.	M520, T504						

(Key: 1001-1300 = Oral, O = Oral Poster, S = Sunday Plenary poster, M = Monday poster, T = Tuesday Poster, W = Wednesday Poster, WG = Working Group Abstract)

Taketani, S.	M097	Tenenhouse, A.	M336, M371, S336, S371, T333	Tommasini, S. M.	1241, T204	Turner, I.	M151
Taketani, Y.	T395, T493, W130	Tenero, D.	M427, S427	Tomoe, Y.	1115, M214, S214	Turner, N.	W467
Takeuchi, K.	M302, T263, T405	Teng, Y.	M080	Tomura, S.	W394, WG12	Turner, P. J.	M510
Takeuchi, T.	W431	Tenne, M.	T227	Tong, J.	T058	Turner, R. T.	1263, M148, M152, M196, M391, M482, S148, S152, S482, T254, W311
Takeyama, K.	M260, W022	Teplyuk, N.	M047, S047	Torchia, J.	1291	Turner, S.	M200
Takigawa, M.	T125	Teplyuk, V.	M047, S047	Torner, J. C.	M528, M529, S528	Twomey, T.	W315
Takita, M.	O262, M262, S262, W196	Terada, K.	M132	Torrekens, S.	1101	Tyagi, I.	WG18
Takito, J.	M136, M251, S136	Terai, H.	W286	Torres, A.	T050	Tylavsky, F.	1083, M533, S533, T346, W506, W506, W515, W520
Talavera, J.	M380	Teraki, Y.	W090	Torres, B.	T454		
Tam, H.	T448	Teramachi, J.	O099, M099, S099, M108	Torres, M.	T335		
Tam, S.	1150			Torres Cerino, M. Gabriela	T327, W149		
Tamai, N.	T264	Terauchi, M.	1136, 1298	Torti, F. M.	W189		
Tamaki, J.	T334, T352	Terkeltaub, R.	1236, 1259	Toss, G.	M213, W391		
Tamara, S.	T088	Terwedow, H.	T217	Tosteson, A. N. A.	M355		
Tamura, I.	M144, W014, W162	Tetta, J.	M287	Totty, W. G.	W425	Uchida, A.	1002
Tamura, M.	M031, S031	Teter, P.	T275	Touby, F.	M453	Uchida, T.	M091
Tamura, T.	1145, M416	Teti, A.	T170, W080	Toulson, S.	T140	Uchikura, C.	M395
Tamura, Y.	W470	Tetradis, S.	T179	Toussiot, E.	T281	Uchiyama, S.	W389
Tan, H.	1088, 1122, 1231, 1232	Tezuka, K.	M201	Towler, D. A.	1140, O185, M185, S185, T036, T165	Ucran, J.	1230
Tan, L. Jun	W244	Thabane, L.	M436, T332, T396	Towne, B.	W174, W179	Udagawa, N.	1149, M082, M106, M239, S082, S239, T085, W071, W072, W332, W492
Tan, T.	T511	Thalhammer, T.	T262	Towns, W.	T045	Udesky, J.	W145, W261
Tan, W.	M516	The Genomos Study Group	1199	Toyama, Y.	M016, M089, M136, M251, S016, S136, T016, T072, T308	Ueda, A.	T243
Tanabe, M.	T176, WG21	The Hellenic HORTHON Study Group	W388	Toyosawa, S.	M176, S176	Ueda, T.	T264
Tanabe, N.	T084	The LAVOS Group	M380	Tozer, R.	M328	Uehara, J.	T125
Tanaka, H.	T084, T146, T159, W371	The STOPP Consortium	M489, S489	Tracy, K.	M301	Uehara, M.	W389
Tanaka, I.	W220	Thiel, S.	M340	Tragl, K.	W024	Uehara, S.	T085
Tanaka, J.	T231	Thiruchelvam, D.	1275	Tran, B. H.	1201	Uenishi, K.	T311, W159, W260
Tanaka, K.	M365, T311, W004, W336, W394, WG12	Thomas, B. E.	1299	Travers, R.	W426	Ueno, T.	W389
Tanaka, M.	M303, S303	Thomas, C. Colleen	1119	Travers-Gustafson, D.	T359	Uetani, M.	T465
Tanaka, O.	T263	Thomas, D. L.	M069	Travison, T. G.	M337, M338, W259, W471	Uitterlinden, A.	1199, W329
Tanaka, R.	T493	Thomas, L.	M207	Trebec, D. P.	M087, T105	Ulvieri, F. Massimo	M422
Tanaka, S.	1098, 1181, 1290, M186, T102	Thomas, M.	T376	Trevisiol, C. H.	M391	Ulla, M. R.	T472
Tanaka, S.	W004, W336	Thomas, T.	M522	Triffitt, J. T.	W320, W325	Umino, K.	W141
Tanaka, Y.	T433, T491, W005, W439, W447	Thompson, B.	M051	Trikalinos, T. A.	1199	Undale, A. H.	T054
Tang, C.	T511	Thompson, D. D.	T435	Trimpou, P.	M194, T343, W288	Underwood, K.	1132, 1230, M394, S394, W312
Tang, D.	T114	Thompson, L.	M399, S399	Troen, B. R.	M414	Uoshima, K.	T127
Tang, H.	T156	Thorne, C.	W372	Trokhan, D.	W325	Urbanetz, A. A.	T342
Tang, P. L. F.	T214	Thornhill, T. S.	T407	Tron, F.	M500	Urganus, A. L.	W091
Tang, W.	1227	Thorsdottir, I.	W408	Trotta, F.	T370	Urso, M. L.	W056
Tang, Y.	1032, 1072	Thraillkill, K. M.	W348	Truong, V.	W334	Ushita, M.	1175, 1182, W101
Tang, Z. Hui	W263	Thrall, E.	W224	Trybulski, E. J.	1010	Uusi-Rasi, K.	T319
Tangpricha, V.	M483	Thurstun, R.	M368, S368	Trzeciakiewicz, A.	W407	Uveges, T. E.	W166
Tanikawa, R.	W005, W447	Tian, X. Yan.	M417	Tsang, J. F.	1078, 1080, 1163, M321, S321	Uyama, A.	W513
Tanikawa, T.	T491, W005, W447	Tiegs, R. D.	T479, WG16	Tsang, P. K.	1133	Uzawa, M.	T398
Tanimura, A.	T493	Tile, L. E.	M399, S399	Tsuboi, H.	W013		
Tanini, A.	T053, T213, W230	Timm, W.	M325, T287	Tsuboyama, T.	W181		
Tankó, L. B.	M356, S356	Tinahones, F.	W405	Tsuchiya, S.	T390		
Tanner, B.	M324	Tineo, A.	M481, W145, W146	Tsuchiya, Y.	T439		
Tanno, K.	W419	Ting, K.	1105, M200	Tsugawa, N.	T261, T311, T318, T439, W159		
Tannous, Z.	T289	Tintut, Y.	1117	Tsuhji, W.	1208		
Tanzilli, L.	T514	Titus, L.	T038	Tsujio, T.	W286		
Taquahashi, Y.	M402	Tkachenko, E. V.	W481	Tsujioka, K.	W061		
Tarantino, U.	T419	Tóbiás, B.	T226	Tsukamoto, K.	O262, M262, S262		
Targownik, L. E.	M351, S351	Tobimatsu, H.	T340, WG31	Tsukamoto, M.	W434		
Tarrés, M.	T472	Toda, T.	W389	Tsumaki, N.	M130, S130, T119		
Taskar, V. R.	M458	Tognarini, I.	T028, T053, T213	Tsushima, Y.	W022		
Tassabehji, M.	M032	Togo, F.	W343	Tu, C.	1176, 1284, O223, M223, S223		
Tataczuch, L.	M120	Toh, K.	T147	Tu, S.	M238, T401		
Tateishi, S.	T128	Toh, S.	M273	Tuan, R. S.	T048, W039		
Tatsumi, S.	M214, S214	Tohma, S.	M186	Tucker, K. L.	T309, T317, W266, W267		
Taylor, A. F.	1285	Tohma, T.	W358	Tuerk, J.	M453		
Taylor, B. C.	1076, M355	Tohima, T.	W358	Tuma, R. F.	M008		
Taylor, K.	T375, W303, W384	Toivaiainen-Salo, S.	M281, S281	Tunophon, S.	M258		
Taylor, R. H.	W224	Tokita, A.	T434	Tuppurainen, M.	1270, M344, M452, S452, S344, W291		
Tebben, P. J.	T479, WG16	Tokunaga, K.	T017, W411	Turan, S.	W165		
Techasurungkul, S.	T315, T320	Tokutomi, K.	T147	Turner, C.	W485		
Techawiboonwong, A.	M329	Toma, C. D.	T262	Turner, C. H.	1084, 1245, M406, M526, W050, W171, W176, W178, W185, W308, W456, W494		
Tei, K.	T161	Tometsko, M.	M307, S307				
Teichert, A. E.	W158, WG3	Tomida, K.	M215				
Teilmann, J.	W345	Tomimori, Y.	W332				
Teitelbaum, S. L.	1146, W359	Tomin, E.	T171				
Tejedor, D.	M275, S275	Tominaga, H.	W029				
Telford, R.	W486	Tominaga, Y.	T496				
Tell, G. S.	T272	Tominari, T.	O262, M262, S262				
ten Dijke, P.	W044	Tomita, M.	T457				
Tenenbaum, H. Charles	T106	Tomizuka, K.	T356				
		Tomlinson, G.	M399, S399				
		Tomlinson, R. E.	W481				

(Key: 1001-1300 = Oral, O = Oral Poster, S = Sunday Plenary poster, M = Monday poster, T = Tuesday Poster, W = Wednesday Poster, WG = Working Group Abstract)

(Key: 1001-1300 = Oral, O = Oral Poster, S = Sunday Plenary poster, M = Monday poster, T = Tuesday Poster, W = Wednesday Poster, WG = Working Group Abstract)

Westover, A. J.	M389	Wong, M.	W342	Xie, Z.	T505	Yamauchi, M.	M003
Wettschreck, N.	1123	Wong, M.	W384	Xing, L.	1100, 1148	Yamauchi, M.	M011
Wetzsteon, R. J.	T187, W521	Wong, M. Sau	W337	Xing, W.	1107, M005, T080	Yamauchi, M.	M056, M059, S056
Whang, J.	M200	Woo, J.	M343	Xing, X.	W168	Yamauchi, M.	M203, M270, S270
Wheeler, V. W.	T353	Woo, K.	M020	Xing, X.	W170	Yamauchi, M.	M316, M484, S316, S484
White, K. E.	1113, 1116	Woo, K.	T139	Xing, X.	W323	Yamauchi, M.	T142, T147
Whited, B.	W187	Woo, S. M.	T179	Xing, Y.	1225	Yamauchi, M.	W030
Whitehead, J. P.	T056	Wood, D.	M050	Xing, Y.	T060	Yamazaki, K.	M131
Whitfield, G. K.	M255, M259, S255, S259, W161	Woodhouse, A.	T376	Xing, Y.	T159	Yamazaki, M.	W131
Whitford, G. M.	W425	Woodruff, K.	T039, W082	Xing, Z.	M163, S163	Yamoah, K.	1153
Whitlow, H. James	W009	Woodson, G.	1209, T386	Xiong, J. Xian	W244	Yamoah, K.	T071
Whitlow, M.	W057	Woolf, P. J.	W109	Xiong, Q.	M280	Yan, D.	W350
Whyte, M. P.	1259, T474, T475, W169, W425, W430	Workman, S.	T097	Xiong, W.	M079	Yan, S.	T206
Wicker, C. A.	1058, 1086	Worton, L. E.	T056	Xu, A.	T174	Yanagi, H.	W394, WG12
Wieland, M.	W002	Wosje, K. S.	M536	Xu, J.	1293, M103, M104, S103	Yanagisawa, R.	T071
Wieringa, B.	M083	Wotton, D.	1286	Xu, J.	M192	Yanagisawa, T.	M006, T173, W480
Wigner, N. A.	W102	Wraae, K.	M467	Xu, L.	M412	Yanagita, T.	T125
Wilburn, C.	W187	Wren, T.	T449	Xu, L.	W009	Yang, C.	1297
Wilhelmsen, L. W.	M194, T343, W288	Wren, T. A. L.	W514	Xu, M.	1151	Yang, D.	1119
Wilkins, L.	W338	Wright, D.	W182	Xu, M.	1234, M180	Yang, D.	1188
Willey, J. S.	M464	Wright, J. Timothy	T148	Xu, M.	T478	Yang, D.	O142, M142, S142
Willheim, M.	T164	Wright, L. E.	W349	Xu, X.	T217	Yang, D.	T100
Williams, B. O.	1108	Wright, N. C.	1207, W306	Xue, M.	1251	Yang, D.	W083
Williams, D. S.	T290	Wright, T. M.	T366	Xue, Y.	1025	Yang, F.	W244
Williams, G. A.	T174	Wronski, T. J.	1021, 1265, M385, M393, W311	Xuei, X.	T215	Yang, J.	T157
Williams, J. A.	W103	Wu, A. C. K.	T140			Yang, J.	T506
Williams, L. J.	T354	Wu, B.	M200			Yang, J. Y.	M044
Williams, M. I.	T266	Wu, C.	M357			Yang, J. Yeon	M209
Williams, N. I.	T200, W062	Wu, D.	M098, M412			Yang, K.	T409, W282
Willing, M. C.	M528, M529, S258	Wu, G.	O373, M373, M381, S373, S381			Yang, L.	1004
Willinger, U.	W203	Wu, H.	1104			Yang, L.	1146
Willson, K.	M366, S366	Wu, J.	1008			Yang, L.	M332, S332
Wilson, D. L.	W481	Wu, J.	1255			Yang, M.	M235, S235
Wilson, K. E.	1076, W224, W226	Wu, J. Y.	1020			Yang, M.	W193
Wilson, M. A.	1010	Wu, L.	1202			Yang, N.	T180
Wilson, P. M.	M065	Wu, L.	M471, S471			Yang, R.	T364, T511, W491
Wilson, P. W. F.	M483	Wu, L.	T325			Yang, S.	M093, S093
Wilson, S. G.	1203	Wu, M.	1250			Yang, S.	T122
Wilson, S. Ruth	W065	Wu, M.	M476			Yang, S.	T306
Wimalawansa, S. J.	W081, W375, W400	Wu, S.	1029			Yang, T.	1212, M202, S202
Windahl, S. H.	T201	Wu, S.	W244			Yang, T. Lin	W263
Windle, J. J.	1099, M477, M479, S477	Wu, T.	M234			Yang, W.	1106
Windolf, J.	M211, W369	Wu, X.	1032, 1072, 1256, 1297			Yang, W.	M140
Winer, K. K.	WG6	Wu, Y.	1291			Yang, W.	W010
Winkelmann, C.	M175	Wu, Z.	M108			Yang, W.	W017, W050
Winkles, J. A.	M043, S043	Wuester, C.	T518			Yang, X.	1063
Winters-Stone, K. M.	M1158, M299	Wylie, C.	M124, M125, M126			Yang, X.	1136
Winzenberg, T.	M366, S366	Wynne, R.	1011, M002, S002			Yang, X.	1183
Wiren, K. M.	M013, T202, T203	Wynnyckj, C.	W474			Yang, X.	1298
Wirth, A. J.	1164	Wysolmerski, J. J.	M219, M220, S219			Yang, X.	T027
Wiseman, M.	T450	Wysolmerski, R. B.	W069			Yang, X. Fang	M257
Wisher, C. D.	W222					Yang, Y.	1171
Wiswall, A.	W324					Yano, F.	1112, 1123, 1175, 1182
Wittelsberger, A.	1299, W147					Yano, S.	M056, M059, M316, M484, S056, S316, S484
Wittrant, Y.	T039, W082					Yanovich, R.	W487
Witzke, K.	M299, W448					Yantorno, M. Pablo D.	T327, W149
Wixted, J. J.	1258					Yao, G.	1255
Wobraschek, P.	W271					Yao, W.	1291, M392, S392, T181, W331
Wolf, G.	W414					Yao, X.	W342
Wolf, L.	M167					Yao, X. Sheng	W337
Wolf, O.	W473					Yao, Z.	1148, 1212
Wolf, U.	M459, S459, T416					Yasuda, H.	M096, M136, S096, S136, W072, W332
Wolfe, F.	T436					Yasuhara, R.	T121, W084
Wolff, A. M.	T208					Yasui, N.	M188, T155, T456
Wollén, C.	T001					Yasui, T.	1098, 1290
Wolos, J. A.	1277					Yasunaga, A.	W343
Womack, C.	M324, M352					Yaszkowski, M. J.	M306, T254
Won, Y.	M398, M503					Yata, K.	T263
Won, Y.	W262					Yatani, H.	T243
Won, Y.	W451					Yaturu, S.	T355
Wong, B. Y. L.	WG7					Yawaka, Y.	M031, S031
Wong, D. H.	M305, S305					Yaworsky, P. J.	1048
Wong, J.	1105					Yayon, A.	T009
Wong, M.	T375, W303					Ye, L.	M270, S270
						Yee, Y. K.	1012

(Key: 1001-1300 = Oral, O = Oral Poster, S = Sunday Plenary poster, M = Monday poster, T = Tuesday Poster, W = Wednesday Poster, WG = Working Group Abstract)

Yeh, J. K.	W313	Yun, K.	T130	Zhao, B.	1145, T121
Yeo, H.	1283	Yun, S.	M398	Zhao, H.	1146
Yeung, D. K. W.	1133	Yuzawa, H.	M206	Zhao, J.	1177
Yi, S.	M398			Zhao, J. J.	T059
Yim, C.	M247, W344			Zhao, L.	1072
Yin, J.	M301	Z		Zhao, L.	M062, S062, T157
Yin, L.	T157	Zabel, B.	W106	Zhao, M.	1257, T115
Yin, M. T.	W444	Zack, D.	W445	Zhao, S.	T270
Yingling, V. R.	W510	Zahed, L.	1194, M283	Zhao, Y.	T032
Yip, K. H. M.	M104	Zahner, L.	W519, WG30	Zhao, Y.	W091
Ylönén, S.	T239	Zaidi, M.	1153, M198	Zheng, H.	1212
Yoda, M.	T072	Zaidi, S. K.	M047, S047	Zheng, J.	M412
Yoda, T.	W117	Zainabadi, K.	1097	Zheng, M. Hao	1293, M103, M104, S103
Yoffe- Sheinman, H.	W197	Zajac, J. D.	1217	Zheng, Q.	1184, M032, W106
Yoh, K.	M365	Zalutskaya, A. A.	W104	Zheng, R. Min	M034
Yokota, H.	M526	Zaman, F.	M121, S121	Zheng, T. S.	M009
Yokoyama, A.	T066, T138	Zaman, G.	O064, M036, M064, S036, S064, T067	Zheng, Y.	1006
Yokoyama, T.	M273			Zheng, Y.	1146
Yoneda, M.	T030	Zambon, S.	W302	Zheng, Y.	T182
Yoneda, T.	1002, 1224, O293, M176, M293, S176, S293, T055, T243, W020, W092	Zanatta, M.	M147	Zhong, Y.	1027
Yoneshima, H.	T352	Zanchetta, J. R.	1206, M380, T382	Zhou, C.	W150
Yoo, M.	T378	Zanduetta, C.	1001	Zhou, G.	1180, 1212, M032, W106
Yook, J.	T033	Zanello, L. P.	1030	Zhou, H.	1006, 1018
Yoon, B.	T423	Zangari, M.	1172, 1173	Zhou, H.	1096, 1164, M388, M477, S388, S477
Yoon, H.	M247	Zanotti, S.	1178, T019, T172, W122	Zhou, H.	T062, T182, T183
Yoon, H.	M398	Zapata, M.	W235	Zhou, H.	T486
Yoon, H.	W344	Zappoli Thyron, G.	T053	Zhou, J.	1227, 1296
Yoon, W.	M199	Zarnitsky, C.	M500	Zhou, L.	1208
Yopshikawa, H.	T264	Zayzafoon, A.	W070	Zhou, L.	M234
Yoshida, C.	M123, S123	Zayzafoon, M.	1283, T208	Zhou, L.	T206
Yoshida, C. A.	1066	Zebaze, R.	1039, M333, M334, T289	Zhou, Q.	1013
Yoshida, H.	T072	Zeitz, U.	1009	Zhou, Q.	T116, T117
Yoshida, H.	W438	Zella, L. A.	1067	Zhou, Q.	T512, W232, W260
Yoshida, M.	W438	Zemel, B. S.	M329	Zhou, S.	W031
Yoshida, N.	M107	Zenari, S.	M147	Zhou, X.	1249, M432, M438, S432
Yoshida, T.	1192	Zeng, L.	W105	Zhou, X.	M508, S508
Yoshihara, A.	T439	Zeng, Q.	1012	Zhou, X.	T386
Yoshikata, H.	W186	Zeng, Y.	M040	Zhou, X.	W170
Yoshikata, R.	W256, W517	Zeni, S. N.	W223	Zhou, X.	W317, W351, W374
Yoshikawa, H.	1224, M130, S130, T119, W013, W431	Zerbini, C.	M274, T209, W264, T387, W354, W442	Zhou, Z.	M079
Yoshikawa, Y.	M144, W014, W162	Zernicke, R. F.	M069, T360, W086	Zhu, E.	W032
Yoshiko, Y.	M210, S210	Zerwekh, J. E.	M491, T365	Zhu, J.	T175
Yoshimatsu, M.	M107	Zhan, P.	M180	Zhu, K.	1038
Yoshimoto, T.	T076	Zhang, C.	1249	Zhu, K.	T269
Yoshimura, A.	M089	Zhang, F.	1256	Zhu, K.	T321
Yoshimura, N.	W307, W438	Zhang, G.	T178	Zhu, K.	W226
Yoshioka, T.	T231	Zhang, J.	1007	Zhu, L. L.	1153
Yoshiuchi, K.	W343	Zhang, J.	1055	Zhu, S.	T141
Yost, J. Gantt	T149	Zhang, J.	M007, M037	Zhu, T.	1108
You, J.	T060	Zhang, J.	M140	Zhu, X. Zhen	W244
You, J.	W202	Zhang, J.	M310, T115	Zhu, Y.	1013
Young, C. M.	M524	Zhang, J.	T247, T248	Zhuang, J.	1004
Young, C. S.	W316	Zhang, J.	T357	Ziegler, T. R.	M483
Young, D. W.	M047, S047	Zhang, L.	W011	Zielenski, J.	W315
Young, K.	M190, W116	Zhang, M.	T116, T117	Zimmer, W. E.	T507
Young, M. Francis	1174, O157, M157, S157	Zhang, P.	M526	Zion, M.	T373
	T399, T400	Zhang, Q.	1038, 1100	Zivny, P.	W245
Yu, B.	T452	Zhang, Q.	W143	Zmierczak, H. G.	T228
Yu, C.	M115	Zhang, S. Qin	1142	Zmuda, J. M.	1053, T268, T353
Yu, H.	W170	Zhang, W.	1070	Zoeger, N.	W271
Yu, L.	1007	Zhang, W.	T057	Zoeherer, R.	M447, S447, T486
Yu, S.	1296	Zhang, X.	1105	Zonefrati, R.	T053
Yu, S.	M007, M037	Zhang, X.	1108	Zou, L.	T365
Yu, S.	T123	Zhang, X.	1251	Zouch, M.	M522
Yu, S.	W433	Zhang, X.	M200	Zuk, P. A.	T051
Yu, V. W. C.	M033, S033	Zhang, X.	M403, S403	Zulliger, M.	M330, S330
Yu, X.	1113, 1116	Zhang, X.	T202, T203	Zuo, J.	M092, M094
Yuan, B.	1225, T159	Zhang, X. Henry	1164, M327	Zustin, J.	W477
Yuan, H.	1297	Zhang, Y.	1062	Zwerina, J.	W443
Yuan, H.	M205	Zhang, Y.	1285	Zysset, P.	1165, 1267, T368, W475, W476
Yuasa, T.	T082	Zhang, Y.	M412		
Yukata, K.	T155, T456	Zhang, Y.	T265		
Yull, F.	1097, 1147	Zhang, Z.	1117		
Yun, H.	M378	Zhang, Z.	M010, S010		
		Zhang, Z.	T058		
		Zhang, Z.	T230		
		Zhang, Z.	W323		

(Key: 1001-1300 = Oral, O = Oral Poster, S = Sunday Plenary poster, M = Monday poster, T = Tuesday Poster, W = Wednesday Poster, WG = Working Group Abstract)

Key: 1000-1300 = Oral, O = Oral Poster, S = Sunday Plenary Poster, M = Monday Poster, T = Tuesday Poster, W = Wednesday Poster, WG = Working Group Abstract
***(Asterisk) Denotes Non-ASBMR Membership**

Numeric

$\alpha 5$

Integrin association with Cx43 regulates the function of osteocyte hemichannels in response to shear stress, T504

$\alpha_9\beta_1$

ADAM8 binds to increase osteoclast formation and function by interacting with Pyk2 and activating paxillin, 1099

$\beta 2$

Adrenergic receptor deficiency enhances bone mass in by antagonizing against aging-induced bone loss and blunts anabolic effects of PTH on osteoblasts, M390, O390, S390
 Modify RANKL/OPG expression and cell proliferation in human osteoblasts and osteoblastic cells, T006

A

A disintegrin and metalloproteinase 8 (ADAM8)

Binds $\alpha_9\beta_1$ to increase osteoclast formation and function by interacting with Pyk2 and activating paxillin, 1099

A-raf

Dispensable for endochondral bone development, W095

Abbott Diagnostics

Development of an assay for 25OH(D) on the ARCHITECT Analyzer, W156

Ac45

Cytoplasmic terminus is required for proper interaction with V0 domain subunits and efficient osteoclastic bone resorption, M104

Actin

Binding activity in the B subunit is required for sorting V-ATPase in osteoclasts, M092
 HMGB1 regulates cytoskeleton organization and RANKL-induced osteoclastogenesis in a manner dependent on RAGE, M079
 Polymerization through activation of RhoA, mechanosensitivity of osteoblasts is regulated by, W010

Activating transcription factor 4 (ATF4)

ATF4 is required for the anabolic actions of PTH on bone in vivo, 1007
 Synergistically activates osteoblast-specific osteocalcin gene expression, M037

Activation domain 3 (AD3)

Supports synergistic Runx2-MINT activation of the osteocalcin FGF response element via a DMAT-sensitive kinase, T036

Activin

Novel nodal-binding protein G11 inhibits matrix mineralization in osteoblasts, M203

ADAM. See A disintegrin and metalloproteinase

ADAMTS-7/12

α_2 M is a novel substrate for, and inhibits degradation of COMP, M166

Adenomas. See adenomas by type

Adenosine receptors (AR)

Adenosine A_1 receptor blockade reverses bone loss in OVX mice and deletion of adenosine A_{2A} receptors leads to diminished bone density, 1124
 In the osteoclast, W078

Adipocyte differentiation

Combination of Vitamin D and BADGE potentiates their pharmacological inhibition of PPAR γ and increases osteogenic differentiation of adipocyte precursors, W155
 Inhibiting, GILZ enhances osteoblast differentiation of bone marrow mesenchymal stem cells by, T057
 From MSC, CLA regulates, T047
 And osteoblast differentiation, opposing effects of GH and alcohol reveal a critical role in the relationship between, M196

Adipocytes

Bone marrow, secretion of adipokines and hypertrophic changes in, M473
 RANKL is produced by and stimulates osteoclastogenesis, W079

Adipogenesis

Accelerated, misexpressions of SOX9 during skeletogenesis lead to, 1180
 Bone marrow, effect of estrogens on, M243
 Classical ER signaling is essential for estrogen mediated enhancement of osteogenesis but not for inhibition of, M250, S250
 Differentially modulated by PTH and the N- and C-terminal fragments of PTHrP, T050
 Estrogen suppression is mediated by TGF β , M024
 Factors produced in ovary inhibit musculoskeletal growth and promote adipogenesis during puberty, M246, S246
 Marrow, reflects global energy utilization through activation of PPARG and modulation by "clock" genes in a genotype-specific manner, M021, O021, S021

Adipokines

Secretion and hypertrophic changes in bone marrow adipocytes, M473

Adiponectin

Action influences osteoblast-related gene expression, W014
 Anabolic to bone in vitro but negative effects in vivo, T174
 Changes in adiponectin and leptin serum levels in osteoporotic postmenopausal women after treatment with raloxifene or ALN, T454

Adiponectin receptor 1 (ADIPOR1)

Association of ADIPOR1 and ADIPOR2 gene polymorphisms with BMD in postmenopausal Korean women, T220

Adipose-derived stem cells (ASC). See Stem cells, adipose-derived

Adipose tissue

Accuracy and precision of adipose tissue cross-sectional area measured using pQCT, T268
 MSC from, osteogenic differentiation and interaction with Ti6Al4V, T053
 Overexpression of Δ FosB decreases, in a non-cell autonomous manner by increasing energy expenditure independently of bone cells, 1248
 Pericytes derived from, characterization and evaluation of their osteogenic potential, 1215

Adolescence. See Puberty

Adolescent idiopathic scoliosis (AIS). See Scoliosis, adolescent idiopathic

Adrenomedullin (AM)

Development of small molecule AM antagonists for treatment of bone metastases, T260

Advanced glycation end products (AGE)

AGEs induce vascular calcification through the RAGE/p38 MAPK signaling pathway, W447
 Comprehensive analysis of bone-related gene expression induced by acute oxidative stress, W413

Aft4

Inhibiting the transactivation activity of, vimentin negatively regulates osteoblast differentiation by, T027

AG490

Regulates osteoclast survival via distinct signaling pathways, T100

Aggrecan

Tissue-specific expression is regulated through both regulatory enhancer and repressor elements, W102

Aging, premature

Homozygous missense mutation in *KLOTHO* causes severe tumoral calcinosis but not, 1113

AIDS. See HIV/AIDS

Akt

Contributes to maintenance of bone mass and turnover by inhibiting apoptosis of osteoblasts through FoxO3a/Bim axis, 1211
 Effects on β -catenin regulate osteoblasts' responses to mechanical strain and PTH, T067
 PC1 selective activation of *Runx2*-II isoform transcription is mediated through, 1142
 Signaling, Osx mediates the feedback regulation of BMP-2 via, T029
 Signaling pathways, regulation of chondrocyte proliferation, function, and differentiation by, M123, S123

Akt inhibitor

Ultrasound induces HIF-1 activation and iNOS expression through, T511

Albuminuria

Predicts bone loss in older adults, M495

Alcoholism

Effects of low-dose PTH on body composition, bone mass and turnover and ectopic osteoinduction in chronic alcohol abuse, M391
 Opposing effects of GH reveal a critical role in the reciprocal relationship between adipocyte and osteoblast differentiation, M196

Alendronate (ALN)

Change of bone markers after once-weekly low dose ALN in postmenopausal women with moderate bone loss, T379

Comparison of ALN and strontium ranelate in men with established primary osteoporosis, T374

Comparison of effects of ALN and raloxifene on the lumbar BMD, bone turnover, and lipid metabolism in elderly women with osteoporosis, T398

Effect of combined treatment of ALN and Vitamin K $_2$ on BMD and strength, W328

Efficacy of ALN for the treatment of osteoporosis in postmenopausal women with subclinical hyperthyroidism, W364

Efficacy of continued ALN for fractures in women without prevalent vertebral fracture, 1057

- Impairs angiogenesis and bone formation during the early stages of bone healing in an animal model for ONJ, 1265
- Improved tendency in esophageal-gastroduodenal mucosal effect of enterocoating ALN combined with calcitriol drug compared with ALN only in Korean postmenopausal women, T378
- Induced bone matrix changes on resorption and turnover, effects of, W330
- Lipid profile and BMD changes in postmenopausal Korean women treated with ALN, T400
- Low-energy femoral diaphyseal fractures associated with ALN use, M430, S430
- Mechanistic bases of BMD increase during ALN therapy, M435, O435, S435
- Mineralization status of bone matrix in postmenopausal women during a 10-year ALN treatment period, M437, S437
- Pretreatments abolish this process, GC suppresses the differentiation of osteoblasts by enhancing the expressions of BMP antagonists, M059
- Prevention of bone loss in acute spinal cord patients over one year with ALN, T392
- Prior ALN treatment does not inhibit the early stimulation of osteoblast activity in response to TPTD, M388, S388
- Randomized, active-controlled, 6-month study of once weekly 280 mg oral buffered ALN solution for treatment of PDB, M476
- Alfacalcidol (ALF)**
Differential effects of ALF in the distal tibial metaphyses, M417
Effect of ALF on volumetric BMD measured by pQCT in ALN-treated postmenopausal women with osteopenia or osteoporosis, M453
- Alkali therapy**
Biochemical and histological assessment of the effects of alkali therapy on bone during high animal protein intake, T365
- Allantoin**
Percutaneous injection of allantoin accelerates fracture repair, W258
- Alox5**
Alox5 null mice have reduced cortical bone density, altered bone turnover and low serum IGF-1, 1228
- Alpha-2**
Osteoblast response to titanium microtopography is dependent on, W002
- Alpha lipoic acid**
Alpha lipoic acid attenuates vascular smooth muscle calcification via the expressional regulation of genes related to apoptosis and oxidative stress, W436
- Alpha1**
Modify RANKL/OPG expression and cell proliferation in human osteoblasts and osteoblastic cells, T006
- Atherosclerosis**
Bone formation in atherosclerotic vessels, T473
Does low bone mass predict carotid atherosclerosis in postmenopausal women?, T352
- AluI**
Polymorphism in ESR2 is associated with reduced risk of osteoporotic fractures, T218
- Aluminum (Al)**
Distribution and localization of Al in bone tissues of aluminum osteopathy, W090
- Ameloblast**
Differentiation and proliferation, CAII regulates via intracellular pH-dependent mechanism, T121
- Amelogenesis**
Identification of calcein expression using ACP DDRT-PCR method, T129
- Amenorrhea.** See also *Menarche*
Bone formation is predicted by resting metabolic rate and leptin in exercising women with hypothalamic amenorrhea, T197
Fracture risk factors in breast cancer survivors with chemotherapy-induced amenorrhea, M299
Increased caloric intake is associated with reversal of amenorrhea and favorable changes in metabolic and bone markers, T200
Model of secondary amenorrhea in the adolescent female rat, W510
- Amino terminal domain (NTD)**
Identification of proteins that interact with the collagen type XI ($\alpha 1$), M149
- Aminobisphosphonate**
Giant osteoclast formation after long-term oral aminobisphosphonate therapy for postmenopausal osteoporosis, 1058
- Aminoimidazole-4-carboxamide ribonucleoside (AICAR)**
AMPK activator in vivo, osteoclast formation and osteolysis are promoted by, 1150
Induce the differentiation and mineralization of osteoblastic MC3T3-E1 cells via inhibiting the mevalonate pathway and enhancing BMP-2 expression, M056, S056
- AMP-activated protein kinase (AMPK)**
Activator AICAR in vivo, osteoclast formation and osteolysis are promoted by, 1150
- Amputees**
BMD and bone quality in unilateral lower limb amputees, W504
- Amyloid precursor protein (APP)**
Cleavage products of, regulate osteoblast function, T145
- ANA**
Responses of bone in ANA knock-out mice to ovariectomy, T030
- Anagen**
Induction, similar effects of proteasome inhibition on osteoblast differentiation and, W111
- Androgens**
Act directly via the AR in mineralizing osteoblasts to regulate bone turnover and maintain trabecular bone, 1217
Alpha/beta-T cells do not modulate androgen withdrawal-induced bone loss in aged rats, M466, S466
Attenuate p66^{shc} phosphorylation via an ERK and PKC β signaling cascade, T185
- Androgen receptors (AR)**
Androgenic effects on bone and body composition depend on concerted and additive activation of, M244, S244
Androgens act directly in mineralizing osteoblasts to regulate bone turnover and maintain trabecular bone, 1217
Gene, association of tri-nucleotide (CAG and GGC) repeat polymorphism in Taiwanese women with refractory or remission RA, W433
Role in the lineage commitment of BMSCs, T198
Signaling, dissection of, T203
- Anemia**
Hip geometric structure is weaker in anemic women, M381, S381
Lower hip BMD among ethnically diverse postmenopausal women with anemia, W255
- Angiogenesis**
Chondrostatin as a new inhibitor of, T259
Dramatic increase in bone marrow of rescued RANKL-deficient mice by expression of soluble RANKL transgene, M096, S096
Genetic and pharmacologic activation of the HIF-1 pathway promotes, 1065
- Angiopoietin 1 (Angpt1)**
Overexpression of osteoblast specific, increases bone mass, M016, S016
- Angiotensin converting enzyme (ACE)**
ACE-011 increases BMD and improves microarchitecture in cynomolgus monkeys, 1230
ACE inhibitor use is not associated with serum concentrations of bone related hormones in older men, T469
Single dose of ACE-011 is associated with increases in bone formation and decreases in bone resorption markers in healthy, postmenopausal women, 1132
- Angiotensin II (Ang II)**
Receptor in osteoclasts and its roles on differentiation and survival, expression of, W073
Suppresses bone mass via AT1 receptor in long bones of adult mice, M141
- Angiotensin II type 1 (AT1)**
Receptor in long bones of adult mice, Ang II suppresses bone mass via, M141
- ank.** See *Progressive ankylosis gene*
- Ankylosing spondylitis (AS)**
Bone metabolism in an animal model of, W441
Increased expression of RANKL in stimulated T-cells from patients with, W446
- Annealing controlled primers (ACP)**
Identification of calcein expression in rat amelogenesis using, T129
- Annexin V/VI/VIII**
Collagen interactions regulate growth plate chondrocyte mineralization, 1111
Critical bone matrix-dependent osteoclast gene transcriptionally regulated by RANKL and NFATc1, W068
Loss affects endochondral bone formation, T131
- Annulus fibrosis**
Effect of removal of nucleus pulposus cells on, M124
- Anoikis**
Small GTPase RhoA and its effector kinase ROCK mediate actin cytoskeleton reorganization leading to, M233, S233
- Anorexia nervosa**
BMD in Japanese adolescent girls with anorexia nervosa, T308
Thin healthy women have a similar low bone mass as women with anorexia nervosa, W405
- Anterior cruciate ligament (ACL)**
Tibial insertion after rupture, cell death and cell proliferation of cartilage layer in, W096
- Anti-epileptic drugs (AED).** See *Epilepsy*
- Anticoagulants**
Long-term use of oral anticoagulants and risk for osteoporosis, W300
- Antidepressants**
Fragility fracture increases antidepressant use among women 65 years of age and older, M429

- Is antidepressant use associated with bone loss or fractures in postmenopausal women?, 1272
- Antiresorptive agents**
Treatment with increases circulating FGF-23, decreases renal expression of 25OH(D) 1(OH)ase, and reduces circulating 1,25(OH)₂D, W127
- Anulus fibrosus cells**
IGF-1-treated, activation of Erk1/2 prevents the FasL-induced apoptosis in, T117
- AP-1**
M-CSF stimulates bone resorbing activity of mature human osteoclasts via increased activation of, T075
- Apatite-wollastonite (A-W)**
Bespoke bioceramic scaffolds support MSC growth and osteogenic differentiation, M050
- APC^{min}**
Evaluation of bone phenotype in mice carrying APC^{min} gene mutation, M175
- Apoptogenesis**
Smad4 has a direct apoptogenic role at the mitochondria, M205
- Apoptosis**
Captured under a microscope connected with time-lapse motion video picture, decisive moment of, M072
Cementoblast cultured on fibrin induces fibrinolysis and, T139
17β-Estradiol abrogates in skeletal muscle cells through extra-nuclear estrogen receptors, T196
Evaluation in GC-induced osteoporosis in rats treated with Ris, W318
FasL-induced, activation of Erk1/2 prevents in IGF-1-treated anulus fibrosus cells, T117
Hormonal regulation of hypertrophic chondrocyte, W094
Osteoblast, regulation by estrogens is preserved when the ER cannot directly interact with DNA, T184
Osteoclast, FADD-caspase-8 axis regulates, T102
Proteasome inhibition induces apoptosis in growth plate chondrocytes, M121, S121
Regulation of skeletal homeostasis by anti-apoptotic molecule Bcl-2, 1290
In young and old mice, comparative analysis of osteoclast bone resorption activity and, W081
- 2-Arachidonyl glyceryl (2-AG)**
Long-term effect of 2-AG ether on body weight and bone mass, W344
- ARCHITECT Analyzer**
Development of an assay for 25OH(D) on the, W156
- Arkadia**
Represses skeletal muscle differentiation through enhancement of Myostatin and TGFβ signaling, M206
- Aromatase**. See also *CYP19*
Characterization of regions upstream of exon II of, that mediate regulation by cAMP in murine osteoblasts, T032
Local overexpression in osteoblasts leads to clearly increased bone mass, 1218
- Arthritis**. See also *Osteoarthritis*
Adjuvant-induced, possible suppressive role of Galectin-3 in osteoclastic bone destruction accompanying, M108
Periarticular bone loss in arthritis, WG23
Periarticular bone loss in, role of synovial GC generation, M232
- Value of bone and cartilage markers in the conservatively treated community-based inception VERA cohort, M500
- Arthritis, autoimmune**
Immunoregulatory role of RANKL-stimulated dendritic cells on, T162
- Arthritis, collagen-induced (CIA)**
Anti-GGT antibody attenuates osteoclastic bone erosion, T090
Effects of HO-1 on, T130
Small molecule inducer of activated CD4⁺ T cell death inhibits disease progression in, M499
Therapeutic effect of KHB9 on cartilage degradation and inflammation in, M135
- Arthritis, inflammatory**
Osteoblast-mediated bone formation is suppressed at sites of focal bone erosion in inflammatory arthritis, W007
- Arthritis, juvenile chronic (JCA)**
Prevalence of osteopenia in children with early JCA, T515
- Arthritis, KRN**
Serum-induced, transgenic disruption of GC signaling in mature osteoblasts attenuates, T183
- Arthritis, psoriatic (PsA)**
BMD and prevalence of osteoporosis and fractures in PsA, M470
- Arthritis, rheumatoid (RA)**
Anti-TNF treatment in RA patients does not alter the one-year change in spine and hip BMD compared to control patients, M497
Effect of ETN on bone metabolism in patients with, W434
Evaluation of the BMD and body composition in early RA, W440
Importance of biochemical markers of bone and cartilage turnover as the predictors of radiographic progression in patients with early RA, W431
Joint destruction, treatment with anti-TNFα antibody recovers osteoclast maturation deviated from bone remodeling cycle, W439
Osteoporosis and RA, which nutritional factors are associated?, W442
Refractory or remission, association of tri-nucleotide (CAG and GGC) repeat polymorphism of AR gene in Taiwanese women with, W433
Rheumatoid synovial fibroblasts promote osteoclastogenic activity by activating RANKL via TLR-2 and TLR-4 activation, W435
TRACP isoform 5a as a marker of disease severity in RA, W432
- Arthritis, TNF-mediated**
VDR deficiency aggravates, W443
- Aryl hydrocarbon receptor (AhR)**
Crosstalk in BaP-mediated inhibition of osteoclastogenesis, NF-κB but not NFATc1 is involved in, T106
- ASARM-peptides**
Directly responsible for defective mineralization in HYP, 1155
SIBLING (minhibins), degradation of MEPE, DMP1 and release of, 1155
- Ataxia telangiectasia mutated (Atm)**
Genetic interaction between, p53 in bone development, M271
Regulates osteoblast differentiation through the BMP-Smad1/5/8 pathway, M017
- ATDC5**
Gene-trap mutagenesis revealed the involvement of vinculin in chondrogenic differentiation in, M137
Identification of a novel chondrogenic factor SNX19 using a real-time fluorescence monitoring cell line, 1185
- ATF4**
As a crucial partner of c/EBP in osteoblast differentiation, W029
Regulates chondrocyte proliferation and differentiation by direct targeting Ihh transcription, 1183
- Athletes**. See also *Exercise*
Effect of combined strength and speed training on cortical bone geometry and mass distribution in master athletes, W505
Relationship between serum 25OH(D) and bone markers in professional football players, W503
- Atomic layer deposition (ALD)**
Derived HA surface, attachment of osteoblast-like cell on, W009
- Atorvastatin**
Inhibits lipid induced aortic valve calcification and osteoporosis via the Lrp5/Wnt mediated pathways in vivo and in vitro, 1154
- ATP**
1,25(OH)₂ Vitamin D₃-induced release, molecular mechanisms in osteoblasts, 1030
Modulation of MAPKs and c-fos expression in osteoblastic and breast cancer cells, T064
PTH enhances induced ERK1/2 activation via a competitive mechanism involving GRK2 in osteoblastic cells, T060
Released from human osteoblasts by multiple mechanisms, M065
- Autocrine mechanism**
RANKL stimulates osteoclasts to release VEGF-C and enhances osteoclastic bone resorption through, 1100
- Autosomal recessive hypophosphatemic rickets (ARHR)**. See *Rickets*
- AZD0530**
Phase II pilot study of safety and effects on bone resorption of AZD0530 in prostate or breast cancer patients with bone metastases, W189
- B**
- B-raf**
Dispensable for endochondral bone development, W095
- B₁**
Induction of kinin receptor in osteoarthritis is performed by vasoactive peptide ET-1, M117
- BAG-1**
Role as an intracellular binding protein for 1,25-dihydroxyvitamin D₃, M252
- Basic multicellular unit (BMU)**
Activity, lacunocanalicular fluid flow and regulation of, M069
- Bax deficiency**
Bax-deficient mice exhibit marked increase in callus size and cartilage during endochondral repair of femur fractures, 1223
- Bazedoxifene**
Efficacy of bazedoxifene for prevention of postmenopausal osteoporosis, 1209
Efficacy of bazedoxifene in reducing new vertebral fracture risk in postmenopausal women with osteoporosis, 1206

- Safety and tolerability of bazedoxifene in postmenopausal women with osteoporosis, W385
- Bazedoxifene acetate (BZA)**
Effects of BZA on bone loss, M404
Safety and tolerability of BZA for the prevention of postmenopausal osteoporosis, W387
- bcl-x**
Osteoclast-specific deletion of gene, functional analysis of Bcl-xL in osteoclasts by, 1098
- Bcl-xL**
Functional analysis in osteoclasts by osteoclast-specific deletion of bcl-x gene in mice, 1098
Molecular interaction with Bnip3 determines the cell fate of hypertrophic chondrocytes, 1181
- Bcl2**
Anti-apoptotic molecule, regulation of skeletal homeostasis by, 1290
In osteoclastogenesis ex vivo, role of, W083
- Benzo[a]pyrene (BaP)**
Mediated inhibition of osteoclastogenesis, NF- κ B but not NFATc1 is involved in AhR-RANKL crosstalk in, T106
- Beta-adrenergic receptors**
Beta-adrenergic receptor agonist administration during hindlimb unloading attenuates losses in bone geometry, structure, and mechanical properties, M514, S514
- Beta blockade**
Mitigates bone loss during energy restriction partially via leptin, 1110
- BHH9**
Effects on expression of VEGF and their receptors during osteoblast differentiation, W042
- Biglycan (bgn)**
And fmod control bone mass by regulating osteoclast differentiation through BMSC, M157, O157, S157
- Bim**
Akt1 contributes to maintenance of bone mass and turnover by inhibiting apoptosis of osteoblasts through, 1211
- Bioceramics**
Scaffolds support MSC growth and osteogenic differentiation, M050
- Bioluminescence**
Application in stem cell-based bone formation, W046
- Biomechanics**
Biomechanical testing in experimental bone interventions, W457
And body size quantitative trait loci in HcB/8 and HcB/23 F2 mice, W466
Correlation between growth patterns and material composition leads to preferred sets of adult bone traits, 1242
Functional muscle-bone unit in young active women, W488
Technique for calculating area moment of inertia of long bones using CT data, W225
Topological analysis and spatial distribution of apparent trabecular bone in radiographs correlate to biomechanical bone properties, W229
- Bioreactors**
Design for osteochondral tissue, M151
- Birth weight**
Birth weight predicts lean body mass and thus BMC in healthy men at peak bone mass, M467
Impact of birth weight and age at menarche on skeletal growth in young women, W256
- Bisphenol-A-diglycidyl ether (BADGE)**
Combination with Vitamin D potentiates their pharmacological inhibition of PPAR γ and increases osteogenic differentiation of adipocyte precursors, W155
- Bisphosphonates**
Adherence and fracture risk, M440, S440
Affinity to hydroxyapatite and farnesyl pyrophosphate inhibitory potency, together, drive in vivo efficacy, W325
Analog that lacks anti-remodeling activity prevents osteocyte and osteoblast apoptosis in vivo, 1011
Are bone resorption markers during osteoporosis treatment with bisphosphonates within the lower half of the premenopausal range?, M314
Case of GI side effects or contraindications for oral bisphosphonates treatment with intravenous pamidronate is a good alternative, T388
Cause inflammatory response in vivo and in human peripheral blood mononuclear and polymorphonuclear cells in vitro, W361
Changes in bone resorption markers during osteoporosis treatment with oral bisphosphonates, M315
Convenience and preference perceptions after one year of oral bisphosphonate treatment in a group of Brazilian women, W383
Essential mechanistic studies of the esophagogastric transit of oral bisphosphonates, W327
FDPS, *GGPS1* and *FDFT1* gene polymorphisms as pharmacogenetic markers for the response to bisphosphonates, T213
How quickly do oral bisphosphonates work, and are there differences between them?, T380
Impact of GI medication usage with regard to discontinuation and restart behavior with oral bisphosphonates in three large U.S. Physician groups, M442
Long-term bisphosphonates therapy and increase fracture risks, W375
Longitudinal patterns of adherence with bisphosphonates, M444
Modeling the contribution of long-term persistence with weekly or yearly bisphosphonate treatment to fracture outcomes, M443, S443
Therapy and hip fractures within the Ris and ALN (REAL) Cohort Study, T384
Three-year effects of bisphosphonates on treatment of osteoporosis and on reducing the risk for vertebral fractures of RA patients, W358
Treatment during long-term disuse blunts the recovery response of bone to restored weight-bearing, M403, S403
Use increases in patients with osteopenia and prior fractures following a multifaceted osteoporosis educational intervention, T396
Use increases in patients with osteoporosis following an integrated osteoporosis educational intervention, M436
Women are more persistent with monthly bisphosphonate therapy compared to weekly bisphosphonates, W366
Year 3 effects on bone mass in women using bisphosphonates after PTH therapy, 1094
- BK channels**
In human osteoblast-like cells, properties and function, W045
- Black cohosh**
Effects of black cohosh root extract on the vasomotor symptom and bone metabolism of menopausal women, T423
- Bleaching**
Changes in dental enamel crystals by, W480
- BMIL**
Evaluation of bone area in the BMIL QA/QC phantom on the Norland system, T276
- BMP** See *Bone morphogenic protein*
- BMP and activin membrane-bound inhibitor (BAMBI)**
Regulation of mouse gene expression, W113
- Bnip3**
Molecular interaction with Bcl-xL determines the cell fate of hypertrophic chondrocytes, 1181
- Body mass index (BMI)**
High cholesterol, smoking and coffee consumption but low BMI are risk factors for fractures, T343
High leisure time physical activity and high BMI protect against fractures, but heavy work and smoking increase risk, W288
- Bone accretion**
Skeletal muscle-specific overexpression PAPP-A increases, T080
- Bone adaptation**
Bone adaptation to impact loading, M525, S525
Functional, comparison of in vivo model to the calculated mechanical environment, W086
Inadequate, in bone cell specific Cx43 deficient mice, 1285
Site specific, modulation by signaling in osteocytic networks, W060
- Bone area**
Increased due to mechanical loading gradually decreased following cessation of loading, T151
- Bone cells** See also Bone marrow stromal cells; Fetal bone cells
Evidence for lineage dependent non-canonical Wnt signal transduction by, 1139
Induced proliferation and recruitment, effects of mechanical strain on osteocytes, W054
Mechanical loading of, collagen and osteopontin upregulation by, T154
PHD1 and PHD3 are expressed but are not essential for bone homeostasis, T132
Specific Cx43 deficient mice, inadequate bone adaptation in, 1285
- Bone density**
At age of peak bone mass in women is not associated with history of childhood fractures, M535, S535
And body composition values in healthy Japanese girls, T512
Clinical evaluation of jaw bone density with a newly developed "jaw bone density evaluation system," T280
EPO as a regulator of in elderly men, M177
Muscle cross section and muscular power in the lower limbs in healthy postmenopausal women, patients on corticosteroids and fracture patients, M367
Use of s-RANKL, s-FREE RANKL and OPG serum levels for prediction of bone density, W219
- Bone destruction**
Osteoclastic, possible suppressive role of Galectin-3 accompanying adjuvant-induced arthritis in rats, M108

Bone development

Embryonic, BMP signaling in osteoblasts negatively regulates canonical Wnt signaling to reduce bone mass during, M270, S270
 Endochondral, A-raf and B-raf are dispensable for, W095
 Genetic interaction between p53 and Atm in, M271
 Intramembranous, osteoblast-targeted disruption of GC signaling delays, T182

Bone erosion

NEMO (IKK) modulates, T098

Bone fillers

Development of novel mini-tetrapod bone fillers, T356

Bone formation

In 2D and 3D tissue engineered constructs, use of statins to enhance, T003
 Deletion of Cnb1 in osteoblast reveals novel role for calcineurin in, T283
 Ectopic, functional RNAi screening for Runx2-regulated genes corresponding to, M273
 Effects of CIB on, W006
 Effects of traumatic brain injury on, during fracture healing in a rat model, M008
 Endochondral, BMP canonical signaling through receptor Smad 1 and Smad 5 is required for, M171, S171
 Endochondral during embryonic development, CITED1 ablation impairs, M142, O142, S142
 Endochondral, loss of annexin VI affects, T131
 Endochondral, osteogenic stem cell homing to sites of, T071
 Endochondral, role of the transcription factor Lbh in, M122
 Haversian-type bone and blood vessels guided by the artificial ECM of vasculature-inducing geometry, M154
 Imatinib mesylate inhibits and decreases bone mass in vivo by inhibiting PDGFR-mediated osteoblast mitogenesis, T018
 Impaired in mice lacking Gs α in early osteoblasts leads to marked bone fragility, T020
 NELL-1 promotes in a spinal fusion model, M200
 New approach to assess rates and IHC/ISH in the same bone specimen, T115
 New, TGF β stimulates in neonatal calvariae via suppression of DKK1, M197
 OASIS is involved in, M029, S029
 OsM is an essential stimulus of osteoclastogenesis and, T068
 Osteal macrophages, novel regulators of, T186
 In osteoblastic cells, osteoclasts secrete an activity promoting, T005
 Osx as a regulator of, M010, S010
 Over-expression of Runx2 in mesenchymal cells enhanced, T066
 Point mutation of endofin at PP1c-binding domain (F872A) stimulates, T256
 Rate falls after puberty in Brlt OI mouse due to cellular uncoupling, W166
 In skeletal remodeling, TRIP-1 as an important co-regulator of, T252
 Stem cell-based, application of bioluminescence in, W046
 TGF β 1 induces migration of MSCs in coupling bone resorption and formation, T072
 In vitro and in vivo, Zfp521 is a novel inhibitor of Runx2 activity with opposite effects on, T250

In vivo ectopic induced by BMP-2, noggin siRNA gene transfer enhances, W121

In vivo, PGD₂ in, T001

In vivo tibial compression stimulates bone formation, M521

Bone fragility

Impaired bone formation in mice lacking Gs α in early osteoblasts leads to, T020
 Knockout of CatK in adult mice does not result in, W063
 May be caused by mechanostress inequality in transitional period from a steady-state bone metabolism to another state, W470

Bone geometry

Dok-1 and Dok-2 deficiency enhances bone resorption and modulates in vivo, M086, S086
 Heritability of the principal components of a statistical shape model describing midshaft femur geometry, W172
 Load-specific differences in femoral neck cortical geometry, WG32

Bone growth

Local CNP clearance system as a regulator of CNP-GC-B system for, T168
 Rapid site-specific bone growth by a combination of bone marrow ablation, PTH and bisphosphonate therapy, W143
 Reduced, deficiency of GPR30 leads to, T201
 Sexual dimorphism in radial and longitudinal bone growth differ by tempo and magnitude, T039

Bone healing

Implication of OPN and BSP in, M160, S160
 Intramembranous, local application of GH and IGF-1 have a similar effect on, M193
 Normal endochondral bone healing follows continuous bisphosphonate pre-treatment, T089

Bone health

Approach for screening natural plant ingredients for development of nutraceutical supplements to support bone health, W338
 Bringing bone health to seniors' communities, W376

Bone homeostasis

Dimorphic effects of Notch signaling in, T212
 PHD1 and PHD3 are expressed in bone cells but are not essential for, T132

Bone loss

Antiepileptic drugs affect bone loss via reproductive hormones, W415
 Beta blockade mitigates during energy restriction partially via leptin, T110
 Comparative analysis of expression profile in the anatomically separated parts of femurs prepared from unloading induced bone loss model, T153
 Comparison of a soluble ACTRIIA, PTH and ZOL for treatment of established bone loss, T233
 DEX-induced in vitro, silencing *Dkk1* expression rescues, M057
 Following small bowel transplantation, T497
 Of lactation, estrogen deficiency and PTHrP infusion do not fully reproduce, M220
 Ovariectomy-induced, purinergic P2X₂ receptor is responsible for, M248, S248
 Overexpression of low molecular weight isoform of FGF-2 partly prevents, T160
 Periarticular in arthritis, role of synovial GC generation, M232

Selective deletion of the membrane-bound CSF1 isoform in vivo does not affect estrogen-deficiency, T255

Tri-partite relationships between bone, cartilage and adipogenic changes contribute to bone loss, T277

Use of RAP-011 in combination with PTH or ZOL using a mouse model of established bone loss, M394, S394

In vivo, I κ B α -deficient mice display increased, T147

Bone markers

Relationship with serum 25OH(D) in professional football players, W503
 Responses to short-term training, W056

Bone marrow

Adipogenesis, effect of estrogens on, M243
 Adiposity, opposing effects of GH and alcohol reveal a critical role in the reciprocal relationship between adipocyte and osteoblast differentiation, M196
 Cell culture, differentiation during medullary bone formation period in Japanese quail, M091
 Dramatic increase in hematopoiesis and angiogenesis of rescued RANKL-deficient mice by expression of soluble RANKL transgene, M096, S096
 IGF-1 engineered MSCs improve the fracture healing process, M191, S191
 Long-term follow up of BMD, bone turnover markers and 25-hydroxyvitamin D in bone marrow transplant survivors, T499
 MSC from, osteogenic differentiation and interaction with Ti6Al4V, T053
 Secretion of adipokines and hypertrophic changes in adipocytes, M473

Bone marrow-derived mesenchymal stem cells (bmMSC). See Mesenchymal stem cells, bone marrow-derived**Bone marrow fat cells**

Temporal feature in the process of steroid-associated ON development, T178

Bone marrow stromal cells (BMSC)

Activation of LXR inhibits hedgehog signaling and osteogenic differentiation of, W023
 bgn and fmod control bone mass by regulating osteoclast differentiation through, M157, O157, S157
 Calcitriol inhibits differentiation into osteoblasts in a manner cooperative with but independent of TGF β , T069
 Differentiated cell line, PTHrP induces MKP-1 in, M001
 FGF2 and TGF β 1 have opposite effects on the mural cell phenotype of CD146⁺, M178
 Nondestructive evaluation of cell numbers in BMSCs, T043
 PTH/PTHrP receptor modulates the pool of, W138
 Rapamycin inhibits osteoblast proliferation and differentiation in, M007
 Role of AR in the lineage commitment of, T198
 Role of EphB/ephrin-B interactions in cell attachment and spreading of mesenchymal precursors derived from, W033

Bone mass

Ang II suppresses via AT1 receptor in long bones of adult mice, M141
 Body mass influences bone mass independent of leptin signaling, M148, S148

- Bone varies the spatial distribution of its mass, rather than its mass, to optimize strength and minimize bulk, M333
- Cancellous, opposing effects of GH and alcohol reveal a critical role in the reciprocal relationship between adipocyte and osteoblast differentiation, M196
- Determinants of bone mass and fracture in adolescent children, 1042
- Determinants of bone mass and size in term, near-term, and preterm boys, M532
- During embryonic bone development, BMP signaling in osteoblasts negatively regulates canonical Wnt signaling to reduce, M270, S270
- Expression of *OCZF* directed by the CatK promoter affects, M099, O099, S099
- Imatinib mesylate inhibits bone formation and decreases in vivo by inhibiting PDGFR-mediated osteoblast mitogenesis, T018
- Increased, transgenic expression of an engineered Gs-coupled receptor in osteoblasts produces, 1019
- Interaction between dietary fat and polymorphisms in a previously undetected, alternate 3 UTR of the PPARG gene influences bone mass, M285
- Local overexpression of aromatase in osteoblasts leads to clearly increased, 1218
- Low, transgenic mice overexpressing sFRP-4 have, but do not exhibit disturbed phosphate homeostasis, M209
- Low, with null mutation in TGIF, 1286
- Maintenance of by inhibiting apoptosis of osteoblasts through FoxO3a/Bim axis, Akt1 contributes to, 1211
- Osteoclast specific ablation of *dicer* increases, 1292
- Overexpression of osteoblast specific *Angpt1* increases, M016, S016
- Peak spine and hip bone mass in Korean women, W262
- Reference graphs of age-related changes in bone mass, volumetric density, design and strength and of muscle-bone interactions in normal men and women, W235
- Targeted deletion of a distant transcriptional enhancer of the RANKL gene increases, 1067
- Theoretical analysis of current density to increase bone mass with low-frequency interferential electrical stimulation, T429
- In vivo, aging-associated gene SIRT-1 regulates, 1097
- Bone mass measurement (BMM)**
Longitudinal patterns in BMM among U.S. Medicare beneficiaries, M324
- Bone matrix**
Microstructural variation in, modifies strain amplification on the osteocyte, M066
- Bone matrix, demineralized.** See *Demineralized bone matrix*
- Bone measures**
Distribution of bone measures in children at 11 years of age, M529
- Bone mechanotransduction**
Novel role for NFATc1 in, M519
Role of CaV1.3 in, W494
- Bone metabolism**
After posterolateral lumbar fusion using OP-1, W119
In an animal model of AS, W441
- Dietary Ca, P, protein and bone metabolism in Korean postmenopausal women, M343
- Effect of ETN in patients with RA, W434
- Effects of Pit-1 type III Na-dependent phosphate transporter overexpression on, W128
- Bone microstructure**
Heritability of bone microstructure in women, 1243
Micro-architectural changes of developing bone in male and female rats, W450
Role of microarchitecture on whole-vertebral body biomechanical behavior, M506
- Bone mineral content (BMC)**
Accrual of lean mass has more impact than the accrual of fat mass on BMC during growth, W520
Correlation of isokinetic knee and trunk muscular strength with BMC in female soccer players, W518
Gender related differences in bone mineral quality, T314
Posterior cortical BMC in the femoral neck predicts proximal femur failure load, W461
In postmenopausal women, relationship of serum cytokines and monocyte gene expression to, M183
- Bone mineral density (BMD)**
Age, gender and region related changes in BMD of Korean adult, W243
Association of self-reported frailty with BMD and incident fractures in an elderly population, W297
Associations between BMD and SOS, T298
Clinical comparison in BMD gains with monthly oral IBN and weekly oral ALN, W354
Clusters of dietary protein and relation to BMD in men and women of the Framingham Offspring Study, W267
Combination therapy of ALN and calcitriol increases in BMD by keeping intact Ca metabolism for the treatment of osteoporosis, T434
Comparison of changes in BMD and bone turnover marker with ALN once-weekly and bi-weekly in postmenopausal Korean women, T399
Comparison of QCT and DXA derived areal BMD, T269
Correlations between bone and body composition in post-pubertal daughters and their premenopausal mothers, W260
Declines with age in zebrafish (*Danio rerio*), T452
Effect of BMD measurement of hip bilateral in clinical practice, T273
Effects of functional single nucleotide polymorphism in the tissue-nonspecific alkaline phosphatase gene (787T>C) Associated with BMD, M342, S342
Evaluation of forearm BMD measurement for diagnosis and treatment monitoring, T282
Examination of the effect of dietary habits on BMD in healthy men aged 15-49 years living in Debrecen, Hungary, M341
FGF-23 is an independent predictor in a population-based cohort of elderly men, W125
Gene polymorphisms, BMD and BMC in children, M528, S528
How discrepancies in BMD changes and fracture risk may be explained, W478
- Increased BMD in transgenic mice over-expressing tissue-nonspecific alkaline phosphatase, 1236
- Increased, targeted deletion of E11/gp38 results in, 1043
- Investigating the role of Mesp2 in the epigenetic regulation of BMD, T208
- Linkage screen for BMD phenotypes in male and female COP and DA rat strains, W178
- Longitudinal rate of change in BMD by age for men and women, M336, S336
- Longitudinal study of changes in BMD in women undergoing screening for osteoporosis, W252
- Multifactor dimensionality reduction reveals antagonistic epistasis between ESR1 and ESR2 with BMD variation in Southern Chinese women, T229
- No-vertebral fracture rates are lower in Hong Kong Chinese men than American Caucasians but BMD predicts fracture risk similarly in the two groups, W253
- Nutrient intakes related to BMD in Brazilian men and women, T312
- Phalangeal BMD assessment using radiographic absorptiometry from hand x-rays taken with digital mammography, T279
- In postmenopausal women, relationship of serum cytokines and monocyte gene expression to, M183
- Prediction of 24-month change in BMD on PTH followed by ALN, 1090
- Prevalence of high BMD T-scores in a community population, T455
- Recognition of postmenopausal women at risk of fracture using BMD and clinical risk factors, M379, S379
- Reduced, deficiency of GPR30 leads to, T201
- Regulation by MATN3 through modulating BMP signaling pathways, 1063
- Relationships between diaphyseal geometry and cortical mineral density as assessed by pQCT in the tibia, W236
- Relationships between to lower-limb physical function and BMD in community-dwelling older people, M375, S375
- Relative contribution of body composition to BMD in young Chinese and Caucasians, T458
- Seasonal changes in the BMD of a non-hibernating arctic rodent species, M515
- Selective deletion of FN in osteoblasts affects, 1179
- Similar improvements in hip BMD with monthly oral IBN versus weekly oral ALN in postmenopausal osteoporosis, T377
- Single chromosome substitutions alter functional interactions among femoral morphological traits and, W173
- Solid-state 31P MRI quantifies decreased mineralization density in OVX rat bone, T267
- Spine BMD predicted incident new vertebral fractures in postmenopausal Korean women, W251
- Threshold associations between aspects of body composition and bone mineral mass, W259
- Tibial BMD and geometric properties in females of three generations, W516
- Unilateral osteoarthritic hips have lower trochanteric BMD and higher femoral neck BMD compared with the unaffected side, W473
- Vasomotor symptoms are related to lower BMD, M368, S368

- Volumetric, increased due to mechanical loading gradually decreased following cessation of loading, T151
- Women and men with a recent clinical fracture have bone and fall related fracture risks far beyond the presence of low BMD, WG28
- Bone mineral density, volumetric (vBMD)**
- Determinants of change in bone volumetric density and geometry differ between boys and girls in a multiethnic population, W521
- pQCT reproducibility of vBMD measurements at the radius and tibia in healthy women, M328
- Premenopausal women with short LPL have reduced vBMD but normal bone bending strength at the tibial midshaft, T187
- Bone morphogenetic protein (BMP)**
- Acid swelling overcomes osteogenesis inhibition of xenogeneic collagenous matrix delivery system used for naturally-derived, M172
- Activated osteoblast differentiation with nanopatterned surfaces, assessing, W120
- Antagonists increased expression during distraction osteogenesis, W112
- Atm regulates osteoblast differentiation through, M017
- Canonical signaling through receptor Smad1 and Smad5 is required for endochondral bone formation, M171, S171
- Directed osteoblastogenesis, Spp24 is converted from an inhibitor to a functional enhancer during, M156
- Enhancing the expressions of antagonists, GC suppresses the differentiation of osteoblasts by, M059
- Induced transcription, unliganded ER α or ER β , but not the AR, potentiates osteoblastogenesis and, T190
- Mediated adult bone marrow-derived MSC, active fragment of Spp24 enhances differentiation to osteoblasts, T144
- Point mutation of endofin at PP1c-binding domain (F872A) stimulates bone formation in transgenic mice, 1256
- Proinflammatory control of Smad-driven transcription and osteogenesis, W044
- Signal pathways, CCN3/NOV inhibits BMP-2-induced osteoblast differentiation by interacting with, T070
- Signaling in osteoblasts negatively regulates canonical Wnt signaling to reduce bone mass during embryonic bone development, M270, S270
- Signaling, oxidative stress suppresses osteoblastogenesis by antagonizing, M174
- Signaling pathway in osteoblastic Saos-2 cells, Ubc9 promotes stability of Smad4 and regulates, T065
- Signaling pathways, regulation of chondrocyte hypertrophy and BMD by MATN3 through modulating, 1063
- Smad-mediated signaling, endogenous CREB signaling enhances, W118
- Spatial and temporal localization of components of signaling pathways in the postnatal LVGP, M125
- Type III TGF β receptor regulates signaling in differentiating osteoblasts in vitro and in vivo, W114
- Xenogeneic complex enhances allogeneic DBM osteoinductivity in rats, M173
- Bone morphogenetic protein 2 (BMP-2)**
- Auto-expression via PI3K/Akt signaling, Osx mediates the feedback regulation of, T029
- Co-stimulation with 1,25-(OH) $_2$ D $_3$ enhances the expression of VDR and RANKL mRNA in osteoblasts, W162
- Conditional knockout using the 3.6 Coll1a1-Cre model, 1106
- Craniofacial reconstruction with, M170
- Effects of GC on expressions in bone and kidney, M234
- Enhancing expression, differentiation and mineralization of osteoblastic MC3T3-E1 cells via inhibiting the mevalonate pathway and, M056, S056
- Induced osteoblast differentiation, CCN3/NOV inhibits by interacting with BMP and Notch signaling pathways, T070
- Induced osteogenic transcription factors in NIH3T3 cells, downstream signal transactivation by FGF-4/Osx transgene partially imitates changes of, W016
- Induced osteogenesis, diverse effects of noggin on, W107
- Induces sustained expression of COX-2 in MC3T3-E1 osteoblasts, M168
- Inducible Osx increases osteoblastic CSF-1 and RANKL/OPG ratio to induce osteoclast maturation, M100
- Molecular mechanisms for transcription by the hedgehog pathway, 1257
- Noggin siRNA gene transfer enhances the in vivo ectopic bone formation induced by, W121
- Regulated osteoblastogenesis, Osx functions as downstream of Runx2 and Msx2 during, W020
- Role in postnatal bone biology, 1106
- Signaling, identification of a novel Wnt/ β -catenin response element in the OPG gene promoter and its regulation with, M031, S031
- Bone morphogenetic protein 4 (BMP-4)**
- And BMP-4 are overexpressed in the multiple myeloma bone marrow samples, W110
- In postnatal alveolar bone formation and tooth cytodifferentiation, M140
- Bone morphogenetic protein 6 (BMP-6)**
- And BMP-4 are overexpressed in the multiple myeloma bone marrow samples, W110
- Bone morphogenetic protein 7 (BMP-7)**
- Effects of GC on expressions in bone and kidney, M234
- Bone phenotype**
- Characterization in CIC-7 deficient mice, M272, O272, S272
- Bone regeneration**
- Analysis and quantification of spontaneous bone regeneration, W508
- Bone regeneration with local controlled application of G-CSF in bone defects, T161
- Genetic and pharmacologic activation of the HIF-1 α pathway promotes angiogenesis and accelerates, 1065
- With local controlled application of G-CSF in a bone defect of rabbit ulna, T161
- Osteoblasts in adult bone use *Slug* for, but not remodeling, 1213
- Bone remodeling**
- After achievement of osseointegration by Ti implantation in rat maxillae, T127
- Of bone microarchitecture in aging mice is associated with changes in ephrins gene expression, M455
- Central control by NMU, 1061
- Cycle in RA joint destruction, treatment with anti-TNF α antibody recovers osteoclast maturation deviated from, W439
- Delayed during fracture healing in MMP-13 null mutant mice, M163, S163
- Effects of traumatic brain injury on, during fracture healing in a rat model, M008
- ESWT stimulates in the rat, evaluated with in vivo micro-SPECT scanning, W347
- Hard callus, osteopetrotic *ia/ia* rat exhibits reduced osteoclast activity, resulting in normal endochondral fracture union but delayed, T088
- Osteoblasts in adult bone use *Slug* for regeneration and repair but not, 1213
- Phenotypical heterogeneity between osteoclasts involved in, T083
- Role of PLF following injury, T020
- Spatio-temporal dynamics of a single bone remodeling unit, 1244
- Targeted deletion of a distant transcriptional enhancer of the RANKL gene reduces, 1067
- TRIP-1, an important co-regulator of bone formation in, 1252
- TRPV4 affects by regulating Ca signaling required for osteoclast activity, 1101
- TSG-6 as a new regulator of, T092
- In various bony microenvironments, distinct roles of ITAM signaling in, 1291
- In vivo, PGD $_2$ in, T001
- Bone repair**
- Endochondral, SDF-1/CXCR4 is essential for in vivo, T163
- Interest of platelet-derived products for bone reparation, T498
- Osteoblasts in adult bone use *Slug* for, but not remodeling, 1213
- Bone resorption**
- Activity and apoptosis in young and old mice, comparative analysis of, W081
- Conditional inactivation of the CTSK gene in adult mice results in osteopetrosis without activation of compensatory mechanisms for, W064
- Defects in osteoclasts, disruption of WASP-associated signaling complex formation leads to, M113
- Development of cell-based assays for identifying antiresorptive compounds targeting RANK signaling through HTS, M102
- Diphyllin abrogates acidification of, T093
- Dok-1 and Dok-2 deficiency enhances and modulates the geometry of bone in vivo, M086, S086
- Effect of food intake on bone resorption in cynomolgus monkeys, W221
- Effects of ALN-induced bone matrix changes on, W330
- High cardiovascular risk in men with increased bone resorption or low bone mass, M468, S468
- Increased activity of large osteoclasts in inflammation, mechanisms leading to, T105
- Increased, transgenic overexpression of PTP-oc in cells of osteoclastic lineage led to, M112, O112, S112
- Inflammatory induced by LPS in vivo, TNFR1 and TNFR2 differentially regulate, M110, S110
- Inflammatory, TNF α /CCL3-5/CCR5 cascade mediates RANKL $^+$ cells migration in, M181
- M-CSF stimulates activity of mature human osteoclasts via increased activation of AP-1 and NFB, T075

- Modeling role of ER in transcellular Ca flux in, M105
- Murine model, use of nanogels as a drug delivery system for TNF α antagonist in, M101
- Osteoclast activity by regulating the V-ATPase and Rho activity, CK-B involves, M083
- Osteoclast activity, canonical NF- κ B pathway mediates, T094
- Osteoclast specific ablation of dicer suppresses, T292
- Osteoclastic, cytoplasmic terminus of a V-ATPase accessory subunit Ac45 is required for proper interaction with V0 domain subunits and, M104
- Osteoclastic, potential role of Rab3D-calmodulin interaction in, M103, S103
- Osteoclastic through an autocrine mechanism, RANKL stimulates osteoclasts to release VEGF-C and enhance, I100
- Osteoclastic, VGLUT1 knockout mice develop osteopenia due to an increase in, T085
- Osteoclasts secrete an activity promoting bone formation and canonical Wnt signaling in osteoblastic cells, T005
- Small GTPase cdc42 enhances, I146
- TGF β 1 induces migration of MSCs in coupling bone resorption and formation, I072
- in vitro, homogenous fluorescence-based Ca assay for the rapid determination of, T096
- Bone sialoprotein (BSP)**
- Implication in bone healing, M160, S160
- Mediated osteoblast differentiation and mineralization is principally dependent on the intrinsic characteristics of responding cells, T149
- Post-translationally modified, NFATc1 mediates the stimulatory effects on the resorptive activity of rabbit osteoclasts, T099
- Bone size**
- Coadaptation among trabecular and cortical traits contribute to genetic variation affecting bone size in recombinant inbred mouse vertebrae, T241
- ENU mutation mapped to a distal region of Chromosome 11 is major determinant of bone size independent of body growth, T211
- Genetic control of by regulating the differentiated function of periosteal cells, locus on Chr 4 exerts, W008
- IGFBP-3, 4 and 5 triple knock-out mice have larger bones, M189
- Targeted disruption of Efnb1 in osteoblasts reduces, I107
- Bone-specific alkaline phosphatase (BAP)**
- Development of an assay for the LIAISON[®] Analyzer, W217
- Bone strength**
- Assumptions and limitations in image-based strength assessment of bone, M509
- DXA and QCT geometric structural measurements of proximal femoral strength, T291
- Genetic and environmental effects on muscle cross-sectional area and structural strength of tibia in older female twins, T204
- Genetic loci for bone structure and strength identified in inbred COP and DA rats, W185
- Genome-wide scan of metacarpal bone geometric strength indices in the Framingham Study, W177
- Is bone strength a simple function of muscle, or does other mechanical loading play a role?, I037
- Lean and not fat mass is associated with male proximal femur strength, W471
- And toughness are reduced by loss of architecture, W240
- Trends in femur structural strength with aging in Canadian adults, W233
- Bone strength indices (BSI)**
- Longitudinal change in BSIs, T285
- Bone surface**
- Mast cell migration precedes and appears essential for PTH-induced peritrabecular fibrosis, M482, S482
- Sex-specific changes during adolescent growth, pQCT analysis of the mid-tibia, M527
- Bone texture**
- Laws' masks descriptors applied to bone texture analysis, T295
- Morphological texture analysis of radiographs of the proximal femur, W449
- Bone tissue**
- Effects of GC on BMP-2 and BMP-7 expressions in, M234
- Bone turnover**
- Age-related changes in bone turnover in men, W218
- Androgens act directly via the AR in mineralizing osteoblasts to regulate, I217
- Association of dietary Ca, BMD and biochemical markers of bone turnover among rural Thai women, T313
- Biochemical markers of bone turnover, hip bone loss and non-spine fracture in men, I074
- Cancellous, opposing effects of GH and alcohol reveal a critical role in the reciprocal relationship between adipocyte and osteoblast differentiation, M196
- Effect of energy restriction on bone turnover in physically active females, W001
- Effects of ALN-induced bone matrix changes on, W330
- Effects on bone turnover of the potent, once-daily, oral Src inhibitor AZD0530 in patients with advanced solid malignancies, W192
- Environmental influences on variability in levels of bone turnover markers, M313
- Establishing a reference range for bone turnover markers in 635 healthy, young, premenopausal women, I168
- Fluctuation of the normal values of the biochemical markers of bone turnover in Greek premenopausal women, W208
- GLP-1 action in normal and type 2 diabetic state, T207
- In late gestation and six months postpartum, T002
- Maintenance of by inhibiting apoptosis of osteoblasts through FoxO3a/Bim axis, Akt1 contributes to, I211
- Markers and prediction of fracture, I073
- Markers of bone turnover in peripubertal girls, M317
- Prevalence of severe suppression of bone turnover among patients with atypical osteoporotic fractures, W359
- Reproducibility of biochemical markers of bone turnover in clinical practice, W215
- Serum IGFBP-2 is a marker of, I253
- Bortezomib**
- Anti-myeloma response of bortezomib is associated with reduced osteoclastogenesis and increased osteoblastogenesis and bone mass in myelomatous bones, I173
- Brain injury, traumatic**
- Effects on bone formation/remodeling during fracture healing in a rat model, M008
- Breast cancer**
- Accelerated bone resorption, due to dietary Ca deficiency, promotes tumor growth in a murine model of breast cancer bone metastasis, I006
- Cell lines, activation of FXR by bone-derived lipid, M249
- Components of native bone environment involved in breast cancer metastasis, T252
- Conditional ablation of PTHrP in mammary epithelial cells inhibits progression, I295
- Fracture threshold in breast cancer patients treated with adjuvant aromatase inhibitors, M147
- Heparin-like polysaccharides markedly reduce osteolytic bone destruction and tumor growth in a mouse model of breast cancer bone metastasis, T241
- High extracellular Ca directly stimulates MDA-MB 231 breast cancer cell by a mechanism involving the CaR, T250
- Oral bisphosphonate treatment prevents the changes of BMD and bone biomarkers in postmenopausal Japanese women with early breast cancer treated with aromatase inhibitor, W186
- Runx2 regulates the Ihh-PTHrP pathway in breast cancer cells, M295, S295
- Sclerotic bone changes found on densitometry testing in a patient with a remote history of breast cancer, W13
- Serum TRACP 5b increases with advancement of osteolysis in a nude mouse model of breast cancer bone metastasis, T239
- Breast cancer cells**
- MAPKs and c-fos expression in, ATP modulation of, T064
- Btk**
- Lack of Btk results in osteoporosis, despite defects in osteoclast function, T097
- C**
- c/EBP α**
- Reciprocal regulation of Dkk1 gene transcription by, I140
- c/EBP β**
- As a crucial partner of ATF4 in osteoblast differentiation, W029
- c-fms**
- Antibody inhibits mechanical stress-induced root resorption, M107
- c-Fos**
- Activation, endogenous TNF in osteoclast precursor cells promotes osteoclastogenesis via, T077
- ATP modulation of, in osteoblastic and breast cancer cells, T064
- Expression in osteoclastogenesis, POZ-Zn transcriptional regulator OCZF/LRF is induced by RANKL and increases, W067
- C-reactive protein (CRP)**
- BMD and hip fracture risk in elderly men and women, T347

- In patients with osteoporotic non-traumatic fractures, W203
- c-Src**
Activation of MAPKs by 17 β -estradiol is mediated in skeletal muscle cells, T194
Interaction of galectin-9 with lipid rafts induces osteoblast proliferation through, W005
Mediated osteoblast differentiation, role of IL-6 signaling in, T170
- C-terminal**
Regulatory domain, growth inhibition of osteoblast progenitors by Runx2 depends on, M047, S047
- C2C12**
TNF α stimulated Msx2 expression in, M020
- C3H10T1/2**
Mineralization of murine mesenchymal cells in micromass culture, W088
- C57BL/6**
Aging, exhibit increased oxidative stress and defective replication, M052, S052
Effect of age on bone mass and bone material properties in C57BL/6 mice, T464
- C57BL/6J**
Seasonal changes in bone and body mass are gender and compartment specific, M269
- CaCl₂**
Hydrothermal treatment with, improving bone bonding ability of Ti, W011
- Calbindin-D_{9k}**
Studies using nullmutant mice reveal active intestinal Ca transport in the absence of calbindin-D_{9k} or TRPV6, 1026
- Calcaneal speed of sound (SOS)**
Improved standardization of calcaneal SOS measurements, T304
- Calcification**
Role of Fe³⁺ ion and ferritin on differentiation of chondrocytes at the stage of, M131
- Calcification, abdominal aortic (AAC)**
On VFA images predicts incident myocardial infarction and stroke independent of clinical cardiovascular disease risk factors, 1076
- Calcification, vascular**
And aortic gene expression are consistent with hyperphosphatemia in OPG-deficient mice, 1117
Associated with increased expression of receptor activator of NF- κ B ligand (RANKL), oxidative stress-induced, 1216
Establishment of model using high dose of Vitamin D, T431
- Calcilytics**
Block the suppressive effect of calcimimetics on PTH mRNA levels in parathyroid cells, M228
- Calcimimetics**
Calcilytics block the suppressive effect on PTH mRNA levels in parathyroid cells, M228
- Calcineurin (Cn)**
Deletion of Cnbl in osteoblast reveals novel role for, in bone formation, 1283
- Calcinosis**
Acro-osteolysis and calcinosis, M490
Homozygous missense mutation in *KLOTHO* causes, 1113
- Calcitonin (CT)**
Analgesic efficacy of CT for vertebral fracture pain, M446
Deletion of the CGRP gene causes a profound cortical resorption phenotype, 1120
And TPTD for vertebral fracture pain, M012
- Calcitonin-gene related peptides (CGRP)**
Deletion of the CT gene causes a profound cortical resorption phenotype, 1120
- Calcitriol (CaI)**
Combination of calcitriol shows more bone sparing effect by suppressing secondary increment of PTH in raloxifene therapy, T433
Inhibits BMSC differentiation into osteoblasts in a mannner cooperative with but independent of TGF β , T069
And its analog successfully elongate survival period and improve the skeletal growth via independent pathway of VDR, W157
Treatment of XLH increases FGF-23 concentration, W123
- Calcium (Ca)**
Absorption from commonly consumed vegetables in healthy Thai women, M396
Comparison of the effects of Ca as carbonate or citrate on bone resorption markers in early postmenopausal women, T417
Density of bone correlates with trabecular bone architecture, M505
Dietary protein and BMD in the presence of low versus high Ca in men and women of the Framingham Study, W266
Effect of Ca channel antagonists on bone metabolism in aged male and female brown Norway rats, M018
Effect of Ca plus Vitamin D supplement on hip geometric structures, 1207
Effect of low-Ca diet on bone properties, W136
Effect of nutritional Ca on the risk of postmenopausal fractures varies with age, M344, S344
Effect of plasma 1,25(OH)₂D concentration or intake on negative correlation between plasma 25OH(D) and PTH concentrations in Japanese adolescents, W159
Effects of Ca sources and soluble silicate on bone metabolism and the related gene expression, W409
Efficiency of dietary Ca use for skeletal growth and mineralization in young pigs fed diets with various phosphorus concentrations, M400
EPO as a regulator of in elderly men, M177
Higher dietary Ca intake along with higher Vitamin D status could suppress bone turnover and BMD decrease in Asian osteoporotic patients, W270
Homogenous fluorescence-based assay for the rapid determination of in vitro bone resorption, T096
Independent and 1,25-dihydroxyvitamin D₃-dependent regulation of the RAS in 25(OH)D 1 α -hydroxylase knockout mice, W150
Intact CaR and PTH genes are required to regulate extracellular concentrations independently, M230
Intake and the risk of osteoporosis and fractures in French women, M345
Intake of Ca and other minerals through water, T307
Low Ca intake and insufficient serum Vitamin D status in treated and non-treated postmenopausal osteoporotic women, T316
Nothing works without Vitamin D and, T393
PC1 selective activation of *Runx2*-II isoform transcription is mediated through, 1142
And phospholipase C γ 2 signaling regulates RANKL-induced osteoclastogenesis, 1104
- PTH upregulates placental transfer in response to fetal hypocalcemia while PTHrP does not, W137
- RANKL-induced expression of TRPV2 is involved in osteoclastogenesis via Ca signaling activation, T103
- Serum Ca values after 4 and 24 weeks of treatment with full-length PTH(1-84) of postmenopausal women with primary osteoporosis, M426
- Signaling required for osteoclast activity, TRPV4 affects bone remodeling by regulating, 1101
- Studies using nullmutant mice reveal active intestinal Ca transport in the absence of calbindin-D_{9k} or TRPV6, 1026
- Supplementation improves lipid profile but does not decrease the incidence of cardiovascular events in postmenopausal women, M449
- Transcellular flux, modeling role of ER in bone resorbing osteoclasts, M105
- Transgenic expression of the hVDR in the proximal small intestine of VDR-null mice improves the utilization of rescue diet in young mice, W154
- Uptake in intestinal epithelial cells, role of TRPV6 and β -glucuronidase in 1,25(OH)₂D₃- and PTH-stimulated, M258
- Urinary excretion of ⁴⁵Ca in mice, T236
- Validation of a simple isotope method for estimating true Ca fractional absorption in adolescent girls, T134
- And Vitamin D supplementation improves bone health in a population-based sample of postmenopausal women, T359
- Calcium (Ca²⁺)**
Presence of, non-adherent circulating progenitor cells with osteoblastic potential become adherent and are able to mineralize, T040
RANKL-evoked oscillations mediated by RGS10 in osteoclast differentiation, mechanism of, M093, S093
- Calcium/creatinine clearance ratio (CCCR)**
24h-urine, discriminative power for the separation between FHH and PHPT, M222
- Calcium excretion (CE)**
24h-urine, discriminative power for the separation between FHH and PHPT, M222
- Calcium phosphate (CaP)**
Effects of Pit-1 type III Na-dependent phosphate transporter overexpression on, W128
Layers, Co incorporation stimulates osteoclast differentiation and activation via HIF pathway, W075
Regulating hormone STC-2 is positively and negatively regulated by 1,25(OH)₂D₃ and PTH in renal proximal tubular cells, W130
- Calcium-sensitive receptors (CaR)**
Activation with cinacalcet increases serum gastrin levels in healthy older subjects, M221
Antagonism of CaR stimulates dose-related release of endogenous PTH in normal volunteers, M427, S427
Conditional ablation causes abnormalities in skeletal development and mineralization, M223, O223, S223
Critical role in bone development, conditional knockouts in early and mature osteoblasts reveal, 1284
Dampens the calcemic response to exogenous 1,25-(OH)₂ Vitamin D in vivo independent of PTH, M224

- Deletion of the 25OH(D) 1 α (OH)ase from mice expressing the null mutation converts a hypercalcemic to a hypocalcemic hyperparathyroid phenotype, M231
- Dose-dependent increases in endogenous PTH concentrations after administration of a CaR antagonist to normal volunteers, I131
- Expression in cartilage is essential for embryonic skeletal development in vivo, I176
- Genetic mosaicism for de novo mutations of the *CASR* gene, WG7
- Intact genes are required to regulate the extracellular Mg and Ca concentrations independently, M230
- Plays a significant role in protection against hypercalcemia, M227, S227
- Regulates PMCA2 activity in mammary epithelial cells, M219, S219
- Regulation by Gcm2 in hyperplastic parathyroid cells, M226
- Testin as a novel binding partner of, M225
- Upregulation of gene expression by the proinflammatory cytokine, IL-6, I187
- Calcyclin**
Expression, identification in rat amelogenesis using ACP DDRT-PCR method, T129
- Calmodulin (CaM)**
CaMK-CREB pathway regulates osteoclast differentiation and function, M114, S114
- Diverging pathways of regulation of osteoclastogenesis, W070
- Potential role in osteoclastic bone resorption, M103, S103
- Calmodulin-dependent kinases (CaMK)**
CREB pathway regulates osteoclast differentiation and function, M114, S114
- Calvariae**
Bone defects, induction of mineralized tissues by in vivo transplantation of cultured dental pulp cells in, T017
- Dynamic imaging reveals the motile properties of osteoblasts and osteocytes and suggests heterogeneity of osteoblasts in bone, I045
- Neonatal, TGF β stimulates new bone formation via suppression of DKK1, M197
- Osteoblast cultures, 1,25(OH) $_2$ D $_3$ inhibits bone nodule mineralization through the FGF-23-mediating ERK pathway in, M210, S210
- cAMP response element binding (CREB) protein.** See also *Cyclic adenosine 3,5-monophosphate*
CaMK-CREB pathway regulates osteoclast differentiation and function, M114, S114
- Endogenous signaling enhances Smad-mediated BMP signaling, W118
- Phosphorylation and DNA binding along with demethylation and deacetylation are required for ultimate activation of CYP27B1 promoter by PTH, W132
- cAMP response element (CRE).** See also *Cyclic adenosine 3,5-monophosphate*
Endogenous CREB signaling enhances Smad-mediated BMP signaling, W118
- Camurati-Engelmann Disease (CED)**
T β RI inhibitor rescues uncoupled bone resorption and formation caused by TGF- β 1 mutations in CED, I032
- Cancer.** See also cancer by type
Computed microtomography of bone specimens in the diagnosis of bone metastases, W201
- Examination of RXR α phosphorylation at serine 260 using specific antibodies in cancer cell lines and tumor tissues, M257
- New urine assay for sensitive detection and assessment of cancer-induced skeletal perturbations, W193
- Non-canonical hedgehog signaling regulates Gli2 and PTHrP expression in osteolytic cancer cells, M296
- capn4**
Knockout mice, characterization of osteoblast-specific, I024
- Carbonic anhydrase II (CAII)**
Regulates differentiation and proliferation of ameloblast via intracellular pH-dependent mechanism, T121
- Carcinogenesis**
Epidermal, VDR, HH signaling and, W158
- VDR, hedgehog signaling and epidermal carcinogenesis, WG3
- Carcinoma**
Gender differences on PTHR1 in non-small cell lung carcinoma, M240
- Non-small cell lung, sex effects on PTHR1 in, M240
- Carcinoma, squamous cell (SCC)**
Role of CXCL13 in associated osteolysis in athymic mice, T257
- Carcinoma, thyroid**
Change of BMD and biochemical markers of bone turnover in patients on suppressive L-thyroxine therapy for differentiated thyroid carcinoma, T339
- Carney Complex (CNC)**
Characterization of bone tumors in a mouse model for CNC, T045
- Carotenoid**
Lack of association of carotenoid intake with BMD in older adults, T317
- Cartilage**
Articular, differential accumulation of Pb and Zn in the tidemark of normal and osteoarthritic human, W271
- Calcified, alterations in collagen structure and mineral composition in a monkey model of OA, W089
- Cell death and cell proliferation in human ACL tibial insertion after rupture, W096
- Degeneration, intra-articular OCIF/OPG prevents in a murine model of osteoarthritis, W097
- Degradation and inflammation, therapeutic effect of KHB9 in CIA, M135
- Delayed remodeling during fracture healing in MMP-13 null mutant mice, M163, S163
- Development, p63 plays a central role by directly regulating key genes for chondrogenesis, I182
- Differentiation, targeted overexpression of PTH2R in chondrocytes impairs, W139
- Does increased local bone resorption result in increased cartilage degradation?, T135
- ECM homeostasis is regulated by RAR γ repression function, W103
- Epiphyseal, mice overexpressing nucleolar PTHrP driven by type II collagen promoter show disordered distribution of chondrocytes in, M116
- Expression of CaR is essential for embryonic skeletal development in vivo, I176
- Formation, inhibitory Smad6 and Smad7 differently regulate, M130, S130
- Formation, over-expression of Runx2 in mesenchymal cells enhanced bone formation but inhibited, I066
- Growth plate, Per1 modulates FGF and VEGF signaling and is essential for vascularization in the development of, I064
- Matrix proteins, effect of IL-6 and sIL-6R on the expression of, T146
- Novel TNF α responsive C/EBP site regulates *Cd-rap* expression, M132
- OPG inhibits degradation in a knee instability mouse model, M134
- Cartilage cells**
Role of Nkx3.2 in muscle/cartilage cell fate determination, W105
- Cartilage oligomeric matrix protein (COMP)**
 α_2 M is a novel substrate for ADAMTS-7 and ADAMTS-12 and inhibits their degradation of, M166
- Cas interacting zinc finger protein (CIZ).** See *Nuclear matrix protein 4/cas interacting zinc finger protein (Nmp4/CIZ)*
- Caspase-3**
Role in the anabolic actions of PTH in bone, I188
- Targeted inactivation of the VDR by, M265, S265
- Targeted inactivation of the VDR by caspase-3, WG2
- Caspase-8**
FADD axis regulates osteoclast apoptosis, T102
- β -Catenin**
AKT's effects regulate osteoblasts' responses to mechanical strain and PTH, T067
- Identification of a novel Wnt response element in the OPG gene promoter and its regulation with BMP-2 signaling, M031, S031
- Mechanical activation of is enhanced after caveolin-1 knock-down, T505
- Pathways, protective effects of mechanical strain on osteocyte viability is mediated by the effects of prostaglandin on, M237
- PTH activates signaling through LRP5/6, I297
- Signaling, FFSS and PE $_2$ activates in MLO-Y4 osteocytic and 2T3 osteoblastic cells, W053
- Signaling, greater sensitivity of osteocytes to shear stress as compared to osteoblasts, W052
- Signaling in osteoblasts, ER α is required for strain-related, M064, O064, S064
- Signaling is compromised in ER α -/- mouse tibia, mechanical loading induced, M036, S036
- Signaling, oxidative stress suppresses osteoblastogenesis by antagonizing, M174
- Cathepsin K (CatK)**
Bone effects of CatK inhibitor in OVX rhesus monkeys, M411, S411
- Conditional inactivation in adult mice results in osteopetrosis without activation of compensatory mechanisms for impaired bone resorption, W064
- Dual-action inhibitors, modulation of human osteoclast function, M389
- Dual-action inhibitors, regulation of human MSC lineage commitment, W315
- Generated type I collagen fragments, regulation of osteoclast activity by, W065
- Inhibition of osteolytic bone metastases in breast cancer with a CatK inhibitor, M291, S291
- Inhibitors for the treatment of osteoporosis, M408
- Inhibitors prevent matrix-derived growth factor degradation by human osteoclasts, W335
- Knockout in adult mice does not result in bone fragility, W063

- MK-0822 is a potent and selective CatK inhibitor that maintains its high selectivity in whole cell assays, W334
- Promoter affects bone mass and osteoclast formation in transgenic mice, expression of *OCZF* directed by, M099, O099, S099
- Randomized, double-blind, placebo-controlled study of a CatK inhibitor in the treatment of postmenopausal women with low BMD, 1128
- CaV1.3**
In bone mechanotransduction, role of, W494
- Caveolin-1**
Knock-down, mechanical activation of β -catenin is enhanced after, T505
Phosphorylation in response to fluid shear in osteoblasts is mediated by P2X7 activation, T061
- CCAAT/enhancer binding protein (C/EBP)**
Novel TNF α responsive site regulates cartilage *Cd-rap* expression, M132
- CCL3/4/5**
Cascade of gene expression indicates essential for osteoclast formation, T073
TNF α /CCR5 cascade mediates RANKL⁺ cells migration in inflammatory bone resorption, M181
- CCN2**. See *Connective tissue growth factor*
- CCR1/5**
Deficient mice have a high turnover osteoporosis that is greater in females than in males, 1254
TNF α /CCL3-5 cascade mediates RANKL⁺ cells migration in inflammatory bone resorption, M181
- CD-1**
Mice, demonstration of an anabolic effect of PGE₂ on bone in, M180
- Cd-rap**
Expression, novel TNF α responsive C/EBP site regulates cartilage, M132
- CD34⁺ cells**
Contributes to fracture healing, local transplantation of G-CSF mobilized, W048
- CD40L**
Mediated cross-talk between T cells and stromal cells is required for estrogen deficiency and PTH to induce bone loss, 1136
- CD146⁺**
BMSCs, FGF2 and TGF β 1 have opposite effects on the mural cell phenotype of, M178
- CD155**
Expression and possible role in osteoclastogenesis, M077
- CDC42**
Small GTPase enhances osteoclastogenesis and bone resorption, 1146
- Cell adhesion**
Rho GTPase signaling pathways in osteoclasts, Wrch1/RhoU role in, M073, S073
- Cell attachment**
Role of EphB/ephrin-B interactions in, W033
- Cell death**
And cell proliferation of cartilage layer in human ACL tibial insertion after rupture, W096
Role in injury-induced calcification from TNF α receptor p55/- p75/- mice, W091
Small molecule inducer of activated CD4⁺ T cell death inhibits disease progression in CIA models, M499
- Cell differentiation**
Microarray expression analyses to examine the effects of DEX on, T048
- Cell proliferation**
And cell death of cartilage layer in human ACL tibial insertion after rupture, W096
Mediation of musculoskeletal tumor cells by an IFI16 protein, T265
Osr2 functions in, M003
- Cementoblasts**
Cell lines, PTHrP induces MKP-1 in, M001
NOX expression in NOS knock-out mice, T173
- Cementum**
Cementoblast cultured on fibrin induces fibrinolysis and its apoptosis, T139
- Cerebral palsy (CP)**
Evaluation of the muscle-bone relationship in the midhigh of children with CP, T516
- cEts1**
Identification as potential primary target in the secondary gene regulation of the FGF-23 gene by 1,25-dihydroxyvitamin D3, W161
- Chemotaxis**
Molecular mechanisms of LPA-stimulated osteoblastic cell, M058, S058
- Chloride channel 7 (CIC-7)**
Deficient mice, characterization of the bone phenotype in, M272, O272
- Chloride channel 7 (CLCN7)**
Association study of *CLCN7* polymorphisms and areal BMD in white or black women or white men, T215
Deficient mice, characterization of the bone phenotype in, S272
- Chlorobenzenes (CIB)**
Effects on bone formation, W006
- Cholecalciferol**
Age modifies the impact of Vitamin D3 supplementation on the 25OH(D)/PTH ratio, M414
Comparison of three high-dose oral Vitamin D₃ supplementation regimens, M415, S415
Effect of a single large oral dose of cholecalciferol on serum 25-hydroxyvitamin D levels, 1210
Effect of four weeks of Vitamin D3 supplementation during late winter on markers of the Vitamin D endocrine system and bone turnover, W272
Effect of Vitamin-D3 and Ca on fracture risk in 65-71 year old women in a 3-year randomized clinical trial, 1270
Modulation of RANKL gene expression by Runx2 and Vitamin D3, 1219
Supplementation, age modifies the impact on the 25OH(D)/PTH ratio, M414
- Cholestatic liver**. See *Liver*
- Chondroclasts**
Formation and recruitment, OPG negatively regulates in endochondral ossification, M136, S136
- Chondrocytes**
Analysis of the role of Runx1 in chondrocyte differentiation using chondrocyte-specific Runx1 deficient mice, M133, S133
Articular in vitro, epigenetic mechanisms are involved in the cytokine-induced de novo expression of IL-1 β in, M184
Articular, regulation of MMP expression by EPAS1 in, T122
Articular specific gene, identification of Hs.43125 as, T120
Atf4 regulates proliferation and differentiation by direct targeting *Ihh* transcription, 1183
Chondrocytic phenotype, epigenetic modulatory agents suppress, W099
- Collagen/annexin V interactions regulate growth plate chondrocyte mineralization, 1111
- Differentiation, *Msx2* promotes late stages by up-regulating *Ihh* expression, W092
- Differentiation, role of Fe³⁺ ion and ferritin at the stage of calcification, M131
- Differentiation, *Twist1* stage-specifically regulates downstream of TGF β and Wnt signaling, M129
- Differentiation, *Zfp521* regulates downstream of PTHrP, 1069
- Disordered distribution in the epiphyseal cartilage, mice overexpressing nucleolar PTHrP driven by type II collagen promoter show, M116
- Endplate, IGF-1 regulation of collagen II and MMP-13 gene expression via distinct signaling pathways in, T116
- Growth plate, hydrostatic loading in vitro, M119
- Growth plate, proteasome inhibition induces permanent growth retardation and apoptosis in, M121, S121
- Growth plate, thyroid hormone-induced terminal differentiation involves IGF-1 modulation of canonical Wnt signaling, M118, S118
- HIF2A induces COL10A1 and promotes hypertrophic differentiation of, 1175
- IL-1 β -treated articular, regulation of MMP-9 expression by MMP-12 in, M139
- Rat growth plate, LPA promotes maturation and survival in, M187
- Regulation of proliferation, function, and differentiation by Akt signaling pathways, M123, S123
- Targeted overexpression of PTH2R impairs cartilage differentiation and trabecular bone growth, W139
- Chondrocytes, hypertrophic**
Establishment of a rat culture system for studying the morphological diversity of, M120
Hormonal regulation of apoptosis, W094
Identification of novel transcription factors necessary for, M164
Localization of the *Cis*-enhancer element for mouse *Col10a1* expression in vivo, W106
Molecular interaction between Bcl-xL and Bnip3 determines the cell fate of, 1181
Molecular network underlying chondrocyte hypertrophy causing osteoarthritis, M127, S127
Non-covalent interaction of MMP-13 and LTBP1 in a unique TGF β large latent complex produced by, M128
PTHrP suppresses ERK activation in, W095
Regulation by MATN3 through modulating BMP signaling pathways, 1063
Trps1 transcription factor regulates chondrocyte hypertrophy and perichondrial mineralization through repression of Runx2, 1184
- Chondrocytic cells**
ENC1 is expressed in, T056
- Chondrogenesis**
ECM1 is a novel potent mediator of, 1062
Epigenetic status monitored by DNA methylation in the 5-flanking regions of CpG-rich promoters are stable during, T126
Gene-trap mutagenesis revealed the involvement of vinculin in chondrogenic differentiation in ATDC5 cells, M137
Of mesenchymal cells, identification and characterization of miRNAs expressed during, T123

- p63 plays a central role in cartilage development by directly regulating key genes for, T182
Transcriptional induction of SOX9 by NF- κ B subunit p65 during, W101
- Chondrogenic differentiation**
Runx1 regulates, T112
- Chondrostatin**
New inhibitor of angiogenesis, tumor invasion and osteoclast activity, T259
- Chr 4**
Locus on exerts genetic control of bone size by regulating the differentiated function of periosteal cells, W008
- Chromatin immunoprecipitation (ChIP)**
On-chip analysis reveals novel GC response genes adjacent to genomic binding sites for SHREs in osteoblastic cells, M061
- Chromatin remodeling**
Complex, positive and negative regulation of osteoblast differentiation by the SWI/SNF, M030
- Chromosomes**
Single substitutions alter functional interactions among femoral morphological traits and mineral density in inbred mice, W173
- Cinacalcet**
Activation of the CaR increases serum gastrin levels in healthy older subjects, M221
- Cis-enhancer**
Localization for mouse *Col10a1* expression in hypertrophic chondrocytes in vivo, W106
- CITED1**
Ablation impairs endochondral bone formation during embryonic development, M142, O142, S142
- Ciz**
Interacts with ECM proteins, W012
- Clodronate**
Efficacy of clodronate on fracture risk in women selected by 10-year fracture probability, T060
- Cloning.** See *Molecular cloning*
- Clostridium histolyticum***
Class I collagenase, collagen binding characteristics of CBD from, M204
- Cnb1**
Deletion reveals novel role for calcineurin in bone formation, T283
- CNP**
Local clearance system as a regulator of CNP-GC-B system for bone growth, T168
- Co-culture system**
Spacio-temporal analysis of osteoclastogenesis using, M078
- Cobalt (Co)**
Incorporation into CaP layers stimulates osteoclast differentiation and activation via HIF pathway, W075
- Col3.6-HSD2**
GC loss-of-function model spanning early and late osteoblast differentiation, M235, S235
- COL10A1.** See *Collagen, type X*
- Collagen**
Alterations in structure and mineral composition in calcified cartilage and subchondral bone in a monkey model of OA, W089
Annexin V interactions regulate growth plate chondrocyte mineralization, T111
Binding characteristics of CBD from *Clostridium histolyticum* class I collagenase, M204
Effect of collagen degradation on the stiffness of bone, W474
New surface modified DBM by rhBMP-2 hybrid coating, T133
Quality and quantity in MC3T3-E1 cell culture system, LOX regulates, M011
Upregulation by mechanical loading of bone cells, T154
- Collagen, type I**
Abnormal production by human osteoarthritic osteoblasts, T143
Conditional knockout of BMP-2 using the 3.6 Col1a1-Cre model, T106
Regulation of osteoclast activity by CatK-generated fragments, W065
- Collagen, type II**
IGF-1 regulation of gene expression in endplate chondrocytes via distinct signaling pathways, T116
Promoter, mice overexpressing nucleolar PTHrP show disordered distribution of chondrocytes in the epiphyseal cartilage, M116
- Collagen, type X (COL10)**
Expression, localization of the *Cis*-enhancer element in hypertrophic chondrocytes in vivo, W106
HIF2A induces and promotes hypertrophic differentiation of chondrocytes, T175
Transcriptional regulation by Runx2, M127, S127
- Collagen, type XI**
Analysis of the function of the CTCF-binding site between *Rxb* and, T119
Identification of proteins that interact with the NTD, M149
- Collagen, type XII.** See also *Fibril-associated collagen*
Expression of splice variants of collagen XII in human osteoblast-like cells, M144
- Collagen binding domain (CBD)**
Collagen binding characteristics from *Clostridium histolyticum* class I collagenase, M204
- Collagen-induced arthritis (CIA).** See *Arthritis, collagen-induced*
- Collagenase**
Collagen binding characteristics of CBD from *Clostridium histolyticum* class I, M204
Limited digestion increases solubility and induction potential of human DBM in vitro, T156
- Colon cancer**
Chemoprevention, novel nutritionally-derived ligand of the VDR with implications for bone health and, M255, S255
- Colony stimulating factor 1 (CSF-1)**
BMP-2-inducible *Osx* increases osteoblastic ratio to induce osteoclast maturation, M100
Osteoblasts express CSF-1R and are a target for, T039
Selective deletion of the membrane-bound isoform in vivo does not affect estrogen-deficiency bone loss in mice, T255
Tumor cells metastatic to bone express CSF-1 and support osteoclast survival, T086
- Colony stimulating factor 1 receptor (CSF-1R)**
Osteoblasts express and are a target for CSF-1, T039
- Computed posturography**
Fracture and sway analyzed by computed posturography, W290
- Computed tomography, high-resolution peripheral quantitative (HR-pQCT)**
Assessment of cortical bone, W228
Bone microarchitecture as assessed by HRpQCT in chronic kidney disease, T490
- Bone microarchitecture as assessed by HRpQCT in HIV⁺ postmenopausal women, W444
Correlations between HR-pQCT and high-field MR in vivo bone imaging, T286
Densitometric derived structural indices in HR-pQCT are independent of cortical geometry, T107
High-resolution CT images yield accurate microstructural information if processed by 3-D extensions of standard histomorphometric analysis or fuzzy segmentation approaches, T287
HRpQCT of the radius reflects iliac crest biopsy measures of microstructure and mechanical competence, T164
In vivo assessment of 3-D bone microarchitecture with HR-pQCT in patients with and without fractures, M330, S330
- Computed tomography, micro (μ CT)**
Comparison of bone architecture via micro-CT after long-term treatment with Ris and ALN, T386
Evaluation of polychromatic μ CT mineralization measurement by comparison to synchrotron radiation CT, T110
- Computed tomography, multi-detector (MDCT)**
Trabecular bone structural analysis using 64 MDCT, M326
- Computed tomography, peripheral quantitative (pQCT)**
Comparison of pQCT-based measures of radial bone geometry and apparent trabecular structure acquired using different algorithms, T284
Model effects in the OVX rhesus monkey as measured with pQCT, T290
Sex-specific bone surface changes during adolescent growth, analysis of the mid-tibia, M527
Using pQCT to assess regional bone changes resulting from short-term exercise interventions, W496
- Computed tomography, quantitative (QCT)**
BMD in hip and spine by quantitative CT and previous history as predictors of incidental low trauma fractures in elderly men and women, T278
Of the forearm using clinical CT scanners, M325
And high-resolution CT are better surrogate measures of bone strength than DXA for patients on TPTD treatment, T165
- Conductive heart failure (CHF)**
Spironolactone use and risk of fraction in men with CHF, M352
- Conjugated linoleic acid (CLA)**
Regulates osteoblast and adipocyte differentiation from MSC, T047
- Connective tissue growth factor (CTGF)**
Causes osteopenia in vivo, T178
Crosstalk with TGF β 1 in MSC condensation, M158
Induces NFAT and osteoblastogenesis in vitro, T172
Inhibits BMP-2-induced osteoblast differentiation by interacting with BMP and Notch signaling pathways, T070
Novel transcription factor-like function of MMP-3/stromelysin-1 that regulates gene transcription, T125
Over-expressing in cells of the osteoblast lineage, skeletal phenotype in transgenic mice, T287

Connexin43 (Cx43)

- Amplifies FGF2-responsiveness in a Runx2/PKC δ -dependent manner, W027
- Channels in osteocytes, FFSS promotes intracellular assembly and formation of, M520
- Deficiency, alteration of ET1 effects on calvarial osteoblastic cells, M054
- Deficiency, attenuated response to skeletal load in, M518, S518
- Deficiency, inadequate bone adaptation in bone cell specific, 1285
- $\alpha 5$ integrin association regulates the function of osteocyte hemichannels in response to shear stress, T504
- Involvement in IL-1 β -induced osteoarthritis-associated changes in synovial fibroblasts, T169

Contraceptives

- Does oral contraceptive use adversely impact bone density in young women?, T351

Copenhagen 2331 (COP) rats

- Identification of sex-specific QTL for femoral neck density and strength in inbred, W171

Cortical bone

- Deletion of the CT/CGRP gene causes a profound cortical resorption phenotype, 1120
- Differences in regional femoral neck cortical thickness with aging, T460
- Dimensions, serum PTH is associated with, W135
- Evolution of the crack-growth resistance and toughening mechanisms of human cortical bone via in-situ electron microscopy, W455
- High-dose estradiol treatment causes destruction and is associated with an increased death rate in old WT and ERKO male mice, T193
- Iliac cortical bone structure in osteoporotic women, T296
- Load-specific differences in femoral neck cortical geometry, W497
- Long-distance runners have greater cortical thickness of distal tibia but not of distal radius, T466
- Novel MRI-based technique for quantifying cortical bone water and porosity in-vivo, M329
- Osteoblast-specific knockout of *Igf1r* alters mechanical properties of, W464
- Positively associated with serum IGF-1 and testosterone and negatively with fibrinogen, M194
- Quality and strength in both OVX and sham-operated rats are lowered by limiting physical activity, W479
- Quality and strength of cortical bone are lowered by limiting physical activity, 1160
- Regional thinning of cortical bone in the femoral neck with age, T294
- Size, UGT2B7 H²⁶⁸Y polymorphism is associated with in young adult men, T199

Corticosteroids

- Modulation of P2X₇R in osteoblasts by estrogen and, M055

CpG

- Rich promoters, epigenetic status monitored by DNA methylation in the 5-flanking regions are stable during chondrogenesis, T126

Cranial sutures

- Hypoplastic, spontaneous mutation in the mouse *Lmna* gene results in, M146, S146

Craniofacial bones

- Development, temporal regulation of histogenesis by mesenchyme during, W040

Craniofacial defects

- Analysis of cranial defect healing in CXCR2^{-/-} mice, M276
- Craniofacial reconstruction with BMP-2, M170
- Nell-1 partially rescues in *Runx2* haploinsufficient mice, 1105

Cranio metaphyseal dysplasia (CMD)

- Phe377del Mutation in the Ank gene causes CMD-like phenotype, M268, S268

cre

- Conditional knockout of BMP-2 using the 3.6 Col1a1-Cre model, 1106
- Mediated Dlx3 inactivation in mice, study of inducible, M027, S027

Creatine kinase brain type (CK-B)

- Involves the bone resorptive activity of osteoclast activity by regulating the V-ATPase and Rho activity, M083

Creatinine clearance (CrCl)

- Significant lower balance and muscle power performance and higher risk for falls in elderly people with a decreasing CrCl, M278
- Significantly higher risk for fall-associated fractures with a CrCl below 65, M256

CTCF

- Binding site, analysis of the function between the *Kxrb* and the *Col11a2* genes, T119

 α CTX

- Comparison of α CTX levels in healthy prepubertal children, adolescent, pre- and postmenopausal women, W223

Curcumin (CM)

- Novel nutritionally-derived ligand of the VDR with implications for colon cancer chemoprevention and bone health, M255, S255

CUSUM

- New CUSUM method for simultaneous quality control of BMD, BMC, and area for DXA scanners, T270

CXC chemokine ligand 13 (CXCL13)

- Role in SCC associated osteolysis in athymic mice, T257

CXCR4

- SDF-1 is essential for in vivo endochondral bone repair, T163

CXR

- Prevalence of vertebral fractures on CXR in elderly African-American and Caucasian women, M340

Cyclic adenosine 3,5-monophosphate (cAMP).

- See also *cAMP response element*
- Endogenous CREB signaling enhances Smad-mediated BMP signaling, W118
- Pathways, protective effects of mechanical strain on osteocyte viability is mediated by the effects of prostaglandin on, M237
- Regulation by, characterization of regions upstream of exon II of the human CYP19 gene that mediate in murine osteoblasts, T032

Cyclodextrins

- Osteotropic cyclodextrins as novel bone anabolic agents, W324

Cyclooxygenase 2 (COX-2)

- Acid-induced stimulation of, in osteoblasts mediated by IP₃, M063
- BMP-2 induces sustained expression in MC3T3-E1 osteoblasts, M168
- Deficiency impairs periosteal progenitor cell activation and differentiation, rescued by Ep4 agonist, 1251
- Expression, evaluation in GC-induced osteoporosis in rats treated with Ris, W318

- Transcription by GILZ, novel mechanism of GC action-inhibition of, T180

CYP19. See also Aromatase

- Aromatase deficiency in an adult Chinese male caused by heterozygote for two new point mutations in the CYP19 gene, W168
- Characterization of regions upstream of exon II of, that mediate regulation by cAMP in murine osteoblasts, T032

CYP21B1

- Promoter, CREB phosphorylation and DNA binding along with demethylation and deacetylation are required for ultimate activation by PTH, W132

CYP27B1

- Derepression of gene expression mediates DNA-demethylation, M260

Cystic fibrosis (CF)

- ALN once weekly for the prevention and treatment of osteoporosis in Canadian adult cystic fibrosis patients, W360

Cytokines

- Induced de novo expression of IL-1 β in human articular chondrocytes in vitro, epigenetic mechanisms are involved in, M184
 - Interactions between PTH and the gp130 pathway in differentiating osteoblasts, W025
 - Intracellular profile of RANKL expressing lymphocytes, T164
 - Pro-inflammatory, effects on SOCS-2 expression in the growth plate, W093
 - Regulation of human osteoclast precursor generation by, T079
 - Serum, relationship to BMD and BMC in postmenopausal women, M183
 - Upregulation of CASR gene expression by the proinflammatory cytokine, IL-6, 1187
- Cytoskeleton organization/reorganization**
- HMBG1 regulates actin and RANKL-induced osteoclastogenesis in a manner dependent on RAGE, M079
 - Small GTPase RhoA and its effector kinase ROCK mediate, leading to osteocyte anoikis by GC, M233, S233

D**Dan**

- Enhancing the expressions of BMP antagonists, GC suppresses the differentiation of osteoblasts by, M059

DANCE Study

- Direct Assessment of Non-vertebral Fracture in Community Experience (DANCE) Study, W303

DDOC

- CD11c⁺ dendritic cells-derived osteoclasts, precursor analyses of, M080

Dehydroepiandrosterone (DHEA)

- Serum DHEA is independent of estradiol and testosterone related to incident fractures in elderly men, 1200

Deminerized bone matrix (DBM)

- Allogeneic osteoinductivity, xenogeneic BMP complex enhances, M173
- Limited collagenase digestion increases solubility and induction potential in vitro, T156
- New surface modified by rhBMP-2-collagen hybrid coating, T133
- Osteogenesis of the human LF by, T008

Dendritic cell-specific transmembrane protein (DC-STAMP)

Transgenic mice, cell-cell fusion of osteoclasts is stimulated in, 1102

Dendritic cells

CD11c⁺-derived osteoclasts, precursor analyses of, M080

In myeloma, up-regulation of TACE in monocytes ameliorates their deflected differentiation into, M302

RANKL-stimulated, immunoregulatory role on autoimmune arthritis in MRL/*lpr* mice, T162

Denosumab (DMab)

Comparison of DMab and ALN in combination with PTH in OVX knockin mice expressing humanized RANKL, 1126

Decreased bone turnover and porosity are associated with improved bone strength in OVX cynomolgus monkeys treated with DMab, M409, O409, S409

Effect of DMab on BMD and bone turnover markers, 1205

Improves cortical and cancellous bone mass and bone strength in OVX cynomolgus monkeys, 1082

Increases BMD in patients with RA, 1208

RANKL inhibition by DMab prevents cortical bone loss in a murine model of GIO, 1009

Densitometers

Reliability of two consecutive prodigy densitometers, T278

Dental enamel

Changes in dental enamel crystals by bleaching, W480

Dental pulp cells

In vivo transplantation in calvarial bone defects, induction of mineralized tissues by, T017

Dental pulp stem cells (DPSC). See Stem cells, dental pulp**Dentin**

Enamel phenotype and sexual dimorphism in dentin of *dssp*-null mouse molars, T148

Dentin matrix protein 1 (DMP1)

57 kDa C-terminal fragment of DMP1 retains all biological activity, 1296

Degradation of, and release of SIBLING ASARM-peptides (minhibins), 1155

Identification of novel DMP1 mutations in two unrelated kindreds with ARHP, W165

Mutants causing ARHR, molecular analyses of, 1116

Osteocyte specific expression after mechanical stimulation in the mouse ulnae loading model, W050

Dentine

Organic matrix down-regulate osteoclastic activity in root resorption, T095

Deoxyribonucleic acid (DNA)

Binding and CREB phosphorylation along with demethylation and deacetylation are required for ultimate activation of CYP27B1 promoter by PTH, W132

Demethylation, derepression of CYP27B1 gene expression mediates, M260

Methylation, epigenetic status monitored in the 5-flanking regions of CpG-rich promoters are stable during chondrogenesis, T126

Dexamethasone (DEX)

Effect of, on the osteoblastic differentiation of human ASC, T051

Induced bone loss in vitro, silencing *Dkk1* expression rescues, M057

Microarray expression analyses to examine the effects on cell differentiation, T048

Dhe (dominant hair and ears)

Spontaneous mutation in the mouse *Lmna* gene results in hypoplastic cranial sutures and under-mineralization of the skeleton, M146, S146

Diabetes mellitus

Correlation between cortical bone structure and biomechanics and metabolic indicators in spontaneously diabetic, eSS rats, T472

And fracture risk in older men, 1161

GLP-1 action on bone turnover in, T207

Vitamin D status and infection frequency in diabetic patients, W153

Diabetes mellitus, type 1

Bone-muscle disconnect during pubertal-driven skeletal growth in type 1 diabetes, WG41

Multifactorial etiology of weak bones in type 1 diabetes, M457

Poor long-term glycemic control is not associated with decreased BMD in type 1 diabetes, W414

Diabetes mellitus, type 2

BMD changes in male veterans with type 2 diabetes, T355

GLP-1 action on bone turnover in, T207

Low vitamin D level and high bone turnover in aged type 2 diabetic patient, M456

OPG as cardiovascular risk marker in patients with, T167

Serum pentosidine level is positively associated with the presence of vertebral fractures in postmenopausal women with type 2 diabetes, M316, S316

Type 2 diabetic patients with charcot arthropathy display reduced calcaneal stiffness despite normal foot BMD, W448

Dicer

Osteoclast specific ablation suppresses bone resorption and increases bone mass, 1292

Dickkopf-1 (DKK1)

TGF β stimulates new bone formation in neonatal calvariae via suppression of, M197

Differential display PCR screening (DDRT-PCR)

Identification of calcein expression in rat amelogenesis using, T129

Dihydrotestosterone (DHT)

Treatment reverses gonadectomy-induced changes in fat and lean mass in male but not female mice, T202

1,25-Dihydroxyvitamin D (1,25(OH)₂D)

Automated measurement on the LIAISON[®] Analyzer, W211

Effect of plasma concentration or Ca intake on negative correlation between plasma 25OH(D) and PTH concentrations in Japanese adolescents, W159

Intracrine synthesis and action of rescues TLR suppression of innate immunity, 1028

Treatment with antiresorptive agents reduces circulating 1,25(OH)₂D, W127

1,25-Dihydroxyvitamin D₃ (1,25(OH)₂D₃). See also Vitamin D

CaP regulating hormone STC-2 is positively and negatively regulated by, in renal proximal tubular cells, W130

Co-stimulation with BMP-2 enhances the expression of VDR and RANKL mRNA in osteoblasts, W162

Dependent and Ca-independent regulation of the RAS in 25(OH)D 1 α -hydroxylase knockout mice, W150

Effect of, on the osteoblastic differentiation of human ASC, T051

Identification of cEts1 and STAT1 as potential primary targets in the secondary gene regulation of the FGF-23 gene by, W161

Inhibits bone nodule mineralization through the FGF-23-mediating ERK pathway in calvaria osteoblast cultures, M210, S210

PTH(7-84) inhibits PTH(1-34)-induced production in primary cultured murine renal tubules, T482

Role for BAG-1 as an intracellular binding protein for, M252

Role of TRPV 6 and β -glucuronidase in stimulated Ca uptake in intestinal epithelial cells, M258

1,25-Dihydroxyvitamin D₃ (1,25(OH)₂D₃)

Hypersensitivity in MVNP expressing cells, changes in VDR coregulator recruitment result in, W152

Induced ATP release, molecular mechanisms in osteoblasts, 1030

2-Dimethylamino-4,5,6,7-tetrabromo-1H-benzimidazole (DMAT)

Sensitive kinase, Runx2 transcriptional AD3 supports synergistic Runx2-MINT activation of the osteocalcin FGF response element via, T036

Diphyllin

Abrogates acidification of the osteoclastic resorption lacunae and bone resorption, T093

Distraction osteogenesis. See Osteogenesis, distraction**Dkk1**

Reciprocal regulation of gene transcription by Mx2 and c/EBP α , 1140

Silencing expression rescues DEX-induced bone loss in vitro, M057

DLAM

DLAMs antagonize bone resorption via suppressing RANKL expression in osteoblasts, M262, O262, S262

Dlx3/5

Gene family, gene networks in osteoblasts that are regulated by, W017

Inactivation in mice, study of inducible cre mediated, M027, S027

Overexpression promotes early odontoblast maturation, M028

Dok-1/2

Deficiency enhances bone resorption and modulates the geometry of bone in vivo, M086, S086

Doxorubicin (DOX)

Effectively inhibits osteoclast differentiation and function, M106

Effects of DOX on BMC and density, W299

Duodenum

Rapidly senses and modulates renal phosphate reabsorption via novel PTH- and phosphatonin-independent pathways, M207

Dup(3q) syndrome

Microdeletion involving TNIK alters the phenotype of Dup(3q) syndrome, T470

Dwarfism

A comparative analysis of BMD, M274
Body composition and BMD analysis, T209
Effect of treatment with depot GH on bone remodeling and heel ultrasonometry in dwarfism due to mutation in the GHRH-R gene, T428

Dynein/dynactin complex

Rab3D recruits to secretory vesicles in osteoclasts through direct interaction with Tctex-1, 1293

E

e-NOS. See *Nitric oxygen synthetase*

E-Selectin ligand-1 (ESL-1)

Negatively regulates TGF β in the Golgi during skeletogenesis, M202, S202

E2F1

Repression of gene expression, TIEG suppresses osteoblast cell proliferation through, M035

E4bp4

Induced by GCs and represses promoter activity in osteoblasts, T179

E11

Targeted deletion in osteocytes results in increased skeletal size and BMD, 1043

Ecto-nucleotide pyrophosphatase phosphodiesterase 1 (ENPP1)

ENPP1 as a candidate gene for femoral bone geometry, T219

Ectoderm neural cortex 1 (ENC1)

Expressed in chondrocytic and osteoblastic cells, T056

Ectopic bone

Osteoclasts generated in are derived from pOCs, W071

Efnb1. See *Ephrin B1*

Egr2

Novel pro-survival functions in promotion of M-CSF-mediated osteoclast survival downstream of the MEK/ERK pathway, M111

Elasticity

New method to determine variation of the elasticity of single trabeculae, W459
Osteoblasts and osteocytes, W061

Elcatonin

Injections after drill-hole injury inhibits osteoclast differentiation and prevents the decrease of BMD in non-injured bones with promotion of repair in the cortical bone defect, W336

Electrophoresis, two-dimensional (2-DE)

Skeletal development analysis by 2-DE in white bream (*Diplodus sargus*), T210

Embryogenesis

Using RCAN to deliver short hairpin siRNA to silence gene expression of Wdr5 in chicken limb bud during, T141

Embryonic development

CITED1 ablation impairs endochondral bone formation during, M142, O142, S142

End-stage renal disease (ESRD)

Tartrate-resistant acid phosphatase isoforms in ESRD, M494

Endochondral fracture union

Osteopetrotic *ia/ia* rat exhibits reduced osteoclast activity, resulting in normal endochondral fracture union but delayed hard callus remodeling, T088

Endochondral ossification. See *Ossification, endochondral*

Endofin

Point mutation at PP1c-binding domain (F872A) stimulates bone formation, 1256

Endoplasmic reticulum (ER)

Modeling role in transcellular Ca flux in bone resorbing osteoclasts, M105

Endothelial cells. See *Human bone marrow endothelial cells*

Endothelial PAS domain protein 1 (EPAS1)

Regulation of MMP expression in articular chondrocytes, T122

Endothelial progenitor cells (EPC)

Healing of critical-sized bone defects by EPC, T009
Osteogenic differentiation of circulating, M042

Endothelin-1 (ET-1)

Effects on calvarial osteoblastic cells from Cx43-deficient mice, alteration of, M054
Induction of kinin B₁ receptor in osteoarthritis is performed by vasoactive peptide ET-1, M117

Enhancer binding protein. See also *CCAAT/enhancer binding protein*

EP2

Receptors to upregulate RGS2 expression in osteoblasts, PGE₂ acts through, T063

EP4

COX-2 deficiency impairs periosteal progenitor cell activation and differentiation, rescued by, 1251

Receptors to upregulate RGS2 expression in osteoblasts, PGE₂ acts through, T063

EphB

Role in cell attachment and spreading of mesenchymal precursors derived from human BMSC and DPSC, W033

Ephrin-B1/2

Anabolic action of PTH in osteoblasts, potential involvement of, T012

Role in cell attachment and spreading of mesenchymal precursors derived from human BMSC and DPSC, W033

Targeted disruption in osteoblasts reduces bone size, 1107

Ephrins

PTH-regulated gene expression in the mouse skeleton suggest a role for ephrins in PTH anabolism versus catabolism, 1121

Epidermal growth factor (EGF)

Like ligands stimulate osteoclastogenesis by regulating expression of osteoclast regulatory factors by osteoblasts, T175

Epigenome

Epigenetic mechanisms are involved in the cytokine-induced de novo expression of IL-1 β in human articular chondrocytes in vitro, M184

Epigenetic modulatory agents suppress the chondrocytic phenotype, W099

Epigenetic status monitored by DNA methylation in the 5-flanking regions of CpG-rich promoters are stable during chondrogenesis, T126

Epilepsy

AED affect bone loss via reproductive hormones, W415

Effect of AED on BMD, T349

Epithelial cells

Intestinal, role of TRPV 6 and β -glucuronidase in 1,25(OH)₂D₃- and PTH-stimulated Ca uptake in, M258

Mammary, CaR regulates PMCA2 activity in, M219, S219

Mammary, conditional ablation of PTHrP inhibits breast cancer progression, 1295

Equol

Possible role of equol status in the effects of isoflavone on bone and fat mass in postmenopausal Japanese women, W389

Producers after soy challenge is related to high bone turnover in premenopausal women, M247

Ergocalciferol

Daily versus monthly oral Vitamin D2 and D3, M451

Measurement by the LIAISON[®] 25 OH Vitamin D TOTAL assay, W216

Vitamin D₂ supplementation suppresses endogenous levels of 25-hydroxyvitamin D₃, M264

ERK

Activation in hypertrophic chondrocytes, PTHrP suppresses, W095

Estrogens or androgens attenuate p66^{shc} phosphorylation via a signaling cascade, T185

FGF-23-mediating pathway, 1,25(OH)₂D₃ inhibits bone nodule mineralization through, M210, S210

Interaction of galectin-9 with lipid rafts induces osteoblast proliferation through, W005

Pathway, novel pro-survival functions of Egr2 in promotion of M-CSF-mediated osteoclast survival downstream of, M111

ERK1/2

Activation prevents the FasL-induced apoptosis in IGF-1-treated anulus fibrosus cells, T117

ATP induced activation, PTH enhances via a competitive mechanism involving GRK2 in osteoblastic cells, T060

Essential for osteoblast differentiation, 1141

Extracellular inorganic Pi induces phosphorylation and up-regulates a target gene of FGF-23 in renal proximal tubule cells via NaPi-IIa, W131

ERKO mice

High-dose estradiol treatment causes destruction of cortical bone and is associated with an increased death rate in, T193

Erythropoietin (EPO)

As a regulator of bone density and serum Ca in elderly men, M177

Escherichia coli

Molecular analysis of two novel mutations in the VDR corepressor *hr* and expression of rHr in, M259, S259

ESR2

AluI polymorphism is associated with reduced risk of osteoporotic fractures, T218

Estradiol

Directed gene transactivation, control by an IEBP and an ERE-BP, 1221

Genetic determinants of serum levels of free estradiol and free testosterone in young adult Swedish men, M245

Mediates rescue of the dominant-negative effects of ERE-BP in vivo, 1222

17 β -Estradiol

Abrogates apoptosis in skeletal muscle cells through extra-nuclear estrogen receptors, T196

Activation of MAPKs is mediated by PKC and c-Src in skeletal muscle cells, T194

Additive and synergistic effects of 17 β -estradiol and DHA on bone post-ovariectomy, T362

Estrogen

Attenuate IL-6 and TNF α production in osteoblastic cells by decreasing oxidative stress and its effects on NF- κ B activation, T186

Attenuate p66^{shc} phosphorylation via an ERK and PKC β signaling cascade, T185

Comparison of early-stage immobilization and estrogen-deficiency induced bone loss assessed by in vivo micro-CT, T462

- Deficiency and PTHrP infusion do not fully reproduce the bone loss of lactation, M220
- Deletion of TIF-2 results in skeletal resistance to estrogen but a high bone mass phenotype due to concomitant resistance to PPAR γ , 1235
- Down-regulation of klotho protein expression by, T192
- Effect of estrogen deficiency on gene expression pattern in the bone tissue of postmenopausal versus premenopausal healthy women, T124
- Effect on bone marrow adipogenesis, M243
- Effects of estrogen on circulating dlk1/pref-1/FA1 levels in postmenopausal women and correlations with bone turnover and volumetric BMD, W418
- High-dose estradiol treatment causes destruction of cortical bone and is associated with an increased death rate in old WT and ERKO male mice, T193
- Identification of primary target cells for the classical genomic effects of raloxifene and, T188
- Low-dose estrogen oral contraceptive use and BMD in adolescents and young adult women, W292
- Mediated enhancement, classical signaling is essential for osteogenesis but not for inhibition of adipogenesis, M250, S250
- Metabolite-mediated inhibitions, regulation of protein synthesis factors in osteosarcoma cells, T254
- Modulation of P2X₇R in osteoblasts by corticosteroids and, M055
- Periosteal and endosteal modeling process is affected differently in response to fatigue loading than during development, M463
- Preferentially suppresses osteogenic gene expression in mice lacking classical ERE signaling, T195
- Regulation of oxidative stress and osteoblast apoptosis is preserved when the ER cannot directly interact with DNA, T184
- Some but not all estrogen-like molecules have both bone and cartilage protective effects, W205
- Suppression of adipogenesis is mediated by TGF β , M024
- Estrogen deficiency**
Bone loss, selective deletion of the membrane-bound CSF1 isoform in vivo does not affect, 1255
- Estrogen receptors (ER)**
In AIS, T189
Cannot directly interact with DNA, regulation of oxidative stress and osteoblast apoptosis by estrogens is preserved, T184
Extra-nuclear, 17 β -estradiol abrogates apoptosis in skeletal muscle cells through, T196
Liganded versus unliganded ER, T044
- Estrogen receptor (ER)**
Androgenic effects on bone and body composition depend on concerted and additive activation of, M244, S244
Classical signaling is essential for estrogen mediated enhancement of osteogenesis but not for inhibition of adipogenesis, M250, S250
Mouse tibia, mechanical loading induced Wnt/ β -catenin signaling is compromised in, M036, S036
Required for strain-related β -catenin signaling in osteoblasts, M064, O064, S064
- Unliganded potentiates BMP-induced transcription and osteoblastogenesis, T190
- Estrogen receptor β (ER β)**
Role for ER β in trabecular bone mechanotransduction, 1084
Unliganded potentiates BMP-induced transcription and osteoblastogenesis, T190
- Estrogen receptor-related receptor gamma (ERR γ)**
Negatively regulates osteoblast differentiation and mineralization through Runx2- and Smad-dependent pathway, W015
- Estrogen response element binding protein (ERE-BP)**
Control of estradiol-directed gene transactivation by, 1221
Estradiol mediates rescue of the dominant-negative effects of, 1222
- Estrogen response element (ERE)**
Classical signaling, estrogen preferentially suppresses osteogenic gene expression in mice lacking, T195
- Etanercept (ETN)**
Effect of ETN on bone metabolism in patients with RA, W434
- Etidronate**
Inhibits progression of vascular calcification and decrease in BMD in chronic dialysis patients, T491
- Exercise.** See also *Athletes*
Association of body weight and daily walking steps with QUS parameters and urinary DPD in elderly Japanese women, W493
Bone biomarker responses to short-term training, W056
Bone increases from jumping exercise persist seven years post intervention, WG29, M530, S530
Bone turnover response of men and women to a strenuous gender-integrated recruit training regimen, W487
Characterization of muscle disuse atrophy and recovery in mice using an in vivo casting model, W489
Comparison of Rehabilitation of Osteoporosis Program-Exercise (ROPE) versus No-ROPE, with or without pharmacotherapy, W393
Effect of resistance exercise on in vivo-derived tomography measures and mechanical properties of rodent bone, W498
Effect of vibration resistance exercise during 56 days of bed rest on different muscle properties, W484
Effects of 3 months of aerobic exercise on bone turnover in premenopausal non-obese women, W062
Effects of daily muscle trainings on falls and vertebral fractures in the elderly osteoporotic women, WG31, T340
Effects of endurance running training on bone quality in growing rats, W491
Effects of vibration plus resistance training on bone metabolism in postmenopausal women, W501
Eight months of twice-weekly ten-minute jumping activity for PE warm up improves bone in adolescent boys and girls, M524
Electrically stimulated eccentric muscle contraction benefits bone in the tibia of hindlimb unloaded rats at both the mid-diaphysis and proximal metaphysis, W490
Flexible multibody simulation approach in the analysis of tibial strains during walking, W502
- Gold standard measurement of physical activity energy expenditure and BMD in older adults, T346
- Independent contribution of physical activity to bone mass during growth, M531
- Induced changes in the macro-architectural parameters of cortical bone as boys progress through puberty, W485
- Influence of exercise and low dose oral contraceptives on vertebral and femoral bone mass in young adult women, T450
- Is golf a good sport for bone health in the elderly?, M522
- Long-term macro-architectural benefits of high impact exercise during growth, W483
- Measures of fitness and body composition in childhood are associated with calcaneal quantitative ultrasound in adulthood, W265
- Physical activity in young adulthood is an independent predictor of BMD in elderly Swedish men, T310
- Positive association of physical exercise and coffee consumption with BMD in postmenopausal women, T336
- Prevents falls and maintains BMD in elderly postmenopausal women, WG11, T415
- Quality and strength of cortical bone are lowered by limiting physical activity, W381
- Quality and strength of cortical bone in both OVX and sham-operated rats are lowered by limiting physical activity, W479
- Regular physical activity has only a temporary effect on bone gain in pubertal girls, M533, S533
- Role of dynamic muscle contractions on inhibition of bone loss and muscle atrophy in a functional disuse mouse model, W482
- School-based physical activity intervention positively affects change in I_{max} in pre- and early pubertal boys, 1040
- Timing of peak bone mass and BMD are influenced by high-level physical activity in young adults of both sex, WG10
- Timing of peak bone mass and BMD are influenced by high-level physical activity in young adults of both sexes, M534
- Weight bearing bones are more sensitive to physical exercise in boys than in girls during pre- and early puberty, WG30
- exon II**
Regions upstream of, characterization of the human CYP19 gene that mediate regulation by cAMP in murine osteoblasts, T032
- External apical root resorption (EARR)**
in vitro, hypoxia contributes to the formation of, T010
- Extracellular matrix (ECM)**
Artificial vasculature-inducing geometry, formation of haversian-type bone and blood vessels guided by, M154
Cartilage homeostasis is regulated by RAR γ repression function, W103
Conditional deletion of FN in osteoblasts reveals distinct roles in orchestrating assembly of proteins and in osteoblast differentiation, 1177
Proteins affect both osteoclast formation and resorptive activity, M087
Proteins, Ciz interacts with, W012
Provision of, correction of increased oxidative stress and defective replication in MSC from aging C57BL/6, M052, S052

Extracellular matrix protein 1 (ECM1)

Novel potent mediator of chondrogenesis, 1062

Extracorporeal shockwave therapy (ESWT)

Stimulates bone remodeling in the rat, evaluated with in vivo micro-SPECT scanning, W347
Unfocused ESW therapy diminishes bone loss in OVX rats, W346

F**F872A**

Point mutation of endofin at PP1c-binding domain stimulates bone formation, 1256

Factor inhibiting ATF4-mediated transcription (FIAT)

Expression of a hypomorphic allele improves long bone mechanical properties, M033, S033

Familial hypocalciuric hypercalcemia (FHH).

See *Hypercalcemia, familial hypocalciuric*

Farnesoid X receptor (FXR)

Activation in breast cancer cell lines by bone-derived lipid, M249

Farnesyl pyrophosphate synthase (FPPS)

Mode of binding of N-containing bisphosphonates in FPPS, W320

FAS-associating death domain-containing protein (FADD)

Caspase-8 axis regulates osteoclast apoptosis, T102

FasL

Activation of Erk1/2 prevents the induced apoptosis in IGF-1-treated anulus fibrosus cells, T117

Fat-1 transgene

Endogenously produced n-3 fatty acids (Fat-1 transgene) protects bone after ovariectomy in mice, M397, S397

Fatty acids

Interrelation between dietary fatty acids and fibers in modulating bone quantity and quality during skeletal growth, W467

Fc gamma receptor II B (FcR)

Osteoclast precursor cells, characterization of OIP-1/hSca binding to, 1103

Femoral bones

Determinants of femoral neck bone loss in the HORIZON-PFT study, T387

Ferritin

Role on differentiation of chondrocytes at the stage of calcification, M131

Fetal bone cells. See also *Bone cells*

For tissue engineering, T041

Fibril-associated collagen (FACIT)

Expression of splice variants of collagen XII in human osteoblast-like cells, M144

Fibrin

Cementoblast cultured on, induces fibrinolysis and its apoptosis, T139

Fibrinogen

Cortical bone is positively associated with serum IGF-1 and testosterone and negatively with, M194

Fibrinolysis

Cementoblast cultured on fibrin induces, T139

Fibroblasts

Continuous local infusion of basic growth factor enhances consolidation of the bone segment lengthened by distraction osteogenesis, T155
Rheumatoid synovial, promote osteoclastogenic activity by activating RANKL via TLR-2 and TLR-4 activation, W435
Synovial, involvement of Cx43 in IL-1 β -induced osteoarthritis-associated changes in, T169

Fibroblast growth factors (FGF)

Runx2 transcriptional AD3 supports synergistic Runx2-MINT activation of the osteocalcin response element via a DMAT-sensitive kinase, T036

Signaling, Perl modulates and is essential for vascularization in the development of the cartilage growth plate, 1064

Spatial and temporal localization of components of signaling pathways in the postnatal LVGP, M125

Fibroblast growth factor 2 (FGF-2)

Overexpression of low molecular weight isoform partly prevents bone loss, T160

Responsiveness, Cx43 amplifies in a Runx2/PKC δ -dependent manner, W027

And TGF β 1 have opposite effects on the mural cell phenotype of CD146⁺ BMSCs, M178

Fibroblast growth factor 4 (FGF-4)

Downstream signal transactivation by transgene partially imitates changes of BMP-2 induced osteogenic transcription factors in NIH3T3 cells, W016

Fibroblast growth factor 7 (FGF-7)

As a potent in vivo phosphaturic agent, M212, S212

Fibroblast growth factor 23 (FGF-23)

Age-dependent regulation of FGF-23 production in murine bone, T159

Association of serum FGF-23 and urinary GGT with BMD, M318

Concentration, treatment of XLH with calcitriol and phosphate increases, W123

Controls NaPi-IIa trafficking via crosstalk between the PI-3 kinase and MAPK pathways, T158

Evaluation of FGF-23 (c-terminal and intact)

ELISA kits in end-stage renal disease patients, M211

Extracellular inorganic Pi induces ERK1/2 phosphorylation and up-regulates a target gene in renal proximal tubule cells via NaPi-IIa, W131

Gene, identification of cEts1 and STAT1 as potential primary targets in the secondary gene regulation of, W161

As an independent predictor of BMD in a population-based cohort of elderly men, W125

Is an independent predictor of BMD in a population-based cohort of elderly men, W125

Klotho ablation completely reverses the biochemical and skeletal alterations in R176Q transgenic mice, M208, S208

Mediating ERK pathway, 1,25(OH) $_2$ D $_3$ inhibits bone nodule mineralization through, M210, S210

Osteocytic regulation of Pi homeostasis through, 1296

Phosphate-independent effects on skeletogenesis, 1114

Possible direct regulatory role of active Vitamin D increased by ultraviolet B on, W126

Protein, analysis and importance of glycosylation status in, W129

PTH expression is negatively regulated in primary parathyroid cells, 1191

Regulatory mechanism of production and circulatory level of, W124

Rise in FGF-23 precedes 1-84PTH and linear decline in calcitriol precedes rise in FGF-23 in non-diabetic predialysis patients, M215

Treatment with antiresorptive agents increases circulating, W127

Venous sampling as a tool for pre-operative localization of tumors giving rise to TIO, M213

Fibroblast growth factor receptors (FGFR)

Continued enhanced function delayed fracture healing, T157

FGFR 3 and FGFR 4 are not physiologically relevant FGF-23 targets in the kidney, 1227

In silico identification of selective FGFR modulators, M393

Fibrodysplasia ossificans progressiva (FOP)

Activation of BMP signaling by the FOP

ACVR1 R206H mutation, 1151

ALK2 induces heterotopic bone formation in patients with FOP, 1034

Diagnosis of FOP prior to the onset of heterotopic ossification, T478

Fibromodulin (fmod)

And bgn control bone mass by regulating osteoclast differentiation through BMSC, M157, O157, S157

Fibronectin (FN)

Conditional deletion in osteoblasts reveals distinct roles in orchestrating assembly of bone ECM proteins and in osteoblast differentiation, 1177

Isoform of FN is responsible for decreased bone formation in patients with primary biliary cirrhosis and this effect is not exclusively mediated by beta1 integrins, T007

Matrix, PAI-1 increases femoral mineralization independent of estrogen status through modulation of, T137

Selective deletion in osteoblasts affects bone density and osteoblast function, 1179

Filamin B (FLNB)

Variation in the *FLNB* gene regulates bone density in two populations of Caucasian women, 1203

Finite element analysis/modeling (FEA/FEM)

Based on in vivo HR-pQCT images of the radius tend to improve wrist fracture prediction, 1280

Combined axial compression and flexion loading mode to evaluate strength of vertebral bodies using a voxel-based FEM, W476

Correlation between the mechanical properties of trabecular bone assessed by FEA and experimental test, W451

Fracture strength of the distal radius can be estimated by nonlinear FEA using 3D HR-pQCT, W460

Methodology for bone strength prediction using parametric statistical shape and density FEM, W452

More accurately predict structural behavior of human cancellous bone when using specimen-specific tissue properties, M502

Novel patient-specific FEM to predict damage accumulation in vertebral bodies under axial compression, W475

Flavanones, citrus

Effect of citrus flavanones on bone metabolism, W407

Fluid flow shear stress (FFSS). See also *Shear stress*

Activates β -catenin signaling in MLO-Y4 osteocytic and 2T3 osteoblastic cells, W053

And mechanical strain induce a similar osteogenic gene response via divergent signaling pathways, M517

- Promotes intracellular assembly and formation of Cx43-forming channels in osteocytes, M520
- Fluorescence resonance energy transfer (FRET)**
Analysis reveals selective binding of long- and short-acting PTH(1-28) analogs to distinct PTH receptor conformations, W144
- Fluoride**
Phenotypic variations of fluoride responses between inbred strains of mice, W350
- 5-Fluorouracil (5-FU)**
Insensitive osteoclast precursors in vivo, osteoclast niche is composed of, M082, S082
- Follicle-stimulating hormone (FSH)**
Association between FSH and bone mass in postmenopausal women, T467
Elevated FSH predicts increased hip fracture risk, T468
- Follistatin**
Enhancing the expressions of BMP antagonists, GC suppresses the differentiation of osteoblasts by, M059
- ΔFosB**
Overexpression of decreases adipose mass in a non-cell autonomous manner by increasing energy expenditure independently of bone cells, 1248
- Δ2FosB**
Zfp521 regulates chondrocyte differentiation downstream of PTHrP, 1069
- FoxO3a**
Akt1 contributes to maintenance of bone mass and turnover by inhibiting apoptosis of osteoblasts through, 1211
- Fracture healing**
Absence of sFRP1 accelerates, 1258
Analysis of differing approaches for the assessment of large scale transcriptional profiling of, T111
Continued enhanced Fgfr2 function delayed, T157
Effects of traumatic brain injury on bone formation/remodeling during, M008
IGF-1 engineered bone marrow MSCs improve, M191, S191
Local transplantation of G-CSF mobilized CD34+ cells contributes to, W048
Local transplantation of hMADS cells improve, W003
Novel model of impaired, M153
rhPDGF-BB and βTCP accelerate fracture healing, W316
Shh in osteoclast formation and, T082
Temporal pattern of gene expression and histology of stress fracture healing in the rat ulna-loading model, 1246
- Fracture risk**
Age increases the risk of subsequent fractures following an initial fracture among women in managed care population, W296
Assessment in dialysis patients, WG40
Asymmetry in leg power increases non-spine and hip fracture risk in older men, 1158
Clinical and nonvertebral fracture risk is reduced with the use of IBN in women with postmenopausal osteoporosis, W355
Clinical low-trauma fractures cluster in time in postmenopausal women, 1276
Clinical risk factors for fracture are additive in postmenopausal women who are at risk for fracture in a primary care setting, W294
Clinical validation of a simplified absolute fracture risk algorithm in Canadian women, 1080
- Development of a clinical nomogram for individualizing 5-year and 10-year risks of fracture, 1166
- Development of a high-resolution 3-D micro-CT based model to predict fracture callus histological architecture, W472
- Does low subjective well-being predict falls and fractures in postmenopausal women?, W291
- Effect of anti-resorptive agents on fracture rates in subjects selected for therapy on the basis of clinical risk factors or low BMD, T404
- Effect of various substances on the reduction of fractures, T381
- Endogenous sex hormones and incident fracture risk in older men, M358, O358, S358
- Epidemiology of children's fractures, M361
- Five-year incidence of fractures in patients with severe osteoporosis, W281
- Five-year longitudinal study of health related quality of life in individuals with and without incident fractures, T333
- Hip geometry and bone fragility among postmenopausal women with RA, W306
- Impact of adherence to osteoporosis medications on fracture rates, 1275
- Incidence estimates of non-traumatic fractures in older women and men, M349, S349
- Increases after cancer diagnosis in postmenopausal women, 1274
- Index after falling, 1279
- Low magnitude mechanical signals reduce risk-factors for fracture during 90-day bed rest, T426
- Mapping the prescriptome to fractures in men, 1162
- National differences in the risk for falls and fractures, W284
- Outreach program improved osteoporosis management after a fracture, WG38
- Pattern of fractures in men, T324
- Peak vertical impact forces during backward falls onto the buttocks and the influence of compliant flooring, W399
- Randomized controlled trial of a falls clinic for prevention of falls and related fractures, T331
- RCT of the OEP to ameliorate fall risk factor profile in patients at high risk of falls, T413
- Risk factors for falls in older community-dwelling women, 1053
- Risk factors for osteoporotic fractures in Brazilian men and women, W283
- Risk of subsequent fracture depends on BMD and fracture type, 1050
- Serum 25(OH)D Levels and falls, frailty, and fractures among postmenopausal women in the Hawaii Osteoporosis Study, T320
- Study of seven polymorphisms genes previously described as linked to osteoporotic fractures, M287
- Use of a web-based fracture risk assessment tool, W278
- Validation of a clinical definition for fragility fracture, M350
- Validation of ten-year fracture risk prediction in a large clinical cohort, 1078
- Vertebral fracture risk, W242
- Vitamin-D plus Ca supplementation decreases the risk of falling among postmenopausal ambulatory women, M452, S452
- ## G
- G-protein**
Coupled signaling pathways, growth inhibition of osteoblast progenitors by Runx2 is accompanied by changes in, M047, S047
- G-protein-coupled estrogen receptor 30 (GPR30)**
Deficiency leads to reduced bone growth and BMD, T201
- G-protein coupled receptors (GPCR)**
Designer, suggest opposing roles for Gs and Gi signaling in osteoblasts, 1021
Peptide ligand interactions, distance restraints and resolution limit in molecular modeling of, W147
- G-protein coupled receptor kinase 2 (GRK2)**
In osteoblastic cells, PTH enhances ATP induced ERK1/2 activation via a competitive mechanism involving, T060
- G11**
Novel activin/nodal-binding protein inhibits matrix mineralization in osteoblasts, M203
- Galectin-3/9**
Interaction of with lipid rafts induces osteoblast proliferation through the c-Src/ERK signaling pathway, W005
Possible suppressive role in osteoclastic bone destruction accompanying adjuvant-induced arthritis in rats, M108
- Gq**
Role in parathyroid gland function elucidated by genetic approaches, M229
Signaling in osteoblasts inhibits bone formation, 1123
- Gamma-glutamyl transpeptidase (GGT)**
Anti-GGT antibody attenuates osteoclastic bone erosion in CIA mice, T090
- Gap junctional intercellular communication (GJIC)**
In living bone and its regulation factor, W051
- Gastrin**
Activation of the CaR with cinacalcet increases serum levels in healthy older subjects, M221
- GCMB**
Expression is normal in parathyroid neoplasia, T480
- Gene-trap mutagenesis.** See *Mutagenesis, gene-trap*
- Genetically engineered cells**
In vitro assay to assess secreted osteogenic factors from, T038
- Geranylgeranylpyrophosphate (GGPP)**
Promotes osteoblast survival and is involved in anti-apoptotic effects of PTH, 1192
- Gi**
Signaling in osteoblasts, Designer GPCRs suggest opposing roles for, 1021
- Gli2**
Ubiquitination, βTrop1 ubiquitin complex regulates Ihh-promoted osteoblast differentiation through, T055
- Glial cells missing 2 (Gem2)**
Regulation of CaR in hyperplastic parathyroid cells, M226
- Glucagon-like peptide 1 (GLP-1)**
Action on bone turnover in normal and type 2 diabetic state, T207
- Glucagon-like peptide 2 (GLP-2)**
Marked abnormality in myeloid and mesenchymal somatic stem cells explains the skeletal defect in GLP2 receptor knockout mice, W412

- Significantly increases hip BMD in postmenopausal women, 1127
- Glucocorticoids (GC)**
Aging and bone hydration, 1086
ChIP-on-chip analysis reveals novel response genes adjacent to genomic binding sites for SHREs in osteoblastic cells, M061
Effects on BMP-2 and BMP-7 expressions in bone and kidney, M234
Enhances the expression of sFRP3 in cultured osteoblasts, T176
Excess in mice leads to early activation of osteoclastogenesis and prolonged suppression of osteogenesis through gene expression profiling, T181
Induced growth retardation, identification and functional involvement of lipocalin 2 in, T177
Induced osteoporosis in rats treated with Ris, evaluation of cell apoptosis and COX-2 expression in, W318
Loss-of-function model spanning early and late osteoblast differentiation, M235, S235
Novel mechanism of action-inhibition of COX-2 transcription by GILZ, T180
Opposing effects of, on Krox20 and mineral deposition in osteoblast cultures, T026
Osteoblast-targeted disruption of signaling delays intramembranous bone development in vivo, T182
Periarticular bone loss in arthritis, role of synovial generation, M232
Regulation of RANKL expression in osteoblast-like cells, T068
Small GTPase RhoA and its effector kinase ROCK mediate actin cytoskeleton reorganization leading to osteocyte anoikis by, M233, S233
Stimulate Wnt expression in mature osteoblasts, T062
Suppresses the differentiation of osteoblasts by enhancing the expressions of BMP antagonists and pretreatments with ALN and PTH abolish this process, M059
Transcription factor E4bp4 is induced by and represses promoter activity in osteoblasts, T179
Transgenic disruption of signaling in mature osteoblasts attenuates KRN serum-induced arthritis in vivo, T183
- Glucocorticoid-induced leucine-zipper (GILZ)**
Enhancement of osteoblast differentiation of bone marrow mesenchymal stem cell by inhibiting adipocyte differentiation, T057
Novel mechanism of GC action-inhibition of COX-2 transcription by, T180
- Glucocorticoid-induced osteoporosis (GIO).** See *Osteoporosis, glucocorticoid-induced*
- Glucose**
High D(+)glucose concentration inhibits RANKL-induced osteoclastogenesis, W082
- β -Glucuronidase**
Role in 1,25(OH)₂D₃- and PTH-stimulated Ca uptake in intestinal epithelial cells, M258
- Glycoprotein nmb (gpnmb).** See also *Osteoactivin*
Bone cell autonomous effects of, in vivo, 1023
- Glycosylation**
Status, analysis and importance in FGF-23 protein, W129
- Golgi**
ESL-1 negatively regulates TGF in the Golgi during skeletogenesis, M202, S202
- Gonadectomy**
DHT treatment reverses induced changes in fat and lean mass in male but not female mice, T202
- Gonadotropins**
Associated with BMD in males, W250
- Gothenburg Osteoporosis and Obesity Determinants (GOOD) study**
Serum PTH is associated with cortical bone dimensions, W135
- gp38**
Targeted deletion in osteocytes results in increased skeletal size and BMD, 1043
- gp130**
Interactions with PTH in differentiating osteoblasts, W025
- Granulocyte colony stimulating factor (G-CSF).** See also *Colony stimulating factor*
Bone regeneration with local controlled application in a bone defect of rabbit ulna, T161
Enhances osteoclast differentiation and function, T074
- Gravity, partial**
Novel partial weight suspension system simulating Mars gravity leads to reduced bone mass and strength in mice, M516
- Gremlin**
Induces MAPK signaling in osteoblasts, W122
- Growth factors**
Matrix-derived, CatK inhibitors prevent degradation by human osteoclasts, W335
- Growth hormone (GH)**
Exostoses after pediatric stem cell transplant are associated with growth hormone treatment, W427
Local application has a similar effect on intramembranous bone healing, M193
Opposing effects of alcohol reveal a critical role in the reciprocal relationship between adipocyte and osteoblast differentiation, M196
Treatment increases cortical thickness by stimulating endosteal bone growth in young adults with childhood onset GH-deficiency, T369
- Growth hormone receptor (GHR)**
Expression of and biomechanical studies in experimental model of cholestatic liver, W416
- Growth plate.** See also *Lumbar vertebral growth plate*
Chondrocytes, thyroid hormone-induced terminal differentiation involves IGF-1 modulation of canonical Wnt signaling, M118, S118
Effects of pro-inflammatory cytokines on SOCS-2 expression in, W093
Postnatal development, IGF-1 signaling is required for, 1109
- Growth retardation**
GC-induced, identification and functional involvement of lipocalin 2 in, T177
- Grx5**
Regulates osteoblast cell functions by protecting against oxidative stress, M005
- Gs**
Signaling in osteoblasts, Designer GPCRs suggest opposing roles for, 1021
- Gsa**
Ability of XLs to mimic in mediating PTH signaling in vivo, M218
Mice lacking in early osteoblasts leads to marked bone fragility, impaired bone formation in, 1020
- GSK-3 β**
Inhibits osteoblastic bone formation through suppression of Runx2 transcriptional activity by the phosphorylation at a specific site, 1247
- GTPase.** See also *Rho GTPase*
RhoA and its effector kinase ROCK mediate actin cytoskeleton reorganization leading to osteocyte anoikis by GC, M233, S233
Small cdc42 enhances osteoclastogenesis and bone resorption, 1146
- Guanylyl cyclase B (GC-B)**
Local CNP clearance system as a regulator of CNP-GC-B system for bone growth, T168
- GW bodies**
Alterations are associated with osteoclastogenesis, M094
- ## H
- H3 lysine 9 methyltransferase**
Histone is a transcriptional coactivator for VDR, 1027
- Hairless (hr)**
Molecular analysis of two novel mutations in the VDR corepressor and expression of rHr in *E. coli*, M259, S259
- Hairy enhancer of split 1 (HES-1)**
An anti-adipogenic mediator of osteogenic oxysterols and hedgehog signaling, W043
- Hajdu-Cheney Syndrome (HCS)**
TPD therapy in HCS, T479
Use of TPD in HCS, WG16
- Haploinsufficiency**
Modeling BMP and bisphosphonate combination therapy in wild type and Nf1 haploinsufficient mice, W164
Nell-1 partially rescues craniofacial defects in *Runx2* haploinsufficient mice, 1105
- Haplotype association mapping (HAM)**
Genome-wide HAM leads to an identification of a genetic variant in CER1 associated with BMD in premenopausal women, T214
- HcB/8/23**
Biomechanics and body size quantitative trait loci in mice, W466
- Hedgehog homolog (HH).** See also *Indian hedgehog homolog*; *Sonic hedgehog homolog*
Activation of LXR inhibits hedgehog signaling and osteogenic differentiation of BMSC, W023
HES-1 is an anti-adipogenic mediator of osteogenic oxysterols and hedgehog signaling, W043
Pathway, molecular mechanisms for BMP-2 transcription by, 1257
Signaling, VDR and epidermal carcinogenesis, W158
- Height loss**
And decreased physical function in Japanese women, M346
Is associated with impaired quality of life in the elderly, M365
Predicts fractures in middle aged and older men and women, 1281
- Hematopoiesis**
Dramatic increase in bone marrow of rescued RANKL-deficient mice by expression of soluble RANKL transgene, M096, S096
- Hematopoietic cells**
PGE₂ increases a specific subset of primitive hematopoietic cells in vivo, M039, S039

- Hematopoietic stem cells (HSC).** See *Stem cells, hematopoietic*
- Heme oxygenase-1 (HO-1)**
Effects on CIA model, T130
- Hemodialysis**
Non-invasive study of bone and cardiovascular disease in chronic hemodialysis subjects, T488
Prospective controlled study assessing the clinical benefit of evening administration of Vitamin D in hemodialysis patients, T494
- Heparan sulfate proteoglycans (HSPG)**
Sulfation during in vitro osteogenesis, W036
- Hepatic osteodystrophy.** See *Osteodystrophy, hepatic*
- Hesr**
Endogenous, redundantly support osteoblast differentiation, W019
- Heterotopic ossification (HO).** See *Ossification, heterotopic*
- Hey**
Endogenous, redundantly support osteoblast differentiation, W019
- High-mobility group box 1 (HMGB1)**
Regulates actin cytoskeleton organization and RANKL-induced osteoclastogenesis in a manner dependent on RAGE, M079
- High-mobility group proteins (HMGs)**
Coupled with TNF α production are essential for osteoclastogenesis, T071
- High throughput screening (HTS)**
Development of cell-based assays for identifying antiresorptive compounds targeting RANK signaling through, M102
- Highly active anti-retroviral therapy (HAART)**
Aberrations in Wnt/ β -catenin signaling driving HAART-induced bone loss in vitro, M469
- Hip axis length (HAL)**
Association between peak HAL and polymorphisms of the VDR and ER1 genes in healthy Chinese men, T230
- Hip fractures**
BMD and hip fracture, 1079
Competing risk of subsequent fracture and death after hip fracture in nursing home residents, M362, S362
Compliance with osteoporosis treatment and incidence of hip and wrist fracture after forearm BMD screening, WG37
Decline in age adjusted hip fracture incidence but a drastic increase in hip fractures among the very oldest, 1051
An epidemiological study of hip fractures in Korean women, W282
Hip muscle cross-sectional area and attenuation, 1282
Hip structural geometry and incidence of osteoporotic fractures in the WHI-BMD cohort, T288
Impact of incident hip fracture on quality of life in older men, M355
Increased mortality in patients with a hip fracture, 1049
Leg lean mass and risk of hip fracture, M347, S347
Loss of follow up after fragility hip fractures in some regions in Czech Republic, W245
Novel, integrated approach to the management of patients following hip fracture, T328
Relationships between leptin, PTH, Vitamin D and bone metabolism markers in patients with hip fracture, M460
Serum 25(OH)D and the risk of hip fractures, 1202
- Using a case-manager to improve osteoporosis treatment after hip fracture, T329
What are the characteristics of postmenopausal women with the T-score of the total hip that is lower than that of the lumbar spine?, W248
- Hip strength**
Comparison of the effects of TPTD and ALN on parameters of total hip strength as assessed by FEA, 1089
- Hip structure analysis (HSA)**
Age effects on hip structure, 1054
Changes in hip geometric structures with aging, M373, O373, S373
Heterogeneity in structure is not captured using the hip structural analysis, M334
In vivo comparison of CT and DXA methods of proximal femur cross-sectional geometry measurement using HSA, W226
- Histogenesis**
Temporal regulation of, by mesenchyme during craniofacial bone development, W040
- Histomorphometry**
Image processing for 3-D dynamic histomorphometry, W481
- HIV/AIDS**
Osteopenia and lipodistrophy in HIV-infected patients, M496
TREM2 pathway is involved in osteoclastogenesis induced by NRTIs in AIDS, W074
- Homeobox protein**
Identification of as a regulator of Osx expression and mediator of TNF action, 1143
- Homocysteine**
Levels and risk of hip fracture in postmenopausal women with poor renal function, M471, S471
- Hormones**
Bone relationship in females is hormonal stage dependent, W515
Concerted growth of bone length and width, influence of sex hormones, IGF-1 and muscle size, 1083
Hormonal regulation of hypertrophic chondrocyte apoptosis, W094
- Hormone therapy**
Methods of transition from hormone therapy to raloxifene or other regimens administered to postmenopausal women for the prevention or treatment of osteoporosis, W388
- HRT**
Postmenopausal osteoporosis HRT and weight gain, M401
- Hs.43125**
Identification as an articular chondrocyte-specific gene, T120
- hSca.** See *Osteoclast inhibitory peptide-1*
- Human adipose tissue-derived stem cells (hADSC).** See *Stem cells, adipose-derived*
- Human bone marrow endothelial (HBME) cells**
PTHrP-induced MCP-1 production promotes osteoclast differentiation in vitro, T247
- Human mesenchymal stem cells (hMSC).** See *Mesenchymal stem cells, human*
- Human multipotent adipose-derived stem (hMADS) cells**
Local transplantation of, improve fracture healing, W003
- Human osteoprogenitor (HOP) cells**
Cell cooperation between, and HUVEC in tissue engineering, M041, S041
- Human osteosarcoma cells (U2OS)**
PDTC inhibits SOD1 gene and cell growth by activating JNK pathway in, W018
- Human type 1a2 procollagen promoter (hCol1a2)**
Nuclear targeting sequence together with human Runx2 enhancer elements drives robust expression in transgenic mouse osteoblasts, 1288
- Human umbilical vein endothelial cells (HUVEC)**
Cell cooperation between HOP and, in tissue engineering, M041, S041
- Human Vitamin D receptor (hVDR).** See *Vitamin D receptor*
- Hyaluronic acid (HA)**
Biological trials of HA acid on osteoclast differentiation induced by IL-1, M161
- Hybridization, in situ (ISH)**
New approach to assess bone formation rates and, T115
- Hydrostatic loading**
Of growth plate chondrocytes in vitro, M119
- Hydroxyapatite (Hap)**
Attachment of cell on ALD-derived surface, W009
Increase of the mechanical strength of novel unidirectional porous ceramics in vivo, T128
- Hydroxyfasudil**
Induce the differentiation and mineralization of osteoblastic MC3T3-E1 cells via inhibiting the mevalonate pathway and enhancing BMP-2 expression, M056, S056
- 1 α -Hydroxylase (1(OH)ase)**
Deletion of the 25OH(D) from mice expressing the null mutation for the CaSR converts a hypercalcemic to a hypocalcemic hyperparathyroid phenotype, M231
Gene knockout mice by transplantation of wild-type NA-BM-MSC, partial rescue of the Vitamin D deficient phenotype of, T058
Knockout mice, Ca-independent and 1,25-dihydroxyvitamin D3-dependent regulation of the RAS in, W150
Treatment with antiresorptive agents decreases renal expression of 25OH(D), W127
- 25-Hydroxyvitamin D (25OH(D))**
Age modifies the impact of Vitamin D3 supplementation on the PTH ratio, M414
Deletion of the 1 α (OH)ase from mice expressing the null mutation for the CaSR converts a hypercalcemic to a hypocalcemic hyperparathyroid phenotype, M231
Development of an assay on the Abbott ARCHITECT Analyzer, W156
Effect of plasma 1,25(OH) $_2$ D concentration or Ca intake on negative correlation with PTH concentrations in Japanese adolescents, W159
Reduction in serum 25(OH)D during PTH treatment, T373
Serum, relationship with bone markers in professional football players, W503
Treatment with antiresorptive agents decreases renal expression of 1 α (OH)ase, W127
- 25-Hydroxyvitamin D $_3$ (25OH(D) $_3$).** See also *Vitamin D*
Relationship between serum 25-hydroxyvitamin D $_3$ concentration and walking ability, leg strength, or balance in community-dwelling Japanese frail elderlies, W394
Relationship between serum 25(OH)D $_3$ concentration and walking ability, leg strength, or balance in community-dwelling Japanese frail elderlies, WG12

- Vitamin D₂ supplementation suppresses endogenous levels of 25-hydroxyvitamin D₃, M264
- Hydroxyapatite ceramics**
Surgical treatment for benign bone tumors with fully interconnected porous hydroxyapatite ceramics, T264
- HYP**
ASARM-peptides are directly responsible for defective mineralization in, I155
- Hypercalcemia**
CaR plays a significant role in protection against, M227, S227
Deletion of the 25OH(D) 1(OH)ase from mice expressing the null mutation for the CaSR converts a hypercalcemic to a hypocalcemic hyperparathyroid phenotype, WG1, M231
Orally-active nonsecosteroidal Vitamin D agonists increased bone mass without causing hypercalcemia, M416
Role of Npt2c, involved in HHRH, I115
Tissue-selective, non-secosteroidal VDRM with improved therapeutic window of bone efficacy over hypercalcemia, I012
- Hypercalcemia, familial hypocalciuric (FHH)**
Discriminative power of the 24h-urine CCCR, the 24h-urine CR and the 24h-urine CE for the separation between PHPT and, M222
- Hypercalciuria**
Effect of hypercalciuria on bone density and strength in genetic hypercalciuria stone-forming rats, M267
How should hypercalciuria be defined?, M383, S383
- Hypercholesterolemia**
LRP5 mutations are associated with osteoporosis, impaired glucose tolerance and hypercholesterolemia, M281, S281
- Hypergravity**
Prevents bone loss in rats following ovariectomy, W492
- Hyperkyphosis**
And physical function in older community dwelling women, M363
To what extent do vertebral fractures, disc height loss, low bone density, and poor muscle strength contribute to hyperkyphosis in older women?, W280
- Hyperparathyroidism**
Comparison of rapid iPTH to IRMA in patients with, M216
Deletion of the 25OH(D) 1(OH)ase from mice expressing the null mutation for the CaSR converts a hypercalcemic to a hypocalcemic hyperparathyroid phenotype, M231
Secondary, role in relation to osteoporosis, M195
- Hyperparathyroidism, childhood**
Childhood hyperparathyroidism with bilateral slipped femoral epiphysis, severe bone disease and Vitamin D deficiency, WG4
- Hyperparathyroidism, normocalcaemic primary (NPHPT)**
Asymptomatic, screening in the United States, T481
Effect of bisphosphonates on BMD in subjects with NPHPT, T403
- Hyperparathyroidism, primary (PHPT, I-HPT)**
Bone quality in mild PHPT, T486
Cardiovascular manifestations of PHPT, M481
Discriminative power of the 24h-urine CCCR, the 24h-urine CR and the 24h-urine CE for the separation between FHH and, M222
- Long-term morbidity and mortality in untreated mild PHPT, T484
Marked improvement of cortical bone geometry after parathyroidectomy in postmenopausal women with primary hyperparathyroidism, M484, S484
Neurocognitive changes in mild, W146
Phosphate stimulates greater PTH release and parathyroid cell proliferation in organ cultures of parathyroid tissue from patients with II-HPT than with I-HPT, W141
- Hyperparathyroidism, secondary (II-HPT)**
Impact of cinacalcet HCL on bone remodeling and minimodeling in patients with secondary hyperparathyroidism, T495
Minimodeling reduces the rate of cortical bone loss in patients with secondary hyperparathyroidism, T496
Phosphate stimulates greater PTH release and parathyroid cell proliferation in organ cultures of parathyroid tissue from patients with II-HPT than with I-HPT, W141
And postpartum Vitamin D insufficiency in healthy Danish women, W151
Protein-PTH mRNA interactions that determine PTH mRNA stability in, M217, S217
- Hyperphosphatemia**
Mediates oxidative stress in bovine aortic endothelial cells, T493
Vascular calcification and aortic gene expression are consistent with, in OPG-deficient mice, I117
- Hypertension**
Activation of renin-angiotensin system induces osteoporosis independently of hypertension, I238
Vitamin D status is inversely associated with blood pressure, M483
- Hypertrophic chondrocytes.** See *Chondrocytes, hypertrophic*
- Hypervitaminosis D**
Fetal, results in neonatal lethality, M266
- Hypocalcemia**
Deletion of the 25OH(D) 1α(OH)ase from mice expressing the null mutation for the CaSR converts a hypercalcemic to a hypocalcemic hyperparathyroid phenotype, M231
Fetal, PTH upregulates placental Ca transfer in response to, W137
Related phenotype of VDR knockout mice, overexpression of human VDR in the intestine rescues, I025
- Hypogonadism**
Prevention and treatment of hypogonadism-associated bone loss and bone metastases by OPG-Fc in a model of mixed osteolytic/osteoblastic metastases, M311, S311
- Hyponatremia**
Induces bone loss and prevents fat accumulation in aged F344 Brown Norway rats, T448
- Hypoparathyroidism**
Bone mass in adults and children with hypoparathyroidism, WG6
Dominant-negative GCMB mutations cause hypoparathyroidism, I031
Protein-PTH mRNA interactions that determine PTH mRNA stability in, M217, S217
Use of PTH in hypoparathyroidism, T485
- Hypophosphatasia (HPP)**
Enzyme replacement therapy for murine HPP, I259
- Possible hypophosphatasia in a man with hypophosphatasemia, spinal ankylosis, and recurrent fractures, T474
- Hypophosphatemic rickets.** See *Rickets, hypophosphatemic*
- Hypovitaminosis D**
Prevalence of hypovitaminosis D and its correlation with different PTH values in a sample of postmenopausal women in Buenos Aires, W149
Prevalence of hypovitaminosis D and male hypogonadism in prednisone-treated rheumatic disease patients, T436
Severe hypovitaminosis D, associated with hyperparathyroidism and osteopenia/osteoporosis in a cohort of long-term kidney transplant recipients with excellent kidney function, T500
- Hypoxia**
Accelerates the transformation of osteoblasts to osteocytes, W013
Contributes to the formation of the EARR in vitro, T010
Role of hypoxia in cancers that metastasize to bone, I003
- Hypoxia-inducible factor (HIF)**
Pathway, Co incorporation into CaP layers stimulates osteoclast differentiation and activation via, W075
- Hypoxia-inducible factor 1 (HIF-1)**
Activation through integrin/ILK/Akt pathway in cultured osteoblasts, ultrasound induces, T511
- Hypoxia-inducible factor 1α (HIF-1)α**
Disruption of HIF-1α in osteoblasts exacerbates ovariectomy induced bone loss in mice, I013
Genetic and pharmacologic activation promotes angiogenesis and accelerates bone regeneration, I065
- Hypoxia-inducible factor 2α (HIF2A)**
Induces COL10A1 and promotes hypertrophic differentiation of chondrocytes, I175

I

I-HPT. See *Hyperparathyroidism*
i-NOS. See *Nitric oxygen synthetase*
Ibandronate (IBN)

- Benefits of oral IBN on non-vertebral fracture risk in postmenopausal osteoporosis, T389
Ca enhances anti-tumor effects of IBN in breast cancer cells, T240
Comparable adherence and improvement in GI tolerability with monthly oral and quarterly intravenous IBN in patients who discontinued previous bisphosphonates because of GI intolerance, W362
Daily and monthly IBN restores bone loss in androgen-deficient male rats, W319
Daily or intermittent oral IBN preserves trabecular microarchitecture, W368
Effect of oral IBN following weekly PTH, M418
Efficacy and safety of intravenous IBN for Chinese primary osteoporotic women, W323
Monthly IBN is associated with reduced risk of serious GI events compared with weekly bisphosphonates, W353
Monthly oral IBN is well tolerated and efficacious in Japanese osteoporotic subjects, T405
Oral monthly IBN is associated with rapid suppression of serum CTX within three days of treatment initiation, W367

- Quarterly intravenous IBN injections provide continuing benefits in women with postmenopausal osteoporosis, W363
- Relationship between increasing annual cumulative exposure to IBN, increases in BMD and reductions in clinical fractures, W365
- Significant reduction in non-vertebral fractures with high- versus low-dose IBN, M428
- Tolerability of once-monthly IBN across different age groups of women switched from once-weekly bisphosphonates, W352
- Icariin**
Icariin exerts bone protective effects in vivo and in vitro, W337
- ICSBP**. See *IRF-8*
- IGF**. See *Insulin-like growth factor*
- IHH**
Spatial and temporal localization of components of signaling pathways in the postnatal LVGP, M125
- II-HPT**. See *Hyperparathyroidism*
- IKB kinase β (IKK β)**
Mice with a myeloid lineage-specific deletion demonstrate both in vivo and in vitro defects in osteoclastogenesis, 1294
- IKB kinase γ (IKK γ)**
Modulates osteoclastogenesis and bone erosion, T098
- IKB α**
Deficient mice display increased osteoclast formation and activity and bone loss in vivo, 1147
- Ikaros**
Transcription factors, *Osr1* gene expression is regulated by, W030
- Ile-Pro-Pro (IPP)**
Enhance osteoblast function in vitro, W038
- Imatinib mesylate**
Inhibits bone formation and decreases bone mass in vivo by inhibiting PDGFR-mediated osteoblast mitogenesis, T018
Suppresses bone metastases by inhibiting osteoclasts through blockade of M-CSF signals, 1170
- Immunohistochemistry (IHC)**
New approach to assess bone formation rates and, T115
- Immunoradiometric PTH assay (IRMA)**
Comparison of rapid iPTH in patients with hyperparathyroidism, M216
- Immunoreceptor tyrosine-based activation motif (ITAM)**
Signaling in bone remodeling in various bony microenvironments, distinct roles of, 1291
- Immunosuppressants**
Effects of immunosuppressants on bone metabolism, T503
- Incisor absent (*ia/ia*) rats**
Osteopetrotic rat exhibits reduced osteoclast activity, resulting in normal endochondral fracture union but delayed hard callus remodeling, T088
- Indian hedgehog homolog (Ihh)**. See also *Hedgehog homolog*
Essential for postnatal bone, T011
Expression, *Msx2* promotes late stages of chondrocyte differentiation by up-regulating, W092
Promoted osteoblast differentiation through Gli2 ubiquitination, *Trep1* ubiquitin complex regulates, T055
- Transcription, *Atf4* regulates chondrocyte proliferation and differentiation by direct targeting, 1183
- Inducible nitric oxide synthase (iNOS)**
Expression through integrin/ILK/Akt pathway in cultured osteoblasts, ultrasound induces, T511
- Inflammation**
Mechanisms leading to increased resorptive activity of large osteoclasts in, T105
- Inflammatory bowel disease (IBD)**
Barrier site metabolism of Vitamin D, 1029
- Inorganic phosphate**. See *Phosphate, inorganic*
- Insoluble collagenous bone matrix (ICBM)**
Acid swelling overcomes osteogenesis inhibition of xenogeneic collagenous matrix delivery system used for naturally-derived BMP complex, M172
- Insulin**
Promotes osteoblast differentiation independent from IGF-1 signaling and its receptor is required for normal postnatal bone acquisition, 1070
- Insulin-like growth factor (IGF)**
LMP-1 accelerates MC3T3-E1 osteoblast differentiation in part through modulation of, T037
- Insulin-like growth factor 1 (IGF-1)**
Ablation of signaling disrupts the communication between osteoblasts and osteoclasts, M241, S241
Carrier components determine skeletal integrity via direct and indirect mechanisms, 1138
Continuous infusion into the epiphysis of the tibia, M188
Cortical bone is positively associated with, and negatively with fibrinogen, M194
Engineered bone marrow MSCs improve the fracture healing process, M191, S191
Expression of and biomechanical studies in experimental model of cholestatic liver, W416
Local application has a similar effect on intramembranous bone healing, M193
Low serum IGF-1 levels results in cortical osteopenia but increased life span in elderly mice, W314
Modulation of canonical Wnt signaling, thyroid hormone-induced terminal differentiation of growth plate chondrocytes involves, M118, S118
Overexpression of osteoblast IGF-1 blunts the deleterious effects of low protein intake on bone strength, W401
Regulation of collagen II and MMP-13 gene expression in endplate chondrocytes via distinct signaling pathways, T116
Role of status and secondary hyperparathyroidism in relation to osteoporosis, M195
Signaling, insulin promotes osteoblast differentiation independent from, 1070
Signaling is required for postnatal growth plate development, T109
Systemic, shows concerted anabolic actions on bone and muscle, M192
Treated anulus fibrosus cells, activation of *Erk1/2* prevents the FasL-induced apoptosis in, T117
In vivo models to study receptor dynamics of bone stem cells, M190
- Insulin-like growth factor binding protein 1/2/3/4/5 (IGFBP-1/2/3/4/5)**
Regulation of and osteocalcin expression in mouse osteoblasts, role of NFI-X transcription factor in, T034
Role of status and secondary hyperparathyroidism in relation to osteoporosis, M195
Serum, a marker of bone turnover, 1253
Triple knock-out mice have larger bones, M189
- Insulin-like growth factor receptor gene (*Igf1r*)**
Osteoblast-specific knockout alters mechanical properties of cortical bone, W464
- Intact parathyroid hormone**. See *Parathyroid hormone, intact*
- Integrin**
Association with Cx43 regulates the function of osteocyte hemichannels in response to shear stress, T504
Bone metastases select for integrin $\alpha 2\beta 1$ negative cells in prostate cancer cell line DU145, M301
Osteoblast response to titanium microtopography is dependent on $\alpha 2$, W002
Regulation of expression by NFATc1 and PU.1 in osteoclasts, M071
Ultrasound induces HIF-1 activation and iNOS expression through, T511
- Integrin-linked kinase (ILK) inhibitor**
Ultrasound induces HIF-1 activation and iNOS expression through, T511
- Interferon-inducible protein 16 (IFI16)**
Mediation of cell proliferation and tumorigenicity of musculoskeletal tumor cells by, T265
- Interleukin-1 (IL-1)**
Induced osteoclastogenesis, *IVVY*⁵³⁵⁻⁵³⁸ plays an essential role in, M084, S084
- Interleukin-1 β (IL-1 β)**
Epigenetic mechanisms are involved in the cytokine-induced de novo expression in human articular chondrocytes in vitro, M184
Induced osteoarthritis-associated changes in synovial fibroblasts, involvement of Cx43 in, T169
Treated articular chondrocytes, regulation of MMP-9 expression by MMP-12 in, M139
- Interleukin-6 (IL-6)**
Effect on the expression of cartilage matrix proteins, T146
Estrogens attenuate production in osteoblastic cells by decreasing oxidative stress and its effects on NF- κ B activation, T186
Signalling, role in c-Src-mediated osteoblast differentiation, T170
Upregulation of CASR gene expression by IL-6, 1187
- Interleukin-8 (IL-8)**
Human breast stem cell transformation and invasiveness is mediated upregulation by *TWIST* interactions with NF- κ B, T242
- Interleukin-12 (IL-12)**
Related cytokines on osteoclast formation and T cell properties, effects of, T076
- Interleukin-15 (IL-15)**
Association study of IL-15 polymorphisms with BMD and fracture risk in postmenopausal Korean women, W257
- Interleukin-23 (IL-23)**
Effects on osteoclast formation and T cell properties, T076
Enhanced osteoclastogenesis is mediated by STAT3 and NF- κ B via upregulation of RANKL from CD4⁺T cells, T078

Interleukin-27 (IL-27)

- Effects on osteoclast formation and T cell properties, T076
- Suppressive effect in osteoclastogenesis, T072

Interleukin-33 (IL-33)

- Inhibits osteoclast formation indirectly through osteoblastic cells, T081

Intervertebral disc (IVD)

- Degeneration in OVX rats, M251
- Effect of removal of nucleus pulposus cells on the annulus fibrosis of, M124
- Lumbar, histological and molecular analysis of the growth and differentiation of, M126

Intracellular assembly

- FFSS promotes, and formation of Cx43-forming channels in osteocytes, M520

Intracellular estradiol binding protein (IEBP)

- Control of estradiol-directed gene transactivation by, 1221

Intracellular scaffold

- Osteoclasts, Tm-2/3 regulate, M074

Intracrine

- Synthesis and action of 1,25-dihydroxyvitamin D rescues TLR suppression of innate immunity, 1028

IP₃

- Acid-induced stimulation of COX2 and RANKL in osteoblasts is mediated by, M063

IRF-8

- As negative regulator of osteoclast differentiation in vitro and in vivo, 1145

Iron (Fe)

- Uptake through the Tfr1 promotes osteoclast differentiation and function, M097

Iron (Fe³⁺)

- Role on differentiation of chondrocytes at the stage of calcification, M131

Isoflavone

- Isoflavone and soya foods intakes in Brazilian population, W275

IVVY⁵³⁵⁻⁵³⁸

- RANK cytoplasmic motif plays an essential role in TNF- and IL-1-induced osteoclastogenesis, M084, S084

J**Jagged1**

- Signaling promotes osteoclast differentiation in vitro, M085

Jak2 specific inhibitor. See *AG490***JNK**

- Activating pathway in U2OS, PDTC inhibits SOD1 gene and cell growth by, W018

K**KCI**

- Cotransport expression in canine osteosarcoma cell lines, investigation of, T031

Keratinocytes

- Skin, PTHrP regulates antimicrobial peptide production by, M238

KHBJ9

- Therapeutic effect on cartilage degradation and inflammation in CIA, M135

Kidneys

- Effects of GC on BMP-2 and BMP-7 expressions in, M234
- FGFR 3 and FGFR 4 are not physiologically relevant FGF-23 targets in, 1227

Kidney disease, chronic (CKD)

- Mechanism of skeletal involvement in cardiovascular mortality in CKD, T489
- Stages classified by serum cystatin-C and incidence of hip fracture in the WHI-OS, T325

Kidney stones

- Reduced formation and altered renal phosphate-homeostasis in mice overexpressing murine-MEPE, 1118

Klotho

- Ablation completely reverses the biochemical and skeletal alterations in FGF-23 (R176Q) transgenic mice, M208, S208
- Homozygous missense mutation causes severe tumoral calcinosis but not premature aging, 1113
- Protein, down-regulation of expression by estrogen, T192

KR62980

- Enhances bone formation through promoting osteoblastogenesis and inhibiting osteoclastogenesis, M387

KRN arthritis. See *Arthritis, KRN***Krox20**

- Analysis of gene regulation reveals Srf function in bone and cooperation with NFAT1, M025, S025
- Opposing effects of GCs and Wnt signaling on, T026

Kyphoplasty

- Adjacent fractures in the thoracic and lumbar spine after the treatment with balloon kyphoplasty, W397
- Balloon kyphoplasty in the treatment of osteolytic lesions in the thoracic and lumbar spine due to cancer, T258
- Importance of balloon kyphoplasty in the management of vertebral fractures, W392
- Interdisciplinary approach to improve pain and mobility in patients with osteoporosis and painful vertebral fractures by kyphoplasty, W26
- Three-year outcome after kyphoplasty in a prospective controlled trial role of initial bone edema and selection of cement type, T416
- Treatment of osteoporotic vertebral body fractures by means of percutaneous balloon kyphoplasty, W395

Kyphosis

- Computer-based measure of kyphosis predicts fractures in the thoracic spine of postmenopausal women, M356, S356
- X-ray ordering improves in patients with height loss or kyphosis following an osteoporosis educational intervention, T332

L**Lactase phlorizin hydrolase**

- Decreased activity of lactase phlorizin hydrolase and BMD in postmenopausal women, M284

Lactation

- Estrogen deficiency and PTHrP infusion do not fully reproduce the bone loss of, M220

Lactose

- Transgenic expression of the hVDR in the proximal small intestine of VDR-null mice improves the utilization of rescue diet in young mice, W154

Lacunae

- Estimation of osteocyte density from total lacunar population, W058

- Histochemical assessments on the distribution of OLCS, W059

- Osteoclastic resorption and bone resorption, diphyllin abrogates acidification of, T093
- Prednisolone induces osteocyte's death and erosion of osteocytic lacunae walls, W458

Lacunocanalicular fluid flow

- And regulation of BMU activity, M069

Lamin A/C

- Inhibits osteogenic differentiation of human MSC, siRNA specific knockdown of, M038

Lasofloxifene

- Lasofloxifene preserves lumbar vertebral strength by preventing bone loss and the deterioration of bone architecture and geometry, T435

Latent TGFβ binding protein (LTBP1)

- Non-covalent interaction with MMP-13 in a unique TGFβ large latent complex produced by hypertrophic chondrocytes, M128

Lbh (limb, bud and heart)

- Role in endochondral bone formation, M122

Lead (Pb)

- Differential accumulation in the tidemark of normal and osteoarthritic human articular cartilage and subchondral bone, W271

Lead (Pb²⁺)

- Bovine ion-bound osteocalcin and implications for toxicity, three-dimensional ¹H NMR structure of, M159

Left

- Nuclear interactions are ligand independent, W148

Leptin

- Beta blockade mitigates bone loss during energy restriction partially via, 1110
- Central control of bone remodelling by NMU, mediator of the leptin-dependent regulation of bone formation, 1061
- Deficient (ob/ob) mice exhibit increased bone mechanosensitivity and corresponding osteoblasts show increased anabolic shear stress responses in vitro, 1081
- Sexual dimorphism in the relationship between serum leptin and skeletal health in healthy adolescents, W507

Leu-Lys-Pro (LKP)

- Enhance osteoblast function in vitro, W038

Leukemia, lymphoblastic (ALL)

- BMD, body composition, BMI and height in children treated for ALL, T513
- Bone morbidity at diagnosis among children with ALL, M489, S489

Leupaxin (LPXN)

- Characterization of LPXN as a focal adhesion-associated protein in prostate cancer cells, W191

LIAISON® Analyzer

- Automated measurement of 1,25(OH)₂D on the, W211
- Development of a BAP assay for, W217
- Measurement of 25OH Vitamin D₂ by, W216

Ligamentum flavum (LF)

- Effect of pore size and surface modification of the circular PEG polymer scaffold on adhesion of cultured, M075
- Osteogenesis of, by demineralized bone matrix, T008

LIM mineralization protein 1 (LMP-1)

- Accelerates MC3T3-E1 osteoblast differentiation in part through modulation of the IGF system, T037

Limb development

Over-expression of Runx2 in mesenchymal cells enhanced bone formation but inhibited cartilage formation and, 1066
SOST overexpression impairs, M179, O179, S179

LIMD1

Modulates osteoblast differentiation and function, W047

Lipids

Bone-derived, activation of FXR in breast cancer cell lines by, M249

Lipocalin 2

Identification and functional involvement in GC-induced growth retardation, T177

Lipopolysaccharide (LPS)

Stimulates the formation of osteoclast-like cells by increasing M-CSF and PGE₂ production by osteoclasts, T084
Synergistically induces osteoclast differentiation, W084
TNFR1 and TNFR2 differentially regulate inflammatory bone resorption induced by, M110, S110

Lipoprotein lipase (LPL)

Association of LPL Hind III polymorphism with lumbar BMD in Korean premenopausal women, T224

Lipoproteins

Metabolism of postprandial, bone plays an important role in mice, T015

Liver

Cholestatic, expression of IGF-1 and GHR and biomechanical studies in experimental model of, W416

Liver X receptors (LXR)

Activation of inhibits hedgehog signaling and osteogenic differentiation of BMSC, W023

Lmna

Spontaneous mutation results in hypoplastic cranial sutures and under-mineralization of the skeleton, M146, S146

Long bones

Ang II suppresses bone mass via AT1 receptor in, M141
Growth plates, analysis of matrix vesicle proteins from, W085
Mechanical properties, expression of a hypomorphic allele of FIAT improves, S033

Lovastatin

Local delivery of lovastatin by a biodegradable polymer increases callus strength in rats, W341

LRF

Induced by RANKL and increases c-Fos expression in osteoclastogenesis, W067

LRP5

Compromised fracture healing in Lrp5 null mice, W456
Gain of function mutation is associated with an increased osteogenic response to loading in trabecular bone, M523, S523
Gene expression and bone turnover with disuse, M511
Haplotype-based analysis of the LRP5 gene in relation to osteoporosis phenotypes, M289
Influence of A1330V LRP5 gene polymorphism on volumetric BMD and structural parameters of bone in men and women, W230
Large-scale analysis of association between polymorphisms in the LRP-5 and LRP-6 genes and BMD and fracture, T199
Mineral and matrix characteristics in mice with LRP5 G171V mutation, M155

PTH activates β -catenin signaling through, 1297
Signals in U2OS osteoblast-like cells, mutations in LRP5 β -propeller 1 block SOST-mediated inhibition of, 1048

LRP5 β -propeller 1

Mutations in block SOST-mediated inhibition of the LRP5-Wnt-TCF signals in U2OS osteoblast-like cells, 1048

LRP5 G171V

Mutation and age-related bone fragility, M279, S279

Mutation protects against disuse-related trabecular bone fragility, M512, S512

Lumbar fusion

After posterolateral, bone metabolism using OP-1, W119

Lumbar vertebral growth plate (LVGP)

Postnatal, spatial and temporal localization of components of the TGF, BMP, IHH and FGF signaling pathways in, M125

Luminex xMAP

Development of multiplex immunoassay panels for simultaneous quantification of bone metabolism markers using Luminex xMAP technology, W206

Lung cancer

RANKL inhibition blocks lung cancer-induced osteolytic lesions and reduces skeletal tumor burden in both RANK-expressing and RANK-negative lung cancers, M307, S307

Lupus

BMD in Hispanic lupus patients, W254

Lupus erythematosus, systemic (SLE)

Low bone mass is common in premenopausal black women with SLE on prednisone, W247

Luteinizing hormone receptor (LHR)

Association of LHR polymorphism with BMD in young men, M286

Lymphatic growth factor

RANKL stimulates osteoclasts to release VEGF-C and enhances osteoclastic bone resorption through an autocrine mechanism, T100

Lymphocytes

RANKL expressing, intracellular cytokine profile of, T164

Lymphoid enhancer binding factor (Lef) 1

Isoform regulates osteoblast maturation, T023

Lymphoma, non-Hodgkin's (NHL)

Chemotherapy is associated with increased risk of fracture in elderly patients with NHL, T345
Elderly patients with NHL who receive chemotherapy at higher risk for osteopenia and osteoporosis, M374

Lysine-specific gingipain (Kgp)

Synergistically induces osteoclast differentiation, W084

Lysophosphatidic acid (LPA)

Induces osteocyte dendrite outgrowth, M182, S182
Production of, P2X7 receptors couple to, M062, S062
Promotes maturation and survival in rat growth plate chondrocytes, M187
Stimulated osteoblastic cell chemotaxis, molecular mechanisms of, M058, S058

Lysyl oxidase (LOX)

Regulates collagen quality and quantity in MC3T3-E1 cell culture system, M011

M **α_2 -Macroglobulin (α_2 M)**

Novel substrate for ADAMTS-7 and ADAMTS-12 and inhibits their degradation of COMP, M166

Macrophages

Identification of TNF α shedding enzyme in, M186

Osteal, novel regulators of bone formation, T186
That enhance osteoblast mineralization, primary murine osteoblast cultures contain, M015

Macrophage colony-stimulating factor (M-CSF)

Independent mechanisms for osteoclastogenesis, W072

Mediated osteoclast survival downstream of the MEK/ERK pathway, novel pro-survival functions of Egr2 in promotion of, M111
Production by osteoclasts, nicotine and LPS stimulate the formation of osteoclast-like cells by increasing, T084

Stimulates bone resorbing activity of mature human osteoclasts via increased activation of AP-1 and NF κ B, T075

Magnesium (Mg)

Intact CaR and PTH genes are required to regulate extracellular concentrations independently, M230

Mammalian P bodies. See GW bodies**Mammalian target of rapamycin (mTOR)**

Signaling, a novel molecular mechanism underlying Wnt's anabolic effects on osteogenesis, T108

Mandibular bones

Histological and biochemical characterization of mandibular bones in senile osteoporotic mice, T147

MAP kinase phosphatase-1 (MKP-1)

PTHrP induces in differentiated BMSC, osteoblast and cementoblast cell lines, M001

MAPK. See Mitogen-activated protein kinases**Marrow**

Marrow fat and peak bone mass, T449

Mast cells

Migration to bone surfaces precedes and appears essential for PTH-induced peritrabecular fibrosis, M482, S482

Matrilin-3 (MATN3)

Regulation of chondrocyte hypertrophy and BMD by, T063

Matrix metalloproteinase (MMP)

Expression of is pleiotropic on alkaline phosphatase expression in osteogenic differentiation, T019
MT3-MMP is a major mesenchymal collagenase essential for skeletal development, M167
Novel transcription factor-like function of stromelysin-1 that regulates CTGF/CCN2 gene transcription, T125
Regulation of expression by EPAS1 in articular chondrocytes, T122
Regulation of expression by MMP-12 in IL-1 β -treated articular chondrocytes, M139
Regulation of MMP-9 expression in IL-1 β -treated articular chondrocytes, M139
Rescue of MT1-MMP expression in cartilage increases survival, chondrocyte proliferation and bone formation, M165, O165, S165

Matrix metalloproteinase 13 (MMP-13)

IGF-1 regulation of gene expression in endplate chondrocytes via distinct signaling pathways, T116

- Induction in osteoblasts, Nmp4/CIZ contributes to fluid shear stress induced, T506
- Non-covalent interaction with LTBP1 in a unique TGF β large latent complex produced by hypertrophic chondrocytes, M128
- Null mutant mice, delayed cartilage and bone remodeling during fracture healing in, M163, S163
- Promoter activation, identification and characterization of Runx2 phosphorylation sites involved in, W026
- Matrix vesicles**
Poteins from long bone growth plates, analysis of, W085
- MC3T3-E1 cells**
BMP-2 induces sustained expression of COX-2 in, M168
- Differentiation and mineralization of osteoblastic via inhibiting the mevalonate pathway and enhancing BMP-2 expression, M056, S056
- LMP-1 accelerates osteoblast differentiation in part through modulation of the IGF system, T037
- LOX regulates collagen quality and quantity in culture system, M011
- Podn affects cell proliferation and in vitro mineralization possibly by inducing cellular senescence in, T142
- Rapamycin inhibits osteoblast proliferation and differentiation in, M007
- McCune-Albright syndrome (MAS)**
Severe hypertension, a possible complication of MAS, M488
- MCP-1**
Cascade of gene expression indicates CCL2 is essential for osteoclast formation, T073
- PTHrP-induced production by HBME cells and osteoblasts promotes osteoclast differentiation in vitro, T247
- Mean carotid plaque thickness (MCPT)**
PTH levels are associated with, W145
- Measles virus nucleocapsid protein (MVNP)**
Enhances NFATc1 activation during osteoclastogenesis in PD, M479
- Expressing cells, changes in VDR coregulator recruitment result in $1\alpha,25(\text{OH})_2\text{D}_3$ hypersensitivity in, W152
- Mechanical loading**
Bone adaptation to impact loading, WG9
- Bone traits are determined early in life but adapt during growth to accommodate local loading circumstances, I197
- Do periosteal and intracortical responses to ulnar fatigue loading differ between old and young rats?, M461
- Effect of hindlimb unloading on bone in two strains of mature mice, M513
- Effects of mechanical loading and estrogen are structurally distinct, I087
- Effects on matrix production by osteoblastic cells cultured in polyurethane scaffolds, T508
- Identification of genes that may modulate the musculoskeletal system's early response to unloading, T510
- Increased vBMD and bone area due to mechanical loading gradually decreased following cessation of loading, T151
- Knee loading stimulates wound healing in mouse femora, M526
- Males have an enhanced osteogenic responsiveness to loading versus females, W500
- Mechanical properties**
Of cortical bone, osteoblast-specific knockout of *Igf1r* alters, W464
- Heritability of lumbar trabecular bone mechanical properties in baboons, W176
- Improved analysis of bone nano-mechanical properties using a novel nanoindentation technique, W463
- Mechanical enhancement of bone quality is paralleled by suppression of fat production, W495
- Testing of mechanical properties of hip protectors using high-tech materials, T418
- Mechanical strength**
Increase of novel unidirectional porous HAp ceramics in vivo, T128
- Mechanical stress/strain**
AKT's effects on β -catenin regulate osteoblasts' responses to, T067
- Effects on osteocytes, induced bone cell proliferation and recruitment, W054
- And fluid shear stress induce a similar osteogenic gene response via divergent signaling pathways, M517
- Induced root resorption, M-CSF receptor c-fms antibody inhibits, M107
- Protective effects on osteocyte viability is mediated by the effects of prostaglandin on the cAMP/PKA and the β -catenin pathways, M237
- Medullary bone**
Formation, osteoclast differentiation in Japanese quail bone marrow cell culture, M091
- MEK**
Pathway, novel pro-survival functions of Egr2 in promotion of M-CSF-mediated osteoclast survival downstream of, M111
- Melanoma**
Melanoma bone metastasis, W188
- TGF β receptor I kinase inhibitor reduces the development and progression of melanoma bone metastases, M305, S305
- Melatonin (Mel)**
Hormonal and pharmacological modulation of MT2 receptor inhibits osteoclast maturation and activity, T087
- Melatonin receptor isoform 1 (MT1)**
Benign and malignant bone tumors express the MT1, T262
- MEN1**
In MEN1 the estimated ratio of mutated p27 versus mutated MEN1 genes is below 1:100, T483
- Menadione (K_3)**
Biosynthesis of MK-4 from PK and, T136
- Menaquinone-4 (MK-4)**
Biosynthesis from PK and K_3 in bone, T136
- Effect of Vitamin K2 in addition to Ris on the patients with postmenopausal osteoporosis, T424
- Synthesis and biological evaluation of Vitamin K_2 metabolites, T261
- Menarche.** See also *Amenorrhea*
Influence of menarcheal age on microstructural constituents of distal tibia in 20-year-old women and their middle-aged mothers, T463
- Menopause**
Impact of herbal remedies for menopause on BMD, M339, S339
- Postmenopausal osteoporosis and weight gain, W386
- Relationship of bone turnover markers, ovarian hormones and cytokines during menopause, M458
- Relationship of serum cytokines and monocyte gene expression to BMD and BMC in postmenopausal women, M183
- MEPE**
Abnormal bone-mineralization, osteoclastogenesis and bone-turnover in transgenic-mice overexpressing MEPE, I226
- Degradation of, and release of SIBLING ASARM-peptides (minhibins), I155
- Murine, reduced kidney-stone formation and altered renal phosphate-homeostasis in mice overexpressing, I118
- Osteocyte specific expression after mechanical stimulation in the mouse ulnae loading model, W050
- Mesenchymal cells**
Differentiation and mineralization, temporal expression of PHOSPHO1 during chick limb bud, W087
- Identification and characterization of miRNAs expressed during chondrogenesis of, T123
- Murine, mineralization of C3H10T1/2 cells in micromass culture, W088
- Over-expression of Runx2 enhanced bone formation but inhibited cartilage formation and limb development, I066
- Mesenchymal stem cells (MSC)**
Adipocyte differentiation of, osteoblast differentiation by inhibiting, T057
- Age-related intrinsic changes in human bone marrow-derived MSC and their differentiation to osteoblasts, W031
- BMP-Mediated adult bone marrow-derived MSC, active fragment of Spp24 enhances differentiation to osteoblasts, T144
- CLA regulates osteoblast and adipocyte differentiation from, T047
- Concentration and bone repair, M046
- Condensation, crosstalk between CTGF and TGF1 in, M158
- Cytoplasmic interaction of p21 with Runx2 during osteogenic differentiation of, T049
- Differentiation to osteoblasts, Snail inhibits, T033
- Enhanced properties in dynamic three-dimensional cultures, M051
- Fom aging C57BL/6 exhibit increased oxidative stress and defective replication, M052, S052
- Growth and osteogenic differentiation, bespoke bioceramic scaffolds support, M050
- From human adipose tissue and bone marrow, osteogenic differentiation and interaction with Ti6Al4V, T053
- IGF-1 engineered bone marrow improve the fracture healing process, M191, S191
- Precursors derived from human BMSC and DPSC, role of EphB/ephrin-B interactions in cell attachment and spreading of, W033
- siRNA specific knockdown of lamin A/C inhibits osteogenic differentiation of, M038
- TGF β 1 induces migration in coupling bone resorption and formation, I072
- Mesenchymal stem cells, bone marrow-derived (bmMSC)**
Progenitor cells in tmMPC have characteristic similarities to, W039
- Mesenchymal stem cells, human (hMSC)**
Derived osteoblasts, effects of PDE7 and PDE8A inhibition on the differentiation of, T046

- Osteogenesis, activation of the non-canonical Wnt pathway during, T048
- Regulation of lineage commitment, dual-action CTSK inhibitors, W315
- Mesenchymal stem cells, non-adherent bone marrow-derived (NA-BM-MSD)**
- Wild-type, partial rescue of the Vitamin D deficient phenotype of 1 α -hydroxylase gene knockout mice by transplantation of, T058
- Mesenchyme**
- During craniofacial bone development, temporal regulation of histogenesis by, W040
- Messenger RNA (mRNA).** See *Ribonucleic acid*
- Metabolic bone diseases**
- Relationship between bone formation rate and bone marrow adipocytes in pediatric metabolic bone diseases, W426
- Metachondromatosis**
- Molecular exclusion of mutations in EXT1 and EXT2 as the cause of metachondromatosis, T475
- Methadone maintenance therapy (MMT)**
- High prevalence of abnormal lumbar spinal DXA scans in men receiving MMT for opiate dependence, W305
- 2-Methoxyestradiol (2-ME)**
- Anti-tumor actions are accompanied by an increase in OPG expression in osteosarcoma cells, M306
- Skeletal effects of 2-ME in combination with other prostate cancer therapies, T251
- Methylglyoxal (MG)**
- Comprehensive analysis of bone-related gene expression induced by acute oxidative stress, W413
- METRNL**
- New secreted protein inhibits differentiation of MG63, M034
- Mevalonate**
- Inhibiting, differentiation and mineralization of osteoblastic MC3T3-E1 cells via, M056, S056
- MG63**
- Differentiation, METRNL secreted protein inhibits, M034
- MHox.** See also Homeobox protein; Prx1
- Identification of as a regulator of Osx expression and mediator of TNF action, I143
- Micro-SPECT scanning**
- ESWT stimulates bone remodeling in the rat, evaluated with in vivo, W347
- Microenvironments**
- Bony, distinct roles of ITAM signaling in bone remodeling in various, I291
- Microgravity**
- Effects of, on osteoblast and osteoclast differentiation, T052
- Microphthalmia-associated transcription factor (Mittf)**
- Isoforms, expression and transcriptional activity during osteoclastogenesis, T101
- MicroRNA (miRNA).** See also *Ribonucleic acid*
- Alterations are associated with osteoclastogenesis, M094
- Expression profiling and function during in vitro osteogenesis, I214
- Identification and characterization expressed during chondrogenesis of mesenchymal cells, T123
- miR-26a targets the SMAD1 protein of hADSCs, T028
- Regulation of osteoblast differentiation by, M049, S049
- Microspectroscopy, synchrotron infrared**
- Microscopic imaging of bone composition en block with synchrotron infrared microspectroscopy, T112
- Microtopography**
- Osteoblast response to, is dependent on integrin α -2, W002
- Microtubules**
- myo10 regulates osteoclast adhesion through linkage of podosomes and, M076
- Milk basic protein (MBP)**
- Interactive effects of MBP supplementation and habitual physical activity on bone health in older women, W343
- Mineral Metabolism Osteoporosis in Abruzzo (MIMOSA-G) project**
- Vitamin D deficiency in a central Italian town normal population, M236
- Mineralization**
- In 2D and 3D tissue engineered constructs, use of statins to enhance, T003
- Bone nodule, 1,25(OH) $_2$ D $_3$ inhibits through the FGF-23-mediating ERK pathway in calvaria osteoblast cultures, M210, S210
- BSP-mediated osteoblast, principally dependent on the intrinsic characteristics of responding cells, T149
- Capacity, osteoblasts from 5-HTT knockout mice display reduced growth and, M013
- Collagen/annexin V interactions regulate growth plate chondrocyte mineralization, I111
- Conditional ablation of the osteoblast CaR causes abnormalities in, M223, O223, S223
- Defective, ASARM-peptides are directly responsible in HYP, I155
- Integration with osteoblast to osteocyte transition, dynamic imaging of fluorescently tagged osteoblast and osteocyte populations, I044
- Matrix, novel activin/nodal-binding protein G11 inhibits, M203
- Of murine mesenchymal C3H10T1/2 cells in micromass culture, W088
- Non-adherent circulating progenitor cells with osteoblastic potential become adherent in the presence of Ca $^{2+}$ and are able to mineralize, T040
- Osteoblasts, androgens act directly via the AR to regulate bone turnover and maintain trabecular bone, I217
- Osteocyte specific expression after mechanical stimulation in the mouse ulnae loading model, W050
- PAI-1 increases femoral mineralization independent of estrogen status through modulation of FN matrix, T137
- Perichondrial, Trps1 transcription factor regulates through repression of Runx2, I184
- Primary murine osteoblast cultures contain macrophages that enhance, M015
- PTH and Ris prevented GC induced reduction in bone mineralization through different mechanisms, W331
- Time sequence of secondary mineralization and microhardness of bone in an ewe model, M504, O504, S504
- Under-mineralization of the skeleton, spontaneous mutation in the mouse *Lmna* gene results in, M146, S146
- And Vitamin D inadequacy, I300
- In vitro, Podn affects by inducing cellular senescence in MC3T3-E1 cell, T142
- Mineralized tissues**
- Induction of by in vivo transplantation of cultured dental pulp cells in rat calvarial bone defects, T017
- Minocycline (Mino)**
- Effectively inhibits osteoclast differentiation and function, M106
- Minodronate**
- Comparison of the effect of daily minodronate with ALN in Japanese women with postmenopausal osteoporosis, T395
- Effect of daily oral minodronate on vertebral fractures in Japanese postmenopausal women with established osteoporosis, I059
- MINT**
- Runx2 transcriptional AD3 supports synergistic activation of the osteocalcin FGF response element via a DMAT-sensitive kinase, T036
- miR-26a**
- Targets the SMAD1 protein of hADSCs, T028
- Mitochondria**
- Smad4 has a direct apoptogenic role at, M205
- Mitogen-activated protein kinases (MAPK)**
- Activation by 17 β -estradiol is mediated by PKC and c-Src in skeletal muscle cells, T194
- ATP modulation of, in osteoblastic and breast cancer cells, T064
- FGF-23 controls NaPi-IIa trafficking via crosstalk with the PI-3 kinase pathway, T158
- RANKL-induced activation by ROS, M115
- Signaling in osteoblasts, gremlin induces, W122
- Mitogenesis**
- PDGFR-mediated osteoblast, imatinib mesylate inhibits bone formation and decreases bone mass in vivo by inhibiting, T018
- MK-0429**
- α , β $_3$ integrin antagonist (MK-0429) inhibits osteolytic lesions in breast cancer and melanoma lung metastases, M290
- MLO-Y4**
- Osteocytic cells, FFSS and PE $_2$ activates β -catenin signaling in, W053
- MMP.** See *Matrix metalloproteinase*
- Molecular cloning**
- Characterization of mouse RANK gene promoter region, M095
- Monoclonal gammopathy of undetermined significance (MGUS)**
- Open-label study on the effects of ALN in osteoporotic patients affected by MGUS, W356
- Monocytes**
- Internalization of DBP by, M253, S253
- In vivo proteomic analysis of circulating monocytes in Chinese pre-menopausal females with extremely discordant BMD, W244
- Morphological traits**
- Single chromosome substitutions alter functional interactions among and mineral density in inbred mice, W173
- Morphometry, quantitative (QM)**
- Magnification correction of vertebral body heights during QM, M357
- MrOS Study (Sweden)**
- FGF-23 is an independent predictor of BMD in a population-based cohort of elderly men, W125
- Msx2**
- Gene transcription, TNF dependent redox signals upregulate via stress activated protein kinases in arterial myofibroblasts, T165
- TNF α stimulated expression in C2C12 cells, M020

- MT2**
Mel receptor inhibits osteoclast maturation and activity, hormonal and pharmacological modulation of, T087
- Multiple myeloma (MM).** See *Myeloma, multiple*
- Multiple sclerosis (MS)**
Survey on the effect of immunomodulatory therapy on bone in MS, W437
- Mural cells**
FGF2 and TGF1 have opposite effects on the phenotype of CD146⁺ BMSCs, M178
- Murine bone**
Age-dependent regulation of FGF-23 production in murine bone, T159
PTH(7-84) inhibits PTH(1-34)-induced production of 1,25-(OH)₂D₃ in primary cultured murine renal tubules, T482
- Muscle cells**
Role of Nkx3.2 in muscle/cartilage cell fate determination, W105
- Muscle segment homeobox 2 (Msx2)**
During BMP2-regulated osteoblastogenesis, *Osx* functions as downstream of, W020
Promotes late stages of chondrocyte differentiation by up-regulating *Ihh* expression, W092
Reciprocal regulation of *Dkk1* gene transcription by, I140
- Musculoskeletal response**
To altered mechanical demand is tissue specific and influenced by genetic make-up, W499
- Mutagenesis, gene-trap**
Revealed the involvement of vinculin in chondrogenic differentiation in ATDC5 cells, M137
- Myeloid cells**
Identification of a novel stem cell for bone and cartilage of, M169, S169
- Myeloma**
Cells decrease EphB4 expression in osteoblasts, M309, O309, S309
Intermittent PTH treatment inhibits development and progression of primary myeloma by promoting bone formation, I172
Mice with a myeloid lineage-specific deletion of *IKKβ* demonstrate both in vivo and in vitro defects in osteoclastogenesis, I294
Osteoclasts in myeloma are derived from Gr-1⁺CD11b⁺ mononuclear cells of the bone marrow niche, I004
Treatment with HepIII inhibits the growth of myeloma tumors in bone, I171
Ubiquitin-proteasome pathway is dysregulated in myeloma cells in the bone microenvironment in vivo, M310
Up-regulation of TACE in monocytes ameliorates their deflected differentiation into osteoclasts and dendritic cells in, M302
- Myeloma, multiple (MM)**
Activity of the Akt inhibitor perifosine and HSP-90 inhibitor 17-DMAG in modulating osteoclastogenesis and the BMM in MM, W195
BMP-4 and BMP-6 are overexpressed in the bone marrow samples, W110
ZOL decreases serum low-density lipoprotein cholesterol in MM patients, W190
- Myoblasts**
Pitx2 inhibits osteoblastic conversion of, through interfering the promoter activity of *Osx* gene, T021
- Smad1 and Smad4 differentially regulate osteoblast differentiation and myogenesis in, W117
- Myocyte enhancer factor 2 (MEF2)**
Control of the *SOST* bone enhancer by PTH via, I046
- Myofibroblasts**
Arterial, TNFα dependent redox signals upregulate *Msx2* gene transcription via stress activated protein kinases in, T165
- Myogenesis**
Differentiation, *Zfp64* is a downstream target of *Runx2* and regulates as a coactivator of *Notch1*, T035
Smad1 and Smad4 differentially regulate osteoblast differentiation and, W117
- Myosin IIA (myoIIA)**
Regulates precursor cell fusion and osteoclast motility, W069
- Myosin X (myo10)**
Regulates osteoclast adhesion through linkage of podosomes and microtubules, M076
- Myostatin**
Signaling, Arkadia represses skeletal muscle differentiation through enhancement of, M206
- N**
- N-telopeptide**
Optimum testing strategy for urinary N-telopeptide, W204
- Nanogels**
Use as a drug delivery system for TNFα antagonist in murine bone resorption model, M101
- Nanopatterned surfaces**
Assessing BMP-2 activated osteoblast differentiation with, W120
- NBCn1**
Expressed in rat osteoclast ruffled border membrane, T091
- Necl-5**
Expression and possible role in osteoclastogenesis, M077
- NELL-1**
Partially rescues craniofacial defects in *Runx2* haploinsufficient mice, I105
Promotes bone formation in a spinal fusion model, M200
- Nephrotic syndrome**
Overexpression of Pit-1 in rats develops the progressive nephrotic syndrome, T138
- Net endogenous acid production (NEAP)**
NEAP and BMD in men and women, T309
- Neurocognitive changes**
In mild PHPT, W146
- Neuromedin U (NMU)**
Central control of bone remodelling by, I061
- Neuropeptide Y (NPY)**
NPY protects the skeleton from stress-induced bone loss, I134
- NF-κB.** See *Nuclear factor-κB*
- NF-κB essential modulator (NEMO)**
Modulates osteoclastogenesis and bone erosion, T098
- Nicotine**
Stimulates the formation of osteoclast-like cells by increasing M-CSF and PGE₂ production by osteoclasts, T084
- NIH3T3 cells**
Downstream signal transactivation by FGF-4/*Osx* transgene partially imitates changes of BMP-2 induced osteogenic transcription factors in, W016
- Nitrates**
And BMD among Canadian men and women, I266
Organic nitrate use, bone loss and fractures in older men, T420
- Nitric oxide (NOX)**
Expression in odontoblasts and cementoblasts of NOS knock-out mice, T173
- Nitric oxygen synthetase (NOS)**
NOX expression in odontoblasts and cementoblasts of NOS knock-out mice, T173
ROS expression in osteoblasts of, in knockout mice, M006
- Nitrous oxide (NO)**
Role of NO in the preventive effects of electrical stimulation on OVX-induced bone loss in rats, W339
- Nkx3.2**
Role in muscle/cartilage cell fate determination, W105
- NMR**
Three-dimensional ¹H structure of bovine lead ion-bound osteocalcin and implications for lead toxicity, M159
- N,N-Dimethyl-D-erythro-sphingosine (DMS)**
Suppression of osteoclastogenesis by, a SPHK inhibition-independent action, M088
- Noggin**
Diverse effects on BMP-2-induced osteogenesis, W107
siRNA gene transfer enhances the in vivo ectopic bone formation induced by BMP-2, W121
- Non-adherent bone marrow-derived mesenchymal stem cells.** See *Mesenchymal stem cells, non-adherent bone marrow-derived*
- Non-Hodgkin's lymphoma.** See *Lymphoma, non-Hodgkin's*
- Normocalcemic hyperparathyroidism.** See *Hyperparathyroidism, normocalcemic*
- Notch**
Signal pathways, CCN3/NOV inhibits BMP-2-induced osteoblast differentiation by interacting with, T070
Signaling in bone homeostasis, dimorphic effects of, I212
- Notch1/2**
Signaling promotes osteoclast differentiation in vitro, M085
Zfp64 is a downstream target of *Runx2* and regulates myogenic and osteogenic differentiation as a coactivator of, T035
- Npt2a.** See *Sodium-phosphate co-transporter; type IIa*
- Npt2c.** See *Sodium-dependent phosphate transporter; type IIc*
- Nuclear factor I-X (NFI-X)**
Transcription factor in regulation of IGFBP-5 and osteocalcin expression in mouse osteoblasts, role of, T034
- Nuclear factor κB (NF-κB)**
But not NFATc1 is involved in AhR-RANKL crosstalk in BaP-mediated inhibition of osteoclastogenesis, T106
Canonical pathway mediates osteoclast bone resorption activity, T094
Constitutive activity of the NF-κB p65/p50 transcriptional complex is critical for bone metastasis in breast cancer, T249

Estrogens attenuate IL-6 and TNF α production in osteoblastic cells by decreasing oxidative stress and its effects on, T186

Human breast stem cell transformation and invasiveness is mediated upregulation of IL-8 by *TWIST* interactions with, T242

IL-23-enhanced osteoclastogenesis is mediated by via upregulation of RANKL from CD4⁺T cells, T078

M-CSF stimulates bone resorbing activity of mature human osteoclasts via increased activation of, T075

Matrix PRELP inhibits osteoclastogenesis inactivating, W080

Oxidative stress-induced vascular calcification is associated with increased expression of receptor activator of, 1216

Regulated gene expression and kinase phosphorylation oscillate rapidly over time, M198

Transcriptional induction of SOX9 by subunit p65 during chondrogenesis, W101

Nuclear factor κ B2 (NF- κ B2)
Limits TNF-induced osteoclastogenesis through precursor cell cycle regulation, 1148

Nuclear factor of activated T cells (NFAT)
Activation during osteoclastogenesis in PD, MVNP enhances, M479

Activation, endogenous TNF in osteoclast precursor cells promotes osteoclastogenesis via, T077

Analysis of Krox20 gene regulation reveals Srf function in bone and cooperation with, M025, S025

AnxA8 is a critical bone matrix-dependent osteoclast gene transcriptionally regulated by, W068

In bone mechanotransduction, a novel role for, M519

CTGF induces in vitro, T172

Down-regulation of, PIAS3 modulates osteoclastogenesis by, W066

Mediates the stimulatory effects of post-translationally modified BSP on the resorptive activity of rabbit osteoclasts, T099

NF- κ B but not NFATc1 is involved in AhR-RANKL crosstalk in BaP-mediated inhibition of osteoclastogenesis, T106

In osteoclasts, regulation of integrin expression by, M071

Nuclear matrix protein 4/cas interacting zinc finger protein (Nmp4/CIZ)
Contributes to fluid shear stress induced *MMP-13* gene induction in osteoblasts, T506

Nucleocytoplasmic shuttling
Ciz, a nucleocytoplasmic shuttling protein, interacts with ECM proteins, W012

Nucleoside reverse transcriptase inhibitors (NRTI)
TREM2 pathway is involved in osteoclastogenesis induced by, W074

Nucleus pulposus (NP) cells
Effect of removal on the annulus fibrosis of the IVD, M124

Nutrition
Diet effects on bone mechanical and molecular markers, T360

Effect of a high-protein diet on bone and body composition, W410

Effect of home parenteral nutrition on BMD, W249

Effect of the dietary habit of skipping breakfast on bone metabolism, skeleton and nutritional status in young Japanese women, W517

High protein intake enhances the positive influence of physical activity on BMC in pre-pubertal boys, 1041

More alkaline diet may enhance the favorable impact of dietary protein on lean tissue mass in older adults, W403

Negative effect of dietary protein intake on bone mass accretion in Chinese pubertal girls with low Ca intake, 1038

Negative impact of caloric restriction on the BMD, T457

Nutrition survey about the status of fat-soluble vitamins in Japanese women, T311

Propensity to accumulate bone microdamages is increased in adult female rats fed an isocaloric low protein diet, W404

Restricting dietary protein may improve skeletal integrity in exercising female rats, T361

O

Obesity

A stronger marker than body weight for BMD in Caucasian women but not in men, M335

Bone growth, adipocytokines and physical training in obese children, T477

Effect of diet and exercise-induced weight loss on regional and total body BMD of obese subjects, M320

Effects of weight reduction on bone mass and structure in obese women, T319

Increased markers of bone formation seen following bariatric surgery in morbidly obese patients, T444

Influence of moderate energy restriction and seafood consumption on bone turnover in overweight young adults, W408

Influence of overweight/obesity on BMD of various skeletal sites in early-postmenopausal women, W274

Relative efficacy of Vitamin D2 or D3 treatment for D-insufficiency in morbidly obese subjects, T445

OCT-1547

OCT-1547 inhibits osteoclast differentiation through inhibition of PLC γ 2 activation and NFATc1 induction, M410

OCZF

Expression directed by the CatK promoter affects bone mass and osteoclast formation in transgenic mice, M099, O099, S099

Odd-skipped related 1/2 (Osr1/2)

Functions in cell proliferation, M003

Gene expression is regulated by Runx2 and Ikaros transcription factors, W030

Odontoblasts

Maturation, Dlx5 overexpression promotes early, M028

NOX expression in NOS knock-out mice, T173

Old astrocyte specifically induced substance (OASIS)

Involved in normal bone formation, M029, S029

Olpadronate

Novel effects of high doses of olpadronate on cortical bone and mechanism of fracture in young rat femurs, W321

Oncogenic osteomalacia. See *Osteomalacia, oncogenic*

Oncostatin M (OsM)

An essential stimulus of bone formation and osteoclastogenesis, 1068

Osseointegration

Ti implantation in rat maxillae, bone remodeling after, T127

Ossification, endochondral

Mechanisms of Osx control of, W098

OPG negatively regulates chondroclast formation and recruitment in, M136, S136

Phenotypical heterogeneity between osteoclasts involved in, T083

Pit-1 controls endochondral ossification through regulating chondrocyte apoptosis, 1224

Ossification, heterotopic (HO)

Characterization of a new traumatic mouse model of, T171

Progenitor cells in tmMPC have characteristic similarities to bmMSCs, W039

Ossification of the posterior longitudinal ligament (OPLL)

Functional RNAi screening for Runx2-regulated genes corresponding to ectopic bone formation in human spinal ligaments, M273

Runx2 haploinsufficiency ameliorates the ectopic calcification in a mouse model OPLL, W100

Ostabolin-CTM

Increases lumbar spine and hip BMD after one year of therapy, 1130

Pulmonary delivery of the PTH analogue Ostabolin-CTM stimulates markers of bone formation in postmenopausal women, M421, S421

Osteoactivin (OA).

See also *Glycoprotein nmb*

Bone cell autonomous effects of, in vivo, 1023

Osteoarthritis (OA).

See also *Arthritis*

Abnormal collagen type 1 production by human osteoarthritic osteoblasts, T143

Alterations in collagen structure and mineral composition in calcified cartilage and subchondral bone in a monkey model of, W089

Associated changes in synovial fibroblasts, involvement of Cx43 in IL-1 β -induced, T169

Back-scattered electron imaging of bone mineralization in osteoarthritis, T113

Differential accumulation of Pb and Zn in the tidemark of normal and osteoarthritic human articular cartilage and subchondral bone, W271

Increased bone resorption in knee osteoarthritis with severe joint surface wear, W207

Induction of kinin B₁ receptor is performed by vasoactive peptide ET-1, M117

Intra-articular OCIF/OPG prevents cartilage degeneration in a murine model of, W097

Of knee decreases regional and total BMD in Japanese women, T456

Molecular network underlying chondrocyte hypertrophy causing, M127, S127

OPG inhibits cartilage degradation in a knee instability mouse model, M134

Prevalence of radiographic osteoarthritis of knee and lumbar spine and its association with pain, W438

Regulation of the transcription factor Pitx1 and its role in OA pathogenesis, 1035

Osteoblasts

From 5-HTT knockout mice display reduced growth and mineralization capacity, M013

Ablation of IGF-1 signaling disrupts the communication between osteoblasts and, M241, S241

- Abnormal collagen type 1 production by human osteoarthritic, T143
- Acid-induced stimulation of COX2 and RANKL in, mediated by IP₃, M063
- Active fragment of Spp24 enhances but is not indispensable for BMP-mediated adult bone marrow-derived MSC differentiation to, T144
- In adult bone use *Slug* for regeneration and repair but not remodeling, 1213
- Alpha1 and beta2 adrenergic agents modify RANKL/OPG expression and cell proliferation in, T006
- ATP is released from, by multiple mechanisms, M065
- Calcitriol inhibits BMSC differentiation into, in a manner cooperative with but independent of TGFβ, T069
- Calvaria cultures, 1,25(OH)₂D₃ inhibits bone nodule mineralization through the FGF-23-mediating ERK pathway in, M210, S210
- Cell lines, PTHrP induces MKP-1 in, M001
- Characterization of regions upstream of exon II of the human CYP19 gene that mediate regulation by cAMP in murine, T032
- Cleavage products of APP regulate function of, T145
- Co-stimulation of 1,25-(OH)₂D₃ and BMP-2 enhances the expression of VDR and RANKL mRNA in, W162
- Conditional ablation of the CaR causes abnormalities in skeletal development and mineralization, M223, O223, S223
- Conditional deletion of FN reveals distinct roles in orchestrating assembly of bone ECM proteins and in osteoblast differentiation, 1177
- Conditional knockouts in early and mature, reveal a critical role for CaRs in bone development, 1284
- Cultured, GC enhances the expression of sFRP3 in, T176
- Cultures, opposing effects of GCs and Wnt signaling on Krox20 and mineral deposition in, T026
- Deletion of Cnb1 reveals novel role for calcineurin in bone formation, 1283
- Designer GPCRs suggest opposing roles for Gs and Gi signaling in, 1021
- Dynamic imaging in living calvaria reveals the motile properties and suggests heterogeneity in bone, 1045
- Dynamic imaging of fluorescently tagged populations integrates mineralization dynamics with osteoblast to osteocyte transition, 1044
- Early, impaired bone formation in mice lacking Gs leads to marked bone fragility, 1020
- EGF-like ligands stimulate osteoclastogenesis by regulating expression of osteoclast regulatory factors by, T175
- Elastic modulus of, W061
- ERα is required for strain-related β-catenin signaling in, M064, O064, S064
- Express CSF-1R and are a target for CSF-1, T039
- Expression of osteoblast-specific transcription factors in aged mice, W024
- Function, bone plays an important role in the metabolism of postprandial lipoproteins in mice, T015
- Function in vitro, bioactive tripeptides enhance, W038
- Function, TWEAK is a regulator of, M009
- Gene networks that are regulated by the *Dlx* gene family, W017
- GGPP promotes survival and is involved in anti-apoptotic effects of PTH, 1192
- Greater sensitivity of osteocytes to shear stress as compared to, PGE₂ production and Wnt/β-catenin signaling, W052
- Gremlin induces MAPK signaling in, W122
- Growth inhibition by Runx2 depends on its C-terminal regulatory domain and is accompanied by changes in G-protein coupled signaling pathways, M047, S047
- GSK-3 inhibits osteoblastic bone formation through suppression of Runx2 transcriptional activity by the phosphorylation at a specific site, 1247
- hCol1a2 nuclear targeting sequence together with human Runx2 enhancer elements drives robust expression in, 1288
- Identification of specific co-regulator complex for VDR, W022
- Identification of TCTP as a nuclear matrix protein in, M143
- Increasing number is not sufficient to enhance the function of the HSC niche, M053
- Inhibiting apoptosis of through FoxO3a/Bim axis, Akt1 contributes to maintenance of bone mass and turnover by, 1211
- Inhibiting proliferation and differentiation in MC3T3-E1 cells and primary mouse BMSCs, rapamycin, M007
- Isolation and immunohistochemical analysis of OMD expressed in, T016
- Local overexpression of aromatase leads to clearly increased bone mass, 1218
- Maturation, Lef 1 isoform regulates, T023
- Mature, GC stimulate Wnt expression in, T062
- Mature, transgenic disruption of GC signaling attenuates KRN serum-induced arthritis in vivo, T183
- MC3T3-E1, BMP-2 induces sustained expression of COX-2 in, M168
- Mineralization, primary murine cultures contain macrophages that enhance, M015
- Mineralizing, androgens act directly via the AR to regulate bone turnover and maintain trabecular bone, 1217
- Modulation of P2X₇R by estrogen and corticosteroids, M055
- Molecular mechanisms of 1α,25(OH)₂ Vitamin D₃-induced ATP release in, 1030
- Nmp4/CIZ contributes to fluid shear stress induced *MMP-13* gene induction, T506
- Novel activin/nodal-binding protein G11 inhibits matrix mineralization in, M203
- P2X₇ receptors couple to production of LPA, a novel signaling axis promoting osteogenesis, M062, S062
- PDGFR-mediated mitogenesis, imatinib mesylate inhibits bone formation and decreases bone mass in vivo by inhibiting, T018
- PGE₂ acts through EP2/EP4 receptors to upregulate RGS2 expression in, T063
- Phosphorylation of caveolin-1 in response to fluid shear is mediated by P2X₇ activation, T061
- Pitx2 inhibits osteoblastic conversion of myoblasts through interfering the promoter activity of *Osx* gene, T021
- Potential involvement of Ephrin B2 in the anabolic action of PTH in, T012
- Proliferation through the c-Src/ERK signaling pathway, interaction of galectin-9 with lipid rafts induces, W005
- PTHrP-induced MCP-1 production promotes osteoclast differentiation in vitro, T247
- Regulation of oxidative stress and osteoblast apoptosis by estrogens is preserved when the ER cannot directly interact with DNA, T184
- Related gene expression, adiponectin action influences, W014
- Response to titanium microtopography is dependent on integrin alpha-2, W002
- Responses to mechanical strain and PTH, AKT's effects on β-catenin regulate, T067
- Role of NF1-X transcription factor in regulation of IGFBP-5 and osteocalcin expression in, T034
- Role of Wnt3A signaling in maturation of, T166
- ROS expression of NOS1, 2 and 3 in knockout mice, M006
- Selective deletion of FN affects bone density and osteoblast function, 1179
- Skeletal phenotype in transgenic mice over-expressing CTGF in cells of the lineage, 1287
- Snail inhibits the differentiation of MSC to, T033
- Specific knockout of *Igf1r* alters mechanical properties of cortical bone, W464
- Targeted disruption of *Efnb1* reduces bone size, 1107
- Targeted disruption of GC signaling delays intramembranous bone development in vivo, T182
- TGFβ suppresses POEM expression in, M201
- TIEG as a novel mediator of Runx2 expression and activity in, 1144
- TIEG directly binds to and represses the OPG promoter, resulting in decreased support of osteoclast differentiation, W028
- Transcription factor E4bp4 is induced by GCs and represses promoter activity in, T179
- Transformation to osteocytes, hypoxia accelerates, W013
- Transgenic expression of an engineered Gs-coupled receptor in, produces increased bone mass, 1019
- Ultrasound induces HIF-1 activation and iNOS expression, T511
- In vitro and in vivo, *Zfp521* is a novel inhibitor of Runx2 activity with opposite effects on, 1250
- Osteoblast differentiation**
- And adipocyte differentiation, opposing effects of GH and alcohol reveal a critical role in the reciprocal relationship between, M196
- And anagen induction, aimilar effects of proteasome inhibition on, W111
- Atm regulates through the BMP-Smad1/5/8 pathway, M017
- bmMSC by inhibiting adipocyte differentiation, T057
- Breast cancer cells inhibit osteoblast differentiation, T237
- BSP-mediated and mineralization is principally dependent on the intrinsic characteristics of responding cells, T149
- c/EBPβ is a crucial partner of ATF4 in, W029
- c-Src-mediated, role of IL-6 signalling in, T170
- CCN3/NOV inhibits BMP-2-induced by interacting with BMP and Notch signaling pathways, T070

- Conditional deletion of FN in osteoblasts reveals distinct roles in orchestrating assembly of bone ECM proteins and in, 1177
- Differential effects of sFRPs and WIF-1 on, M044
- Early and late, GC loss-of-function model spanning, M235, S235
- Effects of BHH9 on expression of VEGF and their receptors during, W042
- Effects of modeled microgravity on, T052
- Endogenous Hesr/Hey genes redundantly support, W019
- ERK1 and ERK2 are essential for, 1141
- And function, LIMD1 modulates, W047
- GC suppresses by enhancing the expressions of BMP antagonists and pretreatments with ALN and PTH abolish this process, M059
- hMSC-derived, effects of PDE7 and PDE8A inhibition on, T046
- Human ASC, effect of VD, RA, and Dex on, T051
- Identification of novel factors associated with, W109
- Insulin promotes independent from IGF-1 signaling and its receptor is required for normal postnatal bone acquisition, 1070
- Interactions between PTH and the gp130 cytokine pathway in, W025
- LMP-1 accelerates MC3T3-E1 in part through modulation of the IGF system, T037
- Membrane domain dynamics during, W116
- And mineralization through Runx2- and Smad-dependent pathway, ERK γ negatively regulates, W015
- miRNA, regulation of, M049, S049
- From MSC, CLA regulates, T047
- And myogenesis in myoblasts, Smad1 and Smad4 differentially regulate, W117
- With nanopatterned surfaces, assessing BMP-2 activated, W120
- Natural plant extracts, Gs-Ac and -H, induce osteoblast differentiation and reduce osteoclast differentiation, M398
- PRDC is expressed in skeletogenesis and prevents, W115
- Progressive ankylosis gene (ank) regulates, M043, S043
- Protein kinase D is an essential mediator during, M019
- Regulation of Runx2 activity, orphan nuclear receptor SHP promotes, T024
- Role of type III NaPi transporters in, W035
- SWI/SNF chromatin remodeling complex, positive and negative regulation of, M030
- Through Gli2 ubiquitination, β Trcp1 ubiquitin complex regulates Ihh-promoted, T055
- TRAP is a negative regulator of, T004
- Vimentin negatively regulates by inhibiting the transactivation activity of Atf4, T027
- In vitro and in vivo, type III TGF receptor regulates BMP signaling in, W114
- Wdr5 is essential for, W032
- Osteoblast-like cells**
- Attachment of cell on ALD-derived HA surface, W009
- BK channels in, properties and function, W045
- Effect of PGD₂ on Na-dependent phosphate transport activity in, T066
- Expression of splice variants of collagen XII in, M144
- Mutations in LRP5 β -propeller 1 block SOST-mediated inhibition of the LRP5-Wnt-TCF signals in, 1048
- Regulation of RANKL expression by GC in, T068
- TRP channels are both present and functional in, T022
- Osteoblastic cells**
- AICAR and hydroxyfasudil induce the differentiation and mineralization of osteoblastic MC3T3-E1 cells via inhibiting the mevalonate pathway and enhancing BMP-2 expression, M056, S056
- Alpha1 and beta2 adrenergic agents modify RANKL/OPG expression and cell proliferation in, T006
- ATP modulation of MAPKs and c-fos expression in, T064
- Chemotaxis, molecular mechanisms of LPA-stimulated, M058, S058
- ChIP-on-chip analysis reveals novel GC response genes adjacent to genomic binding sites for SHREs in, M061
- Cultured in polyurethane scaffolds, effects of compressive loading on matrix production by, T508
- From Cx43-deficient mice, alteration of ET1 effects on calvarial, M054
- Effects of testosterone and estrogen on bone resorption markers and RANKL mRNA levels in bone marrow osteoblastic cells, 1239
- ENC1 is expressed in, T056
- Estrogens attenuate IL-6 and TNF α production in, by decreasing oxidative stress and its effects on NF- κ B activation, T186
- FFSS and PE₂ activates β -catenin signaling in MLO-Y4 osteocytic and 2T3, W053
- Grx5 regulates by protecting against oxidative stress, M005
- IL-33 inhibits osteoclast formation indirectly through, T081
- Intermittent PTH stimulates, even in the absence of osteoclasts, M239, S239
- Non-adherent circulating progenitor cells with osteoblastic potential become adherent in the presence of Ca²⁺ and are able to mineralize, T040
- Osteoclasts secrete an activity promoting bone formation and canonical Wnt signaling in, T005
- Osteoformin enhances gap junction communication of human preosteoblastic cells, M040
- PTH enhances ATP induced ERK1/2 activation via a competitive mechanism involving GRK2 in, T060
- TIEG suppresses cell proliferation through modulation of the TGF β /Smad signaling pathway and repression of E2F1 gene expression, M035
- Ubc9 promotes stability of Smad4 and regulates BMP signaling pathway in, T065
- Osteoblastogenesis**
- BMP-directed, Spp24 is converted from an inhibitor to a functional enhancer during, M156
- CTGF induces in vitro, T172
- Marrow, reflects global energy utilization through activation of PPAR γ and modulation by "clock" genes in a genotype-specific manner, M021, O021, S021
- Osx functions as downstream of Runx2 and Msx2 during regulated, W020
- Oxidative stress suppresses by antagonizing Wnt/ β -catenin and BMP signaling, M174
- Promoting, Wnt5A signals through Ror2, M045, S045
- PTEN and, W034
- Restoration of regenerative osteoblastogenesis, W348
- Unliganded ER α ER β , but not the AR, potentiates BMP-induced transcription and, T190
- Osteocalcin (OC)**
- Analytical and clinical performance of an automated assay for the measurement of OC on the LIAISON[®] Analyzer, W212
- Association of serum OC with bone gain in pubertal girls and bone loss in postmenopausal women, W506
- Expression in mouse osteoblasts, role of NF1-X transcription factor in regulation of, T034
- Expression of osteocalcin by circulating endothelial progenitor cells predicts endothelial dysfunction or structural coronary artery disease, 1262
- Gene expression, TFIIA, ATF4, and Runx2 synergistically activate osteoblast-specific, M037
- Runx2 transcriptional AD3 supports synergistic Runx2-MINT activation of the FGF response element via a DMAT-sensitive kinase, T036
- Specificity of mouse and rat circulating serological osteocalcin values using a novel immunoassay, W222
- Three-dimensional ¹H NMR structure of bovine lead ion-bound, and implications for lead toxicity, M159
- Osteochondral tissue**
- Bioreactor design for, M151
- Osteoclasts**
- Ablation of IGF-1 signaling disrupts the communication between osteoclasts and, M241, S241
- Actin binding activity in the B subunit is required for sorting V-ATPase in, M092
- Activity by regulating the V-ATPase and Rho activity, CK-B involves the bone resorptive activity of, M083
- Activity, chondrostatin as a new inhibitor of, T259
- Activity, TRPV4 affects bone remodeling by regulating Ca signaling required for, 1101
- Adenosine receptors in, W078
- Adhesion, myo10 regulates through linkage of podosomes and microtubules, M076
- Anti-GGT antibody attenuates osteoclastic bone erosion in CIA mice, T090
- AnxA8 is a critical bone matrix-dependent gene transcriptionally regulated by RANKL and NFATc1, W068
- Apoptosis, FADD-caspase-8 axis regulates, T102
- Bone resorbing, modeling role of ER in transcellular Ca flux in, M105
- Bone resorption activity, canonical NF- κ B pathway mediates, T094
- Cascade of gene expression indicates CCL2 is essential for, T073
- CatK inhibitors prevent matrix-derived growth factor degradation by, W335
- CD11c⁺ dendritic cells-derived, precursor analyses of, M080

- Cell-cell fusion is stimulated in DC-STAMP transgenic mice, T102
- Characterization of the signaling complex that mediates activation, T104
- Delays formation and reduces size, increased expression of anti-adhesive PODXL in TIEG knockout precursors, M070
- Dentine organic matrix down-regulate activity in root resorption, T095
- Disruption of WASP-associated signaling complex formation leads to defects in sealing ring formation and bone resorption in, M113
- Expression of Ang II receptor and its roles on differentiation and survival, W073
- Formation and activity and bone loss in vivo, $\text{I}\kappa\text{B}\alpha$ -deficient mice display increased, I147
- Formation and bone mass in vivo, aging-associated gene SIRT-1 regulates, T097
- Formation and osteolysis are promoted by the AMPK activator AICAR in vivo, I150
- Formation and resorptive activity, ECM proteins affect, M087
- Formation and T cell properties, effects of IL-12 related cytokines on, T076
- Formation in transgenic mice, expression of *OCZF* directed by the CatK promoter affects bone mass and osteoclast, M099, O099, S099
- Formation, Shh in fracture repair and, T082
- Formation, T-lymphocytes amplify the anabolic action of intermittent PTH treatment by regulating, I298
- Function, dual-action CTSK inhibitors, modulation of, M389
- Functional analysis of Bcl-xL by osteoclast-specific deletion of bcl-x gene in mice, I098
- Functional consequences of p62 mutations in PDB, M475
- Fusion and apoptosis captured under a microscope connected with time-lapse motion video picture, decisive moment of, M072
- Generated in ectopic bone are derived from pOCPs, W071
- IL-33 inhibits formation indirectly through osteoblastic cells, T081
- Intermittent PTH stimulates osteoblastic cells even in the absence of, M239, S239
- Large, mechanisms leading to increased resorptive activity in inflammation, T105
- M-CSF stimulates bone resorbing activity via increased activation of AP-1 and NF κ B, T075
- Maturation and activity, hormonal and pharmacological modulation of MT2 Mel receptor inhibits, T087
- Maturation, BMP-2-inducible *Osx* increases osteoblastic CSF-1 and RANKL/OPG ratio to induce, M100
- Maturation deviated from bone remodeling cycle in RA joint destruction, treatment with anti-TNF- α antibody recovers, W439
- Motility, myoIIA regulates precursor cell fusion and, W069
- In myeloma, up-regulation of TACE in monocytes ameliorates their deflected differentiation into, M302
- NFATc1 mediates the stimulatory effects of post-translationally modified BSP on the resorptive activity of rabbit, T099
- Niche is composed of 5-FU-insensitive osteoclast precursors in vivo, M082, S082
- Novel pro-survival functions of *Egr2* in promotion of M-CSF-mediated osteoclast survival downstream of the MEK/ERK pathway, M111
- Osteopetrotic *ia/ia* rat exhibits reduced activity, resulting in normal endochondral fracture union but delayed hard callus remodeling, T088
- P2X7 nucleotide receptors couple to isoform-specific activation of PKC in, M109
- Phenotypical heterogeneity involved in the endochondral ossification and bone remodeling, T083
- Possible suppressive role of Galectin-3 in osteoclastic bone destruction accompanying adjuvant-induced arthritis in rats, M108
- Rab3D recruits the dynein complex to secretory vesicles through direct interaction with Tctex-1, I293
- RANKL signaling in, effect of p62 mutations, M474
- RANKL stimulates, to release VEGF-C and enhance bone resorption through an autocrine mechanism, I100
- Regulation of activity by CatK-generated type I collagen fragments, W065
- Regulation of integrin expression by NFATc1 and PU.1 in, M071
- Regulatory factors, EGF-like ligands stimulate osteoclastogenesis by regulating expression of, T175
- Rho GTPase signaling pathways, *Wrch1/RhoU* role in cell adhesion and osteolysis, M073, S073
- Ruffled border membrane, electroneutral sodium/bicarbonate cotransporter NBCn1 is expressed in, T091
- Secrete an activity promoting bone formation and canonical Wnt signaling in osteoblastic cells, T005
- Sex steroids hormone receptors mediate osteoprotective effects by regulating its life cycle, I220
- Specific ablation of *dicer* suppresses bone resorption and increases bone mass, I292
- Survival via distinct signaling pathways, AG490 regulates, T100
- Tm-2/3 regulate the intracellular scaffold of, M074
- Transgenic overexpression of PTP-oc in cells of osteoclastic lineage led to increased bone resorption and marked reduction in trabecular bone mass and density in adult mice, M112, O112, S112
- Osteoclast-associated receptor (OSCAR)**
Down-regulation of, PIAS3 modulates osteoclastogenesis by, W066
- Osteoclast-derived zinc finger (OCZF)**
Induced by RANKL and increases c-Fos expression in osteoclastogenesis, W067
- Osteoclast differentiation**
And activation via HIF pathway, Co incorporation into CaP layers stimulates, W075
- bgn and *fnod* control bone mass by regulation through BMSC, M157, O157, S157
- Effects of modeled microgravity on, T052
- And function, CaMK-CREB pathway regulates, M114, S114
- And function, G-CSF enhances, T074
- And function, iron uptake through the TfR1 promotes, M097
- And function, tetracyclines Dox and Mino effectively inhibit, M106
- Kgp and LPS synergistically induce, W084
- Mechanism of RANKL-evoked $[\text{Ca}^{2+}]_i$ oscillations mediated by RGS10 in, M093, S093
- During medullary bone formation period in Japanese quail bone marrow cell culture, M091
- Role of P-Rex1 in, M098
- And survival, expression of Ang II receptor and its roles on, W073
- Tec tyrosine kinases are essential for, I289
- TIEG directly binds to and represses the OPG promoter in osteoblasts resulting in decreased support of, W028
- In vitro and in vivo, transcription factor IRF-8 is a negative regulator of, I145
- In vitro, Jagged1-Notch2 signaling promotes, M085
- In vitro, PTHrP-induced MCP-1 production by HBME cells and osteoblasts promotes, T247
- Osteoclast inhibitory peptide-1 (OIP-1)**
Characterization of binding to FcR γ on osteoclast precursor cells, I103
- Osteoclast-like cells**
Formation, nicotine and LPS stimulate by increasing M-CSF and PGE₂ production, T084
- Osteoclast precursor cells (pOC)**
Characterization of OIP-1/hSca binding to FcR γ on, I103
- Endogenous TNF α promotes osteoclastogenesis via c-Fos and NFATc1 activation, T077
- Generation, regulation by type II cytokines and STATs, T079
- Osteoclastic protein-tyrosine phosphatase (PTP-oc)**
Transgenic overexpression in cells of osteoclastic lineage led to increased bone resorption and marked reduction in trabecular bone mass and density in adult mice, M112, O112, S112
- Osteoclastogenesis**
Alterations in MicroRNAs and GW bodies are associated with, M094
- Diverging pathways of CaM regulation of osteoclastogenesis, W070
- EGF-like ligands stimulate by regulating expression of osteoclast regulatory factors by osteoblasts, T175
- Ex vivo, role of *Bcl2* in, W083
- Expression and possible role of PVR/CD155/Necl-5 in, M077
- Expression and transcriptional activity of Mitf isoforms during, T101
- Fat-1* gene prevents ovariectomy induced bone loss by modulating osteoclastogenesis, I135
- HMGs coupled with TNF α production are essential for, T071
- IL-23-enhanced is mediated by STAT3 and NF- κ B via upregulation of RANKL from CD4⁺T cells, T078
- Induced by NRTIs in AIDS, TREM2 pathway is involved in, W074
- Inhibition by prosthetic wear debris involves suppression of RANK expression, W076
- M-CSF independent mechanisms for, W072
- Matrix PRELP inhibits, inactivating the NF- κ B signal, W080
- Mice with a myeloid lineage-specific deletion of IKK β demonstrate both in vivo and in vitro defects in, I294
- MVNP enhances NFATc1 activation during, M479

- NEMO (IKK γ) modulates, T098
 NF- κ B but not NFATc1 is involved in AhR-RANKL crosstalk in BaP-mediated inhibition of, T106
 OsM is an essential stimulus of bone formation and, 1068
 PIAS3 modulates by down-regulation of NFATc1 and OSCAR, W066
 POZ-Zn transcriptional regulator OCZF/LRF is induced by RANKL and increases c-Fos expression, W067
 RANKL-induced, Ca and phospholipase C γ 2 signaling regulates, 1104
 RANKL-induced, high D(+)glucose concentration inhibits, W082
 RANKL-induced, HMGB1 regulates actin cytoskeleton organization in a manner dependent on RAGE, M079
 RANKL-induced, PIAS3 negatively regulates, M089
 RANKL-induced, Wnt5a enhances, 1149
 RANKL is produced by adipocytes and stimulates, W079
 Rheumatoid synovial fibroblasts promote osteoclastogenic activity by activating RANKL via TLR-2 and TLR-4 activation, W435
 RNAi machinery is essential for, M090, S090
 Small GTPase cdc42 enhances, 1146
 Spacio-temporal analysis using co-culture system, M078
 Suboptimal 25(OH)D $_3$ levels causes increased osteoclastogenesis and bone loss, W402
 Suppression by DMS, a SPHK inhibition-independent action, M088
 Suppressive effect of IL-27 in, T072
 TNF-induced, NF- κ B2 limits through precursor cell cycle regulation, 1148
 TNF α - and IL-1-induced, IVVY⁵³⁵⁻⁵³⁸ plays an essential role in, M084, S084
 Via c-Fos and NFATc1 activation, endogenous TNF in osteoclast precursor cells promotes, T077
 Via Ca signaling activation, RANKL-induced expression of TRPV2 is involved in, T103
 In vivo activation of TLR9 modulates, M081
- Osteoclastogenesis inhibitory factor (OCIF)**
 Intra-articular, prevents cartilage degeneration in a murine model of osteoarthritis, W097
- Osteocyte-lacunar canalicular system (OLCS)**
 Histochemical assessments on the distribution of, W059
- Osteocytes**
 Density, estimation from total lacunar population, W058
 DMP1 and MEPE expression after mechanical stimulation in the mouse ulnae loading model, W050
 Dynamic imaging in living calvaria reveals the motile properties and suggests heterogeneity of osteoblasts in bone, 1045
 Dynamic imaging of fluorescently tagged populations integrates mineralization dynamics with osteoblast to osteocyte transition, 1044
 Effects of mechanical strain on, induced bone cell proliferation and recruitment, W054
 Elastic modulus of, W061
 FFSS promotes intracellular assembly and formation of Cx43-forming channels in, M520
 Greater sensitivity to shear stress as compared to osteoblasts, PGE $_2$ production and Wnt/ β -catenin signaling, W052
 Hemichannels, α 5 integrin association with Cx43 regulates in response to shear stress, T504
 Hypoxia accelerates the transformation of osteoblasts to, W013
 LPA induces dendrite outgrowth, M182, S182
 Microstructural variation in the bone matrix and cell attachments modify strain amplification on, M066
 Osteocytic regulation of Pi homeostasis through FGF-23, 1296
 Prednisolone induces death and erosion of osteocytic lacunae walls, W458
 Presence of p120-catenin in, T507
 Primary, effects of PTH(1-34) on, M068, S068
 Protective effects of mechanical strain on viability is mediated by the effects of prostaglandin on the cAMP/PKA and the β -catenin pathways, M237
 Small GTPase RhoA and its effector kinase ROCK mediate actin cytoskeleton reorganization leading to anoikis by GC, M233, S233
 Target ablation of PTH/PTHrP receptor in, 1047
 Targeted deletion of E11/gp38 results in increased skeletal size and BMD, 1043
 Viability, ex vivo model in trabecular bone, W055
- Osteocytic cells**
 FFSS and PE $_2$ activates -catenin signaling in MLO-Y4, W053
 Nanoprobe osteocytic subcellular compartments by SERS, W057
- Osteocytic networks**
 Modulation of site specific bone adaptation by signaling in, W060
- Osteodystrophy, hepatic**
 Expression of IGF-1 and GHR and biomechanical studies in experimental model of cholestatic liver, W416
- Osteodystrophy, renal (ROD)**
 Structural implications of low-magnitude mechanical stimulation in a pilot study of patients with ROD, M493, S493
- Osteoformin**
 Enhances gap junction communication of human preosteoblastic cells in culture, M040
- Osteogenesis**
 Acceleration of fracture healing via enhanced, through SCF/cKit pathway, T013
 Acid swelling overcomes inhibition of xenogeneic collagenous matrix delivery system used for naturally-derived BMP complex, M172
 BMP-2-induced, diverse effects of noggin on, W107
 Circulating osteogenic precursor cells of hematopoietic origin, 1156
 Classical ER α signaling is essential for estrogen mediated enhancement of, M250, S250
 Combination of Vitamin D and BADGE potentiates their pharmacological inhibition of PPAR and increases osteogenic differentiation of adipocyte precursors, W155
 Differentially modulated by PTH and the N- and C-terminal fragments of PTHrP, T050
 Downstream signal transactivation by FGF-4/Osx transgene partially imitates changes of BMP-2 induced transcription factors in NIH3T3 cells, W016
 Estrogen preferentially suppresses osteogenic gene expression in mice lacking classical ERE signaling, T195
 Gene response via divergent signaling pathways, fluid shear stress and mechanical strain induce a similar, M517
 HES-1 is an anti-adipogenic mediator of osteogenic oxysterols and hedgehog signaling, W043
 Of the human LF by demineralized bone matrix, T008
 Induced, tension stress/stain in canine leg lengthening procedures, T059
 mTOR signaling, a novel molecular mechanism underlying Wnt's anabolic effects on, 1108
 P2X7 receptors on osteoblasts couple to production of LPA, a novel signaling axis promoting, M062, S062
 Pericytes derived from adipose tissue, characterization and evaluation of their osteogenic potential, 1215
 Proinflammatory control of BMP-Smad-driven transcription and, W044
 Role in injury-induced calcification from TNF α receptor p55/- p75/- mice, W091
 In vitro assay to assess secreted osteogenic factors from genetically engineered cells, T038
 In vitro, HSPG sulfation during, W036
 In vitro, miRNA expression profiling and function during, 1214
- Osteogenesis, distraction**
 Continuous local infusion of basic fibroblast growth factor enhances consolidation of the bone segment lengthened by, T155
 Increased expression of BMP antagonists during, W112
- Osteogenesis imperfecta (OI)**
 Carrier frequency of recurring mutation causing severe/lethal recessive type VIII OI in African-Americans, T471
 Influence of the gene polymorphisms of collagenase-1 in OI, T216
 Mutations in CRTAP or P3H1 cause dysregulation of Prolyl-3-hydroxylation and recessive OI, 1261
 Phenotypic analysis of the Crtap $^{-/-}$ mice, first animal model for recessive OI, M150, S150
 Sequencing of Col1 in three patients with multiple fractures of unknown aetiology reveals novel mutations causing OI with normal to high BMD, 1196
 Treatment of OI in adults with TPTD, 1260
 Vitamin D deficiency in OI, T437
- Osteogenic differentiation**
 Bespoke bioceramic scaffolds support MSC growth and, M050
 Of BMSC, activation of LXR inhibits hedgehog signaling and, W023
 Of circulating EPC, M042
 Expression of MMP-14 is pleiotropic on alkaline phosphatase expression in, T019
 Of human MSC, siRNA specific knockdown of lamin A/C inhibits, M038
 And interaction with Ti6Al4V, MSC from human adipose tissue and bone marrow, T053
 Of MSC, cytoplasmic interaction of p21 with Runx2 during, T049
 Zfp64 is a downstream target of Runx2 and regulates as a coactivator of Notch1, T035
- Osteogenic index (OI)**
 Bone biomarker responses to short-term training, W056

Osteogenic protein-1 (OP-1)

Bone metabolism after posterolateral lumbar fusion using, W119

Osteogenic stem cells. See *Stem cells, osteogenic Osteoinductivity*

Allogeneic DBM, xenogeneic BMP complex enhances, M173

Osteolysis

Collapse of the vascular bone remodeling compartment is a key process in the development of myeloma-induced osteolysis, 1005

Comparative study of anti-resorptive and anti-cancer treatments in the geometrical and biomechanical properties of rat femurs with tumor-induced osteolysis, W199

Osteoclast formation and, promoted by the AMPK activator AICAR in vivo, 1150

Rho GTPase signaling pathways in osteoclasts, Wrch1/RhoU role in, M073, S073

Role of CXCL13 in SCC associated osteolysis in, T257

Osteomalacia

Following gastric bypass and biliopancreatic diversion surgery, WG14, W420

Unusual presentation of severe Vitamin D deficiency osteomalacia in a patient with congenital hypophosphatemia, WG15

Osteomalacia, oncogenic (OOM)

Minimally invasive treatment by radiofrequency ablation, W422

Osteomalacia, tumor-induced (TIO)

Lack of efficacy of octreotide in the treatment of TIO, W424

Novel algorithm using ^{99m}Tc-MIBI scintigraphy, sequential whole body MRI and venous sampling for FGF-23 for tumor localization in, WG18

Venous sampling for FGF-23 as a tool for pre-operative localization of tumors giving rise to, M213

Osteomodulin (OMD)

Expressed in osteoblast, isolation and immunohistochemical analysis of, T016

Osteonecrosis (ON)

Experimental rabbit model of lunette-like osteonecrosis, T502

Steroid-associated development, temporal feature of bone marrow fat cells in the process of, T178

Osteonecrosis of femoral head (ONFH)

Association study of catalase gene polymorphisms with an ONFH in Korean population, T223

Osteonecrosis of the jaw (ONJ)

ONJ under bisphosphonate therapy, M298, S298
Progression of ONJ in breast cancer patients even with discontinuation of intravenous BP therapy, T233

ZOL delayed the wound healing of tooth extraction socket but failed to cause ONJ in mice, T243

Osteons

Within osteons infrared parameters linked to specific bone properties vary as a function of tissue and animal age, T109

Osteopenia

Comparison of estrogen, raloxifene and bisphosphonate administration for prevention of bone loss in climacteric women complicated with osteopenia, M431

Effect of onion on ovariectomy-induced osteopenia, T364

Female, but not male, TIEG-null mice display severe osteopenia and abnormal cancellous bone microarchitecture, M152, S152

Longitudinal changes in bone density and management in men with osteopenia, T266

One-week evaluation of pharmaceuticals in sRANKL-injected osteopenia model mice, W332

Severe, in PERK-knockout mice is due to impaired osteoblast differentiation associated with reduction of type II RUNX2 expression, 1022

VGLUT1 knockout mice develop, due to an increase in osteoclastic bone resorption, T085

In vivo, CTGF causes, 1178

Osteopenia, diabetic

TRX-1 overexpression attenuates streptozotocin-induced diabetic osteopenia, M498, O498, S498

Osteopetrosis

Conditional inactivation of the CTSK gene in adult mice results in, without activation of compensatory mechanisms for impaired bone resorption, W064

Osteopontin (OPN)

β-Adrenergic signaling requires bone matrix protein OPN to suppress bone formation and to activate bone resorption, 1015

Implication in bone healing, M160, S160

Upregulation by mechanical loading of bone cells, T154

Osteoporosis

AluI polymorphism in ESR2 is associated with reduced risk of osteoporotic fractures, T218

Antifracture efficacy of combined treatment with ALN and ALF for osteoporosis in early-phase treatment, T438

Associations of osteoporotic spinal deformity with back strength among elderly women, M472

Back extensor strength, lumbar spine mobility and spinal inclination as related factors for falls in osteoporotic patients, T341

Basis for osteoporosis in the aldehyde reductase knockout mouse, 1016

Bringing bone health to seniors' communities, WG39

Care pathways for hospital patients with fragility fractures, T407

Clinical factors associated with osteoporotic fractures in a representative population of French women, T344

Community-based program to minimize osteoporosis and fractures risks, W400

Comparative efficacy of osteoporosis treatment in postmenopausal women, T397

Compliance with osteoporosis treatment and incidence of hip and wrist fracture after forearm BMD screening, W377

Compromised bone marrow perfusion in osteoporosis, 1133

Dental status, low bone mass, and other osteoporosis-related conditions as predictors of adverse outcomes in an elderly population, W302

To determine serum fluoride levels in patients with osteoporosis is quite useful for the judgment of effectiveness of osteoporosis treatment, W419

Enhancement of prognosis of osteoporotic fractures by genetic marker, 1201

Evaluation of vertebrae fragility by osteoporosis, W462

Factors associated with lack of osteoporosis care at the time of fragility fracture, W295

Factors influencing the diagnosis and the treatment of osteoporosis following a fragility fracture, M364, S364

Factors influencing women persistence with osteoporosis treatment after 6 months of treatment, M372

Factors predicting osteoporosis treatment initiation in a regionally-based clinical cohort, M321, S321

Fosamax® (ALN sodium) and cholecalciferol (Vitamin D₃) in the treatment of men and postmenopausal women with osteoporosis, T432

GC-induced in rats treated with Ris, evaluation of cell apoptosis and COX-2 expression in, W318

Group-based patient-education program increases knowledge of osteoporosis and adherence to pharmacological treatment, W382

High turnover, incidence in CCR1-deficient mice is greater in females than in males, 1254

Identification of the CACNA2D2 gene on chromosome 3p21 as a novel susceptibility gene for osteoporosis, M282

Identifying the treatment care gap in postmenopausal women at the Southlake Regional Health Centre, W372

Integrated model for evaluation and simulation of therapeutic responses to bone-related therapies, W417

Is osteoporosis related to future incidence of osteoarthritis over 10 years, or vice-versa?, W307

Knowledge of osteoporosis among tertiary students in Vietnam, W340

Long-term retention of knowledge from an osteoporosis education program, T337

Material properties of osteoporotic ewes, M501

Mouse model for diabetes-mediated

osteoporosis, T206

Osteoporotic fragility fractures in older adults admitted in a French primary care department, W287

Outreach program improved osteoporosis management after a fracture, W378

Patient opinions on osteoporosis interventions in the fracture clinic setting, WG35, M439

Post-fracture screening program, T323

Postmenopausal, and weight gain, W386

Prevalence of osteoporosis and Vitamin D deficiency/insufficiency among elderly people with falls in Denmark, T446

Prevalence of secondary causes of osteoporosis among breast cancer patients with osteoporosis and osteopenia, M312

Qualitative method and the method based on the concept of 10 years probability of bone fracture in qualifying patients for pharmacological treatment of osteoporosis, T275

Randomized controlled assessment for effectiveness of an evidence-based guideline for osteoporosis and osteoporotic fracture prevention, T334

- Relationship between the knowledge on osteoporosis in females and BMD at hip, spine and forearm, T274
- Risk factors for osteoporosis and BMD in late postpartum women, T342
- Risk factors for osteoporosis and fragility fractures in postmenopausal women and men older than 50 attended in a primary care center of Spain, T348
- Role of Fas/Fas ligand system in estrogen deficiency-induced osteoporosis, M004, S004
- Role of IGF-1 and IGFBP-1 status and secondary hyperparathyroidism in relation to, M195
- Secondary causes of osteoporosis in fracture patients, T322
- Socioeconomic burden of osteoporotic fractures in Korea, T409
- Southern California Hispanic Women Osteoporosis Education and Screening Project, M384
- Stage-of-change model applied to osteoporosis medication use at the time of fragility fracture, M382
- Study subjects and ordinary patients in treatment of osteoporosis, T406
- Ten-year probability of osteoporotic hip fracture in elderly women combining clinical factors and heel bone ultrasound, I167
- Tolerability of monthly IBN and weekly ALN in women with postmenopausal osteoporosis, T383
- VDR, ESR1, and COL1A1 associations with osteoporosis phenotypes at baseline and after Ris treatment in the IMPACT trial, W329
- In vivo genome-wide expression study of human blood B cells suggests a novel ESR1 and MAPK3 network for postmenopausal osteoporosis, W263
- Osteoporosis, glucocorticoid-induced (GIO)**
- Bone effects of 17 β -estradiol and dihydrotestosterone on bone turnover in a mouse model of GIO, M407
- Correlations between bone turnover markers and BMD in patients treated with TPTD or ALN for GIO, M425, S425
- Efficacy and safety of ALN for the treatment of GIO in children, W371
- GC enhances the expression of sFRP3 in cultured osteoblasts, T176
- GC suppresses the differentiation of osteoblasts by enhancing the expressions of BMP antagonists and pretreatments with ALN and PTH abolish this process, M059
- Osteoporosis, idiopathic (IOP)**
- Abnormal trabecular microarchitecture and mechanical competence in premenopausal women with IOP can be detected by HRpQCT, M327
- Reduced levels of serum IGF-1 in male with idiopathic osteoporosis, M465
- Sixteen-year-old male with idiopathic juvenile osteoporosis, WG20
- Osteoporosis, postmenopausal (PMO)**
- Impact of bonemarker feedback on adherence to once monthly IBN treatment for PMO in Mexican and Chilean patients (BOHEMIA Study), T391
- Osteoporosis, pregnancy-associated (PAO)**
- Ten-years-follow-up of a PAO, W369
- Osteoporosis, presumed (PO)**
- Prevalence and patterns of OP among older Americans based on Medicare data, M378
- Osteoporosis Self-Assessment Tool (OST)**
- Versus alternative triage tests, W301
- Osteoprobe II**
- New bone diagnostic instrument, the Osteoprobe II, M510
- Osteoprotegerin (OPG)**
- Anti-inflammatory role of OPG in the pathophysiology of osteoporosis and arteriosclerosis, M459, S459
- Anti-tumor actions of 2-ME are accompanied by an increase in expression in osteosarcoma cells, M306
- Association study between polymorphism across the OPG gene and osteoporotic phenotypes, M288, S288
- BMP-2-inducible Osx increases osteoblastic ratio to induce osteoclast maturation, M100
- As cardiovascular risk marker in patients with type 2 diabetes mellitus, T167
- Deficient mice, vascular calcification and aortic gene expression are consistent with hyperphosphatemia in, I117
- Expression and cell proliferation in human osteoblasts and osteoblastic cells, alpha1 and beta2 adrenergic agents modify, T006
- Identification of a novel Wnt/ β -catenin response element in the gene promoter and its regulation with BMP-2 signaling, M031, S031
- Increased plasma OPG concentrations are associated with indices of bone strength of the hip, I240
- Inhibits cartilage degradation in a knee instability mouse model, M134
- Intra-articular, prevents cartilage degeneration in a murine model of osteoarthritis, W097
- Negatively regulates chondroclast formation and recruitment in endochondral ossification, M136, S136
- Prevents osteopenia via different mechanisms than bisphosphonate therapy, W445
- Promoter in osteoblasts, TIEG directly binds to and represses for decreased support of osteoclast differentiation, W028
- Transgenic overexpression of OPG results in increased bone mass and strength and decreased bone turnover in one-year-old female rats, I088
- Osteosarcoma**
- Anti-tumor actions of 2-ME are accompanied by an increase in OPG expression in, M306
- Dynamic genomic and proteomic patterns of osteosarcoma metastasis to lung, W187
- Five years results of bisphosphonate treatment in long-term survivors of highly-malignant osteosarcoma, W194
- Investigation of KCl cotransport expression in canine cell lines, T031
- Microarray analysis of craniofacial and appendicular osteosarcoma, W198
- PDTC inhibits SOD1 gene and cell growth by activating JNK pathway in U2OS, W018
- Regulation of protein synthesis factors in estrogen metabolite-mediated inhibitions of, T254
- Tyrosine kinase inhibitors slow motility of osteosarcoma cells in vitro, T255
- In vivo inhibition of osteosarcoma growth by Notch pathway inhibition, M303, S303
- Osterix (Osx)**
- As a regulator of bone formation and maintenance, M010, S010
- BMP-2-inducible increases osteoblastic CSF-1 and RANKL/OPG ratio to induce osteoclast maturation, M100
- Downstream signal transactivation by transgene partially imitates changes of BMP-2 induced osteogenic transcription factors in NIH3T3 cells, W016
- Expression, identification of Prx1, MHOx, as a regulator of, I143
- Functions as downstream of Runx2 and Msx2 during BMP2-regulated osteoblastogenesis, W020
- Inhibition of Wnt signaling by, I249
- Mechanisms of control of endochondral ossification, W098
- Mediates mesenchymal progenitor cell differentiation into osteoblasts downstream of PTH during bone repair, M023, S023
- Mediates the feedback regulation of BMP-2 auto-expression via PI3K/Akt signaling, T029
- Promoter activity of, Pitx2 inhibits osteoblastic conversion of myoblasts through interfering with, T021
- Osthon**
- Osthon stimulates pre-osteoblast proliferation and differentiation via BMP-2/RUNX2/SMAD1 pathway, T114
- Ovariectomy (OVX)**
- Decreases bone mass in young and old female athymic mice, I137
- Degeneration of intervertebral disc in OVX rats, M251
- Effect on bone properties, W136
- Overexpression of low molecular weight isoform of FGF2 partly prevents bone loss in OVX mice, T160
- Quality and strength in OVX rats are lowered by limiting physical activity, W479
- Oxidative stress**
- Grx5 regulates osteoblast cell functions by protecting against, M005
- Oxygen saturation, arterial**
- Arterial oxygen saturation during sleep and the risk of fractures, falls and mortality in older men, I157
- Oxysterols**
- Osteogenic, HES-1 is an anti-adipogenic mediator of, W043
- P**
- P-Rex1**
- Role in osteoclast differentiation, M098
- P2X₇**
- Activation, phosphorylation of caveolin-1 in response to fluid shear in osteoblasts is mediated by, T061
- Agonist reduce ovariectomy-induced bone loss in a murine model, W345
- Nucleotide receptors couple to isoform-specific activation of PKC in osteoclasts, M109
- Purinergic receptor is responsible for ovariectomy-induced bone loss, M248, S248
- Receptors on osteoblasts couple to production of LPA, a novel signaling axis promoting osteogenesis, M062, S062
- P2X₇ receptor (P2X₇R)**
- Modulation in osteoblasts by estrogen and corticosteroids, M055
- p21**
- Cytoplasmic interaction of, with Runx2 during osteogenic differentiation of MSC, T049

- 1p36**
Mouse Chromosome 4 homologous with human 1p36, W183
- p53**
Genetic interaction between, Atm in bone development, M271
- p55--/--**
Role of cell death and osteogenic activity in injury-induced calcification from, W091
- p62**
Effect of mutations, RANKL signaling in human osteoclasts, M474
Mutations, functional consequences in PDB osteoclasts, M475
- p63**
Plays a central role in cartilage development by directly regulating key genes for chondrogenesis, I182
- p65**
Transcriptional induction of SOX9 by NF- κ B subunit during chondrogenesis, W101
- p66^{shc}**
Phosphorylation, estrogens or androgens attenuate via an ERK and PKC signaling cascade, T185
- p75--/--**
Role of cell death and osteogenic activity in injury-induced calcification from, W091
- p120-catenin**
Presence in osteocytes and other bone cells, T507
- Paget's Disease (PD)**
Cells cultured from bone lesions of patients with PD show no evidence of measles virus RNA or somatic mutations in SQSTM1, T205
Enhanced levels of FGF-2 and SOCS signaling modulates RANK ligand expression in patients with PD, M480
Measles virus nucleocapsid gene expression is required for abnormal osteoclast activity in PD, I152
Mice with a truncation mutation affecting the UBA domain of SQSTM1 develop several phenotypic features PD including focal lytic lesions, and increased bone turnover in vivo, I036
Mutations in p62 linked to PD make the bone microenvironment highly osteoclastogenic, M477, S477
MVNP enhances NFATc1 activation during osteoclastogenesis in, M479
- Paget's Disease (PD), juvenile**
OPG deficiency, Juvenile Paget's Disease, W169
- Paget's Disease of the bone (PDB)**
Functional consequences of p62 mutations in osteoclasts, M475
Long-term effects of single zoledronate or neridronate infusion in PDB, M478
No role for polymorphisms in the gene encoding RANKL in the development of sporadic PDB in contrast to some OPG polymorphisms, T228
- Pamidronate**
Extraction socket healing in pediatric patients treated with pamidronate, I198
Intravenous administration of pamidronate decreases serum levels of FGF-23 rapidly in patients with OI, M486
Low doses of pamidronate for children with metabolic and genetic diseases, T519
Pamidronate is effective for children with severe GIO, T390
- Paralysis, muscle**
Focal bone loss in mice with transient muscle paralysis, T150
- Paraoxonase (PONI)**
Associations of *PONI* promoter polymorphisms with vertebral fractures risk independently of BMD in postmenopausal women, T221
- Parathyroid**
Response to Vitamin D insufficiency, T453
Vitamin D insufficiency and normal parathyroid function, W406
- Parathyroid adenomas**
Molecular analysis of histologically atypical parathyroid adenomas, M485
- Parathyroid cells**
Calcilytics block the suppressive effect of calcimimetics on PTH mRNA levels in, M228
Hyperplastic, regulation of CaR by Gcm2 in, M226
Phosphate stimulates greater proliferation in organ cultures of parathyroid tissue from patients with II-HPT than with I-HPT, W141
Primary, PTH expression is negatively regulated by FGF-23 in, I191
Tissue-specific knockout of CaRs in parathyroid cells, WG5
- Parathyroid gland**
Function, role of Gq elucidated by genetic approaches, M229
Identification of distinct, functional domains in the hyperplastic rat parathyroid gland, W140
- Parathyroid hormone (PTH)**
Activates β -catenin signaling through LRP5/6, I297
Age modifies the impact of Vitamin D3 supplementation on the 25OH(D) ratio, M414
AKT's effects on β -catenin regulate osteoblasts' responses to, T067
Anabolic action of, potential involvement of Ephrin B2 in, T012
Analysis of PTHR interaction mechanisms using a new, long-acting PTH(1-28) analog reveals selective binding to distinct receptor conformations and biological consequences in vivo, I190
Binding, movements within the PTH1R upon, I299
Biomarker effect of daily dosing of human PTH1-34 on intact cynomolgus monkeys for 12 days, W134
Calcilytics block the suppressive effect of calcimimetics on mRNA levels in parathyroid cells, M228
CaP regulating hormone STC-2 is positively and negatively regulated by, in renal proximal tubular cells, W130
CaR dampens the calcemic response to exogenous 1,25(OH)₂D in vivo independent of, M224
Changes in circulating osteoblast lineage cells following PTH(1-34) therapy and correlation with changes in trabecular bone mass, I268
Characteristics of postmenopausal women treated with PTH(1-84) in the TOP study, M420
Continuous treatment with PTH is anabolic in cultured osteoblasts from COX-2 knockout mice, W037
Control of the *SOST* bone enhancer by, I046
CREB phosphorylation and DNA binding along with demethylation and deacetylation are required for ultimate activation of CYP27B1 promoter by, W132
- Dissection of the mechanisms of mediated inhibition of sodium-dependent phosphate transporter using a long-acting PTH(1-28) analog, I189
Dynamic bone changes in PTH(1-34) treated OVX rats, evaluated by in-vivo micro-CT scanning, W142
Effect of plasma 1,25(OH)₂D concentration or Ca intake on negative correlation with plasma 25OH(D) concentrations in Japanese adolescents, W159
Effects of cyclic and daily PTH in combination with OPG, I125
Effects of one year treatment with PTH(1-34) on bone microstructure at the ultradistal radius, I085
Effects of PTH(1-34) on primary osteocytes, M068, S068
Effects of treatment of OVX adult rhesus monkeys with PTH(1-84) on trabecular and cortical bone structure and biomechanical properties of the proximal femur, W308
Endogenous measurements in cynomolgus monkey serum, W133
Enhances ATP induced ERK1/2 activation via a competitive mechanism involving GRK2 in osteoblastic cells, T060
Expression is negatively regulated by FGF-23 in primary parathyroid cells, I191
FRET analysis reveals selective binding of long- and short-acting PTH(1-28) analogs to distinct receptor conformations, W144
GGPP promotes osteoblast survival and is involved in anti-apoptotic effects of, I192
Improves bone strength in an osteoporosis model through increasing mineralized matrix, M392, S392
Independent pathways, duodenum rapidly senses and modulates renal phosphate reabsorption via, M207
Intact genes are required to regulate the extracellular Mg and Ca concentrations independently, M230
Interactions with the gp130 cytokine pathway in differentiating osteoblasts, W025
Intermittent PTH has increased anabolic effects in COX2 knockout mice, I234
Intermittent, stimulates osteoblastic cells even in the absence of osteoclasts, M239, S239
Intermittent treatment, T-lymphocytes amplify the anabolic action by regulating osteoclast formation, I298
Intratrabeular tunneling increases trabecular number at multiple skeletal locations in OVX rhesus monkeys treated with PTH(1-84), W310
Levels are associated with MCPT and number, W145
Mast cell migration to bone surfaces precedes and appears essential for induced peritrabecular fibrosis, M482, S482
mRNA interactions that determine mRNA stability in secondary hyperparathyroidism and hypoparathyroidism, M217, S217
Osteogenesis and adipogenesis are differentially modulated by, T050
Pharmacokinetics and pharmacodynamics of human PTH(1-84) in adult OVX rhesus monkeys, W309
Phosphate stimulates greater release in organ cultures of parathyroid tissue from patients with II-HPT than with I-HPT, W141

- PLC signaling via the PTHrP receptor is essential for normal full response in both bone and kidney, 1119
- Pretreatments abolish this process, GC suppresses the differentiation of osteoblasts by enhancing the expressions of BMP antagonists, M059
- PTH(7-84) inhibits PTH(1-34)-induced production of 1,25-(OH)₂D₃ in primary cultured murine renal tubules, T482
- PTHrP receptor modulates the pool of BMSCs, W138
- Receptor, target ablation in osteocytes, 1047
- Relationship between variation in the PTH, PTHrP and the PTHR1 and PTHR2 genes and BMD and fracture in elderly women, T227
- Role of *caspase-3* in the anabolic actions of, 1188
- Role of TRPV 6 and β -glucuronidase in stimulated Ca uptake in intestinal epithelial cells, M258
- Serum, endogenous PTH measurements in cynomolgus monkeys, W133
- Serum is associated with cortical bone dimensions, W135
- Signaling in vivo, ability of XLAs to mimic Gas in mediating, M218
- Upregulates placental Ca transfer in response to fetal hypocalcemia while PTHrP does not, W137
- Very low or undetectable intact parathyroid hormone levels in patients with surgically verified parathyroid adenomas, WG17
- Weekly administration of a novel PTH-CBD fusion protein increases BMD by more than 15% in normal mice, 1229
- Parathyroid hormone, human (hPTH)**
Effects of intermittent administration of hPTH(1-34) on distraction osteogenesis in rabbits, M395
- Transdermally-delivered hPTH(1-34), T371
- Parathyroid hormone, intact (iPTH)**
Rapid, comparison to IRMA in patients with hyperparathyroidism, M216
- Relationship between iPTH and bone metabolic markers, T487
- Parathyroid hormone-related protein (PTHrP)**
Both N- and C-terminal fragments of PTHrP exert pro-survival effects on prostate cancer cells through transcription factor Runx-2, T232
- C-terminal PTHrP(109-119) in serum and urine is a useful biomarker for malignancies, M308
- Conditional ablation in mammary epithelial cells inhibits breast cancer progression, 1295
- ECM1 is a novel potent mediator of chondrogenesis, 1062
- Estrogen deficiency and infusion do not fully reproduce the bone loss of lactation, M220
- Induced MCP-1 production by HBME cells and osteoblasts promotes osteoclast differentiation in vitro, T247
- Induces bone pain through stimulation of proton-secretion in osteoclasts, M293, O293, S293
- Induces MKP-1 in differentiated BMSC, osteoblast and cementoblast cell lines, M001
- Nucleolar, mice overexpressing driven by type II collagen promoter show disordered distribution of chondrocytes in the epiphyseal cartilage, M116
- Osteogenesis and adipogenesis are differentially modulated by the N- and C-terminal fragments of, T050
- PLC signaling via the PTH receptor is essential for normal full response to PTH in both bone and kidney, 1119
- PTH receptor modulates the pool of BMSCs, W138
- PTH upregulates placental Ca transfer in response to fetal hypocalcemia while PTHrP does not, W137
- Receptor, target ablation in osteocytes, 1047
- Regulates antimicrobial peptide production by skin keratinocytes, M238
- Suppresses ERK activation in hypertrophic chondrocytes, W095
- Zfp521 regulates chondrocyte differentiation downstream of, 1069
- Parathyroid hormone type 1/2 receptor (PTH1/2R)**
Movements within upon PTH binding, 1299
- Sex effects in non-small cell lung carcinoma, M240
- Targeted overexpression in chondrocytes impairs cartilage differentiation and trabecular bone growth, W139
- Parathyroid neoplasia**
Expression of *GCMB* is normal in, T480
- Paxillin**
ADAM8 binds $\alpha\beta$ 1 to increase osteoclast formation and function by interacting with Pyk2 and activating, 1099
- PDE7/8A**
Inhibition on the differentiation of hMSC-derived osteoblasts, effects of, T046
- Pentsidine (PEN)**
Clinical significance of PEN in GIO, W220
- Peptides**
Antimicrobial production, PTHrP regulates by skin keratinocytes, M238
- Percutaneous vertebroplasty (PVP)**
Success and complication rate of PVP in patients with osteoporosis, W390
- Pericytes**
Derived from adipose tissue, characterization and evaluation of their osteogenic potential, 1215
- Periodontal ligament (PDL) cells**
Flow cytometric immunophenotyping of, W041
- Periodontitis**
Low Ca diet accelerates alveolar bone resorption in rat experimental periodontitis, W411
- Small organic molecule compound protects against inflammatory bone loss in periodontitis, M412
- Periosteal cells**
Locus on Chr 4 exerts genetic control of bone size by regulating the differentiated function of, W008
- Periostin-like factor (PLF)**
Role in remodeling of bone following injury, T020
- Peripheral artery disease (PAD)**
And osteoporosis in older adults, W304
- Peritrabecular fibrosis**
PTH-induced, mast cell migration to bone surfaces precedes and appears essential for, M482, S482
- PERK**
Severe osteopenia in, due to impaired osteoblast differentiation associated with reduction of type II RUNX2 expression, 1022
- Perlecan**
Modulates FGF and VEGF signaling and is essential for vascularization in the development of the cartilage growth plate, 1064
- Peroxisome proliferator activator γ 2 (PPAR γ 2)**
Combination of Vitamin D and BADGE potentiates the pharmacological inhibition and increases osteogenic differentiation of adipocyte precursors, W155
- PHD1/3**
PHD1/3 are expressed in bone cells but are not essential for bone homeostasis, T132
- PHEX**
Dominant XLH, a new mutation of PHEX gene, T118
- Phosphatases**
Dual-specificity, modulation of WNT3A-induced signaling through, T042
- Phosphate**
Disturbed homeostasis, transgenic mice overexpressing sFRP-4 have low bone mass but do not exhibit, M209
- FGF-7 is a potent in vivo phosphaturic agent, M212, S212
- Independent effects of FGF-23 on skeletogenesis, 1114
- Reduced kidney-stone formation and altered renal homeostasis in mice overexpressing murine-MEPE, 1118
- Regulates chondrocyte differentiation in a model of embryonic endochondral bone formation, W104
- Renal, duodenum rapidly senses and modulates reabsorption via novel PTH- and phosphatonin-independent pathways, M207
- Stimulates greater PTH release and parathyroid cell proliferation in organ cultures of parathyroid tissue from patients with II-HPT than with I-HPT, W141
- Treatment of XLH increases FGF-23 concentration, W123
- Phosphate, inorganic (Pi)**
Effect of PGD₂ on Na-dependent phosphate transport activity in osteoblast-like cells, T066
- Extracellular, induces ERK1/2 phosphorylation and up-regulates a target gene of FGF-23 in renal proximal tubule cells via NaPi-IIa, W131
- Osteocytic regulation of homeostasis through FGF-23, 1296
- Renal reabsorptive process of Npt2a, role of Npt2c in, M214, S214
- Role of type III NaPi transporters in osteoblastic differentiation, W035
- Phosphate, Pit-1 type III**
Na-dependent, effects of transporter overexpression on Ca phosphate and bone metabolism, W128
- Phosphatidylinositol 3 kinase (PI3K)**
FGF-23 controls NaPi-IIa trafficking via crosstalk with the MAPK pathway, T158
- PC1 selective activation of *Runx2*-II isoform transcription is mediated through, 1142
- Signaling, Osx mediates the feedback regulation of BMP-2 via, T029
- Phosphatonin**
Independent pathways, duodenum rapidly senses and modulates renal phosphate reabsorption via, M207
- PHOSPHOI**
Temporal expression during chick limb bud mesenchymal cell differentiation and mineralization, W087
- Phospholipase C (PLC)**
Signaling via the PTH/PTHrP receptor is essential for normal full response to PTH in both bone and kidney, 1119

Phospholipase C γ 2

Signaling regulates RANKL-induced osteoclastogenesis, I104

Phosphoprotein-24 (Spp24), secreted

Active fragment enhances BMP-mediated adult bone marrow-derived MSC differentiation to osteoblasts, T144

Converted from an inhibitor to a functional enhancer during BMP-directed osteoblastogenesis, M156

Phosphorous (P)

Addition of P to Cd exacerbate the compromised BMD gain in OVX rats, T451

Phosphorylation

Of caveolin-1 in response to fluid shear in osteoblasts is mediated by P2X7 activation, T061

CREB and DNA binding along with demethylation and deacetylation are required for ultimate activation of CYP27B1 promoter by PTH, W132

ERK1/2, extracellular inorganic Pi induces and up-regulates a target gene of FGF-23 in renal proximal tubule cells via NaPi-IIa, W131

Oscillate rapidly over time, NF- κ B-regulated gene expression and, M198

RXR α , examination at serine 260 using specific antibodies in cancer cell lines and tumor tissues, M257

Sites involved in matrix MMP-13 promoter activation, identification and characterization of Runx2, W026

PHPT. See Hyperparathyroidism, primary**Phylloquinone (PK)**

Biosynthesis of MK-4 from K $_2$ and, T136

Physical activity. See Exercise**Pitx2**

Inhibits osteoblastic conversion of myoblasts through interfering the promoter activity of Osx gene, T021

PKA. See Protein kinase A**PKC μ . See Protein kinase D****Placental growth factor (PIGF)**

Specific inhibition of the VEGF homologue PIGF is protective against osteolytic bone metastasis, I169

Plasma membrane calcium ATPase, isoform 2 (PMCA2)

CaR regulates activity in mammary epithelial cells, M219, S219

Plasminogen activator inhibitors (PAI)

Increases femoral mineralization independent of estrogen status through modulation of FN matrix, T137

PAI-1 deficiency enhances fracture callus size but reduces cartilage remodeling during fracture repair, W163

Platelet-derived growth factor receptor (PDGFR)

Mediated osteoblast mitogenesis, imatinib mesylate inhibits bone formation and decreases bone mass in vivo by inhibiting, T018

Pleiotropy

Genome-wide measure of pleiotropy among osteoporosis-related traits in the Framingham Study, M277, S277

Plums

Dried plum polyphenols stimulate osteoblast activity and attenuate detrimental effects of TNF on Runx2, Osx and IGF-1 in MC3T3-E1 cells, T363

Year-long study to demonstrate the bone reversal efficacy of dried plums in postmenopausal women, M445

Podocalyxin (PODXL)

Increased expression in TIEG knockout osteoclast precursors delays osteoclast formation and reduces osteoclast size, M070

Podocan (Podn)

Affects cell proliferation and in vitro mineralization by inducing cellular senescence in MC3T3-E1 cell, T142

Podosomes

myo10 regulates osteoclast adhesion through linkage of microtubules and, M076

Poliovirus receptor (PVR)

Expression and possible role in osteoclastogenesis, M077

Poly(3-hydroxybutyrate-co-3-hydroxyvalerate) (PHBV)

Biomaterial implanted in a murine tibial defect, analysis of in vivo responses to hydrogen peroxide purified, T140

Polycystin-1 (PC1)

Selective activation of Runx2-II isoform transcription is mediated through the Ca-PI3K-Akt pathway, I142

Polyethylene glycol (PEG)

Effect of pore size and surface modification of the circular polymer scaffold on adhesion of cultured human LF cells, M075

Polymorphism

Alu polymorphism in ESR2 is associated with reduced risk of osteoporotic fractures, T218

Association of tri-nucleotide (CAG and GGC) repeat polymorphism of AR gene in Taiwanese women with refractory or remission RA, W433

H²⁶⁸Y, UGT2B7 is associated with serum sex steroid levels and cortical bone size in young adult men, T199

Polyunsaturated fatty acids

Oxidized metabolites of polyunsaturated fatty acids stimulate osteoblast apoptosis via both PPAR γ -dependent and independent mechanisms, M002, S002

Polyurethane

Scaffolds, effects of compressive loading on matrix production by osteoblastic cells cultured in, T508

Postmitotic osteoclast precursors (pOCP)

Osteoclast niche is composed of 5-FU-insensitive osteoclast precursors in vivo, M082, S082

Osteoclasts generated in ectopic bone are derived from, W071

Postnatal bone

Biology, role of BMP-2 in, I106

Ihh is essential for, T011

Normal acquisition, insulin promotes osteoblast differentiation independent from IGF-1 signaling and its receptor is required for, I070

Potassium (K)

Association between urinary K and hip bone mass in a prospective cohort study of elderly postmenopausal women, T321

Poverty

As a risk factor for osteoporotic fractures, T335

POZ-Zn

Transcriptional regulator OCZF/LRF is induced by RANKL and increases c-Fos expression in osteoclastogenesis, W067

PPARG

Marrow adipogenesis and osteoblastogenesis reflect global energy utilization through activation of, M021, O021, S021

Pravastatin

Administration of pravastatin inhibits suppressed osteoblast dysfunction and bone turnover in uremic rats, M492

Prednisolone

Induces osteocyte's death and erosion of osteocytic lacunae walls, W458

Pregnancy-associated plasma protein-A (PAPP-A)

Skeletal muscle-specific overexpression increases bone accretion, T080

Premature aging. See Aging, premature**Preosteoblast epidermal growth factor-like repeat protein with MAM domain (POEM)**

TGF β suppresses expression in osteoblasts, M201

Primary hyperparathyroidism (PHPT). See Hyperparathyroidism, primary**Procollagen aminoterminal propeptide (PINP)**

Development of a highly sensitive high-throughput mass spectrometry-based assay for PINP, W202

Non-radioactive immunoassay for PINP, W214

Serum PINP is a useful marker of bone formation, W210

Progenitor cells

Activation and differentiation, COX-2 deficiency impairs periosteal, I251

Non-adherent circulating, with osteoblastic potential become adherent in the presence of Ca²⁺ and are able to mineralize, T040

In tmMPC have characteristic similarities to bmMSCs, W039

Progressive ankylosis gene (ank)

Regulates osteoblast differentiation, M043, S043

Proline/arginine-rich end leucine-rich repeat protein (PRELP)

Matrix inhibits osteoclastogenesis inactivating the NF- κ B signal, W080

Propranolol

Long-term propranolol improves BMC and lean body mass in pediatric burn patients, M487, S487

Prostaglandins

Role of prostaglandins in strontium ranelate effects on osteoblastic differentiation and growth factor production, W333

Prostaglandin D₂ (PGD₂)

In bone formation and remodeling in vivo, T001

Effect of, on Na-dependent phosphate transport activity in osteoblast-like cells, T066

Prostaglandin E₂ (PGE₂)

Activates β -catenin signaling in MLO-Y4 osteocytic and 2T3 osteoblastic cells, W053

Acts through EP2/EP4 receptors to upregulate RGS2 expression in osteoblasts, T063

Demonstration of an anabolic effect on bone in CD-1 mice, M180

Effects of long-term treatment with a PGE₂

receptor subtype 4 agonist and PTH at skeletal sites with moderate osteopenia, M385

Effects on the cAMP/PKA and the β -catenin pathways, protective effects of mechanical strain on osteocyte viability is mediated by, M237

Increases a specific subset of primitive

hematopoietic cells in vivo, M039, S039

Production and Wnt/ β -catenin signaling, greater sensitivity of osteocytes to shear stress as compared to osteoblasts, W052

Production by osteoclasts, nicotine and LPS stimulate the formation of osteoclast-like cells by increasing, T084

Receptor EP4 antagonist attenuates osteolysis due to cancer metastasis, W196

Prostate cancer

Activation of MCP-1/CCR2 axis promotes prostate cancer invasion and the tumor-induced osteoclast activity in vitro, T248

Fracture risk is increased in Danish men with prostate cancer, T256

MTA1 was highly expressed and localized in nucleus in prostate cancer bone metastasis, T253

Non-isomerized C-telopeptides of Type I collagen (ALPHA CTX) for early detection and treatment monitoring of bone metastases secondary to prostate cancer, T245

Osteoblast-prostate cancer cell signaling, T244

PTHrP-induced MCP-1 production by HBME cells and osteoblasts promotes osteoclast differentiation in vitro, T247

PTHrP regulation of AKR1C1-3 and growth in prostate cancer cells, T234

TGF β increases osteolytic prostate cancer bone metastases and expression of pro-metastatic genes, T238

WISP-1/CCN-4, a novel target for inhibiting prostate cancer growth in bone, I174

Wnts increase osteoblast activity in prostate cancer through BMP, T235

Prostate cancer, hormone-refractory (HRPC)

$\alpha_v\beta_3$ integrin inhibitor MK-0429 is generally safe and decreases bone turnover in men with HRPC and MBD, T246

Prosthetic wear

Inhibition of osteoclastogenesis involves suppression of RANK expression, W076

Proteasome

Inhibition induces permanent growth retardation and apoptosis in growth plate chondrocytes, M121, S121

Inhibition on osteoblast differentiation and anagen induction, similar effects of, W111

Protein inhibitor of activated STAT3 (PIAS3)

Modulates osteoclastogenesis by down-regulation of NFATc1 and OSCAR, W066

Negatively regulates RANKL-induced osteoclastogenesis, M089

Protein kinases

Stress activated, TNF α dependent redox signals upregulate Mx2 gene transcription via, T165

Protein kinase A (PKA)

Pathways, protective effects of mechanical strain on osteocyte viability is mediated by the effects of prostaglandin on, M237

Protein kinase C β (PKC β)

Estrogens or androgens attenuate p66^{shc} phosphorylation via a signaling cascade, T185

Protein kinase C delta (PKC δ)

Cx43 amplifies FGF2-responsiveness in a dependent manner, W027

Protein kinase C (PKC)

Activation of MAPKs by 17 β -estradiol is mediated in skeletal muscle cells, T194

Isoform-specific activation in osteoclasts, P2X7 nucleotide receptors couple to, M109

Translocation revealed by live-cell imaging, spatio-temporal patterning of, M109

Protein kinase D

As an essential mediator during osteoblast differentiation, M019

Protein phosphatase 1 (PP1c)

Binding domain (F872A), point mutation of endofin stimulates bone formation, I256

Protein related to DAN and cerberus (PRDC)

Expressed in skeletogenesis and prevents osteoblastic differentiation, W115

Protein synthesis

Regulation in estrogen metabolite-mediated inhibitions of osteosarcoma cells, T254

Protein tyrosine kinase 2 (Pyk2)

ADAM8 binds $\alpha_v\beta_1$ to increase osteoclast formation and function by interacting with, I099

Proton pump inhibitors (PPI)

Chronic PPI use is not associated with an increased risk of osteoporotic fra, M351, S351

Prx1. See also *Homeobox protein; MHox*

Identification of as a regulator of Osx expression and mediator of TNF action, I143

Pseudoarthritis. See also *Arthritis*

Prognostic factor on MRI findings inducing prolonged intractable pain due to pseudoarthrosis following osteoporotic vertebral fracture, W286

Pseudohypoparathyroidism. See also *Hypoparathyroidism*

Hyperparathyroid bone disease in two sisters with pseudohypoparathyroidism 1b, W429

Psychiatric illness

Association between psychiatric illness and falls, T354

PTEN

And osteoblastogenesis, W034

PTH. See *Parathyroid hormone*

PTH/PTHrP receptor (PTHR)

Analysis of interaction mechanisms using a new, long-acting PTH(1-28) analog reveals selective binding to distinct PTH receptor conformations and biological consequences in vivo, I190

PU.1

In osteoclasts, regulation of integrin expression by, M071

Puberty

Decreases in cortical thickness are associated with the pubertal increase in forearm fractures in girls, I193

Effect of plasma 1,25(OH) $_2$ D concentration or Ca intake on negative correlation between plasma 25OH(D) and PTH concentrations in Japanese adolescents, W159

Fat mass is inversely related to subsequent change in bone size and mass in young prepubertal children, M536

Five-year follow-up of bone mineral distribution and bending strength changes across puberty, W512

Is development of ovulatory cycles in adolescence important for peak bone mass?, W511

Optimising bone health in pre-pubertal children, W486

Sex-specific bone surface changes during, pQCT analysis of the mid-tibia, M527

Tempo and timing of bone mineral accrual during the pre-, peri- and post-adolescent growth periods, W509

Weight bearing bones are more sensitive to physical exercise in boys than in girls during pre- and early puberty, W519

Pulmonary disease, chronic obstructive (COPD)

BMD and serum Vitamin D levels in patients with COPD without GC use, M454

Epidemiology of COPD and osteoporosis, W298

Prevalence and risk factors of osteoporosis and vertebral fractures in COPD males, M376

Vertebral fractures in patients with COPD patients, T330

Pulposus cells

Effect of vertebroplasty filler materials on viability and gene expression of mouse and human, M138

Pulse wave velocity (PWV)

Association of PWV and BMD, W293

PYK2

Deletion of PYK2 led to high bone mass through a positive balance between bone formation and resorption, I014

Pyrrolidine dithiocarbamate (PDTC)

Inhibits SOD1 gene and cell growth by activating JNK pathway in U2OS, W018

Q

Quantitative trait loci (QTL)

Candidate genes of every known QTL of BMD in whole mouse genome, M280

On Chr 11 regulates bone shape in SAMP6 mice, W181

Evidence for QTL underlying normal variation in calcaneal QUS measures, W179

For femoral BMD identified in two separate chicken intercrosses are syntenic to loci controlling human BMD, W182

Genome-wide scan for QTL influencing BMD, W174

In HcB/8 and HcB/23 F2 mice, W466

Identification of sex-specific for femoral neck density and strength in inbred COP and DA rats, W171

Identification of sex-specific QTL for femoral neck density and strength in inbred Dark Agouti (DA) rats, W171

Identifying mechanical loading QTL by gene expression changes for alkaline phosphatase and bone sialoprotein, T152

Mapping to Chromosome 2p influences variation in bending resistance of bone, W180

Positional cloning identified ESR2, ESRRB, BMP4 and LTBP2 as the candidate genes for the QTL in Chromosome 14 for BMD variation, W175

Serum alkaline phosphatase QTLs provide evidence that genes on Chromosome 5 and 11 regulate bone formation and affect bone size and strength, T212

R

R176Q. See *Fibroblast growth factor 23*

R325Q

Single nucleotide polymorphism R325Q in the Vitamin K-dependent GGCC gene has effects on the correlation between dietary Vitamin K intake and gamma-carboxylation of serum osteocalcin, T318

Rab3D

Potential role in osteoclastic bone resorption, M103, S103

Recruits the dynein complex to secretory vesicles in osteoclasts through direct interaction with Tctex-1, I293

Rac2

Knockout mice have an augmented anabolic response to PTH, I008

Radiation

- Acute 7 gray dose of gamma-radiation induces a profound and rapid loss of trabecular bone, M464
- Bone microarchitecture of irradiated and bone marrow transplanted mice, M067
- Low-level radiation can enhance trabecular bone quantity and architecture, W276
- Murine bone loss following local irradiation, M145

Radiation, electromagnetic

- Bone density changes with pulsing EM field treatment of the forearm after disuse, T430

Radiation, ionizing

- Increased active osteoclasts are associated with acute cancellous bone loss in adult mice exposed to ionizing radiation and musculoskeletal disuse, M462

Radiation, ultraviolet

- Effects of UV-B light on serum Vitamin D levels, M450
- Personal exposure and Vitamin D synthesis, M261
- Possible direct regulatory role of active Vitamin D increased by ultraviolet B on FGF-23, W126

Radiofrequency ablation

- Minimally invasive treatment of OOM by, W422

Radiographic texture analysis (RTA)

- Clinical utility of RTA performed on densitometric calcaneal images, M331

Radiography

- Texture analysis and geometry measurements on plain radiographic femurs, W231

Raloxifene

- Adherence to raloxifene therapy, W379
- Comparison of serum TRACP type 5b assays and other bone resorption markers for monitoring raloxifene therapy, W209
- Identification of primary target cells for the classical genomic effects of estrogen and, T188

Raman spectroscopy

- Measurement protocols for the noninvasive assessment of bone constituent properties by Raman spectroscopy, T108

RAP-011

- Increases BMD in combination with prior antiresorptive therapy, W312

Rapamycin

- Differentially alters the skeletal response to PTH and mechanical loading, 1245
- Inhibits osteoblast proliferation and differentiation in MC3T3-E1 cells and primary mouse BMSCs, M007

RAR γ

- Repression function, cartilage ECM homeostasis is regulated by, W103

Reactive oxygen species (ROS)

- Estrogens attenuate IL-6 and TNF α production in osteoblastic cells by decreasing oxidative stress and its effects on NF- κ B activation, T186
- Expression in osteoblasts of NOS1, 2 and 3 in knockout mice, M006
- Grx5 regulates osteoblast cell functions by protecting against oxidative stress, M005
- Oxidative stress suppresses osteoblastogenesis by antagonizing Wnt/ β -catenin and BMP signaling, M174
- Regulation of RANKL-induced MAPK activation by, M115

Receptor activator of NF- κ B (RANK)

- Characterization of gene promoter region, molecular cloning and, M095
- Expression, inhibition of osteoclastogenesis by prosthetic wear debris involves suppression of, W076
- IVVY⁵³⁵⁻⁵³⁸ plays an essential role in TNF α - and IL-1-induced osteoclastogenesis, M084, S084
- Signaling in human osteoclasts, effect of p62 mutations, M474
- Signaling through HTS, development of cell-based assays for identifying antiresorptive compounds targeting, M102

Receptor activator of NF- κ B ligand (RANKL).

- See also *Nuclear factor B*
- Acid-induced stimulation of, in osteoblasts mediated by IP₃, M063
- Activating via TLR-2 and TLR-4 activation, rheumatoid synovial fibroblasts promote osteoclastogenic activity by, W435
- AnxA8 is a critical bone matrix-dependent osteoclast gene transcriptionally regulated by, W068
- BMP-2-inducible Osx increases osteoblastic ratio to induce osteoclast maturation, M100
- Cells migration in inflammatory bone resorption, TNF α /CCL3-5/CCR5 cascade mediates, M181
- Crosstalk in BaP-mediated inhibition of osteoclastogenesis, NF- κ B but not NFATc1 is involved in, T106
- Deficient mice by expression of soluble RANKL transgene, dramatic increase in hematopoiesis and angiogenesis in bone marrow of rescued, M096, S096
- Evoked [Ca²⁺]_i oscillations mediated by RGS10 in osteoclast differentiation, mechanism of, M093, S093
- Expressing lymphocytes, intracellular cytokine profile of, T164
- Expression and cell proliferation in human osteoblasts and osteoblastic cells, alpha 1 and beta2 adrenergic agents modify, T006
- Gene, targeted deletion of a distant transcriptional enhancer reduces bone remodeling and increases bone mass, 1067
- High D(+)glucose concentration inhibits RANKL-induced osteoclastogenesis, W082
- Increased expression in stimulated T-cells from patients with AS, W446
- Induced expression of TRPV2 is involved in osteoclastogenesis via Ca signaling activation, T103
- Induced MAPK activation by ROS, regulation of, M115
- Induced osteoclastogenesis, Ca and phospholipase C γ 2 signaling regulates, 1104
- Induced osteoclastogenesis, HMGB1 regulates actin cytoskeleton organization in a manner dependent on RAGE, M079
- Induced osteoclastogenesis, PIAS3 negatively regulates, M089
- Induced osteoclastogenesis, Wnt5a enhances, 1149
- Modulation of RANKL gene expression by Runx2 and Vitamin D3, 1219
- mRNA, co-stimulation of 1,25-(OH)₂D₃ and BMP-2 enhances the expression in osteoblasts, W162
- Oxidative stress-induced vascular calcification is associated with increased expression of receptor activator of, 1216

- POZ-Zn transcriptional regulator OCZF/LRF is induced by, W067

- Produced by adipocytes and stimulates osteoclastogenesis, W079

- Regulation of expression by GC in osteoblast-like cells, T068

- Regulation of RANKL expression by GC in human osteoblast-like cells, WG22

- Stimulated dendritic cells on autoimmune arthritis in MRL/*lpr* mice, immunoregulatory role of, T162

- Stimulates osteoclasts to release VEGF-C and enhance osteoclastic bone resorption through an autocrine mechanism, 1100

- Upregulation from CD4⁺T cells, IL-23-enhanced osteoclastogenesis is mediated by STAT3 and NF-B via, T078

Receptor for advanced glycation endproducts (RAGE)

- HMGB1 regulates actin cytoskeleton organization and RANKL-induced osteoclastogenesis in a manner dependent on, M079

Regulator of G-protein signaling 10 (RGS10)

- Osteoclast differentiation, mechanism of RANKL-evoked [Ca²⁺]_i oscillations mediated by, M093, S093

Renin-angiotension system (RAS)

- Ca-independent and 1,25-dihydroxyvitamin D₃-dependent regulation in 25(OH)D 1 α -hydroxylase knockout mice, W150

Replication

- Defective, MSC from aging C57BL/6 exhibit increased oxidative stress and, M052, S052

Replication competent avian virus system (RCAN)

- Using to deliver short hairpin siRNA to silence gene expression of Wdr5 in chicken limb bud during embryogenesis, T141

Retinoblastoma

- Related pocket protein Rbl2 is a candidate gene for a QTL affecting peak bone mass and strength, 1237

Retinoblastoma binding protein 1 (RBP-1)

- A novel factor critical for Runx2 expression and transcriptional activation, W021

Retinoic acid (RA)

- Effect of, on the osteoblastic differentiation of human ASC, T051

Retinoid X receptor α (RXR α)

- Examination of phosphorylation at serine 260 using specific antibodies in cancer cell lines and tumor tissues, M257

Rett's syndrome

- Bone mass determination in girls and mice, WG8
- Bone ultrasonography in the longitudinal monitoring of bone status in patient with Rett's syndrome, T514

RGS2

- Expression in, PGE₂ acts through EP2/EP4 receptors to upregulate, T063

rhBMP-2

- New surface modified DBM by collagen hybrid coating, T133

Rheumatoid arthritis (RA). See Arthritis, rheumatoid**Rhizoma drynaria (RD)**

- Total flavonoid fraction of RD and its active ingredient, naringin, exert bone protective effect in vivo and in vitro, W342

- Rho**
Activity, CK-B involves the bone resorptive activity of osteoclast activity by regulating, M083
- Rho GTPase**. See also *GTPase*
Signaling pathways in osteoclasts, *Wrch1/RhoU* role in cell adhesion and osteolysis, M073, S073
- Rho-kinase (ROK) inhibitor**. See *Hydroxyfasudil*
- RhoA**
Activation of, mechanosensitivity of osteoblasts is regulated by actin polymerization through, W010
Small GTPase and its effector kinase ROCK mediate actin cytoskeleton reorganization leading to osteocyte anoikis by GC, M233, S233
- RhoU**
Role in cell adhesion and osteolysis, Rho GTPase signaling pathways in osteoclasts, M073, S073
- Ribonucleic acid, messenger (mRNA)**
Protein-PTH interactions that determine PTH stability in secondary hyperparathyroidism and hypoparathyroidism, M217, S217
PTH, calcilytics block the suppressive effect of calcimimetics on levels in parathyroid cells, M228
RANKL, co-stimulation of 1,25-(OH)₂D₃ and BMP-2 enhances the expression in osteoblasts, W162
- Ribonucleic acid, short hairpin (shRNA)**
Using RCAN to deliver short hairpin siRNA to silence gene expression of *Wdr5* in chicken limb bud during embryogenesis, T141
- Ribonucleic acid, small interfering (siRNA)**
Noggin gene transfer enhances the in vivo ectopic bone formation induced by BMP-2, W121
Specific knockdown of lamin A/C inhibits osteogenic differentiation of human MSC, M038
Using RCAN to deliver short hairpin siRNA to silence gene expression of *Wdr5* in chicken limb bud during embryogenesis, T141
- Rickets**
Is associated with failure of epiphyseal/metaphyseal bone tether formation, W421
- Rickets, autosomal recessive hypophosphatemic (ARHR)**
Molecular analyses of DMP1 mutants causing, I116
- Rickets, hereditary hypophosphatemic with hypercalciuria, (HHRH)**
Role of *Npt2c*, involved in, I115
- Rickets, X-linked hypophosphatemic (XLH)**
7B2 protein regulates FGF-23 degradation and production in XLH, I225
Dominant XLH, a new mutation of *PHEX* gene, T118
Growth and response to active Vitamin D and P treatment is highly associated with haplotype of the VD promoter in XLR, I195
Three novel mutations of the *Phex* in three Chinese families with XLH, W170
Treatment with calcitriol and phosphate increases FGF-23 concentration, W123
- Risedronate (Ris)**
Cost-effectiveness of Ris versus IBN, W322
Early and sustained non-vertebral fracture efficacy with Ris, M438
Effect of Ris on bone loss associated with liver transplantation, T501
- Effect of Ris on risk of clinical fracture among patients with prior hip fracture, M432, S432
Effects of Ris and raloxifene on serum lipid levels in postmenopausal women, W370
Effects of Ris on bone change at children with OI, T520
Efficacy and tolerability of a once-a-month dosing regimen of Ris for the treatment of postmenopausal osteoporosis, T382
Efficacy for non-vertebral fractures is consistent across age groups, W351
Evaluation of cell apoptosis and COX-2 expression in GC-induced osteoporosis in rats treated with, W318
Patients previously treated with Ris demonstrate greater responsiveness to TPTD than those previously treated with ALN, I091
Patient's satisfaction and compliance for Ris, once-weekly versus once-daily, T401
Patients treated with Ris have a fracture risk similar to patients 20 years younger in age, W317
Persistence with Ris therapy is already high and further improved by a patient educational program, T394
Preserves bone turnover as measured by biochemical markers after 5 years treatment in postmenopausal Greek women, WG19, T402
Prevents bone loss in breast cancer survivors, I017
Reduces osteonal cortical porosity in osteoporotic women, M508, S508
Therapeutic effects of Ris for two years on bone metabolic markers, especially on TRACP-5b, W357
Treatment in type 2 diabetic men with primary osteoporosis, M433
Two-consecutive days-a-month Ris reduces vertebral fracture risk at one year, W373
Vertebral fracture efficacy with Ris is apparent early and is sustained, W374
- RNA interference (RNAi)**
Functional screening for *Runx2*-regulated genes corresponding to ectopic bone formation in human spinal ligaments, M273
Machinery is essential for osteoclastogenesis, M090, S090
- ROCK**
Effector kinase mediate actin cytoskeleton reorganization leading to osteocyte anoikis by GC, M233, S233
- Ror2**
Promoting osteoblastogenesis, *Wnt5A* signals through, M045, S045
- Ruffled border membrane**
Osteoclast, electroneutral sodium/bicarbonate cotransporter *NBCn1* is expressed in, T091
- Runx1**
Analysis of the role in chondrocyte differentiation using chondrocyte-specific *Runx1* deficient mice, M133, S133
Regulates chondrogenic differentiation, I112
- Runx2**
Activity, *Zfp521* is a novel inhibitor of with opposite effects on osteoblasts and bone formation in vitro and in vivo, I250
During BMP2-regulated osteoblastogenesis, *Osx* functions as downstream of, W020
Cx43 amplifies FGF2-responsiveness in a dependent manner, W027
Cytoplasmic interaction of p21 with, during osteogenic differentiation of MSC, T049
- Enhancer elements drives robust expression in transgenic mouse osteoblasts, *hCol1a2* nuclear targeting sequence together with, I288
ERRγ negatively regulates osteoblast differentiation and mineralization through, W015
Expression and activity in osteoblasts, TIEG as a novel mediator of, I144
Expression and transcriptional activation, *RBP1* as a novel factor critical for, W021
Growth inhibition of osteoblast progenitors depends on its C-terminal regulatory domain and is accompanied by changes in G-protein coupled signaling pathways, M047, S047
Haploinsufficient mice, *Nell-1* partially rescues craniofacial defects in, I105
Modulation of RANKL gene expression by *Runx2* and Vitamin D3, I219
Nell-1 partially rescues craniofacial defects in *Runx2* haploinsufficient mice, I105
Novel R131G *RUNX2* mutation causing cleidocranial dysplasia disrupts heterodimerization with core binding factor-β, M022
Over-expression in mesenchymal cells enhanced bone formation but inhibited cartilage formation and limb development, I066
Phosphorylation sites involved in matrix MMP-13 promoter activation, identification and characterization of, W026
Regulated genes corresponding to ectopic bone formation in human spinal ligaments, functional RNAi screening for, M273
Regulation of activity, orphan nuclear receptor *SHP* promotes osteoblast differentiation by, T024
Regulation of at the nuclear lamina, M032
Synergistically activates osteoblast-specific osteocalcin gene expression, M037
Transcription factors, *Osr1* gene expression is regulated by, W030
Transcriptional activity by the phosphorylation at a specific site, *GSK-3β* inhibits osteoblastic bone formation through suppression of, I247
Transcriptional AD3 supports synergistic MINT activation of the osteocalcin FGF response element via a *DMAT*-sensitive kinase, T036
Transcriptional regulation of *COL10* by, M127, S127
Translation, regulation by 5- and 3-UTR binding proteins, M026
Trinucleotide repeat mutations are associated with decreased bone density and altered protein function, I033
Trps1 transcription factor regulates chondrocyte hypertrophy and perichondrial mineralization through repression of, I184
Zfp64 is a downstream target of, and regulates myogenic and osteogenic differentiation as a coactivator of *Notch1*, T035
- RUNX2-II**
Isoform transcription is mediated through the *Ca-PI3K-Akt* pathway, *PC1* selective activation of, I142
Reduction of expression, severe osteopenia in *PERK*-knockout mice is due to impaired osteoblast differentiation associated with, I022
- Rxrb**
Analysis of the function of the CTCF-binding site between *Col11a2* and, T119

S**SABRE Study**

Study of Anastrozole with the Bisphosphonate Ris (SABRE Study), M300, S300

Saos-2

Ubc9 promotes stability of Smad4 and regulates BMP signaling pathway in, T065

Sarcoidosis

Progression of vertebral deformities but no change in BMD in patients with sarcoidosis, W279

Sarcopenia

In ageing men with osteopenia, osteoporosis and normal BMD, W264

SB-423557

Oral treatment with SB-423557 causes PTH release in multiple species and positive bone forming effects in the rat, M386, O386, S386

Sclerosis

Of the principal medial compressive trabeculae in the osteoporotic femur may mask the bone mineral loss of the femoral cortex, T293

Sclerostin (SOST)

Anti-sclerostin antibody increases markers of bone formation in healthy postmenopausal women, I129

Bone enhancer, control of by PTH via MEF2 transcription factors, I046

Inhibition leads to increased periosteal and endocortical bone formation as well as decreased cortical porosity, I232

Mediated inhibition of the LRP5-Wnt-TCF signals in U2OS osteoblast-like cells, mutations in LRP5 β -propeller 1 block, I048

Overexpression impairs limb patterning, M179, O179, S179

Treatment with an anti-sclerostin antibody directly stimulates bone formation in a dose-dependent manner, I231

Treatment with an anti-sclerostin antibody increased bone mass by stimulating bone formation without increasing bone resorption, I122

Scoliosis, adolescent idiopathic (AIS)

Estrogen receptors in, T189

SDF-1

CXCR4 is essential for in vivo endochondral bone repair, T163

Sealing ring

Defects in formation in osteoclasts, disruption of WASP-associated signaling complex formation leads to, M113

Secondary hyperparathyroidism (II-HPT). See Hyperparathyroidism, secondary**Secreted frizzled related proteins (SFRP)**

Differential effects on osteoblastic differentiation of mouse pluripotent mesenchymal cell line, M044

Secreted frizzled related protein 1 (sFRP1)

Absence of accelerates fracture healing, I258
Small molecule inhibitor of the Wnt antagonist SFRP-1 stimulates bone formation, I010

Secreted frizzled related protein 3/4 (sFRP3/4)

GC enhances the expression in cultured osteoblasts, T176
GC enhances the expression of a Wnt antagonist, sFRP3, in cultured human osteoblasts, WG21
Transgenic mice overexpressing have low bone mass but do not exhibit disturbed phosphate homeostasis, M209

In vitro and in vivo effects of sFRP3 overexpressed by Phi 31 integrase strategy, W049

Secretory vesicles

Rab3D recruits the dynein complex through direct interaction with Tctex-1, I293

Selective androgen receptor modulator (SARM)

Bone specific SARMS Increased BMD in a different manner from anti-resorptive agent raloxifene with minimum effects on the uterus, M402

Combination treatment with a bisphosphonate has additive effects in osteopenic female rats, M405, S405

Selective serotonin reuptake inhibitors (SSRI)

SSRI use is associated with increased risk of fracture among older men, I159

Senescence

Cellular, Podn affects cell proliferation and in vitro mineralization by inducing in MC3T3-E1 cell, T142

Serine 260

Examination of RXR phosphorylation using specific antibodies in cancer cell lines and tumor tissues, M257

Serotonin transporter (5-HTT)

Osteoblasts from knockout mice display reduced growth and mineralization capacity, M013

Serum response factor (Srf)

Function in bone and cooperation with NFAT1, analysis of Krox20 gene regulation reveals, M025, S025

Sham-operated rats

Quality and strength of cortical bone are lowered by limiting physical activity, W479

Shear stress. See also Fluid flow shear stress

$\alpha 5$ integrin association with Cx43 regulates the function of osteocyte hemichannels in response to, T504

Greater sensitivity of osteocytes as compared to osteoblasts, PGE₂ production and Wnt/ β -catenin signaling, W052

Short hairpin RNA (shRNA). See Ribonucleic acid, short hairpin**SIBLING**

Degradation of MEPE, DMP1 and release of ASARM-peptides (minhibins), I155

Side population (SP) cells

Co-expressing Stro-1, identification of, T054

Silent information regulator T-1 (SIRT-1)

Aging-associated gene regulates osteoclast formation and bone mass in vivo, I097

Single nucleotide polymorphisms (SNP)

Association of bone mass with SNPs of frizzled genes in Wnt system and circulating OPG, T222

Identification of SNPs contributing to BMD and fractures, M275, S275

Multiplex SNP genotyping and data analysis on 360 Hungarian postmenopausal women, T226

Sirtuins

Effect of caloric restriction on bone is exerted through the stimulation of sirtuins, M048

Skeletal development

Conditional ablation of the osteoblast CaR causes abnormalities in, M223, O223, S223

In vivo, expression of CaR in cartilage is essential for embryonic, I176

Skeletal growth

CAL and its analog successfully elongate survival period and improve via independent pathway of VDR, W157

Genetic variation in post-natal skeletal growth defines functional interactions among adult bone traits and fragility, T204

Skeletal health

Racial differences in skeletal health, W261
Between two different groups of Hispanic American women, T283

Skeletal homeostasis

Regulation by anti-apoptotic molecule Bcl-2, I290

Skeletal load

Attenuated response in Cx43 deficient mice, M518, S518

Skeletal muscle

Activation of MAPKs by 17 β -estradiol is mediated by PKC and c-Src in, T194

Arkadia represses differentiation through enhancement of Myostatin and TGF β signaling, M206

Comparison between gene expression in skeletal muscle and bone of postmenopausal osteoporotic females and their controls, W213
17 β -Estradiol abrogates apoptosis through extra-nuclear estrogen receptors, T196

Specific overexpression PAPP-A increases bone accretion, T080

Skeletal parameters

Age-related distribution of bone and skeletal parameters in 1322 young women, W513

Skeletal phenotype

In transgenic mice over-expressing CTGF in cells of the osteoblast lineage, I287

Skeletal remodeling. See Bone remodeling**Skeletal size**

And fracture risk in a large clinical cohort, I163
Increased, targeted deletion of E11/gp38 results in, I043

Skeletogenesis

ESL-1 negatively regulates TGF β in the Golgi during, M202, S202

Misexpressions of SOX9 lead to accelerated adipogenesis in transgenic mice, I180

Phosphate-independent effects of FGF-23 on, I114

PRDC is expressed in, and prevents osteoblastic differentiation, W115

Skeleton

Under-mineralization, spontaneous mutation in the mouse *Lmna* gene results in, M146, S146

Skin color

Seasonal variations and the impact on Vitamin D status, M263

Slug

Osteoblasts in adult bone use, for regeneration and repair but not remodeling, I213

Smad

ERR γ negatively regulates osteoblast differentiation and mineralization through, W015

Mediated BMP signaling, endogenous CREB signaling enhances, W118

Modulation of the signaling pathway, TIEG suppresses osteoblast cell proliferation through, M035

Proinflammatory control of BMP-driven transcription and osteogenesis, W044

Signaling, new insights into the determination of, by TGF β superfamily, M199

Smad1

Atm regulates osteoblast differentiation through, M017

Differentially regulate osteoblast differentiation and myogenesis in myoblasts, W117

- Protein, miR-26a targets of hADSCs, T028
Required for endochondral bone formation, BMP canonical signaling through, M171, S171
- Smad4**
Differentially regulate osteoblast differentiation and myogenesis in myoblasts, W117
Has a direct apoptogenic role at the mitochondria, M205
Ubc9 promotes stability of, and regulates BMP signaling pathway in osteoblastic Saos-2 cells, T065
- Smad5/6/7/8**
Atm regulates osteoblast differentiation through, M017
Inhibitory Smad6 and Smad7 differently regulate cartilage formation, M130, S130
Required for endochondral bone formation, BMP canonical signaling through, M171, S171
- Small heterodimer partner (SHP)**
Promotes osteoblast differentiation by regulation of Runx2 activity, T024
- Small interfering RNA (siRNA).** See *Ribonucleic acid, small interfering*
- Small leucine-rich proteoglycan (SLRP)**
bgn and fnod control bone mass by regulating osteoclast differentiation through BMSC, M157, O157, S157
- Snail**
Inhibits the differentiation of MSC to osteoblasts, T033
- SNF**
Chromatin remodeling complex, positive and negative regulation of osteoblast differentiation by, M030
- SOD1**
PDTC inhibits gene and cell growth by activating JNK pathway in U2OS, W018
- Sodium-dependent phosphate transporter, type IIc (Npt2c)**
Role in renal Pi reabsorptive process of Npt2a, M214, S214
Role of, involved in HHRH, 1115
- Sodium-phosphate co-transporter, type IIa (NaPi-IIa)**
Extracellular inorganic Pi induces ERK1/2 phosphorylation and up-regulates a target gene of FGF-23 in renal proximal tubule cells via, W131
FGF-23 controls trafficking via crosstalk between the PI-3 kinase and MAPK pathways, T158
Role of Npt2c in renal Pi reabsorptive process of, M214, S214
- Soluble interleukin-6 receptor (sIL-6R)**
Effect on the expression of cartilage matrix proteins, T146
- Sonic hedgehog homolog (Shh).** See also *Hedgehog homolog*
In fracture repair and osteoclast formation, T082
- Sorting nexin 19 (SNX19)**
Identification of a novel chondrogenic factor using a real-time fluorescence monitoring cell line ATDC5-S2RD5, 1185
- SOSTDC1**
Common variant of SOSTDC1 is associated with increased risks of fractures and osteoporosis, T217
- Sox5/6**
Runx1, co-activator of Sox5/6, regulates chondrogenic differentiation, 1112
- SOX9**
Misexpressions during skeletogenesis lead to accelerated adipogenesis in transgenic mice, 1180
- Runx1, co-activator of Sox9, regulates chondrogenic differentiation, 1112
Transcriptional induction by NF-κB subunit p65 during chondrogenesis, W101
- Soy**
Does pre- or post-menopausal soy consumption affect postmenopausal bone loss?, W277
- SPARE Study**
Baseline characteristics of participants in the Soy Phytoestrogens as Replacement Estrogen (SPARE) Study, T425
- Sphingosine kinase (SPHK)**
Inhibition-independent action, suppression of osteoclastogenesis by DMS, M088
- Spinal Curvature Irregularity Index (SCII)**
SCII discriminates hip fractures, T289
- Spinal defects**
Associations of osteoporotic spinal deformity with back strength among elderly women in Japan and the United States, WG24
Double KO of HIP1 and HIP1r lead to an osteopenic phenotype with severe spinal defects, W167
- Spinal muscular atrophy (SMA)**
Functional role for SMA gene expression in bone remodeling, W077
- Spine**
Limits for exclusion of individual vertebra from the L2-L4 AP spine assessment, T277
- Spine cancer**
Paclitaxel-loaded hydroxyapatite-alginate beads for local chemotherapy of metastatic spine cancer, T231
- Squamous cell carcinoma (SCC).** See *Carcinoma, squamous cell*
- Stanniocalcin 2 (STC-2)**
CaP regulating hormone is positively and negatively regulated by 1,25(OH)₂D₃ and PTH in renal proximal tubular cells, W130
- STAT**
Identification as potential primary target in the secondary gene regulation of the FGF-23 gene by 1,25-dihydroxyvitamin D₃, W161
IL-23-enhanced osteoclastogenesis is mediated by via upregulation of RANKL from CD4⁺T cells, T078
Regulation of human osteoclast precursor generation by, T079
- Statins**
Decrease bone turnover markers in postmenopausal women, W326
Use of to enhance bone mineralization and formation in 2D and 3D tissue engineered constructs, T003
- Stem cell factor (SCF)-cKit signaling pathway**
Acceleration of fracture healing via enhanced vasculogenesis and osteogenesis through, T013
- Stem cells**
Application of bioluminescence in bone formation, W046
- Stem cells, adipose-derived (ASC, hADSC)**
Differentiation of, effect of VD, RA, and Dex on human, T051
miR-26a targets the SMAD1 protein of, T028
- Stem cells, bone**
In vivo models to study IGF-1 receptor dynamics of, M190
- Stem cells, breast**
Transformation and invasiveness is mediated upregulation of IL-8 by *TWIST* interactions with NF-κB, T242
- Stem cells, dental pulp (DPSC)**
Role of EphB/ephrin-B interactions in cell attachment and spreading of mesenchymal precursors derived from, W033
- Stem cells, hematopoietic (HSC)**
Identification for bone and cartilage of the myeloid lineage, M169, S169
Increasing osteoblast number is not sufficient to enhance the function of, M053
- Stem cells, mesenchymal.** See *Mesenchymal stem cells*
- Stem cells, osteogenic**
Homing to sites of endochondral bone formation, 1071
- Steroid hormone receptor elements (SHRE)**
ChIP-on-chip analysis reveals novel GC response genes adjacent to genomic binding sites for, M061
- Steroidogenesis**
Wwox knockout mice reveal impaired steroidogenesis, defects in bone metabolism, and formation of osteosarcomas, W200
- Steroids, sex.** See also *Androgen; Estrogen*
Comparison of sex steroid measurements in men by mass spectroscopy versus immunoassay, M369, S369
Hormone receptors in osteoclasts mediate osteoprotective effects by regulating its life cycle, 1220
Proliferation and differentiation of periosteal osteoblast progenitors are differentially regulated by sex steroids and intermittent PTH administration, M060, S060
Serum levels, UGT2B7 H²⁶⁸Y polymorphism is associated with in young adult men, T199
- Strain amplification**
On the osteocyte, microstructural variation in the bone matrix and cell attachments modify, M066
- Stress shielding**
Ex vivo model in trabecular bone, W055
- Stro-1**
Co-expressing, identification of human circulating SP cells, T054
- Stromal cells.** See *Bone marrow stromal cells*
- Stromelysin-1**
Novel transcription factor-like function of MMP-3 that regulates CTGF/CCN2 gene transcription, T125
- Strontium (Sr)**
Correction of BMD measurements for bone Sr content, M448
Improved Sr bioavailability in a new tablet formulated Sr salt, T411
Non-pharmaceutical Sr and Ca supplements have inconsistent mineral analyses and DXA imaging analyses, T357
- Strontium ranelate**
Bone material characteristics in osteoporotic postmenopausal women after 3-year treatment with strontium ranelate, M447, S447
Effects in human osteoblasts support its uncoupling effect on bone formation and bone resorption, M014
Effects of strontium ranelate on biochemical bone markers in elderly women and men with reduced BMD, T414
Effects of strontium ranelate therapy after long term bisphosphonate treatment, W477
Reduces the risk of vertebral fracture in young postmenopausal women with severe osteoporosis, T412

Subchondral bone

Alterations in collagen structure and mineral composition in a monkey model of OA, W089
 Differential accumulation of Pb and Zn in the tidemark of normal and osteoarthritic human articular cartilage and, W271

Suppressor of cytokine signalling-2 (SOCS-2)

Expression, effects of pro-inflammatory cytokines in the growth plate, W093

Surface-enhanced Raman spectroscopy (SERS)

Nanoprobng osteocytic subcellular compartments by, W057

SWI

Chromatin remodeling complex, positive and negative regulation of osteoblast differentiation by, M030

T**T cells**

Activated, small molecule inducer of cell death inhibits disease progression in CIA models, M499
 IL-23-enhanced osteoclastogenesis is mediated by STAT3 and NF- κ B via upregulation of RANKL from, T078
 Properties, effects of IL-12 related cytokines on osteoclast formation and, T076
 Stimulated from patients with AS, increased expression of RANKL in, W446

T-lymphocytes

Amplify the anabolic action of intermittent PTH treatment by regulating osteoclast formation, 1298

2T3

Osteoblastic cells, FFSS and PE₂ activates β -catenin signaling in, W053

Tartrate-resistant acid phosphatase (TRAP)

Negative regulator of osteoblast differentiation, T004

TCF

Signals in U2OS osteoblast-like cells, mutations in LRP5 β -propeller 1 block SOST-mediated inhibition of, 1048

Tctex-1

Rab3D recruits the dynein complex to secretory vesicles in osteoclasts through direct interaction with, 1293

Tea, green polyphenols (GTP)

Protective role of GTP in bone microarchitecture, W313

Tea, instant

Skeletal fluorosis from instant tea, W425

Tec

Tec tyrosine kinases are essential for osteoclast differentiation, 1289

Teriparatide (TPTD)

Adherence and persistence with TPTD therapy in commercial insurance plans and managed medicare, W380
 Administration following antiresorptive therapy (BBB-Study), M419, S419
 BMD response to TPTD in treatment naïve patients versus patients previously treated with a bisphosphonate, T367
 Bone apposition in patients on TPTD treatment is preferably directed to skeletal regions of local structural weakness, 1267
 Bone turnover markers demonstrate greater earlier responsiveness to TPTD following treatment with Ris compared with ALN, 1092

Changes in 25-hydroxy- and 1,25-dihydroxyvitamin D during treatment with TPTD, M424

In clinical practice, T427

Early adjuvant therapy with TPTD after major orthopaedic surgery of complicated fractures of long bones in postmenopausal women, M422

Effects of 2 year TPTD treatment on 3-D femoral neck bone distribution, geometry and bone strength, 1269

Effects of two years of TPTD treatment on bone strength assessed by HRCT based finite element analysis of human vertebrae in vivo, T368

Efficacy of adding TPTD versus switching to TPTD in postmenopausal women with osteoporosis previously treated with RLX or ALN, M423, O423, S423

Improvement of the persistence with TPTD in postmenopausal osteoporosis, WG36, M441

Improves bone microarchitecture in postmenopausal women previously treated with ALN, 1095

Monitoring BMD during the course of TPTD therapy in a community setting, T375

Persistence with TPTD therapy among participants in the DANCE trial, W384

Rapid and robust biochemical response to TPTD therapy for osteoporosis, T366

Reduces bone microdamage accumulation in postmenopausal women previously treated with ALN, 1093

Skeletal effects of TPTD in GC-treated mice, W311

Speeds fracture healing and initiates healing of non-unions in humans, M242

Treatment following bisphosphonate-resistant osteoporosis, T372

Treatment in osteoporotic patients treated with GC for chronic inflammatory/autoimmune rheumatic diseases, T370

Unusual osteoclast morphology in TPTD, 1096

Testin

As a novel binding partner of the CaR, M225

Testosterone

Cortical bone is positively associated with, and negatively with fibrinogen, M194

Low total and bioavailable testosterone does not play a role in renal bone disease in men on hemodialysis, M491

Presence of symptoms in men with low testosterone levels improves prediction of low BMD, M337

Serum testosterone in elderly men measured by liquid chromatography-tandem mass spectrometry and RIA, T191

Therapy increases vertebral and hip strength via complex changes in bone mass and structure, T476

Tet

Inducible expression systems for bone tissue engineering, in vitro characterization of bidirectional, W108

Tetracyclines

Dox and Mino effectively inhibit osteoclast differentiation and function, M106

TFIIA

Synergistically activates osteoblast-specific osteocalcin gene expression, M037

TG interacting factor (TGIF)

Null mutation in, low bone mass with, 1286

TGF. See *Transforming growth factor*

TGF β inducible early gene-1 (TIEG)

As a novel mediator of Runx2 expression and activity in osteoblasts, 1144

Directly binds to and represses the OPG promoter in osteoblasts, resulting in decreased support of osteoclast differentiation, W028

Increased expression of anti-adhesive PODXL delays osteoclast formation and reduces osteoclast size, M070

Suppresses osteoblast cell proliferation through modulation of the TGF β /Smad signaling pathway and repression of E2F1 gene expression, M035

TGF β receptor interacting protein (TRIP-1)

An important co-regulator of bone formation in skeletal remodeling, 1252

Thalassemia

Evaluation of bone microarchitecture with HR-pQCT in patients with thalassemia, W238

Thiazide

Comparison of the effects of thiazide diuretics and ACE inhibitors on fracture risk, M366, S366

6-Thioguanine

Acts on Gli2 to decrease PTHrP expression and osteolysis, M294

Threonine 137

Is an important determinant of sodium-phosphate co-transport in human NaPi-IIc, 1264

Thyroid hormone

Induced terminal differentiation of growth plate chondrocytes involves IGF-1 modulation of canonical Wnt signaling, M118, S118

Thyroid stimulating hormone (TSH)

Associations of TSH receptor gene polymorphisms with BMD in postmenopausal women, T225

Is both anti-resorptive and anabolic in vivo, 1153

Ti6Al4V alloy

MSC from human adipose tissue and bone marrow, osteogenic differentiation and interaction with, T053

Tibia

Continuous infusion of IGF-1 into the epiphysis of, M188

Sex-specific bone surface changes during adolescent growth, pQCT analysis of, M527

Tibial insertion

After rupture, cell death and cell proliferation of cartilage layer in human ACL, W096

Tissue engineering

Cell cooperation between HOP cells and HUVEC in, M041, S041

Human fetal bone cells for, T041

Use of statins to enhance bone mineralization and formation in 2D and 3D constructs, T003

In vitro characterization of bidirectional Tet-inducible expression systems for, W108

Tissue inhibitor of metalloproteinase 1 (TIMP-1)

Inhibitor of metalloproteinases TIMP-1 rescues the strong bone loss induced by Runx2 overexpression, M162

Titanium (Ti)

Implantation in rat maxillae, bone remodeling after achievement of osseointegration by, T127

Improving bone bonding ability of, by hydrothermal treatment with CaCl₂, W011

Osteoblast response to microtopography is dependent on integrin α -2, W002

TNF. See *Tumor necrosis factor*

TNF-like weak inducer of apoptosis (TWEAK)

As regulator of osteoblast function, M009

TNF-mediated arthritis. See *Arthritis, TNF-mediated***TNF-stimulated gene-6 (TSG-6)**

As a new regulator of bone remodeling, T092

TNF α converting enzyme (TACE)

Up-regulation in monocytes ameliorates their deflected differentiation into osteoclasts and dendritic cells in myeloma, M302

Toll-like receptor (TLR)

Activation, rheumatoid synovial fibroblasts promote osteoclastogenic activity by activating RANKL via, W435

Suppression of innate immunity, intracrine synthesis and action of 1,25-dihydroxyvitamin D rescues, 1028

In vivo activation modulates osteoclastogenesis, M081

Tooth development

Role of TROY in, M176, S176

Tooth roots

Resorption, dentine organic matrix down-regulate osteoclastic activity in, T095

Resorption, mechanical stress-induced, M-CSF receptor c-fms antibody inhibits, M107

Toremifene

Preserves bone architecture and strength in aged ORX rat, M406

Trabecular bone

Age-related changes in vertebral trabecular architecture in female macaques, T459

Androgens act directly via the AR in mineralizing osteoblasts to maintain, 1217

Ex vivo model of stress shielding and osteocyte viability in, W055

Growth, targeted overexpression of PTH2R in chondrocytes impairs cartilage differentiation and, W139

Increased age and a rod-like trabecular architecture are independently associated with accumulation of microdamage in human vertebral trabecular bone, T461

Marked reduction in mass and density, transgenic overexpression of PTP-oc in cells of osteoclastic lineage led to, M112, O112, S112

Mass evaluation as related to cortical mass in the human leg, W237

Microarchitecture assessed by micro-MRI in postmenopausal women with osteoporosis on therapy, W239

Microstructure assessments of the distal radius using a compact MRI, W241

Radiographic analysis of trabecular bone structure and bone geometry in the prediction of hip fracture load, W454

Regional variations in three-dimensional microstructural properties of proximal femoral trabeculae with aging, M503

Structure in men of African heritage, T353

Three-dimensional in vivo trabecular microstructure analysis of spine, calcaneus, and femoral head/neck/trochanter in Japanese postmenopausal women, T465

TRACP5b

New specific immunoassay for intact serum TRACP5b demonstrates increased sensitivity in osteoporosis, M319

Transcription factors

Necessary for chondrocyte hypertrophy, identification of novel, M164

Transcutaneous electrical nerve stimulation (TENS)

In the management of osteoporosis-related pain, WG33, T421

Transferrin receptor 1 (TfR1)

Iron uptake promotes osteoclast differentiation and function, M097

Transforming growth factor β (TGF β)

Calcitriol inhibits BMSC differentiation into osteoblasts in a manner cooperative with but independent of, T069

Drives expression of osteogenic molecules in bone metastatic breast cancer cells, M297

ESL-1 negatively regulates in the Golgi during skeletogenesis, M202, S202

Estrogen suppression of adipogenesis is mediated by, M024

Identification of a novel TGF β dependent-prometastatic signature mediating bone colonization, 1001

Inhibition suppresses myeloma cell growth via enhancement of osteoblast differentiation, T263

Large latent complex produced by hypertrophic chondrocytes, non-covalent interaction of MMP-13 and LTBP1 in, M128

Modulation of the signaling pathway, TIEG suppresses osteoblast cell proliferation through, M035

Signaling, Arkadia represses skeletal muscle differentiation through enhancement of, M206

Signaling, Twist1 stage-specifically regulates chondrocyte differentiation downstream of, M129

Spatial and temporal localization of components of signaling pathways in the postnatal LVGP, M125

Stimulates new bone formation in neonatal calvariae via suppression of DKK1, M197

Superfamily, new insights into the determination of Smads signaling by, M199

Suppresses POEM expression in osteoblasts, M201

Type III receptor regulates BMP signaling in differentiating osteoblasts in vitro and in vivo, W114

Transforming growth factor β 1 (TGF β 1)

Crosstalk with CTGF in MSC condensation, M158

And FGF2 have opposite effects on the mural cell phenotype of CD146⁺ BMSCs, M178

Induces migration of MSCs in coupling bone resorption and formation, 1072

Transgenic mice

DC-STAMP, cell-cell fusion of osteoclasts is stimulated in, 1102

Expression of *OCZF* directed by the CatK promoter affects bone mass and osteoclast formation in, M099, O099, S099

hCol1a2 nuclear targeting sequence together with human Runx2 enhancer elements drives robust expression in, 1288

Transient receptor potential (TRP)

Affects bone remodeling by regulating Ca signaling required for osteoclast activity, 1101

Channels are both present and functional in human osteoblast-like cells, T022

RANKL-induced expression is involved in osteoclastogenesis via Ca signaling activation, T103

Translationally controlled tumor protein (TCTP)

As a nuclear matrix protein in osteoblasts, identification of, M143

TRAP5b

Profiles in children with chronic kidney disease, T492

Traumatized muscle (tmMPC)

Progenitor cells have characteristic similarities to bmMSCs, W039

 β Trep1

Ubiquitin complex regulates Ihh-promoted osteoblast differentiation through Gli2 ubiquitination, T055

Triggering receptor expressed on myeloid cells 2 (TREM2)

Pathway is involved in osteoclastogenesis induced by NRTIs in AIDS, W074

Tripeptides, bioactive. See also *Ile-Pro-Pro; Leu-Lys-Pro; Val-Pro-Pro*

Enhance osteoblast function in vitro, W038

Tropomyosin-2/3 (Tm-2/3)

Regulate the intracellular scaffold of osteoclasts, M074

TROY

Role in tooth development, M176, S176

Trps1

Transcription factor regulates chondrocyte hypertrophy and perichondrial mineralization through repression of Runx2, 1184

TRPV4/6

Osmosensing receptor TRPV4 mediates cancer-induced bone pain, 1002

Role in 1,25(OH)₂D₃- and PTH-stimulated Ca uptake in intestinal epithelial cells, M258

Studies using nullmutant mice reveal active intestinal Ca transport in the absence of calbindin-D_{9k} or TRPV6, 1026

Tumor-induced hypophosphatemic osteomalacia (TIO). See *Osteomalacia, tumor-induced***Tumor invasion**

Chondrostatin as a new inhibitor of, T259

Tumor necrosis factor (TNF)

Identification of Prx1, MHOx, as a regulator of Osx expression and mediator of, 1143

Tumor necrosis factor α (TNF α)

Antagonist in murine bone resorption model, use of nanogels as a drug delivery system for, M101

Anti-TNF α antibody, treatment with recovers osteoclast maturation deviated from bone remodeling cycle in RA joint destruction, W439

CCL3-5/CCR5 cascade mediates RANKL⁺ cells migration in inflammatory bone resorption, M181

Dependent redox signals upregulate Mx2 gene transcription via stress activated protein kinases in arterial myofibroblasts, T165

Endogenous in osteoclast precursor cells promotes osteoclastogenesis via c-Fos and NFATc1 activation, T077

Estrogens attenuate production in osteoblastic cells by decreasing oxidative stress and its effects on NF- κ B activation, T186

Induced osteoclastogenesis, IVVY⁵³⁵⁻⁵³⁸ plays an essential role in, M084, S084

Induced osteoclastogenesis through precursor cell cycle regulation, NF- κ B2 limits, 1148

Novel responsive C/EBP site regulates cartilage *Cd-rap* expression, M132

Production coupled with HMGs are essential for osteoclastogenesis, T071

Role of cell death and osteogenic activity in injury-induced calcification from, W091
 Shedding enzyme, identification in macrophages, M186
 Stimulated *Msx2* expression in C2C12 cells, M020
 Upregulates aortic BMP2-*Msx2*-Wnt signaling in diabetic LDLR-/- mice, M185, O185, S185

Tumor necrosis factor receptor 1/2 (TNFR1/2)

Differentially regulate inflammatory bone resorption induced by LPS in vivo, M110, S110

Tumoral calcinosis. See *Calcinosis, tumoral*

Tumorigenesis

Mediation of musculoskeletal tumor cells by an IFI16 protein, T265

Turmeric

Extracts for postmenopausal osteoporosis treatment, W349

TWIST

Interactions with NF- κ B, human breast stem cell transformation and invasiveness is mediated upregulation of IL-8 by, T242

Twist1

Stage-specifically regulates chondrocyte differentiation downstream of TGF β and Wnt signaling, M129

Txnip

Deficient HcB/19 mice have decreased BMD and femoral strength, W465

Tyrosine kinases. See also *Protein tyrosine kinase*

Tec, essential for osteoclast differentiation, 1289

U

U2OS. See also Human osteosarcoma cells

Mutations in LRP5 β -propeller 1 block SOST-mediated inhibition of the LRP5-Wnt-TCF signals in, 1048

Ubc9

Promotes stability of Smad4 and regulates BMP signaling pathway in osteoblastic Saos-2 cells, T065

Ubiquitin

β Trcp1 complex regulates *Ihh*-promoted osteoblast differentiation through Gli2 ubiquitination, T055

UDP glucuronosyltransferase (UGT) 2B7

H²⁶⁸Y polymorphism is associated with serum sex steroid levels and cortical bone size in young adult men, T199

Ultrasound

Bone age measurements by ultrasound are equivalent to radiological assessments, T518
 Induces HIF-1 activation and iNOS expression through integrin/ILK/Akt pathway, T511
 New through-transmission approach for ultrasonic assessment of the radius, T301
 Respiratory function is associated with bone ultrasound measures and hip fracture, M360, O360, S360

Ultrasound, broadband attenuation (BUA)

Calcaneal BUA and risk factors for osteoporotic fractures in postmenopausal South Asian and Caucasian women, T302
 Improved accuracy of BUA measurement using phase insensitive detection, T305

Ultrasound, quantitative (QUS)

Canadian normative data for sunlight omniscense QUS, T303
 Newly developed QUS scanner for the proximal femur, T297

Precision study of QUS and DXA in Korean women, T306

Predicts incident vertebral and hip fractures at least as strongly as DXA, 1075

Ultraviolet radiation. See *Radiation, ultraviolet*

Uremic bone disease

Novel central mechanism in uremic bone disease, 1263

3/5-UTR

Binding proteins, regulation of RUNX2 translation by, M026

V

Vacuolar H⁺-ATPase (V-ATPase)

Actin binding activity in the B subunit is required for sorting, M092

CK-B involves the bone resorptive activity of osteoclast activity by regulating, M083

Cytoplasmic terminus of accessory subunit Ac45 is required for proper interaction with V0 domain subunits and efficient osteoclastic bone resorption, M104

Diphyllin abrogates acidification of the osteoclastic resorption lacunae and bone resorption, T093

Domain subunits and efficient osteoclastic bone resorption, cCytoplasmic terminus of a V-ATPase accessory subunit Ac45 is required for proper interaction with, M104

Val.Pro-Pro (VPP)

Enhance osteoblast function in vitro, W038

Vascular calcification. See *Calcification, vascular*

Vascular endothelial growth factor (VEGF)

Effects of BHH9 on expression and their receptors during osteoblast differentiation, W042

Vascularization

Perl modulates FGF and VEGF signaling and is essential in the development of the cartilage growth plate, 1064

Vasculogenesis

Acceleration of fracture healing via enhanced, through SCF/cKit pathway, T013

Veganism

Bone health of vegans, T300

VEGF

RANKL stimulates osteoclasts to release and enhance osteoclastic bone resorption through an autocrine mechanism, 1100

Signaling, Perl modulates and is essential for vascularization in the development of the cartilage growth plate, 1064

Vertebral fractures

Assessment of vertebral fracture threshold and ALN therapeutic effects by a QCT-based nonlinear FEM in postmenopausal women, W453

Clinical risk factors for incident vertebral fractures, 1077

Detection of prevalent vertebral fractures using a combination of physical examination maneuvers, W285

Health-related quality of life 7 years after hip or vertebral fractures, W391

Identifying clinical vertebral fractures using administrative claims data, M354

Impact of incident vertebral fractures on health-related quality of life in postmenopausal women, M359

Improving trunk strength and endurance in older women with vertebral fractures, WG27, W398

Long-term risk factors for incident vertebral fractures in healthy older women after 15 years of follow-up, 1271

Low levels of 25-hydroxyvitamin D associated with moderate/severe vertebral fractures, T326

Morphometric vertebral fracture status and WHO predictors of fracture risk, M371, S371

No ethnic differences in vertebral fractures were found between Caucasians, Mestizos and other ethnic background in the Latin-American Vertebral Osteoporosis Study (LAVOS), M380

Physical impact of morphometric vertebral fractures in me, W289

Prevalence of asymptomatic vertebral fractures in postmenopausal women with osteoporosis in Buenos Aires, T327

Proportion of clinical vertebral and nonvertebral fractures among women in a managed care population, T408

Significant reduction of vertebral fractures, ROPE versus No-ROPE, with or without pharmacotherapy, WG25

Vertebral compression fractures in patients with poor bone quality, T419

Vertebral fracture lines are not smooth, but mixtures of multiple Schmorl's nodes and endplate perforations, M353, S353

Vertebral shape

Automated assessment of vertebral shape by statistical shape modelling on lateral radiographs, W227

MRI-based measurement of vertebral shape in Japanese women, T292

Vertebral stenosis

Life quality in patients with surgically treated vertebral stenosis and the relation with bone quality, W396

Vertebroplasty

Effect of filler materials on viability and gene expression of mouse and human nucleus pulposus cells, M138

Vesicular glutamate transporter (VGLUT)

Knockout mice develop osteopenia due to an increase in osteoclastic bone resorption, T085

Vimentin

Negatively regulates osteoblast differentiation by inhibiting the transactivation activity of Atf4, T027

Vinculin

Involvement in chondrogenic differentiation in ATDC5 cells, gene-trap mutagenesis revealed, M137

Vitamin A

Deficiency delays healing process after cortical bone and bone marrow injury, W004
 Physical closure from chronic Vitamin A intoxication, W430

Vitamin D

Absence of toxicity despite high dietary Vitamin D and Ca intake in non-human primates, T358
 Active, possible direct regulatory role increased by ultraviolet B on FGF-23, W126

Association of Vitamin D status with BMD considering seasonal changes of Vitamin D, M322

Automated measurement of 1,25(OH)₂D on the LIAISON[®] Analyzer, W211

Barrier site metabolism of, 1029

CaSR dampens the calcemic response to exogenous 1,25-(OH)₂ Vitamin D in vivo independent of PTH, M224

Combination with BADGE potentiates their pharmacological inhibition of PPAR γ and increases osteogenic differentiation of adipocyte precursors, W155

Deficiency, a common occurrence in both high and low energy fractures, W468

Deficiency in a central Italian town normal population (MIMOSA-G project), M236

Deficiency in oncologic patients, W197

Deficiency, low BMD, and acculturation in Hispanic men, M338

Deficient phenotype of 1 α -hydroxylase gene knockout mice by transplantation of wild-type NA-BM-MSC, partial rescue of, T058

Effects of UV-B light on serum levels, M450

Establishment of vascular calcification model using high dose of, T431

Evidence for plain Vitamin D and active D-hormone analogs for prevention of falls and fractures, T442

Global Vitamin D levels in relation to age, gender, ethnicity, and latitude, W160

Heritability of serum 25-hydroxyvitamin D suggests genetic factors contribute to endogenous Vitamin D production, W184

Inadequacy, bone mineralization and, 1300

Incidence of osteoporotic fractures and Vitamin D status in hip-fracture patients, T350

Insufficiency in the adult, low-energy fracture population, T443

Insufficiency is associated with lower bone density in African-American men, M370

Measurement of 25OH Vitamin D₂ by the LIAISON[®] 25 OH Vitamin D TOTAL assay, W216

Nothing works without Ca and, T393

Patient and physician attitudes toward Vitamin D in osteoporosis treatment, WG34, T447

Postnatal Vitamin D supplementation normalized neonatal bone and lean mass following maternal dietary Vitamin D deficiency, W428

Postpartum insufficiency and secondary hyperparathyroidism in healthy Danish women, W151

Prevalence of Vitamin D and Ca supplementation following low impact hip fracture, T440

Prevalence of Vitamin D deficiency in women age 45 and older in a small Michigan community and the effect of Vitamin D supplementation on myalgia, T441

Prevalence of Vitamin D insufficiency in patients with breast cancer, M292

Severe depletion in Arab-American women living in Dearborn, MI, USA, W423

Skeletal and Vitamin D status in two indigenous North American populations, W246

Status and bone health in adolescents, W269

Status and infection frequency in diabetic patients, W153

Status, bone mass, and bone metabolism in postmenopausal Japanese women, T439

Status in postmenopausal Japanese-American women living in Hawaii, T315

Status/insufficiency may predict physical performance in a group of osteopenic/osteoporotic women, T271

Status of apparently healthy schoolgirls from two different socioeconomic strata in Delhi, T521

Status, seasonal skin color variations and the impact on, M263

Supplementation and 25OHD levels in long-term care residents, M413

Synthesis, personal ultraviolet exposure and, M261

Vitamin D binding protein (DBP)
Internalization by monocytes, M253, S253

Vitamin D receptor (VDR)
CAL and its analog successfully elongate survival period and improve the skeletal growth via independent pathway of, W157

Changes in coregulator recruitment result in 1,25(OH)₂D₃ hypersensitivity in MVNP expressing cells, W152

Co-stimulation of 1,25-(OH)₂D₃ and BMP-2 enhances the expression in osteoblasts, W162

Deficiency aggravates TNF-mediated arthritis, W443

Expression in multiple tissues in adult and developing *Danio rerio* (zebrafish), M254

Gene polymorphisms modulate the musculo-skeletal response to Vitamin D supplementation in healthy girls, 1194

HH signaling and epidermal carcinogenesis, W158

Histone H3 lysine 9 methyltransferase is a transcriptional coactivator for, 1027

Identification of osteoblast-specific co-regulator complex for, W022

Lack of major survival benefit of VDR gene polymorphisms, M283

Molecular analysis of two novel mutations in the corepressor *hr* and expression of rHr in *E. coli*, M259, S259

Novel nutritionally-derived ligand with implications for colon cancer chemoprevention and bone health, M255, S255

Nuclear interactions are ligand independent, W148

Overexpression of human VDR in the intestine rescues the hypocalcaemia-related phenotype of VDR knockout mice, 1025

Targeted inactivation by caspase-3, M265, S265

Transgenic expression in the proximal small intestine of VDR-null mice improves the utilization of Ca- and lactose-rich (rescue) diet in young mice, W154

Vitamin D₂. See *Ergocalciferol*

Vitamin D₃. See *Cholecalciferol*

Vitamin E

High dose Vitamin E prevents the formation atherosclerotic lesions but does not reverse loss of bone due to orchidectomy, T410

Vitamin K

Supplementation in postmenopausal women with osteopenia, M399, S399

Vitamin K₁. See *Phylloquinone*

Vitamin K₂. See *Menaquinone-4*

Vitamin K₃. See *Menadione*

W

Walcott-Rallison Syndrome. See *PERK*

Wdr5

In chicken limb bud during embryogenesis, using RCAN to deliver short hairpin siRNA to silence gene expression of, T141

Essential for osteoblast differentiation, W032

Weight gain/loss

Influence of prior and current weight change on forearm bone loss in menopausal women, T338

Postmenopausal osteoporosis and, W386

Wiscott-Aldrich Syndrome protein (WASP)

Disruption of signaling complex formation leads to defects in sealing ring formation and bone resorption in osteoclasts, M113

Wnt

Absence of sFRP1 accelerates fracture healing, 1258

Activation of the non-canonical pathway during hMSC osteogenesis, T048

BMP signaling in osteoblasts negatively regulates canonical signaling to reduce bone mass during embryonic bone development, M270, S270

Canonical signaling, thyroid hormone-induced terminal differentiation of growth plate chondrocytes involves IGF-1 modulation of, M118, S118

ENC1 is expressed in chondrocytic and osteoblastic cells, T056

GC enhances the expression of sFRP3 in cultured osteoblasts, T176

GC stimulate expression in mature osteoblasts, T062

Identification of a novel β -catenin response element in the OPG gene promoter and its regulation with BMP-2 signaling, M031, S031

Inhibition of signaling by Osx, 1249

Lineage dependent non-canonical signal transduction by bone cells, evidence for, 1139

mTOR signaling, a novel molecular mechanism underlying anabolic effects on osteogenesis, 1108

Signaling, greater sensitivity of osteocytes to shear stress as compared to osteoblasts, W052

Signaling in osteoblastic cells, osteoclasts secrete an activity promoting bone formation and canonical, T005

Signaling is compromised in ER-/- mouse tibia, mechanical loading induced, M036, S036

Signaling on Krox20 and mineral deposition in osteoblast cultures, opposing effects of, T026

Signaling, oxidative stress suppresses osteoblastogenesis by antagonizing, M174

Signaling, Twist1 stage-specifically regulates chondrocyte differentiation downstream of, M129

Signals in U2OS osteoblast-like cells, mutations in LRP5 β -propeller 1 block SOST-mediated inhibition of, 1048

Wnt inhibitory factor 1 (WIF-1)

Differential effects on osteoblastic differentiation of mouse pluripotent mesenchymal cell line, M044

Wnt3A

Induced signaling through dual-specificity phosphatases, modulation of, T042

Signaling, role in maturation of osteoblasts, T166

Wnt5A

Enhances RANKL-induced osteoclastogenesis, 1149

Signals through Ror2 to promote osteoblastogenesis, M045, S045

Women's Health Initiative (WHI)

Associations between body composition and hip geometry in postmenopausal women in the WHI, M377, S377

Comparisons of load normalized section modulus among women with and without fracture history in the WHI, M348

Ethnic variations in hip geometry among women at baseline from the WHI, 1052

Wrch1

Role in cell adhesion and osteolysis, Rho GTPase signaling pathways in osteoclasts, M073, S073

Wrist fracture

Functional decline after incident wrist fracture, 1273

X

X-linked hypophosphatemic rickets (XLH). See *Rickets*

X-ray absorptiometry, dual (DXA)

Association between DXA-assessed muscle-bone proportionality and fractures in pre- and postmenopausal women, W234

Body composition measurements with lunar iDXA, T281

Comparison of femur structure measurements derived from DXA and QCT, W232

Comparison of iDXA measurements of mid-body fat mass and tape-measured circumferences in overweight women, W273

Correcting DXA pediatric BMD measurements to account for fat inhomogeneity, W514

Poor bone growth in children with CP is underestimated by dual-energy x-ray absorptiometry, T517

Ultrasound and dual-energy x-ray absorptiometry comparisons at the distal radius, T299

Use of DXA-based structural engineering models of the proximal femur to predict hip fracture, M332, S332

Utility of lumbar spine DXA scanning in women undergoing asymptomatic osteoporosis screening, M323, S323

In vivo and in vitro comparison of DXA scanners, T272

X-ray absorptiometry, volumetric dual (VXA)

Hip geometry and density parameters derived from VXA correlate strongly with 3D QCT, W224

XLs

Ability to mimic Gsln mediating PTH signaling in vivo, M218

XXY mice

Have an osteoporotic phenotype, 1018

Y**Young's modulus**

Variation of the Young's modulus of single trabeculae in a sheep femur, W469

Z**ZETOS system**

Calibration of the ZETOS bone loading system, T509

Zfp521

Novel inhibitor of Runx2 activity with opposite effects on osteoblasts and bone formation in vitro and in vivo, 1250

Zinc finger protein 64 (Zfp64)

As a downstream target of Runx2 and regulates myogenic and osteogenic differentiation as a coactivator of Notch1, T035

Zinc finger protein 521 (Zfp521)

Regulates chondrocyte differentiation downstream of PTHrP, 1069

Zinc (Zn)

Differential accumulation in the tidemark of normal and osteoarthritic human articular cartilage and subchondral bone, W271

Zoledronate

Effects of intravenous zoledronate on bone turnover and BMD persist for at least 24 months, T376

Zoledronic acid (ZOL)

Effects of ZOL once-yearly on bone remodeling and structure in osteoporotic women are consistent across age, M434, S434

Efficacy and safety of ZOL in preventing fractures in men and women with prevalent hip fracture, 1055

Reduction of bone turnover markers with annual infusion of ZOL in postmenopausal osteoporosis, T385

Risk factors for serious adverse events of atrial fibrillation in the HORIZON-PFT trial of ZOL, 1056

In vitro effects of ZOL alone or in combination with radiation therapy on cells of the metastatic bone environment, M304